nature

INTERNATIONAL WEEKLY JOURNAL OF SCIENCE

Vol 311 No 5981 6-11 September 1984 £1.80 $4.50

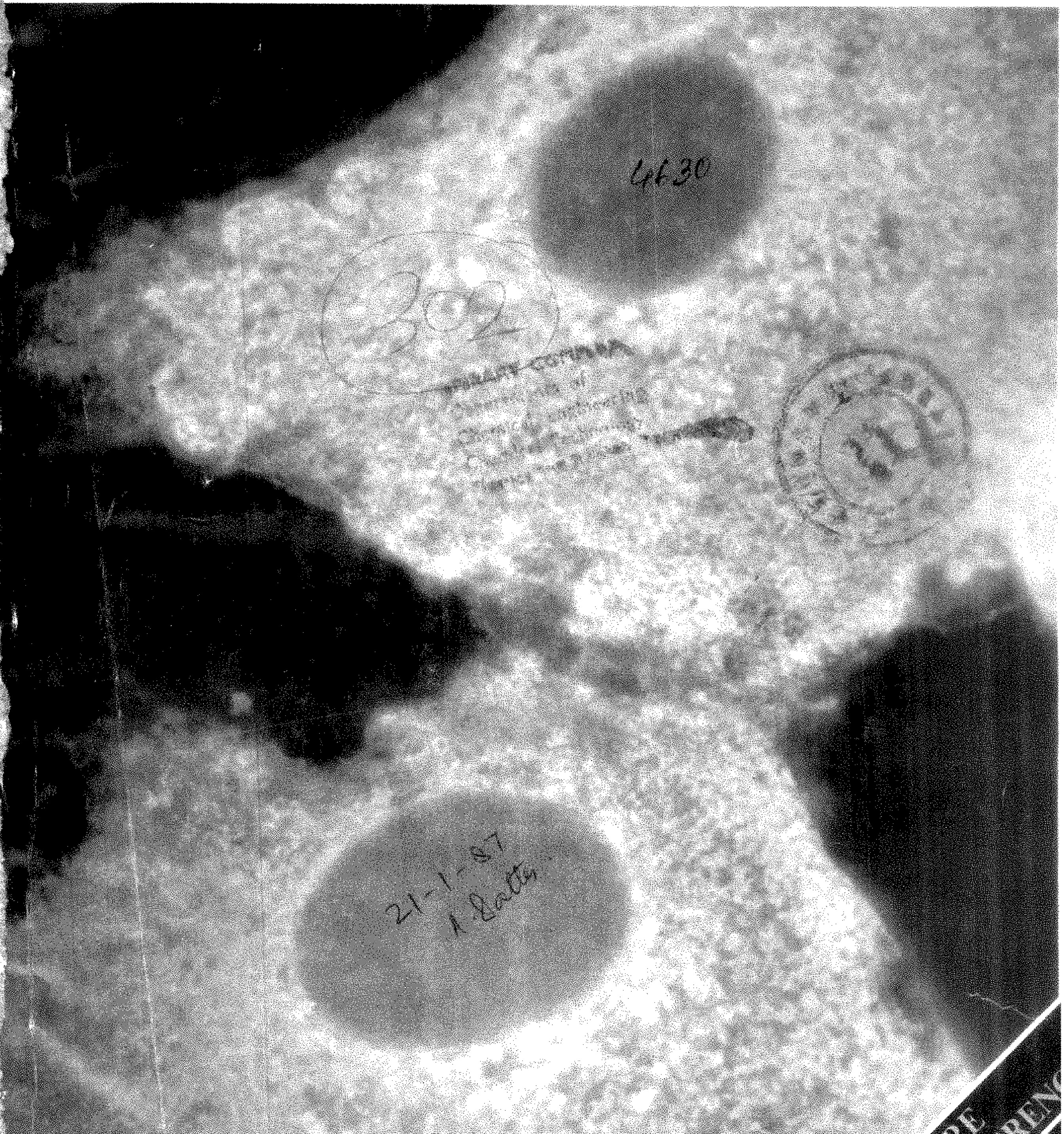

4430

302

21-1-87

HOW PROTEINS FIND THE NUCLEUS

NATURE
BOSTON CONFERENC
product review

Promega's Riboprobe System...
...Easier Then Ever To Use

erformance Guaranteed and erifiable

Ve provide a positive control template vhich is specifically constructed to en- ure that you get good transcription eaction performance.

his mixture of Riboprobe system plas- nid constructs simultaneously synthe- izes three discrete transcripts: 0.225 kb, .557 kb, and 1.386 kb. The labeled anscription products are shown in el A.

lso, under nonlimiting synthesis condi- ons the amount of RNA synthesized is o high that detection of transcripts is ossible without radioisotopes (gel B).

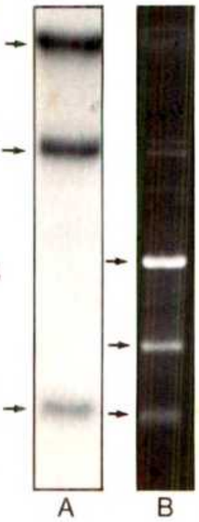

New Reaction Conditions

romega provides up-to-date information on the best onditions for transcription reactions and for the subse- uent use of the RNA products made. For example, we ecently determined that the addition of 5-20 mM NaCl ncreases transcription product synthesis as much as fold. A salt curve analysis of transcription on two ifferent templates is presented below.

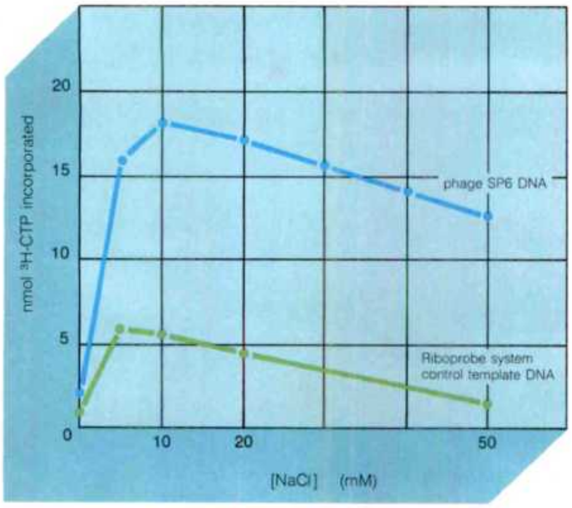

s we test and experiment with the Riboprobe system, ve are finding new applications and conditions for its ise all the time. Promega customers will receive all of is information as it becomes available.

Introducing Riboprobe™ *System II*

Minimizes Reaction Set Up Time

This product contains all the reagents (excluding radioisotopes) required for performing up to 50 efficient transcription reactions. The availability of these pretested and qualified reagents reduces your reaction set up time a great deal and helps assure consistent results:

- Riboprobe System RNA polymerase
- 20 μg pSP64 plasmid
- 20 μg pSP65 plasmid
- 10 μg Riboprobe system positive control transcription template
- RNasin® ribonuclease inhibitor
- lot qualified solutions of all 4 cold ribonucleotides
- transcription optimized 5X buffer
- 100mM DTT

Other Benefits Of Using Riboprobe™ *System II:*

Guaranteed performance
With the purchase of our *System II,* we provide all the test data obtained on the lot of reagents you recei You can quickly verify the system's effectiveness yourself.

Cost effectiveness
This system is very cost effective. When you add up the real cost for your lab to buy and test all the reagents involved, it is actually cheaper to buy our Riboprobe™ *System II.*

Proven protocols
With our system you will receive up-to-date, detailed protocols including:

- plasmid preparation procedures
- transcription reaction conditions
- blot hybridization techniques

Components also available separately
All components of the Riboprobe *System II* are available separately, as needed, including Riboprob system polymerase and RNasin® ribonuclease inhibitor.

Promega Biotec

Circle No.22 on Reader Service Card

f you have already received an informational packet on the Riboprobe system, but got it before July, 1984, ou can call us again to get a copy of the updated applications information and new product configura- ons described above.

Riboprobe™

Gene Analysis System

- ☐ **May make nick translation obsolete.**
- ☐ **Increases Northern/Southern blot sensitivity up to 10 fold.**
  (and/or reduces exposure times up to 10 fold)
- ☐ **Eliminates the need to isolate probes from gels.**
- ☐ **Increases *in situ* hybridization sensitivity.**
- ☐ **Eliminates the need to end label probes in many applications.**

Current research confirms that RNA can be used successfully for gene probing, providing greater sensitivity than can be achieved with similar DNA probes (see our technical information sheets for references). The **Riboprobe**™ gene analysis system offers a convenient vector/enzyme system for the preparation of microgram quantities of high specific activity single-stranded RNA's. These RNA's are suitable for use as probes, as RNA processing substrates, and for other applications where large amounts of hot specific RNA's or enhanced probing sensitivity is required.

The **Riboprobe** system consists of: **1)** highly purified, RNase-free bacteriophage SP6 RNA polymerase, **2)** the latest **Riboprobe** system SP6 vectors (pSP64, pSP65) as developed by Melton, Krieg, and Green, *et al.* (see technical information sheets for references), and **3)** a **Riboprobe** system RNA marker template for use as a positive control.

With the **Riboprobe** system, simply ligate your DNA into one of the **Riboprobe** system plasmids, prepare a recombinant plasmid by standard plasmid propagation and purification techniques, linearize the recombinant plasmid with the appropriate restriction enzyme, add the **Riboprobe** system polymerase with labelled ribonucleotides, and incubate the reaction.

The **Riboprobe** system does the rest. It is exceedingly efficient and, depending on conditions, can synthesize up to 10 μg of RNA from 1 μg of plasmid template. **The use of this RNA will improve or replace many important analytical procedures in molecular biology.**

Circle No.21 on Reader Service Card.

Promega Biotec

A complete Riboprobe system technical information packet is available, including:

- **—References**
- **—Applications data**
- **—Plasmid maps**
- **—Schematic protocols**
- **—Product specifications**
- **—Ordering information**

Promega Biotec
2800 S. Fish Hatchery Road
Madison, WI 53711 U.S.A.

Toll Free	800-356-9526
Telephone	608-274-4330
TWX	910-286-2738

Riboprobe, Promega, TOPO I, GammaPrep, and ○ are all trademarks of Promega Biotec, Madison, WI, U.S.A. RNasin and Packagene are trademarks registered in the U.S. Patent and Trademark office by Promega Biotec, Madison, WI, U.S.A.

4630

Routine Detection of Single Copy Genes with RNA Probes

Side by side comparison demonstrates superior performance.

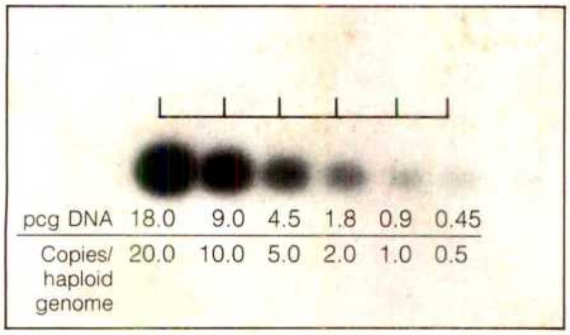

RNA Probe

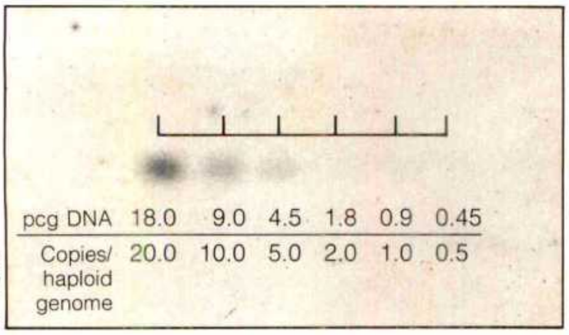

Nick Translated Probe

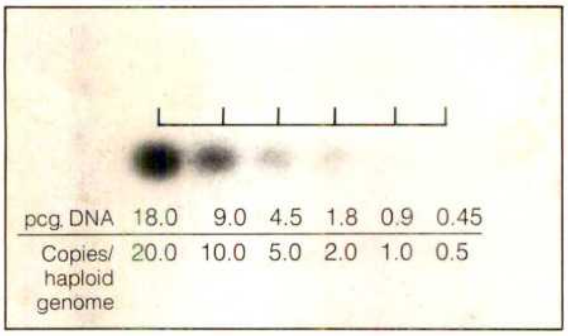

M-13 Probe

Riboprobe system synthesized RNA probes were directly compared with similarly labeled nick translated DNA probes and primer extended M-13 probes. Significant sensitivity increases (up to 10 fold in favor of the RNA probe) were observed in detection of relevant sequences.

Under comparable conditions, the Riboprobe system detected 0.45 picograms of the target sequence, the nick translated DNA probe shows 4.5 picograms and the M-13 probe 1.8 picograms. (Data provided by E. Schenborn and J. Mitchen, University of Wisconsin). Standardized for the number of gene copies detected, the Riboprobe system synthesized probe easily detects 0.5 copies/haploid genome, demonstrating its effectiveness for analyzing single copy genes.

In situ hybridizations: Results demonstrate high signal to noise ratios and efficient detection of target sequences.

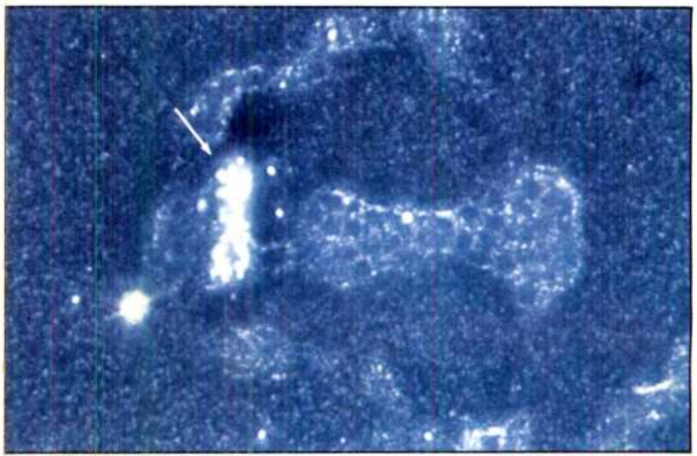

Sea Urchin tissue

Sea urchin plutei tissue sections were analyzed by *in situ* hybridization using an RNA probe specific for muscle actin message (Schott *et al.*, 1984). A high signal is detected in the few cells synthesizing the actin message (see arrow). The absence of noise over cells not expressing the gene demonstrates the specificity of the system (Data provided by L. Angerer, University of Rochester).

Sensitivity is increased at least eight fold when the detection capabilities of these single stranded RNA probes are compared with those of comparable double stranded probes. A detailed technical information sheet on *in situ* hybridization is available on request from Promega Biotec.

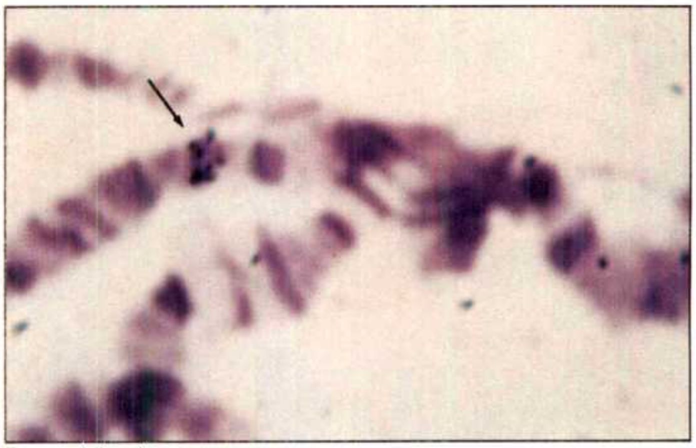

Drosophila chromosome

Drosophila salivary gland chromosomes were analyzed for the location of a cloned drosophila genomic DNA fragment. (Data provided by K. Loughney and B. Ganetzky, University of Wisconsin). Specific signals were detected after the short exposure time of 5-7 days (see arrow). The results indicate very high signal to noise ratios.

nature

NATURE VOL. 311 6 SEPTEMBER 1984

21-1-87 [illegible] 4630

COVER

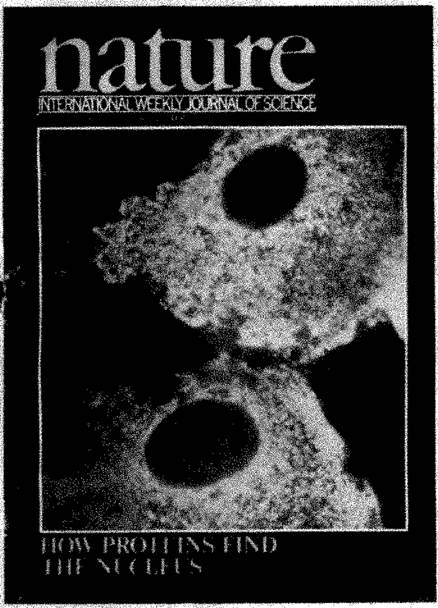
nature
INTERNATIONAL WEEKLY JOURNAL OF SCIENCE
HOW PROTEINS FIND THE NUCLEUS

An immunofluorescence micrograph demonstrating ge-T antigen in the cytoplasm of Vero cells. A point tion in the gene encoding this antigen causes the nally nuclear protein to be dispersed in the plasm (see page 33).

OPINION

oor show for aviation industry 1
Too brief encounter 2
Academic divisions

NEWS

Biotechnology 3
Industrial training
European high-energy physics 4
European dimension
Japanese astronomy 5
Open University cuts
pace shuttle 6
oviet space programme
roduct contamination 7
ench nuclear energy
ench universities

CORRESPONDENCE

ence in India/Red Sirius 8

NEWS AND VIEWS

olecular biology and cancer
John Maddox 9
Nitrate leaching from grassland
R E White 10
Galaxies in collision
M G Edmunds 10
Electron microscopy 50 years on
Colin J Humphreys 12
Recombinant vaccinia for prevention of hepatitis B
John Beale
The cupic map in theory and practice
Robert M May 13
Ozone increases in ground-level European air
S A Penkett 14
Novel helical conformation in a nylon
Edward Atkins 16
Glycine receptor protein the solution?
W Graham Richards

SCIENTIFIC CORRESPONDENCE

Mass extinctions and missing matter
R B Stothers 17
The case against impact extinctions
L M Van Valen
Did komatiitic lavas erode channels on Mars?
A K Baird & B C Clark 18
A question of chirality
N W Pirie

BOOK REVIEWS

302

Begotten or Made?
by O O'Donovan
John Habgood 85
Molecular Evolution and Organization of the Chromosome
by A Lima-de-Faria
J R S Fincham
Science and Civilisation in China, Volume 6 Part II: Agriculture
by F Bray
Charles Higham 86
Chondrules and Their Origins
E A King, ed.
Derek W G Sears 88
Amphibian Morphogenesis
by H Fox
Jonathan Slack

REVIEW ARTICLE

Origins of biomolecular handedness
S F Mason 19

ARTICLES

A general circulation model of water isotope cycles in the atmosphere
S Joussaume, R Sadourny & J Jouzel 24
lecular cloning of a new transforming gene from a chemically transformed human cell line
C S Cooper, M Park, D G Blair, M A Tainsky, K Huebner, C M Croce & G F Vande Woude 29
Sequence requirements for nuclear location of simian virus 40 large-T antigen
D Kalderon, W D Richardson, A F Markham & A E Smith 33

LETTERS TO NATURE

The boundary of the Solar System
R Smoluchowski & M Torbett 38
Emission of large hydrocarbons from frozen CH_4 by keV proton irradiation
A E de Vries, R Pedrys, R A Haring, A Haring & F W Saris 39
Diffuse reflectance pulse radiolysis of opaque samples
F Wilkinson, C J Willsher, P Warwick, E J Land & F A P Rushton 40
Measurements of hydrogen peroxide in polar samples
A Neftel, P Jacob & D Klockow 43
Age differing between polar ice and the air trapped in its bubbles
J Schwander & B Stauffer 45
Chronology of palaeoclimatic change at the end of the last glaciation
R B Stewart & V E Neall 47
Turbulent motions may control phytoplankton photosynthesis in the upper ocean
M R Lewis, E P W Horne, J J Cullen, N S Oakey & T Platt 49
Nitrate leaching from grassland
J C Ryden, P R Ball & E A Garwood 50
A pseudo α-helix from poly(α-isobutyl-L-aspartate), a nylon-3 derivative
J M Fernández-Santín, J Aymamí, A Rodríguez-Galán, S Muñoz-Guerra & J A Subirana 53
Replacement of oak forest with pine in the Himalaya affects the nitrogen cycle
J S Singh, Y S Rawat & O P Chaturvedi 54
Species variation and the mechanism of pressure–anaesthetic interactions
E B Smith, F Bowser-Riley, S Daniels, I T Dunbar, C B Harrison & W D M Paton 56

Contents continued overleaf

Nature® (ISSN 0028-0836) is published weekly on Thursday, except the last week in December, by Macmillan Journals Ltd and includes the Annual Index (mailed in February). Annual subscription for USA and Canada US $230 (for subscription prices elsewhere, see next page). USA and Canadian orders only to: *Nature*, Subscription Dept, PO Box 1018, Manasquan, New Jersey 08736, USA. All other orders to *Nature*, Brunel Road, Basingstoke, Hants RG21 2XS, UK. Second class postage paid at New York, NY 10010 and additional mailing offices. Authorization to photocopy material for internal or personal use, or the internal or personal use of specific clients, is granted by *Nature* to libraries and other users registered with the Copyright Clearance Center (CCC) Transactional Reporting Service, provided that the base fee of $1.00 per copy plus $0.10 per page is paid directly to CCC, 21 Congress Street, Salem, Massachusetts 01970, USA. The identification code for *Nature* is 0028-0836/84 $1.00 + $0.10. US Postmaster send form 3579 to: *Nature*, 15 East 26 Street, New York, NY 10010. Published in Japan by Macmillan Shuppan K.K., 5th Floor Eikow Building, 1-10-9 Hongo, Bunkyo-ku, Tokyo, Japan. © 1984 Macmillan Journals Ltd.

Leukotriene B_4 [^3H] assay reagents system

This exclusive system from Amersham comprises:
- [^3H] LTB_4 tracer
- High specificity antiserum*
- LTB_4 standard*
- Detailed assay protocol

*By arrangement with Wellcome Diagnostics

Also available from Amersham: assay systems for TxB_2, 6-Keto-$PGF_{1\alpha}$ and bicyclic PGE_2

For research use only

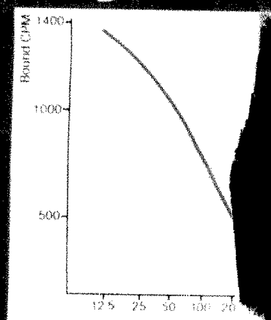

Amersham Corporation
2636 South Clearbrook Drive, Arlington Heights, IL 60005
(312) 364-7100 or (800) 323-9750 (Toll Free)

In Canada 505 Iroquois Shore Road, Oakville ONT L6H 2R3 (416) 842-2720/(800) 268-5061

Amersham

Amersham Australia PTY Ltd Sydney (2) 211 4399/4489 **Amersham Belgium SA/NV** Brussels (2) 538 9194 **Amersham Buchler GmbH & Co KG** Braunschweig, West Germany (05307) 8080
Amersham Canada Ltd Ontario (416) 842 2720 **Amersham Corporation** Arlington Heights USA (312) 364 7100 **Amersham Denmark ApS** Birkerød (02) 82 0222
Amersham France SA Paris (6) 928 8300 **Amersham Japan** Tokyo (3) 543 0777 **Amersham Nederland BV** Utrecht (30) 7308 31 **Amersham Sweden AB** Solna (8) 734 0800

Circle No.51 on Reader Service Card.

Index

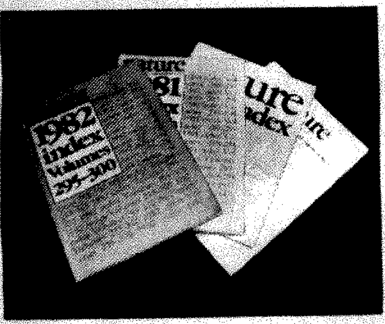

Comprehensive annual indexes of subject and author are available for all issues of **Nature** from 1971 to 1983.

Prices and address for orders are set out below.

Annual Subscription Prices

UK & Irish Republic		£98
USA & Canada		US$230
Australia & NZ	Airspeed	£150
Continental Europe	Airspeed	£120
India	Airspeed	£115
Japan	Airspeed	Y85000
Rest of World*	Surface	£120
Rest of World*	Airmail	£180

**(not USA, Canada, Europe & Japan)*

Orders (with remittance) to:

USA & Canada
Nature
Subscription Dept
PO Box 1018
Manasquan
NJ 08736
USA

UK & Rest of World
Nature
Circulation Dept
Brunel Road
Basingstoke
Hants RG21 2XS, UK
Tel: 0256 29242

(The addresses of Nature's editorial offices are shown facing the first editorial page)

Japanese subscription enquiries to:
Japan Publications Trading Company Ltd
2-1 Sarugaku-cho 1-chome
Chiyoda-ku, Tokyo, Japan
Tel: (03) 292 3755

Personal subscription rates
These are available in some countries to subscribers paying by personal cheque or credit card. Details from:

USA & Canada
Nature
15 East 26 Street
New York,
NY 10010, USA
el: (212) 689-5900

UK & Europe
Felicity Parker, Nature
Brunel Road
Basingstoke
Hants RG21 2XS, UK
Tel: 0256 29242

edit card orders only (in USA):
all toll-free: (800) 824-7888 (Operator 246)
in California: (800) 852-7777 (Operator 246)

Back issues
UK, £2.50; USA & Canada, US$6.00 (surface), US$9.00 (air); Rest of World, £3.00 (surface), £4.00 (air)

Binders
Single Binders: UK, £4.50; Rest of World, $10.00
Set(s) of 3 Binders; UK, £12.00; Rest of World, $25.00

Annual indexes (1971–1983)
UK, £5.00 each; Rest of World, $10.00

Nature First Issue Facsimile
UK, 75p; Rest of World (surface), $1.50; (air) $2.00

Nature in microform
For Information:
University Microfilms International, 300 North Zeeb Road, Ann Arbor, MI 48106, USA

Rules for neural development revealed by chimaeric sensory systems in crickets
W W Walthall & R K Murphey 57

Evidence for neurotensin as a non-adrenergic, non-cholinergic neurotransmitter in guinea pig ileum
M Goedert, J C Hunter & M Ninkovic 59

Adenosine mediates a slow hyperpolarizing synaptic potential in autonomic neurones
T Akasu, P Shinnick-Gallagher & J P Gallagher 62

Partial correction of murine hereditary growth disorder by germ-line incorporation of a new gene
R E Hammer, R D Palmiter & R L Brinster 65

Live recombinant vaccinia virus protects chimpanzees against hepatitis B
B Moss, G L Smith, J L Gerin & R H Purcell 67

Defect in the generation of light-chain diversity in bursectomized chickens
S Jalkanen, M Jalkanen, K Granfors & P Toivanen 69

Direct evidence for an integrated function of J chain and secretary component in epithelial transport of immunoglobulins
P Brandtzaeg & H Prydz 71

Immunoglobulin κ light-chain diversity in rabbit is based on the 3′ length heterogeneity of germ-line variable genes
O Heidmann & F Rougeon 74

Transcription of plant defence genes in response to UV light or fungal elicitor
J Chappell & K Hahlbrock 76

Inhibition of mRNA binding to ribosomes by localized activation of dsRNA-dependent protein kinase
A De Benedetti & C Baglioni 79

Activating protein factor binds *in vitro* to upstream control sequences in heat shock gene chromatin
C Wu 81

Corrigendum. . . page 84
Turbulence in an oceanic convective mixed layer
T J Shay & M C Greg

MISCELLANY

100 years ago 15
Product review: *Nature*'s Boston conference 89

NATURE CLASSIFIED

Professional appointments — Research posts — Studentships — Fellowships — Conferences — Courses — Seminars — Symposia: Back pages

Next week in *Nature*:

- Transposition between human X and Y chromosomes during evolution
- Chromatin structure of lysozyme gene
- Trypanosomal variable surface glycoproteins
- Messengers in the process of vision
- Primary structure and antigenic reactivity in proteins
- Cell-cell communication in amphibian embryo
- Bismuth in interplanetary dust
- Gravitation and galaxy formation
- Molecular hydrogen in merging galaxies
- Superparamagnetic iron in Orgueil meteorite
- Structural disruption in Himalayas and Hindu Kush
- Tree rings and climate

GUIDE TO AUTHORS

Authors should be aware of the diversity of *Nature*'s readership and should strive to be as widely understood as possible.

Review articles should be accessible to the whole readership. Most are commissioned, but unsolicited reviews are welcome (in which case prior consultation with the office is desirable).

Scientific articles are research reports whose conclusions are of general interest or which represent substantial advances of understanding. The text should not exceed 3,000 words and six displayed items (figures plus tables). The article should include an abstract of about 50 words.

Letters to *Nature* are ordinarily 1,000 words long with no more than four displayed items. The first paragraph (not exceeding 150 words) should say what the letter is about, why the study it reports was undertaken and what the conclusions are.

Matters arising are brief comments (up to 500 words) on articles and letters recently published in *Nature*. The originator of a Matters Arising contribution should initially send his manuscript to the author of the original paper and both parties should, wherever possible, agree on what is to be submitted.

Manuscripts may be submitted either to London or Washington (decisions being made only in London). Manuscripts should be typed (double spacing) on one side of the paper only. Three copies are required, each accompanied by copies of lettered artwork. No title should exceed 80 characters in length. Reference lists, figure legends, etc. should be on separate sheets, all of which should be numbered. Abbreviations, symbols, units, etc. should be identified on one copy of the manuscript at their first appearance.

References should appear sequentially indicated by superscripts in the text and should be abbreviated according to the *World List of Scientific Periodicals*, fourth edition (Butterworth 1963–65). The first and last page numbers of each reference should be cited. References to books should clearly indicate the publisher and the date and place of publication. Unpublished articles should not be formally referred to unless accepted or submitted for publication, but may be mentioned in the text.

Each piece of artwork should be clearly marked with the author's name and the figure number. Original artwork should be unlettered. Suggestions for cover illustrations are welcome. Original artwork (and one copy of the manuscript) will be returned when manuscripts cannot be published.

Requests for permission to reproduce material from Nature *should be accompanied by a self-addressed (and, in the case of the United Kingdom and United States, stamped) envelope.*

Close your eyes.

Imagine you're creating a weekly current awareness service for scientists and scholars—one that would alert you to just those articles you were interested in. You think to yourself, this is a good idea...but impossible.

Now open your eyes. Such a service is available right now. It's called ASCA®. ASCA is custom-designed ...for each individual...anywhere in the world...in any discipline. And your individualized ASCA reports can cost as little as $3.00 per week. Intrigued? Want more information? Fill out the coupon and mail it. You'll be glad you did.

Let ASCA Open Your Eyes.

☐ Send me more information about ASCA®.

Name / Title

Address

City State Country

Organization / Department

Zip Phone

ISI® Institute for Scientific Information®
Customer Services Department
3501 Market Street, Philadelphia, PA 19104 U.S.A.
Tel: (215) 386-0100 ext. 1371, Cable: SCINFO, Telex: 84-5305
European Office: 132 High Street, Uxbridge,
Middlesex UB8 1DP, United Kingdom
Tel: 44-895-70016, Telex: 933693 UKISI

21-3522
©1984 ISI

Circle No.10 on Reader Service Card.

Rp429

nature

21-1-87

NATURE VOL. 311 13 SEPTEMBER 1984

COVER

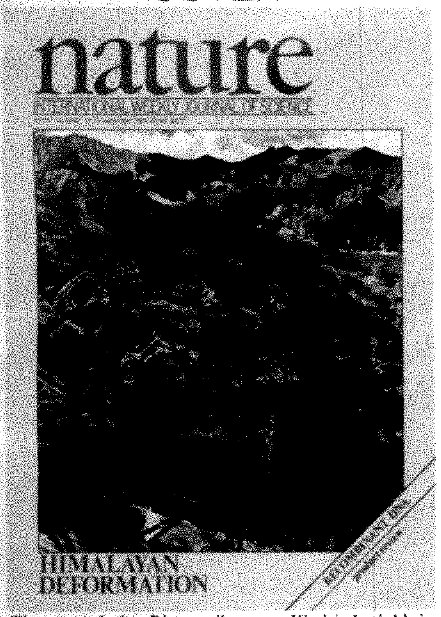

The upper Indus River valley near Khalsi, Ladakh in northwestern India. The dark rocks in the foreground are serpentinites and peridotites of the Indus suture zone. The continuing convergence of India with Eurasia has produced the Late Cenozoic deformation described in the article on page 114.

OPINION

New joint ventures in Europe 91
Election irrelevant 92

NEWS

Space shuttle 93
British aerospace
Acid rain 94
Laboratory animals 95
Bird books safe
Oceanography 96
European solar energy
BA gets under way
Science in India 97
Mongolia
Siberia 98
UK research
Defence department money on offer
US agricultural research 99
New US genetics centre goes west
Nature index of biotechnology stocks

CORRESPONDENCE

Fast food/Cancer at Sellafield/ Literature explosion 100

NEWS AND VIEWS

Brownian and quantum motion
John Maddox 101
Windscale effluent as a tracer for continental shelf circulation
J T F Zimmerman 102
Excision of introns in lariat form
Charles Weissmann 103
Cystic fibrosis — in search of the gene
Veronica van Heyningen 104
Cellulose synthesis — another brick in the wall
Keith Roberts 105
Sharing outside of pairing
R P Erickson & P N Goodfellow 106
Cell communication in early embryos
Jonathan Slack 107
Geological problems of north-east Africa
Robert Bowen 108

BOOK REVIEWS

The Environmental Crisis: A Handbook for all Friends of the Earth
D Wilson, ed. and
Crisis and Conservation: Conflict in the British Countryside
by C Pye-Smith and C Rose
Gordon Conway 181
Ascent to Orbit: The Technical Writings of Arthur C Clarke
by A C Clarke
David E H Jones 182
Interferons and Their Applications
P E Came and W A Carter, eds
Robert M Friedman
Materials Science of the Earth's Interior
I Sunagawa, ed.
Raymond Jeanloz 183
Animal Architecture and Building Behaviour
by M H Hansell
W C McGrew
The Primary Source: Tropical Forests and Our Future
by N Myers
Paul Richards 184

ARTICLES

Gravitational interactions of cosmic strings
C J Hogan & M J Rees 109
Sequential late Cenozoic structural disruption of the northern Himalayan foredeep
D W Burbank & R G H Reynolds 114
Occurrence of a transposition from the X-chromosome long arm to the Y-chromosome short arm during human evolution
D C Page, M E Harper, J Love & D Botstein 119
Correlation between segmental mobility and the location of antigenic determinants in proteins
E Westhof, D Altschuh, D Moras, A C Bloomer, A Mondragon, A Klug & M H V Van Regenmortel 123
Antibodies to gap-junctional protein selectively disrupt junctional communication in the early amphibian embryo
A E Warner, S C Guthrie & N B Gilula 127

LETTERS TO NATURE

Detection of molecular hydrogen in two merging galaxies
R D Joseph, G S Wright & R Wade 132
Detection of radiation from a heated and modulated equatorial electrojet current system
R J Lunnen, H S Lee, A J Ferraro, T W Collins & R F Woodman 134
Bismuth in interplanetary dust
I D R Mackinnon & F J M Rietmeijer 135
Occurrence of oxidated components in Qingzhen enstatite chrondite
E R Rambaldi, R M Housley & R S Rajan 138
Presence of a superparamagnetic component in the Orgueil meteorite
T J Wdowiak & D G Agresti 140
The ability of small molecules to form clathrate hydrates of structure II
D W Davidson, Y P Handa, C I Ratcliffe, J S Tse & B M Powell 142
Reflected turbidity currents on an Ordovician basin floor, Canadian Appalachians
R N Hiscott & K T Pickering 143
Sampling strategy for stable carbon isotope analysis of tree rings in pine
S W Leavitt & A Long 145
Correlation of marine and continental glacial and interglacial events, Arctic Ocean and Banks Island
D L Clark, J-S Vincent, G A Jones & W A Morris 147
Patterns of junctional communication in the early amphibian embryo
S C Guthrie 149
Transient expression of a surface antigen on a small subset of neurones during ring embryonic development
K J Kotrla & C S Goodman 151

Contents continued overleaf

Nature® (ISSN 0028-0836) is published weekly on Thursday, except the last week in December, by Macmillan Journals Ltd and includes the Annual Index (mailed in February). Annual subscription for USA and Canada US $230 (for subscription prices elsewhere, see next page). USA and Canadian orders only to: *Nature*, Subscription Dept, PO Box 1018, Manasquan, New Jersey 08736, USA. All other orders to *Nature*, Brunel Road, Basingstoke, Hants RG21 2XS, UK. Second class postage paid at New York, NY 10010 and additional mailing offices. Authorization to photocopy material for internal or personal use, or the internal or personal use of specific clients, is granted by *Nature* to libraries and other users registered with the Copyright Clearance Center (CCC) Transactional Reporting Service, provided that the base fee of $1.00 per copy plus $0.10 per page is paid directly to CCC, 21 Congress Street, Salem, Massachusetts 01970, USA. The identification code for *Nature* is 0028-0836/84 $1.00 + $0.10. US Postmaster send form 3579 to: *Nature*, 15 East 26 Street, New York, NY 10010. Published in Japan by Macmillan Shuppan K.K., 5th Floor Eikow Building, 1-10-9 Hongo, Bunkyo-ku, Tokyo, Japan. © 1984 Macmillan Journals Ltd.

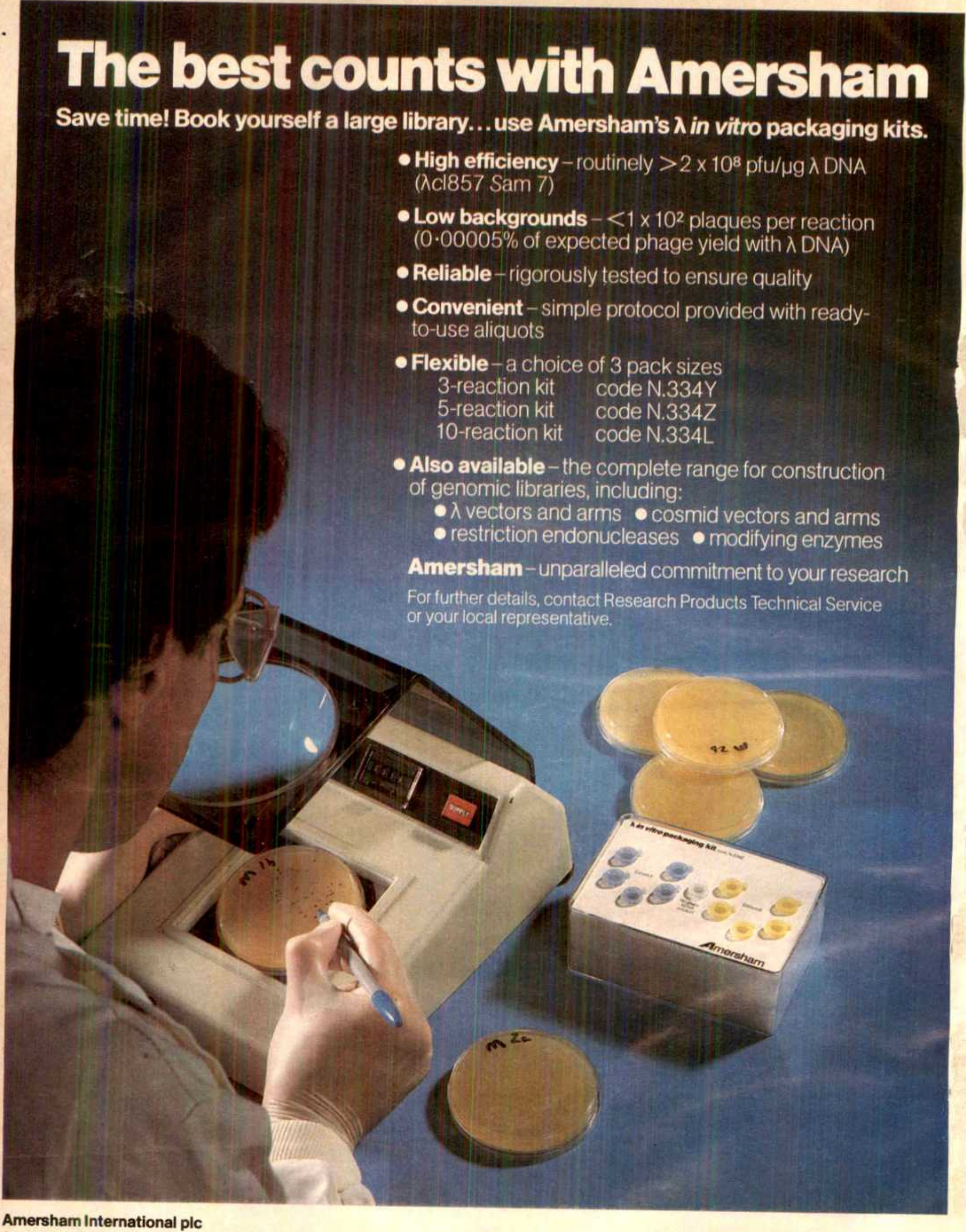

The best counts with Amersham

Save time! Book yourself a large library... use Amersham's λ *in vitro* packaging kits.

- **High efficiency** – routinely $>2 \times 10^8$ pfu/µg λ DNA (λcI857 *Sam* 7)
- **Low backgrounds** – $<1 \times 10^2$ plaques per reaction (0·00005% of expected phage yield with λ DNA)
- **Reliable** – rigorously tested to ensure quality
- **Convenient** – simple protocol provided with ready-to-use aliquots
- **Flexible** – a choice of 3 pack sizes

3-reaction kit	code N.334Y
5-reaction kit	code N.334Z
10-reaction kit	code N.334L

- **Also available** – the complete range for construction of genomic libraries, including:
  - λ vectors and arms
  - cosmid vectors and arms
  - restriction endonucleases
  - modifying enzymes

Amersham – unparalleled commitment to your research

For further details, contact Research Products Technical Service or your local representative.

Amersham International plc
Amersham England HP7 9LL
telephone Little Chalfont (024 04) 4444
telex 83141 ACTIVA G

Amersham

Amersham Australia PTY Ltd Sydney (2) 211 4399/4489 **Amersham Belgium SA/NV** Brussels (2) 538 9194 **Amersham Buchler GmbH & Co KG** Braunschweig, West Germany (05307) 8080 **Amersham Canada Ltd** Ontario (416) 842 2720 **Amersham Corporation** Arlington Heights USA (312) 364 7100 **Amersham Denmark ApS** Birkerød (02) 82 0222 **Amersham France SA** Paris (6) 928 8300 **Amersham Japan** Tokyo (3) 543 0777 **Amersham Nederland BV** Utrecht (30) 7308 31 **Amersham Sweden AB** Solna (8) 734 0800

Circle No.50 on Reader Service Card.

Index

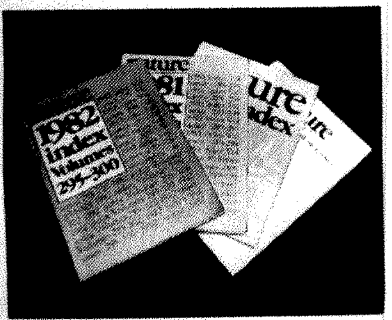

Comprehensive annual indexes of subject and author are available for all issues of **Nature** from 1971 to 1983.

Prices and address for orders are set out below.

Annual Subscription Prices

UK & Irish Republic		£98
USA & Canada		US$230
Australia & NZ	Airspeed	£150
Continental Europe	Airspeed	£120
India	Airspeed	£115
Japan	Airspeed	Y85000
Rest of World*	Surface	£120
Rest of World*	Airmail	£180

**(not USA, Canada, Europe & Japan)*

Orders (with remittance) to:

USA & Canada
Nature
Subscription Dept
PO Box 1018
Manasquan
NJ 08736
USA

UK & Rest of World
Nature
Circulation Dept
Brunel Road
Basingstoke
Hants RG21 2XS, UK
Tel: 0256 29242

(The addresses of Nature's editorial offices are shown facing the first editorial page)

Japanese subscription enquiries to:
Japan Publications Trading Company Ltd
2-1 Sarugaku-cho 1-chome
Chiyoda-ku, Tokyo, Japan
Tel: (03) 292 3755

Personal subscription rates
These are available in some countries to subscribers paying by personal cheque or credit card. Details from:

USA & Canada
Nature
15 East 26 Street
New York,
NY 10010, USA
Tel: (212) 689-5900

UK & Europe
Felicity Parker, Nature
Brunel Road
Basingstoke
Hants RG21 2XS, UK
Tel: 0256 29242

Credit card orders only (in USA):
Call toll-free: (800) 824-7888 (Operator 246)
In California: (800) 852-7777 (Operator 246)

Back issues
UK, £2.50; USA & Canada, US$6.00 (surface), US$9.00 (air); Rest of World, £3.00 (surface), £4.00 (air)

Binders
Single Binders: UK, £4.50; Rest of World, $10.00
Set(s) of 3 Binders; UK, £12.00; Rest of World, $25.00

Annual indexes (1971–1983)
UK, £5.00 each; Rest of World, $10.00

Nature First Issue Facsimile
UK, 75p; Rest of World (surface), $1.50; (air) $2.00

Nature in microform
For Information:
University Microfilms International, 300 North Zeeb Road, Ann Arbor, MI 48106, USA

Neural cell adhesion molecules and myelin-associated glycoprotein share a common carbohydrate moiety recognized by monoclonal antibodies L2 and HNK-1
J Kruse, R Mailhammer, H Wernecke, A Faissner, I Sommer, C Goridis & M Schachner 153

Neuronal-type Na$^+$ and K$^+$ channels in rabbit cultured Schwann cells
S Y Chiu, P Schrager & J M Ritchie 156

Photoreceptor excitation and adaptation by inositol 1,4,5-triphosphate
A Fein, R Payne, D W Corson, M J Berridge & R F Irvine 157

***myo*-inositol polyphosphate may be a messenger for visual excitation in *Limulus* photoreceptors**
J E Brown, L J Rubin, A J Ghalayini, A P Tarver, R F Irvine, M J Berridge & R E Anderson 160

Alternative sets of DNase I-hypersensitive sites characterize the various functional states of the chicken lysozyme gene
H P Fritton, T Igo-Kemenes, J Nowock, U Strech-Jurk, M Theisen & A E Sippel 163

High rates of *in vitro* synthesis of 1,4-β-D-glucan in cell-free preparations from *Phaseolus aureus*
T Callaghan & M Benziman 165

6Å-Resolution X-ray structure of a variable surface glycoprotein from *Trypanosoma brucei*
D M Freymann, P Metcalf, M Turner & D C Wiley 167

α-Helical coiled-coil structures of *Trypanosoma brucei* variable surface glycoproteins
C Cohen, B Reinhardt, D A D Parry, G E Roelants, W Hirsch & B Kanwé 169

Mutant viral RNAs synthesized *in vitro* show altered aminoacylation and replicase template activities
T W Dreher, J J Bujarski & T C Hall 171

Plasma protease inhibitors in mouse and man: divergence within the reactive centre regions
R E Hill, P H Shaw, P A Boyd, H Baumann & N D Hastie 175

Erythrocyte spectrin is comprised of many homologous helical segments
D W Speicher & V T Marchesi 177

MISCELLANY

Books received 185
Product review: Recombinant DNA 187
Announcements 191
Employment: How valuable is the student grant?
R Pearson 192

NATURE CLASSIFIED

Professional appointments — Research posts — Studentships — Fellowships — Conferences — Courses — Seminars — Symposia: Back pages

Next week in *Nature*:

- India–Asia suture mapped
- North American gravity map
- Volcanic gravity variations
- Deci-Ångstrom electron microscopy
- Atmospheric toluene degradation
- Back-front in *Drosophila* embryos
- X and Y chromosomal similarity
- Defective *ras* gene activity
- Polyoma and papilloma similarities
- Evolution of ratites

GUIDE TO AUTHORS

Authors should be aware of the diversity of *Nature*'s readership and should strive to be as widely understood as possible.

Review articles should be accessible to the whole readership. Most are commissioned, but unsolicited reviews are welcome (in which case prior consultation with the office is desirable).

Scientific articles are research reports whose conclusions are of general interest or which represent substantial advances of understanding. The text should not exceed 3,000 words and six displayed items (figures plus tables). The article should include an abstract of about 50 words.

Letters to *Nature* are ordinarily 1,000 words long with no more than four displayed items. The first paragraph (not exceeding 150 words) should say what the letter is about, why the study it reports was undertaken and what the conclusions are.

Matters arising are brief comments (up to 500 words) on articles and letters recently published in *Nature*. The originator of a Matters Arising contribution should initially send his manuscript to the author of the original paper and both parties should, wherever possible, agree on what is to be submitted.

Manuscripts may be submitted either to London or Washington (decisions being made only in London). Manuscripts should be typed (double spacing) on one side of the paper only. Three copies are required, each accompanied by copies of lettered artwork. No title should exceed 80 characters in length. Reference lists, figure legends, etc. should be on separate sheets, all of which should be numbered. Abbreviations, symbols, units, etc. should be identified on one copy of the manuscript at their first appearance.

References should appear sequentially indicated by superscripts in the text and should be abbreviated according to the *World List of Scientific Periodicals*, fourth edition (Butterworth 1963–65). The first and last page numbers of each reference should be cited. References to books should clearly indicate the publisher and the date and place of publication. Unpublished articles should not be formally referred to unless accepted or submitted for publication, but may be mentioned in the text.

Each piece of artwork should be clearly marked with the author's name and the figure number. Original artwork should be unlettered. Suggestions for cover illustrations are welcome. Original artwork (and one copy of the manuscript) will be returned when manuscripts cannot be published.

Requests for permission to reproduce material from Nature *should be accompanied by a self-addressed (and, in the case of the United Kingdom and United States, stamped) envelope.*

THERE'S NO OTHER PROTEIN A LIKE ASORB™

The charts tell it all.

First, look at purity. Note that only one competitive brand even approaches Asorb.™

Then compare the prices.* That "pure-looking" competitor charges you almost three times what we do. And look how high the others are.

By any comparison, the clear winner is Asorb. Created by the maker of IgGsorb.®

Asorb is stable as a lyophilized powder for two years at 4°C. We're ready to ship at 24 hours' notice.

So call us today.

TOLL FREE 1-800-343-2170

THE ENZYME CENTER, INC.
36 Franklin Street, Malden, MA 02148
(617) 322-4885

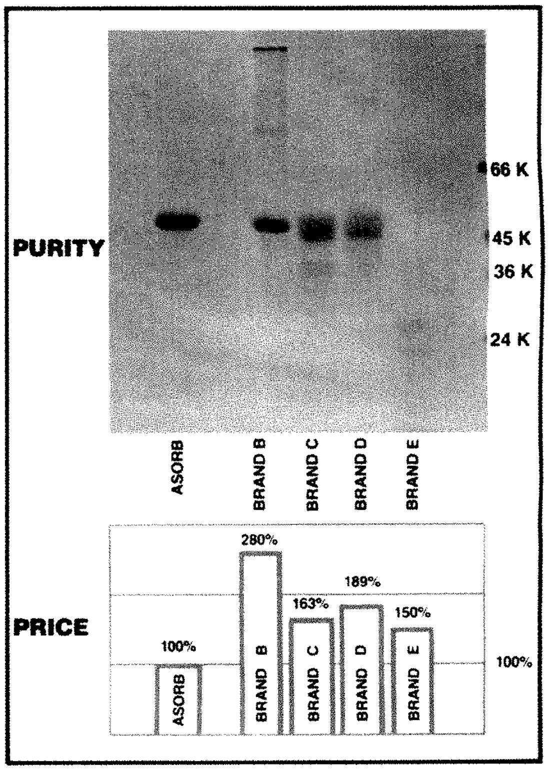

*Based on 6-84 published prices for 5mg

© The Enzyme Center Inc 1984

Circle No.41 on Reader Service Card.

YOUR NEW PARTNER

Fine Biochemicals
- Thyroxin binding globulin (Human TBG).
- Testosterone binding globulin (Human TEBG).
- Fibroblast growth factor (bovine FGF).
- Fibronectin (human - bovine - mouse - rat).
- Protein A.
- Protein A - solid phase.
- Gelatin - solid phase.
- Antisera (list available on request).

Diagnostic

hPL	R.I.A. Kit
hCGβ	R.I.A. Kit
hLH	R.I.A. Kit
hFSH	R.I.A. Kit
hPRL	R.I.A. Kit
hTSH	R.I.A. Kit
T3	R.I.A. Kit
T4	R.I.A. Kit
hTBG	R.I.A. Kit
Monotech hGH (monoclonal antibody).	R.I.A. Kit

Catalog available on request

TECHLAND S.A.
Parc Industriel de Recherches du Sart-Tilman - B-4900 Liège - Belgium
Tel. 32 (41) 67 44 64 - Telex 42384 TTC

Circle No.23 on Reader Service Card.

nature

21-1-87
A·Latts

NATURE VOL. 311 20 SEPTEMBER 1984

COVER

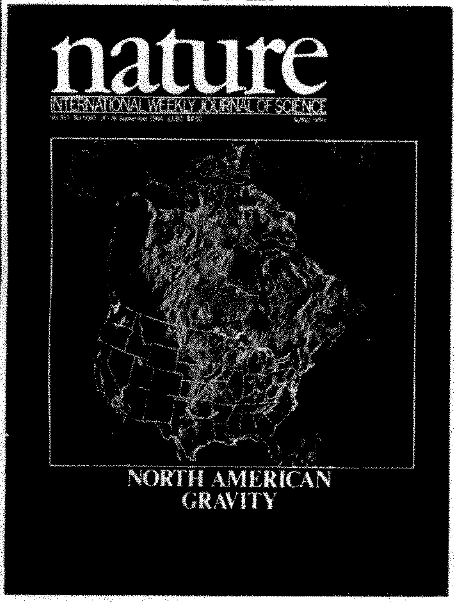

A Bouguer anomaly image for North America generated using 750,000 anomalies computed from ground readings and interpolations between stations. The processed data were converted to shaded relief form and overlain with colour-coded anomaly values from purple (−343 in mGal) to pink (316 mGal). A simulated sun was placed at 20° above the western horizon. The image is in a Lambert equal area projection, centred at 52° N latitude, 90° W longitude. See p.241. (Data Defense Mapping Agency Aerospace Center, St Louis, and the Department of Energy, Mines and Resources, Canada.)

OPINION

Past defended, future unforeseen 193
Help for Argentina? 194

NEWS

Restraints on publication
AIDS 195
Entrance standards on increase
British universities 196
French research
Merger resisted 197
European science
Amazon to yield more secrets?
Patent rights
US pharmaceuticals 198
British association at Norwich 199

CORRESPONDENCE

Whither gene therapy?/
Jumping the gun on publication 200

COMMENTARY

Army pall over Argentine science
S Budiansky 201

NEWS AND VIEWS

The molecular biology of cancer 205
Plans for future space missions
Alan Johnstone 209
Diabetes — on the track of viruses
Abner Louis Notkins 209
Nearly the 'top' conference
David J Miller 210
Open season for magmatic fractional crystallization
Bob Thompson 211
First clue to biological role of clathrin light chains
Ernst Ungewickell 213
How to make a fruitfly
Geoffrey North 214

SCIENTIFIC CORRESPONDENCE

Laying down the −3/2 power law
R Whittington 217
Repetitive sequences in structural genes
R P Erickson
Fourier's law and thermal conduction
H Büttner & F Mokross
On the hand of *Archaeopteryx*
R A Thulborn & T L Hamley 218

BOOK REVIEWS

Religion and Empire: The Dynamics of Aztec and Inca Expansionism
by G W Conrad and A A Demarest
Warwick Bray 281
Techniques in Nucleic Acid Biochemistry
Jeffrey Williams 282
In the Presence of the Creator: Isaac Newton and His Times
by G E Christianson
A Rupert Hall
The Logic of Perception
by I Rock
Horace B Barlow 283
The Rock Art of Africa
by A R Willcox
Patricia Vinnicombe 284

ARTICLES

Tectonics and structural zonation of southern Tibet, China
J P Burg & G M Chen 219

Information for the dorsal–ventral pattern of the *Drosophila* embryo is stored as maternal mRNA
K V Anderson & C Nüsslein-Volhard 223

A role for clathrin light chains in the recognition of clathrin cages by 'uncoating ATPase'
S L Schmid, W A Braell,
D M Schlossman & J E Rothman 228

Mutations that alter the DNA sequence specificity of the catabolite gene activator protein of *E. coli*
R H Ebright, P Cossart,
B Gicquel-Sanzey & J Beckwith 232

LETTERS TO NATURE

Molecular hydrogen jets from the Orion nebula
K N R Taylor, J W V Storey, G Sandell,
P M Williams & W J Zealey 236

IR observations of the peculiar galaxy Arp220
I P Emerson, P E Clegg, G Gee,
C T Cunningham, M J Griffin,
L M J Brown, E I Robson
& A J Longmore 237

Accurate atomic positions from electron microscopy
S Hovmöller, A Sjögren, G Farrants,
M Sundberg & B-O Marinder 238

Bouguer images of the North American craton and its structural evolution
R E Arvidson, D Bindschadler,
S Bowring, M Eddy, E Guinness
& C Leff 241

Periodic gravity changes at Poás volcano, Costa Rica
H Rymer & G C Brown 243

Timing the increase in atmospheric sulphur deposition in the Adirondack Mountains
G R Holdren Jr, T M Brunelle,
G Matisoff & M Wahlen 245

Toluene degradation products in simulated atmospheric conditions
B E Dumdei & R J O'Brien 248

Natural ^{15}N abundance measurements and atmospheric nitrogen standard calibration
A Mariotti 251

Microplankton productivity in the oligotrophic ocean
R E H Smith, R J Geider
& T Platt 252

Contents continued overleaf

Nature® (ISSN 0028-0836) is published weekly on Thursday, except the last week in December, by Macmillan Journals Ltd and includes the Annual Index (mailed in February). Annual subscription for USA and Canada US $230 (for subscription prices elsewhere, see next page). USA and Canadian orders only to: *Nature*, Subscription Dept, PO Box 1018, Manasquan, New Jersey 08736, USA. All other orders to *Nature*, Brunel Road, Basingstoke, Hants RG21 2XS, UK. Second class postage paid at New York, NY 10010 and additional mailing offices. Authorization to photocopy material for internal or personal use, or the internal or personal use of specific clients, is granted by *Nature* to libraries and other users registered with the Copyright Clearance Center (CCC) Transactional Reporting Service, provided that the base fee of $1.00 per copy plus $0.10 per page is paid directly to CCC, 21 Congress Street, Salem, Massachusetts 01970, USA. The identification code for *Nature* is 0028-0836/84 $1.00 + $0.10. US Postmaster send form 3579 to: *Nature*, 15 East 26 Street, New York, NY 10010. Published in Japan by Macmillan Shuppan K.K., 5th Floor Eikow Building, 1-10-9 Hongo, Bunkyo-ku, Tokyo, Japan. © 1984 Macmillan Journals Ltd.

Do your fluorescent problems need sorting?

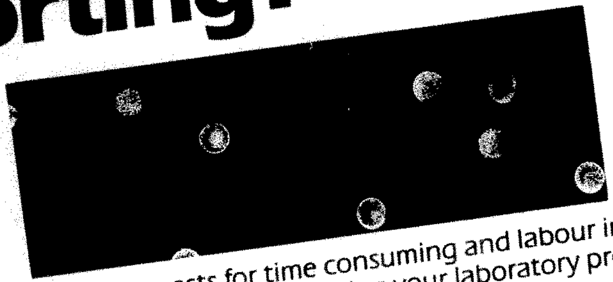

Increasing requests for time consuming and labour intensive fluorescent analysis may be causing your laboratory problems.

If so, the following news should help:

The COULTER EPICS® 'C' flow cytometer will:—

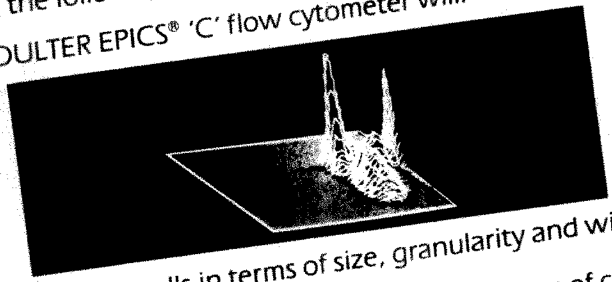

- Characterise cells in terms of size, granularity and with fluorescent probes.
- Carry out high speed analysis on large numbers of cells.
- Sort populations of interest for positive identification and further examination.

It will do this:—

Quickly — on up to 10,000 cells per second

Simply — with user definable 'profiles'

Economically — low capital outlay and running costs

Epics® C

Automatic cell analyser and sorter at an 'analyser only' price. Let Coulter help to sort your problem!

PIONEERING 25 YEARS TECHNOLOGY 1959 1984

Coulter Electronics

Coulter Electronics Limited,
Northwell Drive, Luton, Beds, LU3 3RH, England.
Tel: (0582) 582442. Telex: 825074.

Circle No.01 on Reader Service Card.

Please send me details of the EPICS® C clinical flow cytometer.

NAME ____

COMPANY/HOSPITAL ____

ADDRESS ____

____ TEL: ____

NUK 9/84

CONTENTS

SCIENCE IN THE LOW COUNTRIES

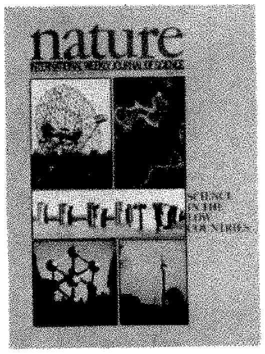

- *Will the policy of "concentrating" the universities in Holland and Belgium create more problems than it solves?*
- *Is Belgian science stagnating?*
- *What would be the effect of increased government control over Dutch research policy?*

These and other questions are examined in *Nature*'s special supplement on Science in the Low Countries.
Extra copies of this issue are available now from the address given below.

Annual Subscription Prices

UK & Irish Republic		£98
USA & Canada		US$230
Australia & NZ	Airspeed	£150
Continental Europe	Airspeed	£120
India	Airspeed	£115
Japan	Airspeed	Y85000
Rest of World*	Surface	£120
Rest of World*	Airmail	£180

**(not USA, Canada, Europe & Japan)*

Orders (with remittance) to:

USA & Canada
Nature
Subscription Dept
PO Box 1018
Manasquan
NJ 08736
USA

UK & Rest of World
Nature
Circulation Dept
Brunel Road
Basingstoke
Hants RG21 2XS, UK
Tel: 0256 29242

(The addresses of Nature's editorial offices are shown facing the first editorial page)

Japanese subscription enquiries to:
Japan Publications Trading Company Ltd
2-1 Sarugaku-cho 1-chome
Chiyoda-ku, Tokyo, Japan
Tel: (03) 292 3755

Personal subscription rates
These are available in some countries to subscribers paying by personal cheque or credit card. Details from:

USA & Canada
Nature
15 East 26 Street
New York,
NY 10010, USA
Tel: (212) 689-5900

UK & Europe
Felicity Parker, Nature
Brunel Road
Basingstoke
Hants RG21 2XS, UK
Tel: 0256 29242

Credit card orders only (in USA):
Call toll-free: (800) 824-7888 (Operator 246)
In California: (800) 852-7777 (Operator 246)

Back issues
UK, £2.50; USA & Canada, US$6.00 (surface), US$9.00 (air); Rest of World, £3.00 (surface), £4.00 (air)

Binders
Single Binders: UK, £4.50; Rest of World, $10.00
Set(s) of 3 Binders; UK, £12.00; Rest of World, $25.00

Annual indexes (1971–1983)
UK, £5.00 each; Rest of World, $10.00

Nature First Issue Facsimile
UK, 75p; Rest of World (surface), $1.50; (air) $2.00

Nature in microform
For Information:
University Microfilms International, 300 North Zeeb Road, Ann Arbor, MI 48106, USA

Immuno-gold localization of leghaemoglobin in cytoplasm in nitrogen-fixing root nodules of pea
J G Robertson, B Wells, T Bisseling, K J F Farnden & A W B Johnston 254

Ratites as oldest offshoot of avian stem — evidence from α-crystallin A sequences
S O Stapel, J A M Leunissen, M Versteeg, J Wattel & W W de Jong 257

Closely related sequences on human X and Y chromosomes outside the pairing region
H J Cooke, W A R Brown & G A Rappold 259

Isolation of the *dorsal* locus of *Drosophila*
R Steward, F J McNally & P Schedl 262

Internal control of the coated vesicle pp50-specific kinase complex
A Pauloin & P Jollès 265

A six-armed oligomer isolated from cell surface fibronectin preparations
H P Erickson & J L Inglesias 267

Lowering of pH_i inhibits Ca^{2+}-activated K^+ channels in pancreatic B-cells
D L Cook, M Ikeuchi & W Y Fujimoto 269

Intracellular ATP directly blocks K^+ channels in pancreatic B-cells
D L Cook & C N Hales 271

The product of *ras* is a GTPase and the T24 oncogenic mutant is deficient in this activity
R W Sweet, S Yokoyama, T Kamata, J R Feramisco, M Rosenberg & M Gross 273

A common function for polyoma virus large-T and papillomavirus El proteins?
P Clertant & I Seif 276

Reduction of the minimal sequence for initiation of DNA synthesis by qualitative or quantitative changes of an initiator protein
G P Dotto & N D Zinder 279

Errata . . . page 280
Constraints on the neutron lifetime from triton β decay
J Byrne
Unusual DNA sequences associated with the ends of yeast chromosomes
R M Walmsley, C S M Chan, B-K Tye & T D Petes

—NATURE CLASSIFIED—

Professional appointments — Research posts — Studentships — Fellowships — Conferences — Courses — Seminars — Symposia: **Back pages**

Next week in *Nature*:

- Polyacetylene for rechargeable batteries
- Neptune's moons
- X-ray haloes around supernova remnants
- Photon forces
- Optical arcs from airborne ice
- Enrichment in the Earth's mantle
- Thermoluminescence as a palaeo-thermometer
- T-cell receptor gene rearrangement
- Malarial antigen clone expressed
- The lot of laboratory animals in the United States
- New journals reviewed

—GUIDE TO AUTHORS—

Authors should be aware of the diversity of *Nature*'s readership and should strive to be as widely understood as possible.

Review articles should be accessible to the whole readership. Most are commissioned, but unsolicited reviews are welcome (in which case prior consultation with the office is desirable).

Scientific articles are research reports whose conclusions are of general interest or which represent substantial advances of understanding. The text should not exceed 3,000 words and six displayed items (figures plus tables). The article should include an abstract of about 50 words.

Letters to *Nature* are ordinarily 1,000 words long with no more than four displayed items. The first paragraph (not exceeding 150 words) should say what the letter is about, why the study it reports was undertaken and what the conclusions are.

Matters arising are brief comments (up to 500 words) on articles and letters recently published in *Nature*. The originator of a Matters Arising contribution should initially send his manuscript to the author of the original paper and both parties should, wherever possible, agree on what is to be submitted.

Manuscripts may be submitted either to London or Washington (decisions being made only in London). Manuscripts should be typed (double spacing) on one side of the paper only. Three copies are required, each accompanied by copies of lettered artwork. No title should exceed 80 characters in length. Reference lists, figure legends, etc. should be on separate sheets, all of which should be numbered. Abbreviations, symbols, units, etc. should be identified on one copy of the manuscript at their first appearance.

References should appear sequentially indicated by superscripts in the text and should be abbreviated according to the *World List of Scientific Periodicals*, fourth edition (Butterworth 1963–65). The first and last page numbers of each reference should be cited. References to books should clearly indicate the publisher and the date and place of publication. Unpublished articles should not be formally referred to unless accepted or submitted for publication, but may be mentioned in the text.

Each piece of artwork should be clearly marked with the author's name and the figure number. Original artwork should be unlettered. Suggestions for cover illustrations are welcome. Original artwork (and one copy of the manuscript) will be returned when manuscripts cannot be published.

Requests for permission to reproduce material from Nature *should be accompanied by a self-addressed (and, in the case of the United Kingdom and United States, stamped) envelope.*

SIMPLY WORTH PAYING FOR

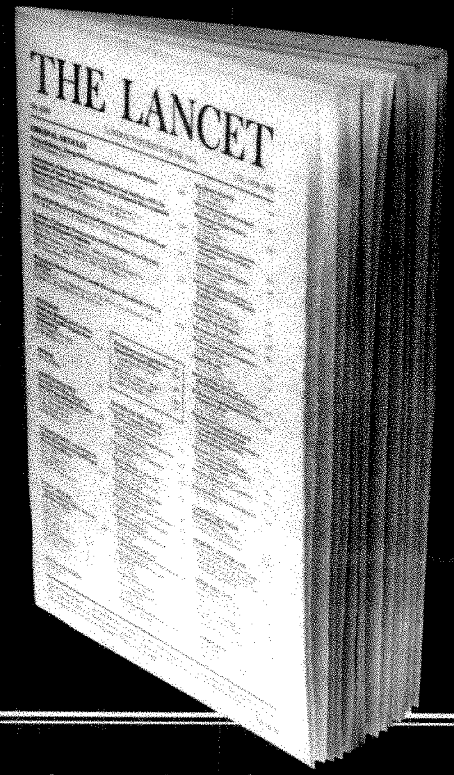

The most cited medical journal in the world

To: The Lancet Ltd., 7 Adam Street, Adelphi, London WC2N 6AD

Please send me The Lancet each week for one year
☐ £42 in UK and Eire ☐ Cheque enclosed or
Charge to my Access/Visa No. (UK only)
☐☐☐☐☐☐☐☐☐☐☐☐☐☐☐☐☐

☐ £61 Overseas (Airspeeded)
☐ Please invoice me

☐ £24 special rate (UK and Eire only) for doctors within 5 years of registration or graduation and for medical students.
Date of registration: ____________

NAME ____________
ADDRESS ____________
____
____
SIGNATURE ____________
DATE ____________
N

BLOCK CAPITALS PLEASE

nature

21-1-87
A. Datta

NATURE VOL. 311 27 SEPTEMBER 1984

COVER

A pillar of light at the anthelic point (opposite the Sun) photographed on 28 March 1978 at Point Barrow, Alaska. This effect is caused by light from the Sun (at an elevation of 6°) undergoing up to four internal reflections within airborne ice crystals. See page 339.

OPINION

Poor control for US in formation 285
Orphaned academy 286
Redundant agency

NEWS

Nuclear winter 287
Netherlands budget
Publication controls 288
***In vitro* fertilization**
Information technology 289
Model zoo
Arms control 290
Toxic hazards in Britain
Archaeology
UN biotechnology 291
Badgers at bay
Sellafield
French research 292
UK biotechnology
Florida citrus 293
Danube environment

CORRESPONDENCE

On "Science for the people"/How to name genes 294

COMMENTARY

Mistreatment of laboratory animals endangers biomedical research
C Stevens 295

NEWS AND VIEWS

New ways with solar neutrinos
John Maddox 298
Implications of Arctic air pollution
S A Penkett 299
Malaria parasite blood-stage antigens cloned
K N Brown 300
A step closer to the principles of eukaryotic transcriptional control
Tim Reudelhuber 301
Polyacetylene and organic superconductors lead the field
Martin R Bryce and Munir M Ahmad 301
Messenger RNA pieced together
H D Robertson 302
Giant tortoises down under
Michael J Benton 303
Continental area and elevation
A G Smith 304
Receptor gene rearrangement and ontogeny of T lymphocytes, and **The Snark was a Boojum, probably**
Miranda Robertson 305

SCIENTIFIC CORRESPONDENCE

"Nuclear winter" to be taken seriously
R P Turco, O B Toon, T P Ackerman, J B Pollack & C Sagan 307
Reply: J Maddox 308
Amino acid transport systems
S Bannai *et al.*

NEW JOURNALS

Where is the revolution?
Michael Buckingham evaluates the promise and the problems of electronic publishing in science 309

This issue contains reviews of new journals which have appeared between June 1982 and May 1983. The reviews begin on p. 311, with an introduction and index on p. 310.

REVIEW ARTICLE

Mantle enrichment processes
C J Hawkesworth, N W Rogers, P W C van Calsteren & M A Menzies 331

ARTICLES

Casimir effect for massive photons
G Barton & N Dombey 336

Anthelic arcs from airborne ice crystals
R G Greenler & E Tränkle 339

The structure, rearrangement and expression of D_β gene segments of the murine T-cell antigen receptor
G Siu, M Kronenberg, E Strauss, R Haars, T W Mak & L Hood 344

Apparent discontinuous transcription of *Trypanosoma brucei* variant surface antigen genes
D A Campbell, D A Thornton & J C Boothroyd 350

LETTERS TO NATURE

On the origin of Triton and Pluto
W B McKinnon 355

X-ray haloes around supernova remnants
G E Morfill, L O'C Drury & B Aschenbach 358

Spectral feature of 31 December 1981 γ-ray burst not confirmed
P L Nolan, G H Share, E L Chupp, D J Forrest & S M Matz 360

Limiting battery performance parameters for polyacetylene
J C W Chien & J B Schlenoff 362

Thermoluminescence as a palaeothermometer
R K Guimon, K S Weeks, B D Keck & D W G Sears 363

Seismic reflectors and unconformities at passive continental margins
J Thorne & A B Watts 365

Evolution of the lower continental crust: granulite facies xenoliths from the Eifel, West Germany
H-G Stosch & G W Lugmair 368

Relationship between continental area and elevation
A R Wyatt 370

A lower crustal origin for massif-type anorthosites
S R Taylor, I H Campbell, M T McCulloch & S M McLennan 372

Role of paternal and maternal genomes in mouse development
S C Barton, M A H Surani & M L Norris 374

A biological consequence of variation in the site of D-J_H gene rearrangement
B A Pollok, J F Kearney, M Vakil & R P Perry 376

Contents continued overleaf

Nature® (ISSN 0028-0836) is published weekly on Thursday, except the last week in December, by Macmillan Journals Ltd and includes the Annual Index (mailed in February). Annual subscription for USA and Canada US $230 (for subscription prices elsewhere, see next page). USA and Canadian orders only to: *Nature*, Subscription Dept, PO Box 1018, Manasquan, New Jersey 08736, USA. All other orders to *Nature*, Brunel Road, Basingstoke, Hants RG21 2XS, UK. Second class postage paid at New York, NY 10010 and additional mailing offices. Authorization to photocopy material for internal or personal use, or the internal or personal use of specific clients, is granted by *Nature* to libraries and other users registered with the Copyright Clearance Center (CCC) Transactional Reporting Service, provided that the base fee of $1.00 per copy plus $0.10 per page is paid directly to CCC, 21 Congress Street, Salem, Massachusetts 01970, USA. The identification code for *Nature* is 0028-0836/84 $1.00 + $0.10. US Postmaster send form 3579 to: *Nature*, 15 East 26 Street, New York, NY 10010. Published in Japan by Macmillan Shuppan K.K., 5th Floor Eikow Building, 1-10-9 Hongo, Bunkyo-ku, Tokyo, Japan. © 1984 Macmillan Journals Ltd.

Setting the standard...

$[^3H]$ Micro-scales

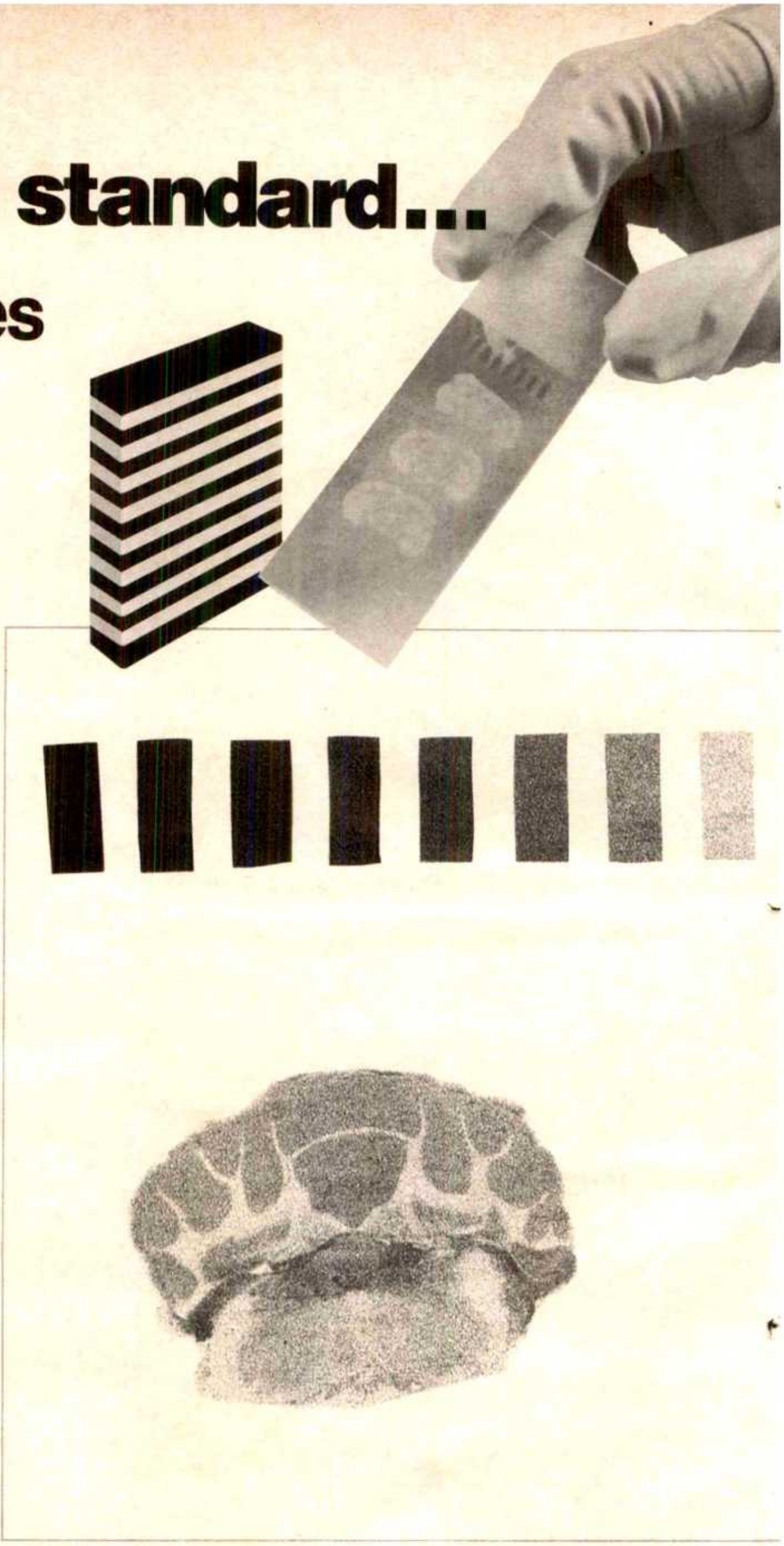

Easy, accurate way to quantify tritium distribution by autoradiography

Compare $[^3H]$ Micro-scales with your current quantification procedure for ease of use, speed, dependable uniformity and accuracy. Micro-scales from Amersham set the standard by which all others will be measured.

That's because each Micro-scale block consists of eight layers of tritiated polymer, arranged in order of increasing specific activity—from 3 to 110nCi/mg—and separated by inactive layers. Using a standard microtome, the block can be sliced into hundreds of sections . . . each sized to fit on a standard microscope slide along with tissue sections. Then, when an autoradiogram is exposed and developed, tissue radioactivity levels can be calibrated directly against the Micro-scale.

Because hundreds of slices can be cut from each Micro-scale block, the cost per calibration is very low. And, potential applications extend to anyone currently performing $[^3H]$ autoradiography of cells, tissues or other substrates. For details, write or call for literature on $[^3H]$ Micro-scales. The new standard for autoradiography.

Amersham International plc
Amersham England HP7 9LL
telephone Little Chalfont (024 04) 4444
telex 83141 ACTIVA G

Amersham

Amersham Australia PTY Limited Sydney **Amersham Belgium SA/NV** Brussels **Amersham Buchler GmbH & Co. KG** Braunschweig W Germany **Amersham Canada Ltd.** Ontario **Amersham Corporation** Arlington Heights USA **Amersham Denmark ApS** Birkerød **Amersham France SA** Paris **Amersham Japan** Tokyo **Amersham Nederland BV** Utrecht

Circle No.51 on Reader Service Card.

CONTENTS

SCIENCE IN THE LOW COUNTRIES

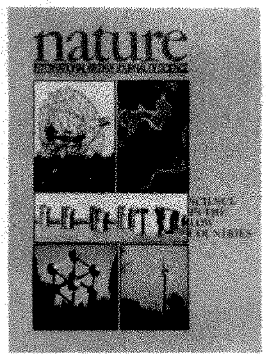

- *Will the policy of "concentrating" the universities in Holland and Belgium create more problems than it solves?*
- *Is Belgian science stagnating?*
- *What would be the effect of increased government control over Dutch research policy?*

These and other questions are examined in *Nature*'s special supplement on Science in the Low Countries.
Extra copies of this issue are available now from the address given below.

Annual Subscription Prices

UK & Irish Republic		£98
USA & Canada		US$230
Australia & NZ	Airspeed	£150
Continental Europe	Airspeed	£120
India	Airspeed	£115
Japan	Airspeed	Y85000
Rest of World*	Surface	£120
Rest of World*	Airmail	£180

***(not USA, Canada, Europe & Japan)*

Orders (with remittance) to:

USA & Canada
Nature
Subscription Dept
PO Box 1018
Manasquan
NJ 08736
USA

UK & Rest of World
Nature
Circulation Dept
Brunel Road
Basingstoke
Hants RG21 2XS, UK
Tel: 0256 29242

(The addresses of Nature's editorial offices are shown facing the first editorial page)

Japanese subscription enquiries to:
Japan Publications Trading Company Ltd
2-1 Sarugaku-cho 1-chome
Chiyoda-ku, Tokyo, Japan
Tel: (03) 292 3755

Personal subscription rates
These are available in some countries to subscribers paying by personal cheque or credit card. Details from:

USA & Canada
Nature
15 East 26 Street
New York,
NY 10010, USA
Tel: (212) 689-5900

UK & Europe
Felicity Parker, Nature
Brunel Road
Basingstoke
Hants RG21 2XS, UK
Tel: 0256 29242

Credit card orders only (in USA):
Call toll-free: (800) 824-7888 (Operator 246)
In California: (800) 852-7777 (Operator 246)

Back issues
UK, £2.50; USA & Canada, US$6.00 (surface), US$9.00 (air); Rest of World, £3.00 (surface), £4.00 (air)

Binders
Single Binders: UK, £5.25; Rest of World, $11.50
Set of 3 Binders; UK, £14.00; Rest of World, $31.00

Annual indexes (1971–1983)
UK, £5.00 each; Rest of World, $10.00

Nature First Issue Facsimile
UK, 75p; Rest of World (surface), $1.50; (air) $2.00

Nature in microform
For Information:
University Microfilms International, 300 North Zeeb Road, Ann Arbor, MI 48106, USA

Major surface antigen gene of a human malaria parasite cloned and expressed in bacteria
R Hall, J E Hyde, M Goman, D L Simmons, I A Hope, M Mackay, J Scaife, B Merkli, R Richle & J Stocker 379

Human antisera detect a *Plasmodium falciparum* genomic clone encoding a nonapeptide repeat
M Koenen, A Scherf, O Mercereau, G Langsley, L Sibilli, P Dubois, L Pereira da Silva & B Müller-Hill 382

Rearrangements of T-cell receptor gene *YT35* in human DNA from thymic leukaemia T-cell lines and functional T-cell clones
B Toyonaga, Y Yanagi, N Suciu-Foca, M Minden & T W Mak 385

Identification of a diversity segment of human T-cell receptor β-chain, and comparison with the analogous murine element
S P Clark, Y Yoshikai, S Taylor, G Siu, L Hood & T W Mak 387

Isolation of UV-resistant revertants from a xeroderma pigmentosum complementation group A cell line
B Royer-Pokora & W A Haseltine 390

Genetic effects of injection of Rous sarcoma virus DNA into polar plasm of early *Drosophila melanogaster* embryos
K G Gazaryan, S D Nabirochkin, A G Tatosyan, A K Shakhbazyan & E N Shibanova 392

Detection of virus-specific sequences in *Drosophila melanogaster* mutants induced by injection of RSV DNA into early embryos
A G Tatosyan, S D Nabirochkin, A K Shakhbazyan, K G Gazaryan & F L Kisseljov 394

MATTERS ARISING

15-Myr periodicity in the frequency of geomagnetic reversals since 100 Myr
P L McFadden
Reply: A Mazaud, C Laj, L de Sèze & K L Verosub 396

MISCELLANY

100 years ago 304
Announcements 397

NATURE CLASSIFIED

Professional appointments — Research posts — Studentships — Fellowships — Conferences — Courses — Seminars — Symposia: Back pages

Next week in *Nature*:

- Cell-cycle oncogenes
- Oncogene phosphorylation
- Neuronal replacement
- Giant synaptosomes
- Neurone classification by antibodies
- Neostriatal patch/matrix interplay
- Parkinsonism and monoamine oxidase
- Deep-sea helium-3
- Noiseless NMR
- Boltzmann's ultraviolet conjecture
- Stress in tectonic plates
- Cellular automata

GUIDE TO AUTHORS

Authors should be aware of the diversity of *Nature*'s readership and should strive to be as widely understood as possible.

Review articles should be accessible to the whole readership. Most are commissioned, but unsolicited reviews are welcome (in which case prior consultation with the office is desirable).

Scientific articles are research reports whose conclusions are of general interest or which represent substantial advances of understanding. The text should not exceed 3,000 words and six displayed items (figures plus tables). The article should include an abstract of about 50 words.

Letters to *Nature* are ordinarily 1,000 words long with no more than four displayed items. The first paragraph (not exceeding 150 words) should say what the letter is about, why the study it reports was undertaken and what the conclusions are.

Matters arising are brief comments (up to 500 words) on articles and letters recently published in *Nature*. The originator of a Matters Arising contribution should initially send his manuscript to the author of the original paper and both parties should, wherever possible, agree on what is to be submitted.

Manuscripts may be submitted either to London or Washington (decisions being made only in London). Manuscripts should be typed (double spacing) on one side of the paper only. Three copies are required, each accompanied by copies of lettered artwork. No title should exceed 80 characters in length. Reference lists, figure legends, etc. should be on separate sheets, all of which should be numbered. Abbreviations, symbols, units, etc. should be identified on one copy of the manuscript at their first appearance.

References should appear sequentially indicated by superscripts in the text and should be abbreviated according to the *World List of Scientific Periodicals*, fourth edition (Butterworth 1963–65). The first and last page numbers of each reference should be cited. References to books should clearly indicate the publisher and the date and place of publication. Unpublished articles should not be formally referred to unless accepted or submitted for publication, but may be mentioned in the text.

Each piece of artwork should be clearly marked with the author's name and the figure number. Original artwork should be unlettered. Suggestions for cover illustrations are welcome. Original artwork (and one copy of the manuscript) will be returned when manuscripts cannot be published.

Requests for permission to reproduce material from Nature *should be accompanied by a self-addressed (and, in the case of the United Kingdom and United States, stamped) envelope.*

andès

16, rue Claude-Bernard
75231 PARIS CEDEX 05
Tél. : (1) 337.51.12 (matin)

POURQUOI ?

L'Association nationale des Docteurs ès-Sciences (ANDES) a été créée en 1970. Reconnue d'utilité publique en 1975, elle est une association pluridisciplinaire et multiprofessionnelle servant de ralliement à des scientifiques très diversifiés dans leur devenir post-doctoral. Elle a pour buts essentiels :

- **d'agir en faveur de la diffusion de la culture scientifique et de l'expansion de la Recherche,**
- **d'affirmer le rôle des scientifiques dans la France et le monde de demain, répartis dans le monde entier,**
- **d'associer, dans une structure de dialogue, les Docteurs ès-Sciences de l'Université, des Organismes de recherche, de l'Administration et de l'Industrie,**
- **d'accroître la participation des scientifiques à la vie de la Nation et de les aider à contribuer au développement des activités socio-économiques qui transforment la société,**
- **de développer les contacts et l'information entre l'Université et l'Industrie,**
- **d'aider les Docteurs ès-Sciences dans la recherche d'un emploi et de réfléchir, d'une manière générale, au problème de l'emploi et des carrières des Docteurs ès-Sciences.**

COMMENT ?

- par la diffusion d'un Bulletin de liaison, ANDES-Informations, qui tient informés les membres de l'Association de tout texte administratif les concernant,
- par la publication de dossiers, de documents ou libres blancs destinés à la réflexion de la communauté des Docteurs ès-Sciences sur les problèmes d'actualité,
- par un annuaire informatisé bisannuel qui contient à ce jour 2530 noms de Docteurs ès-Sciences français ou étrangers, formés en France par la Recherche, donc francophones. Répartis dans le monde entier, ils sont universitaires, chercheurs, agents économiques, industriels, coopérants, membres de services diplomatiques ou d'organisations internationales. Un classement par disciplines scientifiques permet de faire appel à leur compétence pour le traitement de problèmes scientifiques ou techniques spécifiques,
- par des contacts suivis avec le (ou les) ministères chargé de la Recherche et de l'Industrie, les ministères de l'Éducation nationale, de la Formation professionnelle, du Travail et des Relations extérieures, en vue d'une information constructive et réciproque, condition du maintien élevé du niveau du Doctorat français,
- par des conférences et des tables rondes organisées périodiquement sur des sujets divers intéressant la vie de l'ANDES, les activités et le rôle des Docteurs ès-Sciences dans l'économie nationale et internationale, et les grands thèmes liés à la prospective scientifique,
- par l'organisation de rencontres entre Docteurs ès-Sciences de l'Industrie, de l'Université et des grands organismes publics.

DOCUMENTS DISPONIBLES sur demande au siège de l'ANDES, règlement à la commande par chèque bancaire ou postal à l'ordre de l'ANDES (CCP PARIS 7692-77 B).

1. **Étude sommaire comparative des diplômes universitaires scientifiques dans divers pays industrialisés,** 53 pages, Janvier 1980, 20 FF plus port (— de 250 g).
2. **Annuaire des Docteurs ès-Sciences** (n° ISSN 0761-1587), 5e édition, Mars 1984, 120 FF plus port (+ de 500 g). 2530 noms en 4 listes : alphabétique, géographique, professionnelle, scientifique.
3. **Document sur les Bourses ou contrats de recherche pour français ou étrangers,** Numéro spécial 32 du Bulletin d'ANDES-Informations, 18 pages, Juin 1984, 30 FF plus port (— de 100 g).
4. **Minicatalogue des Thèses de Doctorat ès-Sciences,** 108 titres, 80 pages, Juillet 1984, 30 FF plus port (— de 250 g).

CONDITIONS D'ADHÉSION : Membres ordinaires **170 FF** (demi-tarif pour retraité, conjoint et docteurs ès-sciences depuis moins de 3 ans) - Membres bienfaiteurs **850 FF** - Membres à vie **2 040 FF.**

BULLETIN D'ADHÉSION donne droit à l'envoi gratuit de l'Annuaire en cours, et des Bulletins d'ANDES-Informations récents - l'adresser au siège de l'ANDES, 16, rue Claude-Bernard, 75231 Paris Cedex 05, France. Les documents à remplir pour figurer dans le fichier seront envoyés par retour.

NOM, Prénoms ____________________
Adresse ____________________
____________________ Pays ____________
THÈSE de Doctorat d'État français, soutenue le ____________
à ____________________
Règlement par Chèque bancaire à l'ordre de l'ANDES à joindre au présent bulletin.

Circle No.43 on Reader Service Card.

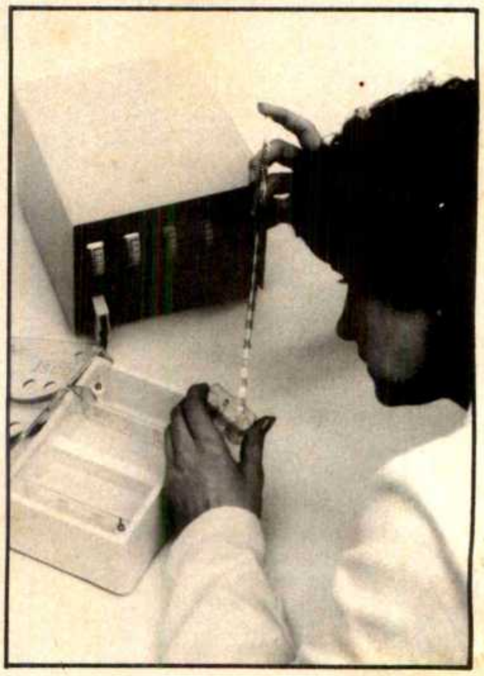

RECOVER SAMPLES FROM GELS AND GRADIENTS.

CONCENTRATE SMALL SAMPLES FAST.

Concentrate and separate samples from non-ionic media such as polyacrylamide gels or density gradient sugar solutions. You can use an Isco concentrator for proteins, nucleic acids, certain whole cells and fragments, or any other water soluble macromolecule larger than 3500 MW and having electrophoretic mobility

The Isco concentrator gives you 50-fold concentration of up to sixteen 10 ml samples in 90 minutes or less. To learn more, write or phone toll-free **[800]228-4250.**

ISCO

Isco
Box 5347
Lincoln, NE 68505
USA

Circle No.40 on Reader Service Card.

nature

21-1-87
A. Batty

COVER

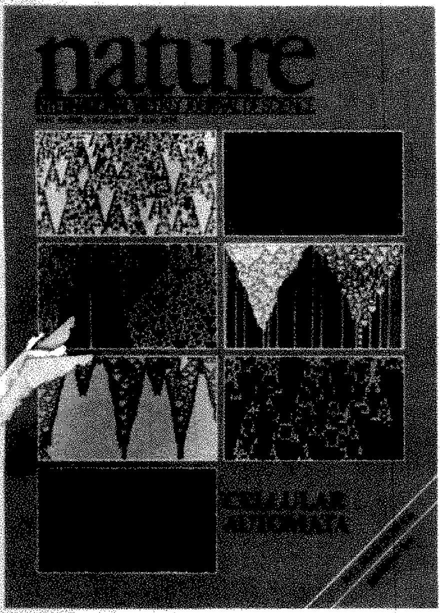

The origin of complex patterns developed by natural systems can be investigated by using mathematical models termed 'cellular automata'. Each consists of many simple identical components, together capable of complex behaviour. (See page 419.)

OPINION

Mr Gromyko and Mr Reagan 397
Another culprit

NEWS

European synchrotron source 399
Marinov
Canadian science 400
Looking south
Microscope acquired
European pollution 401
Lead and pollution
Weinberg *et al.* threat from animal lib
ICSU 402
Visas denied
Drugs in athletics
Heavy-ion research 403
Japanese research 404
Virus diseases
Australian science 405
US election

CORRESPONDENCE

Peer review/Brazilian science/ Era of bio companies/etc. 406

NEWS AND VIEWS

Jumping the smoking gun
Stephen Budiansky 407
Making fuel for inertially confined fusion reactors
Robert W Cahn 408
Seismic reflections of the continental crust Simon L Klemperer 409
Regulation by anti-sense RNA
Andrew Travers 410
Control of dolomite formation
M Kastner 410
Meteorites from Mars
David W Hughes 411
Forest history from pollen
Peter D Moore 412
Aurora seen in daylight
Alan Johnstone 413
Plant molecular studies forge ahead
John Ingle 413
The epidermal growth factor receptor gene and its product
Tony Hunter 414

SCIENTIFIC CORRESPONDENCE

Malignant cell lines — why use APUDoma? G E Moore 417
Mechanism for heritability of intelligence
T E Reed
Atmospheric humidity and the nuclear winter J Katz
DNA can be a selfish parasite
D A Hickey
Primroses and self fertilization
J G Piper, B Charlesworth & D Charlesworth 418
Herpes simplex transforming fragments
E Zuckerkandl
Chinese sources no guide to Geminga
F Verbunt

BOOK REVIEWS

Strong Medicine
by A Hailey John Treherne 489
Chemical Ecology of Insects
W J Bell and R T Cardé, eds
C T David
Development and the Environmental Crisis: Red or Green Alternatives?
by M Redclift
Stephen Cotgrove 490
Late-Quaternary Environments of the United State, 2 vols
S C Porter and H E Wright Jr, eds
D Q Bowen
Physics of Bioenergetic Processes
by L A Blumenfeld
Hans V Westerhoff 491
Conceptual Issues in Evolutionary Biology: An Anthology
E Sober, ed. Mark Ridley
Matter at Low Temperatures
by P V E McClintock, D J Meredith and J K Wigmore H M Rosenberg 492

REVIEW ARTICLE

Cellular automata as models of complexity
S Wolfram 419

ARTICLES

Orientation of *in situ* stresses in the oceanic crust
R L Newmark, M D Zoback & R N Anderson 424
Mantle upflow under North America and plate dynamics
D I Gough 428
Stimulation of 3T3 cells induces transcription of the *c-fos* proto-oncogene
M E Greenberg & E B Ziff 433
Differentiation of F9 teratocarcinoma stem cells after transfer of *c-fos* proto-oncogenes
R Müller & E F Wagner 438

LETTERS TO NATURE

Accretion disk limit cycle mechanism in twin-degenerate interacting binaries
J K Cannizzo 443
Boltzmann's ultraviolet cut off and Nekhoroshev's theorem on Arnold diffusion
G Benettin, L Galgani & A Giorgilli 444
Maximum entropy signal processing in practical NMR spectroscopy
S Sibisi, J Skilling, R G Brereton, E D Laue & J Staunton 446
High ^{3}He/^{4}He ratio in ocean sediments
M Ozima, M Takayanagi, S Zashu & S Amari 448
Occurrence of subtidal dolomite in a hypersaline lagoon, Kuwait
A Gunatilaka, A Saleh, A Al-Temeemi & N Nassar 450
Cobalt in pore waters of marine sediments
D Heggie & T Lewis 453
Contribution of gaseous sulphur from salt marshes to the global sulphur cycle
P A Steudler & B J Peterson 455

Contents continued overleaf

Nature® (ISSN 0028-0836) is published weekly on Thursday, except the last week in December, by Macmillan Journals Ltd and includes the Annual Index (mailed in February). Annual subscription for USA and Canada US $230 (for subscription prices elsewhere, see next page). USA and Canadian orders only to: *Nature*, Subscription Dept, PO Box 1018, Manasquan, New Jersey 08736, USA. All other orders to *Nature*, Brunel Road, Basingstoke, Hants RG21 2XS, UK. Second class postage paid at New York, NY 10010 and additional mailing offices. Authorization to photocopy material for internal or personal use, or the internal or personal use of specific clients, is granted by *Nature* to libraries and other users registered with the Copyright Clearance Center (CCC) Transactional Reporting Service, provided that the base fee of $1.00 per copy plus $0.10 per page is paid directly to CCC, 21 Congress Street, Salem, Massachusetts 01970, USA. The identification code for *Nature* is 0028-0836/84 $1.00 + $0.10. US Postmaster send form 3579 to: *Nature*, 15 East 26 Street, New York, NY 10010. Published in Japan by Macmillan Shuppan K.K., 5th Floor Eikow Building, 1-10-9 Hongo, Bunkyo-ku, Tokyo, Japan. © 1984 Macmillan Journals Ltd.

New biotin-streptavidin systems from Amersham

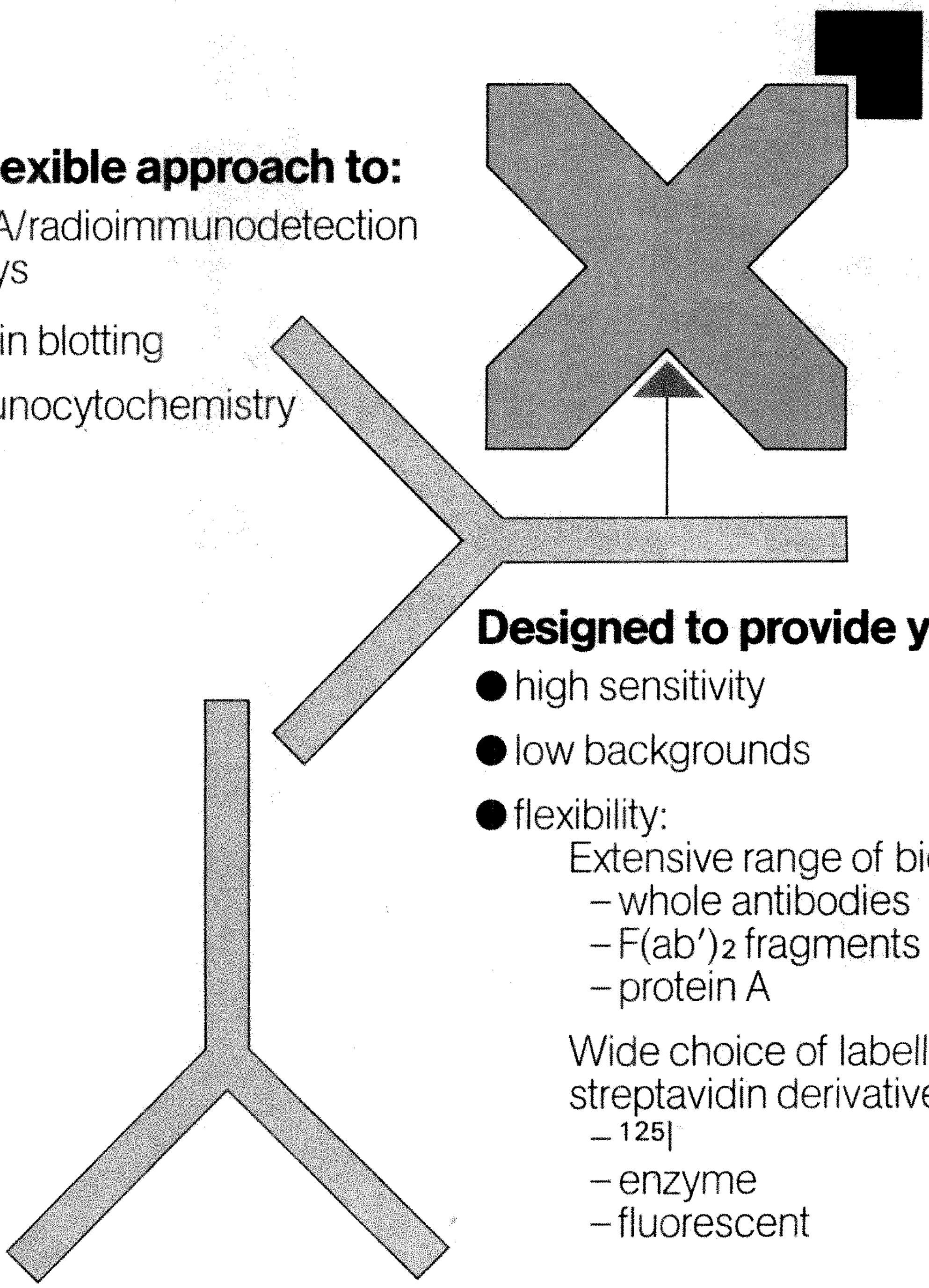

Your flexible approach to:

- ELISA/radioimmunodetection assays
- protein blotting
- immunocytochemistry

Designed to provide you with:

- high sensitivity
- low backgrounds
- flexibility:
  Extensive range of biotinylated
  - whole antibodies
  - $F(ab')_2$ fragments
  - protein A

  Wide choice of labelled streptavidin derivatives
  - $^{125}\mathrm{I}$
  - enzyme
  - fluorescent

For more details of this high performance detection system, please contact our Research Products Technical Service department or your local representative.

Amersham International plc
Amersham England HP7 9LL
telephone Little Chalfont (024 04) 4444
telex 83141 ACTIVA G

Amersham

Amersham Australia PTY Limited Sydney **Amersham Belgium SA/NV** Brussels **Amersham Buchler GmbH & Co. KG** Braunschweig W. Germany **Amersham Canada Ltd** Ontario **Amersham Corporation** Arlington Heights USA **Amersham Denmark ApS** Birkerød **Amersham France SA** Paris **Amersham Japan** Tokyo **Amersham Nederland BV** Utrecht

Circle No.50 on Reader Service Card.

CONTENTS

Index

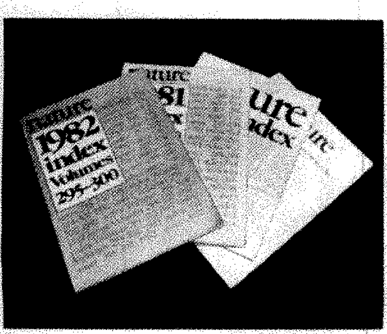

Comprehensive annual indexes of subject and author are available for all issues of **Nature** from 1971 to 1983.

Prices and address for orders are set out below.

Annual Subscription Prices

UK & Irish Republic		£98
USA & Canada		US$230
Australia & NZ	Airspeed	£150
Continental Europe	Airspeed	£120
India	Airspeed	£115
Japan	Airspeed	Y85000
Rest of World*	Surface	£120
Rest of World*	Airmail	£180

**(not USA, Canada, Europe & Japan)*

Orders (with remittance) to:

USA & Canada
Nature
Subscription Dept
PO Box 1018
Manasquan
NJ 08736
USA

UK & Rest of World
Nature
Circulation Dept
Brunel Road
Basingstoke
Hants RG21 2XS, UK
Tel: 0256 29242

(The addresses of Nature's editorial offices are shown facing the first editorial page)

Japanese subscription enquiries to:
Japan Publications Trading Company Ltd
2-1 Sarugaku-cho 1-chome
Chiyoda-ku, Tokyo, Japan
Tel: (03) 292 3755

Personal subscription rates
These are available in some countries to subscribers paying by personal cheque or credit card. Details from:

USA & Canada
Nature
15 East 26 Street
New York,
NY 10010, USA
Tel: (212) 689-5900

UK & Europe
Felicity Parker, Nature
Brunel Road
Basingstoke
Hants RG21 2XS, UK
Tel: 0256 29242

Credit card orders only (in USA):
Call toll-free: (800) 824-7888 (Operator 246)
In California: (800) 852-7777 (Operator 246)

Back issues
UK, £2.50; USA & Canada, US$6.00 (surface), US$9.00 (air); Rest of World, £3.00 (surface), £4.00 (air)

Binders
Single Binders: UK, £5.25; Rest of World, £7.75
Set of 3 Binders: UK, £14.00; Rest of World, £21.00

Annual indexes (1971–1983)
UK, £5.00 each; Rest of World, $10.00

Nature First Issue Facsimile
UK, 75p; Rest of World (surface), $1.50; (air) $2.00

Nature in microform
For Information:
University Microfilms International, 300 North Zeeb Road, Ann Arbor, MI 48106, USA

Functional neuronal replacement by grafted striatal neurones in the ibotenic acid-lesioned rat striatum
O Isacson, P Brundin, P A T Kelly, F H Gage & A Björklund 458

The neostriatal mosaic: compartmentalization of corticostriatal input and striatonigral output systems
C R Gerfen 461

Intraneuronal generation of a pyridinium metabolite may cause drug-induced parkinsonism
S P Markey, J N Johannessen C C Chiurh, R S Burns & M A Herkenham 464

Protection against the dopaminergic neurotoxicity of 1-methyl-4-phenyl-1,2,5,6-tetrahydropyridine by monoamine oxidase inhibitors
R E Heikkila, L Manzino, F S Cabbat & R C Duvoisin 467

Monoclonal antibodies against carbohydrate differentiation antigens identify subsets of primary sensory neurones
J Dodd, D Solter & T M Jessel 469

Pattern of presynaptic nerve activity can determine the type of neurotransmitter regulating a postsynaptic event
N Y Ip & R E Zigmond 472

Giant synaptosomes
J A Umbach, C B Gundersen & P F Baker 474

42,000-molecular weight EGF receptor has protein kinase activity
M Basu, R Biswas & M Das 477

Protein kinase C phosphorylation of the EGF receptor at a threonine residue close to the cytoplasmic face of the plasma membrane
T Hunter, N Ling & J A Cooper 480

Autophosphorylation sites on the epidermal growth factor receptor
J Downward, P Parker & M D Waterfield 483

Isolation of the closed circular form of the transposable element *Tc1* in *Caenorhabditis elegans*
A M Rose & T P Snutch 485

MISCELLANY

Product review: Neurosciences 491

NATURE CLASSIFIED

Professional appointments — Research posts — Studentships — Fellowships — Conferences — Courses — Seminars — Symposia: **Back pages**

Next week in *Nature*:

- Axion dark matter
- Laser particle accelerators
- Meteoritic interstellar dust
- Magnetic field reversing patterns
- Nucleosome particle structure
- Ca channel regulation
- Colonic *ras* gene expression
- Vaccinia immunogenicity
- Left-handed RNA helices

GUIDE TO AUTHORS

Authors should be aware of the diversity of *Nature*'s readership and should strive to be as widely understood as possible.

Review articles should be accessible to the whole readership. Most are commissioned, but unsolicited reviews are welcome (in which case prior consultation with the office is desirable).

Scientific articles are research reports whose conclusions are of general interest or which represent substantial advances of understanding. The text should not exceed 3,000 words and six displayed items (figures plus tables). The article should include an abstract of about 50 words.

Letters to *Nature* are ordinarily 1,000 words long with no more than four displayed items. The first paragraph (not exceeding 150 words) should say what the letter is about, why the study it reports was undertaken and what the conclusions are.

Matters arising are brief comments (up to 500 words) on articles and letters recently published in *Nature*. The originator of a Matters Arising contribution should initially send his manuscript to the author of the original paper and both parties should, wherever possible, agree on what is to be submitted.

Manuscripts may be submitted either to London or Washington (decisions being made only in London). Manuscripts should be typed (double spacing) on one side of the paper only. Three copies are required, each accompanied by copies of lettered artwork. No title should exceed 80 characters in length. Reference lists, figure legends, etc. should be on separate sheets, all of which should be numbered. Abbreviations, symbols, units, etc. should be identified on one copy of the manuscript at their first appearance.

References should appear sequentially indicated by superscripts in the text and should be abbreviated according to the *World List of Scientific Periodicals*, fourth edition (Butterworth 1963–65). The first and last page numbers of each reference should be cited. References to books should clearly indicate the publisher and the date and place of publication. Unpublished articles should not be formally referred to unless accepted or submitted for publication, but may be mentioned in the text.

Each piece of artwork should be clearly marked with the author's name and the figure number. Original artwork should be unlettered. Suggestions for cover illustrations are welcome. Original artwork (and one copy of the manuscript) will be returned when manuscripts cannot be published.

Requests for permission to reproduce material from Nature *should be accompanied by a self-addressed (and, in the case of the United Kingdom and United States, stamped) envelope.*

Good News!

to all European Scientists:

You can now order Peninsula Labs' quality synthetic peptides from

PENINSULA LABORATORIES EUROPE, LTD.

- Stock Inventory
- Immediate Delivery from U.K.
- Avoid Custom-clearing Problems

Peninsula Laboratories, Inc. has formed a subsidiary in U.K. to serve all European countries. Please contact:

PENINSULA LABORATORIES EUROPE, LTD.
Dr. Stanley Moore
Box 62, 17K Westside Ind. Estate
Jackson St., St. Helens
Merseyside, England WA9 3AJ
Telephone: St. Helens 612108 (0744)

Circle No.17 on Reader Service Card.

nature

21-1-87
[illegible]

COVER

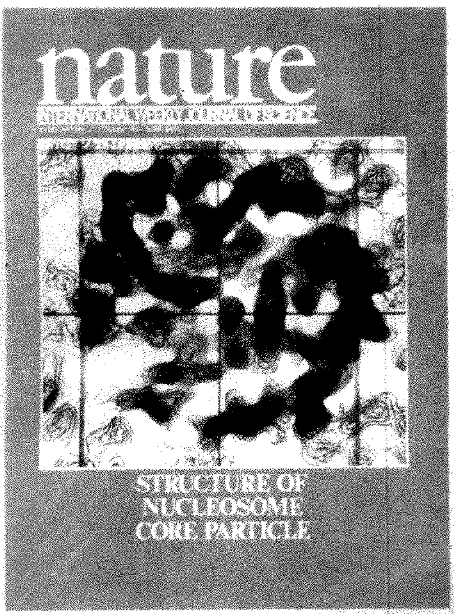
nature
INTERNATIONAL WEEKLY JOURNAL OF SCIENCE
STRUCTURE OF NUCLEOSOME CORE PARTICLE

A portion of the electron density map of the nucleosome core particle, showing one-half of the protein tetramer and central turn of DNA superhelix viewed down the axis of the superhelix. See page 532.

OPINION

A council ripe for abolition 493
Australia's problem 494
Conservation cheers

NEWS

Genetic manipulation 495
Dutch universities
French medical institutes 496
Soviet geology
Polish universities 497
US–Japanese education
Japanese universities 498
US basic research
British geology 499
UK atomic energy 500
UNESCO
Australian array
Italy 501
US Army research
Nature index of biotechnology stocks

CORRESPONDENCE

Persistence of miracles/Sequence databases/Nuclear power 502

COMMENTARY

Ethics, ethical committees and animal experimentation
D Britt 503

NEWS AND VIEWS

Thunder and electric storms
John Maddox 507
Cosmologists in the dark
Joseph Silk 508
Oscillations of degenerate stars
Arthur N Cox 509
In search of novel immunogens
Peter Newmark 510
Flight of fancy planned for the largest pterosaur
Kevin Padian 511
Continental interior in view
Roger N Anderson 512
Kin-groups in megalithic burials
C J Scarre 512
Clues to aetiology of Parkinson's disease from a toxin
Solomon H Snyder 514

SCIENTIFIC CORRESPONDENCE

Similarity between p154E of murine and feline leukaemia viruses and p21 of HTLV
G J Cianciolo, R J Kipnis & R Snyderman 515
Islet activating protein analogous to p21 *ras*?
R K Ralph
Heritable IQ — a reason to bother
J Hartung
Raising the tone of DNA sequences
M Pembrey & D Hart 516

BOOK REVIEWS

Evolution: The History of an Idea
by P J Bowler
Colin Patterson 587
The Dawn of Animal Life: A Biohistorical Study
by M F Glaessner
Steven M Stanley
Quarks and Leptons: An Introductory Course in Modern Particle Physics
by F Halzen and A D Martin
Gauge Theories of the Strong, Weak, and Electromagnetic Interactions
by C Quigg
Gauge Theory of Elementary Particle Physics
by T-P Cheng and L-F Li
Gauge Theories of Strong and Electroweak Interactions
by P Becher, M Böhm and H Joos
Graham G Ross 588
Muscles, Reflexes, and Locomotion
by T A McMahon
D R Wilkie 589

REVIEW ARTICLE

Formation of galaxies and large-scale structure with cold dark matter
G R Blumenthal, S M Faber, J R Primack & M J Rees 517

ARTICLES

Ultrahigh gradient particle acceleration by intense laser-driven plasma density waves
C Joshi, W B Mori, T Katsouleas, J M Dawson, J M Kindel & D W Forslund 525
Is there a climatic attractor?
C Nicolas & G Nicolis 529
Structure of the nucleosome core particle at 7Å resolution
T J Richmond, J T Finch, B Rushton, D Rhodes & A Klug 532
Different modes of Ca channel gating behaviour favoured by dihydropyridine Ca agonists and antagonists
P Hess, J B Lansman & R W Tsien 538
Relic interstellar grains in Murchison meteorite
J Yang & S Epstein 544

LETTERS TO NATURE

Improved positive-ion composition measurements in the upper troposphere and lower stratosphere and the detection of acetone
G Hauck & F Arnold 547
Microdomains observed at the ferroelectric/paraelectric phase transition of barium titanate
L A Bursill & Peng Ju Lin 550
Invariant and changing transitional field configurations in a sequence of geomagnetic reversals
J-P Valet & C Laj 552
Density of the ocean crust
R L Carlson & G S Rasin 555
Growing season precipitation from D/H ratios of Eastern White Pine
J R Lawrence & J W C White 558
Induction of hair growth by implementation of cultured dermal papilla cells
C A B Jahoda, K A Horne & R F Oliver 560

Contents continued overleaf

Nature® (ISSN 0028-0836) is published weekly on Thursday, except the last week in December, by Macmillan Journals Ltd and includes the Annual Index (mailed in February). Annual subscription for USA and Canada US $230 (for subscription prices elsewhere, see next page). USA and Canadian orders only to: *Nature*, Subscription Dept, PO Box 1018, Manasquan, New Jersey 08736, USA. All other orders to *Nature*, Brunel Road, Basingstoke, Hants RG21 2XS, UK. Second class postage paid at New York, NY 10010 and additional mailing offices. Authorization to photocopy material for internal or personal use, or the internal or personal use of specific clients, is granted by *Nature* to libraries and other users registered with the Copyright Clearance Center (CCC) Transactional Reporting Service, provided that the base fee of $1.00 per copy plus $0.10 per page is paid directly to CCC, 21 Congress Street, Salem, Massachusetts 01970, USA. The identification code for *Nature* is 0028-0836/84 $1.00 + $0.10. US Postmaster send form 3579 to: *Nature*, 15 East 26 Street, New York, NY 10010. Published in Japan by Macmillan Shuppan K.K., 5th Floor Eikow Building, 1-10-9 Hongo, Bunkyo-ku, Tokyo, Japan. © 1984 Macmillan Journals Ltd.

Tachykinin receptor studies

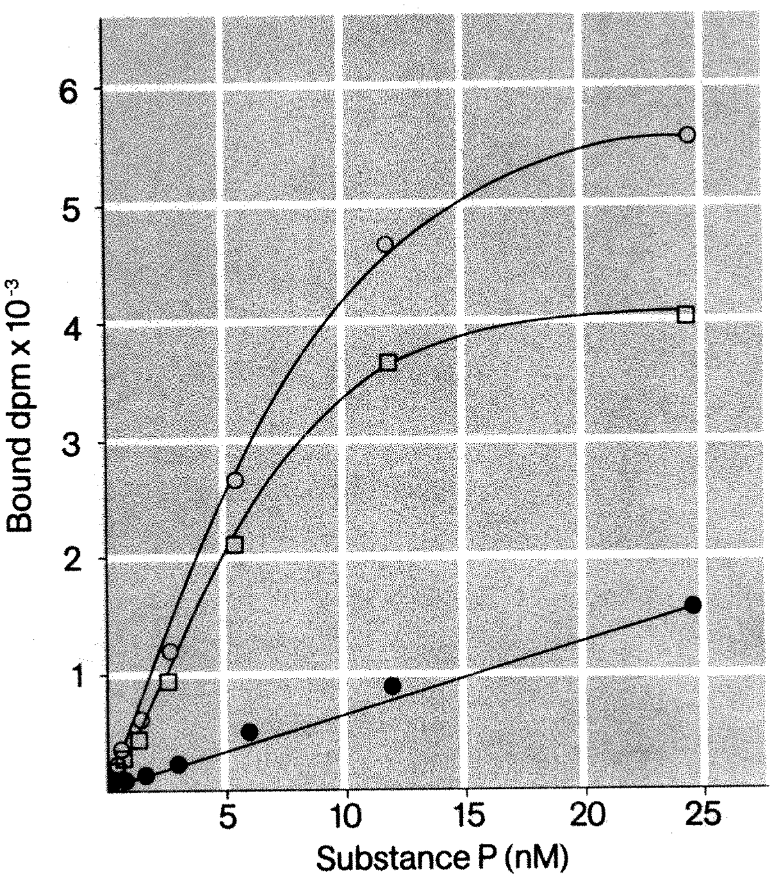

Binding of ^{3}H-Substance P to human Girardi heart cells.
○ Total binding
□ Specific binding
● Non-specific binding

Amersham provides the following high quality, proven products:

● [*prolyl*^{2,4}-3,4(n)-^{3}H]**Substance P**	TRK.786
● **Substance P, ^{125}I-labelled with Bolton and Hunter reagent**	IM.157
● **Substance P antiserum for RIA**	N.1571
● **Substance P antiserum for immunocytochemistry**	RPN.1572
● **Substance K,** *N*-[*propionyl*-^{3}H]**propionylated**	TRK.816
● (3-[^{125}I]*iodohistidyl*^{1})**Substance K**	IM.168
● [*prolyl*-3,4(n)-^{3}H]**Eledoisin**	TRK.811
● [*prolyl*-3,4(n)-^{3}H]**Physalaemin**	TRK.817

Please contact our Research Products Technical Service Department or your local representative for further details.

Amersham International plc
Amersham England HP7 9LL
telephone Little Chalfont (024 04) 4444
telex 83141 ACTIVA G

Amersham

Amersham Australia PTY Ltd Sydney (2) 211 4399/4489 **Amersham Belgium SA/NV** Brussels (2) 538 9194 **Amersham Buchler GmbH & Co KG** Braunschweig, West Germany (05307) 8080
Amersham Canada Ltd Ontario (416) 842 2720 **Amersham Corporation** Arlington Heights USA (312) 364 7100 **Amersham Denmark ApS** Birkerød (02) 82 0222
Amersham France SA Paris (6) 928 8300 **Amersham Japan** Tokyo (3) 543 0777 **Amersham Nederland BV** Utrecht (30) 7308 31 **Amersham Sweden AB** Solna (8) 734 0800

Circle No.52 on Reader Service Card.

CONTENTS

● HOW BRITAIN RUNS ITS SCIENCE

The new edition is available now. Nature's successful wallchart has been updated to take account of the changes in structure and personnel since the previous edition was published in 1981.
It includes the ministerial and other changes which followed the 1983 British General Election and provides a comprehensive survey of the administration of British science. Designed as a fold-out sheet, it can be carried easily to meetings or hung as a poster for permanent reference.

The new wallchart is available at £3.50 or US$7.95 from Nature's offices in Basingstoke or New York.

Annual Subscription Prices

UK & Irish Republic		£98
USA & Canada		US$230
Australia & NZ	Airspeed	£150
Continental Europe	Airspeed	£120
India	Airspeed	£115
Japan	Airspeed	Y85000
Rest of World*	Surface	£120
Rest of World*	Airmail	£180

**(not USA, Canada, Europe & Japan)*

Orders (with remittance) to:

USA & Canada
Nature
Subscription Dept
PO Box 1018
Manasquan
NJ 08736
USA

UK & Rest of World
Nature
Circulation Dept
Brunel Road
Basingstoke
Hants RG21 2XS, UK
Tel: 0256 29242

(The addresses of Nature's editorial offices are shown facing the first editorial page)

Japanese subscription enquiries to:
Japan Publications Trading Company Ltd
2-1 Sarugaku-cho 1-chome
Chiyoda-ku, Tokyo, Japan
Tel: (03) 292 3755

Personal subscription rates
These are available in some countries to subscribers paying by personal cheque or credit card. Details from:

USA & Canada
Nature
15 East 26 Street
New York,
NY 10010, USA
Tel: (212) 689-5900

UK & Europe
Felicity Parker, Nature
Brunel Road
Basingstoke
Hants RG21 2XS, UK
Tel: 0256 29242

Credit card orders only (in USA):
Call toll-free: (800) 824-7888 (Operator 246)
In California: (800) 852-7777 (Operator 246)

Back issues
UK, £2.50; USA & Canada, US$6.00 (surface), US$9.00 (air); Rest of World, £3.00 (surface), £4.00 (air)

Binders
Single Binders: UK, £5.25; Rest of World, £7.75
Set of 3 Binders; UK, £14.00; Rest of World, £21.00

Annual indexes (1971–1983)
UK, £5.00 each; Rest of World, $10.00

Nature First Issue Facsimile
UK, 75p; Rest of World (surface), $1.50; (air) $2.00

Nature in microform
For Information:
University Microfilms International, 300 North Zeeb Road, Ann Arbor, MI 48106, USA

Monoclonal antibodies define differential *ras* gene expression in malignant and benign colonic diseases
A Thor, P H Hand, D Wunderlich, A Caruso, R Muraro & J Schlom 562

T3-Ti receptor triggering of T8+ suppressor T cells leads to unresponsiveness to interleukin-2
A Bensussan, O Acuto, R E Hussey, C Milanese & E L Reinherz 565

A Ca-dependent Cl^- conductance in cultured mouse spinal neurones
D G Owen, M Segal & J L Barker 567

The agonist effect of dihydropyridines on Ca channels
A M Brown, D L Kunze & A Yatani 570

Immunochemical tests of acetylcholine receptor subunit models
J Lindstrom, M Criado, S Hochschwender, J L Fox & V Sarin 573

Photoreceptor-specific degeneration caused by tunicamycin
S J Fliesler L M Rapp & J G Hollyfield 575

Recombinant vaccinia virus primes and stimulates influenza haemagglutinin-specific cytotoxic T cells
J R Bennink, J W Yewdell, G L Smith, C Moller & B Moss 578

Transposition without duplication of infecting bacteriophage Mu DNA
R M Harshey 580

Effect of protein packing structure on side-chain methyl rotor conformations
A A Kossiakoff & S Shteyn 582

'Z-RNA' — a left-handed RNA double helix
K Hall, P Cruz, I Tinoco Jr, T M Jovin & J H van de Sande 584

Erratum . . . page 586
Dynamics of meltwater discharge from Northern Hemisphere ice sheets during the last deglaciation
R H Fillon & D F Williams

MISCELLANY

100 years ago 513
Employment: Job prospects in the United States
R Pearson 590

NATURE CLASSIFIED

Professional appointments — Research posts — Studentships — Fellowships — Conferences — Courses — Seminars — Symposia: Back pages

Next week in *Nature*:

- Nemesis for Nemesis
- India — Eurasia collision
- Deep-sea stratigraphy
- Human LHR hormone precursor
- Interleukin receptor cloned
- Transferrin receptors and oncogenes
- Influenza haemagglutin
- Transducin activation

GUIDE TO AUTHORS

Authors should be aware of the diversity of *Nature*'s readership and should strive to be as widely understood as possible.

Review articles should be accessible to the whole readership. Most are commissioned, but unsolicited reviews are welcome (in which case prior consultation with the office is desirable).

Scientific articles are research reports whose conclusions are of general interest or which represent substantial advances of understanding. The text should not exceed 3,000 words and six displayed items (figures plus tables). The article should include an abstract of about 50 words.

Letters to *Nature* are ordinarily 1,000 words long with no more than four displayed items. The first paragraph (not exceeding 150 words) should say what the letter is about, why the study it reports was undertaken and what the conclusions are.

Matters arising are brief comments (up to 500 words) on articles and letters recently published in *Nature*. The originator of a Matters Arising contribution should initially send his manuscript to the author of the original paper and both parties should, wherever possible, agree on what is to be submitted.

Manuscripts may be submitted either to London or Washington (decisions being made only in London). Manuscripts should be typed (double spacing) on one side of the paper only. Three copies are required, each accompanied by copies of lettered artwork. No title should exceed 80 characters in length. Reference lists, figure legends, etc. should be on separate sheets, all of which should be numbered. Abbreviations, symbols, units, etc. should be identified on one copy of the manuscript at their first appearance.

References should appear sequentially indicated by superscripts in the text and should be abbreviated according to the *World List of Scientific Periodicals*, fourth edition (Butterworth 1963–65). The first and last page numbers of each reference should be cited. References to books should clearly indicate the publisher and the date and place of publication. Unpublished articles should not be formally referred to unless accepted or submitted for publication, but may be mentioned in the text.

Each piece of artwork should be clearly marked with the author's name and the figure number. Original artwork should be unlettered. Suggestions for cover illustrations are welcome. Original artwork (and one copy of the manuscript) will be returned when manuscripts cannot be published.

Requests for permission to reproduce material from Nature *should be accompanied by a self-addressed (and, in the case of the United Kingdom and United States, stamped) envelope.*

BRITAIN AFTER NUCLEAR WAR

A NATIONAL BRIEFING ON THE 'NUCLEAR WINTER'
BY THREE OF THE WORLD S LEADING AUTHORITIES ON THE SUBJECT.
PROF. PAUL EHRLICH (USA) • DR. RICHARD TURCO (USA) • DR. ANNE EHRLICH (USA)

5·15 NOVEMBER · 1984

5 Nov.	**LONDON**
All day	Press, T.V., radio interviews.
6 Nov.	**SHEFFIELD**
1.30 pm	Local Authority Briefing.
7.30 pm	Public Meeting, Octagon Centre, Sheffield University Campus, Western Bank.
	LEEDS
Afternoon	University Seminar
7.30 pm	Public Meeting, Main Hall, Kitson College of Technology, Cookridge Street.
7 Nov.	**NEWCASTLE**
1.30 pm	Local Authority Briefing.
7.30 pm	Public Meeting, New Tyne Theatre, Westgate Road.
	EDINBURGH
1.30 pm	Seminar/lecture, Edinburgh University.
7.30 pm	Public meeting, Music Hall, Assembly Rooms, George Street.
8 Nov.	**GLASGOW**
All day	Civil Defence/Emergency Planning Conference.
7.30 pm	Public Meeting, Henry Wood Centre, Berkeley Street.
9 Nov.	**BIRMINGHAM**
1.30 pm	Local Authority Briefing.
Afternoon	Seminar/lecture, Birmingham University.
7.30 pm	Public Meeting, Great Hall, Aston University.
10 Nov.	**OXFORD**
All day	SANA Symposium on 'The Global Effects of Nuclear War'.
12 Nov.	**CAMBRIDGE**
Afternoon	Seminar/lecture, Cambridge University.
	NORWICH
Afternoon	Seminar/lecture, University of East Anglia.
7.30 pm	Public Meeting, Blackfriars Hall, St. Andrews Street.
13 Nov.	**BRISTOL**
1.30 pm	Local Authority Briefing.
Afternoon	Seminar/lecture, Bristol University.
7.30 pm	Public Meeting, Watershed, Bristol Exhibition Centre.
14 Nov.	**LONDON**
Morning	Consultations, GLC.
Afternoon	Seminar/lecture, University of London, Imperial College.
15 Nov.	**LONDON**
Morning	Briefing for MPs, House of Commons.
1.30 pm	Local Authority Briefing.
7.30 pm	Public Meeting, Lecture Hall, Central Hall, Westminster.

For further information
about the Speakers, the Nuclear Winter,
the University Seminars and the
Scientific Symposium or about SANA,
contact Rebecca Miles.
SANA, London Production Centre,
Broomhill Road, Wandsworth,
London SW18 4JQ

For further information
about the Local Authority Briefings,
Public Meetings or Nuclear Free Zone Authorities
contact Jim Coleman,
Nuclear Free Zone Officer,
Central Policy Unit,
Sheffield City Council,
Town Hall, Sheffield S1 2HH.

ORGANISED BY:
Steering Committee of Nuclear Free Zone Local Authorities and Scientists against Nuclear Arms

Circle No.04 on Reader Service Card.

New from...

MACMILLAN PRESS
SCIENTIFIC & MEDICAL

CLINICAL TESTS OF RESPIRATORY FUNCTION

G. J. Gibson

Contents:
Preface Acknowledgements 1. Equipment 2. Tests of Mechanical Function 3. Tests of Gas Exchange Function 4. Tests of Ventilatory Control 5. Exercise Tests 6. Physiological Variation 7. Airway Diseases 8. Alveolar Diseases 9. Diseases of Pleura and Chest Wall 10. Pulmonary Vascular Disease 11. Cardiac Disease 12. Blood Disorders 13. Neuromuscular Diseases 14. Renal Diseases 15. Hepatic and Bowel Disease 16. Metabolic and Endocrine Disorders 17. Systemic Vasculitis and Collagen Diseases 18. Clinical Application of Respiratory Function Tests Glossary of Terms, Abbreviations and Units Index.

1984 £30.00 0 333 32568 0 352pp

MOVEMENT DISORDERS – TREMOR

ed. Leslie J. Findley and Rudy Capildeo

This new volume provides the most comprehensive study of normal and pathological tremor currently available. It is interdisciplinary in its approach and contains contributions from all the leading researchers in this field, including C. D. Marsden, R. Young and K. E. Hagbarth. The 35 chapters are arranged under the broad headings: 1. General Aspects 2. Neurophysiology of Tremor 3. Essential Tremor 4. The Tremors of Parkinson's Disease 5. Cerebellar Tremor 6. Tremors in Peripheral Neuropathy 7. Tremulous and Tremor-Like Movements of the Eyes 8. Diverse Tremulous States.

1984 £55.00 0 333 35040 5 512pp

SCIENTIFIC & MEDICAL **M** **MACMILLAN PRESS LTD**

Please order these new titles from your bookseller or from Charlotte Wollocombe, Product Manager, Macmillan Press Ltd, FREEPOST, Houndmills, Basingstoke, Hants RG21 2BR, UK.

Postage free if payment with order. Credit cards accepted.

LIBRARY COMPLEX
Departments of
Chemical Engineering
Chemical Technology
Plastics and Rubber Technology

nature

21-1-87
A. Batts

NATURE VOL.311 18 OCTOBER 1984

COVER

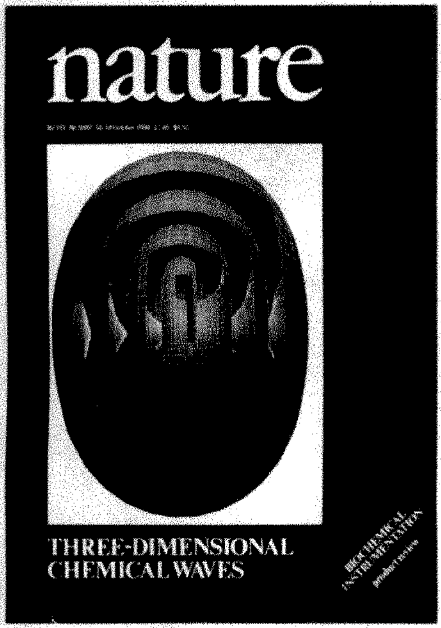

Computer image of a periodic wave of chemical activity moving through an excitable medium. Such waves can be seen in many biological and chemical environments. The three-dimensional nature of chemical waves is reviewed on page 611.

OPINION

Targets for future arms control 591
New academic tests
Irish disunity 592

NEWS

Fast reactors 593
Danish physics
European biotechnology 594
Danish collaboration
Japanese conservation 595
US patents
Soviet astronomy 596
US health research
Acid rain 597
Health advice
Chip pirates hit
Israeli aid 598
Israelis visiting China
Democratic elitism

CORRESPONDENCE

CERN/Mental arithmetic/Animal rights 599

NEWS AND VIEWS

Prizes (at last) for immunology
Peter Newmark 601
A continent in a grain of sand
Bruce W Sellwood 602
Nemesis for Nemesis?
Mark E Bailey 602
Optimal foraging theory tested
Jared M Diamond 603
Autocrine control of growth?
C D Stiles 604
Many guises of biophysics in Bristol
Maxine Clarke 605
Submersible study of the East Pacific Rise
Members of the Geocyarise expedition 606
Details of Soviet cosmodrome from space shuttle photographs
Grant H Thomson 607
Neutrinos and the Sun
Virginia Trimble 608
Sodium channels in invertebrate muscle
P R Stanfield 609

SCIENTIFIC CORRESPONDENCE

The nature of tumour cell proliferation
D A Gilbert 610
Machine-readable DNA sequences
R Lathe & R Findlay

BOOK REVIEWS

Man-Made Carbon Dioxide and Climatic Change: A Review of the Scientific Problems
by P S Liss and A J Crane
Carbon Dioxide — Emissions and Effects
by I M Smith
Climate and Energy Systems: A Review of their Interactions
by J Jäger
Our Threatened Climate: Ways of Averting the CO_2 Problem through Rational Energy Use
by W Bach
John S Perry 681
In Search of the Physical Basis of Life
by G N Ling
D A T Dick 682
Science and Medicine in France: The Emergence of Experimental Physiology, 1790–1855
by J E Lesch
W F Bynum 683
Geomagnetism of Baked Clays and Recent Sediments
K M Creer, P Tucholka and C E Barton, eds
Robert S Coe 684
Microcomputers and Laboratory Instrumentation
by D J Malcolme-Lawes
Alan Braithwaite

REVIEW ARTICLE

Organizing centres for three-dimensional chemical waves
A T Winfree & S H Strogatz 611

ARTICLES

India–Eurasia collision chronology has implications for crustal shortening and driving mechanism of plates
P Patriat & J Achache 615
Palaeomagnetic estimates of crustal shortening in the Himalayan thrusts and Zangbo suture
J Besse, V Courtillot, J P Pozzi, M Westphal & Y X Zhou 621
Molecular cloning and expression of cDNAs for the human interleukin-2 receptor
W J Leonard, J M Depper, G R Crabtree, S Rudikoff, J Pumphrey, R J Robb, M Krönke, P B Svetlik, N J Peffer, T A Waldmann & W C Greene 626
Molecular cloning of cDNA encoding human interleukin-2 receptor
T Nikaido, A Shimizu, N Ishida, H Sabe, K Teshigawara, M Maeda, T Uchiyama, J Yodoi & T Honjo 631

LETTERS TO NATURE

Terrestrial catastrophism — Nemesis or Galaxy?
S V M Clube & W M Napier 635
Dynamical constraints on the mass and perihelion distance of Nemesis and the stability of its orbit
J G Hills 636
How stable is an astronomical clock that can trigger mass extinctions on Earth?
P Hut 638
Orbital stability of the unseen solar companion linked to periodic extinction events
M V Torbett & R Smoluchowski 641
Nitryl perchlorate as the essential intermediate in the thermal decomposition of ammonium perchlorate
A K Galwey & M A Mohamed 642
South American modern beach sand and plate tectonics
P E Potter 645

Contents continued overleaf

Nature® (ISSN 0028-0836) is published weekly on Thursday, except the last week in December, by Macmillan Journals Ltd and includes the Annual Index (mailed in February). Annual subscription for USA and Canada US $230 (for subscription prices elsewhere, see next page). USA and Canadian orders only to: *Nature*, Subscription Dept, PO Box 1018, Manasquan, New Jersey 08736, USA. All other orders to *Nature*, Brunel Road, Basingstoke, Hants RG21 2XS, UK. Second class postage paid at New York, NY 10010 and additional mailing offices. Authorization to photocopy material for internal or personal use, or the internal or personal use of specific clients, is granted by *Nature* to libraries and other users registered with the Copyright Clearance Center (CCC) Transactional Reporting Service, provided that the base fee of $1.00 per copy plus $0.10 per page is paid directly to CCC, 21 Congress Street, Salem, Massachusetts 01970, USA. The identification code for *Nature* is 0028-0836/84 $1.00 + $0.10. US Postmaster send form 3579 to: *Nature*, 15 East 26 Street, New York, NY 10010. Published in Japan by Macmillan Shuppan K.K., 5th Floor Eikow Building, 1-10-9 Hongo, Bunkyo-ku, Tokyo, Japan. © 1984 Macmillan Journals Ltd.

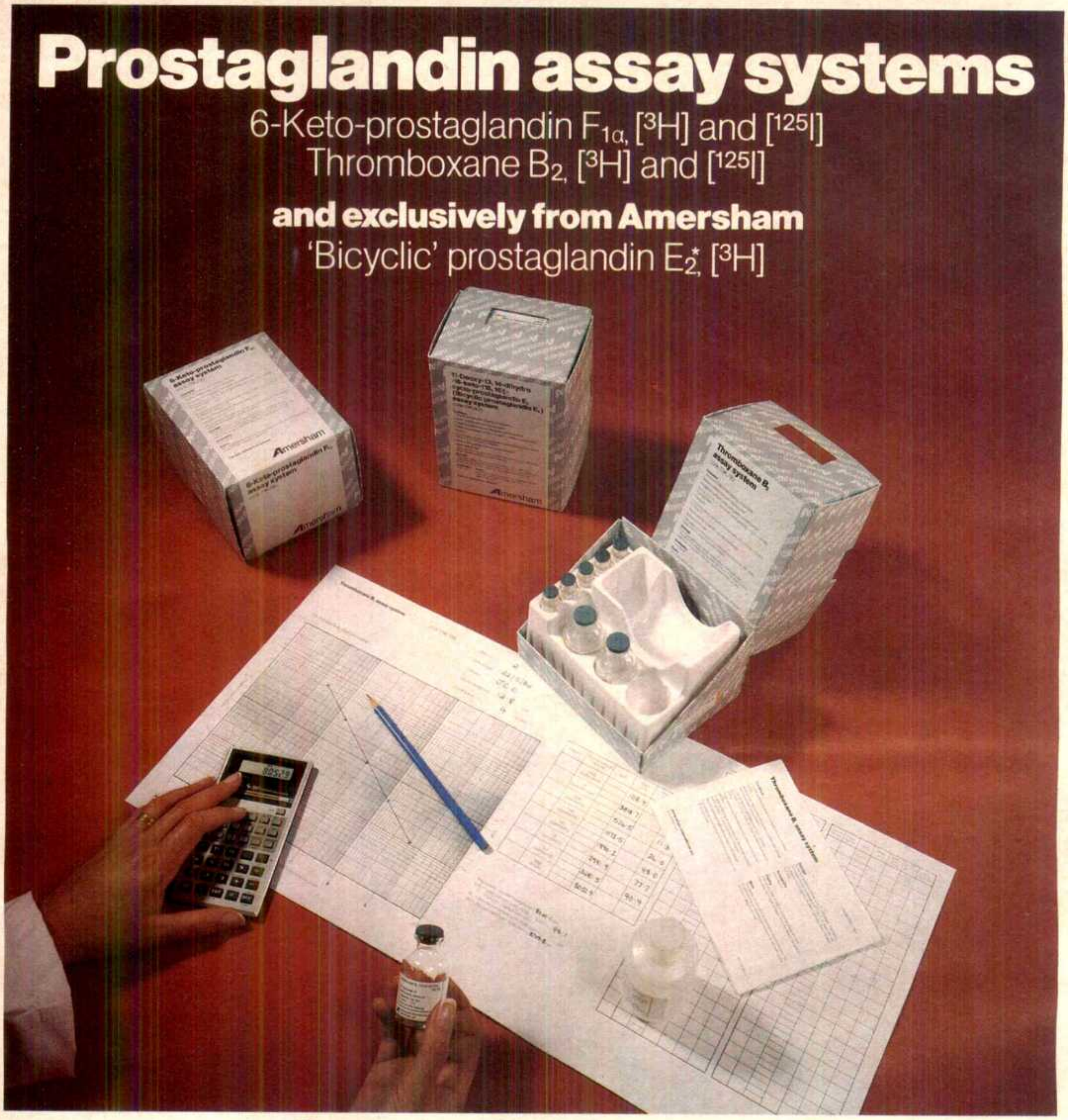

Prostaglandin assay systems

6-Keto-prostaglandin $F_{1\alpha}$, $[^3H]$ and $[^{125}I]$
Thromboxane B_2, $[^3H]$ and $[^{125}I]$

and exclusively from Amersham
'Bicyclic' prostaglandin E_2^*, $[^3H]$

...for rapid results

Amersham's new radioimmunoassay systems are the fast, accurate approach to measuring key prostaglandin metabolites reliably and consistently.

*11-Deoxy-13,14-dihydro-15-keto-11β,16ξ-cyclo-prostaglandin E_2, the high stability PGE_2 metabolite.

For research use only.

Amersham International plc
Amersham England HP7 9LL
telephone Little Chalfont (024 04) 4444
telex 83141 ACTIVA G

Amersham

Amersham Australia PTY Limited Sydney **Amersham Belgium SA/NV** Brussels **Amersham Buchler GmbH & Co. KG** Braunschweig W. Germany **Amersham Canada Ltd** Ontario **Amersham Corporation** Arlington Heights USA **Amersham Denmark ApS** Birkerød **Amersham France SA** Paris **Amersham Japan** Tokyo **Amersham Nederland BV** Utrecht

Circle No.51 on Reader Service Card.

CONTENTS

Keep your copies of *Nature* protected in these tough black PVC binders

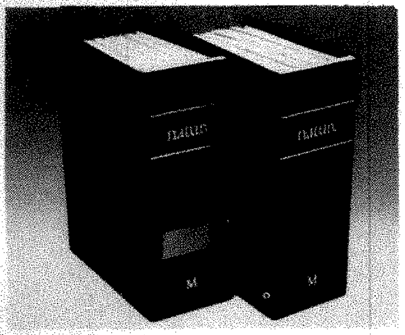

- Each binder is supplied with a set of wires for the easiest possible loading
- *Nature* logo blocked in gold on spine
- Transparent plastic pocket provided for your own reference
- Each binder takes two volumes of *Nature;* three binders will serve for a year
- Prices and address for orders are set out below

Annual Subscription Prices

UK & Irish Republic		£98
USA & Canada		US$230
Australia & NZ	Airspeed	£150
Continental Europe	Airspeed	£120
India	Airspeed	£115
Japan	Airspeed	Y85000
Rest of World*	Surface	£120
Rest of World*	Airmail	£180

**(not USA, Canada, Europe & Japan)*

Orders (with remittance) to:

USA & Canada
Nature
Subscription Dept
PO Box 1018
Manasquan
NJ 08736
USA

UK & Rest of World
Nature
Circulation Dept
Brunel Road
Basingstoke
Hants RG21 2XS, UK
Tel: 0256 29242

(The addresses of Nature's editorial offices are shown facing the first editorial page)

Japanese subscription enquiries to:
Japan Publications Trading Company Ltd
2-1 Sarugaku-cho 1-chome
Chiyoda-ku, Tokyo, Japan
Tel: (03) 292 3755

Personal subscription rates
These are available in some countries to subscribers paying by personal cheque or credit card. Details from:

USA & Canada
Nature
15 East 26 Street
New York,
NY 10010, USA
Tel: (212) 689-5900

UK & Europe
Felicity Parker, Nature
Brunel Road
Basingstoke
Hants RG21 2XS, UK
Tel: 0256 29242

Credit card orders only (in USA):
Call toll-free: (800) 824-7888 (Operator 246)
In California: (800) 852-7777 (Operator 246)

Back issues
UK, £2.50; USA & Canada, US$6.00 (surface), US$9.00 (air); Rest of World, £3.00 (surface), £4.00 (air)

Binders
Single Binders: UK, £5.25; Rest of World, £7.75
Set of 3 Binders: UK, £14.00; Rest of World, £21.00

Annual indexes (1971–1983)
UK, £5.00 each; Rest of World, $10.00

Nature First Issue Facsimile
UK, 75p; Rest of World (surface), $1.50; (air) $2.00

Nature in microform
For Information:
University Microfilms International, 300 North Zeeb Road, Ann Arbor, MI 48106, USA

A new method for environmental analysis of particle size distribution data from shoreline sediments
N R J Fieller, D D Gilbertson & W Olbricht 648

Effect of benthic mixing on the information content of deep-sea stratigraphical signals
P Schiffelbein 651

Pre-Columbian age for North American *Corispermum* L. (Chenopodiaceae) confirmed by accelerator radiocarbon dating
J L Betancourt, A Long, D J Donahue, A J T Jull & T H Zabel 653

Seabird colony distributions suggest competition for food supplies during the breeding season
R W Furness & T R Birkhead 655

Excitatory amino acids directly depolarize rat brain astrocytes in primary culture
C L Bowman & H K Kimelberg 656

Millisecond activation of transducin in the cyclic nucleotide cascade of vision
T M Vuong, M Chabre & L Stryer 659

Electrogenic Na–Ca exchange in retinal rod outer segment
K-W Yau & K Nakatani 661

Abrogation of resistance to bone marrow transplantation by induction of specific tolerance in natural killer cells?
M Waterfall, L S Rayfield & L Brent 663

Characterization of cDNA for precursor of human luteinizing hormone releasing hormone
P H Seeburg & J P Adelman 666

Developmentally regulated production of platelet-derived growth-like molecules
R A Seifert, S M Schwartz & D F Bowen-Pope 669

A novel transforming gene in a human malignant melanoma cell line
R A Padua, N Barrass & G A Currie 671

An artefact explains the apparent association of the transferrin receptor with a *ras* gene product
J Harford 673

Primary structure of human transferrin receptor deduced from the mRNA sequence
C Schneider, M J Owen, D Banville & J G Williams 675

Three-dimensional structure of an antigenic mutant of the influenza virus haemagglutinin
M Knossow, R S Daniels, A R Douglas, J J Skehel & D C Wiley 678

Errata . . . page 680

A general circulation model of water isotope cycles in the atmosphere
S Joussaume, J Jouzel & R Sadourny

Sequential late Cenozoic structural disruption of the northern Himalayan foredeep
D W Burbank & R G H Raynolds

MISCELLANY

100 years ago 606
Books received 685
Product review: Biochemistry laboratory equipment 687
Announcements 690

NATURE CLASSIFIED

Professional appointments — Research posts — Studentships — Fellowships — Conferences — Courses — Seminars — Symposia: Back pages

Next week in *Nature*:

- Geomagnetic secular variation
- Nuclear glass corrosion
- Volcanic climate
- Embryonic actin activation
- Algal phototactic rhodospin
- Monocot *Agrobacterium* plasmid
- B-cell differentiation
- No life in space
- New sparking-plugs

GUIDE TO AUTHORS

Authors should be aware of the diversity of *Nature*'s readership and should strive to be as widely understood as possible.

Review articles should be accessible to the whole readership. Most are commissioned, but unsolicited reviews are welcome (in which case prior consultation with the office is desirable).

Scientific articles are research reports whose conclusions are of general interest or which represent substantial advances of understanding. The text should not exceed 3,000 words and six displayed items (figures plus tables). The article should include an abstract of about 50 words.

Letters to *Nature* are ordinarily 1,000 words long with no more than four displayed items. The first paragraph (not exceeding 150 words) should say what the letter is about, why the study it reports was undertaken and what the conclusions are.

Matters arising are brief comments (up to 500 words) on articles and letters recently published in *Nature*. The originator of a Matters Arising contribution should initially send his manuscript to the author of the original paper and both parties should, wherever possible, agree on what is to be submitted.

Manuscripts may be submitted either to London or Washington (decisions being made only in London). Manuscripts should be typed (double spacing) on one side of the paper only. Three copies are required, each accompanied by copies of lettered artwork. No title should exceed 80 characters in length. Reference lists, figure legends, etc. should be on separate sheets, all of which should be numbered. Abbreviations, symbols, units, etc. should be identified on one copy of the manuscript at their first appearance.

References should appear sequentially indicated by superscripts in the text and should be abbreviated according to the *World List of Scientific Periodicals*, fourth edition (Butterworth 1963–65). The first and last page numbers of each reference should be cited. References to books should clearly indicate the publisher and the date and place of publication. Unpublished articles should not be formally referred to unless accepted or submitted for publication, but may be mentioned in the text.

Each piece of artwork should be clearly marked with the author's name and the figure number. Original artwork should be unlettered. Suggestions for cover illustrations are welcome. Original artwork (and one copy of the manuscript) will be returned when manuscripts cannot be published.

Requests for permission to reproduce material from Nature *should be accompanied by a self-addressed (and, in the case of the United Kingdom and United States, stamped) envelope.*

Fermentation engineering tailored to your specifications

You get better results in laboratory and production scale fermentations by using equipment with incorporated know-how. And when this equipment is tailored to your special tasks, you'll be another step ahead. B. Braun offers both. With their expertise and pragmatic approach, B. Braun utilizes the latest technology to plan and set up your fermenter – meeting your requirements exactly. Try us.

Picture: Custom made BIOSTAT® 300 D and BIOSTAT® U 30 D

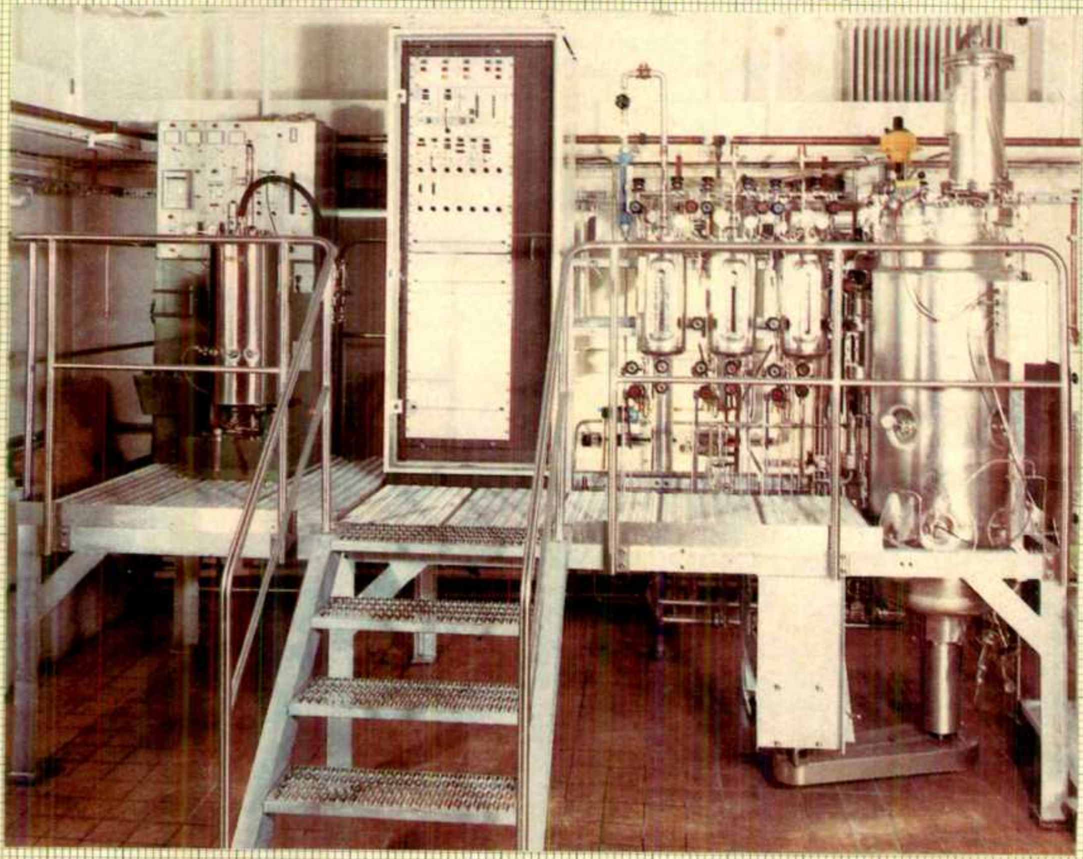

America headquarters
B. Braun Instruments
875, Stanton Road
Burlingame, Ca. 94010
Phone: 415-692-6022
Telex: 0176532 aic-bbi brgm

Japan headquarters
Japan BBM Co., Ltd.
1-20-5, Inokashira, Mitaka
Tokyo, Japan 181
Phone: 0422-43-4626
Telex: 02822375 nbbm j

European headquarters
B. Braun Melsungen AG
Postfach 110 + 120
D-3508 Melsungen
Phone: (05661) 71-0
Telex: 99937 bbraun d

Far East headquarters
B. Braun Medica Industries Sdn. Bhd.
Bayan Lepas Free Trade Zone
P.O. Box 880
Penang, Malaysia
Phone: 04-831511
Telex: 40401 bmi ma

B. Braun Flexible Fermentation Technology

B. Braun Melsungen AG
P.O.B. 110 + 120
D-3508 Melsungen/W.-Germany
Telephone: (05661) 71-0
Telex: 99937 bbraun d
Cable: INTERBRAUN Melsungen

B.BRAUN

Circle No. 16 on Reader Service Card.

nature

NATURE VOL. 311 25 OCTOBER 1984

21-1-87
R. Laiten

COVER

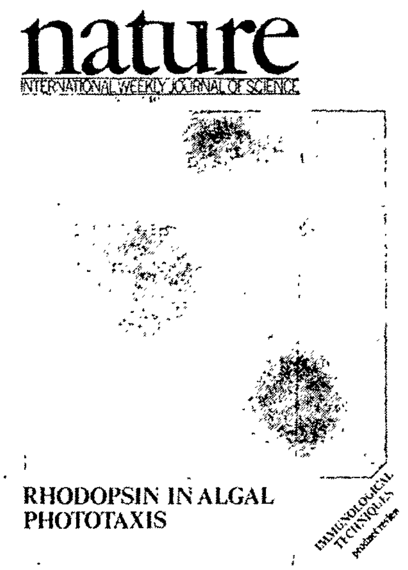
nature
INTERNATIONAL WEEKLY JOURNAL OF SCIENCE
RHODOPSIN IN ALGAL PHOTOTAXIS
IMMUNOLOGICAL TECHNIQUES
product review

Rhodopsin, a visual pigment ubiquitous in multicellular organisms, is also present in the unicellular alga *Chlamydomonas*. This supports the idea that visual pigments have a common ancient origin (see p.756, and News and Views p.702). Cover shows the related multicellular alga *Volvox carteri f. weismannia*. Each cell has a blue "eye" which reflects light; magenta is chloroplast fluorescence. (Photo: K.W. Foster and R. Birchem.)

OPINION

Causes of the British disease 691
Argument too formal 692
Truth will out (if late)

NEWS

British research council 693
Medical shoestring pared down
US Congress sweeps up remaining bills 694
Carlsberg Foundation 695
Synchrotron radiation
Genetic manipulation
US space station 696
UK Australian nuclear tests
European telecommunications 697
US policies offend Europeans
North Sea records
Thermonuclear fusion 698
Conservation in Japan
Nobel prize 699
Animal welfare

CORRESPONDENCE

NERC's virtues/Nuclear winter/ US federal deficit /Last word on Homer's wine. 700

NEWS AND VIEWS

CERN's first Nobel prize 701
Robert Walgate
Bovine-like rhodopsin in algae
Howard C Berg 702
Andean guide to Pliocene-Quaternary climate
J R Flenley 702
Creationism in confusion
Michael E Howgate & Alan J Lewis 703
Supertramps at sea
Jared M Diamond & William F Keegan 704
Chaotic spinning of Hyperion?
Carl D Murray 705
More prospects for Ti plasmids
M H Drummond 706
Resolution of intermediates in DNA recombination
Nancy L Craig 706
Origins of stony-iron meteorites
Edward R D Scott 708
Shiro Kakiuchi 1929-1984
A R Means 708

BOOK REVIEWS

International Environmental Policy: Emergence and Dimensions
by L K Caldwell
Eric Ashby 765
Amedeo Avogadro: A Scientific Biography
by M Morselli and
Boussingault: Chemist and Agriculturist
by F W J McCosh
Colin A Russell 766
Artificial Intelligence: Tools, Techniques, and Applications
T O'Shea and M Eisenstadt, eds
Wendy G Lehnert 767
Contractile Mechanisms in Muscle
G H Pollack and H Sugi, eds
Michael Spencer
Foundations of Laser Spectroscopy
by S Stenholm
G R Wilkinson 768

REVIEW ARTICLE

Geomagnetic secular variation impulses
V Courtillot & J L Le Mouël 709

ARTICLES

Cell type-specific activation of actin genes in the early amphibian embryo
T J Mohun, S Brennan, N Dathan, S Fairman & J B Gurdon 716

Resolution of synthetic *att*-site Holliday structures by the integrase protein of bacteriophage λ
P L Hsu & A Landy 721

Preferential utilization of the most J_H-proximal V_H gene segments in pre-B-cell lines
G D Yancopoulos, S V Desiderio, M Paskind, J F Kearney, D Baltimore & F W Alt 727

LETTERS TO NATURE

Rapid variability in optical polarization of the quasar-like object OJ287
A K Kulshrestha, U C Joshi & M R Deshpande 733

Outer-core geostrophic flow and secular variation of Earth's geomagnetic field
J L Le Mouël 734

Stress corrosion in a borosilicate glass nuclear wasteform
A E Ringwood & P Willis 735

A novel ignition device for the internal combustion engine
A J J Lee & F J Weinberg 738

Climatic impact of explosive volcanic eruptions
P M Kelly & C B Sear 740

Nd-Sr isotopic and REE constraints on the genesis of hydrothermal manganese crusts in the Galapagos
N Clauer, P Stille, C Bonnot-Courtois & W S Moore 743

Efficiency of petroleum expulsion from shale source rocks
D Leythaeuser, M Radke & R G Schaefer 745

Investigation of claims for interstellar organisms and complex organic molecules
R E Davies, A M Delluva & R H Koch 748

Rejection of transplantable AKR leukaemia cells following MHC DNA-mediated cell transformation
K Hui, F Grosveld & H Festenstein 750

Insertion of *N* into heavy-chain genes is correlated with expression of terminal deoxytransferase in B cells
S V Desiderio, G D Yancopoulos, M Paskind, E Thomas, M A Boss, N Landau, F W Alt & D Baltimore 752

Contents continued overleaf

Nature® (ISSN 0028-0836) is published weekly on Thursday, except the last week in December, by Macmillan Journals Ltd and includes the Annual Index (mailed in February) Annual subscription for USA and Canada US $230 (for subscription prices elsewhere, see next page). USA and Canadian orders only to: *Nature*, Subscription Dept, PO Box 1018, Manasquan, New Jersey 08736, USA. All other orders to *Nature*, Brunel Road, Basingstoke, Hants RG21 2XS, UK. Second class postage paid at New York, NY 10010 and additional mailing offices. Authorization to photocopy material for internal or personal use, or the internal or personal use of specific clients, is granted by *Nature* to libraries and other users registered with the Copyright Clearance Center (CCC) Transactional Reporting Service, provided that the base fee of $1.00 per copy plus $0.10 per page is paid directly to CCC, 21 Congress Street, Salem, Massachusetts 01970, USA. The identification code for *Nature* is 0028-0836/84 $1.00 + $0.10. US Postmaster send form 3579 to: *Nature*, 15 East 26 Street, New York, NY 10010. Published in Japan by Macmillan Shuppan K.K., 5th Floor Eikow Building, 1-10-9 Hongo, Bunkyo-ku, Tokyo, Japan. © 1984 Macmillan Journals Ltd.

New biotin-streptavidin systems from Amersham

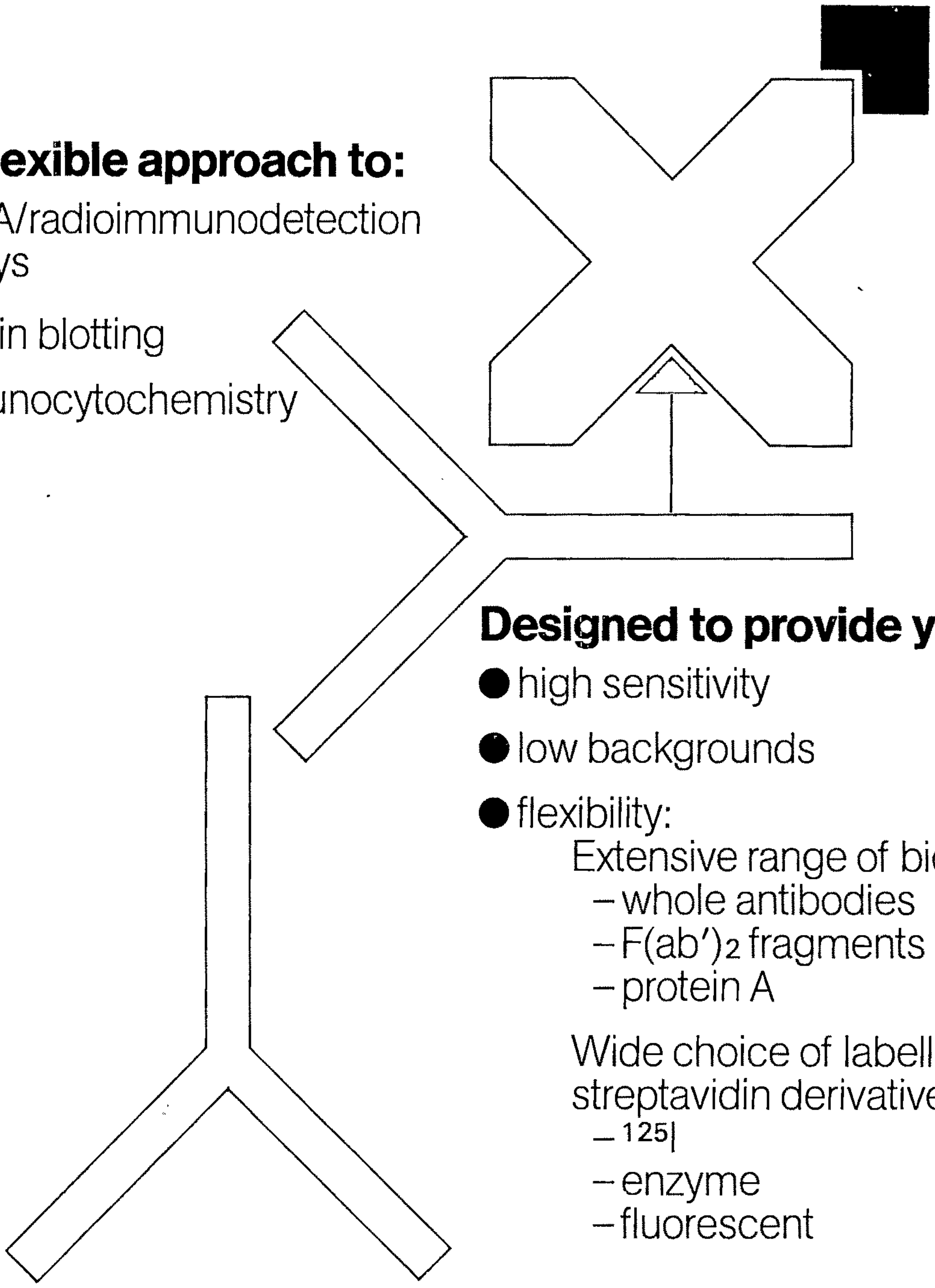

Your flexible approach to:

- ELISA/radioimmunodetection assays
- protein blotting
- immunocytochemistry

Designed to provide you with:

- high sensitivity
- low backgrounds
- flexibility:
  Extensive range of biotinylated
    - whole antibodies
    - F(ab')$_2$ fragments
    - protein A

  Wide choice of labelled streptavidin derivatives
    - ^{125}I
    - enzyme
    - fluorescent

For more details of this high performance detection system, please contact our Research Products Technical Service department or your local representative.

Amersham International plc
Amersham England HP7 9LL
telephone Little Chalfont (024 04) 4444
telex 83141 ACTIVA G

Amersham

Amersham Australia PTY Limited Sydney **Amersham Belgium SA/NV** Brussels **Amersham Buchler GmbH & Co. KG** Braunschweig W. Germany **Amersham Canada Ltd** Ontario **Amersham Corporation** Arlington Heights USA **Amersham Denmark ApS** Birkerød **Amersham France SA** Paris **Amersham Japan** Tokyo **Amersham Nederland BV** Utrecht

Circle No.50 on Reader Service Card.

● HOW BRITAIN RUNS ITS SCIENCE

The latest edition is available now. Nature's successful wallchart has been updated to take account of the changes in structure and personnel since the previous edition was published in 1981.
It includes the ministerial and other changes which followed the 1983 British General Election and provides a comprehensive survey of the administration of British science.
Designed as a fold-out sheet, it can be carried easily to meetings or hung as a poster for permanent reference.

The wallchart is available at £3.50 or US$7.95 from Nature's offices in Basingstoke or New York.

Annual Subscription Prices

UK & Irish Republic		£98
USA & Canada		US$230
Australia & NZ	Airspeed	£150
Continental Europe	Airspeed	£120
India	Airspeed	£115
Japan	Airspeed	Y85000
Rest of World*	Surface	£120
Rest of World*	Airmail	£180

**(not USA, Canada, Europe & Japan)*

Orders (with remittance) to:

USA & Canada	UK & Rest of World
Nature	Nature
Subscription Dept	Circulation Dept
PO Box 1018	Brunel Road
Manasquan	Basingstoke
NJ 08736	Hants RG21 2XS, UK
USA	Tel: 0256 29242

(The addresses of Nature's editorial offices are shown facing the first editorial page)

Japanese subscription enquiries to:
Japan Publications Trading Company Ltd
2-1 Sarugaku-cho 1-chome
Chiyoda-ku, Tokyo, Japan
Tel: (03) 292 3755

Personal subscription rates
These are available in some countries to subscribers paying by personal cheque or credit card. Details from:

USA & Canada	UK & Europe
Nature	Felicity Parker, Nature
15 East 26 Street	Brunel Road
New York,	Basingstoke
NY 10010, USA	Hants RG21 2XS, UK
Tel: (212) 689-5900	Tel: 0256 29242

Credit card orders only (in USA):
Call toll-free: (800) 824-7888 (Operator 246)
In California: (800) 852-7777 (Operator 246)

Back issues
UK, £2.50; USA & Canada, US$6.00 (surface), US$9.00 (air); Rest of World, £3.00 (surface), £4.00 (air)

Binders
Single Binders: UK, £5.25; USA & Canada $11.50; Rest of World, £7.75
Set of 3 Binders; UK, £14.00; USA & Canada $31.00; Rest of World, £21.00

Annual indexes (1971–1983)
UK, £5.00 each; Rest of World, $10.00

Nature First Issue Facsimile
UK, 75p; Rest of World (surface), $1.50; (air) $2.00

Nature in microform
For Information:
University Microfilms International, 300 North Zeeb Road, Ann Arbor, MI 48106, USA

A rhodopsin is the functional photoreceptor for phototaxis in the unicellular eukaryote *Chlamydomonas*
K W Foster, J Saranak, N Patel, G Zarilli, M Okabe, T Kline & K Nakanishi 756

Co-localization of neurotensin-like immunoreactivity and ^{3}H-glycine uptake system in sustained amacrine cells of turtle retina
R Weiler & A K Ball 759

Interactions between enkephalin and GABA in avian retina
C B Watt, Y-yu Tsu & D M-K Lam 761

Expression of Ti plasmid genes in monocotyledonous plants infected with *Agrobacterium tumefaciens*
G M S Hooykaas-Van Slogteren, P J J Hooykaas & R A Schilperoort 763

MISCELLANY

100 years ago 703
Books received 769
Product review: Immunological techniques 771
Announcements 774

NATURE CLASSIFIED

Professional appointments — Research posts — Studentships — Fellowships — Conferences — Courses — Seminars — Symposia: **Back pages**

Next week in *Nature*:

- T-cell receptor α chains
- Activation of ras gene-product
- Mapping of *src* oncogene
- Yeast growth control
- Potential emphysema cure
- Cygnus X-3
- Optical γ-ray source?
- Geminga
- Heliopause radio emission

GUIDE TO AUTHORS

Authors should be aware of the diversity of *Nature*'s readership and should strive to be as widely understood as possible.

Review articles should be accessible to the whole readership. Most are commissioned, but unsolicited reviews are welcome (in which case prior consultation with the office is desirable).

Scientific articles are research reports whose conclusions are of general interest or which represent substantial advances of understanding. The text should not exceed 3,000 words and six displayed items (figures plus tables). The article should include an abstract of about 50 words.

Letters to *Nature* are ordinarily 1,000 words long with no more than four displayed items. The first paragraph (not exceeding 150 words) should say what the letter is about, why the study it reports was undertaken and what the conclusions are.

Matters arising are brief comments (up to 500 words) on articles and letters recently published in *Nature*. The originator of a Matters Arising contribution should initially send his manuscript to the author of the original paper and both parties should, wherever possible, agree on what is to be submitted.

Manuscripts may be submitted either to London or Washington (decisions being made only in London). Manuscripts should be typed (double spacing) on one side of the paper only. Three copies are required, each accompanied by copies of lettered artwork. No title should exceed 80 characters in length. Reference lists, figure legends, etc. should be on separate sheets, all of which should be numbered. Abbreviations, symbols, units, etc. should be identified on one copy of the manuscript at their first appearance.

References should appear sequentially indicated by superscripts in the text and should be abbreviated according to the *World List of Scientific Periodicals*, fourth edition (Butterworth 1963-65). The first and last page numbers of each reference should be cited. References to books should clearly indicate the publisher and the date and place of publication. Unpublished articles should not be formally referred to unless accepted or submitted for publication, but may be mentioned in the text.

Each piece of artwork should be clearly marked with the author's name and the figure number. Original artwork should be unlettered. Suggestions for cover illustrations are welcome. Original artwork (and one copy of the manuscript) will be returned when manuscripts cannot be published.

Requests for permission to reproduce material from Nature *should be accompanied by a self-addressed (and, in the case of the United Kingdom and United States, stamped) envelope.*

Waters™ HPLC Systems for Amino Acid Analysis.

Now analyze primary and secondary amino acids with one picomole sensitivity.

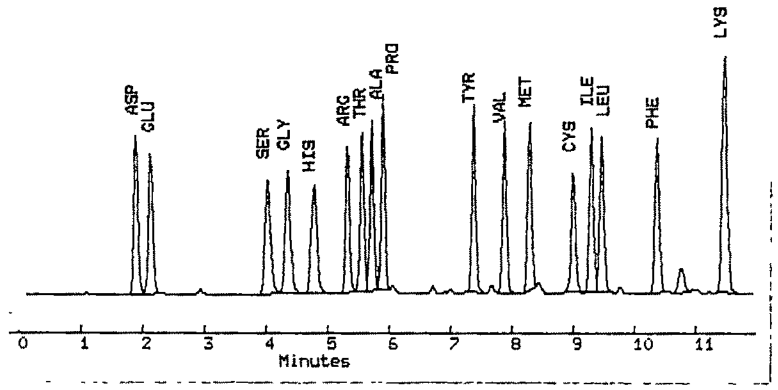

Introducing Waters high-speed PICO·TAG™ method. This innovative pre-column derivatization method is pre-packaged for guaranteed results. In 15 minutes, you can run a complete compositional analysis from as little as 100 nanograms of protein, with a detection limit of one picomole. Waters provides the complete methodology, plus reagents, buffers, column, Waters HPLC System and PICO·TAG Work Station.

With Waters Systems, choose the method that best meets your needs.

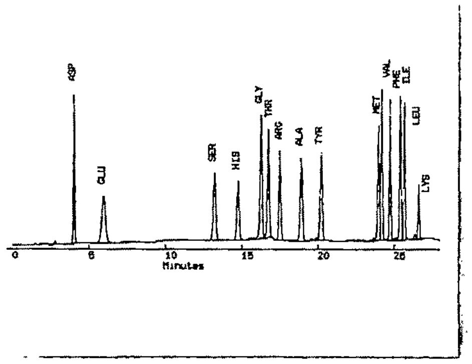

Waters AUTO·TAG™ OPA fully automated derivatization method. This exclusive method offers fully automated pre-column derivatization, separation and data reduction for high sensitivity analysis of primary amino acids. Perfect for process monitoring of amino acids in fermentation broths and cell cultures.

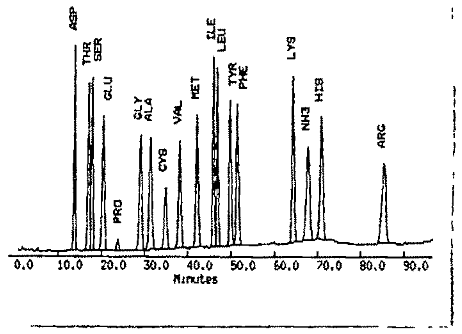

Classical Ion Exchange method with better quantitation. Waters improves this high resolution method with raw chromatographic data storage and re-integration capability for better quantitation, and full documentation of method, chromatography and integration.

More than offering just a choice of methodologies, Waters helps you get results.

For more information, contact Waters Life Science Dept., 34 Maple Street, Milford, MA 01757, 617-478-2000 (X 2665).

Circle No.05 on Reader Service Card.

MILLIPORE
Waters Chromatography Division

nature

21-1-87
A. Zatti
4630

Poor show for aviation industry

This week's Farnborough show of the aircraft industry is not so much a trade fair as a reminder that the industry's chief product, civil air transport, is not as accessible or cheap as it should be.

THE English place-name Farnborough means two things — a research establishment (the Royal Aircraft Research Establishment) and an air show (mounted every other year on the establishment's private airfield by the Society of British Aircraft Constructors). Once, the air show was what the name suggests, an opportunity for the wider public to see and inspect the latest wonders of aviation — aircraft with six wings and then with two; aircraft with metal wings and enclosed cockpits; aircraft capable of carrying passengers; and so on. Now, as this week's show will have amply demonstrated, the biannual show is nothing of the kind. Most of the exhibitors are not plane-makers but would-be manufacturers of bits and pieces from which aircraft may eventually be assembled. Those who make navigation equipment, or who provide fast-food for airline passengers, may even turn out to have done enough business at this year's show to justify the cost of being present. But in spite of the ritual flying display by familiar flying machines, most of them military, the show should be, for most of those who attend it, a reminder that the aircraft business is in a mess. And that it will remain so unless drastic steps are taken towards reform.

The problems are mostly political, deriving from the way in which governments of most countries seek short-term gains from technology at the expense of the potential beneficiaries — ordinary people, either as air-travellers or as taxpayers. Since the days when biplanes were made robust enough reliably to cross the narrow strip of water between England and France during the First World War, the aircraft business has become thoroughly international in the particular sense that international travel has become habitual and largely beneficial. Families split by emigration half a century ago unexpectedly find themselves reunited. People who choose to work in two continents can do so. People bored with vacations at Morecambe or Martha's Vineyard can hope to swim off Marrakesh instead. Even though groups of malcontents occasionally seize civil aircraft and force them to fly to places not on their flight-plans, the general influence of civil air transport is rightly to be welcomed. The tragedy is that the benefits of this important technology would be even more widely shared if it were properly exploited.

Problems

There are three ingredients of the muddle afflicting aircraft technology, all of them familiar. The chief is the practice by which most governments connive at the distortion of the air travel market by subsidizing national airlines and then by seeking to minimize the costs of that malpractice by bartering the right to fly over international routes with other governments. Second is the argument, even by governments guiltless on the first count, that aircraft technology is so closely bound up with military security that self-sufficiency is essential. Finally, the cost of developing new flying machines has been allowed, by lax governments and extravagant manufacturers, to become so large that the cost of equipment — and the risks in making it — are needlessly great. This is how governments and manufacturers should set out to put this ramshackle industry in order.

The distortion in the market for air travel is sanctified by an international conference in Ottawa in 1944, in the heady days when people hoped the United Nations would replace chauvinism by international charity. For much of the past 40 years, the International Air Transport Authority (IATA) which was a direct result has functioned as a simple cartel, allowing airlines to fix the prices charged for tickets on international routes. The same experience, working on the principle that the slice of the lower atmosphere above each country is part of its sovereign territory, launched the iniquitous doctrine that governments should be required to negotiate bilaterally how many flights by which airlines there should be between one and the other. In most parts of the world, the result has been that prices have been too high and services too few. That there would be problems in the outright deregulation of international air transport is not denied. Maverick governments willing indefinitely to support their national airlines could easily drive into bankruptcy competing airlines enjoying reciprocal rights but organized commercially. It would simply be necessary to drive down fares. The short-term remedy is the scheme the British and Dutch Governments have imaginatively drawn up for deregulating traffic between London and Amsterdam — there is a low minimum fare, but restrictions on frequency and the onward destinations of passengers are abolished. Other governments should follow suit — and in Europe, the European Commission should prod them more vigorously. Further ahead, there is a crying need that all airlines should operate on near-commercial principles. In Europe, the best solution would be a European fund specially created to finance airline operations in the inevitable years of deficit — and an agreement that airlines that cannot survive prudent bankers' investigation should go to the wall.

Chauvinism

The chauvinism that runs through the aircraft manufacturing business with disastrous consequences must somehow be moderated. Outside the Soviet Union and China, there are only three practical suppliers of large civil aircraft (Boeing, McDonnell-Douglas and Airbus Industrie, the European consortium) and three manufacturers of large jet engines (Rolls-Royce, General Electric and Pratt and Whitney). This is probably as many as a thin market will support, yet these companies are increasingly under pressure to make deals with local manufacturers in the countries whose national airlines agree to buy their wares, sometimes to abate the purchase price, more often to acquire unfamiliar skills. In military aircraft, the consequences of chauvinism are even worse. The widespread practice, even among military allies, of manufacturing as much as possible of their service aircraft is a means of increasing the great cost of these machines, and of keeping together groups of workers which are already too large. The excuse is that indigenous technology and manufacturing capacity are strategic necessities, a particularly thin excuse when military planners say that future wars will be unpleasantly nasty but mercilessly short. The economic consequences of these arrangements are easily guessed. Modern aircraft are assembled from bits and pieces themselves manufactured by companies which are smaller than they need be, and often too small to be fully skilled. Flying the flag, as the saying goes, is a way of making aircraft more expensive, and therefore less useful, than they might be.

The technical extravagance of the major manufacturers tends in the same direction. The unit of accounting in the development of a new aircraft or of its engines seems to have settled down at

£1,000 million or thereabouts. (Boeing's past successes may owe something to its economical ways of working.) Even allowing for the technical sophistication of the new machines and their power plants, and for the value of the potential prizes to be won, it is hard to see how costs on this scale can be justified. Part of the explanation is the ambition of most manufacturers to keep in being the small armies of skilled people which constitute their design teams. It would do no harm, and indeed might even benefit the aircraft industry itself, if the wisdom of these practices were closely examined by people skilled at telling not merely whether carbon-fibre composites are better for some technical purpose than the new aluminium-lithium alloys, but whether the processes of design and development need be as expensive as they have become. The economic benefits could be substantial — more flexibility in too tightly hierarchical an industry, easier access by the people to a technology whose benefits are already great, but which could be huge. Governments will not attempt the hard-eyed scrutiny that the aircraft industry needs, but would undoubtedly welcome the results. The responsibility falls squarely on the technical community. Why not (for Britain) Farnborough? ☐

Too brief encounter

The likely outcome of the space weapons talks is that the negotiators will meet only to adjourn.

THOSE who believe diplomacy a dull business should think again. Some weeks ago, the Soviet Union invited — some would say challenged — the United States to a conference at Vienna on the use of the space above the atmosphere for the siting of military weapons. The date suggested for the opening of the conference is 18 September, less than two weeks from now. Yet as things were earlier this week, nobody knew for certain whether two small armies of diplomats would actually arrive, ready to begin talking to each other. Careful people that they are, the potential members of the negotiating teams have arranged for hotel rooms to be booked on their behalf.

But Mr Konstantin Chernenko is clearly a little anxious that nothing at all will happen. In his interview with *Pravda* published at the weekend, he made noises apparently designed to soften the quarrel there has been with the United States about the agenda for the talks. If, he suggested, the United States would agree to talk about space weapons only at Vienna, he might ensure that there would be negotiations at another place and time about the issues the United States says it must discuss — the disposal of nuclear weapons in Europe and more broadly. Unfortunately, Mr Chernenko seems to have reckoned without the American calendar, temporal and electoral. Last weekend was Labor Day weekend, when citizens of the United States do not labour. And with President Ronald Reagan off to a good start in his campaign for re-election only two months from now, giving hostages to fortune in a negotiation that could not be complete before election day was bound to go against the electoral grain. So the State Department quickly announced that there was nothing new in what Mr Chernenko had to say, even though it is clear that it provided an opportunity that could have been exploited if anybody had felt so inclined.

What happens next? The most serious danger is that the preoccupation of even enlightened spirits in the United States with the election will blind one partner in the talks to the importance of what needs doing. Meanwhile, even the President and his advisers might prudently calculate (as they should have done during the last election campaign) that talks with the Soviet Union will be necessary once the dust has settled. Just as well to get something started before the election, but not to get too deeply embroiled in negotiations until the polls have taken place. So the likely calculation, at the State Department, is to aim at a preliminary encounter over space weapons, a polite statement of the need to talk about other things as well and an offer to adjourn the impending negotiation until something can be arranged. Whether Mr Chernenko and his colleagues will agree is entirely unclear. ☐

Academic divisions

Polytechnics should be made into universities or otherwise transformed.

THESE are busy but depressing days for polytechnics, the Cinderellas of the British system of higher education. For this is the season of the year at which would-be students denied places at universities turn to the polytechnics in the hope of being fitted in. On past form (and the figures released earlier this week by the Universities' Central Council on Admissions), something like 100,000 applicants for university places will be refused (but 75,000 will be accepted). Those turning to the polytechnics for an undergraduate education will, however, be douched with cold water by the report now published of a study of *Expectations of Higher Education* commissioned in 1980 by the Department of Education and Science and carried out by the Department of Government at Brunel University, the head of which (Professor Maurice Kogan) is as much an educationalist as anything else. The short message of a formless document is simple — employers are biased against the recruitment of graduates from the polytechnics, preferring the products they are used to — graduates from universities and especially from Oxford and Cambridge. This unsurprising news will be a slap in the face for many of the young hopefuls now hurrying off to the public sector in the hope of finding places as undergraduates. For those concerned with the future of British higher education, however, it should be a reminder that present arrangements are far from being sensible, and should urgently be scrapped.

Britain is not unique among industrialized nations in maintaining two kinds of institutions of higher education. Usually there are more vocational educational institutions. The distinctiveness of the British system is that the polytechnics were established overtly as an alternative to the university system, and have ever since been advertised as such. Whether the motives of the minister responsible, the late Mr Anthony Crosland, were political (British universities were already becoming unpopular with politicians), economic (the technical colleges from which the polytechnics emerged were thought to be cheaper) or pragmatic (what else could have so quickly increased the supply of graduates?), the designation of 26 polytechnics as graduating institutions within what is called the binary system turns out to have been a mistake. If there are two classes of institutions, one of which is seen to attract less highly qualified students (and probably less talented teachers), yet which has failed in nearly twenty years to make a characteristic mark, who can be surprised if that one continues to seem second-rate?

The prejudice of employers of all kinds against polytechnic graduates is understandable, even forgivable, on the basis of the data collected by the Kogan study. The school-leaving qualifications of polytechnic students, which span a spectrum overlapping with that of university entrants, are in general and on the average lower than those of new university undergraduates. While any process of education must somehow be capable of improving on people's attainment at the outset of their academic careers, nobody should be surprised that some of these measurable characteristics persist — and that when jobs are hard to find, employers take the easy way out. But all this is unfair to the polytechnics, many of which are in every way at least as competent as fully-fledged universities, and as successful in preparing their students for valuable careers. Especially because of the way that, in Britain, the sharpness of the binary division is accentuated by the academic snobbery which is rife, there is the strongest possible reason for its abolition. The sensible course would be to set a term, say five years from now, when all these institutions would be freed from the apron-strings of the local authorities that now watch over them, some to become rounded institutions of higher education, others to make their way in the world in different ways, perhaps by providing the distinctively vocational higher education that was originally, and inconsistently, part of the reason for their creation. Others might have to sink without trace. ☐

Biotechnology

Cohen–Boyer patent finally confirmed

Washington

AFTER 10 years of legal argument, Stanford University has finally been granted a "groundbreaking" product patent covering recombinant DNA molecules as produced by the Cohen–Boyer gene cloning technique. The Cohen–Boyer technique is fundamental to most genetic engineering research, and the new patent, which includes the uses of recombinant DNA in bacterial cells, confirms Stanford's proprietary hold on the fledgling biotechnology industry. A process patent covering Cohen–Boyer was granted to the university in 1980, and is considerably strengthened by the new product patent.

At present 66 companies are licensed to use the technology by Stanford, which shares rights with the University of California at San Francisco. Others have been holding back from paying the $10,000 annual licence fee until the status of the product patent became clear. The university will from now on enforce both, and it is likely that most industrial users of the technique will pay up: as one patent attorney put it, "you'd have to be out of your mind to challenge a $10,000 licence" since legal costs would inevitably be much greater than the licence fee.

The Cohen–Boyer technique uses a bacterial plasmid to transfer foreign DNA into a host cell. While the cost to licensees of using the technique might be modest, the value of the patents to Stanford and the University of California, San Francisco, is likely to be considerable, especially when genetically engineered products become more widely available. The universities will share royalties at the rate of 1 per cent for the first $5 million of sales, decreasing to ½ per cent on sales over $10 million. Use of the Cohen–Boyer technique in pure research is not restricted, but the partners have already earned almost $3 million on the process patent from commercial companies. The two inventors, Dr Stanley Cohen of Stanford's school of medicine and Dr Herbert Boyer, professor of biochemistry at the University of California, San Francisco, have both waived their rights to a one-third share of revenues. The income is used by the universities to support graduate student programmes. The new patent will prevent, for example, companies avoiding royalty payments by manufacturing abroad and importing into the United States.

The Cohen–Boyer saga has been controversial on several counts. In 1982, the Patent and Trademark Office tentatively rejected the product patent on the grounds that the original application incorrectly specified the origin of the plasmid called pSC101. The plasmid was described in the application as arising from a naturally occurring plasmid by recircularization of a fragment itself produced by hydrodynamic shear. A later paper by Cohen and a co-author revised this view and left open several possibilities for the plasmid's origin.

A patent specification must under US law provide sufficient information to enable a person "skilled in the art" to reproduce the invention. In granting the new product patent the patent office seems to have recognized that a description of how to make a product contains sufficient disclosure if it is operationally accurate, even if the proposed interpretation is incorrect.

Also related to the disclosure requirement was the objection that Cohen and Boyer failed to deposit samples of their plasmid in a public repository at the time the application was filed. They did, however, make samples available to qualified investigators, and the patent office seems now to have accepted that this practice was not unduly restrictive. This aspect of the case has caused some consternation to lawyers, who see dangers in allowing an organism in a private repository to suffice as a patent standard. Not least of these dangers is the natural inclination of a scientist to replace a strain isolated for a specific purpose with a better specimen should one turn up.

Other issues raised have included that of whether the invention was non-obvious and whether the scope of the application was too broad. Despite some fleeting references to the possibility of artificially recombining DNA published more than a year before the application, the new ruling confirms the originality of the idea. Stanford has withdrawn an earlier claim over the use of recombinant molecules in eukaryotic cells to expedite the present patent, but is still pursuing that claim in a separate undisclosed application.

The patent office usually declines comment on interpretation of its decisions, although an official said the judgement did "not represent a change of policy". A detailed policy statement on biotechnology is now being prepared by the patent office and is expected to clear up much of the confusion left in the wake of the Cohen–Boyer patent. **Tim Beardsley**

Industrial training

Britain lags well behind

A NEW approach to vocational training and education in Britain is essential if British industry is to compete successfully in world markets. This is the major conclusion of a report entitled *Competence and Competitions* prepared by the Institute of Manpower Studies for the National Economic Development Council (NEDC) and the Manpower Services Commission which compares, for the first time, British investment in training and human resources with that of West Germany, Japan and the United States. All three of these countries clearly recognize education and work competence as an important key to their economic success, some major companies in Japan and the United States, for example, investing between 2.5 per cent and 3 per cent of their sales revenue in training.

Young people in Germany, Japan and the United States are better equipped for working life than their British counterparts, the report says, because more of them participate in education and training programmes and for longer periods. In Japan, 84 per cent of school leavers voluntarily continue their education to the age of 18, in Germany the figure is 70 per cent, and in the United States 73 per cent of those aged between 16 and 24 are enrolled in some form of further education. It is quite sobering to realize that, in Britain, education beyond 16 is the exception rather than the rule; two-thirds of all 16 year olds enter the labour market.

Britain trains only 15,000 graduate engineers a year compared with Japan's 70,000. But, the report says, the most acute shortage is among craftsmen, technicians and middle-level engineers, and Britain must counteract the decline in apprenticeship training by creating alternative training routes.

Education and training in Germany, Japan and the United States is funded primarily by industry. In Germany, for example, employers bear 80 per cent of the cost of the 1.67 million apprentices under training. All three countries have responded to the recession by accelerating their training programmes and so investing money in the future.

The report makes twenty-four specific recommendations. Among other things, it calls for measures to enable 80 per cent of young people in Britain to enter the job arena with qualifications relevant to their employers and for Britain to emulate Germany's achievement of having 12 per cent of its adult workforce on work-related education and training. Industry, it says, must take the responsibility for funding new engineering training facilities. The report calls on the government, trade unions and employers to make a positive commitment to these aims.

Marcus Chown

European high-energy physics

Poor marks for enterprise

In the thirty years since the establishment of CERN, the European Organisation for Nuclear Research near Geneva, the laboratory has produced only two "crucial discoveries" compared with a dozen or more at United States laboratories, whose total cost is similar, and may even be less.

This is the bottom line of a lengthy balance sheet, with many other conclusions and observations, drawn up in nearly two years' work by social scientists Ben Martin and John Irvine, of the Science Policy Research Unit at the University of Sussex, and published today (6 September). The two-part report is certain to be influential in this particular reappraisal of its membership of CERN.

The first CERN discovery categorized as "crucial" was in 1973 ("neutral currents", a new form of weak interaction). By then, US laboratories had discovered a second neutrino, the omega-minus (the beginning of the quark model), charge-parity-violating interactions, deep inelastic scattering (which indicated that the proton really had components, now known to be quarks) and more. CERN, on the whole, has been thorough but dull, say Martin and Irvine — CERN lacked "bzazz". But the second of CERN's crucial discoveries is very recent (the intermediate vector bosons W and Z found last year), is attributable to a new adventurousness at CERN and, according to the review, "to a certain extent the balance of power in experimental high-energy physics between North America and Western Europe seems to have reached a turning point".

Martin and Irvine are famed (or notorious) for their previous critical assessments of the Jodrell Bank radiotelescope, British astronomy (notably the Isaac Newton telescope) and the Daresbury electron synchrotron NINA. But their review of CERN is more important as it may affect real policy in two ways: first, a British scientific committee (see box) is studying whether Britain should remain a member of CERN, given the present £27-million price tag; and there are indications that Martin and Irvine's much-improved approach to scientific assessment in the CERN report is finding favour among British policy-makers, and could be applied to other fields. (A study has already been made of protein crystallography, for example, and delivered to Sir David Phillips, chairman of the Advisory Board for the Research Councils, which allocates basic research funds among the different research councils in Britain.)

But does the Irvine and Martin method work? The two researchers' earlier reviews drew criticism that in assessing scientific productivity (or the lack of it) in terms of indicators of publication volume, citation frequency and peer ranking of laboratories, they ended up with too bleak a picture of what began to seem "targets" rather than mere subjects for research. There were mitigating circumstances, and forms of productivity unmeasured by the indicators.

But Martin and Irvine's present effort — two papers published in *Research Policy* — can hardly be criticized on those grounds. The CERN survey is sophisticated, and the two investigators clearly recognize a development in their technique. For example, they previously described their method as one of "converging" indicators, thus begging the question of whether or not the indicators do indeed converge on a single black-or-white assessment of a laboratory. In the case of CERN, the indicators clearly do not converge, and, write the researchers, "the results based on each indicator need to be carefully interpreted". Interpret they do, basing their analysis on 182 interviews with particle physicists from the Soviet Union to the United States.

High-energy physicists, even those at CERN, who have seen draft versions of the papers describe the analysis as fair, balanced and (mostly) accurate. CERN is admitted to have just missed the boat on many occasions. The two quarks called charm and bottom, which highlighted a revolution in physics in the 1970s described by Martin and Irvine as "the American Revolution", could have been found at CERN, the study claims. Missing the discovery of these particles was described by one physicist interviewed by Martin and Irvine as "a tremendous failure".

CERN even produced serious errors. One particle, the $A2$, was claimed — falsely, as it turned out — to be split, or twofold, creating a puzzle which absorbed theoreticians for nearly five years during the late 1960s. But similar errors were made in the United States (the "high-y" anomaly of Fermilab which caused equal consternation in the 1970s). Here the balance sheet is even.

European dimension

Sir John Kendrew, the molecular biologist who is chairing a committee looking into Britain's future commitment to CERN, said last week that the Irvine and Martin report (see above) will be distributed to all the members of the committee — but along with many other papers it had received ("too many actually", said Sir John).

His committee will report "early next year" to the Science and Engineering Research Council, together with the Advisory Board for the Research Councils, and the committee plans to visit CERN in October, Sir John said.

Just what impact the committee's views will have remains to be seen — Sir Keith Joseph, Secretary of State for Education and Science, announced on setting up this committee that its scientific review would be "without prejudice" to a final (political) decision on CERN membership. The final decision will have to be taken in the wider context of Britain's whole relationship to Europe. Robert Walgate

In terms of positive results, CERN's first big machine, the 28 GeV proton synchrotron(PS), though on line before the equivalent alternating gradient synchrotron (AGS) at Brookhaven, was nowhere near as productive at the beginning. Physicists attribute this, above all, to lack of experience in the design of high-energy physics experiments in Europe. Then the intersecting storage rings (ISR), designed to collide PS protons with each other head on, was a brilliant technical success — but failed to produce revolutionary physics. (It helped in understanding the quark structure of nuclear particles, but could have seen and not missed charm and bottom.) Martin and Irvine suggest the machine was underexploited by CERN management. The 400 GeV super proton synchrotron (SPS) that followed came too late — more than four years after Fermilab in the United States had creamed the energy region — and had to rely on tidying-up (which, nevertheless, it did well, with resources that were considerably greater than Fermilab's).

Dr Herwig Schopper

The lesson, if there is a single one, is that Europe's laboratory was run too much by committee, whereas American laboratories owed more to individual flair. (Maurice Goldhaber at Brookhaven, R. R. Wilson at Fermilab and Pief Panofsky at Stanford Linear Accelerator Center are singled out.) But Martin and Irvine say that things are changing at CERN under director-general Herwig Schopper and that a more individualistic style has emerged.

Nevertheless, CERN has committed itself now to just one future machine and its 15-mile tunnel, the electron accelerator LEP now under construction. A future and more controversial report by Irvine and Martin will discuss the prospects for LEP, and at lease one official involved in the British decision to support it has said he wishes he had had the report before him when he said yes. **Robert Walgate**

Japanese astronomy

Plan for telescope on Hawaii

JAPAN's astronomers, led by Professor Kei-ichi Kodaira of the Tokyo Astronomical Observatory, have announced plans to build what could be the world's largest optical telescope on Mauna Kea in Hawaii. A 7.5-metre single-mirror telescope is being called for — a considerable advance on the Mount Palomar 5-metre, or the 6-metre telescope now apparently operating at Zelenchukskaya in the Soviet Union.

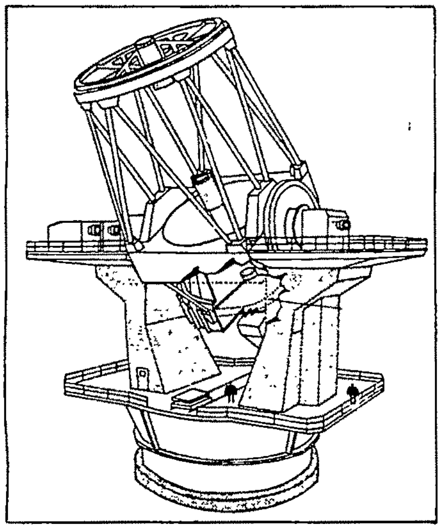

Whether the Japanese telescope turns out to be the world's largest depends upon how US plans for a multiple-mirror 15-metre telescope (the NTT, new technology telescope), possibly on the same site, come along. Records, anyway, are not what the Japanese are after: the telescope is being designed to complement, not compete with, NTT and to mesh neatly with Japan's proven capability in millimetre-wave astronomy and X-ray satellite astronomy.

Although the telescope plan has only just been made public, it has been vigorously discussed for some years. Ten years ago, the astronomy committee of the Science Council of Japan — the major representative body for scientists through which virtually all plans for large-scale facilities must pass — recommended building a 4-metre telescope. In those days, as now, Japan's biggest optical instrument was the 1.88 metre installed in 1960 at Okayama.

The 4-metre telescope was not built, however, and much of the astronomical community's energy went instead into backing the construction of the world's largest millimetre-wave telescope at Nobeyama. By the time attention had turned back to the need for an optical telescope, technological advances had been made and a 4-metre telescope was clearly too small, given that it will be 1990 before it is in operation.

Over the years two kinds of obstacles had also surfaced. First, Japan lacks any kind of central astronomical institute. The "Tokyo Astronomical Observatory", which has the major share of top-class facilities with seven observatories including Nobeyama, is actually a part of the University of Tokyo and does not have the authority to speak for all universities and astronomers, either to the government or to those in foreign countries from whom cooperation is necessary. Second, Japan has no history of large optical telescope building. Although there is no bar to foreign manufacturers, the newness of the design means it will be essential to have engineers close by to work with — and to charm with the technical challenge of the problems, rather than potential profits, for telescopes are not going to sell in bulk.

While neither of these problems has actually been solved, there is confidence that the Tokyo Astronomical Observatory can gradually move towards a central institute status similar to that held by ISAS and KEK (the space and high-energy physics research institutes) and that while international cooperation may be needed for the mirror design, Japanese engineers can handle the tracking and mounting.

The next question, which must be settled this year, is mirror design itself. There are advocates of both the honeycomb type pioneered at the Steward Observatory of the University of Arizona and a solid meniscus. Either way, the telescope aims at high performance not only in the optical region of the spectrum but also well into the infra red, with a resolving power around 0.1 arc seconds and a field of view wide enough (around 0.5 degrees) for efficient observation of 20th magnitude stars. This performance will complement that of NTT, which in aiming for a very large collecting area that will allow spectroscopy of extremely faint stars, will inevitably sacrifice some resolution (0.3 arc seconds has been cited), and the space telescope, which will have no infra red facility (at least to begin with) nor the combination of high resolution and wide field of view that the Japanese telescope will be able to offer.

Prime scientific objectives for the new telescope will obviously be stellar and planetary formation and the formation and evolution of galaxies. As astronomy is getting "redder and redder", the infra-red capacity will be of vital importance and allow a look back to early evolutionary stages of great cosmological significance. As two-dimensional infra-red detectors become available, the capacity of the telescope can be further expanded.

If the project gets the go-ahead, it will break political as well as scientific ground. At present, the Japanese Government owns no major research facilities abroad (other than Antarctic bases) and a move to Hawaii will be a major piece of "internationalization" requiring legal changes and the passage of a couple of bills through the Diet. Contacts have already been made with the University of Hawaii and the state governor for there is not much space left on Mauna Kea: with a proposed limit of 13 telescopes, six have been built, two planned and more are expected to be listed soon.

The astronomical community is expecting that all the basic plans for the telescope will be complete in a few months. Beyond that it is up to the University of Tokyo, rather than the observatory, to submit the request officially to the Ministry of Education, Culture and Science and for it to press for funds — estimated at around 20,000 million yen — from the government. If all goes well, money for a two-year evaluation programme will be granted beginning in 1986 and will be followed by five years of construction.

There is no official word yet, but the astronomical community seems confident that the money will be found. Behind-the-scenes opinion sampling which always precedes the emergence of a decision in Japan appears to have been going well. By 1986 they should know for sure. **Alun Anderson**

Open University cuts

THE Open University (OU), in common with other British universities, is facing a cutback in government financial support. The proposed cut comes after four successive years in which OU has seen its state aid shrink in real terms. Meanwhile, its efforts to economize have resulted, over the same period, in an increase in the proportion of total university expenditure met by non-government sources from 15 to 25 per cent.

OU is concerned that the cuts will lead to a reduction in its student numbers and its courses and will also seriously limit its ability to provide teaching through television and radio programmes, and it disputes the goverment's assessment of the precise magnitude of the planned cut. Sir Keith Joseph, Secretary of State for Education and Science, has insisted that the cut, over the three-year period until 1986, will amount to just £4.5 million. OU claims, however, that it will have to make a total reduction in expenditure of some £13.2 million by 1986, and has gone to some lengths to prove its point.

In arriving at its figure, OU has estimated the net increase in its costs (1983–86) due to inflation and "unavoidable" costs (equipment renewals, superannuation increases, etc.), after taking into account the expected rise in income from student fees during the period.

About 100,000 students were enrolled at the Open University last year, Britain's only university with no formal entrance requirements and open to people who, through financial or job constraints, cannot attend a full-time institution.

Marcus Chown

Space shuttle

Discovery takes off at last

Washington

OFFICIALS of the National Aeronautical and Space Administration (NASA) could almost be heard breathing a collective sigh of relief last week when the temperamental shuttle orbiter *Discovery* finally cleared the launch tower at Kennedy Space Center, Florida, on 30 August. Two previous launch attempts were aborted with the crew already strapped in and ready to go, and a scheduled launch on 29 August was called off after deficiencies were found in computer software controlling critical flight functions. NASA has tried to keep its commercial customers happy by rescheduling satellite deployments, but at the back of everyone's mind is the knowledge that NASA will now be able to launch only 6 shuttle flights this year even if there are no further problems. Originally 10 were planned.

The 29 August attempt was abandoned because simulations confirmed that under certain emergency conditions (such as the failure of one of the five on-board general-purpose computers), commands to the shuttle's "major event controller" could be delayed by as much as one second, enough for them to be rejected. The controller switches such critical events as the separation of the shuttle's external fuel tank and solid-fuel booster rockets, not to mention the bolts that secure the orbiter to the launch pad. NASA stresses that the postponement was a "safety first" decision and that a launch on 29 August would probably have been successful.

The difficulty appears to have been caused ultimately by inadequate testing procedures, since NASA insists that the on-board computers and the event controller had consistently performed to expectation in pre-flight simulations. The timing problem was first noticed during separate tests on software under development for a future shuttle mission. Parallel tests were then run on *Discovery's* computers and a similar effect confirmed: delays arose when the system had to deal with several events occurring almost simultaneously. The difficulty was rectified by a software patch, and go-ahead for the 30 August launch was given after a hastily-convened telephone conference of engineers. The inability to foresee exactly how a system of interacting computers will behave under non-standard conditions is presumably a problem that will not easily go away, because programs and hardware are continually being modified.

NASA was putting a brave face on the delay before last week's successful launch, and spokesmen were keen to point out that the last fault was only a potential one, and then only under worst-case conditions. Indeed, one suggested, it was to NASA's credit that it employed engineers able to raise such hypothetical problems. Whether NASA's customers will be able to see further delays to the shuttle programme in quite this light remains to be seen. American Telephone and Telegraph (AT&T), whose Telstar 3 satellite was reassigned to the present mission after the original failure to launch *Discovery* in June, declares itself content with the service given by NASA so far. However, AT&T has not directly lost out as a result of NASA's latest rescheduling, which involved combining parts of the payloads of two separate missions. Less pleased, presumably, is Hughes Communications Services Inc., whose LEASAT-1 satellite has been held up by shuttle breakdowns, and a movie company whose cameras have had to be left behind.

Besides three commercial satellites, *Discovery* was carrying three major NASA experiments to provide information that will be needed for designing a space station. These employ a 30-metre long folding panel such as might be used for solar cells; on the present flight, however, most of the cells will be dummies. Besides characterizing the test cells' performance, the array will be used to gather information on structural vibrations. The shuttle is also carrying a continuous flow electrophoresis system belonging to McDonnell Douglas and Ortho Pharmaceuticals Inc., which will further examine the feasibility of commercial pharmaceutical manufacture in the zero-gravity environment of space. Earlier versions of this experiment flown in previous shuttle missions have given encouraging results, but the partners are not telling what exactly they have in mind to produce.

Tim Beardsley

Soviet space programme

Remote sensing in prospect

FURTHER Comecon participation in the Soviet manned space programme is not foreseen in the "near future", Academician Vladimir Kotel'nikov told a press conference in Moscow last month. "Very broad and successful" international cooperation of the socialist countries of the world would, however, continue, he said. The "most impressive", he noted, will be the planned Vega mission to be launched in December, in which a two-part probe will be sent to Venus, one part then making a soft-landing on the planet and the rest continuing the rendezvous with Halley's comet, passing through the tail (at some 10,000 km from the head) in March 1986. The 130-kg Venus payload will include equipment developed in Bulgaria, Hungary, Poland and Czechoslovakia, and also Austria, France and West Germany. East Germany will provide the ground equipment for decoding the signals.

Apart from Vega, future *Interkosmos* projects seem likely to concentrate on what has always been one of the main aims of the programme: the use of remote sensing to aid the economies of the member nations. Photography from space of the homeland of the "guest" cosmonaut always formed part of the manned *Interkosmos* flights (although in the case of the Cuban cosmonaut this was apparently carried out by his Soviet "hosts" after he had returned to Earth). An *Interkosmos* symposium in Dushanbe last November, in which the Interkosmos cosmonauts took part, summed up the experience of the manned programme with particular emphasis on the value of remote sensing for locating mineral deposition and "enhancing" agricultural productivity.

The annual conference of leaders of the national coordinating bodies of *Interkosmos*, which met in Prague shortly before the Dushanbe conference, had likewise come out strongly in favour of remote sensing, the most practical route to making cooperation in space "more efficient".

A major step in implementing this joint remote sensing programme began last week in north-west Azerbaijan, involving representatives of all the European Comecon countries except Romania, working in conjunction with the three Soviet cosmonauts aboard Salyut-7. The ground team will make observations of the "spectral characteristics" of natural objects in the area (including the Mingechaur reservoir), which would be coordinated with aerial photographs and also photographs and spectrographs taken from the Salyut station. The orbital and airborne data are received by a special automated data-processing unit developed in Baku. The experiment is intended both to develop the "fundamentals of remote sensing of the environment" and also to provide practical recommendations for the utilization of agricultural land, pasture and reservoirs. For the Comecon participants, it is primarily a training exercise for future projects in which they will cooperate with Soviet space-crew passing over their homelands.

Interestingly, the experiment is co-ordinated not from Moscow or Baikonur, but by the Institute for the Remote Sensing of Natural Resources of the Azerbaijan Academy of Sciences. This institute has already obtained good results in predicting floods and mudslides in Azerbaijan, monitoring the state of the pastureland and forecasting the yield of the cotton crop. Delegation of coordination to the Academies of the Union Republics seems to be becoming a feature of the *Interkosmos* programme; the Vega mission is being coordinated by the Ukranian Academy.

Vera Rich

Product contamination

FDA sends in the marshals

Washington

US MARSHALS acting for the Food and Drug Administration (FDA) last week seized $4 million-worth of tissue culture and related products belonging to Flow Laboratories Inc., a major supplier to clinicians and researchers. The FDA action was taken following an inspection in April that found numerous instances of bacterial contamination of products and violations of FDA's code of good practice.

A federal judge later allowed Flow to recover raw materials and products used only for research. Flow attorneys argued that the FDA action was unlawful because marshals took "everything they could lay their hands on", and that cell lines would quickly die without attention. The company had been forced by the FDA action to close its manufacturing facility at McLean, Virginia.

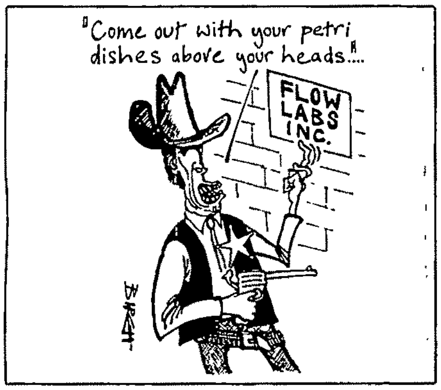
"Come out with your petri dishes above your heads!..."
FLOW LABS INC.

Flow does not dispute most of the hundred or so complaints listed by FDA in April, but, according to Douglas Poretz, director of corporate affairs, the company has since made vigorous efforts to comply with the FDA observations. The complaints originally made by FDA allege that procedures for testing contamination were inadequate, that "clean" and "dirty" areas were not kept separate and that sterilization equipment failed to work to specification. Several products were not routinely tested in the manner claimed and significant contamination was present in others. In some instances, according to FDA, the company had failed to notify customers after a faulty batch was detected.

Flow says that after the April inspection, several senior staff were fired and outside consultants were brought in. But problems continued, and more than 10 product recalls were made during July. An anonymous Flow employee telephoned FDA to say that some products known to be contaminated were being shipped to customers. FDA finally acted on the basis of the product recalls without carrying out a second inspection.

Flow General Inc., the parent company, has been through a disastrous 2 years and has sold off parts of its operation after sustaining losses last year of $10 million on sales of $129 million. Legal difficulties over a defence contract led to many staff resigning, and Flow Laboratories' factory in Scotland had to recall many products because of mycoplasma contamination from the water supply. A trial to examine the legality of the FDA action will be held on 12 September. **Tim Beardsley**

French nuclear energy

Overpowered

FRENCH pressurized water reactors (PWRs) now provide more than half of French electric power, and last year "had the best performance ever" after a rather worrisome year in 1982, according to a spokeswoman for Electricité de France (EDF), the French national utility.

In 1982, French reactors were troubled by problems with the radiation embrittlement of certain clips ("*broches*") which held fuel in place, which resulted in long shutdowns for repairs and consequently very poor operating figures for that year. It was feared that the French method of large batch production of a very small number of designs might have been cheap, but risky. If there were a fundamental flaw in the design, at worst all the reactors could go down, and French electricity production would be halved. What had seemed like sense began to seem like foolhardiness.

But all along EDF claimed that these were mere teething troubles. The French nuclear system had grown so rapidly, most of it was very new: the *broches* problem was a problem of running-in, said EDF (crossing its collective fingers meanwhile).

Now, however, the *broches* problem is past and all is well. In the first half of 1984, French PWRs have turned in availabilities (energy produced divided by energy theoretically capable of production, if the reactors all ran full-time) of over 80 per cent, compared with figures around and under 60 per cent a year earlier. West Germany and Japan are said to be showing similar good results.

But the problem in France now is what to do with all that electricity. The French Government, in announcing a slimmed-down nuclear construction programme last year, asked EDF to aim at increasing French electricity consumption by 40 per cent by 1990, a task which requires finding some inventive new uses for electricity. Domestic electricity consumption has indeed risen this year by about one per cent a month — but there are no obvious reasons why (the French economy has been stagnant). The other possible opportunity of filling the gap is export. Given the tardiness of the other European power programmes in substituting for coal and oil, this must be the greatest opportunity facing the French utility in 1990.

Robert Walgate

French universities

Now one for Le Havre

THE new French minister of education, M. Jean-Pierre Chevènement, is conforming to his old, expansionist style, and belief in investment in "grey matter". He has created a new university.

This will be the Université du Havre, a university for the channel port of Le Havre, the third port of Europe, the twentieth city in France and one that has been seeking university status for its various colleges for some fifteen years.

But "the university of where?" asked a surprised spokesman for the Centre National de la Recherche Scientifique (CNRS), France's principal source of funds for basic research, when confronted with the news on Monday. Admittedly the university had been created during her holiday (last Tuesday in fact), but this may be a small indication that the university is not immediately going to startle the world.

Actually, Le Havre will be the 64th French university, counting the vast 13-university University of Paris as one, to compare with 48 in Britain (counting the University of London as one), for about equal populations in the two countries. The comparison reflects the effects of the troubles of May 1968, when student pressure and political expediency led to the creation of many new universities in France and elsewhere on mainland Europe, but few in Britain.

The expansion might have been thought to be over in France, but that was reckoning without M. Chevènement — and the fact that the new Prime Minister, Laurent Fabius, owes his seat in the national assembly to the electorate of the Seine-Maritime department, which includes Le Havre.

The university is expected to concentrate on matters concerning international trade, and will begin with a £3 million cash grant to create a 6,300 sq. metre campus. It will combine an existing IUT (an institut universitaire de technologie, something like a British polytechnic) of 1,000 students, and other units that have previously depended on the Université de Rouen, 40 miles up the Seine. Its creation thus runs counter to policies observable in other countries (notably Britain), which tend towards a combination of facilities among universities.

According to figures collected by UNESCO, the United Nations Educational, Scientific and Cultural Organisation, France ranks fifth in the world in terms of the proportion of the population studying at university after the United States, Sweden, Japan and the Soviet Union. West Germany and Britain follow after France.

Robert Walgate

Too little Indian zeal

Sir — To my mind, the basic problem with Indian academics is that their sense of social responsibility is often regrettably poor. Only a very few educated people are ready to produce an amount of work that will justify their salaries. Even in a research institution such as the Tata Institute of Fundamental Research, where the annual input is equivalent to US$6 million, the annual output is about 270 research publications in the journals, shared by more than 300 top-level scientists. These scientists are potentially as capable as their counterparts in the West, but we become lazy in our home country. The very same people, when abroad, are compelled (possibly by example) to work hard, each producing as many as 5–10 papers a year. I am not saying that quantity is a measure of quality, but I certainly believe that, for the average research worker, quantity does beget quality.

The situation is much worse in Indian universities and other research organizations, which submit thousands of eyewashing project reports to their financiers, in preference to publication in one of the standard journals. Mainly on the basis of these obscure reports, however, the government measures national progress. Notwithstanding the rosiness of any such picture, the country seems to receive a poor return for its heavy investment. People are adequately paid for working, but the moral sense of their official responsibility fails to meet the minimum standard.

Mrs Indira Gandhi made a very brave attempt to improve matters by imposing emergency rule in 1976. All officials in positions of responsibility were forced to keep full office hours and to carry out their duties properly. This obviously irked all the educated parasites, who successfully brought about a ballot-paper revolution against her. So the poor lady has now learned that morality cannot be taught by force. We must rely on an appeal to people's individual consciences for any improvement — and I have written this letter in order to make such an appeal. A country can progress only if every citizen is willing to carry out his or her job responsibilities with sincerity and commitment. That is all that is needed in the first place, a step which has already proved to be the prime key to success in the West, the Soviet Union, China and Japan.

Many important plans in India have already failed because neither the planners nor the executors did their jobs properly. People are willing, for as long as a year if necessary, to weigh all the pros and cons before for example buying a motor car for themselves, but will lay out a hundred times as much on an expensive official project after as little as two weeks consideration. If that project is doomed to fail, it is not because of any failure of hands or brain, but because of a lack of commitment. The chance of success depends much more on this factor than merely saying later that the project had been too ambitious. One must go for ambitious projects, but wholeheartedly.

Another problem for India is that it is producing more specialists than it needs. In the United Kingdom, only 2.5 per cent of students go to university, but in India, the fraction is about 15 per cent. This means not only that some incompetent students sneak into higher education, but also promotes a brain drain to other countries or to other types of lucrative jobs. The aim of the universities is quite lost in the burden of teaching, while the research institutions fail to hold the meritorious scholars, because of either poor rewards or poor guidance. The latter seems to be the greater problem. Unless the professor or director is prepared to do more brain work than his subordinates, there is no justification for either his rank or the wastage of national money on him. Only a very committed leader can create an atmosphere conducive to equal commitment from his staff. Will the right people ever set the right examples?

Department of Physics, N.C. Rana
Science Laboratories,
University of Durham,
Durham DH1 3LE, UK
(On leave from Tata Institute of Fundamental Research, Bombay 400 005, India.)

Suggested remedies

Sir — For the sake of completeness of your appraisal of Indian universities (*Nature* **308**, 581-600; 1984), I would like to add the following comments on higher education in India.

Since independence in 1947, India has taken big strides in higher education, especially in science and technology. In the past two decades, the number of institutes of higher learning has increased enormously, but the provision of new institutes without consolidating the existing ones has had an undesirable effect on the quality of education. Indeed, many institutes have become degree-granting bodies rather than places of learning.

Almost all universities suffer from the age-old problem of "inbreeding". Unlike those elsewhere, Indian students after graduation are usually employed at their own *alma mater*, and even a very bright graduate will have a tough time getting a job at any other university. As a result, some universities have certain departments specializing in only one discipline — that of the preceptor. This has essentially stifled the influx of new ideas and progress and also creates a situation in which the head of a department, being senior to the rest of the faculty, has an absolute say in the running of his department. His colleagues, most of whom were his own students, do not dare to voice their feelings. Since the fate of an individual faculty member is decided by only one person, the spirit of competition is lost at the very beginning of tenure and every faculty member has. to promote himself by means other than teaching and research. With the increasing linguistic chauvinism in the universities, science education has suffered a great deal. A developing country such as India needs ideas and literature from the advanced countries. But since education in English has been trimmed to promote one of the fourteen official languages of India, students cannot grasp the progress of developed nations. This is a self-defeating and shortsighted approach which has been forced on the country by self-promoting educationists and politicians. The effect has inevitably been an overall decline of science and technology education in India.

Striking has become a pastime for Indian students. Students go on strike for a difficult question paper, for failing grades or for compulsory promotion, but never for better teachers. Since the strikes are almost invariably resolved to the students' advantage, they have become an important tool in obtaining degrees, mainly because many students are admitted to university who are not sufficiently well qualified to be there.

India must find ways to eliminate the pitfalls inherent in the existing system. To start with, there should be a ban on appointments to a faculty from among its own graduates. English should be made essential for prospective scientists and technologists. There should be a nationwide qualifying test for university entrance. Educationalists and politicians should do everything they can to formulate progressive and farsighted policies on education and should rise above petty political advantage. It is after all education which eventually leads a nation.

3420 Wythe Road, Kailash C. Gupta
Memphis, Tennessee 38134, USA

Red Sirius

Sir — The correspondence about Homer's wine-coloured sea reminds me about red Sirius. Several ancient authors call Sirius red, even though it is white with a slight bluish tint. This is another object which seems to have been called red even though blue would have been a better description.

Göran H. I. Johansson
Lund Observatory,
Box 1107,
S-22104 Lund, Sweden

Sir — Homer's wine-dark sea is not the only such problem in Greek culture. It is well-known by astronomers that in Ptolemy's *Almagest*, Sirius is described as a red star, and there is no explanation on modern astrophysical grounds for such obvious disagreement.

Carlos Alberto P.C.O. Torres
Observatório Astrofísico Brasileiro,
Caixa Postal 21,
37.500 Itajuba MG, Brazil

Worldwide Scientific Progress from Plenum

BEHAVIOR OF MARINE ANIMALS

Volumes 5 & 6

SHOREBIRDS

edited by **Joanna Burger**, *Rutgers University*, and **Bori Olla**, *Oregon State University, Newport*

Volume 5

Breeding Behavior and Populations

The first volume of this outstanding two-volume set is a selection of current research in shorebird classification and breeding behavior: breeding site fidelity; polyandrous mating systems; communication; parental and antipredator behavior.
0-306-41590-9/454 pp./ill./1984
$59.50 ($71.40 outside US & Canada)

Volume 6

Migration and Foraging Behavior

This second volume covers behavior aspects during the nonbreeding season, focusing on abiotic factors affecting migration, migratory behavior in the Western Palearctic and New World, foraging and activity patterns, food supplies, and spacing patterns of nonbreeding migrants.
0-306-41591-7/344 pp./ill./1984
$49.50 ($59.40 outside US & Canada)

two-volume set: $89.50 ($107.40 outside US & Canada)
Circle No. on Reader Service Card.

SYNTHETIC ORGANIC PHOTOCHEMISTRY

edited by **William M. Horspool**,
The University of Dundee, UK

This brand-new volume provides a broadly based account of the exciting opportunities arising from the application of photochemical methods in organic synthesis. Highlighting the synthetic value of the reactions discussed, the book deals with aromatic compounds, enones, electron-transfer reactions, phthalimides, heterocycles, azirines, photo-protecting groups, and oxetan formation and gives a brief outline of equipment and techniques.
0-306-41449-X/552 pp./ill./1984
$75.00 ($90.00 outside US & Canada)
Circle No. on Reader Service Card.

THE PHYSICIAN'S GUIDE TO DIVING MEDICINE

edited by **Charles W. Shilling, Catherine B. Carlston,** and **Rosemary A. Mathias,**
Undersea Medical Society, Bethesda, Md.

A practitioner's guide to the medical care of scuba divers and others who are exposed to hyperbaric environments. Covers physical, physiological, and behavioral effects of diving; diving equipment and procedures; how to diagnose and treat decompression sickness, gas embolism, and near-drowning; medical examination and evaluation of divers; and investigation of diving accidents.
0-306-41428-7/721 pp. + index/ill.
1984/$95.00 ($114.00 outside US & Canada)
Circle No. on Reader Service Card.

HANDBOOK OF MENTAL ILLNESS IN THE MENTALLY RETARDED

edited by **Frank J. Menolascino** and **Jack A. Stark**, *University of Nebraska Medical Center, Omaha*

The movement to deinstitutionalize the mentally retarded has created new challenges for mental health professionals responsible for the care of the enormous number of citizens who are both mentally ill and mentally retarded. This book offers a variety of ways to effectively treat and manage these patients, including individual therapy, group therapy, vocational training, and psychopharmacological approaches.
0-306-41648-4/437 pp. + index/ill.
1984/$39.50 ($47.40 outside US & Canada)
Circle No. on Reader Service Card.

PLENUM PUBLISHING CORPORATION
233 Spring Street, New York, N.Y. 10013
In United Kingdom:
88/90 Middlesex Street
London E1 7EZ, England

Plenum

Circle No.01 on Reader Service Card.

Aeronomy of the Middle Atmosphere

Chemistry and Physics of the Stratosphere and Mesosphere

GUY BRASSEUR and SUSAN SOLOMON

1984, xvi + 441 pp.
Cloth Dfl. 120,–/US $ 44.00/£ 30.50
ISBN 90-277-1767-2
ATMOSPHERIC SCIENCES LIBRARY

Aeronomy of the Middle Atmosphere is a comprehensive review of the authors' understanding of the natural and anthropogenic processes that influence the chemical composition of the stratosphere and mesosphere. Thermal and photochemical aspects of radiation are discussed, as well as atmospheric transport, and ion and neutral chemistry. The important coupling mechanisms between radiation, transport, and chemistry are emphasized. This volume will be a useful text for graduate level courses in aeronomy, and a source and reference work for researchers in atmospheric chemistry and physics, meteorology, and environmental science.

D. Reidel Publishing Company
Dordrecht/Boston/Lancaster

Circle No.29 on Reader Service Card.

nature
is available in Microform.

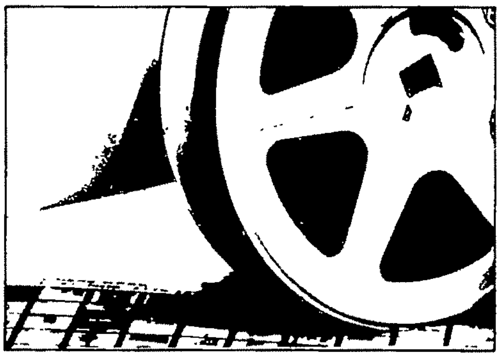

University Microfilms International

Please send additional information
for ______
Name ______
Institution ______
Street ______
City ______
State ______ Zip ______
300 North Zeeb Road, Dept. P.R., Ann Arbor, MI 48106

New from
Pharmacia P-L Biochemicals

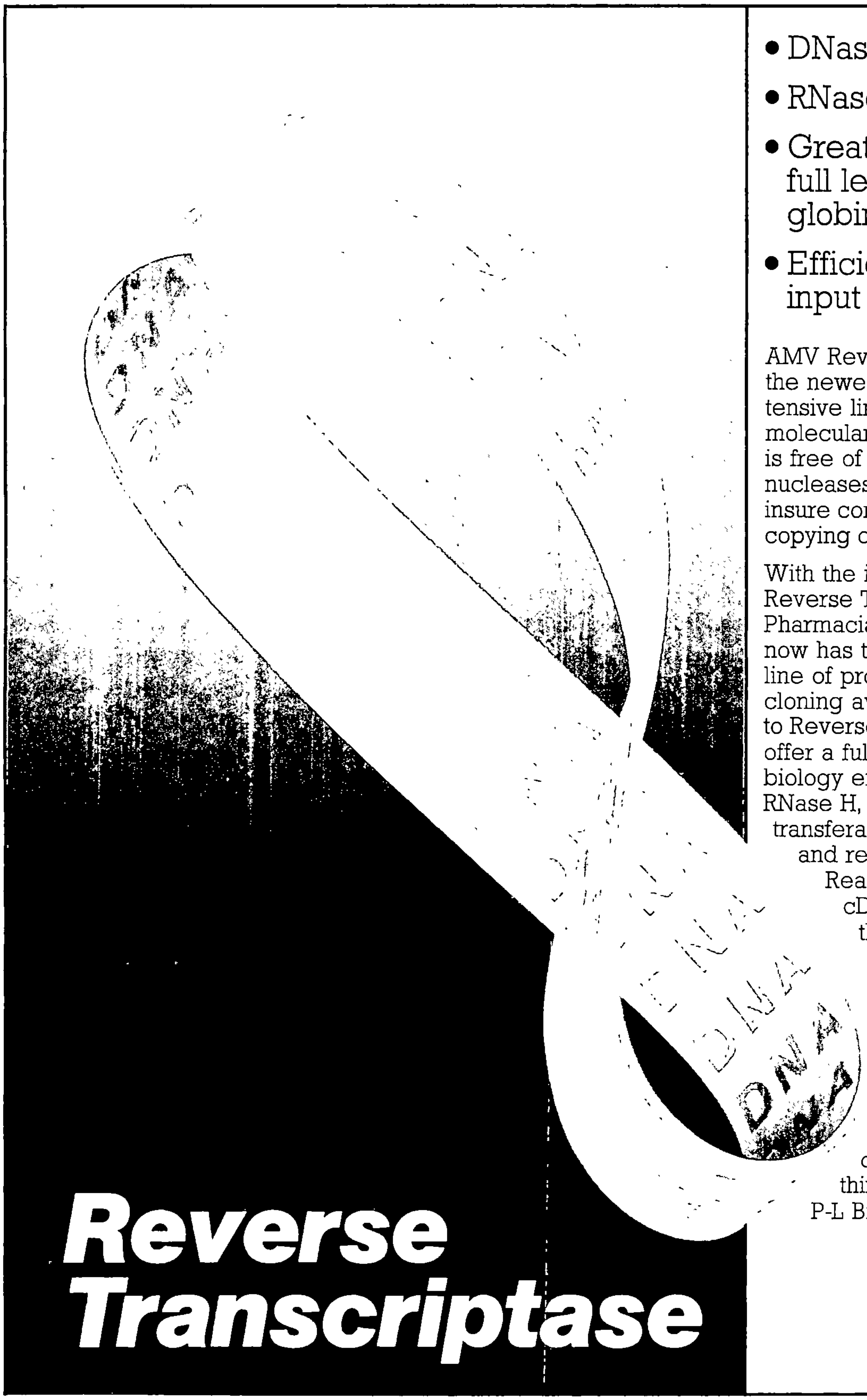

- DNase free
- RNase free
- Greater than 90% full length globin transcripts
- Efficient copying of input mRNA

AMV Reverse Transcriptase is the newest addition to our extensive line of enzymes for molecular biology. The enzyme is free of all contaminating nucleases and is tested to insure complete and efficient copying of mRNA.

With the introduction of Reverse Transcriptase, Pharmacia P-L Biochemicals now has the most complete line of products for cDNA cloning available. In addition to Reverse Transcriptase, we offer a full line of molecular biology enzymes including RNase H, DNA ligase, terminal transferase, DNA polymerases and restriction nucleases. Ready-to-use vectors for cDNA cloning by either the Okayama-Berg or Heidecker-Messing cDNA cloning procedures are also available.

For Reverse Transcriptase and cDNA cloning, think of Pharmacia P-L Biochemicals!

Pharmacia P-L Biochemicals, Inc.
Subsidiary of Pharmacia Inc.
800 Centennial Ave.
Piscataway, New Jersey 08854

Pharmacia P-L Biochemicals, Inc.
S-751 02 Uppsala
Sweden

Pharmacia
P-L Biochemicals

Pharmacia products will be on display at the NATURE Conference — Booth 35
Circle No.09 on Reader Service Card.

Molecular biology and cancer

A Nature *conference next week is a modest celebration of the prospect that cancer will soon be understood. It does not imply that practical oncology will be transformed overnight.*

THE question whether molecular biology has a contribution to make to the practice of medicine has now been answered. And positively. The half-dozen or so techniques for the diagnosis of genetic conditions and infection which are already in the hands of physicians are a sufficient proof of that. But when will molecular biology contribute something important to the practice of medicine, perhaps by helping to cure a disease and not by merely recognizing it?

For the past few years, there has been widespread excitement over the opportunities which seem to lie ahead for the treatment of genetic diseases and, more immediately, for the understanding if not the treatment of some of the many different forms of human cancer, which are in part at least genetic aberrations. That is one of the reasons why *Nature* is next week holding a conference on the subject in Boston, Massachusetts.

The opportunities in the field of cancer for molecular biologists are literally fascinating. They do cast a spell as can be told from the now wide currency of the word *oncogene*, which almost everybody knows of — and misuses. And there is a general opinion that oncogenes have something to do with viruses, whence the somewhat chilling suspicion that some forms of human cancer may yet turn out to be infectious (as, indeed, it seems that adult T-cell leukaemia is, at least in the coastal regions of southern Japan).

At times like these, it is therefore important to remember how long and tortuous is the history of the field that now seems so full of promise. It is well over half a century since the late Dr Peyton Rous, then a young man, first claimed that a sarcoma (in chickens) could be caused by a transmissible agent, an old-fashioned synonym for a virus. Rous persisted in the face of the sceptical politeness owed such a modest man and was rewarded, although not vindicated, by Richard Shope's discovery of the cell-transforming papilloma virus in the early 1930s. Only with development of techniques in the post-war decades was the reality of oncogenic viruses proved up to the hilt, first in rodents with polyoma (a DNA virus), then with the subset of the RNA viruses (collectively known as retroviruses) shown to cause cancer in animals.

More recently, the possibility of a connection between the retroviruses and the causation of human cancer has been answered with yes and no in an illuminating way. The recognition within the past decade that there is often a close similarity between the nucleotide sequence of oncogenic retroviruses and certain unidentified genes in vertebrate cells was naturally a stimulus to investigation. Just over two years ago, three separate groups in the United States were able to show that a close similarity existed between the genetic structure of one strain of the ras retrovirus and a genetic structure in the DNA of cells taken from human bladder carcinomas.

By November of that year, two separate groups in the United States (at the Massachusetts Institute of Technology and at the National Institutes of Health) had been able to show that the aberrant structure, apparently that responsible for the causation of cancer, differed from that of a gene normally present in all human cells in apparently trivial ways. The normal version of the gene carries the code for a protein, called p21, whose existence had already been catalogued but whose function was unknown. The abnormal version of the protein, inferred from the structure of the abnormal gene, differs in only two amino acids in the sequence. From that point on, the attention of molecular biologists has been directed squarely at the human (and vertebrate) genome.

The picture that has emerged illustrates why the term oncogene is so commonly misused. At least in the case of the human bladder cancer (but probably many others), there is a normal gene which plays a crucial part in the biochemistry of all normal cells, and an aberrant version associated with the cancer. Strictly speaking, only the aberrant version deserves to be called an oncogene. In a careful world, the normal version would be called by a name indicative of its function.

So great has been the excitement since November 1982, that *Nature*, in a leading article on the outlook for 1983, offered the prospect that the causation of at least some forms of cancer would be understood within the year. In retrospect, that hope was over-optimistic; the function of p21 and its aberrant form have been glimpsed only in the past few weeks (see *Nature* 23 August, p.628, and references therein). But there have been other remarkable developments to make up for such disappointments as there may have been — the recognition that the oncogene called *myc* does appear to migrate from one chromosome to another in cases of human leukaemia and the startling recognition of a similarity of structure of the gene responsible for the normal receptor for human epidermal growth factor and a true oncogene carried by the retrovirus known as erb-B. Whether the laboratory and clinical versions of the aberrant gene also interact with the biochemical system involving p21 remains to be determined, but it is hard to suppress the suspicion that the time is fast approaching when it will be worked out which properties of the cell surface have gone awry in cases of human malignancy.

These are only some of the reasons why the present is a time for modest celebration. But even now, it is far from self-evident that a better understanding of malignancy will help with the treatment of the human disease. That is a question that physicians rightly ask. They do so in the knowledge that even now, in other fields of human therapy, the development of successful drugs has ridden on the back of an understanding of how a disease is caused biochemically. It is only a hope that the field of cancer may be different, or that, say, the new techniques of molecular biology will provide a full understanding of the mechanism by which cells acquire genetic resistance to cytotoxic drugs.

The long history of people's attempts to deal with human cancer counsels caution. There have been too many crude disappointments for any other course to be safe. But even if the only certainty is that there will soon be a rounded understanding of the processes leading to overt disease, and ultimately perhaps of the interaction between genetic and environmental influences, it should at least be possible to put present strategies for the avoidance of cancer on a much sounder footing.

The role of *Nature* in such developments should not be misunderstood. Even a journal which enjoys the privilege of publishing many of the most important discoveries in such a field is not a scientific society in the strict sense but a vehicle for communication among active investigators and between them and the wider body of professional people. But the process of communication, in this field just as in any other, is more than the mere publication of information. The sense of excitement shared by those working in a promising field is also relevant. And there is much value in a forum in which those working at the bench can meet those whose work may be affected by what emerges. That is the spirit in which this conference has been designed.

John Maddox

Nitrogen cycle

Nitrate leaching from grassland

from R.E. White

RECENTLY, interest has revived in the effect that nitrate leached from agricultural land may have on the quality of surface and underground water used for human consumption. The consensus of scientific opinion, as presented in The Royal Society Study Group's report 'The nitrogen cycle of the United Kingdom', published in December 1983, is that most of the nitrate leached comes from arable land and represents approximately one-third of the nitrogen (N) applied annually to that land as fertilizer. The report concludes that little of the 900,000 tonnes of fertilizer N spread on grassland is leached out of the root zone. By contrast, results published in *Nature* this week (page 50), from J.C. Ryden, P.R. Ball and E.A. Garwood of the Grassland Research Institute at Hurley, suggest that loss of nitrate by leaching from intensively-managed grazed grassland may be five to six times higher than losses from comparable swards cut for hay or silage. The average annual loss from the grazed sward was 162 kg N per ha, which exceeded by far the range of 52–93 kg N per ha per year quoted in The Royal Society report for nitrate leached from arable land into the unsaturated zone of Chalk aquifers.

The Hurley researchers took soil and subsoil samples at 0.33 m intervals to a depth of 8 m from two adjacent plots (0.123 ha) on a loamy soil of the Frilsham series on Upper Chalk near Hurley. Both plots were sown to perennial ryegrass in the year April 1976 to March 1977 and fertilized with ammonium nitrate at the rate of 420 kg N per ha per year between April 1977 and December 1982. The 'cut' sward was mown every 4 weeks during the growing season while the 'grazed' sward was stocked with yearling steers for 1 week in 4 at an average stocking rate of 9.3 head per ha. From measurements of the drainage rate of nearby lysimeters, it was estimated that percolating water from the drainage season immediately following 1976–77 should have reached a depth of 5.5–5.8 m by December 1982. This coincided very closely with the depth of 6 m at which nitrate concentrations in the soil water below the cut and grazed swards were not significantly different. Above that depth, nitrate concentrations under the cut sward ranged from 5.4 to 13.3 mg N per litre, whereas the concentrations beneath the grazed sward exceeded the 'acceptable' range of 11.3–22.6 mg N per litre set by the World Health Organization.

Following the December 1982 sampling, the swards were ploughed and cropped to spring barley and winter wheat. A further sampling to 3 m depth in December 1983 confirmed the pronounced mineralization of soil organic N that occurs when grassland is ploughed. Allowing for the 80 kg per ha of fertilizer N applied in 1983, some 275–310 kg per ha of N in excess of crop requirements were mineralized, most of it being nitrified and therefore vulnerable to leaching.

Ryden and co-workers attribute the greater loss of N from the grazed sward to the inefficiency of ruminant animals in converting fertilizer N to protein, less than 20 per cent of the N input to grassland being recovered in animal products. The return of much of the ingested N in dung and urine creates 'hot spots' in the soil where the uptake of N by the grass fails to match the supply. The excess mineral N is then vulnerable to leaching.

The results of the new study are especially interesting because most previous work has been done on cut swards exposed to smaller amounts of N fertilizer (<250 kg N per ha per year). The Royal Society report makes passing reference to nitrate concentrations of 10–100 mg N per litre in profiles beneath grass receiving >400 kg N per ha per year, but adheres to the central view that nitrate concentrations in water percolating below grassland are generally < 10 mg N per litre. Even so, much of the drainage water from less heavily-fertilized grassland will exceed the new European Community guide level of 5.7 mg N per litre. Grazing and fertilizer combined are likely to push the average concentrations above the new maximum level of 11.3 mg N per litre. As Ryden *et al.* point out, 37 per cent of the grassland of England and Wales now receives >200 kg N per ha per year and 5 per cent receives >400 kg N per ha per year. Further intensification of livestock farming is therefore likely to exacerbate the problem of nitrate pollution of water supplies at a time when politicians and the public are becoming more concerned about the potential health hazard of high nitrate in drinking water. □

R.E. White is in the Department of Agricultural Science, Parks Road, Oxford OX1 3PF.

Astrophysics

Galaxies in collision

from M.G. Edmunds

GRAVITY never fails to suprise. The exotic predictions of general relativity have perhaps rather overshadowed the quite remarkable effects that can occur with nothing more than simple inverse square Newtonian force. Interesting things happen when galaxies collide, and recent dynamical simulations suggest that some quite strange morphological features of galaxies can be attributed simply to gravitational interaction.

The discovery of 'shells' — sharply defined extended arcs of low brightness — around elliptical galaxies was first reported in *Nature* four years ago (ref. 1 and see Fig. 1). The features were so unexpected that at first sight it seemed that they must be some kind of false diffraction image. Familiar artefacts of this type are the spikes seen on photographs around the images of bright stars, caused by diffraction at the structural supports of the telescope's prime focus. Nevertheless, investigations using different telescopes and of many galaxies have shown that the shells are real and occur around about 11 per cent of elliptical galaxies. No spiral galaxy has so far been found to have them.

The shells are generally aligned with the major axis of the galaxy, but do not completely surround it. Around a single galaxy there can be up to twenty shells, ranging over a factor of 30 in radius. Particularly intriguing is the observation that where several shells occur, they are generally interleaved, such that the next shell out in radius from the centre is on the opposite side of the nucleus. The colours of the shells[2] are consistent with the colours of the population of stars in the galaxies, so it seems that the shells are composed of stars, though not particularly young ones.

How do stars come to be organized into such sharp-edged configurations? One possible explanation is that they formed there. Gas lost from stars in the main body of the galaxy[3] or from an active galactic nucleus[4] could blow out of the galaxy, cool and suddenly form into a narrow shell of stars as conditions became suitable. But why the regular spacing of multiple shells (unless it is the result of recurrent events) and, even more strange, why the alternation of shells on either side of the galaxy? An argument against the suggestion of an active nucleus is that the galaxies with shells seem, on average, to show radio emission less often than do similar galaxies without shells.

An explanation of shells on purely dynamical grounds[5] was examined by P.J. Quinn (formerly of the Australian National University and now at Caltech) in his thesis work, and has now been published[6]. The basic idea is that a disc galaxy collides with a very much more massive — perhaps by a factor of 10 or 100 — elliptical galaxy. The massive elliptical acts as a potential well in which the stars from the disc become trapped. Computer simulations, performed with certain simplifying assumptions, show that the

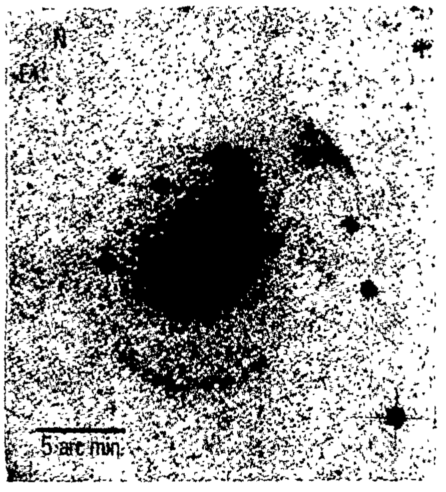

Fig. 1 The elliptical galaxy NGC 1344, showing sharp-edged shells which may be the result of gravitational interactions in a galactic collision (UK Schmidt plate, from ref. 1).

disc breaks up and the stars oscillate around in the potential. Provided the collision parameters are set correctly, and provided the original disc was dynamically 'cold' (did not have much random motion in the stars), then shell-like structures do occur. The number of stars per unit volume inside a galaxy is in general far too small for actual physical impact of the stars — they merely pass by each other and scatter off the gravitational potential of the system. The stars from the ruptured disc spend a lot of time at the ends of the radial motion of their orbits — rather as a simple harmonic oscillating pendulum spends most of its time at the ends of its swing — and the bunching of stellar orbits there is visible as a shell. The orbits evolve with time and more shells (essentially density waves) appear, interlaced on opposite sides of the centre, as is observed. The lifetime of a shell system, which ends when its structure becomes washed out by internal velocity dispersion, is predicted from these models to be some 2×10^9 years from the collision, during which time 10 - 30 shells would appear.

Astronomy still has a skeleton, not merely in its closet but actually knocking at the closet door, in the form of non-luminous mass in and around galaxies which we know must exist but cannot see. If correct, this gravitational-interaction picture could provide a most useful means of approaching the problem. Since the spacings of the time-evolving shells depend on the form of the gravitational potential, they can be used to probe the total (seen and unseen) mass distribution of the elliptical.

Despite their apparent success, Quinn's models face two major problems. The first is observational, the second theoretical. It might be expected that shell galaxies would occur where there was opportunity for plenty of collisions, but the reverse is observed: galaxies with shells are found preferentially in regions of low space density of galaxies. This objection can be weakened slightly by claiming that in groups or clusters of galaxies, the velocities of collision would be too high for production of shells, or that subsequent collisions might destroy the shells.

The second, and probably more serious, problem is that shells are produced in the simulations only for a rather restricted type of collision. As Quinn is at pains to point out, other collision conditions lead to a veritable Modern Art gallery of structures. In a classic investigation some years ago[7], Toomre and Toomre showed that the tidal gravitational interaction between two galaxies could lead to very peculiar structures — filaments, jets, arcs, bridges and tails — composed simply of stars pulled out in the collision. But in ellipticals, regular shell structure is found far more frequently than the complex structures that might be expected to result from arbitrary collision parameters. Undoubtedly some very strange structures do exist; sensitive photographic techniques and electronic light-sensitive arrays are beginning to reveal increasing numbers of jet-like structures in both spiral and elliptical galaxies. Just how many features can be accounted for on the basis of gravitational tidal interaction remains to be seen. Much more work can be done on dynamical simulations, although the almost unlimited range of masses, potentials, relative velocity vectors and internal dynamical states of the colliding galaxies makes this approach rather open-ended. Quinn's use of a fixed potential for the more massive galaxy must inevitably have suppressed collective effects — although it was sensible for computational convenience in an initial investigation.

The effects of collision on spiral galaxies have also been the focus of attention, with recent accurate mapping of the velocity field of a 'ring' galaxy in the direction of the Vela constellation by Taylor and Atherton[8]. Ring galaxies are fairly rare structures, characterized by a bright annulus, typically of young stars and associated glowing gas (Fig. 2). Two rival schemes have been put forward to explain their origins. Both explanations involve a normal spiral galaxy, with one scheme requiring collision with an intergalactic gas cloud, and the other collision with an elliptical (by contrast with the mechanism of shell formation, in the scheme for forming ring galaxies, the elliptical is much smaller than the disc galaxy). The critical ingredient is the gas, which is physically shocked and much of it forced over into gravitational collapse to form new stars.

The new velocity data, obtained with the novel 'Taurus' imaging Fabry–Perot system on the Anglo-Australian Telescope, are rather ambiguous. The velocity field is not what would be predicted in a head-on collision with an elliptical, that is, an expanding rotating ring. It may well be that the ring is actually folded back on itself, which could occur in collision with a gas cloud, as has previously been suspected in another peculiar galaxy, Arp 144. The main difficulty, though, is that there are not enough intergalactic gas clouds to produce even the small number of ring galaxies known. Taylor and Atherton hedge their bets, and suggest both schemes may produce a share of the objects.

Colliding galaxies certainly seem to be coming back into vogue. Back in the 1950s, Baade and Minkowski proposed galactic collisions as the origin of strong radio sources. Although now it is massive black holes in galactic nuclei that are the preferred power source, it is becoming popular to attribute enhanced activity to the effects of collisions spilling fresh gaseous fuel down into the nuclei. The sudden 'starburst' of star formation that is induced by collision in the presence of a large amount of gas will in itself generate significant radio emission from new supernovae remnants. If there is a large amount of dust as well, absorption of visible and ultraviolet radiation and its re-emission at infrared wavelengths may give rise to the very strong infrared luminosities (up to 100 times the optical output) detected by the IRAS satellite in several apparently interacting systems. Infrared excesses from interacting pairs, seen in ground-based studies[9], suggest that only one of the pair undergoes a sudden starburst.

©1977 Royal Observatory, Edinburgh

Fig. 2 The Cartwheel galaxy, a giant ring galaxy, which may have been formed by collision. (Photograph by Photolabs, ROE, from an original negative by the UK 1.2 m Schmidt telescope.)

A new catalogue[10] of elliptical galaxies with shells has been prepared by the original discoverers, D.F. Malin and D. Carter, and contains over 130 candidates for further study. What an exciting prospect, given the rich diversity of complicated structures that can be generated by a low-velocity galactic collision. !

1. Malin, D.F. & Carter D. *Nature* **258**, 643 (1980)
2. Carter, D., Allen, D.A. & Malin, D.F. *Nature* **295**, 126 (1982).
3. Fabian, A.C., Nulsen, P.E.J. & Stewart, G C *Nature* **287**, 613 (1980).
4. Williams, R.E. & Christiansen, W.A. *Eur. Southern Observ. Preprint*, no. 322 (1984).
5. Schweizer, F. *Astrophys. J.* **237**, 303 (1980)
6. Quinn, P.J. *Astrophys. J.* **279**, 596 (1984).
7. Toomre, A. & Toomre, J. *Astophys. J.* **178**, 623 (1972)
8. Taylor, K. & Atherton, P.D. *Mon. Not. R. astr Soc.* **208**, 601 (1984).
9. Joseph, R.D., Meikle, W.P.S., Robertson, N.A & Wright, G.S. *Mon. Not. R. astr. Soc.* **209**, 111 (1984).
10. Malin, D.F. & Carter, D. *Anglo-Australian Observ. Preprint* (1983).

M.G. Edmunds is at University College, Cardiff, PO Box 78, Cardiff CF1 1XL.

MICRO-84

Electron microscopy 50 years on

from Colin J. Humphreys

IN 1934, *Nature* published the first electron micrographs of biological material. Fifty years later, the Royal Microscopical Society, in association with *Nature*, organized MICRO-84, an international microscopy conference and exhibition held in London from 9 to 13 July 1984. The conference was attended by about 800 scientists from all over the world.

One of the highlights of the meeting was a description by Albert Crewe (University of Chicago) of a revolutionary 0.6 Å point resolution scanning transmission electron microscope he has recently started to build. This represents a dramatic advance in resolution over existing electron microscopes, the best of which have a point resolution of about 1.7 Å. Modern electron microscopes have computer control added on, as it were. Crewe proposes to reverse this procedure and build his microscope around a computer system large enough to operate and control the microscope, and process and store the images. His computer system, comprising four computers with 3.6 Giga bytes of storage, has been donated by IBM, which demonstrates the importance that major microelectronics companies attach to high-resolution electron microscopy. If successfully built, Crewe's microscope should have major applications in biology, chemistry, materials science and physics.

Many microelectronic circuits are now so small that they cannot be resolved using an optical microscope, and an electron microscope is necessary simply to see them. D. Cherns (University of Bristol) and W.M. Stobbs and D.J. Smith (University of Cambridge) demonstrated how high-resolution electron microscopy can be used to determine the positions of atoms lying in and near the interfaces of semiconductor devices, so that their electrical properties can be understood.

In recent years, not only the resolution but also the analytical capabilities of electron microscopes have dramatically improved. It is now possible to analyse chemically very small regions of materials using an electron beam less than 10 Å in diameter, by detecting the signals (for example, characteristic X rays) generated when the incident electron beam is inelastically scattered by the specimen. Moreover, it is possible to measure the energy spectrum of the transmitted electrons by a technique called electron energy loss spectroscopy, which is sensitive to all elements and is increasingly being used for the analysis of both biological and non-biological materials.

If the fine structure of an electron energy spectrum is studied, a technique known as electron loss near edge structure (ELNES), results can be obtained equivalent to those achieved on a synchrotron source, but for any atomic number element and with far higher spatial resolution (C. Colliex, University of Paris). ELNES tells us not only what atoms are present in a sample, but also their environment. Mick Brown (University of Cambridge) described some novel applications of electron energy loss spectroscopy which exploit the very high spatial resolution available, for example, the measurement of energy band gaps in insulators.

Topics covered in the wide-ranging programme included microsurgery, forensic science, archaeology and art. Among the relatively new fields, C.F. Quate (Stanford University) gave an outstanding review of the advances in acoustic microscopy from a resolution of 10 µm 10 years ago to one of 300 Å, using helium, today, and G. Schmahl (University of Göttingen) described the latest results from his 500 Å resolution X-ray microscope, which is probably the best in the world. X-ray microscopy offers the prospect of studying living biological material with a resolution far better than that of optical microscopy, and with much less damage than is produced in an electron microscope. To be really useful, however, its resolution will have to be improved still further. Perhaps this will be achieved by the next meeting of MICRO, in 2 years time. ☐

Colin J. Humphreys is in the Department of Metallurgy and Science of Materials, University of Oxford, Parks Road, Oxford OX1 3PH.

Vaccine development

Recombinant vaccinia for prevention of hepatitis B

from John Beale

THE idea of using vaccinia virus as a means of carrying other immunogens for the purpose of vaccination has seemed very attractive since Paoletti and Moss and their colleagues started to investigate the use of vaccinia recombinants in 1982 (Panicali, D. & Paoletti, E. *Proc. natn. Acad. Sci. U.S.A.* **79**, 4927; 1982 and Mackett, M., Smith, G.L. & Moss, B. *op. cit.* **79**, 7415; 1982). The rationale is that the live virus will express a foreign gene inserted into its DNA when it is applied to an animal, which will subsequently produce an immunological response to the foreign gene product. So far, recombinant DNA technology has been used successfully to express various antigens in vaccinia, including hepatitis B virus surface antigen (HBsAg), malaria sporozoite antigen, and influenza and herpes glycoproteins, and the list is growing all the time. On page 67 of this week's *Nature*, Moss and his colleagues take the hepatitis story a stage closer to a practical vaccine by showing that chimpanzees can be protected against hepatitis by vaccination with live recombinant vaccinia virus.

Last year, Smith, Mackett and Moss reported the construction of a fusion gene between DNA encoding HBsAg and an early vaccinia promoter (*UCLA Symp. molec. cell. Biol.*, New Ser. **8**, 543; 1983). By inserting the fusion product into the thymidine kinase-encoding portion of the vaccinia genome such that thymidine kinase activity was no longer expressed, they could select the new recombinant virus by growth in the presence of 5-bromodeoxyuridine. The plaques were tested for HBsAg expression by dot-blot hybridization and for HBsAg gene expression by immunological methods.

What Moss and his colleagues have now done is to vaccinate two chimpanzees with the HBsAg-containing recombinant vaccinia virus and one chimpanzee with wild-type normal vaccinia virus, and then challenge them with living hepatitis B virus. They find that treatment with HBsAg–vaccinia hybrids produces smaller lesions and lower antibody titres to vaccinia than does treatment with vaccinia alone. None of the animals produced antibodies to HBsAg after vaccination. On challenge with hepatitis B virus, however, the chimpanzee given vaccinia alone developed typical signs of hepatitis B virus infection: hepatitis surface antigenaemia, antibodies to the core antigen as well as to the surface antigen of hepatitis B (the production of core antibodies indicates some hepatitis B virus replication had occurred in the primed animal) and biochemical evidence of hepatitis. By contrast, the two HBsAg–vaccinia-treated chimpanzees, although producing no antibodies before challenge, were protected against the challenge, as shown by the lack of biochemical evidence of liver damage and of antigenaemia, and the rapid onset of antibodies to the surface antigen. They had thus been immunologically primed by the expression of HBsAg when the recombinant vaccinia was growing in the skin.

These are impressive results that pose in a sharper form the policy implications of this approach. The attraction is that the accepted and proven instrument of smallpox eradication can be adapted to the formidable task of hepatitis B prevention.

Indeed, as a result of the success of the World Health Organisation (WHO) smallpox eradication campaign, vaccinia has had magical powers conferred on it, not only by the populations that have benefitted; but also by some public health officials.

At the time of the first publication by Smith, Mackett and Moss, two problems were foreseen: immunity to vaccinia and the question of safety. These two issues remain. On any rational consideration of cost versus benefit, vaccinia should be acceptable in Third World countries for the prevention of hepatitis B. Such decisions are not always made rationally, however, and the use of a vaccinia hybrid for the control of hepatitis B in the USA, for example, would probably be more convincing to governments in Third World countries than hours of debate. For western countries, however, there is no incentive to use vaccinia with its known hazards, which caused it to be abandoned for smallpox control around the time that the WHO started its smallpox eradication scheme. Moss *et al.*'s finding that the lesions in the chimpanzees were less for the recombinant than for the wild vaccinia is encouraging, although more work is clearly needed. The problems of effectiveness and of interference from vaccinia antibodies during booster doses remain to be overcome.

As large amounts of hepatitis B surface antigens become available using recombinant DNA techniques of expression in yeasts and in mammalian cells, there may be no need to use a vaccinia carrier. Instead, it may be possible to combine hepatitis B vaccine with other nonliving childhood vaccines, and to give the combination at birth or soon thereafter.

Priming of the immune response so that immunological memory is induced is one aim of a vaccination programme. Recently, Salk *et al.* (*Ann. clin. Res.* **14**, 204 ; 1982) have argued forcibly that this would justify consideration of a single dose of killed poliovaccine for poliomyelitis control in tropical areas. The problem is the uncertain duration of memory in the absence of an adequate primary stimulus to produce antibody of both IgM and IgG classes. Further experimental data should soon be available to answer these outstanding questions for poliovaccine.

As to future research into the use of vaccinia as a carrier of immunogens, increased expression of the inserted DNA so that larger quantities of immunogen are produced is an important goal. Certainly, there is sufficient evidence to warrant continued research and the cautious extension of experiments in man. It is, however, much too early to think this promising line of research is a panacea for all the vaccine problems in developing countries. ☐

John Beale is at Wellcome Biotechnology Ltd, Langley Court, Beckenham, Kent BR3 3BS.

Mathematical modelling

The cubic map in theory and practice

from Robert M. May

FOR many populations of temperate-zone insects, the adults emerge, mate, reproduce and die over a brief interval in the summer. The dynamical behaviour of such a population, with discrete nonoverlapping generations, may be described by a first-order difference equation of the form $x_{t+1} = f(x_t)$; the population density in generation $t + 1$, x_{t+1}, is given as some function, f, of the density in generation t, x_t. If this equation were linear ($f = \lambda x$), the population would simply increase (or decrease if $\lambda < 1$) in familiar exponential fashion. More commonly, however, the population will tend to increase when at low densities and to crash at high densities, corresponding to some non-linear function or 'map' with a hump (of which the quadratic $f = \lambda x(1-x)$ is the mathematically simplest example). It is now widely appreciated that such non-linear first-order difference equations with a single hump or critical point can unfold an astonishing richness of dynamical behaviour: as nonlinearities become more severe (specifically, as λ increases in the quadratic example), the original stable point gives way to a cascade of period-doubling bifurcations, successively producing cycles of periods 2, 4, 8, 16, ..., 2^n; eventually an apparently 'chaotic' regime is entered, in which the trajectories generated by this deterministic process can be effectively indistinguishable from random noise[1,2]. Many features of this bifurcation phenomenon are reproduced in a self-similar manner, on even finer scales, in successive period doublings, in ways that are generic to essentially all maps with one critical point[1-3]. This subject, which first came to prominence in the early 1970s in studies of biological populations[4,5], has grown dramatically as more possible applications are found in the physical and engineering sciences.

What are the properties of maps with two humps? The canonical example of a map with two critical points is the symmetrical cubic $x_{t+1} = \lambda x_t + (1-\lambda)x_t^3$ (which is chosen such that + 1 maps to + 1, 0 to 0 and −1 to −1). A hint that the dynamics of the cubic are likely to be messier than those of the quadratic is provided by a theorem saying that maps with n critical points can have up to n distinct stable orbits for any given set of parameter values[6]. For maps with one hump, this means at most one stable state or attractor; for generically cubic maps, however, there can be two alternative attractors. Several authors have set out how two such alternative stable orbits can arise for the cubic map[7-9]: when the originally stable point at $x = 0$ becomes unstable (for $\lambda > 2$), it first bifurcates to give a single symmetrical cycle with period 2; as the map becomes more significantly nonlinear ($\lambda > 3$), this cycle does not bifurcate to give a 4-cycle, but rather splits to give two distinctly different (and unsymmetrical) 2-point cycles. Each of the separate 2-point cycles then unfolds the familiar cascade of period doublings to cycles with periods 4, 8, 16, ..., 2^n as λ continues to increase. These cascades display the self-similar properties emphasized by Feigenbaum[3] for the quadratic map. For yet larger values of λ we enter the apparently 'chaotic' regime, where, again, there are two separate attractors for most values of λ. A detailed catalogue of all the possible cycles that lurk as a kind of kaleidoscopic fine structure within the apparently chaotic regime is much more complicated than for the quadratic map[1,2], though an explicit such catalogue has been given for all cycles with periods up to 10, in their order of appearance[9]. Methods for computing the total number of distinct cycles with period k have also been given[7].

The motive behind the first studies of the cubic map was simply that it represented the next logical step beyond the quadratic[7]. Since then, however, the cubic map has come to people's attention in a variety of practical contexts.

Holmes[10] studied equations that arise as the simplest description of a buckled beam that is subjected to forced lateral vibrations. This led him naturally to consider the cubic equation given above, as being the simplest dynamical relationship satisfying the symmetry requirements of his problem. Holmes then established that, for a wide

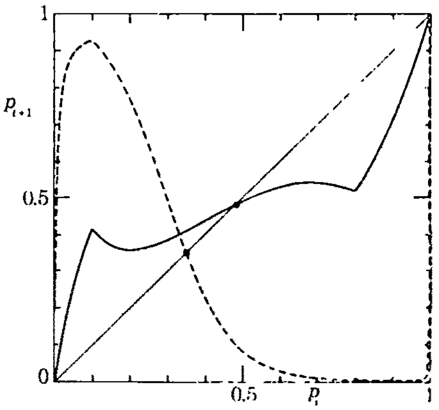

Relationship between the frequency of allele A in successive generations, p_{t+1} to p_t, for a system in which the fitness of host genotypes are determined by associations with pathogens. It is the general propensity to increase at low values and decrease at high values that is the characteristic of the cubic map. (From ref. 16.)

range of parameter values, "two distinct non-periodic attractors exist". His numerical studies of the more complicated buckled beam problem — using both a digital and an analogue computer — corroborated that, indeed, two distinct attracting states exist.

Perez, Jeffries and Testa[11] have experimented with an electronic circuit consisting of a harmonically driven *p–n* junction. They find this system to be characterized by period doublings and chaos of a kind that cannot be modelled by a map with one critical point. Guided by the numerical studies of Testa and Held[8], they believe the symmetric cubic map may describe the essentials of their observations. Perez *et al.* also discuss similar dynamical phenomena, again possibly corresponding to a cubic map, arising in the Belousov–Zhabotinsky chemical reaction.

More generally, Pikovsky[12] has observed that the dynamical properties exhibited by the cubic map may help explain the kinds of transitions to chaos that are observed in systems with a particular symmetry: an example could be the transition to turbulence in a hydrodynamic system with symmetrical boundary conditions. An independent and more explicit example of this sort is provided by Coste and Peyraud's[13] study of the Poincare map generated by a model for Rayleigh–Benard convection. For this symmetrical system, these authors find a bifurcation sequence of the kind described for the cubic equation above (and elsewhere they give an independent analysis of the bifurcation structure of the cubic map[14]).

To my mind, the most interesting application of the cubic map and its friends and relatives with two critical points lies in population genetics. In many situations, it can be that rarer genotypes — and hence rarer alleles — enjoy a selective advantage in the natural world. When this happens, the frequency, p, of the allele A at a diallelic locus will tend to increase when it is rare, and to decrease when the allele is common; that is, the map expressing p_{t+1} as a function of p_t will tend to have two humps. If the frequency-dependent effects are exactly symmetrical, we will have the symmetrical cubic map discussed above, and more generally we will have some unsymmetrical map with two critical points. The ensuing frequency of the allele A may settle to a stable constant value ('balanced polymorphism'), or it may oscillate (in a unique cycle, or in one of two alternative cycles), or we may have apparently chaotic dynamics.

Hamilton[15] has observed that the selective forces exerted by pathogens on their host genotypes are likely to be of just this frequency-dependent kind, with rarer genotypes being at an advantage because their particular diseases are less effectively transmitted by virtue of their low host densities. Hence host-parasite evolution may produce cyclic or chaotic variation in the prevailing host genotype from generation to generation. Hamilton goes further to observe that sexually recombining host populations will undergo less severe oscillations or chaos than corresponding asexual ones, essentially because the existence of heterozygotes and of crossing-over in multilocus situations endows the sexual system with greater dynamical inertia than the asexual one. It can then be that, under strong frequency-dependent selection of the kind possibly associated with pathogens, sexual systems enjoy an average fitness more than twice that of the corresponding asexual system, due to this dynamical mechanism. (The detailed argument is complex, but I believe the basic mechanism is as set out here.) Hamilton's calculations use plausible phenomenological expressions for the frequency-dependence in host fitness produced by pathogens; later studies employing epidemiologically-derived fitness functions find that sexual systems can overcome their intrinsic twofold disadvantage only in the most exceptional circumstances, which tends to undercut the theoretical basis for the suggestion that parasites are responsible for the evolution and maintenance of sex[16]. The idea, however, remains a fascinating one, and it will ultimately stand or fall on the basis of empirical tests of its predictions, several of which are underway[17-19]. Courting couples may feel that sex and the cubic map have little in common, but the fact remains that these two topics are intimately linked in current research on population genetics. ☐

1. May, R.M. *Nature* **261**, 459 (1976).
2. Collet, P. & Eckmann, J.P. in *Iterated Maps on the Interval as Dynamical Systems* (Birkhauser, Boston, 1980).
3. Feigenbaum, M. *J. Stat. Phys.* **19**, 25 (1978).
4. Li, T.Y. & Yorke, J.M. *Am. Math. Month.* **82**, 985 (1975).
5. May, R.M. & Oster, G.F. *Am. Nat.* **110**, 573 (1976).
6. Guckenheimer, J. *et al. J. math. Biol.* **4**, 101 (1976).
7. May, R.M. *Ann. N.Y. Acad. Sci.* **316**, 517 (1979).
8. Testa, J. & Held, G.A. *Bull. Am. phys. Soc.* **28**, 383 (1983).
9. Chavoya-Aceves, O., Angulo-Brown, F. & Pina, E. *Preprint* (Departmento de Fisica, Univ. Metropolitana Iztapalapa, Mexico, 1984).
10. Holmes, P. *Phil. Trans. R. Soc.* **A292**, 419 (1979).
11. Perez, J., Jeffries, C. & Testa, J. *Bull. Am. phys. Soc.* **28**, 383 (1983).
12. Pikovsky, A.S. *J. Phys.* **A16**, 109 (1983).
13. Coste, J. & Peyraud, N. *Phys. Lett.* **84**A, 17 (1981).
14. Coste, J. & Peyraud, N. *Physica* 5D, 415 (1982).
15. Hamilton, W.D. *Oikos* **35**, 282 (1980).
16. May, R.M. & Anderson, R.M. *Proc. R. Soc.* **B219**, 281 (1983).
17. Hamilton, W.D. & Zuk, M. *Science* **218**, 384 (1982).
18. Harvey, P.H. & Partridge, L. *Nature* **300**, 480 (1982).
19. Levin, B.R. *et al.* in *Population Biology of Infectious Diseases* (eds Anderson, R.M. & May, R.M.) 213 (Springer, New York, 1982).

Robert M. May is Class of 1877 Professor of Zoology at Princeton University, New Jersey 08544.

Atmospheric chemistry

Ozone increases in ground-level European air

from S.A. Penkett

EPISODES of photochemically generated ozone are now a common form of acute air pollution in Europe, whilst smoke fogs, which were typical of winter in London and other cities in the 1950s, have largely disappeared. The reasons are complex and are concerned with the changing emission patterns of primary pollutants and with the chemical changes that occur in the atmosphere. High ozone concentrations caused by photochemical pollution were first detected in Los Angeles in the 1940s. It was not until more than twenty years later that the first indications were found of a similar problem in Europe. Measurements of ground-level ozone then commenced, in Holland and at Harwell in southern England. These have produced clear evidence of the production of large amounts of ozone at ground level under anticyclonic conditions.

It is unfortunate that ozone measurements in western Europe started only recently, because it is difficult to detect a trend. By contrast, systematic measurements have been made at both urban and rural sites in the German Democratic Republic (GDR) since 1952. The results show a dramatic increase in the yearly average ozone concentration with the largest increase being observed at rural sites. Data from five sites located throughout the GDR were published in 1979 but attracted little attention at the time (Warmbt, W. *Z.Met.* **29**, no.1, 24; 1979). Recent interest in ozone as a possible cause of damage to forests has highlighted the importance of this unique data set.

The measurements were made using the classical technique of iodometry in solution, which is subject to interference from other atmospheric gases. Modern methods of ozone measurement utilize an absolute optical absorption method to avoid these problems. The same technique was used consistently in the GDR measurements, however, and the imperfections were recognized. Interference from sulphur dioxide was particularly bad at urban sites until a chemical filter was introduced in 1972. At rural sites the interference was less and at one site, Cape Arkona on the Baltic Coast, it was totally absent.

The average ground-level ozone concentration at Cape Arkona showed an increase in the yearly mean from ~ 15 parts per 10^9 by volume (p.p.b.v.) in 1956 to ~ 24 p.p.b.v. in 1977, the most recent year for which data are reported. The mean summer ozone concentration almost doubled, from ~ 18 p.p.b.v. to ~ 32 p.p.b.v. over the 21 year period. The maximum levels observed in photochemical episodes were considerably greater, reaching values of over 100 p.p.b.v.

There are no other ground-level observations of ozone in Europe going back so far. Nevertheless, data collected on the Hohenpeissenberg in southern FRG from 1971 to 1976 show a similar trend to those from the nearest GDR station over the same period. Probably the most numerous data for Western Europe have been collected in Holland. These measurements started in 1969 but are mostly urban and will be affected by large emissions of nitric oxide in the immediate vicinity. This gas reacts rapidly with ozone with the result that levels in urban areas tend to be lower than those in rural areas. The Dutch data show no overall increase during the 1970s.

The continuous upward trend in ground-level ozone concentration, seen particularly at rural sites, is unlikely to be a result of increased transfer of ozone from the stratosphere, which provides much of the ozone in the troposphere, but rather of a change in the efficiency of production *in situ* in the boundary layer. Photochemical production of ozone in the lower atmosphere occurs through a complex chain reaction involving free radicals. The essential precursors are oxides of nitrogen and hydrocarbons; emissions of both these species in Europe have increased substantially over the period covered by the ozone data. If Britain is typical, nitrogen oxide emissions have increased by about 50 per cent and emissions of hydrocarbons have more than doubled. Motor vehicles are the largest source of the chemically reactive hydrocarbons that are the most effective in producing ozone, and between 1953 and 1975 fuel usage in Britain increased about threefold. Most of the increase occurred before 1970, during a time when no systematic measurements were made either of the primary pollutants or of their effects on the ozone concentration. This emphasizes the unique nature of the GDR data.

The observed increase in ozone is indicative of an increase in chemical reactivity in the atmosphere which will probably be reflected in an increased rate of acid production. Indeed, amounts of other potentially acid species may be correlated with ozone. For example, the nitrate content of atmospheric aerosol and of rainwater in England has increased roughly by a factor of three since the mid 1950s. The nitrate aerosol and ozone trends both show peaks and troughs which are associated with meteorological factors, in particular with the amount of sunlight. There is, in fact, some correlation between high oxidant levels and good vintage years, particularly for the Rhine and Mosel wines grown at a similar latitude to the stations where the data were collected. Clearly, there is a strong case for sustained research into the nature of all chemical changes in the atmosphere that lead to the formation of strong oxidants and free acidity. These two chemical properties are strongly linked, as the German word for oxygen, *sauerstoff* (literally 'acid stuff'), shows.

The known aspects of ozone chemistry in the troposphere have recently been discussed in the Swedish journal, *Ambio* (**13**, no.2, 61; 1984). The phytotoxic properties of ozone are emphasized, particularly in the context of forest damage in central Europe. The influence on climate of an increase in ozone concentration throughout the Northern Hemisphere is also considered, as it is possible that emissions of oxides of nitrogen and carbon compounds, such as carbon monoxide and hydrocarbons, from a variety of sources now affect the distribution of tropospheric ozone on a hemispheric scale. Thus, data from the global ozonesonde network show, for the period 1968–1979, an annual increase in ozone concentration of 1 per cent in the height range 2 – 8 km at mid latitudes in the Northern Hemisphere. Ozone behaves as a greenhouse gas, that is, it absorbs infrared radiation from the Earth's surface and thus acts as a thermal blanket. Calculations suggest that a doubling in the tropospheric ozone concentration will increase the global surface temperature by approximately 1°C; this is of a similar magnitude to the value of 3°C calculated for a doubling in the CO_2 concentration. □

S.A. Penkett is in the Environmental and Medical Sciences Division, AERE Harwell, Oxfordshire OX11 0RA.

---

100 years ago

THE TEMPERATURE OF THE SOLAR SURFACE

THE power developed by the sun motor, recorded in *Nature*, has established relations between diffusion and energy of solar radiation which prove that the temperature of the surface of the sun is extremely high. I have, therefore, during the summer solstice of 1884, carried out an experimental investigation for the purpose of demonstrating the temperature of the solar surface corresponding with the temperature transmitted to the sun motor. I have accordingly constructed an instrument of large dimensions, a polygonal reflector (see Fig. 1), composed of a series of inclined mirrors, and provided with a central heater of conical form, acted upon by the reflected radiation in such a manner that each point of its surface receives an equal amount of radiant heat in a given time. The said reflector is contained within two regular polygonal planes twelve inches apart, each having ninety-six sides, the perimeter of the upper plane corresponding with a circle of eight feet diameter, that of the lower plane being six feet. The corresponding sides of these planes are connected by flat taper mirrors composed of thin glass silvered on the outside. When the reflector faces the sun at right angles, each mirror interprets a pencil of rays of 32.61 square inches section, hence the entire reflecting surface receives the radiant heat of an annular sunbeam of 32.61 × 96 = 3130 square inches section. The reflector and conical heater are sustained by a flat hub and eight radial spokes bent upwards towards the ends at an angle of 45°. The heater is composed of rolled plate iron, and provided with head and bottom formed of non-conducting material. A short tube passes through the upper head of the heater, through which a thermometer is inserted for measuring the internal temperature. The stem being somewhat less than the bore of the tube, a small opening is formed by which the necessary equilibrium of pressure will be established with the external atmosphere. It should be mentioned that the indications of the thermometer during the experiment have been remarkably prompt.

The result of the experimental investigation carried out during the summer solstice of 1884 may be thus briefly stated. The diffusion of the solar rays acting on the 20-inch heater being in the ratio of 1 to 10,241, the temperature of the solar surface cannot be less than 298°.87 × 10,241 = 3,060,727° F. This underrated computation must be accepted unless it can be shown that the temperature produced by radiant heat is not inversely as the diffusion of the rays. Physicists who question the existence of such high solar temperature should bear in mind that in consequence of the great attraction of the solar mass, hydrogen on the sun's surface raised to a temperature of 4000°C., will be nearly twice as heavy as hydrogen on the surface of the earth at ordinary atmospheric temperatures; and that, owing to the immense depth of the solar atmosphere, its density would be so enormous at the stated low temperature that the observed rapid movements within the solar envelope could not possibly take place. These facts warrant the conclusion that the high temperature established by our investigation is requisite to prevent undue density of the solar atmosphere.

J. ERICCSON

From *Nature* **30**, 465 (1884).

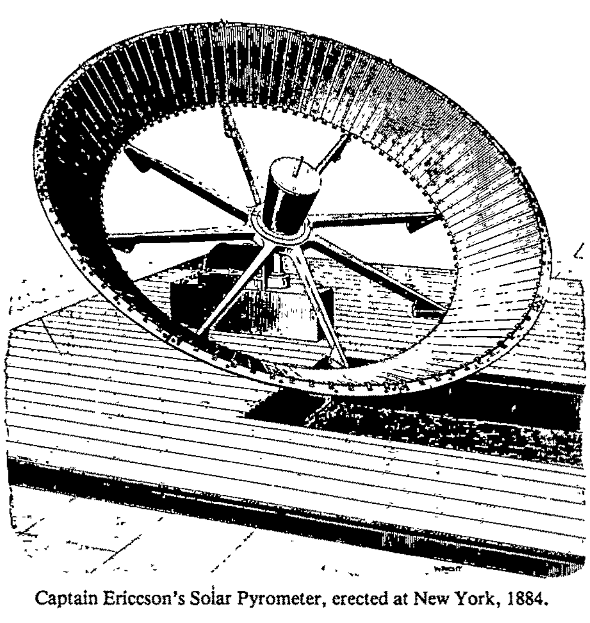

Captain Ericcson's Solar Pyrometer, erected at New York, 1884.

Polymer science

Novel helical conformation in a nylon

from Edward Atkins

X-RAY structure determinations undertaken so far on different nylons have shown that the chains crystallize in an extended planar zig-zag conformation. In the crystals, the vital amide groups (-NH-CO-) participate in interchain hydrogen-bonding in the plane of the zig-zag, generating hydrogen-bonded sheets which stack to form the three-dimensional crystalline structure. The properties and behaviour of the nylons examined until now all relate to this type of molecular architecture. In this issue of *Nature* (page 53), Fernández-Santin, Aymamí, Rodriguez-Galán, Muñoz-Guerra and Subirana describe a novel structure for a nylon derivative, poly(α-isobutil-L-aspartate) : a contracted spring-like helix, stabilized by intrachain hydrogen bonds, which exhibits a number of similarities with the well-known α-helix found in proteins and polypeptides (see Fig.3 on page 53). This novel spring-like conformation is of interest not only for its own sake and because of the implications it has for the properties of a nylon, but also because it highlights the link nylons can provide between synthetic polymers and proteins.

The nylons or polyamides represent a spectrum of synthetic polymers in which amide groups introduce a hydrogen-bonding capability into the structure. At one extreme, the amide groups occur very infrequently, and the nylons approach the conformation, behaviour and properties of polyethylene: an extended planar zig-zag chain associating with neighbouring chains through relatively weak van der Waals' interactions. Near the other end of the spectrum, where the amide groups are separated only by one or a few CH_2 units, is the structure, known as nylon-2, which is chemically identical to polyglycine — a polypeptide or simple protein — in which two carbon atoms ($-CH_2-CO-$) occur between successive nitrogen atoms in the chain. (The ultimate polyamide is nylon-1.) The bulk of the nylons used industrially have amide groups distributed with a frequency intermediate between these two extremes. A common polyamide is nylon-6 with six carbon atoms between successive nitrogens. It might be predicted, *a priori*, that as the frequency of amide groups increases and the nylons take on a similar chemistry to that of polypeptides and proteins, they would be capable of mimicking their biopolymeric counterparts.

In proteins, only a relatively small number of regular conformations have been found, of which the α-helix, the 3-fold or collagen-like helix and the β-sheet are the most prominent. These regular structures are ubiquitous in fibrous proteins (Fraser, R.D.B. & MacRae, T.P. *Conformation in Fibrous Proteins*, Academic, New York; 1973) and occur as domains, connected by less regular segments, in the convoluted conformations found in globular proteins, for example myoglobin, haemoglobin and the enzymes. β-sheets are extended protein chains, hydrogen-bonded together to form sheets. They occur in many insect silks, and can be thought of as the biopolymeric analogues to the traditional nylon structures. Unlike the β-structures, which are stabilized by interchain hydrogen-bonding, the α-helix is a contracted spring-like helix stabilized by intrachain hydrogen bonds, and is found in many keratinous tissues such as hair.

The novel structure discovered by Fernández-Satin *et al.* for nylon-3, which closely approaches the frequency of amide groups in proteins (variants of nylon-2 backbone), is a departure from the traditional nylon structures and represents the first of what is hoped to be a family of self-stabilized spring-like helices for nylons. These substances should exhibit behaviour and properties quite different from those of previous nylons, but similar to those of the extensively studied α-polypeptides and α-proteins. □

Edward Atkins is Professor of Physics at the H.H. Wills Physics Laboratory, University of Bristol, Tyndall Avenue, Bristol B88 1TL.

Anaesthesia

Glycine receptor protein the solution?

from W. Graham Richards

ALCOHOL added to a fish tank containing newts will anaesthetize the newts and they will keel over unconscious. Surprisingly, a subsequent increase of the hydrostatic pressure on the water of the tank reverses this anaesthesia and the unconscious creatures revive and will swim normally under the increased pressure. This is an example of the pressure-reversal of anaesthesia which is widely observed across a huge range of species and ought to provide some clue as to the mechanism of general anaesthesia. Work described in this issue of *Nature* (page 56) uses this approach and comes up with some intriguing results which may implicate glycine-mediated synaptic inhibition in the action of anaesthetics.

In pharmacological terms, general anaesthesia seems to be a rather crude affair not involving very specific molecular receptors: large concentrations of anaesthetic are used and almost any gas, even an inert gas such as helium, will act as an anaesthetic if applied at sufficient pressure. A vital practical ramification of this is the narcosis suffered by divers who can be made semiconscious as a result of the anaesthetic effects of nitrogen in air when they reach depths at which the anaesthetic pressure becomes significant.

The traditional interpretation of this lack of specificity and the influence of pressure has been that the effect of anaesthetic has a relatively simple physical origin. Since anaesthetic potency correlates with solubility in fat, it has been held that the results are achieved by solubility of the gas in lipid membranes; swelling produces anaesthesia reversible by compressing the membranes. Alternatively, the hydrophobic part of a specific protein could be the site of solution.

In this week's *Nature*, Smith *et al.* provide a significant step forwards in elucidating the mechanism of anaesthesia in more precise molecular terms. The key observation is a complete difference in response to pressure between anaesthetized tadpoles and shrimps with anaesthetics chloroform, ether, ethanol, halothane and sodium pentabarbitone. Thus, whereas the relative potencies of these anaesthetics in the two species are very similar, the influence of pressure is totally opposite in the two cases: shrimps show no sign of pressure-reversal, indeed pressure can potentiate anaesthesia, while in tadpoles, the effects of anaesthetic are reversed by the application of pressure in otherwise identical circumstances.

The authors' preferred explanation of this dramatic difference derives from the fact that crustaceans, such as the freshwater shrimp, have a nervous system which is insensitive to strychnine. This implies they do not use glycine as a neurotransmitter. Thus, it is possible that the site of the solution of an anaesthetic is a hydrophobic part of the glycine receptor protein. Support for this notion comes from the fact that the pharmacology of pressure, as elucidated from pressure-induced convulsions in mammals, closely parallels that of strychnine which is believed to act on postsynaptic inhibition mediated by glycine. □

W. Graham Richards is a lecturer in the Physical Chemistry Laboratory, University of Oxford, South Parks Road, Oxford OX1 3QZ.

Mass extinctions and missing matter

SIR — The approximate 30-Myr periodicity that appears to exist in the record of mass biological extinctions and terrestrial impact cratering has been interpreted by Rampino and myself[1] as evidence of a quasi-periodic bombardment of the Earth by comets that have been perturbed into Earth-crossing orbits by close gravitational encounters of the Solar System with massive interstellar clouds of gas and dust. In this model, the underlying clockwork is the Solar System's vertical oscillation through the midplane of the Galaxy, towards which most of the massive interstellar clouds are concentrated.

The downward force exerted by the Galaxy will also perturb the Solar System's comet halo, but will not produce any periodicity. To see why, first observe that the Solar System's vertical orbit[2] lies wholly within the linear domain of the galactic force law[3,4], so that the vertical galactic acceleration is simply $K(z) = -4\pi G\varrho_0 z$, where ϱ_0 represents the local mass density of material near the galactic plane. It follows that the difference between the galactic acceleration of the Sun at galactic height z and that of a comet at a distance r from the Sun in the direction of the galactic plane is $K(z) - K(z-r) = -4\pi G\varrho_0 r$. By equating this small galactic tidal acceleration to the local acceleration of the comet towards the Sun, $-GM_\odot/r^2$, a 'tidal radius' for the comet halo is readily obtained: $r_t = (M_\odot/4\pi\varrho_0)^{1/3} = 1.5 \times 10^5$ AU. (For comparison, the Galaxy's central force field and differential rotation impose a tidal limit[5] of 3×10^5 AU.) Because of its independence of galactic height, r_t differs from the tidal radius that is derived for an inverse-square galactic force law, valid very far from the galactic plane[6]. Thus, the comet halo, unlike a far-ranging globular star cluster[7], never experiences a periodic 'gravitational shock' as it passes up and down through the galactic disk (contrary to ref. 8), although it does suffer a constant amount of compression in the vertical direction. For this reason, individual objects like interstellar gas and dust clouds seem to be needed as perturbers.

Could other dark perturbing objects also be important? The disk of our Galaxy probably contains a large quantity of 'invisible matter'. Kinematical studies have produced a range of estimates for the total mass density ϱ_0 in the solar neighbourhood (believed to be typical of the part of the galactic plane that is accessible to the Solar System) equal to 0.14–0.24 $M_\odot$ pc^{-3} (refs 3, 4, 9–12). Direct counts of observed stars, gas, and dust have turned up only 0.10–0.11 $M_\odot$ pc^{-3} (refs 4, 10), and so the missing disk material could amount to as much as ~ 0.14 $M_\odot$ pc^{-3}.

The effectiveness of any seen or unseen matter in perturbing the Solar System's comet halo depends only on the local mass density of this matter, ϱ_0. From equations (11) and (12) of Hills[13], the mean time interval between random encounters of the Solar System with objects of mass density ϱ is given by $\tau_s = \varrho^{-1} a^{-2}_{\min}$ Myr, if ϱ is in units of $M_\odot$ pc^{-3} and $a_{\min}$ in units of 2×10^4 AU, where $a_{\min}$ is the minimum semimajor axis of those comets for which the loss cone is filled by an encounter. (This result depends on the impulse approximation and point-mass approximation, which turn out to be adequate assumptions for all cases considered here.) Hills' equations (13) and (19) (ref.13) (with $n = 2$) provide the total number of comet collisions with the Earth during an encounter, $N = N_0 a^{-2}_{\min}$, where $N_0 = 4$ or $N_0 = 0.2$ depending on whether Everhart's[14] or Weissman's[15] rate of present-day comet impacts is assumed. In either case, the shower of comets[13] lasts $\tau_1 = 11 a^{3/2}_{\min}$ Myr. Because the outer radius of the main comet reservoir probably lies at ~ 2×10^4 AU (refs 13, 16–19), $a_{\min}$ is not likely to exceed 1.

For the Solar System's vertical motion within the Galaxy to significantly modulate the background comet flux arising from random showers, the most important perturbing objects must not only have a high mass density but must also be concentrated fairly strongly towards the galactic plane. The total comet flux into the inner Solar System is due to solar encounters with known stars (~ 0.05 $M_\odot$ pc^{-3}) (ref.4), known interstellar gas and dust clouds (~ 0.05 $M_\odot$ pc^{-3}(ref.20), interstellar comets (< 6×10^{-4} $M_\odot$ pc^{-3} (ref.21), and invisible matter (≤ 0.14 $M_\odot$ pc^{-3}). If the invisible matter consists of small (or cold) interstellar molecular clouds, which would probably be concentrated strongly toward the galactic plane like the known molecular clouds and the youngest stars (~ 0.04 $M_\odot$ pc^{-3}) (refs 4,20), then the total percentage of local material lying in the flat subsystem could be as high as 75%. Even without invisible matter, the total percentage would still be fairly high, 40%. In all cases, the encounter time τ_s would be acceptably shorter than the Solar System's galactovertical half-period, $P_{1/2} = (\pi/4G\varrho_0)^{1/2} \approx 30$ Myr, and so galactic modulation could arise.

If, however, the invisible material consists of a large population of old, dead stars, with a relatively small galactic concentration, the percentage of local matter belonging to the flat subsystem could be as low as 17%. This would be insufficient to modulate the background comet flux into the inner Solar System. It might be argued that most of these dead stars are young objects, not yet kinematically dispersed far from the galactic plane. However, they would also have to be old enough to have migrated into the area between the star-forming spiral arms (so as to adequately cover the region of the galactic plane that the Solar System traverses in its revolution around the galactic centre). Their ages would consequently[22] need to lie in the narrow range 10^8–10^9 yr. Yet it is very unlikely that much of the invisible matter consists of dead stars; the space densities of faint white dwarfs[23] and of black dwarfs[24–26] are observed to fall off rapidly with declining luminosity (at least to $M_V = 21$), while most neutron stars and stellar black holes are expected to be derivatives of massive main-sequence stars, whose space densities, at least today, are observed to be extremely low[4].

If future observations reveal a large secondary maximum in the luminosity functioin of dead stars at a lower light level (perhaps because star formation has been very sporadic), the implications for the present hypothesis of Galaxy-modulated comet impacts on Earth[1] could be profound.

RICHARD B. STOTHERS
National Aeronautics and Space Administration,
Goddard Space Flight Center,
Institute for Space Studies,
New York, New York 10025, USA

1. Rampino, M.R. & Stothers, R.B. *Nature* **308**, 709-712 (1984).
2. Innanen, K.A., Patrick, A.T. & Duley, W.W. *Astrophys. Space Sci.* **57**, 511-515 (1978).
3. Oort, J.H. in *Galactic Structure* (eds Blaauw, A. & Schmidt, M.) 455-511 (University of Chicago, 1965).
4. Bahcall, J.N. *Astrophys. J.* **276**, 169-181 (1984).
5. Wyatt, S.P. & Faintich, M.B. *Bull. Am. astr. Soc.* **3**, 368 (1971).
6. von Hoerner, S. *Astrophys. J.* **125**, 451-469 (1957).
7. Ostriker, J.P., Spitzer, L. Jr & Chevalier, R.A. *Astrophys. J.* **176**, L51-56 (1972).
8. Scalo, J.M. & Smoluchowski, R. *Bull. Am. astr. Soc.* **16**, 493-494 (1984).
9. Krisciunas, K. *Astrophys. J.* **82**, 195-197 (1977).
10. Hill, G., Hilditch, R.W. & Barnes, J.V. *Mon. Not. R. astr. Soc.* **186**, 813-830 (1979).
11. Rohlfs, K. & Kreitschmann, J. *Astrophys. Space Sci.* **79**, 289-319 (1981).
12. Eggen, O.J. *Publs. astr. Soc. Pacif.* **81**, 741-753 (1969).
13. Hills, J. G. *Astrophys. J.* **86**, 1730 1740 (1981).
14. Everhart, E. *Astrophys. J.* **74**, 735-750 (1969).
15. Weissman, P.R. *Astr. Astrophys.* **85**, 191-196 (1980).
16. Fernandez, J.A. *Icarus* **42**, 406-421 (1980).
17. Napier, W.M. & Staniucha, M. *Mon. Not. R. astr. Soc.* **198**, 723-735 (1982).
18. van den Bergh, S. *J. R. astr. Soc. Can.* **76**, 303-305 (1982).
19. Bailey, M.E. *Mon. Not. R. astr. Soc.* **204**, 603-633 (1983).
20. Sanders, D.B., Solomon, P.M. & Scoville, N.Z. *Astrophys. J.* **276**, 182-203 (1984).
21. Sekanina, Z. *Icarus* **27**, 123-133 (1976).
22. Wielen, R. *Astr. Astrophys.* **60**, 263-275 (1977).
23. Liebert, J., Dahn, C.C., Gresham, M. & Strittmatter, P.A. *Astrophys. J.* **233**, 226-238 (1979).
24. Probst, R.G. & O'Connell, R.W. *Astrophys. J. Lett.* **252**, L69-L72 (1982).
25. Jameson, R.F., Sherrington, M.R. & Giles, A.B. *Mon. Not. R. astr. Soc.* **205**, 39P-41P (1983).
26. Reid, N. *Mon. Not. R. astr. Soc.* **206**, 1-17 (1984).

The case against impact extinctions

SIR — Some people think that the impact hypothesis for the mass extinction at the Cretaceous–Paleogene boundary is 'proved'[1,2]. So it is, if one considers selectively one set of evidence. However, it is equally convincingly disproved if one considers selectively another set of evidence. I have recently reviewed this topic[3], evaluating the literature through 1983; no valid later work known to me materially affects any of the many arugements in each direction given in that paper and only one adds a useful new argument. The best evidence in each direction does not impinge on that for the other, and neither side has a satisfactory explanation for the opposing evidence.

The arguments against the effect of an impact, all discussed in my review, are:

(1) A *Protunqulatum* community lacking dinosaurs.
(2) Appearance and progressive evolution of the *Protunqulatum* community just before the boundary.
(3) Freshwater community unaffected.
(4) Last occurrence of dinosaurs being detectably below boundary in Montana and vicinity
(5) Existence of transitional floras below boundary.
(6) Putatively extraterrestrial material below boundary.
(7) Absence of effects of elimination of stratospheric ozone.
(8) Coincidence with culmination of very large regression.
(9) Marsupials but not placentals nearly eliminated; most arboreal multituberculates and birds survived.
(10) Darkness expected to occur too often.
(11) Concentration of Ir, etc., in reduced material, with associated timing anomaly.
(12) Dinosaurs occurring well above the palynological boundary in New Mexico.
(13) Effect of predicted cooling not seen.
(14) Effects of predicted acid rain not seen.
(15) Absence of turbidites at boundary (if marine impact) and apparent absence of large terrestrial crater.

The first two items refer to a community of Paleocene aspect, whose members were ancestral to much of the Paleocene fauna and which appeared in Montana 4 × 10^5 yr before the boundary. Smit and van der Kaars[5] claim that the sediments involved postdate the boundary, but their work ignores the field relationships given in a detailed geological map[6] (other evidence and will be refuted more adequately in a paper in preparation by several people). That my list of evidence is one-sided, reflects merely the greater publicity which given to evidence favouring an impact as the cause of the extinction.

The results of Bohor *et al.*[4], who found quartz fragments at the boundary which had been shocked at very high pressure, are at first sight strongly favourable to an impact. But until possible alternatives such as a uniquely powerful explosion (perhaps analogous to the smaller ones of kimberlites) are considered, some scepticism seems appropriate. Unless there were mutliple impacts[2], for which there is no evidence (despite considerable search) except an unconvincing [3] interpretation of osmium isotope ratios[7], it is not apparent how the impact hypothesis can be modified to resolve the major conflicting evidence. Yet volcanism, even broadly conceived, has equally severe problems[3,4]. Coincidence is not a satisfactory basis for theory.

On the "late Eocene mass extinction", I know of no evidence that it exists. For instance, there are as many last appearances of marine families recorded in the middle Eocene as in the late Eocene[8], neither value being unusually large; species extinctions are not concentrated at one horizon[9]; and the mammalian turnover is later[9] and clearly involves at least a major biogeographic interchange[10].

LEIGH M. VAN VALEN

Biology Department (Whitman),
University of Chicago,
915 East 57th Street,
Chicago, Illinois 60637, USA

1. Maddox, J. *Nature* 308, 685 (1984).
2. Davis, M., Hut, P. & Muller, E.A. *Nature* **308**, 715-717 (1984).
3. Van Valen, L.M. *Paleobiology* **10**, 121-137 (1984).
4. Bohor, B.F., Foord, E.E., Modreski, P.J. & Triplehorn, D.M. *Science* **221**, 867-869 (1984).
5. Smit, J. & van der Kaars, S. *Science* **223**, 1177-1179 (1984).
6. Bell, R.E. thesis, Univ. Minnesota (1965).
7. Luck, J.M. & Turekian, K.K. *Science* **222**, 613-615 (1983).
8. Van Valen, L.M. *Nature* 307, 50-52 (1984).
9. Keller, G., D'Hondt, S. & Vallier, T.L. *Science* **221**, 150-152 (1983).
10. Russell, D.E. *et al. Palaeovertebrata, Mem. Extraord. (1982).*

Did komatiitic lavas erode channels on Mars?

SIR — Huppert *et al.*[1] show that terrestrial Precambrian komatiitic lavas may have erupted as very hot, highly fluid, turbulent flows capable of eroding deep channels and melting and assimilating rocks over which they flowed. We have argued[2] that the chemical composition of martian fines, measured by Viking Lander spacecraft[3], indicate derivation from mafic igneous rock, that terrestrial Precambrian komatiitic lava would be a good candidate for an analogue. Using our derived Mars composition, Schonfeld[4] calculated that martian lavas had viscosities of about 0.5 Pa s. The new findings of Huppert *et al.*, that komatiitic lavas could have been as hot as 1,700° C and as low in viscosity as 0.1 Pa s, renew our interest in the possibility of martian channel formation by lava[5].

Various channels on Mars have been ascribed to tectonism, earthflows, wind action, glacial ice, and flowing basaltic lava, but the majority have features (braided channels, terraced walls, sculpted islands, dendritic tributaries, meanders, increase in size downstream) that have forced most observers to conclude they were formed by running water. However, the source of the water, and where the water is today, remain vexing problems. (Most workers believe that water had to be more abundant on Precambrian Mars and what water remains is locked principally in ground ice). Most of the previous objections to lava as the principal erosive agent on Mars (see ref.6) are based on observed characteristics of basalt. Such lavas erupt at around 1,200° C and have viscosities more than fifty times that found by Huppert *et al.* for komatiites. If martian lavas were komatiitic, however, a water-like fluid would have been available and such a fluid would explain not only channel formation, but also the enormous lateral extent of martian flows and the absence of apparent outflow deposits (sediments) in the basins into which the large channels discharge. Finally, if water did not carve martian channels, the complex schemes to explain the present lack of surface water, including gross changes in the atmosphere/climate of the planet, are not needed.

ALEX K. BAIRD

Geology Department,
Pomona College,
Claremont, California 91711, USA

BENTON C. CLARK

Martin Marietta Aerospace,
Denver, Colorado 80201, USA

1. Huppert, H.E., Sparks, R.S.J., Turner, J.S. & Arndt, N.T. *Nature* **309**, 19 (1984).
2. Baird, A.K. & Clark, B.C. *Icarus* **45**, 113 (1981).
3. Clark, B.C. *et al. Science* 194, 1283 (1976).
4. Schonfeld, E. *EOS* **57**, 948 (1977).
5. Cutts, J.A., Roberts, W.J. & Blassius, K.R. *Lunar planet. Sci.* **209** (1978).
6. Baker, V.R. *The Channels of Mars* Ch. 3, 34-55 (University of Texas Press, Austin, 1982).

A question of chirality

SIR — Hanke writes (*Nature* **310** 272; 1984) "It is quite remarkable that immunoglobulins should be able to discriminate between the enantiomers because, as can be seen from the diagram, the molecule of abscisic acid is almost symmetrical...".

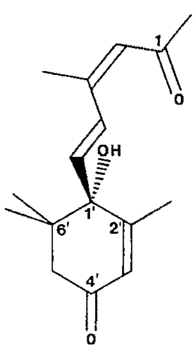

To my eye, the degree of chirality shown by abscisic acid is almost exactly the same as that between my feet. Perhaps Hanke is more supple than me, but I cannot put my right foot into a left shoe. Why should a globulin be more flexible?

N.W. PIRIE

42 Leyton Rd,
Harpenden, Herts, UK

Scientific Correspondence

Scientific Correspondence is intended to provide a forum in which readers may raise points of a rather technical character which are not provoked by articles or letters previously published (where Matters Arising remains appropriate).

Origins of biomolecular handedness

Stephen F. Mason

Chemistry Department, King's College, London WC2R 2LS, UK

Classical mechanisms proposed for the transition from racemic geochemistry to homochiral biochemistry in terrestrial evolution generally ascribe to chance the particular handed choice of the L-amino acids and the D-sugars by self-replicating systems. The parity-violating weak neutral current interaction gives rise to an energy difference between a chiral molecule and its mirror-image isomer, resulting in a small stabilization of the L-amino acids and the L-peptides in the α-helix and the β-sheet conformation relative to the corresponding enantiomer. The energy difference suffices to break the chiral symmetry of autocatalytic racemic reaction sequences in an open non-equilibrium system.

THE class of handed or enantiomorphous molecules (see Fig. 1) was first identified in 1848 by Pasteur[1] from his study of optical activity, the rotation of the plane of polarized light by natural products in the fluid state or in solution. As a student, Pasteur found that the crystals of the sodium ammonium salt of an optically inactive tartaric acid, then termed racemic acid, are separable into two morphological classes, distinguished by hemihedral crystal facets which, in the one set, have a non-superposable mirror image relation to the corresponding facets of the other set of crystals. One set proved to be isomorphous with the sodium ammonium salt of the major naturally occurring isomer, (+)tartaric acid, and gave the same positive specific optical rotation in aqueous solution. The other set, morphologically enantiomorphous, gave a specific rotation of the same magnitude but negative in sign, and liberated the optical isomer, (−)tartaric acid, on acid treatment.

From the view then generally prevailing (see ref. 2), that a crystal and its constituent molecules are morphologically 'images of each other', Pasteur[1] concluded that the individual (+) and (−)tartaric acid molecules are structurally dissymmetric, related as non-superposable mirror-image forms, like the macroscopic hemihedral crystals of the corresponding sodium ammonium salts. While still current in France,[3] Pasteur's term *dissymétrie* became generally supplanted elsewhere by Kelvin's expression 'chirality'[4] from the familiar analogy of the morphological mirror-image relation between the left and the right hand.

Pasteur soon came to the view that chiral molecules, characterized by their fluid-state optical activity, and hemihedral crystals are the product of universal dissymmetric influences, exemplified by the polar fields of electricity and magnetism, or composite rotations, such as those of the inherently-chiral solar system[5]. Following the discovery by Faraday[6] of magnetically-induced optical activity in isotropic transparent media, Pasteur grew normally holohedral crystals in a magnetic field with the object of inducing hemihedral crystal forms. Not discouraged by the negative results, Pasteur attempted to induce optical activity in synthetic products by running reactions in a centrifuge, and to modify the optical activity of natural products by rotating the plants producing them with a clockwork mechanism. These experiments, and their negative results, were reported by Pasteur[5,7] in his later years (1884), in the course of a restatement of his views on the universality of dissymmetric forces and structures in nature. Previously, in his lectures on molecular dissymmetry, Pasteur[8] (1860) had proposed that optical activity provides a demarcation criterion between the products of laboratory synthesis and the natural products synthesized biochemically by living organisms.

Chiral synthesis

Le Bel[9] (1874), in his pioneer work parallel to that of van't Hoff[10] on the connection between optical activity in the fluid phase and enantiomorphous three-dimensional molecular structures, proposed forces of dissymmetry additional to those considered by Pasteur. The reactions of symmetrical substrates, whether achiral or a racemic mixture of enantiomers, carried out photochemically with left- or right-circularly polarized electromagnetic radiation, or thermally with a chiral catalyst, would be expected to produce an excess of a particular enantiomeric product[9].

The differential absorption of left- and right-circularly polarized light by chiral molecules in solution, isotropic circular dichroism, was discovered by Cotton[11] (1895). It provided a physical basis for the proposed chiral photodiscrimination, which however eluded Cotton[12] himself. The first unambiguous photoresolutions of fluid racemic mixtures were achieved by Kuhn and co-workers[13,14] (1929), and the first chiral photosyntheses from achiral precursors, notably, the helicene enantiomers[15–17], are relatively recent.

The second of the dissymmetric influences on reactivity considered by Le Bel[9], the use of chiral reagents in thermal reactions, was implicit in Pasteur's[18] (1853) discovery of diastereomers. The introduction of a second chiral centre into an enantiomer gives two diastereomers with different chemical and physical properties, apart from optical activity. In general, the yields of the two diastereomers are unequal, as Fischer[19] (1894) showed in the step-wise synthesis of the D-series of sugars from (+)glyceraldehyde, and the L-series from the corresponding (−)enantiomer. Fischer[19] found the reactions of diastereomers mediated by naturally-occurring chiral catalysts to be particularly selective, showing that α-methyl-D-glucoside is hydrolysed by maltase, but not by emulsin, whereas β-methyl-D-glucoside is cleaved by emulsin, but not by maltase, although neither of the corresponding L-glucosides are affected by either enzyme preparation.

The stereochemical 'key and lock' hypothesis of Fischer[19,20], based upon these and analogous observations, went far to account for the substantial homochiral biochemistry of living organisms, the general adoption of only one of the two enantiomeric series of the α-amino acids and, equally, of the sugars. Subsequent developments of the 'key and lock' hypothesis suggest a more dynamic relation, a mutual stereochemical adaptation between the catalyst and the substrate. Pauling[21] proposed that the catalytic activity of an enzyme derives from the steric distortion of the substrate when it binds, towards the structure

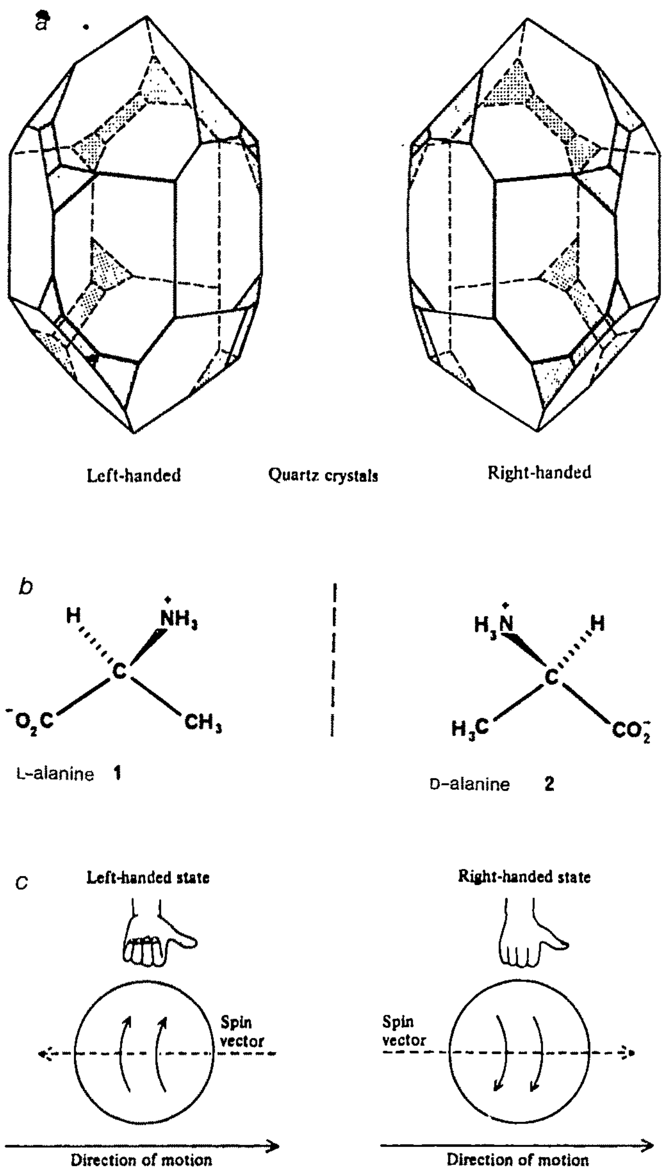

Fig. 1 A chiral or handed structure is not superposable upon the corresponding mirror-image form, its enantiomer. Chirality appears macroscopically (*a*), as in quartz crystals, in which the minor crystal facets follow either a left-handed or a right-handed sequence when viewed in a direction along the three-fold crystal axis. At the molecular level, chirality is exhibited by organic compounds (*b*), such as L-alanine (1) and D-alanine (2), in the respective left-handed (anticlockwise) or right-handed (clockwise) sequence of the NH$_3^+$, CO$_2^-$, and CH$_3$ groups attached to the central carbon atom, when viewed with the bonded hydrogen atom remote from the observer. In the case of a particle (*c*), such as an electron, the left-handed or right-handed chirality derives from the respective antiparallel, or parallel, relation between the linear momentum vector and the angular momentum axial vector.

of the transition state for reaction, a view supported by X-ray structural studies of crystalline enzyme-substrate complexes and by a range of related fluid-state investigations[22].

The results of kinetic studies and product analyses of the synthesis and hydrolysis of polypeptides provide further grounds for the adoption of a homochiral biochemistry by living systems. The polymerisation of a given enantiomer of an α-amino acid, in the form of the *N*-carboxyanhydride derivative, proceeds at a rate faster by a factor of ~20 than that of the corresponding racemic mixture in the same conditions[23]. The partial polymerization of near-racemic mixtures of D- and L-leucine-*N*-carboxyanhydride, containing a small excess of one of the enantiomers, gives a polyleucine in which the original enantiomeric excess is enhanced and, when the polymer product is partially hydrolysed, the degree of homochirality in the residual polymer is further increased[24].

Although the general stereochemical and energetic bases, if not the detailed mechanisms, are clear for the natural selection of an efficient homochiral biochemistry by living organisms, the particular choice of the L-amino acids and the D-sugars appears generally to be a matter of chance[25]. The classical dissymmetric influences, based on electromagnetism or gravitation and the Coriolis force of rotation, might have equally generated an initial enantiomeric excess of D-amino acids or L-sugars which propagated to an enantiomeric homochiral biochemistry.

Chiral fields

In an application of his general principle, that the symmetry of a physical effect implies a corresponding symmetry in the causes, Curie[26] pointed out that each of the polar fields which Pasteur had taken to be dissymmetric has mirror symmetry individually. Any type of chiral field is necessarily composite, with collinear axial and polar vector components, or corresponding higher-rank tensor components. The simultaneous application of a magnetic field and a parallel or an antiparallel electric field provides such a chiral combination, the parallel relation being transformed into the enantiomeric antiparallel relation by mirror-reflection or, equivalently, by space inversion.

Curie[26] conjectured that the synthesis of an optically-active substance from an achiral substrate might be feasible by running the reaction in a chiral combination of an electric and a magnetic field. The conjecture was refuted, at least for the case of uniform static fields, by applications[27–29] of Wigner's general principle[30], that a complete experiment subject to space-inversion and time-reversal should give a transformed experiment which is possible in principle. The application of the parity operator, space-inversion, to a chiral molecule in parallel, static, and uniform electric and magnetic fields transforms the molecule into its mirror-image isomer and the fields into the enantiomeric antiparallel combination. The reversal of the direction of the circular electric current producing the magnetic field, equivalent to time-reversal, leaves the mirror-image isomer unchanged but restores the parallel relation of the electric and the magnetic field. The cycle implies that the fields do not discriminate between a chiral molecule and its enantiomer, both substances having an identical energy in the same combination of environmental fields, so that a racemic mixture inevitably results from a reaction carried to equilibrium in the field combination.

Similar conclusions are derived for the chiral products of reactions run in a centrifuge rotating clockwise or anticlockwise horizontally in a vertical gravitational field[28,29]. The simultaneous application of three uniform fields, electric, magnetic, and gravitation, for example, is required to discriminate between the enantiomeric products from achiral reactants. The discrimination with realistically attainable fields is, however, vanishingly small[28,29]. The most significant of the classical chiral fields is that of circularly polarized electromagnetic radiation, but the discrimination is even-handed, and the pure electromagnetic circular dichroism of a D-isomer, while opposite in sign, is of equal magnitude to that of its L-enantiomer.

Parity non-conservation

A group of anomalies in elementary particle physics led Lee and Yang[31] to conclude that parity, space-inversion equivalence, is not conserved in the weak nuclear interaction, contrary to the original principle of Wigner[30]. A consequence of parity violation, the asymmetric β-decay of radionucleides, was observed in the decay of cobalt-60 to nickel-60 with the emission of an electron[32], and in the emission of the corresponding antiparticle, the positron[33], in the decay of cobalt-58 to iron-58. These and other studies of the weak interaction establish an intrinsic left-chirality for the electron, antiparallel momentum and spin vectors, and right-chirality for the positron, parallel momentum and spin vectors, in proportion to the ratio of the velocity of the particle, or the antiparticle, to the velocity of light.

The discovery of parity non-conservation in the weak interaction led to the chemical expectation that the β-decay of nucleides should give rise to an enantio-differentiating radiolysis of racemic mixtures, or to the corresponding photolysis by the circularly-polarized electromagnetic radiation arising from the progressive retardation of the emitted spin-polarized electron or positron[34]. As yet, no unequivocal enantio-selective radiolyses of racemic mixtures have been reported by the agency of β-radionucleides[35], or of spin-polarized electrons[36] or spin-polarized positrons[37] produced by particle accelerators.

The weak interactions initially investigated, notably β-decay, are mediated by the charged massive bosons, $W^{\pm}$, in the weak charged currents, which have only a minor, high-order, significance for charge-retaining atomic and molecular properties. An additional weak neutral current interaction, involving the massive neutral boson, Z^0, recently detected, together with its charged counterparts, $W^{\pm}$, at CERN[38], emerged from the unification of the weak with the electromagnetic interaction by Weinberg[39] and Salam[40]. The weak neutral current (WNC) is more significant for charge-retaining properties of atoms and molecules, including the stationary state properties, as the perturbation of the state properties by the parity-violating electro-weak interaction between each valence or inner-shell electron and the nucleus or other electrons of an atom remains finite in the non-relativistic limit.

Due to the WNC interaction, all atoms and achiral molecules, as well as enantiomers, are expected to be optically active to electromagnetic radiation and to polarized matter waves. Further, enantiomeric molecules have different electronic binding energies, owing to the dependence of the WNC interaction between different atomic centres on the particular handedness of the molecular stereochemistry. Just as the electron and the positron have intrinsic enantiomeric chirality, so a D-isomer composed of electrons and other particles has a true isoenergetic mirror-image L-enantiomer made up of positrons and other antiparticles in a hypothetical counter-world of antimatter, but the natural particulate L-isomer is not energetically equivalent[41].

The optical rotation of electromagnetic radiation by a free atom, due to the WNC interaction, is expected to be proportional to Z^6, where Z is the atomic number[42,43]. Accordingly, vapours of heavy metal atoms have been investigated, and an optical rotatory dispersion of the correct sign and order of magnitude has been reported for electronic transitions of atomic bismuth, lead, thallium and caesium in the vapour phase[42–44]. Similarly, the matter wave analogue of optical rotation, due to the WNC interaction, has been observed in the rotation of the spin-polarization of a cold neutron beam by crystals of metallic tin, the tin-117 isotope giving a particularly large rotation[45].

The WNC interaction in chiral molecules gives rise to a parity-violating energy shift, E_{pv}, which is positive for one isomer and negative for its enantiomer. Early estimates[46,47] gave a magnitude order, $E_{pv} \sim 10^{-12}$ eV, based upon a crystal field model where a single heavy atom is perturbed by a chiral electrostatic field. More fundamental estimates of E_{pv}, based upon the molecular orbital wavefunctions, are substantially smaller for chiral molecules composed of light atoms[48]. The wave functions of a model chiral ethylene molecule, twisted through 10° to dihedral symmetry[49], provide an energy shift, E_{pv}, of $\sim \pm 5 \times 10^{-19}$ eV, positive for the (R)-isomer and negative for the (S)-enantiomer[48].

Ab initio calculations on a simple chiral molecule, hydrogen peroxide[50], show that the energy shift, E_{pv}, is sensitive to the molecular conformation, with an optimum value of the same magnitude, $\sim \pm 5 \times 10^{-19}$ eV. The energy shift, E_{pv}, for the α-amino acids is also sensitive to the molecular conformation and, at the conformation preferred in aqueous solution, L-alanine is more stable than the D-enantiomer by $\sim -6 \times 10^{-19}$ eV. The extension of the calculations to a peptide unit of a polypeptide in the α-helix or the β-sheet conformation shows that the polypeptides from the L-amino acids are stabilized relative to the corresponding D-enantiomers in both conformations by $\sim -9 \times 10^{-20}$ eV for each peptide unit[51,52].

These parity-violating energy differences between enantiomers amount to no more than $\sim -2 \times 10^{-14}$ J mol^{-1} per amino acid residue in the polymer, corresponding to an enantiomeric excess of some 10^6 L-peptide molecules per mole of racemate in thermodynamic equilibrium at ambient temperature. Although small, the enantiomeric excess indicates a determinate intrinsic bias in organic nature for the particular handedness which evolved historically into homochiral dominance. The sign and the magnitude of the parity-violating energy shift for a sugar enantiomer remains undetermined as yet. Chemically, however, the D-sugars are connected with the L-amino acids through the conversion of D-glucosamine to L-alanine[53].

Chiral symmetry breaking

Observable consequences of the parity-violating energy difference between enantiomeric molecules, owing to the small magnitudes involved, require either an extended, cumulative, amplification mechanism, or an open, dynamic, metastable system with a selection between alternative outputs triggered by a very small perturbation. Systems of the latter type involve the catastrophe theory of symmetry-breaking, in which ordered dissymmetry emerges from an open non-equilibrium process[54]. Kinetic reaction sequences designed to produce a spontaneous transition from a racemic reaction process to the one or the other of the two constituent homochiral reaction sequences postulate autocatalytic branched-chain kinetics in each reaction channel, accompanied by competitive cross-reactions between the two enantiomeric sequences that are mutually inhibitory and form inactive products[55–61]. An open reaction scheme proposed recently has the general form[59],

$$\mathrm{A}+\mathrm{B} \underset{k_{-1}}{\overset{k_1}{\rightleftharpoons}} \mathrm{L} \qquad (1a)$$

$$\mathrm{A}+\mathrm{B} \underset{k_{-1}}{\overset{k'_1}{\rightleftharpoons}} \mathrm{D} \qquad (1b)$$

$$\mathrm{L}+\mathrm{A}+\mathrm{B} \underset{k_{-2}}{\overset{k_2}{\rightleftharpoons}} 2\mathrm{L} \qquad (2a)$$

$$\mathrm{D}+A+B \underset{k_{-2}}{\overset{k'_2}{\rightleftharpoons}} 2\mathrm{D} \qquad (2b)$$

and,

$$\mathrm{L}+\mathrm{D} \xrightarrow{k_3} \mathrm{P} \qquad (3)$$

In an open non-equilibrium system with an input of achiral substrates A and B, and an output composed of the enantiomers L and D, together with the inactive product P, formed irreversibly, the overall process remains racemic if corresponding primed and unprimed rate constants are equal and the input remains small. As the input concentrations of A and B are increased, the racemic process becomes metastable and switches spontaneously into the one or the other enantiomeric homochiral reaction sequence, ($1a$) and ($2a$) or ($1b$) and ($2b$), breaking the racemic chiral symmetry[59]. In a collection of such systems, it is expected that the L-channel would be adopted by one half of the reaction sequences and the D-channel by the other half.

At the onset of racemic metastability in the reaction sequence (1), (2) and (3), the bifurcation point dependent on the substrate input, the system becomes hypersensitive to small chiral perturbations, which determine the particular homochiral channel adopted by the system. The chiral perturbation may be external to the system, or intrinsic, such as a small difference, ΔE, between the activation energy of corresponding primed and unprimed reactions in the processes (1) and (2). Thermal fluctuations, which increase with a rise in temperature, offset the hypersensitivity of the reaction sequence at the bifurcation to chiral perturbations, and the overall chiral discrimination governing the choice of a homochiral channel becomes proportional to $(\Delta E/kT)$. The critical magnitude order, $(\Delta E/kT) \geq 10^{-17}$, is

21-1-87 A. Laite 4630

R 429

found[59] to govern the selection of a particular enantiomeric reaction sequence in the series (1), (2) and (3).

At ambient temperature, the estimated parity-violating energy differences between enantiomers composed of light atoms correspond to the lower limit of the criterion, $(E_{pv}/kT) \sim 10^{-17}$. The determinate selection of the lower-energy homochiral reaction sequence is promoted by a slow passage through the transitional point where the racemic reaction process bifurcates into the two homochiral reaction channels, that is, by small increments of the input concentrations of the substrates A and B, extended over long time periods. From the parity-violating energy differences between the enantiomers of the α-amino acids and of the polypeptides, it is estimated that the selection of the lower-energy L-series occupied a minimum time of $\sim 10^3$ years[61].

An external chiral perturbation, ΔE_{ext}, of the reaction sequence (1), (2) and (3), made up from the combination of three macroscopic vector fields, electric, magnetic, and gravitation, does not meet the above mentioned criterion because, even with extreme field strengths, the ambient temperature ratio amounts to no more[59] than $(\Delta E_{ext}/kT) \sim 10^{-19}$. The external perturbation of circularly polarized light is not eliminated however. While the pure electromagnetic circular dichroism of two enantiomers is equal in magnitude and opposite in sign, the electro-weak interaction gives each atom in the two molecules a small additional optical activity which is of the same sign for each enantiomer. The magnitude-symmetry of the differential absorption of left and right circularly polarized light by enantiomeric molecules is broken by the WNC interaction, and even equally alternating opposite circular components in the solar radiation would tend to favour one of the two enantiomeric reaction channels in the long run. Owing to multiple aerosol scattering, twilight is ~0.1% circularly polarized, particularly in the near infrared region, with one circular component in excess at sunrise and the other at sunset[62].

A uniformitarian model, alternative to that of the catastrophic bifurcation of competitive reaction sequences, depends upon the progressive accumulation of small differences between each successive enantiomeric stage in a manifold chemical or physical process, starting from an achiral or racemic substrate and terminating with an enantiomerically enriched or homochiral product[63–69]. The accumulation model, proposed initially to account for the prevalence of homochiral biopolymers among the natural products[63], postulates that a small difference between the activation parameters of the enantiomeric monomers, ΔE, effective in relation to the thermal fluctuations, kT, through the ratio, $\varepsilon = (\Delta E/kT)$, at each of the n stages of the polymerization, results in an excess of one of the homochiral n-fold polymers. The relative enantiomeric excess of the favoured n-fold polymer, $\mathrm{L}(n)$, say, is dependent upon the degree of polymerization, n, and the advantage ratio, ε,

$$[\mathrm{L}(n) - \mathrm{D}(n)]/[\mathrm{L}(n) + \mathrm{D}(n)] \simeq n\varepsilon \qquad (4)$$

Subsequent applications of the accumulation model include cases of the spontaneous optical resolution of racemic substances by crystallization[66–69]. By the use of the relation (4), the advantage ratio is estimated at $\varepsilon \sim 10^{-10}$ from the distribution of (+) and (−) crystals formed in 63 recrystallizations of racemic sodium ammonium tartrate[69], compared to a value, $\varepsilon \sim 10^{-6}$, obtained from the polymerization of monomeric alanine derivatives[64]. Both values are substantially larger than the minimum ratio, $\varepsilon \sim 10^{-17}$, required by the bifurcation model[59], and approximately equal to the ambient temperature ratio, E_{pv}/kT, for the parity-violating energy difference between enantiomers composed of the lighter elements[50–52].

The condensation of optically-impure monomeric α-amino acid derivatives gives heterochiral polymers[23,24], not the homochiral polymers as required by the progressive accumulation model[63]. Further, no equilibrated racemate is expected to be truly equimolecular in its constituent enantiomers, owing to the parity-violating energy difference between them, so that neither the polymerization of enantiomeric monomers, nor an optical resolution by crystallization, begin with exactly equal enantiomer concentrations. Synthetic racemic camphor is reported to contain an excess of up to 3 or 4% of (+)camphor[68], and, after four successive recrystallizations of racemic tartaric acid, a minor excess of the (+)isomer was found to remain in the final crop of crystals and in the last of the mother liquors[70].

In a general criticism of the progressive accumulation model, it is argued that the condensation of an exactly equimolecular mixture of enantiomeric monomers would necessarily terminate with an equimolecular mixture of homochiral n-fold polymers, the enantiomeric enrichment of the incomplete process being transient[58]. The objection is applicable to a closed system of optically-stable enantiomers in a racemic process, but not to an open system, with a continuous input of substrate and output of chiral product, nor to a closed system in which a stable chiral product forms from an achiral or optically-labile substrate.

Sometimes, the formation of enantiomorphous crystals by an achiral substance, for example sodium chlorate[71], or an optically-labile racemate, for example allylethylmethyl-anilinium iodide[72], gives, in a single experiment, crystals predominantly of one hand. As a result of many experiments, involving 46 crystallizations and 3,206 crystals in the case of sodium chlorate[71], the weighted mean of the number of (+) and (−) crystals approaches equality. However because the departure from equality attains the 90% confidence level, it is not a matter of chance in the case of the terrestrial distribution of quartz where, over a total collection of 16,807 crystals, a 1% enantiomeric excess of (−)quartz is documented[73]. The (−)quartz bias is common to all the locations sampled in the Americas, Europe, and Asia, and the collection excludes 931 unrepresentative sets of crystals, in which the mean enantiomeric excess of (−)quartz rises to 9.8%.

The excess of (−)crystals in the quartz laid down in the post-biotic period may arise from chiral biomolecular influences, although the elevated temperatures favouring the hydrothermal crystallization of quartz do not support this. While L-analine is preferentially absorbed from the corresponding racemic mixture by (−)quartz[74,75], this and other α-amino acids are racemised at 142 °C in aqueous solution with a halflife of no more than a few days[76]. If a significant proportion of crystalline quartz was laid down in the prebiotic era, the excess of (−)quartz provides not only a possible perturbation of determinate chirality in the bifurcation or the accumulation model for the generation of biomolecular homochirality, but also evidence for a small intrinsic parity non-conservation in the physical world at large.

Conclusion

The significance of the electro-weak interaction is established in particle physics, through the detection of the massive neutral boson, Z^0, mediating the weak neutral current[38], and in atomic physics, by measurements of the optical activity of heavy metal atoms[42–44]. The importance of the WNC interaction for chiral systems, particularly biomolecules, is confined as yet to small enantiomers, composed of the lighter elements, for which reliable *ab initio* computations are currently feasible. The calculations to date of the parity violating energy difference between the enantiomers of the α-amino acids and the polypeptides in the α-helix and the β-sheet conformation provide a basis for the viewpoint that the adoption of the L-α-amino acid series, at least, in the homochiral biochemistry of living organisms was fully determinate, and not merely a matter of chance.

The current calculations refer to the range of molecular conformations stereochemically permitted for a small enantiomer in its electronic ground state. Corresponding computations of the potential energy surfaces for the stereoisomeric transition states connecting an archiral set of substrates with an enantiomeric pair of products are required, for example the reaction surfaces linking an aldehyde and ammonia or hydrogen cyanide with the enantiomeric aldehyde-ammonia or cyanohydrin products. These component reactions make up the traditional

Strecker synthesis of α-amino acids from carbonyl compounds, a synthesis which is considered to be significant in biogeochemical evolution. The evaluation of the potential energy surfaces for enantiomeric reactions, including the parity-violating energy shift, has importance for both the bifurcation and the accumulation mechanism proposed for the emergence of biochemical homochirality.

As yet, an open, flow-reactor, reaction sequence, involving the autocatalytic chain-branching of enantiomeric intermediates, has not been devised for an experimental investigation of the triggered bifurcation model for the spontaneous development of homochiral from racemic reaction systems. The nearest analogous reaction sequences characterized, although rather remote, involve the autocatalytic chain-branching of atomic radicals and other achiral intermediates, notably, the oscillatory chemical reactions of the Belousov-Zhabotinsky type, in which the reaction system switches spontaneously from one quasi steady state to another[54,77–79].

The alternative accumulation model for the emergence of homochirality from racemic systems is the more readily testable in principle at present. The practical limitation of the investigation of racemic monomer condensations, namely, the formation of heterochiral polymers, has an analogue, the formation of heterochirally twinned crystals, in studies of the spontaneous optical resolution of racemates by crystallization. The heterochiral Brazil twinning of quartz crystals provides an example, although the twinning is readily identified and the homochiral crystals are the more generally prevalent[73].

A study of the relative abundance of the (+) and the (−) crystals formed by solutions of an optically-labile racemate, or an achiral substance, affords an immediately practicable method of investigating the parity-violating energy difference between enantiomers, due to the electroweak interaction. Although the energy difference is small, it is multiplied by the number of molecules, or the number of unit cells, in a macroscopic crystal, as prescribed by relation (4). Further, the parity violating energy difference between enantiomers is expected to be proportional to Z^5, where Z is the atomic number of the heavy atom or atoms in the molecule[47,48], and there are indications, from the *ab initio* calculations of the energy differences carried out to date, that such a proportionality holds to a fair approximation[52].

Reports in the literature describe the formation of predominantly dextro-rotatory crystals from aqueous solutions of potassium dodecatungstosilicate[80–82], and of the corresponding dodecamolybdosilicate with a smaller, but still substantial, enantiomeric excess[82]. A similar substantial excess of dextro-rotatory crystals is reported for 21 recrystallizations of allylethylmethylanilinium iodide[72]. These salts contain relatively heavy elements, Mo ($Z = 42$), I ($Z = 53$), and W ($Z = 74$). The heaviest element readily available, uranium ($Z = 92$), provides, in the form of sodium uranyl acetate, which crystallizes[83] in the chiral cubic space group, $P2_13$, a promising material for an investigation of the parity-violating energy difference between enantiomorphous structures due to the electro-weak interaction from the relative and absolute abundance of (+) and (−) crystals formed in a spontaneous optical resolution by crystallization.

1. Pasteur, L. *C.r. hebd. Séanc. Acad. Sci. Paris* **26**, 535 (1848); *Oeuvres de Pasteur* Vol. 1 (ed. Pasteur Valery-Radot) 61–64 (Masson, Paris, 1922).
2. Haüy, R. J. *Tableau Comparatif des Resultats de la Cristallographie et de l'Analyse Chimique*, xvii (Courcier, Paris, 1809).
3. Caillois, R. *La Dissymétrie*, 33–64 (Gallimard, Paris, 1973).
4. Kelvin, Ld. *Baltimore Lectures*, 618–619 (Clay, London, 1904).
5. Pasteur, L. *Rev. Scient.* 7, 2 (1884); *Oeuvres* Vol. 1, 369–380 (1922).
6. Faraday, M. *Phil. Mag.* **28**, 294 (1846).
7. Pasteur, L. *Bull. Soc. Chim. Fr*, **41**, 215 (1884); *Oeuvres* Vol. 1, 385 (1922).
8. Pasteur, L. *Recherches sur la Dissymétrie Moleculaire* (1860); *Oeuvres* Vol. 1, 314–344; English trans., *Alembic Club Reprint*, No. 14 (Livingstone, Edinburgh, 1948).
9. Le Bel, J. A. *Bull. Soc. Chim. Fr.* **22**, 337 (1874).
10. Van't Hoff, J. H. *Arch. Neéland Sci. Exact. Nat.* 9, 445 (1874).
11. Cotton, A. *C.r. hebd. Séanc. Acad. Sci. Paris* **120**, 989 & 1044 (1895).
12. Cotton, A. *J. Chim. phys.* **7**, 81 (1909).
13. Kuhn, W. & Braun, F. *Naturwissenschaften* **17**, 227 (1929).
14. Kuhn, W. & Knopf, E. *Z. phys. Chem.* **B7**, 292 (1930).
15. Burchardt, O. *Angew. Chem. int. Edn.* **13**, 179 (1974).
16. Martin, R. H. *Angew. Chem. int. Edn.* **13**, 649 (1974).
17. Kagan, H. & Fiaud, J. C. *Topics Stereochem.* **10**, 175 (1978).
18. Pasteur, L. *Annls Chim. Phys.* **38**, 437 (1853); *Oeuvres* Vol. 1, 203–241 (1922).
19. Fischer, E. *Chem. Ber.* **27**, 2985 & 3231 (1894).
20. Fischer, E. *J. chem. Soc.* **91**, 1749 (1907).
21. Pauling, L. *Nature* **161**, 707 (1948).
22. Dodson, G., Glusker, J. P. & Sayre, D. (eds) *Structural Studies on Molecules of Biological Interest: A Volume in Honour of Dorothy Hodgkin*, Sections IV & V (Clarendon, Oxford, 1981).
23. Blout, E. R. & Idelson, M. *J. Am. chem. Soc.* **80**, 2387 (1958).
24. Blair, N. E., Dirbas, F. M. & Bonner, W. A. *Tetrahedron*, **37**, 27 (1981).
25. Miller, S. L. & Orgel, L. E. *The Origins of Life on the Earth*, 171 (Prentice Hall, Englewood Cliffs, 1974).
26. Curie, P. *J. Physique théor. appl.* Ser 3, **3**, 393 (1894).
27. De Gennes, P.-G. *C.r. hébd. Séanc. Acad. Sci. Paris* **B270**, 891 (1970).
28. Mead, C. A. & Moscowitz, A. *J. Am. chem. Soc.* **102**, 7301 (1980).
29. Peres, A. *J. Am. chem. Soc.* **102**, 7390 (1980).
30. Wigner, E. P. *Z. Phys.* **43**, 624 (1927).
31. Lee, T. D. & Yang, C. N. *Phys. Rev.* **104**, 254 (1956).
32. Wu, C. S., Ambler, E., Hayward, R. W., Hoppes, D. D. & Hudson, R. P. *Phys. Rev.* **105**, 1413 (1957).
33. Rodberg, L. S. & Weisskopf, V. F. *Science* **125**, 627 (1957).
34. Ulbricht, T. L. V. *Q. Rev. chem. Soc.* **13**, 48 (1959).
35. Ulbricht, T. L. V. *Origins Life* **11**, 35 (1981).
36. Bonner, W. A., Blair, N. E. & Dirbas, F. M. *Origins Life* **11**, 119 (1981).
37. Gidley, D. W., Rich, A., Van House, J. & Zitzewitz, P. W. *Nature* **297**, 629 (1982).
38. Walgate, R. *Nature* **303**, 473 (1983).
39. Weinberg, S., *Phys. Rev. Lett.* **19**, 1264 (1967); *Rev. mod. Phys.* **52**, 515 (1980).
40. Salam, A. in *Proc. 8th Nobel Symposium: Elementary Particle Theory* (ed. Svartholm, N.) (Almquist and Wiksell, Stockholm, 1968); *Rev. mod. Phys.* **52**, 525 (1980).
41. Barron, L. D. *Molec. Phys.* **43**, 1395 (1981).
42. Sanders, P. G. H. in *Fundamental Interactions and the Structure of Matter* (eds Crowe, K., Duclos, J., Fiorentini, G. & Torelli, G.) Vol. 57 (Plenum, New York, 1980)
43. Fortson, E. N. & Wilets, L. *Adv. atom. molec. Phys.* **16**, 319 (1980).
44. Emmons, T. P., Reeves, J. M. & Fortson, E. N. *Phys. Rev. Lett.* **51**, 2089 (1983), **52**, 351 (1984)
45. Stodolsky, L. *Nature* **290**, 735 (1981).
46. Rein, D. W. *J. molec. Evol.* **4**, 15 (1974).
47. Zel'dovich, B. Ya., Saakyan, D. B. & Sobel'man, I. I. *JETP Lett* **25**, 94 (1977)
48. Hegstrom, R. A., Rein, D. W. & Sanders, P. G. H. *J. chem. Phys.* **73**, 2329 (1980)
49. Bouman, T. D. & Hansen, A. E. *J. chem. Phys.* **66**, 3460 (1977).
50. Mason, S. F. & Tranter, G. E. *Chem. Phys. Lett.* **94**, 34 (1983).
51. Mason, S. F. & Tranter, G. E. *JCS Chem. Commun.* 117 (1983).
52. Mason, S. F. & Tranter, G. E. *Molec. Phys.* (in the press).
53. Wolfrom, M. L., Lemieux, R. U. & Olin, S. M. *J. Am. chem. Soc.* **71**, 2870 (1949)
54. Nicolis, G. & Prigogine, I. *Self-organisation in Non-equilibrium Systems* (Wiley, New York, 1977).
55. Frank, F. C. *Biochim. biophys. Acta* **11**, 459 (1953).
56. Seelig, F. F. *J. theor. Biol.* **31**, 355 (1971).
57. Decker, F. *Nature new Biol.* **241**, 72 (1973); *J. molec. Evol.* **4**, 49 (1974)
58. Fajszi, Cs. & Czege, J. *Origins of Life* **11**, 143 (1981).
59. Kondepudi, D. K. & Nelson, G. W. *Phys. Rev. Lett.* **50**, 1023 (1983); *Physica A* (in the press)
60. Tennakone, K. *Chem. Phys. Lett.* **105**, 444 (1984).
61. Kondepudi, D. K. & Nelson, G. W. *Phys. Rev. Lett.* **52** (in the press).
62. Angel, J. R. P., Illing, R. & Martin, P. G. *Nature* **238**, 389 (1972).
63. Yamagata, Y. *J. theor. Biol.* **11**, 495 (1966).
64. Thiemann, W. & Darge, W., *Origins of Life* **5**, 263 (1974).
65. Letokhov, V. S. *Phys. Lett.* **53A**, 275 (1975); *Nuovo Cimento Lett.* **20**, 107 (1977)
66. Thiemann, W. & Wagener, K. *Angew. Chem. int. Edn.* **9**, 740 (1970).
67. Wagener, K. *J. molec. Evol.* **4**, 77 (1974).
68. Thiemann, W. *J. molec. Evol.* **4**, 85 (1974).
69. Keszthelyi, L. *Phys. Lett.* **64A**, 287 (1977).
70. Kipping, F. S. & Pope, W. J. *J. chem. Soc.* **95**, 103 (1909).
71. Kipping, F. S. & Pope, W. J. *J. chem. Soc.* **73**, 606 (1898).
72. Havinga, E. *Biochim. biophys. Acta* **13**, 171 (1954).
73. Palache, C., Berman, H. & Frondel, C. *Dana's System of Mineralogy*, 7th edn, Vol 3, 16 (Wiley, New York, 1962).
74. Kavasmaneck, P. R. & Bonner, W. A. *J. Am. chem. Soc.* **99**, 44 (1977).
75. Furuyama, S., Sawada, M., Machiya, K. & Morimoto, T. *Bull. chem. Soc. Japan* **55**, 3394 (1982).
76. Bada, J. L. & Shou, M. Y. in *Biogeochemistry of Amino Acids* (eds Hare, P. E., Hoering, T. C. & King, K.) 235 (Wiley, New York, 1980).
77. *Physical Chemistry of Oscillatory Phenomena, Faraday Symp. chem. Soc.* No 9 (1974)
78. Noyes, R. M. & Field, R. J. *Accts chem. Res.* **10**, 214 & 273 (1977).
79. Epstein, I. R. *J. phys. Chem.*, **88**, 187 (1984).
80. Wyrouboff, G. *Bull. Soc. Fr. Minér. Cristallogr.* **19**, 219 (1896).
81. Soret, C. *Arch. Sci. phys. nat.* **7**, 80 (1899).
82. Copaux, H., *Bull. Soc. Fr. Minér Cristallogr.* **18**, 219 (1910).
83. Zachariasen, W. H. & Plettinger, G., *Acta crystallogr.* **12**, 527 (1959)

LIBRARY COPY
Departments of
Chemical Engineering
Chemical Technology
Plastics and Rubber Technology

A general circulation model of water isotope cycles in the atmosphere

Sylvie Joussaume*, Robert Sadourny* & Jean Jouzel†

* Laboratoire de Météorologie Dynamique, 24, rue Lhomond, 75231 Paris Cedex 05, France
† Laboratoire de Géochimie Isotopique DPC-CEN Saclay, BP 2-91191 Gif sur Yvette Cedex, France

$H_2{}^{18}O$ and HDO are important climatic tracers largely used to reconstruct continental palaeoclimates. The only thorough way to compare isotopic distributions in precipitation for modern and palaeoconditions is to simulate isotope cycles using atmospheric general circulation models. $H_2{}^{18}O$ and HDO cycles incorporated into our atmospheric general circulation model show good agreement between observed and predicted values for modern conditions.

THE water isotopes $H_2{}^{18}O$ and HDO are important climatic tracers for several reasons. First, on a worldwide scale, ^{18}O and deuterium contents of precipitation decrease with the mean surface-air temperature at the sampling site[1]; this relationship can be used to reconstruct palaeotemperatures, especially at high latitudes where it is particularly well obeyed[2–5]. Second, the relationship between ^{18}O and deuterium contents of precipitation, $\delta D - 8\delta^{18}O = d$ (where d is 10‰ at present[6], with $\delta^{18}O$ and δD expressed in ‰ versus the standard mean ocean water, SMOW, reference), appears to be climate dependent, with smaller values of deuterium excess d during the last ice age (18,000 yr BP)[7,8]; the smaller ice age values found in Antarctic ice cores have been interpreted[7], using a simple model, as reflecting higher relative humidity over the corresponding moisture source regions. Third, spatial and temporal variability of isotope contents of precipitation depends not only on temperature, but also on other atmospheric or geographical parameters[1], such as intensity of precipitation and air mass origin; these further dependencies make climate reconstructions more difficult, but at the same time could be useful as additional climatic information.

Simple models have been derived to study the dependency of isotope contents of vapour and precipitation on atmospheric parameters. These models take into account all the details of fractionation processes but they only deal with prescribed trajectories of isolated air masses. They yield results consistent with the mean temperature–isotope and δD–$\delta^{18}O$ relationships[1,9,10] and can also be used to study more complex dependencies, such as amount of precipitation, air mass origin or meteorological path[11]. The only way, however, to reconstruct the full space–time variations of isotope contents of vapour and precipitation is to include the isotope cycle modelling in atmospheric general circulation models (AGCMs) which explicitly simulate the global and regional features of atmospheric dynamics and thermodynamics, with fully detailed hydrological cycles. Such AGCM modelling of isotope cycles must be tested first on modern conditions for which reasonably good documentation of isotope contents is available: vertical profiles have been measured[12–14], spatial and seasonal distributions in precipitation are reasonably well known, mainly from the IAEA network[15]. Once it has been validated against modern data, AGCM isotope modelling can be used in palaeoclimatic simulations; this may be a first step towards a better interpretation of isotope changes from ancient to present times in terms of changes in atmospheric parameters.

Model description

The AGCM[16] of the Laboratoire de Météorologie Dynamique (LMD) is an 11-layer gridpoint general circulation model with a regular longitude–sine-of-latitude grid, based on primitive equations (horizontal equation of motion, hydrostatic equation, equation of continuity and thermodynamic equation). It includes a fully interactive hydrological cycle as well as prognostic equations for soil moisture, land- and ice-surface temperature and snow depth. Radiative fluxes are calculated taking into account model predicted cloud cover[17]. Orography, land and sea-ice extent, sea-surface temperature and ocean-surface albedo are prescribed external parameters; in the present experiments, land-surface albedo is a prescribed function of soil moisture and snow depth, based on the CLIMAP data set[18].

The basic hydrological cycle of the LMD AGCM[16] includes: surface evaporation over oceans and continents, vertical turbulent diffusion within the planetary boundary layer, horizontal and vertical transport, condensation processes, vertical diffusion in convective clouds and re-evaporation under cloud base. Within this basic hydrological cycle, differentiation between the water isotope species occurs at each phase change through fractionation processes resulting from differences in water vapour pressures and molecular diffusivities. Because HDO and $H_2{}^{18}O$ have lower vapour pressures than $H_2{}^{16}O$, the condensed phase in equilibrium with vapour is enriched in heavy isotopes up to a fractionation coefficient $\alpha (\alpha > 1)$ (refs 19–21). On the other hand, differences in molecular diffusivities[22] lead to kinetic fractionation which changes the relative behaviour of $H_2{}^{18}O$ and HDO for non-equilibrium processes.

Surface evaporation in the basic water cycle is proportional to a drag coefficient C_D, surface wind speed and the difference between the saturated mixing ratio at ground-surface temperature and the air mixing ratio at 10 m above the surface. Over land without snow or ice cover, surface moisture fluxes are limited through an evapo-transpiration coefficient which is a simple increasing function of soil moisture[16]. For $H_2{}^{18}O$ and HDO, the parameterization used for surface evaporation[23] differs over ocean, snow or ice, and land. At the air–ocean interface, water isotope fluxes are treated in the same way as the water vapour flux: that is, they are proportional to the difference between isotopic mixing ratio at ocean surface (in equilibrium with the ocean) and at 10 m. Isotopic drag coefficients are formulated according to Merlivat and Jouzel[9] in order to represent kinetic effects. Over snow and ice, no fractionation is assumed because the time scale of isotope exchanges inside snow or ice crystals is large; therefore, water evaporates with the isotopic ratio of the ground surface. Over land without snow or ice, evaporation is also assumed to occur without fractionation. This assumption, which seemed reasonable from the experimental results of Zimmermann *et al.*[24], has also been used by Rozanski *et al.*[25]; it was recently supported by a simple model and confirmed in studies under controlled environmental and natural conditions[26,27]. Condensation, however, is not treated like evaporation (except over oceans): isotopic equilibrium is always assumed between condensed water and surface vapour.

The basic hydrological cycle uses two ground water reservoirs[16], snow depth and soil moisture, whose evolution is governed by precipitation, surface evaporation or condensation, snowmelt and runoff. Soil moisture is defined as a single-layer parameter without differentiating surface and deep soil contents; runoff occurs whenever soil moisture exceeds a maximum value of 15 cm. Although the isotopic ratio of the soil moisture reservoir is not in reality constant with depth, we use a single ratio for the entire soil water reservoir[23], the evolution of which is governed only by precipitation and condensation, as surface evaporation, snowmelt and runoff have no fractionation effects. This 'mixed single layer' approach is, in fact, the simplest way to retain a memory of the past precipitation–condensation processes without using an expensive multilayer formulation. This simplification is, to some extent, equivalent to a kind of time averaging of precipitations; therefore, it is likely to yield a systematic underestimation of surface variability, and distortions of time lag effects (which may not be too important as long as seasonal variations are not considered). In the case of snow or ice cover, a similar 'mixed single layer' approach is used[23], although the molecular exchanges inside snow or ice are very slow. Furthermore, as there is no fractionation during snowmelt and surface evaporation, we do not distinguish snow and soil liquid water isotope contents. Over land ice, the single mixed-layer reservoir for snow and ice used for isotope budgets has an equivalent water depth of only 1 cm, in order to average precipitations over seasonal time scales. In the case of sea ice, the single reservoir is limited to the snow layer; over bare sea ice, we assume constant isotopic ratios[28]: +3‰ for $H_2{}^{18}O$ and +20‰ for HDO.

Like $H_2{}^{16}O$, the two isotope species HDO and $H_2{}^{18}O$ are diffused vertically across the planetary boundary layer with a turbulent diffusion coefficient depending on static stability and vertical wind shear[16].

Transport is a critical process in isotope modelling[23]. Ordinary second-order finite difference schemes applied to the transport equation are not effective for treating positive quantities which may have large variations from one gridpoint to the next; in particular, they can produce unrealistic negative values. The problem is not very serious when only water vapour is advected, as negative values can be corrected *a posteriori*. When isotope species are simultaneously modelled, however, the occurrence of negative values must be avoided because of resulting dramatic inconsistencies in isotopic ratios (preliminary tests have shown that values up to 10^8‰ are easily generated). In the present simulation, horizontal transport is modelled, using a first-order upstream flux form. All isotope species are, therefore, transported consistently in horizontal directions. The upstream scheme is strongly diffusive along the flow streamlines, but it has the advantage of producing more coherent precipitation patterns when it interacts with convective parameterizations. However, this upstream scheme cannot be applied in the vertical direction because it would lead to an unrealistically humid stratosphere. Vertical transport of water vapour is, therefore, modelled using a second-order flux form based on harmonic means between neighbouring points[23]; this scheme is not diffusive and ensures positive values of the water vapour mixing ratio. The fluxes of HDO and $H_2{}^{18}O$ are computed from the product of the water vapour flux and the arithmetic means of isotopic ratios. This technique ensures a consistent treatment of all isotope species and keeps isotopic ratios within reasonable bounds[12,13]. More elaborate methods, such as 'flux corrected techniques'[29], should also be considered for future simulations.

The LMD AGCM distinguishes two kinds of condensation processes, large-scale condensation and small-scale convection[16]. The first case occurs when the air is supersaturated and the temperature lapse rate is less than the moist adiabatic lapse rate (non-convective clouds). Water vapour is condensed and temperature rises due to the release of latent heat until the mixing ratios reach the saturation value at the new temperature. Supersaturation is then tested downwards, starting from the top layer, and condensed water vapour is eventually re-evaporated in the next layer down when the air is undersaturated. The second case occurs when the air is conditionally unstable, with a temperature lapse rate exceeding the moist adiabatic lapse rate (convective clouds). For supersaturated air, the moist convective adjustment technique[30] is used: the temperature is adjusted to the previous estimate of the moist adiabatic lapse rate, with energy being conserved in the process over the whole unstable range. The mixing ratios are then set equal to saturation values at the adjusted temperature and the excess precipitates. For unsaturated layers, condensation may occur in moisture convergence areas. Here we follow Kuo's parametrization[31] of cumulus convection: we assume a moist adiabatic profile within the cloud with a moist static energy equal to its saturation value at cloud base, that is at the top of the mixed layer; the fractional area occupied by the cloud is determined as the ratio of latent heat available from moisture convergence at cloud base, to the energy necessary to generate the whole cloud on the mesh size. Temperature and humidity are then homogenized within the mesh, and the excess of moisture precipitates. In the present simulations, precipitating water re-evaporates under convective cloud base until the air becomes saturated.

At each phase change, isotopic fractionation is modelled[21] according to the type of phase change and the nature of the phase formed. Two phase transitions can lead to ice formation: direct deposition of vapour onto a solid phase, which actually occurs below −15 °C, and the freezing of liquid droplets. In the first case, as the molecular exchanges are very slow inside solid crystals, the classical Rayleigh or open system model is assumed[32]: the condensed phase is immediately removed after its formation and leaves the air parcel in isotopic equilibrium with the vapour phase. The second case occurs between −15 and 0 °C without any isotopic fractionation, since, whatever their size, the freezing time of droplets and drops is negligible in comparison with their isotopic relaxation time[31]. The case of liquid formation, above −15 °C, is more difficult to model: the Rayleigh model is more reasonable for drops, as their isotopic relaxation time is large[32], while the closed system model, which assumes isotopic equilibrium between all the condensed phase and the vapour, is more adequate for droplets. Indeed, an accurate model[34] should take into account the isotopic interactions between the water species coexisting in a cloud (vapour, cloud water, rainwater, cloud ice and graupel), the partial removal of precipitation and the variations with time of these parameters. Instead, we have chosen the two extreme hypotheses (open and closed system) by performing two parallel experiments (B and A respectively) in which one of the two assumptions is used. During evaporation, we simply assume no fractionation for solid water, because the molecular exchanges are extremely slow, and isotopic equilibrium for liquid water, which is a reasonable approximation when liquid water is mainly composed of droplets with a radius <100 μm (ref. 33).

The parameterization of convective clouds presently used in the LMD AGCM only provides the total change of water vapour mixing ratio at each layer without separating convective diffusion from condensation. For isotope modelling[21], however, we need to separate the two processes. We assume an intermediate step where water vapour and all isotope species are uniformly mixed throughout the vertical extension of the cloud; this assumption, associated with the cloud budget already computed, uniquely determines the vertical distribution of condensation. This seemingly excessive vertical diffusion is, in fact, compensated by intensive condensation in the upper cloud layers, associated with re-evaporation in the lower cloud layers (in this step isotopic equilibrium between liquid and vapour is assumed at the end of the process). Another necessary parameter is the fractionation coefficient at the location of phase changes. To take into account the complexity of convective diffusion, we define the fractionation coefficient as the arithmetic average of its 'initial' value (determined by the temperature at the source regions—mainly cloud base) and its final value (determined by the final temperature of the layer). This scheme was first tested on isolated clouds. It yields acceptable results but with a

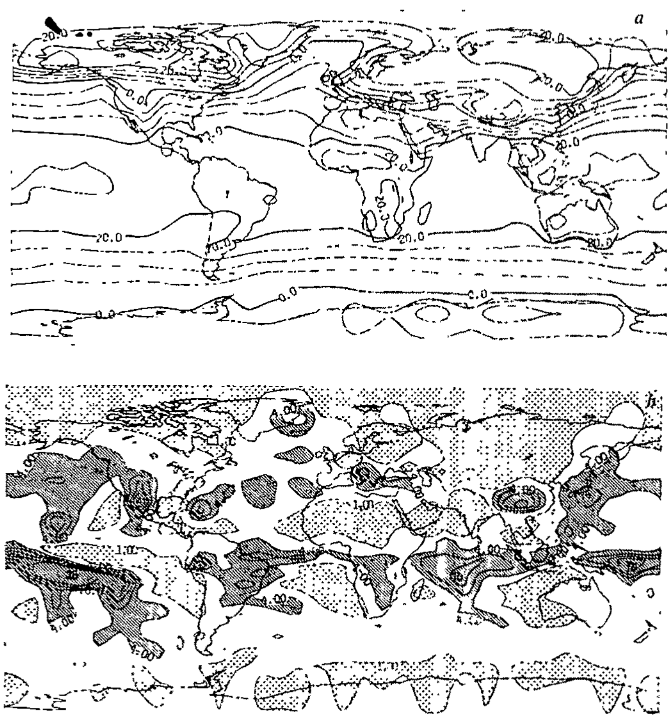

Fig. 1 Mean January simulated: *a*, surface-air temperature (°C; isolines every 5 °C); *b*, precipitation. Isolines every 3 mm day^{-1} up to 16 mm day^{-1}; dotted areas, <1 mm day^{-1}; hatched areas, >4 mm day^{-1}.

tendency to systematically underestimate isotopic ratios at cloud top; this effect, however, is not too serious because it is noticeable only when clouds extend up to higher tropospheric levels where mixing ratios are, in any case, small.

Usually the supersaturation S with respect to the liquid phase is <1% in clouds[35] and so kinetic effects are completely negligible. However, they may become important when S is far from zero. This occurs in the case of snow crystal formation, where the supersaturation S with respect to the solid phase may reach values up to 20% (ref. 36). During re-evaporation, kinetic effects are negligible for droplets but become important for drops[32], which prevail mainly in precipitating water from convective clouds. Kinetic effects at snow formation can be simply parameterized using an equivalent fractionation coefficient α_e (ref. 10) which is a decreasing function of S; therefore, compared with equilibrium values, they tend to decrease the enrichment of falling snow and to enhance their δD–δ^{18}O slope. Inclusion of these effects in a dynamically simple model leads to predicted snow isotopic values in very good agreement with observed values in polar areas, both concerning the isotope–temperature and δD–δ^{18}O relationships[10]. To test the impact of kinetic effects on snow formation with our isotope modelling[23], we introduced these effects on snow formation with clouds below −15 °C in only one experiment (experiment B); however, the supersaturation function used $S = 0.906 \exp(-0.008\, t_c)$, t_c being the condensation temperature in °C, is slightly lower than the one leading to the best agreement between observed and predicted isotopic ratios over East Antarctica[10]. Kinetic effects during re-evaporation of drops lead to a further enrichment of precipitating water[37,38] and to a decrease of the δD–δ^{18}O slope[1]. The formulation used to model these effects[23] is based on the treatment developed by Stewart[37] for a single drop, assuming that stationary δD and δ^{18}O values are reached at the end of re-evaporation; the enrichment increases as the relative humidity decreases. These effects have been introduced for re-evaporation of precipitating water under a convective cloud base in one experiment (B) only; the relative humidity value determining the enrichment of drops is chosen as an average of the initial and final relative humidity values of the layer.

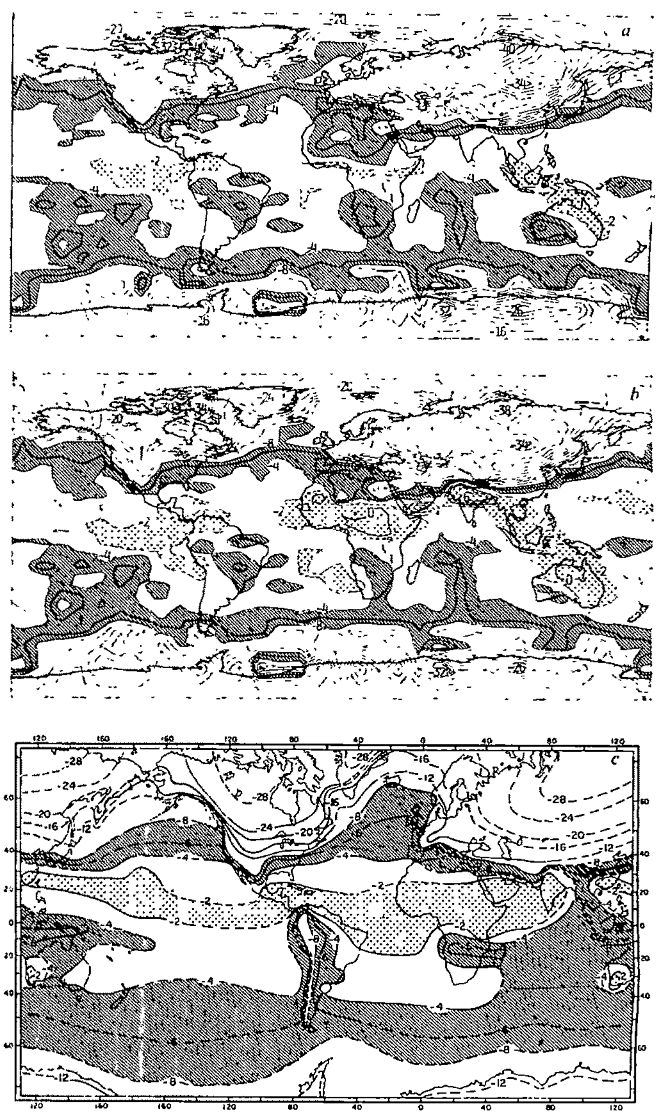

Fig. 2 Mean ^{18}O content of precipitation charts, experiments A(*a*) and B(*b*) for January to be compared with *c*, mean January observations (from J. R. Lawrence, work in preparation). Isolines every 2‰, for *c* isolines every 4‰ below −8‰; dotted areas, >−2‰; hatched areas, between −8 and −4‰.

Numerical experiment

The preliminary tests of isotope modelling described here have been performed with a low-resolution version of the LMD AGCM: 32 points in longitude, 24 points in latitude, 11 levels, which corresponds to a horizontal mesh size of the order of 800 × 800 km^2 around 50° and 1,250 × 450 km^2 at the Equator. The numerical experiment was a simulation of the present day January climate. Initial values of atmospheric and ground variables were taken from an earlier January simulation. The initial values for vapour isotopic ratios were chosen as constant in the whole atmosphere and smaller than the observed values (−80‰ for $H_2{}^{18}O$ and −600‰ for HDO, that is a deuterium excess of 40‰). Surface isotope ratios were set initially at the climatological mean precipitation ratios deduced from the local surface-air temperature[1]. During all the simulation, the oceanic surface-isotopic ratio was prescribed at 0‰ for both isotopes. All results presented here are averages over the last 20 days of this 80-day run.

The climatology of the present experiment is reasonably realistic, although it suffers from the coarse horizontal resolution. The surface-air temperature pattern (Fig. 1*a*) is well simulated, especially in the tropics[39]. The continental gradients in the Northern Hemisphere are realistic. However, the high-latitude temperatures in both hemispheres are markedly too warm, a defect common to all AGCMs but possibly emphasized by the low resolution used here; the particularly strong warming observed over north east Siberia is clearly associated with the low CLIMAP surface albedo value in this area. In the precipitation field (Fig. 1*b*), the Inter-Tropical Convergence Zone is fairly well resolved, with realistic values of 6–10 mm day^{-1} (ref. 40), except for the Pacific branch which is underestimated and slightly shifted to the north, associated with a strongly developed South Pacific Convergence Zone with values up to 28 mm day^{-1}. These anomalous Pacific features have been noticed in other numerical experiments, using the same model; they correspond to a transient episode in the model climatology. In middle latitudes, the coarse resolution of the model yields a systematic underestimation of baroclinic instability processes and the associated low pressures and rainfall, especially in the 'roaring forties'. A related defect is an underestimation of the extent of the subtropical dry regions associated with very weak high pressures.

Concerning the isotopes, we shall mainly discuss experiment A (involving the closed-system assumption for liquid formation and no kinetic fractionation, except for evaporation at the ocean–air interface) and mention experiment B (involving the open system assumption for liquid formation and kinetic fractionation) only when major differences between A and B are observed.

Figure 2*a* displays the 20-day average ^{18}O content of precipitation as simulated by experiment A. We observe a good agreement with January mean observations (Fig. 2*c*), with high ratios in the tropics and a decrease with increasing latitude modulated by a Northern Hemisphere planetary wave pattern. In middle to high latitudes, Figs 1*a* and 2*a* clearly show the expected positive correlation between δ^{18}O and temperature fields, low ratios being associated with low temperatures. When we look into geographical distributions in more detail, we have to be cautious because the rather large variability in space and time tends to limit the significance of 20-day averages; moreover, observations are missing in some areas (dashed contour lines on Fig. 2*c*). In middle latitudes, the simulated ratios are quite realistic, with values in the −8, −14‰ range in Western Europe for example. In higher latitudes, simulated ratios down to −40‰ are obtained in the coldest areas (−20, −25 °C). The accuracy of the model is not easy to verify there because observations are scarce: for instance, in Yakutsk, the simulated ratio is around −30‰ against an observed value of −34‰ (ref. 41) in December; but in Fort Smith and Edmonton, the model yields −20‰ against a range of January values from −25 to −33‰ (refs 42–47). Thus we may overestimate isotopic ratios at some locations in higher latitudes. This is especially true over ice sheet: in Greenland, our minimum simulated ratio is −22‰ whereas winter values registered in recent snow can be down to −40‰ (ref. 48); over the Antarctic Plateau, the minimum simulated value is −32‰ compared with observed values of −40 to −55‰ (refs 2, 49–51). This tendency to overestimate isotopic ratios is partially related to the unrealistic warming already observed in the model climate at high latitudes; but the values obtained over Siberia, for instance, show that the correlation between isotope and temperature biases may be disturbed by other factors such as fluctuations or biases in the origin and path of air masses. In middle to high latitudes, experiment B tends to simulate lower isotopic ratios with a difference down to −4‰, probably induced by kinetic fractionation during formation of snow crystals, as will be seen with the analysis of deuterium excess.

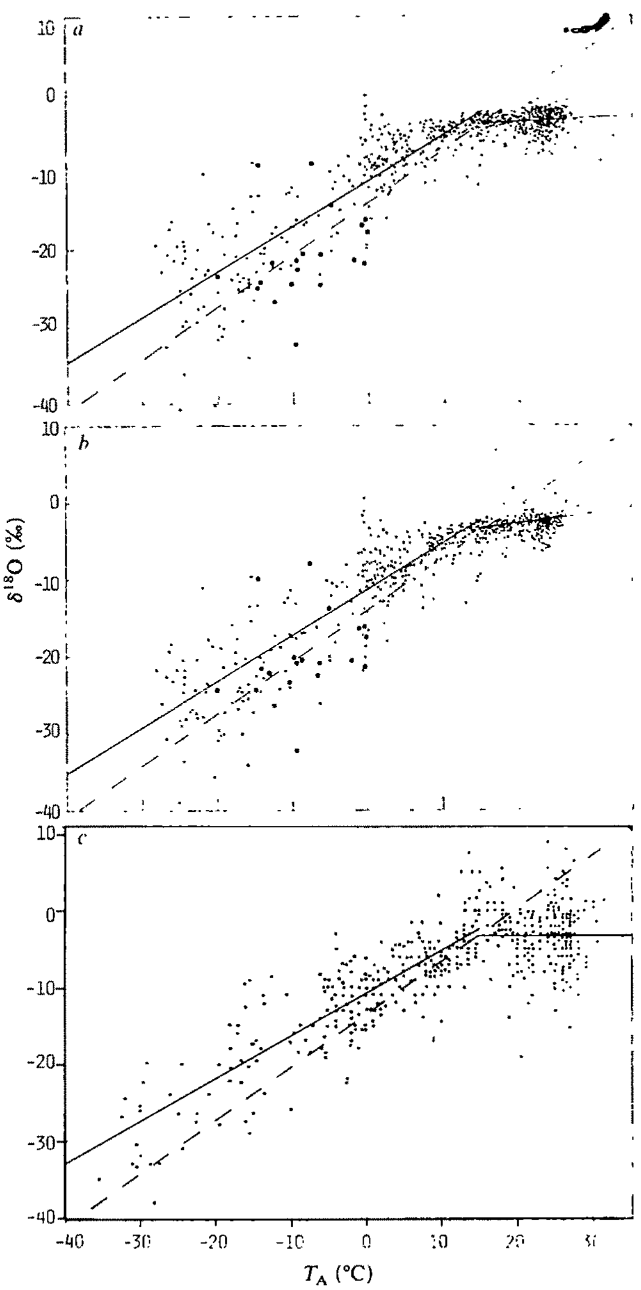

Fig. 3 Mean ^{18}O content of precipitation as a function of mean surface-air temperature, experiments A (*a*) and B (*b*) to be compared with *c*, monthly mean observations for January from the IAEA network[42–47]. Solid lines, regression lines for $T_A < 15$ °C: *a*, $\delta^{18}O = 0.59\ T_A - 11.1$, $r = 0.86$ (correlation coefficient); *b*, $\delta^{18}O = 0.60\ T_A - 11.5$, $r = 0.87$; *c*, $\delta^{18}O = 0.55\ T_A - 10.7$, $r = 0.85$. For $T_A >$ 15 °C: *a*, $\delta^{18}O = 0.05\ T_A - 4.6$, $r = 0.12$; *b*, $\delta^{18}O = 0.13\ T_A - 5.6$, $r = 0.22$; *c*, $\delta^{18}O = 0.006\ T_A - 3.4$, $r = 0.007$. Dashed line, Dansgaard's observations[1]: $\delta^{18}O = 0.69\ T_A - 13.6$. Simulated Antarctica and Greenland grid point values are identified (large dots).

In the tropics, where there is little variation in temperature, the simulated δ^{18}O field exhibits a strong spatial variability, further enhanced in experiment B. These patterns are closely correlated to the precipitation field (Fig. 1*b*). Dansgaard[1] has already observed this 'amount effect' in tropical data sets and explained it on the one hand, by an enrichment of precipitation ratios in regions of undersaturated air or low precipitation rates, and on the other hand, by an impoverishment of water vapour in regions of intensive condensation or high precipitation rates. The first mechanism is confirmed by comparing experiments A and B: in experiment B, higher ratio regions correspond to higher enrichment by kinetic fractionation during re-evaporation under cloud base (this interpretation is corroborated by the comparative analysis of deuterium excess). Note that the closed or open system assumptions during liquid formation do not seem to have any appreciable impact on the results. More quantitatively, the simulated results are in good agreement with observations with ratios down to −4, −10‰ for high precipitation rates and up to 0–1‰ for low precipitation rates[41]. The best agreement is with experiment B, which corroborates the importance of kinetic fractionation during re-evaporation under cloud base: simulated ratios as high as 6‰ may seem to be overesti-

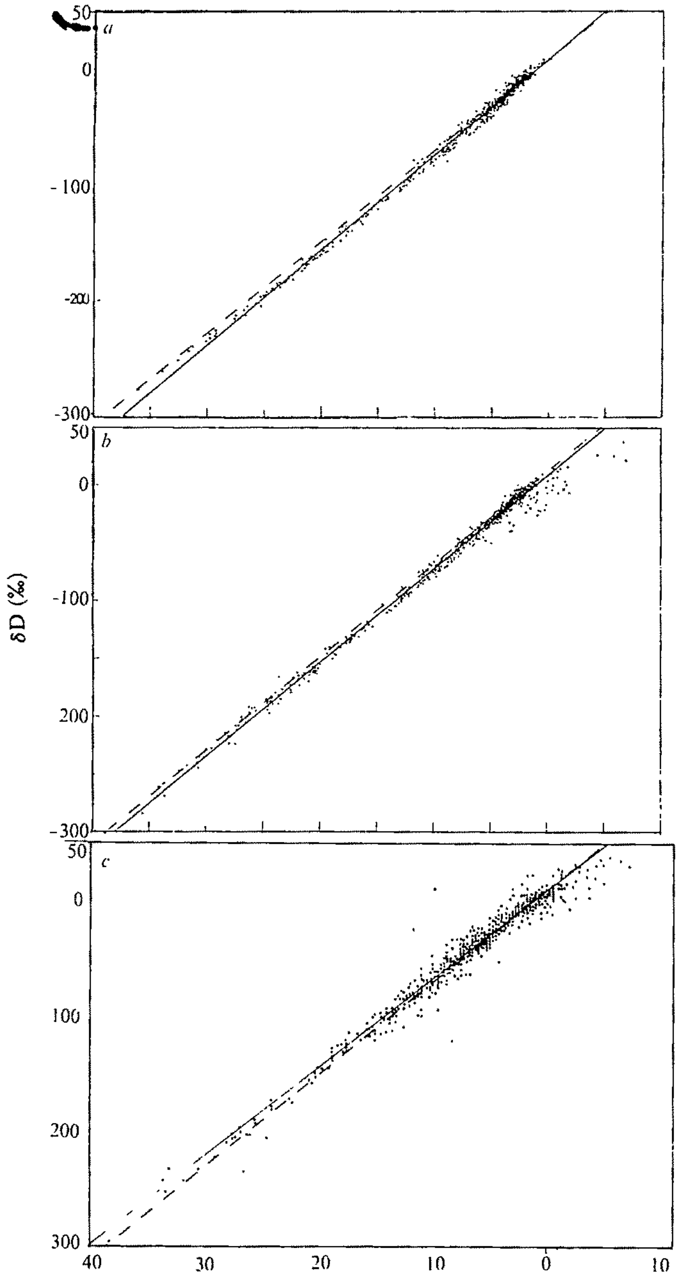

Fig. 4 Mean ^{18}O content of precipitation as a function of mean D content of precipitation, experiments A (*a*) and B (*b*) to be compared with *c*, monthly mean observations for January from the IAEA network[42–47]. Solid lines, regression lines: *a*, $\delta D = 8.3\ \delta^{18}O + 11.2$, $r = 0.99$; *b*, $\delta D = 8.0\ \delta^{18}O + 8.3$, $r = 0.99$; *c*, $\delta D = 7.7\ \delta^{18}O + 8.5$, $r = 0.98$. Dashed line, Craig's observations[6]: $\delta D = 8\ \delta^{18}O + 10$.

mated, but ratios around 8‰ are actually observed, for example, in Bamako in February or in Adelaide in January[41–47]. Major discrepancies with observations come mainly from a displacement of some precipitation patterns in the model's climatology, for example, in central Indonesia and northern Australia, where our 20-day average 'climate' happens to be drier than normally observed and the simulated isotopic ratios are consequently higher than observed, or in the southern Pacific. Note that the dispersion in the $\delta^{18}O$–precipitation relationship can be important; in some observations[41–47], or in simulated results over Australia, a positive correlation with precipitation can even occur locally. This feature probably reflects the impact of atmospheric circulation patterns on isotope contents of precipitation; simulated results over Australia are quite similar to observations in 1973, but differ from mean observations. It would be hazardous, however, to explain all our isotope deficiencies by model climatic drifts. To test our isotope modelling, we need to investigate in greater detail the dependency of ^{18}O content of precipitation on both temperature and precipitation; the impact of atmospheric circulation patterns will be roughly deduced.

Figure 3*a*, *b* shows a good correlation between surface-air temperature and the 20-day average ^{18}O content of precipitation simulated in experiments A and B respectively; Fig. 3*c* displays the corresponding monthly average observed field for January, extracted from IAEA data over the 1953–75 period[42–47]. At temperatures <15 °C, the correlation is quite significant in all of Fig. 3, with correlation coefficients around 0.85. The simulated and observed regression lines and dispersions are also quite similar. The differences noted in the geographical charts between experiments A and B do not affect the $\delta^{18}O$–temperature relationship. This seems to contradict earlier conclusions obtained from simple models[10,32], which do not, however, include dispersion effects such as the origin and path of air masses; the reason could also be that the model produces temperatures that are too warm and a relatively large proportion of convective precipitation in polar areas, thus underestimating the importance of kinetic effects during formation of snow crystals, which are taken into account in non-convective systems only and for snow formed below −15 °C. Dansgaard's[1] linear relation between $\delta^{18}O$ and temperature below 15 °C has also been plotted in Fig. 3. We observe that both IAEA-observed and simulated ratios are, on average, higher than Dansgaard's values, with an increasing discrepancy in colder regions. Dansgaard's data are more reliable at high latitudes where IAEA stations are scarce; the low values he obtained there have been confirmed by more recent studies[2,52]. Note that all ice cap data to which we refer[1,2,48,52] concern annual means; for Antarctica, the displacement could be further enhanced when considering January values[49,50]. These relatively low values over polar regions (Antarctica and Greenland) associated with an enhanced dependency on temperature could be due to (1) increased distance from water isotope source regions, inducing a larger amount of fractionation processes, and (2) altitude, which causes precipitations to originate from higher tropospheric levels. Such a systematic polar cap effect is actually simulated by the model as can be seen by the large dots on Fig. 3*a*, *b*, corresponding to Antarctica and Greenland grid point values; these values are indeed close to ice cap data[48]. It is, however, difficult to assess the efficiency of our isotope modelling in these regions as temperatures there are systematically too high.

At temperatures above 15 °C, both correlation and dependency on temperature totally disappear in observed data and decrease strongly in our simulation. The weakening of the temperature–isotope relation is mainly due to the predominance of convective systems, accompanied by intense mixing of water originating from different layers. The dispersion (further enhanced in experiment B by kinetic effects under cloud base) mainly reflects dependency on precipitation amount. The general dependency of $\delta^{18}O$ on precipitation for temperatures higher than 15 °C clearly appears on both experiments with correlation coefficients around −0.4 and simulated regression lines: $\delta^{18}O = -0.50P - 2.8$ for experiment A and $\delta^{18}O = -0.79P - 2.0$ for experiment B, with $\delta^{18}O$ in ‰ and precipitations P in 100 mm per month. The results of experiment B are in particularly good agreement with January mean observations: $\delta^{18}O = -0.93P - 1.8$ with a similar correlation coefficient. This again pinpoints the importance of kinetic fractionation during re-evaporation under cloud base.

Deuterium content of precipitation has similar dependencies on temperature and precipitation; therefore, at this stage, we just need to study its relation with ^{18}O content of precipitation (Fig. 4*a*, *b*, *c*). Correlation is high in all of Fig. 4, with correlation coefficients around 0.98. The simulated ratios are in close agreement with observations and their dispersion around Craig's meteoric water line[6] $d = \delta D - 8\delta^{18}O = 10‰$ is similar. In the high ratio range, the observed decrease in slope and increase in dispersion (Fig. 4*c*) is well simulated only by experiment B: this supports the importance of kinetic fractionation during re-evaporation under cloud base[1]. In the low ratio range, experiment B with kinetic fractionation during snow crystal formation shows a better agreement with observations, with a slightly greater δD–$\delta^{18}O$ slope than in experiment A. Although they have a smaller amplitude, these features corroborate simple model results[10].

Conclusion

We have presented the first simulation of the atmospheric cycles of HDO and $H_2{}^{18}O$. Many features of our simulations are in good agreement with real conditions. Most of the differences we have observed on geographical charts seem mainly due to local differences between simulated and observed climate; this is confirmed by the fact that the $\delta^{18}O$–temperature, $\delta^{18}O$–precipitation and δD–$\delta^{18}O$ relations are realistically simulated. The use of higher resolution in future experiments will improve the climatology of the model and, therefore, many aspects of the isotope simulations. The model in its present form looks accurate enough to be used for palaeoclimatic reconstructions.

This work was supported by the Programme National de la Dynamique du Climat. We thank L. Merlivat (LGI) for helpful discussions, J. R. Lawrence (Lamont Doherty Geological Observatory) for providing the geographical chart of mean observed January ^{18}O content of precipitation, M. Fonchon (LMD) for developing the graphics and M. Gangloff (LMD) for processing CLIMAP data. We particularly thank P. Le Van (LMD) for his essential contribution to the programming work.

Received 22 March; accepted 20 June 1984.

1. Dansgaard, W. *Tellus* **16**, 436–468 (1964).
2. Lorius, C. & Merlivat, L. *IAHS-AISH Publ.* **118**, 127–137 (1977).
3. Lorius, C., Merlivat, L., Jouzel, J. & Pourchet, M. *Nature* **280**, 644–648 (1979).
4. Dansgaard, W., Johnsen, S. F., Moeller, J. & Langway, C. C. *Science* **166**, 377–381 (1969).
5. Dansgaard, W. *et al. Science* **218**, 1273–1277 (1982).
6. Craig, H. *Science* **133**, 1702–1703 (1961).
7. Jouzel, J., Merlivat, L. & Lorius, C. *Nature* **299**, 688–691 (1982).
8. Sonntag, C. *et al. Isotope Hydrology*, 569–581 (IAEA, Vienna, 1978).
9. Merlivat, L. & Jouzel, J. *J. geophys. Res.* **84**, 5029–5033 (1979).
10. Jouzel, J. & Merlivat, L. *J. geophys. Res.* (in the press).
11. Covey, C. & Haagenson, P. L. *J. geophys. Res.* (in the press).
12. Ehhalt, D. H. *Vertical Profiles of HTO, HDO and H_2O in the Troposphere* (NCAR Tech. note, NCAR-TN/STR100, 1974).
13. Taylor, C. B. *N.Z. Dept. Sci. Ind. Res., Inst. nucl. Sci.*, Rep INS-R-107 (1972).
14. Jouzel, J. *J. Rech. Atmos.* **13**, 261–269 (1979).
15. Yurtsever, Y. & Gat, J. R. *Stable Isotope Hydrology, Tech. Rep. Ser.* No. 210 (IAEA, Vienna, 1981).
16. Sadourny, R. & Laval, K. in *New Perspectives in Climate Modelling* (ed. Berger, A.), 173–198 (Elsevier, Amsterdam, 1984).
17. Le Treut, H. & Laval, K. in *New Perspectives in Climate Modelling* (ed. Berger, A.), 199–222 (Elsevier, Amsterdam, 1984).
18. CLIMAP Project Members *Seasonal Reconstructions of the Earth's Surface at the Last Glacial Maximum* (Geological Society of America, Map and Chart Series MC-36, 1981).
19. Majoube, M. *J. chim. Phys.* **10**, 1423–1436 (1971).
20. Majoube, M. *J. chim. Phys.* **10**, 625–636 (1971).
21. Merlivat, L. & Nief, G. *Tellus* **19**, 122–127 (1967).
22. Merlivat, L. *J. chim. Phys.* **69**, 2864–2871 (1978).
23. Joussaume, S. Thesis, Univ. Paris (1983).
24. Zimmerman, V., Ehhalt, D. & Münnich, K. O. *Isotopes in Hydrology*, 567–584 (IAEA, Vienna, 1967).
25. Rozanski, K., Sonntag, C. & Münnich, K. O. *Tellus* **34**, 142–150 (1982).
26. White, J. W. C. Thesis, Lamont-Doherty Geological Observatory, Palisades (1983).
27. White, J. W. C. & Gedelzman, S. *J. geophys. Res.* (submitted).
28. O'Neil, J. *J. chem. Phys.* **72**, 3683–3684 (1968).
29. Zalesak, S. T. *J. comp. Phys.* **31**, 335–362 (1979).
30. Manabe, S. & Strickler, R. F. *J. atmos. Sci.* **21**, 361–385 (1965).
31. Kuo, H. L. *J. atmos. Sci.* **22**, 40–63 (1965).
32. Jouzel, J. *Handbook of Environmental Isotope Geochemistry* Vol. 2 (eds Fritz, P. & Fontes, J. C. (Elsevier, Amsterdam, in the press).
33. Jouzel, J., Merlivat, L. & Roth, E. *J. geophys. Res.* **80**, 5015–5029 (1975)
34. Federer, B., Brichet, N. & Jouzel, J. *J. atmos. Sci.* **39**, 1323–1335 (1982)
35. Mason, B. J., *The Physics of Clouds* (Clarendon, Oxford, 1971).
36. Miller, S. & Schwerdtfeger, W. *Antarct. J. US.* **7**, 170–171 (1972)
37. Stewart, M. K., *J. geophys. Res.* **80**, 1138–1146 (1975).
38. Ehhalt, D. H., Knott, K., Nagel, J. F. & Vogel, J. C. *J. geophys. Res.* **68**, 3775–3780 (1963)
39. Crutcher, H. L. & Jenne, R. J. *An Interim Note on Northerm Hemisphere Climatological Grid Data tape NOAA* (Environmental Data Service, Ashville, 1970)
40. Jaeger, L. *Monatskarten des Niederschlages für die ganze Erde* (Ber. Dtsch. Wetterd., Offenbach/Main No. 139, 18, 1976).
41. *Statistical Treatment of Environmental Isotope Data in Precipitation* (Tech. Rep. Ser. 206, IAEA, Vienna, 1981).
42. *Environmental Isotope Data No. 1: World Survey of Isotope Concentration in Precipitation (1953–1963)* (Tech. Rep. Ser. No. 96, IAEA, Vienna, 1969).
43. *Environmental Isotope Data No. 2: World Survey of Isotope Concentration in Precipitation (1964–1965)* (Tech. Rep. Ser. No. 117, IAEA, Vienna, 1970).
44. *Environmental Isotope Data No. 3: World Survey of Isotope Concentration in Precipitation (1966–1967)* (Tech. Rep. Ser. No. 129, IAEA, Vienna, 1971).
45. *Environmental Isotope Data No. 4: World Survey of Isotope Concentration in Precipitation (1968–1969)* (Tech. Rep. Ser. No. 147, IAEA, Vienna, 1973).
46. *Environmental Isotope Data No. 5: World Survey of Isotope Concentration in Precipitation (1970–1971)* (Tech. Rep. Ser. No. 165, IAEA, Vienna, 1975).
47. *Environmental Isotope Data No. 6: World Survey of Isotope Concentration in Precipitation (1972–1975)* (Tech. Rep. Ser. No. 192, IAEA, Vienna, 1979).
48. Dansgaard, W., Johnsen, S. J., Clausen, J. B. & Gundestrup, N. *Meddr Grønland* 197 (1973).
49. Jouzel, J., Merlivat, L., Petit, J. R. & Lorius, C. *J. geophys. Res.* **88**, 2693–2703 (1983)
50. Aldaz, L. & Deutsch, S. *Earth planet. Sci. Lett.* 3, 2667–2674 (1967).
51. Petit, J. R., Jouzel, J., Pourchet, M. & Merlivat, L. *J. geophys. Res.* **87**, 4301–4308 (1982)
52. Lorius, C., Merlivat, L. & Hageman, R. *J. geophys. Res.* **74**, 7027–7031 (1969)

Molecular cloning of a new transforming gene from a chemically transformed human cell line

Colin S. Cooper[*], Morag Park[†], Donald G. Blair[†], Michael A. Tainsky[†], Kay Huebner[‡], Carlo M. Croce[‡] & George F. Vande Woude[§]

[*] Laboratory of Molecular Carcinogenesis, Dana-Farber Cancer Institute, Boston, Massachusetts 02115, USA
[†] Laboratory of Molecular Oncology, National Cancer Institute, Frederick Cancer Research Facility, Frederick, Maryland 21701, USA
[‡] The Wistar Institute, 36th and Spruce, Philadelphia, Pennsylvania 19104, USA
[§] Basic Research Program, Litton Bionetics, Inc., Frederick, Maryland 21701, USA

Molecular cloning of the transforming gene from a chemically transformed human osteosarcoma-derived cell line enables the gene to be mapped to chromosome 7 (7p11.4–7qter) and by this criterion and by direct hybridization to be shown to be unrelated to known oncogenes.

DOMINANT transforming genes have been detected in several different types of chemically induced tumours and in cells transformed *in vitro* by chemical carcinogens. Many of the transforming genes identified in these studies were members of the *ras* family of oncogenes. Cellular homologues of the oncogene of Harvey sarcoma virus (*ras*^{H}) were activated in chemically induced squamous cell carcinomas and papillomas in mice[1,2], chemically induced mammary tumours in rats[3] and guinea pig cells transformed *in vitro* by chemical carcinogens[4]. Similarly, cellular homologues of the oncogene of Kirsten sarcoma virus (*ras*^{K}) were activated in 3-methylcholanthrene-induced mouse sarcomas[5] and in mouse fibroblasts[6] transformed *in vitro* by chemical carcinogens. A third member of the *ras* gene family (*ras*^{N}) was activated in chemically induced thymic lymphomas of mice[7]. Studies of these systems should reveal the mechanisms of activation of *ras* genes by classes of chemical carcinogens

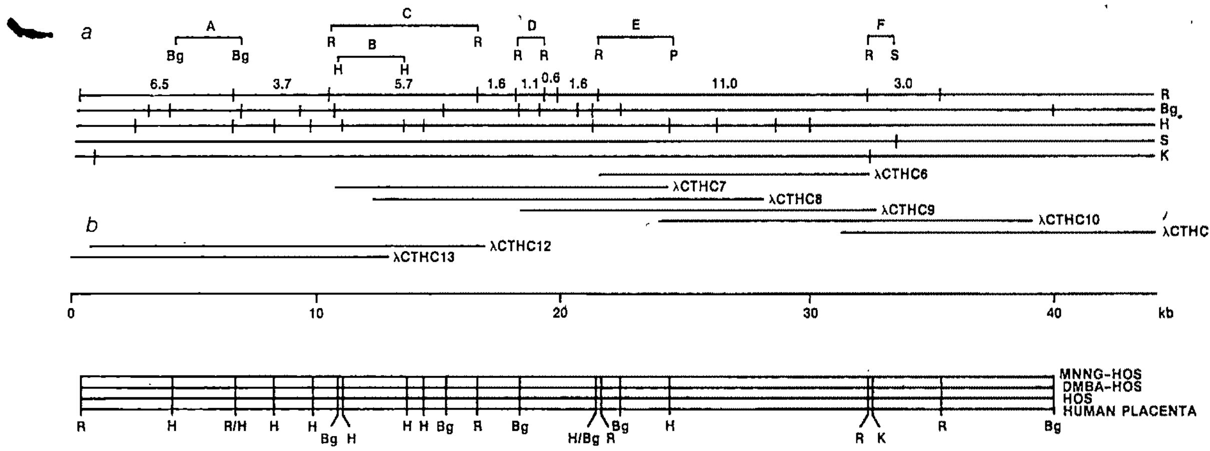

Fig. 1 *a*, Transforming DNA sequences of MNNG–HOS cells. An 11.0-kb human DNA fragment present in *Eco*RI-digested DNA from a MNNG–HOS secondary transfectant (λCTHC6) was cloned from a library constructed in the λgtWES cloning vector. Phage libraries were constructed by the method of Hohn and Murray[49]. The library was screened, without prior amplification, by the method of Benton and Davis[50] using Blur8 plasmid DNA[18] which was labelled with ^{32}P by nick-translation[51] as a probe. The 11.0-kb *Eco*RI fragment was subcloned into pBR322 and the subclone was used as a probe to isolate recombinant DNA clones (λCTHC7–11) that contained adjacent DNA sequences from a second library. The latter was constructed by first partially digesting DNA from an MNNG–HOS transfectant with *Sau*3A and then introducing the partially digested DNA into the EMBL3 cloning vector[52]. Clones λCTHC-12 and -13 were isolated from the same EMBL3 library using a probe prepared from a restriction fragment (fragment B) produced by digesting λCTHC7 with *Hin*dIII. A restriction map of the cloned cellular DNA is presented. Six specific restriction fragments (fragments A–F) were subcloned into pBR322. The sizes in kilobases of the *Eco*RI fragments are indicated. *b*, Partial restriction maps of the gene present in human placenta, MNNG–HOS cells, DMBA–HOS cells and HOS cells. The maps were determined from the results of hybridization analysis in which restriction fragments A–F (*a*) were used to detect related sequences in human DNAs that had been digested either with *Eco*RI, *Hin*dIII and *Bgl*II or with *Kpn*I and *Bgl*II. DNAs were prepared exactly as described previously[16], digested with three to fivefold excess of restriction enzyme, electrophoresed in agarose (1% w/v) gels and blotted onto nitrocellulose as described by Southern[17]. Filters were hybridized to DNA fragments labelled with ^{32}P by nick translation[51], in stringent conditions (50% formamide, 5×SSC, 42 °C) for 24 h and washed with a final stringency of 0.2×SSC at 68 °C. Restriction endonucleases used were *Eco*RI (R), *Bgl*II (Bg), *Hin*dIII (H), *Sal*I (S), *Kpn*I (K) and *Pst*I (P).

which, as environmental and dietary contaminants, are suspected of contributing to the incidence of cancer in man[8–10].

In contrast to the abundance of studies on chemically transformed rodent cells, there are only a few reported examples of human cells transformed by direct treatment with chemical carcinogens[11–14]. The transformation of human fibroblasts[11] and human osteosarcoma (HOS)[12,13] cells by chemical carcinogens *in vitro* has been reported and in initial studies we examined the ability of DNA prepared from these chemically transformed human cell lines to transform NIH 3T3 cells[15,16]. Our results showed that DNA from a HOS cell line that had been chemically transformed *in vitro* with *N*-methyl-*N*′-nitro-*N*-nitrosoguanidine (MNNG)[12] could transform NIH 3T3 cells. In contrast, DNA from 7,12-dimethylbenz(*a*)anthracene (DMBA) transformed HOS cells[13], parental HOS cells or 4-nitroquinoline-1-oxide transformed human fibroblasts (HUT14) did not transform NIH 3T3 cells[15], suggesting that MNNG may have caused genetic alterations in HOS cells that gave rise to a transferable transforming gene. Recently, we have demonstrated that this transforming gene is not a member of the *ras* family of genes[16], and we now report the molecular cloning of the MNNG–HOS transforming gene, its comparison with known oncogenes and its human chromosomal localization.

Molecular cloning

High molecular weight DNA from MNNG–HOS cells can efficiently transform mouse NIH 3T3 cells, and DNA from the transformed NIH 3T3 cells (primary transfectants) can be used in a second round of transfection to induce secondary transfectants[15,16]. Southern analysis[17] of *Eco*RI-digested transfectant DNA with a probe specific for human highly repeated *Alu* DNA sequences (Blur8)[18] showed that the secondary transfectants contained conserved human *Eco*RI DNA fragments of 11.0, 5.7 and 3.7 kilobases (kb). This observation suggested that these three human DNA fragments are closely associated with the transforming gene. In our strategy for the molecular cloning of the MNNG–HOS transforming gene, we first used the probe specific for human highly repeated DNA sequences to isolate the 11.0-kb *Eco*RI DNA fragment. The 11.0-kb human DNA fragment present in *Eco*RI-digested DNA from an MNNG–HOS secondary transfectant was enriched by centrifugation through a sucrose gradient and cloned into the EK2 vector λgtWES. From a library of 400,000 recombinant phage, we obtained one isolate (λCTHC-6, Fig. 1*a*) that possessed human repeated DNA sequences and contained an 11.0-kb *Eco*RI DNA fragment.

Regions of the transforming gene which were adjacent to the 11.0-kb *Eco*RI fragment were isolated from a library obtained using DNA from an MNNG–HOS secondary transfectant. The DNA was first partially digested with *Sau*3A and then cloned into the EMBL3 cloning vector. A library of 2×10^6 recombinant phage was amplified and phage that contained regions of the transforming gene immediately adjacent to the 11.0-kb *Eco*RI fragment were isolated from portions of the amplified library using the cloned 11.0-kb *Eco*RI human DNA fragment as a probe. More distant regions of the transforming gene were isolated in genomic library 'walking' experiments (Fig. 1*a*). Figure 1*a* shows restriction map of 44 kb of cellular DNA present in seven recombinant clones isolated from the library.

To determine which parts of the cloned DNA represented the MNNG–HOS transforming gene, the λ clones (λCTHC6–13) and specific restriction fragments (fragments A–F, Fig. 1*a*) were used as probes in Southern analyses[17] to detect related sequences in DNA from MNNG–HOS secondary transfectants. The results of these analyses indicated that 26 kb of DNA which includes *Eco*RI human DNA fragments of 11.0, 5.7, 3.7, two 1.6, 1.1 and 0.6 kb (Fig. 1*a*) is part of the transforming gene, as these DNA sequences are invariably present in DNA from MNNG–HOS secondary transfectants. For example, probes prepared from the cloned 11.0-kb *Eco*RI fragment present in λCTHC6 and from fragment D (Fig. 1*a*) both detected an 11.0-kb DNA fragment in *Eco*RI-digested genomic DNA from secondary transfectants. In contrast, the 3.0- and 6.5-kb *Eco*RI fragments that occur respectively at the right and left ends of the cloned DNA (Fig. 1*a*) were not detected in all of the secondary transfectants. Thus, the data presented in Fig. 3 show that a probe prepared from λCTHC10 only detected the 3.0-kb *Eco*RI DNA fragment in two of the four secondary transfectants. In addition, the results of similar studies in which λCTHC13 was used as a probe showed that only 7 of 10 secondary transfectants examined contained the 6.5-kb DNA fragment (data not shown). When taken together, these observations indicate that the 6.5- and 3.0-kb *Eco*RI DNA fragments contain flanking DNA sequences that can be removed during transfection without affecting the activity of the MNNG–HOS transforming gene.

In transfection experiments, when examined individually, none of the λ clones (λCTHC6–13) could transform NIH 3T3 cells. However, this result was not unexpected as each clone contains only part of the transforming gene. Examination of the biological activity of the cloned MNNG–HOS transforming gene must await the reconstruction of the intact gene.

Arrangement of the MNNG–HOS gene

To determine whether the transforming gene was rearranged in MNNG–HOS cells, portions of the cloned gene (Fig. 1*a*, fragments A–F) were used as probes to detect related sequences in DNA prepared from several different human cell lines and from human placenta. A probe prepared from an *Eco*RI–*Pst*I restriction fragment (fragment E, Fig. 1*a*) hybridized to an 11.0-kb DNA fragment in *Eco*RI-digested human placental DNA (Fig. 2*B*, lane *h*), as well as DNA prepared from other human cell lines (Fig. 2*B*, lanes *f*, *g*, *i*–*m*). Data obtained in this experiment and in other Southern analyses of DNA digested either with *Eco*RI, *Hin*dIII, *Bgl*II and *Kpn*I or with *Kpn*I and *Bgl*II allowed us to construct partial restriction maps of the related DNA sequences present in human placenta, MNNG–HOS cells, DMBA–HOS cells and HOS cells. The partial restriction maps obtained for all four human DNAs are identical and are shown in Fig. 1*b*. Thus, at this level of resolution there are no detectable rearrangements of these DNA sequences in the MNNG–HOS cell line.

Relationship to oncogenes and location

We reported previously that the MNNG–HOS transforming gene is not a member of the *ras* family of oncogenes[16]. Hybridization of the cloned MNNG–HOS transforming gene to cloned viral and cellular oncogenes confirmed this result and also showed that the transforming gene is not homologous by DNA hybridization to *mos*, *myc*, *myb*, *src*, *sis*, *rel* and *Blym* (data not shown). Furthermore, the restriction map of the MNNG–HOS transforming gene is not the same as those of *ras*$^{\mathrm{N}}$ (refs 19, 20) and *Blym* (ref. 21) or of the human homologues of *ras*$^{\mathrm{H}}$ (ref. 22), *ras*$^{\mathrm{K}}$ (ref. 19), *mos* (ref. 23), *myc* (ref. 24), *abl* (ref. 25), *sis* (ref. 26) and *fes* (ref. 27).

As a further characterization of the MNNG–HOS gene, we determined its human chromosomal location. Southern analysis of DNA from 12 different rodent–human somatic cell hybrids containing unique complements of human chromosomes (Table 1) was used to determine the chromosomal location of the MNNG–HOS transforming gene. Cell hybrids were characterized by karyotype analysis and by expression of isozyme markers that have been previously assigned to each of the human chromosomes[28–31]. DNA prepared from each cell hybrid was digested with *Hin*dIII and subjected to Southern analysis using the *Eco*RI–*Pst*I DNA fragment (fragment E, Fig. 1*a*) as a probe. In stringent conditions of hybridization, probe E detects a single 3.2-kb human *Hin*dIII restriction fragment (Fig. 4*A*, lanes *g*, *i*) but does not hybridize to rodent DNA (Fig. 4*A*, lane *h*). Figure 4 gives examples of these analyses while Table 1 shows the human chromosome complement of the hybrid cell lines and the results obtained when the DNAs from these hybrids were scored for the presence of the 3.2-kb *Hin*dIII restriction fragment. The results are consistent only with assignment of the MNNG–HOS transforming gene to chromosome 7. To refine this initial result, we have analysed a human–mouse hybrid cell line (53-87-3 c136 is c12 sub7) which retains only the portion of human chromosome 7 from 7p11.4 to 7qter (ref. 30) and has

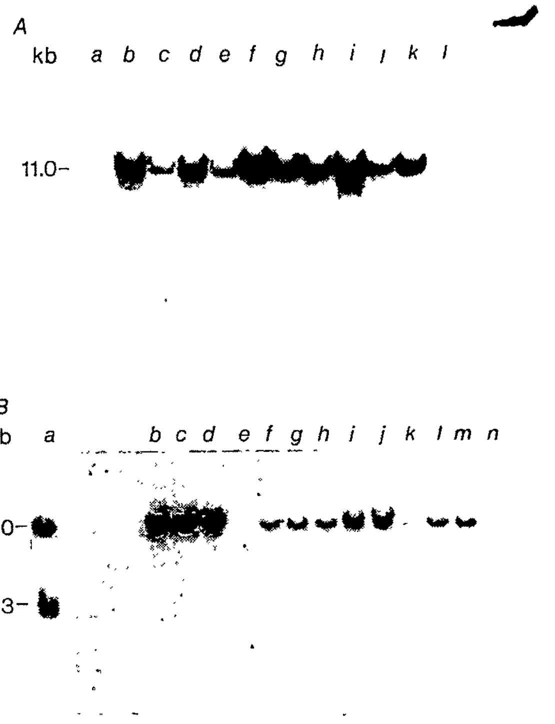

Fig. 2 Hybridization of human DNA and DNA from MNNG–HOS secondary transfectants to cloned DNA sequences. *A*, 10 μg of each DNA (lane *a*, NIH 3T3; lanes *b*–*l*, independent MNNG–HOS secondary transfectants) was digested with *Eco*RI, subjected to electrophoresis in agarose gels (0.8 w/v) and transferred to a nitrocellulose filter as described by Southern[17]. The filters were hybridized (50% formamide, 5×SSC, 42 °C) for 21 h to a ^{32}P-labelled probe that was prepared from the 11.0-kb *Eco*RI restriction fragment present in clone λCTHC6 (Fig. 1*a*) by nick translation[51]. The 11.0-kb *Eco*RI restriction fragment was first subcloned into pBR322. The plasmid DNA was digested with *Eco*RI and the 11.0-kb restriction fragment was purified by electrophoresis in agarose gels. *B*, 10 μg of each DNA (lane *a*, NIH 3T3 DNA containing 5 genomic equivalents of the 11.0-kb *Eco*RI restriction fragment cloned into pBR322; lanes *b*–*d*, independent MNNG–HOS secondary transfectants; lane *e*, NIH 3T3; lane *f*, DMBA–HOS[16]; lane g, MNNG–HOS[16]; lane *h*, HOS[16]; lane *i*, human placenta; lane *j*, human fibrosarcoma HT1080 (ref. 15); lane *k*, human teratocarcinoma, PA1 (ref. 16); lane *l*, human nasopharyngeal carcinoma; lane *m*, Wilms' tumour; lane *n*, human fibrosarcoma NF-1 (ref. 16)) was digested with *Eco*RI and subjected to Southern analysis as described in *A*. The nitrocellulose filters were hybridized to a ^{32}P-labelled probe prepared from an *Eco*RI–*Pst*I restriction fragment (fragment E, Fig. 1*a*).

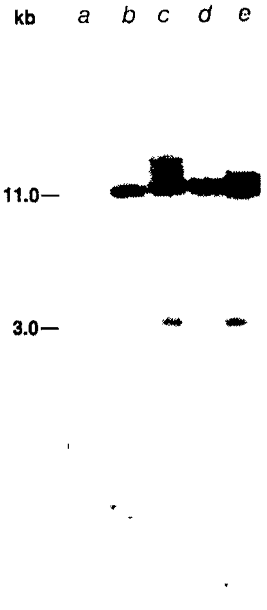

Fig. 3 Hybridization of DNA from MNNG–HOS secondary transfectants to cloned DNA sequences. 10 μg of each DNA (lane *a*, NIH 3T3, lanes *b*–*e*, independent secondary transfectants) was digested with *Eco*RI, subjected to electrophoresis in agarose gels (0.8% w/v) and transferred to a nitrocellulose filter as described by Southern[17]. Filters were hybridized (50% formamide, 5× SSC, 42 °C) for 21 h to a ^{32}P-labelled probe prepared from the recombinant bacteriophage λCTHC10 by nick translation[51].

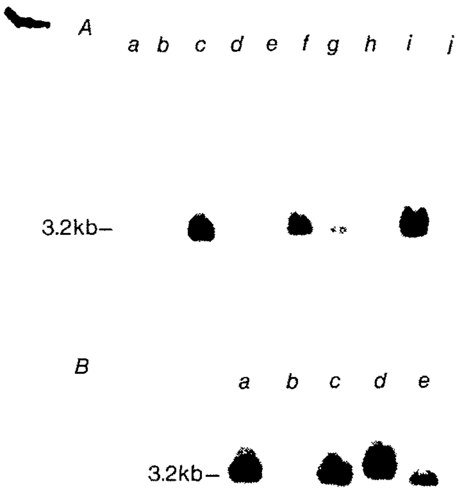

Fig. 4 Hybridization of a probe specific for the MNNG–HOS transforming gene to DNA from rodent–human cell hybrids. *A*, Segregation of the MNNG–HOS transforming gene in rodent–human hybrids. High molecular weight DNA (10 μg) isolated from 77-B10 cl26 (lane *a*), DSK 1B2A5 cl20 (lane *b*), Nude 9 (lane *c*), PAF×BALB IV cl5 (lane *d*), M44 cl2S5 (lane *e*), 53-87-1 cl21 (lane *f*), HL60 human promyelocytic leukaemia cell line (lane *g*), F9 mouse strain 129 teratocarcinoma cell line (lane *h*), JD-38 human Burkitt lymphoma cell line (lane *i*), 706B6-40 cl17 (lane *j*), 77 B10 cl8 (lane *k*) and 77 B10 cl33 (lane *l*) cell lines was digested with a fivefold excess of restriction endonuclease *Hin*dIII, subjected to electrophoresis in 1% agarose gels, then blotted onto nitrocellulose filters. Filters were hybridized in stringent conditions, (50% formamide, 5×SSC, 10% dextran sulphate at 42 °C) for 20 h with ^{32}P-labelled, nick-translated fragment E (Fig. 1*a*). Hybridized blots were exposed to Kodak XAR-5 film at −70 °C in the presence of Kodak intensifier screens for 18 h. *B*, High molecular weight DNA (10 μg) isolated from Ag876II human Burkitt's lymphoma cell line (lane *a*), NP3, BALB/c mouse myeloma cell line (lane *b*), Nude 9 (lane *c*), 53-87-1 cl21 (lane *d*), 53-87-3 cl36 is cl2 sub7 (lane *e*) cell lines was digested with a fivefold excess of *Hin*dIII and subjected to Southern analysis[17] as described above. The rodent–human cell lines used in these experiments have been described previously[28–31].

lost the distal part of the short arm. This analysis (Fig. 4*B*) shows that hybrids containing only human chromosome 7 (Fig. 4*B*, lane *d*) or only 7p11.4 to 7qter (Fig. 4*B*, lane *e*) have retained the MNNG–HOS transforming gene. Thus, this gene is located on chromosome 7 between 7p11.4 and 7qter.

The localization of the MNNG–HOS transforming gene on chromosome 7 provides additional evidence that this gene is not a human homologue of *ras*$^{\mathrm{H}}$, *ras*$^{\mathrm{K}}$, *fos, mos, myb, myc, raf, abl, fes, src* or *sis*, and does not represent an activated human *ras*$^{\mathrm{N}}$, *Blym* or *myc*$^{\mathrm{N}}$ locus because these human proto-oncogenes are located on different human chromosomes (reviewed in ref. 32). The human homologue of the avian erythroblastosis virus (AEV) transforming gene (*erbB*) has been assigned to chromosome 7 (7pter−7q22)[33]. Because the MNNG–HOS transforming gene is located between 7p11.4 and 7qter, chromosomal assignment could not exclude the possibility that it is related to *erbB*. However, the MNNG–HOS transforming gene failed to hybridize to probes prepared from the *erbB* portion of AEV (the 2.5-kb *Pvu*II–*Pvu*II fragment described in ref. 34) or from part of the human homologue of *erbB* (the 2.5-kb *Hin*dIII–*Eco*RI fragment he-B, described in ref. 35; data not shown). These data demonstrate that the MNNG–HOS transforming gene is not directly homologous to *erbB*. However, the cloned he-B and viral *erbB* DNA sequences only represent parts of the cellular gene that show homology to *erbB* (ref. 35) and we cannot exclude the possibility that the MNNG–HOS transforming gene may be related to other parts of this cellular gene.

Assuming that the MNNG–HOS transforming gene is unrelated to other transforming genes, we suggest that the three-letter abbreviation, *met*, should be used when referring to this gene.

Table 1 Detection of the MNNG–HOS transforming gene in rodent–human hybrid cells

Hybrid	Human Chromosomes																							Human met Gene
	1	2	3	4	5	6	7	8	9	10	11	12	13	14	15	16	17	18	19	20	21	22	X	
DSK 1B2A5 cl2 Suba			■					■						■		■	■					■		-
DSK 1B2A5 cl20														■	■		■	■			■	■	■	-
Nu 9						■	■																	+
PAF × Balb IV cl5		■			■			■				■							■					-
706B6-40 cl17								■																-
77-B10 cl8	■		■		■			■	■				■	■				■		■			■	-
77-B10 cl12	■				■			■	■					■				■		■			■	-
77-B10 cl26	■		■		■			■	■	■				■				■		■			■	-
77-B10 cl33	■		■		■			■	■	■			■	■				■		■			■	-
GM × LM cl3a				■			■								■		■			■				+
GM × LM cl6b				■			■				■	■				■				■		■		+
M44 cl2S5														■										-
53-87-1 cl21							■																	+
53-87-3 cl36 is cl2 sub 7							■																	+

The rodent–human hybrid cells have been described previously and the presence of particular human chromosomes was determined by chromosomal and isoenzyme analyses[28–31]. The presence of the transforming gene in each hybrid cell line was determined by Southern analysis[17] as described in Fig. 4 legend. The black squares indicate the presence of a particular human chromosome. Hybrid cell line M44 cl2S5 contains only a 14q^{+} t(8;14) human chromosome[47] and hybrid cell line 52-87-3 cl36 is cl2 sub7 contains only a portion of a human chromosome 7, from 7p11.4 to 7qter (ref. 30).

Discussion

This new transforming gene has been mapped to human chromosome 7 (7p11.4 to 7qter) and by these criteria or by direct hybridization seems to be unrelated to other known oncogenes.

The presence of *met* on chromosome 7 is of interest because several different types of human neoplasia are associated with alterations in chromosome 7. Monosomy of chromosome 7, alone or in combination with other chromosomal abnormalities in the same cell, is one of the nonrandom aberrations seen in most subtypes of acute non-lymphocytic leukaemia[36–38]. Several types of rearrangements involving chromosome 7 have also been detected in cells from individuals with ataxia telangiectasia. These include both translocations [t(7;7) and t(7;p14)] and chromosomal inversions[39]. A more detailed localization of the position of the *met* transforming gene on chromosome 7 by *in situ* hybridization may allow a better assessment of the possible involvement of this transforming gene in specific disorders.

The activation of a non-*ras* transforming gene in MNNG–HOS cells is at variance with the observations that most of the transforming genes activated in chemically transformed rodent cells are members of the *ras* family of oncogenes[1–7], and that activated *ras* genes are detected in a variety of human neoplasias, such as lung and colon tumours[40–42], which are believed, at least in part, to result from exposure to environmental carcinogens. Because we have been able to examine only a limited number of human cell lines, it is not yet possible to determine whether the activation of non-*ras* transforming genes is a consistent feature of human cells that are transformed *in vitro* by chemical carcinogens or whether the HOS cell line possesses a unique predisposition to activation of the *met* transforming gene. Some of the transforming genes detected in chemically transformed rodent cells were, however, also unrelated to *ras*. These include genes from DMBA-induced transplantable mammary tumours[43] and mineral oil induced B- and T-cell neoplasms[44].

No detectable rearrangements were observed in the restriction map comparison of the *met* gene in genomic DNA of MNNG–HOS with other human DNA samples. Activation of the transforming gene might therefore involve more subtle changes in the DNA such as the activation of the human *ras*$^{\mathrm{H}}$ gene in the EJ and T24 bladder carcinoma cell lines which involves a single G→T point mutation[45–47]. It is conceivable that a point mutation is also involved in the activation of the MNNG–HOS transforming gene. Alternatively, there may be small insertions, deletions or rearrangements that were not detected in these analyses. As DNA, RNA and proteins can be easily prepared from MNNG–

HOS cells and as the chemistry of the interaction of simple methylating carcinogens such as MNNG is particularly well defined[48], a comparison of the *met* gene from MNNG–HOS cells with the parental HOS cell gene may provide a model system with which to study the mechanisms of transformation of human cells by this carcinogen.

In at least one *N*-nitroso-*N*-methylurea (NMU) induced rat mammary tumour, activation of the ras^{H} transforming gene involves a simple G→A point mutation[3]. Notably, this is precisely the mutation that NMU would be predicted to induce if it reacted directly with the transforming gene. It will be interesting to see whether the precise method of activation of this transforming gene and of other transforming genes detected in chemically transformed cells also reflects the particular chemicals used to induce transformation. Further characterization of the *met* transforming gene and its comparison with the non-transforming allele may provide an interesting insight into one of the ways in which chemical carcinogens can activate proto-oncogenes in human cells.

We thank Dr M. Wigler for the gift of the ras^{N} clone, Drs C. Der, A. Diamond, G. M. Cooper and M.-A. Lane for providing the *Blym, sis, myb, src, erb* and *rel* clones, Dr B. Vennstrom for the human *erbB* clone, Dr Barbara Knowles for the 53-87-3 c136 is c12 sub7 cell lines, Dr David Patterson for 706B6-40 c117 DNA, and Debbie Dugan and Josephine Romano for technical assistance. This work was in part supported by the NCI, DHHS, under contract N01-C0-23909 to G.V.W. and NIH grants CA16685, CA21124 and HD17561 to K.H. and C.M.C.

Received 7 March; accepted 6 June 1984.

1. Balmain, A. & Pragnell, I. B. *Nature* **303**, 72–74 (1983).
2. Balmain, A., Ramsden, M., Bowden, G. T. & Smith, V. *Nature* **307**, 658–660 (1984).
3. Sukumar, S., Notario, V., Martin-Zarca, D. & Barbacid, M. *Nature* **306**, 658–661 (1983).
4. Sukumar, S. *et al. Science* **223**, 1197–1199 (1984).
5. Eva, A. & Aaronson, S. A. *Science* **220**, 955–956 (1983).
6. Parada, L. F. & Weinberg, R. A. *Molec. cell. Biol.* **3**, 2298–2301 (1983).
7. Guerrero, I., Caleada, P., Mayer, A. & Pellicer, A. *Proc. natn. Acad. Sci. U.S.A.* **81**, 202–205 (1984).
8. Henry, S. A. *Br. med. Bull.* **4**, 389–401 (1947).
9. USPHS Publ. (HEW) 79-50066 (US Dept of Health, Education and Welfare, Washington, DC, 1979).
10. Renwick, A. G. & Drasan, B. S. *Nature* **263**, 234–235 (1976).
11. Kakunaga, T. *Proc. natn. Acad. Sci. U.S.A.* **75**, 1334–1338 (1978).
12. Rhim, J. S. *et al. J. natn. Cancer Inst.* **55**, 1291–1294 (1975).
13. Rhim, J. S., Park, D. K., Arnstein, P., Huebner, R. J. & Weisburger, E. K. *Nature* **256**, 751–753 (1975).
14. DiPaolo, J. A. *J. natn. Cancer Inst.* **70**, 3–8 (1983).
15. Blair, D. G., Cooper, C. S., Oskarsson, M. K., Eader, L. A. & Vande Woude, G. F. *Science* **218**, 1122–1125 (1982).
16. Cooper, C. S. *et al. Cancer Res.* **44**, 1–10 (1984).
17. Southern, E. M. *J. molec. Biol.* **98**, 503–517 (1975).
18. Jelinek, W. R. *et al. Proc. natn. Acad. Sci. U.S.A.* **77**, 1398–1402 (1980).
19. Shimizu, K. *et al. Proc. natn. Acad. Sci. U.S.A.* **80**, 2112–2116 (1983).
20. Hall, A., Marshall, C. J., Spurr, N. K. & Weiss, R. *Nature* **303**, 376–400 (1983).
21. Diamond, A., Cooper, G. M., Ritz, J. & Lane, M. A. *Nature* **305**, 112–116 (1983).
22. Chang, E. H., Gonda, M. A., Ellis, R. W., Scolnick, E. M. & Lowy, D. R. *Proc. natn. Acad. Sci. U.S.A.* **79**, 4848–4852 (1982).
23. Watson, R., Oskarsson, M. & Vande Woude, G. F. *Proc. natn. Acad. Sci. U.S.A.* **79**, 4078–4082 (1982).
24. Dalla Favera, R. *et al. Proc. natn. Acad. Sci. U.S.A.* **79**, 6497–6501 (1982).
25. Heisterkamp, N., Groffen, J. & Stephenson, J. R. *J. molec. appl. Genet.* **2**, 57–68 (1983).
26. Josephs, S. F., Dalla Favera, R., Gelmann, E. P., Gallo, R. C. & Wong-Staal, F. *Science* **219**, 503–505 (1983).
27. Groffen, J., Heisterkamp, N., Grosveld, F., Van de Ven, W. & Stephenson, J. R. *Science* **216**, 1136–1138 (1983).
28. Dalla-Favera, R. *et al. Proc. natn. Acad. Sci. U.S.A.* **79**, 7824–7827 (1982).
29. Croce, C. M. & Koprowski, H. *J. exp. Med.* **139**, 1350–1353 (1974).
30. Knowles, B. A. *et al. J. exp. Med.* **145**, 314–326 (1977).
31. Croce, C. M., Aden, D. & Koprowski, H. *Science* **190**, 1200–1202 (1975).
32. Gilden, R. V., Rice, N. R. & McAllister, R. M. *Gene Analysis Tech.* **1**, 23–33 (1984).
33. Spurr, N. K. *et al. EMBO J.* **3**, 159–163 (1984).
34. Vennstrom, B., Fanshier, L., Moscovici, C. & Bishop, J. M. *J. Virol.* **36**, 575–585 (1980).
35. Jansson, M., Philipson, L. & Vennstrom, B. *EMBO J.* **2**, 561–565 (1983).
36. Rowley, J. D. & Testa, J. R. *Adv. Cancer Res.* **36**, 103–148 (1982).
37. Appendix 1: *Cancer Genet. Cytogenet.* **11**, 300–303 (1984).
38. Yunis, J. J. *Cancer Genet. Cytogenet.* **11**, 125–137 (1984).
39. Ray, J. H. & German, J. in *Genes, Chromosomes and Neoplasia* (eds Arrighi, F. E., Rao, P. N. & Stubblefield, E.) 351–376 (Raven, New York, 1981).
40. Pulciani, S. *et al. Nature* **300**, 539–542 (1982).
41. Der, C. J. & Cooper, G. M., *Cell* **32**, 201–208 (1983).
42. Perucho, M. *et al. Cell* **27**, 467–476 (1981).
43. Lane, M.-A., Sainten, A. & Cooper, G. M. *Proc. natn. Acad. Sci. U.S.A.* **78**, 5185–5189 (1981).
44. Lane, M. A., Sainten, A. & Cooper, G. M. *Cell* **28**, 873–880 (1982).
45. Reddy, E. P., Reynolds, R. K., Santos, E. & Barbacid, M. *Nature* **300**, 149–152 (1982).
46. Taposowsky, E. *et al. Nature* **300**, 762–764 (1982).
47. Tabin, C. J. *et al. Nature* **300**, 143–148 (1982).
48. Margison, G. P. & O'Conner, P. J. in *Chemical Carcinogens and DNA* Vol. 1 (ed. Grover, P. L.) 111–159 (CRC Press, Boca Raton, Florida, 1979).
49. Hohn, B. & Murray, K. *Proc. natn. Acad. Sci. U.S.A.* **74**, 3259–3263 (1977).
50. Benton, W. D. & Davis, R. W. *Science* **196**, 180–182 (1977).
51. Rigby, P. W. J., Dieckmann, M., Rhodes, C. & Berg, P. *J. molec. Biol.* **113**, 237–251 (1977).
52. Frischauf, A.-M., Lehrach, H., Poustka, A. & Murray, N. *J. molec. Biol.* **170**, 827–843 (1983).

Sequence requirements for nuclear location of simian virus 40 large-T antigen

Daniel Kalderon, William D. Richardson, Alexander F. Markham* & Alan E. Smith

Biochemistry Division, National Institute for Medical Research, Mill Hill, London NW7 1AA, UK
*ICI Pharmaceuticals Division, Alderley Park, Macclesfield, Cheshire SK10 4TG, UK

A point mutation in the simian virus 40 large-T gene, which was generated by mixed oligonucleotide mutagenesis and resulted in the conversion of Lys 128 to Thr, produced a large-T antigen that was detected in the cytoplasm but not the nucleus of cells. Deletions within the surrounding sequence Lys-^{128}Lys-Lys-Arg-Lys-Val-Glu also produce cytoplasmic large-T and define a region of the protein involved in nuclear location.

THE large-T antigen of simian virus 40 (SV40), molecular weight M_r 94,000, is sufficient to transform established and non-established rodent cells *in vitro* and to induce tumours in newborn hamsters[1]. It is also required for the productive infection of simian cells by SV40[2].

Large-T is a predominantly nuclear protein[3] but is also found in a modified form in the plasma membrane[4,5]. During a productive infection the nuclear form of large-T regulates the level of viral gene expression and stimulates viral DNA replication through an interaction with the viral origin of DNA replication[6–8]. To investigate whether DNA binding by large-T is also involved in transformation we have introduced mutations[9] into a region coding for a putative DNA binding domain of the protein[6,10–13]. Within this domain is a striking tract of five basic amino acids (^{127}Lys-Lys-Lys-Arg-Lys^{131}) just downstream from a cluster of serine and threonine phosphorylation sites[14]. As the sense of the codons for lysine is unaffected by the action of the commonly used mutagen, sodium bisulphite, to mutate this region we devised a modification of oligonucleotide-directed mutagenesis[15,16] that allows the introduction of several defined point mutations in a single experiment.

The large-T protein encoded by one of the mutants generated in this manner contains a threonine residue in place of Lys 128. This mutant large-T, although able to transform Rat-1 cells with wild-type efficiency as measured by focus formation in high serum, accumulates in the cytoplasm rather than the nucleus of

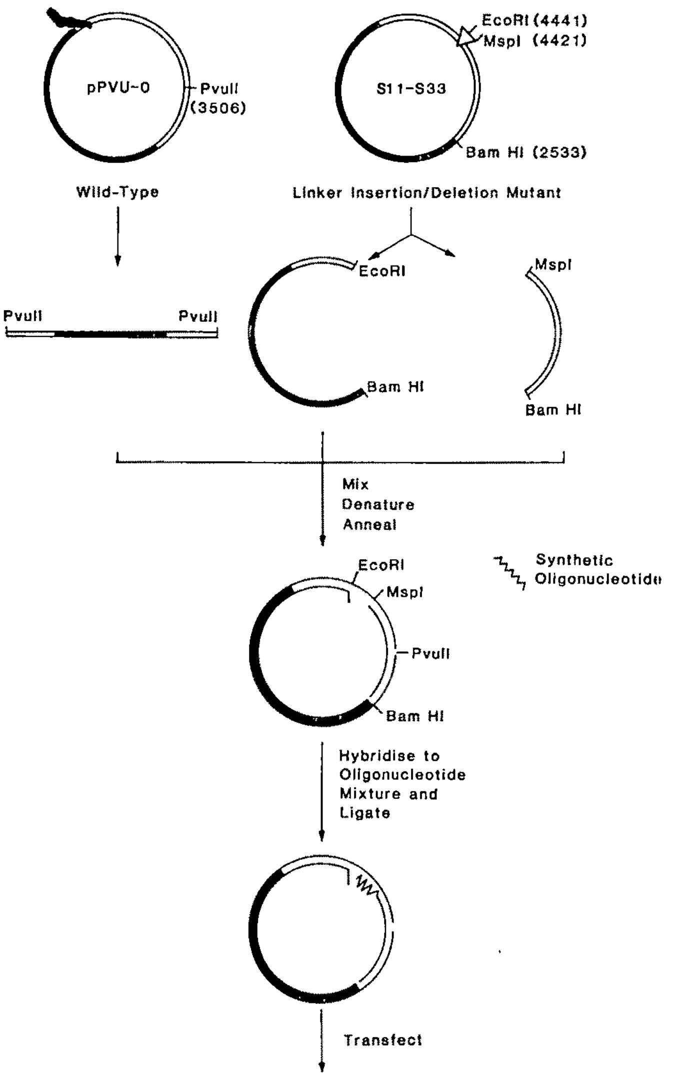

Fig. 1 Mixed oligonucleotide mutagenesis. Plasmid pPVU-0 (ref. 23) contains the wild-type SV40 early region from *Bam*HI (2,533) to *Pvu*II (270) between the *Bam*HI (375) and *Pvu*II (4,676) sites of pBR328 (ref. 37) but with a deletion of 3 base-pairs at the junction of *Pvu*II sites, thus destroying the enzyme recognition site at this point. In the figure, plasmid DNA sequences are shaded whereas the SV40-derived sequences are not. S11-S33 (ref. 9) is a derivative of pPVU-0 that contains a 10 bp *Eco*RI linker (CGGAATTCCG) spanning a deletion between SV40 nucleotides 4441 and 4421. An *Msp*I site is created at the junction of linker and SV40 nucleotide sequences around position 4421. *Msp*I–*Bam*HI and *Bam*HI–*Eco*RI restriction fragments from S11-S33 were purified by agarose gel electrophoresis followed by phenol extraction[9] and were mixed in equimolar proportions with pPVU-0 DNA linearized at its unique *Pvu*II site. After denaturation with alkali and subsequent renaturation[23] about 10–20% of the products migrated as form II (open duplex circles) during agarose gel electrophoresis and were presumed to be circular heteroduplexes of the form shown above. The hybridization products (2.5 μg DNA) were dissolved, after ethanol precipitation in 10 μl of ligation buffer (50 mM Tris-HCl *p*H 8.0, 7.5 mM $MgCl_2$, 1 mM ATP, 10 mM dithiothreitol (DTT) and 0.02% gelatin) and to this was added 2.5 μg of the oligonucleotide mixture (synthesized as in ref. 38) and phosphorylated by T4 polynucleotide kinase, also in 10 μl of ligation buffer. The components were mixed initially at 60 °C, the temperature was then gradually reduced to 0 °C over a 6 h period, after which additional dithiothreitol (to 5 mM) and T4 DNA ligase (6 units) were added. After 1 h at 0 °C, ligation was continued for 4 h at 15 °C. Some of the ligated material was then used directly for transfection. Alternatively, after phenol extraction and ethanol precipitation aliquots were treated with S_1 nuclease (50 units per 10 μl/0.4 μg DNA for 20 min at 37 °C) before neutralization and transfection. S_1 nuclease treatment reduced the number of transfectants about 10-fold. Parallel experiments showed that significant cleavage of nicked circular plasmid DNA did not occur at the S_1 nuclease concentration used.

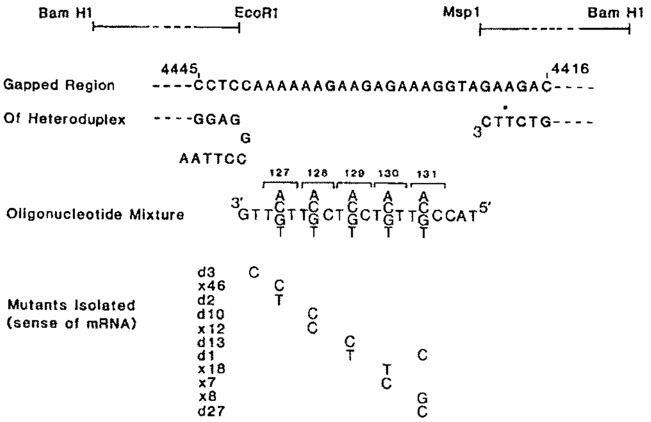

Fig. 2 Mutants obtained using mixed oligonucleotide mutagenesis. The composition of the synthetic oligonucleotide mixture is shown above together with the single-stranded region of the gapped heteroduplex, formed as in Fig. 1, to which the oligonucleotides were hybridized. Note that after hybridization the synthetic oligonucleotides are exactly apposed at their 5' ends to the double-stranded region of the heteroduplex and can therefore be ligated directly into the heteroduplex. The nucleotide sequence alterations in mutant plamids recoverd from the procedure described in Fig. 1 are shown. The inferred alterations to the amino acid sequence of large-T are presented in Table 1. The mutation found in plasmid d3 should not theoretically have been introduced by the oligonucleotide mixture used. It was not studied further because it does not alter the amino acid sequence of large-T.

the transformed cells. The phenotypes of other mutants with lesions in the same area help to define a region around Lys 128 which is required for the nuclear localization of large-T.

Mixed oligonucleotide mutagenesis

Oligonucleotide-directed mutagenesis is currently the method of choice for the introduction of single, precisely defined mutations. However, this method is not generally used for the creation of large families of point mutants because of the labour or expense involved in obtaining a large number of individual synthetic oligonucleotides. In the procedure described here a mixture of oligonucleotides synthesized on a single resin was used as the mutagen.

The mixture of oligonucleotides, each of 20 residues, was synthesized by including an equimolar mixture of all four nucleotides at five selected positions along its length (Fig. 2). The degenerate positions correspond to the second nucleotides in the codons for the basic sequence ^{127}Lys-Lys-Lys-Arg-Lys^{131}, thereby potentially allowing the conversion of each of these residues to any of three different amino acid residues. Thus the oligonucleotide mixture contained 4^5 components, one of which was an exact copy of the wild-type SV40 large-T coding sequence in this region and 15 of which contained a single base change. The oligonucleotide mixture was incorporated into plasmid DNA bearing a cloned wild-type large-T gene by direct ligation into a gapped heteroduplex, formed between wild-type plasmid DNA and two restriction fragments of a linker insertion/deletion mutant derivative of the plasmid (Fig. 1).

After transfection, colony hybridization[17] using a 19-nucleotide long probe of sequence corresponding to the wild-type gene in this region (4,423–4,441:ACCTTTCTCTTCTTTTTTG) was used to detect plasmids bearing mutations within this sequence. Washing filters at increasing temperatures[18] following hybridization at room temperature clearly distinguished between wild-type plasmids in which hybrids were stable up to about 55 °C (in 6 × SSC) and others which showed no detectable hybridization beyond about 45 °C. Although this latter class could itself be resolved into two distinct categories because of differences in the stability of hybridization to the oligonucleotide probe, plasmid DNA was isolated from all poorly hybridizing colonies and examined by restriction enzyme mapping. All plasmids for which hybrids were not stable above ~37 °C, contained large

Table 1 Biological properties of mutant large-T proteins produced by mixed oligonucleotide mutagenesis

						Transformation Focus formation on Rat-1 cells				Replication		
Wild-type plasmid	127 Lys	128 Lys	129 Lys	130 Arg	131 Lys	10 µg DNA Expt	10 µg DNA % wt	1 µg DNA Expt	1 µg DNA % wt	Plasmid DNA	Virus	Location of large-T in transformed Rat-1 cells
X46	Thr					(1)	59	(A)	67	–	–	Nuclear
						(2)	73	(A)	80			
d2	Ile					(3)	28	(A)	135	–	–	Nuclear
						(4)	112	(C)	164	–	–	
d10		Thr				(6)	107	(A)	140	–	–	Cytoplasmic
						(7)	101					
X12		Thr				(2)	16	(A)	83	–	–	Cytoplasmic
						(4)	48					
d13			Thr			(3)	14	(A)	40	+	D*	Mixed
						(5)	23	(B)	61			
d1			Met		Thr	(3)	190	(A)	105	–	–	Mixed
						(7)	96	(E)	378			
X18				Ile		(1)	54	(A)	54	–	–	Mixed
X7				Thr		(2)	33	(A)	31	D†	D‡	Mixed
X8					Arg	(1)	56	(A)	37	+	+	Nuclear
d27					Thr	(3)	24	(D)	74	+	+	Mixed
						(4)	40	(C)	103			

Transformation assays: Plasmid DNA (10 µg or 1 µg + 9 µg salmon sperm DNA) was transfected into semi-confluent Rat-1 cells by the calcium phosphate method[20]. Cells were grown in Dulbecco's modified Eagle's medium supplemented with 10% fetal calf serum. Dense foci were visible after about 14 days post-transfection and were counted 3–9 days after their first apperance. The numbers above represent the mean of duplicate assays expressed as a percentage of the number of foci induced by the wild-type plasmid, pPVU-0, in the same experiment. The numbers of foci induced by pPVU-0 in these experiments were as follows: Experiment (1) 1,220; (2) 1,150; (3) 446; (4) 500; (5) 464; (6) 694; (7) 634. (A) 170; (B) 94; (C) 50; (D) 76; (E) 62. The deletion mutants RL6 and S5-S32 (ref. 9) which encode a wild-type small-t but severely truncated large-T proteins of 175 and 142 amino acids, respectively, failed to induce any foci in these assays.

Replication assays: Plasmid DNA and viral replication assays were performed as described elsewhere[9]. (–) Indicates that no DNA was detectable in an experiment that would detect 0.1% of wild-type DNA accumulation or that no plaques were detectable within 4 weeks (wild-type plaques are normally visible by 10 days); (+) indicates behaviour indistinguishable from wild-type and (D) (defective) behaviour intermediate between these extremes.

Subcellular localization: Cells derived from transformed foci of Rat-1 cells were grown on glass coverslips, fixed in 4% formaldehyde in phosphate-buffered saline (20 min at room temperature), permeabilized with 1% Nonidet P40 (5 min at room temperature) and incubated with hamster anti-tumour serum followed by fluorescein isothiocyanate-labelled rabbit anti-hamster antibody (Nordic). d10 and X12 transformed cells were also examined using monoclonal antibody PAb423 (ref. 21), followed by rhodamine isothiocyanate-conjugated rabbit anti-mouse antibody. Controls using normal Rat-1 cells and normal hamster serum were included. Normal Rat-1 cells were also generally still present in the population of cells derived from dense foci and thus acted as internal controls for non-specific staining. Immunofluorescence was scored as nuclear, cytoplasmic or mixed. Mixed indicates that three different patterns of staining could be seen in individual cells within a population of transformed cells. Some cells were stained only in the nucleus, others only in the cytoplasm and the rest in both compartments. The most extreme example of this phenotype is d1. Similar localization patterns were seen by staining with the large-T specific monoclonal antibody PAb423 following manual microinjection of each of the mutant plasmids into Vero cells.

* Plaques visible 3 days later than wild-type. † Less than 10% of wild-type DNA accumulation. ‡ Plaques visible 6 days later than wild-type.

deletions (about 2 kb) that included the target for mutagenesis. In contrast, all plasmids for which hybrids were stable to between 40 °C and 45 °C were of wild-type size, indicating the presence of point mutations within the target area. This was confirmed by determining the DNA sequence in this region of all plasmids which formed hybrids of intermediate stability, using the oligonucleotide primed dideoxy procedure applied to double-stranded DNA[19].

Nine of the eleven plasmids sequenced in this way were found to have single point mutations of the wild-type sequence at positions corresponding to the degeneracies in the oligonucleotide mixture (Fig. 2). One mutant plasmid (d1) contained two such alterations and another contained an A to C transversion at a position that should have been invariant (and wild-type) in the oligonucleotide mixture. Two independent isolates of one mutant plasmid (X12; d10) were recovered. In a subsequent experiment using the same oligonucleotide mixture, three further single point mutants were isolated (W. H. Colledge, personal communication). Thus, 12 of the 15 possible point mutants have been obtained. Mutants were recovered corresponding to each of the degenerate positions in the oligonucleotide mixture and examples of each kind of mutagenic change (A → C, G, T) were found. The overall efficiency of production of point mutants was enhanced from 0.7% to 3% by the inclusion of an S_1 nuclease digestion step immediately before transfection, designed to linearize those gapped heteroduplexes to which no oligonucleotide had hybridized. The ease with which large numbers of plasmids can be reliably screened for the presence of point mutations by hybridization to an oligonucleotide of wild-type sequence compensates for the relatively low rate at which mutant plasmids are produced. The genotype of the mutants recovered demonstrates that the mutagenic procedure selects for the incorporation of synthetic oligonucleotides containing single deviations from the wild-type sequence, from a large excess of oligonucleotides with multiple alterations. The principle of mixed oligonucleotide mutagenesis should be applicable to all methods of conventional oligonucleotide-directed mutagenesis currently in use[16].

Transforming activity

The transforming potential of mutant plasmids was assayed by measuring the induction of dense foci on a monolayer of Rat-1 cells following calcium phosphate transfection[20]. The formation of dense foci was large-T dependent, as shown by the failure of deletion mutants that encode a wild-type small-t but severely truncated large-T proteins, to produce dense foci (Table 1). However, all point mutants examined showed a transforming activity similar to wild-type. Although slight differences in specific transforming activity were observed, the latent period before foci became visible was never significantly different from wild-type (13–14 days).

Subcellular localization

Individual foci of transformed Rat-1 cells were picked, the cell population expanded and the subcellular location of large-T assessed by indirect immunofluorescence of permeabilized fixed cells using serum from hamsters bearing SV40-induced tumours as the first antibody.

Rat-1 cells transformed by wild-type large-T, encoded by the plasmid pPVU-0, exhibited a typical nuclear staining with no detectable nucleolar or cytoplasmic staining (Fig. 3*a*). A strikingly different staining pattern was seen for cells transformed by the point mutants, d10 and X12, both of which encode a threonine residue in place of Lys 128 (Fig. 3*c*). The nuclei appear dark against a bright cytoplasmic background. An identical pattern was seen using a monoclonal antibody (PAb423; ref. 21) directed to the carboxy-terminal region of large-T as first

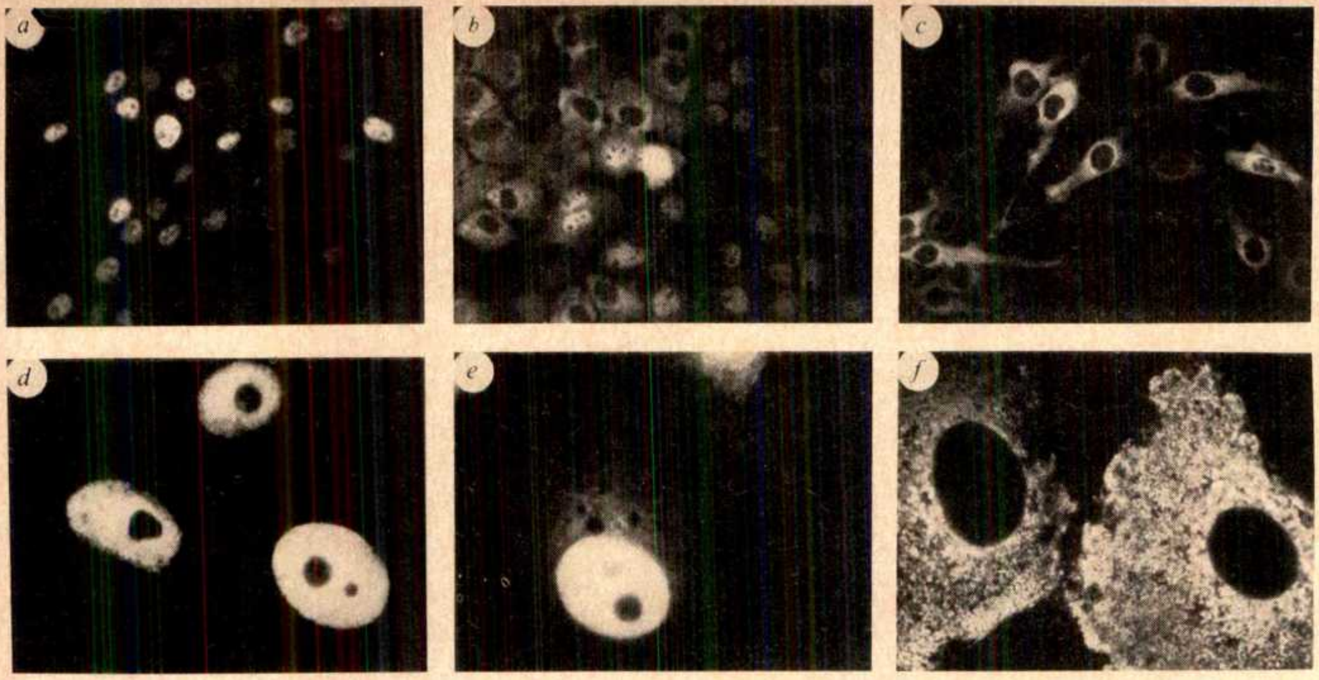

Fig. 3 Nuclear accumulation of large-T in transformed Rat-1 cells and in Vero cells is abolished by alteration of Lys 128 to Thr and impaired by mutation of the surrounding basic amino acid residues. Individual dense foci of Rat-1 cells transformed by wild-type pPVU-0 (panel *a*), the double point mutant d1 (Lys 129→Met, Lys 131→Thr) (panel *b*) and the point mutant d10 (Lys 128→Thr) (panel *c*) were picked and expanded. Cells transformed by d1 were then cloned successively by passage through soft agar and by dilution. Cell lines were fixed and stained by indirect immunofluorescence as described in the legend for Table 1, using hamster anti-tumour serum as the first antibody. The location of large-T in Vero cells was examined by the same indirect immunofluorescence procedure using the monoclonal PAb423 as first antibody, 18 hr after manual microinjection[22] of about 200 copies of plasmid DNA into the nucleus of confluent cells growing on glass coverslips. The plasmids injected were wild-type pPVU-0 (panel *d*), d1 (panel *e*) and d10 (panel *f*). The fields shown in *d–f* are of confluent monolayers and include some cells that have not been microinjected and show no immunofluorescent staining.

antibody. This antibody, unlike anti-tumour serum, does not recognize SV40 small-t antigen which should be expressed in wild-type form by all mutant plasmids used in this study. The same cytoplasmic staining pattern was seen in Rat-1 cells transformed by d10 that were isolated as colonies growing in soft agar.

The exclusion of large-T from the nuclei of transformed Rat-1 cells consequent to mutation of Lys 128 is not observed for similar mutation of individual adjacent amino acid residues that form part of the five residue basic tract ([127]Lys-Lys-Lys-Arg-Lys[131]). Cells transformed by each of these mutants exhibit predominantly nuclear staining. In some cases (d2, X8, X46), the subcellular distribution of large-T appears indistinguishable from that of the wild-type protein. In other cases (X7, X18, d13, d27), a slight defect in nuclear accumulation of large-T is manifest by the presence of some cytoplasmic, in addition to nuclear, staining in the majority of cells derived from an individual focus. Furthermore, a minority of cells from the same focus show predominantly cytoplasmic staining.

The heterogeneous staining pattern (Fig. 3*b*) is even more obvious for the double mutant, d1 (Lys 129→Met, Lys 131→Thr). To date, the subcellular distribution of d1 large-T has been examined in 16 foci, derived from two independent transformation assays. In only one of these was a homogeneous staining pattern observed, with the mutant large-T apparently confined to the cytoplasm of the transformed cells. In all other cases, nuclear staining exceeded cytoplasmic staining in the majority of cells (60–95%); some cells clearly exhibited both nuclear and cytoplasmic staining, whereas in others large-T was apparently either wholly cytoplasmic or wholly nuclear. Cells derived from three of these foci were cloned further either by limiting dilution or by passage through soft agar. In each case, the heterogeneous staining pattern was preserved, indicating that clonally derived sibling cells express a large-T antigen that can, at any one time, be present predominantly in either cytoplasmic or nuclear compartments.

The variable distribution of the large-T protein encoded by the mutants d1, d13, d27, X7 and X18 shows that mutations close to Lys 128 can modulate but do not prevent the accumulation of large-T in the nucleus. Although other interpretations are possible, the heterogeneous localization of large-T in cells transformed by these mutants may reflect a deficiency in the rate of nuclear accumulation less extreme than that observed for d10, which allows the visualization of intermediate stages in the nuclear accumulation of large-T, for example following the breakdown of the nuclear envelope at mitosis.

Transient expression

The wild-type plasmid, pPVU-0, and mutant derivatives were manually microinjected into the nucleus of semi-confluent Vero cells[22] and the location of the encoded large-T products assessed by indirect immunofluorescence 18 h post-injection. The staining patterns observed were virtually identical to those seen for transformed cells but were of much greater intensity, presumably due to the large number of gene copies available for transcription. Thus, large-T coded by wild-type pPVU-0 was exclusively nuclear (Fig. 3*d*) and that encoded by d10 was seen only in the cytoplasm (Fig. 3*f*). Both nuclear and cytoplasmic staining was observed for the mutants d1, d13, d27, X7 and X18 (Fig. 3*e*) but the heterogeneity in this staining pattern between individual cells in a population was not as marked as for transformed cell lines.

Replicative activity

As all mutations were introduced into a plasmid, pPVU-0 (ref. 23) that contains the viral origin of DNA replication as well as the entire large-T gene, the ability of the mutant large-T proteins to stimulate the replication of viral origin-bearing episomes in permissive cells could be tested directly by transfection of mutant plasmids into CV-1 cells and quantitation of intracellular plasmid DNA 72 h later[24]. In addition, the mutant large-T coding sequences from these plasmids were reconstructed into viral DNA and the viability of mutant virus tested by plaque assay[25]. The two assays gave similar results (Table 1), indicating that several of the mutants were unable to support viral DNA replication. Many other mutants[9] with lesions either side of those

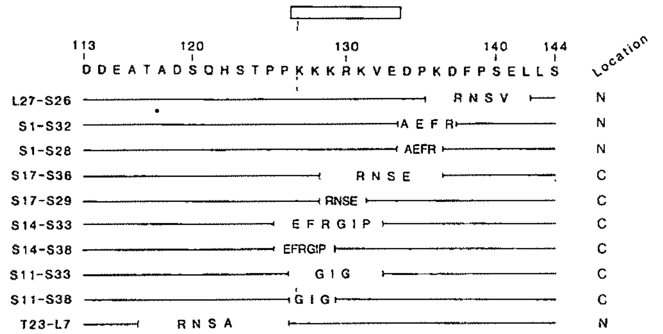

Fig. 4 Amino acid sequence of large-T proteins with deletions in the vicinity of Lys 128. Mutants were constructed from wild-type pPVU-0 containing one or two *Eco*RI linkers CGGAATTCCG at the site of a small deletion[9]. The consequent inferred alterations to the wild-type amino acid sequence are shown. Subcellular localization of mutant large-T antigens in transformed cells was determined as in Table 1 and Fig. 3. (+) (−) indicate the presence or absence, respectively, of nuclear immunofluorescence. Some of the large-T coded by T23-L7 was also detected in the cytoplasm. The box above the amino acid sequence of large-T indicates those residues which cannot be deleted without preventing nuclear localization of the mutants described here. Abbreviations used are: A, alanine; D, aspartic acid; E, glutamic acid; F, phenylalanine; G, glycine; H, histidine; I, isoleucine; K, lysine; L, leucine; N, asparagine; P, proline; Q, glutamine; R, arginine; S, serine; V, valine.

described here also appear to be unable to stimulate viral DNA replication, indicating that this is a common phenotype of mutants from this region.

The viability of mutants altered at Lys 129 and Lys 131, respectively, implies that these (heterogeneously localized) mutant large-T antigens must be able to interact effectively with DNA sequences around the viral origin of replication. Direct measurement of DNA-binding activity *in vitro* by the McKay assay[26] suggests that the non-viable cytoplasmic (d10) and partially cytoplasmic (d1) mutants can also recognize SV40 origin DNA (E. Paucha, D.K. and A.E.S., manuscript in preparation), suggesting that the aberrant localization of these proteins is not related to their ability to interact with SV40 DNA.

Sequences around Lys 128

The data above show that alteration of Lys 128 and, to a lesser extent, the surrounding basic amino acid residues either modulates or abolishes the nuclear accumulation of large-T. The properties of a large number of single, double and triple point mutants with lesions either side of this region between amino acids 106 and 158, by contrast, do not exhibit any impairment in the nuclear accumulation of large-T[9]. The importance of Lys 128 to the localization of large-T is highlighted further by the recent observation of R. G. Lanford and J. S. Butel (personal communication) that the only lesion in the large-T coding sequence of the PARA-cT variant[27], isolated several years ago on the basis of its cytoplasmic phenotype, is the conversion of the codon for Lys 128 to that for Asn.

It is likely, therefore, that Lys 128 forms an essential part of some structural feature of the wild-type large-T protein that allows it either to be transported to or retained within the nucleus. The other possibility that the variant large-T proteins coded by d10 and PARA-cT have acquired an affinity for cytoplasmic components seems improbable, in that a novel specificity of binding is unlikely to be endowed by two different amino acid changes.

The context in which Lys 128 serves to localize large-T to the nucleus has been probed further by examining the properties of a number of insertion/deletion mutants with lesions in the immediate vicinity of Lys 128 (Fig. 4). These were made by standard procedures as part of a more comprehensive mutagenic analysis of large-T[9]. As all of the mutants shown in Fig. 4 were able to transform Rat-1 cells (Table 2), the subcellular distribution of the mutant large-T antigens could be examined in cells derived from transformed foci. In all cases where any part of the basic tract of amino acid residues (127–131) is interrupted, even if this does not include Lys 128, large-T is seen only in the cytoplasm of transformed cells (Fig. 4). However, the normal nuclear accumulation of large-T was not detectably impaired by the alteration of as many as four consecutive amino acid residues distal to Glu 133 and was only marginally affected by changing as many as ten residues proximal to Lys 127. Thus, if there exists a region of primary amino acid sequence around Lys 128 that directs large-T to the nucleus, it probably does not extend beyond Lys 127 or Glu 133. The tolerance of the nuclear large-T mutants L27-S26 and T23-L7 to variation in the length of polypeptide chain separating this sequence from the rest of the molecule perhaps also suggests that the function of Lys 128 is not dependent on a precisely structured three-dimensional configuration within the protein. The cytoplasmic location of several different insertion/deletion mutants supports the argument presented earlier that this phenotype does not result from a novel retention of large-T in the cytoplasm but rather from a defect in transport to or retention within the nucleus.

Table 2 Transforming activity and subcellular localization of large-T proteins with deletions in the vicinity of Lys 128

	Net change in no. of amino acid residues	Nuclear large-T	Transformation of Rat-1 cells	
			No. of foci % wt 10 µg DNA	No. of foci % wt 1 µg DNA
L27-S26	−3	+	81	44
S1-S32	0	+	3, 20, 35*	30
S1-S28	+1	+	30	40
S17-S36	−4	−	66, 50	36
S17-S29	+1	−	38, 53	17
S14-S33	+1	−		
S14-S38	+2	−		
S11-S33	−3	−	72	75
S11-S38	0	−	110	35
T23-L7	−6	+	21	75

The transforming activity and subcellular locations of the mutant large-T proteins in transformed cells is given. These parameters were assayed as described in Table 1.

* These foci appeared 7, 3 and 6 days later than wild-type, respectively.

All of the cytoplasmic insertion/deletion mutants, like d10, transform Rat-1 cells according to dense focus formation in high serum with an efficiency and latent period similar to wild-type (Table 2).

Transformation by non-nuclear T

SV40 large-T is an unusual transforming protein in that it can transform primary cells as well as established cell lines[28] and gives rise to a gradation of transformed phenotypes[29]. In this study only the ability of large-T to transform an established cell line, Rat-1, in high serum was measured by the criterion of dense focus formation. None of the cytoplasmic large-T deletion or point mutants showed a significant deficiency in transforming activity relative to wild-type in this assay. Preliminary experiments indicate that the point mutant, d10, also transforms Rat-1 cells, by the criterion of colony formation in soft agar at high serum concentration with an efficiency similar to wild-type. However, any implication that large-T need not be nuclear to transform, must be tempered by two considerations. First, although large-T is seen by immunofluorescence only in the cytoplasm of cells transformed by d10 or by any of several deletion mutants, some large-T may nevertheless be present in the nucleus but remain undetected, either because of its very low abundance or because it is in a form that is not accessible to the antibodies used for its detection. Second, it is possible that differences in the transforming activity of nuclear and non-nuclear large-T species may be revealed by more stringent assays. By using such assays, R. G. Lanford and J. S. Butel concluded that the cytoplasmic large-T encoded by the PARA-cT mutant induces a partially transformed phenotype in hamster cells, although it can induce colony formation in semi-solid medium and tumour formation *in vivo*[30]. In view of the notion that the transformation of primary cells involves the combined action of a nucelar immortalizing gene product (such as polyoma virus large-T, adenovirus E1a protein, the *myc* gene product) and a membrane-associated protein[31] (such as the *ras* gene product, polyoma virus middle-T), it might be predicted that a non-nuclear large-T would be unable to immortalize or transform primary cells, whereas the plasma-membrane associated form of large-T[5] may suffice to transform established cell lines. These predictions are being tested using the cytoplasmic mutants described here.

Mechanisms of nuclear localization

The nuclear envelope differs from other cellular membranes in that it allows the free passage of virtually all proteins below a certain size (corresponding to approximately 18,000 M_r) in addition to some larger proteins[32–34]. Thus, for any given protein it is not clear whether nuclear accumulation results from a specific mechanism that either facilitates or drives transport across the envelope or whether the protein is free to diffuse, for instance through nuclear pores and is then retained in the nucleus by virtue of an affinity for elements that are themselves confined to the nucleus. This distinction has not been made for SV40 large-T, though the large size of the monomer may favour a specific transport mechanism.

The accumulation of nucleoplasmin in the nucleus of *Xenopus laevis* oocytes[35] is the only case for which there is good evidence for the involvement of a nuclear transport system. Proteolytic digestion of the native pentameric protein has shown that a 16,000 M_r fragment derived from a single 33,000 M_r monomeric unit is sufficient to allow the nuclear accumulation of partial proteolytic cleavage products as large as 101,000 M_r, and is therefore presumed also to specify the nuclear location of the native protein.

Whatever the mechanism of nuclear accumulation, the evidence presented here heralds the possibility that a very restricted region of the SV40 large-T amino acid sequence around Lys 128 may be sufficient to ensure the nuclear location of this protein. Further experiments are in progress to determine more precisely to what extent this putative signal is independent of the rest of the large-T molecule and whether the signal can act in the context of other proteins that are normally cytoplasmic so as to direct them to the nucleus. The availability of the d10 mutant will be invaluable as a control for such studies. When this manuscript was in preparation, M. N. Hall *et al.* reported that restricted sequences derived from the yeast Mat $\alpha 2$ gene product can direct another protein to the nucleus in yeast[36].

We thank Robert Lanford, Janet Butel and Lynna Hereford for communication of results prior to publication, Ed Harlow for monoclonal antibody PAb423, Roger Morris for the gift of rhodamine-isothiocyanate-conjugated rabbit anti-mouse antibody, Joe Brock for help with illustrations and Lydia Pearson for typing the manuscript.

Received 24 April; accepted 3 July 1984.

1. Tooze, J. *Molecular Biology of Tumor Viruses* Part 2, 2nd edn (Cold Spring Harbor Laboratory, New York, 1981).
2. Tegtmeyer, P. *J. Virol.* **10**, 591–598 (1972).
3. Pope, J. H. & Rowe, W. P. *J. exp. Med.* **120**, 121–128 (1964).
4. Santos, M. & Butel, J. S. *Virology* **120**, 1–17 (1982).
5. Klockmann, U. & Deppert, W. *EMBO J.* **2**, 1151–1157 (1983).
6. Tjian, R. *Cell* **13**, 165–179 (1978).
7. Shortle, D. R., Margolskee, R. F. & Nathans, D. *Proc. natn. Acad. Sci. U.S.A.* **76**, 6128–6131 (1979).
8. Rio, D., Robbins, A., Myers, R. & Tjian, R. *Proc. natn. Acad. Sci. U.S.A.* **77**, 5706–5710 (1980).
9. Kalderon, D. & Smith, A. E. *Virology* (in the press).
10. Prives, C., Beck, Y. & Shure, H. *J. Virol.* **33**, 689–696 (1980).
11. Chaudry, F., Harvey, R. & Smith, A. E. *J. Virol.* **44**, 54–66 (1982).
12. Clark, C., Peden, K., Pipas, J. M., Nathans, D. & Tjian, R. *Molec. cell. Biol.* **3**, 220–228 (1983).
13. Morrisson, B., Kress, M., Khoury, G. & Jay, G. *J. Virol.* **47**, 106–114 (1983).
14. Scheidtmann, K. H., Echle, B. & Walter, G. *J. Virol.* **44**, 116–133 (1981).
15. Hutchinson, C. A. III *et al. J. biol. Chem.* **253**, 6551–6560 (1978).
16. Smith, M. & Gillam, S. in *Genetic Engineering, Principles and Methods*, Vol. 3 (eds Setlow, J. K. & Hollaender, A.) (Plenum, New York, 1981).
17. Grunstein, M. & Hogness, D. *Proc. natn. Acad. Sci. U.S.A.* **72**, 3961–3965 (1975).
18. Wallace, R. B. *et al. Nucleic Acids Res.* **6**, 3543–3557 (1979).
19. Wallace, R. B. *et al. Gene* **16**, 21–26 (1981).
20. Graham, F. L. & van der Eb, A. J. *Virology* **52**, 456–467 (1973).
21. Harlow, E., Crawford, L. V., Pim, D. C. & Williamson, N. M. *J. Virol.* **39**, 861–869 (1981).
22. Richardson, W. D. & Westphal, H. *Cell* **27**, 133–141 (1981).
23. Kalderon, D., Oostra, B. A., Ely, B. K. & Smith, A. E. *Nucleic Acids Res.* **10**, 5161–5171 (1982).
24. Myers, R. M. & Tjian, R. *Proc. natn. Acad. Sci. U.S.A.* **77**, 6491–6495 (1980).
25. Dulbecco, R. & Freeman, G. *Virology* **8**, 396–397 (1959).
26. McKay, R. D. G. *J. molec. Biol.* **145**, 471–488 (1981).
27. Rapp, F., Pauluzzi, S. & Butel, J. S. *J. Virol.* **4**, 626–631 (1969).
28. Pollack, R., Risser, R., Conlon, S. & Rifkin, D. *Proc. natn. Acad. Sci. U.S.A.* **71**, 4792–4796 (1974).
29. Risser, R. & Pollack, R. *Virology* **59**, 477–489 (1974).
30. Lanford, R. G. & Butel, J. S. *Virology* **110**, 147–158 (1981).
31. Land, H., Parada, L. F. & Weinberg, R. A. *Science* **222**, 771–778 (1983).
32. Paine, P. L & Feldherr, C. M. *Expl Cell Res.* **74**, 81–98 (1972).
33. Paine, P. L., Moore, L. C. & Horowitz, S. B. *Nature* **254**, 109–114 (1975).
34. De Robertis, E. M. *Cell* **32**, 1021–1025 (1983).
35. Dingwall, C., Sharnick, S. V. & Laskey, R. A. *Cell* **30**, 449–458 (1982).
36. Hall, M. N , Hereford, L. & Herskowitz, I. *Cell* **36**, 1057–1065 (1984).
37. Prentki, P., Karch, F., Iida, S. & Meyer, J. *Gene* **14**, 289–299 (1981).
38. Edge, M. D. *et al. Nature* **292**, 756–761 (1981).

LETTERS TO NATURE

The boundary of the Solar System

R. Smoluchowski

University of Texas, Austin, Texas 78712, USA

M. Torbett

Carnegie Institution, Department of Terrestrial Magnetism,
Washington DC 20005, USA

The shape of the boundary of the Solar System, defined as the surface within which the gravitational attraction of the Sun, rather than that of the rest of the Galaxy, controls the orbital motion of bodies such as planets and comets, has been determined. Outside of this surface, the dominant factors are the radial tides due to the galactic centre and, especially, the vertical tides caused by the galactic disk. Orbits which are direct with respect to the galactic plane, have a boundary which differs from that for retrograde orbits, both being 10–20% oblate and both larger than the, usually assumed, present Oort cloud. The surface may have been the boundary of the early cloud of comets which was later reduced by the passages of stars and molecular clouds.

Losses of bodies from the Solar System are caused by: sporadic perturbations by passing stars or giant molecular clouds, which occur at a rate of several per 10^6 or 10^9 yr respectively, perturbations by giant planets and the steady gravitational perturbation by the galaxy. The first two kinds of perturbations have been extensively studied[1–4]. We now describe the results of a three-dimensional stability study (inertial coordinates) of a system consisting of a comet and the Sun rotating[5] around the galactic centre [mass $1.3 \times 10^{11}\ M_{\odot}$, distance 8.2 kpc (ref. 6)] and periodically traversing the nearly harmonic field of the galactic mid-plane (GMP)[7]. A two-dimensional model of a greatly simplified version of this problem has been studied previously[5] and a corresponding three-dimensional Hill surface is also known[8]. To get an indication of the extent and structure of the boundary of stability[9] paths of comets were integrated numerically for various initial parameters using Cowell's method and fourth-order Runge–Kutta integration. Near the boundary of stability the orbit of a comet is non-keplerian, its semimajor axis a, average inclination i, eccentricity e and the direction of perihelion $\tilde{\omega}$ are highly variable. Thus, for an initial i, the values of e and a were so chosen as to obtain an orbit which was bound for the age of the Solar System. The value of $\tilde{\omega}$ had essentially no effect on the results.

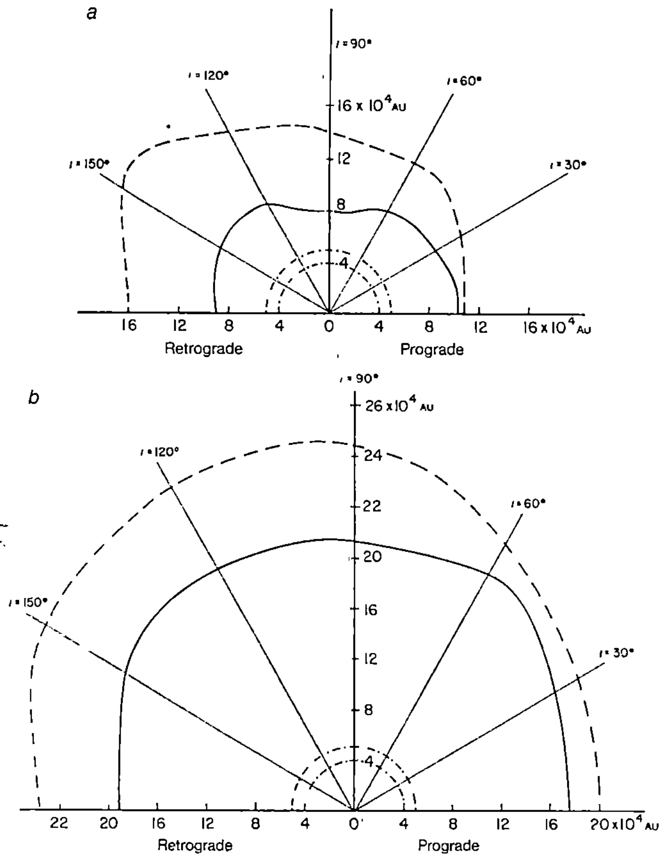

Fig. 1 *a*, Maximum stable semi-major axes of orbits perturbed by the galactic centre alone (dashed line) and by the galactic centre and the mid-plane (solid line). The usually assumed size of the Oort cloud is also indicated (dash-dot line). *b*, Maximum aphelia of orbits perturbed.

The effect of the galactic centre was investigated first and then the influence of the GMP was included. Without such an influence, a cometary orbit is, in general, more stable for high eccentricities and inclinations near 90° as it then senses less of the tidal field of the galactic centre[10] and thus the stability boundary has a proloid shape as shown by dashed lines in Fig. 1. When the effect of the gravitational compression[7] caused by the oscillations of the Sun through the GMP is added, the results indicate a strong destabilization of all orbits especially for i higher than 90°. As shown in Fig. 1, the boundaries of stability then become oblate by 10–20%.

For large a, the periods of orbits are comparable to a substantial fraction of 1.9×10^8 yr, the period of the Sun around the galactic centre or to the shorter period of motion of the Sun across the GMP, so that the directions of the galactic tidal forces change significantly and a resonance can occur between the period of the comet and the other two. The three-dimensional shape of the limits of the stable Solar System, taking both the GC and GMP into account, is obtained by rotating the curves shown in Fig. 1 around the z-axis perpendicular to the plane of the galaxy. This leads to two rather similar co-axial surfaces: the inner one, enclosing the prograde orbits and the outer one, limiting the extent of the retrograde orbits. A rough estimate of the volume of these surfaces suggests that if the density of comets per unit volume were uniform, there would be ~20% more retrograde than prograde comets. The assumption of a uniform density is, however, questionable. Both surfaces have dimensions that are appreciably larger than the commonly assumed radii of the Oort cloud whether based on observation or on other theoretical estimates[1,2,10–13].

Among the stars which penetrate and perturb the Oort cloud those in the mass range of 0.15–0.85 $M_\odot$, have higher velocities than those with masses in the 0.85–1.15 $M_\odot$ range. Taking the mass[14] and velocity distribution into account indicates that the velocity impulse produced by one of the smaller stars is, on average, one-third of that caused by a more massive star. The smaller stars are, however, sufficiently more numerous so that the net perturbations are comparable. The frequency of encounters with the region of stable pro- and retrograde orbits is about 10 per 10^6 yr while for the present Oort cloud it is, depending on the assumed radius, 2–6 per 10^6 yr.

Comets spend most of the time near their aphelia where they are weakly bound and thus the outer regions of both clouds will be severely depleted in spite of continuous redistribution of comets by weak perturbations. It is possible that the early Oort cloud, whatever its origin was comparable in size to the volume of stability here described or, if it were initially smaller, it would have been spread by early perturbations. Later perturbations especially by molecular clouds[3,15,16] decreased the cloud to its present size with a roughly comparable number of prograde and retrograde comets. Such a sequence of events may have an important role in explaining the primordial bombardment of the Solar System. An estimate of the total number of comets in this early cloud and its subsequent changes is beyond the scope of this letter.

We thank V. Szebehely for valuable discussions. Supported in part by NASA grant NSG 7505 Sup 5.

Received 3 April; accepted 28 June 1984.

1. Oort, J. H. *Bull. astr. Inst. Neth.* **11**, 91–110 (1950).
2. Everhart, E. *Astr. J.* **73**, 1039–1052 (1968).
3. Weissman, P. R. in *Comets* (ed. Wilkening, L. L.) (University of Arizona Press, Tucson, 1982).
4. Bierman, L., Huebner, W. F. & Lust, Rh. *Proc. natn. Acad. Sci. U.S.A.* **80**, 5151–5155 (1983).
5. Chebotarev, G. A. *Soviet Astr. J.* **8**, 787–792 (1965), **10**, 341–344 (1966).
6. deVaucouleurs, G. *Astrophys. J.* **268**, 451–467 (1983).
7. Bahcall, J. N. *Astrophys. J.* **276**, 169–181 (1984).
8. Antonov, V. A. & Latyshev, I. N. *IAU Symp.* No. 45, 341–345 (1972).
9. Szebehely, V. *Theory of Orbits* (Academic, New York, 1967).
10. Keenan, D. W. & Innanen, K. A. *Astr. J.* **80**, 290–302 (1975).
11. Weissman, P. R. *Nature* **288**, 242–243 (1980).
12. Sekanina, Z., *Bull. astr. Inst. Czech.* **19**, 223–229 (1968).
13. Marsden, B. G. & Sekanina, Z. *Astr. J.* **78**, 1118–1124 (1973).
14. Scalo, J. M. *Fund. Cos. Phys.* (in the press).
15. Fernández, J. A. & Jockers, K. *Rep. Progr. Phys.* **46**, 665–772 (1983).
16. Napier, W. M. & Clube, V. M. *Nature* **282**, 455–459 (1979).

Emission of large hydrocarbons from frozen CH_4 by keV proton irradiation

A. E. de Vries*, R. Pedrys†, R. A. Haring*, A. Haring* & F. W. Saris*

* FOM Institute for Atomic and Molecular Physics, Kruislaan 407, 1098 SJ Amsterdam, The Netherlands
† Instytut Fizyki, Uniwersytet Jagiellonski, PL 30-059 Krakow, Poland

Ever since the first description of the synthesis of molecules by impinging protons on ices[1], the possibility of formation of various molecules on cold surfaces by particle radiation has been widely discussed[2–5]. Because fluxes of light ions with energies of ~1 keV AMU^{-1} exist in a wide variety of astrophysical sites[6] there has been a dispute over whether molecules in space are formed by such a process or by gaseous reactions[7]. We have recently studied sputtering of species by bombarding simple frozen gases such as water, carbon monoxide and ammonia with light ions[2]. With these substances, only rather simple molecules were found. However, when bombarding methane, we detected much larger molecules in the sputtered beam—hydrocarbons containing up to at least 13 atoms. We propose, therefore, that bombardment of frozen methane by keV protons may produce large molecules in the Solar system.

Frozen methane at 15 K was bombarded with 6-keV H_3^+ ions and the sputtered flux was analysed by mass spectrometry. The frozen layer had a thickness of ~10 μm (much larger than the range of the projectiles). The ion-beam flux was 50–100 μA cm^{-2}.

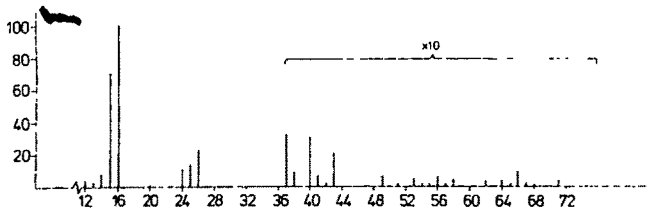

Fig. 1 Mass spectrum of the neutral species sputtered from frozen methane at 15 K by 6-keV H_2^+ ions.

H_2^+ ions were chosen instead of H^+ ions because of achievable ion beam intensity, and on entering the target surface, the H_2^+ ions dissociate at the first collision.

The kinetic energy of the sputtered species was determined by a time-of-flight method[2]. Sputtering of various hydrocarbons was inferred from the spectrum shown in Fig. 1. This gives the signals found in phase with the ion beam modulation, so that continuous background contributions, including those from evaporation, are subtracted.

The signals of sputtered species drastically decrease as the size of molecules increases, and are too low to detect when molecules contain more than five carbon atoms. On the other hand, the total sputtering yield in these experiments is about 1–10, that is, for every incoming ion a few neutral molecules are sputtered. The low fluxes of the larger molecules prohibited time-of-flight measurements, but this was possible for C_2H_2. We found a median energy of 0.063 eV, although 10% of the sputtered C_2H_2 had an energy of >0.28 eV. These energies are far in excess of what can be expected for a volatile substance at 15 K. In addition, the energy distribution is not maxwellian and agrees with that of a collision cascade mechanism[2].

After bombardment, a residue was found which was later warmed up and analysed by pyrolysis mass spectrometry[8]. The resulting spectrum, (Fig. 2) shows masses of up to about 170 indicating that the residue contains molecules with at least 12 carbon atoms. The technique used was the so-called 'open-system flash-pyrolysis mass spectrometry' in which the products from the pyrolysis immediately escape and cannot react with the substrate. Thus synthesis cannot take place but fragmentation clearly does. Note that during the initial warming up of the bombarded layer to room temperature, reactions may have occurred and, therefore, the results from the pyrolysis mass spectrometry only hint that larger molecules may be present in the bombarded sample.

In both the sputtered flux and the residue the largest molecules found were present in concentrations approaching the limit of the sensitivity of our measurements, and thus even larger molecules may have been formed and sputtered by a collisions-cascade mechanism. Obviously some polymerization takes place in the process, producing very large molecules. Polymerization of CH_4 may be caused by electrical discharges, UV light or MeV protons[9], and we conclude from the present measurements that large molecules are also formed by keV ions and infer that a considerable fraction of these is sputtered.

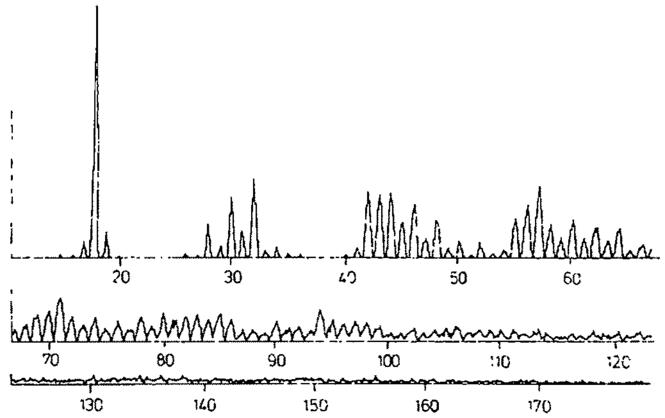

Fig. 2 Pyrolysis mass spectrum of the residue obtained from frozen CD_4 by bombardment with 6-keV H_2^+ ions after warming up to room temperature.

Note that such a process may occur on the most outer planet Pluto and its moon Charon which are covered with methane ice[10,11]. The escape velocity v is given by $v = (2GM/R)^{1/2}$ in which M, R and G are the mass and radius of the planet and G is the gravitation constant, 6.6732×10^{-11} N m^2 kg^{-2}. For Pluto $M = 1.13 \times 10^{22}$ kg and $R = 1{,}800$ km and the escape velocity becomes 917 m s^{-1} (<10% of that of the Earth). The escape energy is then 0.0043 eV AMU^{-1}. For Charon $M = 1.0 \times 10^{21}$ kg and $R = 800$ km. This gives an escape energy of <0.001 eV AMU^{-1}. Therefore, large molecules formed and sputtered from these small planets may turn up in the Solar System. From the above measurements we can infer that the total flux of sputtered molecules is of the same order of magnitude as the incident flux of the solar wind.

This work is sponsored by FOM with financial support by ZWO.

Received 21 March; accepted 18 July 1984.

1. Berger, R. *Proc. natn. Acad. Sci. U.S.A.* **47**, 1434–1436 (1961).
2. Haring, R. A., Haring, A., Klein, F. S., Kummel, A. C. & de Vries, A. E. *Nucl. Instrum. Meth.* **211**, 529–533 (1983).
3. Haring, R. A., Kolfschoten, A. W. & de Vries, A. E. *Nucl. Instrum. Meth.* (in the press).
4. Brown, W. L., Lanzerotti, L. J. & Johnson, R. E. *Science* **218**, 525–531 (1982).
5. Strazulla, G., Pirronello, V & Foti, G. *Astr. Astrophys.* **123**, 93–97 (1983).
6. Maurette, M. *Nucl. Instrum. Meth.* **132**, 579–586 (1976).
7. Wickramasinghe, N. C. in *Early Solar System Processes and the Present Solar System* (ed. Lal, D.) 122–139 (North Holland Amsterdam, 1980).
8. Meuzelaar, H. L. C., Haverkamp, J. & Hileman, F. D. *Techniques and Instrumentation in Analytical Chemistry* Vol. 3 (Elsevier, Amsterdam, 1982).
9. Strazulla, G., Calcagno, L. & Foti, G. *Mon. Not. R. astr. Soc.* **204**, 59P–62P (1983).
10. Arnold, S. J., Boksenberg, A. & Sargent, W. L. W. *Astrophys. J. Lett.* **234**, L159–L163 (1979).
11. Namba, G. *Zenit* **7**, 52–55 (1980).

Diffuse reflectance pulse radiolysis of opaque samples

F. Wilkinson*, C. J. Willsher*, P. Warwick*, E. J. Land† & F. A. P. Rushton†

* Department of Chemistry, Loughborough University of Technology, Loughborough, Leicestershire LE11 3TU, UK
† Paterson Laboratories, Christie Hospital and Holt Radium Institute, Manchester M20 9BX, UK

Flash photolysis and pulse radiolysis techniques[1] have contributed substantially to our understanding of the harmful and beneficial effects of radiation. The development of extremely short pulsed excitation sources means that time resolution is no longer a serious limitation to the application of these methods[2,3]. However, these methods have previously been restricted to transparent samples because changes in transmission of analysing light were measured following pulsed excitation. Recently[4–6], we have established that photochemical processes within opaque and highly scattering systems can be studied by observing changes in diffusely-reflected analysing light following laser excitation. Many of the most important radiation-induced processes involve non-transparent, heterogeneous systems, for example, most biological systems. We report here the first successful 'diffuse-reflectance pulse radiolysis' experiments in which we demonstrate that time-dependent absorption spectra of short-lived species can now be measured for opaque samples following pulse radiolysis.

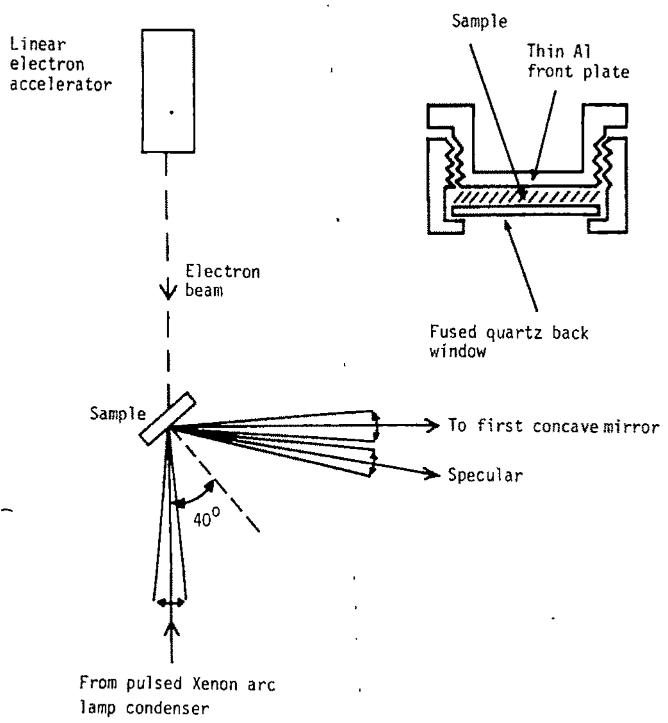

Fig. 1 Schematic diagram of the equipment used for studying diffuse reflectance pulse radiolysis of opaque samples. (Inset shows sample holder in more detail.) Diffusely reflected monitoring light diverging from the sample into a cone of solid angle 0.07 sr is imaged on to the entrance slit of a monochromator (outside the accelerator area at unit magnification) by means of two concave mirrors of 23-cm diameter and 77-cm focal length spaced about 10 m apart.

The pulse radiolysis apparatus has been described previously[7]. Typically 200 ns pulses of 10-MeV electrons were used which delivered doses of up to 100 Gy to the sample through a thin aluminium front plate. Analysing light was obtained from a pulsed xenon arc[8] which was triggered ~750 μs before the excitation pulse fired. This gave a steady reproducible intensity of analysing light which was reflected off the sample through the optically-transparent 'back' face of the irradiation sample holder (see Fig. 1). Collection of specular reflected light with angle of incidence equal to angle of reflection was avoided as far as possible as it contains little transient information. 10-MeV electrons in the excitation pulse are not strongly attenuated on passing through the opaque samples which typically had path lengths of ~1 mm. Thus, 'back' face analysis, which did not require major modification of the pulse radiolysis apparatus designed for normal transmission detection, proved successful (see Fig. 1). This contrasts with the situation when excitation is by pulses of light which are usually substantially attenuated, resulting in a much smaller penetrating depth. Thus, with light excitation, analysis of diffusely-reflected analysing light at the front irradiated surface is essential. The diffusely-reflected light before pulse radiolysis gives a perfect blank in these experiments. A Tektronix 7912 transient digitizer was used to capture the transient information which was then transferred to a minicomputer for analysis. Figure 2 shows a typical set of traces for pulsed radiolysis of microcrystals of benzil analysed at 510 nm. Trace *c* can be corrected for any observed emission, and, by making measurements at different wavelengths, time-dependent absorption spectra of short-lived species produced by pulsed ionizing radiation can be obtained.

The first experiments were performed with opaque samples of organic microcrystals which have already been shown to give transient intermediates in diffuse reflectance laser flash photolysis experiments. Diffuse reflectance pulse radiolysis of benzophenone and benzil give transient absorption spectra which have similar spectra and similar half lives to those obtained by laser flash photolysis[5,6]. Figure 3 shows a comparison of the transient absorption spectra for benzophenone observed from pulse radiolysis and laser photolysis. Phosphorescence decay following pulse radiolysis was also measured and differences were observed between the decay of the transient absorption and the phosphorescence in the case of benzil. This may mean that there is more than one transient absorption, possibly there is some contribution from the negative radical ion of this ketone which would be expected to absorb in the same region as the triplet state.

Several other samples were subjected to the technique and most gave weak transient absorption of <2%. Oxygen was not excluded from any of these samples as the transients observed when microcrystals of benzil and benzophenone are subjected to diffuse reflectance laser flash photolysis are not sensitive to gas phase oxygen. The transient spectrum obtained following pulse radiolysis for naphthalene crystals is shown in Fig. 4*a*.

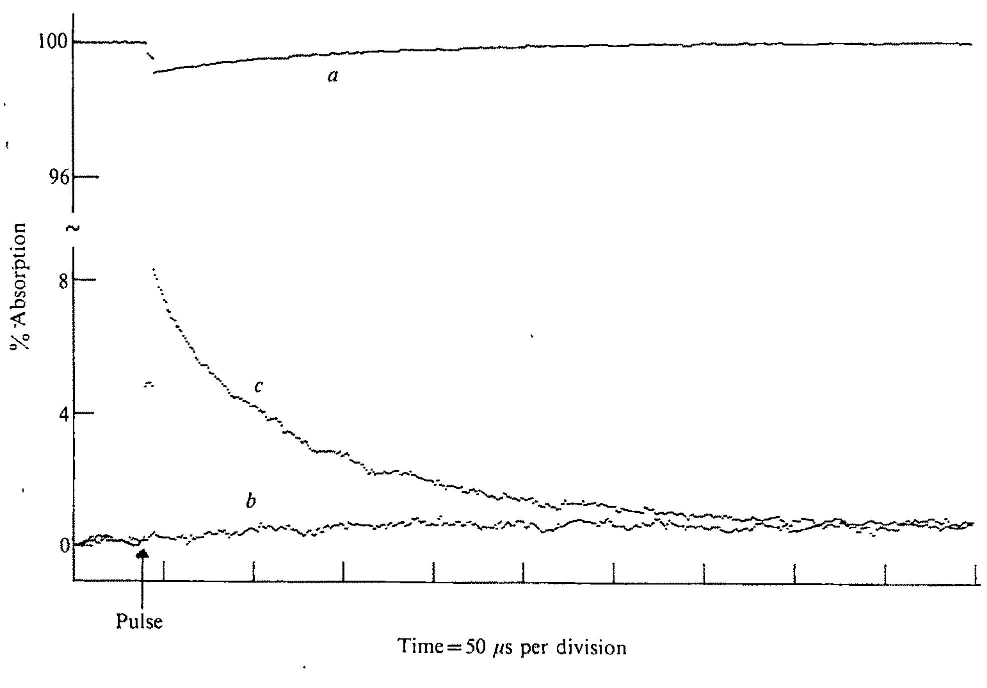

Fig. 2 Transient absorption of microcrystalline benzil, excited by 10-MeV electrons (200 ns pulse), monitored at 510 nm, as a function of time. (Sample thickness = 1 mm, dose ≈ 100 Gy, pulse duration ≈ 200 ns.) *a*, The signal observed following excitation in the absence of analysing light resulting from emission at the analysing wavelength. *b*, The diffusely reflected analysing light in the absence of excitation. *c*, The substantial transient absorption of diffusely reflected light following the pulsed electron excitation.

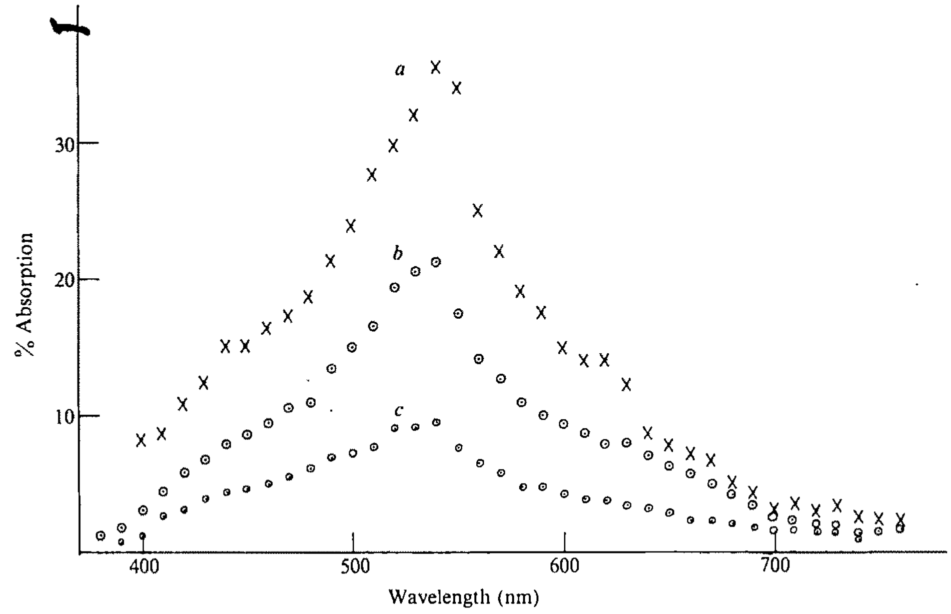

Fig. 3 Excited state absorption spectra of microcrystalline benzophenone. Sample thickness, 1 mm; dose ≈ 100 Gy; pulse duration ≈ 200 ns. *a*, From pulsed laser excitation at 354 nm (ref. 5). *b*, From electron excitation, 3 μs after the end of excitation. *c*, From electron excitation, 13 μs after the end of excitation.

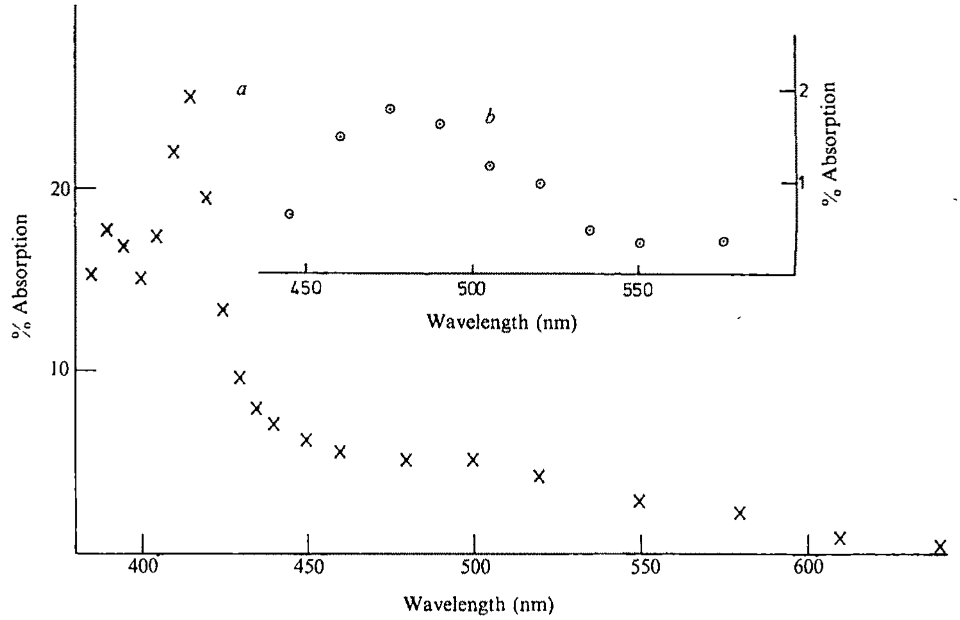

Fig. 4 *a*, Transient absorption spectrum of microcrystalline naphthalene, following pulse radiolysis ($t_{1/2} \approx 20$ μs; sample thickness = 1 mm; dose ≈ 80 Gy; pulse duration ≈ 200 ns). *b*, Transient absorption spectrum of bovine muscle tissue following pulsed radiolysis ($t_{1/2} \approx 20$ μs; sample thickness = 5 mm; dose ≈ 100 Gy; pulse duration ≈ 200 ns).

The absorption spectra in the range 380–440 nm shows strong similarities to the triplet–triplet absorption spectrum of naphthalene obtained in dilute solution using transmission flash photolysis[9]. We tentatively assign the transient absorption in this region to the triplet state of naphthalene. Note that quite a wide distribution of optical absorption path lengths is possible in different samples and that this should be considered in any interpretation of spectra or kinetics.

We stress that pulse radiolysis using diffusely reflected light for analysis extends considerably the range of systems that can be studied by this technique. Diffuse reflectance spectroscopy has been used to probe the effects of radiolysis on, for example, polycrystalline selenites[10], but we believe our work is the first to use diffusely-reflected light to monitor the decay of excited states produced by pulse radiolysis. We feel that this development has most potential for studies of biological systems which are non-transparent. To illustrate this, we have subjected a sample of bovine muscle tissue to this technique and observed the unassigned transient shown in Fig. 4*b*. We consider that our preliminary measurements provide an important step in helping to unravel the mechanism of radiation-induced processes in complicated biological systems and for non-transparent systems in general.

We thank the Cancer Research Campaign for financial support to E.J.L. and F.A.P.R., Loughborough University for support to C.J.W., and Dr J. P. Keene for helpful discussions.

Received 25 April; accepted 11 July 1984.

1. Bensasson, R. V., Land, E. J. & Truscott, T. G. *Flash Photolysis and Pulse Radiolysis: Contributions to the Chemistry and Biology of Medicine* (Pergamon, Oxford, 1983).
2. Porter, G. & West, M. A. *Techniques of Chemistry* Vol. 6, pt II (Wiley, New York, 1974).
3. Kobayashi, H. *et al. Radiat. phys. Chem.* **21**, 13–19 (1983).
4. Kessler, R. W. & Wilkinson, F. *JCS Faraday Trans. I*, **77**, 309–320 (1981).
5. Wilkinson, F. & Willsher, C. J. *Chem. phys. Lett.* **104**, 272–276 (1984).
6. Wilkinson, F. & Willsher, C. J. *Appl. Spectrosc.* (in the press).
7. Keene, J. P. *J. scient. Instrum.* **41**, 493–496 (1964).
8. Hodgson, B. W. & Keene, J. P. *Rev. scient. Instrum.* **43**, 493–496 (1972).
9. Porter, G. & Wilkinson, F. *Proc. R. Soc.* **264A**, 1–18 (1961).
10. Contineau, M. *Rev. Chim. Bucharest* **34**, 61—612 (1983).

Measurements of hydrogen peroxide in polar ice samples

A. Neftel*, P. Jacob† & D. Klockow†

* Physics Institute, University of Bern, Switzerland
† Department of Chemistry, University of Dortmund, FRG

Hydrogen peroxide, a powerful oxidant, is believed to be a key component in the oxidation of SO_2 to H_2SO_4 in clouds[1]. The first quantitative H_2O_2 measurements in snow, rain, hoarfrost and fog were reported in 1874 (ref. 2), however, systematic investigations of H_2O_2 concentrations in precipitation and hydrometeors began only a few years ago[3,4]. We report here measurements of hydrogen peroxide in polar ice samples. To our knowledge, chemically-reactive species have not been previously analysed in ice core samples. Our measurements show that H_2O_2 is a dominant trace compound present in clouds over remote and clean areas.

The cores from Greenland were drilled as part of the US–Danish–Swiss Greenland Ice Sheet Program. The North Central core, drilled in 1977, and the Dye 3 deep core drilled in 1979–81 were mechanically drilled and are in perfect condition. The Greenland sample series corresponded to a precipitation period of ~1 yr. The locations from which the samples were taken are listed in Table 1 together with their glaciological characteristics.

The analytical system is described in detail elsewhere[5]. Hydrogen peroxide is measured through the chemiluminescence radiation emitted during its reaction with bis-trichlorophenyloxalic ester (TCPO)[6]. Perylene is used as a fluorescing agent. Both the perylene and the TCPO are dissolved in purified acetone. The reaction between the H_2O_2 solution and the TCPO reagent (acetone to water ratio 3:1) takes place in a mixing chamber placed in fromt of a photomultiplier. The emission of the chemiluminescent reaction is linear with H_2O_2 concentration in the range between 0.5 p.p.b. (parts per 10^9) (w/w), detection limit and 30 p.p.m. (parts per 10^6) (w/w).

Because the reaction of hydrogen peroxide with TCPO strongly depends on the *p*H of the solution, the samples were adjusted to a *p*H of 8 using a borate buffer.

Ice cubes (2–5 cm³) were cut in a cold room (−20 °C) with a band saw, so that at least a 1 cm layer was removed from each surface. The cubes were cleaned with a Teflon brush and placed in polyethylene containers. The ice cubes were melted in the containers in a warm water bath (~40 °C). As soon as a whole cube was melted, a sample was taken, mixed with the buffer, and injected into the analytical system. To check whether the handling introduced any noticeable background contamination, ice cubes from a laboratory-grown pure single crystal, purified three times by zone melting, were analysed. The H_2O_2 concentration of such samples were below or close to the detection limit of 0.5 p.p.b.

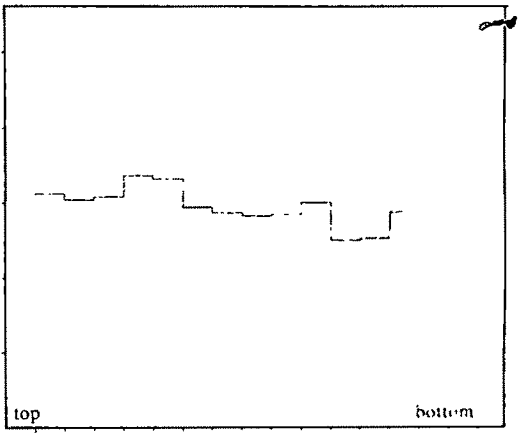

Fig. 1 H_2O_2 concentration along a 26-cm segment from North Central Greenland at a depth of 101 m below the surface. The ice is ~650 yr-old.

Table 1 also shows the measure of mean values of H_2O_2 concentrations with their standard deviation. Figures 1–3 show detailed records from the Dye 3 core and the North Central core.

At Dye 3, melted layers are formed almost every summer[7]. The occurrence of such melted layers may change the H_2O_2 concentration dramatically. In melted layers of the Dye 3 core, concentrations up to 400 p.p.b. H_2O_2 were found (Fig. 2). Figure 2 also shows the distribution of H_2O_2 across a single winter layer of the Dye 3 firn core. A few samples were also analysed from two cores from Antarctica (Byrd and South Pole). (The Byrd core was drilled in 1968–69 and the South Pole core in 1981–82 by the Polar Ice Core Office (PICO).

Because precipitation is stored in the frozen state in ice sheets, chemical trace substances are relatively well preserved and chemical reactions occur extremely slowly. H_2O_2 is produced in the gas phase by the reaction of two HO_2 radicals. The formation of HO_2 radicals in the clean atmosphere starts with the photolysis of O_3 producing O^1 (D), which further reacts with H_2O to form OH radicals[8]. The latter are extremely reactive and several reaction mechanisms, including hydrocarbons and CO as reactants, may lead to the production of HO_2.

A substantial amount of H_2O_2, found in cloud droplets, may have been produced in the liquid phase, due to dissolved OH and HO_2 radicals[9]. It is not known whether H_2O_2 is produced or destroyed at the surface of, or inside, snowflakes, either in clouds or on the ground after deposition.

A small amount of H_2O_2 in the ice could have been produced as a consequence of ionization processes caused by cosmic rays. To estimate an upper limit of this production for the South Pole

Table 1 Locations and glaciological characteristics of samples

Station	Geographical location	Mean annual temperature (°C)	Mean accumulation rate (cm water equiv. yr^{-1})	Measured samples	Depth below surface (m)	Age (yr BP)	Mean H_2O_2 concentration (µg H_2O_2 per kg ice)
Dye 3	65°11′ N 43°50′ W	−19.6	50	20	26	30	92 ± 76*
Dye 3	65°11′ N 43°50′ W	−19.6	50	16	85	115	103 ± 46*
Dye 3	65°11′ N 43°50′ W	−19.6	50	12	1,724	~9,000	28.9 ± 9.1
Dye 3	65°11′ N 43°50′ W	−19.6	50	6	1,830	~25,000	< 0.5
North central	74°37′ N 39°36′ W	−31.7	11	13	101	650	149 ± 15
Byrd	79°59′ S 120°01′ W	−28	16	3	297	1,300	8 ± 0.8
Byrd	79°59′ S 120°01′ W	−28	16	3	1,652	~22,000	2.8 ± 0.24
South Pole	90° S	−51	7	3	91	650	17.3 ± 1.0
South Pole	90° S	−51	7	3	160	1,600	11.6 ± 0.6
South Pole	90° S	−51	7	3	191	2,000	16.7 ± 1.6

* The standard deviation reflects the seasonal variation and melt layer influence (see Figs 2 and 3).

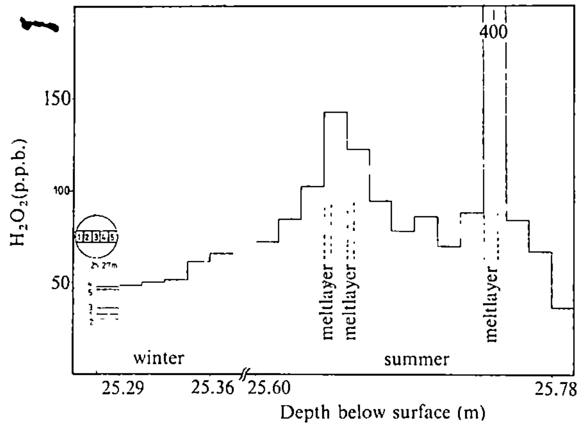

Fig. 2 H_2O_2 concentration in a 30-yr old firn segment from Dye 3 at a depth of 26 m below the surface including melt layers. Summer and winter layers were identified by visual stratigraphy.

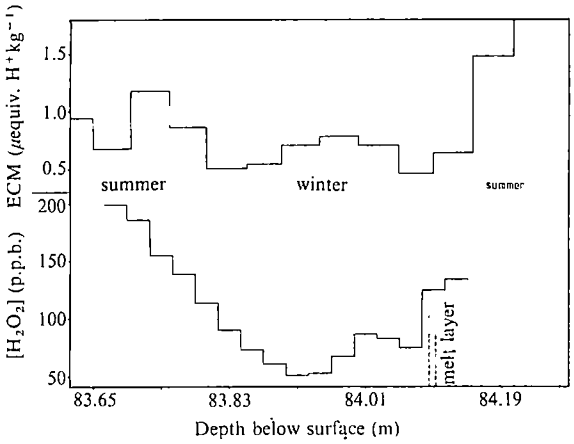

Fig. 3 H_2O_2 concentration and acidity in a 1-yr layer from Dye 3 at a depth of 85 m below the surface, corresponding to an age of 115 yr. Winter and summer layers were identified by the acidity and visual stratigraphy.

core, we assume an ion-pair production of 5×10^3 pairs $g^{-1} s^{-1}$ in the ice[10] and H_2O_2 generation of one molecule per ion pair. Furthermore, we assume that the cosmic ray flux is attenuated exponentially with a damping constant of 0.023 m^{-1} in the first 100 m water equivalent of the ice sheet. With this assumption, 5 p.p.b. H_2O_2 could have been built up in 1,500-yr ice from the South Pole. This crude approximation shows that such a mechanism may be of importance at the South Pole. It has little relevance for Greenland however, because here significantly larger H_2O_2 concentrations have been found in the ice cores.

H_2O_2 is one of the dominant trace compounds in the Greenland cores. In comparison, Table 2 shows mean concentrations of other impurities found in Greenland ice[11] and South Pole firn[12]. The Antarctic samples have a significantly lower H_2O_2 concentration. The annual H_2O_2 deposition rate at Dye 3 would, according to our results, be roughly 30 times higher than at South Pole. This ratio is clearly higher than the one observed for NO_3^- and SO_4^{2-}.

There are three possible causes for the lower H_2O_2 deposition rate at the South Pole:

(1) Transport of H_2O_2 or precursors from mid-latitude sources. Dye 3 is at a much lower latitude than the South Pole, and is meteorologically connected to the continental regions of America and Europe, whereas the whole Antarctic continent is shielded by the circumpolar vortex from lower latitudes.

(2) The stratospheric ozone input to the Southern Hemisphere is lower by a factor of about two[13]. The lower stratospheric–tropospheric air mass exchange in the Southern Hemisphere is also evident from measurements[14,15] of the cosmic ray produced radioisotopes ^7Be and ^{10}Be.

Table 2 Chemical impurities in natural polar ice

Species	Greenland ice sheet* (μmol kg^{-1})	South Pole† (μmol kg^{-1})
Cl^-	0.5	1.25
NO_3^-	1.0	1.44
SO_4^{2-}	0.25	0.75
H^+	1.2	3.37
Na^+	0.4	0.63
K^+, Mg^{2+}, Ca^{2+}	0.1	0.2
NH_4^+	0.3	0.16
H_2O_2‡	3.2	0.5

* Ref. 11.

† M. Legrand (personal communication), mean values from samples covering the time 1968–78.

‡ This paper.

(3) Snow formation and heterogeneous removal mechanisms may differ at South Pole and Dye 3, especially when the lower temperature at the South Pole is taken into account.

The findings, presented in Figs 2 and 3, may be explained by physical and air chemical processes, respectively. High H_2O_2 levels in melt-layers (Fig. 2) indicate that conditions change, if meltwater is present. However, the change of phase of water from the liquid to the solid state decreases the solubility of dissolved impurities by several orders of magnitude[16]. Liquid water in equilibrium with an atmospheric H_2O_2 concentration of 0.5 p.p.b. (v/v), which corresponds to a typical background value[9], would contain 500 p.p.b. (wt/wt) H_2O_2. During the freezing process, H_2O_2 will accumulate in the liquid phase adjacent to the freezing front and will gradually be captured in the ice matrix. Concentrations of H_2O_2 in previously melted layers will, therefore, depend on the mode of refreezing. In addition, any chemical reactions that occur while the water is in the liquid state, as well as increased H_2O_2 deposition during the summer, may also alter H_2O_2 concentrations.

The selected core segment from a depth of 83 m below the surface (Fig. 3) contains only a small melt layer. Nevertheless, the H_2O_2 concentration shows a clear variation, which we interpret as a seasonal variation with high H_2O_2 contents in the summer half year and low contents in the winter half year. The summer and winter layers, respectively, were identified by visual stratigraphy and electrical conductivity measurements (ECM), which give the total acidity in ice[17]. The ECM results show an almost perfect seasonal variation in the Dye 3 core[11]. Indeed, model calculations predict a seasonal variation of the H_2O_2 mixing ratio in the atmosphere for high latitudes, with a maximum in summer[18].

Sublimation and recrystallization smooth out such factors as seasonal variations in $\delta^{18}O$ during the earlier lifetime of the firn from stations with low snow accumulation rates, such as North Central[19]. Thus, we did not expect to see a seasonal variation of the H_2O_2 concentration in the North Central core, and this was confirmed by measurements (Fig. 1).

H_2O_2 is a reactive substance and it is not yet known whether chemical conversions occur in ice. Even if they proceed slowly, they could have affected the H_2O_2 concentration during the hundreds of years since snow formation. Samples from the Dye 3 core from 1,724 m below surface, corresponding to an age of 9,000 yr, gave a mean H_2O_2 concentration of 28.9 p.p.b. Ice samples from the same core with an age of 30,000 yr (ice from the last glaciation) showed H_2O_2 levels at or below the detection limit of 0.5 p.p.b. During the cold periods of the last glaciation, the dust content in the ice was 10–100 times higher than during the Holocene[11]. Perhaps dust was responsible for a catalytic destruction of the H_2O_2 during the snow formation. We cannot decide, however, whether these low concentrations are due to specific atmospheric conditions, or whether they reflect a slow decay of H_2O_2 in the natural ice sheet.

Our measurements show that chemically reactive species, such as H_2O_2, are conserved in polar ice samples. The observed concentrations are not surprising if one takes into account that measurements and model calculations predict similar mixing ratios in ambient air for HNO_3 and H_2O_2 (0.1–1 p.p.b.) and that both trace gases have comparable solubilities in water. If, therefore NO_3^- is found in ice cores, we can also expect H_2O_2 to be present. Although natural ice sheets seem to provide a record of the atmospheric chemical reactor, it is, however, not yet possible to establish any quantitative relationship between the H_2O_2 content of ice and that in the Arctic and Antarctic atmospheres. In the near future, we intend to investigate the effect of sample age on H_2O_2 concentrations to determine more precisely the interhemispheric differences.

We thank H. Oeschger for the opportunity to do this work and his continuing interest. D. Raynaud, R. Delmas and S. Penkett reviewed the manuscript and made valuable suggestions. C. Hammer provided the ECM results from the Dye 3 core segments. P. Warneck gave us much good advice. The development of the analytical system was supported by the Ministry of Science and Research, Nordrhein-Westfalen, FRG.

Received 12 March; accepted 13 June 1984.

1. Penkett, S. A., Jones, B. M. R., Brice, Y. A. & Eggleton, A. E. J. *Atmos. Envir.* **13**, 123–137 (1979).
2. Schöne E. *Berichte* **7**, 1693–1708 (1874).
3. Kok, G. L. *Atmos. Envir.* **14**, 653–656 (1980).
4. Zika, R., Saltzmann, E., Chameides, W. L. & Davis, D. D. *J. geophys. Res.* **87**, 5015–5017 (1982).
5. Klockow, D. & Jacob, P. *Proc. NATO Advanced Study Institute, Summer School on Chemistry of Multiphase Atmospheric Systems*, Corfu (in the press).
6. Scott, G. & Seitz, W. R. *Analyt. chim. Acta* **115**, 221–228 (1980).
7. Herron, M. M., Herron, S. L. & Langway, C. C. *Nature* **293**, 389–391 (1981).
8. Chameides, W. L. & Davis, D. D. *Chem. Engng News* **60**, 38–52 (1982).
9. Chameides, W. L. & Davis, D. D. *J. geophys. Res.* **87**, 4863–4877 (1982).
10. Lal, D. & Peters, B. *Handb. Phys.* XLVI/2, 551–612 (1967).
11. Hammer, C. U. *J. phys. Chem.* **87**, 4099–4103 (1983).
12. Legrand, M. & Delmas, R. J. *Atmos. Envir.* (in the press).
13. Fabian, P. & Pruchniewicz, P. G. *J. geophys. Res.* **85**, 2063–2073 (1977).
14. Raisbeck, G. M. *et al Nature* **292**, 825–826 (1981).
15. Beer, J. *et al. Radiocarbon* **25**, 269–278 (1983).
16. Neftel, A., Oeschger, H., Schwander, J. & Stauffer, B. *J. phys. Chem.* **87**, 4116–4120 (1983).
17. Neftel, A. *et al. Greenland Ice Sheet Program*, Philadelphia (American Geophysical Union Monogr., in the press).
18. Logan, J. A., Prather, M. J., Wofsy, S. C. & McElroy, M. B. *J. geophys. Res.* **86**, 7210–7254 (1981).
19. Johnsen, S. J. *IAHS Publ.* No. 118, 210–219 (1977).

Age difference between polar ice and the air trapped in its bubbles

J. Schwander & B. Stauffer

Physics Institute, University of Bern, CH-3012 Bern, Switzerland

Air entrapped in bubbles formed in cold ice has essentially the same composition as that of the atmosphere at the time of bubble formation. The analysis of dated ice samples therefore enables the history of atmospheric composition to be investigated.[1–3] The age of the entrapped air is, however, not the same as that of the surrounding ice because air bubbles only become isolated from the atmosphere during the transition from firn to ice. Typically the age of the ice at this transition is between 100 and 3,000 yr, depending mainly on firn temperature and snow accumulation rate. The mean age difference between ice and enclosed air, as well as the age distribution width for a given sample, are especially important for the investigation of the anthropogenic increase of CO_2 and trace gases in the atmosphere over the last centuries, and for the comparison of climatic parameters recorded in the ice with parameters recorded in the bubbles. For Siple Station (Antarctica), this age difference and age distribution width were deduced from the bubble volume measured as a function of depth. The values are 95 yr and 22 yr respectively.

In polar regions, snow is compacted to firn, which is connected to the atmosphere through a system of interconnected pores. The thickness of the firn layer is typically 50–120 m, depending on the temperature and snow accumulation rate. At the depth of the firn–ice transition, the pores are closed-off and individual bubbles are formed. The amount of enclosed air in firn as a function of depth has been measured previously by first removing and discarding the air from open pores, then melting the sample and measuring the amount of gas extracted during melting[4,5]. Two methods have been used to remove the air from the open pores. In the first, the container is evacuated with the ice sample inside; however, this technique carries the risk that some air from closed, but still fragile, bubbles may also be extracted. For the other method, the air in the open pores is displaced by slow immersion of the sample. In this case, however, some of the air from open but dead-ended channels will not be removed.

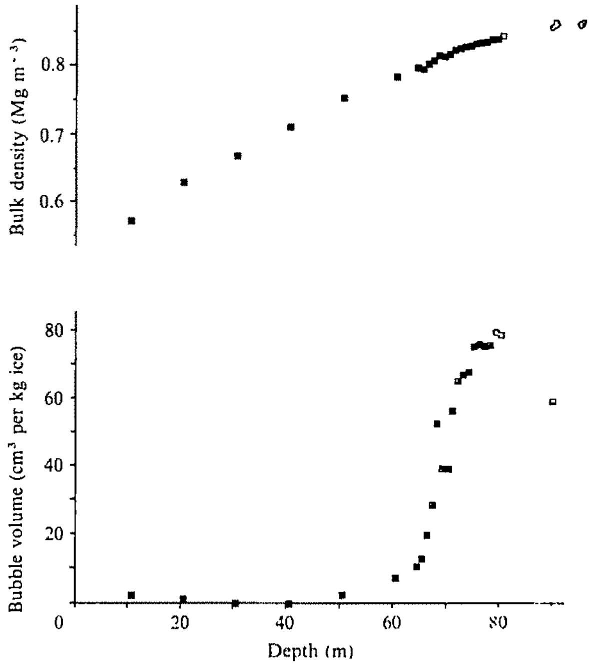

Fig. 1 Bulk density and bubble volume versus depth at Siple Station. Each point represents a 1 m average.

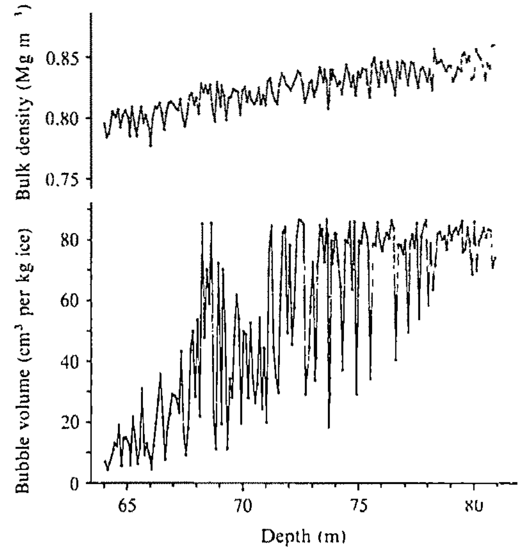

Fig. 2 Detailed bulk density and bubble volume profile of the Siple Station core at the firn–ice transition. Data points are connected by straight lines to illustrate their sequential order

To avoid the problems associated with removing the air first from open pores, we applied the classical method based on the law of Boyle–Mariotte for ideal gases: pressure × volume = constant at constant temperature. Samples are cut to a cylindrical shape of ~35 cm³. The bulk volume is measured with an

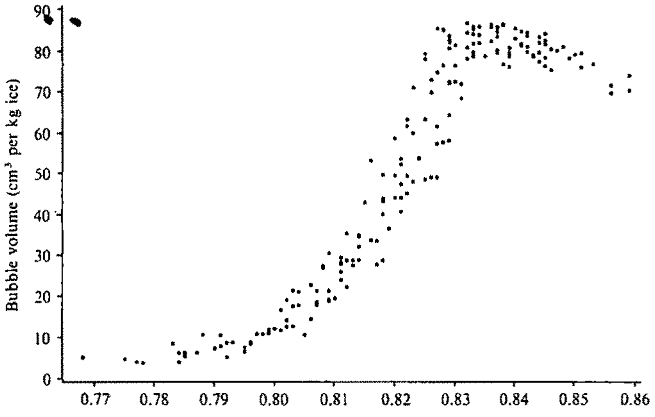

Fig. 3 Bubble volume versus bulk density from all samples between 60 and 81 m depth.

accuracy of 0.1%; the weight is measured with an absolute accuracy of 0.02 g. A calibrated cell containing the firn or ice sample at atmospheric pressure is isolated from the atmosphere and connected to a second, previously-evacuated cell. The pressure decrease, caused by the expansion at constant temperature, allows the volume of the closed bubbles to be calculated. We assumed a pure ice density of 0.919 Mg m^{-3} at −25 °C. There is no danger of disrupting closed but fragile bubbles as the pressure drop is small (5,000–7,000 Pa). The accuracy of the density and bubble volume measurement is ±0.002 Mg m^{-3} and ±2 cm^3 kg^{-1} respectively.

Measurements using this method were made on samples from an ice core drilled in November 1983 at Siple Station (75.92° S; 83.92° W). The main objective for drilling this 192 m core was to determine quantitatively the increase in CO_2 content of the atmosphere since 1800 by analysing air extracted from samples at different depths. The core from Siple Station is especially well suited for this analysis because this location combines a low mean-annual air temperature (−24 °C) with a rather high annual accumulation rate (0.5 Mg m^{-2}). Due to the low temperature, there is only a minimal risk, that the gas composition could be altered by meltwater[6]. A single meltlayer, of 10 mm thickness, was observed in the entire ice core. The high accumulation rate allows a good time resolution and the ice core was dated by counting the seasonal variations of the electrical conductivity of the ice[7]. The age error is <2 yr over the past 200 yr. CO_2 analyses on the Siple ice core will be carried out in the near future. We now focus on measurements which allow the age difference between ice and the enclosed air to be estimated.

All measurements on the ice core were done in a snow trench at South Pole Station[8], where the temperature was very stable (−25 °C). Density and bubble volume of 257 samples from 10 to 91 m depth below the 1982 snow surface were determined. Each point in Fig. 1 represents a 1-m section average, obtained from 10 measurements at 0.1-m intervals. Eighty per cent of the enclosure process takes place between the depths of 64 and 76 m. Only 10% of the final bubble volume is already enclosed above 64 m, and the remaining 10% is trapped below a depth of 76 m. Although at Siple Station (elevation 1,054 m) we expect a mean air content of the ice of 120 cm^3 (STP) kg^{-1} (ref. 5), the measured bubble volume is only 80 cm^3 kg^{-1} at the end of the pore close off (Fig. 1). We deduce a mean bubble pressure at this depth of 140 kPa. The pressure in the bubbles exceeds atmospheric pressure as soon as the bubbles are closed off due to the large local hydrostatic pressure. Detailed results for the depth interval 64–81 m are shown in Fig. 2. The cause of the variations in bubble volume and core density must be seasonal because these variations follow the pattern of the electrical conductivity measurements that distinguish between summer and winter deposits. The summer layers are characterized by low-density and low-bubble volume. The functional dependence between density and bubble volume is shown in Fig. 3 where only measurements between 60 m and 81 m are represented.

To calculate the mean age difference between the ice and the enclosed air, and the age distribution width, we have to assume an age of the air in the open pore volume at the transition zone which is connected to the atmosphere by many meters of permeable firn. ^{39}Ar measurements provide evidence that the air in the open pore volume is well mixed at least down to the beginning of the firn–ice transition[9]. Whether the air in the permeable layers sandwiched between almost impermeable layers is also well mixed with the atmopshere is uncertain. Assuming that the air is well mixed with the atmosphere in all permeable layers, then the mean difference between the age of the ice and the age of the air entrapped in its bubbles is about equal to the age of the ice at a depth where half of the final amount of air is closed off. For Siple Station the mean age difference obtained this way is 95 yr. The age distribution width, defined as the time interval during which the amount of entrapped air rises from 10 to 90% of the final value, is 22 yr. If impermeable layers such as the one from 72.0 to 72.5 m (Fig. 2) have a sealing effect, the mean age difference will be smaller, estimated to be ~90 yr; the age distribution width should also be smaller, although it is difficult to estimate by how much.

Only 10% of the bubble volume is formed at a bulk density of <0.795 Mg m^{-3}, while the final 10% is formed at densities above 0.83 Mg m^{-3}. Results from ice samples from Dye 3 (unpublished data) and North Central, Greenland[10], suggest that these values might be valid for most polar sites. A semi-

Table 1 Measured values for Siple Station, and calculated values for other important sites, of the difference between the age of the ice and the mean age of the air trapped in its bubbles as well as the age distribution width

Site	Location		Mean annual air temperature (°C)	Annual accumulation (m water equivalent)	Width of age distribution (yr)	Difference between mean age of ice and year (yr)
					Measured	
Siple	75°55′ S,	83°55′ W	−24	0.5	22	95
					Calculated	
Vostok	78°28′ S,	106°48′ E	−57	0.022	590	2,800
Dome C	74°39′ S,	124°10′ E	−53	0.036	370	1,700
Southpole	90°00′ S		−51	0.084	220	950
Byrd Station	79°59′ S,	120°01′ W	−28	0.16	54	240
North Central	74°37′ N,	39°36′ W	−31.7	0.11	76	350
Crête	71°07′ N,	37°19′ W	−30	0.265	46	200
Camp Century	77°11′ N,	61°09′ W	−24	0.34	31	130
Dye 3	65°11′ N,	43°50′ W	−19.6	0.5	22	90

empirical formula by Herron *et al.*[11] allows the density and age of the firn to be calculated as a function of depth if mean firn temperature, yearly accumulation rate, and snow density at the surface are known. We calculated the mean age difference between the enclosed air and ice, and the age distribution width using this formula for different stations, assuming that the air is of zero age in all open pores at any depth, and that 80% of the air is enclosed between the densities 0.795 and 0.83 Mg m^{-3}. The results are given in Table 1. The width of the age distribution limits the time resolution for the detection of variations of the past atmospheric composition obtained from ice core analysis.

If the air is well mixed, even in permeable layers sandwiched between impermeable ones, then it should be of different ages in neighbouring seasonal layers. In periods showing an increase in the concentration of an atmospheric component we would expect summer layers to show higher concentrations than winter layers because bubbles in the winter layers close off earlier than those in the summer layers. Measurements of such a seasonal modulation of CO_2 concentration during a period of industrial CO_2 proliferation should provide detailed information on the CO_2 increase and the mixing of the air in the permeable layers at the firn–ice transition.

This work has been supported by the US NSF and by the Swiss NSF. The ice core at Siple Station was drilled by the Polar Ice Coring Office, Nebraska.

Received 21 March; accepted 28 June 1984.

1. Delmas, R. J., Ascencio, J.-M. & Legrand, M. *Nature* **284**, 155–157 (1980).
2. Neftel, A., Oeschger, H., Schwander, J., Stauffer, B. & Zumbrunn, R. *Nature* **295**, 220–223 (1982).
3. Stauffer, B., Hofer, H., Oeschger, H., Schwander, J. & Siegenthaler, U. *Ann. Glaciol.* (in the press).
4. Langway, C. C. Jr *Physics of the Movement of the Ice*, Chamonix (IUGG Meet., IAHS Publ. No. 47, 336–349, 1958).
5. Raynaud, D. & Lebel, B. *Nature* **281**, 289–291 (1979).
6. Neftel, A., Oeschger, H., Schwander, J. & Stauffer, B. *J. phys. Chem.* **87**, 4116–4120 (1983).
7. Hammer, C. U. *J. Glaciol.* **25**, 359–372 (1980).
8. Stauffer, B. & Schwander, J. *Antarct. J.* **18**, No. 5 (1983).
9. Loosli, H. H. *Earth planet. Sci. Lett.* **63**, 51–62 (1983).
10. Stauffer, B. *Z. Gletscherk. Glazialgeol.* **17**, 17–56 (1981).
11. Herron, M. M. & Langway, C. C. *J. Glaciol.* **25**, 373–385 (1980).

Chronology of palaeoclimatic change at the end of the last glaciation

R. B. Stewart & V. E. Neall

Department of Soil Science, Massey University, Palmerston North, New Zealand

Analysis of sediments recorded in a piston core, located east of southern North Island, New Zealand, gives a detailed record of climate change at the end of the last glacial. Accumulation rates[1] of both detrital (quartz) and biological (carbonate and biogenic silica) components of the sediment are much higher during glacial than post-glacial time and they all show a synchronous, rapid decline at 14,700 yr BP. We attribute this to a decline in intensity of the strong glacial westerly winds in the New Zealand region as the polar winds contracted to their present latitudes[2–6]. The greatest rate of quartz accumulation occurs between 16,200 and 14,700 yr BP and is not matched by any change in carbonate or silica accumulation. We believe this reflects accelerated fluvial transport of detritus out of the mountain ranges and consequently increased aeolian dust transport before the decline of the polar westerlies.

Accumulation of greater amounts of quartz in deep-sea sediments during glacial periods than during times of warmer climate has been recognized[7,8] and been attributed to increased wind erosion from arid regions during those cold periods[7–11]. A marked change in global atmospheric circulation at the end of the last glaciation has also been inferred from changes in manganese abundance in east-equatorial Pacific deep-sea sediments[12] and from changes in the microparticle content of polar ice[13,14]. In the New Zealand region, differences in the distribution of quartz between surface sediments and those deposited ~18,000 yr BP have been used to infer that the westerly winds in the south-west Pacific were more intense and extended further north during the last glacial than they do today[6].

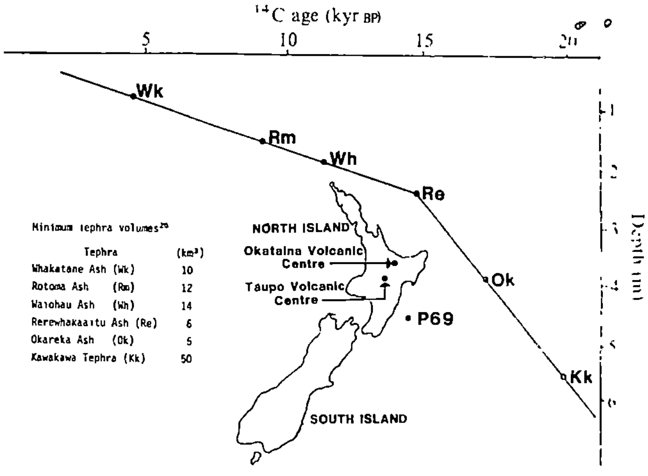

Fig. 1 Depth versus radiocarbon age of tephras in core P69 collected on cruise no 1059, Northland Plateau sediments, 17–31 March 1977 (from R/V *Tangaroa*), located at 40°23′ S, 177°59.8′ E. Mean pre-and post-Rerewhakaaitu Ash sedimentation rates are 594 mm kyr^{-1} and 156 mm kyr^{-1} respectively. Wk, Whakatane Ash (4,640±90 yr BP, NZ 3949A); Rm, Rotoma Ash[37] (9,120 ± 30 yr BP, NZ 1945A) Wh, Waiohau Ash (11,250±200 yr BP, NZ 568A); Re, Rerewhakaaitu Ash (14,700±200 yr BP, NZ 716A); Ok, Okareka Ash (estimated age of ~17,000 yr BP from terrestrial sequences); Kk, Kawakawa Tephra (19,850±310 yr BP, NZ 1056A). NZ numbers are New Zealand radiocarbon numbers. All tephras are from Okataina Volcanic Centre except Kawakawa Tephra, a Taupo Volcanic Centre eruptive.

As part of a wider project examining the accumulation of aerosolic dust in New Zealand we obtained a piston core from 2,195 m depth of hemipelagic sediment from a location 110 km east of southern North Island, New Zealand (Fig. 1). Quartz content in selected size fractions was determined by pyrosulphate fusion and hydrofluorsilicic acid digestion[15], carbonate was determined by a titrimetric method[16] and biogenic silica content by X-ray diffraction[17]. Time control is provided by six identifiable rhyolitic tephras[18,19] erupted from the central North Island during the late Quaternary, five of which have been reliably radiocarbon dated in terrestrial sequences[20] (Fig. 1).

Rerewhakaaitu Ash (14,700 yr BP) occurs in a stratigraphical position marking major changes in sedimentation in the core. The mean sedimentation rate before this age is 594 mm kyr^{-1}, markedly greater than that of the younger sediment at 150 mm kyr^{-1} (Fig. 1). As there is no evidence of major erosion or turbidites in the core, we believe that this change in sedimentation reflects the change in climatic conditions (especially a change in the westerly wind system) at the end of the last glaciation, influencing the supply of terrestrial sediment to the marine environment.

To elucidate the nature of this change in more detail the accumulation of three components of the sediment, one detrital (quartz) and two biological (carbonate and silica) were determined (Fig. 2). Quartz accumulation in both the 62–20 μm (representing loess) and 5–2 μm (representing aerosolic dust)[21] size fractions showed a consistent, abrupt decrease in accumulation at ~14,700 yr BP. Quartz accumulation in both size fractions shows a maximum between ~16,200 and 14,700 yr BP. It is generally recognized that the glacial maximum occurred at about 18,000 yr BP in New Zealand[22] and the period of maximum rate of quartz accumulation in the core clearly postdates this time. We interpret these data as showing that during and after the

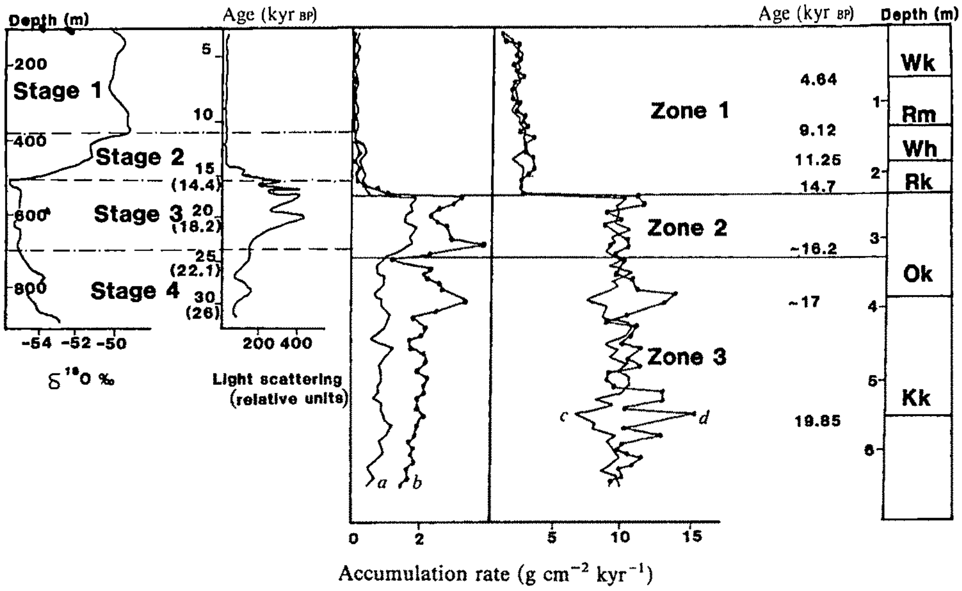

Fig. 2 Accumulation rates of: *a*, 5–2 μm quartz; *b*, 63–20 μm quartz; *c*, biogenic silica; *d*, carbonate. Tephra nomenclature is that described in Fig. 1. Zone 1 represents post-glacial sedimentation, zone 2 the period of accelerated erosion at the end of the last glaciation, and zone 3 the sedimentation during part of the last glaciation itself. The secondary maximum in 63–20-μm sized quartz is in part attributed to volcanic quartz from Okareka Ash, which occurs in this stratigraphical position. The oxygen isotope and microparticle (from light scattering in relative units) distribution curves are from Dome C ice core[14] for comparison.

glacial maximum, a strong westerly wind system existed across the southern North Island. During the period 16,200–14,700 yr BP (zone 2, Fig. 1) we postulate an increase in fluvial activity in the early part of the climatic amelioration following the glacial maximum. This would increase transportation of erosion detritus stored in the mountain ranges during the cold, dry, glacial climate, to form the extensive aggradational surfaces of the lowlands. The continuing strong westerlies would have caused substantial wind erosion from these aggradational surfaces and resulted in increased aeolian transport of detritus to the marine environment east of the southern North Island. At ~14,700 yr BP the contracting westerly wind system passed to the south of the region and the abrupt decrease in wind erosion and transport resulted in a large decrease in the detrital component of sedimentation at this time (zone 1, Fig. 1).

The change in wind regime at 14,700 yr BP is also correlated with palynological evidence from central North Island where forest expansion began after this time[23,24]. The change is also consistent with observations of the Rerewhakaaitu Ash overlying a widespread erosion break in terrestrial tephra sequences of central North Island[23–25] and the cessation of tephric loess accumulation.

This interpretation of the quartz accumulation data is supported by the changes in accumulation of the biological components. These also show an abrupt decrease in accumulation rate at ~14,700 yr BP (Fig. 2), indicating a marked change in the marine biological environment at this time. Biological productivity in the oceans is a function of nutrient content, particularly phosphorus[26,27], of surface waters and nutrient concentration is generally higher in cold polar and sub-polar waters. Upwelling of these nutrient-rich waters is predominantly caused by strong winds[27–31] and so patterns of biological detritus accumulation in the oceans are closely related to global wind patterns[17,27,29]. The abrupt change in accumulation rate in biological components in the core at 14,700 yr BP is thus interpreted as a response to the strong glacial westerly wind system decreasing in intensity and contracting poleward at the end of the last glaciation. As the factors which caused increased accumulation of quartz between the glacial maximum and 14,700 yr BP would have had little effect on biological activity in the marine environment, no change occurred in the glacial accumulation rate of the biological components until the decline of the glacial westerly wind system ~14,700 yr BP.

Our data are consistent with a climatic amelioration beginning at ~16,200 yr BP, corresponding to initiation of a global rise in sea level[32,33] following the glacial maximum. By ~14,700 yr BP the energy balance of the ocean–atmosphere system was such that the glacial circumpolar wind systems began to contract towards their present post-glacial latitudes. Evidence of a change in particle transport at about this time has been found in both Arctic and Antarctic ice cores, concomitant with evidence of a change from cooler to warmer climate shown by oxygen isotope ratios of ice from the same cores[13,14,34]. Comparison with the Dome C ice core[14] shows that our zone 1/2 boundary correlates closely with their isotope stage 2/3 boundary and a similar distribution in microparticle content occurs (Fig. 2). Thus our inferred palaeoclimatic history from core P69 appears to be consistent with evidence from both deep-sea sediments and ice cores, suggesting that these changes were global. Finally, the terrestrial climatic changes reported here for New Zealand are for a maritime environment which may have responded more rapidly to global climatic variation than continentally glaciated areas on which ice sheets persisted into Holocene time[35,36].

This research is part of a wider study into the provenance of quartz in soils and sediments in New Zealand and we thank the New Zealand Department of Scientific and Industrial Research for funding.

Received 13 December 1983; accepted 28 June 1984.

1. van Andel, Tj., H., Heath, G. R. & Moore, T. C. Jr *Geol. Soc. Am. Mem.* 143 (1975).
2. Climap Project Members *Science* **191**, 1131–1137 (1976).
3. Lamb, H. H. & Woodroffe, A. *Quat. Res.* **1**, 29–58 (1970).
4. Gardner, J. V. & Hays, J. D. *Geol. Soc. Am. Mem.* **145**, 221–246 (1976).
5. Gates, W. L. *Nature* **191**, 1138–1144 (1976).
6. Thiede, J. *Geology* **7**, 259–262 (1979).
7. Bowles, F. A. *Quat. Res.* **5**, 225–235 (1975).
8. Kolla, V., Biscaye, P. E. & Hanley, A. F. *Quat. Res.* **11**, 261–277 (1979).
9. Parkin, D. W. *Proc. R. Soc.* **A337**, 73–100 (1974).
10. Parkin, D. W. & Padgeham, R. C. *Proc. R. Soc.* **A346**, 245–260 (1975).
11. Janecek, T. R. & Rea, D. K. *Bull. geol. Soc. Am.* **94**, 730–738 (1983).
12. Berger, W. H., Finkel, R. C., Killingley, J. C. & Marchig, V. *Nature* **303**, 231–233 (1983).
13. Thompson, L. G., Hamilton, W. L. & Bull, C. *J. Glaciol.* **14**, 433–444 (1975).
14. Petit, J. R., Briat, M. & Royer, A. *Nature* **293**, 391–394 (1981).
15. Sridhar, K., Jackson, M. L. & Clayton, R. N. *Soil Sci. Am. Proc.* **39**, 1209–1213 (1975).
16. van der Linden, W. J. M. *Misc. Publ. N.Z. Oceanogr. Inst.* **39**, (1968).
17. Ellis, D. B. & Moore, T. C. J. *J. mar. Res.* **31**, 742–746 (1973).
18. Healy, J., Vucetich, C. G. & Pullar, W. A. *Bull. NZ. geol. Surv.* n.s. **73** (1964).
19. Kohn, B. P. *Lithos* **3**, 361–368 (1970).
20. Pullar, W. A. & Birrell, K. S. *N.Z. Soil Surv. Rep.* **1** (1973).
21. Jackson, M. L. *et al. Soil Sci.* **116**, 135–145 (1973).
22. Suggate, R. P. & Moar, N. T. *N.Z. J. Geol. Geophys.* **13**, 742–746 (1970).
23. McGlone, M. S. & Topping, W. W. *N.Z. J. Bot.* **11**, 283–290 (1973).
24. McGlone, M. S. and Topping, W. W. *N.Z. J. Bot.* **15**, 749–760 (1977).
25. Vucetich, C. G. *9th int. Congr. Soil Science Trans.* **4**, 121–130 (1968).
26. Broecker, W. S. in *Late Cenozoic Glacial Ages* (ed. Turekian, K. K.) 239–265 (Yale University Press, 1971).
27. Molina-Cruz, A. *Quat. Res.* **8**, 324–338 (1977).
28. Quinn, W. H. *Nature* **229**, 330–331 (1971).
29. Diester-Haass, L. *Quat. Res.* **6**, 299–314 (1976).
30. Sarntheim, M., Tetzlaff, G., Koopermann, B., Wolter, K. & Pflaumann, U. *Nature* **293**, 193–196 (1981).
31. Parkin, D. W. & Shackleton, N. J. *Nature* **245**, 455–457 (1973).
32. Shackleton, N. J. & Opdyke, N. D. *Quat. Res.* **3**, 39–55 (1973).
33. Bloom, A. L., Broecker, W. S., Chappell, J. M. A., Matthews, R. K. & Mesolella, K. J. *Quat. Res.* **4**, 185–205 (1974).
34. Fisher, D. A. *Quat. Res.* **11**, 299–305 (1979).
35. Saarnisto, M. *Quat. Res.* **4**, 316–339 (1974).
36. Kukla, G. J. *Earth Sci. Rev.* **13**, 307–374 (1977).
37. Nairn, I. A. thesis, Victoria Univ. Wellington (1981).

Turbulent motions may control phytoplankton photosynthesis in the upper ocean

M. R. Lewis*†, E. P. W. Horne†, J. J. Cullen†, N. S. Oakey‡ & T. Platt†

* Department of Biology, Dalhousie University, Halifax, Nova Scotia, Canada B3H 4J1
† Marine Ecology Laboratory, and ‡ Atlantic Oceanographic Laboratory, Bedford Institute of Oceanography, Dartmouth, Nova Scotia, Canada B2Y 4A2

In their natural environment, algal cells may experience large amplitude variations in incident light on time scales shorter than those associated with the reproductive rate. A major source of variability is due to vertical mixing of water masses: turbulence in the upper mixing layer of the ocean transports algae through a light field that decreases exponentially from the sea surface. Several attempts have been made to discover how the physiological adaptation of algae to fluctuating light[1–9] might affect the magnitude of marine primary production[10–16,17], but it has proved difficult to estimate the vertical mixing rate at sea, and hence the time scales of irradiance variability [18,19]. We recently succeeded, for the first time to our knowledge, in making direct measurement of rates of turbulent kinetic energy (TKE) dissipation, simultaneously with those of photoadaptation properties of natural phytoplankton populations. Dissipation of TKE in these experiments was a strong determinant of algal photosynthetic rate in the upper mixing layer; we conclude that the vertical mixing induced by turbulence to a large degree controls the photosynthetic performance of algae in nature.

The experiment attempted to test hypotheses generated by a recent theoretical analysis of algal photoadaptation in a mixing water column[20], where the significance of photoadaptation was evaluated by considering the time scales at which algal cells would be exposed to changing light intensity. As a first approximation, a simplified bulk view of the turbulent velocity field was taken. It is assumed that the algal cells remain uniformly distributed with depth. Then, any changes in a measurable index of photoadaptation (for example, maximum photosynthetic rate, *in vivo* fluorescence), at a particular depth, can be separated into two terms, one denoting physiological adaptation, and the other changes which result from turbulent fluid motion. As cells are transported in the vertical, irradiance incident on the cells varies. When the rate of photoadaptation is high relative to the rate of turbulence-induced light fluctuation, photoadaptation should produce variations in the photoadaptive property with depth. Conversely, when the rate of photoadaptation is low relative to that of turbulence, photadaptive variations in depth should be smoothed out by turbulence and consequently algal populations throughout the water column should be physiologically homogeneous. The physiological index, for a sample from a particular depth horizon, is an ensemble average of all cells present: it also contains (weighted) information about the recent light history of the cells. For fluid motions sufficiently rapid, samples taken anywhere in the mixing region should have the same average light history and therefore should be indistinguishable with respect to the magnitude of the physiological index. To test these hypotheses,a reliable and independent estimate of the rate of vertical mixing is required.

We therefore designed an experiment where the rate of turbulent mixing was determined simultaneously with the vertical distribution of photoadaptive indices. The experiment was carried out in Bedford Basin, a coastal marine inlet adjacent to the laboratory. Stations were occupied twice a day every 2–3 days for a one-month period during the spring. At each occupation samples were taken from the surface and bottom of a near surface mixing region distinguished from a temperature trace (Guildline SCTD) taken at time of sampling (Fig. 1). Maximum

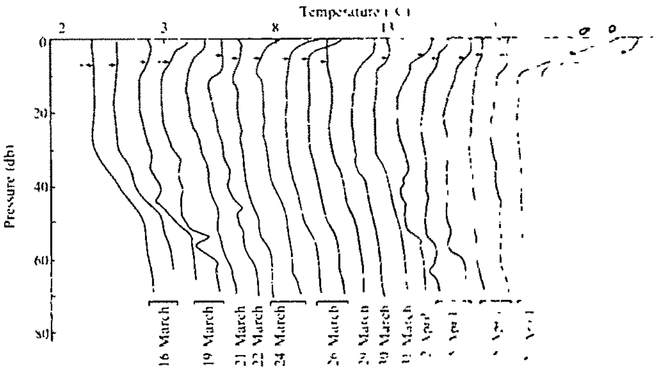

Fig. 1 Profiles of temperature during the study with the dates and sampling depth indicated. Profiles are offset by 1 °C. When two profiles are indicated for a single day, the first is a.m., the second is p.m.

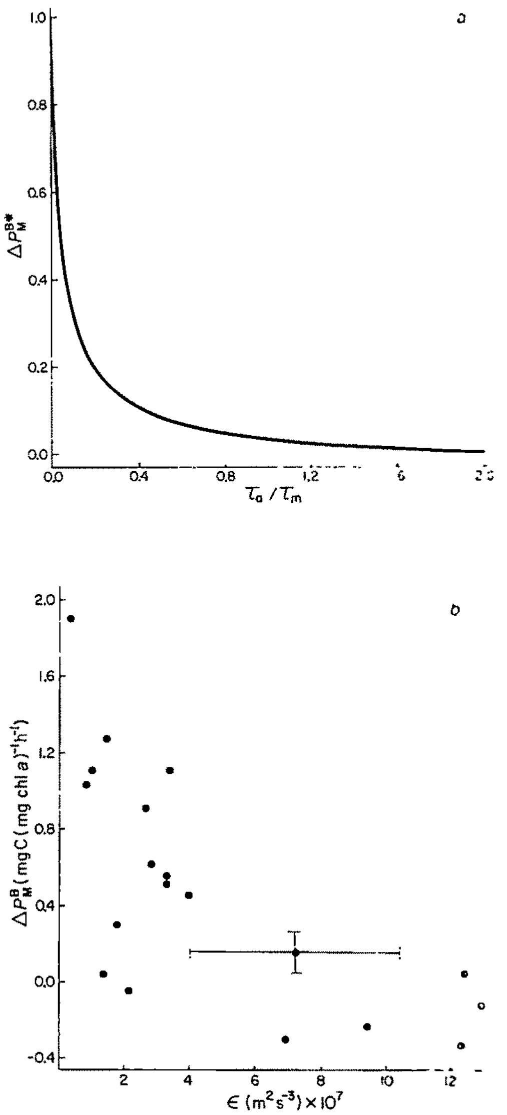

Fig. 2 *a*, Results from analytical solution[20]. ΔP_m^{B*} is the normalized difference between surface samples and those at the base of the mixing region. The irradiance gradient is the same as that in the field study. τ_a/τ_m is the ratio of the photoadaptation time scale to the mixing time scale. *b*, Measured differences between P_m^B at the surface and P_m^B at the base of the mixing region as a function of turbulent energy dissipation rate, ε. Error bars are ±1 s.d.

potential photosynthetic rate normalized to chlorophyll a, P^B_m, was determined by methods described previously[21,22] *In vivo* fluorescence per unit chlorophyll, a photoadaptive index with a rapid response to irradiance changes[23-25], was also measured after a 15-min dark adaptation time. Rates of TKE dissipation, $\varepsilon(m^2\,s^{-3})$, were determined from direct measurements of velocity shear microstructure[26-29] from the recently-developed microscale profiler, Octuprobe[28] according to,

$$\varepsilon = 7.5\nu\overline{\left(\frac{\partial u'}{\partial z}\right)^2} \qquad (2)$$

where $\overline{(\partial u'/\partial z)^2}$ is the averaged variance in turbulent velocity shear and ν is the kinematic viscosity. The numerical constant is a factor for isotropy. Values of ε over the depth interval 2–10 m were averaged over 6 or 7 realizations spanning 25 min. These values of ε were compared with differences between P^B_m and fluorescence parameters over the mixing region.

Results, shown in Fig. 2*b*, were consistent with the expectation of prior[20] theoretical analysis (Fig. 2*a*). At high TKE dissipation rates, little depth variation in P^B_m was observed; on days when energy dissipation rates were low, surface samples showed higher values of P^B_m (Fig. 2*b*). This strong inverse correlation between ΔP^B_m, which measures the physiological homogeneity of plankters over the mixing region, and ε, which is determined from dissipation scale fluctuations in velocity shear, does not result from an inconsistency of scales. The large-scale processes generating TKE may well be of the scale of the mixing region. Variations between days in the irradiance gradient were not significant. Order of magnitude mixing time scales to compare with those in Fig. 2*a* can be estimated from,

$$\tau_m = l^2 K_v^{-1} \approx 4 l^2 \varepsilon^{-1} N^2 \qquad (3)$$

where l is the depth of the mixing layer, K_v is the eddy diffusivity and N is the Brunt–Väisälä frequency[28,30-32]. Algal populations became physiologically more uniform throughout the mixing region as ε became larger. With $\varepsilon = 4\times10^{-7}\,m^2\,s^{-3}$ and with measured values of $l \approx 5$ m, and $N \approx 10^{-2}\,s^{-1}$, the corresponding mixing time scale is ≈ 10 h. This value is consistent with laboratory estimates of the photoadaptation time of P^B_m ($= \tau_a$; Fig. 2*a*) of 6–10 h (refs 9, 20). Some of the observed residual scatter could be due to other environmental factors such as temperature, nutrient supply and grazing (see ref. 19). The relationship in Fig. 2*b* would suggest that the dominant source of variation responsible for the observed difference in physiological performance is turbulence-induced fluctuations in light incident on the algal cell.

Few motile cells were observed; the dominant species was the diatom *Melosira*. Populations of motile cells could potentially resist the vertical displacement induced by turbulence. If the swimming velocity is $\bar{w}$, a 'swimming time scale' can be estimated as $l\bar{w}^{-1}$ and compared with τ_m to determine which vertical motion would dominate. For a typical swimming velocity[33] of the order of $10^{-4}\,m\,s^{-1}$, and the parameter values used here, ε would have to exceed $\approx 10^{-7}\,m^2\,s^{-3}$ for the mixing process to dominate, as it does here (Fig. 2*b*).

In-vivo fluorescence, when normalized to unit chlorophyll concentration, was less at the surface in the afternoon on all days except one—the day of highest measured dissipation. This was also consistent with our hypotheses; the time scale for variation in *in vivo*, chlorophyll-specific fluorescence on exposure to high light ($>100\,W\,m^{-2}$) is ≈ 1 h (refs 23–25), comparable with our highest estimate of $\tau_m \approx 1$h. The sea-surface irradiance (400–700 nm) varied between 100 and 400 $W\,m^{-2}$ at noon. The observation of decreased fluorescence yield for most days at the surface is therefore consistent with a mixing time scale for these days greater that ~ 1 h.

We conclude that turbulent fluid motion in the upper layer of the ocean controls to a large degree the physiological performance of algal cells. Only when energy dissipation rates are high can algal populations in the upper 'mixed' layer be considered physiologically homogeneous. It also appears from these data that the rate of vertical mixing in the upper layer may be inferred from the vertical distributions of appropriate algal physiological indicators.

We thank Mr B. Irwin, Mr P. Dickie, and Mr M. Hodgson for field assistance and Dr K. H. Mann for critical reading of the manuscript. M.R.L. was supported by the Natural Sciences and Engineering Research Council (Canada) and by a Dalhousie University Fellowship.

Received 6 February; accepted 26 June 1984.

1. Steeman Nielsen, E. & Jorgensen, E. G. *Physiol. Pl.* **21,** 647–654 (1968).
2. Beardall J. & Morris, I. *Mar. Biol.* **37,** 377–387 (1976).
3. Marra, J. *Mar. Biol.* **46,** 191–202 (1978).
4. Harris G. P. *Can. J. Fish. aquat. Sci.* **37,** 877–900 (1980).
5. Marra, J. *Mar. Biol. Lett.* **1,** 175–183 (1980).
6. Falkowski, P. G. in *Primary Production in the Sea* (ed. Falkowski, P. G.) 99–119 (Plenum, New York, 1980).
7. Falkowski, P. G. *J. Plankton Res.* **3,** 203–216 (1981).
8. Rivkin, R. B., Seliger, H. H., Swift, E. & Biggley, W. H. *Mar. Biol.* **68,** 181–191 (1982).
9. Berseneva, G. P., Krupatkina, D. K. & Sergeeva, L. M. *Ėkologiya* **3,** 12–16 (1982).
10. Harris, G. P. & Lott, J. N. A. *J. Fish. Res. Bd Can.* **30,** 1771–1778 (1973).
11. Jewson D. H. & Wood, R. B. *Verh. int. Verein. theor. angew. Limnol.* **19,** 1037–1044 (1975).
12. Kremer, J. N. & Nixon, S. W. *A Coastal Marine Ecosytem: Simulation and Analysis* (Springer, Berlin, 1978).
13. Marra, J. *Mar. Biol.* **46,** 203–208 (1978).
14. Platt, T. & Gallegos, C. L. in *Primary Production in the Sea* (ed. Falkowski, P. G.) 339–362 (Plenum, New York, 1980).
15. Falkowski, P. G. & Wirick, C. D. *Mar. Biol.* **65,** 69–75 (1981).
16. Gallegos C. L. & Platt, T. *Deep-Sea Res.* **29,** 65–76 (1982).
17. Falkowski, P. G. & Wirick, C. D. *Mar. Biol.* **65,** 69–75 (1981).
18. Denman K. L. & Gargett; A. *Limnol. Oceanogr.* **28,** 801–815 (1983).
19. Falkowski, P. G. *J. mar. Res.* **41,** 215–237 (1983).
20. Lewis, M. R., Cullen, J. J. & Platt, T. *Mar. Ecol. Prog. Ser.* **15,** 141–149 (1984).
21. Platt, T., Gallegos, C. L. & Harrison, W. G. *J. mar. Res.* **38,** 687–701 (1980).
22. Lewis, M. R. & Smith, J. C. *Mar. Ecol. Prog. Ser.* **13,** 99–102 (1983).
23. Cullen, J. J. & Renger, E. H. *Mar. Biol.* **53,** 13–20 (1979).
24. Vincent, W. F. *J. Phycol.* **15,** 429–434 (1979).
25. Vincent, W. F. *J. Phycol.* **16,** 568–577 (1980).
26. Osborn, T. R. *J. phys. Oceanogr.* **4,** 109–115 (1974).
27. Osborn, T. R. *J. geophys. Res.* **83,** 2939–2957 (1978).
28. Oakey, N. S. *J. phys. Oceanogr.* **12,** 256–271 (1982).
29. Oakey, N. S. & Elliott, J. A. *J. phys. Oceanog.* **12,** 171–185 (1982).
30. Lilly, D. K., Waco, D. E. & Adelfang, S. I. *J. appl. Met.* **13,** 488–493 (1974).
31. Weinstock, J. *J. atmos. Sci.* **35,** 1022–1027 (1978).
32. Osborn, T. R. *J. phys. Oceanogr.* **10,** 83–89 (1980).
33. Cullen, J. J. & Horrigan, S. G. *Mar. Biol.* **62,** 81–89 (1981).

Nitrate leaching from grassland

J. C. Ryden*, P. R. Ball† & E. A. Garwood*

* The Grassland Research Institute, Hurley, Maidenhead,
Berkshire SL6 5LR, UK
† Grassland Division, DSIR, Private Bag, Palmerston North,
New Zealand

Increased awareness of the economic importance of losses of nitrogen (N) from agricultural land, together with the recognition that nitrate in drinking water is potentially detrimental to human health, have stimulated research on nitrate leaching[1-4]. Various reports[5-7] have suggested that the leaching of nitrate from arable land is the major source of nitrate to water supplies in east and south-east England. In contrast, leaching from grassland is thought to be small[5,8-10]. However, this conclusion has been based largely on studies of leaching below cut swards, which exclude the effect of ruminants (cattle and sheep) on nitrate loss. This effect is likely to be substantial as <20% of the input of N to grassland systems is recovered in products of the ruminant animal[11]. Our study demonstrates that the amount of nitrate leached below a grass sward grazed by cattle was 5.6 times greater than that leached below a comparable cut sward and exceeded the losses normally observed from arable land.

The extent of leaching was assessed by measuring the nitrate content of samples of soil or chalk removed in successive 0.33 m increments to a depth of 8 m below an experimental site at Hurley, Berkshire, UK. Management of the site is summarized in Table 1. The site was on a loam of the Frilsham series[12] overlying Upper Chalk which occurs at a variable depth between 0.7 and 1.3 m. Some properties of the top soil (0–20 cm) are:

Table 1 Management of the experimental site

Date	Plot 1 Cut ryegrass sward	Plot 2 Grazed ryegrass sward
January 1974–April 1976	Fodder maize* which received cattle slurry and farm-yard manure; annual input of N was estimated to be 450 kg ha^{-1}	
April 1976–April 1977	Year during which the swards (each 0.123 ha) described below were established	
April 1977–December 1982	Cut perennial ryegrass† sward to which 420 kg N ha^{-1} as ammonia nitrate was applied annually. The sward was cut once very 4 weeks during the season April to October	Grazed perennial ryegrass† sward to which 420 kg N ha^{-1} as ammonium nitrate was applied annually. The sward was grazed rotationally (1 week in 4, April to October) by yearling steers. Average stocking rate was 9.3 head ha^{-1}
December 1982–present	Swards ploughed and planted to spring barley‡ (April 1983) and winter wheat§ (September 1983). A total of 80 kg N ha^{-1} was applied in 1983	

* *Zea mays* L.; † *Lolium perenne* L.; ‡ *Triticum aestivum* L.; § *Hordeum vulgare* L.

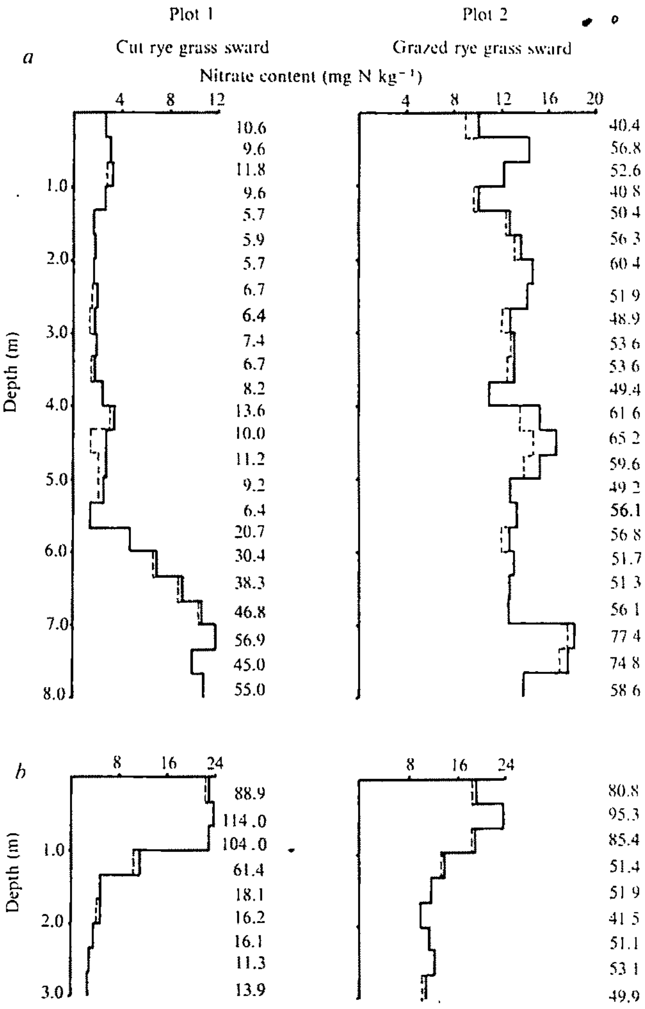

Fig. 1 Nitrate content (mg N kg^{-1}) of samples from successive depths below cut and grazed ryegrass swards (details in Table 1); *a*, before the swards were ploughed in December 1982; *b*, 12 months after ploughing and one crop of spring barley. The numbers alongside each profile are the nitrate concentrations in solution (mg N l^{-1}) at each depth. Values are the arithmetic means of five observations at each depth. The dashed lines indicate the geometric mean where this differed from the corresponding arithmetic mean by more than 0.3 mg N kg^{-1}. The mean values of nitrate content within the 0–1 m depth of each profile derived from the five replicates obtained in the present study were not significantly different from those derived from up to 39 samples removed from a similar depth in a preliminary study[19]. Samples for nitrate analysis were obtained using a power-driven flighted auger drill (Mobil Drilling Co., Indianpolis, USA) mounted on a Land Rover. Nitrate was extracted within 2 h of collection by blending 100-g sub-samples with 200 ml 2 M KCl. The supernatant solution was recovered after 2 h by filtration (Whatman No. 1) and its content of nitrate plus nitrite was determined using an automated colorimetric procedure based on the Griess-Ilosvay Cd-reduction method[21]. Nitrate comprised >99% of the nitrate plus nitrite content of extracts. The water content of samples was determined gravimetrically by drying in a forced air oven at 90 °C for 4 days.

*p*H, 6.0–6.5; bulk density, 1,250 kg m^{-3}; organic carbon, 2.2–2.4%; total N, 0.25–0.28% (ref. 13). The bulk density of the sub-soil to a depth of ~1 m was 1,410 kg m^{-3} while that of chalk at depths >1 m ranged from 1,370 to 1,610 kg m^{-3} with a mean of 1,530 kg m^{-3} for 10 samples. The mean annual precipitation and potential evapotranspiration since 1974 were 694 and 500 mm, respectively[14,15].

The nitrate content of samples removed from below the grazed sward to a depth of ~6 m in December 1982, was consistently greater than that in samples below the cut sward to the same depth (Fig. 1*a*). Although Macduff and White[16] have shown a log-normal distribution of nitrate content in soil, little evidence for this was found for the samples of chalk analysed in the present study. There were only small differences between the arithmetic and geometric means of nitrate content in the five replicates from each depth (Fig. 1 and Table 2). Consequently, a normal distribution was assumed during interpretation of the data obtained.

The differences between the mean nitrate contents of each profile to a depth of 6 m were significant at $P<0.01$; the 95% confidence limits on each mean value were generally in the range ±20–30% (Table 2). The nitrate contents of samples from successive depths to 6 m within a particular profile were not significantly different ($P>0.05$). At depths >6 m, the mean nitrate contents below the cut sward increased to values in the range 8.5–12.0 mg N kg^{-1} and were not significantly different from those observed at the same depths below the grazed swards ($P>0.05$).

Between April 1976 and December 1982, a total of 2,155 mm drainage was measured from lysimeters containing profiles of the Frilsham soil and installed within 500 m of the experimental site[14]. Based on a mean volumetric water content of 0.38 (95% confidence limits ±0.011) in the samples removed and assuming simple piston flow, it is estimated that the 1976–77 leaching front associated with the first drainage season following establishment of the experimental swards should have reached a depth between 5.5 and 5.8 m. It was at about this depth that the nitrate content below the cut sward increased to values similar to those observed below the grazed sward. Thus, the similarity in nitrate content below both swards at depths >6 m apparently reflected the uniformity in management of the site before April 1976, when substantial amounts of waste from winter-housed cattle were applied (Table 1).

The average annual loss of nitrate from the experimental swards can be estimated by relating the mean nitrate content of samples from depths <5 m to the bulk density of material removed and to an estimate of the annual rate of water movement through the profile. Based on the above considerations, the rate of water movement between 1976 and 1982 was ~0.8 m yr^{-1}, a value similar to others derived in studies at sites overlying chalk in south-east England[6,10]. Hence, the average amounts of nitrate leached (nitrate content × bulk density × 8 × 10^{-3}) were 29 and 162 kg N ha^{-1} yr^{-1} for the cut and grazed swards, respectively. Nitrate leaching associated with the return of cattle slurry and farmyard manure during 1974 and 1975 was ~152 kg N ha^{-1} yr^{-1} based on the mean nitrate content of samples from below 6 m.

A substantial increase in the nitrate content of the upper 1.3 m of each profile was observed in December 1983, 12 months after

Table 2 Typical data for the nitrate content of samples from selected depth intervals within the profiles of nitrate content (Fig. 1) below cut and grazed swards

Depth interval (m)	Range	Arithmetic mean (mg N kg^{-1})	s.e.m.	Geometric mean
Cut ryegrass		**December 1982**		
0.33–0.67	1.3–5.1	3.3	0.63	3.0
3.00–3.33	1.1–2.8	2.0	0.35	1.9
7.00–7.33	9.7–15.4	13.1	1.09	12.9
		December 1983		
0.33–0.67	21.8–25.9	24.1	1.71	24.0
2.33–2.67	2.8–3.6	3.2	0.29	3.3
Grazed ryegrass		**December 1982**		
1.00–1.33	9.1–17.4	12.6	1.68	12.2
3.67–4.00	8.8–14.7	10.6	1.06	10.5
7.33–7.67	10.2–20.2	17.2	1.81	16.7
		December 1983		
0.33–0.67	21.4–25.7	23.4	1.69	23.4
2.33–2.67	7.9–12.5	10.5	2.14	10.3

the experimental site was ploughed and cropped with spring barley (Fig. 1*b*; Table 1). Mean nitrate contents in the top metre of each profile ranged from 19.4 to 24.0 mg N kg^{-1} dry soil, but differences within this depth and between profiles were not significant and did not reflect the differences in previous management. A discontinuity in the nitrate content of each profile occurred between 1.0 and 1.3 m, an observation in broad agreement with the estimated rate of water movement through the profiles. Although the nitrate front had spread into the upper part of the second metre, probably due to above average rainfall during spring 1983, nitrate contents below this depth were not significantly different from those measured in the corresponding profiles before ploughing (Fig. 1*a*). As 138 kg N ha^{-1} were removed in harvested grain and straw in August 1983, the bulk densities and nitrate contents of the samples removed indicate that between 275 and 310 kg N ha^{-1} in excess of crop requirements was mineralized and nitrified during the first 12 months following ploughing. A further 50 kg N ha^{-1} was present as NH_4^+ at the time of sampling. Much of this inorganic N is expected to be leached below 1 m during the 1983–84 drainage season.

The nitrate concentration in the water moving within each profile can be calculated from the nitrate contents (Fig. 1) and water contents (0.23–0.32 wt/wt) of the samples removed. Concentrations in water draining below the cut sward were in the range 5.4–13.3 mg N l^{-1}, and were above the 'guide level' (5.7 mg N l^{-1}) but generally below the maximum (11.3 mg N l^{-1}) set by the European Community[17] for water for human consumption. Concentrations of nitrate in water draining below: (1) the grazed sward; (2) the experimental area when slurry and farmyard manure were applied; and (3) both plots after they were ploughed, greatly exceeded the upper limit of the range 11.3–22.6 mg N l^{-1} set by the World Health Organisation as 'acceptable'[18].

The present study has shown that substantial amounts of nitrate can be leached from intensively farmed grassland as well as when grassland is ploughed in a ley–arable system. The most striking feature is the effect of ruminant production on nitrate leaching. The annual loss of nitrate from the grazed grass sward was 5.6 times greater than that below the comparable cut sward, despite a common input of fertilizer N and defoliation frequency. The enhanced nitrate movement below the grazed sward can be attributed mainly to the return in urine and dung of as much as 90% of the N in the herbage consumed by cattle[11]. The effect of this is illustrated by the data in Table 3. At the end of the grazing season in October 1982, the mean nitrate content of soil below urine- and dung-affected areas of pasture was 3.2–7.7 times greater than that observed during random sampling across the grazed sward. Additional inorganic N was present as NH_4^+ at this time, much of which had been nitrified by the time the profile was sampled in December at the onset of the drainage season (Fig. 1 and ref. 19). The small amount of residual inorganic N below the cut sward reflected the removal of at least 75% of the applied N in the harvested herbage. However, the cutting and conservation of herbage, and its subsequent use as feed, merely serves to delay the loss of nitrate that can occur after the disposal of slurry and farm-yard manure from winter-housed cattle (Fig. 1*a* and ref. 20).

The effect of ruminant production on the N cycle has received only limited attention in much of the recent work on the use of N in agricultural production[1,5]. The present study and other reports[21–23] show that this effect is substantial, particularly in intensive systems. The amount of fertilizer N applied to the swards used in the present study is typical of the amounts applied to intensively farmed grassland in north-west Europe[24,25]. In England and Wales, 37% of the total area of grass leys now receives >200 kg N ha^{-1} yr^{-1}, with 5% receiving >400 kg N ha^{-1} (ref. 26); responses in animal production have been recorded for inputs up to 600 kg N ha^{-1} (R. D. Baker, personal communication). The data indicate that as the management of grassland is intensified, the amounts of nitrate leached are likely to equal or exceed the range observed for continual arable production (40–100 kg N ha^{-1} yr^{-1}, refs 10 and 27), the losses being greatly accentuated by ruminant production.

Table 3 Nitrate and ammonium contents of soil (0–30 cm) removed from below the cut and grazed swards at the end of the grazing season in October 1982

Sampling position	Number of samples	Nitrate content* Arithmetic mean (mg N kg^{-1} dry soil)	s.e.m.	Geometric mean	s.e.m.†	Ammonium content* Arithmetic mean (mg N kg^{-1} dry soil)	s.e.m.	Geometric mean	s.e.m.†
At random across cut sward	15	2.2	0.29	2.0	1.72–2.22	2.2	0.25	2.0	1.75–2.18
At random across grazed sward	15	7.5	2.23	5.6	4.64–6.63	4.4	2.23	2.2	1.69–2.83
Below urine-affected areas	8	53.5	14.79	43.8	37.11–51.7	56.3	12.56	41.7	33.25–52.25
Below dung-affected areas	8	26.2	8.22	17.8	12.58–25.23	15.1	3.76	10.4	7.09–15.18

* Although the arithmetic and geometric means of the nitrate and ammonium contents of soil below the grazed sward differed by a factor of 1.3–2.0, this was reduced to 1.1–1.2 when individual contents of each form of N were summed for each replicate sample and the mean values of total inorganic N calculated. Hence, the distribution of total N content in October was similar to that of nitrate in December by which time much of the ammonium had been nitrified (see Fig. 1 and ref. 19).

† Lower and upper values on the geometric mean.

We thank J. E. McNeill for technical assistance, K. C. Tyson and D. H. Roberts for help in managing the experimental site and M. S. Dhanoa for advice on the statistical treatment of data. This work was conducted while P.R.B. was a visiting research worker at the Grassland Research Institute and partly supported by the National Research Advisory Council (NZ). The Grassland Research Institute is financed through the Agricultural and Food Research Council, London, and the work was commissioned in part by the Ministry of Agriculture, Fisheries and Food.

Received 13 April; accepted 11 July 1984.

1. Stewart, W. D. P. & Rosswall, T. *The Nitrogen Cycle* (The Royal Society, London, 1982).
2. Cooke, G. W. *Phil. Trans. R. Soc.* B281, 231–241 (1977).
3. Magee, P. N. *Ambio* 6, 123–125 (1977).
4. Frazer, P. & Chilvers, C. *Sci. Total Envir.* 18, 103–116 (1981).
5. *The Nitrogen Cycle of the United Kingdom, A Study Group Report* (The Royal Society, London, 1983).
6. Young, C. P. & Gray, E. M. *Nitrate in Groundwater—the Distribution of Nitrate in the Chalk and Traissic Sandstone Aquifers* (Tech. Rep. No. TR 69, The Water Research Centre, Marlow, 1978).
7. Wilkinson, W. B. & Green, L. A. *Phil. Trans. R. Soc.* B296, 459–475 (1982).
8. Tomlinson, T. E. *Outlook Agric.* 6, 272–277 (1971).
9. Dowdell, R. J. & Webster, C. P. *J. Soil Sci.* 31, 65–75 (1980).
10. Foster, S. S. D., Cripps, A. C. & Smith-Carrington, A. *Phil. Trans R. Soc. Lond.* B296, 477–489 (1982).
11. Henzell, E. F. & Ross, P. J. in *Chemistry and Biochemistry of Herbage* Vol. 2 (eds Butler, G. W. & Bailey, R. W.) 227–246 (Academic, London, 1973).
12. Jarvis, M. G., Hazelden, J. & Mackney, D. *Soils of Berkshire* (Soil Survey of England and Wales, Harpenden, 1979).
13. Ryden, J. C. & Dawson, K. P. *J. Sci. Food Agric.* 33, 1197–1206 (1982).
14. *A Reps. The Grassland Res. Inst.* (1974–1982).
15. Garwood, E. A. & Tyson, K. C. *J. agric. Sci., Camb.* 80, 303–312 (1973).
16. Macduff, J. H. & White, R. E. *Pl. Soil* 76, 35–47 (1984).
17. *Council Directive on the Quality of Water for Human Consumption Official J.* No. 80/778 EEC L229, 11 (European Economic Community, 1980).
18. *European Standards for Drinking Water* 2nd edn (World Health Organisation, Copenhagen, 1970).
19. Ball, P. R. & Ryden, J. C. *Pl. Soil* 76, 23–33 (1984).
20. Vetter, H. & Steffens, G. in *Nitrogen Losses and Surface Run-off from Landspreading of Manures* (ed. Brogan, J. C.) 251–269 (Nijhoff/Junk, The Hague, 1981).
21. Hendriksen, A. & Selmer-Olsen, A. R. *Analyst* 95, 514–518 (1970).
22. Field, T. R. O. & Ball, P. R. *Proc. N.Z. Grassld Ass.* 43, 64–69 (1982).
23. Ball, P. R. & Keeney, D. R. *Proc. 14th int. Grassld Congr.*, Lexington, 342–344 (Westview Press, Boulder, Colorado, 1983).
24. Van der Meer, H. G. *Proc. 9th Eur. Grassld Fed. Meet.*, Reading, 61–68 (The British Grassland Society, Hurley, 1983).
25. Gasser, J. K. R. *Phil. Trans. R. Soc.* B296, 303–314 (1982).
26. Church, B. M. *Rothamsted Experimental Station Rep. for 1982* Part II, 161–168 (Rothmansted Experimental Station, Harpenden, 1983).
27. Dowdell, R. J., Webster, C. P., Mercer, E. R. & Hill, D. *Agricultural Research Council Letcombe Lab. A. Rep., 1979* 40–42 (1980).

A pseudo α-helix from poly(α-isobutyl-L-aspartate), a nylon-3 derivative

J. M. Fernández-Santín, J. Aymamí, A. Rodríguez-Galán, S. Muñoz-Guerra & J. A. Subirana

Unidad de Química Macromolecular del Consejo Superior de Investigaciones Científicas, Escuela T. S. de Ingenieros Industriales de Barcelona, Diagonal 647, Barcelona 08028, Spain

Derivatives of nylon-3, with the general formula given in Fig. 1, crystallize as extended chains, producing sheets similar to those found in polypeptides in the β-conformation[1–3]. Nylon-3 itself (R=H, poly-β-alanine) crystallizes as extended chains[4]. However, given the similarity of the chemical structure, we decided to search for conformations related to the α-helix in this type of compounds. We show here that the nylon-3 derivative poly(α-isobutyl-L-aspartate) can adopt a helical structure similar to an α-helix. The turn has 3.25 residues, equicalent to 13 main chain atoms, whereas the α-helix has 10.8 atoms per turn. This is the first time that a helical structure has been observed in a polyamide, other than in the conventional polypeptides and proteins.

Poly(α-isobutyl-L-aspartate) was prepared using the method described by Yuki *et al.*[3]. A stretched fibre of this compound gave the X-ray diffraction pattern shown in Fig. 2 which can be

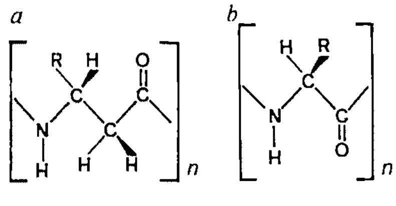

Fig. 1 Comparison of a segment of a nylon-3 derivative of the type described here (*a*) with a peptide unit in a protein (*b*). In *a*, $R{=}COOCH_2CH(CH_3)_2$. The lateral group R is on the opposite side to that in proteins, as it would be in polypeptide chains prepared from D-amino acids. The polymer was obtained by polycondensation of the pentachlorophenyl ester of α-isobutyl-L-aspartate hydrobromide according to Yuki *et al.*[3]. Its intrinsic viscosity is 0.57 dl g^{-1} in dichloroacetic acid at 25° which corresponds to a molecular weight of 90,000 if the equation for poly(γ-benzyl-*L*-glutamate) is applied[6].

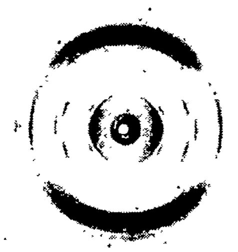

Fig. 2 X-ray diffraction pattern of a fibre of poly(α-isobutyl-L-aspartate) stretched from a chloroform solution. The stretching direction is on the meridian. Equatorial reflections correspond to an hexagonal unit cell with $a = 13.50$ Å. This crystallographic system provides additional evidence for a helical structure, because an extended structure should not pack in the hexagonal system. The first and fourth layer lines are clearly visible in the picture, with spacings of 19.9 and 4.98 Å respectively, which indicate a pitch for the helix of 4.98 Å. The structure contains 13 monomer units in four turns of the helix.

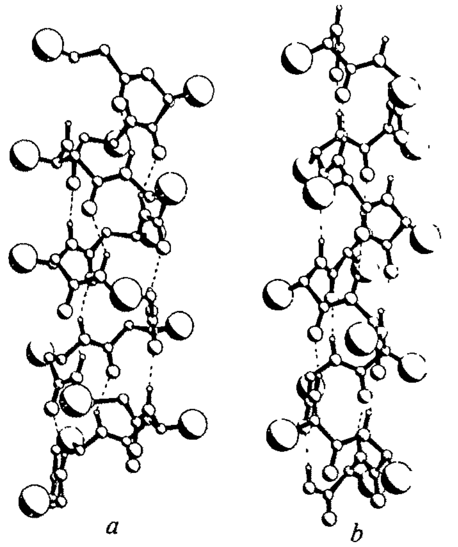

Fig. 3 Comparison between the left-handed helix observed in poly(α-isobutyl-L-aspartate) (*a*) and the conventional α-helix (*b*), constructed in this case with D-amino acids for a more adequate comparison. The larger spheres indicate the side chains. The smallest spheres correspond to the hydrogen atoms involved in hydrogen bonds, which are indicated as dotted lines. The rest of the hydrogen atoms are not shown. The model was built and refined using linked-atom-least-squares methodology[7].

Table 1 Cylindrical atomic coordinates of a residue in the helical conformation of poly(α-isobutyl-L-aspartate)

z (Å)	r (Å)	ϕ (deg)	z (Å)
O	2.54	−35.8	0.81
C′	2.28	−29.6	1.99
N	2.14	3.4	2.39
H	2.11	11.1	3.35
Cα	2.70	26.3	1.42
Cβ	2.72	59.1	1.59
C1 (R)	4.2	24.4	1.66
O1 (R)	5.06	27.1	0.83
O2 (R)	4.46	19.5	2.90
C2 (R)	5.60	9.6	2.90
C3 (R)	5.49	−5.6	2.46
C4 (R)	6.89	−8.0	1.87
C5 (R)	5.33	−15.5	3.68

Helix parameters: unit height $h = 1.53$ Å; unit twist = 110.8°; pitch, 4.98 Å. r, ϕ and z are the cylindrical coordinates.

interpreted as a helix. The main argument in favour of such interpretation is that a weak layer line is observed with a spacing of 19.9 Å, together with a strong layer line at 4.98 Å. The first spacing corresponds to the true repeat of the structure, whereas the 4.98-Å spacing corresponds to the pitch of the helix. There should be a whole number of units in the 19.9-Å spacing. Model building indicates that there are 3.25 units in a complete turn of the helix and 13 units in the true repeat of four turns. Additional support for this interpretation comes from the hexagonal packing system found, which is typical of helical structures. The calculated density for such structure is 1.19, which is in reasonable agreement with the measured density of 1.17.

A model of the suggested structure was built and its coordinates are given in Table 1. It is shown in Fig. 3 together with the conventional α helix found in polypeptides. The following conclusions can be made from such a comparison: (1) The α helix has 10.8 main chain atoms per turn whereas the helix described here has 13. (2) The orientation of the hydrogen bonds is the same in both helices, so that they both have a polar structure. (3) To achieve such orientation, the nylon-3 derivatives maintain in the helix a conformation similar to that found in the extended chain, whereas in the α-helix there is a considerable rotation around the N–C and C–C bonds of the main chain so that consecutive peptide units have the same orientation. (4) The orientation of the side group with respect to the main chain in poly(α-isobutyl-L-aspartate) is similar to that found in a left-handed α-helix built from D-amino acids, in fact, our calculations show that there are fewer steric hindrances in a left-handed rather than a right-handed helix. (5) The average radius of the main chain atoms in the helix we have described is 2.4 Å, a value significantly larger than that found in the α-helix (1.8 Å), as it is apparent from Fig. 3.

Our studies show, therefore that it is possible to obtain conformations similar to the α-helix in nylon-3 derivatives. In fact, given the higher degree of flexibility provided by the additional carbon atom in the main chain, it is likely that other conformations (similar to either ω or π helices[5]) may be found in these compounds. To our knowledge it is the first time that a helical conformation has been found in a nylon derivative.

Received 29 May; accepted 29 June 1984.

1. Bestian, H. *Angew. Chem. Int. Edn.* **7**, 278–285 (1968).
2. Schmidt, E. *Angew. Makromolek. Chem.* **14**, 185–202 (1970).
3. Yuki, H., Okamoto, Y., Taketani, Y., Tsubota, T. & Marubayashi, Y. *J. Polym. Sci. Polym. Chem.* **16**, 2237–2251 (1978).
4. Masamoto, J., Sasaguri, K., Ohizumi, Ch. & Kobayashi, H. *J. Polym. Sci.* A-2, **8**, 1703–1711 (1970).
5. Colonna-Cesari, F., Premilat, S., Heitz, F., Spach, G. & Lotz, B. *Macromolecules* **10**, 1284–1288 (1977).
6. Doty, P., Bradbury, J. H. & Holtzer, A. M. *J. Am. chem. Soc.* **78**, 947 (1956).
7. Campbell-Smith, P. J. & Arnott, S. *Acta crystallogr.* **A34**, 3–11 (1978).

Replacement of oak forest with pine in the Himalaya affects the nitrogen cycle

J. S. Singh, Y. S. Rawat & O. P. Chaturvedi

Department of Botany, Kumaun University, Naini Tal 263 002, India

Pine and oak are the two predominant evergreen forests in the central and western Himalaya between altitudes 1,200 and 2,200 m. The pine is a light-demanding, fire-adapted but fire-promoting species. The surface fires averaging once every 2 or 3 years cause substantial nitrogen losses in pine forest. Pine forest naturally occurs on the driest and rockiest slopes, and has spread greatly under the influence of cutting and burning, replacing oak forest in vast areas. Oak forest is non-inflammable but has suffered a good deal from fire spreading from the pine forest[1]. Deforestation has also accounted for loss of oak forest[1–3], and although the replacement of oak by pine is common[1,2], the reverse has not been observed. Our studies indicate that the greater nutrient-conserving ability of pine and the creation of a nitrogen shortage makes it difficult for oak to re-invade areas occupied by pine[4–8].

The pine (*Pinus roxburghii* Sarg.) forest was studied on four sites and the oak (*Quercus leucotrichophora* A. Camus & *Q. floribunda* Lindl.) forest on three sites, between 1,300 and 2,100 m altitude, 29°24′–29°37′ N lat. and 79°28′–79°38′ E long. The annual rainfall is 1,160–2,298 mm, and mean annual temperature 13–18 °C. All sites have mature (60–200-yr old) forests with uneven-aged trees. Soil in the pine forest is residue from chlorite–sericite schists and micaceous quartzites, weakly podzolic (*p*H 5.7), and sandy loam of composition 15.2% clay, 18.3% silt, 66.5% sand, 2.28% organic carbon and 0.18% total nitrogen. Oak forest soil is residual brown earth (*p*H 6.0), derived from limestone, quartzite and shales, and sandy loam (sand 76%, silt 13% and clay 11%) with 4.51% organic carbon and 0.51% N.

Biomass was estimated using allometric equations, and the density and diameter of trees. Net production was calculated from diameter increments and litter fall. One-fifth of the leaf fall was assumed to be equal to fine root mortality[9], and this was added to the estimate of net production. All plant components were analysed for nitrogen and phosphorous. Gross uptake was calculated by multiplying the net production of different components by their respective nutrient concentration. The amounts of N and P transferred to the forest floor were estimated from litter fall and its nutrient concentration, and from canopy leaching. Standard error ranged between 3 and 6% of the mean values. The differences in nutrient concentration and dry weight of mature live and freshly senescent leaves were used to calculate the per cent withdrawal of N and P.

Dry matter, and the amounts of N and P for the two forests are given in Table 1. Dry weight of the standing vegetation in the oak forest was 1.8 times and N 3 times that of the pine forest. The amount of P was roughly similar. Soil (to a depth of 20 cm) under oak forest had 1.5 times as much N as in pine forest. The C:N ratio of oak soil was 8.5 and of pine soil 14.

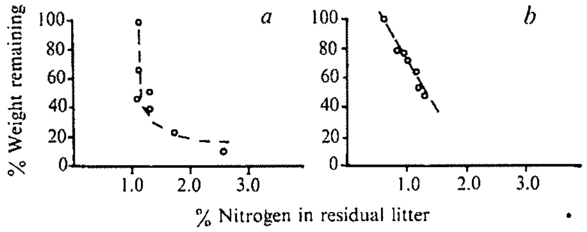

Fig. 1 Relationship between per cent weight remaining and N concentration of residual leaf litter after different time intervals during a year. *a*, Oak (*Q. leucotrichophora*) leaf litter enclosed in litter bags and placed on the forest floor of an oak forest; *b*, pine leaf litter enclosed in litter bag and placed on the forest floor of a pine forest.

Table 1 Dry matter and N and P abundances for the tree layer of pine and oak forests

	Pine forest			Oak forest		
	Dry matter	N	P	Dry matter	N	P
Compartment pools (tonne ha^{-1})						
Vegetation						
Foliage	7.40	0.149	0.012	13.90	0.285	0.012
Branch	33.50	0.254	0.031	134.20*	1.571	0.065
Bole	131.10	0.656	0.092	153.40	0.966	0.046
Root	38.50	0.047	0.010	75.60	0.477	0.012
Total	210.50†	1.106	0.145	377.10	3.299	0.135
Litter	10.62	0.131	0.011	5.70	0.094	0.004
Soil (to 20 cm)	—	3.964	0.218†	—	5.819	0.186‡
Total	221.12	5.201	0.374	382.80	9.212	0.325
Accumulation in net production (tonne ha^{-1} yr^{-1})						
Foliage	4.67	0.087	0.007	5.06	0.093	0.006
Branch	3.72	0.026	0.003	4.19	0.052	0.002
Bole	5.50	0.027	0.004	3.52	0.022	0.001
Root	2.81	0.003	0.006	2.33	0.018	0.0007
Total	16.70	0.143	0.920	15.10	0.185	0.010
Reabsorption before senescence (tonne ha^{-1} yr^{-1})						
Foliage	—	0.045	0.004	—	0.012	0.0005
Wood	—	0.008	0.001	—	0.006	0.0005
Total	—	0.053	0.005	—	0.018	0.0010
Net uptake from soil (tonne ha^{-1} yr^{-1})	—	0.091	0.010	—	0.167	0.009
Return (tonne ha^{1} yr^{-1})						
Leaf litter	4.66	0.044	0.004	4.75	0.079	0.005
Wood litter§	2.05	0.010	0.001	1.38	0.014	0.001
Removal from canopy in through fall	—	0.004	0.0006	—	0.005	0.0004
Removal from canopy in stem flow	—	0.00006	0.00003	—	0.0001	0.0001
Root mortality	0.94	0.0009	0.0002	0.95	0.0076	0.0005
Total	7.65	0.060	0.006	7.08	0.107	0.007
Retention in vegetation compartments (tonne ha^{-1} yr^{-1})	9.05	0.031	0.004	8.02	0.060	0.002
Ratios						
Reabsorption : accumulation	—	0.37	0.33	—	0.10	0.11
Return : vegetation pool	0.04	0.05	0.04	0.02	0.03	0.06
Litter : litter fall	1.58	2.40	2.10	0.93	1.00	0.61

* Reproductive biomass was weighed with twigs and values are included in branch components.

† Cones in pine average 0.300 tonne dry wt ha^{-1}, 0.008 tonne N ha^{-1} and 0.0007 tonne P ha^{-1}.

‡ Available P.

§ Includes reproductive litter.

Of the total N and P in the system, pine vegetation had, respectively, 22 and 40%, and oak vegetation 37 and 41%.

Net production was 8% of the tree layer biomass for the pine forest and 4% for the oak forest. Gross uptake of nitrogen was higher for the oak forest.

Substantial quantities of N and P were reabsorbed from old leaves before abscission in pine. Thus, 37% and 33% of gross uptake of N and P, respectively, were derived from nutrients reused from previous years in pine compared with 10% N and 11% P in oak. For foliage alone, 51% N and 52% P were reused for production of new leaves in pine, but 13.2% N and 8.5% P in oak. The withdrawal of nutrients before abscission maintains a relatively mobile pool within the living biomass of the ecosystem, and allows the plant to use the same unit of nutrient to build successively new leaves or plant parts[10,11]. Increased internal redistribution of nutrients is considered to be an adaptation to impoverished soils[12–15].

The net uptake of N and P from the soil is lower than the nutrient pool accumulated in net production (gross uptake) by the amount reused from previous years[16]. Net uptake in oak was relatively low for P, but for N it was considerably higher than in pine.

The return of N and P amounted to 3–6% of the quantities in the vegetation pool. The dry matter : nitrogen ratio of leaf litter fall was 105 in pine and 60 in oak. Thus the efficiency of litter production per unit of N was greater in pine compared with oak. Vitousek[11] suggested that nitrogen efficiency of litter production varies as an inverse function of the nitrogen available.

The high, dry matter : nitrogen ratio of the litter and high, C:N ratio of the soil in pine forest reduce the rate of litter decomposition and increase the fuel load on the forest floor. In addition, the decomposers of litter of a high, dry matter : nitrogen ratio may immobilize available N from the soil solution. Weight loss and the N concentration of residual litter of pine and oak enclosed in litter bags and placed on respective forest floors were studied for 1 yr. Figure 1 clearly indicates a marked immobilization of N in decomposing pine litter. The dynamic available N pool in the soil at any point in time is usually only a small proportion of total N[10,17] and its immobilization by microbes may intensify the N shortage in nitrogen-poor ecosystems. We suggest that this is the main reason why pine is able to resist reinvasion by oaks. As argued by Vitousek[11], low N availability caused by the immobilization by microbes may lead to increased efficiency of N use and production of litter with still higher dry matter : nitrogen ratio. Recurring fires in the pine forest lead to marked N losses through volatilization, augmenting the N shortage.

Oak has a relatively heavy demand for N and cannot succeed in N-poor soil. Through the return of N-rich litter and rapid mineralization, oaks maintain high soil fertility. Heavy lopping of oaks for fodder and cutting for fuel cause large canopy gaps and reduce leaf fall and hence N return, making the conditions suitable for invasion by pine.

The retention of N is specially pronounced in the oak forest (Table 1). Thus, in this forest the N pool may be more severely altered by deforestation. In such systems, replacement of N reserves will be essential to avert a long-term decline in productivity following deforestation[10]. In view of the above, the widespread replacement of mixed rain forests with plantations of conifers in the tropics and subtropics should be viewed with caution.

This research was supported by the University Grants Commission, New Delhi.

Received 16 March; accepted 3 July 1984.

1. Champion, H. G. & Seth, S. K. *A Revised Survey of the Forest Types of India*, 297–299 (Govt of India Publications, New Delhi, 1968).
2. Dwivedi, B. N. & Mathur, R. S. *Working plan for the Naini Tal Forest Division, Kumaun Circle, Uttar Pradesh*, 521 (Working Plan Circle, U.P. Forest Department, Naini Tal, 1978–79 to 1987–88).
3. Singh, J. S., Pandey, U. & Tiwari, A. K. *Ambio* **13**, 80–87 (1984).
4. Chaturvedi, O. P. thesis, Kumaun Univ., Naini Tal (1983).
5. Rawat, Y. S. thesis, Kumaun Univ., Naini Tal (1983).
6. Chaturvedi, O. P. & Singh, J. S. *Biomass* (in the press).
7. Negi, K. S., Rawat, Y. S. & Singh, J. S. *Can. J. For. Res.* **13**, 1185–1196 (1983).
8. Pathak, P. C. & Singh, J. S. *Tellus*, **36**, 44–49 (1984).
9. Ogino, K. *Primary productivity of Japanese forests* (eds Shidei, T. and Kira, T.) 172–186 (University of Tokyo Press, 1977).
10. Bormann, F. H., Likens, G. E. & Melillo, J. M. *Science* **196**, 981–983 (1977).
11. Vitousek, P. *Am. Nat.* **119**, 553–572 (1982).
12. Nye, P. H. *Plant Soil* **13**, 333–346 (1961).
13. Small, E. *Can. J. Bot.* **50**, 2227–2233 (1972).
14. Grubb, P. J. *Ann. Rev. Ecol. Syst.* **8**, 83–107 (1977).
15. Gosz, J. R. *Ecol. Bull.* (Stockholm) **33**, 405–426 (1981).
16. Schlesinger, W. H., Gray, J. T., Gill, D. S. & Mahall, B. E. *Bot. Rev.* **48**, 71–117 (1982).
17. Robertson, G. P. & Vitousek, P. M. *Ecology* **62**, 376–386 (1981).

Species variation and the mechanism of pressure–anaesthetic interactions

E. B. Smith, F. Bowser-Riley, S. Daniels, I. T. Dunbar, C. B. Harrison & W. D. M. Paton*

Physical Chemistry Laboratory, South Parks Road,
Oxford OX1 3QZ, UK
* Department of Pharmacology, South Parks Road,
Oxford OX1 3QT, UK

The mechanism of general anaesthesia has proved difficult to elucidate (see ref. 1 for a review), although the relative potencies of anaesthetic agents have been used to establish that the site at which anaesthetics act is hydrophobic in nature[2]. One further clue to their mode of action is that the effects of anaesthetics on vertebrates can be eliminated by pressures of ~100 atm (refs 3, 4). However, the effects of anaesthetics are not always reversed in model systems, where there is evidence that the pattern of pressure reversal varies significantly[5–10]. We now find that pressure fails to reverse the effects of anaesthetics on the freshwater shrimp (*Gammarus pulex*), although the sensitivity of these crustaceans to anaesthetics is comparable with that of higher animals. This is hard to reconcile with traditional bio-physical mechanisms and indicates that anaesthetics may act at a specific protein site rather than having a general effect on cell membranes. The pharmacology of pressure in mammals seems to be more similar to that of strychnine than of any other central stimulant[11]. As glycine, whose action is blocked by strychnine, is absent as a neurotransmitter in the arthropod central nervous system, we believe that this substance may be involved in determining pressure–anaesthetic interactions in vertebrates.

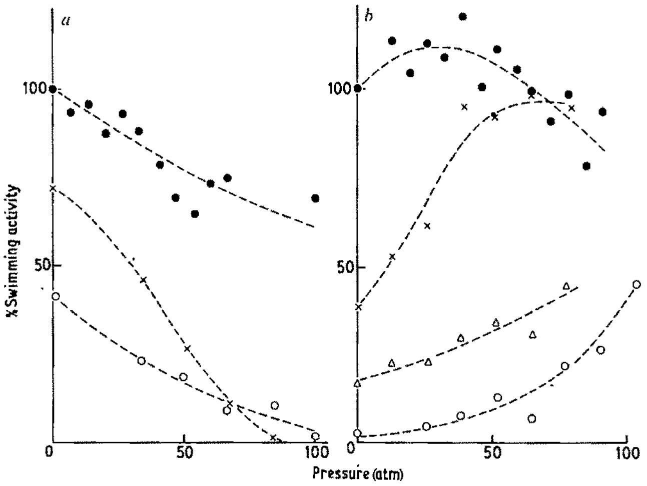

Fig. 1 *a*, Effect of pressure on *G. pulex* in the presence of ethanol (the lines are merely visual aids). *b*, Effect of pressure on larvae of *R. temporaria* in the presence of ethanol. ●, No anaesthetic; ×, 0.02 M ethanol; △, 0.265 M ethanol; ○, 0.275 M ethanol.

The effects of pressure and anaesthetics on the stimulated swimming activity of freshwater shrimps (*G. pulex*) and tadpoles (the larvae of *Rana temporaria*) were compared in similar experimental conditions. The animals were observed in glass cells, 5 cm long, designed to fit into a high-pressure chamber. The lower portion of the cells consisted of a trough of 1 cm^2 cross-section fitted with tungsten electrodes. Above the trough was a larger volume with steep sides so that anaesthetized animals fell into the trough which, when an electrical stimulus was applied, was a region not favoured by unanaesthetized animals. Five animals were placed in the cell and each determination of activity consisted of 20 observations taken at 10-s intervals. The fraction of the total population remaining above the trough was taken as a measure of swimming activity. Optimum swimming activity was obtained by the application of 5-V pulses of 0.1 s duration every 2 s for shrimps and similar pulses of 10 V for tadpoles. In these conditions the standard deviation of the measurements of activity was found to be ±7%. The experiments were carried out at 18 °C. Anaesthetics were added directly to the cell and up to 30 min was allowed for equilibration. Pressure was applied using helium gas; this is an acceptable agent because any anaesthetic effects that it might induce are not significant at the pressures used here[12].

For shrimps, the relative potencies of the anaesthetics studied—ethanol, ether, chloroform, halothane and sodium pentabarbitone—were very similar to those determined with other organisms (Table 1). Furthermore, the absolute potencies for shrimps and tadpoles are close to those reported for other species. The effect of pressure, in the absence of anaesthetics, on the swimming of the shrimps was moderately to reduce activity by ~30% at 100 atm and no hyperactivity was observed (Fig. 1). With all the anaesthetics used, the application of pressure further reduced swimming activity. In no instance was there any evidence of pressure reversal; indeed, the decrease in activity seemed greater than would be predicted by the simple addition of the effects of pressure and anaesthesia. Tests were made to confirm that the effects of both pressure and the anaesthetics were reversible.

The experiments with tadpoles were carried out in a similar manner. Pressure alone caused moderate hyperexcitability. When anaesthetics were present, the application of pressure dramatically restored swimming activity (Fig. 2). This effect had been previously observed qualitatively with tadpoles[13] and also with mice and newts[3]. Because tadpoles behave as expected in the same experimental conditions, it is unlikely that the anomalous behaviour of the shrimps is due to the experimental procedure.

This behaviour of the shrimps parallels that of the pleopod frequency of *Marinogrammarus marinus* which exhibits a gradual decline when exposed to 3.9 mm Hg pressure of halothane and which is potentiated by pressure[5]. For the brine shrimp, *Artemia salina*, the locomotor activity showed a lower relative decline on the application of pressure in the presence of anaesthetics than occurred in their absence. However, it was concluded that neither pressure reversal of anaesthesia nor a narcotic amelioration of the pressure effect had occurred[14].

Table 1 Anaesthetic potencies

	*Gammarus** (swimming activity)		*Goldfish*† (swimming activity)		*Mouse*‡ (righting reflex)		*Tadpoles*§ (swimming activity)	
	ED_{50}	Ratio	ED_{50}	Ratio	ED_{50}	Ratio	ED_{50}	Ratio
Chloroform	0.0008 ± 0.0002	1	0.0014	1	0.0011	1	0.0008	1
Ether	0.020 ± 0.003	25	0.029	21	0.20	18	0.024	30
Ethanol	0.25 ± 0.02	310					0.21 ± 0.02	260
Halothane	0.0004 ± 0.001	0.5	0.0038	0.3	0.00048	0.4		
Sodium pentabarbitone	0.0020 ± 0.003	2.5						

ED_{50} doses expressed as molarities.

* This work; † ref. 23; ‡ data from ref. 24 corrected to molarity by method given in ref. 23; § ethanol; this work. Other data from ref. 25

The relative potencies of the anaesthetics for shrimps, as for other organisms, point clearly to a hydrophobic site of action. The absolute potencies for shrimps and tadpoles are sufficiently close to suggest that in both species the anaesthetics act at physically similar sites by a common mechanism. However, the effects of pressure on anaesthesia in the two species suggests that very different mechanisms are involved. The effects of pressure on a process can be interpreted in terms of an associated volume change, ΔV (ref. 15). For a simple equilibrium, defined by equilibrium constant K,

$$\frac{\mathrm{d}\ln K}{\mathrm{d}P}=\frac{\Delta V}{RT} \qquad (1)$$

The association of ΔV with physical changes in the system depends on the model adopted[1]. For vertebrates the volumes calculated from this equation, or obtained from more sophisticated models such as the constant volume hypothesis[3], are positive and in the range 50–100 cm^3 per mole of anaesthetic[1,16]. This range is in keeping with the volume change associated with anaesthetic interaction at a hydrophobic region[14]. Conversely, the data for the shrimps, though not sufficiently precise to define quantitatively the associated volume change, indicate that the ΔV obtained from equation (1) is small and possibly negative.

Serious consideration has been given to two types of sites at which general anaesthetics might act. Traditionally, anaesthetics have been thought to act by a general perturbation of the lipid bilayers of the cellular membrane[17]. More recently, hydrophobic sites associated with protein molecules have been proposed[1]. This idea has drawn support from investigations of the complex responses of bacterial luciferases to clinical concentrations of general anaesthetics[18]. Anaesthetics at low concentrations can enhance light production from the enzyme by facilitating substrate binding and at higher concentrations can decrease the light emission by blocking the binding of an aldehyde necessary for luminescence[19]. The effects are observed both *in vivo* and with the extracted enzyme. The reduction of light intensity caused by anaesthetics can be reversed by the application of pressure. The very different responses observed in shrimps and tadpoles are not easily explained in terms of general membrane sites, but the differences could be consistent with more specific binding at protein sites if, for shrimps, anaesthetics induce a conformational change in a protein which leads to a negative ΔV.

The pharmacology of pressure, as elucidated from studies of pressure-induced convulsions in mammals, has been found closely to parallel that of strychnine[11]. This compound is believed to act primarily on postsynaptic inhibition, which is mediated by the neurotransmitter glycine. Crustaceans are insensitive to strychnine[20] and have a central nervous system in which glycine is not present as a neurotransmitter[21,22]. Thus, we propose that pressure reversal of anaesthesia, as observed in vertebrates, may involve effects of pressure on strychnine-sensitive processes, possibly through changes brought about in the glycine receptor protein. Although we cannot rule out the possibility that pressure reversal results from an independent action of pressure leading to a physiological rather than pharmacological antagonism of anaesthesia, most models of pressure reversal assume that pressure and anaesthetics act at the same site[1,4]. This suggests that in vertebrates, as in luminous bacteria, both pressure and anaesthetics act on the same relevant protein. By analogy with the luciferase model, anaesthetics could facilitate the binding of glycine to its receptor protein, a process that could play a part in determining those aspects of general anaesthesia which are reversed by pressure, including loss of consciousness in mammals.

Received 13 March; accepted 12 June 1984.

1. Franks, N. P. & Lieb, W. R. *Nature* **300**, 487–493 (1982).
2. Miller, K. W., Paton, W. D. M. & Smith, E. B. *Nature* **206**, 574–577 (1965)
3. Lever, M. J., Miller, K. W., Paton, W. D. M. & Smith, E. B. *Nature* **231**, 368–371 (1971).
4. Miller, K. W., Paton, W. D. M., Smith, R. A. & Smith, E. B. *Molec. Pharmac.* **9**, 131–143 (1973).
5. Youngson, A. F. & McDonald, A. G. *Br. J. Anaesth.*, **42**, 801–802 (1970)
6. Little, H. J., *Br. J. Pharmac.* **77**, 209–215 (1982).
7. Roth, S. M., Smith, R. A. & Paton, W. D. M. *Br. J. Anaesth.* **48**, 621–625 (1976)
8. Halsey, M. J. *Physiol. Rev.* **62**, 1341–1377 (1982).
9. Kendig, J. J., Tindell, J. R. & Cohen, E. N. *J. Pharmac. exp. Ther.* **195**, 215–244 (1975)
10. Little, J. H. & Paton, W. D. M. *Br. J. Pharmac.* **67**, 221–228 (1979)
11. Bowser-Riley, F. *Phil. Trans. R. Soc.* **B304**, 31–41 (1984)
12. Miller, K. W., Paton, W. D. M., Streett, W. B. & Smith, E. B. *Science* **157**, 97–98 (1967
13. Johnson, F. H. & Flagler, E. A. *Science* **112**, 91–92 (1951).
14. Simon, S. A., Parmentier, J. L. & Bennett, P. B. *Comp. Biochem. Physiol* **75A**, 193–198 (1983)
15. Johnson, F. H., Eyring, H. & Polissar, M. J. *The Kinetic Basis of Molecular Biology* (Wiley New York, 1954).
16. Smith, E. B. *Phil. Trans. R. Soc.* **B304**, 5–16 (1984).
17. Janoff, A. A. & Miller, K. W. in *Biological Membranes* (ed. Chapman, D.) 417–476 (Academic, London, 1982).
18. Johnson, F. H., Brown, D. E. S. & Marsland, D. A. *J. cell. comp. Physiol* **20**, 269–272 (1942).
19. Middleton, A. J. & Smith, E. B. *Proc. R. Soc.* **B193**, 159, 173–190 (1976)
20. Florey, E. *A. Rev. Physiol.* **23**, 501–528 (1961).
21. Gerschenfeld, H. M. *Physiol. Rev.* **53**, 1–119 (1973).
22. Johnston, G. A. R. *A. Rev. Pharmac. Tox.* **18**, 269–289 (1978).
23. Cherkin, A. & Catchpool, J. F. *Science* **144**, 1460–1462 (1963).
24. Miller, K. W., Paton, W. D. M. & Smith, E. B. *Anaesthesiology* **36**, 339–351 (1972)
25. Meyer, K. H. *Trans. Faraday Soc.* **33**, 1062–1068 (1937).

Rules for neural development revealed by chimaeric sensory systems in crickets

W. W. Walthall & R. K. Murphey

Neurobiology Research Center, State University of New York at
Albany, 1400 Washington Avenue, Albany, New York 12222, USA

Many sensory systems are organized so that the afferent projection forms a topographic map of the sensory surface within the central nervous system (CNS)[1,2]. The information necessary to create such a map may be available to the neuronal cell body based on its position in the receptor array, and this 'positional information' is translated into an axonal arborization in the proper part of the CNS[3–6]. To study how the location of a cell body within the sensory surface determines the termination pattern of its axon within the CNS, we have transplanted epidermis, containing identified sensory neurones, from a black cricket to a tan cricket. As we report here, when epidermis is transplanted to an unusual location in the receptor array, newly generated neurones are produced along the borders of the graft. These neurones arborize in locations that are appropriate neither to their new position nor to their original position in the array, but rather to a position somewhere in between. This is direct evidence for the idea that positional information guides the differentiation and ultimately the synaptic connections of insect sensory neurones.

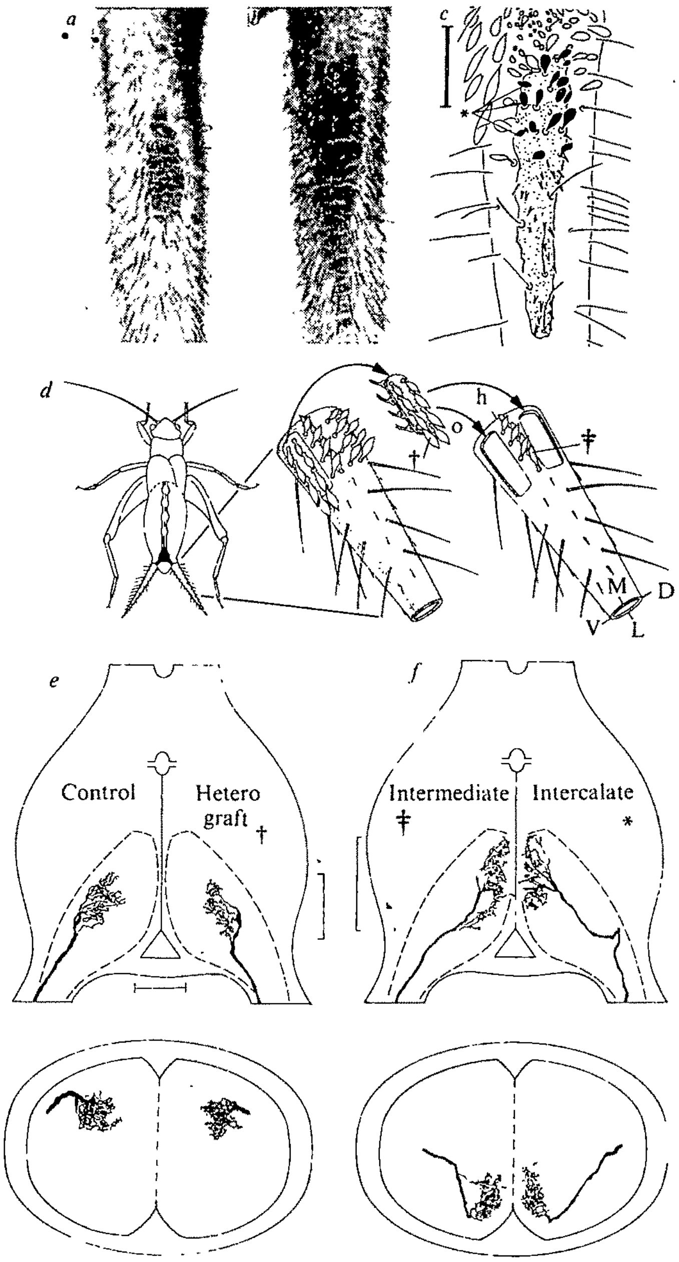

Fig. 1 Transplantation of neurones and characterization of their axonal arborizations. *a*, *b*, Light micrographs of chimaeric cerci. *a*, Ventral view of a cercus showing an orthotopic graft. The graft is schematized and indicated by 'o' in part *d*. *b*, Dorsal view of a cercus showing a heterotopic graft. This graft is schematized and indicated by 'h' in part *d*. *c*, Camera lucida drawing of the heterotopic graft shown in *b*. Transplanted clavate hairs (club-shaped) lie in the centre and to the right of the graft. *, Intercalated clavate hairs, as shown by their smaller size and by examining the graft for new hairs, after each moult. *a* and *c* are shown at the same magnification; scale bar, 500 μm. *d*, Schematic diagram illustrating the methods. The cutaway view of a cricket outlines the abdominal nervous system. The last abdominal ganglion, site of termination for all clavate neurones, is darkened. In each graft the two most ventral rows of clavate hairs and the surrounding epidermis were moved from a donor *G. bimaculatus* to a host *A. domesticus*. The graft consisted of a piece of tissue, 100 μm × 250 μm, transplanted when both crickets were in the 6th instar. Phenyl thiocarbamide (Sigma grade II), penicillin G (Sigma) and streptomycin sulphate (Sigma) powders were combined by weight in a ratio of 2:1:1 and added directly to the wound to guard against infection and melanization. *e*, *f*, Comparison of the axonal arborizations of normal and transplanted neurones. *e*, The axonal arborization of a neurone transplanted to a foreign location (hetero-graft), indicated by † in *d*, is compared with the equivalent neurone on an unoperated cercus (control). *f*, The terminal arborization of an intercalated sensory neurone (intercalate) innervating a clavate hair along the ventral margin of the dark epidermis (not actually grafted but intercalated) (*c*, *) is compared with a neurone (intermediate) normally found between the new graft site and its site of origin (*d*, ‡). The upper panels in *e*, *f* represent dorsal views; the lower panels represent transverse views. The transverse views were reconstructed from serial sections (the region reconstructed is indicated by a bracket next to the dorsal view). The dashed lines in the dorsal views outline the target area, the cercal glomerulus, for clavate neurones. *e* and *f* are shown at the same magnification; scale bar, 100 μm.

An orderly array of club-shaped sensilla called clavate hairs, located on the cercus of crickets[7,8], forms the initial stage of a neuronal circuit that apprises the insect of its position with respect to the gravitational field[9]. Each clavate hair is innervated by a single epidermally derived sensory neurone whose axon projects into the CNS. As a group, these sensory neurones form a topographically ordered neuronal projection[8]. Analogous individual receptors can be identified on two species of cricket, *Acheta domesticus* and *Gryllus bimaculatus*. The only detectable difference is one of colour; *A. domesticus* epidermis is tan, whereas *G. bimaculatus* is black. To demonstrate the similarity of the two species, we transplanted strips of tissue containing the cuticle, underlying epidermis and receptors and associated sensory neurones from the cercus of a black cricket, the donor, to an analogous position (orthotopic graft, Fig. 1*d*, 'o') on the cercus of a tan cricket, the host. The transplanted tissue survived as a contiguous sheet of black epidermis; the borders between donor and host were sharply delineated and the hairs retained their colour differences (Fig. 1*a*), thus allowing donor-derived clavate hairs to be readily distinguished from their host-derived neighbours.

Because a stereotyped series of cell divisions produces a hair cell and its associated sensory neurone from a single epidermal cell[10], a marked hair is always innervated by a sensory neurone of the same genotype. Thus, *G. bimaculatus* epidermis provides a marker not only for cuticle, but also for the underlying sensory neurone. When identified donor neurones within the graft were stained, they possessed axonal arborizations indistinguishable in size and location from the equivalent host neurone on the undisturbed cercus (Table 1). Apparently, there are no species-specific differences between donor sensory neurones and the host CNS to prevent regeneration of normal axonal arborizations.

We have taken advantage of these similarities to study whether the position of the soma on the body surface determines the axonal arbor within the CNS. Donor sensory neurones were transplanted into non-equivalent areas of the cercus (heterotopic grafts), and they then regenerated arbors characteristic of their original position. For example, when ventro-medial donor tissue was transplanted to a dorso-medial location on the host (Fig. 1*d*, 'h'), the donor tissue healed into place and transplanted neurones terminated in a location within the CNS appropriate to their position of origin (Fig. 1*e*, hetero-graft). In fact, these heterotopic neurones are virtually indistinguishable from the equivalent neurone on the undisturbed cercus (Fig. 1*e*, control). Thus, some intrinsic property of the neurone allows it to regenerate an axonal arbor to its former location even after its soma has been transplanted to a foreign location.

How does a neurone obtain this instruction about where to terminate? If the position of origin of the soma is important in assigning the axonal arborization of a neurone to the proper target area, a translocation of the neurone or its precursor before differentiation (or determination) should assign it a new identity and lead to an axonal arbor in a location appropriate to its new position[6,11]. Heterotopic grafts trigger the proliferation of new epidermal cells along the border between donor and host tissue[12–14], as is suggested in Fig. 1*a* and *b*, which compare an orthotopic and a heterotopic graft: even though the donor tissues were initially the same size (0.025 mm^2), the heterotopic graft grew significantly larger (0.343 mm^2) than the orthotopic graft (0.139 mm^2, Table 1). It has been demonstrated, using external cuticular markers, that this new tissue represents positions normally located between the donor and the host and the epidermis is thus said to 'intercalate' the intermediate positions[12–14].

When a heterotopic graft was created by transplanting a piece of donor epidermis containing identified clavate hairs to an unusual position on the host (Fig. 1*d*, 'h'), we noticed that new receptors often differentiated along the margins of the graft (Fig. 1*c*, asterisk). These new receptors could be identified by examining the graft after each moult; they were smaller and were not present at the time of the transplantation. Staining the axonal arbors of the sensory neurones associated with these intercalated receptors provides a critical test of the idea that sensory neurones are specified by positional information: if donor-derived neurones of 'intermediate' phenotype are produced, this supports the hypothesis that position of origin determines target area. When donor-derived neurones, associated with black hairs along the ventral border of the heterotopic graft (Fig. 1*c*, hairs indicated by an asterisk) were stained (Fig. 1*f*, 'Intercalate'), they projected to an area normally associated with neurones located in an area between that of the apposed host and the donor tissue (such as those innervating the hair indicated in Fig. 1*d*,‡). Of 11 intercalated neurones stained in 11 different specimens, 10 could be recognized as having intermediate phenotypes (Table 1). Equally important, none of these neurones had the phenotype of the transplanted neurones (located more centrally in the graft, for example, Fig. 1*e*, heterograft). This result strongly supports the idea that relative position of the neuronal cell body, at or near the time of its terminal mitotic division, determines the shape and location of the neurone's axonal arborization in the CNS.

Bate[6,15] suggested, from physiological determinations of neuronal connections, that the position of a sensory neurone on the epidermis of an insect regulates the central connections it makes. The present results and related work[7,8,16] provide strong support for Bate's hypothesis because they show first that the axonal arborizations are physically distinguishable within the CNS, and second that the topography of the afferent projection is controlled by the position of origin of the cell body. The idea is very similar to Sperry's chemoaffinity hypothesis[3], developed to explain results regarding the development of the projection from eye to brain in amphibians and fish. Subsequent work has led to considerable debate[4,17–19] over the exact role of positional information in the formation of the retinal projection, primarily because it is so difficult to identify and keep track of the neurones involved. In contrast, the individual sensory neurones of the cricket cercus, which are easily identifiable, have allowed us to demonstrate clearly that soma position is translated into a property that guides the elaboration of an axonal arborization in a particular location of the CNS. Because the location of the axonal arborization is ultimately associated with synaptic connectivity[16], we conclude that positional information guides connectivity.

Table 1 Results of grafts between *A. domesticus* and *G. bimaculatus*

Type of graft	No. of successful grafts	Average size (mm^2)	Successfully stained neurones	Type of arbor
Orthotopic	11	0.139 ± 0.063 ($n = 8$)	5 Transplanted neurones	Normal
Heterotopic	30	0.343 ± 0.214 ($n = 17$)	6 Transplanted neurones	Normal
			11 Intercalated neurones	Intermediate*

The difference in average size between the two groups was significant at the 0.05 level ($t = 2.08$, d.f. = 22). Some of the chimaeric cerci were used for histological work and could not be included here.

* This arbor is located ventro-medially in the neuropil (see Fig. 1*f*, 'intermediate').

We thank Professor F. Huber for providing the *G. bimaculatus*, Dr J. P. Bacon, L. Eisele, G. A. Jacobs, S. E. Johnson, H. Rothenberg and D. S. Sakaguchi for advice, and R. Loos, R. Speck and L. Welch for assistance in preparing the manuscript. This work was supported by NIH award NS-15571 to R.K.M.

Received 12 March; accepted 18 June 1984.

1. Gaze, R. M. in *The Formation of Nerve Connections* (Academic, New York, 1970).
2. Sperry, R. W. *J. exp. Zool.* **92,** 263–279 (1943).
3. Sperry, R. W. *Proc. natn. Acad. Sci. U.S.A.* **50,** 703–710 (1963).
4. Jacobson, M. *Devl Biol.* **17,** 202–218 (1968).
5. Wolpert, L. *J. theor. Biol.* **25,** 1–47 (1969).
6. Bate, C. M. *J. exp. Biol.* **59,** 95–107 (1973).
7. Murphey, R. K., Jacklet, A. & Schuster, L. *J. comp. Neurol.* **191,** 53–64 (1980).
8. Murphey, R. K. *Devl Biol.* **88,** 236–246 (1981).
9. Sakaguchi, D. S. & Murphey, R. K. *J. comp. Physiol.* **150,** 141–152 (1983).
10. Lawrence, P. A. *J. Cell Sci.* **1,** 475–498 (1966).
11. Bate, C. M. in *Handbook of Sensory Physiology* (ed. Jacobson, M.) 2–53 (Springer, New York, 1978).
12. Marcus, W. *Wilhelm Roux Arch. EntwMech. Org.* **154,** 56–102 (1962).
13. Locke, M. *J. Insect Physiol.* **12,** 397–402 (1966).
14. French, V., Bryant, P. & Bryant, S. *Science* **193,** 969–981 (1976).
15. Bate, C. M. & Lawrence, P. A. in *Developmental Neurobiology of Arthropods* (Cambridge University Press, 1973).
16. Bacon, J. & Murphey, R. K. *J. Physiol., Lond.* (in the press).
17. Schmidt, J. T. *Trends Neurosci.* **5,** 111–116 (1982).
18. Cooke, J. *Trends Neurosci.* **3,** 45–48 (1980).
19. Schmidt, J. T., Cicerone, C. M. & Easter, S. S. *J. comp. Neorol.* **177,** 257–278 (1978).

Evidence for neurotensin as a non-adrenergic, non-cholinergic neurotransmitter in guinea pig ileum

Michel Goedert, John C. Hunter & Mary Ninkovic

MRC Neurochemical Pharmacology Unit,
Medical Research Council Centre, Medical School, Hills Road,
Cambridge CB2 2QH, UK

Neurotensin is a 13-amino acid peptide that is widely distributed in central and peripheral tissues of various mammalian species[1]. In peripheral tissues, the highest concentration of neurotensin-like immunoreactivity is found in the ileum, where it is present in endocrine-like cells and nerve fibres[2–4]. The longitudinal smooth muscle layer of the guinea pig ileum, where neurotensin has both a direct relaxant and an indirect contractile action, has been used extensively as a biological assay system for neurotensin[5]. We report here that the majority of specific ^{3}H-neurotensin binding sites is present in the guinea pig ileum circular smooth muscle layer, which is known to be innervated by a large proportion of the ileal non-adrenergic inhibitory nerves[6]. Neurotensin produces a dose-dependent, tetrodotoxin-resistant relaxation, whereas the relaxation produced by field stimulation of the inhibitory nerves is frequency-dependent and tetrodotoxin-sensitive. The calcium-dependent potassium channel blocker apamin[7,8] inhibits both the neurotensin- and nerve stimulation-induced muscle relaxation. Incubation of the circular smooth muscle preparation with a neurotensin antiserum substantially inhibited the nerve stimulation-induced relaxation, indicating a direct relationship between the effects of neurotensin and of nerve stimulation.

For receptor autoradiography, adult male guinea pigs (250–400 g, Hartley strain) were stunned, a portion of their terminal ileum was dissected, flushed with cold saline, frozen and sectioned in the transverse plane at 13 μm using a cryostat. The sections were incubated with 2 nM ^{3}H-neurotensin and non-specific binding was defined as that in the presence of 1 μM neurotensin. Following incubation, they were apposed to emulsion-coated coverslips and kept at −20 °C for 2 months. The coverslips were then developed and the tissue sections Nissl-stained. Test-tube binding for ^{3}H-neurotensin was performed by using washed membranes prepared from whole guinea pig ileum. The guinea pig ileum circular smooth muscle preparation was set up as described previously[9]. Contraction of the muscle tone was induced by the tachykinin kassinin (10 nM) and all experiments were performed in the presence of atropine (5 μM), guanethidine (20 μM), indomethacin (1 μM) and mepyramine (5 μM).

When sections through the guinea pig ileum were incubated with ^{3}H-neurotensin, labelling was found in the smooth muscle layers, with a dense band of silver grains in the circular muscle layer and a band of lesser density in the longitudinal muscle layer (Fig. 1). The neurotensin binding sites were further characterized by using a test-tube binding assay for ^{3}H-neurotensin performed on washed membranes of whole guinea pig ileum.

The binding was saturable (Fig. 2*a*) and Scatchard transformation of the specific binding data (Fig. 2*b*) indicated the presence of a single population of binding sites with an equilibrium dissociation constant of 3.4±0.7 nM ($n = 4$) and a maximum number of binding sites of 14±2.6 fmol per mg protein ($n = 4$). The relative potencies of various neurotensin fragments in competing with ^{3}H-neurotensin for its specific binding site were similar to the potencies obtained for these fragments in the circular smooth muscle preparation (Table 1), indicating that the binding properties of ^{3}H-neurotensin were consistent with binding to a physiological receptor.

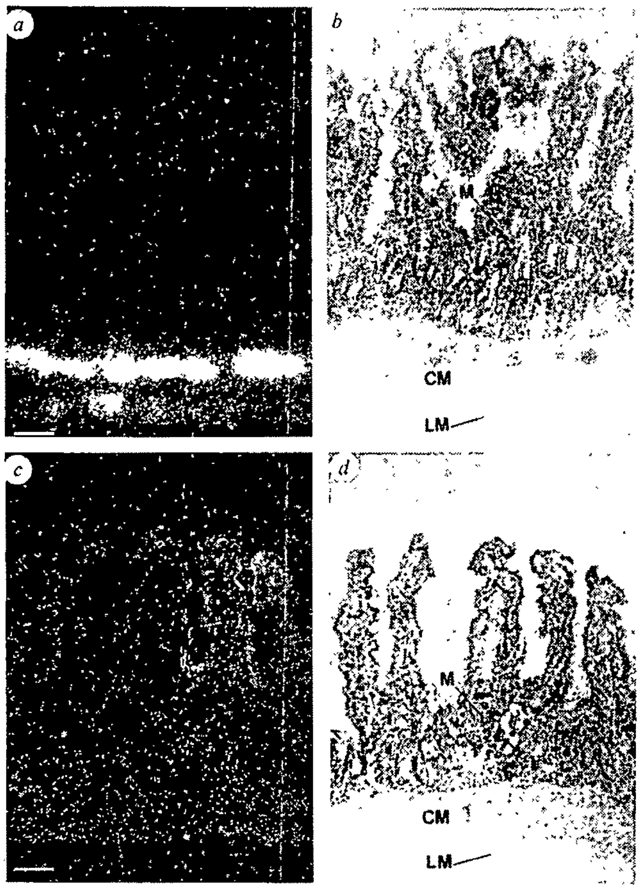

Fig. 1 Autoradiographic localization of ^{3}H-neurotensin binding sites in the guinea pig ileum. *a*, Dark-field photomicrograph of a section incubated in the presence of 2 nM ^{3}H-neurotensin. *b*, Light-field photomicrograph of the Nissl stain of the same section as in *a*. *c*, Dark-field photomicrograph of an adjacent 13-μm section to *a* incubated in the presence of 2 nM ^{3}H-neurotensin and 1 μM unlabelled neurotensin. *d*, Light-field photomicrograph of the Nissl stain of the same section as in *c*. M, mucosa; CM, circular muscle; LM, longitudinal muscle. Note the labelling of the circular and longitudinal muscle layers in *a*. Similar results were obtained for the ilea from six different animals. Scale bar, 100 μm.

Methods: Sections (13 μm) of the guinea pig ileum were pressed onto gelatin-coated slides, melted in place and dried overnight at 4 °C in air-tight boxes with desiccant. The thawed sections were incubated for 10 min at 25 °C in 2 nM [3,11-tyrosyl-3,5-^{3}H]neurotensin (56.3 Ci mmol^{-1}, NEN) in 50 mM Tris-HCl *p*H 7.4, containing 0.1% bovine serum albumin (radioimmunoassay grade, Sigma), 40 mg l^{-1} bacitracin (Sigma) and 1 mM EDTA. Nonspecific binding was defined in adjacent sections as binding in the presence of 1 μM unlabelled neurotensin (Cambridge Research Biochemicals). Following the incubation, the sections were washed twice in cold buffer (2 min each time), dipped into cold water and dried under a stream of cold air. They were then apposed to emulsion-coated coverslips[26] and kept at −20 °C for 2 months. The coverslips were developed in safe-light conditions using Kodak D19 developer and the tissue sections put into Carnoy's fixative, Nissl stained and mounted using Depex. Dark-field photomicrographs were taken of the silver grains and the Nissl stain, respectively. In some experiments, following the incubation with 2 nM ^{3}H-neurotensin, the dried tissue sections were scraped off the slides and the bound radioactivity determined by liquid scintillation spectrometry. The specific binding was 77±9% ($n = 3$) of the total (taken as 100%). The binding of ^{3}H-neurotensin was not affected by 1 μM of the following peptides: neurotensin(1–6), neurotensin(10–13), substance P, vasoactive intestinal polypeptide, somatostatin(15–28) and dynorphin(1–17).

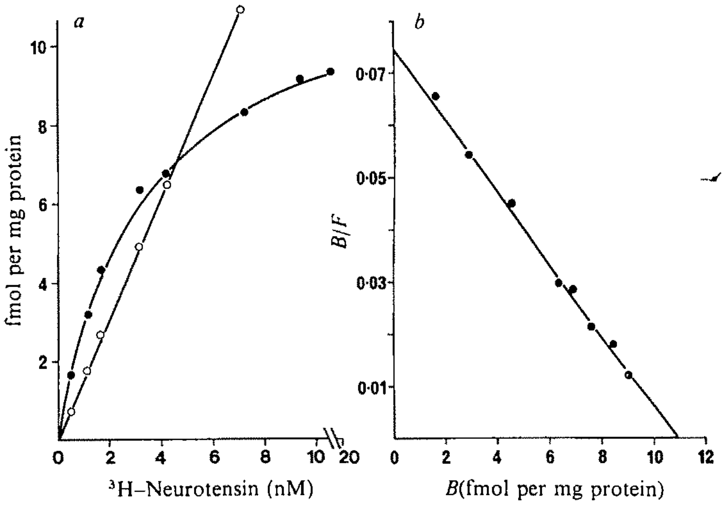

Fig. 2 ^{3}H-Neurotensin binding to a membrane preparation of guinea pig ileum. *a*, ^{3}H-Neurotensin as a function of the radiolabelled peptide concentration. Values were obtained in a single experiment; similar results were obtained in four separate experiments. Nonspecific binding (○) was defined as binding in the presence of 1 μM neurotensin and specific binding (●) was obtained by subtracting the nonspecific from the total binding. *b*, Scatchard transformation of the specific binding data.

Methods: The ileum from adult male guinea pigs was dissected, flushed with cold saline, weighed and homogenized in 10 vol (w/v) of cold 50 mM Tris-HCl *p*H 7.4, with a Polytron at setting 7 for 15 s. After 20 min centrifugation at 50,000*g*, the pellet was resuspended in 10 vol 50 mM Tris-HCl, incubated at 37 °C for 30 min and centrifuged again. The washed pellet was resuspended in 50 mM Tris-HCl *p*H 7.4, containing 0.1% bovine serum albumin, 40 mg l^{-1} bacitracin and 1 mM EDTA to yield a concentration of 10 mg tissue per ml buffer. 1 ml of homogenate was incubated in the presence of ^{3}H-neurotensin at 25 °C for 10 min. At the end of the incubation period the tubes were transferred to ice and filtered immediately under reduced pressure through GF/B glass fibre filters (Whatman) pretreated with 0.2% polyethyleneimine (Sigma) in water. Each of the filters was washed four times with 5 ml cold buffer and the radioactivity determined by liquid scintillation spectrometry. A detailed characterization of the binding assay has been published elsewhere[25]. Proteins were determined according to Lowry *et al.*[27] using bovine serum albumin as the standard.

In the guinea pig ileum circular smooth muscle preparation, neurotensin produced a dose-dependent relaxation of the muscle tone, with an IC_{50} value of 3.6 ± 0.6 nM ($n = 12$, Fig. 3*a*), whereas the relaxation following field stimulation was frequency dependent (Fig. 3*b*). The latter was inhibited by 0.6 μM tetrodotoxin, whereas the muscle relaxation effected by neurotensin was tetrodotoxin-resistant. Both the neurotensin-mediated smooth muscle relaxation (1–30 nM) and the relaxation produced by inhibitory nerve stimulation (1, 2 and 5 Hz) were completely inhibited by 30 nM of the bee venom apamin.

The possibility that the smooth muscle relaxation effected by inhibitory nerve stimulation is due to the release of a neurotensin-like substance was investigated by incubating the circular smooth muscle preparation with a previously described antiserum directed against the carboxy-terminus of neurotensin[10]. Incubation with the neurotensin antiserum (1 in 20 dilution) for 3 h not only prevented the action of neurotensin, but also inhibited the nerve stimulation-induced smooth muscle relaxation at all frequencies tested (Figs 3, 4). Higher dilutions of the antiserum at 1:50 and 1:100 were ineffective. Controls consisted of using the same dilution of either preimmune serum (Fig. 4) or an antiserum raised against [Lys^{8}Asn^9]neurotensin(8–13) a peptide sequenced from chicken small intestine which shares marked sequence homologies with neurotensin[11], but is not present in mammalian tissues[12]. This antiserum, which was raised in the same way as the neurotensin antiserum and had a similar antibody titre, did not cross-react with synthetic neurotensin. Neither the preimmune serum (Fig. 4) nor the antiserum raised against [Lys^{8}Asn^9] neurotensin(8–13) affected the smooth muscle relaxation produced by either neurotensin or inhibitory nerve stimulation.

It was possible that the effect of the neurotensin antiserum was due to a non-selective postsynaptic action on the circular smooth muscle. However, the antiserum did not affect the contractile response to 10 nM kassinin (Fig. 4), nor the reduction

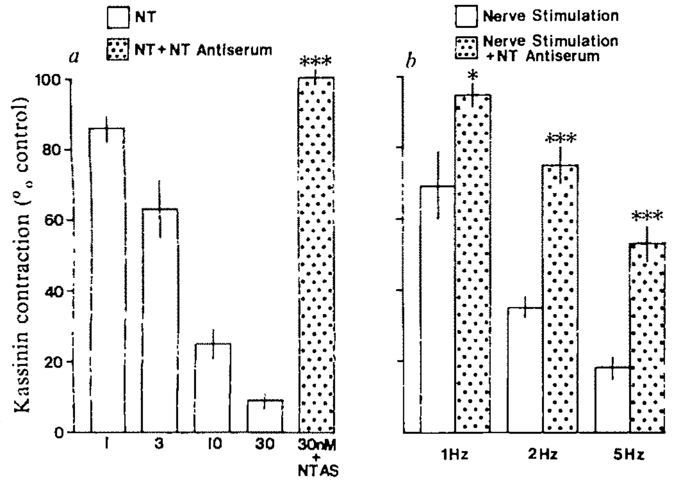

Fig. 3 Effect of neurotensin antiserum on the dose– and frequency–response curves to neurotensin (*a*) and non-adrenergic inhibitory nerve stimulation (*b*) in the guinea pig ileum circular smooth muscle. Note that the neurotensin antiserum completely reversed the inhibitory effect of neurotensin at all dose levels, with the effect on the maximum response of neurotensin (30 nM) shown above. The neurotensin antiserum also significantly antagonized the response to inhibitory nerve stimulation at all frequencies tested. All values have been expressed as a percentage of the control response to kassinin (100%). Open columns represent the controls and stippled columns the effects of neurotensin and inhibitory nerve stimulation in the presence of neurotensin antiserum. In each preparation, control responses were obtained before incubation of the tissues with the neurotensin antiserum (1:20 dilution) for 3 h at 37 °C. Each value represents the mean ± s.e.m. of 4–10 observations. * $P < 0.05$; *** $P < 0.001$ (Student's *t*-test).

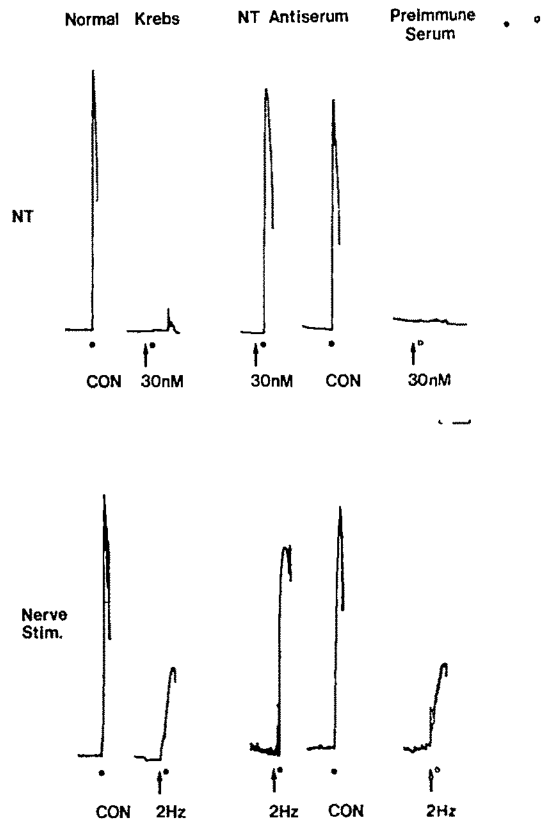

Fig. 4 Effect of neurotensin antiserum on the inhibitory responses of the guinea pig ileum circular smooth muscle to neurotensin and non-adrenergic inhibitory nerve stimulation. The upper row of records illustrates the effect of neurotensin (NT, 30 nM) and the lower row the effect of inhibitory nerve stimulation on the kassinin-induced tone of the guinea pig ileum circular smooth muscle preparation. Intramural nerve fibres were stimulated with 0.5-ms pulses at supramaximal voltage and at a frequency of 2 Hz. The first pair of responses are in normal Krebs and represent, respectively, a control dose of 10 nM kassinin (CON) followed by a subsequent dose in the presence of either NT or nerve stimulation. The second pair of responses are in the presence of the neurotensin antiserum (1:20 dilution) following prior incubation of the tissues with the antiserum for 3 h at 37 °C and the last response in each row shows the effect of prior incubation with preimmune serum (1:20 dilution) for 3 h at 37 °C. Time bar, 2 min. Note that the neurotensin antiserum completely antagonized the inhibitory effect of neurotensin and substantially reversed the effect of inhibitory nerve stimulation, whereas the preimmune serum had no effect on either parameter.

Methods: Male guinea pigs (250–400 g, Hartley strain) were stunned, the terminal ileum was dissected, flushed with Krebs saline at 37 °C and the circular smooth muscle preparation set up as previously described[9]. The tissues were suspended under a tension of 1 g in 2 ml organ baths containing Krebs saline at 37 °C and aerated with a mixture of 95% O_2 and 5% CO_2. The saline composition was (in mM): NaCl 118, KCl 4.7, $CaCl_2$ 2.5, $MgSO_4$ 1.2, $NaHCO_3$ 25, KH_2PO_4 1.2 and glucose 11. In all preparations tension was recorded with isotonic transducers. Contraction of the muscle tone was induced by 10 nM kassinin (CON) and all experiments were performed in the presence of atropine (5 μM), guanethidine (20 μM), indomethacin (1 μM) and mepyramine (5 μM). However, the contractile response to kassinin was found to be transient and hence inconvenient for the study of inhibitory responses in the conventional manner. The protocol of the present study was therefore similar to that of the anti-assay previously described by Burn[28]. Briefly, neurotensin was added (arrow) 20 s (optimal) before the addition of kassinin (●). Similarly, field stimulation of the inhibitory nerves was started (arrow) 20 s before the addition of kassinin (●) and was continued until the peak of the response to kassinin was reached, normally 25–30 s. The direct inhibitory effects of neurotensin and inhibitory nerve stimulation on the circular smooth muscle have therefore been observed as a reduction in the contractile response to kassinin.

Table 1 Relative potencies of neurotensin fragments in a binding and a biological assay

Peptide	Binding assay		Biological assay	
	IC_{50} (nM)	Potency (%)	IC_{50} (nM)	Potency (%)
NT(1–13)	3.2 ± 0.5	100	3.3 ± 0.3	100
NT(8–13)	7.3 ± 0.7	43	11.5 ± 0.8	29
NT(9–13)	633 ± 90	0.50	344 ± 75	0.95
NT(10–13)	>10,000	<0.04	>10,000	<0.04
NT(1–6)	>10,000	<0.04	>10,000	<0.04

The binding assay was the inhibition of specific ^{3}H-neurotensin binding to guinea pig ileum membranes and the biological assay the inhibition of kassinin-induced tone of the guinea pig ileum circular smooth muscle preparation. The binding of tritiated neurotensin (NT) was assayed at a concentration of 2 nM. The IC_{50} was defined as the concentration of unlabelled peptide required to inhibit the specific binding of ^{3}H-neurotensin by 50%. In the biological assay the IC_{50} was defined as the concentration of peptide required to produce 50% inhibition of the contractile response to 10 nM kassinin. The relative potencies were calculated by comparing the IC_{50} values with that of NT(1–13), taken as 100%. The results represent the means ± s.e.m. of between three and five separate experiments. The concentrations of NT(1–13) and of all NT fragments were determined by amino acid analysis. The purity of ^{3}H-NT was determined by subjecting an aliquot from each batch to reverse-phase HPLC[25]. NT(9–13) and NT(10–13) were synthesized by Dr B. J. Williams, NT(8–13) was purchased from Peninsula Laboratories and all other peptides were obtained from Cambridge Research Biochemicals.

($74.5 \pm 5.3\%$, $n = 4$) in this response which was produced by the β-adrenoceptor agonist isoprenaline (500 nM).

The present results indicate that neurotensin has a potent direct relaxant effect on the guinea pig ileum circular smooth muscle layer, where a dense accumulation of specific ^{3}H-neurotensin binding sites is found. The circular smooth muscle preparation may therefore constitute a favourable biological assay system for neurotensin. Electrophysiological studies have indicated that the circular smooth muscle layer of the guinea pig ileum is innervated by non-adrenergic, non-cholinergic inhibitory nerve fibres whose action is blocked by apamin[13,14]. In addition, it has been shown that ATP and vasoactive intestinal polypeptide are unlikely mediators of this inhibitory non-adrenergic effect[14]. In the present study, the relaxant effects of nerve stimulation and neurotensin were both apamin-sensitive; a similar effect has previously been noted for the relaxant effect of neurotensin in the guinea pig colon and the rabbit ileum longitudinal smooth muscle[15,16].

This parallelism suggested that neurotensin may be released from non-adrenergic inhibitory nerve fibres following nerve stimulation. In the absence of neurotensin receptor antagonists, we have made use of a specific neurotensin antiserum to neutralize the endogenous peptide. Specific antisera have been used to study the physiological function of hypothalamic releasing hormones[17–19]; more recently, both polyclonal and monoclonal antibodies have also been successfully used to prevent the actions of neuropeptides in both the peripheral and the central nervous system[20–24]. In the present study, the neurotensin antiserum inhibited the nerve stimulation-induced smooth muscle relaxation to a significant extent, whereas both the preimmune serum and a control immune serum were without effect. The residual smooth muscle relaxation observed after exposure to the neurotensin antiserum may be due to the inability of the antiserum to neutralize rapidly all of the neurotensin released; alternatively, a substance distinct from neurotensin may contribute to the relaxation of the circular smooth muscle. In conclusion, the present results are consistent with the hypothesis that neurotensin functions as an inhibitory non-adrenergic, non-cholinergic neurotransmitter in the guinea pig ileum.

We thank Dr P. C. Emson for the gift of the neurotensin antiserum, Dr S. P. Hunt for his advice and Mrs M. Wynn for help with the preparation of the manuscript.

Received 1 June; accepted 2 July 1984.

1. Nemeroff, C. F., Luttinger, D. & Prange, A. J. *Handbk Psychopharmac.* **16**, 363–466 (1983).
2. Sundler, F., Håkanson, R., Leander, S. & Uddman, D. *Ann. N.Y. Acad. Sci.* **400**, 94–104 (1982).
3. Schultzberg, M. *et al. Neuroscience* **5**, 689–744 (1980).
4. Reinecke, M., Forssmann, W. G., Thiekötter, G. & Triepel, J. *Neurosci. Lett.* **37**, 37–42 (1983).
5. Kitabgi, P. *Ann. N.Y. Acad. Sci.* **400**, 37–55 (1982).
6. Hirst, G. D. S. & McKirdy, H. C. *J. Physiol., Lond.* **238**, 129–143 (1974).
7. Vladimirova, A. I. & Shuba, M. F. *Neurofiziologija* **10**, 295–299 (1978).
8. Banks, B. E. C. *et al. Nature* **282**, 415–417 (1979).
9. Harry, J. *Br. J. Pharmac.* **20**, 399–417 (1963).
10. Emson, P. C., Goedert, M., Williams, B. J., Ninkovic, M. & Hunt, S. P. *Ann. N.Y. Acad. Sci.* **400**, 198–215 (1982).
11. Carraway, R. & Ferris, C. F. *J. biol. Chem.* **258**, 2475–2479 (1983).
12. Goedert, M., Schwartz, W. N. & Williams, B. J. *Brain Res.* (submitted).
13. Bauer, V. & Kuriyama, H. *J. Physiol., Lond.* **330**, 95–110 (1982).
14. Bauer, V. & Kuriyama, H. *J. Physiol., Lond.* **332**, 375–391 (1982).
15. Kitabgi, P. & Vincent, J. P. *Eur. J. Pharmac.* **74**, 311–318 (1981).
16. Huidobro-Toro, J. P. & Yoshimura, K. *Br. J. Pharmac.* **80**, 645–653 (1983).
17. Arimura, A., Debeljuk, L. & Schally, A. V. *Endocrinology* **95**, 323–325 (1974).
18. Arimura, A., Smith, W. D. & Schally, A. V. *Endocrinology* **98**, 540–543 (1976).
19. Rivier, C., Rivier, J. & Vale, W. *Science* **218**, 337–339 (1982).
20. Goyal, R. K., Rattan, S. & Said, S. I. *Nature* **288**, 378–380 (1980).
21. Matsuzaki, Y., Hamasaki, Y. & Said, S. I. *Science* **210**, 1252–1253 (1980).
22. Lundberg, J. M. *Acta physiol. scand. Suppl.* **496**, 1–57 (1981).
23. Bannon, M. J. *et al. Nature* **307**, 791–792 (1983).
24. Han, J. S. & Xie, G. X. *Pain* **18**, 367–376 (1984).
25. Goedert, M., Pittaway, K., Williams, B. J. & Emson, P. C. *Brain Res.* **304**, 71–81 (1984).
26. Ninkovic, M., Hunt, S. P. & Kelly, J. S. *Brain Res.* **230**, 111–119 (1981).
27. Lowry, D. H., Rosebrough, N. H., Farr, A. L. & Randall, R. J. *J. biol. Chem.* **193**, 265–275 (1951).
28. Burn, J. H. *Biological Standardization* (Oxford University Press, 1937).

Adenosine mediates a slow hyperpolarizing synaptic potential in autonomic neurones

T. Akasu, P. Shinnick-Gallagher & J. P. Gallagher

Department of Pharmacology and Toxicology, The University of Texas Medical Branch, Galveston, Texas 77550, USA

Considerable evidence has accumulated suggesting that purines, adenosine and ATP function as neurotransmitters in the central and peripheral nervous systems[1–4]. Burnstock[2] has proposed that purinergic receptors be classified into two types, P_1 and P_2, having adenosine and ATP, respectively, as agonist prototypes. Recent data suggest that ATP may mediate a synaptic potential in guinea pig vas deferens[5,6], but no such evidence exists for adenosine. The presence of a non-cholinergic, non-adrenergic nerve supply to the urinary bladder has been postulated[7,8] and termed purinergic[1,2], as these nerves have been shown to release ATP[7]. Furthermore, atropine-resistant contractions of bladder smooth muscle are thought to be mediated by ATP, while *in situ* experiments[9,10] in vesical parasympathetic ganglia have suggested that a purinergic modulatory mechanism may control urinary bladder function. We now report the presence of a slow hyperpolarizing synaptic potential (slow-h.s.p.) in neurones of cat vesical parasympathetic ganglia, produced by stimulating the preganglionic nerves, and provide evidence that the slow-h.s.p. is mediated by adenosine.

Vesical parasympathetic ganglia isolated from the surface of the urinary bladder were placed in a chamber superfused with oxygenated (95% O_2/5% CO_2) Krebs' solution of the following composition (mM): NaCl, 117; KCl, 4.7; $MgCl_2$, 1.2; $CaCl_2$, 2.54; NaH_2PO_4, 1.19; $NaHCO_3$, 25 and glucose, 11. We employed conventional intracellular recording methods using glass microelectrodes (50–80 MΩ) filled with 2 M K_2SO_4 (ref. 11).

Vesical parasympathetic ganglion cells were superfused with a solution containing hexamethonium (1 mM) to block nicotinic responses to synaptically released acetylcholine in all experiments[11]. Supramaximal stimulation (3–10 V) of the preganglionic nerve at 40 Hz for 250 ms in hexamethonium-containing solution revealed the presence of the slow-inhibitory postsynaptic potential (slow-i.p.s.p.), mediated through monosynaptic activation of muscarinic receptors[11] (Fig. 1*a*). When the stimulus

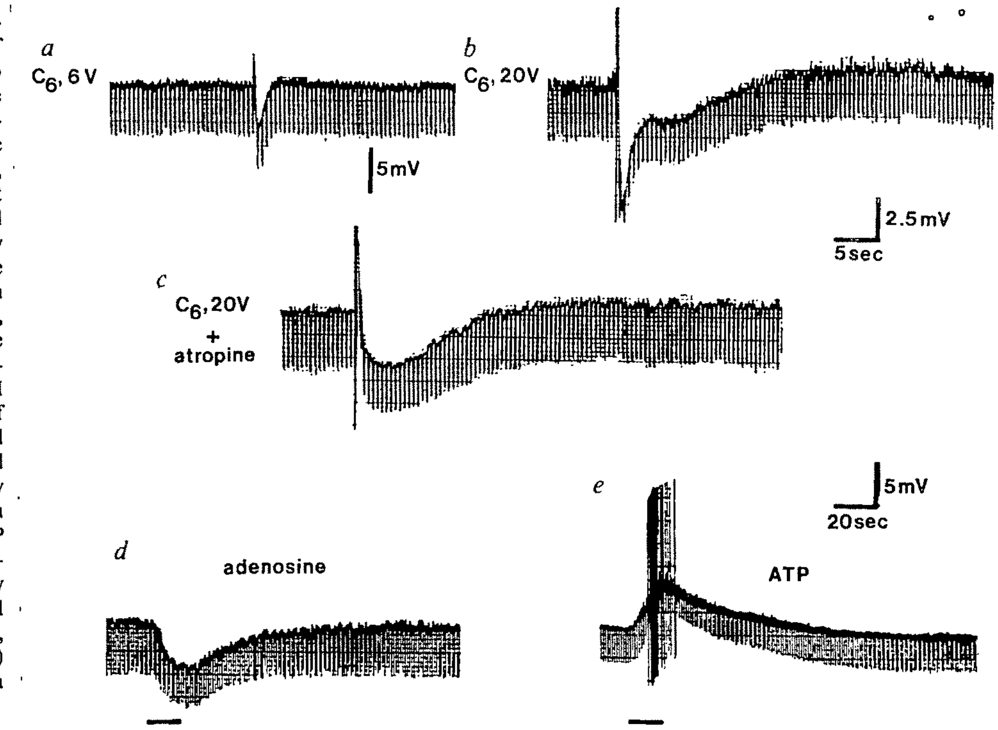

Fig. 1 Responses to nerve stimulation recorded in the presence of hexamethonium (C_6; 1 mM) and to exogenous application of adenosine (100 μM) and ATP (50 μM). *a*, Slow-i.p.s.p. elicited by preganglionic nerve stimulation (6 V, 40 Hz, 250 ms). *b*, Slow-i.p.s.p. recorded at a higher sensitivity in the same cell as in *a* after the stimulus intensity had been raised to 20 V; note the slower hyperpolarizing response on the falling phase of the slow-h.s.p. *c*, The slow-h.s.p., recorded from same cell as in *b*, remained after the slow-i.p.s.p. had been blocked with 1 μM atropine. Note that the sensitivity of the recording was increased in *b* and *c*. *d*, *e*, Adenosine (100 μM; *d*) and ATP (50 μM; *e*) were applied by superfusion as indicated. Action potentials recorded in the ATP response were truncated. The downward deflections were produced by injecting constant-current anodal pulses of 100 ms and 1.4 nA (*a*), 0.7 nA (*b*, *c*) and 0.5 nA (*d*, *e*) through the recording electrode as a measure of membrane resistance.

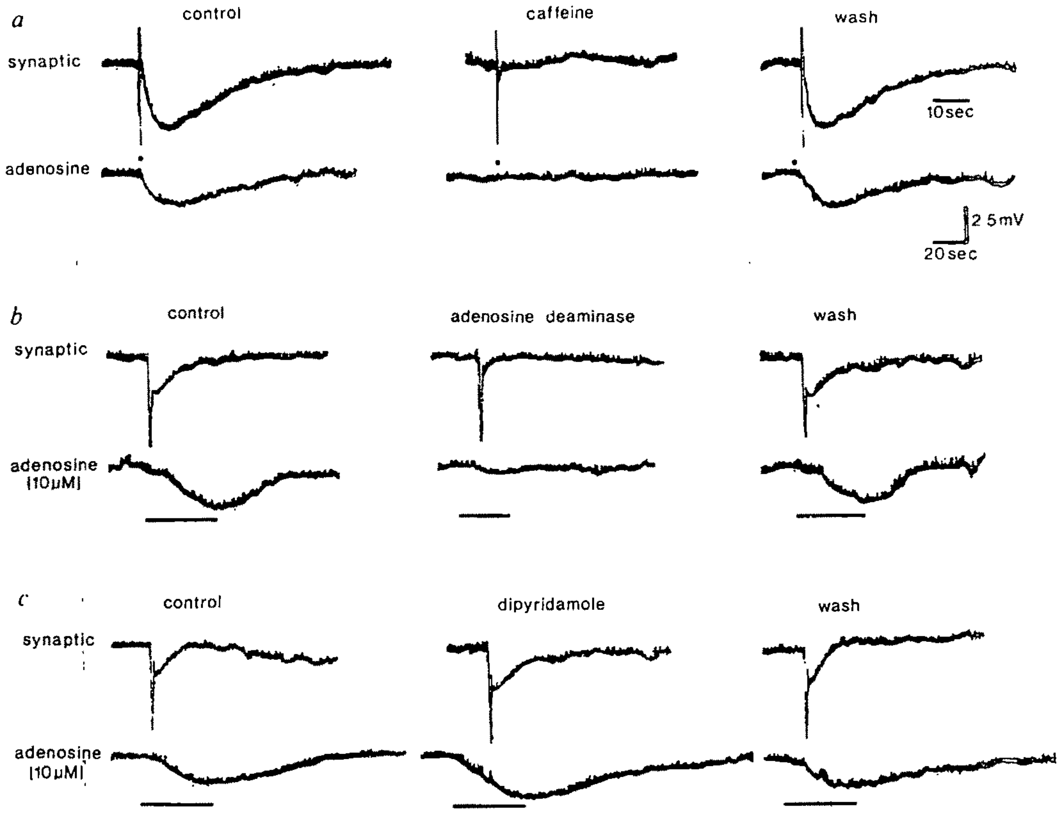

Fig. 2 Comparison of the pharmacology of the slow-h.s.p. and the adenosine hyperpolarization. *a*, The slow-h.s.p. and adenosine hyperpolarization in control conditions (left panels) and after 10 and 5 min treatment, respectively (middle panels), with 1 mM caffeine. The responses returned to control levels after a 15-min wash with normal Krebs' solution (right panels). Adenosine (100 μM) was applied to the bath in a drop from an 18-gauge needle attached to a 1-ml glass syringe as indicated (dot). Resting potentials were −66 mV and −62 mV, respectively. *b*, The slow-h.s.p. and adenosine hyperpolarization in control (left panels) and 10 min after treatment with 0.25 IU ml^{-1} adenosine deaminase (middle panels). The responses returned to control amplitude after 15 min washing with normal Krebs' solution (right panels). Resting potentials were −68 mV. Adenosine was applied by superfusion as indicated (bar). *c*, Slow-h.s.p. and adenosine response in control (left panels), 8 min after treatment with dipyridamole (1 μM; middle panels) and 10 min after washing with control Krebs' solution (right panels). Resting potentials were −59 mV and −60 mV, respectively.

intensity was increased (8–30 V), a slower hyperpolarizing potential appeared on the falling phase of the slow-i.p.s.p. (Fig. 1*b*). Treatment with atropine (0.5–1 μM) completely abolished the slow-i.p.s.p.[11] and revealed the presence of the slow-h.s.p. (Fig. 1*c*). This potential was quickly abolished in a low Ca^{2+} (0.25 mM), high Mg^{2+} (3.74 mM) solution, suggesting that the slow-h.s.p. was produced by a neurotransmitter released from the terminals of neurones whose axons were present in the preganglionic nerve trunk. The amplitude of the non-cholinergic slow-h.s.p. varied from 2 to 13 mV in individual neurones, with a mean amplitude obtained from 58 neurones of 4.1 ± 1.7 mV (mean ±s.d.), recorded at a mean resting membrane potential of 62.3 ± 3.4 mV. The mean duration of the slow-h.s.p. was 31.6 ± 5.5 s, an order of magnitude greater than that of the muscarinic slow-i.p.s.p.[11].

Adenosine (5 μM–1 mM) hyperpolarized (2–10 mV) most (92%) ganglion cells ($n = 71$, Fig. 1*d*); other neurones (8%) were slightly depolarized by or did not respond to adenosine. The adenosine hyperpolarization persisted in low Ca^{2+} (0.25 mM), high Mg^{2+} (3.74 mM) solution for more than 25 min,

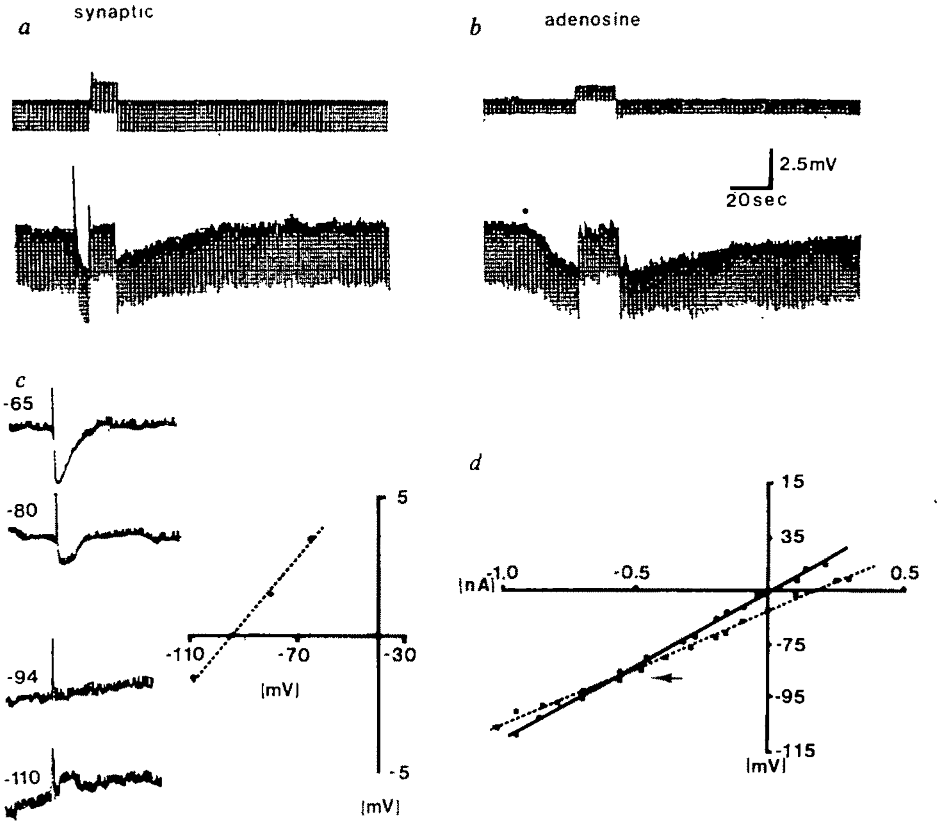

Fig. 3 Comparison of the membrane mechanism of the slow-h.s.p. and the adenosine hyperpolarization. *a*, *b*, Upper trace, the transmembrane current passed by means of a bridge circuit; lower trace, the membrane potential during the slow-h.s.p. (*a*) or during superfusion of adenosine (50 μM) applied in a drop to the organ bath as indicated (dot). Resting potential = −68 mV in *a* and −60 mV in *b*. *c*, Left panel, slow-h.s.p. recorded at different membrane potentials in the presence of hexamethonium (1 mM) and atropine (1 μM); right panel, graph of the relationship between the amplitude of the slow-h.s.p. (ordinate; 40 Hz, 250 ms) illustrated in left panels and membrane potential (abscissa). The slow-h.s.p. was nullified here, around −94 mV; the slow-h.s.p. reversed polarity with further hyperpolarization of the membrane. *d*, Hyperpolarizing and depolarizing current pulses of constant duration (100 ms) and varying amplitude were passed across the membrane in control solution (solid line; circles) and in the presence (dashed lines; squares) of a solution containing adenosine (50 μM). The difference in the slope of the lines indicates a decrease in resistance during adenosine superfusion. The intersection point of the lines (arrow) represents the estimated reversal potential of the response, here −90 mV for adenosine. Lines were fitted by eye.

suggesting a direct action of adenosine on vesical neurones. The adenosine hyperpolarization also persisted in the presence of hexamethonium (1 mM) and atropine (0.5–1 μM). On the other hand, bath application of ATP (100 nM–1 mM) produced a depolarization (3–12 mV) in 62% of vesical parasympathetic neurones tested ($n = 63$, Fig. 1*e*). Some parasympathetic neurones (14%) showed a hyperpolarizing response to ATP (100 nM–1 mM) application, while others (24%) were not affected by ATP at these concentrations. In many cases, ATP and adenosine were applied to the same cells. These data suggested that the response to exogenous adenosine application is similar to the slow hyperpolarizing synaptic response.

Pharmacological analyses were performed to examine the possibility that the slow-h.s.p. is mediated by a purinergic neurotransmitter[7,8]. Caffeine, known to be an antagonist of the P_1 purinoceptor[2], depressed the slow-h.s.p. recorded in 11 (73.3%) out of 15 neurones tested (Fig. 2*a*). The slow-h.s.p. was decreased 89.3 ± 7.7% ($n = 8$) by caffeine (1 mM) in 5 min and abolished in 10 min. The effect of caffeine was concentration dependent, 100 and 10 μM caffeine depressing the slow-h.s.p. by 64.4 ± 7.1% ($n = 7$) and 41.8 ± 5.2% ($n = 5$), respectively, after 5 min of treatment. In four neurones (26.7%), the slow-h.s.p. was relatively insensitive to the effect of caffeine (1 mM), being depressed by only ~22% after 10 min of treatment. Caffeine at these concentrations slightly hyperpolarized (1–3 mV) the membrane but did not significantly affect membrane resistance or directly evoked action potentials. Bath application of caffeine (1 mM) decreased the amplitude of the adenosine hyperpolarization by 92.6 ± 4.3% ($n = 11$) after 5 min of treatment. The adenosine hyperpolarization was subsequently blocked reversibly by caffeine (Fig. 2*a*), but the response to ATP was not affected (not shown). These data suggest that the receptor underlying the synaptic response is similar to that mediating the response to adenosine—a P_1 purinoceptor.

Adenosine deaminase, the enzyme which catabolizes adenosine to inosine and NH_3, depressed the amplitude of the slow-h.s.p. by 82.4 ± 8.6% (5 cells) after 5–10 min of treatment (Fig. 2*b*) and depressed the response to exogenous adenosine by 92.3 ± 7.4% ($n = 7$). Bath application of adenosine deaminase (0.25 IU ml^{-1}) produced no significant changes in the membrane potential or resistance. All the effects of this enzyme were reversible. The application of dipyridamole (3 μM), which has been reported to block the uptake of adenosine[12] and augment adenosine effects in heart muscle[13] and in neurones of sympathetic ganglia[14], produced a slight hyperpolarization of parasympathetic neurones (2–4 mV), with no appreciable change in membrane resistance. At 1 μM, dipyridamole increased the amplitude and duration of the slow-h.s.p. by 45.7 ± 5.3% ($n = 6$) and 185.1 ± 0.3% ($n = 6$), respectively (Fig. 2*c*), while the amplitude and duration of the response to exogenous adenosine were enhanced by 128.3 ± 10.3% ($n = 6$) and 136.6 ± 15.4% ($n = 6$), respectively. These data suggest that the synaptic response, the slow-h.s.p., and adenosine hyperpolarization are affected by pharmacological agents in a similar manner.

We compared the membrane mechanism of the slow-h.s.p. with that of the adenosine hyperpolarization (Fig. 3). The slow-h.s.p. was associated with a decrease in membrane resistance (Fig. 3*a*). The changes in membrane resistance could be separated from membrane rectification by passing a cathodal current through the recording electrodes and returning the membrane to its original resting level during the peak of the slow-h.s.p. or adenosine hyperpolarization. The mean decrease in resistance during the slow-h.s.p. was 35.8 ± 8.8% ($n = 12$). Adenosine (100 μM) induced hyperpolarization was also associated with a decrease in membrane resistance (Fig. 3*b*), to 33.7 ± 5.6% ($n = 9$) of that at original resting potential levels. We also compared the reversal potential for the synaptic response with that of the adenosine hyperpolarization. The amplitude of the slow-h.s.p. was decreased by membrane hyperpolarization and eventually reversed in polarity at a membrane potential of −95 mV (Fig. 3*c*). The mean reversal potential of the slow-h.s.p. obtained in five neurones was −93.7 ± 7.4 mV. As Fig. 3*d* shows, the slope of the current-voltage (*I*–*V*) curve was decreased in the presence of adenosine (100 μM). The reversal potential of the adenosine hyperpolarization estimated by the intersection of *I*–*V* curves determined in control and adenosine (50 μM) containing Krebs' solution[15] was −90 mV; the mean reversal potential of the adenosine hyperpolarization obtained from nine neurones was

−93.5 ± 4.3 mV. The amplitude of the adenosine hyperpolarization was increased in K^+-free solution to 175.5 ± 10.3% of the control response ($n = 9$). The slow-h.s.p. was also augmented in a low-K^+ (0.5 mM) solution, to 156.1 ± 8.1% of the control value ($n = 7$). Neither the slow-h.s.p. nor the adenosine hyperpolarization was affected by prolonged injection of Cl^- ion, applied by passage of outward current through an electrode filled with 2 M KCl. This indicates that Cl^- ions are probably not involved in the responses. These data suggest that both the slow-h.s.p. and the adenosine hyperpolarization are mediated primarily through activation of a K^+ conductance. A similar ionic mechanism for a purinergic hyperpolarization has been reported in guinea pig taenia coli[16], frog heart muscle[13] and *Xenopus* oocyte[17].

Our data demonstrate that a synaptic response, a slow-h.s.p., produced by preganglionic nerve stimulation in vesical parasympathetic neurones in the presence of cholinergic blocking agents, can be most closely mimicked by exogenous application of adenosine. The present results seem to satisfy the pharmacological and electrophysiological criteria for establishing adenosine as a neurotransmitter in vesical parasympathetic ganglia. These data provide the first evidence for a synaptic response mediated by adenosine and lend further support to the mounting evidence that purines function as neurotransmitters in the autonomic nervous system.

We thank Drs Gil Hillman, Betty Williams and James Blankenship for their careful review of the manuscript. This work was supported by NS 16228, to P.S.G.

Received 15 May; accepted 20 June 1984.

1. Burnstock, G. *J. Physiol. Lond.* **313**, 1–35 (1981).
2. Burnstock, G. *Cell Membrane Receptors for Drugs and Hormones: A Multidisciplinary Approach* (eds Smith, R. W. & Bolis, L.) 107–118 (Raven, New York, 1978).
3. Stone, T. W. *Neuroscience* **6**, 523–555 (1981).
4. Phillis, J. W. & Wu, P. H. *Prog. Neurobiol.* **16**, 187–239 (1981).
5. Sneddon, P. and Westfall, D. P. & Fedan, J. S. *Science* **218**, 693–695 (1982).
6. Sneddon, P. & Westfall, D. P. *J. Physiol., Lond.* **347**, 561–580 (1984).
7. Burnstock, G., Cocks, T., Kasakov, L. & Wong, H. K. *Eur. J. Pharmac.* **49**, 145–149 (1978).
8. Burnstock, G., Cocks, T., Crowe, R. & Kasakov, L. *Br. J. pharmac.* **63**, 125–138 (1978).
9. DeGroat, W. C. & Booth, A. M. *Fedn. Proc.* **39**, 2990–2996 (1980).
10. DeGroat, W. C., Booth, A. M. & Krier, J. in *Integrative Functions of the Autonomic Nervous Systems* (eds Brooks, C. M., Koizumi, K. & Sato, A.) 234–247 (University of Tokyo Press, 1979).
11. Gallagher, J. P., Griffith, W. H. & Shinnick-Gallagher, P. *J. Physiol., Lond.* **332**, 473–486 (1982).
12. Nimit, Y., Skolnick, P. & Daly, J. W. *J. Neurochem.* **36**, 908–912 (1981).
13. Hartzell, N. C. *J. Physiol., Lond.* **293**, 23–50 (1979).
14. Henon, B. K. & McAfee, D. A. *J. Physiol., Lond.* **336**, 607–620 (1983).
15. Ginsborg, B. L., House, C. R. & Silinsky, E. M. *J. Physiol., Lond.* **236**, 723–731 (1974).
16. Tomita, T. & Wantanabe, H. *J. Physiol., Lond.* **231**, 167–178 (1973).
17. Lotan, I., Dascal, N., Cohen, S. & Lass, Y. *Nature* **298**, 572–574 (1982).

Partial correction of murine hereditary growth disorder by germ-line incorporation of a new gene

Robert E. Hammer, Richard D. Palmiter* & Ralph L. Brinster

Laboratory of Reproductive Physiology,
School of Veterinary Medicine, University of Pennsylvania,
Philadelphia, Pennsylvania 19104, USA
* Howard Hughes Medical Institute, Department of Biochemistry,
University of Washington, Seattle, Washington 98195, USA

The dwarf little (*lit*) mouse is a model for the human hereditary disorder, isolated growth hormone (GH) deficiency type I[1]. In these animals, dwarfism results from an autosomal recessively inherited gene mutation. The *GH* gene is present[2] but production of *GH* mRNA is deficient[3], resulting in reduced serum GH and concomitantly decreased serum somatomedin[4–6]. Growth retardation is evident by 15 days of age and adult animals reach approximately one-half normal size[1]. Mutant mice of both sexes also exhibit a delayed onset of puberty, with males having a high degree of infertility[1]. As administration of GH restores growth[7], we reasoned that growth failure in the mutant mice might be corrected by providing them with sufficient GH by gene therapy. Here we demonstrate that although the rat and human *GH* genes alone do not restore growth in transgenic mutants, a metallothionein–rat growth hormone fusion gene (*MT–rGH*) does. Moreover, the fertility of transgenic mutant males is improved; however, female fertility is impaired.

As one approach to gene therapy, we tested the feasibility of introducing either rat or human *GH* genes that contained normal 5′ and 3′-flanking sequences[8,9]. Because mutant eggs are difficult to obtain, we piloted this approach with normal mice. Thirty-two transgenic mice carrying one or more copies of the foreign *GH* genes were produced, and despite low levels of human growth hormone (*hGH*) mRNA transcripts in the liver and pituitary of some mice carrying the hGH_N and *cGH4* genes (data not shown), no foreign GH was detectable and none of the mice grew larger than normal (Table 1). This lack of *hGH* gene expression has occurred in other *hGH* mice[10] and may reflect a requirement for precise chromosomal localization[11,12], insufficient flanking sequences or highly species-specific regulation of *GH* gene expression. The absence of detectable serum hGH and increased growth suggested that introducing normal *GH* genes into mutant eggs would be ineffective; therefore, we attempted to correct the growth disorder of mutant *lit*/*lit* animals by introducing a *MT–rGH* fusion gene into mutant eggs, as this construct has been shown to stimulate growth of normal mice[13]. Forty-one animals developed from microinjected eggs; seven *lit*/*lit* mice carried the foreign gene (Table 2).

By 5 weeks of age, six of the seven transgenic *lit*/*lit* mice were already twice mutant size, and by 16 weeks were approximately 1.5 times the size of *lit*/+ mice (Table 2). Thus *MT–rGH*

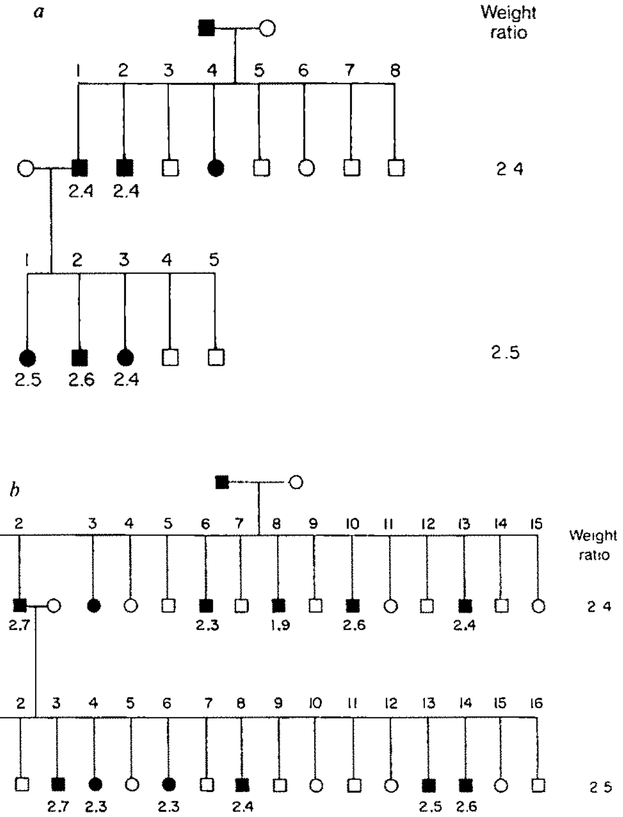

Fig. 1 Pedigree from: *a*, 41-1; *b*, 54-1 males. Mice that carry the *MT–rGH* genes are indicated by the solid symbols. Squares represent males and circles females. Numbers above symbols designate animal number and numbers below solid symbols the weight ratio of a MT-rGH mouse to control littermates at 6 weeks of age. Female 3 in the F_1 generation of 54-1 and female 4 in the F_1 generation of 41-1 died before body weights were taken.

Table 1 Transfer of *GH* structural genes to mice

Injected genes	DNA length (kb)	No. of transgenic mice	No. of gene copies	Rat or human GH in serum	Body weight ♂	Body weight ♀
rGH	7.6	8	1–250	ND	27.4 ± 2.1	22.3 ± 1.8
hGH_N	2.6	8	1–10	ND	27.1 ± 2.3	22.7 ± 1.1
hGH_N, hPL_L, hPL_A	43.0	16	1–50	ND	27.6 ± 1.2	21.5 ± 1.5
Control	—	—	—	—	27.5 ± 3.2	22.2 ± 1.7

A 7.6-kilobase (kb) *Bam*HI linearized fragment containing the entire *rGH* structural gene[8,19] was isolated and about 1,000 copies were microinjected into the male pronucleus of eggs from C57 × SJL hybrid crosses[20]. The 2.6-kb *Eco*RI linearized fragment containing the entire hGH structural gene (hGN_N)[9,21] or a cosmid fragment containing three genes of the *hGH* gene family (hGN_N and two human placental lactogen genes, hPL_L and hPL_A; *cGH4*, 43 kb)[21] were isolated and about 1,000 copies microinjected. The number of foreign structural genes per cell was estimated by DNA dot hybridization with a nick-translated 1.0-kb *Pst*I probe for *rGH* and a 1.0-kb *Pvu*II probe for hGH_N and *cGH4*. The radioactivity was then measured by scintillation counting[11,13]. Serum rat GH or hGH were determined by radioimmunoassay of duplicate samples using either rat[19] or human[11] GH standards respectively. The GH antiserum used interacts with both rat and mouse GH; therefore 'ND' indicates no significant difference between the serum GH concentration of rGH transgenic (mean ± s.d. 254 ± 54) and control (319 ± 50) mice. The concentration of hGH in hGH_N and cGH4 mice was lower than the limit of detection (~10 ng ml^{-1}) and is listed as 'ND'. Body weight is given as mean ± s.d. at 11 weeks of age; $n = 42$ animals.

Table 2 Expression of *MT–rGH* fusion gene in transgenic *little* mice

Animal	Sex	Genotype	Gene copy (No. per cell)	Serum GH (ng ml^{-1})	Body weight (g)	Ratio
20-1	♀	*lit/lit*^{1}	4	2,600	50.0	4.0
41-1	♂	*lit/lit*^{2}	17	31,200	41.8	2.9
41-2	♀	*lit/lit*^{2}	98	29,300	38.0	3.0
41-3	♀	*lit/lit*^{2}	1	1,463	12.9	1.0
54-1	♂	*lit/lit*^{1}	8	2,764	43.7	3.0
65-1	♀	*lit/lit*^{1}	10	1,630	39.0	3.1
65-2	♀	*lit/lit*^{1}	12	6,540	37.5	3.0
Control	♂	*lit/lit*	—	66 ± 11	14.6 ± 1.8	
Control	♀	*lit/lit*	—	76 ± 8	12.6 ± 0.4	
Control	♂	*lit/+*	—	254 ± 90	28.8 ± 2.3	
Control	♀	*lit/+*	—	254 ± 60	23.0 ± 1.9	
Control	♂	*+/+*	—	110 ± 18	31.0 ± 0.7	
Control	♀	*+/+*	—	240 ± 55	25.9 ± 1.0	

A 5.0-kb linear fragment of the fusion gene *MT–rGH*[13] containing the mouse *MT-I* regulator/promoter region fused to *rGH* gene was injected into fertilized one-cell eggs collected from superovulated[22] *lit/lit* females crossed with either *lit/lit* males or hypodactyl males carrying the little gene (*Hd+/+lit*). The male pronuclei of 690 fertilized eggs were microinjected with approximately 2 pl of buffer containing 300–600 copies of DNA, and 494 eggs were transferred into the oviducts of pseudopregnant recipients[20]. The animals were weaned and total nucleic acids extracted from a piece of tail and used for dot hybridization with a probe corresponding to exons 1 and 2 of *rGH* gene. Digestion of the DNA by *Sst*I or *Stu*I and Southern blotting confirmed the presence of *MT–rGH* genes and indicated that, in all animals with multiple copies, the foreign genes were integrated as tandem arrays (data not shown)[20]. For the genotype, mice that developed from eggs obtained from the cross mutant *lit/lit* females × *lit/lit* males are indicated by superscript 1 and those developing from crosses between *lit/lit* females and *Hd+/+lit* males (hypodactyl males carrying the little gene) are indicated by superscript 2. Mutant males have delayed sexual maturation and show a marked degree of infertility[1]. This suboptimal fertility was improved by implanting pituitaries from heterozygous mice into mutant males, thereby allowing us to make homozygous crosses for egg collection. The hypodactyl gene which is closely linked to *little* gene locus[1] was introduced into the little colony by crossing *lit/lit* females with *Hd+/++* males and using the resulting hypodactyl male offspring (*Hd+/+lit*) for stud with *lit/lit* females. Mice resulting from this cross are either *+lit/+lit* (five-toed and dwarf) or *Hd+/+lit* (hypodactyl and normal). The number of *MT–rGH* genes per cell was estimated by DNA dot hybridization with a nick-translated *Sst*I–*Bgl*II probe corresponding to the mouse *MT-I* promoter/regulator, and scintillation counting[23]. Serum GH levels were determined by radioimmunoassay of duplicate samples using GH standards[19]. The antibody used for rGH determinations binds both rat and mouse GH; therefore appropriate control values should be subtracted from transgenic GH values. Body weights were compared at 16 weeks of age. The weight ratio compares transgenic mutant body weight to control mutant mice of the same sex. Values for controls are mean ± s.e.m., with $n \geq 8$ in each group.

expression in transgenic mutants not only restores growth but changes their phenotype from dwarfs to giants. The absence of a correlation between copy number or gene dosage and growth rate has also been observed in other *MT–rGH* mice (unpublished) and *MT–hGH* mice[11] and may result, at least in part, from only one or a few genes in the tandem arrays actually being expressed.

Serum GH levels in *MT–rGH* transgenic and control mice were quantified to see whether the accelerated growth correlated with elevated serum GH (Table 2). Mutant mice had approximately one-third the quantity of GH found in *lit/+* mice. All seven of the transgenic mutant mice had elevated serum GH ranging between 20 and 400 times greater than *lit/lit* control mice and 5 and 120 times greater than *lit/+* and *+/+* controls. The one transgenic mouse which failed to grow also had elevated serum GH. Transgenic mice with this characteristic have occurred previously in both *MT–rGH* (unpublished) and *MT–hGH*[11] experiments, indicating that although an immunoreactive product is produced, its biological potency is not assured.

To determine whether *MT–rGH* was stably integrated into the host chromosome making the phenotype heritable, two transgenic *lit/lit* males, 41-1 and 54-1 (Table 2), were bred with *lit/lit* females (Fig. 1). Both males transmitted their characteristic number of copies of fusion gene (data not shown) to approximately half of their offspring, indicating that multiple copies were integrated into a single chromosomal location. In both lines, the fusion gene has been transmitted into the second generation as well; every animal carrying *MT–rGH* genes was more than twice mutant size by 6 weeks of age.

To establish when transgenic mutants develop a sensitivity to elevated serum GH, we bred 54-1-2 ♂ with *lit/lit* females (Fig. 1) and compared the growth rates of transgenic and normal mutant offspring and *+/+* controls (Fig. 2). At about 40 days of age the growth of mutant mice essentially ceases. In contrast, transgenic mutant mice enter an accelerated growth phase at about 20 days of age and by 90 days they are approximately three times the size of nontransgenic littermates. Transgenic mutants surpass normal body weight by 30 days of age and by 90 days are more than 1.5 times normal weight.

All the transgenic males in the F_1 generation of 54-1 have been bred and have sired at least two litters. Thus in contrast to mutant males where only 50% sire one litter, 30% sire second litters and third litters are rare; the fertility of transgenic mutant males is improved by *MT–rGH* expression. Transgenic mutant females (with the exception of 41-3, Table 2) were also bred to *+/+* males and all four were infertile. Although control *lit/lit* females show delayed sexual maturation, they eventually reach full fertility[1]. We also assessed the effects of extra-pituitary GH production on the fertility of *MT–GH* transgenic C57 × SJL hybrid mice. F_0 males exhibited slightly reduced fertility (15 out of 20 were fertile). The fertility of F_1 *MT–GH* male mice was

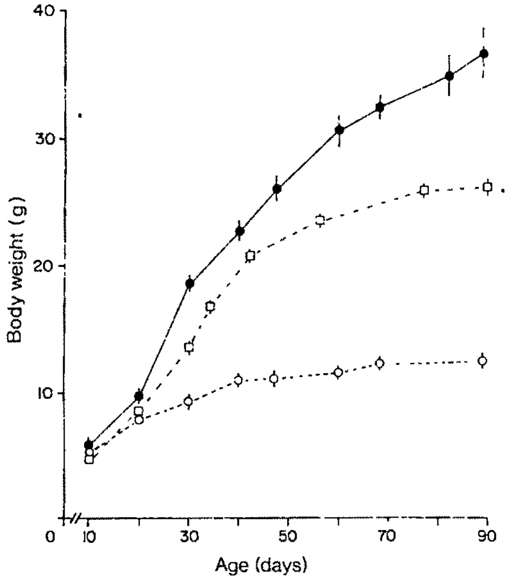

Fig. 2 Growth curves of MT–rGH *lit/lit* mice, nontransgenic littermates and control C57Bl/6J mice. One litter (eight pups) from the F_2 generation of 54-1 (see Fig. 1) was marked 1 week after birth and their weights were recorded periodically. Hybridization of tail DNA with a 0.38-kb *Xho*I–*Pvu*II *rGH* probe revealed five offspring inherited the *MT–rGH* gene (●) and three did not (○). □, Weights of C57Bl/6J mice. Mean body weights ± s.e.m. are indicated at each point.

normal with 11 out of 12 siring multiple litters. In contrast, the fecundity of F_0 transgenic females was dramatically reduced: only 1 of 10 of the *MT–GH* females bred was fertile. Thus whereas excess GH in transgenic mutant males improves fertility and has a negligible effect on the fertility of other *MT–GH* males, it dramatically reduces the fertility of both transgenic mutant and +/+ females. The mechanisms by which GH influences fertility are unexplored.

Several different *Drosophila* null mutants have been corrected recently by introducing wild-type gene counterparts into the germ line by their injection as part of P-element vectors into mutant eggs[14–16]. In the case described here, the primary defect is unknown. The *lit* mutation probably affects the regulation of expression of *GH* gene rather than gene itself[2,3]. Therefore, we attempted to correct the phenotypic defect in GH production by supplying a *GH* gene attached to an alternate promoter so that it would be independent of normal *GH* regulation. Although this approach has remedied the diminutive size of *lit/lit* mice as well as improved the fertility of males, we have uncovered an unsuspected deleterious effect of chronic elevated GH production on female fertility.

Although it seems feasible to correct certain genetic defects in animals, the application of the present technology to humans is inappropriate for several practical reasons. First, the techniques are inefficient; only about 1% of the injected eggs develop into mice that express the gene. Second, because the integration site of the foreign DNA is unpredictable, it is not possible to replace mutant DNA sequences with normal sequences. Thus the mutant gene will not be eliminated from the gene pool and will probably segregate independently of the foreign gene in the next generation. Furthermore, the unpredictability of integration means that it is possible that the foreign DNA could disrupt a normal gene, thereby creating a new mutation[10,17,18]. Current estimates are that about 20% of transgenic mice harbour recessive mutations[10,17]. These considerations, coupled with the fact that for most genetic diseases only one of four offspring are at risk, argue against application to humans.

We thank Dr Ronald Evans for continued interest and help, Myrna Trumbauer and Mary Yagle for experimental assistance, Dr Eva Eicher and Linda Washburn for assistance in setting up our *little* and *hypodactyl* colonies, and April Hamel for secretarial help. The cosmid containing the human *GH* gene family was provided by Greg Barsh and Richard Gelinas. R.E.H. was supported by NIH training grant HD 07155, and the work by research grants from NIH (HD 17321 and HD 09172) and NSF (PCM 81 07172).

Received 28 March; accepted 1 June 1984.

1. Eicher, E. M. & Beamer, W. G. *J. Hered.* 67, 87–91 (1976).
2. Phillips, J. A., Beamer, W. G. & Bartke, A. *J. Endocr.* 92, 405–407 (1982).
3. Cheng, T. C., Beamer, W. G., Phillips, J. A., Bartke, A. & Mallonee, R. L. *Endocrinology* 113, 1669–1678 (1983).
4. Herington, A. C., Harrison, D. & Graystone, *J. Endocr.* 112, 2032–2038 (1983).
5. Nissley, S. P., Knazek, R. A. & Wolff, G. L. *Horm. Metab. Res.* 12, 158–164 (1980).
6. McKern, N. M., Cheek, D. B. & Crewther, W. G. *Aust. J. biol. Sci.* 34, 221–230 (1981).
7. Beamer, W. G. & Eicher, E. M. *J. Endocr.* 71, 37–45 (1976).
8. Barta, A., Richards, R. I., Baxter, J. D. & Shine, J. *Proc. natn. Acad. Sci. U.S.A.* 78, 4867–4871 (1981).
9. Seeburg, P. H. *DNA* 1, 239–249 (1982).
10. Wagner, E. F., Covarrubias, L., Stewart, T. A. & Mintz, B. *Cell* 35, 647–655 (1983).
11. Palmiter, R. D., Norstedt, G., Gelinas, R. E., Hammer, R. E. & Brinster, R. L. *Science* 222, 809–814 (1983).
12. Jaenisch, R. *et al. Cell* 24, 519–529 (1981).
13. Palmiter, R. D. *et al. Nature* 300, 611–615 (1982).
14. Scholnick, S. B., Morgan, B. A. & Hirsh, J. *Cell* 34, 37–45 (1983).
15. Spradling, A. C. & Rubin, G. M. *Cell* 34, 47–57 (1983).
16. Goldberg, D. A., Posakony, J. W. & Maniatis, T. *Cell* 34, 59–73 (1983).
17. Schnieke, A., Harbers, K. & Jaenisch, R. *Nature* 304, 315–320 (1983).
18. Palmiter, R. D., Wilkie, T. M., Chen, H. Y. & Brinster, R. L. *Cell* 36, 869–877 (1984).
19. Doehmer, J. *et al. Proc. natn. Acad. Sci. U.S.A.* 79, 2268–2272 (1982).
20. Brinster, R. L. *et al. Cell* 27, 223–231 (1981).
21. Barsh, G. S., Seeburg, P. H. & Gelinas, R. E. *Nucleic Acids Res.* 11, 3939–3958 (1983).
22. Brinster, R. L. in *Growth, Nutrition and Metabolism of Cells in Culture* Vol. 2 (eds Rothblat, G. & Cristofalo, V.) 251–286 (Academic, New York, 1972).
23. Palmiter, R. D., Chen, H. Y. & Brinster, R. L. *Cell* 29, 701–710 (1982).

Live recombinant vaccinia virus protects chimpanzees against hepatitis B

Bernard Moss*, Geoffrey L. Smith*, John L. Gerin† & Robert H. Purcell‡

* Laboratory of Viral Diseases, and ‡ Laboratory of Infectious Diseases, National Institute of Allergy and Infectious Diseases, National Institutes of Health, Bethesda, Maryland 20205, USA
† Division of Molecular Virology and Immunology, Georgetown University Medical Center, Rockville, Maryland 20852, USA

Hepatitis B virus (HBV) is an important human pathogen responsible for over 200 million cases of chronic infection, many of which progress to hepatocellular carcinoma. Although HBV cannot be propagated in tissue culture, highly effective subunit vaccines obtained from the plasma of chronically infected patients have been developed and licensed[1–3]. Such vaccines are safe but their expense and limited quantities make them unavailable to most Third World countries. Other approaches to vaccine construction, including purification of the HBV surface antigen (HBsAg) from genetically engineered eukaryotic cells[4–13] and the synthesis of peptides predicted from the nucleotide sequence of the HBsAg gene[14–19], are still under evaluation. Another potential application of recombinant DNA technology to vaccine development is the use of live virus vectors to express foreign genes[20–25]. An infectious vaccinia virus recombinant that expressed the HBsAg in animal cells and which stimulated the production of antibody to HBsAg (anti-HBs) in rabbits represented a novel candidate vaccine of this class[22,23]. As a continuation of our earlier study, we now present evidence that chimpanzees vaccinated with a live recombinant vaccinia virus were protected against hepatitis following challenge with HBV.

The construction of vHBs4, the recombinant vaccinia virus used for these experiments, has been described elsewhere[22]. Briefly, a 1,350-base pair DNA fragment of HBV strain *adw*, containing the entire gene coding for HBsAg, was fused to an early vaccinia virus promoter and inserted into the coding sequence of the vaccinia virus thymidine kinase (*tk*) gene. The chimaeric gene was inserted into vaccinia virus by homologous recombination *in vivo* and infectious TK^- recombinant virus was isolated.

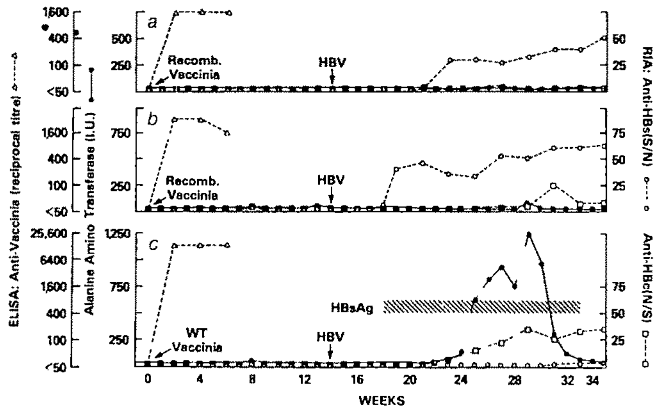

Fig. 1 Response of chimpanzees to intradermal vaccination with live recombianant virus vHBs4 or wild-type vaccinia virus, followed by challenge with live HBV. Chimpanzee 66 (*a*) and chimpanzee 67 (*b*) received recombinant vaccinia virus; chimpanzee A-98 (*c*) received wild-type vaccinia virus. Alanine aminotransferase activity is expressed in IU l^{-1}. Antibodies to vaccinia are expressed as reciprocal dilutions; anti-HBs and anti-HBc are expressed as the ratio of sample c.p.m. to negative control c.p.m. (S/N) and negative control c.p.m. to sample c.p.m. (N/S) respectively. Positive HBsAg values (>2.1 P/N) are shown as cross-hatching; between weeks 19 and 32, chimpanzee A-98 had P/N values ranging from 56 to 155.

Three chimpanzees (*Pan troglodytes*) weighing 14–25 kg were housed and maintained as described previously[26]. None showed serological evidence of prior exposure to HBV, as determined with commercial radioimmunoassays for HBV markers (HBsAg, AUSRIA; anti-HBs, AUSAB; anti-HB core antigen, anti-HBc, CORAB; anti-HBc IgM, CORZYME-M, Abbott Laboratories). Also, the animals had no other evidence of hepatitis, as judged by normal levels of alanine aminotransferase, aspartate aminotransferase and isocitric dehydrogenase enzymes.

To test the ability of vaccinia virus recombinant vHBs4 to protect chimpanzees against hepatitis, 10^8 plaque forming units (PFU) in 0.1 ml were administered intradermally in the upper back of two animals (66 and 67). A third chimpanzee (A-98) was vaccinated with 10^8 PFU of wild-type vaccinia virus. All three chimpanzees developed primary vaccinia lesions at the sites of vaccination. The two chimpanzees vaccinated with the recombinant virus had dermal lesions of diameters 24 and 22 mm, respectively. The chimpanzee vaccinated with the wild-type vaccinia developed a larger primary lesion of 37 mm diameter. A secondary vaccinia lesion developed in the right axilla of this animal. The greater severity of infection in the chimpanzee receiving wild-type virus, compared with that of chimpanzees receiving recombinant virus, was also reflected in a four- to eight-fold higher antibody titre to vaccinia virus when tested by enzyme-linked immunosorbent assay (ELISA)[27] (Fig. 1). Correlation of the TK^- phenotype of recombinant vaccinia virus with attenuated pathogenecity will be presented elsewhere.

Following vaccination, weekly serum samples were obtained from the three chimpanzees and tested for biochemical evidence of liver disease and serological evidence of exposure to hepatitis B viral antigens as described above. All sera were negative for elevations of liver enzyme activity and for evidence of exposure to HBV antigen except for one weak positive but repeatable 2.5 P/N value (ratio of positive c.p.m. to negative control c.p.m.) for anti-HBs 8 weeks after vaccination of chimpanzee 67 (Fig. 1).

Fourteen weeks after vaccination, all three animals were challenged intravenously with $10^{3.5}$ chimpanzee ID_{50} units of live HBV (subtype *ayw*, strain MS-2), a dose and strain of HBV which has consistently produced hepatitis B in chimpanzees[26,28]. Figure 1 shows that chimpanzee A-98 (vaccinated with wild-type vaccinia) developed typical hepatitis B. Circulating HBsAg appeared 4 weeks after HBV challenge and reached a peak P/N value of 155. Anti-HBc and biochemical evidence of hepatitis occurred after 8 and 9 weeks, respectively. HBsAg levels declined and disappeared by 19 weeks after challenge, coincident with the appearance of anti-HBs.

In contrast, chimpanzees 66 and 67 (vaccinated with recombinant virus) had no detectable HBsAg or biochemical evidence of hepatitis. Instead, anti-HBs appeared at 4–7 weeks after challenge and rapidly rose to high levels that persisted throughout the experiment. Both chimpanzees developed low levels (3.8–8.8 N/P) of anti-HBc, 21 or 27 weeks post-challenge, indicating that they had experienced inapparent infections with HBV. As a follow-up, the livers of the two chimpanzees inoculated with recombinant vaccinia virus were biopsied at 11 months after HBV challenge. There was no evidence of acute or chronic hepatitis.

Sera from chimpanzees 66 and 67 were analysed for the immunoglobulin class of anti-HBs by sucrose gradient centrifugation followed by radioimmunoassay of the fractions containing IgM or IgG immunoglobulins for anti-HBs activity. Two weeks after detection of anti-HBs in chimpanzees 66 and 67, IgM and IgG anti-HBs activities were present in approximately equal proportions (data not shown). Late convalescent sera (14–17 weeks after seroconversion) contained only IgG anti-HBs. Thus, the immune reaction had features characteristic of both primary and anamnestic responses. Sera obtained from chimpanzees 66 and 67 during the early phase of the immune response (2–6 weeks after seroconversion) were tested by radioimmunoassay[29] for the subtype specificity of the anti-HBs: only anti-*a* was detected.

This study demonstrated that chimpanzees receiving a single intradermal vaccination with a live recombinant vaccinia virus that expresses HBsAg were protected against hepatitis B. Following a challenge with HBV of a heterologous subtype, the vaccinated animals experienced a mild inapparent infection characterized only by seroconversion to anti-HBs and anti-HBc. The marginal primary antibody response of chimpanzees 66 and 67, when compared with the anti-HBs response of rabbits following vaccination with this same recombinant vaccinia virus, is in keeping with the relatively poor response of primates to a single dose of HBsAg in the absence of adjuvants[30]. Although the chimpanzees had little or no circulating anti-HBs after vaccination, they were immunologically 'primed'. Consequently, they showed a brisk and sustained antibody response, presumably due to newly synthesized HBsAg, following challenge with live HBV. The early detection of IgG anti-HBs and the anti-*a* subtype specificity are consistent with the anamnestic nature of the response. Priming of neutralizing antibody production by vaccination of rabbits with synthetic peptides of poliovirus structural protein VP1 has been reported[31], but has not been demonstrated previously for HBV.

In conclusion, these studies indicate the feasibility of using a recombinant vaccinia virus as a live hepatitis B vaccine. Current research is directed towards increasing HBsAg expression by using stronger vaccinia virus promoters.

Since submission of this manuscript, additional vaccinia virus recombinants that express prokaryotic chloramphenicol acetyltransferase[32], herpesvirus glycoprotein D (ref. 33), HBsAg[33] and malaria sporozoite antigen[34] have been described.

We thank R. L. M. Buller for vaccinia virus antibody determinations, H. Popper for evaluation of liver biopsies, W. T. London and J. Cicmanec for care and management of the chimpanzees and R. Engel for technical assistance.

Received 21 May; accepted 26 June 1984.

1. Szmuness, W. *et al. New Engl. J. Med.* **303**, 833–841 (1980).
2. Crosnier, J. *et al. Lancet* **i**, 455–459 (1981).
3. Reesink, H. W. *et al. Antiviral Res.* **1**, 13–25 (1981).
4. Moriarty, A. M., Hoyer, B. H., Shih, J. W.-K., Gerin, J. L. & Hamer, D. H. *Proc. natn. Acad. Sci. U.S.A.* **78**, 2606–2610 (1981).
5. Dubois, M. F., Pourcel, C., Rousset, S., Chany, C. & Tiollais, P. *Proc. natn. Acad. Sci. U.S.A.* **77**, 4549–4553 (1980).
6. Gough, N. & Murray, K. J. *Molec. Biol.* **162**, 43–67 (1983).
7. Wang, Y., Schafer-Ridder, M., Stratoma, C., Wong, T. K. & Hofschneider, P. H. *EMBO J.* **1**, 1213–1216 (1982).
8. Colbere-Garapin, F., Horodniceanu, F., Kourilsky, P. & Garapin, A. C. *EMBO J.* **2**, 21–25 (1983).
9. Crowley, C. W., Liu, C.-C. & Levinson, A. D. *Molec. cell. Biol.* **3**, 44–55 (1983).
10. Laub, O. *et al. J. Virol.* **48**, 271–280 (1983).

11. Valenzuela, P., Medina, A., Rutter, W. J., Ammerer, G. & Hall, B. D. *Nature* **298**, 347–350 (1982).
12. Miyanohara, A. *et al. Proc. natn. Acad. Sci. U.S.A.* **80**, 1–5 (1983).
13. Hitzeman, R. A. *et al. Nucleic Acids Res.* **11**, 2745–2763 (1983).
14. Lerner, R. A. *et al. Proc. natn. Acad. Sci. U.S.A.* **78**, 3403–3407 (1981).
15. Hopp, T. P. & Woods, K. R. *Proc. natn. Acad. Sci. U.S.A.* **78**, 3824–3828 (1981).
16. Dreesman, G. R. *et al. Nature* **295**, 158–160 (1982).
17. Bhatnagar, P. K. *et al. Proc. natn. Acad. Sci. U.S.A.* **79**, 4400–4404 (1982).
18. Prince, A. M., Ikram, H. & Hopp, T. P. *Proc. natn. Acad. Sci. U.S.A.* **79**, 579–582 (1982).
19. Neurath, A. R., Kent, S. B. & Strick, N. *Proc. natn. Acad. Sci. U.S.A.* **79**, 7871–7875 (1982).
20. Panicali, D. & Paoletti, E. *Proc. natn. Acad. Sci. U.S.A.* **79**, 4927–4931 (1982).
21. Mackett, M., Smith, G. L. & Moss, B. *Proc. natn. Acad. Sci. U.S.A.* **79**, 7415–7419 (1982).
22. Smith, G. L., Mackett, M. & Moss, B. *Nature* **302**, 490–495 (1983).
23. Smith, G. L., Mackett, M. & Moss, B. *UCLA Symp. molec. cell. Biol., new Ser.* **8**, 543–554 (1983).
24. Panicali, D., Davis, S. W., Weinberg, R. L. & Paoletti, E. *Proc. natn. Acad. Sci. U.S.A.* **80**, 5364–5368 (1983).
25. Smith, G. L., Murphy, B. R. & Moss, B. *Proc. natn. Acad. Sci. U.S.A.* **80**, 7155–7159 (1983).
26. Barker, L. F. *et al. J. infect. Dis.* **132**, 451–458 (1975).
27. Buller, R. M. L., Bhatt, P. N. & Wallace, G. D. *J. clin. Microbiol.* **18**, 1220–1225 (1983).
28. Tabor, E., Purcell, R. H., London, W. T. & Gerety, R. J. *J. infect. Dis.* **147**, 531–534 (1983).
29. Hoofnagle, J. H., Gerety, R. J., Smallwood, L. A. & Barker, L. F. *Gastroenterology* **72**, 290–296 (1977).
30. McAuliffe, V. J., Purcell, R. H., Gerin, J. L. & Tyeryar, F. J. in *Viral Hepatitis: 1981 int. Symp.* Philadelphia, 295–304 (Franklin Institute Press, 1982).
31. Emini, E., A., Jameson, B. A. & Wimmer, E., *Nature* **304**, 699–703 (1983).
32. Mackett, M., Smith, G. L. & Moss, B. *J. Virol.* **49**, 857–864 (1984).
33. Paoletti, E., Lipinskas, B. R., Samsonoff, C., Mercer, S. & Panicali, D. *Proc. natn. Acad. Sci. U.S.A.* **81**, 193–197 (1984).
34. Smith, G. L. *et al. Science* **224**, 397–399 (1984).

Defect in the generation of light-chain diversity in bursectomized chickens

Sirpa Jalkanen*‡, Markku Jalkanen†‡, Kaisa Granfors* & Paavo Toivanen*

* Departments of Medical Microbiology and †Medical Chemistry, Turku University, SF-20520 Turku, Finland

The avian bursa of Fabricius has been regarded as a central organ for B-cell development[1,2], but there is controversy about the existence of other sites for differentiation of B cells[3–6]. We have recently shown that chickens surgically bursectomized as early embryos, before the bursal primordium appears, can produce cytoplasmic, surface and serum immunoglobulins of IgM, IgG and IgA classes but are unable to generate specific antibodies in response to antigen[7–9]. We have therefore examined the structure and diversity of immunoglobulins of bursectomized chickens. Analysis of serum IgG revealed normal γ-heavy chains but altered light chains with more basic and less diverse isoelectric points than normal. These light chains may represent germ-line specificities not diversified by somatic mutations. Thus the bursa of Fabricius appears not to be necessary for the production of immunoglobulin molecules as such but to function in the creation and expansion of the antibody repertoire, possibly by providing a microenvironment for somatic mutations.

Chickens were surgically bursectomized after 60 h incubation by cutting off the tail caudally to the leg buds. Bursectomy was ascertained by careful microscopic examination at the autopsy at 10 weeks of age[7,8]. All bursectomized chickens had detectable amounts of serum immunoglobulins; mean concentrations of serum IgM and IgA were normal, whereas that of serum IgG was 1/10 of the control value[9]. In spite of immunoglobulin production, the bursectomized chickens did not respond to repeated immunizations with levan, *Escherichia coli* lipopolysaccharide, tetanus toxoid, dinitrophenyl-bovine serum albumin, brucella, diphtheria, pertussis, salmonella, sheep red blood cells and human γ-globulin[7,9]. Also all the tests made to detect natural antibodies to major histocompatibility complex (MHC) products, rabbit red blood cells, faecal bacteria and phosphorylcholine, and autoantibodies to the kidney, thyroids and liver, were totally negative. Antibodies to bursal structures were not observed[9]. The total lack of inducible or spontaneous antigen-specific antibody responses, given near normal immunoglobulin levels, suggested that the immunoglobulins produced by bursectomized chickens might be abnormal in structure. To examine this possibility, we compared serum IgG of the bursectomized and control chickens at the age of 10 weeks. Serum proteins were electrophoresed in SDS-polyacrylamide gel electrophoresis (PAGE)[10] or electrofocused in thin layer agarose gel[11], and then

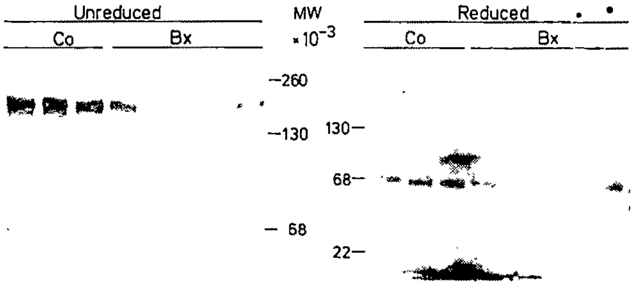

Fig. 1 Molecular weight of serum IgG and γ-chain of the control (Co) and bursectomized (Bx) chickens. Serum samples (1 µl) were examined in non-reducing (left) or reducing (right) conditions by SDS–PAGE[10] by using a 5% homogeneous or 5–22.5% gradient gel, respectively. After electrophoresis, proteins were transferred to a nitrocellulose sheet[12] (HAWP 000 10; Millipore). The sheet was saturated for 1 h with 20% fetal calf serum (FCS) diluted in Tris-buffered 0.9% NaCl (TBS) and then incubated for 2 h with rabbit antiserum against chicken γ-chain[8] diluted in 20% FCS–TBS. After extensive washings with 0.1% Triton-X-100-TBS for 1 h, alkaline phosphatase conjugated pig anti-rabbit IgG (Orion Diagnostica) was added and incubation was continued overnight. After washings with 0.1% Triton-X-100–TBS phosphatase activity on the sheet was visualized with α-naphthyl phosphate as a substrate and 4-amino-diphenylamine diazonium sulphate as a staining dye[11]. Pepsin-digested collagen β- and α-chains of type I of molecular weight (MW) 260,000 (260K) and 135K, bovine serum albumin (68K) and trypsin inhibitor (22K) were used as molecular weight standards.

Fig. 2 γ-Chain fragments of one control (Co) and one bursectomized (Bx) bird after enzymatic digestion with *Staphylococcus aureus* V-8 protease (V-8), chymotrypsin (CH) or trypsin (T): control incubation without any enzyme (C). Sodium sulphate precipitated serum immunoglobulins in SDS-buffer were subjected to enzymatic digestion for 2 h at 37 °C according to Cleveland *et al.*[21] All enzymes were used in concentrations of 25 µg ml⁻¹. After digestion proteins were fractionated by using a 15% homogeneous SDS–PAGE. Transfer to a nitrocellulose sheet and identification of γ-chain fragments were performed as described in Fig. 1 legend.

---

‡ Present addresses: Departments of Pathology (S.J.) and Pediatrics (M.J.), Stanford University Medical Center, Stanford, California 94305, USA.

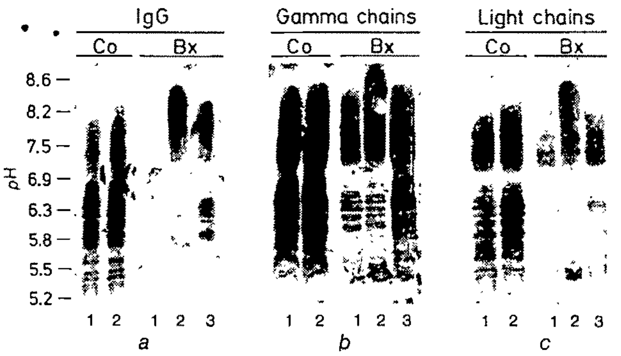

Fig. 3 *a*, Diversity of IgG; *b*, γ-chains; *c*, light chains of the control (Co) and bursectomized (Bx) chickens. Only bursectomized birds with serum IgG > 10% of the control value were selected for diversity analysis. Serum samples (2 μl) were electrofocused in 1% agarose gel in the absence (*a*) or presence (*b*, *c*) of 0.1 M mercaptoethanol[11]. After electrofocusing, proteins were transferred to a nitrocellulose sheet[11] and then the sheet was stained with the following antibodies. *a*, *b* Stained with the same procedure as in Figs 1 and 2 using rabbit antiserum against chicken γ-chain[8] at the first step. *c*, First incubated with monoclonal mouse anti-chicken light chain[13], then with rabbit anti-mouse IgG (Dako-immunoglobulins) and finally with alkaline phosphatase-conjugated pig anti-rabbit IgG (Orion Diagnostica). The *p*H gradient of the gel as measured with a surface electrode is indicated on the left. Light chains of both normal chickens reveal 26 separate bands at *p*H values 5.2–6.9 (concentration of total serum immunoglobulins 20.4 and 12.3 mg ml^{-1}) whereas two of the bursectomized chickens show 11 bands (concentration of total serum immunoglobulins 6.8 and 2.3 mg ml^{-1}) and the third showed 20 bands (concentration of total serum immunoglobulins 14.3 mg ml^{-1}) in this same area, indicating limited diversity of bursectomized birds show the same or even greater light-chain diversity than the controls. The mean isoelectric points of the light chains of bursectomized chickens are more basic than normal. In contrast, γ-chains of the bursectomized chickens have normal diversity.

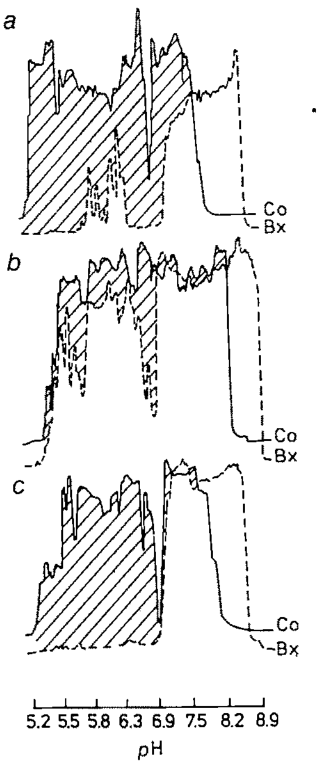

Fig. 4 Densitograms of the isoelectric focusing patterns of: *a*, whole IgG; *b*, gamma chains; *c*, light chains of one control (Co) and one bursectomized (Bx) chicken. These densitograms are made from isoelectric focusing patterns of the chickens Co 1 and Bx 2 in Fig. 3.

transferred to nitrocellulose sheets[11,12]. Immunoglobulins on the sheets were identified by an indirect immunoenzymatic staining[11] using polyclonal rabbit antibodies to γ-chain[8] and monoclonal mouse antibodies to light chain[13] (gift from Dr Max Cooper).

Bursectomized chickens had entire IgG molecules containing both heavy and light chains of apparently normal molecular weight (for γ-chain ~70,000 and for whole molecule ~190,000; Fig. 1). γ-chains of the bursectomized and control chickens showed identical cleavage patterns with three different proteases (Fig. 2), which suggests that their major structural fragments are similar and that they are expressed after similar gene rearrangement. Thus, IgG from bursectomized chickens exhibited no detectable structural abnormalities. However, whole IgG molecules of the bursectomized chickens had more basic isoelectric points than those of the controls (Fig. 3*a*). This was not due to a change in γ-chains, because they showed a normal diversity in isoelectric points (Fig. 3*b*). Instead, bursectomy decreased the amount of acidic light chains to an almost undetectable level without having any corresponding effect on the amount of basic light chains (Fig. 3*c*). Thus, alterations in the isoelectric spectra of the whole bursectomized IgG result from alterations in the light chains. This finding is clarified further in Fig. 4. The results clearly suggest abnormally limited diversity in these light chains.

Normal concentration of serum immunoglobulins does not necessarily imply normal immunoglobulin diversity and antigen binding capacity[14]. In this respect, the bursectomized chickens closely resemble human patients suffering from antibody deficiency with normal serum immunoglobulins[15,16]. Our finding of limited diversity of light chains in the bursectomized chickens is supported by the previous findings of Huang and Dreyer[17], who used testosterone bursectomy *in ovo* at day 11 of incubation. They concluded that bursectomy at day 11 of incubation blocks the generation of new clones of B cells. However, when bursectomy is performed 4 days after hatching a normal diversity of antibodies to human serum albumin develops[18].

Both somatic recombination and somatic mutation diversify the genetic information coded by the germ line genome. Somatic mutation, which alters bases throughout the sequences coding for the variable region, amplifies the diversity arising through recombination[19]. The isoelectric spectra of light chains of bursectomized chickens indicate that they consist of more basic amino acids than normal and may represent germ-line specificities. The antigen specificities of these antibodies have not yet been determined. The number of genes coding light-chain variable regions is not known in the chicken, but it is very probable that the number is small as in the human, and the diversity is generated mostly by somatic mutations[20]. Abnormality only in the light chains of the bursectomized chickens, on the other hand, indicates either that the specific influence of the bursa of Fabricius on B-cell development occurs late in the history of the B-cell clones, or that the normal diversity of the γ-chains observed in isoelectric focusing is generated with high numbers of variable-region genes.

Thus, our findings in bursectomized chickens of immunoglobulins without detectable antigen specificities and of abnormal diversity of light chains suggests that the bursa of Fabricius creates and expands the antibody repertoire by regulating somatic diversification, especially somatic mutations.

We thank Dr Max Cooper for monoclonal mouse anti-chicken light chain antiserum and him and Drs Irving Weissman, Matthias Wabl and Eugene Butcher for critical reading of this manuscript, Soile Niittoaho for technical assistance and Dr Timo Hyypiä for advice. This work was supported by grants from the Sigrid Jusélius Foundation and the Finnish Cancer Union.

Received 26 March; accepted 19 June 1984.

1. Lawton, A. R., Kincade, P. W. & Cooper, M. D. *Fedn Proc.* **34,** 33–39 (1975).
2. Toivanen, A., Toivanen, P., Eskola, J. & Lassila, O. in *Avian Immunology* (eds) Rose, M. E., Payne, L. N. & Freeman, B. M.) 45–62 (British Poultry Science Ltd, Edinburgh, 1981).
3. Lerner, K. G., Glick, B. & McDuffie, F. C. *J. Immun.* **107,** 493–503 (1971).
4. Sato, K. & Abe, S. *Immunology* **28,** 293–299 (1975).
5. Fitzsimmons, R. C., Garrod, E. M. F. & Garnett, I. *Cell. Immun.* **9,** 377–383 (1973).
6. Janković, B. D. *et al. Eur. J. Immun.* **5,** 656–659 (1975).
7. Granfors, K. *et al. Clin. Immun. Immunopath.* **23,** 459–469 (1982).
8. Jalkanen, S., Granfors, K., Jalkanen, M. & Toivanen, P. *J. Immun.* **130,** 2038–2041 (1983).
9. Jalkanen, S., Granfors, K., Jalkanen, M. & Toivanen, P. *Cell. Immun.* **80,** 363–373 (1983).
10. O'Farrell, P. H. *J. biol. Chem.* **250,** 4007–4021 (1975).
11. Jalkanen, M. & Jalkanen, S. *J. clin. Lab. Immun.* **10,** 225–228 (1983).
12. Towbin, H., Staehelin, T. & Gordon, J. *Proc. natn. Acad. Sci. U.S.A.* **76,** 4350–4354 (1979).
13. Chen, C. L., Lehmeyer, J. E. & Cooper, M. D. *J. Immun.* **129,** 2580–2585 (1982).
14. Van Meter, R., Good, R. A. & Cooper, M. D. *J. Immun.* **102,** 370–374 (1969).
15. Rothbach, C., Nagel, J., Rabin, B. & Fireman, P. *J. Pediat.* **94,** 250–253 (1979).
16. Saxon, A., *et al. Clin. Immun. Immunopath.* **17,** 235–244 (1980).
17. Huang, H. V. & Dreyer, W. J. *J. Immun.* **121,** 1738–1747 (1978).
18. Ivanyi, J. & Moreno, C. in *Developmental Immunobiology* (eds Solomon, J. B. & Horton, J. D.) 419–426 (Elsevier, Amsterdam, 1977).
19. Tonegawa, S. *Nature* **302,** 575–581 (1983).
20. Bentley, D. L. *Nature* **307,** 77–80 (1984).
21. Cleveland, D. W., Fischer, S. G., Kirschner, M. W. & Laemmli, U. K. *J. biol. Chem.* **252,** 1102–1106 (1977).

Direct evidence for an integrated function of J chain and secretory component in epithelial transport of immunoglobulins

P. Brandtzaeg* & H. Prydz†

* Laboratory for Immunohistochemistry and Immunopathology, Institute of Pathology, and † Research Institute for Internal Medicine, University of Oslo; The National Hospital, Rikshospitalet, Oslo 1, Norway

J chain is a polypeptide of molecular weight (M_r) ~ 15,000 common to human dimeric IgA and pentameric IgM[1,2]. These immunoglobulin polymers show a high affinity for secretory component (SC) *in vitro*[3,4], a feature that, in some studies, has been claimed to be a function of the J chain[5,6]. SC is a glycoprotein of M_r ~80,000 which is expressed on the basolateral surfaces of secretory epithelial cells[7,8] where, according to a current hypothesis, it may act as a receptor for dimeric IgA and pentameric IgM[9] which are selectively transported through secretory epithelial cells into exocrine fluids[10,11]. Previous studies, however, have not excluded the possibility that secretory cells express isotype-specific Fc receptors for IgA and IgM which may be involved in epithelial transport. We now report that the adsorption of immunoglobulin polymers to SC-expressing epithelial cells depends solely on a J chain-determined binding site. This finding lends biological significance to the striking J-chain expression shown by immunoglobulin-producing immunocytes in secretory tissues[12–14].

Almost 20 years ago Tomasi *et al.*[15] showed that the major immunoglobulin class present in human secretions is dimeric IgA covalently bound to an epithelial component now called SC. Pentameric IgM is similarly enriched in most exocrine fluids in contrast to IgG[10]; and secretory IgM is also associated with SC, although not in a covalently stabilized complex[11].

At least seven models have been proposed for the epithelial transport of IgA (reviewed in ref. 9). The common transport model for dimeric IgA and pentameric IgM proposed by one of us in the early 1970s[16,17] has subsequently gained considerable support from observations of both normal[8] and neoplastic[18,19] living epithelial cells. This model postulates that the J chain and SC represent the 'lock and key' in the selective external transport. It has recently been shown that SC is synthesized as a transmembrane protein of M_r ~95,000 (ref. 20). This larger SC precursor may alone, or in combination with other binding factors, constitute the actual receptor.

As it is known that human hepatocytes contain an IgA-binding site unrelated to SC[9] and that subsets of T and B lymphocytes[21,22], monocytes[23], alveolar macrophages[24] and granulocytes[23] express Fcα receptors, we believed it important to examine whether this is the case also for human secretory epithelial cells. In addition, we wanted to test directly the role of J chain in immunoglobulin binding to cell membrane-associated SC.

Experiments were performed with cells from the colonic carcinoma line designated H29 (ref. 25). The subclone HT29.E10 (used with the permission of Dr K. E. Mostov; ref. 20) was maintained as monolayers in 75 cm^2 Costar flasks at 37 °C with an atmosphere of 5% CO_2 in McCoy's Modified 5A medium supplemented with 15% fetal bovine serum, 2 mM glutamine, 50 units ml^{-1} penicillin and 50 µg ml^{-1} streptomycin. The cultures were split by 7-min treatment with 0.05% (w/v) trypsin and 0.02% (w/v) EDTA (Trypsin–EDTA; Flow), washed and seeded into Leighton tubes. Coverslips from 2–6-day-old cultures were divided into small areas that were subjected to tests with various human protein preparations (Table 1).

Direct immunofluorescence showed that only 20–40% of the living cells expressed substantial amounts of SC. After preincubation with polymeric IgA containing appropriate amounts of J chain (>4 mg per 100 mg), paired staining showed strict correspondence between SC expression and IgA binding (Fig. 1*a*); a positive result was obtained with staining end points of $<0.02\ \mathrm{g\,l^{-1}}$ for unlabelled and $<0.01\ \mathrm{g\,l^{-1}}$ for fluorescein-labelled preparations (Fig. 2). The only exception was colostral IgA which did not produce binding below 1 g l^{-1} (Fig. 1*c*). Monomers of IgA having no J chain showed no adsorption to the cells (Fig. 2*b*), even when tested at $\geqslant 3.5\ \mathrm{g\,l^{-1}}$ (Fig. 2). Conversely, three monomer preparations with small amounts of J chain showed binding between 0.3 and 1.8 g l^{-1} (Fig. 2), probably reflecting the presence of contaminating polymers. Four IgA polymers deficient in J chain produced staining end points comparable to the latter three monomer preparations when J-chain content and percentage SC-binding capacity were taken into account (Figs 1*d*, 2). The same was true for a J chain-deficient polymeric IgM in contrast to the three pentamers with normal J-chain content (Figs 1*e*, *f*, 2). On the whole, there was good agreement between the SC-binding capacity of the various preparations and their staining end points when tested on living cells (Fig. 2).

No binding of IgA or IgM was observed with epithelial cells lacking SC (Fig. 1*a*, *e*). Conversely, IgG at 4 g l^{-1} was largely adsorbed to such cells (Fig. 1*g*), probably reflecting the presence of Fcγ receptors, which may be expressed by carcinoma cells[26]. This finding indicated that the amount of these receptors might be related to cellular de-differentiation resulting from clonal diversification as preservation of SC expression is found mainly in well-differentiated colonic carcinomas[27].

In previous binding studies with the HT29 cell line, no dose–response analyses were performed. One study included dimeric IgA, monomeric IgA and IgG only at 0.2 g l^{-1} (ref. 19) and another used a much higher (4 g l^{-1}) concentration[18]. Although no binding was reported for monomeric IgA, the possibility could not be excluded that the positive results obtained with polymers were due to isotype receptors because paired staining for ligand and SC was not performed. Indeed, it has been shown that the Fcα receptors present on granulocytes show much higher (~10 times) binding activity for dimeric than for monomeric IgA[23]. We do not believe that tests with colostral IgA are an appropriate control; its incorporated SC could, by steric hindrance, have interfered with binding to putative Fcα receptors. Blocking by preincubation with antibodies to SC[5,6] is, using a similar reasoning, an unsatisfactory control.

Thus, for the first time we have excluded the possibility that 'conventional' Fcα and Fcμ receptors are significantly involved in the adsorption of immunoglobulin polymers to human secretory epithelial cells; a J chain-determined binding site specific for SC seems to be the decisive structure. Although much work has been done to elucidate a role for the J chain in B-cell differentiation, there is as yet no clue to this end[28]. Immunoglobulin-producing cells may express cytoplasmic J chain regardless of concurrent isotype[12]; but the combination

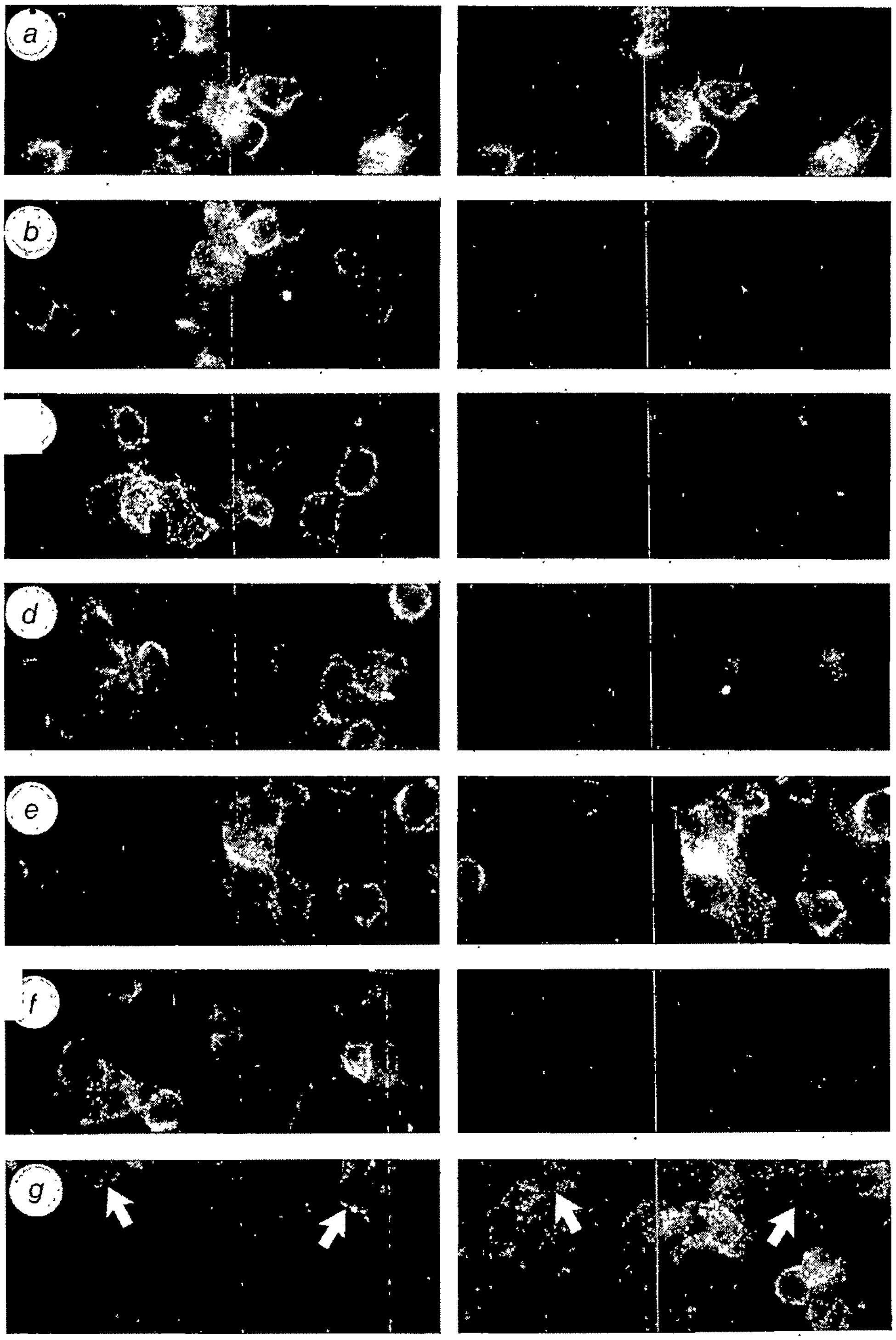

Fig. 1 Paired immunofluorescence staining of vital HT29.E10 monolayer preparations to demonstrate concurrent surface expression of SC (left panel, 10-s exposure of rhodamine emission) and binding of IgA, IgM or IgG (right panel, 20-s exposure of fluorescein emission). *a*, Binding of fluorescein-labelled polymeric IgA at 0.15 g l^{-1}. *b*, Lack of binding of fluorescein-labelled monomeric IgA at 1.2 g l^{-1}. *c*, Absence of binding of fluorescein-labelled colostral IgA at 1.0 g l^{-1}. *d*, Lack of binding of J chain-deficient polymeric IgA at 2.9 g l^{-1}. *e*, Binding of polymeric IgM at 0.25 g l^{-1}. *f*, Absence of binding of J chain-deficient polymeric IgM at 0.25 g l^{-1}. *g*, Binding of IgG at 4.0 g l^{-1} obtained mainly with SC-negative cells; the locations of two SC-positive cells are indicated by arrows. ×390.

Methods: Protein binding to living cells was tested by incubating unfixed monolayers at room temperature for 45 min with various concentrations of human immunoglobulin preparations which were applied either unlabelled or conjugated with fluorescein isothiocyanate as indicated. Dilutions (4.0–0.005 g l^{-1}) were done in phosphate-buffered isotonic saline (PBS), *p*H 7.5, containing bovine serum albumin (120 g l^{-1}). After washing in PBS (10 min), the monolayers were incubated (30 min) with a combination of rhodamine conjugate specific for SC and fluorescein conjugate specific for the appropriate immunoglobulin isotype. The characteristics of these fluorochrome conjugates have been reported previously[39]. After a final wash in PBS, all preparations were fixed in 96% ethanol (15 min), rinsed in PBS, and mounted in a polyvinyl alcohol medium for fluorescence microscopy[8].

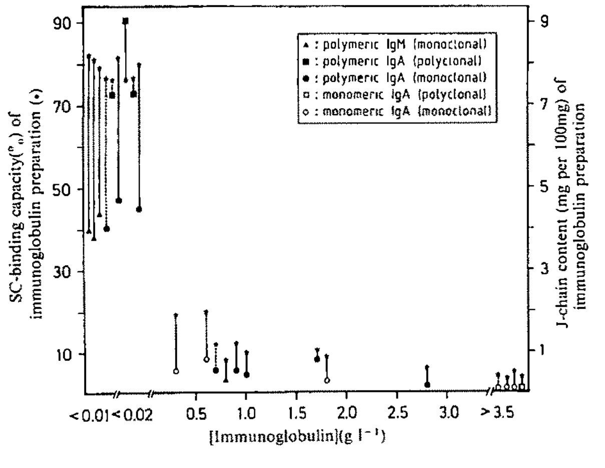

Fig. 2 Staining end points for binding of various human immunoglobulin preparations to the surface of HT29.E10 cells as determined by indirect immunofluorescence (see Fig. 1). The results were based on microscopic evaluation of 175 monolayer preparations incubated with IgA and 45 incubated with IgM. The abscissa gives the concentration of immunoglobulin needed for binding to SC-expressing epithelial cells. The plots of SC-binding capacity (*) and J-chain content (different symbols as indicated) are connected by vertical lines (broken for fluorescein-labelled IgA preparations); these data were obtained as described in Table 1.

Table 1 Characteristics of human immunoglobulin preparations used in binding studies with HT29.E10 cells

No. and type of preparation		Approximate composition	Molar *F*/*P* ratio	J-chain content (mg per 100 mg)	SC-binding capacity (%)*
1	Pc Pm IgA	78% Dimers 15% Larger polymers 7% Monomers	4.0	7.3	76
1	Pc Pm IgA	78% Dimers 15% Larger polymers 7% Monomers	None	7.3	76
2	Pc Pm IgA	70% Dimers 25% Larger polymers 5% Monomers	None	9.3	76
3	Mc Pm IgA	70% Dimers 20% Larger polymers 10% Monomers	0.9	4.0	77
4, 5	Mc Pm IgA	Mainly trimers 5–10% Monomers	None	4.5–4.7	80
6	Mc Pm IgA	20% Dimers 40% Trimers 40% Larger polymers	3.0	0.6	12
6	Mc Pm IgA	20% Dimers 40% Trimers 40% Larger polymers	None	0.6	12
7–9	Mc Pm IgA	40–60% Dimers 25–50% Larger polymers 10–20% Monomers	None	0.2–0.8	7–10
10	Colostral IgA	75% Dimers 25% Larger polymers	3.2	ND	19
11	Mc Mm IgA	Mainly monomers	3.6	0	4
12	Pc Mm IgA	Mainly monomers	None	0	4
13,14	Mc Mm IgA	Mainly monomers	None	0	4–5
15–17	Mc Mm IgA	Mainly monomers	None	0.3–0.8	9–20
18–20	Mc Pm IgM	Mainly pentamers	None	3.9–4.4	80–82
21	Mc Pm IgM	Mainly hexamers	None	0.5	8

Pc, polyclonal; Pm, polymeric; Mc, monoclonal; Mm, monomeric. Purification was achieved by anion-exchange chromatography and gel filtration[6]. It is unknown whether the J chain-deficient polymers had been produced as such or whether the J chain had been removed by selective proteolysis *in vivo* or *in vitro*[36]. The fact that preparation 21 consisted mainly of hexamers[33] suggests the former possibility. The approximate composition of each preparation was determined by density gradient centrifugation[6]. The *F*/*P* (fluorochrome/protein) ratio was determined as described previously for preparations labelled with fluorescein isothiocyanate[37]. The conjugation method and purification of the conjugates by anion-exchange chromatography followed standardized procedures[37]. J-chain content was measured for reduced preparations by an immunochemical method described previously[38]. ND, not determined.

* Percentage of 2.5 μg iodinated SC spontaneously associated with 100 μg protein as determined by density gradient centrifugation[3].

of J chain and immunoglobulin occurs only in IgA and IgM cells, thereby generating functional SC-binding sites already at the intracellular level[14]. Several studies have shown that the cytoplasmic appearance of J chain depends on B-cell stimulation[28,29]; clonal maturity may, on the other hand, result in repression of J chain synthesis[30]. The immunocytes populating secretory tissues apparently belong to relatively immature memory clones[31]; this feature probably explains the fact that not only do more than 90% of their IgA- and IgM-producing cells express J chain but so do most of the IgD-producing cells and 50–70% of the IgG-producing cells at these sites[14].

The obvious functional goal of J-chain expression at a certain stage of clonal B-cell differentiation is generation of SC-binding IgA and IgM locally where external transport through SC-positive epithelium can occur readily. However, it is not clear how the J chain is involved in the binding site; it may act solely by causing structural modification of the α and μ chains present in the immunoglobulin polymers. Studies both *in vitro* and *in vivo* have suggested that the J chain is not required absolutely for polymerization[32–34], but it clearly facilitates intracellular formation of selected polymer species that can combine with SC[14]. Despite the fact that purified dimeric J chain affords only marginal blocking of SC binding to dimeric IgA and pentameric IgM[35], the possibility of direct non-covalent interactions between polymer-associated J chain and SC cannot be excluded.

This study was supported by the Norwegian Cancer Society, the Norwegian Research Council for Science and the Humanities, the Norwegian Council for Cardiovascular Diseases, and Anders Jahre's Foundation. We thank Drs Sylvia Crago and Jiri Mestecky for providing the HT29.E10 cells.

Received 26 March; accepted 28 June 1984.

1. Halpern, M. S. & Koshland, M. E. *Nature* **228**, 1276–1278 (1970).
2. Mestecky, J., Zikan, J. & Butler, W. T. *Science* **171**, 1163–1165 (1971).
3. Brandtzaeg, P. *Immunochemistry* **14**, 179–188 (1977).
4. Socken, D. J. & Underdown, B. J. *Immunochemistry* **15**, 499–506 (1978).
5. Eskeland, T. & Brandtzaeg, P. *Immunochemistry* **11**, 161–163 (1974).
6. Brandtzaeg, P. *Scand. J. Immun.* **5**, 411–419 (1976).
7. Brandtzaeg, P. *J. Immun.* **122**, 1553–1559 (1974).
8. Brandtzaeg, P. *Scand. J. Immun.* **8**, 39–52 (1978).
9. Brandtzaeg, P. in *Recent Advances in Mucosal Immunity* (eds Strober, W., Hanson, L. A. & Sell, K. W.) 267–285 (Raven, New York, 1982).
10. Brandtzaeg, P., Fjellanger, I. & Gjeruldsen, S. T. *Scand. J. Haemat. Suppl.* **12**, 1–83 (1970).
11. Brandtzaeg, P. *Immunology* **29**, 559–570 (1975).
12. Brandtzaeg, P. *Nature* **252**, 418–420 (1974).
13. Brandtzaeg, P. *et al. J. Immun.* **122**, 503–510 (1979).
14. Brandtzaeg, P. *Molec. Immun.* **20**, 941–966 (1983).
15. Tomasi, T. B., Tan, E. M., Solomon, A. & Prendergast, R. A. *J. exp. Med.* **121**, 101–124 (1965).
16. Brandtzaeg, P. *Nature new Biol.* **243**, 142–143 (1973).
17. Brandtzaeg, P. *Immunology* **26**, 1101–1114 (1974).
18. Crago, S. S., Kulhavy, R., Prince, S. J. & Mestecky, J. *J. exp. Med.* **147**, 1832–1837 (1978).
19. Nagura, H., Nakane, P. K. & Brown, W. R. *J. Immun.* **123**, 2359–2368 (1979).
20. Mostov, K. E. & Blobel, G. *J. biol. Chem.* **257**, 11816–11821 (1982).
21. Lum, L. G. *et al. J. Immun.* **123**, 714–719 (1979).
22. Hoover, R. G., Dieckgraefe, B. K. & Lynch, R. G. *J. Immun.* **127**, 1560–1563 (1981).
23. Fanger, M. W., Shen, L., Pugh, J. & Bermier, G. M. *Proc. natn. Acad. Sci. U.S.A.* **77**, 3640–3644 (1980).
24. Gauldie, J., Richards, C. & Lamontagne, L. *Molec. Immun.* **20**, 1029–1037 (1983).
25. Huang, S. W., Fogh, J. & Hong, R. *Scand. J. Immun.* **2**, 263–268 (1976).
26. Tønder, O., Matre, R. & Wesenberg, F. *Contemp. Topics Immunobiol.* **10**, 167–176 (1980).
27. Rognum, T. O. *et al. J. clin. Path.* **35**, 922–933 (1982).
28. Koshland, M. E. *J. Immun.* **131**, 1–IX (1983).
29. Hajdu, I., Moldoveanu, Z., Cooper, M. & Mestecky, J. *J. exp. Med.* **158**, 1993–2006 (1983).
30. Korsrud, F. R. & Brandtzaeg, P. *Scand. J. Immun.* **13**, 281–287 (1981).
31. Cebra, J. J., Fuhrman, J. A., Horsfall, D. J. & Shahin, R. D. *Semin. infect. Dis.* **4**, 6–12 (1982).
32. Kownatzki, E. *Immun. Commun.* **2**, 105–113 (1973).
33. Eskeland, T. *Scand. J. Immun.* **3**, 757–763 (1974).
34. Stott, D. I. *Immunochemistry* **13**, 157–163 (1976).
35. Brandtzaeg, P. *Scand. J. Immun.* **4**, 837–842 (1975).
36. Koshland, M. E., Chapuis, R. M., Recht, B. & Brown, J. C. *J. Immun.* **118**, 775–781 (1977).
37. Brandtzaeg, P. *Scand. J. Immun.* **2**, 273–290 (1973).
38. Brandtzaeg, P. *Scand. J. Immun.* **4**, 439–450 (1975).
39. Brandtzaeg, P. *J. Histochem. Cytochem.* **29**, 1302–1315 (1981).

Immunoglobulin κ light-chain diversity in rabbit is based on the 3′ length heterogeneity of germ-line variable genes

Odile Heidmann & François Rougeon

Unité de Génétique et Biochimie du Développement, Institut Pasteur,
Institut Pasteur, ERA CNRS 851, 25, rue du Docteur Roux,
75724 Paris Cedex 15, France

Antibody diversity is generated by the combinatorial association of multiple distinct genetic segments (variable (V), joining (J) and diversity (D) light (L) and heavy (H) chains—V_L, J_L and V_H, D, J_H) and amplified somatically by three or four different mechanisms[1–6]. The κ system in mouse and human consists of 50–100 V_κ segments associated with a cluster of four or five functional J_κ segments, located 2.5 kilobases (kb) 5′ to a single C_κ gene[7–10]. The third hypervariable region (CDR3), which is part of the antibody combining site, is usually nine amino acids long in human and mouse κ chains. It is encoded by the last seven codons of the V_κ segment and the first two of the J_κ segment, one codon sometimes being added or deleted between V and J by junctional variation[2]. In the rabbit, the $C_\kappa1$ gene which encodes the major isotype[11–14], is associated with a cluster of five J_κ segments, only one of which seems to be functional[11], thus significantly decreasing the combinatorial potential. However, amino acid sequence comparison has revealed extensive heterogeneity in the length of rabbit CDR3 (ref. 15), suggesting the existence of a D segment analogous to that in the heavy-chain system. We show here that rabbit V_κ genes have several additional nucleotides at their 3′ ends. Thus, even with a single functional J_κ segment, high CDR3 diversity can be generated based on the length heterogeneity of V_κ germ-line segments and their greater length, which might leave scope for an increased junctional deletion.

We have isolated many recombinant cosmids from a rabbit liver genomic library[13] and find that each DNA insert of ~35 kb contains four to six *Eco*RI fragments that hybridize to a V_κ probe; this suggests that rabbit V_κ genes are clustered and spaced 6–8 kb apart. Human and mouse V_κ genes, with few exceptions[16], seem to be separated by 15 or 20 kb[17,18]. By Southern genomic blot experiments (Fig. 1), a single V_κ probe can detect as many as 25–30 restriction fragments displaying different intensities, and reveals little restriction site polymorphism between four independent individuals. Compared with mouse and human, where a single V_κ probe detects, respectively, 1–15 and 15–20 restriction fragments[19,20], in the rabbit at least one group of cross-hybridizing V_κ genes is greatly amplified. However, V_κ subgroups are not clearly defined[21,22]. It remains to be determined whether the probe can detect a large proportion of the V_κ gene repertoire, as in human, or only a small subset of this repertoire, as in mouse.

Figure 2 shows the nucleotide sequences of four unrearranged V_κ segments, isolated by pairs on two independent recombinant cosmids. They contain two exons, as in human and mouse[23,24], a small exon encoding most of the peptide leader sequence, separated by a 123-base pair (bp) intron from a large exon encoding the end of the signal peptide and the V_κ region. Whereas many human and mouse V_κ and V_H pseudogenes have been reported[23–25], these four rabbit V_κ genes show apparently normal signal peptide and V_κ coding sequences. The deduced amino acid sequences are 85% homologous (apart from CDR3, see also Fig. 3), the most common amino acid sequence being that defined by Kabat *et al.*[15]. As in mouse and human where signal peptides are usually 20 or 22 amino acids long[23,24], the ATG codon (position 143 in Fig. 2) gives a 22 amino acid signal peptide. We also note, 30 bp upstream, another in-phase ATG codon giving rise to a 32 amino acid signal peptide[26]. The promoter sequences (CAAT-like and TATA-like boxes) are located at the same distance from the ATG codon-22 as in the human HK102 V_κ gene (Fig. 2). Percentages of similarity given in Table 1 show that signal peptides are highly conserved and that rabbit flanking sequences and introns are more conserved than the V_κ coding regions. Furthermore, as shown in Fig. 2, base pair substitutions are preferentially clustered in the first third and in the CDR3 regions of the V_κ genes. Such patterns of segmental homology are highly characteristic of gene conversion events[17,27–31].

As in human and mouse, the recombination signal at the end of the V_κ coding sequence consists of the heptamer CACAGTG separated from the nonamer ACAAAAACC by a 12-bp nonconserved spacer[1]. The signal sequences of V18a and V19a are perfectly conserved. V18b and V19b have, respectively, one base pair deletion and three base pair substitutions in the nonamer.

Table 1 Percentages of similarity between V_κ genes

	5′	P_L	Int	V_κ	3′
V18a/V18b		95.4 (90.9)	95.9	88.4 (79.2)	95.0
V19a/V19b	89.0	93.9 (90.9)	92.7	86.4 (80.6)	92.0
V18/V19	90–95	95–97 (91–100)	94–97	81–88 (71–81)	91–96
V18a/HK102	72.9	92.4 (81.8)	62.1	74.0 (61.0)	72.4

Nucleotide sequences of the 5′ flanking (5′), leader peptide (P_L), intron (Int), V_κ coding (V_κ) and 3′ flanking (3′) regions were compared and percentages were calculated as: number of substitutions to number of nucleotides compared. Each deletion or insertion of nucleotide (whatever the number) was scored as a single mutation. Numbers in parentheses correspond to percentages of similarity at the amino acid level. Numbers given for 18/19 (lane 3) correspond to the minimum and maximum values obtained when a V18 gene (a or b) was compared with a V19 gene (a or b). Human V_κ HK102 is from ref. 23.

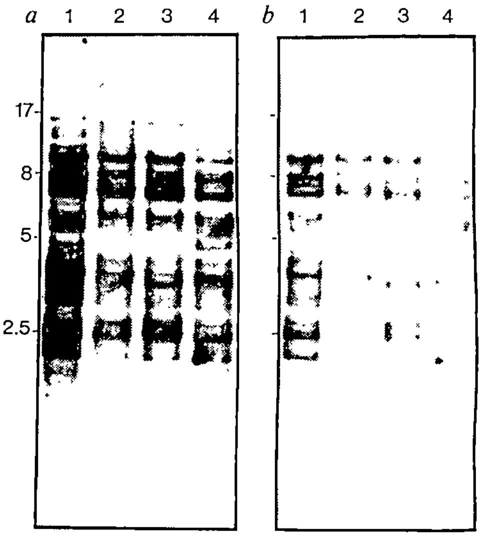

Fig. 1 Southern blot analysis of four individual rabbit DNAs using the V19a gene as a probe. Liver DNAs of homozygous *b9/b9* (lane 1), *b4/b4* (lane 2), *b5/b5* (lane 3) and *b6/b6* (lane 4) rabbits were digested with *Eco*RI, electrophoresed on a 0.7% agarose gel and transferred to nitrocellulose[34]. Hybridization was according to ref. 35. The probe was the 1.5 kb V19a *Eco*RI insert (see Fig. 2 legend); this was purified, ligated to itself and nick-translated, as already described[35]. *a*, The blot was washed in low-stringency conditions, at 65 °C in 2×SSC, 0.1% SDS for 90 min with three changes, and autoradiographed for 2 days. *b*, The same blot was then washed in high-stringency conditions, at 65 °C in 0.1×SSC, 0.1% SDS for 30 min, and autoradiographed for 15 days.

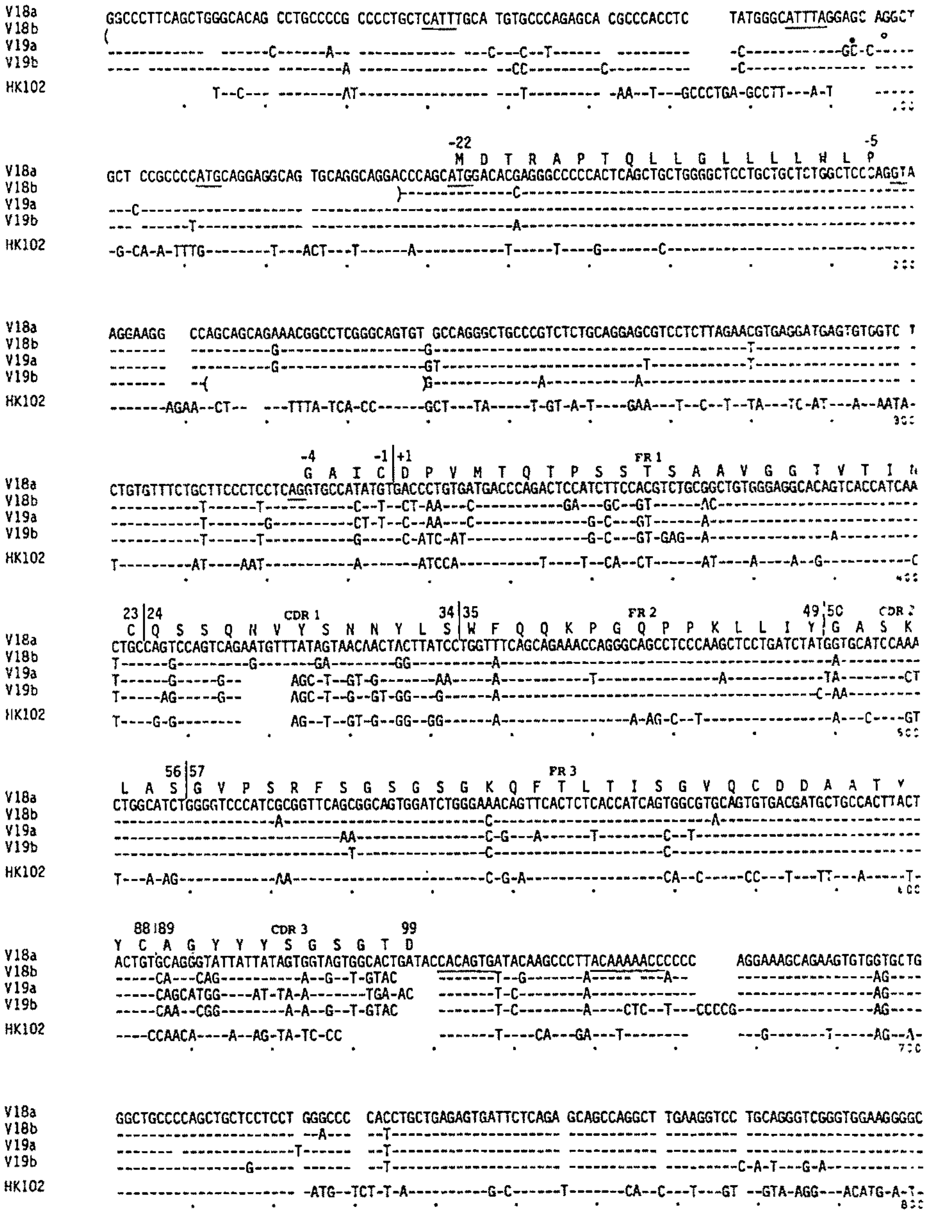

Fig. 2 DNA sequence comparison of four germ-line rabbit V_κ genes and the human HK102 V_κ gene[23]. A rabbit $V_\kappa + C_\kappa$ cDNA probe was constructed from *b5/b5* rabbit spleen mRNA, as previously described[36]. A cosmid library of adult *b4/b4/* rabbit liver DNA fragments[13] was screened by *in situ* hybridization with the nick-translated $V_\kappa + C_\kappa$ cDNA insert, as already reported[13]. Two recombinant cosmids, V4R-18 and V4R-19, were digested with *Eco*RI and analysed by Southern blot hybridization[34] with the cDNA probe. Two positive *Eco*RI restriction fragments were chosen from each cosmid (2.1 kb (V18a) and 2.9 kb (V18b) from V4R-18; 1.3 kb (V19a) and 2.2 kb (V19b) from V4R-19). *Sau*3A, *Hae*III or *Ava*II restriction digests of the four *Eco*RI fragments were subcloned into M13mp701 vector and sequenced on both strands by the chain-termination method[37–39]. The amino acid translation of the V18a gene is given in the one-letter code[40] and the numbering is according to ref. 15. The frameworks (FR) and complementarity-determining regions (CDR) are indicated. Dashes indicate nucleotide identities with the V18a nucleotide sequence. Blank spaces have been introduced to maximize homology. Parentheses in V18b and V19b genes correspond to unidentified residues, and alignments have been made in accordance with V18a gene and restriction mapping analysis. Promoter signal sequences, translational initiation codons, splicing signal and recombination recognition signal sequences are underlined.

Because the rabbit κ genes conform to the 12/23-bp rule, we can exclude the possibility that an intermediate *D* segment accounts for the high heterogeneity in CDR3 length. As shown in Fig. 2, the rabbit V_κ genes are very heterogeneous in length and sequence in their CDR3 regions, and are longer than in human and mouse. They vary from 30 to 35 bp and can code for 10 or 11 amino acids, whereas in human and mouse, CDR3 regions are usually 22–23 bp encoding 7 amino acids, with two exceptions being 25 bp long[32,33].

In fact, the rabbit CDR3 region has been shown to contain up to six more amino acids than human and mouse[11]. However, in the two cases where there are six extra amino acids, the sixth (Thr or Gly) could be derived from the J_κ codon (Ala) by a single (somatic?) point mutation. The four rabbit V_κ germ-line genes in the present study can code for three or four extra amino acids, or four or five, depending on junctional variation[2]. It is thus very likely from our data, that the extra amino acids found in the rabbit κ-chains are entirely encoded by the V_κ genes, without the need for an N region as in the heavy-chain system[3].

Recombination between V_κ and J_κ segments may delete nucleotides in the V_κ genes, as in the J_κ segment. Junctional deletions have been observed mainly at the V_H–*D* and *D*–J_H junctions, with only rare exceptions in the light-chain system[32]. As the signal sequences involved in the V_κ–J_κ junction are identical in rabbit and mouse or human, the junctional deletion or variation must follow the strand cut during recombination. This deletion mechanism is probably of the same kind as in the heavy-chain system. It might have been selected in the rabbit because of structural constraints linked to the length of J_κ and V_κ segments. Thus, the additional nucleotides at the 3′ end of rabbit V_κ genes are somewhat analogous to the *D* segment of the heavy-chain system. They leave scope for an increased junctional deletion mechanism during rearrangement, which in turn generates high CDR3 diversity.

Junctional deletion of the rabbit J_κ codons means that they are no longer involved in the formation of CDR3 (ref. 11) and thus J_κ segments can be inactivated during evolution, without serious consequences, provided, of course, that one J_κ segment remains functional. The rabbit V_κ genes may correspond to an ancestral system from which the human and mouse V_κ genes have been derived by nucleotide deletions during evolution of these species. In this respect, it is interesting that human λ light chains also show CDR3 length heterogeneity[15], suggesting a possible common origin for the human V_λ and rabbit V_κ genes.

In conclusion, immunoglobulin genetic segments can to variable extents use the mechanisms available for the generation of antibody diversity. κ Light-chain CDR3 diversity in human and mouse is based on combinatorial potential and is amplified by a limited junctional variation mechanism. Our data show that in the rabbit only a single functional J_κ segment is required.

```
        -22                 1         10        20        30
V18a    MDTRAPTQLLGLLLLWLP  GAICDPVHTQTPSSTSAAVGGTVTINCQSSQNVYSHNYLSWFQ
V18b    ------------------  --TFAQ-L---E-PV--P---------A--S--D--W---Y-
V19a    ------------------  --TFAQ-L----A-Y------------A-E  SISS--N-Y-
V19b    ------------------  --R-AID-----A-VE------I----A-E  SISSW-A-Y-
HK102   --M-V-A-----------  --K--IQ-I-S--TL--S--DR---T-RA--  SISSW-A-Y-

Kabat                        -I--------V------------A--S-SI--R-A-Y-
                                         FR1              CDR1

        40        50        60        70        80        90       99
V18a    QKPGQPPKLLIYGASKLASGVPSRFSGSGSGKQFTLTISGVQCDDAATYYCAGYYYSGSGTD
V18b    ------------D------------------T-------------------Q-S---SGWY
V19a    --L---------Y--T-----------K-----TEY-----------------QHG-IYS--D
V19b    ------------E------------------T-------------------Q-G--NSGWY
HK102   ----KA------D--S-E-------------TE------SL-P--F-----QQ-NSYS

Kabat   ------------K--T-----------K-----T-------D-----------Q-AN--STVV
           FR2        CDR2             FR3                   CDR3
```

Fig. 3 Deduced amino acid sequences of the four rabbit germline V_κ genes. The one-letter code is used[40] and numbering is according to ref. 15. Dashes indicated identities with the amino acid sequence of the V18a gene. Gaps have been introduced to maximize homology. Also given is the deduced amino acid sequence of the human HK102 V_κ gene[23]. Kabat's sequence is a compilation of rabbit κ light-chain amino acid sequences and represents for each residue the most common amino acid observed at that position[15].

The diversity is based on the greater length and length heterogeneity of germ-line V_κ-CDR3 regions, and is highly amplified by nucleotide deletions in the J_κ and perhaps V_κ segments, during *V–J* recombination. Diversity in rabbit κ light chains mimics the mechanisms of CDR3 diversity in human and mouse heavy-chain systems, where V_H segments are highly conserved at their 3′ ends, and heterogeneity in length and sequence is provided by the *D* segments, the N region and the junctional deletion.

We thank Dr J. J. Panthier for helpful discussions and Drs C. Henderson and G. Langsley for critical reading of this manuscript. This work was supported by grants from the CNRS (ATP AI-5054, CP 960008), the Ministère de la Recherche et de l'Industrie (L.P. 82.L.1311) and the Fondation pour la Recherche Médicale Française.

Received 24 April; accepted 21 June 1984.

1. Tonegawa, S. *Nature* **302**, 575–581 (1983).
2. Weigert, M. *et al. Nature* **283**, 497–499 (1980).
3. Alt, F. W. & Baltimore, D. *Proc. natn. Acad. Sci. U.S.A.* **79**, 4118–4122 (1982).
4. Kim, S., Davis, M., Sinn, E., Patten, P. & Hood, L. *Cell* **27**, 573–581 (1981).
5. Gearhart, P. J. & Bogenhagen, D. F. *Proc. natn. Acad. Sci. U.S.A.* **80**, 3439–3443 (1983).
6. Krawinkel, U., Zoebelein, G., Brüggemann, M., Radbruch, A. & Rajewsky, K. *Proc. natn. Acad. Sci. U.S.A.* **80**, 4997–5001 (1983).
7. Max, E. E., Seidman, J. G. & Leder, P. *Proc. natn. Acad. Sci. U.S.A.* **76**, 3450–3454 (1979).
8. Sakano, H., Hüppi, K., Heinrich, G. & Tonegawa, S. *Nature* **280**, 288–294 (1979).
9. Hieter, P. A., Max, E. E., Seidman, J. G., Maizel, J. V. Jr & Leder, P. *Cell* **22**, 197–207 (1980).
10. Hieter, P. A., Maizel, J. V. & Leder, P. *J. biol. Chem.* **257**, 1516–1522 (1982).
11. Heidmann, O. & Rougeon, F. *Cell* **34**, 767–777 (1983).
12. Emorine, L. & Max, E. E. *Nucleic Acids Res.* **11**, 8877–8890 (1983).
13. Heidmann, O. & Rougeon, F. *EMBO J.* **2**, 437–441 (1983).
14. Benammar, A. & Cazenave, P.-A. *J. exp. Med.* **156**, 585–595 (1982).
15. Kabat, E. A., Wu, T. T. & Bilowsky, W. in *Sequences of Immunoglobulin Chains* (NIH, Bethesda, Maryland, 1979).
16. Heinrich, G., Traunecker, A. & Tonegawa, S. *J. exp. Med.* **159**, 417–435 (1984).
17. Bentley, D. L. & Rabbitts, T. H. *Cell* **32**, 181–189 (1983).
18. Cattaneo, R., Gorski, J. & Mach, B. *Nucleic Acids Res.* **9**, 2777–2790 (1981).
19. Joho, R., Weissman, I. L., Early, P., Cole, J. & Hood, L. *Proc. natn. Acad. Sci. U.S.A.* **77**, 1106–1110 (1980).
20. Bentley, D. L. & Rabbitts, T. H. *Cell* **24**, 613–623 (1981).
21. Hood, L., Eichmann, K., Lackland, H., Krause, R. M. & Ohms, J. J. *Nature* **228**, 1040–1044 (1970).
22. Braun, D. G. & Jaton, J. C. *Immunochemistry* **10**, 387–395 (1973).
23. Bentley, D. L. & Rabbitts, T. H. *Nature* **288**, 730–733 (1980).
24. Joho, R., Gershenfeld, H. & Weissman, I. L. *EMBO J.* **3**, 185–191 (1984).
25. Givol, D. *et al. Nature* **292**, 426–430 (1981).
26. Kelley, D. E., Coleclough, C. & Perry, R. P. *Cell* **29**, 681–689 (1982).
27. Seidman, J. G., Leder, A., Nau, M., Norman, B. & Leder, P. *Science* **202**, 11–17 (1978).
28. Egel, R. *Nature* **290**, 191–192 (1981).
29. Baltimore, D. *Cell* **24**, 592–594 (1981).
30. Schreier, P. H., Bothwell, A. L., Mueller-Hill, B. & Baltimore, D. *Proc. natn. Acad. Sci. U.S.A.* **78**, 4495–4499 (1981).
31. Ollo, R. & Rougeon, F. *Cell* **32**, 515–523 (1983).
32. Kwan, S.-P., Max, E. E., Seidman, J. G., Leder, P. & Scharff, M. D. *Cell* **26**, 57–66 (1981).
33. Höchtl, J., Müller, C. R. & Zachau, H. G. *Proc. natn. Acad. Sci. U.S.A.* **79**, 1383–1387 (1982).
34. Southern, E. M. *J. molec. Biol.* **98**, 503–517 (1978).
35. Heidmann, O. & Rougeon, F. *Cell* **28**, 507–513 (1982).
36. Heidmann, O., Auffray, C., Cazenave, P.-A. & Rougeon, F. *Proc. natn. Acad. Sci. U.S.A.* **78**, 5802–5806 (1981).
37. Sanger, F., Nicklen, S. & Coulson, A. R. *Proc. natn. Acad. Sci. U.S.A.* **74**, 5463–5467 (1977).
38. Messing, J., Crea, R. & Seeburg, P. H. *Nucleic Acids Res.* **9**, 309–321 (1981).
39. Biggin, M. D., Gibson, T. J. & Hong, G. F. *Proc. natn. Acad. Sci. U.S.A.* **80**, 3963–3965 (1983).
40. Dayhoff, M. O. in *Atlas of Protein Sequence and Structure* (National Biochemical Research Foundation, Silver Spring, Maryland, 1978).

Transcription of plant defence genes in response to UV light or fungal elicitor

Joseph Chappell* & Klaus Hahlbrock

Biologisches Institut II der Universität, D-7800 Freiburg, and
Max-Planck-Institut für Züchtungsforschung, D-5000 Köln 30, FRG

The synthesis of secondary metabolites in response to stress conditions has been implicated as a major defence response of higher plants[1]. Cell suspension cultures of parsley (*Petroselinum hortense*) have been studied extensively as a model system and shown to respond to UV irradiation and treatment with fungal elicitor by the synthesis of flavonoids and furanocoumarins, respectively[2,3]. The induced synthesis of these compounds might afford the plant protection against the respective environmental hazards, because flavonoids strongly absorb UV light and furanocoumarins possess fungitoxic properties[4]. The production of each class of compound is preceded by the induction of groups of coordinately regulated enzymes[2,5–8], based on rapid changes in amounts and activities of the corresponding messenger RNAs[9,10]. We now report that these changes are due to transient increases in the transcription rates of the respective genes, which indicates that gene activation has an important role in UV and disease resistance in higher plants.

The three enzymes of general phenylpropanoid metabolism (group I) are co-induced in cultured parsley cells with either the flavonoid glycoside pathway, comprising some 16 enzymes, (group II) or the less clearly defined furanocoumarin pathway (group III), depending on whether UV light or a pathogen-derived elicitor[11] is used as inducing agent[2,4,6,8]. The effect of UV light is highly selective for the synthesis of flavonoids, whereas various metabolic changes are induced by the elicitor[4,10]. Cloned complementary DNA copies of mRNAs coding for two enzymes of group I, phenylalanine ammonia-lyase (PAL; EC 4.3.1.5) and 4-coumarate: CoA ligase (4CL; EC 6.2.1.1.2), and for chalcone synthase (CHS), a member of group II, have recently been used to show that the accumulation of flavonoids or furanocoumarins is associated with rapid increases in the respective mRNAs[9,10]. The same cDNAs were used in the present study, where nuclei were isolated from UV-irradiated and elicitor-treated cells, and RNA synthesis was continued *in vitro* in the presence of ^{32}P-UTP. The radioactive RNA was then hybridized to the cDNA inserts bound to diazobenzyloxymethyl (DBM) filters or to DNA–nitrocellulose blots. The amount of ^{32}P-UTP incorporated into a specific mRNA is taken as a measure of the polymerase activity associated with the respective gene at the specific time of nuclei isolation. Because it is unlikely that initiation of transcription takes place in these conditions[12], we are measuring only the completion of transcripts initiated *in vivo* before the nuclei were isolated.

Irradiation of the cell cultures with UV light for a standard 2.5-h period[5,7] induced transient increases in the transcription rates of the genes coding for PAL, 4CL and CHS mRNAs. Figure 1 shows the results for PAL and CHS, confirming the previously observed small, but distinct, difference in the timing of induction of groups I and II[4,5,10]. Changes in the rates of 4CL mRNA synthesis were similar to those obtained for PAL, but as expected[7], the amounts of hybridizable material were much smaller and more difficult to determine accurately (~2 parts per million (p.p.m.) at the peak around 4 h after the onset of induction).

Similar results were obtained in both types of determination, DNA blot (Fig. 1*a*) and DBM filter (Fig. 1*b*) hybridizations. The CHS cDNA used here encompasses the entire coding sequence of the mRNA[13] and contains an internal *Pst*I site. On isolation of the cDNA insert from the *Pst*I site of the cloning vector, plasmid pBR322, two fragments of 720 and 780 base pairs were obtained (Fig. 1*a*).

---

* Present address: Department of Biology, C-016, University of California, San Diego, La Jolla, California 92093, USA.

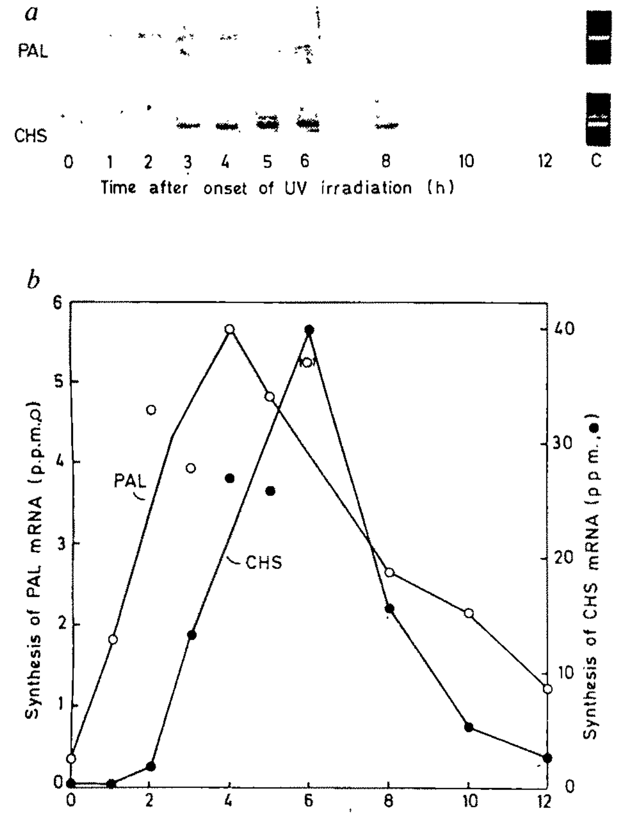

Fig. 1 Changes in the transcription rates of PAL and CHS genes in nuclei isolated from parsely cell cultures at various times after the onset of UV irradiation for 2.5 h. The ^{32}P-RNA synthesized by isolated nuclei was hybridized either to DNA blots (*a*) or to DBM filters (*b*) containing cDNA inserts complementary to PAL and CHS mRNAs. The amount of RNA hybridizing to a specific cDNA was determined by autoradiography (*a*) or by scintillation spectrometry (*b*). A control (C) shows the cDNA inserts stained with ethidium bromide.

Methods: A cell suspension culture of parsley (*Petroselinum hortense*) was grown in continuous darkness for 7 days after subculturing in a simple, synthetic medium[7] and then irradiated with UV light[5,7] for 2.5 h. Cells were collected at the indicated times after the onset of irradiation. Nuclei were isolated from the cells according to Willmitzer and Wagner[14] with the following modifications. Cells (25–40 g) were gently stirred in 100 ml of 0.7 M mannitol, 10 mM methane ethane sulphonate (MES) *p*H 5.8, 5 mM EDTA, 0.1% bovine serum albumin (BSA) (w/v), 0.2 mM phenyl methylsulphonyl fluoride (PMSF) containing 50 mg cellulase (Onozuka) and 10 mg Macarzyme (Onozuka) for 15 min at 25 °C, and the partial protoplastic cells were homogenized three times with an Ultra-turrax for 15 s in 0.25 M sucrose, 10 mM NaCl, 10 mM MES *p*H 6.0, 5 mM EDTA, 0.25 mM spermine-HCl, 0.5 mM spermidine-phosphate, 20 mM mercaptoethanol, 0.2 mM PMSF, 0.6% Triton X-100 (w/v) and 2% dextran (40,000) (w/v). In 100-μl reaction volumes, 10^7 isolated nuclei completed transcripts initiated *in vivo* in 75 mM $(NH_4)_2SO_4$, 8 mM $MgCl_2$, 0.5 mM each of GTP, ATP and CTP, 8% glycerol (v/v), 20 mM Tris-HCl *p*H 7.8 and 100 μCi ^{32}P-UTP (400 Ci $mmol^{-1}$) for 30 min at 30 °C. The reaction was linear in these conditions for about 60 min. The RNA synthesized *in vitro* was isolated[15] and dissolved in 50% formamide, 4×SSPE, 0.02% each of Ficoll, polyvinylpyrrolidone and BSA (w/v), 200 μg ml^{-1} each of transfer RNA and poly(A)$^+$ RNA, and 0.2% SDS (w/v). The radiolabelled RNA (2×10^7 c.p.m. per sample) was then hybridized to 200 ng insert DNA transferred to GeneScreen (NEN) filters (*a*) or to DBM filters[16] containing 200 ng insert DNA (*b*). Hybridization was done in the same buffer containing 8% dextran sulphate (w/v) at 42 °C for 40–62 h. The filters were then washed three times with 2×SSC, 0.5% SDS at 60 °C for 30 min, once with 0.5×SSC, 0.5% SDS at 60 °C for 30 min, twice with 2×SSC and subsequently treated with 20 μg ml^{-1} RNAse A in the same buffer for 30 min at room temperature. The filters were finally washed twice in 2×SSC with 0.5% SDS and twice in the same buffer without SDS. Additional amounts of DNA did not increase the amount of RNA hybridization, and a linear relationship existed between the amount of RNA used and RNA hybridization. The ^{32}P-RNA hybridized was visualized by autoradiography of the DNA blots (*a*) or quantified by scintillation spectrometry of the radioactivity released by treating the DBM filter with 0.4 M NaOH (*b*). The lanes on the far right in *a* show the ethidium bromide-stained agarose gel before transfer of the cDNA insert to GeneScreen (NEN). Hybridization to DBM filters was corrected for background by subtracting the radioactivity released from a filter containing 200 ng λ dV DNA. Specific hybridization is presented as p.p.m. of input RNA. 3×10^7 c.p.m. of ^{32}P-RNA was used for each hybridization shown and the background hybridization was an average of 112 c.p.m. No corrections were made for the hybridization efficiency or size of the hybridization probe.

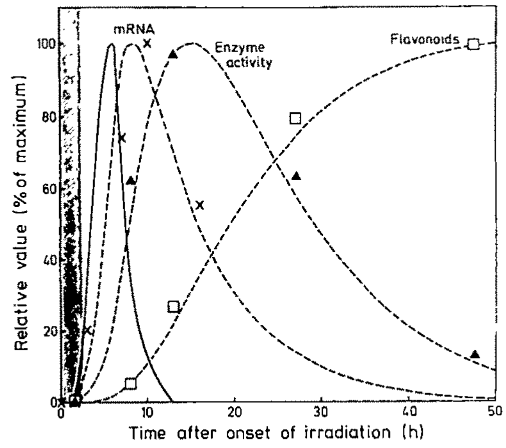

Fig. 2 Comparison of predicted and measured changes in CHS mRNA and enzyme activities and in flavonoid glycoside concentrations in UV-irradiated parsley cells. The shaded area indicates the length of the UV irradiation period. The solid curve represents the data shown in Fig. 1 for UV light-induced CHS gene transcription; this curve was used to calculate (broken curves) the expected changes in CHS mRNA and enzyme activity, and the accumulation of flavonoid glycosides, in the previously established conditions in which both the mRNA and the enzyme were rapidly degraded[5] but the flavonoids were not further metabolized[17]. In these conditions, the equation

$$dx(t)/dt = {}^0k_s(t) - {}^1k_d x(t) \qquad (1)$$

can be applied to calculate mRNA or enzyme activity changes (x) with time (t) from the respective zero-order rate constants of synthesis (${}^0k_s$) and the first-order rate constants of degradation (${}^1k_d$), and the equation

$$P(t) = \int_0^t E(\tau)\,d\tau \qquad (2)$$

describes the changes in the amount of products (P) accumulated with time(t; τ) as a result of changes in the rate-limiting enzyme activity (E)[4,5,18]. The symbols represent mean values of two measurements each of CHS mRNA (×), CHS activity (▲) and total flavonoids (□). Changes in levels of CHS mRNA and translational activity have previously been shown to follow the same kinetics[9,10].

Methods: Propagation and collection of cells at the indicated times, extraction procedures and measurements of hybridizable mRNA amounts[9,10], enzyme activity[19] and amounts of total flavone and flavonol glycosides[20] have been reported previously.

The apparent changes in the rates of transcription were not due to an attenuation of the transcription rates of particular genes in control cells, because the same results were obtained in conditions where the nuclei had been lysed and the DNA superstructure disrupted by high salt concentrations (data not shown). Furthermore, the transcription rate of a constitutively expressed mRNA, which is complementary to cloned cDNA from the plasmid pLF14 and codes for a protein of unknown function (J.C. and K.H., unpublished results), was constant throughout the experiment (Fig. 1) at ~20 p.p.m. Ribosomal RNA synthesis, measured using a cloned maize genomic fragment comprising a cluster of ribosomal genes (P. Schulze-Lefert and G. Feix, manuscript in preparation), showed an approximate doubling over controls with 4 h. The *in vitro* transcription of the PAL, 4CL and CHS genes was sensitive to 0.1–0.4 μg ml^{-1} α-amanitin, suggesting that these genes are transcribed by RNA polymerase II.

The UV light-induced changes in the rates of PAL and CHS mRNA synthesis have also been measured *in vivo* (Table 1). Both mRNAs were synthesized at much higher rates 3–4 h after the onset of UV irradiation than in control cells or at a later stage after induction. These changes were basically the same as those measured *in vitro* and further demonstrate that the PAL and CHS genes are under transcriptional control in UV-irradiated cells.

Figure 2 shows the causal relationship between the timing of changes in the rate of CHS mRNA synthesis and the kinetics of flavonoid accumulation. The timing of the entire sequence of events, as predicted from the induced changes in the rates of CHS gene transcription and the rates of mRNA and enzyme degradation (which are easily calculated from the respective half lives[4,5]), agrees with corresponding experimental results. Only a few time points are shown here for the changes in the

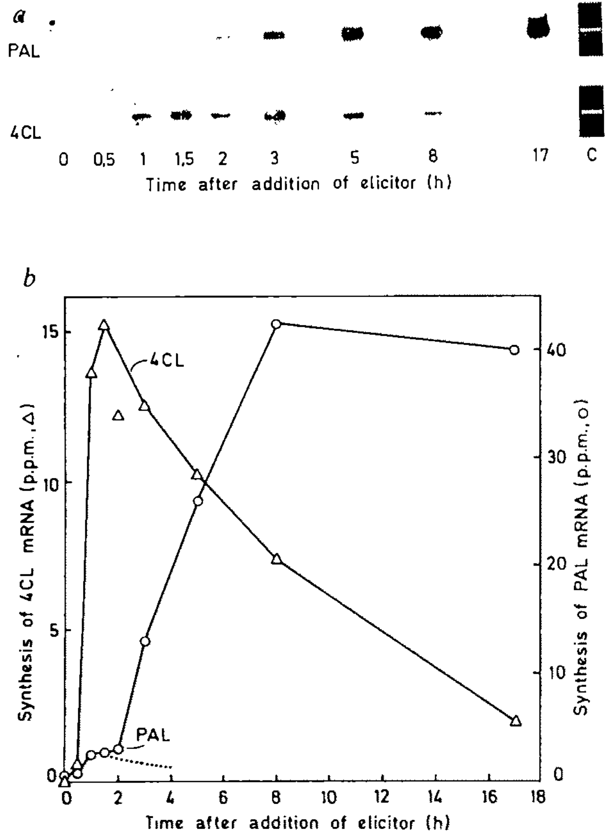

Fig. 3 Changes in the transcription rates of PAL and 4CL genes in nuclei isolated from cultured parsley cells at various times after the addition of elicitor. The ^{32}P-RNA synthesized by isolated nuclei was hybridized either to DNA blots (*a*) or to DBM filters (*b*) containing cDNA inserts complementary to the respective mRNA. The amount of RNA hybridizing to a specific cDNA was determined by autoradiography (*a*) or by scintillation spectrometry (*b*). A control (C) shows the cDNA inserts stained with ethidium bromide. The dotted line in *b* represents possible alternative changes in the rate of PAL mRNA synthesis (see text for discussion).

Methods: A cell suspension culture of parsley was treated at time 0 with $\sim 25\ \mu g\ ml^{-1}$ of a fungal elicitor prepared from the cell wall of *Phytophthora megasperma* f. sp. *glycinea*[11]. Culture conditions, nuclei isolation, RNA synthesis and hybridizations with PAL and 4CL cDNAs were as described for Fig. 1, except that 1.5×10^7 c.p.m. per hybridization were used. Specific hybridization, obtained by correction for an average background of 178 c.p.m., is expressed as p.p.m. of input RNA. No corrections for hybridization efficiency or the size of the hybridization probe were made.

amount of hybridizable mRNA and in enzyme activity, but a more detailed analysis has been reported previously[5,9,10]. We conclude from the coincidence of the calculated and the experimentally derived data that the timing of flavonoid glycoside accumulation in UV-irradiated parsley cells is determined solely, or at least predominantly, by the kinetics of gene transcription. It is impossible, however, to deduce from our present data whether one particular enzyme of the two UV light-induced pathways is rate-limiting. Although PAL transcription follows different kinetics from CHS transcription, the apparent half lives of PAL and CHS mRNA and enzyme activities are also different[5], resulting in a similar flavonoid accumulation curve when PAL rather than CHS is used for the calculations described above.

Table 1 UV light-induced *in vivo* PAL and CHS mRNA

Time of labelling	Total RNA used (c.p.m.)	PAL		CHS	
		c.p.m.*	p.p.m.	•c.p.m.*	p.p.m.
−1–0 h	430,000	4	9	1	0
3–4 h	560,000	17	30	76	136
8–9 h	410,000	6	15	16	39

At the indicated times before or after the onset of 2.5 h UV irradiation, cell cultures were concentrated from 5 g per 40 ml to 5 g per 5 ml medium by gentle filtration and labelled for 1 h with 0.5 mCi each of [5,6-^{3}H]uridine (40–60 Ci $mmol^{-1}$), [5-^{3}H]cytosine (25–30 Ci $mmol^{-1}$) and [5′-^{3}H]guanosine (20–40 Ci $mmol^{-1}$). The cells were collected by suction filtration, washed with sterile water and frozen in liquid nitrogen. Polyribosomal RNA and poly(A)$^+$ RNA were isolated from the cells as described previously[9]. The poly(A)$^+$ RNA (specific activity 35,000–70,000 c.p.m. per μg RNA) was hybridized to DBM filters containing 200 ng of the appropriate cDNA insert. Hybridization, washes and release of selected RNAs were as described in Fig. 1 legend. Specific hybridization was determined by subtracting background hybridization to a filter containing 200 ng of λ dV DNA, which gave a mean value of 15 c.p.m. Specific hybridization is also presented as p.p.m. of the input RNA. dV = defective virulent.

* Corrected for non-specific hybridization.

We have recently shown that either the same or very similar PAL and 4CL mRNAs were induced by treatment of parsley cells with UV light or with a fungal elicitor[10]. We therefore measured the transcription rates *in vitro* of the PAL and 4CL genes in nuclei isolated from elicitor-treated cells (Fig. 3). In agreement with observations at the level of changes in amounts of mRNA[10], apparent differential rates of PAL and 4CL gene transcription in elicitor-treated cells were observed, and the elicitor-induced changes in the transcription rate of the 4CL gene were transient but more rapid than those induced by UV irradiation. The transcription rate of a mRNA constitutively expressed in other conditions and monitored with the cDNA insert from pLF14 (see above) declined slowly after elicitor treatment from 20 p.p.m. to 10 p.p.m. within the period of the experiment. Flavonoids are not synthesized in elicitor-treated cells, and the elicitor has no effect on CHS[6].

The relatively high rate of 4CL gene transcription and the low initial rate of PAL gene transcription in elicitor-treated cells, as compared with UV-irradiated cells, are consistent with similar relative levels of both the enzyme activities and the mRNA levels[6,10]. As discussed elsewhere[10], the apparent late and large increase in the transcription rate of the PAL gene and the corresponding accumulation of PAL, or PAL-like, mRNA in elicitor-treated cells are unexpected in view of the rapid, transient changes in the translational activity of PAL mRNA and might be due in part to cross-hybridization of the PAL cDNA with other elicitor-induced mRNA(s) of similar size. The actual changes in the rate of PAL gene transcription responsible for the coordination of the PAL and 4CL mRNA and enzyme activity changes[6,10] might follow a time course similar to that indicated by the dotted line in Fig. 3. Experiments are in progress to clarify this point. In any case, we have shown here for the first time that both types of stress, UV light or pathogen-derived elicitor, induce the respective defence response of the challenged plant cells by transcriptional control of genes involved in the biosynthesis of resistance-related compounds.

We thank Ms G. Braun for technical assistance, Dr G. Feix for cloned maize rDNA and Dr E. Schäfer for valuable help with the mathematical calculations. The work was supported by the Deutsche Forschungsgemeinschaft (SFB 46), the Fonds der Chemischen Industrie, and the Max-Planck-Society.

Received 2 April; accepted 18 June 1984.

1. Bell, E. A. in *Biochemistry of Plants* Vol. 7 (ed. Conn, E. E.) 1–19 (Academic, New York, 1981).
2. Hahlbrock, K. in *Biochemistry of Plants* Vol. 7 (ed. Conn, E. E.) 425–456 (Academic, New York, 1981).
3. Tietjen, K. G., Hunkler, D. & Matern, U. *Eur. J. Biochem.* **131**, 401–407 (1983).
4. Hahlbrock, K., Kreuzaler, F., Ragg, H., Fautz, E. & Kuhn, D. N. in *Biochemistry of Differentiation and Morphogenesis* (ed. Jaenicke, L.) 34–43 (Springer, Berlin, 1982).
5. Schröder, J., Kreuzaler, F., Schäfer, E. & Hahlbrock, K. *J. biol. Chem.* **254**, 57–65 (1979).
6. Hahlbrock, K. *et al. Pl. Physiol.* **67**, 768–773 (1981).
7. Ragg, H., Kuhn, D. N. & Hahlbrock, K. *J. biol. Chem.* **256**, 10061–10065 (1981).
8. Tietjen, K. G. & Matern, U. *Eur. J. Biochem.* **131**, 409–413 (1983).
9. Kreuzaler, F., Ragg, H., Fautz, E., Kuhn, D. N. & Hahlbrock, K. *Proc. natn. Acad. Sci. U.S.A.* **80**, 2591–2593 (1983).
10. Kuhn, D. N., Chappell, J., Boudet, A. & Hahlbrock, K. *Proc. natn. Acad. Sci. U.S.A.* **81**, 1102–1106 (1984).
11. Ayers, A. R., Ebel, J., Finelli, F., Berger, N. & Albersheim, P. *Pl. Physiol.* **57**, 751–759 (1976).
12. Darnell, J. E. Jr *Nature* **297**, 365–371 (1982).
13. Reimold, U., Kröger, M., Kreuzaler, F. & Hahlbrock, K. *EMBO J.* **2**, 1801–1805 (1983).
14. Willmitzer, L. & Wagner, K. G. *Expl. Cell Res.* **135**, 69–77 (1981).
15. McKnight, G. S. & Palmiter, R. D. *J. biol. Chem.* **254**, 9050–9058 (1979).
16. Alwine, J. C. *et al. Meth. Enzym.* **68**, 220–242 (1980).
17. Mühle, E. thesis, Univ. Münster (1975).
18. Schimke, R. T. *MTP int. Rev. Sci. Biochem. Ser. 1* **9**, 183–221 (1974).
19. Heller, W. & Hahlbrock, K. *Archs Biochem. Biophys.* **200**, 617–619 (1980).
20. Hahlbrock, K., Knobloch, K.-H., Kreuzaler, F., Potts, J. R. M. & Wellmann, E. *Eur. J. Biochem.* **61**, 199–206 (1976).

Inhibition of mRNA binding to ribosomes by localized activation of dsRNA-dependent protein kinase

Arrigo De Benedetti & Corrado Baglioni

Department of Biological Sciences, State University of New York at Albany, Albany, New York 12222, USA

The initiation of protein synthesis can be regulated in mammalian cells by protein kinases which phosphorylate the α subunit of initiation factor eIF-2 (ref. 1). This phosphorylation results in a block in the recycling of eIF-2 (refs 2, 3) and in the inhibition of messenger RNA binding to 80S initiation complexes[4,5]. After eIF-2α is phosphorylated, the mRNA becomes associated with 48S complexes consisting of a 40S ribosomal subunit[4], eIF-2(αP), GDP and Met-tRNA$_f$ (ref. 5). One of the eIF-2α kinases is activated by low concentrations of double-stranded RNA (dsRNA)[6]. This kinase (PK$_{ds}$) is present at a basal level in all mammalian cells investigated[7] and its synthesis is induced in cells treated with interferon[8]. The PK$_{ds}$ may be involved in the inhibition of translation of viral mRNA in interferon-treated cells infected with RNA viruses, as it is activated by viral replicative complexes. It is not known, however, if the activated PK$_{ds}$ preferentially inhibits the translation of viral mRNA when cellular protein synthesis proceeds at a normal rate in infected cells[9]. We now report that mRNA covalently linked to dsRNA is preferentially inhibited from binding to 80S complexes by a localized activation of PK$_{ds}$. This suggests that in interferon-treated cells the binding of some nascent viral mRNAs to functional initiation complexes may be preferentially inhibited by a similar mechanism.

The initial experiments were carried out with ^{3}H-uridine-labelled mRNA from[5] vesicular stomatitis virus (VSV). This was purified by absorption to nitrocellulose filters to obtain mRNA with poly(A) sequences longer than 60 nucleotides[10]. This mRNA was incubated with reticulocyte lysate to determine its binding to initiation complexes, which were fractionated by centrifugation on sucrose gradients[5]. After incubation at 0 °C, unbound mRNA sedimented more slowly than 40S ribosomal subunits (Fig. 1*a*), whereas after incubation at 30 °C the mRNA was quantitatively bound to 80S initiation complexes (Fig. 1*b*). Further addition of ribosomes to 80S complexes was prevented by the inclusion of emetine, an inhibitor of elongation[5]. When the lysate was incubated with 750 ng ml^{-1} of the dsRNA poly(A). poly(U) for 7 min before the addition of VSV mRNA, the assembly of 80S complexes was inhibited and the mRNA sedimented instead at 48S (Fig. 1*c*). When the mRNA and dsRNA were added together, however, most of the mRNA bound to 80S complexes (Fig. 1*d*). This finding could be explained by the observation that it takes up to 5 min after the addition of dsRNA to obtain extensive phosphorylation of eIF-2 (refs 5, 11). The mRNA could bind to 80S complexes within 90 s[12], before a significant fraction of eIF-2 was phosphorylated.

A completely different result was obtained when the dsRNA was covalently linked to mRNA. This dsRNA was formed by annealing poly(U) to the poly(A) sequence of VSV mRNA, as previously described[13], to form dsRNA longer than 60 base pairs which can activate the PK$_{ds}$ (ref. 14). The mRNA containing poly(A)·poly(U) did not bind to 80S initiation complexes, but sedimented instead at 48S (Fig. 1*e*). In this experiment, the poly(A)·poly(U) linked to mRNA was present at the same concetration as 'free' poly(A)·poly(U) in the experiment shown in Fig. 1*d*. The dsRNA linked to mRNA was apparently responsible for inhibiting its binding to 80S initiation complexes. This may have been due to a localized activation of the eIF-2 kinase by the poly(A)·poly(U) in mRNA and the phosphorylation of a fraction of eIF-2 which became associated with this mRNA in 48S complexes. In support of this explanation, when 2-aminopurine, an inhibitor of the eIF-2α kinase[5,6] was added to a binding assay of mRNA containing the poly(A)·poly(U) duplex, the mRNA bound quantitatively to 80S complexes (Fig. 1*f*).

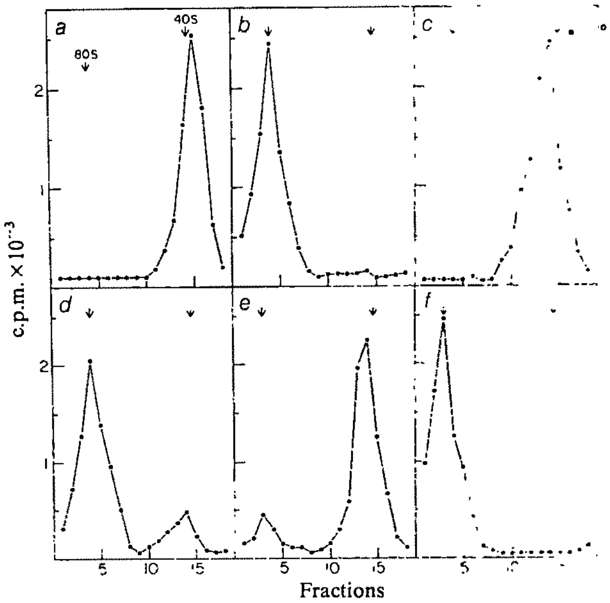

Fig. 1 Binding of VSV mRNA to initiation complexes. *a*, Incubation was at 0 °C. All the other incubations were at 30 °C and were stopped 3 min after the addition of mRNA. The ^{3}H-mRNA was added after a 7-min preincubation without (*b*) or with 750 ng ml^{-1} of poly(A)·poly(U) (*c*). This dsRNA was added together with ^{3}H-mRNA in *d*. The mRNA contained a poly(A)·poly(U) duplex in *e* and *f*; 10 mM 2-aminopurine was added in *f*. The position of the 80S and 40S peaks is indicated by arrows. The VSV mRNA was labelled with ^{3}H-uridine in infected cells, fractionated to obtain a 12–16S fraction[5] and absorbed to nitrocellulose filters to select mRNA with poly(A) sequences longer than 60 nucleotides[10]. This mRNA was either directly used in binding assays or annealed with sufficient poly(U) to prevent its retention by oligo(dT)–cellulose[13]. The average size of the poly(U) (purchased from Miles Biochemicals) was 120 nucleotides. The binding assays were carried out in 0.1 ml reactions which contained 60 µl of reticulocyte lysate supplemented with 50 µM haemin, 10,000 c.p.m. of ^{3}H-mRNA, 0.1 mM emetine and the other additions described elsewhere[5]. At the end of the incubation the assays were diluted with 3 vol of 0.5 M NaCl, 30 mM Mg(OAc)$_2$ and 20 mM Tris, *p*H 7.6 (buffer A) and centrifuged for 5 h at 38,000 r.p.m. through 12-ml gradients of 15–30% sucrose in buffer A. The gradient fractions were counted directly[5].

Figure 2 presents direct evidence for the activation of eIF-2α kinase by dsRNA linked to mRNA. Lysate was incubated with [γ-^{32}P]ATP and 750 ng ml^{-1} of free poly(A)·poly(U) or mRNA-linked poly(A)·poly(U). With no added dsRNA or after 3 min incubation with free poly(A)·poly(U), there was no detectable eIF-2α phosphorylation (Fig. 2*a*, *b*). After 7 min of incubation with poly(A)·poly(U) or 3 min incubation with mRNA-linked poly(A)·poly(U), eIF-2α was clearly phosphorylated (Fig. 2*c*, *d*). When 48S complexes were isolated and analysed by gel electrophoresis[5], some eIF-2(αP) was found associated with these complexes (Fig. 2*e*, *f*). It appeared that eIF-2α was phosphorylated at a faster rate with mRNA-linked poly(A)·poly(U) than with free poly(A)·poly(U). This could be explained by a slow rate of dephosphorylation of eIF-2(αP) bound to 48S complexes relative to unbound eIF 2(αP)[15]. In one incubation, the PK$_{ds}$ bound to mRNA-linked poly(A)·poly(U) preferentially phosphorylated eIF-2α associated with 48S complexes, whereas in the other the PK$_{ds}$ bound to free poly(A)·poly(U) phosphorylated eIF-2α which could be readily dephosphorylated by lysate phosphatases[15]. In fact, a 70,000 molecular weight polypeptide previously identified[16] with PK$_{ds}$ was detected in 48S complexes isolated from the incubation with mRNA-linked poly(A)·poly(U) (Fig. 2*f*). This polypeptide could represent PK$_{ds}$ bound to the 3'-terminal duplex of mRNA in these complexes.

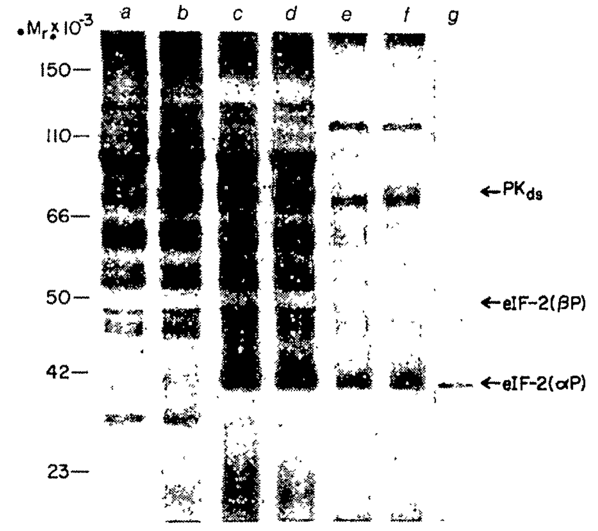

Fig. 2 Electrophoretic analysis of the phosphoproteins labelled: *a*, in 7 min incubation with no added dsRNA; *b*, *c*, in 3 and 7 min with 750 ng ml^{-1} of poly(A)·poly(U); *d*, in 3 min with mRNA annealed to poly(U) as described in Fig. 1*e* (750 ng ml^{-1} of dsRNA). The incubations were assembled as in Fig. 1, except that ATP was substituted with 10 μCi of [γ-^{32}P]ATP; 20 μl of each reaction were directly analysed (*a*–*d*), whereas 80 μl of the incubations shown in *c* and *d* were fractionated by gradient sedimentation to isolate the 48S peak. Gradient fractions were combined and proteins precipitated with 2 vol of acetone (*e*, *f*). The proteins were fractionated on 10% polyacrylamide–0.26% bisacrylamide gels. Authentic eIF-2 phosphorylated in a separate reaction is shown in *g*. To activate eIF-2 kinase, reticulocyte lysate was incubated for 15 min without added haemin[6]; 3 μl of this lysate were incubated for 4 min with 2 μg of purified eIF-2 (a gift of Dr William C. Merrick), 50 μM (γ-^{32}P]ATP (1 μCi), 15 μg of bovine serum albumin and 1.5 mM Mg(OAc)$_2$. 0.2 μg of eIF-2 were analysed. The position of the PK$_{ds}$, eIF-2(αP), eIF-2(βP) and molecular weight markers is indicated.

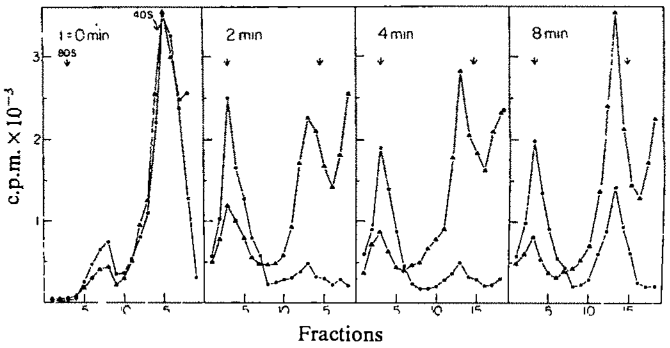

Fig. 3 Binding of HeLa cell mRNA to initiation complexes. Each 0.1-ml binding assay contained 17,500 c.p.m. of ^{3}H-mRNA (●) and ^{32}P-mRNA (▲) with a poly(A)·poly(U) duplex. The reactions were incubated at 30 °C for the time indicated in the panel and analysed as described in Fig. 1 legend, except that the gradient pellets containing polyribosomes were also counted. The ratio of c.p.m. in polyribosomes and 80S initiation complexes over c.p.m. in 48S complexes was 8.6, 6.7 and 2.5 for the ^{3}H-mRNA, and 0.7, 0.4 and 0.3 for the ^{32}P-mRNA at 2, 4 and 8 min, respectively. The ^{3}H-mRNA (58,000 c.p.m. per μg) was obtained from HeLa cells labelled with ^{3}H-uridine[13] and the ^{32}P-mRNA by annealing 200 ng of unlabelled HeLa cells mRNA with 2 ng of poly(U) labelled by 3′-terminal addition of [γ-^{32}P]dATP. In a 2-μl reaction, 200 ng of poly(U) were incubated for 4 h with 50 μM (α-^{32}P]dATP (150 μCi), 2.5 U of calf thymus deoxynucleotide terminal transferase and 0.5 μg of bovine serum albumin in 0.2 M K-cacodylate, 2 mM dithiothreitol, 0.5 mM CoCl$_2$ and 25 mM Tris, *p*H 6.9 (ref. 17). The reaction was stopped by the addition of 0.1 ml of NaOAc buffer, *p*H 5.2, containing 5 μg of yeast tRNA. The RNA was precipitated with 0.4 ml of 3% cetyltrimethylammonium bromide, washed with this solution and 75% ethanol, and dissolved in 0.125 M KOAc and 20 mM HEPES buffer, *p*H 7.4. The poly(U) had a specific activity of 1.3 × 10^5 c.p.m. per ng and the specific activity of the mRNA annealed with this poly(U) was ~1 × 10^4 c.p.m. per ng.

In subsequent experiments, we demonstrated a preferential inhibition of the initiation of mRNA containing a poly(A)·poly(U) duplex by including in the same incubation mRNA not annealed with poly(A)·poly(U) and labelled with a different isotope. In these experiments, poly(U) was labelled to high specific activity with terminal transferase[17] and annealed with unlabelled HeLa cell mRNA (Fig. 3). Only the mRNA containing a poly(A)·poly(U) duplex was thus labelled with ^{32}P. Very small amounts of this mRNA were added to binding assays together with uniformly ^{3}H-labelled HeLa mRNA. The concentration of added dsRNA was reduced to 3 ng ml^{-1} to delay the generalized inhibition of initiation observed in the experiment shown in Fig. 1*c*. Therefore, we carried out the binding assays without added emetine and allowed multiple cycles of initiation to take place. When an incubation was kept at 0 °C, the two mRNAs sedimented more slowly than 40S ribosomal subunits (Fig. 3*a*). The ^{3}H-mRNA was bound to 80S initiation complexes and to polyribosomes after 2–8 min incubation at 30 °C, whereas the mRNA containing the poly(A)·poly(U) duplex sedimented predominantly at 48S (Fig. 2*b*–*d*). The ratio of ^{3}H-mRNA bound to polyribosomes and 80S complexes to that sedimenting at 48S was always much greater than that of the ^{32}P–mRNA with the poly(A)·poly(U) duplex. It should be pointed out that even with as little as 3 ng ml^{-1} of dsRNA, the initiation of protein synthesis was inhibited after 8 min of incubation[6] and a significant fraction of ^{3}H-mRNA sedimented in 48S complexes.

To demonstrate that the inhibition of binding of this mRNA was caused by the activation of PK$_{ds}$, a binding assay was performed using a high concentration of added dsRNA, thus specifically preventing the activation of this kinase[6]. When HeLa cell mRNA annealed with labelled poly(U) was incubated with lysate, its binding to 80S initiation complexes was inhibited (Fig. 4*a*). With 10 μg ml^{-1} of poly(I)·poly(C) present, however, this mRNA was quantitatively bound to 80S complexes (Fig. 4*b*). Two other experiments provided additional evidence that the inhibition of binding of mRNA covalently linked to dsRNA required the activation of PK$_{ds}$. A mRNA containing a hybrid poly(A)·poly(dT) duplex was quantitatively bound to 80S initiation complexes (Fig. 4*c*). This showed that an RNA/DNA duplex, which could not activate the PK$_{ds}$ (ref. 18), had no effect on mRNA binding. Another experiment, based on the observation that 50 μM ethidium bromide prevented the activation of PK$_{ds}$ by poly(A)·poly(U) (ref. 19), showed that the inhibition of binding of mRNA with the poly(A)·(U) duplex was largely abolished by adding this concentration of ethidium bromide to a binding assay (Fig. 4*d*).

The inhibition of binding of mRNAs covalently linked to dsRNA was discovered with model polynucleotides constructed for the present experiments. The mechanism involved in this inhibition, however, is of general interest as it may function in interferon-treated cells preferentially to inhibit translation of viral mRNA. This mechanism involves the activation of PK$_{ds}$, the phosphorylation of eIF-2α and the binding of mRNA and eIF-2(αP) to 48S complexes. In the experiments with two mRNAs labelled with different isotopes present in the same incubation, only the binding of mRNA linked to dsRNA was inhibited. Therefore, eIF-2(αP) presumably associated with mRNA close to the site of activation of PK$_{ds}$. This could result from the binding of this kinase to the mRNA-linked poly(A)·poly(U) and the phosphorylation of eIF-2 interacting with this mRNA during the formation of 48S initiation complexes. The association of eIF-2 with specific nucleotide sequences near the 5′-terminus of mRNA has been reported[20], but it is not known whether these sequences interact with eIF-2 already bound to 40S ribosomal subunits during the assembly of initiation complexes.

On addition of 2-aminopurine and dephosphorylation of eIF-

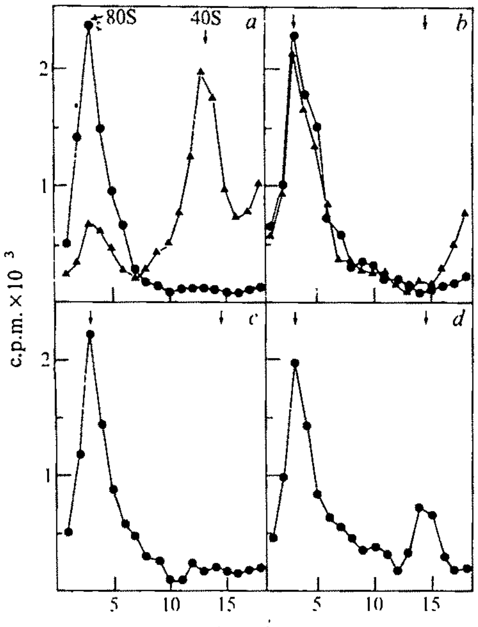

Fig. 4 Binding of HeLa cell mRNA to initiation complexes. The binding was carried out for 3 min after the addition of mRNA and analysed as described in Fig. 1 legend. The assays were incubated for 7 min without (a) or with (b) 10 μg ml^{-1} of poly(I)·poly(C) before the addition of 10,000 c.p.m. of HeLa cell ^{3}H-mRNA (●) and of mRNA containing a poly(A)·(U) duplex labelled with ^{32}P (▲) as described in Fig. 3 legend. The other assays contained mRNA with a poly(A)·poly(dT) duplex (c) or with a poly(A)·poly(U) duplex (d). Poly(dT) and poly(U) were labelled with terminal transferase as described in Fig. 3 legend, except that 2 μg of polynucleotide and 10 μCi of ^{3}H-dCTP were used. The polynucleotides were labelled to a specific activity of 5×10^3 c.p.m. per ng and 10 ng were annealed with 1 μg of HeLa cell mRNA. 50 μM ethidium bromide was added to the binding assay in d.

2(αP) by phosphatases[21], the mRNA binds slowly to 80S initiation complexes[5], indicating that mRNA in 48S complexes is not inactivated. It seems possible that mRNA synthesized by viral replicative complexes which activate the PK$_{ds}$ becomes bound to 48S complexes. Comparison of the rate of cleavage of mRNA in polyribosomes with that of mRNA associated with 48S complexes shows that the latter is cleaved significantly faster by the endonuclease activated by 2′,5′-oligo(A) (ref. 15). As these oligonucleotides may be synthesized by an interferon-induced enzyme bound to viral replicative complexes[22] and can activate the endonuclease in a localized way[13], it seems possible that mRNA in 48S complexes formed during transcirption of viral templates is preferentially degraded. Experiments are in progress to investigate this in intact cells. It is also conceivable that PK$_{ds}$ is involved in translational control of cellular mRNA if duplexes which can activate this kinase are formed.

We thank Drs Connie R. Faltynek and Timothy W. Nilsen for discussions and criticism of this manuscript, and Dr William C. Merrick for the gift of purified eIF-2. This work was supported by American Cancer Society grant CD-103, and NIH grants CA29895 and AI16076.

Received 25 April; accepted 27 June 1984.

1. Jagus, R., Anderson, W. F. & Safer, B. *Prog. Nucleic Acids Res. molec. Biol.* **25**, 127–185 (1981).
2. Grace, M., Ralston, R. D., Banerjee, A. C. & Gupta, N. K. *Proc. natn. Acad. Sci. U.S.A.* **79**, 6517–6521 (1982).
3. Siekierka, J., Mauser, L. & Ochoa, S. *Proc. natn. Acad. Sci. U.S.A.* **79**, 2537–2540 (1982).
4. Kaplañsky, D. A., Kwan, A. & Gross, M. *J. biol. Chem.* **257**, 5722–5729 (1982).
5. De Benedetti, A. & Baglioni, C. *J. biol. Chem.* **258**, 14556–14562 (1983).
6. Farrell, P. J. *et al. Cell* **11**, 187–200 (1977).
7. Lenz, J. R. & Baglioni, C. *J. biol. Chem.* **253**, 4219–4223 (1978).
8. Baglioni, C. *Cell* **17**, 255–264 (1979).
9. Nilsen, T. W., Maroney, P. A. & Baglioni, C. *Molec. cell. Biol.* **3**, 64–69 (1983).
10. Gorski, J., Morrison, M. R., Merkel, C. G. & Lingrel, J. B. *J. molec. Biol.* **86**, 363–371 (1974).
11. Leroux, A. & London, I. *Proc. natn. Acad. Sci. U.S.A.* **79**, 2147–2151 (1982).
12. Baglioni, C., Simili, M. & Schafritz, D. A. *Nature* **275**, 249–243 (1978).
13. Nilsen, T. W. & Baglioni, C. *Proc. natn. Acad. Sci. U.S.A* **76**, 2600–2604 (1979).
14. Minks, M. A., West, D. K., Benvin, S. & Baglioni, C. *J. biol. Chem* **254**, 10180–10183 (1979).
15. De Benedetti, A. & Baglioni, C. *J. biol. Chem.* (submitted).
16. Ranu, R. S. *Biochem, biophys. Res. Commun.* **97**, 252–262 (1980)
17. Wu, R., Jay, E. & Roychoudburg, R. *Meth. Cancer Res.* **12**, 87–91 (1976)
18. Hunter, T., Hunt, T. & Jackson, R. J. *J. biol Chem.* **250**, 409–417 (1975)
19. Baglioni, C. & Maroney, P. A. *Biochemistry* **20**, 758–765 (1981)
20. Kaempfer, R., Van Emmelo, J. & Fiers, W. *Proc. natn. Acad. Sci. U.S.A* **78**, 1542–1546 (1981)
21. Crouch, D. & Safer, B. *J. biol. Chem.* **255**, 7918–7924 (1980).
22. Nilsen, T. W., Maroney, P. A. & Baglioni, C. in *Regulation of Macromolecular Synthesis by Low Molecular Weight Mediators* (eds Koch, H. & Richter, D.) 329–339 (Academic, New York, 1979).

Activating protein factor binds *in vitro* to upstream control sequences in heat shock gene chromatin

Carl Wu

Laboratory of Biochemistry, Developmental Biochemistry Section,
National Cancer Institute, National Institutes of Health, Bethesda,
Maryland 20205, USA

DNA sequences, important for the control of *Drosophila* heat shock gene expression, are packaged in chromatin in a nuclease hypersensitive configuration[1]. Recently, two protein-binding (exonuclease-resistant) sites which cover the TATA box sequence and an upstream control element were shown to occur *in vivo* amidst the 5′ terminal hypersensitive regions of several heat shock genes[2]. Protein-binding at the TATA box is independent of heat shock, but the binding at the upstream element is heat shock dependent, and it was proposed that a heat shock activator protein, HAP, positively regulates the genes[2]. Here, I report the detection of HAP activity in heat shocked cell extracts by reconstituting specific binding to *hsp*82 gene chromatin *in vitro*. Inhibition of the binding by free DNA from the 5′ region of heat shock genes implies a coordinate regulation of the gene family through HAP interaction with the upstream heat shock consensus sequence[3]. Furthermore, the special ease of induction of the *hsp*82 gene over other heat shock genes can be explained in molecular terms by the higher affinity of HAP for the *hsp*82 binding site, which contains a 28 base sequence with almost perfect dyad symmetry, GAAGCCTCTAGAAG|TTTCTAGAGACTTC.

We reasoned that promoter DNA in its naturally 'hypersensitive' state in chromatin should be a superior substrate to purified DNA for the *in vitro* binding of specific protein factors extracted from *Drosophila* cell nuclei. The binding to the target in chromatin can be revealed by the resistance to exonuclease digestion starting at an appropriate restriction endonuclease cut in the 5′ hypersensitive region. We chose to monitor the binding activity of heat shocked cell extracts on the single-copy gene encoding the heat shock protein of molecular weight 81,858 (ref. 4–8) (*hsp*82; formerly referred to as *hsp*83), because of the exceptionally strong resistance to exonuclease digestion observed previously *in vivo*[2]; for experimental strategy, see Fig. 1.

The *in vivo* binding of HAP factor to the *hsp*82 gene promoter in heat shocked *Drosophila* embryos is shown in Fig. 2. Purified nuclei from normal (lane a) or heat shocked (lanes b, c) embryos were digested with *Eco*RI and an exhaustive amount of *Escherichia coli* exonuclease III (exoIII). (ExoIII is unable to proceed with digestion from fragment ends made by those restriction enzymes, for example *Pst*I, which leave a 4-base, 3′ protrusion; S. Henikoff, personal communication.) DNA was purified and the single-stranded DNA tails were trimmed with S$_1$ nuclease. After repurification, the DNA was cut with two restriction enzymes, *Xho*I and *Hin*dIII, and was sized by electrophoresis on agarose gels. The *hsp*82 gene fragments resulting from *Eco*RI and exonuclease digestion were visualized with an indirect end-labelling probe after Southern transfer. Thus, the barrier to exonuclease digestion downstream from the *Eco*RI cut in the active gene was located at position −86, the distal border of the HAP binding site (Fig. 2, lanes b, c) whilst that

Fig. 1 The *in vitro*, chromatin binding assay. The nuclease hypersensitive site in the noninduced *hsp*82 gene 5′ region is represented as a stretch of DNA associated with the TATA box binding protein, (TAB)[2]. Circles represent neighbouring nucleosomes whose precise positions have not been determined. HAP (+) and HAP (−) refer to the heat shocked and nonshocked condition, respectively.

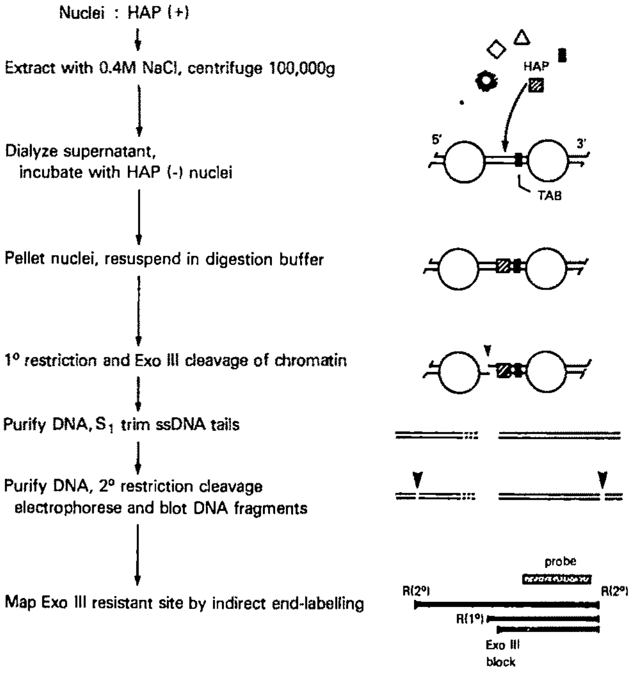
Nuclei : HAP (+)
Extract with 0.4M NaCl, centrifuge 100,000g
Dialyze supernatant, incubate with HAP (-) nuclei
Pellet nuclei, resuspend in digestion buffer
1° restriction and Exo III cleavage of chromatin
Purify DNA, S₁ trim ssDNA tails
Purify DNA, 2° restriction cleavage electrophorese and blot DNA fragments
Map Exo III resistant site by indirect end-labelling
HAP
5′
3′
TAB
probe
R(2°)
R(2°)
R(1°)
Exo III block

at position −39 in the inactive gene reveals a boundary of the TATA box binding protein (TAB) (lane *a*)[2].

To assay for HAP factor *in vitro*, nuclei purified from non-heat-shocked *Drosophila* embryos were incubated with a 0.4 M NaCl extract of nuclei from heat-shocked embryos or cultured cells (Schneider line 2, SL2). After incubation with the extract, the nuclei were pelleted and resuspended for digestion with *Eco*RI and exoIII, and the exonuclease-resistant sites were mapped as above. When using buffer alone, or an extract from non-heat-shocked embryos, or when histone H1 protein was used for the incubation, no resistance at position −86 was observed. However, distinct resistance at −86 was observed using extracts from heat-shocked embryos, and from two preparations of shocked SL2 cells. We are thus able to detect HAP binding *in vitro* using crude nuclear extracts without having to resort to previous purification.

HAP binding activity in shocked embryonic extracts is low compared to that observed in shocked SL2 cell extracts; this is

Fig. 2 Chromatin binding activity of extracted factors at the *hsp*82 gene promoter. *a–c*, exoIII digestion downstream from an *Eco*RI cut at position −166 in chromatin from non-heat-shocked (nhs) *Drosophila* embryos, and from embryos heat-shocked (hs) at 36 °C for 15 min. (+1) is the transcriptional start indicated on the partial restriction map by the arrow pointed in the direction of transcription. Arrowheads indicate the positions of the barriers to exoIII digestion. Purified nuclei from 2–7-h-old *D. melanogaster* (Oregon R) embryos were digested with *Eco*RI and exoIII; the DNA was purified, trimmed with S_1 nuclease, repurified, digested with *Hin*dIII and *Xho*I, electrophoresed, blotted to nitrocellulose and hybridized with an indirect end-labelling probe (solid bar) as described previously[2]. *c*, From the same gel as *d–j*. *d–j*, exoII digestion from the *Eco*RI cut at position −166 in normal chromatin incubated with the indicated extracts and reagents.

Methods: Nuclei were purified from 2–7-h-old *Drosophila* embryos grown at 24 °C as previously described[2]. The pelleted nuclei were resuspended in nuclear buffer[2] at 5×10^8 per ml, transferred to 1.5 ml Eppendorf tubes and centrifuged briefly in the microfuge. After removal of the supernatant, the pellet was resuspended in buffer alone (Solution III; see below), in extract plus 5 mM $MgCl_2$, or in 50 μg histone HI protein (Boehringer–Mannheim) per ml of nuclear buffer, and incubated at room temperature, 24 °C, for 20 min. The nuclei were pelleted again and the supernatant was removed. Nuclei were then resuspended for digestion at 30 °C for 15 min in nuclear buffer—5% glycerol containing 3,500–6,100 U ml^{-1} *Eco*RI and 9,000 U ml^{-1} *E. coli* exonuclease III and $MgCl_2$ adjusted to 6 mM. The reactions were terminated with EDTA and SDS, and nucleic acids were purified by organic extraction and precipitated in EtOH. S_1 nuclease trimming of ssDNA tails was performed essentially as described[2], using 2,500 U ml^{-1} S_1 nuclease for a DNA concentration of ~0.1 mg ml^{-1}. DNA was repurified and digested with *Hin*dIII and *Xho*I, electrophoresed on a 25 cm long 1.4% agarose Tris-acetate EDTA (TAE) gel, blotted to nitrocellulose and hybridized as above. Extracts were prepared using a modification of the procedure of Dignam *et al.*[21]. Schneider line 2 tissue culture cells were grown in suspension[22] at 23–24 °C, to a density of 5×10^6–1×10^6 cells ml^{-1}. After washing in saline, pelleted cells were frozen in dry ice-EtOH and stored at −70 °C until use. Pellets containing about 10^{10} cells were thawed, and resuspended at 4 °C, the subsequent operating temperature, in two packed cell volumes of Solution I (0.3 M sucrose, 10 mM HEPES, *p*H 7.9, 10 mM KCl, 1.5 mM $MgCl_2$, 0.1 mM EGTA, 0.5 mM dithiothreitol (DTT), 0.5 mM phenylmethanesulphonyl fluoride (PMSF).) Cells were lysed in a Dounce homogenizer using about 15 strokes of the tight pestle. Breakage of cells was about 95% by microscopic inspection. The homogenate was centrifuged in a clinical centrifuge at top speed for 7.5 min (1,600*g*) to pellet crude nuclei. The nuclei were resuspended in 2 packed nuclei volumes of Solution II (10 mM HEPES, *p*H 7.9, 400 mM NaCl, 1.5 mM $MgCl_2$, 0.1 mM EGTA, 0.5 mM DTT, 5% glycerol, 0.5 mM PMSF) and the final NaCl concentration was re-adjusted to 0.4 M. The crude nuclei were extracted at 4 °C for 30 min with continuous stirring, followed by centrifugation at 100,000*g* for 1 h. The supernatant was transferred into a colloidon bag (Schleicher and Schuell UH 100/10) for dialysis in Solution III (20 mM HEPES, *p*H 7.9, 75 mM NaCl, 0.1 mM EDTA, 0.5 mM DTT, 20% glycerol, 0.5 mM PMSF) for about 5 h. A vacuum was applied for some time during dialysis to concentrate the extract to the original packed cell volume. The extract was cleared by centrifugation at 10,000*g* for 10 min. The supernatant (~50 mg protein per 10^{10} cells) was frozen in aliquots in liquid N_2, and stored at −70 °C; the extracts retained their activity for at least two months after storage. A 1/5 dilution of active extract still gave 'full' occupancy of the binding site, but further dilutions up to 1/40 reduced binding activity to undetectable levels. Embryonic extracts from 15 g each of normal and heat shocked (36 °C, 20 min) 0–18-h-old *Drosophila* embryos were prepared from nuclei purified by centrifugation through Solution I (1.7 M sucrose) as described previously[2] except that the homogenizing buffer was Solution I supplemented with leupeptin, 5 μg ml^{-1}, pepsfatin, 2 μg ml^{-1}, and aprotinin, 0.2 TI U ml^{-1}. Embryonic nuclei were extracted for 30 min at 4 °C, with stirring, in 10 ml Solution II; NaCl was re-adjusted to 0.4 M to account for the volume of the purified nuclear pellet. The embryonic extract was centrifuged, dialysed, clarified and stored essentially as for extracts from cultured SL2 cells.

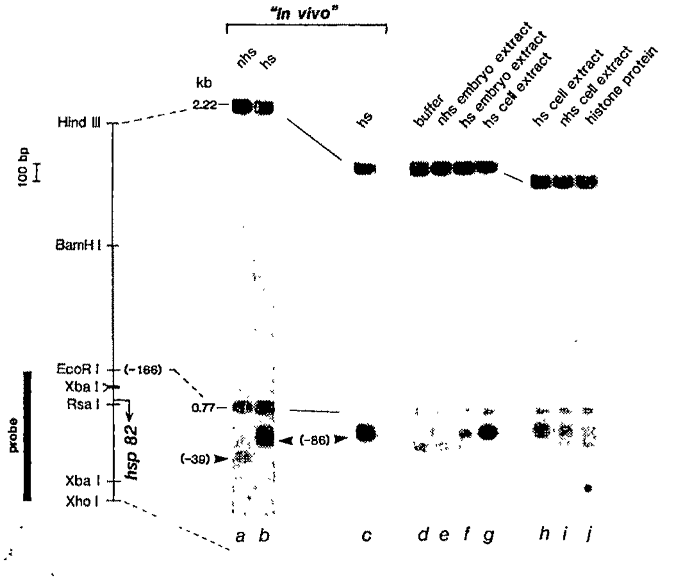

presumably due to high protease activity associated with the former. A non-heat-shocked SL2 cell extract also contains HAP binding activity (Fig. 2, lane *i*) (roughly 20-fold less than shocked cell extracts, as seen by dilution experiments, data not shown). This result is not unexpected as the *hsp*82 gene is expressed at some level in *Drosophila* cell lines cultured under normal laboratory conditions[6,9–11] and as HAP binding *in vivo* can be observed even in nonshocked SL2 cells (C.W., unpublished observations).

To map the proximal boundary of HAP binding *in vitro* we analysed the resistance to exonuclease digestion upstream from a *Rsa*I cut at position +20 in the chromatin (Fig. 3). As shown previously[2], the weaker *in vivo* exonuclease resistance of the non-heat-shocked *hsp*82 gene at position −17, the proximal border of the TAB binding site, is largely overcome in limit-digestion conditions, and the bulk of the *Rsa*I-cleaved fragments are further degraded to a smear (not well reproduced in Fig. 3, lane *b*). On heat shock (lane *c*), HAP binding poses an impenetrable barrier at position −50, and also retards the kinetics of digestion through the TAB site. When non-heat-shocked nuclei are incubated with the indicated extracts, pelleted, and resuspended for digestion with *Rsa*I and exoIII, the position of resistance to exoIII generated by *in vitro* HAP binding is identical to that shown *in vivo* (Fig. 3, lanes *d–i*). The specific variation in the binding activity of the extracts from embryos and cultured cells also parallels the analysis of exonuclease resistance from the *Eco*RI cut in Fig. 2.

We can assay for this binding independently by measuring the sensitivity to *Xba*I cleavage in chromatin at two sites positioned at −74 and −64, within the HAP binding site. When non-heat-shocked embryonic nuclei are incubated with the extract from heat-shocked SL2 cells, the *Xba*I sites at positions −74 and −64 are clearly protected from cleavage (Fig. 3, lane *m*). Interestingly, the other *Xba*I site at position +484, inside the *hsp*82 transcriptional unit, does not become more sensitive upon shock as it does *in vivo*, suggesting that the extract may be unable to effect the secondary phenomenon associated with chromatin activation.

The chromatin binding activity is unaffected by treatment of active extract with RNase A+T1, or with micrococcal nuclease. However, when extracts are treated with trypsin or proteinase K (subsequently inactivated with protease inhibitors), HAP binding activity is abolished using the exonuclease protection

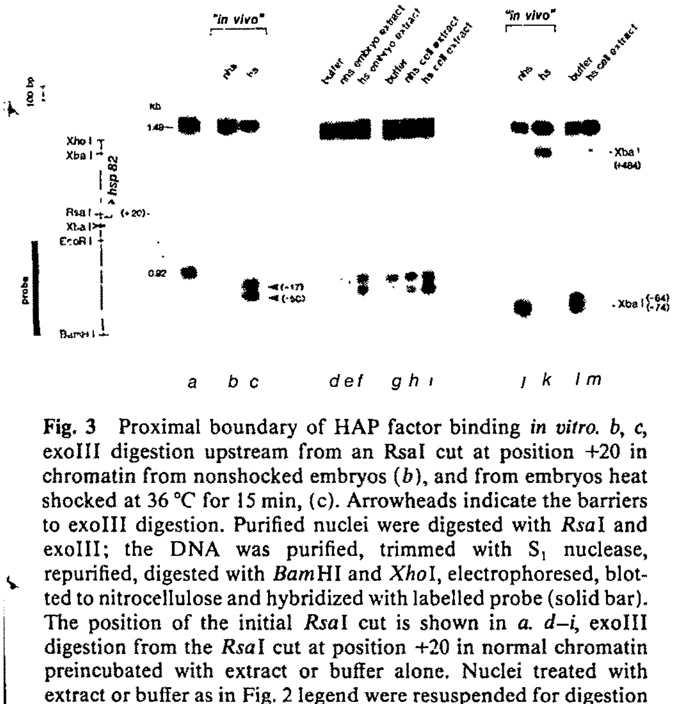

Fig. 3 Proximal boundary of HAP factor binding *in vitro*. *b*, *c*, exoIII digestion upstream from an RsaI cut at position +20 in chromatin from nonshocked embryos (*b*), and from embryos heat shocked at 36 °C for 15 min, (c). Arrowheads indicate the barriers to exoIII digestion. Purified nuclei were digested with *Rsa*I and exoIII; the DNA was purified, trimmed with S_1 nuclease, repurified, digested with *Bam*HI and *Xho*I, electrophoresed, blotted to nitrocellulose and hybridized with labelled probe (solid bar). The position of the initial *Rsa*I cut is shown in *a*. *d–i*, exoIII digestion from the *Rsa*I cut at position +20 in normal chromatin preincubated with extract or buffer alone. Nuclei treated with extract or buffer as in Fig. 2 legend were resuspended for digestion at 35 °C for 12 min in nuclear buffer-5% glycerol containing 1,300 U ml^{-1} *Rsa*I plus 9,000 U mol^{-1} exoIII (*d–f*), or 2,300 U ml^{-1} *Rsa*I plus 9,000 U ml^{-1} *exo*III (*g–i*). The reactions were stopped, the purified DNA treated with S_1 nuclease, repurified, restricted with *Bam*HI and *Xho*I, electrophoresed on a 40-cm-long TAE agarose gel, blotted to nitrocellulose and hybridized as above. *j–m*, *Xba*I sensitivity of the *hsp*82 gene at positions −64, −74 and +484 in chromatin from nonshocked embryos (*j*), from embryos heat shocked at 36 °C for 15 min (*k*), and in nonshocked embryonic chromatin incubated with buffer alone (*l*), or with an extract made from heat shocked SL2 cells (*m*). Nuclei purified from 2–7-h-old *Drosophila* embryos were digested with 1,400 U ml^{-1} *Xba*I at 35 °C for 15 min (*j*, *k*), and with 1,700 U ml^{-1} *Xba*I at 35 °C for 12 min for the nuclei incubated with buffer or extract (*l*, *m*). DNA was purified and restricted for blot analysis as above.

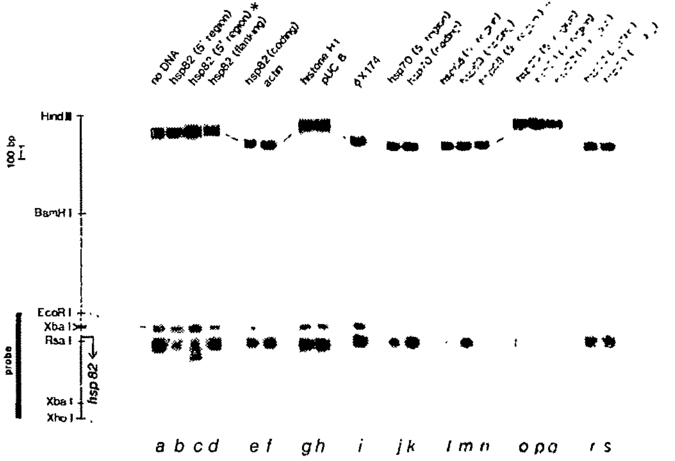

Fig. 4 DNA inhibition of HAP binding to *hsp*82 gene chromatin. Extracts from heat shocked SL2 cells were diluted 5-fold; 100 µl was incubated with the indicated DNA's for 10 min at 24 °C, followed by incubation with nuclei purified from nonshocked *Drosophila* embryos. The DNA templates were linearized by restriction cleavage before incubation. The inhibition produced by different parts of each heat shock gene is compared using approximately equivalent DNA concentrations for the particular sequence Specific chromatin-binding activity was assayed by exonuclease protection as in Fig. 2 legend. *b*, *hsp*82 (5′ region); 0.05 µg of 186 bp, *Eco*RI (−166) to *Rsa*I (+20) fragment, with 0.95 µg of ϕX174-*Hae*III as carrier DNA. *c*, DNA as in (*b*) was incubated with extract as above. $CaCl_2$ was added to 0.4 mM, micrococcal nuclease to 300 U ml^{-1} and free DNA was digested for 5 min at 24 °C. Micrococcal nuclease was inactivated with EGTA to 1 mM and the extract was then incubated with noninduced nuclei as above. *d*, *hsp*82 (flanking); 0.2 µg of 0.7 kb upstream *Bam*HI to *Eco*RI (−166) fragment with carrier DNA as above. *e*, *hsp*82 (coding); 0.25 µg of 1.8 kb *Xho*I (+584) to *Sal*I (+2,400) fragment with carrier DNA as above. *f*, Actin gene; 1 µg of linearized plasmid DNA consisting of pBR322 vector and a 3.8 kb *Bam*HI–*Eco*RI insert containing coding and upstream sequences for the *Drosophila* actin gene at chromosomal locus 57A (E. Fryberg, personal communication). g, Histone HI gene; 0.75 µg of a 1.3 kb *Bam*HI–*Hpa*I fragment containing roughly the 5′ half of the coding sequence plus upstream DNA[23]. *h*, pUC8; 1 µg of the linearized plasmid DNA. *i*, ϕX174; 1 µg of duplex phage DNA cut with *Hae*III. *j*, *hsp*70 (5′ region); 0.4 µg of 279 bp *Xho*I (−194) to *Pst*I (+85) fragment. *k*, *hsp*70 (coding); 1 µg of 1.1 kb *Pst*I (+85) to *Pst*I (+1,187) fragment. *l*, *hsp*68 (5′ region); 1 µg of 0.4 kb upstream *Pst*I to *Hpa*II (+44) fragment[24]. *m*, *hsp*68 (coding); 1 µg of 0.6 kb *Pst*I–*Pst*I fragment of coding sequence[24]. *n*, 1 µg of *hsp*68 0.4 kb 5′ *Pst*I–*Hpa*II fragment was incubated with extract, digested with micrococcal nuclease and processed as in (*c*). *o*, *hsp*26 (5′ region); 1 µg of linearized plasmid DNA consisting of pUC9 vector and a 0.7 kb upstream *Pst*I–*Eco*RI (+7) fragment[25–28]. *p*, *hsp*23 (5′ region); 1 µg of linearized plasmid DNA consisting of pUC9 vector and a 0.7 kb upstream *Pst*I–*Eco*RI (+7) fragment[25–28]. *q*, *hsp*22 (5′ region); 1 µg of linearized plasmid DNA consisting of pUC9 vector and a 0.6 kb *Hin*dIII (−402) to *Hin*dIII (−213) fragment[25–28]. *r*, *hsp*22 (coding); 1 µg of linearized plasmid DNA consisting of pUC9 vector and a 0.8 kb downstream *Bam*HI to *Hin*dIII (+213) fragment[23–28]. *s*, *hsp*26 (coding); 1 µg of linearized plasmid DNA consisting of pUC9 vector and a 0.6 kb downstream *Pvu*II to *Eco*RI (+7) fragment[25–28].

assay as above (data not shown). This confirms that the specific binding component of HAP is protein.

Specific HAP binding to *hsp*82 gene chromatin is almost totally inhibited by pretreating active extracts with a short *hsp*82 DNA fragment containing the binding site (Fig. 4, lane *b*). No inhibition on pretreatment is observed using further upstream flanking sequences or sequences in the *hsp*82 coding region, nor when other DNAs are used (lanes *d*–*i*). On the other hand, purified DNA from the 5′ region of the other heat shock genes: *hsp*70, *hsp*68, *hsp*26, *hsp*23, *hsp*22 do inhibit to a partial extent the binding of HAP factor to *hsp*82 gene chromatin (lanes *j*, *l*, *o*–*q*), whereas purified DNA from the coding sequences of *hsp*70, *hsp*68, *hsp*22 and *hsp*26 do not (lanes *k*, *m*, *r*, *s*). To demonstrate that the HAP activity we have measured in the extract is a primary DNA binding activity and not a secondary enzymatic activity with converts an ineffective HAP to its specific DNA binding mode, we pretreated active extract with target DNA and digested excess DNA with micrococcal nuclease. The resultant extract has no HAP binding activity towards the *hsp*82 gene chromatin (Fig. 4, lanes *c*, *n*); the activity should have been retained were the active component secondary to DNA binding. (Effective removal of excess DNA by micrococcal nuclease is demonstrated by the recovery of HAP binding activity to chromatin on readdition of active extract; data not shown.)

We infer from these inhibition experiments that HAP factor for the *hsp*82 gene is able to bind to purified DNA, not only to its own target sequence but also to the upstream consensus sequence[3] shared by other heat shock genes. The simplest model consistent with the data is that HAP, in concert with bound TAB, can coordinately activate the whole heat shock gene family by binding to each upstream element, and that the variation in the kinetics of activation among these genes reflects differential binding affinities of HAP for individual upstream elements that are similar but not identical in sequence. Such a model would predict a direct relationship between decreasing HAP binding affinities and the increasing order of transcriptional activation. The available evidence supports this prediction. The *hsp*82 gene is most easily activated[6,9–11,12], whilst HAP binding strength *in vivo* (ref. 2 and unpublished data), or *in vitro* (Fig. 4) is greater for the *hsp*82 gene than for other heat shock genes. It will be of interest to investigate further the correlation between binding strength and activation kinetics.

We re-examined the sequence of the 36 bp HAP binding site[2] for *hsp*82 and found that it covers a central 28 base sequence with almost perfect dyad symmetry (24 bases out of 28): (−81) GAAGCCTCTAGAAG|TTTCTAGAGACTTC (−54). None of the upstream elements of the other heat shock genes have this high degree of symmetry. The exceptionally strong binding affinity of HAP to this symmetrical dyad suggests that it may be the canonical recognition sequence for HAP binding (as a protein dimer or tetramer like prokaryotic DNA binding proteins).

We do not believe that HAP is synthesized *de novo* upon heat shock, because the response can be brought on within minutes after stimulation, and can occur in the absence of protein synthesis[13]. It seems that HAP should either be decompartmentalized upon heat shock or more likely, be converted from a pre-existing inactive form to a specific DNA binding form. Our finding that HAP activity in the crude extract binds DNA directly does not preclude the presence of secondary modifying activities in the extract. We are currently devising appropriate assays to retrace the physiological pathway from the terminal events of heat shock.

Others have shown the presence of eukaryotic sequence-specific DNA binding proteins[14,15], and activators of heat shock genes have been reported in studies employing different methods[16–19]. HAP factor appears to be unrelated to these activities. During the preparation of this manuscript, Parker and Topol[20] published a report on a *Drosophila* transcription factor designated HSTF that is specific for the *hsp*70 gene; partially purified preparations of this factor bind to a 55 bp region upstream of the TATA box. HAP and HSTF bind roughly to the same DNA sequence, but their binding activities in non-heat-shocked cells appear to be very different; further work should illuminate the relationship between the two factors.

We believe that the *in vitro* chromatin binding, exonuclease protection assay reported here is a powerful method for analysing eukaryotic DNA binding proteins for the following reasons: (1) precision in delimiting the binding site, (2) confidence in the physiological relevance of the binding provided by *in vivo* comparison, and (3) exceptional sensitivity, as seen by detection of binding activity in crude extracts with no fractionation whatsoever. This feature permits binding activity to be tracked from the start of the purification; at later stages, more traditional assays could be used to increase experimental efficiency.

I thank B. Sauer, C. Klee, P. Wagner and S. Wilson for helpful suggestions on protein analysis, E. Craig, E. Fyrberg, R. Holmgren, R. Blackman, R. Morimoto and M. Meselson for gifts of cloned DNA, T. Paisley for technical assistance and B. Miller for typing the manuscript.

Received 5 June; accepted 26 July 1984.

1. Wu, C. *Nature* **286**, 854–860 (1980).
2. Wu, C. *Nature* **309**, 229–234 (1984).
3. Pelham, H. R. B. *Cell* **30**, 517–528 (1982).
4. Holmgren, R., Livak, K., Morimoto, R., Freund, R. & Meselson, M. *Cell* **18**, 1359–1370 (1979).
5. Holmgren, R., Corces, V., Morimoto, R., Blackman, R. & Meselson, M. *Proc. natn. Acad. Sci. U.S.A.* **78**, 3775–3778 (1981).
6. O'Connor, D. & Lis, J. T. *Nucleic Acids Res.* **9**, 5075–5092 (1981).
7. Hackett, R. W. & Lis, J. T. *Nucleic Acids Res.* **11**, 7011–7030 (1983).
8. Blackman, R. K. thesis, Harvard Univ. (1983).
9. Storti, R. V., Scott, M. P., Rich, A. & Pardue, M. L. *Cell* **22**, 825–834 (1980).
10. Lindquist, S. *Devl Biol.* **77**, 463–479 (1980).
11. Buzin, C. M. and Petersen, N. S. *J. molec. Biol.* **158**, 181–201 (1982).
12. Spradling, A., Pardue, M. L. & Penman, S. *J. molec. Biol.* **109**, 559–587 (1977).
13. Ashburner, M. *Chromosoma* **31**, 356–376 (1970).
14. Emerson, B. M. & Felsenfeld, G. *Proc. natn. Acad. Sci. U.S.A.* **81**, 95–99 (1984).
15. Jack, R. S., Gehring, W. J. & Brack, C. *Cell* **24**, 321–331 (1981).
16. Compton, J. L. & Bonner, J. J. *Cold Spring Harb. Symp. quant. Biol.* **42**, 835–838 (1978).
17. Compton, J. L. & McCarthy, B. J. *Cell* **14**, 191–201 (1979).
18. Bonner, J. J. *Devl Biol.* **86**, 409–418 (1981).
19. Craine, B. L. & Kornberg, T. *Cell* **25**, 671–681 (1981).
20. Parker, C. S. & Topol, J. *Cell* **37**, 273–283 (1984).
21. Dignam, A. D., Martin, P. L., Shastry, B. S. & Roeder, R. G. *Meth. Enzym.* **101**, 582–598 (1983).
22. McKenzie, S. L., Henikoff, S. & Meselson, M. *Proc. natn. Acad. Sci. U.S.A.* **72**, 1117–1121 (1975).
23. Lifton, R. P., Goldberg, M. L., Karp, R. W. & Hogness, D. S. *Cold Spring Harb. Symp. quant. Biol.* **42**, 1047–1051 (1978).
24. Holmgren, R. thesis, Harvard Univ. (1980).
25. Craig, E. A. & McCarthy, B. J. *Nucleic Acids Res.* **8**, 4441–4457 (1980).
26. Corces, V., Holmgren, R., Freund, R., Morimoto, R. & Meselson, M. *Proc. natn. Acad. Sci. U.S.A.* **77**, 5390–5393 (1980).
27. Ingolia, T. D. & Craig, E. A. *Nucleic Acids Res.* **9**, 1627–1642 (1981).
28. Southgate, R., Ayme, A. & Voellmy, R. *J. molec. Biol.* **165**, 35–57 (1983).

Turbulence in an oceanic convective mixed layer—Corrigendum

T. J. Shay & M. C. Greg

Nature 310, 282–285 (1984)

In the above letter it was stated that the mixed layer mean value of ε/J_b^0 in the ocean was a factor of two lower than that in the atmosphere, and that difference was left unexplained. The difference was the result of a computational error. When that error is corrected, the two cases are in much better agreement, as seen in the figure. For the region $0.4 < z/D < 1.0$, the mean value of ε/J_b^0 in both the ocean and atmosphere is 0.45. The difference in scatter may be due to more restrictive editing of the atmospheric data as well as the influence of lateral processes in the ocean.

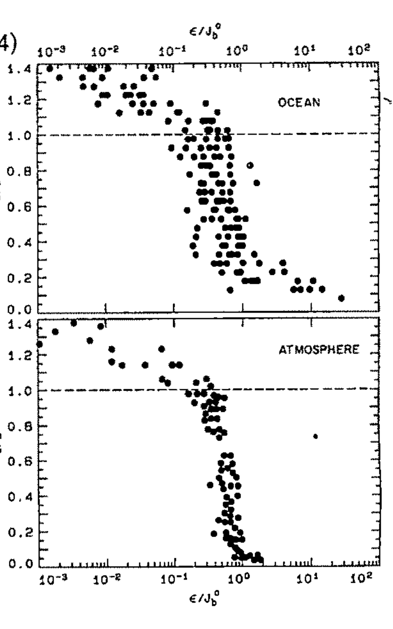

Theology *in vitro*

John Habgood

Begotten or Made? By Oliver O'Donovan.
Clarendon: 1984. Pp.88. Pbk £2.50, $4.95.

THE debate sparked off by the Warnock Committee report on human fertilization should benefit from this unusual contribution by Professor O'Donovan. As befits the Regius Professor of Moral and Pastoral Theology in the University of Oxford he approaches the topic at a high level of generality, in sharp contrast to the pragmatic and piecemeal procedure often favoured by practising scientists. He modestly claims to make no more than a contribution to the discussion, but his main argument, if accepted, would radically change the thrust of much current practice in this field. I hope that scientific readers who find it hard to cope with his style of argument, and in particular with his Christian presuppositions, will nevertheless persevere with the book if only for the sake of the fresh perspective it opens up.

One of the discouraging and perplexing features of many of the moral choices facing medical practitioners is not the fact that difficult decisions have to be made, but the sense that medical practice is part of a vast and seemingly inevitable process of social change. It is the pre-emption of choice which is worrying, and this is why no amount of analysis of particular cases, and no attempts to specify legal limits in relation to this or that technique, can fully resolve the underlying dilemmas. Effective moral comment entails criticism of the cultural assumptions which make it easy and natural to look for one kind of solution to our practical problems in preference to another. Only by tackling the issues at this level is it possible to see, and maybe begin to counteract, the full implications of runaway technology.

The impact of living in a technological culture carries particular threats for the process of human begetting. What distinguishes our relationship with human beings in such an environment is precisely the fact that they are not "made".

> A being who is the 'maker' of any other being is alienated from that which he has made, transcending it by his will and acting as the law of its being. To speak of 'begetting' is to speak of quite another possibility than this: the possibility that one may form another being who will share one's own nature, and with whom one will enjoy a fellowship based on radical equality [p.2].

It is this radical equality, this deep set of assumptions about the status and being of persons, which Professor O'Donovan believes is eroded by reproductive techniques which break up the act of begetting into a series of manipulations. If it is objected that science and medicine are doing no more than to supplement natural processes which have gone wrong, then the reply is that it is precisely this assumption — that every human ill has a technological answer — which in the end threatens our humanity.

The theme is illustrated by reference to trans-sexual surgery, artificial insemination by donor, experimentation on embryos and *in vitro* fertilization. The first of these raises important questions about the degree to which social perceptions of a person's sex can be used to justify surgical interference with the given characteristics of their body. The second highlights the erosion and confusion of the role of parents. The third leads to an illuminating discussion of the meaning of the word "person", and the tendency to convert a concept whose primary reference is ontological and historical into a qualitative term, indicating the possession of a particular quality, "personality". Embryos, on this latter view, do not yet possess personality and so may be experimented on as being interestingly human but not yet persons to be respected. O'Donovan comments,

> The practice of producing embryos by IVF with the intention of exploiting their special status for use in research is the clearest possible demonstration of the principle that when we start making human beings we necessarily stop loving them; that that which is made rather than begotten becomes something that we have at our disposal...[p.65].

On IVF itself he accepts the arguments for "assisted reproduction", but wonders whether the price in terms of research and risk-taking is morally too high.

This is not a book which will please those who follow their scientific and technological noses wherever the evidence and opportunities lead them. Even a sympathetic reader like myself spattered the margins with question-marks. Its merit is that it raises some fundamental issues about the character of the civilization we are making (the word is significant) for ourselves, in a way which gives current dicussions of particular techniques a new sense of urgency. The fact that its title echoes a phrase in one of the Christian creeds, referring to Christ as "begotten not made", is a reminder of the extent to which traditional Western assumptions about the nature and value of human life have been rooted in Christian theology. I suspect that theology still provides the best defence against the dehumanizing tendencies of a technological culture, but it has to be admitted that, humanly speaking, the defence looks uncomfortably fragile.

John Habgood is Archbishop of York.

The orderly chromosome

J.R.S. Fincham

Molecular Evolution and Organization of the Chromosome.
By A. Lima-de-Faria.
Elsevier Science: 1984. Pp.1, 186. Dfl. 450, $191.50.

THE scope of this book is broader than its title might suggest; it provides a reappraisal of genetics and a very individual view of life. Its main weight lies in an extensive review of many aspects of chromosome behaviour, especially those involving interactions between different parts of genomes. The author has for many years promoted the idea of the "chromosome field", the essence of which is that the arrangement of sequences within chromosomes matters for function. There is therefore much emphasis on such topics as *Drosophila* variegation-type position effects, control of the activity of nucleolus-organizer regions, the activity of centromeres and neocentromeres, and inter-chromosomal effects on crossover frequency. None of these has yet been explained in molecular terms, but the author is quite clear that they are molecular phenomena.

In his preface, Professor Lima-de-Faria remarks that his book is mainly based on the 25,000 reprints in his personal collection, supplemented by over 3,000 photocopies. Many of these have been drawn upon to supply the book's copious tables and figures which, for the most part, appear with legends reproduced verbatim from the originals. This does not always conduce to close integration with the text but at least helps, I suppose, to minimize error. In preparing a book of the magnitude, it is obviously difficult to be up-to-the-minute in every area; of the (approximately) 2,000 references in fact fewer than 10 per cent date from within the past five years. Thus we find only a brief mention of the nucleosome and little or nothing on non-histone proteins, the sequences of eukaryotic promoters and enhancers, methylation and the relationships of all these to states of transcriptional activity and inactivity.

It is clear that Lima-de-Faria's object in writing this book was not only to review a field but also to correct a number of what he sees as misconceived notions in modern biology. In nuclear cytology he considers that much harm has been done by the concept of chromosome *mechanics*. He looks to molecular rather than mechanical explanations of chromosome behaviour, and evidently sees a conflict between the two. More generally, he is in profound opposition to the idea of randomness, and upholds the principle of order in all things.

This attitude emerges in a number of striking passages. Discussing meiosis (p. 923), he dismisses the view that disjunction of different bivalents occurs at random, making the point that, if this were so, there would be nothing to prevent whole parental chromosome sets from segregating out together. Rather, he says, the bivalents are *directed* to segregate independently of one another. Earlier in the book (p. 415) he criticizes Ohno for his speculation that many segmental rearrangements have been fixed in evolution by chance, being in themselves neutral or "harmless". Lima-de-Faria maintains that to say that a rearrangement is harmless is to imply that there is an organization in the chromosome that could in principle be harmed and so Ohno is contradicting himself — a formidable logical trap indeed! Naturally, Lima-de-Faria has no time for the concept of "junk" DNA, disposing of it with another brief argument (p. 1,030). When one actually looks at such a piece of putative junk, he says, one finds that it has a definite sequence and definite locations in the genome — it clearly is not accidental at all! It is not surprising to find him also opposed to the idea of mutations occurring at random; he points out that they are now known to have causes, including that new class of directive agents the transposable elements. Indeed, nothing is accidental in Lima-de-Faria's view of the world. Everything is determined by the laws of physics and chemistry.

As a corollary of his belief of physico-chemical determinism, Lima-de-Faria considers that natural selection is a greatly over-rated concept. "Selection", he says (p. 147), "appears to be impotent in producing major changes in the face of the molecular determination locked in the chromosome and the cell". As a means of explaining evolution, natural selection is largely redundant in any case, since there is not that much evolution to explain. Organisms use their genes in so many ways that they do not need to have many of them, and most of those that they do have they have in common. Thus (pp. 1,060) the bee orchid is able to imitate the bee, and a grasshopper is able to camouflage itself as a leaf, because insects and plants share many of their genes!

Those who have access to this book will find it useful in at least two ways. First as an extensive and generally interesting collection of snippets from Professor Lima-de-Faria's reprint library, second as a rich source of quotations suitable for use as provocative essay topics for first-year students. ☐

J.R.S. Fincham is Balfour Professor of Genetics at the University of Cambridge.

China under the plough

Charles Higham

Science and Civilisation in China. Volume 6, Part II Agriculture.
By Francesca Bray.
Cambridge University Press: 1984. Pp. 724, £50, $99.50.

THE vastness and longevity of Chinese civilization are the joint themes of one of the great scholarly adventures of the century: Joseph Needham's *Science and Civilisation in China*. Even the most casual acquaintance with the successive volumes will rapidly dispel any ethnocentric smugness on the part of the Westerner in the priority or superiority of his Graeco-Roman heritage. For the sinophile, each new volume is, by definition, the basic reference in English. The latest to appear is arresting not only because it is the first to be written by one of Needham's research associates, but also because its theme, agriculture, is basic to any appreciation of the productive forces which underwrote Chinese civilization.

Let it be said that this is a massive compilation: the references alone run to 50 crowded pages, and 38 are necessary to contain the index. The preceding text follows an almost military step. The first section stresses China's geographic and climatic diversity, setting the stage for the subsequent contrast between the dryland systems of the north and the wet rice cultivation which characterized the warmer terrain south of the Yangtze. We are then introduced to the source materials, their potential and deficiencies. Literary sources begin with the Shang oracle texts and proceed through three-and-a-half millennia of expansion, addition and recension. The growing body of archaeological evidence illuminates the earlier half of the history of Chinese agriculture, and supplements the historic sources for the later phases.

The main empirical thrust is reserved for a detailed and analytical review of cultivation systems, land tenure, classes of tools, crops and techniques of soil preparation, husbandry and, of course, harvesting, processing and storage. Apparent blind spots, such as the methods of water control, have been considered in earlier volumes or are promised for later ones.

It could be argued that the vast array of facts would have revealed more structure had the author treated her subject holistically, reviewing, for example, first the prehistoric and then the dynastic phases sequentially rather than taking specific implements or techniques and following their development through the millennia. The non-specialist must be nimble-minded to be aware, all the time, where he is chronologically. This possible source of confusion is not mitigated by the illustrative material. It is true that many of the original Chinese drawings of agricultural scenes are charming and highly informative. They would have been more so had the author placed a date or at least a dynasty in the caption. Many of the author's illustrations are most uneven in quality; many also lack a scale, and those scales which are provided vary between the imperial and the metric.

Yet it must be remembered that this is but one of a series of volumes which aims to detail Chinese achievements in all fields, blow by blow. It is not, by definition, an entity with the aim of synthesizing Chinese agriculture within its social and technological contexts. It is, therefore, refreshing to find that we are not denied some contextual analyses.

Agriculture is the engine which sustains statehood. The polity out of step with its agricultural system will soon trip. Through the millennia of population growth, territorial expansion and external threat, the Chinese farmer has displayed a necessary blend of innovation and conservatism. We are invited to consider three instances of the articulation between society and subsistence.

The first concerns agriculture under the Shang. Shang civilization is regarded as the earliest complex society in China, flourishing for five centuries from *c.* 1500 BC. The basic issue is how the Shang rulers, bureaucrats and craft specialists were sustained in such centres as An-Yang. The agricultural techniques of the Shang peasantry are hardly known: archaeologists have concentrated on royal tombs and élite residences, and oracle bones are not concerned with the minutiae of agriculture. Bray favours a system based on plough cultivation. Now the plough is a very important implement. Goody, whose basic text on the social implications of ploughing is absent from the bibliography, has stressed the adhesions which exist between the extra productive capacity of ploughing and social organization, generation of surplus and the organization of marriage and inheritance. Archaeological sources are silent on the issue of Shang ploughing, however, and it could be argued that Bray has tried unduly hard to extract the necessary evidence. For example she is in error when describing the bronze ploughshares from Tonkin as being contemporary with Shang. Vietnamese archaeologists are unanimous in ascribing them to the Dong Son culture, which is a millennium later. Again, Wheatley's view is that the Shang centres were more ceremonial and élitist than centres of dense population. If he is right, then the need to invoke ploughing to produce large food surpluses is reduced.

The author is more assured when handling documentary sources. As a second example, we are given a revealing glimpse of the changing basis of land tenure under the Han — the state-sponsored aid to improve output provides so many parallels with recent Western attempts that one needs reminding that Han events took place 2,000 years since.

During the Sung the political centre of China moved south to the wet rice lands, and this introduces Bray's third instance of the articulation between social and agricultural variables. The wet rice agricultural technique involves parcelling the land into level plots separated by bunds. The soil in these fields — which are always small and often minute — is turned by the plough, then converted by harrowing to a creamy consistency prior to the transplanting of rice from a seed bed. The labour input during the planting and harvesting seasons is very high, and the regulation of water flow during the growing season is crucial. During the off-season, however, peasants may turn to cottage industry or, given the surpluses produced by farmers, some may specialize in craft production or exchange.

A basic tenet of this work is that such an essentially small-scale individual or family system is not susceptible to the revolutionary changes in productivity and intensification which characterized Europe's industrial revolution. So we encounter an intriguing paradox: growing European familiarity with Chinese agricultural technology, particularly the efficient curved metal mouldboard and the multiple seed drill, had a revolutionary impact when applied to European agriculture. In China, however, intensification in the face of a rising population involved not mechanization, but subtle refinements in wet rice agriculture which, of its very nature, failed to enter into a multiplier effect with the social or technological systems. This interplay did not stop with Mao's revolution: in effect modern production teams are a close image of the Sung communal unit, the backbone of wet rice cultivation.

The debate which such hypotheses will surely stimulate requires the full availability of data, an axiom which has been scrupulously adhered to. The portrayal of Chinese agriculture requires the broad brush of generality and the miniaturist's stroke of critical detail. This monumental and important book has both in full measure. ☐

Charles Higham is Professor of Anthropology at the University of Otago, New Zealand.

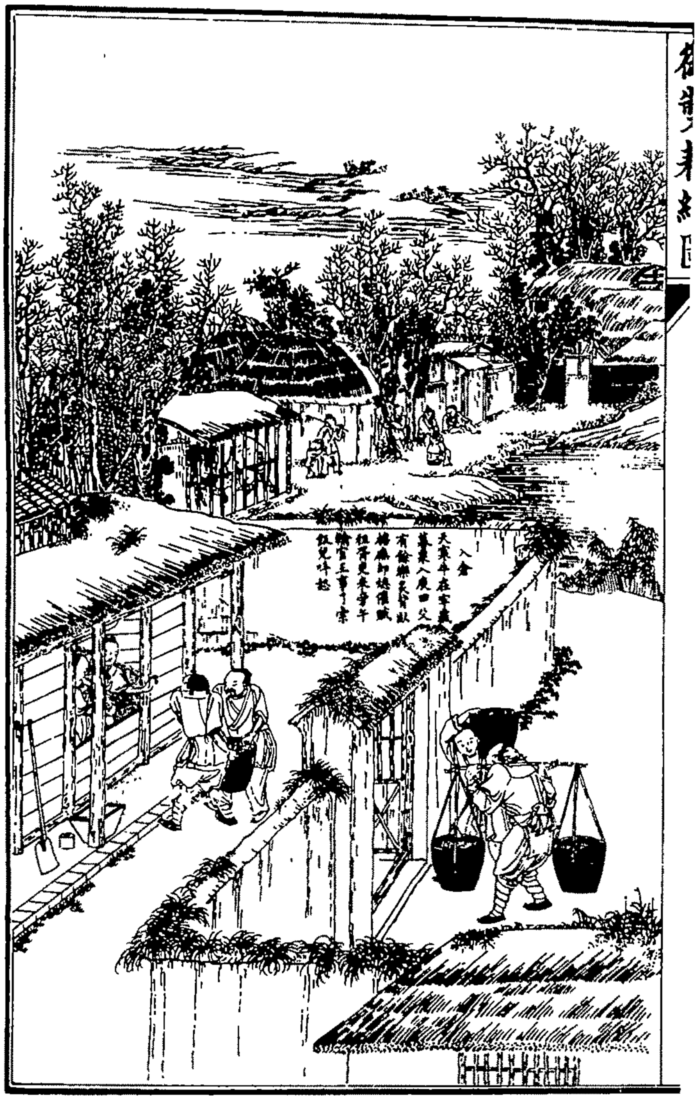

The illustration is taken from *Science and Civilisation in China* depicting a thatched village granary.

ADVERTISEMENTS

ACID PRECIPITATION DIGEST

Each monthly issue provides capsule summaries of

- news items
- books
- technical reports
- periodical reports
- conference proceedings
- peer reviewed literature
- calendar of upcoming conferences and events
- documents

"Current...concise... comprehensive — the single best source for information on acid rain." **Dr. Chris Bernabo,** Executive Director *National Acid Precipitation Assessment Program*

Subscriptions (one year) Corporate, For-Profit Firms, $125; Government Agencies, $65; Nonprofit organizations (including public and academic libraries), $30. Non-affiliated individuals -inquire for rates. Add $15 for foreign airmail postage ($5 for Canada) Make checks/money orders payable to: **Acid Precipitation Digest.**

Published by the nonprofit, non-advocacy
Acid Rain Information Clearinghouse
a project of the
Center for Environmental Information, Inc.
Department N, 33 South Washington Street
Rochester, New York 14608 (716)546-3796

Circle No.33 on Reader Service Card.

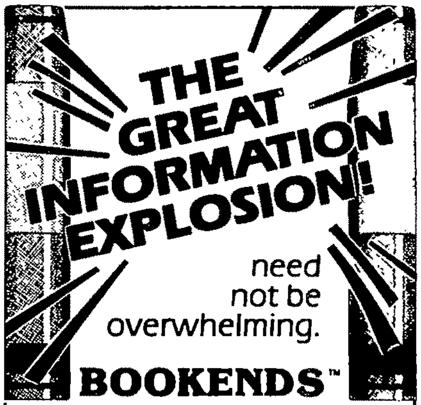
THE GREAT INFORMATION EXPLOSION!
need not be overwhelming.
BOOKENDS™

can prevent the frustration and delay which is otherwise inevitable when searching for elusive reference information in your bulging files BOOKENDS lets you "put your finger" on specific information, articles, magazine or books almost instantly in your database BOOKENDS lets you rearrange this data in virtually any configuration to create professional bibliographies It edits like a word processor It's the way of the Eighties to save, retrieve and format

BOOKENDS™
The Reference Management
Software System
is available for Apple computers for $124 95

Apple is a trademark of
Apple Computer Inc

Sensible Software, Inc.
24011 Seneca, Oak Park, MI 48237
(313) 399-8877

Circle No.06 on Reader Service Card.

Out of the blue

Derek W.G. Sears

Chondrules and Their Origins.
Edited by Elbert A. King.
Lunar and Planetary Institute, Houston: 1984. Pp.377. $33.

CHONDRULES are millimetre-sized silicate assemblages found in meteorites and, like their hosts, they have a unique story to tell about the conditions in the early Solar System. Hitherto, information about them has been spread through a vast literature. So an entire book devoted to the topic is long overdue.

Chondrules and their Origins is essentially the proceedings of a two-day workshop held at the Lunar and Planetary Institute, Houston, in November 1982. It suffers all the strengths and weaknesses typical of such books. The contributed papers are highly variable in approach and quality — some are significant new contributions, a few are useful reviews, and some are brief re-statements of particular views — and the coverage of the subject is rather patchy. Several prominent contributors to the field are conspicuous by their absence and, while petrologic studies abound, chemical and isotopic papers are under-represented; of the 25 papers included, 14 deal with petrology, 3 with chemistry and 3 with isotopic studies (of which only one is on radiometry). There are also 5 which deal with model-making, qualitative and quantitative.

Examples of the useful reviews are the summary of radiometric work by Swindle, Caffee and Hohenberg, who conclude that the chrondrule-forming epoch was brief and occurred at the time of the formation of the meteorites (and the Solar System), and the masterly synthesis of compositional data by Grossman and Wasson. The latter authors argue for a view that has become popular within the past few years, namely that chondrules were formed by the melting of pre-existing, fine-grained dust. The once-popular idea that chondrules could form directly by condensation from the nebular gas has almost no supporters now, although Blander advocates a modification of the idea. In a somewhat more narrowly-focused, but equally worthwhile review, Taylor, Scott and Keil amass arguments against the idea that chondrules could form by impact, volcanism or accretional heating.

One notable example of an original contribution is the paper by Nagahara, who describes another major line of evidence that chondrules were made by melting pre-existing dust; she describes several grains which survived melting. Another is the article by R.N. Clayton and co-workers; on the basis of oxygen isotope data, they argue that although the chondrules from different classes of meteorite formed from different solid material, they were melted in a common gas. There are also two brief but fascinating accounts of astronomical data relevant to chondrule formation by D.D. Clayton and D. Heymann.

In his foreword, Elbert King, the editor, states that his aim was to provide a broad overview of current ideas. I am not convinced that the book succeeds totally, being top-heavy in specialized contributions and leaving certain areas devoid of attention. For example, a review of ideas on the heat-source which melted the chondrules would have been welcome. The book might also have come closer to achieving its aims had it been organized differently — the sequence of papers, alphabetical by first author, is probably the least helpful possible. Surely it would have been better to have gathered the papers by subject area, with each section being led by a review. Still, the book has served as a vehicle for many valuable papers which might not otherwise have been written, and for that Elbert King is to be congratulated.

Derek W.G. Sears is a Professor of Chemistry at the University of Arkansas, Fayetteville.

New in paperback

- *Plurality of Worlds: The Origins of the Extraterrestrial Life Debate from Democritus to Kant,* by Steven J. Dick. Publisher is Cambridge University Press, price is £7.50, $12.95. For review see *Nature* **298**, 588; 1982.
- *Endangered Lives: Public Health in Victorian Britain* by Anthony S. Wohl. Publisher is Methuen/Harvard University Press, price is £7.95, $7.95. For review see *Nature* **305**, 164; 1983.

Amphibian's book of lists

Jonathan Slack

Amphibian Morphogenesis.
By Harold Fox
Humana: 1984. Pp.301. $59.50 (US), $69.50 (elsewhere).

TABLES of standard stages enable embryologists to know precisely at which point in development their experiments have been conducted and to communicate this information to others. But anyone who has worked with amphibian embryos probably feels that stage series are somewhat arbitrary and do not capture the true intrinsic periodization of development. Embryos seem to spend hours at stage 9 (late blastula) and then gallop through gastrulation to stage 13. There they wait for even longer and then race even faster through neurulation to stage 20. Presumably the springs which drive the morphogenetic movements are being coiled at stage 9 and stage 13 and the subsequent events represent the mechanical consequences.

Amphibian Morphogenesis must be the first book to list stage series for 192 species of amphibia, a more or less comprehensive collection. Alas it is just a list. None of the potentially interesting features of stage series are critically discussed, for example the question of intrinsic periodization or the extent to which the timing of one event can be altered relative to another in evolution. The list-like quality pervades the whole book and makes one aware of the difference in approach to a problem adopted by biomedical scientists on the one hand, who are chiefly interested in developmental mechanisms and regard amphibia as useful models for experimental work, and zoologists on the other who would like to catalogue the anatomy, physiology, ecology and evolutionary history of all 2,850 amphibian species.

This book will probably fail to satisfy either audience. Its core is Section III which reviews organ development in larvae. This is the best part and although it is dull reading it will be useful in laboratories such as mine where occasionally we suddenly want to know all about the development of the lateral line, the cement gland or the blood. It contains a useful collection of references but would have benefited from more diagrams and more light microscope photographs. It is full of electron micrographs but these are relatively uninformative because the magnification is too great to show the specific features of the tissues.

There are three other sections in the book, dealing with evolution (I), stage series (II) and embryogenesis (IV). Curiously enough, on close inspection, all of them seem to be mainly about hormones and metamorphosis just like Section III. The full and meticulous references to metamorphosis contrast strangely with the casual treatment of other subjects; for example on p. 4 we read that

> During the warm, moist period of the Carboniferous era, the earth was covered by swampy forests and giant ferns, which later fossilized into coal. Conditions were favorable for amphibian development and a great variety of them evolved in this great age of the "Amphibia," for they required warmth to maintain a high enough body temperature, the prevailing moist atmosphere hindered desiccation and food was plentiful.

We must conclude that this is essentially a review article about metamorphosis onto which has been grafted some rather subjective passages about other aspects of amphibian biology. Only those with a passionate interest in metamorphosis are likely to be tempted to acquire it. □

Jonathan Slack is the Head of the Experimental Morphology Laboratory at the Imperial Cancer Research Fund Laboratory, Mill Hill, London.

New at the Boston show

The products covered this week include some on view at Nature's *Boston conference, and some recent introductions in the field of biotechnology.*

- A new C-tailing and cloning system intended to bring convenience and reproducibility to the construction of DNA recombinants, capable of transforming *Escherichia coli* cells at high levels of efficiency, has been introduced by New England Nuclear (NEN). NEN's new C-tailing and cloning system is self-contained and provides an oligo (dG)-tailed cloning vector, all critical chemical reagents, ready to use competent cells, control DNAs and procedures for successful, reproducible incorporation of DNA into the *E.coli*-pBR322 host-vector system. The method can be used to clone any double-stranded DNA, but is especially useful in cloning cDNA and DNA not suited to cloning by other methods. The results provided with the kit confirm that a control *Hae*III digest of M13mp8 DNA receives uniform, compact C-tail distribution in the biologically active range (15–25 residues). And, following annealing of the C-tailed digest to the system's oligo (dG) tailed pBR322 vector, transformation levels in competent cells are between 2×10^5 and 1×10^6 transformants per μg vector.

Circle No. 100 on Reader Service Card.

- For convenience in precasting 14×16 cm gels for use in Hoefer vertical slab gel units SE400, SE600, and SE700, Hoefer Scientific Instruments now offers a multiple casting chamber, the SE615. Up to ten 1.5-mm thick gels, or eleven 0.75-mm gels may be cast simultaneously. This greatly reduces gel preparation time and ensures unformity in pore size and/or gradient shape from one gel to another. Gradient gels are poured from the bottom of the chamber. Precast gels can be stored for two weeks at a time. The unit is made of sturdy acrylic plastic, and the front panel is removable to facilitate assembly and disassembly of the stack of glass plate sandwiches.

Circle No. 101 on Reader Service Card.

- Triton Biosciences Inc. now manufacture affinity purified antibodies to an oncogene protein and a transforming growth factor. Each antibody is generated against a synthetic peptide corresponding to an amino acid sequence in the native protein. The antibodies are purified by affinity chromatography, and Western blot and immunoprecipitation analyses are used to verify reactivity and specificity. Anti-ras$^{\text{Ha}}$p21 antibody is the first in a new series of oncogene analysis products from Triton. Ultimately such antibodies could be used in diagnostic tests to detect human malignancies.

Circle No. 102 on Reader Service Card.

- New England Biolabs has developed an *in vitro* method for creating novel DNA cleavage specificities by using DNA methylases in conjunction with restriction endonucleases as a valuable new tool for gene cloning and DNA sequence analysis. Added to the New England list of 78 restriction endonucleases are: *Dpn*I (GmA/TC), *Xho*II (Pu/GATCPy), *Sna*BI (TAC/GTA), *Hin*PI (G/CGC), *Nla*III (CATG/), *Nla*IV (GGN/NCC), *Ssp*I (AAT/ATT), *Spe*I (A/CTAGT), *Nhe*I (G/CTAGC), *Nsi*I (ATGCA/T) (isoschizomer of *Ava*III), and *Dra*I (TTT/AAA) (isoschizomer of *Aha*III). New DNA methylases include: M.*Alu*I, M.*Cla*I, M.*Taq*I, M.*Hph*I and *Dam*. New M13 cloning vectors now available are: M13mp10w RF I DNA, M13mp11w RF I DNA, M13mp18w RF I DNA and M13mp19w RF I DNA. Among the new products from the range of New England Biolabs' Organic Synthesis Division are the following phosphorylated linkers: p*Xba*I, d(pCTCTAGAG) and p*Bcl*I, d(pCTGATCAG).

Circle No. 103 on Reader Service Card.

- A new product data sheet from Schleicher & Schuell gives specifications and selection guidelines for S&S pure NC nitrocellulose, the standard immobilization matrix in nucleic acid and protein research. S&S nitrocellulose is highly selective and offers high binding capacity, low background radiation, and lot-to-lot consistency. S&S NC is suitable for the transfer of RNA, DNA, and protein, capillary and electrophoretic transfers as well as plaque and colony hybridization studies. It can also be used in trichloroacetic acid precipitations and dissolved for scintillation counting. The illustrated fact sheet includes a selection guide for choosing the most suitable dimension, pore size, and format. S&S pure nitrocellulose is available in a wide variety of sizes of circles, squares, sheets, and rolls, with special grid patterns, and in pore sizes ranging from 0.45 μm to 0.025 μm.

Circle No. 104 on Reader Service Card.

- Monoclonal anti-human kappa (Clone TB28), a new antibody from Becton Dickinson, is specific for the kappa light chains of all classes of human immunoglobulins and Bence–Jones kappa does not react with lambda light chains, giving superior results in tissue staining of frozen sections. Anti-kappa reacts with 50 to 70% of normal B lymphocytes and with Ig2 leukaemic cells, and can be used to study the clonality of B cells in tissues by indirect immunoperoxidase techniques.

Circle No. 105 on Reader Service Card.

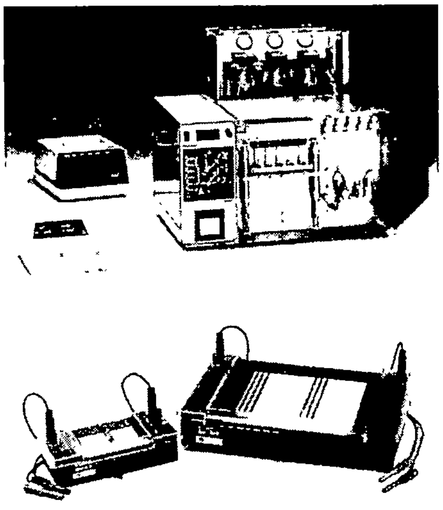

The Systec DNA synthesizer (top) and Pharmacia's electrophoresis system.

- The Systec Microsyn-1460 dual-cell DNA synthesizer permits the continuous synthesis of DNA oligomers with a coupling efficiency of 99%, or more, per step and a cycle time of 6 min using the phosphoramidite method. Two synthesis cells allow the continuous sequential synthesis of multiple oligomers, maximizing DNA production while minimizing operation time and cost. The Microsyn uses flexible RAM-based control software making possible the automation of all phosphate and phosphite methods, as well as user modification of Systec's standard methods. Sequence programming is simplified by an "ACGT" keyset, allowing the rapid entry of single and mixed probe base additions. Valves have been tested to 1 million cycles, the equivalent of 10 years of use, and all parts and labour are fully warranted for one year.

Circle No. 106 on Reader Service Card.

- New from Pharmacia Fine Chemicals are two new injection-molded nucleic acid electrophoresis systems of the classic "submarine" design. The "mini", GNA-100 apparatus gives rapid separations (0.5–2 h) and allows detection of very small amounts of material. The larger, full-size submarine format, GNA-200, allows many samples to be run on one gel (up to 60) with maximal resolution. Other features include UV, transparent lids and gel trays, rugged titanium-based electrodes, and buffer circulation ports with interconnecting stop-cock. Especially suited for analysis of restriction enzyme digests, the new GNA-100 and GNA-200 are complete and ready-to-use.

Circle No. 107 on Reader Service Card.

- First introduced at the European Congress on Biotechnology in Munich last month, the ISF fermenter from Infors AG is available in three sizes of 1 - 70 litres working volume. It is compact and features either a top or bottom drive. Drive characteristics can be selected without special tools. The bottom valve with high current flow is combined with the sampling port which allows extraction of very small probes. Sterilization *in situ* is guaranteed. Sterilization of the air inlet and outlet systems can be effected independently of the vessel. Specially designed systems are built into the fermenters to avoid by-pass lines and during sterilization the air inlet and outlet lines are automatically separated from the vessel. A programmable sterilization sequence controller reduces waiting time.

21-1-85
A. Gatto

Circle No. 108 on Reader Service Card.

ADVERTISEMENT

Ideal for microinjection of xenopus oocytes

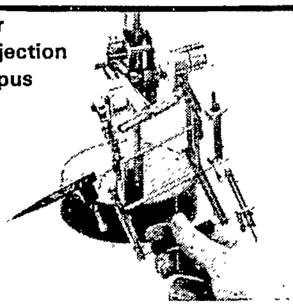

SINGER MICROMANIPULATORS ARE FAMOUS BECAUSE

Singer Micromanipulators enable anyone to make exact movements without tremor or lost motion, in three dimensions, using a single control handle under low or high power magnification.
A varied range available. All simple to operate.

SINGER INSTRUMENT CO. LTD.,
Treborough Lodge, Roadwater, Somerset.
Tel: Washford (0984) 40226/325

Circle No.23 on Reader Service Card.

PHORBOL ESTERS

MEZEREIN
Co-Inducer of Interferon

Cat. # M4600 . .... 5mg/$55

L C SERVICES CORPORATION
165 New Boston Street
[illegible]
(617) [illegible]

Circle No.24 on Reader Service Card.

AUTHORS WANTED BY N.Y. PUBLISHER

A well-known New York subsidy book publisher is searching for manuscripts worthy of publication. Fiction, non-fiction, poetry, juveniles, travel, scientific, specialized and even controversial subjects will be considered. If you have a book-length manuscript ready for publication (or are still working on it), and would like more information and a free booklet, please write:

Vantage Press, Dept. D-69
516 W. 34th St., New York, N.Y. 10001

Circle No.32 on Reader Service Card.

- An immunofixation electrophoresis (IFE) assay kit is now available in the Paragon electrophoresis product line from Beckman Instruments. The new Paragon IFE test provides a fast, sensitive and easy-to-read method for diagnostic identification of monoclonal gammapathies, immunoglobulin deficiencies and other immunoglobulin anomalies; IFE is a procedure combining protein electrophoresis and immunoprecipitation.

Circle No. 109 on Reader Service Card.

- Using Bio-Rad's mini vertical slab cell it is possible to analyse protein and nucleic acid samples two or three times faster than with conventional 16 cm cells, while maintaining comparable resolution. The cell controls heat related artefacts, and a variety of spacers and combs allows one to produce exactly the gel configuration needed for each specific application.

Circle No. 110 on Reader Service Card.

- The New Brunswick Scientific GEN II microprocessor-controlled instrumentation system provides fully distributed P I D or on/off control of fermentation processes. Up to 11 modules, each dedicated to the control of a specific fermentation parameter, can communicate with each other to provide dynamic control of the process as metabolic conditions change. The GEN II system is entirely self-contained, but can be operated by a supervisory computer or through remote terminal communications.

Circle No. 111 on Reader Service Card.

- The RF-1 incubation system from Bioengineering Associates Inc. is a virtually noiseless incubator shaker of a compact, space-saving design. The magnetic drive assures maintenance-free operation. A digital panel display indicates actual and set-point speed which is continuously adjustable from 40 to 400 r.p.m. (± 1%). The incubator is fitted with a Pt 100 sensor for precise temperature control (± 0.1°C). Should temperature deviate 0.8°C from set point, the digital display starts flashing and an accoustical alarm sounds every two minutes until the condition is corrected. A humidification system, operating on the evaporation principle, is built in. All materials are selected for resistance to corrosion and will withstand continuous operation.

Circle No. 112 on Reader Service Card.

- The mixed sequence hexadeoxynucleotides used by Feinberg and Vogelstein in the development of their new method of generating radio-labelled DNA probes are now available from Pharmacia P-L Biochemicals. Also available are di-, tri-, tetra- and pentadeoxynucleotides. The random sequence hexadeoxynucleotides hybridize to any isolated restriction fragment. The hexadeoxynucleotides then act as primers for DNA synthesis using the DNA polymerase 1 Klenow fragment in the presence of radioactive deoxynucleotide triphosphates, thus generating radiolabelled copies of the fragment.

Circle No. 113 on Reader Service Card.

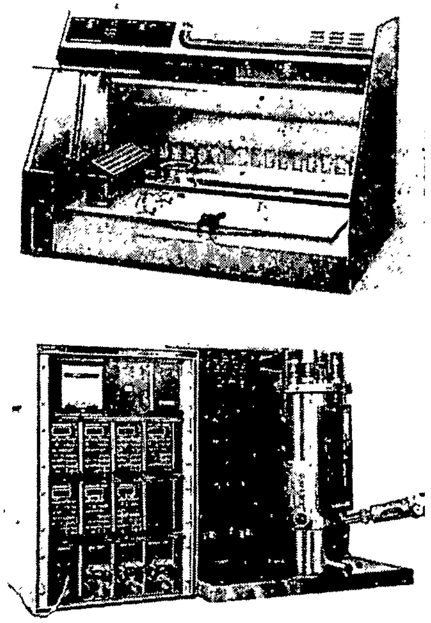

The RF-1 incubation system from Bioengineering Associates (top) and New Brunswick's fermentation controller.

- Two full-range, hand-held *p*H meters with clear digital displays have recently been introduced by Corning. Constructed to cope with indoor and outdoor working environments, the new meters — Models 103 and 105 — can be used with either remote or clip-on electrodes and offer a resolution of 0.01 *p*H units. The meters can also be used for ion selective electrode work.

Circle No. 114 on Reader Service Card.

- The LKB Transphor 2005 electroblotting unit uses the principles of electrophoresis to transfer proteins or nucleic acids from polyacrylamide or agarose gels onto nitrocellulose, DBM, or other immobilizing matrices. By binding molecules in concentrated bands on one of these matrices, electrophoretic bands are made easily accessible for faster, more sensitive and more quantitative visualization than possible on the original gel or even on a non-electrophoretic blot. Detection procedures are also more economical as they require smaller amounts of reagents.

Circle No. 115 on Reader Service Card.

- An applications laboratory is now available at Microfluidics Corporation, Newton, Massachusetts, for processing customer samples and for demonstrations in the fields of fine emulsions, liposomes and dispersions. Prototype formulation work is also underway, utilizing the company's latest Microfluidizer equipment. Samples as small as 15 ml can be processed and flow rates up to 350 ml min^{-1} are available. Particle size and distribution analysis of processed samples is provided.

Circle No. 116 on Reader Service Card.

These notes are based on information provided by the manufacturers. For further details circle the appropriate numbers on the Reader Service Card bound inside the journal.

nature

21-1-87
A. Battey

New joint ventures in Europe

Next week's meeting of European science ministers at Paris is unlikely to accomplish much, but at least it makes a start on the improvement of science collaboration. Where next?

THE Council of Europe can hardly be accused of being bossy. Its faults are rather those of ineffectiveness. The council (which, with twenty-one members, covers a wider swathe in Europe than, say, the European Communities) is best known as the source of international conventions which have the force of law in Europe when ratified by member governments. (The human rights convention works well, the convention on laboratory animals has been five years in negotiation and is still not complete.) The council also stages large inter-governmental conferences of monumental banality such as that labelled "Education 2000" at Strasbourg (the council's home base) last November and that on communications and society. So how does such an organization come to be staging an important meeting of European ministers responsible for research at Paris this weekend? And can it be trusted with the responsibility?

The oddest feature of the meeting is not the agenda, which is excessively modest, but that there is one of any kind. The origin of next week's meeting goes back to the stirring speech to the council's parliamentary assembly by M. François Mitterrand, the President of France, on what has become the characteristic French theme in Europe (and in France) — that Europe's economic future rests on the better use of science and technology. What Charlemagne once did by conquest, to create economic and political power out of unity, M. Mitterrand would accomplish by the coordination of European research and development. M. Mitterrand can congratulate himself that he has been listened to so well. And if the agenda for next weekend is only modest, there is always a chance that it will lead to better things.

Objectives

The omens are encouraging. Even governments such as the British, whose hostility to much of the council's work stems not so much from insularity as from the wish not to be distracted from preoccupations of its own choosing, seems willing to go along with what is proposed. Two objectives dominate the agenda — the improvement of the networks linking research people in Europe, and providing encouragement to the mobility of scientists. If all turns out as planned, the chief beneficiary of the conference next week will be the European Science Foundation (also Strasbourg-based), which will be urged to encourage the development of research networks on a European basis (but told to raise the money for that from its members, mostly European research councils). This is a timely recognition of the foundation's success, during the past decade, in creating mechanisms of collaboration in fields as different as neurophysiology and the uses of synchrotron radiation (and the development of sources thereof). The other theme, mobility, is necessarily more nebulous. Everybody recognizes that the free movement of research people within Europe would be good for science as well as for the economies of Europe, but there are serious barriers to mobility, deriving from chauvinism and pettifogging administration, to be overcome. The hope seems to be that the Council of Europe and the European Commission can jointly embark on the removal of some of these obstacles once the weekend is over.

That, for those who attend, is the applause. The other side of the coin, of which they should be made aware, is that the agenda on which they will be brooding is about as modest as any that could have been devised. In the spirit of M. Mitterrand's rhetoric, and no doubt against the background of the many high-sounding things that will be said in Paris, the agreements that will be reached are bound to seem like an anticlimax. Charlemagne made the Rhine into the axis of economic power. But the science ministers — on the same metaphor — will be invited next weekend merely to test the salinity of the river at a few selected points. European politics being what they are, there may be no other choice. But the ministers (and M. Mitterrand) should acknowledge how wide a gulf separates their ambitions and what is likely to be achieved.

The problem

The European dilemma is simply stated. Many Europeans think it prudent to opt out of the ambition of making Europe into an integrated economic power, counting institutions such as the European Communities and the Council of Europe as institutions whose value must continually be reassessed. Even the others, those who hold that European integration in some form may be more than a pragmatic benefit, are divided into separate groups — those who hold that the forging of economic strength in Europe must be an evolutionary process, one small thing leading to another hardly any bigger, and those (numerically fewer) who would prefer to take the bull by its constitutional horns (which is what the signatories of the Treaty of Rome thought they were doing thirty years ago). Rhetoric apart, this weekend's meeting is squarely but limply in the evolutionary tradition.

The present difficulty in Europe is that both approaches are likely to be ineffectual. Softly-softly is too slow. But even constitutional change is frustrated by what are known in the European Communities as "non-tariff barriers to trade". People pay lip-service to the notion that it would be good for Europe if the most efficient manufacturers of, say, mousetraps enjoyed the best sales but they are also willing to bend the rules so as to make sure that only nationally manufactured mousetraps really succeed. In this spirit, one of the European Communities' collaborative projects in technology, the Esprit computer development programme will be a simple and a shocking waste of quite a lot of money if its outcome has to contend with the long-standing chauvinism of European governments towards the products of high technology. Even the modest proposals being discussed in Paris at the weekend will be frustrated if approval for the greater mobility of technical people is alloyed with too much concern that public research funds should always be spent by those who have contributed towards them as taxpayers or that public laboratories should employ only local nationals.

President Mitterrand's ambition will never be achieved if Europe insists on putting the cart before the horse in ways like that. The logic is impeccable. Numerically, even the European Communities are large and rich enough to be an economic unit comparable in size with any others in the world, while the populations concerned are amongst the most literate and skilled that are anywhere to be found. Moreover, Europe is blessed with modern social and economic institutions — universities, for example, or commercial companies and investment institutions. But as things are, the dream is belied by the reality. European governments are these days being repeatedly reminded of how they are slipping in their performance. The British Government, for example, after four years of energetic sponsorship of what it calls information technology, should have been shattered two weeks ago to have been told by a committee of the National Economic Development Office under Professor John Ashworth that this same period has seen a steady deterioration in the balance of external trade in equipment such as computing machinery. The difficulty is that a home-grown industry only poorly supported by research and development, and facilities for education and training, is being exhorted to compete across the board with stronger organizations overseas.

What next weekend's meeting should also recognize is that there is a sharp difference of timing between the urgency of these problems of industrial competitiveness and the time-scale implied by its own agenda. Stronger networks in research are, to be sure, desirable, but will they help with the problems of industrial survival cropping up all over Europe? The simple answer is that they will not. The Council of Europe is, in any case, out of its depth in fields such as this. But the recognition that opportunities are being lost with every year should at least give those assembling in Paris a sense that if their weekend is to be usefully spent they had better look further ahead.

What might the council achieve? New actors can always hope to breathe new life into old parts especially because, since the council's constituency extends between the European Communities, evolutionary and not constitutional approaches are unavoidable. One worthwhile ambition, however, would be to embark on the encouragement of integration in higher education, both in teaching and academic research. Why not seek to engineer the return to the fourteenth century, when it was commonplace that both the students and teachers of European universities were recruited from the whole continent? Why not even go one step further and acknowledge that if the objective is true European scholarship, it will at some stage be necessary that public spending on the support of scholarship, even by national governments, should be channelled always to teachers and people most likely to make use of it? It is unreasonable to expect all scholastic steps in this direction to be taken quickly, but it is illogical not to prepare for it while otherwise behaving as if President Mitterrand's speeches should be taken seriously. □

Election irrelevant

Something must be done about the federal deficit, whatever the outcome of the US election.

WILL interest rates go up or down after the November presidential election in the United States? And will the dollar, now (with the yen) the strongest of international currencies, then lose some of its recent shine? Voters in the United States should know that these questions (together with the administration's policy on arms control) are elsewhere more absorbing and more important than the intricacies of the candidates' relationships with the Inland Revenue Service. Future prosperity in the rest of the world, industrialized and poverty-stricken alike, will be determined by the economic fall-out of the election. The crucial question is how the paradox of US economic policy is eventually to be unscrambled.

The essence of the paradox is now boringly familiar. The federal government has failed to balance its budget to the tune of $200,000 million a year, and seems likely to continue in that way. Only last weekend, President Reagan told an election audience that he had no special plans to act on the deficit after the election, saying that continued growth might automatically redress the balance by increasing tax revenues. The result is that the US Treasury has had to borrow from the money markets to finance its research, to pay salaries to those who work in government laboratories, for example. High interest rates are not, however, necessarily a precondition for successful borrowing, but they are the only way of financing a huge deficit while keeping inflation in check. Everybody agrees about that.

It is also agreed that US policy has been successful within its lights. Inflation has indeed been kept at bay, which is why not only US citizens but people and institutions from overseas are eager to lend to the US Government. So money has been rushing into the United States. The penalty, a consequence of short-term confidence in the dollar, is that goods and services in the United States have become relatively less competitive, so that the trade balance has deteriorated. This year, the United States will not be paying in the usual way for $85,000 million of the goods and services it will be importing, a deficit comparable in scale with the surpluses earned by the oil exporters in the 1970s. That, the United States demonstrated at the end of the 1960s, when part of the cost of the Vietnam war was paid for with paper money printed on the Eurodollar market, which turned out to be a way of exporting inflation. Since then, however, other governments have learned a thing or two, but their only defence against the resurgence of inflation is to keep their own interest rates at a level determined by those in the United States. The paradox is that those who lend money internationally do not usually do so with confidence when a creditor country is in the red both on its fiscal accounts and its balance of trade. Circumstances such as these have dictated retrenchment in an emergency.

Instability

Even in the United States, the strongest economy in the world, this state of affairs cannot last indefinitely. Two British economists, Professor M.J. Artis (University of Manchester) and Mr M.V. Posner (until last year the chairman of the Social Science Research Council) have given elegant explanations of the reasons in the autumn issue of *The Midland Bank Review*. Writing as members of a group of independent economists called the Clare group (after the Cambridge college of that name), they argue that the crucial question for lenders to the United States is not now whether they have confidence in the management of the US economy but whether they consider that other lenders will retain that sense. And since, on arithmetical grounds, the accumulation of both deficits cannot continue indefinitely, lenders have no choice but to second-guess other lenders. Sooner or later, the argument continues, the lenders will begin to lose their nerve, and then there will be only two choices for the US authorities — to increase interest rates still further in the possibly vain hope of continuing to finance the federal deficit or to let inflation run riot again. Either way, the economic recovery of the past two years would be stopped in its tracks.

This argument is not, of course, unfamiliar. It has been repeated endlessly in the past three years, especially in relation to the debts of the developing countries whose financial problems, serious enough a decade ago in the wake of the oil crises of 1983 and 1979, are aggravated as the rate of interest of foreign loans which cannot be serviced is converted to that prevailing in New York. So much, indeed, has been made of the instability of the present situation, and so little has come of these predictions of disaster, that it is tempting to think the general air of gloom must be mistaken. But that cannot be the case. Simple arithmetic decrees otherwise. The question is not whether both deficits can continue indefinitely, but when one or other or both of them must be eliminated, and how.

Obviously the best solution is that the US Administration should recognize the truth of what economists elsewhere are saying, that this state of affairs cannot persist indefinitely. The alternative to action is to wait for it to be resolved catastrophically. The Reagan Administration, whatever its faults, is fiscally well-managed and thus equipped to know when the time has come to change tack. Indeed, *The Midland Bank Review* (not the Clare group as such) takes the line that the change must come within the next twelve months. On the assumption that the administration (whatever its colour) may then have changed course, it guesses that interest rates in New York (and thus elsewhere) will have fallen by two per cent by the end of 1985 — and that the value of the dollar relative to other currencies will also have fallen by 20 per cent. Mr Walter Mondale, the Democratic candidate, has been promising such a change of tack, but for the time being the incumbent President dissents. What the economists are saying is that neither has a free choice. □

Space shuttle

Pentagon gains ground in battle for alternative

Washington

DESPITE a near-perfect maiden flight by the space shuttle orbiter *Discovery* last week, doubts over the shuttle's commercial prospects seem to be increasing. The shuttle successfully placed all its satellites into orbit, and the crew again demonstrated the possibilities of in-flight maintenance. But the day before *Discovery* touched down in California, an expert panel of the US National Research Council told Congress it was "not clear" that the shuttle would ever be competitive with an expendable launcher for military payloads and agreed with the air force's argument that a new launch vehicle would provide it with greater operational flexibility.

This leaves the National Aeronautical and Space Administration (NASA) with a major problem, because NASA had been counting on the military to pay for more than one third of projected future shuttle flights. If the US Air Force insists on developing its own expendable launcher for some of these flights, NASA may well have to increase its prices to civilian customers.

The National Research Council, the research arm of the National Academy of Sciences, was asked by appropriations committees of both houses of Congress to compare options for expendable launch vehicles capable of lifting large payloads into orbit. Its report echoes previous criticisms of the shuttle — main engine and fuel pump performance are still below specification, turn-around times are still too long and, says the committee, "a sustained engineering programme will be required to realize the full benefit" of the shuttle concept.

The air force has been unhappy with the shuttle for some time. Apart from the question of reliability, the Department of Defense has been concerned about the limited number of launch sites and the security difficulties should it wish to launch a sensitive satellite "without the public exposure that has become the norm in NASA flight operations". The research council panel also points out that in time of crisis the shuttle would have to overfly Soviet territory in order to put a satellite into a polar orbit suitable for reconnaissance: here, an unmanned launcher offers obvious advantages. And commercial companies might be happier if the Department of Defense were less likely to requisition planned shuttle flights, as it has the right to do.

The panel examined three possible expendable launchers being considered by the Department of Defense — the Titan 34D7/Centaur, the Atlas II and the SRB-X, which is derived from the shuttle. All are based on existing technology. Any of these would be capable of meeting immediate requirements but none offers the possibility of expansion to carry loads much heavier than 10,000 pounds to geosynchronous orbit, the panel concludes. The cost of developing one of the alternatives would be around $2,000 million.

The research council panel avoids addressing in detail how the prospect of a new competitor to the shuttle would affect NASA finances. NASA at present charges its customers only "out-of-pocket expenses", although there is pressure for it to move to a full-cost policy. But already the European *Ariane* launcher "appears to be competitive" with the shuttle.

While apparently accepting all the military's arguments for a new expendable launcher, the National Research Council panel stops short of giving the project an unconditional endorsement. The main need, it concludes, is for further study of a new class of heavyweight launch vehicle capable of taking payloads of up to 450,000 pounds into low Earth orbit. Both NASA and the air force are already working on plans for such a system, thought likely to be necessary for President Reagan's "strategic defence initiative", better known as Star Wars. Such a system could be designed using motors developed for the shuttle programme with the aim of reducing costs without loss of reliability.

Tim Beardsley

British aerospace

Per atmosphaera ad astra

A BRITISH space shuttle? Surely a joke? Perhaps, perhaps not. A study by British Aerospace of a new concept for the launch of large payloads (up to 7 tonnes) into low Earth orbit comes as the British Government finds itself under increasing pressure from its high-technology companies and its European Space Agency partners to make a positive commitment to space or pass up for ever the chance to keep a presence on the "high frontier".

The new concept, dubbed HOTOL (Horizontal Take-Off and Land Satellite Launcher), is of a vehicle of aircraft type with the ability to take off horizontally and land on a conventional runway. The vehicle would use a combination of air breathing and rocket propulsion.

An ideal re-usable launch vehicle, says British Aerospace, should have no expendable parts (unlike the US space shuttle), should be capable of repeated operations with a minimum turn-around between missions, accommodate payloads in the 4–7 tonnes range and, if necessary, should be capable of unmanned operation.

At present vertical take-off into Earth orbit is impossible because even the highest-performance chemical fuels give a single-stage rocket insufficient impulse. A two-stage lift is essential, so that expensive equipment is irrevocably lost in re-entry or at sea.

British Aerospace proposes to overcome this apparently insurmountable difficulty by economizing on the supply of liquid oxygen, which may account for 85 per cent of the propellant mass of a booster rocket. If air scooped from the atmosphere were to supplement a rocket's supplies of liquid oxygen during the early phases of flight, its dead weight might be substantially reduced. Add wings for additional lift and there it is — HOTOL. British Aerospace believes the system capable of revolutionalizing the space industry.

It is unlikely that Britain would have the resources to undertake such a major project on its own. If life were to be breathed into the idea, a collaborative effort, perhaps with other European countries, would seem the most prudent course to take.

It is just such a collaboration that European ministers are now pressing Britain to join, chiefly in the form of a European consortium to take part in the US manned space platform. Britain would be expected to contribute an extra £15 million a year compared with its present spending of just £80 million a year (and France's £400 million), principally for membership of the European Space Agency.

"You'd think we'd have our own departure lounge."
SPAIN
BIRCH

British Aerospace is eager for government support for its space effort. But in the realm of fact rather than fancy, the company has announced a contract, from the US corporation Scott Science and Technology Inc., to design a Satellite Transfer Vehicle needed to carry satellites from shuttle orbits to geosynchronous orbit. The vehicle will be propelled by liquid fuels which, as well as being more efficient than solid fuel, will allow a range of burn strategies tailored to individual missions.

Marcus Chown

Acid rain

CEGB takes a pasting from MPs

BRITAIN should cut back drastically in its emissions of sulphur dioxide and other gases contributing to the problem of "acid rain", with most of the burden falling on the Central Electricity Generating Board (CEGB), according to a report published last week by an all-party committee of Members of Parliament. If the MPs recomendations were put into effect, they would force the CEGB to cut sulphur dioxide emissions by 85 per cent. This would cost "many thousands of millions of pounds" and raise electricity bills "up to 10 per cent", according to CEGB. Moreover, there is no guarantee that the measures (flue gas desulphurization, or in the long term fluidized bed combustion) to reduce sulphur emissions would have any commensurate effect on acid rain itself, the board claims.

But the MPs, after many months' taking of evidence from scientists and politicians in Britain, West Germany and Scandinavia, are convinced that scientific understanding is sufficiently advanced to demand action now. By this they mean that while a direct and proportional link between sulphur emissions and environmental damage is not scientifically proven, the case against sulphur dioxide is telling enough and the damage severe enough that action must be taken before all the evidence is in. In this they agree with a recently-published report by a committee of the House of Lords (see *Nature* **310**, 535; 1984), but the bottom line of the Commons report — its demands — is far more punishing. And the MPs lay less stress than the Lords on the question of "linearity" between sulphur emissions and acid rain effects, a key scientific issue which is generally assumed to remain open. Moreover they quote modelling by Swedish professor of meteorology Henning Rodhe which supports linearity. Rodhe's models indicate that a decline in the acidity of Swedish rain since 1975 was attributable to a corresponding decline in European emissions — if depositions were linearly related to emissions.

Impressed by this and other evidence, and "appalled" by lack of action in Britain, the MPs say Britain must (among other measures):

- Join the "30 per cent club" of nations committed to reductions of 30 per cent in total national emissions of sulphur dioxide by 1990, a target to be achieved solely by cutbacks in CEGB emissions.
- Refit CEGB power stations to achieve a national 60 per cent reduction in sulpur dioxide emissions by 1995.

The second measure is broadly in line with an existing draft directive on "large combustion plant" from the Commission of the European Communities (CEC), but whereas CEC says that the measure should be applied to all plant of output greater than 50 MW, the British MPs have singled out electricity supply for attack. "We don't want to affect manufacturing industry", a member of the Commons committee explained last week. As a result, he admitted, the measure would imply that CEGB cut its own emissions by 85 per cent, to achieve the net national reduction of 60 per cent.

Why should manufacturing industry be feather-bedded? To protect its fledgling rebirth in Britain, the MPs imply, and because CEGB's sulphur dioxide emissions have remained constant since 1970, whereas net British emissions have fallen 37 per cent. This fall was largely due to industry turning away from coal to natural gas (and to the recession).

Overall, it is difficult to avoid the impression that the MPs are singling out CEGB for punishment. Yet the punishment may be deserved. The MPs claim that CEGB "dismissed" the effects of acid emissions on stonework with the remark "to dissolve an inch of limestone would take 5,000–20,000 years", whereas, say the MPs, it is "well-understood" that dry deposition and the formation of calcium sulphate leads to the much more rapid process of flaking. In this context the report quotes the cathedral architect at Cologne as saying that none of the original stonework of Cologne cathedral will remain within five years, and that the constantly-repaired cathedral will become "a copy". The same process is at work in Britain, say the MPs.

In other areas CEGB has "begun work only two years ago" or "made no attempt to monitor effects". And, say the MPs, while CEGB is spending £1.5 million a year on research on the environmental effects of acid rain, it is spending only £200,000 on research on flue gas desulphurization "largely on paper studies of foreign systems".

As for scientific evidence, the committee claims it took pains to get balanced and detailed views in the UK and abroad. "I shouldn't comment on the Lords", said committee chairman Sir Hugh Rossi, "but they didn't do their homework — they didn't go abroad". The Lords' report was consequently superficial, he implied.

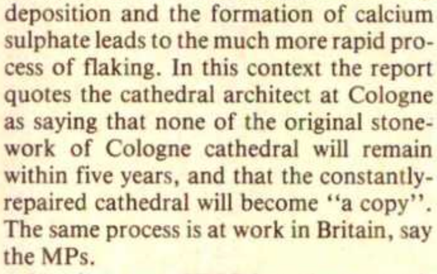

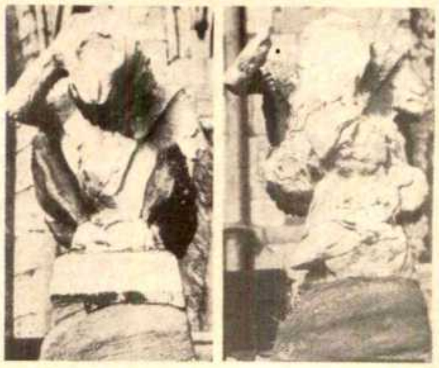

Stonework on Lincoln Cathedral, in the plume path of Trentside power stations. "Despite... the knowledge of CEGB research staff that the cathedral was suffering from the effects of sulphur dioxide, CEGB has made no effort to monitor those effects", say British MPs in a new report on acid rain. On the left, a photograph from 1910; on the right, 1984.

The evidence of UK Natural Environment Research Council (NERC) scientists impressed the MPs. These scientists "independent of any manufacturing or industrial interests... told us that scientific work had advanced far enough for a decision to be taken". The minutes of evidence show, indeed, that NERC secretary John Bowman volunteered that although the next five years' research would provide "a good many answers to the questions you have been putting to us... I do not think that should be used as an argument for doing nothing now".

And as for the liming of acidified lakes in Scandinavia — as recommended by the Watt committee on energy (see *Nature* **310**, 535; 1984) — this showed ignorance of Scandinavian research, and mere geography, which made liming impractical even as a short-term measure, committee members said last week. "Anyone who has flown over southern Norway and seen the number of damaged lakes in remote areas where there is no indigenous source of lime would realize this" the report says.

The only solution is for Britain to put its own house in order, say the MPs. But will their advice be taken? The next political step in Britain will be a debate on the report. According to Sir Hugh Rossi the government has promised such a debate before the end of the year. **Robert Walgate**

- Britain's Social Democratic Party (SDP) announced their own solution to the problem last week: energy conservation. "Substantial reductions [in sulphur dioxide emissions] could be achieved rapidly even without the costly installation of desulphurization equipment in power stations if the government invested more in energy efficiency measures. A five per cent cut in electricity gneration would enable Britain to meet the Select Committee's targets by the early 1990s, at half the cost estimated by the CEGB. It would also improve the competitiveness of industry", the SDP claims. □

Laboratory animals

Animal rights lobby cashes in

THERE is still no word from the British Government on the progress of its new animal experimentation legislation. More than a year has passed since the release of the White Paper — "Scientific Procedures on Living Animals" (see *Nature* **303**, 191; 1984) — containing draft proposals for the replacement of the Cruelty to Animals Act of 1876 with more effective and less anachronistic controls. In that year, the views and critical comments of concerned organizations have been collected and assimilated. Moderate animal rights groups are now hoping that a suitable response, in the form of a supplementary White Paper, will be published by the end of the year.

Meanwhile, the more extreme animal rights groups, including the Animal Liberation Front (ALF), have stepped up their campaign against animal experimentation with paramilitary style attacks on selected institutions. Government laboratories have been forcibly entered, equipment damaged and records essential to research stolen. Pharmaceutical companies have also suffered harassment and intimidation of their employees. And Mr David Mellor, Under-Secretary at the Home Office and the man principally responsible for preparing the new legislation, has become the object of escalating harassment which, he says, has included threats on his life. Meanwhile, a coalition of organizations including Animal Aid and the British Union for the Abolition of Vivisection, has drawn up a list of minimum requirements which, it says, must be part of the legislation to replace the archaic 1876 act. It wants to see a complete ban on tests of cosmetics, alcohol and tobacco, behavioural and psychological tests, warfare experiments and, more specifically, two routine tests it considers particularly offensive: the Draize eye test in which irritants are put in the eyes, usually of rabbits, until damage is caused, and the so-called LD50 toxicity test in which animals are given increasing doses of a test substance until half have died.

The coalition is unlikely to be satisfied with the proposed measures which, in order not to hamstring British companies by prohibiting experiments that competing foreign companies would be free to carry out, avoids a complete research ban. The proposals differ from the old act in the following ways:

- The 1876 law, which only governs experiments, will be extended in scope to address procedures such as the production of antisera and the passaging of tumours.
- A statutory Animal Procedures Committee will replace the previous non-statutory body.
- Laboratory animals will have to be obtained from registered establishments, outlawing the use of strays.
- The 1876 law required all animals recovering from anaesthesia to be compulsorily killed but, today, some surgical procedures are relatively mild and anaesthesia is used principally to immobilize a subject. This requirement is to be waived in such circumstances.
- The conditions in which animals are maintained will be regulated.
- Home Office inspectors will need to be satisfied that a procedure is justifiable and that no satisfactory alternative to the use of animals is feasible, that the minimum number of animals is used and that the least possible suffering is caused.

The Royal Society for the Prevention of Cruelty to Animals (RSPCA) is generally critical of these proposals. The White Paper advocates the continuation of the present rule that "if an animal is found to be suffering severe pain which is likely to endure, it shall at once be killed". But, RSPCA points out, since the Home Office itself admits it cannot define the terms "pain", "severe" or "enduring", the inclusion of these words in such a pivotal role undermines the credibility of the proposals. Other organizations are also insistent that the pain question be dealt with. The Fund for the Replacement of Animals in Medical Experiments (FRAME) is commited to reducing animal experiments to a minimum and to finding alternatives to animals. In a study, prepared in conjunction with the British Veterinary Association (BVA) and the Committee for the Reform of Animal Experimentation (CRAE) and supplied to the Home Office, it distinguishes two types of pain: unexpected pain inflicted during an experiment, and pain and suffering which is the inevitable consequence of an experiment. In the former situation, FRAME says, the animal should be killed as required by the 1876 act. In the latter situation, permission should be given only in very special circumstances when the experiment is of great importance to human or animal health.

Both the RSPCA and FRAME are unwilling to be too critical of the Home Office until they see its revised proposals and can assess to what extent their advice has been heeded. The new bill could reach Parliament during next year or in 1986.

Marcus Chown

Britain leads the way

DESPITE the flak aimed at the government by animal rights organizations, Britain is ahead of most other European countries in the area of animal experimentation reform. The 21-nation Council of Europe has been trying, since 1978, to perfect a "Convention for the protection of animals used for experimental purposes" (*Nature* **302**, 284; 1983) and the convention is likely to be less strict than the British law. Nevertheless, a European accord on the political horizon could go some way to allaying the fears of pharmaceutical companies that what they perceive as an over-zealous British initiative.

The ageing British act also has admirers in the United States. In a Commentary appearing in *Nature* later this month, an animal rights campaigner argues that the British approach to animal experimentation is much more humane than the US approach. Two bills aiming to improve matters are at present bogged down in the US Congress, with the powerful industrial lobby content to keep them there. □

Bird books safe

Washington

A UNIQUE collection of environmental and natural history documents, including the only known intact copy of the "elephant folio" edition of John Audubon's *Birds of America*, has been granted a reprieve from the auction block. The National Audubon Society had planned to close the library and sell off part of it to raise funds, but the society has now changed its mind after word of the plan leaked out and provoked a minor squall among members and the American Library Association. Many were upset that the board of directors of the society did not consult its membership before taking the decision at its May meeting, and that the society has in fact still made no official announcement on the subject.

According to the library association, the collection, which is housed in the society's New York offices, contains many works on ornithology, wildlife preservation and conservation which can be found together in no other library. It also includes a number of unduplicated nineteenth century works.

The library dispute appears to be part of larger tensions that have been growing between the society's membership and its staff on the one hand and its leadership on the other. Under the presidency of Russell Peterson, the society has become increasingly involved in what is known in the trade association business as "government affairs", that is, lobbying. Peterson attempted to move the entire office to Washington several years ago, but abandoned the plan. Peterson has also involved the society in such issues as global population and nuclear war. Many staff members are known to be displeased with what they see as a swelling bureaucracy — including some 25 vice-presidents — which has grown at the expense of basic programmes.

Although the library will remain intact for the time being, it has been closed to the public and its full-time librarian assigned to new duties within the society.

Stephen Budiansky

Oceanography

Excitement on the seabed

THE US oceanographic and geological community has been "set alight" by a quarter-million-square-mile survey of the Pacific Ocean floor off the west coast of the United States — a survey, completed three weeks ago with the British side-scanning sonar system GLORIA, of the 200-mile exclusive economic zone (EEZ) declared by President Reagan last year under the international Law of the Sea. The survey, says Dr Jim Gardner of the US Geological Survey (USGS) at Menlo Park, has for the first time provided a "road map" of the whole area stretching from the Mexican border in the south to the Canadian in the north, and outwards into the Pacific from the edge of the narrow continental shelf. This map reveals some 200 previously unknown volcanic sea-mounts, "spectacular canyons" 300–500 km long — apparently carrying meandering rivers of sediment along the ocean floor — and almost every kind of plate tectonic boundary.

Economically, the sea-mounts may offer sources of strategic minerals, and the canyons and ocean-floor fans will interest the oil industry both as models of older sources of oil, and as possible drilling sites. There are no indications of sea-floor manganese nodules, but these were not expected so far north.

The survey, says Gardner, who headed the American side of the US–British team that did the work, will lead to half-a-dozen priority research projects for more detailed investigation, and already $60 million is inscribed in the USGS budget for fiscal year 1986 (yet to be approved) to pay for the work (over five years). This will be done jointly with universities, Gardner says.

In Britain, the excitement matches Gardner's, with the extra twist that the mission's success offers a real opportunity for British enterprise. GLORIA was developed at the Institute of Oceanographic Sciences (IOS) at Wormley, Surrey, and has a uniquely long range, which makes it extremely cost-effective for the survey of the 200-mile EEZs which almost every nation has declared since the 'Law of the Sea' agreement. According to Neil Kenyon of IOS, who with another British oceanographer Douglas Masson took charge of the British side of the recent GLORIA mission, GLORIA can perform an area survey 10 times faster than any competing system. It can survey an area half the size of Wales every day at a cost of $5 per square mile, IOS claims.

As a result there is now likely to be a flood of interest in using the torpedo-like instrument to survey EEZs around the world. Already USGS is negotiating for a further five years' work with GLORIA, says Gardner, starting next year in the Gulf of Mexico, and later covering Alaska and Hawaii; and, says Dr Tony Laughton, the director of IOS, to judge by reaction from the recent second international hydrographic technical conference in Plymouth, there are already indications of real interest in many other countries.

But that leaves IOS with an interesting problem. There is only one GLORIA. The USGS programme, if agreed, would occupy it nearly full-time. Apart from the interest of other nations, IOS scientists must have their own time with the instrument. And IOS funds, provided through the Natural Environment Research Council (NERC), are so short it would seem impossible to find the financial and human resources to build a second instrument, costing around £1 million. "If we were a commercial company, we would borrow money to build a new GLORIA on the prospect of making a profit", said Lawton. And, says IOS administrator Dr Tony Rees, "with ten GLORIAs we could cover the world in ten years".

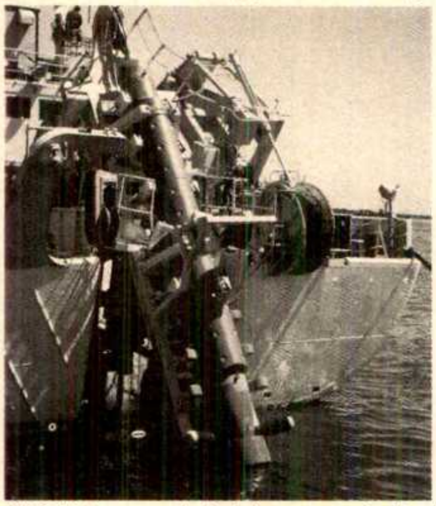

GLORIA — geological long-range inclined ASDIC — is an acronym of an acronym. Dating from the second world war, ASDIC stood for "anti-submarine detection investigation committee". The acronym came to be used to describe the acoustic echo system developed in Britain to detect German U-boats. The achievements of GLORIA represent a 40-year development of ASDIC. The photograph shows GLORIA being launched from the Farnella *research vessel — a converted trawler.*

Treasury rules, under which NERC (and hence IOS) operate, make borrowing difficult. But since the present government is in favour of enterprise, Dr Lawton is hopeful something might be arranged. Other possibilities he is considering are to establish a private company to exploit GLORIA or to license the technology to an existing company. However, too much has been published about the instrument for it to be patentable, he thinks. The potential profits are large. But IOS will have to strike the right balance between commerce and science, says Lawton. "It clearly poses some big problems in terms of our role."

Robert Walgate

European solar energy

Off to sunny Sicily

Brussels

HELPED by the European Commission, a consortium of European companies will next month launch an experiment, in Sicily, to test four types of photovoltaic cells "in the field" for the first time. According to Commission officials, the data collected could play an important role in developing cheaper and more efficient solar cells.

The project will compare fixed and sun-tracking systems of monocrystalline and polycrystalline silicon modules, and two alternative modules: flat-plate amorphous silicon cells and concentrator gallium arsenide cells. The electricity produced by the 5 kW systems will be used in small local applications. The companies involved in the design and manufacture of the components are the Italian companies

BA gets under way

THE 146th annual meeting of the British Association for the Advancement of Science (BA) opened at the University of East Anglia in Norwich on Monday, with over 3,000 visitors expected — 700 more than last year's conference in Brighton. In recent years the BA has been seeking a new identity; it may have found it at Norwich in a mix of science popularization, science politics (whither Britain?), due concern for the place of science in the developing world, and increasing efforts to link science and industry in the minds of its visitors.

To paraphrase the outgoing president Sir Alastair Pilkington (the glassmaker) the BA represents an effort to put science to work in Britain: it has a utilitarian, constructive goal. According to the incoming president, biochemist Sir Hans Kornberg — a man closer to the cuts that British science has suffered recently — next year's BA meeting at the University of Strathclyde will see a greater emphasis on basic science (and perhaps a little more polemic on its behalf) than at Norwich.

But BA officers are very pleased with the £450,000 that Norwich has raised locally to support the meeting (covering more than half its costs) and with the buoyancy of the BA young scientists scheme (BAYS), with its 130 local branches (ever increasing) which hold local meetings throughout the year. And this year there is a new departure: the BA is launching a glossy new magazine, *Link-up*, edited by John Stansell, which will aim to link university science with industrial problems.

Robert Walgate

ENEL and Pragma, and MAN and Siemens of West Germany. Only a dozen or so European companies have been seriously developing solar energy components, including photovoltaic cells. In 1981, Europe had only a 12 per cent share of the world photovoltaics markets which then totalled 6 MWP (megawatts at peak). According to Commission estimates, the world market is expected to reach 400 MWP by 1990, and Commission officials believe that Europe could corner up to 40 per cent of that market. But Europe's main competitors, the United States and Japan, have a head start because of the extensive governmental support given to work on solar energy in those countries.

The solar energy industry is well-established in the United States. The photovoltaics market is worth an annual turnover of $55 million to the fifteen companies involved in component and systems production. The US research and development programme is extensive, while Japanese companies are forging ahead with the development of large-area low-cost amorphous silicon cells, encouraged by a MITI subsidiary, the New Energy Development Organization (NEDO).

National non-nuclear energy budgets in Europe are less generous to research in this field. Tax incentives to encourage the production of electricity using solar energy are becoming more and more frequent in the United States, but in Europe such stimulants have so far only been introduced in Denmark.

The European Community's non-nuclear energy research and development programme has contributed to bringing the cost of silicon cells down to one-fifth of their 1973 cost. According to those working in the field, the cost could be down to one dollar per watt by the year 2000.

However, the community's second pluri-annual programme came to an end in June 1983, while the ambitious budget of 379 million European Currency Units (2 ECU = £1) which the European Commission proposed for the third programme — a tripling of the previous budget — has been held up by the Community's unresolved budgetary wrangles.

In the meantime the delay continues to take its toll of research operations. Far-seeing officials earmarked funds from the 1979–83 budget to keep certain projects ticking over. But lack of funds in other projects will mean that research teams may be moved to other fields. Calls for tenders have also been delayed, so that it may be another year before work on new contracts can get under way.

In addition, extra investments allocated to the Community's advanced information technology programme (Esprit), launched this year, mean that cuts have to be made in other areas in 1984 and 1985. Solar energy research is no exception. The three largest EEC member states, West Germany, France and the United Kingdom, have opposed the draft budget proposed by the Commission at successive research councils. The proposal is not likely to fare any better when the ten's research ministers take their next look at it in mid-October.

The potential of photovoltaics is reflected in the funds earmarked for it under the third non-nuclear energy research and development programme proposed by the Commission — half of the solar energy sub-programme (80 million ECU) which also includes developing solar architecture, passive solar heating and cooling systems, and instruments for analysis, testing solar energy systems and looking at the problems of storage and performance.

As far as photovoltaics are concerned, the Commission wants to lower the costs of cells and develop competitive large-area power supply systems during the next four years. The second area of priority is biomass. It is estimated that the conversion of biomass could eventually provide 5 per cent of the Community's energy requirement, and half a millon extra jobs. The Community has a 38 per cent energy deficit at the moment. Eight of the ten member countries have to import between 48 per cent (Greece) and 81 per cent (Italy) of their energy requirement from abroad — the two energy exporters are the United Kingdom and the Netherlands.

The third area on which research is to be concentrated is geothermal energy. The Commission has proposed spending 39 million ECU to develop low temperature source applications, and look at the problems of reservoir management, fluid extraction, energy conversion and develop the feasibility of the hot dry rocks process.

The final area of research and development is wind energy. In addition to monitoring the performance of some 200 wind generators, which are scattered throughout the ten member states, Community research would be centred on the development of multiwatt machines, the improvement of blade design and engineering, improving the technology of small and medium sized machines, solving the problems of site aerodynamics, subsystem concepts and integration into the overall electrical supply system.

Anna Lubinska

Science in India

In the special issue on science in India (*Nature* **308**, 581-600; 1984), in an article dealing with the administration of research (pp.591 *et seq.*), there is a reference to an academic's complaint that he had to negotiate with his university to spend Rs100. The same paragraph mentioned the Madurai Kamaraj University, and the vice-chancellor, Dr J. Ramachandran, asks us to point out that the reference was not to his university. □

Mongolia

New man backs science

The new general secretary of the Central Committee of the Mongolian People's Revolutionary Party, Dr Jambyn Batmonh, is something of a rarity among communist leaders. The usual route to political power involves rising through the ranks of the party or military apparatus. But Dr Jambyn is a former academic with good links with the scientific community.

Educated at the Mongolian State University and at the Academy of Social Sciences of the Central Committee of the Communist Party of the Soviet Union, Dr Batmonh worked for more than twenty years in Mongolia's higher education system. In 1967 he became pro-rector, and subsequently rector, of the Mongolian State University.

In 1973, he transferred to party work as head of the central committee's Department of Science and Education. In 1974, he became chairman of the Council of Ministers of the Mongolian People's Republic. Given his background, it is not surprising that his inaugural speech as general secretary stressed the importance of science and technology in raising the efficiency of Mongolian agriculture and the need to improve education and health facilities.

Dr Batmonh — academic makes good.

The son of north-Mongolian cattle-herders, Dr Batmonh's *curriculum vitae* illustrates the rapid development of education in Mongolia which (apart from lamasery schools) began only five years before his birth with the foundation of a 40-pupil elementary school in Urga (now Ulan Bator). The Mongolian State University was founded only in 1942 and the Mongolian Academy of Sciences in 1941. As a result of the lack of opportunity at home, a strong tradition has developed that Mongolian scholars do at least a part of their postgraduate studies in the Soviet Union, and in many fields of research, including the application of radioisotopes, the development of the Mongolian chemical industry and the geophysical survey, Soviet scientists continue to play an important role.

Vera Rich

Siberia

Canals to feed saline lake

SOVIET plans to divert the north-flowing Siberian rivers southward have received a new impetus, with the launch of a scheme to replenish the waters of the landlocked Aral Sea. Increasing irrigation demands on the Rivers Amudarya and Syrdarya which feed the Aral have led to a drop in the water level of 3 metres in the past two decades. The consequent rise in salinity has had an adverse effect on the fish-stocks of the lake.

As the Aral basin is the main source of Soviet cotton and the 1982 Food Programme envisages further irrigation projects in the area, a massive rescue operation has been planned, requiring the construction of a 2,550 km canal from the confluence of the Ob' and Irtysh rivers to the Amudarya. This will not only replenish the Aral Sea to its optimum level, but also permit the irrigation of an additional 4 million hectares of land. The fall in water-level is undoubtedly worrying to ecologists, who, until the canal is ready, plan to regulate evaporation losses by building two dams, which will cut off Adzhibai Bay and the gulf known as the Little Sea and thus keep those areas close to the river mouths at a salinity level suitable for fisheries.

Dam-construction in Soviet seas is, however, a sensitive issue. A dam completed five years ago, which was meant to halt evaporation losses in the Caspian Sea has instead caused disastrous changes in the subterranean brines which form the feedstock of the Karbogazsulfat chemical industry, and have turned the region east of the gulf into a salt desert. (The Caspian level, meanwhile, has risen through apparently natural causes.)

The proposed use of the Irtysh water for the diversion scheme, too, is not without its problems. Although the proposed canal will draw off only 6 per cent of the Ob'-Irtysh water resources, even this small proportion could raise difficulties. Recently there has been a continuing dispute on the upper Irtysh between the farmers, fishermen and river-boatmen who depend on a plentiful water-supply, and the Kazakhstan Ministry of Land Reclamation and Water Resources which withheld supplies at the request of the electrical generating authorities. According to *Kazakhstanskaya Pravda,* there have been serious planning errors in the construction of hydroelectric works on the upper Irtysh which will require further major engineering works to put right. Yet all public statements on the proposed canal to the Amudarya tacitly assume that the Ob' and Irtysh have no difficulties with their "water budgets".

The emphasis on the small percentage of water to be drawn off by the canal, and the consequent assurances that its diversion will not affect the ecology of the region is a fairly new approach. Earlier plans spoke grandiosely of turning whole rivers back in their courses. When, however, the schemes were revived in the early 1970s, there was a worldwide outcry from ecologists, who feared that the loss of water to the Arctic Ocean might change the world's weather patterns. The Soviet planners issued vehement denials that such a disaster might occur, but postponed their plans until further surveys could be carried out.

As a result, they have introduced a major modification into the "diversions" announced during the 1970s. The plan originally involved replenishing the feeder rivers of both the Azov and Caspian Seas. To do this, however, would necessitate the transfer of more than 20 km^3 of water a year, too great an amount, according to planners, for the environmental changes to be predictable. (The Amudarya canal will transfer 27.2 km^3 a year.) Accordingly, it was decided to concentrate on the Caspian, not only because its present "water-budget" is still fairly close to equilibrium as regards inflow but also because of the particular economic importance of the Caspian as the largest producer of sturgeon in the world.

Vera Rich

UK research

Councils hunting for heads

BRITISH research councils appear to be increasingly hamstrung in their attempts to recruit new chief executives, at least in part because suitable candidates now consider senior positions with the research councils to be uncomfortable beds of nails. Three of the five councils will need to appoint new chairmen within the next twelve months.

The Natural Environment Research Council is in the most urgent need now that its chairman for the past three years, Sir Hermann Bondi, has become Master of Churchill College, Cambridge. Apparently the council has been rebuffed by the two candidates first approached, but has now recommended (to the Secretary of State for Education and Science) that Dr Hugh Fish, chairman of the London Water Board and one of its own members, should be appointed chairman on a short-term basis.

The Agricultural and Food Research Council, whose secretary Sir Ralph Riley is on the point of retirement, is by contrast using the services of an executive recruitment agency to appoint a successor. By all accounts, however, the Science and Engineering Research Council plans to go one substantial step further and to use a head-hunting company as a means of identifying possible candidates. In this case, there is a suitable breathing space. The present chairman of the council, Professor John Kingman, is due to become vice-chancellor of the University of Bristol only at the beginning of the academic year 1985-86. □

Defence department money on offer

Washington,

THE US Department of Defense is putting its money where its mouth has been on biological warfare, and a major beneficiary may be academic researchers. A series of full-page advertisements have recently appeared in *Science* magazine, placed by the US Army Medical Research Acquisition Agency, calling for proposals in a broad range of areas related to protection against biological agents.

A spokesman for the US Army Medical Research Institute of Infectious Diseases (USAMRIID), the old biological warfare establishment at Fort Detrick, Maryland, said that the solicitations are part of a general effort to expand its research programmes on biological defence in four areas: parasitic diseases, low-molecular-weight toxins, rickettsial diseases and bacterial diseases. The most recent advertisement seeks research proposals on biochemical, immunological, genetic, pathophysiological and therapeutic studies of bacterial diseases, with special emphasis on anthrax, botulin, diarrhoeal diseases and "other bacteria or toxins capable of eroding combat strengths" or "agents of potential biological warfare importance".

The USAMRIID spokesman said that the advertising campaign was simply a way of letting scientists who are probably already familiar with the institute's work learn how they can submit proposals. All of the work is unclassified.

Support for USAMRIID has risen dramatically in the past few years, from $17 million in fiscal year 1982 to approximately $40 million this year. The current plan is to double that figure over the next three years. The entire Army Medical Research Command, of which USAMRIID is a part, is now spending more than $100 million a year on extramural research, although this figure includes not only biological warfare defence research but other topics relating to soldiers' health.

The USAMRIID spokesman attributed the new emphasis on medical research both to a heightened concern with preparedness — the Secretary of Defense, Caspar Weinberger, has cited medical care as a critical element in US war-fighting capability — and also to the biological warfare threat perceived in the Soviet Union's supposed proxy use of "yellow rain" in South-East Asia.

Stephen Budiansky

US agricultural research

Competition reaps rewards

Washington

A STUDY of US agricultural research now being circulated to colleges and universities offers encouragement to scientists and may pave the way for more coherent planning. The report* emphasizes the need for improved communications between Congress and the executive so that scientific projects do not become hostages to political fortune, and may lead to an expansion of competitive grant funding. This would bring benefits to the underdeveloped plant biotechnology research programme.

The timing of the report is apt: next year's agriculture appropriations bill remains jammed in Congress. The Senate has restored the administration's $50 million budget request for the Department of Agriculture's competitive grants programme after the House sought to cut this to $17.5 million. The $50 million includes $28.5 million allocated to the administration's new biotechnology initiative. Although no conference committee has yet been appointed to bridge the gap, much behind-the-scenes negotiating is going on. But despite the generally favourable light in which science is regarded in Congress, prominent figures in the House consider basic research in agriculture irrelevant to the immediate needs of farmers.

The report now being circulated was prepared under contract for the Department of Agriculture as an "action research programme", involving scores of interviews. It is heavy with sociological theorizing and even ventures some speculations on philosophical issues: for example, the "logical positivistic" underpinnings of agricultural research are blamed for the "paradox of faith in science leading to doubt and distrust". But there are also some more concrete suggestions, chief among which is a proposal for a new National Agricultural Issues Commission based within the National Academy of Sciences which would define long-term research goals.

Ironically, that proposal is the one that seems least likely to get anywhere. A majority of the key decision makers who reviewed a draft of the report felt that two existing bodies — the Joint Council on Food and Agricultural Sciences and the Users Advisory Board — could do the job.

Many of the report's other conclusions have been well received, although a proposal for new centres of excellence in agricultural research is contentious. The report urges efforts to broaden recruitment to bring in more students from non-farm backgrounds, and argues for increased prominence and status for scientists. A separate study being completed by Professor Irwin Feller of Pennsylvania State University, shortly to be delivered to the agriculture department, is thought to have a similarly up-beat approach towards future contributions of research.

The combined impact of both studies is likely to have a "slow but significant effect" on policy, according to Dr John Jordan, administrator of the agriculture department's cooperative state research service. The activity of recent months has brought together congressmen and scientists "who would never normally see each other". The use of competitive grants to fund research is now likely to increase, thus allowing major research centres outside the land-grant system to make bids. And even the land-grant colleges are starting to make more use of competitive schemes and joint schemes with non-land-grant institutions, says Jordan.

Tim Beardsley

The Paradox of Success: The Impact of Priority Setting in Agricultural Research and Extension, (US Department of Agriculture).

New US genetics centre goes west

San Francisco

A NEW research centre concerned with genetic engineering of crop plants has been established jointly by the US Department of Agriculture (USDA) and the University of California. The centre hopes to attract university and industry researchers from all over the world to work on basic research projects in plant genetics and gene expression.

The Plant Gene Expression Center, with an initial annual budget of $4 million, will be housed in USDA's Western Regional Research Center in Albany, near the Berkeley campus of the university. The facility has laboratory space for about 40 researchers and is expected to be operational within a year. Ten senior scientists will form the foundation of the centre, including two senior scientist programme leaders holding university appointments. The remaining eight core scientists will hold positions with USDA's Agricultural Research Service (ARS).

The core group will be supported by a consortium of public and private researchers. The consortium serves as a source of expertise and provides an important link with other research institutions and industry. In addition, a science advisory committee will be formed to help set research priorities.

The centre will investigate basic questions in plant molecular biology, using and further developing new tools of plant genetic engineering. The centre wants to make its research findings available to anyone, including those interested in developing marketable products. Details of publication policy have not yet been worked out, according to Gerald Still, acting director of the centre. Usually the centre will follow the ARS practice of establishing public patents and refusing industry support that stipulates secrecy and exclusive rights. Dr Still, formerly National Program Leader at ARS in Beltsville, Maryland, has the task of coordinating research activities, arranging cooperative agreements and recruiting financial support. He hopes to supplement the annual budget provided by ARS with grants from other public and private agencies and industry.

Bruni Kobbe

Nature index of biotechnology stocks

12-Month high	12-Month low	Company	Close previous month	Close 31 August	Change
14	6	**Biogen (Switzerland)**	6¾	8	+1¼
2	1	**Bio-Logicals (Canada)**	1⅛	1¼	+⅛
14⅜	7⅝	**Bio-Response (USA)**	8⅞	9½	+⅝
14	9¾	**Cetus (USA)**	9⅜	11⅜	+2
10⅜	4¼	**Collaborative Research (USA)**	5¼	6¼	+1
19⅞	11½	**Damon (USA)**	13	14½	+1½
26¼	11¾	**Enzo-Biochem (USA)**	12½	14¼	+1¾
10⅛	4¼	**Flow General (USA)**	4¾	5⅜	+⅝
42¼	28¾	**Genentech (USA)**	33	33¼	+¼
10¾	4½	**Genetic Systems (USA)**	5	6⅞	+1⅞
17¼	8¼	**Genex (USA)**	11⅛	12	+⅞
23	11	**Hybritech (USA)**	11¼	14¼	+3
16¼	7¾	**Molecular Genetics (USA)**	8¾	10¼	+1½
15½	8¼	**Monoclonal Antibodies (USA)**	8¼	10	+1¾
60⅞	39	**Novo Industri A/S (Denmark)**	40⅝	37¼	−3⅜
22¾	14½	**Pharmacia (Sweden)**	17⅛	19	+1⅞

Closing prices are for the last Friday of the month. For over-the-counter stocks, bid price is quoted; for stocks on the American and New York exchanges, the transaction price. *Nature*'s weighted index of biotechnology stocks stood at **149** on 31 August, compared with **138** a month earlier. Data from E.F. Hutton, Inc.

Roman food not so fast

SIR — As a pioneer in the study of animal remains from archaeological sites, I counsel caution in concluding that a high proportion of pig bones indicates the decline of Rome into a fast-food empire (*Nature* 17 May, p.211). First, the bones indicate the proportions in which the different species were eaten rather than kept. Although in a peasant economy the two are probably the same, it is noteworthy that whereas the Cistercian monks kept thousands of sheep but relatively few cattle, 90 per cent of the medieval bone remains from Kirkstall Abbey were from cattle[1].

Although it is true that the greatest proportion of pig bones from a Roman site in Britain (for comparison) was 26 per cent, the figures of 40 per cent and even 65 per cent pigs quoted by Hodges from Italy hardly indicate overwhelming predominance when one notes that cattle remains ranged up to 78 per cent and sheep remains up to 95 per cent on Roman sites, again in Britain[2].

The term "fast food" used by Hodges is used in a modern context for food preparation rather than for food production. Since the pig was a scavenger in the past, pork was certainly cheap to produce, but not "fast" or "short term" as Hodges implies, since until after the Middle Ages pigs were slow-maturing animals. If the production of pigmeat is relatively "fast" today (as a major component of "fast" or convenience foods) it is because pigs have been bred for early maturity and are fed concentrated cereal-based diets.

M.L. RYDER
Hill Farming Research Organisation,
Bush Estate,
Penicuik, Midlothian EH26 OPY, UK

1. Ryder, M.L. *Animal bones in Archaeology* 2nd edn (Blackwell, Oxford, 1969).
2. Ryder, M.L. "Livestock" in *The Agrarian History of England and Wales* Vol. 1, Pt 1 (ed. Piggott, S.) (Cambridge University Press, 1981).

Richard Hodges replies:

SIR — Dr Ryder is making a mountain out of a molehill. My short review in *Nature* placed in a wider historical context a collection of recently published studies by archaeozoologists, in whom I have every confidence.

First, I made exactly the point (the main thrust of my note) that it was consumption of pig rather than any assumptions about production directly that made the data so historically interesting. I agree with him. However, I suspect his Kirkstall Abbey example is a poor illustration of his point, since I would imagine his high cattle bone is merely an indication of the sampling procedures (or lack of them) used when the site was excavated.

Second, I do not follow his point about Roman sites in Britain. To make such comparisons without considering historical and ecological contexts for the sites concerned is quite unscientific.

Third, I like the term "fast-food", suggested to me by your assistant editor. Of course, Ryder is strictly right. The term should have been qualified — and would have been in a *long* article — by precisely the comments he makes, effectively endorsing the reason for drawing attention to high pig numbers in the first place.

RICHARD HODGES
Department of Prehistory &
Archaeology,
University of Sheffield,
Sheffield S10 2TN, UK

Cancer incidence at Sellafield

SIR — The investigation by Sir Douglas Black (see *Nature* 26 July, p.263) into the alleged increased incidence of cancer in West Cumbria usefully suggested what further research is needed, especially the measurement of radiation dose actually received and whether metabolic differences between children and adults alter the effects of radiation. However, on the evidence already available, doubts must be raised about the report's judgement that the incidence of leukaemia in Seascale is "unusual but not unique".

Ward rank order	Cases	Children	Poisson probability	Rate per 1,000
1*	4	411	0.0001	9.73
2	4	976	0.0032	4.09
3	2	144	0.0036	13.88
4	4	1,207	0.0068	3.31
5	4	1,353	0.0100	2.95

Top five wards ranked by Poisson probability for incidence of lymphoid malignancy in under 15 year olds, 1968–82 (from Craft *et al.*[2]).

*Seascale.

The report examines the occurrence of lymphoid malignancy, in children under 15, in the 765 electoral wards of Cumbria, from 1968 to 1982. Incidence in the wards was ranked by rate per 1,000. Seascale (9.73/1,000) is ranked third. Although well above average (0.61/1,000), Seascale appears to lie within the normal pattern of variation.

However, rate so measured is an uninformative index. As most wards have only 0 or 1 cases, all that is reflected in rate is ward size, which varies twenty-fold (from 100 to 2,000). A more appropriate measure is the cumulative Poisson probability. This gives the probability of occurrence in a ward of 0,1,2. . . cases, if the cases are randomly distributed in the region. The incidence seen in Seascale is 1.3×10^{-4}, which when ranked lies first (see table and ref. 2). This incidence is expected to occur once in a sample of 8,000 wards.

Even more disturbing are the two further cases of lymphoma registered in Seascale in 1983 (ref. 1). By updating the survey to 1983, the Poisson probability for such an occurrence falls to approximately 1.0×10^{-6}. This can only be described as unique, lying well beyond the expected variation.

The two simple points raised here must make the "qualified reassurance" given by the Black report less acceptable. Seascale has an extraordinarily high incidence of lymphoid malignancy. Its proximity to the Sellafield reprocessing plant, a potential source of mutagenic radiation, is disquieting.

ANDREW POMIANKOWSKI
School of Biological Sciences,
University of Sussex,
Falmer,
Brighton, Sussex, UK

1. Report of the Independent Advisory Group, *Investigation of the Possible Increased Incidence of Cancer in West Cumbria* (HMSO, London, 1984).
2. Craft, A.W. Openshaw, S. & Birch, J. *Lancet* ii, 96-97 (1984).

Too many papers?

SIR — For some years there has been talk of there being too many scientific journals but now it appears that there are too many papers. An informal sampling suggests that, in science and medicine, journals of reasonable status are experiencing an increase of around 10 per cent in submissions while editors in the area of whole organism biology or traditional life science disciplines have reported increases of up to 30 per cent, and even 50 per cent in the case of certain high status titles.

There are several possible explanations. (1) A demographic factor; as a result of the growth in tertiary education in the 1960s, a large number of scientists are now in their most productive period and could be making a last effort to gain promotion. (2) Support of research in some areas, especially "soft" science, has been severely cut, heightening the struggle for grants. (3) Information technology has made it easier to store and process research data. This could be having an effect in astrophysics and geophysics in particular. (4) The decline in the publication of multi-author review volumes, resulting from library cutbacks, may have diverted longer review articles, or just the writing effort involved, towards refereed journals.

At present, smaller journals are being forced to restrict page budgets and there is the prospect of worthwhile if specialized papers going unpublished. Whatever the underlying reasons for the apparent increase in papers, the signs indicate a developing problem in the publication of research, especially in non-commercial areas such as ecology.

ROBERT CAMPBELL
Blackwell Scientific Publications,
Osney Mead,
Oxford OX2 OEL, UK
TIM HALLIDAY
Department of Biology,
Open University,
Milton Keynes MK7 6AA, UK

Brownian and quantum motion

A recent demonstration that a classical problem in brownian motion belies Dirac's relativistic equations of quantum mechanics is a reminder of many things that students should be taught.

THE connection between brownian motion and quantum mechanics should be better known, at least to those brought up in the days before the full implications of Feynman's reformulation of quantum mechanics (in 1948) were fully appreciated, perhaps 15 years ago. That will be people's reaction to the neat argument, now published by B. Gaveau *et al.* (*Phys. Rev. Lett.* **53**, 419; 1984) which sets out to provide a demonstration that Dirac's relativistic wave equation can be derived from a consideration of a simple classical problem in brownian motion. Others will however note that the authors include Mark Kac, now at the University of Southern California, Los Angeles, who first derived the Schrödinger equation from a brownian motion problem in 1959, as well as T. Jacobson (University of Texas, Austin) and L.S. Schulman (Technion, Haifa), who have more recently made important contributions to similar problems.

The starting point for the argument is simple but evocative. Consider a particle moving in one dimension only at some fixed velocity, and let it suffer reversals of direction at random intervals, themselves distributed statistically according to some suitable law, most simply a Poisson distribution. Practitioners in brownian motion problems will readily write down expressions for the probability density (per unit length and per unit time) that the particle is at some place along the line at a certain time, and moving in one direction or the other. Most simply, there is a different function for each direction. The next step is to relate these probability densities to each other by taking account of the conservation in number of the particles moving along the line. The outcome is a set of differential equations which must be satisfied by the two probability densities. (In the sequel, these correspond to the two states of chirality or handedness which alone are accessible to relativistic Dirac particles in one dimension.) What the authors assert (and then prove) is that these equations are in an appropriate sense equivalent to Dirac's equation in one dimension. They then show that the same technique can be extended to the full relativistic problem (with three space dimensions).

The origin of this problem is intriguing, for it seems first to have appeared as an exercise for students in the elegent textbook *Quantum Mechanics and Path Integrals*, by R. P. Feynman and A.R. Hibbs, published in 1965. There, users of the book are invited to calculate the evolution in time of a system consisting of a particle moving with the velocity of light in a single dimension, and suffering random reversals of direction. To Feynman and Hibbs, this would merely have been a test of what students had been told in the first thirty pages of the book. To Kac and company, the challenge has been to demonstrate that the connection between quantum mechanics and brownian motion that applies in non-relativistic mechanics also applies to Dirac's equation. That they succeed will not surprise those already in the know.

For the rest of us, there are several missing elements of which the least excusable is Feynman's use of the concept of the path integral. That, of course, is also familiar from classical mechanics. Since de Maupertuis and the principle of least action in the eighteenth century, it has been understood that the path that will actually be followed, and which is thus that dictated by the laws of motion, will be that for which the action (force multiplied by time) is least. For simple systems, forces can be calculated as a function of time from the function of the system called the lagrangian, essentially the difference between the kinetic and potential energies. Given initial and final states, and starting and finishing times, it is then possible to calculate (in principle at least) the action for all possible paths and to choose that for which the action is least.

The difference between this and quantum mechanics is that there is no unique path for the evolution of a system but that all possible paths must be counted. As Bohr and his disciples were always telling us, a photon confronted with two slits in a screen cannot be said to use one slit or the other, but both.

Each path is relevant; the only meaningful question to ask about the outcome is not where the particle finishes up, but the probability that it should finish up here or there and, to that end, that it is necessary to add together probability amplitudes (one for each possible path), taking account of plus and minus signs, and of imaginery as well as real parts, before calculating the probability (by squaring the amplitude). The essence of Feynman's quantum mechanics is a powerful prescription for calculating the evolution of the amplitude for each possible path. Inevitably, the outcome is a line integral. Although the integrals are not the same as those appearing in classical mechanics, their relationship is plain to see. In passing, it is worth asking whether quantum mechanics would ever be presented to students in other terms, necessarily less direct, if it were not that so much energy had been invested in teaching them to solve differential equations.

The connection with brownian motion is harder to discern. The formal resemblance with quantum mechanics is simple enough. Because the process is statistical, the most one can hope to do is to calculate the probability that a particle starting from one place on the line will finish up at another. Thus, if a particle is to start at one place and finish at another after a specified length of time, there is a large (even infinite) number of paths which it may traverse in doing so. The first to recognize this deeper relationship with Feynman's quantum mechanics — the existence of a multitude of paths — seems to have been K. Ito, working on brownian motion in 1951.

In reality a connection between the quantum mechanics of brownian motion gets even more specific. Put briefly, while the probability amplitudes in the brownian motion problem are all real and positive (and are thus simply additive), those which conspire in the calculation of Feynman's propagation functions are not. The quantum version of the calculations can be turned into the other version simply by replacing *i* (the square root of minus 1) by minus 1 whenever it occurs. The similarity is even more striking when one sees it demonstrated that a specific path in Feynman's formulism can be boiled down to calculating the chances that a brownian particle makes its way along the same such trajectory by random process.

The implication is simply grasped. The propagation of the probability amplitude along an arbitrarily chosen trajectory is indeed to be likened to brownian motion. One of the quirks of that process, the fact that the average displacement of a particle is proportional to the square root of the time elapsed, accounts for some of the computational complexity of Feynman's formulism. Taken together, the whole box of tricks makes it intelligible that there should be a correspondence between the theory of quantum fields and that of phase transitions on a lattice. This is yet another part of the case for changing tack on teaching.

John Maddox

Oceanography

Windscale effluent as a tracer for continental shelf circulation

from J.T.F. Zimmerman

CONCERN about the radioactive effluent from plants reprocessing nuclear fuel, primarily Sellafield (formerly Windscale) in Cumbria, UK, and to a lesser extent Cape la Hague near Cherbourg, France, has led to regular surveying, over more than a decade, of the radioactivity of the west European continental shelf waters, particularly by the Fisheries Research Laboratory in Lowestoft, UK, and by the Deutsche Hydrographische Institut in Hamburg. The results of the survey are not simply a means of monitoring a pollutant, but can be put to scientific use. As the flushing time scale of the Irish Sea–North Sea–English Channel system is of the order of several years, the outfall should by now have spread over the entire area. Tracing the fate of the radionuclides should therefore provide a method of testing hypotheses about the general circulation of these shelf seas. In a recent paper, D. Prandle of Bidston Observatory, Merseyside, UK, uses the radionuclide data to provide a numerical model of the water circulation of the area[1].

The radionuclide caesium-137 is an ideal conservative trace because its half life of about 30 years is long compared to the transport time scales on the shelf and because, being highly soluble, it is not easily removed from the water column by sedimentation. ^{137}Cs does not occur in nature. By the time the discharges from the reprocessing plants started, however, nuclear bomb tests had already created a background level in the Atlantic Ocean of 0.14 pCil^{-1}, rising to 0.4 pCil^{-1} in the North Sea[2]. The latter level has now been increased to 1–5 pCil^{-1}, though this is still well below the permissible limit of 900 pCil^{-1} set by the International Atomic Energy Agency[3].

What can be learned from the spread of ^{137}Cs over the contaminated shelf and even beyond that in the arctic waters of the North Atlantic Ocean? Early surveys[2-4] already confirmed the traditional view[5] of major transport routes of the water masses in the North Sea, Irish Sea and English Channel. Thus, generally, water from the Atlantic Ocean enters the English Channel, where its splits into two branches, one of which flows through the Straits of Dover, along the Dutch, German and Danish coasts to the Skagerrak area and finally is removed to the northern Atlantic Ocean by a northward current through the deeper Norwegian trench. A second branch splits off between Cornwall and Ireland, flows northwards through the Irish Sea, turns around Scotland, mixes with Atlantic water and then enters the North Sea near the Shetland–Orkney Islands. From there it flows southwards in a broad band on the western side of the North Sea to about 53°N, the latitude of the Wash, where it finally joins the flow from the Straits of Dover.

The distribution of radioactive effluent shows[2-4] that the discharge from Windscale enters the North Sea through its northern entrance and gradually spreads over all of its area before being flushed to the northern Atlantic Ocean, whereas that from Cape la Hague primarily influences the eastern side of the North Sea basin.

What are the velocities along these pathways? What is the dilution rate of a patch that follows a specific transport route and what kind of mechanism drives circulation and diffusion? Some of these questions could be tentatively answered by looking at the evolution with time of the ^{137}Cs distribution pattern[2-4] or by using simple box models for subregions of the shelf, particularly the North Channel and Irish Sea[6-8]. In a much more ambitious use of the ^{137}Cs data, Prandle has now employed the recorded time evolution of the ^{137}Cs distribution over the continental shelf to calibrate a complete two-dimensional (vertically integrated) numerical model of its water circulation.

The model supports the 'traditional view' of the general circulation but also, more importantly, identifies the primary driving forces of the water movement and their relative strength. Thus, Prandle shows that windstress over the area, which is, on average, southwesterly in direction, sets the water on its course and that this circulation is reinforced and its speed increased by 10–50 per cent, by tidal rectification. Together, these driving forces create a more or less steady current with velocities of 1–6 cm s^{-1}, giving annual displacements of 500–1,000 km along the transport routes described above. This gives a transit time of 5 years for the Cornwall–Skagerrak route that passes the Irish Sea and recirculates into the North Sea and about half that time for the 'direct' route through the Straits of Dover.

Advection by currents is only half of the story, however. The tracer is also diffused by turbulent eddies, which cannot be resolved by a model. Turbulent diffusion coefficients have, therefore, to be introduced and it is here that the observed ^{137}Cs distribution can be used for calibration. The best way to parametrize turbulent diffusion coefficients in these areas is controversial. Prandle prefers to express them in the tidal current velocities, probably the safest choice. Calibration of the model with the aid of ^{137}Cs data gives values for the diffusion coefficients ranging from 50 m^2 s^{-1} for the quiescent regions of the central North Sea to 600 m^2 s^{-1} for the 'turbulent' Irish Sea. Thus, advection dominates diffusion over much of the North Sea area, whereas in the Irish Sea and English Channel the two transport processes are equally important.

Once supplied with diffusion coefficients, Prandle's model is able to predict a variety of time scales for the flushing of the shelf waters and the discharges from Windscale and Cape la Hague. It predicts that effluent from Windscale takes about 4 years to travel around the North Sea before entering the Atlantic Ocean through the Norwegian trench. The calculated bimodal distribution of transit times for Windscale, however, suggests that after 1 year about one-third of the discharge has escaped to the Atlantic Ocean by mixing during its passage through the waters around northern Scotland. The discharge from Cape la Hague — which is an order of magnitude less than that from Windscale — needs about 2 years to reach the Skagerrak via the

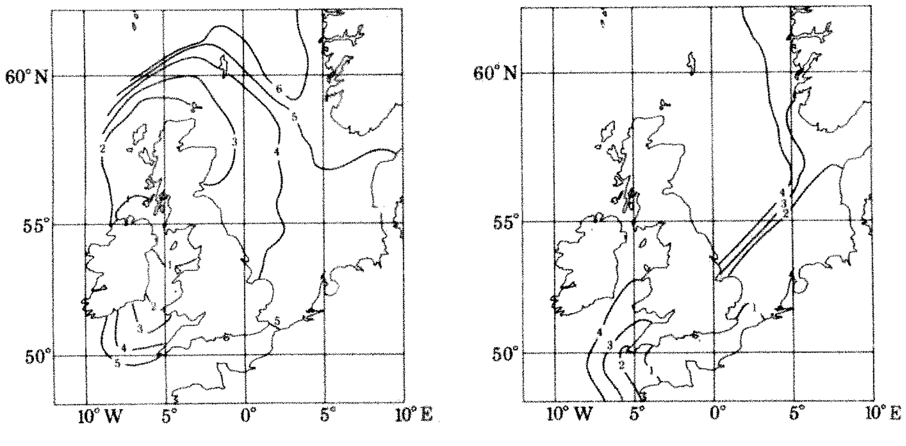

'Age' distribution (in years), as calculated by Prandle[1], for the effluent of Windscale (left) and Cape la Hague (right), where the 'age' of a constituent of a watermass is the average time it needs to travel from its discharge position to another arbitrary position in the area of consideration.

eastern North Sea. These values are of course related to the *e*-folding time for flushing of separate basins by the fluxes through their boundaries. For the North Sea and Irish Sea as a whole, Prandle's estimates for these scales are 530 and 328 days respectively.

For various subregions of the North Sea it is tempting to compare Prandle's estimates of the flushing time scale with those reported last year[9] by a working group of the International Council for the Exploration of the Sea (ICES) led by L. Otto from KNMI, de Bilt, Netherlands. There are notable discrepancies: ICES observations suggest much more stagnant water masses along the east coast of England and in the centre of the North Sea gyre and more rapid flushing in the deep Norwegian trench than are predicted by Prandle's model (and others). Clearly the details of the circulation pattern are still open to question; nonetheless, Prandle's tuning of a circulation model with a suitable tracer has improved our understanding of the west-European shelf.

What happens to the radioactive effluent once it has left the shelf? At a recent symposium on 'Contaminant fluxes through the coastal zone' held in Nantes in May, Dahlgaard and co-workers from the Riso National Laboratory, Denmark, and the University of Lund, Sweden, presented an updated version[10] of their earlier conclusions[11] that the Windscale effluent reaches the East Greenland Current in about 6–8 years, probably after being transported northwards along the Norwegian coast and across the Atlantic south of Spitsbergen. Although crude, this picture fits in very well with Dahlgaard's results for the North Sea. These predict transport times and a dilution rate of the Windscale effluent as follows. If its concentration is set at 1,000 in the northern Irish Sea where the material stays for 1 year, say, it will take about 3 years to cross the North Sea during which time its concentration drops to 100. The passage along the Norwegian coast takes another year, with a dilution of another 50 per cent, and by the time the material reaches the waters near Greenland, within 2–4 years, its concentration will be about a thousandth of its original value. ☐

1. Prundle, D. *Phil. Trans. R. Soc.* **A310**, 407 (1984).
2. Kautsky, H. *Dt. hydrogr. Z.* **26**, 241 (1973).
3. Kautsky, H. *Dt. hydrogr. Z.* **29**, 217 (1976).
4. Kautsky, H., Jefferies, D.F. & Steele, A.K. *Dt. hydrogr. Z.* **33**, 152 (1980).
5. Otto, L. in *North Sea Dynamics* (eds Sundermann, J. & Lenz, W.) 26 (Springer, Berlin, 1983).
6. Jefferies, D.F., Preston, A. & Steele, A.K. *Mar. poll. Bull.* **4**, 118 (1973).
7. Jefferies, D.F., Steele, A.K. & Preston, A. *Deep Sea Res.* **29**, 713 (1982).
8. Livingston, H.D., Bowen, V.T. & Kupferman, S.L.J. *Mar. Res.* **40**, 253 & 1227 (1982).
9. ICES *Co-oper. Res. Rep.* **123**, 159 (1983).
10. Dahlgaard, H., Aarkrog, A., Hallstadius, L., Holm, E. & Eioseco, J. *Preprint Symp. Contaminant Fluxes through the Coastal Zone*, Nantes, 14–16 May (1984).
11. Aarkrog, A., Dahlgaard, H., Hallstadius, L., Hansen, H. & Holm, E. *Nature* **304**, 49 (1983).

J.T.F. Zimmerman is at the Netherlands Institute for Sea Research, PO Box 59, 1790 Abden Burg, Texel, and at the University of Utrecht, The Netherlands.

Molecular biology

Excision of introns in lariat form

from Charles Weissmann

SEVEN years after the discovery that the protein-coding sequences of most genes are disrupted by introns, an astonishing pathway has been revealed for the splicing (that is, excision) of introns from gene transcripts. In short, both Sharp's group[1,2] and Maniatis, Green and their colleagues[3] have shown that, contrary to expectation, the introns that are excised in the production of messenger RNA (mRNA) from its precursors (ultimately the gene transcripts) are recovered as lariat-like structures rather than as linear or circular RNA. The lariats are formed by attachment of one end (5′) of the intron to a site close to the other (3′).

This discovery has followed the recent development of cell-free systems for the splicing of preformed mRNA precursors[4-6]. As a substrate for their cell-free system Sharp and his colleagues used a ^{32}P-labelled RNA, prepared by the Manley system[7], that consisted of the major adenovirus 'late' exons (L1 and L2) separated by an abbreviated intron and with a short second intron following L2. This substrate is schematized as 'S' in Fig. 1. Earlier this year they had reported[4] that prolonged incubation of the substrate with a HeLa cell extract in the presence of ATP and Mg^{2+} gave rise to four major products (now identified as structures II to V in Fig. 1), three of which accumulated, while one (II) appeared transiently with the kinetics expected of an intermediate. The sequences of these products were investigated by fingerprint analyses and hybridization experiments. III was one of the expected splice products, with L1 joined to L2 and followed by the second intron; V resembled III but lacked most or all of the second intron (it is believed to be a degradation product of III).

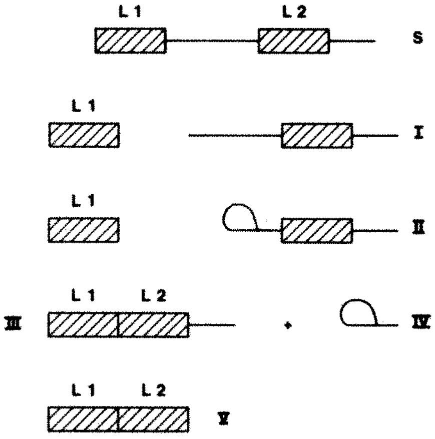

Fig. 1 Structures of the products (I–V) of cell-free splicing of a substrate (S) RNA composed of two exons (L1 and L2) and two introns. IV is the excised intron in lariat form.

As judged by its oligonucleotide map, IV corresponded to the intron, but it showed two unexpected features. First, it had an abnormally low electrophoretic mobility for its molecular weight and when subjected to limited RNase T$_1$ digestion gave rise to a discrete product with a lower mobility. Second, its complete digestion by RNase T$_1$ gave rise to a modified oligonucleotide not present in the precursor RNA. The putative intermediate II contained the sequences of the first intron, the second exon and the second intron; it too showed an abnormal mobility and was digested by RNase T$_1$ to the same modified oligonucleotide as IV. The modified oligonucleotide resisted complete digestion by nuclease P$_1$, suggesting to Grabowski *et al.* that it might contain a branchpoint of the kind previously found in total polyadenylated nuclear RNA by Wallace and Edmonds[8], who, interestingly, suggested that the branched RNA species could be splicing intermediates. To explain its properties, Grabowski *et al.* suggested that IV contained a circular moiety.

The new papers by Padgett *et al.*[2] and Ruskin *et al.*[3] show beyond reasonable doubt that product IV and putative intermediate II have the lariat-like structures indicated in Fig. 1. The additional evidence offered by Padgett *et al.* for the structures of IV and II is as follows: the intron-derived product IV has a free non-phosphorylated 3′ terminus; complete digestion of the modified oligonucleotide with RNase T$_2$ gives rise to a nuclease-resistant oligonucleotide, namely 2′, 3′-ADP linked to two nucleotides (presumed to be 3′-UMP and 3′-GMP) by 3′–5′ and 2′–5′ phosphodiester bonds respectively, as shown in Fig. 2; and in both II and IV, the 5′-terminal region of the intron is linked to the modified oligonucleotide, which contains the sequence running from nucleotides 19 to 32 upstream of the 3′ splice site.

Ruskin *et al.*, employing a technically distinct approach, used as their substrate a truncated β-globin RNA, prepared by the SP6 RNA polymerase system[9] and consisting of the first exon, the small intron and part of the second exon, to which was added a 5′ cap using vaccinia virus guanylyltransferase. With an extract of cell nuclei as the source of splicing activity, the species corresponding to I (mentioned in passing by Sharp and his colleagues) and II were produced during the early stages of the reaction, while those corresponding to III and IV accumulated later. Ruskin *et al.* characterized the lariat-like structures on the following basis: first, reverse transcriptase elongation of a primer complementary to a segment of the second exon was blocked about 37 nucleotides

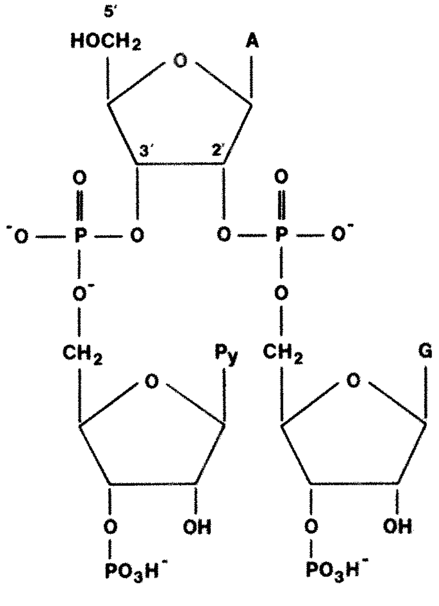

Fig.2 Digestion product of the modified oligonucleotide formed at the attachment site of the lariat-like structure of an excised intron.

upstream of the 3′ splice site, while a primer complementary to a segment of the first intron upstream of the block was elongated to the 5′ end of the intron; second, when (and only when) an oligodeoxyribonucleotide complementary to the intron was hybridized to the globin counterpart of IV, RNase H treatment led to a strong shift in electrophoretic mobility but did not give rise to a second RNA fragment, showing that cleavage must have occurred within a circular entity (an analogous result was obtained for intermediate II); third, a nuclease-resistant branched oligonucleotide with the structure shown in Fig. 2 (where Py = cytosine) was characterized, and the branchpoint located at the thirty-seventh nucleotide upstream of the 3′ splice site.

What does all this mean? It is quite likely that products I and II represent intermediates on the way to the final product. The suggestion is that splicing involves cleavage at the 5′ splice site of the intron, yielding a 5′-phosphorylated guanosine residue at the 5′ terminus of the intron which then becomes joined to the 2′ hydroxyl group of the branch acceptor nucleotide (an adenosine residue) within the intron. The reaction may be concerted in the sense that the attack of the branch acceptor site on the 5′ terminus of the intron cleaves off the first exon while forming the lariat. In the next step, the cleaved 3′ end of the first exon, which is presumed to remain bound to a putative splicing complex, attacks the phosphate between the last (3′) nucleotide of the first intron and the first (5′) nucleotide of the second exon, releasing the intron as a lariat while joining the two exons.

Several questions are raised by the new findings. Are there further intermediates? As an incubation of 15 min in the presence of ATP is required before intermediates I and II are first detected, it is likely that some essential, as yet uncharacterized, event must occur before the cleavage at the 5′ splice site. This could, for example, be either the formation of a nucleoprotein particle in which the precursor RNA would asume the conformation necessary for splicing, or an ATP-dependent activation of the branchpoint acceptor.

Is the branch acceptor nucleotide (usually an adenosine residue[8]) embedded in a highly specific sequence? This is unlikely in the case of eukaryotic introns, because, as shown by Wieringa *et al.*[10], deletions or substitutions that remove all but 15 nucleotides adjoining the 3′ splice site of the large β-globin intron do not impair splicing. In the case of the intron in yeast nuclear genes, however, an internal sequence (TACTAAC) is essential for splicing[11] and Pikielny *et al.*[12] have in fact mapped what may be a reverse transcription stop in this region. Ruskin *et al.* note that all β-globin introns contain a 'consensus sequence', of which the TACTAAC sequence is a subset, located in the region between 19 and 37 nucleotides upstream of the 3′ splice site. The consensus sequence is: Py-X-Py-T-Pu-A-Py (the underlined A represents the branchpoint in β-globin). The sequence in which the branchpoint identified by Padgett *et al.* for adenovirus is embedded conforms to this consensus sequence except that the fifth residue is a pyrimidine (Py) rather than a purine (Pu).

Since at least some of the intron deletions examined by Wieringa *et al.* do not contain a reasonable facsimile of the consensus sequence but are nonetheless efficiently spliced, it would seem that even if branch formation preferentially occurs within the consensus sequence, it may occur elsewhere if a consensus sequence is lacking; moreover, it remains to be proved that branch formation is essential for splicing.

Why does the 5′ end of the intron become joined to an internal nucleotide? It is striking that the introns of *Tetrahymena* ribosomal RNA and of yeast mitochondrial precursor mRNAs are released in circular form. Perhaps, as Ruskin *et al.* suggest, the initial cleavage may be reversible, and branch or circle formation are required to sequester the 5′ intron definitively, allowing the next reaction step to occur. Thus, although splicing in higher eukaryotes differs in many important respects from that in lower eukaryotes, they may have some mechanistic principles in common. ☐

1. Gabrowski, P.J. *et al. Cell* **37**, 415 (1984).
2. Padgett, R.A. *et al. Science* **225**, 898 (1984).
3. Ruskin, B. *et al. Cell* **38**, 317 (1984).
4. Padgett, R.A. *et al. Cell* **35**, 101 (1983).
5. Hernandez, N. & Keller, W. *Cell* **35**, 89 (1983).
6. Krainer, A.R. *et al. Cell* **36**, 993 (1984).
7. Manley, J.L. *et al. Meth. Enzym.* **101**, 568 (1983).
8. Wallace, J.C. & Edmonds, M. *Proc. natn. Acad. Sci. U.S.A.* **80**, 950 (1983).
9. Green, M.R. *et al. Cell* **32**, 681 (1983).
10. Wieringa, B. *et al. Cell* **37**, 915 (1984).
11. Langford, C.J. *et al. Cell* **36**, 645 (1984).
12. Pikielny, C.W. *et al. Cell* **34**, 395 (1983).

Charles Weissmann is at the Institute für Molekularbiologie I, Universität Zürich, 8093 Zürich, Switzerland.

Cystic fibrosis

In search of the gene

from Veronica van Heyningen

SADLY, the future of the 10th International Cystic Fibrosis Congress seems assured. The enigma of the primary gene defect in cystic fibrosis — the most common genetic disease in Caucasian populations (1 in 2,000 births) — has not yielded to the wide-ranging biochemical, physiological and molecular genetic approaches described at the 9th Congress*.

Cystic fibrosis is a disease of the exocrine glands which is inherited in an autosomal recessive fashion. It is characterized by the production of abnormally thick mucus in many organs, resulting typically in chronic obstructive lung disease; by pancreatic insufficiency often leading to malabsorption; and by abnormally high levels of sodium and chloride in sweat. This last feature is the basis for definitive diagnosis.

Despite the steadily improving prospects for afflicted individuals, the social implications of the disease are still serious, as was reflected in a study of parental attitudes in Californian cystic fibrosis families (M. Kaback *et al.*, University of California, Los Angeles). In 65 per cent of the 183 families studied, the affected child was the last born to the couple and more than a quarter of the couples resorted to surgical sterilization to avoid the possibility of having further offspring with the disease. Reliable prenatal diagnosis would clearly be welcome to such families.

Brock (*Lancet* **ii**, 941; 1983) and colleagues have found reduced levels of intestinal microvillar enzymes in amniotic fluid if an affected fetus is being carried in a pregnancy 'at risk' (previous cystic fibrosis child born to the parents). The reduced levels are thought to be secondary to the impaired passage of meconium in the cystic fibrosis fetus. Following the failure of an earlier prospective trial for reduced amniotic fluid protease activity (Nadler, H.L. & Walsh, M.M.J. *Pediatrics* **66**, 690; 1980) great caution is being exercised in confirming and extending these findings. Nonetheless, groups in Rotterdam (W.J. Kleijer *et al.*, Erasmus University), Paris

---

*9th International Cystic Fibrosis Congress, Brighton, 9-15 June 1984. The proceedings will be published this year (*Cystic Fibrosis: Horizons*; ed. Lawson, D., Wiley, Chichester; 1984).

(A. Boué *et al.*, Inserm U73) and Glasgow (D.A. Aitken *et al.*, University of Glasgow) are successfully applying microvillar enzyme estimations prospectively. Validation of this approach to prenatal diagnosis would be speeded up if definitive diagnosis of cystic fibrosis were possible in the fetuses declared abnormal and aborted on parental request. Confirmation of normal outcome in pregnancies carried to term is also difficult because there is considerable variability in severity and age of onset of overt disease, although neonatal sweat testing and immune-reactive trypsin measurement of newborns may help.

While there is every indication that prenatal diagnosis of this kind will help prevent the birth of a second affected child in families at risk, the assays are based on what is almost certainly a secondary phenomenon and the race to identify the basic gene defect is still on. Considerable excitement has been generated by recent work on isolated sweat glands (Quinton, P.M. *Nature* **301**, 421; 1983) and on nasal epithelium (M.R. Knowles, R.C. Boucher *et al.*, University of North Carolina). In both cases, there appears to be a defect in ion transport in affected individuals. Thus, raised potential differences across the apical membrane of epithelial cells suggest reduced chloride permeability, and this is accompanied by reduced responsiveness to β-adrenergic stimulus by isoproterenol. The possibility that the abnormal β-adrenergic responsiveness and secretion in cystic fibrosis results from a defective calcium-dependent regulatory protein was suggested by several workers, for a variety of tissues (R.M. Case, University of Manchester; G. Cabrini *et al.*, Centro Fibrosi Cistica, Verona; M. McPherson *et al.*, University of Cardiff). One of the few groups to study heterozygote as well as homozygote red cells observes a calcium transport defect in both (C.A. Seymour and J.A. Davis, University of Cambridge).

As long as the basic gene defect remains unidentified, the choice of tissue for study will be arbitrary and often made on the basis of availability. The ability to culture sweat gland epithelia (P.S. Pedersen, Rigshospitale, Copenhagen) may prove a useful stimulus in this field. Meanwhile, considerable effort is being made to set up reliable heterozygote detection using serum samples (Manson, J.C. & Brock, D.J.H. *Lancet* **i**, 330; 1980) as this would help in the search for the defective metabolic pathway and ultimately the primary mutant gene locus (A. Jamieson *et al.*, University of Glasgow; V. van Heyningen *et al.*, MRC Clinical and Population Cytogenetics Unit, Edinburgh; O. Guy-Crotte *et al.*, Inserm U31, Marseille). Various teams (R. Williamson *et al.*, St Mary's Hospital Medical School, London; K.W. Klinger, Case Western Reserve University, Cleveland; Lap-Chee Tsui *et al.*, Hospital for Sick Children, Toronto; and R.H. Schwartz *et al.*, University of Rochester) are setting up DNA banks or permanent cell lines from cystic fibrosis families with two or more affected children.

The only available method of searching for the cystic fibrosis gene is linkage analysis by exclusion mapping using polymorphic DNA probes that have been mapped to a known chromosome region. In this way, using samples only from affected individuals and obligate heterozygotes, a number of chromosome regions have been found not to be linked to cystic fibrosis. Just before the congress took place, there was excitement about the possibility of assigning the cystic fibrosis gene to the tip of the long arm of chromosome 13 on the basis of an informative family with a segregating translocation (Edwards J.H., Jonasson J.A. & Black N.L. *Lancet* **i**, 1020; 1984), but this now seems unlikely. Nonetheless, an air of optimism pervaded the conference because the introduction of new methods such as electrophysiology and gene cloning brings some promise of breakthrough. □

Veronica van Heyningen is in the MRC Clinical and Population Cytogenetics Unit, Crewe Road, Edinburgh EH4 2XU.

Cellulose synthesis

Another brick in the wall

from Keith Roberts

IT is estimated that almost 2 × 10^{12} tonnes of carbon are wrapped up in organic molecules on the landmasses of this planet. The most abundant of these molecules, accounting for just over one-third of the dry weight of plants, is cellulose. Indeed, there is so much of it that cellulose forms the major buffer for the levels of carbon dioxide in the atmosphere. For a macromolecule of such abundance and economic importance (wood, paper, cotton), it is really rather astonishing that we still do not know in detail how it is made (Colvin, J.R. in *The Biochemistry of Plants*, ed. Preiss, J., 543, Academic, New York; 1980). What is clear is that higher plants have a remarkably complex and delicate machinery for synthesizing the basic building blocks of cellulose, the glucan chains, and for ordering their crystallization and orientation in the cell wall. The difficulty in trying to dissect the complexity of this machinery has been in obtaining an *in vitro* system that will make identifiable cellulose (Delmer, D.P. *Adv. Carbohyd. Chem. Biochem.* **41**, 105; 1983). Until now, despite many false alarms in the literature, no one has managed to do this. However, a report in this issue of *Nature* at last holds out some promise by describing the production of cellulose *in vitro* using a membrane preparation from a higher plant.

Cellulose is a (1→4)-β-D-glucan, consisting of many long parallel polysaccharide chains held together by inter- and intramolecular hydrogen bonds to form microfibrils, typically 10–40 nm in diameter. The microfibrils are extremely insoluble and form the high-tensile-strength skeletal framework of the plant cell wall (see the figure). The consensus of opinion is that the enzyme or enzyme complex that produces cellulose is an integral protein(s) of the plasma membrane. Most efforts to achieve cellulose synthesis *in vitro* have therefore started with isolated membrane preparations, usually either from rapidly elongating tissue such as the hypocotyl, or from cells laying down large amounts of cellulose, such as those that make cotton fibres.

Why has none of the previous attempts to mimic *in vivo* cellulose synthesis with *in vitro* membrane preparations been completely successful? The answer, at least in part, lies in the complexity of the process itself and in the structural constraints on the system which have to be preserved *in vitro*. Initially, even the precursors that the plant uses to make cellulose were the subject of dispute, with opinion slowly shifting from GDP-glucose to UDP-glucose. Intact cells take up and use exogenous UDP-glucose very poorly, the cellulose synthase complex accepting UDP-glucose only on its cytoplasmic face. Somewhow UDP-glucose has to gain access to the inner face of the membrane and, in general, cell breakage leads to inactivation of the synthetic complex. There has also been disagreement about the role, if any, of various intermediates. Both lipid-linked intermediates and glycopro-

The complex texture of cellulose microfibrils *in vivo* is revealed in this metal-shadowed specimen of an extracted primary cell wall. The specimen comes from a root hair cell of an onion. (Micrograph by B. Wells.)

tein intermediates have been invoked at various times, but neither has been conclusively shown to be involved. Uncertainty also prevails over the requirements for Ca^{2+} and Mg^{2+}, GTP and various other soluble cofactors. The biggest stumbling block and the greatest puzzle have been that *in vitro* systems used so far have invariably been able to incorporate glucose into high-molecular-weight material, but the product always seems predominantly to be $(1\rightarrow3)$-β-D-glucan (callose) and not $(1\rightarrow4)$-β-D-glucan (cellulose). The reasons for this are unclear but it was suggested at two recent meetings* that cell damage or wounding stimulates callose production at the expense of cellulose, possibly because of altered Ca^{2+} access to each side of the membrane. It was even suggested by D. Delmer (ARCO, California) at the Fribourg meeting, and by D.H. Northcote (University of Cambridge) at the Glasgow meeting, that the same enzyme complex, regulated by Ca^{2+}, may be involved in the synthesis of both polymers.

Clearly, the complexity of the synthetic system is great and a model system is required. In this case, as in so many branches of cell biology, the model system is a bacterium, *Acetobacter xylinum*, which produces a cellulosic pellicle in liquid culture. Two years ago, a collaboration between D. Delmer and M. Benziman's group in Israel resulted in high rates of *in vitro* synthesis of cellulose using a stabilized membrane fraction from this bacterium (Aloni Y. *et al. Proc. natn. Acad. Sci. U.S.A.* **79**, 6448; 1982). Success appeared to depend crucially on the presence of polyethylene glycol 4000 (PEG) which stabilizes sealed membrane vesicles and aggregates proteins.

Now, in another attempt with higher plants, T. Callaghan, working with Benziman, has elegantly applied the same basic methodology to membrane fractions from mung bean hypocotyls, apparently with remarkable success (see page 165 of this issue). Using a PEG-stabilized preparation, they are able to achieve rates of cellulose synthesis that approach those found *in vivo*. Notably, no detectable $(1\rightarrow3)$-β-D-glucan is formed, Ca^{2+} and Mg^{2+} are both essential, no intermediates are formed and cellobiose and another low-molecular-weight soluble factor increase the rate of synthesis. Although the crucial final X-ray demonstration of authentic cellulose has not been done, the notoriously difficult chemical characterization of the product appears convincing.

At present it is hard to identify the reasons for this success where previous attempts had failed. One reason put forward is that because the system is very complex, it makes sense to tamper with it as little as possible; thus high-speed spins and any attempt to 'clean up' the membrane fraction have been avoided. This, together with the use of stabilizing PEG and the correct choice of cofactors, may have tipped the scales in Callaghan's and Benziman's favour. It will be interesting to see whether the new methodology is repeatable and whether it can be used with other plant material.

If it does prove to be a viable system for the *in vitro* synthesis of cellulose and not, for example, a way simply of making the glucan backbone of hemicellulose molecules, the door is opened for exploring a whole range of extremely important issues in higher-plant cell biology. As well as being able to investigate the factors that control the width and length of cellulose microfibrils, the separation or otherwise of the synthesis and crystallization processes and the true relationship between callose and cellulose synthesis, it should also be possible to attack one particularly thorny critical problem. For many years it has been suggested that particular plasma membrane complexes seen in the electron microscope correspond to cellulose synthase assemblies (Giddings, T.H. *et al. J Cell Biol.* **84**, 327; 1980). An extension of this idea, which still has no strong experimental backing, is that the complexes move through the plane of the membrane, spinning out microfibrils into the extracellular matrix as they go. Elements of the plant cytoskeleton, the cortical microtubule array, are thought to define membrane channels in which the complexes are free to move, and may therefore control the orientation of cell-wall microfibril deposition. As wall texture is fundamental to organized cell expansion, this phenomenon is at the heart of many fundamental problems of plant cell growth and differentiation. It looks as though at least one possible avenue for attacking them has been opened up. □

Keith Roberts is Head of the Department of Cell Biology, John Innes Institute, Colney Lane, Norwich NR4 7UH.

---

*'Third cell wall meeting', 26–29 March, Fribourg, Switzerland, and SEB Seminar Series symposium 'Plant cell walls', 10–11 July, Glasgow.

Sex chromosome evolution

Sharing outside of pairing

from R.P. Erickson and P.N. Goodfellow

THE human X and Y chromosomes are very different in appearance and genetic content and yet are believed to be derived from an ancestral pair of chromosomes differing only at a single sex-determining locus. Several models for the evolution of mammalian sex chromosomes have been proposed to explain sex chromosomal differentiation but experimental evidence to decide between the models has been lacking. Analysis of cloned DNA sequences from the human sex chromosomes, particularly the Y chromosome, should eventually solve the problem of how the X and Y chromosome have evolved and should provide clues to the mechanism of sex determination. This approach has been used by two groups who report their results in *Nature* this week and next.

Genes determining testicular and ovarian development predate fixed chromosomal sex determination in evolution. One can imagine that two nonhomologous chromosomes separately accumulated genes for sexual differentiation, genes for male development on an ancestral Y and genes for female development on a nonhomologous ancestral X. However, evolution of sex chromosomes from a homologous pair appears frequently in vertebrate evolution and is the usually accepted mechanism.

Given a pair of homologues, one with male-determining genes, two theories have been proposed to explain the evolution of sex chromosome differentiation. The classic model of sex chromosome evolution from homologues places cross-over suppression between the ancestral pair as the primary event with a slow accumulation of differences by mutation[1]. Later, X-chromosome inactivation occurs to maintain the gene dosage for genes now found only on the X chromosome. An alternative theory puts chromosomal inactivation of the non-sex-determining portion of the sex chromosomes first[2], solving the male/female sex-chromosomal dosage problem at the start. The selective force hypothesized in the classic model is the need to keep a block of sex differentiation genes intact. The selective force in the alternative model is the still obscure advantage of chromosomal sex determination. Both models assume continued crossing-over between homologous Xs and, thus, explain the observation that while the X chromosome has retained many structural genes apparently unconnected with the process of sexual differentiation, the much smaller Y chromosome seems to have lost all but a small number of genes directly concerned with sex determination and male gametogenesis.

There are two major limitations on sex chromosome differentiation. First, sex chromosome pairing must occur at meiosis for normal chromosomal disjunction. Chromosomal pairing is thought to depend on sequence similarity and this implies that the X and Y chromosomes should show sequence homology in the X–Y pairing region. Light microscopic studies of human meiosis have shown that the pairing region includes the terminal third of the X-chromosome short arm and most of the Y-chromosome short arm[3]. Second, the sex-determining region must not be disrupted by recombination with the X chromosome. The consequences of transfer of sex-determining genes from the Y to the X chromosome can be seen in the generation of sterile XX males by the transfer of the *Sxr* fragment in the mouse[4,5]. A similar event has been demonstrated in some XX human males who have inherited Y-derived sequences[6]. Correlation of clinical and cytogenetic findings in patients with rearranged Y chromosomes has localized the sex-determining region to around the centromere of the Y chromosome, well outside the pairing region[7]. Thus, it would be predicted that homologous sequences shared by the X and Y chromosomes would be restricted to the X–Y pairing region. This prediction is compatible with the localizations of the only expressed gene known to be homologous between the X and Y chromosomes[8]. Studies with cloned sequences derived from the Y chromosome, however, have found considerable sequence homology between the X and Y chromosomes outside the pairing region.

Early studies of human Y-chromosomal DNA emphasized the large amount of relatively Y-specific repeat elements (reviewed in ref. 9). The cloning of Y-chromosomal DNA in cosmid vectors, however, has led to the isolation of unique-sequence sub-clones[10-13], many, but not all, of which also hybridize to the X chromosome. Furthermore, several clones from X-chromosome libraries have been found to hybridize with the Y[13,14]. Many of the X and Y shared sequences have been mapped to the short arm of the Y and the long arm of the X[11-15]: the homology does not fit the pairing seen at meiosis. The simple prediction is also not supported by the two new studies reported in *Nature*. One of the first sequences shown to be shared by the X and Y chromosomes was isolated as a random fragment from a total human genomic library[16]. On page 119 of this issue, Page *et al.* show that the homology region extends for at least 36 kilobases (kb) and maps to the short arm of the Y chromosome and the long arm of the X chromosome (Xq13–Xq21), well outside the X–Y pairing region[17]. Careful restriction mapping suggests that the X and Y sequences are at least 98 per cent homologous. An even greater degree of homology has been found by Cooke and Rappold (next week's *Nature*) for a sequence first isolated from a genomic library made from flow-sorted Y chromosomes[18]. Direct sequencing of the X- and Y-derived clones shows no differences in over 1 kb. This DNA segment too maps to the long arm of the X chromosome, but it maps to the heterochromatic region of the Y chromosome, well outside the pairing region.

Page *et al.* have gone on to study the origin of their homologous sequence by investigating DNA from male and female primates[17]. They find that in chimpanzees, gorilla and orang-utan, the sequence is found only on the X chromosome. Genomic mobility may be a feature of many Y-chromosome sequences and has been documented previously both for the Y-specific repeats and unique sequences. The 3.4-kb repeat, which may constitute as much as 40 per cent of the human Y chromosome, may have an autosomal origin[9]. In this case, transfer of a few repeats followed by rapid expansion mediated by unequal crossing-over or gene duplication (or both) could be envisaged. For other sequences found on the X, Y and autosomes, such as actin[19] and arginsuccinase[20] pseudogenes, a mRNA origin is likely. It is not clear that such mechanisms can explain the transfer of the 36 kb segment described by Page *et al.*, nor the other X–Y homologous sequences reported to map outside the pairing region. At least one of these other sequences also spans greater than 20 kb (ref. 13). The high degree of sequence conservation suggests that the X–Y exchange must have occurred relatively recently, perhaps as the result of double recombination events facilitated by normal X–Y pairing or as a function of an ancient pre-existing homology. It is also possible that a new mechanism analogous to gene conversion but occurring on a larger scale may be operating. ☐

P.N. Goodfellow is at the Imperial Cancer Research Fund, Lincoln's Inn Fields, London WC2A 3PX. R.P. Erickson is currently of the same address; his permanent address is the Departments of Human Genetics and Pediatrics, University of Michigan School of Medicine, Ann Arbor, Michigan 48108.

1. Muller, H.J. *Genetics* **3**, 422 (1918).
2. Jones, K.W. *Chromosomes Today* (in the press).
3. Pearson, P.L. & Bobrow, M. *Nature* **226**, 959 (1970).
4. Singh, L. & Jones, K.W. *Cell* **28**, 205 (1982).
5. Shapiro, M. *et al. J. Reprod. Immun.* **4**, 191 (1982).
6. Guellaen, G. *et al. Nature* **307**, 172 (1984).
7. Davies, R.M. *J. med. Genet.* **18**, 161 (1981).
8. Goodfellow, P.N. *et al. Nature* **302**, 346 (1983).
9. Cooke, H.J., Fantes, J. & Green, D. *Differentiation* **23** (Suppl.), 5548 (1983).
10. Bishop, C.E. *et al. Nature* **303**, 831 (1983).
11. Bishop, C. *et al. J. molec. Biol.* **173**, 403 (1984).
12. Wolfe, J. *et al. Ann. hum. Genet.* **48**, 253 (1984).
13. Kunkel, L.M. *et al. Nucleic. Acids. Res.* **11**, 7961 (1983).
14. Koenig, M. *et al. Nucleic Acids. Res.* **12**, 4097 (1984).
15. Page, D., Wyman, A. & Botstein, D. in *Recombinant DNA Applications to Human Disease* (eds Caskey, C.T. & White, R.) (Cold Spring Harbor Laboratory, New York, 1983).
16. Page, D. *et al. Proc. natn. Acad. Sci. U.S.A.* **79**, 5352 (1982).
17. Page, D.C., Harper, M.E., Love, J. & Botstein, D. *Nature* **311**, 119 (1984).
18. Cooke, H.J. & Rappold, G.A. *Nature* **311** (in the press).
19. Heilig, R. *et al. EMBO J.* **3**, 1083 (1984).
20. Daiger, S.P. *et al. Nature* **298**, 682 (1982).

Embryonic development

Cell communication in early embryos

from Jonathan Slack

'LOW-RESISTANCE' junctions between cells in embryos and many adult tissues were discovered in the 1960s by their ability to pass electric current[1]. Later it became clear that they were the same as the 'gap junctions' seen under the electron microscope as open channels connecting adjacent cells, and that they were capable of passing most substances of molecular weight less than about 1,000 (ref. 2). A popular view has been that gap junctions transmit the inductive signals that control regional specification in the early embryo. But although the junctions have been mapped in embryos of various types[3-6], functional evidence for this interpretation has so far been lacking because there has been no method of blocking the junctions *in vivo* without unacceptable side effects. Now, in this week's *Nature*, Warner, Guthrie and Gilula describe a means of doing just this by injection of antibody against gap junction protein into early *Xenopus* embryos[7]. The authors are very cautious in their interpretation; nonetheless, the experiments provide the first direct evidence that gap junctions indeed have a role in early embryonic development.

Before these experiments could be done, it was necessary to know the normal disposition of junctions in the *Xenopus* embryo. Previous electrophysiological studies had shown that cells of the early embryo were coupled[3], but the work was done without reference to the positions of the cells studied. In the paper by Guthrie in this week's *Nature*[8], each of the blastomeres in the animal hemisphere of the 32-cell stage has been injected with the fluorescent dye Lucifer Yellow and it is shown that dye transfer is much more frequent between the cells on the dorsal side than between those on the ventral side.

Warner *et al.* therefore selected a dorsal blastomere of the 8-cell stage for injection of antibody to gap junction protein, and then studied dye-coupling at the 32-cell stage between the progeny of the injected cell[7]. They find that the frequency of dye-coupling is substantially less than in untreated embryos and in most cases cells which fail to transfer dye are also uncoupled electrically. By contrast, injection with preimmune serum or an unrelated antibody is without effect.

At later developmental stages the injected embryos show substantial morphological defects in the region derived from the injected blastomere: the brain and eyes being absent or reduced. These defects do not arise from cell death, which would be very obvious in an embryo type which develops without increase in size. Rather, they appear to be due to a failure of neural induction since in normal development the neural tube is induced from dorsal ectoderm by the action of the underlying mesoderm. This might be because the tissue movements during gastrulation have been disturbed so that the disposition of ectoderm and mesoderm is abnormal; alternatively, it might be the result of a direct blockage of the transmission of the inducing signal. It should be possible to distinguish between these possibilities by co-injecting a lineage label[9] with the antibody to enable movements of the affected cells to be followed.

A direct role for gap junctions as channels for the neural inducing signal is perhaps unlikely in view of the fact that at least the early steps of neural induction can occur in the absence of any cell contact[10], implying that the active substances can diffuse across extracellular spaces. Nonetheless, neural induction shows considerable regional specificity, particular regions of the archenteron roof inducing corresponding regions of the nervous system[11], so the whole process is probably more complex than the transmission of a single substance. Clearly, gap junctions are involved in some way but more work is needed on the unfashionable problem of the biochemistry of inducing factors before we can make a final assessment. ☐

1. Furshpan, E.J. & Potter, D.D. *Curr. Top. dev. Biol.* **3**, 95 (1968).
2. Feldman, J., Gilula, N.B. & Pitts, J.D. *Intercellular Junctions and Synapses* (Chapman & Hall, London, 1978).
3. Slack, C. & Palmer, J.F. *Expl Cell Res.* **55**, 416 (1969).
4. Lo, C.W. & Gilula, N.B. *Cell* **18**, 411 (1979).
5. Warner, A.E. & Lawrence, P.A. *Cell* **28**, 243 (1982).
6. Weir, M.E. & Lo, C.W. *Devl Biol.* **102**, 130 (1984).
7. Warner, A.W., Guthrie, S.C. & Gilula, N.B. *Nature* **311**, 127 (1984).
8. Guthrie, S.C. *Nature* **311**, 149 (1984).
9. Slack, J.M.W. *Bioessays* **1**, 5 (1984).
10. Toivonen, S. *et al. Differentiation* **4**, 1 (1975).
11. Mangold, O. *Naturwissenschaften* **21**, 761 (1933).

Jonathan Slack is at the Imperial Cancer Research Fund Mill Hill Laboratories, Burtonhole Lane, London NW7 1AD.

Geology

Geological problems of north-east Africa

from Robert Bowen

EARTH satellites are helping to uncover valuable data about the sub-surface topography of arid regions such as the western Sahara and the Mojave deserts. So much was clear from an international meeting* on the geography of north-east Africa earlier this year, in advance of the launch on the US NASA shuttle later this year of the second shuttle imaging radar (SIR-B) designed by the Jet Propulsion Laboratory (Pasadena).

The first SIR experiment in 1982 led to the still remarkable reports of 'radar river' deposits, described by J. McCauley and C. Breed for themselves and G. Schaber (U S G S, Flagstaff, Arizona). They occur as buried channels in the Western Desert of Egypt, where broad valleys and younger inset channels have been identified using radar responses from surface and subsurface materials including caliche horizons in fluviatile sediments. Such features have promoted a new understanding of the regional role of running water in shaping the hyperarid core of the Sahara, before the onset of the periodic Quaternary aridity, and have made it possible to understand fluviatile environments including some containing 'Acheulian' artefacts of presumed late Pleistocene age, which have been located incidentally to stratigraphic investigations in backhoe trenches.

In an extension of the radar technology (R. Blom, JPL), igneous dykes beneath as much as 2 m of alluvium were detected in the Mojave Desert by the Seasat L-band (23.5 cm) synthetic aperture radar in 1978, when soil moisture probably fell below the 1 per cent critical microwave absorption level. Blom pointed out that the Mojave is a 'swamp' compared to the hyperarid eastern Sahara, and can be examined only when moisture content declines sufficiently. Other factors such as the roughness and the dihedral configuration of the dykes were significant because they helped in the generation of strong radar echoes. Clearly, conditions suitable for the detection of subsurface features may exist intermittently in places previously considered unsuitable, although the definitive interpretation of radar tracking image data may need subsequent field work.

There was some controversy at this meeting over Egyptian and Sudanese stratigraphy, a supracratonic arenaceous sequence extending through most of the Phanerozoic. Until recently, access has been difficult while the marginal interest of the petroleum companies has reduced further the number of geologists actively working in these countries. However, in the last couple of decades, progress has been made by attempts to clarify the so-called Nubian sandstone (B. Issawi, Egyptian Geological Survey; E. Klitzsch, Technical University of Berlin).

The disagreement derives from correlation of clastic beds, especially those of supposed Palaeozoic age. The stratigraphic position of fluvio-glacial deposits occurring both in Egypt and in Sudan, originally given as Ordovician by Klitzsch, has been traced laterally from Libya across to Saudi Arabia by U. Jux (University of Cologne). The situation is now unsatisfactory because Klitzsch (*J. Afr. Earth Sci.* **1**, no.1, 17; 1983) re-assigned the deposits to the Permo-Carboniferous ('karroo-type'), which implies an equivalence to the Dwyka glaciation of southern and south-central Africa and of course a totally new concept of Gondwana and its biotas. The pre-Carboniferous Palaeozoic column in southern Egypt is devoid of index fossils, so that the stratigraphy is to a large extent based on ichnofossils such as Cruziana and Bifungites, the identity and reliability of which were disputed.

Proper correlation is presently impossible in this vast terrain which was previously considered to embody a 'pancake'-type geology but, because of epeirogenic movements of the Uweinat-Aswan geanticlinal arch, is now known to have been marked by cyclic transgression and regression events involving deposition and erosion (D. Bhattacharryya, Washington University; B. Issawi). Klitzsch takes the view that there was a change in the fluviatile discharge direction in Egypt and Sudan, reversing an earlier north–south flow, but more data are needed to resolve this question.

Obtaining more detailed geological information is even more necessary in Sudan where, as R. Stern (University of Texas, Dallas) pointed out, sampling is hardly richer than on the Moon. He presented some interesting chronometric results supporting a model for the tectonic evolution of the Sudanese basement in the late Proterozoic.

Another very controversial subject is that of the aquifer systems of Libya and Egypt, where the occurrence of recharge and groundwater flow are in dispute. M.U. Ahmad (University of Ohio) presented a steady-state groundwater flow model for the southern Libyan basins which has been applied to test the existence of recharge through the past five thousand years. Ahmad believes this to have occurred, in which case the water problems of the region can be solved. The flow rate from Libya to Egypt is given as almost 4 million m^3 daily, a figure with which Issawi strongly disagrees.

The meeting ended with a lively discussion of the Libyan glass enigma. J. Underwood Jr (Kansas State University) and R. Giegengack (University of Pennsylvania) cited various unacceptable explanations and an unpublished paper by U. Jux which deals with the differing origins of Libyan astroblemes and the glass. Underwood, Giegengack and Jux agree on a terrestrial origin, and the only viable model appears to be that suggested by Jux in 1983 — a diagenetic silcrete-type mechanism of formation under early Neogene semiarid conditions resulting from reaction between superficial waters containing carbon dioxide and alkaline highly-siliceous subterranean and groundwaters. ☐

Robert Bowen is an ICCROM Expert and can be contacted at 21 Kings Gardens, Huntingdon, Camb. PE18 7LL.

---

*14-16 May, Whittier College, California.

Gravitational interactions of cosmic strings

21-1-87
A. [illegible]

C. J. Hogan
Theoretical Astrophysics 130-33, California Institute of Technology, Pasadena, California 91125, USA
M. J. Rees
Institute of Astronomy, Madingley Road, Cambridge CB3 0HA, UK
and Institute of Theoretical Physics, University of California, Santa Barbara, California 93106, USA

Breaking a Yang–Mills symmetry at very high energy could lead to macroscopic structures in the vacuum called 'strings', which may be the cause of galaxy formation and clustering. Dissipative gravitational interactions of string loops can produce unusual astrophysical side effects. Such scenarios generally predict a stochastic background of gravitational radiation which should be observable using the millisecond pulsar 1937+21. Gravitational radiation recoil accelerates loops, but dynamical friction on ordinary matter tends to slow them down so they may be able to accrete matter. Internal oscillations of loops produce a time-varying shear perturbation which may lead to an observable heating of stellar or gaseous systems in their immediate neighbourhood.

THE general acceptance of Yang–Mills theories of fundamental interactions, and the associated idea of their intrinsic symmetries being 'broken' by an asymmetric vacuum, have led physicists to endow the vacuum with an ever-increasing number of degrees of freedom and intrinsic structural properties. The vacuum, as now envisaged, can sustain long-lived and even macroscopic structures. A vacuum in three-dimensional space can have three types of topologically stable 'defects'—monopoles, strings, and domain walls, corresponding to zero-, one-, and two-dimensional surfaces in which the vacuum is 'trapped' in its high-energy symmetric state[1]. Astrophysical effects of magnetic monopoles have attracted much attention recently because of their possible revolutionary implications for a 'grand unified' Yang–Mills theory and for cosmological models[2]. The possibility of relic cosmic strings has also been studied, primarily with a view towards using them to produce the density fluctuations leading to galaxy and galaxy–cluster formation[3–5].

Here, we study various other astrophysical consequences of such string scenarios. One of the most serious observational constraints on strings (or conversely, their most promising distinctive observational signature) is the background of gravitational radiation they would produce[6], which is now detectable because of the precision of the millisecond pulsar. Within a few years, measurements will probably be sensitive enough to exclude any scenario which suggests that strings produce galaxy clustering using only their direct gravitational effects.

We also study some other unusual interrelated consequences of the string picture, including: (1) recoil reaction of gravitational radiation on oscillating loops; (2) damping of the translational energy of such loops by dynamical friction on ordinary matter; (3) accretion of ordinary matter bound to a loop and the motion of a loop within its potential well; and (4) the dissipative coupling of the internal energy of loops to ordinary matter. In some situations, loop oscillations can noticeably affect bound stellar or gaseous systems, although as far as the loops are concerned there are generally no comparable energy-loss mechanisms to the gravitational radiation.

Finally, we consider the possibility of using strings as 'seeds' in an alternative theory of galaxy formation, in which they are required only to produce some pregalactic energy sources instead of the whole of the observed clustering energy. This allows the use of much lighter strings and hence avoids, for the time being at least, the gravitational-wave constraint. The minimum value of the string mass expected to have significant astrophysical effects has some interest because string production is predicted in association with a Peccei–Quinn symmetry breaking, generally thought to occur at well below the grand unification scale ($\simeq 10^{12}$ GeV to close the Universe with axions)[7].

General properties of strings

Strings are topologically-stable structures which may appear in the vacuum as a result of domains formed during the breaking of a Yang–Mills symmetry, if the topology of the manifold of degenerate vacua in the broken phase is appropriate. They have a mass per unit length $\mu \equiv \varepsilon / G$, where $\varepsilon \simeq (\langle\varphi\rangle / m_p)^2$ is the dimensionless amplitude of their gravitational potential, m_p is the Planck mass, and the vacuum expectation value of the Higgs field is $\langle\varphi\rangle$. Because of their enormous tension ε / G the network of strings formed in the transition, which may be thought of as a superposition of random walks, strives to reduce its length by ironing out small scale wrinkles at close to the speed of light and allowing strings, when they cross, to intercommute or exchange partners. Strings are forbidden to have ends (at least in the simplest models) so they must either be in closed 'loops' or in infinite 'open' strings.

A closed loop whose radius matches the current horizon size t_i has a good chance of not intercommuting further with the rest of the network. The behaviour of isolated closed loops is still open to question. They tend to undergo oscillations in which the transverse inertia acts as a 'weight' and the restoring force is provided by longitudinal tension. What is not known is how frequently an initial loop configuration chosen 'at random' (from the network of self-avoiding random walks) will cross itself and bifurcate into smaller loops, and how frequently it will oscillate indefinitely as a stable object. If the latter case is not very unlikely, the network produces debris of stable oscillating loops smaller than the current horizon which are effectively decoupled from each other and from the rest of the network. These loops eventually decay by gravitational radiation at a time $t_{dec} \simeq \varepsilon^{-1} t_i$. At a time t loops which are larger than $R_{dec} \simeq \varepsilon t$ (the ones currently decaying), and which separated out at $\simeq t_i$ have a mean separation (in the long-lived case) of the order of $R_{sep}(t) \simeq (a(t)/a(t_i))t_i$, where a is the Friedmann scale factor. During the matter-dominated era (for $t > t_{eq}$), loops in each logarithmic interval of loop size $R_l \geqslant t_{eq}$ contribute a fraction $\sim\varepsilon$ of the mean cosmological density; for $R_l < t_{eq}$, the fraction increases as $R_l^{-1/2}$ (because of the change in the expansion law when these loops entered the horizon), down to R_{dec}, below which it falls off like R.

Although many properties of loops can be estimated only in an order-of-magnitude sense, it is sometimes useful to be reasonably definite in normalization of certain quantities.

(1) We assume that loops form when their radius is equal to H^{-1} (the current Hubble time), and that, on average, one half of such a loop appears in a typical spherical volume of radius cH^{-1}. This leads to an estimate of the mass–density perturbation

by the loops at horizon crossing $(\delta\rho/\rho)_{\mathrm{hc}} = 2\pi\varepsilon$.

(2) The value of ε required to produce galaxy clustering by gravitational interaction alone depends on the composition of the dark matter, because of the usual damping processes which can take place at high redshift. However, a useful estimate of a lower limit for ε can be obtained by assuming a matter-dominated universe of cold particles. Simple scaling derived from the linear-growth model for the perturbations $(\delta\rho/\rho)_{\mathrm{hc}}$ after they enter the horizon gives

$$(\delta\rho/\rho)_{\mathrm{hc}} = (r_0/ct_0)^2 \qquad (1)$$

where r_0 is the radius for which randomly sampled spherical volumes have unit variance in density at the present epoch, $\langle\delta\rho^2\rangle_{r=r_0} \equiv \langle\rho^2\rangle$. Estimates of the galaxy correlation function show that $r_0 \simeq 10\ \mathrm{Mpc}\ h_{100}^{-1}$ where $h_{100} = H_0/100\ \mathrm{km\ s^{-1}\ Mpc^{-1}}$ (for a more detailed discussion see ref. 9), so

$$2\pi\varepsilon \gtrsim 10^{-5} r_{10}^2 \qquad (2)$$

if strings are to produce galaxy clustering by gravity alone. (This estimate applies independently of the probability of loop formation because it only relies on linear growth after t_{hc}.) In what follows we use a fiducial value $\varepsilon_{-6} \equiv \varepsilon/10^{-6} \gtrsim 1$.

(3) Oscillating loops, in their gravitational interaction with normal matter, behave like a mass $M_1 \cong 2\pi\mu R_1$ spread out over the volume covered by the oscillations (in a sense to be described below). It is useful to associate loops with a virial velocity $v_{\mathrm{vir}} \simeq \varepsilon^{1/2}$, a virial time $t_{\mathrm{vir}} \simeq \varepsilon^{-1/2} R_1$ and a virial temperature $T_{\mathrm{vir}} \simeq \varepsilon m_{\mathrm{pr}}$ where m_{pr} is the proton mass. The circular orbital velocity of a particle around a circular loop at the loop radius is

$$v_{\mathrm{vir}} = \sqrt{2GM_1/R_1} \cong 1{,}000\,\varepsilon_{-6}^{1/2}\ \mathrm{km\ s^{-1}} \qquad (3)$$

(4) Turok[5] has found exact solutions for which the simple order-of-magnitude estimate for the gravitational-wave decay half-life, τ_{dec}, of loops is remarkably accurate:

$$\tau_{\mathrm{dec}} \simeq \varepsilon^{-1} R_1 \qquad (4)$$

to within a factor of two for various modes.

Since loops have a constant $GM/R \simeq \varepsilon$, smaller loops have a higher effective local density contrast $M_1/(\rho_{\mathrm{m}} R_1^3) \propto M_1^{-2}$ where ρ_{m} is the matter density. Loops whose mean density matches the background have a mass $\simeq \varepsilon^{3/2} M_{\mathrm{H}}$, where $M_{\mathrm{H}} = 4\pi\rho_{\mathrm{m}} t^3/3 = t/2G \simeq 10^{23} M_\odot h_{100}^{-1}\Omega$ is the current horizon mass Ω is the cosmic density parameter); loops which are currently decaying have a density contrast $\simeq \varepsilon^{-1}$, and are very much denser than background matter in their vicinity. Their mass is $M_{\mathrm{dec}} \sim 2\pi\varepsilon^2 M_{\mathrm{H}} \simeq 6\times10^{11}\varepsilon_{-6}^2 \Omega h_{100}^{-1} M_\odot$, their radius is $R_{\mathrm{dec}} \simeq 3h_{100}^{-1}\varepsilon_{-6}$ kpc, and their mean separation is $\simeq \varepsilon^{1/3} t \simeq 30 h_{100}^{-1}\varepsilon_{-6}^{1/3}$ Mpc (loops of this size are the most numerous). If these loops are present in the Universe today, the discussion below indicates that some, at least, should be found in clusters of galaxies, and we expect roughly one loop per rich cluster.

Gravitational wave background

Vilenkin[6] has sketched out the gravitational wave background expected in the loop scenario. Here we consider several regimes and compare the predictions with current limits from the millisecond pulsar.

Let us suppose that newly-formed loops fall with probability W into the set of infinite-non-self-intersecting trajectories[8]. A fraction W of horizon-sized loops form a long-lived stable population as described above, and all of their rest mass is released eventually as gravitational radiation at z_{dec}. Let the differential energy spectrum of gravitational waves of frequency ω be $\rho_{\mathrm{g}}(\omega)$; define a logarithmic spectrum Ω_{g} by

$$\rho_{\mathrm{g}}(\omega)\,\mathrm{d}\omega \equiv \Omega_{\mathrm{g}}(\omega)(d\omega/\omega)\rho_{\mathrm{c}} \qquad (5)$$

where ρ_{c} is the critical density. Gravitational waves redshift in exactly the same way as electromagnetic ones, so loops which formed and decayed during the radiation-dominated era produce a background with

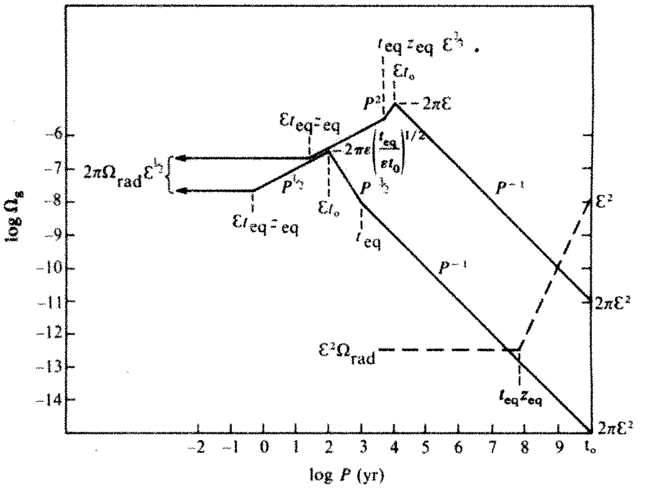

Fig. 1 Spectrum of stochastic gravitational radiation background produced by population of oscillating loops. Logarithmic energy density is plotted against period for two cases, $\varepsilon = 10^{-8}$ and 10^{-6}. Inflection points between different power-laws correspond to waves emitted by loops which decayed or entered the horizon at t_{eq}, and loops which are now decaying. The upper curve corresponds to the case of strings important for galaxy clustering, and can be tested against data at $P \sim 1$ yr. The dashed line represents the background produced by primordial tensor perturbations in the metric.

$$\Omega_{\mathrm{g}} \cong W\Omega_{\mathrm{rad}}\left(\frac{\delta\rho}{\rho}\right)_{\mathrm{hc}}\left(\frac{z_{\mathrm{i}}}{z_{\mathrm{dec}}}\right) \simeq 2\pi W\Omega_{\mathrm{rad}}\varepsilon^{1/2} \simeq 2\times10^{-7} W\varepsilon_{-6}^{1/2} h_{100}^{-2} \qquad (6)$$

where z_{i} is the redshift of loop formation, the z factor is the amount $\approx \varepsilon^{1/2}$ by which the radiation redshifted between z_{i} and z_{dec}, and we have used $\Omega_{\mathrm{rad}} \simeq 10^{-4.5} h_{100}^{-2}$ and $(\delta\rho/\rho)_{\mathrm{hc}} \simeq 2\pi\varepsilon$. This flat specimen extends down to waves emitted by loops which formed near the time of the phase transition itself, at temperature $\simeq \varepsilon^{1/2} m_{\mathrm{p}}$. This corresponds to a present-day period $P_{\min} \simeq 10^{-11.5} N^{-1/2}$ s (independent of ε), where N is the number of particle degrees of freedom. The shape of the spectrum at longer wavelengths depends on whether the loops currently decaying formed before or after t_{eq} (whether $t_{\mathrm{eq}} < \varepsilon t_0$ or $t_{\mathrm{eq}} > \varepsilon t_0$, the latter case being more likely); these spectra are summarized in Fig. 1, which includes the case considered by Vilenkin. The waves observable with the millisecond pulsar, with periods P of the order of 1 yr, were emitted at a redshift

$$z_{\mathrm{dec}} \simeq 2\times10^6 \varepsilon_{-6} P_{\mathrm{y}}^{-1} N^{-1/6} \qquad (7)$$

and originally had a period

$$t_{\mathrm{i}} \simeq P_{\mathrm{y}}^2 \varepsilon_{-6}^{-1} N^{1/3} \times 10\ \mathrm{s} \qquad (8)$$

Therefore, the waves in this scenario are relics of the early stages of the expansion, emitted by loops which formed shortly after nucleosynthesis.

Note, however, that the strings give a gravitational wave background very different from a primordial spectrum of curvature fluctuations (produced at the end of inflation[10], say); in this case, if scalar and tensor modes have comparable metric perturbations $|h_{\mu\nu}|$, the gravitational wave density $\Omega_{\mathrm{g}} \simeq h^2(P/t_0)^{-2}$ is of the order of $(\delta\rho/\rho)_{\mathrm{hc}}^2$. Another semi-classical source of perturbations might be the Starobinsky[11,12] effect, which produces gravitational waves (without scalar fluctuations) which enter the horizon with $\Omega_{\mathrm{g}} \simeq (\delta\rho/\rho)_{\mathrm{hc}}^2 \simeq (H_{\mathrm{inf}}/m_{\mathrm{p}})^2$, where H_{inf} is the Hubble constant during inflation. The spectrum from these effects is also plotted in Fig. 1. The short-wave cutoff in this case is $\simeq (H_{\mathrm{inf}}/m_{\mathrm{p}})^{-1/2} P_{\min}$. One can set constraints on H_{inf} using microwave anisotropy measurements (because in this case the waves are already present when the relevant scales enter the horizon), and the millisecond pulsar can only set more severe constraints if its Ω_g sensitivity goes below $\Omega_{rad}(\delta T/T)^2$ where $\delta T/T$ is the sensitivity of anisotropy measurements. In these scenarios, the microwave background isotropy is likely to remain a more sensitive constraint.

If W is sufficiently less than 1 there will also be a contribution from recently-formed loops. Let us consider a scenario in which an oscillating loop bifurcates frequently, leading to a 'cascade' of loop divisions to successively smaller scales. A loop of mass M will on average bifurcate $\simeq \log_2 W$ times until there are $\sim W^{-1}$ daughters and there is a good chance that one of its progeny, of total energy $\approx MW$, is oscillating in a mode where it is stable. Each successive division of the remaining progeny will leave behind some stable loops, which contain a total mass $\simeq MW$ in each logarithmic 'generation'. In general, each division converts some fraction $1-f$ of the loop length into translational motion of the succeeding generation, so that after n divisions loops are moving with relativistic γ-factors $\sim f^{-n}$. The stable loops radiate their rest mass into gravitational waves, as usual, but their radiation, even if emitted isotropically in their rest frame, is now beamed into a solid angle γ^{-2} and blueshifted (within the beam) in frequency by a factor γ. The resulting background has a spectrum

$$\Omega_g \simeq \min\left[\varepsilon^2 W(P/t_0)^{1/\log_2(f^2/2)}, \varepsilon W\right]$$

which at sufficiently high frequencies could, in principle, be larger than the 'primordial' contribution of equation (6). However, in general, this background is not stochastic; only a small fraction of observers lie within the beam of a radiating loop. In principle, Earth-based gravitational wave antennas might pick up occasional events from loop events of this type, coming from redshifts $\leqslant 10^6$, if W is moderately small. There is, however, only a small range of W in which these events could occur where one would not encounter a more serious constraint from the γ-ray background, as we now explain.

After $n \sim W^{-1}$ bifurcations, the entire rest mass of the original loop is locked up in non-self-intersecting loops. For $W \leqslant -\log(f/2)/\log(\langle\varphi\rangle t_0)$, most of the rest mass of the original loop remains when the daughter loops become so small that non-gravitational interactions become important at $R_l \simeq \langle\varphi\rangle^{-1}$, at which point the energy is presumably radiated in a complicated mixture of coherent vacuum phase waves and high-energy particles. Thus for very small W, the best constraint is likely to come from the γ-ray background produced by the smallest loops in the cascade. Particles with energy of the order of $\langle\varphi\rangle$ would be degraded in $\ll t_0$ down to $\sim 10^5$GeV by pair production on the non-thermal radio-wave background and microwave background; below this energy (corresponding to pairs produced just over the peak of the blackbody) the mean free path for this process exceeds a Hubble length, and pairs lose most of their energy by inverse Compton scattering on the microwave photons. The resulting γ-ray spectrum peaks at 10^5GeV with $\Omega_\gamma \simeq \varepsilon$ and falls off like $\Omega_\gamma \propto E_{pair} \propto E_\gamma^{1/2}$ at smaller energies. Observations of cosmic rays near the peak energy constrain ε to be $<\Omega_\gamma \leqslant 10^{-7}$.

Thus very small values of W are already ruled out if the string scenario is to work at all. Recent simulations also indicate that W is probably not smaller than about 10% (A. Albrecht and N. Turok, in preparation), so the gravitational wave background given by equation (6) is a fairly firm prediction of the string scenario. Apart from the uncertainty associated with W, the other major numerical uncertainty in estimating their backgrounds lies in the probability of loop formation. We have assumed above that 1/2 loop of radius ct forms, per spherical volume of radius ct, when the expansion rate is $H = t^{-1}$. The actual number could be smaller than this, but not by very much; this is another question which can be answered using numerical simulations.

Detection of gravitational waves

We base our discussion on detecting gravitational waves using the millisecond pulsar from earlier work[13–15]. Suppose we observe a clean pulsar for a time T, and, after allowing for known intrinsic period variations of the pulsar ($\dot{P}$ and $\ddot{P}$) and for standard ephemeris corrections, we find a mean-square timing residual $\langle R^2\rangle$ (that is, a mean square phase residual $\langle R^2\rangle (P/2\pi)^{-2}$, where P is the pulsar period). Such a residual can be produced by a stochastic background of gravitational waves; in fact the residual produced by waves with angular frequencies higher than α/T is[14]:

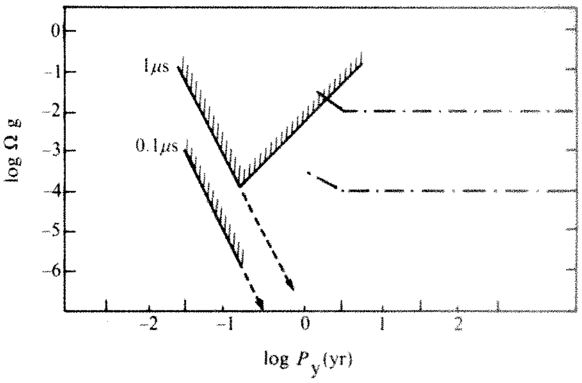

Fig. 2 Current and projected sensitivity of millisecond pulsar timing to gravitational wave background at different wavelengths. Curves are plotted for $\alpha = 2\pi$, $T_y = 1$, and $R = 1$ and 0.1 μs; dotted lines show expected improvement as data accumulation time T increases, for constant R. Improvement at shorter periods may also be expected by distinguishing various forms of noise in the timing residuals. Limits at larger periods arise from cubic residuals induced by long-wavelength waves. Also shown is the projected optimal sensitivity (dot-dash lines) of the binary pulsar if its orbital clock can be calibrated (the two estimates correspond to different signs for the clock residuals, which are limited by different effects[14,15].)

$$\langle R^2\rangle = \frac{32\pi}{3}\rho_c \int_{\alpha/T}^{\infty} d\omega \frac{\Omega_g(\omega)}{\omega^5}\left(1 - \frac{\sin \omega T}{\omega T}\right) \tag{9}$$

assuming isotropy and averaging over random phases and polarizations.

Using $H^2 = 8\pi G\rho_c/3$, and assuming $\Omega_g = \text{const}$ and $\alpha > 1$, this becomes

$$\Omega_g = \langle R^2\rangle T^{-4}\alpha^4 H^{-2} \tag{10}$$

(where all of the numerical coefficients have cancelled), or in units appropriate to the millisecond pulsar 1937+21 (refs 16, 17, and J. H. Taylor, personal communication)

$$\Omega_g = 10^{-7} h_{100}^{-2} \alpha^4 T_y^{-4} R_{\mu s}^2 \tag{11}$$

where T is measured in yr, and R in μs. Currently, pulse arrivals are only measured to an accuracy of $R_{\mu s} \sim 1$ because of time variations in the pulse spectrum induced by interstellar scintillation, which lead to imperfect removal of the effects of interstellar dispersion. However, instrumental improvements will probably reduce $R_{\mu s}$ to $\leqslant 0.1$.

Even the millisecond pulsar is not 'clean' in the above sense, because of residuals introduced by secular effects whose intrinsic parameters are unknown, such as the $\dot{P}$ of the pulsar, which must be fit to the data. One really needs to know the value of Ω_g which would be likely (at a given confidence level) to have produced residuals in excess of those which remain after one has subtracted a best-fit quadratic from the raw residuals. Thus, in using real pulsar data to set an upper limit on Ω_g, the 'safe' choice of α, and that of ref. 14, is $\alpha = 2\pi$ (wave period at cutoff = period of observation), because waves of this high a frequency could not accurately mimic a simple quadratic fit. This is perhaps the first instance in which a precise statistical analysis[23] of these limits is worthwhile, as the constraint on string models is such a sensitive function of α. Meanwhile, Fig. 2 presents an estimate of the current and projected sensitivity of the pulsar observations.

The prospects for achieving levels where string models will be seriously constrained are apparent from the above formulae, which yield

$$\varepsilon < 2.5 \times 10^{-7} (T_y/\alpha)^{-8} R_{\mu s}^4 \qquad (12)$$

In this formula, R is the residual after fitting for known secular effects, and may begin to increase with time due to some source of noise other than gravitational waves. However, if R does not increase too rapidly, even safe choices of α only require longer integrations (of the order of α yr) to reach the level where values of ε required to produce galaxy clustering gravitationally could be ruled out with a high level of confidence.

The predicted spectrum of gravitational radiation leads to residuals increasing quite rapidly with time—at least as fast as $R \propto t^2$, somewhat faster for $\varepsilon \leqslant 10^{-6}$. Variations in interstellar electron density lead to residuals which increase only as $R \propto t^{0.8}$, and in any event have a spectral signature which aids in their removal[18]. Imperfections in the terrestrial clock standards and Solar System ephemeris are an important source of error; they are currently at the level of ~0.3 μs over 1 yr) (D. C. Backer, personal communication). A confident detection of gravitational waves probably requires correlating residuals with other equally clean pulsars so the possibility of intrinsic pulsar variations, and the effects just mentioned, can be removed.

It is also possible that the generation of Earth-based gravitational-wave detectors (~5-km laser interferomers) could detect a stochastic background with $\Omega_g \simeq 10^{-7}$ at $P \sim 10^{-2}$–10^{-3} s. With $\Omega_g \simeq h^2(PH_0)^{-2}$, this requires a broad-band sensitivity to metric deformations $h \simeq 10^{-23}$–10^{-24}.

Dynamical friction

Loops are born with initial centre of mass velocities v_i close to the speed of light, because of the acceleration given by the last intercommute which formed them and subsequently slow time $v \propto a^{-1}$ due to the expansion. Loops also suffer dynamical friction on cold collisionless matter[19,20]. The dynamical friction rate is about

$$t_{df}^{-1} \simeq 2\pi^{3/2} G^2 \rho M \ln \Lambda / v^3 \qquad (13)$$

where v is the peculiar velocity of the loop and $\Lambda \cong v/R_l$ is the range of relevant impact parameters. If $t_{df} < H^{-1}$, the peculiar velocity of a loop decays rapidly to the velocity dispersion of the background material. This occurs if

$$(Ht_{df})^{-1} \cong v_i^{-3} R_l H(a(t)/a(t_i))^3 \varepsilon \ln \Lambda \qquad (14)$$

exceeds unity. For a matter-dominated universe of cold matter, loops with initial γ factors of the order of unity stop just before they decay at $t \simeq \varepsilon^{-1} R_l$.

(There is also an additional direct dynamical friction on strings moving through matter due to the 'wake' of material deflected behind it[20]. This dissipation is important only for one or two oscillations after a loop enters the horizon, although it may produce observable discontinuities in the microwave background temperature[21].)

However, the dynamical friction is much less effective during the early radiation-dominated phase. If the background medium is treated as collisionless particles with speed $\tilde{v}$, then the dynamical friction slowdown time scale for a loop moving with speed $v < \tilde{v}$ is independent of v (and proportional to $\rho^{-1} \propto t^2$). For a given ρ this time scale is longer by $(\tilde{v}/v)^3$ than it would be if the background particles were cold. Dynamical friction is reduced further for subsonic motion of a shallow potential well through a collisional gas[22] (such as the baryon + photon fluid before recombination). Thus, in the early universe it is the neutrinos, and not the photon-plus-baryon fluid, which produce the main drag. Dynamical friction is never efficient before recombination except in a model containing cold dark matter.

The anisotropy in the gravitational wave energy (and momentum) radiated in a single oscillation may be of the order of unity and, therefore, a recoil velocity of $\Delta v_s \cong \varepsilon$ is induced by each oscillation[5]. The cumulative effect depends on whether there is long-term stability in the mode of oscillation and its orientation. If the oscillations are strictly periodic (at least for a time comparable with the gravitational wave decay time scale), then the radiation is repeatedly beamed in exactly the same direction producing an acceleration $\simeq c/t_{dec}$. Thus a loop initially slows down like $v \propto a^{-1}$, reaches a minimum velocity $v_{min} \simeq \varepsilon^{2/5} v_i^{3/5}$, and shoots up to a velocity $\sim c$. In this case, loops with $v_i \simeq c$ never slow down sufficiently for dynamical friction to have any effect. In the opposite extreme, when successive oscillations are completely uncorrelated, the velocity random walks, and can build up only to $\sim \varepsilon^{1/2} c$ on the overall gravitational wave time scale. Real loops lie between these extremes.

Consider now what happens if we include both dynamical friction and recoil forces on a loop. The recoil velocity attainable in a time $t_{df}(< t_{dec})$ is of the order

$$v_c = c(t_{df}/t_{dec}) \min[1, (t_{coh}/t_{df})^{1/2}] \qquad (15)$$

where t_{coh} is the effective coherence time for the oscillations. If this velocity exceeds $\tilde{v}$, then the loop can run away in the sense that dynamical friction will never again be important. In the opposite case, where $\tilde{v} > v_c$, recoil will accelerate a loop to the point where the dynamical friction just damps the energy being added by recoil, rather like brownian motion in a viscous fluid. The actual value of $\tilde{v}$ is unknown, but in the case of cold dark matter such as axions could be arbitrarily small.

A loop whose gravitational radiation recoil is $\ll c/t_{dec}$, or whose initial velocity is sufficiently small, may 'accrete' a halo of matter around it. A loop can accrete its own mass when it slows to the Hubble velocity across a mass of matter equal to the loop mass. For $v_i \leqslant \varepsilon_c^{1/6}$ this occurs by redshifting before coherent recoil begins to take effect, but for $v_i \simeq c$ it occurs at $\simeq t_{dec}$, and even then only if $v_c < \tilde{v}$. The depth of the potential, and the total mass accumulated, depend on the details of when a loop actually slows.

Would the recoil from gravitational radiation eject a string loop from a virialized system? Even if recoil acts in a constant direction, this requires the recoil to produce an acceleration which is sufficient for it to break out of the potential well—that is $\varepsilon/l > v_{vir}^2/l = (M_{matt}/M_l)\varepsilon/l$. Thus a string cannot (unless it breaks into two) escape from a potential well which it does not dominate, although the recoil may cause it to reside away from the centre of the potential well. The effect of the beaming would be to cause the entire virialized system to recoil.

Dissipative heating by oscillating string

After accreting a halo of matter around itself, how does a loop interact with the ordinary matter bound to it? Can gravitational coupling of a loop to ordinary matter enable it to dissipate its rest mass more quickly than an isolated loop?

Goddard *et al.*[24] discovered that, surprisingly, strings of constant invariant length—for our purposes, this means perfectly nondissipative loops, with no gravitational interactions—obey a perfect nondissipative linear wave equation, even for large-amplitude waves. The physical reason for this behaviour is that, locally, the inertia and the tension of the string must always be exactly orthogonal because of restrictions imposed by Lorentz covariance. As a consequence, Kibble and Turok[8] showed that the motion of such a perfect loop is described by advanced and retarded waves travelling with arbitrary waveforms (except that some will lead to self-intersection) in the two directions around the loop. Because the solutions are exactly periodic, the loop traces out repeatedly the same contorted surface, and in fact has a time-averaged gravitational field equivalent to a surface whose local mass density acts like the square of the local transverse velocity[25]. Perfect coherence is maintained indefinitely, so the orientation of this surface is stationary for a perfect loop in a particular Lorentz frame of reference.

We have already seen that the long-term coherence of the direction of gravitational beaming makes a crucial difference in their behaviour (whether they rocket off or whether they stop and accrete matter). Now we find that this coherence is also of crucial importance for the dissipative interaction of loops with matter, because whereas a perfect loop has vanishing power at frequencies $\ll R_l^{-1}$ even a slight perturbation can generate components which vary over a longer time scale, comparable to the orbital time scales of stars. This allows for much more efficient coupling.

A string undergoing exactly periodic oscillations will, in effect, produce a quadrupole (newtonian) component of the gravitational potential which oscillates on a time scale R_l. This time scale is very short compared with the dynamical time scale (in most applications), so the effect is merely to produce small amplitude quasi-periodic shear distortions. Let the mass of (non-string) material within a sphere of diameter R_l be $x \times$ (mass of string loop). Then if $x < 1$, the gravitational binding is due to the string; otherwise the string is just a perturbation:

$$v_{\rm vir} \cong \varepsilon^{1/2} \times \max\,[1, x^{1/2}]c \qquad (16)$$

The velocity perturbation induced by the string in a time R_l is $\Delta v = \varepsilon$ (this is true for all values of x, though not completely obviously so). The corresponding shear amplitude is $\sigma \simeq \varepsilon$.

The amount of dissipation depends on the ratio $y = t_{\rm coll}/R_l$ where $t_{\rm coll}$ is the particle collision time. If this is $\gg 1$ (as, for instance, in stellar-dynamical systems) then the dissipation is small; also, if it is $\ll 1$, so that the pressure remains isotropic, there is again no dissipation. The dissipation is maximized if $y \simeq 1$, but even then the internal energy of the cloud is increased by only $\Delta\sigma/\sigma \simeq \sigma^2$ per oscillation. There are two contexts when we would indeed expect $y \simeq 1$: hot gas in clusters of galaxies, when the ions and electrons have mean free times against Coulomb scattering of order l/c; and pre-combination baryon clouds of $\simeq 10^6 M_\odot$ where the photons provide the main internal pressure, and have mean free paths of order the scale of the system. The motion of the loop also leaves a 'wake'[20], or shear-free velocity perturbation $\Delta v \simeq \varepsilon$ normal to the swath swept out by the string. The energy dissipated from this effect would also be of order ε^2 per oscillation, for $y \geqslant 1$ and $x \leqslant 1$.

As the strings decay through gravitational radiation after $\sim \varepsilon^{-1}$ oscillations, this suggests that fractional change in the energy content of a virialized system due to the oscillations of a perfect loop is negligible (a fraction $\leqslant \varepsilon^{1/2}$ of the binding energy of the matter).

Gravitational interactions of the loop's mean newtonian quadrupole field are likely to have much stronger effects, but their character depends strongly on the long-term coherence over many oscillations. For strings of the type discussed by Kibble and Turok, the orientation and amplitude of the time-averaged newtonian quadrupole moment probably remains coherent over a time $\sim t_{\rm dec}$ if gravitational radiation losses dominate. The surface swept out by the string thus forms a rigidly fixed gravitating shell. If matter in its vicinity has a rotating ellipsoidal figure, the loop will torque the matter through dynamical friction (even if $x > 1$) until it is rotating by an angle $\simeq \varepsilon^{1/2}$ per orbital time.

Other types of string not obeying strict local covariance are likely to be less coherent than these loops. The optimum time scale $t_{\rm coh}$ for the coherent variation of the newtonian quadrupole to interact most strongly with matter is, of course, $t_{\rm coh} \simeq t_{\rm vir}$; in this case the string could, in principle, disperse the matter within one orbital time, if $x \leqslant 1$. However, it is possible that the coherence time is very short compared with $t_{\rm vir}$. The extreme case—and the case of weakest coupling for short $t_{\rm coh}$—is to set $t_{\rm coh} \sim R_l$. The main effect is then contributed by variations in the loop's quadrupole moment averaged over time $T \simeq t_{\rm vir}$; the matter now experiences a randomly oriented shear distortion $\sigma \simeq \varepsilon^{1/4}/\max\,(1, x^{3/4})$ every orbital time. Moreover, the distortion is dissipative even if $t_{\rm coll} \gg t_{\rm vir}$ because of violent relaxation. We then have a fractional increase in the matter's energy of order $\sigma^2 \simeq \varepsilon^{1/2}/\max\,(1, x^{3/2})$ every orbital time, which for $x \leqslant 1$ amounts to its entire binding energy during the lifetime of the loop. The interaction of a loop with the central galaxy in a cluster, for example, would be sufficient to evaporate a substantial fraction of its matter in a Hubble time into an extended envelope. The loop could also provide a significant heat source for the cluster gas, although maximal dissipation would now occur for $t_{\rm coll} \simeq t_{\rm vir}$.

Minimum value of ε

It is possible that loops would establish 'seeds' of some kind (meaning astrophysical sources of energy) even if ε were too small to have a direct influence on galaxy clustering. The energy sources could then be used to generate clustering by some secondary process.

A minimum value of ε for which anything would happen even after decoupling is that for which $T_{\rm vir} \simeq T_{\rm rad}$, because matter cannot cool radiatively below $T_{\rm rad}$ and if it can be pressure supported at that temperature against a loop's gravity no collapse occurs. Thus at $z = 30$ (say) $T_{\rm rad} \cong 100$ K so baryon clouds with $\delta\rho/\rho > 1$ form around loops even if $\varepsilon \simeq 10^{-12}$ and the vacuum expectation value is as small as $\langle\varphi\rangle \simeq 10^{-6} m_{\rm p} \simeq 10^{13}$ GeV; it is sufficient to have $v_{\rm vir} \simeq 1$ km s^{-1}. However, this condition is not sufficient for further collapse and fragmentation. The matter heats up to $T_{\rm vir}$ and again nothing happens unless there is a cooling mechanism at that temperature which can permit the gas to radiate its binding energy in a free-fall time. Various authors have considered rates for cooling in primordial gas, in which cooling is dominated by molecular hydrogen, whose abundance is determined by a charge-exchange reaction catalysed by free electrons. We use the formula given by Blumenthal *et al.*[26], $t_{\rm cool} < t_{\rm dyn}$ if

$$M > M_{\rm cool} = 4.1 \times 10^7 M_\odot \left(\frac{n_{\rm e}/n_{\rm H}}{10^{-4}}\right)^{-0.625} (\Omega h^2)^{-0.917} \times \left(\frac{\Omega_{\rm g}/\Omega}{0.1}\right)^{-1.04} \left(\frac{1+z}{10}\right)^{-2.75} \qquad (17)$$

Strings characteristically generate density fluctuations leading to systems which collapse when $M \simeq \varepsilon^{3/2} M_{\rm H}(z)$. Now $M_{\rm H} \propto z^{-3/2}$ so it is clear that a lower ε is permitted by the cooling argument for higher z. The lowest interesting value of ε will be that which has $M_{\rm cool} \simeq \varepsilon^{3/2} M_{\rm H}(z)$ at the epoch when $T_{\rm vir} = T_{\rm rad}$. This works out to be a redshift $z \approx 100$ and $\varepsilon \approx 10^{-11}$, which may be low enough to be attributable to Peccei–Quinn symmetry breaking. The gravitational wave background for this low an ε is probably (though not necessarily) inaccessible to the millisecond pulsar.

Conclusions

If pulsar limits on $\Omega_{\rm g}$ go below $\sim 10^{-7}$, as it seems will happen soon, then cosmic strings will be pretty well ruled out as candidate sources for any large-scale fluctuations having a significant direct impact on galaxy clustering. At present, however, there is still the possibility that their gravitational waves will start to appear in timing residuals during the next few years. This motivation provides a strong incentive to find at least one other very clean pulsar (preferably several) so that a more definitive signature may be established.

We thank J. Preskill, R. Narayan and M. Wise for helpful discussions, and, particularly, D. C. Backer, N. Kaiser, and N. Turok for important suggestions. This work was supported by a Bantrell Fellowship and by NSF grant 82-14126 at Caltech, and was completed while the authors were participants in the Program on the Formation of Structure in the Universe at the Institute for Theoretical Physics, Santa Barbara.

Received 1 May; accepted 28 June 1984.

1. Kibble, T. W. B. *J. Phys. A* **9,** 1387–1398 (1976); *Phys. Rep.* **67,** 183–199 (1983).
2. Preskill, J. *The Very Early Universe* (eds Gibbons, G. W., Hawking, S. W. & Siklos, S. T. C.) pp. 119–146 (Cambridge University Press, 1983).
3. Zeldovich, Ya. B. *Mon. Not. R. astr. Soc.* **192,** 663–667 (1980).
4. Vilenkin, A. *Phys. Rev. Lett.* **46,** 1169–1172 (1981); *Phys. Rev.* **D24,** 2082–2089 (1981).
5. Turok, N. *Grand Unified Strings and Galaxy Formation.* Preprint (Univ. California, Santa Barbara, UCSB TH-3, 1984).
6. Vilenkin, A. *Phys. Lett.* **107B,** 47–50 (1982).
7. Wilczek, F. *The U(1) Problem: Instantons, Axions and Familons,* Preprint (ITP-84-14, Santa Barbara, 1984).
8. Kibble, T. W. B. & Turok, N. *Phys. Lett.* **116B,** 141–146 (1982).
9. Fall, S. M. *Rev. mod. Phys.* **51,** 21–42 (1979).

10. Gibbons, G. W., Hawking, S. W. & Siklos, S. T. C. (eds) *The Very Early Universe* (Cambridge University Press, 1983).
11. Starobinsky, A. *JETP Lett.* **30,** 682–685 (1979).
12. Rubakov, V., Sazhin, M. & Veryaskin, A. *Phys. Lett.* **115B**, 189–192 (1982).
13. Detweiler, S. *Astrophys. J.* **234,** 1100–1104 (1979).
14. Bertotti, B., Carr, B. J. & Rees, M. J. *Mon. Not. R. astr. Soc.* **203,** 945–954 (1983).
15. Rees, M. J. in *Gravitational Radiation* (eds Deruelle, N. & Piran, T., 297 (North-Holland, Amsterdam, 1983).
16. Cordes, J. M. & Stinebring, D. R. *Astrophys. J. Lett.* **277,** L53–L56 (1984).
17. Backer, D. C. *J. Astrophys. Astr.* (1984).
18. Armstrong, J. W. *Nature* **307,** 527–528 (1984).
19. Hogan, C. *Phys. Lett.* (in the press).
20. Silk, J. & Vilenkin, A. *Cosmic Strings and Galaxy Formation*, Preprint (Univ. California, Berkeley, 1984).
21. Kaiser, N. & Stebbins, A. *Nature* **310,** 391–393 (1984).
22. Rephaeli, Y. & Salpeter, E. E. *Astrophys. J.* **240,** 20–24 (1980).
23. Blandford, R., Narayan, R. & Romani, R. W. *J. Astrophys. Astr.* (in the press).
24. Goddard, P., Goldstone, J., Rebbi, C. & Thorn, C. B. *Nuclear Phys.* **B56,** 109–135 (1973).
25. Turock, N. *Phys. Lett.* **126B**, 437–440 (1983).
26. Blumenthal, G. R., Faber, S. M., Primack, J. R. & Rees, M. J. *Nature* (in the press).

Sequential late Cenozoic structural disruption of the northern Himalayan foredeep

Douglas W. Burbank* & **Robert G. H. Reynolds**†

* Department of Geological Sciences, University of Southern California, Los Angeles, California 90089-0741, USA
† AMOCO International, PO Box 4381, Houston, Texas 77210, USA

Chronologies for the Siwalik molasse and intermontane basins along the southern margin of the Himalaya and Hindu Kush Ranges constrain the timing and pattern of facies migration and structural disruption of the Indo-Gangetic foredeep. This synthesis indicates that quiescent intervals are punctuated by pulses of rapid deformation as thrusting migrates in a stepwise fashion across the foredeep.

THE large-scale southward migration of tectonic deformation away from the axis of the Himalayan orogen has long been recognized[1-4]. Extensive thrusting and nappe development in the vicinity of the Main Central Thrust in the Himalayas and of the Main Mantle Thrust in the Hindu Kush occurred primarily during the middle Cenozoic[4-10]. In contrast, the development of the Main Boundary Thrust (MBT) and related thrusts along the northwestern margin of the Indo-Gangetic foredeep (Fig. 1) has been largely confined to the Plio-Pleistocene[1,2,4,10]. Using magnetic-polarity stratigraphy and fission-track dating, Johnson *et al.*[11] and Opdyke *et al.*[12] have shown that close temporal constraints can be placed on tectonic events recorded by the molasse sediments of the western Himalaya. However, a precise chronology for the succession of events by which thrust faulting disrupted sedimentation within the molasse basin has not been previously delineated. The synthesis presented here is based on the analysis of lithofacies, provenance, and accumulation rates of strata in 14 recently dated sections. Integration of these data reveals the detailed timing of the progressive migration of deformation across the proximal foredeep margin in northern Pakistan and northwestern India during the past 5 Myr (Fig. 1).

Two distinct depositional settings, the largely undisturbed foredeep and the intermontane basins, are found adjacent to the deformational front. In the Indo-Gangetic foredeep, molasse sediments are typically characterized by sheet sandstones representing low-sinuosity, laterally-migrating rivers[13,14], siltstones

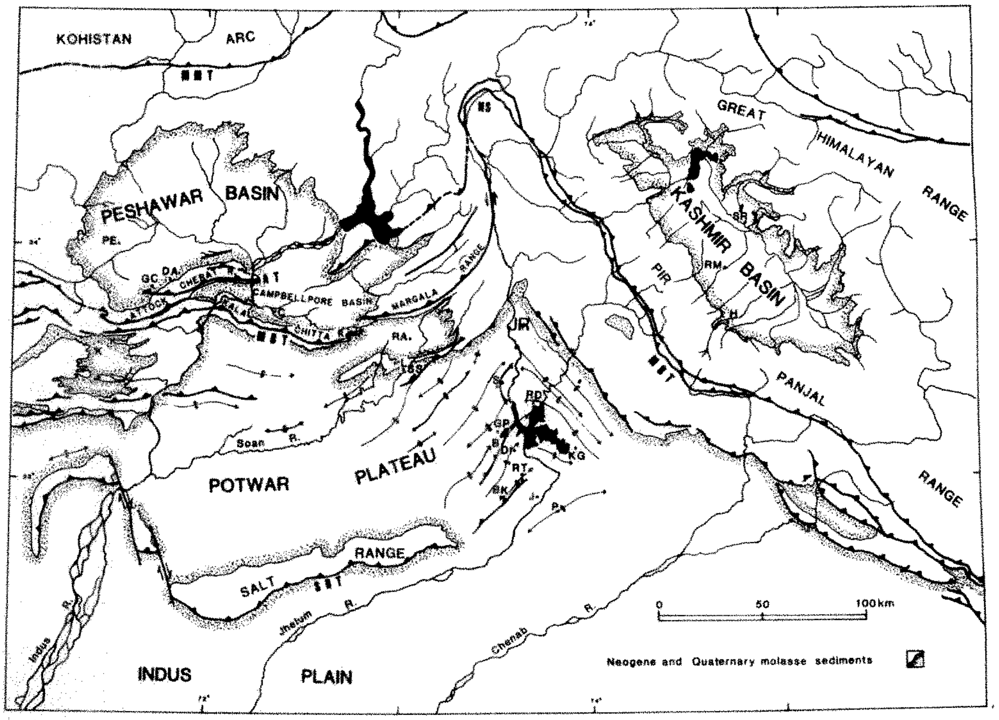

Fig. 1 Map of the northwestern portion of the Indo-Gangetic foredeep, the southern margin of the Himalaya and Hindu Kush, and the major intermontane basins in the vicinity of the North-west Syntaxis (NS). The major anticlinal axes in the deformed molasse sediments, as well as major thrust faults (barbed lines) and strike-slip faults in the region surrounding the Jhelum Re-entrant (JR), are delineated. During the Plio-Pleistocene, structural deformation has progressively migrated southwards across the foredeep in response to the ongoing Indo-Asian collision. Major thrust faults: AT, Attock Thrust; MBT, Main Boundary Thrust; MMT, Main Mantle Thrust; SRT, Salt Range Thrust. Locations of measured and dated stratigraphical sections: B, Bangala; C, Campbellpore; DA, Dag; DI, Dina; GP, Ganda Paik; GC, Garhi Chandan; H, Hirpur; KG, Kas Guma; L, Lei; RD, Rata-Dadial; RT, Rohtas; RM, Romushi; S, Sakrana; SS, Soan Syncline. Other localities: BK, Basawa Kas; J, Jhelum; P, Pabbi; PE, Peshawar; RA, Rawalpindi; SR, Srinagar.

Department of Chemical Engineering Chemical Technology Plastics and Rubber Technology

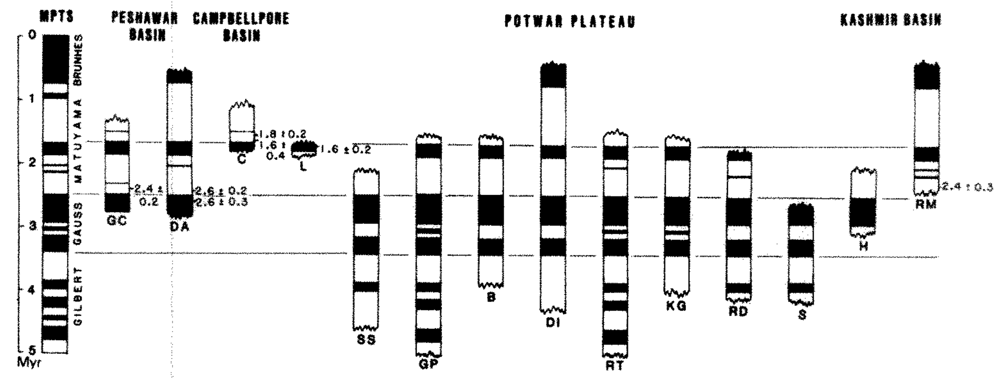

Fig. 2 Comparisons of locally determined magnetic-polarity stratigraphies (MPSs) with the magnetic-polarity time scale[41,42]. Fission-track dates on volcanic ashes are shown with 2σ errors at their appropriate stratigraphical positions. The magnetostratigraphical correlations are based on recognition of identifiable chrons or subchrons and are aided by both fossil occurrences and the frequent presence of prominent ashes straddling the Gauss–Matuyama transition. The fission-track dates from Lei and from the lower ash at Campbellpore are reported in ref. 29. The Soan Syncline section is from ref. 31. For a detailed discussion of other sections and fission-track dates, see refs 13 and 24. The local MPSs are arranged as they would be encountered along a traverse from the Peshawar Basin southeastwards to the Potwar Plateau and then northeastwards to the Kashmir Basin. In order: MPTS, magnetic-polarity time scale; GC, Garhi Chandan; DA, Dag; C, Campbellpore; L, Lei conglomerate; SS, Soan Syncline; GP, Ganda Paik; B, Bangala; DI, Dina; RT, Rohtas; KG, Kas Guma; RD, Rata-Dadial; S, Sakrana; H, Hirpur; RM, Romushi. Note that based on the sediment accumulation rates in the dated portion of the Hirpur sequence, the base of the underlying conglomeratic and mudstone section is interpreted to be ~4 Myr old[19].

with numerous palaeosol horizons developed on broad, interfluvial floodplains[15–17], and subsidiary ribbon sandstones representing higher sinuosity rivers[17]. Lacustrine strata are virtually absent within the molasse sediments[11–17]. The molasse sequence, 6,000 m thick, is exposed in the Himalayan foothills, where it is termed the Siwalik and Rawalpindi Groups[18]. In contrast, the intermontane basins, such as the Kashmir and Peshawar Basins, are dominated by proximal alluvial-fan facies, intermediate braided-river sediments, and extensive high-sinuosity fluvial and shallow lacustrine sediments that extend across the central portion of the basins[19–21]. These sequences occur in tectonically ponded valleys that lie inside the deformational front of the Himalayan fold-and-thrust belt. It is the predominant control on the style and rate of sediment accumulation exerted by the tectonic environment that permits us to unravel the patterns of regional tectonic evolution by dating strategically located stratigraphical sections.

Western limb of Jhelum Re-entrant

The Potwar Plateau represents the outermost and youngest of the series of intermontane basins in the western Himalaya. It is separated from the southernmost ranges of the Hindu Kush by the Peshwar and Campbellpore intermontane basins (Fig. 1). Earthquake-hypocentre distributions suggest that the Peshawar Basin is underlain by a subhorizontal, detachment surface[22,23]. This surface is inferred to continue southward as a largely aseismic detachment beneath the Potwar Plateau and to break the surface at the southern edge of the Salt Range. The Attock Thrust and the MBT (Fig. 1) are inferred to represent splays off this detachment surface[22,23]. Late Cenozoic movement along these thrusts has uplifted the Attock–Cherat Range and the Kala Chitta–Margala Range which define the southern margins of the Peshawar and Campbellpore Basins, respectively (Fig. 1). To constrain the deformational chronology of the northern foredeep, we have dated sections: (1) within the Peshawar and Campbellpore Basins; (2) near the bounding faults; and (3) across the Potwar Plateau.

Along the northern flank of the Attock Range in the Peshawar Basin (Fig. 1), mid-to-late Pleistocene uplift has exposed intermittently the uncomformable contact of the basin-filling sediments with the underlying Oligocene–Miocene bedrock[24,25,43]. Two magnetostratigraphical sections from this area commence in the upper Gauss chron, as indicated by three fission-track dates on ashes straddling the overlying reversal interpreted as

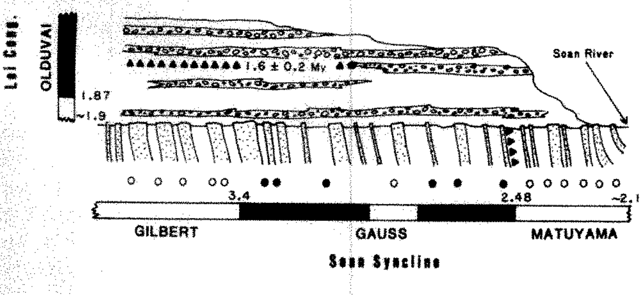

Fig. 3 The northern limb of the Soan Syncline, where nearly vertical strata of typical Siwalik molasse sediments are truncated and overlain by the generally underformed Lei conglomerate. Only the upper portion of >3,000 m of molasse sediments is shown. ▲, Enclosed volcanic ashes. The magnetostratigraphy[31] indicates that these strata encompass the Gauss chron and that the youngest preserved sediments extend into the lower Matuyama chron, probably to ~2.1 Myr. The overlying Lei conglomerate includes an ash dated at 1.6 ± 0.2 Myr (ref. 29) on the basis of which the normal-polarity magnetozone is interpreted as the Olduvai subchron. The base of the Lei conglomerate must predate the Olduvai and is interpreted as ~1.9 Myr. Thus, between 2.1 and 1.9 Myr ago, >3,000 m of uplift and erosion (mean minimum rate of 15 mm yr^{-1}) occurred as the Soan Syncline was strongly compressed in response to thrusting along the MBT.

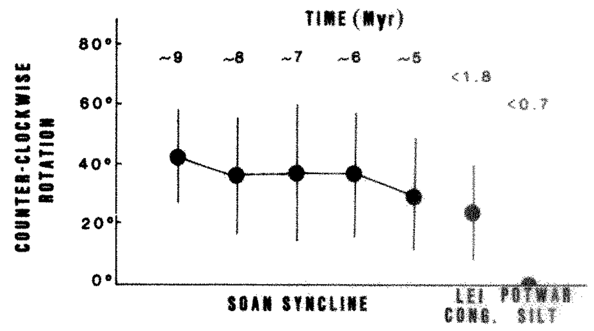

Fig. 4 Post-depositional rotation of foredeep sediments in the vicinity of the Soan Syncline. Amount of rotation is based on the deviation of the mean orientation of the normal and reversed magnetic sites from a given time interval with respect to the theoretical north–south axial dipole. The chronologically constrained data indicate that up to 15° of counterclockwise rotation occurred between 9 and 2 Myr ago. However, the most rapid rotation of over 20° occurred between 1.8 Myr and the present, following the development of the Soan Syncline.

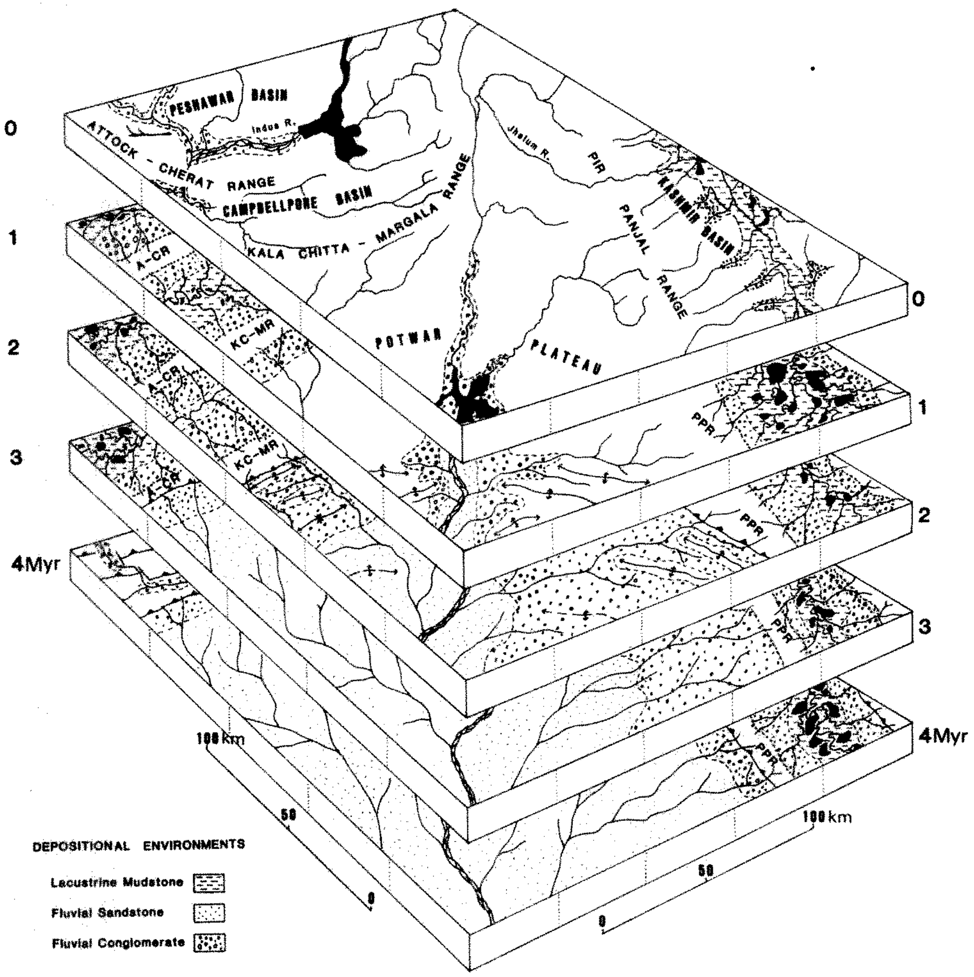

Fig. 5 Reconstructed structural and depositional relationships in the vicinity of the North-west Syntaxis at 1-Myr intervals during the past 4 Myr. Changes in facies relationships and the pattern of structural deformation are depicted adjacent to thrusts active at each interval. The zone of molasse deposition beyond the intermontane basins becomes increasingly restricted as thrusting and anticlinal growth migrate across the foredeep. Conglomerate facies and strong structural deformation in positions proximal to active faults grade laterally to indisturbed sheet sandstones in distal settings. A–CR, Attock–Cherat Range; KC–MR, Kala Chitta–Margala Range; PPR, Pir Panjal Range.

the Gauss–Matuyama transition (Fig. 2). Based on the estimated age of the basal depositional contact at Garhi Chandan, intermontane sedimentation in the Peshawar Basin is inferred to have begun ~3.0 Myr ago. Before this, movement along the Attock Thrust (Fig. 1) had caused uplift of the ancestral Attock Range and generated a tectonic depression on the northern side of the uplifted terrane. This tectonic event ponded the fluvial systems which had previously drained across the region and localized sediment accumulation in the newly formed basin.

The Campbellpore Basin is an elongate depression enclosed by the Attock Range to the north and the Kala Chitta–Margala Range to the south (Fig. 1). Despite the brevity of the sections along the western Haro River[24,26–28] (Fig. 2), the presence of several volcanic ashes permits precise dating of the basin fill[24,29] and indicates that sedimentation in the Campbellpore Basin had commenced by ~1.8–1.7 Myr ago. We can conclude that the thrusting along the MBT (Fig. 1) which uplifted the Kala Chitta Range and delimited the southern margin of the Campbellpore Basin had commenced at least 1.9 Myr ago.

Further information on the onset and duration of thrusting is provided by a section on the southern side of the MBT. The Soan Syncline (Fig. 1) is located ~20 km south of the MBT near Rawalpindi, where it is developed in sediments of the Upper Siwalik Group. The Soan Syncline is strongly asymmetric with a vertically standing northern limb and a gently dipping southern limb[30]. The magnetostratigraphy of the Upper Siwalik sediments in the northern synclinal limb[31] indicates that the youngest deformed strata are ~2.1 Myr old (Figs 2 and 3) and that the sequence, which is >3,000 m thick, extends well into the Upper Miocene[13]. The horizontally-bedded Lei conglomerate unconformably overlies the vertical strata of the northern limb of the syncline. A fission-track date of 1.6 ± 0.2 Myr on an enclosed ash[29] indicates that the normal-polarity interval is the Olduvai subchron and that the oldest strata of the Lei conglomerate are likely to be ~1.9 Myr old (Figs 2, 3).

These chronological data delineate a very brief interval of rapid tectonic deformation in the latest Pliocene. During a period of ~200,000 yr beginning around 2.1 Myr ago, >3,000 m of structural relief was developed and was accompanied by rapid erosion. By 1.9 Myr ago, the deformed sequence had been truncated by erosion, and the Lei conglomerate spread southward across the area (Fig. 3).

We interpret the deformation of the Soan Syncline as a response to the initiation of major movement along the MBT around 2.1 Myr ago. The Lei conglomerate represents the proximal, transgressive facies shed from the rising Kala Chitta–Margala Range to the north. The horizontal aspect of the Lei conglomerate today, the gentle dips (<5°) found in the intermontane sediments of the Campbellpore Basin[22,25,26], and the absence of conglomerates younger than 1.6 Myr (Fig. 2) suggest that major movement along the MBT was short lived and had largely ceased by the end of the Pliocene. Following deposition of the Lei conglomerate, major rotation of the Soan area began (Fig. 4). We view this rotation as coincident with the propagation of the detachment surface[22,23] beneath the Potwar Plateau towards the modern Salt Range and with the resulting development of the Potwar Plateau as an allochthonous unit.

During the Pleistocene, tectonic disruption migrated systematically southwards across the central and eastern Potwar Plateau. Three magnetostratigraphical sections[13,32] from the eastern Potwar (Fig. 2) constrain this history of tectonism. Two intervals of conglomeratic sedimentation are present in most sections: one in the upper portion of the comformable molasse sequence (sometimes intraformational in nature) and one overlying the deformed and eroded molasse strata. The first appearances of conglomerates are time-transgressive events related to either an influx from extrabasinal, bedrock uplifts or intrabasinal deformation. In addition, the timing of initiation of conglomeratic sedimentation at a given section is a function of the spatial relationship between the section and the former axis of

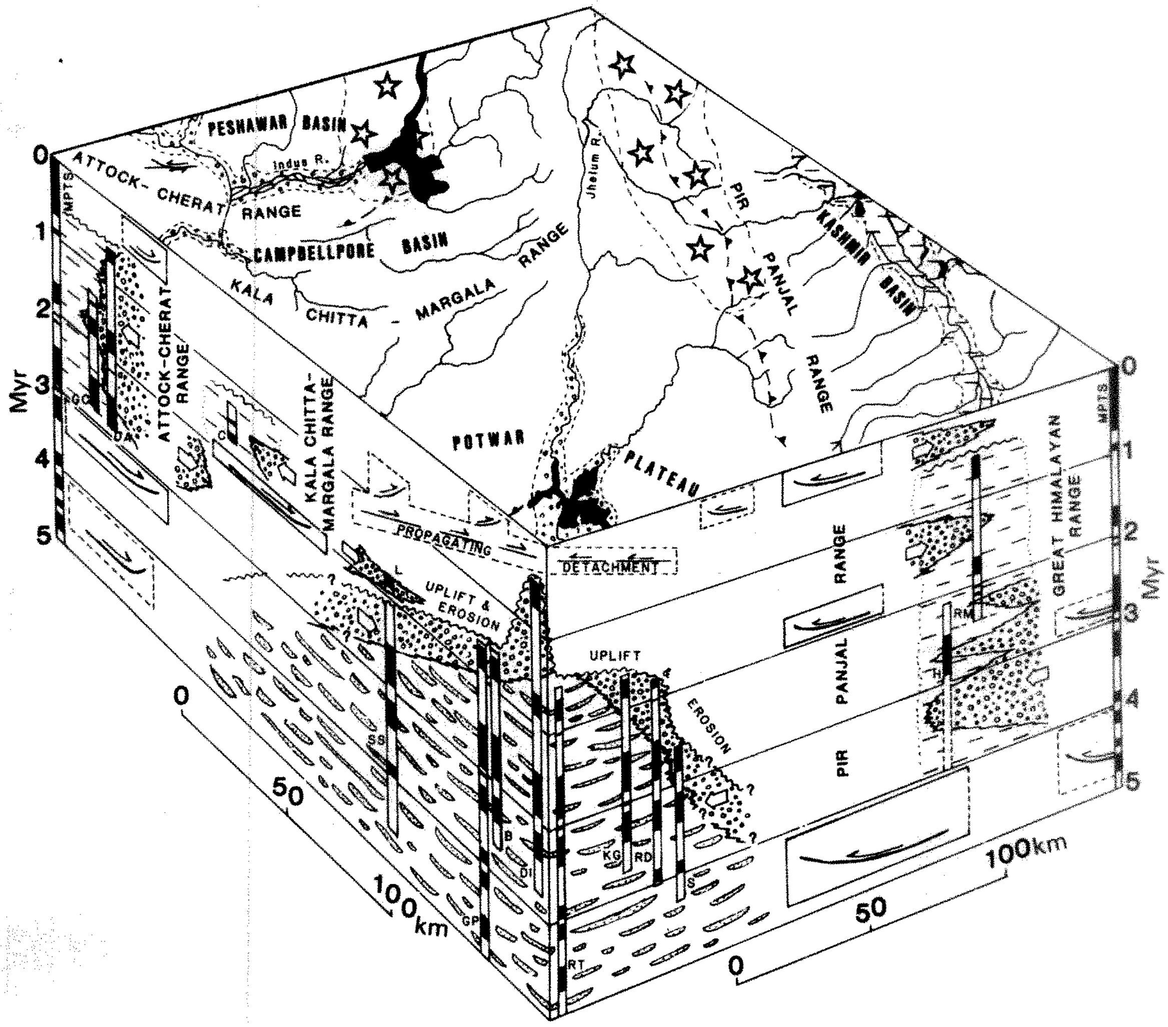

Fig. 6 Time–distance block diagram of the Himalayan foredeep and adjacent ranges in the vicinity of the North-west Syntaxis. The vertical dimension extends back to 5 Myr. The dated sequences described in this study and shown in Fig. 2 are depicted in their chronological range and are projected from their geographical location on to the transects defining the sides of the block. The abbreviations next to each magnetic column are as in Figs 1 and 2. Medial sections such as Sakrana (S) could be projected onto either face. The northeastern face is chosen here based on the affinities of the conglomerates at Sakrana with those from Rata–Dadial (RD) and Kas Guma (KG). For each of the stratigraphical sections, generalized depositional and facies relationships are shown in their proper chronological position (for example, the southward progradation of conglomerates from Sakrana across the eastern Potwar Plateau after 3 Myr). The intermontane basins are dominated by low-energy (largely lacrustine) facies punctuated by conglomeratic influxes. Two broad phases of molasse sedimentation across the Potwar Plateau are shown: a channel-and-floodplain interval succeeded by late-stage polymictic conglomerates. Large, open arrows indicate the prevailing palaeocurrent directions at different times. The boxes enclosing a thrust-fault symbol delineate both the spatial and chronological intervals over which the thrusts are interpreted to have been active. Dashed boxes show less well constrained periods of thrusting. On the left-hand panel, thrusting, folding and intermontane basin formation are seen to progress in a stepwise fashion from the Peshawar Basin to the south-east between 4 and 1 Myr ago. On the right-hand panel, three intervals of uplift in the vicinity of the Pir Panjal Range have defined the Kashmir Basin, controlled palaeocurrent patterns, and deformed the adjacent foredeep to the south-west. The surface of the block illustrates active, present-day processes. Deposition is largely restricted to the axial portions of the intermontane basins and narrow floodplains. Regions of high seismicity within 10–15 km of the surface[22] are shown by stars. Presently- or recently-active faults that break the surface seem to be associated with shallow seismicity.

local fluvial deposition. Intraformational conglomerates first appear at Ganda Paik and Bangala (Fig. 1) about 2.0–1.9 Myr ago, synchronous with the inferred movement along the MBT. At the same time, decreasing rates of sedimentation are observed at Ganda Paik, Bangala, and, farther to the south, at Dina (Fig. 1), where extrabasinal conglomerates first appear around 1.6 Myr ago. The youngest comformable molasse strata in each section provide a limiting date on the cessation of sedimentation, as a wave of folding, uplift and erosion traversed the region. Thus, to the south-east of the Soan Syncline where deformation began around 2.1 Myr ago, the topmost conformable strata are progressively younger at Ganda Paik and Bangala (~1.6–1.5 Myr) and at Dina (~0.5 Myr). The youngest strata preserved farther south-east at Rohtas (Fig. 1) are ~1.5 Myr old. However, the presence of molasse strata as young as 0.4 Myr on the Rohtas anticline some 10–15 km farther south-west[11,12] (BK, Fig. 1) suggests significant truncation of the Rohtas section.

Eastern limb of Jhelum Re-entrant

The Kashmir intermontane basin is separated from the Indo-Gangetic foredeep by the thrust-faulted Pir Panjal Range (Fig. 1). South of the Pir Panjal, the Siwalik molasse is well exposed in a series of thrust-cored anticlines where measured and dated stratigraphical sections record the history of fluvial systems flowing from the Himalayas. Although the detailed timing of tectonic events in the enclosing ranges and the bounding foredeep cannot be delineated as precisely as in the region to the west, three intervals of deformation can be discerned in both the intermontane sediments of Kashmir and the molasse sediments to the south.

In Kashmir, the basin-filling Karewa Formation[19,21,33–36] is >1,300 m thick. Magnetostratigraphical sections from Hirpur and Romushi (Figs 1 and 2) indicate that Karewa sedimentation spans the interval from ~4 Myr to the present[19]. This deposition began as a response to the initial emergence of the ancestral Pir Panjal Range $\sim$4.5 Myr ago. Although molasse sedimentation across the Potwar region to the south continued uninterruptedly during this interval[13], major changes in clast lithologies in the molasse and in drainage patterns (from east-flowing to south-flowing)[13,37] signal the concomitant onset of structural development of the Jhelum Re-entrant[38]. In addition, for the first time in Upper Siwalik sediments, polymictic conglomerates appear in abundance, reaching Sakrana (Fig. 1) by 3.1 Myr ago and prograding southwards across Rata-Dadial (2.5 Myr) and Kas Guma (2.1 Myr). This onslaught of conglomeratic sedimentation appears to be a time-transgressive response to the initial uplift of the Pir Panjal Range.

Concurrently in Kashmir, palaeocurrent indicators[19] suggest that pulses of uplift, presumably thrust-related, occurred along the northeastern margin of the basin until $\sim$2 Myr ago. Subsequently, diminution of this thrusting[38] and accelerated uplift of the Pir Panjal Range redirected palaeocurrents towards the north-east. This interval of tectonism is synchronous with that previously described in the north-central Potwar and is recorded concurrently by a deceleration in molasse sedimentation rates at Rata-Dadial and Kas Guma (Fig. 1). This deceleration is likely to signal the onset of development of the thrust-cored anticlines in the foredeep in response to intensified thrusting and uplift to the north. Subsequently, progressive uplift and erosion spread southwards across the eastern Potwar, as evidenced by the youngest comformable strata at Sakrana ($<$2.7 Myr), Rata-Dadial ($<$1.8 Myr) and Kas Guma ($<$1.4 Myr). The youngest deformation in the Potwar is recorded in sections at Pabbi[32,39], Basawa Kas[11,12] (P, BK; Fig. 1) and Dina, where erosion supplanted sedimentation $<$0.5–0.4 Myr ago. This third phase of tectonism is contemporaneous with the most recent interval of rapid uplift, totalling 1,300–3,000 m, of the Pir Panjal Range in southern Kashmir[19].

Synthesis

The use of magnetostratigraphy in conjunction with fission-track dating provides an insight into the chronology of the late Cenozoic structural disruption of the northern margin of the Indo-Gangetic foredeep in northern Pakistan and India. Figure 5 illustrates the reconstructed depositional and tectonic conditions in 1-Myr increments between 4 Myr and the present. The time–space perspective diagram in Fig. 6 illustrates the concurrent evolution of both arms of the North-west Syntaxis.

Intermontane basin development commenced in Kashmir 4–5 Myr ago and progressed contemporaneously with major changes in palaeocurrents and provenance in the adjacent foredeep. Dated sequences in the Peshawar and Cambellpore intermontane basins and in the Soan Syncline delineate the sequential southward migration between $\sim$3.0 and 1.8 Myr ago of major thrust faulting, uplift, and the concurrent development of intermontane basins on the back side of the uplifted terranes. During this time interval, the locus of thrusting shifted some 50 km to the south. The duration of significant movement along the major thrusts (Attock, MBT) is envisaged as rather brief ($<$0.5 Myr). Contemporaneous deformation and erosion of sedimentary sequences in front of the thrusts often occurred at rapid rates ($\geq$15 mm yr^{-1}). Subsequent to the development of the imbricated, thrust-bounded ranges and basins in northern Pakistan and to a second pulse of uplift in Kashmir, the locus of major deformation continued migrating towards the south, where it caused folding, faulting and rotation of the Potwar Plateau[13,32,40], and propagation of the detachment surface to the Salt Range.

Whereas the initial development of the Kashmir and Peshwar Basins does not appear to be synchronous, a pulse of deformation associated with thrusting along the MBT is manifested across a broad region of the northwestern foredeep around 2–1.5 Myr ago. Development of the Campbellpore Basin, snapping shut of the Soan Syncline, and renewed uplift of the Pir Panjal Range were apparently contemporaneous with the disruption of molasse sedimentation across the Potwar Plateau as thrust-cored anticlines began to grow along the northern foredeep margin.

Conclusions

Because of the temporal resolution provided by magnetostratigraphical studies, the timing and duration of tectonic and sedimentary events in the northern Himalayan foredeep can now be reconstructed with greater detail than was previously possible. The chronological data emphasize the sporadic nature of tectonism in this collisional setting. Although the rate of convergence of the Indian subcontinent with Eurasia[41] appears steady during the studied time interval, this detailed reconstruction of the northwestern Himalayan foredeep indicates that prolonged periods of quiescence and uniform sedimentation were punctuated by brief, intense intervals of deformation as the locus of thrust faulting encroached in a stepwise fashion on the adjacent foredeep. This sporadic tectonism may be regarded as the pulse of an orogenic process which, when integrated over time intervals in excess of 1 Myr seems to be continuous.

This research was suppoted by grants from the Geological Society of America, Marathon Oil, the Shell Foundation and Amoco International to D.W.B. and the NSF (INT 8019373 and EAR 8018779) to Dartmouth College. The assistance of R. A. K. Tahirkheli of Peshawar University is gratefully acknowledged. Many of these results are derived from doctoral studies completed by us while at Dartmouth College. Discussions with G. D. Johnson, N. M. Johnson and P. K. Zeitler contributed greatly to this research.

Received 4 May; accepted 18 June 1984.

1. Gansser, A. *Geology of the Himalayas* (Wiley, London, 1964).
2. Wadia, D. N. *The Geology of India* (McGraw-Hill, New York, 1966).
3. Powell, C. McA. *Geodynamics of Pakistan* (eds Farah, A. & de Jong, K.) 5–24 (Geological Survey of Pakistan, Quetta, 1979).
4. Le Fort, P. *Am. J. Sci.* **275A**, 1–44 (1975).
5. Bard, J. P., Maluski, H., Matte, P. & Proust, F. *Spec. Iss. geol. Bull. Univ. Peshawar* **13**, 87–94 (1980).
6. Bordet, P., Colchen, M., Le Fort, P. & Pecher, A. in *Zagros, Hindu Kush, Himalaya, Geodynamic Evolution* (eds Gupta, H. K. & Delaney, F. M.) 149–168 (American Geophysical Union, Washington, 1981).
7. Coward, M. P. *et al. Nature* **295**, 22–24 (1982).
8. Seeber, L., Armbruster, J. C. & Quittmeyer, R. C. in *Zagros, Hindu Kush, Himalaya, Geodynamic Evolution* (eds Gupta, H. K. & Delaney, F. M.) 215–242 (American Geophysical Union, Washington, 1981).
9. Zeitler, P. K. thesis, Dartmouth College, Hanover (1983).
10. Tahirkheli, R. A. K. *Spec. Iss. geol. Bull. Univ. Peshawar* **13**, 39–46 (1980).
11. Johnson, G. D., Johnson, N. M., Opdyke, N. D. & Tahirkheli, R. A. K. in *Geodynamics of Pakistan* (eds Farah, A. & de Jong, K.) 149–165 (Geological Survey of Pakistan, Quetta, 1979).
12. Opdyke, N. D., Johnson, N. M., Johnson, G. D., Lindsay, E. H. & Tahirkheli, R. A. K. *Palaeogeogr., Palaeoclimatol., Palaeoecol.* **37**, 1–15 (1982).
13. Raynolds, R. G. H. thesis, Dartmouth College, Hanover (1980).
14. Johnson, G. D. & Vondra, C. F. *Himalayan Geol.* **2**, 118–144 (1972).
15. Johnson, G. D. *et al.* in *Hominoid Sites: Their Paleoenvironmental Settings* (eds Rapp, G. & Vondra, C. F.) 197–254 (American Association for the Advancement of Science, Washington, 1981).
16. Johnson, G. D. *Geol. Rdsch.* **66**, 192–216 (1977).
17. Behrensmeyer, A. K. & Tauxe, L. *Sedimentology* **29**, 331–352 (1982).
18. Pilbeam, D. R. *et al. Nature* **270**, 684–689 (1977).
19. Burbank, D. W. & Johnson, G. D. *Palaeogeogr., Palaeoclimatol., Palaeoecol.* **43**, 205–235 (1983).
20. Singh, I. B. *J. Paleont. Soc. Ind.* **27**, 71–110 (1982).
21. Bhatt, D. K. *Misc. Publ. geol. Surv. Ind.* **24**, 188–204 (1975).
22. Seeber, L. & Armbruster, J. in *Geodynamics of Pakistan* (eds Farah, A. & de Jong, K.) 131–142 (Geological Survey of Pakistan, Quetta, 1979).
23. Seeber, L., Armbruster, J. & Quittmeyer, R. C. in *Zagros, Hindu Kush, Himalaya, Geodynamic Evolution* (eds Gupta, H. K. & Delaney, F. M.) 215–242 (American Geophysics Union, Washington, 1981).
24. Burbank, D. W. thesis, Dartmouth College, Hanover (1982).
25. Meissner, C. R., Master, J. M., Rashid, M. A. & Hussain, M. *U.S. geol. Surv. Prof. Pap.* 716-D (1974).
26. de Terra, H. & de Chardin, P. T. *Proc. Am. phil. Soc.* **76**, 792–822 (1936).
27. Opdyke, N. D. *et al. Palaeogeogr., Palaeoclimatol., Palaeoecol.* **27**, 1–34 (1979).
28. Bloch, R. B., thesis, Dartmouth College, Hanover (1982).
29. Johnson, G. D. *et al. Palaeogeogr., Palaeoclimatol., Palaeoecol.* **37**, 63–93 (1982).
30. Gill, W. D. *Q. Jl geol. Soc., Lond.* **107**, 395–421 (1951).
31. Moragne, J. H. thesis, Dartmouth College, Hanover (1979).
32. Raynolds, R. G. H. & Johnson, G. D. *Geol. Soc. Lond. Spec. Publ.* (in the press).
33. Godwin-Austin, H. H. *Q. Jl geol. Soc. Lond.* **15**, 221–229 (1859).
34. de Terra, H. & Paterson, T. T. *Studies on the Ice Age in India and Associated Human Cultures* (Carnegie Institution of Washington, 1939).
35. Farooqi, I. A. & Desai, R. N. *Geol. Soc. Ind.* **15**, 299–305 (1974).
36. Bhatt, D. K. *Himalayan Geol.* **6**, 197–208 (1976).
37. Raynolds, R. G. H. *Geol. Bull. Univ. Peshawar* **14**, 141–150 (1982).
38. Burbank, D. W. *Earth planet. Sci. Lett.* **64**, 77–92 (1983).
39. Keller, H. M. *et al. Earth planet. Sci. Lett.* **36**, 187–201 (1977).
40. Minster, J. B. & Jordan, T. H. *J. geophys. Res.* **83**, 5331–5354 (1978).
41. Mankinen, E. A. & Dalrymple, G. B. *J. geophys. Res.* **84**, 615–626 (1979).
42. Harland, W. B. *et al. A Geologic Time Scale* (Cambridge University Press, 1982).
43. Burbank, D. W. & Tahirkheli, R. A. K. *Bull. geol. Soc. Am.* (in the press).

Occurrence of a transposition from the X-chromosome long arm to the Y-chromosome short arm during human evolution

David C. Page*‡, Mary E. Harper†§, Jamie Love† & David Botstein*

* Department of Biology, Massachusetts Institute of Technology, Cambridge, Massachusetts 02139, USA
† The Agouron Institute, 505 Coast Boulevard South, La Jolla, California 92037, USA
‡ Present address: Whiteside Institute for Biomedical Research, Nine Cambridge Center, Cambridge, Massachusetts 02142, USA
§ Present address: Laboratory of Tumor Cell Biology, National Cancer Institute, Bethesda, Maryland 20205, USA

DXYS1, *a site showing greater than 99% DNA sequence homology between the human X and Y chromosomes, maps to the X long arm and to the Y short arm. In great apes, sequences homologous to* DXYS1 *are found only on the X chromosome. These findings suggest an X–Y transposition during human evolution.*

IT is widely held that the mammalian X and Y chromosomes are in part homologous as a consequence of their evolution from a completely homologous pair[1,2]. Terminal pairing of the short arms of the human X and Y chromosomes during meiosis is taken as evidence of such partial homology[1,3–8]. Here we demonstrate that human X–Y sequence homology is not limited to the pairing portions of the sex chromosomes. Moreover, X–Y homology at the locus *DXYS1* appears to be the result of a recent transposition from the X to the Y chromosome.

Chromosomal sublocalization of *DXYS1*

DXYS1 was the first site of single-copy DNA sequence homology to be found between the human X and Y chromosomes[9,10]. A *Taq*I restriction fragment length polymorphism (RFLP)[11] at *DXYS1* consists of allelic X-linked fragments of 11 and 12 kilobases (kb) and a male-specific (Y-specific) 15-kb fragment. The complete association of the 15-kb fragment with the Y chromosome and the strictly X-linked inheritance of the 11- and 12-kb fragments imply that X–Y recombination does not normally occur (or is lethal) at *DXYS1*. Given the long-standing hypothesis that meiotic recombination between the pairing regions of X and Y chromosomes occurs frequently[12], we set out to determine whether *DXYS1* maps to the pairing regions of the sex chromosomes.

To localize *DXYS1* on the X and Y chromosomes, we carried out *in situ* hybridization of a probe defining *DXYS1* [pDP31, a subclone of probe 5 (Fig. 2*a*) into pBR322; ref. 9] to human metaphase chromosomes. As illustrated by the representative cell in Fig. 1*a*, pDP31 showed significant hybridization to the proximal portion of the long arm of the X chromosome and to the short arm of the Y chromosome. Of 72 cells hybridized at 100 ng ml^{-1} probe DNA and exposed for 5–11 days, 47% exhibited grains on the proximal long arm of the X chromosome and/or on the short arm of the Y chromosome. These grains represented 20% of all label observed in the 72 cells. Experiments were then done to refine the sublocalization of *DXYS1* by hybridization of the ^{3}H-labelled probe at a low concentration (12 ng ml^{-1}) followed by exposure for 46 days. Analysis of grains on labelled X and Y chromosomes (Fig. 1*b*) indicated sublocalization of *DXYS1* to Yp and to a region on the X that includes the lower half of band q13 and the upper half of q21 (most likely Xq13.2–q21.2).

To provide a second, independent sublocalization of *DXYS1* on the human X and Y chromosomes, genomic DNAs were

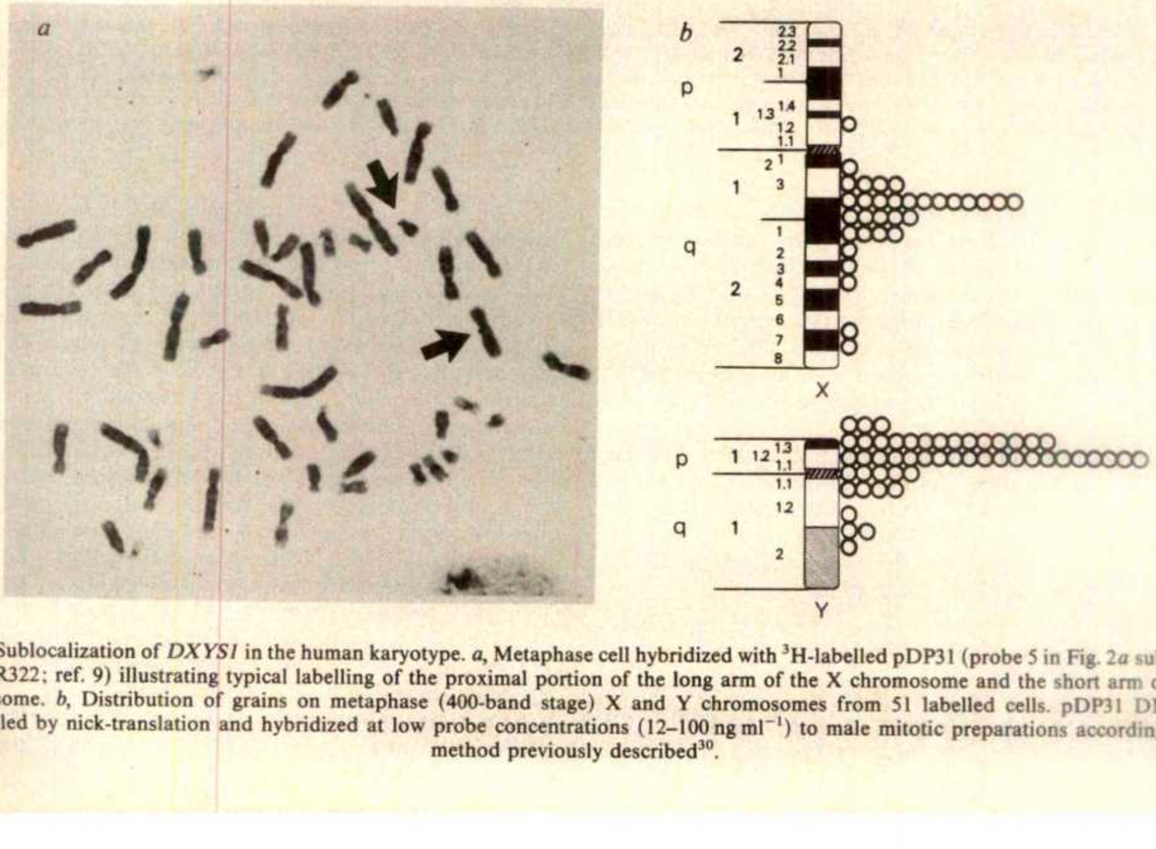

Fig. 1 Sublocalization of *DXYS1* in the human karyotype. *a*, Metaphase cell hybridized with ^{3}H-labelled pDP31 (probe 5 in Fig. 2*a* subcloned into pBR322; ref. 9) illustrating typical labelling of the proximal portion of the long arm of the X chromosome and the short arm of the Y chromosome. *b*, Distribution of grains on metaphase (400-band stage) X and Y chromosomes from 51 labelled cells. pDP31 DNA was ^{3}H-labelled by nick-translation and hybridized at low probe concentrations (12–100 ng ml^{-1}) to male mitotic preparations according to the method previously described[30].

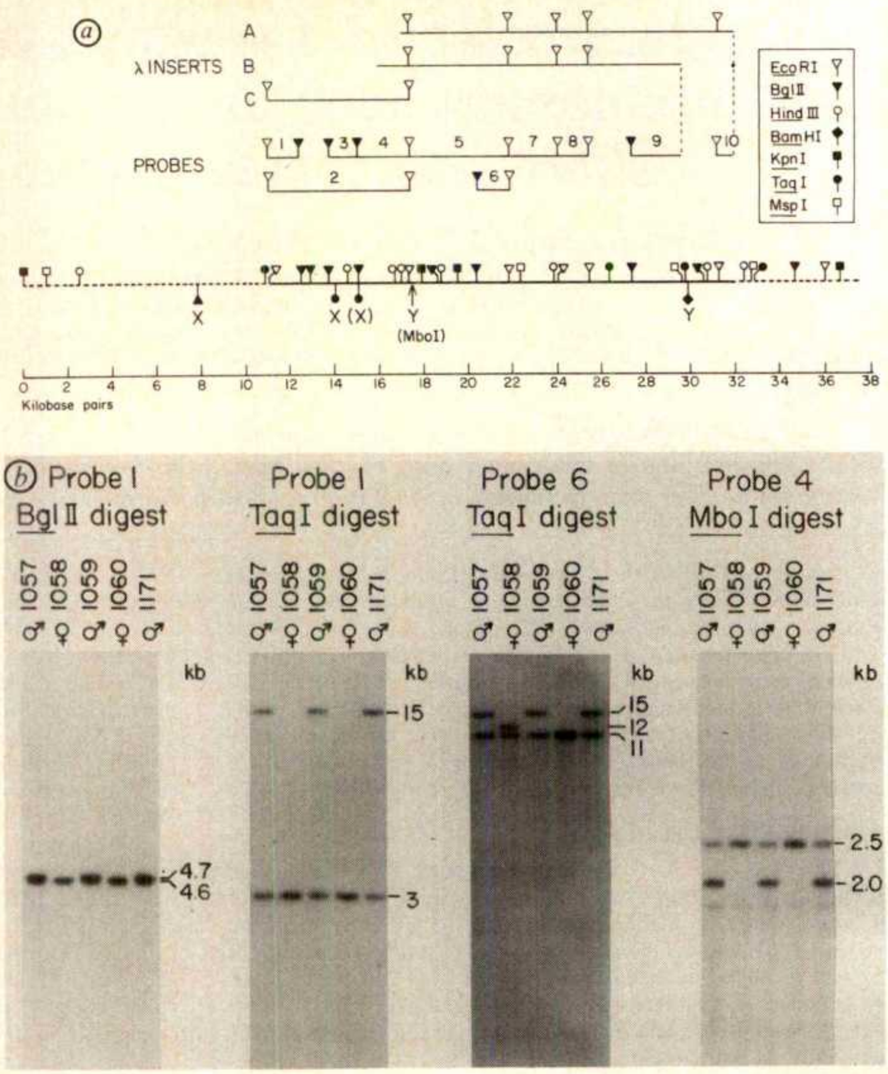

Fig. 2 ***a***, Restriction endonuclease mapping of 36 kb of the human X and Y chromosomes at *DXYS1*. At the top are shown the overlapping human DNA inserts of three recombinant λ phage: A, λ-rHs-3-1; B, λ-rHs-4813; and C, λ-rHs-X6.3. The locations of *Eco*RI restriction sites are indicated. Below the phage inserts are 10 restriction fragments purified from these inserts for use as hybridization probes; terminal restriction sites are indicated. Below the probes is shown the restriction map of the X and Y chromosomes at *DXYS1*. Restriction endonuclease cleavage sites common to the X and Y chromosomes are indicated by symbols above the line. Sites specific to either the X or the Y chromosome are indicated below the line. A Y-specific *Mbo*I site (see text) is shown. Sites within the 21-kb region (solid line) spanned by the three λ clones were mapped by direct analysis of those clones and confirmed by blot hybridization using probes 1–10. Sites outside the region (dotted line) were mapped by blot hybridization using probes 1 and 10. Every site was detected or confirmed by blot hybridization of DNAs from at least nine unrelated males and two unrelated females (nine Y chromosomes and 13 X chromosomes). We have previously reported a Y-linked *Msp*I/*Bgl*II restriction fragment length polymorphism at *DXYS1* (ref. 9); this polymorphism is the result of a tandem duplication on the Y chromosome in some males (D.C.P., in preparation). The map of the Y chromosome shown here is that of the nonduplicated form. No new RFLPs were detected during this study. ***b***, Differential patterns of hybridization of human male and female DNAs with DNA probes for *DXYS1*. These hybridizations detected restriction sites specific to either the X or the Y chromosome.
Methods: Recombinant phage λ-rHs-4813, purified from a human genomic library[31], was the original source of hybridization probes for *DXYS1* (ref. 9). Recombinant phages λ-rHs-3-1 and λ-rHs-X6.3 derive from the same genomic library[31] and from an X-specific library[32], respectively. These two phage were identified by plaque hybridization screening[33] using DNA probes purified from the human insert of λ-rHs-4813. Some of these restriction fragments were subcloned into plasmid pBR322 or an abbreviated derivative (pDP322; D.C.P., unpublished) before use as hybridization probes. Human genomic DNAs were prepared from peripheral leukocytes by the method of Kunkel *et al.*[13]. DNA samples were digested with restriction endonuclease, electrophoresed on 0.75% agarose gels, and transferred[34] to AMF Zetapore paper. Restriction fragments purified from phage λ-rHs-3-1, λ-rHs-4813 and λ-rHs-X6.3 were labelled with ^{32}P by nick-translation[35] and hybridized overnight to the filter-bound genomic DNAs at 47 °C in 50% formamide, 5× SSC (1× SSC = 0.15M NaCl, 15 mM Na citrate *p*H 7.4), 1× Denhardt's (0.02% Ficoll 400, 0.02% polyvinyl pyrrolidone, 0.02% bovine serum albumin), 20 mM $NaPO_4$ *p*H 6.6, 50 μg ml^{-1} denatured salmon sperm DNA, and 10% dextran sulphate. Following hybridization, filters were washed three times for 15 min each at 55–60 °C in 0.1× SSC, 0.1% SDS and exposed at −70 °C for 1–7 days with Kodak XAR-5 film backed by a DuPont Lightning-Plus intensifying screen.

obtained from three rodent–human cell hybrids (characterized by G. Bruns, unpublished results) containing portions of the human X chromosome and from three humans whose cells contain portions of the Y chromosome (ref. 13 and K. Smith and collaborators, unpublished results). Gel transfers of *Taq*I digests of these DNAs were hybridized with *DXYS1* probe 5 (see Fig. 2*a*) and scored for the presence or absence of the X- and Y-specific *Taq*I fragments detected by probe 5. The results of these studies map *DXYS1* to Xq1–q22 and to Ycen–pter (data not shown). In addition, *DXYS1* probe 9 (Fig. 2*a*) was applied to the dosage panel used by Kunkel *et al.*[14] to assign DNA segments to regions of the human X chromosome. By this method, *DXYS1* was mapped to Xq13–q24 (data not shown). These results are consistent with the assignment of *DXYS1* to Xq13-q21 and Yp by *in situ* hybridization.

X–Y restriction mapping

The homology between the X and Y chromosomes at *DXYS1* extends for at least 28 kb[9]. In order to quantitate further the X–Y homology at *DXYS1*, we made a comparative restriction map of the X and Y chromosomes at this locus. A series of neighbouring single-copy restriction fragments were hybridized to gel transfers of restriction endonuclease-digested human male and female DNAs (Fig. 2). In this way, a stretch of 36 kb was mapped in this region. Where no differences were detected in the patterns of hybridization with male and female DNA, it was assumed that the X and Y chromosomes share a common restriction fragment. Indeed, most restriction fragments were found to be identical on the X and Y chromosomes. Of 40 *Eco*RI, *Bgl*II, *Hin*dIII, *Bam*HI, *Kpn*I, *Taq*I and *Msp*I restriction sites that we mapped at *DXYS1*, 36 sites are common to the X and Y chromosomes, one site is specific to the Y, two sites are specific to the X, and one (*Taq*I) site gives rise to the X-linked RFLP which is present on about half of the X chromosomes in Northern European populations, but absent from the Y chromosome. These results establish that the X and Y chromosomes are homologous over an expanse of at least 36 kb at *DXYS1*. We have not detected the termination of this X–Y sequence homology.

Analysis of this region with the restriction enzyme *Mbo*I yields similar results. Of 11 *Mbo*I restriction fragments observed over

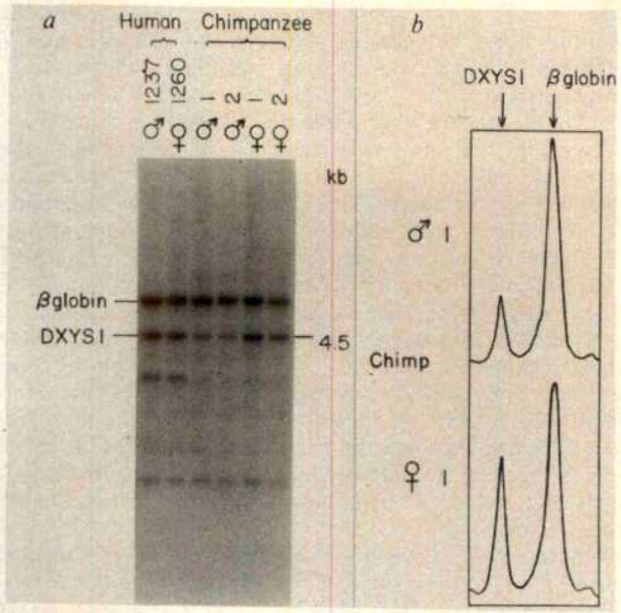

Fig. 3 Male–female dosage at a *DXYS1*-homologous locus in chimpanzee. *a*, Hybridization of *Eco*RI-digested human and chimpanzee male and female DNAs to probes for *DXYS1* and β-globin. Genomic human and chimpanzee DNAs were digested with the restriction endonuclease *Eco*RI, blotted, and hybridized as in Fig. 2*b* with ^{32}P-labelled probe 5 (Fig. 2*a*) and plasmid πSVβ (containing 3.7 kb of human genomic sequence from the β-globin locus; ref. 36). Probe detects a 4.5-kb human genomic *Eco*RI fragment common to the human X and Y chromosomes (Fig. 2*a*). It is also homologous to a 4.5-kb *Eco*RI fragment in chimpanzee. Plasmid πSVβ detects a 5.3–kb *Eco*RI fragment in both human and chimpanzee. In the human, this *Eco*RI fragment contains most of the β-globin gene and derives from chromosome 11. πSBβ also hybridizes to two smaller *Eco*RI fragments in both human and chimpanzee (in man, these are known to correspond to the remainder of the β-globin locus and to the δ-globin locus). *b*, Densitometric tracings of portions of two lanes (chimpanzee male no. 1 and female no. 1) of an autoradiogram produced without an intensifying screen but otherwise identical to that in *a*.

Table 1 Calculations of X–Y sequence divergence at *DXYS1*

Distribution of restriction sites on the X and Y chromosomes

6-base enzymes	m_X	m_Y	m_{XY}	4-base enzymes	m_X	m_Y	m_{XY}
*Eco*RI	6	6	6	*Taq*I	3.5	2	2
*Bgl*II	8	8	8	*Msp*I	2	2	2
*Hin*dIII	6	6	6	Total	5.5	4	4
*Bam*HI	0	1	0				
*Kpn*I	2	2	2	$\bar{m} = 4.75$			
Total	22	23	22				

$\bar{m} = 22.5$

Combined 6- and 4-base enzyme data: $d = 0.0083 \pm 0.0054$

6-base enzyme data only: $d = 0.0037 \pm 0.0038$

The fraction of nucleotides at which the X and Y chromosomes differ at *DXYS1* was estimated using data drawn from the X–Y comparative restriction map of Fig. 2*a* and formulae for 'nucleotide counting' of Nei and Tajima[15]:

$$d = d_1 \frac{\sum_i r_i(\bar{m}_i - m_{XYi})/[\{1-(1-d_1)^{r_i}\}\{2-(1-d_1)^{r_i}\}]}{\sum_i r_i \bar{m}_i/[2-(1-d_1)^{r_i}]}$$

where $d_1 = 1 - \hat{S}^{1/r}$,

$$\hat{S} = \frac{2m_{XY}}{m_X + m_Y},$$

i refers to the ith type of enzyme (in this case there are two types, 4-base and 6-base enzymes),

$$\bar{m} = (m_X + m_Y)/2$$

and where the standard error of d is

$$s_d = \left(\frac{1}{\sum_i \frac{2r_i^2 \bar{m}_i S_i}{(2-S_i)(1-S_i)}} \right)^{1/2}$$

where

$$S_i = e^{-r_i d}$$

where d is the estimated fraction of nucleotides at which X and Y differ; r, the number of base pairs recognized by a given restriction enzyme (in this case, 6 or 4); m_X and m_Y, the number of restriction sites on, respectively, the X and Y chromosomes; m_{XY}, the number of restriction sites shared by the X and Y chromosomes. Note that the polymorphic *Taq*I site on the X chromosome contributes 0.5 to the value of m_X for *Taq*I.

~22 kb at *DXYS1*, nine are common to the X and Y chromosomes, one is specific to the Y chromosome, and one is specific to the X chromosome. Thus, of at least 12 *Mbo*I sites represented by these fragments, one site is specific to the Y (Fig. 2*a*), and all other sites are common to the X and Y chromosomes. The results of several hybridization experiments that revealed restriction sites specific to either the X or the Y chromosome are shown in Fig. 2*b*.

Sequence divergence

The fraction of nucleotides at which a pair of homologous DNAs differ can be estimated by comparing the restriction maps of the two sequences. Given the comparative X–Y restriction map of *DXYS1* (Fig. 2*a*), we set out to determine the fraction of nucleotides at which the X and Y chromosomes differ in this region. This fraction was estimated using the iterative 'nucleotide counting' method of Nei and Tajima[15]. In using this method, we assume that restriction cleavage sites are created or eliminated solely by substitutions of base pairs. The calculation involves only those mapped restriction sites which fall within the 21 kb at *DXYS1* which we have cloned, and which is mapped in its entirety for seven enzymes (Fig. 2*a*). The data on *Mbo*I fragments are not included in the calculation as they do not represent mapped sites. Drawing on data for the seven other enzymes, we estimate that the human X and Y chromosomes differ at 0.83 ± 0.54% of their nucleotides at *DXYS1* (Table 1). It has been argued that CpG nucleotide dimers (such as occur within the recognition sequences of the enzymes *Taq*I and *Msp*I) are remarkably prone to mutation in humans[16]. If the *Taq*I and *Msp*I data are eliminated from the calculation of X–Y sequence divergence, the estimate of that divergence falls to 0.37 ± 0.38%.

Homologous sequences in great apes

Our estimate of X–Y sequence divergence at *DXYS1* (0.37 ± 0.38%) is lower than estimates of the divergence of the human and chimpanzee genomes as a whole (1–3%)[17–20]. Assuming that the X and Y chromosomes do not evolve more slowly than the autosomes, this suggests one of two possibilities. First, *DXYS1* could represent an evolutionarily ancient homology between the X and Y chromosomes and some mechanism could retard or repair X–Y divergence at that locus. Alternatively, the presence of *DXYS1* sequences on both the X and Y chromosomes might be a phenomenon limited to recent evolutionary times. According to this hypothesis, *DXYS1* sequences have been present on both the X and Y chromosomes only for a period comparable to or shorter than that since humans diverged from chimpanzees.

To distinguish between the two possibilities, genomic DNAs from the great apes were examined for sequences homologous to *DXYS1*. If *DXYS1* represents an ancient homology between the X and Y chromosomes, one would expect to find *DXYS1*-homologous sequences on both the X and Y chromosomes in all the great apes. However, if X–Y homology at *DXYS1* is of recent origin, one would expect to find *DXYS1*-homologous sequences on either the X or Y chromosome, but not on both.

Filter hybridization experiments revealed that the great apes have *DXYS1*-homologous sequences only on their X chromosomes. Gel transfers of *Eco*RI digests of human and ape DNAs were hybridized with probe 5 (Fig. 2*a*) at moderately high stringency as described in Fig. 2 legend. At least one male and one female of each of three ape species (chimpanzee, gorilla

Table 2 Dosage of *DXYS1*-homologous sequences in male and female ape DNAs

	Sex	Autosomal standard: Ratio of areas *DXYS1*/β-globin	X-linked standard: Ratio of areas *DXYS1*/*DXS9*	No. of *DXYS1* copies per cell
Chimpanzee	M	0.30 (0.5)	0.83 (0.9)	1
	M	0.33 (0.6)	0.88 (1.0)	1
	F	0.59 (1.0*)	0.92 (1.0*)	2
	F	0.60 (1.0)	0.89 (1.0)	2
Gorilla	M	0.36 (0.6)	1.06 (1.1)	1
	F	0.62 (1.0*)	0.96 (1.0*)	2
	F	0.75 (1.2)	0.97 (1.0)	2
Orangutan	M	—	1.17 (1.2)	1
	F	—	1.00 (1.0*)	2
Human	M	0.60 (1.1)	1.95 (2.4)	2
	F	0.55 (1.0*)	0.83 (1.0*)	2

Genomic human, chimpanzee, gorilla and orangutan DNAS were digested with *Eco*RI, blotted and hybridized with probes for *DXYS1* and β-globin or *DXYS1* and *DXS9* (RC8, ref. 21) as described in Fig. 3 legend. To ensure a linear relationship of filter-bound radioactivity to absorbance on the autoradiogram, no intensifying screen was used. As in Fig. 3*b*, densitometric scans of the autoradiograms were made. The areas under the peaks corresponding to *DXYS1* and β-globin or *DXYS1* and *DXS9* were integrated, and, for each species, the ratios of these areas were normalized to the female, indicated by an asterisk. (*DXYS1*/β-globin ratios could not be calculated for the orangutans because of poor separation of the *DXYS1* and β-globin peaks.) The number of copies of *DXYS1* per cell was calculated assuming that females have two copies per cell of both β-globin and *DXS9* and that males have two copies per cell of β-globin and one of *DXS9*.

and orangutan) were examined. In humans, probe 5 detects a 4.5-kb *Eco*RI fragment that is common to the X and Y chromosomes. Thus there are two copies per cell in both males and females. All ape DNAs contained sequences homologous to *DXYS1* (for example, Fig. 3*a*). In the gorilla and chimpanzee, probe 5 detects a 4.5-kb *Eco*RI fragment, and in the orangutan, probe 5 detects two *Eco*RI fragments of 3.4 and 5.3 kb. Unlike the human, however, in all three ape species the dosage of *DXYS1*-homologous sequences is a function of sex. As judged using an autosomal (β-globin) or X-linked (*DXS9*, probe RC8; ref. 21) reference standard, in each of the three ape species, females contain twice as many copies of the *DXYS1*-homologous sequence as do males (Table 2, Fig. 3); no male-specific *Eco*RI (or *Taq*I, data not shown) fragment was found in any of the apes. The most economical interpretation of these findings is that *DXYS*1-homologous sequences occur only on the X chromosome among the great apes. Thus, it seems that X–Y homology at *DXYS1* is of recent origin and, among extant species, is found only in man.

Conclusions

Homology of single-copy DNA sequences on mammalian X and Y chromosomes was first reported at the human locus *DXYS1* (ref. 9), and there is now increasing evidence of substantial homology of single-copy sequences of no known function on the human X and Y chromosomes[22]. However, although a monoclonal antibody elicited by an antigen (12E7) encoded by the human X chromosome cross-reacts with an antigen coded for by the human Y chromosome[23], there is little rigorous evidence of homologous functional genes on the X and Y chromosomes of any mammal.

Our mapping of *DXYS1* to Xq13–q21 is consistent with the findings of other workers. J. Weissenbach (personal communication) has, by means of a different panel of rodent–human cell hybrids containing portions of the human X chromosome, assigned *DXYS1* to Xq12–q22. Drayna *et al.*[24] have recently demonstrated a genetic distance of about 12 centimorgans between *DXYS1* and *DXS17* (S21), which in turn has been mapped to Xq21–q22.

The findings reported here are not consistent with a model that limits X–Y sequence homology to the short arms of the X and Y chromosomes. Terminal portions of the short arms of the X and Y chromosomes pair during meiosis in human spermatogenesis[3–7], and this observation provided the basis for the prevailing model of homology between the human X and Y chromosomes[1,8]. According to this hypothesis, the terminal, pairing portions of the X and Y chromosomes are homologous at the DNA sequence level, while the non-pairing, or 'differential', portions are not. However, we have demonstrated the presence of single-copy DNA sequences (*DXYS1*) homologous to the Y chromosome at Xq13–q21, far outside the pairing region of the X chromosome. In addition, there seem to be numerous other single- or low-copy number[22] and repetitive[25] sequences on Xq which are homologous to the Y chromosome. Thus, although single-copy sequence homology between Xp and Yp may exist, X-Y homologous sequences are clearly not limited to those regions. Furthermore, *DXYS1* sequences on the short arm of the Y chromosome, virtually all of which is thought to pair with the X (ref. 26), have no homologue on the short arm of the X. Thus, although the pairing regions of the X and Y chromosomes may be partially homologous, it is unlikely that there is continuous X–Y homology throughout the length of the pairing region.

We have previously reported[9] our failure to observe meiotic recombination between the X and Y chromosomes at *DXYS*1. Given the location of *DXYS1* at Xq13–q21, it is now clear that single reciprocal cross-overs between the X and Y at *DXYS1* would destroy the integrity of both the X and Y chromosomes.

It is widely accepted that the mammalian X and Y chromosomes evolved from a completely homologous pair[2]. It has been assumed, as a corollary, that if limited homology of the human X and Y chromosomes exists, the homology should be ancient in an evolutionary sense[1]. The findings reported here demonstrate that this need not be the case. Among extant species, *DXYS1*-homologous sequences apparently occur on both the X and Y chromosomes only in man; in chimpanzee, gorilla and orangutan, *DXYS1*-homologous sequences are found only on the X chromosome. Thus, the simplest explanation is that *DXYS1*-homologous sequences were transposed from the X chromosome to the Y chromosome after the human line diverged. (To argue that the common ancestor of all four species had *DXYS1*-homologous sequences on both X and Y chromosomes, one must appeal to the loss of *DXYS1*-homologous sequences from the Y chromosome three times during evolution.) This hypothesis is consistent with the finding that the divergence of human X and Y DNA sequences at *DXYS1* is somewhat less than the divergence of the human genome from that of its closest relative, the chimpanzee. It is estimated that the human and chimpanzee lines diverged between 4 and 8 Myr ago[20,27,28]. Thus, *DXYS1* sequences have been present on both the X and Y chromosomes for less than—perhaps much less than—8 Myr.

The full extent of the X-to-Y transposition that occurred at *DXYS1* during human evolution is unknown, but it is clear that at least 36 kb of DNA was involved. To our knowledge, this X-to-Y transposition has not been detected by comparative light microscopic examination of banded human and ape chromosomes[29]. The recent finding[22,25] of other human X–Y homologous sequences on Xq suggests either that the transposition was much larger than 36 kb or that it was in some way directed by preexisting X–Y homologies.

We thank Tom Mañiatis for a human genomic DNA library; Kay Davies for a human X chromosome library and for phage RC8; Gail Bruns for cell hybrid DNAs; Kirby Smith for ape and human DNAs; Lou Kunkel for human DNAs; Stu Orkin for plasmid πSVβ; and Arlene Wyman and Linda Wolfe for preparing some of the human DNAs and Southern blots. We particularly thank Masatoshi Nei for assistance with the calculations of nucleotide divergence, and we appreciate the advice of Luca Cavalli-Sforza. We thank Connie Holm, Arlene Wyman and Linda Wolfe for useful criticisms of the manuscript. This work was aided by grants from the NIH (to D.B., Arlene Wyman and Melvin Simon) and from the Wills Foundation (to Arlene Wyman). D.C.P. received research stipends from Harvard Medical School, and M.E.H. received a NIH National Research Service Award.

Received 2 April; accepted 2 July 1984.

1. Polani, P. E. *Hum. Genet.* **60,** 207–211 (1982).
2. Ohno, S. *Sex Chromosomes and Sex-linked Genes* (Springer, New York, 1967).
3. Koller, P. C. *Proc. R. Soc. Edinb.* **B57,** 194–214 (1937).
4. Ford, C. E. & Hamerton, J. L. *Nature* **178,** 1020–1023 (1956).
5. Solari, A. J. & Tres, L. L. *J. Cell Biol.* **45,** 43–53 (1970).
6. Pearson, P. L. & Bobrow, M. *Nature* **226,** 959–961 (1970).
7. Moses, M. J., Counce, S. J. & Paulson, D. F. *Science* **187,** 363–365 (1975).
8. Burgoyne, P. S. *Hum. Genet.* **61,** 85–90 (1982).
9. Page, D. *et al. Proc. natn. Acad. Sci. U.S.A.* **79,** 5352–5356 (1982).
10. Page, D., Wyman, A. & Botstein, D. in *Banbury Rep. 14: Recombinant DNA Applications to Human Disease* (eds Caskey, C. & White, R.) 267–273 (Cold Spring Harbor, New York, 1983).
11. Botstein, D., White, R. L., Skolnick, M. & Davis, R. W. *Am. J. hum. Genet.* **32,** 317–331 (1980).
12. Darlington, C. D., Haldane, J. B. S. & Koller, P. C. *Nature* **133,** 417 (1934).
13. Kunkel, L. M. *et al. Proc. natn. Acad. Sci. U.S.A.* **74,** 1245–1249 (1977).
14. Kunkel, L. M., Tantravahi, U., Eisenhard, M. & Latt, S. A. *Nucleic Acids Res.* **10,** 1557–1578 (1982).
15. Nei, M. & Tajima, F. *Genetics* **105,** 207–217 (1983).
16. Barker, D., Schafer, M. & White, R. *Cell* **36,** 131–138 (1984).
17. King, M.-C. & Wilson, A. C. *Science* **188,** 107–116 (1975).
18. Benveniste, R. E. & Todaro, G. J. *Nature* **261,** 101–108 (1976).
19. Deininger, P. L. & Schmid, C. W. *Science* **194,** 846–848 (1976).
20. Sibley, C. & Allquist, J. E. *J. molec. Evol.* **20,** 2–15 (1984).
21. Murray, J. M. *et al. Nature* **300,** 69–71 (1982).
22. Weissenbach, J., Geldwerth, D., Guellan, G., Fellous, M. & Bishop, C. *Cytogenet. Cell Genet.* **37,** 604 (1984).
23. Goodfellow, P. *et al. Nature* **302,** 346–349 (1983).
24. Drayna, D. *et al. Proc. natn. Acad. Sci. U.S.A.* **81,** 2836–2839 (1984).
25. Mueller, C. R., Davies, K. E. & Ropers, H. H. *Cytogenet. Cell Genet.* 37, 545 (1984).
26. Solari, A. J. *Chromosoma* **81,** 315–337 (1980).
27. Sarich, V. M. & Cronin, J. E. in *Molecular Anthropology* (eds Goodman, M. & Tashian, R. E.) 141–170 (Plenum, New York, 1976).
28. Johanson, D. C. & White, T. D. *Science* **203,** 321–330 (1979).
29. Yunis, J. J. & Prakash, O. *Science* **215,** 1525–1530 (1982).
30. Harper, M. E. & Saunders, G. F. *Chromosoma* **83,** 431–439 (1981).
31. Lawn, R. M., Fritsch, E. F., Parker, R. C., Blake, G. & Maniatis, T. *Cell* **15,** 1157–1174 (1978).
32. Davies, K. E., Young, B. D., Elles, R. G., Hill, M. E. & Williamson, R. *Nature* **293,** 374–376 (1981).
33. Benton, W. & Davis, R. *Science* **196,** 180–182 (1977).
34. Southern, E. M. *J. molec. Biol.* **98,** 503–517 (1975).
35. Rigby, P. W. J., Dieckmann, M., Rhodes, C. & Berg, P. *J. molec. Biol.* **113,** 237–251 (1977).
36. Triesman, R., Orkin, S. H. & Maniatis, T. *Nature* **302,** 591–596 (1983).

Correlation between segmental mobility and the location of antigenic determinants in proteins

E. Westhof[*], D. Altschuh[*], D. Moras[*], A. C. Bloomer[†], A. Mondragon[†], A. Klug[†] & M. H. V. Van Regenmortel[*]

[*] Institut de Biologie Moleculaire et Cellulaire, CNRS, 15 rue Descartes, 67000 Strasbourg, France
[†] MRC Laboratory of Molecular Biology, Hills Road, Cambridge CB2 2QH, UK

Most continuous antigenic determinants of tobacco mosaic virus protein (TMVP), myoglobin and lysozyme correspond to those surface regions in the protein structure, as determined by X-ray crystallography, which possess a run of high-temperature factors along the polypeptide backbone, that is, a high segmental mobility. The mobility of an antigenic determinant may make it easier to adjust to a pre-existing antibody site not fashioned to fit the exact geometry of a protein. The correlation found between temperature factors and antigenicity is better than that between hydrophilicity and antigenicity.

THE antigenic reactivity of proteins resides in restricted parts of the molecule known as antigenic determinants or epitopes. Antigenic determinants represent the accessible patches on the surface of a native protein that interact with the binding sites of antibody molecules. Epitopes made up of a continuous sequence of amino acid residues are called 'continuous determinants' while 'discontinuous determinants' consist of residues that are not contiguous in the primary structure but which are brought together by the folding of the polypeptide chain[1]. The continuous epitopes comprise five to eight residues and their uniform size in different proteins reflects the constant size of the complementary antibody combining sites.

The localization of continuous determinants in proteins is based on measurements of the antigenic reactivity of natural or synthetic peptides of the molecule[2,3]. Usually, the fragments are tested for their ability to inhibit the reaction between antibodies and the whole antigen, and very high molar ratios of peptide to intact antigen are often required to achieve significant inhibition; this is usually explained by assuming that peptides exist in solution in a variety of random conformations and that only the rare conformations which approximate to that found in the native protein will bind to the antibody[4,5]. Both the N- and C-termini of different proteins often show higher than average antigenic activity[6–14], presumably because they are located at the surface and have a high relative flexibility[15].

In the last few years, the importance of the internal dynamics of protein molecules in relation to function has been emphasized[16–18]. This appreciation prompted us to examine whether there is a more general link between the local mobility of short segments of proteins and the antigenic structure. For this study we selected three proteins: the coat protein of tobacco mosaic virus (TMVP), myoglobin and lysozyme, which have been studied extensively by X-ray crystallography[19–21]. Present refinement methods[22,23] give not only precise atomic coordinates but also atomic temperature factors (B values). The temperature factor represents the mean-square displacement of each atom and, when plotted against residue number, provides a graphic image of the degree of mobility existing along the polypeptide chain. Such plots were used to examine the possible correlation between the mobile segments of these proteins and the locations of their epitopes.

Tobacco mosaic virus protein

The antigenic properties of the coat protein of tobacco mosaic virus have been extensively studied by several groups[24]. Milton and Van Regenmortel[25] originally reported that TMVP possesses five continuous antigenic determinants situated in tryptic peptides I, IV, VIII and XII. Peptide I contains two epitopes located in residues 1–10 and 34–39. The epitope in peptide VIII has been studied extensively by Benjamini[26], who located it in residues 105–112, although some residual activity is also found in the shorter pentapeptide, 108–112. Two additional antigenic determinants were recently identified[10] in residues 55–61 and 80–90, by comparing the inhibitory activity of tryptic peptides II, III (42–61) and VI (72–90) from three strains of the virus. Three peptides corresponding to residues 72–77, 129–134 and 142–147 that were synthesized because they correspond to accessible regions on the surface of the TMVP molecule were found to have no significant (that is, above the 10% level) antigenic activity in enzyme-linked immunosorbent assay (ELISA) inhibition tests.

Thus, the many studies of the antigenic structure of TMV[10,26,27] have so far revealed only seven continuous epitopes in the protein. The immunoassays were carried out at very low

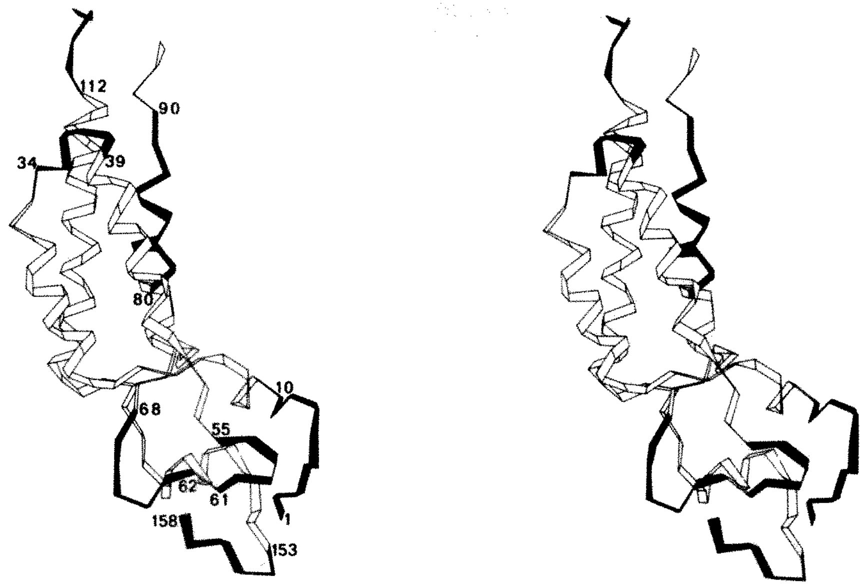

Fig. 1 Stereo drawing of the α-carbon backbone of the TMVP subunit at the present stage of refinement of the protein disk (A-ring). All residues (1–158) are shown except for 94–106, which are omitted because this region of the polypeptide has no specific conformation in the disk. The locations of the seven continuous antigenic determinants are indicated by solid lines.

concentrations where the protein is almost totally dissociated into monomers. The presence of very small amounts of other species would, in any case, not influence the measured degree of inhibition.

The seven epitopes are situated in the vicinity of residues 1–10, 34–39, 55–61, 62–68, 80–90, 105–112 and 153–158. Their positions in the TMVP molecule are shown in Fig. 1. The starting model of the TMVP subunit as seen in the protein disk at 2.8 Å resolution[19] has been subjected to constrained crystallographic refinement[22] to produce these coordinates and temperature factors (A.M. and A.C.B., in preparation). When the positions of the epitopes of TMVP were superimposed on a plot of the temperature factors of main-chain atoms in each residue (Fig. 2), it was found that all seven antigenic regions correspond to local maxima of the *B* value. Furthermore, the positions of six of the seven epitopes correlate with the major peaks, whereas only one epitope corresponds to a minor peak (residues 55–61); the lack of mobility in this seventh epitope can perhaps be explained by the fact that, in the crystal, residues 55–61 are constrained, in both layers of the TMV protein disk, by strong intermolecular contacts involving hydrogen bonding, hence they show a lower *B* value than would occur in an isolated monomer. A similar plot of the overall temperature factor for each residue (thus including the side-chain atoms) displays additional peaks which do not correspond to observed antigenic determinants. Thus, side-chain mobility does not correlate with antigenicity whereas that in the main chain does.

It is well known that the N- and C-termini of many proteins are flexible and accessible on the molecular surface[15]. In several cases (reviewed in 28, 29) the termini are known to be antigenic determinants (for example, the carboxy-terminal of histone H3 (ref. 9), TMVP[10], simian virus 40 T-antigen[30]). However, we did not expect that all the other known epitopes of TMVP would also belong to regions having higher than average flexibility. The three antigenically inactive peptides (residues 72–77, 129–134 and 142–147) lie in surface regions but do not have *B* values significantly different from the mean. This last finding shows that the correlation in Fig. 2 is not based solely on the high surface accessibility of these regions.

The locations of the seven TMVP epitopes were also superimposed on a plot (Fig. 3) of the hydrophilicity values of the protein residues calculated according to Hopp and Woods[31,32]. These plots have been used to predict positions of epitopes in proteins for which only the sequence is known[32–34]; their predictive value stems from the fact that hydrophilic residues lie predominantly at the surface and are therefore more likely to belong to epitopes. Although Fig. 3 shows a good correlation between antigenicity and some of the hydrophilicity peaks (for example, residues 62–68), several of the maxima correspond to regions with no proven antigenic activity, and the agreement with hydrophilicity is thus less striking than that with *B* values.

Myoglobin

The antigenic structure of myoglobin has been studied extensively by Atassi and collaborators[35], who identified five epitopes in residues 15–22, 56–62, 94–99, 113–119 and 145–151. Although it was claimed that these five sequences accounted for all the antigenic properties of myoglobin[36], subsequent work showed that additional continuous epitopes are present in regions 1–6, 22–55, 72–89 and 121–127 (refs 37–40).

The temperature factors plotted in Fig. 4*a* are taken from the restrained least-squares refinement[22] of oxymyoglobin at 1.6 Å resolution[20] using diffraction data collected at −12 °C. The *B* values are, in general, low in helical regions and high at bends and chain termini, but it is clear that in myoglobin the deviations from the mean are small[20] and few distinctive peaks are present (Fig. 4*a*). This observation is related to the high helix content and compact nature of the protein, which has no long flexible

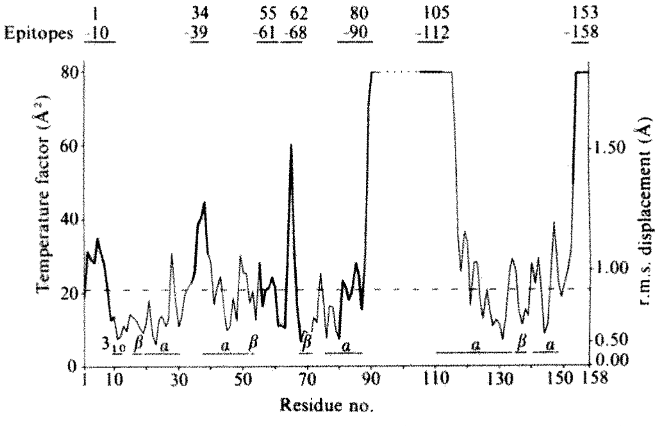

Fig. 2 The mean temperature factor of the main-chain atoms in each residue plotted against residue number for the TMVP disk. These temperature factors are from the constrained crystallographic refinement[22] of the disk of TMVP at 2.8 Å resolution. Strict 17-fold non-crystallographic symmetry constraints were applied throughout the refinement. Temperature factors for the A-ring are shown here although those for the B-ring are esentially the same (A.M. and A.C.B., in preparation). The mean value of the temperature factor (omitting residues for which $B > 80$) is shown by a dashed line. The locations of the seven continuous antigenic determinants are indicated by thick lines. Regions of secondary structure are denoted α, β, 3_{10}. The r.m.s. value of the displacement is calculated from $\overline{U^2} = \overline{U_x^2} + \overline{U_y^2} + \overline{U_z^2} = 3B/8\pi^2$, where U is the total displacement and U_x, U_y, U_z are the components.

loops. The positions of six of the nine epitopes correlate with local maxima; however, one epitope (residues 56–62 at the tight corner between helices D and E) corresponds to a minimum. No conclusion can be made about the epitopes in peptides 22–55 and 72–89 (ref. 40) because of the uncertainty in their location.

Lysozyme

The antigenic structure of lysozyme has been studied by Atassi and colleagues[41] who identified three discontinuous epitopes centred around the disulphide bridges 30–115, 76–94 and 6–127. It was claimed that these three epitopes account for all the antigenicity of lysozyme[42], although other investigators have shown that the loop formed by the residues lying between the disulphide bridge at 64–80 (refs 43–46) and also residues 38–54 possess antigenic activity[47]. The antigenic reactivity of the loop depends on the preservation of the disulphide bridge.

Figure 4*b* shows the variation of the temperature factor along the polypeptide chain of lysozyme[21]. The mean main-chain temperature factors are from the restrained least-squares refinement[23] of the tetragonal hen egg white lysozyme (HEWL) at 2 Å resolution. Three peaks are seen in Fig. 4*b* around residues 47, 70 and 101. The peaks at 47 and 70 correlate with the known epitopes, but are not found in a corresponding plot for the orthorhombic form of HEWL, where these residues are involved in molecular contacts within the crystal[21]. The third peak, 99–102 (which corresponds to one tip of the active site), is found in both forms of HEWL[21] and also in human lysozyme[20]. No antigenic activity has been reported to involve these residues, but there is a discontinuous epitope nearby on the sides of the active site cleft, which, as noted by Artymiuk *et al.*[18], lies in a region of relatively high flexibility. We have isolated, by HPLC, a tryptic peptide that encompasses the region 99–102, but found that it possessed no antigenic reactivity in ELISA inhibition tests[11].

Conformational dependence of epitopes

Several opposing views of the nature of protein epitopes have emerged recently[48]. In one picture, proteins contain only a small number of discrete antigenic regions situated in highly accessible surface locations[36,42]. The presence of antigenic reactivity when these parts are excised from the intact molecule is then ascribed to the preservation of specific conformational features. That the antigenic reactivity of proteins is dependent on the native conformation is corroborated by the finding that there is usually very little cross-reactivity between the native and denatured forms of the molecule.

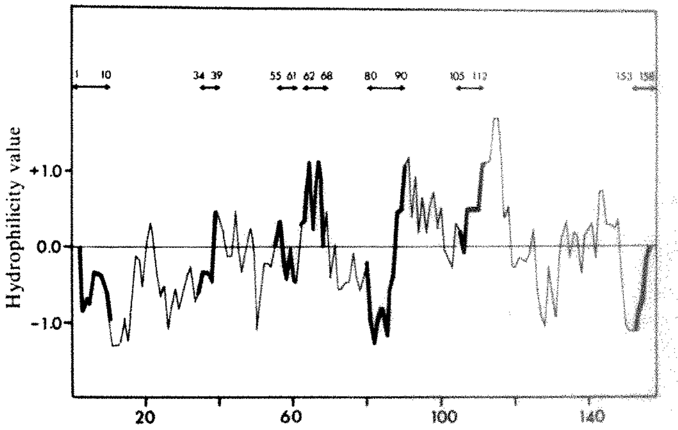

Fig. 3 The hydrophilicity value of each residue of TMVP (calculated after Hopp and Woods[31]) plotted against residue number, after averaging the value over six residues. The locations of the seven continuous epitopes are indicated by thick lines.

From studies of the immunological cross-reactivity between related proteins, a contrasting view has emerged—that virtually the entire accessible surface of a protein can combine with appropriate antibodies[49,50]. Consequently a considerable proportion of the antigenic determinants of globular proteins must be discontinuous in character as only a small part of the surface of a globular protein is made up of linear arrays of residues[40,48]. Indeed, attempts to locate protein epitopes by using monoclonal antibodies directed against the native molecule have led to the identification of mainly discontinuous epitopes[51–54]. It seems that as monoclonal antibodies recognize a small sample of all antigenic specificities, they are more likely to be directed against the numerous surface patches of a protein made up of residues distant in the sequence, rather than against continuous determinants.

Clearly, discontinuous epitopes cannot be studied with antibodies specific for short linear peptides and cannot be identified in linear plots of flexibility along the protein chain. Although the correlation we have demonstrated between segmental mobility and the location of epitopes pertains only to continuous epitopes, the notion of flexibility in epitopes is of considerable interest in the current debate on what constitutes an antigenic determinant.

The classical method of localizing epitopes by measuring the antigenic reactivity of cleaved fragments of the protein with anti-protein antibodies is now being increasingly replaced by an analysis of the specificity of antibodies raised against various fragments. It was originally believed that antibodies reactive with the native protein would be produced only if the fragment used for immunization closely reproduced the tertiary conformation of the protein. However, recent work shows that many

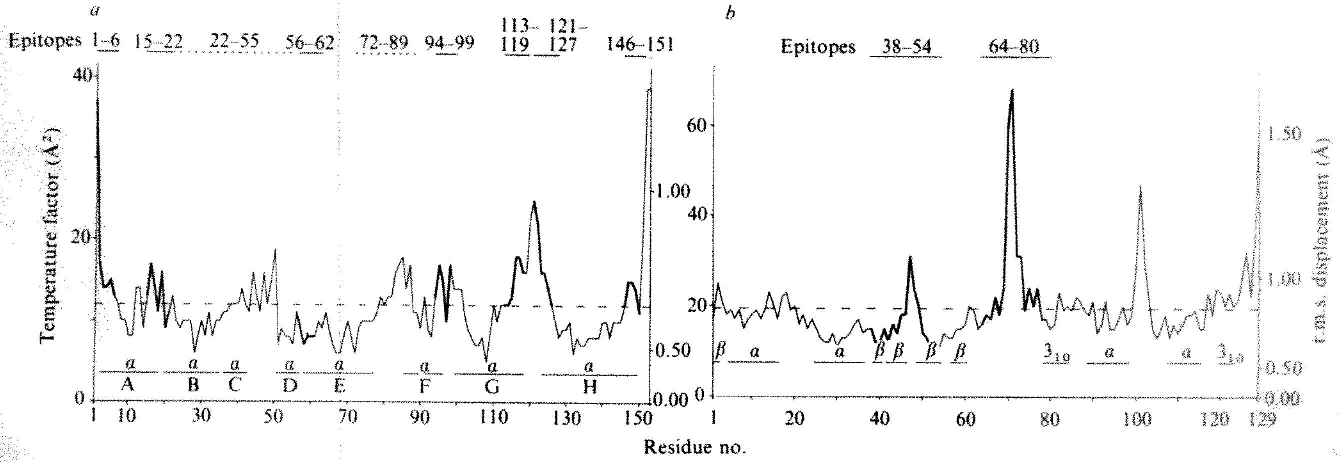

Fig. 4 The mean temperature factor of main-chain atoms plotted against residue number for: *a*, oxymyoglobin (redrawn after ref. 20) and *b*, lysozyme (redrawn after ref. 21). The mean temperature factor is shown by a dashed line. The first and last residue numbers are given for each continuous epitope and the mean displacement is calculated from $\overline{U^2} = 3B/8\pi^2$.

linear synthetic peptides corresponding to parts of proteins are able to elicit antibodies that react with the intact antigen[28–30,33,55]. One explanation is that synthetic peptides are able to mimic the corresponding regions of the native protein because one of the conformations adopted in solution approximates that in the native molecule[33]. In the so-called stochastic model, this native-like conformation of the peptide is assumed to be rare. An attempt to test this model involved estimating the frequency with which monoclonal antibodies directed against peptides recognize the corresponding intact protein[56]; of 21 hybridomas that synthesized antibody against an influenza haemagglutinin peptide, 16 produced antibodies that reacted with the complete molecule. Such a high frequency seems to refute the view that the immunogenic form of the peptide corresponds to a rare conformational occurrence. However, the results described for haemagglutinin are rather unusual, as conventional antibodies raised against the complete molecule did not react with any of 20 peptides representing nearly the entire sequence of the molecule[55]. Furthermore, it is also possible that the anti-peptide monoclonal antibodies recognized the intact haemagglutinin because this molecule had been partly denatured by the immunoassay procedures used in the experiments. It seems, therefore, that the stochastic model has not yet been adequately tested.

There is also an apparent contradiction between the finding that, on the one hand, monoclonal antibodies raised against a native protein are so conformation-specific that they usually do not bind to peptide fragments of the molecule, while, on the other hand, the majority of monoclonal antibodies raised against a peptide fragment also recognize the intact molecule[48,54,56]. This contradiction might disappear if truly native, that is, correctly folded, intact, molecules were tested for their ability to react with anti-peptide monoclonal antibodies.

The obverse explanation offered for the finding that anti-peptide antibodies specific for different conformations of the peptide bind to the complete molecule is that local disorder in short segments of the protein mimics the flexibility of the peptide in solution[56]. The data shown in Figs 2 and 4 represent the first concrete evidence of a link between high local mobility in proteins and the location of (continuous) antigenic determinants, but it should be stressed that this motion is generally one about a well-determined average conformation, even though the r.m.s. displacements in the cases of TMVP and lysozyme are of the order of 1–1.5 Å (Figs 2, 4*b*). The mobility in the epitope may make it easier to adjust to an antibody site which after all has not been fashioned to fit the exact geometry of a particular protein. It may be necessary, therefore, to discard one of the assumptions of protein immunochemistry according to which epitopes in intact proteins are conformationally rigid while epitopes in short peptides are highly flexible.

The view that linear peptides in solution necessarily comprise a very large number of conformers, only some of which are recognized by protein-specific antibodies, arose from the finding that large molar excesses (of the order of 10^3–10^4) of peptide over intact protein are needed to reveal their antigenic reactivity[4,5]. However, it is also possible that most antigenically active linear synthetic peptides contribute only a short stretch within them to a larger discontinuous antigenic region, and thus that the low level of antigenicity is not simply due to incorrect folding of the peptide.

Thus, the question remains of explaining the success that has been achieved in raising anti-peptide antibodies that are able to recognize apparently native proteins. It is conceivable that the extremes of segmental motion of proteins of the kind demonstrated here may provide the necessary degree of conformational similarity between the isolated peptide and the same region in the intact molecule. Epitopes located in flexible segments of the protein would be recognized in the form of peptides when the conformational prerequisites for building the antigenic structure are not very stringent—this is the case for the epitopes of TMVP and myoglobin that were identified by measuring the antigenicity (Fig. 2) and/or immunogenicity (Fig. 4*a*) of short peptides by using polyclonal antisera. In general, therefore, antibodies raised against a peptide would have a high probability of recognizing the corresponding epitope in the complete protein, whereas monoclonal antibodies raised against the intact protein would tend to be directed against the discontinuous epitopes which are more numerous[51,52,54].

Although segmental flexibility in proteins emphasizes only one type of antigenic determinant, its understanding is of crucial importance as it is probably on this type of epitope that present hopes for successful synthetic vaccines are ultimately based. Methods for predicting the secondary structure of proteins achieve a better success rate for loops and turns than for helices and sheets[57]. As loops and turns are more likely to correspond to flexible segments of proteins, peptides corresponding to sequences predicted to lie in these positions should be good candidates for synthetic vaccines.

A.M. thanks the National University of Mexico and ORS for support.

Received 24 April; accepted 27 June 1984.

1. Atassi, M. Z. & Smith, J. A. *Immunochemistry* **15**, 609–610 (1978).
2. Crumpton, M. J. in *The Antigens* Vol. 2 (ed. Sela, M.) 1–78 (Academic, New York, 1974).
3. Goodman, J. W. in *The Antigens* Vol. 3 (ed. Sela, M.) 127–187 (Academic, New York, 1975).
4. Sachs, D. H., Schechter, A. N., Bastlake, A. & Anfinsen, C. B. *Proc. natn. Acad. Sci. U.S.A.* **69**, 3790–3794 (1972).
5. Furie, B., Schechter, A. N., Sachs, D. H. & Anfinsen, C. B. *J. molec. Biol.* **92**, 497–506 (1975).
6. Anderer, F. A. *Biochim. biophys. Acta* **71**, 246–248 (1963).
7. Anderer, F. A. & Schlumberger, H. D. *Biochim. biophys. Acta* **97**, 503–509 (1965).
8. Absolom, D. & Van Regenmortel, M. H. V. *FEBS Lett.* **81**, 419–422 (1977).
9. Muller, S., Himmelspach, K. & Van Regenmortel, M. H. V. *EMBO J.* **1**, 421–425 (1982).
10. Altschuh, D., Hartman, D., Reinbolt, J. & Van Regenmortel, M. H. V. *Molec. Immun.* **20**, 271–278 (1983).
11. Altschuh, D. & Van Regenmortel, M. H. V. *J. immunol. Meth.* **50**, 99–108 (1982).
12. Bittle, J. L. *et al. Nature* **298**, 30–33 (1982).
13. Quesniaux, V., Briand, J. P. & Van Regenmortel, M. H. V. *Molec. Immun.* **20**, 179–185 (1983).
14. Quesniaux, V., Jaegle, M. & Van Regenmortel, M. H. V. *Biochim. biophys. Acta* **743**, 226–231 (1983).
15. Thornton, J. M. & Sibanda, B. L. *J. molec. Biol.* **167**, 443–460 (1983).
16. Gurd, F. R. N. & Rothgeb, T. M. *Adv. Protein Chem.* **33**, 73–165 (1979).
17. Karplus, M. & McCammon, J. A. *CRC Crit. Rev. Biochem.* **9**, 293–349 (1981).
18. Artymiuk, P. J. *et al. Nature* **280**, 563–568 (1979).
19. Bloomer, A. C., Champness, J. N., Bricogne, G., Staden, R. & Klug, A. *Nature* **276**, 362–368 (1978).
20. Phillips, S. E. V. *J. molec. Biol.* **142**, 531–554 (1980).
21. Berthou, J., Lifchitz, A., Artymiuk, P. & Jolles, P. *Proc. R. Soc.* **B217**, 471–489 (1983).
22. Jack, A. & Levitt, M. *Acta crystallogr.* **A34**, 931–935 (1978).
23. Hendrickson, W. A. & Konnert, J. H. in *Biomolecular Structure, Function, Conformation and Evolution* Vol. 1 (ed. Srinivasan, R.) 43–59 (Pergamon, Oxford, 1980).
24. Van Regenmortel, M. H. V. *Serology and Immunochemistry of Plant Viruses*, 302 (Academic, New York, 1982).
25. Milton, L. R. C. & Van Regenmortel, M. H. V. *Molec. Immun.* **16**, 179–184 (1979).
26. Benjamini, E. in *Immunochemistry of Proteins* Vol. 2 (ed. Atassi, M. Z.) 265–310 (Plenum, New York, 1977).
27. Van Regenmortel, M. H. V., Altschuh, D. & Briand, J. P. in *Protein Conformation as an Immunological Signal* (eds Celada, F., Schumaker, V. N. & Sercarz, E. E.) 181–190 (Plenum, New York, 1983).
28. Sutcliffe, J. G., Shinnick, T. M., Green, N. & Lerner, R. A. *Science* **219**, 660–666 (1982).
29. Shinnick, T. M., Sutcliffe, J. G., Green, N. & Lerner, R. A. *A. Rev. Microbiol.* **37**, 425–446 (1983).
30. Walter, G., Scheidtmann, K. H., Carbone, A., Laudano, A. & Doolittle, R. F. *Proc. natn. Acad. Sci. U.S.A.* **77**, 5197–5200 (1980).
31. Hopp, T. P. & Woods, K. R. *Proc. natn. Acad. Sci. U.S.A.* **78**, 3824–3828 (1981).
32. Hopp, T. P. & Woods, K. R. *Molec. Immun.* **20**, 483–489 (1983).
33. Lerner, R. A. *Nature* **299**, 592–596 (1982).
34. Tamura, T., Bauer, H., Birr, C. & Pipkorn, R. *Cell* **34**, 587–596 (1983).
35. Atassi, M. Z. *Immunochemistry* **12**, 423–438 (1975).
36. Atassi, M. Z. *CRC Crit. Rev. Biochem.* **6**, 337–369 (1979).
37. Schmitz, H. E., Atassi, H. & Atassi, M. Z. *Molec. Immun.* **19**, 1699–1702 (1982).
38. Young, C. R., Schmitz, H. E. & Atassi, M. Z. *Molec. Immun.* **20**, 567–570 (1983).
39. Schmitz, H. E., Atassi, H. & Atassi, M. Z. *Immun. Commun.* **12**, 161–175 (1983).
40. Leach, S. J. *Biopolymers* **22**, 425–440 (1983).
41. Atassi, M. Z. & Habeeb, A. F. S. A. in *Immunochemistry of Proteins* Vol. 2 (ed. Atassi, M. Z.) 177–264 (Plenum, New York, 1977).
42. Atassi, M. Z. & Lee, C. L. *Biochem. J.* **171**, 429–434 (1978).
43. Arnon, R. & Sela, M. *Proc. natn. Acad. Sci. U.S.A.* **62**, 163–170 (1969).
44. Arnon, R., Maron, E., Sela, M. & Anfinsen, C. B. *Proc. natn. Acad. Sci. U.S.A.* **68**, 1450–1455 (1971).
45. Teicher, E., Maron, E. & Arnon, R. *Immunochemistry* **10**, 265–271 (1973).
46. Ibrahimi, I. M., Eder, J., Prager, E. M., Wilson, A. C. & Arnon, R. *Molec. Immun.* **17**, 37–46 (1980).
47. Takagaki, Y., Hirayama, A., Fujio, H. & Amano, T. *Biochemistry* **19**, 2498–2505 (1980).
48. Todd, P. E. E., East, I. J. & Leach, S. J. *Trends biochem. Sci.* **7**, 212–216 (1982).
49. White, T. J., Ibrahimi, I. M. & Wilson, A. C. *Nature* **274**, 92–94 (1978).
50. East, I. J., Todd, P. E. & Leach, S. J. *Molec. Immun.* **17**, 519–525 (1980).
51. Berzofsky, J. A. *et al. J. biol. Chem.* **257**, 3189–3198 (1982).
52. East, I. J., Hurrell, J. G. R., Todd, P. E. E. & Leach, S. J. *J. biol. Chem.* **257**, 3199–3202 (1982).
53. Smith-Gill, S. J. *et al. J. Immun.* **128**, 314–322 (1982).
54. Van Regenmortel, M. H. V. in *Hybridoma Technology in Agricultural and Veterinary Research* (eds Stern, N. & Gamble, H. R.) 42–80 (Rowman and Allenheld, Totowa, New Jersey, 1984).
55. Green, N. *et al. Cell* **28**, 477–487 (1982).
56. Niman, H. L. *et al. Proc. natn. Acad. Sci. U.S.A.* **80**, 4949–4953 (1983).
57. Kabsch, W. & Sander, W. *FEBS Lett.* **155**, 179–182 (1983).

Antibodies to gap-junctional protein selectively disrupt junctional communication in the early amphibian embryo

Anne E. Warner, Sarah C. Guthrie & Norton B. Gilula*

Department of Anatomy & Embryology, University College London, Gower Street, London WC1E 6BT, UK
* Department of Cell Biology, Baylor College of Medicine, Houston, Texas, USA

Antibodies to the major protein of rat liver gap junctions, molecular weight 27,000 (27K), have been microinjected into one identified cell of 8-cell stage Xenopus *embryos. This treatment selectively disrupts both dye transfer and electrical coupling between the progeny cells. These results provide evidence that the 27K protein is an integral component of the cell-to-cell junctional channel. The disruption of junctional communication at early stages results in specific developmental defects, suggesting that blocking intercellular communication can have a pronounced influence on embryonic development.*

CELLS within the embryos of most species are able to communicate directly with each other through a low electrical resistance pathway. This pathway, which probably reflects the presence of the morphological structure, the gap junction[1], has been described in all embryos so far studied, both vertebrate and invertebrate[2]. Communicating junctions are found between embryonic cells, regardless of their eventual developmental fate, at times when other evidence suggests that they are capable of influencing each other. This has led to the suggestion[3] that the direct communication pathway mediated by gap junctions is responsible for the cell-to-cell transfer of information involved in directing embryonic development. Despite widespread support for this view, there is little evidence to indicate that gap junctions play a pivotal role in embryonic development.

There are a number of methods for reducing the permeability of gap junctions: raising intracellular calcium[4], lowering intracellular *p*H (ref. 5) or treatment with alcohols[6]. However, all of these methods elicit secondary metabolic effects, making it difficult to relate unequivocally any effects these agents might have on development with their ability to lower gap-junctional permeability.

In recent years it has become possible to isolate and characterize constituent proteins from isolated gap junction preparations[7,8]. This offers the opportunity to generate gap junction-specific antibodies which may be used to study the physiological properties of gap junctions. Here, we report the results of experiments to test whether antibodies raised against the major gap-junctional protein are able to interfere with cell–cell communication. In addition we have examined the developmental consequences of treatment with such antibodies.

Antibodies

For this analysis, three different affinity-purified rabbit polyclonal antibodies were selected. Polyclonal antibodies were preferred, as monoclonal antibodies are generally highly species-specific and rarely directed against functional portions of the molecule. Two of the antibodies (A and B) were generated by immunizing rabbits with a 27,000 molecular weight (27K) protein, the major protein present in rat liver gap junctions. The 27K protein was electrophoretically eluted from rat liver gap junctions which had been prepared as described in ref. 9. The sera from these two rabbits were purified on an affinity column containing only the eluted 27K protein. The resulting affinity-purified reagents bound specifically to the denatured 27K protein on immunoblots, as well as to 47K and 54K proteins present in homogenates of rat liver (Fig. 1*a* (1–3), *b* (1–3)). The 47K protein represents a 'dimeric' form of the 27K protein[7,8], while the relationship between the 54K and the 27K proteins in rat liver has not yet been clarified. All three of these molecules are recognized by the antibody that was affinity purified on the 27K column, as absorption with the 27K protein removes staining of the 47K and 54K bands. In addition, the affinity-purified antibodies bind to the cytoplasmic surface of intact rat liver gap junctions as indicated by electron microscopic immunolocalization both on isolated gap junctions and in intact liver. A detailed description of the preparation and characterization of the antibodies will be published elsewhere (N.B.G. *et al.*, in preparation). Immunochemical evidence for the existence of related determinants in *Xenopus* embryos was obtained by applying antibody B to a nitrocellulose blot containing the 27K rat liver gap junction protein, a rat liver homogenate, and homogenates of various stage *Xenopus* embryos (see legend to Fig. 1). The immunoblot in Fig. 1 provides direct evidence that antigenically related proteins, comparable in size to those found in rat liver, are present in unfertilized *Xenopus* eggs and embryos. The 54K molecule, present in homogenates of both rat liver and *Xenopus* embryos, is the most abundant antigenic species that has been detected in immunoblots of *Xenopus* homogenates (unfertilized eggs, fertilized eggs, 8-cell, and 32-cell embryos). As noted earlier, the relationship between the 27K protein and the 54K antigenic species has yet to be clarified both in rat liver and in *Xenopus*. The 54K protein could represent a biosynthetic precursor of the gap junction, as indicated by Epstein *et al.*[10] on the basis of the speed with which junctions can form between communication competent cells, and the ability to form junctions in the prolonged absence of protein synthesis and ATP production. Alternatively, the 54K protein may represent the undegraded gap-junctional protein as elimination of endogenous protease activity when preparing plasma membranes is very difficult. However, this uncertainty does not invalidate conclusions about the ability of the antibody raised against gap junctional protein to interfere with cell to cell communication, which are drawn from the results given below. The third antibody (C) was generated against, and specifically interacted with, an extracellular matrix glycoprotein that is synthesized and secreted by rat liver and *Xenopus* embryos. There was no cross-reactivity between this antibody and any of the species recognized by the antibody raised against gap junction protein, or with gap junctions. Conversely, the gap-junction antibody does not recognize the extracellular matrix glycoprotein. The 54K protein recognized by the gap junctional antibody cannot, therefore, be a contaminant from the extracellular matrix glycoprotein. Antibody C was therefore used as a control antibody that did not interact with gap junctions or the 27K gap-junctional protein.

The presence of gap-junctional proteins in the unfertilized egg may seem surprising. However, in the early *Xenopus* embryo, zygotic RNA and protein synthesis does not begin until the 'midblastula transition' (ref. 11). All material necessary for progression through development to the blastula stage must, therefore, be available in the unfertilized egg. This would include the production of gap junctions, as well as many other cellular products. For example, it has been reported that fibronectin is present in early *Xenopus* embryos 2 h after fertilization and subsequently as a product of maternal transcripts[12], and large quantities of sodium are sequestered in the egg for subsequent transfer to the blastocoel fluid as the blastocoel cavity forms[13].

To test whether these antibodies were capable of interfering with intercellular communication, they were injected into *Xenopus* embryos at the 8-cell stage. The injections were always made into the same cell, located in the region of the grey crescent (Fig. 2*a*). Assays of intercellular transfer were made two cleavage divisions later at the 32-cell stage (Fig. 2*b*), which allowed sufficient time for the antibody to diffuse throughout the four daughter cells. To confirm that the cells contained the injected antibody, a second reagent, fluorescein isothiocyanate, (FITC)-conjugated goat anti-rabbit IgG, was applied directly to the antibody-injected region on frozen sections. The localization of antibody at the edge of the injected region is illustrated in Fig. 3*c*.

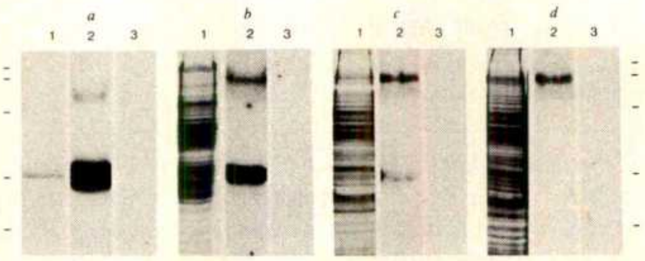

Fig. 1 Immunoblot analysis of rat liver gap-junction protein, rat liver homogenate, and *Xenopus* homogenates with pre-immune and immune affinity-purified antibody B. Lanes *a* (1–3) contained electrophoretically eluted rat liver 27K gap-junction protein, *b* (1–3) contained a protein homogenate from rat liver, *c* (1–3) contained a protein homogenate from *Xenopus* unfertilized eggs and *d* (1–3) contained a protein homogenate from 8-cell stage *Xenopus* embryos. The protein in lanes labelled 1 was separated electrophoretically and stained with Coomassie brilliant blue. Samples in all other lanes were transferred to nitrocellulose paper and treated with either the immune antibody B at 1:100 dilution (lanes 2), or with pre-immune antibody B at 1:100 dilution (lanes 3). The bound immunoglobulin was detected with an autoradiogram following treatment with ^{125}I-labelled *Staphylococcus* protein A. Molecular weight standards are indicated by lines to the left and right of the figure; they represent (from top to bottom) 68K (bovine serum albumin), 57.5K (catalase), 43K (ovalbumin), 25.7K (chymotrypsinogen), and 21.5K (soybean trypsin inhibitor). Note that the 27K junction protein was detected in both the Coomassie blue stained material (lane *a*, 1) and the autoradiograms of the immune antibody-treated material from the eluted 27K protein (*a*, 2), the liver homogenate (*b*, 2), and *Xenopus* unfertilized eggs (*c*, 2). The dimeric form of the 27K protein was readily detected in the eluted 27K preparation (*a*, 2), and minor amounts were detected in the other samples (*b*-*d*, 2). With the same reagent, a slightly larger molecule (about 54K) was detected in rat liver homogenates (lane *b*, 2). The 54K protein was also observed in *Xenopus*, and it was the most abundant antigenic species detected (lanes 2, *b*, *d*). No antigens were detected in any of the samples by the pre-immune reagents, lanes 3.

Methods: The *Xenopus* samples were prepared by collecting at appropriate stages (unfertilized eggs, fertilized eggs, 8-cell stage, and 32-cell stage), removing the vitelline membranes and jelly by dissection, and homogenizing material in 1 mM $NaHCO_3$ with a loose-fitting Dounce homogenizer. The homogenate was spun at 500*g* for 10 min in a Beckman TJ-6 centrifuge to remove most the yolk and pigment granules. The remaining supernatant was spun at 12,900*g* for 15 min in an Eppendorf centrifuge. Both pellets and supernatants from these samples were analysed immunochemically and found to contain immunoreactive material. The samples in this figure represent the 12,900*g* supernatants from the specimens of unfertilized eggs and 8-cell stage embryos. The different protein samples were solubilized in a SDS sample buffer[22] and electrophoretically separated with a 12.5% SDS-polyacrylamide slab gel. The gel was stained with Coomassie blue (2.5% Coomassie blue (w/v), 50% methanol, 7% glacial acetic acid) for about 15–20 min and then destained (40% methanol, 7% glacial acetic acid). For immunoblotting, the protein was electrophoretically transferred from the gel to nitrocellulose paper (BA85; Schleicher and Schuell) according to the published procedure[23]. The paper was initially 'blocked' by treatment with 3% bovine serum albumin (BSA) in Tris buffered saline (TBS) overnight at 4 °C, and then the appropriate antibody was added at a 1:100 dilution in 3% BSA–TBS for 2 h at room temperature. Following several washes in TBS containing 0.1% Nonidet P-40 (NP40), the blot was incubated for 1 h at room temperature with ^{125}I-labelled *Staphylococcus* protein A (ICN) (35 Ci g^{-1} protein). The blot was then washed with TBS–NP40, then TBS alone, dried, and placed on Kodak XAR film with an intensifying screen at −70 °C. The film was exposed for 3 days.

Transfer of Lucifer yellow

The pattern of cell–cell transfer of Lucifer yellow in the 32-cell *Xenopus* embryo is described elsewhere in this issue[14]. In the present experiments, injection of Lucifer yellow were made into one of the cells showing widespread transfer of dye to its lateral neighbours, cell *d* (see Fig. 2*b*), which is one of the progeny of the antibody injected cell. Following injection of either gap-junctional antibody A or B, cell *d* rarely transferred dye to its neighbours. Figure 3*b* is a photograph of an intact embryo after injection of Lucifer yellow into cell *d* of an embryo previously injected with antibody B. The adjacent frozen section (Fig. 3*a*) confirms that the Lucifer yellow remains confined to the injected cell. For comparison, a frozen section taken through an embryo initially injected with pre-immune serum B is shown in Fig. 3*d*, demonstrating extensive transfer of Lucifer yellow to its lateral neighbours. The results of all assays of Lucifer yellow transfer in this series of experiments are shown in Table 1. None of the injected reagents influenced cell membrane potential or cell division. In each set of control embryos, failure to transfer to one or more cells, other than the sister of the previous cleavage, was only observed in about 30% of the embryos tested. In contrast, between 70 and 80% of the embryos injected with antibody A or B failed to transfer dye; transfer failed to take place into cells lying on both sides of the injected cell (see Fig. 3*a*). This implies that the antibodies can block, or reduce, the permeability both of junctions formed before antibody injection, that is, those present at the 8-cell stage, and possibly of junctions formed during the subsequent cleavage to 16 cells. It is also possible that the antibody can inhibit the formation of junctions in later cleavage stages.

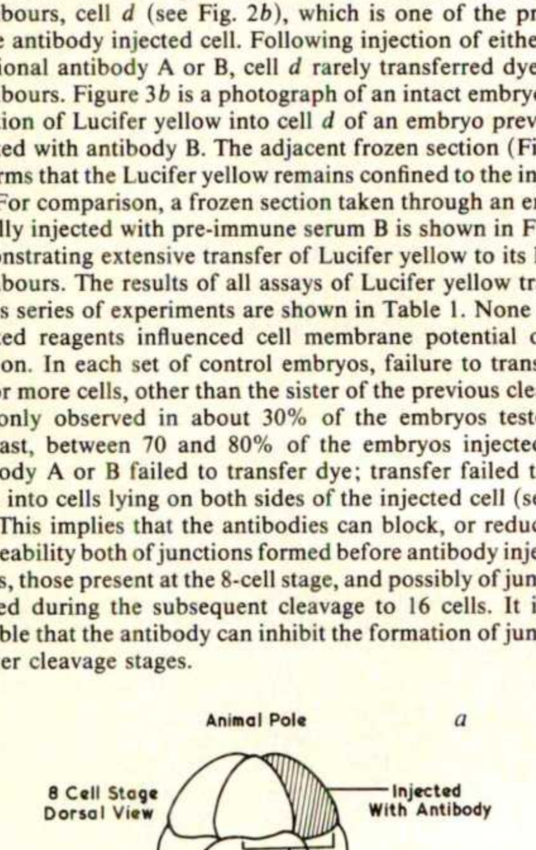

Fig. 2 The location of the cell injected with antibody at the 8-cell stage (*a*) and subsequently with Lucifer yellow, cell *d* (*b*). Hatched region indicates the presence of injected antibody. Cross-hatched region the presence of injected Lucifer yellow. ~15 nl antibody was pressure-injected using a Picospritzer. Lucifer yellow was injected ionophoretically at a current of 100 nA for 5 min with 30 s pulses at 10 Hz. Transfer of Lucifer yellow was assayed at the end of the injection period.

Table 1 Incidence of dye passage in 32-cell stage *Xenopus* embryos after injection of gap-junction antibodies

Condition	Transfer to more than one cell, excluding sister % (n)*	No transfer, or to sister cell only % (n)
Control 1	69 (11)	31 (5)
Control 2	63 (10)	38 (6)
Control 3	79 (11)	21 (3)
Pre-immune A	86 (12)	14 (2)
Pre-immune B	75 (12)	25 (4)
Immune A (I+II)	26 (13)	74 (37)†
Immune B (I+II)	18 (9)	82 (41)†
Immune C (I+II)	76 (40)	34 (21)

Control 1, values taken from ref. 14. Control 2, buffer containing 7.5 mM NaCl, 2.5 mM Na borate, 10 mM boric acid, pH 7.4. Control 3, buffer containing 5 mM Tris, 75 mm KCl, pH 7.6. Pre-immune A, IgG from rabbit A serum obtained prior to immunization injected at 1.5 mg ml^{-1}. Pre-immune B, IgG from rabbit B serum obtained prior to immunization injected at 1.5 mg ml^{-1}. Immune A, affinity-purified IgG from rabbit A after immunization with electrophoretically eluted 27K protein from rat liver gap junctions. Immune B, affinity-purified IgG from rabbit B after immunization with electrophoretically eluted 27K protein from rat liver gap junctions. Immune C, affinity-purified IgG from rabbit C after immunization with electrophoretically eluted glycoprotein from rat liver extracellular matrix. I, reagent affinity-purified X1, injected at a concentration of 1 mg ml^{-1} in buffer 2 or 3. II, reagent affinity purified X2, injected at a concentration of 1.5 mg ml^{-1} in buffer 2 or 3. Results with I and II were identical and were therefore combined in the table.

Methods: All injections were made at the 8-cell stage, in a volume of ~15 nl. Transfer of Lucifer yellow out of cell *d* (for nomenclature see ref. 14) was assessed at the 32-cell stage. Transfer to sister cell only was scored 'no transfer' because of cytoplasmic bridges remaining after cleavage. Transfer was assessed immediately after injection of the dye (5–7 min of injection). The affinity purified reagents were prepared chromatographically[21] using either the 27K protein (antibodies A and B) or the glycoprotein (antibody C) conjugated to CNBr-activated Sepharose 4B (Pharmacia). The sera were applied to the columns and the bound IgG reagents were eluted by treatment with 200 mM glycine, pH 2.6. The reagents were then dialysed against either 0.1 × control buffer 2 or 3, and concentrated 10-fold with a Savant Speed-Vac before use. IgG was obtained from the pre-immune sera by using a Protein A-Sepharose 4B (Pharmacia) column; the bound IgG was eluted by treatment with 100 mM glycine, pH 3.0.

* n = no. of embryos tested.

† Incidence of transfer significantly different from controls (χ^2 test, $P < 0.005$).

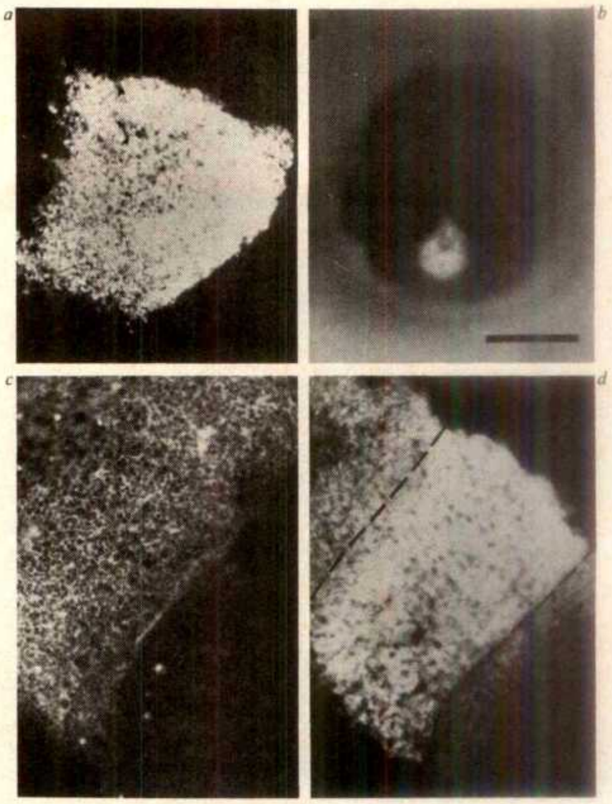

Fig. 3 *a*, Frozen section taken at the 32-cell stage through cell *d* to show restriction of Lucifer yellow to the injected cell after prior injection of antibody B at the 8-cell stage. *b*, Whole embryo injected with antibody B at the 8-cell stage, showing restriction of Lucifer yellow subsequently injected at the 32-cell stage. *c*, Frozen section at the 32-cell stage through embryo injected with antibody B at the 8-cell stage showing antibody stained with FITC-labelled goat anti-rabbit antibody (Nordic Laboratories) applied directly to the frozen section. Note clear restriction of antibody to one of the progeny of the cell injected at the 8-cell stage. *d*, Frozen section through cell injected with Lucifer yellow at the 32-cell stage after injection of pre-immune serum B at the 8-cell stage. Note extensive transfer to both lateral neighbours. Cell borders are indicated by dotted lines. Compare with *a*. Scale bar, 150 μm for *a*; 500 μm for *b*; 100 μm for *c* and 250 μm for *d*. For frozen sectioning, embryos were briefly fixed (1 h) in 4% formaldehyde, frozen in isopentane and 20 μm serial sections were taken on a Bright 5030 cryostat.

To confirm that the antibody was able to block junctions that were already formed, antibody B was injected into cell *d* at the 32-cell stage; this was immediately followed by injection of Lucifer yellow. Subsequent assay for dye transfer took place within 5 min of antibody injection (the minimum time for ionophoretic injection of Lucifer yellow). Of 12 embryos tested, 10 failed to transfer dye. This is significantly less than in control embryos ($0.01 > P > 0.005$). We therefore conclude that the antibody blocks transfer through intact junctions within a short time. It is unlikely that the block is the result of an increase in intracellular calcium, since direct injection of calcium ions will not block gap junctions in *Xenopus*[15]. A fall in intracellular pH ($p\mathrm{H_i}$) is also unlikely, as cell division is inhibited when $p\mathrm{H_i}$ falls sufficiently to block cell–cell communication[5]; cleavage was not affected by injection of antibody. The question of whether the antibody also inhibits the formation of new gap junctions in subsequent developmental stages is more difficult to resolve. This issue must await further experiments designed to analyse the structure of gap junctions in antibody-injected cells several cleavage stages later.

To confirm that these effects were the consequence of the presence of gap-junctional antibody, a number of other controls were carried out. Injection of an antibody to an extracellular matrix glycoprotein (antibody C) had no effect on the transfer pattern (Table 1). Injection of pre-immune sera from the rabbits used to raise antibodies A and B also did not interfere with the pattern of transfer, which was similar to that observed in control embryos (Table 1). Thus only injection of antibodies raised against gap-junctional protein interfered with dye transfer.

Similar experiments were carried out with monovalent fragments of the affinity-purified immunoglobulins, prepared from immune antibody B (refs 16, 17), in order to determine whether the disruption of communication was due to cross-linking of the multivalent IgG on the cytoplasmic surface of the junction, or to a direct interaction of the immunoglobulin with the 27K protein in the channel region. With non-immune Fab fragments (Cappel Laboratories; injected at 1.5 mg ml^{-1}) dye transfer failed in only 20% of the embryos, whereas with the immune fragments (injected at 1.5 mg ml^{-1}) dye transfer failed in 52% of the embryos tested. The incidence of failure to transfer observed after injection of the immune fragments is significantly greater than that observed with the non-immune fragments ($0.1 > P > 0.05$), suggesting that disruption of the channel permeability results from a direct interaction of the antibody with the 27K protein.

Effects on electrical coupling

Dye transfer provides a relatively insensitive measure of cell–cell communication, as low levels of transferred dye may not reach the threshold for detection. To confirm that failure of dye

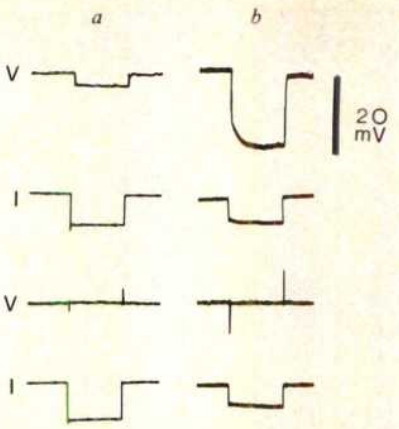

Fig. 4 Electrical coupling between cells injected with either antibody A (*a*) or antibody B (*b*). Embryos were released from the vitelline membrane and the seal between the blastocoel and extracellular fluid mechanically broken to prevent current flow through the extracellular space. One electrode injected hyperpolarizing current pulses (1 s long, 1×10^{-8} A in *a* and 3×10^{-8} A in *b*; current was recorded at different gains in *a* and *b*) into one cell while a second electrode inserted into a lateral neighbour recorded the resultant voltage deflection. Current and voltage recorded using conventional electrophysiological techniques and displayed on an oscilloscope and Gould-Brush pen recorder. Upper pairs of traces show electrical coupling between two cells in the uninjected region. Lower pairs show the absence of electrical coupling in the antibody containing region of each embryo; in both cases only capacitative artefact remains on the voltage trace. Membrane potential was −40 mV (*a*) or −30 mV (*b*). Membrane potentials in the injected and uninjected regions were within 5 mV of each other.

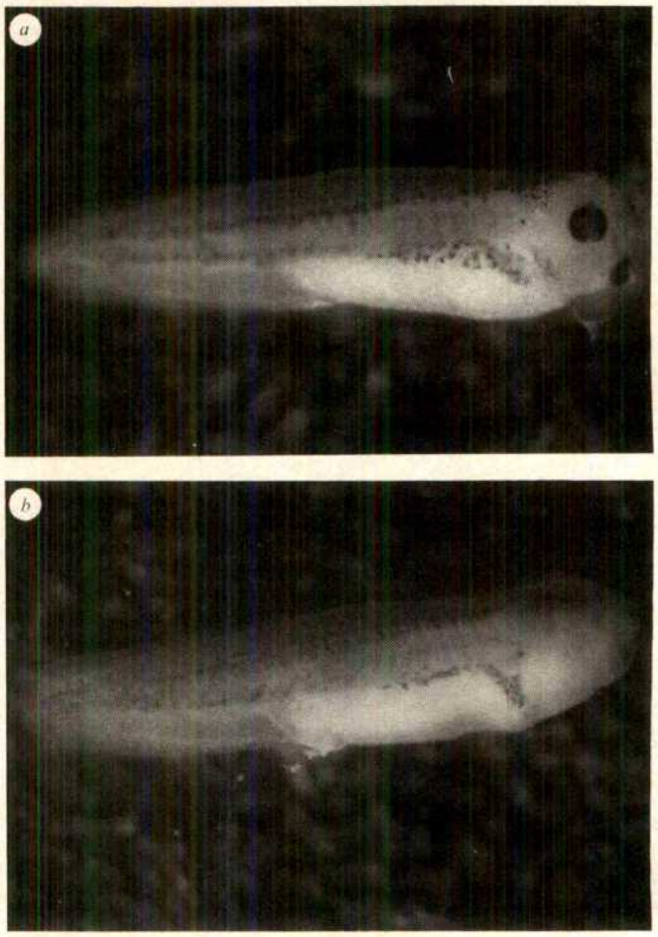

Fig. 5 A control embryo (*a*) and an embryo injected with antibody A at the 8-cell stage (*b*) photographed by S. E. Fraser prior to fixation, when the control had reached stage 36. The embryos are viewed from the right hand side. Note absence of the eye and deformed shape of the head in the antibody injected embryo. Note that the tail of the injected embryo is fairly normal. Sections through these two embryos to show the internal head structures are shown in Fig. 6.

transfer was accompanied by a reduction in electrical coupling, embryos which had been injected with Lucifer yellow and scored for failure to transfer dye were tested for the presence or absence of electrical coupling. In the whole embryo current can flow from one cell to the next through the restricted extracellular space because of the presence of tight junctions joining the outer edges of the cells. To avoid this complication, the embryos were released from their vitelline membranes and the seal into the blastocoel was broken mechanically before testing for electrical coupling. In each embryo, coupling was tested between cells lying in the uninjected animal pole region of the embryo for comparison with coupling between cells containing either antibody A or B. Figure 4 shows the results for two embryos. Injection with either antibody A (Fig. 4*a*) or antibody B (Fig. 4*b*) reduced electrical coupling to below the limits of detection. Similar measurements on 10 other embryos revealed either complete abolition of electrical coupling (8 cases), or a reduction to just above the detectable level (2 cases), between cells containing either gap-junction antibody.

The occasional failure of the antibodies to cause complete block of both dye transfer and electrical coupling is almost certainly the consequence of a large, potentially variable, amount of unassembled junction protein available in the egg. Undoubtedly, variability in the amount of antibody injected also contributes. Presumably all of the protein available to form junctional channels must combine with the antibody in order for the block to be completely effective.

These results show that two antibodies raised against a protein extracted from rat liver gap junctions are capable of blocking functional transfer of both a low molecular weight dye and small ions in the early *Xenopus* embryo. Since preliminary experiments to test the efficacy of such antibodies in a cultured rat liver cell line showed that antibody A prevented cell to cell transfer of 6-carboxyfluorescein, the results suggest that gap junctions in both *Xenopus* and rats share a determinant which is closely involved in controlling the transfer of molecules from cell to cell. This is consistent with the observed immunochemical homology (Fig. 1) and a previous report on the lack of specificity for generating cell to cell channels between heterologous vertebrate cells[18].

Developmental consequences

Cells injected with all the reagents tested, maintained normal resting potentials through many rounds of cell division and continued to divide at the same rate as other cells in the embryo. The injected embryos were examined for signs of cell death and extrusion throughout their development but no signs of death were observed. Embryos in which the injected cell was killed or injured (by deliberate over-irradiation after injection of Lucifer yellow) showed gradual failure of cleavage and cytolysis of the progeny of the injured cell. Such effects were never seen in embryos injected with gap junction antibody. Furthermore, the progeny of the cell which had been injected with Lucifer yellow at the 32-cell stage to test for dye transfer after antibody injection, were clearly visible in the living tadpole for at least 3 days. The progeny of the cell injected at the 8-cell stage contribute to both ectodermal and mesodermal derivatives on the right hand side of the embryo. Injection of either antibody A or B generated a high proportion of tadpoles with a characteristic set of abnormalities which were related to the developmental fate of the injected cell. The most frequently occurring defects were varying degrees of right/left asymmetry (63%), although some embryos (19%) failed to form brains and eyes on both sides. In asymmetric embryos the right eye frequently failed to form altogether; this was accompanied by gross underdevelopment of the brain on the right hand side. An example

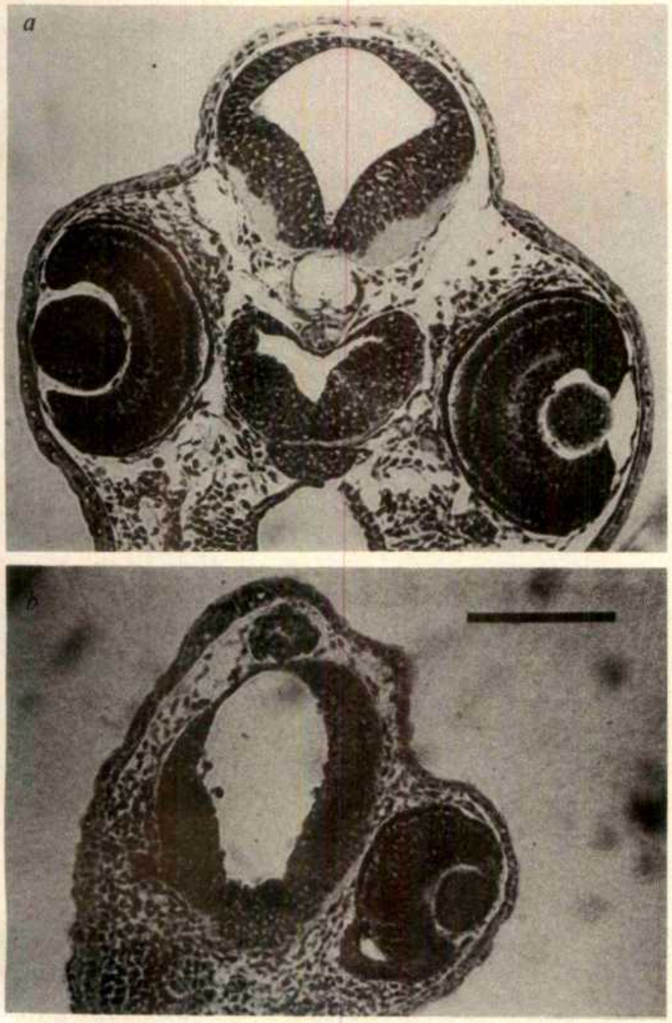

Fig. 6 Transverse section at the level of the developing eyes in a control embryo at Nieuwkoop and Faber stage 36 (ref. 24) (*a*) and an embryo of the same age which had been injected with antibody A at the 8-cell stage (*b*). Scale bar, 500 μm. The plane of section through the two eyes of the control embryo is not exactly the same because of a slight tilt in orientation. The experimental embryo shows three features of note: (1) the eye is missing on the side previously injected with gap-junction antibody; (2) the brain is the shape normally found anterior to the eyes and (3) the brain is particularly underveloped on the injected side. Embryos fixed in 2.5% glutaraldehyde in Ringer's solution overnight, washed in buffer, dehydrated in alcohols and embedded in methacrylate resin. 7 μm serial sections were cut on a Sorvall JB4 microtome and stained with haematoxylin and eosin.

of this defect in the intact embryo, produced by injection of antibody A, is shown in Fig. 5, along with a photograph of its sibling control (Fig. 5*a*). Figure 6 shows sections taken at the level of the eyes through these two embryos. In milder cases of impaired development, the notochord was shifted from its central position to the uninjected side and the brain and eyes on the right hand side were then much smaller than those on the left. Attempts to produce completely communication-incompetent embryos, by injecting antibody just before the first cleavage, or into both cells at the two cell stage, were unsuccessful; all such embryos died before gastrulation. None of the control reagents induced abnormalities above the spontaneous, low level. The abnormalities observed in control embryos were highly variable and rarely asymmetric.

Until we know how long the injected gap-junction antibody remains effective in blocking cell to cell communication and how the embryo responds to the presence of a group of non-communicating cells, it is difficult to relate the observed developmental defects directly to a role for gap-junctional communication. Nevertheless, the developmental defects induced by injection of antibodies to gap-junctional protein clearly warrant careful and detailed analysis.

Our studies show that two antibodies raised against the 27K gap-junction protein extracted from rat liver, are able to inhibit functional cell to cell communication in the early *Xenopus* embryo, assessed either as transfer of the dye Lucifer yellow or by electrical coupling. These observations provide direct evidence that the 27K protein in gap junctions is an integral component of the functional channel for cell–cell communication. Several studies have suggested that the channel is formed by the oligomeric arrangement of proteins[19,20]; this suggestion is clearly consistent with our findings. Furthermore, the disruption of intercellular communication caused by injection of antibodies to the 27K protein produces characteristic developmental defects. It should therefore now be possible: (1) to identify a molecular determinant(s) which controls the functional properties of gap junctions; (2) to further analyse the developmental consequences of blocking cell to cell transfer, in order to determine the developmental role of intercellular communication.

A.E.W. thanks the Wellcome Trust for a travel grant to enable preliminary experiments to be carried out, Scott Fraser for the hospitality and facilities of his laboratory and the MRC for support. S.G. is in receipt of an MRC Studentship. N.B.G. has received support from the NIH (grants GM 32230 and HL 28446). We thank Rosa Earls, Nigel Messenger, Lisa Satterwhite and Danna Zimmer for assistance, W. W. Stewart for a gift of Lucifer yellow and J. Hollyfield and L. Etkin for access to *Xenopus* materials in Houston.

Received 23 March; accepted 24 July 1984.

1. Gilula, N. B., Reeves, O. R. & Steinbach, A. *Nature* **235**, 262–265 (1972).
2. Spray, D. C., Harris, A. L. & Bennett, M. V. L. in *Cellular Communication During Ocular Development* (eds Sheffield, J. B. & Hilfer, S. R.) 57–84 (Springer, New York, 1982).
3. Potter, D. D., Furshpan, E. J. & Lennox, E. *Proc. natn. Acad. Sci. U.S.A.* **55**, 328–336 (1966).
4. Rose, B. & Loewenstein, W. R. *J. Membrane Biol.* **28**, 87–119 (1976).
5. Turin, L. & Warner, A. E. *J. Physiol.*, Lond. **300**, 489–504 (1980).
6. Johnston, M. F., Simon, S. A. & Ramon, F. *Nature* **286**, 498–500 (1980).
7. Henderson, D., Eibl, H. & Weber, K. *J. molec. Biol.* **132**, 193–218 (1979).
8. Hertzberg, E. L. & Gilula, N. B. *J. biol. Chem.* **254**, 2138–2147 (1979).
9. Hertzberg, E. L. *J. biol. Chem.* **259**, 9936–9943 (1984).
10. Epstein, M. L., Sheridan, J. D. & Johnson, R. G. *Expl Cell Res.* **104**, 25–30 (1977).
11. Newport, J. & Kirschner, M. *Cell* **30**, 675–686 (1982).
12. Lee, G., Hynes, R., Kirschner, M. *Cell* **36**, 729–740 (1984).
13. Slack, C., Warner, A. E. & Warren, R. L. *J. Physiol., Lond.* **232**, 297–312 (1973).
14. Guthrie, S. C. *Nature* **310**, 149–151 (1984).
15. Rink, T. J., Tsien, R. Y. & Warner, A. E. *Nature* **283**, 658–660 (1980).
16. Porter, R. R. *Biochem. J.* **73**, 119–126 (1959).
17. Slemmon, J. R., Salvaterra, P. M. & Saito, K. *J. Histochem. Cytochem.* **28**, 10–15 (1980).
18. Epstein, M. L. & Gilula, N. B. *J. Cell Biol.* **75**, 769–787 (1977).
19. Makowski, L. Caspar, D. L. D., Phillips, W. C. & Goodenough, D. A. *J. Cell Biol.* **74**, 629–645 (1977).
20. Unwin, P. N. T. & Zampighi, G. *Nature* **283**, 545–549 (1980).
21. Parikh, I., March, S. & Cuatrecasas, P. *Meth. Enzym.* **346**, 77–102 (1974).
22. Laemmli, U. K. *Nature* **227**, 680–695 (1970).
23. Towbin, H., Staehelin, T. & Gordon, J. *Proc. natn. Acad. Sci. U.S.A.* **76**, 4350–4354 (1979).
24. Nieuwkoop, P. D. & Faber, J. *Normal Table of Xenopus laevis* (*Daudin*) (North-Holland, Amsterdam, 1956).

Detection of molecular hydrogen in two merging galaxies

R. D. Joseph & G. S. Wright
Blackett Laboratory, Imperial College, London SW7 2BZ, UK

Richard Wade
Royal Observatory, Blackford Hill, Edinburgh EH9 3HJ, UK

NGC6240 and Arp 220 (IC4553) are two of the most luminous IR galaxies known[1,2]. They are also both thought to be examples of galaxy–galaxy mergers. As part of our study of interacting and merging galaxies[1,3,4] we have obtained IR spectra in the 2-μm region of NGC6240 and Arp 220 and detected the $v = 1\text{–}0$ S(1) quadrupole rotation–vibration emission line of H_2 (rest wavelength 2.122 μm) in both galaxies. (This line in NGC6240 has also recently been detected by E. E. Becklin *et al.*, personal communication.) These detections, which double the number of previously published measurements of extragalactic H_2 (refs 5, 6) suggest that the merger of two galaxies results in the production of massive quantities of shocked molecular gas. This shocked gas must cool and collapse, leading to an enormous burst of star formation. These measurements of shocked H_2 thus strengthen our earlier interpretation[1] of the extremely large IR luminosity of NGC6240 in terms of a 'super-starburst'. Arp 220 may be undergoing similar activity. We suggest that merging galaxies are a unique new class of ultra-luminous IR galaxies.

The spectra were measured on the UK Infrared Telescope (UKIRT) on the nights of 10 and 11 April 1984 using a seven-channel cooled grating spectrometer (CGS-2) with a 5 arc s aperture[7]. Wavelength calibration and the instrumental resolution of 550 km s^{-1} were derived from observations of Brackett γ (λ 2.166 μm) in the planetary nebula NGC7027. Spectra of the star BS5447 provided flux calibration. The spectra were measured at positions defined by the peak of the IR emission for NGC6240, and by the peak of the optical emission for Arp 220. The spectral coverage of the seven-channel spectrometer, ~0.023 μm, was centred on the $v = 1\text{–}0$ S(1) line of H_2 (hereafter, the S(1) line) redshifted to the recessional velocities of the galaxies. The full spectra obtained are shown in Fig. 1. The S(1) line is clearly detected in both galaxies and probably also resolved in both. The corresponding fluxes and luminosities, for $H_0 = 50$ km s^{-1} Mpc^{-1}, are given in Table 1. The luminosity in the S(1) line for NGC6240 of 10^8 $L_{\odot}$ may be compared with luminosities of 3×10^6 $L_{\odot}$ and 3×10^7 $L_{\odot}$ in this line for NGC1068 (ref. 5) and NGC3690 (ref. 6) respectively.

Using the data in Table 1 we can develop the following physical picture of the H_2 excitation in these two merging galaxies. First, this gas is almost certainly excited by shock-heating, as is the case for virtually all known examples of H_2 quadrupole emission[8]. In NGC6240, the width of the S(1) line, ~800 km s^{-1}, is identical to the widths of optical emission lines seen in a similar aperture on the nucleus, and which are thought to be shock-excited[9]. Fluorescence following absorption of UV photons is considered to be the most plausible alternative mechanism for excitation of these rotation–vibration levels. In this case, the $v = 2\text{–}1$ S(1) line should have about half the intensity of the $v = 1\text{–}0$ S(1) line[10]. Our failure to detect the $v = 2\text{–}1$ S(1) line in NGC6240 at a sensitivity similar to that reached for the $v = 1\text{–}0$ S(1) line detection, suggests that UV pumping does not contribute significantly to the excitation, and shocks remain as the most likely excitation mechanism.

Second, the mass of hot gas may be estimated by assuming local thermodynamic equilibrium at a temperature of 2,000 K (ref. 8). The luminosities in Table 1 then imply masses of excited molecular gas of ~10^5 $M_{\odot}$ and ~10^4 $M_{\odot}$ for NGC6240 and Arp 220 respectively.

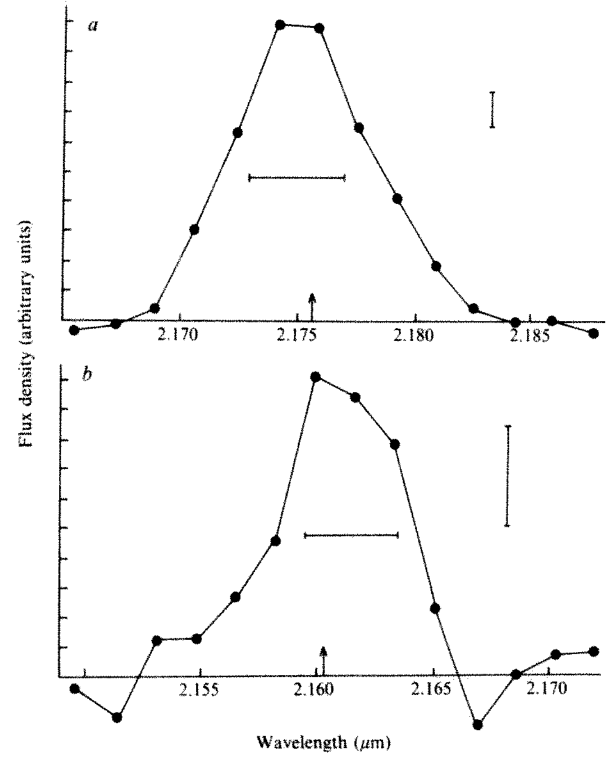

Fig. 1 Near IR spectrum of the nucleus of *a*, NGC6240; *b*, Arp 220 in a 5 arc s aperture. The arrow shows the wavelength of the 2.122 μm S(1) line redshifted to the radial velocity of the respective galaxies. The spectrum has been ratioed with the standard, smoothed using a triangular function, and the baseline has been subtracted off. The vertical bar represents the 1σ error per point, and the horizontal bar represents the instrumental resolution.

Third, we can use simple energetic arguments to investigate the underlying source driving the shocks. The gas cools to a temperature <1,000 K in about 3 yr (ref. 11), so in NGC6240 the shock excites about 3×10^4 $M_{\odot}$ of gas per year. The force, $\dot{m}v$, required to drive such a shock at a speed of ~20 km s^{-1} is ~5×10^{36} dynes. By comparison, the radiation pressure, L/c, of these ultra-luminous galaxies, with L_{IR} ~10^{12} $L_{\odot}$, is ~10^{35} dynes. Despite the high luminosities, radiation pressure is clearly insufficient to drive the shocks which we infer are present in these galaxies.

These objects are the results of galaxy–galaxy mergers, and are both likely to be examples of 'super-starbursts'[1,2]. Two obvious mechanisms for driving the shocks are either the relative kinetic energy of the collision, or mass outflow from the early-type stars in the starbursts. To investigate the relative contributions of these two processes we can use the ratios of the luminosities in the S(1) lines to the total IR luminosities. This ratio should have a characteristic value if the H_2 is excited by mass outflow from young stars, and the IR luminosity is provided by the luminosity of the early-type stars which is thermalized by dust and re-radiated in the IR. These ratios are presented in Table 2, along with that for Orion, a 'typical' star formation

Table 1 Fluxes and luminosities in the S(1) line

Galaxy	Flux (W m^{-2})	$L(L_{\odot})$
NGC6240	$(15\pm1)\times10^{-17}$	1×10^8
Arp 220	$(2.5\pm0.5)\times10^{-17}$	9×10^6

Table 2 The ratio of luminosity in the S(1) line to total, IR luminosity

Object	Ratio $(L(\mathrm{S}(1))/L_{\mathrm{IR}})$
NGC6240	20×10^{-5}
Arp 220*	1.2×10^{-5}
Orion	1.2×10^{-5}
NGC3690	3×10^{-5}
NGC1068	0.9×10^{-5}

* See comments in text.

region in the Galaxy[12]. For comparison, we have also included these ratios for the other two galaxies in which H_2 has been detected, NGC1068 and NGC3690 (refs 6 and 12). We have used our 10–20 μm UKIRT photometry[1] to obtain the appropriate IR luminosity for the nucleus of NGC6240 in a 5 arc s aperture, similar to that used for the S(1) observations. These measurements give an IR continuum spectrum of similar shape to the large aperture IRAS photometry[1] and imply a luminosity $L_{\mathrm{IR}} \sim 5\times10^{11}\ L_{\odot}$, a factor of 4 less than that inferred from the IRAS results. We have, therefore, used a similar factor to scale the IRAS luminosity for Arp 220 (ref. 2) to that expected in a 5 arc s aperture.

Table 2 shows that all the galaxies, with the exception of NGC6240, could be excited by mass outflow from star formation regions similar to Orion. NGC6240 is clearly the exception, by a factor of more than 10, and it is likely that mechanical energy in the galaxy–galaxy collision has provided most of the energy required to heat the H_2 gas. If we assume a galaxy mass of $\sim10^{12}\ M_{\odot}$, 10% of which is gas, and a relative velocity between the colliding galaxies of ~300 km s^{-1}, then this process supplies an energy of $\sim10^{59}$ ergs. For an efficiency of 0.002 in coupling shock energy into the S(1) line[13], the mechanical energy in the collision can excite the gas at the observed rate for a time $\sim2\times10^{7}$ yr. For Arp 220 the luminosity ratio in Table 2 is entirely consistent with excitation by mass outflow from star formation regions. However, it is very likely that we have not measured the maximum S(1) line intensity in Arp 220, since we observed only the optical nucleus. Given the physical similarity between NGC6240 and Arp 220, it would be surprising if a better measurement of the S(1) line flux did not result in a luminosity ratio closer to that for NGC6240.

There are several important conclusions to be drawn from these measurements. First, the existence of massive quantities of shocked molecular gas, in excess of that expected for star formation regions alone, is consistent with what might be expected when galaxies merge, and tends further to confirm other indications that NGC6240 is indeed the merger of two gas-rich galaxies. Second, both these galaxies are probably undergoing an episode of star formation of exceptional intensity, with shocked, and, therefore, dense H_2 produced at the rate of 3×10^{3} to $3\times10^{4}\ M_{\odot}\ \mathrm{yr}^{-1}$. This gas will cool rapidly, collapse and fragment, and result in a burst of star formation. The enormous mass of molecular gas that is shocked over any reasonable lifetime for this process, and its expected spatial extent on a scale of kpc if the shocks are merger-driven, as seems to be the case for NGC6240 at least, will produce an episode of rapid star formation of unusual spatial extent and intensity, that is, a 'super-starburst'. Finally, because dust is required to form the H_2 molecules[14], there must be dust present. It will thermalize the radiation from the newly-formed stars and re-radiate it in the IR. Thus these super-starbursts are likely to produce ultra-luminous IR galaxies. We have suggested previously[1] that NGC6240 is a paradigmatic example of such a process, and the detection of shocked H_2 strongly supports this interpretation. As a consequence, merging galaxies may be a unique new class of galaxies exhibiting super-starbursts and ultra-large IR luminosities.

This picture of interaction-induced shocks, which then trigger a super-starburst in merging galaxies, is physically coherent and plausible. However, there remain some fundamental unanswered questions concerning the details of these processes. First, how common might such a phase of vigorous H_2 excitation be among merging galaxies generally? As these two galaxies were selected for study on the basis of their large IR luminosities, it is difficult to attempt generalizations about the time scale of the phase of luminous H_2 emission on the basis of these measurements alone. However, the fact that the S(1) line is so luminous in two merging galaxies suggests that the episode of this activity may be a significantly large fraction of the time over which the morphological disturbance would be recognized as a merger. The dynamical simulations of Toomre and Toomre[15] and Wright[16] suggest that the tidal 'tails' resulting from an interaction persist for periods of the order of 10^{9} yr. This is longer than the 2×10^{7} yr estimated above for the time merger-driven shocks can excite the gas in NGC6240 at the observed rate. Despite the rather large uncertainties in this estimate, the duration of luminous H_2 emission powered by the merger is unlikely to be more than 10^{8} yr. Even if the H_2 were mostly excited by mass outflows from star formation regions, the time scale for such starbursts is probably $\lesssim10^{8}$ yr (ref. 17). This is also rather short compared with the merger lifetime. So, if these time scales are approximately correct, we would expect that only ~10% of the galaxies recognizable as mergers from their morphologies are currently undergoing a phase of activity similar to that in NGC6240.

Perhaps even more intriguing is the fact that we failed to detect the Paschen α hydrogen recombination line in NGC6240 at a comparable sensitivity to that reached in the S(1) line measurements. (We measured Paschen α because Brackett α, at a rest wavelength of 4.051 μm, is at the edge of the atmospheric transmission window at the redshift of NGC6240.) For those objects in which the H_2 excitation is thought to be due to mass outflows in star formation regions—NGC1068, NGC3690, and Orion—the Brackett γ line flux is within a factor of 2 of the S(1) line flux. Although we have shown that in NGC6240 the S(1) line is ~20 times stronger than expected for excitation from star formation regions, the Paschen α line is also expected to be about 12 times stronger than Brackett γ from recombination theory[18,19]. Because it is difficult to avoid the conclusion that the high IR luminosity of NGC6240 is due to a massive burst of star formation[1], our failure to detect the Paschen α recombination line is indeed surprising. Whether this can be understood in terms of a complex geometry for dust extinction, self-shielding by the H_2, or perhaps a starburst initial mass function with fewer high mass stars, requires further detailed analysis. Such an analysis, supplemented by additional spectroscopic results for these and other interacting galaxies, is in preparation.

We thank Charles Telesco, James Graham and especially Ian Gatley for stimulating and informative discussions. G.S.W. is a research student supported by the UK SERC.

Note added in proof: Molecular hydrogen emission has been discovered in these two galaxies by several independent observers as listed in IAU Circ. No. 3968.

Received 20 June; accepted 8 August 1984.

1. Wright, G. S., Joseph, R. D. & Meikle, W. P. S. *Nature* **309**, 430–431 (1984).
2. Soifer, B. T. *et al. Astrophys. J.* (submitted).
3. Joseph, R. D., Meikle, W. P. S., Robertson, N. A. & Wright, G. S. *Mon. Not. R. astr. Soc.* **209**, 111–122 (1984).
4. Graham, J. R., Wright, G. S., Meikle, W. P. S., Joseph, R. D. & Bode, M. F. *Nature* **310**, 213–214 (1984).
5. Thompson, R. I., Lebofsky, M. J. & Rieke, G. H. *Astrophys. J. Lett.* **222**, L49–L53 (1978).
6. Fischer, J., Simon, M., Benson, J. & Solomon, P. M. *Astrophys. J. Lett.* **273**, L27–L30 (1983).
7. Wade, R. *Proc. S.P.I.E.* **445**, 47–50 (1983).
8. Shull, J. M. & Beckwith, S. *A. Rev. Astr. Astrophys.* **20**, 163–190 (1982).
9. Fosbury, R. A. E. & Wall, J. V. *Mon. Not. R. astr. Soc.* **189**, 79–88 (1979).
10. Black, J. H. & Dalgarno, A. *Astrophys. J.* **203**, 132–142 (1976).
11. Kwan, J. *Astrophys. J.* **216**, 713–723 (1977).
12. Beckwith, S. in *Infrared Astronomy* (eds Wynn-Williams, C. G. & Cruikshank, D. P.) 167–178 (Reidel, Dordrecht, 1981).
13. Kwan, J. & Scoville, N. *Astrophys. J. Lett.* **210**, L39–L43 (1976).
14. Hollenbach, D. & McKee, C. F. *Astrophys. J. Suppl.* **41**, 555–592 (1979).
15. Toomre, A. & Toomre, J. *Astrophys. J.* **178**, 623–666 (1972).
16. Wright, A. E. *Mon. Not. R. astr. Soc.* **157**, 309–333 (1972).
17. Rieke, G. H., Leboksky, M. J., Thompson, R. I., Low, F. J. & Tokunaga, A. *Astrophys. J.* **238**, 24–40 (1980).
18. Giles, K. *Mon. Not. R. astr. Soc.* **180**, 57P–59P (1977).
19. Osterbrock, D. E. *Astrophysics of Gaseous Nebulae*, 65–66 (Freeman, San Francisco, 1974).

Detection of radiation from a heated and modulated equatorial electrojet current system

R. J. Lunnen*, H. S. Lee*, A. J. Ferraro*, T. W. Collins† & R. F. Woodman‡

* The Communications and Space Sciences Laboratory and
† Electronic Design Services, Department of Electrical Engineering, Pennsylvania State University, University Park, Pennsylvania, USA
‡ Geophysical Institute of Peru, Apartado 3747, Lima, Peru

In May 1983, ionospheric heating experiments were conducted using the Jicamarca very high frequency (VHF) radar facility located ~11 km east of Lima, Peru. Experiments involving high frequency (HF) heating of the lower *D*-region of the ionosphere were successfully conducted during 1982 using the Arecibo, Puerto Rico HF transmitter located 5 km east at Islote, Puerto Rico. These local experiments had characterized the signal radiated from a heated and modulated ionospheric current system near the mid-latitudes. A long-path signal had also been received in September 1982 at Salinas, Puerto Rico from a mid-day equatorial electrojet, heated and modulated by the Jicamarca facility. We have investigated the characteristics of the local signal that would be radiated from a strong equatorial electrojet when heated and modulated, and report here that at the geomagnetic equator they were similar to, but less intense than, those observed at Arecibo, Puerto Rico due to parameter differences. This radiation is believed to be the first detected from a heated and modulated equatorial electrojet current system in the Western Hemisphere.

The VHF heating experiments involved a research team from The Pennsylvania State University working in close cooperation with the Jicamarca Radar Observatory of the Geophysical Institute of Peru. Stubbe *et al.*[1] successfully detected radiation from the polar electrojet above Tromso, Norway and Ferraro *et al.*[2] have detected radiation from the dynamo current system above Arecibo, Puerto Rico. The Peruvian experiment involved heating the equatorial electrojet current system with the Jicamarca radar (76°52′ W, 11°57′ S, dip 2° N). ~5,547 MW of effective radiated power (with linear polarization at 49.920 MHz and a 2° beamwidth, modulated at a 5% duty cycle with a square wave at a frequency of 2.5 KHz) was radiated vertically into the atmosphere. The radar was then operated on a heating and cooling cycle of 2 min on and 2 min off. This type of experiment has been repeated many times using the Islote, Puerto Rico heating transmitter of the Arecibo Observatory; however, the parameters of the Islote transmitter differ from those of Jicamarca. Specifically, the usual Isolote heating frequency is 3.170 MHz and the duty cycle of the modulating signal is 50%. The two transmitting facilities are compared in Table 1.

The basic physics of electromagnetic radiation from a heated, modulated ionosphere at frequencies <30 KHz is influenced by the fact that ionospheric conductivity depends on the temperature of the electrons. The conductivity of the heated ionosphere varies periodically with the frequency of the heating radiation. The natural currents (such as, dynamo, polar electrojet, and equatorial electrojet) which pass through the heated region are modulated by conductivity changes, with radiation of energy at the modulating frequency having been detected.

The receiving system used a synchronous detector to measure the in-phase and quadrature components of the signal. A balanced loop 1 m in diameter consisting of 200 turns of number 14 wire with a tuned Q of ~55 at 2.5 KHz was used. A 0.5-m one-turn coaxially mounted loop was used for calibration using the procedure outlined in ref. 3. The signal was amplified, filtered, sampled and stored using a microcomputer with floppy diskette storage. Subsequent signal processing on the VAX 11/780 revealed the signal amplitude and phase as well as the Fast Fourier Transform (FFT) of the 2 min on–2 min off signal envelope.

Table 1 Comparison of transmitting facilities

	Islote, Puerto Rico	*Jicamarca, Peru
Geographical location	18°28′33″ N 66°39′57″ W	11°57′ S 76°52′ W
Magnetic lat.	32° N	0°
Magnetic dip	51° N	2° N
Frequency (MHz)	3–12	49.920
Antenna	4×8 array of orthogonal planer log-periodic	96×96 array of orthogonal half wave dipoles
Antenna zenith gain (D)	23–26	42
Antenna beamwidth (deg)	5–10	2
Duty cycle (%)	Variable	5
Power (maximum) (kW)	800	350
Effective radiated power (MW)	160–320	5,547

* Values present during experiment.

The long-path experiment was conducted on 17 September, 1982 with the Jicamarca radar operating as previously described. The receiving equipment was located at Salinas, Puerto Rico (17°59′ N, 66°16′45″ W). Salinas is located ~67 km south east of the Isolate transmitter and ~3,532 km from the Jicamarca Peru facility.

Figure 1 shows the 2.5 KHz FFT received on 17 September 1982 at Salinas, Puerto Rico. The dominant amplitude of 4.17 mHz corresponds to the on/off period of 240 s. The conversion of the amplitude to magnetic field strength at the loop was not accomplished for these data; however, when compared with the local primary component of 4.17 mHz, in volts, the local signal is stronger.

In May 1983 the receiving equipment was installed ~9 km south of the Jicamarca Observatory as shown in Fig. 2. A mountain range of several thousand feet separated the transmitter and the receiver. The transmitter was operated as previously described with two of four transmitters feeding the entire array. This limited the effective radiated power to 5,547 MW throughout the experiment. The high-power radiation capabilities were not utilized as the transmitter was undergoing modification at the time of the experiment. The radiation was linearly polarized with the electrical field in the north–south direction. The electrojet echo strength was monitored during the experiment with maximum returns near local noon. An antenna trap at 49.920 MHz was used to ensure that direct ground radiation would not affect the data. A VHF receiver was used to check the tone of the received signal from the transmitter. The tone scintillation on the 50 MHz receiver verified that there was a strong electrojet current during the received signal period.

The VHF heating test was conducted on 4, 5 and 9 May 1983.The dominant modulating frequency used was 2.5 KHz. Four hours of testing at 2.5 KHz during the first day were consumed in technical considerations of tuning receiving system calibration and general coordination to ensure valid test results. The receiving loop has its strongest quality factor at 2.5 KHz and a solid data base at this frequency from Arecibo testing was available for comparison. Only 1 h of testing was devoted to 5.0 KHz, 1.0 KHz and 0.08 KHz to complete a limited overall test schedule. No signals were found at these three frequencies; however, limited testing coupled with system parameters, past experience, and the need for tuning and calibration makes premature conclusions unwise.

The results at 2.5 KHz on 5 and 9 May 1983 were similar so only the latter are shown in Fig. 3. The signal radiated from the heated and modulated electrojet was observed within a few-hours window at local noon, chosen to coincide with a strong electrojet current. The received signal exhibited a cyclic character where it was visible in some portions of data and submerged in noise during others.

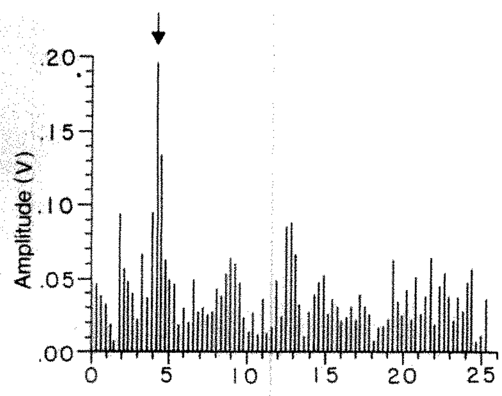

Fig. 1 Long-path amplitude spectrum, 2,500 Hz, Jicamarca, Peru to Salinas, Puerto Rico, 1600–1700 UT, September 1982.

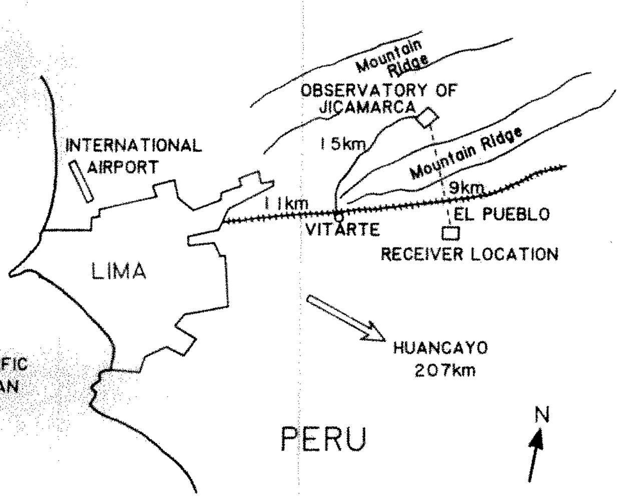

Fig. 2 Relative locations of the Radar Observatory of Jicamarca, Peru and the VLF/ELF receiver location.

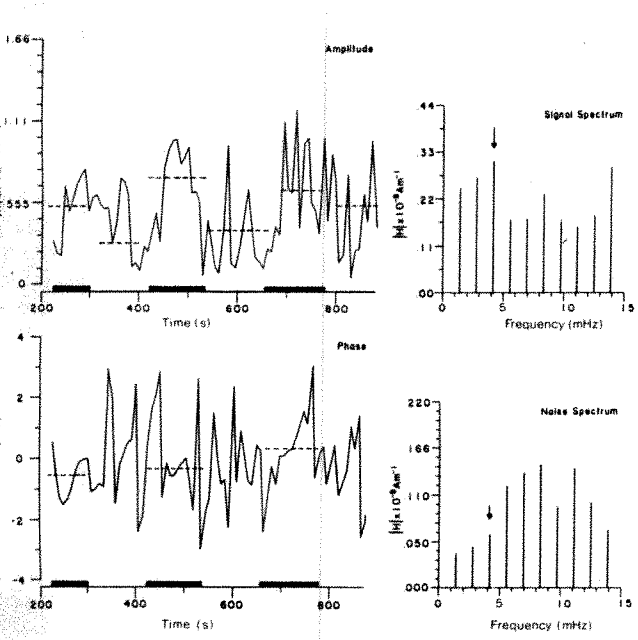

Fig. 3 Amplitude, phase and spectrum of a local Jicamarca, Peru signal at 2,500 Hz, 1345–1400 UT, 9 May 1983, compared with noise spectrum.

In Fig. 3, the amplitude and phase of the 2.5 KHz on 9 May are augmented with dashed lines to show average values. The intensity of the amplitude during the 2-min heating cycle, indicated by the dark portion of the time axis, was an order of magnitude less than a typical signal recorded at Arecibo. This is primarily attributed to the narrow beamwidth, higher heating frequency, and lower duty cycle of the Jicamarca radar compared with the Islote facility where parameters are closer to ideal. The phase tracking while the signal was being received is also characteristic of the Arecibo signal received. The amplitude spectrum shows the predominance of the 4.17-mHz spectral line. A pure noise spectrum is shown for comparison. The noise sample was recorded the day before testing because it could not be done while the experiment was in progress. This explains the apparent difference in amplitude of anything other than the primary frequency component. In this case, the calibration procedure was used to calculate the magnetic field strength at the loop, for comparison with Arecibo data recorded in 1983 and 1984.

Received 1 May; accepted 4 July 1984.

1. Stubbe, P., Kopka, H., Tructveld, M. & Dowden, R. L. *J. atmos. terr. Phys.* **44**, 1123–1135 (1982).
2. Ferraro, A. J. *et al. J. atmos. terr. Phys.* **44**, 1113–1122 (1982).
3. Jean, A. G., Taggart, H. E. & Wait, J. R. *J. res.* **65**, 189–193 (1961).

Bismuth in interplanetary dust

Ian D. R. Mackinnon & Frans J. M. Rietmeijer

Microbeam Inc., Mail Code SN4, NASA Johnson Space Center, Houston, Texas 77058, USA

Samples of a large (~60 μm) chondritic porous (CP) aggregate collected from the stratosphere have been analysed in detail by analytical electron microscopy (AEM). Previous studies of CP aggregates have shown that they are extraterrestrial in origin[1–3] and may be related to cometary debris[4]. CP aggregates are dissimilar to C1 and C2 carbonaceous chondrite matrices and many have not been significantly altered by thermal or radiation processes since their assembly[5]. We report here a high concentration of Bi_2O_3 grains within the large CP aggregate designated W7029*A (~60 μm) and suggest they formed by rapid heating (~300 °C) of elemental Bi grains within the aggregate during atmospheric entry. We examine the possibilities for terrestrial Bi contamination of CP aggregate W7029*A but judge them unlikely. Enrichment of elemental Bi within components of extraterrestrial materials is consistent with a nebula condensation model[6] and implies that Bi within CP aggregate W7029*A may have formed at a late stage of the condensation process.

W7029*A was collected from the stratosphere as part of the Cosmic Dust Program at Johnson Space Center[7]. Before allocation, a small (<10 μm) fragment of W7029*A was removed from the collection surface for preliminary examination. Scanning electron microscopy (SEM) and bulk chemical analysis by the Cosmic Dust Preliminary Examination Team[7] indicate that aggregate properties follow the criteria for a typical CP aggregate[4]. Portions of the aggregate were transferred from the collection surface to holey carbon films mounted on Be grids and gently washed with hexane in order to minimize contamination by the silicone oil used in the collection process. CP aggregate W7029*A is fragile and readily disaggregated on removal from the collection surface. Thus, individual fragments of the aggregate were suitably dispersed on carbon films for detailed AEM investigations. Electron microscopy on the allocated sample was performed with a modified JEOL 100CX AEM and with a Phillips EM420 AEM. Accelerating voltages of 100 and 120 kV, respectively, were used for all samples analysed. Each individual fragment or grain from this portion of the aggregate was then identified by a combination of high-resolution imaging, electron diffraction, electron energy-loss spectroscopy or energy dispersive spectroscopy (EDS). Modal analysis of CP aggregate W7029*A indicates that the following phases are predominant: carbon-rich phases (~47%), layer silicates (~11%), other silicates (~12%) and metals and/or oxides (~8%). Nine Bi grains (comprising ~50% of the metals or oxides) have been identified.

A typical example of a Bi grain from CP aggregate W7029*A is shown in Fig. 1. This conventional transmission electron microscopy (TEM) image shows an angular grain, ~350 × 400 nm in size, with a small (<2 nm) rim of less electron-dense material. The nature of the rim is unknown, but thin rims of a similar nature have been observed on individual crystals of cohenite[5] and (Fe, Ni) carbides[8] in other CP aggregates collected from the stratosphere. All Bi grains show a narrow size range between 0.5 and 0.25 μm. EDS analyses of all grains show the characteristic M and L lines for secondary X-ray fluorescence of Bi (Fig. 2). Determination of Bi from EDS spectra within the 0–10 kV range is difficult due to overlap of the Bi M line with the K line for sulphur (ref. 9). However, the higher energy-line positions (between 10 and 20 kV) and intensities ($L\alpha > L\beta > L\gamma$) provide an unambiguous identification of Bi. The inset in Fig. 2 shows the lower energy end of an EDS spectrum taken with a windowless energy dispersive spectrometer. A small peak for the oxygen K line is evident. The intensity of the O peak is significantly higher than that observed in spectra from carbon substrates containing residual silicone oil. The lower intensity of the O peak relative to the Bi M line is probably due to self absorption of the soft oxygen X rays.

Electron diffraction (inset, Fig. 1) from all Bi grains indicates that they are single crystals and confirm the oxide composition from EDS data[10]. Bi metal forms in space group R$\bar{3}$m with cell dimensions $a = 4.537$, $c = 11.838$ Å. Bi forms two oxides, Bi_2O_3 and Bi_2O_5, the former occurring as three well defined polymorphs[11]: monoclinic, tetragonal and body centred cubic. Two other polymorphic forms of Bi_2O_3 have also been described: oxide (I) and oxide (II)[12]. The structures of these latter forms are not well determined, but oxide (I) has a simple cubic structure with $a = 5.65$ Å (refs 12, 13). All grains observed in CP aggregate W7029*A index according to this simple cubic cell for Bi_2O_3 (ref. 12).

The geochemical properties of elemental Bi are unique and provide a convenient set of independent criteria to argue against terrestrial contamination of CP aggregate W7029*A during its entry into the stratosphere or after collection. Terrestrial Bi may enter the stratosphere by natural or anthroprogenic processes. However, we shall present arguments which show that, at the time, neither of these processes was significant for the collection of CP aggregate W7029*A.

Bi is not abundant in the terrestrial crust (ranges between 0.1 and 0.2 p.p.m.)[14] and is commonly found in the native state with traces of As, S and Te (ref. 15). Bi can also be found in sulphide minerals in veins associated with Ag–Pb ore deposits or in replacement deposits formed by hydrothermal solutions[15]. Although Bi minerals occur in pneumatolytic deposits associated with volcanic action, the Bi content of volcanic plumes is not known with any degree of certainty. Nevertheless, the collection period for flights which sampled W7029*A does not correlate with any reported volcanic eruption, still less a volcanic plume which penetrated the Northern Hemisphere tropospheric–stratospheric boundary. Thus, the lack of sulphur or other commonly associated elements within these Bi grains and the low concentrations of Bi minerals in the Earth's crust argue against a natural terrestrial origin for Bi in W7029*A.

Anthropogenic Bi contamination may occur through infall of debris from higher altitudes[16], atmospheric nuclear explosion plumes, or at a later stage of the collection and curation process. Alloys and oxides of Bi are used in the space and materials science industries[17]. However, in the most common applications (cosmetic and medicinal preparations) Bi is not used in great volumes, and even in low melting temperature alloys the metal is consumed in small quantities[15]. Bi within W7029*A derived from either of these sources should show trace or remnant compositions characteristic of the relevant alloy or oxide used in space or on Earth. Such compositional variety is not observed for any Bi particle in CP aggregate W7029*A. Furthermore, a survey of the collection and curation procedures at Johnson Space Center indicates that Bi metals, oxides or alloys are not contaminants at any stage of the process. An extensive survey of all possible forms of contamination within our sample preparation and analysis procedures has been undertaken during the past 2 yr. This survey has included detailed mapping of TEM grids before and after supply to the Curatorial Facility, SEM and AEM analysis of all forms of plastic, epoxy and mounting materials. Grains containing Bi have not been observed within these potential laboratory contaminants or unusual non-chondritic stratospheric particles.

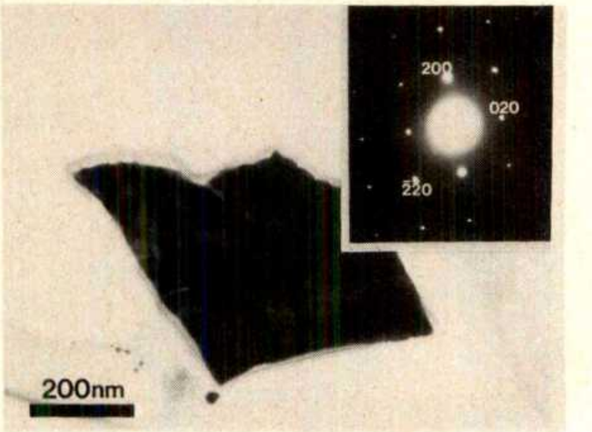

Fig. 1 TEM image of a typical Bi grain (mounted on holey carbon film) from CP aggregate W7029*A. The electron diffraction pattern (inset) is indexed according to a simple cubic form of Bi_2O_3.

Bi has one naturally occurring isotope (^{209}Bi) with a half life of 2×10^{18} yr (ref. 15). Five other isotopes of Bi occur as the daughter products of uranium or thorium decay. However, the longest half-life for any daughter product from these decay chains is ~5 days (ref. 15). The most recent recorded atmospheric nuclear test in the Northern Hemisphere occurred in late 1974[18,19]. Artificial tritium fallout studies at the South Pole indicate that stratospheric half residence times for gaseous species (for transport from the Northern Hemisphere to the South Pole) is ~20 months. Therefore, we infer that particulates will remain in the Northern Hemisphere stratosphere in normal conditions for less than 20 months. Any daughter Bi from a nuclear explosion plume in the Northern Hemisphere would have decayed and been transported from the stratosphere by the time CP aggregate W7029*A entered the stratosphere. If the aggregate itself was a product of an atmospheric nuclear explosion, this set of observations would be inconsistent with the present consensus of opinion in the field of interplanetary dust[1–5]. In addition, transport times[19] and settling rates for stratospheric particles of irregular shape[20] do not support a nuclear blast origin for CP aggregate W7029*A.

Terrestrial Bi from natural or anthropogenic sources may contaminate CP aggregates within the stratosphere during the limited time they settle from rest velocity height to the collecting altitude. (This time period is calculated[20] to be <150 days.) In addition, for a terrestrial origin of Bi, particle clustering must be shown to be significant during the period of collection of CP aggregate W7029*A. Clustering of particles is primarily dependent on the relative concentration of particles within the stratosphere and is significant for anomalous conditions such as the El Chichón stratospheric cloud[20]. However, during normal collection periods, particle concentrations within the stratosphere are significantly lower than during the collection period through the El Chichón cloud[20,21]. Evidence for particle clustering during

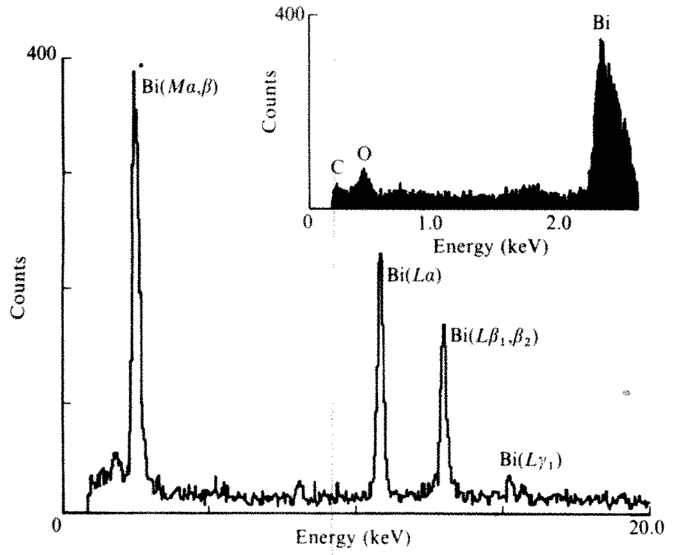

Fig. 2 Energy dispersive spectra from the grain shown in Fig. 1. Only Bi *M* and *L* lines are present with a conventional Be window detector. The windowless energy dispersive spectrum (inset) reveals a significant oxygen peak above background from the substrate. See text for details.

ambient stratospheric conditions has never been reported since the inception of the flat-plate collection process. We believe that particle clustering can occur in these conditions, but in very limited circumstances. These circumstances would primarily involve the most abundant stratospheric particles (such as Al spheres and fragments from solid rocket fuels[22,23] and would tend to include the abundant smaller size fractions[24,25]. Al-rich spheres or fragments from rocket debris have not been observed in the complete W7029*A aggregate, nor in any portion allocated for this study. Therefore, we suggest that particle clustering (and contamination by terrestrial Bi grains) is not significant for CP aggregate W7029*A.

Bismuth oxide may form from elemental Bi in a variety of conditions involving heating and oxidation. Throughout the lifetime of CP aggregate W7029*A, major periods of heating may have occurred during interplanetary passage or on entry into the Earth's atmosphere. During the latter process, oxidation may also occur. An understanding of the formation conditions for Bi_2O_3 and probable temperature profiles for micrometeors in Earth-crossing orbits may place constraints on the transformation of elemental Bi to Bi_2O_3 within CP aggregate W7029*A.

Fraundorf[26] has used typical entry parameters for micrometeors in Earth-crossing orbit to calculate temperature profiles for different size particles at different densities as they enter the stratosphere. Although the model does not strictly apply to CP aggregate particles, we use this formulation to estimate that a 60-μm size CP aggregate may have experienced maximum temperatures between 800 and 950 °C for a few seconds during atmospheric passage to 20 km altitude. Fraundorf's model[26] does not account for the complex shapes and heat capacities inherent in a typical CP aggregate. Calculations are based on an aggregate size ~60 μm and bulk densities ranging between 0.5 and $1.0\ g\ cm^{-3}$. Aggarwal and Goswami[12] have produced the simple cubic form of Bi_2O_3 by rapidly heating Bi film in air or in partial vacuum ($\sim 10^{-2}$ atm) between 250 and 300 °C. Oxides formed at higher temperatures (using a Bunsen burner flame) melted during oxidation[12]. This method for simple cubic Bi_2O_3 formation is kinetically favourable and suggests that the Bi grains in CP W7029*A were heated to ~300 °C during atmospheric entry. The apparent absence of tetragonal Bi_2O_3, which forms at higher temperatures (~900 °C; ref. 11), suggests that the range of temperatures experienced by Bi grains on entry is between 300 and 900 °C. Interpretation of data from associated minerals within this aggregate[27] indicates that many particles did not experience temperatures as high as 800 °C. We have shown that on average, temperatures on entry for CP aggregate W7029*A did not exceed 400 °C (ref. 27). These results are consistent with a known mechanism and our temperature estimate for heating Bi grains on atmospheric entry. Limited periods of pulse heating may also occur during interplanetary orbit, but with less certainty and a lower probability of oxidation. Therefore, we believe that CP aggregate W7029*A contained elemental Bi which transformed to Bi_2O_3 by pulse heating to 300–400 °C on entering the Earth's atmosphere.

In cosmochemistry, Bi is important because it is the heaviest stable element and it is highly volatile. Bi is present in variable, trace concentrations in meteorites and is most abundant in carbonaceous chondrites[28]. Individual meteorites from other groups also show high abundances of Bi (for example, the unequilibrated ordinary chondrite (UOC) Meso-Madaras[28]) though, in general, the average bulk analysis for each group is less than carbonaceous chondrites. Individual grains of Bi or Bi_2O_3 have not yet been observed in any meteorite. All previous attempts to determine the presence of Bi within meteorites have used optical microscopy, electron microprobe or bulk chemical techniques. These techniques cannot provide the same spatial resolution as AEM and therefore do not allow direct mineralogical comparisons between CP aggregate W7029*A and Bi-rich meteorites. With further AEM studies, it may be possible to identify the form and nature of Bi minerals in meteorites. Nevertheless, we use bulk meteorite data and current theories of Solar System evolution to provide some insight on the possible cosmochemical significance of Bi within CP aggregate W7029*A.

The unique properties of Bi have been used to predict its relative abundance within meteorites using a two-component model for condensation from a nebula gas[6]. The two-component model correctly predicts the mean abundances of Bi in carbonaceous chondrites (relative to Cl chondrites)[6,29,30]. This fractionation model has also been used to calculate accretion temperatures for ordinary chondrite meteorites[29–31], based on the abundances of volatile elements including Bi. In addition, the predicted siderophile nature of Bi in nebula conditions[31] has been confirmed by a study of Bi distribution in kamacites in the UOC Kohar[32]. (Note that both Meso-Madaras and Kohar are mildly metamorphosed Class II, L3 ordinary chondrites[33].) A material termed 'mysterite' has been proposed for ordinary chondrites with unusually high Bi abundances (such as Suphee) and low petrological type[34]. Mysterite is associated with dark clasts within these chondrites and occurs as a Tl-poor or a Tl-rich variety[34]. Higuchi *et al.*[34] suggest that these two components formed as late condensates from a solar nebula that collected volatiles which were left behind by earlier generations of chondrites. Independent evidence that these processes may occur in the region of the solar nebula sampled by these clasts has been provided by Davis *et al.*[35].

The agreement between theory and observations for the nebula condensation of Bi within the frame of reference provided by chondritic meteorites suggests that the implicit assumptions made by Larimer[31] for two-component model calculations may also apply to other primitive materials within our Solar System. The absolute age of CP aggregates has proved difficult to determine experimentally. CP aggregates may prove to have a cometary origin[4], and thus, some individual aggregate grains may have formed during our early Solar System evolution[36]. For the purposes of this study, we assume that CP aggregates are potentially primitive extraterrestrial materials, that Bi will occur in primitive materials as a metal and that the condensation temperature for Bi at nebula pressures between 10^{-3} and 10^{-6} atm is between 180 and 225 °C (ref. 31). To estimate the minimum abundance value for Bi within CP aggregate W7029*A, we assume the bulk density of the aggregate is $0.5\ g\ cm^{-3}$ and that its mass is 10^{-8} g. Using these values, we estimate the abundance of Bi within CP aggregate W7029*A to be at least in the p.p.m. range. This value for Bi suggests a considerable localized enrichment relative to cosmic abundance values[31]. Enrichment of Bi within components of extraterrestrial materials is consistent with a nebula condensation model[6] and implies that Bi within CP aggregate W7029*A formed at a late stage of the condensation process.

Richard McConnville and John Fahey of the Applications Laboratory, Philips Electronic Instruments Inc. are acknowledged for provision of the windowless energy dispersive spectrum shown in Fig. 2. F.J.M.R. is an NRC Research Associate at the Johnson Space Center.

Received 13 February; accepted 27 June 1984.

1. Rajan, R. S. *et al. Nature* **267,** 133–134 (1977).
2. Hudson, B., Flynn, G. J., Fraundorf, P., Hohenberg, C. M. & Shirck, J. *Science* **211,** 383–386 (1981).
3. Zinner, E., McKeegan, K. D. & Walker, R. M. *Nature* **305,** 119–121 (1983).
4. Fraundorf, P., Brownlee, D. E. & Walker, R. M. in *Comets* (ed. Wilkening, L. L.) 383–409 (University of Arizona Press, 1982).
5. Fraundorf, P. *Geochim. cosmochim. Acta* **45,** 915–943 (1981).
6. Anders, E. *Accts chem. Res.* **1,** 289–298 (1968).
7. Clanton, U. S. *et al. Cosmic Dust Catalog* Vol 2 (Curatorial Branch Publ. no. 62, NASA Johnson Space Center, Houston, 1982).
8. Bradley, J. P., Brownlee, D. E. & Fraundorf, P. *Science* **223,** 56–58 (1984).
9. Jenkins, R. & De Vries, J. L. *Practical X-ray Spectrometry* (Springer, New York, 1969).
10. Donnay, J. D. H. & Nowacki, W. *Geol. Soc. Am. Mem.* **60,** (1954).
11. Elliot, R. P. *Constitution of Binary Alloys* (McGraw-Hill, New York, 1965).
12. Aggarwal, P. S. & Goswami, A. *Z. Naturf.* **13a,** 885–887 (1958).
13. Sillen, L. G. *Ark. Kem. Miner. Geol.* **12A,** 1–15 (1937).
14. Kupick, V. in *Handbook of Geochemistry* Vol. 11 (ed. Wedepohl, K. H.) 83A1–83A7 (Springer, New York, 1972).
15. Angino, E. E. in *Geochemistry of Bismuth* (eds Angino, E. E. & Long, D. T.) 9–12 (Dowden, Hutchinson & Ross, Stroudsberg, 1979).
16. Kessler, D. J. & Cour-Palais, B. G. *J. geophys. Res.* **83,** 2637–2646 (1978).
17. Weast, R. C. (ed.) *Handbook of Chemistry and Physics, The Elements,* 53rd edn (Chemical Rubber Co., 1972).
18. Carter, M. W. & Mogishi, A. A. *Hlth Phys.* **33,** 55–71 (1977).
19. Jouzal, J., Merlivat, L., Pourchet, M. & Lorius, C. *Earth planet. Sci. Lett.* **45,** 188–200 (1979).
20. Mackinnon, I. D. R., Gooding, J. L., McKay, D. S. & Clanton, U. S. *J. Volcan. geotherm. Res.* (in the press).
21. Gooding, J. L., Clanton, U. S., Gabel, E. M. & Warren, J. *Geophys. Res. Lett.* **10,** 1033–1036 (1983).
22. Brownlee, D. E., Ferry, G. V. & Tomandl, D. *Science* **191,** 1270–1271 (1976).
23. Mackinnon, I. D. R., McKay, D. S., Nace, G. A. & Isaacs, A. M. *J. geophys. Res.* **87,** A413–A421 (1982).
24. Zolensky, M. E., Mackinnon, I. D. R. & McKay, D. S. *Lunar planet. Sci.* **15,** 963–964 (1984).
25. Rietmeijer, F. J. M. *Meteoritics* (in the press).
26. Fraundorf, P. *Geophys. Res. Lett.* **10,** 765–768 (1980).
27. Rietmeijer, F. J. M. & Mackinnon, I. D. R. *Lunar planet. Sci.* **15,** 687–688 (1984) *J. geophys. Res.* (in the press).
28. Lipschutz, M. E. in *Handbook of Elemental Abundances in Meteorites* (ed. Mason, B.) 511–517 (Gordon & Breach, New York, 1971).
29. Laul, J. C., Case, D. R., Schmidt-Bleek, F. & Lipschutz, M. E. *Geochim. cosmochim. Acta* **34,** 89–103 (1970).
30. Keays, R. R., Ganapathy, R. & Anders, E. *Geochim. cosmochim. Acta* **35,** 337–363 (1971).
31. Larimer, J. W. *Geochim. cosmochim. Acta* **37,** 1603–1623 (1973).
32. Woolum, D. S., Mascitelli, R., Burnett, D. S. & August, L. S. *Proc. 9th lunar planet. Sci. Conf.,* 1173–1186 (1978).
33. Huss, G. R., Keil, K. & Taylor, G. J. *Geochim. cosmochim.* Acta **45,** 33–51 (1981).
34. Higuchi, H., Ganapathy, R., Morgan, J. W. & Anders, E. *Geochim. cosmochim. Acta* **41,** 843–852 (1977).
35. Davis, A. M., Grossman, L. & Ganapathy, R. *Geochim. cosmochim. Acta* **41,** 853–856 (1977).
36. Weissman, P. R. in *Comets* (ed. Wilkening, L. L.) 637–658 (University of Arizona Press, 1982).

Occurrence of oxidized components in Qingzhen enstatite chondrite

E. R. Rambaldi*, R. M. Housley† & R. S. Rajan*

* Jet Propulsion Laboratory, California Institute of Technology, Pasadena, California 91109, USA
† Rockwell International Science Center, Thousand Oaks, California 91360, USA

Clues to the early history of the Solar System can be acquired by studying the properties of highly unequilibrated chondrites. These chondrites are thought to preserve an almost unaltered record of nebular processes[1–3]. Here we show that the most unequilibrated enstatite chondrite[4], Qingzhen, contains a population of enstatite grains which appear to have formed under more oxidizing nebular conditions than the bulk of the meteorite, which is highly reduced. These grains are black in transmitted light because of the presence of micrometre-sized inclusions of Ni-poor, Cr-rich metal and occur either isolated within the matrix or in chondrule interiors. Even though subsequent *in situ* reduction has led to the nucleation of metal, in most cases the FeO content of the enstatite grains still falls above the range found in the reduced portion of the meteorite. The textural occurrence of these grains argues against their having been introduced during collision of Qingzhen with an oxidized meteorite. Most likely, they originated in the same general nebular neighbourhood as the reduced bulk Qingzhen material and were subsequently transported into the reducing environment either before or during the process of chondrule formation. The discovery of this once-oxidized material in Qingzhen poses significant constraints on the existing models of formation of reduced matter in the Solar System.

The enstatite chondrites are characterized by an assemblage of highly reduced mineral phases[5–7]. Elements which are predominantly lithophile in other chondrite groups, display in enstatite chondrites, chalcophilic or siderophilic properties. Part of the Si is present in solid solution in the metal or as the Ni–Fe silicide perryite, and the bulk of the Fe occurs as the metal kamacite and the sulphide troilite. The ferromagnesian silicates (low-Ca clino- and orthopyroxene) have very low FeO contents. The FeO/(FeO+MgO) ratio in these minerals ranges from 0.0004 to 0.1, in contrast to values of 0.15 to 0.30 found in the olivine and pyroxene of ordinary chondrites[7,8].

The Qingzhen meteorite contains well defined chondrules and chondrule fragments surrounded by a population of metal, sulphide and enstatite grains. Some of the latter are black in transmitted light and have an average FeO content three to five times higher than enstatite in the chondrule interior[9], indicating formation under more oxidizing conditions than the bulk of the Qingzhen meteorite.

Sample A is an 80×120 μm black enstatite grain which contains fine-grained metallic inclusions (Fig. 1*a*) oriented subparallel to the crystallographic planes of the mineral. An enlarged portion of sample A (Fig. 1*b*) shows that the metallic inclusions tend to form small clusters or coalesce into larger grains surrounded by optically metal-free enstatite. Glass inclusions are also present. The composition of the enstatite in the metal-free areas is given in Table 1 (A1). The rather high total of this analysis (101.87) indicates an excess FeO (~2%) due to the presence of ultrafine metallic inclusions. The metal particles consist of almost pure Fe, and are Cr-rich and Ni-poor (Table 2, A4) relative to the average metal composition in the Qingzhen matrix. Nickel-poor metal can be produced during reduction of ferrosilite ($FeSiO_3$) originally present in solid solution within the pyroxene. The reduction reaction: $FeSiO_3 \rightarrow Fe^0 + SiO_2 + 1/2O_2$ produces free SiO_2. Inclusions of SiO_2-rich glass are found within the enstatite (Table 1, A3).

An approximate estimate of the FeO content of sample A before reduction was obtained by means of broad beam analyses of large areas of the grain (Table 1, A2), assuming absence of pre-existing metal and no metal loss after reduction. The analytical techniques used in this study do not allow for resolving the amount of Fe present as metal from that present as FeO within the enstatite. The bulk Fe present in the area analysed, given as FeO, is 8.6%.

In sample B a set of coarse metal grains is oriented along one of the crystallographic planes of the enstatite and the areas immediately adjacent to the coarsest grains are relatively free of metal (B1, Table 1). The original FeO content of the grain, obtained by broad beam analysis, is 9.3% (B2 in Table 1). Glass inclusions are present, but are too small to be analysed. The metal (B3, Table 2) has higher Cr and lower Ni contents than the metal within Sample A.

Sample C (60×80 μm) consists of a fine-grained intergrowth of metal, enstatite, glass and sulphide, surrounded by clear enstatite (Fig. 1*c*). The reduction process was accompanied by a significant degree of melting followed by crystallization of clear enstatite (Fig. 1*d*). Broad beam analyses of optically metal-poor areas within the intergrowth (C1, Table 1) reveal a high FeO content (17.3%) in spite of only a slightly high total

Table 1 Chemical data on oxidized components in Qingzhen (in weight %)

	Sample A			Sample B		Sample C			Sample D		
	A1	A2	A3	B1	B2	C1*	C2	C3	D1†	D2	D3
SiO_2	56.6	58.1	79.3	57.9	56.2	51.1	59.7	63.8	55.1	59.0	98.9
Al_2O_3	—	—	5.1	—	—	—	—	14.7	2.0	—	—
Cr_2O_3	0.73	0.90	0.38	0.71	0.78	1.32	—	—	0.91	—	—
CaO	0.27	0.13	1.22	—	—	2.3	—	—	0.86	0.23	—
MgO	39.2	36.8	10.9	38.9	38.0	29.9	40.5	7.7	33.8	39.0	—
FeO	4.9	8.6	2.9	2.4	9.3	17.3	1.07	1.4	7.6	1.76	1.10
Na_2O	—	—	1.92	—	—	—	—	9.9	—	—	—
Total	101.70	104.53	101.72	99.91	104.28	101.92	101.27	97.50	100.27	99.99	100.00

* Also MnO (0.41%) and S (0.8%).
† Also S (0.35%).

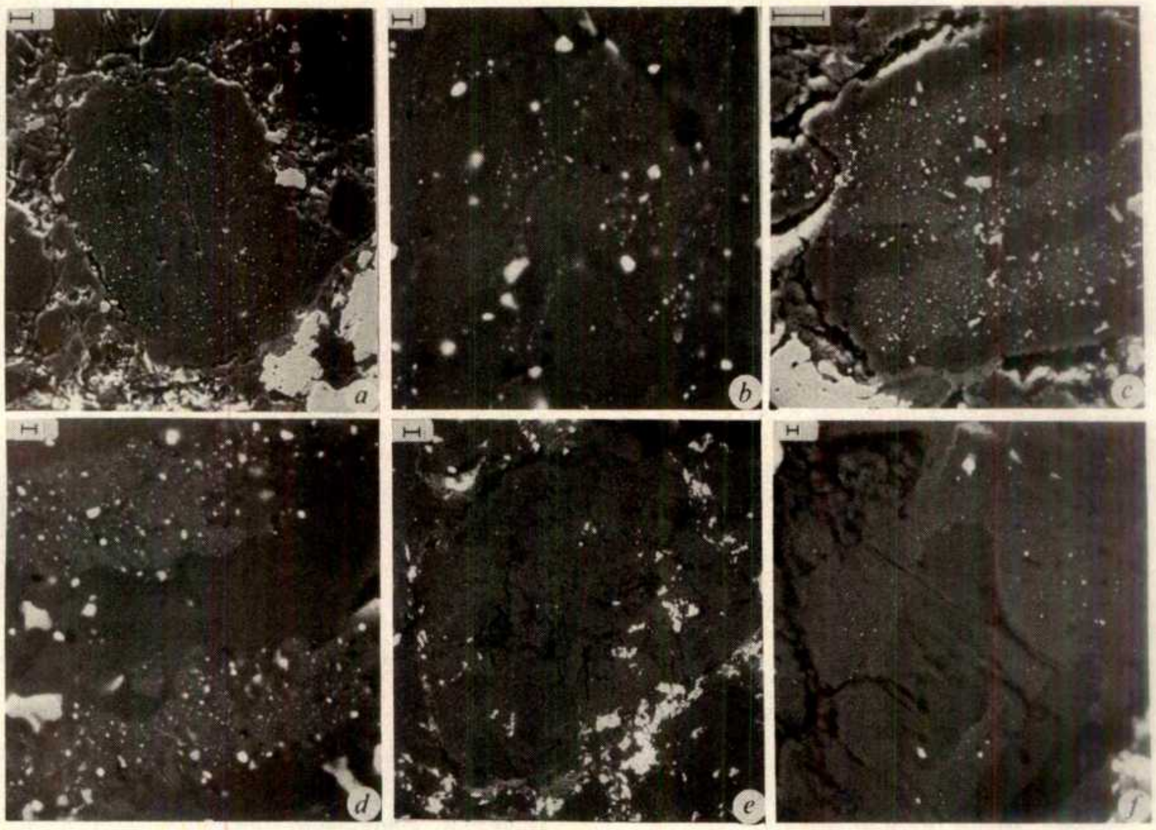

Fig. 1 *a*, A 80 × 120 μm grain of black enstatite (sample A) in Qingzhen, containing inclusions of Ni-poor metal, oriented subparallel to the crystallographic planes of the mineral. *b*, Enlargement of a portion of sample A, showing clustering and coalescing of the metallic particles. SiO_2-rich glass inclusions (dark gray) are also visible. *c*, Sample C (60 × 80 μm) consists of fine-grained intergrowth of metal, enstatite, glass and sulphide, surrounded by inclusion-free enstatite. *d*, Enlargement of sample C, showing textural evidence that melting has occurred. *e*, A 150 × 200 μm chondrule fragment (sample D) consisting of enstatite (light grey) and tridymite (dark grey). *f*, An enlargement of a portion of sample D showing that the enstatite contains sub-micrometre inclusions of metal and vugs. Metal and vug-free enstatite (medium grey) has crystallized in the interior of SiO_2-rich glass areas. Scale bars: *a*, *c*, *e*, 10 μm; *b*, *d*, *f*, 1 μm.

(101.92%). The clear enstatite (C2) has a low FeO content and is Cr_2O_3- and CaO-free. Droplets of glass of prevalently albitic composition (C3, Fig. 1*d*) have segregated into the clear enstatite, suggesting the presence of a feldspathic component within the metal-rich intergrowth. Most metal is Ni-poor (C4, Table 2), but a few grains of Ni-rich metal have been found (C5) indicating that some metal was originally present within the precursor assemblage.

Sample E is a 150 × 200 μm chondrule fragment consisting of enstatite and tridymite in an approximately 1 : 1 ratio (Fig. 1*e*). The enstatite crystals contain sparse sub-micrometre metal inclusions and abundant vugs (Fig. 1*f*) suggesting loss of a volatile component during chondrule formation. SiO_2-rich glass included within the pyroxene is coated with clear enstatite which is vug-free (Fig. 1*f*). The enstatite has a high FeO content (7.6%) and contains significant amounts of Al_2O_3, Cr_2O_3 and CaO (D1, Table 1). This is the highest FeO content ever reported in pyroxenes from enstatite chondrites. It is about 10 times higher than the FeO content of enstatite within 'reduced' chondrules of Qingzhen. The clear enstatite is FeO-poor and Al_2O_3- and Cr_2O_3-free (D2) and the tridymite contains only minor amounts of FeO (D3). The metallic inclusions within the enstatite are too small to be analyzed, but metal grains, interstitial among enstatite and tridymite, are Ni-rich (D4, Table 2). The high FeO content of the enstatite, and the small number of metal inclusions strongly suggest that only minor reduction has occurred within this chondrule.

Qingzhen also contains a population of porphyritic chondrules containing grains of olivine with micron-size inclusions of metal[10,11]. The metal is Ni-poor and was probably produced by *in situ* reduction of the fayalitic (Fe_2SiO_4) component of the olivine[12]. The original fayalitic content of the grains (15–25 mol %) is inconsistent with the composition of materials formed under strongly reducing conditions.

Table 2 Chromium and Ni content of metal within matrix and oxidized components in Qingzhen (in weight %)

	Matrix	A4	B3	C4	C5	D4
Cr	<0.05	1.94	4.4	0.96	0.50	0.50
Ni	3.4	0.95	0.60	1.02	4.1	5.4

Ni-poor metal might represent the condensation product of Fe vapour produced during shock reheating and introduced within the enstatite grains along cracks and crystallographic planes (D. W. Sears, personal communication). As discussed by Sears[13,14], the vapour to form first when Fe, Ni alloy is evaporated is Ni-free because of the lesser volatility of Ni. As shown in Table 2, the Ni-poor metal contains substantial amounts of Cr, while the matrix metal is Cr-free. Therefore, evaporation of the latter could not produce a Cr-rich vapour. Furthermore, the metallic inclusions occur within enstatite grains which in most cases still retain FeO contents significantly higher than the 'reduced' enstatite in the surrounding matrix and chondrules. Incomplete reduction of precursor oxidized silicates appears to be the only possible mode of formation of the Ni-poor metal.

The observed range of FeO contents in the ferromagnesian silicates of Qingzhen (0.15–7.6%) represents a lower limit, because reduction has occurred. The highest calculated FeO content is 18% for relict olivines inside incompletely melted chondrules. Even though the bulk of the Qingzhen meteorite is highly reduced, such high ranges of FeO contents are comparable to those observed in highly unequilibrated ordinary chondrites.

We exclude the possibility that the oxidized components in Qingzhen were introduced during collision with a more oxidized body and subsequently reduced. These components occur as single grains or chondrules surrounded by highly reduced material, not as xenolithic clasts. Furthermore, the presence of FeO-rich enstatite in chondrule interiors indicates that these components were already present prior to or during the process of chondrule formation, and therefore long before the accretional event that culminated with the formation of the parent body of Qingzhen.

Various reheating mechanisms could have triggered the reduction process and the melting (often incomplete) of these oxidized components. Reheating during shock is a possibility. Wang and Xie[15] describe some features in Qingzhen which are suggestive of shock. But shock features are absent in the coarse grained sulphide minerals in the matrix, which are always monocrystalline, and not polycrystalline as one would expect had they been shocked (A. El Goresy, personal communication). Thermal metamorphism in the parent body interior is another possibility. This process, which is recorded in the texture and chemistry of ordinary chondrites of increasing petrologic type, brings about mineral recrystallization and equilibration leading ultimately to mineral phases with uniform FeO/(FeO/MgO) ratios. But thermal metamorphism cannot be responsible for the reduction of the oxidized components in Qingzhen for the following reasons: (1) Qingzhen is highly unequilibrated and contains neither the textural nor the chemical evidence of metamorphic processes; (2) in many cases the grains were accompanied by melting, while the bulk of Qingzhen was never melted.

Thus, a reheating event outside the parent body is required, leaving the chondrule formation process as the only plausible alternative. It has been recently shown that this process may lead to incomplete melting of chondrule precursor assemblages and reduction during chondrule formation has been well documented in highly unequilibrated ordinary chondrites[2,12,16]. We suggest that oxidized ferromagnesian silicates occurring either isolated or as clusters of grains were reheated and melted to various degrees during the chondrule formation event that produced the main population of highly reduced chondrules in Qingzhen.

The less reducing nebular conditions required for the stability of the oxidized components found in Qingzhen could be obtained by assuming local fluctuations in the degree of reduction of the nebular gas possibly related to inhomogeneous admixture of a reducing component.

It has been recently suggested that the onset of the reducing conditions required for the formation of enstatite chondrites may be produced by loss of O-bearing compounds, in the form of high temperature condensates (refractory compounds of Ca, Al and Ti)[14], or by a process of dust-gas fractionation followed by evaporation and condensation in the dust-(and O) depleted nebular region[17]. According to these models, failure of the residual solids to equilibrate with the nebular gas or incomplete evaporation of solids in the dust-depleted region, could allow the preservation of oxidized material. Alternatively, the oxidized components found in Qingzhen might represent materials originated in dust-enriched nebular regions[17], which were subsequently transported into an adjacent more reducing environment.

We thank D. Wang for making samples of the Qingzhen meteorite available. The work described in this paper was carried out at the Jet Propulsion Laboratory, California Institute of Technology, under contract with the National Aeronautics and Space Administration.

Received 8 December 1983; accepted 4 July 1984.

1. Afiattalab, F. & Wasson, J. T. *Geochim. cosmochim. Acta* **44,** 431–446 (1981).
2. Rambaldi, E. R. & Wasson, J. T. *Geochim. cosmochim. Acta* **45,** 1001–1015 (1981).
3. Sears, D. W., Grossman, J. N., Melcher, C. L., Ross, L. M. & Mills, A. A. *Nature* **287,** 791–795 (1980).
4. Rambaldi, E. R., Rajan, R. S. & Wang, D. *Lunar planet Sci.* **14,** 626–627 (1983).
5. Anders, E. *Space Sci. Rev.* **3,** 583–714 (1964).
6. Mason, B. *Geochim. cosmochim. Acta* **30**, 23–39 (1966).
7. Keil, K. *J. geophys. Res.* **73,** 6945–6979 (1968).
8. Keil, K. & Fredricksson, K. *J. geophys. Res.* **69,** 3487–3515 (1964).
9. Housley, R. M., Rajan, R. S., Rambaldi, E. R. & Wang, D. *Meteoritics* **18,** 317–318 (1983).
10. Rambaldi, E. R. & Wang, D. *Meteoritics* **17,** 272 (1982).
11. Rambaldi, E. R., Rajan, R. S. Wang, D. & Housley, R. M. *Earth planet. Sci. Lett.* **66,** 11–24 (1983).
12. Rambaldi, E. R. & Wasson, J. T. *Geochim. cosmochim. Acta* **46,** 929–939 (1981).
13. Sears, D. W. *Earth planet. Sci. Lett.* **41,** 128–138 (1978).
14. Sears, D. W. *Icarus,* 184–202 (1980).
15. Wang, D. & Xie, X. *Geochemistry* **1,** 69–81 (1982).
16. Rambaldi, E. R. & Wasson, J. T. *Geochim. cosmochim. Acta* (in the press).
17. Bartholomay, H. A. & Larimer, J. W. *Meteoritics* **17,** 180–181 (1982).

Presence of a superparamagnetic component in the Orgueil meteorite

Thomas J. Wdowiak & David G. Agresti

Department of Physics, University of Alabama in Birmingham,
Birmingham, Alabama 35294, USA

The Orgueil CI carbonaceous chondrite meteorite fall of 14 May 1864 is of particular interest because of the presence of an organic component which included amino acids. Using Mössbauer spectroscopy, we have determined that the Orgueil meteorite contains an appreciable fraction of its iron in the superparamagnetic state. This result implies that the superparamagnetic iron component was formed during an aqueous phase in the history of the parent body, and that the superparamagnetic component may have served as a catalyst for formation of the organic component.

A 52.4-mg sample from the Smithsonian National collection (Orgueil USNM-234) was ground into a powder and dispersed into 78.4 mg of molten parafin. On cooling, the parafin was moulded, while plastic, into a 6-mm diameter pellet that was then supported by a 25-mm lead annulus. The sample was cooled to temperatures between 21 and 295 K by transferring heat by gaseous helium from the sample to an Air Products closed-cycle refrigerator. This method of heat transfer was used to prevent mechanical vibration of the sample by the closed-cycle refrigerator. The Mössbauer spectrometer employs a liquid-nitrogen cooled Si(Li) detector for the 14.4-keV ^{57}Fe γ rays.

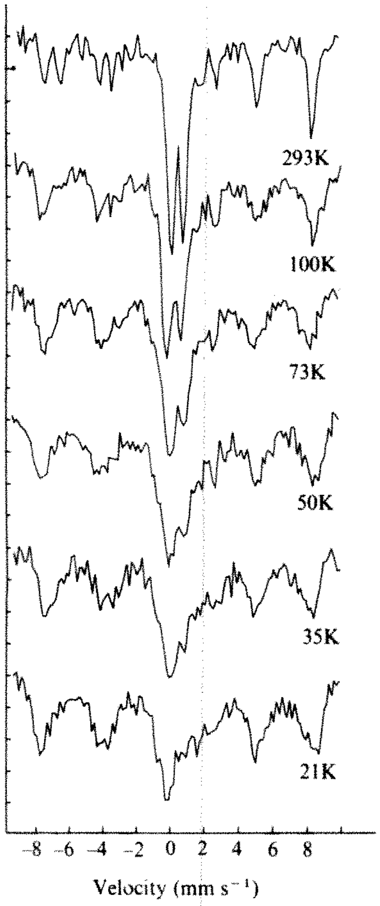

Fig. 1 Mössbauer spectra of the Orgueil CI carbonaceous chondrite. The 293 K spectrum shows the presence of ferromagnetic magnetite and two paramagnetic absorptions near 0 mm s^{-1}. Spectra obtained below the Verwey transition at 119–116 K, at 100 K, 73 K, 50 K, 35 K and 21 K show a gradual diminishing of the paramagnetic absorption and enhancement of the ferromagnetic absorptions indicating the presence of a superparamagnetic magnetite component.

A spectrum was obtained at 295 K in order to characterize the sample. This spectrum, similar to that obtained by Gerard and Delmelle[1], shows a blending of paramagnetic features with the ferromagnetic spectrum of magnetite[2]. Subsequent measurements were made at temperatures of 100, 73, 50, 35, and 21 K. This range is below the Verwey transition that occurs in Fe_3O_4 between 119 and 116 K, and was chosen because previous studies[3] have shown that the Fe_3O_4 ferromagnetic spectrum does not alter between 100 and 7 K. Each spectral measurement required ~5 days of counting because of sample size and source strength. The spectra obtained between 100 and 21 K show the same gradual diminishing of the paramagnetic absorptions and enhancement of the ferromagnetic features as observed for superparamagnetic materials where the particles are of subdomain size[4–6].

Such particles are in a state of uniform magnetization with a net magnetic moment possibly 10^5 times that of a single atom (hence 'superparamagnetic'). For sufficiently small particles at higher temperatures, the relaxation time of the magnetic moments of these particles is smaller than the nuclear Larmor precession time, and the Zeeman splitting collapses to the two-peak spectrum characteristic of the paramagnetic state[5]. As temperature decreases for a given particle size, the relaxation time increases to the point where the Zeeman splitting can be observed (ferromagnetic state). When a distribution of subdomain particles exists, as is usual, that distribution can be determined from the Mössbauer spectrum[4,5]. We plan to carry out such determinations in the future. By taking the ratio of the integrated paramagnetic iron absorption between 100 and 21 K and the total integrated absorption of all forms of iron, we estimate that ~30% of the iron of the meteorite is in the superparamagnetic subdomain form. The remaining iron is ~45% ferromagnetic and 25% paramagnetic. The magnetite is thus ~40% superparamagnetic and 60% ferromagnetic. Characteristically, superparamagnetic particles are <300 Å in size, which indicates that the Orgueil contains an appreciable portion of iron as Fe_3O_4 in this size range. The magnetite content of the Orgueil meteorite has been determined using the Faraday balance and the vibrating sample magnetometer to 11.0 ± 0.4 wt% (ref. 7). Combined with the present results, this suggests the superparamagnetic magnetite component is ~4.5 wt%.

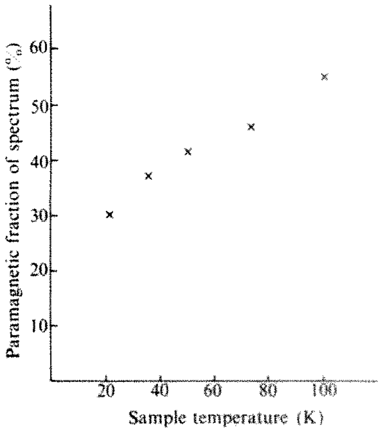

Fig. 2 Paramagnetic fraction of spectrum versus sample temperature. The decrease between 100 and 21 K indicates the superparamagnetic magnetite component held by ~30% of all iron.

The presence of a superparamagnetic component in the Orgueil meteorite requires a discussion of its origin and its impact on the origin of the organic component. Particles having sizes in the <300 Å range are almost certainly not the result of size reduction processes. Superparamagnetic particles can be produced by precipitation from aqueous solutions[5], vapour condensation[8], and crystallization from a melt[6]. The last mechanism is unlikely for a CI carbonaceous chondrite such as the Orgueil. There is evidence for aqueous activity in the parent body of the Orgueil meteorite[9–11], as well as those of other carbonaceous chondrites. The magnetite superparamagnetic particles could be the result of precipitation from an aqueous solution or they may be a secondary product arising from the oxidation of iron sulphides in aqueous conditions, although oxidation in the solar nebula is also a possibility[7].

While aqueous processes are those most likely to be responsible for the superparamagnetic magnetite component of the Orgueil meteorite, either directly through precipitation or indirectly through oxidation of iron sulphide, an alternate hypothesis for superparamagnetic particles has been put forward by Cameron[12]. He argued that superparamagnetic magnetite relict cores of interstellar grains, such as proposed by Jones and Spitzer[13], might be found in carbonaceous chrondites of type I. This hypothesis needs to be re-examined in the light of the result presented here. It may be that the Orgueil superparamagnetic component is a solar nebula analogue to interstellar grain cores.

The possibility that catalytic activity of magnetite in meteorites and in the solar nebula is responsible for meteorite organics has been reviewed by Anders *et al.*[14]. The organic component of the Orgueil includes amino acids[15], fatty acids[16], alkanes[14], heterocyclics[17], and polymeric material[18]. Nickel–silica catalysts prepared by coprecipitation and exhibiting superparamagnetic properties[19,20] are utilized in laboratory and industrial organic synthesis. A superparamagnetic magnetite component would thus be an attractive candidate as a catalyst for the formation of organics in the Orgueil meteorite.

A preliminary examination of bulk samples and separated magnetic fractions of the Allende meteorite has not revealed any superparamagnetism in the iron minerals. The bulk of the iron was paramagnetic and only a small separated fraction exhibited ferromagnetism. Sears and Marshall[21] have pointed out that while Mössbauer spectroscopy does not reveal magnetite in the Tieschitz unequilibrated ordinary chondrite[22], X-ray diffraction indicates its presence. The difference between those results may be due to the magnetite in the Tieschitz being entirely superparamagnetic, and hence not appearing in the expected ferromagnetic absorption pattern of a 293 K Mössbauer measurement, while X-ray diffraction would show the lattice structure of particles ≪300 Å in size. This question, coupled with the results of our preliminary examination of the Orgueil meteorite at a range of cryogenic temperatures, suggests that the Mössbauer technique has broader applications in meteoritics than previous studies have indicated.

We thank Roy Clarke Jr for assistance in obtaining the Orgueil meteorite sample and acknowledge the Graduate School of the University of Alabama in Birmingham for its support.

Received 25 May; accepted 25 June 1984.

1. Gerard, A. & Delmelle, M. *C. r. hebd Séanc Acad. Sci., Paris* **259,** 1756–1759 (1964).
2. Muir, A. H. & Blander, M. in *Proc. Conf. Application of the Mössbauer Effect* (ed. Dezsi, I.) 61–72 (Akademiai Kiado, Budapest, 1971).
3. Sawatzky, G. A., Coey, J. M. D. & Morrish, A. H. *J. appl. Phys.* **40,** 1402–1403 (1969).
4. Kundig, W., Bommel, H., Constabaris, G. & Lindquist, R. H. *Phys. Rev.* **142,** 327–333 (1966).
5. van der Kraan, A. M. *Phys. Stat. Sol.* **a18,** 215–226 (1973).
6. Helgason, O., Steinthorsson, S., Morup, S., Lipka, J. & Knudsen, J. E. *J. phys. Colloq.* **C6,** Suppl. 12, **37,** 829–832 (1976).
7. Hyman, M. & Rowe, M. W. *J. geophys. Res. Suppl.* **88,** A736–A740 (1983).
8. Haneda, K. & Morrish, A. H. *Nature* **282,** 186–188 (1979).
9. Kerridge, J. F. & Bunch, T. E. in *Asteroids* (ed. Gehrels, T.) 745–764 (University of Arizona Press, Tucson, 1979).
10. Bunch, T. E. & Chang, S. *Geochim. cosmochim, Acta* **44,** 1543–1578 (1980).
11. Macdougall, J. D., Lugmair, G. W. & Kerridge, J. F. *Nature* **307,** 249–251 (1984).
12. Cameron, A. G. W. in *Interstellar Dust and Related Topics* (eds Greenberg, J. M. & Van de Hulst, H. D.) 545–547 (Reidel, Dordrecht, 1973).
13. Jones, R. V. & Spitzer, L. *Astrophys. J.* **147,** 943–964 (1967).
14. Anders, E., Hayatsu, R. & Studier, M. H. *Science* **182,** 781–790 (1973).
15. Lawless, J. G., Kvenvolden, K. A., Peterson, E., Ponnamperuma, C. & Moore, G. *Nature* **236,** 66–67 (1972).
16. Nagy, B. & Bitz, C. M. *Arch. Biochem. Biophys.* **101,** 240–248 (1963).
17. Foldsome, C. E., Lawless, J. G., Romiez, M. & Ponnamperuma, C. *Geochim. cosmochim. Acta* **37,** 455–465 (1973).
18. Bandurski, E. L. & Nagy, B. *Geochim. cosmochim. Acta* **40,** 1397–1406 (1976).
19. Dietz, R. E. & Selwood, P. W. *J. appl. Phys.* **30,** 101S–102S (1959).
20. Selwood, P. W. in *Structure and Properties of Thin Films* (eds Neugebauer, C. A., Newkirk, J. B. & Vermilyea, D. A.) 490–494 (Wiley, New York, 1960).
21. Sears, D. W. & Marshall, C. *Meteoritics* **15,** 364 (1980).
22. Sprenkel-Segel, E. L. in *Meteorite Research* (ed. Millman, P.) 93–105 (Reidel, Dordrecht, 1969).

The ability of small molecules to form clathrate hydrates of structure II

D. W. Davidson, Y. P. Handa, C. I. Ratcliffe & J. S. Tse

Division of Chemistry, National Research Council of Canada,
Ottawa, Canada K1A 0R9

B. M. Powell

Atomic Energy of Canada Limited, Chalk River Nuclear
Laboratories, Chalk River, Ontario, Canada K0J 1J0

Since gas hydrates were shown in the mid-1950s[1] to be water clathrates of two distinct crystallographic structures (Table 1), it has been generally accepted that structure I hydrates are formed by molecules with maximum van der Waals diameters of up to about 5.8 Å while structure II hydrates are formed by larger molecules, up to about 7.0 Å in size. No exception to this general rule has been observed among more than 100 individual species of molecules known to form clathrate hydrates[2,3]. From X-ray and neutron diffraction studies we now find, however, that the two smallest molecules which form clathrate hydrates—argon and krypton—do so in the structure II modification. This finding supports a suggestion of Holder and Manganiello[4].

One of the reasons for the shortage of crystallographic data for gas hydrates of small guest molecules is because such hydrates are stable near 0 °C only at relatively high pressures.

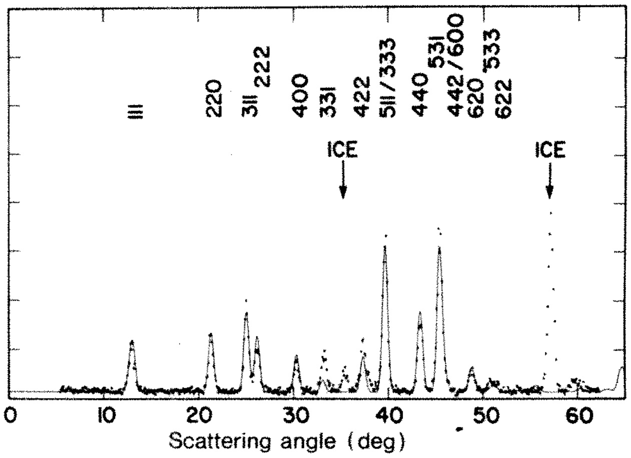

Fig. 1 Comparison of the observed (points) and fitted neutron scattering profile of krypton deuteriohydrate at 5.7 K.

Powder diffraction patterns, however, may be recorded at low temperatures (≤100 K) without appreciable hydrate decomposition. For the X-ray and neutron diffraction studies described here, powdered samples were prepared by grinding H_2O or D_2O ice in a rotating rod mill at −30 °C for several days under gas pressures (2 MPa for Kr and CH_4, 10 MPa for Ar) twice as high as required for hydrate stability.

X-ray powder photographs of Ar and Kr hydrate samples were taken with MoK_α radiation, as previously described[5]. Lines were readily indexed in the structure II cubic Fd3m space group, with observed intensities in good agreement with structure factor calculations which assumed full occupancy of the 12- and 16-hedral cages.

Elastic neutron scattering measurements on Kr and CH_4 D_2O hydrates were made on the C5 spectrometer operated in a two-axis mode at the NRU reactor, Chalk River. The monochromator was Si(111) and the neutron wavelength 2.22374 Å. A sapphire filter in the incident beam and a Si(111) analyser set for elastic scattering were used to reduce the background. The powder diffraction profile of Kr deuteriohydrate at 5.7 K is shown in Fig. 1. Except for two peaks from hexagonal ice the observed peaks are indexed on the basis of space group Fd3m. No peaks from structure I were observed. Integrated intensities were fitted to a structure II hydrate lattice, with all cages filled and zero thermal parameters for O and D. Because of the limited range of scattering angle, the fit was not very sensitive to these two assumptions.

The results are summarized in Table 2. The lattice parameters *a* found for Ar and Kr hydrates at 100 K are similar to those found for other structure II hydrates[5,6], which average less than 0.1 Å larger at comparable temperatures. Methane hydrate is established as structure I. In the hydrates of N_2 and O_2, which require higher pressures for stability than any other known hydrate[7], the guest molecules are smaller than methane: the structures of these hydrates must now be considered uncertain.

Except for small compressibility effects, the ideal solid–solution theory of clathrate hydrates[8] gives for the chemical potentials of water molecules in structures I and II

$$\mu(\mathrm{I}) = \mu^0(\mathrm{I}) - \frac{kT}{23}[\ln\{1 + C_\mathrm{S}(\mathrm{I})P\} + 3\ln\{1 + C_\mathrm{L}(\mathrm{I})P\}]$$

$$\mu(\mathrm{II}) = \mu^0(\mathrm{II}) - \frac{kT}{17}[2\ln\{1 + C_\mathrm{S}(\mathrm{II})P\} + \ln\{1 + C_\mathrm{L}(\mathrm{II})P\}]$$

where μ^0 refers to water in the hypothetical empty lattice, C_S is the Langmuir constant which relates the extent of occupancy by the gas of the small 12-hedral cages to the pressure P (strictly, the fugacity) of the hydrate-forming gas, and $C_\mathrm{L}(\mathrm{I})$, $C_\mathrm{L}(\mathrm{II})$ are corresponding Langmuir constants for the 14- and 16-hedra. The 12-hedra being similar in the two structures, $C_\mathrm{S}(\mathrm{I}) \sim C_\mathrm{S}(\mathrm{II})$.

Table 1 Unit cells of cubic clathrate hydrates

	Structure I	Structure II
Cell size *a*, symmetry	12.0 Å, Pm3n	17.2 Å, Fd3m
No. of water molecules	46	136
No. of 12-hedra, diameter*	2, 5.0 Å	16, 5.0 Å
No. of 14-hedra, diameter	6, 5.8 Å	—
No. of 16-hedra, diameter	—	8, 6.6 Å
Limiting compositions:		
All cages filled	$M\cdot 5\frac{3}{4}\,H_2O$	$M\cdot 5\frac{2}{3}\,H_2O$
Only large cages filled	$M\cdot 7\frac{2}{3}\,H_2O$	$M\cdot 17\,H_2O$

* Average free diameter of cage.

Table 2 Clathrate hydrates formed by small molecules

Guest/host	Diameter of guest	Structure	X-ray lattice parameter *a*
Ar/H_2O	3.83 Å	II	17.07 ± 0.04 Å (100 K)
Kr/H_2O	4.04	II	17.08 ± 0.08 (100 K)
Kr/D_2O		II	17.01 ± 0.05 (100 K)
Kr/D_2O		II	17.01 ± 0.01 (5.7 K)*
CH_4/D_2O	4.58	I	11.77 ± 0.01 (5.2 K)*
H_2S/H_2O	4.58	I	11.96 ± 0.05 (125 K)†
Xe/H_2O	4.57	I	11.84 ± 0.02 (110 K)‡

* From neutron diffraction.
† S. R. Gough, unpublished data.
‡ Ref. 12.

The lowest gas pressure P_0 at which a hydrate can exist is the pressure which lowers its chemical potential to that of ice or liquid water at the same temperature: whether structure I or structure II is stabler depends on which has the smaller value of P_0. Although accurate values of μ^0 are not known, $\mu^0(\mathrm{II}) < \mu^0(\mathrm{I})$ because of the greater similarity to ice of the hydrogen bonding between the water molecules in the structure II lattice[2].

For relatively large guest molecules (M) structure II is more stable because $C_L(\mathrm{II}) \gg C_S$, $C_L(\mathrm{I})$, only the 16-hedra are occupied by M molecules, and the compositions approach $M\cdot 17H_2O$. For very small guest molecules, on the other hand, structure II stability results from the condition $C_S > C_L(\mathrm{I})$, $C_L(\mathrm{II})$, that is, from a preference for the small cages, and the composition is much different, about $M\cdot 6H_2O$. Structure I will generally be preferred when $C_L(\mathrm{I}) > C_S$, $C_L(\mathrm{II})$ or $C_L(\mathrm{I}) \approx C_S > C_L(\mathrm{II})$. The former condition appears to apply to most structure I hydrates since even for a guest molecule as small as Xe (Table 2) NMR studies have shown[9] that $C_L(\mathrm{I})$ is an order of magnitude larger than C_S near 0 °C.

The limited success of past calculations of hydrate dissociation pressures from assumed intermolecular potentials[2,8,10] now appears to be due, at least in part, to the erroneous assignment of structure I to the model hydrates of argon and krypton. Accurate experimental determination of the compositions of Ar and Kr hydrates should prove of importance in the evaluation of $\mu^0(\mathrm{II})$. Values of $C_S(\mathrm{II})$ for Ar and Kr in the double hydrates of $CHCl_3$ have already been measured by Barrer and Edge[11].

This manuscript is issued as NRCC no. 23110.

Received 18 May; accepted 29 June 1984.

1. von Stackelberg, M. & Müller, H. R. *Z. Elektrochem.* **58,** 25–39 (1954).
2. Davidson, D. W. in *Water: A Comprehensive Treatise* Vol. 2 (ed. Franks, F.) 115–234 (Plenum, New York, 1973).
3. Ripmeester, J. A. & Davidson, D. W. *Molec. Cryst. Liquid Cryst.* **43,** 189–195 (1977).
4. Holder, G. D. & Manganiello, D. J. *Chem. Engng Sci.* **37,** 9–16 (1982).
5. Sargent, D. F. & Calvert, L. D. *J. Phys. Chem.* **70,** 2689–2691 (1966).
6. Bertie, J. E. & Jacobs, S. M. *J. chem. Phys.* **69,** 4105–4113 (1978).
7. van Cleeff, A. & Diepen, G. A. M. *Rec. Trav. Chim. Pays-bas* **84,** 1085–1093 (1965).
8. van der Waals, J. H. & Platteeuw, J. C. *Adv. Chem. Phys.* **2,** 1–57 (1959).
9. Ripmeester, J. A. & Davidson, D. W. *J. molec. Struct.* **75,** 67–72 (1981).
10. Tse, J. S. & Davidson, D. W. *Proc. 4th Can. Permafrost Conf.*, Calgary, Alberta (ed. French, H. M.) 329–334 (National Research Council, Ottawa, 1982).
11. Barrer, R. M. & Edge, A. V. J. *Proc. R. Soc.* **A300,** 1–24 (1967).
12. Bertie, J. E. & Jacobs, S. M. *J. chem. Phys.* **77,** 3230–3232 (1982).

Reflected turbidity currents on an Ordovician basin floor, Canadian Appalachians

R. N. Hiscott* & K. T. Pickering†

* Earth Sciences Department, Memorial University, St John's, Newfoundland A1B 3X5, Canada
† Department of Geology, Goldsmiths' College, University of London, London SE8 3BU, UK

Sedimentary structures associated with turbidity current deposits show either partial or complete Bouma T_{a-e} sequences[1] that suggest deposition of sediment from a waning (decelerating) unidirectional flow[2]. Bathymetric highs and basin margins can cause turbidity currents to reflect back along their original flow paths, a rare situation in both ancient[3,4] and modern[5] marine basins. The internal structures of such contained, or reflected, turbidites have only been described in one case, the Contessa bed (ref. 4 pp. 268, 300). Our data from 1–6-m thick graded, mud-dominated turbidites from the Quebec Appalachians, using mainly sole marks, megaripple, ripple and grain fabric data, suggest that during the deposition of these beds the turbidity currents were reflected several times from either internal basin highs or basin slopes. The recognition of such beds not only provides an insight into the depositional environment (deep-water basin floor), but also allows detailed bed-by-bed correlations over tens of kilometres of coastal sections since the beds are reliable chronostratigraphical datum lines.

The beds form part of the 1.5-km thick $\beta 1$ and $\beta 2$ members of the Middle Ordovician Cloridorme Formation[6], a flysch unit deposited in a constricted foreland basin during the Taconic Orogeny[7]. The $\beta 1$ and $\beta 2$ sequence consists of thinly-bedded classic turbidites and hemipelagic shales, punctuated about every 10 m by a thick bipartite bed consisting of a lower, graded sandstone (1/4) and a texturally homogeneous, structureless, silty mudstone cap (3/4). These beds range in thickness from 1 to 5.5 m, and can easily be correlated with little apparent thickness change between localities 25 km apart.

Most beds have basal flute casts that indicate flow from east to west. This led earlier workers[8] to interpret the beds as deposits of unusual, unidirectional turbidity currents. Internal sedimentary structures consist of parallel lamination, cross-lamination, small-scale megaripple and ripple forms, climbing ripple lamination, wavy and convolute lamination, and pseudonodules[8]. Grading in the lower sandstone part is not continuous, but is punctuated by mud-draped partings across which grain size may decrease abruptly. Between these grain-size breaks, or muddy

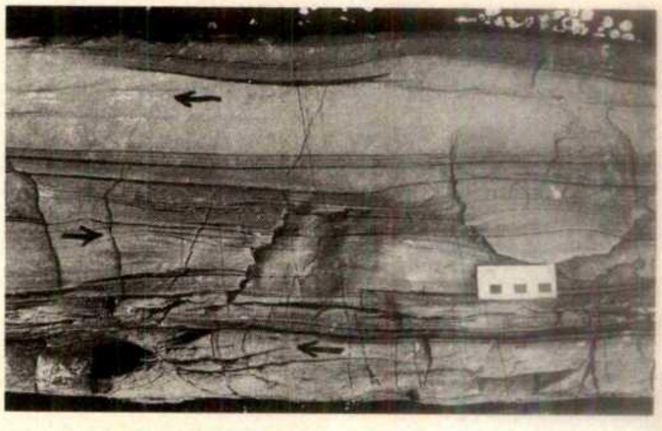

Fig. 1 Sandstone divisions deposited by a reflected turbidity current. The sandstone part of the turbidite is ~30 cm thick. The mudstone cap (not shown) is 105 cm thick (bed PF-2, Fig. 2). Arrows indicate flow directions through the bed.

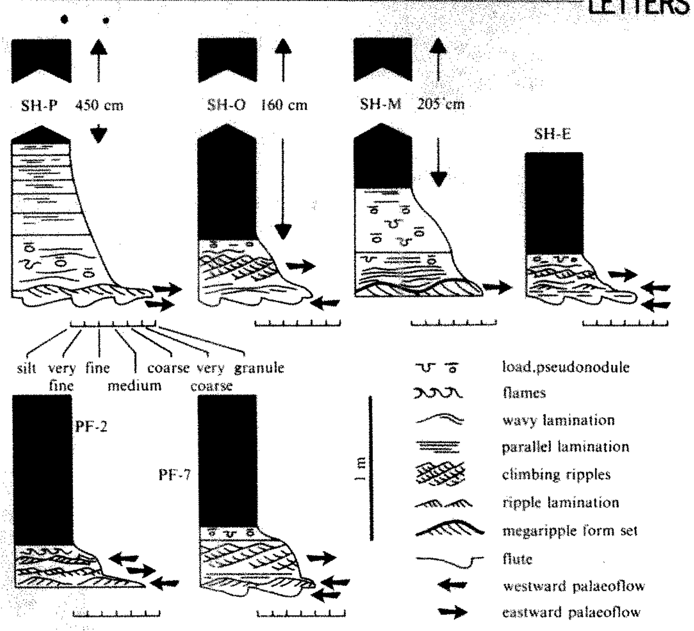

Fig. 2 Sketches of six beds deposited by reflected flows. Structures are accurately drawn to show observed eastward or westward flow.

partings, sedimentary structures or grain imbrication indicate flow from either east to west, or from west to east, with measured palaeoflow azimuths frequently 160°–180° opposed to one another in the same bed (Fig. 1). At the top of the sandy part of a few beds, alternating divisions of muddy lamination and pseudonodules may repeat several times, each couplet being finer and thinner than the one below. The uppermost sandy division, in all beds, consists of pseudonodules. Sketches of the internal features of six beds appear in Fig. 2. We have observed about 50 such beds in members $\beta 1$ and $\beta 2$.

The form set of cross-stratification at the base of bed SH-M (Fig. 2) has been interpreted as the deposit of antidunes migrating upcurrent[9,10], due to the 180° difference between; (1) cross-bed dip direction; and (2) palaeoflow direction indicated by flute casts in surrounding beds. Our discovery of both eastward and westward palaeoflows in single beds removes the original impetus for the antidune hypothesis. In addition, the grain fabric of the cross-strata[11] indicates that the depositing current flowed from west to east, opposite to the direction required by the antidune hypothesis. We interpret this form set, therefore, as a mud-draped megaripple train; the megaripples were migrating from west to east.

Each graded bed was deposited by a large volume turbidity current. The thick, poorly-graded mudstone caps suggest flows with enormous amounts of entrained mud. Despite the palaeoflow reversals in the sandy parts of beds, deposition was rapid. as suggested by both abundant climbing ripples and loading (pseudonodules).

We explain the details of sedimentation of these beds as follows (Fig. 3). The large-volume, mud-rich flows were generated along steep, tectonically-formed slopes on the south side of the foreland basin[6]. On reaching the base of the slope, the powerful flows were constrained to flow westward into the area where our sections are now located; most flutes were eroded by this first westward pass of the current. The lowest sand division was either deposited by the initial westward-flowing current, or by the first return flow. There is often a sharp grain-size break above the lower division, followed by a thin mud drape. We believe this sequence indicates: (1) deposition of a coarse basal division; (2) passage of the main flow across the basin floor; (3) suspension fallout of mud from thick, residual, suspended-sediment cloud; and (4) return of the reflected current to deposit the next sandy division. The return flow was always less competent than the first westward flow, due to frictional energy losses and loss of sediment load and, therefore, transported sand significantly finer than that in the lower division (Fig. 2).

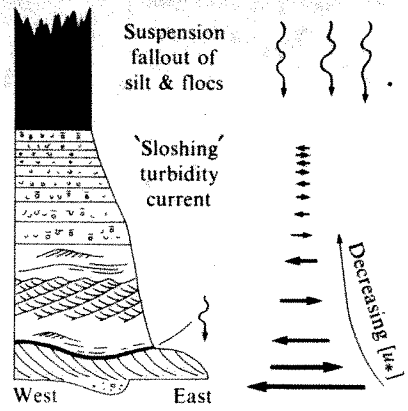
Suspension fallout of silt & flocs
'Sloshing' turbidity current
Decreasing [u*]
West
East

Fig. 3 Depositional model and a representative structure sequence for contained, reflected flows. The length of east–west arrows indicate relative current speeds as the flow decelerates. See Fig. 2 for key.

Several beds have a basal division of coarse to granule grade sand with a fabric or sedimentary structures indicating eastward sediment transport. Included in this category is the bed with basal megaripple cross-stratification (bed SH-M, Fig. 2). These coarse divisions are better sorted than overlying sand, and may not have been deposited entirely by the first reflected current. The sand, due to its coarse grain size, was probably deposited by the initial westward-flowing current, and later reworked as bedload beneath the first reflected flow.

After sand deposition, the ponded, residual, silt-mud suspension was probably still moving slowly back and forth across the basin floor, gradually losing momentum. We believe that it was at this time that the fine-grained pseudonodule divisions were deposited. The silt was deposited quickly, leading to extensive loading and disruption of lamination by liquefaction. In the case of the largest flows (bed SH-P, Fig. 2), the periodic, decaying oscillation of the current led to the deposition of alternating laminated (current deposited) and pseudonoduled (liquefied) layers of decreasing thickness.

The final phase of sedimentation was the fallout of mud from the ponded suspension to form a thick, homogeneous, mudstone cap. The concentrated mud cloud deposited rapidly, perhaps in the same way that shelf muds are rapidly deposited in areas of high concentration, regardless of the competence of local currents[12]. Lack of grading in the caps is also consistent with rapid deposition. Clay minerals probably formed particle aggregates (flocs) that settled much more quickly than single particles.

Unlike Bouma-type turbidites, these contained, or reflected, turbidites do not have a predictable sequence of internal sedimentary structures. In particular, ripple lamination, wavy lamination, convolution, pseudonodules and parallel lamination may alternate in an unpredictable way in the upper division of the sandstone part of these beds. Flow direction in these divisions may change one or more times up through a single bed. For each bed, the exact details of deposition depend on: (1) the importance of flow reflection; (2) the distance that the flow travelled before returning to deposit more sediment; and (3) the importance of interference and collisions between separated parts (offspring) of the single primary flow (parent) that could be moving along different paths and, perhaps, overriding one another because of density differences.

Contained, reflected turbidites can, with care, be distinguished from classic Bouma-type turbidites, based primarily on palaeoflow reversals and thick mudstone caps produced by ponding of the residual mud-silt cloud[3]. These unusual beds are widespread, and provide compelling evidence for deposition in a confined basin. Contained turbidites have only been described from deep-sea sediments, but thinner and perhaps finer-grained examples should also be expected in turbidite sequences of glacial or alpine lakes and arctic fjords with suitable geometry.

Received 3 April; accepted 11 July 1984.

1. Bouma, A. H. *Sedimentology of Some Flysch Deposits* (Elsevier, Amsterdam, 1962).
2. Walker, R. G. *Proc. Yorks. geol. Soc.* **33,** 1–29 (1965).
3. Ricci Lucchi, F. & Valmori, E. *Sedimentology* **27,** 241–270 (1980).
4. Ricci Lucchi, F. in *Excursion Guidebook with Contributions on Sedimentology of some Italian Basins* (ed. Ricci Lucchi, F.) 229–303 (International Association of Sedimentologists, 1981).
5. van Andel, T. H. & Komar, P. D. *Bull. geol. Soc. Am.* **80,** 1163–1190 (1969).
6. Enos, P. *Spec. Pap. geol. Soc. Am.* 117 (1969).
7. St-Julien, P. & Hubert, C. *Am. J. Sci.* **275A,** 337–362 (1975).
8. Skipper, K. & Middleton, G. V. *Can. J. Earth Sci.* **12,** 1934–1952 (1975).
9. Skipper, K. *Sedimentology* **17,** 51–68 (1971).
10. Hand, B. M., Middleton, G. V. & Skipper, K. *Sedimentology* **18,** 135–138 (1972).
11. Pickering, K. T. & Hiscott, R. N. *Sedimentology* (in the press).
12. McCave, I. N. & Swift, S. A. *Bull. geol. Soc. Am.* **87,** 541–546 (1976).

Sampling strategy for stable carbon isotope analysis of tree rings in pine

Steven W. Leavitt & Austin Long

Department of Geosciences, University of Arizona,
Tuscon, Arizona 85721, USA

Stable carbon isotope measurements in tree rings have been explored as potential indicators of past climate[1,2], and as proxy data for reconstructions of the history of $^{13}C/^{12}C$ variations of atmospheric carbon dioxide as related to the global carbon cycle[3–6]. Results of these studies are often conflicting, perhaps partly due to the limited style of sampling natural systems with large inherent spatial variability. We have examined stable carbon isotopic trends in tree rings among several radii of the same tree (*Pinus edulis* Engelm.) and among several trees from the same site, to determine the extent of this variability. The circumferential range in $\delta^{13}C$ values of cellulose is ~1–1.5‰, whereas among individuals it is ~2–3‰. Tests to determine how well various combinations of cores fit the trend of an individual tree or of the site as a whole indicate that pooling four cores from four trees accurately represent site $\delta^{13}C$ trends and absolute values.

Whereas dendroclimatological studies commonly sample several tens of trees at each site with two cores per tree[7], the time and expense of carbon isotopic analysis precludes such density of sampling at each site, and often limits analysis to groups of years rather than individual years. The potential weaknesses of single radius (or core) sampling in isotopic studies was revealed by the $\delta^{13}C$ results of Tans and Mook[8] for two radii of the same *Quercus rubra* L. cross-section which showed not only different isotopic trends but up to 4‰ differences between corresponding rings. The factors which influence carbon isotopic fractionation in trees have already been addressed in models such as that of Francey and Farquhar[9]. However, the patterns and magnitude of this fractionation in natural settings have not been discussed in such detail. To test for circumferential variability we obtained two cross-sections from a pinyon pine tree (*Pinus edulis* Engelm.) located at a site 30 km south of Flagstaff, Arizona, cut at the end of the 1981 growing season. To test for intrasite variability we collected cores from eight other *P. edulis* individuals from the same site at the end of the 1982 growing season.

The wood materials were dated at the Laboratory of Tree-Ring Research of the University of Arizona. One cross-section was divided into eight equally spaced radii which were cut out as 'cores' 5 mm wide. The rings were separated into 5-yr groups from 1900–04 to 1975–79, plus 1980–81 for the cross-section samples and 1980–82 for the cores. The ring intervals from the second cross-section were milled from the full circumference. The cellulose (holocellulose) component of the wood was isolated in a method modified after Green[10] (details of preparation and analysis are given in refs 5, 11). The $^{13}C/^{12}C$ isotopic ratios are expressed with respect to the international PDB standard[12]. Overall reproducibility, including sample preparation, combustion and mass-spectrometric analysis, is estimated to be ~0.1‰.

Several studies have reported on circumferential $\delta^{13}C$ variability in leaves[11,13,14] and rings[3,6,8,13,15,16–18]. Despite a variety of species and localities, the range of $\delta^{13}C$ around the circumference of tree rings is typically 1–2‰. Except for the Tans and Mook[8] results, the isotopic trend from a single core has generally been found to parallel that of others, even though absolute values may differ. From the standpoint of practical sampling and efficiency of analysis, the relevant question is what minimum number of cores from a single tree is required to represent

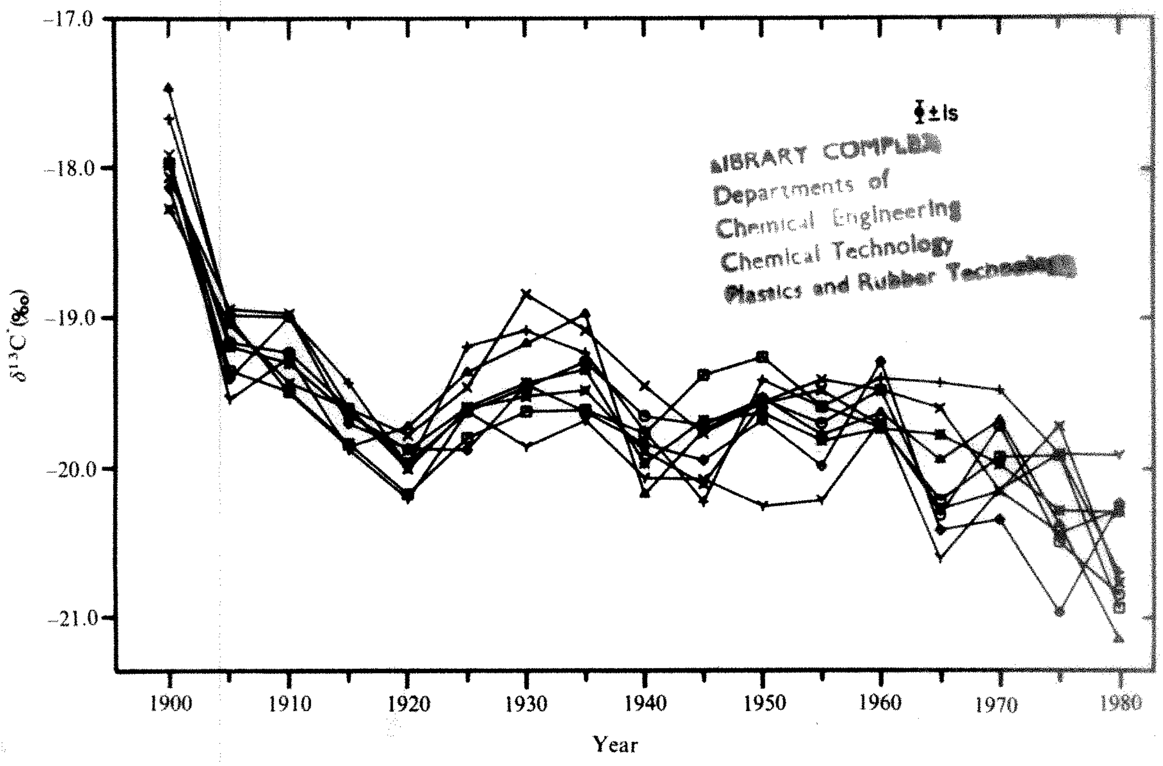

LIBRARY COMPLEX
Departments of
Chemical Engineering
Chemical Technology
Plastics and Rubber Technology

Fig. 1 The $\delta^{13}C$ trends of 5-yr ring groups (values plotted at the beginning of each 5-yr interval) from eight radii of a *P. edulis* tree sampled south of Flagstaff, Arizona. *, The $\delta^{13}C$ trend from an adjacent cross-section whose ring-groups were collected from the full circumference.

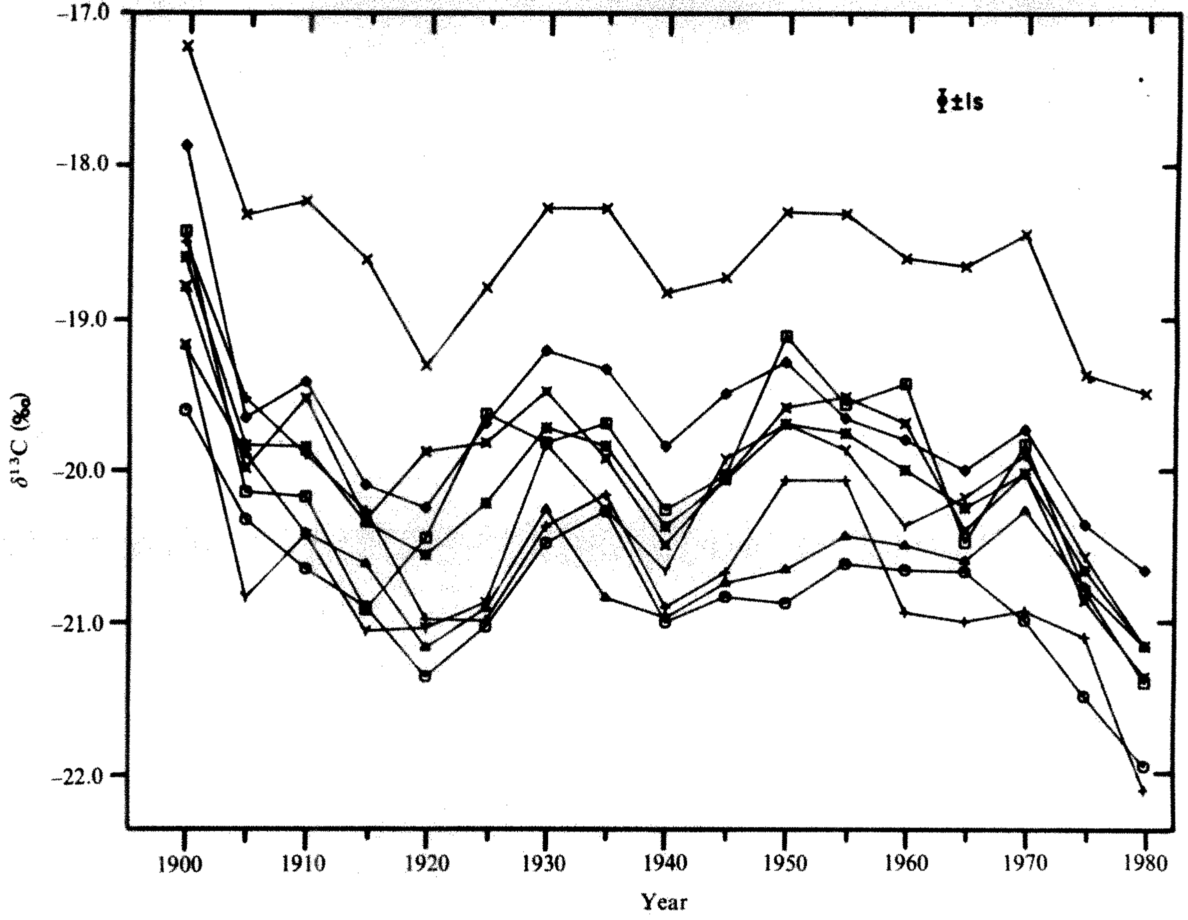

Fig. 2 The $\delta^{13}C$ trends from eight trees at the site where the tree in Fig. 1 was collected. Each tree is represented with four cores whose 5-yr ring groups were pooled before analysis. *, The eight-tree mean.

accurately the $\delta^{13}C$ of cellulose fixed in a tree-ring sequence, although the answer may actually differ among species and local environments.

The *P. edulis* cross-sections we used to help resolve this question for one environment had nearly circular, concentric rings. Furthermore, the ring series had only 1.5% missing rings over the growth period 1795–1981. Figure 1 shows the comparison between the $\delta^{13}C$ trends of the eight radial slices (simulating cores) and 'whole-ring' trend derived from full-circumference analysis of the adjacent cross-section. The $\delta^{13}C$ differences among radii at any interval range from ~0.5 to 1.2‰.

An assessment of the minimum number of cores needed must involve a compromise between effort involved and proximity to the true value. To evaluate this trade-off, we compared combinations of cores with the full-circumference $\delta^{13}C$ results taken as the true value, using two tests. The Pearson correlation coefficient (r) measures the strength of the linear relationship between mean data of a given core combination and that of the cross-section, and the sum of the squares of the differences (SS) between the mean core combination and the true trend is a measure of the absolute $\delta^{13}C$ differences between the curves.

These tests were performed on selected combinations of 1–8 radii. Sampling of a given number of cores from a tree in the field would normally be done equidistantly about the tree circumference, and it is these combinations which were examined. For the eight radii of this study at 45° intervals, equidistant combinations of 2, 4 and 8 cores exist. For combinations of three, five, six and seven cores, however, equidistance could only be approximated with this set of cores. The lowest r found was 0.84 for a single radius (west) versus the true values, yet it is actually significant at 99%. However, close examination of such $\delta^{13}C$ trends with relatively low r values reveals significant differences between some of the short-term variations of the core trend and the true trend. This would limit reconstruction of fine-scale features with single cores. Both parameters improve greatly as the number of cores increases from one to four ($\bar{r}$ increases from 0.89 to 0.96 and $\overline{SS}$ decreases from 1.54 to 0.47), but beyond four cores the improvement tails off. Two cores show a marked improvement over single cores in that not only are the correlation coefficients of each two core combination >0.90, but the largest SS values are only slightly >1. SS values of <1 indicate the mean deviation between core combination and true trend at each interval is <0.25‰, close to a non-statistical difference in light of analytical precision.

We performed this statistical analysis using (1) unweighted $\delta^{13}C$ means of the core combinations, and (2) $\delta^{13}C$ means of the core combinations weighted for the respective 5-yr ring thickness contribution of each of the selected cores, and found the results to be nearly identical, despite two- to threefold differences in ring thickness among radii for a given interval. This implies that, in application, cores may be pooled before analysis (equivalent to weighting the mean) and the results will not be distinguishable from the much more involved process of analysing each core separately and calculating a mean (equivalent to the unweighted mean). We had also tested the eight possible combinations of four cores from the same side of the tree and found they show an appreciably higher SS ($\overline{SS}=0.62$, range 0.42–0.74) than those taken from opposite directions ($\overline{SS}=0.35$, range 0.19–0.51), which suggests that orthogonal cores yield more representative samples. Based on these results we are now sampling four cores per tree wherever possible, because they represent short-term variations well and they offer an extra margin of safety over two cores.

Adequate representation of a $\delta^{13}C$ trend from a given locality requires a knowledge of the $\delta^{13}C$ variability among individuals. Very few studies have examined intra-site variation of $\delta^{13}C$ in tree rings, with results in the general range of 1–2‰ (refs 3, 6, 16, 18, 19). Unfortunately, single cores were generally taken as representative of each tree in these studies. Our study compares δ^{13}C trends in eight trees from a single site sampled with four orthogonal cores per tree. These trees were within an area of ~2 ha of an open pinyon–juniper woodland with typical distances of 5–10 m between individuals. The goal was not to sample eight identical trees, but to sample eight trees having no obvious characteristics which would disqualify them in routine sampling. The physical setting was uniform in that the terrane was nearly flat or sloping slightly WNW, and the soil was developed on basalt bedrock. We selected pinyons of apparent good health although each had a different canopy configuration. The heights of the sampled trees ranged from 5 to 7 m, the diameters (1 m above ground) were ~20–45 cm, and the ages varied from ~130 to 300 yr. For each tree, 5-yr ring groups from the four cores were combined before chemical preparation and analysis.

Figure 2 shows the δ^{13}C trends from these eight trees and the mean trend. The δ^{13}C values for each time interval range over 2.5‰ among the trees. If not for the one tree which shows distinctly heavy isotopic values, the range would be more of the order of 1.5‰. We found no relationship between the absolute δ^{13}C values of the trends and the respective ages, heights, diameters, crown shapes, or proximity to neighbours of the trees.

As in the case of the radial results, it is important to determine how many trees would be required to give an accurate representation of both the δ^{13}C trend and absolute δ^{13}C values registered in the trees of the site. No absolute reference value exists for comparison, so we have used the mean of the eight trees as the true value. The unweighted mean seems logical as there is no *a priori* reason to suspect that any one tree is a more reliable recorder than the next. It was also necessary to examine many more combinations of individuals in the site test than in the circumferential test in order to simulate all field collection possibilities.

The δ values of each tree were first weighted for their respective mean 5-yr group ring widths, which typically varied 3-to 4-fold among trees, before calculating the mean trend of each combination of trees. This is equivalent to pooling trees before analysis. The pattern of r and SS results is similar to those from the intra-tree analysis, although due to the wider range in δ^{13}C values among the trees, the SS values are higher. As in the intra-tree analysis, it appears possible for a single tree to be highly representative of the site (high r, low SS), but in the mean ($\bar{r} = 0.91$, $\overline{SS} = 8.51$) and extreme, individual trees will be much less representative than larger combinations. Sampling four trees per site yields highly significant r values ($\bar{r} = 0.98$) and low SS ($\overline{SS} = 0.80$), making it a good choice for practical application. The diminishing returns of larger samples may not justify the added sampling expense and energy. We are now collecting cores from six to eight trees per site and choosing four trees with the best dating, fewest missing rings, fewest obscured rings, and so on, for a pooled sample to represent the site δ^{13}C trend. These pooled test results show no significant differences from a similar compilation comparing unweighted means of the selected trees with the true value trend. Furthermore, these results differ little from those of similar tests where we used a weighted (by ring thickness) mean trend of the eight trees as the 'true' trend.

In addition to tree-ring isotope studies for reconstruction of climate and past atmospheric carbon dioxide, these results may be useful in designing and interpreting growth-chamber experiments where environmental effects on δ^{13}C are tested, or to food-web studies where stable isotopic compositions of organic matter are used to determine carbon sources and contributions. However, we must warn against extrapolating circumferential relationships developed from one pinyon pine to all species and environments. In view of the factors influencing δ^{13}C in plants described by Francey and Farquhar[9], microenvironmental factors such as shading may enhance circumferential variability. Perhaps the δ^{13}C differences among radii of any tree may ultimately be used to quantify the microenvironmental differences in the crown which produce the circumferential variability.

Within a site, the range of 2–3‰ among pinyon pine is actually quite similar to other studies with other species, despite their being sampled with single cores and representing site environments often quite distinct from the semi-arid sites in which pinyon commonly occur. This range of δ^{13}C values at a site must be considered in sampling, particularly when attempting to relate the differences in absolute δ^{13}C values among sites to the different climates of the respective sites. We had found such a δ^{13}C-climate relationship in a study with juniper[5], but we had represented the δ^{12}C values of each site with only one tree.

We thank J. Dean and D. Bowden (Laboratory of Tree-Ring Research, University of Arizona) for dating the pinyon pine tree rings. C. Sullivan and M. Leavitt assisted in field sampling, E. Sutherland assisted in mechanical preparation, and L. Warneke helped prepare and analyse the cellulose. This research was supported under the US Department of Energy Carbon Cycle Research Program through Oak Ridge-Martin Marietta Subcontract No. 19X-22290C.

Received 9 January; accepted 27 June 1984.

1. Farmer, J. G. *Nature* **279**, 229–231 (1979).
2. Grinsted, M. J., Wilson, A. T. & Ferguson, C. W. *Earth planet. Sci. Lett.* **42**, 251–253 (1979).
3. Francey, R. J. *Nature* **290**, 232–235 (1981).
4. Stuiver, M. *Science* **199**, 253–258 (1978).
5. Leavitt, S. W. & Long, A. *Tellus* **35B**, 92–102 (1983).
6. Freyer, H. D. & Belacy, N. *J. geophys. Res.* **88**, 6844–6852 (1983).
7. Fritts, H. C. *Tree Rings and Climate* (Academic, London, 1976).
8. Tans, P. P. & Mook, W. G. *Tellus* **32**, 268–283 (1980).
9. Francey, R. J. & Farquhar, G. D. *Nature* **297**, 28–31 (1982).
10. Green, J. W. in *Methods of Carbohydrate Chemistry* (ed. Whistler, R. L.) 9–21 (Academic, New York, 1963).
11. Leavitt, S. W. & Long, A. *Isot. Geosci.* **1**, 169–180 (1983).
12. Craig, H. *Geochim. cosmochim. Acta* **12**, 133–149 (1957).
13. Leavitt, S. W. thesis, Univ. Arizona (1982).
14. Arnold, L. D. thesis, Univ. Arizona (1979).
15. Freyer, H. D. & Wiesberg, L. in *Isotope Ratios as Pollutant Source and Behavior Indicators*, 49–62 (IAEA, Vienna, 1975).
16. De Silva, M. P. thesis, Rheinisch-Westfalische Hochschule Aachen (1978).
17. Mazany, T., Lerman, J. C. & Long, A. *Nature* **287**, 432–435 (1980).
18. Bender, M. M. & Berge, A. J. *Tellus* **34**, 500–504 (1982).
19. Freyer, H. D. *Tellus* **31**, 124–137 (1979).

Correlation of marine and continental glacial and interglacial events, Arctic Ocean and Banks Island

David L. Clark*, Jean-Serge Vincent†, Glenn A. Jones‡ & William A. Morris§

* Department of Geology and Geophysics, University of Wisconsin, Madison, Wisconsin 53706, USA
† Geological Survey of Canada, 601 Booth Street, Ottawa, Ontario, Canada K1A 0E8
‡ Woods Hole Oceanographic Institute, Woods Hole, Massachusetts 02543, USA
§ Morris Magnetics, R.R. No. 2, Lucan, Ontario N0M 2J0, Canada

Correlation of Pleistocene glacial and interglacial sediments deposited on land with sediments deposited synchronously in the ocean basins is rarely accomplished[1–3]. A significant exception is the correlation of continental shelf Bay of Biscay interglacial deposits with interglacial sediments from north-east France using δ^{18}O and pollen[4]. In the Arctic Ocean, the definition of a partial magnetic stratigraphy for a Pleistocene sequence on Banks Island, western Arctic Archipelago[5], permits correlation with magnetically defined marine sediment of the Chukchi–Alpha Ridge[6–8] (Fig. 1). We report here the details of this first Arctic Ocean glacial-marine to continental-glacial deposit correlation, and its climatic interpretation. Arctic Ocean sediment texture is climatically controlled and fine-grained textured sediment was deposited in the ocean at the same time as interglacial deposits formed on the adjacent land. The occurrence of coarse-grained Arctic Ocean sediment on the other hand is synchronous with glacial advances on land and also represents periods of deglaciation.

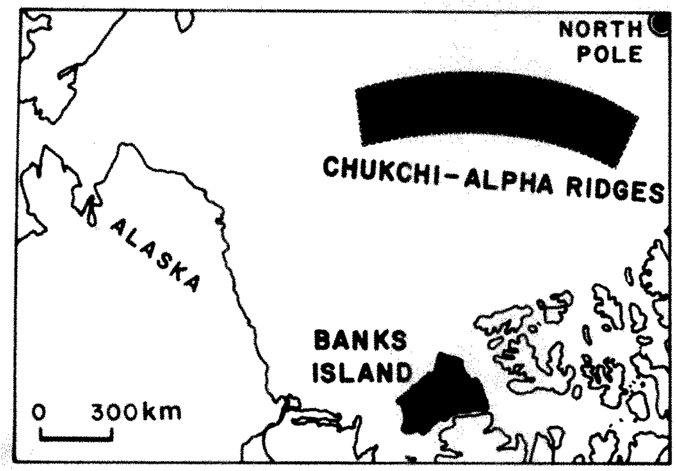

Fig. 1 Location of Banks Island and the area of glacial–marine stratigraphy developed for the Chukchi–Alpha Ridges.

Palaeomagnetic interpretations of Arctic Ocean sediment have been based primarily on polarity signatures (+ or −) published without supporting inclination, intensity or virtual geomagnetic pole (VGP) latitude data[6,9]. However, these data have been discussed recently[8], with inclination data for a representative Arctic core (and similar data for the Banks Island record) (Fig. 2) confirming the validity of previous interpretations. Demagnetization and VGP data have been published for Banks Island[5]. Supporting data on demagnetization, inclination and intensity of the marine cores not considered here, will be published elsewhere[10].

The Bruhnes–Matuyama magnetic boundary, interpreted to be 730 kyr, has been recognized in numerous sediment cores taken from ice-island T-3. The reversal from normal to reversed polarity occurs consistently in stratigraphical unit K[7], which is widely recognized throughout the Amerasian Basin of the Central Arctic Ocean and also reliably correlates with sediment of the Lomonosov Ridge[11]. Unit K is a dark yellowish-brown foraminifera-rich, silty lutite that ranges in thickness from 14 to 53 cm, is intensively burrowed and is finer-grained than adjacent units. It has been interpreted as representing an interval of reduced glacial ice influx in the Arctic (that is, the glacial ice minimum).

Sediments on Banks Island provide the best record of Pleistocene events in the western Canadian Arctic Archipelago. Three continental glaciations (Banks, Thomsen and Amundsen) as well as preglacial and intervening interglacial periods (Morgan Bluffs and Cape Collinson) have been documented[12,13] (Fig. 3).

A preliminary palaeomagnetic investigation[5] of the Duck Hawk Bluffs of southwestern Banks Island, where all recognized glacial and nonglacial events are recorded[14], indicates that the preglacial sediments, and the glacial and marine deposits laid down during the oldest and most extensive Banks Glaciation, and during part of the Morgan Bluffs Interglacial, are probably of Matuyama age (>730 kyr) (Fig. 3). Younger terrestrial deposits associated with the Morgan Bluffs and Cape Collinson interglacials, and the glacial and marine deposits associated with the Thomsen and Amundsen glaciations, are normally magnetized and probably of Brunhes age (<730 kyr). The Banks Glaciation is the only one in which continental ice overrode most of Banks Island and probably large areas of other western Arctic Islands, extending some distance in the ocean. During the younger glacial stages the ice filled some of the inter-island channels and impinged on coastal areas but may have not extended very far into the ocean.

Figure 3 is a tentative correlation of the glacial and interglacial deposits of Banks Island with the lithostratigraphical units recognized in the central Arctic Ocean. The Morgan Bluffs Formation includes terrestrial interglacial deposits and unit K represents a time of reduced glacial ice activity in the ocean. The younger Thomsen and Amundsen glaciations, the Cape Collinson Interglaciation, and Holocene deposits from Banks Island correlate with the upper part of unit K, and units L and M, which are glacial–marine units that include alternating coarse- and fine-textured sediment; these represent alternating intensive and less intensive ice rafting.

The older Banks Glaciation glacial and associated marine deposits, represented by the Duck Hawk Bluffs Formation (Fig. 2), record the strongest advance of a continental ice sheet in the western Canadian Arctic Archipelago and are probably correlative with unit J in the oceanic record. Unit J is one of the coarsest grained units of the late Cenozoic stratigraphy and commonly shows a large coarse peak on graphs of texture (Fig. 4). Because the Banks Glaciation is the strongest glacial advance recognized in the western Canadian Arctic, it is reasonable to expect that the ocean record of this event was a very pronounced increase in coarse sediment. In detail, unit J (Fig. 4) commonly has two prominent coarse zones separated by a finer-grained interval. This suggests that if a correlation with the Banks Glaciation is real, the Banks interval may have included more than one surge of ice, a fact which should be recorded on southern Banks Island by the presence of multiple stacked and distinct Banks Glaciation tills[13]. Because terrestrial glacial and interglacial deposits could experience more erosion than their equivalents in the ocean, the marine record should be more complete. It has also been suggested that unit J can be correlated with oxygen isotope glacial stage 22 (ref. 7).

The recognition of the Bruhnes–Matuyama magnetic signature in Pleistocene sediments of Banks Island permits the first correlation of Canadian continental glacial and interglacial deposits with Arctic Ocean sediment. The Morgan Bluffs Formation is interpreted to be an interglacial deposit and its correlative, unit K, is a silty lutite that has been interpreted to have been deposited during time of reduced continental glacial ice activity[3].

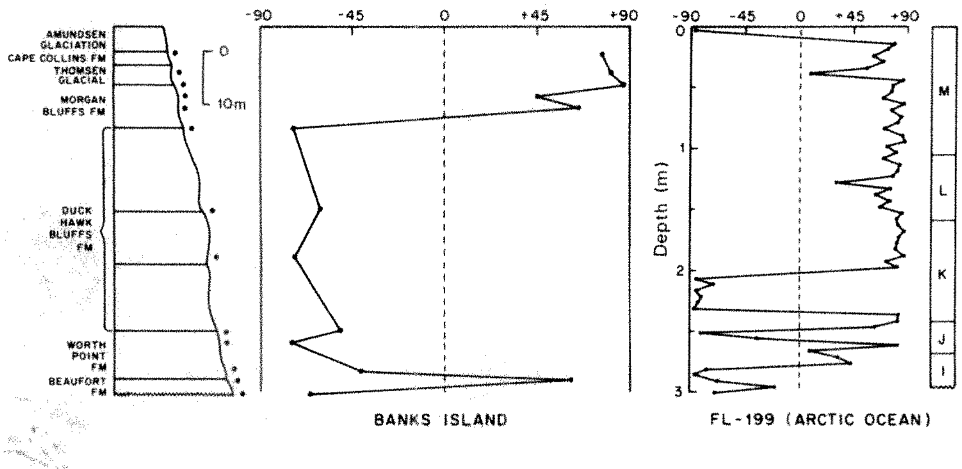

Fig. 2 Magnetic inclination plots for a representative Central Arctic Ocean core compared with a similar plot for Banks Island; the Arctic plot is representative of cores[8,10], and the Banks Island data are based on multiple samples[5]. Note that Banks Glaciation is represented by Duck Hawk Bluffs Formation.

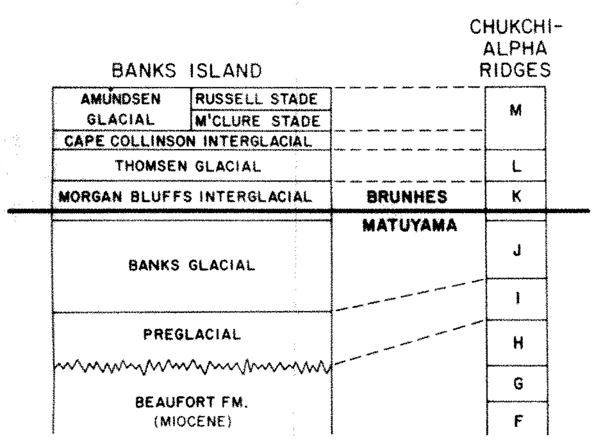

Fig. 3 Correlation of the Banks Island terrestrial deposits[8,9] and glacial–marine stratigraphy of the central Arctic Ocean[7]. The Brunhes normal and Matuyama reversed magnetic intervals in terrestrial and marine sequences are indicated. Marine unit K has previously been interpreted to be of interglacial marine origin[7].

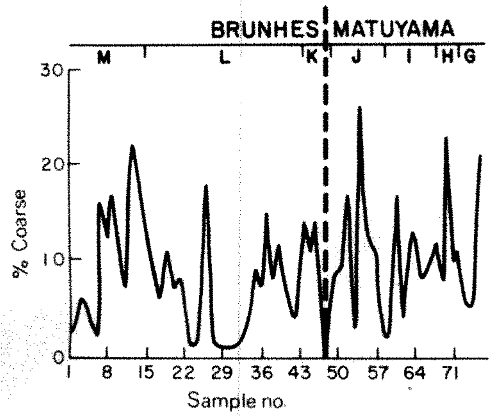

Fig. 4 Per cent coarse sediment (>62 μm) in Arctic Ocean core FI-196, at 80°33′ N, 171°34′ W, from 3,327 m depth. '1', is the core top with samples at 1-cm intervals. The Brunhes–Matuyama magnetic boundary (730 kyr) is indicated as is M, L, K, J, I, H, and G stratigraphy for the core[7]. Coarse peak in J probably correlates with Banks Glacial (Duck Hawk Bluffs Formation, Figs 2, 3).

The other stratigraphical units identified in the Arctic Ocean and differentiated by texture provide a record of glacial and interglacial events that can be correlated with the terrestrial deposits. This apparent confirmation of the significance of oceanic glacial–marine textural relationships with continental glacial and interglacial sediments provides a powerful tool for marine–terrestrial–glacial correlations. This Arctic terrestrial–marine correlation should permit significant palaeoclimatic interpretations that are based on sediment texture.

Received 14 February; accepted 4 July 1984.

1. Turekian, K. K. (ed.) *The Late Cenozoic Glacial Ages* (Yale University Press, New Haven, 1971).
2. Berggren, W. A. & van Couvering, J. A. *The Late Neogene* (Elsevier, Amsterdam, 1974).
3. Bowen, D. Q. *Quaternary Geology, a Stratigraphic Framework for Multidisciplinary Work*, 77 (Pergamon, Oxford, 1978).
4. Turon, J.-L. *Nature* **309**, 673–676 (1984).
5. Vincent, J-S., Morris, W. A. & Occhietti, S. *Geology* **12**, 139–142 (1984).
6. Clark, D. L. *Bull. geol. Soc. Am.* **81**, 3129–3134 (1970).
7. Clark, D. L., Whitman, R. R., Morgan, K. A. & Mackey, S. D. *Geol. Soc. Am. Spec. Pap.* **181** (1980).
8. Jones, G. A. *13th A. Arctic Workshop Abstr.* 44–45 (1984).
9. Linkova, T. I. *Moscow Nauka Press* 279–281 (English transl., Directorate Scientific Infor. Serv. DBR Can., 1966).
10. Jones, G. A. & Clark, D. L. Preprint, *Arctic Ocean paleomagnetic Studies* (Woods Hole Oceanographic Institute, and University of Wisconsin, 1984).
11. Clark, D. L., Morris, T. H. & Blasco, S. M. *Geol. Soc. Am. Abstr.* **15,** 545 (1983).
12. Vincent, J. S. in *Quaternary Stratigraphy of Canada* (ed. Fulton, R. F.) (Geol. Surv. Can. Pap. 84–10, in the press).
13. Vincent, J. S. *Geol. Surv. Can. Mem.* **405** (1983).
14. Vincent, J. S. *et al. Can. J. Earth Sci.* **20,** 1694–1712 (1983).

Patterns of junctional communication in the early amphibian embryo

Sarah C. Guthrie

Department of Anatomy and Embryology,
University College London, Gower Street, London WC1E 6BT, UK

It has long been recognized that cells in early embryos can communicate with each other via a direct cell-to-cell pathway, probably mediated by gap junctions. Low electrical resistance pathways, detected electrophysiologically, have been identified in all species examined so far. However, studies in various embryos on the transfer of molecules larger than small ions (for example, fluorescent dyes in the molecular weight range 350–500) have given conflicting results[1–5]. In all these studies the ability to transfer dyes from cell to cell was determined without reference to the position of the injected cell in the embryo. In the experiments reported here, cell–cell transfer of the fluorescent dye, Lucifer yellow[6] (molecular weight (M_r) 450) was re-examined in the early *Xenopus laevis* embryo by injecting the dye into identified cells, as the position of the injected cell within the embryo may be important. At the 32-cell stage, we found that dye transfer often occurred between animal pole blastomeres which were not sisters, as well as between sister cells, and also that Lucifer yellow was indeed transferred via gap junctions. The cell–cell transfer was not uniform within the animal pole; transfer was maximal near the dorsal side and minimal at the ventral side. This pattern may reflect differences in permeability or numbers of gap junctions across the embryo, and could be related to early events in development.

Previous studies[1–5] investigating the transfer from cell to cell of fluorescent dyes in the molecular weight range 300–500 in various embryos have yielded inconsistent results. Dye transfer has been reported in *Fundulus* embryos[1], mouse embryos[2] and blastomeres from axolotl embryos[1]. Conversely, the absence of cell–cell transfer of such dyes has also been demonstrated in *Fundulus*[3], and in starfish embryo[4] and blastomeres of early *Xenopus* embryos[5]. These studies failed to identify the position of the injected cell within the embryo, and it is now clear that restriction of dye transfer can occur at the site of a developmental boundary, for example, the segmental border in the insect *Oncopeltus*[7]. This has also been suggested by experiments in the mouse embryo[2] and in *Drosophila* imaginal disk[8]. Thus it is possible that transfer between cells of molecules in this molecular weight range depends on the position of the injected cell in the early embryo. This possibility has now been tested in the early *Xenopus* embryo.

All injections were made at the 32-cell stage of development. In preliminary studies, where animal pole cells were injected randomly with respect to position, Lucifer yellow was often found to pass between cells which were not sisters, frequently filling two or more other cells, but not often more than four or five. However, instances of no transfer within the observation period (up to 20 min after injection) were also observed, consistent with previous observations in this embryo[5]. In whole embryos the visual assessment of failure to transfer was sometimes complicated by pigmentation, scatter and autofluorescence. Scatter was largely eliminated by closing down the diaphragm, and scanning across cells appearing to contain dye. Frozen sections were then used to confirm the determination made on the whole embryo (see Fig. 2).

In order to eliminate complications introduced by the persistence of cytoplasmic bridges from the previous cleavage, several injections used fluorescein isothiocyanate (FITC)-conjugated dextrans, whose high molecular weight (10,000) prevents their passage through gap junctions[9]. The results showed that FITC–dextrans were often present in two cells which were daughters of the previous cleavage (that is, sisters at the 32-cell stage) but never in more than these two cells. As Lucifer yellow frequently filled cells that were not sisters, it was assumed to transfer via gap junctions. The timing of the disappearance of

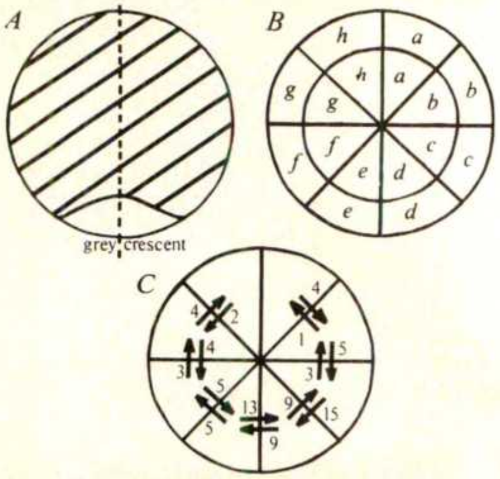

Fig. 1 Map of the *Xenopus* embryo. *A*, The pigmentation pattern of the animal pole of the *Xenopus* egg, at the time when the lifting of the pigment at the grey crescent becomes apparent. The grey crescent is bisected by the primary cleavage axis, and is fated to become the future dorsal side of the embryo, while the opposite side will be ventral. Eggs were obtained by inducing pairs of *Xenopus laevis* to lay by injection of chorionic gonadotropin. *B*, The nomenclature of the cells used in these experiments in a 32-cell embryo, viewed from the animal pole. Embryos at the 32-cell stage, with regular cleavage pattern and identifiable grey crescent were mechanically dejellied and placed in a wax bath filled with half-strength Ringer's solution (60 mM NaCl, 1.25 mM KCl, 4 mM $CaCl_2$, 1 mM Tris, *p*H 7.4) in their normal orientation with the animal pole upwards. Sixteen radical cells were then visible, with pairs of sister cells lying in the same segment, and position identifiable with respect to the grey crescent. *C*, The predominant dye movements in the 32-cell embryo, labelled with the direction and number of instances of transfer. Because of the unknown duration of cytoplasmic bridges between sister cells, dye movements are shown between segments of the animal pole, each consisting of two sisters of the previous cleavage. Note that transfer was bidirectional across all segments except across the primary cleavage axis at the ventral end. The high incidence of transfer across the axis at the dorsal side, from segment *d* to *e* and vice versa, emphasized this asymmetry.

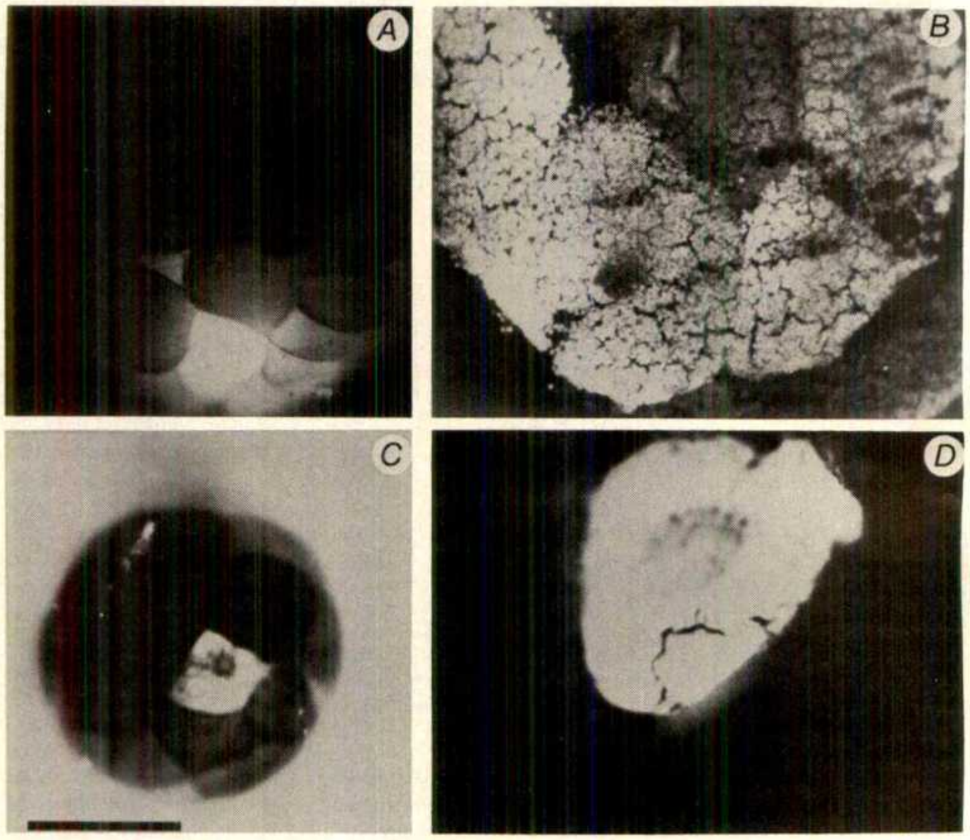

Fig. 2 Photographs of Lucifer yellow-injected embryos. *A*, A whole embryo injected with Lucifer yellow into cell *d* (inner ring) at the 32-cell stage. The embryo has begun to cleave to 64 cells, and there is extensive transfer into several other cells. Scale bar, 500 μm. *B*, A frozen section of an embryo with dye injected into cell *d*. The injected cell is the largest in the field of view with a prominent nucleus, and has transferred dye in the lateral direction to three other cells. Scale bar, 200 μm. *C*, A whole embryo with dye injected into cell *a* (inner ring) at the 32-cell stage with no transfer apparent. Scale bar, 600 μm. *D*, A frozen section of an embryo with dye injected into cell *a*, with sharp restriction of dye to the injected cell. Scale bar, 200 μm.

Methods: For Lucifer yellow injection, microelectrodes were filled with 2% Lucifer yellow, and backfilled with 1% LiCl (resistance 20 MΩ). After impalement and sealing, indicated by a good resting potential (20 mV), rectangular hyperpolarizing pulses (100 nA, 30 ms duration, 10 Hz) were used to iontophorese dye into cells, using a standard injection time of 5 min. To inject 4% FITC–dextran (Sigma) I used a hand syringe or pressure injection unit (Picospritzer II). Immediately after injection, embryos were examined by fluorescence microscopy, and the pattern of dye spread out from the injected cell was noted diagrammatically. The injected cell was often slightly swollen, but this had no deleterious effects, as injected embryos could be grown into normal tadpoles in tap-water. Some embryos were fixed in 4% formaldehyde for frozen sectioning (1 h fixation followed by freezing in isopentane and sectioning at 20 μm on a Bright 5030 microtome) or plastic sectioning (4–5 h fixation followed by dehydration in alcohols, overnight infiltration and embedding in methacrylate resin, then sectioning at 10 μm on a Du Pont Sorvall UB4 microtome).

cytoplasmic bridges varied from embryo to embryo; all cases of transfer of Lucifer yellow into the sister cell only were therefore scored as instances of failure to transfer.

To test whether the non-uniform transfer of dye between cells was related to the position of the cell within the animal pole, injections were made into cells whose position had been reliably identified with respect to the primary cleavage axis and the grey crescent. Figure 1*A* and *B* shows the nomenclature used. Sixteen injections were made into cells at each position, so that 256 embryos were injected in all. Photographs of whole embryos and sections showing examples of presence and absence of transfer are shown in Fig. 2.

The pattern which emerged was that cells near the grey crescent transferred dye in a majority of cases, but those distant from it transferred little dye. The data from all these experiments are given in Fig. 3, as plots of the number of embryos (out of a total of 16) for each identified cell, which showed no transfer, transfer to sister cell only, or transfer to one or more other cells, not including the sister. For the inner ring, cells *c*, *d* and *e*, at the grey crescent side (future dorsal), clearly exhibited the best transfer. By contrast, cells *a* and *h* (at the future ventral side) rarely transferred dye into their lateral neighbours. The pattern of transfer was shifted slightly to the right of the primary cleavage axis at the grey crescent end. A similar pattern was seen for the outer ring of cells, although the total amount of transfer was substantially greater. Table 1 summarizes the data from these experiments, giving the percentage of observed cases of transfer and no transfer for each cell. From this it is clear that even cells which frequently transferred dye, for example cell *c*, could sometimes fail to transfer, just as cells which seldom transferred dye occasionally showed the opposite behaviour. There is no evidence for corresponding differences in electrical coupling across the embryo, though accurate quantitative measurements of the extent of electrical coupling are difficult to obtain. Using

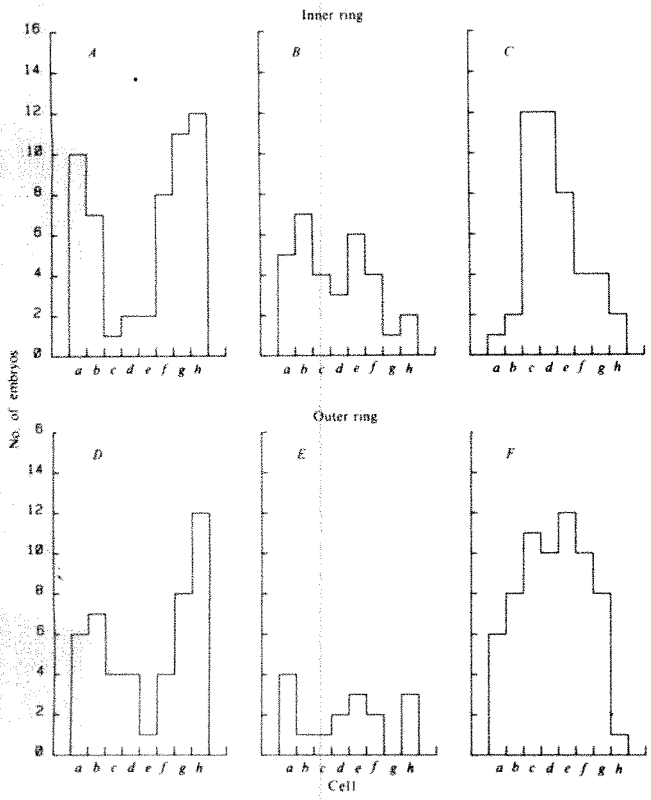

Fig. 3 Graphs showing distribution of Lucifer yellow transfer in the 32-cell embryo. Plots *A* and *D* show the number of instances of no transfer from cells in the inner and outer ring respectively. *B* and *E* show incidence of transfer to sister cell only, and *C* and *F* incidence of transfer to one or more other cells not including the sister cell. The irregularity of graphs *B* and *E* reflects the finding that transfer between sister cells appears to be random with respect to position. Graphs *A* and *D* show that the least transfer occurred at the non-grey crescent side of the embryo, while the predominance of transfer at the grey crescent is evident from graphs *C* and *F*, especially for cells *c* and *d* in the inner ring, and cell *e* in the outer ring.

the χ^2 test, statistical comparison of the observed patterns of transfer on the assumption that there was an equal probability of observing transfer throughout the embryo showed that the chance of these patterns occurring at random is $<1\%$.

Examination of the qualitative nature of the pattern of dye transfer showed preferences in the direction of transfer from individual cells. The major dye movements in the 32-cell embryo are mapped in Fig. 1*C*. As noted above, dye transfer occurred predominantly at the grey crescent side of the embryo, especially between segments *d* and *e*. A striking finding was the presence of bidirectional transfer between all segments except at the ventral side between *a* and *h*, where no instance of transfer was observed.

The data presented here suggest that there were pronounced asymmetries in the degree and direction of spread of dye from cells of the early *Xenopus* embryo. Differences in number or permeability of gap junctions could be responsible for the gradient of transfer from the dorsal to ventral side, though the factors which govern direct cell–cell communication in embryonic systems are as yet unknown. The more interesting question raised by these findings, however, is whether this phenomenon has developmental implications; evidence of stage-dependent changes in the pattern of dye transfer would support this. Further experiments on the early *Xenopus* embryo have shown a progressive restriction of dye transfer from the 16-cell through to the 32- and 64-cell stages, followed by an increase at the early blastula stage. These results will be elaborated elsewhere, together with data from injections using probes of different sizes. Manipulations which disrupt the pattern of cell to cell communication, and produce a parallel disruption in development, would also provide persuasive evidence for a developmental link. One such manipulation is described elsewhere in this issue[10].

Table 1 Dye transfer between identified animal pole cells at the 32-cell stage

Inner ring	Instances of no transfer or transfer to sister cell only % (*n*)	Instances of transfer to one or more other cells, not sister cells % (*n*)
Cell *a*	94 (15)	6 (1)
b	87.5 (14)	12.5 (2)
c	31 (5)	69 (11)
d	31 (5)	69 (11)
e	50 (8)	50 (8)
f	75 (12)	25 (4)
g	75 (12)	25 (4)
h	87.5 (14)	12.5 (2)
Outer ring		
a	62.5 (10)	37.5 (6)
b	50 (8)	50 (8)
c	31 (5)	69 (11)
d	37.5 (6)	62.5 (10)
e	25 (4)	75 (12)
f	37.5 (6)	62.5 (10)
g	50 (8)	50 (8)
h	94 (15)	6 (1)

The numbers and percentages of transfer and cases of no transfer observed for each cell. Instances of transfer to the sister cell only were regarded as no transfer, as sister cell transfer depended on the time in the cleavage cycle when the injection was made. The observed distribution of transfer from all cells examined was compared with a distribution in which the probability of transfer from all cells was taken to be 50%, by the χ^2 test. The observed distribution was shown to be significantly different $(0.01 > P > 0.005)$. For a comparison between the observed results and a distribution in which the probability of transfer is 100%, $0.005 \gg P$. *n*, Number of embryos.

I thank Anne E. Warner for advice. I am in receipt of an MRC studentship. Lucifer yellow was kindly donated by W. W. Stewart.

Received 23 March; accepted 24 July 1984.

1. Bennett, M. V. L., Spira, M. E. & Spray, D. C. *Devl Biol.* **65**, 114–125 (1978).
2. Lo, C. W. & Gilula, N. B. *Cell* **18**, 411–422 (1979).
3. Bennett, M. V. L. in *Intracellular Staining Techniques in Neurobiology* (eds Kater, S. D. & Nicholson, C.) 115–142 (Chapman & Hall, London, 1973).
4. Tupper, J. T. & Saunders, J. W. *Devl Biol.* **27**, 546–554 (1972).
5. Slack, C. & Palmer, J. P. *Expl Cell Res.* **55**, 416–419 (1969).
6. Stewart, W. W. *Cell* **14**, 741–759 (1978).
7. Warner, A. E. & Lawrence, P. A. *Cell* **28**, 243–252 (1982).
8. Weir, M. P. & Lo, C. *Proc. natn. Acad. Sci. U.S.A.* **79**, 3232–3235 (1982).
9. Simpson, I., Rose, B. & Loewenstein, W. R. *Science* **195**, 294–296 (1977).
10. Warner, A. E., Guthrie, S. C. & Gilula, N. B. *Nature* **310**, 127–131 (1984).

Transient expression of a surface antigen on a small subset of neurones during embryonic development

Kathryn J. Kotrla & Corey S. Goodman

Department of Biological Sciences, Stanford University, Stanford, California 94305, USA

During development, neurones find and interconnect with their targets in a remarkably precise way. The unfolding of neuronal specificity involves a series of highly specific recognition events which are likely to be coordinated by the spatial and temporal expression of many different surface molecules. At early stages of development, neuronal recognition occurs most dramatically at the tips of growing axons, at growth cones and their filopodia[1,2]. Previous studies on the grasshopper embryo suggest that specific filopodial contacts lead to the stereotyped patterns of selective

axonal fasciculation; these results support the 'labelled pathways' hypothesis which predicts that the different neighbouring axon fascicles in the embryonic neuropil within filopodial grasp are differentially labelled[3–8]. To uncover the molecular labels on fasciculating embryonic axons, we screened 2,000 monoclonal antibodies generated against the embryonic neuroepithelium[9]. Here we describe three antibodies which reveal surface antigens whose temporal and spatial expression during embryogenesis correlate with the predictions of the model. In particular, the Mes-2 antibody recognizes an antigen which is transiently expressed on the surface of only 4 out of ~1,000 neurones in each metathoracic hemisegment during a short period of embryogenesis. The growth cones of two of these neurones fasciculate in the periphery and innervate the same target. Moreover, they transiently express the Mes-2 surface antigen while doing so.

In the 40% grasshopper embryo, the G growth cone is within filopodial grasp of ~25 different longitudinal axon fascicles (made up of ~100 different axons), and yet invariably fasciculates on the A/P fascicle; when the A/P fascicle is ablated, the G growth cone does not show a high affinity for any other fascicle[5–8]. Furthermore, extensive ultrastructural[7] and experimental[8] analysis demonstrates that G is able to distinguish the two P axons from the two A axons within the A/P fascicle. Given this specificity, it seems reasonable to hypothesize that each of the ~25 longitudinal axon fascicles, and perhaps subsets of axons within the fascicles, are differentially labelled.

To identify molecules whose temporal and spatial expression correlate with this prediction, we generated monoclonal antibodies against the grasshopper embryo central nervous system (CNS)[9]. In three fusions (NS-1 myeloma cells), BALB/c mice were immunized with 40% grasshopper neuroepithelium; in a fourth fusion (from which monoclonal antibody Mes-2 was generated), mice were first immunized with whole *Drosophila* embryos and boosted with 40% grasshopper neuroepithelium. Approximately 2,000 wells were screened on lightly fixed wholemount embryos.

The Mes-3 and Mes-4 monoclonal antibodies stain only one longitudinal axon bundle (that pioneered by the MP1 and dMP2 axons) out of ~25 different fascicles in each hemisegment in the 40% embryo (Fig. 1*d*); the antigens recognized by these antibodies are expressed from the beginning of axonogenesis to the end of embryogenesis. This demonstrates that an individual fascicle is antigenically distinct from all other fascicles within filopodial grasp at the time growth cones are choosing between them. The Mes-3 and Mes-4 antigens (as well as the Mes-2 antigen described below) are also expressed on the surface of the muscle pioneers, large mesodermal cells which provide guidance cues for mononeurone growth cones[10]. The finding that all three antibodies recognize the surfaces of the muscle pioneers is striking, but its significance is unclear.

The Mes-2 antigen is transiently expressed on only 4 out of ~1,000 neurones in each metathoracic (T3) hemisegment (Fig. 1*a*, *b*) during a short period of development (Table 1). The four neurones comprise two interneurones (IN X and IN Y; little is known about their central axon pathways), and the two excitatory motoneurones that innervate the extensor tibiae (ETi) muscle in the leg–FETi (F in Fig. 1*a*, *b*; from neuroblast 4-4) and SETi (S in Fig. 1*b*, *c*; from neuroblast 2-3). Staining of the cells with Mes-2 antibody in either highly dissected living preparations or fixed but unpermeabilized preparations (cytoplasmic antigens require detergent treatment in these whole-mount preparations) indicates that the Mes-2 antigen is on the cell surface.

The growth cones of FETi and SETi follow the same final axonal pathway and innervate the same muscle. Of the ~100 motoneurones in each T3 hemisegment whose growth cones innervate muscles in the body wall or limb bud, only FETi and SETi express the Mes-2 antigen. Although these two motoneurones arise from different neuroblasts, they alone amongst their two families share a final axonal pathway and target, and express Mes-2. Two other neurones also innervate this muscle later in development: they are the CI inhibitory

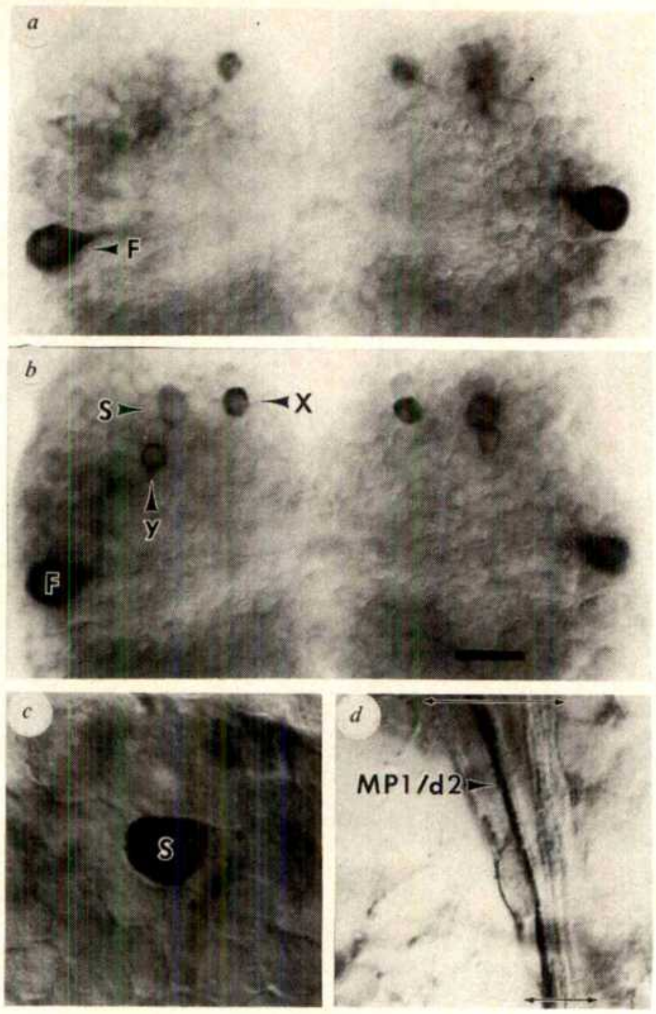

Fig. 1 Binding of Mes-2 (*a*–*c*) and Mes-3 (*d*) monoclonal antibodies to small subsets of neurones in the grasshopper embryo. *a*, *b*, Two different focal planes of a 60% metathoracic (T3) ganglion showing four cell bodies (out of 1,000 on each side) labelled by Mes-2 antibody: F, FETi, fast extensor tibiae motoneurone; S, SETi, slow extensor tibiae motoneurone; X, interneurone X; Y, interneurone Y. The Mes-2 recognizes a surface antigen that is transiently expressed on the axons and cell bodies of these four neurones. *c*, Transient expression of Mes-2 antigen (see Table 1). At 55% of development shown here, SETi expresses the antigen at a high level, whereas by 60% (*b*), SETi's expression is already declining, in contrast to that of FETi and interneurone X. *d*, The MP1/dMP2 fascicle is specifically labelled by the Mes-3 antibody. Only one out of ~20 axon bundles is stained in the longitudinal connective at 38% of development. Lines with arrows shown at the top and bottom of the figure mark the medial (left) and lateral (right) extent of the longitudinal axon fascicles as shown here on the right side of a single segment. Horseradish peroxidase (HRP) immunohistochemistry was performed by fixing embryos in 2% paraformaldehyde for 1/2 h, followed by incubation with antibody supernatant and subsequent protocol for the biotin/avidin HRP system (Vectastain ABC kit, Vector Laboratories). Although the Mes-2 and Mes-3 antibodies bind to surface antigens in living embryos, in all photographs shown here, 0.2% saponin was added for better visualization. Such detergent treatment reveals that the Mes-2 antigen is also within the cytoplasm in the cell bodies of the four neurones. Calibration bar: *a*, *b*, 40 μm; *c*, *d*, 15 μm.

Table 1 Transient expression of Mes-2 surface antigen

	Staining at (% embryonic development):								
Cell	40	45	50	55	60	65	70	80	Adult
SETi	−	−	++	++	+	+	−	−	−
FETi	−	−	++	++	++	−	−	−	−
In X	−	−	+	+	++	++	++	++	−
In Y	−	−	−	−	+	++	+	+	−

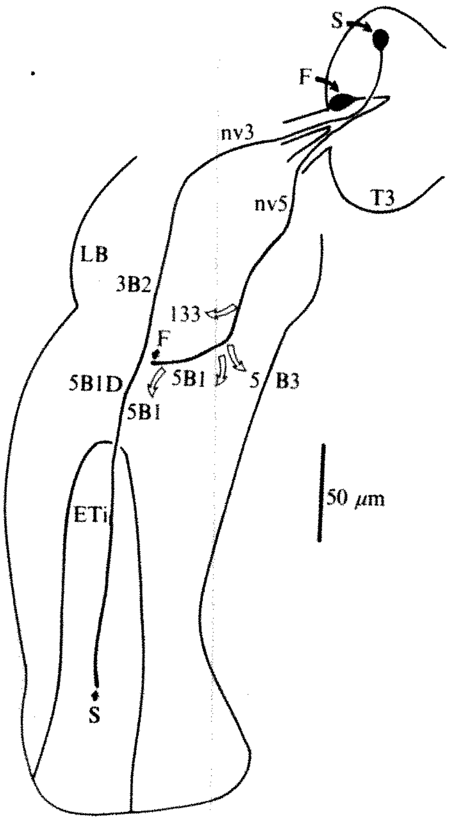

Fig. 2 Camera lucida drawing of the axons of the SETi and FETi motoneurones at 48.5% of development. At this stage, both FETi and SETi have just begun to express the Mes-2 antigen on their surface, as indicated by double labelling experiments using the Mes-2 monoclonal antibody and intracellular dye injections of Lucifer yellow followed by HRP immunocytochemistry with the anti-Lucifer yellow antibody[12]. At this stage, FETi's growth cone is just about to contact SETi's axon in the femur of the limb bud (LB). The cell bodies of both motoneurones are in the T3 ganglion and SETi's growth cone at this stage is already extending across the extensor tibiae (ETi) muscle pioneers[10]. On its way to its target, FETi's growth cone came within 2 µm of SETi's axon as it left the CNS; at that stage, neither cell expressed the Mes-2 antigen. On its way out as nerve 5, FETi's growth cone extended past the muscle pioneer for coxal muscle 133a, where the growth cones of three motoneurones branch off. It then reached a pathway trifurcation in the limb bud, in which it extended along nerve 5B1 instead of nerves 5B3 (followed by flexor motoneurones) or nerve 5B2 (followed by tarsal motoneurones). It then extended off from nerve 5B1 towards SETi's axon in nerve 3B2 (which becomes 5B1D). After the time shown in this figure, FETi fasciculates on SETi's axon and extends distally towards the ETi muscle. For implications, see text. Unfortunately, technical difficulties of antibody access in the 48.5% limb bud prevented us from using antibodies to block function in the living embryo.

motoneurone which also innervates several other muscles, and the DUMETi modulatory neurone which innervates other targets as well.

The Mes-2 antigen is not expressed on either FETi or SETi at the time their growth cones are extending along different central and peripheral axonal pathways. SETi's growth cone pioneers nerve 3 (ref. 11) and extends distally into the femur of the metathoracic limb bud where it extends along the ETi muscle pioneers[10]. At about this time, the FETi growth cone reaches the exit point of the CNS where several axon fascicles diverge as they extend distally as peripheral nerves. Although FETi's growth cone is within short filopodial grasp (2 µm) of SETi's axon, it does not fascilitate with SETi but instead extends out nerve 5 (Fig. 2). At this stage (~40%), neither cell expresses the Mes-2. FETi's growth cone extends out into the limb bud and then makes several other pathway choices.

At 49% of development, FETi's growth cone once again comes into contact with SETi's axon in the femur of the limb bud, and now fasciculates with SETi's axon, following it distally to the ETi muscle pioneers; at this stage of development it is the only axon to do this. Clearly, one or both of the cells has changed since their previous encounter over 24 h earlier.

Double labelling of the neurones with the Mes-2 antibody and intracellular injections of the dye Lucifer yellow reveal that expression of Mes-2 on the processes and cell bodies of both cells begins at 48.5%, just before FETi's growth cone reaches SETi's axon. Their expression of Mes-2 is transient (Table 1; compare S in Fig. 1*c* at 55% and *b* at 60%). After reaching and innervating their common muscle, expression of the Mes-2 antigen decreases dramatically and eventually disappears, and does not reappear during larval and adult life.

The data suggest that the Mes-2 antigen may be involved in the selective fasciculation of FETi's growth cone onto SETi's axon. Only when both cells express the antigen on their surface do they fasciculate. The Mes-2 antibody demonstrates (1) the remarkable specificity of a surface antigen on a very small subset of neurones (4 out of 1,000, 2 of which fasciculate in the periphery) and (2) the transient expression of a surface antigen during the narrow time window of development in which axon outgrowth and cell recognition occurs. It will thus be of interest to isolate the surface molecules recognized by such antibodies as Mes-2, Mes-3 and Mes-4, and to characterize their function during neuronal development.

We thank Lily Jan and Yuh Nung Jan for help in the grasshopper/*Drosophila* fusion from which Mes-2 was isolated, Amy Sater for help in isolating Mes-4,, Pauline Sallata and John Berlot for technical assistance, and John Thomas for criticizing the manuscript. The work was supported by NIH grant and McKnight Scholars Award to C.S.G.

Received 19 March; accepted 26 June 1984.

1. Bray, D. in *Cell Behavior* (eds Bellairs, R., Curtis, A. & Dunn, G.) 299–318 (Cambridge University Press, 1982).
2. Letourneau, P. C. in *Neuronal Development* (ed Spitzer, N. C.) 213–259 (Plenum, 1982).
3. Goodman, C. S., Raper, J. A., Ho, R. & Chang, S. *Symp. Soc. Deu. Biol.* **40**, 275–316 (1982).
4. Raper, J. A., Bastiani, M. J. & Goodman, C. S. *J. Neurosci.* **3**, 20–30 (1983a).
5. Raper, J. A., Bastiani, M. J. & Goodman, C. S. *J. Neurosci.* **3**, 31–41 (1983b).
6. Raper, J. A., Bastiani, M. J. & Goodman, C. S. *Cold Spring Harb. Symp. quant. Biol.* **48**, 587–598 (1983).
7. Bastiani, M. J., Raper, J. A. & Goodman, C. S. *J. Neurosci.* (in the press).
8. Raper, J. A., Bastiani, M. J. & Goodman, C. S. *J. Neurosci.* (in the press).
9. Kotrla, K. J. & Goodman, C. S. *Soc. Neurosci.* **9**, 1045 (1983).
10. Ho, R. K., Ball, E. E. & Goodman, C. S. *Nature* **301**, 66–69 (1983).
11. Ho, R. K. & Goodman, C. S. *Nature* **297**, 404–406 (1982).
12. Taghert, P. H., Bastiani, M. J., Ho, R. K. & Goodman, C. S. *Devl Biol.* **94**, 391–399 (1982).

Neural cell adhesion molecules and myelin-associated glycoprotein share a common carbohydrate moiety recognized by monoclonal antibodies L2 and HNK-1

J. Kruse*, R. Mailhammer*, H. Wernecke*,
A. Faissner*, I. Sommer*, C. Goridis†
& M. Schachner*

* Department of Neurobiology, University of Heidelberg,
Im Neuenheimer Feld 504, 6900 Heidelberg, FRG
† Centre d'Immunologie, INSERM–CNRS de Marseille Luminy,
13288 Marseille Cedex 9, France

Cell surface molecules have been implicated in cell interactions which underlie formation of the nervous system. The analysis of the functional properties of such molecules has profited from the combined use of antibodies and cell culture systems. It has been suggested that the interplay between these molecules modulates cell-to-cell interaction at critical developmental stages[1,2]. In the mouse, N-CAM[1,3] and L1 antigen[4] have been shown to mediate Ca^{2+}-independent adhesion among neural cells. N-CAM plays a role in fasciculation of neurites and formation of neuromuscular

junction. L1 is apparently not involved in synaptogenesis, but in migration of granule cell neurones in the developing mouse cerebellar cortex[5]. The two antigens are distinct molecular and functional entities which act synergistically in aggregation of neuroblastoma[6] and early postnatal cerebellar cells[7]. In view of a certain similarity in function between the two groups of molecules, it was not surprising to find that structural similarities are detectable by the monoclonal antibody L2. We show here that a carbohydrate moiety recognized by L2 and HNK-1 monoclonal antibodies, is present in mouse N-CAM and L1. The L2 epitope appears on all major neural cell types but not all N-CAM molecules express it. This heterogeneity points to a previously undetected molecular diversity which may have functional implications for modulating cell adhesion during development.

To demonstrate that L2 antibodies react with L1 antigen and mouse N-CAM Western blots were performed with the two antigens which had been immunoaffinity purified on the respective monoclonal antibody columns. In this study, monoclonal antibody BSP-2 was used to purify and test mouse N-CAM[8,9]. L2 and HNK-1[10–12] antibodies recognized the 200 and 140 kilodalton (kd) constituents of L1 and the 180 and 140, but not the 120 kd band of N-CAM isolated from adult mouse brain. In contrast, the 120 kd band of N-CAM was clearly visualized by polyclonal antiserum to BSP-2/N-CAM (Fig. 1). The two antibodies reacted with additional polypeptides present in an Nonidet P40 solubilized crude membrane fraction of adult mouse brain including two bands at 160 and 100 kd and several fainter ones in higher and lower molecular weight regions. The 160 and 100 kd bands were more clearly visualized when L1 and mouse N-CAM were removed from the membrane fraction by sequential immunoaffinity chromatography and the residual polypeptides (designated 'rest L2') recovered by L2 antibody immunoaffinity chromatography (Fig. 1). Polyclonal antiserum to MAG[13] reacted with the 100 kd component, but not with any other polypeptide of 'rest L2' (Fig. 1).

To determine whether the L2/HNK-1 epitopes resided in the carbohydrate or protein moieties, biochemical modifications of the total glycoproteins expressing the L2 epitope were carried out. All L2 positive glycoproteins were obtained from adult mouse brain by affinity chromatography with a monoclonal L2 antibody column and will be designated 'L2 antigen'. The L2/HNK-1 epitopes were found to be heat resistant (95 °C, 15 min) and destroyed by periodate treatment (1 μg antigen in 46 μl 0.07 M Na *m*-periodate, *p*H 5.0, 16 h, 37 °C in the dark, according to ref. 14). Also, when 'L2 antigen' was treated extensively with pronase in denaturating conditions, the carbohydrate containing fraction was isolated by gel filtration and used to compete for L2 and HNK-1 antibody binding to purified 'L2 antigen' in immunospot binding (not shown) and enzyme-linked immunosorbant assay (ELISA) test (Table 1). The results obtained by both techniques and with both antibodies were similar. (It will be shown later by immunocytological methods that the two antibodies compete with each other for binding.) While similar amounts of 'L2 antigen' competed for both antibodies, inhibition by carbohydrate fraction was less efficient and 60 times less for HNK-1 (IgM) than for L2 (IgG) antibodies. Controls for the reaction consisted of carbohydrate fraction obtained in identical conditions from fetuin and used for competition in L2 antibody binding. Furthermore, the carbohydrate fraction from 'L2 antigen' was used for competition in an unrelated antibody-antigen reaction (human haemoglobin). No inhibition of antibody binding was observed in these controls. In an alternate experiment, purified 'L2 antigen' was treated with endoglycosidase F in denaturating conditions[15]. The digested product was then spotted onto nitrocellulose filters which do not permit the adsorption of free carbohydrate chains. L2 and HNK-1 antibodies did not react, while polyclonal L2 antibodies prepared in rabbits against 'L2 antigen' showed maximal binding.

To determine which cell types express the L2 epitope, immunocytochemical studies were carried out on cultured cells using double immunolabelling techniques with established cell

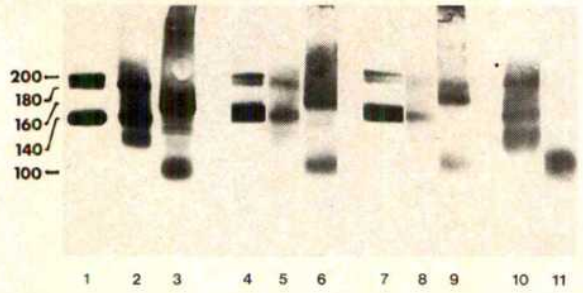

Fig. 1 Western blot analysis of immunoaffinity purified antigens L1, mouse N-CAM/BSP-2 and 'rest L2' from adult mouse brain using monoclonal antibodies L2 and HNK-1 and polyclonal antisera to BSP-2/N-CAM and MAG. Antibodies were described previously[2,3,4,10,13]. L2 antibodies were obtained from two hybridoma clones resulting from an immunization and fusion as described for L1[4]. Another L2 antibody was obtained from a hybridoma clone resulting from an immunization with a glycoprotein enriched membrane fraction from adult mouse brain which showed neutralizing activity towards Fab fragments from antibodies to crude membranes from adult mouse cerebellum in reaggregation of dispase-treated[7] postnatal cerebellar cells. Preparation of crude membrane fraction, immunoaffinity purification of antigens on monoclonal antibody columns and Western blot techniques have been described[4,7]. Immunopurified antigens (visualized by reduced silver staining[4]): lane 1, L1; 2, N-CAM; 3, 'rest L2'. Antigens for Western blots (lanes 4–11): 4 and 7, L1; 5, 8 and 10, N-CAM; 6, 9 and 11, 'rest L2' obtained by sequential immunoaffinity removal of L1 and N-CAM before immunoaffinity chromatography on an L2 antibody column. Antibodies: 4–6, L2 antibody; 7–9, HNK-1 antibody; 10, polyclonal anti-BSP-2/N-CAM antiserum; 11, polyclonal anti-MAG antiserum.

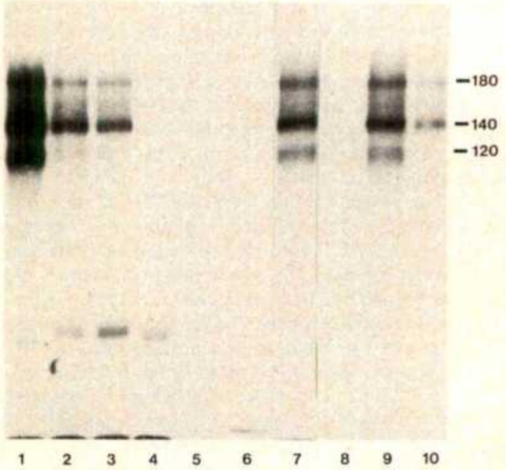

Fig. 2 Sequential immunoprecipitation of immunopurified, iodinated mouse N-CAM with two monoclonal antibodies to N-CAM (H28.123 and P61 (ref. 33) 1, 2, respectively), L2 antibody (3) and L1 antibody (4). Antibody P61 does not recognize the 120 kd band[33]; 5, precipitation with H28.123 after preclearing with H28.123; 6, anti-L2 after preclearing with H28.123; 7, H28.123 after preclearing with anti-L2; 8, anti-L2 after preclearing with anti-L2; 9, H28.123 after preclearing with anti-L1; 10, anti-L2 after precleaning with anti-L1. N-CAM was immunopurified from adult mouse brain membrane in presence of 2-deoxy-2,3-dehydro-*N*-acetyl neuraminic acid (Boehringer, Mannheim) to prevent possible degradation of terminal sugars. Since endogenous endoglycosidase activities in eucaryotic cells are negligible, it is unlikely that the N-CAM preparation contains degraded carbohydrate chains. Immunoprecipitation was carried out with mouse anti-rat kappa mouse Ig coupled to Sepharose as described[7]. N-CAM (5×10^5 c.p.m.) was incubated for 1 h at 0 °C with first antibodies and for 4 h at 4 °C with Sepharose beads. After four washings, supernatants from the precipitates were again treated identically with antibodies and Sepharose beads. Treatment of supernatants with Separose beads was repeated to remove potentially present soluble complexes.

Table 1 Inhibitory capacity of carbohydrate moiety of 'L2 antigen' for binding of L2 and HNK-1 antibodies to immunopurified 'L2 antigen'

Antibodies	Competing compounds			
	'L2 antigen'		Carbohydrate fraction of 'L2 antigen'	
	Half-maximal inhibition	Maximal inhibition	Half-maximal inhibition	Maximal inhibition
L2	0.176 μg	1.76 μg	0.28 μg	1.4 μg
HNK-1	0.176 μg	1.76 μg	16.8 μg	ND

An ELISA test[29] was performed with L2 and HNK-1 antibodies on immunoaffinity purified 'L2 antigen' (20 ng per spot on nitrocellulose filters) in the presence of competing 'L2 antigen' and carbohydrate fraction obtained from 'L2 antigen' by proteolytic digest. Treatment of 'L2 antigen' (2 mg ml^{-1}) in 50 mM Tris, *p*H 8.2 containing 0.1% SDS and 4 mM $CaCl_2$ with pronase (three consecutive additions of 30 μg ml^{-1}, 30 h, 37 °C), subsequent redigestion with pronase (27 h, 37 °C, 2 mM $CaCl_2$) or proteinase K (27 h, 37 °C, 10 mM EDTA), isolation by gel filtration on Biogel P4 and chromatographic analysis of carbohydrate fraction were carried out as described elsewhere[14,30]. Antibodies were used at a concentration of 2 serial dilutions before titre endpoint, 1:200,000 from a 14 mg ml^{-1} stock for L2 and 1:100,000 for HNK-1 and incubated with 'L2 antigen' or carbohydrate fraction (1 h, room temperature) before the ELISA test. Amounts of competing compounds are given in μg protein for 'L2 antigen'[31] and μg carbohydrate for carbohydrate fraction[32] which give half maximal and maximal inhibition of antibody binding. ND, not determined.

type-specific neural markers. In monolayer cultures of early postnatal cerebellar cells the L2 and HNK-1 antibodies reacted with a fraction of tetanus toxin[16], N-CAM and L1 positive neurones, glial fibrillary acidic protein (GFA) and vimentin-positive astrocytes[17] and 04 and 01 antigen-positive oligodendrocytes[18–20], but not with fibronectin-positive fibroblast-like cells[21]. The two antibodies were able to block each other in binding. With time in culture the percentage of N-CAM positive neurones that were also L2/HNK-1 positive decreased from 49±8% or 52±2% after 1 day to 18±5% or 13±3% after 7 days in culture for L2 or HNK-1, respectively.

To investigate the paradoxical finding that only some neurones that are recognized by polyclonal and monoclonal N-CAM antibodies express the L2 epitope, sequential immunoprecipitation of iodinated N-CAM immunopurified from adult mouse brain (see Fig. 1) was performed with antibodies to N-CAM and L2 (Fig. 2). Antibodies to N-CAM removed all further reactivity for the same or for L2 antibody. In contrast, two clearings with anti-L2 removed all material reacting with the same antibody, but left considerable amounts of the 180, 140 and 120 kd bands in solution which could be precipitated by N-CAM antibodies. L2 antibodies removed only 15–20% of the N-CAM that is precipitable by N-CAM antibodies. Similar results were obtained, when the embryonic form of N-CAM was used for immunoprecipitation (not shown). These results support the conclusion that not all N-CAM molecules of both the adult and embryonic forms express the L2 epitope. Furthermore, the L2 antibody did not bind the 120 kd band (Fig. 2).

Since two bands of N-CAM are heterogeneous with respect to expression of the L2 epitope, the most likely explanation for the absence of L2 on N-CAM bearing neurones is a heterogeneity among N-CAM molecules which is distinct from the molecular heterogeneity represented by the adult and embryonic forms. On the other hand, some neurones may express only the 120 kd component. A similar heterogeneity may also exist for L1, since in this case also not all L1 positive neurones were found to express the L2 epitope.

The present study has shown that two cell adhesion molecules share a common carbohydrate moiety also present on myelin-associated glycoprotein. From our experiments we cannot determine whether the two antibodies recognize the same epitope or two distinct epitopes closely associated with each other on the carbohydrate chains so that the antibodies compete with each other for binding. In any case, the L2/HNK-1 epitopes are simultaneously expressed on the same select group of molecules. It has been suggested that myelin associated glycoprotein mediates the interaction of the periaxonal membrane of myelin with the axon[22]. It is possible, therefore, that the common moiety is not only a sign of fortuitous structural homologies between neural cell surface constituents, but implicates that the L2 expressing molecules perform similar functional tasks.

The role of the L2/HNK-1 carbohydrate moiety in cell interactions remains at present unknown. Variations in carbohydrate composition of the embryonic and adult forms of N-CAM underlie differences in adhesive properties[23,24] and it is conceivable that the L2 epitope represents an additional possibility to modulate cell interactions among neural cells. Heterogeneity in expression of the L2 epitope in the population of N-CAM molecules on individual neurones would provide particular cells with the capability to superimpose other tuning modes of adhesion between cell surface receptors and their ligands as they have been described in non-neural systems (see, for instance, ref. 25). Whether adhesive properties are affected in human gammopathies with demyelinating neuropathy and antibodies to myelin associated glycoprotein[26–28] remains an open question.

We thank Andrea Kalkhoff, Magdalena Schlotter and Sabine Ullrich for technical assistance, F. G. Rathjen for producing L2 monoclonal antibodies, R. C. McGarry and J. C. Roder for HNK-1 hybridoma clone, N. Sternberger for MAG antiserum, and Deutsche Forschungsgemeinschaft and Centre National de la Recherche Scientifique for support.

Received 16 March; accepted 17 July 1984.

1. Edelman, G. M. *et al. Cold Spring Harb. Symp. quant. Biol.* **48,** 515–526 (1983).
2. Schachner, M. *et al. Cold Spring Harb. Symp. quant. Biol.* **48,** 557–568 (1983).
3. Goridis, C. *et al. Cold Spring Harb. Symp. quant. Biol.* **48,** 527–538 (1983).
4. Rathjen, F. G. & Schachner, M. *EMBO J.* **3,** 1–10 (1984).
5. Lindner, J., Rathjen, F. G. & Schachner, M. *Nature* **305,** 427–430 (1983).
6. Rathjen, F. G. & Rutishauser, U. *EMBO J.* **3,** 461–465 (1984).
7. Faissner, A., Kruse, J., Goridis, C., Bock, E. & Schachner, M. *EMBO J.* **3,** 733–737 (1984).
8. Hirn, M., Pierres, M., Deagostini-Bazin, H., Hirsch., M. & Goridis, C. *Brain Res.* **214,** 433–439 (1981).
9. Hirn, M., Ghandour, M. S., Deagostini–Bazin, H. & Goridis, C. *Brain Res.* **265,** 87–100 (1983).
10. Abo, T. & Balch, C. M. *J. Immun.* **127,** 1024–1029 (1981).
11. McGarry, R. C., Helfand, S. L., Quarles, R. H. & Roder, J. C. *Nature* **306,** 376–378 (1983).
12. Schuller-Petrovic, S., Gebhart, W., Lassmann, H., Rumpold, H. & Kraft, D. *Nature* **306,** 179–181 (1983).
13. Quarles, R. H., Johnson, D., Brady, R. O. & Sternberger, N. H. *Neurochem. Res.* **6,** 1115–1127 (1981).
14. Spiro, R. G. *Meth. Enzym.* **8,** 26–52 (1966).
15. Elder, J. H. & Alexander, S. *Proc. natn. Acad. Sci. U.S.A.* **79,** 4540–4544 (1982).
16. Schnitzer, J. & Schachner, M. *J. Neuroimmun.* **1,** 429–456 (1981).
17. Schnitzer, J., Franke, W. W. & Schachner, M. *J. Cell Biol.* **90,** 447–475 (1981).
18. Sommer, I. & Schachner, M. *Devl Biol.* **83,** 311–327 (1981).
19. Schachner, M., Kim, S. U. & Zehnle, R. *Devl. Biol.* **83,** 328–338 (1981).
20. Sommer, I. & Schachner, M. *Neurosci. Lett.* **29,** 183–188 (1982).
21. Schachner, M., Schoonmaker, G. & Hynes, R. O. *Brain Res.* **158,** 149–158 (1978).
22. Itoyama, Y. *et al. Ann. Neurol.* **7,** 167–177 (1980).
23. Sadoul, R., Hirn, M., Deagostini-Bazin, H., Rougon, G. & Goridis, C. *Nature* **304,** 347–349 (1983).
24. Hoffman, S. & Edelman, G. M. *Proc. natn. Acad. Sci. U.S.A.* **80,** 5762–5766 (1983).
25. Reutter, W., Köttgen, E., Bauer, C. & Gehrock, W., in *Sialic acids; Chemistry, Metabolism and Function* (ed. Schauer, R.) 263–305 (Springer, Berlin, 1982).
26. Latov, N. *et al. Proc. natn. Acad. Sci. U.S.A.* **75,** 7139–7142 (1981).
27. Steck, A. J., Murray, N., Vandevelde, M. & Zurbriggen, A. *J. Neuroimmunology* **5,** 145–156 (1983).
28. Stefansson, K. *et al. Acta neuropath. (Berl.)* **59,** 255–261 (1983).
29. Palfree, R. G. E. & Elliot, B. E. *J. immun. Meth.* **52,** 395–408 (1982).
30. Holmes, E. W. & O'Brien, J. S. *Analyt. Biochem.* **93,** 167–170 (1979).
31. Neuhoff, V., Phillipp, K., Zimmer, H. G. & Mesecke, S. *Hoppe-Seyler's Z. physiol. Chem.* **360,** 1657–1670 (1979).
32. Hirs, C. H. N. *Meth. Enzym.* **11,** 411–413 (1967).
33. Gennarini, G., Hirn, M., Deagostini-Bazin, H. & Goridis, C. *Eur. J. Biochem.* (in the press).

Neuronal-type Na$^+$ and K$^+$ channels in rabbit cultured Schwann cells

S. Y. Chiu*, P. Schrager† & J. M. Ritchie*

* Department of Pharmacology, Yale University School of Medicine, 333 Cedar Street, New Haven, Connecticut 06510, USA
† Department of Physiology, University of Rochester Medical Center, Rochester, New York 14642, USA

Nerve axons in the central and peripheral nervous system are normally surrounded by satellite cells. These cells, known as Schwann cells in the peripheral nervous system, interact with axons to form a myelin sheath, so allowing nerve impulses to proceed at high speed. Schwann cells are thought to differ from neurones in their membrane properties in one important aspect: they lack excitability. Using the patch-clamp technique we have now measured directly the ionic currents across the membrane of single Schwann cells cultured from newborn rabbits. Surprisingly, we found that these Schwann cells possess voltage-gated sodium and potassium channels that are similar to those present in neuronal membranes.

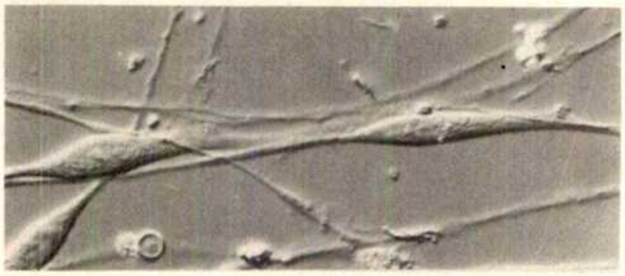

Fig. 1 Two-day-old cultured rabbit Schwann cells under Nomarski optics. (×610).

Figure 1 shows 2-day-old Schwann cells cultured from the sciatic nerves of newborn rabbits[1]. Although markers (such as RAN-1) exist for rat Schwann cells, no such marker is readily available for the rabbit. Schwann cells in the present study were therefore identified morphologically by their characteristic bipolar spindle shape; this is distinct from the flat multipolar appearance of the contaminating fibroblasts that form the only other cellular component of the primary cultures used (and which were not studied electrophysiologically in the present experiments). Although Schwann cells in culture may come to resemble fibroblasts in shape in certain conditions[2], fibroblasts are unlikely to be mistaken for Schwann cells. Proliferation of fibroblasts was inhibited in some cultures by adding cytosine arabinoside to the medium.

Ionic currents were recorded using the patch-clamp technique of Hamill *et al.*[3] in the whole cell configuration. Following formation of a gigohm seal to the cell surface, the patch membrane was broken by excess suction, allowing access to the cell interior. Patch pipettes were filled with solutions in which the primary salt was KCl, CsCl or CsF, together with Ca^{2+} buffered to low concentrations by EGTA. In this system, ion concentrations inside the cell equilibrate with those in the pipette with a time constant of about 5 s (ref. 4). Over 60 cells were studied in cultures for 2–10 days.

Figure 2*a* shows ionic currents recorded from a rabbit Schwann cell with KCl in the patch pipette. The cell was held at −75 mV and test pulses, each preceded by a prepulse to −115 mV, were applied in 10-mV increments, the final potential ranging from −75 mV to +25 mV. The records consist of two components, an early inward current and a delayed outward current. They thus resemble responses found in a number of neurones. We have used pharmacological compounds of known specificities to characterize these Schwann cell currents further. Figure 2*b* shows the effect of the K$^+$ channel blocker 4-aminopyridine (4-AP)[5,6]. Two minutes after adding 6 mM 4-AP to the solution bathing the cell, the delayed outward current was selectively blocked. In other experiments in which the pipette was filled with CsCl, another blocker of K$^+$ channels, only inward currents were observed. We thus conclude that the delayed outward current is a K$^+$ current similar to that found in squid and frog nerves.

The nature of the initial inward current was studied with tetrodotoxin (TTX), a highly selective blocker of Na$^+$ channels[7]. Figure 3 shows inward currents before (*a*) and 30 s after (*b*) the introduction of 60 nM TTX into the bathing solution. Potassium currents in this cell had been eliminated by using a pipette containing CsF. It can be seen that the transient inward current was virtually abolished by TTX. Figure 3*c* illustrates a family of ionic currents which includes depolarizations sufficiently strong to elicit outward transient currents. The pipette solution contained primarily CsCl to block current through K$^+$ channels but included 29 mM Na$^+$. We consistently found that the apparent reversal potential was about +70 mV, which is about 30 mV more positive than the Na$^+$ equilibrium potential. There are at least two possible explanations for this discrepancy. First, most of the steady-state current in Fig. 3*c* was not blocked by TTX or Cs and may thus be flowing through a third ionic channel. This suggestion is supported by the recent findings of anionic[1] and non-selective cationic[8] channels in rat Schwann cells; and we have found single channels in rabbit cells which appear similar to these but will require further characterization. This current would have little effect on our estimate of maximum peak inward current, but might be significant at +70 mV. A second possibility is that the spindle shape of these cells may lead to spatial non-uniformity and poor control of the internal potential by the voltage-clamp.

Although all cells exhibited Na$^+$ currents, the amplitude of the currents varied considerably among different cells (compare Figs 2*a* and 3*a*). For example, the maximum peak inward Na$^+$ current ranged from 50 to 2,100 pA, with an average value of 498 ± 84 pA (±s.e.m., $n = 28$). This variation did not seem to be

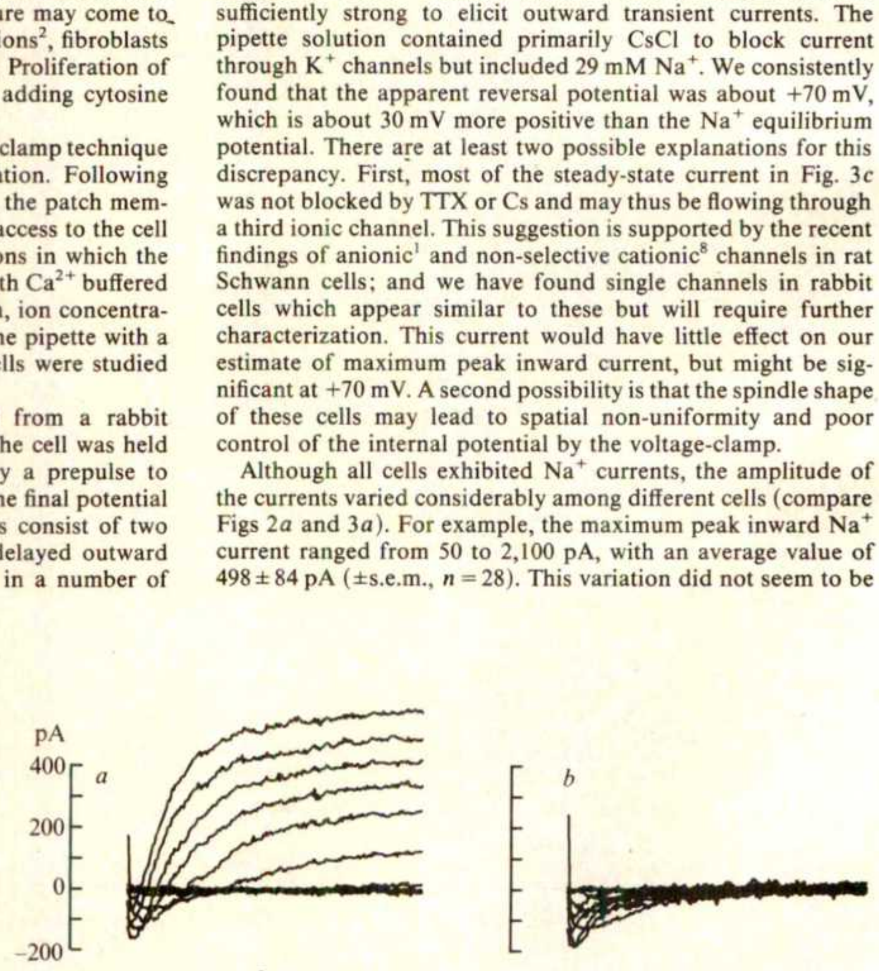

Fig. 2 Ionic currents in 8-day-old cultured rabbit Schwann cells in normal Locke's solution. Records were made using the whole cell configuration of the patch-clamp technique before (*a*) and after (*b*) adding 6 mM 4-aminopyridine externally. The patch pipette was filled with (mM): KCl, 140; CaCl$_2$, 1; MgCl$_2$, 2; EGTA, 11; HEPES, 10; NaOH, 29 to *p*H 7.2. The Locke's solution contained (mM): NaCl, 154; KCl, 5.6; CaCl$_2$, 2.4; MOPS, 10; *p*H 7.4. Test depolarizations were applied in 10-mV steps from −75 mV to +25 mV. The cell was held at −75 mV and 300-ms prepulses to −115 mV preceded each test step. Linear contributions to leak and capacitative currents were removed by scaling and adding the average of several traces elicited by a hyperpolarization to −120 mV. Currents were sampled and digitized at 50-μs intervals. Temperature, 23 °C.

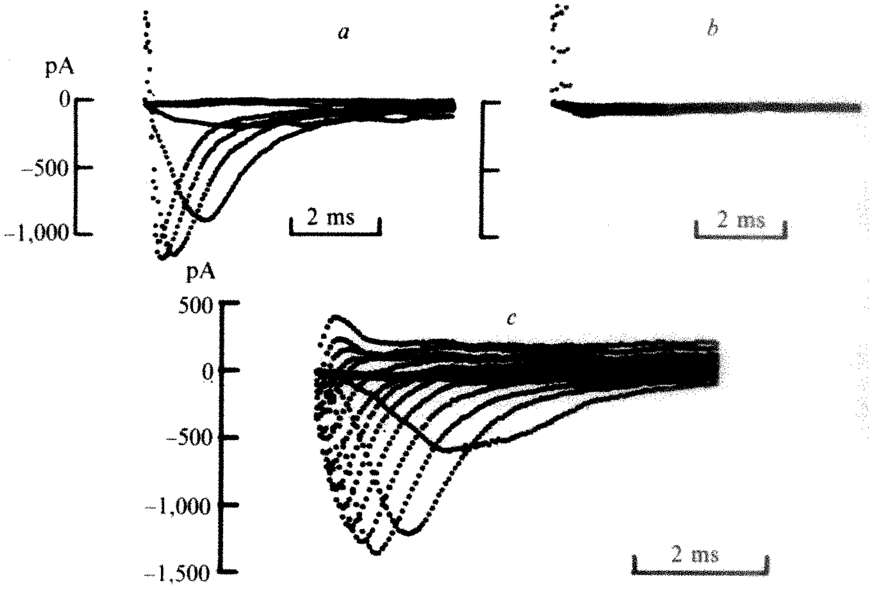

Fig. 3 Ionic currents in 7-day-old cultured rabbit Schwann cells in normal Locke's solution obtained before (*a*) and after (*b*) addition of 60 nM TTX externally. The patch pipette was filled with (mM): CsF, 140; $CaCl_2$, 1; $MgCl_2$, 2; EGTA, 11; HEPES, 10; NaOH, 29 to *p*H 7.2. Holding potential, −74 mV. Prepulses to −114 mV were applied for 300 ms. Test depolarizations were made in 10-mV steps to final potentials ranging from −64 mV to −4 mV. *c*, A family of ionic currents recorded from another (3-day-old) Schwann cell. The feedback resistor in the patch-clamp headstage was reduced to 1 GΩ to allow strong test pulse depolarizations. The pipette solution was identical to that of *a*, *b* except that CsCl was used in place of CsF. The cell was held at −75 mV. Test pulses were applied in 10-mV steps from −55 to +105 mV and were preceded by 300-ms hyperpolarizations to −115 mV. The external medium was normal rabbit Locke's solution.

correlated with the age of the culture. Other factors, such as cell shape or phase of the mitotic cycle, were not examined. The cell capacitance was measured in several experiments by integrating the change in the capacity transient on rupture of the patch membrane. The average value was 20 ± 2 pF ($n = 14$) and the corresponding peak current 30 ± 9 pA pF^{-1} ($n = 14$). Examination of a typical Schwann cell under light microscopy showed the cell to be spindle shaped, about 50 μm from pole to pole, and about 10 μm in diameter in the middle. If any contribution from the small processes at either end are ignored, an upper limit of about 3 μF cm^{-2} is obtained for the membrane capacity of the Schwann cell.

Ritchie and Rang[9] have recently measured the uptake of tritiated saxitoxin (STX) by rat and rabbit sciatic nerves that had undergone axonal degeneration resulting from excision of a small segment of the trunk. In peripheral nerves of rabbit, but not rat, the saturable binding of STX (which blocks Na^+ channels in a manner similar to that of TTX) increases dramatically from about 5 days after sectioning, a time coincident with the known proliferation of Schwann cells in regions distal to the excision. The results presented here thus provide strong support for the idea that these STX binding sites are indeed voltage-sensitive Na^+ channels of the kind generally believed to be restricted to excitable tissue. Glial cells (and fibroblasts) are already known to possess channels that are opened by veratridine and blocked by TTX[10,11]. However, in such experiments there is no evidence of voltage sensitivity; and, in fact, glial cells in particular have long been thought to be inexcitable. Intracellular recording from satellite cells in the leech central nervous system[12] and the squid giant axon[13] has failed to detect any regenerative response. Furthermore, *Necturus* central glia lack a specific, saturable component of binding of STX[14]. By contrast, rabbit Schwann cells do seem to possess the machinery necessary for action potential generation. However, their resting potential, which we have measured to be about −30 to −40 mV, probably inactivates most Na^+ channels, rendering these cells effectively inexcitable. Whether these Na^+ and K^+ channels are included in the myelin lamellae generated by Schwann cells, whether they have any role in remyelination or axonal regeneration, or whether they are conceivably a source of axolemmal Na^+ (and K^+) channels, pose interesting questions for future investigation.

We thank Drs Richard Aldrich and David Corey for invaluable help with patch-clamp techniques, and Ms Bhagya Subramanian for technical assistance in cell culturing. This work has been supported by USPHS grants NS08304, NS12327 and NS17965 and by grant RG 1162 from the US National Multiple Sclerosis Society.

Received 10 April; accepted 26 June 1984.

1. Gray, P. T. A., Bevan, S. & Ritchie, J. M. *Proc. R. Soc.* (in the press).
2. Brockes, J. P., Fryxell, K. J. & Lemke, G. E. *J. exp. Biol.* **95**, 215–230 (1981).
3. Hamill, O. P., Marty, A., Neher, E., Sakmann, B. & Sigworth, F. J. *Eur. J. Physiol.* **391**, 85–100 (1981).
4. Fenwick, E. M., Marty, A. & Neher, E. *J. Physiol., Lond.* **331**, 577–597 (1982).
5. Yeh, J. Z., Oxford, G. S., Wu, C. H. & Narahashi, T. *Biophys. J.* **16**, 77–81 (1976).
6. Meves, H. & Pichon, Y. *J. Physiol., Lond.* **251**, 60P–62P (1975).
7. Narahashi, T., Moore, J. W. & Scott, W. R. *J. gen. Physiol.* **47**, 965–974 (1964).
8. Bevan, S., Gray, P. T. A., Rang, H. P. & Ritchie, J. M. *J. Physiol., Lond.* **348**, 17P (1984).
9. Ritchie, J. M. & Rang, H. P. *Proc. natn. Acad. Sci. U.S.A.* **80**, 2803–2807 (1983).
10. Munson, R., Westermark, B. & Glaser, L. *Proc. natn. Acad. Sci. U.S.A.* **76**, 6425–6429 (1979).
11. Pouyssegur, J., Jacques, Y. & Lazdunski, M. *Nature* **286**, 162–164 (1980).
12. Kuffler, S. W., Nicholls, J. G. & Orkand, R. K. *J. Neurophysiol.* **29**, 768–787 (1966).
13. Villegas, J., Sevcik, C., Barnola, F. V. & Villegas, R. *J. gen. Physiol.* **67**, 369–380 (1976).
14. Tang, C. M., Strichartz, G. R. & Orkand, R. K. *J. gen. Physiol.* **74**, 629–542 (1979).

Photoreceptor excitation and adaptation by inositol 1,4,5-trisphosphate

Alan Fein*†, Richard Payne*, D. Wesley Corson*†, Michael J. Berridge‡ & Robin F. Irvine§

* Laboratory of Sensory Physiology, Marine Biological Laboratory, Woods Hole, Massachusetts 02543, USA
† Department of Physiology, Boston University School of Medicine, Boston, Massachusetts 02118, USA
‡ ARC Unit of Invertebrate Chemistry and Physiology, Department of Zoology, University of Cambridge, Downing Street, Cambridge CB2 3EJ, UK
§ Department of Biochemistry, ARC Institute of Animal Physiology, Babraham, Cambridge CB2 4AT, UK

A central question concerning vision is the identity of the biochemical pathway that underlies phototransduction. The large size of the ventral photoreceptors of *Limulus polyphemus* renders them a favourite preparation for investigating this problem[1]. The fact that a single photon opens approximately 1,000 ionic channels in these photoreceptors[2,3] suggests the need for an internal transmitter. We have investigated whether inositol 1,4,5-trisphosphate ($InsP_3$) functions as such an internal transmitter, given that $InsP_3$ may act as an intracellular messenger in other cellular processes[4,5]. Here we report that in *Limulus*, intracellular pressure injection of $InsP_3$ both excites and adapts ventral photoreceptors in a manner similar to light.

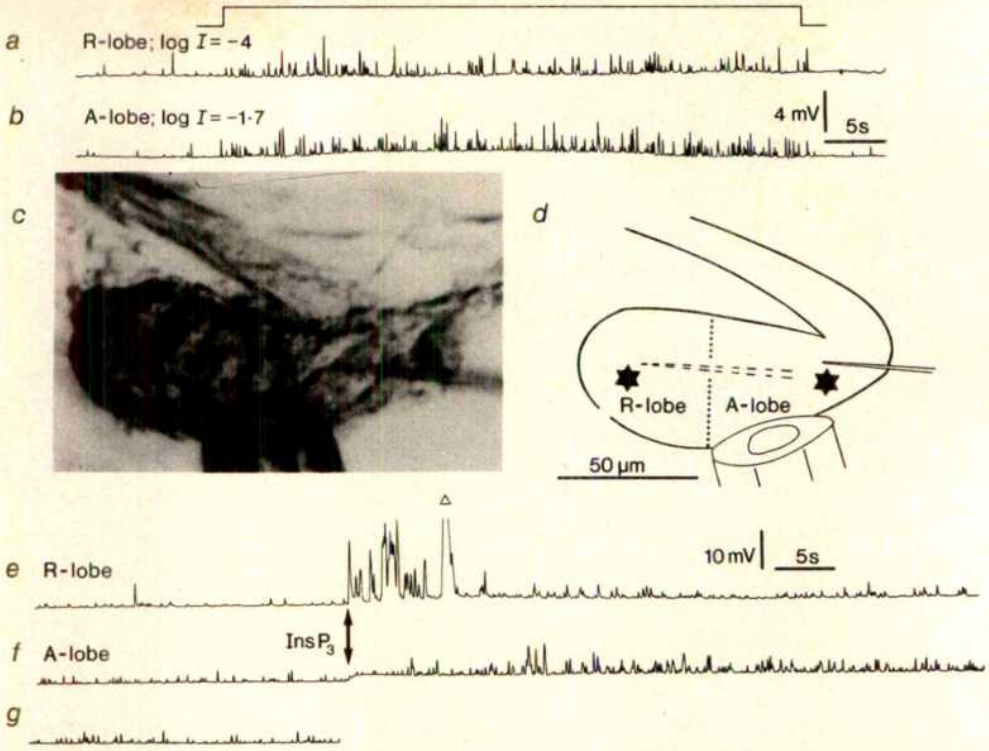

Fig. 1 $InsP_3$-induced excitation of *Limulus* ventral photoreceptor. The photomicrograph (*c*) shows the receptor after the connective tissue had been stripped away[11]. The tip of the suction pipette, which was used for stripping and holding the cell, can be seen in the micrograph. Recordings and injections were made through a pipette, filled with a stock solution containing (in mM): 100 K aspartate, 10 HEPES, *p*H 7.0 in which 20 μM $InsP_3$ was dissolved. Injections of stock solution alone were found to have no effect (30 cells). The cell was first impaled in the A-lobe and the extent of the A-lobe and R-lobe determined by scanning the cell with a 10-μm spot of light[9]. Records *a* and *b* show the response of the R-lobe and A-lobe respectively to steady illumination (square pulse at the top of the traces) with a spot of the indicated $\log_{10}$ attenuation from the maximum available intensity. The R-lobe was found to be approximately 200 times more sensitive to light than the A-lobe[11]. Record *f* shows the response to an $InsP_3$ injection (15 p.s.i., 200-ms pulse at the arrow) into the A-lobe and record *g* shows the recovery 150 s after the injection. Following this injection, the same electrode was inserted into the R-lobe. Sensitivity in the R-lobe was then checked and found to be unchanged relative to *a*. Record *e* shows the response to an $InsP_3$ injection (15 p.s.i., 200-ms pulse at the arrow) into the R-lobe. (The open triangles in the records of this figure and the solid ones in subsequent figures indicate when the recordings went off the scale of the chart recorder.) The sketch of the cell in *d* shows the location of the pipette during injections into the R-lobe and A-lobe. ★ Indicates the location of the spot of light, when centred on the A- and R-lobes. The dotted line indicates the probable demarcation of the R-lobe and A-lobe, as determined by a large change in sensitivity to a spot of light. After record *e* was obtained, the electrode was withdrawn and the A-lobe re-impaled. Results similar to *f* were again obtained (not shown). Similar results were obtained in nine other cells. $InsP_3$, $Ins(1,4)P_2$ and $Ins(4,5)P_2$ were prepared essentially by the method of Grado and Ballou[21] as adapted by R.F.I., M.J.B. and K. D. Brown (in preparation). Briefly, a crude inositide fraction from ox brain was hydrolysed by 1M NaOH and, after neutralization with formic acid, the hydrolysate was fractionated into crude $InsP_1$, $InsP_2$ and $InsP_3$ on Dowex–formate columns[22]. $InsP_3$, $Ins(1,4)P_2$ and $Ins(4,5)P_2$ were further purified by paper chromotography[21] and their identities and purities checked by ionophoresis. A blank region from a paper chromatograph was also eluted and, like the inositol phosphates, de-cationized, followed by neutralization with KOH.

We have previously described the methods for intracellular recording, stimulating and reliably pressure-injecting aliquots of solution of the order of 10 pl (refs 6–9). Injected solutions are specified by the concentration in the pipette. $InsP_3$, inositol 1,4-bisphosphate ($Ins(1,4)P_2$) and inositol 4,5-bisphosphate ($Ins(4,5)P_2$) were prepared as described in Fig. 1 legend; *myo*-inositol, potassium phosphate, *myo*-inositol 2-monophosphate and phytic acid (inositol hexaphosphoric acid) were from Sigma.

The ventral photoreceptors of *Limulus* are segmented into two lobes, a rhabdomeral lobe (R-lobe), specialized for phototransduction, and an arhabdomeral lobe (A-lobe)[10,11], the R-lobe being approximately 100 times more sensitive to light than the A-lobe (Fig. 1*a*, *b*)[11]. When injected into the R-lobe, 20 μM $InsP_3$ reversibly induced, with no detectable latency, the production of discrete waves of depolarization and bursts of waves (Fig. 1*e*). The individual $InsP_3$-induced waves have a similar waveform to the 'quantum bumps' that are evoked by single photons (Fig. 1*a*). Injection of $InsP_3$ into the A-lobe resulted in a response that was both greatly delayed and much smaller (Fig. 1*f*, *g*), as would be expected if the injected $InsP_3$ had to diffuse into the R-lobe in order to produce an effect. The greater sensitivity to $InsP_3$ of the R-lobe, coupled with a similar effect to that of light, suggests that $InsP_3$ acts on the structures of the R-lobe that are specialized for phototransduction.

When measured under voltage clamp, the response to $InsP_3$ (Fig. 2*a*, *c*) is an inward current, as is the light response (Fig. 2*b*). When cells were stimulated with a dim flash (Fig. 2*d*, arrow) followed by an injection of $InsP_3$ (Fig. 2*d*, solid bar), the currents due to light and $InsP_3$ both reversed at approximately +18 mV; this result would be expected if light and $InsP_3$ opened the same ionic channels. Light-adaptation by a bright flash desensitizes the photoreceptor and decreases the $InsP_3$-induced current (Fig. 2*a*–*c*); thus, the response to $InsP_3$ can be light-adapted.

The specificity of the excitatory effect of $InsP_3$ was checked by injecting related compounds. The following had no effect: *myo*-inositol (1 mM, 11 cells), phosphate (1 mM, 10 cells), *myo*-inositol-2-monophosphate (1 mM, 9 cells), phytic acid (1 mM, 6 cells) and a blank from the paper chromatograph (10 cells) (see Fig. 1 legend). $Ins(1,4)P_2$, the degradation product of $InsP_3$, had no effect at concentrations of 20 μM (14 cells) and 100 μM (12 cells); however, two out of three cells exhibited an excitatory effect when 500 μM $Ins(1,4)P_2$ was injected. $Ins(4,5)P_2$ had an excitatory effect at 20 μM (9 cells), indicating that the site of $InsP_3$ action is not selective for $InsP_3$ over $Ins(4,5)P_2$.

As $InsP_3$ excites the receptor, it might initiate other processes that follow excitation, such as adaptation. Figure 3*a* shows localized adaptation by light, in which a prolonged stimulus at position 1 reduced subsequent responses at this position more than at position 2. Similarly, injecting $InsP_3$ at position 1 reduced subsequent responses to light flashes at this position more than at position 2 (Fig. 3*c*, *d*). Desensitization following $InsP_3$ injection under voltage clamp is shown in Fig. 3*e*. We have also observed desensitization of responses to $InsP_3$ following injection of $InsP_3$ (not shown). We have not seen in any cell an $InsP_3$-induced desensitization that was not preceeded by excitation resulting from $InsP_3$ injections. The similarity of the desensitizing effect of $InsP_3$ to that of light suggests that $InsP_3$, or a related compound, initiates processes leading to adaptation as well as to excitation.

A rise in intracellular calcium has been implicated in the adaptation of ventral photoreceptors[12]. The desensitizing effect of $InsP_3$ injection shown in Fig. 3*c*–*e* might be caused by calcium

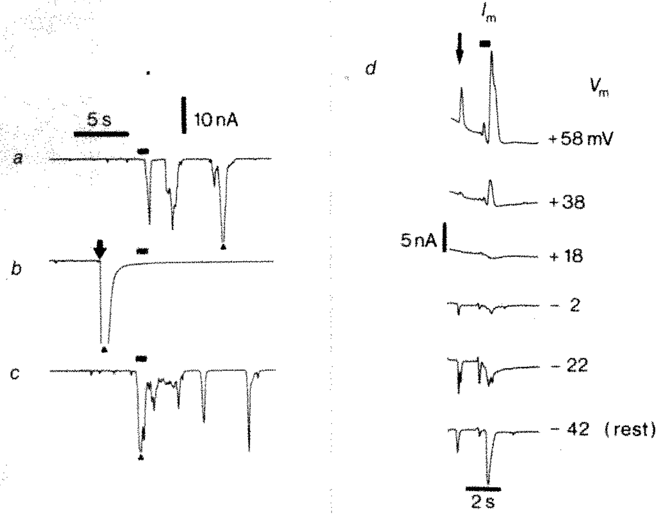

Fig. 2 Light adaptation and reversal potential of $InsP_3$-induced currents. The currents in *a*, *b*, and *c* were obtained from a cell voltage-clamped to its membrane potential (−50 mV) in the dark. The bar above the records indicates the duration of injection with 20 μM $InsP_3$. The arrow above the records indicates a 20-ms flash of uniform white light attenuated by 1.5 log units in *b* and by 5.0 log units in *d*. In *b*, light adaptation blocks the $InsP_3$ response. Spontaneous quantum bumps are present in record *b* before the flash, but not after, indicating that the cell was adapted by the flash. The record in *c* was obtained after the cell recovered sensitivity, following the adapting flash in *b*. A video recording of the injection made under IR illumination[8] allows us to determine that a successful injection occurred in *b* even though there was no effect of the injection. Record *d*, taken from a different cell, shows that the reversal potential of the $InsP_3$-induced current coincides with that of the light-induced current. These voltage-clamp recordings were made in artificial seawater in which the Ca^{2+} was reduced from 10 mM to 1 mM to avoid desensitization produced by voltage-dependent Ca^{2+} entry[23]. The membrane potential (V_m) was moved in 20-mV steps through the reversal potential by a series of 15 s-long command pulses, each beginning 10 s before the test flash. The large steady-state component of the transmembrane current resulting from the voltage step was subtracted from the current records.

contamination of the injection solution; de-cationization of the $InsP_3$ preparation (see Fig. 1 legend) minimized such contamination. Also, six cells were injected with 100 μM $InsP_3$ to which 500 μM EGTA had been added to reduce the free Ca^{2+} to $<10^{-7}$ M; this solution produced the same effects as in Fig. 3 *c–e*. Therefore, it is unlikely that the observed desensitization is due to calcium contamination of the injection solution.

Illumination can facilitate or enhance a photoreceptor's response to a flash of light[7,13–15]. Figure 3*d* shows that the light response at spot 2 was transiently facilitated immediately after $InsP_3$ injection. At a site (spot 1) closer to the injection, this facilitation may be masked by adaptation (Fig. 3*c*). The voltage-clamp recording in Fig. 3*f* was obtained from another cell to demonstrate that the $InsP_3$-induced facilitation could be experimentally separated from $InsP_3$-induced desensitization. Multiple injections of $InsP_3$ produced an approximately threefold facilitation of the light response. Comparison of Fig. 3*e* and *f* illustrates our notion that a sustained facilitation of the light response is associated with a weaker excitation than accompanies desensitization. $InsP_3$ or a related compound may, therefore, initiate facilitation as well as excitation and adaptation.

It is unlikely that $InsP_3$ is the sole messenger in the pathway of adaptation and excitation. Light is thought to release calcium from internal stores so as to adapt the light response in ventral photoreceptors[12,16]. It has been suggested that $InsP_3$ causes the release of calcium from an intracellular compartment in pancreatic acinar cells[5] and in hepatocytes[17,18]. $InsP_3$ might, therefore, release calcium from intracellular stores in ventral photoreceptors to induce adaptation. The inability of 500 μM EGTA, injected with 100 μM $InsP_3$, to block desensitization may be due to the inability of this amount of EGTA to significantly increase the existing calcium buffering capacity of the cell. Further investigation is needed to determine whether $InsP_3$ directly releases calcium from within the cell.

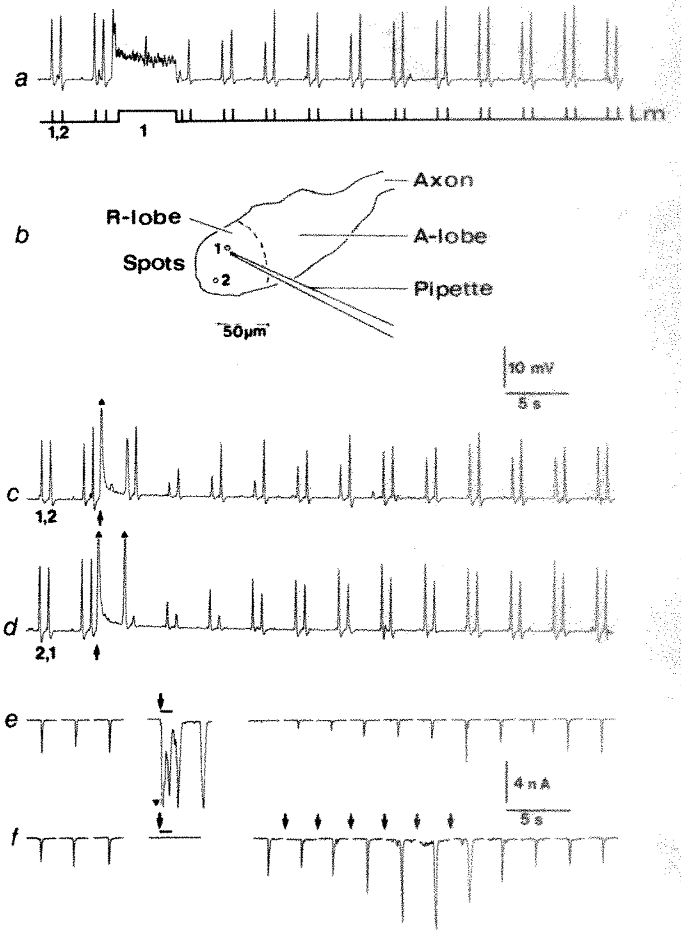

Fig. 3 $InsP_3$-induced desensitization. Localized desensitization was produced both by light (***a***) and by injection of 100 μM $InsP_3$ (***c*** and ***d***) in a cell whose outline is shown in ***b***. In record *a*, the light monitor (Lm) denotes the time of occurrence of the light stimuli at spots 1 and 2. Record *a* demonstrates that light adaptation at spot 1 produces a stronger desensitization of subsequent responses at spot 1 than at spot 2 (ref. 9). Similarly, injection of 100 μM $InsP_3$ at spot 1 produces a greater desensitization of subsequent responses at spot 1 compared with spot 2 (records *c* and *d*). The sequence of light flashes in *c* and *d* was reversed to exclude the possibility that the localized desensitization was in any way related to the sequence in which the two regions of the cell were illuminated. Similar findings were obtained in two other cells with injections of 100 μM $InsP_3$ and in three further cells with 100 μM $InsP_3$ and 500 μM EGTA (see text). The same experiment was performed with 20 μM $InsP_3$; three out of four cells showed a localized desensitization. As controls, four cells were injected with 20 μM $Ins(1,4)P_2$; none showed a localized desensitization. Of six cells injected with 100 μM $Ins(1,4)P_2$, none showed localized desensitization for single injections. Multiple injections, however, did induce a localized desensitization in two of these cells. The voltage-clamp recording in ***e***, from another cell, demonstrates $InsP_3$-induced desensitization of the light response following the excitatory effect of $InsP_3$ injection (arrow). Record *f* demonstrates facilitation of the light response following multiple injections (arrow) of $InsP_3$ into another voltage-clamped cell; in this cell, the electrode was probably in the A-lobe as there was only a slowly developing excitatory effect with each $InsP_3$ injection (not shown). In *e* and *f*, the bars indicate the injection duration; the test flash was 20 ms, the intensity was attenuated by 5.0 log units and the illumination was uniform. A portion of the record between each light response was deleted in *e* and *f* for ease of presentation.

Although $InsP_3$ may adapt the receptor by means of stimulating the release of calcium, it is unlikely that the excitatory effect of $InsP_3$ is mediated solely by a rise in calcium. Ionophoretic injection of calcium does not excite ventral photoreceptors[12]. In addition, we must also explain the correlated opening of the thousands of channels that underlie the $InsP_3$-induced discrete waves and bursts. If these channels open independently of each other then $InsP_3$ must initiate the correlated release of many molecules of another transmitter which opens the individual channels.

If visual excitation and adaptation involve $InsP_3$, one might reasonably expect that the level of $InsP_3$, and of its precursor, phosphatidylinositol-4,5-bisphosphate [$PtdIns(4,5)P_2$], would change during illumination. Light causes a drop in the incorporation of ^{32}P into $PtdIns(4,5)P_2$ of the octopus eye[19] and the 'no receptor potential' (norp A) mutant of *Drosophila* exhibits increased incorporation of ^{32}P into $PtdIns(4,5)P_2$ (ref. 20). Our physiological findings taken together with these biochemical data, suggest an important role for $InsP_3$ in phototransduction.

This research was supported by NIH grants EY01362 and EY03793. We thank Dr Simon Levy for help with the calcium measurements.

Received 18 April; accepted 21 June 1984.

1. Clark, A. W., Millecchia, R. & Mauro, A. *J. gen. Physiol.* **54**, 289–309 (1969).
2. Wong, F. *Nature* **276**, 76–79 (1978).
3. Bacigalupo, J. & Lisman, J. *Nature* **304**, 268–270 (1983).
4. Berridge, M. J. *Biochem. J.* **212**, 849–858 (1983).
5. Streb, H., Irvine, R. F., Berridge, M. J. & Schulz, I. *Nature* **306**, 67–69 (1983).
6. Fein, A. & Charlton, J. S. *J. gen. Physiol.* **66**, 823–836 (1975).
7. Fein, A. & Charlton, J. S. *J. gen. Physiol.* **69**, 553–569 (1977).
8. Corson, D. W. & Fein, A. *Biophys. J.* **44**, 299–304 (1983).
9. Payne, R. & Fein, A. *J. gen. Physiol.* **81**, 767–769 (1983).
10. Calman, B. G. & Chamberlain, S. C. *J. gen. Physiol.* **80**, 839–862 (1982).
11. Stern, J., Chinn, K., Bacigalupo, J. & Lisman, J. *J. gen. Physiol.* **80**, 825–837 (1982).
12. Brown, J. E. & Lisman, J. E. *Nature* **258**, 252–254 (1975).
13. Hagins, W. A., Robinson, W. E. & Yoshikami, S. *Ciba Fdn Symp.* **31**, 169–189 (1975).
14. Hanani, M. & Hillman, P. J. *J. gen. Physiol.* **67**, 235–249 (1976).
15. Ventura, D. F. & Puglia, N. M. *J. comp. Physiol.* **114**, 35–49 (1977).
16. Brown, J. E. & Blinks, J. R. *J. gen. Physiol.* **64**, 643–665 (1974).
17. Burgess, G. M. *et al. Nature* **309**, 63–66 (1984).
18. Joseph, S. K., Thomas, A. P., Williams, R. J., Irvine, R. F. & Williams, J. R. *J. biol. Chem.* **259**, 3077–3081 (1984).
19. Yoshioka, T., Inoue, H., Takagi, M., Hayashi, F. & Amakawa, T. *Biochim. biophys. Acta* **755**, 50–55 (1983).
20. Yoshioka, T., Inoue, H. & Hotta, Y. *Biochem. biophys. Res. Commun.* **111**, 567–573 (1983).
21. Grado, C. & Ballou, C. E. *J. biol. Chem.* **236**, 54–60 (1961).
22. Ellis, R. B., Galliard, T. & Hawthorne, J. N. *Biochem. J.* **88**, 125–131 (1963).
23. O'Day, P. M., Lisman, J. E. & Goldring, M. *J. gen. Physiol.* **79**, 211–232 (1982).

---

myo-inositol polyphosphate may be a messenger for visual excitation in *Limulus* photoreceptors

J. E. Brown*, L. J. Rubin*, A. J. Ghalayini†, A. P. Tarver†, R. F. Irvine‡, M. J. Berridge§ & R. E. Anderson†

* Department of Ophthalmology, Washington University, St Louis, Missouri 63110, USA
† The Cullen Eye Institute, Baylor College of Medicine, Houston, Texas 77030, USA
‡ Department of Biochemistry, ARC Institute of Animal Physiology, Babraham, Cambridge CB2 4AT, UK
§ AFRC Unit of Insect Neurophysiology and Pharmacology, Department of Zoology, University of Cambridge, Downing Street, Cambridge CB2 3EJ, UK

Photoreceptor excitation begins with the absorption of a photon by rhodopsin and proceeds through an unknown sequence of steps that leads to changes in specific ionic conductances. These conductance changes produce the receptor potential. It has been proposed[1–3] that hydrolysis of phosphoinositides is involved in the control of a variety of physiological processes. Recent studies have implicated inositol 1,4,5-trisphosphate as an intracellular messenger in the cascade mediating hormone-stimulated secretion[4–7]. We propose that one of the steps in the excitatory cascade[8,9] in *Limulus* ventral photoreceptors may be an increase in intracellular concentration of *myo*-inositol polyphosphates, derived from hydrolysis of the membrane component phosphatidylinositol bisphosphate by a phospholipase. Here we present biochemical and electrophysiological evidence that an inositol polyphosphate may be an intracellular messenger in the cascade mediating excitation, based on the following criteria: (1) the cells possess the synthetic and degradative metabolism for the messenger; (2) the natural stimulus leads to a change in the concentration of the messenger within the cells; and (3) intracellular injection of exogenous messenger mimics naturally occurring electrophysiological events.

Limulus ventral rudimentary eyes[10,11] were dissected out of the blood vessels that ensheath them. The cluster of photoreceptor cell bodies at the distal end of the nerve was assayed for the effects of illumination on phosphoinositide metabolism. Steady illumination increased the incorporation of $^{32}PO_4$ and ^3H-inositol into phosphatidylinositol (compare the light/dark ratio for paired ventral eyes, Table 1). However, the amount of ^3H-inositol incorporated into phosphatidyl inositol bisphosphate ($PtdInsP_2$) decreased with steady illumination while there was no effect on $^{32}PO_4$ incorporation (Table 1). Fisher and Agranoff[12] reported a similar finding from synaptosomes in

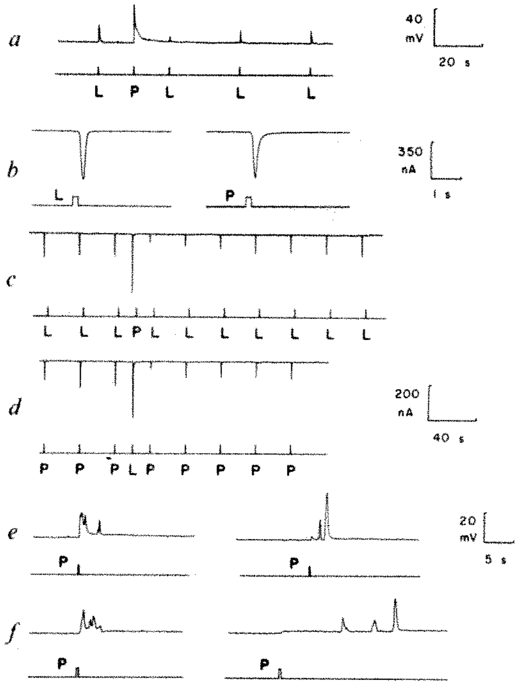

Fig. 1 Electrophysiological effects of intracellular injections of inositol polyphosphates. *Limulus* ventral photoreceptors were impaled with either one micropipette to measure membrane voltage[35] or two micropipettes to measure voltage-clamp currents[36,37]. The electrodes were inserted into the rhabdomeric lobe except where noted. The lower of each pair of traces is a monitor for stimuli: L denotes illumination. Injections (denoted P) were made by applying pressure to the back of the micropipette. *a*, Membrane voltage recorded from an electrode filled with 400 μM $Ins(1,4,5)P_3$ plus 200 mM KCl. Light intensity 3×10^{-7} W cm^{-2}. Pressure injections of $Ins(1,4,5)P_3$ induced large depolarizations and attenuated the subsequent responses to illumination. *b–d*, Currents recorded by a voltage clamp. *b*, Light stimulus 2.1×10^{-5} W cm^{-2}, duration 200 ms. *c*, Note that pressure injection of $Ins(1,4,5)P_3$ induced an inward current and desensitized the light response (light intensity 1.3×10^{-6} W cm^{-2}). *d*, Conversely, light (1.3×10^{-3} W cm^{-2}) desensitized the response of the photoreceptor to the injection of $Ins(1,4,5)P_3$ (same scales for *c* and *d*). Records *a–d* were from the same cell. *e, f*, Membrane voltage recorded by micropipettes filled with 400 μM $Ins(1,4)P_2$ in each of two cells. The left-hand records were obtained with the micropipettes placed in the rhabdomeric lobe; the right-hand records were obtained with the micropipette placed near the rhabdomeric lobe (in *e*) and far from the rhabdomeric lobe (in *f*). Note that the $Ins(1,4)P_2$-induced depolarizations appear to be summated 'discrete events'[21,22] and are more delayed when the injection pipette is impaled farther from the rhabdomeric lobe (same scales for *e* and *f*).

Table 1 Effect of light on the incorporation of labelled precursors into phosphoinositides

	Precursor	Product	Total d.p.m. radioactivity (mean ± s.e.m.) Light	Dark	Ratio light/dark per animal (mean ± s.e.m.)	*P* value for ratio
a	^{3}H-inositol	InsP$_3$	930 ± 157	563 ± 122	1.76 ± 0.22	0.005 (25)
b	^{3}H-inositol	PtdIns	3,660 ± 388	3,232 ± 345	1.20 ± 0.09	0.05 (10)
	^{3}H-inositol	PtdInsP	344 ± 56	456 ± 50	0.84 ± 0.16	>0.1 (10)
	^{3}H-inositol	PtdInsP$_2$	1,928 ± 262*	3,001 ± 289*	0.66 ± 0.09	0.01 (10)
	^{32}PO$_4$	PtdIns	4,558 ± 583*	2,008 ± 277*	2.37 ± 0.23	0.01 (10)
	^{32}PO$_4$	PtdInsP	710 ± 183	546 ± 57	1.46 ± 0.45	>0.4 (10)
	^{32}PO$_4$	PtdInsP$_2$	3,466 ± 545	3,425 ± 411	1.01 ± 0.17	>0.5 (10)

a, Isolated ventral eyes were incubated on three separate occasions in the dark at 21 °C for 6–8 h in *Limulus* serum containing [2-^{3}H]-inositol (300–500 μCi ml^{-1}). Each ventral eye was washed twice with artificial seawater[23]. One ventral eye of each pair was exposed to light (1–3×10^{-3} W cm^{-2}) for 30 s, followed immediately by the addition of chloroform/methanol (1:2, v/v). The dark-maintained ventral eye from the same animal was extracted in the same way. Water-soluble inositol phosphates were separated by either ion-exchange chromatography[28] or TLC on PEI cellulose[29] and counted for radioactivity. Statistical comparisons were made between the ventral eyes from the same animal using a paired Student's *t*-test. *b*, Each isolated ventral eye was incubated in 0.1 ml *Limulus* serum containing [2-^{3}H]-inositol (500 μCi ml^{-1}) and ^{32}PO$_4$ (250 μCi ml^{-1}) in light or dark at 21 °C for 3 h. The incubation was stopped by adding 2 ml of chloroform/methanol/HCl (100:100:6, by vol.), followed by 0.3 ml of 0.2 M HCl. The lower phase was evaporated to near dryness. Phospholipids were separated by TLC using silica gel HR plates in a solvent system of chloroform/methanol/methylamine (40%)/water (60:36:5:5, by vol.). Areas that contained ^{32}P were identified by autoradiography on X-ray film, scraped off and counted. When the total radioactivities from each group were averaged, only those dark/light values marked by an asterisk were significantly different (at the 0.02 confidence level, two-tailed *t*-test). These data are confounded by large between-animal variations. To minimize the effects of these variations, comparisons of light–dark differences in the incorporation of label were made between the ventral eyes isolated from the same animal, using a paired Student's *t*-test (the number of pairs is given in parentheses).

which acetylcholine stimulated ^{32}PO$_4$ incorporation into phosphatidylinositol but reduced the incorporation into polyphosphoinositides. In addition, Yoshioka *et al.* (in *Octopus*)[13] and Vandenberg and Montal (in squid)[14] have shown that light causes a reduction of ^{32}PO$_4$ incorporation into polyphosphoinositides in preparations of broken photoreceptor cells. We interpret our findings as evidence that phosphoinositides are synthesized in the photoreceptor cells and that the turnover of phosphatidylinositol is increased by illumination, but that the pool of PtdInsP$_2$ is reduced due to enzymatic release of inositol trisphosphate (InSP$_3$) into the cytosol. We found that dark-adapted *Limulus* ventral eyes contained InsP$_3$ and that the content of InsP$_3$ was increased by illumination (Table 1). Taken together, these data show that *Limulus* ventral eyes contain metabolic mechanisms for the synthesis of polyphosphoinositides and for the light-induced increase in the concentration of InsP$_3$. Therefore, *Limulus* photoreceptors contain the metabolic mechanisms necessary for the synthesis of the putative excitatory messenger, InsP$_3$.

We examined the electrophysiological effects of intracellular injection of inositol phosphates into single *Limulus* ventral photoreceptors. Photoreceptors whose cell bodies are isolated from neighbouring photoreceptor cell bodies are found scattered along the ventral eye nerve[15,16]. The adhering glia and axons were peeled away from these cells by the procedure of Stern *et al.*[17]. The location of the rhabdomeric lobe of a peeled cell can usually be identified visually; the rhabdomeric lobe is the region of the cell that contains most of the rhodopsin[18] (G. Murray, personal communication) and which shows the maximum sensitivity to light[17]. It is the region of the cell in which both excitation and adaptation occur[17,19].

The rhabdomeric lobe was impaled with a micropipette containing InsP$_3$ (0.004–0.4 mM). The location of the micropipette was viewed using an IR television camera. Successful intracellular injection of a solution caused a local disturbance in optical transmission through the cell, which could be observed on a television monitor[20]. Brief pressure injections of the InsP$_3$ solution elicited a depolarization (in 48 cells) that resembled the response of the cell to a flash of light (Fig. 1*a* and Table 2). Moreover, brief injections of InsP$_3$ elicited an inward positive membrane current measured by a voltage-clamp technique (19 cells) (Fig. 1*b*). Injections of some samples of InsP$_3$ elicited responses that appeared to be the summation of discrete events[21,22] (28 cells) (Table 2); injections of other samples most often elicited smooth responses. The causes of these differences between samples of InsP$_3$ are unknown. Injection of InsP$_3$ was found to cause a subsequent decrease in the sensitivity of the photoreceptor to light (Fig. 1*a*, *c*). Furthermore, light caused a subsequent attenuation in the responses elicited by repetitive injections of InsP$_3$ (22 cells) (Fig. 1*d*), that is, light caused an apparent adaptation of the responses elicited by InsP$_3$ (and vice versa). Injection of InsP$_3$ into the cell at some distance from the rhabdomeric lobe sometimes elicited little or no smooth depolarization (or smooth inward positive membrane current), sometimes elicited delayed, summated discrete events such as those evoked by the absorption of a small number of photons[21,22], but often led to a profound desensitization of the cell.

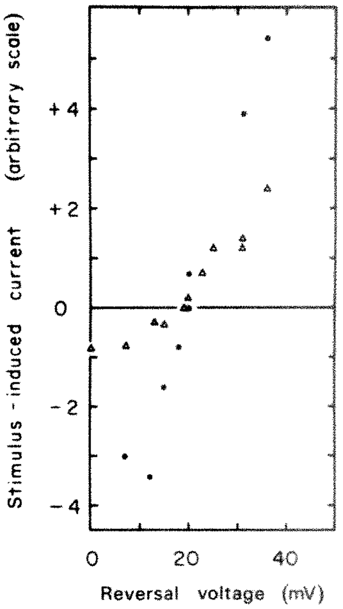

Fig. 2 Reversal voltages of light-induced and Ins(1,4,5)P$_3$-induced currents. The amplitude of currents recorded by a voltage clamp are plotted against membrane voltage. Note that the two nonlinear curves cross the zero-current axis at approximately the same voltage; that is, the reversal voltage for light-induced currents (●) is approximately the same as that for Ins(1,4,5)P$_3$-induced currents (△).

Injection of inositol 1,4–bisphosphate [Ins(1,4)P$_2$] or inositol 4,5-bisphosphate [Ins(4,5)P$_2$] (Table 2) into the rhabdomeric lobe of *Limulus* photoreceptors also induced transient depolarizations. These responses sometimes appeared to be identical to

Table 2 Effects of intracellular injections of *myo*-inositol phosphates

Substance injected	Effect Smooth depolarization or inward current	Discrete events	Total number of cells
400 µM Ins(1,4,5)P_3* (Irvine; human red cell ghosts)	+++ (19)	+ (1)	20
40–400 µM Ins(1,4,5)P_3† (Irvine; bovine brain)	+++ (11)	–	11
4 µM Ins(1,4,5)P_3† (Irvine; bovine brain)	–	–	5
2 mM InsP_3‡ (Tarver; bovine brain)	+++ (25)	+++ (27)	27
400 µM Ins(1,4,5)$P_3{}^+$Ins(2,4,5)P_3†§ (Irvine; bovine brain)	+++ (2)	–	2
0.4–4.0 mM Ins(1,4)P_2† (Irvine; bovine brain)	++ (3)	++ (6)	8
0.4–4.0 mM Ins(4,5)P_2† (Irvine; bovine brain)	++ (9)	++++ (14)	15
Chromatography blank‖¶ (Irvine; elution from paper)	–	–	5
1.6 mM glycerol-P-Ins(4,5)P_2# (Ballou; bovine brain, deacylation)	+++ (9)	+++ (10)	12
400 µM DL-InsP_1**¶ (Sherman; synthetic)	–	–	4
4 mM InsP_6†† (Sigma; corn)	–	–	6

The concentrations of compounds shown were those contained in the injection pipettes. The volumes of injections were estimated to be always less than 1% of the cell volume. For each compound, the person who prepared the substance and the source used are given. The numbers in parentheses are the number of cells from which each type of event was observed; some cells showed both types of events. The number of 'plus' signs indicates the relative efficacy of the injections; – indicates no effect.

* Potassium salt prepared as described by Streb *et al.*[5].

† Potassium salt prepared by the method of Grado and Ballou[30] as modified by Irvine *et al.*[31]. All three inositol polyphosphates were checked for purity (>99%) and identified by iontophoresis[32].

‡ Potassium salt prepared by mild alkaline hydrolysis[33] of phosphatidylinositol-4,5-bisphosphate, followed by oxidation with periodate and treatment with 1,1-dimethylhydrazine[34].

§ Ratio of Ins(1,4,5)P_3 to Ins(2,4,5)P_3 was 3:1.

‖ Material that had been eluted from the same paper chromatogram on which InsP_3, Ins(1,4)P_2 and Ins(4,5)P_2 were separated but which did not contain inositol polyphosphates.

¶ These injections did not induce responses such as those shown in Fig. 1, but did produce small, often irreversible depolarizations that we attribute to either artefacts of the injection procedure or cell damage.

# Potassium salt; ** cyclohexylammonium salt; †† sodium salt.

those induced by InsP_3 injections but more often appeared to be the summation of discrete events (Fig. 1*e*, *f*). The responses induced by injections of inositol bisphosphate into a region of the cell not containing rhabdomere were more delayed (Fig. 1*e*, *f*); the delay qualitatively depended on the apparent distance between the injection micropipette and the rhabdomeric lobe of the cell. Responses induced by injections of inositol bisphosphate also apparently could be adapted by light, and vice versa.

It is difficult to estimate the intracellular concentration of inositol polyphosphates that is necessary to induce the physiological events that we describe, for two reasons. First, the amplitude of the injection-induced responses depends strongly on the location of the pipette within the cell, for both InsP_3 and InsP_2 compounds. Second, the details of diffusion from the tip of the injection pipette to the site or sites of action are unknown. For the same reasons, it is difficult to compare quantitatively the efficacy of different compounds or solutions of the same compounds at different concentrations.

The injection of DL-inositol 1-phosphate into the rhabdomeric lobe had no noticeable effect on the cell (Table 2). For each of these cells, InsP_3 was injected from a second pipette placed close to the pipette containing inositol-1-phosphate, to verify that the cell responded. Also, the injection of inositol hexaphosphate (phytic acid, InsP_6) had no noticeable effect on the cells (Table 2).

A stringent criterion for a putative messenger for excitation is that it must change the same specific ionic conductances as light. We tested InsP_3 according to this criterion by measuring the reversal voltages for both light-induced currents and InsP_3-induced currents; Fig. 2 shows that the reversal voltages were very similar. In five cells, the reversal voltages did not differ by more than 5 mV. Moreover, in one cell the reversal voltages for both light-induced currents and InsP_3-induced currents were measured at each of two concentrations of extracellular Na^+ (425 mM and 106 mM, sucrose replacing NaCl)[23]; in each solution, the reversal voltages differed by 4 mV. Thus, injection of InsP_3 into the rhabdomeric lobe mimics several of the electrophysiological effects of a flash of light. We note that responses with the properties shown in Figs 1 and 2 are not induced by intracellular iontophoretic injections of calcium ions[24], or pressure injections of EGTA[25], ATP, cyclic AMP, GTP, cyclic GMP[26], or *p*H buffers[27].

Our biochemical and electrophysiological findings, reported here, are consistent with some criteria for the identification of InsP_3 as an authentic messenger for excitation in *Limulus* ventral photoreceptor cells. Our electrophysiological evidence also is consistent with an inositol bisphosphate or glycerol-1-phosphoinositol-4,5-bisphosphate being an excitatory messenger; the biochemistry necessary to test these compounds is incomplete at present. We do not yet know whether the magnitude or the kinetics of the light-induced changes in either the concentrations or the turnover rates of the intracellular inositol polyphosphates is consistent with the hypothesis; nor do we know whether the inositol bisphosphates have direct actions in the excitation process or cause a change in InsP_3 concentration, or have some other action on the cell's metabolism. Therefore, we tentatively suggest that light leads to the release of an inositol polyphosphate by the hydrolysis of PtdInsP_2 in the membranes of the photoreceptors; the inositol polyphosphate is diffusible within the cytosol and is one messenger in the cascade of excitation.

We thank Drs S. R. Bolsover, G. D. Fischbach, J. Korenbrot, P. W. Majerus, B. M. Salzberg and W. R. Sherman for helpful discussions; Dr W. R. Sherman for a gift of DL-inositol-1-phosphate and Dr C. E. Ballou for gifts of glycerol-P-Ins(4,5)P_2 and authentic inositol phosphates; and Dr R. Sundler for a preprint of his description of the PEI chromatographic system. The work was supported by NIH grants EY-01914 and EY-05166 to J.E.B., and EY-00871 and EY-04149 to R.E.A.

Received 18 April; accepted 11 July 1984.

1. Michell, R. H. *Biochim. biophys. Acta* **415,** 81–147 (1975).
2. Berridge, M. J. *Biochem. J.* **220,** 345–360 (1984).
3. Hokin, M. R. & Hokin, L. E. *J. biol. Chem.* **203,** 967–977 (1953).
4. Berridge, M. J. *Biochem. J.* **212,** 849–858 (1983).
5. Streb, H., Irvine, R. F., Berridge, M. J. & Schulz, I. *Nature* **306,** 67–69 (1983).
6. Burgess, G. M. *et al. Nature* **309,** 63–66 (1984).
7. Joseph, S. K., Thomas, A. P., Williams, R. J., Irvine, R. F. & Williamson, J. R. *J. biol. Chem.* **259,** 3077–3081 (1984).
8. Fuortes, M. G. F. *Proc. Symp. Inf. Processing in Sight Sensory Systems*, Calif. Inst. Technol., Pasadena, 37–47 (1965).
9. Wong, F., Knight, B. W. & Dodge, F. A. *J. gen. Physiol.* **76,** 517–537 (1980).
10. Demoll, R. *Zool. Jb.* **38,** 443–464 (1914).
11. Clark, A. W., Millecchia, R. & Mauro, A. *J. gen. Physiol.* **54,** 289–309 (1969).
12. Fisher, S. K. & Agranoff, B. J. *J. Neurochem.* **37,** 968–977 (1981).
13. Yoshioka, T., Inoue, H., Takagi, M., Hayashi, F. & Amakawa, T. *Biochim. biophys. Acta* **755,** 50–55 (1983).
14. Vandenberg, C. A. & Montal, M. *Biochemistry* **23,** 2347–2353 (1984).
15. Holt, C. E. & Brown, J. E. *Biochim. biophys. Acta* **274,** 140–157 (1972).
16. Calman, B. & Chamberlain, S. *J. gen. Physiol.* **80,** 839–862 (1982).
17. Stern, J., Chinn, K., Bacigalupo, J. & Lisman, J. *J. gen. Physiol.* **80,** 825–837 (1982).
18. Murray, G. *Science* **154,** 1182–1183 (1966).
19. Harary, H. H. & Brown, J. E. *Science* **224,** 292–294 (1984).
20. Corson, D. W. & Fein, A. *Biophys. J.* **44,** 299–304 (1983).
21. Yeandle, S. S. thesis, The Johns Hopkins, University (1957).
22. Borsellino, A. & Fuortes, M. G. F. *J. Physiol., Lond.* **196,** 507–539 (1968).
23. Brown, J. E. & Mote, M. I. *J. gen. Physiol.* **63,** 337–350 (1974).
24. Brown, J. E. & Lisman, J. E. *Nature* **258,** 252–254 (1975).
25. Lisman, J. E. & Brown, J. E. *J. gen. Physiol.* **66,** 489–506 (1975).
26. Bolsover, S. R. & Brown, J. E. *J. Physiol., Lond.* **332,** 325–342 (1982).
27. Coles, J. A. & Brown, J. E. *Biochim. biophys. Acta* **436,** 140–153 (1976).
28. Downes, C. P. & Michell, R. H. *Biochem. J.* **198,** 133–140 (1981).
29. Emilsson, A. & Sundler, R. *J. biol. Chem.* **259,** 3111–3116 (1984).

30. Grado, C. & Ballou, C. E. *J. biol. Chem.* **236**, 54–60 (1961).
31. Irvine, R. F., Brown, K. D. & Berridge, M. J. *Biochem. J.* (in the press).
32. Irvine, R. F., Hemington, N. & Dawson, R. M. C. *Biochem. J.* **176**, 475–484 (1978).
33. Creba, J. A. *et al. Biochem. J.* **212**, 733–747 (1983).
34. Brown, D. M. & Stewart, J. C. *Biochim. biophys. Acta* **125**, 413–421 (1966).
35. Millecchia, R. & Mauro, A. *J. gen. Physiol.* **54**, 310–330 (1969).
36. Millecchia, R. & Mauro, A. *J. gen. Physiol.* **54**, 331–351 (1969).
37. Brown, J. E., Harary, H. H. & Waggoner, A. *J. Physiol., Lond.* **296**, 357–372 (1979).

Alternative sets of DNase I-hypersensitive sites characterize the various functional states of the chicken lysozyme gene

Hans P. Fritton*, Tibor Igo-Kemenes*, Joachim Nowock†, Ute Strech-Jurk†, Manfred Theisen† & Albrecht E. Sippel†‡

* Institut für Physiologische Chemie, Physikalische Biochemie
und Zellbiologie der Universität, Goethestrasse 33,
D-8000 München 2, FRG
† ZMBH, Im Neuenheimer Feld 364, D-6900 Heidelberg 1, FRG

The structural organization of chromatin is thought to determine the state of differentiation and activity of eukaryotic genes. Local interruptions of the regular nucleosomal array, the so-called DNase-hypersensitive sites, may indicate regions of the genome which play a critical part in regulation of differential gene activity[1–4]. We present here two new observations on the chromatin structure of the chicken lysozyme gene, which strongly support a regulatory function for these sites. First, different sets of DNase I-hypersensitive sites have been found upstream from the promoter, depending on whether the gene is constitutively expressed (cultured macrophages) or in the steroid hormone-controlled state (oviduct). It seems, therefore, that diverse modes of regulation of the same gene are associated with discrete patterns of DNase I hypersensitivity. Second, one of the DNase I-hypersensitive sites in the oviduct chromatin disappears and reappears on steroid hormone withdrawal and secondary induction. These reversible changes in a narrow chromatin region reflect the transition from the potentially active to the active state of the lysozyme gene.

Nuclease hypersensitivity in chromatin involves short regions of approximately 50–400 base pairs that are roughly one order of magnitude more susceptible to nuclease cutting than is active chromatin as a whole[1–5]. These regions are generally referred to as DNase-hypersensitive sites[4] and have mostly been localized to the region near the 5′ end of actively transcribed genes. Genes which are subject to complex regulatory mechanisms, such as developmentally controlled genes[5–7] or genes under hormonal control[7–9], often display a more complex pattern of DNase hypersensitivity with multiple sites upstream and downstream from the gene.

The chicken lysozyme gene offers attractive features for studying the role of chromatin structure in activation and inactivation of a eukaryotic gene. In the chicken oviduct, synthesis of lysozyme mRNA is under the control of steroid hormones[10] and can be reversibly induced in immature chickens by oestrogen administration or withdrawal[11]. Expression of the same lysozyme gene in mature chicken macrophages is constitutive and transcription proceeds from the same promoter at a relatively low rate (ref. 12 and our unpublished S_1-mapping experiments). Liver cells, like most other cell types in the organism, do not express lysozyme mRNA (data not shown). It was conceivable that the chromatin might be organized differently depending on whether the cell in question is steroid hormone-responsive, nonresponsive or dormant.

We examined the chromatin structure of a 7.1-kilobase(kb) *Eco*RI fragment containing 4.6 kb of DNA sequences upstream from the promoter of the chicken lysozyme gene, the first two exons and part of the second intron (see scheme in Fig. 3). Previously, we demonstrated that in the mature oviduct of egg-laying hens this region is marked by three hypersensitive sites referred to as HS3, HS4 and HS5 (ref. 8). As subsequent investigations have revealed a more complex pattern, we have re-named them according to their position with respect to the promoter of the gene (in kb) as HS − 2.4, HS − 1.9 and HS − 0.1. Potentially active genes are often found to have hypersensitive sites independent of the transcription process *per se*[3,4,7]. We therefore anticipated that only some of the sites upstream of the lysozyme gene might appear and disappear in correlation with steroid-mediated control of the transcriptional activity of the gene. To investigate this possibility, nuclei were prepared from the oviducts of immature chickens induced for 3 and 12 days with diethylstilboestrol, a synthetic oestrogen (primary induction). The small amount of oviduct cell mass in uninduced chickens precluded an assay for hypersensitive sites in birds with induction periods shorter than 3 days. Nuclei were mildly digested to varying extents by DNase I. DNA was then isolated and digested with *Eco*RI and analysed by the Southern blot technique using an indirect end-labelling procedure[13,14]. After 3 days of exposure to oestrogen, the three sites HS −2.4, HS −1.9 and HS −0.1, characteristic of the mature oviduct of the egg-laying hen, are fully established and do not change during an additional 9-day period of primary induction (Fig. 1). If hormone administration is interrupted after 11 days, one of the hypersensitive sites (HS −1.9) disappears; on secondary induction with the oestrogen analogue it reappears. Thus, a close correlation can be demonstrated between the presence of the steroid hormone and the formation of the DNase I-hypersensitive site about 1.9 kb upstream of the transcriptional start site of the gene[15]. A similar observation was made in the chromatin of the vitellogenin gene[7]. The formation of a particular chromatin structure at a position far upstream appears to be associated with oestrogen activation of transcription. The site at −1.9 kb may be due to binding of the hormone–receptor complex, or to other DNA-binding proteins related to steroid action.

The hypersensitive site at −0.1 kb is only slightly less prominent 6 days after hormone withdrawal, indicating that the promoter region does not show considerable structural changes in response to the varying extents of oestrogenic induction and withdrawal.

To gain more information about functional aspects of the chromatin structure, we performed a second set of experiments in which the chromatin pattern was examined in various tissues of the egg-laying hen which do or do not express lysozyme (Fig. 2). The most striking result is that there are marked differences in the structural organization of chromatin between nuclei from two lysozyme-producing cell types. In mature macrophages, which constitutively express the gene, neither of the oviduct sites HS −1.9 or HS −2.4 is present; instead two new sites, HS −0.7 and HS −2.7, can be seen. This finding shows for the first time that different modes of transcriptional regulation of a eukaryotic gene correlate with different chromatin structures and supports the notion that the chromatin structure itself determines the functional state of a gene. The result further supports our finding that HS −1.9 is involved in steroid-dependent gene expression, as it is obviously not used for constitutive expression of the lysozyme gene. The formation of HS −1.9, however, cannot be the result of the mere presence of a functional oestrogen receptor complex because in liver, an oestrogen target organ[7], this hypersensitive site is not formed (Fig. 2).

The hypersensitive site immediately upstream of the cap site, HS −0.1, is only present in cells which either express or have the potential to express the lysozyme gene (Figs 2 and 3). In tissues which do not express the lysozyme gene, the promoter region is buried within an inaccessible chromatin structure.

The hypersensitive site HS −2.4 is present in oviduct, liver, kidney, brain and in 5-day-old embryos, but is absent in macrophages and erythrocytes. There is no obvious function which correlates with this hypersensitive site. Based on its

---

‡ To whom correspondence should be addressed.

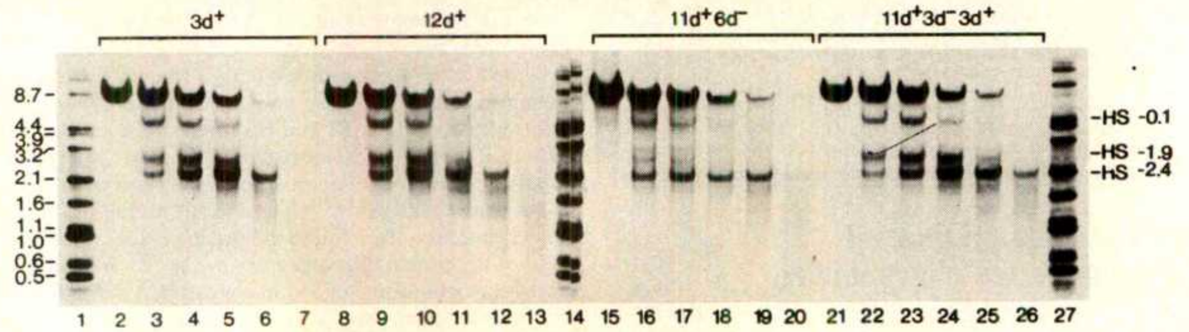

Fig. 1 Mapping of DNase I-hypersensitive sites in the 5′ flanking region of the lysozyme gene in oviducts of diethylstilboestrol-induced, deinduced and reinduced immature chickens. Silicon tubes filled with crystalline diethylstilboestrol (DES) were implanted subcutaneously in 5-week-old female chickens[17]. Groups of chickens were either killed 3 and 12 days after implantation or hormone was withdrawn by removal of the tubes after 11 days. After 3 days of hormone withdrawal, one group of chickens was injected with 2 mg DES in sesame oil (secondary stimulation) while control chickens remained uninduced. Reinduced chickens and those in which hormone was withdrawn were killed 6 days after the start of the withdrawal period. Oviduct nuclei were prepared as described previously[8] except that 2 mM EDTA and 0.5 mM EGTA were present in the isolation buffers. Digestion was with increasing concentrations of DNase I. Nuclear DNA was then isolated and completely digested with *Eco*RI. Southern blots were probed with radioactively labelled nick-translated plasmid DNA containing sequences between *Hin*dIII sites 4 and 5 (ref. 18) essentially as described previously[8]. The autoradiograph shows oviduct hypersensitive sites on the *Eco*RI fragment E4E5 (compare with scheme in Fig. 3) from 3-day-induced (3d$^+$, tracks 2–7), 12-day-induced (12d$^+$, tracks 8–13), 11-day-induced plus 6 days' hormone withdrawal (11d$^+$6d$^-$, tracks 15–20), and 11-day-induced/3 days' hormone withdrawal/3-day-reinduced (11d$^+$3d$^-$3d$^+$, tracks 21–26) chickens. Tracks 1, 14 and 27 show DNA size markers, their length indicated in kb. The same results as seen in tracks 15–26 were obtained when oviduct chromatin was mapped from 12-day-induced followed by 3 or 6 days' hormone withdrawal, chickens (12d$^+$3d$^-$, 12d$^+$6d$^-$) and from 12-day-induced, 6 days' withdrawal, 3-day-reinduced chickens (12d$^+$6d$^-$3d$^+$, data not shown). Hypersensitive sites (HS) were named according to their approximate location upstream of the cap site of the gene (in kb).

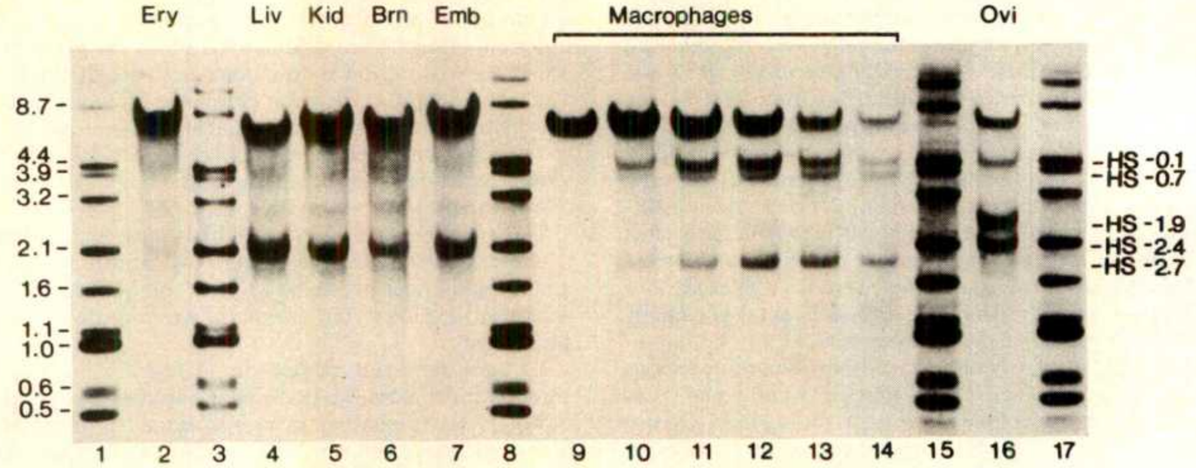

Fig. 2 Mapping of DNase I-hypersensitive sites in the 5′ flanking region of the lysozyme gene in various lysozyme-producing and -nonproducing tissues of egg-laying hens and in tissue of total embryos. The autoradiograph shows hypersensitive sites mapped in nuclear chromatin of erythrocytes (track 2), liver (track 4), kidney (track 5), brain (track 6), mature oviduct (track 16) and whole 5-day-old embryos (track 7). Tracks 9–14 show the pattern obtained when nuclear chromatin of mature macrophages was mapped with increasing concentrations of DNase I. Mapping was done in all cases as described previously[8]. Tracks 1, 3, 8, 15 and 17 show DNA size markers (in kb). Macrophages were obtained from cultured white blood cells. Blood was collected by heart puncture and the buffy coat separated by centrifugation at 800g for 10 min through a Ficoll solution (lymphocyte separation medium, density 1.077; Flow) and seeded at 1×10^8 cells per 150 cm^2 flask in growth medium (MEM-Iscove; 8% fetal calf serum, 2% chicken serum; Boehringer). The adherent cell fraction was scraped off after 5 days and lysed by Dounce homogenization at 2×10^7 cells ml^{-1} in homogenization buffer[8] modified as described in Fig. 1 legend.

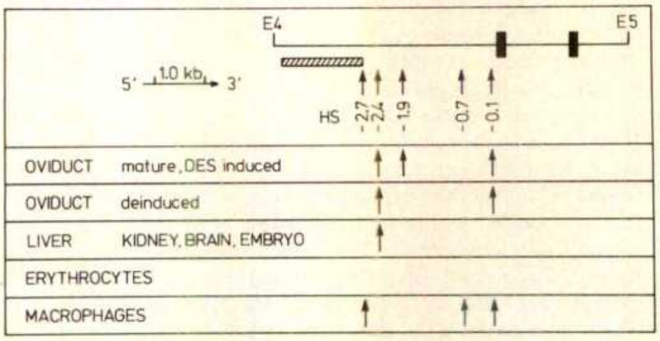

Fig. 3 Scheme showing the positions of DNase I-hypersensitive sites in the 5′ flanking region of the lysozyme gene in various chicken tissues. E4 and E5 denote relevant *Eco*RI sites 4.6 kb upstream and 2.5 kb downstream of the promoter of the gene[18]. Solid boxes represent exon regions and the hatched bar shows the position of the subcloned *Hin*dIII fragment (H4H5 in ref. 18) used as radioactive probe in the procedure for mapping DNase I-hypersensitive sites. Arrows indicate the positions of hypersensitive sites as shown in Figs 1 and 2.

absence or presence in the various tissues, we propose that HS −2.4 has a role in suppressing lysozyme gene activity. Such a function should not be present in macrophages which express the lysozyme gene constitutively, but would be required in the oviduct, in which transcription occurs in a reversible fashion depending on the hormonal state. In the latter case, the steroid-inducible site HS − 1.9 would override the presumed function of HS −2.4.

Implicit in our interpretation is the assumption that the upstream hypersensitive sites are involved in the control of the lysozyme gene itself rather than being indicative of a yet unidentified adjacent transcription unit. As *in vitro* transcription analyses of the respective DNA sequences revealed transcripts starting only at the lysozyme promoter (M. Theisen, unpublished), we feel this bias to be tenable.

DNase I-hypersensitive sites are believed to be short nucleosome-free regions which mark sites where regulatory proteins gain access to specific DNA sequences[16]. Evidence is accumulating that these structures not only signal the actual transcriptional state of a gene but also the state of differentiation. The correct formation of these structures during differentiation seems to be crucial for differential expression. It remains to be shown how chromatin structural changes observed kilobases away from the transcriptional initiation point can determine the state of differentiation and activity of a eukaryotic gene.

This work was supported by the Deutsche Forschungsgemeinschaft (Forschergruppe Genomorganisation und SFB 74) and the Bundesministerium für Forschung und Technologie (BCT 0364/1).

Received 4 June; accepted 6 July 1984.

1. Mathis, D., Oudet, P. & Chambon, P. *Prog. Nucleic Acid Res. Mol. Biol.* **24,** 1–55 (1980).
2. Igo-Kemenes, T., Hörz, W. & Zachau, H. G. *A. Rev. Biochem.* **51,** 89–121 (1982).
3. Cartwright *et al. CRC Crit. Rev. Biochem.* **13,** 1–86 (1982).
4. Elgin, S. C. R. *Cell* **27,** 413–415 (1981).
5. Groudine, M. & Weintraub, H. *Cell* **24,** 393–401 (1981).
6. Bryan, P. N., Olah, J. & Birnstiel, M. L. *Cell* **33,** 843–848 (1983).
7. Burch, J. B. E. & Weintraub, H. *Cell* **33,** 65–76 (1983).
8. Fritton, H. P., Sippel, A. E. & Igo–Kemenes, T. *Nucleic Acids Res.* **11,** 3467–3485 (1983).
9. Kaye, J. S., Bellard, M., Dretzen, G., Bellard, F. & Chambon, P. *EMBO J.* **3,** 1137–1144 (1984).
10. Schütz, G. *et al. Cold Spring Harb. Symp. quant. Biol.* **42,** 617–624 (1978).
11. Sippel, A. E. *et al.* in *Steroid Induced Uterine Proteins* (ed. Beato, M.) 297–314 (Elsevier, Amsterdam, 1980).
12. Hauser, H. *et al.* in *Haematology and Blood Transfusion* Vol. 26 (eds Neth, R., Gallo, R. C., Graf, T., Mannweiler, K. & Winkler, K.) 175–178 (Springer, Berlin, 1981).
13. Wu, C. *Nature* **286,** 854–860 (1980).
14. Nedospasov, S. A. & Georgiev, G. P. *Biochem. biophys. Res. Commun.* **92,** 532–539 (1980).
15. Grez, M. *et al. Cell* **25,** 743–752 (1981).
16. McGhee, J. D., Wood, W. I., Dolan, M., Engel, J. D. & Felsenfeld, G. *Cell* **27,** 45–55 (1981).
17. Hynes, N. *et al. Biochemistry* **18,** 616–624 (1979).
18. Nowock, J. & Sippel, A. E. *Cell* **30,** 607–615 (1982).

High rates of *in vitro* synthesis of 1,4-*β*-D-glucan in cell-free preparations from *Phaseolus aureus*

T. Callaghan & M. Benziman

Department of Biological Chemistry, Institute of Life Sciences,
The Hebrew University of Jerusalem, 91904 Jerusalem, Israel

Progress in the study of biosynthesis of cellulose (1,4-*β*-D-glucan) has been persistently hampered by the low rates of *in vitro* synthesis obtained using cell-free preparations derived from plant or bacterial cells capable of ample cellulose synthesis *in vivo*[1]. We recently reported the achievement of high rates of synthesis of 1,4-*β*-D-glucan from UDP-glucose, using membrane preparations obtained from the bacterium *Acetobacter xylinum*. The key to the success lay in the discovery of a complex GTP-Ca^{2+}-protein factor-mediated regulatory system for the *A. xylinum* UDP-glucose-*β*-D-glucosyltransferase (cellulose synthase)[2,3]. We now describe conditions found for an extremely efficient transfer of glucose from UDP-glucose to a cellulosic 1,4-*β*-D-glucan product using enzyme preparations derived from a higher plant, seedlings of mung beans (*Phaseolus aureus*). The rates of enzyme activity achieved approach those of cellulose synthesis observed *in vivo*.

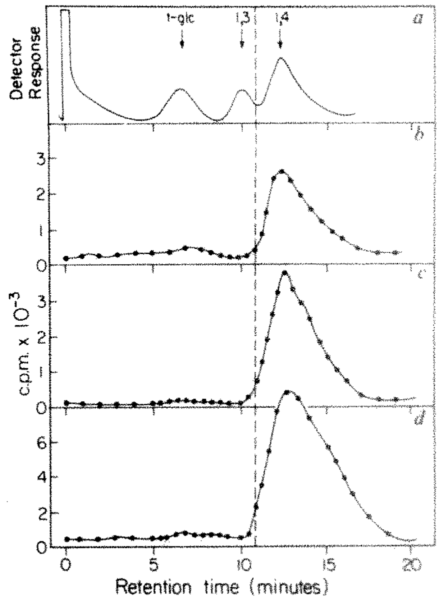

Fig. 1 Gas liquid chromatography of permethylated derivatives of the ^{14}C-labelled-24% KOH-insoluble product formed from UDP-[^{14}C]glucose. *a*, Recorder tracing of derivatives obtained from a mixture of laminarin and cellobiose. Peaks were identified by comparison with derivatives of the individual compounds (1,3 = permethylated derivative of laminarin; 1,4 = permethylated derivative of cellobiose; t-glc = terminal glucose). The lower three curves represent elution profiles of radioactivity of permethylated derivatives from products formed in standard assay mixtures, 5 μM (*b*), 500 μM (*c*) and 1 mM UDP-[^{14}C]glucose (*d*).

In all the studies described here, data are presented only for the radioactive 24% KOH-insoluble glucan product formed from UDP-[^{14}C]glucose, which has been characterized as 1,4-*β*-D-glucan by the following criteria: (1) Total acid hydrolysis converted >90% of the radioactivity to ^{14}C-glucose. (2) The product was more than 95% digested by either highly purified *Trichoderma reesei* exocellobiohydrolase or by highly purified *Trichoderma* endo-1,4-*β*-glucanase (on chromatography of the exocellobiohydrolase digest, on Whatman No. 4 paper in *n*-propanol/ethyl acetate/water, 7:1:2, v/v, >80% of the soluble radioactivity co-chromatographed with a cellobiose standard and the remainder was found at the origin and in glucose). (3) Methylation analysis[2] of the products formed either from 5 μM, 500 μM or 1 mM UDP-glucose, yielded exclusively 1,4,5-trioctyl-2,3,5-tri-*O*-methyl-[^{14}C]glucitol, the derivative expected for 1,4-linked glucosyl moieties (Fig. 1). (4) periodate oxidation[4], followed by borohydride reduction, complete acid hydrolysis and paper chromatography yielded primarily erythritol (indicative of 1,4-linkages), a trace of glycerol and some material which remained at the origin. In no case could a significant peak of glucose (indicative of 1,3-linkages) be detected. The small peak of glycerol detected amounted to 1–3% of the labelling of the major erythritol peak. Assuming that this glycerol arises from terminal glucose residues, it indicates that the enzyme is producing long chains and is not a chain-terminating enzyme adding just single glucose residues to pre-existing polysaccharides.

The procedure for preparing the enzyme is summarized in Fig. 2. If cells were ruptured in an extracting medium containing 20% polyethylene glycol 4000 (PEG), the membranes and all associated glucan synthase activity (when assayed under standard assay condtions, see below) pelleted at relatively low centrifugal forces (12,000*g* for 10 min). In contrast, in the absence of PEG, higher centrifugal forces (150,000*g* for 60 min) were needed to sediment membranes and the enzyme activity. A similar effect of PEG has been observed with other plant glucan synthases[1] and with *A. xylinum* 1,4-*β*-D-glucan synthase[2],

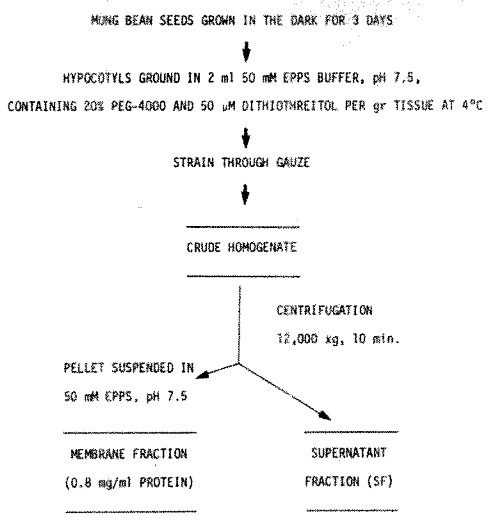
MUNG BEAN SEEDS GROWN IN THE DARK FOR 3 DAYS
HYPOCOTYLS GROUND IN 2 ml 50 mM EPPS BUFFER, pH 7.5,
CONTAINING 20% PEG-4000 AND 50 μM DITHIOTHREITOL PER gr TISSUE AT 4°C
STRAIN THROUGH GAUZE
CRUDE HOMOGENATE
CENTRIFUGATION
12,000 xg, 10 min.
PELLET SUSPENDED IN
50 mM EPPS, pH 7.5
MEMBRANE FRACTION
(0.8 mg/ml PROTEIN)
SUPERNATANT
FRACTION (SF)

Fig. 2 Protocol for preparation of enzyme.

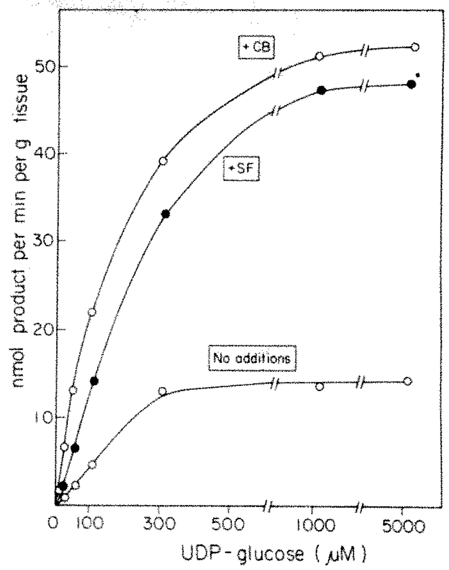

Fig. 3 The effect of varying the concentration of UDP-glucose on enzyme activity. UDP-glucose concentrations were as indicated, and membrane fraction derived from 10 mg fresh weight of tissue (0.04 mg protein) was used per assay. Additions indicated were: 5 mM cellobiose (+CB) and 25 μl of supernatant fraction (+SF).

and may be attributed to the known effect of PEG in promoting membrane fusion and protein coagulation[5]. PEG treatment also enhanced 4–5-fold, the rate of product formation by the membrane preparation. This effect could involve protection of the enzyme during cell breakage and/or promotion of interaction of enzyme subunits. Activity was retained in PEG preparations for two months when these were frozen in liquid nitrogen and kept at −70 °C.

Standard assays performed at 20 °C contained in a final volume of 0.2 ml: 50 mM *N*-(2-hydroxyethyl)-piperazine-*N'*-3-propanesulphonic acid buffer, *p*H 7.5, 5 μM UDP-[^{14}C]glucose (320 c.p.m. pmol^{-1}), 6 mM $MgCl_2$, 4 mM $CaCl_2$, 5 mM cellobiose and enzyme. Reactions were terminated by addition of 2 ml 24% KOH. Aproximately 20 mg of carrier cellulose was added, and the mixture incubated for 12 h at 40 °C (ref. 6). The mixtures were then filtered onto Whatman GF/A glass fibre filters, and washed consecutively with water and methanol. The filters containing alkali-insoluble product were dried and counted. Under these conditions, reactions were linear with time for up to 30 min and proportional to enzyme concentration up to 100 μg protein. At *p*H 8.6, activity was considerably lower and linearity with time ceased after 2–5 min.

Requirements for the reaction are shown in Table 1. The enzyme has an absolute requirement for both Mg^{2+} and Ca^{2+}. Whereas the dependence on Mg^{2+} was demonstrable with regular enzyme preparations, the effect of Ca^{2+} was much more pronounced when EGTA was included in the medium used for extracting the enzyme. The particulate membrane fraction sedimenting from centrifuged crude homogenates exhibits low activity. Activity is restored on re-addition of the supernatant fraction (SF). The supernatant alone was found to contain no synthase activity (data not shown). Product formation is markedly increased by the addition of cellobiose to the incubation mixture. However, the extent of this effect is dependent on the enzyme preparation. Whereas addition of cellobiose to centrifuged fractions results in a tenfold increase in activity, in the presence of the SF only a twofold increase is observed. Activity of the particulate fraction increases with increasing cellobiose concentrations and with varying levels of SF. Half-maximal stimulations are achieved with 0.75 mM cellobiose and 1.5 μl of SF (an amount of supernatant derived from 0.8 mg fresh weight of tissue). The enzyme displays normal Michaelis–Menten kinetics with respect to UDP-glucose (Fig. 3). The presence of saturating amounts of cellobiose or SF does not alter the apparent K_m for the substrate (100 μM) but the V_{max} is enhanced about fivefold (compare refs 7 and 8). Preliminary characterization of the stimulatory factor in SF, based on stability studies, indicate that it is an organic dialysable, alkali-labile compound which is absorbed by charcoal. It is resistant to heat and acid treatment (0.1 M HCl, 10 min at 100 °C) and to digestion by exocellobiohydrose, endo-1,4-*β*-glucanase, *β*-glucosidase, crude cellulase and alkaline and acid phosphatases. Unlike the 1,4-*β*-glucan synthase of *A. xylinum*[2], the plant enzyme has not been found to respond to the addition of GTP. The SF, however, strongly interferes with GTP activation of the bacterial enzyme.

Table 1 Factors affecting UDP-glucose: 1,4-*β*-D-glucan synthase activity

Incubation mixture	Activity (pmol product per min per g tissue)
Complete system	1,700
Minus Mg^{2+}	50
Minus Ca^{2+}	40
Minus SF minus cellobiose	170
Minus cellobiose	850
Minus SF	1,700
Plus DCB (6 μM)	120
Plus coumarin (2 mM)	40

The complete system contains: crude homogenate derived from 10 mg of tissue in the presence of 5 mM EGTA; 6 mM $MgCl_2$; 4 mM $CaCl_2$; 5 mM cellobiose; and 5 μM UDP-[^{14}C]glucose. DCB = 2,6-dichlorobenzonitrile.

Incorporation of labelled glucose from UDP-[^{14}C]glucose into the cellulosic product was neither stimulated nor inhibited by the addition of an up to 100-fold excess of unlabelled UDP-xylose or GDP-glucose (compare refs 6, 9–11). Coumarin and dichlorobenzonitrile, specific inhibitors of plant *in vivo* cellulose synthesis[12] strongly inhibit our enzyme (Table 1). Note that these compounds inhibit GTP activation of the *A. xylinum* 1,4-*β*-glucan synthase (Y. Aloni and M.B., unpublished results).

Because the reaction product is clearly a 1,4-*β*-D-glucan, we presume that we are dealing with a true cellulose synthase; however, lacking information on the crystalline structure and microfibrillar nature of the product, we referred to it at present simply as a 1,4-*β*-D-glucan synthase. The rates of synthesis of 1,4-*β*-glucan *in vitro* reported here far exceed those previously reported[13–17], and approach those of cellulose synthesis observed *in vivo* during primary cell wall formation (12–30 nmol per min per g fresh weight of tissue)[15,17,18]. Thus, the long awaited goal of obtaining from a plant source a highly active system for 1,4-β-D-glucan synthesis *in vitro* has been accomplished. This system with its interesting properties, especially in relation to the bacterial synthase system, should be of great value for exploring further the details of the mechanism and regulation of cellulose synthesis.

Received 15 May; accepted 4 July 1984.

1. Delmer, D. P. *Adv. Carbohydr. Chem. Biochem.* **41**, 105–153 (1983).
2. Aloni, Y., Delmer, D. P. & Benziman, M. *Proc. natn. Acad. Sci. U.S.A.* **79**, 6448–6452 (1982).
3. Aloni, Y., Cohen, R., Benziman, M. & Delmer, D. P. *J. biol. Chem.* **258**, 4419–4423 (1983).
4. Heiniger, U. & Delmar, D. P. *Pl. Physiol.* **59**, 719–723 (1977).
5. Boni, L. T., Stewart, T. P., Alderfer, J. L. & Hui, S. W. *J. Membrane Biol.* **62**, 65–70 (1981).
6. Hayashi, T. & Matsuda, K. *Pl. Cell Physiol.* **22**, 1571–1584 (1981).
7. Delmer, D. P., Heiniger, U. & Kulow, C. *Pl. Physiol.* **59**, 713–718 (1977).
8. Delmer, D. P. *Recent Adv. Phytochem.* **11**, 45–77 (1977).
9. Ray, P. M. *Pl. Physiol.* **56**, Suppl. 84 (1975).
10. Villemez, C. L. & Hinman, M. *Pl. Physiol.* **56**, Suppl. 79 (1975).
11. Ray, P. M. *Biochim. biophys. Acta.* **629**, 431–444 (1980).
12. Montezinos, D. & Delmer, D. P. *Planta* **148**, 305–311 (1980).
13. Barber, G. A., Elbein., A. D. & Hassid, W. Z. *J. biol. Chem.* **239**, 4056–4061 (1964).
14. Villemez, C. L., Franz, G. & Hassid, W. Z. *Pl. Physiol.* **42**, 1219–1223 (1967).
15. Shore, G., Raymond, Y. & Maclachlan, G. *Pl. Physiol.* **56**, 34–38 (1975).
16. Carpita, N. C. & Delmer, D. P. *Pl. Physiol.* **66**, 911–916 (1980).
17. Abdul-Baki, A. A. & Ray, P. M. *Pl. Physiol.* **47**, 537–544 (1971).
18. Meinert, M. C. & Delmer, D. P. *Pl. Physiol.* **59**, 1088–1097 (1977).

6 Å-Resolution X-ray structure of a variable surface glycoprotein from *Trypanosoma brucei*

D. M. Freymann, P. Metcalf, M. Turner* & D. C. Wiley

Department of Biochemistry and Molecular Biology,
Harvard University, Cambridge, Massachusetts 012138, USA
* MRC Biochemical Parasitology Unit, The Molteno Institute,
Downing Street, Cambridge CB2 3EE, UK

The variable surface glycoprotein (VSG) is the predominant component of the surface coat of the African trypanosome[1]. The expression of antigenically distinct VSGs on minor populations during infection allows the parasite to escape the host immune response[2,3]. Purification of the protein is facilitated by the enzymatic release of a soluble form of VSG (sVSG) which occurs on cell lysis[4]. The soluble form is a dimer with an approximate molecular weight of 120,000–130,000[5]. Partial proteolysis of sVSG[6] reveals a protease-sensitive link between an amino-terminal domain which comprises about two-thirds of the molecule, and a C-terminal domain which contains the membrane attachment site[7]. We have obtained crystals suitable for high-resolution structural analysis from preparations of three sVSG: MITat 1.2, ILTat 1.25 and ILTat 1.22. The crystal structure of the dimer of the MITat 1.2 amino-terminal domain has been solved to 6 Å resolution. We report here that the dimer is an unusual 90 Å rod-like molecule composed of a helical bundle of at least four 80 Å-long α-helices.

sVSG was purified from *Trypanosoma brucei* as described previously[1]. MITat 1.2 was crystallized by vapour diffusion of a 40 mg ml^{-1} solution in 50 mM Tris-HCl/0.1% sodium azide, *p*H 7.5 against 9% polyethylene glycol (PEG) 8000/10% ethylene glycol in the same buffer. Tetragonal bipyramidal crystals, which diffract to 2.9 Å, appear within a week and grow to a maximum dimension of 1 mm. The space group is $P4_12_12$, with $a = 96.3$, $c = 111.3$ Å; the asymmetric unit contains one monomer of the amino-terminal domain. Details of the crystallization of ILTat 1.22 and ILTat 1.25 will be published elsewhere.

Protein recovered from MITat 1.2 crystals has an apparent molecular weight (MW) of 43,000 (43 K) on SDS-polyacrylamide gel electrophoresis (PAGE), co-migrating with the amino-terminal domain identified by Johnson and Cross[6] (Fig. 1). The amino-terminal sequence of the recovered protein is Ala-Ala-Glu-Lys, consistent with the previously published N-terminal sequence[6]. By using 'immuno-blots'[8], (data not shown) we have demonstrated that the protein recovered from the crystal does not contain the C-terminal 'cross-reacting determinant'[9] of the intact VSG. Thus, it seems that adventitious proteolysis from a contaminating protease releases an N-terminal crystallizable domain. On gel permeation HPLC (data not shown) protein recovered from MITat 1.2 crystals elutes with an approximate molecular weight of 80,000, clearly distinguishable from the intact native dimer at around 120,000, suggesting that the crystalline protein is a dimer of two 43K domains.

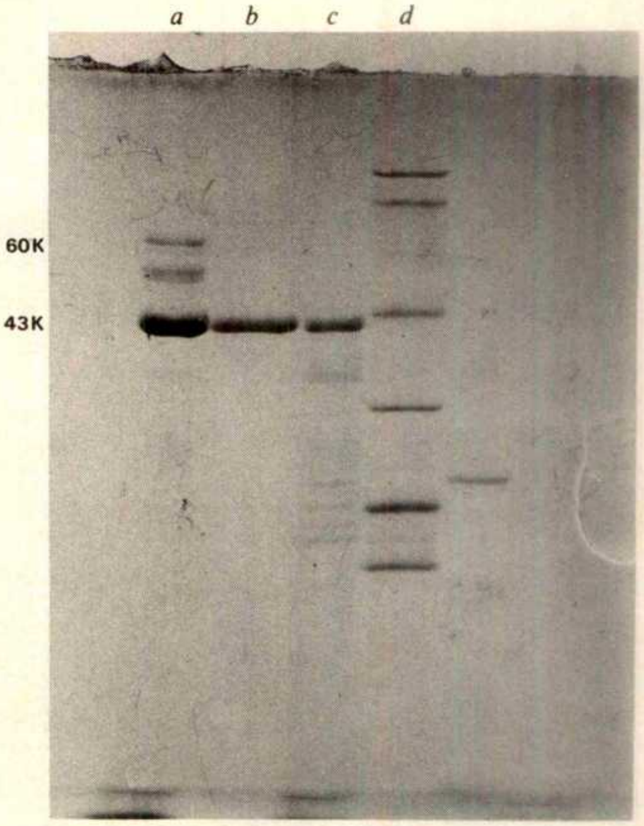

Fig. 1 Protein recovered from MITat 1.2 crystals migrates with an apparent MW of 43,000 (43K) on a 12% SDS polyacrylamide gel. *a*, 5 μg MITat 1.2 from a solution used for crystallization. The intact polypeptide migrates with an apparent MW of 60,000 (60K); the fragment at 43K corresponds to protein recovered from the crystal. *b*, Two large (0.5, 1 mm) crystals were washed in 2 ml 12% PEG, 10 mM TrisHCl, 0.1% azide, *p*H 7.5, and dissolved in a capillary with 30 μl 10 mM TrisHCl *p*H 7.5. The dissolved protein was boiled for 3 min after addition of 90 μl sample buffer; an aliquot of 20 μl was loaded on the gel. *c*, 5 μg MITat 1.2 was digested with trypsin, using the conditions of Johnson and Cross[6]; the digestion was stopped by adding excess phenylmethanesulphony fluoride and boiling after addition of sample buffer. The amino-terminal protease-resistant fragment co-migrates with the crystallized protein. *d*, Bio-Rad molecular weight standards: 92.5K, 66.2K, 45.0K, 31.0K, 21.5K and 14.5K.

A mercury derivative was obtained after a 1-day soak in a 12% PEG solution (otherwise identical to the mother liquor) saturated with K_2HgI_4. Data from one native crystal and one Hg derivative crystal were collected by diffractometer. Data were corrected for Lorentz polarization effects and radiation damage, and an empirical absorption correction was applied[10]. Friedel equivalents were scaled together in blocks of reciprocal space[11]. Data collection statistics are summarized in Table 1.

Harker sections of isomorphous and anomalous difference Pattersons showed identical peaks, and were interpretable in terms of a single Hg site at 0.20, 0.19, 0.50. After 10 cycles of refinement of the heavy-atom parameters, including the anomolous scattering data, 1,211 reflections (89% of the 15–6 Å shell) were phased with a mean figure of merit of 0.72 (Table 1). A difference Fourier showed no additional Hg sites.

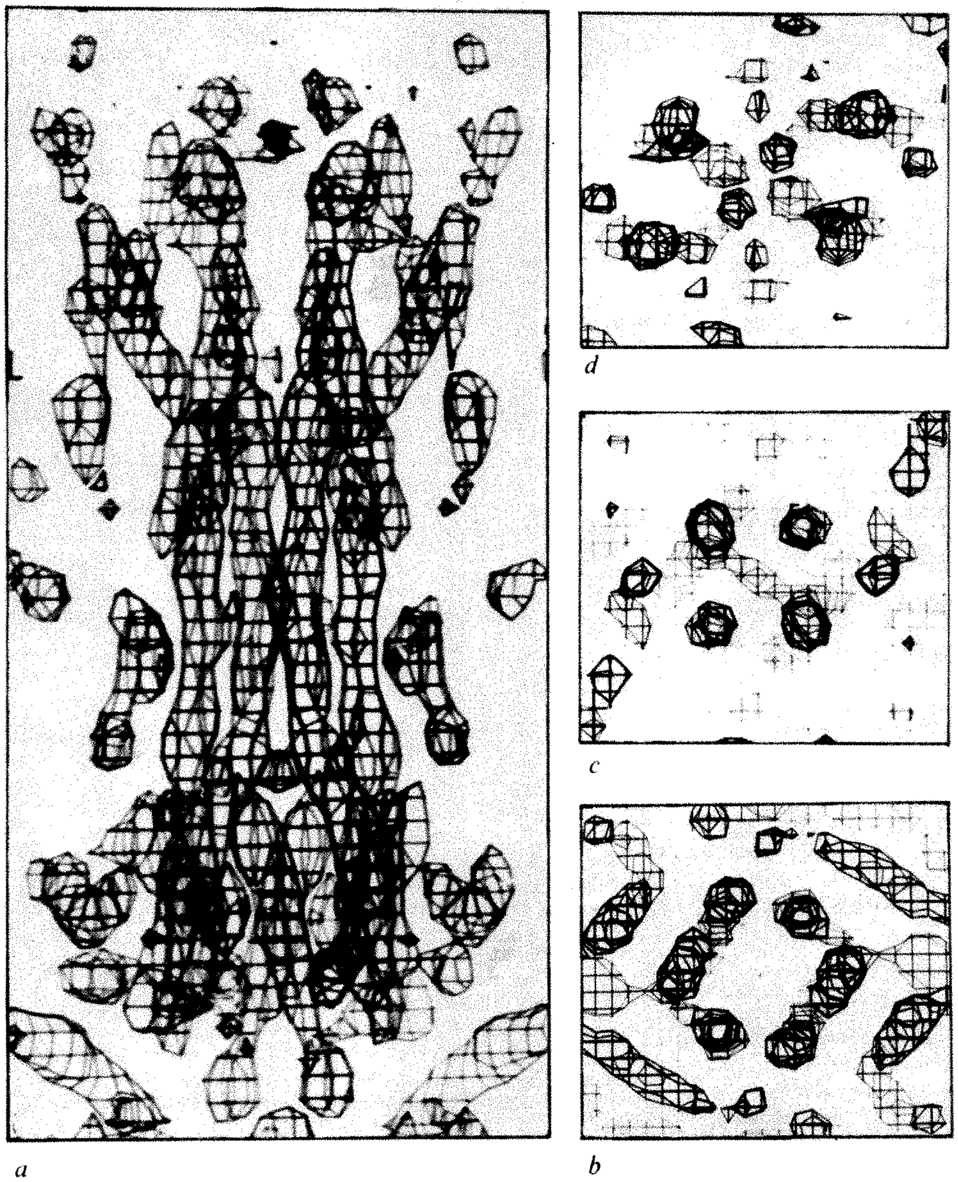

Fig. 2 *a*, View of the electron density map perpendicular to the dimer axis, which is vertical in the figure. The map was contoured two standard deviations above mean density and displayed on an Evans and Sutherland PS300 using the FRODO molecular graphics program by J. W. Pflugrath, M. A. Saper, B. Bush and A. Jones. At the bottom is the 6-fold bundle extending about 25 Å along the dimer axis. At the top, the density diverges, forming a 'two-headed' structure. (Symmetry-related density is seen in the lower corners.) *b–d*, Regions of the map shown in *a*, viewed along the dimer 2-fold axis. *b*, Approximately 20 Å from the 'bottom'. The 6-fold bundle of electron-dense rods is apparent. The distance between rods of density is ~10 Å. Unconnected density occurs adjacent to the bundle. *c*, Approximately 50 Å from the 'bottom'. The 4-fold bundle is the continuation of density which begins in *b*. *d*, Approximately 80 Å from the 'bottom'. Density from each monomer diverges and appears to form two distinct bundles.

The native electron density map calculated using the 'best' phases[12] shows that the unit cell contains four dimers packed along the crystallographic 2-fold axes. At this resolution, rods of high electron density ~10 Å apart are clearly resolved, forming a bundle which extends about 80 Å. We interpret this as an α-helical 'core' of the dimeric molecule.

The dimer is elongated, with approximate dimensions of 40×40×90 Å (Fig. 2*a*). When viewed down the dimer axis, the helical bundle is apparent (Fig. 2b–d). The connectivity of two α-helices in each monomer can be traced for about 80 Å. At one end (bottom of Fig. 2*a*) density connects the two helices, which form a 25 Å-long left-handed 6-fold bundle with another, unconnected, helical segment (Fig. 2*b*). The two helices from each subunit extend past this region to form a fairly straight four-α-helical bundle which extends about 30 Å (Fig. 2*c*). A third rod of high electron density begins adjacent to this structure. The strands then diverge to form two left-twisted structures, about 30 Å long, each of which clearly involves three helices, and possibly other adjacent density , at the 'top' of each subunit (Fig. 2*d*).

We estimate, by crude fitting of polyalanine α-helices, that about 175 residues are accounted for by the well defined helical regions of the low-resolution map. This is about 50% of the expected length of the polypeptide based on its migration on SDS-PAGE, and its consistent with circular dichroism results (M.J.T. and T. Bayley, unpublished data). We have not yet established the connectivity of additional density which occurs at the end of the dimer and around the helical bundle.

The long rod-like α-helical core of the VSG is similar, in principle, to the trimeric α-helical coiled-coil in the stem region of the influenza virus haemagglutinin (HA)[13]. The occurrence of helical motifs in other surface glycoproteins has been discussed[14]. The connectivity observed here between the two long helices in the MITat 1.2 amino-terminal domain implies a helical region extending about 120 residues with only one break. If such a structure were common to VSGs of diverse sequences, it might be revealed by analysis of secondary structure predictions. Alternatively, this feature might readily be recognized in the low-resolution structure of a second VSG. Although interesting sequence homology among VSGs has been observed in the C-terminal region[15–18], the extent of structural homology is unknown[19].

Recent work[20] has shown that the N-terminal domain of another VSG, MITat 1.6, binds most monoclonal antibodies against the intact VSG molecule; that only a subset of the monoclonal antibodies which bind to isolated intact VSG will interact with the VSG when it is in the trypanosome surface coat; and that the subset of monoclonal antibodies which bind to the trypanosome coat also bind to the N-terminal domain. These results suggest that the N-terminal domain contains the regions of the VSG which are responsible for the antigenic variation recognized by antisera against live trypanosomes. Thus

Table 1 6 Å data collection and phase refinement for MITat 1.2 VSG

	Native		Hg	
Cell dimensions (Å)	96.3, 111.2		96.4, 111.6	
No. of reflections collected	2,781		2,812	
Friedel *R* factor		No. of pairs		No. of pairs
Centric	1.7%	381	1.4%	387
Acentric	2.2%	950	3.9%	979
No. of reflections phased	1,211			
Mean figure of merit	0.72			
Kraut *R*	7.39			
$\langle Fh\rangle/\langle E\rangle$	2.97			

Friedel *R* factor: $\mathrm{sum}(|I^{+}-I^{-}|)/\mathrm{sum}(I^{+}+I^{-})$

Kraut *R*: $\dfrac{\mathrm{sum}[|Fph(\mathrm{obs})-Fph(\mathrm{calc})|]}{\mathrm{sum}[Fph(\mathrm{obs})]}\times 100\%$

Fph = derivative structure factor

$\langle Fh\rangle/\langle E\rangle$: $\dfrac{\text{r.m.s. heavy-atom structure factor}}{\text{r.m.s lack of closure error}}$

Before data collection, MITat 1.2 crystals were transferred to a solution containing 12% PEG, 10% ethylene glycol, 0.1% azide, 50 mM Tris HCl *p*H 7.5. Data were collected using a Wyckoff step scan[21] on a Syntex P3/F diffractometer equipped with a 50-cm helium-filled extension tube. About 3,000 reflections, including Friedel pairs, were collected in the 15–6 Å shell. Four reference reflections were collected every hundred reflections; the mean decay was 26% (native) and 21% (Hg) over the 3 days of data collection. The length of the *c* axis was observed to change by 1% during the data collection. Difference Patterson maps were calculated using coefficients $(Fph-Fp)$**2 and (Kemp**2/4)$(Fph^{+}-Fph^{-})$**2, where Kemp[22] was 6.43. The heavy-atom position and occupancy were refined using the program PHARE3, which alternates cycles of parameter refinement and phase calculation[23]. The anomalous scattering information was included in the refinement[24], and was used to distinguish the correct space group, $P4_12_12$, from its enantiomer[25]. B was held at 25 Å**2. The final mercury position, after 10 cycles, was $x/a=0.22$, $y/b=0.19$, $z/c=0.50$ with occupancy 0.58. The iodine atoms were not included in the refinement.

the three-dimensional structure of the N-terminal domain should contribute to establishing which parts of the sequence are implicated in the generation of antigenically distinct trypanosomes and to determining the structure of the variable epitope(s).

We thank Judith Creighton for technical assistance in the preparation of VSGs. Both laboratories have received support from the UNDP/World Bank/WHO Special Program for Research and Training in Tropical Diseases (Project No. 810278 to D.C.W. and Project No. 800328 to M.J.T.). M.J.T. also received support from ILRAD, Nairobi, Kenya).

Received 27 April; accepted 5 July 1984.

1. Cross, G. A. M. *Parasitology* **71,** 393–417 (1975).
2. Vickerman, K. *Nature* **273,** 613–617 (1978).
3. Turner, M. J. *Adv. Parasit.* **21,** 69–153 (1982).
4. Cardoso de Almeida, M. L. & Turner, M. J. *Nature* **302,** 349–352 (1983).
5. Auffret, C. A. & Turner, M. J. *Biochem J.* **193,** 647–650 (1981).
6. Johnson, J. G. & Cross, G. A. M. *Biochem. J.* **178,** 689–697 (1979).
7. Ferguson, M. A. J. & Cross, G. A. M. *J. biol. Chem.* **259,** 3011–3015 (1984).
8. Towbin, H., Staehelin, T. & Gordon, J. *Proc. natn. Acad. Sci. U.S.A.* **76,** 4350–4354 (1979).
9. Barbet, A. F., Musoke, A. J., Shapiro, S. Z., Mpimbaza, G. & McGuire, T. C. *Parasitology* **83,** 623–637 (1981).
10. North, A. C. T., Phillips, D. C. & Mathews, F. S. *Acta crystallogr.* **A24,** 351–359 (1968).
11. Matthews, B. W. & Czerwinski, E. W. *Acta crystallogr.* **A31,** 480–487 (1975).
12. Blow, D. M. & Crick, F. H. C. *Acta crystallogr.* **12,** 794–802 (1959).
13. Wilson, I. A., Skehel, J. J. & Wiley, D. C. *Nature* **289,** 366–373 (1981).
14. Cohen, C. & Phillips, G. N. *Proc. natn. Acad. Sci. U.S.A.* **78,** 5303–5304 (1981).
15. Rice-Ficht, A. C., Chen, K. K. & Donelson, J. E. *Nature* **294,** 53–57 (1981).
16. Bridgen, P. J., Cross, G. A. M. & Bridges, J. *Nature* **263,** 613–614 (1976).
17. Mathyssens, G., Michiels, F., Hamers, R., Pays, E. & Steinert, M. *Nature* **293,** 230–233 (1981).
18. Holder, A. A. & Cross, G. A. M. *Molec. biochem. Parasit.* **2,** 135–150 (1981).
19. Lalor, T. M. *et al. Proc. natn. Acad. Sci. U.S.A.* **81,** 998–1002 (1984).
20. Miller, E. N., Allan, L. M. & Turner, M. J. *Molec. biochem. Parasit.* (in the press).
21. Wyckoff, H. W. *et al. J. molec. Biol.* **27,** 563–578 (1967).
22. Matthews, B. W. *Acta crystallogr.* **20,** 230–239 (1966).
23. Dickerson, R. E., Weinzierl, J. E. & Palmer, R. A. *Acta crystallogr.* **B24,** 997–1003 (1968).
24. Matthews, B. W. *Acta crystallogr.* **20,** 82–86 (1966).
25. Blow, D. M. & Rossmann, M. G. *Acta crystallogr.* **14,** 1195–1202 (1961).

α-Helical coiled-coil structures of *Trypanosoma brucei* variable surface glycoproteins

Carolyn Cohen*, Bruce Reinhardt*, David A. D. Parry†, Georges E. Roelants‡, Wolfgang Hirsch‡ & Babine Kanwé‡

* Rosenstiel Basic Medical Sciences Research Center,
Brandeis University, Waltham, Massachusetts 02254, USA
† Department of Chemistry, Biochemistry and Biophysics,
Massey University, Palmerston North, New Zealand
‡ Centre de Recherches sur les Trypanosomoses Animales,
Bobo-Dioulasso, Haute-Volta

We have used electron microscopy to examine purified intact variable surface glycoproteins (VSGs) from clones derived from two distinct stocks of *Trypanosoma brucei*. The VSG molecule from MITat 1.2 has a large elongated domain consistent with the shape of the dimeric N-terminal domain determined by X-ray analysis (see preceding paper[1]), and a heretofore unseen short, thin fibrous tail presumed to be the C-terminal domain. Electron microscopy on DiTat 1.3, however, indicates a morphology quite distinct from that of MITat 1.2. Analysis of four VSG amino acid sequences reveals 7-fold periodicities (heptad repeats) which indicate that α-helical coiled-coil secondary structure elements occur in all of these VSGs, consistent with the observation of helical bundles in one VSG[1]. These results suggest the possibility that VSG antigenic diversity may be related to a diversity in length and disposition of α-helical bundles and coiled-coil domains.

We have determined the overall morphology of certain VSG molecules in the electron microscope by rotary shadowing with platinum. The first observations were carried out on DiTat 1.3. Although the material obtained from lyophilized preparations shows considerable heterogeneity, many molecules in the field display a distinctive shape; these are ~180 Å long and consist of a globular 'head' region (~60 Å diameter) attached to a narrower 'stem' about 100 Å long and 30 Å thick that can often be seen to terminate in a small globular domain (Fig. 1). A variety of smaller fragments related to this form may also be seen (Fig. 1). SDS gels of this material indicate that most of the sample has an apparent molecular weight of 64,000 (Fig. 2). Shadowing of mixtures of VSG and tropomyosin (MW 66,000) suggests that the molecules we have observed are VSG dimers (MW 130,000). Digestion with trypsin (data not shown) indicates that the large globular head region contains the N-terminus.

We then examined intact MITat 1.2 VSG molecules whose N-terminal dimer structure has recently been solved[1]. This VSG species appears to have a markedly different morphology: particles with a major domain about 100 Å × 70 Å are observed. No clear 'stem' region is apparent, but a short tail can sometimes be seen (Fig. 3). Dissolved crystals of the dimer of the N-terminal domain show similar compact particles that lack tail regions (Fig. 3). These images agree well with the results of the X-ray structure determination, considering that particle flattening often occurs in rotary-shadowed preparations. The presence of the slender tail regions may account for difficulties in crystallizing the intact molecules[1].

Sequence information is not yet available for either of the VSG molecules that we have examined, but we have carried out conformational analyses of the published sequences of four other VSGs from the two C-terminal subsets that have been distinguished[2,3] (including VSG 117 (MITat 1.4) (ref. 4), AnTat 1.1 (ref. 5), ILTat 1.1 (ref. 6), and ILTat 1.4 (ref. 7)). Detailed findings will be reported elsewhere, but the major conclusions are summarized here. Secondary structure analyses were based on modifications of the procedures of Chou and Fasman[8], Robson and Suzuki[9] and Garnier *et al.*[10]. On this basis, some

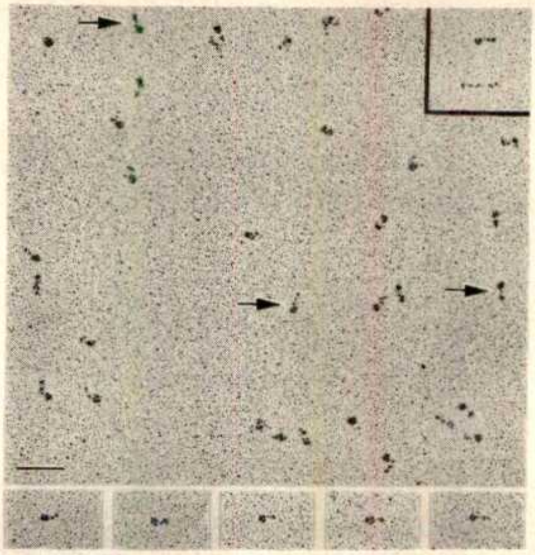

Fig. 1 Electron micrographs of rotary-shadowed VSG (*T. brucei brucei* clone T45R10, antigenic type DiTat 1.3). The molecules are ~180 Å long and show three distinct domains: a large 'globular' head region about 60 Å in diameter; a 'stem' ~100 Å long and 30 Å wide; and a smaller globular region ~40 Å in diameter. Molecules are also observed that lack the small globular region, thus appearing to have a 'tail' about 140 Å long. The field and selected molecules illustrate both types of image. Inset, a cardiac tropomyosin molecule (MW 66,000; dimensions 400 Å × 20 Å) shadowed together with VSG. The VSG molecules probably correspond to dimers. Replicas were prepared by rotary shadowing with platinum[17]. Measured dimensions may vary by ±20 Å depending on the thickness of the platinum deposit. Scale bar, 500 Å.

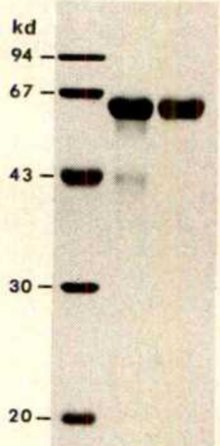

Fig. 2 Intact DiTat 1.3 monomer has an apparent molecular weight of ~64,000 by SDS-polyacrylamide gel electrophoresis. Lanes *b* and *c* show two different VSG samples, both purified from *T. brucei brucei* clone T45R10, antigenic type DiTat 1.3. The material was prepared by the method of Cross[18] and Roelants *et al.*[19] with affinity chromatography on concanavalin A–Sepharose as the final purification step, followed by lyophilization. Lane *a* shows a mixture of low-molecular weight markers (phosphorylase *b*, albumin, ovalbumin, carbonic anhydrase, trypsin inhibitor and α-lactalbumin; supplied by Pharmacia Fine Chemicals). Laemmli SDS-polyacrylamide gel (12.5%) electrophoresis.

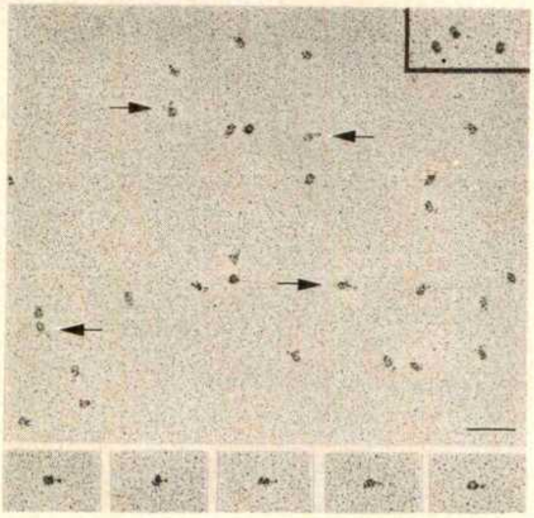

Fig. 3 Electron micrographs of rotary-shadowed VSG (*T. brucei brucei*, antigenic type MITat 1.2). The dimeric molecules display a large 'globular' domain about 110 Å × 70 Å and often a shorter (~50–100 Å) 'tail' region. Occasionally, the tail terminates in a very small globular domain. Inset, the N-terminal dimer portion of the molecule from redissolved crystals of this domain prepared as described by Freymann *et al.*[1]. Experimental details of shadowing as for Fig. 1. Scale bar, 500 Å.

50% of the VSG conformation may be α-helical. We also carried out a search for quasi-repeating heptads of the form $(a\text{-}b\text{-}c\text{-}d\text{-}e\text{-}f\text{-}g)_n$ where *a* and *d* are apolar residues[11,12] that allow an interlocking of α-helices, as envisaged by Crick, to form a coiled-coil structure[13]. Our analysis reveals that the N-terminal domains show extended 7-fold periodicity indicative of a high proportion of α-helical coiled-coil structure which differs, however, in extent and disposition between the subsets. Examples of such 7-fold repeats in two subset I VSG sequences are shown in Table 1. The extent of the regions exhibiting the heptad repeat is such that *n* commonly lies between 2 and 7, which is much less than that found for tropomyosin (where $n = 40$), but comparable to that in the rod segments of fibrinogen[11]. It should be stressed that 'broken heptads' of the type found here (with discontinuities in regularity) are compatible both with a long stretch of coiled-coil or with shorter stretches of α-helices interlocking in a more compact structure (such as a 4-α-helical motif[14]). For example, the coiled-coils could form a compact region followed by an extended stem (perhaps as in DiTat 1.3) or a more elongated bundle (as in MITat 1.2). The heptads found in the sequences have a markedly higher content of hydrophobic residues in positions *b*, *c*, *e*, *f* and *g* than those of α-helical coiled-coil muscle proteins (Table 1). This feature may be related to the characteristic dimerization of these molecules (see also 1). Although the C-terminal domains of VSG molecules may be morphologically distinct in different species (as in DiTat 1.3 and MITat 1.2), a highly charged 25-residue segment appears to be conserved in both subsets and is likely to have a membrane-binding role. Our results on α-helix content are in general agreement with the recent study of Lalor *et al.*[15]; we believe, however, that consideration of the heptad regularity is a critical aspect of the sequence analysis and one which has important structural and functional implications.

At present only parts of the puzzle are available to establish strict morphology/sequence/function relations in the VSGs. Nevertheless, our results, taken together with the recent X-ray crystallographic studies of Freymann *et al.*[1], suggest some design principles for these surface glycoproteins. As described by Cohen and Phillips[16], the α-helical coiled-coil is a fundamental feature of the structure. The length and disposition of α-helices in the exposed N-terminal variable region may differ, however, in different species of VSG (see also ref. 15). It is also possible that the broken heptad repeats in the sequences provide a device for generating structural diversity. Thus, the α-helical segments

Table 1 Heptad regularities in α-helical regions of the N-terminal domains of two subset I VSGs

Residue	*a*	*b*	*c*	*d*	*e*	*f*	*g*
VSG 117 (MITat 1.4)							
7 heptads		Cys	Gly	Leu	Ala	Ala	Thr
	Leu	Arg	Lys	Val	Ala	Gly	Gly
	Val	Leu	Thr	Lys	Leu	Lys	Ser
	His	Ile	Ser	Tyr	Arg	Lys	Lys
	Leu	Glu	Glu	Met	Glu	Thr	Lys
	Leu	Arg	Ile	Tyr	Ala	Leu	Lys
	Gly	Asp	Gly	Val	Gly	Glu	Gln (Lys Ser)
2½ heptads	Ala	Glu	Ile	Leu	Ala	Thr	Thr
	Ala	Ala	Leu	Met	Arg	Gln	Lys
	Ala	Leu	Thr	(Pro	Glu	Glu	Ala Asn)
3½ heptads	Leu	Lys	Thr	Ala	Leu	Lys	Ala
	Ala	Gly	Phe	Ala	Gly	Glu	Gly
	Ala	Ala	Ala	Val	Ser	Ser	Tyr
	Leu	Met	Thr	Leu	(Gly	Thr	Leu
	Thr	Thr	Ser	Gly	Ser	Ala	His Cys)
AnTat 1.1							
6 heptads		Cys	Thr	Tyr	Ser	Lys	Thr
	Ala	Lys	Arg	Gln	Ala	Ala	Asn
	Leu	Ala	Gln	Thr	Leu	Gln	Arg
	Ala	Ser	Ser	Ala	Ala	Lys	Gln
	Ser	Arg	Gln	Ala	Gln	Gln	Leu
	Ala	Ala	Leu	Ala	Leu	Ala	Lys
	Leu	(Pro	Asp)				
2 heptads	Tyr	Lys	Glu	Ala	Ala	Ala	Thr
	Leu	Leu	Ile	Tyr	Ala	Thr	His (Lys)
5 heptads	Ile	Gln	Asp	Ala	Gln	Ala	Ser
	Ile	Glu	Asn	Trp	Thr	Gly	Glu
	Asn	Thr	Lys	Leu	Val	Gly	Gln
	Ala	Met	Tyr	Ser	Ser	Gly	Arg
	Ile	Asp	Glu	Leu	Met	Leu	Leu
	Leu	Glu	(Gly	His	Arg	Glu	Asp
	Gly	Ala	Asn	Gly	Gln	Asp	Lys Thr Cys)

Apolar residues in positions *a* and *d* permit the adoption of a coiled-coil structure. Residues in parentheses introduce a discontinuity in the heptad repeat, represented by a space in the sequence. The upper sequence is from VSG 117 (MITat 1.4) between Cys 14 and Cys 121. The lower sequence is from AnTat 1.1 between Cys 45 and Cys 154. The sequences of AnTat 1.10 and 1.1B give similar results. Subset II VSGs appear to be somewhat different: broken heptad runs occur farther along in the sequence—for example, between residues 237 and 339 in ILTat 1.1 and 151 and 277 in ILTat 1.4.

may adopt a variety of closely related forms, from extended to compact, that depend as well on the constraints imposed by disulphide bridges. Such a range of possible conformations (unlikely for α-helical regions lacking heptad repeats) may have implications for the antigenic variability of these proteins. Although the antigenic diversity may arise from amino acid replacements *per se*, it could also depend on structural changes, possibly gross, controlled by broken heptad repeats that can result from a small change of sequence.

This work was supported by grants from NIH (AM17346), NSF (PCM82-02516), and the Muscular Dystrophy Association (to C.C.); the Deutsche Gessellschaft für Technische Zusammenarbeit (PN 77.2227.5) and the Institut d'Elevage et de Médecine Vétérinaire des Pays Tropicaux, France (to G.E.R.). We thank Louise Seidel for secretarial assistance, Daniel Hellerstein for computing assistance, Drs Don Wiley and Mervyn Turner for samples of VSG MITat 1.2 and Dr Don Wiley for discussions and aid with the manuscript.

Received 18 June; accepted 5 July 1984.

1. Freymann, D., Metcalf, P., Turner, M. & Wiley, D. C. *Nature* **310,** 167–169 (1984).
2. Holder, A. A. & Cross, G. A. M. *Molec. biochem. Parasit.* **2,** 135–150 (1981).
3. Rice-Ficht, A. C., Chen, K. C. & Donelson, J. E. *Nature* **294,** 53–57 (1981).
4. Allen, G., Gurnett, L. P. & Cross, G. A. M. *J. molec. Biol.* **157,** 527–546 (1982).
5. Pays, E. *et al. Cell* **34,** 371–381 (1983).
6. Rice-Ficht, A. C., Chen, K. C. & Donelson, J. E. *Nature* **298,** 676–679 (1982).
7. Donelson, J. E., Young, J. R., Dorfman, D., Majiwa, P. A. O. & Williams, R. O. *Nucleic Acids Res.* **10,** 6581–6595 (1982).
8. Chou, P. Y. & Fasman, G. D. *A. Rev. Biochem.* **47,** 251–276 (1978).
9. Robson, B. & Suzuki, E. *J. molec. Biol.* **107,** 327–356 (1976).
10. Garnier, J., Osguthrope, D. J. & Robson, B. *J. molec. Biol.* **120,** 97–120 (1978).
11. Parry, D. A. D. in *Fibrous Proteins: Scientific, Industrial and Medical Aspects* Vol. 1 (eds Parry, D. A. D. & Creamer, L. K.) 393–427 (Academic, London, 1979).
12. Parry, D. A. D. *Biosci. Rep.* **2,** 1017–1024 (1982).
13. Crick, F. H. C. *Acta crystallogr.* **6,** 689–697 (1953).
14. Weber, P. C. & Salemme, F. R. *Nature* **287,** 82–84 (1980).
15. Lalor, T. M. *et al. Proc. natn. Acad. Sci. U.S.A.* **81,** 998–1002 (1984).
16. Cohen, C. & Phillips, G. N. Jr *Proc. natn. Acad. Sci. U.S.A.* **78,** 5303–5304 (1981).
17. Flicker, P. F., Wallimann, T. & Vibert, P. *J. molec. Biol.* **169,** 723–741 (1983).
18. Cross, G. A. M. *Parasitology* **71,** 393–417 (1975).
19. Roelants, G. E. *et al. Expl Parasit.* (submitted).

Mutant viral RNAs synthesized *in vitro* show altered aminoacylation and replicase template activities

T. W. Dreher*, J. J. Bujarski & T. C. Hall*

Biophysics Laboratory of the Graduate School, University of Wisconsin-Madison, Madison, Wisconsin 53706, USA

A remarkable feature of the genomic RNAs of several plant viruses is the presence at the 3′ end of a region that exhibits tRNA-like functions, including aminoacylation[1–3]. The three genomic and single subgenomic RNAs of brome mosaic virus (BMV) accept tyrosine *in vitro*[4] and *in vivo*[5], the smallest 3′ fragment that can be aminoacylated being about 135 nucleotides long[6]. The roles of the tRNA-like properties are incompletely understood, but an involvement in replication rather than translational functions is likely[3,7,8]. We have recently shown (J.J.B. *et al.*, in preparation) that the features recognized by the BMV RNA-specific RNA-dependent RNA polymerase (replicase)[9,10] for the use of BMV RNA for complementary strand synthesis also lie within the tRNA-like structure. To distinguish between the roles of BMV RNA as a substrate for tyrosyl-tRNA synthetase and BMV replicase, we have now produced BMV RNAs with mutations at two separate loci within the tRNA-like structure. This has been achieved by transcription *in vitro* from specifically mutagenized cDNA, an approach permitting the generation of targeted mutants without regard to their viability *in vivo*.

The synthesis of RNAs active in aminoacylation, a function known to be stringently dependent on a correct 3′-CCA terminus[11,12], required the extension of existing *in vitro* transcription techniques[13,14]. Correct 3′ termini were obtained by transcription from a template linearized at a position corresponding to the 3′ end of the BMV cDNA sequence; a *Tth*111I restriction site was created at such a location within a 201-base pair (bp) BMV RNA3 cDNA clone containing the tRNA-like structure (Fig. 1*a*). After placing the BMV sequence under the control of an SP6 promoter[13,15] (Fig. 1*b*), microgram quantities of BMV RNA transcript of the expected size (207 nucleotides) were prepared from *Tth*111I-linearized template DNA. The transcribed RNA was active in two assays characteristic of the tRNA-like structure of BMV RNA: aminoacylation and complementary strand synthesis by BMV replicase. The behaviour of BMV RNA transcripts in both assays was comparable to that of native virion RNA. These activities are discussed below in comparison with those of mutated RNAs.

Point mutations were introduced into the BMV cDNA segment of clone mpTD11 by oligonucleotide-directed mutagenesis[16]. Mixed oligonucleotide primers[17], containing sequence ambiguities at two adjacent bases, were used to construct libraries expected to contain all possible single and double base mutants for each dinucleotide target. This procedure was applied to two loci in the BMV sequence, the 3′ end and the –AUA–tyrosyl anticodon triplet. Figure 2*a* identifies the sequence substitutions of BMV RNAs produced from clones selected from mutant libraries.

---

* Present address: Department of Biology, Texas A & M University, College Station, Texas 77843, USA.

Transcripts representing the wild-type and mutant BMV RNAs (207 nucleotides) migrated identically during electrophoresis (Fig. 2*b*). Termination of transcription did, however, show some heterogeneity, as indicated by the poorly resolved doublets. The 3′ termini of all transcripts studied here were analysed by 3′-terminal labelling with 5′-^{32}P-pCp (ref. 18), followed by complete digestion with alkali or specific ribonucleases (data not shown). Although transcriptional termination on such linear templates gave rise to a limited range of products, it was clear that the heterogeneity existed beyond the required 3′ end, that no significant premature termination was caused by the end of the DNA template, and that about one-third of transcript molecules consistently contained the expected 3′ end. The run-off transcription system described here is thus capable of producing faithfully terminated RNA molecules.

Wild-type transcripts were aminoacylated with kinetics similar to those of virion RNA; about 40% of transcribed molecules were tyrosylated (Fig. 3*a*). This is consistent with an estimated one-third of transcribed molecules having a correct 3′ terminus (see above). All five mutants in which the anticodon was changed to that of three different amino acids, or to the amber nonsense triplet, were as active in tyrosylation assays as were wild-type transcripts, and displayed indistinguishable kinetics (Fig. 3*a*). In contrast, all four mutations at the 3′ terminus abolished aminoacylation. The low level of tyrosylation observed after longer incubations with mutant RNAs containing single base changes at the far 3′ end was due to turnover of the 3′ nucleotide[12], which generated some molecules with a correct −CCA end. tRNA nucleotidyl transferase and low levels of nuclease are known to be present in the partially purified synthetase preparations used.

The above sets of RNAs were assayed for their abilities to act as templates for BMV replicase (Fig. 3*b*). Wild-type transcripts showed similar activity to BMV RNA4, yielding full-length, double-stranded RNA. All of the point mutations studied

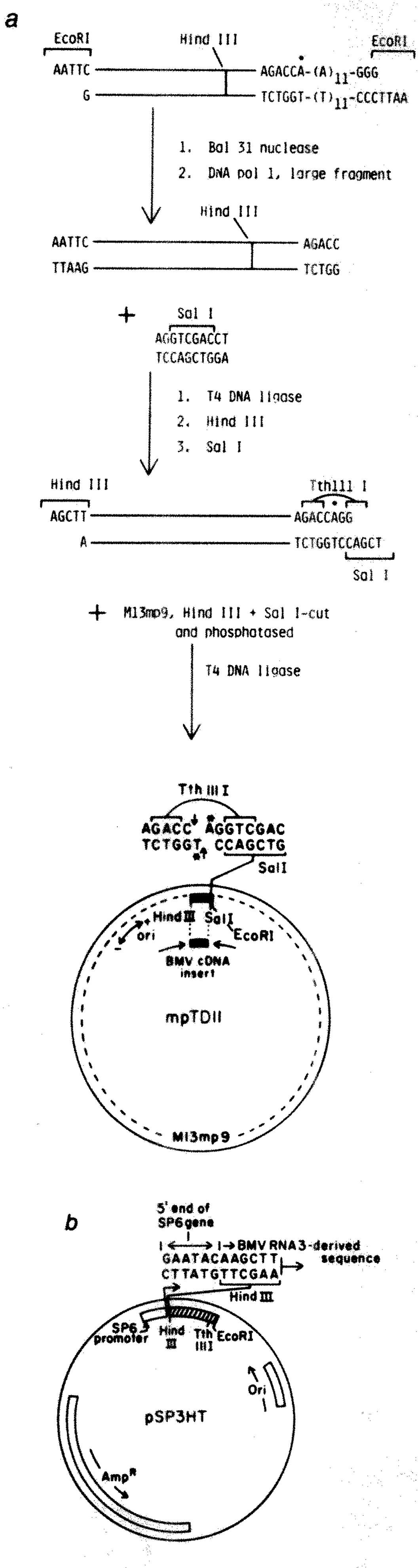

Fig. 1 Construction of a plasmid allowing the synthesis by transcription of RNA molecules comprising the tRNA-like region of BMV RNA3 and terminating in correct 3′ ends. *a*, Scheme for the creation of a *Tth*111I site with the cleavage position coincident with the 3′ end of the BMV RNA3 cDNA sequence. Clone mpTD11 contains the cDNA sequence corresponding to the 201 3′ nucleotides of BMV RNA3. *Marks the 3′ end of the BMV cDNA sequence. The cleavage positions for the *Tth*111I restriction endonuclease are indicated by arrows. *b*, Diagram of the transcriptional plasmid pSP3HT, obtained by subcloning the *Hin*dIII to *Eco*RI insert of mpTD11 (cross-hatched) into plasmid pSP64, a pUC12 (refs 25, 26) derivative containing an SP6 promoter fragment, and constructed in the laboratory of D. Melton. The 5′ region of the DNA sequence transcribed by the SP6 RNA polymerase is shown; transcripts possess six bases at their 5′ ends originating from the SP6 gene.

Methods: A fragment comprising the cDNA sequence corresponding to BMV RNA3 was released by *Eco*RI cleavage of 10 μg of a plasmid supplied by P. Ahlquist. To remove the poly(dA) tail added during cDNA cloning, the DNA mixture was treated with *Bal*31 nuclease (0.6 units, BRL) at 16 °C in a reaction containing 20 mM Tris-HCl (*p*H 8.1), 0.6 M NaCl, 12 mM $CaCl_2$, 12 mM $MgCl_2$, 1 mM EDTA and 250 μg ml^{-1} bovine serum albumin (BSA)[27]. Portions of the reaction, taken at 7, 10 and 13 min, were pooled and the reaction was stopped in 20 mM EGTA, phenol extracted and ethanol precipitated. Treatment with *Escherichia coli* DNA polymerase I (large fragment, BRL)[28] was used to increase the proportion of fragments with blunt ends before linker addition. A decameric self-complementary oligodeoxynucleotide d(AGGTCGACCT), which contained an internal *Sal*I site and was capable of creating a *Tth*111I site when ligated to the desired *Bal*31-deleted DNA, was synthesized by the phosphite triester procedure[29] using a DNA Synthesis Kit from New England Biolabs. The oligomer (0.6 μg) was phosphorylated to completion using T4 polynucleotide kinase (Pharmacia-P/L) in a reaction containing 200 μCi[γ-^{32}P]ATP (3,000 Ci mmol^{-1}; Amersham) chased with 500 μM unlabelled ATP[30]. After ligation of the ^{32}P-labelled decameric linker to the *Bal*31-treated DNA, the DNA was digested with *Hin*dIII (BRL) and linkers were depolymerized by complete digestion with *Sal*I (Pharmacia-P/L). Digestion products were electrophoresed through a 1.5% low melting point agarose gel, and a band (~200 bp) was extracted. The DNA was ligated to *Hin*dIII + *Sal*I-digested, phosphatased M13mp9 vector[26] using T4 DNA ligase. Following transfection into *E. coli* JM101, clone mpTD11 (shown) was isolated by screening plaques for the presence of a *Tth*111I restriction site in replicative form DNA.

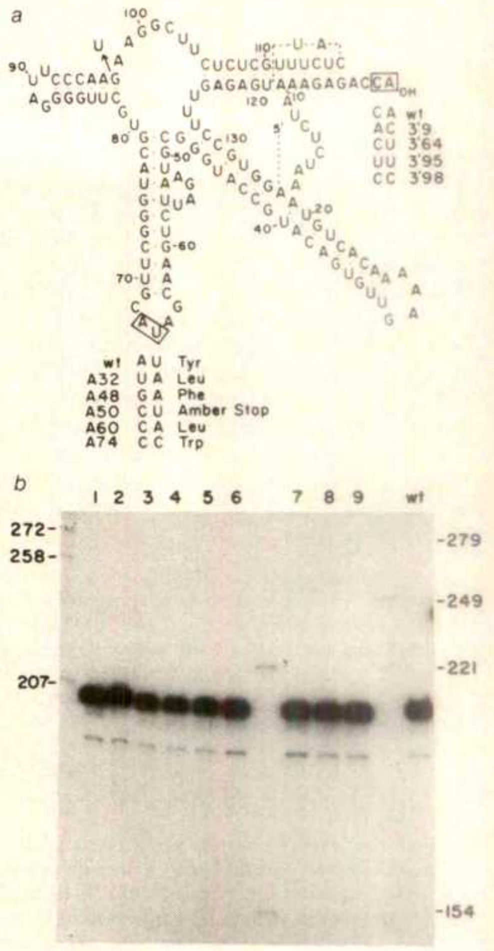

Fig. 2 Synthesis of BMV RNAs with mutations within the tRNA-like structure. ***a***, Two-dimensional representation of the postulated conformation of the tRNA-like structure of BMV RNA3 (after Rietveld *et al.*[31]). Nucleotide positions are numbered from the 3′ end, and the two pairs of adjacent nucleotides at which mutations have been introduced are boxed: the 3′ terminus and the putative anticodon. Mutant clones were sequenced both before and after subcloning into the transcriptional plasmids, and the sequences of their transcripts are indicated for each locus; the amino acid corresponding to each anticodon triplet is also shown. The wild-type transcripts studied here varied from the RNA consensus sequence shown by the single base change G97 to U97 (indicated), which was also present in mutant transcripts. This substitution appeared neutral with respect to aminoacylation and BMV replicase template activity. Note that the split recognition sequence of *Tth*111I GACN′NNGTC permits 3′ mutations. ***b***, Analysis of transcripts arising from mutated BMV cDNA clones on a 5% polyacrylamide-7 M urea sequencing gel. The migrations of DNA markers are indicated. Lanes 1–9, mutant transcripts 3′9, 3′64, 3′95, 3′98, A32, A48, A50, A60 and A74 respectively; wt is the wild-type transcript. Transcripts labelled with [α-^{32}P]UTP were synthesized from *Tth*111I-linearized transcriptional plasmids using SP6 RNA polymerase[13].

Methods: Construction of mutant clones: Libraries of all possible double and single mutants at each locus were generated in a single mutagenizing experiment from single-stranded phage DNA (clone mpTD11), by an extension of published methods[16,17]. 3′-Terminal mutations: A hexadecameric deoxyoligonucleotide mixture of sequence d(GTCGACCXYGTCTCTT) was synthesized as above. The positions designated X and Y were the sites directing the mutagenesis, where X = dT and Y = dG in the wild-type sequence. During synthesis, the condensation reaction at position Y contained a molar ratio of 3dC:3dA:3dT:dG of the protected nucleotide reagents. At position X, the molar ratios were 3dC:3dA:3dG:dT. In this synthesis system, molar ratios of condensation products are roughly proportional to the concentration of reagents in the reaction. The low proportion of the wild-type nucleotide was used to depress the ratio of recreated wild-type clones after mutagenesis. Conditions expected to allow priming of second strand synthesis by oligomers with double and single mismatches were established in pilot dideoxy sequencing reactions with the synthetic hexadecameric mixture as primer. The oligomer mixture was kinased and mixed with 1.5 μg of single-stranded mpTD11 template (~15-fold molar excess of primer) in 9 μl containing 20 mM Tris-HCl (*p*H 7.5), 10 mM $MgCl_2$, 50 mM NaCl and 1 μM dithiothreitol. After boiling for 2 min, the mixture was annealed at 37 °C for 15 min, chilled on ice and brought to room temperature just before second strand synthesis. The reaction proceeded as recommended[16]. 100 phage clones were screened by temperature-shift hybridization, in which M13 phage was applied directly onto nitrocellulose (Schleicher & Schuell) and the [γ-^{32}P]-labelled synthetic oligomer mixture was used as probe[16,17]. Hybridization was carried out at room temperature overnight, and was followed by 5-min washes at successively higher temperatures (37, 45, 55 and 60 °C), alternating with exposure of the dot blots to film. Suspected mutant phage were analysed by dideoxy sequencing[32] using the M13 universal primer (17mer, New England Biolabs). Some phage selected on the basis of hybridization results did prove to be wild type. Because the blotted phage were not screened exhaustively, the proportion of mutants achieved was not determined. Anticodon mutations: The 21mer oligomer mixture used for mutagenesis at this locus was synthesized as above. The sequence was d(GACTTGCTWZGCAAGCCCATG), where W = dA and Z = dT in the wild-type sequence. The molar ratios at position W were 3dG:3dC:3dT:dA and at position Z were 3dG:3dC:3dA:dT. Mutagenesis was performed as above, except that the annealing temperature was 50 °C. During screening, washes were for 5 min at 50, 57, 67 and 72 °C. At least 8% of phage were mutants. Mutant clones were plaque purified, and the *Hin*dIII–*Eco*RI insert was subcloned into pSP64 as for the wild-type clone (see Fig. 1).

Table 1 Relative activities of mutant transcripts as templates for BMV replicase and in aminoacylation

Transcript	Relative replicase template activity	Relative aminoacylation activity
wt	1.00	1.00
3′9	0.05	0.00
3′64	0.34	0.02
3′95	0.05	0.01
3′98	0.32	0.01
A32	0.15	1.00
A48	0.15	0.97
A50	0.20	0.82
A60	0.18	0.94
A74	0.14	0.99

Replicase template activities were estimated by determining the ratio of ^{32}P c.p.m. incorporated into product by BMV replicase to ^{3}H c.p.m., a measure of the amount of synthetic template (transcript) present. Replicase reaction products were phenol extracted and electrophoresed through 5% sequencing gels, conditions in which product and template co-migrate. Bands located by exposure to film were excised from the gel, and the RNA present was base hydrolysed using Soluene 100 (Packard), and analysed in a liquid scintillation spectrometer for ^{32}P and ^{3}H c.p.m. Aminoacylation activities were derived from the amounts of ^{3}H-tyrosine bound after 5-min incubations (Fig. 3*a*). This avoids the confusion with the end-group repair which occurs for transcripts 3′64 and 3′98 during longer incubations. Aminoacylation differences between anticodon mutants were not significant. wt, Wild type.

within the anticodon uniformly and markedly inhibited the template activity of the RNA. The template activity of 3′ end mutants was governed by the location of the substitution. Transcripts with mutations only at the terminal position were active templates, although their activity was about one-third that of the wild-type transcript. In contrast, transcripts with substitutions at both the penultimate and terminal positions were very poor templates. The lowered activity of 3′ mutant RNAs probably results from interference with the normal initiation of RNA synthesis.

The relative aminoacylation and replicase template activities of wild-type and mutant transcripts are compared in Table 1. Aminoacylation results were derived from charging levels after 5-min incubations, at which time 3′ nucleotide turnover is undetectable (Fig. 3*a*). Replication activities were quantified by determining the ratio of product to template RNA in replicase reactions. Mutations at each locus had differential effects on the two activities. Several mutations within the anticodon triplet show that BMV replicase, and not tyrosyl-tRNA synthetase, interacts with this sequence, which exists in an exposed loop of the tRNA-like structure. The anticodon residues may thus be involved in the specific recognition of BMV RNA by the replicase.

The indifference of tyrosyl-tRNA synthetase to mutations in the anticodon of BMV RNA requires comment. Chemical modifications and mutations of the anticodons of tRNAs have not inhibited aminoacylation in all systems studied (compare refs 19, 20). Further, although anticodons corresponding to the specifically bound amino acid are present in several plant viral RNAs[2,3], their occurrence is not universal; some viruses closely related to BMV, and whose RNAs bind tyrosine[21], do not have analogous anticodons[6,22,23]. This variation is compatible with the anticodon residues representing important determinants of replicase specificity. However, such observations leave open the question of the significance of the correspondence between bound amino acid and anticodon in RNAs from viruses such as BMV.

Four different mutations at the 3′ terminus of BMV RNA abolished tyrosine-accepting activity. Thus, the −CCA terminus is as necessary for the aminoacylation of BMV RNAs as it is for tRNAs[1,12]. In contrast, BMV replicase is not as stringent in its requirement for a correct 3′ terminus, and mutants with substitutions in the terminal position retained 33% of replicase template activity. However, substitutions at both of the 3′-terminal positions resulted in 95% loss of activity. These results are consistent with initiation of (−)strand synthesis very close to the 3′ end (J.J.B. *et al.*, in preparation), possibly at the penultimate C residue.

The approach described here for rapidly obtaining mutant RNA molecules with defined 3′ termini is likely to be useful for studying the functions of various RNA molecules, including tRNAs, especially when the desired mutations cannot be obtained by traditional means or when the mutations are likely to be lethal. This system offers clear advantages over an RNA synthesizing system based on Qβ replicase[24], which requires substantial Qβ sequences at the 3′ end of the RNA. Placement of cloned DNA sequences immediately adjacent to the SP6 promoter will permit the synthesis of RNAs with both authentic 5′ and 3′ ends.

We thank Dr M. Wickens for supplying SP6 RNA polymerase before its commercial availability, and for helpful discussions. Dr D. Melton supplied the transcriptional plasmid pSP64 and Dr P. Ahlquist supplied the BMV cDNA clone used. We thank Allen Miller for discussions, Dr L. A. Ball for help with the manuscript, Chris Harkin for technical assistance, and Professor

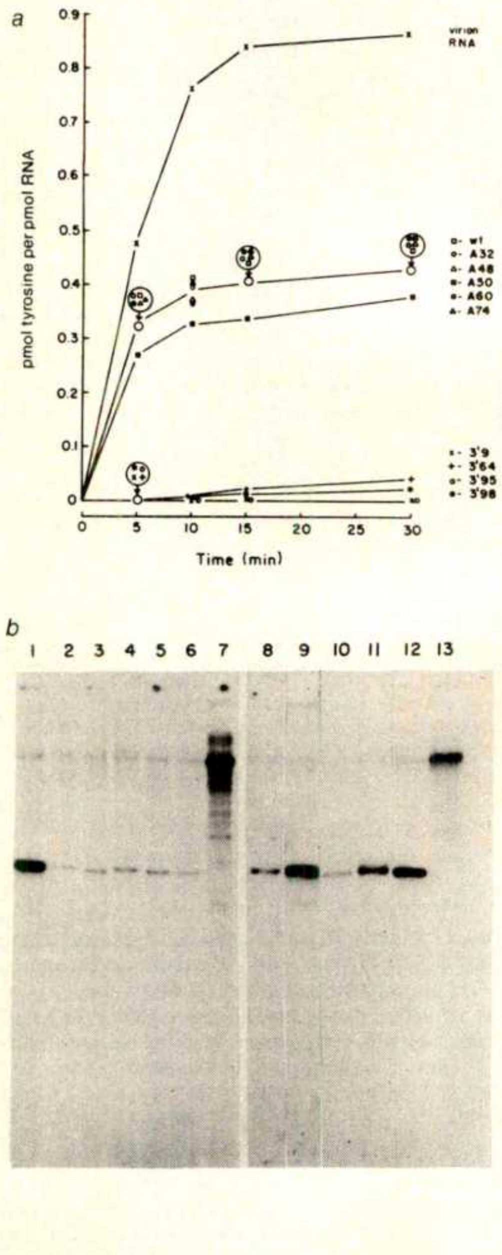

Fig. 3 Biological activity of wild-type and mutant BMV RNAs synthesized *in vitro*. *a*, Aminoacylation of transcripts. *b*, Activity of transcripts as templates for BMV replicase. Lanes 1 and 12, replicase reaction product with wild-type transcript as template; lanes 2–6, products with anticodon mutant transcripts as templates, A32, A48, A50, A60, A74 respectively; lanes 8–11, products with 3′ mutant transcripts as templates, 3′9, 3′64, 3′95, 3′98 respectively. Lanes 7 and 13 are products obtained using 1.2 μg BMV RNA4 as template; low levels of products synthesized from endogenous RNA4 are evident in the other lanes, and are useful internal controls.

Methods: *a*, BMV RNA was prepared as previously reported[21]. Transcripts were labelled to a known specific activity of ~60,000 d.p.m. per μg with [α-^{32}P]UTP (Amersham), allowing calculation of the amount of RNA used in each aminoacylation reaction. Reactions (50 μl) containing 3 μg of *Tth*111I-linearized DNA, 3.5 units of SP6 RNA polymerase and 500 μM each nucleotide triphosphate typically yielded 3–5 μg of transcribed RNA. RNA was phenol extracted and purified either using DEAE-Sephacel (Pharmacia) followed by ethanol precipitation, or by two successive ethanol precipitations in the presence of ammonium acetate. In both cases unincorporated nucleotides were completely removed. Because template DNA was shown not to interfere with the aminoacylation assay, it was not removed. Aminoacylation (tyrosylation) assays used a partially purified preparation of aminoacyl-tRNA synthetases from wheat germ[33]. Reactions (50 μl) contained 0.5–0.7 μg of ^{32}P-labelled transcript RNA, 7.3 μCi ^{3}H-tyrosine (54.6 Ci mmol^{-1}; NEN), 48 mM KCl, 5 mM MgCl$_2$, 0.64 mM ATP and 5 μl of synthetase preparation and were incubated at 30 °C. Aliquots were taken at the times indicated, and incorporation of ^{3}H-tyrosine was determined by precipitation of RNAs onto filter paper with trichloroacetic acid. Radioactivity was counted in a liquid scintillation spectrometer in conditions suitable for ^{32}P/^{3}H double counting. The results shown are averages from two experiments for virion RNA, and of duplicate assays on at least two independently synthesized sets of transcripts. The altered sequences for mutant transcripts are identified in Fig. 2*a*. The results for transcript A50 were not significantly different from those of wild type or other anticodon mutants. *b*, Template activities of mutant and wild-type transcripts were assayed by incubation with BMV replicase, prepared from BMV-infected barley leaves and treated with micrococcal nuclease[9,10]. Labelled complementary strand was synthesized in 25 μl reactions containing 1 μM [α-^{32}P]UTP (80 Ci mmol^{-1}; Amersham), 80 μg ml^{-1} actinomycin D, 20 μl of BMV replicase preparation and template RNA. The reaction mixture was incubated at 30 °C for 30 min, extracted twice with phenol–chloroform, ether extracted and ethanol precipitated in the presence of ammonium acetate. A portion of the replicase reaction products was treated with ribonuclease[9] before electrophoresis to confirm the presence of double-stranded products (not shown). Transcripts were prepared as above, but were labelled with [α-^{3}H]UTP (NEN) to a specific activity of about 3×10^5 d.p.m. per μg. Replicase reaction products with mutant and wild-type BMV transcripts and virion BMV RNA4 as templates were run on a 5% nondenaturing polyacrylamide gel and autoradiographed. Replicase reactions contained 0.9 μg of transcript for 3′9 and 3′64 (lanes 8, 9), and 0.3 μg for all others.

P. Kaesberg for laboratory space. This work was funded by NIH grant AI 11572.

Received 16 April; accepted 19 June 1984.

1. Pinck, M., Yot, P., Chapeville, F. & Duranton, H. *Nature* **226,** 954–956 (1970).
2. Hall, T. C. *Int. Rev. Cytol.* **60,** 1–26 (1979).
3. Haenni, A. L., Joshi, S. & Chapeville, F. *Prog. Nucleic Acid Res. molec. Biol.* **27,** 85–104 (1982).
4. Hall, T. C., Shih, D. S. & Kaesberg, P. *Biochem. J.* **129,** 969–976 (1972).
5. Loesch-Fries, L. S. & Hall, T. C. *Nature* **298,** 771–773 (1982).
6. Joshi, R. L., Joshi, S., Chapeville, F. & Haenni, A. L. *EMBO J.* **2,** 1123–1127 (1983).
7. Chen, J. M. & Hall, T. C. *Biochemistry* **12,** 4570–4574 (1973).
8. Hall, T. C., Pinck, M., Ma, Y., Duranton, H. M. & German, T. L. *Virology* **97,** 354–365 (1979).
9. Bujarski, J. J., Hardy, S. F., Miller, W. A. & Hall, T. C. *Virology* **119,** 465–473 (1982).
10. Miller, W. A. & Hall, T. C. *Virology* **125,** 236–241 (1983).
11. Sprinzl, M. & Cramer, F. *Prog. Nucleic Acid Res. molec. Biol.* **22,** 1–69 (1979).
12. Deutscher, M. P. *Enzymes of Nucleic Acid Synthesis and Modification* Vol. 2 (ed. Jacob, S. T.) 159–183 (CRC Press, Boca Raton, Florida, 1983).
13. Green, M. R., Maniatis, T. & Melton, D. A. *Cell* **32,** 681–694 (1983).
14. Contreras, R., Cheroutre, H., Degrave, W. & Fiers, W. *Nucleic Acids Res.* **10,** 6353–6362 (1982).
15. Butler, E. T. & Chamberlin, M. J. *J. biol. Chem.* **257,** 5772–5778 (1982).
16. Zoller, M. J. & Smith, M. *Meth. Enzym.* **100,** 468–500 (1983).
17. Zarucki-Schulz, T. *et al. J. biol. Chem.* **257,** 11070–11077 (1982).
18. England, T. E., Bruce, A. G. & Uhlenbeck, O. C. *Meth. Enzym.* **65,** 65–74 (1980).
19. Schimmel, P. R. & Söll, D. *A. Rev. Biochem.* **48,** 601–648 (1979).
20. Bruce, A. G. & Uhlenbeck, O. C. *Biochemistry* **21,** 3921–3926 (1982).
21. Kohl, R. J. & Hall, T. C. *J. gen. Virol.* **25,** 257–261 (1974).
22. Ahlquist, P., Dasgupta, R. & Kaesberg, P. *Cell* **23,** 183–189 (1981).
23. Wilson, P. A. & Symons, R. H. *Virology* **112,** 342–345 (1981).
24. Miele, E. A., Mills, D. R. & Kramer, F. R. *J. molec. Biol.* **171,** 281–295 (1983).
25. Vieira, J. & Messing, J. *Gene* **19,** 259–268 (1982).
26. Messing, J. *Meth. Enzym.* **101,** 20–78 (1983).
27. Guo, L.-H. & Wu, R. *Meth. Enzym.* **100,** 60–96 (1983).
28. Maniatis, T., Fritsch, E. F. & Sambrook, J. *Molecular Cloning* (Cold Spring Harbor Laboratory, New York, 1982).
29. Beaucage, S. L. & Caruthers, M. H. *Tetrahedron Lett.* **22,** 1859–1862 (1981).
30. Goodman, H. M. & MacDonald, R. J. *Meth. Enzym.* **68,** 75–90 (1979).
31. Rietveld, K., Pleij, W. A. & Bosch, L. *EMBO J.* **2,** 1079–1085 (1983).
32. Sanger, F., Coulsen, A. R., Barrell, B. G., Smith, A. J. H. & Roe, B. A. *J. molec. Biol.* **143,** 161–178 (1980).
33. Kiberstis, P. A. & Hall, T. C. *J. gen. Virol.* **64,** 2073–2077 (1983).

Plasma protease inhibitors in mouse and man: divergence within the reactive centre regions

Robert E. Hill, Phillip H. Shaw*, Patricia A. Boyd, Heinz Baumann† & Nicholas D. Hastie

Molecular Genetics Section, MRC Clinical and Population
Cytogenetics Unit, Western General Hospital,
Edinburgh EH4 2XU, UK
* Swiss Institute for Experimental Cancer Research, Ch-des
Boveresses, CH-1066 Epalinges, Lausanne, Switzerland
† Department of Cell and Tumor Biology, Roswell Park Memorial
Institute, Buffalo, New York 14263, USA

The plasma protease inhibitors control a wide variety of physiological functions including blood coagulation, complement activation and aspects of the inflammatory response. The inhibitors function by forming a 1:1 complex with a specific protease within the reactive centre region of the inhibitor. Little is known about the evolutionary relationships of these inhibitors. We report here the sequences of cDNAs which represent the C-terminal halves of the two major murine plasma protease inhibitors. One of these, murine α_1-antitrypsin, more appropriately called α_1-proteinase inhibitor (α_1-PI), has diverged from its human counterpart at a vital position in the reactive centre but this has not led to a physiologically significant change in function. Also, we have determined the partial sequence of a recently characterized protein termed contrapsin, which inhibits trypsin-like proteases[1,2]. We show, surprisingly, that contrapsin is highly homologous to human α_1-antichymotrypsin, an inhibitor of chymotrypsin-like proteases. The reactive centre regions of these two inhibitors have diverged considerably, which may account for the differences in specificity. We propose that the genes for contrapsin and human α_1-antichymotrypsin are the descendents of a single gene that have evolved since rodent and primate divergence to encode proteins with different functions.

Previously, we have isolated cDNA clones corresponding to abundant liver-specific mRNA sequences[3]. Two of these clones, p1796 and p54, are complementary to mRNA encoding, respectively, the protease inhibitors α_1-PI and contrapsin (our unpublished data and Jack Gauldie, personal communication). Figure 1 shows the DNA sequence analysis of the p1796 and p54 inserts. The two cDNA inserts are approximately 800 nucleotides long, representing the 3′ half of the corresponding mRNA. Figure 1*a* compares the nucleotide and derived amino acid sequences of murine α_1-PI with those published for the primate α_1-PI (ref. 4). Over the region analysed, the mouse sequence is 70% homologous with the primate α_1-PI at the nucleotide level, and 60% at the amino acid level. This degree of evolutionary divergence is common among many of the serum proteins studied[5,6].

Comparison of the sequence of mouse contrapsin (Fig. 1*b*) with that of murine α_1-PI (Fig. 1*a*) reveals that the two inhibitors are related, sharing 59% homology at the nucleotide level and 44% at the amino acid level. This suggests that the two proteins diverged from a common ancestral gene probably some 200–300 Myr ago.

Contrapsin is a major component of the protease inhibitory activity of mouse plasma; however, this activity is not detected in human plasma[1]. To search for a possible human counterpart, we screened a human liver cDNA library for complementary sequences[7]; approximately 0.1% of the clones screened gave a strong positive signal with the mouse contrapsin insert. One representative clone, pHL6.1, was selected and the region corresponding to the mouse cDNA insert sequenced. Figure 1*b* compares the mouse and human sequences, which are 70% homologous at the nucleotide level and 60% homologous at the amino acid level—the same degree of homology that murine α_1-PI shares with its human counterpart. Analysis of the human sequence shows that it is identical to the published sequence of human α_1-antichymotrypsin[8,9] except for two amino acid differences. One of the amino acid differences places the termination codon 32 nucleotides upstream of the published triplet due to the addition of an A at nucleotide position 659. Therefore, murine contrapsin and human α_1-antichymotrypsin are highly homologous.

Recently, a protease inhibitor 'superfamily' has been described which includes the human serine protease inhibitors α_1-PI (ref. 10), antithrombin III (ref. 11) and α_1-antichymotrypsin[9] and two proteins having no reported inhibitor activities—chicken ovalbumin[12] and rat angiotensinogen[13]. We would now include mouse contrapsin in this 'superfamily'. We have aligned the sequences of all the members of this superfamily with our sequences and find that they have 15 amino acids in common. It is of interest that in all the members, except angiotensinogen, there is conservation of the two glutamic acid residues designated by arrows in Fig. 1*a*. Angiotensinogen contains only the first of the two residues. Two well characterized mutations[14–17] that occur in human α_1-PI, the S and Z polymorphisms which lead to low serum levels of the protein, result from substitutions at these sites. Conservation of these two amino acids suggests that these residues have an important role in the stabilization and secretion of this family of proteins.

Protease inhibitors are traditionally described according to their reactivity to proteases *in vitro* and the specificity of the inhibitor is determined by the reactive centre region of the protein. *In vitro* the protease may specifically cleave within the reactive centre between two amino acids at positions designated P_1 and P_1'. Studies involving substitution of different amino acids within the reactive centre suggest that the residue at the P_1 position is consistently the most important in determining the specificity of the inhibitor[18]; this was substantiated by a naturally occurring mutation in α_1-PI called α-PI Pittsburgh, in which a single amino acid change at the P_1 position produced a protein having no α_1-PI activity but possessing a several thousand-fold increase in antithrombin activity[19] (Fig. 2).

The reactive centre regions of human α_1-PI and α_1-antichymotrypsin are located towards the C-termini of the proteins. Alignment of the mouse inhibitor sequences with the related

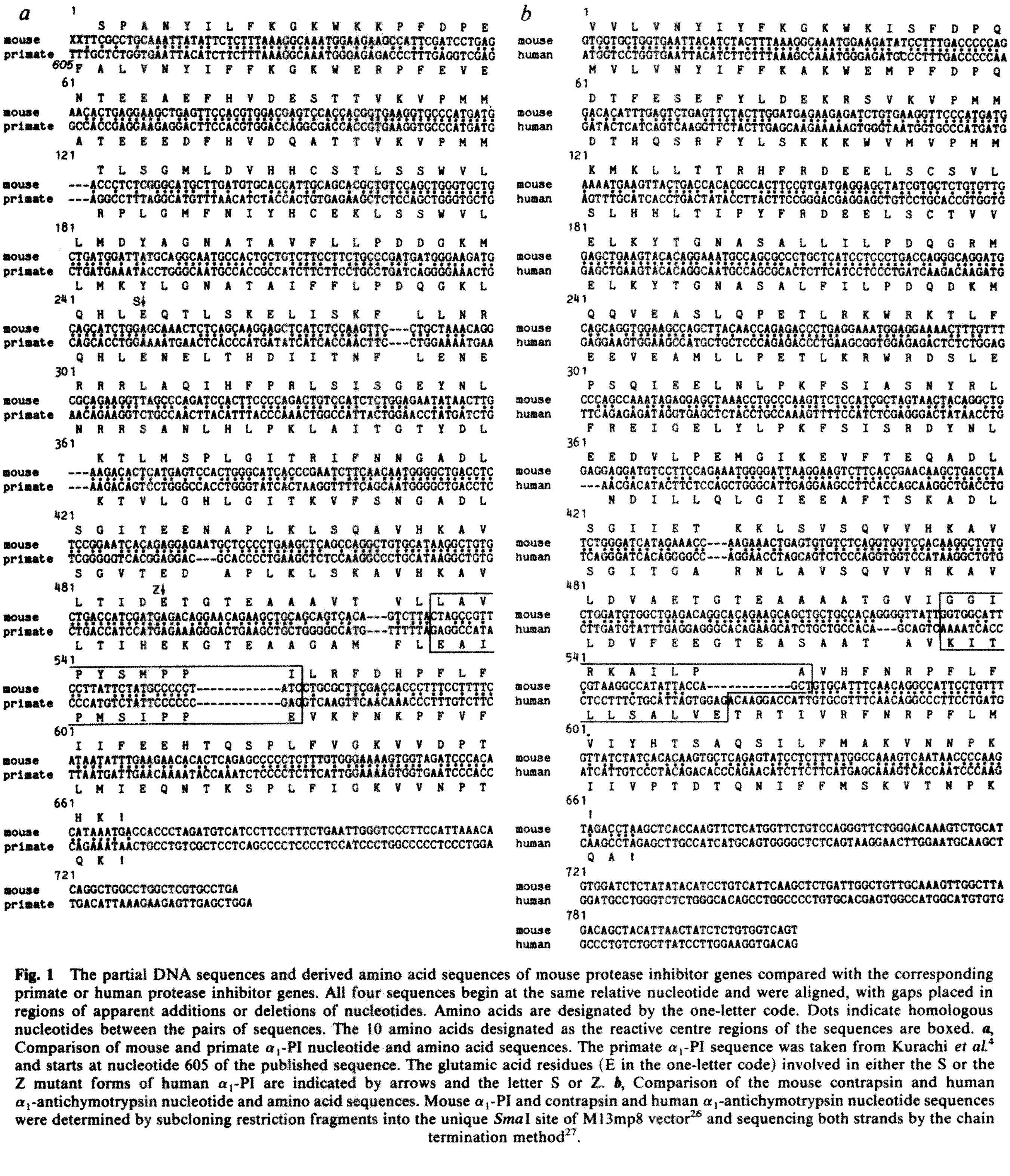

Fig. 1 The partial DNA sequences and derived amino acid sequences of mouse protease inhibitor genes compared with the corresponding primate or human protease inhibitor genes. All four sequences begin at the same relative nucleotide and were aligned, with gaps placed in regions of apparent additions or deletions of nucleotides. Amino acids are designated by the one-letter code. Dots indicate homologous nucleotides between the pairs of sequences. The 10 amino acids designated as the reactive centre regions of the sequences are boxed. *a*, Comparison of mouse and primate α_1-PI nucleotide and amino acid sequences. The primate α_1-PI sequence was taken from Kurachi *et al.*[4] and starts at nucleotide 605 of the published sequence. The glutamic acid residues (E in the one-letter code) involved in either the S or the Z mutant forms of human α_1-PI are indicated by arrows and the letter S or Z. *b*, Comparison of the mouse contrapsin and human α_1-antichymotrypsin nucleotide and amino acid sequences. Mouse α_1-PI and contrapsin and human α_1-antichymotrypsin nucleotide sequences were determined by subcloning restriction fragments into the unique *Sma*I site of M13mp8 vector[26] and sequencing both strands by the chain termination method[27].

human sequences allowed us to predict the positions of the reactive centre regions in the mouse inhibitor (Fig. 1). The reactive centre regions of the human and mouse α_1-PI differ by several amino acids (Fig. 2), most importantly, perhaps, at the P_1 position which in the human is a methionine and in the mouse a tyrosine. A major function of the human α_1-PI is the inhibition of neutrophil-secreted elastase[20,21]. Similarly, murine α_1-PI is a potent inhibitor of mouse elastase ($K_i = 2.1 \times 10^{-11}$)[2], suggesting that the physiological specificity of these inhibitors is the same. However, the specificity of the murine α_1-PI against some proteases *in vitro* differs from that of the human inhibitor. In this case, the difference at the P_1 position may affect the inhibitory properties of these two proteins *in vitro* but is probably of no physiological consequence.

In contrast, mouse contrapsin and human α_1-antichymotrypsin differ greatly in their specificities; that is, contrapsin is active against trypsin-like proteases[1,2] and α_1-antichymotrypsin inhibits chymotrypsin-like proteases[20,22,23]. Consistent with this, the reactive centre regions of these sequences differ substantially. Over the stretch of 10 amino acids that encompasses the reactive centre, one amino acid is shared (Fig. 2), with only 30% homology at the nucleotide level (Fig. 1*b*), whereas the nucleotide homology surrounding this region is strikingly high. At the P_1–P_1' position, the mouse inhibitor contains Lys-Ala residues in contrast to the human Leu-Ser residues. It has been predicted that an inhibitor with a lysine residue at the P_1 position would be more effective against trypsin-like proteases[24] than chymotrypsin-like proteases. The P_1' position

Protease inhibitor	P_5	P_4	P_3	P_2	P_1	P_1'	P_2'	P_3'	P_4'	P_5'
mouse contrapsin	GLY	GLY	ILE	ARG	LYS /	ALA	ILE	LEU	PRO	ALA
human α_1-achy	LYS	ILE	THR	LEU	LEU /	SER	ALA	LEU	VAL	GLU
mouse α_1-PI	LEU	ALA	VAL	PRO	TYR /	SER	MET	PRO	PRO	ILE
human α_1-PI	GLU	ALA	ILE	PRO	MET /	SER	ILE	PRO	PRO	GLU
α_1-PI Pittsburgh					(ARG)					
human ATIII	VAL	ILE	ALA	GLY	ARG /	SER	LEU	ASN	PRO	ASN
BPTI	THR	GLY	PRO	CYS	LYS /	ALA	ARG	ILE	ILE	ARG

Fig. 2 Comparison of the reactive centre regions of several protease inhibitors. α_1-PI Pittsburgh[18], a mutant form of human α_1-PI differing by one amino acid situated at the P_1 site and which has acquired antithrombin activity, is compared with human antithrombin III (ATIII)[9-11] which has the same amino acid at the P_1 site as α_1-PI Pittsburgh. Bovine pancreatic trypsin inhibitor (BPTI)[25,28] is an example of a protein with trypsin inhibitory activity having a P_1–P_1' site identical to that of mouse contrapsin. α_1-achy, α_1-antichymotrypsin.

is of interest here as the mouse protein is the only member of this family of inhibitors that does not have a serine at this position[18]; the functional significance of this is not known. However, a protein (bovine pancreatic trypsin inhibitor) (Fig. 2) from an unrelated family of protease inhibitors also has Lys-Ala at the P_1–P_1' position and, as predicted, exhibits antitrypsin activity[24,25]. We propose, therefore, that mouse contrapsin is closely related to human α_1-antichymotrypsin but has different inhibitory activity due to divergence within this short, functionally important stretch of amino acid residues.

In man, α_1-PI and α_1-antichymotrypsin are two of the most abundant serum protease inhibitors. In the mouse, the two most prevalent inhibitors are α_1-PI and contrapsin. Attempts to demonstrate a contrapsin-like protein in man[1,2] and an α_1-antichymotrypsin-like inhibitor in rodents (H. Bauman, unpublished results) have failed. Thus, contrapsin and α_1-antichymotrypsin are probably equivalent, and we propose that the genes for contrapsin and α_1-antichymotrypsin are descendants of a single gene that have evolved, specifically within the reactive centre regions, to encode proteins with different activities. This has occurred since the time of rodent and primate divergence.

We thank Dr Jack Gauldie for helpful discussions and for communicating data, and Dr Lowell Sheflin for teaching the DNA sequencing techniques. We also thank Dr Derek Woods for supplying the human cDNA library.

Received 29 May; accepted 4 July 1984.

1. Takahori, H. & Sinohara, H. *J. biol. Chem.* **257**, 2438–2446 (1982).
2. Takahori, H. & Sinohara, H. *J. Biochem.* **93**, 1411–1419 (1983).
3. Barth, R. K., Gross, K. W., Gremke, L. C. & Hastie, N. D. *Proc. natn. Acad. Sci. U.S.A.* **79**, 500–504 (1982).
4. Kurachi, K. *et al. Proc. natn. Acad. Sci. U.S.A.* **78**, 6826–6830 (1981).
5. Sarich, V. *Nature* **265**, 24–28 (1977).
6. Wilson, A. C., Carlson, S. S. & White, T. J. *A. Rev. Biochem.* **46**, 573–639 (1977).
7. Woods, D. E., Markham, A. F., Ricker, A. T., Goldberger, G. & Colton, H. R. *Proc. natn. Acad. Sci. U.S.A.* **79**, 5661–5665 (1982).
8. Morii, M. & Travis, J. *J. biol. Chem.* **258**, 12749–12752 (1983).
9. Chandra, T., Stackhouse, R., Kidd, V., Robson, J. & Woo, S. *Biochemistry* **22**, 5055–5061 (1983).
10. Travis, J., Garner, D. & Bowen, J. *Biochemistry* **17**, 5647–5651 (1978).
11. Carrell, R., Owen, M., Brennan, S. & Vaughn, L. *Biochem. biophys. Res. Commun.* **91**, 1032–1037 (1979).
12. Hunt, L. T. & Dayhoff, M. O. *Biochem. biophys. Res. Commun.* **95**, 864–871 (1980).
13. Doolittle, R. F. *Science* **222**, 417–419 (1983).
14. Owen, M. C. & Carrell, R. W. *Br. med. J.* **i**, 130–131 (1976).
15. Jeppsson, J. O. *FEBS Lett.* **65**, 195–197 (1976).
16. Yoshida, A., Lieberman, J. J., Gaidulis, L. & Ewing, C. *Proc. natn. Acad. Sci. U.S.A.* **73**, 1324–1328 (1976).
17. Carrell, R. W. *et al. Nature* **298**, 329–334 (1982).
18. Laskowski, M. & Kato, I. *A. Rev. Biochem.* **49**, 593–626 (1980).
19. Owen, M. C., Brennan, S. O., Lewis, J. H. & Carrell, R. W. *New Engl. J. Med.* **309**, 694–698 (1983).
20. Beatty, K., Bieth, J. & Travis, J. *J. biol. Chem.* **255**, 3931–3934 (1980).
21. Gauthier, F., Fryskmak, U., Ohlsson, L. & Bieth, J. *Biochim. biophys. Acta* **700**, 178–183 (1982).
22. Travis, J., Bowen, J. & Baugh, R. *Biochemistry* **17**, 5651–5656 (1978).
23. Laine, A., Davril, M. & Hayem, A. *Biochem. biophys. Res. Commun.* **105**, 186–193 (1982).
24. Laskowski, M. & Sealock, R. W. *Enzymes* **3**, 375–473 (1971).
25. Anderson, S. & Kingston, I. B. *Proc. natn. Acad. Sci. U.S.A.* **80**, 6838–6842 (1983).
26. Messing, J. & Veira, J. *Gene* **19**, 269–276 (1982).
27. Sanger, F., Nicklen, S. & Coulson, A. R. *Proc. natn. Acad. Sci. U.S.A.* **74**, 5463–5467 (1977).
28. Kassel, B., Radicevic, M., Ansfield, M. J. & Laskowski, M. *Biochem. biophys. Res. Commun.* **18**, 225–258 (1965).

Erythrocyte spectrin is comprised of many homologous triple helical segments

David W. Speicher & Vincent T. Marchesi

Department of Pathology, Yale University,
Yale University School of Medicine,
PO Box 3333, New Haven, Connecticut 06510, USA

Spectrin is an $\alpha\beta$ heterodimeric protein (molecular weight (M_r) = 460,000) which is a major component of the erythrocyte membrane skeleton[1-8]. The membrane skeleton also includes actin (band 5) and is attached to the membrane via non-covalent associations with two linking proteins[9-12]. Recently we have reported the amino acid sequence of a peptide of molecular weight 80,000 which comprises the NH_2-terminal one-third of the α subunit[13,14]. This α-subunit peptide contains multiple homologous non-identical sequences with a periodicity of 106 amino acids and an approximate molecular weight of 12,000. It was also established that spectrin is not related to any other proteins whose sequence was known. We now report additional amino acid sequence of peptides representative of other domains of both spectrin subunits. The results suggest that most of the human erythrocyte spectrin molecule is comprised of homologous segments with a 106 amino acid (M_r 12,000) length per segment. Each homologous 106-amino acid segment may be folded into a triple helical structure with a short non-helical region connecting adjacent units.

Amino acid sequences from the α and β subunits which exhibit homologous structure are presented in Fig. 1. The sequences of the first nine repeats are derived from the α-1 and α-2 domains and provide nearly complete sequence information on the NH_2-terminal half of the α subunit.

The degrees of homology between each of the sequences in Fig. 1 were analysed using the computer programs ALIGN and RELATE with either an identity or mutational data matrix. In all pairwise comparisons of sequences, homology was statistically significant (s.d. > 5), and there was no evidence for any repetitive structure smaller than 106 amino acids.

When all homologous sequences are compared as a group, only a single amino acid, tryptophan at position 45, is completely invariant in all sequences. A number of other positions (indicated by arrows in Fig. 1*a*) are strongly conserved and might have critical structural roles. A single amino acid predominates in each of these positions with occasional conservative substitutions. Positions 1, 12, 15, 26, 35 and 46 contain hydrophobic residues, but unlike other positions where any hydrophobic residue is permitted, these six positions exhibit a strong preference for I, W, L, L, F and I respectively (single-letter amino acid code). Several other highly conserved positions involve charged residues which might be involved in critical salt bridges. Arginine is preferred at position 22, lysine occurs at position 71 and aspartate predominates at positions 38 and 41. Either glutamate or aspartate occurs at position 48 in most sequences. Histidine is strongly conserved at positions 72 and 101.

Figure 2 summarizes available sequence information. So far, the sequence of 1,435 residues or 35% of the total molecule has been determined. If most of the spectrin molecule is composed of 106-amino acid repeat units, approximately 38 repeat units would be present. Evidence of 22 homologous repeat units throughout both subunits has already been obtained, thus it is likely that most of the spectrin molecule is made up of a single type of repetitive structure. The positions of known sequences are schematically represented in Fig. 2*b* and *c*. Repeat units have been numbered starting at the NH_2-terminal ends of the α and β subunits. The two subunits are aligned antiparallel with respect to NH_2-terminal orientation when in the dimer form[14-16]. The NH_2-terminals of both subunits are blocked but these blocked termini are removed during mild trypsin treatment, and both the α-T80 peptide and the β-T74 peptide have free NH_2-termini. The COOH-terminal region of the β subunit beyond repeat 18 in Fig. 2 contains the four covalent

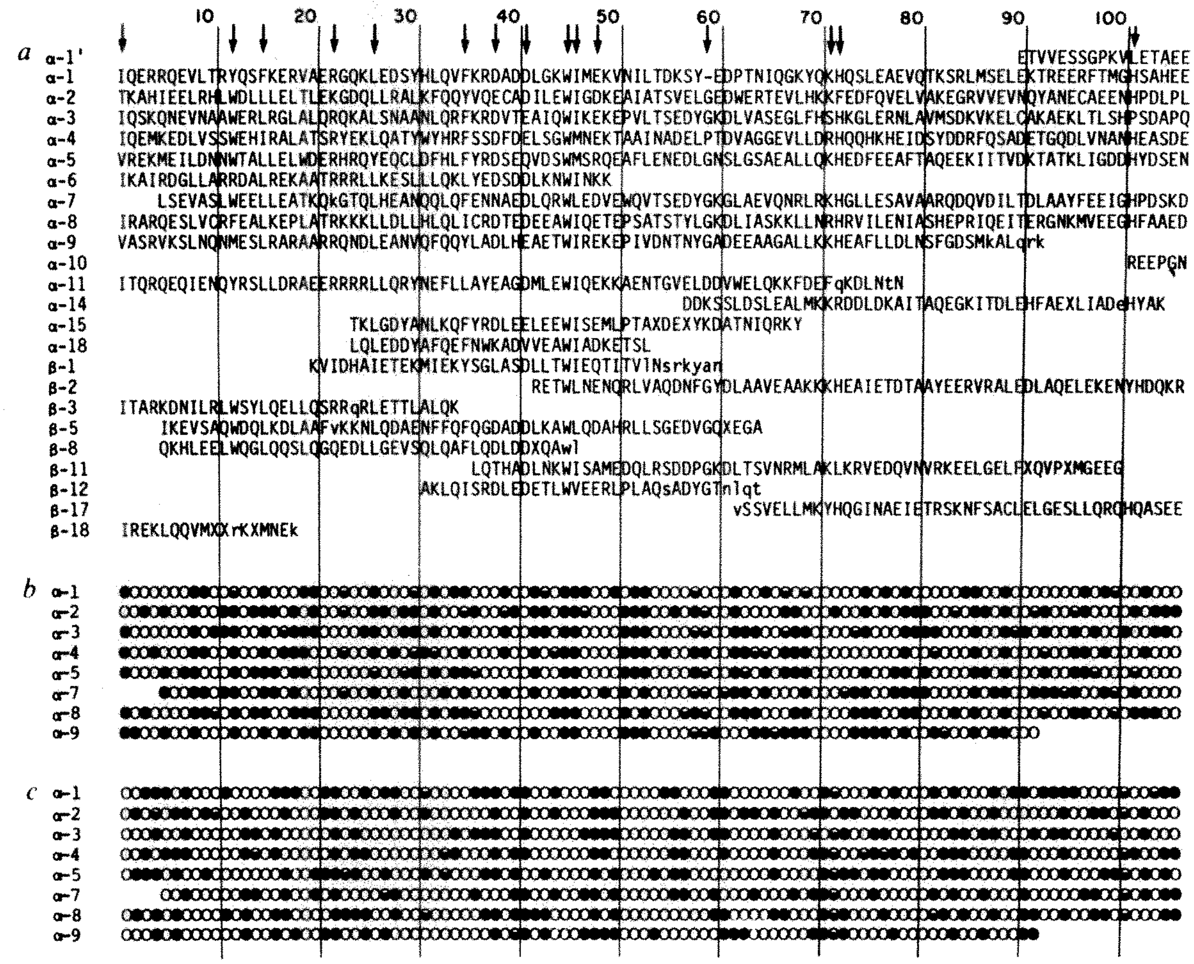
10 20 30 40 50 60 70 80 90 100
a
α-1' ETVVESSGPKVLETAEE
α-1 IQERRQEVLTRYQSFKERVAERGQKLEDSYHLQVFKRDADDLGKWIMEKVNILTDKSY-EDPTNIQGKYQKHQSLEAEVQTKSRLMSELEKTREERFTMGHSAHEE
α-2 TKAHIEELRHLWDLLLELTLEKGDQLLRALKFQQYVQECADILEWIGDKEAIATSVELGEDWERTEVLHKKFEDFQVELVAKEGRVVEVNQYANECAEENHPDLPL
α-3 IQSKQNEVNAAWERLRGLALQRQKALSNAANLQRFKRDVTEAIQWIKEKEPVLTSEDYGKDLVASEGLFHSHKGLERNLAVMSDKVKELCAKAEKLTLSHPSDAPQ
α-4 IQEMKEDLVSSWEHIRALATSRYEKLQATYWYHRFSSDFDELSGWMNEKTAAINADELPTDVAGGEVLLDRHQQHKHEIDSYDDRFQSADETGQDLVNANHEASDE
α-5 VREKMEILDNNWTALLELWDERHRQYEQCLDFHLFYRDSEQVDSWMSRQEAFLENEDLGNSLGSAEALLQKHEDFEEAFTAQEEKIITVDKTATKLIGDDHYDSEN
α-6 IKAIRDGLLARRDALREKAATRRRLLKESLLLQKLYEDSDDLKNWINKK
α-7 LSEVASLWEELLEATKQkGTQLHEANQQLQFENNAEDLQRWLEDVEWQVTSEDYGKGLAEVQNRLRKHGLLESAVAARQDQVDILTDLAAYFEEIGHPDSKD
α-8 IRARQESLVCRFEALKEPLATRKKKLLDLLHLQLICRDTEDEEAWIQETEPSATSTYLGKDLIASKKLLNRHRVILENIASHEPRIQEITERGNKMVEEGHFAAED
α-9 VASRVKSLNQNMESLRARAARRQNDLEANVQFQQYLADLHEAETWIREKEPIVDNTNYGADEEAAGALLKKHEAFLLDLNSFGDSMkALqrk
α-10 REEPGN
α-11 ITQRQEQIENQYRSLLDRAEERRRRLLQRYNEFLLAYEAGDMLEWIQEKKAENTGVELDDVWELQKKFDEFqKDLNtN
α-14 DDKSSLDSLEALMKKRDDLDKAITAQEGKITDLEHFAEXLIADeHYAK
α-15 TKLGDYANLKQFYRDLEELEEWISEMLPTAXDEXYKDATNIQRKY
α-18 LQLEDDYAFQEFNWKADVVEAWIADKETSL
β-1 KVIDHAIETEKMIEKYSGLASDLLTWIEQTIITVlNsrkyan
β-2 RETWLNENQRLVAQDNFGYDLAAVEAAKKKHEAIETDTAAYEERVRALEDLAQELEKENYHDQKR
β-3 ITARKDNILRLWSYLQELLQSRRqRLETTLALQK
β-5 IKEVSAQWDQLKDLAAFvKKNLQDAENFFQFQGDADDLKAWLQDAHRLLSGEDVGQXEGA
β-8 QKHLEELWQGLQQSLQGQEDLLGEVSQLQAFLQDLDDXQAwl
β-11 LQTHADLNKWISAMEDQLRSDDPGKDLTSVNRMLAKLKRVEDQVNVRKEELGELFXQVPXMGEEG
β-12 AKLQISRDLEDETLWVEERLPLAQsADYGTnlqt
β-17 vSSVELLMKYHQGINAEIETRSKNFSACLELGESLLQRCHQASEE
β-18 IREKLQQVMXXrKXMNEk
b
α-1
α-2
α-3
α-4
α-5
α-7
α-8
α-9
c
α-1
α-2
α-3
α-4
α-5
α-7
α-8
α-9

Fig. 1 The 106-amino acid repeat unit. *a*, Homologous sequences of the α and β subunits were aligned using the computer programs ALIGN and RELATE as previously described[14] and are represented using the single-letter code. *b*, The locations of hydrophobic residues within the indicated α-subunit repeat units are represented. An extended hydrophobic series was used: ●—I, V, W, F, L, M, A, P; ◒—Y, C, G. *c*, The locations of charged residues in the indicated eight repeat units are represented. ●—E, D, K, R; ◒—H. The sequence (α-1' to α-6) of an α-subunit 80,000-dalton tryptic peptide previously named the α-I domain[13] and the sequence (α-7 to α-10) of a peptide of molecular weight 46,000 representing the α-II domain were determined using several overlapping groups of proteolytically cleaved peptides (D.W.S., G. Davis, V.T.M., manuscript in preparation). The remaining sequences with the exception of β-2, β-3 were obtained by extended automated Edman degradation of peptides which had previously been aligned by peptide mapping[15,28]. The sequencing methodology used here has been described previously[13]. The peptides were produced by mild proteolytic treatment[15], purified on two-dimensional gels and electroeluted[29], desalted by HPLC gel filtration in the presence of 0.2 M Tris-HCl, 8 M urea, 10 mM 2-mercaptoethanol *p*H 7.0 and dialysed extensively before sequence analysis. The amount of peptide used for sequencing ranged from 0.5 to 5 nmoles per run. Because some of these sequences represent a single extended run, the COOH-terminal portions of these sequences should be regarded as tentative. The β-2, β-3 sequence is from an 11,000-M_r CNBr fragment near the NH_2-terminal of the β subunit which bound to calmodulin columns in the presence of 6 M urea (D. E. Sears, J. S. Morrow, D.W.S. and V.T.M., manuscript in preparation). Unidentified residues are represented as X and tentatively identified residues are represented by lower case letters. Sequences from each subunit are presented in the order in which they occur in the total sequence, starting from the NH_2-terminal end of the polypeptide chain. Optimal alignment of all the illustrated sequences within the 106-residue repeat unit required only a single one residue gap in α-1 at position 59. There is no simple way to define the start point or phase of the repeat unit without knowledge of the gene structure. We had initially assigned the start point based on the tentative hypothesis that the first 17 residues of the α-T80 peptide (α-1') were unrelated to the rest of the molecule[14]. We have since found that statistically significant correlations of homology cannot be made on 17-residue segments. It is unlikely that this phasing correlates precisely with either the gene structure or protein conformational units (see text and Fig. 3), but the current convention will be retained until more definitive data are available. Many sequences illustrated here are continuous with the next line and can be read in the same manner as text that is, sequences which extend to the right end of a repeat unit are contiguous with the left end of the consecutively numbered repeat. This continuity and the approximate placement of remaining sequence segments within the two spectrin subunits is diagrammatically represented in Fig. 2. Arrows indicate positions within the repeat unit which are especially well conserved in all sequences presented.

phosphorylation sites characterized by Harris and Lux[16]. This region is ~10,000 daltons and has not been sequenced. It may be unrelated to the general spectrin repeat unit, because its amino acid composition is quite different from the compositions of peptides having homologous structure (refs 14, 16 and data not given). One segment of the α-subunit (α-10) also appears to be unrelated to the basic 106-repeat unit.

The presence of repetitive sequences within the spectrin molecule is not novel although the large number of intramolecular repeats is somewhat unusual. A number of proteins with internal repetitive structure have been identified, and current concepts of molecular evolution indicate that larger proteins have probably evolved from smaller precursors via gene fusions involving either unrelated genes or duplicated genes[17–20]. In the latter case the resulting larger proteins have internal repeats which undergo independent mutation, evolving to non-identical but homologous sequences. Presumably spectrin has evolved in such a manner, and the large number of repeats suggests that spectrin evolution involved many gene duplication and fusion stages.

a

Subunit	Total Residues	Residues Sequenced	Repeat Size	Total Possible Repeats	Identified Repeats
ALPHA	2100	1080	106	20	14
BETA	1950	355	106	18	9
TOTAL	4050	1435	106	38	23

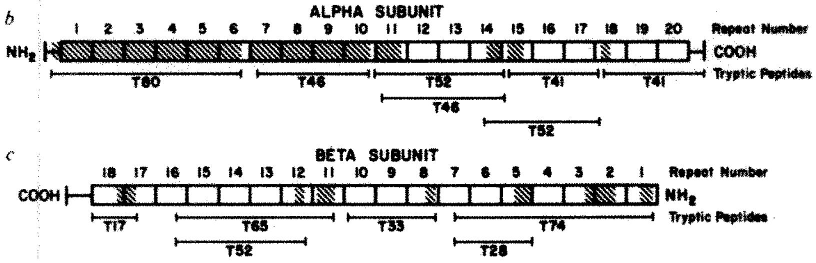

Fig. 2 Schematic representation of sequence positions within the spectrin subunits. ***a***, Summary of sequence analysis. Several sequences are known in addition to the sequences represented in Fig. 1. These include 90 residues of the sequence from the α-10 segment which is not homologous to the rest of the molecule, partial sequence of the remainder of α-6, and several other short sequences. For simplicity each of the 106-amino acid segments will be referred to here as a repeat unit, and the apparently unique α-10 which may have been related to the remainder of the molecule at one time (see text) will be referred to as a non-homologous repeat unit. ***b***, The α subunit (M_r 240,000) is represented as being made up of 20 repeat units (106 amino acids and 12,000 daltons per repeat) numbered starting at the amino-terminal end. Small regions near the NH_2- and COOH-termini are believed to contain binding sites and these may be unique and unrelated to the repeat unit (ref. 14 and text). The positions of known sequences are represented by the cross-hatched areas. The tryptic peptides which were used for sequence analysis are represented and have been aligned based on previous peptide mapping analysis[15,28]. The exact positions of sequences near the COOH-terminus of the α subunit are necessarily approximate and are based on three assumptions; (1) the α subunit is approximately 240,000 daltons and contains 20 repeats, (2) each repeat is 106 amino acids and approximately 12,000 daltons, and (3) several tryptic peptides overlap in repeat 14. This last assumption is the most tentative and is based on the consistently low yield of the T52 peptide encompassing repeats 14–17, the small number of spots on peptide maps involving repeat 14, and the fact that combined masses of the previously described domain peptides exceed the mass of the intact chain[15,28]. There may also be additional overlaps between peptides represented here which have not yet been detected. Therefore the assignment of the indicated sequence to repeats 14, 15 and 18 are provisional but their relative order should be accurate. ***c***, The β subunit (M_r 220,000) is comprised of 18 repeat units plus the phosphorylated region on the COOH-terminal end of the polypeptide chain. This subunit has been positioned antiparallel to the α subunit to illustrate their relative arrangement in the dimer, as the subunits associate side to side in an antiparallel orientation (see text). Repeats have been numbered starting at the NH_2-terminal end. The positions of known sequences shown are represented by the cross-hatched areas and tryptic peptides which were used as sources of material for sequence analysis are also represented. The most ambiguous location of sequence segments in this subunit is the placement of the 11,000-dalton CNBr fragment in repeats 2 and 3. Based on mapping data, this sequence could either occupy the indicated position or be translocated 106 amino acids towards the COOH-terminal end and occupy corresponding portions of repeats 3 and 4. Remaining assignments of sequences seem to be unambiguous based on repeat size, peptide size and previous mapping data.

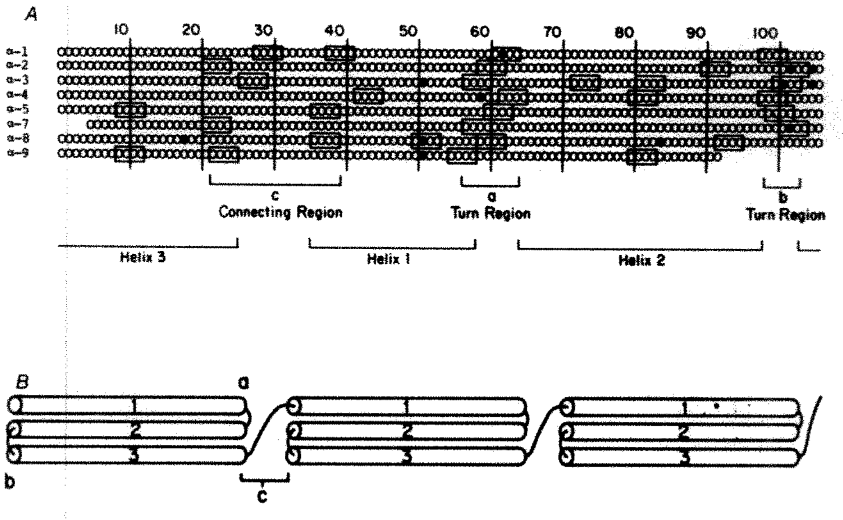

Fig. 3 Localization of reverse turns and connecting region within the 106-amino acid repeat unit. *A*, Diagrammatic representation of the eight repeat units of the α subunit corresponding to the sequences in Fig. 1. *B*, Three consecutive triple helical segments. The arrangement of helices, reverse turns (a and b), and the connecting region (c) between triple helical segments correspond to the similarly labelled regions of *A*. **Methods**: Reverse turns were calculated using P_α, P_β and P_T values, and positional frequencies for reverse turns as given by Chou and Fasman[22]. Average values of P_α, P_β and P_T were calculated over all possible 4-residue segments. Positional frequencies for reverse turns were calculated for 4-residue sequences with $P_\alpha < P_T > P_\beta$ and sequences with positional frequencies greater than 0.70×10^{-4} were scored as reverse turns if no other reverse turns with higher positional frequency values were predicted to occur within six residues. Two turn regions (a and b) were identified where most of the repeat units contained a predicted turn. A connecting region is also indicated where the helices probably break but are not in a turn configuration. Proline residues are indicated by shaded dots and the approximate locations of helical segments are given. It is quite likely that small amounts of other types of secondary structure also exist in the areas designated here as helices. One particularly interesting segment is between position 50 and 60 of the repeat unit. The entire segment between region c and turn a cannot be a single continuous helix in all repeats because three of the eight repeats in Fig. 4 have a proline at position 51. This would necessitate at least a kink in the helix at this point for these three repeats or it may signal a transition to another type of structure. Note that most of the repeats have a high β potential in this area[14].

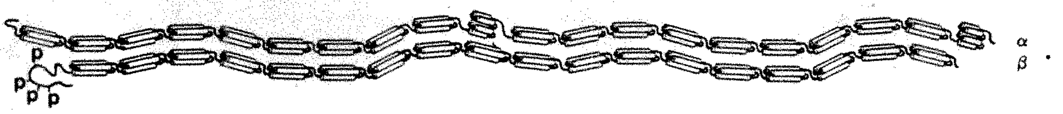

Fig. 4 A model of the spectrin dimer. The α and β subunits are composed of multiple triple helical segments connected by short non-helical regions. The subunits are antiparallel with the NH_2-terminus of the α subunit on the left. Each triple helical segment contains ~106 amino acids, corresponding to the periodicity observed from sequence data (Fig. 1). The tenth segment in the α subunit is not homologous and probably has a more compact globular structure and is represented here by shorter helices simply to illustrate a more globular structure. The twentieth segment of the α subunit may have a common evolutionary origin to the tenth repeat (data not given) and hence is represented in a similar manner. The COOH-terminal region of the β subunit contains four phosphorylation sites and may also be unrelated to the triple helical repetitive structure.

The Chou and Fasman predictive method[21,22] has previously been applied to an analysis of 595 residues of the α-1 domain[14]. This model can now be refined further, taking into account the existence of the 106-amino acid repeat throughout all domains of the molecule. Each of these repeats should have approximately the same conformation, as they were derived from a single ancestral gene, and it is well established that chain folding of related gene products is even more strongly conserved than amino acid sequence[19,20]. This preservation of chain folding within spectrin repeat units is also suggested by the well defined zones occupied by either hydrophobic or charged residues (Fig. 1*b*, *c*). In most positions where hydrophobic residues occur, the zones are especially well defined. Two additional properties of spectrin provide essential information on the nature of spectrin secondary structure. The intact molecule and the isolated subunits are highly α-helical (60–80%), with little or no β structure as determined by circular dichroism measurements[23,24]. In addition, the molecule is a long, thin, highly flexible rod ~1,000 Å in length[25,26], and this flexibility seems to be imparted by the presence of many hinge points throughout the length of the molecule. We also know that the NH_2-terminus is near one physical end of each subunit and the COOH-terminal is near the opposite end[14,15,27].

The eight repeat units presented in Fig. 1*b*, *c* were analysed further to determine a protein conformational model (Fig. 3). Turn regions (a and b) have been assigned to the two areas in the repeat unit where turns were predicted in most of the repeats. A connecting region c, corresponding to at least part of the region centred at residue 30, is probably a short non-helical loop. These three regions (a, b, c) divide the 106-amino acid repeat into three parts corresponding to the helices of a triple helical segment. The size of the basic structural unit coincides with the basic genetic unit.

A model emphasizing important structural features of the spectrin molecule is given in Fig. 4. The α and β subunits are both made up of many homologous segments. Each segment, which contains 106 amino acids (~12,000 daltons) is composed of a triple helical segment. The connecting region between adjacent triple helical segments is not helical and may provide the observed flexibility of the molecule. The two subunits are oriented in an antiparallel manner with the NH_2-termini at opposite ends of the dimeric molecule.

This work was supported by USPHS grants GM21714 and AM27932. We thank Gary Davis and Marcia Bologna for their assistance and collaboration, Anthony Lanzetti for technical assistance and, Toni Suarez for secretarial assistance.

Received 12 March; accepted 28 June 1984.

1. Marchesi, V. T. *Blood* **61**, 1–11 (1983).
2. Haest, C. W. M. *Biochim. biophys. Acta* **694**, 331–352 (1982).
3. Goodman, S. R. & Shiffer, K. *Am. J. Physiol.* **244**, C121–C141 (1983).
4. Calvert, R., Bennett, P. & Gratzer, W. *Eur. J. Biochem.* **107**, 355–361 (1980).
5. Ralston, G. B. *Biochim. biophys. Acta* **455**, 163–172 (1976).
6. Morrow, J. S. & Marchesi, V. T. *J. Cell Biol.* **88**, 463–468 (1981).
7. Zweig, S. E. & Singer, S. J. *Biochem. biophys. Res. Commun.* **88**, 1147–1157 (1979).
8. Speicher, D. W. & Marchesi, V. T. *J. Cell Biochem.* **18**, 479–492 (1982).
9. Ungewickell, E., Bennett, P. M., Calvert, R., Ohanian, V. & Gratzer, W. B. *Nature* **280**, 811–814 (1979).
10. Cohen, C. & Branton, D. *Nature* **279**, 163–165 (1979).
11. Tyler, J., Hargreaves, W. & Branton D. *Proc. natn. Acad. Sci. U.S.A.* **76**, 5192–5196 (1979).
12. Bennett, V. & Stenbuck, P. J. *J. biol. Chem.* **254**, 2533–2541 (1979).
13. Speicher, D. W., Davis, G., Yurchenco, P. D. & Marchesi, V. T. *J. biol. Chem.* **258**, 14931–14937 (1983).
14. Speicher, D. W., Davis, G. & Marchesi, V. T. *J. biol. Chem.* **258**, 14938–14947 (1983).
15. Speicher, D. W., Morrow, J. S., Knowles, W. J. & Marchesi, V. T. *J. biol. Chem.* **257**, 9093–9101 (1982).
16. Harris, H. W. Jr & Lux, S. E. *J. biol. Chem.* **255**, 11512–11520 (1980).
17. Barker, W. C., Ketcham, L. K. & Dayoff, M. O. in *Atlas of Protein Sequences and Structure* Vol. 5, Suppl. 3 (ed. Dayhoff, M. O.) 359–362 (National Biomedical Research Foundation, Washington DC, 1978).
18. Schwartz, R. M. & Dayhoff, M. O. in *Atlas of Protein Sequences and Structure* Vol. 5, Suppl. 3 (ed. Dayhoff, M. O.) 353–358 (National Biomedical Research Foundation, Washington DC, 1978).
19. Schulz, G. E. & Schirmner, R. H. in *Principles of Protein Structure* (ed. Cantor, C. R.) 166–205 (Springer, New York, 1979).
20. Pink, J. R. L. in *Biochemical Evolution* (ed. Gutfreund, H.) 231–260 (Cambridge University Press, 1981).
21. Chou, P. Y. & Fasman, G. D. *A. Rev. Biochem.* **47**, 251–276 (1978).
22. Chou, P. Y. & Fasman, G. D. *Adv. Enzym. Related Areas molec. Biol.* **47**, 45–148 (1978).
23. Hudson, J. R. & Ralston G. B. *Biochim. biophys. Acta* **535**, 169–177 (1978).
24. Calvert, R., Ungewickell, E. & Gratzer, W. *Eur. J. Biochem.* **107**, 363–367 (1980).
25. Shotten, D., Burke, B. & Branton, D. *Biochim. biophys. Acta* **536**, 313–317 (1978).
26. Shotten, D., Burke, B. & Branton, D. *J. molec. Biol.* **181**, 303–329 (1979).
27. Morrow, J. S., Speicher, D. W., Knowles, W. J., Hsu, C. J. & Marchesi, V. T. *Proc. natn. Acad. Sci. U.S.A.* **77**, 6592–6596 (1980).
28. Speicher, D. W., Morrow, J. S., Knowles, W. J. & Marchesi, V. T. *Proc. natn. Acad. Sci. U.S.A.* **77**, 5673–5677 (1980).
29. Knowles, W. J. & Bologna, M. L. *Meth. Enzym.* **965**, 305–313 (1983).

Friends and their foes

Gordon Conway

The Environmental Crisis: A Handbook for all Friends of the Earth.
Edited by Des Wilson.
Heinemann Educational: 1984. Pp. 196. Hbk £13.95; pbk £4.50, $10.
Crisis and Conservation: Conflict in the British Countryside.
By Charlie Pye-Smith and Chris Rose.
Penguin: 1984. Pp.213. Pbk £3.95.

FOURTEEN years ago, when the British arm of Friends of the Earth (FoE) was founded, the world seemed to be heading for environmental disaster. The Friends were a tiny band, valiantly trying to stem the surging tide of pollution and bring wisdom to the management of dwindling resources. Fortunately, things have not turned out to be quite as bad as was forecast. Food production per capita has significantly increased in many Third World countries and birth rates are falling. We still have oil and coal in abundance. The end of the world is not going to come from ozone depletion and although increasing carbon dioxide and acid deposition may result in severe local disruption, the effects are unlikely to amount to a global catastrophe. There is still much to be worried about but, given the political will, solutions to most environmental problems seem feasible.

If the Earth is likely to scrape by, it might be presumed that the environmentalists would lose their mission and momentum. But FoE, although remaining a relatively small group of activists, is still a force to be reckoned with. In Britain, today's environmental crisis is more about the kind of world people want to live in, how desires can be satisfied, hazards and nuisances removed and fears allayed, than it is about imminent global catastrophe. It is a shift in emphasis to which the campaigners have adjusted and the politicians are beginning to respond. The British Government has announced its intention to reduce lead in petrol and to introduce pesticide legislation. David Owen and David Steel, leaders of the Social Democratic and Liberal parties, have recently signed a Greenpeace statement on radioactive discharges, and in William Waldegrave we now have a minister who gives the impression of being for, and not merely of, the environment. Industry too is accommodating. Pesticide legislation has been welcomed by the British Agrochemicals Association and the Confederation of British Industry is agreeable to much greater public access to information on polluting discharges.

Britain has been fortunate in the style and leadership of its environmental lobby. Targets are chosen with care, the homework is done and the propaganda contains no greater misrepresentation or oversimplification than is the norm for more respectable and traditional lobbies. Although fundamentally serious, the campaigns have been witty and attractive, gaining broad public support.

In two of the chapters in *The Environmental Crisis*, Walter Patterson and Des Wilson recount the early and recent history of FoE. The battle roll extends from Rio Tinto Zinc, Schweppes returnable bottles, trade in endangered species, Save the Whale, recycled paper, allotments, Windscale, the Wildlife and Countryside Act and lead-free petrol to today's campaigns against Sizewell and pesticides, and for greater freedom of information. Many of them have been successful and most people would agree we are better off as a result.

Courtesy FoE.

The Friends at work, defending the Somerset Levels against agricultural interests in 1983.

The book is subtitled *A Handbook...* but this is a misnomer. Facts and figures are included but are only sufficient to get the campaigner into an argument; there is not enough to sustain a case against well-informed opposition. There is little new in the book for anyone expert in the field. It is better read as a series of essays — on pollution, wildlife, land use, transport, energy, conservation and waste — by leading figures in FoE.

The most eloquent contribution is Richard Sandbrook's chapter on the environmental debate. Whereas much of the rest of the book is parochial in scope, Sandbrook addresses the global issues. He attacks those in the environmental movement who seek the salvation of the world through the creation of numerous small, self-contained islands. The reality, he argues, is ecological and economic interdependence and, in consequence, there are few, if any, simple solutions to our problems. If we are to achieve a more sustainable and equitable world then there is no alternative to the hard grind of analysis and the energetic pursuit of solutions which, while not perfect, are at least a step in the right direction. One such step would be a sensible, long-term energy policy for Britain, and this proposal is well argued and supported in another chapter by Czech Conroy.

The most strident of the essays is by Chris Rose on "The Battle for the British Countryside". His arguments are elaborated in the second book reviewed here, *Crisis and Conservation*, co-written by Rose and Charlie Pye-Smith. This is a book about villains. Not surprisingly, chief among them are the farmers, forestry commissioners and water-authority members, together with their allies in the research institutes and universities. Less expectedly the Conservation Movement also comes under bitter attack. The Nature Conservancy Council, the Countryside Commissions and the Naturalists' Trusts are characterized as "dominated by people who are themselves farmers, foresters and landowners". Even FoE is criticized for being lured onto government committees.

The crime of this so-called "Old Guard" is that they believe farming and conservation can be reconciled. They seek consensus, cooperation and compromise while wildlife is being lost at an unprecedented rate. This seems to me unfair. There has been a long, and reasonably successful, tradition of voluntary agreements in British environmental policy. Such agreements, for example over the use of pesticides, can work providing the economic dice are not loaded against them. What *has* changed in the past few years has been the massive increase in the incentives for intensive farming consequent on Britain being subject to the Common Agricultural Policy (CAP). It is this which is making a policy of voluntary agreements ineffective and destroying the efforts of those who are working towards a compromise.

Pye-Smith and Rose provide a disturbing account of the destruction of British wildlife and habitats, but their book is weak on solutions. They believe planning controls are likely to be ineffective and they ignore the potential for changing the CAP. Their principal solution seems to be a land tax with exemptions for land of conservation or amenity value, yet there is no analysis of how this might work and it is not proposed with any confidence. The book ends with what amounts to a call for direct action: "Disorder, then, looks like being the order of the day". But disorder without policy or concrete solutions to put in place when the battle is won seems a mindless exercise. It will be a sad day if the environmental movement takes this road. ☐

Gordon Conway is Professor of Environmental Technology at Imperial College, University of London.

Foundations: fiction in fact

David E. H. Jones

Ascent to Orbit: The Technical Writings of Arthur C. Clarke.
By Arthur C. Clarke.
Wiley: 1984. Pp.226. £14.95, $19.95.

WHAT makes a good science fiction writer? Apart from literary talent and uninhibited imagination, he needs one special gift. He must have a great knowledge and love of science, and yet not feel guilty if he is occasionally unfaithful to her. He must imagine, delight in and develop the consequences of things he knows to be scientifically incredible; yet to make them real he must embed them in a matrix of sound scientific understanding.

Few writers have these attributes, but Arthur C. Clarke is one of them. In dozens of stories, some of them major achievements of the genre, he has displayed his unruly imagination. Now in *Ascent to Orbit*, his collected technical works, he shows us his grasp of the rules.

The book brings together 24 technical articles spanning the years 1938–1981, on topics from electronics and astronomy to rocket theory and mathematical recreations. At its core is a cluster of about a dozen papers written between 1945 and 1950 on aspects of space technology. They form a sort of Old Testament in Dr Clarke's literary output: a foundation of rigorous theory in contrast to the later New Testament of wildly visionary science fiction. In them Dr Clarke, as a member of the British Interplanetary Society, is spokesman for a small band of enthusiasts preparing the way for a new technology. Escape velocities, the theory of rockets and their mass-ratio, transmitter powers necessary for interplanetary communication, theory of optimal orbital-transfer manoeuvres, are all here.

Among these papers is the brief, almost throw-away note which caused the whole book to be published. It is a privately-circulated two-page document dated May 1945 and entitled "The Space-station: Its Radio Applications". A few months later an expanded and now-famous version was published in *Wireless World*. In this paper Dr Clarke proposes the geostationary communications satellite, 20 years before the first one was put into orbit. This wonderful prevision of what is now the central technology of the "global electronic village" won him the 1982 Marconi Award for communication technology, which in turn inspired him to assemble the book. Dr Clarke modestly disclaims the title of "Father of Satellite Communications". He was, he insists, only its godfather.

It is tempting to scan this book for the seeds that were later to flower in his science fiction. There are some overt themes, of course: space travel itself, ion-drive rockets, lunar colonies. But more subtly, the grain and detail of his fiction seem informed by the same respect for scientific and technical truth that is shown here. My favourite piece is not on space travel at all: it is "You're on the Glide Path — I Think", an account of his wartime experience as a development engineer with the first ground-controlled approach radar for aircraft landing. Dr Clarke describes the authentic feel of development work: the cams that revolved once during every approach unless they fell off their shafts, the calibration markers that vanished or were mis-identified, the aerial-rotation unit that chose the precise crucial moment to strip its gears. This is the sort of formative experience, I suspect, that gives his science fiction stories their credibility.

Arthur C. Clarke is, of course, an excellent writer. His style is effortlessly lucid and humorous, his papers always a pleasure to read. Some of them (for example his "Dynamics of Space Flight", first published in 1949) might well form a good introduction to their topics even today. His comments on them, interspersed throughout the book, constitute an informal scientific autobiography which has a charm and interest of its own. One section describes his work as a physics-abstractor in 1949 and 1950: "I am proud of the fact that I appear as a distinct second-order differential coefficient on the curve 'Thousands of *Physics Abstracts* since 1900' in Derek J. de Solla Price's *Science Since Babylon*".

That was the last salaried job he held. His income from writing and broadcasting was rising, and he decided to make it his full-time career. His New Testament period was about to commence.

One might define a truly great science fiction writer as one who makes a dramatic technical prediction, incredible or absurdly visionary at the time, which within his lifetime actually comes true. By this criterion, Arthur C. Clarke and the communications satellite is up there with H. G. Wells and the atomic bomb. □

David E.H. Jones is a guest staff member of the Physical Chemistry Department, University of Newcastle upon Tyne, and a science consultant to industry and the media. He is author of The Inventions of Daedalus: A Compendium of Plausible Schemes, *published by W.H. Freeman in 1982.*

Mixed interferons

Robert M. Friedman

Interferons and Their Applications.
Edited by P.E. Came and W.A. Carter.
Springer-Verlag: 1984. Pp.575. DM 460, $178.50.

IN THE past few years the cloning of the genes for human beta and gamma interferon, and for the subtypes of genes for alpha interferon, has both increased the supply of these interferons for clinical studies and led to the initiation of critical experiments on the control of the expression of this gene family. Many groups are now investigating the biological roles of the already well-characterized enzymes and active metabolites associated with the interferon system. Relatively recently, interferons have also been recognized as important immunomodulators and cell growth inhibitory substances.

Because of this wide range of biological activities, the publication of *Interferons and their Applications* is timely. The volume attempts "to catalogue the current understanding of interferons from different biomedical disciplines" in order "to assist the growing community of laboratory researchers and students who may come to share [the editors'] enthusiasm for long term, in-depth study of the interferon systems".

Sadly, however, the book does not attain these objectives, because of the manner in which it has been compiled; it is made up of 27 chapters of widely varied character and quality. Some chapters are excellent reviews, some are for the most part reports of the author's own work, and others are philosophical discussions, but almost all of the contributions are too short to be really useful.

The difficulty of coordinating a large number of authors has also led to omissions, numerous repetitions and sometimes, even more unfortunately, to contradictions in the material presented. For instance, there is almost no discussion of the interesting effects of interferons on the replication of retroviruses. Extensive sections of Chapter 3 which deals with the evolution of interferon genes are repeated in Chapter 4 on comparative analysis of interferon structural genes. On p.73 of the latter chapter we read that: "It has clearly shown that the other human IFN-β genes are widely dispersed in the human genome", while the following chapter states: "In the contrast to the multigene family of Hu IFN-α, only a single Hu IFN-β gene has been found (p.85). Authors of other chapters specifically agree or disagree with each of these comments, thus compounding the confusion. Clearly a single discussion of the pros and cons of the thesis that there are multiple β interferon genes would have been more helpful.

Finally, the book has numerous typographical errors. All of the authors and the editors are culpable to varying degrees — but not many of them to the extent that they discuss work on "New Zeal and black (NZB) mice" (p.309). □

Robert M. Friedman is Professor and Chairman of the Department of Pathology at the Uniformed Services University of the Health Sciences, Bethesda, Maryland.

Mineral physics from Japan

Raymond Jeanloz

Materials Science of the Earth's Interior.
Edited by Ichiro Sunagawa.
Terra Scientific, Tokyo/Reidel: 1984.
Pp.653. Dfl. 340, $120, £80.

HOW much good science can be purchased for 8×10^8 yen (approximately $4 million at current rates)? Judging from this book, the answer is a lot.

Much of the leading research in mineral physics is being done in Japan, the work involving application of tools and principles from physics, chemistry, geology and materials science to the complex materials that make up our planet. *Materials Science of the Earth's Interior* summarizes research in mineral physics that was carried out during a three-year programme funded (with the amount mentioned) by the Japanese Ministry of Education. The programme was completed in 1981, and the book written in 1982, yet this volume is a remarkably up-to-date summary of work on the subject.

Although it emphasizes experiments over theoretical investigations, the book manages to cover a broad range of topics. For example, X-ray diffraction studies of silicate crystals and melts at temperatures up to $\sim$ 2,000°C are complemented by accounts of molecular dynamics calculations on molten silicates. Descriptions of techniques available for growing high-quality crystals, including diamond and other high-pressure phases, are followed by a number of studies on defects, rheology, diffusion and natural occurrences of the same minerals. High-pressure research is well represented, particularly in the areas in which the Japanese have excelled: the development and application of large-volume presses, *in situ* studies of phase transformations and determinations of complex phase equilibria. Also notable are individual contributions summarizing recent work on the theory of transition-metal compounds (Sugano and Ohnishi), the noble-gas geochemistry of natural diamonds (Ozima and co-workers), and the use of shock waves in high-pressure experiments (Syono and Goto). Overall, the articles bring together a great deal of material that was hitherto widely scattered or unavailable elsewhere in the literature.

The book will be especially interesting to the earth scientist who wants to know about advanced techniques that are now available and will become increasingly important in the study of geological materials. For the materials scientist or condensed-matter physicist, however, few clues are provided regarding the geological motivation for carrying out these studies; the connection between material properties and the evolution of planetary interiors is not explicitly examined. Still, the properties of complex inorganic systems such as minerals are of broad interest, and this book has allowed some of the leaders in mineral physics to describe frontier research in their field. ☐

Raymond Jeanloz is in the Department of Geology and Geophysics, University of California, Berkeley.

Beavering away

W.C. McGrew

Animal Architecture and Building Behaviour.
By Michael H. Hansell.
Longman: 1984. Pp.324. £25, $60.

TWENTY-THREE families of birds, from bulbuls to wrens, gather and use spider silk in constructing their nests. Beetles living in the Namib desert dig shallow trenches in the sand to trap dew for drinking water. Mole-rats burrow as a team, from the excavator in front, through the "conveyor belt" of intermediates, to the soil-expeller at the end of the queue. These are some of the splendid examples of animals building, as recounted by Michael Hansell. His book would be welcome if it were just an encyclopaedia of such habits, but it is much more.

A fifth of the text is taken up with a survey of animal architecture, across the minor builders from protozoa to chimpanzees, but focusing on the three main classes of major builders: spiders, insects and birds. The rest is devoted to analysis of architecture as action. As an ethologist, the author considers the structure to be inseparable from the behaviour which creates it. He is a great lister: artefacts may serve four functions, namely, protection from the elements, defence against other organisms, aids to subsistence, and communication and display. (A beaver's dam may perform all four.) There are seven methods of construction — sculpting, piling-up, moulding, rolling and folding, sticking-together, weaving, and sewing — birds, apparently, having the widest range. With such classificatory schemes, the author makes neat sense of a diverse array of knowledge, so that unexpected generalizations emerge; for example, the same properties of mud are exploited by organisms from termites to house martins.

For the scientist, animal artefacts have many uses. As products of behaviour they can be used to infer the qualities of the minds that produced them. They can persist long after the acts were performed, thus providing "frozen" or "fossilized" behavioural data. Some artefacts are sufficient to describe taxa the characteristics of which are otherwise completely unknown. Perhaps most impressive is that building has ramifications throughout the whole complexity of adaptation. Hansell argues convincingly that evolutionary changes in the choice of building materials may effect changes even in social structure; for example, in wasps the change from building with mud to building with vegetation allowed group sizes to increase and so for sociality to emerge.

The book is not without flaws. The author's special field of study is the house-building of caddis-fly larvae, and occasionally one feels that the book contains more than one ever wanted to know about these insects. By and large, vertebrates are under-represented compared with spiders and wasps — the use of hammer-stones by *Ammophila* wasps is mentioned four times, hammer-stone use by sea otters or chimpanzees not at all. The sleeping-nests of great apes rate only two sentences, despite an extensive literature which includes details of such things as the apparent use of dung as insulation against the cold by mountain gorillas!

A recurring problem is how wide to cast one's net, so to speak, in dealing with artefacts. The author is mostly interested in dwellings or other fixed structures, as his title suggests. Yet, at times, and seemingly arbitrarily, he inserts material on tool-use. The use of cafeteria-style trays by *Aphaenogaster* ants to carry off food is memorable, but why was this included when (for instance) probing with a cactus spine for insect prey by Galapagos finches was omitted? The author might better have left out tool-use altogether, as this has already been definitively dealt with in Benjamin Beck's *Animal Tool Behavior*, published by Garland in 1980 (for review see *Nature* **289**, 616; 1982). In fact, the two books are largely complementary and show many resemblances in emphasis and viewpoint.

Overall, this is a book of thoughtful analysis, always enlivened with entrancing details of natural history. Everyone knows of the marvellous bower-birds of the Antipodes. But who was aware that one species changes the flowers in its bower daily, or that another spends hours trimming leaves above its arena so that sunlight can penetrate, enabling the bird to show off its plumage? ☐

W.C. McGrew is Senior Lecturer in Psychology at the University of Stirling.

New in paperback

- *History of the British Flora: A Factual Basis for Phytogeography*, 2nd Edn, by Sir Harry Godwin. Publisher is Cambridge University Press, price is £18, $36. For review see *Nature* **261**, 527; 1976.
- *The Illustrated Natural History of Selborne*, an attractively-produced edition of Gilbert White's classic book, compiled by Ronald Davidson-Houston. Publisher is Papermac, price is £8.95.

If you go down to the woods today...

Paul Richards

The Primary Source: Tropical Forests and Our Future.
By Norman Myers.
W. W. Norton: 1984. Pp.399. $17.95, £13.50.

TROPICAL forests are shrinking fast. Many believe that they may hardly survive into the next century, but books about them continue to multiply. Dr Myers's is only the latest in an outburst of publications which range from specialist volumes and authoritative texts, such as T.C. Whitmore's *Tropical Rain Forests of the Far East**, to semi-popular illustrated books and magazine articles.

The Primary Source is aimed mainly at non-specialists, but will also hold the interest of specialists. It is very readable and the author has the gift of explaining complex matters, such as the hydrological cycle of Amazonia, in simple, comprehensible language. Unlike most books on tropical forests, it is mainly concerned, not with the forests themselves, but with the impact of modern man on them — their destruction by commercial loggers, fuelwood gatherers, cattle raisers and shifting cultivators — as well as with their actual (and potentially much greater) contribution to human welfare. Dr Myers is well qualified to write about this topic: he has spent many years in Africa and more recently made a comprehensive survey of the current state of "forest conversion" in the humid tropical countries on behalf of the U.S. National Research Council's Committee on Research Priorities in Tropical Biology.

Dr Myers interprets the term "tropical forests" very widely; indeed, when he writes about the economic possibilities of water hyacinths and capybaras one wonders whether his subject is not really the whole flora and fauna of the tropics. The opening chapters ("Bio-ecological Background") are the only ones dealing with the forest as such; they emphasize its richness in species and its ecological complexity. Some statements here are questionable, for example that on p.81 that the seeds of very few tropical trees are wind-dispersed; this is not true and overlooks the function of natural gaps in rain-forest regeneration. Overall the purpose of these early chapters might have been better served had more space been given to illustrations and less to trying to convey a written picture of what a rain forest is "really" like.

In the next section we are on firmer ground. Much of the chapter on commercial logging is fairly familiar, but Dr Myers gives figures on the insatiable demand of the United States, Japan and other advanced countries for tropical hardwoods which are both striking and disquieting, not least because it is evident that present rates of consumption cannot be maintained; already some tropical countries, such as Nigeria, are reserving what remains of their hardwood stocks for their own use. It is even more disturbing that less than one-twentieth of tropical forests are under management of any kind. A survey of logging companies showed that not one of them leaves enough trees to act as seed-parents for natural regeneration. The accounts of the cattle ranchers and fuel gatherers are also full of information but are no more reassuring.

Still more horrifying is the chapter on shifting cultivators (whom Dr Myers calls "forest farmers"). At least 200 million people depend for survival on the temporary and relatively unproductive farming of small plots won by felling and burning tropical forests. Their numbers are rapidly increasing and have been swollen by incursions of squatters and dispossessed people who lack the simple skills of the traditional forest farmers and are thus even more damaging to the environment.

The effects of human demands on tropical forests might be less tragic if their resources were used fully and rationally. But as the chapters on "Contributions to our Welfare" show, this is far from true. In conventional tropical forestry, resources are classified into timber and "minor forest products". The latter now include such things as the steroid-yielding tubers of Mexican species of *Dioscorea* (yams) which are collected from wild plants in the forest and are an export worth millions of dollars. The future possibilities of discovering new drugs and insecticides in tropical forest plants may be enormous and others may provide templates or blue-prints from which such substances could be synthesized. Forest plants may also have uses as sources of protein and of "green gasoline" and other energy-yielding products. In order that the forest resources should be more completely, and less wastefully, used, Dr Myers suggests the establishment of "forest industrial complexes". Of course the products yielded by forests are not their only contribution to human welfare. Other chapters discuss their part in maintaining water supplies, and checking soil erosion and the silting of reservoirs, as well as their effects on the hydrological cycle, albedo and the carbon dioxide content of the atmosphere. The references on these and other topics are up to date and will be very useful for most readers, however expert.

Many readers will turn most eagerly to the final section of the book, "What We Can Do". The political, economic and biological problems are formidable, but Dr Myers thinks that there is much that can be done both by the citizens of tropical countries and by "outsiders". Basically he believes that the outlook would be brighter if tropical forests were valued at their true worth. Because they are undervalued, forestry departments have always been the Cinderellas of governments in tropical countries; agricultural departments are better supported, but often are more interested in cutting down than in conserving forests. More money is needed for forest protection and for research, and those who understand the importance of forests need to have an effective voice in governments.

Dr Myers sets out what all this implies in some detail, and even provides a "shopping list" for us outsiders which includes such activities as persuading giant corporations to do a better job for tropical forests. Gloomy though the prospects may seem, he remains optimistic, and points to success stories such as the more enlightened attitude to forestry in Indonesia and a change of policy in favour of forestry at the World Bank. But perhaps the most apposite message is the motto from Edmund Burke on the first page of the book: "Nobody makes a greater mistake than he who did nothing because he could do only a little". ☐

Paul Richards is Emeritus Professor of Botany in the University of Wales. He is author of The Tropical Rain Forest, *reprinted by Cambridge University Press in 1979.*

---

*The second edition of this book has just been published by Oxford University Press, price £40, $67.50.

ADVERTISEMENT

ACID PRECIPITATION DIGEST

Each monthly issue provides capsule summaries of —

- news items
- books
- technical reports
- periodical reports
- conference proceedings
- peer reviewed literature
- calendar of upcoming conferences and events
- documents

"Current...concise... comprehensive — the single best source for information on acid rain." **Dr. Chris Bernabo,** Executive Director, *National Acid Precipitation Assessment Program*

Subscriptions (one year): Corporate, For-Profit Firms, $125; Government Agencies, $65; Nonprofit organizations (including public and academic libraries), $30. Non-affiliated individuals -inquire for rates. Add $15 for foreign airmail postage ($5 for Canada). Make checks/money orders payable to: **Acid Precipitation Digest.**

Published by the nonprofit,
non-advocacy
Acid Rain Information Clearinghouse
a project of the
Center for Environmental Information, Inc.
Department N, 33 South Washington Street
Rochester, New York 14608 (716)546-3796

Circle No.19 on Reader Service Card.

BOOKS RECEIVED

Mathematics

Algebra. By LARRY C. GROVE. *Academic: 1983. Pp.229. ISBN 0-12-304620-3. $32.*

Physics

Applied Charged Particle Optics Part C. A. SEPTIER (ed). *Academic: 1983. Pp.545. ISBN 0-12-014576-6. $74.50.*

Advances in Electronics and Electron Physics, Vol.61. PETER W. HAWKES (ed). *Academic: 1983. Pp.408. ISBN 0-12-0414661-4. $60.00.*

Light Scattering Near Phase Transitions. H.Z. CUMMINS and A.P. LEVANYUK (eds). *North-Holland: 1984. Pp.666. ISBN 0-444-86466-0. Np.*

Magnetic Fields in Astrophysics. By YA. B. ZELDOVICH, A. A. RUZMAIKEN and D. D. SOKOLOFF. *Gordon & Breach: 1983. Pp.365. ISBN 0-667-05530-7. Np.*

Methods of Experimental Physics, Vol.21. J.N. MUNDY, S.J. ROTHMAN, M.J. FLUSS and L.C. SMEDSKJAER (eds). *Academic: 1983. Pp.504. ISBN 0-12-475963-7. $69.00.*

Microwave and Optical Ray Geometry. By S. CORNBLEET. *Wiley: 1984. Pp.152. ISBN 0-471-90315-9. £19.*

Optical System Design. By RUDOLF KINGSLAKE. *Academic: 1983. Pp.323. ISBN 0-12-408660-8. $32.*

Quantum Gravity. M.A. MARKOV and P.C. WEST (eds). *Plenum: 1984. Pp.548. ISBN 0-306-41513-5. Np.*

Quantum Statistics of Linear and Nonlinear Optical Phenomena. By JAN PERINA. *Reidel: 1984. Pp.310. ISBN 90-277-1512-2. $54.*

Quantum Theory of Gravity. Essays in Honor of the 60th Birthday of Bryce S. DeWitt. STEVEN M. CHRISTENSEN (ed.). *Adam Hilger, Bristol: 1984. Pp.483. ISBN 0-85274-755-1. Np.*

Radiation Physics and Chemistry: The International Journal for Radiation Reactions, Processes and Industrial Applications. Volume 23, No. 1–2. A.J. SWALLOW (ed.). *Pergamon: 1984. Pp.291. Np.*

Recirculating Electron Accelerators. By ROY E. RAND. *Harwood: 1984. Pp.236. ISBN 3-7186-0183-4. $60.00.*

Chemistry

Structure and Bonding: New Developments. MJ. CLARKE *et al.* (eds). *Springer-Verlag: 1984. Pp.155. ISBN 3-540-13106-X/0-387-13106-X. $30.60.*

The Sulphur Electrode: Fused Salts and Solid Electrolytes. RAGNAR P. TISCHER (ed.). *Academic: 1983. Pp.375. ISBN 0-12-691680-2. $ 68.*

Topics in Current Chemistry. Host Guest Complex Chemistry III. F. VÖGTLE and E. WEBER (eds). *Springer-Verlag: 1984. Pp.224. ISBN 3-540-12821-2/0-387-12821-2. $36.60.*

Computer Science

The Cartoon Guide to Computer Science. By LARRY GONICK. *Harper & Row: 1984. Pp.248. Pbk ISBN 0-06-460417-9. Pbk £3.95.*

Very Basic Basic. By D. ELLERSHAW and P. SCHOFIELD. 3 Volumes ZX Spectrum, Commodore 64, Electron. *Century: 1984. Pp.120. Pbk ISBN 0-7126-0410-3, 0-7126-0412-X, 0-7126-0411-1. Pbk £2.95.*

Biological Sciences

Aging and Cell Function. JOHN E. JOHNSON (ed.). *Plenum: 1984. Pp.283. ISBN 0-306-41420-1. $42.50.*

Aging and Cell Structure, Vol. 2. JOHN E. JOHNSON (ed.). *Plenum: 1984. Pp.223. ISBN 0-306-41455-4. Np.*

Animal Behavior: Neurophysiological and Ethological Approaches. KIYOSHI AOKI, SUSUMU ISHII and HIROMICHI MORITA (eds). *Springer-Verlag: 1984. Pp.274. ISBN 3-540-13046-2/0-387-13046-2. DM 98, $36.60.*

Antarctic Ecology, Vol.2. R.M. LAWS (ed.). *Academic: 1984. Pp.850. ISBN 0-12-439-502-3. £45, $75.*

Cellular and Molecular Biology of Neuronal Development. IRA B. BLACK (ed.). *Plenum: 1984. Pp.353. ISBN 0-306-41550-X. Np.*

Effects of Aging on Regulation of Cerebral Blood Flow and Metabolism. C. FIESCHI, G.I. LENZI and C.W. LOEB (eds). *Karger: 1984. Pp.258. ISBN 3-8055-3805-7. $98.25.*

Enzyme Regulation by Reversible Phosphorylation — Further Advances (Molecular Aspects of Cellular Regulation Volume 3). P. COHEN (ed.). *Elsevier: 1984. Pp.250. ISBN 0-444-80525-7. $75.00.*

Essentials of Human Anatomy and Physiology. By ELAINE NICPON MARIEB. *Addison-Wesley: 1984. Pp.355. ISBN 0-201-15882-5. £16.15.*

Evolutionary Genetics of Fishes. BRUCE J. TURNER (ed.) *Plenum: 1984. Pp.636. ISBN 0-306-41520-8. Np.*

Family Physique and Fortune: A Study in Multifactorial Inheritance. By RICHARD W. PARNELL. *Parnell Publications: 1984. Pp.232. ISBN 0-9509466-0-5. £11.75.*

Fatty Acid Metabolism and Its Regulation. New Comprehensive Biochemistry, Vol.7 S. NUMA (ed.). *Elsevier: 1984. Pp.209. ISBN 0-444-805281. Np.*

Fetal Nutrition, Metabolism, and Immunology: The Role of the Placenta. RICHARD K. MILLER and HENRY A. THIEDE (eds). *Planum: 1984. Pp.387. ISBN 0-306-41639-5. Np.*

Flora of the British Isles. Illustrations. Vol.I Pteridophyta to Papilionaceau, Vol.II Rosaceae, Vol.III Boraginaceae to Compositae, Vol.IV Monocotyledons. By A.R. CLAPHAM *et al.* *Cambridge University Press: 1984. Pp.144, 119, 115, 119. Pbk ISBN 0-521-26962-8, 0-521-26963-6, 0-521-26964-4, 0-521-26965-2. Pbk £8.95, $17.95.*

Frogs of Western Australia. By M.J. TYLER *et al.* *Advance Press, Australia: 1984. Pp.109. Pbk ISBN 0-7244-9482-0. Pbk $A9.95.*

Function and Dysfunction of the Small Intestine: Proceedings of the Second George Durrant Memorial Symposium. By R.M. BATT and T.L.J. LAWRENCE. *Liverpool University Press: 1984. Pp.264. ISBN 0-85323-454-X. £22.50.*

Gas Chromatography, Mass Spectrometry, Applications in Microbiology. GORAN ODHAM *et al.* (eds). *Plenum: 1984. Pp.444. ISBN 0-306-41314-0. Np.*

General Microbiology: A Laboratory Manual. By JANE ANN PHILLIPS and THOMAS D. BROCK. *Prentice-Hall: 1984. Pp.234. ISBN 0-13-35062-6. Np.*

Genes and Antigens — The Monoclonal Antibody Approach. Contributions to Oncology 19. *Karger: 1984. Pp.192. ISBN 3-8055-3843-X. DM75, $37.75.*

Genetic and Environmental Factors during the Growth Period. C. SUSANNE (ed.). *Plenum: 1984. Pp.248. ISBN 0-306-41479-1. Np.*

La Genetique du Development. By JEAN-CLAUDE BEETSCHEN. *Presses Universitaires de France: 1984. Pp.127. ISBN 2-13-038052-2. Np.*

Giardia and Giardiasis: Biology, Pathogenesis, and Epidemiology. STANLEY L. ERLANDSEN and ERNEST A. MEYER (eds). *Plenum: 1984. Pp.407. ISBN 0-306-41539-9. Np.*

Humoral Factors in Host Defense. YUICHI YAMAMURA *et al.* (eds). *Academic: 1983. Pp.364. ISBN 0-127-68220-1. $32.*

Hydrocephalus. KENNETH SHAPRIO, ANTHONY MARMAROU and HAROLD PORTNOY (eds). *Raven: 1984. Pp.415. ISBN 0-89004-337-7. $93.*

Immunoassays of Steroids in Saliva. Ninth Tenovus Workshop. G.F. READ *et al.* (eds). *Alpha Omega Publishing: 1984. Pp.346. ISBN 0-900663-13.8. £15, $30.*

Inset Neurochemistry and Neurophysiology. ALEXEJ B. BORKOVEC and THOMAS J. KELLY (eds). *Plenum: 1984. Pp.523. ISBN 0-306-41511-9. Np.*

Insects on Plants: Community Patterns and Mechanisms. By D.R. STRONG, J.H. LAWTON and RICHARD SOUTHWOOD. *Blackwell Scientific: 1984. Pp.313. Hbk ISBN 0-632-00907-1; pbk ISBN 0-632-00909-8. Hbk £22, pbk £11.80.*

Integration of Ecological Aspects in Coastal Engineering Projects Part 1. B.A. BANNINK (ed.). *Pergamon: 1984. Pp.336. Pbk ISBN 0-08-031036-2. Pbk £88, $160.*

Isotopes and Radiation in Agriculture. Vol.2 Animals, Plants, Food and the Environment. M.F. L'ANNUNZIATA and J.O. LEGG (eds). *Academic: 1984. Pp.356. ISBN 0-12-436602-3. $75, £49.*

Learning, 2nd Edn. By A. CHARLES CATANIA. *Prentice/Hall: 1984. Pp.406. ISBN 0-13-527697-7. £24.65.*

Pineal Research Reviews, Vol. 1. R.J. REITER (ed.). *Alan R. Liss: 1983. Pp.276. ISBN 0-8451-3600-3. $56.*

The Role of Terrestrial Vegetation in the Global Carbon Cycle: Measurement by Remote Sensing. G.M. WOODWELL (ed.). *Wiley: 1984. Pp.247. ISBN 0-471-90262-4. £27.50.*

Science and Gender: A Critique of Biology and Its Theories on Women. By RUTH BLEIER. *Pergamon: 1984. Pp.220. Pbk ISBN 0-08030971-2. Hbk $25; pbk $12.50.*

Sensation and Perception, 2nd Edn. By STANLEY COREN, CLARE PORAC and LAWRENCE M. WARD. *Academic: 1984. Pp.606. Pbk ISBN 0-12-188554-2. Pbk $15, £10.50.*

The Shell Guide to Britain's Threatened Wildlife. By NIGEL SITWELL. *Collins: 1984. Pp.208. ISBN 0-00-219050-8. £8.95.*

Sleep and Breathing. NICHOLAS A. SAUNDERS and COLIN E. SULLIVAN (eds). *Marcel Dekker: 1984. Pp.613. ISBN 0-8247-7064-1. SwFr.213.*

Sudden Infant Death Syndrome. J. TYSON TILDON *et al.* (eds). *Academic: 1983. Pp.731. ISBN 0-12-691050-2. $45.*

Toxins and Plant Pathogenesis. J.M. DALY and B.J. DEVERALL (eds). *Academic: 1983. Pp.181. ISBN 0-12-200780-8. $21.50.*

Applied Biological Sciences

The Addictive Behaviours. HOWARD SHAFFER and BARRY STIMMEL (eds). *Haworth Press: 1984. Pp.172. ISBN 0-86656-243-5. $22.95.*

Advances in Clinical Neuropsychology, Vol. 1. GERALD GOLDSTEIN (ed.). *Plenum: 1984. Pp.189. ISBN 0-306-41502-X. Np.*

Advances in Immunobiology: Blood Cell Antigens and Bone Marrow Transplantation. JEFFREY McCULLOUGH and S. GERALD SNADLER (eds) *Alan R. Liss: 1984. Pp.462. ISBN 0-8451-0149-8. £44.00.*

Advances in World Diabetes Resarch: Reviewed Contents of 1982's Major Diabetes Congresses. By FRANCESCO BELFIORE and SILVIA IANNELLO. *Karger: 1984. Pp.258. ISBN 3-8055-3810-3. $99.00.*

Angiology: New Developments. P. BALAS (ed.). *Plenum: 1984. Pp.1288. ISBN 0-306-41349-3. Np.*

Antimalarial Drugs 1. Biological Background, Experimental Methods, and Drug Resistance. W. PETERS and W.H.G. RICHARDS (eds). *Springer-Verlag: 1984. Pp.484. ISBN 3-540-12616-3/0-387-12616-3. DM 370, $138.10.*

Antimalarial Drugs II. Current Antimalarials and New Drug Developments. W. PETERS and W.H.G. RICHARDS (eds). *Springer-Verlag: 1984. Pp.520. ISBN 3-540-12617-1/0-387-12617-1. DM 390, $145.50.*

Antineoplastic, Immunogenic and Other Effects of the Tetrapeptide Tuftsin: A Natural Macrophage Activator. V. NAJJAR and M. FRIDKIN (eds). *The New York Academy of Sciences: 1983. Pp.273. Hbk ISBN 0-89766-233-6; pbk ISBN 0-89766-233-4. Np.*

Aspirin and the Salicylates. By K.D. RAINSFORD. *Butterworths: 1984. Pp.335. ISBN 0-407-00316-9. £36.*

Bacterial Adhesion and Preventive Dentistry. S.A. LEACH *et al.* (eds). *IRL Press: 1984. Pp.230. Pbk ISBN 0-904147-63-0. Pbk £20, $40.*

Bacterial Infections of Humans: Epidemiology and Control. ALFRED S. EVANS and HARRY A. FELDMAN (eds). *Plenum: 1982. Pp.702. Pbk ISBN 0-306-41705-7. Np.*

Benzoidazepine Recognition Site Ligands: Biochemistry and Pharmacology. Advances in Biochemical Psychopharmacology, Vol.38. G. BIGGIO and E. COSTS (eds). *Raven: 1983. Pp.272. ISBN 0-89004-432-5. $38.50.*

Biochemical Basis of Chemical Carcinogenesis. HELMUT GREIM *et al.* (eds). *Raven: 1983. Pp.325. ISBN 0-89004-961-0. $68.50.*

The Biochemical Mode of Action of Pesticides 2nd edn. By J.R. CORBETT, K. WRIGHT and A.C. BAILLIE. *Academic: 1984. Pp.382. ISBN 0-12-187860-0. £35.00, $59.00.*

Biological Responses in Cancer: Progress Toward Potential Applications. Volume 2. ENRICO MIHICH (ed.). *Plenum: 1984. Pp.245. ISBN 0-306-41583-6. Np.*

Cancer Invasion and Metastasis: Biologic and Therapeutic Aspects. G. NICOLSON and L. MILAS (eds). *Raven: 1984. Pp.501. ISBN 0-89004-896-7. $81.*

Central Cardiovascular Control: Basic and Clinical Aspects. Current Topics in Neuroendocrinology. D. GANTEN and D. PFAFF (eds). *Springer-Verlag: 1983. Pp.192. ISBN 3-540-11350-9/0-387-11350-9. DM 90, $35.*

Chronic Diarrhoea in Children (Nestle Nutrition Workshop Series, Volume 6). EMANUEL LEBENTHAL (ed.). *Raven: 1984. Pp.588. ISBN 0-89004-319-1. $49.00.*

Contemporary Hematology/Oncology, Vol.3. ALBERT S. GORDON, JOSEPH LOBUE and ROBERT SILBER (eds). *Plenum: 1984. Pp.271. ISBN 0-306-41535-6. Np.*

Continuous Culture: Biotechnology, Medicine and the Environment. A.C.R. DEAN, D.C. ELLWOOD and C.G.T. EVANS (eds). *Wiley: 1984. Pp.322. £35, $60.50.*

Control of Virus Diseases. EDOUARD KURSTAK (ed.). *Marcel Dekker: 1984. Pp.584. ISBN 0-8247-7066-8. SwFr. 320.*

Current Issues in Toxicology: Age-Associated (Geriatric) Pathology. Its Impact on Long-Term Toxicity Studies. H.C. GRICE (ed.). *Springer-Verlag: 1984. Pp.114. Pbk ISBN 3-540-12845-X/0-387-12845-X. Pbk DM 35, $13.60.*

Diseases of the Lymphatic System: Diagnosis and Therapy. DAVID W. MOLANDER (ed.). *Springer-Verlag: 1984. Pp.340. ISBN 3-540-90850-1/0-387-90850-1. DM 192, $71.70.*

End-Stage Renal Disease: An Integrated Approach. W.J. STONE and P.L. RABIN (eds). *Academic: 1983. Pp.373. ISBN 0-12-672280-3. $55.*

Environmental Aspects of Cancer: The Role of Macro and Micro Components of Foods. ERNST L. WYNDER *et al.* (eds). *American Health Foundation: 1983. Pp.295. ISBN 0-917678-17-6. $65.*

Experimental Allergic Encephalomyelitis: A Useful Model for Multiple Sclerosis. Progress in Clinical and Biological Research, Vol.146. ELLSWORTH C. ALVORD, MARIAN W. KIES and ANTHONY J. SUCKLING (eds). *Alan R. Liss: 1984. Pp.554. ISBN 0-8451-0146-3. Np.*

Growth of the Heart in Health and Disease. RADOVAN ZAK (ed). *Raven: 1984. Pp.490. ISBN 0-89004-734-1. $98.*

Human *in Vitro* Fertilization and Embryo Transfer. DON P. WOLF and MARTIN M. QUIGLEY (eds). *Plenum: 1984. Pp.440. ISBN 0-306-41623-9. Np.*

Hydroxyanisole: Recent Advances in Anti-Melanoma Therapy. P.A. RILEY (ed.). *IRL Press: 1984. Pp.248. Pbk ISBN 0-904147-64-9. Pbk £19, $38.*

Hypertension and the Angiotensin System: Therapeutic Approaches. AUSTIN E. DOYLE and ALEXANDER G. BEARN (eds). *Raven: 1984. Pp.320. ISBN 0-89004-309-4. $49.*

Manipulation and Expression of Genes in Eukaryotes. PHILIP NAGLEY *et al.* (eds). *Academic: 1983. Pp.386. ISBN 0-12-513780-X. $41.*

Measurement in Clincal Respiratory Physiology. By GABRIEL LASZLO and MICHAEL F. SUDLOW. *Academic: 1983. Pp.337. ISBN 0-124-37080-2. $60.*

Nucleic Acid Research: Future Development. KIYOSHI MIZOBUCHI, ITARU WATANABE and JAMES D. WATSON (eds). *Academic: 1983. Pp.586. ISBN 0-125-01650-6. $65.*

Perspectives in Cardiovascular Research, Vol. 10. Clinical Pharmacology of Antiarrhythmic Therapy. BENEDICT R. LUCCHESI, JAMES V. DINGELL and RICHARD P. SCHWARZ (eds). *Raven: 1984. Pp.275. ISBN 0-89004-966-1. $56.*

Pituitary Hyperfunction: Physiopathology and Clinical Aspects. F. CAMANNI and E.E. MULLER (eds). *Raven: 1984. Pp.448. ISBN 0-89004-968-8. $99.50.*

Recent Results in Cancer Research: Early Detection of Breast Cancer. S. BRUNNER, B. LANGFELDT and P.E. ANDERSEN (eds). *Springer-Verlag: 1984. Pp.214. ISBN 3-540-12348-2/0-387-12348-2. DM 108, $40.30.*

Recombinant DNA and Medical Genetics. ANNE MESSER and IAN H. PORTER (eds). *Academic: 1983. Pp.207. ISBN 0-124-92220-1. $29.*

The Reproduction Revolution: New Ways of Making Babies. By PETER SINGER and DEANE WELLS. *Oxford University press: 1984. Pp.273. Hbk ISBN 0-19-217736-2; pbk ISBN 0-19-286044-5. Pbk £2.95; hbk £12.50.*

Respiratory Medicine for Primary Care. CHARLES W. DRAGE (ed.). *Academic: 1983. Pp.231. ISBN 0-127-88165-4. $29.95.*

Targets for the Design of Antiviral Agents. E. DE CLERCQ and R.T. WALKER (eds). *Plenum: 1984. Pp.378. ISBN 0-306-41618-2. Np.*

Treatment of Hyperlipoproteinemia. LARS A. CARLSON and ANDERS G. OLSSON (eds). *Raven: 1984. Pp.304. ISBN 0-89004-341-8. $60.00.*

Ultrasound: Biological Effects and Potential Hazards. By A. ROY WILLIAMS. *Academic: 1983. Pp.321. ISBN 0-12-756960-X. $49.50.*

Viral Hepatitis and Delta Infection. Progress in Clinical and Biological Research, Vol. 143. GIORGIO VERME *et al.* (eds). *Alan R. Liss: 1984. Pp.448. ISBN 0-8451-0143-9. £41.*

Visual Disorders in the Handicapped Child. Pediatric Habilitation, Vol.5. By JOHN L. GOBLE. *Marcel Dekker: 1984. Pp.287. ISBN 0-8247-7109-5. SwFr. 127.*

History of Science

Darwin, Marx and Freud: Their Influence on Moral Theory. ARTHUR L. CAPLAN and BRUCE JENNINGS (eds). *Plenum: 1984. Pp.230. ISBN 0-306-41530-5. Np.*

General

Black Apollo of Science: The Life of Ernest Everett Just. By K.R. MANNING. *Oxford University Press: 1983. Pp.397. ISBN 0-19-503299-3. $29.95.*

Bulimarexia: The Binge/Purge Cycle. By MARLANE BOSKING-WHITE and WILLIAM C WHITE Jr. *W.W. Norton: 1984. Pp.219. ISBN 0-393-01650-1. £12.50, $18.00.*

Cancer Rehabilitation. ALBERT E. GUNN (ed.) *Raven: 1984. Pp.237. ISBN 0-89004-989-0. $47.50.*

Centrifugation 2nd edn.: A Practical Approach. D. RICKWOOD (ed.). *IRL Press: Pp.352. ISBN 0-904147-55-X. £10.00, $20.00.*

Coconut Research & Development. N.M. NAYAR (ed.). *Wiley: 1983. Pp.518. ISBN 0-85226-607-3. Np.*

Conflict Processes and the Breakdown of International Systems: Merriam Seminar Series on Research Frontiers. DINA A. ZINNES (ed). *University of Denver: 1983. Pp.160. ISBN 0-87940-073-0. Np.*

An Elementary Primer for Gauge Theory. By K. MORIYASU. *World Scientific: 1983. Pp.177, Hbk ISBN 9971-950-83-9; pbk ISBN 9971-950-94-4. Np.*

The Experience of Science: An Interdisciplinary Approach. By MARTIN GOLDSTEIN and INGE GOLDSTEIN. *Plenum: 1984 Pp.400. ISBN 0-306-41538-0. Np.*

Exploring the Earth and the Cosmos. By ISAAC ASIMOV. *Penguin: 1984. Pp.339. Pbk ISBN 0-14-022512-9. Pbk £3.95.*

Exploring the Universe, 3rd Edn. By WM. PROTHEROE, E.R. CAPRIOTI and G.H. NEWSOM (eds). Charles E. Merrill: 1984. Pp.586. ISBN 0-675-20145-4. Np.

Extinctions. M.H. NITECKI (ed.) *University of Chicago Press; 1984. Pp.354. Pbk ISBN 0-226-58690-1. Hbk $30.00, £25.50, Pbk $16.00, £13.60.*

Genesis on Planet Earth : The Search for Life's Beginning, 2nd Edn. BY WILLIAM DAY. *Yale University Press: 1984. Pp.299. IBN Hbk 0-300-02954-3; pbk 0-300-03202-1. Np.*

Higher Perspective. By HAROLD W.G. ALLEN. *Image Publishing, 752 King Street, Hamilton, Ontario L8M 1A5, Canada: 1984. Pp.252. ISBN 0-919357-01-6. $19.95.*

Instructor's Manual to Accompany Exploring the Universe 3rd edn. By W.M. PROTHEROE, E.R. CAPRIOTTI and G.H. NEWSOM. *Charles E Merrill: 1984. Pp.116. Np.*

An Introduction to The Life of the Rev Thomas Birch D.D. F.R.S. 1705-1766. By A.E. GUNTHER. *Halesworth Press: 1984. Pp.188. ISBN 0-9507276-1-X. £7.90.*

Lecture Notes on Coastal and Estuarine Studies: Remote Assessment of Ocean Color for Interpretation of Satellite Visible Imagery : A Review. By HOWARD R. GORDON and ANDRE Y. MOREL. *Springer-Verlag: 1983. Pp.114. ISBN 3-540-90923-0. $22.50.*

Leibniz. By G. MACDONALD ROSS. *Oxford University Press: 1984. Pp.121. HBk ISBN 0-19-287621-X, pbk ISBN 0-19-287620-1. Hbk £7.95, pbk £1.95.*

Looking Glass Universe: The Emerging Science of Wholeness. By JOHN P. BRIGGS and F. DAVID PEAT. *Simon & Schuster: 1984. Pp.290. Pbk ISBN 0-346-12594-4. Pbk $9.95.*

Management and Office Information Systems. SHI-KUO CHANG (ed.). *Plenum: 1984. Pp.476. ISBN 0-306-41447-3. Np.*

Managing Solid Wastes in Developing Countries. JOHN R. HOLMES (ed.). *Wiley: 1984. Pp.304. ISBN 0-471-90234-9. £23.50, $44.50.*

Maximum Lifespan. By ROY L. WALFORD. *Avon: 1984. Pp.256. Pbk ISBN 0-380-65524-1. Pbk $3.95.*

Mechanical Engineering at the National Research Council of Canada, 1929–1951. By W.E. KNOWLES. *Wilfrid Laurier University Press, Ontario, Canada: 1984. Pp. 286. ISBN 0-88920-164-1. $19.50 (Canada), $22.50 (US).*

Megalithic Astronomy: A New Archaeological and Statistical Study of 300 Western Scottish Sites. By C.L.N. RUGGLES. *BAR British Series 123: 1984. Pp.320. ISBN 0-86054-253-X. £15.00.*

The Miracle of Existence. By HENRY MARGENAU. *Ox Bow Press: 1984. Pp.143. ISBN 0-918024-26-9. $16.00.*

The Nature of Prosocial Development: Interdisciplinary Theories and Strategies. DIANE L. BRIDGEMAN (ed.). *Academic: 1984. Pp.358. ISBN 0-12-133980-7. $34.*

Nitrogen in the Marine Environment. EDWARD J. CARPENTER and DOUBLAS G. CAPONE (eds). *Academic: 1983. Pp.900. ISBN 0-12-160280-X. $59.*

Peace for Beginners. By IAN KELLAS. *Writers & Readers: 1984. Pp.183. ISBN 0-86316-009-3. Pbk £2.95.*

People of the Ice: Eskimos, White Men and the Whale. DAVID BOERI. *Dutton: 1984. Pp.285. ISBN 0-525-24206-6. $19.95.*

Personal Identity. By SYDNEY SHOEMAKER & RICHARD SWINBURNE. *Basil Blackwell: 1984. Pp.158. Hbk ISBN 0-631-13208-2; pbk ISBN 0-631-13432-8. Hbk £15.00; pbk £5.50.*

Physiological Chemistry of Training and Detraining. P. MARCONNET, J. POORTMANS and L. HERMANSEN (eds). *Karger: 1984. Pp.262. ISBN 3-8055-3764-6. $118.75.*

Planned Beef Production, 2nd Edn. By DAVID ALLEN and BRIAN KILKENNY, *Granada: 1984. Pp.228. Pbk ISBN 0-246-12194-7. Pbk £8.95.*

The Platte: Channels in Time: By PAUL A. JONSGARD. *University of Nebraska Press: 1984. Pp.154. ISBN 0-8032-2560-1. £13.25.*

Prospero Drill. By CARL A. POSEY. *Robert Hale: 1984. Pp.192. ISBN 0-7090-1546-1. £7.95.*

Time, Space and Things. 2nd Edn. By B.K. RIDLEY. *Cambridge University Press: 1984. Pp.182. Hbk, ISBN 0-521-26293-3; pbk ISBN 0-521-26920-2. Hbk £15, $29.95; pbk £5.95, $9.95.*

Total Synthesis of Natural Products: The 'Chiron' Approach. By S. HANESSIAN. *Pergamon: 1983. Pp.291. Hbk ISBN 0-08-029247-X; pbk ISBN 0-08-030715-9. Hbk np; pbk £11.25, $20.*

Trialectics: Toward a Practical Logic of Unity. ROBERT E. HORN (ed.). *Information Resources, PO Box 417, Lexington, MA 02173: 1984. Pp.190. Pbk ISBN 0-912864-10-9. Pbk $16.95.*

Unreality and Time. By ROBERT S. BRUMBAUGH. *State University of New York Press: 1984. Pp.164. Hbk ISBN 0-87395-613-3; pbk ISBN 0-87395-614-1. Hbk $29.50; pbk $12.95.*

Voiceless Victims. By REBECCA HALL. *Wildwood House, Chapel Road, Hounslow, Middlesex: 1984. Pp.304. Pbk ISBN 0-7045-0500-2. Pbk £5.95.*

Varroa Jacobsoni OUD. Affecting Honey Bees: Present Status and Needs. Proceedings of a Meeting of the EC Experts' Group/Wageningen. R. CAVALLORCO (ed.). *A.A. Balkema: 1983. Pp.107. ISBN 90-6191-524-4. £11.*

Warday and the Journey Onward. By WHITLEY STRIEBER and JAMES KUNETKA. *Hodder and Stoughton: 1984. Pp.380. Pbk ISBN 0-340-35849-1. Hbk £8.95; pbk £4.95.*

A Wealth of Wild Species: Storehouse for Human Welfare. By N. MYERS. *Westview Press: 1983. Pp.272. Hbk ISBN 0-86531-132-3; pbk ISBN 0-86531-133-1. Hbk £19.50; pbk £8.75.*

Wood and Agricultural Residues: Research on Use for Feed, Fuels and Chemicals. E.J. SOLTES (ed.). *Academic: 1983. Pp.615. ISBN 0-12-654560-X. $57.*

Wood: Chemistry, Ultrastructure, Reactions. By D. FENGEL and G. WEGENER. *Walter de Gruyter: 1984. Pp.613. ISBN 3-11-008481-3. DM 245.*

Nucleic acids and related areas

The new chemicals and apparatus described this week are mainly for those working with recombinant DNA technology.

- Now available from Worthington, the Type II restriction endonuclease *Cpf*I (from *Clostridium perfringens*) is an isoschizomner of *Sau*3AI and *Mbo*I which cleaves DNA leaving the 5′ terminal extension GATC like *Sau*3AI, *Bam*HI, *Bgl*II and several other enzymes. Like *Sau*3AI, *Cpf*I cleaves DNA that is adenine methylated. The best conditions are 10 mM Tris-HCl, *p*H 7.5, 100 mM NaCl, 10 mM $MgCl_2$, 10 mM β-mercaptoethanol and 100 $\mu g\ ml^{-1}$ bovine serum albumin at 37°C. It is supplied at 5–10 units μl^{-1} in package sizes of 200 units, 500 units or 1,000 units.

Circle No. 100 on Reader Service Card.

- Boehringer Mannheim has recently introduced three DNA-affinity ligands which have been developed specially for the sequence specific electrophoretic separation of DNA fragments. By the use of two-dimensional gel systems, DNA fragments of differing base composition may be separated according to their retarded mobilities in the presence of a particular ligand. After separation the ligand can be removed, yielding the unmodified DNA. Also available from Boehringer Mannheim is a top quality Ribonuclease H. The enzyme is particularly suited to cDNA preparation. The absence of endonucleases and nicking actively is routinely checked by incubation with λ DNA and pBR322 DNA followed by gel electrophoresis. Absence of RNaseIII and RNase is checked by incubation of the enzyme with tritiated poly (U) poly (A) and MS 2RNA.

Circle No. 101 on Reader Service Card.

- Bio-Rad's new Mini-Sub submarine electrophoresis cell speeds the separation of DNA restriction fragments and other nucleic acids. Using very small sample loads, high resolution is obtained in runs of only 10 cm, taking only 30 min to 2 h. Effective separations of *Eco*RI or *Hin*dIII digest of λ phage DNA have been performed at 175V in as little as 20 min. Using sample loads as small as 50 ng, as little as 1–5 ng of DNA can be detected in agarose gels with ethidium bromide, while as little as 500 pg of DNA can be detected in polyacrylamide gels using the Bio-Rad Silver Stain. The Mini-Sub cell's increased speed and sensitivity simplifies many procedures. For example, clones can be screened rapidly for proper recombinant inserts, DNA enzymes can be assessed for activity, and DNA ligations, and other DNA modifying reactions can be monitored quickly.

Circle No. 102 on Reader Service Card.

- Terminal transferase and AMV reverse transcriptase are now available from Boehringer Mannheim. Both enzymes are extensively tested for the absence of endonucleases, exonucleases and nicking activities. Boehringer also markets SP-6 polymerase and SP-62 PL plasmid DNA. The SP-6 polymerase system generates single RNA species of known genetic origin in large quantities. These RNAs may be used as highly specific probes in blot and *in situ* hybridizations and as substrates in RNA transcription studies and S_1 mapping experiments. The enzyme is supplied free of contaminating endonucleases, exonucleases, nicking activities and ribonucleases. Restrictions endonuclease *Asp*718 (G/GTACC) is also available from Boehringer Mannheim. *Asp*718 is an isochizomer to *Kpn*1, but produces fragments with 5′-cohesive ends as opposed to the 3′-cohesive ends from *Kpn*1.

Circle No. 103 on Reader Service Card.

- A new 24-page catalogue includes detailed descriptions and prices for Becton Dickinson's complete line of monoclonal reagents, kits and panels for enumerating and identifying human and mouse leukocytes and immunoglobulins. Second-step reagents and monoclonal controls are also listed.

Circle No. 104 on Reader Service Card.

- A comprehensive range of restriction endonucleases, DNA vectors and modifying enzymes is marketed by Genetic Research Instrumentation of Bishop's Stortford, UK. The company also offers a complete range of instruments and biochemicals for all aspects of molecular biology — for plant cells as well as animals and microbes. The new range of enzymes is added to the existing range of plant protoplast enzymes.

Circle No. 105 on Reader Service Card.

- The new Schleicher and Schuell Mini-Collodion Membrane is designed for quick, efficient, and simultaneous concentration and dialysis of protein and nucleic acids in small sample quantities. A microtapered collection tip yields sample recoveries of up to 98% with concentrations down to 10 μl. The Mini-Collodion Membrane has a volume of 2 ml and molecular weight cut-off at 25,000. Simultaneous concentration and dialysis can be achieved simply by using the membrane in conjunction with an easy-to-assemble S&S all-glass apparatus and the membrane can also be used without the specialized apparatus for dialysis. Short sample preparation times are possible because of the high surface area-to-volume ratio.

Circle No. 106 on Reader Service Card.

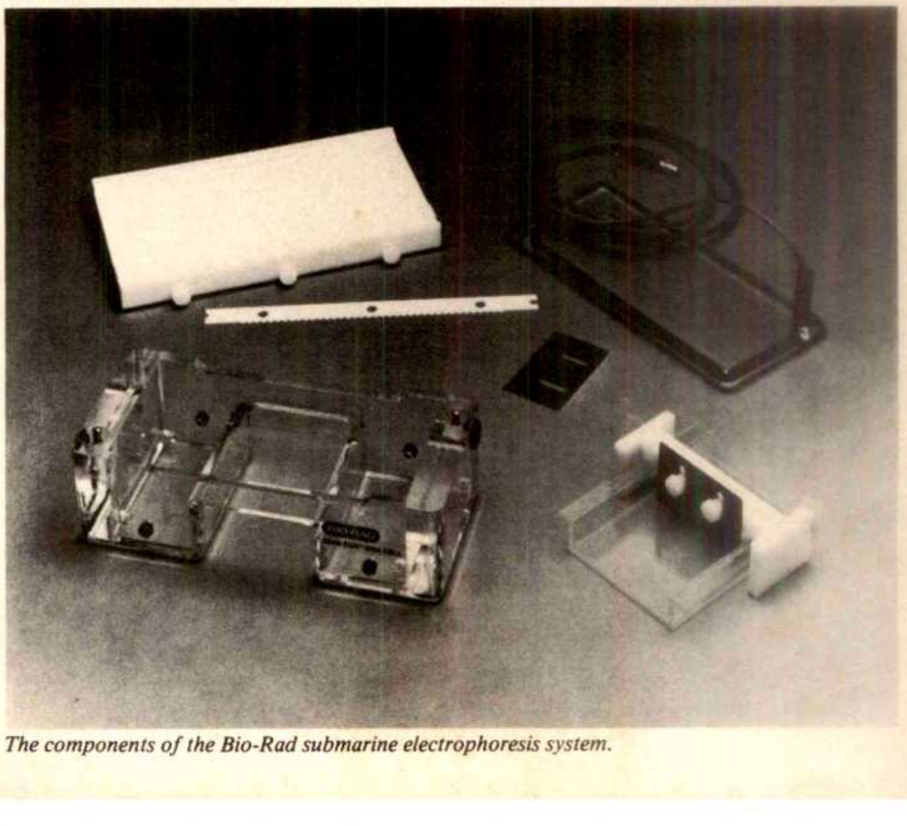

The components of the Bio-Rad submarine electrophoresis system.

TWO NEW reliable, up-to-date and complete biotechnology information resources.

EXAMINE ON FREE APPROVAL WITHOUT COMMITMENT

Detailed information on every aspect of biotechnology worldwide

An indispensable guide to: ★ Products, services and research ★ Companies ★ Government and international agencies ★ Information sources

THE INTERNATIONAL BIOTECHNOLOGY DIRECTORY 1984 —

- is thoroughly international
- features a unique BUYER'S GUIDE to products, research and services
- covers both the old and new biotechnologies

The Directory tells you:

★ Who your competition is, and what they are doing.

★ Who are potential customers and suppliers.

★ Where to buy equipment, chemicals and services.

★ Where culture collections are located and what cultures they hold.

★ Who imports/exports biotechnology products in over 20 countries.

★ Which government departments are associated with biotechnology.

All compiled by the eminent biotechnologist Dr. Jim Coombs and now available to you on **FREE APPROVAL.**

Macmillan Hardcover 400pp
November 1983
ISBN 0 333 35140 1
£50.00/A$100.00

Information Sources in Biotechnology

★ covers both old and new technologies

★ covers technical and commercial literature

★ covers difficult and hard to trace sources

★ includes over 20 at-a-glance evaluation tables

★ provides an Index of publishers and their addresses

Dr. Crafts-Lighty, Head of Information and Library Services at Celtech Limited, systematically and critically reviews all the important information sources:

• books • conferences • trade periodicals • research periodicals • computer databases • patent • market surveys • directories • organisations • secondary sources

Macmillan Paperback 320pp
September 1983
ISBN 0 333 36178 4
£40.00/$80.00

Send no money now. Examine on FREE APPROVAL

You can take these new books for 30 days examination without commitment. If you are not completely satisfied, just return the book(s) in good condition within 30 days and we will cancel your invoice.

Globe

Globe Book Services Limited,
Brunel Road, Houndmills,
Basingstoke, Hants RG21 2XS England
Telephone: Basingstoke (0256) 26222
A DIVISION OF MACMILLAN PUBLISHERS LTD.

The Nature Press,
15 E 26 Street, New York, N.Y. 10010
Telephone: 212-532-4811

FREE APPROVAL ORDER FORM

To: Ian Jacobs, Globe Book Services Ltd., FREEPOST, Brunel Road, Houndmills, Basingstoke, Hants RG21 2BR, England.

The Nature Press, 15 E 26 Street, New York, N.Y. 10010. Credit card callers call toll-free 800-221-2123 (or in New York: 212-532-4811)

Please send me on 30 days FREE APPROVAL ______ copies of *The International Biotechnology Directory 1984* at £50.00/$100.00 each, and/or ______ copies of *Information Sources in Biotechnology* at £40.00/$80.00 each.

If I am not entirely satisfied. I may return any book in good condition within 30 days and you will cancel my invoice.

Postage and Packing

UK subscribers £2.00 (Overseas £3.00) US Subscribers $1.50

Tick preferred method of payment

☐ Bill me. I need send no money now.
☐ I enclose cheque for £/$ ______
☐ Charge my credit card on publication £/$ ______
☐ Visa ☐ Access/Mastercharge ☐ Am. Express ☐ Diners

Card No. ______ Expiry Date ______
Signature ______
(Orders cannot be accepted without a signature)
Name ______
(PLEASE PRINT)
Address ______

Postcode/Zip Code ______
Books will be delivered to you on publication. N3
UK Subscribers POST TODAY — NO STAMP NEEDED

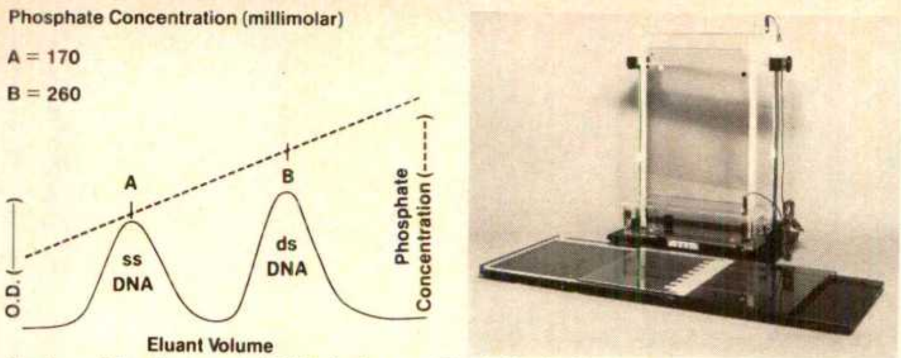

Single- and double-stranded DNA eluting on a Bio-Gel hydroxlapatatite column, and a new DNA sequencing device from Atto.

• Hydroxylapatite is often used to characterize DNA hybrids and to study reassociation kinetics. To simplify its use in these applications, each bottle of Bio-Gel hydroxylapatite shows the conditions for optimal separation of single and double-stranded DNA on the label. To find the conditions, heat-denatured (single-stranded) and native (double-stranded) calf thymus DNA are combined, applied to the hydroxylapatite colulmn in 0.01M sodium phosphate, *p*H 6.8 at 25°C, and eluted with a gradient of increasing phosphate concentration. On the above graph, point A is the concentration at which single-stranded DNA elutes. Double-stranded DNA elutes at point B. The numerical value for the phosphate concentration at both points is given. Because all the information needed for the selection of the right conditions for each separation comes with the hydroxylapatite, it is possible to perform procedures faster by eliminating the use of a continuous gradient.

Circle No. 107 on Reader Service Card.

• American Bionuclear's DNA Synthesis Grade diisopropyl phosphoramidites is suitable for preparing synthetic oligonucleotides using either manual or automated procedures. Each preparation is more than 98% pure based on ^{31}P NMR and TLC analysis. Functional tests conducted on each lot guarantee greater than 95% coupling efficiency. A detailed quality control assay report is included with each shipment. The diisopropyl phosphoramidites are distributed in septum vials designed to fit commercially available automated DNA synthesizers.

Circle No. 108 on Reader Service Card.

• Atto's new DNA sequencing apparatus is highly versatile, being adjustable for both width and height. It accommodates plates from 200 mm high by 100 mm wide to 1 m high by 300 mm wide. The air cooling system controls 'smile' effects, and avoids the 'hot spots' common to fully enclosed systems. Large 1.5 litre compartments avoid problems of buffer breakdown and circulation ports are provided. A single acrylic clamp bar retains the plates securely in position, assuring leak-free sealing and ease of operation. Physical make/break safety lids are standard and connect to taut protectively housed platinum electrodes. The separation unit is of the functional sliding type, extremely effective in preventing discontinuities caused by air bubbles, to aid gel preparation.

Circle No. 109 on Reader Service Card.

• Schleicher & Schuell's "Quick Blot Kit" is a highly selective, quantitative and rapid method for the purification and immobilization of multiple samples of mRNA onto nitrocellulose. mRNA isolated from small volumes of whole cells, bacteria and virus can be hybridized, translated, reverse-transcribed or released and manipulated. The mRNA is tightly bound and always remains biologically active as no baking of the membrane is required. The system takes advantage of the high selectivity of nitrocellulose for mRNA which has been dissolved in concentrated NaI. Under these conditions and at low temperatures, adsorption of mRNA is very high whilst rRNA, tRNA, tRNA, native and denatured DNA, as well as proteins do not co-immobilize.

Circle No. 110 on Reader Service Card.

ABN
Adenosine Diisopropyl Phosphoramidite
ABN
Cytidine Diisopropyl Phosphoramidite
ABN
Guanosine Diisopropyl Phosphoramidite
ABN
Thymidine Diisopropyl Phosphoramidite
ABN
DMT-dA-(N-Bz)-Suc-LCAA-CPG
ABN
DMT-dC-(N-Bz)-Suc-LCAA-CPG
ABN
DMT-dG-(N-iBu)-Suc-LCAA-CPG
ABN
DMT-T-Suc-LCAA-CPG

The raw material for oligonucleotide synthesis, from American Bionuclear.

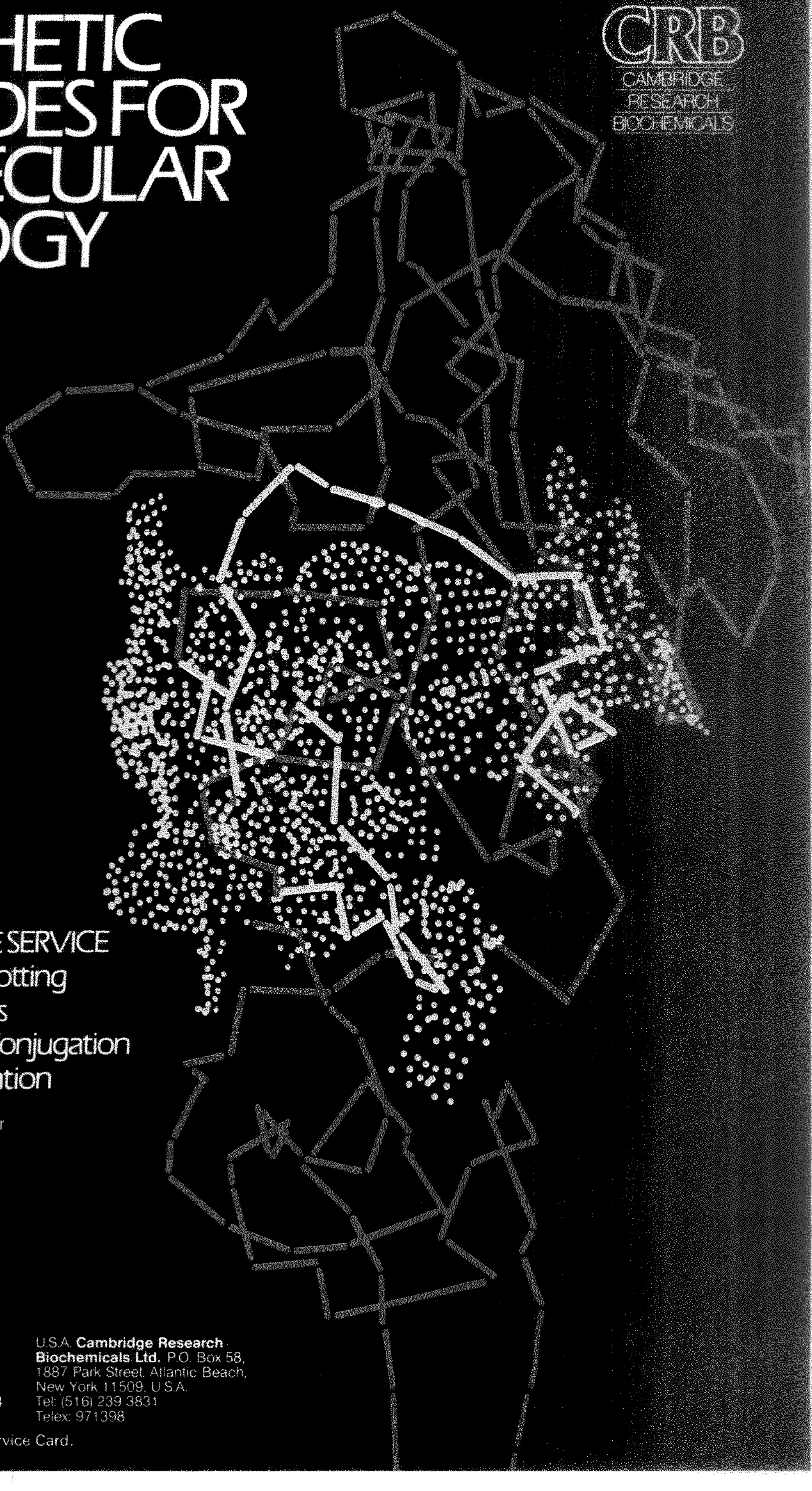

SYNTHETIC PEPTIDES FOR MOLECULAR BIOLOGY

CRB
CAMBRIDGE
RESEARCH
BIOCHEMICALS

THE COMPLETE SERVICE
Hydrophilicity Plotting
Peptide Synthesis
Peptide Carrier Conjugation
Structure Elucidation

For further details, or for any information concerning the use of synthetic peptides in research please do not hesitate to contact:

Dr Paul W Sheppard
Contract Research Director
Cambridge (0223) 871674/5

Cambridge Research Biochemicals Ltd,
Button End Industrial Estate,
Harston, Cambridge
CB2 5NX
ENGLAND
Tel: Cambridge (0223) 871674
Telex: 817694 CRBLTD G

U.S.A. **Cambridge Research Biochemicals Ltd.** P.O. Box 58,
1887 Park Street, Atlantic Beach,
New York 11509, U.S.A.
Tel: (516) 239 3831
Telex: 971398

Circle No.32 on Reader Service Card.

● D-Gel, a new product from Tekmar, will rapidly and efficiently extract nucleic acids from gels. This electrophoretic transfer system will directly transfer nucleic acids to DEAE-cellulose, or DEAE anion-exchange resin. DNA can then be recovered rapidly and intact in a quantitative yield, free from contaminating gel impurities, for assured biological activity in subsequent enzymatic reactions. The system ensures a high recovery efficiency — nanogram to submilligram quantities — with no danger of cross contamination. Utilizing isolated and removable transfer chambers, the D-Gel system is compatible with standard laboratory power supplies.

Circle No. 111 on Reader Service Card.

● New additions to Cappel's range of affinity gells are anti-mouse IgG(H&L) coupled to Sepharose 4B and anti-rat IgG(H&L) coupled to Sepharose 4B. The antibodies are affinity purified and the mouse affinity gel will bind mouse IgG1, IgG2a, IgG2b, IgG3, IgM and IgA; the rat IgG affinity gel will bind rat IgG1, IgG2a, IgG2b, IgG2c and IgM. Affinity gels are useful for purification of mouse or rat immunoglobulin as well as immunoprecipitation of any IgG subclass mouse or rat monoclonal antibodies. These gels may also be used in columns for the same purposes. Each millilitre of gel has bound to it 2.0 mg of active affinity purified antibody resulting in a binding capacity of 1.0 to 1.75 mg ml^{-1} of IgG.

Circle No. 112 on Reader Service Card.

● The new DNA sequencing system from American Bionuclear is available in two versions: SQU-1000 (20 cm width) and SQU-2000 (33 cm width). Both are fully adjustable to provide the flexibility of running sequencing gels from 20 cm to 1 m in length. Both models feature adjustable upper buffer reservoirs, a 'no leak' gasket system of high compression silicone tubing that guarantees a tight seal and leak-free direct buffer–gel contact. Ports on both the upper and lower reservoirs permit buffer re-circulation, and a wide range of accessories is available for both models.

Circle No. 113 on Reader Service Card.

● The LKB 2301 Macrodrive 1 power supply is intended for low-voltage electrophoresis applications. Using a few simple switches and clear, easy-to-read LED displays, the required constant voltage (0–1,000 V), current (0–400 mA) and integral digital timer (0–60 hours) can be quickly set. The Macrodrive 1 is well suited for routine PAGE, SDS, disc and gradient gel electrophoresis, as well as immunoelectrophoresis.

Circle No. 114 on Reader Service Card.

● Purpose-built for the new blotting techniques the Desatronic 200/1000 (0–200 V/O-1,000 mA) power supply is available from Desaga GmbH of Heidelberg. Also new is the Desatronic 6000/100 for isoelectric focusing. Voltage, current and wattage are regulated automatically; all parameters are digitally displayed.

Circle No. 115 on Reader Service Card.

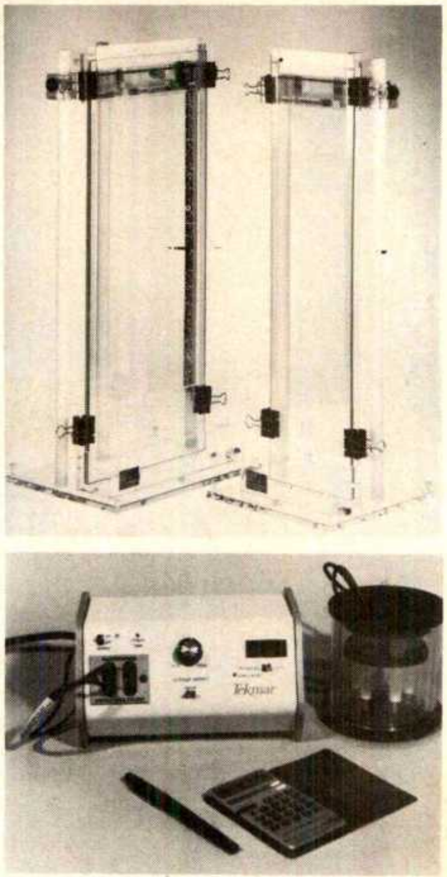

Top: American Bionuclear's DNA sequencing apparatus comes in two sizes. Bottom: Tekmar's D-Gel for extracting nucleic acids from gels.

ANY U.V. PROBLEMS?

CALL UPON OUR LIGHTS!

A complete range of 254-302-365nm and multiband U.V. lamps and generators for your FLUORESCENT ANALYSIS

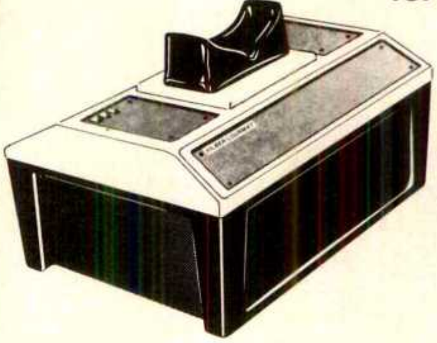

CN-15 U.V. darkroom

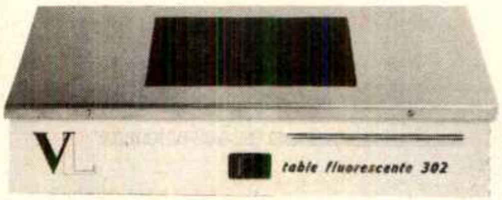

Fluorescent table

V.L. lamp with stand

Esquisse

FIRST FRENCH MANUFACTURER

☐ 254-302-365nm lamps
☐ Multiband lamps
☐ Portable lamps
☐ U.V. darkrooms
☐ Fluorescent tables
☐ U.V. radiometers
☐ Eprom erasers

VL VILBER LOURMAT

BP 66 - Torcy. Z.I. Sud. 77202 Marne-la-Vallée Cedex 2
France - Tél. : (6) 006.07.71 + - Télex VILBER 691062 F

LOOKING FOR EXPORT AGENTS

Circle No.31 on Reader Service Card.

ANNOUNCEMENTS

Awards

Professor K.D. Cole of Latrobe University, Melbourne, Australia, has been awarded the 1984 **Appleton Prize** for Ionospheric Physics by the Royal Society UK, in recognition for his contributions to understanding the fundamental processes taking place in the magnetosphere.

The Royal Society has also elected the following as new Foreign Members: **Professor P-G. De Gennes**, Professor at the Collège de France, Paris, in recognition of his many major contributions to theoretical physics — in the fields of magnetism, superconductivity, liquid crystals, polymers and mixed fluid flows; **Professor R. Hoffmann**, John A. Newman Professor of Physical Science at Cornell University, Ithaca, New York, USA, in recognition of his contributions to theoretical chemistry, particularly as originator of the extended Huckel theory; **Professor M. Meselson**, Cabot Professor of Natural Science, Harvard University, Cambridge, Massachusetts, USA, in recognition of his first demonstration of semiconservative DNA replication and for his studies on the mechanism of genetic recombination; **Professor G.E. Palade**, Professor of Cell Biology at Yale Univesity, New Haven, Connecticut, USA, in recognition of his investigations of the ultrastructure of biological cells, and notably the description and the delineation of the functions of the endoplasmic reticulum; **Professor C. Rubbia**, Professor of Physics, Harvard University, Cambridge, Massachusetts, USA, and Senior Research Officer, CERN, Geneva, Switzerland, in recognition of his work as an initiator of important experiments in new areas of high energy physics, and **Professor H.H. Ussing**, Professor of Biochemistry at the University of Copenhagen, Denmark, in recognition of his work on the active and passive transport of ions across cell membranes and on the functioning of secretory epithelia.

Emeritus Professor Sir Alan Harris, FEng of Imperial College London, has been awarded the Gold Medal of the Institution of Structural Engineers.

Professor J.T. Stuart, FRS, Head of the Department of Mathematics at Imperial College, has been awarded the Whitehead Prize of the London Mathematical Society.

Professor Michael Sela, President of the Weizmann Institute of Science, **Professor Louis Chedid** of the Pasteur Institute, Paris and **Professor Edgar Lederer** of the French Academy of Science, have been jointly awarded the Prix de l'Institut de la Vie by the Fondation Electricité in France for their elucidation and perfection of the production of synthetic vaccines and the adjuvants of immunity.

Mr Erik Quistgaard, Director General of the European Space Agency, has been presented with the NASA Distinguished Public Service Medal.

Dr Richard Beasley of Wellington University, New Zealand, has been awarded the first two-year fellowship by the Wellcome Trust in association with the Medical Research Council of New Zealand, to study factors underlying asthma — at the Department of Medicine, Southampton University.

Appointments

Sir Alec Merrison and **Professor L.A. Thomas** have been elected President and Vice-president, respectively, of the Institute of Physics, London.

Dr John Midwinter, Head of the Optical Communications Technology Division of British Telecom, has been elected to the British Telecom Chair of Optoelectrics at the Department of Electronic and Electrical Engineering, University College London.

Professor Brian May, Head of Silsoe College, Bedfordshire, UK, has been elected President of the Institution of Agricultural Engineers.

Professor Guillermo Soberón Acevedo, Secretary of Health and Welfare, Mexico, has been elected President of the 37th Annual Session of the World Health Assembly (WHO), Geneva, Switzerland.

Professor Edwin C. Cadman, MD, Professor of Medicine at the University College of San Francisco, has been elected to the presidency of the American Federation of Clinical Research.

Dr Gordon H. Sato, Director of the W. Alton Jones Cell Science Center, has been elected a Member of the National Academy of Sciences, USA.

James F. McDonald has been elected President and chief operating officer of Gould Electronics, Illinois, USA, while **David Simpson** has been elected vice-chairman of the board.

Professor Roderick N.M. McSween has been appointed to the Chair of Pathology at the University of Glasgow; also at Glasgow University, **Professor Kenneth C. Calman** has been appointed to the Chair of Postgraduate Medical Education and the Deanship of Postgraduate Medicine, and **Dr Miles D. Hounsley** has been appointed to the Gardiner Chair of Biochemistry.

Professor Gilmour Toner has been appointed to the Musgrave Chair of Pathology, and **Dr Ronald Henry Perrott** to the Chair of Software Engineering at the Queen's University of Belfast, Northern Ireland.

Professor Bryan Carsberg of the London School of Economics has been appointed as Director General of Telecommunications, UK.

Dr John Rose, a Director of Dainichi Sykes Robotics Ltd, has been appointed to the United Kingdom's first University chair in automated manufacturing technology at the University of Salford.

Arnold Allen, CBE, a Chief Executive at the UK Atomic Energy Authority, has been appointed its full-time Chairman.

Michael Bown, formerly Group President in charge of International Operations at Peabody International Corporation, has been appointed as the the first Director of CEED – the UK Centre for Economic and Environmental Development.

Dr George Russell, Senior Lecturer in the Department of Electrical and Electronic Engineering, Heriot–Watt University, has been appointed to a new Professorship within that Department.

Dr Bernard Wegener has been appointed Managing Director of Merrell Dow Pharmaceuticals GmBH, Ruesselsheim, West Germany.

Dr Bernard Hyams of the UK has been appointed by the Council of CERN – The European Laboratory for Particle Physics near Geneva, Switzerland – as the new head of the Experimental Physics Division.

Erich Bloch, currently Vice President for Technical Personnel Development at IBM, has been appointed Director of the National Science Foundation (NSF).

Dr Moustafa T. Chahine has been appointed to the position of Chief Scientist at the Jet Propulsion Laboratory (JPL), NASA, California; he is currently Manager of the Earth and Space Sciences Division at JPL.

Paul F. Engstrom, MD, has been named vice-president of Cancer Control and Continuing Education at the Fox Chase Cancer Center in Philadelphia, USA.

Paul Beeson MD, **Charles K. Donegan MD**, **Adrian Ostfeld MD**, **James Neel MD**, and **Dr Martha Storandt** have been appointed as new members of the National Advisory Council on Aging, USA.

Short Courses

Autumn 1984, **Continuing Engineering Education Program** organised by the George Washington University; London, Copenhagen, Dusseldorf, Frankfurt (Mr Michael Keenan, Manager, The George Washington University Continuing Engineering Education Program, 18 St. George's Street, Hanover Square, Mayfair, London W1R 9DE, UK).

18-20 September, **Introduction to Reinforced Plastics**, (Short Course Office (IFRP), Department of Mechanical Engineering, University of Sheffield, Mappin Street, Sheffield S1 3JD, UK).

24-27 September, **Programming in Pascal** and 23-25 October, **Control of Mechanical Systems** (The Registrar, The University of Manchester Institute of Science and Technology, PO Box 88, Manchester M60 1QD, UK).

17-19 October, **Basic High Performance Liquid Chromatography Course**, (Chrompack UK Ltd., Unit 4, Indescon Court, Millharbour, London E14 9TN).

19-22 November, **Training Course in Fluid Rheology** (Mr L.J. Viney, Warren Spring Laboratory, Gunnels Wood Road, Stevenage, Hertfordshire SG1 2BX, UK).

21-1-87
A. Batty

How valuable is the student grant?

from Richard Pearson

The student grant in the United Kingdom has been severely devalued by the effects of inflation. But individual circumstances vary widely.

ALTHOUGH graduate employment prospects are improving rapidly from the doldrums of the early 1980s, many will still not find an easy or speedy transition from higher education into employment (*Nature* **310**, 260; 1984). With the government and its critics continuing to debate the likely level of future demand for places in the light of the declining numbers of 18-year-olds in the population, and with the apparent falling "rate of return" to studying many subjects in higher education, how attractive is the student grant in terms of supporting three years' investment in higher education?

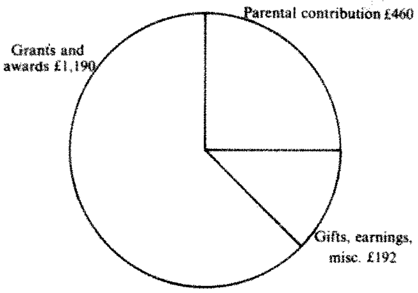

Fig. 1 Sources of student income for UK university and polytechnic students in 1982–83. (Source: NUS survey).

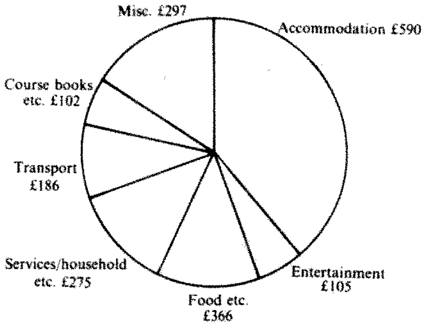

Fig. 2 Student expenditure for the academic year 1982–83. (Source: NUS survey).

In order to encourage student interest in subjects in demand by employers, the UK Department of Education and Science has announced that the amount undergraduates can receive from a sponsoring employer before their grant is affected will rise to £1,200 together with a £400 earnings allowance. For the lucky few who can combine sponsorship (see *Nature* **307**, 488; 1984) with a full grant, this means a student income of nearly £3,500 for the academic year, double the basic grant. A recent survey for the National Union of Students (*Undergraduate Income and Expenditure*, NUS, 1984) has, however, shown that for most students half this figure may be unattainable, with many parents not making up their means-tested contribution. Although the basic grant in 1982–83 was £1,595, the average student received only £1,167, and there has been growing concern about the adequacy of this grant whose value has fallen behind the inflation rate over the past few years.

In the United Kingdom, grants are payable to the majority of students on a means-tested basis; a student living away from home at a college outside London in 1982–83 could have received a maximum grant of £1,595 plus tuition fees from his local education authority. Various supplements are also payable, for example, to those studying in London, or on a course that is longer than normal , while mature students receive a full grant with no means test. One in eight students, however, received only the minimum grant payable of £410, some because they, or their parents, refused to take the means test, while a further 5 per cent received less than £600 because their parental income was too high. Half received under £1,200 and only one in four students received the maximum grant. The total amount saved by the means test was estimated to be over £150 million in 1982–83 compared with a total public expenditure on grants of about £500 million. Just over half the parents paid their assessed contribution, a rather higher proportion than in 1974–75 when only just over a quarter did so. Interestingly almost as many parents paid more than the assessed contribution as paid less than the total due and the size of the sum due from parents did not seem to affect the likelihood of the student receiving more or less than that assessed. In terms of basic grant, science and social science students got slightly higher amounts than the engineers and arts students. Average income for the academic year, including additions such as gifts and term-time earnings was £1,842, two thirds coming from the basic grant (Fig. 1).

A significant additional source of student income, outside term time, was vacation jobs, which gave an average income of £251 per student, with 10 per cent earning in excess of £700, and a few earning over £200 per week, although nearly half had no vacation job. By contrast ten years earlier 80 per cent of students had vacation jobs in the summer. Men received rather higher vacation income than women, while engineers and technology students received significantly more than the average, aided by sponsorship and enhanced prospects of vacation work. This latter factor also boosted term-time incomes of these students. Supplementary benefit and vacation grants were further sources of income out of term time for a minority of students, the average sum overall being around £100 per student.

Where then does the money go? Accommodation is the biggest outgoing. Only one in ten undergraduates in the United Kingdom lives in the parental home, while nearly half live in "official" college halls or hostels. College premises are particularly important for university students while for those at polytechnics, rented flats were the most common form of accommodation. In London, more students live in their parents' home because of easier travel conditions and larger college catchment areas and the lower availability of halls of residence. The average cost of college accommodation was £24 per week, with the polytechnics cheaper than the universities, most college accommodation including some food and services. Those in private rented accommodation paid an average of £14 per week each for rent alone.

Other living costs included food and household expenses, travel and recreational. Course-related expenditure included books and course equipment; average annual expenditure was to be around £100 with university students spending most (Fig. 2) and 10 per cent apparently spending nothing at all on books. On a subject basis, medical students spent most on course equipment with social science and language students also spending above the average.

The study showed that the majority of students relied on parental support or supplementary income to support part of their studies. While for the "average" student such supplementary income was usually forthcoming, some receiving more than the notionally required sum, many had to restrict expenditure significantly to sustain themselves. The survey, by revealing the many sources of income and grants available and the various patterns of expenditure, highlights the complexities of an informed debate about student finance. Perhaps the one clear message that comes through is that to plan grants, loans and finance around a notional average case will lead to very different outcomes for different individuals. Student finance is not an exact science. ☐

Richard Pearson is at the Institute of Manpower Studies, Mantell Building, University of Sussex, Brighton BN1 9RF, UK.

nature

21-1-87
A. Batten

Past defended, future unforeseen

British higher education is once more under scrutiny. Both sectors of the binary system have now made claims and the government will soon decide. But constitutional questions are still begging.

THE elementary principle that he who pays the piper calls the tune is often nullified because the paymasters do not know what they would like to hear, which is why they often find it necessary to pay not just a piper but on pipe-music. This part of the reason why, in the administration of British higher education (and of that in many other parts of the world), relations between central government and the publicly supported universities are channelled through some intermediary — in the British case, the organisation called ther University Grants Committee. Some of the troubles that now afflict the British system of higher education have arisen because the present British Government differs from many of its predecessors in knowing — or in believing that it knows — what the system of higher education should be doing. For close on five years, the paymaster has been pipe-master as well, with disastrous consequences. By the end of this year, with the appearance of the promised reappraisal of policy, it should be clear whether there is now to be a return to normalcy and good sense.

In normal times, last week's argument by the University Grants Committee (see page 196) would have been taken as a sign that the future must now be brighter than it has seemed. The committee has put forward a case that is at once cogent and combative. It is on sure ground in pointing to the errors in the calculations by the government (and others) of the way in which the demand for student places will decline, for demographic reasons, in the years ahead. It is right to protest that if the present system and further planned reductions of expenditure continue, the university system will not be able to adapt without structural damage, certainly to the quality of institutions, perhaps to the survival of some of them. The committee is also on firm ground in arguing for some means of rejuvenating the teaching staffs of British universities, asking that at least 3.5 per cent of academics should be replaced each year, if necessary by the continuation of schemes for persuading older people to retire early. All these proposals will make eminent sense to British academics, who will recognize that they again have an intelligent and robust friend at court. This is precisely what would have been expected from Sir Peter Swinnerton-Dyer, the committee's chairman for only the past year.

Dissension

On the committee's long list of practical proposals for change, there are several that should not cause dissension even in its relations with the government. Most obviously, it is hard to see how the present British Government, which is forever urging that the universities should raise a greater share of their income from other than public sources, can continue to resist reforms that would simplify that task. The notion that gifts by corporations to British universities should be tax-free only if they can be shown to further the donor's corporate interests (the present position) is absurd, and should be abandoned promptly. The present tax regulation that allows no relief from personal taxation in respect of the payment of fees for higher education is both a restraint on the ability of universities and other institutions to attract students and a foolish fiscal economy when the need for added skill is as great as even the government acknowledges it to be. The way in which the British Treasury is empowered to play a game of cat and mouse with supposedly autonomous universities wishing to dispose of physical assets, and which cannot know in advance what proportion of the proceeds they will be able to keep for new development and reorganization, is both inequitable and an encouragement of sloth. The general suspicion that institutions that succeed in raising outside funds, perhaps by benefactions, will then get less from public funds, which the committee says is not the case, should be formally denied by the government which has helped to create this false impression. It will be discreditable if a government that has been preaching self-reliance for the universities for the past five years cannot meet this reasonable demand by the grants committee. That is the small change of what the committee asks on the universities' behalf.

Trouble

The bigger questions will not be answered as readily, as the grants committee must know full well. The issue of who shall become a student, for example, is certain to cause trouble. Pointing out that the government has made elementary errors in its calculations of changing demographic patterns of demand is bad enough, which no doubt is why the grants committee has not taken the obvious further step of reminding it that many of the economies decreed in higher education in the past five years have been literally a waste of resources — academics have been tempted into not teaching students seeking higher education by an early retirement scheme that will have to be paid for out of future budgets. What the committee has done, in concert with the National Advisory Body, is to rewrite the standard criterion for telling whether a would-be student should be eligible for a place at a university or polytechnic. Liberally, the committee holds that the words "qualified by ability and attainment" are too obvious an invitation to over-specialization in the preparation of school-leaving examinations, and too discriminatory against those who would come to higher education later in their careers. The snag is that the alternative form of words now put forward — "able to benefit" — will seem to the government to be a demand for a blank cheque. And the demand will easily be denied. The government will merely have to repeat what it has creditably said of high-school education about the importance of objective as distinct from relative measurements of attainment. It need not confess that its real anxiety is that open access, or access determined by other people's assessment of who would benefit, will in principle bring into play the government's obligation to pay students a pittance of a salary (called a maintenance grant).

The grants committee's proposals on academic staffs at British universities are similarly vulnerable to government obtuseness. If it is asserted that younger academics are in some sense more desirable than older experienced teachers, why (the government will ask) should older people generally speaking be better paid? The grants committee, unfortunately, cannot put into words what it knows to be the truth, that even the most careful assessment of people's quality at the outset of their careers cannot predetermine excellence, and that what it wishes to do is to operate an informal and unspoken system whereby academics can generously be put out to grass at widely different stages in their personal development. The case for that is strong, and equitable in spite of the appearances. But the British Government, and even the academic professions, are unlikely to accept it in its unvarnished form. A guileful statement of the case would have been barely saleable if the grants committee had been able to suggest a compromise with the government on academic tenure, but the best it has been able to muster is a proposal that probationary periods should last for five years, not three. The committee's reminder that universities individually are always free to dismiss academics whose work is less than satisfactory will not satisfy a government persuaded that academic tenure is a charter for wrong-thinking layabouts.

The committee's arguments on research are similarly ambiguous. It is right to say that British universities are responsible for well over half of British basic research. It could have claimed the more interesting half. But it will cut very little ice with a sceptical government that, having accepted the universities' view that money should not be allocated separately for teaching and research, the committee should not be able to say how it will "be more selective" without further consultation. Worse still, the committee has to confess that its efforts will not succeed unless universities themselves become more self-conscious about their prosecution of research.

Much the same is true of the committee's case for extra funds within the university system. The case is overwhelming when the need for industrial change has become as clamant as in Britain now, yet outwardly the universities' case is little different from that of other claimants on the public purse. The coalminers of Britain, for example, are flush with arguments about the strategic importance of stable mining communities. The best hope for the immediate future is that the government may listen to what the grants committee has been saying for long enough to provide a chance for internal change to be engendered. The danger is that the government will lose patience.

The most serious gap, and thus the most serious weakness, of the universities' claim on the British Government is that the committee has so little to say on their behalf about their constitution, and about relationships between the public and private sectors. Yet the greatest iniquities of the past few years are embodied in the ways in which universities have been told how many students they may teach and are now being moulded on patterns specified from without. Academics apparently willing to go to the stake in defence of academic freedom supposedly bound up in the rules of tenure seem much less eager to defend their institutions on these more important counts. The only remedy is that constitutional autonomy should be backed by financial autonomy, and that academic institutions — public as well as private — should be allowed to make their way in the world by the reputations they are able to acquire in the eyes of students and students' employers. If, in the arrangement of financial autonomy for universities (and polytechnics), it were possible also to solve the government's problem of the blank cheque — the fear that more students must mean extra maintenance costs — it might be possible to look forward in Britain to a system of higher education that would change to meet external needs without external prodding, and which would be free from the attributes of academic class-distinction that now compromise the good work that individual institutions do.

In due course, the grants committee and its opposite number for the public sector will come to recognize that such a solution is inevitable. So, too, will the government. For the time being, however, the best that can be hoped for is that higher educational institutions, public as well as private, will recognize the potential value of diversity and their masters the importance of autonomy. The grants committee's document refers to a scheme the British Government was canvassing earlier this year that would have given some universities a fixed budget, no other marching orders but an exhortation to make what they could of their resources. Cryptically, the committee says it will give its opinion on the scheme "if asked". Appearances to the contrary, its opinion should be that everybody would stand to gain from an experiment in autonomy along lines like these. Why not offer an opportunity for one university and one polytechnic to try their hands at freedom within the confines of an inflation-proofed public subvention? Or is everybody afraid of being overwhelmed by the rush of applicants? ☐

Help for Argentina?

The plight of Argentinian science (see page 201) deserves widely to be recognized.

IT is easy for those in developed countries to regard the sorry state of Argentinian science with the contempt familiarly accorded the efforts of developing countries to appear scientifically sophisticated; building biotechnology centres without biotechnologists to populate them, or research reactors when there are no nuclear physicists. But Argentina is different. It has produced a large number of first-rate scientists (many of whom now work in the United States or Europe) and it has made a not unrespectable start at industrialization, helped by near self-sufficiency in petroleum and a major surplus in agricultural products. Argentina is not a banana republic — indeed, until December of last year, it was not even a republic. And that is crucial to understanding the special nature of Argentinian science, and why it is in a different mess from that of other developing countries.

In addition to its major credentials of repression, murder and the Falklands war, the military regime that seized power in 1976 can claim credit for the dismantling of Argentina's scientific institutions, the universities in particular. The potential remains, but its realization is further away than ever. The return to democracy, still a source of wonder and justifiable admiration in the Western world, has brought with it a sweeping change of attitudes. Some of the most competent and knowledgeable people one could expect to find in any government have been put in charge of repairing Argentine science, but the task requires more than clear thinking. It is difficult to have a science policy without money, and Argentina has none. And the new government will not indulge the luxury of investing long-term in science and higher education while its overseas debt amounts to $50,000 million — and while it has to keep borrowing more to pay the outstanding interest.

So what can others do to help? And why should they bother? External financial aid for scientific institutions would be invaluable, but is unlikely to materialize quickly. Yet that is no reason why the question should not be considered. In the past few days, the World Bank has made a loan of $25 million to the People's Republic of China to help with the foundation of a network of institutes for agricultural research. Even allowing for the way in which China has become the apple of Western eyes, and for the fact that Argentina still has to meet the tough monetary conditions prescribed by the World Bank's sister organization, the International Monetary Fund, the case for a special loan is powerful.

The extent of the damage done to Argentinian science — and the real potential for excellence — has magnified the value of more informal contributions. People in the United States and Europe will do far more than they can perhaps imagine possible for restoring science in Argentina simply by participating in conferences there, by spending time there as visiting professors or teaching short courses, or simply by keeping in contact with Argentinian scientists who have been isolated by the recent events, and who face enormous difficulties in what is elsewhere the effortless task of keeping up with current scientific information. The shortage of foreign journals, always a problem in developing countries, has been greatly exacerbated by the military regime's policy of choking off the universities.

To those in Britain who may mumble about the Falklands war and about cooperation with a nation still technically at war, it is worth noting that the best assurance of peace and reasonableness on all sides is the presence of a democracy in Argentina. It was a desparate totalitarian regime that launched the Falklands war, an awkward legacy for the new government. And at least among educated Argentinians, one is more likely to hear joking references to Britain's "enemy" status than talk of vengeance. Anything that can be done to bolster Argentina's democracy, and its commitment under President Raul Alfonsin to make education, rather than weapons, the foundation of its national security, is a step in the right direction for everyone concerned. ☐

Restraints on publication

Deal in prospect on US export rules

Washington

A WORKING group headed by the President's Office of Science and Technology Policy has recommended that draft export control regulations be altered to provide greater freedom for scientific communications. This was announced by Charles Herz, general counsel of the National Science Foundation and a member of the group, speaking at a meeting of the Department of Defense-University Forum last week. The forum had made several specific suggestions to the Department of Commerce, the agency charged with writing the regulations, chief among them being the idea that fundamental research should be controlled only through national security classification and not through any rules requiring universities to obtain an export licence before publishing research results.

The group also recommended that when export controls are applied to university research, research contracts — rather than licensing procedures — should be the enforcement mechanism. The point is an important one to universities, which have demanded to know in advance of accepting research contracts whether their freedom to publish will be restricted. Many universities as a matter of policy refuse to accept such restrictions.

Under the working group's proposed changes, any research at universities that complies with contract terms would automatically be granted a "general licence" for "export" — a term which includes publication. The situation now is that universities in principle could find themselves in double jeopardy in that publication may be cleared by the Department of Defense (DOD), but still be held a violation of export rules by the Department of Commerce.

An earlier plan to establish a broad category of "sensitive" but unclassified research that could be subject to export controls was abandoned by DOD in May in the face of stiff university opposition. DOD's revised policy exempts "fundamental" research from controls.

But questions remain over just how DOD and the other federal agencies plan to apply export controls to publication other than fundamental research. David Wilson, the universities' co-chairman of the DOD-University Forum committee on export controls, recommended that export controls incorporated in research contracts should permit DOD only a 60-day review before publication. DOD could then advise the university of information in the proposed publication that would violate the export act if published, but the ultimate decision whether or not to publish would remain with the university.

The definition of "fundamental" research remains unclear. DOD officials and Wilson seem to agree that a reasonable approach would be to define as fundamental on-campus research in what DOD calls categories 6.1 or 6.2, which correspond to basic research and "advanced technology development" respectively. More than 99 per cent of on-campus research supported by DOD is said to fall in these two categories, while the remainder is in category 6.3, "strategic programmes". That, as well as 6.2 research conducted at off-campus facilities such as Johns Hopkins University's Applied Physics Laboratory, could be subject to contract restrictions based on export control authority. (An exception is to be made for star wars research which, although categorized as 6.3, will for the most part be considered fundamental.)

DOD officials say they need the "flexibility" to apply restrictions to sensitive research that does not warrant classification, which they say is "a pain in the neck", because classified documents are subject to security restrictions — they must be kept in locked cabinets, for example, and cannot leave offices or be left lying on desks.

Stephen Budiansky

● Meanwhile, a revised Export Administration Act — needed to implement the regulations — remains stalled in Congress. At a conference committee meeting last week, House members refused to accept compromises offered by the Senate on contract sanctity and national security. More meetings are planned this week. The commerce department, however, has shifted its position on high-technology exports of equipment (as opposed to information). Its latest proposals would allow the exporting companies themselves to enforce the regulations, subject to audit by the departments. □

AIDS

Virus clones multiply

Washington

YET another US genetic engineering company has jumped on the bandwagon of acquired immune deficiency syndrome (AIDS). The Chiron Corporation, of Emeryville, California, announced last week that its researchers had succeeded in cloning the entire genome of a putative AIDS virus isolated by Dr Jay Levy of the University of California at San Francisco. Earlier this year, Chiron was not among those companies selected by the federal government to develop a diagnostic blood test for AIDS from virus isolated at the National Institutes of Health by Dr Robert Gallo.

Following the frequent practice of some genetic engineering companies, Chiron made its announcement without at the same time publishing details of its accomplishment. Lacey Overby, a vice-president of Chiron, said that a scientific manuscript describing the process was essentially complete and ready to be submitted for publication. Overby averred that scientific journals seemed not to mind publishing previously announced findings. Chiron plans to work on expressing the viral proteins in yeast cells, a field in which it already has expertise.

Chiron says it assumes that the virus isolate it is using is the same as the human T-cell leukaemia virus III isolated by Gallo. The cloning of the virus paves the way for a widely available diagnostic test that does not require the intact virus to be used, as well as, perhaps, a vaccine.

But Chiron is not alone in the race to produce an AIDS diagnostic nor the first to have cloned an AIDS-linked virus. Gallo has also now cloned his viral isolate, and probably others have done the same without making an announcement.

Chiron says its public statement is justified by the "intense competition" in the field. Chiron expects to be making a profit within the next 18 months (it was incorporated only in 1981) and reports that clinical trials on what is likely to be its first commercially available product, a genetically engineered hepatitis B vaccine, are going well.

Tim Beardsley

Entrance standards on increase

BRITISH universities are demanding higher examination grades from prospective students than they did in 1980. This conclusion can be drawn from Universities Central Council on Admissions (UCCA) statistics recently released. Entrance requirements for each of the 24 main university subjects have risen with those for electrical engineering and computer sciences showing the most marked rise.

UCCA believes that the increasingly high standards required for university entrance are deterring marginal candidates — those who may not have attended good secondary schools but might, nevertheless thrive at university — from applying. The statistics also show that young people from wealthier families are still over-represented among successful applicants.

Marcus Chown

British universities

Champion springs to life

THE University Grants Committee (UGC) has told the British Government that, on present financial policies, it may be necessary for one or more universities to be closed. And UGC goes on to say, in its document *Strategy for Higher Education in the 1990s*, published last week, that it will leave to the government the invidious choice of institutions to be shut, on the grounds that it is not itself competent to assess non-academic considerations and that, in any case, its relationship with universities generally "would not survive" the act of pointing the fatal finger.

UGC's document, like the parallel document also published last week by the National Advisory Body (NAB, responsible for non-university higher education, especially the polytechnics), is formally a response to a government request for advice in advance of the reappraisal of higher education strategy, advertised for later in the year.

UGC's gloomy forecast arises from its calculation that published estimates of spending on higher education in the years to 1986–87 entail an annual reduction of 0.5 per cent, and from experience in recent years that university pay settlements have exceeded the amount allowed for to an extent that will impoverish the universities by a further 1 per cent a year. Tartly, UGC says that universities conformed more closely to the guidelines on public sector pay than government itself.

UGC's gloomy forecast stems partly from its view that the budget cuts of 1981 have already forced universities to mortgage their "freedom of manoeuvre", and that further cuts will require commensurate staff reductions. Faced with that need, UGC says, it would prefer to recommend contraction on a discriminatory basis rather than letting the cuts fall equally across universities. But that course could prove impossible, in which case it would be forced to recommend "with extreme reluctance" that some universities should be shut.

UGC adds that it cannot understand the implications of such a development, for the institutions closed would probably have "better" students, staff and facilities than "most institutions in the public sector", and says that closing a university would entail a waste of assets that "could not be defended".

For the years ahead, what UGC pleads for is "level funding" at the very least. As things are, its document argues, shrinking budgets will mean that fewer students can be taught. Stability, on the other hand, could mean that universities could provide more education for the same cost.

Even level funding will not, however, allow British universities to finance a substantial increase in the number of student places in science and technology, an expansion of continuing education and the rejuvenation of university teaching staffs by the replacement of older people by newer recruits. And the strategy document makes a strong case for each objective, the first of which at least is that of the British Government as well.

Both UGC and NAB also quarrel with earlier government estimates of student demand over the remainder of the century. UGC argues for an increase (to 170,000 a year) in the number of British students entering full-time education, and for a total full-time student population of 600,000 by the end of the decade. UGC asks that, when the British Government finally picks a number, there should be consultation on the distribution of students between "private" and "public" sectors.

NAB is more bullish, largely on the basis of a redefinition of the criteria for access to higher education agreed with UGC, that higher education should be open to "those able to benefit" from it, and who wish to do so. As things are, the guiding principle, laid down in 1963, is that students should be "qualified by ability and attainment".

UGC includes a discussion of the statistical errors of earlier estimates of student demand, and asks that the basic data should be refined before estimates are calculated for the 1990s, saying that demand will not diminish "just because there are fewer 18 year olds". It fears that there will be shortages of graduates "across the board" as "the country moves out of recession".

On government pleas for a "switch" from the arts and humanities to science and technology, UGC argues that the pace of change will be determined by the "supply of good students", saying that the problem would be transformed if more "girls" (*sic*) could be persuaded to "develop an interest in mathematics and physical sciences". UGC says that extra funds would in any case be necessary, and that extra science places at universities should not be provided at the expense of the arts and humanities.

On research, UGC says that it proposes to accept the general university opinion that individual budgets should not deal separately with teaching and research, although it accepts that universities deserve a fuller account of how their budgets are determined. The document says UGC will be "more selective" in favour of strong research universities, but only after further consultation. UGC adds that its policy will succeed only if universities equip themselves to decide strategies on research.

By its tone and in what it says, the UGC document should help restore UGC's reputation among academics as their defence against the government. Whether the latest defence will prove sufficient remains to be seen. □

French research

Growth rate is checked

Paris

THE French research budget for 1985, published last week, is good. But not so good as last year, or the year before. Research spending in France, previously buoyant, is reaching the top of the S-curve. At the same time, some of the more ambitious ministerial efforts at linking French research with industry are now deemed failures. Science policy-makers should reflect on how best to continue the French experiment of "solving the economic crisis through science".

In 1983, the first big year for science in the Mitterrand presidency, the budget for fundamental research leapt by nearly 25 per cent in current francs, and applied research by 18 per cent, compared with a net government budget increase of 13 per cent. In 1984, as the recession began to bite, growth slowed to 12 per cent in fundamental research and the same in applied research, against a net government budget increase of 4 per cent (and 7 per cent inflation). This was not enough, researchers began to complain, to cope with the franc falling rapidly against the dollar and other currencies in which materials and equipment are usually purchased. (The franc has fallen 25 per cent even against the pound since 1982.)

This year, increases will be less again (but at least they are increases). Fundamental and applied research should each grow by 10 per cent against the net budget growth of 3 per cent and projected inflation of 4.5 per cent in 1985, research minister Hubert Curien announced last week.

CNRS, the principal research council for basic science in France, will see an increase of nearly 8 per cent in its operating budget next year. This, however, will be fully taken up, says director Pierre Papon, by existing CNRS expansion programmes in microelectronics — a new major laboratory is planned at Bajneux to the south of Paris — and other areas.

Yet Papon is pleased by the new posts offered by Curien. The minister will create 536 new posts for fundamental researchers, of which 300 will go to CNRS. Combined with vacancies arising from departures and retirements, CNRS will have 500 posts, around 5 per cent of its total research staff, to play with this year. This gives some real room for policy-making, Papon says, allowing for expansion in priority areas (life science, engineering and social science) and even in some "second order" priorities (such as high-energy physics, which will be favoured over low-energy nuclear physics next year).

Linking researchers with French industry remains one of Curien's highest priorities, but the more centralist exercises of the ex-research minister Jean-Pierre

LIBRARY COMP
Departments of
Chemical Engineering
Chemical Technology
Plastics and Rubber Technology

Chevènement are now being described by policy-makers as "70 per cent failures". These were "*programmes mobilisateurs*" designed to stimulate action in fields like bio-technology and information technology. The problem: the French penchant for autocracy. The *programmes mobilisateurs* were to be run at arm's length by small groups at the Ministry of Research (responsive to the needs of industry and research). But these small groups grew too large, and developed ideas and programmes of their own. Industry saw them as socialist interventionalism. Papon himself admits he is anxious.

Meanwhile, Curien hopes to respond next year with a new and somewhat wiser "law for research" — wiser indeed than the Chevènement version of 1982, which aimed at an increase in French national research and development spending from 1.8 per cent of gross national product in 1981 to 2.5 per cent by 1985. That will not be reached, but the ratio will be 2.8 per cent. Now France is waiting for industry to respond.

Robert Walgate

Merger resisted

Düsseldorf

THE Social-Democratic (SPD) Government of Nordrhein-Westfalen in Düsseldorf has protested vigorously against the plans of the federal Minister for Research and Technology, the Christian Democratic (CDU) Dr Heinz Riesenhuber, who has proposed that the main thrust of biotechnology research in West Germany should be concentrated in future in one, rather than two, research centres.

Last year (see *Nature* 106, 305; 1983), an investigating committee suggested that the two major centres at Jülich (Nordrhein-Westfalen) and Braunschweig-Stöckheim (Niedersachsen, CDU government) would be better amalgated into one, thus improving the efficiency of research and reducing its cost. The new committee recommended that the new centre should be based in Braunschweig despite the committee's poor opinion of the standard of the work of the 350 research workers at Braunschweig, and its praise for the work of the 100 researchers at Jülich.

Rolf Krumsiek, Minister for Research in Nordrhein-Westfalen, has now promised to retain the Jülich institute at its present size, and in this he has the full support of the two directors of this research centre, Professor Hermann Sahm and Professor Christian Wandrey, both of whom wish to stay in Nordrhein-Westfalen. This difference of opinion between the central government and that of Nordrhein-Westfalen may bring difficulties should the central government decide to withdraw its financial support for Jülich, at present 90 per cent of the total cost. Retention of an interest in this promising research sector would then require an enormous financial intervention from the *Land* government.

Jürgen Neffe

European science

Forging stronger research links

Paris

THE European Science Foundation (ESF), a cooperative focus for over 50 national science funding agencies in Europe, has received broad political backing for a $1 million increase in its $2½ million budget — to help European researchers to keep in touch with one another.

This was one of the more concrete results of a unique meeting in Paris on Monday of 21 European research ministers under the auspices of the Council of Europe. The meeting, which had taken nearly a year of preparation, aimed at creating a "fresh political impetus" to European scientific co-operation, and this it has clearly done. However, although it recommended $1 million for ESF, the meeting had no power actually to define a budget. ESF must wait to see if its member agencies can find the cash.

Certainly, better cooperation as would be developed by ESF in a number of specified research areas is necessary, if any real life is to be given to the concept of "European research". The French Centre National de la Recherche Scientifique (CNRS), for example, annually sends more scientists to California than it does to the whole of Europe put together. And CNRS is not alone, either in its Atlanticism or in the need it feels to balance this by increasing cooperation within Europe.

In Paris on Monday, ESF was recommended to create "networks" of exchange in, for example, oceanography, Earth sciences, materials sciences, epidemiology and, altogether, 18 other fields of research. Although the money required would be a considerable sum for ESF, it would be small in relation to total European research budgets (a "per cent of a per cent", says ESF).

Now, ESF will make a detailed study of the 18 network proposals, themselves already filtered by ESF from around 200 originally received from national bodies before the conference. ESF will make specific recommendations for action within five months. The networks would differ from the superficially similar stimulation programme of the European Economic Community in one important respect, said ESF vice-president Professor Roger van Lieshout: they would be aimed at individual scientists, offering them mobility and choice, rather than at specific institutions. "If you create a centre of excellence, it will always remain a centre but not always remain excellent", said van Lieshout.

Also on Monday, the Council of Europe was instructed to consider the introduction of a "researcher's card". The card would be a kind of passport to Europe allowing accredited researchers certain privileges (such as help in getting electronic equipment past inquisitive customs officers). The Council of Europe should also consider, said the ministers, other moves to improve mobility by removing certain trivial but cumulatively important obstacles to free exchange — such as freedom to open a bank account.

Peter Brooke, the British research minister, also made a surprising and last minute proposal: to create a prestigious European academy like, for example, the Royal Society and the US National Academy of Sciences. This would foster a sense of identity among European scientists, said Brooke. Conference president, Frenchman Hubert Curien, described the proposal as "very interesting", but it was not among the official recommendations of the meeting. Britain may take the proposal further on its own initiative, said Brooke after the meeting.

Robert Walgate

Amazon to yield more secrets?

THE government of Brazil has invited a team of Soviet oceanologists to carry out a survey of the Amazon and its estuary. This is a follow-up to last year's expedition aboard the Soviet oceanological research vessel, *Professor Shtokman*, in February–April 1983, in which a joint Soviet-Brazilian scientific team took part and which penetrated far up the Amazon as well as surveying the ocean around its outfall.

The 1983 expedition concentrated on the geological sampling of the bed, ichthyological studies, and also some hydrographic work. The exceptional depth of the Amazon (as much as 100 m in places) — a consequence of the river lying on the boundary of two geological plates — made it necessary to use an ocean-going vessel. Much of the data from the 1983 expedition remains to be fully worked out. Nevertheless, according to Academician Aleksandr Yanshin, a vice-president of the Soviet Academy of Sciences, much has already been discovered.

Numerical data from the 1983 expedition include figures for the annual outflow of the Amazon (6,000 km^3, some 50 per cent more than the total of all Soviet rivers apparently) and the annual sediment burden (300 million tonnes). Theories have been developed to explain how the sediments became spread out all along the coast of South America rather than forming a delta as with most major rivers.

One notable discovery, the Soviet hydrobiologists claim, was that the Amazonian river water retains its brown colour even after the precipitation of all sediments. This, it is thought, is due to the presence of dissolved organic compounds, reminiscent of swamp water.

Vera Rich

Patent rights

Patient sues for title to own cells

Los Angeles

A FORMER leukaemia patient last week sued doctors at the University of California, Los Angeles (UCLA), for patenting and marketing a cell line derived from his spleen, removed to save his life. The suit, said to be the first of its kind, raises the ethical question of who has the right to profit from biological discoveries made by physicians using patients' organs.

The cell line, named "Mo" after patient John Moore, has potential commercial value in treating or perhaps even curing blood diseases including cancer and acquired immune deficiency syndrome (AIDS), according to Mr Moore and his Beverly Hills attorney, Sanford Gage.

In the lawsuit, filed in Los Angeles Superior Court on 11 September, Mr Moore asserts his ownership of his blood and bodily substances and of any by-products produced from them. The University of California patented the cell line without his permission, he says, but could conceivably make millions of dollars from it.

The UCLA researchers, Dr David W. Golde (chief of haematology and oncology) and medical technician Shirley Quan, say, however, that the cell line has not proved to have any commercial value, even though it is an "enormously valuable research tool". For example, Mo is the cell line which provided the supernatant from which Dr Robert Gallo of the National Cancer Institute isolated a human T-cell lymphotrophic virus, called HTLV-II. This virus, which is rare, evidently caused Mr Moore's disease, a T-cell variant of hairy cell leukaemia. A similar virus isolated in 1980 from other cell lines, called HTLV-I, is recognized as the cause of adult T-cell leukaemia, while HTLV-III, discovered in recent months, is the cause of AIDS.

...and Mr Doe reserves full rights to his tumour...
CONTRACT
ATTORNEY
BIRCH

The potential commercial value of the Mo cell line lies in its unusual lymphokine activity. Lymphokines are hormone-like substances secreted by lymphocytes with wide-ranging biological activity. They act locally to modulate cells responsive to them. They include interleukin-2, colony-stimulating factor, neutrophil migration inhibition factor and an erythroid-potentiating protein.

Mr Moore's spleen cells provide an unusually rich source of these proteins, which is why the University of California took out a patent, granted in March 1984, on the line. When the patent was applied for in 1976, there was growing commercial interest in producing interferon as an antiviral agent.

There are now nearly one hundred other cell lines, many of them not patented, which are also rich lymphokine sources. Lymphokines are still defined phenomenologically, and their potential in treating viral diseases is still highly speculative. But according to Dr Golde and others, Mr Moore's spleen cell line and his blood serum are still especially interesting because of the rarity of his leukaemia and the virus that caused it. **Sandra Blakeslee**

- The question of availability of the Mo T-lymphoblast cell line has caused some controversy. The complexities of the situation were touched upon by Dr Golde (*Nature* **308**, 19; 1984), responding to the various requests for the cells. He explains that the cells would become available from the American Type Tissue Culture Collection when UCLA's application for a patent had been processed. Those wanting the B-lymphoblasts from patient Mo, however, are not, it seems, affected by the patent. ☐

US pharmaceuticals

Patents extended, generics agreed

Washington

A DEFT legislative compromise appears to have pleased both research-based and "generic" pharmaceutical manufacturers in the United States. The two houses of Congress last week agreed on a bill that will extend the lives of patents on new drugs to compensate for the years spent by their manufacturers in seeking regulatory approval. Manufacturers of generic drugs have also won, in that they will in future be able to rely on the original testing data of a drug to back applications to market a generic equivalent once the patent term has expired. The Drug Price Competition and Patent Term Restoration Act, as it will be known, is backed by the administration and is likely to be signed into law within the next few weeks.

The research-based drug companies, represented by the Pharmaceutical Manufacturers Association, have long argued that the lengthy process of obtaining approval for a drug from the Food and Drug Administration (FDA) seriously reduces the incentive to search for new therapeutic compounds. In 1983, according to the association, each new drug brought to the market had soaked up an average of $91 million in direct and indirect costs, typically over 7 to 10 years. Only one in three drugs provides a reasonable return on this investment, and by the time all regulatory hurdles have been cleared, on average only 9 years of patent life remain out of the total of 17 years.

The new bill will allow an extension of the patent term by up to 5 years, with the proviso that the total remaining patent life after extension cannot exceed 14 years. The extension comprises one half of all the time the company spends testing, plus all the time the FDA spends processing applications. The special needs of genetic engineering companies are recognized in the bill: though normally there can be no more than one patent term extension for each product, substances made by recombinant DNA technology are treated for this purpose as if they differ from the same substance made by conventional means.

On the other side of the coin, generic brand manufacturers can often sell their products at very much lower prices than the original versions. These manufacturers argue that the public interest is best served by maximizing competition, but they also complain that, as things stand, they are caught in a "paperchase" when seeking regulatory approval for their products. Although, in principle, generic manufacturers may support their applications with data from previous tests on the same substance, the original data are often not published in the open literature, and many tests have to be repeated.

The new act introduces an "abbreviated new drug application" (ANDA) which simply requires the generic manufacturer to show that a product is essentially identical with an existing approved drug in terms of dosage and bioavailability. Senator Orrin Hatch (Republican, Utah), who sponsored the bill, quotes $1,000 million as the likely savings by consumers over the next 10 years as more generic drugs become available, although more cautious observers say it is impossible to make estimates of this kind.

The wheeling and dealing that went into the bill has led to an unusually complex set of rules on when ANDAs may be filed. An earlier version caused serious divisions within the Pharmaceutical Manufacturers Association because it would have allowed a generic drug manufacturer to obtain approval for a copied drug only 18 months after challenging the validity of a patent covering the product. The result could have been that research-based manufacturers would have had repeatedly to defend themselves against patent challenges. In the final version of the bill, ANDAs linked to patent challenges may be submitted to FDA 4 years after approval of an original drug, though marketing approval for the generic version must wait 7½ years from the original approval. **Tim Beardsley**

British Association for the Advancement of Science — Norwich

Accountability and the future

SIR Hans Kornberg's new blue-and-white insignia, whose glorious silver pendant marks him as next year's president of the British Association for the Advancement of Science, match his pyjamas. So, with glee, Sir Hans revealed to his neighbours at the British Association (BA) "science audit" last Friday. The pyjamas were not, however, on display.

The other delights at the University of East Anglia (Norwich) last week included a "Santa Claus machine", and the founder of the Open University proposing a £400,000 experiment to simulate a Martian colony on Earth and a delegation from China. There were also scientific submeetings galore, prizes, reviews of oncogenes and opiates, the first of Richard Gregory's exploratorium experiments, accounts of the environmental rape of the developing world and the terrors of future war. . . .

Fie to figures

AT least one industry in Britain will be booming next year — the industry of research on research. The beginnings of the industry were on display at Norwich in the BA audit of science spending and in the forthcoming Annual Review of Research by the Cabinet Office, introduced by cabinet science advisor, Robin Nicholson.

Nicholson's figures were preliminary: a collation of departmental projections. But they confirm that there will be a real reduction of a few per cent in the British Government's science spending in the next few years. Sir Bruce Williams, director of the Technical Change Centre (whose researcher Ted Butler was lent to the BA for the audit) found Nicholson's figures "very disturbing". He was also disturbed by the present scale of British civil research and development spending which, when measured per capita, begins to look "very small indeed" (half that of Switzerland, two-thirds of West Germany).

The BA audit also shows that Britain's military spending, usually taken to be half the British research and development effort, is "considerably overstated". As for the universities, a little embarrassment could be detected at Norwich. The figures on university research revealed by the audit show reductions since 1980 "nowhere near as severe" (said Sir Bruce) as had been claimed earlier by the Advisory Board for the Research Councils (ABRC). In the fifteen years up to 1981, funds for British university research (including salaries) doubled in real buying power. From 1964 to 1983, university research and development rose from six per cent to ten per cent of total British research and development. (But the real resources of the research councils were static between 1976 and 1980, and fell about five per cent in the next three years.)

After that doubling, is there not dead wood to prune? Sir Keith Joseph, Secretary of State for Education and Science, keeps asking that. Research chums together, as at Norwich, know there is more to it than that; the doubling has been needed "to stand still", to keep up with techniques and instrumentation and to pay for entry into new branches of research. These costs could not have been covered by pruning old branches, said Sir Bruce. But yes, there is dead wood, admitted Sir Geoffrey Allen (ex-chairman of the Science and Engineering Research Council), chairman of the BA science audit for a second year.

The perception in the community is that things are much worse than the figures show.But there seems a dawning realization that university researchers must explain themselves more clearly. And it should be a major impetus for more research on research.

The Technical Change Centre would like to help with that, Sir Bruce Williams says, but its funds are limited. But Nicholson was more forthcoming; perhaps £250,000 a year would suffice in the medium term. The ABRC could find the money "within the errors" of counting the science budget, he said.

Taking measures

HOW to measure science? Notoriously, it is much easier to measure inputs (money) than outputs (science). But now ABRC chairman Sir David Phillips has been converted to the measurement of scientific output by citation indices suitably modified by interviews, peer ranking and other indicators.

Where from this light on the road to Damascus? The Science Policy Research Unit (SPRU) of the University of Sussex, where two social science renegades have charmed Sir David with their analysis of research in protein crystallography (his own field). Sir David has prodded the Royal Society to head a pilot study of the health of British science using the SPRU techniques. With £25,000 from ABRC and £15,000 from the Economic and Social Research Council, whose chairman Sir Douglas Hague is also a convert, the Royal Society is to assess the productivity of British geneticists, solid state physicists and chemists.

The two renegades now brought in from the cold are Ben Martin and John Irvine (who recently reviewed the work of the European centre for nuclear research, CERN — see *Nature* 6 September, p. 4). Royal Society officials were visiting them last week.

"Martin and Irvine", names that will soon be as familiarly linked as "Laurel and Hardy" in British science policy, first shook the world with a citation and peer-review attack on the Jodrell Bank radio telescope at Manchester.

Future-watching

ONE of the more playful themes at Norwich was 2010, or 2050, or whatever: the distant future. There were plenty of predictions: a chip with numbers of components to match the number of neurones in the human brain by 2000 (Brian Oakley, director of Britain's information technology programme) and NATO (the North Atlantic Treaty Organization) turning from defence to offence in Europe in the next few years (Frank Barnaby, peace researcher). Barnaby said the future has lost its flavour because everybody is concentrating on getting through 1984 or 1985.

It was different 20 years ago, when broadcaster Nigel Calder was editor of the popular science magazine, *New Scientist*. He asked scientists to predict 20 years ahead (George Orwell's 1984) and, said Calder, on the whole they got it right. Nevertheless Werner von Braun erred on the optimistic side (nuclear-powered rockets and men on Mars) as did hovercraft inventor Christopher Cockerell (hovercraft everywhere). Others foresaw home video-recorders, optical cables and the new biotechnology.

What of our future now? Calder listed a few machines — the total information machine (everything accessible with a chip) and the Big Brother machine (total surveillance). A little further off may be the Santa Claus machine, "a large, self-governing device that eats rocks and excretes anything that human beings care to specify: coffee cups, Porsche cars, spaceships, or other Santa Claus machines".

Colonies on Mars

LORD Young (Michael Young) is also worried about the future. But he has plans. Founder of the Consumers' Association (publisher of *Which?*) and the Open University, he now aims to found something out of this world: a colony on Mars. He says it should be the goal of the European Space Agency and that, though a century or so off, the prospect of a Martian colony could raise the sights of mankind above our petty squabbles.

Meanwhile Lord Young is seeking £400,000 to build two domes. One dome would have a simulated Martian desert, permafrost and landscape to test the theory of atmospheric chemist James Lovelock that an injection of fluorocarbons into the Martian atmosphere could do a lot to make it more Earth-like, melt the permafrost and so on. The other dome would be a social experiment which smacks of nineteenth century idealists creating utopias in the Amazon: people would live there as if on Mars (with as little communication with Earthlings) and try to set up social democracy or whatever to prove to the rest of us that everyone can live in peace.

Lord Young will get his money, it was confidently predicted. **Robert Walgate**

Do we need gene therapy?

SIR — A serious imbalance is creeping into discussions on human embryo research and the direction of clinical genetics.

The first paragraph of the Warnock report on human fertilization and embryology (para 1.1) says "It is now possible to observe the very earliest stages of human development, and with these discoveries came the hope of remedying defects at this very early stage"; a theme developed in paragraph 12.15. Edwards and Puxon (*Nature* **310**, 179; 1984) suggest that "such research could open undreamt-of-vistas of improvement and amelioration for mankind"; and Weatherall concludes his comment on gene transfection (*Nature* **310**, 451; 1984) with the statement "offers major encouragement to those who believe that the ultimate goal of clinical genetics is gene replacement therapy, rather than termination of pregnancy".

The belief that the ultimate goal of all clinical practice is to remedy the defect seems to be common among molecular geneticists as well as physicians involved in the treatment of genetic and partly genetic disorders. Patients and parents usually go along with this philosophy when the diagnosis is made after birth, or late in pregnancy, but it would be wrong to assume that this traditional goal of clinicians is necessarily appropriate for embryos with genetic defects.

Physicians and surgeons tend to forget that no matter how grateful patients or parents are for the effort and skill put into treatment, or how desperately they long for the research "breakthrough" that will allow improved treatment, they would much prefer to have no need of doctors at all. People do not want their babies to be medical successes, they want them to be normal. It will be argued that treatment will make them normal. But complete success can rarely be guaranteed in advance, and there is usually a considerable gap between what doctors and what patients regard as a success (although the latter may be too polite to say so).

The goal of correction of genetic defects rather than termination of pregnancy implies detection of the affected embryo in the first trimester of pregnancy even if therapy is carried out later. However, as someone who has close contact with couples making decisions about prenatal diagnosis and selective abortion, I believe that once the abnormality has been detected, most couples will opt for termination of pregnancy and "trying again", rather than chance treatment of the embryo or fetus. There is already widespread acceptance of selective abortion in early pregnancy, which can only be enhanced with the general realization that about 40 per cent of conceptions are lost as natural miscarriages (D.K. Edmunds *et al. Fertil. Steril.* **38**, 447; 1982), and close on half of early miscarriages are chromosomally abnormal (E.D. Alberman and M.R. Creasy *J. med. Genet.* **14**, 313; 1977). The advent of home pregnancy testing kits that confirm a pregnancy within two weeks of conception can only encourage the view that selective abortion is Nature's way.

It seems quite wrong for clinicians and scientists to assert that the goal for clinical genetics is gene replacement, when many, probably the majority of couples would not choose this option. It can only be one of several aims of clinical genetics. Certainly "the need to develop methods of gene replacement in embryos" cannot be regarded as a reason for allowing the creation of human embryos specifically for research purposes, until such a need has been demonstrated. It should also be remembered that 7 out of 16 members of the Warnock committee were against the creation of human embryos specifically for research purposes.

MARCUS E. PEMBREY

Mothercare Unit of Paediatric Genetics,
Institute of Child Health,
University of London,
30 Guilford Street,
London WC1N 1EH, UK

Science journalism

SIR — The editorial policy of *Nature* in declining for publication material that has already been communicated to lay or popular news media has provoked hostile reaction from those media, as exemplified by Mr Leif Robinson's letter (*Nature* 16 August, p. 536).

When I was first engaged in scientific research, it was accepted without question that one did nothing to invite publication of one's work outside the scientific literature-of-record, not only for fear of misrepresentation but also because it was regarded as unprofessional self-advertisement. Mr Robinson claims that by adhering to this ethic *Nature* is guilty of restricting the public's right to know the results of research.

He attempts to justify this assertion by arguing first that misrepresentation has become less of a danger with the recruitment of better qualified scientific journalists, and then that they can misrepresent research results just as easily after proper scientific publication as before. Clearly the two arguments largely nullify each other. The fact is that misrepresentation is less harmful if the true record has been published so that anyone who really cares about the truth can refer to it. As an aside, I do agree that there are now some excellent and professional scientific journalists, but the fact that coverage of science by the lay media in general still leaves much to be desired is illustrated by the example of the ludicrous reports of Soviet science which sometimes appear in otherwise respected newspapers "from our Moscow Correspondent".

Mr Robinson then destroys his own case by stating that science journalists will "ferret out stories", since to make a scientific result into a journalist's story is in itself distortion of a fundamental kind; there can of course be legitimate stories about science but that is different. Denial of the public right to information lies in giving the public a substitute account, not in insistence that what is published is a true professional and authentic record.

I conclude that *Nature*'s policy is correct even in relation to the considerations raised by Mr Robinson. In addition, and despite scientists who have attracted repeated press notice having behaved with integrity in not exploiting this attention unfairly, the climate for scientific research will remain healthier to the extent that young scientists are encouraged to publish for peer-judgement not public acclaim.

PETER FELLGETT

Department of Cybernetics,
University of Reading,
Reading RG6 2AL, UK

SIR — It ill becomes Leif Robinson (*Nature* 16 August, p.536) to upbraid John Maddox for reminding scientists and others of the fundamental importance of their voluntary code of practice regarding the announcement and publication of new results. It is natural of course that Robinson should do so, given that he evidently regards peer review as a potentially restrictive practice obstructing the free flow of information between scientists, the public and the press. The fact that scientific peers today often *do* look upon themselves as a kind of thought police, imperially appointed to defend some imagined consensus view rather than subjecting arguments to independent rational review, may partially condone the error. Nevertheless, it is sad that Leif Robinson, editor of a widely read popular journal of science, so fails to appreciate the true role of peer review in the scientific process that he appears to advocate its omission.

At the same time, another problem exists which Robinson's complaint does perhaps more directly address, namely the ethical dilemma that sometimes confronts scientists concerning publicity between the instant of acceptance and the instant of actual publication. In this age, there are scientists and institutions who no longer feel restrained by traditional practices and who seek increasingly to pre-empt such kudos as might otherwise accrue to the publishing journal by organizing their own publicity. If the editors of *Nature* wish to maintain their reputation as publishers of original new scientific results, it seems that they can succeed in this aim only by so marshalling modern technology as to reduce the interval between acceptance and publication to the absolute minimum.

S.V.M. CLUBE
W.M. NAPIER

Royal Observatory,
Blackford Hill,
Edinburgh EH9 3HJ, UK

Army pall over Argentine science

The destruction of science in Argentina will probably never be more than a footnote to the history of the recent military government, whose major accomplishment was the kidnapping, torture and murder of 30,000 of its citizens in the name of Christian and Western civilization. Official neglect of Argentina's dogged potential for scientific excellence is nothing new; inevitably, there is a tendency to see even the most deliberate and calculatingly destructive acts of the military as a mere extension of what passed before.

Buenos Aires, August

SCIENCE in Argentina has always mirrored the paradox of the country as a whole: a vast potential, occasional glimmers of greatness (which, in the case of science, include two Nobel prizes and an impressive home-grown expertise in nuclear engineering). But, overall, chaos. And scientists in Argentina have always sought out better opportunities in the United States and Western Europe.

However, it is the completeness of the military's crusade against the academic and intellectual life of the country that is so striking today when one visits Argentina's universities and research institutions. Research at the major universities is at a halt. Under the military regime, which seized power in 1976 during a rapidly deteriorating political situation that included frequent terrorist attacks, hundreds of academically unqualified — though politically acceptable — professors were appointed. More than 90 per cent of the faculty of natural and exact science at Buenos Aires University have been appointed since 1976; none can be fired. The selective persecution of individuals, but more importantly a general policy based on the premise that the universities were centres of subversion, accelerated the brain drain to the point where now almost an entire generation of Argentine scientists have been lost to the developed countries. The efforts of Argentina's new democratic government to reestablish contacts with its expatriate scientists has only now revealed the true extent of this loss: a list being compiled by the Argentine embassy in Washington of Argentine scientists who hold research positions in the United States now stands at 500. One is struck not only by the sheer size of the list, but by the quality of the positions as well. Massachusetts Institute of Technology, Princeton University, the University of Chicago and the University of California appear repeatedly.

Legacy

Although the election of Raul Alfonsin as president last December has brought about a remarkable and sweeping change in spirit within the academic world in Argentina, the legacies of seven years of military rule will be much harder if not impossible to eradicate. Bureaucrats left over from the military government remain within the agencies responsible for science; they cannot be fired and at least some are a continuing source of resistance to the reforms of the new government. A swollen organization of government-controlled research institutes is another onerous legacy. And then there is one inescapable reality that confronts every attempt at policy-making: Argentina's economy is a shambles. The external debt, to which the military government added more than its share, is $50,000 million. Inflation reached 22 per cent for the month of August alone, equivalent to an annual rate of almost 1,000 per cent. All business transactions are calculated in dollars; the recent revaluation in which four zeroes were dropped off the end of the currency has encouraged no one.

The Peronist legacy persists even in 1984.

Economics is the heart of the problem for the universities. The military's attempts to turn the universities into little more than secondary schools is readily apparent in its budget. The entire research budget for the faculty of exact and natural sciences at Buenos Aires is $200,000 a year, roughly one-fifth of its historical level. The budget for teaching expenses is $50,000. (These figures do not include salaries, nor research funds channelled through "institutes" that were set up at a frantic pace during the military government as a substitute channel for research.

Spending is being held at 1983 levels as the legislature has failed to act on the 1984 budget requests. The universities have been promised additional funding by the end of the year by President Alfonsin.

The other part of the universities' problem is personnel. According to Gregorio Klimovsky, dean of exact and natural sciences at Buenos Aires, one-third of his faculty simply would not have received their appointments during normal times. Klimovsky's effort to annul the appointments made during the military government has been blocked by the university's governing council. Klimovsky also complains that the university administration has taken no steps to rehire professors improperly dismissed, as provided for under a new law passed this year.

In the unlikely event that all of those dismissed do ask for their jobs back, there will not be much that the university could actually do. The problems go back a long way. In 1966, some 300 members of the science faculty resigned in the wake of a bloody seizure of the faculty by the military government (an earlier military government) that had come to power one month earlier.

In 1974, the unstable Peronist Government fired 400 faculty members and teaching assistants. And during the 1976 military government, all faculty and staff were required annually to fill out forms providing personal and background information to the various branches of the military and police in order to obtain clearance. In practice, the system lent itself not only to political persecution but to personal vendettas as well.

Klimovsky, who was one of the few who spoke out against the human-rights abuses of the military regime and who is now serving on the national commission investigating the "disappeared", says that approximately 60 scientists, mostly from the universities of Buenos Aires and La Plata, are believed to have been killed by the military regime. Some were politically active, others victims of denunciations. Klimovsky says that the commission believes that as many as half of the victims overall had been taken for questioning and either died under torture or were killed to conceal what was happening.

A huge banner hangs in the atrium of the faculty of sciences listing the names of the several dozen faculty members, students and graduates who disappeared, an overwhelming reminder of the brutality born of Argentina's political instability. That instability has not disappeared with the coming of the new government; and it is the major obstacle to Klimovsky's hope that many good scientists who left will return, eventually diluting the mediocrities who now flourish.

A certain amount of volunteerism has sprung up, to be sure. Many professors are working without pay while holding regular jobs elsewhere, often in industry. Some are paying for equipment and maintenance and subscriptions to foreign journals — two items especially squeezed by tight budgets — out of their own pockets.

But the prospects of attracting scientists who have settled in the United States or Europe to return seem slim even with the best will in the world. If nothing else, salaries are very low; a full professor earns about $700 per month; many senior researchers earn as little as $400 per month.

Some universities fared better than others under the military. At one extreme, Lujan University, which had been created only a decade earlier, was shut down completely in 1977. At the other extreme, Mar de la Plata University actually reaped the benefits of persecution elsewhere by hiring scientists fired from the University of Buenos Aires or other institutions. A major research group in biology was "rescued" in 1979 when Mar de la Plata hired four senior scientists, Horacio Pontis, Rafael Pont Lezice, Ruben Conde, and Gistavo Daleo, who had been dismissed three years earlier from the Bariloche Foundation.

How Argentina spends its research money

Atomic Energy Commission (CNEA)	22%
Ministry of Defence; Armed Forces	4%
National Institute of Industrial Technology (INTI)	10%
National Institute of Agricultural Technology (INTA)	22%
Universities	9%
National Research Council (CONICET)	32%
Total: $350 million	

Everywhere, however, certain disciplines suffered. Sociology and psychiatry departments were shut down across the board; they were, in the eyes of the military, lending "ideological support" to the leftist guerillas that the government was fighting. Psychiatry was suppressed, Freud being an "ideological criminal". In Cordoba, the military government's ideological enemies included the "new math", the teaching of which was banned by decree.

And even in those universities that were able to maintain research programmes, those programmes were circumscribed. At Mar de la Plata, materials research and agriculture continued; but a major fisheries research institute was taken over by the military under a new Secretary of Marine Interests. An agreement is now being worked out to allow Mar de la Plata to use the institute's three research vessels once again.

Some similar bits of reorganization are being attempted at Mar de la Plata and elsewhere to undo the damage done by the military, but without significant new funds they may accomplish little. Dr Enrique Schneck, secretary of science and technology at Mar de la Plata, has for example established a new programme of graduate fellowships — a signal of the intent to reestablish research at the university. But the funds for these fellowships have had to come out of undergraduate scholarships.

Universities

The efforts to return the universities to research is surely not going to be made any easier by the open admissions policies that the universities are adopting. Under the military government, applicants to the universities competed for a predetermined, limited number of places. This year, admission has been granted to any applicant who scores above a fixed qualifying level on entrance examinations. Next year, admission will be guaranteed to any student who has graduated from high school.

Perhaps the greatest obstacle to the restoration of research to the universities is, paradoxically, the generosity that the military regime showed for science elsewhere. The National Research Council (CONICET — Consejo Nacional de Investigaciones Cientifica y Technica) expanded rapidly during the seven years of military rule; from 1976 to 1983 the number of CONICET scholarships jumped from 233 to 2,222, the number of researchers (who are paid salaries, as in the French system) from 752 to 1,525 and the number of technicians from 569 to 2,185. During the 1970s, CONICET's budget increased sevenfold.

The military government's motive is not hard to find. CONICET, unlike the universities, is under direct government administration. An expansion of CONICET fitted in nicely with the military's objective of removing research from the universities. This is most evident in the proliferation of CONICET institutes that took place. In 1976, CONICET supported 48 institutes and centres; today, the number is 210.

The proliferation of institutes has balkanized the research effort. The individual institutes go their own ways, divorced from the universities and from each other. Many were clearly created to reward politically correct persons; many show a striking disparity between the elaborateness of their buildings and the meagreness of the research that goes on within. Several institutes are being examined by the federal prosecutor for misappropriation of funds, kickbacks and other questionable expenditures.

Because the universities have so few research funds of their own, CONICET is in the view of the new government the major tool for bringing research back to the universities. (CONICET has a budget of $120 million, or about one-third of the total government research and development budget. The universities altogether have a "research" budget of $30 million, or 9 per cent of the total, almost all of which goes for salaries.) Dismantling the institutes is harder than it might seem; as in the case of the universities, people cannot be fired. The Secretary of Science and Technology, Manuel Sadosky, has said that there will be no special investigation of individuals, but that over the next few years the institutes will be reviewed on the basis of their performance and that some may be shut down; Sadosky hopes, too, that new good scientists will dilute the mediocre.

Not surprisingly, CONICET is facing some stiff opposition from the many researchers who established comfortable fiefdoms in the existing system of institutes. Some discontents are circulating anonymous newsletters to hundreds of scientists, denouncing Dr Carlos Abeledo, the president of CONICET, Sadosky, and other officials as being part of the "antinational" Marxist left, which, in this version, apparently also includes imperialism and the international Jewish conspiracy. Several of these letters, signed by "Ameba Loca" (the crazy amoeba), make less veiled antisemitic references to Sadosky, who is Jewish. (The crazy amoeba calls himself director of the Organization of Information to the Scientific Community; another group calls itself the Committee for the Defence of CONICET. Several of the letters carry the message: "reproduction permitted only within the territory of Argentina".)

These groups, which apparently have no shortage of funds for printing and mailing these letters, have also recently taken to fabricating and distributing documents that seem quite damaging to CONICET officials. A recent one purported to be a blacklist of scientists who were not to be supported by CONICET in the future; most of the names are of scientists who were close to the military government.

Scepticism

These provocations are calculated to play upon the deep-seated scepticism that this government will be any different from its predecessors. CONICET officials say they are determined to avoid any favouritism in the award of research grants this autumn; the difference will be that all research groups will have to apply individually for grants — under the military, institute directors received grants in a lump sum, which they then distributed within their institutes as they saw fit. Proposals are due next month for 1985 grants.

Despite the military's support for CONICET, salaries slipped considerably. Earlier this month, President Alfonsin signed a decree bringing CONICET salaries up to par with those of comparable university positions; they had been about 30 per cent lower.

Amid all of the chaos of recent years, pockets of scientific research have enjoyed relative tranquillity. The most prominent of these is the laboratory of Dr Luis Leloir, Argentina's only living Nobel laureate. Leloir's institute, the Fundacion Campomar, has its own modern building, with an excellent research library and that most rare of Argentine scientific commodities, ample laboratory space. With an annual budget of $100,000 (not including salaries), the institute's 25 PhD researchers are considerably better off than most of their counterparts elsewhere in the country. A private endowment provides one-third of the funding; the remainder comes from about 100 private companies and foundations, CONICET, and the University of Buenos Aires, which pays most of the salaries.

Leloir's reputation, and the institute's private endowment, unquestionably helped to shield the institute from political turmoil. Leloir has directed the institute since its inception in 1947; he is a man who professes to have no opinions and indeed who has made a career of having no opinions; "Here we do not mix up in politics", he says.

Another organization that weathered the storm, though not so easily, is the National Institute for Research and Diagnosis of Chagas Disease. Chagas' disease, the South American equivalent of trypanosomiasis, affects more than 25 per cent of 18-year olds in Argentina. Although research came to a halt in 1981 when funds were shifted to a misguided effort by an army colonel in Cordoba to eradicate the disease, the institute has recovered well. A $90,000 capital grant from the World Health Organization has helped, and the government provides $400,000 per year, 25 per cent of which is used for salaries of the 70 staff members.

The mission-oriented research of the Chagas institute is an exception to the rule of Argentina's scientific expertise. Despite a considerable industrial potential (especially in food and petroleum), applied research is very weak; the best minds have consistently gone into very basic research. Industry in Argentina uses foreign technology almost exclusively; there is virtually no industry-supported research within the country. The scientists employed in industry perform routine quality control and engineering tasks.

Agriculture

Foreign technology has nevertheless proved remarkably successful in the agricultural sector, which remains the backbone of Argentina's export economy. The role of the National Institute of Agricultural Technology (INTA) has been to adapt foreign innovations to local conditions. Its 42 experiment stations and 240 extension agencies have few links with the universities or with basic research in general; arguably, there has been no need.

INTA's new president, Carlos Lopez Saubidet, is concerned, however, that this process of adaptation has reached its limit. Uniquely Argentine problems are emerging that will demand indigenous solutions; he points to the need for new methods of production in arid regions, for example, a necessity forced by the shift of cattle to these marginal regions as the productive lands of the pampas are increasingly put under continuous cropping of grains.

Lopez Saubidet is looking to the United States model of the land grant colleges, both to improve basic research and to institute training programmes. No universities offer PhDs in agricultural science; masters programmes have been in place only since the 1970s. Lopez Saubidet says that with the proper organization, existing expertise can be tapped to establish masters programmes at universities that do not now have them, in the areas of plant production, animal production, soil fertility and agricultural economics.

Biotechnology

Saubidet is also planning to tap the universities' expertise to start a new programme in biotechnology research. INTA has until now carried out all of its research in its own laboratories (which employ about 60 PhD scientists); this new scheme, Saubidet says, will probably involve outside researchers who will be supported by grants. The major goals of the biotechnology effort would be genetic improvement of plants, nitrogen fixation, drought resistance and vaccines.

INTA's budget has had ups and downs. In 1980, the military government eliminated a series of taxes and tariffs, including a 1.5 per cent levy on agricultural exports that had provided INTA's direct support. The tax has only now been restored, and should provide $90 million a year. In the meantime, the budget fell to half its historical level, with a staggering 80 per cent of the budget going to salaries. That proportion should fall to 60 per cent with the restoration of the tax base.

Saubidet has plans to free additional funds for research by phasing out activities that he believes can be assumed by private farmers. But one potential strain on the budget is the 150 or so employees who were dismissed for political reasons in 1976 and who now want their jobs back. (A total of 500 were dismissed in 1976.)

Efforts to bolster the ties between research and other industries face similar obstacles. The only PhD-level training programme is in chemical engineering; it began only in 1980. Most process plants are turnkey operations bought from abroad. The research departments that did exist in the chemical, food processing, and metal industries were the first things to go when economic problems intensified.

The National Institute for Industrial Technology (INTI) follows the familiar pattern of Argentine research organizations — fragmentation into small laboratories (about 40), a large proportion of the budget going for salaries (65 per cent), and isolation from basic science. INTI laboratories have drifted into the relatively easy business of providing technical services, such as chemical analyses, to industry; this now makes up 70 per cent of its activities.

Although INTI laboratories are well equipped by Argentine standards — they own $500 million worth of equipment and employ a staff of 1,500, including 500 scientists — operating funds have been tightly squeezed. The same 1980 tax reform that eliminated INTA's tax base wiped out INTI's — a 0.25 per cent levy on bank loans to industry. The budget fell from $40 million to half that: the tax base has not yet been restored. Nearly 300 of its staff were dismissed following this budget cut.

CONICET president Abeledo — under pressure.

INTI's current plan calls for concentrating on fewer areas, specifically food processing, electronics, fine chemicals, textiles, metrology and civil engineering.

The Research Committee of the Province of Buenos Aires (CIC) is shaping up to be another significant promoter of applied research. Under the new administration, CIC is, apparently for the first time, living up to its legal mandate of applying 60 per cent of its funds to mission-oriented research of local importance. The five areas chosen are natural resources, food technology, clinical research, non-conventional building technology and energy.

Angel Plastino, president of CIC, is also attempting to channel more of CIC's funds outside its six laboratories, to the universities. A major project under the natural resources programme is the first geological survey of the province's mineral resources. The project, which began in February in cooperation with the University of La Plata, is to cover the important mineral areas of the province in the first two years; the entire survey will take perhaps 10 years.

CIC's budget now stands at 0.5 per cent of the total provincial budget, twice its previous level; current plans call for a further doubling of the budget and of the number of scientists (now 250) supported by CIC. Plastino said that one key function of CIC in support of the universities will be the purchase of foreign books and journals for university libraries, which have deteriorated badly.

Several agencies of the federal government are trying to promote an initiative in biotechnology as a basis for future industrial growth. An acute shortage of microbiologists and fermentation scientists, and the pressure of economic realities have thrown cold water on some of the more optimistic plans (such as the proposal to build a $20 million biotechnology research centre). A more modest effort is now being planned by CONICET, in which investigator-initiated proposals will determine the scope and size of the programme.

The public health ministry is also interested in biotechnology, as a way for Argentina to get a foothold in the pharmaceutical industry. Although many international companies manufacture drugs in Argentina — 45 per cent of the market is locally produced — research activity is nil. Carlos Canitrot, the undersecretary for regulation (equivalent to the commissioner of the Food and Drug Administration in the United States), notes that to develop a new drug costs about $40 million; the largest pharmaceutical company in Argentina has sales of only $60 million a year. He sees biotechnology as a way of competing at lower costs, particularly in biologicals, vaccines and diagnostics.

Channelling local efforts into productive avenues is not going to be easy; much of the local "innovation" consists of formulating new combinations of drugs — some containing as many as five different active ingredients. And the drug regulation system suffered a near total breakdown under the military government.

Nuclear worries

The one area of applied science where Argentina is doing quite well is nuclear engineering. The concern in the rest of the world is that Argentina is doing a little too well. Last autumn, the outgoing director of the National Atomic Energy Commission (CNEA), Admiral Raul Castro Madero, revealed that Argentina had built its own uranium enrichment plant at the nuclear centre in Bariloche, in the south. Argentina has an abundant natural supply of uranium; it has long had its own fuel fabrication plant; it is in the process of building a plutonium reprocessing plant at the Ezeiza Atomic Centre near Buenos Aires, and, with Swiss help, a heavy-water plant with Arroyito.

Although the two power plants are under International Atomic Energy Agency safeguards, as are Argentina's research reactors (a necessity, since the enriched uranium fuel that powers the research reactors was provided by the United States), Argentina has consistently refused to sign the Nuclear Non-Proliferation Treaty (NPT). Mario Mariscotti, chief of research and development for CNEA, and widely considered to be the next in line as director of the agency, raises the familiar arguments that NPT discriminates against non-weapons states. He also complains of foot-dragging in technology transfer by the United States, particularly since India exploded its nuclear bomb. He argues that if Argentina can become independent in its fuel cycle, why should it give that up for the questionable and uncertain benefits of American aid? He tells of the United States backing out of an arrangement to supply enriched fuel for a plant that Argentina was building for Peru as an illustration.

Opinions differ about Argentina's technical capability to build a bomb. But there seems to be little doubt that it either has or could eventually produce the materials for one. The enrichment plant, which is not under safeguards — Mariscotti says that opening it to international inspection would itself constitute a proliferation risk — has a capacity of "less than a ton" of 8 per cent enriched uranium per year, according to Mariscotti. The maximum enrichment it can yield is 20 per cent. In principle, the unsafeguarded fuel from this plant could be burned in a research reactor to produce plutonium, which could then be reprocessed to yield bomb-grade material. Argentina is legally bound to accept safeguards only on the fuel (and the plutonium derived from it) that was originally supplied by the United States. Once the research reactors are being fuelled by its own uranium and heavy water — which is the offical plan — safeguards could legally be dropped.

Mariscotti asserts that Argentina currently has only "laboratory-scale" amounts of unsafeguarded uranium and plutonium. And he says that despite widespread speculation to the contrary, there never was a weapons programme under the military regime. He said he has not found it necessary to alter any research programmes out of concern that they were directed towards building a bomb.

But Argentina's fascination with nuclear research and development has always attracted suspicion. The programme was established in 1950 by President Juan Peron, and has enjoyed the special favour of every government since. Despite an erratic start under the direction of a German scientist, Ronald Richter, who at one point claimed to have developed a fusion reactor, the programme has produced results. Argentine physicists in the mid-1950s discovered several new radioisotopes using a state-of-the-art cyclosynchrotron; research programmes today show significant strengths in reactor chemistry, low-temperature physics, and radiobiology. A 20 MeV heavy-ion electrostatic accelerator (which cost $30 million) is nearing completion, and should permit state-of-the-art investigations. Yet it is frankly difficult to see how the benefits of CNEA's activities justify the costs. The two operating power plants (Atucha I near Buenos Aires, a 300 MW station and Embalse Nuclear Centre near Cordoba, 600 MW) supply about 10 per cent of the nation's electricity demand. A third plant now under construction (Atucha II) will supply an additional 700 MW. If three additional plants are built as planned, nuclear power will be supplying 15 per cent of the electricity by the year 2000.

All of the plants are of the heavy-water variety, which means they can use natural-enrichment uranium, although a better burn is achieved with 1 per cent-enriched fuel; the official plan is to use the enrichment plant to produce enough fuel to supply 1,000-MW-worth of power reactors, in addition to the 8 per cent enriched fuel needed for the research reactors.

CNEA's budget is $500 million per year, 10 per cent of which goes for research of which 10 per cent is basic research. National pride, the usual excuse given for this emphasis, is a less persuasive justification than it might be if the rest of Argentina's scientific and technical endeavours were in good shape.

The future

The difficulties that Argentina faces in rebuilding the scientific institutions it once had, in exploiting a potential that has never been significantly tapped, and in putting science to use for development are so enormous that they approach the absurd at moments. If it is no longer political persecution, it is low salaries; if the salaries are raised, there is still the shortage of equipment and foreign journals; if those problems should somehow be solved, there is still the mass of incompetents in high places; and the lack of the needed training programmes; and the brain drain; and, to top it off, the strike of clerical and janitorial help at the university that leaves the corridors ankle deep in trash and the phones unanswered.

That those now in charge of running Argentina's science have the best of intentions — and a sober vision of the problems — there can be no doubt. The emphasis on repairing the damage to the universities and on providing opportunities for the next generation of Argentine scientists is clearly the right one; there can be little hope that the many Argentines living in the United States and Europe will give up the security and prestige of their current positions in favour of the uncertainty in a country from which they not long ago fled.

If Argentina's leaders are a cause for optimism, though, its economy is surely a cause for pessimism. Sad to say that the future of Argentine science will probably have more to do with Argentina's woeful economy than with all of the careful planning and clear thinking of its new science administrators. ☐

Stephen Budiansky is Washington Editor of Nature.

Molecular biology of cancer

Last week's Nature *conference in Boston suggests that the study of oncogenes will provide a route to general understanding as well as a powerful insight into normal cell biology.*

THE molecular biology of cancer may almost be synonymous with the molecular biology of the cell. That is one of the impressions formed by last week's conference on the molecular biology of cancer. What seems to be happening is that the exceptional circumstances of malignancy (or of transformed cells in culture) is throwing a clear light on many aspects of the normal functioning of normal cells. Who would have guessed, even a few years ago, that so much would now be known about the biochemistry of the previously shadowy materials known as growth factors, for example?

So is the molecular biology of cancer merely another way of tackling longstanding problems of an academic character? That is the naturally impatient question asked by physicians, epidemiologists and the managers of public health. Patients also ask questions on the subject, and for good reason.

The answer, which is in the negative, is nevertheless a little roundabout. That the best cure for cancer is avoidance is undeniable. The worry, for now and for some time to come, is whether avoidance is feasible on the scale and at the speed to which agencies such as the US National Cancer Institute are committing themselves. Everybody will be delighted if the objective of reducing cancer mortality in the United States by half by the year 2000 can be attained. But even if the programme succeeds, there will still be more than 250,000 deaths a year from cancer in the United States. So the need for better treatment will still be as clamant, for which purpose only a better understanding of the manifestations of forms of the disease can provide.

In this sense, the two approaches to the problem of cancer—avoidance and understanding—are complementary. But they are more closely linked even than that. The strategy that emphasizes avoidance (the best course) requires that people should change their ways, sometimes radically. Public authorities, which have a constitutional licence to fix tax rates and speed limits, are conspicuously successful at changing their electors' habits. Understanding, however, may in the long run accomplish what exhortation cannot. And the molecular biology of cancer is more likely to provide persuasive general understanding than some of the advertising campaigns manned for the years ahead.

John Maddox

Speakers

S. Broder (National Institutes of Health); J. Cairns (Harvard University); R. Gallo (National Institutes of Health); F. Gilbert (Mt Sinai School of Medicine); P. Greenwald (National Institutes of Health); J. Gutterman (M. D. Anderson Hospital, Texas); P. Leder (Harvard University); R. Peto (University of Oxford); M. Sporn (National Institutes of Health); G. Todaro (Oncogen Inc.); J. Uhr (University of Texas); A. Varshavsky (Massachusetts Institute of Technology); R. Weinberg (Massachusetts Institute of Technology); I. B. Weinstein (Columbia University); R. White (University of Utah).

Synthetic genes

Transgenic mice inherit cancer

MAKE your own oncogene, Dr Philip Leder's recipe for grafting the regulatory sequences of the mouse mammary tumour virus (MMTV) onto the coding sequences of the c-*myc* gene, was the biggest sensation last week.

The circumstances are clearer than the full significance. The c-*myc* gene appears to be responsible for human lymphomas when translocated from its normal position on chromosome 8 to somewhere among the immunoglobin genes on chromosomes 2, 14 and 22, presumably because the regulatory environment then allows it to be activated. But the *myc* gene is a curious structure, with a long (more than 100 base-pair) sequence upstream of the first of three exons, which is duly transcribed into RNA but which (together with a short stretch at the beginning of the second exon) plays no part in coding for the gene product. So why not equip the gene with indigenous control elements by replacing the upstream end by a known regulatory element?

Fusion genes on this pattern are made from the regulatory elements of MMTV and the *myc* gene from which various upstream regions have been removed. In fertilized mouse oocytes, the synthetic genes become part of the genetic constitution of transgenic mice. In adult females, the gene should be turned on during pregnancy, as MMTV is activated by hormonal influences.

The offspring of two of the transgenic mice produced in this series of experiments turn out to have inherited MMTV-*myc* fusion genes, most remarkably in the case of four daughters of a transgenic mouse provided with the bare minimum of c-*myc*—the coding parts of the second and third exons, the intervening sequence and the downstream tail of the gene.

The pathological effects of the synthetic oncogene are distinct from those of MMTV and of c-*myc* but result, rather, in a distinctive adenocarcinoma of the breast tissue appearing only after pregnancy (confirming the influence of the lactational hormones). Offspring have been salvaged from these pregnancies (transgenic females are bad mothers, perhaps not coincidentally) by fostering, and the females turn out to have inherited both the fusion genes and the characteristic pathology of their mothers.

The mere development of this mouse strain confirms current notions that c-*myc* gene in the human genome is, in its normal position on chromosome 8, repressed (by some unknown mechanism), but that translocation to some other site allows it to be expressed. In this respect, c-*myc* differs from the *ras* oncogene, the activated form of which is now known to produce a protein distinct from the normal variety.

Potentially, the new strain of transgenic mice is a valuable model for the study of gene regulation and of oncogenesis, or at least of that for which *myc* is responsible.

The view that *myc* is normally suppressed, which Leder describes as a speculation, is consistent with the association of human lymphoma (and its mouse equivalent) with translocation but also with comparisons of the structure of the long leader sequence ahead of the three *myc* exons in the genes from mouse and human beings. These have substantially diverged from each other in the course of evolution except for a short region of some 200 base-pairs, most graphically seen in heteroduplex structures made from a DNA strand from each species, which may be the site of repression.

Functionally, c-*myc* normally appears to be active only in the cell cycling of precursor white blood cells. In culture, the cell products appear 3–6 hours after the treatment of resting cells with platelet-derived growth factor (PGDF). Of the importance of its abnormal functions in differentiated lymphocytes, there is however no question. Leder was one of several speakers who last week drew attention to the demographic importance of Burkitt's lymphoma in, for example, West Africa. □

Longer list

ROBERT WEINBERG, much involved with the characterization of the activated form of the H-ras oncogene, now has another. Last week, Weinberg described the isolation from a chemically initiated neuroblastoma in rats of an oncogene different from those already known.

Neither the sequence of the new gene nor the function of its product is known as yet. Indeed, the 85,000 molecular weight protein identified on the neuroblastoma cell surfaces may not be coded for directly by the oncogene, but could in principle be a secondary product thereof.

But the protein and the epidermal growth factor receptor are cross reactive, suggesting similarity falling short of identity.

So how many more oncogenes will be found? Weinberg reckons that the next three or four years will bring a further dozen. Obviously the effort will yield diminishing returns, but nobody can know how long the list will be.

Already the list is long enough for classification to be meaningful. Weinberg would divide them into transforming oncogenes (such as the ras genes) and the immortalizing genes (such as myc). And the effects on cells are similarly categorized—some (e.g. sis) allow cells to make their own growth factors, some (erb-B) alter growth factor receptors and other (H-ras) may change the regulation of cell biochemistry. □

Binary toxin

COUPLING cytotoxic drugs to antibodies has during the past few years been a commonly favoured strategy for killing specific cells. Dr J. Uhr explained last week his strategy for the development of immunotoxins from the natural product ricin—a constituent of the castor bean. The protein molecule consists of two chains (A and B) which are separated within cells, whereupon A becomes lethal (one molecule, one cell).

Uhr's objective is to couple ricin, and ricin A chains, separately to immunoglobin molecules raised against specific antibodies on circulating B-cells. The objective is the high cell specificity that would promise the avoidance of side-effects in therapy. A spontaneously arising B-cell clone is being used as a test system for telling whether the effects of A-chains might be potentiated by the manipulation of intracellular conditions or even the use of ricin B-chains also tagged to immunoglobin molecules. □

AIDS

Bad news, good news

ROBERT Gallo spread a sense of urgency last week about the HTLV group of retroviruses, and especially about HTLV–III, which he and his associates have done most to establish as the agent of AIDS (autoimmune deficiency syndrome). Since the publication of the evidence for the identification of the virus earlier in the summer, complications have arisen.

Gallo's bad news, derived from nucleotide mapping and sequencing, is that HTLV–III may vary considerably in its nucleotide sequence from one patient to another; whether this will affect the outlook for the preparation of vaccines will depend on whether the antigenic sites are affected. The news that AIDS has been recognized among adults with only heterosexual partners, and that (according to some reports) up to 5 per cent of blood offered for transfusion in the United States may be contaminated, suggests that the virus may already be more widespread among the human population than its overt manifestation implies.

The good news is that Gallo and others have cloned the gene, and that its nucleotide sequence is nearly complete. The development of diagnostic tests for AIDS is also well advanced—so much so that physicians are already worrying what they will tell their patients when they have concrete information to give them. And, small comfort though it is, the association of HTLV–III with AIDS, and the prevalence of the disease, is such that Gallo was able to say last week that "we no longer need an animal model for AIDS".

Why should a virus whose effect on the T cells it infects is to kill them feature among oncogenes? Gallo's sober answer is that HTLV–III, like the two other human T-cell viruses now known, is a retrovirus with similar specificity, with HTLV–I now emerging as the agent of the adult T-cell leukaemias (ATL). The more memorable way of putting it is the rhetorical question "Why not use HTLV–III to treat the leukaemias and HTLV–I to cure AIDS?" (The suggestion will not work because different "subsets of subsets of T cells" are responsible for the deficiencies of the immune system that characterize the two groups of diseases.)

Gallo's obsession is to see a vaccine in trials and eventually in general use. Like everybody else, he is infuriated by the knowledge that as things are, it is possible only to treat the adventitious aspects of the syndrome, Kaposi's sarcoma or whatever. The evidence, as he sees it, that the disease is spreading beyond the groups of male homosexuals and haemophiliacs dependent on injected Factor VIII makes the search more urgent. □

Some success with interferon

SUCCESS in the use of interferon in the treatment of serious cancers is beginning to trickle in. That was the burden of the report by Dr J. Gutterman of his own group's use of interferon, both alpha and gamma interferon and naturally occurring (and thus heterogeneous) and genetically-engineered material. But the development of therapeutic regimes is painfully slow.

Gutterman described the use of alpha interferon in a group of 27 patients with chronic myeloid leukaemia (CML) in which the underlying defect is a translocation from chromosomes 9 to 22. Only 3 of the 27 patients had failed to go into remission after the administration of interferon, although the question cannot yet be regarded as resolved, given the long duration (3.2 years average) of the chronic phase. But Gutterman says it is encouraging that in many of the patients treated, the proportion of cells with abnormal chromosomes in bone marrow had been markedly reduced, in some cases apparently to zero.

Gutterman also described the successful treatment with gamma interferon of 10 (out of 11) patients suffering from hairy cell leukaemia, and the generally successful amelioration of Kaposi's sarcoma (an accompaniment of AIDS) with alpha interferon.

Even so, the development of effective means of using genetically-engineered and naturally occurring interferon will be an enormous task. Alpha and beta interferon (which share the same cell receptors) do not potentiate each other, but alpha and gamma interferon are mutually synergistic, which argues for appropriate mixtures, not yet defined.

Even more daunting is the need somehow to distinguish between the constitutional genetic variants of three types of interferon specified by the human genes. Clinically, for the time being, this problem has been left on one side.

On the side-effects of interferon therapy, Gutterman says that the chief effect seems to be a loss of "executive function", a lassitude, which psychologists describe as a reversible biochemical lobotomy.

With the need to distinguish between all the possible variants of interferon, Gutterman considers there is an urgent need to define various types of cancer in terms of "early molecular events" so as to be able to make use of accumulating knowledge of the role of interferon and of other lymphokines in the physiology of body cells. □

Growth factors

Ambivalence in plenty

GROWTH factors may inhibit growth, and inhibitors may sometimes have the opposite effect. This ambivalence of the compounds on the steadily lengthening list of the gene products of the known oncogenes emerged most clearly from Dr Michael Sporn's survey of the field last week.

Much of the interest at last week's conference has been stimulated by the recognition that the interaction between growth factors and oncogenes may be crucial to the development of malignancy. Notable among these are the links between the *sis* oncogene and platelet-derived growth factor (PDGF) and between the *erb*-B and the receptor for epidermal growth factor.

Dr P. Newmark (Deputy Editor of Nature*), Dr P. Leder and Dr R. White.*

Sporn emphasized last week the common features of the architecture of many of the growth factors whose role in carcinogenesis is coming to light. Although similarities of amino-acid sequences ("homologies" in slang) are many fewer than might have been expected, Sporn and Dr George Todaro agreed that the character of the molecules is determined by three disulphide bonds between as many pairs of cysteine molecules. (Insulin, two peptides held together by two disulphide bonds, is—significantly—not very different.)

So the hunt for growth factors which are somehow linked with oncogenes is now fast and furious. Sporn reported last week a significant difference between the two versions of the growth factor TGF (for tumour growth factor) called alpha and beta, which have been isolated from rat tissues (among others). Heroically, Sporn and his colleagues have been able to determine the sequence of beta-TGF by wringing 40 micrograms of pure substance from 14 kg of bovine kidney.

Although similar in their architecture, the two molecules differ profoundly in their effects on cells: alpha-TGF is always stimulatory of cell metabolism, beta-TGF may be inhibitory. This argues for distinct receptors but also for the more philosophical view that growth factors are regulatory elements in the same category as some hormones (insulin), the lymphokines (interleukin I and II for example) and the interferons which are recognized as "growth factors" only in relation to malignant cells.

Sporn and Todaro agree on the importance of deciding how the growth factors produced by transformed cells play a part in malignancy as such. On the autocrine model, cells produce growth factors which stimulate themselves. Todaro thinks the circumstances may be rare, perhaps occurring in Weinberg's transformed neuroblastoma cell-line. Whatever the detailed mechanism, Todaro thinks it likely that the effects of the secreted products of oncogenes on cells (including themselves) may be to activate proteases (perhaps by phosphorylating tyrosine residues) which then cleave precursor molecules to yield activated growth factors, much as proinsulin is converted into insulin.

The interest of Todaro, now more than a year with the company Oncogen, is guided by the suspicion that the common recognition of growth factors produced by transformed cells may conceal the way in which, in normal tissues, their stimulatory effects are balanced by those of inhibitory factors. Against some of the odds called in recent years, shadowy materials such as tumour necrosis factor (TNF) are now well on the way to being characterized. Todaro's people are embarking on assays of these and other materials in the urine of cancer patients, processing up to a litre of urine at a time in what seems to have been a successful if preliminary demonstration that TGF is secreted in cancers of the lung, breast and colon, and in melanoma, but not by leukaemic patients or normal controls. Who said that molecular biology is picobiochemistry? □

Front end virus

CLINICIANS, these days, are as often as not closet molecular biologists. Dr Samuel Broder said last week that working with T-cell leukaemia virus is the "front end of cancer". There is, he said, a "basic duality" in knowing whether the conditions that arise are direct consequences of the neoplasm or secondary consequences of the immune suppression accompanying T-cell leukaemia. □

Biology

No genuflection

CANCER may not be what it seems even now, oncogenes notwithstanding. That was the theme of the iconoclastic message delivered by Dr John Cairns (now at the Harvard School of Public Health) in a clear English accent.

After "genuflecting" towards the oncogene, Cairns faced the conference with interlocking pieces of evidence that the development of malignancy in a cell is a long-term process, as follows.

- Irradiate cells in culture, allow them to grow to fill up the culture dish and, after 10–12 generations, the number of malignant foci will be that determined by the Poisson statistics describing the distribution of rare events. In a parallel experiment, remove part of the cell mass; the average number of malignant foci will be the same. But trypsinize the cells to break up the cell mass at an intermediate stage, and the number of foci will increase, suggesting that the progeny of a large proportion of the original cells have inherited the propensity to malignancy.
- Paint rabbits' ears with coal-tar (following 1920s' experiments by Peyton Rous), sampling tissue by some traumatic procedure (such as using a punch); the outcome suggests that many more cells are rendered by the trauma susceptible to transformation than become malignant under the influence of the promoter.
- The incidence of lung cancer and smoking in human beings argues that the development of malignancy must require both early events (because lung cancer develops only after long exposure) and late events (because giving up the practice sharply reduces the relative risk within two or three years).

In the interpretation of these and other data, Cairns said that "we have been brainwashed by current ideas of evolution and mutagenesis". In his view, both the arguments of Gould and others in favour of "punctuated equilibrium" in evolution and Barbara McClintock's work on the occurrence of mobile genetic elements in maize suggest that "mutation rates are not constant" but are, instead, increased by "genomic stress".

To molecular biologists, Cairns commended the study of long terminal repeats and of parvoviruses. In his opinion, the study of the role of hepatitis-B virus infection as the stimulant of liver cancer is, numerically, the most valuable contribution that could be made. But for those who would reduce the mortality from cancer, the objective should be prevention of cancers with known causes. The role of diet is obscure and needs urgent investigation.

Oncogenes, Cairns says, will "give us a fascinating insight into how cells manage their affairs" but will not contribute to public health in the near future. □

Somatic genes

Ways with drug resistance

ONCOGENES are merely the frosting on the cake of the application of molecular biology to the problem of cancer. By common consent, last week, the need to trace the effects of the gene products through the biochemical apparatus of the cell is plainly urgent. Why does the activated (mutated) *ras* gene have such profound effects? The first steps in what may be a long cascade have been described (see *Nature passim*). Other areas cry out for attention.

Alexander Varshavsky's account of the phenomenon of the acquired resistance of cancer cells to not just one but several cytotoxic drugs suggested a fruitful field for investigation. The problem all too often presents itself in the chemotherapy of cancer patients. Although Varshavsky was at pains last week to emphasize that multi-drug resistance can be acquired in several different ways (mutation of the target gene which may make its product less susceptible to attack by cytotoxic drugs, other mutations which may affect the regulation of the gene or the import and export of the cytotoxic drug through the cell membrane), the mechanism of gene amplification is the most commonly discussed.

Whatever genes are amplified may be up to 600 times more common in drug-resistant cells, for which reason Varshavsky argued strongly for direct interaction between drug and DNA rather than for the evolution of a labile genome under selective pressure. Many of his audience were eager to know why hydroxyurea should apparently be a powerful stimulus to resistant cells (in culture) to shed copies of the resistant genes (but could not be satisfied). The practitioners' concern is to characterize those genes which are amplified in resistant cells and whose functions are not already known. (Resistance to methotrexate usually entails the amplification of the gene for dehydrofolate reductase, but multi-drug resistance seems often to involve a decrease of membrane permeability to the drug associated with amplification.) Varshavsky and his associates are struggling with genetic fragments more than 1,000 base-pairs in length, but Dr John R. Riordan (Hospital for Sick Children, Toronto) offered the information that a relatively small glycoprotein (molecular weight about 20,000) has been consistently isolated from multi-resistant cells.

Genetic amplification causing drug resistance is one thing—genetic changes in somatic cells associated with cancer, or in germ cells which carry a predisposition to certain forms of cancer, are another. R. White left his audience last week with two clear impressions. First, the map of the human genome is now reasonably well sprinkled with potential genetic markers so that the identification of the usually rare genes carrying a predisposition to hereditary cancers may often be successful. Second, the interlocking familial studies of cancer incidence and genetic constitution based in Utah (whose large Mormon population makes the construction of kindred trees more feasible) has already provided an invaluable resource for the investigation of the genetics of cancer incidence. Dr F. Gilbert confirmed the practical potential of such developments.

The genetics of carcinogenesis, and of tumour promoters, is in a different ballpark. I. B. Weinstein was anxious that people should understand that the effects of tumour promoters on the cells in which they engender malignancy are usually direct, not via the genome. So much is clear from studies with protein kinase C (PKC), whose targets include a growing list of the molecular components of cells such as growth factor and insulin receptors and even myelin basic protein.

These lines of development are quite distinct from the pursuit of oncogenes. They offer the prospect that even when the list of oncogenes is complete, there will remain as vast a canvas as that which now appears to stretch ahead for the exploration of how malignant cells are the products of their genes. □

Avoidance is the best cure

CANCER as a preventable disease, the ideological basis of the National Cancer Institute's National Cancer Control Program, was urged on the conference last week by Dr Richard Peto. He urged a clear distinction between the identification of causes and of mechanisms, and that "it is possible to show that the disease is avoidable without knowing how to avoid it".

The argument is epidemiological: if cancer rates vary over a wide range from one part of the world to another, and if people migrating to new dwelling places acquire the cancer rates of their new surroundings, it follows that cancer is not an externally determined fate.

Within developed countries, Peto says, tobacco consumption is responsible for 35 per cent of cancer mortality, and for one million deaths a year worldwide. Peto's rearrangement of priorities on the international demographic canvas puts liver cancer following hepatitis-B infection high on the list—100,000 liver cancer deaths a year in China alone. □

Strategy

How to reduce mortality?

REDUCING the rate of cancer mortality in the United States by half by the end of the century, the National Cancer Institute (NCI)'s promise to the US Congress last November, requires only the application of knowledge now available according to Dr Peter Greenwald of NCI. With present cancer rates, and allowing for the age-structure of the increased population of the United States by the year 2000, annual cancer deaths would increase from 414,000 to 575,000. So NCI's goal is to reduce the annual mortality to 288,000.

Reduction of cigarette smoking should yield a 15 per cent reduction in mortality, as should the extension of improved methods of treatment to the whole country and the use of techniques (such as body scanning) for the detection of micrometastases. Perhaps the most controversial element of NCI's prospectus is the calculation that cancer mortality will be reduced by 5 per cent by changes in US diet (more fibre, less fat), chiefly by effecting a reduction of mortality from colon cancer. Persuading people to change their diet is uncharted territory. Continuing professional disputes about the efficacy of fibre in reducing colon cancer should, however, in Greenwald's opinion, be outweighed by the number of reports tending in this direction.

Greenwald says that NCI's new objective is deliberately to apply present knowledge in the avoidance and treatment of cancer. Hitherto, he says, reports identifying the causes of cancer have been published, but little has been done to show that agencies such as NCI can successfully intervene. The objective for the coming decades will be to mount demonstration projects which can thereafter be applied elsewhere in the United States. In this programme, Greenwald says, molecular biology may have important functions to perform as, for example, in the identification of the mutagens presumed responsible for cancer of the colon, now the second cause of cancer mortality in the United States.

The cost of the Cancer Control Program is necessarily speculative at this stage. Greenwald hopes that funds will begin to appear in NCI's budget with the beginning of the next administration next January. By the end of the century, the cost will be $10,000 million. The spur is that for each of the known causes of cancer in the United States, there is some society elsewhere which seems successfully to have avoided it. And even within the United States, the mortality from cancer among Seventh Day Adventists in the western states is only two-thirds of the national average. □

Cometary exploration

Plans for future space missions

from Alan Johnstone

IT may seem premature to plan more space missions to comets before any of the group of five now scheduled to meet Halley's comet in 1986 have even left the ground, but such is the interest in this comet and so long is the time required to prepare a new space probe, that planning for the next generation of spacecraft is already underway.

All the missions planned so far are flyby ones, that is, they will make one pass through the coma at the high velocity of 67 km s^{-1}. Giotto, the European Space Agency's (ESA) mission, which will be aimed closer to the nucleus than any of the two Russian and two Japanese spacecraft, will collect data on the composition of the comet over only four hours. These data will be collected by automatic instruments, set up beforehand to operate in the conditions believed to exist near the nucleus. There will be no opportunity to make adjustments during the flight. Despite the difficulties, a flyby mission is the proper first step in cometary exploration and the first measurements actually made within the coma of a comet, rather than on the radiation coming from it, will revolutionize cometary science.

A consensus now exists among cometary physicists about the form that the next steps in cometary exploration should take. First priority is a rendezvous mission in which the spacecraft is manoeuvered to be in the same orbit around the Sun as the comet. This will enable the comet to be studied as it passes from several astronomical units into perihelion and out again. Furthermore, as the spacecraft observes the development of the coma, it will be able to move at leisure through all the important regions. The difficulties are that such a programme requires advanced propulsion systems and is limited to the study of an unimpressive group of comets — those deflected by the gravitational effect of Jupiter into orbits which keep them in the inner Solar System. Nonetheless, one is being planned for the mid 1990s as a joint US-FRG venture.

For those interested in the composition of the comet and the origin of comets and the Solar System, the ultimate aim is to bring back to Earth a sample of cometary material — ideally, a piece of the nucleus — to be analysed in the laboratory using a formidable array of sophisticated techniques (Niehoff, J. *Comet Sample Return Mission Techniques*, Eur. planet. Sci. Symp., Heidelberg, April 1984). This kind of mission involves all the difficulties of a rendezvous mission, with the additional problems of acquiring and returning a solid sample. It will not be undertaken this century.

A much less difficult mission is to collect coma dust and a gas sample. The samples are collected on special plates carried on a simple flyby spacecraft which then returns to the Earth in its natural orbit and ejects the samples in a re-entry probe to be recovered as it descends through the atmosphere on a parachute. Engineers and scientists from NASA and ESA are currently studying the feasibility of a mission using a second model of the Giotto spacecraft. Its dust shield would be modified to carry the collectors, consisting of a number of cells or compartments covered by a thin diaphragm. Dust grains vaporize when they strike the diaphragm and the resulting gas condenses on the specially coated walls of the cell from where it can be recovered and studied in laboratories on the ground. Plane coated surfaces would be used to collect coma gas molecules. It is even possible to collect dust particles nearly intact by decelerating them slowly in a foam material that does not overheat the particle. Although some of the outer layers are removed in the process, 80 per cent of the particle can be recovered and its mineralogy studied. After encounter, the collectors would be retracted and stowed within a re-entry capsule mounted within the space now occupied by the rocket motor. This rocket injects the spacecraft into an orbit around the Sun; the need for it in Giotta 2 could be removed by using an appropriate launch vehicle. The rest of the instrumentation on Giotto would remain the same and would be used to study a second comet.

Several targets have been identified in the years 1989–1994. For example, a probe launched on 14 December 1989 would encounter Comet Schwassmann — Wachmann 3 on 4 May 1990 and return to the Earth on 14 December 1990 (see the figure).

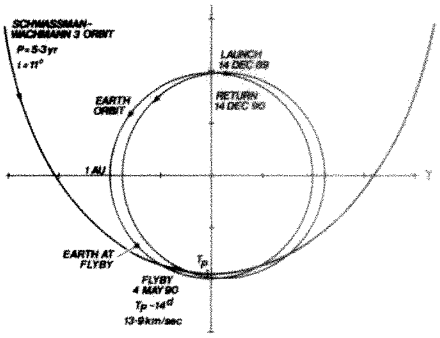

The trajectory profile for Schwassman-Wachmann 3 coma sample return. *P*, period; *i*, inclination; T_p, time of perihelion.

The provision of the spacecraft by ESA would be much less expensive than usual since the spacecraft would be made to an existing proven design as a continuation of the present project. NASA would provide the re-entry probe and the launcher. Thus an exciting new mission could be achieved quickly, at a fraction of the cost of developing a planetary mission from scratch. ☐

Alan Johnstone is at the Mullard Space Science Laboratory, Holmbury St Mary, Dorking, Surrey RH5 6NT.

Diabetes

On the track of viruses

from Abner Louis Notkins

THERE are two major forms of diabetes mellitus: the insulin-dependent (IDDM) type, often referred to as juvenile diabetes, and the noninsulin-dependent (NIDDM) type, also known as maturity-onset diabetes[1]. IDDM is caused by destruction of the insulin-producing β cells in the pancreas which results in hypoinsulinaemia and hyperglycaemia. The pathogenesis of NIDDM is less well understood. In this form of diabetes, there is little evidence of β-cell destruction and insulin levels in the blood are generally within the normal range. There is evidence, however, that in some cases the functional capacity of β cells, as measured by glucose-stimulated insulin release and/or the capacity of peripheral tissues to metabolize glucose, is impaired. It has been known for several years that in experimental animals, the destruction of β cells by acute viral infections can cause IDDM[1,2]. Now, in a recent issue of *Science*, Michael Oldstone and his colleagues show that in mice, a nondestructive but persistent viral infection of β cells can result in a condition resembling NIDDM[3].

Extensive studies over the last decade, especially with encephalomyocarditis (EMC) virus, have shown that the development of virus-induced IDDM in mice depends on the genetic background of the host (only certain inbred strains of mice develop virus-induced diabetes) and the genetic make-up of the virus[1,2]. The severity of the disease is directly related to the number of β cells destroyed by the infection and, in some cases, several insults are required to produce sufficient β-cell damage to result in clinically apparent diabetes. Variants of Coxsackie B viruses, Mengo virus and reoviruses also have been shown to damage β cells and produce diabetes. In humans, several lines of evidence including sero-epidemiological data, histological surveys of human pancreas, virus isolation and animal inoculation studies suggest that viruses, especially members of the Coxsackie B group, can actually cause or at least serve as the final insult in causing some cases of IDDM[1,2]. The number of well documented cases is small, however, and if an acute destructive viral infection is a major cause of IDDM, then that virus has not yet been isolated.

Recently, it has been observed that many patients with newly diagnosed IDDM, but not NIDDM, have autoantibodies in their sera that react with cells in the pancreatic islets of Langerhans. In fact, in some patients, these islet cell autoantibodies appear many months and even years before the development of clinically apparent IDDM[4], suggesting that this disease may have a slower or more chronic course than previously suspected. Whether these autoantibodies cause the disease or are the result of it and whether their appearance is genetically programmed and/or triggered by environmental agents, such as viruses, is not known. The possibility that viruses might sometimes trigger the production of autoantibodies is receiving considerable attention and several models exist[5]. For example, reovirus causes an autoimmune polyendocrine disease in mice; human B lymphocytes immortalized by Epstein–Barr virus make autoantibodies that react with a variety of human cells, including β cells; and some monoclonal antiviral antibodies cross-react with normal tissues (that is, molecular mimicry), including β cells.

The experiments of Oldstone and co-workers provide still another mechanism by which viruses might cause diabetes, particularly NIDDM. In earlier work, they showed that lymphocytic choriomeningitis (LCM) virus, which produces a persistent infection in mice, could shut off the luxury functions of differentiated cells (for example, the capacity of pituitary cells to make growth hormone), while leaving their vital function intact[6]. In the present work, by hybridization *in situ*, immunofluorescence and electron microscopy, they show that LCM virus produces a persistent infection in β cells. The infected cells appear to have normal morphology, their insulin content remains within the normal range and there is no inflammation. Nonetheless, glucose levels are elevated and glucose tolerance tests are markedly impaired. Precisely how LCM virus alters glucose tolerance tests has not yet been determined, but based on Oldstone's earlier work, impairment of the luxury function of β cells would seem a likely possibility. Careful studies *in vivo* of the function of hormone-secreting cells, especially glucose-stimulated insulin release, should be revealing.

The idea that viruses, and, more particularly, persistent viral infections, might sometimes be involved in NIDDM is supported by other lines of evidence[2,7]. In mice, retroviruses have been observed in β cells and herpesviruses have been found in the islets of several species. In hamsters, infection with Venezuelan encephalitis virus causes impairment of glucose-stimulated insulin release for several months in the absence of permanent morphological changes in the islets. *In vitro*, this virus-induced β-cell defect can be corrected by analogues of cyclic AMP or by inhibitors of phosphodiesterase[7], but whether the virus actually persists in β cells has not been determined. At the human level, some of the most convincing evidence for a viral involvement in diabetes comes from studies with rubella, a virus that sometimes produces a persistent infection. In patients born with congenital rubella the likelihood of developing diabetes in the first several decades of life (predominantly IDDM, but also NIDDM) is 10–20 per cent, compared to 0.1–0.2 per cent in the control population[8,9]. How the infection actually causes diabetes is not known.

Clearly, much remains to be learned. Nonetheless the concept of virus-induced alterations in luxury function and the demonstration that viruses can establish a persistent infection in β cells opens up a whole new area of exploration concerning the possible aetiology of both IDDM and NIDDM.

1. Notkins, A.L. *Scient. Am.* **241**, 62 (1979).
2. Toniolo, A. & Onodera, T. in *Immunology in Diabetes* (eds Andreani, D., Di Mario, U., Federlin, K.F. & Heding, L.G.) 71 (Kimpton Medical Publications, London, 1984).
3. Oldstone, M.B.A., Southern, P., Rodriguez, M. & Lampert, P. *Science* **224**, 1440 (1984).
4. Gorsuch, A.N. *et al. Lancet* **ii**, 1363 (1981).
5. Notkins, A.L. & Srinivasappa, J. *Proc. 7th int. Congr. Endocr.* (Elsevier, Amsterdam, in the press).
6. Oldstone, M.B.A., Rodriguez, M., Daughaday, W.H. & Lampert, P.W. *Nature* **307**, 278 (1984).
7. Rayfield, E.J. & Mento, S.J. *Rev. infect. Dis.* **5**, 341 (1983).
8. Menser, M.A., Forrest, J.M. & Bransby, R.D. *Lancet* **i**, 57 (1978).
9. Ginsberg-Fellner, F. *et al. Rev. infect. Dis.* (in the press).

Abner Louis Notkins is Chief of the Laboratory of Oral Medicine, National Institute of Dental Research, National Institutes of Health, Bethesda, Maryland 20205.

Particle physics

Nearly the 'top' conference

from David J. Miller

DISCUSSION at the 22nd International Conference on High-Energy Physics held in Leipzig, GDR, on 19–25 July, centred round the possible detection of two so far unobserved components of elementary particle theory. Very recent experiments at CERN, Geneva, and at the Deutsches Elektronen Synchrotron, Hamburg, have discovered what may be the heavy 'top' quark and Higgs particle respectively, and the conference was the first opportunity for many in the high-energy physics community to form their own opinions as to the strength of the evidence.

The top quark was predicted to exist. Physicists do not yet know why the fundamental spin-1/2 particles are arranged in three 'generations', each with a larger mass, but the pattern is clear. Normal matter contains only the first generation: two light quarks, 'up' and 'down', along with a lepton, the electron. In nuclear β-decay, up and down quarks can transform into one another, producing a positive or negative electron which forms the β-radiation and the electron's neutral partner, the neutrino. The 'strange' quark, the 'charmed' quark, the muon and its neutrino form the second generation. Particles carrying strangeness or charm eventually decay to normal matter and muons decay to electrons. The third generation is so far incomplete. The 'bottom' (or 'beauty') quark is securely established as a heavy equivalent of the down and strange quarks. The tau lepton is just like a heavy electron or muon, and in its decays it behaves as if it had its own kind of neutrino, though the tau-neutrino has not yet been directly observed. To complete the conventional picture of the quarks we need the top (or 'truth') quark, which should be like a very heavy equivalent of the up and charm quarks.

R. Bock (CERN) presented the UA1 collaboration's result. In proton–antiproton collisions at the CERN collider, the group has seen several events that contain a high-energy lepton (an electron or a muon) and two narrow 'jets' of high-energy particles, together with an apparent 'missing energy'. The group claims these events could be a result of the production of the W^+ boson (discovered last year at the same machine by the UA1 and UA2 experiments) which is predicted sometimes to decay to a top quark and a bottom antiquark. The energy of the lepton, and its angle to the jets, requires that it be produced by the decay of a very heavy particle, consistent with the top quark. The evidence is only circumstantial and there is room for other explanations. The number of events observed (three with muons and three with electrons) is a little larger than predicted and UA2 has not yet reported a clear signal for the process. If the top mass is eventually established to be between 30 and 50 GeV, then UA1 may well be credited with the discovery, but many would say "not yet".

The Higgs particle is another unobserved component of the conventional picture of elementary particles. It is a spin-zero object, postulated to provide a basis for the properties of the other integer-spin particles which generate the electroweak forces, the photon, the W^+, W^- and the Z. Perhaps the best candidate for the Higgs particle so far was reported at Leipzig by those involved in the crystal ball collaboration, working on the DORIS II machine in

Hamburg (see Walgate, R. *Nature, News & Views* **310**, 546; 1984).

They use a hollow sphere of sodium-iodide detectors, which gives unequalled acceptance and energy resolution for γ-rays, to look for line spectra in the decay of the 'upsilon' states, the 'bottom–antibottom' analogues of the J/psi particles. They see the expected spectrum of lines representing transitions to intermediate states between the first and second upsilon states (the upsilon-1S and the radially excited upsilon-2S). Their new observation is a line in the upsilon-1S decay spectrum corresponding to a transition to a novel 'zeta' particle with a mass of 8.3 GeV. If a Higgs particle exists, theory predicts it will associate most strongly with the heaviest of the other available particles. Thus, if the zeta particle is the Higgs particle, it should decay most commonly to a pair of the heaviest leptons, a tau and an antitau, and only rarely to a muon- or electron-pair. So far, however, taus have not been detected so there is no proof that the zeta is a Higgs particle. Moreover, the upsilon-2S also should decay into the Higgs particle and that has not been seen.

In the conventional picture, quantum chromodynamics (QCD) is the force which confines quarks and gives rise to the properties of the strongly interacting particles (hadrons). Before it can be proved, QCD needs to make a clear and specific prediction that can be tested. One such prediction is the existence of 'glueballs', particles which would have strong interactions but contain no quarks. Candidates exist, and the evidence is consistent with their being composed only of the self-interacting quanta of the QCD field, the vector gluons. In reviewing the subject, A.M. Zaitsev (Dubna, USSR) suggested that the theta-meson, seen in J/psi decay by the Mark III collaboration at Stanford, is most likely to be composed of gluons, but no one has been able to prove it.

Another explicit test may still be possible in photon–photon scattering, though theorists last year were despairing at infinities in the higher-order QCD calculations. Now Gluck, Grassie, Reya and Rossi, as reported by S. Brodsky (California Institute of Technology), have shown how to avoid these troubles. Experimenters are not surprised, since the data from PETRA and PEP already looked very close to the lowest-order QCD predictions. In fact, QCD looks increasingly satisfactory, even without a firm proof, just because it can be made to work without special pleading for such a wide range of processes.

The most memorable talk at the conference came from the speaker furthest removed from laboratory science, the Russian cosmologist A.D. Linde (Moscow). He displayed a breathtaking lucidity in dealing with the most complex of topics, 'inflationary models' of the early Universe. In his picture of the big bang, the first stage may be a quantum tunnelling from 'nothing'. In the very first moment of its existence, the Universe cannot have had a precisely defined energy, according to the Heisenberg uncertainty principle. It cannot therefore have been in the most stable possible state, and must have taken a while to stabilize, during which time expansion would start. According to Linde, this initial expansion is sufficient to 'explain' the isotropy of our visible Universe, together with its great asymmetry between particles and antiparticles. For 'explanation' he gave an impressive succession of arguments based on supersymmetry and other current speculative elementary particle theory.

The cosmologists are no longer as pleased as they were with one concept they inherited from particle theory — the possibility that neutrinos have mass, and therefore might account for the unseen mass of the Universe. Now they would rather that the unseen mass be carried by some of the hypothetical supersymmetric particles. M. Srednicki suggested that decay of these particles might account for the surprising number of antiprotons which have been observed in the cosmic radiation.

Terrestrial experimenters continue to look for the effects of finite-mass neutrinos. Two positive results were reported at the conference. B.A. Ljubimov (Novosibersk) reported an improved version of his group's earlier result on the end point of the β-decay spectrum of tritium. They obtain limits of between 20 and 45 eV for the mass of the neutrino produced in this decay. Of course, if a neutrino has mass, then it will not travel at the speed of light and the question of what happens in its rest-frame becomes relevant. One possibility is transitions between the three generations of neutrinos — the electron-, the muon- and the tau-neutrino. Searches have been going on for some years to establish the existence of such transitions, which might explain the continued shortfall in the number of solar neutrino interactions observed in the Brookhaven experiment of Davis and co-workers. A group working at the Le Bugey reactor in France reported evidence for the disappearance of neutrinos from their beam and gave a range of limits on the possible mass and transition rate which could cause this. But their result is incompatible over almost all of this range with an experiment at the Gösgen reactor in Switzerland, leaving only a tiny allowed region at a neutrino mass much lower than that measured by the Russian tritium experiment. Most observers are reserving their judgement on neutrino masses until some agreement is found between independent measurements. ☐

David J. Miller is in the Department of Physics and Astronomy, University College London, Gower Street, London WC1E 6BT.

Geophysics

Open season for magmatic fractional crystallization

from Bob Thompson

PHASE-equilibria studies have for many years been a popular approach to studying the course of chemical evolution of a basic magma undergoing fractional crystallization. Analyses of volcanic rock suites suggest that a mildly-silica-undersaturated olivine–tholeiite magma may give rise to residues which are either Fe-rich and relatively Si-poor or vice-versa. On the basis of phase-equilibria data, P.L. Grove and M.B. Baker have recently proposed an ingenious mechanism whereby these alternatives may come about (*J. geophys. Res.* **89**, 3253; 1984).

They have made a detailed study of the crystallization of olivine–tholeiite melt at 1 atmosphere pressure, using electron-probe microanalysis to determine the compositions of all the solid and liquid (glass) phases. They find that when the liquids reach the stage of cotectic co-precipitation of plagioclase, olivine and Ca-rich clinopyroxene, the mineral assemblage shows a high ratio of the relatively siliceous phase, plagioclase, to the two ferromagnesian silicates, and relative Fe enrichment of the residue occurs. Enrichment is carried further when, with rising silica activity in the system, any crystals of olivine (a relatively Fe-rich and Si-poor phase) suspended in the liquid dissolve and are replaced by the Ca-poor clinopyroxene pigeonite.

Grove and Baker have not conducted experiments to elucidate the alternative so-called calc-alkaline fractionation trend towards Si enrichment and Fe depletion, but on the basis of published data, they propose that the key factors are crystallization of the magma under a moderate pressure (~ 5 kbar) and the presence of dissolved water in amounts less than sufficient to saturate the liquid. The field boundary between olivine and Ca-rich clinopyroxene is very sensitive to the first of these factors, whilst the second influences both the stability field and the composition of the precipitating feldspar. As a result, a hydrous (undersaturated) olivine–tholeiite magma fractionating at mid-crust depths may precipitate a high ratio of olivine and pyroxene to plagioclase, and the latter may be substantially more Ca-rich (and therefore Si-poor) than in the anhydrous system. The combination of these effects leads inexorably to siliceous Fe-poor residua.

The two fractionation schemes proposed by Grove and Baker may help to resolve a controversy which has rumbled along ever since Bowen produced a meticulously documented case that basic liquids proceed down the calc-alkaline trend during fractional crystallization (*The Evolution of the Igneous Rocks*, Princeton University Press; 1928), while Fenner showed in equally impressive detail that their chemistry evolved in an entirely different direction (*Mineral Mag.* **22**, 539; 1931). For many years attempts to reconcile these views focused on phase-equilibria experiments by Osborn and his co-workers (for example, *Am.J.Sci.* **264**, 428; 1966), who varied the oxidation states of Fe-bearing simplified basaltic systems and thus, by altering the proportion of magnetite to silicates in the precipitating phases, produced either Fe enrichment or Fe depletion. Grove and Baker accept the current widespread opinion that magnetite is an important phase separating during the later stages of fractional crystallization of basaltic melts, but that it is probably not a crucial trend-determining factor during the initial high-temperature stages. They take the same view of amphibole, another relatively Si-poor silicate, which has been canvassed by Green (in *Andesites*, Wiley, New York; 1982) and many others as the crucial phase to precipitate from a hydrous mafic magma and set it on a calc-alkaline trend, although Wyllie (*Phil.Trans.R.Soc.* **A310**, 439; 1984) has stressed that natural hydrous but undersaturated mafic liquids do not contain amphibole as a liquidus phase at the high temperatures of the basaltic composition range. Nonetheless, there seems to be incontrovertible petrographic evidence from xenoliths that amphibole precipitates with anorthite, magnesian olivine and Cr-rich diopsidic clinopyroxene from hydrous mafic liquids at depths corresponding to the crustal base in the island arcs of the Lesser Antilles (Arculus, R.J. & Wills, K.J.A. *J. Petrol.* **21**, 742; 1980), Aleutians (Conrad, W., Kay, R.W. & Kay, S.M. *J. Volcanol. geotherm. Res.* **18**, 279; 1983) and elsewhere. Perhaps, as Green suggests, the discrepancy between observational and experimental petrology is related to the fact that halogens in the natural systems would increase the thermal stability of amphibole.

Once removed from the pressures and temperatures at which they are stable, magmatic amphiboles dissolve rapidly. Their absence as phenocrysts from a suite of lavas is therefore probably no guarantee that amphibole was not fractionating at depth. Fortunately, the separation of this mineral leaves a distinctive imprint on the trace-element geochemistry of a suite of comagmatic rocks because the distribution coefficients of heavy rare-earth elements (HREE) between amphibole and mafic silicate liquids are so large that HREE concentrations fall with progressive fractional crystallization if amphibole is a major separating phase, whereas olivine, plagioclase and pyroxenes incorporate near-negligible amounts of HREE. REE data show the importance of amphibole separation in forcing basic magmas in the Aleutian Arc to follow calc-alkaline fractionation trends (Kay, S.M. *et al. J.geophys.Res.* **87**, 4051; 1982).

Grove and Baker use two subduction-related magmatic suites to illustrate their model for the genesis of calc-alkaline residua. In the oceanic example, the Witu Islands, Papua New Guinea, closed-system fractional crystallization can explain all the available chemical data for the lavas. By contrast, the continental margin suite — from Medicine Lake Highland volcano, California — shows increases in various trace elements and $^{87}Sr/^{86}Sr$ ratio with magmatic evolution that cannot result from closed-system processes and require an open-system model, with concomitant fractional crystallization and assimilation of small amounts of fused sialic crust. This type of scenario appeals to the authors of most recent detailed geochemical studies of magmatic provinces where large volumes of basic liquid have invaded continental crust over a short time span (for example, James, D.E. *Yb.Carnegie Inst. Wash.* **82**, 486; 1983; Cox, K.G. & Hawkesworth, C.J. *Phil. Trans. R.Soc.* **A310**, 627; 1984), although the details of the relationship between fractional crystallization and sial assimilation seem to vary from case to case (Thomson, R.N., Morrison, M.A., Dickin, A.P. & Hendry, G.L. in *Continental Basalts and Mantle Xenoliths*, Shiva Press; 1983). □

Bob Thompson is in the Department of Geology, Royal School of Mines, Prince Consort Road, London SW7 2BP.

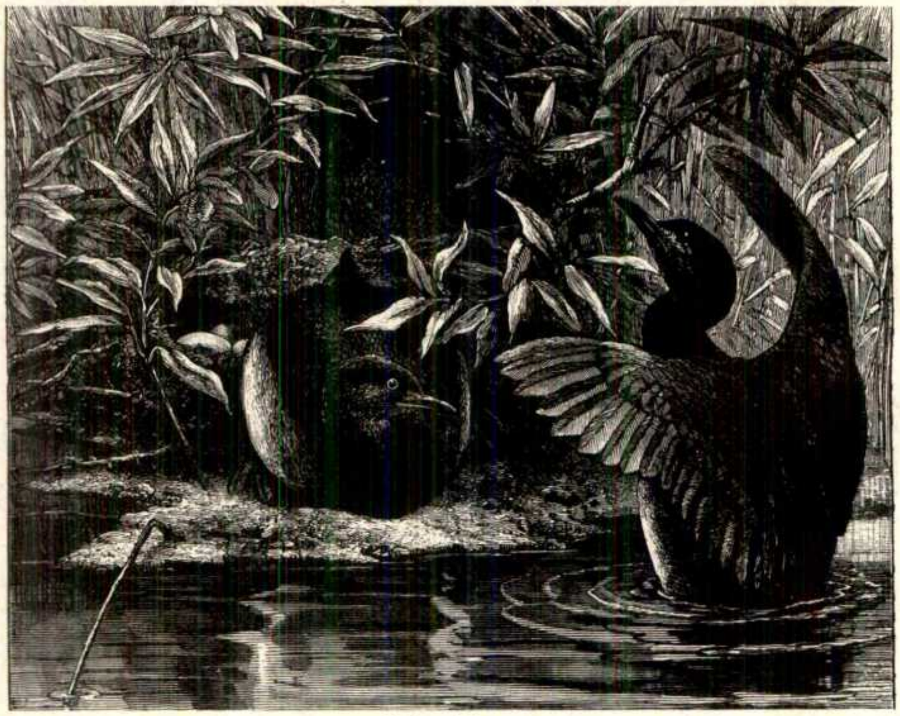

Grebes and Nest.

100 years ago

BRITISH BIRDS AT THE NATURAL HISTORY MUSEUM

VISITORS to the new Natural History Museum can scarcely have failed to notice the many improvements which have been made in the rearrangement of the zoology collections since their removal from Bloomsbury to South Kensington. Here the visitor finds a collection of British birds, in which each species is separately represented by a pair of old birds in the plumage peculiar to the breeding season, with its nest and eggs, not merely in a natural position, but in the actual position in which they were found.

Not very long since Mr. H. Seebohm gave a lecture at the Zoological Gardens on "Birds' Nests" From an attentive study of the subject he considered that nests might be roughly grouped into five classes, according as the birds which owned them relied for the safety of their eggs: (1) on the concealed position of the nest; (2) upon the inaccessible position of the nest; (3) upon the protective colour of the eggs; (4) upon the protective colour of the sitting hen; (5) upon their own ability, either singly, in pairs or in colonies to defend their eggs.

Amongst birds which rely for safety on the inaccessible position of their nest may be mentioned the hawks and owls, raven, chough, kingfisher, sandmartin, moorhen, coot, and grebe. There are few eggs more difficult to take than those of the peregrine falcon, raven, and chough, from the habit of these birds to nest in precipitous cliffs; while moorhens, coots, and grebes, make slovenly-constructed nests upon soft, treacherous ground, or amongst sedges, flags, and other water plants which are unapproachable without the aid of a boat. One cannot fail to note that the more slovenly the nest of these water-birds the more likely is it to escape detection, for, were it well shaped and neat in appearance, its very neatness amidst a mass of wind-strewn rushes or tangled growth of water-weeds would be sure to attract attention towards it.

From *Nature* **30**, 491, 18 September 1884.

Cell biology

First clue to biological role of clathrin light chains

21.1.87
A. Baltz

from Ernst Ungewickell

Two papers[1,2] in this week's *Nature* shed new light on the nature and mechanism of action of coated pits and coated vesicles, two related cell organelles responsible for selective ingestion and specific intracellular transport of membrane proteins by eukaryotic cells[3].

We now know a good deal about the structure of these apparatuses. Their cytoplasmic sides are coated by polyhedal constructions, made up of clathrin (molecular weight 180,000) and several associated polypeptides with subunit molecular weights of 100,000 - 130,000, ~ 50,000 and 30,000–40,000. The building blocks or protomers of the coats are three-legged complexes commonly referred to as clathrin triskelions, constructed from three 180K polypeptide chains. Tightly associated with the triskelions are three of the 30K–40K polypeptides, usually referred to as clathrin light chains or sometimes clathrin-associated proteins (CAPs). Each vertex in the polyhedral coat structure is the centre of a triskelion and the edges of the polygons are formed by extensively overlapping legs of adjoining triskelions (for details see ref. 4).

Both coated pits and coated vesicles are highly dynamic structures. According to a widely accepted working hypothesis the latter derive from the former by a kind of budding process that is accompanied by a rearrangement of the coat structure, whereby some hexagonal facets turn into pentagons so that the polyhedra then possess twelve pentagonal faces amongst the hexagons. Upon budding, coated vesicles rapidly shed their coats to allow them to fuse with their target membranes. The liberated triskelions are thought to return to the membrane to reassociate with an incipient coated pit. This cycle requires a sophisticated regulatory mechanism that must orchestrate assembly, disassembly and reorganization of the coat structure.

Two years ago Patzer *et al.* discovered in the cytosol from bovine brains a protein factor, which in the presence of ATP was able to strip coated vesicles of their coats[5]. The same group has now purified this factor almost to homogeneity by a sequence of steps, of which the most important is affinity chromatography on coupled ATP[6].

This 70K protein turns out to have a latent ATPase activity, which is activated by coated vesicles or indeed by the empty cage-like structures generated by purified triskelions. In ionic milieus, in which the clathrin polyhedron is marginally unstable, the factor causes dissociation of the vesicle coat or disruption of the empty cage, with formation of a complex that contains one molecule of factor per triskelion leg. The triskelions thus sequestered will not reassociate to cages, even under the most favourable ionic conditions.

A recent exciting extension of this work, reported on page 228 of this issue of *Nature*, is the demonstration that the presence of clathrin light chains on the assembled triskelions is a prerequisite for the interaction of the uncoating protein with clathrin and hence for the expression of ATPase activity, and disintegration of the structure into triskelions[1]. Neither free triskelions with bound light chains nor free light chains alone are recognized by the uncoating protein. This result gives us the first indication of a biological role for clathrin light chains.

The mechanistic details of the uncoating reaction remain to be elucidated. The observation that factor-dependent uncoating is most effective under conditions in which cages or coats are not very stable suggests that the action of the uncoating protein is contingent on the prior dissociation of interacting triskelion legs. Normally, a single transient dissociation event has no ill-effects, for the two remaining legs of the triskelion will suffice to hold it securely in place. As judged by electron microscopy[6], the uncoating protein seems to bind near the centre of the triskelion, yet it evidently disrupts a clathrin–clathrin interaction that extends over 18 nm or so. It is here that the light chains may intervene, since they have been shown to extend from the triskelion centre to a point at least 16 nm along the leg[7]. It may be conjectured, then, that binding of uncoating protein and concomitant ATP hydrolysis induces a conformational change in the light chains or a change in their binding site on the heavy chain, such that when two legs dissociate, they will no longer recombine. The dissociation of the last of the three legs of a given triskelion will then result in its release from the cage. In order to restore the ability of the liberated triskelions to enter into a new round of coating and uncoating, other, as yet unrecognized factors may be required.

But to denude coated vesicles of their coats it is not sufficient merely to impede clathrin–clathrin interactions, since triskelions are also anchored by way of protease-sensitive sites to the vesicle membrane itself. For the present it is not altogether clear whether this interaction is also perturbed by the uncoating protein or whether release of triskelions from the membrane involves two unrelated, but simultaneous events.

In this connection one should take note of the intriguing results of Pauloin *et al.*[8], concerning a coated vesicle-associated Ca^{2+}- and cyclic AMP-independent protein kinase that phosphorylates specifically a 50K polypeptide in coated vesicles. This group has now shown (see page 265) that after extraction of purified coated vesicles with 0.5 M Tris, the 50K substrate co-elutes from gel-filtration columns together with the 100K - 130K polypeptide cluster. This fraction also contains the kinase activity. Chemical cross-linking experiments support the idea of a stoichiometric interaction between the 50K phosphoprotein and probably a single member of the 100K–130K subunit group. Even before this finding, there were reasons enough for homing in on this polypeptide mixture, since Zaremba and Keen have shown that it promotes the self-association of purified clathrin triskelions into a relatively uniform population of 78 nm cages, under conditions that otherwise prohibit assembly[9]. Furthermore, some of these polypeptides are suspected to mediate the interaction of clathrin with the coated vesicle membrane[10].

When Pauloin and Jollès[2] investigated the effect of purified triskelions on the kinase activity, they noted a fourfold stimulation, which they were able to ascribe uniquely to the clathrin light chains.

The conditions employed for the phosphorylation of the 50K polypeptide are similar to those in the uncoating experiments of the Stanford group and one should therefore expect both events to occur simultaneously (though the sceptical reader may feel a trifle uneasy at the low ionic strength of the media preferred by both groups). It would be pleasing if it should turn out that the phosphorylation of the 50K polypeptides weakens the interaction of triskelions with the membrane, but this is perhaps too much to hope for at this stage.

Nevertheless, I would expect that the undoubted breakthrough by Rothman and his group on the uncoating reaction will provoke some workers in the field to leap onto the accelerating bandwagon before its speed becomes dangerously high. At all events, further rapid progress in uncovering the details of the coated pit/coated vesicle pathway can be confidently predicted. □

1. Schmid, S.L., Braell, W.A., Schlossman, D.M. & Rothman, J.E. *Nature* **311**, 228 (1984).
2. Pauloin, A. & Jollès, P. *Nature* **311**, 265 (1984).
3. Pearse, B. & Bretscher, M. *A. Rev. Biochem.* **50**, 85 (1981).
4. Slayter, H. *Nature* **298**, 228 (1982).
5. Patzer, E.J., Schlossman, D.M. & Rothman, J.E. *J. Cell Biol.* **93**, 230 (1982).
6. Schlossman, D.M., Schmid, S.C., Braell, W.A. & Rothman, J.E. *J. Cell Biol.* (in the press).
7. Ungewickell, E. *EMBO J.* **2**, 1401 (1983).
8. Pauloin, A., Bernier, I. & Jollès, P. *Nature* **298**, 574 (1982).
9. Zaremba, S. & Keen, J.H. *J. Cell Biol.* **97**, 1339 (1983).
10. Unanue, E.R., Ungewickell, E. & Branton, D. *Cell* **27**, 439 (1981).

Ernst Ungewickell is at the Max Planck Institute for Biophysical Chemistry, Postfach 968, Am Fassberg, D-3400 Goettingen, FRG.

Developmental biology

How to make a fruitfly

from Geoffrey North

In recent issues of *Nature*, Gary Struhl[1] and Jonathan Slack[2] have explained how the discovery of the 'homoeo box' may have provided the first link between genes known to regulate the development of the fruitfly *Drosophila melanogaster* and previously unknown sets of analogous genes in vertebrates. The 'homoeo box' is a short DNA sequence present in several of the homoeotic genes that specify the character of the different parts of the fruitfly body[3,4] and it has now turned up in a highly conserved form in the genomes of vertebrates[5,6].

If the promise of this startling discovery is fulfilled, the great gap that has separated the genetic understanding of *Drosophila* development from that of the higher vertebrates will soon begin to close. In the meantime, as became clear at a recent meeting*, it continues to widen rapidly. Nearly all of the genes concerned with regulating the early development of *Drosophila* will soon have been identified, while the analysis of the later-acting homoeotic genes has already reached the stage at which their protein products are coming in for scrutiny.

Establishing polarity

The earliest genes involved in regulating embryonic development are those that determine the polarity of the three axes of the embryo: anterior–posterior, dorsal–ventral and left–right. These genes are defined by mutations that affect the establishment of pattern along one axis independently of the others, and establish polarity of the egg even before fertilization; thus their effects on the embryo reflect only the maternal genotype and mutations in these genes are known as 'maternal-effect' mutations.

The establishment of the dorsal–ventral polarity has been studied in most detail. The prototype gene affecting this polarity is called *dorsal*, and females homozygous for the most extreme *dorsal* mutations produce what are known as 'dorsalized' embryos, which lack ventral and lateral structures, and have dorsal structures extending all around the body. Weaker *dorsal* mutations allow the development of more lateral structures, which is consistent with the existence of a gradient of some morphogen that determines polarity.

A total of eleven genes, recessive mutations of which have effects identical to that of *dorsal*, has now been identified (K. Anderson, Friedrich-Miescher Laboratorium, Tübingen). The implication is that each of these genes, which are distributed throughout the genome of *Drosophila*, encodes a component of a unified process of pattern formation. According to recent evidence reported by Anderson, the component contributed by one of them, a gene named *Toll*, may actually be a physiological morphogen.

As with the other ten genes, recessive mutations in *Toll* cause 'dorsalized' embryos. But dominant mutations in the same gene produce the reverse effect: the extension of ventral structures to the dorsal side of the embryo. And females that not only have a dominant *Toll* allele, but are also homozygous for mutations of all but *dorsal* itself of the ten other genes, produce 'lateralized' embryos, which lack structures characteristic of the dorsal-most and ventral-most regions of the embryo.

The evidence that *Toll* encodes a morphogen comes from experiments in which components of wild-type embryos are injected into mutant embryos. Some of the recessive dorsalized mutants, including *Toll*, can be rescued by injections of wild-type cytoplasm into the embryo (ref. 7 and Anderson). But only in the case of *Toll* can the polarity of the embryo be reversed by such injections. In mutant embryos the egg retains a visible dorsal–ventral asymmetry, even when the embryo into which it eventually develops does not. In all 'rescue' cases other than *Toll*, the rescued embryo has the same polarity as the egg. This shows that these mutant embryos must retain an intrinsic polarity that can be expressed only in the presence of some factor in the wild-type cytoplasm. In the case of *Toll*, however, the polarity of the rescued embryo is determined by the site of injection of the wild-type cytoplasm. The implication is that unlike the other dorsalized mutants, recessive *Toll* mutant embryos really are apolar, and that the product of the *Toll* gene, by its differential localization in the embryo, is a direct determinant of dorsal–ventral polarity. A possible explanation of the dominant 'ventralizing' *Toll* alleles, then, might be that they result in the overproduction of the *Toll* gene product, so that levels are elevated in more dorsal regions of the embryo leading to the determination of ventral structures in the wrong place.

In this issue of *Nature*, two papers report further important steps in understanding the molecular nature of the mother fruitfly's legacy to its offspring. On page 223, Christiane Nüsslein-Volhard and Anderson show that for many of the genes involved in establishing dorsal–ventral polarity, a substantial fraction of the rescuing activity is in the form of stored maternal poly(A)$^+$ RNA[8]. And the cloning of the first of these genes, *dorsal*, together with evidence that the gene encodes a 2.8 kilobase (kb) RNA present in ovaries and 0–2.5 h embryos, is reported by Steward *et al.*[9] on page 262.

Dividing up the embryo

Apart from its overall symmetry and polarities, the other obvious feature of the body of a fruitfly is that it is divided into segments along its anterior–posterior axis. Segmental patterns have fascinated theoreticians of pattern formation for many years, but the mechanistic basis of the periodicity they imply has remained elusive. This may change with the characterization of the genes controlling segmentation of *Drosophila*.

In 1980, Nüsslein-Volhard and Wieschaus reported the identification of fifteen genes, mutations of which caused an alteration of the segmental pattern of homozygous larvae[10]. The mutations fall into three classes, defined by the kind of pattern alteration they cause (see the figure). Two of the classes have a periodic effect on the segmental pattern, one with a periodicity of a single segment (segment polarity mutations), the other with a two-segment periodicity (pair-rule mutations). Mutations of the third class (gap mutations) have an aperiodic effect, causing the loss of groups of adjacent segments.

Of the three classes, the gap genes are thought likely to work the earliest in development, possibly having a primary role in interpreting an anterior–posterior gradient of positional information and determining large regions of the early

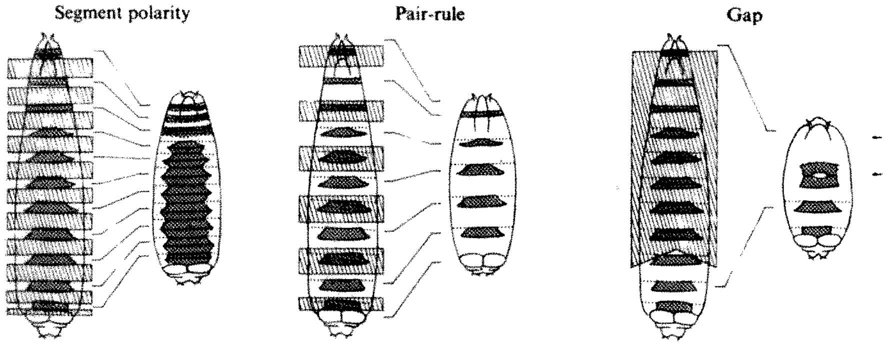

One example of each of the three classes of *Drosophila* mutations which alter the segmented pattern of homozygous larvae. The hatched bars on the normal larvae (left) indicate the regions missing in the mutant larvae (right). From ref. 10.

---

*The fourth EMBO Workshop on the molecular and developmental biology of *Drosophila* was held in the Orthodox Academy of Kolymbari, Crete, from 24 to 29 June 1984.

embryo (H. Meinhardt, Max Planck Institut fur Entwicklungsbiologie, Tübingen). There are three zygotic gap genes, which differ with respect to the region of the embryo affected by mutations of them: *hunchback* mutations delete thoracic segments; *knirps* mutations delete abdominal segments; and *Krüppel* mutations delete thoracic and anterior abdominal segments. It seems that in the absence of the appropriate gap gene, large regions of the embryo simply fail to develop, the remaining segments developing normally. Further insight into their workings should be forthcoming, now that the *Krüppel* gene has been cloned (H. Jäckle, Max Planck Institut fur Entwicklungsbiologie, Tübingen). The partial rescue of mutant embryos by injecting the cloned DNA into the prospective thoracic and anterior abdominal region suggests that the product of the *Krüppel* gene is active in the region of the embryo affected by *Krüppel* mutations. The major RNA transcript detected by hybridization with the cloned *Krüppel* DNA is expressed specifically at the blastoderm stage of development, which is the time when the *Krüppel* gene product seems to be required.

By the time that signs of segmentation first become apparent in the life of a fruitfly, the embryo's nuclei have become transcriptionally active and its development is no longer dominated by its maternal inheritance. However, although most of the segmentation genes are strictly zygotic, several of the *knirps* group of gap genes, including *oskar*, are actually maternal-effect genes. Nüsslein-Volhard (Friedrich-Miescher Laboratorium, Tübingen) reported that the phenotype of *oskar* mutant embryos (which would normally fail to develop an abdomen) can be completely rescued by the injection of wild-type cytoplasm as long as the cytoplasm is taken from the posterior pole of a wild-type embryo and injected into the prospective abdominal region of the mutant embryo. The implication is that the rescuing activity is actually stored at the posterior pole and transported anteriorly, in some way influencing the development of cells in the abdominal region of the embryo.

Of the genes that have a periodic effect on the segmentation pattern when mutated, most is known of the pair-rule gene *fushi tarazu* (*ftz*). In homozygous *ftz* mutant embryos, roughly the posterior half of every even-numbered segment and the anterior half of every odd-numbered segment is deleted; the remaining half-segments are fused, so that the mutant embryos have half the usual number of segments. Interestingly, in normal embryos, *ftz* RNA is distributed periodically, with a periodicity roughly corresponding to that of the deleted parts of *ftz* mutant embryos, before the first morphological signs of segmentation (A. Kuraiwa, Biozentrium, Basel; refs 2, 11, 12).

Another pair-rule gene, *Hairy*, seems to be the complement of *ftz* in that *Hairy* mutations lead to the deletion of the parts not deleted in *ftz* mutants. An important point made by D. Ish-Horowicz (Imperial Cancer Research Fund, London) is that the parts of the embryo not deleted in *Hairy* mutants retain their wild-type segment identity. By combining *Hairy* and homoeotic mutations it has also been shown that the requirement for a wild-type *Hairy* gene depends upon the position of a group of cells in the embryo, and not upon the character of the segment of which the cells will form a part. So it would seem that segment specification — the domain of the homoeotic genes — and whatever genes such as *ftz* and *Hairy* are doing, are to some extent independent processes. Ish-Horowicz revealed that the *Hairy* gene has been cloned and shown to be expressed early in development, so it will be interesting to see how the spatial distribution of *Hairy* transcripts compares with that of *ftz* transcripts.

Homoeo box latest

Walter Gehring revealed at the European Developmental Biology Congress in Southampton two weeks ago that his group in Basle, in collaboration with Tom Kornberg in San Francisco, has now identified the first gene in *Drosophila* outside of the bithorax and Antennapedia complexes to contain a homoeo box sequence. The gene is ***engrailed***, which keeps up the association of the homoeo box with genes that specify the development of different parts of the fruitfly as *engrailed* is also a homoeotic gene, with the particular role of distinguishing the posterior from the anterior compartments of each segment. Gehring also reported that it is now clear that at least nine homoeo boxes fall within the bithorax and Antennapedia complexes: three have been mapped within the bithorax complex (two by Welcome Bender's group at Harvard), and there are at least six in the Antennapedia complex, of which three have been assigned to known genes (see the figure; note that further genes are believed to exist within Antennapedia, left of *pb*).

The disposition of the three homoeo boxes within the bithorax complex may be especially significant in the light of some recent results of Gines Morata (University of Madrid). Morata reported at the Crete meeting that on the basis of complementation analyses the bithorax complex seems to consist of three distinct genes: *Ultrabithorax* (*Ubx*), *abdominal-A* (*abd-A*) and *Abdominal-B* (*Abd-B*). Each of these genes is concerned with specifying the development of a different region of the fruitfly: thus, the *Ubx* domain extends from the posterior compartment of the second thoracic segment to the anterior compartment of the first abdominal segment; the *abd-A* gene then takes over as far as the fourth abdominal segment; and the *Abd-B* gene specifies the four most posterior segments. As can be seen in the figure, the three homoeo boxes have fallen neatly one into each genetically defined unit.

Although evidence is still lacking that the highly-conserved homoeo box sequences that have been found in the genomes of vertebrates really are markers of genes involved in regulating development, the assumption has now received further support from the first studies of the expression of such a gene. The crucial finding reported by Eddy de Robertis (Basle) in Southampton is that the second homoeo box-containing gene his group has identified in the genome of the frog *Xenopus laevis* is expressed at high levels in oocytes, and that transcripts of the gene disappear in early (blastula-phase) embryos. Transcripts of the gene can again be detected at gastrulation, but at a much lower level than in oocytes. The exciting possibility suggested by these observations is that they have identified a gene that encodes a stored maternal mRNA that may be involved in specifying the early development of the frog embryo.

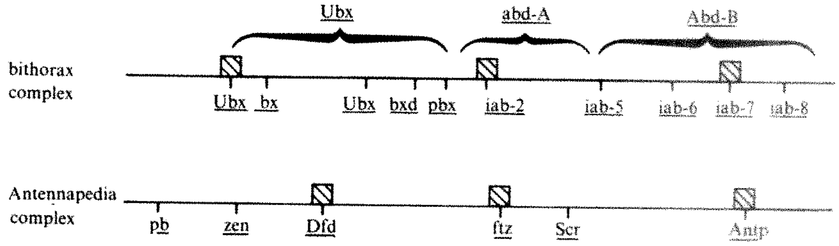

Specifying the parts

The importance as units of development of the parts into which segmentation divides the body of a fruitfly is clearly shown by the effects of homoeotic mutations, which cause specific parts of the body to develop in ways characteristic of other parts. The affected parts are usually delineated by either two segment boundaries, or a segment boundary and a line that divides a segment into anterior and posterior halves. Homoeotic mutations are thought to identify genes that specify the development of different parts of a fruitfly's body, and their domains of action are known as developmental compartments.

The archetypal homoeotic genes cluster in a region of the *Drosophila* genome known as the bithorax complex, which controls the development of all segments of the *Drosophila* body posterior to the second thoracic segments. Recessive bithorax complex mutations cause segments to develop like more anterior segments, and the genetic order of the mutants roughly corresponds to the spatial order of the affected segments along the anterior–posterior axis[13].

These observations led E.B. Lewis of the California Institute of Technology to propose that, starting with the third thoracic segment, progressively more posterior segments express successively more of the genetic components of the bithorax complex, and that the particular combination of genes expressed by groups of cells early in development is determined by their position in the embryo and directs their subsequent developmental fate. The conceptual framework established by Lewis (and elaborated by others, see ref. 14) has become open to direct testing at the molecular level with the recent cloning of bithorax[15]. This cloning feat has also helped to suggest an explanation for the intriguing genetic phenomenon of *cis*-vection, which was the topic of Lewis's talk in Crete and may turn out to be a reflection of an important aspect of the regulation of expression of bithorax complex genes.

Cis-vection in the bithorax complex is seen in the case of *Ultrabithorax* (*Ubx*) mutations. These mutations are capable of inactivating simultaneously four independent activities mapping in the bithorax complex, each of which is primarily concerned with specifying a different one of the four half-segments from posterior second thoracic to anterior first abdominal. *Ubx* mutations are thus like the sum of the four mutations ***anteriorbithorax*** (***abx***), ***bithorax*** (***bx***), ***postbithorax*** (***pbx***) and ***bithoraxoid*** (***bxd***), each of which transforms one of the four half-segments into the equivalent half-segment of the immediately preceding segment. *Ubx*, *abx* and *bx* mutations all map together in a segment of the bithorax complex which is known to encode a giant 75 kb primary transcript that is processed into several discrete RNA products[3].

Thus the effect of *Ubx* mutations on the activities of *abx* and *bx* functions is relatively easy to explain: either *abx* or *bx* are discretely inactivated by point mutations or both are abolished by a mutation (*Ubx*) affecting the entire unit. *Pbx* and *bxd* mutations, however, map within a separate 25 kb (*bxd*) transcription unit upstream of the *Ubx* transciption unit and which also encodes multiple RNA products. How, then, is the effect of *Ubx* mutations on *pbx* and *bxd* functions to be explained? This is the problem of *cis*-vection, and D. Hogness (Stanford University) and P. O'Farrell (University of California, San Fransisco) independently suggested the following solution.

Although mutations that independently affect the *pbx* and *bxd* functions map to the *bxd* transcription unit, Hogness and O'Farrell suggest that the gene products are encoded, together with the *abx* and *bx* products, in the discrete RNAs produced from the *Ubx* transcription unit. To account for *cis*-vection Hogness and O'Farrell suggest that the *Ubx* and *bxd* primary transcripts interact whilst still attached to the chromosome, and that the interaction is required for correct processing of the *Ubx* transcript to produce the RNAs specifying the four *Ubx* activities. Consistent with this model is the lack of sizeable open reading frames in the sequences of cDNA copies of *bxd* transcripts so far determined by Hogness's group. Although no clear relationship has yet been established between a *Ubx* function and a *Ubx* transcript, the 4.7 kb size class *Ubx* RNA is present only early in development (Hogness), which suggests it may be associated with the *abx* function that has been shown by clonal analysis to be a uniquely early *Ubx* activity (the others are required throughout larval development).

To return to Lewis's model for the bithorax complex, the crucial prediction that has become amenable to testing is that the genes are expressed in a segment-specific fashion. Akam has shown by the technique of hybridization *in situ* that *Ubx* RNAs are indeed expressed only in specific segments of *Drosophila* embryos and larvae, and that, by and large, the highest levels of expression occur in those regions most affected by *Ubx* mutations[16]. But Akam's results extend the conclusions drawn from classical genetic experiments in two important respects. The first is that the spatial pattern of expression actually does differ for different cell types: for example, in larvae the pattern for epidermal cells differs from that for muscle cells. The second is that it is now clear that Lewis's original suggestion that bithorax genes are expressed in all segments posterior of the first segment in which they are expressed is oversimplistic: for example, in embryos the level of *Ubx* expression in central nervous system cells decreases posterior of the first abdominal segment.

Two speakers in Crete, Hogness and R. White (Laboratory of Molecular Biology, Cambridge), reported that the availability of cloned DNA has for the first time allowed the protein products of a homoeotic gene to be identified and localized in a developing fruitfly. The results presented by both speakers relied on antibodies generated against hybrid proteins made by expressing *Ubx* cDNA sequences fused to a β-galactosidase gene in *Escherichia coli*. From what is known of the processing of *Ubx* RNAs the antigenic determinants recognized by the antibodies could be shared by several different protein products, and in fact White has found by protein-blotting experiments that his antibodies recognize at least three proteins, two of molecular weights of approximately 44,000 and one of 41,000.

Both Hogness and White reported immunofluorescence staining experiments carried out to localize the *Ubx* proteins in wild-type and mutant embryos and larvae. An important observation made by both groups is that the proteins are localized in cell nuclei, which is consistent with the suggestion that they have DNA-binding activities, conferred by the basic 'homoeo box' domain[1,17,18].

The distribution of *Ubx* proteins in wild-type embryos and larvae is reasonably consistent with that reported for the RNAs by Akam. However, further complications of the classical model of the bithorax complex have been revealed by the effects of mutations on the distribution. Thus, Hogness reported that mutations of the *Polycomb* gene, which transform all segments into copies of the most posterior abdominal segment, do indeed make all segments stain like the most posterior abdominal segment of wild-type embryos. But this means that in the third thoracic and first abdominal segments the level of *Ubx* proteins actually appears to decrease, in direct contradiction of Lewis's prediction that *Polycomb* mutations simply deregulate bithorax gene expression so that all genes are expressed in all segments.

I think it is fair to say that in general terms Lewis's model is proving remarkably valid. Not surprisingly, the details are proving more complex than can have been predicted solely on the basis of classical genetic experiments, and the hope now is that some of this complexity will become unravelled when the relationship between the multiple mRNA and protein products of the bithorax complex genes and the genetically identified activities becomes clearer.

Caveat

Lest some might infer from the above that developmental biology is close to being solved, I think I should say that even now not a single process of pattern formation in *Drosophila* is understood in mechanistic detail. The position is somewhat akin to that in the study of the molecular basis of cancer: many of the genes involved are known, but how they work is poorly understood.

To take just one example, virtually nothing is known of the origins of asymmetry in the embryo. As I have explained above these origins seem the domain of maternal genes expressed during oogenesis, but it is an open question whether the asymmetries inherent in a *Drosophila* egg are determined explicitly by the asymmetrical nature of meiosis, or are generated *de novo* by the maternal gene products during egg development.

Perhaps the most important conclusion is that the problems can now be seen to be soluble. In the end, we shall know how fruitflies are made. And perhaps, when we do, we shall know in principle how people are made too. □

1. Struhl, G. *Nature, News & Views* **310**, 10 (1984).
2. Slack, J. *Nature, News & Views* **310**, 364 (1984).
3. North, G. *Nature, News & Views* **310**, 364 (1984).
4. Akam, M.E. *Nature, News & Views* **308**, 402 (1984).
5. McGinnis, W. *et al. Cell* **37**, 403 (1984).
6. Carrasco, A.E. *et al. Cell* **37**, 409 (1984).
7. Santamaria, P. & Nüsslein-Volhard, C. *EMBO J.* **2**, 1695 (1983).
8. Andeson, K.V. & Nüsslein-Volhard, C. *Nature* **311**, 223 (1984).
9. Steward, R., McNally, F.J. & Schedl, P. *Nature* **311**, 262 (1984).
10. Nüsslein-Volhard, C. & Wieschaus, E. *Nature* **287**, 795 (1980).
11. Kuroiwa, A., Hafen, E. & Gehring, W.J. *Cell* 37, 825 (1984).
12. Hafen, E., Kuroiwa, A. & Genring, W.J. *Cell* 37, 833 (1984).
13. Lewis, E. *Nature* **276**, 565 (1978).
14. Garcia-Bellido, A., Lawrence, P.A. & Morata, G. *Scient. Am.* **241**, 90 (1979).
15. Bender, W. *et al. Science* **221**, 23 (1983).
16. Akam, M.E. *EMBO J.* **2**, 2075 (1983).
17. Laughon, A. & Scott, M.P. *Nature* **310**, 25 (1984).
18. Shepherd, J.C.W. *et al. Nature* **310**, 70 (1984).

Geoffrey North is an assistant editor of Nature.

Laying down the $-3/2$ power law

SIR — Referring to the ecological -3/2 power law, A.F. Hayton[1] mentions White's belief[2] that the ecological "-3/2 law" has not yet been properly explained. The background to the law is indeed traceable to the Japanese origins[3-5] referred to by Hayton. There its attempted explanation is seen to revolve around the consideration of energetics, the energy flux transferring through the surface of a plant to contribute to the energy encapsulated within its volume. Dimensionally these relate to each other according to the square and cube respectively of a typical dimension. In the form of the "-3/2 law" this reduces to the now-famous gradient. However, reservations regarding rigour persist primarily it would appear because mixing the area of the individual plant surface with that of the territory colonized by the whole population threatens to cloud the issue.

Let us instead explore a purely geometric analysis. The figure represents a plant growing within a population of N individuals occupying a territory of area A. Prior to competition the exclusion zones of each, those volumes of air and soil space adequate to meet the entire needs of the plants, would not interfere with one another and the plants could increase their mass without loss of numbers. At the point of interference and thereafter competition would ensue with the result that increasing biomass would be achieved at the price of decreasing distribution density as follows:

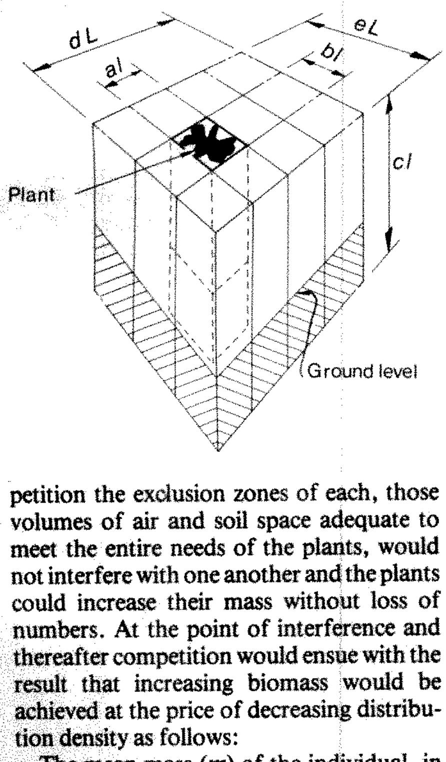

The mean mass (m) of the individual, in this case the typical specimen shown in the figure, is $\varrho\, x\, (al)\, (bl)\, (cl)$ in which ϱ is the density of the plant x is the proportion of the space occupied by the plant within its exclusion zone, l is a typical dimension of the plant and, a, b and c are constants for a particular genera relating the plant to its exclusion zone; a would normally be equal to be in this schematic representation.

Thus we have:

$$m = \varrho\, xabc\, l^3 = kl^3 = k\left(\frac{1}{l_2}\right)^{-3/2} = k\left(\frac{N}{Nl^2}\right)^{-3/2}$$

where $k = \varrho\, xabc$, a combination of constants for a particular genera.

Also, if L is a typical dimension of the total territory occupied by the whole population, the area (A) of that territory is $(dL)\,(eL)$ where d and e are constants determining the shape of the area in this schematic representation. However, in a competing community of N individuals $N\,(al)\,(bl) = (dL)\,(eL)$. Therefore, $Nl^2 = (de/ab)L^2$. Hence:

$$m = k\left(\frac{abN}{deL^2}\right)^{-3/2} = k\,(ab)^{-3/2}\left(\frac{N}{deL^2}\right)^{-3/2}$$

$= K\left(\frac{N}{A}\right)^{-3/2}$ where K is a derived constant for a particular genera.

Therefore, $\log m = -3/2 \log\left(\frac{N}{A}\right) + \log K$

This is the "-3/2 law". Its derivation thus far requires no significant reference to energetics, although any attempt to quantify K would, as it contains ϱ, x, a, b and c, all of which are to some degree genera-dependent with x in particular almost certainly relating to energetics. However, the basic law is a geometrical phenomenon and perhaps now deserves to be regarded as a true law instead of the mere rule correctly noted by Hayton in relation to previous usage.

A final point, the "-3/2 law" relates the distribution density to the *mean* mass and not the *combined* biomass, as implied by Hayton, although in the context of the above item, in which nations of people are considered as separate units of biomass and treated individually, this does not devalue its contribution.

R. WHITTINGTON

Hunter's Way,
Bunkers Lane
Rookley,
Isle of Wight, UK

1. Hayton, A.F. *Nature* **310**, 178 (1984).
2. White, J. *J. theor. Biol.* **89**, 475-500 (1981)
3. Shinozaki, K. & Kira, T. *J. Inst. Polytech, Osaka City Univ.* **D7**, 35 (1956).
4. Todaki, Y. & Shidei, T. *J. Jap. For. Soc.* **41**, 341 (1959).
5. Yoda, K., Kira, T., Ogawa, H. & Hozumi, K. *J. Biol. Osaka City Univ.* **14**, 107 (1963).

Repetitive sequences in structural genes

SIR — In a recent News and Views item[1], Edward Max discusses the implications of CpG clusters in structural genes. He postulates that these CpG clusters will be under-methylated in germ-line DNA and proposes the experiment of determining whether the CpG-rich regions of histocompatibility Class I genes will be found to be under-methylated in sperm DNA. Our recent study in mouse sperm DNA of the state of methylation of *H-2*, Class I CpG sequences recognized by the isoschizomers *Msp* I and *Hpa* II showed them to be highly methylated. The multiplicity of sequences cross-hybridizing to the Class I probe prevents us from determining the 3′ or 5′ location of the few unmethylated sites. The other sequences studied (β-globin, amylase, and a spermatid cDNA clone) were also highly methylated in germ-line DNA, even from immature testes which contain only pre-meiotic cells.

These results are comparable to those reported by others who have found that structural genes are usually highly methylated in sperm DNA (rabbit β-globin[3], ovalbumin[4], α2-collagen[5]). In contrast, those repetitive sequences which have been studied were found to be hypomethylated in sperm DNA[6-8]. Since the two classes of sequences behave differently at meiosis, the alterations in methylation seen in sperm DNA are unlikely to be secondary to the chromatin structure changes which occur during meiosis.

ROBERT P. ERICKSON

Imperial Cancer Research Fund Laboratories,
PO Box No 123,
Lincoln's Inn Fields,
London WC2A 3PX, UK

1. Max, E. *Nature* **310**, 100 (1984).
2. Rahe, B., Erickson, R.P. & Quinto, M. *Nucleic Acids Res.* **11**, 7947 (1984).
3. Waalvaijk, C. & Flavell, R.A. *Nucleic Acids Res.* **5**, 4631 (1978).
4. Mandel, J.L. & Chambon, P. *Nucleic Acids Res.* **7**, 2081 (1979).
5. McKeon, C., Ohkubo, H., Pastan, I & de Crombrugghe, B. *Cell* **29**, 203 (1982).
6. Chapman, V., Forrester, L., Sanford, J., Hastie, N & Rossant, J. *Nature* **307**, 284 (1984).
7. Sanford, J., Forrester, L., Chapman, V., Chandley, A. & Hastie, N. *Nucleic Acids Res.* **12**, 2823 (1984).
8. Ponzetto-Zimmerman, C. & Wolgemuth, D.J. *Nucleic Acids Res.* **12**, 2807 (1984).

Fourier's law and thermal conduction

SIR — Casati *et al.*[1] recently described a many-body system in which the Fourier law for thermal conductivity was shown to result from the deterministically random dynamics of the system. Their conclusions are interesting, and confirm and extend similar results that were found for another one-dimensional system a year ago[2]. In an editorial comment[3] the importance of the results of ref.1 were correctly described, but again there was no reference to our earlier work. We now wish to discuss the numerical calculations which have been done for the diatomic Toda chain, and to outline some of the outstanding problems in this field.

The diatomic Toda lattice is a linear chain with alternating masses which interact by an exponential force[2,4]. The equations of motion for the displacement q_n and the momentum p_n at site n for the mass ratio $\sigma_{2n} = \sigma$ and $\sigma_{2n+1} = 1$ can be written down as:

$$\begin{aligned} dp_n/dt &= \exp(q_{n-1} - q_n) - \exp(q_n - q_{n+1}) \\ dq_n/dt &= \sigma_n V p_n \end{aligned}$$

For equal masses ($\sigma = 1$) this is one of the few discrete lattices which are integrable[5]. For alternating masses the system is not integrable[6] but shows mixing behaviour[2,6].

This diatomic Toda chain was coupled at both ends to two different heat baths containing particles with a maxwellian distribution with which the first as well as the last particle in the chain can exchange momentum by a realistic collision mechanism[7]. The conductivity coefficient was shown to depend on the mass ratio and temperature of the heat bath, but most importantly, it was independent of the chain length and therefore an intrinsic property of the chain. The results in ref.2 are calculated for quite large mass-differences. For the case of only small mass differences the influence of the non-integrability is not strong enough and additional heat transport is possible via slowly decaying solitary excitations.

This effect is most dramatically seen in the case of the monatomic chain where the mean kinetic energy of the particles is constant along the chain. At larger mass-differences, however, and when the heat baths are at high temperatures, there was no influence of solitary transport in the heat current. As well as studying the current through the first particle, we examined the difference of the current through the first and the last particle. This difference became equal to zero with small oscillations after a certain time of integration. Comparisons with experimental values for the conductivity were quite satisfactory. Interestingly, in all our computer-experiments we found a certain surface layer with rather high thermal resistivity.

Both systems[1,2] are coupled to the randomly acting heat baths and therefore the dynamical system itself is only a transport mechanism to these random collisions. It would be very interesting (but much more complicated) to study the behavior of the diatomic Toda chain in phase space without external disturbances. Preliminary results indicate that the system starting from an arbitrary state relaxes to a state with equally distributed kinetic energy, it behaves like a thermodynamical system. But again one has to be very careful in studying this effect since another random influence, namely the numerical errors in the computational procedure, may change the conclusions. It would therefore be desirable to have some analytic results on these systems that can be compared to studies in which thermal conduction is studied in a system of oscillators interacting by a stochastic process[8].

Finally, it should be noted that the two systems so far studied are one-dimensional and the influence of higher dimensions remains to be determined[9]. It is known that in higher dimensions solitary excitations decay much more rapidly and this might help the normal thermal conduction; but numerical computer experiments in this case need much larger computers than we have available.

In summary, we think that some progress has been made in interpreting Fourier's law for thermal conduction. But it is worth remembering Peierls comment in 1960: "It seems there is no problem in modern physics for which there are on record as many false starts and as many theories which overlook some essential features as in the problem of thermal conductivity of non-conducting crystals"[10].

H. BÜTTNER

Physikalisches Institut,
Universität Bayreuth,
D-8580 Bayreuth, FRG

F. MOKROSS

Friedrich & Co.,
D-7022 Leinfelden-Echterdingen,
FRG

1. Casati, G., Ford, J., Vivaldi, F. & Visscher, W.M. *Phys. Rev. Lett.* **52**, 1861 (1984).
2. Mokross, F. & Büttner H. *J. Phys.* C**16**, 4539 (1983).
3. Maddox, J. *Nature* **309**, 511 (1984).
4. Mokross, F. & Büttner, H. *Phys. Rev.* A**24**, 2826 (1981).
5. Toda, M. *Theory of Nonlinear Lattices* (Springer, Berlin, 1981).
6. Casati G. & Ford, J. *Phys. Rev.* A**12**, 1702 (1975).
7. Mokross, F. thesis, Univ. Bayreuth, (1983).
8. Kipnis, C., Marchioro, C. & Presutti, E. *J. Stat. Phys.* **27**, 65 (1982).
9. Tennebaum, A., Ciccotti, G. & Gallico, R. *Phys. Rev.* A**25**, 2778 (1982).
10. Peierls, R.E. in *Theoretical Physics in the Twentieth Century* (eds Fierz, M. & Weisskopf, V.) 140 (Interscience, New York, 1960).

On the hand of *Archaeopteryx*

SIR — Hecht and Tarsitano[1] complain that Howgate[2] has misrepresented their views[3,4] on the structure of the hand in *Archaeopteryx*. Howgate also discussed our interpretation of the *Archaeopteryx* hand[5], yet we find that his inaccuracies are trivial when measured against those of Hecht and Tarsitano.

According to Hecht and Tarsitano[1], palaeontologists unfailingly identify the three hand digits of theropods, *Archaeopteryx* and birds as numbers 1-2-3 (relative to a primitive pentadactyl format). Indeed, they maintain that palaeontologists are "convinced" of this fact in *Archaeopteryx*. This is not entirely true, for we have argued[5] that the digits are numbers 2-3-4. Hecht and Tarsitano are certainly aware of our arguments because they have cited them in their published work[4]. Yet on this occasion[1], in chiding Howgate, they chose to overlook such irksome details. In fact we are justified in claiming that Hecht and Tarsitano have misrepresented our views. We suggested[5] that the longest metacarpal should be identified as number 3 — and not the longest *digit*, as was stated by Hecht and Tarsitano[4]. However, this part of our argument, along with the rest, was dismissed by these authors as "merely changing the numbering of the digits".

Next, Hecht and Tarsitano plead that they "only stated the possibility" of there being a break in the outermost finger of the *Archaeopteryx* hand[1]. Yet their illustrations of the hands in the Berlin specimen (Figs 3,4 in ref.3) show the feature in question unequivocally labelled as "break". Their description (ref.3, p.155) is equally assertive: the feature "is apparently a break, not a joint... contrary to the opinions of Heilmann[6], Wellnhofer[7] and Ostrom[8]". Evidently Howgate did not misrepresent the views of Hecht and Tarsitano.

Hecht and Tarsitano accuse Howgate of attempting to make their explanations appear "ludicrous". But if the problematical feature in the outermost finger is a joint (and not a break) then their explanation *is* ludicrous: it would maintain[1] that a finger-joint "was caused by forces during stalling, impact upon the water, or as a result of preservation".

Finally Hecht and Tarsitano are not accurate in summarizing the issue. The important point is not whether the three digits in question are numbers 1-2-3 or numbers 2-3-4; it is whether or not the three fingers are homologous in theropods, birds and *Archaeopteryx*. Some biologists maintain that they are, whether they be 1-2-3 (ref.9) or 2-3-4 (ref.5). Hecht and Tarsitano disagree, contending that the three fingers of birds (including *Archaeopteryx*) are not homologous with the three fingers of theropods. But their argument is not convincing: it entails a complex explanation (convergence) where a simple one might suffice; it conflicts with the cladistic methodology that Hecht and Tarsitano claim to espouse (ref.5, p.621); and it implies that theropods differed from all other tetrapods (except syndactylous marsupials) in their pattern of digital reduction (ref.3, p.161). Despite these difficulties Hecht and Tarsitano have sought to defend their opinions. It is unfortunate that they should do so by ignoring any arguments to the contrary and by claiming that others have misrepresented and distorted their views.

RICHARD A. THULBORN
TIM L. HAMLEY

Department of Zoology,
University of Queensland,
St Lucia,
Queensland 4067,
Australia

1. Hecht, M.K. & Tarsitano, S.F. *Nature* **309**, 588 (1984).
2. Howgate, M. *Nature* **306**, 644 (1983).
3. Tarsitano, S. & Hecht, M.K. *Zool. J. Linn. Soc.* **69**, 149 (1980).
4. Hecht, M.K. & Tarsitano, S. *Geobios mem. spec.* **6**, 141 (1982).
5. Thulborn, R.A. & Hamley, T.L. *Aust. J. Zool.* **30**, 611 (1982).
6. Heilmann, G. *The Origin of Birds* (Witherby, London, 1926).
7. Wellnhofer, P. *Palaeontographica* A **147**, 169 (1974).
8. Ostrom, J.H. *Biol. J. Linn. Soc.* **8**, 91 (1976).

Scientific Correspondence

Scientific Correspondence is intended to provide a forum in which readers may raise points of a rather technical character which are not provoked by articles or letters previously published (where Matters Arising remains appropriate).

Tectonics and structural zonation of southern Tibet, China

J. P. Burg* & **G. M. Chen**†

* Department of Geology, University of Melbourne, Parkville, 3052, Victoria, Australia
† Geological Institute, Chinese Academy of Geological Sciences, Baiwanzhuang St, Beijing, China

The Yarlung Zangbo suture zone is composed of several thrust sheets with distinct stratigraphies, states of deformation and metamorphic grades. Successive deformations have been produced by persistent north–south shortening since obduction of the ophiolites by late Cretaceous–Palaeocene times. A possible decoupling of the crust may be associated with the intracontinental thrust system which has formed in the subducted Indian plate. This article emphasizes the role of shear deformations in the building of a collision belt.

THE Yarlung Zangbo suture zone (YZSZ) in southern Tibet (China) marks the site of collision of the Eurasian and Indian continental plates after closure of the Tethys Ocean[1–4]. Collision is thought to have occurred in the Eocene[4–6], when the northward motion of India slowed rapidly from 10 cm yr^{-1} to 5 cm yr^{-1} (ref. 7). Since then, India has moved ~2,000 km further northwards relative to Asia[8,9] with underthrusting of continental India beneath Asia[10,11] and lateral expulsion of Asian crustal wedges bounded by strike-slip faults[7,12,13]. The aims of this article are: first, to examine and interpret the structural pattern of the YZSZ; and second, to assess the relative roles of obduction and intracontinental deformation in the tectonic evolution of the area. In the region visited (Figs 1, 2), the three following tectonolithostratigraphical units can be recognized in a north–south direction: the Lhasa Block; the Yarlung Zangbo suture; and the north Indian margin.

Lhasa Block

Before the collision, the northern margin of the Tethyan ocean consisted of Precambrian basement overlain by Carboniferous to Upper Cretaceous shallow water sediments which contain the Cretaceous Cathaysian flora[14,15]. The southern margin of the marine Lower Mesozoic basin may have deposited on an oceanic crust[16]. Shallow water and subaerial sediments associated with a Cretaceous–Palaeocene[17] ignimbritic series overlie eroded folds of the Upper Cretaceous and older rocks. The southern portion of the Lhasa Block is dominated by the Transhimalayan Plutonic Belt[3] in which radiometric ages range between 120 and 40 Myr (ref. 18). We have summarized the geological history of the Lhasa Block as follows[16]: Lower Cretaceous metamorphism probably accompanied the development of small scale isoclinal F_1 folds, an axial planar S_1 foliation and north–south stretching lineation. The intensity of the F_1 fabric and metamorphism increase towards the Yarlung Zangbo suture. The deformation and metamophism are related to northward subduction while calc-alkaline magmatism of the Transhimalayan Belt takes place possibly along a continent–ocean margin, leaving remnants of continental Precambrian crust to the north and of (Triassic?) oceanic crust to the south. A period of continuing crustal shortening associated with further intrusions gave rise to F_2 folding with fanlike S_2 cleavage and subvertical axial surfaces. The F_2 structures steepen the shallow

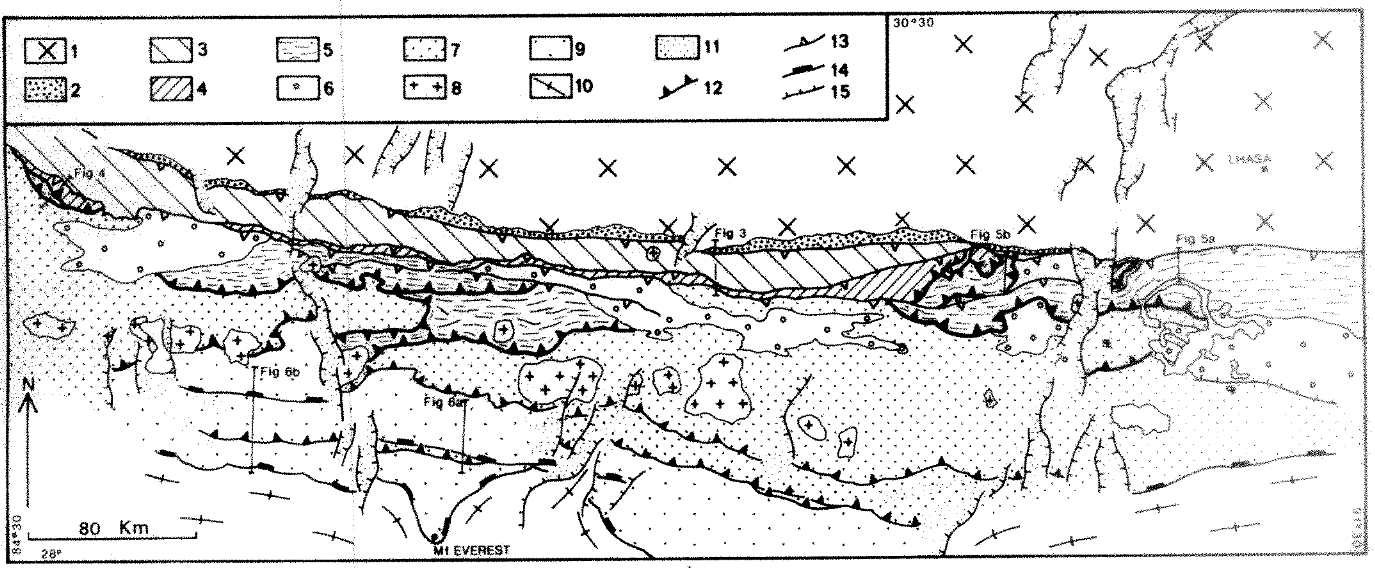

Fig. 1 Locations of the cross-sections on a simplified geological map of the YZSZ in southern Tibet. 1, Upper Palaeozoic to Cenozoic sedimentary rocks, Precambrian basement, calc-alkaline plutons and volcanites of the Lhasa Block; 2, conglomerates (Eocene?) lying unconformably on the Lhasa Block; 3, Cretaceous turbidites (Xigaze series) of the forearc basin; 4, Tsangpo ophiolites; 5, infra-ophiolitic thrust sheets of radiolarites and (Upper Triassic–Liassic?) turbiditic flysch; 6, unconformable (Maestrichtian?) wildflysch with exotic blocks and overlying black shales and quartzite; 7, north Tethyan sediments (with polyphase deformation and metamorphism); 8, North Himalayan two-mica granites and crystalline rocks; 9, south Tethyan sediments (unmetamorphosed and with one major phase of folding); 10, Main Central Crystalline Sheet; 11, Quaternary; 12, southward thrusts; 13, backthrust (post-Miocene); 14, post-Miocene northward normal fault; 15, Quaternary normal faults.

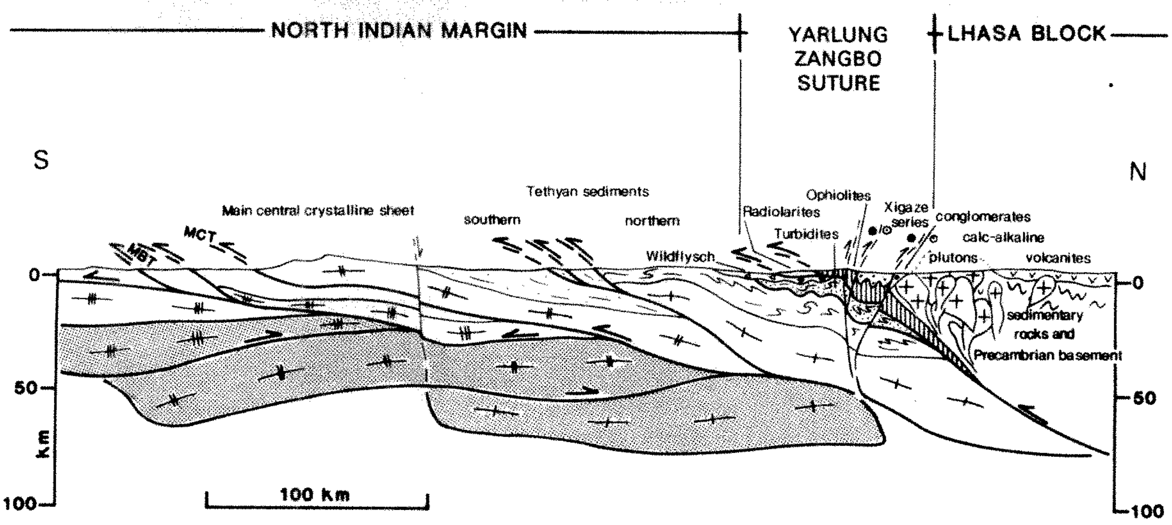

Fig. 2 Synthetic and interpretative cross-section of the YZSZ and relationship to north Indian margin and Lhasa Block. Moho and deep structures adapted from refs 44, 47. Shaded areas are lower crust layers corresponding to the upper crust layers with same gneiss symbols (after refs 44, 47). MCT, Main Central Thrust; MBT, Main Boundary Thrust[1].

dipping S_1 and could be produced from an Andean type orogen. Emersion and erosion by uppermost Cretaceous times truncated all the structures. The uncomfortable Palaeocene has undergone minor shortening with undulations of low amplitude and several kilometres wavelength and low-angle reverse faults with less than a few kilometres displacement. This indicates that significant crustal shortening was completed here by the Palaeocene; late granitic plutons intrude the Palaeocene series.

South of the Transhimalayan Plutonic Belt conglomerates are intercalated with red shales, sandstones and local basaltic and ignimbritic flows. The sequence is comparable with the Indus Molasse of Eocene age in Ladakh[19] and in the Kailas[20] and displays one phase of east–west folding with a northward vergence and a weak steep dipping cleavage. The folds could be related to the near vertical or south dipping fault traced along the southern margin of the Lhasa Block (Fig. 1). Slickenside striation on the fault plane and related fractures indicate dextral wrench faulting before northwards thrusting.

Yarlung Zangbo suture

The YZSZ is traditionally traced along the ophiolite sheets[2,21], which are the eastern continuation of those recognized in southwest Tibet[22] and in Ladakh (western Himalayas[19,23]). We attribute three rock subunits to the suture (Figs 1, 2). They are from the north to the south Cretaceous turbidites (the so-called Xigaze series)[24], ophiolites and associated radiolarites, and allochthonous turbidites. The suture has been reactivated by northward backthrusting and dextral strike-slip movement. The reason why all these rock subunits are not present on every transect may be a primary discordance between their earlier limits and the late faults.

The northern section of the Xigaze series is composed of a turbidite sequence with Aptian–Albian limestones[25] and conglomerates containing pebbles of plutonic and volcanic calc-alkaline rocks[26,27] which show that this sequence was deposited near the Transhimalayan Belt whose erosion was occurring by the late Cretaceous. The southern section is composed of pelagic sediments with Albian–Cenomanian radiolarites forming the sedimentary cover of pillow lavas[28]. The Xigaze series appear within a large east–west trending synclinorium shortened ~40% after the early Cenozoic (Fig. 3) with dominantly southward verging folds, a steep dipping cleavage and no metamorphism. The Xigaze subunit has been interpreted as a forearc basin lying on the plutonic belt to the north and on the ophiolites to the south[26,27]. As we have emphasized the existence of an important fault between the turbidites and the Lhasa Block, the floor of the sediments which overlie pillow-lavas to the south could only be an oceanic crust. To the west we have recognized an Upper Barremian–Lower Cenomanian limestone formation (bearing orbitolinids) interlayered with basaltic and possibly andesitic flows. The formation is squeezed between backthrusts along the southern boundary of the Xigase subunit and could imply that the calc-alkaline lavas have flowed southwards towards the oceanic floor of the Xigaze series. Note that in Ladakh, similar associations of the same age have been found in the Dras formation[29] where calc-alkaline lavas overlie oceanic basalts[30].

Nicolas *et al.*[31] have noted the abundant faults and the normal polarity of the ophiolites which now tectonically overlie the sedimentary series described below with the major faults being north dipping thrusts subparallel to the layering. A tectonic mélange with a matrix of serpentinites locally appears within the thrusts. The infra-ophiolitic sole is a package of Cretaceous (and Jurassic?[26]) slightly metamorphosed radiolarite slices with tuffs and basaltic flows (Fig. 4). The sequence is dominated by numerous contacts subparallel to an S_1 cleavage which is axial planar to small scale isoclinal folds (rarely sheath folds). The N150–220 fold axes are parallel to a stretching lineation L_1 marked by quartz fibres within S_1 and slickensides within the thrust planes. The F_1 folds are refolded by N030–150 south facing chevron folds F_2. Both folding events are attributed to the emplacement of the ophiolitic nappes, the stretching lineation being parallel to the tectonic transport from north to south as indicated by the sense of displacement on thrusts and the direction of vergence.

An uncomfortable polygenic and coarse subaerial conglomerate appears only along the ophiolite–radiolarite outcrops and is considered to be Oligo-Miocene[32]. This conglomerate is deformed in the south-dipping backthrusts (unit 4, Fig. 3 and unit 6, Fig. 4) indicating that this important faulting due to north–south compression is a recent event.

The ophiolites and the radiolarites are thrust onto an allochthonous turbidite sequence (Fig. 2) with late Triassic to Liassic marine fossils[33,34]. This turbidite subunit is comparable to the Indus Flysch[19]. To the west a lower nappe of similar turbidites containing blocks of cherts and crystalline limestones could be equivalent to the Namika La Flysch[35]. Large-scale recumbent F_1 folds (Fig. 5) have inverted the stratigraphical series. Southwest verging mesoscopic F_1 folds trend N030–180 and contain an S_1 slaty cleavage formed in low-grade conditions of metamorphism. Quartz fibres and long axes of pressure fringes are parallel to the N340–030 stretching lineation Le which can be equated with a transport direction (Hansen's method[36]). Basal thrusts of this subunit and of the ophiolites and their sole cut

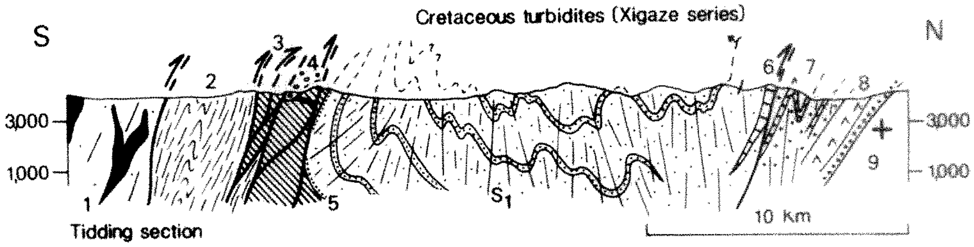

Fig. 3 Tidding cross-section. 1, Late alkaline gabbros intruded into north Tethyan Jurassic calcschists; 2, radiolarites; 3, ophiolites; 4, Oligo-Miocene (Liuqu conglomerate for the Academica Sinica[32]) conglomerates unconformable onto northward dipping thrusts in the ophiolites; 5, stratigraphical contact between Albian–Cenomanian cherts and pillow-lavas; 6, orbitolinid-bearing limestones (Aptian–Albian); 7, Eocene(?) conglomerate (pebbles >50 cm) interlayered with 8, ignimbritic and basaltic flows unconformably lying on calc-alkaline granodiorite (8). S_1 cleavage of the Xigaze series. The arrows indicate the younging direction.

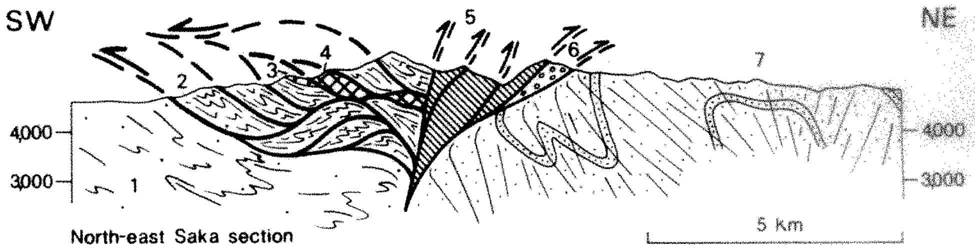

Fig. 4 North Saka cross-section. 1, North Tethyan sediments with isoclinal folding and subhorizontal S_1 cleavage. 2, Radiolarite slices containing recrystallized limestones and imbricate (3) with, basalts and tuffs (4), ophiolites (5) backthrusted onto, Oligo-Miocene (Liuqu) conglomerates (6) and Xigaze series (7).

the F_1 structures and are marked by some crush zones, metres thick, formed in non or very low grade conditions of metamorphism. Both the thrust contacts and the F_1 folds are folded about F_2 structures (Fig. 5) in various ways, as the upright chevron folds (interlimb angles 110–50°) may coexist with subisoclinal folds (interlimb angles ~20°) with rounded hinges and overturned to the south. The F_2 axes are parallel to a N060–120 crenulation lineation. F_2 folding increases in intensity northwards and is contemporaneous with intrusion of two mica granites recognized in the North Himalayan Belt (Fig. 1). Local N040–130 kinks with different axial plane attitudes are attributed to an F_3 event and may be contemporaneous with post-F_2 movement along basal thrusts.

North Indian Margin

The sedimentary sequence which formed in a continental shelf environment on the Indian Shield (carbonates and shales) passed northwards into a deeper water facies (pelites and flyschs). A major thrust separates the northern and southern Tethyan sequences thus defining two subunits (Figs 1 and 2).

The north Tethyan sediments show downward increasing metamorphism from regional low grade to localized staurolite kyanite schist. In the structural section, the lowest rocks are Lower Ordovician orthogneiss[37,38] underlying metamorphosed rocks and recrystallized Permian limestones[33]. Overlying the Permian, the Mesozoic includes a thick and monotonous calcareous flysch of up to Turonian age[39] involved in polyphase deformation. The first major event generated large-scale recumbent folds overturned to the south-west and a well developed slaty cleavage S_1 with a N350–040 stretching lineation. The bulk strain increases northwards towards the YZSZ and upwards under the ophiolitic and associated nappes. An unconformable wildflysch with exotic blocks is lying on these deformations (Figs 1 and 2). The blocks are composed of Permian to Maestrichtian rocks locally more deformed than the matrix and derived from the north. The youngest fossils found in the blocks and in the locally layered matrix are Maestrichtian to Palaeocene which is taken as the age of this synorogenic formation overlain by undated black shales and quartzites. If the age of the wildflysch is correct, the major thrusting events are thus Upper Cretaceous–Palaeocene in age. The wildflysch and the black shales have been folded about upright east–west trending folds (Fig. 5) with a non metamorphic fanning cleavage parallel to the bulk axial plane; this cleavage is a crenulation cleavage in the older rocks. The folding is equated with the F_2 event of the turbidite nappes. The structurally lower metamorphic rocks show a comparable polyphase deformation with an unexpected downward increase in intensity of the fabric contemporaneous with the intermediate pressure metamorphism[40]. The problem which arises is that radiometric ages of micas are 13 Myr (Ar/Ar method, H. Maluski, personal communication) and hence inconsistent with the Maestrichtian–Palaeocene age of the F_1 structures as suggested above. It is proposed that both the deformation and the metamorphism of the lower rocks are associated with a ductile thrust zone whose deformation front does not reach the upper part of the pile but instead produces the thrust and locally a trailing imbricate fan to the south between the northern and southern Tethyan sediments (Fig. 2). The juxtaposition of two areas having comparable fabrics, though they are different in age, is one of the striking features of the northern subunit. This is a consequence of the heterogeneity of the shear deformation during thrusting, which affects areas close to the thrust plane and preserves the sequence away from the thrust. The F_2 upright folding throughout the north Tethyan sediments is contemporaneous with late Miocene emplacement of two-mica granites of the North Himalayan Belt.

The southern Tethyan sediments range in age from Cambrian to Eocene[33] without any significant unconformity and are of the 10-km thick platform type series identical to that known further west in Ladakh[23]. In contrast to the north Tethyan sediments they are non-metamorphosed and have suffered one main phase of east–west trending box and chevron folds (Fig. 6) that can be followed for tens of kilometres along their axial traces. Intensity of shortening decreases southward and a faulted contact separates the southern Tethyan sediments from metamorphosed schists intruded by Miocene leucogranites of the Main Central Crystalline Sheet (Fig. 2). The faulted contact has been interpreted as a thrust[27] which is not consistent with the northward shearing in the leucogranites[41] and the normal faulting suggested by the superposition of unmetamorphosed sediments onto staurolite garnet schists. To the east, the steeply dipping normal fault separates Jurassic schists from gneisses indicating at least 8,000 m of vertical movement.

The basal thrust (MCT) of the Main Central Crystalline Sheet is not exposed in Tibet[27]. The youngest formations overlain by the MCT (Fig. 2) are Miocene thus dating the Main Central Crystalline Sheet emplacement. An underlying thrust sheet is represented by the Main Boundary Thrust (MBT) which continues to produce modern seismicity in a north–south compressive regime[42,43].

Conjectural deep structure

The interpretations and implications of the geophysical data for the deep structure in Tibet are twofold:

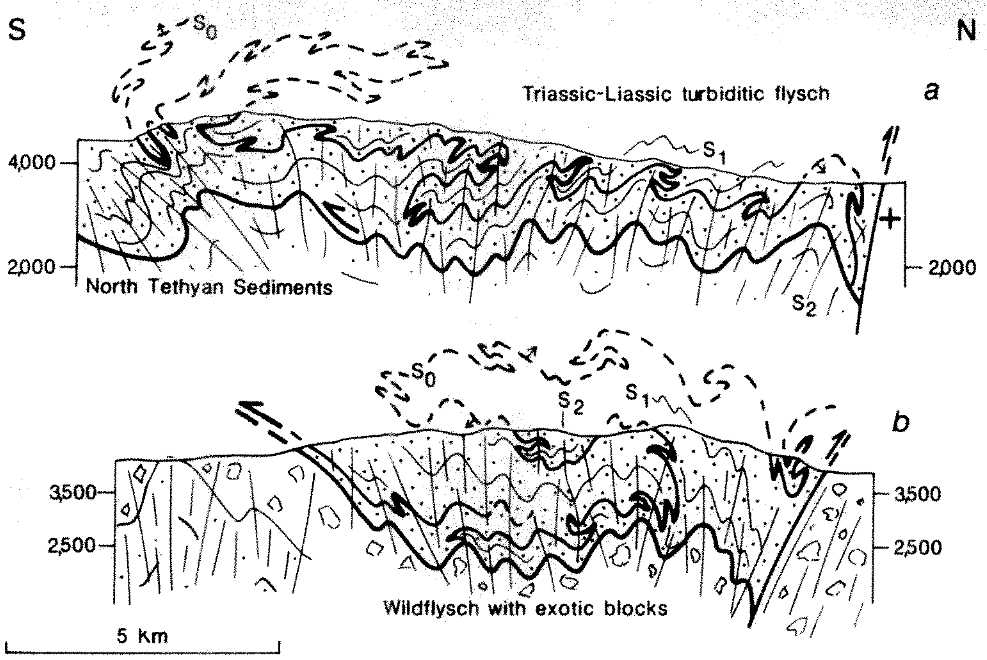

Fig. 5 Two detailed cross-sections in the Triassic–Liassic turbidite flysch. They show polyphase deformation with S_1 cleavage and S_2 crenulation cleavage. Bedding S_0–S_1 relationships and younging directions (arrow) give evidence for several kilometres inverted series. Thickening of F_1 hinges is voluntary exaggerated. Lower Cretaceous calcschists underlie the wildflysch.

(1) The major thrust sheets (MCT, MBT and the northern Tethyan sediments) correspond to the prism-shaped seismic structures reported by Hirn *et al.*[44]. Crustal shortening and thickening of the North Indian Margin is produced by decoupling and thrusting separating lower and upper crustal layers. The superposition of the neighbouring segments of the upper crust occurs along imbricate thrusts with polarity opposite to, though contemporaneous with, thrusts in the lower crust which may involve upper mantle rocks (ref. 44, interpreted in Fig. 2). The upper crust can slide and/or fold independently of the lower crust. A similar situation may have been identified in the Alps[45] and requires splitting of the crust with major thrust zones merging towards the inner part of the belt into a unique shear zone within the crust. The driving force necessary to initiate and develop such a thrust configuration implies a crustal process. Consequently, the origin of the merging shear zones may possibly be connected with the subduction zone itself. The evolution of the thrust system as drawn in Fig. 2 leads to steepening of the inner thrust planes (and the suture) by growth of the underlying outer crystalline sheet. The vertical inner thrust zones and the suture then become rejuvenated as wrench faults, as observed in southern Tibet and as proposed in the Variscan Belt[46].

(2) The geophysical data suggest an almost 20-km step precisely below the surface traces of the boundaries of the Main Central Crystalline Sheet and of the Lhasa Block (Fig. 2), which are both recent and prominent faults. Hirn *et al.*[47] point out that the fault limiting the Lhasa Block is a vertical contact which is consistent with strike-slip movements. Moreover, a variation in the level of the Moho can be identified further north[47] indicating that if the deep crust topography is due to post-Miocene disruptions as suggested by geological data, crustal thickening since the Miocene did not occur through mere underplating of several hundred kilometres of continuous Indian Crust beneath Tibet (600–1000 km with a mean motion of 3–5 cm yr^{-1} since 20 Myr).

Conclusions

In the YZSZ, several thrust sheets have distinct stratigraphies, states of deformation and metamorphic grade. The movement pattern is that the earliest strains are consistent with some oceanic crust being subducted to the north. This was accompanied by Andean type deformation and magmatism south of the Lhasa Block, and possibly by a period of rapid erosion as northly derived rocks were deposited in the forearc Xigase basin. This suggests that the crust of the Lhasa Block might

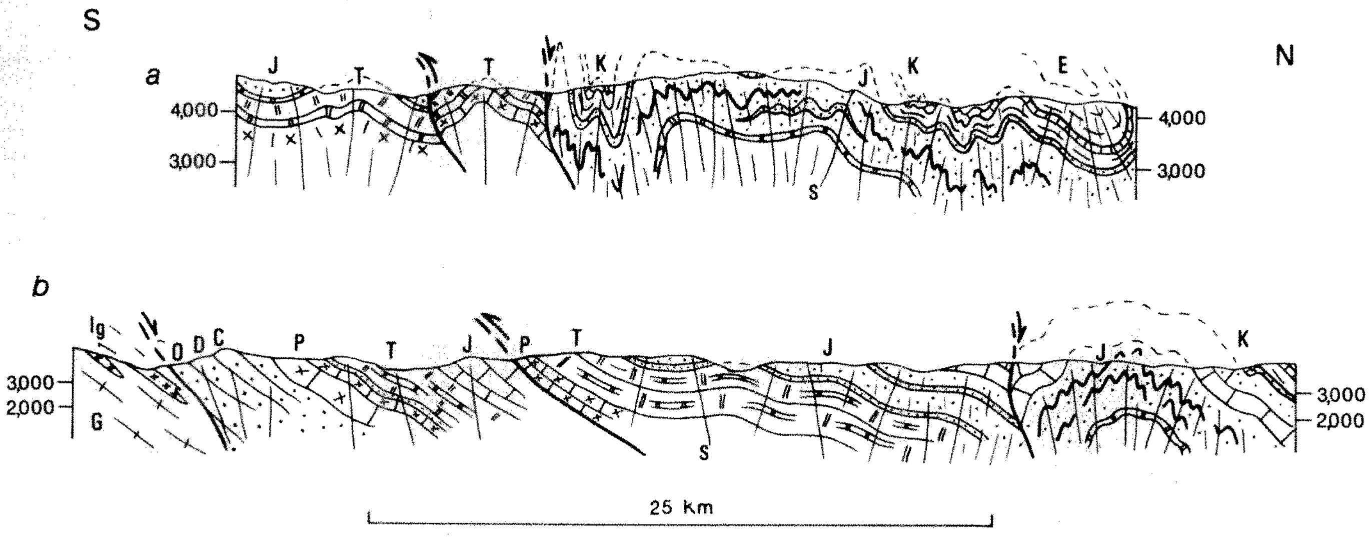

Fig. 6 Two examples of section across the south Tethyan sediments: G, gneisses of the Main Central Crystalline Sheet intruded by lg, Miocene leucogranites; O, Ordovician; D, Devonian; C, Carboniferous; P, Permian reef limestones; T, Triassic; J, Jurassic limestones, shales and sandstones; K, Cretaceous calcschists and limestones; E, Eocene nummulite-bearing limestones; S, weak spaced cleavage.

have been thickened before the India–Asia Collision. The Lhasa Block and the ophiolites which carry the Xigaze series represent the overriding plate in which magmatism terminated in the Eocene. At this time, the deformation of the overriding plate was substantially less than that of the subducted plate except along its southern edge. The southward obduction of the suture rocks took place while the wildflysch was deposited (Maestrichtian–Palaeocene?). The bulk strain of this age increases upwards in the suture region with the development of a subhorizontal cleavage and roughly north–south stretching lineation. A deformation pause may be represented by the unconformity between north Tethyan sediments and the wildflysch, although it is not necessarily an orogenic pause as thrusting and associated shearing may develop in lower parts of the crust. Post-collision deformation involved intracontinental thrust zones in the subducted plate, associated with intermediate pressure metamorphism, two-mica granite intrusions and widespread upright folding. In the North Indian Margin, intracontinental thrust zones with upward decreasing deformation create deformation belts different in ages though having the same fabric feature because they result from persistent north–south compression. Later events include the rejuvenation of the suture into transcurrent movements and post-Miocene backthrusting.

This article is a digest of J.P.B.'s thesis presented in Montpellier in May 1983. The work was carried out within the Cooperative Research Project of the Chinese Geological Academy, Chinese Academy of Sciences, French CNRS and Institut National d'Astronomie et de Geophysique. J.P.B. thanks all his colleagues who participated in the fieldwork in southern Tibet, during which time some of the ideas presented here evolved. We thank C. J. L. Wilson for help with the English and I. Munro who typed the manuscript.

Received 26 April; accepted 20 July 1984.

1. Gansser, A. *Geology of the Himalayas* (Wiley, London, 1964).
2. Gansser, A. *Colloq. int. Cent. natn. Res. Scient.*, Paris **268**, 181–191 (1977).
3. Gansser, A. *Tectonophysics* **62**, 37–52 (1980).
4. Dewey, J. F. & Bird, J. M. *J. geophys. Res.* **75**, 2625–2647 (1970).
5. Dewey, J. F. & Burke, K. C. A. *J. Geol.* **81**, 683–692 (1973).
6. Powell, C. McA. & Conaghan, P. J. *Earth planet. Sci. Lett.* **20**, 1–12 (1973).
7. Molnar, P. H. & Tapponnier, P. E. *Science* **189**, 419–426 (1975).
8. Molnar, P. H. & Wang, P. C. *Nature* **273**, 218–220 (1978).
9. Klootwijk, C. T. & Bingham, D. K. *Earth planet. Sci. Lett.* **51**, 381–405 (1980).
10. Argand, E. *C.R. 13th Cong. Geol. Int. 1922*, 171–372 (1924).
11. Powell, C. McA. & Conaghan, P. J. *Geology* **3**, 727–731 (1975).
12. Taponnier, P. E., Peltzer, G., Le Dain, A. Y., Armijo, R. & Cobbold, P. *Geology* **10**, 611–616 (1982).
13. Tapponnier, P. *et al. Nature* **294**, 405–410 (1981).
14. Allègre, C. J. *et al. Nature* **307**, 17–22 (1984).
15. Jaeger, J. J., Adloff, C., Doubinger, J., Pons, D., Vozenin-Serra, C. & Wang, N. W. *EOS* **63**, 1093–1094 (1982).
16. Burg, J. P., Proust, F., Tapponnier, P. E. & Chen, G. M. *Eclog. geol. Helv.* **76**, 643–665 (1983).
17. Maluski, H., Proust, F. & Xiao, X. C. *Nature* **298**, 152–154 (1982).
18. Zhang, Y. Q., Dai, T. M. & Hong, A. S. *Proc. Symp. on Qinghai-Xizang (Tibet) Plateau* Vol. 1, 493–495 (Gordon and Breach, New York, 1981).
19. Frank, W., Gansser, A. & Trommsdorf, V. *Schweiz. Petrogr. Mitt.* **57**, 89–113 (1977).
20. Honegger, K., Dietrich, V., Frank, W., Gansser, A., Thoni, M. & Trommsdorff, V. *Earth planet. Sci. Lett.* **60**, 253–292 (1982).
21. Chang, C. F. & Cheng, H. L. *Scient. Sinica* **16**, 257–265 (1973).
22. Heim, A. & Gansser, A. *Denkschr. schweiz. naturf. Ges.* **73**, 1–245 (1939).
23. Andrieux, J., Brunel, M. & Shah, S. K. *C.R. hebd Séanc. Acad. Sci., Paris* **284D**, 2327–2330 (1977).
24. Wu, H. R., Wang, D. G. & Wang, L. C. *Scient. Geol. Sinica* **3**, 250–262 (1977).
25. Cherchi, A. & Schroeder, R. *C.R. hebd Séanc. Acad. Sci., Paris* **291D**, 385–388 (1980).
26. Bally, A. W. *et al. U.S. geol. Surv. Open File Rep.* **80–501**, (1980).
27. Shackleton, R. M. *J. struct. geol.* **3**, 97–105 (1981).
28. Marcoux, J. *et al. Ofioliti* Suppl. **6**, 31–32 (1981).
29. Gupta, V. J. & Kumar, S. *Geol. Rdsch.* **64**, 540–563 (1975).
30. Reibel, G. & Juteau, T. *C.R. hebd Séanc Acad. Sci., Paris* **239**, II, 57–60 (1981).
31. Nicolas, A. *et al. Nature* **294**, 414–417 (1981).
32. *A Scientific Guidebook to South Xizang (Tibet)* (Academica Sinica, Beijing, 1980).
33. Mu, A. T., Wen, S. H., Wang, Y. K., Chang, P. K. & Yin, C. H. *Scient. Sinica* **16**, 96–111 (1973).
34. Marcoux, J., Mascle, G. & Cuif, J. P. *Bull. Soc. geol. Fr.* **24**, 971–980 (1982).
35. Bassoullet, J. P., Colchen, M., Marcoux, J. & Mascle, G. *Riv. ital. Paleont. stratigr.* **86**, 825–844 (1981).
36. Hansen, E. *Strain Facies*, (Springer, Berlin, 1971).
37. Debon, F., Sonet, J., Liu, G. H., Jin, G. W. & Xu, R. H. *C.R. hebd Séanc. Acad. Sci., Paris* **295**, II, 213–218 (1983).
38. Xu, R. H., Shärer, U. & Allègre, C. J. *Terra Cognita* **3**, 273 (1983).
39. Wang, T. G., Wang, Y. J. & Wu, H. R. *Scient. Geol. Sinica* **4**, 149–156 (1976).
40. Burg, J. P., Guiraud, M. & Chen. G. M. *Earth planet. Sci. Lett.* **68** (in the press).
41. Burg, J. P., Brunel, M., Gapals, D., Chen, G. M. & Liu, G. H. *J. struct. Geol.* **6** (in the press).
42. Seeber, L., Armbruster, J. G. & Quittmeyer, R. in *Zagros–Indukush–Himalaya Geodynamic Evolution* (eds Gupta, H. K. & Delany, F. M.) 215–242 (Geol. Survey of India, 1981).
43. Barazangi, M. & Ni, J. *Geology* **10**, 179–185 (1982).
44. Hirn, A., *et al. Nature* **307**, 23–25 (1984).
45. Caby, R., Kienast, J. R. & Saliot, P. *Rev. Geograph. Phys. Geol. Dyn.* **20**, 307–322 (1978).
46. Brun, J. P. & Burg, J P. *Earth planet. Sci. Lett.* **61**, 319–332 (1982).
47. Hirn, A. *et al. Nature* **307**, 25–27 (1984).

Information for the dorsal–ventral pattern of the *Drosophila* embryo is stored as maternal mRNA

Kathryn V. Anderson & Christiane Nüsslein-Volhard

Friedrich-Miescher-Laboratorium der Max-Planck-Gesellschaft, Spemannstrasse 37–39, 7400 Tübingen, FRG

Maternal-effect mutations in 10 loci in Drosophila *produce totally 'dorsalized' embryos. Injection of RNA isolated from wild-type embryos into mutants at six loci partially restores dorsal–ventral polarity. For the mutant* snake, *injection of poly(A)$^+$ RNA restores a complete dorsal–ventral pattern.*

DESPITE decades of research, the molecular mechanism underlying pattern formation have eluded developmental biologists. Although several molecules have been identified which clearly elicit specific morphogenetic responses, including retinoic acid, *Dictyostelium* DIF and hydra head activator[1–3], it is not clear whether these are normal *in vivo* morphogens. More significantly, even the identification and characterization of an *in vivo* morphogen cannot, in isolation, explain the position-dependent activity of that molecule within an embryonic field. The genetic dissection of pattern-forming processes provides a means of defining specific morphogenetically active substances, and, at the same time, permits studies of interactions between components of the system which are required for position-dependent development.

The establishment of the dorsal–ventral pattern in the *Drosophila* embryo is a genetically defined system both for the identification of the *in vivo* morphogenetically active molecules and for the study of interactions between regulatory components[4]. The dorsal–ventral embryonic pattern is directed by a defined group of maternal-effect genes dispersed throughout the genome, which have been identified in recent saturation screens for female sterile mutations (refs 5–7; T. Schüpbach, personal communication; C.N.-V., K.V.A., G. Jürgens and R. Lehmann, unpublished observations). Ten loci have been found which are required for the production of lateral and ventral pattern elements. For each locus, lack of gene function in the mother, results in an embryonic phenotype identical to that described for the maternal-effect mutation *dorsal*, where all

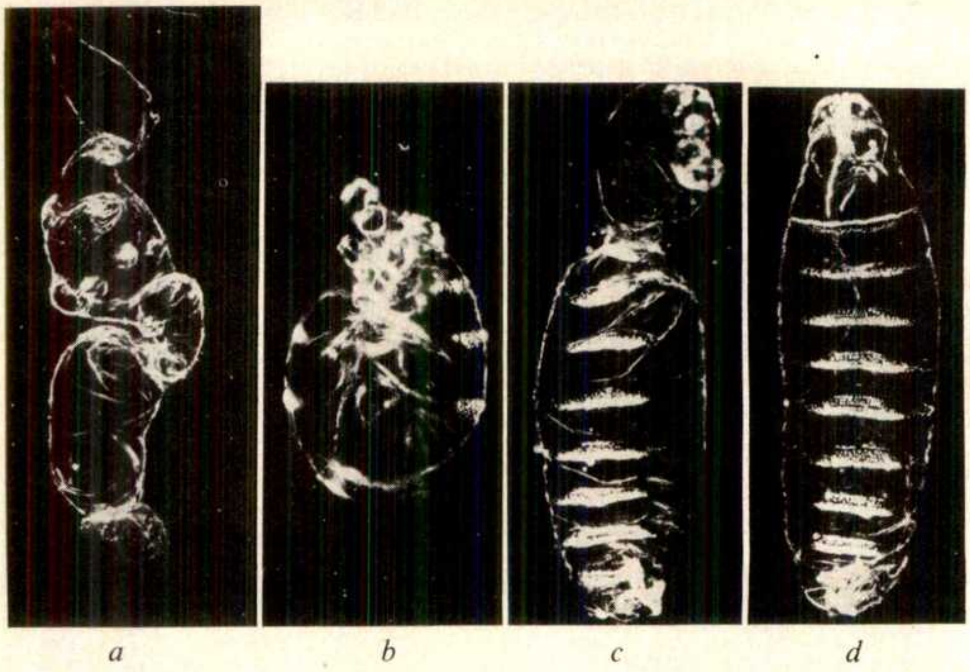

Fig. 1 Rescue by injection of wild-type cytoplasm into *easter*, *tube* and *snake Drosophila* mutants. Cuticle preparations of uninjected *easter*, *tube* and *snake* embryos all show the same tube-like form of dorsal cuticle (*a*, uninjected *snake* embryo). The maximal extent of the phenotypic rescue for each locus, shown here, is characteristic for each locus. Of these three, *easter* (*b*) responds the most weakly to injection, generally developing only filzkörper in addition to dorsal cuticle and occasionally narrowed rows of ventral denticles, as shown here; *tube* (*c*) responds more strongly, typically developing ventral denticles in addition to filzkörper; *snake* embryos (*d*) show a total restoration of dorsal–ventral pattern elements after injection. The embryo in *d* had hatched before being mounted.
Methods: For injection, both mutant embryos and wild-type Oregon R donor embryos were collected for 1 h at 18 °C, dechorionated in 50% bleach and mounted on double-sided sticky tape. Embryos were dried for 20–25 min at 18 °C in a silica gel-containing chamber and were then covered with Voltalef 10S oil. Injections were done at 18 °C with a 5–7 μm diameter glass micropipette. The total content of a single wild-type donor was used to inject into ~30 mutant hosts, thus the volume of cytoplasm injected corresponds to ~3% of the total egg volume. The cytoplasm was injected into the central yolk at a posterior position. Embryos which had formed pole cells and older embryos were not used as donors or hosts. Embryos were allowed to develop for 3 days at 18 °C, and cuticle preparations were made[9]. Mutant *easter* embryos were obtained from ea^{IIR65} homozygous females, *tube* embryos from tub^{238}/tub^{118} females, and *snake* embryos from snk^{073}/snk^{229} females.

embryonic cells develop like the dorsal-most cells of the wild-type embryo[4,8]. The common phenotype produced in the absence of any one of these gene functions indicates that each is an essential component of one pattern-forming process.

The recent demonstration that the phenotype of embryos produced by homozygous *dorsal* females can be partially rescued by injection of wild-type cytoplasm[9] established a specific assay for the molecules required for expression of the embryonic dorsal–ventral pattern. Here we use this phenotypic rescue assay to demonstrate that the information from several of the 'dorsalizing' maternal-effect genes is found in the wild-type egg in the form of poly(A)$^+$ RNA.

Phenotypic rescue of dorsalizing loci

During a saturation screen for female sterile mutations on the third chromosome of *Drosophila*, we identified mutants falling into eight complementation groups which produced dorsalization of the embryo (Table 1). For all loci, the embryonic mutant phenotypes are indistinguishable from those of the previously described loci *dorsal*[8,10] and *gastrulation defective*[11]. Embryos produced by females homozygous for amorphic alleles of any of these genes show no polarity in the dorsal–ventral axis and all cells differentiate like the dorsal-most cells of the normal embryo. The dorsalized phenotype can be seen in cuticle preparations of differentiated, unhatched larvae, where the cuticle is a long tube covered with the fine hairs normally found only dorsally. Early in development, in contrast to the highly asymmetric pattern of normal gastrulation, the mutant pattern of folding at gastrulation is totally symmetrical in the dorsal–ventral axis. As previously shown for *dorsal*[12], this embryonic phenotype apparently results from a shift in the position-dependent fate of cells along the dorsal–ventral axis of the blastoderm embryo.

Pursuing the observation that injection of wild-type cytoplasm partially rescues the *dorsal* phenotype[9], we found that injection of wild-type cytoplasm into young mutant embryos modifies the mutant phenotype for six of the eight newly identified third-chromosomal loci (Fig. 1 and Table 1). Although the phenotypic rescue in all cases results in a partial restoration of the dorsal–ventral pattern, mutants at each locus show a characteristic degree of response to injected cytoplasm. Differentiation of filzkörper was used as the minimum criterion of rescue. This structure, normally derived from a dorso-lateral position in the blastoderm fate map, is easily identifiable in cuticle preparations. Ventral denticles, which are normally derived from a ventro-lateral position, were taken as evidence of stronger rescue. The

Table 1 Maternal-effect dorsalizing loci

Locus	Map position	Cytological localization	No. of recessive alleles	Phenotypic rescue by cytoplasm	by RNA
gastrulation defective	1–37	11A1–7	8	–	ND
dorsal	2–52.9	36C	11	+	–
nudel	3–17	–	8	ND	ND
tube	3–47	–	2	+	+
pipe	3–47	–	2	–	ND
snake	3–52	87D10–12	4	+	+
easter	3–57	88EF	13	+	+
Toll	3–91	97D	28	+	+
spätzle	3–92	97E	2	+	+
pelle	3–92	97F	6	+	+

Gastrulation defective and *dorsal* have been described previously[8,11]. Most alleles of the third chromosomal loci were recovered during a systematic screen for female steriles, described elsewhere (refs 5, 6; T. Schüpbach, personal communication; C.N.V., K.V.A., G. Jürgens and R. Lehmann, unpublished observations) Rice[7] isolated two alleles of *nudel* (his alleles *mel*(3)2 and 5), one allele of *snake* (*mel*(3)4), two alleles of *Toll* (*mel*(3)9 and 10), one allele of *spätzle* (*mel*(3)7), and one allele of pelle (*mel*(3)8). Twenty-four of the *Toll* alleles were recovered as revertants of the dominant female sterile *Toll* mutations (refs 4, 10 and K.V.A., unpublished). Ten alleles of *easter* were isolated by F. Müller-Holtkamp. The cytological location of *snake* is defined by its inclusion in Df(3R)ry^{36} and exclusion from DF(3R)kar^{1G27} (ref. 12); *easter* maps by recombination between *jvl* and *sbd*[23], and is included neither in Df(3R) sbd^{105} (ref. 25) nor in the deficiency from T(3;1)kar^{51} (ref. 26). *Toll*, *spätzle* and *pelle* are defined primarily by aberrations isolated as revertants of the dominant *Toll* alleles (K.V.A., unpublished). ND, not determined.

Table 2 Phenotypic rescue of *snake* by injection of cytoplasm and RNA

Maternal genotype of donor embryos	Material injected	No. of recipient embryos Total	Differentiated	Rescued	% Rescued (of differentiated embryos)
+/+	Cytoplasm	439	122	119	98
snk/snk	Cytoplasm	102	36	0	0
+/+	Total RNA, 18 mg ml^{-1}	116	60	46	77
+/+	Total RNA, treated with RNase A*	97	33	0	0
+/+	Total RNA, alkaline hydrolysate*	113	34	0	0
+/+	Poly(A)$^-$RNA, 16 mg ml^{-1}	166	61	0	0
+/+	Poly(A)$^+$RNA, 6 mg ml^{-1}	208	61	54	89
+/+	Poly(A)$^+$RNA, treated with RNase A*	174	57	0	0
snk/snk	Polt(A)$^+$RNA, 9 mg ml^{-1}	141	54	0	0

Injection and RNA isolation methods are described in the legends to figs 1 and 2. Embryos were considered differentiated when the cuticle phenotype could be unambiguously scored for filzkörper and ventral denticles. Rescue was defined as the development of filzkörper.

* A single RNA preparation was split and used for the samples with and without RNase treatment. RNA was incubated with 2 μg ml^{-1} RNase A for 20 min at 25 °C. RNase was removed by phenol-chloroform extraction. For alkaline hydrolysis, an aliquot of the same RNA sample was incubated for 10 min in 0.2 M NaOH at 25 °C, then neutralized and reprecipiatated with ethanol before injection.

response of *spätzle* is similar to that seen with *dorsal*[9], with many injected embryos developing filzkörper. Most injected *easter* embryos develop filzkörper, and, in addition, ventral denticles are also seen occasionally. Injected *tube*, *pelle* and *Toll*^{rec} embryos respond more strongly: many develop well-organized rows of ventral denticles in addition to filzkörper. The most dramatic effect is seen with *snake*: this is the only case where injection of wild-type cytoplasm completely restores the normal dorsal–ventral pattern.

The characteristic response of mutants in each locus to injected cytoplasm indicates that different components of wild-type cytoplasm produce the rescue response in the different mutants. This is shown directly by the fact that in all cases examined so far, cytoplasm from dorsalized embryos resulting from mutations at one locus can rescue the phenotype of dorsalized embryos from mutations at other loci. For example, *snake* embryos, although not rescued by cytoplasm from other mutant *snake* embryos, are rescued by cytoplasm from mutant embryos of all nine other dorsalizing loci.

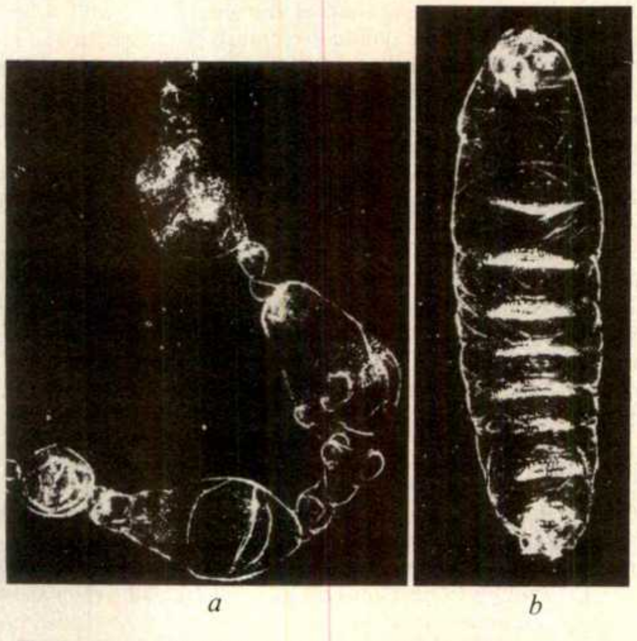

a *b*

Fig. 2 Rescue of *snake* by injection of poly(A)$^+$ RNA. *a*, Cuticle of uninjected *snake* embryo; only the dorsal cuticle is differentiated. *b*, Cuticle of *snake* embryo injected with 10 mg ml^{-1} poly(A)$^+$ RNA isolated from wild-type embryos, showing a full dorsal–ventral pattern including ventral denticle belts of normal width. RNA was isolated from 0–2-h Oregon R embryos by phenol–chloroform extraction and proteinase K treatment[15]. Poly(A)$^+$ RNA was isolated by one cycle of binding to oligo(dT)-cellulose as described elsewhere[15], except that SDS was omitted from the buffers. The concentration of RNA was measured by absorbance at 260 nm. The injection procedure was similar to that described for cytoplasm. RNA was injected in 25 mM KCl, 2.5 mM PIPES, 0.5 mM EDTA, 25% glycerol.

Total rescue of *snake*

A typical dorsalizing maternal-effect gene, both genetically and phenotypically, is *snake*. Four alleles of *snake* have been isolated, three in our laboratory and one by Rice (*mel*(3)4) (ref. 7). By deficiency complementation, *snake* maps in the polytene bands 87D10–12. Only two complementation groups in this cytological interval, *rosy* and *l(3)S12* (ref. 13), have been identified in saturation screens for lethal and visible mutations. Mutants in *snake* are viable, have normal eye colour and are female fertile in *trans* to *rosy* and all alleles of *l(3)S12*, thus it is probable that there are no visible or lethal alleles of *snake*. *Snake* is a pure maternal-effect gene: all allele combinations and all alleles in *trans* to deficiency are fully viable, male fertile, and mutant females produce totally dorsalized embryos, even when fertilized by sperm carrying two copies of the *snake*$^+$ gene.

Snake embryos show a dramatic response to injection of wild-type cytoplasm. Although the total volume of cytoplasm injected is only 3% of the total egg volume, a completely normal dorsal–ventral cuticular pattern is restored in nearly all differentiating embryos (Fig. 1). Over 20% of the rescued embryos hatch into larvae, which can develop further into normal adults. This complete restoration of the dorsal–ventral pattern can be observed within 2 h after injection, when nearly all developing embryos gastrulate normally, including the formation of a ventral furrow. This dramatic response contrasts with the other loci studied, where hatching larvae have not been obtained. The strong response of *snake* to injected cytoplasm makes it ideal for the investigation of the molecular nature of the rescuing activity.

Poly(A)$^+$ RNA rescues *snake*

Mutant *snake* embryos can be rescued by wild-type cytoplasm up to the stage of pole cell formation, indicating that the function of the *snake* gene is required after that time. The information encoded by the *snake* gene is thus synthesized during oogenesis, stored in the egg, and becomes necessary for embryonic pattern formation only some time after fertilization. This observation suggested that the *snake*-rescuing activity might be stored in the egg in the form of maternal mRNA.

In order to test whether the *snake*-rescuing activity is RNA, cytoplasmic RNA purified from cleavage stage wild-type embryos was injected into *snake* embryos. The injection of RNA

Table 3 Characteristics of rescue by cytoplasm and RNA for *snake*, *tube* and *easter*

Maternal genotype of recipient embryos	Stage of wild-type donor embryos	Material injected	% Of differentiated embryos			
			with Filzkörper	with ventral denticles	hatched	(*n*)
snake	Cleavage	Cytoplasm	98	98	20	(122)
		Total RNA	77	15	0	(60)
		Poly $(A)^+$ RNA	85	57	0	(204)
	Extended germ band	Cytoplasm	34	0	0	(139)
		Poly$(A)^+$ RNA	45	0	0	(53)
tube	Cleavage	Cytoplasm	89	48	0	(65)
		Total RNA	59	0	0	(69)
		Poly$(A)^+$ RNA	77	17	0	(100)
	Extended germ band	Cytoplasm	72	49	0	(67)
		Poly$(A)^+$ RNA	18	0	0	(61)
easter	Cleavage	Cytoplasm	83	6	0	(219)
		Total RNA	67	0	0	(67)
		Poly$(A)^+$ RNA	65	1	0	(86)
	Extended germ band	Cytoplasm	0	0	0	(47)
		Poly$(A)^+$ RNA	15	0	0	(34)

For cytoplasmic injections, cytoplasm was taken from wild-type embryos before pole cell formation (cleavage) or from embryos 1–2 h after the onset of gastrulation (extended germ band). Cleavage-stage RNA was isolated from 0–2-h embryos and extended germ band-stage RNA from 3–7-h embryos. The concentration of injected RNA, measured by absorbance at 260 nm, was 18 mg ml^{-1} for total RNA and 6–9 mg ml^{-1} for poly$(A)^+$ RNA preparations. The disappearance of *snake*- and *easter*-rescuing activities from cytoplasm begins at the onset of gastrulation (3.5 h) and falls off steadily to the value shown here 1–2 h later. The extended germ-band RNA was made from 3–7-h embryos, which should be a mixture of embryos that still have significant cytoplasmic rescuing activity and those that do not.

dramatically rescued the *snake* phenotype; the injected embryos developed filzkörper and ventral denticle bands (Fig. 2). The observed rescue is not due to some non-RNA contaminant, because the purified rescuing activity is protease-insensitive, RNase-sensitive and alkali-sensitive (Table 2).

To test whether the rescuing RNA is mRNA, the cytoplasmic RNA was separated on oligo(dT)-cellulose into poly$(A)^+$ and poly$(A)^-$ fractions, and both were tested for rescuing activity. The rescuing activity was recovered exclusively in the poly$(A)^+$ fraction; the *snake*-rescuing RNA is therefore polyadenylated and most probably mRNA (Table 2).

The phenotypic response seen depends on the concentration of the injected RNA. Injection of high concentrations of poly$(A)^+$ RNA restores the complete range of dorsal–ventral pattern elements in *snake* embryos. Although we have not observed hatching, many of these larvae have a full set of ventral denticle belts of normal width, and they exhibit movement inside the egg case. As the concentration is decreased, most rescued embryos have either clearly narrowed ventral denticle belts or develop only filzkörper. Another drop in concentration produces embryos which do not form ventral denticles, but still develop filzkörper. With yet further decreases in RNA concentration, the fraction of injected embryos developing filzkörper falls (Fig. 3). Thus, the highest degree of 'ventralness' achieved is proportional to the concentration of rescuing RNA, with a continuous increase in the qualitative nature of the response over a 50-fold range of RNA concentration. This dose–response curve for *snake* is the biochemical correlate of gene dosage studies with *dorsal*, where the presence of ventral structures is a function of the number of copies of the dl^+ gene[8,14].

The measurement of the dose-dependence of the response makes it possible to compare concentrations of rescuing activity in different preparations. For example, because rescuing activity can still be detected in a 50-fold dilution of poly$(A)^+$ RNA, the absence of activity from the corresponding RNase-treated sample means that more than 98% of the rescuing activity in that sample is RNase-sensitive. As equivalent responses are seen with total RNA and a 10-fold more dilute sample (in mg ml^{-1}) of poly$(A)^+$ RNA, the poly$(A)^+$ fraction is roughly 10-fold enriched in *snake*-rescuing RNA.

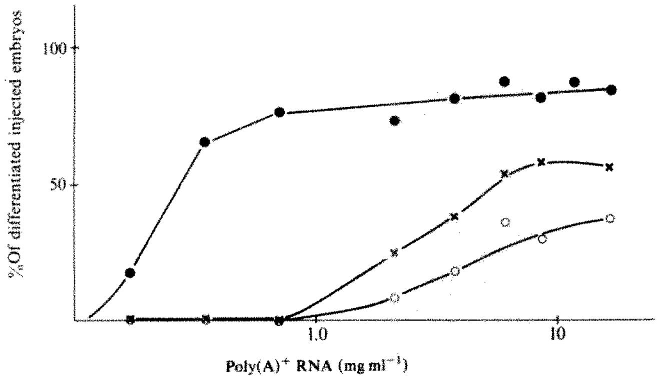

Fig. 3 Dose–response relationship for rescue of *snake* by poly$(A)^+$ RNA. At 0.2 mg ml^{-1} poly$(A)^+$ RNA, filzkörper (●) are developed by 40% of the differentiated injected embryos. At a 10-fold higher concentration, ventral denticles (×) (in addition to filzkörper) are developed by 40% of the differentiating embryos. At even higher RNA concentrations, a high percentage of embryos show a normal cuticular pattern (○), characterized by a full set of thoracic and abdominal ventral denticle belts of normal width in addition to filzkörper and head structures. The poly$(A)^+$ RNA fraction injected was purified by only one cycle of binding to oligo(dT)-cellulose and certainly still contains ribosomal RNA. The concentrations given here, measured by UV absorbance, should therefore be considered as relative, and are not directly comparable with the *in vivo* concentration of poly$(A)^+$ RNA. Each point represents the mean of at least 20 differentiated embryos.

Rescue of other dorsalizing mutants

Table 1 shows that six of the eight third-chromosomal dorsalizing maternal-effect mutants can be partially rescued by the injection of wild-type cytoplasm, with five loci responding strongly enough to develop ventral denticles. All five of these strongly responding loci (*snake, tube, easter, Toll* and *pelle*) are rescued not only by cytoplasmic injection but also by injection of RNA from cleavage stage wild-type embryos. In each case, the rescuing RNA is enriched in the poly$(A)^+$ fraction and is therefore probably mRNA. The rescuing RNA is locus-specific: while poly$(A)^+$ RNA isolated from *snake* embryos does not rescue *snake* embryos, the same preparation does rescue embryos mutant for *tube, easter, Toll* and *pelle.*

Each mutant shows a characteristic degree of response to injected RNA, which shows some parallels with the response of each mutant to cytoplasm. Of the three loci studied in greatest detail (*snake, tube* and *easter*), *snake* responds most strongly to injection of both cytoplasm and RNA (Table 3). The *in vivo* concentration of total RNA is 18 mg ml^{-1} (ref. 15), comparable to the concentration of total RNA injected in the experiment shown in Table 3. Comparing the rescue obtained with cytoplasm and total RNA, it is clear that a large amount of the *snake*- and *tube*-rescuing activities are not recovered in purified RNA, while most of the *easter*-rescuing activity is retained in the RNA. We estimate that 10% of the *snake*- and *tube*- and 70% of the *easter*-rescuing activities are recovered in purified RNA.

The *easter*-rescuing RNA also apparently differs from both the *tube* and *snake* RNAs in its degree of polyadenylation. Both *snake* and *tube* RNAs are roughly 10-fold enriched in the poly(A)$^+$ fraction, while the *easter* RNA is only 3-fold enriched. This is supported by the observation that the poly(A)$^-$ fraction rescues *easter* only slightly more weakly than total RNA (data not shown).

The concentrations of the poly(A)$^+$ RNAs that rescue *snake*, *tube* and *easter* all decrease rapidly during early development. The *tube*- and *easter*-rescuing activities are barely detectable in poly(A)$^+$ RNA isolated from 3–7-h embryos and the rescuing activity for *snake* is 20-fold reduced (by comparison with the dose–response curve of Fig. 3). This loss of rescuing activity in RNA parallels the loss of *snake*- and *easter*-rescuing activities from cytoplasm after the onset of gastrulation. For *tube*, in contrast, cytoplasm from extended germ band stage donors continues to rescue as effectively as cleavage cytoplasm, although RNA isolated from that stage not longer rescues significantly.

Conclusions

Maternal mRNA in *Drosophila* includes messages for abundant proteins like histones, actin and tubulin which are needed in large amounts early in development, as well as a high sequence complexity class of less abundant messages[16–20]. Maternal mRNA could also code for proteins specifically required in early embryonic morphogenesis. Indirect evidence from several systems supports the hypothesis that maternal mRNA is a source of morphogenetic information. In *Smittia* embryos, for example, an RNase-sensitive component prevents double abdomen formation[21]. It has also been shown that poly(A)$^+$ RNA can restore the ability to form pole cells in UV-sterilized *Drosophila* embryos[22]. It is difficult, however, to assess the specificity of these experimental manipulations and their relation to normal pattern-forming processes.

The maternal-effect mutations described here each remove a single, genetically defined component required in embryonic pattern formation. The phenotypic rescue of these mutants by injection of RNA provides a specific assay to probe the molecular basis of the establishment of the embryonic dorsal–ventral pattern. As poly(A)$^+$ RNA isolated from cleavage wild-type embryos rescues *snake*, *tube*, *easter*, *pelle* and *Toll*, these five different RNAs are a normal storage form of the morphogenetic information from these genes.

It is reasonable to assume that the rescuing RNAs are the protein-coding transcripts from the respective mutant genes. In the case of *snake*, the molecular analysis of this hypothesis should be relatively straightforward, because deficiency mapping has localized the *snake* gene within the DNA cloned in the *rosy-Ace* region[23].

The availability of a purified rescuing substance provides a probe for studying the nature of this pattern-forming system. The dose–response relationship between the amount of RNA injected and the phenotypic response of *snake* embryos shows that the level of ventral development achieved in the embryo is a direct, continuous function of the amount of *snake*-rescuing RNA present in the embryo. The rescue responses of *tube* and *easter* show analogous dose–response relationships, although more RNA is required for the same level of response. Thus *snake*, *tube* and *easter* are all essential components of a system of graded, positional information, and, at limiting amounts of gene activity, the effective morphogen activity becomes proportional to the amount of that gene product.

The cytoplasmic rescuing activity of each gene has a unique set of characteristics, which must reflect their unique roles in the establishment of the dorsal–ventral pattern. Not only are there large, quantitative differences in the responses of the mutants to the injection of wild-type cytoplasm, but the molecular nature of the rescuing activity is also characteristic for each mutant. Because more than two-thirds of the cytoplasmic rescuing activity for *easter* is recovered in purified RNA, and as the presence of rescuing activity in cytoplasm is paralleled by the rescuing activity in RNA during development, we suggest that the cytoplasmic rescuing activity for *easter* is exclusively RNA. Only about 10% of the cytoplasmic rescuing activities for *tube* and *snake* are recovered in RNA. Because the RNA could have been subject to differential degradation during purification or after injection, the *snake*-rescuing activity could be either exclusively RNA or a mixture of RNA and protein. Cytoplasm from the extended germ band stage of wild-type embryos rescues the *tube* mutant phenotype (at this stage almost no rescuing activity in RNA can be detected), suggesting that there is also a non-RNA component of the rescue with younger cytoplasm. We have been unable to detect any response of mutant *dorsal* embryos to the injection of RNA, although the *dorsal* RNA is present in young embryos[24]. The response of *dorsal* embryos to cytoplasmic injection is relatively weak, so if the RNA were preferentially labile, or if RNA is only a small fraction of the normal rescuing activity, we might not have detected it in our assay. In contrast *spätzle* embryos also respond weakly to cytoplasmic injection, but are nevertheless rescuable by RNA (F. Müller-Holtkamp and H. Jäckle, personal communication).

The demonstration that a group of morphogenetic mRNAs is present in early wild-type embryos suggests that control of the translation of these mRNAs may be a significant aspect of the mechanism of establishing dorsal–ventral pattern. The investigation of this possibility will require specific molecular probes for both the RNAs and the protein products of these genes. Such probes should elucidate the interaction between the members of this defined group of gene products that give rise to the dorsal–ventral pattern.

We thank Liselotte Bokla for technical assistance, Felix Müller-Holtkamp and Herbert Jäckle for communicating unpublished results, and Renate Brodbeck for typing the manuscript. K.V.A. was supported by the Deutsche Forschungsgemeinschaft.

Received 12 June; accepted 6 July 1984.

1. Tickle, C., Alberts, B., Wolpert, L. & Lee, J. *Nature* **294**, 564–566 (1982).
2. Schaller, H. C., *J. Embryol. exp. Morph.* **29**, 27–39 (1973).
3. Kay, R. R. & Jermyn, K. A. *Nature* **303**, 242–244 (1983).
4. Anderson, K. V. & Nüsslein-Volhard, C. in *Pattern Formation* (eds G. M. Malacinski & Bryant, S.) 269–289 (Macmillan, New York, 1984).
5. Gans, M., Audit, C. & Masson, M. *Genetics* **81**, 683–704 (1975).
6. Mohler, J. D. *Genetics* **85**, 259–272 (1977).
7. Rice, T. B. thesis, Yale Univ. (1973).
8. Nüsslein-Volhard, C. in *Determinants of Spatial Organization* (eds Subtelney, S. & Konigsberg, I. R.) 105–211 (Academic, New York, 1979).
9. Santamaria, P. & Nüsslein-Volhard, C. *EMBO J.* **2**, 1695–1699 (1983).
10. Campos-Ortega, J. A. *Wilhelm Roux Arch. dev. Biol.* **192**, 317–316 (1983).
11. Konrad, K. D. & Mahowald, A. P. in *Molecular Aspects of Early Development* (eds Malacinski, G. M. & Klein, W. H.) 167–188 (Plenum, New York, 1984).
12. Nüsslein-Volhard, C., Lohs-Schardin, M., Sander, K. & Cremer, C. *Nature* **283**, 474–476 (1980).
13. Hilliker, A. J., Clark, S. H., Chovnick, A. & Gelbart, W. M. *Genetics* **95**, 95–110 (1980).
14. Nüsslein-Volhard, C. in *Cell Lineage, Stem Cells and Cell Determination* (ed. Le Douarin, N.) 69–82 (Elsevier, Amsterdam, 1979).
15. Anderson, K. V. & Lengyel, J. A. *Devl Biol.* **70**, 217–231 (1979).
16. Kuo, C.-H. & Garen, A. in *Cancer Biology IV. Differentiation and Carcinogenesis* (eds Borek, C. *et al.*) 97–103 (Stratton Intercontinetal Medical Book Corp. New York, 1977).
17. Arthur, C. G., Weide, C. M., Vincent, W. S. & Goldstein, E. S. *Expl Cell Res.* **121**, 87–94 (1979).
18. Hough-Evans, B. R., Jacobs-Lorena, M., Cummings, M. R., Britten, R. J. & Davidson, E. H. *Genetics* **95**, 81–94 (1980).
19. Raff, E. C. *et al. Cell* **28**, 33–40 (1982).
20. Anderson, K. V. & Lengyel, J. A. in *Histone Genes* (eds Stein, G. & J.) 135–161 (Wiley, New York, 1984).
21. Kandler-Singer, I. & Kalthoff, K. *Proc. natn. Acad. Sci. U.S.A.* **73**, 3739–3743 (1976).
22. Togashi, S. & Okada, M. *Dev. Growth and Different.* **25**, 423 (1983).
23. Spierer, P., Spierer, A., Bender, W. & Hogness, D. S. *J. molec. Biol.* **168**, 35–50 (1983).
24. Steward, R., McNally, F. J. & Schedl, P. *Nature* **311**, 262–265 (1984).
25. Lindsley, D. L. & Grell, E. H. *Genetic Variations of* Drosophila melanogaster (Carnegie, Washington, 1968).
26. Hall, J. & Kankel, D., *Genetics* **83**, 517–535 (1976).

A role for clathrin light chains in the recognition of clathrin cages by 'uncoating ATPase'

Sandra L. Schmid, William A. Braell, David M. Schlossman & James E. Rothman

Department of Biochemistry, Stanford University Medical School, Stanford, California 94305, USA

A cycle of clathrin assembly and disassembly drives the formation of coated vesicles, intermediates in intracellular protein transport. The heavy chain of clathrin is needed for assembly, but the function of the clathrin light chains has remained obscure. An enzyme has now been purified which uses ATP hydrolysis to power the release of clathrin from coated vesicles, presumably recycling the coat protein for repeated rounds of vesicle budding. This 'uncoating ATPase' requires clathrin light chains for its action.

COATED vesicles have a central role in intracellular protein transport[1-3]. Clathrin, the major coat protein, forms a three-legged structure termed a triskelion[4,5] which can self-assemble into cages resembling coats[6-8]. Each triskelion contains three clathrin heavy chains of 180,000 molecular weight (180K) and three noncovalently bound light chains. The molecular weights of the light chains from different species and tissues varies between 30K and 40K (refs 9, 10). Two different light chains are present, LC_α (36K in bovine brain) and LC_β (33K in bovine brain), in a constant molar ratio of 1:2. Both types of light chain can rebind to the same site on heavy chains near the vertex[11-13] and are found randomly distributed among these sites[13].

The function of the light chains has been obscure. The lack of assays in which the *in vivo* functions of clathrin and other coated vesicle proteins are reconstituted has made it difficult to elucidate the role of these components in the clathrin-coated vesicle cycle of assembly and disassembly which drives selective protein transport[14]. Therefore, we have attempted to reconstitute these processes. Here we report that light chains are required for the enzymatic disassembly of clathrin cages.

As an entry point into the cycle, we chose the uncoating step in which clathrin is released for use in repeated rounds of vesicle budding. We found that crude cytosol contained an ATP-dependent activity capable of releasing clathrin from coated vesicles and clathrin cages[15]. Based on this assay, we purified to homogeneity the active 70K protein from bovine brain cytosol[16,17]. This protein, an 'uncoating ATPase', uses ATP hydrolysis to power the release of clathrin from coated vesicles (or from cages reconstituted from triskelions). Clathrin is released as trimers containing stoichiometric amounts of noncovalently bound uncoating ATPase. ATP is hydrolysed in a coupled fashion during this release. Uncoating protein will only hydrolyse ATP when clathrin is also present; that is, uncoating protein is a clathrin-dependent ATPase. Assembled clathrin cages will elicit this ATPase activity but unassembled triskelions will not, as would be appropriate for an uncoating protein.

Clathrin-coupled ATP hydrolysis

The clathrin cage-dependent ATPase activity of the uncoating protein can be exploited as an assay to determine the structural aspects of clathrin needed for its recognition as a substrate. To test for a possible requirement for light chains, we prepared clathrin cages that either contained or lacked light chains, and tested these as substrates for uncoating ATPase.

Figure 1 is an SDS-polyacrylamide gel of these various clathrin substrates and demonstrates the selective removal of light chains in the appropriate forms of clathrin. Heavy chains free of detectable light chains were prepared by limited proteolysis[18,19] of clathrin cages using chymotrypsin or elastase (Fig. 1, lane *b*), or from triskelions following extraction of light chains with NaSCN (Fig. 1, lane *h*) according to Winkler and Stanley[12]. Light chain-depleted coated vesicles (Fig. 1, lane *f*) could be similarly prepared by limited proteolysis using chymotrypsin. Both proteolysis and extraction were used because recent evidence[12] shows that clathrin heavy chains prepared by limited proteolysis lack native assembly properties. Light chains will bind back to light chain-depleted 'heavy chain' cages with high affinity in near stoichiometric amounts to form 'reconstituted' cages, as reported previously[11-13,18]. The heat-stable light chains (Fig. 1, lane *d*) were prepared from supernatants of boiled clathrin[18,21]. Reconstituted cages were prepared by incubating these light chains with chymotrypsin-digested cages (Fig. 1, lane

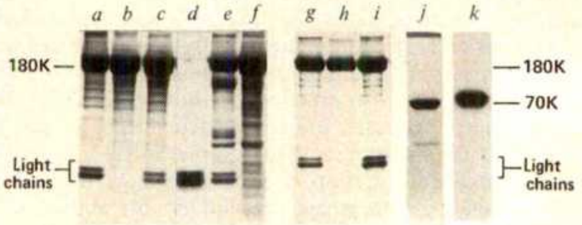

Fig. 1 SDS-polyacrylamide gel of clathrin substrates. Clathrin was purified from bovine brain by the method of Schook *et al.*[23] as previously described[16]. Lanes *a*, *g*, empty cages (12 μg) prepared by overnight dialysis of clathrin (1 mg ml^{-1}) into buffer A (20 mM methane ethane sulphonate, 2 mM $CaCl_2$, 1 mM EDTA *p*H 6.2) at 4 °C and preincubated in buffer B (40 mM HEPES, 75 mM KCl, 4.5 mM MgOAc, 0.8 mM dithiothreitol *p*H 7.0) as described previously[17]. Lane *b*, chymotrypsin-digested cases (12 μg) prepared by incubation of empty cages (1 mg ml^{-1}) in buffer A with 1.5 μg ml^{-1} TLCK-treated α-chymotrypsin (Sigma) for 45 min at 25 °C. Digestions were stopped by addition of phenylmethylsulphonyl fluoride (PMSF) to 1 mM. Chymotrypsin-digested cages were washed twice by centrifugation in a Beckman Airfuge at 100,000 *g* for 10 min and resuspended in buffer A containing 1 mM PMSF. Lane *c*, reconstituted chymotrypsin-digested cages (12 μg) prepared by recombination with light chains as described previously[18,11]. A ratio of 1:0.4 (w/w) heavy chains to light chains (~2-fold molar excess of light chains) was used to obtain stoichiometric reconstitution of light chains. Lane *d*, clathrin light chains (4 μg) prepared by boiling purified clathrin as previously described[18,21]. Lane *e*, coated vesicles (15 μg) purified from bovine brain using D_2O-Ficoll gradients as described by Pearse[24]. Lane *f*, chymotrypsin-digested coated vesicles (15 μg) prepared as described for chymotrypsin-digested empty cages. Lane *h*, clathrin heavy chains (10 μg) derived from NaSCN-extracted triskelions exactly as described by Winkler and Stanley[12]. Lane *i*, reconstituted SCN$^-$-extracted cages (12 μg) prepared by recombination with light chains, as described for lane *c*. Lane *j*, Coomassie blue stained gel and lane *k*, corresponding autoradiograph of ^{3}H-labelled uncoating ATPase (3 μg) prepared by the procedure of Tack *et al.*[22], as described in Fig. 4 legend. SDS-polyacrylamide gel electrophoresis minigels shown were 10% acrylamide and 3.5 cm in length. Samples were boiled in sample buffer and electrophoresed as described by Laemmli[25]. Gels were stained with Coomassie blue.

c) and SCN$^-$-extracted heavy-chain cages (Fig. 1, lane *i*). These various substrates were tested for their ability to elicit ATP hydrolysis by the uncoating enzyme.

Figure 2*a* shows the clathrin-dependent ATP hydrolysis by uncoating protein when intact cages are provided as substrate. The very low rate of clathrin-independent ATP hydrolysis (< 10% of the total) has been subtracted[17]. When cages depleted of light chains (by limited chymotrypsin digestion) were assayed (Fig. 2*a*), little or no hydrolysis was detected above enzyme-only backgrounds. To ensure that this difference was due to removal of light chains and not to some other effect of chymotrypsin, we determined whether adding back light chains would restore clathrin function. We found indeed that reconstitution with light chains quantitatively restored clathrin-dependent ATP hydrolysis (Fig. 2*a*). Uncombined light chains, added in equivalent amounts, did not elicit ATP hydrolysis (Fig. 2*a*). Qualitatively, but not quantitatively, the same results were obtained when we tested cages depleted of light chains by SCN$^-$ extraction (Fig. 2*b*). Again, clathrin function was restored on recombination with light chains (Fig. 2*b*).

The greater residual activity in Fig. 2*b* compared with Fig. 2*a* could be explained by a greater residue of light chains in the SCN$^-$-extracted clathrin, not easily detectable by Coomassie blue staining. To test this, we prepared ^{3}H-labelled clathrin by reductive methylation[16] and used this clathrin to prepare light chain-depleted cages as described above. Even though no residual light chains were detected in stained gels (Fig. 3, lanes *b*, *c*), autoradiography revealed that the SCN$^-$-extracted clathrin (Fig. 3, lane *f*) still retained up to 15% of its light chains (almost exclusively LC$_B$). No such residue could be detected in the chymotrypsin-treated heavy-chain cages (Fig. 3, lane *e*).

The apparent requirement for light chains could be trivially explained if the light chain-depleted cages had dissociated in assay conditions, for we have already shown[17] that dissociated triskelions do not elicit ATP hydrolysis. That the various cage substrates remain assembled during incubation to a comparable degree is demonstrated in Table 1*a*.

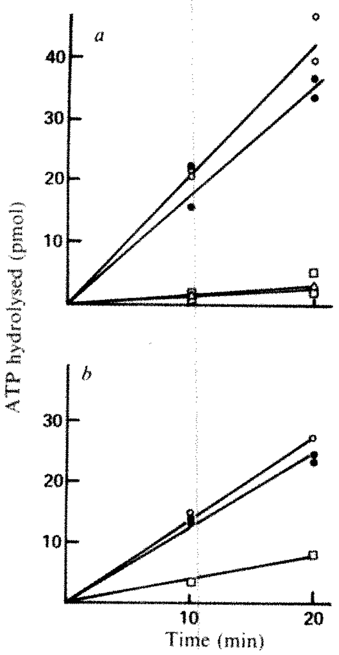

Fig. 2 ATPase activity of uncoating ATPase using various clathrin substrates. ATPase assays were performed as previously described[17]. Each assay contained 160 pmol ^{3}H-ATP, 4 μg clathrin substrate (prepared as described in Fig. 1 legend) or 1.5 μg of free light chains, and 0.2 μg uncoating ATPase in 20 μl buffer B. Data were corrected for backgrounds as described elsewhere[17] and thus reflect clathrin-dependent levels of ATP hydrolysis. Substrates used in *a*: empty cages (●), chymotrypsin-digested empty cages (□), free clathrin light chains (△) and chymotrypsin-digested cages whose light chains had been restored (○). Substrates used in *b*: empty cages (●), cages formed from NaSCN-extracted clathrin (□) and those cages recombined with light chains (○).

Clathrin release from cages

Given that ATP hydrolysis indeed precedes and is a prerequisite of clathrin release[17], uncoating protein-facilitated cage disassembly should also be light chain-dependent. Table 1*b* demonstrates that cages depleted of light chains by chymotrypsin digestion are poor substrates for ATP-dependent dissociation by uncoating ATPase (25 ± 17% of untreated controls). However, when light chains are added back, the ability of the cages to be dissociated by uncoating ATPase is restored (79 ± 16% of untreated controls).

Light-chain dependence is less evident when SCN$^-$-extracted cages are used as substrate (41 ± 9% release relative to controls). Because a few ATP-dependent enzymatic 'hits' may well be all that is needed to disassemble the cages[16], this assay is likely to be much more sensitive to the presence of residual light chains than is the ATPase assay. The 15% residual light chains present in SCN$^-$-extracted cages (~16 light chains per clathrin cage) may therefore be sufficient to facilitate uncoating protein-catalysed cage fragmentation and ensuing clathrin release.

Uncoating ATPase and clathrin cages

The requirement of light chains in clathrin cages to elicit the ATPase activity of uncoating protein implies that they are needed for the productive association of uncoating protein with

Table 1 Release of clathrin cages as a function of their light-chain content

a, Spontaneous release	
Substrate	Clathrin released* (% of total)
Control cages	6.5 ± 1.4 (6)
Chymotrypsin-digested cages	14.6 ± 7.6 (5)
Chymotrypsin-digested cages recombined with light chains	13.7 ± 7.8 (5)
SCN$^-$-extracted clathrin cages	17.7 ± 6.6 (6)
SCN$^-$-extracted clathrin cages recombined with light chains	12.5 ± 4.6 (6)
b, Uncoating ATPase-promoted release	
Substrate	% Release (relative to control cages)
Control cages†	[100]
Chymotrypsin-digested cages	25 ± 17 (7)
Chymotrypsin-digested cages recombined with light chains	79 ± 16 (7)
SCN$^-$-extracted clathrin cages	41 ± 9 (5)
SCN$^-$-extracted clathrin cages recombined with light chains	71 ± 22 (7)

Uncoating assays were performed as described previously[16]. Each assay contained 10 μg of clathrin substrate (prepared as described in Fig. 1 legend), 3 μg of uncoating ATPase and 50 μM ATP in 50 μl buffer B. After incubation at 37 °C for 10 or 20 min, the reaction was stopped by addition of yeast hexokinase (to 10 U ml^{-1}) and glucose (to 5 mM) and centrifuged in a Beckman Airfuge, as described previously[16]. A sample of each supernatant (20 μl) was electrophoresed on 10% polyacrylamide minigels. Release of clathrin into the supernatant was quantitated as described elsewhere[14,16], from densitometric tracings of the 180K clathrin band on the Coomassie blue stained gels. In *a*, incubations were performed in the absence of uncoating enzyme to test the intrinsic stability of each cage substrate to incubations in assay conditions. In *b*, incubations contained 3 μg uncoating ATPase. The rate of ATP-dependent clathrin release is expressed relative to release from untreated cages in parallel incubations to allow comparison between experiments.

* Values are mean ± s.d.

† Uncoating protein-dependent clathrin release from control cages was 46.7 ± 25% ($n = 10$) during 10 min incubations in buffer B.

Table 2 Light chain-dependent association of uncoating protein with clathrin cages

Clathrin substrate	ATP	Uncoating protein bound (% of total)†
None	+	4.5 ± 2.2 (4)
	−	5.3 ± 1.6 (2)
Cages	+	33.8 ± 7.8 (13)
	−	11.0 ± 5.4 (7)
Chymotrypsin-digested cages	+	16.4 ± 4.0 (6)
	−	14.5 ± 0.0 (2)
Chymotrypsin-digested cages recombined with light chains	+	38.0 ± 9.3 (4)
	−	16.3 ± 0.1 (2)
SCN⁻-extracted clathrin cages	+	13.9 ± 3.9 (5)
	−	7.5 ± 5.9 (2)
SCN⁻-extracted clathrin cages recombined with light chains	+	36.7 ± 3.4 (5)
	−	4.0 ± 1.6 (2)
Coated vesicles	+*	28.9 ± 13.2 (5)
	−	9.3 ± 3.9 (3)
Chymotrypsin-digested coated vesicles	+*	15.3 (1)
	−	10.7 (1)

Column elution profiles generated as described in Fig. 4 legend were quantitated by integration of void and included peaks. Data are expressed as the ^{3}H counts recovered in the void peak as a per cent of the total ^{3}H eluted. The mean ± s.d. from several independent experiments is shown. The number of experiments is given in parentheses.

* ATP regenerating system[15] was used instead of ATP.

† Recovered in the void volume of Biogel A1.5m.

cages. The uncoating protein plus bound ATP[17] must clearly interact with cages before ATP hydrolysis and subsequent clathrins release. This interaction could occur first, independently of light chains, followed by light chain-dependent ATP hydrolysis. Alternatively, light chains might be required for the initial recognition of cages by the uncoating enzyme–ATP complexes, leading to subsequent ATP hydrolysis and then clathrin release. To distinguish between these possibilities, we have devised a binding assay to detect any association between uncoating protein and clathrin cages and investigated whether we could detect any binding of uncoating protein to cages depleted of light chains.

^{3}H-labelled uncoating protein (specific activity 0.1–0.2 mCi per mg) was prepared by reductive methylation[22] and was fully active in both clathrin-dependent ATPase and ATP-dependent clathrin release assays (see Fig. 4 legend for details). Figure 1 shows a Coomassie blue stained SDS gel (lane *j*) and corresponding autoradiograph (lane *k*) of a preparation of ^{3}H-labelled uncoating ATPase. The uncoating ATPase was incubated with excess amounts of light chain-depleted clathrin cages with or without ATP, and the products were separated by gel filtration on Biogel A1.5m to distinguish free uncoating protein (^{3}H in the included volume) from that bound to clathrin (^{3}H in the void volume).

It is important to note that this assay will measure binding of uncoating protein to intact cages (when disassembly does not occur) as well as entry of uncoating ATPase into complexes with the released triskelions (when disassembly does occur), as both forms of clathrin elute in the void volume. Therefore, the assay measures any association between uncoating ATPase and clathrin, independent of clathrin release. As expected, incubation of ^{3}H-labelled uncoating protein with empty cages and ATP results in binding (Fig. 4*b*), in this case to the released triskelions (Table 1*b*). This binding does not occur in the absence of ATP (Fig. 4*a*), a condition in which clathrin is not released[16]. We showed previously[17] that preformed uncoating protein–ATP complexes can interact with cages, resulting in ATP hydrolysis. The lack of ATP-independent binding of uncoating protein to cages indicates that the ATP–uncoating protein complexes must form before interaction with cages.

When cages depleted of light chains (by chymotrypsin digestion) were used (Fig. 4*c*), little or no binding to cages occurred above minus clathrin background (Fig. 4*h*), even in the presence of ATP. Therefore, if a light chain-independent interaction of uncoating protein with clathrin cages does precede ATP hydrolysis and cage disassembly, we cannot detect it. ATP-dependent binding could be restored by adding back light chains to the chymotrypsin-treated cages (Fig. 4*d*). As with intact cages, this association represents uncoating protein present in complexes with released calthrin whose ability to be released was restored on recombination with light chains (Table 1*b*). Qualitatively similar results were obtained when we used cages prepared from SCN⁻-extracted heavy chains (Fig. 4*e*), and when these were recombined with light chains (Fig. 4*f*). Again, a greater residue of binding occurs when SCN⁻-extraction rather than proteolysis is used to deplete light chains. As expected, coated vesicles were also substrates for the formation of uncoating protein–clathrin complexes during uncoating (Fig. 4*g*). As with cages, selective chymotrypsin digestion of light chains from coated vesicles greatly reduced the yield of the released complexes (Table 2). Table 2 presents quantitative data on binding calculated as the per cent of ^{3}H-labelled uncoating protein recovered in the void volume.

Altogether, we have found no evidence for interaction of uncoating protein with light chain-free clathrin cages. These experiments suggest that light chains are required by uncoating protein for the initial recognition of clathrin cages as substrate.

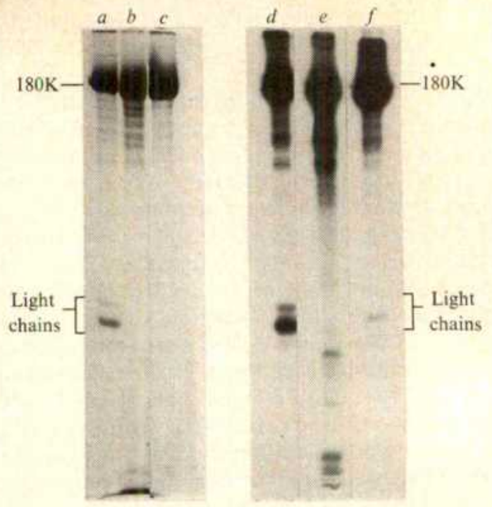

Fig. 3 SDS-polyacrylamide gel and corresponding autoradiograph of ^{3}H-clathrin substrates. ^{3}H-clathrin (~0.2 mCi per mg) was prepared by reductive methylation with formaldehyde and NaB[^{3}H]$_4$ as described previously[16]. ^{3}H-labelled empty cages were prepared by dilution of labelled clathrin with unlabelled clathrin to a final specific activity of 16,000 c.p.m. per μg and dialysis against buffer A as described in Fig. 1 legend. Chymotrypsin-digested cages and SCN⁻-extracted cages were prepared from ^{3}H-labelled empty cages or from the diluted ^{3}H-clathrin. Lanes *a–c*, Coomassie blue stained; lanes *d–f*, the corresponding autoradiograph. Lanes *a*, *d*, ^{3}H-labelled empty cages; lanes *b*, *e*, ^{3}H-chymotrypsin-digested cages; lanes *c*, *f*, ^{3}H-labelled SCN⁻-extracted cages. Each lane contained 25 μg of protein and 400,000 c.p.m.

Conclusions

Our studies of the mechanism of ATP-dependent uncoating in a cell-free system reconstituted from pure components has revealed that light chains are required on clathrin cages for the activation of uncoating ATPase. This is the case for all facets of its activity that we can presently measure—clathrin-dependent ATP hydrolysis, ATP-dependent clathrin release and ATP-dependent enzyme–clathrin complex formation. Two lines of evidence suggest that light chains are needed at an early stage in the uncoating reaction for initial recognition of clathrin cages

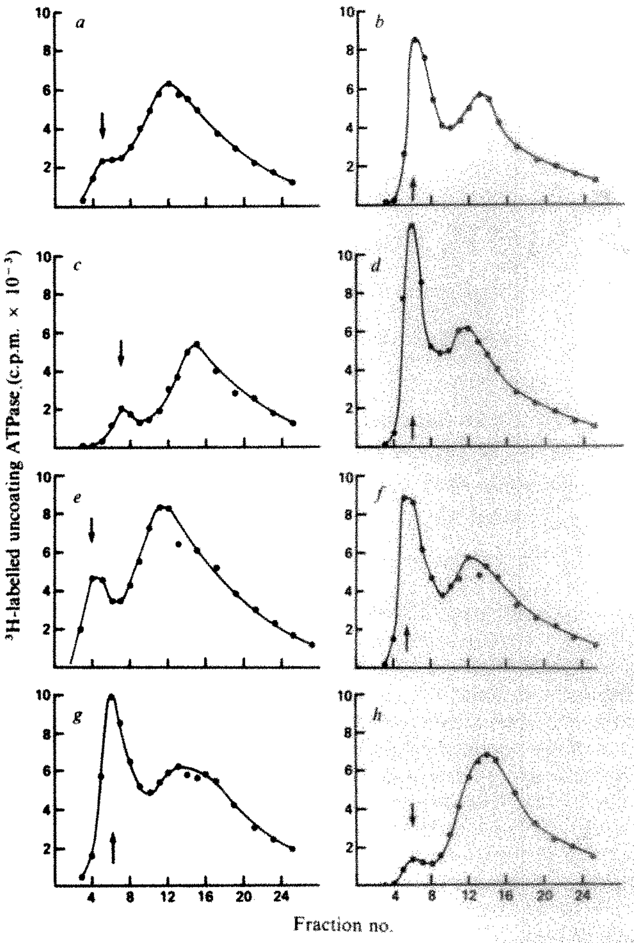

Fig. 4 Gel filtration assay for binding of ^{3}H-uncoating ATPase to clathrin substrates.

Methods: *a*, Empty cages in the absence of ATP which was replaced in the incubation by yeast hexokinase (10 U ml^{-1}) and glucose (5 mM); *b*, empty cages as substrate in the presence of ATP; *c*, chymotrypsin-digested cages, with ATP; *d*, chymotrypsin-digested cages recombined with light chains (with ATP); *e*, cages prepared from SCN$^-$-extracted clathrin; *f*, SCN$^-$-extracted clathrin cages after recombination with light chains; *g*, bovine brain-coated vesicles as substrate with ATP; *h*, incubation of uncoating ATPase in the presence of ATP, without any clathrin. The arrow indicates the void volume. Uncoating ATPase was tritiated using the Tack procedure for reductive methylation[22]. Typically, 150 μg of uncoating ATPase (1–2 mg ml^{-1}, 2.1 nmol) in 0.2 M Na borate *p*H 8.9 was incubated with 0.4 μmol formaldehyde and 0.1–0.2 μmol ^{3}H-NaBH$_4$ (Amersham, 8.7 Ci mmol^{-1}) for 10 min on ice. Free radiolabel was removed by exhaustive dialysis against two changes of 1,000 vols each of buffer B. ^{3}H-labelled uncoating ATPase (~ 0.1 mCi per mg) retained full ATPase and uncoating activities (data not shown) and was stable for 4–6 days at 4 °C and for several months after freezing in liquid N$_2$ and storage at −70 °C. Incubations contained 20 μg clathrin substrate, 1.3 μg of ^{3}H-labelled uncoating ATPase (diluted with unlabelled uncoating protein to achieve a final specific activity of ~30,000 c.p.m. per μg) and 1.25 nmol ATP in 25 μl of buffer B. After 20 min at 37 °C, incubation mixtures were chilled on ice and quickly loaded onto Biogel A1.5 m columns (15 × 0.3 cm) equilibrated in buffer B containing 0.5% bovine serum albumin (BSA) at 4 °C. Columns were eluted at 1.5 ml h^{-1}, collecting 55-μl fractions which were counted for ^{3}H. Representative elution profiles using various clathrin substrates are shown here. The ATP dependence of binding, as well as uncoating[16], varied with uncoating ATPase preparations but was high and reproducible following storage at 4 °C for 1–2 days or after being subjected to the discharging procedure described elsewhere[16]. We believe that ATP independence reflects a variable amount of tightly bound nucleotide obtained on elution of the enzyme from ATP–Sepharose with ATP during purification[16].

by the uncoating enzyme. First, we can detect no interaction of uncoating protein with cages lacking light chains (Fig. 4, Table 2) and second, light chains are required for ATP hydrolysis (Fig. 2), which precedes clathrin release[16,17]. In the simplest view, uncoating protein would bind directly to the light chains on the surface of cages. However, as free light chains do not substitute for whole clathrin (Fig. 2), either light chains exist in a different conformation (recognized by uncoating protein) when bound to heavy chains, or sites on both heavy and light chains are needed for productive binding, or both. In any case, it is clear that light chains are required for the function of clathrin in enzymatic uncoating.

The reason clathrin has two distinct species of light chains is unknown. We found that cages reconstituted so as to contain exclusively LC$_\alpha$ or LC$_\beta$ (refs 11, 12) are equivalent to native cages as substrates for ATPase activity (W.A.B. and J.E.R., unpublished data). This suggests that the functional distinction between LC$_\alpha$ and LC$_\beta$ cannot be detected by the limited assays available, and that additional roles of these components remain to be elucidated. For example, light chains may well function in other stages of the clathrin-coated vesicle cycle. If so, this will only become apparent through the creation of assays that represent reconstitutions of these steps. Such an approach will lead to an understanding of how clathrin and coated vesicles function in the dynamic process of membrane transport.

We thank the Helen Hay Whitney Foundation and Jane Coffin Child Memorial Fund for their support (of D.M.S. and W.A.B., respectively). This research was carried out under NIH grant GM 25662.

Received 27 March; accepted 19 June 1984.

1. Goldstein, J. L., Anderson, R. G. W. & Brown, M. S. *Nature* **279**, 679–685 (1979).
2. Pearse, B. M. F. & Bretscher, M. S. *A. Rev. Biochem.* **50**, 85–101 (1981).
3. Pearse, B. M. F. *Trends biochem. Sci.* **5**, 131–134 (1980).
4. Ungewickell, E. & Branton, D. *Nature* **289**, 420–422 (1981).
5. Kirchhausen, T. & Harrison, S. C. *Cell* **23**, 755–761 (1981).
6. Pearse, B. M. F. *Proc. natn. Acad. Sci. U.S.A.* **73**, 1255–1259 (1976).
7. Woodward, M. P. & Roth, T. F. *Proc. natn. Acad. Sci. U.S.A.* **75**, 4394–4398 (1978).
8. Keen, J. H., Willingham, M. C. & Pastan, I. H. *Cell* **16**, 303–312 (1979).
9. Pearse, B. M. F. *J. molec. Biol.* **126**, 803–812 (1978).
10. Brodsky, F. M. & Parham, P. *J. molec. Biol.* **167**, 197–204 (1983).
11. Ungewickell, E. *EMBO J.* **2**, 1401–1408 (1983).
12. Winkler, F. K. & Stanley, K. K. *EMBO J.* **2**, 1393–1400 (1983).
13. Kirchhausen, T., Harrison, S. C., Parham, P. & Brodsky, F. M. *Proc. natn. Acad. Sci. U.S.A.* **80**, 2481–2485 (1983).
14. Rothman, J. E., Fries, E., Dunphy, W. C. & Urbani, L. J. *Cold Spring Harb. Symp. quant. Biol.* **46**, 797–805 (1982).
15. Patzer, E. J., Schlossman, D. M. & Rothman, J. E. *J. Cell Biol.* **93**, 230–236 (1982).
16. Schlossman, D. M., Schmid, S. L., Braell, W. A. & Rothman, J. E. *J. Cell Biol.* **99**, 723–733 (1984).
17. Braell, W. A., Schlossman, D. M., Schmid, S. L. & Rothman, J. E. *J. Cell Biol.* **99**, 734–741 (1984).
18. Lisanti, M. P. *et al. Eur. J. Biochem.* **125**, 463–470 (1982).
19. Schmid, S. L., Matsumoto, A. K. & Rothman, J. E. *Proc. natn. Acad. Sci. U.S.A.* **79**, 91–95 (1982).
20. Ungewickell, E., Unanue, E. R. & Branton, D. *Cold Spring Harb. Symp. quant. Biol.* **46**, 723–731 (1981).
21. Brodsky, F. M., Holmes, N. J. & Parham, P. *J. Cell Biol.* **96**, 911–914 (1983).
22. Tack, B. F., Dean, J., Eilat, D., Lorenz, P. E. & Schechter, A. N. *J. biol. Chem.* **255**, 8842–8847 (1980).
23. Schook, W., Puszkin, S., Bloom, W., Ores, C. & Kochwa, S. *Proc. natn. Acad. Sci. U.S.A.* **76**, 116–120 (1979).
24. Pearse, B. M. F. *Proc. natn. Acad. Sci. U.S.A.* **79**, 451–455 (1982).
25. Laemmli, U. K. *Nature* **177**, 680–685 (1970).

Mutations that alter the DNA sequence specificity of the catabolite gene activator protein of *E. coli*

Richard H. Ebright*, Pascale Cossart†, Brigitte Gicquel-Sanzey‡ & Jon Beckwith*

* Department of Microbiology and Molecular Genetics, Harvard Medical School, Boston, Massachusetts 02115, USA
† Unité de Biochimie Cellulaire, Institut Pasteur, 28 Rue du Dr Roux, 75724 Paris Cedex 15, France
‡ Unité de Biochimie des Regulations Cellulaires, Institut Pasteur, 28 Rue du Dr Roux, 75724 Paris Cedex 15, France

Three mutations that alter the DNA sequence specificity of the catabolite gene activator protein (CAP) from AA-TGTGA--T---TCA-ATW to AA-TGTAA--T---TCA-ATW have been isolated. All three mutations affect the same amino acid of CAP, glutamic acid 181. We propose that it is this amino acid of CAP that makes contacts with base pairs 7 and 16 of the symmetrical recognition site.

THE catabolite gene activator protein (CAP; also referred to as the cyclic AMP receptor protein, CRP), when complexed with cyclic AMP, binds to specific DNA sites at or near promoters, where it stimulates the initiation of RNA synthesis[1,2]. Figure 1 shows 18 DNA sequences that have been demonstrated to bind to CAP by nuclease protection analysis. The last line presents a consensus sequence (AA-TGTGA--T---TCA-ATW), indicating those bases that are conserved at a statistically significant frequency. The chemical-protection[3,4] and genetic[5–8] data confirm that the bases specified in this sequence are in fact important points of contact between DNA and CAP.

Ultimately we hope to understand how, at the atomic level, each base pair (bp) in the consensus DNA site is recognized by CAP. Our approach here is to isolate a mutationally altered CAP (CAP′) that binds tightly and selectively to a DNA site that differs by one nucleotide from the wild-type recognition site. A mutation that confers this phenotype will do so by altering, directly or indirectly, the contact made by CAP with the base that differs in the 'new' and wild-type recognition sites (Fig. 2). In principle, therefore, this approach has the potential to define individual direct contacts between CAP and DNA.

We describe here a genetic selection that yields mutations of this type. We also describe the characteristics and DNA sequences of three mutations isolated using this selection. The implications of the results for CAP–DNA recognition, and for protein–DNA interaction in general, will be discussed briefly here and in detail elsewhere[9].

Selection procedure

The strategy we used relies on two facts: (1) *lac*, *mal*, *ara*, *rbs*, *tna*, *uhp* and *glpT* are all genes or operons whose expression is dependent on CAP plus cyclic AMP[1,10]. Each of these contains an intact wild-type site for recognition by the CAP–cyclic AMP complex. (2) The *lacL8* mutation is a $G \rightarrow A$ nucleotide substitution within the *lac* recognition site for CAP (Fig. 3)[5,6]. CAP binds to the *lacL8* sequence only $\frac{1}{70}$th as tightly as to lac^+; therefore, strains bearing the *lacL8* mutation exhibit a Lac$^-$ phenotype[5,11].

The objective of our experiments was to obtain a mutationally altered CAP (CAP′) able to bind tightly and selectively to the *lacL8* sequence. We reasoned that the desired class of mutations would confer two identifiable properties: (1) a pleiotropic defect for recognition by CAP of wild-type sequences and (2) the ability to activate *lacL8* (Fig. 2).

We have devised a genetic selection that, on a single plate, imposes both of these criteria. Our selection consists of two steps. In the first step, we select from a *lacL8* parent a pool of 1,000–5,000 independent colonies defective for activation by CAP of the wild-type *uhp* and *glpT* sequences. To do this, we select resistance to the antibiotic phosphonomycin[10,12] on plates containing cyclic AMP. In the second step, we identify the rare colonies within this pool that exhibit a Lac$^+$ phenotype (that is, those that activate *lacL8*). To identify these, the selection with phosphonomycin/cyclic AMP is performed on Lac-EMB (ref. 13) indicator plates; Lac$^+$ colonies are purple on this medium, whereas the Lac$^-$ parent is white.

Isolation of crp′

A population of *lacL8 gal thi* cells was mutagenized by exposure to UV light, grown for 6.5 h at 37 °C and plated (1×10^8 cells) onto selective media of the type described above. Selective plates were Lac-EMB, to which were added 5 μM phosphonomycin, 0.5 mM glucose 6-phosphate, 0.5 mM glycerol (to de-repress *uhp* and *glpT*, respectively), 0.3 mM cyclic AMP and 3 mM thiamine. Eight independent mutageneses/selections were performed, resulting in the isolation of approximately 20,000 independent phosphonomycin-resistant colonies.

Among these, two purple (Lac$^+$) colonies were detected. These isolates, designated *crp′L8-1* and *crp′L8-2*, were found to be

LAC	5'- TAATGTGAGTTAGCTCACTCA
GAL	5'- AAGTGTGACATGGAATAAATT
MALT	5'- AATTGTGACACAGTGCAAATT
ARAB	5'- AAGTGTGACGCCGTGCAAATA
ARAE	5'- AATTGGAATATCCATCACATA
TNA	5'- AAATGTGAATCGAATCACAAT
BGLR	5'- AACTGTGAGCATGGTCATATT
DEOC	5'- AATTGTGATGTGTATCGAAGT
CAT	5'- AAATGAGACGTTGATCGGCAC
ILVB	5'- AATTGAGGGGTTGATCACGTT
CRP	5'- TAATGTGACGTCCTTTGCATA
PBRP4	5'- CGGTGTGAAATACCGCACAGA
OMPA	5'- AAGTGTGAACTCCGTCAGGCA
LAC-SITE 2	5'- AATTGTGAGCGGATAACAATT
ARAB-SITE 2	5'- AAAAGTGTCTATAATCACGGC
DEOC-SITE 2	5'- TAATGCGATCTGGGTCAAATA
CAT-SITE 2	5'- ACCTGTGACGGAAGATCACTT
CRP-SITE 2	5'- GAAGGCGACCTGGGTCATGCT
CONSENSUS	5'- AA-TGTGA--T---TCA-ATW

Fig. 1 DNA sites known to bind to CAP. 18 DNA sequences are shown to which CAP has been demonstrated to bind using nuclease-protection experiments; the last line is a consensus sequence indicating those bases that are conserved at a statistically significant frequency ($P < 0.05$). (W indicates a position that can be either A or T.) The sequences were aligned, and statistical significance calculated, by the method of Ebright[36], where 11 of these sequences were tabulated (compare ref. 2). References for the sequences are supplied in ref. 36, except for *malT* (ref. 37), *araE* (ref. 38), *tna* (ref. 39), *bglR* (A. Wright, A. Reynolds and S. Le Grice, personal communication), *ilvB* (ref. 40), *crp* (ref. 41) and *crp*-site 2 (ref. 41).

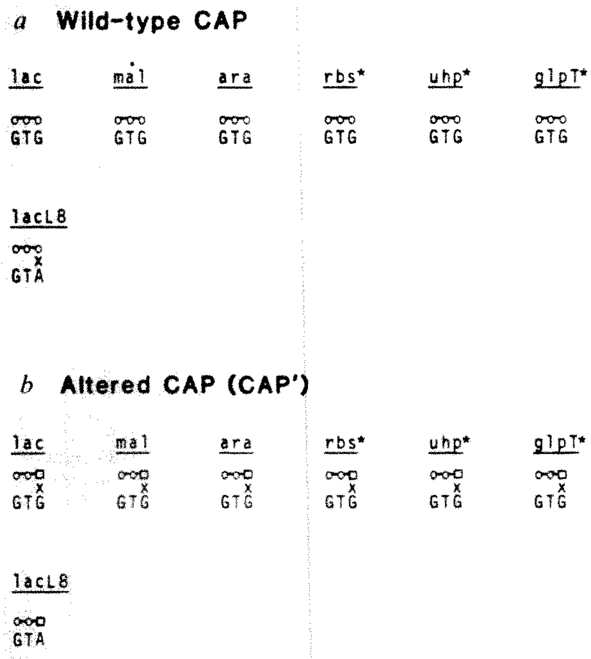

Fig. 2 Logic of the experiment. *a*, Line 1: Wild-type CAP binds tightly to sites contained in *lac*$^+$, *mal*, *ara*, *rbs*, *tna*, *uhp* and *glpT* (refs 1, 2, 10). The sequence GTG is the most highly conserved portion of the consensus recognition site (Fig. 1), the three nucleotides being present in, respectively, 18, 13 and 17 of the 18 known sites. (The actual sequences of *rbs*, *uhp* and *glpT* are not known, but we expect that they will contain this triplet.) The contacts CAP makes with the three nucleotides are illustrated schematically as circles. Line 2: Wild-type CAP does not interact tightly with the *lacL8* site, which contains a G → A nucleotide substitution at position '3' (refs 5–7). The low affinity (1/70th that for *lac*$^+$)[6,11] apparently reflects the inability of the contact CAP makes with position 3 to be satisfied by A. *b*, The object of our experiments was to obtain a mutationally altered CAP, CAP', that exhibits the opposite specificity of binding: that is, defective for interaction with wild-type sequences (line 1), but binds tightly to *lacL8* (line 2). A mutation of this type will alter, directly or indirectly, the contact CAP makes to position 3—changing this contact from one that confers specificity to G, as in wild-type CAP, to one that confers specificity to A.

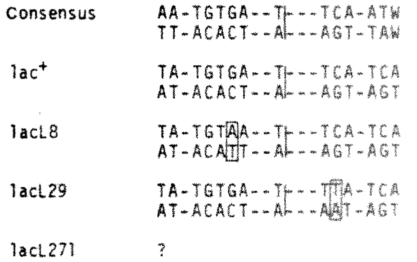

Fig. 3 Sequences of wild-type and mutant *lac* recognition sites. Line 1 shows the consensus site (Fig. 1), indicating both DNA strands. (W indicates a position that can be either A or T.) The axis of 2-fold symmetry in the sequence is located between positions 11 and 12. Lines 2–5 show the *lac*$^+$ site, which is very similar to the consensus, and three mutant recognition sites. Note that the base changes in *lacL8* and *lacL29* (boxed) are symmetrically identical[5,6]. *LacL271* is a *lac* promoter mutation isolated using the same selection that yielded *lacL8* and *lacL29* (ref. 42), but not yet sequenced (sequence analysis presently in progress; W. Reznikoff, personal communication). By two genetic criteria, the mutation is a substitution within the recognition site for CAP: (1) inability to recombine with the *lacL1*[5,6] deletion, and (2) same β-galactosidase level as *lac*$^+$ in a *crp*$^-$ genetic background[42]. However, from its β-galactosidase level in a *crp*$^+$ background (304 units), it is clear that *lacL271* is a different nucleotide substitution from either *lacL8* or *lacL29* (93 and 109 units, respectively). Our results in Table 2 substantiate this point.

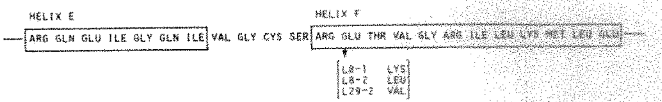
HELIX E
HELIX F
ARG GLN GLU ILE GLY GLN ILE VAL GLY CYS SER ARG GLU THR VAL GLY ARG ILE LEU LYS MET LEU GLU
L8-1 LYS
L8-2 LEU
L29-2 VAL

Fig. 4 Sequences of the *crp'* mutations. The amino acid sequence of CAP between residues 169 and 191 is illustrated[43,44], along with the amino acid substitutions in CAP'L8-1, CAP'L8-2 and CAP'L29-2, as deduced from the DNA sequences. All three mutations affect glutamic acid 181 (GAA) of CAP, substituting it by lysine (AAA), leucine (TTA) or valine (GTA). The positions of α-helices E and F in the crystallographic structure of CAP[17] are also indicated.

Mal$^-$ Ara$^-$ Rbs$^-$ Tna$^-$ Uhp$^-$ and GlpT$^-$, as assessed on indicator plates (Table 1). To quantify the effect on Lac expression in the two isolates, β-galactosidase assays were carried out. Table 1 shows that the two isolates exhibit 2.2 and 34 times the β-galactosidase level of the *lacL8 crp*$^+$ parent. Note that the β-galactosidase level in the *lacL8 crp'L8-2* isolate (3,200 units) actually exceeds that obtained in a *lac*$^+$ *crp*$^+$ strain (2,350 units, Table 2). This suggests that CAP'L8-2 may interact with the *lacL8* site equally or more tightly than wild-type CAP interacts with the *lac*$^+$ recognition site.

A selection identical in scale and protocol was carried out using the *lacL29* (refs 5, 6) mutation (Fig. 3). In this case, from ~18,000 phosphonomycin-resistant colonies, two Lac$^+$ colonies were isolated. One isolate was found to be Mal$^+$ Ara$^+$ Rbs$^+$ Tna$^+$ GlpT$^+$, and therefore was not characterized further. The other isolate, designated *crp'L29-2*, exhibited a pleiotropic Rbs$^-$ Tna$^-$ Uhp$^-$ GlpT$^-$ phenotype (Table 1). Table 1 shows that the *lacL29 crp'L29-2* isolate has 24 times the β-galactosidase level of the *lacL29 crp*$^+$ parent (a level comparable with that obtained in an isogenic *lac*$^+$ *crp*$^+$ strain).

Mapping and transfer to a phage vector

The phage λY1079 (λ *Bam*λ1° *srI*λ[1, 2]Δ cIts857 *int crp*$^+$; S. Adhya, personal communication) carries a 3.5-kilobase (kb) *Bam*HI insert containing the complete *crp* structural gene and promoter. Because λY1079 is *int*$^-$, it integrates into and excises from the chromosome only by homologous recombination within the 3.5-kb insert. We have used this property to demonstrate that the *crp'* mutations in fact map within *crp*. This was done in two ways.

In the first type of experiment, λ$^-$ recombinants ('cures') were selected from *crp'*/λY1079 lysogens by cultivation at 40 °C. For each *crp'* allele, approximately one-half of the cures were Rbs$^+$ (that is, *crp*$^+$), and inspection of 16 of these verified that all were also Lac$^-$. These data demonstrate that both the Lac$^+$ and Rbs$^-$ phenotypes of the three mutants are contained within the region defined by the 3.5-kb *crp* insert of λY1079.

In the second type of experiment, recombinant phage that carry *crp'* were isolated. This was accomplished by thermoinduction of *crp'*/λY1079 lysogens. The procedure gave rise to mixed lysates, each containing approximately equal numbers of λ*crp*$^+$ and λ*crp'*. It was possible to identify λ*crp'* either by plaque colour on a lawn of *lacL8* (or *lacL29*) cells on Lac-tetrazolium plates, or by inability to complement the Rbs$^-$ phenotype of *crp'L29-2*.

Effects on DNA sites

Table 2 presents the results of analyses with the *lac*$^+$ and three mutationally altered *lac* recognition sites. The striking result is that each CAP' interacts approximately equally well with *lacL8* and *lacL29*. Note from Fig. 3 that the base changes in *lacL8* and *lacL29* are symmetrically identical: each is a G → A substitution located 5 bp from the axis of 2-fold symmetry in the recognition site (that is, at base pairs 7 and 16)[6]. The ability of CAP′ to interact tightly with both the *lacL8* and *lacL29* sequences, but not with wild-type sequences (Table 1), indicates that the contact made by CAP to base pair 7 of the recognition site may be identical in detail to the contact it makes to the symmetrical position, base pair 16. The simplest interpretation of the data is that in the CAP–DNA complex the 2-fold axis of the CAP dimer is superimposed on the 2-fold axis of the recognition site (see ref. 9 for detailed discussion).

The control experiments which support this conclusion are presented in Table 2. Column 3 shows that each CAP′ interacts with *lacL271* even less effectively than does wild-type CAP. By both biochemical and genetic criteria, *lacL*271 is a mutation within the recognition site for CAP in *lac*, but is a different nucleotide substitution from either *lacL*8 or *lacL*29 (Fig. 3, legend). The inability of CAP′ to suppress the *lacL271* defect, despite its strong effects on *lacL8* and *lacL29*, is evidence for allele specificity. Thus, the data indicate that CAP′ alters, and does not merely relax, DNA sequence specificity.

Table 2, column 4, shows that each CAP′ is defective for interaction with the wild-type lac^+ sequence. In the case of CAP′L8-1, the quantitative defect for interaction with lac^+ is fivefold. CAP′L8–2 and CAP′L29-2 show a more modest defect, 1.3–1.5-fold, but these effects are reproducible. We point out that the *in vivo* concentration of CAP may approach or exceed the amount required to saturate the lac^+ site. Thus, our *in vivo* data may underestimate the actual defect in affinity of CAP′ for lac^+. The greater defect observed for the interaction of CAP′L8-2 and CAP′L29-2 with the rbs^+ site (7.5- and 2.5-fold; R.H.E. and J. Lopilato, unpublished data) is consistent with this possibility. A rigorous determination of this parameter must await measurement of the binding affinities *in vitro*. Such experiments are in progress.

CAP′ requires cyclic AMP

To assess *in vivo* the dependence of CAP′ on cyclic AMP, we have introduced a cya^- (adenylate cyclase) mutation into each *crp′* strain. Table 3 shows that, in each case, introduction of the cya^- mutation reduced β-galactosidase expression to the basal level of ~130 units. These data demonstrate that, like wild-type CAP, CAP′ requires cyclic AMP, which suggests that the *crp′* mutations alter only DNA sequence recognition, and not the binding of cyclic AMP to CAP or the cyclic AMP-mediated allosteric change.

Fine-structure mapping

To map more precisely the locations of the *crp′* mutations, we used a deletion mapping system, the details of which will be discussed elsewhere. Briefly, the system consists of 20 deletions generated by *Bal*31 (ref. 14) digestion, starting either at the *Hpa*I site located upstream of the *crp* promoter, or at the *Bcl*I site located within *crp* at the position corresponding to isoleucine 51. In addition to the deletions generated *in vitro*, the mapping experiments have also used a *lacZ* insertion–deletion mutation, *D2*, located at the 3′ end of the *crp* gene.

To map the mutations, spot crosses on Rbs-minimal plates were carried out between HfrG6 Δ*crp* strains and the three F^- *crp′* recipients. The data indicate that all three *crp′* mutations map to a single deletion interval within *crp*. This interval, defined by deletions *T22* and *D2*, corresponds to amino acids 122–192 of CAP.

DNA sequence analysis

The entire DNA nucleotide sequence of the region defined by deletions *T22* and *D2* was determined for each mutation. The source of DNA for this analysis was the 3.5-kb *Bam*HI *crp* fragment purified directly from high-titre stocks of λ*crp′*. The sequences were determined by the method of Maxam and Gilbert[15].

Remarkably, all three mutations affect the same codon of *crp*: GAA, corresponding to glutamic acid 181 of CAP (Fig. 4). The *crp′L8-1*, *crp′L8-2* and *crp′L29-2* mutations convert this codon to AAA (lysine), TTA (leucine) and GTA (valine), respectively. No other changes were detected in the appropriate deletion interval or up to 60 bp to either side. This result demonstrates that it is possible to alter the specificity of CAP by a single amino acid substitution. It indicates further that residue 181 is important in determining the specificity of CAP for lac^+ compared with *lacL8* or *lacL29*.

Table 1 Pleiotropic effects of *crp′*

Markers	Lac	Mal	Ara	Rbs	Tna	Uhp	GlpT
Δ*gal165 lacL8* crp^+	−(93)	+	+	+	+	+	+
Δ*gal165 lacL8 crp′L8-1*	+(209)	−	−	−	−	−	−
Δ*gal165 lacL8 crp′L8-2*	+(3,200)	−	−	−	−	−	−
Δ*gal165 lacL29* crp^+	−(108)	+	+	+	+	+	+
Δ*gal165 lacL29 crp′L29-2*	+(2,620)	+	+	−	−	−	−

+ Indicates wild-type phenotype as determined in plate tests; − indicates a defect in expression. The numbers in parentheses are induced β-galactosidase levels expressed in Miller units[32] and are the means of three independent determinations. For *crp′L8-2* and *crp′L29–2*, we have also determined β-galactoside levels in Δ*lac* strains containing a rbs^+–*lacZ* operon fusion (R.H.E. and J. Lopilato, unpublished data). The quantitative data verify that the *crp′* strains are defective for *rbs* expression (144 and 516 units, compared with 1,070 for crp^+).

Methods: Strains contained the Δ*gal165* mutation in order to avoid the complicating effects of *gal* expression, which is CAP-regulated[1,2], on the Lac phenotype. (Lactose is metabolized to glucose and galactose; therefore, in gal^+ strains, colour on Lac indicator plates reflects a composite of lactose and galactose metabolism.) Each strain also contained a thi^- mutation. Lac, Mal, Ara and Rbs phenotypes were assessed on tetrazolium[33] indicator plates; − indicates dark-red colour. Tna phenotype was determined in spot tests on tryptone media using Kovacs' reagent (ref. 34 and J. Felton, personal communication); − in this case refers to white colour. Uhp and GlpT phenotypes were determined by sensitivity to phosphonomycin (ref. 10) and GlpT was independently verified by growth on α-glycerophosphate. β-Galactosidase assays were carried out according to the method of Miller[32], using cells grown in the presence of 1 mM isopropyl-1-thio-β-D-galactoside (IPTG) and 3 mM thiamine.

Model building has previously implicated this region as being involved in DNA recognition. Figure 4 shows that amino acid 181 is the second residue of α-helix F of CAP. In the crystallographic structure of CAP, this helix protudes from the surface of each of the two subunits of the dimer, and is separated across the molecular 2-fold axis by 34 Å from the same helix of the other subunit[16,17]. These features led Steitz and co-workers to propose that helix F could interact with two successive major grooves of either left[16] or right-handed[18] B-DNA. In support of this analysis, is has been shown that the conformation of the 24 α-carbon atoms comprising helices E and F is similar to that of a helix-turn-helix motif contained in both cro and λ-repressor[19,20]. As in the case of CAP helix F, the second of the two α-helices in cro and repressor protrudes from the surface of the molecule, is separated from the same helix in the other subunit by 34 Å across the 2-fold axis, and therefore is a potential candidate to interact with base pairs in successive major grooves of DNA[21,22]. Furthermore, the amino acid sequences of the relevant regions show striking homologies in CAP, cro and repressor, and also in a variety of other prokaryotic DNA-binding proteins[23–25]. From these theoretical considerations, it has been proposed that the helix-turn-helix motif (helices E and F in CAP) is central to the sequence-specific interactions of CAP and other proteins to DNA. The sequences of our three mutations provide strong support for this hypothesis.

In addition, biochemical experiments support the idea that this part of CAP is important for interaction with DNA. Proteolysis by *Staphylococcus aureus* V8 protease removes amino acids 172–209 of CAP, while leaving the rest of the molecule intact[26,27] This treatment has been shown to destroy the DNA-binding activity of CAP, and has been interpreted to imply that amino acids 172–209 may participate in contacts to DNA.

Glutamic acid 181

We have demonstrated that substitution of glutamic acid 181 by lysine, leucine or valine alters the DNA sequence specificity

Table 2 Effects of CAP′ on wild-type and mutant recognition sites

Markers	*lacL8*	*lacL29*	*lacL271*	*lac*$^+$
crp$^+$	93	109	304	2,350
crp′L8-1	275	544	141	504
crp′L8-2	3,110	3,560	189	1,810
crp′L29-2	3,920	2,710	179	1,500

The data are β-galactosidase levels (means of four independent assays) determined as in Table 1. Strains were constructed in two steps. In step one, *lacL8*, *lacL29*, *lacL271* or *lac*$^+$ recipients were lysogenized with λY1079 *crp′* (see text). In step two, λ$^-$ cures were selected from the lysogens by cultivation at 40 °C. Rbs$^-$ (that is, *crp′*) cures were identified on Rbs–tetrazolium agar and were verified to be Uhp$^-$ GlpT$^-$, and where appropriate also Mal$^-$ and Ara$^-$. In addition to the markers indicated, the strains also contained *Δgal165* and *thi*.

Table 3 Dependence of CAP′ on cyclic AMP

Markers	*cya*$^+$	*Δcya854*
lacL8 crp′L8-1	196	132
lacL8 crp′L8-2	2,250	138
lacL29 crp′29-2	2,220	127

The data are the means of four assays of β-galactosidase (method in ref. 32). Cells for the assays were grown in media containing 1 mM IPTG, 3 mM thiamine, 0.5 mM isoleucine and 1.2 mM valine. *Δcya854*, a deletion of the gene for adenylate cyclase[35], was introduced into recipient strains from Table 2 by Pl co-transduction with *ilv*::Tn*5*. The tested strains also were *ilv*::Tn*5* *Δgal165 thi*.

of CAP. The mutationally altered proteins preferentially recognize A·T base pairs at positions 7 and 16 of the symmetrical recognition site, rather than G·C base pairs as is the case with wild-type CAP. The simplest explanation of these results is that amino acid 181, wild-type or mutant, is the side chain of CAP that makes direct contact with base pairs 7 and 16 in the recognition site. By this hypothesis, glutamic acid 181 makes hydrogen bonds to G·C base pairs, whereas lysine leucine and valine at this position selectively hydrogen bond or otherwise interact with A·T base pairs.

In principle, it is possible that the mutations instead could alter DNA sequence recognition through an indirect, conformationally transmitted effect. However, based on several lines of evidence, we consider this alternative hypothesis unlikely.

(1) All three *crp′* mutations affect the same residue of CAP (amino acid 181). This result implies that there is a limited number—possibly only one—of targets at which amino acid substitutions can confer this phenotype. It is difficult to reconcile this result with possible alterations in specificity due to conformational effects, particularly long-range effects, which one would expect on structural grounds to have multiple targets.

(2) In the crystallographic structure of CAP, the side chain of glutamic acid 181 is completely exposed to solvent (ref. 17 and T. Steitz and I. Weber, personal communication). Glutamic acid 181 is located in an α-helix that protrudes from the surface of the protein, and it interacts neither with neighbouring amino acid side chains nor with other parts of the peptide backbone. Model building suggests that the three mutant side chains would similarly be fully exposed. The absence of interactions between amino acid 181 and other CAP residues argues that the mutant side chains would not perturb either local or global CAP conformation (see refs 28, 29).

(3) Glutamic acid 181 in wild-type CAP is in an α-helix[17] (helix F; Fig. 4). By the assignments of Chou and Fasman[30], the mutant side chains lysine, leucine and valine exhibit a probability comparable with that of glutamic acid to maintain α-helical conformation. Thus, the identified mutations are unlikely to alter CAP conformation through peptide backbone effects. (Examples of amino acids that would not fulfil this criterion are proline and glycine.)

Therefore, we propose that the *crp′* mutations alter sequence specificity by substituting the amino acid of CAP that makes direct contact with base pairs 7 and 16 of the DNA site. This conclusion is consistent with previous model building[16,18] and biochemical[27] analyses (see preceding section) which indicate that amino acid 181 is in the region of CAP expected to make contacts with DNA. The implications of our results for the molecular basis of CAP–DNA recognition will be discussed in detail elsewhere[9].

Conclusion

We have devised a simple genetic approach that enables us to identify amino acids of CAP which are directly involved in making sequence-specific contacts with DNA. The advantage of this experiment is that it not only identifies these amino acids, but also correlates them to the specific base pairs within the recognition site with which they make contact.

The genetic techniques described here could be applied with only minor modifications to a variety of other prokaryotic or eukaryotic DNA-binding proteins. In fact, Youderian and co-workers have used a closely analogous approach to isolate a mutant of P22 Mnt protein with altered DNA-binding specificity[31].

We acknowledge S. Adhya for the gift of λY1079 before its publication. We thank M. Ptashne and his co-workers for critical discussion and encouragement, I. Weber and T. Steitz for discussion, unpublished data and comments on the manuscript, Ms. A. McIntosh for typing, and G. Cohen and A. Ullmann for their constant interest in this research. This work was supported by the NIH (GM13017), the CNRS (ATP-960-006, LA-270, GR-30), the Délégation Générale a la Recherche Scientifique et Technique (81-F-1202), the Institut National de la Santé et de la Recherche Médicale (81–1026) and the Ministère de l'Industrie et de la Recherche (584).

Received 15 February; accepted 27 June 1984.

1. Pastan, I. & Adhya, S. *Bact. Rev.* **40,** 527–551 (1976).
2. DeCrombrugghe, B., Busby, S. & Buc, H. *Science* **224,** 831–838 (1984).
3. Majors, J. thesis, Harvard Univ. (1975).
4. Simpson, R. *Nucleic Acids Res.* **8,** 759–766 (1980).
5. Beckwith, J., Grodzicker, T. & Arditti, R. *J. molec. Biol.* **69,** 115–160 (1972).
6. Dickson, R. *et al. J. molec. Biol.* **111,** 65–76 (1977).
7. Majors, J. *Nature* **256,** 672–674 (1975).
8. Kolb, A. *et al. EMBO J.* **2,** 217–222 (1983).
9. Ebright, R., Cossart, P., Gicquel-Sanzey, B. & Beckwith, J. *Proc. natn. Acad. Sci. U.S.A.* (in the press).
10. Alper, M. & Ames, B. *J. Bact.* **133,** 149–157 (1978).
11. Kolb, A. *et al. Nucleic Acids Res.* **11,** 7833–7852 (1983).
12. Kahan, F., Kahan, J., Cassidy, P. & Kropp, H. *Ann. N.Y. Acad. Sci.* **235,** 364–386 (1974).
13. Lederberg, J. *Genetics* **32,** 505–524 (1947).
14. Legerski, R., Hodnett, J. & Gray, H. *Nucleic Acids Res.* **5,** 1445–1463 (1978).
15. Maxam, A. & Gilbert, W. *Meth. Enzym.* **68,** 499–560 (1980).
16. McKay, D. & Steitz, T. *Nature* **290,** 744–749 (1981).
17. McKay, D., Weber, I. & Steitz, T. *J. biol. Chem.* **257,** 9518–9524 (1982).
18. Steitz, T., Weber, I. & Matthew, J. *Cold Spring Harb. Symp. quant. Biol.* **47,** 419–426 (1983).
19. Steitz, T. *et al. Proc. natn. Acad. Sci. U.S.A.* **79,** 3097–3100 (1982).
20. Ohlendorf, D. *et al. J. molec. Biol.* **169,** 757–769 (1983).
21. Anderson, W., Ohlendorf, D., Takeda, Y. & Matthews, B. *Nature* **290,** 754–758 (1981).
22. Pabo, C. & Lewis, M. *Nature* **298,** 443–447 (1982).
23. Anderson, W., Takeda, Y., Ohlendorf, D. & Matthews, B. *J. molec. Biol.* **159,** 745–751 (1982).
24. Sauer, R. *et al. Nature* **298,** 447–451 (1982).
25. Weber, I., McKay, D. & Steitz, T. *Nucleic Acids Res.* **10,** 5085–5102 (1982).
26. Eilen, E., Pampeno, C. & Krakow, J. *Biochemistry* **17,** 2469–2474 (1978).
27. Pampeno, C. & Krakow, J. *Fedn Proc.* **37,** 1830 (1978).
28. Perutz, M. & Lehmann, H. *Nature* **219,** 902–909 (1968).
29. Hecht, M., Nelson, H. & Sauer, R. *Proc. natn. Acad. Sci. U.S.A.* **80,** 2676–2680 (1983).
30. Chou, P. & Fasman, G. *Biochemistry* **13,** 222–245 (1974).
31. Youderian, P. *et al. Cell* **35,** 777–783 (1983).
32. Miller, J. *Experiments in Molecular Genetics* (Cold Spring Harbor Laboratory, New York, 1972).
33. Signer, E., Beckwith, J. & Brenner, S. *J. molec. Biol.* **14,** 153–166 (1965).
34. Kovacs, H. *Z. Immun.* **55,** 311–315 (1928).
35. Brickman, E., Soll, L. & Beckwith, J. *J. Bact.* **116,** 582–587 (1973).
36. Ebright, R. in *Molecular Structure and Biological Activity* (eds Griffen, J. & Duax, W.) 91–100 (Elsevier, New York, 1982).
37. Chapon, C. & Kolb, A. *J. Bact.* **156,** 1135–1143 (1983).
38. Stoner, C. & Schleif, R. *J. molec. Biol.* **171,** 369–381 (1983).
39. Deeley, M. & Yanofsky, C. *J. Bact.* **151,** 942–951 (1982).
40. Friden, D., Newman, T. & Freundlich, M. *Proc. natn. Acad. Sci. U.S.A.* **79,** 6156–6160 (1980).
41. Aiba, H. *Cell* **32,** 141–149 (1983).
42. Hopkins, J. *J. molec. Biol.* **87,** 715–724 (1974).
43. Aiba, H., Fujimoto, S. & Ozaki, N. *Nucleic Acids Res.* **10,** 1345–1362 (1982).
44. Cossart, P. & Gicquel-Sanzey, B. *Nucleic Acids Res.* **10,** 1363–1378 (1982).

Molecular hydrogen jets from the Orion nebula

K. N. R. Taylor*, J. W. V. Storey*, G. Sandell†, P. M. Williams‡ & W. J. Zealey§

* Optical Science and Technology, University of New South Wales, Kensington, 2033 Australia
† Astrophysics Laboratory, University of Helsinki, Helsinki 13, Finland
‡ United Kingdom Infrared Telescope Unit, 900 Leilani Street, Hilo, Hawaii 96720, USA
§ Royal Observatory, Blackford Hill, Edinburgh EH9 3HJ, UK

The environs of interstellar space in which star formation takes place involve high-velocity gas flows. Channelled by embryonic dust toroids, these gas flows culminate in energy-losing shock processes at the interface with the ambient interstellar cloud. The excitation of molecular hydrogen transitions in this gas provides one means of observing these shocked regions and their relation to the well-known indicators of star formation such as the Herbig Haro objects and T Tauri stars. In an attempt to understand the relationship of the recently discovered complex of Herbig Haro objects in Orion[1] to the IR sources in this region, we have carried out a survey of the molecular hydrogen S(1) line distribution. These observations have led to the discovery of a previously unsuspected structure of finger-like filaments of H_2 emission extending radially outwards from a common centre at IRC9.

This survey was carried out using the Anglo-Australian Telescope in conjunction with the IR photometer and spectrometer. Areas of the sky were observed by scanning the telescope in a raster pattern, using the imaging mode with an aperture of 2 arc s diameter and a scan interval (1 pixel) of 1 arc s. The circular variable filter (CVF, resolution 100) was set to the wavelength of the peak of the S(1) transition at 2.12 μm. A total integration time per pixel of 0.2 s produced a limiting detectable flux (3σ level) at S(1) of $\sim 10^{-13}$ erg cm^{-2} s^{-1}. The images obtained in this manner indicate the distribution of the net emission at this wavelength arising from both the continuum and S(1) radiation. A subsequent image at a continuum wavelength (2.09 μm), or at worst a series of spectra taken at strategic positions in the object, can then be used to derive the molcular hydrogen distribution.

Two 100-arc s square images of Orion were obtained, centred on the BN object. One of these was obtained in the S(1) line wavelength and the other was taken to provide a map of the continuum emission. Further images were obtained at 2.12 μm at locations to the north of the BN object (one 100 × 100 arc s centred 90″N, 15″W and a second 64 × 64 arc s centred 72″N, 68″E). Time limitations prevented us from obtaining a continuum map at these new locations; however, we were able to obtain several spectra in the brighter H_2 knots to establish the local S(1) line-to-continuum intensity ratio at these points and also a broad K-band image of the 64-arc s square region. The seeing at the time of these observations was ~1 arc s and our observations resulted in the highest spatial resolution map of H_2 yet obtained for this complex.

The combined images at 2.12 μm taken from the computer graphics display are shown in Fig. 1. Regions of significant continuum emission (2.09 μm) in the southern section are shown. The localized emission sources at 2.12 μm which do not appear on the continuum map are emphasized. In addition, the locations of the known Herbig Haros are indicated. Finally, the positions at which spectra in the 2-μm band were obtained are also shown. The spectra themselves are given in Fig. 2, fluxed with respect to the star BS2007 which was used as a standard[2].

Two immediately striking features are evident from Fig. 1: first, the large spatial extent over which a complex distribution

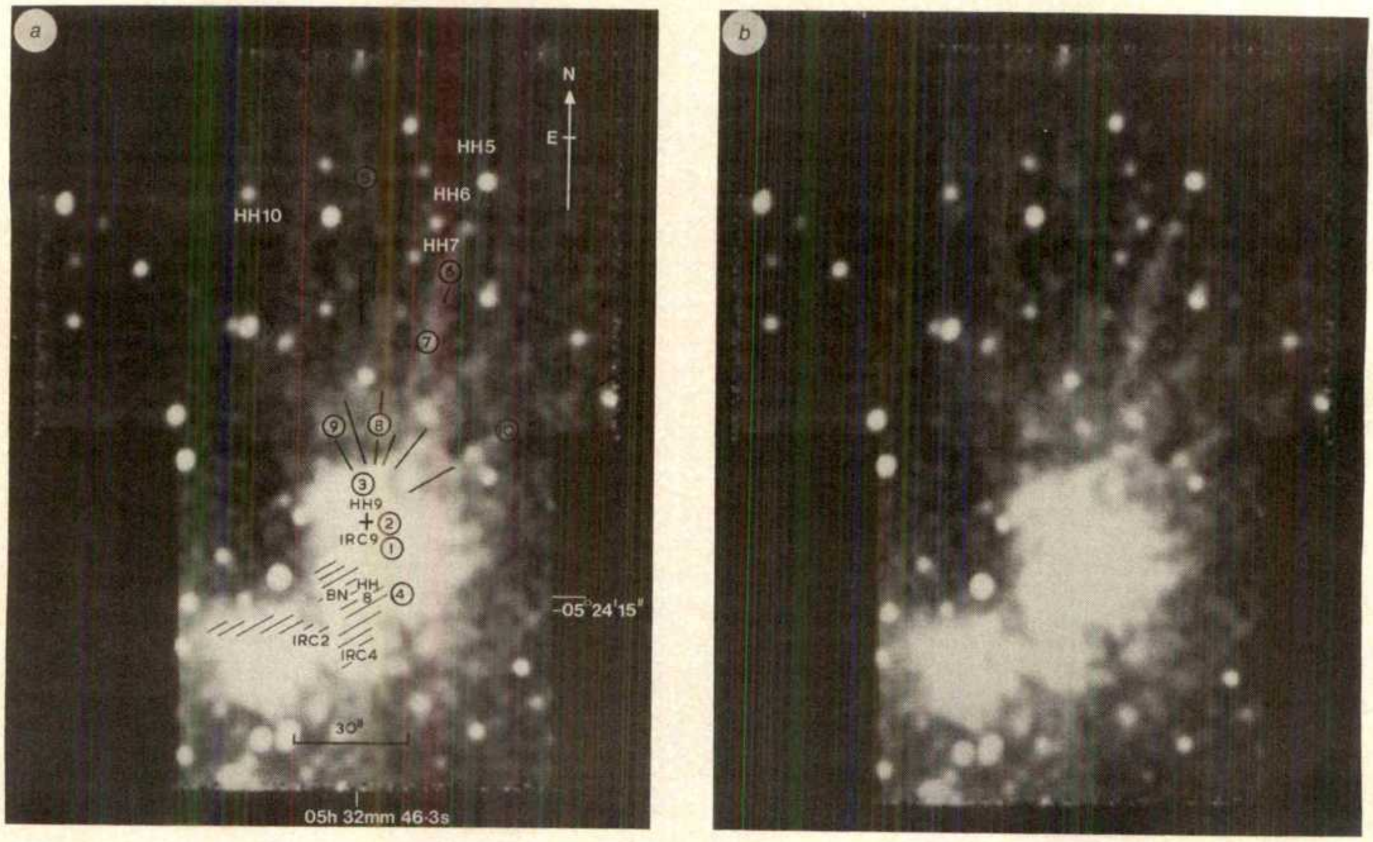

Fig. 1 Photographs of the computer graphics display of a montage of the three images of the molecular hydrogen distribution. The image has been smoothed over five pixels and the display levels have been set to emphasize the low-intensity jet region of the final picture. *a* is annotated, while *b* is untouched to avoid biasing the apparent orientation of the jets. Scale bar, 30 arc s. Regions of significant extended continuum emission are shown hatched. The locations of the Herbig Haro objects HH5, 6, 7, 8, 9 and 10 in M42 are shown along with the sources IRC1, 4 and 9. The positions at which the 2–2.5 μm spectra were obtained are shown by a circled number.

appears at 2.12 μm, which is not, however, evident in the continuum map and second, and more importantly, the appearance of the long fingerlike structures extending radially outwards from the main body of molecular hydrogen.

Although an understanding of the detailed nature of the overall H_2 distribution is of considerable importance to our knowledge of this region, below we only concentrate on the previously unknown, and unsuspected, jet-like structures. That at least a significant fraction of the total emission in these jets arises from the S(1) transition is evident from the spectra of Fig. 2.

While the Orion region is experiencing a bipolar outflow of material[3–7], it has previously been assumed that the envelope of this flow is in the form of a smooth, continuous, bubble. In view of our observations this can only be a broad generalization of the real structure, and there are several explanations for the jet-like structures of Fig. 1. We suggest four below:

(1) The formation of the expanding bipolar bubble by the stellar winds from the central object has resulted in considerable structure on the inner face. Because of the internal dynamics, such structure can take the form of channels initiated by local density fluctuations in the cloud. The outflowing hot gas then illuminates this structure as it strikes the interface. Such a model would require the outer limits of the bipolar flow to extend beyond the limits thought (K. Taylor and D. Axon) to include the Herbig Haro objects M42 HH5, 6, 7 and M42 HH10[1].

(2) The fingers are hot, dense gas breaking through weaker regions of the outer cool material and extending into jets as it penetrates the ambient cloud.

(3) In agreement with the 'interstellar bullet' model of Herbig Haro formation[8–10], small dense clumps of the interstellar medium have been accelerated by the wind from the central star and are now leaving trails of shock-excited molecular hydrogen in their wake.

(4) The structures represent local enhancements in the dust density and the molecular hydrogen is seen by reflection of the emission from the core of the molecular cloud.

In each case, the emission is due to shock excitation rather than UV photoexcitation of the molecular hydrogen, consistent with the observed ratios of the $v = 1$ and $v = 2$ S(1) lines[5].

One feature then remains to be considered. If the lines of the jets of Fig. 1 are extended backwards into the molecular cloud they appear to intersect at IRC9 rather than at IRC2. This is significant, as IRC2 is believed to lie at, or near to, the origin of the bipolar outflow[6]. The possible role of IRC9 in this phenomenon requires further study, a conclusion supported independently by the work of Beck[11].

Furthermore, high-velocity resolution spectra are now needed to allow us to distinguish between the models proposed for those jets, and corresponding searches for similar structures are needed to establish whether this is a general feature of bipolar outflows in star forming regions. Similarly, observations of other molecules normally associated with shocked molecular hydrogen could reveal the ambient conditions of density and temperature at the jets. Finally, a relation between the jets and the Herbig Haro objects M42 HH5, 6 and 7 seems likely and could be verified by measurement of the Doppler-shifted velocities of the S(1) and nebular emission lines.

We thank the Australian Time Allocation Committee for awarding time on the telescope and members of the observatory for their valuable assistance. We also thank David Allen for encouragment, and a referee for drawing our attention to the preprint by Beck (1984) dealing with the object IRC9.

Received 18 April; accepted 3 July 1984.

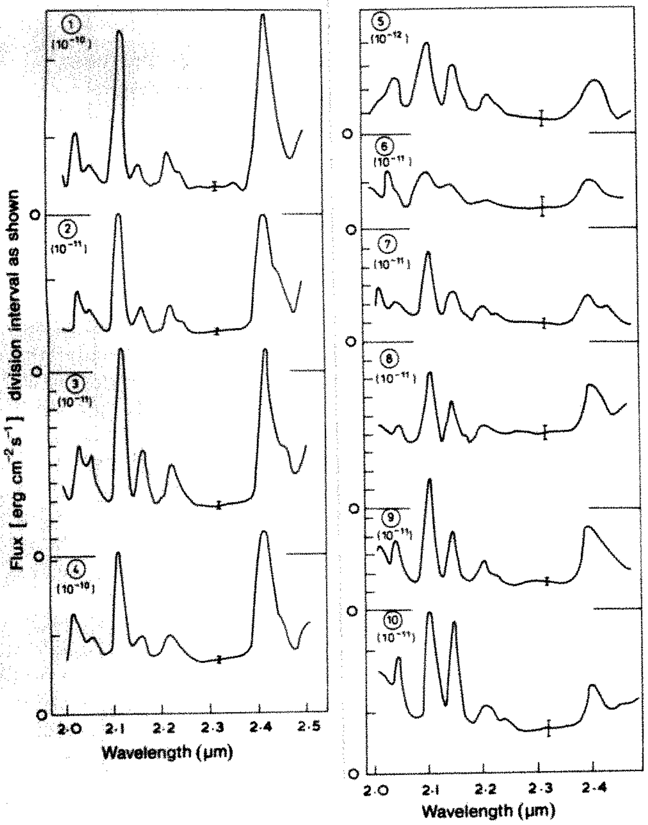

Fig. 2 The 2–2.5 μm spectra taken at the various points shown in Fig. 1. Spectra 1–4 were taken within the extended molecular cloud while spectra 5–10 were observed in the vicinity of the molecular hydrogen jets. The apparently anomalous Q branch to S(1) line ratio almost certainly arises because of rapid fluctuations in the atmospheric absorption which lead to incomplete cancellation when ratioing to the standard star. The 3σ levels are indicated in the continuum region of each curve.

1. Taylor, K. & Axon, D. *Mon. Not. R. astr. Soc.* **207**, 241–261 (1984).
2. Allen, D. A. & Cragg, T. A. *Mon. Not. R. astr. Soc.* **203**, 777–783 (1983).
3. Wright, M. C. H., Plambeck, R. L., Vogel, S. N., Ho, P. T. P. & Welch, W. J. *Astrophys. J. Lett.* **267**, L41–L45 (1983).
4. Nadeau, D., Geballe, T. R. & Neugebauer, G. *Astrophys. J.* **253**, 154–166 (1982).
5. Scoville, N. Z., Hall, D. N. B. Kleinmann, S. G. & Ridgway, S. T. *Astrophys. J.* **253**, 136–148 (1982).
6. Beckwith, S., Persson, S. E., Neugebauer, G. & Becklin, E. E. *Astrophys. J.* **223**, 464–460 (1978).
7. Downes, D., Genzel, R., Becklin, E. E. & Wynn-Williams, C. G. *Astrophys. J.* **244**, 869–883 (1981).
8. Norman, C. & Silk, J. *Astrophys. J.* **228**, 197–205 (1979).
9. Rodriguez, L. F., Moran, J. J., Ho, P. T. P. & Gottlieb, E. W. *Astrophys. J.* **235**, 845–865 (1980).
10. Tenario-Tagle, G. & Rozyczka, M. *Rev. Mex. Astr. Astr.* **7**, 124–125 (1983).
11. Beck, S. C. *Astrophys. J.* (in the press).

IR observations of the peculiar galaxy Arp220

J. P. Emerson*, P. E. Clegg*, G. Gee*,
C. T. Cunningham†, M. J. Griffin*,
L. M. J. Brown‡, E. I. Robson‡, A. J. Longmore§

* Department of Physics, Queen Mary College, Mile End Road,
London E1 4NS, UK
† Rutherford Appleton Laboratory, Chilton, Didcot,
Oxon OX11 0QX, UK
‡ Division of Physics and Astronomy, Preston Polytechnic,
Corporation Street, Preston PR1 2TQ, UK
§ United Kingdom Infrared Telescope, 900 Leilani Street, Hilo,
Hawaii 96720, USA

Observations from IRAS (the Infrared Astronomical Satellite) have shown that the peculiar galaxy Arp220 (=IC4553) has extreme IR properties[1]. Its IR luminosity is 100 times greater than normal spirals and nearly equals that of the most luminous Seyfert known, Mkn231. Its optical appearance suggests that it is either

a recent merger or that it has a prominent central dust lane. Soifer *et al.*[1] have discussed whether a starburst or a Seyfert nucleus can better explain their observations. We report here 20-, 350- and 760-μm observations which constrain the mass and size of the emitting region and compare Arp220 with the archetypal starburst galaxy M82.

The submillimetre observations were made with the United Kingdom Infrared Telescope on 1 May, and the 20-μm observations on 3 June 1984. At 350 μm we find 8.7 ± 1.2 Jy in a 55 arc s beam and at 760 μm a 3 σ upper limit of 3.2 Jy in a 58-arc s beam. The total uncertainty in the 350-μm flux density, including the calibration as well as statistical uncertainties, is 1.9 Jy. The beam sizes used should contain all the submillimetre flux from Arp220 whose size was determined by IRAS as < 25 arc s (ref. 1). At 20 μm we find 1.7 ± 0.2 Jy in a 4-arc s beam, and no significant flux in adjacent 4-arc s beams.

Figure 1 shows the measured submillimetre and IRAS[1] flux densities fitted, except at 12 μm, with a thermal dust spectrum; the absorption coefficient of the dust was taken to vary as frequency squared, which is appropriate for those wavelengths beyond which the source is found to be optically thin[2]. (We did not fit the IRAS 12-μm point because its colour correction[3] is strongly temperature dependent at these low temperatures.) With 1 d.f. the value of χ^2 was 1. The fit yields a value of 61 K for the temperature parameter and a solid angle filled by the source of 3.8×10^{-11} sr. The optical depth is 1 at 180 μm and 0.26 at 350 μm. The IR luminosity is $2 \times 10^{12} L_\odot$ assuming a distance of 90 Mpc (ref. 1).

Assuming that the properties of dust, and the gas-to-dust ratio, are the same in Arp220 as summarized by Hildebrand for the Galaxy[2], our model fit determines the mass of gas in the IR emitting region to be $7 \times 10^9 M_\odot$. Bearing in mind the uncertainties in the properties of the dust, we believe this estimate to be accurate to within a factor of two. Presumably most of this gas is in molecular form.

A lower limit to the size of the emitting region is set by assuming that the observed solid angle is that subtended by a single spherical lump of material; this gives a diameter of 1.4 arc s. Our 20-μm flux density measured in a 4-arc s beam is consistent with extrapolation of our fit to the IRAS 25-μm flux density measured with a much larger beam, and our 20-μm mapping shows no evidence for significant 20-μm flux outside one 4-arc s beam diameter. We conclude, therefore, that the emitting region is between 0.6 and 1.7 kpc in diameter, giving a molecular gas density of between 1×10^2 and 2×10^3 nucleons cm^{-1}.

At the density and temperature deduced for the cloud we would expect star formation to take place. The suggested presence of many OH masers[4] is consistent with this idea. It is interesting to compare Arp220 with the starburst galaxy M82 (ref. 5), whose luminosity is $3 \times 10^{10} L_\odot$ and whose spectrum[6] is similar to many H II region/molecular cloud complexes in our Galaxy. The spectra of the two galaxies are very similar at long wavelengths but at shorter wavelengths the much greater optical depth of A220 is apparent (Fig. 1). The luminosity per nucleon for Arp220 of 9×10^{-29} W per nucleon is similar to the value of 7×10^{-29} W per nucleon in M82 (ref. 7). The ratio of the 6-cm radio flux density (which is a measure of supernova formation and Lyman continuum photon production rates) to the 100-μm flux density is also similar for the two galaxies[1]. It is, therefore, tempting to interpret the IR luminosity of Arp220 as arising from a starburst involving the order of 100 times as much material as that in M82. The equally high IR luminosity of the galaxy NGC6240 has been interpreted as an interaction-induced starburst[8].

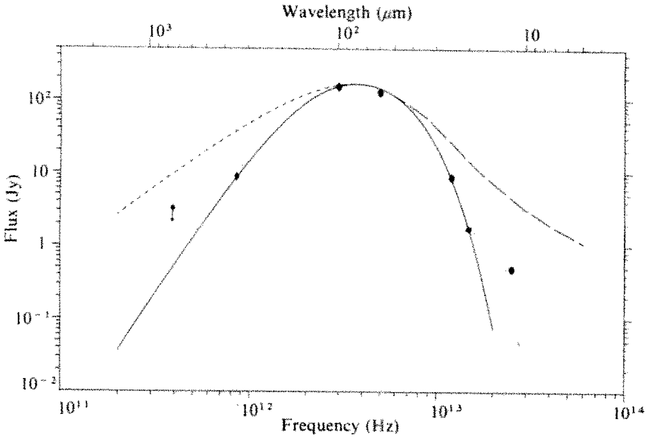

Fig. 1 The IR spectrum of Arp220. Data from: ◆, this paper; ● IRAS flux densities. Solid curve, model fit (see text). Short dashed curve, extrapolation of a 61-K black body. Long dashed curve, short-wavelength spectrum of M82 normalized to 60-μm flux denisty of Arp220.

We thank the SERC's PATT for the allocation of observing time. G.G. and L.M.J.B. acknowledge research studentships and M.J.G. a research assistantship from SERC.

Received 4 June; accepted 16 July 1984.

1. Soifer, B. T. *et al. Astrophys. J.* (in the press).
2. Hildebrand, R. H. *Q. J. R. astr. Soc.* **24,** 267–282 (1983).
3. Neugebauer, G., *et al Astrophys. J. Lett.* **278,** L1–L6 (1984).
4. Baan, W. A., Wood, P. A. D. & Haschick, A. D. *Astrophys. J. Lett.* **260,** L49–L52 (1982).
5. Rieke, G. H., Lebofsky, M. J., Thompson, R. I., Low, F. J. & Tokunaga, A. T. *Astrophys. J.* **238,** 24–40 (1980).
6. Telesco, C. M. & Harper, D. A. *Astrophys. J.* **235,** 392–404 (1980).
7. Stein, W. A. & Soifer, B. T. *A. Rev. Astr. Astrophys.* **21,** 177–207 (1983).
8. Wright, G. S., Joseph, R. D. & Meikle, W. P. S. *Nature* **309,** 430–431 (1984).

Accurate atomic positions from electron microscopy

Sven Hovmöller*, Agneta Sjögren*, George Farrants*, Margareta Sundberg† & Bengt-Olov Marinder†

* Department of Structural Chemistry, and † Department of Inorganic Chemistry, Arrhenius Laboratory, University of Stockholm, S-106 91 Stockholm, Sweden

Modern electron microscopes have resolutions in the range 1.8–2.4 Å which is, in principle, sufficient for structure determination at atomic resolution. High-resolution electron microscopy (HREM) has been widely used for studies of inorganic materials[1], and computerized image processing of electron micrographs has been used for structure determinations of biological macromolecules[2,3]. Klug[4] suggested that image processing could also be applied to electron micrographs of inorganic crystals. By combining the two powerful methods, HREM and computerized image processing, we have determined atomic coordinates (in projection) of metal atoms in a thin inorganic crystal, to an accuracy of 0.1 Å. This high accuracy is mainly due to the noise reduction achieved through averaging over many identical unit cells.

A sample with composition $K_{8-x}Nb_{16-x}W_{12+x}O_{80}$ (where $x \sim 1$) was ground to a fine powder and dispersed in *n*-butanol. A drop of this suspension was collected on a holey carbon film supported by a copper grid and examined in a JEOL JEM 200CX/THG 2 electron microscope equipped with a top entry ultrahigh resolution goniometer and operated at 200 kV. HREM[1] was used to examine a crystal with a very thin edge. The crystal was oriented so that the short unit cell axis was parallel to the electron beam by using the criterion that the electron diffraction pattern should be symmetrical (Fig. 1*a*). In this way, the two longer unit cell axes were both in the plane of projection. Several HREM images were recorded at different defocus values.

The electron micrographs were analysed by eye and in an optical diffractometer equipped with a laser. The diffraction Hpattern of the micrograph is seen in the back focal plane of the objective lens of an optical diffractometer and can be used

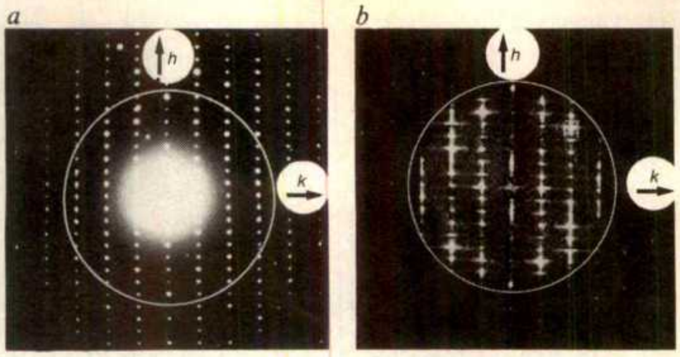

Fig. 1 Diffraction patterns from $K_{8-x}Nb_{16-x}W_{12+x}O_{80}$. Reflections with k odd are systematically absent. The fine rings correspond to 2.4-Å resolution. *a*, Electron diffraction of the microcrystal, a small part of which is shown in Fig. 2. *b*, Amplitude part of the diffraction pattern calculated by computer as the Fourier transform of the digitized electron micrograph. The picture has been photographed from the computer graphics screen. The contrast transfer function is visualized in the background noise. The boxed area is shown in greater detail in Fig. 3*a*.

to evaluate quantitatively the quality of the micrograph. The level of defocus can be determined by the positions of the nodes of the contrast transfer function, which are seen as dark rings in the pattern[5]. The shape of the rings shows the presence or absence of astigmatism in the picture—a non-astigmatic picture will have circular rings, an astigmatic picture will have elliptical rings. The micrographs taken at different defocus values were examined in the optical diffractometer, and one which had been taken very close to Scherzer focus was selected for further analysis. In this micrograph the first node occurred at 2.4 Å resolution.

The contrast in a HREM image, taken at optimum defocus (Scherzer focus), of a properly oriented crystal thin enough to approximate to a phase object, may be directly interpreted in terms of the local projected structure of the crystal[6]. In these conditions, the black features in the micrograph (Fig. 2) represent scattering atoms. This has been verified by computed crystal structure images of the model in Fig. 4*b*. Good agreement was obtained between observed (Fig. 2) and calculated images at a defocus of −633 Å (Scherzer focus) and a crystal thickness of $5\times3.9\sim20$ Å (ref. 7).

The thin area of the crystal showed both a constant local average optical density and a constant optical diffraction pattern, indicating that variations in thickness, structure and orientation were very small in the processed region. These conditions are necessary for applying our method. An area corresponding to 90 unit cells was digitized using a Joyce-Loebl Microdensitometer 6. A raster size of 50×50 μm was used and 256×256 points were scanned. At a magnification of 690,000 times, this corresponds to a sampling interval of 0.72×0.72 Å^2. Such sampling preserves the details of the structure to at least 2.0 Å resolution. The information in the electron micrograph, present as a variation in optical density, was transferred in digital form to a VAX 11/750 computer.

The Fourier transform of the digitized image was calculated. The digital transform is closely related to the analogue optical diffraction pattern. If the optical diffraction pattern is recorded on photographic film, the phase information is lost, whereas the calculated diffraction pattern contains both the amplitude and the phase information of each diffraction point. The amplitude part of the complex numbers of the Fourier transform was displayed on a Digital VS11 raster graphics system (Fig. 1*b*), and the lattice indexed with the aid of a cursor. The diffraction spots were very sharp, and the phases constant over the whole spot (Fig. 3). Lattice parameters were refined from accurate positions of 12 strong diffraction spots. The cell parameters obtained were $a=22.1+/-0.3$ Å, $b=17.8+/-0.3$ Å, $\gamma=89.9+/-0.4°$. The amplitudes and phases for all 47 reflections in the unique half of the diffraction pattern within a resolution of 2.4 Å were obtained automatically by computer. Amplitudes were calculated by integrating over the 3×3 points closest to the predicted position of the lattice point in the Fourier transform followed by subtraction of the local background, and the phases were taken as the phase value of that point in the Fourier transform which was closest to the predicted lattice point. The accuracy of this method was evaluated by comparing the amplitudes and phases from two scans of the same area of the micrograph, one scanned in a direction parallel to the crystal axes, and the other along the diagonal of the unit cell. The two sets of amplitudes and phases were virtually identical.

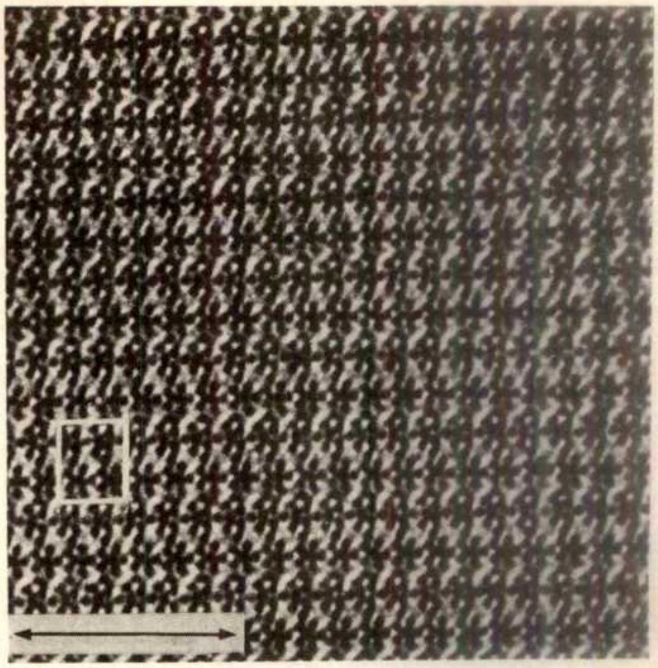

Fig. 2 Electron micrograph of a thin crystal of $K_{8-x}Nb_{16-x}W_{12+x}O_{80}$, projected over a hole in the carbon film. The defocus was about −630 Å. The area shown is the one used for computerized image processing. Atoms appear dark in the picture, and the pentagonal arrangements are clearly visible. One unit cell is indicated. Scale bar, 50 Å. Magnification, $\times4.6\times10^6$.

For the method to be valid, the specimen in the microscope should behave as a weak phase object—a first-order (kinematical) approximation must be sufficiently accurate to describe the image formation process, and the second-order (dynamical) effects should be small. When this condition is satisfied the product of each Fourier component with the zero-order term ($F(000)$) will be much greater than the products of the Fourier terms with each other.

The validity of this assumption was examined using the method described by Erickson and Klug[8]. The difference

Table 1 Atomic coordinates for the heavy metal atoms (Me) in $K_{8-x}Nb_{16-x}W_{12+x}O_{80}$ as determined by electron microscopy and image processing, and in $Na_7Nb_{15}W_{13}O_{80}$ as determined by X-ray diffraction[10]

	Fractional atomic coordinates					
	Electron microscopy		X-ray diffraction		Difference EM/X-ray	
Atom	x/a	y/b	x/a	y/b	x/a	y/b
Me(1)	0.1069	0.4077	0.1060	0.4137	0.0009	0.0060
Me(2)	0.1578	0.2014	0.1616	0.2059	0.0038	0.0045
Me(3)	0	1/4	0	1/4	—	—
Me(4)	1/4	0.3588	1/4	0.3508	—	0.0080
Me(5)	1/4	0.0364	1/4	0.0338	—	0.0026

The unit cell dimensions obtained from electron microscopy are $a=22.1$ Å, $b=17.8$ Å, while those determined from X-ray diffraction are $a=21.963$ Å, $b=17.763$ Å.

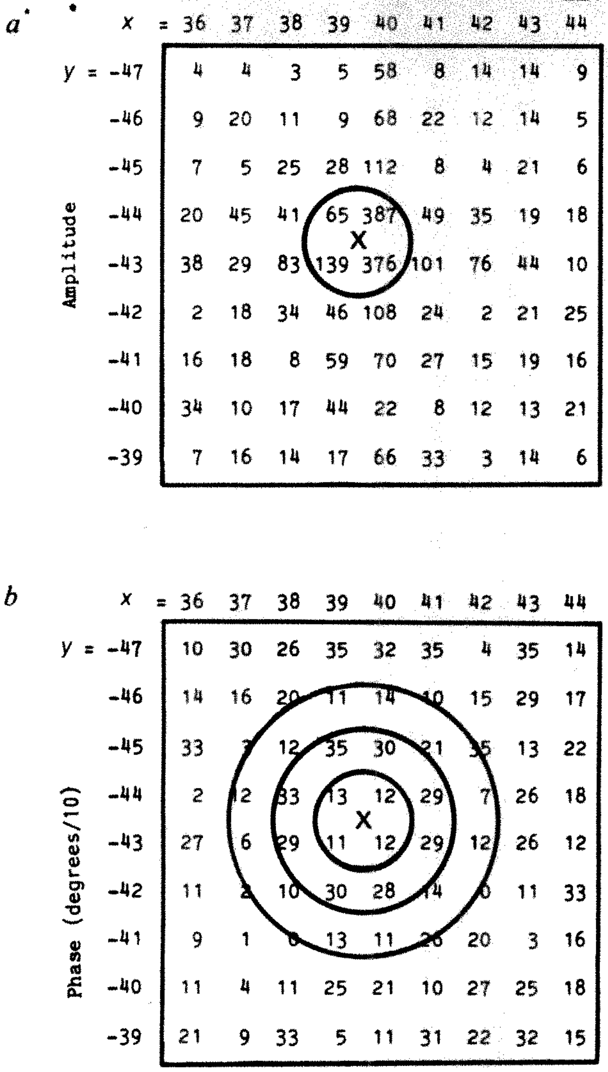
a
Amplitude
X
b
Phase (degrees/10)
X

a

	x = 36	37	38	39	40	41	42	43	44
y = −47	4	4	3	5	58	8	14	14	9
−46	9	20	11	9	68	22	12	14	5
−45	7	5	25	28	112	8	4	21	6
−44	20	45	41	65	387	49	35	19	18
−43	38	29	83	139	376	101	76	44	10
−42	2	18	34	46	108	24	2	21	25
−41	16	18	8	59	70	27	15	19	16
−40	34	10	17	44	22	8	12	13	21
−39	7	16	14	17	66	33	3	14	6

b

	x = 36	37	38	39	40	41	42	43	44
y = −47	10	30	26	35	32	35	4	35	14
−46	14	16	20	11	14	10	15	29	17
−45	33	[illegible]	12	35	30	21	35	13	22
−44	2	12	33	13	12	29	7	26	18
−43	27	6	29	11	12	29	12	26	12
−42	11	2	10	30	28	14	0	11	33
−41	9	1	0	13	11	26	20	3	16
−40	11	4	11	25	21	10	27	25	18
−39	21	9	33	5	11	31	22	32	15

Fig. 3 Extract from the Fourier transform around one diffraction point ($h=5$, $k=4$). This area corresponds to the boxed area in Fig. 1*b*. *a*, Amplitude part, scaled such that the $F(000)$ term has a magnitude of 20,000. *b*, Phase part relative to an arbitrary phase origin, given as (phase in degrees)/10. The predicted position of the lattice point ($X=39.77$, $Y=-43.41$) falls between four sampling points of the Fourier transform. The amplitude is spread over these four sample points, and the phase is constant over the whole diffraction point. The theoretical shape of the diffraction point is a $\sin(x)/x$ function for a perfect single crystal. Deviations from this shape show lack of order in the crystal lattice. It can be seen that the $\sin(x)/x$ behaviour is accurately followed, with the phase changing by 180° in a series of rings around the central maximum. The period of x is two transform units.

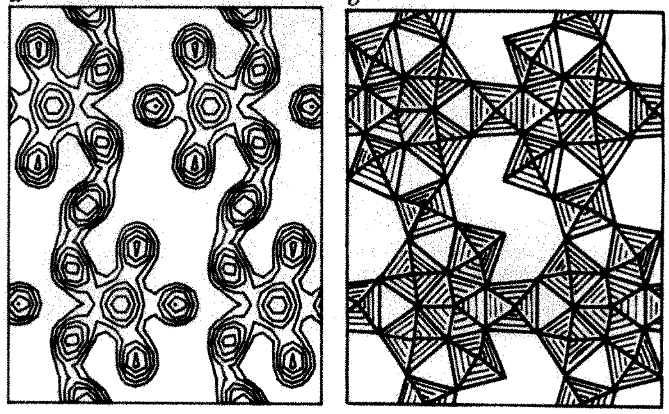

Fig. 4 *a*, Contour map of $K_{8-x}Nb_{16-x}W_{12+x}O_{80}$ after averaging over the 90 unit cells digitized from the electron micrograph, and over the four asymmetric units in the unit cell. One unit cell is shown. The density map was contoured at nine equidistant levels. The five contour levels corresponding to the highest density are shown. The MeO_7 bipyramids and MeO_6 octahedra are seen as circular features of high density. Scale 5 mm per Å. *b*, Model of $Na_7Nb_{15}W_{13}O_{80}$ determined from X-ray diffraction. The MeO_7 bipyramids and MeO_6 octahedra are drawn such that the heavy metal atoms are at the centre of each bipyramid and octahedron. The sodium atoms are not shown. Scale 5 mm per Å.

between the average optical density of the thin area used for reconstruction and the average optical density of the background was used to place the magnitudes of the Fourier components on a scale relative to an $F(000)$ term of 1.00. The strongest reflection is then the (3, −4) with a magnitude of 0.084. The strongest second-order diffraction effect would then be the interaction of this reflection (and equivalent reflections), with a magnitude of $0.084\times0.084=0.0071$. This value is small when one takes into account the fact that 28 out of the 47 reflections had magnitudes greater than 0.01. Thus, any second-order interaction will be small compared with the first-order interactions, and the weak phase object approximation is valid.

The symmetry of the crystal is orthorhombic, space group *Pmab* (no. 57 in ref. 9), as determined from electron diffraction patterns of the three orthogonal views (h, k, 0), (h, 0, l), (0, k, l). Very weak reflections indicating a doubling of the c-axis were observed, but since the processed image represented the projected atomic structure along the c axis, these reflections are unobserved and have no effect on the image processing. Thus, we use here the space group appropriate for the basic structure. In this space group, there is a two-fold axis parallel to the c-axis, a mirror plane perpendicular to a, and 2_1 screw axes parallel to the a and b axes. The effects of these symmetry elements on the amplitudes and phases of the diffraction points are the following: the amplitudes show *mm* symmetry, that is, $|F(hk0)|=|F(\bar{h}k0)|=|F(h\bar{k}0)|=|F(\bar{h}\bar{k}0)|$, all phases are centric with phases of 0° or 180°, $(hk0)$-reflections with k odd and $(h00)$-reflections with h odd are systematically absent, and the phases of the reflections $(hk0)$ and $(\bar{h}k0)$ are equal if h is even, and differ by 180° if h is odd.

The presence of a two-fold axis along c was investigated quantitatively by examining the phase residual between the observed phases and centric values. The phase residual, R, was calculated as:

$$R=\frac{\sum_i w_i\phi_i \ (\mathrm{mod}\ 180)}{\sum_i w_i}$$

where, for i reflections, w_i is a weighting factor (here set to be equal to the amplitude of the reflection), and ϕ_i is the observed phase of the reflection. When the origin of the unit cell is positioned exactly on a two-fold axis, all the reflections have phases of 0° or 180°. The arbitrary origin which comes from the starting position of the densitometer is unlikely to correspond to this two-fold axis, and the observed phases will then take on arbitrary values between 0° and 360°. A computer program moves the position of the origin stepwise along both a and b to a total of 120 × 120 evenly spaced points within the unit cell. For each of these positions, the deviation from the nearest of 0° or 180° is calculated for all reflections. The phase residual is printed out in the form of a map, and the position of the lowest residual is found. For this crystal the lowest phase residual was 17°, which should be compared with the average residual of 45° for positions other than the two-fold axes. The origin of the unit cell was shifted to coincide with this two-fold axis, and the phases of all reflections were recalculated relative to this origin, by applying proper phase shifts to the reflections.

Before calculating the final map, the space group symmetry, determined as outlined above, was imposed. Imperfections in the imaging process, noise in the electron micrograph and deviations from the exact crystallographic orientation with the electron beam going along c, cause the experimentally-determined amplitudes and phases to deviate from the symmetry-constrained values. The phases of all reflections with experimentally-determined phases in the range −90° to +90° were set to 0°; otherwise the phases were set to 180°. Approximate *mm* symmetry was made exact by averaging the amplitudes of the two symmetry related observations of a reflection ($h, k, 0$) and ($h, \bar{k}, 0$). The final map of the unit cell was obtained by calculating the inverse Fourier transform of the symmetry averaged centrosymmetric set of structure factors.

The map was calculated on a grid of 32×32 points along the unit cell edge and contoured at nine equidistant levels. The five contour levels corresponding to the highest scattering potential are shown in Fig. 4*a*. All 28 heavy metal atoms in the unit cell are clearly visible as peaks of density arranged in four pentagons. The symmetry of the crystal is such that there are only five unique heavy metal positions in the unit cell. The coordinates of the heavy metal atoms were determined from the density map. To check the accuracy of the structure determination by image processing, these coordinates were then compared with those found independently by X-ray crystallographic methods on the isostructural sodium compound[10] (Table 1). The structure is built up of pentagonal MeO_7-bipyramids and MeO_6-octahedra (Me = Nb or W) as shown in Fig. 4*b*. Each bipyramid is linked by equatorial edge-sharing to five octahedra forming a star-shaped cluster of polyhedra. Along the *a* axis the units are linked by an MeO_6-octahedron through corner sharing. Four of the 10 atomic coordinates are fixed by symmetry to be 0 or 1/4. All the other six positional parameters agree to within < 1/100 of a unit cell. The average difference in positions found by the two methods was 0.10 Å, with the largest difference being 0.14 Å.

The X-ray structure determination of the isostructural sodium compound showed that the niobium and tungsten atoms were distributed over all five positions, with different site occupancies. In the map reconstructed by image processing, all peaks have the same height to within 10%, but the significance of these differences has not been examined.

We have demonstrated, therefore, that, for a thin and unbent crystal, it is possible to determine the positions of metal atoms in the crystal lattice with an accuracy of 0.1 Å, by combining high-resolution electron microscopy and computerized image processing, without using any previous information about the crystal structure.

This investigation was carried out with financial help from the Swedish National Science Research Council (NFR). A grant from the Knut and Alice Wallenberg Foundation for the electron microscope is gratefully acknowledged.

Received 16 April; accepted 24 July 1984.

1. Spence, J. C. H. *Experimental High Resolution Electron Microscopy* (Clarendon, Oxford, 1981).
2. DeRosier, D. J. & Klug, A. *Nature* **217**, 130–134 (1968).
3. Henderson, R. & Unwin, P. N. T. *Nature* **257**, 28–32 (1975).
4. Klug, A. *Chem. Scr.* **14**, 245–256 (1978–79).
5. Thon, F. *Z. Naturf.* **21a**, 476–478 (1966).
6. Cowley, J. M. & Iijima, S. *Z. Naturf.* **27a**, 445–451 (1972).
7. Sundberg, M. & Marinder, B.-O. (in preparation).
8. Erickson, H. P. & Klug, A. *Phil. Trans. R. Soc.* **B261**, 105–118 (1971).
9. *International Tables for X-ray Crystallography*, Vol. A (Riedel, Dordrecht, 1983).
10. Marinder, B.-O. & Sundberg, M. *Acta Crystallogr.* **C40** (in the press).

Bouguer images of the North American craton and its structural evolution

R. E. Arvidson, D. Bindschadler*, S. Bowring, M. Eddy, E. Guinness & C. Leff

McDonnell Center for the Space Sciences, Department of Earth and Planetary Sciences, Washington University, St Louis, Missouri 63130, USA

Processing of existing gravity and aeromagnetic data with modern methods is providing new insights into crustal and mantle structures for large parts of the United States and Canada[1–3]. More than three-quarters of a million ground station readings of gravity are now available for this region. These data offer a wealth of information on crustal and mantle structures when reduced and displayed as Bouguer anomalies, where lateral variations are controlled by the size, shape and densities of underlying materials. We have used digital image processing techniques to generate Bouguer images that display more of the granularity inherent in the data as compared with existing contour maps. A dominant NW–SE linear trend of highs and lows can be seen extending from South Dakota, through Nebraska, and into Missouri (Fig. 2). The structural trend cuts across the major Precambrian boundary in Missouri, separating younger granites and rhyolites from older sheared granites and gneisses. This trend is probably related to features created during an early and perhaps initial episode of crustal assembly by collisional processes. The younger granitic materials are probably a thin cover over an older crust.

Our processing technique, which is based on local arithmetic averages of Bouguer values, was chosen specifically to preserve local details[4], thus enhancing short wavelength anomalies of probable crustal origin. The data were reduced to Bouguer anomalies using the 1967 International Gravity Formula and a slab density of 2.67 $g\,cm^{-3}$. The interpolated results are displayed in a shaded relief form in Fig. 2 for an area centred on the midcontinent. We concentrate on delineating and interpreting NW–SE trending features in the midcontinent, covering the Dakotas, Nebraska, and Missouri. This area is one where gravity and magnetic data can provide considerable information on crustal structure as much of the region is covered by Phanerozoic sedimentary rocks.

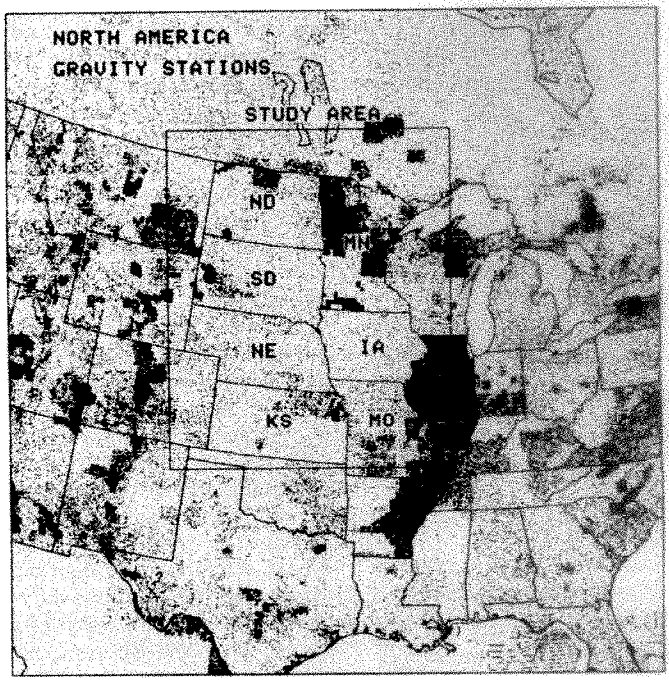

Fig. 1 Gravity station locations are shown as dots in this Lambert equal area projection of part of the United States and southern Canada. Bouguer anomalies for the station locations were utilized with the interpolation technique discussed in the text to generate the Bouguer images shown as the shaded relief map in Fig. 2. ND, North Dakota; SD, South Dakota; NE, Nebraska; KS, Kansas; MN, Minnesota; IA, Iowa; MO, Missouri.

Figure 3 is a sketch map compiled from the Bouguer images and from available geological data. This area includes the Superior Province (2,500–2,700 Myr (ref. 5)), the Churchill

---

* Present address: Department of Geological Sciences, Brown University, Providence, Rhode Island, USA.

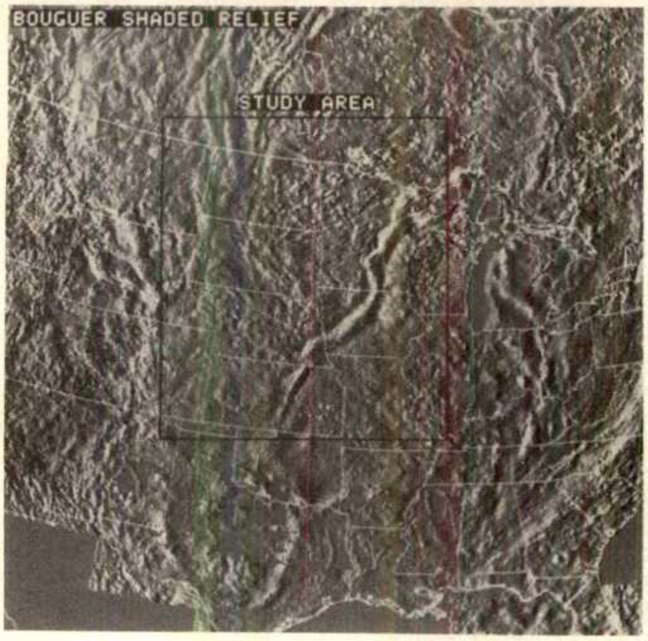

Fig. 2 Shaded relief map of Bouguer anomalies, with simulated sun placed at 20° above the western horizon. The flat, grey areas in the southern United States are places where the areal density of data was too low to allow meaningful interpolations.

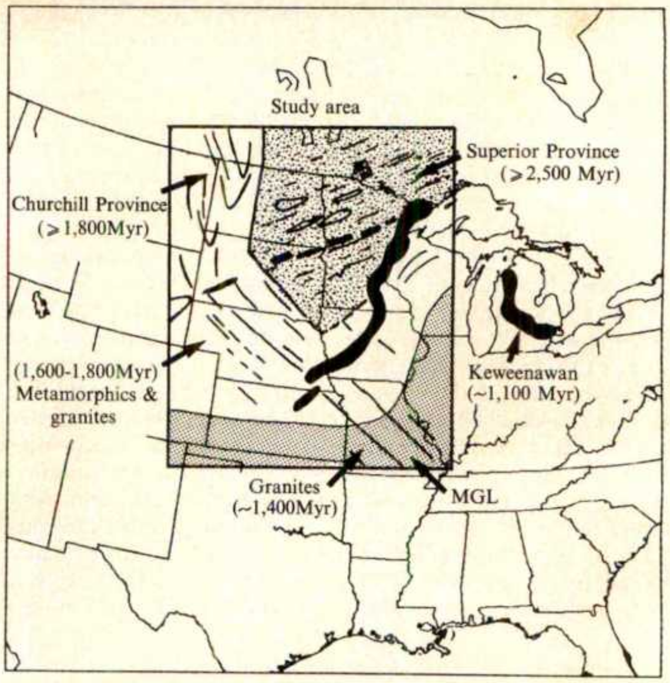

Fig. 3 Interpretation map of the study area. The Great Lakes Tectonic Zone is shown as a series of thick lines running NE–SW in Minnesota. Also shown is the projection of the tectonic zone into Wyoming. The continuity in trend and form of NW–SE structures to the south of the linear zone suggests a common origin. The deep-seated Missouri Gravity Low (MGL) has apparently been covered with a veneer of younger granites in southern Missouri.

Province (1,800–1,900 Myr, with residual Superior ages[5]), and areas to the south. We have included part of Canada because large parts of the Superior and Churchill Provinces are exposed, thereby allowing the Bouguer trends to be interpreted in concert with extensive geological data. Trends within the Superior Province are largely NE–SW, reflecting the presence of belts of mafic metavolcanic rocks[6]. The western boundary between the Superior Province and the younger Churchill Province shows up clearly in the images, partly because the structural fabric has very different wavelengths and trends in the two provinces. The Churchill Province exhibits structures that trend in N–NW directions. These structures consist of curvilinear belts of metamorphic and igneous rocks that are thought to have formed in a series of collisional events associated with convergent plate margins[7,8].

The Churchill trend appears to be truncated along a linear zone extending NE–SW from Minnesota, through South Dakota, and into Wyoming. This zone corresponds to the Great Lakes Tectonic Zone in Minnesota and to the Wyoming Shear Zone in Wyoming[9,10]. The structures to the south of the zone strike more towards the NW and have a finer texture than do the structures in the Churchill Province. Our presentations show that this NW–SE trending fabric extends from South Dakota to the southeastern section of Missouri. The NW–SE trending fabric extending into Missouri has clearly been cut by the younger ∼1,100 Myr basalts emplaced during the Keweenawan rifting event[11]. Within the zone of NW–SE trending fabric, the Precambrian terranes consist of igneous and metamorphic rocks that range in age from 1,600 to 1,700 Myr in South Dakota and Nebraska, to undeformed granitic rocks 1,300–1,400 Myr in age in southern Missouri[12]. As shown in Fig. 3, the northern boundary of the younger granitic rocks runs in an E–W to NE–SW direction, roughly perpendicular to the NW–SE trending fabric.

The dominant NW–SE trending feature in Missouri, the 'Missouri Gravity Low' (MGL)[13,14], is 700 km long, 120 km wide, and has a maximum amplitude of ∼−40 mGal. It is best modelled as a 4–6 km crustal excess at the Moho[15]. The gravity signature of the Missouri feature is similar to those for modern rift valleys. On the other hand, negative Bouguer rift signatures arise because of sediment fill or because of low-density magma ponded at the base of the crust[16]. Neither hypothesis seems valid for the Missouri feature, since: (1) no Precambrian sediments are associated with the gravity low, and (2) the last major magmatic activity was associated with mafic dykes and sills that are unconformably overlain by Cambrian sediments[15]. It is equally difficult to explain the Missouri feature as a shear zone, given the amplitude of the low[15]. The most plausible origin is one involving crustal thickening due to events associated with convergent plate margins[17]. In fact, the signature is not unlike the pattern found in selected regions within the Churchill and Superior Provinces[7,8].

The preservation of the deep-seated MGL beneath the granitic basement of southern Missouri is consistent with the younger granitic rocks being a veneer emplaced over an older igneous and metamorphic crust. Neodymium–samarium data imply that the Missouri granites and rhyolites formed by partial melting of crustal rocks that have a mantle separation age of ∼1,800–1,900 Myr (ref. 18). The mantle separation age is similar to the age of the hypothesized collisional events to the north that produced the Penokean, Trans-Hudson and Wopmay Orogens[5]. Given the cumulative evidence, it is not inconceivable that the NW–SE trends in South Dakota, Nebraska, and Missouri formed by collisional processes similar to those that occurred to the north, during approximately the same time period. We treat such a hypothesis as intriguing and one deserving further scrutiny and evaluation. If true, much of the original Proterozoic craton was assembled in a similar manner over a relatively brief interval.

This work was supported by NASA grant NSG-7087 from the Planetary Geology Program and by a Jet Propulsion Laboratory contract from NASA's Non-Renewable Earth Resources Program.

Received 3 May; accepted 24 July 1984.

1. Arvidson, R. E., Guinness, E. A., Strebeck, J., Davies, G. & Schulz, K. *EOS* **18**, 261–265 (1982).
2. Hildenbrand, T. G., Simpson, R. W., Godson, R. H. & Kane, M. F. *U.S. geol. Surv., Geophys. Inves. Map* GP-953-A (1982).
3. Zietz, I. *U.S. geol. Surv., Geophys. Inves. Map* GP-954-A (1982).
4. Eliason, E. & Soderblom, L. *Proc. 8th Lunar planet. Sci. Conf.* 1163–1170 (1977).
5. McCullogh, T. & Wasserburg, G. *Science* **200**, 1003–1011 (1976).

6. Morey, C. & Sims, P. *Bull. geol. Soc. Am.* **87,** 141–152 (1976).
7. Gibb, R. A. & Thomas, M. D. *Nature* **262,** 199–200 (1976).
8. Lewry, J. F. *Nature* **294,** 69–72 (1981).
9. Sims, P. K., Card, K. D., Morey, G. B. & Peterman, Z. E. *Bull. geol. Soc. Am.* **91,** 690–698 (1980).
10. Warner, L. A. *Bull. geol. Soc. Am.* **89,** 161–171 (1978).
11. Green, J. C. *Geol. Ass. Can. Spec. Pap.* **16,** 407–422 (1977).
12. Van Schmus, W. & Bickford, M. *Precambrian Plate Tectonics* (ed. Kroner, A.), 261–296 (Elsevier, 1981).
13. Guinness, E. A. *et al. J. geophys. Res.* **87,** 8529–8545 (1982).
14. Guinness, E. A., Arvidson, R. E., Leff, C., Edwards, M. & Bindschadler, D. *Econ. Geol.* **78,** 654–663 (1983).
15. Eddy, M. S. thesis, Wash. Univ. (1984).
16. Burke, K. & Whiteman, A. J. in *Implications of Continental Drift to the Earth Sciences* (eds Tarling, D. H. & Runcorn, S. K.) 735–755 (Academic, 1973).
17. Dutch, S. I. *Geology* **11,** 478–481 (1981).
18. Nelson, B. & DePaolo, D. *Geol. Soc. Am. Abstr.* **14,** 575 (1982).

Periodic gravity changes at Poás volcano, Costa Rica

H. Rymer & G. C. Brown

Department of Earth Sciences, The Open University, Walton Hall, Milton Keynes MK7 6AA, UK

The measurement of gravity over active volcanoes is usually aimed either at the development of sub-surface structural models[1–4] or the investigation of temporal changes in gravity associated with magma movements[5–13]. The positive gravity anomaly over Poás volcano, Costa Rica[4] indicates the presence of a cylindrical pipe of denser material extending to several kilometres depth. Although the volcano is active, this feature has remained apparently stable for at least the past four years. However, our programme of high-precision microgravity studies indicates changes with amplitudes of 120 μGal at the crater rim and 50 μGal on the flanks with a periodicty of ~30 days. These data are interpreted in terms of either relative movements of several metres between the magma body and the stable volcanic edifice or of cyclic density change related to the degree of vesiculation or crystallization of the magma: there is a possibility that these variations are tidally induced. Such studies may have wider relevance in analysing previously unrecognized components of microgravity change and in the monitoring of active volcanoes.

Theoretical considerations[8,14,15] may be used to describe mathematically the vertical and horizontal elastic deformation of the crust due to hydrostatic pressure changes associated with sub-volcanic magma movements. In gravitational terms, we may anticipate a cyclic sequence involving pre-eruptive inflation of a volcanic cone, associated with gravity decrease according to the free-air gradient, followed by post-eruptive deflation and gravity increase. Coupled microgravity–elevation studies related to eruptions at Kilauea volcano, Hawaii[7,8], at Pacaya volcano, Guatemala[9,10] and at the Icelandic rift near Krafla[11] record parts of this cycle and show that high precision measurements provide a powerful method for monitoring and locating active areas in a volcanic system. More significantly, in terms of our results on Poás, Eggers[10] has reported evidence for sub-surface magma density changes at Pacaya. In contrast, small changes of gravity and elevation at Etna[12,13] do not record a major inflation–deflation cycle but were related to magma movements through sub-terranean fissures. The gravity–elevation data for these volcanoes raise two interesting questions: (1) how typical are the large (hundreds of μGal) gravity changes associated with eruptions that have been observed at Kilauea, Pacaya and Krafla, and (2) to what extent are the smaller changes (tens of μGal) observed at Etna unambiguously related to magma movements?

Situated at 10°11′ N, 84°13′ W, Poás is the only active member of a NNW–SSE oriented line of dominantly pyroclastic calc-alkaline volcanic centres comprising the Cordillera Central of Costa Rica (see Fig. 1*a*). The volcano is apparently in a state of equilibrium where thermal gains and losses are balanced, yet magma must be present at a shallow depth. A full gravity and elevation survey at 45 stations covering the summit area in February 1979 revealed a closed positive residual Bouguer anomaly of 10 mGal amplitude[4] centred over the north-east corner of the crater (Fig. 1*c*). The anomalous area is approximately circular with the strongest gradients to the north and west but with lesser gradients where the gravity contours extend towards the old crater (south-east). The tight gravity contours define the cross-section of a shallow sub-surface cylindrical pipe extending to several kilometres depth and with a positive density contrast ($>250\ \mathrm{kg\ m^{-3}}$) compared to the ash–lava sequence of the Poás cone (surface density $\sim 2{,}100\ \mathrm{kg\ m^{-3}}$). It has been argued[16,17] that the cylindrical pipe is largely solidified lava but, in view of the geological evidence of shallow magma beneath the dome (Fig. 1*a*), we suggest that unvesiculated magma (density $\sim 2{,}500\text{–}2{,}600\ \mathrm{kg\ m^{-3}}$) may more plausibly occupy much of the cylinder.

Gravity measurements were repeated at selected stations on the crater rim and along a traverse 20 km south of the volcano (Fig. 1*b*) during February 1979, January 1981, at regular inter-

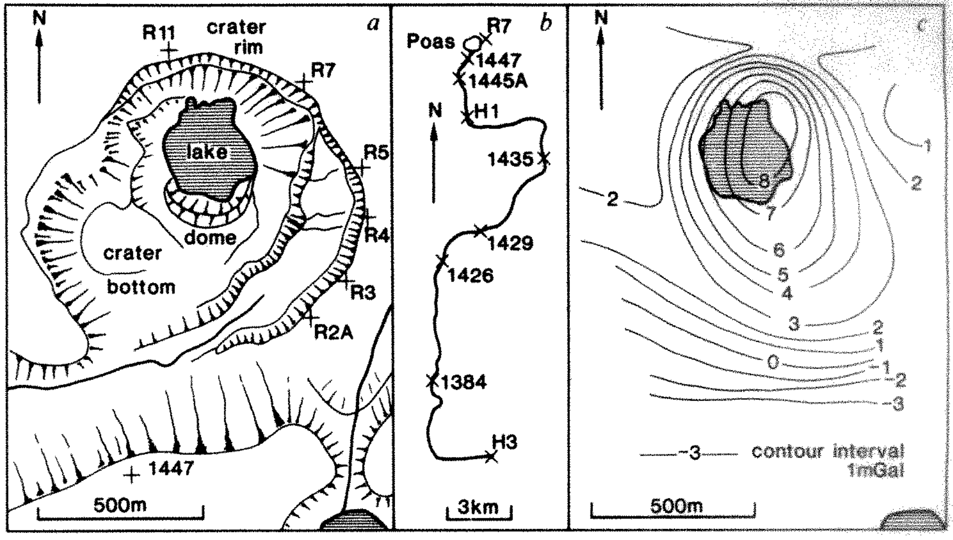

Fig. 1 *a*, Summit morphology of Poás volcano, Costa Rica. The area is characterized by the eroded remains of several calderas and includes an active crater with a steaming convecting lake (top centre) and a prehistoric crater with a cold water lake (bottom right). The active crater is three-sided and, with a floor at 2,320 m elevation, lies some 120 m below the surrounding plateau, or crater rim, where six gravity stations included in Tables 1 and 2 are marked. Activity is centred on an elongate pyroclastic dome (25 m high) with vigorous fumaroles, that stands on the south shore of the lake. The most recent large pyroclastic eruption was in 1953 when the crater floor dropped to its present level[21]; subsequent activity has involved geyser-like plumes of steam and mud, centred on the lake, with occasional ejection of lava blocks and juvenile material[16]. Since 1979, no major eruptions have been recorded although fumarole temperatures rose in 1980 and cracks in the dome have since glowed dull red after dark. *b*, Distribution of gravity stations along the road to the south of Poás used in the April–May 1983 survey. As the volcano approximates to a cone shape, basal diameter 25 km, rising to 1,200 m above the surrounding terrane, stations 1447 to 1435 are classified as flank stations, whereas 1429 to H3 are 'remote' stations. *c*, Residual gravity map of the Poás summit covering the same area and at the same scale as *a*.

Table 1 Gravity data in mGal, corrected for Earth tides and drift, and given with respect to 1445A

Station	Elevation (m)	Distance south from R7(km)	February 1979	January 1981	April 1983	December 1983	Max Δg
R2	2,459	0.5	15.119	15.056	15.050	—	−0.069
R3	2,459	0.4	14.471	14.395	14.411	—	−0.076
R4	2,455	0.3	15.185	15.191	15.195	—	0.010
R5	2,454	0.2	15.364	15.365	15.371	—	0.007
R7	2,443	0	17.090	17.143	17.106	17.159	0.069
1438	1,979	4	115.048	115.034	115.030	115.085	0.055
1435	1,802	6	147.801	—	147.748	148.803	0.055
1426	1,260	10	252.758	—	252.750	252.695	−0.063

vals on 10 occasions throughout April–May 1983, and again in December 1983. All readings were corrected for theoretical Earth tides using the potential prediction programme of Broucke *et al.*[18] and a gravimetric factor for all constituents of 1.16. They were expressed first as gravity differences relative to a base station outside the volcano area, and gravity changes at individual stations were then calculated. The accuracy of the tidal prediction programme at this geographical location was tested by measuring the semidiurnal tide at one location for several days. Residual differences between observed and predicted gravity are a sum of any small programme errors combined with precision errors in meter reading, long-term drift and the effect of ocean loading tides. The standard error of these residual differences was 15 μGal, from which it follows that observed gravity changes exceeding 45 μGal have a 99.7% chance of being significant. A further source of error arising from disturbances due to movement of the meter on survey days is difficulty to assess, but from repeated readings at the base station, it appears to have been similar to the errors quoted above. Our total standard errors are likely to be <30 μGal (compare with the estimate of 35 μGal for Lacoste and Romberg meters[19]), although these exceed those reported in the high precision Etna work[12,13] partly because the meter used on Etna had an electrical readout, whereas G-513 is manual, and also because the observed accuracy of the tidal programme is included in our error estimate.

Gravity data measured in 1979, 1981, early 1983 and late 1983 at eight stations for which we have taken records on at least three occasions are summarized in Table 1. The maximum variation between any two sets of readings at a single station is 0.076 mGal at station R3. No systematic gravity changes occurred either with time or distance from the volcano over four years and it follows that no long-term changes in the Poás magma chamber can be resolved on this time scale. These data confirm the overall equilibrium state of the volcano and the small changes in Table 1 are attributed to the randomizing effect of reading errors (above)—only single readings are represented in the 1981 and December 1983 columns—and disturbance to the meter due to use elsewhere between visits to Poás. The more intensive higher precision studies at 11 stations during April–May 1983, however, have yielded some interesting results (Table 2). Assuming first that gravity is invariant with time, the r.m.s. deviations about the means for each station show a clear systematic decrease with distance from the crater—averages of 58, 48 and 33 μGal respectively for crater rim, flank and remote stations. These observations are statistically significant and imply that the invariant hypothesis is not valid, particularly for stations close to the volcano.

Because a degree of periodicity is observed in the data (Table 2), various simple sine waves were fitted to the data by choosing a period and calculating the amplitude and phase giving the minimum r.m.s. difference between observed and calculated values. From a range of periods, that for 30 days gave the optimum fit for all seven rim and flank stations (Table 2), the r.m.s. differences being distinctly less than for the straight line of the invariant hypothesis. We suggest, therefore, that an anomalous response with an ~30-day period is being recorded (Fig. 2). The effect is larger (~120 ± 60 μGal) at the crater rim stations than at flank stations (~50 ± 25 μGal). If these gravity changes were wholly attributed to elevation changes, then given a Bouguer-corrected free air gradient of 0.2 mGal m^{-1}, rim and flank stations would be rising and falling over 60 and 25 cm respectively during the 43 days of observation. Local tiltmeter data however, constrains elevation changes at rim stations to a few centimetres.

Having excluded elevation changes as the major source of

Table 2 Tidally corrected gravity data (in μGal) relative to values measured on 13 April 1983 which, therefore, are zero for every station

Station	Elevation (m)	Distance south of R7 (km)	Date of reading (1983)									r.m.s. deviation about mean (invariant assumption)	r.m.s. deviation about best-fit sine curve of period		
			18.4	21.4	25.4	2.5	5.5	9.5	13.5	18.5	25.5		20 days	30 days	40 days
Crater rim stations															
R11	2,441	−0.1	30	128	132	138	115	190	90	150	110	56	56	48	57
R7	2,443	0	70	136	162	—	192	132	42	—	72	65	61	35	56
R2A	2,459	0.5	90	90	120	99	150	105	−5	—	58	52	52	40	30
											Means:	58	56	41	48
Flank stations															
1447	2,574	1	41	125	—	120	113	119	38	46	82	46	47	32	32
1445A	2,520	2	70	120	120	96	130	148	38	72	108	46	42	35	35
H1	2,500	4	60	155	129	138	155	115	25	—	115	57	52	39	44
1435	1,802	6	14	6	91	31	91	48	−41	—	18	43	43	33	35
											Means:	48	46	35	37
Remote stations															
1429	1,420	9	19	38	94	60	72	63	8	9	85	34	33	20	27
1426	1,260	10	23	38	105	31	59	—	−11	—	15	37	37	28	23
1384	931	16	−21	−26	−89	−89	−77	−53	7	—	−100	41	37	23	34
H3	951	20	0	−25	−20	−20	15	−25	—	—	25	21	21	20	19
											Means:	33	32	23	26

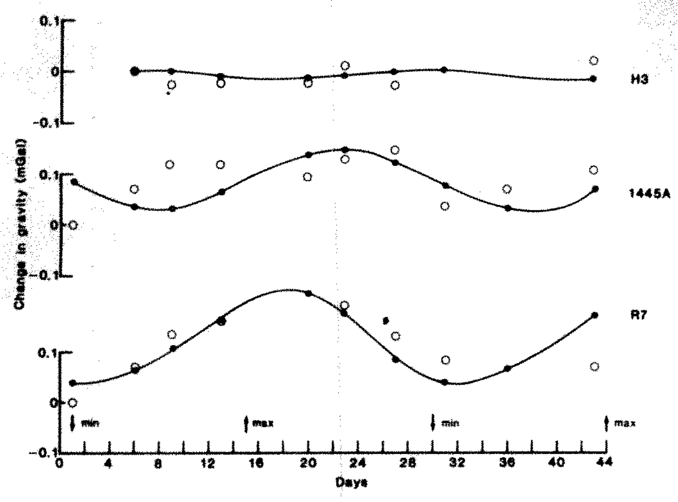

Fig. 2 Observed gravity changes with time at three selected stations (one for each group in Table 2); open circles, observed points; curves with solid circles, the calculated best-fit sine waves (unconstrained amplitude and phase) with a 30-day period. Note that the arrows indicate the maximum and minimum points on the predicted lunar synodic-tide (period 29.53 days) and that these are broadly in phase with the observations at R7. Whether this correlation between gravity change and the synodic tide is purely coincidental remains to be evaluated.

the observed gravity changes we consider next the possible sub-surface causes. (1) Assuming 30% porosity for the volcanic edifice, vertical water table movements of 10–20 m could produce the observed gravity changes. However, observations were made during the dry season; moreover, the crater lake level remained constant, so water table fluctuations are rejected as the cause. (2) A periodic change in shape of the shallow magma body is a possibility, but the similarity of observed gravity changes at the rim stations makes this less likely than changes in the depth and/or density of the magma body. (3) Given a maximum density contrast of 500 kg m^{-3} for the unvesiculated magma of the cylindrical body and the surrounding ash–lava sequence, and a probable depth of 100 m, then a rise and fall of the density interface through 10 m would produce the observed gravity change at R7. However, the contrast in density between the magma body and the overlying solidified rubble is probably less, so that the gravity changes can be explained only partially in terms of independent vertical movement between the magma body and surrounding volcanic cone. (4) The final possibility is that the overall density of the magma body is varying: changes of 5–10 kg m^{-3} throughout the entire body, or greater changes confined to the upper parts are required. In the interpretation of gravity changes related to eruptions at Pacaya, Eggers[10] noted that variations in the degree of vesiculation of the magma (related to the periodic rise of gas bubbles) or in its crystallinity, may cause changes of density, and hence gravity, of the magnitude observed at Poás.

While a more complete analysis would be premature, we conclude that periodic gravity changes at Poás volcano are due to a combination of depth and density changes in the sub-surface magma chamber: the process is cyclic with a period of ~30 days. However, the only appropriate external driving force, the lunar synodic tide, is weak compared with the diurnal and fortnightly tides for which we do not observe a response. The observed periodicity is, therefore, either a primary feature of the Poás volcanic plumbing system, unrelated to tides (compare with natural gravitational oscillations observed elsewhere but of random periodicity[20]), or is due to tidal resonance at a synodic period (Fig. 2).

This work has shown that previously-unrecognized periodic changes in gravity, unrelated to eruptions, can occur over a stable volcano. There are clear implictions for monitoring non-stable volcanic systems in which, for example, catastrophic build-up of pressure may be recorded in dramatic changes to the amplitude and periodicity of steady-state gravitational change.

We thank many friends and colleagues who contributed to this work, particularly R. S. Thorpe, C. A. Locke and M. Randal for field assistance, R. Edge (IOS, Bidston) for discussion of tidal gravity, and A. W. Shelton and A. Eggers for stimulating reviews of an earlier manuscript. Financial assistance from the Royal Society and the co-operation of the Servicio de Parques Nacionales de Costa Rica are gratefully acknowledged.

Received 22 March; accepted 2 July 1984.

1. Kane, M. F., Mabey, D. R. & Brace, R. *J. geophys. Res.* **81**, 754–761 (1976).
2. Finn, C. & Williams, D. L. *Geology* **10**, 503–507 (1982).
3. Yokoyama, I. & Hadikusumo, D. *Bull Earthq. Res. Inst. Tokyo Univ.* **47**, 991–1001 (1969).
4. Thorpe, R. S., Locke, C. A., Brown, G. C., Francis, P. W. & Randal, M. *J. geol. Soc. Lond.* **138**, 367–373 (1981).
5. Iida, K., Hayakawa, M. & Katayose, K. *Geol. Surv. Jap.* Rep. No. 152 (1952).
6. Malone, S. D. *EOS* **57**, 1016 (1976).
7. Jachens, R. C. & Eaton, G. P. *J. Volcan. Geotherm. Res.* **7**, 225–240 (1980).
8. Dzurisin, D. *et al. J. Volcan. Geotherm. Res.* **7**, 241–269 (1980).
9. Eggers, A. A. & Chavez, D. *J. Volcan. Geotherm. Res.* **6**, 391–402 (1979).
10. Eggers, A. A. *J. Volcan. Geotherm. Res.* **19**, 223–237 (1983).
11. Torge, W. *Tectonophysics* **71**, 227–240 (1981).
12. Sanderson, T. J. O. *Nature* **297**, 487–490 (1982).
13. Sanderson, T. J. O., Berrino, G., Corrado, G. & Grimaldi, M. J. *J. Volcan. Geotherm. Res.* **16**, 299–315 (1983).
14. Mogi, K. *Bull. Earthq. Res. Inst. Tokyo Univ.* **36**, 99–134 (1958).
15. Dietrich, J. H. & Decker, R. W. *J. geophys. Res.* **80**, 4094–4102 (1975).
16. Francis, P. W., Thorpe, R. S., Brown, G. C. & Glassock, J. *Nature* **283**, 754–756 (1980).
17. Locke, C. A., Brown, G. C., Thorpe, R. S., Cassidy, J. & Francis, P. W. *Bull. volcan. Costa Rica* (in the press).
18. Broucke, R. A., Zürn, W. E. & Slichter, L. B. *Geophys. Monogr. Ser., Am. geophys. Un.* **16**, 319–324 (1972).
19. Torge, W. *Proc. Gen. Meet. of Int. Ass. Geophys., Tokyo*, 319–324 (1980).
20. Björnsson, A., Johnsen, G., Sigurdsson, S., Thorbergsson, G. & Tryggvason, E. *J. geophys. Res.* **84**, 3029–3038 (1979).
21. Raccichini, S. & Bennett, F. D. *Rev. Geogr. Am. Centr.* **5–6**, 37–53 (1977).

Timing the increase in atmospheric sulphur deposition in the Adirondack Mountains

George R. Holdren Jr*, Thomas M. Brunelle*, Gerald Matisoff† & Martin Wahlen‡

* Department of Geological Sciences, University of Rochester, Rochester, New York 14627, USA
† Department of Geological Sciences, Case Western Reserve University, Cleveland, Ohio 44106, USA
‡ Center for Laboratories and Research, New York State Department of Health, Albany, New York 12201, USA

The timing and magnitude of increases in the flux of atmospherically-derived anthropogenic substances to remote areas can be estimated from their distributions in lake sediments. For transition metals[1–4] or trace organics[5–7], this is done simply by comparing their distributions with that of geochronological tracers. This approach is not directly applicable to species which exhibit significant post-depositional mobility. Diagenetic mobilization must be assessed from the distribution of the species in the sediment pore waters. However, by using this and related information, loading histories can be calculated. We have done this for sulphate, the major anionic component of modern precipitation[8–11], for a watershed located in the Adirondack Mountains of New York State. Our results suggest that previous estimates for the onset of increased sulphur deposition in eastern North America[12,13] are too old by a factor of about two, and that significant increases did not occur until about 1930.

In the sediments of softwater lakes, sulphate is converted to both organo-sulphur compounds[14–16] and mineral sulphides[17,18]. In non-acidic systems[19], the rates of conversion are proportional to the sulphate concentration in the lake water[20]. Sulphate is transformed to these immobile forms over a finite interval within the sediment column[21,22]. As a result, a part of the 'modern' sulphur is transported downward to 'older' sediments before

Table 1 Results of sediment solids and pore water analyses from Grass Pond

Sediment solids					Pore waters			
Depth below sediment–water interface (cm)	Water content (wt %)	Organic carbon (wt %)	Total sulphur (μg per g)	$^{210}Pb_T$* (d.p.m. g^{-1})	Depth below sediment–water interface (cm)	*p*H	$(H_2S + HS)$ (μM)	SO_4^{2-} (μM)
0–1.4	94	22.0	3,700	13.5 ± 5.0 (0.75)†	OW ‡	6.75	<1.0§	78.0‖
1.4–3.0	94	—	—		1–2	5.90	<1.0	68.6
3.0–4.4	93	21.5	5,800	17.9 ± 2.9 (3.30)	3–4	6.27	1.5	56.6
4.4–5.6	93	22.4	5,750		5–6	6.53	4.1	41.2
5.6–6.8	94	22.6	5,350	14.6 ± 1.5 (6.15)	7–8	6.57	6.2	18.8
6.8–8.0	93	22.3	5,150	11.5 ± 2.0 (8.15)	9–10	6.55	15.3	9.8
8.0–9.4	93	20.9	4,900		12–13	6.49	14.7	<5
9.4–10.8	94	20.7	4,700	10.1 ± 2.9 (10.3)	17–19	6.36	32.4	<5
10.8–12.0	92	21.1	4,850		24–26	6.32	18.2	<5
12.0–13.5	90	19.7	3,700		34–36	6.30	15.0	—
13.5–14.8	92	20.1	3,450					
14.8–16.3	92	20.5	3,300	8.8 ± 2.9 (15.95)				
16.3–18.5	91	19.1	3,000					
18.5–20.8	91	18.9	2,400	3.8 ± 0.6 (20.95)				
20.8–23.0	91	18.9	2,700					
23.0–25.3	91	17.7	2,350	2.4 ± 0.6 (26.1)				
25.3–28.6	91	18.7	2,400					
28.6–32.0	91	18.4	2,950	<1.25 (31.10)				
32.0–37.3	90	17.7	2,050					
37.3–42.5	90	18.3	2,100	<1.25 (36.0)				
42.5–48.0	90	18.1	2,200	<1.25 (41.0)				
48.0–53.2	90	17.7	2,000					
53.2–58.6	90	17.8	2,200					
58.6–64.4	90	19.1	2,200					

* Total ^{210}Pb activities. Excess ^{210}Pb values were computed by subtracting 1.2 d.p.m. g^{-1} from each of these values.

† ^{210}Pb activities were measured on a core collected beside the one used for bulk properties and sulphur analyses. The values in parentheses are the midpoint depths in cm of samples taken from that core.

‡ Overlying water.

§ Detection limit of analytical methods used.

‖ Average of three analyses from the overlying core collected by the peeper.

Table 2 Model parameters, their values and the methods of evaluation

Symbols	Definition	Value	Source
$S(z, t)$	Total sedimentary sulphur concentration	Variable	Measured
$S(0, t)$	Detrital sulphur input to sediment	0.16 wt %	Estimated using model
$SO_4(x, t)$	Profile of pore water sulphate concentrations	Variable	Measured for modern values
$SO_4(0, t)$	Lake-water SO_4 concentration	t = 1982–80 μM t < 1920–10 μM	Estimated using model
ω	Sedimentation rate	0.25 cm yr^{-1}	$^{210}Pb_{xs}$
z	Depth below sediment–water interface within sediment column (positive downward)		
X_1	Depth of oxic sediment zone	≈2 cm	Measured
X_2	Depth of bioturbated zone	4 cm	Measured
D_B	Biological mixing coefficient	3×10^{-8} $cm^2 s^{-1}$	Calculated from $^{210}Pb_{xs}$, $S(z)$ and Pb_{Total} profile
D_{SO_4}	SO_4^{2-} diffusion coefficient	4.5×10^{-6} $cm^2 s^{-1}$	Ref. 30
R	SO_4^{2-} reduction rate parameter	0.38 cm^{-1}	Calculated from SO_4^{2-} profile data
Φ	Porosity	0.91	Measured
ρ	Bulk sediment density	1.11 g cm^{-3}	Measured

becoming fixed in the sediment solids. Upward mobilization of the sulphur, as sulphide, also occurs. However, this transport is only a fraction of that observed for sulphate, and, therefore, is not a significant factor in controlling the observed distributions of total sedimentary sulphur.

Because the reactions are microbially mediated—it has been demonstrated that microbial activities can be either enhanced by eutrophication[23], or depressed by acidification[19]—and because of certain constraints needed to do the following calculations, it is important that the study area be only minimally perturbed by encroaching civilization. Our study was conducted in Grass Pond, Herkimer Co., New York State (43°41.5′ N × 75°3.5′ W). The pond has a maximum depth of 5.3 m and an area of ~2 ha. The 210-ha watershed is covered by a predominantly deciduous forest and is largely undisturbed. There are no roads or human dwellings within the watershed. The *p*H of the largest perennial stream in the basin averages ~6.8–6.9, except during snow melt. The smaller, ephemeral streams tend to have lower *p*H values, with at least one which has an average *p*H of ~4.3. In spite of these acidic contributions, typical summer and autumn *p*H values in Grass Pond are in the range 6.4–6.8.

Diver-operated piston cores were retrieved from the pond in May 1981 and in August 1982. The cores were returned to Rochester, sectioned and frozen within 48 h of collection. These samples were used for the determination of several parameters including total sedimentary sulphur, total organic carbon, water content and $^{210}Pb_{xs}$. Pore water data were obtained using a peeper[24] which was placed in the pond in August 1982 and retrieved in November 1982. The results of these measurements are summarized in Table 1.

Because sulphate exhibits post-depositional mobility, it is necessary to use model calculations to extract information regarding the timing and magnitude of increased atmospheric fluxes of sulphur to this basin. This can be accomplished using a mass balance equation in which the diffusion, reaction, burial and biological mixing of the sediments are considered. We have done this using a one-dimensional, diagenetic equation[25] of the form:

$$\frac{\mathrm{d}S(z,t)}{\mathrm{d}t}=\frac{\partial}{\partial z}D_{\mathrm{B}}\frac{\partial S(z,t)}{\partial z}+\omega\frac{\partial S(z,t)}{\partial z}+P(x,t)+\frac{\partial S(0,t)}{\partial t} \quad (1)$$

where

$$P(x,t)=\frac{\Phi D_{\mathrm{SO}_4}}{\rho(1-\Phi)}\frac{\partial^2\mathrm{SO}_4(\mathrm{x},\mathrm{t})}{\partial\mathrm{x}^2} \quad (2)$$

and

$$\mathrm{SO}_4(x,t)=\mathrm{SO}_4(0,t)\exp(-R(z-X_1)) \quad (3)$$

Individual terms are defined in Table 2. Equation (2) describes the instantaneous mass accumulation of solid sulphur based solely on the observed changes in the gradients of dissolved sulphate (equation (3)). By integrating this over time, which we have done numerically, and combining the results with equation (1), a profile of total sedimentary sulphur can be computed for any given sulphate loading history.

Modern-day values for all of the parameters used in the calculations, except the detrital sulphur concentration, can be derived directly from the field data. In the absence of historical information, we have assumed that these have remained time invariant. The two most poorly known, time-dependent parameters include the detrital sulphur concentration and the lake-water sulphate concentration. The detrital sulphur concentration cannot be measured directly because sedimentary sulphur is an admixture of detrital and diagenetically-derived material at all depths in the sediment column[21,22]. The lake-water sulphate concentration is related to the atmospheric loading history, and, ultimately, is the information to be extracted from this calculation.

To evaluate these two parameters, steady-state, sedimentary sulphur profiles[26,27] (curve *a* in Fig. 1) were calculated using various combinations of detrital sulphur and lake-water sulphate concentrations. Based on the results of these mass balance computations, the most reasonable value for preanthropogenic, detrital sulphur is 0.16 wt%, and for lake-water sulphate concentration is 10 ± 2 μM. Compared with the present day sulphate concentration of about 80 μM, this suggests that loadings in the Grass Pond watershed have increased eight- to 10-fold during this century. This is in excellent agreement with estimates made by Galloway and Whelpdale[28]. Changing either of the parameters requires a concurrent change in the value of the other to maintain the mass balance. For example, if preanthropogenic lake-water sulphate concentrations averaged 20 μM, detrital sulphur concentrations would have accounted for only 20% (0.05 wt%) of the total sedimentary sulphur. Alternately, if detrital contributions accounted for 88% (0.22 wt%) of the sedimentary sulphur, then lake-water sulphate concentrations could not have exceeded about 4 μM.

To determine the timing of changes in the sulphate loading rates, presumed loading histories were incorporated into the computation. Steady-state conditions were assumed to prevail into the twentieth century when sulphate concentrations began to increase towards present day values. These modelled increases ceased in 1965, because trend analyses of sulphate loading rates in the region suggest that these values have been constant to within 20% during the past 20 yr (ref. 29).

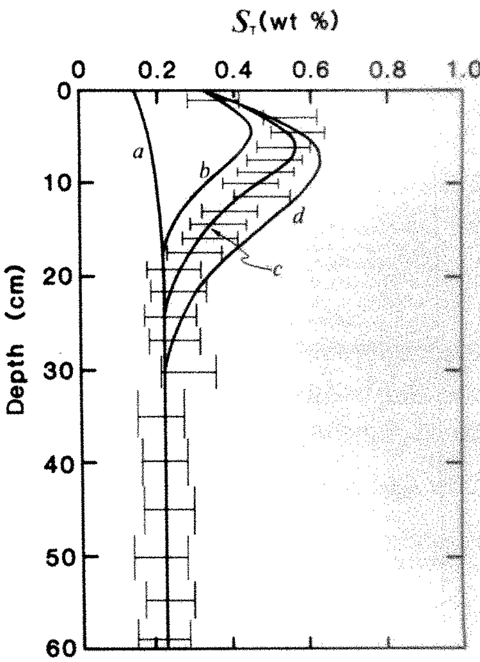

Fig. 1 Comparison of the measured versus model profiles for total sedimentary sulphur in the sediments of Grass Pond. Measured sulphur concentrations are indicated by the barred symbols. The heavy lines represent the results of the model calculations. *a*, Best estimate for the preanthropogenic, steady-state profile. *b*, *c* and *d* show the profiles computed assuming an onset of increased sulphate loading to Grass Pond beginning in 1950, 1935 and 1920, respectively.

Comparison of the model results with the field data permit a clear estimation of the timing of increased sulphur loading to the Grass Pond watershed. Curves *b*–*d* in Fig. 1 illustrate the comparison between three model curves and the field data. Curve 1*b* was calculated assuming that sulphur loading rates began to increase in 1950; curve *c* corresponds to an increase beginning in 1935; and curve *d* to 1920. From these results, it seems that increased sulphur deposition began in Grass Pond during the early to mid-1930s.

This timing estimate contrasts sharply with that which would have been made had the mobility of the sulphate not been taken into consideration. Excess sedimentary sulphur concentrations appear at a depth of ~23 cm in these sediments, or, based on the $^{210}\mathrm{Pb}_{\mathrm{xs}}$ data, in sediments which were being deposited in the 1880s and 1890s. Although these presumed dates are consistent with previous estimates for the onset of increased atmospheric deposition of 'pollution' sulphur in eastern North America[11,12], they are too old by a factor of about two when post-depositional mobility is taken into consideration.

We thank R. C. Aller, R. A. Berner, O. P. Bricker, W. Casey, G. E. Likens, and J. O. Nriagu for helpful comments. S. Matis and A. Pfordresher performed the total sulphur and carbon analyses reported.

Received 6 February; accepted 16 July 1984.

1. Galloway, J. N. & Likens, G. E. *Limnol. Oceanogr.* **24,** 427–433 (1979).
2. Wahlen, M. & Thompson, R. C. *Geochim. cosmochim. Acta* **44,** 333–339 (1980).
3. Johnston, S. E., Norton, S. A., Hess, C. T., Davis, R. B. & Anderson, R. S. *Energy and Environmental Chemistry* Vol. 2 (ed. Keith, L. W.) 177–188 (Ann Arbor Science, 1982).
4. Kahl, J. S., Norton, S. A. & Williams, J. S. *Geologic Aspects of Acid Deposition* Vol. 7 (ed. Bricker, O. P.) (Ann Arbor Science, 1984).
5. Heit, M., Tan, Y., Klusek, C. & Burke, J. C. *Wat., Air Soil Pollut.* **15,** 441–464 (1981).
6. Eisenreich, S. J., Rappaport, R., Urban, N., Capel, P. & Looney, B. *Proc., Paleolimnological Analysis of the Impact of Acidic Precipitation and Related Pollutants on Lake Ecosystems* (ed. Norton, S. A.) (Rockport, Maine, 1984).
7. Hites, R. A. *Proc., Paleolimnological Analysis of the Impact of Acidic Precipitation and Related Pollutants on Lake Ecosystems* (ed. Norton, S. A.) (Rockport, Maine, 1984).
8. Junge, C. E. & Werby, R. T. *J. Met.* **15,** 417–425 (1958).
9. Gambell, A. W. & Fisher, D. W. *J. geophys. Res.* **69,** 4203–4210 (1964).
10. Gambell, A. W. & Fisher, D. W. US *geol. Surv. Wat.-Supply Pap.* 1535-K (1966).
11. Likens, G. E., Bormann, F. H., Pierce, R. S., Eaton, J. S. & Johnson, N. M. *Biogeochemistry of a Forested Ecosystem* (Springer, Berlin, 1977).
12. Nriagu, J. O. & Coker, R. D. *Nature* **303,** 692–694 (1983).
13. Mitchell, M. J., David, M. B. & Uutala, A. J. *Hydrobiology* (in the press).
14. Casagrande, D. J. & Siefert, K. *Science* **195,** 675–676 (1977).

15. Mitchell, M. J., Landers, D. H. & Brodowski, D. F. *Wat., Air Soil Pollut.* **16,** 351–359 (1981).
16. Mitchell, M. J., Landers, D. H., Brodowski, D. F., Lawrence, G. B. & David, M. B. *Wat., Air Soil Pollut.* **21,** 231–245 (1984).
17. Berner, R. A. *Am. J. Sci.* **268,** 1–23 (1970).
18. Nriagu, J. O. *Limnol. Oceanogr.* **13,** 430–439 (1968).
19. Rao, S. S. & Dutka, B. J. *Hydrobiology* **98,** 153–157 (1983).
20. Cook, R. B. & Schindler, D. W. *Ecol. Bull., Stockh.* **35,** 115–127 (1981).
21. Nriagu, J. O. & Coker, R. D. *Limnol. Oceanogr.* **21,** 485–489 (1976).
22. Brunelle, T. M. thesis, Univ. Rochester (1984).
23. Tobin, R. S. & Anthony, D. H. J. *Limnol. Oceanogr.* **23,** 161–165 (1978).
24. Hesslein, R. H. *Limnol. Oceanogr.* **21,** 912–914 (1976).
25. Berner, R. A. *Early Diagenesis* (Princeton University Press, 1980).
26. Goldhaber, M. B. *et al. Am. J. Sci.* **277,** 193–237 (1977).
27. Aller, R. C. *Adv. Geophys.* **22,** 237–350 (1980).
28. Galloway, J. N. & Whelpdale, D. M. *Atmos. Envir.* **14,** 409–417 (1980).
29. Bilonick, R. A. & Nichols, D. G. *Atmos. Envir.* **17,** 1063–1072 (1983).
30. Li, Y.-H. & Gregory, S. *Geochim. cosmochim. Acta* **38,** 703–714 (1974).

Toluene degradation products in simulated atmospheric conditions

Bruce E. Dumdei & Robert J. O'Brien

Chemistry Department and Environmental Sciences Doctoral Program, Portland State University, Portland, Oregon 97207, USA

Atmospheric hydrocarbons have an important influence on the chemistry of the polluted lower atmosphere. Aromatic hydrocarbons or benzene derivatives comprise about 25–40% of gasoline in the US[1] and they are widely employed as solvents. Toluene is the most commonly used aromatic hydrocarbon and is often the most abundant of all non-methane hydrocarbons in urban atmospheres. Typical urban toluene concentrations range from 1 to 50 p.p.b. (parts per 10^9)[2,3] and clean-air concentrations up to 0.4 p.p.b. have been reported[4]. The aromatic hydrocarbons are destroyed by reaction with atmospheric hydroxyl radical (HO) and toluene remains in the atmosphere for about 50 daylight hours before reacting. Despite extensive study, toluene's reaction products are poorly understood[5]. Many reaction products have been identified, but most of these are ring-addition or side-chain oxidation products which retain the aromatic character of toluene. We have conducted a thorough study of toluene's oxidation products in simulated atmospheric conditions and present here an account of the products found and outline their probable formation and destruction mechanisms.

The simulated atmospheric reactions were carried out in hydrocarbon-free Pyrex vessels by black-light irradiation of toluene and nitrogen oxides (1–10 p.p.m. each) in zero-air at 50% relative humidity. This irradiation produces hydroxyl radical, and reaction conditions were adjusted to suppress ozone formation. Past failure to detect ring-opened fragmentation products of the toluene/HO reaction has been due, at least in part, to their precipitation from the gas phase onto the walls of the reaction vessel[6]. In the present experiment, products were recovered by solvent extraction from the vessel walls after 24–30 h irradiation. During this period, 60–80% of the toluene reacted. The solvent extract was concentrated and analysed by direct probe insertion into a Finnigan MAT triple stage quadrupole mass spectrometer/data system[7] (MS/MS)[8]. In addition to normal (H_8) toluene, methyl-deuterated (D_3) and perdeuterated (D_8) toluene were reacted to clarify the mass spectral interpretations. Product identifications were based on collision-induced-dissociation (CID) spectra.

Table 1 lists all compounds identified in this study. Of the 27 compounds, only 10 have been previously identified[9–15]; four others have been proposed[16–18], although never identified. The previously identified products are those amenable to gas-phase sampling and analysis by gas chromatography (GC) or gas chromatography–mass spectrometry (GC/MS).

Products missing from Table 1 are the low molecular weight gaseous compounds, such as carbon monoxide, carbon dioxide, acetylene, methylnitrate, peroxyacetylnitrate, formaldehyde, and formic acid, which have been previously identified as products of toluene. These compounds are either unlikely to partition into the solvent, are expected to be easily lost during the con-

Table 1 Identified products

Compound	H_8 m/z $(M+1)$	References
1. Glyoxal 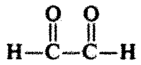 $H-\overset{\overset{O}{\Vert}}{C}-\overset{\overset{O}{\Vert}}{C}-H$	59	(9,15)*
2. Acetic acid 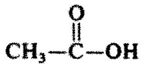 $CH_3-\overset{\overset{O}{\Vert}}{C}-OH$	61	
3. 3-Oxo-butene‡ 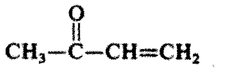 $CH_3-\overset{\overset{O}{\Vert}}{C}-CH=CH_2$	71	
4. Methylglyoxal 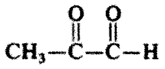 $CH_3-\overset{\overset{O}{\Vert}}{C}-\overset{\overset{O}{\Vert}}{C}-H$	73	(9, 15)*
5. Butenedial 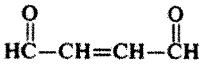 $\overset{\overset{O}{\Vert}}{HC}-CH=CH-\overset{\overset{O}{\Vert}}{CH}$	85	
6. Hydroxy-3-oxobutene‡ 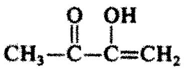 $CH_3-\overset{\overset{O}{\Vert}}{C}-\overset{\overset{OH}{\vert}}{C}=CH_2$	87	
7. Phenol	95	(16–18)†
8. 5-Oxo-1,3-hexadiene‡ 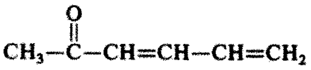 $CH_3-\overset{\overset{O}{\Vert}}{C}-CH=CH-CH=CH_2$	97	
9. 4-Oxo-2-pentenal‡ 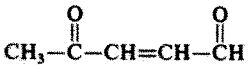 $CH_3-\overset{\overset{O}{\Vert}}{C}-CH=CH-\overset{\overset{O}{\Vert}}{CH}$	99	15*(16, 18)†
10. Hydroxybutenedial 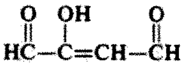 $\overset{\overset{O}{\Vert}}{HC}-\overset{\overset{OH}{\vert}}{C}=CH-\overset{\overset{O}{\Vert}}{CH}$	101	18
11. Hydroxy-3-oxobutanal‡ 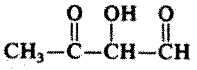 $CH_3-\overset{\overset{O}{\Vert}}{C}-\overset{\overset{OH}{\vert}}{CH}-\overset{\overset{O}{\Vert}}{CH}$	103	
12. Benzaldehyde	107	(11–14, 18)*
13. Cresol‡	109	(11, 12, 14, 15, 18)*
14. Hydroxy-5-oxo-1,3-hexadiene‡ 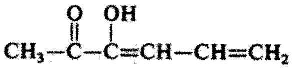 $CH_3-\overset{\overset{O}{\Vert}}{C}-\overset{\overset{OH}{\vert}}{C}=CH-CH=CH_2$	113	
15. Hydroxy-4-oxo-2-pentenal‡ 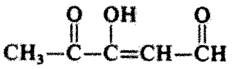 $CH_3-\overset{\overset{O}{\Vert}}{C}-\overset{\overset{OH}{\vert}}{C}=CH-\overset{\overset{O}{\Vert}}{CH}$	115	18†
16. Benzoic acid	123	
17. Hydroxybenzaldehyde‡	123	
18. Dihydroxytoluene‡	125	
19. 6-Oxo-2,4-heptadienal‡ 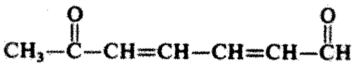 $CH_3-\overset{\overset{O}{\Vert}}{C}-CH=CH-CH=CH-\overset{\overset{O}{\Vert}}{CH}$	125	12
20. 4,5-Dioxo-2-hexenal‡ 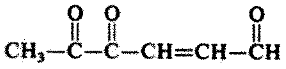 $CH_3-\overset{\overset{O}{\Vert}}{C}-\overset{\overset{O}{\Vert}}{C}-CH=CH-\overset{\overset{O}{\Vert}}{CH}$	127	
21. Nitrotoluene‡	138	(11–15, 18)*
22. Nitrophenol‡	140	14*
23. Hydroxy-6-oxo-2,4-heptadienal‡ 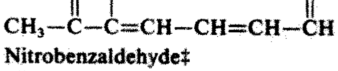 $CH_3-\overset{\overset{O}{\Vert}}{C}-\overset{\overset{OH}{\vert}}{C}=CH-CH=CH-\overset{\overset{O}{\Vert}}{CH}$	141	
24. Nitrobenzaldehyde‡	152	
25. Nitrocresol‡	154	(10–15, 18)*
26. Benzylnitrate	154	(12–15)*
27. Dinitrotoluene‡	183	

* Identified. † Proposed only. ‡ Several isomers possible.

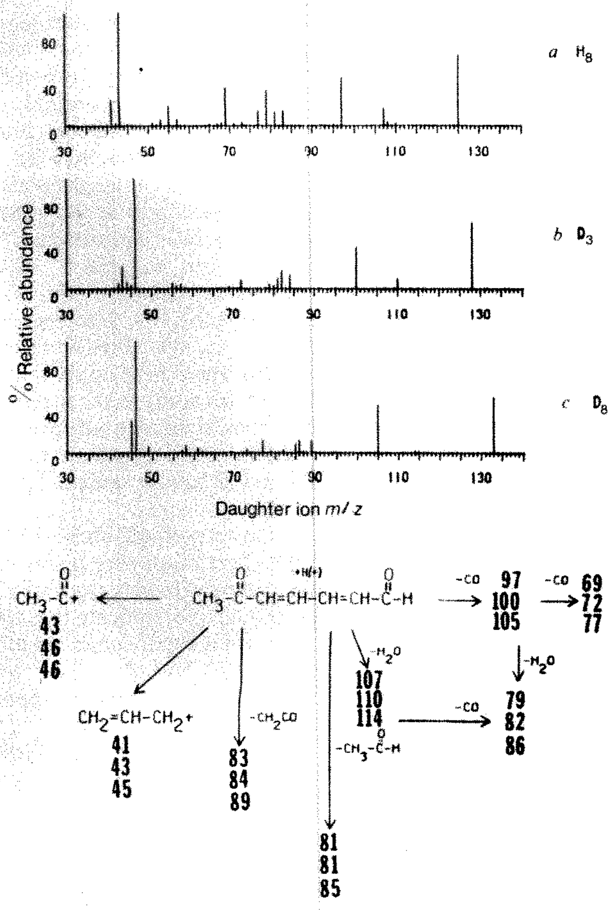

Fig. 1 Identification of 6-oxo-2,4-heptadienal. The $M+H^+$ ion was subjected to collision-induced-dissociation (CID) in its three isotopically-labelled forms. The three daughter-ion spectra are shown in *a, b, c* and the fragments are mass-shifted in agreement with the deuterium labels. *d*, A fragmentation scheme which confirms the identity of the parent molecule.

centration of the solvent, or occur at too low a mass to be scanned in all modes effectively. Six tentatively identified ring fragmentation products found by Schwartz[10] were not found in this study.

With the exception of benzylnitrate, none of the nitrate products hypothesized by Atkinson *et al.*[18] were found by this analysis. This is in agreement with a kinetic study[19] which attributed all NO_x loss before ozone appearance as being due to nitric acid formed in the reaction of HO with NO_2. Daughter spectra were taken at m/z corresponding to the major predicted nitrates. Additionally, neutral loss spectra[8] were taken at the possible major fragmentations: neutral loss of 17(OH), 30(NO), 46(NO_2), and 62(NO_3) mass units. In none of these spectra was there evidence for other nitrate products in the samples analysed. These compounds should have been detected if they were formed in yields as proposed (~25%). Benzoic acid and acetic acid were the only acids identified by MS/MS, and they were minor products. Acids as a group are easily recognized by their predominant fragmentation loss of 44 mass units (CO_2).

The product identification procedure is illustrated by the mass spectra shown in Fig. 1 for the compound 6-oxo-2,4-heptadienal. The three isotopic forms are shown: H_8 in Fig. 1*a*, D_3 in Fig. 1*b*, and D_8 in Fig. 1*c*. The deuterium mass-shifted fragments are in agreement with the proposed CID fragmentation processes shown in Fig. 1*d*. Spectra similar to these were obtained in all three isomeric forms for all compounds reported in Table 1. In some cases, the fragmentation patterns did not allow a choice to be made between several methyl- or hydroxyl-positional isomers, and more than one isomer was often present, as would be expected. Compounds with the same molecular weight but with different numbers of hydrogen atoms will have their molecular weight shifted to a different mass in the deuterium studies. The compounds will be given elsewhere[20].

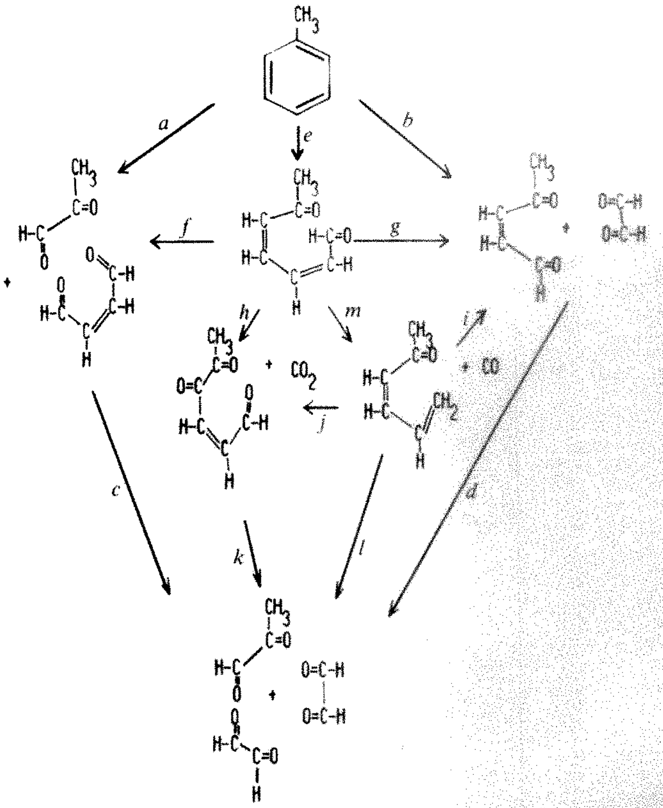

Fig. 2 Reaction pathways for the major ring fragmentation products of toluene which contain only the carbonyl moiety. All processes except *h* and *m* involve attack of hydroxyl radical at a double bond in the reactant. Process *h* involves abstraction of an aldehydic hydrogen. Process *m* is photolysis. Following the rate-determining hydroxyl attack, reactions such as shown in Fig. 3 produce the indicated products.

All of the compounds identified in this study have reasonable production pathways from toluene reacting under simulated atmospheric conditions. Following HO attack, further reactions with molecular oxygen and nitrogen oxides produce stable products and regenerate hydroxyl radicals. The specific reactions to produce the aromatic products are well understood[5,16-18]. Reactions similar to these can be used to explain the other aromatic products; hydroxybenzaldehydes, dihydroxytoluenes, nitrobenzaldehydes, nitrocresols, and dinitrotoluenes. The minor product phenol probably results from secondary reactions of benzaldehyde[17].

Figure 2 presents probable pathways for production of the major ring fragmentation products containing only the carbonyl group. Although many of the compounds in Fig. 2 have not been identified previously, several pathways have been proposed. These pathways are reactions *a–e* in Fig. 2. References for proposed formation of these and other compounds can be found in Table 1. Reactions *f–l* have not been previously proposed. They involve reaction sequences similar to those in *a–e*. Reaction *m* in Fig. 2 is the photolytic loss of carbon monoxide from 6-oxo-2,4-heptadienal. Similarly, hydroxy-5-oxo-1,3-hexadiene, 3-oxobutene and hydroxy-3-oxobutene are possible photolysis products of hydroxy-6-oxo-2,4-heptadienal, 4-oxo-2-pentenal and hydroxy-4-oxo-2-pentenal respectively. The photochemistry of these molecules is unknown. Photolytic loss of CO is common for some aldehydes, but propenal and *trans*-2-butenal do not show significant CO production at normal (25 °C) temperatures[21]. Although this pathway could explain the formation of products with a terminal methylene group, toluene's measured carbon monoxide yields are only 15% (ref. 6).

An alternative mechanism which would lead to these products is a 1,2-hydrogen shift after initial hydroxyl radical attack. This

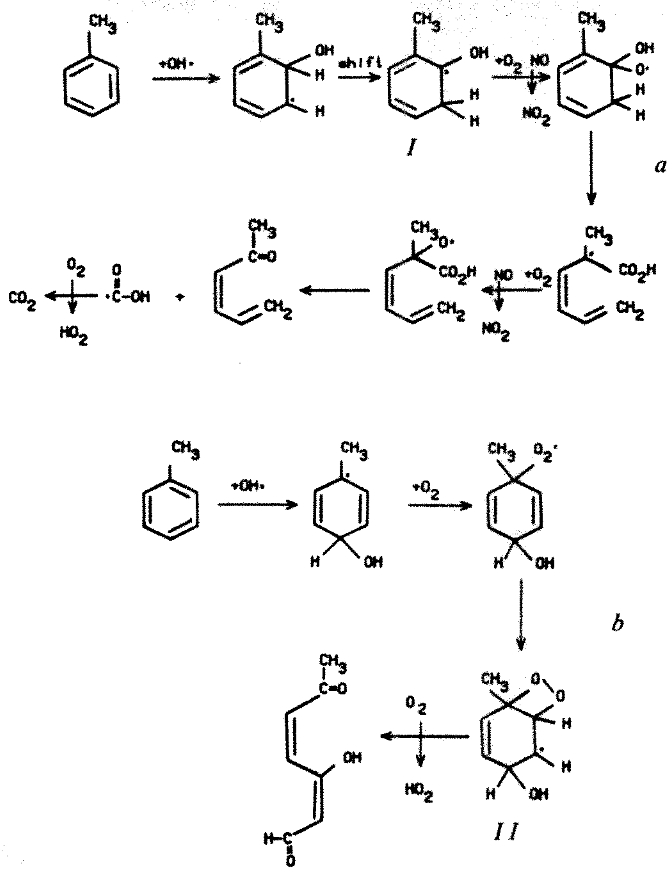

Fig. 3 New reaction pathways for two new toluene products identified. *a*, Reactions producing 5-oxo-1,3-hexadiene involve a initial hydrogen shift and ultimately produce a product containing a terminal methylene group as well as CO_2. *b*, Reactions producing 3-hydroxy-6-oxo-2,4-heptadienal. Mechanisms such as this retain the hydroxyl radical moiety in the ring-opened product.

mechanism is shown in Fig. 3*a*, where the hydrogen-shifted adduct *I* proceeds through reaction sequences similar to those proposed for the other ring fragmentation products. This reaction pathway leads to the production of 5-oxo-1,3-hexadiene and carbon dioxide. The reactions in Fig. 3*a* would help to explain the direct formation of carbon dioxide that we have observed[6]. Similar reaction sequences can be formulated for the other products containing a terminal methylene group. The 1,2-shift proposed in Fig. 3*a* has been observed in the closely related attack of $O(^3P)$ on toluene[22].

The hydroxy products identified in this study have two reasonable formation mechanisms. They may be formed from the primary product cresol reacting along similar fragmentation pathways as toluene. Because the primary cresol yield is low, only small amounts of these products would be expected from this route. An alternative reaction mechanism is shown in Fig. 3*b*. The hydroxy-product results from hydrogen abstraction from the oxygen-cyclized adduct *II*, rather than from oxygen addition leading to methyl glyoxal and glyoxal formation. Such a mechanism probably dominates over cresol reactions in forming products with the alcohol group. Although these compounds are isomeric with the corresponding acids, lack of CO_2 loss in the CID fragmentation argues against this structure.

Although the present work is basically a qualitative study, analysis[20] of the mass spectral product intensities indicates that most of the ring-fragmentation products listed in Table 1 contribute significantly to the reaction mechanism. Current mechanisms[16–18] depict a much simpler scheme, producing only a few of the products in Table 1. Although our structural assignments confirm previously proposed pathways of ring fragmentation, new pathways (Fig. 3) are required to explain the prevalent formation of products containing the terminal methylene group and containing the hydroxyl (alcohol) moiety. The latter class of compound is significantly more polar and will have a much lower vapour pressure than the corresponding carbonyl-containing species which lack the hydroxyl group. Incorporation into aerosols or precipitation may be important. Photolysis of the numerous aldehyde and ketone intermediates may be a significant source of atmospheric free radicals in the gas phase and perhaps also in aerosols or clouds. Failure to detect either nitrates or carboxylic acids in this study has implications for the acidity of precipitation. It has been suggested[23] that carboxylic acids can contribute significantly to such acidity. On the other hand, incorporation of atmospheric NO_x into organic reaction products would lessen the quantity available for oxidation to nitric acid. Note that results presented here apply to the HO/toluene reaction. The extension of this study to the reaction of ozone with the unsaturated products from toluene is desirable, due to the likelihood of acid formation in the ozone reaction[23] and nitrate formation in the reaction with nitrate radical[24] produced from NO_2 and O_3.

The significance of toluene's reactions in polluted air is widely acknowledged, primarily due to the effect of alkylbenzenes on ozone formation in photochemical smog. However, clean-air measurements[4] of toluene as high as 0.4 p.p.b. indicate that the mechanisms inferred here may have wider significance. At this upper concentration, the oxidation rate by HO of toluene represents ~20% of the methane oxidation rate. Although methane has long been presumed to dominate organic clean-air chemistry, products from toluene are more numerous and probably more reactive than the formaldehyde or methylhydroperoxide produced from methane. The very low NO_x concentrations in clean air relative to polluted air will negate formation of nitroaromatic products, and will influence the yields of the ring fragmentation products by curtailing NO reduction of peroxyl radical intermediates. For example, the processes shown in Fig. 3*b* would dominate over those in Fig. 3*a*, which require NO as a reactant. It seems safe to assume that the reactions of toluene and other nonmethane hydrocarbons are making an increasing and probably significant contribution to global tropospheric chemistry.

We thank Dr S. V. Hummel for carrying out the MS/MS analyses, Dr R. P. Yost for use of his instrument, and both for helpful discussions. R.J.O'B. thanks the University of Florida for support and the US Environmental Protection Agency for previous support of this research. P. J. Green provided invaluable assistance in earlier stages of this work.

Received 7 March; accepted 9 July 1984.

1. O'Brien, R. J., Hightower, J. & Crocker, T. D. in *The Alkylbenzenes* Ch. 1 (ed. Peter, F. M.) (National Academy of Sciences, Washington DC, 1981).
2. Pellizzari, E. D. *Information on the Characterization of Ambient Organic Vapors in Areas of High Chemical Pollution* Control No. 68-02-2721 (US Environmental Protection Agency, North Carolina, 1979).
3. Sexton, K. & Westberg, H. *Envir. Sci. Technol.* **14,** 329–332 (1980).
4. Rasmussen, R. A. & Khalil, M. A. K. *Geophys. Res. Lett.* **10,** 1096–1099 (1983).
5. O'Brien, R. J., Johnson, J. E. & Wilkerson, C. in *The Alkylbenzenes* Ch. 4 (ed. Peter, F. M.) (National Academy of Sciences, Washington DC, 1981).
6. O'Brien, R. J., Green, P. J., Nguyen, N-L., Doty, R. A. & Dumdei, B. E. *Envir. Sci. Technol.* **17,** 183–186 (1983).
7. Slayback, J. R. B., Story, M. S. *Ind. Res. Devl* February 129–139 (1981).
8. O'Brien, R. J., Dumdei, B. E., Hummel, S. V. & Yost, R. A. *Analyt. Chem.* (in the press).
9. Nojima, K., Fukaya, K., Fukui, S., Kanno, S. *Chemosphere* **5,** 247–252 (1974).
10. Schwartz, W. *Chemical Characterization of Model Aerosols* (Rep. to U.S. Environmental Protection Agency, NTIS PB-238 557, 1974).
11. Akimoto, H., Hosbino, J., Inone, G., Okuda, M. & Washida, N. *Bull. chem. Soc. Jap.* **51,** 2496–2502 (1978).
12. Hoshino, J., Akimoto, J. & Okuda, M. *Bull chem. Soc. Jap.* **51,** 718–724 (1978).
13. Ishikawa, J., Watanabe, K. & Ando, W. *Bull. chem. Soc. Jap.* **51,** 2174–2178 (1978).
14. O'Brien, R. J. *et al.* in *Nitrogenous Air Pollutants* Ch. 11 (ed. Grosjean, D.) (Ann Arbor Press, 1979).
15. Besemer, A. C. *Atmos. Envir.* **16,** 1599–1602 (1982).
16. Leone, J. A. & Seinfeld, J. H. *Int. J. Chem. Kinet.* **16,** 159–174 (1984).
17. Killus, J. P. & Whitten, G. Z. *Atmos. Envir.* **16,** 1973–1988 (1982).
18. Atkinson, R., Carter, W. P. L., Darnall, K. R., Winer, A. M. & Pitts, J. N. Jr *Int. J. chem. Kinet.* **12,** 799–836 (1980).
19. O'Brien, R. J., Green, P. J. & Doty, R. A. *J. phys. Chem.* **83,** 3302 (1979).
20. O'Brien, R. J., Dumdei, B. E., Hummel, S. V. & Yost, R. A. *38th Northwest Regional Meet. Am. chem. Soc.* Honolulu (submitted for publication).
21. Lee, E. K. C. & Lewis, R. S. *Adv. Photochem.* **12,** 53–55 (1980).
22. Takamuku, S., Matsimoto, H., Hori, A. & Sakurai, H. *J. Am. chem. Soc.* **102,** 1441–1443 (1980).
23. Calvert, J. G. & Stockwell, W. R. *Envir. Sci. Technol.* **17,** 428A–439 (1983).
24. Atkinson, R., Aschmann, S. M., Winer, A. M. & Pitts, J. N. Jr *Envir. Sci. Technol.* **18,** 370–374 (1984).

Natural ^{15}N abundance measurements and atmospheric nitrogen standard calibration

André Mariotti

Université Pierre et Marie Curie, Biogéochimie des Isotopes stables,
Departement de Géologie dynamique T26, 4 Place Jussieu,
75230 Paris Cédex 05, France

Small differences in natural isotope ratios between two compounds can be measured easily and with high precision by using mass spectrometers fitted with double (or triple) ion collectors and dual inlet systems equipped for rapid switching between reference and sample[1–3]. The parameter used to describe these differences in natural ^{15}N abundance is:

$$\delta^{15}N‰ = \frac{R_{sample} - R_{standard}}{R_{standard}} \times 1{,}000$$

where R is the isotopic ratio of $m/z = 29(^{14}N^{15}N^+)$ to $m/z = 28$ ($^{14}N^{14}N^+$). Although an international standard for nitrogen has not yet been defined, atmospheric N_2 had been chosen through practical experience, even before the worldwide homogeneity of its isotopic composition was demonstrated[4–7]. However, the presence of argon ($\simeq 1\%$) in purified air samples may, in some circumstances, modify the apparent isotope ratio of atmospheric N_2. Two different mass spectrometers in our laboratory have been used to assess the magnitude of this 'argon effect', which seems to be essentially an instrumental, presumably pressure-related, effect. Therefore, on mass spectrometers showing this argon effect it is imperative that a correction be applied to measurements of $\delta^{15}N$ of atmospheric N_2. However, in some circumstances (different mass spectrometers, different tuning of the same instrument) this effect can be non-existent or negligible and might require no correction whatsoever.

I have previously described[7] a simple method for the preparation of atmospheric N_2 as a standard for $\delta^{15}N$ measurements. Excellent reproducibility was obtained. This work established the worldwide isotopic homogeneity of atmospheric N_2: the standard deviation in $\delta^{15}N$ of 30 air samples of various origin, measured against one air sample arbitrarily considered as reference, was 0.026‰. Thus, atmospheric N_2 seems to be a reliable standard for ^{15}N natural abundance measurements. In addition, when the variation in ^{15}N abundance is used as the basis for estimating biological N_2 fixation[8], it is essential that an accurate comparison be made between the ^{15}N abundance of plant tissue and of atmospheric N_2. I demonstrated that the various steps in the preparation of atmospheric N_2 as an isotopic standard (deoxygenation, drying, trapping on molecular sieve) did not introduce isotopic enrichments[7]. My data were obtained on a VG 602 D double inlet dual collector mass spectrometer. As it is not possible to eliminate argon in air samples by simple and non-fractionating means, I have used the same instrument to test the side effect of argon on the $\delta^{15}N$ value of nitrogen. No such effect was observed. Some authors (ref. 9 and personal communications from T. Heaton and H. Gerstenberger), however, have found that the presence of atmospheric argon may influence the results of isotopic analyses of atmospheric nitrogen. Heaton (personal communication) pointed out that there is a variable effect which depends on the ion-source focusing of the mass spectrometer. Recently, our laboratory acquired a new triple collector VG SIRA 9 mass spectrometer. During intercalibration between the VG 602 D and SIRA 9 instrument, a small but systematic difference in ^{15}N abundance between atmospheric nitrogen (prepared as described previously[7]) and a secondary working standard (pure tank N_2:99.998%) was observed between the two instruments. No difference, however, was observed between pairs of nitrogen samples without argon. An 'argon effect' was thus suspected. Although Pure tank N_2 is often used as a working standard, data are nearly always reported versus atmospheric N_2. This discrepancy is especially important for precise interlaboratory comparisons. I now suggest a simple method of correcting the measurement of tank N_2 working standard versus atmospheric N_2.

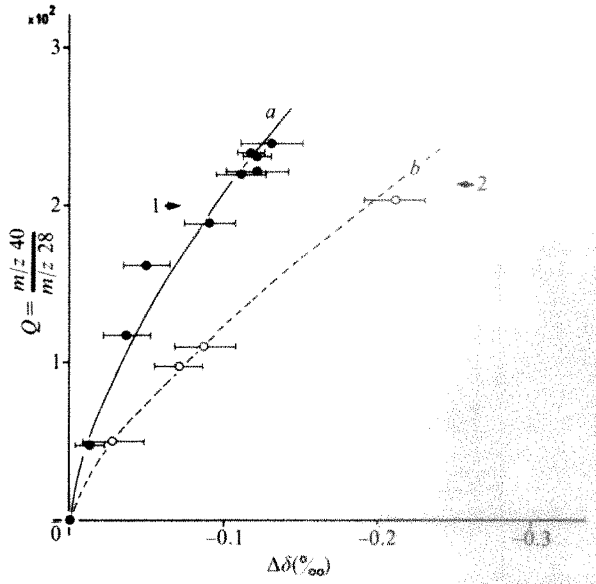

Fig. 1 Effect of increasing quantities of argon on the apparent isotope ratio of nitrogen. Cases *a* and *b* correspond to two different adjustments of the capillary conductance. 1 and 2 represent the *Q* ratio value for atmospheric nitrogen, respectively.

To establish the value of the required correction, pure tank N_2 from the same bottle taken as our daily mass spectrometer standard (N48 pure N_2: 99.998%) was admixed with different proportions (up to 1% v/v) of pure tank argon and stored in evacuated flasks. The ratio, Q, of ion beams in the mass spectrometer corresponding to $m/z = 40$ (argon) and $m/z = 28$ (nitrogen $^{14}N^{14}N^+$) is measured as:

$$Q = \frac{m/z = 40 \text{ ion beam}}{m/z = 28 \text{ ion beam}}$$

For each Q value the apparent isotopic composition of the nitrogen is determined with reference to the same nitrogen when it is argon-free. We define $\Delta\delta$:

$$\Delta\delta = \delta^{15}N \text{ (tank } N_2 \text{ spiked with argon)} \\ -\delta^{15}N \text{ (tank } N_2)$$

These measurements were made on the SIRA 9 mass spectrometer, after optimization of ion-source focusing which was kept constant thereafter. Moreover, all measurements were made with the same gas pressure in the inlet system thus giving the same ion intensity at $m/z = 28$, which is kept as 5×10^{-9}A. These measurements were made for two different capillary conductances, adjusted on both reference and sample sides by means of adjustable crimps[3]. For each Q value, seven or eight measurements of $\Delta\delta$ were made and the mean value determined (standard deviation $\sim \pm 0.02‰$).

An increasing proportion of argon in the nitrogen sample (increasing Q ratio) was associated with a modification of the apparent nitrogen isotope ratio (29/28) which, in the working conditions stated above, was reflected in a lowering of the measured $\delta^{15}N$ value. The relation is not linear (Fig. 1). From these data it is possible to derive an appropriate correction factor to convert the measured $\delta^{15}N$ value to a true $\delta^{15}N$ value. In our present working conditions, this correction is of the order of 0.09‰ for atmospheric nitrogen ($Q \simeq 2 \times 10^{-2}$). Figure 1 also shows that $\Delta\delta$ value as a function of Q is also a function of the capillary conductance. For two different values of this parameter, $\Delta\delta$ is different. In case *a* of Fig. 1 (our present working condition), the capillary conductance, measured by the $m/z = 28$ ion beam value, is 15% lower than in case *b*. On our instrument, the more the capillaries are tightened by means of the crimps, the less is the influence of argon on apparent nitrogen isotope

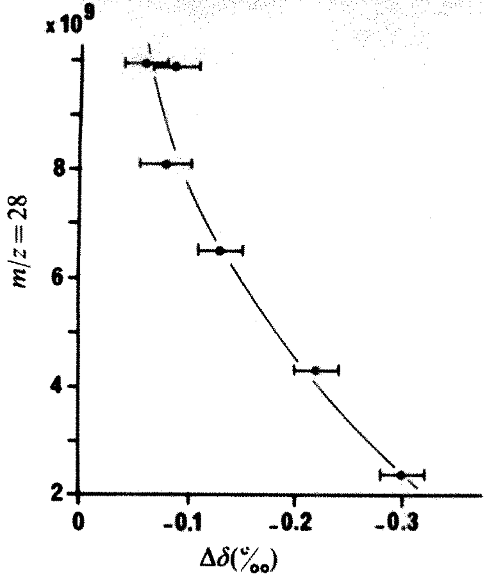

Fig. 2 Effect of the gas pressure in the mass spectrometer inlet system (estimated using $m/e = 28$ v for the ion beam) on the apparent nitrogen isotope ratio in the presence of argon.

ratio. For a pure N_2 sample spiked with argon, we have also tested the influence of gas pressure in the inlet system, adjusted by means of the variable reservoir and estimated through the intensity of ion beam $m/z = 28$. In case *b* (leak rate faster than our present conditions) the increase of gas pressure in the inlet system brings about a reduction of the argon effect on the apparent nitrogen isotope ratio (Fig. 2). With the present condition of capillary conductance (case *a*), this effect is lower. These observations suggest that this effect is presumably pressure related and emphasize the fact that calibration and successive measurements of atmospheric N_2 versus the working standard must be made at the same value of $m/z = 28$ ion current.

Finally, the argon effect may also be modified through tuning of the ion-source focusing. The measured $\delta^{15}N$ value is especially sensitive to the electron trap current (ionizing electron current regulated on the trap electrode) which must be kept at a constant value for the calibration of the correction curve and the further calibration of air nitrogen versus the working standard.

The mean value for several measurements ($n = 30$) using our VG 602 D, an instrument not subject to a detectable argon effect, is 3.4+0.026‰[7] ($\delta^{15}N$ of atmospheric N_2 versus pure tank N_2). The mean of eight different samplings of Paris air measured using the VG SIRA 9 instrument was 3.30±0.02‰ (see Table 1). Air sampled at the same time and at the same location was also measured on the VG 602 instrument (daily procedure); the mean of these measurements (3.39‰) falls within one standard deviation of the value routinely measured on this instrument.

Table 1 Isotopic composition of eight different air samples taken in Paris

Measured $\delta^{15}N_{\text{atmos. }N_2}$ versus bottle N_2	Q ratio ($\times 10^{-2}$)	Corrected $\delta^{15}N$
3.29	1.95	3.38
3.30	1.96	3.39
3.30	1.96	3.39
3.28	1.95	3.37
3.27	1.90	3.37
3.30	2.03	3.42
3.32	1.95	3.40
3.30	1.95	3.39
$\bar{m} = 3.30$		3.39
$\sigma = 0.02$		0.02

The corrected $\delta^{15}N$ is obtained according to curve *a* of Fig. 1.

The value obtained with the SIRA 9 instrument is statistically different ($P < 0.01$) from that obtained on the VG 602 instrument. However, when the argon correction discussed above is applied to the values obtained with the VG SIRA 9 instrument, the mean is 3.39±0.02‰ (Table 1); this corrected value is fully compatible with the previously reported results obtained on the VG 602 instrument.

A correction for possible effects of argon present in atmospheric N_2 prepared as deoxygenated air should be made for each mass spectrometer. Where such effects exist the appropriate steps should be taken to correct for the argon effect to make the precise calibration of a working standard (pure tank N_2 for example, which is very stable with time[7,10]) versus atmospheric N_2. This must be done each time the ion source is adjusted, for example, after a change of filament. This precaution is especially necessary to bring greater validity to the assignment of $\delta^{15}N$ values versus atmospheric N_2 based on interlaboratory comparisons of standards, especially those provided by IAEA (N_1 and N_2 ammonium sulphate[11]).

I thank Professors D. H. Kohl, R. Letolle, F. J. Bergersen and M. C. Clarke for critical reading of and improvements to the manuscript and T. H. E. Heaton and H. Gerstenberger for their personal communications.

Received 2 May; accepted 22 June 1984.

1. Nier, A. O. *Rev. Scient. Instrum.* **18,** 398–411 (1947).
2. McKinney, C. R., McCrea, J. M., Epstein, S., Allen, H. A. & Urey, M. C. *Rev. Scient. Instrum.* **21,** 724–730 (1950).
3. Bridger, N. I., Craig, R. D. & Sercombe, J. S. F. *Adv. Mass Spectrom.* **6,** 365–375 (1974).
4. Dole, M. *et al. Geochim. cosmochim. Acta,* **6,** 65–78 (1954).
5. Junk, G. & Svec. H. J. *Geochim. cosmochim. Acta* **14,** 234–243 (1958).
6. Sweeney, R. E., Liu, K. K. & Kaplan, I. R. *DSIR Bull.* **220,** 9–26 (1978).
7. Mariotti, A. *Nature* **303,** 685–687 (1983).
8. Mariotti, A., Mariotti, F. & Amarger, N. *Physiol. Vég.* **21,** 279–291 (1983).
9. Heaton, T. H. E., Talma, A. S. & Vogel, J. C. *J. Hydrol.* **62,** 243–262 (1983).
10. Mariotti, A. thesis, Mém. Sci. Terre, Univ. Pierre et Marie Curie, Paris, No. 82-13 (1982).
11. Gonfiantini, R. *Nature* **271,** 534–536 (1978).

Microplankton productivity in the oligotrophic ocean

Ralph E. H. Smith*, Richard J. Geider† & Trevor Platt*

* Marine Ecology Laboratory, Bedford Institute of Oceanography, Dartmouth, Nova Scotia, Canada B2Y 4A2
† Department of Oceanography, Dalhousie University, Halifax, Nova Scotia, Canada B3H 4J1

Uncertainty about the absolute levels of biological productivity over vast tracts of the world's oceans is a fundamental limitation to our understanding of the marine ecosystem[1,2]. Various workers have sought clarification through a comparison of the fluxes of oxygen and carbon in the photic layer[3–5]. A re-examination of data[4] used to compare short-term (<1 day) *in vitro* carbon assimilation with long-term (≈100 day) *in situ* oxygen accumulation at a station in the north central Pacific has shown that the molar fluxes of oxygen and carbon are, in fact, consistent within the resolution of the comparison[6]. This test, however, is lacking in discrimination[7]. A recent comparison of short-term *in vitro* carbon and oxygen fluxes off Hawaii has been interpreted[5] as indicating that short-term (≈12 h) carbon uptake in open ocean regions provides an unbiased measure of gross primary production, P_g. We show here that comparisons of short-term oxygen- and carbon-flux measurements do not provide a powerful test of the accuracy of either of the measurements, both of which can be biased by trophic interactions in the microplankton. Consideration of trophic interactions, implicit in the reported data[5], leads to the important new conclusion that the active biomass of microheterotrophic organisms was large compared with that of autotrophs, a situation which may be generally applicable to the pelagic zone of the open ocean.

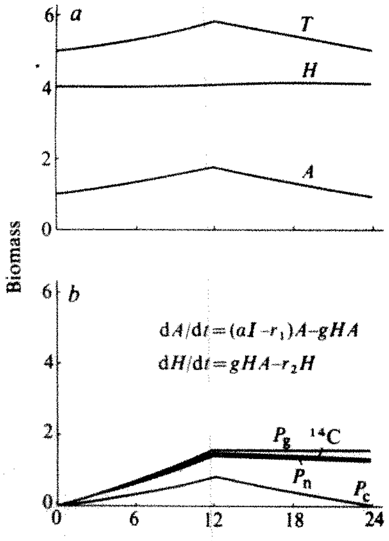

Fig. 1 *a*, The time course (t) of biomass in the total microplankton (T), in autotrophs (A) and in heterotrophs (H) as calculated from the predator–prey model (inset *b*). The photoautotrophic growth rate is αI, set equal to 0.1 h^{-1} for $0 < t \leq 12$ h and zero otherwise. Other parameters were autotroph respiration rate (r_1) = 0.01 h^{-1}; heterotroph respiration rate (r_2) = 0.013 h^{-1}; and grazing rate (g) = 0.0105 h^{-1} biomass^{-1}. Initial autotroph and heterotroph biomasses were 1.0 and 4.0 respectively. *b*, The time dependencies of calculated integral gross (P_g), net autotrophic (P_n), and net community (P_c) productivities and the corresponding productivity which would be calculated from ^{14}C accumulation in the particulate matter. All productivities are expressed in biomass units; parameter and initial values are as in *a*.

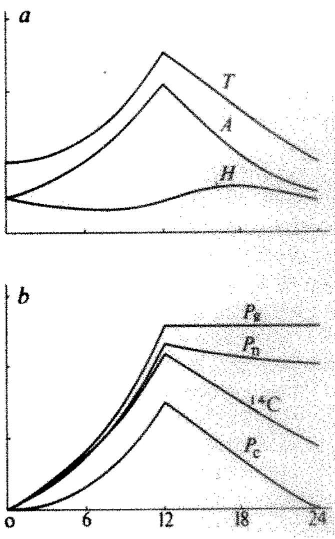

Fig. 2 *a*, The calculated time dependencies of total microplankton, microautotrophic and microheterotrophic biomass. The parameter and initial values used for this simulation are $\alpha I = 0.2\ h^{-1}$ for $0 < t \leq 12$ h and zero otherwise; $r_1 = 0.02\ h^{-1}$, $r_2 = 0.185\ h^{-1}$, $g = 0.080\ h^{-1}$ biomass^{-1}, $A = 1.0$ and $H = 1.0$. *b*, The time dependencies of calculated integral gross, net autotrophic and net community productivities and the corresponding productivity which would be calculated from ^{14}C accumulation in the particulate matter. Parameter and initial values are as in *a*.

The wrong interpretation of *in vitro* molar flux data for biological populations can result from a failure to recognize that a compartmental model of tracer flow through the population is implicit in the calculation of the results[8–10]. The ^{14}C technique[11] depends on measuring the assimilation of tracer inorganic carbon into organic form by photosynthesis, but some of the assimilated tracer carbon may itself be lost due to community respiratory processes. The variability of such losses has long been recognized as a source of uncertainty in the interpretation of ^{14}C-based production estimates[11]. If losses are very small, the ^{14}C estimate can approach P_g, but large losses may greatly reduce the ^{14}C estimate. A particular problem with *in vitro* measurement of autotrophic activity in natural assemblages of open ocean plankton is the lack of discrimination against the activity of microheterotrophs. Their interference with the tracer carbon flux is not the same as their effect on the oxygen flux, and will bias any comparison between the two fluxes. The degree of bias will vary with community structure, in particular with the ratio of the biomasses of microheterotrophs to autotrophs.

The difficulty in accepting the interpretation of Williams *et al.*[5], that 12-h of ^{14}C uptake gives an estimate of P_g, stems from the rapid turnover of microorganisms in the sample they studied. Although the specific growth rate of phytoplankton was as high as 1.2 per day (ref. 12, Table 4) the net change in both pigment biomass and oxygen during 24 h was essentially zero. In other words, the high rate of autotrophic production was in apparent, dynamic balance with consumption and respiration by microplankton. Both autotrophs and heterotrophs contribute to respiration in the incubation bottles. It is easy to show[13] that if autotrophs only were responsible for the respiration, ^{14}C assimilation after 12 h should give a biased estimate of P_g (in fact, a value of ~0.6 P_g). The bias would be less if some physiological mechanism were operating that restricted most of the respiration to the night hours, but then a large diurnal fluctuation in phytoplankton abundance would have been observed. Again, if autotrophic respiration were continuous, but recent assimilate mobilized only at night[14,15], considerable loss of ^{14}C would have been observed during the night hours, which was not the case. If ^{14}C uptake is apparently equal to P_g, as measured by oxygen evolution, the conclusion would seem to be that the high community respiration rate, as implied by a high specific growth rate of autotrophs without biomass accumulation, is predominantly due to microheterotrophs.

We have examined this conclusion using a simple predator–prey model of the Lotka–Volterra type (Fig. 1*b*, inset). We assumed that grazing takes place throughout the 24-h day, but that growth of autotrophs (photosynthesis) occurs only during the light period. The model differs from a recent treatment by Jackson[16] by including the second-order term in heterotrophic and autotrophic biomasses for carbon flow into microherbivores[17]. Both the autotroph and heterotroph pools are assumed to be well-mixed with respect to the tracer, that is, the tracer respires at rates proportional to its specific activity in the pool.

The steady-state solution for constant forcing supplies the initial relationship between the model parameters. Most of the parameters can be fixed through reference to the reported data[5,12]: (1) autotrophic growth rate averaged over 24 h is about 1.2 per day; (2) net biomass change over 24 h (net community productivity, P_c) is about zero; (3) autotrophs comprise only about one-quarter of the total microplankton biomass. Because autotroph respiration rate can be only a small part of P_g, we fixed it at 0.1 P_g, consistent with what is accepted by algal physiologists[18]. The equilibrium conditions can then be solved for the rates of grazing and respiration in the herbivores.

The time course of biomass in autotrophs and heterotrophs was simulated for a 12-h day and 12-h night, and the uptake of ^{14}C (added at the first dawn) calculated over the light–dark cycle. Our simulation reproduces the principal features reported for the natural system: small diel variation in both autotrophic and total microplankton biomass, and little net change in biomass over 24 h (Fig. 1*a*). Despite the rapid system turnover, and the close coupling between autotrophs and heterotrophs, ^{14}C uptake is roughly linear throughout the light period, and is very close to net autotrophic production, P_n, even after 24 h (Fig. 1*b*).

The simulation shows that ^{14}C uptake measured over the light period will yield an apparent carbon assimilation rate practically equal to a simultaneous estimate of P_g by the oxygen method. The oxygen estimate itself will always be too low, due to unequal biomass accumulation in light and dark bottles, which causes respiration to be underestimated (by ~10% in the present case). The considerable and unavoidable random errors in both oxygen- and carbon-flux estimates, together with uncertainty about the true value of the physiologically-variable photosynthetic quotient, will effectively mask the small difference between the two estimates. The uncorrelated, random errors are large, even compared with the difference usually expected between the true, unbiased values of P_g and P_n. It will not, in general, be possible to differentiate between the two (not exhaustive) possibilities that ^{14}C uptake rates measure P_g or P_n, where the standard for P_g derives from changes in oxygen.

Our model, although very simple, accounts for the behaviour of ^{14}C tracer in oligotrophic ocean microplankton near Hawaii. It explains how, in a strictly operational sense, ^{14}C uptake rates might be nearly equal to P_g, in apparent contradiction with the observation that the system is in a state of rapid turnover. But it also reveals that something quite different from P_g is actually measured. A large proportion of the assimilated tracer accumulates in the heterotrophic biomass during the incubation, and ^{14}C uptake measures the retention of carbon in the heterotroph as well as in the autotroph pool. The coincidence in the magnitudes of ^{14}C uptake and P_g is, therefore, a consequence not only of a low autotrophic respiration rate (that is, P_n not very different from P_g) but also of the presence of a large heterotroph population with relatively slow turnover.

Different dynamics may hold in other ocean regions. But because systematic errors scaled to plankton growth rates affect estimates of both carbon and oxygen fluxes, our simple model is not particularly sensitive to the magnitude of its parameters, in so far as the predicted magnitude of apparent photosynthetic quotient is concerned. For example, in the north equatorial current of the Atlantic[3,19,20], pronounced diel fluctuations were reported in oxygen concentration and in particulate carbon concentration. Our model shows (Fig. 2*a*) that large diel fluctuations in biomass may be expected when a relatively small heterotroph population regulates the biomass of a rapidly-growing autotroph population. During the simulated light period, ^{14}C was a reasonable estimate of P_n, in spite of the rapid turnover, but was an underestimate of P_g (Fig. 2*b*). This bias would not have been revealed in a comparison against P_g measured by O_2 evolution *in vitro*, however: respiration in the dark bottle was only ~60% of that in the light bottle, and, therefore P_g would also have been underestimated. The apparent photosynthetic quotient would have been roughly unity, even though both numerator and denominator were biased estimates of P_g. Complete understanding of such a system would require study of the dynamics of both particulate and the ^{14}C tracer throughout the entire 24-h period. Like Jackson, our simulation shows that microplankton grazing alone could not cause ^{14}C uptake during the light period to underestimate P_n by a large factor, as has been suggested[3,19,21].

Our conclusions do not depend on details of the mechanism of carbon transfer from autotrophs to heterotrophs, but on the dominance of the latter in community metabolism and the consequent delay in the respiration of tracer carbon. For example, the microheterotroph biomass at ocean sites is commonly dominated by bacteria[12,22,23] which are presumably nourished indirectly through autotrophic production by a pool of dissolved organic carbon. Despite this difference from our simple predator–prey model mechanism, we may expect that such communities will continue to act as a buffer, delaying the respiration of tracer carbon. Even the detailed kinetics of tracer movement through such communities may be difficult to distinguish from those of a predator–prey model if the coupling between dissolved organic carbon production and consumption is generally as tight as many measurements would suggest[24–26].

We have shown that the presence of a large heterotrophic component, which has been suggested to characterize oceanic plankton[27,28], has a profound regulatory effect on the dynamics of the plankton system, as judged by both the oxygen and the carbon flux. Failure to recognize this in making comparisons betweeen *in vitro* carbon uptake and oxygen·evolution will severely limit the information that can be extracted about the absolute level of productivity in the open ocean. Neither flux provides either a control for the other or an unbiased reference standard for P_g, and an apparent consistency in the observed fluxes is no guarantee that both are free from systematic errors.

Received 7 November 1983; accepted 16 July 1984.

1. Eppley, R. W. & Peterson, B. J. *Nature* **282**, 677–680 (1979).
2. Kerr, R. S. *Science* **220**, 397–398 (1983).
3. Tijssen, S. B. *Neth. J. Sea Res.* **13**, 79–84 (1979).
4. Shulenberger, E. & Reid, J. L. *Deep-Sea Res.* **28A**, 901–919 (1981).
5. Williams, P. J. LeB., Heinemann, K. R., Marra, J. & Purdie, D. A. *Nature* **305**, 49–50 (1983).
6. Platt, T. *Deep-Sea Res.* (in the press).
7. Platt, T., Lewis, M. & Geider, R. *Flows of Energy and Materials in Marine Ecosystems: theory and practice* (ed. Fasham, M. J. R.) (Plenum, London, in the press).
8. Peterson, B. J. *Ann. Rev. Ecol. Syst.* **11**, 369–385 (1980).
9. Smith, D. F. & Horner, S. M. J. *Can. Bull. Fish. Aquat. Sci.* No. 210 (1981).
10. Smith, R. & Platt, T. *Mar. Ecol. Prog. Ser.* **16**, 75–87 (1984).
11. Strickland, J. D. H. *Bull. Fish. Res. Bd. Can.* **122**, Ottawa (1960).
12. Laws, E. A. *et al. Limnol. Oceanogr.* (in the press).
13. Smith, R. E. H. *Mar. Biol. Lett.* **3**, 325–334 (1982).
14. Dring, M. J. & Jewson, D. H. *Proc. R. Soc. Lond.* B **214**, 305–323 (1982).
15. Bidwell, R. G. S. *Can. J. Bot.* **55**, 809–819 (1977).
16. Jackson, G. A. *J. Plankt. Res.* **5**, 83–94 (1983).
17. Landry, M. R. & Hassett, R. P. *Mar. Biol.* **67**, 283–288 (1982).
18. Burris, J. E. *Primary Productivity in The Sea* (ed. Falkowski, P.) (Plenum, New York, 1980).
19. Gieskes, W. W. C., Kraay, G. W. & Beers, M. A. *Neth. J. Sea Res.* **13**, 58–78 (1979).
20. Postma, H. & Rommets, J. W. *Neth. J. Sea Res.* **13**, 85–98 (1979).
21. Sheldon, R. W. & Sutcliffe, W. H. Jr, *Limnol. Oceanogr.* **23**, 1051–1055 (1978).
22. Beers, J. R., Reid, F. M. H. & Stewart, G. L. *Int. Rev. ges. Hydrobiol.* **60**, 607–638 (1975).
23. Azam, F. *et al. Mar. Ecol.-Prog. Ser.* **10**, 257–263 (1983).
24. Billen, G., Joiris, C., Wijnant, J. & Gillian, G. *Est. Coast. Mar. Sci.* **11**, 279–294 (1980).
25. Jensen, L. M. *Mar. Ecol. Prog-Ser.* **11**, 39–48 (1983).
26. Wiebe, W. J. & Smith, D. F. *Mar. Biol.* **42**, 213–223 (1977).
27. Williams, P. J. LeB. *Kieler Meeresforsch. Sonderh.* **5**, 1–28 (1981).
28. Sieburth, J. McN., Smetacek, V. & Lenz, J. *Limnol. Oceanogr.* **23**, 1256–1263 (1978).

Immuno-gold localization of leghaemoglobin in cytoplasm in nitrogen-fixing root nodules of pea

John G. Robertson[*,§], Brian Wells[*], Ton Bisseling[†], Kevin J. F. Farnden[‡] & Andrew W. B. Johnston[*]

[*] John Innes Institute, Norwich NR4 7UH, UK
[†] Laboratory of Molecular Biology, Agricultural University,
De Dreijen 11, 6703 BC Wageningen, The Netherlands
[‡] Department of Biochemistry, University of Otago, Box 56,
Dunedin, New Zealand

A unique feature of nitrogen-fixing nodules formed by association of species of *Rhizobium* and *Frankia* with various legumes and non-legumes is that they contain leghaemoblogin (Lb), an oxygen-carrying myoglobin-like protein[1–6]. Elucidation of the function of Lb, which is thought to facilitate the flow of oxygen to the nitrogen-fixing bacteroid forms of *Rhizobium* within infected nodule cells[7,8], has been hindered by uncertainty regarding its precise intracellular location[9]. Several workers have reported that Lb is located exclusively in the plant cytoplasm in nodules of various legumes[10–12], while others[13–15] have concluded that some of the Lb is located in the peribacteroid spaces in some legumes. Using immuno-gold staining[16] of Lb on thin sections of pea nodules, we demonstrate here that Lb can be detected in the plant cytoplasm and the nucleus of infected cells but not in the peribacteroid spaces.

Good ultrastructual preservation of both nodule and root tip tissue from pea was obtained using the schedule for embedding described in Fig. 1 legend. Immuno-gold staining using anti-pea Lb as the primary antibody on thin sections of 15-day pea nodule tissue revealed specific staining of the cytoplasm of infected

---

[§] Present address: Applied Biochemistry Division, Department of Scientific and Industrial Research, Private Bag, Palmerston North, New Zealand.

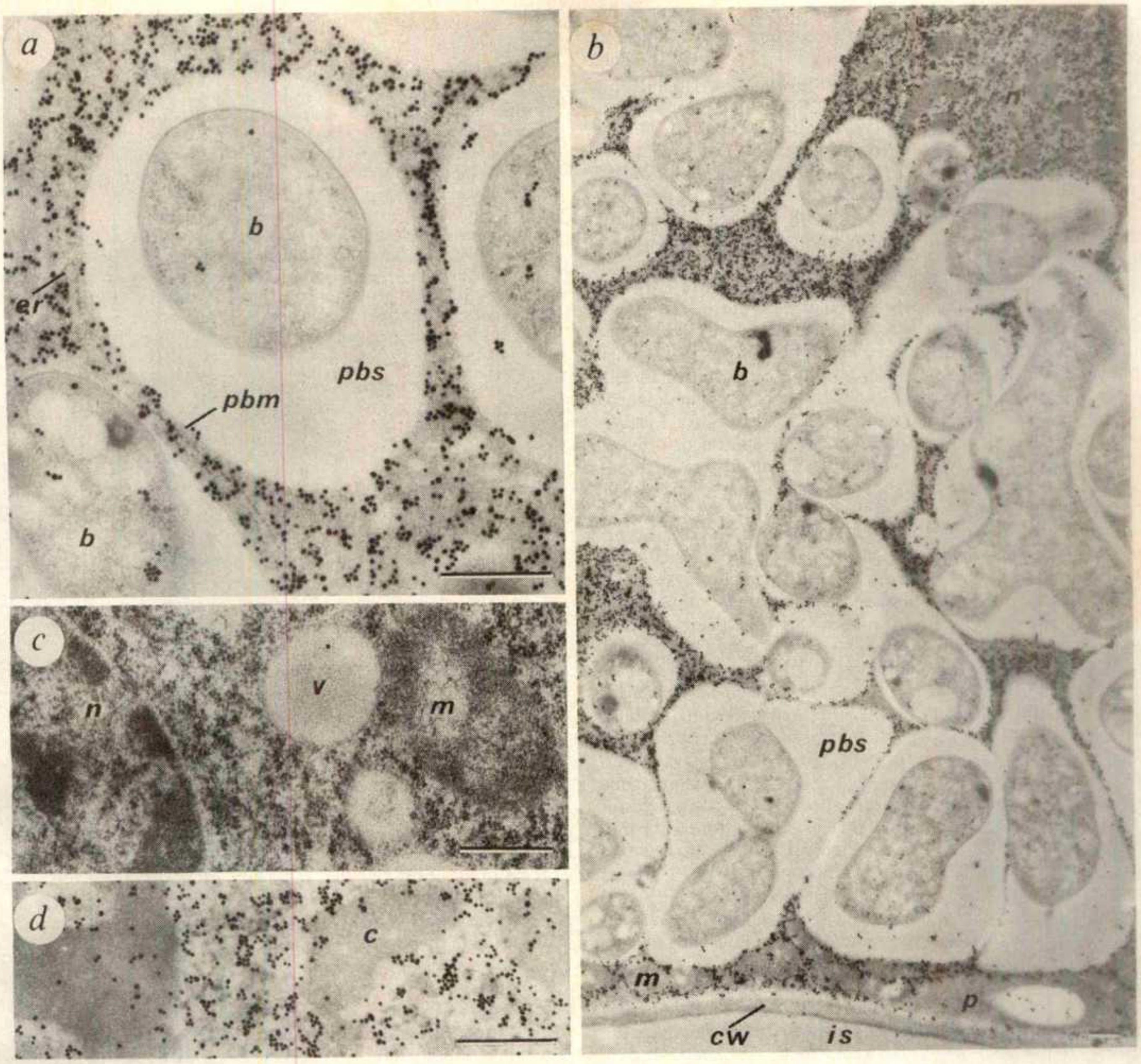

Fig. 1 Immuno-gold staining for Lb of thin sections of 15-day pea nodules and root tips prepared for electron microscopy in Lowicryl K4M. Sections were counterstained with uranium and lead. Scale bars represent 5 µm. *a*, Bacteroid (b) enclosed by a peribacteroid membrane (pbm) in the cytoplasm of an infected nodule cell. Only the plant cytoplasm shows specific immunostaining with gold particles which are sharply delineated from the peribacteroid space (pbs) by the peribacteroid membrane. The endoplasmic reticulum (er) can be distinguished as tracks in the plant cytoplasm which are not generally stained with gold. *b*, Bacteroids distributed in the plant cytoplasm of an infected cell (lower magnification). The nucleus (n) is immunostained with gold. The cell wall (cw), mitochondria (m), plastids (p) and intercellular space (is) show no specific staining. *c*, Section of a non-infected cell from the root tip of pea showing no specific immuno-gold staining of the nucleus, cytoplasm, vacuole (v), or mitochondria. *d*, Section of a nucleus of an infected nodule cell immunostained with gold. The regions of chromatin (c) do not stain as heavily as the non-chromatin regions.

Methods: Nodules were taken from roots of pea plants (*Pisum sativum* var. Wisconsin perfection) grown on agar[27] in a growth cabinet, 11 and 15 days after inoculation of seedlings with *Rhizobium leguminosarum* strain 3688. Nodules of maximum length ~1.5 mm were sliced longitudinally, evacuated and fixed in 2.5% glutaraldehyde, 50 mM cacodylate buffer *p*H 7.2, for 1 h at 22 °C. Dehydration through an ethanol series at 0 °C, −20 °C and −35 °C and infiltration with Lowicryl K4M[26], was done according to the manufacturer's recommendations (Chemische Werke Lowi) in a unit cooled with liquid nitrogen and in which the specimens were rotated at 2 r.p.m. (B.W., in preparation). Polymerization was carried out under UV light (EYE FL20S.BLB) in a −40 °C freezer for 24 h and then at room temperature for 48 h. The pink coloration associated with the presence of Lb in 15-day nodules was visible in the embedded tissue. Root tips ~1 mm long from pea plants were also fixed and embedded. Thin sections were cut on glass knives and processed as follows for immuno-gold staining on 200-mesh gold grids bearing a carbon–Parlodion film which had been glow-discharged. The sections were immersed in bovine serum albumin (BSA, Fraction V; Sigma), 20 mg ml^{-1} in Tris-buffered saline (TBS) containing 10 mM Tris-HCl *p*H 7.4, 9 mg ml^{-1} NaCl, 0.2 mg ml^{-1} NaN_3, 0.5 mg ml^{-1} polyethylene glycol (MW 20,000), for 1 h at 37 °C; immersed in anti-pea Lb antibody (freeze-dried antiserum, 100 µg ml^{-1} in BSA, 20 mg ml^{-1} in TBS) for 1 h at 37 °C; washed with gentle agitation in several changes of BSA, 2 mg ml^{-1} in TBS at room temperature; immersed in goat anti-rabbit IgG–Au(20) (Janssen Pharmaceutica) diluted 1:10 with BSA, 2 mg ml^{-1} in TBS, for 1 h at 37 °C; washed with gentle agitation in several changes of BSA, 2 mg ml^{-1} in TBS at room temperature, followed by the same solution containing 0.1% Triton X-100, and finally with distilled water. Control tests, neither of which gave specific immuno-gold staining, involved the omission of anti-pea Lb antibody from the sequence and inclusion of goat anti-rabbit IgG (Miles) between the anti-pea Lb antibody and the goat anti–rabbit IgG–Au(20). Sections were post-stained with uranyl acetate (20 mg ml^{-1} in distilled water) for 10 min, followed by lead citrate for 2 min[28], and viewed in a Siemens Elmiskop 1A at 80 kV.

Fig. 2 Autoradiogram of an immunoblot showing the specificity of the anti-pea Lb antibody for Lb when blotted against: *a*, the plant cytoplasmic fraction from pea nodules (*Pisum sativum* var. Rhondo); *b*, the peribacteroid space fraction from pea nodules. The methods for purification of Lb, antibody production in rabbits, preparation of the nodule cytoplasmic and peribacteroid space fractions, SDS-gel electrophoresis using 15% polyacrylamide gels and immunoblotting have been previously described[12,17]. 25 μg of protein were applied to each sample well on the gel. SDS-gel electrophoresis of pea Lb yields two components which are only just resolved and which both react with the antibody.

cells (Fig. 1*a*, *b*). No specific immuno-gold staining of the peribacteroid spaces, endoplasmic reticulum, mitochondria or plastids was observed. Determination of the density of gold staining in different cellular compartments (Fig. 1*b*), using a computer programme and graphics tablet (Apple) for measuring the relative areas on electron micrographs, gave a ratio for the plant cytoplasm, peribacteroid spaces and bacteroids of 44 : 1 : 1 gold particles per unit area. This result is consistent with the positive reaction for Lb obtained by immunoblotting the plant cytoplasmic fraction from nodules with anti-pea Lb, and the negative reaction obtained for the peribacteroid space fraction (Fig. 2). Immunoblotting of the bacteroid fraction against anti-pea Lb was also negative (data not shown). Control tests (see Fig. 1 legend) confirmed the specificity of the immuno-gold staining of Lb in the plant cytoplasm of infected cells. No specific immuno-gold staining was observed either in the cytoplasm of pea root tip cells (Fig. 1*c*) or in the cytoplasm of infected cells in the immature 11-day nodules, which were white in colour at the time of harvesting and which contain little Lb[17]. Furthermore, no staining was observed in the cytoplasm of infected cells showing very early signs of senescence in the late symbiotic zone of nodules[18], indicating that Lb was lost very rapidly from such cells.

One unexpected result was that specific staining for Lb occurred in the nuclei of infected cells in 15-day nodules (Fig. 1*b*, *d*). Staining appeared most dense in the non-chromatin areas of the nuclei, and in these areas the density of staining was ~70% of that in the plant cytoplasm of infected cells. Specific immuno-gold staining for Lb was observed neither in the nuclei of infected cells in 11-day nodules nor in nuclei of pea root tip cells (Fig. 1*c*). Staining of Lb in nuclei of infected cells in 15-day nodules was not observed in the control tests used to establish the specificity of immuno-gold staining of Lb in the cytoplasm of infected cells (see Fig. 1 legend). Also, staining for Lb did not occur in nuclei of infected cells in the late symbiotic zone of nodules in which the cells were showing very early signs of senescence. Therefore, it seems that Lb is able to diffuse into and out of the nuclei of the infected cells—this conclusion is consistent with the observation that proteins as large as molecular weight (MW) 150,000 and devoid of specific signal sequences for nuclear transport can penetrate the nuclear envelope[19]. Whether Lb has any functional role in the nuclei is open to conjecture.

The demonstration that Lb could be detected only in the cytoplasm and nuclei of the infected cells in the 15-day nodules substantiates the conclusions of previous studies in which the absence of Lb from the peribacteroid space was established by techniques involving the isolation of bacteroids still enclosed by peribacteroid membranes[10–12]. Localization of Lb in the cytoplasm of infected cells is consistent with studies of *in vitro* synthesis of Lb, demonstrating that newly synthesized soybean Lb does not possess a signal sequence which might allow transport across the peribacteroid membrane[20]. It is also consistent with the finding that the nodule cytosol contains enzymes essential for maintaining Lb in an active state[21,22] and that in some legumes, peribacteroid spaces are not observed[10].

It is apparent from the present results that the role of Lb in facilitating the flow of oxygen to the bacteroids[9] must be restricted to the cytoplasm of the plant cells (Fig. 1*b*). It has been shown that normal rates of nitrogen fixation in nodules from various species of legumes are limited due to resistance to the diffusion of oxygen[23]. Therefore, the spaces between the bacteroids and the peribacteroid membranes might afford a source of resistance to the diffusion of oxygen in some legumes. Also, it has been proposed that the different species of Lb in legume nodules have various functions[24]. Clearly, the mitochondria are bathed in Lb in the plant cytoplasm (Fig. 1*b*) and the implications of this in terms of mitochondrial activity require further study[9]. However, virtually complete development of infected, though non-nitrogen-fixing nodule cells can occur in the absence of functional Lb[25]; although these infected cells tend to senesce prematurely, it follows that the cytoplasmic functions of these plant cells are not strictly dependent on the presence of Lb.

Low-temperature dehydration and embedding techniques[26] coupled with immuno-gold staining[16] have been used previously to localize enzymes in animal tissues but not, to our knowledge, in plant tissues. The present work, together with immuno-gold localization of various enzymes in legume nodules (J.G.R. and B.W., unpublished results), indicates that these techniques have considerable potential for probing the sequence of both plant and bacterial gene expression during infection and nodule development in the legume–*Rhizobium* symbiosis.

We thank E. Carlemalm, J. A. Downie, G. H. Hills, Celia D. Knight and K. Roberts for valuable help and discussions. J.G.R. was supported by a grant from the Trustees of the John Innes Foundation and a Study Award from the Department of Scientific and Industrial Research, New Zealand.

Received 21 May; accepted 17 July 1984.

1. Dilworth, M. J. & Appleby, C. A. in *A Treatise on Dinitrogen Fixation* Sections I–II (eds Hardy, R. W. F., Bottomley, F. & Burns, R. C.) 691–764 (Wiley, New York, 1979).
2. Davenport, H. E. *Nature* **183**, 653–654 (1960).
3. Bogusz, D. in *Advances in Nitrogen Fixation Research* (eds Veeger, C. & Newton, W. E.) 534 (Nijhoff/Junk, The Hague, 1984).
4. Appleby, C. A., Tjepkema, J. D. & Trinick, M. J. *Science* **220**, 951–953 (1983).
5. Gresshoff, P. M. *et al.* in *Advances in Nitrogen Fixation Research* (eds Veeger, C. & Newton, W. E.) 483–489 (Nijhoff/Junk, The Hague, 1984).
6. Tjepkema, J. D. in *Advances in Nitrogen Fixation Research* (eds Veeger, C. & Newton, W. E.) 467–473 (Nijhoff/Junk, The Hague, 1984).
7. Wittenberg, J. B. in *Oxygen and Physiological Function* (ed. Jobsis, F. F.) 228–246 (Professional Information Library, Dallas, 1976).
8. Bergersen, F. J. in *Nitrogen Fixation* (eds Stewart, W. D. P. & Gallon, J. R.) 139–160 (Academic, London 1980).
9. Appleby, C. A. *A. Rev. Pl. Physiol.* **35**, 443–478 (1984).
10. Robertson, J. G., Lyttleton, P. & Tapper, B. A. in *Advances in Nitrogen Fixation Research* (eds Veeger, C. & Newton, W. E.) 475–481 (Nijhoff/Junk, The Hague, 1984).
11. Verma, D. P. S. & Long, S. *Int. Rev. Cytol. Suppl.* **14**, 211–245 (1983).
12. Bisseling, T., Been, C., Klugkist, J., Van Kammen, A. & Nadler, K. *EMBO J.* **2**, 961–966 (1983).
13. Bergersen, F. J. & Appleby, C. A. *Planta* **152**, 534–543 (1981).
14. Bergersen, F. J. in *Root Nodules of Legumes: Structure and Function*, 97–121 (Wiley, Chichester, 1982).
15. Bergersen, F. J. in *Advances in Nitrogen Fixation Research* (eds Veeger, C. & Newton, W. E.) 171–180 (Nijhoff/Junk, The Hague, 1984).
16. De Mey, J. in *Immunocytochemistry: Practical Applications in Pathology and Biology* (eds Polak, J. M. & Van Noorden, S.) 82–112 (Wright PSG, Bristol, 1983).
17. Bisseling, T., Van Den Bos, R. C., Weststrate, M. W., Hakkaart, M. J. J. & Van Kammen, A. *Biochim. biophys. Acta* **562**, 515–526 (1979).
18. Robertson, J. G. & Farnden, K. J. F. in *The Biochemistry of Plants. A Comprehensive Treatise* (eds Stumpf, P. K. & Conn, E. E.) **5**, 65–113 (Academic, New York, 1980).
19. Einck, L. & Bustin, M. *J. Cell Biol.* **98**, 205–213 (1984).
20. Verma, D. P. S., Ball, S., Guerin, C. W. & Wanamaker, L. *Biochemistry* **18**, 476–483 (1979).
21. Puppo, A., Dimitrijevic, L. & Rigaud, J. *Planta* **156**, 374–379 (1982).
22. Saari, L. L. & Klucas, R. V. *Archs Biochem. Biophys.* **231**, 102–113 (1984).
23. Witty, J. F., Minchin, F. R., Sheehy, J. E. & Ines Minguez, M. *Ann. Bot.* **53**, 13–20 (1984).
24. Fuchsman, W. H., Barton, C. R., Stein, M. M., Thompson, J. T. & Willet, R. M. *Biochem. biophys. Res. Commun.* **65**, 387–392 (1976).
25. Ronson, C. W., Lyttleton, P. & Robertson, J. G. *Proc. natn. Acad. Sci. U.S.A.* **78**, 4284–4288 (1981).
26. Carlemalm, E., Garavito, R. M. & Villiger, W. *J. Microsc.* **126**, 123–143 (1982).
27. Beynon, J. L., Beringer, J. E. & Johnston, A. W. B. *J. gen. Microbiol.* **120**, 420–429 (1980).
28. Reynolds, E. S. *J. Cell Biol.* **17**, 208–212 (1963).

Ratites as oldest offshoot of avian stem—evidence from α-crystallin A sequences

Steven O. Stapel*, Jack A. M. Leunissen*, Marlies Versteeg*, Jan Wattel† & Wilfried W. de Jong*

* Department of Biochemistry, University of Nijmegen, Geert Grooteplein Noord 21, 6525 EZ Nijmegen, The Netherlands
† Institute of Taxonomic Zoology, University of Amsterdam, 1018 DC Amsterdam, The Netherlands

One of the most disputed issues in avian phylogeny is the origin of the ratites, the large flightless birds of the Southern Hemisphere (reviewed in refs 1–3). It is still not generally agreed whether the ostriches, rheas, emus and cassowaries, and probably kiwis, form a natural, monophyletic group, although much recent evidence supports this view[4–6]. Also, their phylogenetic relationship with the other avian orders remains unresolved; comparative protein sequence studies *might* shed new light on this problem. Therefore, we determined the amino acid sequence of the eye lens protein α-crystallin A in ostrich, rhea and emu, and in representatives of 13 other avian orders. Comparison of these sequences with known αA sequences of mammals, reptiles, frog and dogfish provides strong evidence that the ratites, as a monophyletic assemblage, represent the first offshoot of the avian line.

The α-crystallin A-chain is a suitable protein for comparative sequence analysis because (1) being a major eye lens constituent in all vertebrate classes[7], it can often be isolated in considerable quantities, and (2) the sequence analysis of the 173-residues αA-chain is relatively simple[8]. There is only a single gene for αA[9], which excludes the possibility of errors resulting from comparing paralogous[10] products of multi-copy genes in different species. The rate of evolution of αA is sufficiently slow to be informative in the study of more distantly related taxa[11]. Sequences of αA-chains have been determined previously in 43 mammalian species[8,9], chicken[8], alligator (W.W. de J., M.V., A. Zweers, H. Dessauer and M. Goodman, unpublished data), and tegu[11], frog[8,12] and dogfish[11]. These studies have already provided useful information about some aspects of mammalian phylogeny[11,13], and allow ample outgroup comparisons for the study of avian phylogeny. In the present study we have included, apart from the large ratites, several other avian orders for which the phylogenetic relationships are disputed. To confirm that closely related species indeed have related αA sequences, which would support the reliability of our approach, we included in our study chicken, turkey (both Galliformes), domestic duck and mute swan (Anseriformes). We obtained sufficient eye lenses to perform sequence analysis of the αA-chains from 21 avian species representing 16 orders (Table 1).

The methods of isolation and sequence analysis of the avian αA-chains and the resulting sequence information, as exemplified by the αA-chain of the rhea, are given in Fig. 1 and its legend. The sequence differences between the avian αA-chains are shown in Table 1; relevant sequence data from outgroup species are included. The six mammalian species represent the major lineages of the mammals investigated previously[11]. Table 1 immediately reveals the common occurrence in the ratite species of the unique substitution, Asp 69 → Glu. Another character shared by the ratites is residue Ala 148, which, however, also occurs in pigeon, gull and guillemot. Because Asp 69 and Ser 148 seem to be the primitive character states present in nearly all outgroups, these substitutions may be considered as shared derived (synapomorphous) characters, in support of a ratite monophyly. Equally conspicuous is the presence of Ala 122 and Pro 147 as apparently shared derived characters in all birds, apart from the ratites. Residues Ala 127 (or Thr) and Asn 135 again seem to be synapomorphies of all birds, with the exception of ratites, galliform and anseriform birds.

It is obvious that parallel and back-substitutions do occur in the evolution of αA, as in all other proteins. This complicates the interpretation of differences between homologous amino acid sequences, and necessitates the use of computer analyses to objectively assess the cladistic relationships among the investigated sequences. The objectives of such computer searches are to find the most parsimonious phylogenetic trees (that is, branching patterns that require the fewest amino acid substitutions) and to calculate the cost, in terms of additional required substitutions, of alternative topologies. By applying different

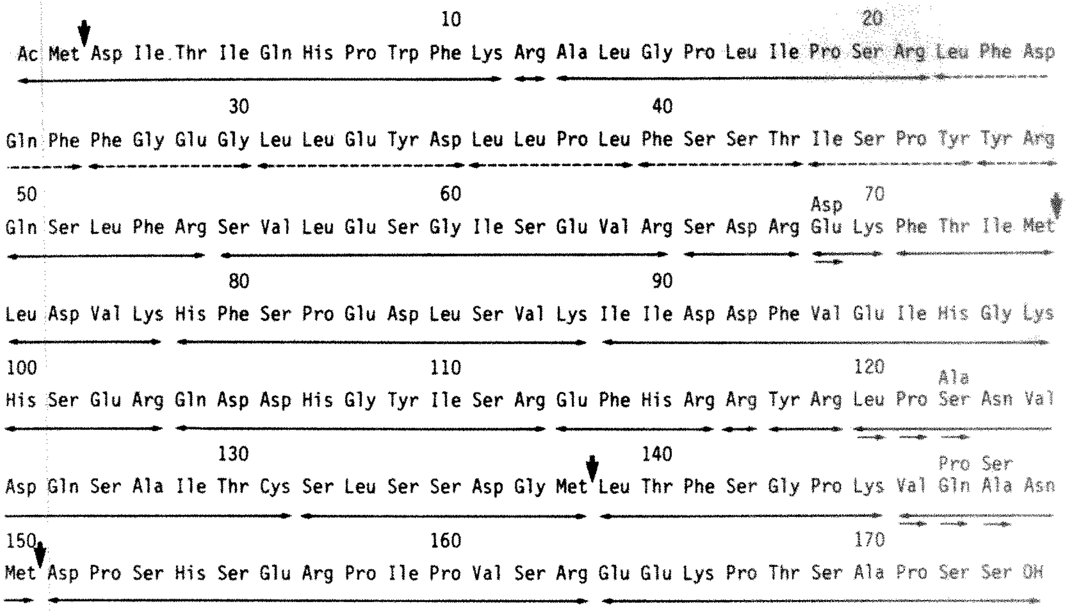
10
20
Ac Met Asp Ile Thr Ile Gln His Pro Trp Phe Lys Arg Ala Leu Gly Pro Leu Ile Pro Ser Arg Leu Phe Asp
30
40
Gln Phe Phe Gly Glu Gly Leu Leu Glu Tyr Asp Leu Leu Pro Leu Phe Ser Ser Thr Ile Ser Pro Tyr Tyr Arg
50
60
Asp
70
Gln Ser Leu Phe Arg Ser Val Leu Glu Ser Gly Ile Ser Glu Val Arg Ser Asp Arg Glu Lys Phe Thr Ile Met
80
90
Leu Asp Val Lys His Phe Ser Pro Glu Asp Leu Ser Val Lys Ile Ile Asp Asp Phe Val Glu Ile His Gly Lys
100
110
120
Ala
His Ser Glu Arg Gln Asp Asp His Gly Tyr Ile Ser Arg Glu Phe His Arg Arg Tyr Arg Leu Pro Ser Asn Val
130
140
Pro Ser
Asp Gln Ser Ala Ile Thr Cys Ser Leu Ser Ser Asp Gly Met Leu Thr Phe Ser Gly Pro Lys Val Gln Ala Asn
150
160
170
Met Asp Pro Ser His Ser Glu Arg Pro Ile Pro Val Ser Arg Glu Glu Lys Pro Thr Ser Ala Pro Ser Ser OH

Fig. 1 Proposed amino acid sequence of the rhea α-crystallin A-chain. The characterization of avian αA chains followed the general procedures described for mammalian and chicken αA chains[8]. α-Crystallin was isolated from four rhea lenses by gel filtration of the water-soluble lens proteins, and the component αA and αB chains were separated by ion-exchange chromatography. Fragments produced by cyanogen bromide cleavage of the *S*-β-aminoethylated αA chain were separated by gel filtration and digested with trypsin. Soluble peptides were isolated by paper electrophoresis and chromatography. The core peptide (22–49) was purified by gel filtration, then subdigested with thermolysin for peptide mapping. Peptide 1–11 was obtained by tryptic digestion of the total αA chain. Amino acid compositions of tryptic (↔) and thermolytic (←- - - -→) peptides were compared with the corresponding ones of the chicken αA chain[8]. When no difference in composition was observed, we assumed identity between the chicken sequences and rhea peptide. Peptides which differed in composition from the corresponding chicken peptides were subjected to dansyl–Edman degradation (→) to localize substitutions. Residues which are different in the chicken αA chain are shown above the rhea αA sequence. Cleavage points of cyanogen bromide are indicated by ↓. The avian αA chains are *N*-terminally blocked, probably by an N^{α}-acetyl group as in bovine αA[7].

Table 1 Phylogenetically informative positions in avian, reptilian and outgroup α-crystallin A sequences

```
                                           1111111111111111111111111111111
POSITION NR         1111133334555567778889990122222223333444444455555556667
                  341367823790056890241690161123456790258234678902345682892

OX                IAKTPFYFELFLQTVDDKVFSTVQEINSSNVDQSLSSAMSGPIPSGVAGHSEASSSS
DOG               |||A|||||||||||||||||||L|||||||||||||||||||V||||||||||||||
RAT               VT|A|||||||||||||||||||L|||||||||||||||||||VQ||L||||||||||
HYRAX             VT|A|||||||||||||QLL|||LD||||||||||||||C||VQ||M|S||||||||
2-TOED SLOTH      VTRA|||||||||||||||||||LD|||TA|||||||||||||---|PS|||T||||
KANGAROO          |T|ASL|||||||||E|||||||LD|S|||||||I||||||||H|DM|S||DS|TL|
CROW              |T|A|LIL||LF|S|E||TM|SIID|S|A||||AIT|N||||V||NM|||||P|T||
EAGLE OWL         |T|A|LIL||LF|S|E||TM|SIID|S|A||||AIT|N||||V||NM|||||P|T||
BUDGERIGAR        |T|A|LIL||LF|S|E||TM..IID|S|A||||AIT|N||||V||NM|S|||P|T||
PIGEON            |T|A|LIL||LF|S|E||TM|SIID|S|.........N||||V|ANM|||||P|T||
GUILLEMOT         |T|A||IL||LF|S|E||.MNSIID|S|A||||AIT|N||H|V|ANMVS|||P|T||
GULL              |T|A|LI|||LF|S|E||.M|SIID|S|A||||AIT|N||||V|ANM|S|||P|T||
CURLEW            |T|A|LI|||LF......TM......S.A||||AIT..||||V||NM|S|||P|T||
OYSTERCATCHER     |T|A|LIL||LF|S|E||TM|SIID|S|A||||AIT|N||||V||NM|S|||P|T||
COOT              |T|A|LIL||LF|S|E||TM|SIID|S|A||||AIT|N||||V||NM|S|||P|T||
BUZZARD           |T|A|LI|||LF|S|E||TM|SIID|S|A||||AIT|N||||V||NM|||||P|T||
HERON             |T|A|LIL||LF|S|E||.M|SIID|S|A||||TIT|N||||V||NM|S|||P|T||
GANNET            |T|A|LIL||LF|S|E||TM|SIID|S|A||||AIT|N||||V||NM|||||P|T||
FULMAR            |T|A|LIL||LF|........S....S|A||||AIT|N||||....M|S|T|P|T||
PENGUIN           |T|A|LIL||LF|S|E||TM|SIID|S|A||||TVT..||V|V||NM|SR||P|T||
DUCK, SWAN        |T|A|LIL||LF|S|E||TM|SIID|S|A|||||IT|S||||V||NMPT|||P|T||
CHICKEN, TURKEY   |T|A|LIL||LF|S|E||TM|SIID|S|A|||||IT|S||||V||NMPS|||P|T||
►OSTRICH          ...A|LIL||LF|S|EE|TM|SIID||||||||||IT|S||||VQANMPS|||P|T||
►RHEA             |T|A|LIL||LF|S|EE|TM|SIID|S||||||||IT|S||||VQANMPS|||P|T||
►EMU              |T|A|LIL||LF|S|EE|TM|SIID|SA|||||||IT|S||||VQANMPS|||P|T||
ALLIGATOR         |T|A|LI|||L|HS|E||TM|SIIDV|||S||||VTV||||SVQ|N|TI||DPAT||
TEGU              |T|A|LI|||LF|||E||T||S|I||||||||||AIT|||AA|VQ|NTPS|N|P|T|P
FROG              |T|A||||DF|||GF||R..||ILD|S|||LNE|I|||I|||LM|SLSS|G|P|T||
DOGFISH           L|RSS|||DF|F|NF||RMN|SIVD|A|||LNE|IA|NLCC|TRP|DSNWQDP|GTE
```

Positions shown are those which are variable in the αA chains of at least two of the species, plus the autapomorphous substitutions in the avian and reptilian sequences. Vertical lines indicate that residues are identical to the topmost sequence. Amino acid sequences have been analysed, as outlined in Fig. 1 legends, for: carrion crow (*Corvus corone*; Passeriformes), eagle owl (*Bubo bubo*; Strigiformes), budgerigar (*Melopsittacus undulatus*; Psittaciformes), domestic pigeon (*Columba livia*; Columbiformes), guillemot (*Uria aalge*; Charadriiformes), black-headed gull (*Larus ridibundus*; Charadriiformes), curlew (*Numenius arquata*; Charadriiformes), oystercatcher (*Haematopus ostralegus*; Charadriiformes), coot (*Fulica atra*; Gruiformes), buzzard (*Buteo buteo*; Falconiformes), heron (*Ardea cinerea*; Ciconiiformes), gannet (*Sula bassana*; Pelecaniformes), fulmar (*Fulmarus glacialis*; Procellariiformes), gentoo penguin (*Pygoscelis papua*; Sphenisciformes), domestic duck (*Anas platyrhynchos*; Anseriformes), mute swan (*Cygnus olor*; Anseriformes), turkey (*Meleagris gallopavo*; Galliformes), ostrich (*Struthio camelus*; Struthioniformes), rhea (*Rhea americana*; Rheiformes), and emu (*Dromaius novae-hollandiae*, Casuariiformes). The αA sequences and scientific names of the mammals, chicken, tegu, frog and dogfish have been given previously[8,11]. The alligator is *Alligator mississippiensis*. The sequences of chicken and turkey αA were found to be identical, as are those of duck and swan. Some αA sequences have been incompletely determined (·). Thr 127 in heron αA has not been ascertained by Edman degradation, and is therefore not taken as a synapomorphy with penguin αA. In sloth αA there is a deletion of three residues (–). The one-letter notation for amino acids is: A, Ala; C, Cys; D, Asp; E, Glu; F, Phe; G, Gly; H, His; I, Ile; K, Lys; L, Leu; M, Met; N, Asn; P, Pro; Q, Gln; R, Arg; S, Ser; T, Thr; V, Val; Y, Tyr.

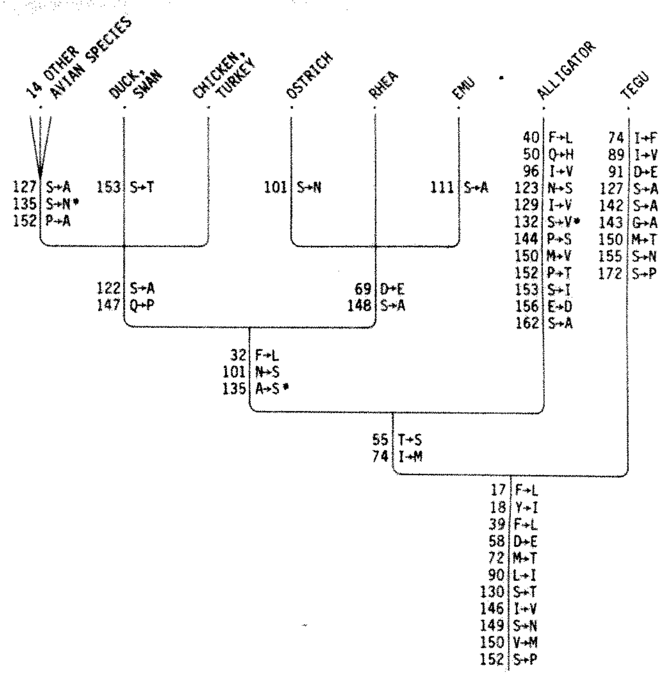

Fig. 2 Avian and reptilian branches of the maximum parsimony tree constructed on the basis of the αA sequence data in Table 1. The procedure starts with the calculation of a matrix of minimum mutation distances for the αA sequences[14], followed by a tree construction programme which begins with an unrooted three-sequence tree to which the other sequences are added one at a time, using a branch-swapping procedure, until a tree of minimal length is found (essentially according to Fitch and Margoliash[14], as modified by J. Felsenstein). The tree construction procedure was repeated several times using different input orders of the αA sequences; this resulted in the same topology in all instances, apart from equally parsimonious minor alternatives in the cluster of 14 'other avian species'. The number of amino acid substitutions required for the most parsimonious tree was 163. The outgroup part of this tree was congruent with the previously constructed topology[11], and is therefore not shown here. Amino acid substitutions in the different branches are deduced from the reconstructed ancestral αA sequences at the nodes[15]. Substitutions that could not be assigned unambiguously to a certain branch were, as far as possible, placed on terminal branches, rather than between ancestral nodes[16]; this minimizes the synapomorphous substitutions characterizing monophyletic groupings in this cladogram. Taking six other mammalian αA sequences (horse, mink, human, elephant, three-toed sloth and opossum)[11] as outgroups in the tree construction procedure resulted in the same topology as shown here. * Substitutions 132 S→V and 135 A→S (or 135 S→N) require two nucleotide replacements.

algorithms[14–16] to the data set of Table 1, we found the most parsimonious tree (see Fig. 2), which requires 163 amino acid substitutions. All changes in the topology presented in Fig. 2 require additional amino acid substitutions (Table 2). On this basis we must conclude that the presence of Ala 148 in ratites and in pigeon, gull and guillemot is due to parallel, or convergent, evolution.

The constructed tree clearly supports the hypothesis that the ratites are monophyletic, and depicts them as the sister group of all other birds. The Galliformes and Anseriformes appear to be the next to branch off from the main avian stem. Our data allow the possibility that Galliformes and Anseriformes are monophyletic[3,4], but conflict with a close relationship between Anseriformes and Charadriiformes[17] (Table 2). The other investigated avian orders are grouped as a monophyletic assemblage, but the scarcity of substitutions in their αA sequences prevents a further, meaningful resolution of their relationships. In fact, several species from different orders are found to have identical symplesiomorphous αA sequences. The most parsimonious tree of αA also stresses the monophyletic origin of the investigated birds and reptiles, and places the crocodiles, represented by the alligator, as a sister group of the birds. These findings conform to the generally held, but not unchallenged, palaeontological views. The recently proposed sister group relationship of birds and mammals[18] would, in the case of αA sequences, result in a considerable loss of parsimony (Table 2).

Also, recent immunological[4] and DNA hybridization studies[6] have provided evidence for a monophyletic origin of the ratites, thus contradicting the suggestion that they are paraphyletic or polyphyletic[2,19]. In fact, Prager and Wilson[20] have suggested a phylogenetic tree, on the basis of immunological comparisons, in which the position of ratites, Galliformes and Anseriformes relative to the other avian orders is essentially as in our αA tree. The primitive, rather than derived, position of the ratites within birds is, among others, also supported by karyological[5] and

Table 2 Numbers of additional amino acid substitutions required to change the topology of Fig. 2

Alternative relationships	Additional substitutions
Polyphyletic origin of ratites from the avian stem	≥4
Ratites within the cluster of 'other avian species'	≥5
Ratites and Galliformes (or Anseriformes) monophyletic	2
Galliformes and Anseriformes monophyletic[3]	0
Anseriformes with Charadriiformes[17]	3
Birds and mammals as sister groups[18]	6

ontogenetic[21] studies. However, a phyletically old origin of the ratites could not be concluded on the basis of morphological and anatomical data[1-3]. Comparative sequence data of avian proteins, including one or more ratite species, are available for cytochrome c[22] and haemoglobin[23]. On the basis of the very few substitutions in seven avian cytochrome c sequences, a cladogram has been proposed in which the ratites are depicted as derived from carinate birds[22]. We found, however, that a more parsimonious tree can be obtained from this cytochrome c data set by assuming the ratites to be a sister group of the other birds. The sequence determinations of avian α and β haemoglobin have not yet led to specific statements about ratite phylogeny[23].

Our αA sequence data may have some bearing on the problem of the time of radiation of the avian orders. Estimates for the time since the last common ancestor of all modern birds range between 130 and 65 Myr[6,24]. Considering that αA evolves at an average rate of three amino acid substitutions per 100 residues in 100 Myr[8], it seems that the small numbers of substitutions in the avian αA chains since their divergence from the last common ancestor (Fig. 2) favour the more recent time of avian radiation. Finally, the branching order in our tree may lend support to the idea that sustained flight developed late in avian evolution, after the divergence of ratites and Galliformes from the main stem.

We thank Mr W. B. Appel and the Klein Karoo Landboukoöperasie for ostrich lenses, Dr S. J. Davies (CSIRO) for emu lenses, Drs Th. Smit and Ms T. Prins for other avian lenses, and Dr J. Felsenstein for supplying his Phylip package. This work was supported by the Foundation for Fundamental Biological Research (BION) with financial aid from the Netherlands Organization for Pure Research (ZWO).

Received 10 April; accepted 17 July 1984.

1. Sibley, G. S. & Ahlquist, J. E. *Bull. Peabody Mus. nat. Hist.* **39,** 44–52 (1972).
2. Feduccia, A. *The Age of Birds* (Harvard University Press, 1980).
3. Cracraft, J. *Auk* **98,** 681–714 (1981).
4. Prager, E. M., Wilson, A. C., Osuga, D. T. & Feeney, R. E. *J. molec. Evol.* **8,** 283–294 (1976).
5. de Boer, L. E. M. *Nature* **287,** 84–85 (1980).
6. Sibley, G. S. & Ahlquist, J. E. in *Evolution Today* (eds Scudder, G. G. E. & Reveal, J. L.) 301–335 (Carnegie-Mellon, Pittsburgh, 1981).
7. Bloemendal, H. (ed.) *Molecular and Cellular Biology of the Eye Lens* (Wiley, New York, 1981).
8. de Jong, W. W., Zweers, A., Versteeg, M. & Nuy-Terwindt, E. C. *Eur. J. Biochem.* **141,** 131–140 (1984).
9. King, C. E. & Piatigorsky, J. *Cell* **32,** 707–712 (1983).
10. Fitch, W. M. *Syst. Zool.* **19,** 99–113 (1970).
11. de Jong, W. W. in *Macromolecular Sequences in Systematic and Evolutionary Biology* (ed. Goodman, M.) 75–114 (Plenum, New York, 1982).
12. Tomarev, S. I. *et al. FEBS Lett.* **162,** 47–51 (1983).
13. de Jong, W. W., Zweers, A. & Goodman, M. *Nature* **292,** 538–540 (1981).
14. Fitch, W. M. & Margoliash, E. *Science* **155,** 279–284 (1967).
15. Dayhoff, M. O., Park, C. M. & McLaughlin, P. J. in *Atlas of Protein Sequence and Structure* Vol. 5 (ed. Dayhoff, M. O.) 7–16 (National Biomedical Research Foundation, Silver Springs, Maryland, 1972).
16. Goodman, M., Moore, G. W., Barnabas, J. & Matsuda, G. *J. molec. Evol.* **3,** 1–48 (1974).
17. Olson, S. L. & Feduccia, A. *Smithson. Contr. Zool.* **323,** 1–24 (1980).
18. Gardiner, B. G. *Zool. J. Linn. Soc.* **74,** 207–232 (1982).
19. Houde, P. & Olsen, S. L. *Science* **214,** 1236–1237 (1981).
20. Prager, E. M. & Wilson, A. C. in *Acta 17th int. Orn. Congr.* (ed. Nöhring, R.) 1209–1214 (Deutsche Ornithologen, Berlin, 1980).
21. McGowan, C. *Nature* **307,** 733–735 (1984).
22. Howard, N. L., Joubert, F. J. & Strydom, D. J. *Comp. Biochem. Physiol.* **48B,** 75–85 (1974).
23. Oberthür, W., Braunitzer, G., Grimm, F. & Kösters, J. *Hoppe-Seyler's Z. physiol. Chem.* **364,** 851–858 (1983).
24. Wyles, J. S., Kunkel, L. G. & Wilson, A. C. *Proc. natn. Acad. Sci. U.S.A.* **80,** 4394–4397 (1983).

Closely related sequences on human X and Y chromosomes outside the pairing region

H. J. Cooke & W. A. R. Brown

MRC Mammalian Genome Unit, King's Buildings,
West Mains Road, Edinburgh EH9 3JT, UK

G. A. Rappold

Institut für Anthropologie und Humangenetik, Universität
Heidelberg, Im Neunheimer Feld 328, D-6900 Heidelberg, FRG

During meiosis the human X and Y chromosomes form a synaptonemal complex which covers most of Yp and the terminal 30% of Xp (ref. 1). By analogy with the autosomes, this is presumed to reflect DNA sequence homology. It has been suggested that these regions of the X and Y chromosomes contain either related or identical loci which are distal to a site of cross-over[2,3], and support for these ideas has come from the finding that an X-linked cell-surface antigen controlling gene *MIC2* is related to a gene on the Y chromosome[4]. A number of DNA sequences have been shown to occur either on the X and Y chromosomes[5] or on the X, Y and autosomes[6,7]. We have now isolated a sequence from the Y chromosome which is present on Xq and Yq. This region lies well outside the pairing segments, and sequence analysis reveals no base change in 1 kilobase pair (kb). This high degree of similarity between the X and Y chromosomes near the tips of the long arms is a strong indication that interchange can occur in this region.

We have isolated a recombinant phage λY2:13 from a library of sorted human Y chromosomes cloned in λgtWES[8]. Initial hybridization studies using somatic cell hybrids containing only human X and Y chromosomes showed that the 8-kb *Eco*RI fragment cloned in this recombinant hybridized to a fragment of the same size in both somatic cell hybrids and was present in equal amounts in DNA from males and females. A background due to repeated sequences in the cloned probe was evident. To generate probes with a lower repeated sequence content, the fragments produced by *Hin*dIII digestion of the human fragment carried by this phage were subcloned into the plasmid vector pUC9 (ref. 9). One of these subclones (pUC9H1, corresponding to the fragment with sequenced regions a and b in Fig. 1) was used for subsequent hybridization studies although a low level of repeated sequences were still detected by this probe. To confirm the apparent identity of these two sequences on the X and Y chromosomes, we hybridized pUC9H1 to digests of three independently derived somatic cell hybrid DNAs, two containing only the human Y chromosome and one containing only a X chromosome. In all of these cell lines the pattern of fragments detected is identical (Fig. 2) and consistent with the map of λY2.13 in Fig. 1. A trivial explanation of this finding would be that these cell lines carry undetected fragments of the X chromosome (in the Y-containing hybrid) or of the Y chromosome (in the X-containing hybrid). We have probed these hybrid

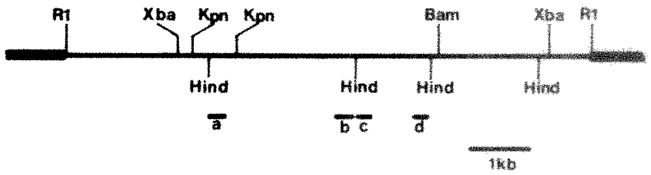

Fig. 1 Restriction map of λY2.13 derived from single and double restriction enzyme digests. Heavy lines are the λgtWES left and right arms. *Eco*RI, *Xba*I, *Kpn*I, *Bam*HI and *Hin*dIII sites are marked. The three *Hin*dIII fragments were subcloned into pUC9, pUC9HI contains the leftmost *Hin*dIII fragment; the lettered regions of these subclones correspond to the sequences in Fig. 3.

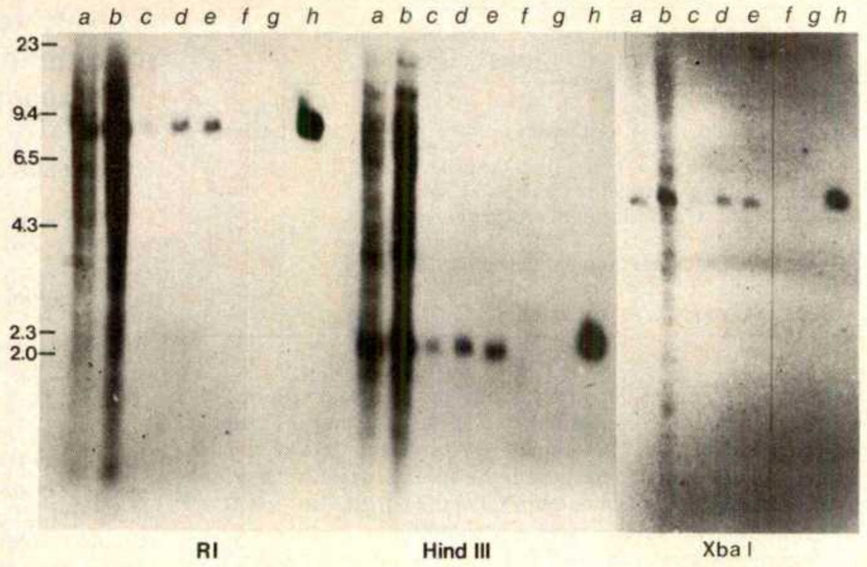

Fig. 2 Hybridization of pUC9H1 to X and Y chromosome sequences. 5 µg of DNA were digested with an excess of *Eco*RI, *Hin*dIII or *Xba*I, fragments separated by electrophoresis on 0.8% agarose gels transferred to nitrocellulose and hybridized with ^{32}P in 5 × SSC, 0.1% SDS 10% dextran sulphate at 65 °C. Final washing conditions were 0.1 × SSC 0.1% SDS at 65 °C. Tracks contain DNA as follows: *a*, human male; *b*, human female; *c*, 3E7—a mouse human hybrid containing only human Y chromosomes; *d*, 853—CHO hybrid with only a Y chromosome; *e*, ThyB1 mouse hybrid with a human X chromosome; *f*, BWS147 mouse control with no human chromosomes; *g*, WG3H chinese hamster control with no human chromosomes; *h*, BWS147 with 75 pg of λY2,13. Differences in intensity of signals are due to differences in loading and additionally in the case of hybrid lines to differences in the percentage of cells containing human chromosomes. Positions of marker fragments are marked with sizes in kb.

a

```
        10         20         30         40         50         60         70
CCAAGCTTTA TCTACAAACT TAAATGTTTC CTTAGGATAA ATGTCATAGG CCGAAAGAAT GAGGGTCGTG

        80         90        100        110        120        130        140
ATCAACTCAG TATACCACTG GAGGCTATAT GAGTGGGCAG CAAACTGTTC TCATCAATGC AGAATGTTGG

       150        160        170        180        190        200        210
TAAACTGACA AACTGCATCT GCTGCCCAGA AGGAATGCTG AGGGTAGTCA CGACCCAAGC ACAGTGTTTC

       220
TTGCGATTAG GTACA
```

b

```
        10         20         30         40         50         60         70
CCAAGCTTTG GTCTGACAGT ATGAAATGGG AAGATTATTT TTCATCAGCC AACTTGGAAA TGGCATTTCA

        80         90        100        110        120        130        140
TATAACATGC TAAGAATTGC ATGAGCATTC ATTTCTTTTT CTTAGGGAAG ATAACAGAAA TCACCTTTTA

       150        160        170        180        190        200        210
ATAGTTTATT TATCTTAAAT ACTTTATCCA AATATAGAAC TACTTCTATC CACAAAGTAC ACACCTAGAA

       220        230        240        250        260        270        280
AGCATTCAAG AATAGAAATA TCCCAGTAAT ATGGAGGCTA GGTTTCAGGC AACCTCAACT ACTTGAAACA

       290
CCACCCGAAA CCTG
```

c

```
        10         20         30         40         50         60         70
CCAAGCTTTT AGCTAGCAGG CTTCAGAAAG AACAGGCTGT AAAATGTTTC TTATCAGACT TAAAGTCTGT

        80         90        100        110        120        130        140
GTTGATGTTC ATGCCAGAGA GGTATAATGA GGCGTGTCCA ACCCCCACTT CCCTTCATGG CCTGAACCAG

       150        160        170        180        190        200        210
TCTTTCAGGT TAAATTTTAA GAGCCTGGCC GAGGAGGAAG TCCATTTAGA TGGTTGAGGG GGCCTTAGCG

       220
TTTTATTTTT GGCATACAC
```

d

```
        10         20         30         40         50         60         70
CCAAGCTTAA TTTAATAATT TTTGGTTTTA GTTTTCTAAA GTCCCAAATA AAACTTCTTT TCTATCATTT

        80         90        100        110        120        130        140
CTGATGAAAT TTTGTTCCCC TATTAAGTTG ATTCCCTTCT GGTGGCATTT TCAGTGCCAG CTGTCCTTGG

       150        160        170        180        190        200        210
ATAATGGGAA CTTTCTGTGT ATGTGTGTGT GTGACATTTT TTAAAACAAA CATTTATTAA TTAGATGCCA

       220        230        240        250        260
GAAATCATAA ATGTCAGAGT TACAGATATA AATTTGGATG TTATGAGCAC ATAGT
```

Fig. 3 Sequences of the regions of λY2,13 and X11 shown in Fig. 1. *Hin*dIII fragments of each recombinant were cloned in pUC9. Clones containing the appropriate insert in each orientation were isolated, labelled with ^{32}P-ATP after cleavage at the *Bam*HI site in pUC9, digested with *Eco*RI and subjected to Maxam–Gilbert sequencing[11]. Only one strand was sequenced where X and Y clones were identical. Second strands were sequenced where base changes were detected or where the sequence could not be unambiguously determined, by end-labelling with ^{32}P-dGTP at the *Bam*HI site, followed by *Eco*RI cleavage and Maxam and Gilbert sequencing.

DNAs with a number of cloned sequences derived from the X or Y chromosomes and have found no inconsistencies which would suggest this to be the case. We conclude that this sequence is highly conserved between X and Y chromosomes.

To establish the extent of sequence conservation between X and Y chromosomal copies, we have isolated the X chromosomal copy of this sequence from a library constructed from sorted X chromosomes (data not shown) by screening the library with pUC9HI. When pooled DNA from this X-derived library is probed with a sequence known to be X-derived, such as RC8 (ref. 10), the amount of hybridization is consistent with degree of enrichment expected from the chromosome sorting, whereas in the Y chromosome library this sequence is not detectable. This shows that the Y chromosome library is relatively free of X chromosome-derived DNA.

Three recombinants with insert sizes and *Hin*dIII restriction sites identical to λY2.13 were isolated from 4 × 10^4 recombinants. One clone, λX11, was used for sequencing studies. *Hin*dIII fragments from λY2.13 and λX.11 were subcloned for Maxam–Gilbert[11] sequencing into pUC9 (ref. 8). The sequences derived are shown in Fig. 3 and their position on the restriction map of λY2.13 in Fig. 1. All four regions sequenced (in total 1,013 bp) are identical in the X and Y chromosome copies. This suggests that this might be a 'pseudoautosomal' sequence which would be expected to map on the X in the region Xp22 − > Xpter.

A collection of somatic cell hybrids containing X − > autosome translocations with break points in different regions of the X and selected for the presence of the hypoxanthine phosphoribosyltransferase (*hprt*) gene[12] has been used for regional assignment of this sequence by blot hybridization. The sequence is present in all hybrids tested (Fig. 4*A*). The minimum common region of the X chromosome which must contain this fragment, is Xq24 − > Xqter. The hybrid line 445 × 393 contains a Xqter-p233 : Yq11-qter chromosome and consistently shows more intense hybridization than the other hybrids which contain a deleted X chromosome but no Y chromosome fragment. This suggests a Yq11-qter localization of the Y chromosome copy of the sequence detected by pUC9H1. Fragments hybridizing with lower intensities are visible in the hybrid DNAs in Fig. 4. These hybrids contain different human chromosomes and it is likely that these fragments show the residual repeated sequence present in the pUC9H1 subclone. Only one additional fragment is detectable in the hybrid which contains X chromosome as the only human chromosome (Fig. 4*B*, Table 1).

We have used *in situ* hybridization to confirm the X and Y chromosome localization of this sequence. Using λY2 : 13 as a probe, 13.5% of grains counted on 30 chromosome spreads were on Xq24-Xqter, this is entirely consistent with the results of blot hybridization to the hybrid lines shown in Fig. 4. Ten per cent of the grains counted were on the Y chromosome, evenly distributed between two sites, one on Yp and one distal site on Yq. No other significant sites of hybridization were detected. Hybridization to Yp could be due to repeated sequences in Y2 : 13 or to a third copy of the 8 kb fragment. In later experiments pUC9H1 was used as probe to hybrid cell lines CH-Y-VII

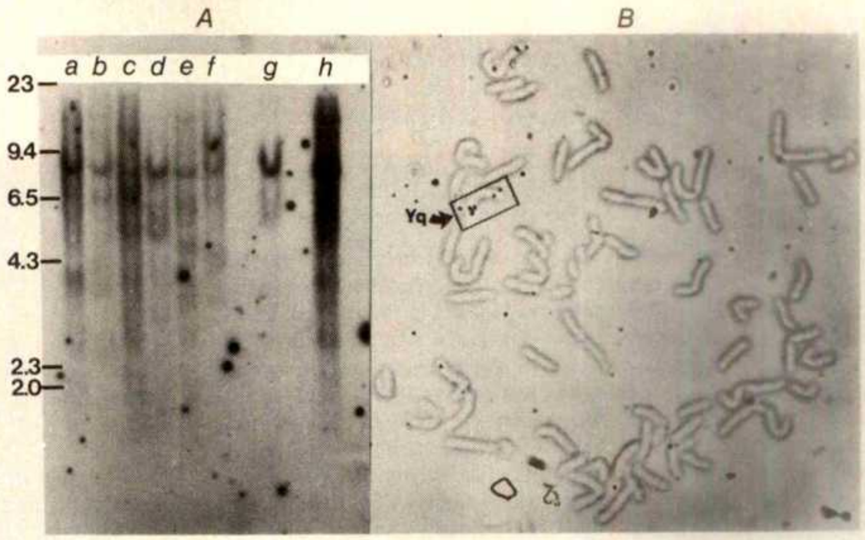

Fig. 4 *A*, Regional assignment of pUC9H1. X chromosome hybrid DNAs with X → autosome translocations were digested with *Eco*RI, transferred to nitrocellulose and hybridized as described in Fig. 2 legend. *a*, 455 × 393, qter-p223; *b*, 697 × 175 qter-p21; *c*, 749, qter-q12; *d*, 676 − 175 qter-q213; *e*, 722 qter p11; *f*, 790 − 175 q24–qter; *g*, ThyB1-33-12–entire X; *h*, Til 46XXXXY human fibroblast. Positions of marker fragments are marked with sizes in kb. *B*, *In situ* hybridization to 445 × 393 chromosomes.

Methods: Chromosome preparations were treated with 70% formamide 2 × SSC at 70 °C for 2 min then dehydrated in ethanol. The slides were then hybridized with 20 ng of ^{3}H-labelled probe with a specific activity of 10^7 d.p.m. per μg in 50% formamide 2 × SSC, 1 × Denhardt's solution, 10% dextran sulphate and 200 μg ml^{-1} salmon sperm DNA at 40 °C for 16–18 h. Slides were washed in 2 × SSC (four 20-min washes) at 68 °C and finally in 0.1 × SSC at room temperature. The slides were dipped in Ilford L4 photographic emulsion and exposed for 2–4 weeks at 4 °C. Chromosomes were identified after autoradiography by quinacrine mustard staining. The boxed area contains the Xqter—p233 : Yq11—qter chromosome. Quantitative evaluation of train distribution was according to ref. 20.

Table 1 *In situ* hybridization of X and Y chromosomes

Clone	Expt no.	Specific activity (c.p.m. per μg DNA)	Cell type	Exposure time (weeks)	No. of metaphase spreads evaluated	Total no. of grains	No. of grains on Y	No. of grains on Yp/Yq	No. of grains on X (%)	No. of grains on Xq2.4–Xqt
2.13	1	2×10^7	CH-Y-VII	1.5	35	140	14 (10%)	7/7	—	—
	2	2×10^7	CH-Y-VII	2.0	35	107	16 (15%)	7/9	—	—
Control	3	—	CH-Y-VII	2.0	35	82	0	0	—	—
	4	2×10^7	CH-Y-VII	2.5	30	298	40 (13.4%)	27/13	—	—
	5	2×10^7	445 × 393	1.0	20	262	19 (7.3%)	−/19	35 (13.5%)	31 (12%)
	6	2×10^7	445 × 393	2.5	30	516	43 (8.3%)	−/43	104 (20.2%)	66 (12.7%)
Control	7	—	445 × 393	2.5	30	171	1 (0.6%)	−/1	5 (2.9%)	2 (1.1%)
pUC 9H1	8	3×10^7	CH-Y-VII	2.0	60	66	11 (16.6%)	0/11	—	—
	9	3×10^7	CH-Y-VII	2.5	30	140	13 (9.3%)	0/13	—	—
	10	3×10^7	445 × 393	2.0	10	58	3 (5.2%)	−/3	14 (24.1%)	13 (22.4%)

Dashes indicate that the chromosome or region of the chromosome is not present in those cells.

(ref. 13) which contains a human Y chromosome and 445 × 393. Ninety CH-Y-VII metaphase spreads were evaluated, 26/206 grains were on Yq. No grains were localized on Yp. This suggests that the Yp localization found for λY2 : 13 is due to the repeated sequences carried by this recombinant. Ten metaphase spreads of 445 × 393 were analysed; of the 58 grains scored, 5% were on the Yq region of the translocation chromosome and 24% on this chromosome in the X region: 23% of the grains were on Xq24-Xqter. It seems likely that the λY2 : 13 sequence is embedded in one or other of the tandemly repeated sequences found on Yq (refs 14, 15).

Such a high degree of sequence conservation between non-homologous chromosomes is striking. Clock rates for base changes in the flanking and non-transcribed regions of the globin genes are about 0.3%–0.4% per million years[16]. Over the 80 million years since the divergence of mammals from a common ancestor, this rate would predict X and Y chromosome homologies of around 70%. If selection were operating to maintain this sequence identity then we would expect to find homologues in the mouse, but hybridization in conditions which should allow detection of sequences with 10% divergence from the human probe reveals no mouse sequences which cross-hybridize. These results show that homologous sequences on the X and Y chromosomes are found in regions which do not form a synaptonemal complex, but the sequence data imply that exchange of DNA sequence between the X and Y chromosomes in the region of this sequence has occurred relatively recently and has resulted in the sequence identity which we have demonstrated. Several homologies between X and Y chromosomes outside the pairing regions have been reported recently[17–19] but the extent of homology varies. This may reflect exchange events of widely different ages.

We thank Edwin Southern for encouragement and comments, Clare Graham for technical assistance and Peter Goodfellow and Ruthi Voss for the gift of cell lines. The work was supported by the MRC and the Deutsche Forschungsgemeinschaft.

Received 13 September 1983; accepted 18 June 1984.

1. Solari, A. J. *Chromosoma* **81,** 315–337 (1980).
2. Burgoyne, P. S. *Hum. Genet.* **61,** 85–90 (1982).
3. Polani, P. E. *Hum. Genet.* **60,** 207–211 (1982).
4. Goodfellow, P. *Differentiation* **23** (Suppl.), 35–39 (1983).
5. Page, *et al. Proc. natn. Acad. Sci. U.S.A.* **79,** 5352–5356 (1982).
6. Daiger, S. P., Wilder, R. S. & Su, T. S. *Nature* **298,** 682–684 (1982).
7. Bishop, C. E. *et al. Nature* **303,** 831–832 (1983).
8. Cooke, H. J., Fantes, J. & Green, D. *Differentiation* **23** (Suppl.) 48–56 (1983).
9. Vieira, J. & Messing, J. *Gene* **19,** 259–264 (1982).
10. Murray, J. M. *et al. Nature* **300,** 69–71 (1982).
11. Maxam, A. M. & Gilberg, W. *Proc. natn. Acad. Sci. U.S.A.* **74,** 560–564 (1977).
12. Wieacker, P. *et al. Am. J. hum. Genet.* **26,** 265 (1984).
13. Cremer, C., Gray, J. W. & Ropers, H. H. *Hum. Genet.* **60,** 262–266 (1982).
14. Cooke, H. J. *Nature* **262,** 182–186 (1976).
15. Cooke, H. J., Schmidtke, J. & Gosden, J. R. *Chromosoma* **87,** 491–502 (1982).
16. Kimura, A. & Takagi, Y. *Nucleic Acids Res.* **11,** 2541–2550 (1983).
17. Mueller, C. R., Davies, K. E. & Ropers, H. H. *Cytogenet. Cell Genet.* **37,** 545 (1984).
18. Bishop, C., Guellaen, G., Geldwerth, D., Fellous, M. & Weissenbach, J. *J. molec. Biol.* **173,** 403–417 (1984).
19. Koenig, M., Camerino, G., Heilig, R. & Mandel, J-L. *Nucleic Acids Res.* **12,** 4097–4109 (1984).
20. Cremer, C. *Cytometry* (in the press).

Isolation of the *dorsal* locus of *Drosophila*

Ruth Steward, Francis J. McNally & Paul Schedl

Department of Biology, Princeton University, Princeton,
New Jersey 08544, USA

The establishment of embryonic polarity is a crucial step in pattern formation and morphogenesis. In the fruitfly *Drosophila melanogaster*, embryonic polarity depends primarily on genes expressed in the female during oogenesis. Mutations in these 'maternal effect' genes can lead to major disruptions in normal pattern formation. Two classes of maternal genes essential for the establishment of polarity in the embryo have been identified. Lesions in one class, the 'bicaudal' genes, disrupt the anterior–posterior axis[1]; lesions in the other class disrupt dorsal–ventral polarity, and in the most extreme cases embryos fail to form any ventral or lateral structures. Genetic studies suggest that the anterior–posterior and dorsal–ventral axes may be independent as the defects observed in mutants from each class seem to be restricted to one axis only[2]. The *dorsal* (*dl*) locus[2] is one of the maternal effect genes involved in the establishment of dorsal–ventral polarity. Homozygous *dl* females produce embryos exhibiting the mutant phenotype—complete lack of dorsal–ventral polarity in the strongest alleles—irrespective of the genotype of the father. Although *dl* is a maternal effect locus and must be expressed during oogenesis, the gene product, or a substance depending on the normal function of the *dl* gene, seems to be active early in embryogenesis, as the *dl* phenotype can be partially rescued by injection of cytoplasm from wild-type cleavage-stage embryos[3,4]. Here we report the molecular cloning of the *dorsal* locus and a study of its expression.

The *dorsal* locus maps in the cytological interval 36C on the left arm of chromosome 2 (ref. 2). To clone this region and identify the *dl* gene, we took advantage of two inversions, $In(2L)dl^H$ and $In(2L)dl^T$, (R.S. and C. Nüsslein-Volhard, unpublished) which inactivate the gene and hence have breakpoints either within or in close proximity to the locus. Females with the genotype $In(2L)dl^H$ or $In(2L)dl^T$ over the deficiency *Df(2L)TW119* (ref. 5), which uncovers the 36C interval (see Fig. 1), produce embryos which display the characteristic *dl* phenotype. Figure 1 also shows that the proximal breakpoint of $In(2L)dl^H$ maps just distally to 37C1,2, which contains the gene for dopa decarboxylase (*Ddc*). The *Ddc* gene and a surrounding 100-kilobase (kb) region have been cloned by Hirsch and Davidson[6]. We were able to 'jump' into the *dl* region by 'walking' from *Ddc* to the $In(2L)dl^H$ breakpoint (for an explanation of walking see ref. 7).

Recombinants containing the rearranged DNA of the inversion chromosome were isolated and characterized (see Fig. 2 legend). As expected, these recombinants hybridized *in situ* to two distinct sites, 36C and 37B-C, in wild-type polytene chromosomes; this is shown for the recombinant iH-6 in Fig. 2*a*. A restriction fragment from iH-6, containing only 36C DNA sequences, was then used to isolate a wild-type genomic recombinant from the *dl* region. Starting from this recombinant, we isolated a 75-kb segment surrounding the dl^H breakpoint (Fig. 3). This 75-kb DNA segment was oriented with respect to the left arm of chromosome 2 by *in situ* hybridization to the $In(2L)dl^H$ chromosome. We also localized the distal edge of the deficiency *Df(2L)TW119* (which uncovers the *dorsal* gene) in the overlapping sequences of recombinants D15 and D31 (see *b* in Fig. 3). These findings indicate that the odd-numbered recombinants map to the distal side of the dl^H breakpoint towards the telomere, but the even-numbered recombinants are proximal or towards the centromere. Moreover, these findings suggest that the *dl* locus is situated within or proximal to phage D15.

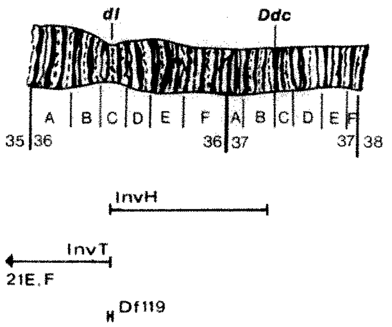

Fig. 1 Chromosome rearrangements on chromosome 2L in the *dorsal* region. *dl*, *dorsal*; *Ddc*, *dopa decarboxylase*; In H, $In(2L)dl^H$; In T, $In(2L)dl^T$; Df119, *Df(2L)TW119*.

As dl^H and dl^T both inactivate the *dl* gene, the localization of the respective breakpoints in the 75-kb walk should permit the identification of DNA sequences essential for normal *dorsal* gene function. Our cloning strategy suggests that the dl^H breakpoint must be located within the recombinant D1. To identify the dl^T breakpoint, we used recombinants from the 75-kb walk to probe genomic blots of dl^T DNA. These experiments showed that the dl^T breakpoint was also contained within the recombinant D1. To map each breakpoint more precisely, we used specific restriction fragments from the phage D1 (Fig. 4*a*) as probes to compare the DNA sequence organization of the two inversions with that of the wild-type parental chromosome. Figure 2*b* shows that both inversion breakpoints map within a small 2.3-kb *Hin*dIII–*Sst*I restriction fragment near the centre of phage D1. Moreover, the breakpoints are localized at different sites within this restriction fragment. These findings indicate that this small DNA segment contains sequences essential for *dl* gene function.

To identify the *dorsal* transcription unit, as well as other genes in the 75-kb region, we probed Northern blots of total and poly(A)$^+$ embryonic RNA with the recombinant phage that spans the *dorsal* region; only three transcription units were detected. Two of these were found to be located in the *Drosophila* DNA segments of phages D31 and D51 and were mapped further using isolated restriction fragments. As indicated in Fig. 3, both transcription units (*c*) are localized distal to the DNA sequences deleted in *Df(2L)TW119*, and hence are unlikely to represent the *dorsal* gene.

The third transcription unit, which encodes a mature poly(A)$^+$ RNA of 2.8 kb (Fig. 4*b*), mapped to the phage D1. We defined the coding region for this 2.8-kb RNA more precisely by probing Northern blots with restriction fragments isolated from D1 and adjacent recombinants. As indicated in Fig. 4*a*, fragments 4–8 were found to contain sequences complementary to the 2.8-kb RNA. Together these fragments span a DNA segment of ~8 kb, which is more than twice the size of the mature RNA, and hence we would expect this transcription unit to contain intervening sequences. As the sequences encoding the 2.8-kb RNA include the *Hin*dIII–*Sst*I fragment (fragment 5 of Fig. 4*a*) which contains the dl^H and dl^T breakpoints, we conclude that this 8-kb transcription unit represents the *dorsal* gene.

To determine the direction of transcription of the *dl* gene, a *Hin*dIII–*Sal*I restriction fragment (fragment 8, Fig. 4*a*) from the proximal end of the transcription unit was subcloned in opposite orientations into the M13 single-strand vectors, mp8 and mp9. The resulting recombinant mp8-8 has the *Sal*I restriction site at the 5′ end of the insert and the *Hin*dIII site at the 3′ end. Conversely, mp9-8 has a 5′ *Hin*dIII and 3′ *Sal*I site. Radioactively-labelled complementary strand DNA was prepared from each recombinant and hybridized to a Northern blot of early embryo poly(A)$^+$ RNA. Figure 4*b* shows that only the complementary strand synthesized from the recombinant mp8-8 hybridized to the RNA. This result shows that the 5′ end of the *dorsal* transcription unit is on the proximal side of the locus, close to the *Sal*I restriction site, while the 3′ end is on the distal side (see Fig. 4*a*).

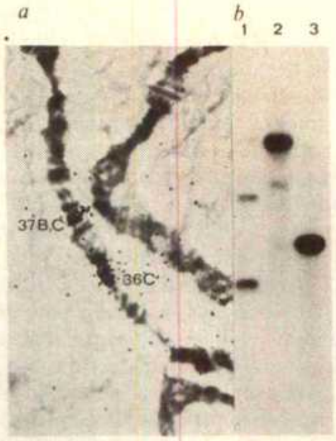

Fig. 2 *a*, *In situ* hybridization of the recombinant phage iH-6 (containing the dl^H breakpoint) to wild-type chromosomes. *b*, Inversion breakpoints in the *dorsal* gene. Lane 1, $In(2L)dl^T/Df(2L)TW119$ DNA. Lane 2, $In(2L)dl^H/Df(2L)TW119$ DNA. Lane 3, DNA of the parental chromosome. The DNAs were digested with *Hin*dIII. The Southern blot was hybridized with fragment 5 (see Fig. 4*a*).

Methods: We used a wild-type Canton S genomic λ phage library[14] to walk[7] approximately 30 kb from the distal edge of the 37C1,2 *Ddc* region, isolated by Hirsch and Davidson[6], to the dl^H breakpoint. A restriction fragment from the phage spanning the breakpoint was then used to screen a recombinant λ phage library prepared from $In(2L)dl^H/CyO$ (ref. 15) fly DNA. The dl^H and dl^T breakpoints were mapped more precisely by using specific restriction fragments from the phage D1 (see Fig. 4*a*) as probes to compare the DNA sequence organization of the two inversions with that of the wild-type parental chromosome in which the inversions have been induced. In the autoradiograph, the DNAs were digested with *Hin*dIII and after gel electrophoresis and blotting, probed with the 2.3-kb *Hin*dIII–*Sst*I fragment from phage D1 (see Fig. 4*a*). In the wild-type parental DNA, fragment 5 hybridizes to a 3.9-kb *Hin*dIII fragment that is missing in both inversions. Two new fragments of 5.5 and 3.6 kb are found in dl^T, while in dl^H there are two fragments of 8.0 and 5.0 kb. *In situ* hybridization was performed using the method of Pardue and Gall[16].

Genetic studies[2,4] have shown that *dorsal* is expressed in females and that the gene product is required during early embryogenesis but does not appear to be essential at later stages in the *Drosophila* life cycle. Therefore, we examined the stage and tissue distribution of the *dorsal* RNA. For this purpose, poly(A)$^+$ RNA was prepared from adult males and females, dissected ovaries, and staged embryos: 0–2.5-h (cleavage and early blastoderm), 2.5–5-h (blastoderm and gastrula), 8–10.5-h (post-gastrula) and 20–24-h embryos collected at 22 °C. Northern blots of these RNAs were then probed with restriction fragment 8 from the *dorsal* gene (see Fig. 4*a*), or with a recombinant containing the 5*C* actin gene[8].

Figure 5*a* shows the developmental profile of the 2.8-kb *dorsal* RNA. We did not detect the *dorsal* transcript in adult males (lane 1) or females (lane 2). Conversely, as expected from genetic studies, the RNA was present in dissected ovaries (lane 3), suggesting that the expression of the *dorsal* gene in adult females may be restricted to ovaries. The *dorsal* RNA is also found immediately after fertilization in the 0–2.5-h cleavage and in early blastoderm embryos (lane 4). Interestingly, this RNA is apparently degraded as it is not detected in either 2.5–5-h embryos (lane 5) or 8–10.5-h embryos (lane 6). In 20–24-h embryos (Fig. 5*a*, lane 7), there are poly(A)$^+$ RNA-containing sequences complementary to the *dorsal* probe. This RNA species is present in low yield and as its mobility appears to be slightly different from that of the 2.8-kb *dorsal* transcript, we are uncertain at present whether it represents a bona fide *dorsal* transcript, or some other RNA which contains homologous sequences.

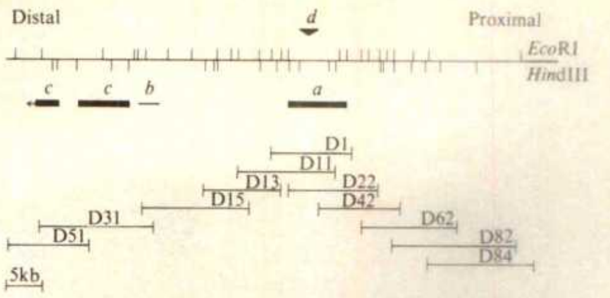

Fig. 3 Restriction map of the *dorsal* region, transcribed regions and chromosomal breakpoints. The D1 to D84 recombinant phages are shown. *a*, *dl* transcript; *b*, location of the distal *Df(2L)TW119* breakpoint; *c*, adjacent transcription units; *d*, location of breakpoints of $In(2L)dl^H$ and $In(2L)dl^T$.

Methods: Overlapping recombinants were isolated from a Charon 4, λ phage library of Canton S genomic DNA[7,14]. Chromosomal breakpoints were localized by hybridization of radioactively-labelled[17] recombinants or isolated restriction fragments to Southern[18] blots containing genomic DNA[19]. Coding regions were identified by hybridizing radioactively-labelled recombinants or isolated restriction fragments to Northern blots containing total or poly(A)$^+$ RNA from early embryos.

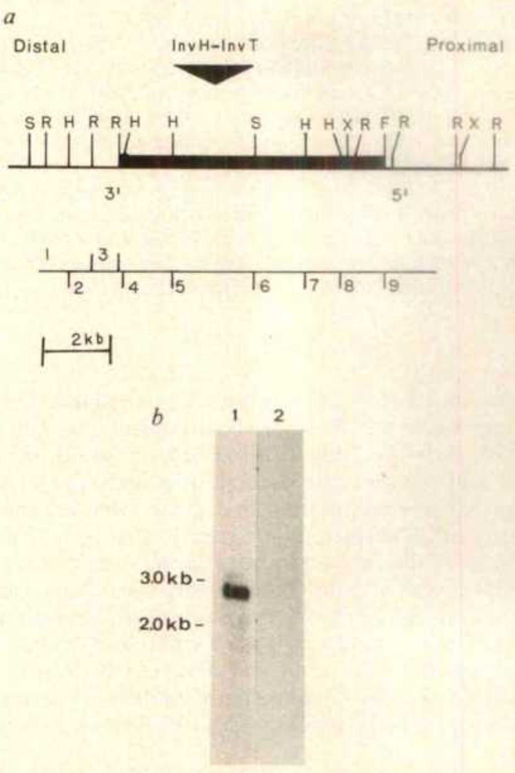

Fig. 4 *a*, Restriction map, transcribed region and chromosomal breakpoints of the *dorsal* gene. R, *Eco*RI; H, *Hin*dIII; S, *Sst*I; *F*, *Sal*I; 1–9, restriction fragments which were isolated and used for hybridization. *b*, The *dorsal* transcript and orientation of transcription. Lane 1, the 2.8-kb *dorsal* transcript. Poly(A)$^+$ embryonic RNA was hybridized with the complementary radioactively-labelled strand of the single-strand recombinant mp8-8. Lane 2, poly(A)$^+$ embryonic RNA hybridized with the complementary radioactively-labelled strand of the single-strand recombinant mp9-8. The size markers were the 3.05-kb, molecular weight (MW) 83,000 heat shock protein mRNA[20] and the 1.95-kb actin mRNA[8].

Methods: Poly(A)$^+$ RNA was isolated from 0–3-h embryos according to the method of O'Hare *et al.*[21], and Northern blots containing this RNA were hybridized with probes containing the *dorsal* coding region and plasmids containing coding sequences for the MW 83,000 heat shock protein or for actin. Fragment 8 was subcloned in opposite orientation into the M13 single-strand vectors mp8 and mp9. Strand-specific radioactively-labelled probes were synthesized[22] and hybridized to Northern blots.

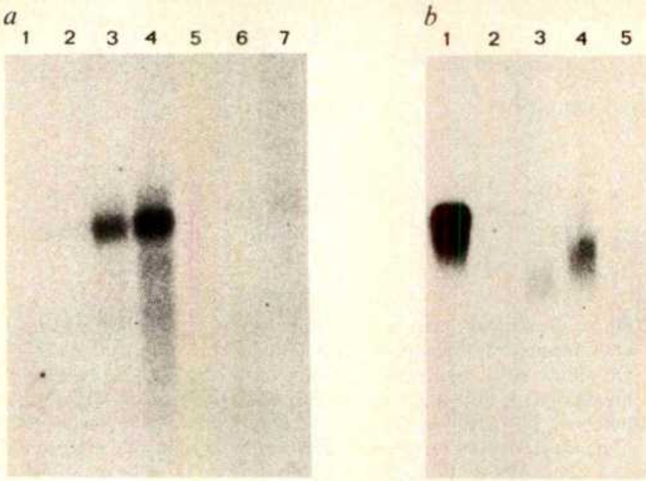

Fig. 5 *a*, Transcripts of the *dorsal* gene during embryonic development. All lanes contain 5 μg of poly(A)$^{+}$ RNA. Lane 1, adult male; lane 2, adult female; lane 3, ovary; lane 4, 0–2.5-h embryo; lane 5, 2.5–5-h embryo; lane 6, 8–10.5-h embryo; lane 7, 20–24 h embryo. *b*, Transcripts of the *dorsal* gene in ovaries from dl^{H} and dl^{T} females. Lane 1, wild-type ovary poly(A)$^{+}$ RNA (5 μg); lane 2, $In(2L)dl^{H}/Df(2L)TW119$ ovary poly(A)$^{+}$ RNA (5 μg); lane 3, $In(2L)dl^{H}/Df(2L)TW119$ ovary total RNA (20 μg); lane 4, $In(2L)dl^{T}/Df(2L)TW119$ ovary total RNA (20 μg); lane 5, $In(2L)dl^{T}/Df(2L)TW119$ ovary poly(A)$^{+}$ RNA (5 μg). The Northern blots were hybridized with fragment 8 (see Fig. 4*a*).
Methods: The RNA samples were run on formaldehyde agarose gels and blotted[23]. After exposure to X-ray film, the filters were rehybridized with a recombinant plasmid (pDmA2) containing part of the coding region of the 5C actin gene[8]. In the Northern blot shown in *a*, low levels of actin message were seen in the lanes containing adult RNA, but consistently high levels were observed in ovaries and during embryogenesis. In the Northern blot shown in *b*, equally high levels of full-length actin message were found in all poly(A)$^{+}$ lanes (results not shown).

To test the integrity of the RNAs, we determined the level of actin message in the different RNA preparations. Although, as expected, there was little actin message in adults, the level in ovaries and during embryogenesis was high and very nearly constant[8]. These results show that the *dl* gene is expressed in the ovary and that there is a dramatic change in the relative abundance of the *dorsal* transcript during early embryogenesis.

The amount of actin mRNA in embryos has been determined by Anderson and Langyel[9], making it possible to estimate the number of *dl* transcripts in 0–2.5-h embryos by comparing the signal intensity of the actin and *dl* RNAs in Northern blots. The *dl* RNA is about 100 times less abundant than actin mRNA and this would correspond to $\sim 5\times10^{4}$ *dl* RNA molecules per embryo.

Because the breakpoints of dl^{H} and dl^{T} are located within the transcription unit for the 2.8-kb RNA, it was of interest to determine whether these mutations affect the transcription of the *dorsal* gene. RNA was prepared from ovaries of females carrying either of the inversion chromosomes over $Df(2L)TW119$. Total and poly(A)$^{+}$ RNA isolated from the mutant ovaries was hybridized with fragment 8 (Fig. 4*a*) from the *dorsal* transcription unit (see Fig. 5*b*). Poly(A)$^{+}$ RNA from wild-type ovaries gives a strong hybridization signal with the dorsal probe (lane 1 of Fig. 5*a*). In contrast, little or no hybridization can be detected in poly(A)$^{+}$ RNA prepared from dl^{H} (lane 2) and dl^{T} (lane 5) ovaries, indicating that these two mutants fail to synthesize the 2.8-kb *dorsal* transcript. Nevertheless, the *dorsal* gene appears to be transcribed in ovaries from both mutants as we observe aberrant poly(A)$^{-}$ RNA species of smaller molecular weight in total RNA (lanes 3 and 4). In a control experiment, RNAs from the two inversion and wild-type ovaries were hybridized with phage D31 which contains the two transcription units distal to the $Df(2L)TW119$ breakpoint (see Fig. 2). As the expected full-length RNAs were found (results not shown) it is unlikely that these distal transcription units (*c* in Fig. 3) are part of the *dorsal* locus.

Here we have described the isolation and characterization of a 75-kb DNA segment from the cytogenetic interval 36C on the left arm of chromosome 2 which contains the *dorsal* locus of *D. melanogaster*. Of the three transcription units identified in the 75-kb *dorsal* region, two map outside the deficiency $Df(2L)TW119$, and are unlikely to be part of the *dorsal* locus. The third transcription unit, which is 8 kb long and encodes a 2.8-kb poly(A)$^{+}$ RNA, lies within the region deleted by $Df(2L)TW119$. This conclusion is based on the finding that inversions dl^{H} and dl^{T}, which are *dorsal* mutations, have breakpoints that disrupt the 8.0-kb transcription unit. Moreover, the 2.8 kb-poly(A)$^{+}$ RNA transcript is absent in ovaries of these mutants, and instead they produce smaller, truncated poly(A)$^{-}$ RNA transcripts from the beginning of the *dorsal* gene.

Although we observe high levels of the 2.8-kb *dorsal* transcript in both dissected ovaries and cleavage-stage embryos, it seems likely that the *dorsal* gene may be transcribed only during oogenesis. First, genetic studies have shown that *dorsal* is not zygotically rescued by wild-type sperm[2]. Second, molecular studies indicate that there is little or no transcription until development of syncytial blastoderm[10,11]. Although the *dorsal* gene is probably not transcribed in early embryos, it is possible that the maternally derived RNA is translated during the initial phase of embryogenesis. Zalokar[10] has shown that translation of stored maternal message starts immediately after fertilization. If the *dl* RNA is translated at this time, this process must be completed before cellular blastoderm formation because the RNA is absent at this stage. Also, the activity of the *dorsal* gene product is presumably required before formation of cellular blastoderm as embryonic polarity seems to be irreversibly determined by that stage[4,12].

The *dorsal* phenotype can be partially rescued by injection of cytoplasm from wild-type cleavage-stage embryos into mutant hosts of the same age[3,4]. The rescuing activity is found on both the dorsal and ventral sides of the wild-type embryos immediately after fertilization and becomes localized in the ventral sides during cleavage[3]. Note that *dorsal*, unlike several other 'dorsalizing' mutants, cannot be rescued by the injection of RNA from early embryos (see accompanying paper[13]). This result is surprising in view of the apparent abundance of the *dl* RNA at this stage. Conceivably, insufficient active *dl* product is synthesized from the injected *dl* RNA. Alternatively, the product either may not function properly or may not be correctly localized. Clearly, it will be of interest to determine how the *dorsal* product (transcript or protein) becomes assymetrically distributed and to study its role in the establishment of dorsal–ventral polarity.

We thank J. Hirsch for providing the recombinant phage from which the cloning work was begun. We also thank E. Fyrberg for the actin clone, Le Nguyen for technical assistance, K. O'Hara for typing the manuscript, and our colleagues, especially Drs D. Coulter and S. Tsubota, for helpful discussions. R.S. also thanks C. Nüsslein-Volhard for her advice and support in the early stages of this work. This work was supported by grants from the NIH and the March of Dimes Birth Defect Foundation.

Received 1 June; accepted 3 August 1984.

1. Nüsslein-Volhard, C. *Wilhelm Roux Arch. dev. Biol.* **183,** 249–268 (1977).
2. Nüsslein-Volhard, C. in *Determination of Spatial Organization* (eds Subtelney, S. & Koenigsberg, I. R.) 185–211 (Academic, New York, 1979).
3. Santamaria, P. & Nüsslein-Volhard, C. *EMBO J.* **2,** 1695–1699 (1983).
4. Anderson, K. V. & Nüsslein-Volhard, C. in *Primers in Developmental Biology* (ed. Malacinski, G.) (Macmillan, New York, 1983).
5. Wright, T. R. F., Hodgetts, R. B. & Sherald, A. F. *Genetics* **84,** 267–285 (1976).
6. Hirsch, J. & Davidson, N. *Molec. cell. Biol.* **1,** 475–485 (1981).
7. Bender, W., Spierer, P. & Hogness, D. S. *J. molec. Biol.* **168,** 17–33 (1983).
8. Fyrberg, E. A., Mahaffey, J. W., Bond, B. J. & Davidson, N. *Cell* **33,** 119–123 (1983).
9. Anderson, K. V. & Lengyel, J. A. in *Histone Genes* (eds Stein, G. & Stein, J.) 135–161 (Wiley, New York, 1984).
10. Zalokar, M. *Devl. Biol.* **49,** 425–432 (1976).
11. McKnight, S. & Miller, O. L. *Cell* **8,** 305–319 (1976).
12. Chan, L.-N. & Gehring, W. *Proc. natn. Acad. Sci. U.S.A.* **68,** 2217–2221 (1971).

13. Anderson, K. V. & Nüsslein-Volhard, C. *Nature* **311**, 223–227 (1984).
14. Maniatis, T. *et al. Cell* **15**, 682–701 (1978).
15. Lindsley, D. & Grell, E. H. in *Genetic Variations of* Drosophila melanogaster (Carnegie, Washington, 1968).
16. Pardue, M. & Gall, J. G. *Meth. cell Biol.* **10**, 1–16 (1975).
17. Maniatis, T., Jeffrey, A. & Kleid, G. D. *Proc. natn. Acad. Sci. U.S.A.* **72**, 1184–1188 (1975).
18. Southern, E. *J. molec. Biol.* **98**, 503–517 (1975).
19. Ish-Horowicz, D., Pinchin, S. M., Schedl, P., Astavanis-Tsakonas, S. & Mirault, M. E. *Cell* **18**, 1351–1358 (1979).
20. Holmgren, R., Croces, V., Morimoto, R., Blackman, R. & Meselson, M. *Proc. natn. Acad. Sci. U.S.A.* **78**, 3757–3761 (1981).
21. O'Hare, K., Levis, R. & Rubin, G. M. *Proc. natn. Acad. Sci. U.S.A.* **80**, 6917–6921 (1983).
22. Hu, N. & Messing, J. *Gene* **17**, 271–277 (1982).
23. Lehrach, H., Diamond, J., Wozney, J. & Boedtker, H. *Biochemistry* **16**, 4743–4751 (1977).

Internal control of the coated vesicle pp50-specific kinase complex

Alain Pauloin & Pierre Jollès

Laboratory of Proteins, University of Paris V,
45 rue des Saints-Pères, 75270 Paris Cedex 06, France

The polyhedral surface lattice of coated vesicles consists of three-legged hexameric protein complexes called triskelions which constitute the basic assembly unit[1]. The triskelion is a molecular complex of molecular weight 630,000 (M_r 630K) composed of three clathrin heavy chains (subunit 180K) and three light chains (subunits 33K and 36K) (refs 2, 3). The presence of additional coated vesicle-specific proteins in the 100–130K and 50–55K range have been reported[4–6]. We previously described the presence of a cyclic nucleotide- and Ca^{2+}-independent protein kinase activity in coated vesicles[7] which was confirmed by others[8,9]. This protein kinase specifically phosphorylates the 50K protein (pp50). In this report, we show that the coated vesicle kinase and its 50K protein substrate are part of a stable multimolecular system. In addition we show that the clathrin–light chain complex stimulates the pp50 phosphorylation and only light chains are implicated in this stimulation and that the pp50 phosphorylation does not seem to be affected by the vesicle.

Coated vesicles were dissociated in a 1 M Tris-buffer, *p*H 7, and applied to a Sepharose CL-4B column[10]. Three peaks (I to III) were characterized (Fig. 1). Peak I contained decoated vesicles. Clathrin with its light chains (triskelions) were the main components of peak II. Peak III contained no clathrin but was greatly enriched in the 50 K protein (pp50) associated with a family of at least six proteins with molecular weights in the range 105–136 K. The most abundant protein was M_r 105K, whereas the others seemed to be present in equal amounts (Fig. 1*a*, III). By comparison with a standard curve prepared with marker proteins, the elution volume of peak III in the Tris buffer corresponded to that of a 400K globular protein. Coated vesicle kinase activity was always present in this peak (Fig. 1*b*, III). The over-exposed autoradiography shows the absence of other phosphorylations in both the decoated vesicle and triskelion fractions (Fig. 1*b*, I and II). The enzymatic activity was stable. In the presence of phenylmethylsulphonyl fluoride (PMSF), a protease inhibitor, activity was preserved for several months in the 1 M Tris-buffer, *p*H 7, at 4 °C or indefinitely at −30 °C in 50% glycerol.

Chemical cross-linking of the previously phosphorylated molecular complex of peak III with dimethyladipimidate (DMA) indicated that pp50 is closely associated with some proteins of the 105–136K group, and forms a 330K labelled complex. No new band appeared in the 100 and 150K regions of the gel suggesting the absence of a pp50 dimer and trimer. Very high molecular weight cross-linked complexes, in particular a 660K complex, were only observed for DMA concentrations above 0.4 mg ml^{-1} (Fig. 2).

We studied the possible interaction of either the triskelions or the decoated vesicles on the kinase activity of the 105–136K complex. Increased concentrations of triskelions had a stimulating effect on pp50-kinase activity. The latter increased the pp50 phosphorylation approximately 4-fold. The light chains seemed responsible for this stimulation, as clathrin had only a very slight effect (Fig. 3). On the other hand, decoated vesicles seemed to inhibit the pp50 phosphorylation, but lost their inhibiting effect when heated (Fig. 3). The inhibition was due to the ATP consumption induced by the ATPase activity present in the decoated vesicles (data not shown).

Keen *et al.*[10] have shown that coated vesicles are dissociated after treatment with protonated amines at neutral *p*H. Gel filtration of their coated vesicle–Tris extract allowed separation of the triskelion fraction from another fraction, described as the basket assembly factor, containing a 110K protein and eluting in a volume corresponding to a molecular weight of 420K. There is a good parallel between this isolation of the basket assembly factor and the kinase-specific substrate complex of coated vesicles. The co-purification of these two biological activities raised the question of whether they share a common molecular support.

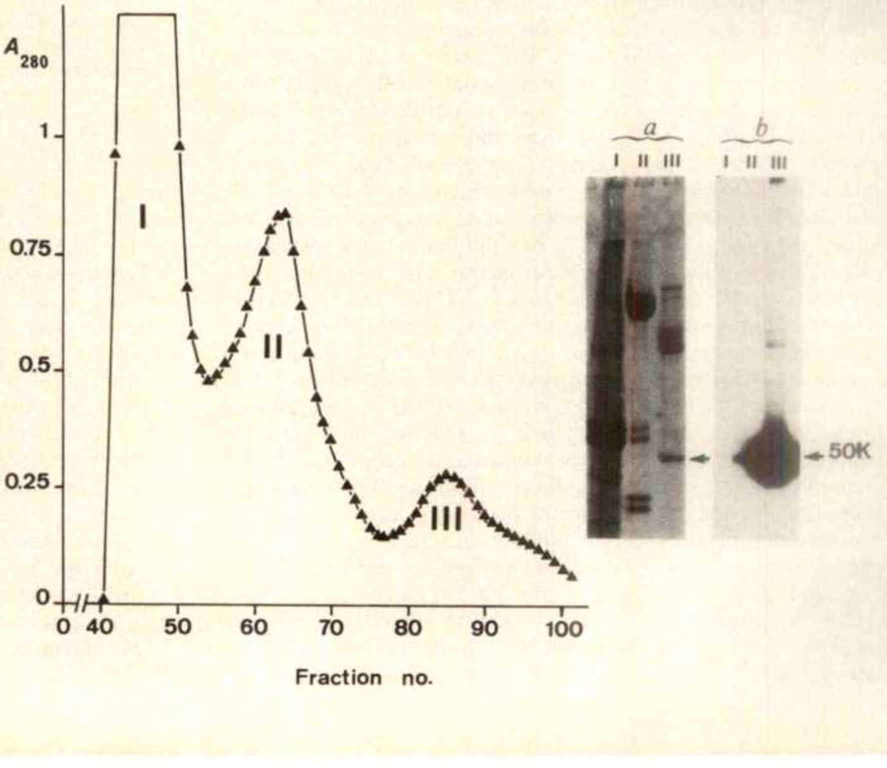

Fig. 1 Gel filtration of Tris-dissociated coated vesicles on Sepharose CL-4B. The gels after Coomassie blue staining *a* and autoradiography *b* are shown in the inserts.
Methods: Coated vesicles were isolated by two successive sucrose gradients[7,10]. The highly enriched upper 5% sucrose solution of the second gradient was used for the final purification using a $^1H_2O/^2H_2O$-8% sucrose step gradient as described[20]. The coated vesicle pellet (50 mg) was solubilized in 3 ml of 1 M Tris buffer, *p*H 7.0, 0.1 mM EGTA, 2 mM $MgCl_2$, 1 mM 2-mercaptoethanol, using a Potter homogenizer, incubated for 30 min at room temperature and applied to a column (2.5 × 120 cm) of Sepharose CL-4B equilibrated and eluted at 20 °C with the Tris buffer. Fractions of 4.5 ml were collected at a flow rate of 22.5 ml h^{-1}. The column was calibrated with ferritine (364K), catalase (240K), human γ-globulins (150K) and albumin (67K). The most enriched fractions of each peak (No. 45, 62, 85 for peaks I, II and III, respectively) were dialysed against 50 mM Tris buffer, *p*H 7.0. Aliquots (30 μl) were taken, phosphorylated with 10 μCi [γ-^{32}P]ATP (specific activity ≃ 3,000 Ci mmol^{-1}) and analysed by SDS-PAGE; autoradiography was performed as described elsewhere[7].

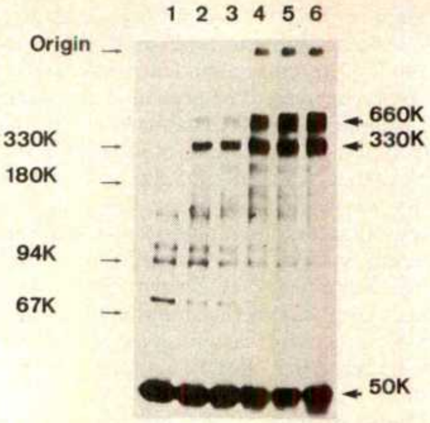

Fig. 2 Cross-linking by the bifunctional reagent dimethyladipimidate (DMA) of the 50/105–136K [^{32}P] molecular complex. Lane 1, purified [^{32}P] 50/105–13K complex without DMA; lanes 2–6, experiments carried out with DMA at 0.2, 0.4, 0.6, 0.8 and 1.0 mg ml^{-1}.

Methods: Cross-linking experiments were performed at room temperature with DMA (Sigma). This reagent was used, in the same conditions as dimethylsuberimidate[21], because it reacted more gently with our material. Cross-linking was performed as follows: 1 vol of 1 M triethanolamine (*p*H 8.5) was added to 4 vol of phosphorylated 50/105–136K molecular complex (0.1 mg ml^{-1}) in 50 mM Tris (*p*H 7.0). DMA was dissolved in 0.5 M triethanolamine (*p*H 8.5) at 15 mg ml^{-1}, and an appropriate volume was added within 1 min to the protein sample in order to obtain a final concentration between 0.2 and 1 mg ml^{-1}. The cross-linking reaction was carried out for 1 h at 25°C, then the cross-linked compounds were analysed by SDS-PAGE and autoradiography.

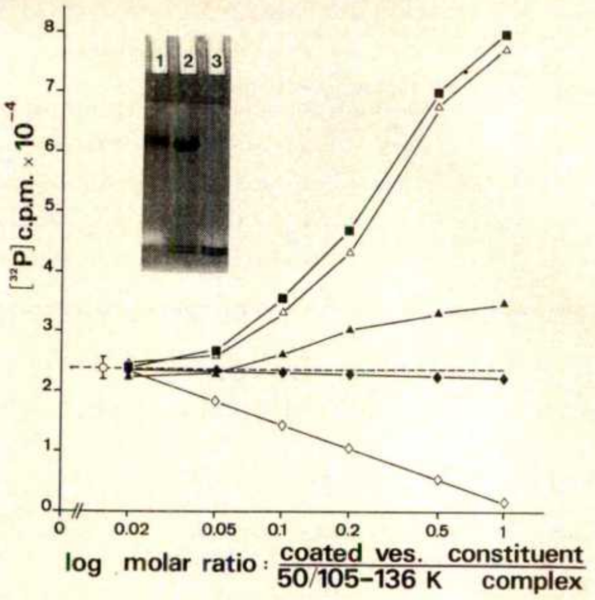

Fig. 3 Action of coated vesicle constituents on the pp50 phosphorylation. Results were expressed as the molar ratio of the concentration of triskelions (■), clathrin (▲), light chains (△), native decoated vesicles (◇) or heated decoated vesicles (◆), to the 50/105–136K molecular complex concentration. Phosphorylation level of the pp50 without effector was indicated (----). Control analysis of both the clathrin and light chains by SDS-PAGE is shown in the insert. Lane 1, clathrin, lane 2, triskelions, lane 3, light chains.

Methods: Decoated vesicles (peak I), triskelions (peak II) and the 50/105–136K complex (peak III), obtained as described (Fig. 1), were dialysed against 50 mM Tris, *p*H 7.0. Dialysed triskelions were concentrated (to ~1 mg ml^{-1}) and divided into three equal fractions. One of these constituted the triskelion sample and was stored at −30 °C in 50% glycerol to prevent proteolysis before using. The second fraction was used to prepare pure clathrin by spontaneous proteolysis of light chains. Their hydrolysis was generally complete after one week at 4 °C. The third fraction was used to prepare pure light chains by thermal denaturation of clathrin as described[17]. Decoated vesicles were divided into two equal fractions. One of these was heated at 50 °C for 5 min, the second was the native decoated vesicles. The protein concentrations[22] were determined before the reassociation experiments. The 50/105–136K complex (15 μl at 75 μg ml^{-1}) was mixed on ice with either 15 μl of various dilutions of triskelions (440 μg ml^{-1}), clathrin (360 μg ml^{-1}), light chains (75 μg ml^{-1}), native decoated vesicles (1,130 μg ml^{-1}) or heated decoated vesicles (1,130 μg ml^{-1}). The pp50 phosphorylations were carried out as previously described[7] and analysed by SDS-PAGE. After Coomassie blue staining, destaining and drying, the 50K bands were cut from the gel and counted by liquid scintillation.

There is no doubt that more than one component was present in the so-called "100–110K band" as shown using SDS-polyacrylamide gel electrophoresis (PAGE) by many authors[1,6,10–13]. Pfeffer and Kelly described a family of one major and seven minor polypeptides in this zone[5]. We agreed with these results and observed one major 105K protein and at least six minor polypeptides from 105K to 136K (ref. 14). This protein complex, whose total molecular weight including all its components, exceeded 1,000K was made up of at least two molecular complex systems possessing the same elution volume corresponding to M_r 400K. One of them might constitute the basket assembly factor (although its molecular composition remains unknown), the other was shown by cross-linking experiments, which demonstrate that pp50 is in close contact with some other proteins, to form a 330K cross-linked compound. Finally the ATP-independence of both the *in vitro* coated vesicle association and dissociation phenomena seemed to indicate that the basket assembly factor was distinct from the kinase-pp50 substrate complex. The phosphorylation of pp50 was under control of several components of the coated vesicles as shown by reassociation experiments. Phosphorylation was greatly enhanced in the presence of triskelions, where the light chains seemed to play the main role. Recently light chains have been shown to contain tightly bound nucleotides (AMP and/or ADP). However, storage of light chains at 4 °C for several days resulted in a large decrease of ADP and an increase in the level of AMP; it appeared that nucleotide hydrolysis had occurred and that ATP was possibly the original bound nucleotide[15]. The presence of this light chain nucleotidic site might facilitate both the ATP capture and its transfer to the kinase and could explain the stimulating effect of the light chains on the pp50 phosphorylation. The light chains have so far been implicated in the cage reassociation[1,6], but recently Winkler and Stanley[17] have suggested that this is not the case. In this present work a biological function related to the light chains has been shown.

The decoated vesicles did not seem to directly inhibit the pp50 phosphorylation. We verified that the apparent phosphorylation inhibition was induced by the previously described vesicular ATPase(s)[12,18,19]. However, the local ATP concentration might be modulated by the vesicles and thus, indirectly regulate the pp50 kinase. It should be noted that the strong ATPase action observed in decoated vesicles was only very slight in native coated vesicles. It is possible that the Tris-dissociating action induces the exposure of some cryptic forms of the ATPases or umasks these enzymes.

Although at present the physiological function of the pp50 phosporylation remains unclear, this activity is present in various different coated vesicle species we have studied[14]. Its activation by triskelions seems to indicate that the pp50-kinase system might be implicated in the control of the coated vesicle working mechanism involving both the membrane and clathrin coat fusion and fission. As we have shown that pp50 phosphorylation is under the positive control of the light chains, a negative control by another part of the coated vesicles or by external stimuli might also exist.

This research was supported by CNRS (ER no. 102) and INSERM (U-116). We thank Dr Fevre (CNRZ) for providing the bovine brains, and Dr I. Bernier (INSERM U-116) and Mrs A. Kropfinger (University of Paris VII) for helpful comments. A part of this work was presented as a poster at the symposium "Médiateurs intracellulaires et phosphorylation des protéines", 5–7 May (1983), Montpellier, France.

Received 27 February; accepted 4 July 1984.

1. Ungewickell, E. & Branton, D. *Trends biochem. Sci.* **7**, 358–361 (1982).
2. Ungewickell, E. & Branton, D. *Nature* **289**, 420–422 (1981).
3. Kirchhausen, T. & Harrison, S. C. *Cell* **23**, 755–761 (1981).
4. Rubenstein, J. L. R., Fine, R. E., Luskey, B. D. & Rothman, J. E. *J. Cell Biol.* **89**, 357–381 (1981).
5. Pfeffer, S. R. & Kelly, R. B. *J. Cell Biol.* **91**, 385–391 (1981).
6. Pearse, B. M. F. *Proc. natn. Acad. Sci. U.S.A.* **79**, 451–455 (1982).
7. Pauloin, A., Bernier, I. & Jollès, P. *Nature* **298**, 574–576 (1982).
8. Kadota, K., Usami, M. & Takahashi, A. *Biomed. Res.* **3**, 575–577 (1982).
9. Pfeffer, S. R., Drubin, D. G. & Kelly, R. B. *J. Cell Biol.* **97**, 40–47 (1983).
10. Keen, J. H., Willingham, M. C. & Pastan, I. H. *Cell* **16**, 303–312 (1979).
11. Unanue, E. R., Ungewickell, E. & Branton, D. *Cell* **26**, 439–446 (1981).
12. Blitz, A. L., Fine, R. E. & Toselli, P. A. *J. Cell Biol.* **75**, 135–147 (1977).
13. Woodward, M. P. & Roth, T. F. *Proc. natn. Acad. Sci. U.S.A.* **75**, 4394–4398 (1978).
14. Pauloin, A., Loeb, J. & Jollès, P. *Biochim. biophys. Acta* **799**, 238–245 (1984).
15. Schook, W. J., Andrès, A. & Puszkin, S. *FEBS Lett.* **164**, 303–306 (1983).
16. Puszkin, S., Maimon, J. & Schook, W. *J. Cell Biol.* **83**, 293a (1979).
17. Winkler, F. K. & Stanley, K. K. *EMBO J.* **2**, 1393–1400 (1983).
18. Stone, D. K., Xie, X.-S. & Racker, E. *J. biol. Chem.* **258**, 4059–4062 (1983).
19. Forgac, M., Cantley, L., Wiedenmann, B., Altstiel, L. & Branton, D. *Proc. natn. Acad. Sci. U.S.A.* **80**, 1300–1303 (1983).
20. Nandi, P. K., Irace, G., Van Jaarsveld, P. P., Lippoldt, R. E. & Edelhoch, H. *Proc. natn. Acad. Sci. U.S.A.* **79**, 5881–5885 (1982).
21. Davies, G. E. & Stark, G. R. *Proc. natn. Acad. Sci. U.S.A.* **66**, 651–656 (1970).
22. Bradford, M. M. *Analyt. Biochem.* **72**, 248–254 (1976).

A six-armed oligomer isolated from cell surface fibronectin preparations

Harold P. Erickson & José L. Inglesias

Department of Anatomy, Duke University Medical Center, Durham, North Carolina 27710, USA

Fibronectins are adhesive glycoproteins thought to mediate the attachment of cells to various substrates[1,2]. Plasma fibronectin (PFN) is a dimer comprising subunits of molecular weight 220,000, connected by one or two disulphide bonds. Electron microscopy shows that PFN is a long, flexible strand, 2–3 nm in diameter and 140 nm long[3,4]. Many cells in tissue culture elaborate an extracellular matrix of insoluble (highly cross-linked by disulphide bonds) fibronectin, and a variable amount of 'cell surface fibronectin' (CSFN) that can be extracted by mild urea treatment. This CSFN, soluble in 1 M urea and at high *p*H, is a mixture of dimers and disulphide-bonded oligomers[5–7]. In the present study we have examined the structure of these molecules by electron microscopy. Oligomers were separated from dimers and contaminating proteins by zone sedimentation through glycerol gradients. We report that the CSFN dimers are identical in structure to PFN. In contrast, the oligomers have an elaborate and well defined structure that we call a 'hexabrachion': six arms emanating from a central globular particle. The arms are similar to PFN in being long, thin and flexible, but have several distinctly different features.

Figure 1 shows the results of SDS-gel electrophoresis of human CSFN fractionated by gradient sedimentation. The only prominent bands were peptides with apparent molecular weights (MWs) of either 285,000 (285K) or 240K, depending on the position in the gradient. The 285K peptide was found in fractions sedimenting at ~13S (Fig. 1, lanes *d, e*), and the 240K peptide in 9S fractions (lanes *g–i*). The 240K molecular weight of the 9S fraction corresponds to the value previously reported for unfractionated human CSFN[8]. The 285K peptide, which can be seen as a faint band in the crude CSFN (Fig. 1, lane *b*), as well as in the oligomeric fractions, has not been reported previously. Note that the amount of oligomeric material varied considerably, and was greatly reduced in older cultures (> 20th passage); this might explain why the 285K band has not been reported previously.

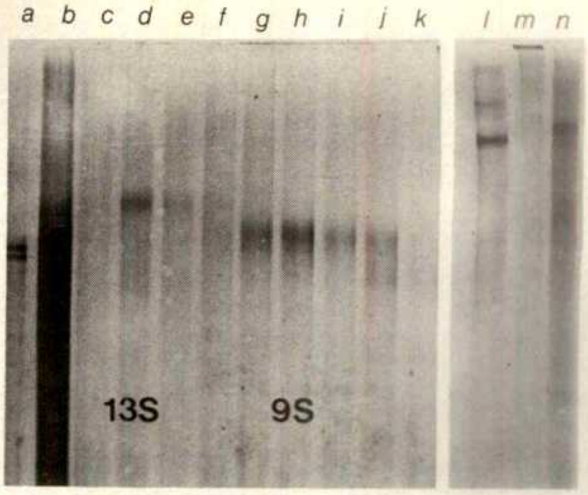

Fig. 1 Analysis of cell surface fibronectin (CSFN) after glycerol gradient sedimentation. CSFN was prepared from cultured human fibroblasts (foreskin, passage 16–18), grown on pads of glass wool in Petri dishes (J.L.I. and H.P.E., in preparation), 2 weeks after subculture. Cultures were extracted with 1 M urea, then CSFN was precipitated with 70% ammonium sulphate and resuspended in 0.15 M NaCl, 10 mM $CaCl_2$, 10 mM cyclohexylaminopropane sulphonic acid, *p*H 11.0 (ref. 5). A 0.5-ml volume of CSFN was layered onto a 12 ml gradient of 15–40% glycerol in 0.2 M ammonium bicarbonate, *p*H 9.5. The gradients were centrifuged at 41,000 r.p.m. for 18 h at 20 °C in a Beckman SW-41 Ti rotor, and 20 fractions of 0.6 ml each were collected. Samples (40 μl) were run on a 5% polyacrylamide gel by the method of Laemmli[12], and the gel was stained by the silver technique[13]. Lanes *a–k* contained β-mercaptoethanol, and lanes *l–n* were run (on the same gel) in non-reducing conditions. *a*, Human PFN (1.25 $\mu g\ ml^{-1}$). *b*, Crude CSFN, a 1:10 dilution of the sample loaded on the glycerol gradient; the weak upper band corresponds to the 285K band in lane *d*. The much stronger 240K band is largely obscured in the photograph by lower-molecular weight contaminants and/or by proteolytic products, but could be clearly distinguished on the gel. *c–k*, Fractions 6–14 from the glycerol gradient. The sedimentation coefficients, determined by comparison with protein standards[9], are indicated at the bottom for the two peak fractions. *l*, PFN (2.5 $\mu g\ ml^{-1}$, non-reduced); the prominent band is the dimer. *m*, 13S fraction (lane *d*), non-reduced; the protein is entirely oligomeric, entering only 0.5 mm into the 5% gel. *n*, 9S fraction (lane *h*), non-reduced; the protein is a dimer, somewhat larger than PFN. Apparent molecular weights were determined by reference to the upper band of the reduced PFN doublet (lane *a*, assumed MW 220K) and to the PFN dimer (lane *l*, assumed MW 430K). Protein concentrations were estimated by visual comparison of band intensities and by scanning the gels, using PFN (1.25 $\mu g\ ml^{-1}$, lane *a*) as a reference. The concentration of 13S protein (lane *d*) is ~1 $\mu g\ ml^{-1}$, and that of 9S protein ~2–3 $\mu g\ ml^{-1}$ (lanes *g, h*). Quantitation of the crude CSFN was more difficult because of the large background of contaminants, but we estimate that ~20–30% of the 285K and 240K peptides were recovered in the gradient fractions.

The 13S and 9S peak fractions were also electrophoresed in non-reducing conditions to determine the size of disulphide-linked structures (Fig. 1, lanes *m* and *n*). The protein in the 13S fraction barely entered the gel, demonstrating that this material comprises entirely disulphide-bonded oligomers. The 9S fraction showed a single band of apparent molecular weight 450K, demonstrating that the material comprises entirely disulphide-bonded dimers.

Protein concentrations were estimated by visual comparison of band intensities as described in Fig. 1 legend. The final recovery of purified protein was low due to losses in gradient sedimentation and to the low concentration of CSFN peptides in the starting material. Perhaps the most important quantitative aspect is a comparison of the protein recovered in the different gradient fractions. The total protein in the 13S fractions represents about one-quarter of that in the 9S fractions. Thus, the

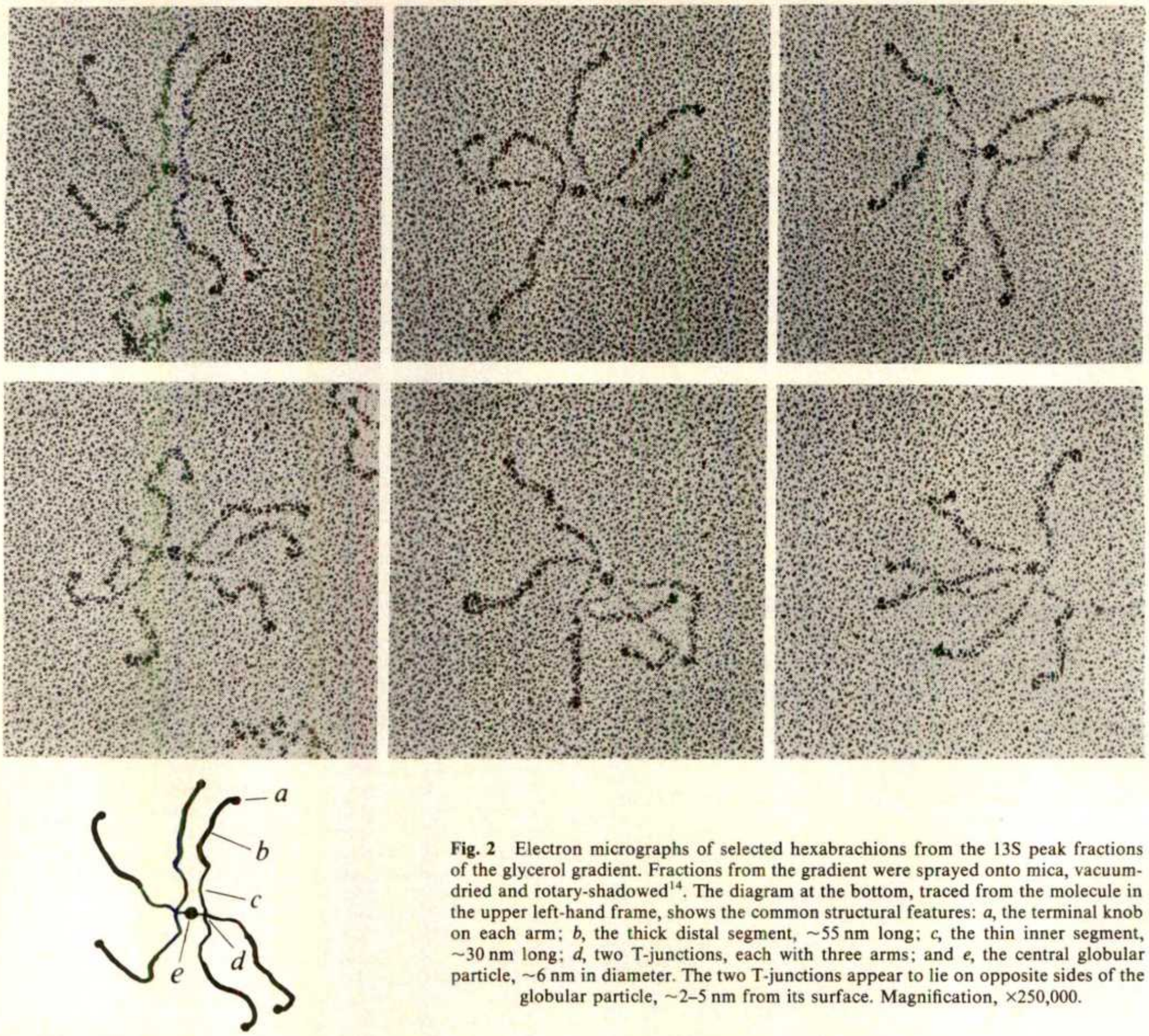

Fig. 2 Electron micrographs of selected hexabrachions from the 13S peak fractions of the glycerol gradient. Fractions from the gradient were sprayed onto mica, vacuum-dried and rotary-shadowed[14]. The diagram at the bottom, traced from the molecule in the upper left-hand frame, shows the common structural features: *a*, the terminal knob on each arm; *b*, the thick distal segment, ~55 nm long; *c*, the thin inner segment, ~30 nm long; *d*, two T-junctions, each with three arms; and *e*, the central globular particle, ~6 nm in diameter. The two T-junctions appear to lie on opposite sides of the globular particle, ~2–5 nm from its surface. Magnification, ×250,000.

oligomers constitute a significant fraction (~20%) of the material recovered after gradient sedimentation.

Electron microscopy of crude CSFN showed a mixture of strands, oligomers of strands, and a variety of globular particles. Oligomers, with the characteristic six-armed structure described below, constituted a significant fraction of the material. Quantitation from the electron microscope specimens was not attempted, but the images were roughly consistent with the 1:4 ratio of protein in the form of oligomers as opposed to dimers estimated above. Specimens prepared after fractionation on the glycerol gradient were much cleaner (no globular particles) and homogeneous. Oligomers were found almost exclusively and in high purity in the 13S fractions. The 9S material consisted largely of single strands, indistinguishable in structure from PFN, with some contamination by fragmented strands.

Electron microscopy showed that the 13S oligomers were not irregular polymers of fibronectin strands. All oligomers had the same structure: six arms emanating from a central globular particle. Figure 2 shows six of the best images obtained; these were selected because the arms were not tangled with each other and could be clearly seen and traced. The same characteristic features were found in over 100 images examined. We found no clear examples with more than six arms. Oligomers with three to five arms, probably the result of proteolysis or incomplete assembly, were found occasionally. As the typical oligomer has six arms we term it a 'hexabrachion'.

The arms are attached to a central globular particle, ~6 nm in diameter (after subtracting for a 1-nm shell of metal). In most images there seem to be two foci or attachment points on opposite sides of the globular core, with three arms extending from each focus; two of the three arms appear to form a continuous strand and the third arm is perpendicular to this strand, forming a 'T' junction. The 'T'-junction appears to lie a few nanometres from the globular particle, suggesting that it is attached to the particle by a short extension.

The arms of the hexabrachions have two structural features that are quite distinct from those of fibronectin dimers. Particularly striking is the small globular domain or knob at the distal tip of each arm. The dimeric molecules, both PFN and the 9S fraction of CSFN, frequently have a kink or forked structure at the ends of the strand[4], but they never show a terminal knob. The second feature peculiar to the hexabrachions is a thickening of the distal two-thirds of the arms. The central 30-nm segment is similar in diameter to the PFN strand but the distal segment, with an average length of 55 nm, appears thicker and more rigid.

The average contour length of the arms was 86.6 nm (s.d. = 5.6 nm, 122 measurements); lengths were measured from the distal knob to the 'T'-junction. When measured from the 'T'-junction, the three arms forming each T-junction were of identical length. The 86.6 nm length is 25% greater than the average length of PFN half-molecules (67–70 nm[4,9]) measured in our laboratory. The additional length of the hexabrachion arms relative to PFN can be accounted for by the higher molecular weight of the polypeptide (285K as opposed to 220K). Some additional protein appears to be needed for the other structural features, especially the central globular particle. The 6 nm diameter particle should contain 50–100K of protein; this might come from the 285K peptides (10K from each arm) or from a separate subunit (which would not have been detected on our lightly loaded gels).

An analysis of CSFN from chicken embryo fibroblasts (supplied by Dr K. Yamada[5], gave a 13S fraction of hexabrachions with essentially the same structural features as those described above. Measurements showed, however, that the arms were substantially shorter (with an average length of 68 nm) than those of the human oligomers. Gel electrophoresis of this material showed bands of 225K (slightly behind the upper band of the human PFN doublet) for both the oligomer and dimer fractions. Thus, the shorter arms of the chicken hexabrachions correspond to their lower subunit molecular weight. It is interesting that in chicken CSFN, which has been studied more extensively than human CSFN, the subunits of the oligomers and dimers have the same apparent molecular weight and are not separated on gels.

Yamada and Kennedy[8] found that CSFN has haemagglutinating activity over 100 times stronger than that of PFN. Our preparation of CSFN had a similarly strong agglutinating activity; when fractions from the glycerol gradient were assayed, the activity was recovered in high yield and exclusively in the 13S oligomer fraction[10]. This fraction agglutinated fixed sheep erythrocytes at a dilution of 1 : 16, that is, at a protein concentration of ~ 50 ng ml^{-1} based on our estimate of 1 μg ml^{-1} for the peak 13S fraction. Thus this activity, ascribed previously to CSFN, is now attributed to the hexabrachions.

Our observations raise the question of whether the hexabrachions, previously considered to be an oligomeric fraction of CSFN, are really fibronectin. Certain features of these oligomers, especially the thin, flexible structure of the arms, are similar to those of PFN and of dimeric CSFN. Other features, such as the terminal knob, central globular particle and the larger subunit size of the human material, strongly suggest that the hexabrachion proteins are distinctly different from fibronectin dimers. We note that several characteristics of the hexabrachions are rather similar to the recently described 'myotendenous antigen', which apparently is different from fibronectin in several other respects[11].

It also seems unlikely that hexabrachions are either precursors or intermediates for fibronectin matrix fibres; they showed no tendency to grow or associate into larger structures, and their architecture, with six arms radiating in all directions, seems poorly adapted to form the parallel array of fine filaments seen in matrix fibres. The elaborate structure of the hexabrachion suggests that it might have some specialized role in cell surface structure or attachment, but its function and its relation to fibronectin remain to be established.

We thank Dr Kenneth Yamada for supplying the preparation of chicken fibroblast fibronectin. The work was supported by NIH grant HL23454.

Received 16 May; accepted 11 July 1984.

1. Yamada, K. M. *A. Rev. Biochem.* **52,** 761–797 (1983).
2. Mosher, D. *Prog. Hemostasis Thrombosis* **5,** 111–150 (1980).
3. Engel, J. *et al. J. molec. Biol.* **150,** 97–120 (1981).
4. Erickson, H. P., Carrell, N. A. & McDonagh, J. *J. Cell Biol.* **91,** 673–678 (1981).
5. Yamada, K. M., Schlesinger, D. H., Kennedy, D. W. & Pastan, I. *Biochemistry* **16,** 5552–5559 (1977).
6. Hynes, R. O. & Destree, A. *Proc. natn. Acad. Sci. U.S.A.* **74,** 2855–2859 (1977).
7. Alexander, S. S., Colonna, G., Yamada, K. M., Pastan, I. & Edelhoch, H. *J. biol. Chem.* **253,** 5820–5824 (1978).
8. Yamada, K. M. & Kennedy, D. W. *J. Cell Biol.* **80,** 492–498 (1979).
9. Erickson, H. P. & Carrell, N. A. *J. biol. Chem.* **258,** 14539–14544 (1983).
10. Iglesias, J. L. & Erickson, H. P. *J. Cell Biol.* **97,** 1233a (1983).
11. Chiquet, M. & Fambrough, D. M. *J. Cell Biol.* **98,** 1926–1936, 1937–1948 (1984).
12. Laemmli, U. K. *Nature* **227,** 600–685 (1970).
13. Oakley, B. R., Kirsch, D. R. & Morris, N. R. *Analyt. Biochem.* **105,** 361–363 (1980).
14. Fowler, W. E. & Erickson, H. P. *J. molec. Biol.* **134,** 241–249 (1979).

Lowering of $p\mathrm{H}_i$ inhibits Ca^{2+}-activated K^+ channels in pancreatic B-cells

Daniel L. Cook, Masatoshi Ikeuchi & Wilfred Y. Fujimoto

Departments of Physiology and Biophysics, and of Medicine,
University of Washington, and Veterans Administration Medical
Center, 1660 Columbian Way S., Seattle, Washington 98108, USA

Glucose-dependent periodic electrical activity of membranes of pancreatic islet cells[1,2] mediates calcium uptake[3,4], which is important for glucose-induced insulin release. As yet there has been no direct evidence identifying the 'second messenger' which couples the uptake and metabolism of glucose[4] to the change of membrane electrical activity. Recent evidence showing that intracellular acidification stimulates islet B-cell electrical activity in a glucose-like manner has suggested that protons produced metabolically may serve as messengers by blocking K^+ channels[5] and depolarizing the membrane. Thus protons have been suggested[6] to inhibit the Ca^{2+}-activated K^+-conductance [$G_\mathrm{K}(\mathrm{Ca})$] which is thought[5–9] to produce the 'pacemaker' current responsible for the rhythmic firing of plateau depolarizations[10] and Ca^{2+} spikes[11]. Although these conductance channels have been characterized at the single channel level in several tissues[12–18], little is known of their response to intracellular *p*H (ref. 19) and they have not yet been characterized in B-cells. We have, therefore, used the patch-clamp method to study identified rat B-cells and show here that the B-cell $G_\mathrm{K}(\mathrm{Ca})$ channel is activated by membrane depolarization as well as by cytoplasmic Ca^{2+}, while it is inhibited by acidification of the cytoplasmic membrane surface.

Monolayer cultures of neonatal rat pancreatic islet cells[20] were perfused at room temperature (22–26 °C). Using the giga-seal method of Hamill *et al.*[21], inside-out patches of B-cell membrane (that is, with the cytoplasmic side of the excised membrane exposed to the bath) were voltage-clampled with a Dagan 8900 patch-clamp amplifier. Sampled cells were photographed *in situ* and subsequently identified immunohistochemically[22] as B-cells. In all experiments the pipette and bath contained a control solution consisting of KCl (140 mM), $\mathrm{MgCl_2}$ (2 mM), HEPES (10 mM). KOH was added to adjust the *p*H to 7.2. EGTA (0.1 mM) was added to reduce background free Ca^{2+} in the water to <1 μM before $\mathrm{CaCl_2}$ was added to bring the free Ca^{2+} concentration ($[\mathrm{Ca}]_i$) to the required levels as measured with an Orion calcium-sensitive electrode calibrated by the method of Bers[23]. Calibration buffers containing nitrilotriacetic acid (NTA, 10 mM), KCl (140 mM) and $\mathrm{MgCl_2}$ (2 mM), calculated to have a free [Ca^{2+}] of 14 μM at *p*H 6.8 (0.283 mM $\mathrm{CaCl_2}$ added) and *p*H 7.6 (1.511 mM $\mathrm{CaCl_2}$ added), changed the *p*Ca by <0.01 unit. Test buffers of different *p*H ($p\mathrm{H}_i$) and $[\mathrm{Ca}]_i$ were rapidly changed on the exposed cytoplasmic surface of the membrane patch by passing the electrode tip into streams of test solution flowing from each of five tubes bound together in the bath[24]. The membrane current responses to holding potentials between -80 and $+60$ mV were recorded for 10–15-s intervals on FM magnetic tape and digitized to construct amplitude histograms. Single channel currents were taken as the current step between peaks of the histograms. The areas under each of the peaks of the histogram were used to calculate the percentage of time that 1, 2, 3, …, *n* channels were simultaneously open. The channels in a patch were assumed to be identical and independent, so that the binomial distribution was used to estimate the per cent open time of each single channel[12].

Figure 1*a* shows membrane currents through a patch with three channels held at a membrane potential of -40 mV. When the cytoplasmic side of the membrane was bathed with $[\mathrm{Ca}]_i =$ 10 μM, the membrane current switched rapidly between the

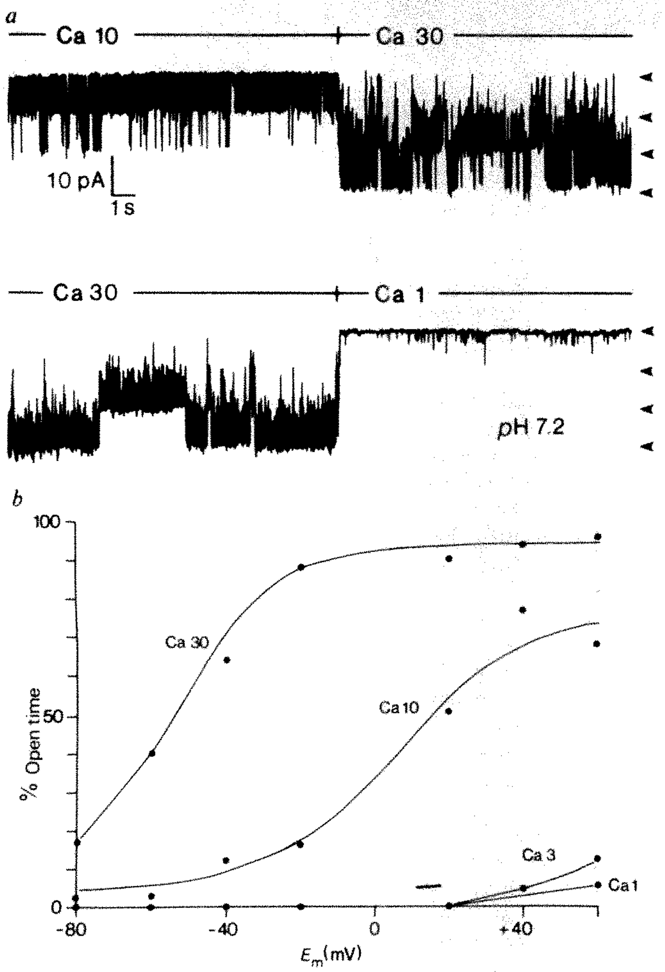

Fig. 1 *a*, Current flow through an inside-out membrane patch from a neonatal rat pancreatic B-cell held −40 mV. The patch was symmetrically bathed in 140 mM KCl solutions with 10 μM free Ca^{2+} ($[Ca]_i$), *p*H 7.2. At the times shown, free $[Ca]_i$ was increased from 10 to 30 μM and then back to 1 μM. Arrowheads mark the current levels corresponding to the leak current (top), and the current flowing with one, two and three channels open. *b*, Plot of the percentage of time that a single channel was open as a function of holding potential for the same patch as in *a* for four levels of $[Ca]_i$ in the range 1–30 μM ($pH_i = 7.2$). The curves are the least-squares fit to the data using equations of the form $y = (a-d)/(1-(x/c)^b)$, where *x* is the free Ca^{2+} level, *c* is the half-maximal activation voltage (corresponding to the E_{50}), *a* and *d* are the activation levels corresponding to 'infinite' hyperpolarization and depolarization, respectively, and *b* is a slope factor which reflects channel sensitivity to membrane potential. As the E_{50} at 10 μM $[Ca]_i$ for these channels was ~+5 mV, they were among the least Ca^{2+}-sensitive of the channels that we have seen.

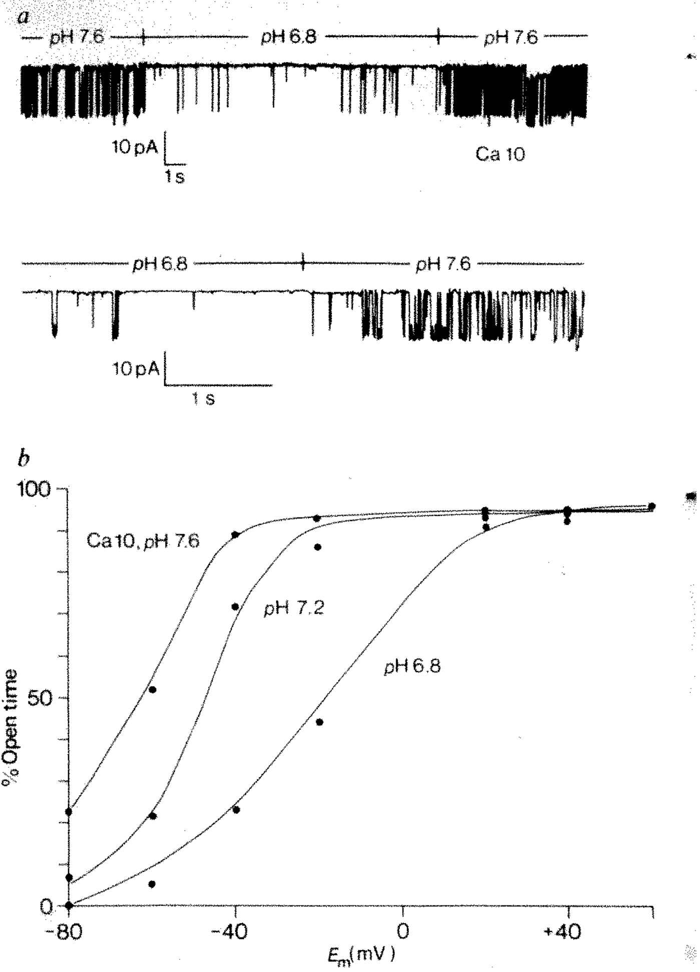

Fig. 2 *a*, Upper trace, current flow through a single channel in another patch held at −60 mV in the presence of 10 μM $[Ca]_i$, *p*H 7.6. Activity was nearly abolished when the *p*H was reduced to 6.8 for 13 s. Lower trace, the transition from *p*H 6.8 to 7.6 shown on an expanded time scale to show details of channel events. *b*, Plot of percentage open time against holding potential for the patch shown in *a*, bathed with $[Ca^{2+}]$ 10 μM (Ca 10) at *p*H 6.8, 7.2 and 7.6. The E_{50} for 10 μM $[Ca]_i$, *p*H 7.2 was ~−49 mV, indicating that this channel was among the most Ca^{2+}-sensitive channels that we have seen.

all-closed state (the top arrow) and two states in which one or two channels were open (the second and third arrows). $[Ca]_i$ was abruptly increased to 30 μM and within 200 ms activity of the channel increased so that two or three channels were open most frequently (the third and fourth arrows). After a further 80 s, reducing the $[Ca]_i$ to 1 μM closed all channels.

Changes in membrane potential produced two effects. First, single channel currents varied with membrane potential in a nearly linear manner with equilibrium potentials near zero and single channel conductances which averaged 244±4 pS ($\bar{x}$ ± s.e.m., *n* = 9). There was no effect of $[Ca]_i$ on channel conductance. Second, membrane depolarization activated the channels (recordings not shown) so that the per cent open time increased in a sigmoid manner (Fig. 1*b*) for constant $[Ca]_i$. As $[Ca]_i$ was increased from 1–30 μM, there was a progressive shift to the left of these activation curves so that at $[Ca]_i = 10$ μM channels are active in the physiological voltage range.

Figure 2*a* shows records from another patch exposed to 10 μM $[Ca]_i$ while pH_i was transiently lowered from 7.6 to 6.8 (upper trace) which blocked channel activity substantially and reversibly. The transition from *p*H 6.8 to 7.6 has been expanded on the time scale to show more detail of the channel activity in the lower trace. As with changes of $[Ca]_i$, pH_i changes had no effect on channel conductance. Acidification of the cytoplasmic side of the membrane shifted the activation curves to the right, away from the physiological voltage range (Fig. 2*b*), while increase in alkalinity shifted the curves to the left.

As a simple method to compare the voltage dependence of channel activation between experiments, we determined the membrane potential required for half-maximal channel activation (E_{50}) from curves fitted to the data as described in Fig. 1 legend. The E_{50} in the presence of 10 μM $[Ca]_i$ varied considerably from patch to patch (from −55 mV to +12 mV, *n* = 9; see also refs 13, 14). For a given patch, the channel sensitivity to changes of $[Ca]_i$ could be assessed by plotting the E_{50} for each Ca_i against log $[Ca]_i$. The slopes of these curves (measures of channel sensitivity to $[Ca]_i$ were highly variable (−84±8, $\bar{x}$ ± s.e.m., range −38 to −115 mV per decade increase of $[Ca]_i$, *n* = 9). The channels had a comparable sensitivity to changes in proton concentration as the slopes of the E_{50} versus pH_i curves had the same range (−61±10, range −31 to −100 mV per *p*H unit, *n* = 5) and were not significantly different from the channel sensitivity to $[Ca]_i$ in the five patches where both were determined. Thus, a 10-fold increase of proton concentration (that is, −1 pH.unit) would be expected to counteract a 10-fold increase of $[Ca]_i$.

This report is the first direct characterization of G_K(Ca) channels in pancreatic B-cells where they are thought to regulate membrane electrical activity and Ca^{2+} uptake[7–9]. The unit conductance and the sensitivities to membrane voltage and to $[Ca]_i$ appear to be comparable with the G_K(Ca) channels described in other systems[12–16] but may be less sensitive to Ca^{2+} than the G_K(Ca) channels in salivary gland[15] and pancreatic acinar cells[18]. This is also the first demonstration that acidification of the cytoplasmic membrane surface can inhibit G_K(Ca) channel activation[19]. This may have important implications; for example, cytoplasmic acidification accompanies Ca^{2+} uptake during the spiking phase of electrical activity in molluscan bursting neurones[25]. If molluscan G_K(Ca) channels, which may be electrical pacemakers in these cells[26], are also pH-sensitive, then their electrical rhythm may depend not only on Ca^{2+} fluxes and buffering, but also on intracellular H^+ buffering and the apparent competition between Ca^{2+} and H^+ for binding sites[27]. Similarly, Ca^{2+}–H^+ interactions at the B-cell membrane may be important determinants of B-cell G_K(Ca) activation and electrical activity.

This observation also provides direct evidence for a possible link between the metabolism of glucose[4] and the changes of electrical activity[1,2] and cation fluxes[3,4] which trigger insulin release. It has been suggested[5,6] that protons produced during glycolysis, which increase with glucose stimulation[28], acidify the cell membrane, block a background K^+ conductance and stimulate electrical activity by depolarizing the membrane. Our observations (Fig. 2*a*, *b*), while consistent with this idea, suggest that protons may do more than simply block a background depolarizing current. Thus, G_K(Ca) channels are thought[7–9] to conduct the dynamic pacemaker current which alternately turns on and off the slow, voltage-dependent plateau current[10] which triggers Ca^{2+} spiking. Proton-mediated inhibition of this pacemaker current may thus explain how glucose prolongs the spiking plateau phase and shortens the silent phase[1,2,6].

We thank Jean Liang and Jeanette Teague for technical assistance. This work was supported by the US Veterans Administration, NIH research grant AM29816, and NSF research grant PCM8108286. D.L.C. was supported by a Juvenile Diabetes Foundation Career Development Award while M.I. was supported in part by an American Diabetes Foundation Fellowship.

Received 8 June; accepted 6 July 1984.

1. Meissner, H. P. & Schmelz, H. *Pflügers Arch. ges. Physiol.* **351**, 195–206 (1974).
2. Cook, D. L., Crill, W. E. & Porte, D. Jr *Diabetes* **30**, 558–561 (1981).
3. Wollheim, C. B. & Sharp, G. W. G. *Physiol. Rev.* **61**, 914–973 (1981).
4. Malaisse, W. J. & Herchuelz, A. *Ann. N. Y. Acad. Sci.* **307**, 562–582 (1978).
5. Pace, C. S., Tarvin, J. T. & Smith, J. S. *Am. J. Physiol.* **244**, E3–E18 (1983).
6. Eddlestone, G. T. & Beigelman, P. M. *Am. J. Physiol* **244**, C188–C197 (1983).
7. Atwater, I., Dawson, C. M., Ribalet, B. & Rojas, E. *J. Physiol., Lond.* **288**, 575–588 (1979).
8. Ribalet, B. & Beigelman, P. M. *Am. J. Physiol.* **237**, C137–C146 (1979).
9. Cook, D. L. *Fedn Proc.* (in the press).
10. Cook, D. L., Crill, W. E. & Porte, D. Jr *Nature* **286**, 404–406 (1980).
11. Ribalet, B. and Beigelman, P. M. *Am. J. Physiol.* **239**, C124–C133 (1980).
12. Barrett, J. N., Magleby, K. L. & Pallotta, B. S. *J. Physiol., Lond.* **331**, 211–230 (1982).
13. Moczydlowski, E. & Latorre, R. *J. gen. Physiol.* **82**, 511–542 (1983).
14. Methfessel, C. & Boheim, G. *Biophys. Struct. Mechanism* **9**, 15–60 (1982).
15. Maruyama, Y., Gallacher, D. V. & Petersen, O. H. *Nature* **302**, 827–829 (1983).
16. Marty, A. *Nature* **291**, 497–500 (1981).
17. Wong, B. S., Lecar, H. & Adler, M. *Biophys. J.* **39**, 313–317 (1982).
18. Maruyama, Y., Petersen, O. H., Flanagan, P. & Pearson, G. T. *Nature* **305**, 228–232 (1983).
19. Moody, W. Jr *A. Rev. Neurosci.* **7**, 257–278 (1984).
20. Fujimoto, W. *Proc. Soc. exp. Biol. Med.* **162**, 241–244 (1979).
21. Hamill, O. P., Marty, A., Neher, E., Sakmann, B. & Sigworth, F. J. *Pflügers Arch. ges. Physiol.* **391**, 85–100 (1981).
22. Baskin, D. G., Gorray, K. C. & Fujimoto, W. Y. *J. Histochem. Cytochem.* **29**, 567–571 (1981).
23. Bers, D. M. *Am. J. Physiol.* **242**, C404–C408 (1982).
24. Yellen, G. *Nature* **296**, 357–359 (1982).
25. Ahmed, Z. & Conner, J. A. *J. gen. Physiol.* **75**, 403–426 (1980).
26. Gorman, A. L. F., Hermann, A. & Thomas, M. V. in *Molluscan Nerve Cells: from Biophysics to Behavior* (eds Koester, J. & Byrne, J. H.) 169–180 (Cold Spring Harbor Laboratory, New York, 1980).
27. Roos, A. & Boron, W. F. *Physiol. Rev.* **61**, 296–434 (1981).
28. Malaisse, W. J. *et al. Diabetologia* **16**, 331–341 (1979).

Intracellular ATP directly blocks K^+ channels in pancreatic B-cells

Daniel L. Cook & C. Nicholas Hales

Departments of Physiology and Biophysics, and of Medicine, and
Howard Hughes Medical Research Laboratories, University of
Washington, and the Seattle Veterans Administration Medical Center,
1660 Columbian Way S., Seattle, Washington 98108, USA

It is known that glucose-induced depolarization[1–4] of pancreatic B-cells is due to reduced membrane K^+-permeability[5–8] and is coupled to an increase in the rate of glycolysis[9], but there has been no direct evidence linking specific metabolic processes or products to the closing of membrane K^+ channels. During patch-clamp studies of proton inhibition of Ca^{2+}-activated K^+ channels [G_K(Ca)] in B-cells[10], we identified a second K^+-selective channel which is rapidly and reversibly inhibited by ATP applied to the cytoplasmic surface of the membrane. This channel is spontaneously active in excised patches and frequently coexists with G_K(Ca) channels yet is insensitive to membrane potential and to intracellular free Ca^{2+} and *p*H. Blocking of the channel is ATP-specific and appears not to require metabolism of the ATP. This ATP-sensitive K^+ channel [G_K(ATP)] may be a link between metabolism and membrane K^+-permeability in pancreatic B-cells.

Figure 1 shows that when ATP (1 mM) is applied to the patches it immediately, completely and reversibly blocks channel activity for the duration of ATP exposure, which in other experiments lasted for several minutes. ATP in the bath was acting on the inner membrane surface as G_K(Ca) channels, when they occurred in the same patch, were activated[10] by membrane depolarization and by increases in bath Ca^{2+} concentration, as expected of an inside-out patch. Bath Ca^{2+} concentration ((10^{-9}–3×10^{-5} M), bath pH (6.8–7.6) and membrane potential had no effect on G_K(ATP) channel activation. Single unit current–voltage curves were nearly linear (Fig. 2) with an average channel conductance at negative voltages of 53.9 ± 1.7 pS ($\bar{x} \pm$ s.e.m., $n = 9$). Increasing the bath concentration of KCl to 210 mM shifted the equilibrium potential to the left (Fig. 2*a*), as expected of a channel which is K^+-, rather than Cl^--permeable. Adding 70 mM NaCl to the bath reduced the K^+ current (Fig. 2*b*) without shifting the equilibrium potential, suggesting that

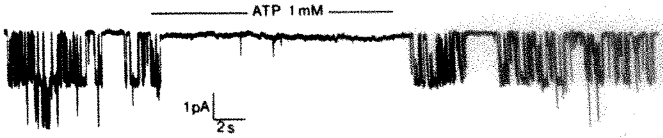

Fig. 1 Effect of 1 mM ATP on K^+-selective ion channel currents in an inside-out patch of membrane excised from a pancreatic B-cell cultured from neonatal rat. The membrane potential was −40 mV. Downward deflections correspond to currents flowing through the membrane patch as if flowing into the cell. Monolayer cultures of neonatal rat islet cells[20] were perfused at room temperature (20–22 °C) in a 0.5-ml chamber. Membrane patches of cells, identified as B-cells using immunohistochemical methods[21,22], were excised (inside-out patches) using the giga-seal method of Hamill *et al*[23]. Patches were perfused on their exposed cytoplasmic surfaces with ionic buffers containing: 140 mM KCl, 2 mM $MgCl_2$, 10 mM HEPES, 0.1 mM EGTA. $CaCl_2$ was added to adjust free Ca^{2+} to 3 μM as measured with an Orion Ca^{2+}-sensitive electrode. Low ((10^{-9} M) Ca^{2+} buffers contained 10 mM EGTA with no added $CaCl_2$. KOH was added to adjust the pH to 7.2. Recording pipettes were filled with this buffer while buffers containing various test substances flowed through each of five tubes (0.2 mm internal diameter) suspended next to each other in the chamber. The solution to which the patch was exposed was changed by moving the electrode tip into the effluent stream at the mouth of each tube[24]. Membrane currents were recorded with a Dagan 8900 patch-clamp amplifier onto FM magnetic tape for computer analysis.

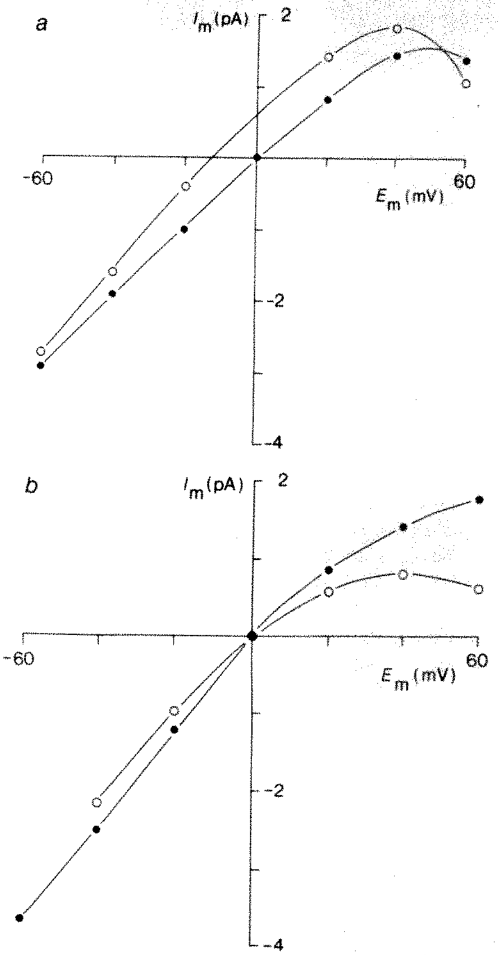

Fig. 2 Current–voltage (I/V) relationships for ATP-sensitive K$^+$ channels. *a*, In symmetrical conditions (140 mM KCl on both sides) the I/V was linear in the negative membrane potential range but showed rectification with deporlarization beyond zero. Increasing the bath KCl concentration from 140 mM (control, ●) to 210 mM (○) shifted the I/V curve to the left, indicating that K$^+$, rather than Cl$^-$, is the permeant ion. The expected equilibrium potential shift was −10.2 mV. The unitary conductances were 48 pS and 59 pS with 140 mM and 210 mM bath KCl, respectively. *b*, Adding 70 mM NaCl to the bath reduced the channel currents, in another patch, without shifting the curve, suggesting that Na$^+$ can block but not permeate the channel. The unitary conductances were 62 pS and 53 pS with control (●) and 70 mM NaCl (○), respectively.

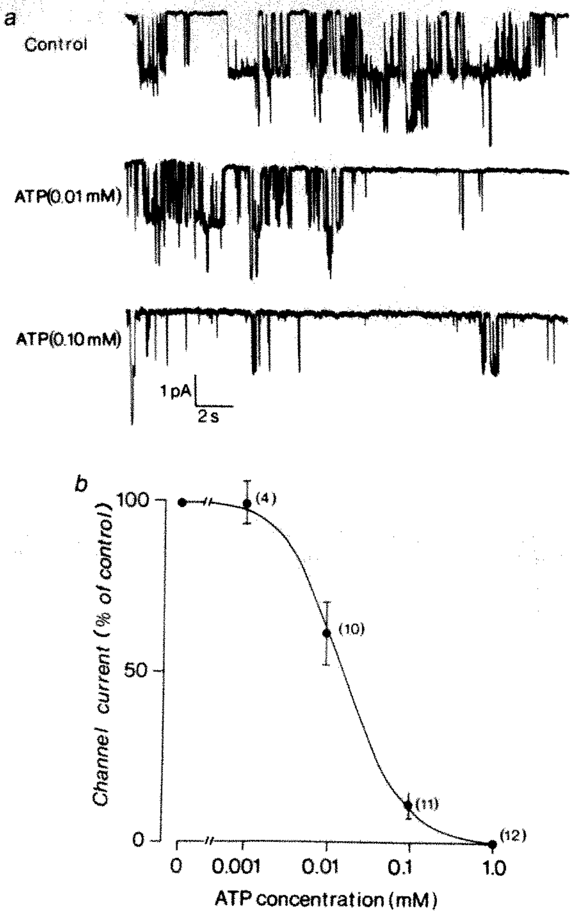

Fig. 3 Dose-dependent effects of ATP on channel activity. *a*, Channel current recordings of a B-cell membrane patch held at −40 mV while exposed to zero (top), 0.01 mM (middle) and 0.10 mM (bottom) ATP. The channels had a decreasing probability of being open and a reduction of average channel current as the ATP concentration was increased. *b*, Average channel currents, expressed as a percentage of the control (no ATP) current ($\bar{x} \pm$ s.e.m.) for 12 patches at four ATP concentrations. The curve is a least-squares fit of the data to the equation $y = 100 - 100/(1+(x/c)^b)$, where $c = 0.015$ (the half-maximal inhibitory concentration of ATP) and $b = 1.18$ (the Hill coefficient).

intracellular Na$^+$ may block but not traverse the channel. The K$^+$ channel blockers, 9-aminoacridine (9-AA 100 μM) and 4-aminopyridine (4-AP, 10 mM), each nearly abolished channel activity. Tetraethylammonium (TEA, 10 mM) and quinine (100 μM) reduced channel conductances by ~30% and 10%, respectively, while reducing channel activity by 80–90%.

Submaximal doses of ATP had graded effects on channel activity (Fig. 3*a*) such that 0.01 mM ATP suppressed activity by ~50% while 0.10 mM ATP nearly abolished activity. To account for time-related variations of activity (for example, middle trace of Fig. 3*a*) the ATP dose–response curve of Fig. 3*b* was constructed by integrating total channel currents for 20–60 s at each of several ATP doses in 12 patches. The half-maximal inhibitory dose of ATP was 0.015 mM. Suppression of channel activity appeared to be specific for ATP as 1 mM each of AMP, GTP or UTP had no effect on channel activity while 1 mM ADP was generally less effective than 0.01 mM ATP. Furthermore, channel suppression appeared not to require metabolism of ATP as Mg^{2+}-free, 1 mM ATP and the ATP analogue, adenylylimidodiphosphate (AMP–PNP, 1 mM), were each as effective and as rapidly active as 1 mM ATP.

These results show that pancreatic islet B-cells possess a K$^+$-selective channel which is rapidly and reversibly blocked by cytoplasmic ATP. The relative potency of adenosine nucleotides (ATP > ADP, with no effect of AMP) differs quantitatively from that described for purinergic receptors[11] but matches the potencies for an ATP-sensitive K$^+$ channel recently described in cardiac tissue[12]. The unit conductance of the B-cell channel, however, was lower (54 compared with 65 pS) while the half-maximal inhibitory concentration of ATP (K_i) was considerably lower (0.015 compared with 0.100 mM). Whether these differences are due to differences of species, tissue or experimental conditions is unclear.

The G_K(ATP) channel may provide a significant component of B-cell K$^+$-permeability as it is observed more commonly than G_K(Ca) channels, and it may explain several findings in B-cells. First, the hyperpolarization by metabolic poisons, ascribed to the intracellular dumping of bound Ca^{2+} and activation of G_K(Ca) channels[13], may also be due to a fall in ATP levels and activation of G_K(ATP) channels. Second, the depolarization and decrease of ^{86}Rb$^+$ efflux seen with TEA[4,14], 9-AA[15] and quinine[13,16] may be partially due to a block of G_K(ATP) channels. Third, the decrease of input impedance and hyperpolarization seen during whole-cell, giga-seal recordings[17] was attributed to an increase in K$^+$-conductance following the loss of a cytoplasmic factor into the recording electrode; our results suggest that ATP may be that factor.

The physiological role of these channels in the B-cell is unclear. Noma[12] has suggested that G_K(ATP) channels may hyperpolarize and inactivate cardiac cells to maintain ATP levels during ischaemia. Although this may occur in B-cells, and perhaps other excitable cells, the extreme channel sensitivity to ATP is puzzling as B-cell electrical and secretory activity cease during glucose withdrawal which lowers islet ATP content by only 20–45% (refs 18, 19). We have two suggestions to explain this: (1) our estimate of the K_i for ATP in these experimental conditions may be artificially low, and (2), cytoplasmic free ATP levels in cells may be lower than generally thought (that is 1–3 mM) since ATP measurements do not account for possible ATP binding or partitioning into organelles. It may be that, given proper ionic gradients, temperature, and intra- and extracellular factors, the K_i for ATP more closely matches free ATP levels in ischaemia. More importantly, the K_i may even approximate physiological ATP levels so that changes of ATP level, or changes of other factors, may modulate G_K(ATP) channels and membrane potential at physiological glucose levels.

We thank Drs E. G. Krebs and D. Porte Jr for their support and encouragement in this project; and Jean Liang for technical assistance. This work was supported by the US Veterans Administration, NIH Research Grant AM29816 and NSF Research Grant PCM8108286. D.L.C. was supported by a Career Development Award from the Juvenile Diabetes Foundation. C.N.H. was on sabbatical leave from the University of Cambridge, UK, and was supported by a Visiting Foreign Scientist Award from the American Heart Association of Washington.

Received 2 April; accepted 6 July 1984.

1. Meissner, H. P., Henquin, J.-C. & Preissler, M. *FEBS Lett.* **94**, 87–89 (1978).
2. Meissner, H. P. *J. Physiol., Lond.* **72**, 757–767 (1976).
3. Dean, P. M. and Matthews, E. K. *J. Physiol., Lond.* **210**, 255–264 (1970).
4. Atwater, I., Ribalet, B. & Rojas, E. *J. Physiol., Lond.* **288**, 561–567 (1979).
5. Atwater, I., Ribalet, B. & Rojas, E. *J. Physiol., Lond.* **278**, 117–139 (1978).
6. Henquin, J.-C. *Nature* **271**, 271–273 (1978).
7. Sehlin, J. & Taljedal, I.-B. *Nature* **253**, 635–636 (1975).
8. Sehlin, J. & Freinkel, N. *Diabetes* **32**, 820–823 (1983).
9. Henquin, J.-C. *Biochem. J.* **186**, 541–550 (1980).
10. Cook, D. L., Ikeuchi, M. & Fujimoto, W. Y. *Nature* **311**, 269–271 (1984).
11. Burnstock, G. *Cell Membrane Receptors for Drugs and Hormones: A Multidisciplinary Approach* (eds Straub, R. W. & Bolis, L.) 107–117 (Raven, New York, 1978).
12. Noma, A. *Nature* **305**, 147–148 (1983).
13. Atwater, I., Dawson, C. M., Ribalet, B. & Rojas, E. *J. Physiol., Lond.* **288**, 575–588 (1979).
14. Henquin, J.-C. *Biochem. biophys. Res. Commun.* **77**, 551–556 (1977).
15. Meissner, H. P., Preissler, M. & Henquin, J.-C. *Proc. 10th Congr. Diabetes Federation* (Excerpta Medica, Amsterdam, 1979) 166–171, (ed. Waldhausl, W. K.).
16. Henquin, J.-C. *Endocrinology* **110**, 1325–1332 (1982).
17. Marty, A. and Neher, E. *Single Channel Recording*, (eds Sakmann, B. & Neher, E.) 117 (Plenum, New York, 1983).
18. Malaisse, W. J. *et al. Diabetologia* **16**, 331–341 (1979).
19. Ashcroft, S. J. H., Chatra, C., Weersinghe, C. & Randle, P. J. *Biochem. J.* **132**, 223–231 (1973).
20. Fujimoto, W. *Proc. Soc. exp. Biol. Med.* **162**, 241–244 (1979).
21. Ikeuchi, M. & Yagi, K. *Jap. J. Physiol.* **32**, 873–878 (1982).
22. Baskin, D. G., Gorray, K. C. & Fukimoto, W. Y. *J. Histochem. Cytochem.* **29**, 567–571 (1981).
23. Hamill, O. P., Marty, A., Neher, E., Sakmann, B. & Sigworth, F. J. *Pflügers Arch. ges. Physiol.* **391**, 85–100 (1981).
24. Yellen, G. *Nature* **296**, 357–359 (1982).

The product of *ras* is a GTPase and the T24 oncogenic mutant is deficient in this activity

Raymond W. Sweet*, Shiro Yokoyama*, Tohru Kamata†, James R. Feramisco†, Martin Rosenberg* & Mitchell Gross*

* Department of Molecular Genetics, Smith Kline & French Laboratories, Philadelphia, Pennsylvania 19101, USA
† Cold Spring Harbor Laboratory, Cold Spring Harbor, New York 11724, USA

Ha-*ras* is a member of a multigene family in man which encode highly related proteins of 189 amino acids (p21)[1–6]. *In vitro*, *ras* proteins bind GTP[7–9], and p21 mutants with threonine at position 59 autophosphorylate at that residue[10–12]. Mutation (at amino acids 12 or 61)[6,13–16] and elevated expression[17] of *ras* genes result in cell transformation in culture, and are also observed in many types of human tumours[18]. Normal and mutant transforming *ras* proteins show no differences in localization, lipidation or GTP binding[9]. However, mutations at position 12 in recombinant (Thr 59) p21 molecules were observed to affect autophosphorylation[12]. We have expressed the full-length normal and T24 transforming (Gly → Val at position 12) Ha-*ras* proteins in Escherichia coli and have purified them to homogeneity (ref. 19 and M.G. *et al.*, in preparation); these proteins bound GTP with approximately molar stoichiometry and with an affinity comparable to partially purified mammalian proteins. Microinjection of the T24 protein into quiescent rodent fibroblasts resulted in a rapid alteration in cell morphology, stimulation of DNA synthesis and cell division[19]; in contrast, little response was observed with the normal protein. We now report that the normal *ras* protein has an intrinsic GTPase activity, yielding GDP and P_i. In contrast, the T24 transforming protein is reduced 10-fold in this activity. We suggest that this deficiency in GTPase is the probable cause for the transforming phenotype of the T24 protein.

Measurement of the GTP-binding properties of *ras* proteins has relied on immunoassays necessitated by the low levels of p21 in normal or transformed mammalian cells[7–9]. Having quantities of essentially pure normal and T24 p21 produced in *E. coli* has allowed us to assess more accurately their GTP binding by standard filter-binding assays (M.G. *et al.*, in preparation). Figure 1*a* shows the kinetics of binding for reactions containing 25 nM [α-^{32}P]GTP and an excess (~300 nM) of either the normal or T24 protein. As measured by retention of ^{32}P on filtration through nitrocellulose, a maximal binding of 15–18 nM was obtained with both proteins within 20 min; no binding was observed in the control reaction containing only bovine serum albumin (BSA). However, the initial rate of binding with the T24 protein was 2–3-fold slower than with the normal protein. This differential rate is reproducible at saturating GTP concentrations and probably reflects a perturbation of the GTP-binding site by the substitution of valine for glycine at position 12. The apparent maximal binding of 70% is characteristic of the filter assay. By a second assay (gel filtration through Sephadex G-25) about 95% binding was observed at the 30-min time point.

The conditions for the rapid complete binding of GTP shown in Fig. 1*a* were specifically chosen to assay our p21 proteins for GTPase activity. To measure hydrolysis of the bound [α-^{32}P]GTP, samples of the reactions described above were analysed by TLC on PEI cellulose (Fig. 1*b*). The normal protein did hydrolyse GTP to GDP with an estimated $t_{1/2}$ of ~2 h (reaction 1). In contrast, a much slower rate of hydrolysis was seen with the T24 transforming protein (reaction 2). No hydrolysis occurred in the control with BSA alone (reaction 3). Most of the GDP product remains associated with p21 as evidenced by the relatively constant level of binding throughout the time course of the assay (Fig. 1). However, the GDP is not covalently bound as it is released on denaturation of the protein (see Fig. 1 legend).

To monitor the fate of the hydrolysed γ-phosphate group of GTP, similar reactions were performed with [γ-^{32}P]GTP. As shown in Fig. 2, the initial binding kinetics were comparable to those observed in Fig. 1 with the α-labelled GTP. However, the amount of ^{32}P associated with the normal protein decayed markedly with time, indicating that the γ-phosphate group was hydrolysed and released from the p21–nucleotide complex. This conclusion was verified by TLC analysis which showed a corresponding increase in free ^{32}P-orthophosphate (Fig. 2). From these results, we estimate that the hydrolytic rate for the GTPase activity of the normal protein is $4\times10^{-5}\ \mathrm{s}^{-1}$. By a comparable

Table 1 Immunoprecipitation of GTPase activity

Reaction no.	Sample	Time (h)	Binding (% unbound)	Hydrolysis (%) GTP	GDP	GMP
(1)	p21 + antibody					
	bound	0.5	—	89	11	0
		1.0	—	81	19	0
	sup	0.4	93	94	5	1
		1.2	81	89	9	2
(2)	Antibody − sup	1.2	100	94	5	1
(3)	p21 − sup	1.2	100	96	3	1
	[α-^{32}P]GTP mix			97	2	1

Purified Ha-*ras* protein (0.8 μg) was incubated with 60 μg of ammonium sulphate fractionated monoclonal antibody 259 (ref. 20) in 100 μl of GTP buffer containing 0.1% Triton X-100, 50 μM phenylmethylsulphonyl fluoride and 0.3 mg ml^{-1} BSA at 0 °C for 60 min. Then 20 μl of protein A–Sepharose beads (Pharmacia), coated with rabbit anti-rat IgG (Cappel) and equilibrated in GTP buffer/0.1% Triton, was added and the sample was mixed for 25 min at 4 °C (sample 1). Similarly, IgC-coated beads were incubated with either 180 μg of monoclonal antibody 259 (sample 2) or 0.8 μg of p21 (sample 3) alone. The beads were washed extensively with GTP buffer containing 0.12 M $(NH_4)_2SO_4$ and 0.1 mg ml^{-1} BSA. The beads were then resuspended in 120 μl of this latter buffer containing 25 nM [α-^{32}P]rGTP and incubated at 25° with occasional mixing. At the indicated times, the beads were pelleted and duplicate aliquots (5 μl) of the supernatant (sup) were counted. The binding results are presented as per cent of ^{32}P remaining in these aliquots relative to the initial concentration. To monitor for hydrolysis of unbound GTP, a third 5-μl aliquot at each time was treated for TLC as described in Fig. 1 legend. Hydrolysis of bound GTP was measured by removing samples of the beads, washing in GTP buffer/0.01% Triton and elution at 65 °C with EDTA/SDS TLC sample buffer. No radioactivity was bound to the beads in reactions 2 and 3 (<0.5% of reaction 1). TLC analysis was as described in Fig. 1 legend and the per cent of ^{32}P as GTP, GDP and GMP was quantitated as in Fig. 2. The extent of hydrolysis in reaction 2 overestimates the contribution of phosphatases contaminating the monoclonal antibody in reaction 1 because the beads were treated with three times as much antibody.

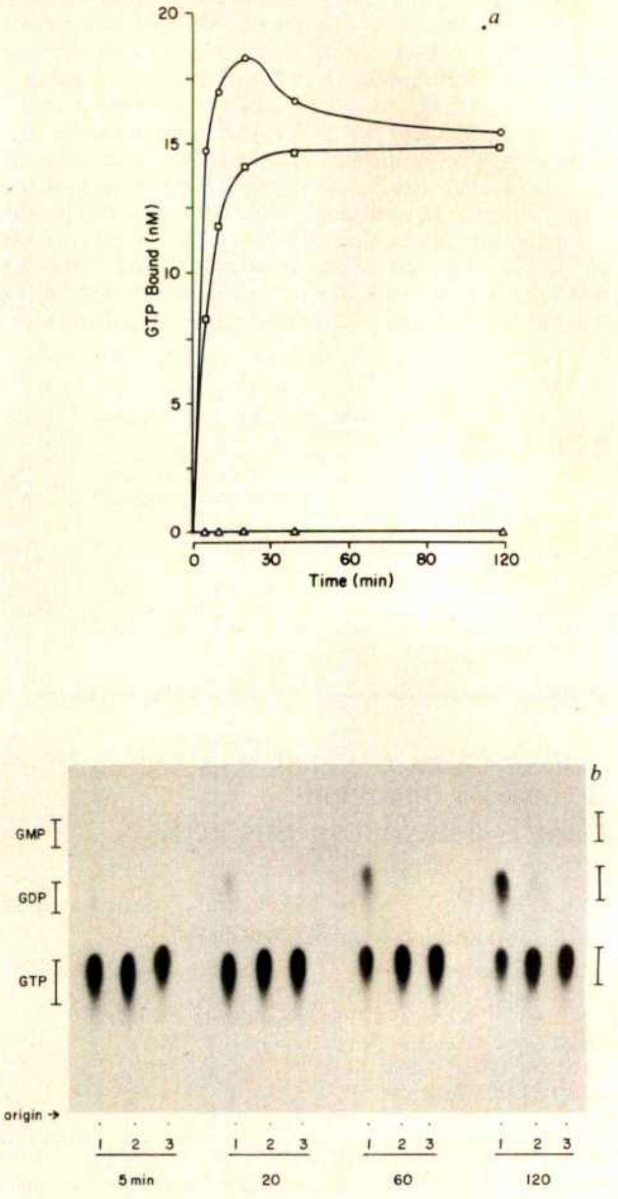

Fig. 1 Binding and hydrolysis of [α-^{32}P]rGTP. *a*, Filter binding of [α-^{32}P]GTP to 0.3 μM normal protein (○, reaction 1), 0.3 μM T24 protein (□, reaction 2) and control (△, no addition). *b*, Thin layer chromatography of samples from reactions 1, 2 and 3 at various times. 1, Normal protein; 2, T24 protein; 3, no addition. **Methods:** *a*, Filter binding reactions were carried out with 25 nM [α-^{32}P]rGTP (15 TBeq mmol^{-1}; Amersham) in 0.25 ml GTP/AS buffer (10 mM Tris-HCl-*p*H 7.5, 100 mM NaCl, 5 mM $MgCl_2$, 0.12 M $(NH_4)_2SO_4$, 0.2 mg ml^{-1} BSA) at 25 °C. At the indicated times, duplicate 20-μl samples were added to 2 ml of cold GTP buffer (Tris-HCl, NaCl, $MgCl_2$ as above) plus 10 μg ml^{-1} BSA. The samples were filtered through nitrocellulose (0.45 μM, Schleicher & Schnell), rinsed with 20 ml of cold GTP buffer and counted. Protein determinations were made with the Bio-Rad Coomassie blue–phosphoric acid reagent with bovine γ-globulin as the standard[30]. Molecular concentrations of *ras* proteins were estimated assuming a molecular weight of 21,000. *b*, At the indicated times, samples (5 μl) of the above reactions were added to an equal volume of 2 mM EDTA/0.5% SDS containing 8 mM each of GTP, GDP and GMP; 2 μl of each sample were spotted onto a prewashed PEI–cellulose plate with fluorescent indicator (Baker) and developed with 1.6 M LiCl. The carrier nucleotide spots were observed by UV illumination and the chromatogram was exposed to X-ray film (Kodak, XAR-5) for 5 h at room temperature.

analysis, the GTPase activity of the T24 protein was 10-fold lower than that of the normal protein (Fig. 2). This quantitation agrees with the autoradiographic results shown in Fig. 1*b*. Thus, we conclude that the normal *ras* protein is a GTPase and that this activity is markedly reduced in the T24 mutant.

It is important to demonstrate that this GTPase activity is intrinsic to p21 rather than arising from a contaminating *E. coli* protein. We can make two strong arguments against a contaminating GTPase. First, the normal and T24 proteins differ 10-fold in GTPase activity, yet both are expressed in the same host/vector system and both purify in a similar manner through identical protocols. In addition, in one preparation of the normal protein, we measured the GTPase activity across the single GTP-binding peak in the final purification step (DEAE–Sephacel column chromatography). The hydrolytic activity co-migrated with binding and the ratio of these two activities was constant throughout the peak (unpublished observations).

Second, and more directly, the GTPase activity of the normal protein was immunoprecipitable by a monoclonal antibody[20] directed against the Harvey virus p21 protein obtained from mammalian cells (Table 1). In this assay, the normal protein was first incubated with the rat monoclonal antibody and then linked to protein A–Sepharose beads coated with an anti-rat IgG antibody. The beads were incubated with [γ-^{32}P]GTP and binding was monitored by measuring the decline of free GTP in the supernatant. As shown in Table 1, ~20% of the GTP was associated with the beads after 70 min (reaction 1). In comparison, no binding occurred in control reactions containing anti-rat antibody-coated beads which had been pretreated with either monoclonal antibody (reaction 2) or the normal p21 (reaction 3) alone. To assess the GTPase activity of the

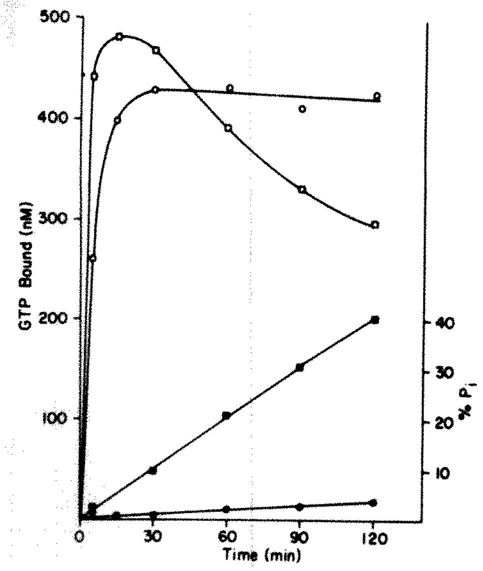

Fig. 2 Binding and hydrolysis of [γ-^{32}P]rGTP. Filter binding for the normal (□) and T24 (○) proteins. % P_i by TLC for the normal (■) and T24 proteins (●).

Methods: The reactions, binding and TLC analysis were as described in Fig. 1 legend except that the labelled nucleotide was [γ-^{32}P]GTP (0.7 μM, 630 MBeq mmol^{-1}; Amersham) Radioactivity on the TLC plate was visualized by exposure to X-ray film (not shown), and the P_i and GTP spots (the only products) were excised and measured in a scintillation counter. As in Fig. 1*b*, no binding or hydrolysis was observed in the control reaction without *ras* protein (not shown).

Sepharose-bound *ras* protein, samples of the beads in reaction 1 were washed extensively, treated with 0.25% SDS to dissociate the bound protein and ^{32}P-labelled nucleotide, then analysed by TLC. The results (Table 1, reaction 1, bound) show that hydrolysis to GDP occurred in a time-dependent manner such that about 20% of the bound nucleotide at 1 h was GDP. This hydrolysis did not result from phospholytic enzymes present in the antibody preparations. In the supernatants of the control reactions containing beads treated with either monoclonal antibody or normal *ras* protein alone (reactions 2 and 3 respectively), <3% conversion to GDP was observed in 70 min. The significant fraction of GDP in the supernatant of reaction 1 must result either from turnover of the hydrolysed GDP on the beads or from release of the nucleotide–p21 complex from the beads during the incubation. In summary, the co-purification of the GTPase and GTP-binding activities and the immunoprecipitation of the GTPase by anti-*ras* monoclonal antibody establish that the GTPase is an intrinsic activity of *ras*.

The GTP-binding and hydrolytic activities of our bacterially produced *ras* proteins occur at very slow rates compared with what might be expected physiologically. Post-translational modifications (for example, lipidation[21]) of the *ras* proteins in mammalian cells may partially account for this discrepancy. However, immunoprecipitated complexes of p21 from mammalian cells show binding kinetics similar to those presented in Table 1 for the bacterially-produced protein (unpublished results). Furthermore, if autophosphorylation is indicative of a GTPase activity (see below), the mammalian proteins have an equally slow hydrolytic activity[10,12]. This situation may be similar to that described for the G_α subunits of the regulatory proteins of adenylate cyclase[22] and for the T_α subunit of transducin[23]. In purified form, these proteins alone or in combination with their partner $\beta\gamma$-subunits exhibit GTP hydrolytic rates similar to that observed with our normal Ha-*ras* protein prepared in *E. coli*[24–27]. However, reconstitution of the G proteins or transducin into lipid vesicles containing appropriate membrane components stimulates their GTPase activity by orders of magnitude[25–27]. As *ras* proteins are membrane-associated[8,28], their reconstitution into membrane complexes may similarly stimulate their binding and hydrolytic activities.

The 10-fold reduction in GTPase activity of the T24 protein represents the first major biochemical differentiation between the products of a normal and a transforming mutant *ras* gene. It is tempting to speculate on the consequence of this altered activity by drawing a functional analogy to transducin and the G stimulatory protein—both of these proteins are activators of enzymes affecting cyclic nucleotide pools[22,23]. This activation requires GTP binding (or exchange of GTP for bound GDP) and appears to terminate on hydrolysis to GDP[23,29]. If the *ras* proteins have an analogous regulatory function in whichever proliferative control pathway they participate, then the deficiency in GTPase activity of the T24 mutant could result in prolonged stimulation of an otherwise regulatable activity. As shown for the G stimulatory protein[22], perhaps modulation of *ras* activity itself occurs through interactions with other proteins, and these interactions may be sensitive to whether GTP and GDP (or neither) occupies the nucleotide binding site.

The autophosphorylating activity of *ras* proteins having threonine at position 59 is probably a consequence of the GTPase activity described here[12]. In a recent characterization of this autophosphorylating activity, Gibbs *et al.*[12] compared the effects of substitutions at position 12 in recombinant (Thr 59) p21 proteins. Interestingly, replacement of glycine with valine increased the rate of autophosphorylation, the opposite of the effect on GTPase activity described here. Thus, we surmise that hydrolysis and autophosphorylation compete for bound GTP and the slower rate of hydrolysis increases the probability of intramolecular phosphorylation.

We thank M. Wigler and J. Stadel for helpful discussions, M. Furth for providing the Y13-259 hybridoma cell line and 0. Finney for typing the manuscript. This work was supported in part by NIH grants GM28277 and CA13106.

Note added in proof: By procedures described in Table 1, we have examined the GTPase activities of the human H-*ras* and T24 gene products synthesized in mammalian cells. The activity of the H-*ras* protein is at least 5-fold greater than that of the T24 mutant and is comparable to the activity of the H-*ras* protein produced in bacteria (S. Yokoyama *et al.*, unpublished results).

LIBRARY COMPLEX
Departments of
Chemical Engineering
Chemical Technology
Plastics and Rubber Technology

Received 6 August; accepted 16 August 1984.

1. Chang, E. H., Gonda, M. A., Ellis, R. W., Scolnick, E. M. & Lowy, D. R. *Proc. natn. Acad. Sci U.S.A.* **79**, 4848–4852 (1982).
2. Shimizu, K. *et al. Proc. natn. Acad. Sci. U.S.A.* **80**, 2112–2116 (1983).
3. Capon, D., Ellson, Y., Levinson, A., Seeburg, P. & Goeddel, D. *Nature* **302**, 33–37 (1983).
4. McGrath, J. P. *et al. Nature* **304**, 501–506 (1983).
5. Shimizu, K. *et al. Nature* **304**, 497–500 (1983).
6. Taparowsky, E., Shimizu, K., Goldfarb, M. & Wigler, M. *Cell* **34**, 581–586 (1983).
7. Scolnick, E. M., Papageorge, A. G. & Shih, T. *Proc. natn. Acad. Sci. U.S.A.* **76**, 5355–5359 (1979).
8. Papageorge, A., Lowy, D. & Scolnick, E. *J. Virol.* **44**, 509–519 (1982).
9. Finkel, T., Der, C. J. & Cooper, G. M. *Cell* **37**, 151–158 (1984).
10. Shih, T. H., Papageorge, A. G., Stokes, P. E., Weeks, M. O. & Scolnick, E. M. *Nature* **287**, 686–691 (1980).
11. Shih, T. Y., Stokes, P. E., Smythers, G. W., Dhar, R. & Oroszlan, S. *J. biol. Chem.* **257**, 11767–11773 (1982).
12. Gibbs, J. B.. Ellis, R. W. & Scolnick, E. M. *Proc. natn. Acad. Sci. U.S.A.* **81**, 2674–2678 (1984).
13. Santos, E., Tronick, S. R., Aaronson, S. A., Pulciani, S. & Barbacid, M. *Nature* **298**, 343–347 (1982).
14. Tabin, C. J. *et al. Nature* **300**, 143–149 (1982).
15. Yuasa, Y. *et al. Nature* **303**, 775–779 (1983).
16. Capon, D. J. *et al. Nature* **304**, 507–513 (1983).
17. DeFeo, D. *et al. Proc. natn. Acad. Sci. U.S.A.* **78**, 3328–3332 (1981).
18. Slamon, D. J., deKemion, J. B., Verma, I. M. & Cline, M. J. *Science* **224**, 256–262 (1984).
19. Feramisco, J. R., Gross, M., Kamata, J., Rosenberg, M. & Sweet, R. W. *Cell* (in the press).
20. Furth, M. E., Davis, L. J., Fleurdelys, B. & Scolnick, E. M. *J. Virol.* **43**, 294–304 (1982).
21. Sefton, B. M., Trowbridge, I. S., Copper, J. A. & Scolnick, E. M. *Cell* **31**, 465–474 (1982).
22. Gilman, A. G. *Cell* **36**, 577–579 (1984).
23. Stryer, L., Hurley, J. B. & Fung, B. K. K. *Trends biochem. Sci.* **6**, 245–247 (1981).
24. Northrup, J. K., Smigel, M. D. & Gilman, A. G. *J. biol Chem.* **257**, 11416–11423 (1982).
25. Brandt, D. R., Asano, T., Pedersen, S. E. & Ross, E. M. *Biochemistry* **22**, 4357–4362 (1983).
26. Fung, B. K. K. *J. biol. Chem.* **258**, 10495–10502 (1983).
27. Kanaho, Y. *et al. J. biol Chem.* **259**, 7378–7381 (1984).
28. Willingham, M. C., Pastan, I., Shih, T. Y. & Scolnick, E. M. *Cell* **19**, 1005–1014 (1980).
29. Cassel, D. & Selinger, Z. *Proc. natn. Acad. Sci. U.S.A.* **74**, 3304–3311 (1977).
30. Bradford, M. *Analyt. Biochem.* **72**, 248–254 (1976).

A common function for polyoma virus large-T and papillomavirus E1 proteins?

Philippe Clertant* & Isabelle Seif†

* INSERM U273, Centre de Biochimie, Université de Nice,
06034 Nice, France
† Laboratoire de Génétique des Virus, CNRS,
91190 Gif-sur-Yvette, France

Nucleotide sequencing has revealed a common genetic organization for three papillomaviruses: BPV-1 (bovine papillomavirus type 1), HPV-1 (human papillomavirus type 1a) and HPV-6 (human papillomavirus type 6b)[1–4]. Several open reading frames, corresponding to as yet uncharacterized proteins, were observed in these genomes in the region that is required for oncogenic transformation by BPV-1 and for plasmidial maintenance of its genome[5]. The longest of these frames, E1, is also the most conserved between the three viruses[3,4]; we have compared the amino acid sequence of its putative product ('E1 protein') with those of the large-T proteins of three polyoma viruses[6–11] and report here significant homologies in their carboxy-terminal halves, extending for over 200 amino acids. Moreover, similar secondary structures were predicted[12,13] in this region, especially in two blocks of homologous residues, which correspond in the large-T proteins of polyoma and simian virus 40 (SV40) viruses to sites involved in the ATPase[14,15] and nucleotide-binding activities[16]. These observations suggest that the papillomavirus E1 proteins might have a function in common with the polyoma virus large-T proteins (which are required for the initiation of viral DNA replication[17]). As it was suggested recently that the E1 gene product is involved in maintaining the BPV-1 genome as a plasmid in transformed cells[18,19], we speculate that the structural features conserved in these otherwise very different viruses are general characteristics of eukaryotic proteins involved in the control of DNA replication.

Similarities between the amino acid sequences of the large-T proteins of SV40 and polyoma[10] or BK[8] viruses have been reported previously. Subsequently, it became possible to compare these sequences with those encoded by the genomes of the papillomaviruses BPV-1 (ref. 1), HPV-1 (ref. 2) and HPV-6 (ref. 3). The overall genetic organization of the papovaviruses and papillomaviruses is very different[4]. We observed, however, significant similarities between part of the large-T proteins and the carboxy-terminal half of the proteins encoded in the largest open reading frame of the three papillomaviruses, designated E1. These homologous regions were detected by comparing the two alignments made within each group (polyoma virus large-T proteins[8,10] and papillomavirus E1 gene products[3]). Starting from the most conserved regions within each class of proteins, we first looked for the best adjustment of either identical or functionally analogous amino acids, and found clusters of homologous or similar residues spanning the entire carboxy-terminal half of the E1 sequences (Figs 1, 2). This region represents the most conserved part of the E1 sequence between the three papillomaviruses[3]. Figure 2 shows the amino acid sequences in this conserved region: two blocks of homology (B and C) are surrounded by two additional zones where the analogy may be extended (A and D). The blocks of homology are in the same relative order in proteins of the two groups.

The validity of this result was confirmed by computer comparison of the proteins, using an alignment program[20] (provided by Dr J. M. Claverie). Pairwise comparisons were made, either for blocks of 100 amino acids centred on the analogous clusters (indicated by A–D in Figs 1, 2), or for larger segments (Table 1). For regions B and C, taken either separately or together, optimal alignments confirmed the alignment described above, except for a few changes due to imprecise gap locations. For the complete (A+B+C) region, the Needleman and Wunsch[21] score was in all cases greater (by >6 s.d.) than the mean value obtained from comparisons with 30 randomly shuffled sequences (see Table 1); this value is higher than the cut-off value of 3 regarded as indicating statistically significant evolutionary relatedness[22]. Region A, when considered alone, was also aligned as expected, with variable statistical significance; when included in a large comparison (A+B+C) which produced a very significant score, an optimal alignment similar to that shown in Fig. 2 was obtained between polyoma large-T and HPV-6 E1 sequences. Only region D was poorly aligned, as might be expected from its small size and from the large gap on its left side. Taken together, these results clearly indicate that the two classes of proteins are related within a region of 120 amino acids (residues 150–270 in Fig. 2) and further suggest significant similarities over at least 210 residues (positions 48–290).

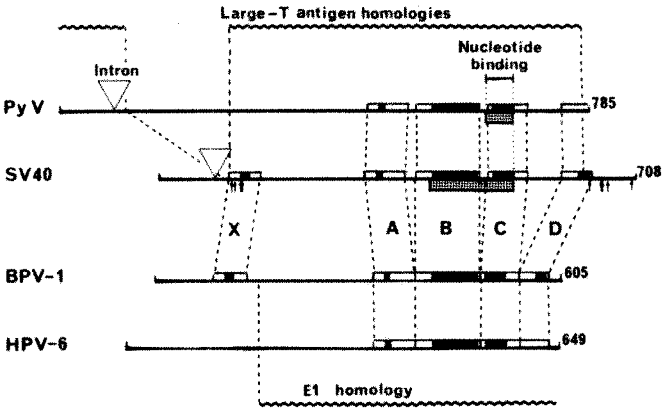

Fig. 1 Comparative maps of the large-T proteins of SV40 and polyoma viruses and the E1 proteins of two papillomaviruses. Sequences were first aligned on the basis of their regions of maximum homology (B; see Fig. 2 for the detailed sequences). Similarities were also detected in region A, C, D and X; solid areas correspond to clusters of homology over 40% analogous residues which were also in the computed optimal alignments (see Table 1). The total number of amino acids is indicated at the carboxy-terminal end of each protein. The positions of the labelled peptides released by CNBr cleavage after affinity-labelling of large-T proteins with periodate-oxidized ATP[16,24] are indicated by stippled areas. The location of the intron in the gene for large-T is indicated by an open triangle, and arrows show the positions of the main phosphorylated amino acids in SV40[25]. Wavy line indicates regions of homology within each class of proteins.

We also noted that residues which have a key role in protein structure, because of their charge (acidic or basic), size (glycine), reactivity or conformation (proline) are the most frequently conserved. For example, throughout the entire (A+B+C) region of homology (see Fig. 2), 53% of prolines, 47% of glycines, 44% of lysines, 40% of phenylalanines and 35% of aspartates are conserved between the E1 protein of PBV-1 and the large-T protein of polyoma. Conservative changes (serine to threonine, arginine to lysine, aspartate to glutamate) were also frequently observed. These observations suggest that the three-dimensional conformation of the E1 and large-T proteins might also be similar in these regions. Comparison of secondary structures and local exposure to solvent, using the methods of Garnier *et al.*[13] and Hopp and Woods[12], supported this hypothesis. Figure 3 shows that the computed hydrophilicity profiles were similar in regions B and C. Although the algorithm that we used to predict secondary conformations gives only a 50% probability[12], we consider it significant that, in regions where it predicts the same conformation for all three proteins of one class, this structure is also encountered in the other class. In region B, an amino-terminal (loop/pleated sheet/loop) pattern and the carboxy-terminal α-helix seem particularly significant. Secondary structure predictions for region C are not uniform, especially for E1 proteins, and thus are difficult to interpret with confidence, but they do suggest a common amino-terminal structure (loop/pleated sheet/loop).

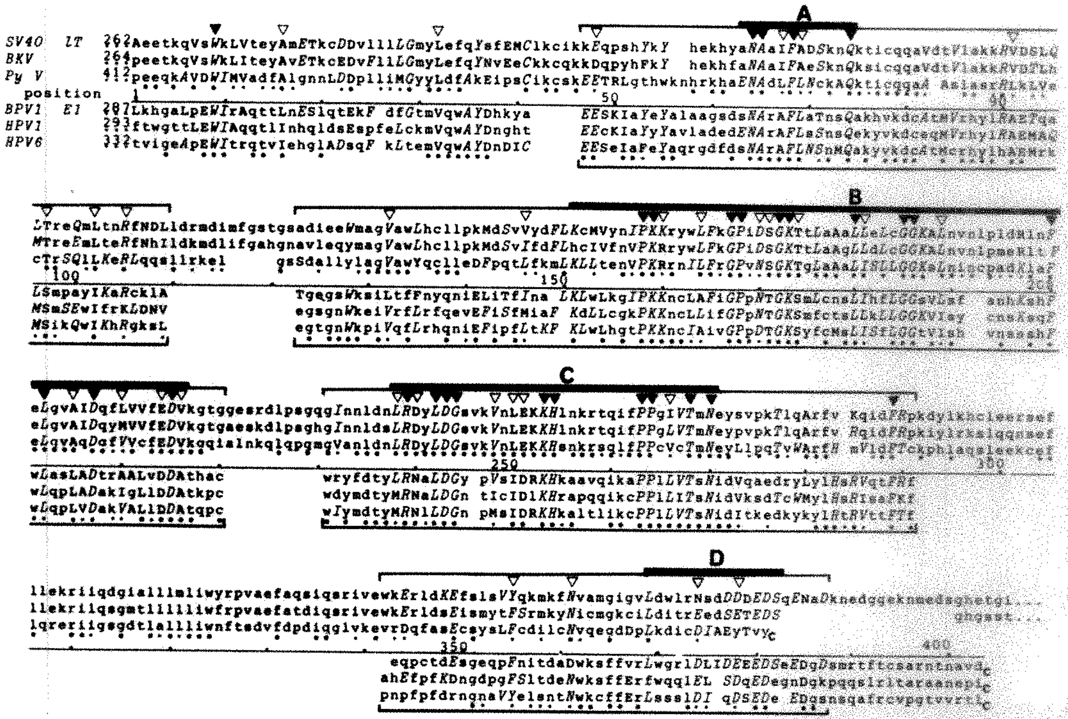

Fig. 2 Alignment of the carboxy-terminal half of the E1 protein from each of three papillomaviruses with the large-T sequences of three polyoma viruses. The more significant optimal alignments made by computer (see Table 1 and text) were retained and slightly modified, especially at the gap borders, to account for the internal homology within each class of proteins. The one-letter amino acid code is used: A, alanine; C, cysteine; D, aspartate; E, glutamate; F, phenylalanine; G, glycine; I, isoleucine; K, lysine; L, leucine; M, methionine; N, asparagine; P, proline; Q, glutamine; R, arginine; S, serine; T, threonine; V, valine; W, tryptophan; Y, tyrosine. Capital letters represent either homology (italics) or analogy (defined as in Table 1) between at least one protein of the large-T class and one of the E1 group. Triangles indicate homology (solid) or analogy (open) between the six sequences. Beneath each set of proteins are also shown homologies (large dots) or analogies (small dots) within a given class. Brackets enclose the regions A, B, C and D (see Fig. 1); the clusters of homology defined in Fig. 1 are underlined. The position in the protein sequence of the first amino acid is indicated at the left-hand side.

Table 1 Comparison of large-T and E1 amino acid sequences

Sequences compared		Agreement with general alignment in region:					
Large-T	E1	A	B	C	D	% Homology	*n* (s.d.)
SV40 295–555	BPV-1 320–550	–	++	++	ND	19.5	+6.28
PyV 440–700	BPV-1 320–550	–	++	++	ND	21.3	+7.18
PyV 440–700	HPV-6 370–600	+	++	++	ND	22.6	+6.13
SV40 390–650	BPV-1 375–605	ND	++	++	–	17.4	+1.84
PyV 525–785	BPV-1 375–605	ND	++	++	–	21.3	+2.74
PyV 525–785	HPV-6 429–649	ND	++	++	–	17.0	+2.51
SV40 305–365	BPV-1 325–385	+	ND	ND	ND	15.7	+0.42
PyV 445–515	HPV-6 370–440	++	ND	ND	ND	18.5	+2.21
SV40 380–480	BPV-1 380–480	ND	++	++	ND	22.0	+9.28
PyV 530–630	HPV-6 430–530	ND	++	++	ND	25.0	+7.73
SV40 440–540	BPV-1 440–540	ND	ND	++	ND	20.0	+2.67
PyV 590–690	HPV-6 480–580	ND	ND	++	ND	18.0	+2.11
SV40 550–650	BPV-1 505–605	ND	ND	ND	+	16.0	+1.61
PyV 685–785	HPV-6 549–649	ND	ND	ND	–	18.0	+2.08
SV40 100–150	BPV-1 80–130	ND	ND	ND	ND	18.0	+1.53

The statistical significance of the homologies shown in Fig. 2 was determined by scoring computer optimal alignments. The program used[20] optimally aligns two sequences and calculates both a value for the distance between them and a Needleman and Wunsch[21] alignment score. The distance value for a pair of residues is thus 0 when they are homologous, 3 when they are unrelated, and 2 when they are analogous. The pairs A-I, A-L, A-V, D-E, D-N, F-Y, I-L, I-M, I-V, K-R, L-M, L-V, M-V and S-T correspond to the most frequent changes observed between pairs of residues from large-T or E1 proteins in their homologous regions; they were considered to be analogous, as they also conserved the charge, size, hydrophilicity or aromatic character of the residue. A penalty value of 6 was applied for each gap, plus the number of residues in the gap. The Needleman and Wunsch score obtained for the optimal alignment between two sequences was then compared with the mean value obtained from 30 comparisons of jumbled sequences of the same length and composition; the difference (*n*) measures the statistical significance of this optimal alignment, expressed as s.d. For this comparison, large-T or E1 polypeptides were cut into segments of various length; these are indicated by the positions in the protein of the first and last residues. Agreement between the optimal alignments that were computed and the general alignment presented in Fig. 2 is indicated as follows: –, <50%; +, 50–80%; ++, >80% correspondence with respect to the different regions defined in Figs 1 and 2 (ND, not determined). The last line refers to region X (see Figs 1 and 4). PyV, polyoma virus.

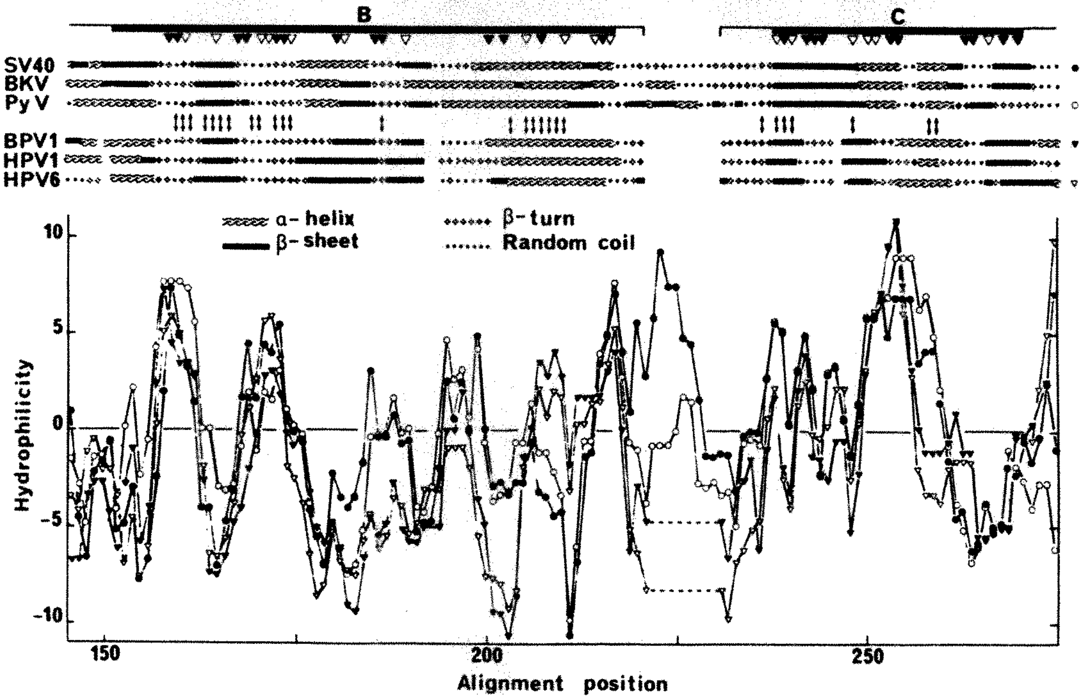

Fig. 3 Predicted secondary structure and exposure to solvent in the homology regions B and C. Local hydrophilicity values were computed from hexapeptide averages as described by Hopp and Woods[12] (●, SV40; ○, polyoma; ▼, BPV-1; ▽, HPV-6). Secondary conformation was predicted according to Garnier *et al.*[13]. Regions B and C, and homologous or analogous positions for the six proteins, are indicated as in Fig. 2. Arrows mark positions of structural identity.

Homologous domains B and C correspond to the segments of highest amino acid similarity within each class of proteins[3,4,10]. These regions probably include the active sites of the large-T molecules. The ATPase activity of SV40 large-T is inhibited by a monoclonal antibody whose epitope is precisely located within B[14,15]. In this region, homologies were also described between the large-T proteins and the *recA* protein of *Escherichia coli*[23], which also carries an ATPase activity. On the other hand, a nucleotide-binding activity for this region was revealed by affinity-labelling of SV40 and polyoma large-T proteins[24]. This binding site appears to be distinct from the ATPase catalytic site on the basis of the differential effects of various antibodies and mutations, and it was mapped to within region C by cyanogen bromide cleavage of the labelled protein (polyoma large-T, peptide 230–269 in Fig. 2; see Fig. 1)[16].

The other homologies detected are not of comparable significance. Region D is not well conserved between the large-T proteins of polyoma and SV40 viruses; it does contain, however, a stretch of acidic residues interspersed with serines that is also found in the large-T proteins of SV40 and BK virus. This is the most hydrophilic region in all these proteins, and one of the two serines in the SV40 large-T protein is phosphorylated[25]. The E1 sequence of BPV-1, but not that of the other papillomaviruses, shows another region of homology with the large-T proteins (region X; see Figs 1, 4) which contains a highly hydrophilic cluster of conserved residues corresponding to the same predicted conformation: a hydrophilic loop around the sequence Thr-Pro-X-Lys-(basic)-(basic)-(basic), followed by an α-helix. The region is rich in serine residues on its amino-terminal side, some of them being phosphorylated in SV40 large-T[25]. One might speculate that these similar features, found at the same relative positions in the different protein sequences, might also be phosphorylated in the E1 protein.

The conservation of functionally significant sequences within a common polypeptide architecture described here suggests that the E1 proteins have a role similar to that of the large-T proteins. The latter are multifunctional, acting in the establishment and maintenance of oncogenic transformation, the initiation of viral DNA replication and the regulation of early transcription during the lytic cycle[17]. The structural similarities observed suggest that, of the known biochemical properties of large-T proteins, at least two (ATPase and nucleotide-binding activities) might also be exhibited by the E1 proteins. At least in the case of polyoma virus, the activity of large-T protein in cell transformation does not require these two properties, as a truncated form which lacks the entire carboxy-terminal half of the molecule (including regions A to D), performs all the functions of the full-length protein[26,27]. This is in agreement with two recent observations on the role of the E1 gene which suggest that it controls the plasmidial maintenance and autonomous replication of papillomavirus genomes in transformed cells[18,19].

Thus, like the large-T proteins, the E1 proteins might be involved in the initiation of viral replication. The 'minichromosomes' of polyoma and papillomaviruses have the same chromatin structure as the cellular genome[17,28,29] and depend on the cellular machinery for their replication. Thus, the common features detected in the E1 and large-T proteins might be general properties of proteins involved in the control of initiation of cellular replicons in higher eukaryotes.

We thank E. Schwartz for communication of the HPV-6 sequence before publication, M. Yaniv and O. Danos for critical

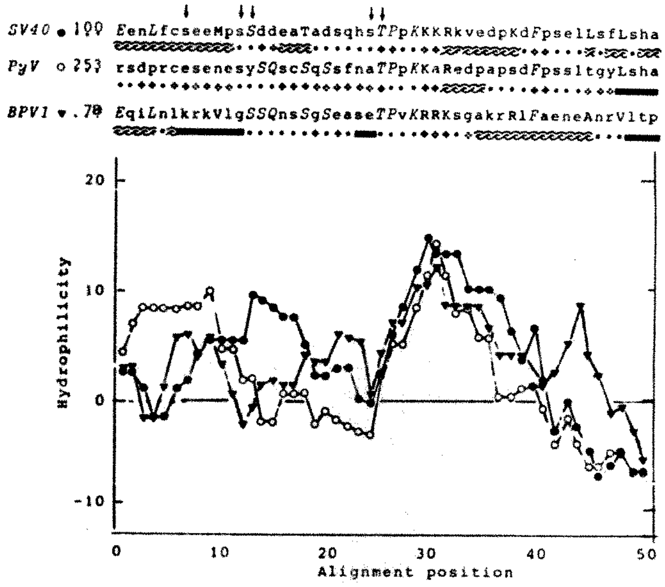

Fig. 4 Region X, another region of similarity between polyoma virus and SV40 large-T proteins and BPV-1 E1 proteins (see Fig. 1). The aligned sequences are given as described for Fig. 2. The predicted secondary structure and hydrophilicity profiles are also presented as in Fig. 3. Arrows above the SV40 sequence indicate the phosphorylated amino acids[25].

reading of the manuscript, R. Seif for helpful discussions, and especially F. Cuzin who wrote the Apple II programs used in this work and helped in the preparation of the manuscript. Special acknowledgements are also due to J. M. Claverie for introducing us to the alignment program used in this work and for hospitality at the Centre de Calcul Scientifique at the Institut Pasteur, Paris. This work was made possible by grants from the CNRS.

Received 11 June; accepted 28 July 1984.

1. Chen, E. Y., Howley, P. M., Levinson, A. D. & Seeburg, P. H. *Nature* **299**, 529–534 (1982).
2. Danos, O., Katinka, M. & Yaniv, M. *EMBO J.* **1**, 231–236 (1982).
3. Schwartz, E., *et al. EMBO J.* **2**, 2341–2348 (1983).
4. Danos, O., Engel, L. W., Chen, E. Y., Yaniv, M. & Howley, P. M. *J. Virol.* **46**, 557–566 (1983).
5. Law, M. F., Lowy, D. R., Dvoretzky, I. & Howley, P. M. *Proc. natn. Acad. Sci. U.S.A.* **78**, 2727–2731 (1981).
6. Fiers, W. *et al. Nature* **273**, 113–120 (1978).
7. Reddy, V. B. *et al. Science* **200**, 494–502 (1978).
8. Seif, I., Khoury, G. & Dhar, R. *Cell* **18**, 963–979 (1979).
9. Yang, R. C. A. & Wu, R. *Proc. natn. Acad. Sci. U.S.A.* **76**, 1179–1183 (1979).
10. Friedman, T., Esty, A., La Porte, P. & Deininger, P. *Cell* **17**, 715–724 (1979).
11. Soeda, E., Arrand, J. R., Smolar, N., Walsh, J. E. & Griffin, B. E. *Nature* **283**, 445–453 (1980).
12. Hopp, T. P. & Woods, K. R. *Proc. natn. Acad. Sci. U.S.A.* **78**, 3824–3828 (1981).
13. Garnier, J., Osguthorpe, D. J. & Robson, B. *J. molec. Biol.*, **120**, 97–120 (1978).
14. Clark, R., Lane, D. P. & Tjian, R. *J. biol. Chem.* **254**, 11854–11858 (1981).
15. Clark, R., Peden, K., Pipas, J. M., Nathans, D. & Tjian, R. *Molec. cell. Biol.* **3**, 220–228 (1983).
16. Clertant, P., Gaudray, P., May, E. & Cuzin, F. *J. biol. Chem.* (in the press).
17. Acheson, N. in *Molecular Biology of Tumor Viruses* Pt 2, 125–204 (ed. Tooze, J.) (Cold Spring Harbor Laboratory, New York, 1980).
18. Nakabayashi, Y., Chattopadhyay, S. K. & Lowy, D. R. *Proc. natn. Acad. Sci. U.S.A.* **80**, 5832–5836 (1983).
19. Lusky, M. & Botchan, M. R. *Cell* **36**, 391–401 (1984).
20. Claverie, J. M. *Nucleic Acids Res.* **12**, 397–407 (1984).
21. Needleman, S. B. & Wunsch, C. D. *J. molec. Biol.* **48**, 443–453 (1970).
22. Doolittle, R. F. *Science* **214**, 149–159 (1981).
23. Seif, R. *Molec. cell. Biol.* **2**, 1463–1471 (1982).
24. Clertant, P. & Cuzin, F. *J. biol. Chem.* **257**, 6300–6305 (1982).
25. Scheidtmann, K., Echle, B. & Walter, G. *J. Virol.* **44**, 116–133 (1982).
26. Rassoulzadegan, M. *et al. Nature* **300**, 713–718 (1982).
27. Rassoulzadegan, M. *et al. Proc. natn. Acad. Sci. U.S.A.* **80**, 4354–4358 (1983).
28. Favre, M., Breitburd, F., Croissant, O. & Orth, G. *J. Virol.* **21**, 1205–1209 (1977).
29. Rösl, F., Waldeck, W. & Sauer, G. *J. Virol.* **46**, 567–574 (1983).

Reduction of the minimal sequence for initiation of DNA synthesis by qualitative or quantitative changes of an initiator protein

Gian Paolo Dotto* & Norton D. Zinder

The Rockefeller University, New York, New York 10021, USA

Initiation of DNA synthesis at an origin of DNA replication involves complex protein–DNA interactions that are still poorly understood. Some of these interactions are highly specific and involve proteins (initiator proteins) thought to be essential for regulation of the initiation process because of their rate-limiting activity[1]. We show here that both qualitative and quantitative changes in one of these proteins have profound effects on protein–DNA interactions at an origin of DNA replication, and are sufficient to reduce to less than one-third the minimal sequence required for initiation. The general implications of these findings are discussed.

Viral strand replication of the filamentous, single-stranded DNA phage f1 (fd, M13) occurs by a rolling circle mechanism[2] which is initiated and terminated by gene II protein, a specific, virus-encoded endonuclease[3]. The levels of this protein inside f1-infected cells remain low through the action of gene V protein, a viral, single-stranded DNA-binding protein that is able to repress gene II mRNA translation[4,5]. Regulation of gene II protein activity (and f1 DNA replication) is crucial to the unique life cycle of the phage[6]; unlike other bacteriophages, the f1-infected cells continue to grow and produce phage indefinitely, f1 growth being finely tuned to that of its host.

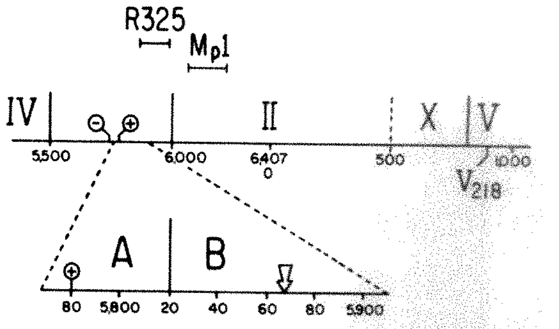

Fig. 1 Map of the f1 genome in the region of interest[6]. Roman numerals, f1 genes; between genes IV and II, intergenic region; ⊕ and ⊖, origin of synthesis of viral (plus) and complementary (minus) strand, respectively. Numbers indicate nucleotide positions on the f1 map[17,18]. V_{218}, map position of the V_{218} mutation in R218[12]. The f1 functional origin is shown in detail (map positions 5,769–5,909)[7,19] with its two domains, A and B[8]. ⇩, *Hae*III G/D site, used to construct R209[10] and Mp1[11]. The upper lines indicate the minimal fragments from Mp1 or R325 that were active in rescuing the R218/f1 phage; they extend, respectively, from map position 5,869 to 5,996 (R325; *Hae*III G/D to *Nci*I site) and from position 6,065 to 6,218 (Mp1; *Dde*I sites). Marker-rescue experiments with purified fragments annealed to R218/f1 single-stranded DNA were performed as described elsewhere[12,20] and fragments were considered positive which induced a 20-fold or more increase in clear-plaque production over background. R218 has been described previously[12]. R325, an independently isolated clear-plaque derivative of R209, was used in all marker-rescue experiments. A clear plaque resulting from one such experiment (using the R325 *Eco*RI to *Bam*HI fragment annealed to R218/f1 single-stranded DNA) was purified as a way of recloning the R325 mutation into an R218 background. The resulting phage (R330) was used for all further experiments.

Gene II protein interacts with the phase 'functional origin'[7,8] (Fig. 1), a region consisting of a stretch of 140 nucleotides required for viral strand replication. Two domains can be identified[8] (Fig. 1). Domain A, about 40 nucleotides long, is absolutely required for replication and can be considered as the 'core' of the origin. It contains three partially overlapping sequences[7–9]: (1) the *in vitro* recognition sequence for gene II protein; (2) a sequence required for initiation of plus-strand synthesis (initiation signal); (3) a sequence required for its termination (termination signal). Domain B, 100 nucleotides long, is required exclusively for initiation. Disruption of domain B by either deletions or insertions does not abolish the origin's function completely but reduces it to ~1% of its original level (biological activity of the origin was measured in a chimaeric ori-plasmid system, using f1 wild type as helper phage)[8].

Paradoxically, the site most frequently used for cloning in the filamentous phage vectors (f1 *Hae*III G/D site) lies within domain B[10,11]. A possible explanation for the good growth of these vectors would be that they contain mutations elsewhere in their genome which can compensate for the disruption of domain B. We have recently confirmed this possibility for one of our cloning vectors, R218 (ref. 12), and have now compared R218 with two other such vectors, R325 and Mp1. R218 and R325 are two independent, clear-plaque derivatives of an original phage, R209, that was constructed in our laboratory by inserting an *Eco*RI site (4 nucleotides) at the f1 *Hae*III G/D site[10]. Mp1 was constructed by Messing *et al.*[11] by inserting a fragment of *lacZ* (800 nucleotides) at the equivalent M13 site. R218, R325 and Mp1 replicate as efficiently as f1 wild type. However, when the 'functional origin' of one of these phages (R218) is extracted from the phage and used to replace the origin of f1 wild type, the resulting recombinant phage (R218/f1) can barely replicate[12]. When plated on normal *Escherichia coli* K38 cells, R218/f1 yields extremely turbid plaques. This property can be exploited in marker-rescue experiments to identify possible compensatory mutations elsewhere in the phage genome.

---

* Present address: Center for Cancer Research and Department of Biology, Massachusetts Institute of Technology, Cambridge, Massachusetts 02139, USA.

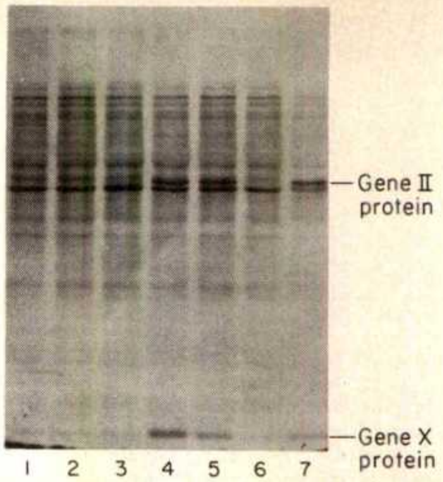

Fig. 2 Gene II protein production in cells infected with various phages. Lane 1, uninfected control; lane 2, R132 (gene II amber); lane 3, f1; lane 4, R13 (gene V amber); lane 5, R218; lane 6, Mp1; lane 7, R330. Exponentially growing *E. coli* K38 cells[21] were infected with various phages and pulse-labelled for 2 min with ^{35}S-methionine as previously described[12]. Samples were immunoprecipitated with gene II protein antiserum and analysed by electrophoresis in SDS/12.5% acrylamide gels[22,23]. The positions of the gene II and X proteins are indicated.

Using this approach, we found[12] that R218 contains a compensatory mutation (V_{218}) within its gene V coding region. The mutated gene V protein seems to retain its single-stranded DNA-binding activity, as phage is made, but loses its ability to repress translation of gene II mRNA. The resulting increased levels of gene II protein (~10-fold) inside the cell could account for the compensatory effect of V_{218} (ref. 12).

Analysis of R325 and its derivative R330 (described in Fig. 1) shows conclusively that increased gene II production is sufficient to overcome the negative effects of insertions in the phage origin. These phages, like R218, contain a mutation in their genome able to restore good growth of R218/f1. Marker-rescue experiments (Fig. 1) and nucleotide sequencing show that the mutation (II_{325}) lies upstream of gene II and consists of a single G to T substitution at position 5,977. This change lies within a sequence of the gene II mRNA leader ($U_5G_4CU_4$) which, because it seems to be unique, was suggested to be the target for translational repression by gene V protein[13]. Here we demonstrate directly the importance of this region for the regulation of gene II expression by showing that II_{325} (in R330, Fig. 2; and R325, data not shown) leads to overproduction of gene II protein in amounts similar to those observed with V_{218} (Fig. 2). Gene X protein, a product of internal initiation within gene II[14], also seems to be overproduced (Fig. 2).

Mp1 also contains a compensatory mutation which, however, does not lead to gene II protein overproduction (Fig. 2). Marker-rescue experiments (Fig. 1) show that the mutation (II_{Mp1}) lies in the gene II coding region. Nucleotide sequencing reveals a G to T substitution at position 6,125, leading to a methionine to isoleucine change (codon 40) in the gene II protein. This structural change in gene II protein has compensatory effects remarkably similar to those observed with increased gene II protein production.

Quite surprisingly, for both types of mutations, not only is the negative effect of insertions in domain B completely overcome, but domain B itself is rendered altogether dispensable. This is revealed by the analysis of chimaeric ori-plasmids containing f1 origins in which domain B is partially or totally deleted[8] (Table 1). These origins show only 1% residual biological activity relative to control (biological activity was measured as described in Table 1 legend), when f1 wild type is used to provide, in *trans*, all the necessary viral gene products. However, when the same origins are tested using R218, R330 or Mp1 as helpers, they are fully active. With Mp1 helper, mutant origins may even be more active than with the other phages.

Table 1 Biological activity of various f1 origins

	Phages (PFU ml^{-1})			
Plasmids	f1	R218	R330	Mp1
pD38 (A^+, B^+)	4×10^{10}	1.8×10^{10}	2×10^{10}	9×10^{8}
pD48 (A^+, B^-)	1.2×10^{12}	4×10^{10}	2.7×10^{10}	2×10^{8}
Δ+41, 70 (A^+, B^-)	2×10^{12}	5×10^{10}	4×10^{10}	6×10^{9}
Δ+29 (A^-, B^-)	3×10^{12}	1×10^{12}	2×10^{12}	1.5×10^{12}

The chimaeric plasmids used, containing the f1 functional origin or some of its parts, have been described previously[8]. A and B refer to the presence of an intact (+) or disrupted (−) domain A and B, respectively, in the various plasmids (see text and Fig. 1 legend). Phage yields were obtained as described previously[7] by infecting K38 cells that harboured the various plasmids. The ability of these plasmids to interfere with phage replication (decreased phage yields) gives a measure of the biological activity of the f1 origins that they contain[16] in the presence of the different phages. PFU, plaque-forming units.

In conclusion, we have shown that both qualitative and quantitative changes in an initiator protein can have a profound effect on the minimal sequence required for initiation of DNA replication. These findings may be of general significance and might even bear on recent, apparently contrasting, speculations concerning the role of increased production or structural alteration of certain key cellular proteins in disrupting the control of cell growth[15].

We thank R. E. Webster for the valuable gift of gene II protein antiserum, and P. Model and K. Horiuchi for critical reading of the manuscript. The work was supported by grants from the NSF and NIH.

Received 19 December 1983; accepted 31 May 1984.

1. Kornberg, A. *DNA Replication* (Freeman, San Francisco, 1980).
2. Gilbert, W. & Dressler, D. *Cold Spring Harb. Symp. quant. Biol.* **33,** 473–485 (1968).
3. Meyer, T. F. & Geider, K. *Nature* **296,** 828–832 (1982).
4. Model, P., McGill, C., Mazur, B. & Fulford, W. D. *Cell* **29,** 329–335 (1982).
5. Yen, T. S. B. & Webster, R. E. *Cell* **29,** 337–345 (1982).
6. Horiuchi, K., Vovis, G. F. & Model, P. in *The Single Stranded DNA Phages* (eds Denhardt, D. T., Dressler, D. & Ray, D. S.) 113–137 (Cold Spring Harbor Laboratory, New York, 1978).
7. Dotto, G. P., Horiuchi, K., Jakes, K. S. & Zinder, N. D. *J. molec. Biol.* **162,** 335–343 (1982).
8. Dotto, G. P., Horiuchi, K. & Zinder, N. D. *J. molec. Biol.* **171,** 507–521 (1984).
9. Dotto, G. P., Horiuchi, K. & Zinder, N. D. *Proc. natn. Acad. Sci. U.S.A.* **79,** 7122–7126 (1982).
10. Boeke, J. D., Vovis, G. F. & Zinder, N. D. *Proc. natn. Acad. Sci. U.S.A.* **76,** 2699–2702 (1979).
11. Messing, J., Gronenborn, B., Muller-Hill, B. & Hofschneider, P. H. *Proc. natn. Acad. Sci. U.S.A.* **74,** 3642–3646 (1977).
12. Dotto, G. P. & Zinder, N. D. *Proc. natn. Acad. Sci. U.S.A.* **81,** 1336–1340 (1984).
13. Fulford, W. D. & Model, P. *J. molec. Biol.* (in the press).
14. Model, P. & Zinder, N. D. *J. molec. Biol.* **83,** 231–251 (1974).
15. Bishop, M. J. *A. Rev. Biochem.* **52,** 301–354 (1983).
16. Dotto, G. P., Enea, V. & Zinder, N. D. *Virology* **114,** 463–473 (1981).
17. Beck, E. & Zink, B. *Gene* **16,** 35–58 (1981).
18. Hill, D. F. & Petersen, G. B. *J. Virol.* **44,** 32–46 (1982).
19. Cleary, J. M. & Ray, D. S. *J. Virol.* **40,** 197–203 (1981).
20. Horiuchi, K., Vovis, G. F., Enea, V. & Zinder, N. D. *J. molec. Biol.* **95,** 147–165 (1975).
21. Lyons, L. B. & Zinder, N. D. *Virology* **49,** 45–60 (1972).
22. Russel, M. & Model, P. *Cell* **28,** 177–184 (1982).
23. Laemmli, U. K. *Nature* **227,** 680–685 (1970).

Errata

Constraints on the neutron lifetime from triton β decay

J. Byrne

Nature 310, 212–213 (1984)

IN the fourth paragraph on page 212, the end of the second sentence is incorrect. It should read 'as a candidate for a neutrino mass search', not 'neutron mass search'.

Unusual DNA sequences associated with the ends of yeast chromosomes

R. M. Walmsley, C. S. M. Chan, Bik-Kwoon Tye & T. D. Petes

Nature 310, 157–160 (1984)

THE first author's name is incorrectly given as Richard W. Walmsley; the initial should be M, not W.

Ideology in archaeology

Warwick Bray

Religion and Empire: The Dynamics of Aztec and Inca Expansionism.
By Geoffrey W. Conrad and Arthur A. Demarest.
Cambridge University Press: 1984. Pp.266. £25, $49.50.

MOST archaeologists, once you come to know them, are quite normal people. They read newspapers, discuss politics, fall in and out of love, and are as irrational and prejudiced as anybody else. In their everyday lives they recognize that the world is a complex and ever-changing place, where human conduct is governed by emotion as well as reason. And yet, these same people, when they write professionally about extinct societies, depict an ordered world in which human behaviour (that is, the raw material of history) develops according to deterministic laws which owe more to Leslie White, Julian Steward or Karl Marx than to evolutionary biology. Ask an anthropologist what caused the industrial revolution, and you will probably get a complicated answer. Ask the same person what caused the urban revolution and the growth of political states, and all too often the reply will be "population pressure", "environmental stress" or some other neat and simple explanation.

At this point a historian (who has read his Machiavelli, and who studies the actions and words of real people, not theoretical abstractions) begins to shake his head and to say that archaeologists have very naive ideas about causality. The archaeologist replies that the historian is unscientific, subjective, and that he corrupts the innocent by passing off creative fiction as historical truth. And there the dialogue usually ends, though each party, in quieter moments, may admit that the other is at least partly right.

Because of the way the subject has developed across the Atlantic, most archaeologists in the United States have little training in history, philosophy or logic. As Conrad and Demarest remark,

> During the past two decades cultural materialism, in one form or another, has been the dominant theoretical approach in New World archaeology. Accordingly, environmental factors involved in state formation and expansion have been much discussed and explored . . . some of the ecological explanations of Precolumbian imperialism have been rather simple-minded deterministic themes which assume environmental pressures to be the *only* major causal forces involved in cultural evolution.

With this complaint I entirely agree, and I applaud the authors' intention to reintroduce ideology (or rather the manipulation of ideology by the governing class) as one of the agencies of social and political change.

The terms of reference are set out in the first half of the book, which describes the rise of the Aztec and Inca empires and their equally dramatic breakup in the face of European invasion. These chapters provide a balanced and well-written survey, though very similar accounts of the Aztec story have been in print for some years, and Conrad's views on "split inheritance" (whereby the Inca ruler's power and title descended to his heir, while his wealth remained the property of the dead man's kin group) have already been the subject of a great deal of discussion in the professional literature.

New or not, these sections are a necessary prelude to the theoretical discussion which follows. The authors conclude that the success of the Aztecs and Incas was due in large part, though not exclusively, to ideological innovation. In particular, they single out the intensification of human sacrifice and the cult of the warrior sun by the Aztecs, and the combination of divine rulership and split inheritance in Inca Peru. I accept Conrad and Demarest's evaluation of these specific phenomena, but, even in societies where there is no clear separation between the religious and the secular, this takes an unduly narrow view of ideology. My dictionary defines the word as "the manner of thinking characteristic of a class or individual". To be effective, a national ideology has first to be made acceptable by a process of enculturation or indoctrination, as any politician well knows (was not Waterloo won on the playing fields of Eton?). A walk around the streets of Belfast will quickly show how difficult it can be to separate religious from political ideology, but I doubt whether any successful empire was built on religion alone. Conrad and Demarest are careful to explain that they are against all monocausal explanations, and that ideology was just one factor in the growth of the Aztec and Inca empires, but they sometimes write as if ideology was the single main stimulus of success. This is arguable, to say the least.

Burden of labour taxation — Incas carrying the produce of state-owned fields to imperial storehouses. An imperial official (centre) directs the work.

Drawing by Guaman Poma, reproduced from *Religion and Empire.*

In their later chapters the authors move from the specific to the more general, in the search for a theoretical framework to explain the emergence of states and the rise of empires. This is one of the bread-and-butter problems of cultural anthropology, so it is fair to ask how — if at all — Conrad and Demarest have improved on previous studies.

In their discussion of socio-political evolution, the biological analogy is never far away. Culture is seen as an adaptive mechanism, responding to particular pressures from the environment (which includes the "climate of opinion" — that is ideology — as well as the physical universe). Thus, "the Mexica and Inca ideological reforms of the early fifteenth century were highly successful adaptive responses to the natural and cultural environments". These responses, successful at first, became maladaptive in the long run, and were instrumental in bringing down the very societies they had helped to create. This is fine, up to a point. But why, given much the same environmental pressures, did the rivals of the Aztecs and Incas not come up with equally effective adaptations? If the answer is simply that the Aztecs and Incas had better leaders (or better theologians), we are back to the Great Man view of history, which is anathema to all processual archaeologists. And why, if the Aztecs and Incas had adapted once, did they not readapt when their reforms had outlived their usefulness? Also, how do the invaders fit into the scheme? Cannot the Spanish conquest be seen as a trial of strength between European and native ideologies, rather than between Spanish and Indian armies?

Most of all, the evolutionary analogy raises questions of "causality" of the kind familiar to historians as well as to anthropologists and archaeologists. Conrad and Demarest give a lot of space to this question, without carrying conviction or offering much hope for the future. In biological evolution the question "What causes elephants?" is meaningless. Perhaps it is just as pointless to ask what "causes" states or empires. Conrad and Demarest do a lengthy demolition job on the ecological determinists, the cultural materialists of the Marvin Harris school, and even on the orthodox Marxist theoreticians (though they show more sympathy for the "structural Marxism" of Godelier and his revisionist colleagues). These criticisms were well worth making, but where do we go from here? To revert to the authors' own biological analogy, we need a theoretical model in which the same phenomenon can simultaneously be an adaptive response (to the previous adaptive responses?) and also a "cause" of change. This, of course, denies the existence of prime movers. Some biologists and anthropologists would argue that, for all its imperfections, some form of systems model comes nearest to satisfying the requirements, but this possibility is never seriously discussed.

Overall, *Religion and Empire* looks backward, to yesterday's problems, rather than forward towards the future. It is a thought-provoking book, but as a contribution to the debate on causality in human history it offers few solutions. Nor does it suggest how the archaeologist, with no documentary information to help him, can even begin to reconstruct the nature of past ideologies, let alone build ideology into his explanatory model. ☐

Warwick Bray is Reader in Latin American Archaeology at the University of London.

Work with nucleic acids

Jeffrey Williams

Techniques in Nucleic Acid Biochemistry.
Techniques in the Life Sciences,
Vol. B5.
Elsevier: 1984. $55.

For those who do not already know the series, it should first be pointed out that *Techniques in the Life Sciences* takes a somewhat unusual form. Each volume consists of a number of pamphlets, loosely held within a plastic box. The rationale is that such a format will allow the publication of supplements and replacements to keep each volume up to date; indeed, with no secure method of retaining individual pamphlets within the box, and with the high loss rate observed for methods sheets in most laboratories, a steady supply of replacements seems likely to prove a necessity.

This is the final volume in the Biochemistry Section of *TLS* (the other, which still continues, deals with physiology, while a Cell Biology Section will be launched next year) and it illustrates the usual advantages and disadvantages of a multi-author technical manual. Because almost all of the authors are recognized experts in their particular techniques, the methods presented are thoroughly tried and tested. The main fault is the enormous variation in the depth of technical detail. Thus the "shotgun" method of DNA sequence analysis is described down to the last salt concentration in a contribution which should find a place above the bench of all aspiring long-distance sequencers. In contrast, the section on RNA sequence analysis is purely a review which, while well written, contains no technical descriptions of any one sequencing method.

These two contributions represent the extremes and most of the articles succeed in the difficult task of combining a literature review with a more-or-less comprehensive methods section. Thus the articles on RPC-5 chromatography of DNA, restriction enzyme purification, restriction enzyme mapping, cosmid cloning, mRNA-DNA hybridization and calcium-phosphate-mediated DNA transformation constitute very useful descriptions of important techniques. There are contributions on genomic cloning in bacteriophage and in yeast which, although predominantly designed to be review articles, give a certain amount of technical information. Finally there are two sections — on bacterial expression vectors and on the analysis of eukaryotic enhancer sequences — which are primarily reviews of work from within the authors' laboratories.

The style of the volume is somewhat akin to the manuals emanating from Cold Spring Harbor Laboratories, but it is a multi-author work and this places it firmly in the mould of a series such as *Methods in Enzymology*. Where the latter is much more successful is in enforcing consistency upon the individual authors and the overall impression is of a valuable concept which in practice still has not quite found its feet. ☐

Jeffrey Williams is at the Mill Hill Laboratories of the Imperial Cancer Research Fund, London.

That strange fellow, Mr Newton

A. Rupert Hall

In the Presence of the Creator: Isaac Newton and His Times.
By Gale E. Christianson.
Free Press, New York: 1984. Pp. 623. $27.50.

ONE OF Isaac Newton's French contemporaries and author of the first textbook on calculus, the Marquis de L'Hôpital, is said to have asked of him: "does he eat & drink & sleep, is he like other men?". Newton's close friend, the philosopher Locke, wrote of him: "Mr Newton is really a valuable man, not only for his wonderful skill in mathematics, but in divinity too . . .". The historian–bishop, Gilbert Burnet, called Newton "the *whitest* soul I ever knew".

Adulation of Newton's character was far from universal in his own lifetime, however: the diaries of Robert Hooke and John Flamsteed, and the letters of Leibniz, contain some of the harshest language a seventeenth-century gentleman (other than Swift) could bear to pen. Newton's successor in the Lucasian Chair, William Whiston, recorded his as "the most fearful, cautious and suspicious temper" he had ever known. Recent writers on Newton the man have, on the whole, taken the side of Newton's enemies rather than that of his friends. At the best they have (following Keynes) emphasized his character as magus, mystic and seer, deducing even the concept of universal physical forces from the mystery of alchemy; at the worst they have found him dictatorial, deceitful, violent, neurotic, a fit subject for the psychohistorian's couch if not the straitjacket.

Gale Christianson is not of the psychoanalytical school, but he discerns another powerful force in Newton's nature: social and personal ambition; "Newton had kept his private pledge to attain the recognition usually denied a lowborn yeoman's son" (p.383). He makes much of Newton's lack of arms, his family illiteracy, his status as a sizar at Trinity, in a way that shows a certain insensitivity to the habits of Newton's society. A sizar was not so very different from a gentle page in a noble household and many gentry could barely sign their names. If one underestimates the likelihood of upward mobility in a society, one is likely also to exaggerate the psychological effects upon those who, like Samuel Pepys and Isaac Newton, rise far in status.

Comparison is inevitable between this new biography and the even ampler one by R.S. Westfall (*Never at Rest*; Cambridge University Press, 1980). Westfall's book is a magisterial study of Newton the scientist based on a quarter-century of steady reading of Newton's manuscripts and publications; Christianson's is a human story in which the scientific achievements are briefly summarized. Rightly, it leans heavily for fact and interpretation on the post-war Newton industry, though Christianson himself must have passed many hours in the Cambridge University Library and other places eliciting obscure information about Newton's life and his relations with his contemporaries.

On the scientific side Christianson is sometimes shaky: Jupiter's were not the only known planetary satellites in Newton's lifetime nor was Descartes seeking, with aspherical lenses, to correct chromatic aberration. Sometimes his eagerness to be in the modern swim verges on absurdity, as when he argues from Robert Boyle's presentation of copies of a book to three Cambridge men (Barrow, More and Newton) in 1673 that all four were "Hartlibians". He spoils a famous story by mistranslation: "I *recognise* the lion by his claw", not "from the claws of the lion" (p.416), is what Johann Bernoulli wrote. Older English readers know that £1.14s and 34s are the same sum.

On the human side Christianson gives a fair picture of Newton's personality, his friendships and enmities, his swift (but not unpainful) ascent to fame and, belatedly, fortune. He dismisses the idea that Newton's character deteriorated with age and power: "The political and professional offices Newton held, in combination with an unassailable reputation, merely enabled him to expand the scale on which his Jovian fits of passion were played out after 1700" (p.500). Combative temper and vindictiveness were present from the start. The picture is gloomy and obsessional, Newton was "a tragic figure of towering dimensions" (p. 499). This is too simple and extreme. Newton was *also* (from evidence Christianson largely omits) a courteous host, a raconteur, indulgent to foreign visitors (even at Cambridge), a man of the world, patient with those labouring under intellectual difficulties, and a Lincolnshire patriot.

Above all, Newton was an intellect; agreed, a formidably serious intellect. To study this, one must go back to Westfall and others. Christianson's is in many ways an excellent, balanced and thorough biography. But the modern tale of Newton the ogre-magician is about as historical as the story of Alfred and the cakes: it is probably not true, and it is certainly not relevant. ☐

A. Rupert Hall is historical adviser to the Wellcome Trust and Emeritus Professor of the History of Science and Technology in the University of London.

New in paperback

Women Scientists in America: Struggles and Strategies to 1940, by Margaret W. Rossiter. Publisher is The Johns Hopkins University Press, price is $10.95, £9.75. For review see *Nature* **302**, 761; 1983.

Intelligence brought into sight

Horace B. Barlow

The Logic of Perception.
By Irvin Rock.
MIT Press: 1984. Pp.365. $22.50, £21.40.

WHEN a sensory physiologist suggests a mechanism for a perceptual phenomenon to a psychologist, the latter's response is usually predictable: he may or may not express polite interest, but sooner or later he will certainly say "Ah, but I'm afraid your idea does not explain XYZ"; XYZ will turn out to be a slight modification of the original phenomenon which seems trivial to the physiologist, but which proves to the psychologist that the explanation offered is of little interest or importance. The good thing about Irvin Rock's book is that it describes explicitly many of the XYZs — the perceptual phenomena that are prominent in the minds of psychologists but not yet explainable in terms of physiological mechanisms. Because physiology, psychology and artificial intelligence are more and more seeking explanations of the same phenomena, the subject matter of the book is very timely.

Irvin Rock describes himself as "originally an ardent advocate of the Gestalt point of view", but in this book he argues that "perception is intelligent in that it is based on operations similar to those that characterize thought". It is tempting and to some extent justifiable to poke fun at him for having finally caught up with Helmholtz, who was emphasizing the importance of unconscious inference in perception well over 100 years ago. But Rock has done a service by describing clearly a large number of the phenomena to which Helmholtz's phrase applies, and he has done elegant experiments to sort out what features of the stimulus are necessary for the intelligent interpretations that the perceptual system makes. Thus he brings together an assortment of material that is potentially of great interest and value to sensory physiologists and those interested in computer simulation of vision. An account of one of these phenomena may give an idea of the subject matter of the book.

Look at a stereo-pair, either through a Wheatstone stereoscope, or better a dichroic pair viewed through red/green spectacles. When a good appearance of depth has been obtained, move your head from side to side: a vivid impression will be obtained that objects in the foreground move relative to objects in the background. The range of head movements possible with a Wheatstone stereoscope is just enough to obtain a good effect, but it is much better with the dichroic stereo-pairs recently available in Britain to eaters of Shredded Wheat. Now shut one eye and repeat the head movements: the relative movement of foreground and background vanish completely.

An explanation for these effects can be reached by considering that depth information from *binocular* parallax is concordant with depth information from *motion* parallax when looking at the real world, but for a stereo-pair both images are in the same plane, so there is no motion parallax regardless of the apparent depth of an object caused by its binocular parallax. One way to reconcile information from the two sources is to suppose that the objects move when the head moves; the required movement of foreground objects relative to background objects is that which will precisely nullify the expected motion parallax, and according to this hypothesis this is what one "sees". This is the explanation Rock gives, and it may be correct; but it is worth noting that the hypothesis has not so far specified the source of information to the perceptual system which leads it to expect motion parallax.

This expectation could arise from the willed head movement, from the vestibular organs or from the visual scene itself. The latter source is suggested by the following observation made by Professor P.A. Merton at his breakfast table, well-equipped with its stereoscopic Shredded Wheat box: rotation of the stereo-pair around a vertical axis gives almost as vivid an impression of relative movement as head motion. Such a rotation, especially if executed by someone other than the observer, could not evoke the expectation of motion parallax from the efferent signal for the movement, nor from the vestibular organs; hence it must arise from changes in the seen images themselves. Since it does not occur monocularly it cannot be the trapezoidal distortions associated with rotation, and (as Dr G. Mitchison points out), the most likely source is the changing gradient of disparities caused by rotation. It is ironic that Mitchison has recently shown (with Professor G. Westheimer) that the perceptual system is extraordinarily insensitive to disparity gradients when tested directly, but this does not prove that they cannot have indirect perceptual consequences.

Another comparable phenomenon described by Rock is the "anorthoscopic display" in which a line moves behind a slit and is therefore shown serially as a succession of short line segments; under appropriate conditions this can be seen as a whole line moving behind the slit aperture. He describes an elegant experimental analysis of the stimulus factors required for the perception of the whole line. Another much-used example with a similar analysis is the "kinetic depth effect", in which a line that changes length as it changes orientation is seen as a rod rotating in three dimensions.

I confess that I found Rock's reasoning about these things less satisfactory than his exposition of them. It is precisely in this sort of area that sensory neurophysiology and artifical intelligence have interesting

21-1-87
A. Beth

things to say, but he has only taken in part of their message. For instance he describes lightness perception without mentioning the separate "on" and "off" system of the mammalian retina, which must surely be relevant to the perception of darkness as well as of lightness. He then goes on to say that the perception of lightness and colour appears to be "based upon information at the edges between regions of differing luminance or hue". That's fine of course, but how is this information extracted from the image and how is it represented in the brain? He talks of the direct detection of relative difference or ratio of luminances, but then suggests that "there is no need to invoke lateral inhibition". This takes one's breath away, for he does not propose any alternative mechanism for the very operations he recognizes are necessary. I think he must fail to realize that, however intelligent or "thought-like" the mechanisms may be, they are ultimately physiological. Surely it is best to proceed by building on the physiological mechanisms we already know about, rather than arguing as if physiological and psychological processes are mutually exclusive alternatives. Neurophysiological explanations are almost always incomplete, but the strength of physiology is that it is a growing science!

For these reasons I fear that Rock's discussions of mechanism are best ignored by physiologists, and I think the same advice can be given to those who approach the problem from the standpoint of image-processing and artificial intelligence. They will have been grappling with the problem of extracting and representing objects in images and will learn little from his reasoning about the phenomena he describes. But the book as a whole should not be ignored, for it gives valuable accounts of perceptual phenomena that are begging for further analysis in terms of neurophysiology and computer simulation. Rock's claim that perception is "shot through with intelligence" does not help much, but both perception and intelligence will be greatly illuminated if we can understand their neurophysiological and computational basis. ☐

Horace B. Barlow is Royal Society Research Professor in the Department of Physiology, University of Cambridge.

Drawn from life

Patricia Vinnicombe

The Rock Art of Africa.
By A.R. Willcox.
Croom Helm, London/Holmes & Meier, New York: 1984. Pp.287.
£45, $69.50.

THE African continent, extending almost 4,000 kilometres both north and south of the Equator, boasts a singularly varied ecology that in turn supports a bewildering diversity of peoples, cultures and belief systems. For millennia the transmission of cultural values from one generation to the next has depended not upon the written word, but upon oral communication reinforced with music, dance, ritual practices and visual representations. It is with one aspect of the latter — paintings and engravings made on rocks — that the book under review is concerned.

The re-discovery and interpretation of African rock art sites, originally painted or graved by Stone Age hunter–gatherers and later by Neolithic pastoralists and Iron Age agriculturalists, has excited the curiosity and imagination of many of the subsequent colonists of the continent. All of them have added their own perspectives as to the age, origin and meaning of the art, resulting in a profusion of data of varying calibre written in many languages and often hidden in obscure journals.

It is against this background that Alex Willcox has marshalled the information for his book. Now in retirement from a career in quantity surveying, his writing has progressed systematically from the particular to the general. His first book was an area study, *Rock Paintings of the Drakensberg* (Max Parrish, London; 1956), followed by a more general *The Rock Art of South Africa* (Wageningen Press, Johannesburg; 1963), and now this compendium covering all of Africa. It is the most systematic and comprehensive amalgamation of data yet presented on the subject. Two previous attempts, *African Rock Art* by Berchard Brentjes (Dent, 1969), and *Rock Art of Africa* by Carson I.A. Ritchie (A.S. Barnes, Cranbury, New Jersey; 1979), were far less successful.

Each of the chapters devoted to a specific region is accompanied by maps, copious line drawings and black-and-white photographs of the predominant art styles, all conveniently juxtaposed to the relevant text. The 67 colour photographs, on the other hand, are sometimes disappointing in quality, and have been crammed onto 24 pages. Even more unfortunately, they have been omitted from the table of contents.

Although Willcox could not be expected to discuss in detail *all* the relevant literature, some omissions are surprising, and viewpoints which do not coincide with his own are somewhat cuttingly and not altogether fairly dismissed. Not everyone will agree with his interpretations, particularly on cultural diffusion and the relationship between the art zones, on the chronological correlation of the art styles, the ethnic identification of the artists and the underlying reasons for the art, but a well-referenced text at least refers readers to the models he eschews. Willcox describes his own model as an Aunt Sally for other archaeologists to shy at (p. 253), and shy they will.

Most contentious of his views is the persuasion, strongly expressed in his first book of almost three decades ago, that the motivation behind the art is essentially the pleasure derived from its execution. Indeed, although Willcox himself refers to a wide range of ethnographic practices connected with rock art, which are summarized and added to by Desmond Clark in an excellent foreword, he is curiously dismissive of this evidence in his final evaluation of the reasons why the art exists. The use of rock art as territorial and ownership marks, in rain-making rituals and in initiation, marriage and burial ceremonies, has been documented from all over Africa. Examples range from the Marghi of northern Nigeria to the Cuissis of Angola, the Oromo of the Harar plateau in Ethiopia to the Guanches of the Canary Islands, the Namia of southern Tanzania to the Bemba, the Butwa and Nyau secret societies of Zaire, Zambia, Zimbabwe and Malawi. Yet when it comes to southern Africa, Willcox is curiously reticent about the considerable amount of ethnographic evidence adduced by Lewis-Williams and others in linking San belief systems to the rock paintings. Whilst Willcox accepts symbolism as a possible component of the non-representational art which he ascribes to the later pastoral peoples, he dismisses the possibility of symbolism in the figurative art of the hunter–gatherers (p. 241). The now classic Levi-Straussian quote that animals are not only *good to eat* but also *good to think* is believed by Willcox to be wrong on both counts. He suggests instead that animals were painted because they were *good to see*. Whilst it is of course true that animals do have a special beauty, it is also undeniable that factors in addition to beauty and pleasure in a task well done were involved in their depiction.

At the start of the book, Willcox claims that the primary purpose of the study of rock art is as a branch of archaeology (p. 9), and here, perhaps, lies the limitation of his approach. As emphasized by Desmond Clark in the foreword, the archaeologist needs to elicit the help of anthropologists, ethnographers, linguists and psychologists in seeking to use the evidence of still-existing peoples the better to understand their prehistoric forebears. Willcox himself observes that the study of art reveals aspects of man's nature not deducible from his material culture (p. 7).

Some idiosyncratic views apart, Alex Willcox's encyclopaedic publication will provide an indispensable source book for professionals and the interested public alike, and will stimulate a deeper awareness of the beauty as well as the scientific and communicative potential of this fascinating body of African art. ☐

Patricia Vinnicombe is in the Aboriginal Sites Department, Western Australian Museum, Perth, and is author of People of the Eland: Rock Paintings of the Drakensberg Bushmen as a Reflection of their Life and Thought *(University of Natal Press, 1976).*

nature

21-1-87
A. Batty

Poor control for US information

The US Congress has put off legislation on the export of high-technology until after the election. Everybody's interest is that it should be given a clear lead from the administration when it returns.

THE US Congress, which leaves Washington to fight the presidential election at the weekend, will leave in a mess the rag-bag of unfinished legislation on the export of high-technology with which it has been wrestling for the past two years. And, for the time being, nobody will care. The universities will be for a few weeks free from anxiety about the interpretation of successive draft regulations from the Pentagon. Societies organizing conferences will be able to live for a few months longer with the practices with which they have become familiar on the participation of foreign nationals. Not even the administration will be deeply disturbed, for on the evidence of the opinion polls, there is every chance that it will be invited to return in January with a more compliant Congress, perhaps one less ready to listen to the doubts of those in the universities and industries of the United States, not to mention their opposite numbers elsewhere in the world, who believe that the past year's attempt to prevent the loss of technical information from the United States is inherently misconceived.

Balancing conflicting aspects of the national interest, any national interest, is always like walking a tightrope. Sure feet and physical fitness are essential (which means that governments must be decisive but also capable of administering what they decide). But it is just as important that the balance organs, with or without the assistance of the eyes (Blondel used to walk in a blindfold) should be keenly tuned, sensitive to the dangers of falling on one side or the other as well as to the signs that the body is out of balance (which means that governments regulating the export of technology must know the dangers of miscalculation in either sense). The worry about the past ten years, and the reason why that experience is a gloomy augury for the future, is that the Reagan Administration has shown flaws in all departments.

That a modern state must have a policy on technical secrecy is not, of course, in question. If there were no secrecy, the benefits of military innovation would flow freely to adversaries and, almost as alarming, to states which are to begin with unaligned but to which the advent of new military technology might seem a challenge. When (as in the eighteenth century) the pace of change in military technology was negligible, but wars were so frequent that new technologies were regularly on display, the need for secrecy (or technical espionage) was hardly noticeable. Now, all that has changed. For the past century, military powers have been compelled to increase their efforts to keep their secrets secret, often with remarkable success. The technology of the manufacture of nuclear weapons is even now less widely spread than it might have been, no doubt in part because nuclear weapons states have an interest that there shall not be too many others like them.

Challenge

The particular challenge of the past few years has been the way in which military and civilian innovations have become intertwined. Even as recently as in the post-war period of 1945–55, when it was already clear that civilian industry had much to learn from the military, civilian innovations were usually by-products of military innovations (jet engines, for example), with the result that the military people were well placed to regulate the speed at which new developments spread. It is too often forgotten that the change which has since come about, only symbolized by the development of transistors, has radically altered the relationship between military and civilian industry. It is now common for the cost of civil development programmes to be comparable with what the military have to spend. Although, historically, the development of the semiconductor industry based on silicon chips and their successors may have been stimulated by the need to miniaturize rocket-borne equipment, only a few years later the incentive came from the civilian side. In the United States, the process has been accelerated by the practice (constitutionally required) of putting military development out to civil contractors. The result has been a quarter of a century of heady technical development from which both partners have profited in their very different ways.

Two further complications have now arisen. First, as the United States is still somewhat disconcerted to discover, civil industry must make its way in markets which are inescapably international. There is no other means by which the technically innovative companies that keep the United States prosperous can pay for the cost of their innovations. So the knick-knacks which the Pentagon wants to buy turn out also to be on sale outside the United States, and in due course become accessible to other people's Pentagons. This circumstance is, of course, entirely maddening. Why should prosperity, on the face of things a just reward for ingenuity, be inescapably alloyed with the wider diffusion of innovation? And why should salt be rubbed in open wounds when it turns out that some of the beneficiaries of this technical diffusion are not potential enemies but, rather, allies who are even faster at organizing production, or piling one innovation on another? In the strictly commercial field, these are the questions that have so plainly irritated the US Administration in its attempts to win legislation on export controls. The same goes for basic research, where the administration has sought the benefits of openness and the security of selective secrecy. Its judgement has as a consequence been distorted — and its knowledge that something is wrong has undermined its capacity for clear action.

Muddle

None of this implies that there should be a bonfire of the regulations. Open licences for military equipment would plainly be absurd. So, too, would be open access to military research. The question of where to draw the line between materials that can and cannot be exported must however depend on a judgement of how much time will be spent by military competitors overseas in using similar techniques for the local manufacturer of comparable equipment, and on the likely relationship of that time-lag to the natural pace of development in the field. Nobody who has seen a micro-chip production line at work will think that the sale of a few of the products to a potential enemy is the equivalent of a gift of the technology, but plainly the architecture of a successful computer may be more sensitive. In the old days, merely four years ago, these were the principles underlying the strategic embargo list then in force. By seeking tougher rules without a philosophical basis for designing them, the Reagan Administration has replaced a workable set of rules which were at a few points absurd with a more comprehensive muddle.

What the United States (together with its military allies and commercial competitors, who are mostly the same) is most in need of is thus an agreed basis on which rules may be worked out as time goes on. The move towards self-regulation by corporations in the United States is a step in the wrong direction — and a recipe for endless uncertainty. The suggestion that there might similarly be a categorization of the research that people attached to universities carry out, with some of it kept secret or semi-secret as other people decide, is not a recipe for "stifling" research but for persuading academic people to pursue uncomplicated goals. On both counts, the result will be less productivity, commercial and intellectual. And the loser will be the United States. Naturally, an openly elected administration is bound to make the choice it thinks the best. On this occasion, unfortunately, the choice is being made irrationally, in the belief that it is possible to keep innovations secret for the rest of time while enjoying the fruits of their sale on the open market. □

Orphaned academy

Britain's scheme for a European academy deserves serious consideration.

THE only squib at last week's predictably somnolent meeting of European science ministers in Paris (see *Nature* 20 September, p. 197) was the British proposal that there should be a European academy of science. And that seems almost to have been an afterthought. The British delegation, embarrassed that its brief called for familiar cautious negativeness on any but the most modest proposals for strengthened collaboration, seems hastily to have hit on this wheeze to demonstrate goodwill. It seems not to have known of the European Academy of Arts, Science and the Humanities, based in Paris, to which Nobelists and some others belong. And by not warning them in advance, the British seem to have embarrassed even its friends. Yet the idea is appealing, even to some of those who regard trans-national institutions as an intolerable threat to national sovereignty. For the truth is that the European community of scholarship is potentially much larger than the sum of its parts, many of which are very small, while the cultural diversity of Europe suggests that such an academy would be an interesting institution. What follows is a recipe for those who would put flesh on the bones the British were rattling.

The first step is to make peace with the European institutions that have, in recent years, thought of themselves as embryonic versions of a European academy. CERN, the high-energy physics laboratory at Geneva, was the first in the field, but the visionaries who in the 1950s dreamed of incorporating other fields of scholarship have long since been replaced by people whose chief concern is where the next 100 million Swiss francs will come from. The European Molecular Biology Organisation (not to be confused with the laboratory of almost the same name at the same place, Heidelberg) has also used language of the same kind, and even has a system of elected personal membership built into its constitution. The European Science Foundation (at Strasbourg), potentially the chief beneficiary of the decision of last week's meeting to encourage stronger European research networks, more openly regards itself as the future European academy, but mistakenly. The foundation, which does splendid work on too small a budget, is as it stands essentially a club for European grant-making organizations, at best an academy of academies. As good a case could be made for the Institut des Hautes Etudes, outside Paris, which is supported by the French Government (with modest help from the European Science Foundation) but which is admirably free from chauvinism in its appointment of people. Whatever their virtues, all these institutions lack the essential attribute of an academy — that of being a self-electing meritocracy.

The designers of the new institution will also have to clear their minds about its function. Academies come in several different forms none of which is a ready model for a European institution. The secular function of academies, that of giving advice to governments, conspicuous in the United States and the Soviet Union but less so elsewhere, cannot apply when there is no single government on which to thrust advice. The conduct of research at a single location is similarly impractical, whatever may have been possible at the academy in St Petersburg in the eighteenth century or in Berlin when the old Kaiser Wilhelm Institute was at its peak. Of the functions of modern academies that could be adapted to a European canvas, the best outlets are the spending of modest sums on the support of scholarship by criteria which are entirely independent, the management of scholarly publications and the pursuit of excellence by repeated demonstration. Such an institution, if properly arranged, could serve to enliven European science in ways not yet foreseen.

But how would it be possible for a European academy to avoid the tokenism to which most kinds of international institutions are prone? Should members of the new institution be elected in proportion to the populations of its sponsor, or to their Gross National Product? Should Nobel prizewinners automatically become members, or be so *ex officio?* Should the presidency rotate among countries? And by alphabetical order or otherwise? Where should the social sciences fit in? Any one of these questions is by itself sufficiently daunting to persuade all but the enthusiasts that the effort would not be worthwhile. There is, however, a way in which these difficulties could be turned. Simply agree that for an initial period of, say, ten years, new members should be elected annually to a European academy by some outside body (for which purpose the European Science Foundation would serve well), but give the existing membership (after the first year) a veto. And then require that for the initial period, no new member should be older than, say, forty. To begin with, it is unlikely that such an organization would be able to do much more than organize occasional scientific meetings. Eventually, however, it might have won enough respect in the outside world, and have learned enough about its own quality, to be able to take independent and less familiar initiatives. And if, by evil chance, luck went the other way, nothing much would have been lost. □

Redundant department

Advocates of new US Government agencies include people who should know better.

RONALD Cape, chairman of Cetus Corporation, president of the Industrial Biotechnology Association and usually a level-headed spokesman for the industry, seems to have been overcome by the excitement of the Biotech '84 conference held earlier this month in Washington, DC. That at least is the kindest interpretation of his talk there, in which he called for the creation of a new federal agency in the United States charged with promoting biotechnology. Its first assignment would be to double the federal government's support for basic research in the life sciences, now some $2,900 million a year.

Cape is sure to qualify for this year's final round of the Bite the Hands That Feed Them Award with his complaint that the National Institutes of Health (which now spend $3,800 million a year on research and development, well over half of that on basic research) are too "fragmented" to meet the needs of biotechnology. The other reason advanced by Cape is, of course, the Japanese Peril. The Soviet Peril was enough to bring about the National Aeronautics and Space Administration, after all, and that was nothing compared with the threat of Japanese competition. "They did it to us in cars", he said. "They did it to us in tape recorders and TVs. And now they say they're going to do it to us again in biotechnology."

Cape may have been asking for trouble in citing these analogies. Once the Department of Biotechnology is established, presumably with Wally Gilbert as Assistant Secretary for Finance and Mark Ptashne as director of the media relations office, the Department of Automobiles, the National Tape Recorder Administration and the Bureau of Cheap Calculators are sure to follow. To avoid the backlog of proposals that is bound to accumulate, *Nature* would like to put forward its own modest suggestion now: a Department of Magazine Mailing whose major function could be the issuance of grants to worthy journals whose competitive position is being hampered by postal rate increases. □

Nuclear winter

US plans for studies proliferate

Washington

A $50 MILLION five-year national research plan for studying "nuclear winter" — possible global cooling following nuclear war — has been drawn up by the National Oceanic and Atmospheric Administration (NOAA). A final draft is now being circulated to an inter-agency review committee before being sent to the White House's Office of Science and Technology Policy (OSTP) by the end of October.

The study plan has been drawn up at OSTP's request by a group headed by Alan Hecht, director of NOAA's National Climate Program Office. It seeks to reduce the principal uncertainties associated with nuclear winter by co-ordinated research in several different areas. The $50 million price tag corresponds to one of several options put forward by NOAA: if the Office of Management and Budget accepts all the study proposals, the cost could be considerably higher. The nominal five years' duration could be extended as necessary.

The proposed study places the highest priority on understanding source inputs of smoke into the atmosphere. Laboratory and field experiments with different fuels would be performed to gain information about the size distribution of smoke particles and their optical properties. Other studies would be designed to investigate how the results from small-scale experiments can be scaled up, first to room size, then to building size and finally to large areas. Ultimately, there would be field experiments entailing managed forest fires instrumented to measure the composition of smoke below, within and above clouds and what happens at the smoke/cloud interface. Some experiments would use areas of clear-felled vegetation.

Hell, there's a much quicker way to find out!
PENTAGON

The number of managed burns the draft plan says, could be contained by studying natural forest fires provided that it is possible to respond rapidly enough in moving equipment and personnel, but some field experiments are thought inevitable. As well as the experimental work, there would be a strengthened modelling effort focusing on further development of mesoscale and cloud models. Optional extras in the plan include studies of the natural transport of Sahara dust and Arctic haze. Also in the high-cost option is work on the biological impact of global temperature changes.

Already, the Department of Energy and the Defense Nuclear Agency (DNA) are managing theoretical studies of nuclear winter. The DNA programme has been allocated $1.5 million in this financial year and will be increased next year; it will be integrated into the national study if and when that is accepted, when DNA may manage some of the work. But, according to Dr C. Gillespie of DNA, the agency's own work is well under way and will not wait for the national plan. DNA concentrates on the chemistry of smoke and on developing modified three-dimensional global climatic models suitable for nuclear winter studies. It also examines likely explosion scenarios and sponsors policy research. All the scientific work, like that in the national programme, will be published in the open literature. Gillespie says the only thing clear so far is that the problems are extremely complex.

Academic scientists who have helped plan this study are pleased by the "unusually good co-operation" and the "non-combative attitude" of government officials from all departments. One commented that nuclear winter is a rare example of an area where disagreements between scientists are noisier than those between bureaucrats. But he fears that the administration may seek to use the scientific uncertainties as an excuse to respond only by commissioning research.

Whatever the political complexion of the administration after November's presidential election, a request for some $50 million of new money over five years will need some justifying. The approval of the President's science adviser (Dr George Keyworth) will be but the first step.

Meanwhile, Congress's Office of Technology Assessment (OTA) is also likely shortly to announce studies connected to nuclear winter. Three broad possibilities are being discussed: a general assessment of what is known about the long-term effects of nuclear war, a survey of all current research relevant to nuclear winter (both in the executive branch and in private institutions) and a more critical study aimed at identifying those areas where further work would be most effective. OTA is unlikely to involve itself in basic research, but feels it does have a role to play in reviewing the efforts of others.

Tim Beardsley

Netherlands budget

Under-the-counter support

THE Netherlands Government budget for 1985, announced last week, contains a few grains of hope for Dutch scientists — and there may be more to come. Science minister Willem Deetman, while broadly protecting the budgets of the national research council (ZWO) and academy of sciences (KNAW), has offered them a little more (just one per cent) to pay for new positions (such as predoctoral and postdoctoral fellowships). Meanwhile, he has continued to tighten the noose on the universities, once considered the best-funded in the world. But, it is said in circles close to the government, he is seeking extra funds to pay for the reinstrumentation of laboratories. But why is he doing this outside the budget, who will benefit from it, and by how much? All these questions are matters for speculation.

At ZWO, the small but respected council for basic science, the budget always contains a few per cent extra for re-equipment, but the sum has been too small "for a number of years", says its director, Professor Robert van Lieshout. In the budget this year, ZWO receives Dfl 15 million (£3.5 million) in this category, around seven per cent of the working budget "but we need ten per cent", says van Lieshout.

Nevertheless van Lieshout is relieved at least to find his net budget uncut. The universities had suffered what they claim to be the maximum possible reductions in recent years, while the research council had been left unscathed; and the Dutch budget minister was demanding more cuts all round. "It's our turn next", said van Lieshout before the budget — but his fears were unfounded.

Moreover, through a budget decision which affects many national institutions, ZWO (and KNAW) find they have a one per cent budget increase to pay for new posts. In ZWO at least, these will be used to provide a few more much-needed postgraduate and postdoctoral fellowships. The Huyghens programme, providing fellowships for high-flyers (20 last year, the first year of the programme), will also be continued by "scraping off" another one per cent of the total ZWO budget. This year, that will pay for around 16 fellowships — although it has been estimated that perhaps another 100 are necessary to maintain the health of science in the Netherlands.

Robert Walgate

Publication controls

State Department raises hackles

Washington

UNIVERSITIES in the United States are mulling over a new threat to freedom of scientific communication, this time from the Department of State. Recent proposed regulations would restrict the export of technical data "directly relevant" to defence. But there is concern that the regulations could be used indiscriminately to curtail export of any general mathematical or engineering knowledge with possible military applications.

The new proposals are to revise the International Traffic in Arms Regulations (ITAR), which have in the past been used to restrict export of information, although less frequently than the Department of Commerce's export regulations (see *Nature* 20 September, p. 195). The arms control regulations are supposed to apply only to military equipment and data. But while much of the research work covered under ITAR is in any event classified, this need not be so. Thus information "directly relevant" to design, development or operation of defence articles is covered.

However, the progress of the new proposals will be rough. The Department of Defense is piqued that some of its own comments on a 1980 draft of the regulations have been excluded from the text, and is preparing a "statement of non-concurrence". This will ensure that the State Department will at the very least have to work hard to justify its proposals, and another draft may be necessary.

Meanwhile, the Office of Science and Technology Policy (OSTP) at the White House is recruiting prominent scientists and industrialists to form an advisory group on the controls on technical data administered by the Department of Commerce. Its job will be to validate and add political clout to proposals drawn up over the summer by an inter-agency working group under Andrew Pettifor of OSTP, which has rejected an earlier suggestion by the Department of Commerce that the existing general export licence for fundamental research should be removed. Fundamental research is defined as anything done on a university campus, and this group says that fundamental research, together with information in the open literature or mentioned at an open conference, should be freely exportable. Details will be circulated for discussion in a few weeks' time.

So far, the Department of Defense, which was represented in Pettifor's group, appears to be bending over backwards to placate academics. Its new declared policy is that fundamental research should be controlled only through national security classification, in marked contrast to its position earlier this year, when its proposals to introduce a new category of "sensitive" research caused widespread protests from universities.

The Pentagon will early next month be publishing a list of "critical technical data" that it wants to see protected. But the new national policy, as it has become known, still has several hurdles to overcome. The proposals of Pettifor's group, which are supposed to provide the nuts and bolts of the new policy, will have to be reviewed both by the White House and by the National Security Council. Any factions in the Pentagon wanting to kill the proposals will still have the opportunity to do so. **Tim Beardsley**

In vitro fertilization

Surrogacy ban by Victoria state

Canberra

THE Victorian state government intends to ban payments for surrogate motherhood and to make surrogacy contracts unenforceable in court following the public release earlier this month of the final report of the committee set up to consider the "social, ethical and legal" issues arising from *in vitro* fertilization (IVF), headed by Victoria Law Reform Commissioner, Professor Louis Waller.

Delivered to the government in August, the report concentrates on the disposition of embryos produced by IVF procedures and should form the basis of widespread discussion throughout Australia. But it approves the techniques which produced the world's first freeze-thaw embryo baby in Melbourne on 28 March this year.

Seven of the nine committee members recommended that the freezing and storage of embryos be permitted to continue, although these procedures should only be undertaken in those hospitals with IVF programmes already approved by the Minister of Health. The hospital itself will not determine the disposition of stored embryos and large embryo banks will not be permitted. Storage, the report says, should be only for short periods, but where a participating IVF couple needs and consents to long-term storage (during chemotherapy, say), storage consent should be reviewed after five years and then may be renewed. The committee also considered that research and development work on procedures for the hitherto unsuccessful freezing and storage of human ova should be encouraged, partly because success would reduce the need for excess embryos in the first place.

According to the Waller recommendations, an embryo should be stored only with the explicit agreement of the couple supplying the gametes, who will have to choose at the outset the embryo's ultimate disposition. If an extra embryo is stored to insure against implantation failure, the couple must decide whether, in the event of a viable pregnancy, their embryo should be donated to another couple in the IVF programme, made available for research or allowed to warm up and perish — to be "removed from storage", in the words of the report. The committee regards the "removal" procedure as morally equivalent to the withdrawal of life-support systems from a mortally ill person.

The embryo should be "removed" if no agreed ultimate provision is made at the time of storage and if, through mischance, the embryo cannot be transferred as initially planned. This appears to seal the fate of the two "orphaned" Rios embryos at present stored at the Queen Victoria Medical Centre in Melbourne, whose parents died last year leaving no directions for the embryos' disposition (see *Nature* **309**, 738; 1984). The government will nevertheless allow three months for further public discussion before the Rios embryos are removed from storage. The committee took the view that untransferred embryos should not be regarded as possessing rights or claims to inheritance.

Two committee members expressed the belief that human embryos should never be used in research at all. Another two members — both medical researchers — claimed that the creation of embryos purely for research purposes was ethically acceptable. The other five members, including the chairman, judged that it was not.

They decided that embryological research in Victoria should be limited to the excess embryos produced by patients in an approved IVF programme. Like the Warnock committee set up to examine the ethics of IVF in Britain, the Melbourne group recommended that experimentation on the embryo should extend only over the first fourteen days, and that all embryo research should be regularly scrutinized. A standing review and advisory body or the state health commission are suggested as bodies capable of the task. As a matter of urgency the committee said that the suggested new review body should examine the practice of *in vivo* fertilization which is already employed in a least one infertility clinic in the United States and which one of the IVF groups in Victoria had stated it would be ready to employ if authorized to do so. Other matters it should consider are embryo cleavage, embryo surgery and genetic manipulation.

The committee's terms of reference were limited to surrogacy in an IVF context. The view was taken that surrogate motherhood arrangements are actually agreements for the purchase of a child, and therefore unacceptable. Non-IVF surrogacy is to be covered in the intended contract-voiding legislation which will then not be uniform throughout Australia. **Jeffrey Sellar**

Information technology

Future reaches Tokyo early

Tokyo

THE first step towards the creation of the "electronic society" took place in Japan this week with the inauguration of a large-scale model Information Network System (INS) in the Mitaka suburb of Tokyo.

The eventual aims of the INS are grandiose: to provide by around the year 2000 a digital network for the whole of Japan which will integrate telephone, telex, facsimile, teletext, computer data and video transmission systems and enable everything from shopping to business management to be carried out from home. If the network is completed, it will require the staggering investment — at present estimates — of 30 million million yen (US$150,000 million).

The model system is rather more modest — about 2,000 households are involved at a cost of Y20,000 million — but it will allow most of the terminal equipment that may be in every household by next century to be tried out. And this stage of the project is going ahead on time, a sure sign that neither criticisms of the INS concept (see *Nature* **305**, 364; 1983) nor the impending privatization of NTT, the telecommunications monopoly, has so far made much impact on the project's future.

Among pieces of equipment not before offered to the public are those exploring the possibilities for increased visual communication. There will be videophones allowing two (or more) people to meet face-to-face on the video screen and a visual circuit service will allow the remote operation of video cameras. This system would, for example, enable an architect to monitor progress on a construction site by dialling the appropriate camera from his home. A totally new visual device is the sketchphone, a telephone that transmits manuscripts and hand-drawn diagrams exactly as they are written or drawn. At first, sketchphones are to be used by the deaf, giving them their first ever opportunity to make telephone calls, and links are to be provided between the Mitaka municipal welfare office and the homes of children with hearing problems.

Other truly new services come from new methods of handling information rather than from new kinds of terminal equipment. If you need to send out the same message to several people, the new network will make that easy: a central voice accumulation device can be used to register the message and the appropriate telephone numbers. The same facility will also be available for facsimile transmission, enabling the chore of sending out New Year greetings cards to be largely automated. The central store may also be used to leave messages for callers, or as a "mailbox" to accumulate calls to be picked up later. Other central facilities will function more like a library. Subscribers will be able to use a videoresponse system to call up still and moving pictures, or to connect with a pre-programmed motion picture service.

A little more mundane are improvements in existing telecommunications services. Subscribers will have new digital telephones that show the number from which a call is coming, the number being dialled and the call charges. High-speed digital facsimile transmission — including multiple address, mailbox and confidential transmission systems — will be available along with access to the CAPTAIN videotext system. In its digital version, CAPTAIN can offer transmission of still pictures with sound or characters and diagrams with voice instructions for terminal use, as well as devices to turn the picture into hard copy. Thousands of pages of information are already available on everything from chess to weather forecasts.

The real excitement over the next 18 months of the system will come, however, not from contemplating new technology but from seeing whether any really new use can be found for information technology. NTT has selected monitors and information providers in order to put the system to as many practical uses as possible and has also connected the Mitaka network to several businesses in Kasumigaseki, one of Tokyo's main office areas, so that some companies with employees living in Mitaka can try letting them work from home or from a satellite office. Obviously the new high-speed facsimile services and videophones will come into their own here and may eventually make unnecessary big offices in central areas with sky-high rents.

For the ordinary citizen, it is the combination of facsimile with CAPTAIN videotext that is likely to be attractive. In the financial field, for example, where 74 separate companies are going to provide services, it will be possible for all the operations for which one would normally need to go to a bank to be carried out at home — information on stocks, shares, exchange rates, insurance, and securities can be provided and transactions carried out. Another 248 companies will use the equipment to provide services in a whole range of fields. Department stores will be able to show goods and collect orders, computer shops advise on operation of personal computers, rail and transport companies provide their timetables and route maps, tour agents conduct potential visitors on pictorial tours of countries overseas, oil companies advise of the nearest open petrol station and power companies facsimile their bills straight into customers' homes.

The real hope (for INS believers) is that subscribers will fight their way through the deluge of unwanted promotional material to a whole new range of applications for telecommunications services. Critics who have looked at the failure of the United Kingdom's Prestel system (which began operation too far ahead of its time in 1979), as well as other nations' viewdata systems, take a somewhat dimmer view. Although INS offers much more than just viewdata, it may still share Prestel's problem of being too stupid to be really useful. Calling up pages of information on a video screen and searching through them is often the slowest and most expensive way to find a particular piece of information, except for special applications such as listing stock exchange prices. What is needed is a truly helpful database, capable of searching for and displaying information specified by its user. No country has yet made available computing power able to handle tasks of that kind.

Whether the Mitaka model system can supply services that customers really want remains to be seen. Those who are desperate for a peek into the future and cannot wait until the end of the preliminary appraisal in 1986 can, of course, simply call up the computerized fortune-telling service that one of the model system companies is offering. And for those who are baffled or simply feel their vocabulary is inadequate for the twentyfirst century, another company is offering explanations of new high-technology terminology as its main service.

Alun Anderson

Model zoo

Washington

THE disclosure that a Texan coral snake on display for the past two years at Houston Zoo is in fact a rubber model has caused consternation in the zoo world. A local newspaper was tipped off by an observant zoo visitor who noticed the snake had not moved in 9 months.

John McLain, assistant curator of reptiles at the zoo, explains that coral snakes are difficult to keep in captivity and tend in any case to hide in litter. As they are venomous, the zoo wanted to educate the public in their appearance, so after several real coral snakes died, the model was substituted. Says McLain: "Many zoos make do with photographs, and we thought we were going one better. We didn't think we were fooling anyone." A zoo official denied that any of the zoo's other animals were models.

Dr Dale Marcellini, a herpetologist at Washington DC's National Zoo, says he has never before heard of a zoo passing off a rubber model snake as the real thing before. But he is sympathetic to Houston's problems and thinks it "not such a bad idea". However, Mr Bob Wagner, executive director of the American Association of Zoological Parks and Aquariums, said his association could not approve of the practice. He intends to take up the matter with the director of Houston Zoo.

Tim Beardsley

Arms control

More Soviet violations alleged

Washington

AN administration report containing the strongest accusations yet of Soviet violations of arms control agreements may finally be released next week. Hardliners both within the administration and in Congress have been pressing President Reagan for almost a year to turn the document over to Congress. Portions already leaked to the press — presumably by members of Congress who have received briefings from the administration — show it to be a strongly ideological statement that mirrors the view of key administration officials, notably Richard Perle and Fred Ikle of the Department of Defense, that the Soviet Union cannot be trusted to abide by any arms limitations treaties. That view has played a major role in the administration's enthusiasm for its Stars Wars concept of a space-based ICBM (intercontinental ballistic missile) defence.

The report was prepared by the General Advisory Committee (GAC) of the Arms Control and Disarmament Agency, a group of outside experts. Although it is formally a report to the President, both houses of Congress have passed amendments to the defence authorization bill requiring that the report should be transmitted to Congress and the signs now are that the administration will not wait for that bill to be enacted before releasing the report. The visit this week of Soviet foreign minister Andrei Gromyko has apparently delayed an earlier planned release date.

In part, the report echoes the major charges that appeared in an administration report to Congress last January — the construction of a possible ABM (anti-ballistic missile) phased-array radar in Siberia, encryption of ICBM telemetry data, testing of more than one new ICBM and the supposed proxy use of chemical and biological agents in South-East Asia. But the GAC report also chronicles other "breaches" going back to 1958. These include "violations of customary international law" (using booby-trap mines and incendiaries against civilians in Afghanistan) and "breaches of unilateral commitments" (atmospheric testing of nuclear weapons in 1961–62, completing construction of SS-20 launchers between March 1982 and December 1983). One lesser known violation cited is the transit of Soviet aircraft carriers through the Turkish straits, a contravention of the Montreux Convention of 1938.

The GAC report is at its most ideological in six "key findings". The Soviet claim during SALT II negotiations that its "backfire" bomber does not have an intercontinental capability, is, for example, cited as evidence in support of the key finding that the "Soviets use deliberate deception in negotiations". Alleged chemical and biological warfare is evidence that "Soviets sign and ratify arms control treaties that they are planning to violate".

The report's authors present a novel theory to explain alleged Soviet breaches since signing SALT II. Because these violations were "done in a fashion which should have at least caused US suspicion", GAC concludes that "a reasonable interpretation . . . is that they are measures designed to test US intelligence capabilities and US political processes relative to arms control" and perhaps "preparation or cover for more extensive violations".

Arms control proponents in the United States have recently argued that both the United States and the Soviet Union are "hedging" on compliance. In an article published in the Fall 1984 issue of *Foreign Policy*, Michael Krepon; director of the verification project of the Carnegie Endowment, notes that the United States is, for example, building a large phased-array radar in Georgia and Texas that could be seen as violating the ABM treaty, as it can cover two-thirds of the continental United States. (The ABM treaty allows only one ABM radar; other radars must point outward to prove that they are early-warning radar only.) Krepon also cites several major weapons construction proposals advanced by the Reagan Administration that would violate existing treaties, including the dense-pack basing mode for the MX, the Midgetman missile and Star Wars. Krepon argues that these actions by the United States signal a "distinct lack of interest in maintaining SALT limitations".

Stephen Budiansky

Toxic hazards in Britain

NEW safety regulations aimed at protecting British workers from exposure to hazardous chemicals have been proposed by the Health and Safety Commission. The commission, having issued the draft regulations in a consultative document, hopes to elicit comments from interested parties before submitting the proposals to the Secretary of State some time in 1985.

The regulations were prepared by a working party composed of members representing the Confederation of British Industry, the Trades Union Congress and independent experts. They require employers to assess any danger their workers face, to take steps to reduce that danger to an acceptable level and, in addition, to provide safety training, to monitor the health of workers and to keep detailed medical records. These measures clarify and extend the terms of the presently enforced Health and Safety at Work Act 1974, a piece of legislation dubbed by critics as vague and too concerned with a small subset of toxic chemicals (lead, asbestos, etc).

Trades unionists are generally delighted with these proposals but some manufacturers believe they will be costly to implement, making British industry less competitive and, consequently, sacrificing jobs. The Health and Safety Commission believes that employers will be helped by a simpler set of regulations applying to all hazardous substances.

Marcus Chown

Archaeology

Cheshire's oldest inhabitant?

THE British Museum is about to take delivery of a remarkable archaeological find — the body, preserved in peat, of a 2,500-year-old Iron Age inhabitant. The body, uncovered unexpectedly by peat workers in Cheshire, has been in the mortuary of a London hospital since its excavation last month by archaeologists from the British Museum and the University of Liverpool.

Researchers at Harwell have attached a tentative date of 550 BC to skin samples supplied, though they hope to refine this estimate after careful calibration of the radio-carbon dating procedure. When allowance is made for fluctuations in the atmospheric $^{14}C/^{12}C$ ratio over past millennia, the technique could possibly yield an earlier Bronze Age date for the body.

Dr Ian Stead of the British Museum's Department of Prehistoric and Romano-British Antiquities is to supervise the work on the body. Until the layers of peat are peeled away, the exact state of preservation of the body will not be known. But there are high hopes that, apart from the skin already found, body hair, clothing and jewellery will also be revealed. With luck it may also be possible to inspect the stomach contents.

This is the first such find in Britain, though similarly preserved bodies have been discovered in Jutland, Denmark. The Danish remains showed signs of violent sacrificial deaths and have ranged in age from 840 BC, the end of the Bronze Age, to as late as AD 95.

Dr Stead believes that, because preservation techniques have become increasingly sophisticated in recent years, the British find could prove the most important yet. The last Jutland body came to light in 1952 and its condition has deteriorated over the years. The British Museum intends to use the more effective technique of freeze-drying. The museum hopes to have its body on display to the public, curled in its original fetal position, within two years.

Marcus Chown

UN biotechnology

Green light for twin lab

THE plan to found a biotechnology organization on behalf of developing countries, masterminded during the past two years by the United Nations Industrial Development Organization (UNIDO), moved one notch ahead last week. The preparatory committee of the International Centre for Genetic Engineering and Biotechnology, meeting in Vienna, heard for the first time what funds the two host countries, India and Italy, are willing to commit. The plan now is that a project leader and a scientific committee should be identified by the committee's next meeting in December.

Opinions are divided about the pace of events beyond that. The two years already spent on the discussion of the project are not thought excessive by the yardsticks of international diplomacy, and because the end-product will be a free-standing international organization to which the 33 member states will be bound by a convention with the legal force of a treaty.

In many cases, the project became tangible only at the beginning of this year, with the decision that the new centre would have two components, one in Italy (Trieste) and one in India (Delhi).

The funds now allocated by the two host governments are substantial but far from sufficient to keep the project going. The Government of India last week offered $5 million towards the cost of the first five years' work at the Delhi site, supplemented by an offer of $8.2 million from the Italian Government, which has also promised $4 million and 13,000 million lire towards the cost of five years' work at Trieste.

The two governments will also contribute towards the cost of equipment (Rs 15 million and 58 million lire for India and Italy respectively). India plans to spend Rs 72 million on land and buildings near Delhi, while Italy will provide a building at Trieste at a token rental.

These bids will demonstrate the seriousness of the two hosts and also serve to encourage the others, as at a charity auction. Whether the other potential contributors will arrive at Vienna with enough promissory notes is, however, less certain. Some will wish to know what people are chosen in the next three months, others the colour of their fellow-members' money, while doubts persist about the decision to split the centre into two components.

A further difficulty is that the centre is planned to be the hub of an international network of "associated centres" that will be nationally located so as to assist with training and exploitation. The obvious danger is that member governments will prefer to commit what funds they can afford to the development at home.

There are also further decisions to be made about the division of work between Delhi and Trieste. The Indian centre will be concerned with developments in agriculture and human health, the Italian with the application of biotechnology in the chemical industry, energy and the like. But where (and how) the dividing line will be drawn is still to be decided in detail. □

Badgers at bay

THE conflict between British farmers and wildlife interests over the badger as a source of bovine tuberculosis will persist, last week's report on the subject from the Ministry of Agriculture, Fisheries and Food (MAFF) notwithstanding. The issue is contentious because the badger is one of the largest native mammals surviving in southern Britain and because wildlife interests dispute the reality of the connection between badgers and bovine tuberculosis. Under present policy, badgers are protected under the Badger Act except in areas (mostly in the south-west) where infection by *Mycobacterium bovis* and badgers coexist, as recommended by Lord Zuckerman in 1980.

The latest report on *Bovine Tuberculosis in Badgers*, the eighth to be published, extends the study of captured badgers up to the end of 1983. It says that 13 per cent of 6,000 carcasses examined at MAFF laboratories between 1971 and 1983 show traces of infection, a higher rate of incidence than in any other common British animal.

But do badgers communicate the disease to cattle? If so, then it is presumably via faeces. Tests for *M.bovis* in faeces over the same eleven-year period were positive in 3 per cent of cases. The evidence implicating the badger population as a reservoir for *M.bovis* remains circumstantial and rests on the coincidence of outbreaks of bovine tuberculosis with concentrations of badgers. The case against badgers is strong but not watertight.

There are, unfortunately, no reliable estimates of the size of Britain's badger population. It is unlikely, the World Wildlife Fund believes, that the species is threatened nationally by culling.

Live trapping has now replaced gassing as the chief method of controlling tuberculosis in badgers, in spite of the extra cost. All cattle are tested regularly for bovine tuberculosis and those reacting to the tests are slaughtered. Research into the link between bovine tuberculosis and badgers and control of the disease continues.

Meanwhile, MAFF has announced a further comprehensive review, as recommended by the Zuckerman report, of the problem of badgers and bovine tuberculosis, to be carried out by a three-man team under Professor G.M. Dunnet (University of Aberdeen), and the ministry now promises that the new findings will be made public. Marcus Chown

Sellafield

BNFL on counter-attack

BRITISH Nuclear Fuels Ltd (BNFL), the focus of public criticism during the past year over its waste-disposal indiscretions, has hit back at its critics in its annual report, *Radioactive Discharges and the Monitoring of the Environment, 1983*. The company hopes that data published in the report will draw the debate on its conduct out of the emotional arena and back into the forum of facts. But this seems unlikely while the argument about high leukaemia incidence near BNFL's Sellafield reprocessing plant continues.

BNFL reports that, during 1983, the quantity of liquid waste discharged from its Sellafield site into the Irish Sea was reduced substantially, continuing the trend of recent years. The total beta discharge was cut by 50 per cent compared with the 1982 level and the alpha discharge was down by 30 per cent. These reductions were achieved despite the contamination of a 15-mile stretch of the Cumbrian coastline, near Sellafield, in 1983 after the accidental transfer of plant washings to a sea tank on site, for which the company is now to be prosecuted. BNFL says that the total radioactivity released as a consequence of this error was negligible, amounting, over an eight-month period, to less than one-tenth of a curie (1 curie $= 3.7 \times 10^{10}$ disintegrations per second). This is to be compared with Sellafield's routine beta discharge in 1983 of 67,000 curie.

BNFL concedes that the contaminated beaches seriously damaged public confidence in the company. To restore that confidence, it is to step up its research efforts to cut liquid discharges to "essentially zero". £190 million is already earmarked for this purpose which will, of course, require an alternative disposal route, most probably to a land site. The company stresses, though, that it now operates well within the government's limits for the dumping of liquid waste.

BNFL has continued its programme of monitoring the environment during 1983. Shellfish eaters near the Sellafield plant have been identified as potentially at risk from radioactive contamination, but tests have verified that their exposure amounts to about one half of the annual limit recommended for members of the public by the International Commission on Radiological Protection (ICRP). According to the report, no other group in the vicinity of any other BNFL installation receives an annual dose even close to this level. These findings are confirmed by an independent study carried out by the Directorate of Fisheries Research of the Ministry of Agriculture, Fisheries and Food (*Radioactivity in Surface and Coastal Waters of the British Isles, 1982*).

Marcus Chown

French research

Pragmatism back in fashion

Paris

DURING the past year of economic crisis, the smile on the official portrait of President François Mitterrand has cast a rather baleful air over government offices. But now that smile is visibly brightening. Mitterrand's new boy, 38-year-old Prime Minister Laurent Fabius, is turning France from socialism to social democracy. Mitterrand looks happier with the new tag, and science may benefit as well.

Fabius's minister of research, M. Hubert Curien, is a technocrat, not a politician, and will not let ideology get in his way. Asked by a newspaper last week to choose his *leitmotif*, he replied "to choose and to act". This may sound banal, but Curien means it. And there is no time to hesitate. General elections are due in 1986, and the electorate has lost its taste for the *Partie Socialiste*. The President needs results.

While the French plan — to base economic growth on research — has life in it yet, the rose-tinted spectacles are gone. There is a new sense of realism, for example, on the French policies on the new technologies, in the past always suspect because they were so centralist (despite efforts to the contrary).

French centralism works beautifully in projects which require the mobilization of France like an army, as Napoleon knew. Thus the French have built the TGV (high speed train), conquered space (with Ariane) and introduced nuclear power (half French electricity is nuclear, and the proportion is rising). The recipe has not worked as well for the multifarious worlds of biotechnology and the microchip. Central projects in biotechnology and electronics launched two years ago have run into the sand.

The big surprise is that technocratic centralist France now admits this. The Prime Minister is now being told influentially that these projects must now be decentralized, made more responsive and various. One lesson learned is that while it may be logical for the Institut Pasteur to have just one company — Institut Pasteur Production — effectively controlling applications of Pasteur research, and for the medical research council INSERM to have a similar body controlling applications of monoclonals (Immunotech), commercial and practical realities make such unique relationships inefficient. So change may be expected there, and in many other places where centralism and "logic" have prevailed.

It helps that Curien has room in which to move. His ministry (research and technology) is rid of the short-term problems of heavy industry, which had begun to dominate the old ministry of industry and research in Fabius's time. But useful links between the industry and research administrations have been retained. Curien's budget has also sensibly increased, and there is a prospect of his having more direct power over the budget of a number of organizations (such as the council of agricultural research, INRA), previously only influenced by the ministry.

One immediate task for Curien's ministry is to prepare the budget for 1986, the first year beyond the 1982–85 "law for research" defined by the first socialist science minister, M. Jean-Pierre Chevènement. That could be important. The law as it stands ties political hands. Curien may wish to try something new, such as abandoning the *programmes mobilisateurs* which centralized policy in, for example, biotechnology and electronics.

Another hopeful sign is that French science has loosened up over the past two years. People are more aware of the outside world and more willing to change where change is needed. Even links between research and industry have improved — from a very low base. According to Philippe Lazar, director-general of the medical research council INSERM, "there's been a real shift in the ideology" both in industry and research.

So Mitterrand's new government has brought a sense of hope. But the Fabius honeymoon will soon be over. Then the marriage must begin.

Robert Walgate

UK biotechnology

Advertisement sails near wind

AN advertisement by the biotechnology group Porton International that appeared in *Nature* on 30 August (and in the US journals *Science* and *Bio/Technology*) appears to have caused a flurry of confusion, even discontent, about the relationship between the company and the Centre for Applied Microbiological Research (CAMR) at Porton, the British government laboratory converted from defence to civil purposes five years ago.

Other commercial companies are offended that the advertisement may have been taken to imply that CAMR is either a subsidiary of Porton International or that it may have an exclusive commercial relationship with Porton International. The Public Health Laboratory Service, whose chief function is to provide pathology services and research for British health services, says it wishes to "make it quite clear" that CAMR is "in no sense a subsidiary company of the advertiser".

Even before the transfer of CAMR from the British Ministry of Defence to the Public Health Service Laboratories, CAMR had been keenly interested in the commercial exploitation of some of its projects, notably that for the production of asparaginase used in cancer chemotherapy. Part of the case for not closing the laboratory five years ago was the argument that the British public investment in biotechnology required a laboratory with Porton's experience in microbiology.

The advertisement has given offence because CAMR is described as a component of several of the company's "ten divisions", in which connection it is listed together with operating subsidiaries of Porton International, and because of the use of an aerial photograph of the CAMR laboratory block and another of a new building as "the new production centre at CAMR, Porton". Complainants say that the achievement gives casual readers the impression that the facilities at Porton are the property of Porton International and not the British Government. The advertisement does, however, say (on the same page) that Porton International "has the largest commitment of any company to research and development at CAMR", implying that the relationship between the two organizations is not exclusive.

Porton International, described in the advertisement as an "independent private group whose shareholders include world leading pension funds and institutional investors", is a company recently created by Wesley Haydon-Baillie with funds from UK and overseas financial institutions. Its British subsidiaries include the well-established company LH Fermentation. Porton International also has a licensing agreement on the herpes vaccine developed jointly at the University of Birmingham and CAMR, now in clinical trials, while other collaborative ventures are in the process of being negotiated.

The laboratory staff's views of the advertisement are mixed. Some point out that Porton International is the largest single customer for CAMR's research services, in which role it supports several members of the laboratory's staff and also has a lien on a proportion of the potential output of the production plant. Others, however, still resent the company's use of the name "Porton", first registered for commercial use in 1982.

By some accounts, the appearance of the advertisement may have complicated a series of negotiations which have been under way for some time between the Department of Health and a number of British companies with interests in biotechnology, the chief effect of which would be to convert part of CAMR into a research facility for a commercial consortium. This is not inconsistent with the insistence of the Public Health Laboratory Service that CAMR is independent and "that there is every intention that this independence should continue".

John Maddox

Florida citrus

Burning bugs sole defence

Washington

WITH the discovery last week that citrus canker has spread to four new nurseries in Florida, drastic measures to halt its further spread seem unavoidable. State agricultural officials have been granted authority to burn all infected trees as well as all trees standing within 125 feet of any tree originating from one of the five infected nurseries. The nursery where the outbreak was first discovered, and which appears to be the source of the other outbreaks, has shipped 89,000 trees since January this year.

Meanwhile, a handful of scientists in Florida and at the Department of Agriculture (USDA) Beltsville laboratory, as well as its Animal and Plant Health Inspection Service, are struggling to discover where the infection originated and whether controls more sophisticated than burning can be effective. According to Dr Ed Civerolo of Beltsville, who has studied citrus canker since 1978, the bacterium responsible for the Florida outbreak appears to differ from those found in recent years in Mexico, Brazil, Argentina and Japan. Although of the same species (*Xanthomonas campestris citri)*, the bacteria in different areas exhibit different host preferences and virulence. The Florida bug is the most virulent, attacking all citrus species. Significantly, the Florida strain does not resemble the Mexican, which is a relatively mild version and which is specific for key lines. Initial studies by Civerolo over the past few weeks indicate that unlike all other known strains, the Florida version contains no plasmids; it also differs in fatty-acid composition and is serologically distinct.

Citrus canker last appeared in the United States in 1912, when it took 15 years to eradicate. On that occasion, the bacteria were carried on rootstocks imported from Japan.

Surprisingly, burning is still the only effective control measure. Bactericides have been singularly ineffective in fighting bacterial plant diseases of all sorts; under favourable environmental conditions (such as a hot moist climate and extensive acreages of suitable hosts), the bacteria simply grow faster than they can be wiped out. Bacterial resistance to antibiotics is also a problem.

An epidemiological study is now beginning to trace the source of the latest outbreak. Contaminated growing stock is the most likely source. Although the United States forbids importation of growing stock except for research (and then only under strict quarantine which requires isolation and propagation in greenhouses for a matter of years), USDA officials say they believe a certain amount of stock circumvents the safeguards, entering the country illegally. Since the bacteria infect stems, leaves and fruits, it is also possible that they were carried in on contaminated fruit or other debris that somehow came in contact with the Florida trees.

The United States has maintained quarantines against the importation of citrus fruits from other countries where the disease is present. So far, none has reciprocated following the Florida outbreak. The US Government has, however, imposed an interstate quarantine; only fruits from inspected groves will be permitted out of Florida, and then only if they are dipped in a chlorine disinfectant and if the destination is a non-citrus-producing area. (Texas and California are the other major citrus-growing states.) The most immediate economic effect on the Florida growers, however, is likely to be that of the eradication programme. Compensation is not being provided to those whose trees are destroyed, and the US Secretary of Agriculture could order compensation only after declaring an "extraordinary emergency", which has never been done for a plant disease.

If the infection should become established in Florida, that would not mean the end of the Florida citrus groves. The immediate consequence of infection is disfiguration of the fruits by raised brown spots and a decline in vigour of the trees and of their yield. But in severe cases, substantial defoliation and premature fruit drop can occur, and the trees may ultimately die.

Stephen Budiansky

Danube environment

Hungarians seek outside support

Budapest

THE Hungarian Government has an environmental battle on its hands over a controversial hydroelectric scheme which, among other things, would entail the diversion of the Danube. Ironically, while the fourth environmental engineering exhibition was being mounted last week, an unofficial Hungarian group called the "Danube Circle" began soliciting Austrian support for its opposition to the project.

The project, which includes the diversion of the major part of the Danube waters through a canal to a power station at Gabcikovo in Czechoslovakia, and the construction of a dam at Nagymaros which would flood the most scenic stretch of the Danube, has been undertaken jointly by Czechoslovakia and Hungary. Hungarian environmentalists fear that the dam would cause irreversible damage to the water table of northern Hungary, endangering the water supply of up to 8 million people, and could lead to the disappearance of many species of flora and fauna from the river and its banks. The agreement between the two governments was signed in 1977, but was based on plans drawn up much earlier, when the long-term environmental consequences were little understood.

Between 1978 and 1983 there was considerable criticism of the scheme in the Hungarian media. Political considerations made it impossible for the Kadar government to withdraw unilaterally from the scheme; nevertheless, in 1981, all work on the Hungarian side stopped, allegedly due to lack of funds. Last autumn, moreover, while signing a new agreement reiterating Hungarian commitment to the scheme, the Kadar government managed to reschedule the completion date from 1990 to 1994.

At this point, the Danube Circle launched a petition, signed not only by Hungary's small community of "dissidents" but also by a number of leading environmentalists, some of whom had actually worked on the official survey of the hazards.

The protesters were particularly irate that the Hungarian public had never been allowed to express an opinion about the project, and that, furthermore, no proper survey had been made to establish the global effects and risk factors. The government responded by clamping down on all media discussion of the project — a somewhat unusual response for Hungary, which in general prefers to stimulate public discussion of environmental issues, so as to bring fears into the open and then allay them with a concerted press campaign.

Upstream, meanwhile, an Austrian proposal to build a similar dam at Hainburg provoked a protest petition with more than 150,000 signatures. Presumably in response to this, the Austrian Government proposed an arrangement by which it would partially finance the construction of the Nagymaros power station in return for a supply of power in the future. But according to the Danube Circle, the whole concept of the scheme, which is to top up electricity supplies at peak hours, is impractical, since the Danube is at its lowest in winter.

It is rumoured in Hungary that the government has had second thoughts on the affair and is trying to find a diplomatically acceptable way of withdrawing. (This view is perhaps substantiated by the fact that the International Danube Commission, based in Budapest, is likewise unwilling to comment on the situation, implying that some kind of negotiations are taking place.) If, however, Mr Kadar has been using the excuse of lack of funds to postpone construction works until such a solution can be established, the Austrian proposal to contribute to the construction costs could prove embarrassing.

Vera Rich

Objectivity versus doctrine

SIR — It has been fashionable for scholars on the periphery of science to attack the idea that science can be objective and value-free. This view stems from confusion between different meanings of the word "science" as a highly subjective activity, a methodology that maximizes objectivity and the resulting body of knowledge. Although we have become more aware that unconscious bias is often hard to avoid, the goal of objectivity remains the foundation on which the success of science rests. No less than in Galileo's day, the deliberate introduction of ideological preconceptions into the scientific process undermines its integrity.

I was therefore dismayed that Sir Peter Medawar reviewed *Not in Our Genes*, by Lewontin, Rose, and Kamin, with enthusiasm (*Nature* 19 July, p. 255). Moreover, he even quoted approvingly part of the authors' frank statement of political purpose: "We share a commitment to the prospect of the creation of a more socially just — a socialist — society. And we recognize that a critical science is an integral part of the struggle to create that society, just as we also believe that the social function of much of today's science is to hinder the creation of that society by acting to preserve the interests of the dominant class, gender, and race." Unfortunately, in admiring the goal of a just society, Medawar overlooks the possibility that the authors' commitment to Marxist doctrine would conflict with their commitment to objectivity.

In fact, the authors skilfully distort the views of scientists interested in human behavioural genetics, intelligence testing and sociobiology, condemning research in these areas as worthless rather than as necessarily limited in precision. Indeed, almost no biomedical research could meet their perfectionist standards. Moreover, they project upon their victims a political motivation equal in intensity, but opposite in direction, to their own. They even condemn Kety's classic demonstration of a major role of heredity in schizophrenia, ignoring the fact that genetic studies on this disease are likely to lead, through the reductionist molecular genetics that they decry, to specific chemical therapy.

Historically, this book must be regarded as part of the long campaign of a group from the radical left, called Science for the People, to outlaw the study of human behavioural genetics. While most of the book repeats this group's earlier arguments, there is one major shift. After many years of trying, with little success, to convince the world that genes have little to do with individual differences in behaviour or in potential, Lewontin *et al.* now deny any such naive cultural determinism and adopt the position long held by their opponents: intelligence is the product of gene–environment interactions. But their turnabout seems to be more a matter of strategy than of convinction: note the title of the book, and the statement that J.B.S. Haldane and H.J. Muller "argued (along lines that we would not) that important aspects of human behavior were influenced by genes" (p. 73). Moreover, instead of gracefully seeking an end to the sterile polemics, they claim the high middle ground of interactionism for themselves, and they cast down their opponents with the epithet "biological determinist" repeated (in a familiar political tactic) on virtually every page.

The authors are unusual not only in the righteousness but also in the manners that they bring to scientific controversy. For example, after quoting Louis Agassiz's assertion (in the nineteenth century) that the human sciences can in principle be freed of politics and religion, they add that "The sentiment was echoed in 1975 by yet another Harvard professor and biological determinist, Bernard Davis, who assures us that 'neither religious nor political fervor can command the laws of nature'". Then follows another quotation from Agassiz: "the brain of the negro is that of the imperfect brain of a seven-month infant in the womb of the white".

As a reviewer has noted, this slur, passing three authors and an editor, says much about the intent of the book (see M. Konner, *Natural History*, August 1984, p. 66).

Why does such doctrinaire and ambiguous rhetoric appeal to many thoughtful people, as it has to Medawar? Obvious reasons include the past misuse of genetic theories to support racism, fear that genetic studies of behavioural traits might reveal differences between races and the belief that it is racist even to entertain that possibility. But this belief, however well intentioned, is profoundly illogical: racism is the willingness to have race, rather than individual qualities, determine a person's social treatment. Moreover, modern genetics has made a major contribution to the struggle to overcome this evil. For the intellectual justification of racism has been the ancient assumption that the differences between races are typological — that all the members of one group differ from all the members of another. But in contrast to the naive support of this view by certain geneticists in the past, modern population genetics has utterly destroyed its typological foundation. We now know that the genetic differences between races (except for some physical traits subject to climatic selection) are statistical and overlapping, and so one cannot infer an individual's potential from his race.

Future advances in understanding human diversity could also help us to reach humanitarian goals, by improving our efforts to develop individual potentials. To be sure, since knowledge of genetic differences, like almost any scientific knowledge, could be used for ill as well as for good, it is understandable that some people focus on the immediate danger. But the shift of genetics from typological to populational thinking encourages confidence that its further advances can have a constructive social impact.

It is sad to see one with Medawar's eminence, and with his credentials as a writer on the philosophy (and on the manners) of science, lending credibility to this book. He does criticize its attack on reductionists, because he finds that they simply do not exist as described. But he does not question the existence of biological determinists, even though they are equally imaginary among modern biologists. He also approves what he terms the "right-thinking" quality of the book. But "right-thinking" (or orthodoxy) is a dangerous concept in matters involving science. If it refers only to the general goal of a just society, or to Medawar's stated belief that the world is in need of change, fine — but if it encompasses or condones political bias in the evaluation of science, it presents a grave challenge.

The extreme positions and the political propaganda presented in *Not in Our Genes* are unlikely to influence the views of many scientists close to the field. Nevertheless, the book may convince lay readers, and it will surely have a distorting influence on the public image of science.

BERNARD D. DAVIS
Bacterial Physiology Unit,
Harvard Medical School,
Boston, Massachussetts 02115, USA

Genes-on

SIR — We now have quite a large number of types of gene. It might be sensible to suggest they are all named in the same way, so that they can be instantly recognized, as enzymes are with their "ase". Maximum simplicity and clarity may be achieved if they all ended with "on", with enough on the front end to indicate their function or status. We have already: recon, muton, replicon, codon, cistron, operon, transposon, regulon, exon, intron operon. There must be others I have not thought of.

Recently a new gene with a widely conserved sequence which may control development in a wide range of segmented animals has been announced, how about "onton"? This would go well with a single oncogene being called an oncon.

Other conversions could be: plasmogene into cyton for cytoplasmic genes; palaeogene into palon; neogene into neogon; regulator into represson (distinct from regulon which means something else).

Perhaps a modern geneticist should define all these terms as proper units, so that we may all express ourselves with precision.

J.R.LLOYD
Westcott House, Sherborne,
Dorset DT9 3HF, UK

Mistreatment of laboratory animals endangers biomedical research

from Christine Stevens

There is now an opportunity for legislators in the United States to rescue medical researchers from themselves.

In the United States, laboratory animals are used in much greater numbers and subjected to far more neglect and mistreatment than elsewhere, in Britain for example. The reason for this is simple: US law does not come to grips with pain prevention. In the absence of an adequate regulatory regime, an all too casual attitude has developed. Pain relief, or indeed any sort of post-operative care, is often omitted in laboratories, test procedures are unnecessarily duplicated and even the minimal standards of care required by current law are routinely ignored. These negligent attitudes are reinforced by a chronically short-staffed and underfunded federal enforcement programme on the one hand and, on the other, an aggressive lobby of commercial animal suppliers whose objective is, simply, to sell as many animals as it can to researchers and testers.

New Bills

An opportunity has now presented itself to bring the federal Animal Welfare Act up to a level roughly comparable with the laws governing the use of laboratory animals in Britain and fourteen European countries. Congress has been presented with two legislative proposals, the Senate with a bill (S.657) introduced by Senator Robert Dole (Republican, Kansas) and the House of Representatives with one (H.R. 5725) introduced by Representative George Brown (Democrat, California), both of which have been endorsed by the American Veterinary Medical Association. Unfortunately, opposition organized largely by the trade association representing laboratory animal breeders has so far prevented these proposals from getting anywhere.

There is no shortage of examples of the current act's deficiencies. The only pain-reducing provision is a deliberately vague phrase included under a general requirement for "adequate veterinary care" which calls for "appropriate use of anaesthetic, analgesic and tranquillizing drugs". Public scrutiny of compliance with this provision is provided only by a requirement that laboratories list the numbers of painful experiments and tests conducted without such drugs, and then note the reason in a one-page annual report.

As a result, compliance even with this vague requirement has been casual in the extreme. The majority of medical schools boldly claim, year after year, that all the pain and distress they cause experimental animals is prevented by pain-killing drugs. (Pharmaceutical houses tend to be more honest in admitting that they inflict suffering; this they usually blame on the testing requirements imposed by the Food and Drug Administration.)

Under the current law, it is entirely up to the researcher to determine whether pain-relieving drugs are necessary. Edward Taub, who received much publicity after the National Institutes of Health (NIH) suspended support for his research on deafferented monkeys, claimed that his superior knowledge made veterinary advice unnecessary. He claimed that no pain-relieving drugs were needed because sensory nerves were cut in the procedure he was using. But Dr William Pryor, the laboratory veterinarian at East Carolina University, testified before a Health and Human Services Department appeals panel to which Taub had taken his case that analogous procedures on humans result in great post-surgical pain, and he recommended an analgesic specifically suited for the purpose.

At the University of California at Berkeley, researchers charged that graduate students conducting major surgery, including the removal of eyes from cats, in Dr Russel DeValois's laboratory, often administered anaesthesia incorrectly. One witness said, "From the high-pitched squealing of the kitten, it was obvious that the animal was experiencing intense pain".

The Dole/Brown proposals would impose the very modest requirement that researchers consult with a veterinarian in the planning of any procedure involving pain to unanaesthetized animals. The bills would also require that post-operative care be provided and that proper staff be available at nights and on weekends. This might do away with the scheduling of surgery at entirely inappropriate times, as happens now. I have seen unconscious post-surgical dogs left in a room with twenty other barking dogs at 3.30 on a Friday afternoon "Been doing some cutting today?" the veterinarian said to a caretaker down the hall. "Yeah", he nodded.

British act

Before giving further examples to illustrate the need for improved legislation in the United States, I should note that about thirty years ago, I went to Britain at the suggestion of my father, Robert Gesell, Chairman of the Physiology Department at the University of Michigan Medical School, to consult those whom he considered the best biomedical scientists to get their views on the British act regulating animal experimentation. I spoke to Sir Alexander Fleming, J.B.S. Haldane and many other distinguished investigators, and visited their animal rooms.

Even though funds were extremely limited at the time (just after the Second World War), I found the animals far better housed and looked after than in most of the American universities I have recently inspected. Fleming's rabbits were fine-looking creatures, at ease in cages big enough for them to take a hop or two and sit up in the classic Easter rabbit pose if they felt so inclined. Haldane's newts lived in large well-furnished aquaria. In the dog laboratories I visited, the dogs occupied good-sized pens — in sharp contrast with the small cages stacked to the ceiling in many US dog rooms of the period, where the cages were commonly hosed with the dogs still inside trying to dodge the stream of water.

No scientist I interviewed during my visit complained of the British Cruelty to Animals Act. Indeed, I was told that it was of much value in bringing home to young research workers their responsibilities to experimental animals. Neither the individual licences nor the pain conditions under which they worked were burdensome. The general attitude was summed up later, when Sir Graham Wilson and Dr Lawrence Abel came to the United States to testify at a Congressional hearing on 30 September 1965. Dr Abel, a former vice-president of the Royal College of Surgeons, said in part: "We do not commit the atrocities which are reported from time to time in some other countries. We do not allow the extravagant cruelty committed by some investigators of stress and shock. We have proved that the desired results can be obtained by less inhumane methods". This testimony was so telling that the subcommittee chairman, to whom a word from NIH was law, decided to suppress it. The second day of the hearing was cancelled, and the hearing record was never published.

I returned from Britain convinced that the British act was a boon to animals, admired by British scientists and altogether most valuable despite its age and the need, in certain respects, for updating.

But on the other side of the Atlantic, there was a violent reaction by groups such as the National Society for Medical Research when a streamlined bill built on the principles of the British act was introduced by 13 leading senators. NIH's public response was less frenetic but equally adamant. NIH even went so far as to withdraw and secrete hundreds of copies of a substantial study it had contracted for because the report clearly showed widespread mistreatment of experimental animals and indicated a need for regulatory legislation.

Blocking tactics

Senator Lister Hill, named after the illustrious British bacteriologist, was NIH's man in the Senate, and he loyally sat on the bill for six years, refusing all attempts to get it to hearings in the committee he chaired. Not until a stolen dalmatian, trucked across state lines by a dealer in laboratory dogs, ignited an unquenchable public interest, did legislation on laboratory animals reach the Senate floor via a different committee. As soon as it did, the vote to protect the animals was unanimous. Unfortunately, the bill (although opposed as fiercely as the better drafted bill based on the British Act) was weak and narrow in its coverage. Amendments passed in 1970 and 1976 finally gave the Secretary of Agriculture authority to include all warm-blooded animals, and required users to report painful experiments and tests conducted without anaesthetic, analgesic or tranquillizing drugs.

Mistreatment of laboratory animals in the United States in some cases involves a failure to provide even basic care, let alone pain-relieving drugs. For example, at the Veterans Administration (VA) Hospital connected with Stanford University Medical School, a medical student working late was startled to find an experimental dog collapsed at the door of his room. He promptly called the VA veterinarian, but she refused to come to treat the obviously suffering animal, so the student took the dog to the veterinarian on duty at the emergency service, who determined that it was past any possible treatment and euthanized the animal. A necropsy showed nothing but hair in the animal's stomach. The festering sores showed no sign of treatment. The hospital's claims that nothing was seriously wrong and that another dog had inflicted the injuries were hopelessly unconvincing.

Refusal to acknowledge error, no matter how grossly evident, appears to be a common weakness among those who neglect and/or mistreat laboratory animals.

The veterinary inspectors of the US Department of Agriculture (USDA) sometimes try to use their limited authority under existing law to require proper procedures. For example, at the University of Chicago, brain surgery was being conducted on squirrel monkeys in an office off a busy corridor. An office table was used as an operating table. Instruments were not properly sterilized. The inspector called for immediate transfer to one of the university's regular operating rooms.

The proliferation of poorly controlled experimentation in dozens of sites on a campus makes USDA's task difficult, and since the financial provision for enforcement of the Animal Welfare Act has never been adequate, it has sometimes been years before every nook and cranny where animals are stowed away has been ferreted out. At the University of California at Berkeley, it took a new inspector to find them all. USDA finally brought a case against the Berkeley campus, charging major violations. The case was recently settled when the university agreed in a "consent decision" to pay a $12,000 fine, establish a training programme for animal handlers and to "cease and desist" from violating the Animal Welfare Act.

The seeming inability of this institution to control its faculty and students is revealing in the light of the thick report of its own specially constituted committee emphasizing that "more diligence on the part of the investigators and better discipline of the caretakers at a minimum of additional costs" would resolve most of the problems. A typical USDA inspection report reads: "Monkeys in room G25 are fed by placing feed in waste pan under floor grill — no feeders present . . . in many rooms a build-up of faeces . . . no regular observation of animals by caretaker under veterinarian's supervision. Some question of DVM [Doctor of Veterinary Medicine] even having access to animal quarters let alone establish an adequate programme of veterinary care."

Reports for all 1,166 Registered Research Facilities in the United States may be obtained under the Freedom of Information Act (FOIA); the Animal Welfare Institute [of which the author is president] has been studying a series of these over the past six months. The reports are astonishing — Harvard, Yale, Johns Hopkins, Vanderbilt, the universities of Utah, Rochester, Pittsburgh, each receiving between $17 and $51 million a year from NIH, all accredited by the American Association for the Accreditation of Laboratory Animal Care, regarded by NIH as an ironclad guarantee of first-class care and treatment of animals, repeatedly violate USDA's minimum standards.

Most frequently recurring are: cages too small for monkeys, dogs and rabbits to make normal postural adjustments, green scum in the water bottles, inadequate ventilation, and just plain filth. These notes on the University of Utah are typical: "Primates have inadequate space . . . filters are pretty well plugged with hair . . . large rabbits [weighing] 9 to 11 pounds have 432 square inches and they should have at least 540 . . . some of the cages are not high enough that rabbits can stand up . . . feed in some feed containers contaminated with urine from top cage." Or from Rochester: "Primates in Room 6-7573B are being kept in cages which have not been sanitized for over 6 weeks." At Pittsburgh: "The [cat] room did not appear to have been cleaned since the last inspection . . . 24 hours for correction." At Harvard a list of 23 different animal rooms housing dogs, cats, guinea pigs, rabbits, gerbils and monkeys used old, rusty, difficult-to-clean cages. The inspector also noted "loose sharp wires" and wrote "it appears sanitation is non-existent while animals are in isolation chambers". One might suppose that correction would be automatic when USDA inspectors write such comments and the institution's attending veterinarian signs off on them. But unless the inspector actually recommends that USDA's General Counsel prepare a case against the institution, the deficiencies frequently drag on, as documented in the Animal Welfare Institute's files.

The USDA inspectors urgently need the increased authority that the Dole and Brown bills would give them, and they need the assistance which institutional committees under this legislation would provide. Key provisions include the appointment of a committee member not employed by the institution "responsible for representing community concerns regarding the welfare of animal subjects", and the requirement that the committee make semi-annual inspections of "all animal study areas and facilities". In addition institutions would be required to inform their employees to report violations of the law to the institutional committee so that prompt corrective action can be taken. Employees would be protected from discrimination against them which many fear at present if they request better treatment of animals.

The basic purpose of the Dole and Brown bills is to prevent needless suffering before it occurs. By putting all personnel on notice that they are not to turn a blind eye to such suffering, the observant and compassionate would occupy the position now frequently usurped by the callous and domineering. All too often, when I visit laboratories I hear the words, "but don't say I told you". This is absurd when the heads of institutions urgently need to know about mistreatment of animals. If they do not know and thus cannot take effective corrective action, they are increasingly likely to find themselves in the embarrassing position that scandals nobody dared to tell them about are publicly revealed. The consequence of that will be increasing erosion of public faith in institutions supported by the tax payers.

Prevention of needless suffering would also be advanced by the provisions of the Dole/Brown bills that aim to eliminate the wasteful duplication of animal experiments and tests. Unintended duplication of government tests was estimated in 1981, by the head of the Interagency Regulatory Liaison Group, to have wasted thousands of millions of tax dollars, yet there is nothing in the Animal Welfare Act as it stands to prevent recurrence of this needless use of animals. The Dole/Brown bills would establish an information service, in cooperation with the National Library of Medicine, to prevent such duplication. (Purposeful replication of research would be unaffected.) This service would also handle information on alternatives to animal experimentation and testing.

Enlightened self-interest alone should cause every medical school to back the Dole and Brown bills. Failure to protect an investment of millions of dollars by supporting reasonable legislation is shortsighted. But such is the prejudice against legislation, especially on the part of those who do not read the words but rely on lobbying organizations' generalizations, that the Dole and Brown bills are still widely resisted. Organizations that fought the 1966 Laboratory Animal Welfare Act with almost hysterical intensity now, having become accustomed to it, join in testimony before Congress to increase support for its enforcement. No doubt they will do the same if the pending amendments to improve the law are passed.

But the opposition is stepping up its activities. At least that is the sinister reading of the recent decision by the executive director of the Association for Biomedical Research (ABR) to move to Washington, DC. ABR was founded in 1979 by a small group of animal breeders (including Henry Foster, founder of Charles River Breeding Laboratories, the largest purveyor of laboratory animals in the world) and biomedical researchers who felt a need for "active representation" on legislation affecting the use of animals. The organization includes about 200 institutions, including medical schools, pharmaceutical companies and breeders, who depend on animal research. Anyone who doubts that animal research is big business should examine the case of Charles River, which began as a two-room rat-breeding facility and which was recently acquired by Bausch and Lomb, the optical company, in a stock transfer that netted Foster nearly $38 million, according to press accounts.

The spectacular growth of the industry might be slowed by the Dole/Brown bills' requirement that investigators consider alternatives to animals, and by the information service that the bills would establish to provide facts on "methods which could reduce or replace animal use".

Not surprisingly, ABR has favoured substitute legislation sponsored by Senator Orrin Hatch (Republican, Utah) and Senator Edward Kennedy (Democrat, Massachusetts) that would call on the National Academy of Sciences to conduct an 18-month study of the current use of animals in research. This legislation has already been passed by the House of Representatives, incorporated as part of the NIH authorization bill.

Although ABR says that a study is needed in order to determine whether problems really do exist in the use of research animals, its director, Frankie Trull, offered a possibly more candid explanation of its support for study legislation in a recent talk she gave to faculty, staff and students at the University of Illinois at Chicago Health Sciences Center. Trull told the audience: "Now, we are criticized for being strong proponents of study legislation by animal welfare organizations who say this is a stalling tactic. Well . . . none of us was born yesterday. The fact of the matter is that, in some ways, it is a stalling tactic." And in response to a question from the audience on how to deal with the media, Trull offered this advice: "You don't answer their questions. In other words, they'll say, 'isn't it true that 83 per cent of all animals had pain-killing drugs withheld during experimentation in your facility last year?' By the way, they know all that stuff. God bless the Freedom of Information Act, they know everything about everything. What you do is you say something like, 'In 1983, in our research institution, we were able to develop a breakthrough in Alzheimer's disease.'" Trull warned that unless researchers take the fight seriously, what happened in Britain could happen in the United States. "England has had horrendous problems, historically, with antivivisectionists . . . there is no question in my mind that the English, in fact, really truly do like their animals better than their people."

In calling on her scientific audiences to do battle with "the other side", Ms Trull deliberately fosters confusion between soundly based regulatory legislation and antivivisectionist sentiment. She emphasizes the rash of break-ins by animal rights groups. "The reason I say please clean up your own shops is that the break-ins are inside jobs, every one of them. By inside jobs, I mean that some sincere, genuine animal technician or cage cleaner or whatever, goes to an animal rights rally or reads an article in a magazine and wants to help the other side. Every single one of the break-ins in the 30 or 40 we're aware of involve inside jobs."

A rational response to this would be to enact the appropriate legal escape valve in the Dole/Brown bills so that personnel who observe mistreatment of animals are protected against reprisals when they blow the whistle — and that a local institutional animal care committee exists to receive such complaints, investigate, and order the problem corrected. But such a sensible procedure is anathema to ABR, which thrives on an "us and them" mentality.

Edmund Burke's advice to choose early reform, which he described as "accommodation with a friend", as against late reform or "capitulation to an enemy," is lost on the lobbyists who fight against proper regulation of animal experimentation. Thus the biomedical community, which needs the Dole/Brown bills as much as the animals do, is listening to badly biased advice inspired by vested interests that seek to increase commercial profits on animals, equipment and services.

Pain clause

Most European countries have legislation which addresses pain prevention, often more specifically and strictly than the Dole/Brown bills. The pain conditions in the British act, for example, which have proved workable over more than a century, have spared great pain to large numbers of animals. The proposed bills require assurances that paralytics may not be used without anaesthesia, and pain relief or euthanasia may not be withheld when not scientifically necessary, much milder provisions than those which obtain in Britain.

At present, it is common for animals to be left to die in agony, and no law requires that they be euthanized even when the experiment is over. Nor does current law specify that dogs must be released for exercise outside their cages. The Mayo Clinic is still hosing cages with the dogs inside. Small wonder that contagion is rife among the more than 500 dogs recently viewed by the 13 owners of stolen dogs that Mayo had purchased, despite repeated warnings that many of the dogs they kept buying seemed to be pets. Before the recent scandal broke, Mayo even bought dogs at the laboratory door. Now a sign is posted: "All please note. We no longer purchase dogs from individuals. But we continue to take them as gifts." It was through this unexpected review of Mayo practices that the dehydration of Mayo dogs came to light. Two owners reported that their dogs immediately drank five-quart pails of water on their return home, so intense was their thirst.

It is only natural for people to become angry when the privilege of using laboratory animals is so grossly abused. The US Congress and people generally want the abuses stopped. Neither Congress nor the overwhelming majority of the public want a ban on experimentation. Scientists of good will should recognize this, reject the paranoia sown by lobbyists and join with legislators such as George Brown, a tried and true friend of science, and Senator Dole, whose record on fiscal responsibility has earned him great respect for sound decision making.

"Those who experiment upon animals", Albert Schweitzer wrote, "by surgery and drugs or innoculate them with diseases in order to be able to help mankind by the results of pain, should never quiet their consciences with the conviction that their cruel action may in general have a worthy purpose. In every single instance, they must consider whether it is really necessary to demand of an animal this sacrifice for men. And they must take anxious care that pain be mitigated as far as possible." □

Christine Stevens is President of the Animal Welfare Institute, Washington, DC, 20007, USA.

New ways with solar neutrinos

The discrepancy between predicted and measured neutrinos from the Sun is an embarrassment. Now there are two schemes for improving on past measurements. They deserve serious backing.

MUCH of the present excitement in cosmology rests on the recognition that there must be a close connection between this conceptually esoteric field and high-energy particle physics, the stamping-ground of those who would push experimental measurement to the limit. The result is that people are always speaking in measured tones about the common ground between the very large and the very small.

And there are successes on the record. Astrophysics shows the neighbourhood of a neutron star to be a kind of natural high-energy physics laboratory. The abundance of deuterium relative to hydrogen in the Universe now is almost exactly that calculated from the assumption that the big bang was a time when particles now unstable were predominant in the Universe. And the temperature of the microwave background, 2.7 K, while it is explicable in other ways, is consistent with the view that the whole world was once a high-energy physics free-for-all. So is it not at least a minor scandal that there persists such uncertainty about the Sun's output of neutrinos? Especially when the energies supposedly carried by those particles are measured in MeV, not the GeV which are now the common coinage of the particle physicists?

It is now more than a decade since R. Davis Jr reported the first results with his unique neutrino detector, essentially a huge tank containing 380 cubic metres of tetrachloroethylene buried deep in the Homestake Mine in Colorado. The simple objective was to count the number of chlorine-37 nuclei converted into argon-37 by interaction with a neutrino (and the subsequent loss of a negative electron). The difficulty, ten years ago, was that the rate of conversion and thus the inferred intensity of the neutrino flux was almost an order of magnitude less than expected from what is known of the nuclear reactions in the Sun. All this is now part of the general lore.

Not much has happened since. Or, rather, there has been much talk and speculation but very little experiment. For a time, there was some hope that the discrepancy might be explained away on the basis of the experiments carried out by F. W. Reines at the University of California, Irvine, whose reports of neutrino "oscillations", the quantum mixing together of different types of neutrinos to form the neutrinos of the real world, also bore on the possibility that neutrinos may have a non-zero mass.

But that line of thought has become unfashionable. The experiments are not easy to repeat, and in any case the cosmologists no longer hope to close the Universe with neutrinos of small mass (a fraction of that of the electron). And while the Davis measurement may be reconciled with expectation by using extremes of several astrophysical parameters, leading in particular to a low core temperature, that seems an ungainly way out of the difficulty.

So what is there left to do? Simply elaborating the Davis measurement would be unprofitable, with a rate of conversion of chlorine into argon only barely above the background. J. Bahcall at Princeton has for the past six years been canvassing the use of gallium-71 as a detector isotope. He would buy a stock of several tons of gallium metal, bury in a mine for several years and then sell it back to the original owners. That device would have the virtue of being sensitive to the least energetic and most abundant neutrinos from the Sun, those produced by the direct interaction of protons. One of these fiscal years, the US Congress may look kindly at the project.

Meanwhile Davis (at the Brookhaven National Laboratory) and a group of colleagues scattered over the United States have suggested yet another neutrino detector. The principle is again the same — convert an isotope of one element into an isotope of another by neutrino interaction, making sure that scores or hundreds of atoms of the product can be measured. The new plan is to convert bromine-81 into krypton-81 (again by the absorption of a neutrino and the loss of an electron). But this time, the product is only weakly radioactive (with a half-life of 200,000 years).

In principle, the experiment (if ever carried out) would have the advantage of being neatly complementary to that proposed by Bahcall. Indeed, bromine-81 nuclei would interact only with neutrinos whose energy exceeded the threshold of 470 keV, which implies that they would be converted into krypton nuclei chiefly by neutrinos arising within the Sun from the radioactive decay of boron-7.

The hope that the quantities of krypton-81 produced can be measured will stretch most people's credulity. If the calculations are correct, krypton isotope atoms should accumulate in the 380 cubic metres of the tank (supposed filled with an organic compound of bromine) at a rate of about two a day, or some hundreds every six months. How are such small quantities of a stable isotope to be detected?

Obviously it helps that krypton is a rare gas, essentially insoluble in organic liquids. Indeed, using their tank filled with its organochlorine liquid, Davis and his group have been able to test the feasibility of what they propose. Having a system for the extraction of argon from the tank, they can just as easily isolate krypton. They find that leakage of atmospheric krypton into the system should not be a serious source of whatever krypton-81 might be produced by neutrino conversion. After say a year, their bromine tank might contain 1,000 atoms of artificial krypton-81.

But how to measure such tiny amounts? Perhaps because they are anxious not to discourage potential backers, the authors make light of the difficulties in their account of a simulation they have carried out (G.S. Hurst *et al. Phys.Rev.Lett.* **53**, 1116; 1984).

The technique consists merely of repetitive mass spectroscopy. Atoms of krypton-81 in what is supposed to be a mixture of krypton isotopes are selectively ionized by a suitable laser and then accelerated selectively and embedded in a silicon target. Since the ionization process will not have been entirely selective, the embedded atoms can be recovered by heating (again with a laser) and put through the process a second time. And, if necessary, a third. Finally, the atoms are embedded in a copper/beryllium target.

Whatever the likelihood that the technique will eventually settle the problem of solar neutrinos, it seems certain to be used widely in other connections. What the authors show, however, is that starting with a sample containing 1,000 atoms of krypton-81 and the contamination expected in a neutrino experiment, they should be able to count as few as 300 atoms. Laser improvements already foreseen should reduce the limit to about 100 atoms.

For many people, this would be sufficient. But plainly Davis and his colleagues intend a renewed assault on the measurement of solar neutrinos. Indeed, they talk of the design of their complementary detectors as the first steps in the spectroscopy of solar neutrinos. They should be given a chance to put their scheme to work and save the nexus of cosmology and physics from the embarrassment on its doorstep.

John Maddox

Atmospheric chemistry

Implications of Arctic air pollution

from S.A. Penkett

IN winter, the southward movement of the polar front allows air from polluted regions of the Northern Hemisphere to be transported into the Arctic, giving rise to a phenomenon known as 'Arctic haze'. This can lead to a visibility in this pristine area of the Earth's atmosphere of as low as 5 km. The scientific community has been aware of the phenomenon for several decades but a detailed study has been impeded by the remoteness and inhospitable nature of the region. Recently, a series of 28 papers has been published (*Geophys. Res. Lett.* **5**; 1984), describing experimental data obtained in a three-dimensional coverage of the atmosphere from Alaska to northern Norway. The papers deal with the meteorology that causes the phenomenon, and with many other aspects which have relevance to such topical concerns as the long-range transport of acidity and climatic change caused by anthropogenic activity.

The results mostly come from the Arctic Gas and Aerosol Sampling Program. It involved the use of six aircraft flying over the Arctic, collecting information on the nature and concentration of the particles making up the haze and on the composition of the associated air. The programme was organized by Russell C. Schnell from the University of Colorado. Scientists came from the United States and Europe, with the majority of the Europeans coming from the Norwegian Institute for Air Research. Funds were provided by the National Oceanic and Atmospheric Administration and by the British Petroleum Company. It is an example of the sort of cooperative programme that has to be mounted if air pollution problems of regional or global significance are to be tackled in detail.

Previous studies at ground level had shown that the aerosol consists mainly of fine particles in a relatively narrow size range (0.2 - 0.4 μm). Its major constituent is sulphate, but because of the presence of substantial amounts of black carbon, it has been referred to as a 'combustion' aerosol. The major source areas are Europe and north-west Asia and the intensity is greatest in March and April. The aircraft surveys took place during this period and showed the presence of a complex layered structure, with well defined 'fronts' dividing clean and polluted air. The structural discontinuities are very similar to those found at the boundaries of cirrus clouds, suggesting high thermal stability and lack of turbulence throughout much of the Arctic atmosphere in winter conditions.

The origin of the fine particulate is thought to be anthropogenic but new evidence is presented of the possible volcanic origin of the giant (>2 μm diameter) particles. These are spread uniformly at latitudes from 0.3 km to 5 km and are not correlated with the haze layers.

Much of the sulphate in the haze layers is in the form of sulphuric acid and by contrast with other anthropogenic aerosols collected in urban areas of Europe and the United States, there is very little nitrate. The same is also true of the composition of snow samples collected in Spitzbergen.

The low abundance of nitrate is very intriguing. It could indicate that the aerosol is directly injected from combustion processes in the source regions and, indeed, evidence is presented to show that during the Arctic winter, particulate sulphate is not formed by atmospheric gas-to-particle conversion on any significant scale. (That is perhaps not unexpected because of the almost complete absence of any atmospheric photochemistry in the region during the winter months.) A photochemical process may be possible, however, in the source regions at lower latitudes, in March and April. A thorough chemical study of Arctic air pollution may shed light on acid formation in the atmosphere in general. Specifically, measurements of nitrogen oxides and peroxyacetylnitrate, as well as sulphur dioxide, would define the emission characteristics of the source region and the nature of the chemical reactivity of its atmosphere in early spring and late winter.

The geographical origin of the air carrying the haze components has been investigated in several ways. One is by analysing the distribution of trace metals. High concentrations of elements such as nickel, lead and zinc may be traceable to smelters at particular locations deep inside the Soviet Union.

Another specific source of particulate material was identified in aircraft flights across a fold in the tropopause: volcanic debris was found to be entering the troposphere from the stratosphere in March 1983, presumably from the eruption of El Chichón in 1982. Considerable evidence of the influence of volcanoes on the particulate content of the Arctic atmosphere is stored in ice cores from Greenland. By contrast with the measurements reported for Spitzbergen, the Greenland ice core data suggest the presence of summer maxima in nitrate concentrations. Extensive studies of the composition of the ice in different parts of the Arctic could provide interesting details on the distribution of source areas.

Measurements of many gaseous species, including sulphur dioxide, ozone, halocarbons and hydrocarbons, are reported. Aircraft measurements show rather small fluctuations in the ozone vertical profiles, and no large changes within or outside the haze layers. The sulphur dioxide concentration peaks in phase with the aerosol in March–April. Large seasonal variations in the concentrations of many other gases were found. In winter, the Soviet Union seems to be a particularly abundant source of hydrocarbons, with the result that the concentrations of propane and butane are as high in March on Spitzbergen, as in air close to London in August. If these values are representative of the whole of the Arctic region, huge reservoirs of these gases could be built up during the winter to be consumed by tropospheric chemistry at lower altitudes as meteorological and sunlight conditions allow. This would probably lead to the production of large amounts of ozone in the troposphere of the Northern Hemisphere and may account for some of the interhemispheric asymmetry observed for this important trace gas.

The profusion of measurable trace gases, including five distinct bromine-containing species, and the absence of photochemical change in the Arctic winter, may allow a specific categorization of air mass sources. It is not unlikely that their relative concentrations will act as a 'fingerprint' for a source area as with no change in distribution during transport, the 'fingerprint' will remain intact over air-mass tracks of many thousands of miles. A detailed examination could form the basis of an effective large-scale tracer experiment.

Many papers deal with the climatological consequences of the Arctic haze. The planetary albedo can be changed significantly by modification of light scattering, such that an increase of 2.5 per cent over the oceans and a decrease of 9 per cent over the icecap is predicted. The presence of graphite particles in the haze layers (at concentrations within a factor of 2 of those recorded in some cities in the United States) has a substantial effect on the optical depth of the atmosphere and is predicted to increase the energy absorbed by the Earth–atmosphere system by as much as 5 per cent. The climatic effects of aerosols of this type, injected into the atmosphere as a result of a large-scale nuclear exchange, are of much current interest. Fortunately, the Arctic haze phenomenon is on a much smaller scale, but studying it may provide quantitative data which can be used to test predictions of the temperature changes likely to be experienced in the aftermath of a large-scale nuclear war. □

S.A. Penkett is in the Environmental and Medical Sciences Division, AERE Harwell, Oxfordshire OX11 0RA.

Malaria

Blood-stage antigens cloned

from K. N. Brown

THE development of DNA cloning and bacterial expression techniques has opened up a new approach to studying the antigenicity of malaria parasite and, perhaps, to developing a malaria vaccine. Five groups[1-5] have recently achieved expression of cloned genes encoding sporozoite and blood-stage proteins of the human malaria parasite (*Plasmodium falciparum*). Intriguingly, four of the antigens contain short repetitive sequences. The significance of these sequences is not known, but they may have a role in generating antigenic diversity and preventing host immunity.

Two papers[1,2] were discussed recently in these columns[6]. Of the others, Coppel *et al.*[3] have cloned an antigen associated with the membrane of infected erythrocytes. Immunoprecipitation and immunoblotting identified the antigen as a 155,000-molecular-weight (155K) acidic protein although some sera also reacted with a 210K polypeptide. The smaller molecule is found predominantly in the immature 'ring'-stage parasites and the 210K antigen in mature parasites. This may indicate a precursor–product relationship, particularly since the mRNA appears to be abundant only in fully mature parasites. Presumably the 155K portion is carried into erythrocytes by invading merozoites. Sequence data show a subunit structure of five repeats encoding Glu-Glu-Asn-Val-Glu-His-Asp-Ala. Immediately C-terminal are repeats of Glu-Glu-Asn-Val codons with Glu-Glu-Val interspersed irregularly. There is so far no evidence that antibody reacting with the membrane antigen of ring-infected cells is protective.

Another gene encoding a repetitive sequence, in this case one of nine amino acids, Glu-Glu-Val-Val-Glu-Glu-Val-Val-Pro, and associated with the membrane of erythrocytes infected with mature parasites, has been isolated by Koenen *et al.*[4] (see page 382 of this issue). Early work showed that erythrocytes infected with mature trophozoites and schizonts had exposed antigens. Two of the antigens on schizont-infected cells have been characterized: an antigentically diverse polypeptide possibly associated with the 'knobs' of *P. falciparum*-infected cells[7] and the phenotypically varying SICA antigen of *P.knowlesi*[8]. Whether the sequence identified by Koenen *et al.* relates to either of these polypeptides, and indeed how these two types of antigen are related, remains to be determined.

Of the cloned antigens of asexual erthrocytic parasites, the only ones known from *in vivo* evidence to have some significance for protective immunity belong to a family of polypeptides occurring in all species of mammalian parasite so far examined and varying in size from 190K to 250K. The effectiveness of protection induced varies greatly with the host–parasite combination used[5,9]. In this issue of *Nature* (page 379), Hall *et al.* report that vaccination of Saimiri monkeys with one member of this family, the *P. falciparum* p190 antigen, provides slight protection[5]. This antigen shows extensive diversity between isolates, although there are common epitopes present on the molecule, and many different serotypes can be isolated from one patient[10]. The antigen, or a processed part of it, is present on the merozoite. Hall *et al.* have cloned what is probably its C-terminal end. The sequence is non-repetitive, but it would be surprising if repetitive sequences did not occur elsewhere in the molecule since merozoites and sporozoites are similar in ultrastructure and in function, both being designed to penetrate cells, and the sporozoite surface antigen has well characterized repeat sequences.

Extensive phenotypic variation during chronic infection has been demonstrated for several surface-exposed parasite antigens, including possibly the 190–250K family. It may well be that variable sequences are inserted into all the exposed antigens of malaria parasites, which would provide a solution to two problems: restriction of numbers to ensure host survival and continued parasite survival for vector transmission. Phenotypic antigenic variability is seen in protozoa other than the malaria parasite. The ciliate *Paramecium* is a classic example of a free-living protozoan which adapts its surface macromolecules to environmental change; the changes are readily detectable serologically and indeed can be triggered by antibody. It seems likely that this immunologically important variation results from a general capacity for genetic rearrangement found throughout the protozoa which is exemplified strikingly in the variant surface glycoprotein genes of *Trypanosoma brucei* and has recently been inferred in other parasites[11-13]. In the case of malaria parasite, some of the diversity detected serologically, whether genotypic or phenotypic, may not necessarily be a response to immune pressure, but rather may reflect the requirement of an obligate parasite to enter and survive in genetically diverse hosts.

If genetic diversity and rearrangement are part and parcel of malaria parasites, what hope is there for a malaria vaccine? Given the epidemiology of malaria it is hardly surprising that with the exception of a few highly-selected laboratory systems, immunization with crude or purified antigen is relatively ineffective. Protection has not so far been achieved with the sporozoite surface antigen — is this a result of antigenic diversity[6], immune evasion by antigen capping or inappropriate vaccination technique? Perhaps immunization with vaccinia virus-containing sporozoite sequences[14] will answer the last question. The requirement for draconian adjuvants and the antigenic diversity of the merozoite surface antigen do not encourage much hope for protective cross-reactivity through common epitopes, although there is preliminary evidence that isolates can be ranked for cross-protective activity. Good immunity to virulent blood-stage infection can, however, be obtained using avirulent K^- *P. falciparum* lines[15] and γ-irradiated non-replicating parasitized cells without adjuvant. These results may indicate that parasite antigen seen in the context of modified erythrocyte is the required immunogen. Could such an immunogen be produced in quantity? Does the report of the insertion of new genetic material into haematopoietic stem cells[16] at last begin to approach the level of technical sophistication which immunization against malaria parasite requires, leading ultimately to *in vitro*-grown erthrocytes derived from precursors containing parasite-antigen-encoding inserts in their DNA?

In order to exploit the developments in the molecular biology, a reliable assay of the protective immunogenicity of and responses elicited by the various forms of malaria parasite immunogens *in vivo* will be essential. This is a difficult problem, however, as protective immunity is rarely complete; for example, around 50 per cent of immune adults in holendemic areas may have parasites detectable in their blood at any one time, and recent or current low-level parasitaemia may be a prerequisite for preventing clinically significant infection. Many attacks of malaria over several years are required to generate clinical immunity, and immunity is in part strain specific. The diversity of malaria parasites and the complexity of the epidemiology also make the interpretation in terms of protective immunity of the new epitope and sequence data on surface antigens extremely speculative at this stage. □

1. Dame, J.B. *et al. Science* **225**, 593 (1984).
2. Enea, V. *et al. Science* **225**, 628 (1984).
3. Coppel, R.L. *et al. Nature* **310**, 789 (1984).
4. Koenen, M. *et al. Nature* **311**, 382 (1984).
5. Hall, R. *et al. Nature* **311**, 379 (1984).
6. Maddox, J. *Nature* **310**, 541 (1984).
7. Leech, J.H. *et al. J. exp. Med.* **159**, 1567 (1984).
8. Howard, R.J. *et al. Proc. natn. Acad. Sci. U.S.A.* **80**, 4129 (1983).
9. Freeman, R.R. & Holder, A.A. *Clin. exp. Immun.* **54**, 609 (1983).
10. Thaithong, S. *et al. Trans. R. Soc. trop. Med. Hyg.* **78**, 242 (1984).
11. Cowman, A.F. *et al. Cell* **37**, 653 (1984).
12. Vaidya, A.B. *et al. J. Immun.* **132**, 3126 (1984).
13. De Lange, T. *et al. Nucleic Acids Res.* **12**, 3777 (1984).
14. Smith, G.L. *et al. Science* **224**, 397 (1984).
15. Langreth, S.G. & Peterson, E. *Proc. 2nd int. Conf. Malaria Babesiosis*, 117 (Marcel Merieux, 1983).
16. Williams, D.A. *et al. Nature* **310**, 476 (1984).

K.N. Brown is at the National Institute for Medical Research, Mill Hill, London NW7 1AA.

Gene regulation

A step closer to the principles of eukaryotic transcriptional control

from Tim Reudelhuber

IN prokaryotes interaction between the genome and sequence-specific DNA-binding proteins has been shown to play an essential part in the control of gene expression. In eukaryotes such a relationship has been much more difficult to prove although evidence is accumulating that certain transcription factors interact with specific promoter elements (see, for example, refs 1, 2). Furthermore, local perturbation of chromatin structure has often been seen over the 5′-flanking sequences of actively transcribed genes. This 'open' chromatin conformation is typified by regions of greatly increased accessibility to cleavage by endonucleases such as DNase I (DNase I hypersensitive sites). These regions have been attracting increasing attention of late, both because they may mark important control regions for gene activity and because we seem to be on the verge of identifying components involved in their generation and, possibly, their function (for an overview of recent advances see ref. 3). To date, the most common finding has been that DNase I hypersensitive sites are missing in the promoter of 'silent' genes and become apparent in tissues which are either expressing or have the potential to express the gene in question. Two weeks ago, Fritton *et al.*[4] reported in *Nature* an interesting new twist to this now familiar story, for the DNase I hypersensitive sites flanking the chicken lysozyme gene.

In the chicken, the gene encoding lysozyme is expressed constitutively at low levels in mature macrophages, and is expressed at high levels in response to steroid hormones in the oviduct. The gene is not expressed in the embryo or in such tissues as brain, liver, kidney and erythrocytes. Fritton *et al.* found that in all the non-expressing tissues studied, with the exception of erythrocytes, there was only one DNase I hypersensitive site (which I shall refer to as B; the other hypersensitive sites are named A, C–E to simplify discussion) upstream of the startsite of transcription. In erythrocytes no hypersensitive sites were detected. In the constitutively expressing macrophages, sites A, D and E were detected while in the hormone-stimulated oviduct an alternate set of sites, B, C and E, was present; site C disappeared when hormone stimulation was withdrawn. What these data suggest is that it is no longer appropriate to refer to the active chromatin conformation of an expressed gene, since different tissues may manipulate the promoter elements in different ways to either 'turn on' or 'turn off' a transcription unit.

An obvious benefit of such a thorough cataloguing of the hypersensitive sites and their correlation with the transcriptional activity of the gene is that it becomes possible to venture an educated guess as to their function. It is known that active transcriptional enhancer elements are capable of inducing regions of DNase I hypersensitivity[5]. In the mouse mammary tumour virus, where an enhancer has been described whose activity is glucocorticoid dependent, a DNase I hypersensitive site appears transiently over this element only during hormonal stimulation[6]. Since site C in the lysozyme gene behaves in an analogous fashion, this region of the promoter is a good place to search for a similar hormone-modulated enhancer whose activation may explain the surge of lysozyme expression in the oviduct. Using similar logic, site B, which appears in most of the non-expressing tissues (but also in the oviduct), may mark the position of the transcriptional repressor element whose effect is overcome by an interaction at site C in the oviduct. The absence of this site in the non-expressing erythrocyte suggests that the cell may have yet another option at its disposal for suppressing lysozyme gene activity. Finally, sites A and D, seen in the macrophage, could mark the position of an alternative set of control elements capable of achieving low-level constitutive expression of the gene.

Of course, the actual function of all these sites remains to be demonstrated. A crucial question to answer will be whether the 'open' chromatin structure of these regions *per se* is important to their function, or whether the sites are simply 'footprints' generated by the interaction of regulatory proteins with the promoter elements. In other words, are the chromatin rearrangements at the hypersensitive sites a prerequisite to the binding of regulatory transcription factors or a consequence of it? *In vitro* systems in which both DNase I hypersensitivity and regulated transcription can be reconstituted will ultimately answer this question. Recent progress has been made in identifying erythrocyte-specific factors involved in generating a DNase I hypersensitive site in the chicken *β*-globin gene promoter[7] and, in a recent issue of *Nature*, Carl Wu described the *in vitro* reconstitution of factors binding in the hypersensitive region of *Drosophila* heat-shock genes[8]. Such advances should take us a step closer to understanding, in molecular terms, the relationship between chromatin structural rearrangements and the control of gene expression at the transcriptional level. □

1. Dynan, W. & Tjian, R. *Cell* **35**, 79 (1983).
2. Parker, C.S. & Topol, J. *Cell* **37**, 273 (1984).
3. Elgin, S.C.R. *Nature* **309**, 213 (1984).
4. Fritton, H.P. *et al. Nature* **311**, 163 (1984).
5. Jongstra, J. *et al. Nature* **307**, 708 (1984).
6. Zaret, K.S. & Yamamoto, K.R. *Cell* **38**, 29 (1984).
7. Emerson, B.M. & Felsenfeld, G. *Proc. natn. Acad. Sci. U.S.A.* **81**, 95 (1984).
8. Wu, C. *Nature* **311**, 81 (1984).

Tim Reudelhuber is in the Laboratoire de Génétique des Eucaryotes du CNRS, Faculté de Médecine, 11 rue Humann, 67085 Strasbourg Cedex, France.

Synthetic metals

Polyacetylene and organic superconductors lead the field

from Martin R. Bryce and Munir M. Ahmad

A RECENT conference* on the 'Physics and chemistry of synthetic metals' confirmed the unabated interest of organic chemists, physical chemists and solid-state physicists in this field (see Bryce, M.R. & Murphy, L.C. *Nature* **309**, 119; 1984 for a review). Significant progress in the two central research themes, conducting polymers and conducting single crystals, has been made since the Les Arcs meeting eighteen months ago.

Polyacetylene remains the most popular compound with the physicists. It is becoming increasingly clear that the quality of the material and the precise nature of any impurities are of central importance to a rationalization of solid-state properties. A two-step synthesis of polyacetylene was described in which a prepolymer is prepared and then purified and cast into films or fibres before conversion to the polymer by elimination (W.J. Feast, University of Durham). This method produces polyacetylene of high purity and overcomes some of the crystallinity and morphology difficulties of the original Shirakawa route. Homogeneous dense films of $(CH)_x$ can now be prepared and iodine-doping proceeds rapidly to 20 molar per cent to yield material with a conductivity of 10 $(\Omega\ \mathrm{cm})^{-1}$. By contrast, AsF_6 doping proceeds only to a level of 14 per cent. Optical, infrared, magnetic and transport properties of these doped films are similar to those measured for Shirakawa polyacetylene. The nature of polarons and solitons, their lifetime and charge storage, were considered for the chemically-induced defects in polyacetylene (J. Schrieffer and A. Heeger, University of Santa Barbara).

---

*Held in Abano Terme, Italy, on 17-22 June.

Several novel polymeric aromatics were discussed. Poly(isothianaphthalene), a transparent organic conductor with a band gap of only 1 eV, attracted special attention (F. Wudl, University of Santa Barbara). Other important polymers were a fluorinated analogue of poly(1,6-heptadiyne), which is an intrinsic semiconductor with enhanced oxidative stability; a new phase of poly-peri-naphthalene; soluble substituted polyacetylenes, such as poly(trimethylsilyl)acetylene, which can be desilylated to a controlled degree to produce a copolymer; and polypyrrole and related polymeric aromatic heterocycles.

Theoretically, there is still controversy over the quantum statistics of fractionally-charged excitations. Schrieffer discussed this topic in the light of proposals that quasi particles of fractional charge are responsible for the fractional Hall effect in low-dimensional materials.

Over the last two years, the field of conducting single crystals has deservedly been dominated by salts of tetramethyltetraselenafulvalene (TMTSF) which are superconducting at very low temperatures and seem to possess many unique remarkable properties. The development of more sophisticated and elaborate theories confirms that no consistent interpretation of this class of conductors can be reached unless one-dimensional physics is used as the starting point (D. Jerome, University of Paris-Sud, Orsay). A clearer understanding of the fascinating phase diagrams is emerging, and for (TMTSF)$_2$PF$_6$ evidence for transitions from metallic to spin-density wave state to superconducting state as temperature is lowered at constant pressure was presented (J. Schirber, University of New Mexico, Albuquerque).

Crystalline salts of bis(ethylenedithiolo)-tetrathiafulvalene (BEDT-TTF) present an exciting new class of materials. (BEDT-TTF)$_2$ReO$_4$ is a high-pressure superconductor. S. Parkin (IBM Labs, San José) correlated the absence of superconductivity in the majority of BEDT-TTF salts with their high dimensionality compared with the 2:1 ReO$_4$ salt. Applications of single-particle-band theory to the electronic structure of the TMTSF and BEDT-TTF salts reveal striking similarities between the two families; (BEDT-TTF)$_2$ReO$_4$ has the lowest anisotropy of any known superconducting charge-transfer salt.

It is more than ten years since the archetypal organic metal, tetrathiafulvalene–tetracyano-*p*-quinodimethane (TTF-TCNQ), was first prepared and, notably, at the conference this complex was hardly mentioned. There were few reports of new donors. The elusive tetratellurafulvalene derivatives have now been prepared, however. D. Cowan (Johns Hopkins University) described the synthetic approaches and pointed out that although TSeF is harder to oxidize than TTF, this trend is reversed on passing to TTeF which has an oxidation potential similar to TTF. K. Bechgaard (University of Copenhagen) has synthesized the donor 1,6-dithiopyrene, which forms a complex with TCNQ that, even at ambient pressure, is metallic down to 4 K with no phase transitions.

Electrocrystallization is now a widely-used technique for preparing metallic salts, including radical cation salts of arenes. Intermolecular interactions in salts based on oligomers of poly-*p*-phenylene, containing segments that carry a charge, were considered as structural models for conducting polymers (V. Enkelmann, University of Freiburg).

Linear chain compounds remain a focus for attention. Metallic, as well as semiconducting, metal–dithiolene complexes are known (A. Underhill and K. Carneivo, Universities of Bangor and Copenhagen respectively), and ferromagnetic compounds comprising ferrocinium and TCNQ units have been characterized by structural, magnetic, spectral and transport data (J. Miller, Dupont Labs).

The industrial future of synthetic metals for technology and applied science seems bright and there is increasing industrial support. Polyacetylene, polyaniline and poly-*p*-phenylene can be used in batteries and fuel cells employing aqueous electrolytes (A. MacDiarmid, University of Pennsylvania). (An account of recent work on battery performance of polyacetylene by J.C.W. Chien and J.B. Schlenoff appears on page 362 of this issue of *Nature*.) The organic metals that are capable of undergoing phase transitions under optical radiation are being used in electro-optic devices for communication and storage of data (K. Yoshino, University of Osaka) and the first erasable switching device capable of processing information using a single laser source was described (R. Potember, Johns Hopkins University). Moreover, there is potential for organic rectifiers based on a donor molecule linked via an insulating carbon bridge to an acceptor molecule, although because of synthetic difficulties this goal has not so far been achieved. □

Martin Bryce is a lecturer and Munir Ahmad a member of research staff in the Department of Chemistry, University of Durham, Durham DH1 3LE.

Molecular biology

Messenger RNA pieced together

from H.D. Robertson

In a provocative paper on page 350 of this issue of *Nature*, Campbell, Thornton and Boothroyd provide evidence that a short segment at the start of a messenger RNA (mRNA) molecule from a trypanosome can be found as part of a discrete transcript, separate from the remainder of the mRNA. They suggest that either the two segments of the mRNA are transcribed separately and subsequently joined or the shorter RNA segment acts as a sort of primer for transcription of the longer segment. The concrete demonstration of either of these mechanisms would be unique for a non-viral system and, particularly in the case of the priming mechanism, would have very important implications for our understanding of how mRNA synthesis can be regulated.

The expression of variant surface glycoprotein (VSG) genes in the African trypanosome *Trypanosoma brucei* is of extraordinary interest because it is responsible for the successive waves of trypanosomes with different surface glycoproteins that allow the parasite to persist in the face of successive attacks by its host's immune system. Recent work has shown that the mode of expression of these genes — at both the DNA and RNA levels — may reveal new molecular pathways.

Leaving aside for the present discussion the fact that the VSG genes can also undergo DNA-level rearrangements which are related to their expression, it has become clear that DNA encoding a 35-nucleotide leader sequence (the 'mini-exon') of all VSG mRNAs and that encoding the remainder of VSG mRNAs can be 30 kilobases or more apart. This great separation, found by several groups of investigators including that of P. Borst, coupled with the investigators' inability to find giant mRNA precursor molecules which would be expected in a conventional synthesis/splicing pathway, have led Campbell, Thornton and Boothroyd to seek and characterize smaller transcripts containing the 35-nucleotide 'mini-exon' RNA with the idea that these might somehow become associated with the remainder of the VSG mRNA after their synthesis.

Since the mini-exon RNA itself occurs in many RNAs of various sizes extracted from infected cells, Campbell *et al.* have used sequence information from cloned DNAs containing the mini-exon and its immediately adjacent regions to seek small transcripts. Using restriction fragments of the cloned DNAs together with a synthetic oligonucleotide complementary to a region about 100 bases downstream from the mini-exon DNA sequence, they have applied three standard indirect tests, all of which have independently pointed to the existence of a 137-base RNA species which contains the mini-exon at its 5′ end.

Regulation of gene expression at the level of RNA transcription is a phenomenon more widely known at present in prokaryotes than eukaryotes. In particular, gene regulatory schemes in which a eukaryotic RNA transcribed at one place in the genome is used to mediate RNA synthesis at a second site have been difficult to support with experimental evidence. Except in the case of a few viruses, proposals from the early 1970s invoking the use of a RNA specifically processed from one gene transcript to stimulate transcription at a second genomic site have remained in limbo. One good reason for this state of affairs was the discovery in 1977 of introns in eukaryotic genes, leading to wide acceptance of the existence of an RNA-splicing mechanism to allow the covalent linkage of non-contiguously coded RNA transcripts. Consequently, there seemed little biochemical need for another way to obtain the same result.

Nevertheless, the idea that RNA primers could be cleaved from one RNA molecule and used to stimulate transcription of another remains an attractive hypothesis, supported in recent years by evidence published by R. Krug and his colleagues at the Sloan-Kettering Institute of the use of host-cell RNA primers for influenza virus mRNA synthesis. They could be sure that their data did not reflect a conventional RNA-processing reaction because the primer RNA sequence linked by the 5′ terminus of each influenza virus-encoded mRNA segment was demonstrably of cellular origin. Thus, mRNA molecules originating both *in vivo* and *in vitro* could be synthesized in controlled conditions and the origins of their segments analysed in detail.

Until recently, the search for such events — with their regulatory potential — in eukaryotes has awaited a system of sufficient interest to make worthwhile the extra effort needed to distinguish transcription-level effects from those at the level of conventional RNA processing, and in which it was feasible to analyse in detail the expression of various RNA segments comprising a candidate mRNA molecule.

A pool of small RNA molecules containing the mini-exon sequence, such as the 137-base RNA reported by Campbell *et al.*, is a pre-requisite for all models of discontinuous transcription of the VSG genes although it presence does not prove that discontinuous transcription is occurring. Similar results have recently been obtained by Borst and his co-workers using several trypanosome strains (*EMBO J.*, in the press). The next step is clearly the direct analysis of the RNA precursors to VSG mRNA, particularly those containing the mini-exon sequence. In this way, it should be possible to tell whether the RNA segments are made separately and then joined by some unconventional mechanism; whether RNA-primed transcription is responsible; or whether some combination of these events in an even more exotic process could be taking place in this system. □

H.D. Robertson is at the Rockefeller University, 1230 York Avenue, New York, NY 10021-6399.

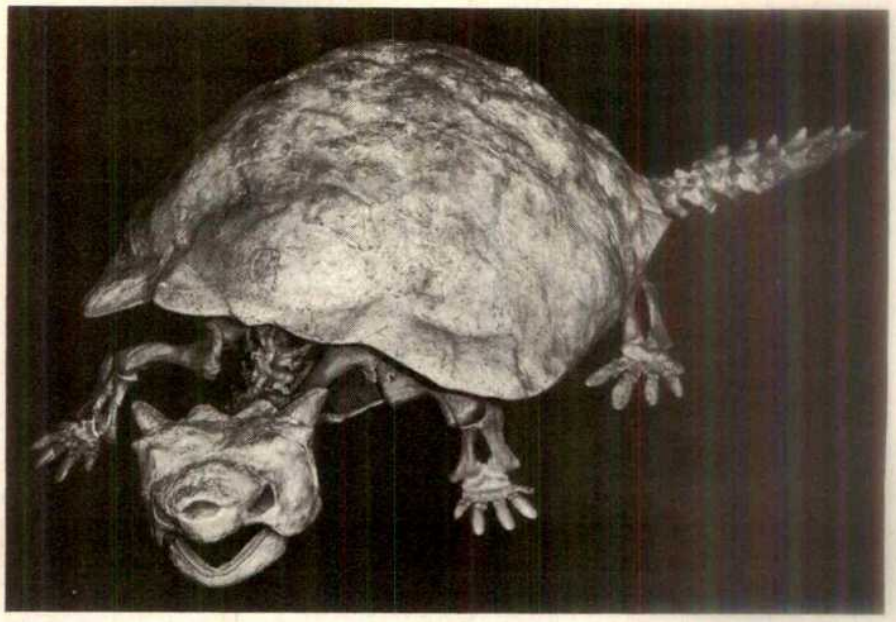

Giant tortoises down under

THE present-day animals of Australia are a peculiar bunch, but those that lived one million years ago, in the Pleistocene, were even stranger. There was a giant wombat called *Diprotodon* which was the size of a rhinoceros, and a monster 3-metre-high kangaroo named *Procoptodon*. This trend to large size was also seen in the turtles. The available specimens of the tortoise *Meiolania* have recently been restudied (Gaffney, E.S. *Bull. Am. Mus. nat. Hist.* **175**, 361; 1983) and some important new finds are reported.

Meiolania platyceps was a 2-metre-long tank-like land tortoise that is known from numerous remains found on Lord Howe Island, New South Wales. Its skull was heavy and covered with an outer armour of plates and horns — no doubt so that it could withstand the impact of a giant kangaroo landing on its head. *Meiolania*, like most turtles, had a relatively small braincase, so it probably wasn't very bright. Its shell was huge, and its arms and legs could be pulled in beneath it. One remarkable feature of *Meiolania* is its tail which was long and carried at its end a bony mass made from rings and spikes. Like certain armoured dinosaurs (the ankylosaurs), *Meiolania* could have swung its tail from side to side to deliver a powerful blow to any potential predator.

All the material has been collected from shoreline and soil deposits on Lord Howe Island, and these have been tentatively dated as 100,000 - 120,000 years old. The first *Meiolania* bones may have been collected in 1844, when John Foulis MD visited the island. He later recommended that it be developed as a penal colony, stating that the island could "support a population of 5,000 souls if under control". One wonders what 'control' he had in mind. The island was not developed in that way. Later, Robert D. Fitzgerald visited the island and found turtle bones in 1869. He sent specimens to Sir Richard Owen, the leading British comparative anatomist of his day. Further bones have been collected since then, with recent finds in 1971, 1980 and 1982; most of these went to the Australian Museum, Sydney.

Richard Owen identified the first skull and tail club of *Meiolania* that he saw as that of a giant lizard (1881, 1882) and, later (1886), other remains as those of a large turtle. It was Thomas H. Huxley, a rival of Owen's, who gleefully pointed out that Owen's 'giant lizard' was in fact a turtle (1887). Since then, other British and Australian scientists have identified various *Meiolania* bones, and speculated wildly about the animal's precise taxonomic relationships.

In the new work, Gaffney redescribes the skull in detail, and concludes that *Meiolania* is a cryptodire turtle, related to present-day soft-shell turtles and tortoises.

Meiolania died out, with the giant wombats and kangaroos, some time ago. This may have been caused partly by climatic changes during and after the Ice Ages, or by the arrival of humans in Australia. Giant tortoises still survive, but only just, on the islands of Aldabra and the Galapagós, but these are not close relatives of *Meiolania*. *Meiolania* would have been a tempting food-source for humans because of its large size, although it would not have been easy to kill because of the heavy armour over its head and body. It was probably very slow-moving and dim-witted, however, and an enterprising group of aborigines could have stood on the tortoise's back to avoid the tail-club, and attacked its unprotected neck with blunt instruments. □

From Michael J. Benton, who is in the Department of Geology, The Queen's University of Belfast, Belfast BT7 1NN.

Geophysics

Continental area and elevation

from A.G. Smith

WHEN all the continents were clustered together as Pangea, a small part of that supercontinent experienced flooding by the sea. By contrast, a much larger area of the smaller continents created by the break-up of Pangea has undergone periodic flooding during global rises in sea level. Because there is no reason to suppose that similar changes in sea level did not take place when Pangea existed, an important aim of geophysicists has been to explain the different flooding frequencies before and after the break-up.

Analyses of the global topography suggest that continental area is correlated with continental height. From this it follows that Pangea, the largest possible continent, would have had the largest average height, thereby reducing the area available to flooding during a global rise in sea level. Two authors[1,2] have recently reassessed the suggested area–height relationship.

On page 370 of this issue of *Nature*, Wyatt[1] discusses some of its implications. In particular, he suggests that the reduction in shelf area that might be expected to have accompanied the formation of Pangea may have been a casual factor in the late Permian extinctions of shelf organisms. Stanley, however, has cited evidence that geologically recent reductions in shelf areas have had little effect on some shallow-water faunas[3].

In a recent paper Cogley[2] makes a more detailed analysis of continental topography, particularly continental margins, than the analyses by Harrison and others[4,5] on which Wyatt's paper is based. Cogley concludes that modal height — as opposed to average height — is not correlated with continental area.

He cites several areas that are much higher than any height–area relationship based on the major continents would predict, including Arabia and India. The tiny mountainous islands of Corsica and Sardinia in the Mediterranean are also anomalous, though this is not unexpected as they are associated with young mountain-building movements. However, were Madagascar regarded as a distinct continent, it too would be anomalously high. It would seem that the correlation of continental elevation with continental area is not as clear as one might like.

Until one has a working model of what determines the thickness of continental crust and why it should change with area, it is difficult to know whether these exceptions are important. In the case of the oceans, there is an excellent quantitative understanding of the relationship between ocean-floor depth and age[5]. Anomalously shallow ocean floor is simply a place where more molten rock has erupted or been injected into the crust than normal. Why this should have happened is not clear, but at least the unexpected increase in thickness is explained.

In the case of the continents there is no generally accepted working model of what determines the thickness of their crust. A suggested mechanism of continental uplift is the injection of carbon dioxide and water into the lower crust, but the volumes involved are so huge that such an explanation seems unlikely, except on a local scale.

The only plausible cause is physical. Analogy with the oceans suggests that the most probable mechanism is an increase in heat flow. This could cause uplift simply by bringing about the thermal expansion of the continental lithosphere. Furthermore, the heat could effect crystalline phase changes in the rock minerals, inducing significant volume changes without any change in bulk composition. Uplift associated with uprising convection currents would be unlikely to be as much as the hundreds or thousands of metres observed in, for example, southern Africa. But one can speculate that convection might be more vigorous under large continents and deliver more heat, and this might partly explain the correlation between area and height.

How can these problems be resolved? An important approach will be to document precisely the changes in continental structure with time. One of the most promising sources of information is the rock fragments brought up from great depths in diamond pipes. It might be possible to infer a continental lithospheric structure from a suite of fragments from an old pipe that is know to have penetrated a continent when it was near sea level and compare it with a suite from a younger pipe that penetrated that continent when it stood at a much higher level. Southern Africa may hold the key to this approach.

It is ironic that our understanding of the continents on which we live is far less advanced that our understanding of the ocean floor, which we rarely see. Discussion of the implications of the correlation between continental area and elevation will help to point the way to changing this state of affairs. ☐

1. Wyatt, A.R. *Nature* **311**, 370 (1984).
2. Cogley, J.G. *Rev. Geophys. Space Phys.* **22**, 101 (1984).
3. Stanley, S.M. *Geology* **12**, 205 (1984).
4. Harrison, C.G.A. *et al. Earth planet. Sci. Lett.* **54**, 1 (1981).
5. Harrison, C.G.A., Miskell, K.J., Brass, G.W., Saltzmann, K.S. & Sloan, J.L. *Tectonics* **2**,357 (1983).
6. Sclater, J.G. & Parsons, B. *J. geophys. Res.* **82**, 803 (1977).

A.G. Smith is in the Department of Earth Sciences, University of Cambridge, Downing Street, Cambridge CB2 3EQ.

NATURE

100 years ago

THE Japanese appear to be determined to render themselves, as far as possible, independent of foreign countries. They have, says the *Pharmaceutical Journal*, established in Tokio a factory for the production of pharmaceutical chemicals on a large scale. A company with a capital of about 40,000*l*. has been formed for this purpose. Of this amount the Government has contributed one-half free of interest for twenty years, besides making a free grant of land and erecting the necessary buildings. A similar company is taking up the utilisation of the waste *saké* from the native breweries in the manufacture of alcohol, and the manufacture of bleaching-powder on a large scale has been commenced. Whether with the object of "protecting" the first of these enterprises or not does not appear, but we learn from the same authority that an increased tax has been placed in Japan on imported patent medicines, and the nature of the articles to which this has been extended is stated to have largely affected the import of some chemicals into that country. Santonin, which was at one time much in request among the Japanese, decreased 20,000 ounces in import last year, although the price was lower; on the other hand, the consumption of quinine showed and increase.

From *Nature* **30**, 512, 25 September 1884.

A SEA MONSTER

A FRIEND of mine, Capt. W. Hopkins, of the schooner *Mary Ogilvie*, who has just returned from a voyage all round Australia, has given me the following information, which I forward you for publication, not so much because of its interesting character, but in order that other travellers may throw some light upon the character of the animal, which, if an Octopus, must be of much larger dimensions than those usually met with. On June 15, when in S. lat. 21° 37′ and E. long .13° 49′, about five miles off the Exmouth Gulf on the western coast of the continent, he saw an immense creature which he took to be a species of Octopus. His attention was drawn to it by a perfect cloud of sea birds, and at first he naturally thought it must be a dead carcass. On approaching it, however, he found it was alive and sluggishly disporting itself. In shape it was like a violin, but of immense size, with some six feelers about the greater diameters of the violin. It lay almost flat upon the water, was of a dark gray above and lighter gray below, and was continually elevating one of its feelers, apparently twice the thickness of a man's arm, to a height of from six to eight feet. It appeared to be vomiting, and as the birds were evidently feeding, that accounted for their presence in such numbers. Its size was so great that, had it grasped the vessel, it could easily have capsized it. The captain therefore got out of the way as quickly as possible, and without making definite measurements; but a large whale in the vicinity looked quite diminutive. It is a pity that something more exact as to size is not available, but I think the description is sufficient to convey an idea of the nature of the monster.

LIBRARY COMPLEX
Departments of
Chemical Engineering
Chemical Technology
Plastics and Rubber Technology

21-1-87
A. Salter

Immunology

Receptor gene rearrangement and ontogeny of T lymphocytes

from Miranda Robertson

MANY of the outstanding questions raised by modern cellular immunology converge on the issue of T-lymphocyte ontogeny. T lymphocytes, so called because they mature in the thymus gland, provide both the cytotoxic effector lymphocytes that eliminate virus-infected cells, and the helper and suppressor lymphocytes that regulate the activities of effector cells including the B lymphocytes that produce antibodies. The exact nature of the thymic maturation process, however, has proved very hard to define, and even the definition of the different subsets of T cells is not altogether unambiguous. Both questions are in part questions about antigen recognition by T cells.

All T lymphocytes, unlike B lymphocytes, recognize foreign antigen in the context of surface molecules encoded in the major histocompatibility complex (MHC), the cytotoxic cells focusing on the class I molecules and the regulatory T cells on the class II molecules. Do T cells 'learn' to recognize 'self' MHC molecules in the thymus, and during this process acquire both tolerance to self alone and the potential to react to self plus foreign antigen? How might that maturation be reflected in the expression of the genes encoding the antigen receptors and how might that vary between different subsets to account for their differential responsiveness to class I and class II molecules? Five recent papers[1-5], three of them published in *Nature* this week[2-4], have an important bearing on these issues.

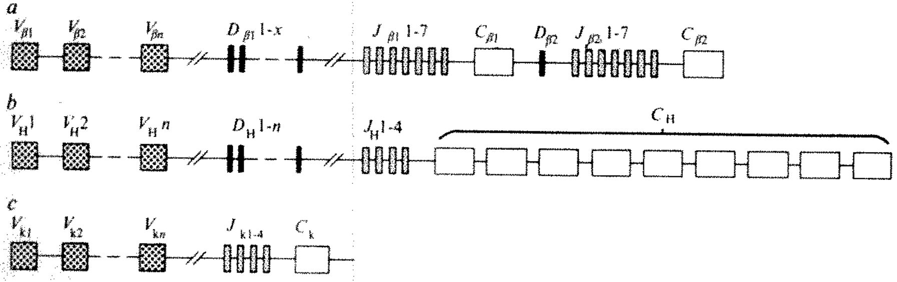

Fig. 1 Gene segments encoding *a*, the β chain of the T-cell antigen receptor; *b*, the heavy chain of immunoglobulin; *c*, the κ light chain of immunoglobulin. Immunoglobulin molecules are made up of four chains, two identical heavy chains that contain a variable antigen-recognition domain and a constant effector domain, and two identical light chains also comprising a variable and a constant region. The variable regions of the light chains, which can be either of two isotypes, known as κ and λ, are assembled from separately-encoded *V* and *J* segments that are brought together by genomic rearrangements during the differentiation of the B lymphocytes that produce antibodies. The final mRNA containing the *VJC* sequence is produced by processing of the primary transcript from the rearranged gene segments. The rearrangements in the heavy-chain gene pool are more complex, in that three separate segments comprise the DNA encoding the variable region: a *V* segment, a *D* segment and a *J* segment which are sequentially rearranged during B-cell ontogeny to produce a continuous *VDJ* DNA sequence. Different combinations of these segments account for much of the diversity of antigen-binding sites in immunoglobulins. The T-cell receptor β chain also contains *D* segments, but is organized differently from that of the immunoglobulin heavy chain in that each of the two constant regions has a set of upstream *D* and *J* segments. Moreover, the two constant regions of the β chain are essentially identical, whereas the immunoglobulin heavy-chain *C* regions are quite different and have different effector functions. The final receptor molecule of the T cell has two chains, known as the α and the β chains; the structure of the α chain is still problematic (see box).

All five papers deal with the genomic rearrangements through which the separate DNA segments encoding the β chain of the T-cell receptor are assembled into a complete gene. Since the β chain is only half of the receptor heterodimer[6], the final answer to the question of antigen recognition will have to await an equivalent analysis of the α-chain DNA. The present position on the α chain (see box on page 306) and the mechanism of antigen recognition will be discussed in more detail in a later article in *News and Views*. I shall here confine myself to the limited but important conclusions that can be drawn from the analysis of β-chain gene organization, and its rearrangement in T lymphocytes of different subsets.

It is now clear that the β-chain DNA shows homology to that of the immunoglobulins not only in sequence but also in general organization: Figure 1 shows how the coding segments compare with immunoglobulin gene segments, and the legend contains a brief recapitulation of how complete molecules are generated from the assembled segments. It was already known the last time this topic was discussed in these columns[7] that the T-cell β chain, like the immunoglobulin heavy chain, is assembled from four separate segments: V_β, D_β, J_β and C_β. Kavaler *et al.*[1] and Siu *et al.*[2] have since cloned genomic D_β segments and are able to demonstrate a significant difference from their immunoglobulin counterparts — not in the coding sequence, though that is of course different — but in the flanking DNA that contains the signals believed to mediate their recombination with the *V* and *J* segments (see Fig. 2). According to the rules that are believed to govern these recombination events (see Fig. 2 legend), neither direct *V–J* joining nor *D–D* joining is allowed in the immunoglobulin heavy-chain gene pool. In the β-chain pool, however, both are possible without violation of the rules. Such flexibility in the assembly of the gene segments might help to compensate for the apparent absence in the β genes of somatic mutations[8] that are known to contribute to the diversity of the immunoglobulins. The structural consequences of the alternative rearrangements in the T-cell pool might however be expected to be more profound than those of scattered point mutations.

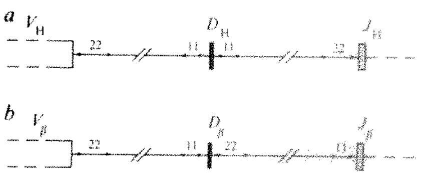

Fig. 2 Recombination signals for the immunoglobulin heavy chain (*a*), and for the T-cell antigen receptor β chain (*b*). The separate DNA segments encoding the variable regions of the immunoglobulin genes are flanked by conserved heptamer and nonamer sequences separated by non-conserved spacer DNA that may be either 11 or 22 nucleotides long, representing either one or two turns of the DNA double helix. These conserved sequences are believed to mediate the genetic recombination by which the separate segments are assembled into the complete coding sequence during B-cell ontogeny, according to a rule known as the 11–22 rule whereby recombination takes place only between a conserved sequence pair separated by an 11-nucleotide spacer and one with a 22-nucleotide spacer. Thus *D–D* or *V–J* joining violates the recombination rules in the heavy-chain gene pool. In the T-cell β-chain gene pool, by contrast, the spacers are so organized that *D–D* and *V–J* joining would be allowed.

So far, however, there is no evidence either for *V–J* or for *D–D* joins. What has emerged from more detailed analyses of the structure and expression of the *D* segments is an entirely unsuspected feature of T-cell ontogeny that has, moreover, been almost simultaneously discovered to have an exact equivalent in B lymphocytes.

In T cells, as in B-cell heavy-chain genes[9], the first joining event is between a *D* and a *J* segment[1]. Siu *et al.* have now discovered that this preliminary joining event results in the production of a *DJC* transcript from a conserved promoter upstream of the *D* segment. The truncated transcripts, which can involve either of the two C_β segments and its associated *D*s and *J*s, are extremely common and indeed account for two of the four cDNA clones originally isolated by Hedrick *et al.*[10]. Siu *et al.* report that the truncated transripts are prevalent in the thymus and are seen very little in peripheral lymph-node T cells[2]. Their prevalence in the thymus could explain why despite the high levels of T-cell receptor RNA in thymocytes[11], Kappler was unable to detect corresponding levels of surface protein (see ref. 7).

Otherwise, however, the importance of the short transcripts is a mystery; though important they must certainly be. First, it is clear from a comparison of mouse and human *D* segments[3] that the *D*-segment promoter is highly conserved, and moreover *DJC* transcripts are highly prevalent in man as well, preliminary data suggesting that they are present in large amounts in thymus and small amounts in periphery; and second, Alt *et al.*[12] have recently shown that equivalent *DJC* transcripts are characteristic of immature B cells in which they are transcribed from a conserved promoter and have also been shown to be translated. No one has been prepared to guess at a possible function for the transcripts, but it must be significant that the *D* segment is the most conserved of all the segments; and it may be significant that both mouse and man have maintained duplicate C_β segments that are almost identical.

Since the near-identity of the $C_{\beta 1}$ and the $C_{\beta 2}$ segments rules out β-chain constant-region isotype as a distinguishing feaure of T-cell subsets, the distinction must be sought elsewhere. One obvious question is whether the same gene pool encodes the β chain of all three major antigen-specific subsets. The original clones were isolated from helper cells. Saito *et al.*[13] have already shown that the same *C* segments are rearranged in cytotoxic cells, and similar analyses have now been extended to other cytotoxic cells and to suppressor cells both in man[4] and in mouse[5]. Hedrick *et al.*[5] have confirmed that the same *C* genes are both rearranged and transcribed in all of six cytotoxic cell lines analysed, and Toyonaga *et al.*[4] find rearrangements of the same *C* sequences in human helper and cytotoxic clones.

The position on suppressor cells is more complex. Toyonaga *et al.* report that their one suppressor clone shows rearrangement of the same C_β sequence; but Hedrick *et al.* find rearrangement in only 2 of 14 suppressor clones: in the remaining 12, C_β segments are deleted, along with very large regions of neighbouring DNA. Moreover, the two rearranged *C* segments lack *V* sequences. The weight of the evidence, then, is that the identified β-chain genes do not participate in antigen-specific suppression of the immune response. The major chromosomal deletions reported by Hedrick *et al.* are unlike anything seen in lymphocyte ontogeny before, and it is not clear what they mean. Saito *et al.*[13] have raised the possibility that if the same C_β segments are expressed in helper and cytotoxic subsets, it remains possible that different V_β pools may be active. This would be consistent with the different MHC-class responsiveness of these two subclasses, and Saito *et al.* point out that the homology between their cytotoxic-cell V_β sequence and the helper V_β sequence of Davis *et al.* is much lower than that between the *V* segments of immunoglobulin genes. It has since turned out, however, that very low homology is characteristic of *V* segments within the helper subset[14]. This discovery, its possible implications for antigen recognition by T cells and the elusive other half of the hererodimer will be the subjects of a second article in *News and Views*. ☐

1. Kavaler, J. *et al.* Nature **310**, 421 (1984).
2. Siu, G. *et al. Nature* **311**, 344 (1984).
3. Clark, S.P. *et al. Nature* **311**, 387 (1984).
4. Toyonaga, N., Yanagi, Y., Suciu-Foca, N. & Mak, T.W. *Nature* **311**, 385 (1984).
5. Hedrick, S.M. *et al. Proc. natn. Acad. Sci. U.S.A.* (in the press).
6. Winchester, G. *Nature* **309**, 750 (1984).
7. Marrack, P. *Nature* **309**, 310 (1984).
8. Chien, Y. *Nature* **309**, 322 (1984).
9. Alt, P.W. *et al. EMBO J.* **3**, 1209 (1984).
10. Hedrick, S.M. *et al. Nature* **308**, 153 (1984).
11. Yoshikai, Y., Yanagi, Y., Suciu-Foca, N. & Mak, T.W. *Nature* **310**, 506 (1984).
12. Reth, M. & Alt, F.W. *Nature* (in the press).
13. Saito, H. *et al. Nature* **309**, 757 (1984).
14. Patten, P. *et al. Nature* (in the press).

Miranda Robertson is Acting Life Sciences Editor of Nature.

The Snark was a Boojum, probably

It would be disingenuous, in an article on the T-cell receptor, not to acknowledge the questions that have been widely raised about the true identity of the cDNA clone isolated in the laboratory of Susumu Tonegawa from a cytotoxic T-cell line and credited with encoding the α chain of the receptor (Saito, H. *et al. Nature* **309**, 757; and Winchester, G. *Nature* **309**, 750; 1984).

Doubts were already being voiced at a conference on 'T-cell receptors, genetics, structure and function,' held at the Given Institute in Aspen, Colorado on 6–8 July, within a week of the appearance of the report in *Nature*, on the following grounds. Protein data on α chains isolated from other kinds of T cells (helper cells) show that they are *N*-glycosylated (Kay, J. & Janeway, C.A. *J. Immun.*, in the press), whereas the sequence reported by Saito *et al.* in *Nature* has no *N*-glycosylation sites. Moreover, Tonegawa reported in Aspen that three 'α' clones isolated from independent cytotoxic lines all contained the same *V* and *J* segments.

Leroy Hood (Caltech) argued in Aspen that such invariance was inconsistent with a role in antigen recognition, although others have pointed out that there is a precedent in the λ light-chain genes of mouse immunoglobulin, which have only two variable-region segments. Moreover, variation in the exact site of the *V–J* join in the cDNA of the three T-cell lines analysed by Tonegawa does in fact generate some diversity that could, as he pointed out, have a significant effect on antigen binding, or on binding of the MHC molecules that form a necessary part of the antigenic stimulus of T cells. And as Tonegawa emphasized, the genomic DNA corresponding to the clone is rearranged and expressed exclusively in T cells and has clear homology to immunoglobulin, both in sequence and in organization, and thus fulfills all the important criteria for a T-cell antigen-receptor gene.

Thus at the time of the Aspen meeting it was unclear how far the discrepancies between the protein and the DNA data on the α chain should be attributed to differences between man and mouse, or cytotoxic and helper cells; and how seriously the small size of the *V*-segment repertoire should be taken.

More definitive evidence is now becoming available and will this be the topic of a later article in *News and Views*.

Erratum

Excisions of introns in lariat form

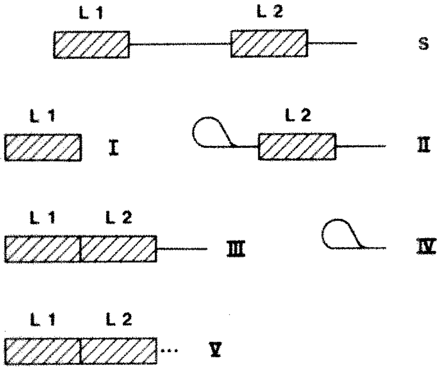

In the article 'Excision of introns in lariat form' by Charles Weissman (*Nature* **311**, 103; 1984), an incorrect version of Figure 1 was used. This was a result of a series of errors in the *Nature* office, for which we apologize. The correct figure is shown here on the left. It illustrates the structures of the products (I–V) of cell-free splicing of a substrate (S) RNA composed of two exons (L1 and L2) and two introns. Structure IV is the excised intron in lariat form.

"Nuclear winter" to be taken seriously

IN two recent articles[1,2] John Maddox has criticized our technical analysis of the long-term worldwide consequences of nuclear war[3]. Our findings on what we have called nuclear winter evolved from, and were partly calibrated by, 12 years of related research on martian dust storms, the climatic consequences of volcanic explosions on Earth and the possible collision of an asteroid or cometary nucleus with the Earth at the time of the Cretaceous/Tertiary extinctions.

Given the importance and sensitivity of the subject, we took extraordinary measures to have our calculations reviewed by a large number of experts in atmospheric physics and chemistry, at a meeting specially convened for this purpose in April 1983, and by other means — well before the submission of the paper for publication. Our article refers to some 95 published scientific papers and reports in which further technical details can be found. We have discussed the technical issues with a large number of recognized experts in a variety of fields (which is not to say that all these experts endorse all of our conclusions). Most of the details of our mathematical models are already published, and a detailed 145-page description of our data sources and methodology has been widely distributed. A much more extensive discussion is in preparation.

Some apparently believe that unless nuclear winter is demonstrated beyond a shadow of a doubt, it is dangerous to discuss it in the scientific literature and in public forums. But this is not a subject amenable to experimental verification — at least not more than once. We hold, to the contrary, that open and informed debate on this issue is the only responsible approach, given the gravity of the potential climatic catastrophe we believe we have uncovered.

Whether Maddox has carefully read the work he is criticizing is open to some doubt. He seems to have missed the point that the major cause of nuclear winter is sooty smoke from fires rather than silicate dust raised from the surface. We clearly state that the greatest climatic effect is from smoke generated in the burning of cities. Nevertheless, in his first article and much of his second, Maddox surprisingly holds that the main climatic perturbation we derive is from dust. That this is not merely a careless use of words is made clear by his repeated comparison of our predictions of the effects of the nuclear war with the frosts produced by volcanic eruptions, exemplified by the work of LaMarche and Hirschboeck[4], who find good agreement between the timing of some volcanic eruptions and temperature declines. Our previous work[5,6] shows that major volcanic explosions in the past few centuries may have produced optical depth perturbations of at most a few tenths, and global temperature declines of at most one degree centigrade. These values are less than even the dust in a nuclear war would probably produce, to say nothing of the soot.

Maddox writes "The chief reason for this huge discrepancy between the consequences of a nuclear war and a volcanic eruption stems from the assumptions made about the quantities of dust carried into the stratosphere by the different events." But our calculations unambiguously show that if there were no dust whatever injected into the atmosphere, and no aerosols of any composition injected into the stratosphere, severe climatic perturbations might nevertheless ensue from upper tropospheric soot. By his statements, Maddox also seems to be unaware that climatic effects of volcanic explosions are caused principally by sulphuric acid aerosols, not by silicate dust. Likewise, our results differ from those of the 1975 National Academy of Sciences report, largely because that study did not consider the injection of soot into the atmosphere from massive fires. But it is also true that the 1975 report did not carefully quantify the dust injection.

Maddox evidently believes that we have not justified or even stated the properties of the dust we employed in our calculation. In fact, we used direct measurements of the particle size distribution of dust produced by nuclear explosions, data on the properties of soils and observations of windblown dust. The log-normal/power law distribution function adopted, the complex refractive index of the dust, and other relevant parameters are explicitly stated.

Nuclear explosions are not volcanic explosions, and the differences between the two kinds of events far outweigh what they have in common. The relative importance of smoke in dominating the attenuation of sunlight in the immediate post-nuclear war environment was first noted by Crutzen and Birks[7]. Our calculations show that smoke is much more effective than dust per unit mass of aerosol, both for optical and for climatic perturbations, because of the greater absorptivity and finer particle size of the former.

Maddox criticizes Covey *et al.*[8] for applying their "new model" to nuclear winter before its applicability has been demonstrated in more conventional calculations of the general circulation. The 'new model' is in fact the Community Climate Model of the National Center for Atmospheric Research, which has been in general use for some years. In our *Science* paper[3] we explicitly noted that the great heat capacity of the oceans will have an ameliorating effect on the post-nuclear war temperature perturbations even in continental interiors, and made a rough estimate of the magnitude of this amelioration. As Covey *et al.* make clear, their three-dimensional general circulation model, as well as one, two and three-dimensional models at Lawrence Livermore National Laboratory and at the Computing Center of the USSR Academy of Sciences, are all in good agreement, in hemispheric average, with our published results. Moreover, Covey *et al.* show that the effects could be significantly worse than we had stated, in that "quick freezes" could occur in a matter of days in areas far distant from the combatant nations, as well as showing that calculated perturbations to the global circulation could bring dust and soot rapidly to the tropics and into the Southern Hemisphere, as we had originally proposed.

There are many points about nuclear winter that require further work, both theoretical and experimental. We have never suggested that the last word has been said on this subject[9]. We have, however, run some 50 different cases, to study uncertainties and sensitivities, in many of which, including those we consider most likely, the climatic effects are very severe.

There are contingencies, which we consider unlikely, that could mitigate the severity — for example, if the smoke is everywhere efficiently scavenged from fire plumes, or if there is persistent mesoscale patchiness in the aerosol cover. But there are also circumstances, some of them very likely, in which the effects could be considerably worse. For example, the smoke from fires set by one nuclear explosion over a city can be propelled rapidly by a later explosion to very high altitudes, where it is immune to scavenging mechanisms. By creating channels for bomblight and by drying, a first nuclear explosions over forests can enhance the burning produced by a subsequent nuclear explosion. We have also entirely ignored the effects of tactical nuclear weapons; there are now almost 35,000 of them in the world inventories, many with yields greater than those of the bombs that destroyed Hiroshima and Nagasaki.

The dramatic restructuring of the Earth's atmosphere by injected aerosols moves the lower atmosphere towards isothermality and the upper atmosphere towards a major thermal inversion, as shown in our *Science* paper. In a fully interactive calculation, this restructuring would significantly prolong the duration of the climatic effects following a nuclear war. The snow/albedo and sea ice/thermal inertia (see ref. 10) feedback effects also act to extend the duration of nuclear winter.

As one measure of the importance of the nuclear winter problem, within the past few months major research efforts, costed at many millions of dollars, have been authorized in the government laboratories of both the United States and the Soviet Union, and still larger programmes are under urgent consideration. Spokesmen for the US Department of Defense have recently testified that they take nuclear winter very seriously[11].

In the closing paragraph of our *Science* paper and elsewhere in the text and notes, we summarize our view of the limitations of this research and express the hope that, because of these new dangers of nuclear war, "the scientific issues raised (here) will be vigorously and critically examined". Many members of the scientific community, ourselves included, are now engaged in such an examination.

RICHARD P. TURCO

R & D Associates,
Marina del Rey, California 90291, USA

O.B. TOON
THOMAS P. ACKERMAN
JAMES B. POLLACK

NASA Ames Research Center,
Moffett Field, California 94035, USA

CARL SAGAN

Cornell University,
Ithaca, New York 14853, USA

1. Maddox, J. *Nature* **307**, 107 (1984).
2. Maddox, J. *Nature* **308**, 11 (1984).
3. Turco, R.P., Toon, O.B., Ackerman, T.P., Pollack, J.B., & Sagan, C. *Science* **222**, 1283-1292 (1983).
4. LaMarche, V.C. Jr & Hirschboeck, K. *Nature* **307**, 121-126 (1984).
5. Pollack, J.B., Toon, O.B., Sagan, C., Summers, A., Baldwin, B., & van Camp, W. *Nature* **263**, 551-555 (1976).
6. Pollack, J. B. *et al. J. geophys. Res.* **81**, 1071-1083 (1976).
7. Crutzen, P.J. & Birks, J.W. *Ambio* **11**, 114-125 (1983).
8. Covey, C.W., Schneider, S.H. & Thompson, S. L. *Nature* **308**, 21-25 (1984).
9. Sagan, C. *Climatic Change* **6** (1), 1-3 (1984).
10. Robock, A. *Nature* **310**, 667-670 (1984).
11. Testimony before the Senate/House Joint Economic Committee, 12 July 1984; *Defense Daily* July 13, 1984; *New York Times* July 13, 1984.

JOHN MADDOX REPLIES — My objective, in the first brief reference to this work and in the second reference, was to remind readers, either of the original works or of *Nature*, that these calculations are uncertain. Plainly I should have made more of the smoke and less of the dust, but the conclusion remains — that the assumptions on which these calculations are based, and the computational techniques themselves, are respectively (but necessarily) so uncertain and imprecise that it would be folly to regard them as more than suggestive, but interesting and even valuable (as I said) on that account.

Uncertainty about the scale on which nuclear war might be waged is probably unavoidable, and I have no complaint at the scenario used; it serves the purpose. The uncertainty about the quantities of smoke generated, the height to which smoke would be carried, the local meteorological effects with which its generation would be attended and the rate at which particles would aggregate and be washed out cannot be processes that could affect the quantity of smoke available for redistribution over the surface of the Earth by one or more orders of magnitude.

Even the climatic modelling is susceptible to sources of error not yet taken account of. The essence of the nuclear winter is a global temperature inversion: how stable is this against lateral variations? The point has not to my knowledge been tested. And there has been no investigation of the likelihood that such an inversion would be formed, by the diffusion of carbon particles over the surface of the Earth, without provoking the vertical movements in the atmosphere whose effect might well be to inhibit the temperature inversion altogether. I acknowledge, of course, that this is a difficult and, for the time being, an intractable problem; the authors have followed other modellers in solving the easy problems first. On such a matter, certain to stir the public imagination, it seems to me improper that the results of calculations should be published even in sober language without a warning to all potential readers of the pitfalls there must be. This is doubly unfortunate when, as on this occasion, a purportedly scientific publication is so fully amplified by popular articles, first in *Parade*, most recently in *Scientific American*.

I do not believe that the authors are politically motivated, except in the most general sense that they believe they may help to save the world. But I think it disingenuous of them to overlook the ways in which their conclusions may be used by politicians in other causes, often of a political character. ☐

Amino acid transport systems

SIR — We are concerned about the problem of making simple and unambiguous reference to well-characterized amino acid transport systems, and we indicate here how we aim to minimize unnecessary further complexities in our use of abbreviations for such systems.

Where a new transport system appears to be simply a variant of a known system, we plan to recognize this close relation with a terminology such as A1, A2, ..., reserving previously unused Roman letters only for more distinctly different systems. In this way we hope to avoid exaggerating complexity. We hope also to avoid evoking any single amino acid where it may be misleading because the system later turns out not to be approximately specific for that amino acid.

For systems for basic amino acids in general, where the mediator appears to accept these amino acids only in a cationic form, we plan to use the symbol y^+, the positive charge indicating the apparent selectivity for the cationic form. (This symbol omits an initial letter L earlier included in Ly^+ (ref. 1), whereby a single amino acid was too strongly evoked.) Conversely, for systems for dicarboxylic amino acids where these appear to be accepted only in their anionic form, we plan to use the symbol x^-. The plus and minus signs do not merely emphasize the requirement that the amino acid substrates have a positively or a negatively charged side chain; they also allow for the possibility that systems will later be found that specifically recognize and require the uncharged side chain group -COOH or $-NH_2$. We plan then to add a single subscript letter such as A, G, or C (for example, x_A) where it seems desirable to indicate that one of these anionic systems is rather specific for aspartate or glutamate, or includes cystine among its substrates. An important Na^+-independent system for anionic amino acids, x^-_C, does indeed include cystine and glutamate among its substrates. When a transport system x^- and y^+ is Na^+-dependent, we propose to indicate it by making x and y capital letters, X^- and Y^+. Specification as to the cell type or organelle under consideration will generally be needed when referring to a particular system, especially for a system apparently peculiar to one or a few tissues.

The terminology x, y may be seen as part of a scheme x, y, z, in which z stands for 'zwitterionic'. This leaves the as yet unassigned letter z for one or all systems for zwitterionic amino acids. The letter N is preempted for another meaning[2].

We do not necessarily mean to complicate matters by these ideas, by changing nonconforming abbreviations which may be regarded as already well established, even the capital L in the classical system[3], although a lower case l (as in l3, l4, ...) will seem appropriate for new similar Na^+-independent systems. We think it is important that a transport system should be characterized in detail before a code is designated for it. The various designations need even then to be regarded as provisional, as the homogeneity of a given component of transport is itself a provisional conclusion, and two components may turn out to be less similar than was at first supposed.

We invite colleagues who come to participate in identifying such transport systems to join us in a general effort for reasonable simplicity.

1. Christensen, H.N. & Liang, M. *J. biol. Chem.* **241**, 5542-5551 (1966).
2. Kilberg, M.S., Handlogten, M.I. & Christensen, H.N. *J. biol. Chem.* **255**, 4011-4019 (1980).
3. Oxender, D.L. & Christensen, H.N. *J. biol. Chem.* **238**, 3686-3699 (1983).

SIGNATORIES: Shiro Bannai (Tsukuba University School of Medicine, Japan); Halvor N. Christensen & Jaydutt V. Vadgama (Dept of Biological Chemistry, The University of Michigan, USA); J. Clive Ellory (Physiology Laboratory, Cambridge University, UK); Ellis Englesberg (Dept of Biological Sciences, University of California at Santa Barbara, USA); Guido G. Guidotti & Gian C. Gazzola (Institute of General Pathology, University of Parma, Italy); Michael S. Kilberg (Dept of Biochemistry and Molecular Biology, University of Florida, USA); Abel Lajtha, (Center for Neurochemistry, Wards Island, New York, USA); Bertram Sacktor (NIH Gerontology Research Center, Baltimore City Hospital Maryland, USA); F.V. Sepúlveda (ARC Institute of Animal Physiology, Babraham, Cambridge, UK); James D. Young (Dept of Biochemistry, The Chinese University of Hong Kong); David Yudilevich & Giovanni Mann (Queen Elizabeth College, University of London, UK).

Where is the revolution?

Electronic publishing will bring a new vitality to science. Michael Buckingham evaluates the promise and the problems.

WHEN Gutenberg invented moveable type, there was no doubt about how the new technology would be applied. Electronic publishing is in no such happy situation. The technology exists and certain benefits have long been clear, not least scientifically. But where, the scientist may reasonably ask, is the revolution in communication which will change his working life?

Electronic information systems such as *Chemical Abstracts, Index Medicus* and *Excerpta Medica* have been with us for some years, and are recognized to offer a better service than their printed equivalents. Hitherto, these services have entailed asking library staffs to conduct a search, but increasingly desk-top computers and word processors are being used to gain entry to them, while managers of the database systems are offering means of access which are simpler and cheaper than before. These developments give scientists freedom and flexibility, as well as the obvious physical convenience of being able to search electronically throughout many years' issues rather than physically to manhandle the printed volumes, while the quality of the searches is improved by using combinations of search terms in a way that would be impracticable with printed text. For these secondary services, electronic access continues to gain ground at the expense of the printed version.

. . . even enthusiastic supporters of electronic publication have to admit that presentation suffers in the process.

But what of the primary literature? For several publishers, the first step has been simply to make the full texts of some of their most important primary journals into computer databases. Thus the American Chemical Society last year made a series of its titles available in this way while, in the biomedical field, Elsevier has offered the rapid-publication journal *IRCS Medical Science* as a full-text database updated simultaneously with the appearance of the printed issues. This year, *The Lancet* and the *British Medical Journal* will become available in database form. Books are not being neglected. Saunders and Churchill Livingstone are active in making their medical textbooks available electronically; the Martindale *Extra Pharmacopeia* is now on-line; and Wiley has made its *Medical Research Directory* into an on-line file which reports work in progress in academic, hospital and government institutions.

The benefits for the reader of electronic access can be substantial. Because of postal delays alone, the advantage of speed is considerable — the reader of a British journal in the United States can see articles up to a month ahead of delivery of the printed issues and can also circumvent the delays of circulation lists. Moreover computers can be used to search past issues and deliver the text of articles immediately, without activating the ponderous processes of inter-library loan. The user of a textbook has the benefit of always reading the latest edition. But even enthusiastic supporters of electronic publication have to admit that presentation suffers in the process. Reading articles on a terminal screen is out of the question. Computer printout, even on the best office printers, lacks the clear, compact presentation of good typography, while the loss of illustrations may be unacceptable. Where papers are short, and rapid publication is a prime objective, then the advantages of electronic publication can be decisive. A 3,000 word paper, on the other hand, is all but totally unmanageable on-line, at least with present technology.

These developments are obvious first steps, but we are still far short of a revolution in scientific communication. Making the text of more journals available electronically is not the answer, nor is the simple speeding up of the information process by making titles, abstracts and bibliographic data accessible through databases. The real task is to develop electronic forms of communication based on a pragmatic understanding of the medium and of the needs of scientists. What can electronic publishing offer that printed journals cannot match? And how can such services better the convenience of dropping into a library at regular intervals to scan favourite titles and look through *Current Contents*?

The early emphasis on converting printed databases to electronic form has tended to overshadow one of the main advantages of computers — the fact that they offer an *interactive* means of communication. Once entered into a system, new information can be collated with existing entries, immediately updating the response to new enquiries. Thus we have an opportunity to introduce a new dynamism into scientific communication, countering the main weakness of the traditional journal.

I have elsewhere said that reading traditional journals is like entering a well kept cemetery; the papers stand in ordered rows, timeless and unchanging. Journals emerged as means of scientific communication when public lecture and debate became impracticable, but much was lost in the process. Scientists continue to talk to each other, of course, at congresses and symposia, but these can be attended only by a small proportion of the workers in any field. And the bibliographic problems associated with recording the proceedings of many meetings mean that much information is effectively lost once the meeting is over.

. . . reading traditional journals is like entering a well-kept cemetery.

The concept of an electronic journal receiving manuscripts by telephone and combining a comment and message service is not, of itself, new. Much of the early work undoubtedly became entrapped in the technology — summed up in the immortal words of John Senders: "I have seen the future and it doesn't work" — but things are changing. In Britain, the BLEND experiment (Birmingham and Loughborough Electronic Network Development), sponsored by the British Library, has provided a successful form of electronic communication for participants, though it has not yet been a vehicle for a great deal of formal original publication. And there are some commercial developments, notably in medicine. In Britain, Elsevier is launching *Clinical Notes On-Line*. This will be an electronic information service, based on submitted and reviewed material, in which

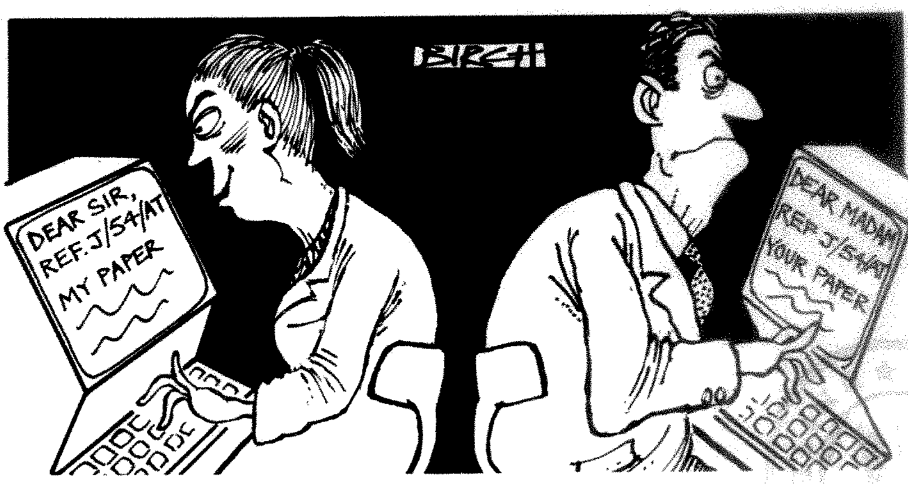

feedback from readers will play a crucial role. In the United States, 3M Inc. is sponsoring the development of a "Bulletin Board" service for the medical profession; the Minnesota Medical Conference Tree has 21 sections ranging from cardiology to general surgery to which physicians can contribute ideas.

These services have emerged to serve particular specialist groups. To meet the needs of the vast range of basic scientific research will be more demanding. In particular, it will be necessary to define the formal status of electronically published work — the role of the peer-review system has to be protected for exactly the same reasons as apply to the printed word. The basis for citation of the work must be equally clear, and some form of archival record must exist. These considerations probably mean that there will still be a need for a printed form of each record, although this need not necessarily be bound and circulated as a conventional journal.

. . . if publishers have to learn new skills, it is reasonable that editors and contributors should do so as well.

Because of the continuing role of printed publications it is entirely possible that electronic debating chambers will grow piecemeal from the electronic publication of existing journals. *IRCS Medical Science* now offers a comment facility, and *The Lancet*, with its strong Letters tradition, is almost an instant electronic forum. But where a journal is not already published electronically, it is arguably easier to start afresh. Whatever the case, contributions will certainly have to be vetted before being made available; editors will still have to edit, and not be seduced by the ease of transmitting the raw material submitted to them; and authors will have to be discouraged from allowing the opportunity to add postscripts to become a substitute for forethought. But if publishers have to adapt and learn new skills, then it is reasonable to ask that editors and contributors should do so as well.

There is a further factor, which being financial may well be decisive. All electronic services charge the reader directly according to the amount of information received. As things are now, a library is a general overhead provided at little direct cost to the individuals using it. Adjusting to a pay-as-you-go system will be traumatic; budgetary responsibility will move away from the librarian to the reader. The true challenge for all concerned, but most of all for the publishers, is to produce services that not only realize the tremendous potential of electronic publication but give immediate value for money. That challenge is a familiar one in selling newspapers but augurs a revolution for scientists and their publishers. ☐

Michael Buckingham is Managing Director of Elsevier-IRCS Ltd, Lancaster, UK.

New journals June 1982 to May 1983

Criteria for journals to be considered for review in this issue were circulated to publishers earlier this year, and were also published in *Nature*. They were that:

(i) the first number appeared, or the journal was re-titled, between June 1982 and May 1983 (although journals not covered in the previous review issues were also considered);*

(ii) the journal appears at least three times a year (two exceptions have been made to this rule);

(iii) the main language used is English;

(iv) where possible four issues should be made available for review, the first, the most recent, plus two others.

Last year's journals review supplement covered publications appearing between June 1981 and May 1982 and the second cut-off date, May 1983, allows for enough issues of a journal to have been published for a reasonable sample to be available for judgement (most are quarterlies). A spread of four different issues is taken as being the usual minimum on which reviewers' comments can be based.

Several journals known to satisfy the above criteria were not submitted for review, or arrived only in August or September, and therefore are not covered in this issue. It proved impossible to find reviewers for other, doubtless worthy journals, while some titles were considered to be of marginal interest to *Nature's* audience.

The brief given to reviewers was to limit themselves to comment on the publications sent to them, and to avoid discussion of general questions of periodical publishing. Opinions expressed in the reviews are based on a sample, and apply to mid-1983 at the latest. As in previous years, the preponderance of journals in the biological sciences reflects the bias of the material submitted for review, and the shortest possible (unconventional) abbreviations of titles have been used in the reviews.

Details of editors and frequency of publication, and the basic annual subscription rates appearing at the top of each review are given in most instances for 1985. These details are not complete in all cases, and readers interested in subscribing to a particular journal should check the rates with the publisher concerned.

---

*See *Nature* **293**, 341-369 (1981); **299**, 491-514 (1982); and **305**, 477-497 (1983).

Index to reviews

Annales Geophysicae 326
ATLA (Alternatives to Laboratory Animals) 321
Behavioral Neuroscience 323
Biological Agriculture & Horticulture 317
Bio/Technology 317
CAL: Computer Applications in the Laboratory 313
Cancer Investigation 318
Cell Biochemistry and Function 320
Chinese Journal of Oceanology and Limnology 325
Clinical & Experimental Metastasis 318
Clinical Physiology and Biochemistry 321
Computer Enhanced Spectroscopy 315
Computer Graphics Forum 312
Computers and Standards 311
Continental Shelf Research 325
Crop Protection 317
Crop Research 317
Diagnostic Immunology 319
Diagnostic Microbiology and Infectious Disease 320
Earthquake Prediction Research 328
Experiments in Fluids 330
First Break 326
Geochemistry 326
Image and Vision Computing 313
Integration: The VLSI Journal 311
Interfaces in Computing 311
International Journal of Developmental Neuroscience 324
Isotope Geoscience 327
Journal of African Earth Sciences 327
Journal of Biological Response Modifiers 318
Journal of Carbohydrate Chemistry 316
Journal of Cereal Science 316
Journal of Comparative Psychology 323
Journal of Metamorphic Geology 326
Journal of Microbiological Methods 320
Journal of Molecular Graphics 314
Journal of Sports Sciences 321
Laser and Particle Beams 328
Lens Research 322
Materials Chemistry and Physics 329
Mechanics of Materials 329
Molecular Biology & Medicine 318
Neurochemical Pathology 323
New Generation Computing 311
New Ideas in Psychology 323
Nucleosides and Nucleotides 316
Nutrition and Behavior 322
Plasma Chemistry and Plasma Processing 329
Quantitative Structure-Activity Relationships in Pharmacology, Chemistry and Biology 314
Reactive Polymers, Ion Exchangers, Sorbents 315
Renewable Sources of Energy 324
Risk Analysis 324
Solvent Extraction and Ion Exchange 315
Sports Medicine 321
Technology and Science of Informatics 311
Trends in Biotechnology 317

Computing communications

W.F. Clocksin

New Generation Computing: An International Journal on Fifth Generation Computers.
Editor-in-chief T. Moto-oka.
Springer-Verlag. 4/yr. DM 250, $96.
Integration: The VLSI Journal. Editor-in-chief L. Spaanenburg.
North-Holland. 4/yr. Dfl. 250.
Technology and Science of Informatics. Editor-in-chief Bertrand Meyer.
North Oxford Academic, 242 Banbury Road, Oxford OX2 7DR, UK. 6/yr. £60, $96.

THE conventional computer designs established by Alan Turing and John von Neumann have begun to encounter numerous difficulties; most particularly, low software productivity and insufficient processing power on non-numerical data have led to the so-called "software crisis". In response, promising new ways of thinking about computation have emerged at the intersection of hardware and software studies. One result has been VLSI (Very Large Scale Integration), a semiconductor technology which makes possible the fabrication of electronic circuits having hundreds of thousands of transistors on an area the size of a fingernail. On the software side, it is becoming increasingly appreciated that the mathematical properties of functional and relational programming languages (such as Prolog) are suitable for specifying logical inferences and computations in an inherently parallel fashion. Such parallelism promises to make effective use of the host of computing elements provided by VLSI technology.

These interconnected technical issues, taken together with planned applications in natural language processing and knowledge engineering, constitute the new generation of computing, and a journal sympathetic to these aims seems sure to be well received. *New Generation Computing* (NGC) shows every sign of fulfilling its potential as the forum for researchers in this area. The need for a new journal is well justified, not the least because of the appalling publication delay in most computer science journals. Credit is due to the Institute for New Generation Computing in Japan for instigating this journal, and for showing from the start a concern for technical and scientific issues.

All of the papers appearing in NGC are in English, but while most of them have thus far originated from Japanese researchers I predict that representation will become more widespread as the field matures. The publisher has done a fine job of packaging and presentation, although in some articles the standard of English (an unfamiliar language to many contributors) leaves much to be desired, requiring considerable imagination on the part of the reader — greater editorial intervention seems to be called for in this regard. Similarly the scientific standard of the papers is somewhat patchy, although this will undoubtedly improve in the future. Each issue of the journal contains about eight papers, many of them short notes of some six pages in length, and there is usually an editorial and a non-technical "leading article" of a more general nature. The journal needs to do some growing up, but my overall impression is that NGC will prove to be indispensable to those who need to be kept informed of developments as the fifth generation approaches.

Integration: The VLSI Journal is a natural partner to NGC. The title *Integration* is an appropriate if unintended *double entendre*, for the coverage of this journal is of interest to the mathematician and computer scientist as well as the electrical engineer. Editorial policy stresses the mutual benefit of communication between these practitioners, and this is a very healthy sentiment which I hope propagates more widely to industry. Certainly, *Integration* will be a valuable addition to the literature serving the computer scientist and engineer.

The papers published in the journal rise to the challenge laid down by the editors and are of high standard. Like NGC, *Integration* has an admirably short publication delay, and also includes a number of departments — letters to the editor, news and a calendar of events, and abstracts of a dozen or so relevant papers published elsewhere. Quality of illustrations is important in reports of VLSI work, and monochrome photographs and half-tones are reproduced to a high standard. As yet, no colour plates are in evidence, however, and no advice on submitting coloured photographs is given, but colour does not seem to be out of the question because both the cover and one advertisement sport the appropriate hues.

Compared with *Integration*, *Technology and Science of Informatics* (TSI) has a wide coverage and is intended to appeal to the more general audience of computer professionals. The journal is a cover-to-cover translation of the French publication, *Technique et Science Informatiques*, and classifies its papers under the three headings "Surveys", "Applications" and "Research". Each paper is introduced by a few paragraphs of commentary by a member of the editorial board. In addition, there are plenty of photographs and line drawings, and there is a relatively large departmental section with correspondence, reviews, bulletins and calendar. The four or five papers appearing in each issue are not dated, giving no obvious clue to publication delay.

It would be natural to find a French emphasis here and, indeed, most of the reviews are of books written in French and the format is identical to that of the parent journal. The publishers have clearly gone to some trouble to translate the papers well, though there is the occasional bloomer; in one article on Unix, for example, the phrase "branching catalogue" should have been rendered "tree-structured directory".

TECHNOLOGY AND SCIENCE OF INFORMATICS

The advantage of TSI is that it offers a direct line to the French computing community, and it will meet the needs of those especially interested in knowing what is happening across the Channel. □

W.F. Clocksin is an Assistant Director of Research at the Computer Laboratory, University of Cambridge.

Standard reading

A.M. Addyman

Computers and Standards.
Editor-in-chief John L. Berg.
North-Holland. 4/yr. Dfl. 262.
Interfaces in Computing.
Editors R.W. Dobinson and P.N. Clout.
Elsevier Sequoia. 4/yr. SwFr. 195, $92.75.

THE advent of *Computers and Standards* (CS) reflects a growing awareness of the need for standards within the computing industry. Unlike most journals in the general area of computing, CS is not limited to one topic such as programming or computer architecture. Rather, it addresses standardization, which affects virtually all aspects of computing. Indeed there is an increasing number of branches of the subject in which the only effective way forward is through the standards process.

Most of the information in CS appears in the form of papers and commentaries; why some contributions are classified as papers and others as commentaries is not clear — to me at least. The quality of the material is, generally, very high, which is only to be expected as many of the authors are well-known and very active in standardization work. Recent issues have contained contributions on the programming language

A choice of new journals from Karger

Acute Care
International Review of Critical Care Medicine
An instructive guidance for all specialists working in intensive care units who require access to the newest developments in emergency care procedures.
Editors: M.H. Weil, North Chicago/Ill.
E.C. Rackow, Chicago/Ill.
1985: Volume 11 with 4 issues
Institutional subscription: SFr. 218.-
Personal subscription: SFr. 109.-

Digestive Surgery
A new reference to basic research as well as advances and technical innovations in a diversity of fields relating to surgery of the alimentary tract.
Editors: E.H. Farthmann, Freiburg i.Br.
L.F. Hollender, Strasbourg
1985: Volume 2 with 4 issues
Institutional subscription: SFr. 246.-
Personal subscription: SFr. 123.-

Experimental and Clinical Immunogenetics
A guide to the explosive growth of research in immunogenetics and its emerging clinical applications.
Editor: K. Bauer, Heidelberg
1985: Volume 2 with 4 issues
Institutional subscription: SFr. 198.-
Personal subscription: SFr. 138.60

Pediatrician
International Journal of Child and Adolescent Health
Problem-orientated topic issues pertinent to practitioners for the maintenance of international expertise on psychological problems and medical disorders with special emphasis on ambulatory pediatrics.
Editor: D.W. Kaplan, Denver/Colo.
1983/85: Volume 12 with 4 issues
Institutional subscription: SFr. 180.-
Personal subscription: SFr. 90.-

Pediatric Neuroscience
Successor to 'Child's Brain'
Experimental and clinical studies featuring new information and observations in pediatric neurosurgery as well as neurology, neuroradiology and neuropathology.
Editors: E.B. Hendrick, Toronto/Ont.
D.H. Reigel, Pittsburgh/Pa.
1985: Volume 12 with 6 issues
Institutional subscription: SFr. 330.-
Personal subscription: SFr. 181.50

Psychopathology
International Journal of Descriptive Psychopathology, Phenomenology and Clinical Diagnostics
Research centered on the concepts, models, and diagnostic categories that guide the practice of psychiatry and help illustrate the dynamics of psychopathologic phenomena.
Editors: P. Berner, Wien, E. Gabriel, Wien
1985: Volume 18 with 6 issues
Institutional subscription: SFr. 254.-
Personal subscription: SFr. 177.80

Free sample copies available on request

KARGER
S. Karger AG, P.O. Box, CH-4009 Basel, Switzerland

KI 84256

Circle No.10 on Reader Service Card.

COBOL, open systems interconnection (OSI) and database management systems, in addition to a number of articles dealing with the process by which standards are produced and the implications of standards production. As well as the main contributions, each issue of the journal contains details of standards activities and standards publications.

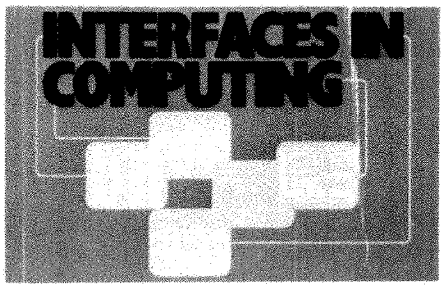

Much of the content of CS will be of particular value to organizations in the computing industry, because the development of standards affects the market for their products. The libraries of educational establishments will find there is less demand for the journal, unless their researchers are active in such fields as programming languages, graphics, databases or computer networks. The key to the success of CS is the fact that the information it contains is generally very difficult to obtain unless one is actively involved with the work. However, the publishers will need to ensure that the delays between the receipt and publication of papers are reduced, because of the perishable nature of much of the information on standards.

Elsevier Sequoia, the publishers of *Interfaces in Computing* (IC), cannot be criticized for tardy publication — the time from receipt of a manuscript to its appearance in print is typically six months. This is essentially a practical journal — like *Software: Practice and Experience*, for example — and it has a fresh, down-to-earth quality. Many of the papers have been written by authors who have created something and are writing from experience; the paper is the result of their work not the reason for it!

Even though there are interfaces in every piece of computer hardware and software, the variety of topics embraced by IC is truly surprising. Subjects covered recently include computer transcription of machine shorthand; device-independent graphics; a pipelined multimicroprocessor system; Cambridge Ring interfaces; CAMAC; and entity relational database systems.

The scope and nature of this journal is such that many computing professionals will find at least one paper of interest in each issue, though the large number of contributions dealing with hardware will probably mean that computer engineers will find more than their software counterparts. Certainly, I will add it to my list of journals to be read. ☐

A.M. Addyman is in the Department of Computer Science at the University of Manchester.

Graphic applications for Europe

Julian Gallop

Computer Graphics Forum.
Editors Günter Enderle and David Duce.
North-Holland. 4/yr. Dfl. 222.

COMPUTER graphics has become accessible to the layman since personal computers with graphics have become more sophisticated and cheaper, and many magazines are available to such readers. The professional user, practitioner or researcher has different requirements, however, and there are far fewer relevant journals available.

Computer Graphics Forum (CGF) is the official publication of the European Association for Computer Graphics (Eurographics) and is now in its third volume. (For an individual, joining Eurographics and thereby obtaining CGF free is cheaper than buying the journal separately.) The text is edited and typeset with computer assistance and the quality of production is good and (after the first volume) uniform.

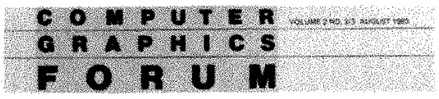

A typical issue contains refereed technical articles; reports and announcements; and Eurographics association news. The technical articles (generally 5–15 pages in length) cover various applications of computer graphics (for example, in chemistry, molecular biology and population planning) and studies in theory or techniques (for example, contouring, picture processing and geometric modelling). The number of articles varies perhaps too widely between one issue and the next; the average is about four to five an issue. This is a rapidly changing field and CGF aims to publish refereed articles quickly. In general, this is achieved, but there has clearly been some publication delay when colour photographs are reproduced on the same pages as text. Occasionally, colour photographs seem to have been included gratuitously and do not add information, notably the pictures of a VDU screen that is virtually a single colour.

Part of CGF is devoted to reports, announcements and surveys. Important events in Europe, and some outside, are announced and reported, including meetings, workshops and conferences. In this part of the journal a book review section has recently been started.

There are parallels between CGF and *Computer Graphics*, published by the Siggraph Association (Special Interest Group on Computer Graphics). However, while international, the latter has a strong North American emphasis and CGF is providing a focal point for refereed technical articles of European origin. In addition, the Siggraph technical contributions are largely concentrated on its conference proceedings and on the very valuable and thorough annual bibliography on computer graphics.

By contrast with other journals in this area, a strong theme in CGF is the standardization of computer graphics. Progress reports, articles on the interpretation and use of standards, and a survey of implementations of the computer graphics programming Standard have been published. Also, an algorithms section has been announced and if successful will encourage the exchange of software using the Standard. □

Julian Gallop is a Senior Scientific Officer in the Central Computing Division of the Rutherford Appleton Laboratory, Chilton, Oxfordshire.

CAL tech

D.J. Malcolme-Lawes

CAL (Computer Applications in the Laboratory).
Editors Lawrence P. Forsley, David W. Grant, Rudolf E. Kaiser and Anthony J. Rackstraw.
*Alfred Heuthig Verlag, PO Box 102869, D-6900 Heidelberg 1, West Germany.**
6/yr. £30, $50.

AMIDST the welter of magazines feeding the public appetite for computing at home, we are now seeing the appearance of publications which attempt to provide a forum for the exchange of information on the scientific uses of microcomputers. One such journal, *Laboratory Microcomputer,* was reviewed in *Nature* last year (**305**, 495; 1983). Another is *Computer Applications in the Laboratory,* launched in March 1983, which apparently wishes to be known as CAL.

As an avid reader of popular computer magazines and a user of laboratory microcomputers, I was moderately excited at my first contact with CAL, and felt that here perhaps was a journal designed for people like me. Sadly this excitement has faded as more issues have appeared.

The publication is well turned out and has many of the features of a popular computer magazine: a glossy colour cover, plenty of photographs, large advertisements, and an editorial and a pattern of sections in each issue. Essentially the magazine is divided into four — news, features, series and "scientific originals". The news items are most commonly one-page articles/advertisements reporting a new computer or program or a conference — FORTH advocates and Perkin-Elmer have dominated so far. Features vary from short reviews of books and programs (e.g. BASIC compilers for Applesoft BASIC), to literature searching, to word processing (although both of the word-processing articles have been on the Apple Writer). The series in the first year have included "Personal computers in the laboratory", "Interfacing", "Learning FORTH" and "6502 made easy". In each case division of the text into different issues was unfortunate because the individual episodes so far have occupied only a small amount of space, and in some instances have contained very little worthwhile information.

The criticisms to be levelled at these three sections are that the hard information content is too low and that selection of topics is too restricted (applications other than chromatography and computers other than the Apple would be of interest). Further, the excessive use of half-page cartoons conveys the impression of a vain attempt to hide a lack of editorial material.

The original work (including short communications) reported in the final section comes from a wider range of contributors and is consequently much more varied. Articles have covered applications of several popular microcomputers, and even the DEC Minc mini. Most of them so far have been on software, covering topics such as the resolution of HPLC peaks, measurement of lung function in babies and children, and electrothermal atomic absorption spectroscopic analysis. The last issue available for review (1/84; volume numbers are not used) contained one scientific original (4 pages) and one short communication (3 pages). That is seven pages out of a total of 60. Not all issues are that low on papers, but even so the serious content is disappointingly small.

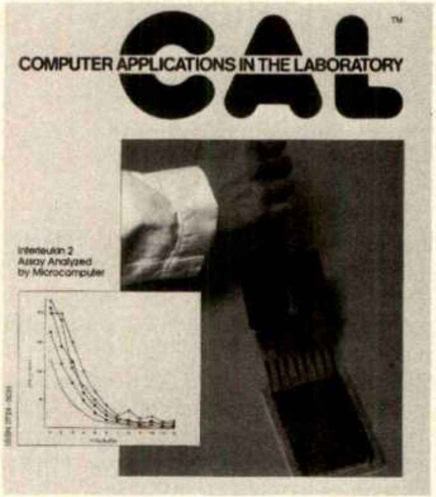
COMPUTER APPLICATIONS IN THE LABORATORY
CAL
TM
Interleukin 2 Assay Analyzed by Microcomputer

There is indeed a place for a publication such as this, half journal and half magazine. But if CAL is to satisfy its readers, and not just its advertisers, the editors will have to include more meat and less froth. □

D.J. Malcolme-Lawes is Royal Society Research Fellow in the Physical Sciences at King's College, University of London.

---

*Also 97 Elgin Crescent, London W11 2JF, and 611 Broadway, New York, NY 10012.

Need for greater vision?

P.W. Hawkes

Image and Vision Computing.
General editor Keith Baker.
Butterworth. 4/yr.
£82, $164.

BRANCHES of science are commonly referred to as fields but the application of computing to imaging and vision is more like a wide sea, spreading over robotics, medicine, military reconnaissance, astronomy, microscopy and a host of other subjects. Thus far it is a shallow sea, however, for despite all the theoretical work there are far more people paddling than swimming. Inevitably, progress is being made on related practical problems in different domains of application. It is in the hope of countering the duplication of results in specialist serials, by collecting together papers of potential interest in several disciplines, that *Image and Vision Computing* (IVC) has been launched by Butterworth.

So far, its success is limited. There are indeed practical papers of general interest but there are others that would have been more widely read in a specialist journal. In particular there are numerous theoretical contributions for which natural homes already exist — the *IEEE Transactions on Pattern Analysis and Machine Intelligence, Computer Vision, Graphics and Image Processing* and *Pattern Recognition* spring to mind. Furthermore, there are only five or six articles per issue, so few that workers in this field will have to look at the other, more-specialized publications anyway. So the case for this new interdisciplinary journal is not very strong.

In addition to original articles, each issue includes a list of related publications in other journals; this list is very short (a dozen or so per issue) but includes long abstracts. It is followed by one or two book reviews (the May 1984 issue contains a review of a book published in 1982), a news feature entitled "Insight", a page or two of "Product News" and a calendar of forthcoming meetings. The latter is useful and easy to consult, though it is not obvious what Applications for Management and Productivity will be discussed at CAMP '84 in Berlin!

It seems to me that there is a serious danger that IVC will attract material difficult to place elsewhere. These first issues do contain some extremely interesting articles—but there will have to be far more of them if the journal is to occupy the place to which its editor aspires. □

P.W. Hawkes is Maître de Recherches at the Laboratoire d'Optique Electronique du CNRS, Toulouse.

Drug design centred

J.M. Midgley

Quantitative Structure-Activity Relationships in Pharmacology, Chemistry and Biology.
Editors Joachim K. Seydel and F. Darvas.
Verlag Chemie. 4/yr. DM 280, $168.

THE elaboration of molecules which will selectively control biochemical processes in a predictable manner is one of the ultimate goals of drug research. Drug design has been defined as the application of rational methodologies which result in a new drug (either through total innovation or via the optimization of a lead compound), and in the past two decades there has been a rapid development in techniques for elucidating quantitative structure-activity relationships (QSAR) for many compounds possessing diverse biological activities.

An indication of the activity in this field is the emergence of a specialist journal, *QSAR in Pharmacology, Chemistry and Biology*, which has a distinguished editorial staff drawn largely from academia in Europe and the United States. The purpose of the journal is "to collect contributions on all aspects of the subject embodied in its title", in particular theoretical and methodological aspects and innovative applications of QSAR. Each of the four issues published annually contains about four refereed contributions (averaging five to six pages in length) of original research, and a balance of subject matter within the editorial remit has been achieved so far. The articles are clear and succinct, and their scientific standard is comparable to those of a similar nature appearing in established journals. The papers largely originate from Europe and the United States, and the significant industrial contribution reflects the growing economic (as well as scientific) importance of QSAR.

ACID PRECIPITATION DIGEST

Each monthly issue provides capsule summaries of —

- news items
- books
- technical reports
- periodical reports
- conference proceedings
- peer reviewed literature
- calendar of upcoming conferences and events
- documents

"Current...concise... comprehensive — the single best source for information on acid rain." **Dr. Chris Bernabo,** Executive Director, *National Acid Precipitation Assessment Program*

Subscriptions (one year): Corporate, For-Profit Firms, $125; Government Agencies, $65; Nonprofit organizations (including public and academic libraries), $30. Non-affiliated individuals -inquire for rates. Add $15 for foreign airmail postage ($5 for Canada). Make checks/money orders payable to: **Acid Precipitation Digest.**

Published by the nonprofit,
non-advocacy
Acid Rain Information Clearinghouse
a project of the
Center for Environmental Information, Inc.
Department N, 33 South Washington Street
Rochester, New York 14608 (716)546-3796

Circle No.34 on Reader Service Card.

Somewhat surprisingly, there is no editorial comment or opportunity for correspondence and the remainder of each issue is taken up with approximately 60 abstracts of publications related to QSAR; these are comprehensive and drawn from diverse sources, but may be too dated to excite the *aficionado*. The whole is produced in a modern two-column format, with clear print and illustrations.

At the price the circulation may be confined to libraries and dedicated investigators in the field. The period from receipt to publication of the articles is variable, often only comparable to that in established international journals, so that research workers may opt to present their more interesting findings to a wider readership rather than preach to the converted. ☐

J.M. Midgley is Professor of Pharmacy and Head of the Pharmaceutical Chemistry Division, Department of Pharmacy, University of Strathclyde.

Picture chemistry!

Peter Kollman

Journal of Molecular Graphics.
Editor A.J. Morffew.
Butterworth. 4/yr. £55, $110.

THE *Journal of Molecular Graphics* (JMG), published in association with the Molecular Graphics Society, was founded to give "computational scientists" a forum to publish their work. The importance of computer graphics in studies of molecular systems, in drug design and in X-ray crystallographic studies of macromolecular structure has begun to be appreciated by many chemists. Indeed I am among the converts to the view that computer graphics is an essential tool for any chemist studying even moderately complex molecules. A corollary to this is that well-written computer software is often crucial in asking the most pertinent questions about a particular molecular system, and in answering them. Thus, there should be mechanisms for publication of software approaches to the solution of chemical problems and for giving due credit to elegant software.

In this context, it should be noted that *Computers and Chemistry* (launched in 1976) and the *Journal of Computational Chemistry* (which first appeared in 1980 and was reviewed in *Nature* **299**, 513; 1982) are journals where descriptions of both computer software and its applications are already welcomed. Of these two, it is significant that the latter has been the more successful because it has attracted a mix of software descriptions and applications of high quality and interest to many scientists.

In its first four issues, JMG has published articles mainly on computer graphics algorithms. Sample applications of the algorithms often occupy a small part at the end of the article and typically the papers do not have a strong scientific punch-line. One cannot blame the authors for saving their scientific message for journals where more chemical scientists will read them, but in my opinion the separation of computer graphics from other areas of computational chemistry is not a good idea. Besides the regular articles, the journal has also included a bibliography of molecular graphics applications, abstracts from the meetings which include computer graphics, and descriptions of new computer products of potential interest to chemists.

One commendable advance made by JMG is to combine colour figures from the individual articles into a central section of colour, thus allowing high-quality colour pictures to be published without charge to the authors. The science itself can often be delivered most effectively with colour figures, yet most journals charge a large amount for publication ($1,000–$2,500 by the *Journal of Medicinal Chemistry, Journal of the American Chemical Society* or *Proceedings of the National Academy of Sciences*) and often also require colour-separated prints (for example the *Journal of Computational Chemistry*).

The appearance of this journal has certainly facilitated the publication of articles dealing with computer graphics, particularly in the approaches requiring examples in colour. Whether it will thrive will depend on many factors, principally whether the field of molecular graphics will emerge as a separate discipline or whether the journal can attract articles which appeal not only to the molecular graphics community but to a broader constituency of chemists. How the focus could be broadened is not clear, but the very title of the journal cannot help but give the impression that papers other than those dealing explicitly with graphics are less likely to be accepted or receive a wide readership. ☐

Peter Kollman is Professor of Pharmaceutical Chemistry in the School of Pharmacy, University of California at San Francisco.

At the interfaces of spectroscopy

K.A. McLauchlan

Computer Enhanced Spectroscopy: An International Journal.
Editor-in-chief H.A. Willis.
Wiley-Heyden. 4/yr. £65, $130.

DATA-handling by computer and computer interfacing to laboratory equipment are very much to the fore in the 1980s, and the basic idea of a new journal to cover such matters is sound. *Computer Enhanced Spectroscopy* (CES) deals with any use of a computer in any branch of spectroscopy. Its contents include data manipulation on- and off-line, library searching, design principles of systems and specific experimental devices; unusually, much software is reported. Authors are invited to publish details which went undescribed in an original scientific paper, a seductive call to double their number of publications.

The problems for the journal, though, are several. Such a range of specialist spectroscopic techniques is involved that the matter dealing with any one topic is dilute. Since in many research fields there exist dedicated journals, it seems unlikely that a seminal paper in, for example, magnetic resonance will make its way to CES. For ideas of inter-disciplinary interest, on the other hand, there exist the well-respected *Reviews of Scientific Instruments* and *Journal of Physics (E)*, which would take most of the material. Many of the practical accounts are device-orientated and concern specific microcomputers and specific types of spectrometer. They are of limited use, for wherever such interfacing is necessary one finds that because of technical advances many problems must be solved afresh. Similarly, software is usually most efficiently written for the precise microcomputer and application in mind, and often not in a high-level language. Some of the basic data manipulation points made in the four issues of Vol. 1 are very straightforward.

The journal is well and attractively produced with excellent reproductions of a wide range of devices, flow diagrams and software. However the first volume does appear to have been short of material, which has perhaps led to the publication of some rather trivial articles. Because of this uncertain start, and the reservations expressed above, I cannot believe that it will become widely read. □

K.A. McLauchlan is a Lecturer in the Physical Chemistry Laboratory, University of Oxford.

Polymer exchange

Philip Hodge

Reactive Polymers, Ion Exchangers, Sorbents.
Editor-in-chief F.G. Helfferich.
Elsevier Scientific. 8/yr. Dfl. 412, $160.

FOR MOST of its history, polymer science has been mainly concerned with polymerization processes, the physical properties of polymers, and their applications in material science. There are many journals that cater for these areas. In contrast relatively little work has been carried out on synthetic reactive polymers. This is surprising, bearing in mind that nature makes extensive use of polymers in various recognition processes and to catalyse and control reactions between low molecular weight species.

In recent years interest in reactive polymers has increased considerably and *Reactive Polymers, Ion Exchangers, Sorbents* seeks to provide a forum for this underdeveloped area of macromolecular science. The journal is well produced and contains original papers, short communications, reviews, book reviews, letters to the editor and a news page. For the first year it appeared quarterly but eight issues will appear in 1984, surely a sign of good health.

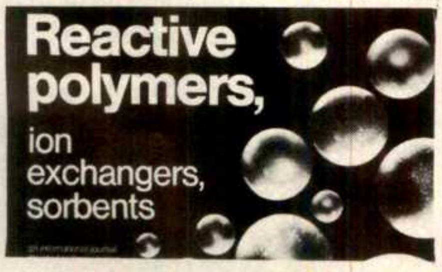

The standard of papers is excellent and there are contributions from many internationally known authors of good reputation. Thus far a rather high proportion of the papers has dealt with ion exchange resins, metal extraction using various sorbents and closely related topics. This bias probably reflects the fact that ion exchange resins are one of the few types of reactive polymers which have been studied for many years and have industrial applications. There are, however, many other areas of interest — polymer-supported catalysts, chemical modifications of synthetic and natural polymers, and biomedical and pharmaceutical applications, for example — and it is to be hoped that the number of papers dealing with these areas will increase to give the journal a better balance.

It is still hard to say how well this journal will fare in the long term. It serves a growing area of polymer science and if it can attract sufficient papers and publish them more frequently, whilst maintaining its present quality, it could do well. □

Philip Hodge is a Reader in Organic Chemistry at the University of Lancaster.

Separate ways

Alwyn McKay

Solvent Extraction and Ion Exchange.
Editors E. Philip Horwitz and James D. Navratil.
Dekker. 6/yr. $150 (US), $166.50 (elsewhere).

THE launching of *Solvent Extraction and Ion Exchange* (SEIE) may well be considered overdue, in view of the enormous expansion in this area since 1945. The journal is a companion to *Separation Science and Technology*, and its appearance follows a questionnaire addressed to specialists in the two related fields.

The first volume of four numbers, published during 1983, contains important material. There are 32 papers, five "notes" (not obviously distinguishable from papers), two valuable review articles and two letters; a bibliography and other items are included in each issue. Volume 2 (1984) will be larger, with eight issues, and it is expected that the journal will be expanded yet further. Certainly, there is plenty of scope for this.

There is, however, a long way to go before the editors' hope of the journal becoming the principal vehicle for papers on solvent extraction and ion exchange can be realized. At present SEIE carries only a small proportion of the total of papers on the subject being published, as the number of entries in the bibliography demonstrates. Moreover the selection is unbalanced in various ways. Academic chemical topics predominate, with emphasis on matters of nuclear interest, and there is little on equipment or industrial processes. On the other hand, the ratio of four solvent extraction papers to one ion exchange paper seems a fair one.

The journal is reproduced directly from the authors' typescripts and diagrams, but despite this it is not particularly cheap. The quality of presentation varies from very good to just adequate; in the worst cases one wishes that the method of printing did not preclude sub-editing to get rid of misprints, poor English and other blemishes. On the positive side, photographic reproduction should speed up publication, and most papers do appear reasonably promptly. The bibliography, however, being based on *Chemical Abstracts* rather than current journal contents lists, is unfortunately somewhat out-of-date.

My verdict is that SEIE indeed fills a gap. But there is some sacrifice of quality to economy and speed of production, and the editors would do well to keep an eye on their standards. □

Alwyn McKay was formerly a Group Leader in the Chemical Technology Division of the Atomic Energy Research Establishment, Harwell, Oxfordshire.

The carbohydrate competition

Neil Baggett

Journal of Carbohydrate Chemistry.
Editor Donald E. Kiely.
Dekker. 4/yr.
$110 (US), $121 (elsewhere).

THE aim of the *Journal of Carbohydrate Chemistry* (JCC), which in part replaces the *Journal of Carbohydrates, Nucleosides, Nucleotides*, is to provide an international forum for aspects of carbohydrate chemistry, excluding polysaccharide studies. This area of chemistry is already served by *Carbohydrate Research*, so that JCC does not fill a vacant niche but competes with the established journal. It is therefore appropriate to compare the two.

The new journal includes original research papers and communications, with some reviews of "timely topics in carbohydrate chemistry". *Carbohydrate Research* does not contain reviews but does cover studies on polysaccharides. Both journals publish articles in English (mainly), but also in French and German. The new journal comprises four issues per year (six were originally promised), so it is much smaller but also much cheaper than its competitor; the two are roughly comparable in terms of price per page. Perhaps the most noticeable difference between the journals is that JCC is reproduced direct from the authors' typescripts, which means that very rapid publication can be achieved but also, on occasions, that minor but necessary editing is not done. Together with the non-uniformity of type, this gives the journal a rather unfinished look, and the principal attraction of JCC for potential authors must be the speed of publication.

The claim to be an international journal is justified. There are representatives from 13 countries on the editorial board and the papers published to date originate from a wide geographical range. There is, however, a bias towards the United States, with almost half of the editorial board and one-third of papers coming from that country.

So far the standard of papers and reviews in the new journal is generally good, perhaps because roughly half of them have been contributed by members of the editorial board. The viability of JCC will depend on whether papers of a similar quality are forthcoming in the future from a broader range of authors, especially if the American Chemical Society continues to expand its range of publications into the area of carbohydrate chemistry. Whilst there are advantages for authors in having two journals to choose between, librarians are not in such a happy position — the standard of the papers in both JCC and *Carbohydrate Research* means that neither can be just ignored. □

Neil Baggett is a Lecturer in the Department of Chemistry, University of Birmingham, UK.

Nucleic acid news

Janet L. Rideout

Nucleosides & Nucleotides.
Executive editor John A. Secrist III.
Dekker. 5/yr. $149.50 (US),
$163.25 (elsewhere).

Nucleosides and Nucleotides (NN) is unashamedly a speciality journal, but one which covers an especially vigorous area of science. Its aim is to concentrate upon the chemistry and biology of nucleosides, nucleotides and closely related compounds, with the chemistry of new entities being emphasized.

Obviously, for this, as for most new journals, success in the long run will depend upon the submission of material from authors who generally send their papers to more established publications. Judging by the eminence of some of the contributors to the first two volumes, NN has made an auspicious beginning. And although the journal is reproduced from camera-ready copy, the standard of production is very high — reviews, original articles and notes are clearly presented, with chemical structures, tables and so on embedded as appropriate in the text.

Submissions are refereed, and must contain experimental details (a refreshing feature to be recommended to the editors of other journals devoted to the rapid publication of scientific research). Authors of review articles are encouraged to include critical comments, and thus far reviewers are responding and are doing more than simply providing compilations of the literature pertaining to a given subject. Lately, abstracts of recent articles and bibliographical data on selected subjects have been added to the journal's contents.

Nucleosides & Nucleotides

Anyone working in this field, or wishing to enter it, will need to refer to NN for information on developments in the chemistry and biology of nucleic acids, for indications of new directions the field is taking, as well as for the comprehensive reviews which appear from time to time. The subscription price is not unreasonable, and altogether the journal seems set for a healthy future. □

Janet L. Rideout is a Group Leader in the Organic Chemistry Department at Burroughs Wellcome, Research Triangle Park, North Carolina.

With the grain

Donald D. Kasarda

Journal of Cereal Science.
Editor T. Galliard.
Academic. 4/yr. £43, $98.

BECAUSE of the enormous importance of cereal grains as food, animal feeds and raw materials, almost every cereal-producing country in the world — from Australia to the USSR — has in recent years made huge investments in cereals research. Such expansion has created a need for extra journals as outlets for the resulting publications. The new *Journal of Cereal Science* (JCS) covers much the same areas as the already well-established journal *Cereal Chemistry*, including research papers (and an occasional review) on topics such as component characterization, nutritional quality, food science and technology, and genetics as they relate to the functional or nutritional quality of cereal grains (unlike *Cereal Chemistry*, however, JCS does not accept papers on legume "grains").

I have the impression that, in addition to a need for more journal space, the impetus for the formation of JCS stemmed partly from dissatisfaction by some scientists (particularly in Britain and France) with what they considered unfortunate reviewing practices by *Cereal Chemistry* that delayed publication of papers. They were also unhappy with the page charges levied by that journal. Since then, it should be said, *Cereal Chemistry* has dealt with many of its problems although the page charges remain.

My examination of five of the six issues out at the time of writing tells me that JCS is doing well; many papers are of a high standard, the quality of editing and of production are good, publication occurs a not-unreasonable six to ten months after receipt of a manuscript, and there are no page charges.

A few papers seem rather pedestrian, however, and such contributions may discourage authors from choosing this journal to publish their better work. On the other hand, authors must contend with the tendency of editors of the better general-science journals to recommend that papers dealing with cereal grains, even reasonably good ones, should be published in speciality journals. Such attitudes, however unfortunate, benefit *Cereal Chemistry* and now, I suspect, JCS as well.

I believe this new journal is here to stay. Not only that, the commitment to improved quality evident in occasional editorials by the editor T. Galliard, and one of his colleagues, J. D. Schofield, should lead to expansion. □

Donald D. Kasarda is Research Leader of the Food Proteins Research Unit, Western Regional Research Center, ARS, US Department of Agriculture, Albany, California.

Agricultural produce

Leonard Broadbent

Crop Protection: An International Journal of Pest, Disease and Weed Control.
Editor G.E. Russell.
Butterworth. 4/yr. £68, $136.
Crop Research.
Editors C.A. Wood, Pauline B. Topham, Jane Bryan-Jones and P.J. Dudney.
Scottish Academic Press.
2/yr. £13.50, $30.
Biological Agriculture & Horticulture An International Journal.
Editor R.D. Hodges.
A B Academic Publishers, PO Box 97, Berkhamsted, Herts HP4 2PX, UK.
4/yr. £19, $33 (personal); £55, $89.50 (institutional).

HORTICULTURE and, in historical terms, its offshoot agriculture, are multi-disciplinary technologies developed during the past 12,000 years. Much more recent is the science-based but energy-intensive production of plants and animals, to which are devoted so many journals. The three well-produced publications reviewed here add to this literature but do not fill gaps in it.

Crop Protection (CP), published since 1982, is attracting good papers from all over the world. An analysis of the four numbers available for review gives 15 papers from Britain, 12 from the United States and 20 from ten other countries, covering every aspect of protection science and practice, including biological, chemical and agronomic control, plant breeding, engineering and economics. It has six well-known and expert editors, and a distinguished advisory board of 15 members drawn from almost as many countries — presumably as bait, as possibly was the initial subscription of £45, which in two years has risen to £68. For this one gets about 48 scientific papers or reviews per volume, averaging ten pages in length, that is, a cost of about £0.14 per page of scientific paper (not counting book reviews). This is expensive: an old-established journal publishes similar papers, with more words per page, profitably at £0.07 per page.

Crop Research (CR) is not new but continues *Horticultural Research*, and remains a journal for the publication of research by the Scottish Crop Research Institute. About half of the papers originate there, and a few are from countries other than Britain. As one would expect from an institute with a good reputation, most of the papers are of high standard, but an editorial board of 17 and five associate editors seems over-weight for an average of ten papers per year; indeed, it has always been difficult to justify the existence of this publication when there are several long-established journals covering the same areas. The advantage of CR is of quick publication, some papers taking only 6-8 weeks from receipt, although the average is nearer 28 weeks (about the same as for CP and for other refereed journals). The cost per page of scientific paper is £0.12 (1984 subscription rate) which again is expensive.

There are many who believe that "biological" or eco-agriculture is distinct from (and better than) "conventional" farming because of its holistic approach. The new journal *Biological Agriculture & Horticulture* (BAH) was started in 1982 by the then seven-year-old International Institute of Biological Husbandry, with the aim of publishing scientifically sound research and reviews "to raise the credibility of the biological system". That this is necessary may reflect sadly upon the blinkered outlook of so many "academic" scientists; on the other hand, applied biologists in agricultural research have long realized the necessity for an ecological approach, and have been publishing sound epidemiological research results for decades.

Eco-agriculture has not, in general, had a good press, because of the tendency of some of its supporters to peddle prejudice as solid scientific fact. The editors of BAH will have to take care that their journal does not follow the precedent, for 58% of the scientific content of the first five numbers consists of reviews and surveys. These, and the 14 papers reporting scientific results, come from ten countries, so the journal justifies its claim to be international. The cost of Vol.2 (1984) is not cheap at £0.16 per small page (if the size remains the same). Four editors are again "advised" by a prestigious board of 23 members, drawn from seven countries. Being a journal of a society it contains conference reports and news, as well as book reviews and notices.

BIOLOGICAL
AGRICULTURE &
HORTICULTURE

There is no doubt that food and fibre production will remain man's greatest challenge for many generations. So there should be ample opportunity for BAH to improve its standing amongst agronomists and scientists in the future. ☐

Leonard Broadbent is Emeritus Professor of Biology and Horticulture in the University of Bath.

Relative value

Julian Davies

Trends in Biotechnology.
Editor John Hodgson.
Elsevier (Cambridge, UK). 12/yr. £28, $49, Dfl. 130 (personal); $165, Dfl.430 (institutional).
Bio/Technology: The International Monthly for Industrial Biology.
Editor Douglas K. McCormick.
Nature Publishing. 12/yr. $78, £70.

FOLLOWING the spate of four-page rumour sheets which accompanied the biotechnology industry in its headlong rush to establish a foothold in the world of commerce, publishers have decided to signal the consolidation of the industry by providing more substantial reading matter for the biotechnologist. In the spring of 1983 Macmillan launched *Bio/Technology* (BT) and Elsevier presented *Trends in Biotechnology* (TBT), both of them intended to create and to meet the need for reliable, intellectual presentations of modern biotechnology. A stablemate of *Nature*, BT will obviously benefit from the association, while TBT is fashioned along the same lines as the excellent *Trends in Biochemistry* (TIBS), a monthly collection of reviews that has a good following in academic circles. The nickname TIBS is well known and a similar mnemonic for TBT would have been a definite advantage. What can we call it? TIBOTS? TOBS? TIBITS?

BIO/TECHNOLOGY
THE INTERNATIONAL MONTHLY FOR INDUSTRIAL BIOLOGY

These newcomers to the biotechnology arena offer higher credibility and scientific acceptability than the other publications presently available in this field (with the exception of *Biofutur*; BT is actually more of an English cousin of this French biotechnology journal than a relative of *Nature*). But their serious approach apart, the two journals are quite different in format, presentation and goals.

TBT concentrates on up-to-date reviews of various aspects and developments in biotechnology and does not concern itself with commercial issues. It is essentially academic and pedagogical in character. By contrast, BT provides much information and comment on issues to do with the regulation, investment, business and international aspects of biotechnology and the products so eagerly anticipated. No other publication provides quite the same scope, though there is some overlap with *Nature* in the presentations of the health of the biotechnology industry. BT also includes a rather perfunctory and generally useless summary of new patents which seems to do nothing more than fill space; other patent review journals such as *Derwent Biotechnology Abstracts* and *Telegen Reporter* do the same thing much better.

Both BT and TBT carry substantial advertising. BT has more glossy advertisements than most journals whereas TBT tends to be more conservative. One infuriating aspect of BT is that the longer and better review articles are often interrupted by as many as six pages of advertising, and in some issues the pages of advertising outnumber the pages of text. However, it is comforting to know that the two journals are well-supported in this way.

Both BT and TBT try to address immediate and future problems of biotechnology in the form of reviews. In recent issues, TBT has carried perceptive articles on delivery systems for drugs and enzyme engineering while BT has presented surveys of novel bioreactor systems and the factors involved in the design of pilot plants. Both have good book reviews and are developing interesting "Letters to the Editor" sections. BT includes two or three original scientific research articles in each issue. The articles are related to recombinant DNA applications and are usually of good quality — more or less equivalent to the type of paper published in *Nature*. In fact they probably could be published in *Nature*, were it not for the fact that this would remove one of the justifications for the existence of BT!

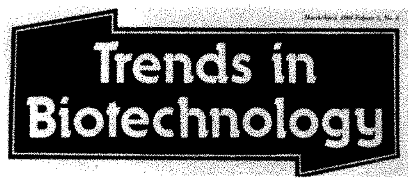

One cannot finish discussion of BT without mention of Bernard Dixon, who is clearly one of the more potent commentators on the science/business scene. His articles are sometimes pungent, usually provocative and always worth reading. Perhaps it is in this respect that BT has the edge over TBT — it invites controversy. Yet the question whether the more academic approach of TBT will win and maintain the necessary readership seems to have been answered already; published six times a year until now, it will go monthly in 1985.

The bottom line comes with the question, are these two journals needed? Indispensability is always hard to justify but BT and TBT have quite obviously created a market for themselves. They are clear advances on the rumour sheets and are likely to be the best media for presentations of the science of biotechnology and its academic and commercial implications. The fact that both of them have distinguished editorial boards to oversee their content and shape their future should guarantee their continued quality in a field of publication where quality is rare. ☐

Julian Davies is President and Research Director of Biogen SA, Geneva.

Journal prices

Details of editors and frequency of publication, and the annual subscription rates appearing at the top of each review are given in most instances for 1985. These details are not complete in all cases, and readers interested in subscribing to a particular journal should check the rates with the publisher concerned.

Common ground for new biologists

Bernard G. Forget

Molecular Biology & Medicine.
Editors E.S. Lennox and S. Brenner.
Academic. 6/yr.

TO QUOTE its editors, *Molecular Biology & Medicine* (MBM)

> takes as its main task the provision of a meeting ground between the basic scientist and the clinician, and to build up connections between molecular biology and clinical medicine.

The focus is therefore on normal and abnormal human biology and related research topics in the disciplines of molecular genetics, cell biology, immunology and biochemistry.

In the first five issues, the subjects that have been particularly emphasized include immunology-related research, ranging from studies of monoclonal antibodies (of human as well as murine origin) to analyses of immunoglobulin and histocompatibility genes; molecular genetics of haemoglobinopathies (thalassaemia and sickle cell anaemia); structural analysis of human viruses; and applications of restriction fragment length polymorphisms (RFLPs) to the study of human genetic disorders. The subject matter of MBM is therefore very broadly based and should be of interest to investigators in a large number of different fields. The article thus far published have originated from leading research laboratories, and although the specific reports have not generally dealt with findings worthy of comment in (say) *Nature's* News and Views section, they nevertheless constitute observations of genuine significance.

In addition to research papers (both long and short), the journal also publishes concise reviews of topical subjects — DNA-based prenatal diagnosis of haemoglobin disorders, chromosome translocations associated with leukaemia, X chromosome inactivation, the relationship of growth factors to cancer, and the association between polymorphisms in the major histocompatibility complex and different disease states, are among the topics covered in the early issues. Meeting reports and book reviews are planned but none have yet appeared.

The editorial in the first issue stressed the importance of rapid publication in the fast-moving fields covered by MBM. However this is an aim that does not appear to have been met. A bimonthly publication schedule was planned, but the most recent issue of the journal, dated December 1983, became available only in August 1984 and contained papers received up to 12 March 1984; the cover date therefore does not accurately reflect the actual publication date.

This journal has a very worthwhile purpose in trying to establish a forum where the basic scientist and the clinician can find common cause; the scope and quality of the papers in the first issues give promise that this goal will be achieved. Overall, MBM will be a very useful addition to the libraries of individuals interested in keeping up to date on advances in the elucidation of the pathogenesis of human diseases as studied by the research technologies of the new biology. ☐

Bernard G. Forget is Professor of Medicine and Human Genetics at Yale University School of Medicine.

Records of cancer control

Tony Davies

Cancer Investigation.
Editor-in-chief Yashar Hirshaut.
Dekker. 6/yr. $95 (US), $111.50 (elsewhere).
Journal of Biological Response Modifiers.
Editor-in-chief Robert K. Oldham.
Raven. 6/yr. $80 (personal); $105 (institutional).
Clinical & Experimental Metastasis.
Editors K. Hellman, G. Nicolson, L. Milas and S.A. Eccles.
Taylor & Francis. 4/yr. £49, $98.

THESE three journals have in common an emphasis on cancer research, two of them obviously so from their titles and the third, covering biological response modifiers, because of its strong affiliation to a programme of the same name which is part of the (American) National Cancer Institute research scheme.

Cancer Investigation (CI) is an all-American effort in that all of its editorial and advisory staff work in institutes in the United States, about 30% of them in the Memorial Sloan-Kettering Cancer Center. The papers reflect this bias fairly accurately. The format is glossy, the illustrations of high quality. There is a deliberate attempt by the editors to include a proportion of review articles both on basic and clinical science, while controversies to do with clinical management are given an airing. For example there is a well-argued account of the virtues or lack thereof of staging laparotomy in Hodgkin's disease, and an article strongly critical of the current practice in the United States of performing mastectomy on the majority of breast cancer patients. Also evident are some pointers to technological advances.

The journal is intended, it seems, to provide a lively account of cancer research for a predominantly clinical readership. The miniseries (*sic*) on oncogenes and cancer led me to believe that here was a splendid archaism, but on reflection I realized that there had been a further enrichment of the English language because of the elision of a hyphen. The editorials are rather pompous and turgid, and censorious of a government which dares to restrict the amount of money put into cancer research. It is not possible to determine how publication time relates to receipt of papers nor is it clear whether or not there is a refereeing system.

The cover of CI displays "Cancer" in big white letters, like its much older antecedent of that name. "Investigation" is added in much smaller black type. As few such journals are likely to attract the casual buyer, such a ploy could hardly be thought deceitful but to a disinterested outsider it seems misleading.

It has always been difficult to define "biological reagents", and the concept of a biological response modifier, apparently coined by Dr Vincent T. DeVita Jr, Director of the National Cancer Institute, is even more complicated. As stated in the *Journal of Biological Response Modifiers* (JBRM), it includes consideration of

> a large number of agents: immunoaugmenting, immunomodulating, and immunorestorative agents; interferon and interferon inducers; lymphokines; cytokines; thymic factors; antitumor and antilymphoid cell antibodies; tumor antigens and modifiers of tumor antigens on cell membranes; antigrowth factors; and maturation and differentiation factors.

Essentially, it means what the Biological Response Modifiers Programme Coordinators want it to mean and anything else for which there is almost a splendid, albeit fictional, precedent. The large editorial board has one or two lonely foreigners known to be sympathetic to the Programme, but the JBRM is so far also predominantly an American effort in content. The argument is advanced, quite fairly, that pressure on other journals makes the new journal inevitable in the welter of "biologicals" emerging from the monoclonal and genetic engineering technological revolutions. Again, no indication is given of publication times.

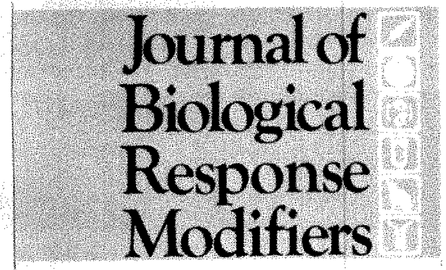
Journal of
Biological
Response
Modifiers

There are published here opinions on contentious issues in science. For example, Harold Hewitt is given the opportunity to air his well-known opposition to the tumour immunology package and in a subsequent issue Ronald B. Herberman fires back a broadside against such temerity. The papers make lively reading if one can swallow an initial anxiety at the rag-bag of topics. If the contributions to JBRM are well refereed the journal could prove to be a useful addition to the literature, and might even act as a quality control device on the burgeoning "biologicals" industry. But it is, I fear, a crusading effort with little chance that impartiality and objectivity will count for much.

K. Hellman and G. Nicolson are prominent members of that part of the scientific community which gives special consideration to the metastasis of cancer cells. Now they have started their own journal, *Clinical & Experimental Metastasis* (CEM). There are others on the same topic but this has not proved a deterrent. A deliberate effort has been taken to make the journal fully international, in that there are representatives on the editorial board from each of a number of countries in which cancer research is funded. The papers published reflect this international flavour. As yet, CEM contains no frills in terms of the airing of controversies, letters to the editor and the like. The illustrations are good, the papers readable and informative. The publication time is difficult to determine on the first few issues but it seems to be coming down from a year or so to about four to six months. It is implied that there is a refereeing system, the submission times being given separately from a time of acceptance. I find it difficult to understand why journals do not state explicitly what their policy is on this important matter. Much of the work of scientists is judged by their output of papers, which in the good old days could reasonably be assumed to be subject to the regulatory influence of studious and independent refereeing. With such a plethora of new journals it is not easy to know if standards are being upheld.

CLINICAL &
EXPERIMENTAL
METASTASIS

There is little doubt that the technological advances of the past few years will, in time, enable us to control malignant cells in the human body (though the difficulties involved should not be underestimated). All three of the journals will contain a part of the record of progress and they are welcome on this score. But to my mind, well before the story is anywhere near complete, the profligate use of trees to act as the vehicle for scientific pronouncements will have ceased and new information will be surveyed on a television screen. It would have been good to have seen at least a hint that these new journals were preparing for the likely change in medium. □

Tony Davies is Chairman of the Section of Biology at the Institute of Cancer Research, London.

Short of practice in immunology

Gordon Reeves

Diagnostic Immunology.
Editor Mariano F. La Via.
Alan R. Liss. 4/yr. $45 (personal); $90 (institutional).

THE immunological literature is both extensive and fabulous. The clinical immunologist has the dual task of keeping abreast of advances in immunobiology, immunochemistry, immunogenetics and immunopathology, and of assessing their relevance to the study of human disease. The first requirement is well served by the excellent *Annual Review of Immunology* and *Immunology Today*. But what of the practice of clinical immunology? Of the various journals which purport to cover this end of the spectrum, only *Clinical and Experimental Immunology*, in my view, maintains a consistently high standard. Nevertheless, the need for a journal which seeks to improve the quality and organization of current practice, as identified in the editorial for the first issue of *Diagnostic Immunology* (DI), is probably a real one.

Unfortunately, little of the content of the first four issues of DI concerns current clinical practice. Although the pitch is often research-and-development orientated, much of this material compares unfavourably with papers appearing in the well-established *Journal of Immunological Methods*. Two useful reviews have appeared on clinical applications of FACS techniques and immunodiagnosis in protozoan and helminthic infections, but there has been little discussion of the practical value of existing methods and ways of delivering a clinical immunology service. Where are the critiques which review how to diagnose and monitor those disorders falling within the prime areas of clinical immunology, i.e. allergy, autoimmunity, immunodeficiency, lympho-proliferative disease and transplantation? The aim to provide "critical evaluation of reagents, quality assurance, standardization of methods and definition of normal ranges" has not been fulfilled. The emphasis of the third issue is on the "goal of providing a forum for discussion of new and promising methodologies", whereas the fifth issue (Vol. 2, No. 1) is the first one to contain a reasonable sprinkling of clinically relevant papers.

To me it seems that DI has undergone an identity crisis. Consistency of content, style and production are important prerequisites, if it is to succeed. □

Gordon Reeves is Consultant Immunologist and Senior Lecturer at the University Hospital, Queen's Medical Centre, Nottingham.

Delving inside the cell

L.G. Lajtha

Cell Biochemistry and Function.
Editor E.M. Crook.
Butterworth. 4/yr. Subscription rates for 1985 not available.

THE admirable editorial in the first issue of *Cell Biochemistry and Function* (CBF) indicates such a wide scope that it is difficult to say what precise niche the journal is attempting to fill. The aim appears to be to cater for studies of a biochemical nature on intact, whole cells. Certainly, although it is not specifically stated, the editors are obviously aware of the current emphasis on compartmental studies and of the biochemical challenges to be found in intracellular micromilieux and microanatomical structures.

An especially useful feature is the commissioned reviews, particularly the multi-authored ones which tackle a particular subject (for instance the five-paper review of mammalian alkaline phosphatase). Also included are short communications, full-length papers (with laudably detailed abstracts), conference reports, calendars of meetings, book reviews and, at the end of each volume, author and subject indexes.

The journal is nicely designed and produced — I particularly like the double-column presentation — but while the paper is of good quality, it does not give as much contrast to electron micrographs as one would like. It is truly an international publication, the papers coming from respectable laboratories all over the world, and the standard of contributions is high, both in science and in writing; the declared rights of the editor to make such editorial amendments as are deemed necessary does result in a pleasant uniformity and clarity of style.

CELL
BIOCHEMISTRY
AND FUNCTION

I think that CBF will appeal to a wide range of readers, although for four issues of about 65 pages each the subscription (£80 in 1984) is on the expensive side. The journal is a sound vehicle for studies of modern intracellular biochemistry and I suspect it will not remain a quarterly for long. ☐

L.G. Lajtha is Emeritus Professor of Experimental Oncology, University of Manchester.

Thinking small

Richard W. Lacey

Journal of Microbiological Methods.
Editor-in-chief D.C. White.
Elsevier Biomedical. 12/yr. Dfl. 510.
Diagnostic Microbiology and Infectious Disease.
Editor-in-chief William J. Martin.
Elsevier Biomedical. 4/yr. $132.

LIKE the cultures which so many of them discuss, journals on microbiological matters are proliferating. Do these two new contenders give readers (and authors) good value?

Each issue of the *Journal of Microbiological Methods* (JMM) contains about six substantial papers on aspects of the physiology, ecology and pathogenicity of bacteria (rather than of any other microorganism). While the science is sound, most of the methods reported are specialized in scope and will appeal largely to workers in each specific field; so while libraries should stock the journal, there will be few individual subscribers. The text is readable — presumably reflecting high editorial standards — and the presentation is good; indeed it is not unlike that of the *Journal of General Microbiology*, to which some of the papers might have found their way. On the debit side, the photographs could perhaps be improved, and I wonder whether enough experimental details are given for the non-expert worker trying to reproduce the experiments.

To date most papers have been published within a few months of acceptance, but quite a number suffered delays due to revision. Was this because authors were not familiar with the journal's style, or did the editors demand improvements in presentation or in scientific content? Whatever the case, prospective authors would certainly not jeopardize their reputation by publication here.

I can be less positive about the stablemate of JMM, *Diagnostic Microbiology and Infectious Disease* (DMID). Each issue contains about eight full-length papers with a variable number of shorter contributions. Most papers are published within six months of receipt, although here, too, many were revised. The standard of detailed editing seems to be high, and the presentation is again good.

The scientific content, however, is variable. The first issue of the journal (March 1983) contains a number of papers commenting on the antibacterial activity and sensitivity-testing of new antibiotics in arbitrary and uncritical ways. In them the objective in the synthesis of new antibiotics is apparently seen to be the identification of an agent with the broadest spectrum and lowest minimum inhibitory concentration. But surely the object of diagnostic microbiology should be rapid and accurate diagnosis, enabling the use of antibiotics wth minimum selection pressure?

Contributions in later issues of DMID do fortunately manifest such an approach. Some of them could have been published in the *Journal of Infectious Disease*, and are of almost comparable standard, but it is difficult to see reasons for some work being undertaken, let alone published. For example, a paper in the January 1984 issue deals with *Pheumocystis carinii* infection in germ-free rats, concluding that "These data have significant implications for the natural history, diagnosis and epidemiology of *P. carinii* with regard to the human host". Such a comment is extremely disturbing, when it is appreciated how much the disease and therapy differ between the rodent and human being.

DIAGNOSTIC
MICROBIOLOGY
AND INFECTIOUS
DISEASE

The journal seeks publications from clinical microbiologists and infectious disease specialists, but I remain unconvinced that members of either of these groups should deflect their energies in this direction, particularly at the expense of their clinical work. How many of our nosocomial infection problems are generated by neglect? Does our interest in novel antibiotics provide the need for these agents? ☐

Richard W. Lacey is a Professor in the Department of Microbiology, University of Leeds.

"THE TRUTH"
THE
ATOMIC COMPLEX
by BERTRAND GOLDSCHMIDT
An accurate, complete and fascinating worldwide political history and personal memoir of nuclear energy — from the development of the bomb in World War II to today's nuclear energy complex and proliferation problems.
NUCLEAR TODAY
Goldschmidt, a leading French scientist turned international statesman, reviews half a century of political moves, countermoves, international intrigue and manipulation. *The Atomic Complex* is a pragmatic look at the nuclear world today, carefully examining the terror nuclear weapons represent, but at the same time stressing the benefits of nuclear energy.
Order this 500 page best seller today.
$31 Hardbound $24 Softbound
American Nuclear Society
555 North Kensington Avenue
La Grange Park, IL 60525 USA
Circle No.41 on Reader Service Card.

One of the places to get together

O.H. Petersen

Clinical Physiology and Biochemistry.
Editors-in-chief J. Rosenthal and M. Rafelson.
Karger. 6/yr. DM 290, $110.

AFTER a long time of ever-increasing specialization, resulting in smaller and smaller branches on the physiology tree, we now seem to have entered a period of reunification. One of the stated aims of *Clinical Physiology and Biochemistry* (CPB), "designed to provide a vehicle for scientific communications amongst clinicians, physiologists and biochemists", is "to re-emphasize those areas of common biologic interest that already exist". To some extent therefore it will be in competition with the older physiological journals, established before the fragmentation of the subject became a problem, of which at least *Pflügers Archiv* and the *Quarterly Journal of Experimental Physiology* deliberately take a broad view of physiology and include pathophysiological papers as long as they serve the purposes of the subject as a basic science.

Clinical Physiology and Biochemistry

Many of the papers so far published in CPB could, at least as far as the subject matter is concerned, have appeared in any of a number of physiological or biochemical journals. These papers are of a reasonable standard without being overexciting — as usual with a new journal only time will tell if it will be possible to attract really high-quality papers away from the broad-based journals covering the whole range of the physiological sciences, or from the journals covering the interface between the basic sciences and clinical investigations (such as the very successful *Journal of Clinical Investigation*), as well as from the many good multidisciplinary "systems" journals.

The editorial board appears to be somewhat narrowly based as an almost exclusive American-German enterprise, but CPB is the official journal of the National Academy of Clinical Biochemistry and presumably has a reasonably secure financial position. Only original papers are considered and there appears to be no wish to publish letters or notes. The delay from manuscript submission to publication seems long, particularly for a new journal; thus most of the papers in the July-August 1984 issue were received in August-September 1983. The quality of the production is good with figures of uniform standard and the text set out in the now-usual two-column format.

The journal faces tough competition from a number of very different but well entrenched rivals. It will undoubtedly, as stated in the first editorial, serve as *a* forum to foster interdisciplinary exchange of information and concepts, but I am not so sure that it will become *the* major platform for this important exercise. □

O.H. Petersen is George Holt Professor of Physiology at the University of Liverpool.

Infant alternatives

W.D.M. Paton

ATLA (Alternatives to Laboratory Animals).
Editors Michael Balls, Rosemary Riddell and Alastair Worden.
FRAME, 5b The Poultry, Bank Place, Nottingham NG1 2JR, UK. 4/yr. £16.

ALTHOUGH labelled Volume 11, the issues of ATLA on which this review is based are indeed the manifestation of a new journal. The original venture, *ATLA Abstracts*, born in 1973, was not a success, probably because it was competing with more professional abstracting services, and perhaps also because it underestimated the extent to which biomedical scientists were already using non-animal methods. But the new journal, backed by an excellent editorial board, is a different proposition. Its policy (outlined in the first issue) remains that of its parent body, the Fund for the Replacement of Animals in Medical Experiments; but instead of abstracts, it includes research papers, general articles, correspondence, news, book reviews, and a list of titles covering all aspects of alternatives to laboratory animals in biomedical research and toxicity testing.

Will the new journal find a niche? It deserves a chance. The news items are really valuable; nowhere else does one find, for instance, rational analysis of animal experiments from around the world, or compact accounts of the innumerable meetings now taking place. The research papers are mixed: some would hardly be published elsewhere, some are worthwhile. Although they would overlap with other journals, why not have a special place where (say) toxicity tests deliberately shaped to reduce animal use can readily be found? It is up to the editors to ensure the merit of such contributions, the only ultimate guarantee of their being read. The correspondence and book reviews could be equally useful. By contrast the melancholy, unorganized caravanserai of selected titles at the end of each issue seems useless; but again, if classified by technique, substance tested or general topic, with an author index, such a list could also be helpful.

The main difficulty for the journal however, may be strategic. One gets the sense of a battle being fought on two fronts: on the one hand a liking for verbal fisticuffs with the biomedical "establishment", of a type perhaps needful to retain support from the more anti-experiment clientele of FRAME; on the other a genuine scientific and critical approach to research, of the type winning respect from the investigator. Fisticuffs are quite fun, and rather encouraged these days, but are boring to re-read and do not wear well (except in the hands of a Housman, Leavis or Medawar). Dr Balls and his colleagues have a tricky task in child-rearing: one hopes that it is an occasional gentle irony (a tutorial with Lewis Thomas would do) along with some meat that finally clothes this promising infant. □

Sir William Paton retires this month as Professor of Pharmacology, University of Oxford.

Science at play

E.C. Frederick

Journal of Sports Sciences.
Editor Thomas Reilly.
E. & F.N. Spon. 3/yr. £39.50, $84.50.
Sports Medicine.
Editor-in-chief Rennie C. Heel.
ADIS Press, PO Box 34-030, Birkenhead, Auckland 10, New Zealand. 6/yr. $95, SwFr. 210.

PUBLISHERS have responded slowly to the furious growth in sports science over the past decade. At a time when the number of researchers was doubling and tripling, the number of journal pages expanded in slow motion. As a consequence, long publication delays and abnormally high rejection rates became the norm.

Although some of the pressure was relieved by the introduction in 1980 of the *International Journal of Sports Medicine*, and by modest increases in issue size and frequency by many existing journals, it was not until the recent spate of new journals that sports science researchers finally found some breathing room. Two contenders for our papers and our subscriptions that should be mentioned in passing are the *International Journal of Sports Biomechanics* (which has just released its first issue and so it is too soon to gauge its scholarly impact), and *Human Movement Science*. The latter espouses an editorial policy encompassing most of the constituent disciplines of sports science, but up to this point has largely published motor-learning papers of somewhat specialist appeal.

The two newcomers that deserve more detailed description, and are reviewed here, are the *Journal of Sports Sciences* (JSS) and *Sports Medicine* (SM). The editors of JSS have shaped their journal into a broadly based, multidisciplinary publication of consistently high standard. Each of the first four issues contains five to six full-length articles, mainly research reports, and an occasional review. In addition, book reviews and a comprehensive listing of forthcoming events appear at the end of each issue. Abstracts from the meetings of the Society of Sports Sciences, the journal's sponsoring body, are published at appropriate times.

Thomas Reilly and his colleagues have clearly avoided the danger of their journal becoming a place to recycle problem manuscripts — a pitfall that traps many new journals — and the high rejection ratio of 70% of submitted manuscripts bespeaks the path they have taken to avoid the problem. No indication is given of the time required for review, but the median time from acceptance to publication is a quick two months.

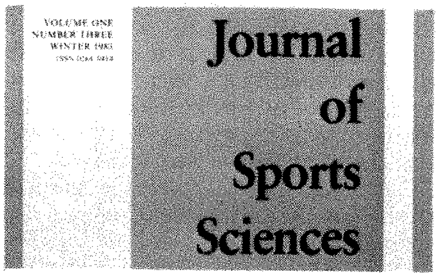
VOLUME ONE
NUMBER THREE
WINTER 1983

Journal of Sports Sciences

In a field of science that is blossoming over such a range of subjects, it can require superhuman dedication to keep track of the trends in areas in which one is not active. *Sports Medicine* helps by publishing six issues annually, each of them containing review articles and "leading articles" which are a forum for the communication of key issues in sports science.

Although the journal's title suggests a clinical emphasis, the term sports medicine is used in a general, multidisciplinary sense; for example, articles in the first three issues cover topics as diverse as ergometry, biological rhythms, sports injury, bicarbonate ingestion, cycling physiology, sex and hereditary effects, and endorphins. The quality and depth of the contributions are uneven, as might be expected given such broad scope, but most are useful and well written.

JSS and SM are welcome additions to an area of science in need of deeper as well as broader journal coverage. These two well-executed newcomers help meet the need on both accounts. ☐

E.C. Frederick is Director of the Nike Sport Research Laboratory, Exeter, New Hampshire.

• A new book of interest to many researchers in sports science is Thomas A. McMahon's *Muscles, Reflexes, and Locomotion.* The book is published by Princeton University Press (price hbk $50, £45.80; pbk $15, £10.70), and will be reviewed in the 11 October issue of *Nature.*

Eye to eyes

George Duncan

Lens Research.
Editor-in-chief Sidney Lerman.
Dekker. 4/yr. $70 (US),
$81 (elsewhere).

Lens Research has been launched upon a stormier sea than are most new journals. Not only do the usual financial stringencies confront it, but the very material that should provide much of the data for the journal — namely, the human lens — is, in many parts of the Western world, removed piecemeal in a messy homogenate rather than as a useful entity. The editor, however, takes a sanguine view of the latter difficulty and believes that it will lead to a rapid improvement in the range of *in vivo* techniques available for lens investigation.

The journal is produced by photo-offset and aimed at the rapid-publication market. It has a distinguished editorial board to steer it, and to set the tone many of them contributed to the first issue. The articles, all derived from a symposium held in Eindhoven in October 1982, are interesting and well produced. They deal with topics as diverse, but equally important, as the X-ray crystallographic structure of lens crystallins and the *in vivo* measurement of light-scattering from human lenses. However, a high proportion of the illustrations (I estimate almost 20%) in this issue were reproduced from previous publications. This is an unwarranted intrusion in the first number of any journal, let alone one which purports to cater for the rapid publication market. (At present, it is in fact impossible to judge how quickly the submitted word is converted to the printed page, since neither submission nor acceptance dates are given in any of the issues so far produced.)

The production standard of the journal had slipped badly by the time the third issue appeared, since one article was published with an average print density of 6 words per line and 22 lines per page. I leave the reader to total up this page for comparison. Another article was photo-offset directly from a low-density dot matrix print-out; apart from contravening the published house rules for submission of articles, it was extremely difficult to read — a great pity in this particular case, since the paper described a good study carried out on those precious intact human cataractous lenses.

One most excellent feature of the journal was the inclusion of a comprehensive index at the end of the third issue. If this sort of care could be extended to the production side, and allowance made for comments on previously published articles, then it might be possible to foresee a calm and fruitful voyage ahead for this particular lens flagship. ☐

George Duncan is Reader in Biophysics at the University of East Anglia.

Between two cultures

John Yudkin

Nutrition and Behavior.
Editor Robin B. Kanarek.
Alan R. Liss. 4/yr. $35 (personal);
$70 (institutional).

IT IS only recently that the traditional nutritionist, concerned with the isolation and description of the nutrients and their effects, began to recognize that the true scope of nutrition embraces the total relationship between people and their food. The subject is therefore based as much on the behavioural sciences as on the experimental sciences. The established journals of nutrition have started to reflect this by publishing occasional papers concerning such matters as food choice and nutrition education. Now comes *Nutrition and Behavior,* devoted wholly to such matters, with papers dealing with the effects of nutritional status on learning, memory and food choice, as well as with the effects of behaviour on nutrition.

A major problem is that those working in the laboratory sciences and those working in the behavioural sciences have developed attitudes and concepts that are often difficult to reconcile. The first paper published in the first number of this new journal illustrates the point. Examining the relationship in children (aged from 5 to 16) between refined carbohydrate intake, hair cadmium and cognition, the authors measure food intake by the totally inadequate method of 24-hour recall. They also ignore the frequent demonstration by laboratory workers that hair analysis for mineral elements is quite unreliable. The tables and figures accompanying the paper contain no recognizable data such as the number of grams of carbohydrate and protein in the diet, or the scores of some of the intelligence tests, but are all derived after one or more mathematical transformations.

Later papers published in the four numbers of Vol. 1 of the journal will not be found so frustratingly incomprehensible; perhaps we can now expect the editors to be more critical of what is submitted to them. There is no point in providing a journal that, as they claim, is aimed at "interdisciplinary communication to researchers in a variety of fields" if what is published fails to communicate anything to most of its readers. Yet, if the journal does fulfil its promise, it will be an important contribution to the literature of nutrition.

John Yudkin is Emeritus Professor of Nutrition in the University of London.

Divers advisers

Stuart Sutherland

New Ideas in Psychology: An International Journal of Innovative Theory in Psychology.
Editors Pierre Moessinger, John Broughton and Richard Kitchener.
Pergamon. 3/yr. £46, $80.

PSYCHOLOGY is becoming a spectator sport. From the terraces a motley crowd of philosophers, linguists, sociologists, anthropologists and artificial intelligencers heckle, cheer and boo. But above all they proffer advice.

The first four issues of *New Ideas in Psychology* (NIP) contain a good many papers of this kind. Some authors advise psychologists to revert to teleological explanations, others urge them to seek salvation in artificial intelligence. Yet others recommend speculative theories provided they are testable, while perhaps the most original piece of advice is contained in a paper which advocates the founding of a science of happiness, to be known as eudology.

Almost all the papers are followed by commentaries, a format that increases the interest of NIP, which is nothing if not eclectic. There are papers on such disparate topics as chimpanzee language, brief psychoanalytic therapy, personal construct theory and the existence of paranormal phenomena, and there is a solitary experimental report that suggests laughing gas operates through the orbital frontal cortex.

Although there is room for a psychological journal of speculation, one wonders whether the fields covered by NIP are not too diverse. Moreover, the quality of the contributions is a little uneven and one commentator's remarks on an article apply to several. He writes,

> Like most programmatic manifestoes it serves the socio-psychological purpose of alerting like-minded scholars to the existence of a community of concern, but it fails to show signs of that rigor of analysis and systematic coverage of the subject matter that the author claims must distinguish a science.

The journal should provide an outlet for articles of this kind and will therefore doubtless serve an important "socio-psychological purpose". □

Stuart Sutherland is Director of the Centre for Research on Perception and Cognition, University of Sussex.

Split psychology

Geoffrey Hall

Journal of Comparative Psychology.
Editor Jerry Hirsch.
American Psychological Association.
4/yr. $36 (US), $39 (elsewhere).
Behavioral Neuroscience.
Editor Richard F. Thompson.
American Psychological Association.
6/yr. $100 (US), $103 (elsewhere).

THE influence of the American Psychological Association is such that when it decides to reorganize its journals the international psychological community has to take notice. If a shift in policy does not reflect a change of emphasis in work in psychology, then it seems probable that one will result.

These two "new" journals are the fission products of the demise of the old *Journal of Comparative and Physiological Psychology* (JCPP) which existed from 1947 to 1982 as the continuation of an earlier (1921-1946) *Journal of Comparative Psychology* (JCP). The original JCP attempted to cover all aspects of the behaviour of non-human animals; its change of title recognized that physiological studies (of brain lesions and, latterly, of the effects of drugs) had come to predominate. When, in 1975, the other main line of work covered by JCPP (laboratory studies of conditioning and learning) was hived off as a special section of the *Journal of Experimental Psychology*, a reconsideration seemed appropriate. What we have now been given in *Behavioral Neuroscience* is a journal devoted to "the broad field of biological bases of behavior" whereas the new version of JCP is concerned with "behavioral patterns... as they relate to evolution, development... and functional significance".

Contributors to a recent symposium on "the place of physiological psychology" saw in this split evidence of an identity crisis in their discipline. But in fact *Behavioral Neuroscience* with its sophisticated behavioural analyses of the effects of lesions and of drugs looks like a direct continuation of JCPP. The work reported is first-rate and this journal will retain its predecessor's reputation as being foremost in its field. JCP is something rather new but seems set to establish itself as a direct competitor to the respected ethological journal *Animal Behaviour*. Given the recent upsurge of interest in North America in what is sometimes called the "ecological" approach to animal behaviour, there is much good work to report and plenty of room for both journals.

These various divisions seem to follow natural fracture lines and are a sensible reaction to the growth of the field. Nonetheless, one looks back on the original JCP with a tinge of regret — ethologists have things of interest to say to learning theorists and both should communicate with physiological psychologists; it would be a pity if any new journal structure were to make such interactions less likely. □

Geoffrey Hall is Senior Lecturer in Psychology at the University of York.

Nervous beginnings

A.G.E. Pearse

Neurochemical Pathology.
Editor-in-chief Lloyd A. Horrocks.
Humana. 4/yr. $100.

CHEMICAL pathology, a term once popular, now has a decidedly antediluvian flavour, following absorption of the subject into clinical biochemistry. So what *is* neurochemical pathology except neuropathology in modern guise?

It comes as no surprise to learn that that is apparently just what the editors of this journal intended. According to their stated terms of reference, the journal is to "serve as the key forum for studies in the rapidly expanding area of biochemical neuropathology" and it "will thus be predominantly devoted to biochemical studies on all those tissues or body fluids that may help to elucidate the etiology or pathogenesis of neurological disorders".

Neurochemical Pathology is sponsored by the International Society for Neurochemistry and the World Federation of Neurology Research Groups on Neurochemistry and Cerebrospinal Fluid. I recognize, on the editorial board, many names derived from these two sources but I doubt if all were consulted in the matter of the creation of the new journal.

It may be pertinent to enquire, in so far as the first volume is concerned, just how far the editors have succeeded in their reasonably justifiable aims. There are 21 papers in the four numbers comprising the volume, and of these no less than 14 come into the category of experimental neuropathology. There are three purely neurochemical papers, each of which contains only a hint of future pathological importance, and three further papers describing chemical aspects of known, little known or unknown syndromes. The one remaining paper is an exercise in clinical neurochemistry.

With so great a preponderance of reports on experimental work — and despite the fact that much of it has some relevance, at least, to deficiencies or overdosages potentially occurring in human beings — one wonders whether the word "experimental" should not have been included in the journal's title. But it is clear enough that the editors did not intend their first year's coverage to present to the reader this predominantly experimental front, nor the virtual exclusion of several of their specifically cited areas of interest.

I conclude that several more years (more volumes) will require surveyance before it is possible to reach a positive conclusion that this journal is a useful one. Sad to say, with its present format and content it fails to justify its existence at all. □

Anthony Pearse is Professor Emeritus of Histochemistry in the University of London.

Society's slice of neuroscience

R. Victoria Stirling

International Journal of Developmental Neuroscience.
Editors-in-chief Antonia Vernadakis and Ezio Giacobini.
Pergamon. 6/yr. £86, $150.

At its annual general meeting in 1983, the International Society for Developmental Neuroscience decided to break an affiliation with Karger, the publishers of *Developmental Neuroscience* (reviewed in *Nature* **293**, 347; 1981), on the grounds of lack of copyright control, excessive page charges, long publication delays and poor illustrations. The new deal with Pergamon, who publish the *International Journal of Developmental Neuroscience* (IJDN) with the same editors-in-chief, seems much more advantageous. Subscription to the Society includes subscription to the journal, and the publisher also prints and distributes the Society's newsletter and collects membership dues. Members are exhorted to contribute to the new journal, the success of which should also accrue to the Society.

The instructions to authors are remarkably similar to those of *Neuroscience* (another society journal, under the editorial board of the International Brain Research Organization). But while the list of editors of IJDN spans many parts of the world, of 33 papers in four issues over half are from the United States, with a quarter from Europe, three from Asia and one each from Venezuela and Finland (i.e. less cosmopolitan a range than *Neuroscience*). In the first issue of Vol. 2 are published an impressive series of abstracts from the Fourth International Congress held in Utah in 1983. I could find only one author who also contributed a paper to IJDN. Most of the contributions to the journal are biochemical in nature, very few being concerned with structural aspects of development. It is therefore difficult to judge the quality of photographic reproduction, but it seems reasonable.

The delay in publication appears to be about six to seven months, though at the start of Vol. 2, the editors announced that to ensure a prompt service they had appointed associate editors in Venezuela and Japan; this was a good idea though the efficiency of the arrangement has yet to manifest itself. Apart from the minutes of the annual general meeting there is no editorial comment, although such a feature (and book reviews) had been suggested at the meeting.

INTERNATIONAL JOURNAL OF
DEVELOPMENTAL
NEUROSCIENCE

This slim journal may potentially be a very useful publication for members of the Society. But unless they contribute meatier material, I cannot see it taking a larger slice of what is now a dwindling cake. ☐

R. Victoria Stirling is a member of the scientific staff at the National Institute for Medical Research, London.

Trends in the risk business

J.R. Ravetz

Risk Analysis: An International Journal.
Editor-in-chief Curtis Travis.
Plenum. 4/yr. $90 (US), $101 (elsewhere).

THE journal *Risk Analysis*, published by the Society for Risk Analysis, reflects the diversity of effort in this area, and also the history of the dominant trends. The attempts at "scientific" studies designed to determine the acceptability of technological risks began in earnest with a classic paper by Chauncey Starr in 1969. The failure of such attempts, first to model "low probability/high cost" hazards, and then also to quantify "acceptability", led to enrichment of the programme by behavioural studies during the 1970s.

The Society was formed rather late in the day, and in its earlier issues the journal still concentrated on a scientistic approach. However, controversy soon broke out in its pages; broader appreciation of the technological and environmental issues found expression in an increasing proportion of its contents. The founding editor, Robert Cumming, contributed to this development by his policy of soliciting articles and insightful editorials.

By now the journal presents a lively picture of current work, all the major articles being accompanied by invited critical comments. For instance, it has recently been the publication point for a seminal paper by Alice S. Whittemore, "Facts and Values in Risk Analysis for Environmental Toxicants" (Vol. 3, No. 1; 1983). In this, it becomes clear that a new methodology, involving the complementarity of "facts and values" and of "knowledge and ignorance", is necessary if an effective discipline of risk analysis is to emerge. ☐

Risk Analysis

J.R. Ravetz is a Senior Fellow at Leeds University, and Co-Director of the SERC-ESRC "Risks" project.

Developing forms of energy

Gordon MacKerron

Renewable Sources of Energy: An International Journal.
Editor-in-chief Essam El-Hinnawi.
Tycooly International, 6 Crofton Terrace, Dun Laoghaire, Co. Dublin, Ireland. 4/yr. Subscription rates for 1985 not available.

ENERGY politics, and therefore energy studies, are bedevilled by an analytically damaging dichotomy between non-renewable and renewable sources. The split will, however, persist, and the latter have generally been served poorly. So there is a real need for a journal devoted to the renewables.

The principal aim of *Renewable Sources of Energy* (RSE) is to "facilitate the flow of information between developed and developing countries", with emphasis on the requirements of developing countries. While the central concern is ostensibly with energy technology, the journal contains a great deal on policy matters, particularly environmental control and local planning. In comparable existing journals (for example *Energy Policy* and *Energy: An International Journal*) renewables have received only sporadic coverage, while among publications dealing specifically with renewables, *Solar Energy* is narrower and more technical, and *World Solar Markets* and *Soft Energy Notes* are less academic. The focus of RSE is therefore unique.

The length of papers published to date has varied between 3 and 28 pages, each issue containing about 6 articles. There are, as yet, no editorials or comments on earlier papers, and only a rather perfunctory review section divided between "News and Views" and some short book reviews.

Articles generally fall into one of two types: semi-technical reportage of devices and projects (for example design optimization of solar water heaters; experience of a rural energy centre) and broader reviews covering such topics as geothermal energy or energy and community development in developing countries. The quality of the former is reasonably good, while that of the reviews is poorer, with some lapses into pious generalities.

Reflecting the editorial objectives, RSE's authorship is centred upon the developing countries, with a third of the early papers coming from India (and one welcome Chinese contribution). The main requirement in this field is for communication between developing countries and this journal should help to provide it. ☐

Gordon MacKerron is a Senior Fellow in the Energy Programme, Science Policy Research Unit, University of Sussex.

Water works

T.R. Parsons

Continental Shelf Research.
Editors Michael Collins and Richard W. Sternberg.
Pergamon. 6/yr. £63, $110.
Chinese Journal of Oceanology and Limnology.
Editor-in-chief C.K. Tseng.
Science Press, Beijing/Springer-Verlag. 2/yr. DM73, $33.

TWENTY-FIVE years ago, oceanographers learned the terms "oceanic" and "neritic" with their vague implication of a discontinuity between plankton species (and therefore, presumably, the physical–chemical environment of the sea) as one approaches a coastline. Not until the past decade, however, has a general understanding emerged of the distinct oceanographic changes which occur as water flows over the continental shelf. Thus I am in complete agreement with Dr Sternberg's statement that research in this area has "come of age", and it is now helpful to think of many oceanographic processes as being either deep-sea or continental shelf phenomena. This is the rationale behind the appearance of *Continental Shelf Research* (CSR), which complements the longer-established journal *Deep-Sea Research.*

The new journal is interdisciplinary in aims and promises to meet a number of needs for oceanographers working on this specialized and, at times, highly variable environment. The first three volumes have contained a wide variety of papers on water movement, frontal zones, microbiology and geological processes. Although in the editorial policy it is not stated that the journal specifically excludes articles on pollution, the early issues are refreshingly devoted to what I would call the pure science of the oceans — studies on the use of the continental shelf as a dumping ground seem either not to have been submitted to date, or to have been excluded. The journal also contains short sections on instruments and methods, and book reviews. Written comments on papers will be considered for publication up to three months after the appearance of the original paper.

There are no Japanese oceanographers on the editorial advisory board and, in fact, one gains an impression from the choice of the associate editors that much of CSR may be given over to discussion of the margins of the Atlantic Ocean. To fulfil the avowed role of a "platform for international research programmes", the editors should have selected their assistants from a wider constituency. On the other hand, the interdisciplinary nature of the subject is reflected both by the composition of the editorial board and by the articles published so far. Clearly CSR has made a good beginning. It should go on to become essential reading for oceanographers.

The Chinese-language journal *Oceanologia et Limnologia Sinica* was first published in 1957 and, by 1982, 410 articles on limnology and oceanology in China had appeared. The other journal reviewed here, the *Chinese Journal of Oceanology and Limnology* (CJOL) is not, as might be thought, a full translation of the Chinese journal. Authors who write in *Oceanologia et Limnologia Sinica* may have their work translated for publication in CJOL, but the journal will also accept articles from other Chinese-language publications as well as original papers written in Chinese. This, then, is how a country of one billion inhabitants and many new institutes of limnology and oceanology intends to present a representative sample of its science on these subjects to the English-speaking world.

Out of the first 23 articles published by CJOL, seven were concerned with physics, six with chemistry, two with geological processes and eight with biology; only two of these papers were limnological in nature. Geographically, most of the authors dealt with scientific problems within China, but one paper was concerned with the Tyne estuary in England.

The papers in physical oceanography do represent an up-to-date approach to the subject. The biological contributions, on the other hand, are mainly keyed to systematics and there is as yet little indication of biological modelling or of more broadly based studies on descriptive ecology. In attempting to carry out their intention of covering a wide spectrum of aquatic science in China, the editors may have gone too far by including at least one paper in the first two numbers which is entirely physiological, while Part II of a paper in physics is promised for another issue — a promise which may be difficult to keep, given the vast amount of Chinese-language science which has to compete for space in the journal.

CHINESE JOURNAL
OF OCEANOLOGY AND LIMNOLOGY
中国海洋湖沼学报

In general, however, Professor Tseng and his colleagues have performed a necessary task in exposing Chinese limnology and oceanology to a wider audience. The journal is well produced, and the text gives little indication that it has been translated. But I have one plea. The editors should ensure that the location of each of the studies is identified. In many of the articles it is not; one example is the paper on the tidal equilibrium of Blue Bay — where in the world is Blue Bay? ☐

T.R. Parsons is a Professor in the Department of Oceanography at the University of British Columbia, Vancouver.

NEW from The Institute of Physics

Inverse Problems

An International Journal on Inverse Problems, Inverse Methods and Computerised Inversion of Data

Editor: P C Sabatier *(Université des Sciences et Techniques du Languedoc, Montpellier, France)*

Inverse Problems will report current research work in this active and expanding field of research and will be of interest particularly to physicists and pure and applied mathematicians, as both contributors and readers. The results of this research are relevant to practitioners in seismology and prospecting, particle scattering, pattern recognition, radar imaging and the many other fields where maximum information needs to be extracted from experimental results.

1985 Vol 1 4 issues £105

Classical and Quantum Gravity

An International Journal of Gravity
Geometry of Field Theories Supergravity Cosmology

Editor: M A H MacCullum *(Queen Mary College, London)*

Launched in 1984, *Classical and Quantum Gravity* reflects current work with implications ranging from particle physics to cosmology, and is aimed at theoretical physicists, mathematicians and cosmologists working in all branches of the theory of space—time and gravitation.

1985 Vol 2 6 issues £95

Further information and specimen copies available from:

The Institute of Physics
Dept I/P, Techno House, Redcliffe Way
Bristol BS1 6NX, England
Telephone: (0272) 297481 Telex: 449149

Circle No.24 on Reader Service Card.

Geophysics: ins and outs of the library

Jean-Claude De Bremaecker

Annales Geophysicae. Editor-in-chief Stephan Mueller.
Gauthier-Villars, 11 rue Gossin, F-92543 Montrouge Cedex, France.
6/yr. FF780.
First Break. Editor Ian Williamson.
Blackwell Scientific. 12/yr. £34.50, $58.

GEOPHYSICALLY, Europe is slowly emerging from the deep: she wears a Latin dress but speaks English. At least, so it seems, for *Annales Geophysicae* (AG) has replaced both the French *Annales de Géophysique* and the Italian *Annali di Geofisica.*

As the official journal of the European Geophysical Society, the future of the journal is promising. It embraces the same subjects as its well-known American counterpart, the *Journal of Geophysical Research*; that is, all the fields covered by the International Union of Geodesy and Geophysics, but with one confusing exception: geochemistry and volcanology are not mentioned in the "scope of the journal". It appears that geodesy may also be excluded, but this is less certain. Further to confuse matters, the president of the EGS states in the first issue that volcanology and geochemistry as well as geodesy are *included.* The "scope" appears inside the front cover, the president's words on the facing right-hand page, and never have the twain met.

One presumes that all articles are refereed, and very speedily too, since the average delay for acceptance is about two months. The editorial board is made up exclusively of western European geophysicists, and very few contributors come from eastern Europe either, a geographical bias which should be corrected. The articles are of a remarkably high quality for a new publication, the abstracts not always so. Thirty-three years have passed since Kenneth Landes's classical "Scrutiny of the Abstract" (*Bull. Am. Ass. petrol. Geol.* **35**, 1660) yet still one finds that "The theory...is developed. An algorithm ... is proposed. Examples...are presented. The possibility of application...is discussed". It seems only reasonable to hope that the editors will in future demand abstracts that are, in Landes's words, "a condensation of the essential qualities of the paper" and "not a mere recital of the subjects covered".

English, we all know, is a good simple international language (except for its spelling). As a non-native speaker residing in the United States, I particularly appreciate the problems which AG's authors and editors have faced and generally overcome. A simple example comes to mind: the French "Pour lever cette difficulté..." does *not* mean "in order to raise the difficulty". There are very few such examples in the journal, and perhaps the best solution to this problem is to forget it; for, as scientists say, "the solution is not entirely clear", which means that it is utterly obscure.

One attractive feature of AG is the absence of page charges, coupled with the supply of 50 free reprints. The format (two-column on approximately 21 × 30 cm paper) is open and pleasant, the printing is of high quality, while the style and typography for the references are the best that I have ever come across. Much as in the *Journal of Geophysical Research*, only articles are published, but short notes are also welcome. So far no "comments" on previously published papers have appeared; presumably they will, eventually. Overall, at a subscription price of FF780 (*c.* $84) outside France, this is a bargain that libraries should not miss.

First Break (FB) is a different sort of beast. It does not aim at being a scientific journal, instead publishing "short non-technical articles...and up-to-date news about the geophysics industry". It is thus not meant to be archived, but does fill a clear need by offering executives and others in the oil industry a means of keeping abreast of events. The industry news consists mostly of publicity releases, and has to be read with a dose of scepticism — that does not make it less valuable. It thus goes without saying that few libraries will want to subscribe to FB, which is to the good of everybody concerned.

The editor is to be commended for dealing exclusively with items connected with geophysics. This may seem obvious, but it is not. Only a little while back its counterpart in the United States, *The Leading Edge,* was launched and unwisely included anything of conceivable interest to geophysicists. As a result its first numbers contained a mish-mash of right-wing propaganda, cross-word puzzles and sports news, with a dash of geophysics added for good measure. *First Break,* it seems, has profited from that sad example.

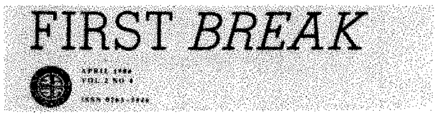

A common temptation with a publication such as this is for the publishers to try to "upgrade" it to a *bona fide* scientific journal. This shoal has not been avoided entirely by FB: at least one paper is reproduced from a well-known geophysical journal. Worse yet would be to fall to the level of taking non-refereed papers which have not been accepted (and could not be) by established journals — far better to publish a slimmer issue than one containing second-rate material. One can only hope that the editor will keep his goal firmly in mind over the next few years; some of the papers are a little disquieting in this respect.

First Break is a readable, informative and reasonably cheap publication. But considering the world-wide scope of the geophysics industry and its currently rather depressed state, as well as the thinness of both FB and *The Leading Edge,* I cannot help but wonder whether these two publications should not merge. It might bruise some editorial egos but the readers of both might well be better served. □

Jean-Claude De Bremaecker is a Professor of Geophysics at Rice University, Texas.

Talk of integration and communication

John Tarney

Journal of Metamorphic Geology.
Editors M. Brown, T.P. Loomis and R.H. Vernon.
Blackwell Scientific. 4/yr.
£47, $97.50.
Geochemistry.
Chairman of the editorial committee Tu Guangchi.
Science Press, Beijing/Springer-Verlag.
4/yr. DM 129, $54.50.

IT WOULD not be exaggerating to say that well over half of the Earth's continental crust is composed of metamorphic rocks, so it is surprising that there has been no specific journal acting as a focal point for research in this area. Until now, observational details have been recorded separately in various national and international journals of mineralogy, petrology, geochemistry or structural geology, of which there are now a great many, and this has put limitations on the possibilities for an integrated approach to the subject.

The new *Journal of Metamorphic Geology* (JMG), titled as it is with the broad term "geology" rather than just "petrology" and so on, should provide an appropriate vehicle for the reporting of broader ranging research on metamorphic rocks, although this may be more commonly achieved through the publication of thematic issues. Certainly, detailed integrated studies are now beginning to tell us a great deal about the past thermal and tectonic histories of metamorphic rocks, and the importance of fluids, which may be of great value in attempts to reconstruct the geological evolution of a province in terms, for instance, of plate tectonics.

During its first year, JMG has attracted contributions from an international group of authors on a wide variety of subjects, dealing with rocks from several continents which extend over an age span of 3,000 Myr. Admittedly, with one or two exceptions, most of these articles could have been published in one or other of the established journals without significant modification, so it remains to be seen whether the new journal will develop a character of its own: only time will tell, but the promise is there. The standard of presentation is high, the style conforms fairly closely to that of other journals published by Blackwell, and altogether JMG represents fairly good value for money.

Geochemistry, a Chinese journal which for the past two years has also appeared in an English-language version, is rather different. Of the several dozen articles which have appeared so far, almost all are written by Chinese authors (although one article has a non-Chinese co-author) and they deal almost entirely with Chinese geological and geochemical problems. Clearly, on the one hand, Chinese geochemists have accepted that English has become, for better or worse, the international language in the geosciences; on the other, we see here implicitly their strong desire to participate fully in geochemical research at international level in future.

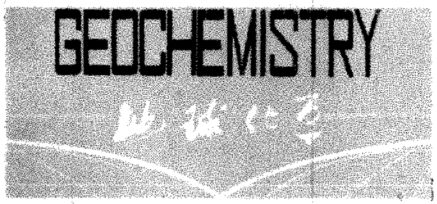

The range of topics covered is comprehensive — various aspects of igneous, metamorphic and sedimentary rock geochemistry, meteorites, marine geochemistry, economic geology and mineralization, organic geochemistry, isotopic dating, experimental studies and new instrumental techniques — and several articles on crystallography and new minerals have also been included. The scope, then, is wider than that of international geochemical journals, and extends into fields normally covered by journals of mineralogy, petrology and economic geology. The standard of presentation and the scientific content of the articles is generally high.

Now that several Chinese institutes have furnished themselves with a range of advanced geochemical instrumentation, comparable with that of any laboratory in the world, we can look forward to an increasing number of important contributions from Chinese geochemists. If that proves to be the case, *Geochemistry* will become necessary reading for many geoscientists. □

John Tarney is F. W. Bennett Professor of Geology at the University of Leicester.

Heart of Gondwana

Paul Mohr

Journal of African Earth Sciences.
Editor-in-chief Cornelius A. Kògbe.
Pergamon. 4/yr. £49, $90.

AFRICA is no longer "the black continent with the big blank spaces on its map" — the description of Hans Cloos en route to his first employment as a geologist in German West Africa. Africa's geology, mostly the preserve of European explorers before the First World War, has painstakingly become revealed through the work of colonial geological surveys and, especially since 1945, by an enthusiastic influx of European and American university personnel. Most of their work has been published in "international" (i.e. European and North American) journals.

Aside from geological survey reports, not notable as repositories for intellectual discussion and new ideas, the African geological literature has been scant (South Africa providing an outstanding exception). Now there appears the *Journal of African Earth Sciences* (JAES). Although published outside Africa, and with its chief and regional editors likewise resident outside the continent, it makes a bold beginning. African geologists and geophysicists have had increasing need for a publishing forum that transcends national boundaries yet keeps to the heart of Gondwana.

The format of JAES is African in its spaciousness (21 × 30cm), it is well produced (the photographic plates are sharp, the line-drawings large and readable), and the print is a boon to eyes overly strained from reading some established journals. The first volume comprises 37 articles, not including book reviews and conference reports. The quality varies, generally in direct proportion to article length. Interestingly, Nigerian and Egyptian geological topics (there are no geophysical articles in this first volume) together make up more than half the volume. Only five articles deal with Francophone Africa, four of these in French. Southern Africa and Zaire are conspicuously unrepresented. Of the authors, about half are based at African institutions, which is a fair achievement.

Clearly the infant journal has some growing up to do before it can justify its continental scope and ambition. On the other hand, one notes that there is as yet no *Journal of European Earth Sciences*. Here, then, is a medium for the propagation of that natural entity, African earth science, and, more than that, for indigenous African geologists and geophysicists to develop their scientific mettle. On this first showing, JAES promises well and deserves every success. Its cost is not too unreasonable by wealthy European standards, but, ironically, it has priced itself out of the greater part of the African market it is designed to serve. □

Paul Mohr is Professor of Geology in the Department of Geology at University College Galway, Ireland.

Birth in decay

Norman K. Grant

Isotope Geoscience: An International Journal.
Editor-in-chief G. Faure.
Elsevier Scientific. 4/yr. Dfl. 237.

IF the distinction and international character of an editorial board are sufficient to ensure the success of a new journal, *Isotope Geoscience* (IG) should do well. The first six issues suggest that the editorial resources available to the editor-in-chief will lead to the publication of critically reviewed descriptive, theoretical and review papers of an attractively high standard. So far about two-thirds of the articles have been on the systematics of radiogenic isotopes, and about one-third on stable isotopes, the average time from manuscript acceptance to publication in the latest number being six to seven months. Book reviews are also published.

Elsevier has introduced IG into our libraries as a daughter journal to *Chemical Geology*. Whether the newcomer can meet its ambitious goals of fostering "scholarly communication between isotope geoscientists of the world", and "form a bridge" between them and other geoscientists remains to be seen. Isotope geoscientists are not a homogeneous group, and the range of interests which the journal proposes to serve is extremely wide — radiogenic and stable isotope and radiochemical systematics in inorganic and organic terrestrial and extraterrestrial materials.

It could be argued that the most fruitful approach for isotope geoscientists is to communicate first of all with scientists in complementary and converging disciplines. For this reason it seems likely that many of the most influential papers in isotope geoscience will continue to be published in established journals of a more general nature, such as *Contributions to Mineralogy and Petrology*, *Journal of Petrology* and *Earth and Planetary Science Letters*. If IG is read only by specialists its importance will be limited. So, for the time being, my advice to librarians is to place the highest priority on the purchase of the journal only when their institution includes staff actively engaged in isotopic research. □

Norman K. Grant is Professor of Geology at Miami University, Oxford, Ohio.

AS WELL AS
TSI
TECHNOLOGY & SCIENCE
OF INFORMATICS
REVIEWED IN
THIS ISSUE
NORTH OXFORD
ACADEMIC
PUBLISHING CO LTD
HAS SOME
FASCINATING
BOOKS FOR
COMPUTER
SCIENTISTS
INCLUDING...

EVALUATING ADA
D. Le Verrand
SOFTWARE ENGINEERING: PRACTICE AND EXPERIENCE E. Girard
SYNCHRONIZATION OF PARALLEL PROGRAMS
F. André et al
ALGORITHMS FOR PATTERN RECOGNITION
J. C. Simon
VARIETIES OF FORMAL LANGUAGES J. E. Pin
RATIONAL SERIES, RATIONAL LANGUAGES
J. Berstel & C. Reutenauer

...AND THE
BEST SELLER
MATRIX
COMPUTATIONS
By G. Golub &
C. F. Van Loan

NORTH OXFORD
ACADEMIC
PUBLISHING CO LTD
242 Banbury Road,
Oxford OX2 7DR, England
Telephone (0865) 51 11 66

Circle No.36 on Reader Service Card.

In the forecasting movement

Chi-Yu King

Earthquake Prediction Research.
Editor Tsuneji Rikitake.
Reidel. 4/yr. Dfl. 90, $36 (personal); Dfl. 180, $72 (institutional).

EARTHQUAKE prediction, the scientific dream once shunned by respectable scientists, has been hotly pursued during the past two decades in such earthquake-prone countries as the USSR, Japan, China and the United States. Because of its interest to the public, and the multi-disciplinary nature of the research effort, many papers on the topic have been presented at a wide variety of scientific and non-scientific meetings, and published in many different journals and reports. Thus the appearance of *Earthquake Prediction Research* (EPR) to serve as a focal point for work on the subject is certainly very welcome.

The journal is published by a Japanese foundation (the Association for the Development of Earthquake Prediction) in cooperation with the Dutch publisher Reidel, with the objective of providing an international medium for original and review papers, reports and other items related to earthquake-prediction research. The editorial board, consisting of most of the current members of the Commission on Earthquake Prediction of the International Association of Seismology and Physics of the Earth's Interior, is strong and internationally well represented.

As of 31 July 1984, five issues of EPR had been published, three of them devoted to a single international symposium. All the issues arrived at our library in Menlo Park much later than scheduled. For example, Vol. 1, No. 1 (1982) and Vol. 2, No. 1 (1983), the last published issue, were received on 1 October 1982 and 9 November 1983, respectively. Thus the speed of publication is significantly less than one might infer from the manuscript receipt dates shown in the individual papers. Writing from personal experience, I submitted a manuscript on 1 November 1982, but was not informed of its acceptance until 9 June 1984.

EPR
EARTHQUAKE PREDICTION RESEARCH Vol.2 No.1 1983
Edited by Tsuneji Rikitake

Published in EPR so far are an introductory editorial, a meeting report and 29 "regular" papers, most of which are seismological (17) and rock-mechanical (9). About half of the papers are not directly relevant to earthquake prediction and could have been published elsewhere. Similarly, the scientific quality of the papers ranges widely, from the mediocre to excellent. Some of the papers (from non-English speaking countries) could have done with additional editorial assistance. The quality of production is very good, comparable to *Pure and Applied Geophysics*, and the cost is reasonable (Vol. 1, which has 391 pages, cost $69 for libraries and $28 for individuals).

Having identified and filled a significant publication gap, EPR has a potential of becoming a fine international journal. Whether it will fulfil its promise depends on the ability of its editorial members to attract and promptly and properly process good, relevant papers from all the different disciplines concerned, including geology, geophysics, geochemistry, hydrology and biology. ☐

Chi-Yu King is a Geophysicist at the US Geological Survey, Menlo Park, California.

Fusion across the fields

G.J. Pert

Laser and Particle Beams: Physics of High Energy Densities.
Editor-in-chief Heinrich Hora.
Cambridge University Press. 4/yr. £50, $135.

IN 1962, the observation of gas breakdown by high-power lasers initiated research into laser-generated plasmas as a possible source of thermonuclear power. However, before the introduction of the concept of near-isentropic compression in 1972 overcame the fundamental limitations, these proposals remained extremely speculative. It was shown that such compression could be generated by the ablation pressure of the blow-off plasma formed by surface heating of a simple deuterium–tritium pellet (sphere or shell). These initial designs have now been shown to be over-simple, in that the nature of the heating process may strongly modify the compression phase, and this problem particularly applies to laser-driven compression. As a result, ion-beam systems have been proposed as alternatives.

Over the past ten years the field has grown considerably, to the extent that probably about a quarter of the fusion effort around the world is now in this direction, and with a commensurate increase not only in number of workers but also in the range of activity. Research in this area now embraces nuclear burn and product studies, hydrodynamics, electromagnetic wave propagation, spectroscopy, and laser construction and design, in addition to the basic plasma physics. The field is thus rooted in several distinct disciplines, which has led to publication of research results in a wide range of journals.

Despite its somewhat misleading title, the object of *Laser and Particle Beams* (LPB) is to serve the inertial fusion and laser-plasma community. Although the creation of yet another contender for our dwindling library budgets may be questioned, this one must be welcomed; it covers a relatively new, multidisciplinary subject which is served by no existing journal.

The new journal is international in character, the editor-in-chief being Australian and the editorial board drawing its members from Britain and the rest of Europe, Russia, the United States and Japan: this same wide distribution is also reflected in the contents. In the first volume, the standard of the papers is generally high, with contributions included or promised from many of the major laboratories, and they cover most of the range of the field. Publication time to date is relatively short (between six and nine months), and the journal is attractively presented, each issue containing 100 pages and about eight papers. No letters or research-notes are included, but there is a useful book review section.

LASER AND PARTICLE BEAMS

The first issues show that LPB has made an encouraging start, but success in the future will depend on the editors' ability to attract the major papers at present published in a variety of specialist journals such as *Physics of Fluids, Journal of Applied Physics* and *Journal of Physics* Parts B and D. This new journal should become required reading for the inertial fusion community, and at its current subscription rate should be within the budget of most libraries. ☐

G.J. Pert is Professor in the Department of Applied Physics at the University of Hull.

Autumn books

Nature's next review supplement is Autumn books, which appears on 15 November. The books to reviewed include:

- *Ideals and Realities*, edited by Z. Hassan and C.H. Lai, a collection of the essays of Abdus Salam.
- *The Limits of Science* by P.B. Medawar.
- *The 4th Dimension: Toward a Geometry of Higher Reality* by Rudy Rucker.
- *The Resourceful Earth*, Julian L. Simon and Herman Kahn's reponse to *Global 2000.*
- *Superforce: The Search for a Grand Unified Theory of Nature* by Paul Davies.
- *From Knowledge to Wisdom: A Revolution in the Aims and Methods of Science* by Nicholas Maxwell.
- The first three volumes in a new series, *Key Environments*, edited by John Treherne.
- *Discoverers of the Lost World*, George Gaylord Simpson's account of palaeontology in South America.

Matter of the fourth state

R.A. Lawes

Plasma Chemistry and Plasma Processing.
Editors Emil Pfender and Stan Veprek.
Plenum. 4/yr. $95 (US), $107 (elsewhere).

Plasma Chemistry and Plasma Processing (PCPP) attempts to cover "the fourth state of matter" — the plasma state — through the publication of research papers and articles on subjects such as plasma physics, fluid dynamics and heat transfer, surface chemistry, materials science and so on. The claim is made that the journal is a major international focal point for the scientific and technical community. It has yet to achieve that status.

The scope of PCPP is very broad and, with only about 20 papers published per annum, there is some evidence of a lack of focus. Viewed from a particular topic, for example plasma technology in microelectronics fabrication, only two or three papers may be of direct interest to an individual reader each year. Thus, for most readers, this journal will be seen as complementary to other, more specific and established publications such as the *Journal of Vacuum Science and Technology.*

The quality of the papers themselves is good, with a strong emphasis on experimental results adequately supported by theory. Their source is world-wide (with a bias towards the United States!) yet firm editorial control has brought all contributions up to a consistent standard. General review papers are avoided and editorial comment is conspicuously absent. There appears to be little encouragement for readers to respond to previously published papers, and this is a failing which the editors would do well to rectify. The quality of production is uniformly excellent with clear text and legible, informative diagrams.

Broadly, PCPP has met most of its objectives as well as can be expected. At an export price of $107 per volume it is probably a little too expensive to reside on personal bookshelves; however, research workers will wish to peruse the contents regularly and should persuade their libraries to take out a subscription. ☐

R.A. Lawes is Head of the SERC Electron Beam Lithography Facility at the Rutherford Appleton Laboratory, Chilton, Oxfordshire.

Albite to zirconium

Robert Cahn

Mechanics of Materials: An International Journal.
Editors S. Nemat-Nasser and J. Weertman.
North-Holland. 4/yr. Dfl. 252.
Materials Chemistry and Physics: An International Journal.
Editor V. Lorenzelli.
Elsevier Sequoia. 12/yr. SwFr. 470, $224.

FLEDGLING engineers are taught a subject generally misnamed "strength of materials", which is mostly elasticity theory applied to the analysis of loaded components and structures. "Mechanics of materials", a more acceptable term, incorporates some of this, but much else besides: it includes the study of plastic flow, fracture, fatigue, the mechanical characteristics of cracks and other precisely defined defects, the mechanics of powders and other porous media, mechanical anisotropy and more. *Mechanics of Materials* (MM) is also the title of a new journal which has got off to a flying start since its first appearance early in 1982, and now publishes some 400 pages each year. Its subheading specifies that it is a "forum for theoretical, experimental, and field advances in mechanics of flow, fracture, and general constitutive behaviour of geophysical, geotechnical and technological materials".

The geological emphasis thus expressed is consistent with the expertise of one of the editors, Professor Johannes Weertman, who is attached to both the Materials and the Geology Departments at Northwestern University, Illinois (while the co-editor is professor of civil engineering at the same university). Up to now, most of the papers in MM have come from the United States, but there have been a number from elsewhere, notably from the geo-mechanical group in Paris headed by J.-P. Poirier and from M.S. Paterson's geophysics group in Australia.

The contributions tend to be strongly theoretical in slant, sometimes to the point of ultra-abstraction, but there are also a few experimental papers, some dealing with powders and porosity; and one intriguing work is concerned with the theory of the drying (seasoning) of wood, treated formally as a porous capillary body. Major theoretical categories include fracture mechanics and the theory of defect aggregates, dislocations in particular.

The new journal has two principal competitors (leaving out of consideration the various specialized fracture journals): the veteran *Journal of Mechanics and Physics of Solids*, now in its thirty-second volume and publishing about 500 pages per annum, a journal with distinct (British) Cambridge connections, and the newer *Res Mechanica* (subtitled *Structural Mechanics and Materials Science*), now on Vol. 11 and publishing around 1,000 pages each year. Both have a strong mathematical bias, like the new journal, and the coverage of all

TWO NEW reliable, up-to-date and complete biotechnology information resources.

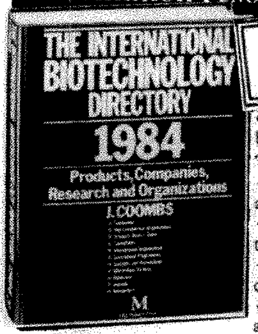
THE INTERNATIONAL BIOTECHNOLOGY DIRECTORY
1984
Products, Companies, Research and Organizations
J. COOMBS
M

EXAMINE ON FREE APPROVAL WITHOUT COMMITMENT

• covers both the old and new biotechnologies

The Directory tells you:

★ Who your competition is, and what they are doing.

★ Who are potential customers and suppliers.

★ Where to buy equipment, chemicals and services.

★ Where culture collections are located and what cultures they hold.

★ Who imports/exports biotechnology products in over 20 countries.

★ Which government departments are associated with biotechnology.

All compiled by the eminent biotechnologist Dr. Jim Coombs and now available to you on **FREE APPROVAL.**

Detailed information on every aspect of biotechnology worldwide

An indispensable guide to: ★ Products, services and research ★ Companies ★ Government and international agencies ★ Information sources

THE INTERNATIONAL BIOTECHNOLOGY DIRECTORY 1984 —

• is thoroughly international

• features a unique BUYER'S GUIDE to products, research and services

Macmillan Hardcover 400pp
November 1983
ISBN 0 333 35140 1
£50.00/A$100.00

Information Sources in Biotechnology

★ covers both old and new technologies

★ covers technical and commercial literature

★ covers difficult and hard to trace sources

★ includes over 20 at-a-glance evaluation tables

★ provides an Index of publishers and their addresses

Dr. Crafts-Lighty, Head of Information and Library Services at Celtech Limited, systematically and critically reviews all the important information sources:

• books • conferences • trade periodicals • research periodicals • computer databases • patent • market surveys • directories • organisations • secondary sources

Macmillan Paperback 320pp
September 1983
ISBN 0 333 36178 4
£40.00/$80.00

Send no money now. Examine on FREE APPROVAL

You can take these new books for 30 days examination without commitment. If you are not completely satisfied, just return the book(s) in good condition within 30 days and we will cancel your invoice.

Globe

Globe Book Services Limited,
Brunel Road, Houndmills,
Basingstoke, Hants RG21 2XS England.
Telephone: Basingstoke (0256) 29222
A DIVISION OF MACMILLAN PUBLISHERS LTD.

The Nature Press,
15 E 26 Street, New York, N.Y. 10010.
Telephone: 212-532-4811

FREE APPROVAL ORDER FORM

To: Ian Jacobs, Globe Book Services Ltd., FREEPOST,
Brunel Road, Houndmills,
Basingstoke,
Hants RG21 2BR, England.

The Nature Press,
15 E 26 Street, New York,
N.Y. 10010. Credit card callers call toll-free
800-221-2123 (or in New York: 212-532-4811)

Please send me on 30 days FREE APPROVAL______ copies of *The International Biotechnology Directory 1984* at £50.00/$100.00 each, and/or______copies of *Information Sources in Biotechnology* at £40.00/$80.00 each.

If I am not entirely satisfied, I may return any book in good condition within 30 days and you will cancel my invoice.

Postage and Packing

UK subscribers £2.00 (Overseas £3.00) US Subscribers $1.50

Tick preferred method of payment

☐ Bill me. I need send no money now.
☐ I enclose cheque for £/$ ______
☐ Charge my credit card on publication £/$ ______
☐ Visa ☐ Access/Mastercharge ☐ Am. Express ☐ Diners

Card No.______ Expiry Date______
Signature ______
(Orders cannot be accepted without a signature)
Name______
(PLEASE PRINT)
Address______

Postcode/Zip Code______
Books will be delivered to you on publication. N3
UK Subscribers POST TODAY — NO STAMP NEEDED

MECHANICS OF MATERIALS

three overlaps considerably. Nevertheless, the geological leanings of MM, combined with the high standard of editing, suggest that it will survive even in the face of the excellent standards of its two immediate rivals.

The other journal, *Materials Chemistry and Physics* (MCP), is a re-titled version of *Materials Chemistry*, transferred to a new publisher from January 1983. In spite of the change of name, it still has a strong chemical bias and indeed the best of the many good papers are all chemical. The authors who fill the annual 1,200 pages or so at present are either Europeans (notably from Italy, France, Spain and eastern Europe) or from India. In this the journal differs from its established rivals, *Journal of Materials Science, JMS Letters, Materials Letters, Journal of Physics and Chemistry of Solids, Solid State Communications* (another letters journal) and *Materials Research Bulletin*. All of these, while international, have a strong American component. Further the new journal has a *de facto* emphasis on electrochemistry, especially photoelectrolysis, and also in general a more applied flavour than does *Journal of Physics and Chemistry of Solids*. It has printed a number of valuable reviews, notably one on oxide electrode materials. Authors are invited to produce camera-ready copy once a typescript has been accepted, and many have availed themselves of this privilege if such it is; unfortunately some had no access to electric typewriters, which should surely be a precondition of acceptance of CRC, in courtesy to readers!

As, say, a journal of applied materials chemistry, I believe that MCP will find a permanent niche. But if it seeks to become a broad-spectrum materials journal (which it is not now), it risks becoming submerged by the competition. ☐

Robert Cahn was formerly Professor of Materials Science at Sussex University and Professor of Metallurgy at the University of Paris-South.

Fluent techniques

G.M. Lilley

Experiments in Fluids: Experimental Methods and their Applications to Fluid Flow.
Editors W. Merzkirch and J.H. Whitelaw.
Springer-Verlag. 6/yr. DM 245, $97.

THE study of theoretical and experimental fluid mechanics relies, as do most fields of science, on the publication in readily available form of good, independent research which has been carefully scrutinized and refereed before reaching print.

For the past 28 years the *Journal of Fluid Mechanics* has been the major forum in this field, and its record has been excellent. Subjects which are embraced by that publication are also among those proposed for this new English-language journal, *Experiments in Fluids* (EF). However, while there is merit in a new journal specifically dealing with experimental fluid mechanics, it would be regrettable if the *Journal of Fluid Mechanics* was thereby to reduce proportionally its number of papers on this important part of the subject; it would appear that there are enough acceptable papers to fill both journals.

The intention of the editors of EF is to publish research papers and technical notes relating to experimental methods and techniques, and to their application to the solution of problems in fluid mechanics. They specify that contributions to the journal should encompass a wide range of applications, including aerodynamics, hydrodynamics, basic fluid dynamics, convective heat transfer, combustion, biological and geophysical flows and turbomachinery.

In the issues published to date there have been no editorial reviews or comments, or book reviews, but there seems to be no editorial policy excluding such features. Currently the publication time for articles appears to be very fast, with about a six-month gap between date of receipt and final publication. Authors receive 50 free off-prints of their published papers, a welcome bonus, but the journal's cost of $97 per year for individuals seems rather expensive. The quality of production of articles is good, although there is nothing exceptional about the standard of illustrations.

The contributions published so far deal with both experimental techniques and detailed flow measurements, and certainly meet the requirements of the editors in respect of range of topics. In at least one paper attention is given to an uncertainty analysis of the measured data, but it cannot be overemphasized that such analysis should be given prominence in all papers published in a journal on experimental methods and measurements.

Although the need for a new journal within fluid mechanics can be questioned, there is probably a place for one specifically associated with experimental techniques and applications. On its early showing, EF appears to be a worthy newcomer in this field. ☐

G.M. Lilley is Emeritus Professor of Aeronautics and Astronautics at the University of Southampton.

REVIEW ARTICLE

LIBRARY COMPL[illegible]
Departments of
Chemical Engineering
Chemical Technology
Plastics and Rubber Technology

Mantle enrichment processes

C. J. Hawkesworth, N. W. Rogers, P. W. C. van Calsteren & M. A. Menzies

Department of Earth Sciences, The Open University, Milton Keynes MK7 6AA, UK

A review of Sr- and Nd-isotope and selected trace element data in both within-plate basalts and mantle xenoliths suggests that at least two enrichment processes are active within the upper mantle. One is consistent with the migration of small volume silicate melts with 'basanitic' trace element distribution patterns, whereas the other is characterized by relatively high ε_{Sr}, Rb/Sr and K/Ti ratios, as observed in K-richterite-bearing periodotite xenoliths.

THE Earth's mantle consists predominantly of Fe, Mg and Al silicates and it is probably fairly homogeneous with respect to major elements. However, mantle trace elements are distributed heterogeneously and these are particularly useful in attempting to describe different domains in the upper mantle and how they may have evolved. Trace elements are only present in very low concentrations and thus they rarely form minerals of their own. Many are termed incompatible because they do not sit readily in the crystal structure of common mantle minerals and so they concentrate in any small volume fluid or melt phase that may be present. Some incompatible elements are radioactive and potentially the changing isotope abundances of their daughter products allow evaluations of the age of individual mantle domains and of the timing of certain upper mantle processes. However, any interpretation of the observed variations in radiogenic isotopes should be allied to an understanding of the processes responsible for the distribution of the parent and daughter elements in the upper mantle. The composition of the mantle may be inferred from studies of basalts, and determined directly on rare samples of mantle rocks transported to the surface either tectonically or as xenoliths (fragments) in mantle-derived magmas. Such samples provide both mineralogical and chemical evidence for the changes that can result from processes that enrich and deplete trace elements in the upper mantle. This review considers the extent to which information on mantle trace-element enrichment processes from mantle xenoliths may be reconciled with some of the trace-element and radiogenic-isotope variations in recent basalts.

Trace elements

The upper mantle is heterogeneous with respect to trace element ratios as well as abundances. Those portions that are enriched in trace elements relative to the mantle source of mid-ocean ridge basalts (MORB) or to best estimates of the primitive mantle testify to processes that scavenge and then concentrate these elements. Moreover, when trace-element enrichment results in changes in Rb/Sr, Sm/Nd and U/Pb, they will with time generate different Sr-, Nd- and Pb-isotope ratios. Yet, ironically, while the evidence for trace-element enriched areas in the upper mantle is generally accepted, there is widespread reluctance to believe that they may develop slightly unusual radiogenic isotope ratios.

The root of this reluctance arguably lies in one of the more spectacular applications of radiogenic isotopes, the models for the chemical evolution of the Earth[1-3], for these models suggest that the chemical evolution of at least the outer portions of the Earth can be reasonably described in terms of a primitive mantle reservoir that differentiates to form the crust and a residual or depleted mantle. With the passage of time, and the radioactive decay of ^{87}Rb and ^{147}Sm, the crust evolves high ^{87}Sr/^{86}Sr and low ^{143}Nd/^{144}Nd ratios and the depleted (MORB-type) mantle has the complementary low ^{87}Sr/^{86}Sr and high ^{143}Nd/^{144}Nd. Consequently, both have similar average model ages of 1,900–1,700 Myr. The problem is how to describe and interpret any compositions intermediate between the selected values for the crust and the depleted mantle. Within the confines of these models, the intermediate compositions can be described in terms of the chosen 'endmembers' of crust and depleted mantle. However, the success of the models has encouraged the two-component approach in other areas, in interpreting both the isotope ratios observed in individual magmatic provinces and the overall array of isotope data on mantle-derived rocks.

Figure 1 summarizes some of the Nd-isotope results available on fragments of the upper mantle brought to the surface as xenoliths in alkali basalts and kimberlites[4-9]. Most were determined on separated minerals that, unlike the whole rocks, appear not to have been contaminated with the host magma en route to the surface. The data range from high ^{143}Nd/^{144}Nd ratios indistinguishable from those of MORB to low values often regarded as typical of crustal rocks. Thus not all mantle-derived rocks are depleted isotopically relative to the bulk Earth, and particularly in continental areas where old segments of mantle may be preserved within the continental lithosphere, it seems that mantle rocks can have comparable radiogenic isotope ratios to those in the overlying crust. For Nd, Sr and even Pb isotopes, caution is needed before arguing that isotope ratios which indicate trace-element-enriched source regions are necessarily derived from the crust. Crustal contamination may be better

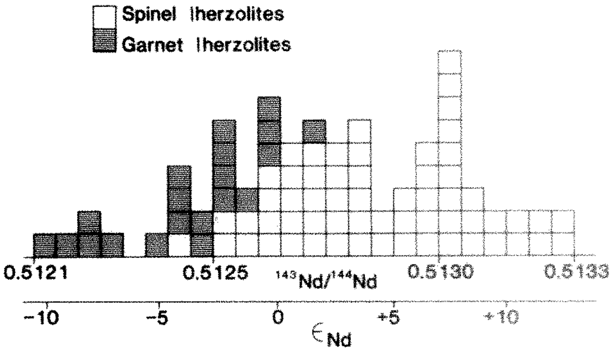

Fig. 1 Present day Nd-isotope composition of clinopyroxenes in spinel and garnet lherzolite inclusions from alkali basalts and kimberlites[4-9]. $\varepsilon_{Nd}(T)$ is the deviation from the value expected in a chondritic reservoir (CHUR) at time T, and is defined as

$$\varepsilon_{Nd}(T) = 10^4 \left[\frac{^{143}\mathrm{Nd}/^{144}\mathrm{Nd}_{\mathrm{rock}}(T)}{^{143}\mathrm{Nd}/^{144}\mathrm{Nd}_{\mathrm{CHUR}}(T)} - 1 \right]$$

where

$$^{143}\mathrm{Nd}/^{144}\mathrm{Nd}_{\mathrm{CHUR}}(T) = 0.51264 - 0.1967[(\exp \lambda_{\mathrm{Sm}} T) - 1].$$

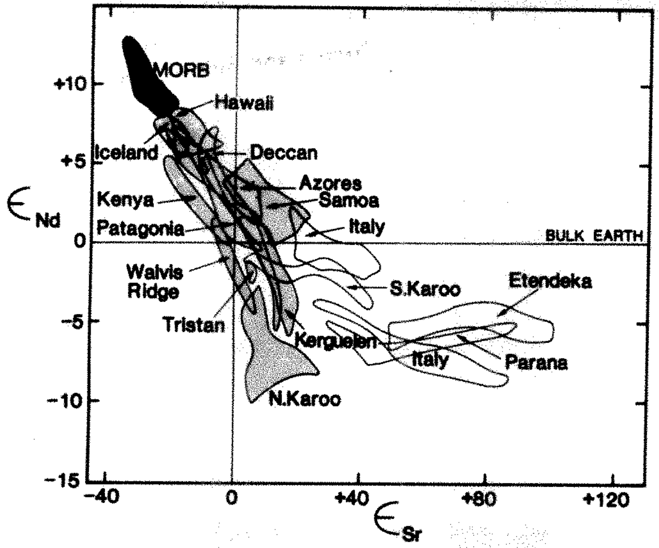

Fig. 2 Nd- and Sr-isotope compositions of selected Jurassic–Recent volcanic rocks[12–28]. The shading identifies MORB and two groups of within-plate basalts which tend to have different minor- and trace-element characteristics (see, for example, Figs 3, 4).

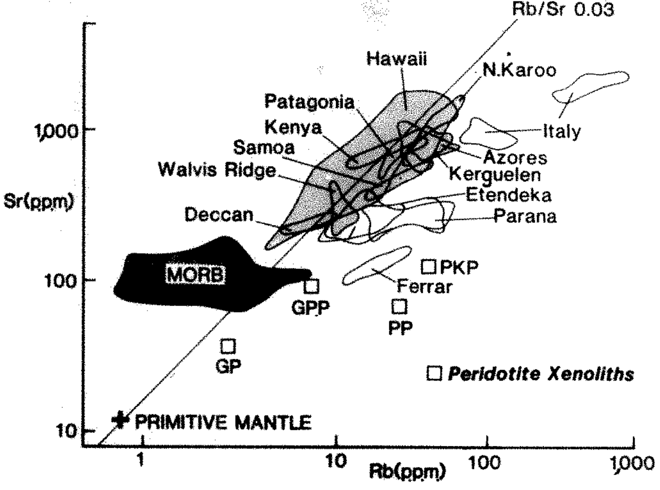

Fig. 3 Rb and Sr variations in selected MORB glasses, peridotite xenoliths and within-plate basalts[5,12–26,35,75–84]. For the peridotites and many basalt provinces average values have been plotted. Ferrar dolerites are included because of their high ε_{Sr} values in primitive rocks[42], even though ε_{Nd} data are not available. Shading as in Fig. 2. GP, garnet peridotites; GPP, garnet phlogopite peridotites; PP, phlogopite peridotites; PKP, phlogopite K-richterite peridotites[5].

demonstrated by the changes in isotope composition that will result from any contamination process, than by appealing to the discriminating powers of specific radiogenic isotope ratios.

The counter argument to such evidence for a mantle relatively enriched in radiogenic isotopes is that while xenoliths in kimberlites are interesting in their own right, they might come from anomalous segments of mantle and so might not be relevant to the study of basalts and their mantle source regions. The evidence from xenoliths need not, therefore, deflect attempts to model the isotope ratios of within-plate basalts in terms of crust and depleted mantle. Moreover, because most xenoliths from kimberlites are too impoverished in those major elements that are enriched in basalt, and are therefore incapable of producing much basaltic melt[10], it is not an argument that can be lightly dismissed.

One way of assessing the significance of mantle enrichment processes is to compare not simply the isotope ratios in basalts and xenoliths, but also variations in minor and trace elements, and hence the coherence between isotope and trace element compositions[11]. This review therefore focuses on certain aspects of the minor- and trace-element variations in mantle xenoliths and basalts which, in conjunction with the Nd- and Sr-isotope data, offer some constraints on the nature of mantle enrichment processes. The discussion is deliberately restricted to Nd and Sr isotopes because their distribution and that of their parents Sm and Rb may be more readily related to that of other commonly analysed trace elements than can, for example, the rare gases or even U and Pb.

Nd and Sr isotopes

Detailed studies have been carried out on a wide range of both oceanic and continental volcanic rocks and some of the results are summarized in Fig. 2 (refs 12–28). Data have been omitted both for clarity, where they exhibit similar trends to those already plotted, and where a reasonable case exists for contamination with continental material as mantle-derived magmas migrate up through the crust (for example, the south Lebombo basalts of the Karoo[24], the lower lavas of the Mahabaleshwar section of the Deccan Traps[20,27] and the British Tertiary[29]. Overall, the inverse correlation of ε_{Nd} and ε_{Sr} defines a broad swathe of results through a point representing the estimated composition of the undifferentiated bulk Earth[28]. Most basalts have positive ε_{Nd} and negative ε_{Sr} (low $^{87}Sr/^{86}Sr$) values and were, therefore, derived from source regions which had low Rb/Sr and Nd/Sm for much of their history; that is, they were relatively depleted in the more incompatible elements such as Rb and the light rare-earth elements (LREEs). Conversely, rocks with negative ε_{Nd} and positive ε_{Sr} contain at least a contribution from sources that had high Nd/Sm and Rb/Sr ratios, and hence by implication were relatively enriched in incompatible elements, for long periods of time. Many crustal rocks have similar ε_{Nd} and ε_{Sr} values, but then so too do some peridotite mantle xenoliths and the diopsides separated from them (refs 4, 5, 30 and Fig. 1).

The issue is the extent to which the broad trend of the Nd- and Sr-isotope data reflects mantle processes operating on the global scale, including the recycling of continental material. The models of Earth evolution rely heavily on the complementary nature of the crustal and depleted (MORB-type) mantle reservoirs, and the shape of the data array is broadly consistent with two-component mixing. Thus, there has been much speculation that this array is due primarily to mixing between continental and depleted mantle material, with the former being introduced either in subducted ocean crust[18,30] or as portions of the continental lithosphere re-assimilated back into the convecting upper mantle[31,32] or by straightforward contamination of mantle-derived magmas en route to the surface in continental areas[33]. However, recent basalts also exhibit a curved negative correlation between Sm/Nd and Rb/Sr (ref. 17). This is consistent with the available information on the distribution of those elements between coexisting mantle phases[34], and it implies that the ε_{Nd}–ε_{Sr} array might equally reflect the fractionation of Sm/Nd and Rb/Sr in a whole series of localized enrichment and depletion events in the upper mantle.

Figure 2 shows the data on intraplate basalts, subdivided on the basis of ε_{Nd} and ε_{Sr}, and the minor and trace element variations illustrated in Figs 3 and 4. One group largely plots on or to the left of the steep portion of the array, with the possible exception of those from Samoa and perhaps the Azores which are discussed below, whereas the samples in the other group are displaced to relatively high ε_{Sr} values. Moreover, while rocks in the first group occur in both oceanic and continental areas, those with relatively high ε_{Sr} seem to be restricted to the continents. This observation suggests that mantle source regions with similar trace element histories are sampled in both environments, and that the high ε_{Sr} values are due to contamination with contiental crust and/or to a different trace-element enrichment process apparently confined to the sub-continental mantle.

Trace-element studies have demonstrated that some basalts have high concentrations of incompatible elements, including

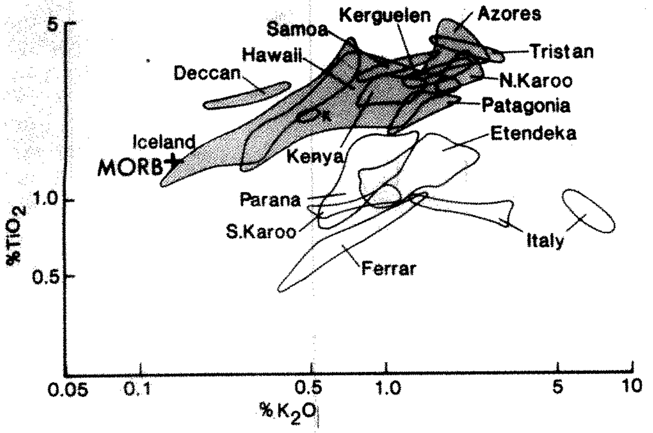

Fig. 4 TiO_2 and K_2O variations in the basic volcanic rock suites for which ε_{Nd} and ε_{Sr} data are plotted in Fig. 2. The exceptions are the Ferrar dolerites which are included because of their high ε_{Sr} values, although ε_{Nd} data have not yet been published. Shading as in Fig. 2. K, small subset of Kerguelen data. Typical MORB from ref. 40.

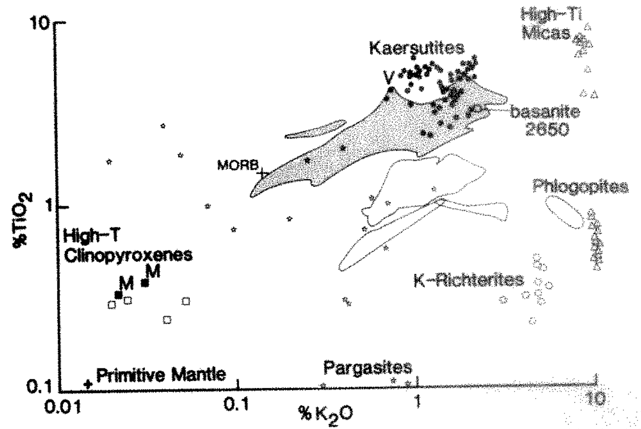

Fig. 5 TiO_2 and K_2O contents of micas, amphiboles and high-temperature clinopyroxenes[45–50,52–61,67–71] compared with trends identified in basalts in Fig. 4. The high Ti-micas, kaersutites and pargasites are from inclusions in alkali basalts, whereas the phlogopites, K-richterites and clinopyroxenes are from inclusions in kimberlite. V, vein sample; M, megacryst from kimberlite. Open squares, diopsides from high-temperature peridotites.

the LREEs, accompanied by comparatively low or unfractionated Rb/Sr ratios, while in others high incompatible element contents are accompanied by high Rb/Sr ratios[17,21,23,24,35]. These differences seem to reflect different trace-element enrichment processes in the upper mantle, and with time they will generate low ε_{Sr}, low ε_{Nd} and high ε_{Sr}, low ε_{Nd} trends respectively on the Nd–Sr isotope diagram.

The case for the existence of different trace-element enrichment processes is supported by studies on garnet- and amphibole-bearing peridotite xenoliths from kimberlite pipes in southern Africa[4,5,36], and by studies on apatite pyroxenite inclusions from south-east Australia[37]. Most cold, coarse peridotites from southern Africa are enriched in LREEs, and hence have low Sm/Nd ratios, but those which contain garnet ± phlogopite are characterized by low Rb/Sr, in contrast to those that are garnet-free and contain phlogopite ± K-richterite and have high Rb/Sr ratios (see average values on Fig. 3). With time the low Sm/Nd, low Rb/Sr rocks have evolved on or to the left of the ε_{Nd}–ε_{Sr} array, and the high Rb/Sr, low Sm/Nd samples have generated relatively high ε_{Sr}, low ε_{Nd} values comparable with those in the Italian and South Karoo basalts in Fig. 2 (refs 11, 23). Furthermore, if mantle-enrichment processes are primarily responsible for such coherent variations in Rb/Sr and Sm/Nd (and hence ε_{Sr} and ε_{Nd}), they should also result in other minor- and trace-element differences that might, for example, be more sensitive to the nature of those enerichment processes.

Rb, Sr and TiO_2, K_2O

There have been surprisingly few attempts to analyse minor- and trace-element variations in mantle-derived rocks in the context of mantle-enrichment processes, and there is only room here for some preliminary speculations. It has been demonstrated[5,11,24] that Rb/Ba ratios were remarkably similar in both garnet and garnet–phlogopite lherzolite xenoliths from Kimberley and in many Karoo basalts, even though average Ba contents ranged from 19 p.p.m. in xenoliths up to 920 p.p.m. in nothern Karoo lavas. All these rocks plotted on or to the left of the ε_{Nd}–ε_{Sr} array, and any group of rocks that had high Rb/Ba ratios also had relatively high ε_{Sr} values (for example, the Etendeka[24] in Fig. 2). However, there are fewer Rb/Ba than Rb/Sr data available in the literature, and since variations in Rb/Sr may also be related more directly to those in $^{87}Sr/^{86}Sr$, Rb and Sr results from some basalts and mantle xenoliths are outlined in Fig. 3 to investigate this line of argument further.

Where possible, the analyses used in compiling Fig. 3 are on the same rocks as those in Fig. 2, although for many provinces, average Rb and Sr values have been plotted. This is partly because in some instances only average values are available, and partly for clarity because it minimizes the scatter. The averages are based on local criteria such as magma type, stratigraphical unit and radiometric age. What is striking is that even though Rb/Sr ratios are highly susceptible to low-pressure effects such as plagioclase fractionation, there are still strong links between Rb/Sr and ε_{Sr} (refs 38, 39). The basalts with high Rb/Sr have relatively high ε_{Sr}, and those with comparatively unfractionated Rb/Sr ratios plot on or to the left of the steep portion of the ε_{Nd}–ε_{Sr} array.

Such consistency between isotope- and trace-element ratios is reassuring, but it is difficult to evaluate by studies of mantle xenoliths because of practical problems in obtaining representative, or even reliable, trace-element data from many mantle rocks. However, several studies have reported high quality microprobe analyses on mantle minerals so that if the inferred styles of trace-element enrichment could be recognized in at least minor element variations, it should be possible to evaluate them by comparison with the minor-element variations in mantle minerals.

The minor elements selected were Ti and K and the results were treated in the same way as the Rb and Sr data. Most basalts from both oceanic and continental areas plot on a broad array within which Ti/K decreases from ~7 in typical MORB[40] to ~1.4 in incompatible element-enriched basalts on oceanic islands such as Sao Miguel in the Azores and Tristan da Cunha (Fig. 4). Significantly, however, those basalts which have relatively high ε_{Sr} (Fig. 2) appear to be characterized by relatively low Ti contents, and hence low Ti/K ratios (~1–0.1). Once again high $^{87}Sr/^{86}Sr$ ratios consistently occur in rocks which have distinctive minor-and trace-element features. Crustal contamination will tend to reduce Ti/K, but significant amounts of contamination are required if that is to be the cause of the observed low Ti/K ratios. For example, to generate a basalt with 1% TiO_2 and 1% K_2O from typical MORB[40] implies 30% contamination, even in the most advantageous conditions of a TiO_2-free contaminant (whereupon the contaminant would have ~2.5% K_2O), and the amount of contamination is not reduced by invoking assimilation with fractional crystallization[41] and/or a contaminant with higher K_2O. Yet both the high Ti and low Ti trends include primitive basalts with so-called 'mantle' $\delta^{18}O$ values of 6.0±0.5‰ (refs 42, 43, and R. S. Harmon, personal communication), suggesting that it is most improbable that the difference between the two trends is due to crustal contamination.

Further evidence for attributing different Ti–K trends to mantle processes comes from the variation of Ti contents, in particular in mantle phases. The textural relations of, for example, phlogopite in mantle xenoliths are extremely complex, and while many authors have identified 'primary' and 'secondary' phlogopite mica[44–50], it is often unclear whether the latter reflect mantle metasomatic processes or interaction with the host kimberlite. In general, secondary micas have higher and more variable Ti contents and in this discussion we have assumed that they reflect kimberlite interaction, and so have not considered them further. Primary phlogopites have $\leq 1\%$ TiO_2 (ref. 46) consistent with the low TiO_2 contents of the amphibole with which they are most often associated K-richterite (see Fig. 5) and the low Ti/K whole rock ratios of the phlogopite–richterite peridotite suite[48]. The identification of Ti-rich accessory phases in association with richterite[51] indicates that Ti is also mobilized in this process, even though the overall character is one of alkali enrichment. Moreover, since these metasomatized xenoliths also exhibit relatively high Rb/Ba, Rb/Sr and ε_{Sr} values[5], they have both minor- and trace-element and Nd–Sr isotope features remarkably similar to those of the low Ti/K, high $^{87}Sr/^{86}Sr$ continental basalts (Figs 2, 4).

Spinel peridotites also exhibit isotope- and trace-element features consistent with trace-element enrichment after some previous major-element depletion episode[49,50]. However, unlike garnet peridotites, spinel peridotites occur predominantly in alkali basalt provinces, and 'metasomatism' tends to be associated with multiple intrusions of alkali-rich or 'basantic' silicate magma[52–61]. Composite xenoliths preserve a record of pyroxenite veins cross-cutting peridotite, and the common amphibole is kaersutite which can occur in veins, poikilitically within the host lherzolite or as megacrysts in alkali-rich basalts. Phlogopite is rare, and when present it is usually Ti-rich, so that both the amphibole and mica commonly associated with trace-element enrichment in the spinel lherzolite facies have the relatively high Ti/K ratios characteristic of most oceanic and continental within-plate basalts. Moreover, both the basalts on the high Ti/K trend and clinopyroxenes and kaersutites from spinel lherzolites tend to have low $^{87}Sr/^{86}Sr$ ratios, <0.7055 (ref. 50).

The amphibole pargasite also occurs as megacrysts and in spinel lherzolites, and yet it is characterized by highly variable K and Ti contents (Fig. 5) and locally it is associated with low-Ti phlogopite[62]. However, the scatter of K and Ti data indicates that pargasite has no simple relationship with the processes responsible for the coherent trends in the basalts. It has been argued, for example, that pargasite may form during wall rock alteration around magma conduits[61].

Magma migration or metasomatism?

The descriptions of trace-element enrichment processes inferred from mantle xenoliths vary significantly from spinel- to garnet-bearing suites. The former emphasize the role of associated magmatism; veins and megacrysts testify to the transfer of material in silicate melts, and chemical metasomatism of the country rocks may be largely restricted to the contacts with veins and conduits. In contrast, discussions of xenoliths from kimberlites, particularly from the Kimberley area where most work has been done on K-richterite bearing rocks[5,46], often appeal to 'pervasive metasomatism and the infiltration of H_2O-rich fluids', and comparatively few vein textures have been reported. Thus, it is very tempting to attribute the low Ti/K, high Rb/Ba, Rb/Sr and subsequently high ε_{Sr} style of enrichment recognized in both basalts and mantle xenoliths in this form of mantle metasomatism, to the infiltration of H_2O- and alkali-rich fluids. Such fluids probably reflect different processes in different areas, but there is increasing evidence from the Italian volcanics (see Figs 2–4) that, at least locally, this style of trace-element enrichment can be related to subduction[62,63]. The more common high Ti/K style of enrichment occurs in both oceanic and continental areas, and the evidence from spinel lherzolites and megacrysts indicates that it reflects the migration of small volumes of silicate melt. It concentrates a spectrum of trace elements from Rb, K, Ba, through Nb, Ta and the LREEs, to Zr and Ti, with the result that within-plate basalts may be characterized on discriminant diagrams intended to distinguish basalts erupted in different tectonic settings[64], and many of the more incompatible element-enriched basalts on the high Ti trend have trace-element-normalized patterns similar to those of basanites. LREE abundances increase, and so Sm/Nd ratios are low, but there is relatively little increase in Rb/Sr and the basalts and xenoliths consistently plot on, or to the left of, the steep part of the ε_{Nd}–ε_{Sr} array.

These features appear to be characteristic of enrichment processes in the convecting upper mantle and they are also observed in discrete nodules (or megacrysts) and high-temperature deformed peridotites from kimberlite pipes[65,66]. Clinopyroxene megacrysts and separates from high-temperature peridotites have both low $^{87}Sr/^{86}Sr = 0.7024$-0.7036 (refs 67–69) and high Ti/K ratios[70,71] comparable with those of the high Ti/K basalt trend (Fig. 4). Thus the isotope- and trace-element compositions, and the pressure–temperature (P–T) conditions of equilibration, of the high-temperature peridotite are predominantly asthenospheric in character; as are the megacrysts which appear to have crystallized from high-temperature Ti-rich magmas derived from the convecting upper mantle. Harte[66] has recently developed this argument to show that using partition coefficients for basaltic magmas the estimated trace-element composition of magma in equilibration with a clinopyroxene megacryst from kimberlite is very similar to that of basanite 2650 from Frey *et al.*[34] (see Fig. 5), which is believed to be a good example of a small-volume mantle melt.

Discussion

This preliminary review of minor- and trace-element and Nd-, Sr-isotope data on within-plate basalts and on xenoliths containing hydrous mantle phases suggests that at least two enrichment processes are active in the upper mantle. In reality there is probably a continuum of enrichment processes. Volcanic rocks with ε_{Nd}–ε_{Sr} values on, or to the left of, the mantle array have trace-element compositions consistent with the migration of small volumes of 'basanitic' melts within their upper mantle source regions. This seems to be the dominant enrichment process in both oceanic and continental areas and it can be observed directly in the composite spinel lherzolite xenoliths which are a feature of many young alkali basalt provinces. In addition, basanitic high-Ti, low $^{87}Sr/^{86}Sr$ magmas have been in equilibrium with the megacryst suite in kimberlites and responsible for the Fe–Ti enrichment in high-temperature deformed peridotites[65]. In contrast, basalts from some provinces are characterized by relatively high ε_{Sr}, Rb/Ba, Rb/Sr and K/Ti—as are metasomatized phlogopite + K-richterite-bearing peridotite xenoliths. These represent a different style of mantle enrichment which is apparently confined to continental areas. It probably results from more than one process, but there is evidence from the Italian volcanics, for example, that, at least locally, it can be related to the release of H_2O- and alkali-rich fluids above a subduction zone[62,63].

There has been some debate over the timing of mantle-enrichment events and their relation to volcanism[72]. In many areas, trace-element enrichment seems to have been closely associated with, and may locally have been responsible for, magma genesis[9,17,73]. Interestingly, however, such magmatic provinces all seem to lie on the high Ti/K trend and it has been suggested that this enrichment reflects the migration of small-volume partial melts. The low Ti/K style of enrichment seems to have no such simple relationship to magma genesis, although in the case of the K-richterite metasomatism in xenoliths from southern Africa, it takes place soon after the widespread Karoo magmatism (ref. 11 and refs therein).

Note that none of the figures used here are intended to be discriminant diagrams, particularly in assessing the effects of crustal contamination. The analyses plotted in Figs 2–4 are from suites in which at least the primitive rocks do not seem to have been affected significantly by crustal contamination. So, although it has been argued that the observed trends are due to mantle-enrichment processes, some of the effects, such as high ε_{Sr}, can also result from crustal contamination. The case for crustal contamination must be reviewed separately for each area, and with the possible exception of high $\delta^{18}O$ values, it leaves few unambiguous fingerprints.

Finally, there is the question of the extent to which these postulated trace-element-enrichment processes are responsible for the observed range in ε_{Nd} and ε_{Sr} in recent basalts, or whether the latter primarily reflect an additional component such as subducted crust[18,30] or re-assimilated continental lithosphere[32]. The coherence between the minor-and trace-element and the isotope trends implies that they are related, and the obseved range in Rb/Sr (Fig. 3) and Sm/Nd (which decreases as Rb and Sr contents increase, Fig. 3) appears to be sufficient to generate the variations in ε_{Nd} and ε_{Sr}. This suggests that an additional (continental) component may not be necessary to explain the trends in ε_{Nd}–ε_{Sr}, except perhaps in areas where inconsistencies exist between the isotope and trace-element data. Such a case may be made for the Azores and Samoa[18] rocks because they have slightly high ε_{Sr} (Fig. 2) and yet still plot on the high Ti/K trend (Fig. 4), but whether that inconsistency is sufficient to require a recycled component to explain the isotope results remains conjectural. It has also been suggested that the ε_{Nd}, ε_{Sr} values of ocean island basalts may primarily reflect the recycling of high ε_{Sr} material from the continental lithosphere[32]. However, such material seems to be characterized by low Ti/K ratios so that it could not control the volumetrically dominant high Ti/K trend in Figs 4, 5—and that would imply that the links between the isotope and minor-element trends identified here are coincidental.

Continental material appears to be recycled into the upper mantle by subduction[18,30], and it may well have influenced the actual ε_{Nd} and ε_{Sr} values estimated for the average upper mantle[74]. However, the systematic minor- and trace-element differences in basalts and mantle xenoliths which exhibit different Nd- and Sr-isotpe trends suggests that the relative fractionation of ε_{Nd} and ε_{Sr} is closely related to the postulated trace-element enrichment processes. The dominant process results in high Ti/K, low Sm/Nd and little fractionation of Rb/Sr, consistent with the migration of small-volume partial melts within the convecting upper mantle. Such melts can be derived from variously depleted and more primitive mantle reservoirs and convection will probably ensure that the enriched portions of mantle are comparatively short-lived, being continually created and destroyed.

We thank K. G. Cox, G. C. Goles, B. Harte, E. Jagoutz and W. P. Leeman for their constructive criticisms of earlier versions of the manuscript. The work was supported in part by NERC grant GR3/4330, and the manuscript was typed by Janet Dryden.

1. Jacobsen, S. B. & Wasserburg, G. J. *J. geophys. Res.* **84**, 7411–7427 (1979).
2. O'Nions, R. K., Evensen, N. M. & Hamilton, P. J. *J. geophys. Res.* **84**, 6091–6101 (1979).
3. Allegre, C. J. *Tectonophysics* **81**, 109–132 (1982).
4. Menzies, M. A. & Murthy, V. R. *Nature* **283**, 634–636 (1980).
5. Erlank, A. J., Allsopp, H. L., Hawkesworth, C. J. & Menzies, M. A. *Terra Cognita* **2**, 261–263 (1982).
6. Menzies, M. A., Kempton, P. & Dungan, M. *Terra Cognita* **2**, 230 (1982).
7. Jagoutz, E., Carlson, R. W. & Lugmair, G. W. *Nature* **284**, 708–710 (1980).
8. Stosch, H. G., Carlson, R. W. & Lugmair, G. W. *Earth planet. Sci. Lett.* **47**, 263–271 (1980).
9. Menzies, M. A. & Murthy, V. R. *Earth planet. Sci. Lett.* **46**, 323–334 (1980).
10. Griffin, W. L. & Murthy, V. R. *Geochim. cosmochim. Acta* **33**, 1389–1414 (1969).
11. Hawkesworth, C. J., Erlank, A. J., March, J. S., Menzies, M. A. & van Calsteren, P. in *Continental Basalts and Mantle Xenoliths* (eds Hawkesworth, C. J. & Norry, M. J.) 111–138 (Shiva, Orpington, 1983).
12. O'Nions, R. K., Evensen, N. M. & Hamilton, P. J. *Earth planet. Sci. Lett.* **34**, 13–22 (1977).
13. Richard, P., Shimizu, N. & Allegre, C. J. *Earth planet. Sci. Lett.* **31**, 269–278 (1976).
14. Cohen, R. S., Evensen, N. M., Hamilton, P. J. & O'Nions, R. K. *Nature* **283**, 149–153 (1980).
15. Stille, P., Unruh, D. M. & Tatsumoto, M. *Nature* **304**, 25–29 (1983).
16. Chen, C. Y. & Frey, F. A. *Nature* **302**, 785–789 (1983).
17. Hawkesworth, C. J., Norry, M. J., Roddick, J. C. & Vollmer, R. *Nature* **280**, 28–31 (1979).
18. White, W. M. & Hofmann, A. W. *Nature* **296**, 821–825 (1982).
19. Norry, M. J., Truckle, P. H., Lippard, S. J., Hawkesworth, C. J. & Marriner, G. F. *Phil. Trans. R. Soc.* **A297**, 259–271 (1980).
20. Cox, K. G. & Hawkesworth, C. J. *Phil. Trans. R. Soc.* **A310**, 627–641 (1984).
21. Richardson, S. H., Erlank, A. J., Duncan, A. R. & Reid, D. L. *Earth planet. Sci. Lett.* **59**, 327–342 (1982).
22. Dosso, L. & Murthy, V. R. *Earth planet. Sci. Lett.* **48**, 268–276 (1980).
23. Hawkesworth, C. J. & Vollmer, R. *Contr. Miner. Petrol.* **69**, 151–169 (1979).
24. Hawkesworth, C. J., Marsh, J. S., Duncan, A. R., Erlank, A. J. & Norry, M. J. *Geol. Soc. S. Afr. Spec. Publ.* (in the press).
25. Hawkesworth, C. J. & Mantovani, M. S. M. Preprint (Open University, 1984).
26. Hawkesworth, C. J. *et al. Earth planet. Sci. Lett.* **42**, 45–57 (1979).
27. Mahoney, J. *et al. Earth planet. Sci. Lett.* **60**, 47–60 (1982).
28. DePaolo, D. J. & Wasserburg, G. J. *Geophys. Res. Lett.* **3, 5**, 249–252, (1976).
29. Carter, S. R., Evensen, N. M., Hamilton, P. J. & O'Nions, R. K. *Science* **202**, 743–747 (1978).
30. Hofman, A. W. & White, W. M. *Earth planet. Sci. Lett.* **57**, 421–436 (1982).
31. McCulloch, M. T., Jaques, A. L., Nelson, D. R. & Lewis, J. D. *Nature* **302**, 400–403 (1983).
32. McKenzie, D. & O'Nions, R. K. *Nature* **301**, 229–231 (1983).
33. Carlson, R. W., Lugmair, G. W. & MacDougall, J. D. *Geochim. cosmochim. Acta* **45**, 2483–2499 (1981).
34. Frey, F. A., Green, D. H. & Roy, S. D. *J. Petrol.* **19**, 463–513 (1978).
35. Clague, D. A. & Frey, F. A. *J. Petrol.* **23**, 447–504 (1982).
36. Basu, A. R. & Tatsumoto, M. *Contr. Miner. Petrol.* **75**, 43–54 (1980).
37. Menzies, M. A. & Wass, S. *Earth planet. Sci. Lett.* **65**, 287–302 (1983).
38. Brooks, C., Hart, S. R., Hofmann, A. & James, D. E. *Earth planet. Sci. Lett.* **32**, 51–61 (1976).
39. Brooks, C., James, D. E. & Hart, S. R. *Science* **193**, 1086–1094 (1976).
40. Pearce, J. A. in *Continental Basalts and Mantle Xenoliths* (eds Hawkesworth, C. J. & Norry, M. J.) 230–249 (Shiva, Orpington 1983).
41. DePaolo, D. J. *Earth planet. Sci. Lett.* **53**, 189–202 (1981).
42. Hoefs, J., Faure, G. & Elliot, D. H. *Contr. Miner. Petrol.* **75**, 199–203 (1980).
43. Taylor, H. P., Giannetti, B. & Turi, B. *Earth planet. Sci. Lett.* **46**, 81–106 (1979).
44. Carswell, D. A. *Phys. Chem. Earth* **9**, 417–429 (1975).
45. Delaney, J. S., Smith, J. V., Carswell, D. A. & Dawson, J. B. *Geochim. cosmochim. Acta* **44**, 857–872 (1980).
46. Jones, A. P., Smith, J. V. & Dawson, J. B. *J. Geol.* **90**, 435–453 (1982).
47. Harte, B., Cox, K. G. & Gurney, J. J. *Phys. Chem. Earth* **9**, 477–506 (1975).
48. Aoki, K. *Contr. Miner. Petrol.* **53**, 145–156 (1975).
49. Frey, F. A. & Prinz, M. *Earth planet. Sci. Lett.* **38**, 129–176 (1978).
50. Menzies, M. A. in *Continental Basalts and Mantle Xenoliths* (eds Hawkesworth, C. J. & Norry, M. J.) 92–110 (Shiva, Orpington, 1983).
51. Haggerty, S. E. *EOS* **64**, 349 (1983).
52. Bergman, S. W., Foland, K. A. & Spera, F. J. *Earth planet. Sci. Lett.* **56**, 343–361 (1981).
53. Best, M. G. *J. geophys. Res.* **79**, 2107–2113 (1974).
54. Wilshire, H. G., Calk, L. C. & Schwarzman, E. C. *Earth planet. Sci. Lett.* **10**, 281–284 (1971).
55. Wass, S. *Am. J. Sci.* **280**A, 639–666 (1980).
56. Boettcher, A. L. & O'Neil, J. R. *Am. J. Sci.* **280**A, 594–621 (1980).
57. Brown, G. M., Pinsent, R. H. & Coisy, P. *Am. J. Sci.* **280**A, 471–498 (1980).
58. Aoki, K. I. & Shiba, I. *J. Jap. Ass. Miner. Petrol. Econ. Geol.* **68**, 303–310 (1973).
69. Vinx, R. & Jung, D. *Contr. Miner. Petrol.* **65**, 135–142 (1977).
60. Francis, D. M. *J. Petrol.* **17**, 357–378 (1976).
61. Wilshire, H. G., Pike, J. E. N., Meyer, C. E. & Schwarzmann, E. C. *Am. J. Sci.* **280A**, 576–593 (1980).
62. Holm, P. M. & Munksgaard, N. C. *Earth planet. Sci. Lett.* **60**, 376–388 (1982).
63. Rogers, N. W., Hawkesworth, C. J., Parker, R. J. & Marsh, J. S. *Contr. Miner. Petrol.* (in the press).
64. Pearce, J. A. & Norry, M. J. *Contr. Miner. Petrol.* **69**, 33–47 (1979).
65. Gurney, J. J. & Harte, B. *Phil. Trans. R. Soc.* **A297**, 273–293 (1980).
66. Harte, B. in *Continental Basalts and Mantle Xenoliths* (eds Hawkesworth, C. J. & Norry, M. J.) 46–91 (Shiva, Orpington, 1983).
67. Kramers, J. D., Smith, C. B., Lock, N. P., Harmon, R. S. & Boyd, F. R. *Nature* **291**, 53–56 (1981).
68. Shimizu, N. *Phys. Chem. Earth* **9**, 655–669 (1975).
69. Allegre, C. J., Shimizu, N. & Rousseau, D. *Nature* **296**, 732–735 (1982).
70. Nixon, P. H. & Boyd, F. R. in *Lesotho Kimberlites, Maseru* (ed. Nixon, P. H.) 67–75 (Lesotho Nat. Dev. Corp., 1973).
71. Boyd, F. R. & Nixon, P. H. *Phys. Chem. Earth* **9**, 431–464 (1975).
72. Menzies, M. A. & Murthy, V. R. *Am. J. Sci.* **280**A, 622–638 (1980).
73. Lloyd, F. E. & Bailey, D. K. *Phys. Chem. Earth* **9**, 389–416 (1975).
74. DePaolo, D. J. *Geophys. Res. Lett.* **10**, 705–708 (1983).
75. Baker, P. E., Rea, W. J., Skarmeta, J., Caminos, R. & Rex, D. C. *Phil. Trans. R. Soc.* **303**, 105–149 (1981).
76. Mantovani, M. S. M., Marques, L. S., de Sousa, M. A., Atalla, L. & Innocenti, F. *J. Petrol.* (in the press).
77. Watkins, N. D., Gunn, B. M., Nougier, J. & Baksi, A. K. *Bull. geol. Soc. Am.* **85**, 201–212 (1974).
78. Erlank, A. J. *et al. Geol. Soc. S. Afr. Spec. Publ.* (in the press).
79. Hedge, C. E., Peterman, Z. E. & Dickinson, W. R. *Bull. geol. Soc. Am.* **83**, 2709–2714 (1972).
80. Kyle, P. R. *Contr. Mineral. Petrol.* **73**, 89–104 (1980).
81. Cohen, R. S. & O'Nions, R. K. *J. Petrol.* **23**, 299–324 (1982).
82. Baker, P. E., Gass, I. G., Harris, P. G. & Le Maitre, R. W. *Phil. Trans. R. Soc.* **256**, 439–578 (1964).
83. Wood, D. A., Joron, J. L., Treuil, M., Norry, M. & Tarney, J. *Contr. Miner. Petrol.* **70**, 319–339 (1979).
84. Duncan, A. R., Erlank, A. J., Marsh, J. S. & Cox, K. G. *Geol. Soc. S. Afr. Spec. Publ.* (in the press).

Casimir effect for massive photons

G. Barton & N. Dombey

School of Mathematical and Physical Sciences, University of Sussex, Falmer, Brighton BN1 9QH, UK

The suggestion that the force between two perfectly conducting plates in quantum electrodynamics depends critically on whether the photon mass is precisely zero or not is false. The solution to this problem involves the discovery of a new class of classical solutions for the electromagnetic field between conducting plates, when the photon has non-zero mass.

THE inverse-power-law forces that act between macroscopic bodies as a consequence of the van der Waals forces between their constituents are not unexpected. They are understood as ordinary electromagnetic forces between charge and current fluctuations at the molecular level. One might then expect a similar interaction between (idealized) perfectly conducting bodies, obtainable from the theory for ordinary conductors and dielectrics by some appropriate limiting procedure.

In contrast to such explanations of these interactions, which focus on charges and currents, the forces between perfect conductors can be understood very simply and directly from an alternative point of view which focuses on the electromagnetic field, and ascribes the forces to changes in the quantum zero-point energy of the field normal modes when the conductors are introduced. The conductors affect the normal modes through the boundary conditions which the fields must satisfy on the conducting surfaces. Accordingly the forces depend only on Planck's constant $\hbar$ (characteristic of quantum mechanics), the speed of light c (characteristic of Maxwell's electromagnetic field equations), and on purely geometrical factors (characteristic of the spatial configuration of the conductors). The archetype of all such phenomena is the Casimir effect[1], the attractive force F (per unit area) between two perfectly conducting slabs separated by a distance $2L$

$$F = -\frac{\pi^2}{240}\frac{\hbar c}{(2L)^4} = -\frac{\partial U}{\partial(2L)}$$

$$U = -\frac{\pi^2}{720}\frac{\hbar c}{(2L)^3}$$

The connection between this approach and the more conventional one has been much discussed by, for instance, Lifshitz and Pitaevskii[2] and Tabor[3]. Here we shall be concerned only with the Casimir approach.

Davies and Unwin[4] considered the problem of the Casimir effect between perfectly conducting plates separated by a gap of length $2L$, assuming that the photon has a small non-zero mass m. This implies that longitudinal modes of the electromagnetic field are present in the gap in addition to the usual transverse modes given by Maxwell's theory. Davies and Unwin conclude that either: (1) the Casimir effect in this case is 3/2 times as large as the effect for $m = 0$ (because an additional longitudinal mode is present as well as the two transverse modes for each allowed frequency), or (2) the quantum-mechanical electromagnetic energy–momentum tensor diverges near a conducting plate, leading to a discontinuous change in the surface energy of the plate as compared with $m = 0$. Case (1) corresponds to an assumption of perfect reflection of the longitudinal modes; case (2) corresponds to the assumption of perfect transmission.

These results, if true, would be surprising. Stueckelberg[5] first investigated quantum electrodynamics (QED) with a massive photon and concluded that amplitudes describing longitudinal modes tended continuously to zero as $m \to 0$, provided that the electromagnetic current were conserved. This result was extended by Goldhaber and Nieto[6] who state that "in the massive photon case the fields and currents of a system are changed only by order $(mD)^2$" where D is the appropriate linear dimension of the system and we now use units $\hbar = c = 1$. It is, therefore, difficult to see how Davies and Unwin's discontinuous results can materialize in a macroscopic system when the situation is continuous on the microscopic level.

On the other hand, if a 'graviton' or Yang-Mills 'photon' is given a small mass, then the resultant theory in the zero mass limit is not the original zero mass theory[7–9]. These matters are of current interest in particle physics because the presence of a small photon mass is not allowed in a non-Abelian grand unified gauge theory such as SU(5) containing electrodynamics but is allowed in a theory which is not unified such as SU(3) × SU(2) × U(1) (ref. 10).

Classical electrodynamics, with finite photon mass, contains a new characteristic length scale, the Compton wavelength $\lambda = m^{-1}$ of the photon. Generally, a small non-zero photon mass will lead to new physical effects over a length scale λ. In particular, the effective range of electromagnetic interactions will be exponentially damped by $e^{-r/\lambda}$ and even for small values of m this leads to important effects over astronomical length scales. Because of this, the strongest indirect limits on m come from astrophysics[11]. They all arise in the same way: by considering astronomical structures in which magnetic fields are known to have a key role in maintaining equilibrium under the assumption that m is zero. The hypothesis that $m \neq 0$ will then destroy the conditions for equilibria over length scales $r > \lambda$, and hence one obtains an upper limit on m. Considerations of the Galactic magnetic field and magneto-acoustic propagation in the Crab Nebula[12–14] lead, in this way, to upper limits on m of order 10^{-20} eV. Magnetized interstellar gas clouds and interstellar gas in the disk of the Milky Way seem to require supporting magnetic field structure and hence[12,13] produce upper limits of about 10^{-25} eV. The strongest published limit on m results from an application of this argument[15,16] to magnetically supported structures in the Small Magellanic Cloud which are claimed to exist over length scales up to about 3 kpc. This leads to an upper limit of $m \leq 10^{-27}$ eV but should be examined in more detail.

Astronomical interest in the question of photon mass has been revived by the suggestion of Georgi *et al.*[17] that photon mass permits photon oscillations which could leave observable traces in the microwave background radiation in the centimetre range. Unfortunately, a high value of $m \sim 5 \times 10^{-18}$ eV seems to be required for an observable sinusoidal distortion of the black-body spectrum of the radiation.

Another area in which photon mass may have important consequences has been discussed by Fargion[18] who points out that the characteristic mass of gravitational Bose condensation in a massive photon gas is $\sim 7.5 \times 10^8 \, (m/10^{-19}\,\text{eV})^{-1} M_\odot$. This mass scale is similar to that of quasars and the nuclei of giant galaxies. It is also a mass scale that would lead to an acceptable picture of gravitational clustering, if it were the scale above which density inhomogeneities could survive damping in the early Universe[19].

This article shows that Stueckelberg *et al.* are right as far as the Casimir effect between two perfectly conducting plates is concerned: there are no discontinuities in photon mass m as $m \to 0$. Neither is there any discontinuity in surface energy. Davies and Unwin obtain incorrect results because they postulate incorrect boundary conditions: they have no freedom to choose boundary conditions because those are determined in advance by the Proca equations describing the classical electrodynamics of a massive photon. The solutions of the Proca equations are unique just as they are in Maxwell's theory.

We, therefore, outline here the solution to the Casimir effect problem assuming a photon of mass m. The details of the calculation will be given elsewhere[20] but we think that the solution involves material of general interest especially in view of the implications for particle physics and astronomy of the existence of a massive photon. The full normal mode analysis of the Proca equations is rather delicate, even in the apparently simple case of slab geometry, and the relations between certain Proca modes and the maxwellian modes are less obvious than they might seem. A systematic treatment is given in ref. 20; the statements that follow are a somewhat simplified version which is not misleading as far as the calculation of the Casimir effect is concerned. We will show that: (1) there are two independent solutions of the Proca equations for the electromagnetic field between two perfectly conducting plates which correspond to the two independent and transverse solutions of Maxwell's theory. The eigenvalue equation which determines the allowed discrete values of the wave number p perpendicular to the plates is unchanged; (2) there is a new class of solutions with a continuous spectrum in p for the Proca equations, which does not exist for Maxwell's equations; (3) the Casimir force receives contributions from both solutions (1) and (2) for non-zero m. We calculate these and show that the $m \to 0$ limit is smooth.

We also demonstrate that the solutions (in class 2) of the Proca equations, which have not been written down before as far as we are aware, are mathematically identical to the one-dimensional square well problem of Schroedinger quantum mechanics. We do not calculate the surface energy here, but we quote the result which is smooth as $m \to 0$.

Proca equations

Potentials A, ϕ are introduced in the Proca equations[11] as in Maxwell's theory satisfying the Lorentz condition

$$\nabla \cdot \mathbf{A} + \frac{\partial \phi}{\partial t} = 0 \qquad (1)$$

and the field strengths are given by

$$\mathbf{E} = -\frac{\partial \mathbf{A}}{\partial t} - \nabla \phi, \quad \mathbf{B} = \nabla \times \mathbf{A} \qquad (2)$$

The energy density T^{00} of the electromagnetic field is given by

$$T^{00} = \{(\mathbf{E}^2 + \mathbf{B}^2) + m^2(\mathbf{A}^2 + \phi^2)\}/8\pi \qquad (3)$$

so that **A** and ϕ are now physical fields which cannot be transformed away. In the presence of sources **j**, ρ satisfying

$$\nabla \cdot \mathbf{j} + \frac{\partial \rho}{\partial t} = 0 \qquad (4)$$

we have

$$\nabla \cdot \mathbf{E} = 4\pi\rho - m^2\phi \qquad (5a)$$

$$\nabla \times \mathbf{B} = 4\pi\mathbf{j} - m^2\mathbf{A} + \frac{\partial \mathbf{E}}{\partial t} \qquad (5b)$$

Following Kroll[21], we can now look for monochromatic plane wave solutions of these equations of positive frequency ω. We must have

$$\nabla \cdot \mathbf{A} - i\omega\phi = 0 \qquad (6)$$

$$\nabla^2\mathbf{A} + \omega^2\mathbf{A} - m^2\mathbf{A} = -4\pi\mathbf{j} \qquad (7a)$$

$$\nabla^2\phi + \omega^2\phi - m^2\phi = -4\pi\rho \qquad (7b)$$

For $\omega < m$, $\mathbf{q}^2 = m^2 - \omega^2$, the solutions of equations (7) can be written as

$$(A(\mathbf{r}), \phi(\mathbf{r})) = \int \frac{(\mathbf{j}(\mathbf{r}'), \rho(\mathbf{r}'))\mathrm{e}^{-q|\mathbf{r}-\mathbf{r}'|}}{|\mathbf{r}-\mathbf{r}'|}\, \mathrm{d}\mathbf{r}' \qquad (8)$$

in terms of sources ρ, **j**. It follows that ϕ and **A** are uniquely determined by the sources and are everywhere continuous provided **j** and ϕ are not too singular. In particular, introducing the conductivity σ as usual through $\mathbf{j} = \sigma\mathbf{E}$, the case of a perfect conductor $\sigma = \infty$ is defined simply by taking $\mathbf{E} = 0$ in the conductor. In this case[21], **A** and ϕ are still continuous across the boundary of the conductor although **E** and **B** may be discontinuous.

It is easy to extend the solutions (8) to $\omega > m$ by analytical continuation. We can now investigate the Proca solutions for the fields between two perfectly conducting plane parallel plates.

Maxwellian solutions

We begin with the treatment of the maxwellian case following ref. 22. Take one conducting plate to be at $z = 0$. Then two independent solutions for $z > 0$ satisfying $\nabla \cdot \mathbf{A} = 0$, and $A_x = A_y = 0$ on the plate are

s-mode:

$$\mathbf{A} = \mathrm{e}^{-i\omega t}\, \mathrm{e}^{i\mathbf{k}\cdot\boldsymbol{\rho}} \sin pz(\mathbf{k} \times \hat{z})/\omega \qquad (9)$$

where **k** is a wave vector parallel to the plates, $\boldsymbol{\rho} = (x, y)$, $\hat{z}$ is the unit vector in the z-direction (perpendicar to the plates) and $\omega^2 = \mathbf{k}^2 + p^2$.

p-mode:

$$\mathbf{A} = \mathrm{e}^{-i\omega t}\, \mathrm{e}^{i\mathbf{k}\cdot\boldsymbol{\rho}}\, (i\mathbf{k}p \sin pz - \hat{z}\mathbf{k}^2 \cos pz)/\omega^2 \qquad (10)$$

Now consider a conducting plate at $z = 2L$. Taking $A_x = A_y = 0$ at $z = 2L$ gives the eigenvalue equation in both cases

$$\sin 2pL = 0 \qquad (11)$$

or

$$p_n = n\pi/2L, \quad \text{integral } n \qquad (12)$$

Thus the allowed frequencies for any **k** are

$$\omega_n^2 = p_n^2 + \mathbf{k}^2 \qquad (13)$$

We turn to the Proca solutions. We must now find **A**, ϕ is continuous across the plates; that is $\phi = 0$, $\mathbf{A} = 0$ for $z < 0$, $z > 2L$ with $\phi = 0$, $\mathbf{A} = 0$ on the plates themselves.

s-mode:

The mode (9) where p is given by equations (11, 12) works provided that in place of equation (13) we have

$$\omega_n^2 = p_n^2 + \mathbf{k}^2 + m^2 \qquad (14)$$

p-mode:

Now **A** of equation (10) is non-zero on $z = 0$. We write

$$\mathbf{A} = \mathbf{A}^{\mathrm{T}} + \mathbf{A}^{\mathrm{L}} \qquad (15)$$

with $\nabla \cdot \mathbf{A}^{\mathrm{T}} = 0$, $\nabla \times \mathbf{A}^{\mathrm{L}} = 0$ and define $\mathbf{A}^{\mathrm{T}}$ by the right-hand side of equation (10). We then need to look for $\mathbf{A}^{\mathrm{L}}$, ϕ, $\nabla \cdot \mathbf{A}^{\mathrm{L}} = i\omega\phi$ such that **A** and ϕ are zero at $z = 0$ and $z = 2L$.

Taking

$$\phi = (i\mathbf{k}^2(\omega^2 - m^2)/\omega^3 p)\, \mathrm{e}^{i\mathbf{k}\cdot\boldsymbol{\rho}}\, \mathrm{e}^{-i\omega t} \sin pz \qquad (16)$$

it is not difficult to show that the cosine term in $\mathbf{A}^{\mathrm{L}}$ cancels with that in $\mathbf{A}^{\mathrm{T}}$ so that **A** is proportional to sin pz. Hence the eigen-

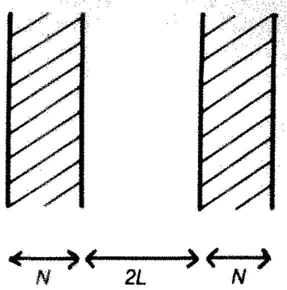

Fig. 1 Reference configuration for the continuum-mode configuration. Shaded area represents conducting plates, each of width N.

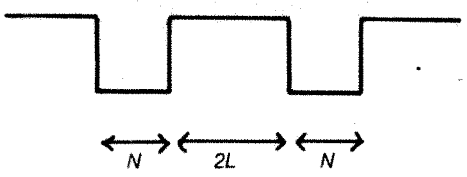

Fig. 2 Equivalent potential well in Schroedinger theory corresponding to the configuration shown in Fig. 1.

value equation for this mode is also $\sin(2pL) = 0$ provided that the dispersion relation (14) holds.

Thus the Proca solutions can be constructed out of the corresponding maxwellian solutions. It is easy to show that there are no other solutions with ϕ, $\mathbf{A}$ vanishing within the conducting plates.

Continuum solutions

We now look for solutions ϕ, $\mathbf{A}^c$ of the Proca equations of frequency ω which are non-zero within the conducting plates satisfying

$$i\omega\phi = \nabla \cdot \mathbf{A}^c \tag{17}$$

For convenience we shift the plates to be at $z = \pm L$ so that we can classify solutions as even and odd. We thus only need to consider the two regions $0 \leq z \leq L$ and $z \geq L$ corresponding to the gap and the conductor. Within a perfect conductor $\mathbf{E} = 0$. Hence

$$-\nabla\phi + i\omega\mathbf{A}^c = 0 \tag{18}$$

Combining equations (17) and (18) gives

$$\nabla^2\phi + \omega^2\phi = 0 \tag{19a}$$

and hence

$$\nabla^2\mathbf{A}^c + \omega^2\mathbf{A}^c = 0 \tag{19b}$$

In the gap, however, we have from equation (7)

$$\nabla^2\phi + (\omega^2 - m^2)\phi = 0 \tag{20a}$$

$$\nabla^2\mathbf{A}^c - (\omega^2 - m^2)\mathbf{A}^c = 0 \tag{20b}$$

From equations (19) and (20) it appears that although the (group) velocity of the photon in the gap is $v = (\omega^2 - m^2)^{1/2}/\omega < 1$ (that is, $v < c$), $v = 1$ (that is, $v = c$) in the conductor. This peculiar result was first noticed by Bass and Schroedinger[23].

The solutions of equations (19) and (20) are straightforward. First restrict motion to the z-direction perpendicular to the plates and consider the even solution

$$A_z^c = \cos pz \tag{21a}$$

$$\phi = (ip/\omega)\sin pz \tag{21b}$$

for $0 < z < L$, $p^2 = \omega^2 - m^2$, corresponding to a field strength $E_z = (im^2/\omega)\cos pz$ in the gap. In the conductor $z > L$ we have

$$A_z^c = A_0 \cos(qz + \delta_e) \tag{22a}$$

$$\phi = iA_0 \sin(qz + \delta_e) \tag{22b}$$

with $q^2 = \omega^2$ and $E_z = 0$. From continuity of $\mathbf{A}^c$ and ϕ at $z = L$, the even phase shift δ_e is determined by

$$\tan(qL + \delta_e) = (p/q)\tan pL \tag{23}$$

Similarly the odd solution for frequency ω determines the odd phase shift δ_0 by

$$\tan(qL + \delta_0) = (q/p)\tan pL \tag{24}$$

Clearly, equations (19b) and (20b) for A_z^c are just the Schroedinger equation for the scattering of a non-relativistic particle of energy E and mass M off a square barrier potential $V(z) = V_0$, $|z| < L$; $V(z) = 0$, $|z| > L$. The solutions (21a, b) and (22a, b) are the even and odd solutions to the square well problem with $p^2 = 2M(E - V_0)$, $q^2 = 2ME$ and the phase shifts δ_e and δ_0 are determined by equations and (23) and (24). The boundary conditions of continuity of A_z^c and ϕ in our case are identical to the Schroedinger conditions of continuity of the wave function and its derivative.

We conclude that an even and an odd continuum-mode solution of the Proca equations exists for any $p > 0$ with $\omega^2 = p^2 + m^2$ which has no counterpart in Maxwell theory. It is not difficult to show that the introduction of any momentum $\mathbf{k}$ parallel to the plates does not change the equations (23) and (24) which determine the phase shifts, except that now

$$\omega_p^2 = \mathbf{k}^2 + p^2 + m^2 = \mathbf{k}^2 + q^2 \tag{25}$$

Casimir effect

We now consider the quantum-mechanical part of the calculation. To calculate the Casimir force we must obtain the dependence of the total zero point energy of the system on the plate separation $2L$. This necessitates a sum over the frequencies of the classical solutions we have found. Again the problem can be separated into the contribution (A) from the maxwellian modes and the contribution (B) from the continuum modes.

The calculation of the contribution from the maxwellian modes is straightforward and has already been performed using dimensional regularization[24,25]. We prefer to use the standard treatment of the effect given in the refs 1, 26. The only change necessary going from $m = 0$ to $m \neq 0$ is that the appropriate dispersion relation for the allowed frequencies ω_n is given by equation (14) rather than (13). This gives a contribution to the L-dependent finite part of the zero point energy $\sum_{n,\mathbf{k}} \frac{1}{2} h\omega_n$ of the maxwellian modes of

$$U(L) = -\frac{\pi^2}{3(2L)^3}\int_\mu^\infty \frac{\mathrm{d}\rho(\rho^2 - \mu^2)^{3/2}}{\mathrm{e}^{2\pi\rho} - 1} \tag{26}$$

where $\mu = 2Lm/\pi$. For $m = 0$, $\mu = 0$ and the normal expression for the Casimir energy in massless QED is obtained. Approximating equation (26) for small μ gives

$$U(L) = \frac{\pi^2}{(2L)^3}\left[-\frac{1}{720} + \frac{1}{48}\mu^2 - \frac{1}{12}\mu^3 - \frac{1}{16}\mu^4 \ln\mu + 0(\mu^4)\right] \tag{27}$$

The first term gives the normal Casimir attractive force. Note that the lowest finite mass correction tends to reduce the effect.

To calculate the contribution from the continuum modes, it is necessary to compute the change in zero point energy for the continuum modes as a result of the gap of length $2L$ from some reference configuration. It is also necessary to pose the problem in such a way as to ensure that the computation gives a finite answer. All total zero point energies are infinite and, therefore, care is needed. In our problem, the reference configuration for the continuum-mode contribution is best taken to be the situation with the two plates touching (that is, $L = 0$). As the longitudinal modes penetrate the conductors we must also consider the two conducting plates to be of finite width N. Thus, we consider the modes of the configuration shown in Fig. 1 when compared with the corresponding modes in a solid slab of conductor of total width $2N$.

The Schroedinger potential well corresponding to Fig. 1 is the double square well of Fig. 2. As the wells are now attractive there is at least one bound state of the system even for arbitrarily small m. The solutions for the bound states are obtained in the usual way for $L=0$ and for $L\neq 0$. The even and odd phase shifts are also computed as in Schroedinger theory. The contributions of any bound states and the phase shifts to the zero point energy can now be calculated using methods developed in the plasmon problem[27]. The general expression for the difference between the zero-point energies of the slab system and of the vacuum is

$$V(L, N)=\sum_b\left(-\frac{1}{12\pi}\right)[(m^2-b^2)^{3/2}-m^3)] + \frac{1}{4\pi^2}\int_0^\infty \mathrm{d}pp(m^2+p^2)^{1/2}(\delta_e+\delta_0) \qquad (28)$$

where $\sum_b$ represents a sum over bound modes having $\omega^2 = \mathbf{k}^2-b^2+m^2$, and δ_e, δ_0 are the even and odd phase shifts calculated for the double square well (Fig. 2). For the difference $U=V(L, N)-V(0, N)$ one finds eventually

$$U=\frac{1}{(2L)^3}f(mL, mN) \qquad (29)$$

where in the most favourable configuration, $L \ll N$, one finds eventually (for the realistic case mL, $mN \ll 1$)

$$f\sim\frac{1}{2\pi^2}(mL)^4\ln\left[\frac{N}{4L}\right] \qquad (30)$$

This contribution to the Casimir force is, therefore, negligible compared with the leading finite-mass correction to the contribution from the transverse modes.

Conclusions

The calculations above follow from the uniqueness of the solutions to the Proca equation. The results demonstrate that the Casimir effect is not sensitive to a small photon mass. We have not discussed surface energies here but Aoyama[28] has worked out the surface energy which results for parallel plate geometry in the case of a scalar field of mass m to be

$$S=\frac{m^3}{18\pi^2}\left(\frac{3\pi}{8}-1\right) \qquad (31)$$

and the same result is true in our case with this surface energy arising from the continuum modes. There is a corresponding term $m^3/24\pi$ from the maxwellian modes[20]. So again this effect is smooth as $m\to 0$, as[29] there is no surface energy in the corresponding problem in QED.

We thank John Barrow, Fawzi Boudjema, David Broadhurst and John Plaskett for assistance.

Received 17 May; accepted 30 July 1984.

1. Casimir, H. B. G. *Proc. K. Ned. Akad. Wet.* **5**, 793 (1948).
2. Lifshitz, E. M. & Pitaevskii, L. P. *Statistical Physics*, Part 2, Ch. 8 (Pergamon, Oxford, 1980).
3. Tabor, D. in *Colloidal dispersions* (ed. Goodwin, J. W.)(Royal Society of Chemistry, London, 1982).
4. Davies P. C. W. & Unwin, S. D. *Phys. Lett.* **98B**, 274 (1981).
5. Stueckelberg, E. C. G. *Helv. Phys. Acta* **14**, 52 (1941); **30**, 209 (1957).
6. Goldhaber, A. S. & Nieto, M. N. *Phys. Rev. Lett.* **26**, 1390 (1971); *Rev. Mod. Phys.* **43**, 277 (1971).
7. Van Dam, H. & Veltman, M. *Nucl. Phys.* **B22**, 397 (1970).
8. Dombey, N. & Vayonakis, C. *J. Phys.* **A9**, 1381 (1976).
9. Barrow, J. D. & Ottewill, A. C. *J. Phys.* **A16**, 2757 (1983).
10. Calogeracos, A., Dombey, N. & Kennedy, A. D. *Phys. Lett.* **104B**, **444** (1981).
11. Barrow, J. D. & Burman, R. R. *Nature* **307**, 14 (1984).
12. Goldhaber, A. S. & Nieto, M. N. *Rev. Mod. Phys.* **43**, 277 (1983).
13. Byrne, J. C. *Astrophys. Space Sci.* **46**, 115 (1977).
14. Barnes A. & Scargle, J. D. *Phys. Rev. Lett.* **35**, 117 (1975).
15. Chibisov, G. B. *Soviet Phy. Usp.* **19**, 624 (1976).
16. Dolgov, A. D. & Zeldovich, Y. B. *Rev. Mod. Phys.* **53**, 1 (1981).
17. Georgi, H., Ginsparg, P. & Glashow, S. L. *Nature* **305**, 765 (1983).
18. Fargion, D. *Phys. Lett.* **141B**, 53 (1984).
19. Barrow, J. D. *Fund. Cosm. Phys.* **8**, 93 (1983).
20. Barton, G. & Dombey, N. *Ann. Phys. N.Y.* (in the press).
21. Kroll, N. *Phys. Rev. Lett.* **26**, 1396 (1971); **27**, 340 (1971).
22. Barton, G. *Proc. R. Soc.* **A320**, 251 (1970).
23. Bass L. & Schroedinger, E. *Proc. R. Soc.* **A232**, 1 (1955).
24. Ambjorn, J. & Wolfram, S. *Annls Phys. N.Y.* **147**, 1 (1983).
25. Boudjema, F. thesis, Univ. Sussex (1983).
26. Boyer, T. H. *Annls Phys. N.Y.* **56**, 474 (1970).
27. Barton, G. *Rep. Prog. Phys.* **42**, 963 (1979).
28. Aoyama, H. *Nucl. Phys.* B (in the press).
29. Balian R. & Bloch, C. *Annls Phys. N.Y.* **64**, 271 (1971).

Anthelic arcs from airborne ice crystals

Robert G. Greenler[*‡] & E. Tränkle[†]

[*] Fritz-Haber-Institut der Max Planck Gesellschaft, Berlin, FRG
[†] Institut für Theoretische Physik, Freie Universitat Berlin, Arnimalee 14, 1000 Berlin 33, FRG
[‡] Permanent address: Department of Physics, University of Wisconsin-Milwaukee, Milwaukee, Wisconsin 53201, USA

A new set of anthelic arcs resulting from hexagonal, pencil-shaped ice crystals that fall with their axes oriented horizontally is revealed by computer simulation. The arcs result from light rays from the Sun that experience two, and sometimes four, internal reflections in the ice crystal.

MANY optical effects result from the interaction of sunlight with airborne ice crystals that have the geometrical form of right, hexagonal prisms[1–5]. Most of the well-known halo phenomena occur within ~50° of the Sun but others do occur in different parts of the sky. An area of the sky where several rare effects are found is the region of the anthelic point. (This is the point on the opposite side of the sky from the Sun, at the same elevation above the horizon as the Sun.) Effects that have been reported in the region of the anthelic point include:

(1) Anthelic arcs—oblique arcs crossing the anthelic point. Photographs[1,6,7] and observations of anthelic arcs have been reported[8–14].

(2) Anthelion—a spot of light at the anthelic point. We know of no photographs that show the anthelion independent of other anthelic phenomena although observations have been reported and mechanisms suggested[1,6,15].

(3) Anthelic pillar—a column of light extending from slightly above the anthelic point down to the horizon. We know of only one published photograph[1,6] but observations have been reported[11,12].

(4) Parhelic circle—a circle of light parallel to the horizon passing through the Sun and anthelic point. This effect is understood to result from reflection from the vertical faces of oriented ice crystals[1–4].

Computer simulation method

All of the anthelic effects must involve at least one reflection to deflect light to the observer. The parhelic circle involves some rays that are externally reflected from the ice crystals; all other effects appear to involve one or more internal reflections.

R.G.G. *et al.* have developed a simulation method for investigating the origins of ice-crystal optical effects[1,16–18]. For a given

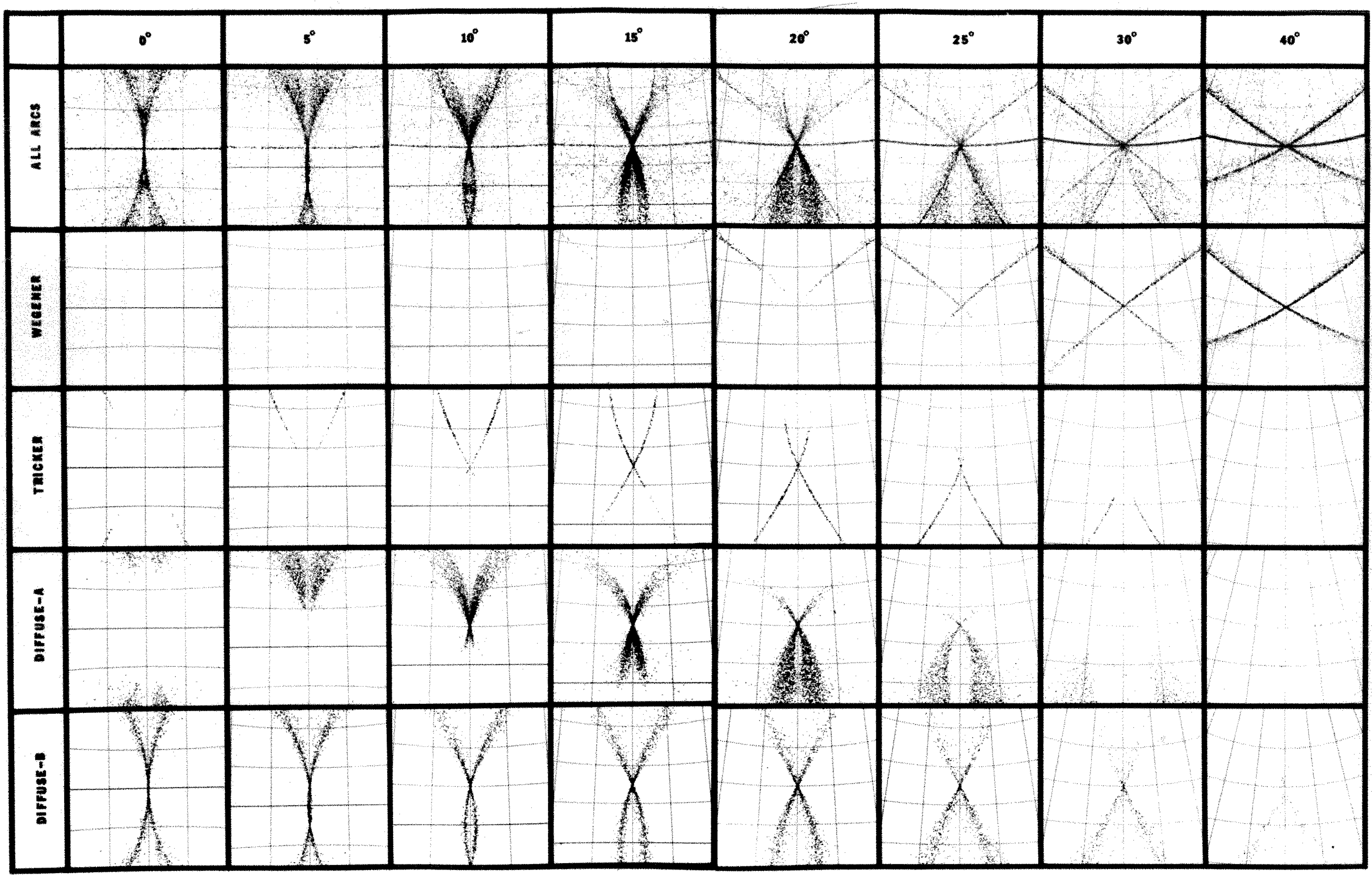

Fig. 1 Intensity patterns that simulate anthelic arcs for various Sun elevations. The grid on each figure consists of lines of constant altitude and of constant elevation, at 10° intervals. The horizon is represented by the darker horizontal line that shows no curvature.

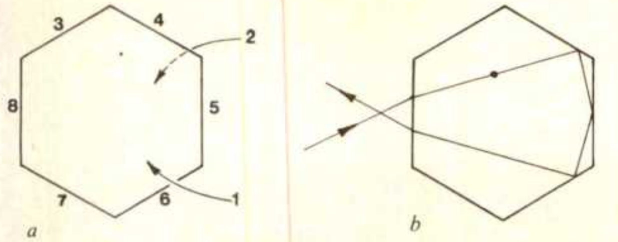

Fig. 2 *a*, Arbitrary numbering of the faces of a right hexagonal prism, representing an ice crystal. *b*, A ray path through the crystal that can be classified (by reference to *a*) as 814568.

orientation of an ice crystal, they calculate the direction of a light ray from the Sun after it has passed through specified entrance and exit faces of the crystal. This direction is translated into a position in the sky where such a crystal would be located to send the ray to the observer's eye and a spot is plotted to represent that position. For refraction phenomena, which require no internal reflections, their method handles intensity effects fairly well. The loss of intensity due to reflection at each face can be calculated. Another factor accounts for the cross-section of the incident light beam that is transmitted by both the entrance and the exit faces. Analytical expressions for both of these factors can be combined into an overall intensity factor which is used to fix the probability of whether a particular spot will be plotted—a high intensity factor yielding a high probability that the spot will be plotted. The collection of many such spots from a variety of crystal orientations gives a representation of the optical effect predicted from the collection of crystals with the given distribution of orientations and with the specified ray path through the crystal. With this method, however, it is difficult to develop the analytical intensity expression for the restriction in beam cross-section resulting from one or more internal reflections. Mallmann and Greenler used this (Monte Carlo) method to simulate anthelic phenomena[6] ignoring the geometrical intensity factor for the internal reflections.

Pattloch and E.T. have extended the Monte Carlo simulation technique so that these intensity effects can be used for any number of internal reflections[19]. They treat the light as a photon that strikes the oriented crystal at a random location. At each encounter with a crystal face, the photon is either transmitted or reflected (with a probability calculated from the Fresnel reflection coefficients). Its path through the crystal is calculated using geometrical optics and followed until it escapes the crystal and can be represented as a spot on a sky diagram. This Monte Carlo approach is used to obtain the intensities and has significant advantages over the previous method:

(1) All the reflection and refraction effects that can result from light interacting with a particular crystal shape are obtained in the simulation. Previously, only those preconceived combinations of entrance, exit, and internal reflection faces would have been investigated.

(2) The relative intensities of all the different arcs and spots are correctly represented for the shape of crystal specified.

(3) Any number of internal reflections are routinely handled. For the results shown here the calculation includes internal reflections up to 17, any more being negligible.

Additional details of the method are given in ref. 19.

Results

Figure 1 shows the simulations of anthelic effects for Sun elevations between 0° and 40°. The top row of simulations show everything predicted to occur for columnar (pencil) crystals with their main axes confined to a horizontal plane but with random orientation of the axes in that plane, and random rotational orientation of the crystals about their axes. The ratio of crystal length-to-width is 2.0. The Sun's angular diameter of 0.5° is taken into account by allowing rays to impinge on the crystal from different directions corresponding to different positions on the Sun's disk.

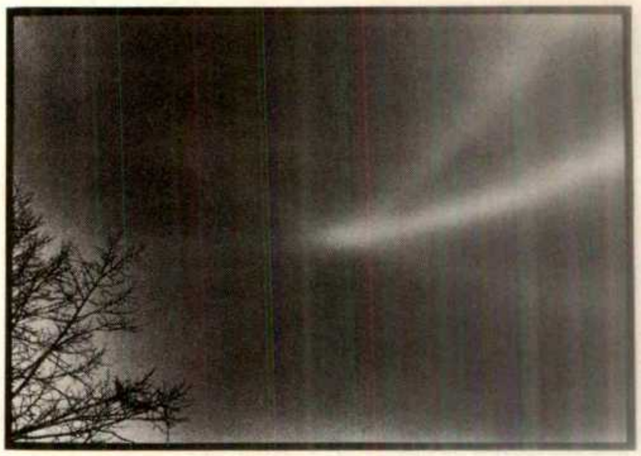

Fig. 3 Photo of the Wegener anthelic arcs and the parhelic circle for a Sun elevation of 50° taken by A. J. Mallmann in Milwaukee, Wisconsin.

If we look at the result for a Sun elevation of 20° we can see the familiar Wegener[6] arcs, the Tricker arc[6], and the parhelic circle but there are more structures that are not familiar. To investigate the source of the additional structures, we modified the computer program so that we can identify the path of a ray that is responsible for a given dot. Figure 2*a* shows an arbitrary assignment of numbers to the hexagonal crystal. The side faces are numbered 3 to 8, with the end faces identified as 1 and 2. The path of a ray through the crystal can be classified by a series of numbers beginning with the entrance face. For example, the path of the ray shown in Fig. 2*b* can be classified as 814568.

The intensity plots in the second to fifth row of Fig. 1 show effects from rays taking particular paths through the crystal. These are subsets of the intensity plots of the first row, which includes all of the effects. In each case, we have plotted all of the contributions from rays whose paths are physically equivalent to the one mentioned. For example, the rays producing the Wegener arcs are called the 814 rays but they would include rays such as 315, 416, 725, and all others that enter a side face, reflect off an end face, and exit from another side face located such that there is one face between the entrance and exit faces. For convenience, we refer to such faces as alternate side faces to distinguish them from adjacent side faces or opposite faces.

The second row represents the effect produced by rays taking the path, 814, through the crystal; these are the Wegener arcs.

We have designated as the Tricker arc, the anthelic arc that is produced by rays that enter the end face of a crystal, make two reflections from adjacent or alternate side faces, are reflected back by the opposite end face, and exit from the same end face by which they enter; for example, 18421. See ref. 1 for the argument that for Tricker's mechanism[20] "... any combination of an even number of side-face reflections plus one end-face reflection, in any order, will produce the same set of arcs". We find that rays of the type, 81463, also lie on the same locus and can contribute intensity to the Tricker arc for higher Sun elevations than those paths requiring exit and entrance through the same end face. The third row of Fig. 1 shows the Tricker arc including most of the possible contributions. The shape of the arc is the same as previously predicted[6] but the intensity distribution is altered.

As we identified the types of rays that contributed to intensity in the anthelic region, it was surprising to find that the class of rays that contribute the most intensity for Sun altitudes in the 5°–25° range had not been investigated before. The ray path is shown in Fig. 2*b*. Although it involves four internal reflections, such rays contribute significant intensity in the anthelic region of the plots of Fig. 1. For a Sun elevation of 20°, for example, with a crystal length-to-width ratio of 2.0, the intensity is greater than that from Wegener-arc rays by a factor of 13 and greater

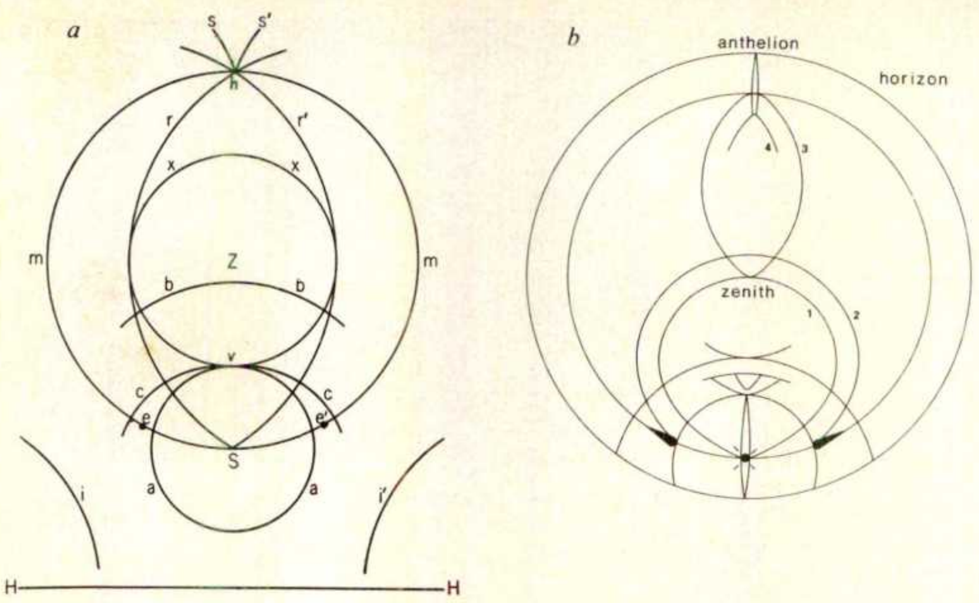

Fig. 4 *a*, Drawing of a complex display in North Dakota by F. J. Bavendick (ref. 22). *b*, Drawing of a complex display in Antarctica by J. R. Blake (ref. 11).

than that from the Tricker arc rays by a factor of 7. It is significant, however, that unlike these latter two arcs, which are quite sharp, the pattern produced by the rays of Fig. 2*b* is much more diffuse. The results are shown in the third row of Fig. 1 labelled diffuse-A.

Another class of rays (8146) also contribute a significant amount of intensity in the anthelic region. The patterns that they produce are shown in the bottom row of Fig. 1, labelled diffuse-B.

These four patterns, together with the parhelic circle, seem to account for all of the intensity patterns that can be seen in the top row. The four sets (and the parhelic circle) account for more than three-quarters of the total number of points for a Sun elevation of 20°. Some ray paths, of course, produce no arcs but add to the general background.

Discussion

The top row of simulations in Fig. 1 shows our predictions of the anthelic optical effects that result from sunlight interacting with pencil crystals with horizontal axes. It seems reasonable to classify separately only those effects that can be separated visually and identified by observation. The Wegener arcs fulfill this requirement. At Sun elevations above 30° they are the only anthelic arcs present and they can be separated from the general display for lower Sun elevations. Figure 3 shows the Wegener anthelic arcs and the parhelic circle for a Sun altitude of 50°. A few other published photos[1,6,7] confirm their reality.

The Tricker arc is seen most distinctly in our simulations for Sun elevations in the range 20°–30°. The photographic evidence for the Tricker arc is not very convincing. The complex display drawn by Bavendick[21] (Fig. 4*a*) shows two sets of anthelic arcs that are well represented by the Wegener and Tricker arcs in the simulation for 30°. (Other problems of interpretation are discussed in ref. 1). The simulations seem to show that for some Sun elevations the Tricker arc may be separated visually from the rest of the anthelic potpourri and thus should be separately classified.

For Sun elevations between 0° and 20°, the anthelic display appears to be dominated by the arcs that we have identified as diffuse arcs-A and B. Because these arcs overlap at all Sun elevations, it seems inappropriate to name them separately. Hence, we refer to the combination as the diffuse anthelic arcs.

The inensity comparison of the diffuse arc with the Tricker arc will depend on the aspect ratio of the crystal. Longer pencil crystals should show diffuse arcs that are relatively more intense than the Tricker arcs. Shorter crystals diminish the relative intensities of the diffuse arcs but as the aspect ratio approaches 1, the crystals will no longer orient with horizontal axes.

Mallmann and Greenler's simulation[6] of anthelic effects considered rays (8146) that we show here to produce the diffuse arc-B component. Their results did not show the diffuse arc but showed a concentration at the anthelic point for Sun elevations above 20° and an anthelic pillar for lower Sun elevations. Apparently, the appropriate intensity factors eliminate rays from well-defined areas of the sky and leave the diffuse arcs rather than the general background seen by Mallmann and Greenler.

Evidence for diffuse arcs

Blake's[11] drawing of the complex sky display he observed in Antarctica in 1958 is reproduced in Fig. 4*b*. Most features have been reproduced quite satisfactorially by computer simulation for a Sun elevation of 11°. The results are shown in ref. 1. The poorest agreement came in trying to match the Y-shaped structure (labelled 4 in Blake's drawing) with a Tricker arc. The diffuse arc simulation (Fig. 1, Sun elevation of 10°) seems to be a much better match for the structure. (Figure 4*b* should be inverted for comparison with the simulation of Fig. 1.)

Figure 5 shows a cusp-like arc extending below the anthelic point for a Sun elevation of 21°. The angle between the arms is consistent with that for Tricker's arc. Compared with the simulation for 20° in Fig. 1, the diffuse arcs appear to give a better representation of the width of the arms. Nothing can be seen above the parhelic circle. The simulation does show that the upper part of the diffuse arcs are less intense.

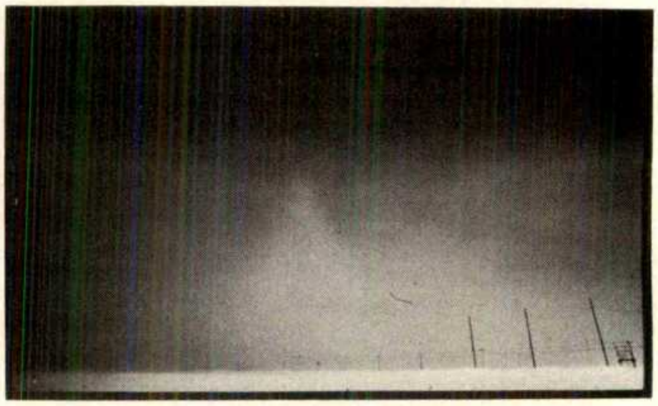

Fig. 5 Photograph of anthelic arcs for a Sun elevation of 21°, taken by R.G.G. at Point Barrow, Alaska.

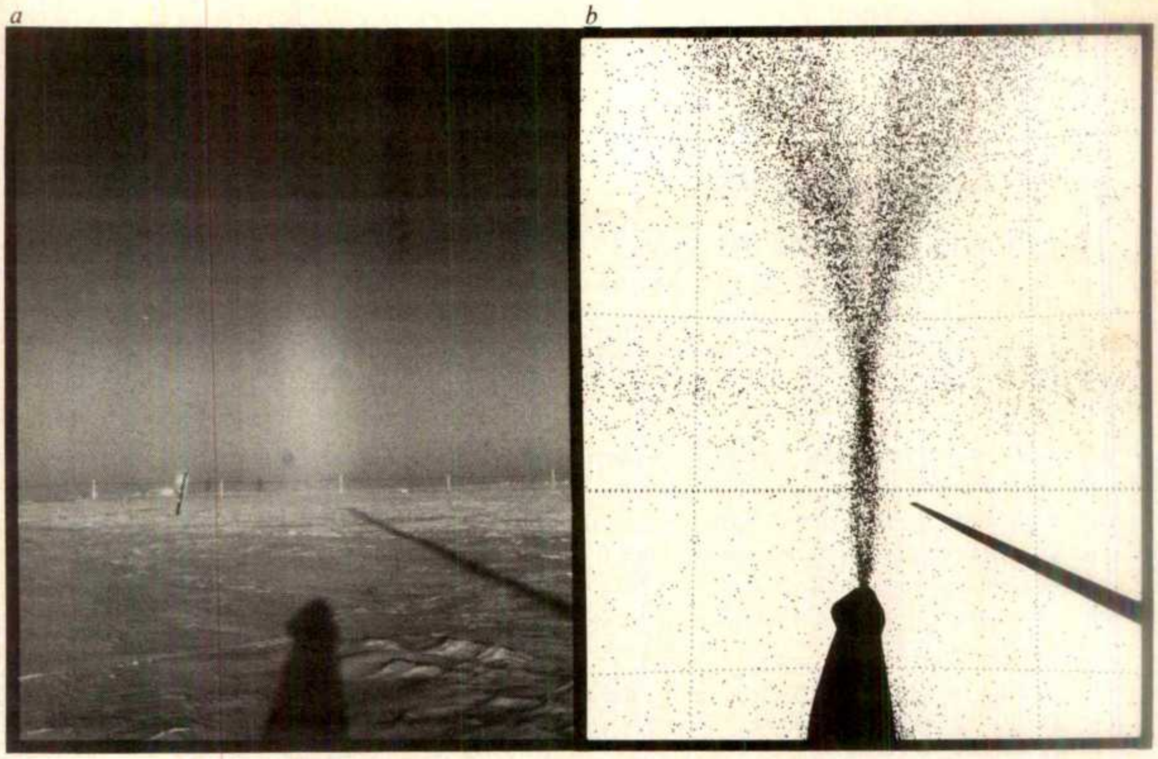

Fig. 6 Photograph (*a*) of an anthelic pillar with a Sun elevation of 6°, taken by R.G.G. at Point Barrow, Alaska. The simulation (*b*) has the same scale as the photo.

Pattloch and E.T. have simulated the effects of Hogan's South Pole photograph[19], in which the structure below the anthelic point is partially obscured by a ghost image of the Sun caused by reflections within the camera lens. The arcs extending above the anthelic point, however, seem to be matched by the combination of diffuse arcs and the Tricker arc.

Figure 6 shows a photo of the anthelic pillar together with an attempt to match it to our simulation for which the pencil crystals have a length-to-width ratio of 1.33, and the crystal axis is permitted to vary by 2° from the horizontal plane. The Sun elevation was 6° during the photo. The most obvious discrepency between photo and simulation is the absence of the upper portion of the predicted display in the photograph. The photo was taken on 28 March 1978 at Point Barrow, Alaska in the evening. Notes taken during the day indicate that various optical effects appeared and disappeared, but that the lower part of the infralateral arcs was quite persistent. Notes made immediately after the sighting and photographing of the anthelic pillar say: "The pillar appeared to be in the same layer that was giving rise to the ILA [infralateral arcs] all day; at least, the angular height of the effect corresponded to the height of the layer." An earlier note says: "The ILA seems to be formed in a cloud layer about 5° high, where it is brighter than the 22° halo." The infralateral arcs are produced by the same distribution of pencil-shaped ice crystals that are being considered for these anthelic effects. We would obviously like to have more (and better) photos of these anthelic effects for comparison with our model predictions.

In this simulation, we do not find any specific contribution that produces an anthelion. There are two possibilities. First, the brightness at the anthelic point may just be the superimposed contribution from the various arcs that intersect there. In cases where the arcs are faint, their intersection at the anthelic point may be the only spot bright enough to be seen. Second, the anthelion may exist independently of these other effects but is not caused by the pencil crystals with the orientations we assume here.

Conclusions

We have used an improved Monte Carlo simulation method to investigate optical effects near the anthelic point that result from sunlight interacting with pencil-shaped ice crystals oriented with their long axes horizontal or nearly horizontal. In addition to the previously described Wegener and Tricker arcs, we find a new set of arcs, the diffuse arcs, that are predicted to dominate the anthelic effects for low Sun elevations.

Received 9 March; accepted 30 July 1984.

1. Greenler, R. *Rainbows, Halos, and Glories* (Cambridge, New York, 1980).
2. Tricker, R. A. R. *Introduction to Meteorological Optics* (American Elsevier, New York, 1970); *Ice Crystal Haloes* (Optical Society of America, Washington DC, 1970).
3. Minneart, M. *The Nature of Light and Colour in the Open Air* (transl. Kremer-Priest, H. M.) (rev. Brian, K. E.) (Dover, New York, 1954).
4. Dietz, G. *Einfuhrung in die Optik der Atmosphaere.* (Akademische Verlagsgesellschaft, Leipzig, 1957).
5. Tape, W. *J. opt. Soc. Am.* **70,** 1175–1192 (1980).
6. Mallmann, A. J. & Greenler, R. G. *J. opt. Soc. Am.* **69,** 1107–1112 (1979); **69,** 1195–1196 (1979); **70,** 1029 (1980).
7. Humphreys, W. J. *Physics of the Air* 3rd edn, 538 (Dover, New York, 1964).
8. Blake, J. R. *Mon. Weath. Rev.* **94,** 599–604 (1966).
9. Hattinga Verschure, P. P. *Weather* **26,** 532–536 (1971); **28,** 300–306 (1973).
10. Robertson, G. W. *Weather* **29,** 113–115 (1974).
11. Blake, J. R. *Australian National Antarctic Res. Expedn Rep.* No. 59, Ser. A, Vol. 4 (Antarctic Division, Melbourne, 1961).
12. Liljequist, G. H. *Norwegian–British–Swedish Antarctic Expedition, 1949–52, Scientific Results* Vol. 2 (Norsk Polarinstitutt, Oslo, 1956).
13. Visser, S. W. *Handbuch der Geophysik,* Band 8, Kapitel 15 (Gebruder Borntraeger, Berlin, 1961).
14. Everhart, E. *Sky Telescope* **21,** 14–15 (1961).
15. Lynch, D. K. & Schwartz, Pt. *J. opt. Soc. Am.* **69,** 383–386 (1979).
16. Greenler, R. G. & Mallmann, A. J. *Science* **176,** 128–131 (1972).
17. Greenler, R. G., Mallmann, A. J., Mueller, J. R. & Romito, R. *Science* **195,** 360–367 (1977).
18. Greenler, R. G., Mueller, J. R., Hahn, W. & Mallmann, A. J. *Science* **206,** 643–644 (1979).
19. Pattloch, E. & Tränkle, E. *J. opt. Soc. Am.* **A1,** 520–526 (1984).
20. Tricker, R. A. R. *Q. Jl R. met. Soc.* **99,** 649–656 (1973).
21. Bavendick, F. J. *Mon. Weath. Rev.* **48,** 330 (1920).

The structure, rearrangement and expression of D_β gene segments of the murine T-cell antigen receptor

Gerald Siu*, Mitchell Kronenberg*, Erich Strauss*, Regina Haars†, Tak W. Mak‡ & Leroy Hood*

* Division of Biology, California Institute of Technology, Pasadena, California 91125, USA
† Department of Pathology, College of Physicians and Surgeons of Columbia University, New York 10032, USA
‡ Department of Medical Biophysics, University of Toronto, Ontario Cancer Institute, Toronto, Canada M4X 1K9

It has been postulated that the variable region of the β-polypeptide of the murine T-cell antigen receptor is encoded by three distinct germ-line gene segments—variable (V_β), *diversity* (D_β) *and joining* (J_β)*—that are rearranged to generate a* V_β *gene. Germ-line* V_β *and* J_β *gene segments have been isolated previously. Here we report the isolation and characterization of two germ-line* D_β *gene segments that have recognition signals for DNA rearrangement strikingly similar to those found in the three immunoglobulin gene families and in* V_β *and* J_β *gene segments. The* D_β *and* J_β *segments can join in the absence of* V_β *gene segment rearrangement and these rearranged sequences are transcribed in some T cells.*

IMMUNOGLOBULINS and T-cell antigen receptor molecules exhibit extensive diversity but the genetic basis and the mechanisms responsible for generating this diversity are well understood only for the immunoglobulin genes[1-3]. Immunoglobulins are heterodimers made up of disulphide-bridged light and heavy chains each of which is divided into variable regions that recognize antigen, and constant regions that control effector functions. Genes that encode the variable region of light chains are created by a DNA rearrangement that joins two distinct gene segments—variable (V_L) and joining (J_L)[4-6]. The variable region genes of heavy chains are created by the joining of three distinct gene segments—variable (V_H), diversity (D_H), and joining (J_H)[7,8]. One mechanism for the generation of immunoglobulin diversity is joining of different V_H, D_H, and J_H, or V_L and J_L gene segments[9,10]. Also gene segments may be joined together at different sites, leading to a junctional variability[10-12] and in the heavy chain gene family, extra nucleotides, not found in V_H, D_H, or J_H gene segments, may be added between these gene segments as a result of the joining process (N-region diversity)[11,13]. The 3′ side of the V gene segments, the 5′ side of the J gene segments, and both sides of the D gene segments are flanked by recognition signals for DNA rearrangements. These signals comprise three components—a highly conserved palindromic heptamer, a nonconserved spacer sequence of 12 or 23 nucleotides, and a relatively conserved A/T-rich nonamer[6-8,14]. It is believed that these recognition sequences play a critical role in DNA rearrangements because they are present in all three of the immunoglobulin gene families and, therefore, have been conserved throughout vertebrate evolution.

The T-cell antigen receptor is a heterodimer composed of two disulphide-bonded polypeptides, α and β, that have a similar molecular weight[15-17]. The genes that encode the β-chain of the T-cell antigen receptor have recently been identified and they share many features with those encoding immunoglobulins. The nucleotide sequence of cDNA clones encoding the β-chain of the T-cell receptor from both mouse and man contains regions similar to V and J gene segments and C genes[18-20]. Distinct germ-line V_β and J_β gene segments and C_β genes have been isolated from genomic libraries[21-23]. Two highly similar and closely-linked C_β genes denoted $C_{\beta1}$ and $C_{\beta2}$ have been isolated on a single cosmid clone of germ-line DNA and each C_β gene has a cluster of J_β gene segments associated with it[23]. The V_β and J_β gene segments have recognition signals for DNA rearrangements that are very similar to those of their immunoglobulin counterparts[21-23].

Both murine and human β cDNA clones encoding a complete variable region contain eight or more nucleotides than their corresponding germ-line V_β and J_β gene segments suggesting that a portion of the β variable region is encoded by a third gene segment analogous to the D_H gene segment of immunoglobulins[21,22]. Indeed, in this paper we present the structure of two germline D_β gene segments. One of these D_β gene segments lies to the 5′ side of the $J_{\beta1}$ gene cluster and the second lies to the 5′ side of the $J_{\beta2}$ gene cluster, between $C_{\beta1}$ and $J_{\beta2}$. Recognition signals for DNA rearrangements on either side of these D gene segments are described, as are rearrangements and transcripts involving the D_β gene segments.

D_β gene segment of each J_β gene cluster

The partial nucleotide sequences of four murine β-chain cDNA clones have been published[19]. Two of them appeared to lack a V_β gene segment but contain joined D_β–J_β sequences. This conclusion was based on several features. First, the published sequences 5′ to the J_β gene segments resemble neither V_β gene segments nor the sequences found 5′ to the germ-line J_β gene segments. Second, in both of these clones the sequences 5′ to the joined J_β gene segment have a recognition signal for DNA joining that includes the heptamer, a 12-nucleotide spacer sequence, and the A/T-rich nonamer sequence, as well as a short sequence that could be a D_β coding segment located between the joining signal and the J_β gene segment. Two 40-base oligonucleotides complementary to a portion of these putative D_β gene segments and their 5′ flanking sequence were synthesized using the technique of Horvath *et al.*[24]. The oligonucleotide T5 is complementary to a region starting at nucleotide position 56 and ending at position 95 of the published sequence of the cDNA clone 86T5 (ref. 19). T6 is complementary to the cDNA clone TM86 at positions 15–54 (ref. 19). We have hybridized these oligonucleotides to Southern blots of a genomic cosmid clone known to contain the $J_{\beta1}$ and $J_{\beta2}$ gene clusters. T6 hybridizes most strongly to a restriction fragment located to the 5′ side of the $J_{\beta2}$ gene cluster, while T5 hybridizes more strongly to the region 5′ to the $J_{\beta1}$ gene cluster (G.S., unpublished observations). We have determined the nucleotide sequence in the vicinity of the hybridizing DNA fragments and have linked them by restriction mapping and DNA sequencing to their respective J_β gene clusters (Fig. 1 and unpublished results).

Each of these hybridizing regions appears to contain a D_β gene segment by the following criteria (Fig. 1). (1) There is a 5′ recognition sequence for DNA joining with a 12-base pair spacer sequence. (2) There is a 3′ recognition sequence for DNA joining with a 23-base pair spacer. Both of these sequences are similar to their immunoglobulin counterparts (Fig. 2). (3) One of these sequences, or a highly similar D_β gene segment, appears

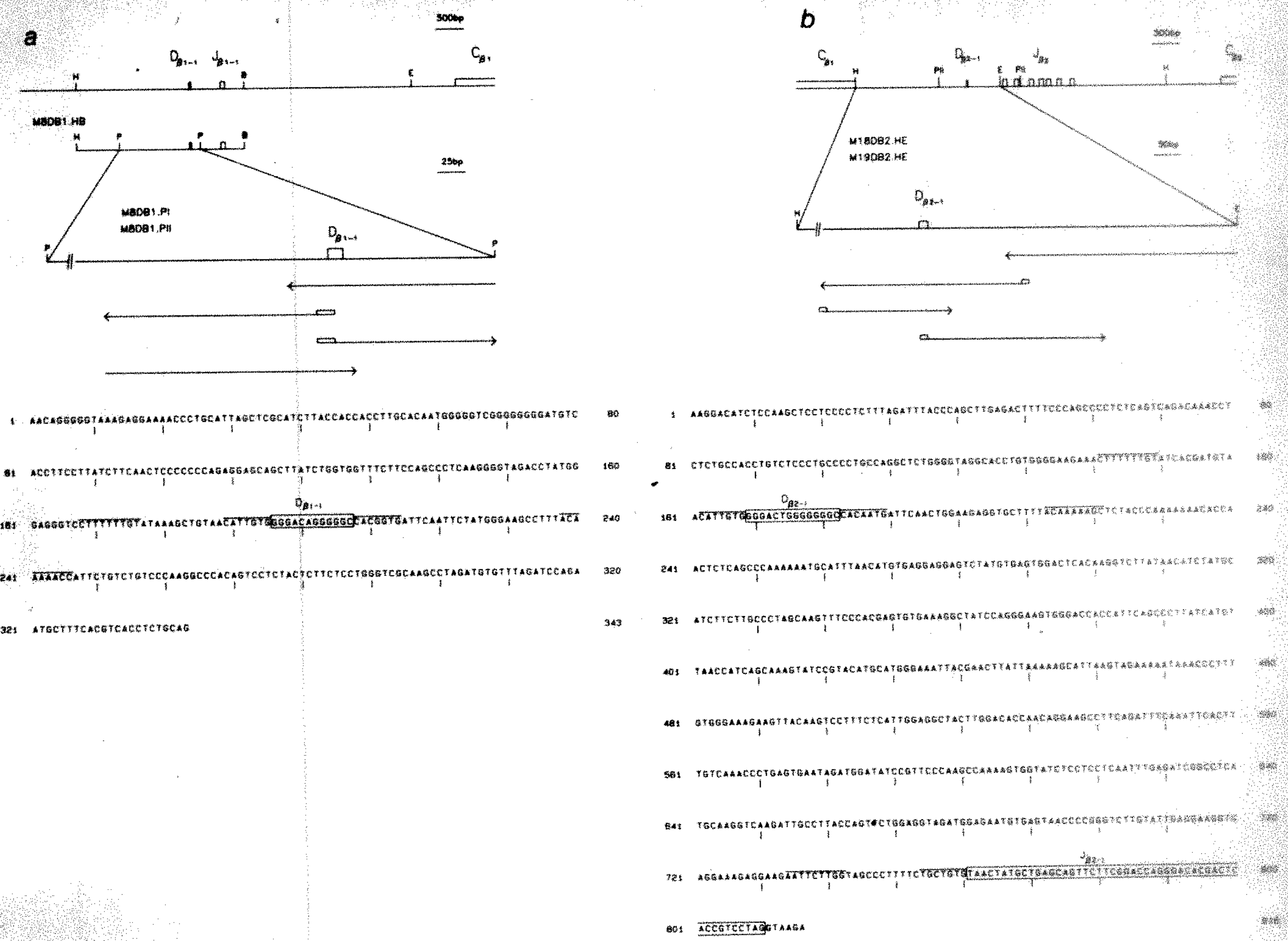

Fig. 1 Nucleotide sequences of germ-line $D_{\beta1\text{-}1}$ and $D_{\beta2\text{-}1}$ gene segments. *a*, The $D_{\beta1\text{-}1}$ subclones sequencing strategy and sequence. *b*, The $D_{\beta2\text{-}1}$ subclones, sequencing strategy and sequence. The sequence from position 410 to position 844 had been previously determined on both strands[23]. The coding regions of the D_β and J_β joining segments are boxed, and the 5′ and 3′ heptamer and nonamer recognition signals are overlined. Sequences were obtained by subcloning restriction fragments into the vectors M13mp8, M13mp18 and M13mp19 (ref. 47) and sequenced using the dideoxynucleotide method[48], as modified by E. Strauss (unpublished). Synthetic oligonucleotides complementary to mouse genomic sequences were utilized as sequencing primers in some cases. The positions of these primers are indicated by the open box at the ends of the arrows. Restriction enzyme sites are abbreviated as follows: B, *Bam*HI; E, *Eco*RI; H, *Hin*dIII; P, *Pst*I; PII, *Pvu*II.

to form part of the variable region of the 86T1β cDNA clone[19]. In addition, the coding sequences for these D_β gene segments are similar to some immunoglobulin D_H gene segments (Fig. 2*a*). We will denote the *D* gene segment to the 5′ side of the $J_{\beta1}$ gene cluster as $D_{\beta1\text{-}1}$ and the *D* gene segment to the 5′ side of the $J_{\beta2}$ gene cluster as $D_{\beta2\text{-}1}$. The $D_{\beta1\text{-}1}$ gene segment is located 647 base pairs (bp) upstream from the 5′-most germ-line $J_{\beta1}$ gene segment (Fig. 1*a*; M.K., R.H., E.S., unpublished results), while the $D_{\beta2\text{-}1}$ gene segment is located 578 bp upstream from the 5′-most germ-line $J_{\beta2}$ gene segment (Fig. 1*b*). Because the murine immunoglobulin heavy chain locus also has a D_H gene segment, D_{Q52}, found 696 bp 5′ to its *J* gene cluster[11], there may be some functional significance of a single *D* gene segment closely linked to the *J* gene cluster in the germline.

There probably are additional D_β gene segments that have not yet been located in the germ-line DNA. With the exception of three nucleotides missing from the 3′ end, the coding and 5′ flanking sequences of the $D_{\beta2\text{-}1}$ gene segment are identical to the D_β gene segment expressed in the TM86 cDNA clone. We believe, therefore, that this cDNA clone includes the $D_{\beta2\text{-}1}$ gene segment. The 86T5 cDNA D_β gene segment is also shorter than the $D_{\beta1\text{-}1}$ gene segment by three base pairs, and in addition it has one difference at its 3′ end and one in the 5′ flanking region out of the 90 base pairs compared. It is therefore possible that the 86T5 D_β gene segment is derived from a different germ-line gene; comparable similarity between members of a family is seen in several immunoglobulin D_H gene segment families[25]. Alternatively, somatic mutation or polymorphism between inbred mouse strains could account for these differences. In addition, the D_β gene segment in 2B4.71, a cDNA clone from a helper T-cell hybridoma[21] specific for cytochrome c, is different from the three other D_β gene segments. Thus the two D_β gene segments identified each lie to the 5′ side of their corresponding J_β gene segment clusters and it appears likely that additional D_β gene segments will lie to the 5′ side of the $J_{\beta1}$ gene cluster.

Structure of germ-line D_β

Figure 2 shows the germ-line $D_{\beta1\text{-}1}$ and $D_{\beta2\text{-}1}$ coding and flanking sequences aligned with each other, with the D_β sequences from several β-chain cDNA clones, and with some representative sequences from the immunoglobulin heavy chain gene family. The $D_{\beta1\text{-}1}$ gene segment has 12 nucleotides while the $D_{\beta2\text{-}1}$ gene segment has 14 nucleotides (Fig. 2*a*) and they therefore resemble murine D_H segments, which range in size from 10–23 nucleotides[25]. The sequences of both the $D_{\beta1\text{-}1}$ and $D_{\beta2\text{-}1}$ gene segments are G-rich and they are similar at 10 out of 12 nucleotides compared; they are also similar to the presumed D_H gene segment found in the heavy chain of some oxazalone-binding immunoglobulins[26], and to the D_H region found in the heavy chain of the 18-81A-2 Abelson murine leukaemia virus (A-MuLV)-transformed cell line[27] (Fig. 2*a*). It has been

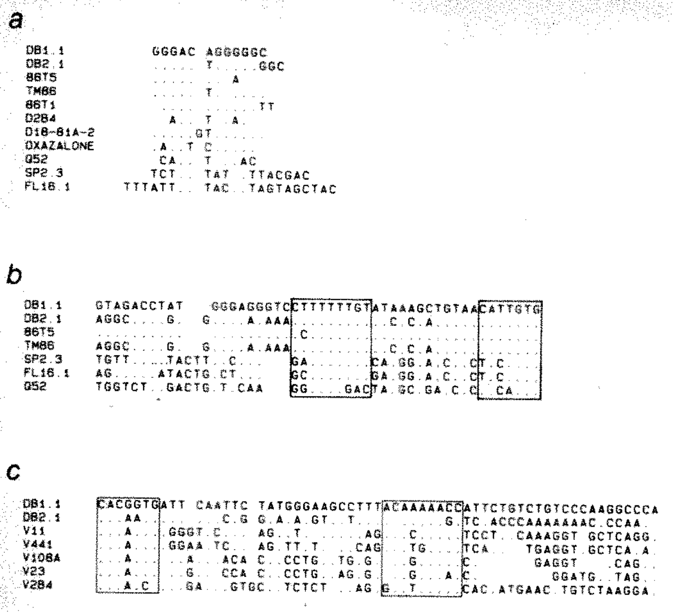
a
DB1.1 GGGAC AGGGGGC
DB2.1 . . . . . T . . . . GGC
86T5 . . . . A
TM86 . . . . . T . . . . .
86T1 . . . . TT
D2B4 A . . T . A .
D18-81A-2 . . . . . GT . . . . .
OXAZALONE . A . . T C . . . . .
Q52 CA . . T . . AC
SP2.3 TCT . . TAT . TTACGAC
FL16.1 TTTATT . . TAC . . TAGTAGCTAC
b
DB1.1 GTAGACCTAT GGGAGGGTC CTTTTTTGT ATAAAGCTGTAA CATTGTG
DB2.1 AGGC . . . G . G . . . A . AAA . . . . C . C . A . . . .
86T5 . C . . . .
TM86 AGGC . . . G . G . . . A . AAA . . . . C . C . A . . . .
SP2.3 TGTT . . . . TACTT . . C . . . GA . . . . . . CA . GG . A . C . . CT . C . . .
FL16.1 AG . . . . ATACTG . CT . . . GC . . . . . . GA . GG . A . C . . CT . C . . .
Q52 TGGTCT . . GACTG . T . CAA GG . . . GAC TA . GC . GA . C . C . . CA . . .
c
DB1.1 CACGGTG ATT CAATTC TATGGGAAGCCTTT ACAAAAACC ATTCTGTCTGTCCCAAGGCCCA
DB2.1 . . . AA . . . . C . G G . A . A . GT . . T . . . . G . TC . ACCCAAAAAAAC . CCAA .
V11 . . . A . . . GGGT . C . . . AG . . T . . . . . AG . . . C . . . . TCCT . CAAAGGT GCTCAGG .
V441 . . . A . . . GGAA . TC . . . AG . TT . T . . . CAG . . TG . . . TCA . . TGAGGT . GCTCA . A .
V108A . . . A . . . . . A . . ACA C . . CCTG . . TG . G . . . G . . . . C . GAGGT . CAG . .
V23 . . . A . . . . G . . CCA C . . CCTG . . AG . G . . . G . . . A . C . GGATG . . TAG .
V2B4 . . . A . C . . . GA . . GTGC . . TCTCT . . AG G . . T . . . . CAC . ATGAAC . TGTCTAAGGA .

Fig. 2 A comparison of the D_β coding and flanking sequences with those found in immunoglobulin gene segments. *a*, Comparison of D_β and D_H gene segment coding regions. 86T5 and 86T1 are from β cDNA clones derived from thymus RNA[19]; TM86 is a cDNA clone from the 3.3T hybridoma[19]; D2B4 is derived from a cDNA clone from a cytochrome c-specific T-helper hybridoma[21]; oxazalone and D18-81A-2 are D_H coding sequences deduced from the sequence of immunoglobulin heavy chain mRNAs[26,40]; Q52, Sp2.3, FL16.1 are germline D_H segments[11,12,25]. *b*, Comparison of D_β and D_H gene segment 5' flanking regions. *c*, Comparison of D_β and V_H gene segment 3' flanking regions. The flanking sequence of four unrelated V_H gene segments that were aligned to each other are shown. The sequences are from the indicated references: V11 (ref. 49), V441 (ref. 50), V108A (ref. 51) and V23 (ref. 52). V2B4 is the V_β region gene from a β-chain cDNA clone from a cytochrome c-specific helper-T hybridoma[21]. Boxed sequences represent the nonamer and heptamer recognition signals for DNA rearrangement. Gaps were inserted to maximize homology.

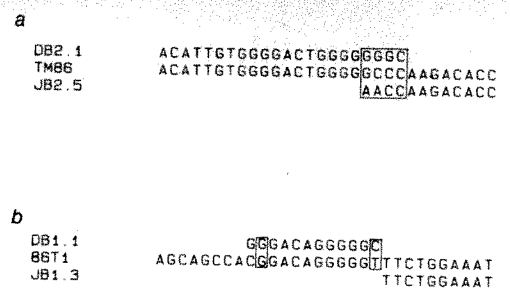
a
DB2.1 ACATTGTGGGGACTGGGG GGGC
TM86 ACATTGTGGGGACTGGGG GCCC AAGACACC
JB2.5 AACC AAGACACC
b
DB1.1 G G GACAGGGGG C
86T1 AGCAGCCAC G GACAGGGGG T TTCTGGAAAT
JB1.3 TTCTGGAAAT

Fig. 3 Junctional and N-region diversity in β-chain rearrangement. Boxed regions indicate gene segment junctions. *a*, The cDNA clone TM86, compared with germline gene segments $D_{\beta 21}$ and $J_{\beta 2\text{-}5}$. The last three nucleotides of $D_{\beta 2\text{-}1}$ and the first two nucleotides of $J_{\beta 2\text{-}5}$ have been deleted in the joining event, and one nucleotide of TM86 (a C at position 20) is not encoded by either germline gene segment. *b*, The cDNA clone 86T1, compared with germline gene segments $D_{\beta 1\text{-}1}$ and $J_{\beta 1\text{-}3}$. One nucleotide at the 5' end of the $D_{\beta 1\text{-}1}$ gene segment has been deleted or substituted in the D_β–J_β joining. One nucleotide of 86T1 (a T at position 20) is not encoded by either the $D_{\beta 1\text{-}1}$or $J_{\beta 1\text{-}3}$ gene segments. No nucleotides were delected from the $J_{\beta 1\text{-}3}$ gene segment during the D_β–J_β joining event; the nucleotide 5' of the first T is a G present in the joining sequence.

previously observed that the D_β gene segment in the 2B4.71 cDNA clone is similar to the immunoglobulin D_H gene segment D_{Q52} (ref. 21). It has also been observed that the coding and flanking regions of the mouse and human $D_{\beta 1\text{-}1}$ gene segments are highly conserved[28]. The significance of the similarity observed between the mouse D_β and D_H gene segments is unclear. Figure 2*b* shows the 5' flanking regions of the $D_{\beta 1\text{-}1}$ and $D_{\beta 2\text{-}1}$ gene segments aligned with each other, with the 86T5 and TM86 β cDNA clones and with representative members of four murine D_H gene segment families[25]. Figure 2*c* shows the aligned 3' flanking sequences of the $D_{\beta 1\text{-}1}$ and $D_{\beta 2\text{-}1}$ gene segments. These 3' flanking sequences are also aligned with immunoglobulin V_H sequences as opposed to D_H gene segments, since the V_H gene segments also have 23-base pair spacers in their 3' joining signals. Gaps were inserted to maximize the similarity between the sequences. The 5' flanking sequences of the $D_{\beta 1\text{-}1}$ and $D_{\beta 2\text{-}1}$ gene segments are similar at 35 out of 47 positions compared. The $D_{\beta 1\text{-}1}$ and $D_{\beta 2\text{-}1}$ 3' flanking sequences share 31 out of 60 nucleotides compared. Comparison of the far-flanking regions of the $D_{\beta 1\text{-}1}$ and $D_{\beta 2\text{-}1}$ gene segments indicates that they share the highest similarity at the recognition signals. Aside from these signals, these flanking regions have little sequence similarity with either the 5' flanking region of D_H gene segments or the 3' flanking region of V_H gene segments.

D_β recognition signals

As was noted by Early *et al.*[7], the 12 and 23 nucleotide spacer sequences of immunoglobulin joining recognition sequences correspond to approximately one and two turns of the DNA helix, respectively. An interesting feature of the recognition sequences for immunoglobulin V_H and V_L gene rearrangements is that the one-turn recognition sequence is always joined to a two-turn recognition sequence. This rule of one- and two-turn joining is followed in the β-gene family of T-cell receptors as well (Fig. 2*b*, *c*)[21–23]. The V_β and J_β gene segments have two-turn and one-turn recognition signals, respectively, and the D_β gene segment has a one-turn recognition signal to its 5' side and a two-turn recognition signal to its 3' side. This organization of recognition sequences permits several types of V_β gene formation consistent with the one- to two-turn joining rule: V_β gene segments may join directly to J_β gene segments, V_β–D_β–J_β joining may occur involving a single D gene segment, or two or more D_β gene segments could join between the V_β and J_β gene segments. Thus, the organization of the recognition sequences for the β-gene family should permit additional combinatorial joining possibilities to be employed in the generation of V_β diversity.

Junctional and N-region diversity

Junctional diversity in immunoglobulin variable regions is caused both by the imprecise joining of V_L and J_L or V_H, D_H, and J_H gene segments that can lead to the deletion of nucleotides from the ends of these gene segments[10–12] and by the addition of nucleotides at the junction between V_H and D_H or D_H and J_H gene segments that are not found in either of the germ-line counterparts (N-region diversity)[11,13]. Analysis of the coding regions of germ-line D_β and J_β gene segments indicates that both mechanisms for generating junctional diversity occur in the β-chain of the T-cell receptor. Figure 3*a* compares the published sequence of the TM86 cDNA clone[19], which contains the $D_{\beta 2\text{-}1}$ sequence joined to the $J_{\beta 2\text{-}5}$ gene segment, to the germ-line sequences of $D_{\beta 2\text{-}1}$ and $J_{\beta 2\text{-}5}$. In the TM86 cDNA three bases have been deleted from the 3' end of the $D_{\beta 2\text{-}1}$ gene segment, and two bases have been deleted from the 5' end of the $J_{\beta 2\text{-}5}$ gene segment. In addition, N-region diversity is indicated by the presence of a cytidine nucleotide not found at the end of either germ-line gene segment that is present at the D–J boundary. A second possible example of both types of diversity can be found by comparing the published sequence of the 86T1 cDNA clone[19] that contains a complete variable region gene segment joined to the $D_{\beta 1\text{-}1}$ and $J_{\beta 1\text{-}3}$ (M.K. and R.H., unpublished) gene segments (Fig. 3*b*). Although the central ten base pairs of the 86T1 D_β gene segment are identical to the germ-line $D_{\beta 1\text{-}1}$ sequence, the end nucleotides have been altered. The first nucleotide of the $D_{\beta 1\text{-}1}$ gene segment at the V_β–D_β boundary has been deleted or substituted, while the last nucleotide at the D_β–J_β boundary has been replaced with a different base. In this latter example, it is also possible that no deletions or additions occur, but instead a D_β gene segment that is slightly different

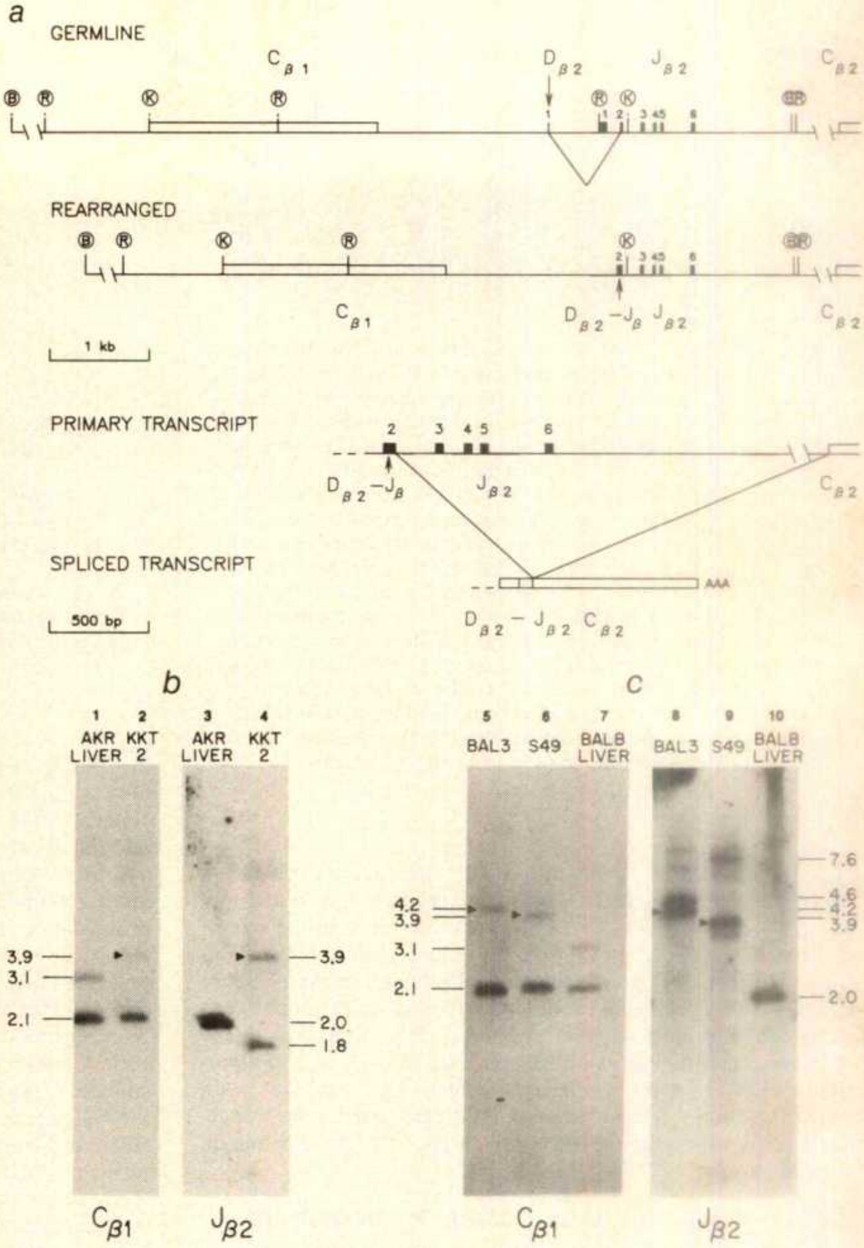

Fig. 4 D_β–J_β joining in T-cell tumour DNA. Southern blots[53] of *Eco*RI digested DNA were hybridized with a $C_{\beta 1}$ cDNA clone[54] and a fragment from a germ-line cosmid clone that contains $J_{\beta 2}$ sequences[23]. Conditions used for the Southern blots have been described previously[55]. *a*, A model for the rearrangement and expression of the partially joined (D_β–J_β) genes. The C_β genes are depicted as open boxes; the separate exons of these genes are not shown. The $D_{\beta 2}$ and $J_{\beta 2}$ gene segments are numbered and are shown as vertical lines or filled boxes. Some relevant restriction sites for the Southern blot analysis are indicated. B, *Bam*HI; K, *Kpn*I; E, *Eco*RI. The rearrangement presented in the figure joins the $D_{\beta 2\text{-}1}$ to the $J_{\beta 2\text{-}2}$ gene segment eliminating the third *Eco*RI site as well as $J_{\beta 2\text{-}1}$ and leading to the rearranged fragments described in the text. Rearrangement to other $J_{\beta 2}$ gene segments is also possible. The scale used to depict the transcripts is expanded twofold. The dotted lines at the 5′ end reflect uncertainty about the structure of this part of the transcript. *b*, Hybridization of the $C_{\beta 1}$ cDNA (lanes 1, 2) and $J_{\beta 2}$ fragment (lanes 3, 4) to AKR strain tumour KKT-2 and to AKR liver DNA. *c*, Hybridization of the $C_{\beta 1}$ (lanes 5–7) and $J_{\beta 2}$ (lanes 8-10) probes with DNA from the BALB/c tumours BAL3 and S49 and with BALB/c liver DNA. In both *b* and *c* the filter was first hybridized with $C_{\beta 1}$ the probe was removed, and the same filter was then hybridized with the $J_{\beta 2}$ probe. The arrows denote the identically-sized rearranged fragment that could be detected by both probes. The estimated sizes in kilobases of the hybridizing fragments are indicated.

from the $D_{\beta 1\text{-}1}$ gene segment may be present in 86T1. It is also possible that inter-strain sequence polymorphisms can account for these differences, since the germ-line sequences are from B10 mice and in this case the cDNA sequence is from BALB/c mice. Because the only differences are at the boundaries between the joined gene segments, we consider these latter possibilities to be less likely.

D_β–J_β joining without *V*–*D*–*J* joining

A productive DNA rearrangement is defined as one in which the *V*, *D* and *J* (or *V*–*J*) joining process occurs in such a way that a functional polypeptide chain can be expressed. In immunoglobulin genes a variety of nonproductive rearrangements may occur, including incomplete rearrangements of D_H and J_H gene segments joined together without a V_H gene segment. Such incomplete heavy chain rearrangements occur frequently in immature B cells[29,30] but are also found in some mature B cells[11,31] and T cells as well[12], and are thought to be the first step in the assembly of heavy-chain variable region genes. The β-gene segments may undergo *D*–*J* rearrangements in the absence of V_β joining in a manner similar to their immunoglobulin counterparts. We have characterized the β-gene rearrangements in a large number of T-cell lines, hybridomas, and tumours (M.K., J. Goverman, M. Malissen, R.H., manuscript in preparation) and have observed several cases in which the DNA from T-cell tumours have undergone an apparent D_β–J_β joining. For example, when germ-line DNA is digested with the restriction enzyme *Eco*RI and hybridized with a $C_{\beta 1}$ cDNA probe, there are two hybridizing fragments of 2.1 and 3.1 kilobases (kb). The 3.1 kb fragment is at the 3′ end of the C_β gene beginning close to the translational stop codon and ending just 5′ to the first $J_{\beta 2}$ gene segment[23] (Fig. 4*a*). In the T-cell tumours S49, BAL3, and KKT-2, the 3.1 kb fragment at the 3′ end of the $C_{\beta 1}$ gene is replaced by a larger fragment that is either 3.9 kb (S49 and KKT-2) or 4.2 kb (BAL3) (Fig. 4*b*, *c*). Hybridization of the same filters with the $J_{\beta 2}$ probe reveals two rearranged fragments in each case, including one fragment identical in size to the one detected with the $C_{\beta 1}$ probe. Southern blots of DNA from these tumours were generated from DNA digested with *Bam*HI and hybridized with the $C_{\beta 1}$ and $J_{\beta 2}$ probes. Digestion of germ-line DNA with this enzyme will generate a single fragment that should hybridize with both probes (Fig. 4*a*). In the DNA from each of the tumours one of the fragments hybridizing with the $J_{\beta 2}$ probe and the only fragment hybridizing with the $C_{\beta 1}$ cDNA are identically sized and approximately 1,000 bp smaller than the germ-line fragment (M.K., R.H., unpublished observations). We therefore conclude that the rearrangements 3′ to the $C_{\beta 1}$ gene in these tumours are small deletions. Since this deletion spans the *Eco*RI site just to

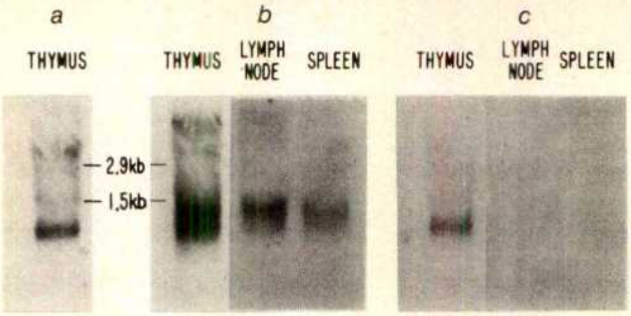

Fig. 5 Hybridization of D_β and C_β probes to RNA from lymphoid tissues. The probes are as follows: *a*, T6 synthetic oligonucleotide; *b*, C_β cDNA clone; *c*, T5 synthetic oligonucleotide. RNA was prepared from thymus, spleen, and lymph node of 4-week-old DBA 1/J female mice by homogenization of the tissues in guanidinium thiocyanate followed by centrifugation through a cushion of CsCl[56]. Northern blots of total cell RNA and hybridization with a C_β probe were performed as described previously[57]. Hybridization with oligonucleotides was done at room temperature with end-labelled synthetic probe at a concentration of 0.5 pmol ml^{-1}. The blots were washed in 2×SSC/0.1% SDS at room temperature followed by washing in the same solution at 37 °C. One filter was used in *a*, *b* and *c*; following hybridization and exposure to film, the probe was removed by stringent washing before retesting with a second probe. The migration distance of *Escherichia coli* ribosomal RNA molecular weight markers is indicated. Other markers included mouse 28+18S ribosomal RNA (4.8 and 1.9 kb) and MS2 phage RNA (3.6 kb).

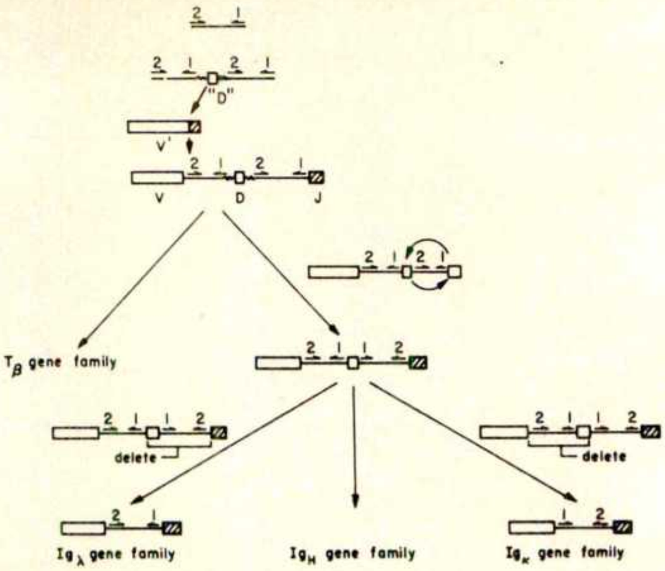

Fig. 6 A model for the evolution of the immunoglobulin and β T-cell receptor gene families. The number 1 represents the one-turn recognition signal; the number 2 represents the two-turn recognition signal.

the 5′ side of the $J_{\beta2}$ gene cluster, the most likely explanation for these events is that the $D_{\beta2\text{-}1}$ gene segment has joined to a $J_{\beta2}$ gene segment (Fig. 4*a*). The slight difference in the size of the rearranged fragment in different tumours could reflect joining to different $J_{\beta2}$ gene segments. We have similar evidence that $D_{\beta1\text{-}1}$ to $J_{\beta1}$ joining events can occur as well (unpublished data). Thus it appears likely that the $D_{\beta1\text{-}1}$ and $D_{\beta2\text{-}1}$ gene segments do participate in both complete (V_β–D_β–J_β) and partial (D_β–J_β) DNA rearrangements. By analogy with immunoglobulin heavy-chain genes, these partial rearrangements may represent the first step in β-chain variable region gene assembly.

D_β–J_β transcription not using V_β promoters

Northern blot analyses have been carried out on RNA from thymus, lymph node, and spleen using both a C_β probe (Fig. 5*b*) and the oligonucleotides T5 and T6 (Fig. 5*a*, *c*). The C_β probe detects two species, approximately 1.3 and 1.0 kb in size, when hybridized to total RNA from the thymus. Similar results have been obtained with poly(A)$^+$ RNA (M.K., G.S., unpublished observations). Spleen and lymph node RNA have a single C_β hybridizing transcript of 1.3 kb. When RNA from these three lymphoid tissues is hybridized with either the T5 or T6 oligonucleotide, only the 1.0 kb thymus RNA is detected. It is important to note that both T5 and T6 are complementary to 6 bases of D_β coding sequences and 34 bases of 5′ flanking sequence. These two probes therefore do not hybridize with fully rearranged V_β–D_β–J_β genes since these rearrangements eliminate the 5′ D_β flanking sequence. Because the probes also do not cross-hybridize with each other, we conclude that at least two D_β gene segments contain 5′ promoters that permit expression in thymus: one is the $D_{\beta2\text{-}1}$ gene segment and the second is the $D_{\beta1\text{-}1}$ gene segment or a highly similar *D* gene segment such as the one found in the 86T5 cDNA clone. It has recently been demonstrated that each immunoglobulin D_H gene segment also has a promoter located in the 5′ flanking DNA[32].

We have hybridized both the C_β probe and the D_β oligonucleotide probes to RNA from the S49 and KKT-2 tumours that are believed to have joined $D_{\beta2}$–$J_{\beta2}$ gene segments. The KKT-2 tumour has only a 1.0 kb transcript that hybridizes with both the T6 D_β oligonucleotide and a probe specific for the 3′ end of $C_{\beta2}$. Several other T-cell tumours and T-cell hybridomas contain 1.0 kb transcripts that hybridize with both C_β probes and the T6 oligonucleotide. However, RNA from S49 does not hybridize with either oligonucleotide, and it contains a 1.3-kb but not a 1.0-kb transcript when hybridized with the C_β cDNA probe (M.K., unpublished observations).

Based on the blot-hybridization and nucleotide sequence data presented here and the partial nucleotide sequences of the TM86 and 86T5 cDNA clones, we have presented a model for the rearrangement and expression of the D_β gene segments and their 5′ flanking sequences (Fig. 5*a*). D_β–J_β rearrangement may stimulate transcription from a promoter located 5′ to several of the D_β gene segments. This transcript is 1.0 kb long, polyadenylated, and contains a joined D_β–J_β gene segment spliced to the exons normally used in the C_β gene. Although we cannot formally rule out transcription from this promoter in the absence of gene rearrangement, it should be noted that the KKT-2 tumour has no germ-line $J_{\beta2}$ clusters (Fig. 4*c*) and that a transcript derived from a promoter 5′ to the $D_{\beta2\text{-}1}$ gene segment that includes the intron between $D_{\beta2\text{-}1}$ and $J_{\beta2\text{-}1}$ as well as the exons of $C_{\beta2}$ would be at least 1.6 kb. No transcript of this length has been detected with any of the probes employed. The prevalence of the 1.0 kb transcript in thymus, as opposed to lymph node and spleen, would suggest that many of the immature cells in this tissue have undergone a partial (D_β–J_β) rearrangement. However, as some functional mature T lymphocytes have a 1.0-kb transcript that hybridizes with the T6 oligonucleotide (M.K., unpublished), there is probably a low level of 1.0-kb transcript in lymph node and spleen that could not be detected on our blots.

Immunoglobulin gene expression in B lymphocytes is thought to result from gene rearrangements that bring into proximity two widely separated elements: a promoter sequence located 5′ to the *V* gene segments[33,34] and an enhancer sequence located in the intron between the *J* gene segments and the *C* genes[35–39]. In the case of the D_β–J_β transcript, however, the location of the promoter relative to any postulated enhancer would not be greatly affected by the relatively small deletions involved in the D_β–J_β joining we have described. Therefore the means by which D_β–J_β joining might stimulate transcription are unknown. Furthermore, Northern blots of RNA from the S49 tumour indicate that rearrangement is necessary but may not be sufficient for transcription. Currently, we are further characterizing the D_β–J_β

DNA rearrangements and D_β transcripts in a number of T-cell tumours in order to understand better the relationship between the rearrangements and the 1.0 kb C_β transcripts that we have described.

Are D_β–J_β transcripts translated?

In the immunoglobulin gene families, transcripts have been described that originate from unrearranged κ[40] and heavy-chain genes[41] or from incompletely rearranged (D_H–J_H) heavy-chain gene segments[27,41]. Some of the RNA molecules do not give rise to detectable polypeptides and are referred to as sterile transcripts[27,42]. These sterile transcripts might not be physiologically significant, or else the RNA molecule itself might have some regulatory function. Similar speculations apply to the 1.0-kb transcripts containing D_β gene segments. In addition, it is also possible that these D_β–J_β transcripts encode functional polypeptides. If the 1.0-kb transcripts use the entire C_β gene and the same 3′ end as is found in the 1.3-kb C_β RNA, then about 100–200 nucleotides remain for the D_β coding region and its 5′ flanking sequence. The nucleotide sequences flanking the $D_{\beta1\text{-}1}$ and $D_{\beta2\text{-}1}$ gene segments have open reading frames for more than 50 codons. A methionine codon that is in frame with the germ-line D_β gene segments is located 5′ to both $D_{\beta1\text{-}1}$ and $D_{\beta2\text{-}1}$ (data not drawn for $D_{\beta2\text{-}1}$). Moreover, the $D_{\beta1\text{-}1}$ flanking sequence has a signal sequence for membrane insertion of a nascent polypeptide[43] 136 nucleotides 5′ to the D_β gene segment (Fig. 1*b*). A possible signal sequence is also located following the methionine codon 5′ of $D_{\beta2\text{-}1}$ (data not shown). Alt and co-workers have demonstrated that most immunoglobulin D_H gene segments have open reading frames in their 5′ flanking sequence that begin with a methionine codon followed by a hydrophobic leader sequence. They have also demonstrated that transcripts derived from partial D_H–J_H rearrangements give rise to truncated C_μ-containing polypeptides[32]. We therefore believe that the D_β–J_β transcripts will in at least some cases give rise to truncated β polypeptides. The function, if any, of these truncated polypeptides is unknown. Because it has been proposed that the synthesis of complete heavy chain and light chain polypeptides derived from productively rearranged genes prevents further *V* gene rearrangement[40,44], we might speculate that the truncated C_μ and C_β polypeptides will in a similar fashion somehow stimulate or facilitate the *V* gene rearrangement process. It is also possible that these truncated proteins provide a stimulatory signal for cell growth similar to that provided by antigen bound to the intact receptor. Alternatively they might function at the cell surface with regard to the development of the repertoire of receptors via network interactions.

Evolution of gene rearrangements

It has been proposed that the ability of the antibody and T-cell receptor gene families to undergo DNA rearrangements evolved from the insertion of a transposable element into a primordial uninterrupted *V* gene exon[6,45] (Fig. 6). This theory proposed the existence of a transposon with asymmetric inverted repeats similar to those found in the joining sequences of the contemporary antigen-receptor gene families. If inserted in the genome, duplication of this transposon along with a short stretch of flanking sequence would lead to a more complex transposon containing a proto-*D* gene segment (Fig. 6). Subsequent insertion of this transposon into a primordial *V* gene would generate a gene segment organization, at least with respect to joining sequences, that is similar to that of the β genes. Duplication of this locus would lead to two separate gene families: the β-chain gene family and the immunoglobulin gene family. As shown in Fig. 6, an inversion bounded by the two right-hand inverted repeats could generate the precursor of the heavy chain gene family. As outlined previously[45], further duplications of this heavy chain gene precursor could have occurred to create precursors of all three immunoglobulin gene families. A deletion on the right hand or 3′ end of the transposon as indicated in Fig. 6 generates the proto-λ gene family with its organization of joining signals. This may have occurred via homologous recombination between these signals. A similar deletion at the 5′ end could give rise to the κ gene family.

This model can account for some of the unique features of variable region genes. The known genes encoding antigen receptors on B and T lymphocytes, cell-surface molecules of the major histocompatibility complex (MHC), β_2-microglobulin and some other cell-surface proteins associated with the immune system, are believed to have evolved in part from a primordial exon that encoded an immunoglobulin-like domain[46]. With the exception of the variable region genes, each domain in these proteins having an immunoglobulin structure is encoded by a single exon. The insertion of a transposon into a primordial variable region gene can account for the fact that all the *V* gene families are split into several exons at a similar location. The theory accounts for the presence of a *D* gene segment in only two of the four antigen-receptor gene families and also explains the different configurations of DNA rearrangement signals in these families. While the evolutionary history outlined above implies that the β-chain gene family arose first, several other pathways beginning with insertion of a slightly different transposon are also possible[45]. Finally, this theory proposes a relatively simple explanation for the evolution of the DNA rearrangement signals in that it proposed these signals evolved from the inverted terminal repeats of a mobile DNA sequence but it remains unclear how these signals and the proteins that recognize them became adapted for the highly regulated rearrangements of the immune system.

This work was supported by grant AI 17565 from the NIH and by a grant from T-cell Sciences, Inc. We thank Dr Irving Weissman, Stanford University, for providing T-cell tumours, Dr Roger Perlmutter for helpful and stimulating discussions, and Dr Suzanna Horvath and Marilyn Seibel for synthesis of the oligonucleotides. We also thank Tim Hunkapiller, Astar Winoto, Drs Rick Barth, Joan Goverman, Joan Kobori, Bernard Malissen, Marie Malissen and Martha Zuniga for critique of the manuscript, Dr Marie Malissen for providing the cosmid clone and plasmid subclones, Debbie Maloney for technical assistance, and Bernita Larsh for preparation of the manuscript.

Note added in proof: While this paper was in the press, the sequence of the $D_{\beta1\text{-}1}$ gene segment and the presence of this gene segment in the 86T1 and 86T5 cDNA clones was reported by Kavaler *et al.*[58].

Received 29 June; accepted 23 July 1984.

1. Early, P. & Hood, L. in *Genetic Engineering* (eds Setlow, J. K. & Hollaender, A.) 157–188 (Plenum, New York, 1981).
2. Tonegawa, S. *Nature* **302,** 575–581 (1983).
3. Honjo, T. *A. Rev. Immun.* **1,** 499–528 (1983).
4. Brack, C., Hirama, M., Lenhard-Schuller, R. & Tonegawa, S. *Cell* **15,** 1–14 (1978).
5. Seidman, J., Max, E. & Leder, P. *Nature* **280,** 370–375 (1979).
6. Sakano, H., Huppi, K., Heinrich, G. & Tonegawa, S. *Nature* **280,** 288–294 (1979).
7. Early, P., Huang, H., Davis, M., Calame, K. & Hood, L. *Cell* **19,** 981–992 (1980).
8. Sakano, H., Maki, R., Kurosawa, Y., Roeder, W. & Tonegawa, S. *Nature* **286,** 676–683 (1980).
9. Schilling, J., Clevinger, B., Davie, J. M. & Hood, L. *Nature* **283,** 35–40 (1980).
10. Weigert, M., Perry, R., Kelley, D., Hunkapiller, T., Schilling, J. & Hood, L. *Nature* **283,** 497–499 (1980).
11. Sakano, H., Kurosawa, Y., Weigert, M. & Tonegawa, S. *Nature* **290,** 562–565 (1981).
12. Kurosawa, Y. *et al. Nature* **290,** 565–570 (1981).
13. Alt, F. & Baltimore, D. *Proc. natn. Acad. Sci. U.S.A.* **79,** 4118–4122 (1982).
14. Max, E. E., Seidman, J. G. & Leder, P. *Proc. natn. Acad. Sci. U.S.A.* **76,** 3450–3454 (1979).
15. Allison, J. P., McIntyre, B. W. & Bloch, D. *J. Immun.* **129,** 2293–2300 (1982).
16. Haskins, K. *et al. J. exp. Med.* **157,** 1149–1169 (1983).
17. Meuer, S. C. *et al. J. exp. Med.* **157,** 705–719 (1983).
18. Hedrick, S. M., Cohen, D. I., Nielsen, E. A. & Davis, M. M. *Nature* **308,** 149–153 (1984).
19. Hedrick, S. M., Nielsen, E. A., Kavaler, J., Cohen, D. I. & Davis, M. M. *Nature* **308,** 153–158 (1984).
20. Yanagi, Y. *et al. Nature* **308,** 145–153 (1984).
21. Chien, Y., Gascoigne, N., Kavaler, J., Lee, N. & Davis, M. *Nature* **309,** 322–326 (1984).
22. Siu, G. *et al. Cell* **37,** 393–401 (1984).
23. Malissen, M. *et al. Cell* **37,** 1101–1110 (1984).
24. Horvath, *J. biol. Chem.* (submitted).
25. Kurosawa, Y. & Tonegawa, S. *J. exp. Med.* **155,** 201 (1982).
26. Kaartinen, M., Griffiths, G., Markham, N. & Milstein, C. *Nature* **304,** 320–324 (1983).
27. Alt, F. W., Rosenberg, N., Enea, V., Siden, E. & Baltimore, D. *Molec. cell. Biol.* **2,** 386–400 (1982).
28. Clark, S. *et al. Nature* **311,** 387–389 (1984).
29. Alt, F., Rosenberg, N., Lewis, S., Thomas, E. & Baltimore, D. *Cell* **27,** 381–390 (1981).
30. Nelson, K., Haimovich, J. & Perry, R. *Molec. cell. biol.* **3,** 1317–1332 (1983).
31. Early, P., Nottenburg, C., Weissman, I. & Hood, L. *Molec. cell. Biol.* **2,** 829–836 (1982).
32. Reth, M. & Alt, F. *Nature* (in the press).

33. Kataoka, T., Niakido, T., Miyata, T., Moriwaki, K. & Honjo, T. *J. biol. Chem.* **257**, 277–285 (1982).
34. Clarke, C. *et al. Nucleic Acids Res.* **10**, 7731–7749 (1982).
35. Rice, D. & Baltimore, D. *Proc. natn. Acad. Sci. U.S.A.* **79**, 7862–7865 (1982).
36. Oi, V., Morrison, S., Herzenberg, L. & Berg, P. *Proc. natn. Acad. Sci. U.S.A.* **80**, 825–829 (1983).
37. Gillies, S., Morrison, S., Oi, V. & Tonegawa, S. *Cell* **33**, 717–728 (1983).
38. Queen, C. & Baltimore, D. *Cell* **33**, 741–748 (1983).
39. Banerji, J., Olson, L. & Schaffner, W. *Cell* **33**, 729–740 (1983).
40. Perry, R. P. *et al. Proc. natn. Acad. Sci. U.S.A.* **77**, 1937–1941 (1980).
41. Kemp, D. J., Harris, A. W. & Adams, J. M. *Proc. natn. Acad. Sci. U.S.A.* **77**, 7400–7404 (1980).
42. Walker, I. D. & Harris, A. W. *Nature* **288**, 290–293 (1980).
43. Silhavy, T. S., Benson, S. A. & Emr, S. D. *Microbiol. Rev.* **47**, 313–344 (1983).
44. Alt, F. W., Enea, V., Bothwell, A. L. M. & Baltimore, D. *Cell* **21**, 1–12 (1980).
45. Hood, L. E., Hunkapiller, T. & Kraig, E. in *Modern Cell Biology* (ed. McIntosh, J. R.) 305–328 (Liss, New York, 1983).
46. Williams, A. F. *Nature* **308**, 108–109 (1984).
47. Messing, J. & Vieira, J. *Gene* **19**, 269–276 (1982).
48. Sanger, F., Coulson, A. R., Barrell, B. G., Smith, A. J. H. & Roe, B. A. *J. molec. Biol.* **143**, 161–178 (1980).
49. Crews, S., Griffin, J., Huang, H., Calame, K. & Hood, L. *Cell* **25**, 59–66 (1981).
50. Ollo, R., Auffray, C., Sikorav, J.-L. & Rougeon, F. *Nucleic Acids Res.* **9**, 4099–4108 (1981).
51. Givol, D., Zakut, R., Effron, K., Rechavi, G., Ram, D. & Cohen, J. B. *Nature* **292**, 426–430 (1981).
52. Bothwell, A. L. M., Paskind, M., Reth, M., Imanishi-Kari, T., Rajewsky, K. & Baltimore, D. *Cell* **24**, 625–637 (1981).
53. Southern, E. M. *J. molec. Biol.* **98**, 503–517 (1975).
54. Caccia, N. *et al. Cell* **37**, 1091–1099 (1984).
55. Steinmetz, M. *et al. Nature* **300**, 35–42 (1982).
56. Chirgwin, J. M., Przybyla, A. E., MacDonald, R. J. & Rutter, W. J. *Biochemistry* **18**, 5294–5299 (1979).
57. Kronenberg, M., Davis, M. M., Early, P. W., Hood, L. E. & Watson, J. D. *J. exp. Med.* **152**, 1745–1761 (1980).
58. Kavaler, J., Davis, M. M. & Chien, Y. *Nature* **310**, 421–424 (1984).

Apparent discontinuous transcription of *Trypanosoma brucei* variant surface antigen genes

David A. Campbell, Deborah A. Thornton & John C. Boothroyd

Department of Medical Microbiology, D-305 Fairchild Building, Stanford University School of Medicine, Stanford, California 94305, USA

The repeated mini-exon sequence that encodes the first 35 base pairs of all variant surface antigen mRNAs of Trypanosoma brucei *directs the synthesis of a discrete 137-nucleotide transcript. It thus seems that variant surface antigen mRNAs are transcribed discontinuously, and we present two alternative models for how this might occur.*

THE ability of African trypanosomes to establish chronic infections in their mammalian hosts depends on a highly developed system of antigenic variation, whereby individual members of the parasite population change the composition of their surface coat[1–3]. This antigenic variation is controlled at the level of gene expression[4,5], each trypanosome possessing a large repertoire of genes (estimated at over 100; refs 6, 7) coding for the antigenically distinct variant surface glycoproteins (VSGs) which comprise the coat. At any one time and on any one trypanosome, only one species of VSG can be detected[8], suggesting that mutual exclusion operates between the VSG genes. Activation of VSG genes occurs by a two-step process requiring first the duplication and transposition of a silent basic copy (BC) of the gene into one of a few telomeric expression sites by a process equivalent to gene conversion, then selection of the expression site over others for transcription[9–15]. The extra copy of the gene thus produced is called the expression-linked copy (ELC). The so-called 'non-duplication-activated' VSG genes described by others probably represent genes which had already undergone the first step in activation (that is, gene conversion into an expression site) before the variants were isolated for study. Although the structure of expression sites and the sequences involved in the gene conversion event have been identified for some variants[16–19], little is known about the second step, particularly how activation occurs and how the mutual exclusion operates between the different expression sites.

Recently, a major clue to this problem has come from the finding that the 5′ 35 nucleotides of VSG mRNAs are not contiguously encoded with the protein-coding portion of the gene[13], and that this spliced leader segment is identical for different VSG mRNAs regardless of which telomeric expression site they occupy[14]. The genomic location of the 35-base pair (bp) mini-exon coding for the spliced leader has recently been reported to be a 1.35-kilobase pair (kb) segment tandemly repeated 100–200 times (as one or more clusters) at an unidentified locus in the genome but at least 30 kb upstream of the active VSG gene[20,21]. Two other important observations concerning the spliced leader are that it is detected on many RNA molecules of varying size in blot analyses using RNA from different life stage forms of *Trypanosoma brucei* (ref. 21 and M. Parsons *et al.*, personal communication) and that homologous sequences have been detected in the genomes of related species and genera[22].

Several models have been proposed to explain how a contiguous mRNA is produced from such an unusual arrangement of exons[20–23] and how the activity of different expression sites is regulated. These have included chromosome end exchange with splicing of very long transcripts, and discontinuous transcription whereby the mini-exon and ELC are flanked by their own initiation and termination sites. To determine how VSG mRNAs are produced and processed, we have studied the 1.35-kb repeats and identified their transcriptional products.

Molecular cloning of a mini-exon repeat

To enable nucleotide sequence analysis of the mini-exon repeat, recombinant plasmids containing individual repeats were generated. This was initially done using a *Pvu*II digest of the genomic DNA of *T. brucei* as this enzyme has been reported to release the mini-exon-containing portion of the repeat as a discrete band at ~720 bp[21]. Such a band was excised from an agarose gel, the DNA purified by electroelution[24] and ligated into the *Pvu*II site of the plasmid vector pBR322 (ref. 25). A sample of this same excised material was radiolabelled by nick-translation[26] and used as a probe in colony hybridization[27], thereby identifying recombinants containing repetitive DNA. Four plasmids thus identified were further characterized and three were found to contain indistinguishable inserts with at least one *Rsa*I site. As the mini-exon should include an *Rsa*I site, nucleotide sequence analysis in the vicinity of this site was performed on one of the plasmids (pMEP.1). The strategy and sequence obtained are shown in Figs 1 and 2, respectively. This demonstrated unambiguously that pMEP.1 contains a portion of the mini-exon repeat.

To obtain a recombinant plasmid containing an insert representative of the complete 1.35-kb repeat, a ligation was performed using the 1.35-kb fraction of trypanosome genomic DNA digested with *Sau*3A and the plasmid vector pAT153 (ref. 28) digested with *Bam*HI. Recombinants were screened with the

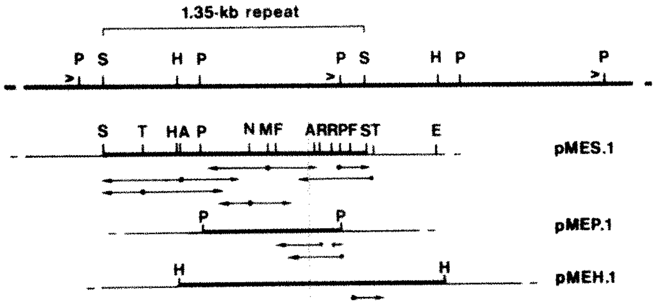

Fig. 1 Restriction maps and sequencing strategies for mini-exon-containing plasmids. The top line of the figure represents a restriction map for the genomic cluster of 1.35-kb tandem mini-exon repeats as deduced from Southern blot analysis (data not shown). The rightward-pointing arrowheads represent the approximate position of the 35-bp mini-exon sequence; beneath this are the recombinant-containing portions of this genomic region as cloned in the plasmid vectors pAT153 (pMES.1 and pMEH.1) and pBR322 (pMEP.1; see text). The restriction sites used in the nucleotide sequencing (by the chemical modification method of Maxam and Gilbert[43]) are shown for each insert. The arrows with solid circles indicate the labelled sites and the region over which unambiguous sequence information was obtained. Restriction sites: A, *Acc*I; E, *Eco*RI; F, *Hin*fI; H, *Sph*I; M, *Mlu*I; N, *Nar*I; P, *Pvu*II; R, *Rsa*I; S, *Sau*3A; T, *Taq*I.

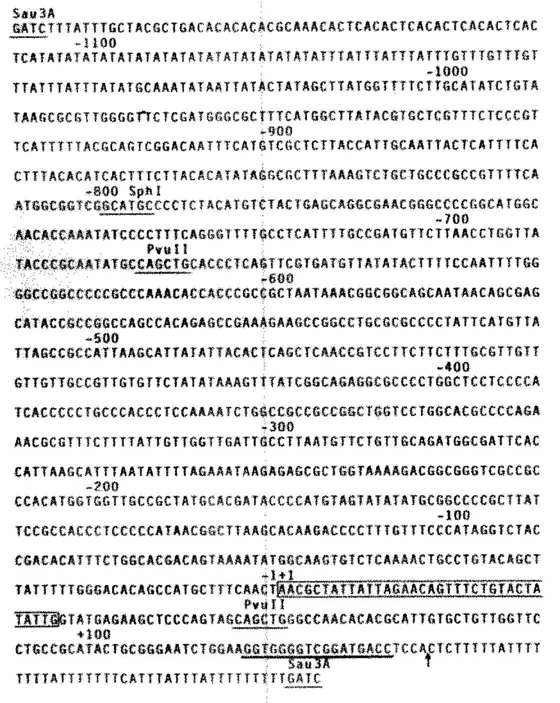

```
Sau3A
GATCTTTATTTGCTACGCTGACACACACACGCAAACACTCACACTCACACTCACACTCAC
         -1100
TCATATATATATATATATATATATATATATATATATATTTATTTATTTATTTGTTTGTTTGT
                                                   -1000
TTATTTATTTATATGCAAATATAATTATACTATAGCTTATGGTTTTCTTGCATATCTGTA

TAAGCGCGTTGGGGTTCTCGATGGGCGCTTTCATGGCTTATACGTGCTCGTTTCTCCCGT
                              -900
TCATTTTTACGCAGTCGGACAATTTCATGTCGCTCTTACCATTGCAATTACTCATTTTCA

CTTTACACATCACTTTCTTACACATATAGGCGCTTTAAAGTCTGCTGCCCGCCGTTTTCA
          -800 SphI
ATGGCGGTCGGCATGCCCCTCTACATGTCTACTGAGCAGGCGAACGGGCCCCGGCATGGC
                                                   -700
AACACCAAATATCCCCTTTCAGGGTTTTGCCTCATTTTGCCGATGTTCTTAACCTGGTTA
                  PvuII
TACCCGCAATATGCCAGCTGCACCCTCAGTTCGTGATGTTATATACTTTTCCAATTTTGG
                               -600
GGCCGGCCCCCGCCCAAACACCACCCGCCGCTAATAAACGGCGGCAGCAATAACAGCGAG

CATACCGCCGGCCAGCCACAGAGCCGAAAGAAGCCGGCCTGCGCGCCCCTATTCATGTTA
          -500
TTAGCCGCCATTAAGCATTATATTACACTCAGCTCAACCGTCCTTCTTCTTTGCGTTGTT
                                                   -400
GTTGTTGCCGTTGTGTTCTATATAAAGTTTATCGGCAGAGGCGCCCCTGGCTCCTCCCCA

TCACCCCCTGCCCACCCTCCAAAATCTGGCCGCCGCCGGCTGGTCCTGGCACGCCCCAGA
                               -300
AACGCGTTTCTTTTATTGTTGGTTGATTGCCTTAATGTTCTGTTGCAGATGGCGATTCAC

CATTAAGCATTTAATATTTTAGAAATAAGAGAGCGCTGGTAAAAGACGGCGGGTCGCCGC
          -200
CCACATGGTGGTTGCCGCTATGCACGATACCCCATGTAGTATATATGCGGCCCCGCTTAT
                                                   -100
TCCGCCACCCTCCCCCATAACGGCTTAAGCACAAGACCCCTTTGTTTCCCATAGGTCTAC

CGACACATTTCTGGCACGACAGTAAAATATGGCAAGTGTCTCAAAACTGCCTGTACAGCT
                              -1+1
TATTTTTGGGACACAGCCATGCTTTCAACTAACGCTATTATTAGAACAGTTTCTGTACTA
                             PvuII
TATTGGTATGAGAAGCTCCCAGTAGCAGCTGGGCCAACACACGCATTGTGCTGTTGGTTC
         +100
CTGCCGCATACTGCGGGAATCTGGAAGGTGGGGTCGGATGACCTCCACTCTTTTTATTTT
                                  Sau3A         ↑
TTTTATTTTTTTCATTTATTTATTTTTTTTGATC
```

Fig. 2 Nucleotide sequence of a complete 1.35-kb mini-exon repeat. The nucleotide sequence of the sense strand of pMES.1 is presented with numbering from the 5′-end of the 35-bp mini-exon, which is boxed. The restriction sites used in the cloning (see Fig. 1) are underlined and annotated. The *Sau*3A site (GATC) used in cloning the insert is duplicated at the beginning and end of the sequence. The thickly underlined segment represents the 17-nucleotide sequence for which a complementary oligonucleotide was synthesized and used in subsequent experiments (see Figs 3 and 5). The arrow between positions 137 and 138 indicates the 3′-terminus of mini-exon-derived RNA as described in the text.

*Pvu*II insert of pMEP.1 and after preliminary restriction mapping, one (pMES.1) was characterized further and found to contain an apparently complete 1.35-kb mini-exon repeat.

Nucleotide sequence of mini-exon repeat

Using the recombinant plasmid pMES.1 and the strategy shown in Fig. 1, the complete nucleotide sequence of one repeat unit containing the mini-exon was determined. This is presented in Fig. 2 with position +1 being the first nucleotide of the mini-exon. The region from −270 to +61 was also sequenced from the independently generated plasmid pMEP.1 (see Fig. 1). The results from the two plasmids were identical in this region.

Although Southern blot analysis suggested that the repeat unit was defined by a single *Sau*3A site (refs 20, 21 and D.A.T. and J.C.B., unpublished results), the possibility remained that two closely adjacent *Sau*3A sites were contained within each repeat and that pMES.1, therefore, lacked a small portion of the repeat. To test this, a further recombinant plasmid containing a mini-exon repeat was generated using an *Sph*I digest of genomic DNA (as cloned in a bacteriophage λ recombinant containing several 1.35-kb repeats; D.A.C., unpublished results) and ligated to *Sph*I-digested pAT153. *Sph*I was known to cut the repeat once (from sequence analysis of pMES.1 and Southern blot analyses; D.A.C., unpublished results) and thus should give a fragment spanning the *Sau*3A site in question. Mini-exon-containing plasmids were identified as above and pMEH.1 was obtained, mapped and sequenced (see Fig. 1). From this plasmid, a contiguous sequence spanning the *Sau*3A site used to construct pMES.1 was obtained (data not shown), demonstrating that the sequence presented in Fig. 2 represents a complete mini-exon repeat.

To ensure that this sequence was not only complete but also representative, we compared its restriction map with the fragment sizes observed on Southern blots of genomic DNA cut with several enzymes, using the *Pvu*II insert of pMEP.1 as a radiolabelled probe (data not shown). The predominant bands obtained in each digest agreed in all cases with the fragment sizes predicted from the sequence; this demonstrated that the mini-exon repeats are highly conserved and that pMES.1 contains a typical member.

Identification of a short transcript

A testable prediction of the model proposing discontinuous transcription is that there should be detectable levels of a small RNA (that is, <1.35 kb) derived from each mini-exon repeat. One of the most sensitive methods for detecting and characterizing particular transcripts is S_1-protection[29], whereby a radiolabelled DNA probe from the region of interest is denatured and renatured in the presence of RNA; the resulting material is then digested with the single-strand-specific S_1 nuclease and the length of any protected fragments measured by gel electrophoresis and autoradiography. The DNA substrate used here was from pMES.1, extending from the [3′-^{32}P]-labelled *Pvu*II site at position +58, downstream through the *Sau*3A site (position +183), to the *Eco*RI site in the vector (see Fig. 1). This fragment was mixed with total trypanosome bloodstream-form RNA (or sucrose-gradient fractions thereof), precipitated, redissolved, denatured and renatured in conditions favouring RNA/DNA hybridization[30]. This mixture was then cooled, diluted and digested with S_1 nuclease, before electrophoresis on a 7 M urea polyacrylamide gel. The resulting autoradiogram (Fig. 3*a*) shows a single major end point of protection by total RNA which corresponds to nucleotide +137 in the sequence presented in Fig. 2. Minor bands immediately flanking this protected region may be indicative of slight heterogeneity at the 3′ end of the RNA or nonspecific digestion by S_1 nuclease at the end of the RNA/DNA duplex.

This result could be interpreted as protection by a short RNA of 137 nucleotides derived from the mini-exon repeats and/or by a longer transcript with a discontinuity at this position in the RNA/DNA duplex. To discriminate between these two alternatives, two procedures were used. The first examined the S_1-protection by different size fractions of RNA produced by sucrose-gradient centrifugation (Fig. 3*b*). Maximal protection was found in fractions 19–21, which possessed RNA with a peak size slightly larger than 4S RNA (that is, ~100–200 nucleotides), with diminishing but detectable protection in the remaining fractions (Fig. 3*a*). This strongly suggested that the protection observed with total RNA was due, at least in part, to the presence of a small RNA. The protection observed with other fractions, particularly those containing larger RNA, may be due

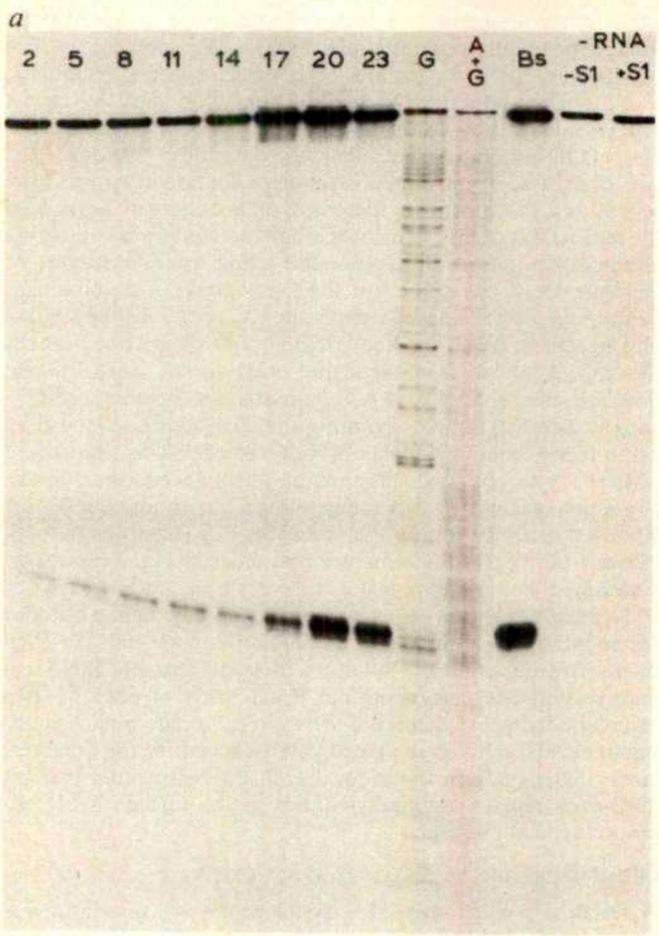

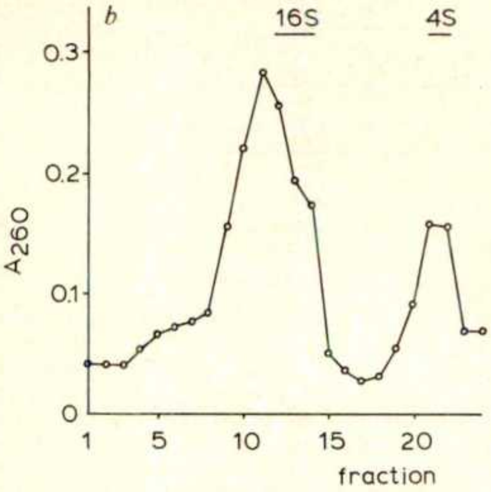

Fig. 3 *a*, S_1 nuclease mapping of the 3′-terminus of medRNA. Lanes 2–23 are reactions performed with RNA from pooled sucrose gradient fractions, as described in *b* below. Next to these are two marker sequencing reactions[43] on the labelled probe. The lane labelled Bs contains the result of a protection experiment with 50 μg of total RNA. The two controls, which contain no added RNA, are with (+S1) or without (−S1) S_1-nuclease, respectively. *b*, A_{260} profile of total trypanosome RNA fractionated by sucrose gradient centrifugation. The size markers are based on samples from each fraction analysed by electrophoresis and ethidium bromide staining (not shown).

Methods: *a*, A [3′-^{32}P]-end-labelled *Pvu*II digest of pMES.1 was re-cut with *Eco*RI to generate a uniquely end-labelled fragment corresponding to positions +59 to +183 plus 375 bp of the vector (see Fig. 1). S_1 protection was done essentially as described elsewhere[30]. Briefly, the probe was mixed with different fractions of bloodstream-form RNA, precipitated, redissolved and denatured in 80% formamide at 80 °C for 10 min. Renaturation of RNA/DNA hybrids was promoted by incubating at 45 °C for 3 h in the same buffer, before diluting with 10 vol of aqueous buffer, cooling to 30 °C and adding 35 units of S_1 nuclease. Digestion was for 30 min, after which the reactions were phenol-extracted, isopropanol-precipitated, resuspended in formamide loading buffer[43] and resolved by PAGE in a 6% polyacrylamide gel with 7 M urea[44]. *b*, A 15–30% linear sucrose gradient was prepared in 0.1 M NaCl, 1 mM EDTA, 20 mM Tris-HCl (*p*H 7.5), 0.1% SDS. About 1 mg of total trypanosome RNA was overlaid with the same buffer and the samples spun in an SW-41 rotor (Beckman) at 40,000 r.p.m. at 20 °C for 9.5 h. Fractions were collected from the bottom of the tube and the A_{260} measured. For the S_1-protection experiments, 5% of each sample was removed and pooled in groups of three (numbered by the middle fraction).

to contamination with the small RNA. Alternatively, they may be a result of protection by hybrid transcripts comprising the small RNA at their 5′ ends linked to RNA from, for example, the ELC region, by the mechanisms discussed below.

The second method to detect and size transcripts from the mini-exon repeat used Northern blot analysis[31]. For this procedure, total trypanosome RNA was resolved by polyacrylamide gel electrophoresis (PAGE) in denaturing conditions, transferred to GeneScreen membrane[32] and hybridized with a [5′-^{32}P]-labelled, synthetic oligonucleotide complementary to positions +117 to +133. This 17-mer was chosen because it excluded the mini-exon itself, which was known to give intense hybridization throughout RNA blots when used as a probe[21] and because the S_1-protection experiments indicated that it should hybridize to mini-exon-derived transcripts. Figure 4*a* shows the ethidium bromide stain of a polyacrylamide/7 M urea gel in which the major small RNA species is readily apparent. Figure 4*b* presents the autoradiogram produced after hybridizing a GeneScreen transfer of a duplicate half of this gel with the 17-mer; only one band is detected in the track containing trypanosome RNA and no signal is observed in the track containing RNA from the unrelated parasitic protozoan, *Toxoplasma gondii.* The size of the band is ~140 nucleotides based on published values for the small ribosomal RNAs of trypanosomes[33], thus confirming that the mini-exon repeats are transcribed to yield a short, discrete RNA which we have termed mini-exon-derived RNA (medRNA). With regard to its precise size, this result is, within experimental error, consistent with medRNA being 137 nucleotides long. We cannot, however, exclude the possibility that medRNA is as many as 4–5 nucleotides longer and that S_1 nuclease nonspecifically digested the 3′ end of the RNA/DNA hybrid. Note, however, that the nucleotides at positions 138 and 140 are cytosines which, as CG pairs, would be less susceptible to such action. A definite answer awaits 3′-sequence analysis of medRNA.

These results also suggest that the 5′-terminus of medRNA is at about position +1 in the mini-exon repeat. To confirm this, we used the synthetic oligonucleotide from the RNA blot analyses as a primer for reverse transcriptase extensions of medRNA. The result (Fig. 5) shows a major band co-migrating with a heterologous DNA marker of 135 nucleotides. Using a different heterologous marker (a *Hin*dIII digest of bacteriophage λ DNA), the size of this band was estimated as 133 nucleotides. This slight discrepancy is probably due to differences in base composition. Allowing for this variation, the extension has an approximate length of 134 ± 1 nucleotides. Given that the 5′-end of the primer represents position +133 of the mini-exon repeat, this result confirms that the 5′-end of medRNA corresponds to position +1, the same as that found for the spliced leader of mature VSG mRNAs[13,14]. The minor band in Fig. 5 at 138 ± 1 nucleotides may be an artefact of reverse transcriptase (for example, loop-back synthesis) or it may be indicative of a minor RNA 4 nucleotides longer than the major species. Such minor heterogeneity might be due to variation in the mini-exon repeat sequences and/or in the site of transcriptional initiation. No other major bands were observed in other loadings of this sample run for longer or shorter periods (data not shown).

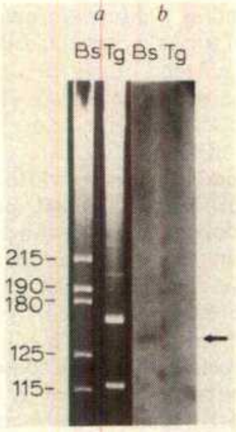

Fig. 4 Detection of the mini-exon-derived RNA. *a*, Ethidium bromide stain of electrophoretically separated trypanosome RNA. Lane Bs contains 10 μg of total RNA from bloodstream-forms of *T. brucei* (strain MITat 1.4). Lane Tg contains 10 μg of RNA from *T. gondii* as a negative control. The major bands in lane Bs are polysome-derived and their sizes in nucleotides are taken from ref. 33. The two major bands in the *T. gondii* RNA are presumably 5S and 5.8S. *b*, Autoradiograph of an RNA blot of the other half of the gel shown in *a*, containing identical samples, and having been probed with [5'-^{32}]-labelled 17-mer complementary to positions +117 to +133 of Fig. 2.

Methods: *a*, Total RNA was separated on an 8% polyacrylamide gel (1.5 mm thick) containing 7 M urea[44]. *b*, The electrophoresed RNA was electroblotted to GeneScreen membrane[32] at 4 V for 18 h at 4 °C in 25 mM Na phosphate (*p*H 6.5). The filter was prehybridized in 50% formamide, 5 × SSC (1 × SSC = 0.15 M NaCl, 0.015 M Na citrate), 1 × Denhardt's, 25 mM Na phosphate (*p*H 6.5), 0.1% SDS, 0.1% Na pyrophosphate, 100 μg ml^{-1} denatured calf thymus DNA at 30 °C for 2 h. A synthetic oligonucleotide complementary to positions +117 to +133 (see Fig. 2) was synthesized by standard means, [5'-^{32}P]-labelled by polynucleotide kinase, added to the prehybridization solution and the incubation continued with gentle shaking for 15 h at 30 °C, followed by 5 h at 22 °C. The filter was washed in four changes of 2 × SSC, 0.5% SDS for 15 min each at 22 °C. Autoradiography was at −70 °C with an intensifying screen for 6 days.

Conclusions

We have cloned and sequenced a complete copy of the 1.35-kb mini-exon repeat of *T. brucei* and identified a short RNA of 137 nucleotides as its transcriptional product. The data indicate that this repeat is a typical member of a highly conserved family—this is demonstrated further by the virtually complete agreement of the sequence presented in Fig. 2 with the partial sequence for the region from −130 to +61 recently published elsewhere[21]; the four differences (three single base changes, one insertion) are all localized to between −115 and −125. As the sequences in both cases were determined from two plasmids, the differences may be indicative of minor, but real, variation in the repeats.

In addition to the region coding for medRNA, each 1.35-kb mini-exon repeat contains about 1,200 nucleotides whose function is not clear; part of this region is presumably involved in the regulation of medRNA expression, but the remainder could be involved in some other aspect of trypanosome gene expression. Of particular note is the repetitive nature of the sequence around the *Sau*3A site, consisting of 1-, 2-, 4- and 6-nucleotide repeats (T, AT/AC, ATTT/GTTT and ACACTC, respectively). It will be interesting to determine whether these regions of the repeat are as exactly conserved as that coding for the medRNA.

The predicted sequence of medRNA can be drawn with several alternative regions of intramolecular base-pairing (data not shown). This suggests that medRNA might adopt a stable conformation with substantial secondary structure, but, as we have no data on RNase sensitivity, we cannot present a reliable structure.

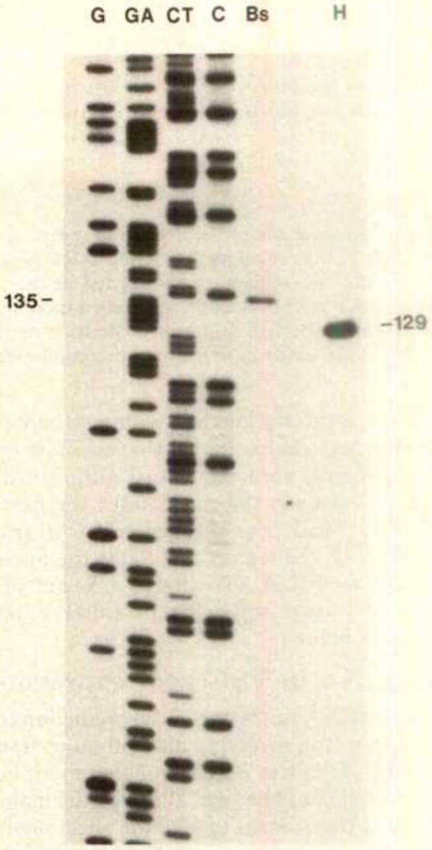

Fig. 5 Identification of the 5'-terminus of the medRNA. Polyacrylamide gel electrophoresis of the reverse transcriptase product primed off medRNA (lane Bs). Marker tracks contained standard sequencing reactions[43] of a mouse cDNA clone (provided by J. Kavaler; lanes G, A+G, C+T and T) or a [3'-^{32}P]-labelled *Hin*dIII digest of λ DNA (lane H).

Methods: The [5'-^{32}P]-labelled synthetic oligonucleotide described in Fig. 4 legend used as a primer in extension reactions using AMV everse transcriptase. About 4 μg of primer were hybridized to 20 μg of total bloodstream-form RNA in 1.2 M Na phosphate buffer (*p*H 6.8), 0.5% SDS, 12.5 mM EDTA at 21 °C for 4 h. After ethanol precipitation, the reverse transcriptase reaction was done in 50 mM Tris-HCl (*p*H 8.3), 6 mM $MgCl_2$, 1 mM dithiothreitol, 60 mM KCl, 0.1 mM dATP, dCTP, dTTP and dGTP, and AMV reverse transcriptase (50 units) at 37 °C for 1 h. The sample was ethanol-precipitated, resuspended in formamide loading dye and electrophoresed on a 7 M urea, 8% polyacrylamide gel. The dried gel was autoradiographed at −70 °C for 72 h.

The detection of medRNA raises questions about the signals directing its transcription. As noted by De Lange *et al.*[21], the octanucleotide centred at position −27 upstream of the putative initiation site for transcription consists of TATTTTTG, similar to the consensus sequence generally found at this position in eukaryotic RNA polymerase II promoters (the so-called TATA box; see ref. 34). Assuming trypanosomes are usual in their types and functions of RNA polymerase and given that the medRNA ultimately forms the 5'-end of the VSG mRNA, the finding of a putative TATA box at this position is expected. Further studies on relative drug sensitivities and 5'-cap structures are needed to confirm medRNA as an RNA polymerase II transcript. The termination site cannot be compared with the general case as too few sequences of eukaryotic transcriptional terminators have been reported to enable consensus sequences to be made.

Recently, the complete sequence of a small nuclear RNA (snR3) and its gene have been reported in yeast[32,35]. This transcription unit shows remarkable similarity to the mini-exon repeat at four critical positions (Fig. 6), the remainder of the two sequences sharing no significant homologies. First, the snR3 gene also has the octanucleotide TATTTTTG centred at position −27 relative to the start site for transcription. Second, the

```
               ?
              TATA      START     SPLICE   END
              -27         +1      +36      +137
mini-exon ...TATTTTTG...AACTAAC...GTATGA...ACTCTTTTTATTTTTTTTTATTTTTTTTCATTTATTTATTTTTT
snR3      ...TATTTTTG...AAGTAAC...GTACGA...TTTTTTTTCTTTTTTTTTTTTTAGTTATGTTTTATTTTTGAACT
              -27         +1      +38        +194
              TATA      START     SPLICE     END
               ?                    ?
```

Fig. 6 Nucleotide sequence of the mini-exon repeat of *T. brucei* compared with that of the small nuclear RNA (snR3) gene of yeast (from ref. 32). The two sequences are aligned at the indicated positions with position +1 in both cases corresponding to the 5′-terminus of their respective transcripts. Question marks designate functions which have not yet been confirmed.

initiation site for transcription lies within a heptanucleotide sequence which is very similar in the two genes (six out of seven bases identical). Third, both sequences, although of different overall length (137 versus 194 nucleotides for medRNA and snR3, respectively), end near the beginning of an extremely T-rich region. Finally, the region containing the putative donor splice site of the medRNA also shares a 5- out of 6-residue homology with the yeast snR3, the potential significance of which is discussed below.

Role of medRNA in VSG gene expression

The finding of medRNA fulfils one of the predictions of a model for VSG gene expression involving discontinuous transcription. However, it is not definitive because of the multiplicity of the mini-exon repeats: it could be that, although the majority of the repeats are indeed transcribed to give the short medRNA, one repeat is used in the initiation of a very long transcript including the VSG coding exon. This is a difficult possibility to exclude because pulse-chase experiments, which have been traditionally used to demonstrate precursor/product relationships, suffer from the same shortcoming—it is impossible to demonstrate that a given mini-exon repeat is used for one purpose compared with another, indistinguishable repeat. Nevertheless, together with published observations regarding the abundance of transcripts containing mini-exon-derived sequences and the inability to detect linkage between a mini-exon sequence and the VSG coding exon, the identification of a short, discrete medRNA strongly supports a model of discontinuous transcription. In this model, the mini-exon-derived leader segment of VSG mRNAs is transcribed as a discrete product of the mini-exon repeats and, by one of several possible mechanisms, is ultimately found attached to the 5′-end of the VSG precursor RNA. The chimaeric intervening sequence is then removed by splicing, bringing together the 35-nucleotide leader with the coding portion to give the final mRNA of ~1.7 kb.

There are two general schemes by which this can most easily be imagined to occur. The first model, presented in Fig. 7*a*, predicts that RNA polymerase transcribes the medRNA and then dissociates from the mini-exon repeat, possibly as a medRNA/polymerase complex; transcription then reinitiates just upstream of the ELC using medRNA as a primer. The second model (Fig. 7*b*) proposed that medRNA and the coding-region RNA are independently produced as discrete transcripts and then post-transcriptionally ligated to each other. In both cases, splicing ultimately removes the intervening sequence to generate the mature mRNA.

The critical difference between the two alternatives is that post-transcriptional ligation requires a functional promoter (in the sense of a site for *de novo* initiation of transcription) upstream of the ELC whereas the reinitiation model proposes a site in this same position where RNA polymerase could only act in the presence of a primer (that is, medRNA). We are now attempting to test for this distinction *in vitro*.

We have previously reported the sequence upstream of an expressed copy of a VSG gene and compared it with a silent copy of that gene[19]. We found that the upstream region of the expressed copy consisted of multiple tandem repeats of ~76 bp flanking an unusual sequence of $(TAA)_{90}$. Although three 76-bp repeats are found upstream of the silent copy, $(TAA)_{90}$ is unique to the expressed copy of this gene and is, therefore, a candidate for the (re)initiation site upstream of expressed VSG genes. If this sequence is unique and mobile, it could be the basis for the mutual exclusion observed between the different expression sites. Equally, another, as yet undetected, mobile control element might have this role.

A critical question raised by the results reported here is whether discontinuous transcription involving a small RNA is a unique property of *T. brucei*. Is it, for example, a special adaptation which has co-evolved with antigenic variation? This is argued against by the finding that the same or similar mini-exon sequences are found in many RNAs (of unknown coding function), not only from bloodstream-forms of the parasite, but also from the procyclic insect forms where VSG genes are not

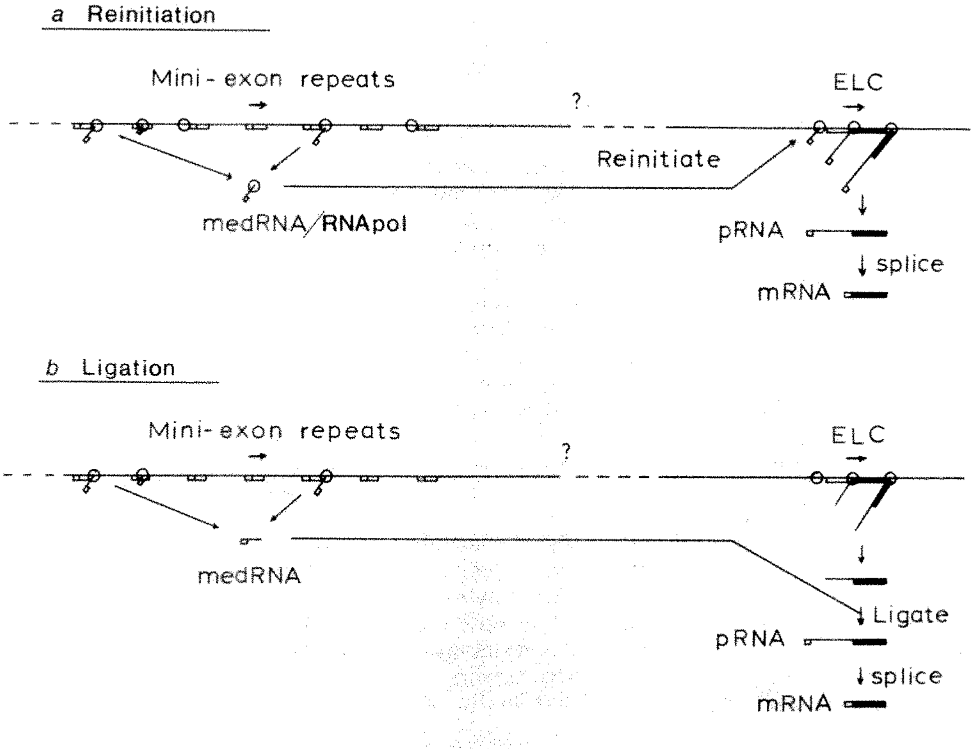

Fig. 7 Two models for discontinuous transcription of VSG mRNAs. *a*, The reinitiation model; *b*, the ligation model. The figure illustrates schematically the important features of the two models which are described in the text. The region of the mini-exon repeat which codes for the medRNA is represented by an open segmented box, the left half indicating the mini-exon coding for the 35-nucleotide spliced leader. The ELC region is also represented as a segmented box with the protein-coding exon shaded. The exon-derived portions of the precursor RNA (pRNA) are boxed in the same way. Uncertainty about whether the mini-exon repeats are linked to the ELC and if so over what distance, is indicated by a question mark over the dashed region. RNA polymerase is represented by an open circle.

expressed (ref. 21 and M. Parsons *et al.*, personal communication). In addition, the mini-exon sequence (or a conserved homologue) has been shown to be present in the genomes of several related species and genera which lack antigenic variation of the type observed for *T. brucei*[22].

Could discontinuous transcription be operating in these other cases? This question cannot, as yet, be answered, but some precedent does exist in systems which are otherwise totally unrelated. Transcription of the influenza virus is known to require a 5′-capped primer (10–15 nucleotides long) derived from cleavage of host mRNAs[36,37]. Coronavirus transcripts, on the other hand, are known to have a common 5′-leader sequence which is seemingly not joined to the coding portion of the RNA by conventional splicing, again strongly suggesting discontinuous transcription[38,39]. The fact that, in both these cases, transcription occurs by an RNA-dependent viral transcriptase may be an important distinction but they do provide a mechanistic precedent for discontinuity in primary transcripts. The observation made in Fig. 6 that a snRNA of yeast has substantial homology with the region known to be a donor splice site in medRNA, suggests that this snRNA (of unknown function) might be similarly involved in discontinuous transcription, albeit on a lesser scale (snR3 is nonessential; ref. 32). Such activity could further provide a molecular basis for the long-standing observation that heterogeneous nuclear RNAs often possess sequences at their 5′-ends which are derived from middle repetitive DNA[40–42] and that such sequences might be important in the control of developmentally regulated gene expression. The testing of this interesting hypothesis in trypanosomes may now be possible.

We thank Mr M. van Bree for technical assistance; Drs N. Agabian, P. Borst, G. Cross, J. Donelson, M. Lai, K. Stuart and their colleagues for exchange of information before publication; Dr M. Fedor for producing the synthetic oligonucleotide; and Ms M. A. Siri for secretarial help. This work was supported in part by a grant from the American Cancer Society (ACS IN 32).

Received 22 March; accepted 22 June 1984.

1. Cross, G. A. M., Holder, A. A., Allen, G. A. & Boothroyd, J. C. *Am. J. trop. Med. Hyg.* **29**(5) Suppl., 393–417 (1980).
2. Englund, P. T., Hajduk, S. L. & Narini, J. C. *A. Rev. Biochem.* **51**, 695–726 (1982).
3. Borst, P. & Cross, G. A. M. *Cell* **29**, 291–303 (1982).
4. Pays, E., Lheureux, M. & Steinert, M. *Nature* **292**, 265–267 (1981).
5. Hoeijmakers, J. H. J., Borst, P., Van den Burg, J., Weissmann, C. & Cross, G. A. M. *Gene* **8**, 391–417 (1980).
6. Van der Ploeg, L. H. T. *et al. Nucleic Acids Res.* **10**, 593–609 (1982).
7. Capbern, A., Giroud, C., Baltz, T. & Mattern, P. *Expl Parasit.* **42**, 6–13 (1977).
8. Cross, G. A. M. *Parasitology* **71**, 393–417 (1975).
9. Hoeijmakers, J. H. J., Frasch, A. C. C., Bernards, A., Borst, P. & Cross, G. A. M. *Nature* **284**, 78–80 (1980).
10. Pays, E., Van Meirvenne, N., Le Ray, D. & Steinert, M. *Proc. natn. Acad. Sci. U.S.A.* **78**, 2673–2677 (1981).
11. Williams, R. O., Marcu, K. B. & Majiwa, P. A. O. *Nature* **282**, 847–849 (1979).
12. Van der Ploeg, L. H. T. *et al. Nucleic Acids Res.* **10**, 3591–3604 (1982).
13. Boothroyd, J. C. & Cross, G. A. M. *Gene* **20**, 281–289 (1982).
14. Longacre, S. *et al. Molec. cell. Biochem.* **3**, 399–409 (1983).
15. Bernards, A. *et al. Cell* **27**, 497–505 (1981).
16. Van der Ploeg, L. H. T., Bernards, A., Rijsewijk, F. A. M. & Borst, P. *Nucleic Acids Res.* **10**, 593–609 (1982).
17. Michiels, F. *et al. EMBO J.* **2**, 1185–1192 (1983).
18. Liu, A. Y. C., van der Ploeg, L. H. T., Rijsewijk, F. A. M. & Borst, P. *J. molec. Biol.* **167**, 57–75 (1983).
19. Campbell, D. A., van Bree, M. & Boothroyd, J. C. *Nucleic Acids Res.* **12**, 2759–2774 (1984).
20. Nelson, R. G. *et al. Cell* **34**, 901–909 (1983).
21. De Lange, T. *et al. Cell* **34**, 891–900 (1983).
22. Nelson, R. G. *et al. Nature* **308**, 665–667 (1984).
23. Borst, P. *et al. Eur. J. Biochem.* **137**, 383–389 (1983).
24. McDonell, M. W., Simon, M. N. & Studier, F. W. *J. molec. Biol.* **110**, 119–146 (1977).
25. Bolivar, F. *et al. Gene* **2**, 95–113 (1977).
26. Rigby, P. W. J., Diekmann, M., Rhodes, C. & Berg, P. *J. molec. Biol.* **113**, 237–251 (1977).
27. Grunstein, M. & Hogness, D. S. *Proc. natn. Acad. Sci. U.S.A.* **72**, 3961–3965 (1975).
28. Twigg, A. J. & Sherratt, D. *Nature* **283**, 216–218 (1980).
29. Berk, A. J. & Sharp, P. A. *Cell* **12**, 721–732 (1977).
30. Maniatis, T., Fritsch, E. F. & Sambrook, J. *Molecular Cloning. A Laboratory Manual* (Cold Spring Harbor Laboratory, New York, 1982).
31. Thomas, P. S. *Proc. natn. Acad. Sci. U.S.A.* **77**, 5201–5205 (1980).
32. Tollervey, D., Wise, J. A. & Guthrie, C. *Cell* **35**, 753–762 (1983).
33. Cordingley, J. S. & Turner, M. J. *Molec. biochem. Parasit.* **1**, 91–96 (1980).
34. Breathnach, R. & Chambon, P. *A. Rev. Biochem.* **50**, 349–383 (1981).
35. Wise, J. A. *et al. Cell* **35**, 743–751 (1983).
36. Plotch, S. H., Bouloy, M., Ulmanen, I. & Krug, R. M. *Cell* **23**, 847–858 (1981).
37. Lamb, R. A. & Choppin, P. W. *A. Rev. Biochem.* **52**, 467–506 (1983).
38. Siddell, S., Wege, H. & ter Meulen, V. *J. gen. Virol.* **64**, 761–776 (1983).
39. Baric, R. S., Stohlman, S. A. & Lai, M. M. C. *J. Virol.* **48**, 633–640 (1983).
40. Firtel, R. A. & Lodish, H. F. *J. molec. Biol.* **79**, 295–314 (1973).
41. Zuker, C. & Lodish, H. F. *Proc. natn. Acad. Sci. U.S.A.* **78**, 5386–5390 (1981).
42. Davidson, E. H. & Posakony, J. W. *Nature* **297**, 633–635 (1982).
43. Maxam, A. M. & Gilbert, W. *Meth. Enzym.* **65**, 499–560 (1980).
44. Sanger, F. & Coulson, A. R. *FEBS Lett.* **87**, 107–110 (1978).

LETTERS TO NATURE

On the origin of Triton and Pluto

William B. McKinnon

Department of Earth and Planetary Sciences, and McDonnell
Center for the Space Sciences, Washington University, Saint Louis,
Missouri 63130, USA

Lyttleton hypothesized long ago that Triton and Pluto originated as adjacent prograde satellites of Neptune[1]. With the presently accepted masses of Triton and Pluto–Charon[2,3], however, the momentum and energy exchange that would be required to set Triton on a retrograde trajectory is impossible. The mass of Triton has probably been seriously overestimated[4,5], but not by enough to relax this restriction. It is implausible that the present angular momentum state of Pluto–Charon has been significantly influenced by Neptune[6]. It could not acquire such angular momentum during an ejection event unless a physical collision was involved, which is quite unlikely. The simplest hypothesis is that Triton and Pluto are independent representatives of large outer Solar System planetesimals. Triton is simply captured, with potentially spectacular consequences that include runaway melting of interior ices and release to the surface of clathrated CH_4, CO and N_2 (ref. 7). Condensed remnants of this proto-atmosphere could account for features in Triton's unique spectrum[8–11].

The dynamics of Triton's orbital evolution are considerably simplified by the fact that its specific dissipation function, Q, at tidal frequencies, is much less than that of Neptune ($Q_T \ll Q_N$). Here I assume a standard solid-body Q for Triton of ~100 (ref. 12). A lower bound on Q_N can be derived by requiring that the outward orbital evolution of a satellite given by

$$\frac{\mathrm{d}a_s}{\mathrm{d}t} = 3k_{2N}\sqrt{\frac{G}{m_N}}\frac{R_s^5 m_s}{Q_N a_s^{11/2}} \tag{1}$$

is not so rapid that the satellite originated at the corotation radius of Neptune 4,500 Myr ago[12] (where m_s and a_s are the satellite's mass and semimajor axis; m_N, R_N and k_{2N} are Neptune's mass, radius, and tidal-effective potential Love number of the second degree; and G is the gravitational constant). k_{2N} is estimated at 0.43, subject to uncertainties in Neptune's rotation rate and J_2 (the coefficient of the second harmonic of the gravitational potential) (see ref. 13); other parameter values are given in Table 1. If Neptune's third satellite[14] is confirmed and proves to be regular and non-commensurate, then $Q_N \gtrsim 10^4$. A lower bound on the Q of Uranus of $\sim 2\times 10^4$ is set using Miranda[15] and a k_2 for Uranus of 0.28. The Qs of both planets should be comparable, and are probably much larger.

Accordingly, the monthly radial tide raised on Triton by Neptune dominates Triton's orbital evolution, except for orbits of very small eccentricity. This tide does not transfer angular momentum for a synchronously-rotating Triton, but in the cases of interest here, such non-synchronous spin angular momentum would be negligible compared with orbital angular momentum. The present fractional rate of change in Triton's orbital angular momentum, due to the tide raised on Neptune by Triton, is

$(\mathrm{d}a_T/\mathrm{d}t)2a_T$, where a_T is Triton's semimajor axis. Using equation (1), the total change over the age of the Solar System is a few per cent for $Q_N \sim 10^5$. Changes in inclination are similarly small.

Lyttleton's hypothesis is evaluated as follows: Triton and Pluto originate as regular direct satellites of Neptune, in circular orbits; orbital evolution brings them into a range of significant gravitational interaction, say, within the sphere of influence of the more massive satellite (the radius of which is given by $s \simeq a_>(m_>/m_N)^{2/5}$ (ref. 16), where $a_>$ and $m_>$ are the semimajor axis and mass of the more massive satellite), and Triton is sent into a retrograde orbit, potentially elliptical, with the same angular momentum as it has today. Conservation of angular momentum requires that the angular momentum of Pluto, l_P, increases to

$$l_P = (Gm_N)^{1/2}\{(\alpha m_T\sqrt{a_T} + m_T\sqrt{a} + m_P\sqrt{a})^2 + \beta^2 m_T^2 a_T\}^{1/2} \quad (2)$$

where m_T and m_P are the masses of Triton and Pluto–Charon, α and β are cos(21.5) and sin(21.5)—accounting for Triton's inclination of 158.5° (ref. 17), and a is the semimajor axis of the interaction. Pluto's post-encounter orbital energy is minimized for velocities perpendicular to its radius vector. The semimajor axis (elliptic or hyperbolic) of the new orbit, with respect to Neptune, is then:

$$a_P = |(l_P^2/Gm_N m_P^2 a) - 2|^{-1} a \quad (3)$$

If $l_P > (2Gm_N a)^{1/2} m_P$, the orbit will be hyperbolic. This is guaranteed for $m_T > (\sqrt{2} - 1)m_P$.

The relationship (3) is illustrated in Fig. 1 for a range of plausible mass ratios m_T/m_P. All the a_P shown correspond to hyperbolic trajectories. Orbits with $a_P < 1.62\ R_N$, however, are so energetic that once Pluto leaves Neptune's sphere of influence, it is not bound to the Solar System. Only for $a_P >$ 54.9 R_N is Pluto definitely bound. The accepted mass of Triton, $1.32\ 0.23 \times 10^{26}$ g, is due to Alden[2]. The combined mass of Pluto and Charon is known more precisely (±5%) (ref. 3) and suggests $m_T/m_P \sim 10$. In this case, momentum conservation alone determines that a Lyttleton-type interaction is not possible, unless the interaction takes place well outside the domain of regular satellites. This domain, $a \leq 60\ R_N$, is defined in analogy with the regular satellite systems of Jupiter, Saturn and Uranus. The outermost regular satellite in each system, Callisto, Iapetus and Oberon, orbits at 27, 59 and 23 units of its respective planetary radius.

Recent radiometric measurements[4,18,19] call Triton's mass estimate into question. Lebofsky's 2σ detection, in particular, yields a radius of 1,750±250 km (ref. 19). In lieu of accepting Triton as a heavy metal satellite, I assume a density appropriate to an ice–rock body of this size (~1.6 cm^{-3}) (ref. 20)—implying that $m_T/m_P \sim 3$. This lower mass ratio, however, does not make Lyttleton's hypothesis more physically acceptable. Note that neither the effect of a non-unity emissivity nor a surrounding atmosphere has been included in the radiometric modelling, and these would have competing effects on the derived radius. A better determination of Triton's mass is needed.

These arguments can be generalized to allow multiple encounters if the conservation of energy is accounted for. The encounters are assumed to be conservative, with the only restriction on Triton's final energy, $-Gm_N m_T/2\tilde{a}_T$, where $\tilde{a}_T$ is Triton's final semimajor axis, being that it exceed Triton's present value. The horizontal curves in Fig. 2 are Pluto's final semilatus rectum, $p_P = l_P^2/Gm_N m_P^2 = a_P|1 - e_P^2|$, where e_P is uto's final eccentricity, for various m_T/m_P. The vertical curves are Pluto's final semimajor axis, given by

$$a_P = a\left\{\frac{m_T}{m_P}\left(\frac{a}{\tilde{a}_T} - 1\right) - 1\right\}^{-1} \quad (4)$$

for $m_T/m_P = 10$ and two representative values of $\tilde{a}_T$. Ascending asymptotes (with increasing a) correspond to bound orbits. For ellipses, however, $p < a$, so only those $a_P \geq p_P$ correspond to possible orbits. In addition, the pericentre distance, $p_P/(1 + e_P)$, has a minimum of $p_P/2$ for $e_P = 1$, and Triton's apocentre distance has a maximum of $\sim 2\tilde{a}_T$. Thus even for $m_T/m_P = 1$, no bound orbits are possible because the final orbits of Triton and Pluto must be ~intersecting ones. A descending branch of a_P, for a given $\tilde{a}_T$, is the locus of unbound states (with respect to Neptune). The top part of the descending branch ($a_P \geq p_P$) corresponds to eccentricities of between $\sqrt{2}$ and 1; hence these orbits are also non-intersecting and are ruled out. The bottom of the descending branch corresponds to hyperbolic orbits with $e_P > \sqrt{2}$; hence, for large enough e_P, a pericentre distance small enough to allow intersecting orbits may appear feasible. The situation is very restricted, however, as a_P has a horizontal asymptote at $\tilde{a}_T m_P/m_T$. This limits e_P to $\{p_P/a_P + 1\}^{1/2}$. Pluto's final pericentre distance remains $> 2\tilde{a}_T$ for $m_T/m_P \geq 1$, regardless of the choice of $\tilde{a}_T$ or initial a. Thus, for plausible mass ratios, and under the stipulated initial conditions, a combination of orbital interactions to reverse Triton's motion cannot be found.

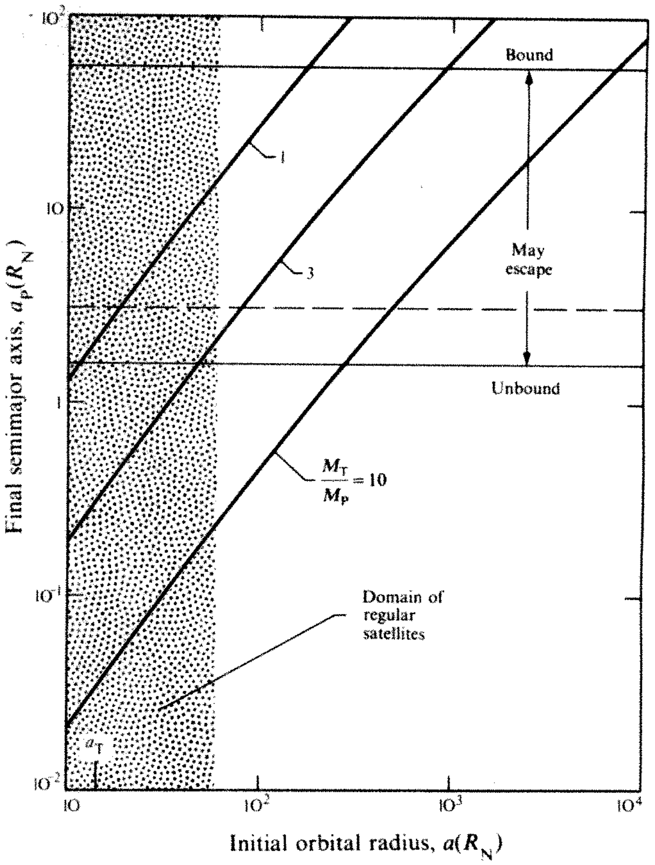

Fig. 1 Hyperbolic semimajor axis of Pluto, with respect to Neptune and after an interaction with Triton, as a function of initial orbital radius for three different mass ratios. These results, derived from angular momentum conservation alone, represent maximum values. Asymptotic velocities from Neptune of 2.25 and 13.1 km s^{-1} ($a_P = 54.9$ and 1.62 R_N) correspond to limits on bound or unbound solar trajectories, if Neptune's orbital velocity is taken into account. The dashed horizontal line is the minimum a_P for ejection into a direct, bound solar orbit. For plausible mass ratios, any interaction to reverse Triton's orbital motion and retain Pluto in the Solar System must take place well outside the domain of regular satellites (see text).

This conclusion, more severe than that due to momentum conservation alone, is not changed by considering tidal interaction with Neptune during the encounters. In addition, allowing the initial conditions to be set when the difference between the semimajor axes of the two 'satellites' closes to within the radius of either the sphere of influence, s, or an even wider sphere of perturbation, can bring Triton and Pluto's final orbits closer together (if Triton is the innermost of the pair), but not

Table 1 Parameter values

Object	Quantity	Value	Reference
Neptune	m_N	1.03×10^{26} kg	36
	R_N	24.75×10^3 km; 1 bar, equatorial	37
	J_2	4.3×10^{-3}	17
	Rotation period	~15 h; dynamical	38
Uranus	Mass	8.67×10^{25} kg	36
	Radius	25.5×10^3 km; 1 bar, equatorial	39, 40
	J_2	3.35×10^{-3}	40
	Rotation period	15.5 h; dynamical	40
Triton	a_T	354.3×10^3 km	17
Pluto	R_P	~1,500 km	41
	Q_P	~100	Assumed
	k_{2P}	$\sim 2.7 \times 10^{-2}$	Based on unity cgs density and water-ice rigidity

sufficiently to have them interacting for $m_T/m_P \geq 1$. Of course, for $m_T \ll m_P$, Triton can be sent retrograde, but Pluto will remain direct.

The present angular momentum state of the Pluto–Charon system (that is, that contained in their mutual orbits and spins) is not consistent with a Neptune satellite origin either. If Pluto–Charon ever orbited Neptune with a semimajor axis a, tides raised on Pluto by Neptune would extract angular momentum from the system at a rate

$$\frac{\mathrm{d}H}{\mathrm{d}t} = \frac{3}{2} \frac{G k_{2P} m_N^2 R_P^2}{a^6 Q_P} \tag{5}$$

where H is the angular momentum, and R_P, Q_P and k_{2P} are, respectively, Pluto's radius, specific dissipation function and potential Love number (see Table 1). The present angular momentum of Pluto–Charon is uncertain due to the difficulty in estimating Charon's mass, but probably lies between 2.4 and 6.6×10^{37} g cm^2 s^{-1}. Extraction of angular momentum would cause the Pluto–Charon system to contract and eventually coalesce. The coalesced object would then be spun down to synchronous rotation[6]. The time scale for 'fusion' and spin-down is

$$\tau = H \bigg/ \left(\frac{\mathrm{d}H}{\mathrm{d}t}\right) \sim 1 \times 10^5 \left(\frac{a}{a_T}\right)^6 \text{ yr} \tag{6}$$

Thus collapse of the Pluto–Charon system and spin-down would occur rapidly unless Pluto–Charon orbited Neptune at a great distance ($\tau \gtrsim 100$ Myr for $a > 45 R_N$). These same arguments apply if the original state of Pluto–Charon was a coalesced, rapidly-rotating proto-Pluto (the angular momentum limits above correspond to primordial rotation periods between ~7 and 11 h; see refs 21, 22).

Only a physical collision could impart the requisite angular momentum to Pluto–Charon prior to its ejection from the Neptune system. A close pass to Pluto by a more massive object could exert an extremely large torque on Pluto but the time scale for the interaction would be severely limited. A grazing pass by an object with even the mass of the Earth would be restricted to last a few 10^3 s, and the angular momentum imparted, according to equation (5), would be only a few per cent of the present total. A larger transfer of angular momentum may be possible for the slowest encounters with a massive grazer, if tidally-induced fission[23] occurs, but the restriction of slow encounters again requires Pluto to initially be in a distant orbit about Neptune.

With regard to ejection dynamics, the reduction of the interaction cross-section from a gravitational one to approximately one of collision makes 'rogue' planet hypotheses such as that of Harrington and Van Flandern[24] probabilistically untenable. Farinella *et al.* call on a captured Triton to eject Pluto as its capture orbit decays[25], but this hypothesis still requires a physical collision with Pluto, following which, gravitationally-bound plutonian debris accretes into a binary and eventually reaches stable, resonant[26] solar orbit; the last requires an additional mechanism. This is an unlikely series of events.

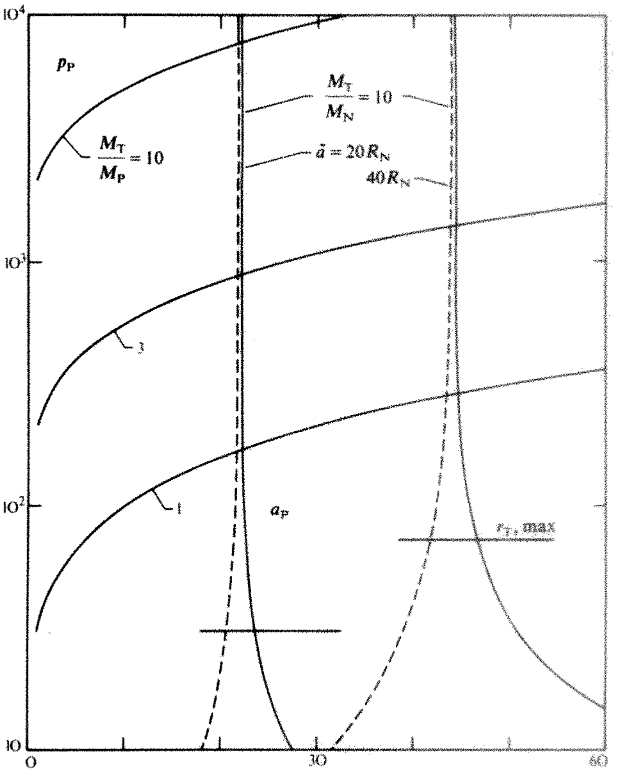

Fig. 2 Semilatus rectum and semimajor axis of Pluto, with respect to Neptune and after interactions with Triton, as a function of initial orbital radius for various mass ratios and final Triton semimajor axes. Only the solid part of the asymptotes represent possible orbits, but none have pericentre distances that approach Triton's final apocentre distance (short horizontal lines). Hence, for mass ratios greater than one, a series of interactions that reverses Triton's orbital motion and that conserve angular momentum and orbital energy cannot be found.

The preceding arguments effectively decouple the origin of Pluto from that of any Neptune satellite. Hence, for Triton to begin as a direct satellite and end up retrograde would require interaction with an unknown and *ad hoc* object. I propose a simple reversal of Lyttleton's hypothesis: instead of beginning as satellites of Neptune, Triton and Pluto originate as satellites of the Sun. The existence of large, outer Solar System planetesimals is consistent with the dynamics of planetary accretion and may even be necessary to explain planetary eccentricities, inclinations, and obliquities (see ref. 27). Pluto–Charon's binary status could be related to hypotheses regarding binary asteroid formation,[21,28–30] and Triton's capture could be effected by the combination of a retrograde, temporary orbit about Neptune[31] and a dissipative mechanism such as gas drag[32,33].

If Triton had been captured, then it should have experienced a spectacular thermal event. As $Q_N \gg Q_T$, nearly all of the orbital energy dissipated during post-capture orbital evolution is deposited in the body of Triton. Gas drag, while potentially important for capture, did not result in a major change in orbital elements, as the evolution of Triton's inclination has been moderate[32]. Calculations[7] show that collapse of an elliptical post-capture orbit, extending to the edge of Neptune's sphere of influence (~3,500 R_N), to one where the semimajor axis is within a few per cent of the present value, requires ~4 Q_T Myr, for a constant Q_T. Most of the energy (~80%), however, is dissipated in an ~1.5 Q_T Myr period near the end. The equivalent surface heat flow, for reasonable Q_T, is far too great for solid-state convection in ice to transport, so it is extremely probable that the icy component of Triton completely melted during the latter phase of capture. Q_T itself would plummet as melting began, accelerating differentiation.

Catastrophic melting of Triton's ices should have released its inventory of clathrated gases to the surface, which for accretion outside a circumplanetary nebula would be CH_4, CO, and N_2 (refs 34, 35). A condensed fraction of this primordial atmosphere may be responsible for Triton's unique surface composition—present spectral identifications include liquid nitrogen[11] and methane ice[9-11].

This work was supported by NASA grant NAGW-432.

Received 27 April; accepted 24 July 1984.

1. Lyttleton, R. A. *Mon. Not. R. astr. Soc.* **97,** 108–115 (1936).
2. Alden, H. L. *Astr. J.* **50,** 110–111 (1943).
3. Harrington, R. S. & Christy, J. W. *Astr. J.* **86,** 442–443 (1981).
4. Cruikshank, D. P., Stockton, A., Dyck, H. M., Becklin, E. E. & Macy, W. Jr *Icarus* **40,** 104–114 (1979).
5. McKinnon, W. B. *Bull. Am. astr. Soc.* **14,** 765 (1982).
6. Lin, D. N. C. *Mon. Not. R. astr. Soc.* **197,** 1081–1085 (1981).
7. McKinnon, W. B. *Bull. Am. astr. Soc.* **15,** 857 (1983).
8. Cruikshank, D. P. & Silvaggio, P. M. *Astrophys. J.* **223,** 1016–1020 (1979).
9. Rieke, G. H., Lebofsky, L. A., Lebofsky, M. J. & Montgomery, E. F. *Nature* **294,** 59–60 (1981).
10. Apt, J., Carleton, N. P. & Mackay, C. D. *Astrophys. J.* **270,** 342–350 (1983).
11. Cruikshank, D. P., Brown, R. H. & Clark, R. N. *Abstr. Natural Satellites, IAU Colloq.* No. 77, 40 (1983).
12. Goldreich, P. & Soter, S. *Icarus* **5,** 375–389 (1966).
13. Munk, W. H. & MacDonald, G. J. F. *The Rotation of the Earth* Ch. 5 (Cambridge University Press, 1975).
14. Reitsma, H. J., Hubbard, W. B., Lebofsky, L. A. & Tholen, D. J. *Science* **215,** 289–291 (1982).
15. Veillet, Ch. thesis, Univ. Paris (1983).
16. Tisserand, F. *Traité de Mécanique Céleste* Vol. 4, Ch. 12 (Gauthier-Villars, Paris, 1896).
17. Harris, A. W. *Abstr. Natural Satellites, IAU Colloq.* **77,** 41 (1983).
18. Morrison, D., Cruikshank, D. P. & Brown, R. H. *Nature* **300,** 425–427 (1982).
19. Lebofsky, L. A., Rieke, G. H., & Lebofsky, M. J. *Bull. Am. astr. Soc.* **14,** 766 (1982).
20. Lupo, M. J. & Lewis, J. S. *Icarus* **40,** 157–170 (1979).
21. Weidenschilling, S. J. *Icarus* **64,** 124–126 (1981).
22. Chandrasekhar, S. *Ellipsoidal Figures of Equilibrium* Chs 5, 6 (Yale University Press, New Haven, 1969).
23. Aggarwal, H. R. & Oberbeck, V. R. *Astrophys. J.* **191,** 577–588 (1974).
24. Harrington, R. S. & Van Flandern, T. C. *Icarus* **39,** 131–136 (1979).
25. Farinella, P., Milani, A., Nobili, A. M. & Valsecchi, G. B. *Moon Planets* **20,** 415–421 (1979); *Icarus* **44,** 810–812 (1980).
26. Nacozy, P. E. & Diehl, R. E. *Astr. J.* **83,** 522–530 (1978).
27. Harris, A. W. & Ward, W. R. *A. Rev. Earth planet. Sci.* **10,** 61–108 (1982).
28. Weidenschilling, S. J. *Icarus* **44,** 807–809 (1980).
29. Farinella, P., Paolicchi, P. & Zappala, V. *Astr. Astrophys.* **104,** 159–165 (1981).
30. Harris, A. W. *Bull. Am. astr. Soc.* **15,** 828 (1983).
31. Huang, T.-Y. & Innanen, K. A. *Astr. J.* **88,** 1537–1547 (1983).
32. Pollack, J. B., Burns, J. A. & Tauber, M. E. *Icarus* **37,** 587–611 (1979).
33. Nakazawa, K., Komuro, T. & Hayashi, C. *Moon Planets* **28,** 311–327 (1983).
34. Lewis, J. S. & Prinn, R. G. *Astrophys. J.* **238,** 357–364 (1980).
35. Prinn, R. G. & Fegley, B. *Astrophys. J.* **249,** 308–317 (1981).
36. *Abstr. Natural Satellites, IAU Colloq.* **77,** 43 (1983).
37. Freeman, K. C. & Lyngå, G. *Astrophys. J.* **160,** 767–780 (1970).
38. Hubbard, W. B. *et al. Astr. J.* (submitted).
39. Elliot, J. L., Dunham, E., Mink, D. J. & Churms, J. *Astrophys. J.* **236,** 1026–1030 (1980).
40. Elliot, J. L. *et al. Astr. J.* **86,** 444–455 (1981).
41. Hege, E. K. *et al. Icarus* **50,** 72–81 (1982).

X-ray haloes around supernova remnants

G. E. Morfill*, L. O'C Drury† & B. Aschenbach*

* Max-Planck-Institut für Physik und Astrophysik, Institut für extraterrestrische Physik, 8046 Garching, FRG
† Max-Planck-Institut für Kernphysik, 6900 Heidelberg, FRG

Recent observations of the Cas-A supernova remnant have shown X-ray emissions not only from the interior, but also from a fainter 'halo' extending beyond what is normally regarded as the outer boundary, or shock front[1]. We suggest here that this may be due to the diffusion of energetic, charged particles out of the remnant giving rise to precursor structure of the type predicted by the theory of diffusive shock acceleration. If this is the case we are seeing thermal emission from ambient gas heated by compression and wave dissipation.

The radio synchrotron emission from supernova remnants is clear evidence that they contain relativistic electrons; it is widely believed that they are also the major source for the galactic cosmic-ray nucleon component, but so far there has been no direct observational evidence for this. Cosmic-ray nuclei have an energy density which exceeds that of the electrons by about two orders of magnitude; for supernova remnants to be responsible for their origin, this implies that a substantial part of the remnant energy must reside in energetic charged particles[2]. This raises the question of how these particles are accelerated. Interstellar plasmas are typically so tenuous that cosmic rays are scattered only by the irregular structure of the magnetic field. Because the field lines are effectively frozen into the background plasma these irregularities can move relative to the bulk fluid at maximum speeds of the order of the magnetosonic speed. As Fermi[3] recognized, this is a rather unusual physical system in that macroscopic degrees of freedom, the magnetic fluctuations and their associated plasma, couple to a few individual particles. If the fluctuations are excited randomly this leads to a diffusion of the particles in momentum space which is the standard second-order Fermi acceleration mechanism. This is normally slow; however, at a shock front where the bulk plasma together with its embedded magnetic structures is suddenly decelerated (in the shock frame) the scatterers, instead of moving randomly, converge, giving rise to a much faster first-order acceleration[4-8]. Perhaps the major attraction of this process, usually called diffusive shock acceleration[9-11], is that an elementary analysis in which the reaction of the particles is neglected, predicts that the accelerated particles should have power-law spectra in momentum with exponents close to those inferred for the sources of the galactic cosmic rays.

It is, however, clear that the reaction of the particles on the scattering irregularities, and through these on the bulk plasma flow, cannot be ignored if the energy density of the particles is significant, as is thought to be the case in supernova remnants[5,12]. The particles diffuse ahead of the shock into the upstream region and produce an adverse pressure gradient which decelerates the flow into the shock. This gradient also works on the scatterers at the rate $-v \cdot \mathrm{grad}\, P_c$, where v is the velocity of the scatterers and P_c is the energetic particle pressure; clearly, and as one would intuitively expect, those fluctuation modes which move upstream relative to the plasma are amplified and those which move downstream are damped. The energy transferred to the amplified modes can be estimated to be of the order of the Alfvén Mach number of the shock times the background magnetic field energy[9,13]. For strong astrophysical shocks, Alfvén Mach numbers of 20 or greater are expected. Thus in the absence of any dissipation, or radical change in the nature of the modes, the energy content of the fluctuations would become many times that of the background field; it seems doubtful that so much energy could be stored without various instabilities setting in which transfer excess energy to the plasma and keep the fluctuation amplitude of the order of unity.

Although the details of this process are very complicated, its main features have been described by a simple model[13-15] in which only the energy and momentum fluxes associated with the thermal particles (treated as an ideal non-relativistic gas), the energetic particles (treated as an ideal relativistic gas) and the magnetic fluctuations (taken to be damped backwards-travelling Alfvén waves) are considered, while the shock structure is taken to be plane and steady.

We have calculated the shock structure and the Bremsstrahlung emissivity predicted by this model. Figure 1 shows an example of a shock with Alfvénic Mach number 20 and equal thermal particle, energetic particle and magnetic pressures far upstream. This high Mach number should be characteristic of young supernova remnant shocks. As can be seen, the shock

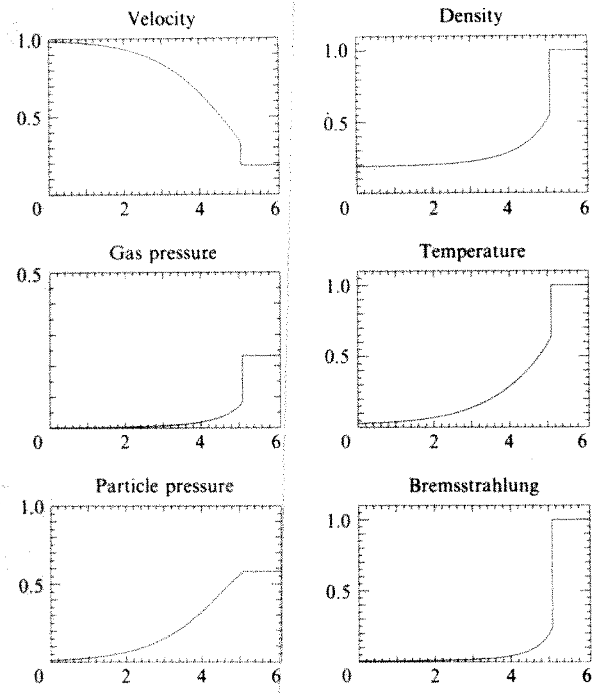

Fig. 1 Effects of cosmic rays on parallel magneto-hydrodynamic shocks. The values of the gas-velocity, gas-pressure and cosmic-ray pressure are normalized such that the total mass and momentum fluxes are unity. All pressures are equal far upstream, and the Alfvén Mach number is 20. The values of the gas-density, gas-temperature and, as a Bremsstrahlung-emissivity measure, $(\text{density})^2 \times \sqrt{\text{temperature}}$ are normalized to the post-shock region. The horizontal axis gives the length scale in units of diffusion coefficient/shock velocity.

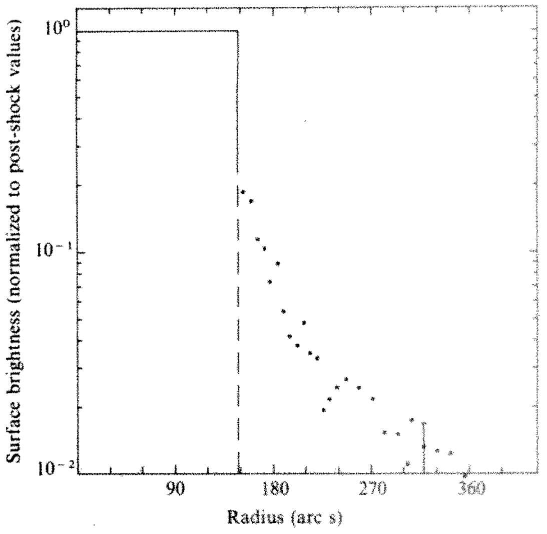

Fig. 2 Surface brightness of the Cas-A 'halo' plotted as a function of distance from the shock. The 'halo' emission is the excess derived by Stewart *et al.*[1]; the data have been normalized to the remnant brightness of the outer ring, and the detailed internal structure of the remnant has not been considered.

acceleration of cosmic rays (predominantly nuclei) is rather important. The cosmic-ray pressure, in the steady model, is about twice the thermal gas pressure and about twice the kinetic energy density. Also, the gas density and velocity profiles are modified ahead of the shock, and the gas is pre-heated by the Alfvén wave decay and the compression in front of the shock. The 'precursor' length scale is rather uncertain because it depends on the (poorly known) diffusion coefficient κ of the particles; however, if they are accelerated at the shock then $\kappa \lesssim R\dot{R}$, where R is the shock radius. The 'precursor' length scale is then less than, or comparable to, the shock radius. The point of interest is that wave dissipation and compression together heat the gas in the precursor to temperatures which are not much lower than those behind the shock.

This implies that the processes described above give rise to extended thermal X-ray (Bremsstrahlung and line) and possibly coronal line (for example, [Fe XIV] 5,303 Å and [Fe X] 6,374 Å) emission outside the shock radius of a young supernova remnant. From an observational point of view this extended halo might be difficult to detect because of its low surface brightness (see Fig. 1). Only Cas-A is definitely known to possess an extended halo, from the Einstein Observatory measurements. Several physical processes for this phenomenon have been discussed, such as, electron 'leakage' ahead of the shock, shock heating by ejecta fragments and scattering by interstellar dust[1]. We present here an alternative interpretation, which could be checked, for instance, by a search for haloes around point sources, and other supernova remnants.

Figure 2 shows the radial variation of the X-ray excess surface brightness outside the shock, in the case of Cas-A. The excess emission outside the shock was normalized to the emission just behind the shock, which, ignoring the complicated internal remnant structure, is simply represented as a constant level. A halo length scale of ~50 arc s is indicated, roughly one-third of the remnant radius. This is in agreement with the upper bound determined from the theory, and, therefore, we tentatively suggest that the faint 'haloes' may be produced by the processes described above. This being the case, we are seeing evidence for a dynamic role of cosmic rays in the interstellar medium, and for the acceleration of nuclei in supernova remnants. A comparison with radio observations of the synchrotron emission may then allow a determination of the relative intensities of the nucleonic and electronic components. If confirmed by further observations, this will have important consequences for the evolution of supernova remnants[16] and the structure of the interstellar medium. Although the model calculations shown in Fig. 1 are based on diffusive shock acceleration at the outer boundary of the remnant, a similar situation will be produced by an efficient acceleration mechanism inside the remnant, provided that the accelerated particles diffuse out (ref. 1 and H. J. Völk, personal communication). In the case of Cas-A, diffusive acceleration at the outer shock seems to work well; however, in view of the complicated and violent internal structure and abnormally high radio luminosity of Cas-A this may not be the only source of cosmic-ray acceleration. To test our interpretation of the X-ray data, and the implied consequences for the interstellar medium, observations in other spectral regions and very deep X-ray exposures are needed.

Received 27 February; accepted 23 July 1984.

1. Stewart, G. C. *et al. Supernova Remnants and their X-ray Emission, IAU Symp. No. 101*, 59 (1983).
2. Ginzburg, V. L. *Phil. Trans. R. Soc.* **A277**, 463, (1974).
3. Fermi, E. *Phys. Rev.* **75**, 1169 (1949).
4. Krimsky, G. F. *Dokl. Akad. Nauk SSSR* **234**, 1306 (1977).
5. Axford, W. I. *et al. Proc. 15th int. Cosmic Ray Conf.*, Plovdiv, **11**, 132 (1977).
6. Bell, A. R. *Mon. Not. R. astr. Soc.* **182**, 147 (1978a).
7. Bell, A. R. *Mon. Not. R. astr. Soc.* **182**, 443 (1978b).
8. Blandford, R. D. & Ostriker, J. P. *Astrophys. J. Lett.* **221**, L29, (1978).
9. Blandford, R. D. *La Jolla. AIP Conf. Proc.* **56**, 335 (1979).
10. Axford, W. I. *Ann. N.Y. Acad. Sci.* **375**, 297 (1981).
11. Drury, L.O'C. *Rep. Prog. Phys.* **46**, 973 (1983).
12. Drury, L.O'C. & Völk, H. J. *Astrophys. J.* **248**, 344 (1981).
13. McKenzie, J. F. & Völk, H. J. *Astr. Astrophys.* **116**, 191 (1982).
14. Völk, H. J. *et al. Astr. Astrophys.* **130**, 19 (1984).
15. Völk, H. J. & McKenzie, J. F. *Proc. 17th Int. Cosmic Ray Conf.*, Paris **9**, 246 (1981).
16. Chevalier, R. *Astrophys. J.* **272**, 765 (1983).

Spectral feature of 31 December 1981 γ-ray burst not confirmed

P. L. Nolan*‡, G. H. Share*, E. L. Chupp†, D. J. Forrest† & S. M. Matz†

* E. O. Hulburt Center for Space Research, Naval Research Laboratory, Washington DC 20375, USA
† Department of Physics, University of New Hampshire, Durham, New Hampshire 03824, USA

The emission lines reported at 400–500 keV in the spectra of γ-ray bursts[1] have been interpreted as redshifted positron annihilation lines, and, together with the lower-energy cyclotron lines[1], are the most direct evidence that bursts occur on the surface of neutron stars[2]. Therefore, it is important to confirm the existence and determine the properties of these features. So far, the most significant detections of emission features have been reported from the Konus experiments on Veneras 11–14. Possible confirmatory observations have suffered from limited statistical significance or difficulties in interpretation. Here we compare measurements of a γ-ray burst at 01:37 UT on 31 December 1981, using the Solar Maximum Mission (SMM) γ-ray spectrometer with those made by the Konus instruments. The SMM spectra exhibit no evidence for the presence of emission features reported by the Konus group[3].

Annihilation lines have been reported in ~5% of the bursts observed by the Konus instruments from 1978 to 1982[1,3]. The typical emission features observed by Konus are centred at 400–450 keV and have widths of ~200 keV (FWHM). The strong feature in the 5 March 1979 burst[2] fits this description; however, that event is so unusual that we are reluctant to include it in the same class as other bursts[4]. There are two other Konus line detections for which simultaneous observations were made with other spectrometers. These bursts occurred on 4 and 19 November 1978. The 4 November line had a width ~200 keV, which is typical of the Konus detections, while the 19 November feature was very broad. Barat[5] confirms the presence of both of these lines. Teegarden and Cline[6] also reported a narrow line at ~420 keV in the spectrum of the 19 November burst, using data from the ISEE 3 germanium spectrometer, but the statistical significance was marginal at best. They found no evidence for a line in the 4 November burst. Fenimore *et al.*[7] analysed the 4 November burst using the scintillation spectrometer on ISEE 3; they found that the apparent strength of the ~400-keV line was strongly dependent on the choice of continuum model, and could be consistent with zero. They also found no evidence for a line in the 19 November burst.

The present observation was made using the Gamma-Ray Spectrometer[8] (GRS) on the SMM spacecraft. The GRS main detector consists of seven NaI scintillators viewing about half of the sky, centred on the Sun. It covers the energy range 0.3–9 MeV with a resolution of 7% FWHM at 0.662 MeV. The gains of the seven crystals are continuously stabilized by ^{60}Co calibration sources. For a burst in the centre of the field-of-view, the effective area is 4–6 times larger than that provided by the Konus system at 0.5 MeV. The time resolution for spectroscopy is 16.384 s. We analyse spectra using a detector response function based on calibrations made before and during flight and on a Monte Carlo computer simulation. The line profiles predicted by this response function have been verified in flight by observation of lines from solar flares and the Earth's atmosphere, including the annihilation line at 0.511 MeV (refs 9, 10).

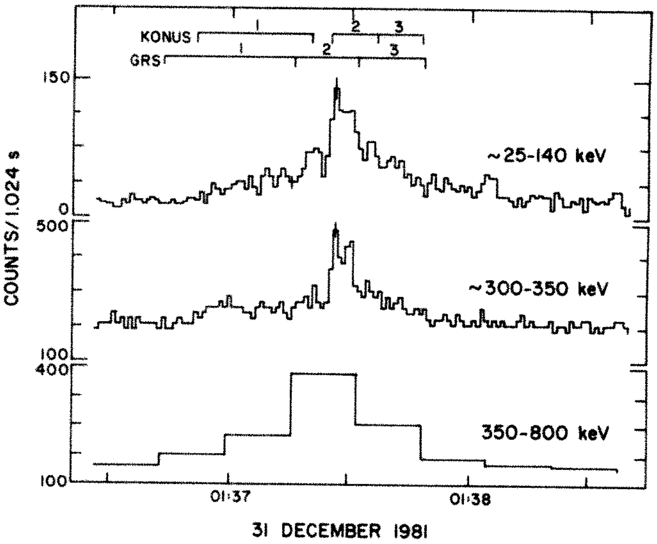

Fig. 1 Time profile of the burst in three GRS energy bands. The top shows the time intervals for which spectra are available from the GRS and Konus instruments.

Figure 1 shows the time profile of the burst, as observed by the GRS auxiliary X-ray detector and main detector. The time resolution for spectroscopic observations is illustrated by the 0.35–0.8 MeV profile. This was an unusually long burst (about 2 min) with several brief subbursts. The time delay between the GRS and Konus detections (about 53 s) was determined by matching the most prominent of these peaks. The report of the Konus observations[3] includes spectra of three time intervals; these are shown at the top of Fig. 1. Broad emission features extending to high energy were reported for intervals 2 and 3. Also shown are the corresponding intervals for which GRS spectra are available. Because the Konus intervals are long (12 s), a direct comparison is possible.

Based on preliminary data from other satellites and from analysis of the response of the GRS shield detectors, we estimate that the position of the burst is ~50° from the GRS viewing direction. This is well within the GRS field of view. As compared with the on-axis response function, the effective detector area at 50° is reduced by about 15% and a small energy-dependent correction is required because of partial screening by the shield and other parts of the instrument. The effect of this correction is to increase the inferred flux near 500 keV by ~5% with respect to higher and lower energies. Thus, applying this correction will enhance any emission features which may be present. The correctness of this procedure will be demonstrated below by the good agreement of the GRS and Konus results in interval 1.

The Konus and GRS spectra for the three intervals are plotted in Fig. 2. The GRS energy channels have been combined to match the Konus channels. For illustrative purposes, the normalizations of the Konus spectra have been adjusted to compensate for the slightly different accumulation intervals of the two instruments. To accomplish this, we compared the average counting rates in the GRS and Konus time intervals, using the 40–140 keV band of the GRS X-ray detectors (1.024 s time resolution). This adjustment is not used in the quantitative analysis described below. The agreement in absolute flux for the two instruments is good to about 30% in the overlapping energy range (0.3 to ~1 MeV). Of course, these power-law functions could not be extended to lower energy; the gradual curvature of the spectra below ~200 keV is evident in Fig. 2.

A single smooth function could fit the spectra from both instruments in interval 1, with a small shift in relative normalization. However, there is no evidence in the GRS spectra for the features which are found in the Konus spectra in intervals 2 and 3. Power-law spectra will fit the GRS data acceptably over the entire 0.3–0.9 MeV range in all three intervals. Of course, these power-law functions could not be extended to lower energy; the gradual curvature of the spectra below 200 keV is evident in Fig. 2.

---

‡ Present address: W. W. Hansen Laboratories, Stanford University, Stanford, California 94305, USA.

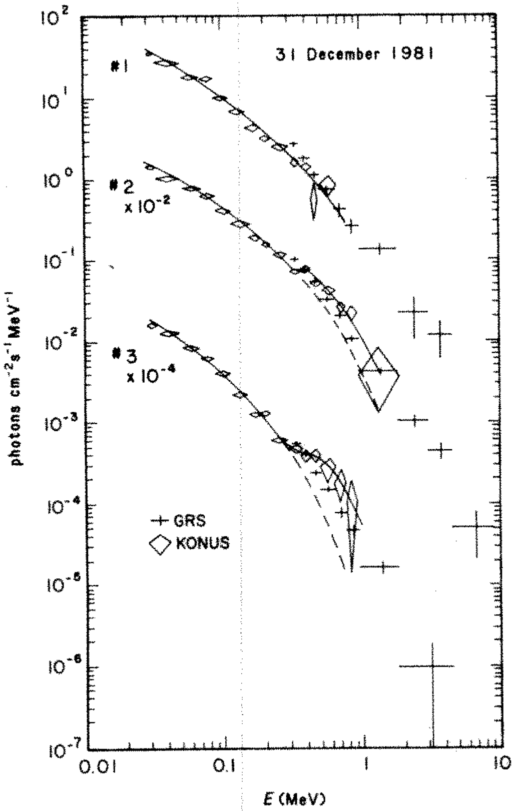

Fig. 2 Photon spectra for the three time intervals from Konus and GRS. The curves represent the models fit to the Konus data by Mazets *et al.*[3]. Solid line, thermal bremsstrahlung + emission feature; dashed line, high-energy extension of bremsstrahlung.

To make direct comparisons between the GRS data and the Konus model spectra, we multiplied the Konus models by the GRS detector response matrix and compared the results with the raw GRS data. We allowed the intensity of the model spectrum to be a free parameter (to account for possible errors in absolute calibration of the instruments), and adjusted it for the best agreement. The comparison was made only in the energy ranges for which both Konus and GRS data are available. In interval 1, the agreement was good: $\chi^2 = 4.3$ for 3 d.f. The best χ^2 values obtained for the other two intervals are unacceptable: 138 for 6 d.f. in interval 2, and 137 for 5 d.f. in interval 3. In both cases the model has a flattening in the 0.3–0.5 MeV range, which is not compatible with the GRS data. Figure 3 illustrates the results for interval 3. It shows, in terms of uncorrected detector counts, the GRS data and the Konus model (adjusted in intensity for the best agreement). The value of the upper limit that we can establish on the flux in a broad line depends on the continuum model chosen. Conservatively, our 99% confidence upper limit is 0.5 photons cm^{-2} s^{-1}, about one-quarter of our estimate of the strength of the Konus feature.

We repeated this analysis, omitting the lowest-energy GRS channel group (~300–350 keV). As we have no energy calibration below a 389 keV background line, it is possible that the assumed width of the lowest channel group could be in error. The agreement in interval 1 continued to be good. Even though the lowest channel group contained the greatest number of counts, the best χ^2 values in the other two intervals remained unacceptable: 44.5 for 5 d.f. in interval 2 and 59.4 for 4 d.f. in interval 3.

The intervals of the two instruments are not identical. However, it is unlikely that a rapid change in the spectrum could have produced the difference in the results. The last two Konus intervals are entirely contained within the combined GRS intervals 2 and 3. The remaining portion of GRS interval 2 is a time of lower burst flux, so its contribution is relatively small. The difference in the results from the two instruments is not subtle.

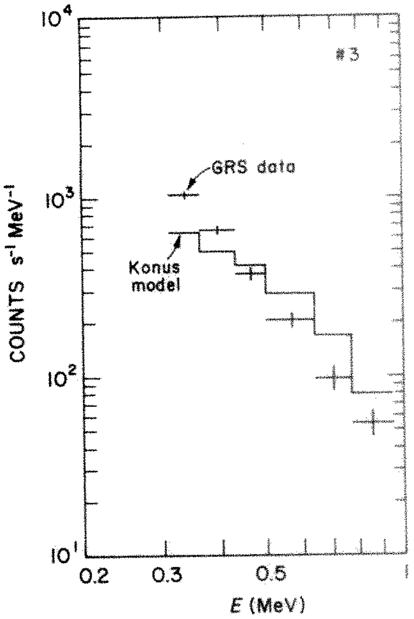

Fig. 3 GRS detector energy loss spectrum of the third interval. The histogram is the Konus model, multiplied by the GRS response matrix, with normalization adjusted for best fit.

There is a flattening of the spectrum in Konus intervals 2 and 3 which is not present in either of the corresponding GRS spectra. In the 0.3–0.5 MeV range, the GRS spectra are fit by power laws with indices of -2.00 ± 0.15 and -2.47 ± 0.23. The two Konus spectra are much flatter, with indices of > -1.2 in this energy range.

It is not certain that we can reconcile the results from the two experiments. As shown above, the continuum shapes are similar, but there are differences in narrow energy bands. We believe that they may be attributed to different data analysis procedures. The Konus data are presented only in the form of 'photon' spectral plots, corrected for the effects of the detector response. The process of producing such graphs is model-dependent, and in many cases, the plotted points tend to move to agree with the model[7]. We do not know to what degree the Konus spectra are prone to such 'compliance', which is due to non-diagonal components in the detector response matrix. The GRS should be less subject to compliance, because the detector is larger and has CsI anticoincidence shields to suppress the detection of Compton-scattered photons. (For example, the derived photon fluxes at 0.3 and 1 MeV vary by only about 20% for a range of input model spectra from $E^{-1.1}$ to E^{-4}.) If this effect is not enough to explain the differences, the only other explanation is a very unlikely fluctuation of the spectrum at just the right time. The best understanding of the nature of a spectrum can be obtained from statistical measures of its agreement with various models. However, the statistical significances of the reported features in the Konus data unfortunately are not given.

We have previously reported a weak (0.4 photon cm^{-2}, 2.5 σ detection) and relatively narrow feature near 475 keV in the first half of GRS interval 1, which contains about 5 s of the burst[11]. But this is not a significant detection, and it is much weaker than the features reported by Konus later in the burst. Indeed, it is about a factor of 4 weaker than the weakest lines detected by Konus in other bursts. Thus this possible feature can have little to do with the features discussed here. We know of only one other burst observed by GRS (28 March 1982) for which Konus spectra have been published. No annihilation lines were found in either the GRS or Konus spectra in that burst.

The GRS observations are inconsistent with the presence of the reported emission features in the burst of 31 December 1981. Because the existence of features such as these is one of the principal pieces of evidence that bursts occur on neutron stars, it is important to assess the significance of all the reported Konus line features.

We thank E. P. Mazets for discussions concerning the Konus observations. Our colleagues Erich Rieger and James Kurfess provided valuable assistance. P.L.N. was supported by a fellowship from the National Research Council. This work was supported by NASA contracts S-70926A at NRL and NAS S-23761 at UNH and by BFFT contract 010K 017-ZA/WS/WRK 0.275.4 at MPI.

Received 5 April; accepted 19 July 1984.

1. Mazets, E. P., Golenetskii, S. V., Aptekar, R. L., Guryan, Yu. A. & Il'inskii, V. N. *Nature* **290**, 378–382 (1981).
2. Mazets, E. P., Golenetskii, S. V., Il'inskii, V. N., Aptekar, R. L. & Guryan, Yu. A. *Nature* **282**, 587–589 (1979).
3. Mazets, E. P. *et al. Positron–Electron Pairs in Astrophysics* (eds Burns, M. L., Harding, A. K. & Ramaty, R.) 36–53 (AIP, New York, 1983).
4. Cline, T. L. *et al. Astrophys. J. Lett.* **237**, L1–L5 (1980).
5. Barat, C. *Positron–Electron Pairs in Astrophysics.* (eds Burns, M. L., Harding, A. K. & Ramaty, R.) 54–58 (AIP, New York, 1983).
6. Teegarden, B. J. & Cline, T. L. *Astrophys. J. Lett.* **236**, L67–L70 (1980).
7. Fenimore, E. E., Klebesadel, R. W., Laros, J. G., Stockdale, R. E. & Kane, S. R. *Nature* **297**, 665–667 (1982).
8. Forrest, D. J. *et al. Sol. Phys.* **65**, 15–23 (1980).
9. Forrest, D. J. *Positron–Electron Pairs in Astrophysics* (eds Burns, M. L., Harding, A. K. & Ramaty, R.) 3–14 (AIP, New York, 1983).
10. Share, G. H. *et al.* in *Positron–Electron Pairs in Astrophysics* (eds Burns, M. L., Harding, A. K. & Ramaty, R.) 15–20 (AIP, New York, 1983).
11. Nolan, P. L. *et al. Positron–Electron Pairs in Astrophysics* (eds Burns, M. L., Harding, A. K. & Ramaty, R.) 59–63 (AIP, New York, 1983).

Limiting battery performance parameters for polyacetylene

James C. W. Chien & Joseph B. Schlenoff

Department of Chemistry, Department of Polymer Science and Engineering, Materials Research Laboratory, University of Massachusetts, Amherst, Massachusetts 01003, USA

The discovery that polyacetylene, $[CH]_x$ could be reversibly electrochemically oxidized or reduced ('doped')[1] has led to its usage as an electrode in light-weight rechargeable storage batteries[2,3]. Using a 100-μm thick electrode comprised of 20–30 nm diameter fibrils[4], performance characteristics slightly superior to those of the lead-acid battery have been achieved. Our cyclic voltammetry study utilizing ultrathin (<0.1 μm) films of $[CH]_x$ comprised of 2–3 nm microfibrils shows significantly improved electrode properties. A current density of 2.4 MA kg^{-1}, power density of 8 MW kg^{-1}, average potential of 3.5 V, maximum energy density of 250 W h kg^{-1} and coulombic efficiency >95% have been obtained with a Li/salt/$[CH]_x$ system. The potential of polyacetylene electrodes for light-weight rechargeable batteries is, therefore, several orders of magnitude higher than presently recognized.

Since the minimum detectable amount of $[CH]_x$ using cyclic voltammetry is ~100 pg, the 20–500 ng of $[CH]_x$ deposited on electron microscopy (EM) grids give excellent signal-to-noise ratios, and quantitative calculations involving doping level (y in mol/mol CH), energy density, efficiency, power density, and current density are possible. These thin films have proved to be ideal for carrying out rapid, numerous electrochemical experiments. The time taken for complete charging and discharging has been accelerated by more than three orders of magnitude. Morphological changes resulting from electrochemical treatment may then be examined directly by electron microscopy and electron diffraction. Because very low currents are involved in our battery experiments, resistive losses in the electrolyte and through the polymer film are negligible, allowing the examination of the limiting charging and discharging characteristics of $[CH]_x$ itself.

The method used to polymerize acetylene directly onto EM grids using a Ziegler–Natta catalyst has been described elsewhere[5–7]. A film of ~0.1 μm thickness was obtained, composed of a network of loosely-packed $[CH]_x$ fibrils of 2–3 nm diameter. Platinum wire contact was made to an EM grid and the grid immersed in 2 ml of 1 M $LiClO_4$ in dry propylene carbonate, 0.35 M $LiBF_4$ in propylene carbonate, or 0.5 M $LiClO_4$ in sulpholane in a dry box. Potential and current was controlled with a Princeton Applied Research (PAR) 173 potentiostat, and charge was recorded with a PAR 179 digital coulometer. Potential ramps for cyclic voltammetry were generated using a PAR 175 programmer and fast discharging transients were recorded on a Tektronix 564B storage oscilloscope.

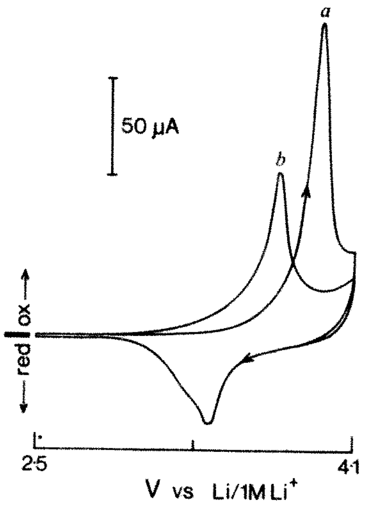

Fig. 1 Cyclic voltammetry of 300 ng $[CH]_x$ on an EM grid in 1 M $LiClO_4$ in propylene carbonate at a 50 mV s^{-1} scan rate: *a*, first scan; *b*, second and subsequent scans.

Cyclic voltammetry of *cis*-rich $[CH]_x$ on EM grids (Fig. 1) gives clear evidence of electrochemical isomerization to the *trans* polymer, a phenomenon that has been inferred from IR studies on electrochemically-doped $[CH]_x$ (ref. 8). The first scan (curve *a*) gives an oxidation peak at 3.96 ± 0.05 V versus $Li^0/1$ M Li^+. The second and all subsequent scans (curve *b*) give a reproducible peak at 3.74 ± 0.03 V. The fact that complete *cis–trans* isomerization occurs on one electrochemical cycle is confirmed by electron diffraction.

Extending the potential range of cyclic voltammetry shows a second, larger peak (Fig. 2*c*). This oxidation is not reversible and, in fact, extended oxidation of $[CH]_x$ leads to the degradation of the electronic properties of doped polyacetylene[9]. Experiments we have done on thicker, previously weighed films show that the stoichiometry of exhaustively oxidized polyacetylene is $[(CH(ClO_4)_{0.5}]_x$. Thus, we are provided with a direct electrochemical way of determining the total quantity of $[CH]_x$ on an EM grid.

The real potential of $[CH]_x$ as a battery material lies in very high power density and current density applications. Figure 3 shows the excellent discharge characteristic of $[CH(ClO_4)_{0.06}]_x$ film on an EM grid, discharged at an average power density of 8 MW kg^{-1} and a current density of 2.4 MA kg^{-1}. These values were obtained at a constant current of 1.0 mA. In the case of the standard thick $[CH]_x$, average power densities of up to 600 W kg^{-1} and current densities of ~20–200 A kg^{-1} have been reported. This large difference in battery performance parameter is due to the resistive potential losses in film and electrolyte, and limited access of counter ion to $[CH]_x$ fibrils. Also, the cyclic volatmmetric scan rates of 2 mV s^{-1} to 200 mV s^{-1} which correspond to charging times of 850 and 8.5 s, respectively, represent an increase of over 1,000-fold in charging rate over that used for thick films[2,3]. Even at these high charging rates, the $[CH]_x$ is doped to saturation, indicating that solid-state diffusion of counter ions into $[CH]_x$ microfibrils is not a limitation[10].

Although a maximum reversible dopant level of 6% was achieved by oxidation of the ~20 nm fibrils found in thick films[2,3], it was generally hoped that by varying the morphology of the polymer or the composition of the electrolyte, higher oxidation levels, and hence energy densities, could be obtained[3].

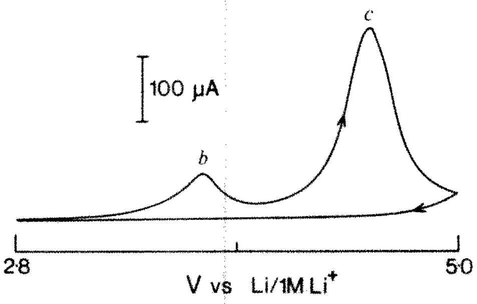

Fig. 2 The exhaustive oxidation of $[CH]_x$ on an EM grid at 50 mV s^{-1} scan rate.

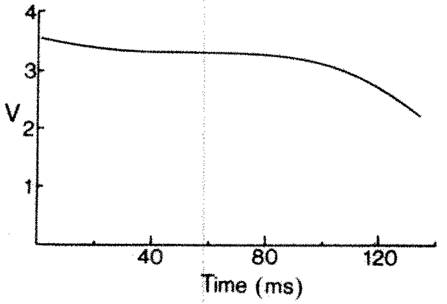

Fig. 3 Fast discharge of a $[CH(ClO_4)_{0.06}]_x$ sample on an EM grid at 2.4×10^6 A kg^{-1}.

For example, if the maximum dopant level were a surface-area related phenomenon, thinner $[CH]_x$ fibrils should lead to a higher energy density. We have found that the maximum reversible oxidation level for the ~3 nm fibril of $[CH]_x$ on EM grids is 6 ± 1% which is relatively insensitive to the counter ion. The average discharge voltage compared with $Li^0/1$ M Li^+ is 3.4 V giving an energy density of 280 Wh kg^{-1} which falls in the range of 176–340 Wh kg^{-1} found for thick films[3,11].

Cycling between 2.5 and 4.2 V, the potential at which $[CH]_x$ starts to degrade, gives coulombic efficiencies in excess of 95% when corrected for background (bare EM grid). This is compared with the 80–90% efficiency for the thick $[CH]_x$ electrodes. Note that the discharge of polyacetylene cannot be represented as the charging of a capacitor[12], as the constant current discharge characteristics of a capacitor would be linear and one would expect the energy density ('capacitance') to be proportional to the surface area of the $[CH]_x$ for ultrathin and thick $[CH]_x$ films.

This study establishes some of the limiting battery performance parameters for $[CH]_x$. Taking average current and power densities obtained with thick $[CH]_x$ films, one can seriously underestimate the true potential of $[CH]_x$. Realization of even fractional gains in these expected current and power densities could improve the technology of light-weight rechargeable batteries.

This work was supported by grants from NSF and ONR.

Received 29 May; accepted 20 July 1984.

1. Nigrey, P. J., MacDiarmid, A. G. & Heeger, A. J. *JCS Chem. Commun.* 594–595 (1979).
2. Kaneto, K., Maxfield, M., Nairns, D. P., MacDiarmid, A. G. & Heeger, A. J. *JCS Faraday. Trans.* **78**, 3417–3429 (1982).
3. Farrington, G. C., Scrosati, B., Frydrych, D. & DeNuzzio, J. *J. electrochem. Soc.* **131**, 7–12 (1984).
4. Ito, I., Shirakawa, H. & Ikeda, S. *J. polym. Sci. Polym. Chem.* **12**, 11–20 (1974).
5. Karasz, F. E. *et al. Nature* **282**, 286–288 (1979).
6. Shimamura, K., Karasz, F. E., Hirsch, J. A. & Chien, J. C. W. *Makromolec. Chem. Rapid Commun.* **2**, 473–480 (1981).
7. Chien, J. C. W., Karasz, F. E. & Shimamura, K. *Macromolecules* **15**, 1012–1017 (1982).
8. Feldblum, A., Heeger, A. J., Chung, T-C. & MacDiarmid, A. G. *J. chem. Phys.* **77**, 5114–5121 (1982).
9. Ahlgren, G., Krische, B., Prón, A. & Zagorska, M. *J. polym. Sci. Polym. Lett.* **22**, 173–183 (1984).
10. Feldblum, A. *et al. Phys. Rev. B* **26**, 815–826 (1982).
11. Nigrey, P. J., MacInnes, D. Jr, Nairns, D. P., MacDiarmid, A. G. & Heeger, A. J. *J. electrochem. Soc.* **128**, 1651–1654 (1981).
12. Schuldiner, S. *J. electrochem. Soc.* **129**, 1270–1271 (1982).

Thermoluminescence as a palaeothermometer

R. K. Guimon, K. S. Weeks, B. D. Keck
& D. W. G. Sears

Department of Chemistry, University of Arkansas, Fayetteville,
Arkansas 72701, USA

Chondritic meteorites are widely regarded as a unique source of information on the chemical and physical processes that occurred in the early Solar System. An important phase in their history is a period of metamorphism[1] and thermoluminescence (TL) has proved a powerful technique for exploring this aspect, especially at the low end of the metamorphic spectrum[2]. The ordinary chondrites as a whole display a 10^5-fold range in TL sensitivity, while the least metamorphosed, or type 3, ordinary chondrites display a 10^3-fold range. Associated with this 10^3-fold range in TL sensitivity are variations in the temperature at which the maximum TL emission occurs, and in the temperature range over which emission occurs[3,4]. We report here the results of annealing experiments on a little-metamorphosed (type 3.5) ordinary chondrite. The TL emission characteristics of the annealed samples show trends very similar to those observed in meteorites which have naturally been metamorphosed to various extents. The trends are also similar to those observed in annealing experiments on terrestrial albite[5–7] where the changes are associated with the low-to high-temperature transformation. These data suggest that the TL phosphor in meteorites is feldspar and that TL can be used to estimate palaeotemperatures for little-metamorphosed and highly-unequilibrated meteorites.

About 1.5 g of the Allan Hills A77011 meteorite was ground (<100 μm) and the magnetic fraction removed. Aliquots weighing 20 mg were then placed in high-purity quartz vials, evacuated to 10^{-5} atmospheres, filled to atmospheric pressure with nitrogen and heat sealed. They were then placed in a wire-wound tube furnace at a variety of temperautres for 100 h. Two vials were annealed at each temperature. After annealing, the vials were allowed to cool in air, reaching room temperature after a few minutes. The TL induced by a 250-mCi ^{90}Sr β source (absorbed dose 25 krad) was then measured 3–5 times. (Our apparatus and techniques are described in ref. 4). Irradiation times were chosen so as to give a signal-to-noise ratio of better than 10, usually it was >50. Data for each vial were averaged and the standard deviation calculated. The data for a given time

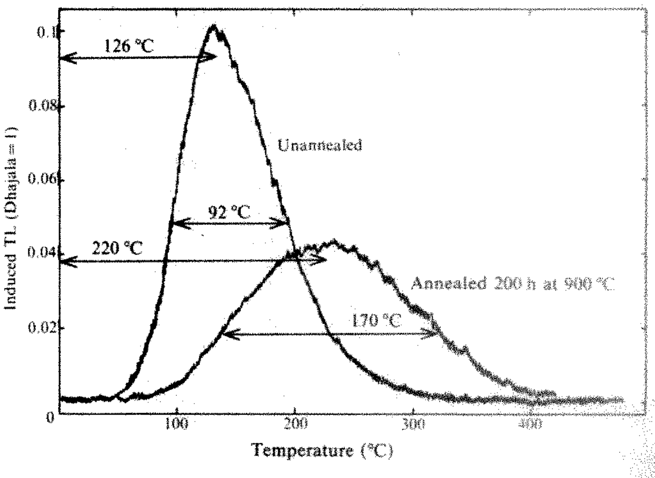

Fig. 1 Plots of the TL, induced by ^{90}Sr β radiation, against temperature for an unannealed sample of the Allan Hills A77011 meteorite, and a sample which has been annealed at 900 °C for 200 h. The annealing treatment has caused the TL peak, in fact, a composite of many smaller individual peaks, to broaden and move to higher temperatures.

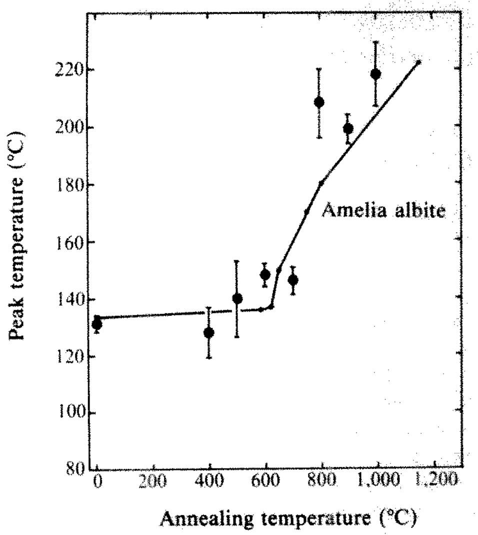

Fig. 2 A plot of the temperature of the TL peak against the temperature at which each sample was annealed for 100 h. The error bars refer to $\pm 1\sigma$ and each data point is the mean of two samples. Also shown are data from ref. 5 for a terrestrial albite from Amelia, Virginia, which was annealed for 24 h in a manner similar to that used here. The change in the TL emission characteristics of the Amelia albite were associated with the low-to-high temperature transformation, suggesting that the TL phosphor in meteorites is feldspar and that the shift in peak temperature on annealing may also be associated with changes in crystallography.

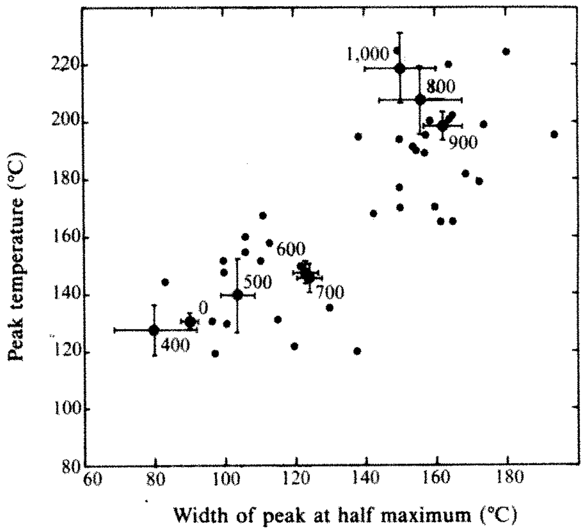

Fig. 3 Peak temperature plotted against the width of the TL peak at half its maximum intensity for the present data (large symbols) and for type 3 ordinary chondrites (small symbols, data from refs 3 and 4). Alongside the present data points are numbers indicating the temperature (°C) at which the samples were annealed for 100 h; 0 indicates the unannealed samples. Errors are $\pm 1\sigma$; two samples were run at each temperature. The meteorites show the same temperature–width relationship as the annealed samples, and the same tendency to bimodality, perhaps associated with the low- and high-temperature forms of the TL phosphor.

and temperature were averaged and the total uncertainty calculated by compounding the 1σ uncertainties for the replicate measurements on each vial and for the standard, Dhajala to facilitate comparison between different laboratories.

Two curves for the TL induced by the β irradiation as a function of glow curve temperature are presented in Fig. 1. Ordinary chondrites display a broad band of TL at 100–300 °C which is composite of many smaller, individual peaks. The glow curves for an unannealed sample and for one of our most severely annealed samples are shown in Fig. 1. The TL peak is relatively sharp in the unannealed sample and appears at a lower temperature in the glow curve than the TL peak of the annealed materials. In the examples in Fig. 1, the annealed sample has its peak 94 °C higher in the glow curve, and its peak is 78 °C wider at half its maximum intensity, than that of the unannealed sample. Our annealed samples in general have glow curves which resemble one or other of the curves in Fig. 1, the less severely annealed samples resembling the unannealed curve—with some variability in the width—and the more severely annealed samples resembling the annealed curve.

Figure 2 shows a plot of the peak temperature of the TL emission as a function of the temperature to which the samples have been annealed. (Peak temperature is that at which the TL emission is at a maximum.) There is a slight indication of a <20 °C increase in the position of the peak as the sample was annealed at temperatures up to 700 °C. The samples annealed at higher temperatures uniformly have TL peaks 80–100 °C higher than in the unannealed sample. We have also indicated on the plot Pasternak's data for samples of low albite from Amelia, Virginia[5–7]. Pasternak's samples were wrapped in Pt foil and annealed in He for 24 h. The agreement is striking and suggests that some change is occurring to the TL phosphor in both the feldspar and the meteorite between 600 and 800 °C. Pasternak performed X-ray diffraction studies on the Amelia albite and found that these changes in TL properties were associated with the transformation from the low-temperature (ordered) form to the high-temperature (disordered) form. However, the association was not a simple one as the TL changes occurred at faster rates than the order–disorder transformation; Pasternak suggests that the TL changes reflect crystallographic changes which precede the transformation, such as the formation of defects. The low to high transformation temperature in albite or meteoritic feldspar (oligoclase in equilibrated meteorites, but unknown in others) is poorly known, but appears to be between 500 and 700 °C in albite[8]. Kinetic factors complicate the comparison of the meteorite and the Amelia anealing data with the feldspar phase diagram, but if the TL changes are associated with known crystallographic changes in the phosphor, the possibility exists that TL can be used for geothermometry.

Feldspar has not been petrographically observed in meteorites of petrologic type 3.5 or lower, except as occasional grains of anorthite usually referred to a 'primary'. However, transmission electron microscope observations of feldspar have been made in meteorites of types >3.7 and feldspar is readily observable in types 5 and 6 where it seems to have formed by the devitrification of glass. Mineral separation experiments have shown that the TL phosphor is located in the low density, feldspar-rich component in equilibrated meteorites[9]. Therefore, we have previously suggested that the TL range in type 3 ordinary chondrites reflects progressive formation of feldspar by the devitrification of glass, and that the peak shape reflects the crystallography of the feldspar[3]. The present data are experimental evidence of that interpretation.

In Fig. 3 we compare the TL peak temperature with the width of the TL peak at half its maximum intensity. The data plot in two fields, the 800, 900 and 1,000 °C annealed samples have peaks at 200–220 °C and widths of 150–170 °C, while the unannealed and <700 °C annealed samples have peaks at 130–150 °C and widths of 80–120 °C. There seems to be a correlation between peak temperature and width for unannealed and <700 °C annealed samples. A ~50% increase in width corresponds to a ~15% increase in peak temperature. The change in peak width caused by the annealing treatment is, therefore, almost as marked as the change in peak position plotted in Fig. 2. We also plot in Fig. 3 data for 39 type 3 ordinary chondrites taken from refs 3 and 4. We have omitted meteorites with TL sensitivities <0.01 because the TL-peak position and TL-peak width relationships break down for these very low TL meteorites where we suspect that a different TL phosphor becomes important. The meteorite samples display the same general trend as our annealed samples, and show a tendency for the peak width and peak position to produce two clumps which may be related to the low- and high-temperature form of the TL phosphor. The data suggest that variations in thermal history are responsible for the peak position–peak width trends observed in type 3 ordinary chondrites[3] and that while some type 3 ordinary chondrites have experienced temperatures above 700 °C others have not. The trends in the chondrites are consistent with the idea that the least metamorphosed meteorites have a low-temperature form of feldspar as their TL phosphor. The implications of these data for our understanding of the metamorphic history of chondrites will be discussed elsewhere. However, one caveat is that our annealing times are very much less than the duration of metamorphism, but if, as we suspect, we are dealing with an equilibrium process, then laboratory measurements will be applicable. A study of the kinetics of the process is required.

Palaeothermometry of type 3 ordinary chondrites has always been a problem. The conventional approach of applying thermodynamic calculations to mineral pairs fails because the meteorites are non-equilibrium assemblages[10]. The oxygen-isotope thermometer works very well for petrologic types 4–6, but the heterogeneity problem is particularly acute for the type 3 chondrites because of the variable amounts of an ^{16}O-rich component[11,12]. We think that TL sensitivity may afford a new means of palaeothermometry in at least one rock type, the type 3 ordinary chondrites, where conventional methods fail. It might be usefully applied to other mildly metamorphosed rocks which contain feldspar as their dominant phosphor.

We thank the Meteorite Working Group of NASA/NSF for supplying the Allan Hills A77011 sample, P. K. Kuroda for interest and encouragement, N. Bakhtiar, B. Brandon, K. Saebo and K. Curtis for technical assistance and R. Hutchison and C. Melcher for constructive reviews. This work is supported by NASA grant NAG 9–81.

Received 8 May; accepted 19 July 1984.

1. Dodd, R. T. *Geochim. cosmochim. Acta* **33**, 161–203 (1969).
2. Sears, D. W., Grossman, J. N., Melcher, C. L., Ross, L. M. & Mills, A. A. *Nature* **287**, 791–795 (1980).
3. Sears, D. W., Grossman, J. N. & Melcher, C. L. *Geochim. cosmochim. Acta* **46**, 2471–2481 (1982).
4. Sears, D. W. G. & Weeks, K. S. *J. geophys. Res. Suppl.* **88**, B301–B311 (1983).
5. Pasternak, E. S. thesis, Univ. Pennsylvania (1978).
6. Pasternak, E. S., Gains, A. M. & Levy, P. W. *Geol. Soc. Am. Abstr. with Program* **8**, 1044 (1976).
7. Levy, P. W. *PACT J.* **3**, 466–480 (1978).
8. Smith, J. V. *J. Geol.* **80**, 505–525 (1972).
9. Lalou, C., Nordmann, D. & Labyrie, J. *C. r. hebd. Séanc. Acad. Sci., Paris* D **270**, 2401–2404 (1970).
10. Dodd, R. T. *Meteorites* (Cambridge University Press, 1981).
11. Onuma, N., Clayton, R. N. & Mayeda, T. K. *Geochim. cosmochim. Acta* **36**, 157–168 (1972).
12. Mayeda, T. K., Clayton, R. N. & Olsen, E. J. *Meteoritics* **15**, 330–331 (1980).

Seismic reflectors and unconformities at passive continental margins

J. Thorne & A. B. Watts

Lamont-Doherty Geological Observatory, and Department of
Geological Sciences, Columbia University, Palisades,
New York 10964, USA

Vail and co-workers[1–3] have recently suggested, based on seismic reflection data available to Exxon, that more than 25 global unconformities occur in Mesozoic–Tertiary age passive continental margins around the world. These data have been used to subdivide the stratigraphical record into several cycles, each of which is controlled by oscillatory changes in sea-level. The resulting scheme has been used as a basis to predict the stratigraphy of passive margins where there is little or no well control[4] or where few reflector terminations can be found[5]. We report here four difficulties with this scheme: (1) during times of minimal continental ice cover changes in the relative rate of sea-level are generally not sufficient to cause unconformities, except in old, slowly subsiding, margins; (2) seismic and biostratigraphical resolution restricts the identification of unconformity-bounded stratigraphical sequences to relatively few in continental shelves; (3) sequence boundaries appear to be best defined on slopes or in regions of active tectonic tilting; and (4) limitations in the sequence analysis technique preclude its use in predictive stratigraphy, especially in shelf and slope regions of margins.

Watts and Steckler[6] used the 'backstripping' equation to determine eustatic changes in sea level from the subsidence history of commercial wells drilled in the margin off North America. Assuming point-wise isostasy this equation can be written:

$$Y = S^* \left(\frac{\rho_m - \rho_s}{\rho_m - \rho_w}\right) + W_d + \Delta_{SL}\left(\frac{\rho_m}{\rho_m - \rho_w}\right) \qquad (1)$$

where Y is the tectonic subsidence of margin in water, W_d the water depth, Δ_{SL} the sea level with respect to present, S^* the uncompacted sedimentary thickness, and ρ_m, ρ_w, ρ_s are mantle, water and sediment densities respectively. Equation (1) can be used to assess the ability of sea-level changes to cause a non-depositional or erosional unconformity. The condition for non-deposition or erosion in submarine or sub-aerial environments is given (assuming an absence of significant variations in the rate of sediment supply to the shelf) by setting the rate of change in sediment thickness, S^*, to $\leqslant 0$. Equation (2) then becomes

$$\dot{\Delta}_{SL} \geqslant (\dot{Y} - \dot{W}_d)\left(\frac{\rho_m - \rho_w}{\rho_m}\right) \qquad (2)$$

where the overdot refers to the derivative with respect to time. Both $\dot{Y}$ and $\dot{W}_d$ can be reasonably well approximated in the case of a passive margin. The variation of tectonic subsidence with time, $\dot{Y}$, follows straightforwardly, for the thermal subsidence stage of a margin[7], from analytical expressions for the cooling by conduction of a plate or half-space[8]. In this study we assume for convenience the half-space approximation $Y = Kt^{1/2}$, where t is the age following rifting and K is a constant. Because of the assumption of a constant sediment supply rate, any deepening of the shelf ($\dot{W}_d > 0$) will necessarily cause sediments to infill. Therefore, the condition for sea-level changes to cause an unconformity on a subsiding margin is given by:

$$\dot{\Delta}_{SL} \geqslant \frac{K(\rho_m - \rho_w)}{2\rho_m}\, t^{-1/2} \qquad (3)$$

Minimum values of $\dot{\Delta}_{SL}$ that are necessary to create an Oligocene unconformity in different age margins are summarized in Table 1. This shows that relatively small values of $\dot{\Delta}_{SL}$ are required to form an Oligocene unconformity in an old passive margin while relatively large values are needed to form the same unconformity in a young margin.

Pitman and Golovchenko[9] have pointed out that among the possible mechanisms, only continental glaciation could cause changes in $\dot{\Delta}_{SL} \geqslant 1.2$ cm kyr^{-1}. Thus, in the absence of continental glaciation, an Oligocene unconformity would be expected at an old margin (for example, East Coast, US) but not at a young margin (for example, Norway). The occurrence of a prominent Oligocene unconformity in the margins of both the East Coast, US[10] and Norway[11] therefore implies continental glaciation during the Oligocene, a suggestion that is in accord with biogeographical evidence of the development of faunas and floras[12] as well as observations of enriched δ^{18}O values in deep-sea sediments[13]. It is unlikely, however, that all the Cenozoic unconformities mapped by Vail *et al.*[1–3] are caused by glaciation. The problem then is to explain the many major unconformities that appear in the Vail *et al.* scheme.

If the sequence boundary technique of Vail *et al.*[1–3] is to be a useful stratigraphical tool, then the major unconformities should be easily recognized within the resolution of seismic and biostratigraphical data.

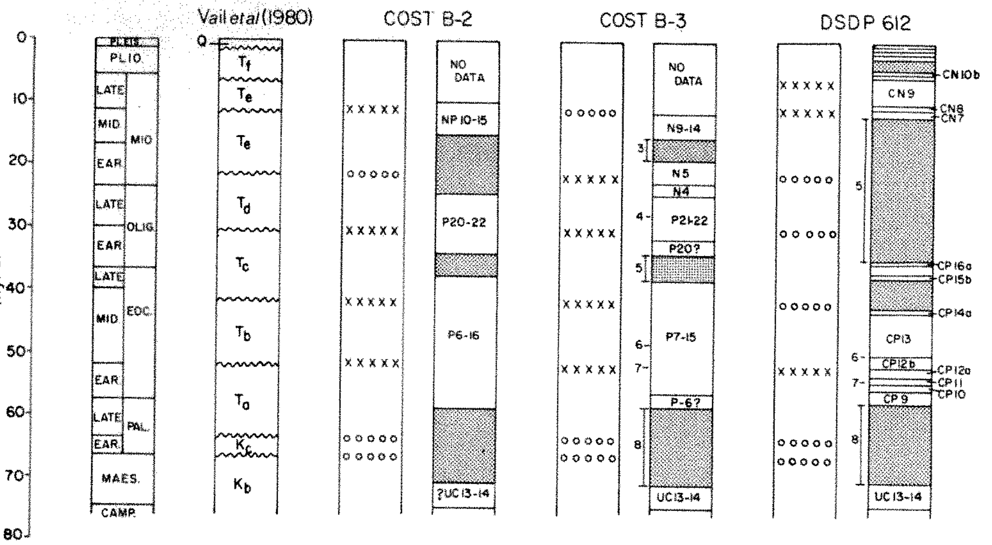

Fig. 1 Comparison of major unconformities predicted by the Vail *et al.*[1-3] scheme to biostratigraphical data at the COST B-2, B-3 and DSDP Site 612: ○ indicates that a short-lived erosional or non-depositional event could be present; × indicates that the predicted unconformity is absent. The position of seismic reflectors 3–8 (see Fig. 2) is also shown at the COST B-3 and DSDP Site 612. The depth to each reflector was computed from synthetic seismograms and travel-depth curves for COST B-3 (ref. 20) and at DSDP site 612 (ref. 21). Bars are used where a reflector spans an unconformity.

The essential problem in seismic sequence analysis is to have the necessary resolution in reflection profiles to identify reflector terminations against other prominent reflectors. Where terminations occur, reflectors split from a single horizon to a reflector pair. If the seismic resolution is poor, then this reflector pair may not be distinguished at any point across the shelf. In the Vail *et al.*[1-3] scheme, it is the differential subsidence across a passive margin during the time gap represented by the sequence boundaries that permits succeeding reflectors to be non-parallel. The average time gap that is observable on the shelf between reflectors above and below a sequence boundary represented by a single reflector termination is equal to the differential subsidence across the shelf divided by two. Table 2 shows the time that is necessary to meet this criteria assuming that the tectonic subsidence of a margin is given either by the half-space ($K = 350\,\mathrm{m\,.\,Myr^{-1/2}}$) or an exponential approximation, sediment loading occurs on an Airy-type crust, porosity falls off exponentially with depth, and the resolution of reflectors in two-way travel time is given by USGS multichannel seismic line 25 (ref. 14) of the US Atlantic shelf. Table 2 shows that within a wide range of assumptions, it is unlikely that seismic sequence analysis can resolve unconformities of ≤4 Myr duration on a thermally-subsiding continental shelf.

Biostratigraphical resolution is limited by the identification of distinct biozones in commercial, COST, and DSDP drill-holes. This is particularly a problem where the identification is based on samples from rotary cuttings. Figure 1 compares the major Cenozoic unconformities in the Vail *et al.*[2] scheme with biostratigraphical data at the COST B-2 (outer shelf), COST B-3 (upper slope) and DSDP Site 612 (middle slope) drill sites off New Jersey. In many cases, the time gap represented by the missing sedimentary section is large (5–10 biozones missing). Although it is relatively easy to identify these unconformities in biostratigraphical data, it would be difficult to estimate the times of the major changes in sea-level that may cause these unconformities with any accuracy. The biostratigraphical data in Fig. 1 is based on Poag[15] for the COST wells and the Scientific Party of DSDP Leg 95 (ref. 16) for Site 612. Since publication of these works, Poag[17] and Miller *et al.*[18] have suggested that the original biostratigraphy at the COST B-2 and B-3 may need to be revised. For example, they suggest that biozones P20 and P21a may be missing at these wells. If this is the case, then the unconformity at the T_c/T_d boundary may, in fact, be present. Figure 1 shows that, with the exception of the unconformities separating cycles T_c/K_b, T_a/K_b and K_c/K_b, the unconformities predicted by the scheme cannot be distinguished in published biostratigraphical data at the three drill sites. Thus, several major unconformities in the Vail *et al.*[2] scheme cannot be recognized in the East Coast US passive margin, even though there is a greater likelihood (Table 1) that sea-level changes will cause major unconformities at old, slowly subsiding, margins.

We have pointed out that rapid changes in sea-level sufficient to satisfy equation (3) are unlikely to create major unconformities that can be distinguished in shelf seismic and biostratigraphical data because of poor resolution. The problem still remains, therefore, that of explaining the large number of unconformities in the Vail *et al.*[1-3] scheme.

A significant number of unconformity-bounded stratigraphical sequences[11] can, in fact, be distinguished in USGS multichannel seismic line 25 of the East Coast, US passive margin. These sequences can only be observed in deep water in the vicinity of the COST B-3 well and Site 612 drill sites. As Fig. 2 shows, more unconformities are predicted by the Vail *et al.* scheme at the drill sites than are actually observed. Furthermore, of the observed sequence boundaries only two of the boundaries (5, 8) correspond to major unconformities. Of the other boundaries, one may represent an unconformity (3), three do not represent unconformities (4, 6, 7) and the remaining five are indeterminate. We call particular attention to sequence boundary 6 which is characterized by the most well defined pattern of reflector terminations on line 25. Evidence at DSDP Site 612 suggests that this reflector represents a post-depositional

Table 1 Rates of sea-level change required to produce a mid-Oligocene unconformity in different age passive continental margins

Age of rifting (Myr BP)	Time since rifting of mid-Oligocene 'event' (Myr)	Rate of change of sea level, Δ_{SL} (cm kyr^{-1}) $K = 295$ (m . Myr$^{-1/2}$)	$K = 350$ (m . Myr$^{-1/2}$)
186	156	0.81	0.97
130	100	1.02	1.21
100	70	1.22	1.44
60	30	1.86	2.20

* The values of K are based on the age–depth curves from refs 8, 19.

Table 2 Minimum length of unconformities for different age passive continental margins

Age of rifting (Myr BP)	Form of subsidence	Compaction depth constant (m)	Minimum length of unconformities (Myr) Age of horizon 30	60	90
186	$t^{1/2}$	2,500	4.1	8.9	9.1
186	Exponential*	2,500	5.5	4.3	5.0
186	Exponential*	1,000	7.8	7.0	8.9
100	$t^{1/2}$	2,500	4.0	7.9	7.2

* The total exponential subsidence was set equal to the $t^{1/2}$ case.

LIBRARY COMPLEX
Department of
Chemical Engineering
Chemical Technology
Plastics and Rubber Technology

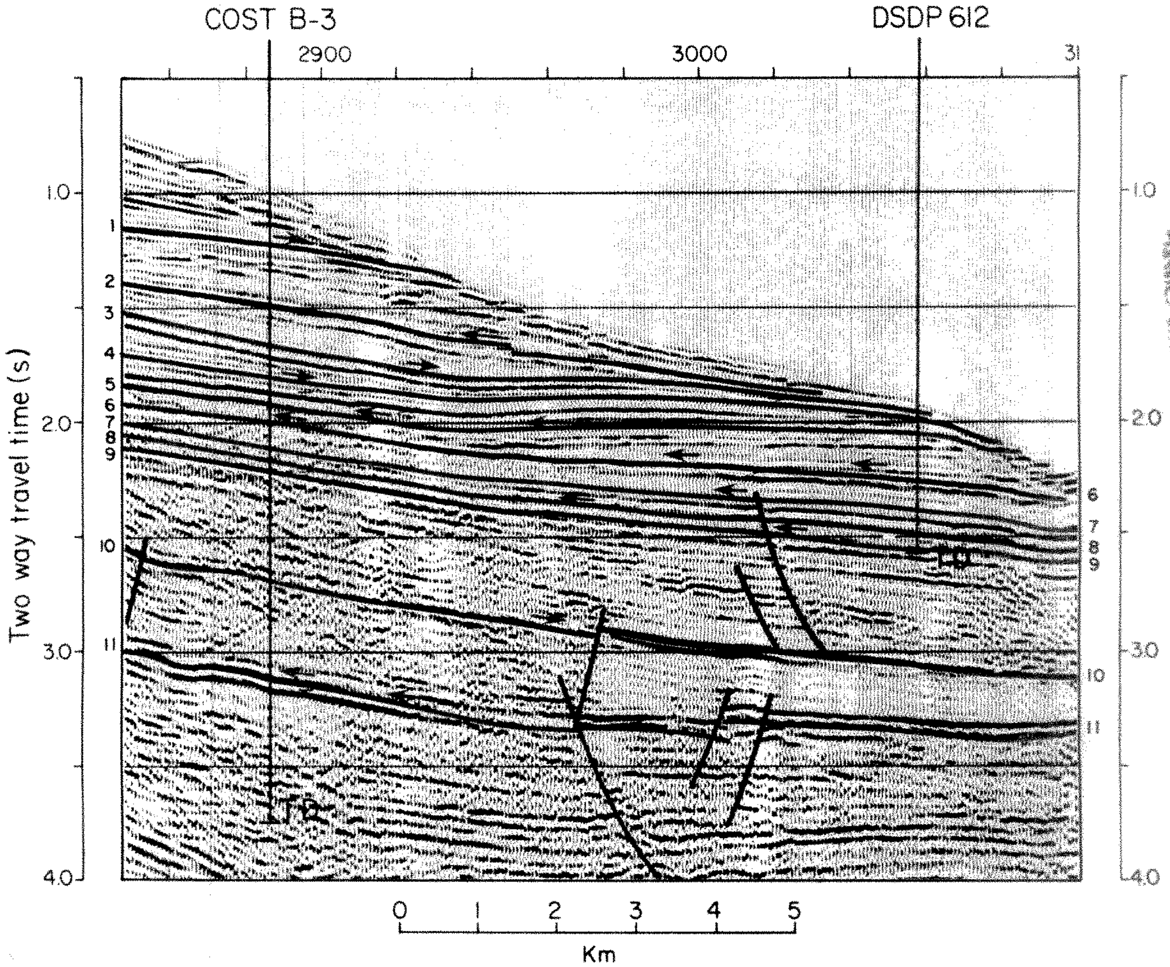

Fig. 2 USGS multichannel seismic line 25 (ref. 14) between shot-points 2847 to 3100. DSDP Site 612 (ref. 16) was drilled at 3558 on line 25. COST B-3 has been projected from 11 km to the north-east to 2885. The coloured reflectors 1–11 represent a preliminary interpretation consistent with the Vail *et al.*[1–3] scheme. Each sequence boundary is defined by reflector terminations (selected terminations shown by an arrow).

diagenetic front separating siliceous nannofossil chalk above from porcellanite below[16]. Although the origin of the front is unknown, it seems to be time-transgressive because it is observed just above the middle–early Eocene boundary at DSDP Site 612 and just below it at DSDP site 613 (ref. 16), drilled 11.5 km downslope of Site 612. The superposition of a diagenetic reflector at an angle to bedding plane reflectors may, therefore, have created the apparent pattern of onlap in Fig. 2. Reflectors should, in theory, be observed to continue across reflector 6. In practice, however, poor seismic resolution makes such an identification difficult.

It is, therefore, unclear which factors control the sequence boundaries on multichannel seismic line 25. We point out, however, that the sequence boundaries can only be easily recognized on the slope part of line 25 and that palaeoceanographic conditions may control at least part of these sequences.

Vail *et al.*[1–3] have repeatedly pointed out the limitations of the seismic sequence analysis technique. We have shown that these limitations may be made more severe by the pattern of subsidence that characterize passive margin development. Because the technique of predictive stratigraphy requires that all or most of the sequence boundaries can be easily recognized in an observed basin section, these limitations suggest caution if they are to be used in age correlation. For example, prominent seismic reflectors of the Barents shelf were 'dated' by Jørgensen and Navrestad[4] based on the Vail *et al.*[1–3] scheme. We caution against too literal an interpretation of these dates until the sedimentary sequences are actually drilled.

As a tool in predictive stratigraphy, it is commonly assumed that the Vail *et al.*[1–3] curve of changes in sea-level is applicable worldwide. We point out, however, that the nature of the control on stratigraphical sequences is unclear. Thus, this assumption should be vigorously tested in the future.

Seismic sequence boundary techniques have proved a valuable tool in quantitative stratigraphy. We have pointed out that the number of sequence boundaries that can be attributed to changes in the rate of sea-level is probably less than previously thought. We have shown that slowly varying changes in sea level can cause major unconformities of wide extent on the shelf, particularly at relatively old passive margins. However, we do not expect that this mechanism can explain many unconformities on the slope. Alternative explanations, therefore, need to be sought for sequence boundaries on the slope, only some of which extend to the shelf. Future studies that include the effects of changes in sediment supply, ocean-wide tectonics, lithospheric mechanics, and palaeoceanographic effects offer the most promise of addressing the unconformity problem in the future.

We thank K. Miller, J. Cochran, G. Mountain, W. Poag, P. Vail, N. Christie-Blick and J. Helwig for their helpful reviews and N. Christie-Blick (formerly at Exxon) for help in constructing Fig. 2. Lamont-Doherty Geological Observatory contribution no. 3705. This work was supported in part by the Office of Naval Research Contract N10014-84-C-0132.

Received 24 January; accepted 11 July 1984.

1. Vail, P. R. *et al. Am. Ass. Petrol. Geol. Mem.* **26**, 49–212 (1977).
2. Vail, P. R., Mitchum, R. M., Shipley, T. H. & Buffler, R. T. *Phil. Trans. R. Soc.* **A294**, 137–155 (1980).
3. Vail, P. R., Hardenbohl, J. & Todd, R. G. *Am. Ass. petrol. Geol. Mem.* (in the press).
4. Jørgensen, F. & Navrestad, T. *Earth Evolut. Sci.* **1**, 43–49 (1981).
5. Schlee, J. *Am. Ass. petrol. Geol. Bull.* **65**, 26–33 (1981).
6. Watts, A. B. & Steckler, M. S. *Am. geophys. Un. Maurice Ewing Symp. Ser.* **3**, 218–234 (1979).
7. Sleep, N. H. *Geophys. J. R. astr. Soc.* **24**, 325–350 (1971).

8. Parsons, B. & Sclater, J. G. *J. geophys. Res.* **82,** 803–827 (1977).
9. Pitman, W. C. & Golovchenko, X. *Soc. Econ. Paleont. Min., Spec. Publ.* **33,** 41–58 (1983).
10. Olson, R. K., Miller, K. G. & Ungrady, T. E. *Geology* **8,** 549–554 (1981).
11. Mutter, J. *Bull. geol. Soc. Am.* (in the press).
12. Kennett, J. P. *J. geophys. Res.* **82,** 3843–3860 (1977).
13. Miller, K. G. & Fairbanks, R. G. *Nature* **306,** 250–253 (1983).
14. Schlee, J. S. & Grow, J. A. *U.S. geol. Surv. Circ.* **833,** 111–116 (1980).
15. Poag, C. W. *U.S. geol. Surv. Circ.* **833,** 44–65 (1980); **833,** 1–3 (1980).
16. Scientific Party. Leg 95, *Geotimes* (in the press).
17. Poag, C. W. in *Geologic Evolution of the United States Atlantic Margin* (ed. Poag, C. W.) (Van Nostrand Reinhold Co., Inc., Stroudsburg, Pennsylvania).
18. Miller, K., Mountain, G. S. & Tucholke, B. E. *Geology* (submitted).
19. Heestand, R. L. & Crough, S. T. *J. geophys. Res.* **86,** 6107–6114 (1981).
20. Wu, C. N. & Nichols, R. R. *U.S. geol. Surv. Circ.* **833,** 26–43 (1980).
21. Goldberg, D. S. *et al. EOS* **65,** 219 (1984).

Evolution of the lower continental crust: granulite facies xenoliths from the Eifel, West Germany

H.-G. Stosch & G. W. Lugmair

Scripps Institution of Oceanography, University of California
at San Diego, La Jolla, California 92093, USA

The lower continental crust is a key region to understanding processes of crust–mantle differentiation and subsequent evolution of the crust. The region is metamorphosed into granulite or amphibolite facies[1,2]. Whereas felsic to mafic granulites with an average intermediate major element composition are typically observed in old exposed lower crustal terranes, mafic compositions are preponderant among granulite facies xenoliths transported by young alkalic basaltic volcanics and kimberlites[1]. Radiometric ages for granulite bulk rocks using the Rb–Sr or U–Pb methods are usually interpreted as metamorphic ages. In contrast, Sm–Nd ages obtained on such metamorphics are interpreted to reflect pre-metamorphic events[3–7], although a case of severe disturbance of the Sm–Nd isotope system during granulite facies metamorphism has also been reported[8]. We present here Sm–Nd and Rb–Sr isotope data for a suite of mafic lower crustal xenoliths from the Hercynian belt. Our data suggest that the igneous precursors of these granulites differentiated from depleted mantle ~1.5 Gyr ago. In most of these granulites this evidence for a mid-Proterozoic age has been obliterated by a young (<172 Myr) metasomatic overprint by mantle derived fluids or melts.

The suite of lower crustal granulite facies xenoliths found in Pleistocene alkalic basaltic tuffs near Engeln/Eifel (Germany) has previously been investigated petrographically and chemically[9,10]. It has been suggested that these granulites are part of the Pleistocene deep crust and form a rather thin layer directly above the Moho[9,10] at ~30 km depth[11]. These xenoliths lack foliation typical of gneiss[9]. Their chemical composition is invariably 'basaltic' favouring an igneous rather than sedimentary origin of the granulite protoliths. On geological grounds the age of the granulite facies metamorphism must have been at least Caledonian[9,10]. A retrograde amphibolite facies metamorphic overprint evidenced by the formation of reaction coronas around garnets was attributed to crustal thinning and/or uplifting during the Hercynian orogeny[9]. The mineralogy of the granulites from Engeln as described by previous investigators is plagioclase ± clinopyroxene ± garnet ± orthopyroxene ± scapolite ± amphibole. Amphibole is ubiquitous in these nominally dry rocks and highly variable in modal abundance (<1–~40%). Texturally the amphibole is clearly secondary in many cases where it formed at the expense of clinopyroxene whereas in other cases amphibole appears to be primary (for example, ref. 9 and own observations).

The results of our analysis of 10 granulites plus one upper mantle spinel peridotite from Engeln/Eifel are presented in Table 1. The presence of amphibole and a pronounced relative light rare earth element (REE) enrichment, classify this mantle xenolith as 'metasomatized', similar to a suite of spinel peridotites from Dreiser Weiher/Eifel[12]. To characterize the local upper crust, we have also analysed one small (~2 cm) sedimentary inclusion (Lower Devonian?) from a basanite flow near Uedersdorf/Eifel as well as one sample of Lower Devonian shale outcropping nearby. The purpose was to possibly obtain information on the crustal residence time of the igneous precursors of these sediments by using the Sm–Nd isotopic system. This follows the approach of McCulloch and Wasserburg[27] and O'Nions and coworkers[21,28].

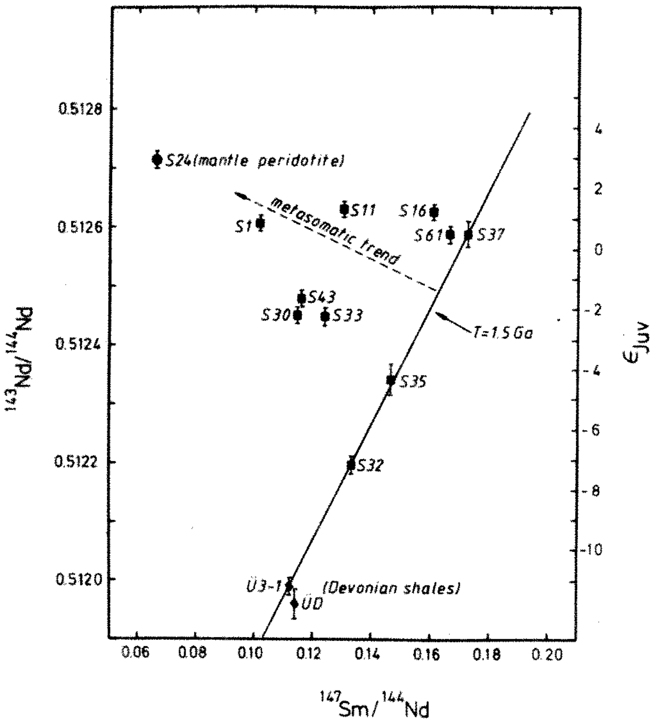

Fig. 1 Sm–Nd isotope evolution diagram for granulites, one peridotite and sediments. An age of ~1.5 Gyr is inferred for a crust forming event involving depleted mantle with $\varepsilon_{JUV}(T) \sim +5$. The arrow indicates the direction of Nd isotopic displacement of parts of the lower crust underneath the Eifel towards mantle values due to metasomatism with mantle derived fluids. This also led to a further light REE enrichment.

The Sr isotopic composition of the mantle peridotite S24 is similar to that reported previously for amphibole-bearing spinel peridotites from Eifel[13]. ^{87}Sr/^{86}Sr of the granulite xenoliths ranges from typical mantle (~0.7036) to crustal values (~0.7095). Rb concentrations and Rb/Sr ratios are among the lowest reported for granulite facies metamorphics so far. The highest Rb concentrations are found in the granulites with the highest modal abundances of amphibole. Due to the overall low Rb/Sr ratios ^{87}Sr/^{86}Sr is essentially frozen, and thus does not allow time constraints to be placed on metamorphic or other events. While the small Rb/Sr ratios of the granulites with low ^{87}Sr/^{86}Sr may have been established during formation of their igneous precursors, high ^{87}Sr/^{86}Sr require that samples like S32 evolved with high Rb/Sr for a considerable time. These data therefore support interpretations similar to those applied to Archaean high-grade metamorphic terranes that Rb, among other elements, can be highly mobile and partly lost during granulite facies metamorphism[14–16]. The two upper crustal sediments have high ^{87}Sr/^{86}Sr and Rb/Sr ratios, attesting to the generally enriched nature of the heavy alkalies in the upper relative to the lower crust.

The Sm–Nd isotopic results given in Table 1 are plotted in Fig. 1 as an isotope evolution diagram. For the granulites two trends can be separated. One trend runs from S35 or from S37 towards the metasomatized spinel peridotite S24, with an inverse correlation between Sm/Nd and ^{143}Nd/^{144}Nd. More specifically, the direction of the trend is from typical crustal Nd isotopic

Table 1 Analysis of Engeln/Eifel samples

		Rb [p.p.m.]*	Sr	$^{87}Rb/^{86}Sr$	$^{87}Sr/^{86}Sr$†	Sm [p.p.m.]*	Nd	$^{147}Sm/^{144}Nd$	$^{143}Nd/^{144}Nd$†	$\varepsilon_{JUV}(0)$‡
Granulites	S1	1.05	690.7	0.0044	0.704922 ± 26	7.16	42.6	0.1015	0.512608 ± 14	+0.8 ± 0.3
	S11	0.73	577.0	0.0037	0.703639 ± 26	1.290	6.01	0.1298	0.512632 ± 14	+1.3 ± 0.3
	S16	0.33	407.6	0.0023	0.705245 ± 26	1.194	4.50	0.1604	0.512628 ± 14	+1.2 ± 0.3
	S30	3.4	916.0	0.0107	0.705790 ± 28	5.82	30.7	0.1145	0.512453 ± 14	−2.2 ± 0.3
	S32	0.94	1325.0	0.00204	0.709478 ± 28	8.07	36.9	0.1323	0.512198 ± 14	−7.2 ± 0.3
	S33	4.64	606.0	0.0222	0.704568 ± 26	9.72	47.5	0.1238	0.512451 ± 14	−2.2 ± 0.3
	S35	1.25	266.1	0.0136	0.705460 ± 26	6.02	24.98	0.1458	0.512343 ± 26	−4.4 ± 0.5
	S37	0.210	406.2	0.00149	0.705207 ± 26	1.500	5.27	0.1720	0.512590 ± 22	+0.5 ± 0.4
	S43	7.1	759.0	0.0270	0.704501 ± 32	9.27	48.4	0.1159	0.512480 ± 14	−1.7 ± 0.3
	S61	0.40	157.8	0.0073	0.704626 ± 28	3.47	12.66	0.1659	0.512591 ± 14	+0.5 ± 0.3
Peridotite	S24	0.051	61.0	0.0024	0.704029 ± 26	0.2924	2.678	0.0660	0.512714 ± 16	+2.9 ± 0.3
Sediments	ÜD	152	119.6	3.69	0.735535 ± 26	7.45	39.7	0.1134	0.511961 ± 26	−11.8 ± 0.5
	Ü3-1	197	146.4	3.90	0.731533 ± 42	7.90	42.7	0.1118	0.511989 ± 16	−11.3 ± 0.3

Isotopic fractionation was corrected to $^{86}Sr/^{88}Sr = 0.1194$ and $^{148}Nd/^{144}Nd = 0.241572$; Nd was measured as NdO^+; $^{87}Sr/^{86}Sr = 0.71026$ measured for NBS987 Sr and $^{143}Nd/^{144}Nd = 0.511859$ for the La Jolla Nd standard.

* Uncertainties for concentrations: [Rb] ± 0.5%, [Sr] < ±0.2%, [Sm] and [Nd] < ±0.1%.

† In most instances actual in-run errors are smaller than quoted; minimum errors given are derived from external precision of standard measurements which are 37 and 27 p.p.m. for $^{87}Sr/^{86}Sr$ and $^{143}Nd/^{144}Nd$, respectively.

‡ Present-day $^{143}Nd/^{144}Nd$ for JUVINAS is 0.512566 ($\varepsilon_{JUV}(0) \equiv 0$).

$$\varepsilon_{JUV}(0) = \left[\frac{^{143}Nd/^{144}Nd^{\text{measured}}_{\text{sample}}}{^{143}Nd/^{144}Nd^{\text{present}}_{\text{JUVINAS}}} - 1 \right] \times 10^4$$

values to values found for metasomatized mantle spinel peridotites (see also ref. 13). Along this trend the modal content of amphibole increases from <5% in S35 to 30–40% in S30. Large ion lithophile element-rich fluids or liquids originating in the mantle probably reacted with the granulites to a variable degree. This trend, therefore, is the result of extensive metasomatism which also is responsible for further light REE enrichment. The time at which the metasomatic modification of an originally dry into hydrous (amphibole and/or phlogopite containing) upper mantle occurred was previously estimated for this region to be <200 Myr ago[13].

Sm–Nd data for plagioclase, clinopyroxene and garnet from granulite S30 (see Table 2 and Fig. 2) form an isochron with a slope corresponding to an age of 172 ± 5 Myr. The data for amphibole as well as the bulk rock, however, are clearly above the isochron. They are displaced towards values for amphibole-bearing mantle peridotites from the Eifel but not towards values for the crust in this area which, at a similar Sm/Nd ratio, would be below the isochron. The same argument holds true for $^{87}Sr/^{86}Sr$. Amphibole (~0.7054) is displaced towards mantle values relative to clinopyroxene and plagioclase (~0.7061 for both minerals). The data point for S30-bulk in Fig. 2 is almost identical to that for S30-amphibole because by mass balance the amphibole accounts for some $\frac{2}{3}$ of this rock's total Nd content. This strongly supports our interpretation that the formation of amphibole in these granulites is due to metasomatism by mantle-derived fluids. The age of this mineral isochron can be regarded as a maximum age for the formation of amphibole and, hence, metasomatism in the lower crust.

The evidence for metasomatic modification of the lower crust clearly indicates that any information on the timing of pre-metasomatic events can only be obtained from those granulite xenoliths which are farthest removed from values for metasomatized mantle in Fig. 1, that is, granulites S32, S35 and S37. These three data points plot along a line with a slope corresponding to an age of 1.5 ± 0.1 Gyr and an initial $\varepsilon_{JUV}(T) = +4.7 \pm 1.9$. We interpret this as evidence that part of the lower crust beneath the Rhenish Shield differentiated from depleted mantle at around this time. Of course, neither the igneous age nor the initial ε_{JUV} of these rocks are tightly constrained by the three data points. Nevertheless, the isochron appears to be real since no mixing relationships can be derived from our isotopic and elemental abundance data. This evidence strongly contradicts the still widely held view that the continental crust in the Hercynian belt in Central Europe is not older than ~700 Myr (refs 17, 18). Additional support comes from U–Pb studies on zircons from the Hercynian fold-belt in Europe which yield even older ages, between 1.9 and 2.2 Gyr (refs 18, 19).

From Fig. 1 it is apparent that the data for the Devonian sediments ÜD and Ü3-1 plot on or close to the line through the data points for granulites S37, S35 and S32, that is their Sm–Nd isotope systematics are consistent with their having about the same 'age' as the granulites. It is worth noting here that loess deposits from Central Europe have Sm–Nd depleted mantle model ages around 1.5 Gyr (ref. 20). Fine-grained clastic sediments from the British Isles south of the late Precambrian to early Palaeozoic Iapetus Ocean have very uniform Sm–Nd depleted mantle model ages around 1.7 Gyr (ref. 21), that is, only slightly higher than the age obtained by us for the Eifel rocks. Both types of sediments probably provide good averages of their upper crustal sources with respect to Sm/Nd ratios, and $^{143}Nd/^{144}Nd$ compositions which can be used to estimate their crustal residence ages. Although it may be fortuitous that the sediment data fall on or close to the line through the data for the granulites in Fig. 1, we consider that the igneous precursors of granulites and sediments have been extracted from the mantle at around the same time, that is towards the end of the ~1.6–2-Gyr tectonothermal event which affected wide parts of the Baltic

Table 2 Sm–Nd results for separated minerals from granulite S30

	Sm [p.p.m.]	Nd	$^{147}Sm/^{144}Nd$	$^{143}Nd/^{144}Nd$	$\varepsilon_{JUV}(0)$
Amphibole	11.81	59.0	0.1211 ± 1	0.512456 ± 14	−2.1 ± 0.3
Clinopyroxene	4.97	22.65	0.1326 ± 1	0.512415 ± 14	−2.9 ± 0.3
Garnet	1.824	1.007	1.095 ± 1	0.513499 ± 30	+18.2 ± 0.6
Plagioclase	0.1831	2.804	0.03946 ± 8	0.512306 ± 24	−5.1 ± 0.5

Conditions and methods as in Table 1.

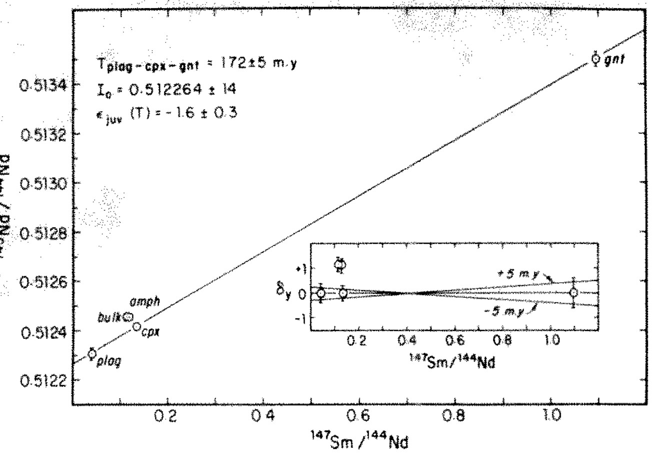

Fig. 2 Sm–Nd isochron diagram for separated minerals from granulite S30 (plag, plagioclase; cpx, clinopyroxene; amph, amphibole; gnt, garnet). All minerals have been hand-picked and etched in dilute HCl and HF prior to dissolution to ensure absence of any contaminants. Inset shows deviation (δy) in parts of 10,000 of the data from the best fit-line through plagioclase, clinopyroxene and garnet.

and Laurentian Shields[22]. Our argument, particularly with regard to involvement of depleted mantle, is further strengthened by the high value of $\varepsilon_{\text{JUV}}(T)$. This value is practically identical to the $\varepsilon_{\text{JUV}}(T)$ indicated for depleted mantle underlying parts of the North American continent[23,24] and Greenland[24] and suggests a relatively large-scale Nd isotopic homogeneity in the upper mantle at around this time. Our isotope data for the Eifel samples add further constraints to the understanding of the derivation through time of continental crust from progressively depleted mantle.

Metamorphic events in the lower crust under the Eifel do not seem to have severely affected the Sm–Nd isotope systematics, in agreement with previous suggestions that the Sm–Nd clock can survive even granulite facies metamorphism[4–7]. The age of the event which metamorphosed the deep crust under the Eifel into granulite facies cannot be disclosed by our Sm–Nd data. However, a Caledonian or older age of the high-grade metamorphism[9,10] cannot be confirmed by our Sm–Nd or Rb–Sr data. In contrast, the results from the mineral isochron (Fig. 2) require Mesozoic ages to be considered as well.

We have suggested that relatively young metasomatism has transported large ion lithophile elements (probably along with volatiles like CO_2 or H_2O) from the mantle into ~1.5 Gyr-old lower crust leading to the formation of amphibole in previously dry granulites. In the case of the Eifel, this has resulted in shifts from crustal to near bulk Earth Sr and Nd isotopic compositions for the majority of the analysed granulites (average $^{87}Sr/^{86}Sr \sim 0.7048$, average $\varepsilon_{\text{JUV}} \sim -1$ for all granulites not lying on the isochron in Fig. 1). This shift represents an isotopic rejuvenation of the lower crust.

Metasomatism is well known from mantle xenoliths of worldwide occurrence, making depleted mantle fertile with respect to its capability to produce alkalic basaltic melts[25]. If, as described here for the Eifel, metasomatic modification by mantle derived fluids or melts is widespread in the lower crust, at least in regions of continental rifting or uplift, it will become necessary to view certain aspects of the evolution of the continental crust (for example, the origin of felsic plutonic rocks, with mantle initial $^{87}Sr/^{86}Sr$ and $^{143}Nd/^{144}Nd$ values) also within the context of derivation from metasomatized lower crust[26].

The granulite xenoliths came from the collection of the Mineralogy-Petrography Institut/University of Cologne. We thank H. A. Seck for valuable discussions and J. Mahoney for help with various analytical aspects. This research was supported by grants from DFG to H. A. Seck and NSF EAR8213670. SIO-IG²L contribution no. 22.

Received 9 January; accepted 29 June 1984.

1. Kay, R. W. & Kay, S. M. *Rev. Geophys. Space Phys.* **19,** 271–297 (1981).
2. Fountain, D. M. & Salisbury, M. H. *Earth planet. Sci. Lett.* **56,** 263–277 (1981).
3. Hamilton, P. J., Evensen, N. M., O'Nions, R. K. & Tarney, J. *Nature* **277,** 25–28 (1979).
4. Jacobsen, S. B. & Wasserburg, G. W. *Earth planet. Sci. Lett.* **41,** 245–253 (1978).
5. Rogers, N. W. & Hawkesworth, C. J. *Nature* **299,** 409–413 (1982).
6. Cliff, R. A., Gray, C. M. & Huhma, H. *Contr. Miner. Petrol.* **82,** 91–98 (1983).
7. McCulloch, M. T., Arculus, R. J., Chappell, B. W. & Ferguson, J. *Nature* **300,** 166–169 (1982).
8. DePaolo, D. J., Manton, W. I., Grew, E. S. & Halpern, M. *Nature* **298,** 614–618 (1982).
9. Okrusch, M., Schröder, B. & Schnütgen, A. *Lithos* **12,** 251–270 (1979).
10. Voll, G. in *Plateau Uplift, The Rhenish Shield—A Case History* (eds Fuchs, K. *et al.*) 336–342 (Springer, Berlin, 1983).
11. Mechie, J., Prodehl, C. & Fuchs, K. in *Plateau Uplift, The Rhenish Shield—A Case History* (eds Fuchs, K. *et al.*) 260–275 (Springer, Berlin, 1983).
12. Stosch, H.-G. & Seck, H. A. *Geochim. Cosmochim. Acta* **44,** 457–470 (1980).
13. Stosch, H.-G., Carlson, R. W. & Lugmair, G. W. *Earth planet. Sci. Lett.* **47,** 263–271 (1980).
14. Heier, K. *Phil. Trans. R. Soc.* **A273,** 429–442 (1973).
15. Weaver, B. & Tarney, J. *Earth planet. Sci. Lett.* **51,** 279–296 (1980).
16. Newton, R. C., Smith, J. V. & Windley, B. F. *Nature* **288,** 45–50 (1980).
17. Jäger, E. *Coll. Int. CNRS, Rennes* **243,** 227–239 (1974).
18. Vidal, P., Auvray, B., Charlot, R. & Cogné, J. *Precamb. Res.* **14,** 1–20 (1981).
19. Gebauer, D. & Grünenfelder, M. *5th Int. Isotope Geology Conf.*, Nikko, Japan, 111–112 (1982).
20. Taylor, S. R., McLennan, S. M. & McCulloch, M. T. *Geochim. cosmochim. Acta* **47,** 1897–1905 (1983).
21. Miller, R. G. & O'Nions, R. K. *EOS* **64,** 906 (1983).
22. Windley, B. F. *The Evolving Continents* (Wiley, London, 1977).
23. DePaolo, D. J. *Nature* **291,** 193–196 (1981).
24. Patchett, J., Arndt, N. T., Chauvel, C. & Todt, W. *Terra Cognita* **4,** 94 (1984).
25. Bailey, D. K. *Nature* **296,** 525–530 (1982).
26. Bell, K. *Nature* **291,** 189–190 (1981).
27. McCulloch, M. T. & Wasserburg, G. J. *Science* 200, 1003–1011 (1978).
28. O'Nions, R. K., Hamilton, P. J. & Hooker, P. J. *Earth planet. Sci. Lett.* **63,** 229–240 (1983).

Relationship between continental area and elevation

Antony R. Wyatt

Department of Geology, University College of Wales, Aberystwyth,
Dyfed SY23 3DB, UK

Continental hypsographic curves, derived from data gathered by Kossinna[1], show a similarity of shape that suggests a correlation between continental area (including the continental shelf) and average height[2,3]. I have considered the varied geological histories of the continental blocks and suggest here that this relationship is not fortuitous, and that changes in continental groupings will have profound effects not only on ocean volumes, and hence sea level, but also on the three-dimensional shapes of the continental blocks.

Harrison *et al.*[2] consider that the apparent link between area and elevation can best be expressed in the form

$$h = -0.4623 + 0.3731 \log_e A \qquad (1)$$

where h is the height (in km) above the continental shelf edge (taken as 200 m below sea level), and A (in Mm^2) is the continental area. This expression was used to derive a theoretical hypsographic curve for Pangaea to explain the lower than otherwise expected areal flooding during eustatic rises of sea level.

This expression was calculated using data from Kossinna[1], but Harrison *et al.*[3] have recently produced more detailed data that would modify this relationship. From a geological point of view the geographer's continental masses have to be regrouped to conform with what is known of crustal movements (see refs 4, 5). The major changes necessary involve the combination of the values for Europe and most of Asia, which appear to have acted as a block for the Mesozoic and Cenozoic, and the removal from Asia of the Arabian Peninsula, which seems to belong more to the African continent. The collision zone of India and Eurasia is complex, and may include other continental fragments[6] and much underthrusting. The data of Harrison *et al.*[3] suggest how the volume of underthrust crust may be estimated, but it is not possible to resolve this into a simple set of area/height data for a separate India. I have, therefore, included India with Eurasia. Details of the hypsographic curves for the rock surfaces of Antarctica and Greenland are not known to

Table 1 Elevation and area data for present continental masses

Continent	Average height (m)	Area (10^{12} m^2)	Average thickness (km)	Volume (10^{12} m^3)
Eurasia	834	59.92	37.2	2,227,750
Afrabia	824	34.82	37.1	1,292,500
North America	699	26.74	36.3	971,250
South America	723	20.10	36.5	733,000
Australia	443	11.12	34.7	385,750
Total		152.70		5,610,250
Antarctica		13.68		484,250
Greenland		2.56		84,500
Total		168.94		6,179,000

Data are based in part on ref. 3. Average heights are above 200 m below present sea level. Average thickness calculated as shown in the text. Volumes given to the nearest 250×10^{12} m^3. Data for Antarctica and Greenland are less reliable than that for the other continental masses.

any great accuracy (estimates of the average elevation of the Antarctic ice cap range from 785 to 2,200 m), and therefore are not used in the calculations below. Harrison *et al.*[3] have separated Madagascar from the rest of Africa. There is still controversy over the nature of the Mozambique channel, and it also looks as if part of the Madagascar Ridge may be thin continental crust[7], which would change the average elevation of the Madagascar block considerably. These data have, therefore, also been left out of the calculations.

The average total thickness of a continental block was calculated assuming that the blocks are in approximate isostatic equilibrium (Fig. 1). Taking average values for the density of continental crust (2.782 g cm^{-3}), oceanic crust (2.9 g cm^{-3}) and seawater (1.03 g cm^{-3})[8] it is possible to derive a simple formula relating the average height of a block to the average depth of its root. For isostatic equilibrium

$$d_w h_4 + d_c h_2 + d_m h_3 = d_c h_1 + d_c h_2 + d_c h_3$$

or

$$h_3 = 5.37 h_1 - 0.398 \qquad (2)$$

It is also possible to derive an expression for the thickness of continental crust below a continent of average height 200 m below sea level. Additional assumptions are the average depth of old oceanic crust (6,400 m below sea level)[9] and the average thickness of oceanic crust (6,600 m)[10]. For isostatic equilibrium

$$d_c(h_5 - h_4) + d_c h_6 + d_c h_7 = d_w(h_5 - h_4) + d_0 h_6 + d_m h_7$$

or

$$h_7 = 19.466 \text{ km}$$

then

$$h_2 = 32.266 \text{ km}$$

Thus, the total thickness of continental crust of a continent of average height h, will be given by the expression

$$\text{Total thickness} = 31.868 + 6.37h \text{ km} \qquad (3)$$

Table 1 lists the revised average height and area figures, the total thickness calculated using equation (3), and the total volume of continental crust for each block. Figure 2 shows average height plotted against area for the blocks with good data, with a curve fitted to these points. Figure 2 suggests that the relationship is better expressed as

$$h = -0.045 + 0.2294 \log_e A \qquad (4)$$

Both the curve fitted to the data in Fig. 2, and the expression derived by Harrison *et al.*[2], have an interesting consequence. If the relationship has held throughout geological time, then the average elevation of the supercontinents must have been greater than that of the fragments we now see. And if the average height

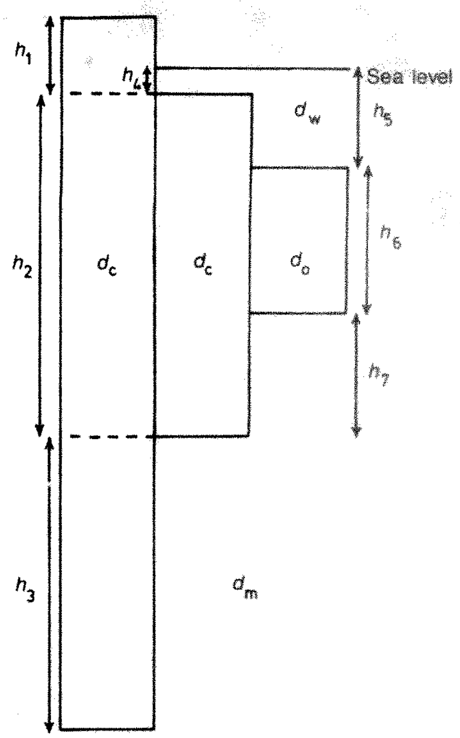

Fig. 1 Blocks in isostatic equilibrium. d_i, Density of material i, where c, continental crust; m, mantle; o, oceanic crust; w, seawater.

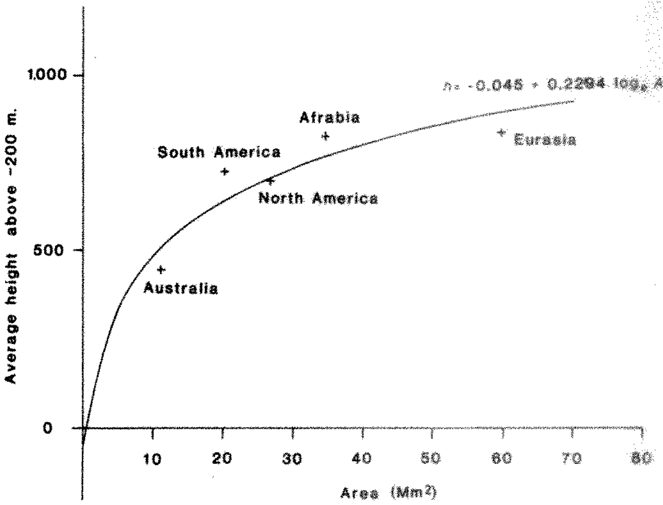

Fig. 2 Relationship between average height and area for those continental blocks with reliable data. The regression line is fitted by least squares.

was greater, the depth of the continental crust must also have been greater to preserve isostatic equilibrium. Unless we invoke changes in the volume of continental crust in parallel with the formation and splitting of continental blocks, this implies changes with time in the area of the globe covered by continental crust. There are sound geochemical arguments showing that the total volume of continental crust has remained almost constant for at least the Phanerozoic, and probably much longer, so it is possible to plot the relationship of volume to area and to calculate the changes in total area of the globe covered by continental crust with different continental groupings.

The relationship of volume to area is given by

$$\begin{aligned} V &= (31.868 + 6.37h)A \\ &= (31.581 + 1.4613 \log_e A)A \qquad (5) \end{aligned}$$

This relationship is plotted on Fig. 3. The numerical values in the expression are dependent on the values for densities and

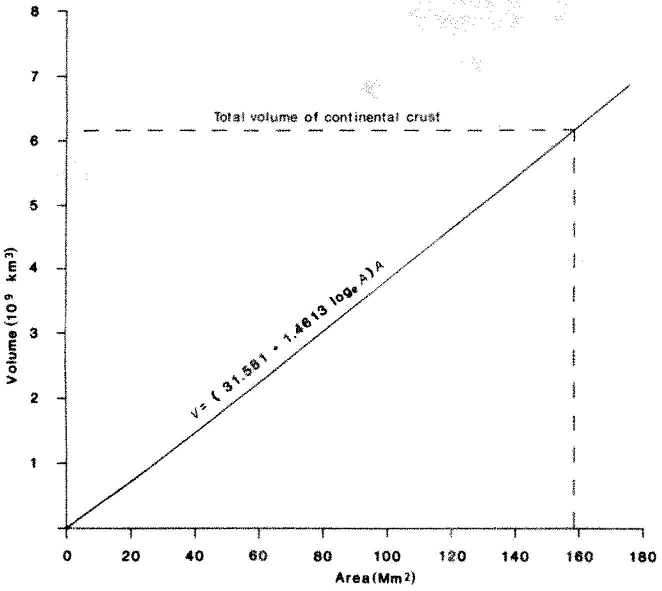

Fig. 3 The theoretical relationship between the volume of a continental block and its surface area.

depths, but slight variation in these values does not affect the conclusions drawn below. From equations (4) and (5) it is possible to calculate theoretical values for the average height and volume of Antarctica and Greenland. These are listed in Table 1, and used simply because they will act in the same way as the other continental blocks.

Figure 3 shows that if all the continental crust formed one block, the total area covered would be ~158.5 Mm^2. This may represent the situation in the early Mesozoic when Pangaea was extant. This is considerably smaller than the present total area covered by continental crust which is about 168.9 Mm^2 (Table 1). This implies that the volume of the ocean basins in the early Mesozoic was ~66.6 × 10^6 km^3 more than it is at present, before allowing for isostatic adjustment due to smaller water load. This is equivalent, after isostatic adjustment, to a sea level some 125 m below the present level.

As Pangaea broke up into smaller fragments these would have altered their configuration to conform with equation (4) that is, the area of a given fragment would increase as its height (and thickness) decreased until it reached a new stable state. Such changes in the area of the continental fragments would have affected the volume of the ocean basins, not only directly, but also by increase in subduction rates and/or decrease in the rate of creation of new crust at ridges, with associated changes in sea level. It may be possible to estimate the rates involved in this flattening process by looking at the history of small fragments of continental crust that have become detached from larger units, as the model suggests that their average height should be much less than that of the parent unit. Berggren[11], for example, suggests, on the basis of microfauna from JOIDES samples, that the Rockall Bank area sank by ~600 m in a time span of some 6 Myr in the Palaeogene. The geological history of some of the microcontinents in the South European Tethys may record the opposite process, as may the late Cenozoic history of the Indian continental crust.

In addition to predicting changes in sea level the model shows that a large continent will have a smaller area of shallow sea than several smaller continents with a total area equal to the large continent. A rough calculation based on a continent of area 158.5 Mm^2 suggests a shallow sea area (that is down to about 200 m below the sea level) of about 13 Mm^2, which is about half the area of modern shallow seas. This has important consequences for evolutionary studies.

The model poses problems for palaeocontinental reconstruction, as it predicts different depth compensation histories for different sized fragments, as well as expansion of the fragments. This may go some way to resolving problems associated with expanding Earth hypotheses, as it suggests that the continents have generally increased their areal extent since the breakup of Pangaea. The Palaeozoic history of the continental blocks should, in general, show the opposite effect.

Cogley[12] has produced an independent reassessment of continental area and height relationships. He recognizes more continental blocks than those used above, suggesting that the total area of continental crust is considerably greater, but his data suggest a similar relationship between mean height and continental area. Modal heights do not show such a simple relationship, suggesting that calculations of shallow sea areas are not as straightforward as might be expected.

I thank Dr. C. G. A. Harrison for useful comments.

Received 17 February; accepted 25 July 1984.

1. Kossinna E. in *Handbuch der Geophysik* Vol. 2 (ed. Gutenberg, B.) (Borntraeger, Berlin, 1933).
2. Harrison C. G. A. *et al. Earth planet. Sci. Lett.* **54**, 1–16 (1981).
3. Harrison C. G. A., Miskell K. J., Brass G. W., Saltzman E. S. & Sloan J. L. II *Tectonics* **2**, 357–377 (1983).
4. Smith A. G., Hurley A. M. & Briden J. C. *Phanerozoic Paleocontinental World Maps* (Cambridge University Press, 1981).
5. Owen H. G. *Atlas of Continental Displacement, 200 Million Years to the Present* (Cambridge University Press, 1983).
6. Allègre, C. J. *et al. Nature* **307**, 17–22, 1984.
7. Schlich, R. in *The Ocean Basins and Margins*, Vol. 6 (eds Nairn A. E. M. & Stehli F. G.) (Plenum, New York, 1982).
8. Brass, G. W. & Harrison, C. G. A. *Icarus* **49**, 86–96 (1982).
9. Sclater J. G., Jaupart C. & Galson D. *Rev. Geophys. Space Phys.* **18**, 269–311 (1980).
10. Raitt R. W. in *The Sea*, Vol. 3 (ed. Hill, M. N.) (Wiley, New York, 1963).
11. Berggren W. A. *Micropaleontology* **20**, 426–448 (1974).
12. Cogley J. G. *Rev. Geophys. Space Phys.* **22**, 101–122 (1984).

A lower crustal origin for massif-type anorthosites

S. R. Taylor, I. H. Campbell, M. T. McCulloch & S. M. McLennan

Research School of Earth Sciences, The Australian National University, Canberra, ACT 2601, Australia

The origin of batholith-sized masses of plagioclase-rich crustal rocks, mainly Proterozoic in age, has mostly been ascribed to aluminous magmas of mantle derivation. Here we propose that such masses are derived by partial melting of an aluminous lower continental crust, which has developed following extraction of a granitic upper crust by intra-crustal melting. This segregation of upper and lower crusts occurred principally in the late Archaean. As the lower crust was depleted in heat-producing elements during the initial melting to produce granites, an external source of heat is required to produce Proterozoic massif-type anorthosites. We speculate that this heat resulted from the continental crust moving over a mantle hotspot or line plume.

Anorthosites may be classified broadly into two types: Archaean and massif. The Archaean anorthosites typically occur as components of layered igneous intrusions[1] of moderate size and are clearly of mantle origin. Plagioclase compositions lie in the range An_{80-95}. In contrast, the massif-type anorthosites which occur as large batholith masses up to 30,000 km^2 in outcrop area, present major petrological and geochemical problems[2–9]. Plagioclase compositions are intermediate, typically An_{40-60} and Mg/(Mg + Fe) ratios are in the range 40–50. Their isotopic characteristics are enigmatic[9]. They are notably depleted in Rb with very low Rb/Sr ratios. Typical initial $^{87}Sr/^{86}Sr$ ratios are low but variable, ranging from 0.7025 to 0.7070, unsupported in many examples by the present Rb/Sr ratios. ε_{Nd} values are even more erratic varying from enriched (−6) to depleted (+4) sources[9]. The bulk composition displays enrichment in Eu relative to the other chondrite-normalized rare-earth elements (REE) (Fig. 1). In addition to their petrological and geochemical

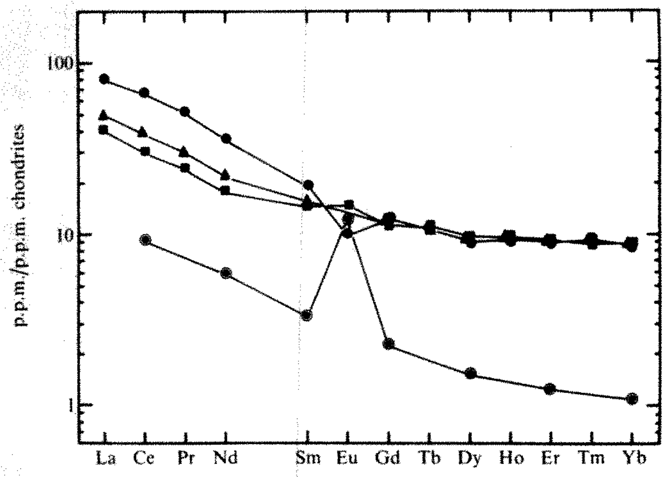

Fig. 1 Chondrite-normalized REE diagram for upper (●), lower (■) and total (▲) continental crust[12]. Also shown is a typical Proterozoic anorthosite pattern (⊙).

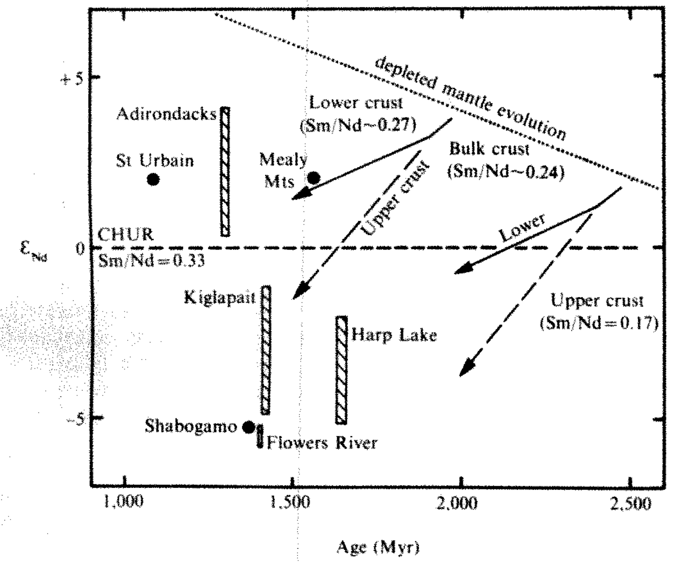

Fig. 2 Fractional deviations from CHUR (chondritic reservoir) in parts per 10^4 of initial ^{143}Nd/^{144}Nd (ε_{Nd}) in Proterozoic anorthosites[1,8]. Also shown are the evolutions of depleted mantle and lower, upper and bulk crust. The range in ε_{Nd} values of the anorthosites is compatible with a 300–500 Myr residence period in the lower crust.

peculiarities, they are primarily a Proterozoic phenomenon, mostly intruded between about 1,700 and 900 Myr ago. Massif-type anorthosites also seem to be related to unique tectonic conditions during the Proterozoic, occurring at sites of incipient or failed continental rifting[5,8,10,11].

We believe that the high Al content, the low An content of the plagioclase and the low Mg/(Mg+Fe) of these rocks is incompatible with a mantle source for Proterozoic massif anorthosites, and now suggest that they are derived from the lower crust. In the model[12–14] that we adopt for the development of the continental crust, a massive increase in continental volume occurred between about 3,000 and 2,500 Myr followed closely by a large intra-crustal melting event which produced enough K-granites to dominate the composition of the upper crust. Thus, the lower crust becomes both dry and depleted in K, Rb, U, Th and the other elements concentrated in granitic melts (Table 1); it also becomes enriched in Al, Sr and Eu (Fig. 1), so that there is an overall enrichment in Eu, relative to chondrite-normalized REE patterns, and the development of low Rb/Sr ratios.

The model composition for the bulk lower crust is given in Table 1. This shows a low quartz and orthoclase content, due to previous extraction of granitic melt. COCORP studies[15] show that the composition of the lower crust is complex. Accordingly, many regions of the lower crust will be even more basic (as shown by many lower crustal xenoliths) and be an appropriate source for the mafic minerals in the massif anorthosites. From our model we predict that anorthosites should possess mineralogical, isotopic and chemical variations which reflect the lower crustal heterogeneity. Although earlier workers[16,17] have suggested that intracrustal melting would produce anorthosites, this proposal differs in specifying an Al- and Eu-rich lower crust residual from the melting episodes which produced a granodioritic upper crust.

Table 1 A model composition of the lower crust[12]

	(%)		(p.p.m.)
SiO_2	54.4	Cs	0.1
TiO_2	1.0	Ba	150
Al_2O_3	16.1	Rb	5.3
FeO_T	10.6	Sr	230
MgO	6.3		
CaO	8.5	La	11
Na_2O	2.8	Ce	23
K_2O	0.33	Nd	12.7
		Sm	3.17
Σ	100.0	Eu	1.17
		Gd	3.3
Norm		Tb	0.59
Q	3.7	Dy	3.6
Or	2.0	Er	2.2
Ab	23.7	Yb	2.2
An	30.4	Lu	0.32
Di	9.8		
Hy	28.6	Th	1.06
Il	1.9	U	0.28
		Hf	2.1
		Ta	0.6
Mg/Mg+Fe	0.51	Cr	235
		Sc	36
		Ni	135
		Co	35

We propose that melting of Al-rich residual lower crustal material in the Proterozoic will produce dry plagioclase-rich melts, enriched in Eu, with low Rb/Sr ratios, unsupported ^{87}Sr/^{86}Sr ratios (inherited from the precursor history) and variable Sm/Nd (and ε_{Nd}) reflecting previous complex crustal history. This typically, but not exclusively, consists of (1) mantle derivation in the late Archaean; (2) extraction of granitic melts by intracrustal melting within 100–200 Myr; (3) residence time in the lower crust in a low Rb/Sr, high Sm/Nd environment for several hundred million years; and (4) a massive melting episode producing the anorthosite magma, which rises and intrudes the upper crust at ~1,500 Myr.

Ashwal and Wooden[8] attributed the ε_{Nd} range between −6.1 and +4.1 for Proterozoic anorthosites from the Nain and Grenville Provinces to derivation from distinct mantle source regions, one enriched (Nain Province) and the other depleted (Grenville Province) in light REE (LREE). A lower crustal origin, however, is more compatible with these data. This is illustrated in Fig. 2 where the evolution of ε_{Nd} values with time is shown for the upper, lower and bulk crustal compositions given in ref. 12. In 500 Myr, ε_{Nd} of the lower crust decreases by two units, while the upper crust decreases by six units. Thus material can reside in the lower crust for extended periods (500 Myr) with only slight decreases in ε_{Nd}, even if a period of 100–200 Myr is allowed following mantle extraction before intra-crustal differentiation occurs. Thus the Nain Province anorthosites considered by Ashwal and Wooden[8] to come from enriched mantle may instead represent melts of older (500 Myr) lower crustal precursors. We note that the Adirondack anorthosites which have highly positive ε_{Nd} (+4) imply derivation from sources more highly depleted in LREE, or from regions with a shorter (<300 Myr) lower crustal residence time. This correlation between crustal provinces and anorthosite Nd isotopic characteristics is consistent with our model, but becomes coincidental if anorthosites are derived from the mantle.

The initial $^{87}Sr/^{86}Sr$ ratios of anorthosites do not directly constrain the crustal prehistory, as anorthosites are characterized by exceedingly low Rb/Sr ratios. The typical $^{87}Rb/^{86}Sr$ ratio (0.03) resembles that of MORB sources and hence the evolution of $^{87}Sr/^{86}Sr$ in the anorthosite source cannot readily be distinguished from that of the mantle. However, the initial Sr ratios for many anorthosites lie in the range 0.7026–0.7066 (ref. 8). The higher values are significantly greater than that expected from a direct mantle origin. This has been attributed to interaction with metasedimentary material or metamorphic fluids. An equally plausible scenario is that the anorthosite protolith existed for a limited period (100–200 Myr) with higher Rb/Sr ratios ($^{87}Rb/^{86}Sr \approx 1$). In our model, this represents the period of crustal residence following mantle extraction, but before intra-crustal differentiation into a granitic upper crust and an Rb depleted lower crust.

Although this postulated sequence of events seems capable of explaining the geological, petrological, geochemical and isotopic characteristics of massif anorthosites, the source of heat required to produce massive lower crustal melting is a major problem. Two heat sources are available for melting continental crust: (1) heat released by the decay of radioactive elements within the crust; and (2) heat released from the underlying mantle and conducted through the crust. The low Rb/Sr ratio of anorthosites indicates that the parent magmas were generated from a source depleted in Rb and other incompatible elements including the heat-producing elements K, U and Th. Most concepts of crustal differentiation, including intracrustal melting and fluid migration models, similarly predict low abundances of the heat producing elements in the lower crust. We suggest that these elements were effectively removed by earlier intracrustal melting episodes which produced the granitic upper crust, and concentrated the bulk of the crustal complement of K, U and Th in the upper 10 km of the continental crust.

Accordingly, it is necessary to invoke a mantle source of heat to generate the anorthositic magmas. Such a heat source must be extensive, linear (to account for the observed geological distribution[3]), operate on a time scale of up to several hundred million years and be capable of heating the base of the crust to temperatures in excess of 1,300 °C. The temperature of basaltic magmas extruded at the surface of the Earth rarely exceeds 1,250 °C, but it has been shown[18,19] that volcanic magmas occupy a density minimum in a tholeiitic fractionation trend with the suggestion that both the crust and crustal magma chambers act as a density filter, preventing dense, primitive magmas from reaching the surface. Parent magmas for mid-ocean ridge basalts (MORB) probably had MgO contents of ~18% (refs 20–22), and liquidus temperatures around 1,400 °C (ref. 23). If a continent migrates over a mantle line plume of the mid-ocean ridge type, then temperatures in excess of 1,400 °C are likely for the upper mantle adjacent to the base of the crust. If such a plume persisted for an extended period of time, as required by our model, temperatures in excess of 1,300 °C do not seem unreasonable for the base of the crust.

Our assessment of the available data reveals that a lower crustal origin for massif-type anorthosites is plausible. On the other hand, if anorthosites can be shown to be derived from mantle sources, then these must have many of the isotopic and chemical characteristics of our lower crustal models. This implies that the magnitude of mantle isotopic and chemical heterogeneity is very much greater than presently recognized.

Received 23 March; accepted 31 July 1984.

1. Ashwal, L. D., Morrison, D. A., Phinney, W. C. & Wood, J. *Contr. Miner. Petrol.* **82,** 259–273 (1983).
2. Simmons, E. C. & Hanson, G. N. *Contr. Miner. Petrol.* **66,** 119–135 (1978).
3. Herz, N. *Science* **164,** 944–947 (1969).
4. Duchesne, J.-C. & Demaiffe, D. *Earth planet. Sci. Lett.* **38,** 249–272 (1978).
5. Emslie, R. F. *Precambr. Res.* **7,** 61–98 (1978).
6. Wiebe, R. A. *Nature* **286,** 564–567 (1980).
7. Fudao, Z. & Guanghong, X. *Geochemistry* **1,** 96–104 (1982).
8. Morse, S. A. *Am. Miner.* **67,** 1087–1100 (1982).
9. Ashwal, L. D. & Wooden, J. L. *Nature* **306,** 679–680 (1983).
10. Bridgwater, D. & Windley, B.F. *Geol. Soc. S. Afr. Spec. Publ.* **3,** 307–317 (1973).
11. Wynne-Edwards, H. R. *Am. J. Sci.* **276,** 927–953 (1976).
12. Taylor, S. R. & McLennan, S. M. *The Continental Crust: its Composition and Evolution* (Blackwell, Oxford, in the press).
13. Taylor, S. R. & McLennan, S. M. *Phil. Trans. R. Soc.* A **301,** 381–399 (1981).
14. McLennan, S. M. & Taylor, S. R. *J. Geol.* **90,** 347–361 (1982).
15. Oliver, J. *J. geophys. Res.* **88,** 3340 (1983).
16. Michot, J. *Norsk Geol. Tidsskr.* **41,** 157–172 (1961).
17. Green, T. H. *Can. J. Earth Sci.* **6,** 427–440 (1969).
18. Sparks, R. S. J., Meyer, P. & Sigurdsson, H. *Earth planet. Sci. Lett.* **46,** 416–430 (1980).
19. Stolper, E. & Walker, D. *Contr. Miner. Petrol.* **74,** 7–12 (1980).
20. O'Hara, M. J. *Nature* **200,** 683–686 (1968).
21. Clarke, D. B. *Contr. Miner. Petrol.* **25,** 203–224 (1970).
22. Elthon, D. *Nature* **278,** 514–518 (1979).
23. Elthon, D. & Scarfe, C. M. *Yb. Carnegie Instn Wash.* **79,** 277–281 (1980).

Role of paternal and maternal genomes in mouse development

Sheila C. Barton, M. A. H. Surani* & M. L. Norris

AFRC Institute of Animal Physiology, 307 Huntingdon Road,
Cambridge CB3 0JQ, UK

There has been much speculation on whether mammalian eggs with two male pronuclei can develop normally. Eggs with two female pronuclei can sometimes develop as far as the 25-somite stage[1–3] but with only very meagre extraembryonic tissues[2,3]. We suggested that the genome undergoes specific imprinting during gametogenesis[3] and that some paternal genes may be necessary for normal development of the extraembryonic tissues[3,4], in which only the maternal X chromosome remains active[5–9]. However, the need for the maternal genome for development to term is not yet unequivocally established. The detailed study described here demonstrates that while between 40 and 50% of heterozygous reconstituted eggs with a male and a female pronucleus develop to term, none of the eggs with two male pronuclei does so. Furthermore, embryos in the latter case are very retarded, even though the trophoblast develops relatively well compared with embryos having two female pronuclei[1–3]. Our combined results indicate that while the paternal genome is essential for the normal development of extraembryonic tissues, the maternal genome may be essential for some stages of embryogenesis.

Fertilized eggs were obtained from (C57BL/6J × CBA/Ca) F_1 females (henceforth called F_1) mated with MF1 albino outbred males or from MF1 ♀ × F_1 ♂ pairings. The female pronucleus was removed from the recipient eggs (usually from F_1 ♀ × MF1 ♂) and replaced with a male pronucleus from MF1 ♀ × F_1 ♂ to yield MF1 ♂ + F_1 ♂ androgenetic eggs. In a small series, F_1 ♂ + F_1 ♂ (MF1 recipient egg) or MF1 ♂ + MF1 ♂ (F_1 donor and recipient eggs) were also prepared. As a control for these experiments, the male MF1 pronucleus from F_1 ♀ × MF1 ♂ eggs was removed and replaced with another F_1 male pronucleus from MF1 ♀ × F_1 ♂ eggs, or the female F_1 pronucleus was removed from F_1 ♀ × MF1 ♂ eggs and replaced with another MF1 female pronucleus from MF1 ♀ × F_1 ♂ eggs (see Table 1). All the reconstituted eggs with two pronuclei were cultured overnight, when the majority of them cleaved to the two-cell stage. These embryos were transferred to the right oviducts and the control MF1 × MF1 eggs (except in the case of the MF1 ♂ + MF1 ♂ experimental eggs, when F_1 ♀ × F_1 ♂ eggs served as controls) to the left oviducts of day 1 pseudopregnant mice (day 1 = day of vaginal plug).

The results (Table 1) demonstrate that 28 androgenetic eggs implanted (23%), and eight of these contained very retarded embryos (4–6 somites) or embryonic remains when examined on day 10 or 11 of pregnancy. All the embryos showed substantially better development of extraembryonic membranes and trophoblast compared with the embryo itself (see Fig. 1 for a description of all the embryos obtained). Poor development of androgenetic embryos cannot be attributed to manipulation of the egg because, in the first series of experiments, three reconstituted eggs out of five containing a male and female pronucleus, developed normally to produce embryos with between 25 and

---

[*] To whom correspondence should be addressed.

Table 1 Development of reconstituted mouse eggs

Eggs			No. transferred to recipients that became pregnant/ total transferred	Implanted	With embryos‡
Recipient	Donor	Reconstituted†			
(1) $F_1 \times$MF1*	MF1 $\times F_1$	Ak MF1 + Ak F_1	90/157	20	6
(2) $F_1 \times$MF1	$F_1 \times$MF1	Ak MF1 + Ak MF1	18/24	5	2
(3) MF1 $\times F_1$	$F_1 \times$MF1	Ak F_1 + Ak MF1	11/17	1	0
(4) MF1 $\times F_1$	MF1 $\times F_1$	Ak F_1 + Ak F_1	3/10	2	0
Total no. of androgenetic eggs			122/208	28	8 Retarded
(5) $F_1 \times$MF1	MF1 $\times F_1$	Gk F_1 + Ak F_1	75/99	46	35 Live young§
(6) $F_1 \times$MF1	MF1 $\times F_1$	Ak MF1 + Gk MF1	71/95	—	27 Live young‖
Total no. of control eggs with a male and female pronucleus			146/194	—	62 Live young
(7) Unoperated control MF1 $\times$ MF1 and $F_1 \times F_1$			190/245	112	102 Normal

Fertilized eggs, F_1 ♀ × MF1 ♂ and MF1 ♀ × F_1 ♂, were recovered 16–21 h after an injection of 5 IU human chorionic gonadotropin (HCG) in animals which had been injected previously with 5 IU pregnant mare's serum (48 h before injection of HCG) to induce superovulation. The cumulus cells were dispersed by incubation in 300 IU ml^{-1} hyaluronidase (ovine testis; Sigma) in phosphate-buffered medium (PBI)[20] +0.4% bovine serum albumin (BSA) for 3–5 min at 37 °C. Eggs were then washed 6–9 times in M16[21] +0.4% BSA and cultured in this medium under paraffin oil at 37 °C in humidified 5% CO_2 in air. Micromanipulation of eggs was done on a Leitz micromanipulator as described previously[2]. The donor and recipient eggs (10–15 of each) were placed in PBI +0.1% BSA containing the cytoskeletal inhibitors cytochalasin D and Nocodazole (Sigma) at a final concentration of 1 $\mu\text{g ml}^{-1}$ and 0.05 $\mu\text{g ml}^{-1}$ respectively, dissolved in 1.5 µl dimethyl sulphoxide[2]. After 30–45 min at 37 °C, the eggs were suspended in hanging drops for micromanipulation. One of the pronuclei was first removed from all the recipient eggs with a 25 µm bevelled needle using the technique described by McGrath and Solter[22], to prepare haploid recipient eggs. Using the same needle, a pronucleus from donor eggs was drawn into the needle and the membrane pinched off to make a small karyoplast fragment[22], followed by approximately 6 pl of β-propiolactone-inactivated Sendai virus[23,24] (3,000 haemagglutination units ml^{-1}) to induce fusion[25]. Virus and karyoplast were then gently released into the perivitelline space underneath the zona pellucida of the recipient egg[22]. The procedure was repeated for each recipient egg. The recipient eggs with adhering karyoplasts were washed twice in PBI +0.1% BSA and cultured in M16 +0.4% BSA at 37 °C as described above. The eggs were checked for fusion of the karyoplast ~4 h after the completion of manipulation on the last group of eggs. Fusion was confirmed by the disappearance of the karyoplast and the appearance of two pronuclei within the recipient egg. The fusion rate was 80–100%. The diploid reconstituted eggs were separated, washed nine times in equilibrated M16 +0.4% BSA and cultured overnight in this medium at 37 °C in 5% CO_2 in air under paraffin oil. The following morning, 98% of the eggs had cleaved and these were transferred to the oviducts of day 1 MF1, CFLP or F_1 pseudopregnant mice which were obtained by mating with vasectomized males of proven sterility.

* The F_1 animals are non-albino homozygous for glucose phosphate isomerase, GPI-*bb*, while the MF1 are outbred albino, GPI-*aa*.

† Ak, androgenetic; Gk, gynogenetic.

‡ Androgenetic embryos were examined on day 10 of pregnancy (groups 1–4) while the reconstituted eggs with a male and a female pronucleus were allowed to proceed to day 19 (group 5) when live young were obtained by autopsy. The embryos were typed for GPI[26] and confirmed as GPI-*ab* (group 1), GPI-*aa* (group 2), GPI-*bb* (group 5) and GPI-*aa* (group 6).

§ Twenty-two females and 13 males were obtained by autopsy on day 19 of pregnancy.

‖ Thirteen females and 14 males were obtained by natural birth. All live young from groups 5 and 6 have reached adulthood and bred normally.

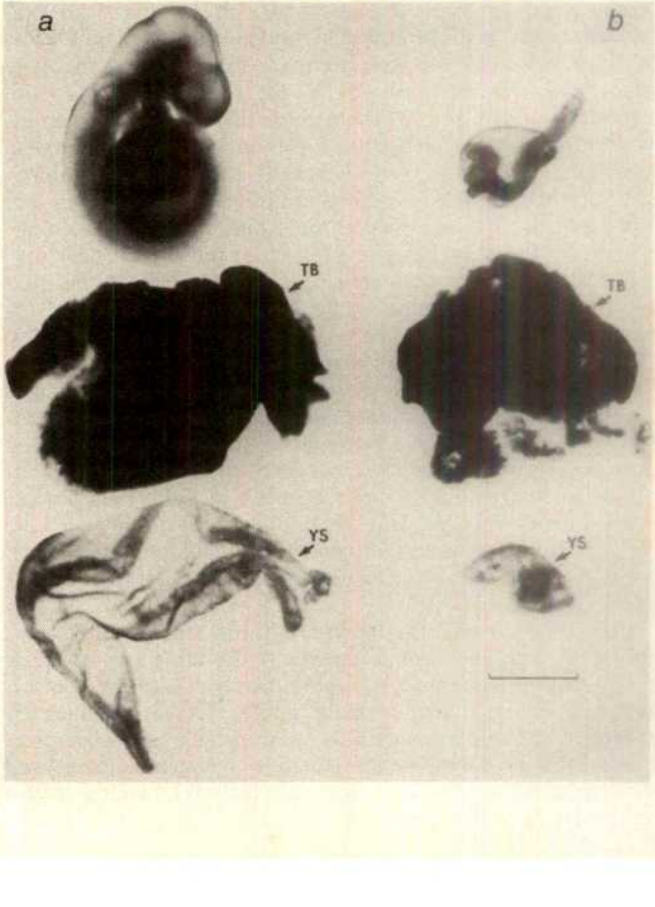

Fig. 1 Normal control embryo (*a*) and androgenetic embryo (*b*) from the same recipient on day 10 of pregnancy, each with its trophoblast (TB) and yolk sac (YS). The retarded androgenetic embryo has ~5 somites and is well formed but rather small for its stage; the trophoblast apparently is normal. The control embryo is at the 25-somite stage (scale bar 1.0 mm). Of the androgenetic embryos transferred, 23% implanted and a quarter of the decidua contained embryos or embryonic tissue at day 10. The decidua were uniformly smaller than those of the concurrent normal controls, whether or not embryos were present. Where embryos were present there was a substantial amount of trophoblastic tissue (giant cells and ectoplacental cone), and the yolk sac was substantial and expanded considering that the embryos were very retarded, unlike embryos from eggs with two female pronuclei[1-3]. Of the embryos present, four had reached the 4–6-somite stage (one of these was examined on day 11 and showed no signs of further development; tissue thickening and the onset of deterioration was evident). The fifth embryo had no somites but was rather large for a headfold embryo. A sixth embryo consisted of substantial but poorly organized neural tissue and somites, and a seventh had ~10 somites from the beating heart downwards, but had no head. One deciduum contained a tiny yolk sac vesicle inside a solid lump of trophoblastic tissue. There were no detectable embryonic remains in the rest of the 20 decidua. The three reconstituted control embryos analysed on day 10 were 25–35-somite embryos of normal size and in normal size decidua, indistinguishable from unoperated controls.

35 somites. The remainder of these normal reconstituted eggs were allowed to proceed to term, when 62 live young (43%) were obtained on day 19 of pregnancy (Table 1).

This study demonstrates that heterozygous androgenetic embryos are unlikely to develop to term. Three different types of androgenetic embryos would be expected, nearly 25% of them containing two Y chromosomes and dying within a few cleavage divisions[8], 25% XX, and 50% XY. It is unknown which of the last two categories of embryos develops better. The maternal X chromosome is preferentially active in the extraembryonic tissue whereas X-inactivation is random in the embryonic ectoderm from which the fetus develops[5–7]; this may partly influence development of androgenetic embryos. In our previous study, homozygous androgenetic embryos (which are YY or XX) had an exceptionally low implantation rate (6%) and no embryonic derivatives were detected[2]. Our results contrast with the reported birth of two homozygous androgenetic females[9], but this and similar findings[9,10] have not yet been substantiated[2,3,11–13]. The embryos with two male pronuclei in this study differ from those with two female pronuclei[2,3], especially with respect to better development of the trophoblast in the former but a better embryo in the latter. There is, however, no consistent development of the experimental embryos. This could be partly due to the necessary interactions between embryonic and extraembryonic tissues[14], which may be impaired to a varying extent.

We have recently suggested that the presence of a male and a female pronucleus is usually necessary for development to term and that this is probably because the paternal and the maternal genomes undergo specific imprinting as a result of epigenetic influences during gametogenesis[3]. There is some evidence to suggest that the differences between the paternal and the maternal genomes are recognized and may be used in embryogenesis. The nonrandom activity of the maternal X chromosome in the extraembryonic tissues is an example of such recognition[5–7]. Furthermore, specific paternal genes may also be necessary for the normal development of the trophoblast, as shown by studies on DDK mutant mice[4]. The absence of a paternal genome in an egg does result in the poor development of extraembryonic tissues[2,3], for example, both triploid and dygynic embryos develop poorly but the latter in addition have meagre extraembryonic tissues, which is attributed to the removal of the male pronucleus[2]. By contrast, we show here that eggs with two male pronuclei have substantial trophoblast but a very retarded embryo. In the human, androgenetic embryos (both XX and XY) sometimes display development as hydatidiform moles which consist of abundant chorionic vesicles and trophoblast, but the fetus is usually absent[15]. Furthermore, studies on the T^{hp}-deletion mutation of chromosome 17 in the mouse suggest that a normal chromosome 17 in the maternal, but not the paternal, genome is essential for normal development[16–18]. Hence, reconstituted eggs lacking entirely the maternal genome, as in this study, would not be expected to complete embryogenesis.

Our studies suggest that eggs with either the paternal or maternal genomes can only develop up to the blastocyst stage; some of these embryos implant and develop to a varying extent partly depending on the genotype. We suggest that the differences in the paternal and maternal genomes are recognized and may be important during embryogenesis in the establishment of the primary lineages. How these differences are involved in the interactions between the paternal and maternal genomes[12] and in gene expression during development remains to be determined.

After submission of this paper, results of a similar study were reported[19], with conclusions essentially the same as ours (refs 2, 3 and the present study); approximately 5% of the control reconstituted eggs with a male and a female pronucleus developed to term but none of the androgenetic or gynogenetic embryos did so. Two post-implantation gynogenetic embryos, one of them with 11 somites, were detected but no androgenetic embryos were obtained.

Received 26 March; accepted 16 July 1984.

1. Kaufman, M. H., Barton, S. C. & Surani, M. A. H. *Nature* **265**, 53–55 (1977).
2. Surani, M. A. H. & Barton, S. C. *Science* **222**, 1034–1036 (1983).
3. Surani, M. A. H., Barton, S. C. & Norris, M. L. *Nature* **308**, 548–550 (1984).
4. Wakasugi, N. *J. Reprod. Fert.* **41**, 85–96 (1974).
5. West, J. D., Frels, W. I., Chapman, V. M. & Papaioannou, V. E. *Cell* **12**, 873–882 (1977).
6. Takagi, N., Wake, N. & Sasaki, M. *Cytogenet. Cell Genet.* **20**, 240–248 (1978).
7. Harper, M. I., Fosten, M. & Monk, M. *J. Embryol. exp. Morph.* **67**, 127–135 (1982).
8. Morris, T. *Genet. Res.* **12**, 125–135 (1968).
9. Hoppe, P. C. & Illmensee, K. *Proc. natn. Acad. Sci. U.S.A.* **74**, 5657–5661 (1977).
10. Hoppe, P. C. & Illmensee, K. *Proc. natn. Acad. Sci. U.S.A.* **79**, 1912–1916 (1982).
11. Modlinski, J. A. *J. Embryol. exp. Morph.* **60**, 153–161 (1980).
12. Markert, C. L. *J. Hered.* **73**, 390–397 (1982).
13. Gulyas, B. J., Wood, M. & Whittingham, D. G. *Devl Biol.* **101**, 246–250 (1984).
14. Gardner, R. L. & Papaioannou, V. E. in *The Early Development of Mammals* (eds Balls, M. & Wild, A. E.) 107–132 (Cambridge University Press, 1975).
15. Bagshawe, K. D. & Lawler, S. D. *Br. J. Obstet. Gynaec.* **89**, 255–257 (1982).
16. Johnson, D. R. *Genetics* **76**, 795–805 (1974).
17. McLaren, A. in *Maternal Effects in Development* (eds Newth, D. R. & Balls, M.) 287–320 (Cambridge University Press, 1979).
18. McGrath, J. & Solter, D. *Nature* **308**, 550–551 (1984).
19. McGrath, J. & Solter, D. *Cell* **37**, 179–183 (1984).
20. Whittingham, D. G. & Wales, R. G. *Aust. J. biol. Sci.* **22**, 1065–1072 (1969).
21. Whittingham, D. G. *J. Reprod. Fert. Suppl.* **14**, 7–21 (1971).
22. McGrath, J. & Solter, D. *Science* **220**, 1300–1302 (1983).
23. Neff, J. M. & Enders, J. F. *Proc. Soc. exp. Biol. Med.* **127**, 260–271 (1968).
24. Giles, R. E. & Ruddle, F. H. *In Vitro* **9**, 103–118 (1973).
25. Graham, C. F. *Acta endocr. Suppl.* **153**, 154–167 (1971).
26. Chapman, V. M., Whitten, W. K. & Ruddle, F. H. *Devl Biol.* **26**, 153–161 (1971).

A biological consequence of variation in the site of D–J_H gene rearrangement

Brian A. Pollok*, John F. Kearney†, Meenal Vakil† & Robert P. Perry*

* Institute for Cancer Research, Fox Chase Cancer Center,
Philadelphia, Pennsylvania 19111, USA
† Cellular Immunobiology Unit, Department of Microbiology,
University of Alabama in Birmingham, Birmingham,
Alabama 35924, USA

One mechanism which generates diversity in immunoglobulin variable (V) regions is flexibility in the site of recombination among the constituent genetic elements[1–7]. Within a specific antibody family (that is, a particular V_H–V_L combination), variability in *V–D–J* rearrangement not only leads to sequence diversity at the boundary of the juxtaposed genes, but also enables the total length of the third complementarity-determining region (CDR-3) of the heavy chain to be conserved[8]. We demonstrate here that the junctional diversity inherent in rearranged immunoglobulin genes can have consequences for the biology of the immune system. Sequence analysis of the expressed immunoglobulin genes of idiotypically variant as opposed to conventional B lymphocytes of a dominant antibody family showed that the variant B cells undergo a novel D–J_H joining event such that an extra amino acid is inserted into the heavy chain CDR-3. The unique D-region conformation possessed by the variant B cells accounts for previous observations which showed that variant and conventional B cells could be differentially regulated *in vivo* by an autologous set of idiotope-specific B lymphocytes[9]. Our findings indicate that D-region structure can determine the expression of regulatory idiotopes and suggest that the conservation of heavy-chain CDR-3 length within an antibody family may reflect regulatory as well as functional constraints.

Serological studies using monoclonal anti-idiotype antibodies and sequence analysis of monoclonal immunoglobulins have shown that there is a significant degree of structural diversity among BALB/c anti-phosphorylcholine (anti-PC) antibodies belonging to the dominant T15 idiotype antibody family[10–12]. Using the A/J anti-T15 monoclonal antibodies AB1-2 and GB4-10, a minor subset of T15$^+$ anti-PC IgM antibodies can be detected in BALB/c mice which do not express the latter idiotope (constituting 0–3% of the normal *in vivo* anti-PC IgM response[10]). The biological significance of this particular idiotypic heterogeneity became apparent when an *in vivo* B-cell counterpart to the GB4-10 anti-T15 hybridoma was found in

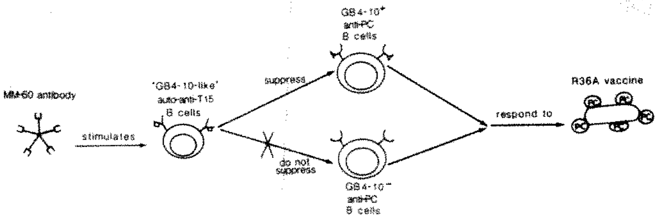

Fig. 1 Schematic diagram of a monoclonal model for idiotype-directed regulation of immunoglobulin production. *In vivo* administration of the auto-anti-(anti-T15) monoclonal antibody, MM-60 (ref. 13) induces proliferation among a restricted, possibly clonal, set of auto-anti-T15 B cells possessing a specificity identical to the A/J anti-T15 hybridoma GB4-10 (ref. 9). Once stimulated, 'GB4-10-like' anti-T15 B cells suppress anti-PC IgM production from only those B cells bearing the GB4–10-defined idiotope; anti-PC IgM production by GB4–10⁻ B cells is unimpaired. The anti-PC humoral response of BALB/c mice is dominated by the GB4-10⁺ component, with 95–100% of all anti-PC serum IgM bearing the GB4–10-defined idiotope[10]. All GB4–10⁺ anti-PC antibodies are also T15⁺, while 40% of GB4–10⁻ anti-PC IgM antibodies in primary immune response are T15⁺ (that is, the variant population studied here), the remainder belonging to the M511 and M603 idiotypic families[10,34].

BALB/c mice and was shown to specifically suppress the production of anti-PC IgM from B cells bearing the GB4-10-defined idiotope[9]. Figure 1 summarizes, from previous work[9,13], the cellular and humoral interactions involved in this differential regulation of the primary *in vivo* B-cell response to PC and how it approximates to a monoclonal model for autologous idiotype-directed immunoregulatory processes. Determining the structural correlate of the GB4-10-defined idiotope would indicate which region(s) of the immunoglobulin molecule are responsible for the expression of regulatory idiotopes and also what genetic changes lead to the loss of such idiotopes, thereby permitting a B lymphocyte to avoid regulation.

To achieve this, four B-cell hybridomas secreting a monoclonal anti-PC IgM of the T15⁺ GB4-10⁻ phenotype (designated 2-21, 5-18, 7-22 & 12-3) were identified following fusion of the nonproductive plasmacytoma Ag8.653 (ref. 14) to spleen cells from BALB/c mice undergoing a primary immune response to R36A pneumococcal vaccine. The monoclonal antibodies from all four variant hybridomas bind PC–protein conjugates and R36A bacterial cells; the purified IgM from the variant 12-3 hybridoma appears to bind PC with an affinity comparable with that of BH8, a monoclonal T15⁺ GB4-10⁺ anti-PC IgM of germ-line sequence (B. A. P., unpublished observation). To prove that those hybridomas from the same fusion (2-21, 5-18, 7-22) were the immortalized products of distinct B-cell clones, the nonproductively rearranged heavy-chain gene of each hybridoma was examined by Southern blot analysis using a J_H region-specific probe[15]. Each hybridoma possessed a different sized J_H-containing *Eco*RI restriction fragment from its nonproductive allele, demonstrating that each hybridoma was derived from independent anti-PC B-cell precursors (data not shown). In addition, no gross structural differences in the T15 V_H–J_H1 gene complex were detected between the variant hybridomas and the prototypic T15⁺ anti-PC plasmacytoma S107 (heavy- and light-chain genes of germ-line sequence[16,17]) as shown by the presence of a 7.5-kilobase (kb) J_H-containing *Eco*RI fragment[5] in all cases.

Loss of expression of GB4-10-defined idiotope could be due to subtle alterations in light- and/or heavy-chain structure as both T15 V_L and V_H regions contribute to idiotope expressions[9,10]. Examination of light-chain structure by isoelectric focusing showed that purified κ light chains from two variant hybridomas (5–18, 7–22) co-migrated with the secreted κ chain of S107 (*p*I 8.0) (ref. 9). The germ-line character of the light chains produced by GB4-10⁻ variant B cells was confirmed by sequencing portions of the κ-chain mRNA from the hybridomas 12–3 and 5–18 (see Fig. 2 legend); the κ mRNA sequence from both variant hybridomas was identical to the S107A κ gene[17] from the beginning of CDR-2 (codon 50) to $J_\kappa1$ (codon 108) (data not shown). The presence of mutations upstream of CDR-2 in the T15 V_L gene of the variant is highly unlikely as somatic mutation in the expressed light-chain genes of IgM-producing B cells (as seen in representative hybridomas) is rare[12,18,19]. In support of this, experiments using recombinant immunoglobulin molecules from GB4–10⁺ and GB4–10⁻ T15⁺ anti-PC hybridomas confirm that expression of the GB4–10-defined idiotope in the T15 family is associated with the heavy chain[9]. Hence, alterations in the T15 V_L structure do not appear to be the basis for the absence of expression of this regulatory idiotope.

```
                                                              V REGION
S107  (+)      GCAAGTAGAAACAAAGCTAATGATTATACAACAGAGTACAGTGCATCTGTGAAGGGTCGGTTCATCGTCTCCAGAGAC
BH8   (+)      GCAAGTAGAAACAAAGCTAATGATTATACAACAGAGTACAGTGCATCTGTGAAGGGTCGGTTCATCGTCTCCAGAGAC
2-21  (-)                              GATTATACAACAGAGTACAGTGCATCTGTGAAGGGTCGGTTCATCGTCTC-AGAGAC
5-18  (-)      GCAAGTAGAAACAAAGCTAATGATTATACAACAGAGTACAGTGCATCTGTGAAGGGTCGGTTCATCGTCTCCAGAGA-
7-22  (-)                                                         AGGGT-GGTT-ATCGTCTCCAGAGAC
12-3  (-)                                            GAGTACAGTGCATCTGTGAAGGGTCGGTTCATCGTCTCCAGAGAC

                                   V REGION                                                   D REGION
ACTTCCCAAAGCATCCTCTACCTTCAGATGAATGCCCTGAGAGCTGAGGACACTGCCATTTATTACTGTGCAAGAGAT  TACTACGGTAGTAGC
ACTTCCCAAAGCATCCTCTACCTTCAGATGAATGCCCTGAGAGCTGAGGACACTGCCATTTATTACTGTGCAAGAGAT  TACTACGGTAGTAGC
ACTTCCCAAAGCATCCTCTACCTTCAGATGAATGCCCTGAGAGCTGAGGACACTGCCATTTATTACTGTGCAAGAGAT  TACTACGGTAGTAGCTAC
ACTT--CAAAG-ATCCTCTACCTTCAGATGAATGCCCTGAGAGCTGAGGACACTGCCATTTATTACTGTGCAAGAGAT  TACTACGGTAGTAGCTAC
ACTT--CAAAGCATCCTCTACCTTCAGATGAATGCCCTGAGAGCTGAGGACACTGC-ATT-ATTACTGTGCAAGAGAT  TACTACGGTAGTAGCTAC
ACTTCCCAAAGCATCCTCTACCTTCAGATGAATGCCCTGAGAGCTGAGGACACTGCCATTTATTACTGTGCAAGAGAT  TACTACGGTAGTAGCTAC

                J REGION                                    Cμ REGION
TACTGGTACTTCGATGTCTGGGGCGCAGGGACCACGGTCACCGTCTCCTCA  GAGAGTCAGTCCTTCCCAAATGTCTTCCCCCTCGTCTCCTGC
TACTGGTACTTCGATGTCTGGGGCGCAGGGACCACGGTCACCGTCTCCTCA  GAGAGTCA
TACTGGTACTTCGATGTCTGGGGCGCAGGGACCACGGTCACCGTCT--TCA  GAGAGTCAGTCCTTC
TACTGGTACTTCGATGTCTGGGG-GCAGGGACCACGGTCACCGTCT--TCA  GAGAGTCAGTCCTTC
TACTGGTACTTCGATGTCTGGGGCGC-GGGACCACGGT-ACCGTCTCCTCA  GAGAGT--GTC
TACTGGTACTTCGATGTCTGGGGCGCAGGGACCACGGTCACCGTCTCCTCA  GAGAGTCAGTC
```

Fig. 2 Nucleotide sequence of the V_H–$5'C_\mu$ region for several idiotypically variant and conventional T15⁺BALB/c monoclonal anti-PC immunoglobulins. The heavy-chain sequence of the S107 plasmacytoma[5] serves as the prototypic sequence for BALB/c anti-PC antibodies as it expresses the germ-line T15 V_H, *D*FL16.1 and J_H1 gene sequences in rearranged form[5,19]. The IgM constant-region gene sequence[35] replaces the IgA constant region in the S107 prototypic sequence as all the immunoglobulins studied here are of the IgM class. Undetermined bases (sequence ambiguities) are denoted by dashes and reactivity with the anti-T15 idiotope antibody GB4–10 is shown as (+) or (−). Sequencing of the hybridoma heavy-chain mRNA was performed as described by Caton *et al.*[36]. A 17-base synthetic oligonucleotide primer complementary to the 5′ end of the first exon of the μ heavy-chain constant gene (underlined nucleotides) was used to initiate reverse transcription of poly(A)⁺ cytoplasmic RNA. Specific dideoxynucleotides were included in the reaction mixtures to create base-specific stops during cDNA synthesis with [$\alpha-{}^{32}$P]dATP or [$\alpha-{}^{35}$S]dATP as the incorporated label. The nucleotide sequence of the cDNA was determined by electrophoresing the labelled cDNA fragments on polyacrylamide gels, followed by autoradiography of the gel. The first 10 bases distal to the primer were consistently indiscernible and the maximum sequence length accurately readable by this method was approximately 250 bases, which permitted sequencing of the entire CDR-2. The confirmatory heavy-chain sequence of the T15⁺ GB4-10⁺ anti-PC IgM-secreting BALB/c hybridoma BH8 (ref. 10) eliminates the possibility that the insertion of the TAC codon at the D–J_H junction is an artefact of our procedure for sequencing μ heavy chains.

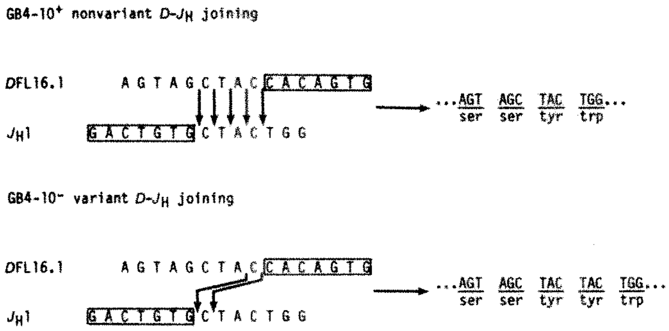
GB4-10$^+$ nonvariant D-J_H joining
DFL16.1
A G T A G C T A C C A C A G T G
J_H1
G A C T G T G C T A C T G G
...AGT AGC TAC TGG...
ser ser tyr trp
GB4-10$^-$ variant D-J_H joining
DFL16.1
A G T A G C T A C C A C A G T G
J_H1
G A C T G T G C T A C T G G
...AGT AGC TAC TAC TGG...
ser ser tyr tyr trp

Fig. 3 Pattern of D–J_H gene rearrangement in GB4–10$^+$ versus GB4–10$^-$ anti-PC B-cell precursors. Rearrangement between the *D*FL16.1 and J_H1 genes could occur at five and two alternate sites in GB4–10$^+$ nonvariant and GB4–10$^-$ variant anti-PC immunoglobulins, respectively (designated by arrows); the two D–J_H joining positions for GB4–10$^-$ variant antibodies are distinct from all the possible sites used by the GB4–10$^+$ nonvariant group. The boxes show the conserved heptamer recognition sequences defined by Sakano *et al.*[7]. The J_H1 and *D*FL16.1 gene sequences have been described previously[5–7,20].

The primary structure of the heavy chain expressed by each variant and a nonvariant hybridoma was examined by sequencing the μ heavy-chain mRNA in the same way (Fig. 2). The heavy chains of all the variant hybridomas are coded by T15 V_H (ref. 6), DFL16.1 (ref. 20) and J_H1 (ref. 5); the same V_H, D and J_H genes as the two nonvariant heavy chains. The heavy-chain gene sequences of the variants are also identical with the germ-line (that is, unmutated) sequence of the constituent T15 V_H, *D*FL16.1 and J_H1 genes (for codons 50–113). The only notable difference in heavy-chain gene structure exhibited by the variant group is the presence of an extra tyrosine codon (TAC) at the D–J_H gene junction. That this structural peculiarity is the sole basis for loss of the GB4–10 regulatory idiotope is strengthened by the finding that amino acid substitutions present throughout V_H of T15$^+$ anti-PC antibodies (including those in regions not sequenced here, such as in CDR-1) have no effect on idiotope expression (ref. 9 and B.P., unpublished data).

Examination of the nucleotide sequence at the 3′ end of the germ-line *D*FL16.1 gene[20] indicates how this insertion might occur (Fig. 3). Although the site of D–J_H joining cannot be precisely defined for either the conventional or the variant T15$^+$ antibody group, generation of the two distinct heavy chains is clearly dependent on different D–J_H gene recombinations. Considering the consistency in length and composition of this site, it is highly unlikely that it derives from an 'N segment'—the non-templated, G+C-rich region often present at the D–J_H boundary[21]. Detection of functional variants within the virgin anti-PC B-cell repertoire of neonatal mice by the clonal splenic focus assay[22,23] (B. A. P. and M. V., unpublished observations), is consistent with the molecular evidence showing that generation of these variant B cells is determined at an early stage of B-cell ontogeny. Although insertion of an extra codon at the site of recombination among immunoglobulin genes is not a rare occurrence, the heavy-chain gene structure of the T15$^+$ GB4–10$^-$ B cells is unusual because the insertion here is not accompanied by a compensating deletion of a codon at the V_H–D junction; this results in a heavy-chain CDR-3 longer by one amino acid residue than the CDR-3 length of all other sequenced T15$^+$ antibodies.

Consistency in heavy-chain CDR-3 length is not unique to the T15 antibody family, but is an apparently universal characteristic among antibody families which dominate a particular antigen response; paucicional systems which exhibit this trait include the anti-α-1, 3 dextran[24], anti-galactan[25], anti-inulin[26], anti-'GAT'[27,28] and anti-phenyloxazalone responses[29]. Although conservation of a particular CDR-3 conformation would most reasonably be based on some functional criterion such as antigen binding activity or light-chain pairing potential, this may not necessarily be the case. Variation in CDR-3 primary structure due to utilization of different D genes and/or flexibility in V_H–D–J_H joining apparently alters neither the antigen specificity nor the ability to pair with the respective light chain for anti-dextran, anti-galactan and anti-PC antibodies[8]. In addition, consistency in CDR-3 length for conventional T15$^+$ anti-PC antibodies cannot be due to a highly preferential V–D–J recombination which precludes all others, as several anti-PC antibodies containing non-T15 light chains and heavy chains coded for by the T15 V_H, *D*FL16.1 and J_H1 genes do exhibit different CDR-3 lengths[12]. Our results indicate that deviation from uniformity in CDR-3 length does not necessarily affect antigen binding or light-chain pairing, but can lead to destruction of a regulatory idiotope and possibly, to the creation of a regulatory idiotope(s) unique to CDR-3 length variants. Conservation of a particular CDR-3 length within a dominant antibody family may be necessary to ensure that target idiotopes responsible for the coordinated regulation of an immune response are properly displayed to the surrounding milieu. The validity of such a model is supported by studies on tertiary structure of V regions of monoclonal anti-PC[30] and anti-galactan[31] antibodies which show that D-region residues are prominently exposed on the external surfaces of the immunoglobulin molecule. Regularity in heavy-chain CDR-3 length within an antibody family may thus reflect a B lymphocyte's niche in the idiotypic network rather than being due solely to antigen binding or light-chain pairing.

It is intriguing that most of the family-specific idiotopes defined so far on mouse immunoglobulins using mouse anti-idiotypic antibodies have been mapped to the D regions[25,32,33]. However, a model of idiotype-specific immunoregulation based on recognition of D-region-determined idiotopes presumably necessitates the existence of an extensive number of anti-idiotypic elements considering the degree of D-region sequence variability often present within an antibody family[25]. Our studies on the 'mini-network' described here suggest an alternative model; the expression of a D-region-determined regulatory idiotope can be resistant to many of the sequence substitutions in a given D-region (ref. 9 and B.P., unpublished data), with loss of idiotope expression brought about by only a few, significant perturbations in D-region tertiary structure (for example, insertion of a bulky, non-polar amino acid at the D–J_H junction). Examination of other autologous idiotype-specific immunoregulatory systems which function *in vivo* should help to resolve whether expression of regulatory idiotopes are generally determined by D-region/CDR-3 conformation.

We thank Dr S. Clarke for instruction on RNA sequencing by primer extension, and Dr M. Weigert for providing the C_μ primer and for valuable discussions. B.A.P. is a recipient of a Damon Runyon–Walter Winchell postdoctoral fellowship. This project was supported by NIH grants 14782, CA 16673 and RCDA 00338, NSF grant PCM80–10972, and an appropriation from the Commonwealth of Pennsylvania.

Received 28 February; accepted 18 July 1984.

1. Weigert, M., Gatmaitan, L., Loh, E., Schilling, J. & Hood, L. *Nature* **276,** 785–790 (1978).
2. Max, E., Seidman, J. & Leder, P. *Proc. natn. Acad. Sci. U.S.A.* **76,** 3450–3454 (1979).
3. Sakano, H., Huppi, K., Heinrich, G. & Tonegawa, S. *Nature* **280,** 288–294 (1979).
4. Weigert, M. *et al. Nature* **283,** 497–499 (1980).
5. Early, P., Huang, H., Davis, M., Calame, K. & Hood, L. *Cell* **19,** 981–992 (1980).
6. Gough, N. & Bernard, O. *Proc. natn. Acad. Sci. U.S.A.* **78,** 509–513 (1981).
7. Sakano, H., Kurosawa, Y., Weigert, M. & Tonegawa, S. *Nature* **290,** 562–565 (1981).
8. Rudikoff, S. *Contemp. Topics molec. Immun.* **9,** 169–198 (1983).
9. Pollok, B. & Kearney, J. *J. Immun.* **132,** 114–122 (1984).
10. Kearney, J., Bartletta, R., Quan, Z. & Quitáns, J. *Eur. J. Immun.* **11,** 877–882 (1981).
11. Cerny, J., Wallich, R. & Hammerling, G. *J. Immun.* **128,** 1885–1891 (1982).
12. Gearhart, P., Johnson, N., Douglas, R. & Hood, L. *Nature* **291,** 29–39 (1981).
13. Pollok, B., Bhown, A. & Kearney, J. *Nature* **299,** 447–449 (1982).
14. Kearney, J., Radbruch, A., Liesgang, B. & Rajewsky, K. *J. Immun.* **123,** 1548–1550 (1979).
15. Marcu, K., Banerji, J., Penncavage, N., Lang, R. & Arnheim, N. *Cell* **22,** 187–196 (1980).
16. Crews, S., Griffin, J., Huang, H., Calame, K. & Hood, L. *Cell* **25,** 59–66 (1981).
17. Kwan, S.-P., Rudikoff, S., Seidman, J., Leder, P. & Scharff, M. *J. exp. Med.* **153,** 1366–1370 (1981).
18. Clarke, S., Claflin, J. L., Potter, M. & Rudikoff, S. *J. exp. med.* **157,** 98–113 (1983).
19. Pawlita, M., Potter, M. & Rudikoff, S. *J. Immun.* **129,** 615–618 (1982).
20. Kurosawa, Y. & Tonegawa, S. *J. exp. Med.* **155,** 201–218 (1982).
21. Alt, F. & Baltimore, D. *Proc. natn. Acad. Sci. U.S.A.* **79,** 4118–4122 (1982).
22. Klinman, N. *J. exp. Med.* **136,** 241–260 (1972).
23. Hurwitz, J., Tagart, V., Schweitzer, P. & Cebra, J. *Eur. J. Immun.* **12,** 342–348 (1982).

24. Schilling, J., Clevinger, B., Davie, J. & Hood, L. *Nature* **283**, 35–40 (1980).
25. Rudikoff, S., Pawlita, M., Pumphrey, J., Musiniski, E. & Potter, M. *J. exp. Med.* **158**, 1358–1400 (1983).
26. Johnson, N., Slankard, J., Paul, L. & Hood, L. *J. Immun.* **128**, 302–307 (1982).
27. Rocca-Serra, J. *et al. EMBO J.* **2**, 867–872 (1983).
28. Tonnelle, C., Rocca-Serra, J., Moulin, A., Moiner, D. & Fongereau, M. *J. exp. Med.* **158**, 1415–1427 (1983).
29. Kaartinen, M., Griffiths, G., Markham, A. & Milstein, C. *Nature* **304**, 320–324 (1983).
30. Potter, M., Pawlita, M., Mushinski, E. & Feldmann, R. in *Immunoglobulin Idiotypes* (eds Janeway, C., Sercarz, E. & Wigzell, H.) 1–19 (Academic, New York, 1981).
31. Feldmann, R., Potter, M. & Glaudemans, C. *Molec. Immun.* **18**, 683–698 (1981).
32. Clevinger, B., Schilling, J., Hood, L. & Davie, J. *J. exp. Med.* **151**, 1059–1070 (1980).
33. Maddalena, A., Hudak, S. & Claflin, J. L. *Anns Immun.* (in the press).
34. Claflin, J., Hudak, S. & Maddalena, A. *J. exp. Med.* **153**, 352–361 (1981).
35. Kawakami, T., Takahaski, N. & Honjo, T. *Nucleic Acids Res.* **8**, 3933–3945 (1980).
36. Caton, A., Brownlee, G., Yewdall, J. & Gerhard, W. *Cell* **31**, 417–427 (1982).

Major surface antigen gene of a human malaria parasite cloned and expressed in bacteria

Roger Hall, John E. Hyde, Mike Goman, David L. Simmons, Ian A. Hope, Martin Mackay & John Scaife

Department of Molecular Biology, University of Edinburgh,
King's Buildings, Mayfield Road, Edinburgh EH9 3JR, UK

Bernhard Merkli, Rolf Richle & John Stocker

Pharmaceutical Research Division, Hoffmann La Roche and Co.,
Basel, Switzerland

The late blood stages of the human malaria parasite, *Plasmodium falciparum*, carry a major surface antigen, p190, of molecular weight (M_r) 190,000 (ref. 1). This antigenically variable protein[1–3] is actively processed, first as the parasite matures and again when it is released into the blood stream and invades a new erythrocyte to initiate a cycle of growth[1]. It elicits a strong immune response in man; all tested adult sera from endemic areas have antibodies against this protein[1]. Our evidence indicates that purified p190 can alter the course of parasitaemia in monkeys with falciparum malaria. We have also succeeded in cloning part of the gene for p190 and expressing it in *Escherichia coli*. To this end we have developed a new technique, antibody select, which greatly simplifies final identification of expressing clones.

The protein p190 was first defined[2] and later purified[1] by monoclonal antibodies. It begins to be made in schizogony as a 190,000 M_r protein. Processing creates smaller peptides, notably major species of approximately 160,000, 125,000, 106,000 and 82,000 M_r (ref. 1 and R.H., unpublished). These and other features strongly suggest that p190 is related to the 195,000 M_r protein studied by Holder and Freeman[4], and to similar proteins in rodent[5–7] and simian[8,9] parasites. One part of p190, defined by monoclonal antibody 2.2, is present in all isolates of *P. falciparum* tested; another part, defined by antibody 7.3, is present in p190 purified from the Thai isolate Kl (ref. 10) but absent from some other isolates[2,3]. Genetically pure lines from a single Thai patient vary in this part of the protein[11]. The antigenically variable part of the protein is cleaved off during release and re-invasion, whilst the constant part survives into the next cycle[1].

Preliminary studies suggest that p190 can protect monkeys against falciparum malaria. Immunization with the affinity-purified native protein modifies the course of infection by the parasite. We treated four control monkeys (Fig. 1) with Freund's complete adjuvant for the first immunization only and with incomplete adjuvant for subsequent immunizations before challenge with the parasite. All show a rapid rise in parasitaemia to the level (20%) at which drug treatment is given to prevent death of the animals. By contrast, two of the three immunized monkeys after an initial rise, rapidly lose detectable parasites and recover. All the immunized monkeys develop antibodies against p190 and show an anamnestic response after challenge (Table 1). Interestingly, the variable part of the p190 protein used in this experiment (purified from isolate K1), was different from its homologue in the challenge parasite (Palo Alto strain)[2,3]. This suggests that the constant part of p190 may have protective value.

Table 1 Antibody response to p190 immunization

Monkey	Inoculated with:	Antibodies against p190 (reciprocal titres) *a*	*b*	*c*
Sven	FCA	<100	<100	100
Uli	FCA	<100	<100	100
Dora	FCA	<100	<100	900
Ronnie	FCA	<100	100	100
Laura	p190+FCA	<100	24,300	>72,900
Anita	p190+FCA	100	8,100	>72,900
Hugo	p190+FCA	<100	24,300	>72,900

Anti-p190 antibodies assayed by ELISA in the treated monkeys. *a*, Before immunization; *b*, after immunization; *c*, 30 days after challenge. FCA, Freund's complete adjuvant. Microtitre plates (Nunc) were coated with affinity-purified p190: 50 μl containing ~100 ng were added to each well and incubated (room temperature; overnight), washed thoroughly (×5) with tap water. Remaining sites were blocked with 100 μl of bovine serum albumin (BSA) solution (3% in phosphate-buffered saline, PBS) for 30 min (room temperature). Threefold dilutions (50 μl) of monkey sera (in 1% BSA in PBS) were incubated (room temperature; 6 h) in each well; the plate was washed (tap water) before adding urease-conjugated rabbit anti-Saimiri IgG antiserum (50 μl of an appropriate dilution in 1% BSA (as above), overnight at room temperature and washed again (×4 in tap water ×2 in distilled water). 150 μl of urease substrate (urea, 0.1%; 0.008% bromocresol purple; 0.2 mM EDTA; *p*H 4.8) was added to each well and incubated (37 °C, 45 min). A positive reaction registers as a change from purple to yellow[27].

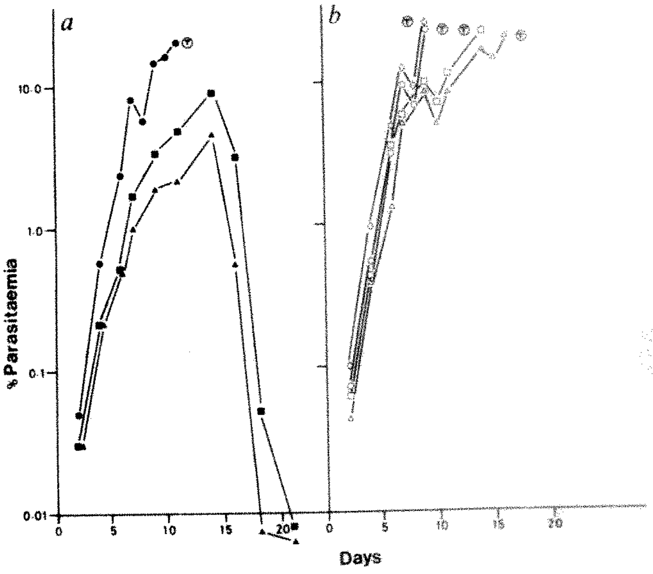

Fig. 1 Effect of p190 on the course of parasitaemia in Saimiri monkeys. *a*, Immunized monkeys. Affinity-purified p190 was injected into three monkeys with Freund's complete adjuvant—Anita (●), Hugo (■) and Laura (▲). Each received subcutaneously 50 μg at day −52, 50 μg at day −39 and 50 μg at day −19. *b*, Controls (open symbols) received adjuvant alone. After immunization, all the monkeys were challenged intravenously with ~2×10^7 parasitized erythrocytes (*P. falciparum*, Palo Alto strain) from a single donor monkey. Ⓣ indicates drug treatment. Parasitaemias were estimated by Giemsa-stained smears.

Much could be learned about this protein from cloning its gene. In addition, clones expressing the gene in bacteria would be a ready source of a protein which is a strong candidate for a subunit vaccine against falciparum malaria. Recently, DNA sequences encoding antigens from both *P. knowlesi*[12] and *P. falciparum*[13] have been cloned. These studies showed that clones

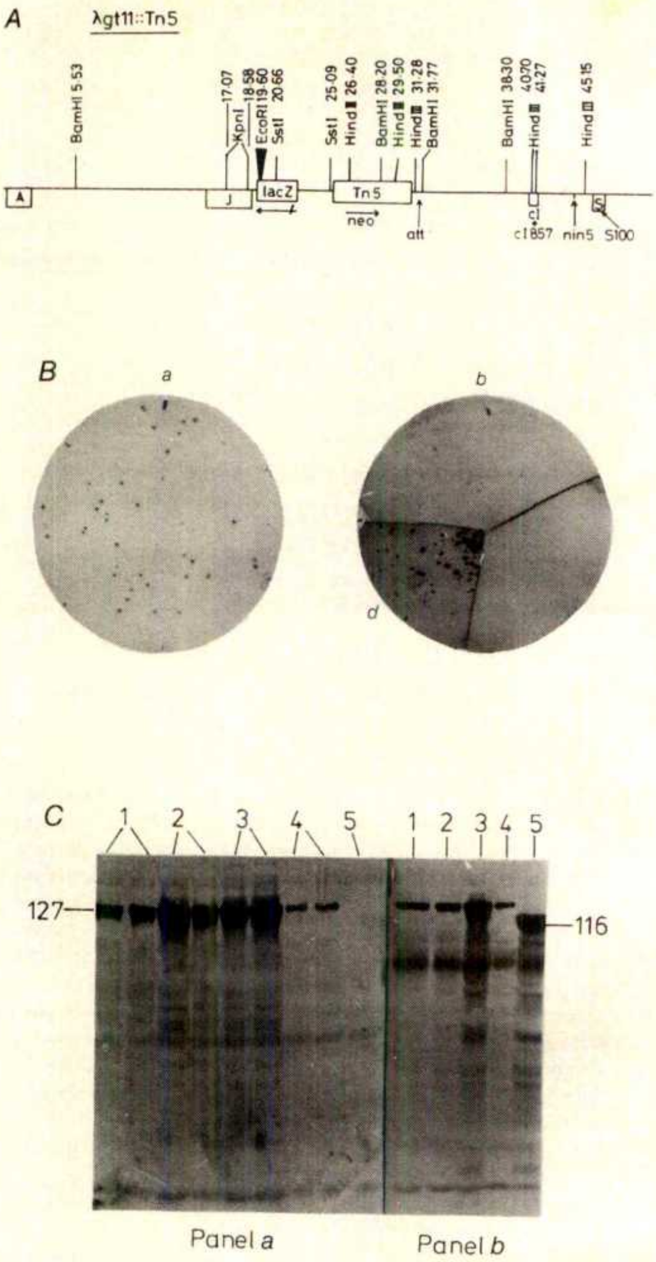

Fig. 2 Isolation of cDNA clones containing p190 sequences. *A*, Cloning vector. Phage $\lambda gt11$ :: Tn*5* was isolated following transposition of Tn*5* to $\lambda gt11$[14]. The cDNA is inserted at the unique *Eco*RI site in *lacZ*, positions of important restriction sites are indicated in kb. The phage is temperature-inducible (cI_{857}) and carries the *nin5* deletion and an amber mutation (S100) preventing lysis in the absence of a suppressor. The presence of Tn*5* greatly simplifies isolation of lysogens, as these derivatives are resistant to kanamycin. *B*, Colony screening of the $\lambda gt11$ :: Tn*5* cDNA expression library by ELISA. *a*, Positive colonies from the primary screen transferred to nitrocellulose and probed again with rabbit anti-p190 serum. *b*, p190 negative colonies from the primary screen probed with anti-p190 serum. *c*, Positive colonies from the primary screen probed with non-immune rabbit serum. *d*, p190-negative colonies from the primary screen probed with anti-β-galactosidase serum. *C*, Western blots of total protein from four p190 lysogens probed with anti-p190 serum (panel *a*, lanes 1–4, each clone run in duplicate) and anti-β-galactosidase serum (panel *b*, lanes 1–4). Lane 5 in each panel shows a control lysogen carrying the vector with no cDNA insert.

Methods: The $\lambda gt11$ :: Tn*5* cDNA library in BTA282, $\Delta lac_{U169}\Delta lon$ *araD*139 str^R *thi hfl* A150 (chr :: Tn*10*) *hsd*R^-M^+ (a derivative of RY1083, see ref. 14) was grown overnight at 30 °C on L-agar with 1555 μg ml^{-1} tetracycline and 40 μg ml^{-1} kanamycin. Colonies were replicated onto nitrocellulose and incubated 2 h at 30 °C. Phage were induced by incubation at 42 °C for 90 min. Colonies were lysed by a modification of the method of Stanley[28]. Nitrocellulose disks were placed on a pad soaked in 5% SDS and heated in a 100 °C oven for 15 min. They were immersed (1 h, 20 °C) in 5% ovalbumin in 10 mM Tris-Cl, *p*H 8.0, 150 mM NaCl (5% OA/TS) containing 0.01% NaN_3, 0.2 mg ml^{-1} henylmethylsulphonyl fluoride (PMSF) and 10 μg ml^{-1} DNase I, washed twice in TS and electroeluted (1 h, 50 V) to remove SDS. The filters were further blocked in 5% OA/TS (15 min, 20 °C) and incubated overnight in rabbit anti-p190 serum diluted 1 : 150 in 5% OA/TS (5 ml). They were washed 5× in TS and incubated in 1 : 1,000 dilution of peroxidase-conjugated goat anti-rabbit IgG in 5% OA/TS (4 h, 20 °C). After a further five washes in TS, the ELISA reaction was developed[29]. The anti-p190 serum was raised in a New Zealand White rabbit against affinity-purified p190 protein[1]. It was extensively preadsorbed on induced $\lambda gt11$ :: Tn*5* lysogens of BTA282 to remove nonspecific anti-*E. coli* antibodies. Total proteins from lysogens for gel analysis were obtained as follows: Young L-broth cultures of lysogens (in BTA282), containing 15 μg ml^{-1} tetracycline and 40 μg ml^{-1} kanamycin, were induced (90 min, 42 °C), centrifuged (1,500*g*, 10 min) and the bacteria ($\sim 2 \times 10^9$) resuspended in 60 μl of 10% SDS, 0.1 mg ml^{-1} PMSF (15 min, 20 °C) and boiled (2 min). 180 μl of Laemmli[30] sample buffer containing 7% 2-mercaptoethanol was added and after further boiling, the samples were electrophoresed on 7.5% SDS-polyacrylamide gels and Western blotted essentially as described previously[29,31]. The filters were probed with antibody as above. Markers used to calibrate the gels were ferritin (220,000 M_r), phosphorylase *b* (94,000 M_r), bovine serum albumin (69,000), catalase (60,000), ovalbumin (46,000), lactate dehydrogenase (36,000) and carbonic anhydrase (30,000).

can be detected using antibody probes to screen bacteria expressing parts of the parasite protein. We report here isolation of a p190 cDNA clone detected by a similar strategy. It includes the 3′ terminus of the messenger RNA and the sequence encoding the final 70 aminoacids at the C-terminus of the protein.

We have made a useful derivative of phage $\lambda gt11$ to serve as the cloning vector for cDNA from cultured *P. falciparum* blood stages. Like its parent,[14,15] our derivative ($\lambda gt11$ :: Tn*5*) facilitates expression of cloned cDNA in *E. coli.* The transposon Tn*5* confers kanamycin resistance on lysogens, which can thus be very easily selected (M.G., N. Bone and J.S., unpublished results). The cDNA was made from total poly$(A)^+$ RNA of blood stage *P. falciparum* isolate Kl, ligated to *Eco*RI linkers and cloned[16] into the unique *Eco*RI site of the vector. The cDNA is thereby inserted into the *lacZ* gene, encoding β-galactosidase (Fig. 2*A*). In the correct frame and orientation at this site, a cDNA molecule is expressed as a hybrid protein comprising most of the β-galactosidase molecule fused to a *P. falciparum* polypeptide (the *Eco*RI site is 153 base pairs (bp) from the C-terminus of the gene)[14,17].

Recombinant phages (~7,000) were screened for synthesis of p190 peptides. Small colonies lysogenic for the phages were transferred to nitrocellulose, induced to stimulate fusion protein synthesis and probed (see Fig. 2) with a polyclonal rabbit antiserum raised against affinity-purified p190[1]. Positive candidate clones were detected by enzyme-linked immunosorbent assay (ELISA) with horseradish peroxidase-conjugated goat anti-rabbit IgG antiserum (Fig. 2*B*). Four apparently identical clones were obtained from this screening. They each encode a hybrid protein (Fig. 2*C*) significantly larger (127,000 M_r) than native β-galactosidase[15]. In Western blots (Fig. 2*C*) they can be seen to have epitopes recognized by both the anti-β-galactosidase (right panel) and the anti-p190 (left panel) probes. By contrast, control clones synthesizing native enzyme only respond to the anti-β-galactosidase probe.

To confirm that our clones encode a p190 sequence, we have developed a rapid and simple technique which we call antibody select. This method eliminates false positive clones which could register in the initial screening if, for example, the anti-p190 probe contained antibodies against other *P. falciparum* pro-

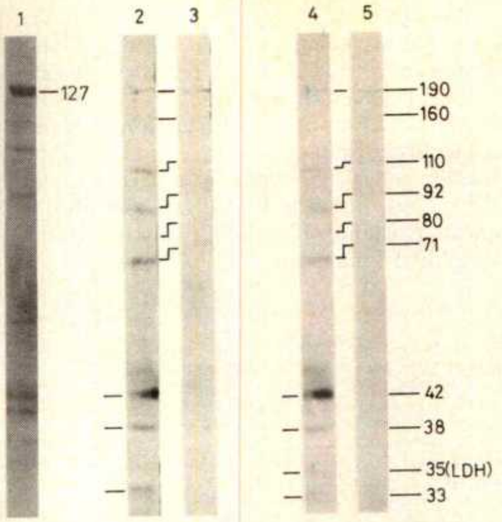

Fig. 3 Confirmation of a λp190 clone by antibody select. Lane 1, p190 hybrid protein used in antibody select (see lanes 3, 5). The protein isolated from an induced lysogen (see below) and run on an SDS-polyacrylamide gel was stained with Coomassie blue. The major band is at 127,000 M_r (see Fig. 2*C*). Lanes 2–5, Western blots of total Kl parasite proteins using the following probes: lane 2, whole anti-p190 serum; lane 3, immunoglobulins affinity-purified from the whole serum by the hybrid protein; lane 4, whole serum with added rabbit antibody against parasite lactate dehydrogenase (LDH); lane 5, immunoglobulins affinity-purified from the mixed sera of lane 4 by the hybrid protein.

Methods: p190 hybrid protein for antibody select was purified as follows: Approximately 10^{11} lysogens (in BTA282) harbouring p190-1 were grown up and collected as described in Fig. 2 legend. The bacterial pellet was resuspended in 4 ml cold 10 mM Tris-Cl, *p*H 8.0, 100 mM NaCl, 1 mM EDTA (TNE) and left on ice 5 min. 4 ml of 50% sucrose in TNE were added, followed 10 min later by 8 ml of 4 mg ml^{-1} lysozyme. After a further 15 min on ice, 4 ml of 0.25 M EDTA, *p*H 8.0 and 2 ml of 10% Nonidet P-40 were added. The suspension was freeze-thawed and the DNA sheared by 5× extrusion through a 19-gauge needle. The extract was then spun at 13,000*g*, 4 °C, 30 min and the pellet suspended in 15 ml of 8 M urea. After a further spin (13,000*g*, 4 °C, 20 min), the supernatant, which contained purified fusion protein, was retained. For antibody select, 4 ml of this supernatant was incubated with 5 cm^2 of nitrocellulose (2 h, 20 °C). After washing and blocking the filter as described for Fig. 2, it was incubated with 5 ml of undiluted rabbit anti-p190 serum plus 5 ml 5% OA/TS overnight at 20 °C. After five washes in TS, specifically bound antibodies were eluted by incubation with 2 ml of 0.1 M glycine-Cl, *p*H 2.6, 0.15 M NaCl (15 min, 20 °C). The eluted material was neutralized with 2 ml 1 M Tris-Cl *p*H 8.0 and 16 ml 5% OA/TS plus 0.01% NaN_3 were added. This solution was used to probe Western blots (lanes 3, 5). Total Kl proteins were prepared from parasite pellets (~2×10^9 mixed stage parasites) after saponin lysis of erythrocytes[1]. The pellets were boiled in 500 μl of Laemmli sample buffer and after spinning on a microfuge (5 min) 80 μl of the supernatant were run on a 7.5% SDS-polyacrylamide gel.

tein(s). Such proteins can be minor contaminants in the p190 preparation used to raise the polyclonal rabbit antiserum.

The hybrid protein of a true p190 clone should be able to bind specific anti-p190 immunoglobulin molecules, permitting them to be affinity purified from the original anti-p190 probe. By contrast, the hybrid proteins of false clones would select immunoglobulin molecules against the contaminating protein.

Hybrid protein from a candidate p190 clone (λp190-1) was bound to nitrocellulose and used to affinity-purify antibodies from the original probe (Fig. 3). The selected antibodies, when eluted and used to probe Western blots of total parasite proteins, prove to bind to p190 and its processed products (160,000, 110,000, 92,000, 80,000 and 71,000 M_r). Moreover, the selection is quite specific. When antibodies against another parasite protein (lactate dehydrogenase, M_r 35,000) were added to the anti-p190 probe, these were not selected (compare lanes 4 and

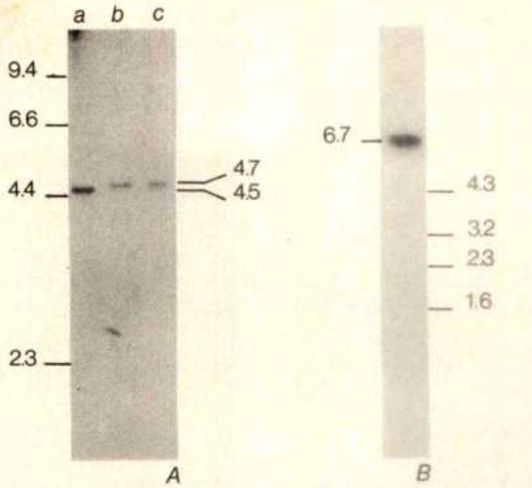

Fig. 4 Parasite sequences hybridizing to the λp190-1 cDNA insert. Panel *A*, Southern blots of *Eco*RI cleaved genomic DNA from different isolates of *P. falciparum*. Lane *a*, isolate Kl (Thailand)[10]; lane *b*, isolate MAD20 (Papua, New Guinea)[3]; lane *c*, Tak9 clone 96 (Thailand)[21]. Markers are *Hin*dIII fragments of λcI_{857} (kb). Panel *B*, Northern blot of total poly(A)$^+$ RNA from isolate Kl. Markers are *E. coli* 16S and 23S RNA and *P. falciparum* '18S' and '28S' RNA[20] (kb).

Methods: For Southern blots 6 μg of genomic DNA were cleaved with 10 U of *Eco*RI (overnight, 37 °C) and electrophoresed on a 0.7% agarose gel. For Northern blots 3 μg of poly(A)$^+$ RNA were run on a 0.8% agarose gel in 2.2 M formaldehyde[20]. Both DNA and RNA were transferred to nitrocellulose in 1 M NH_4Ac, 0.02 M NaOH (1 h). The probe was prepared by digesting λp190-1 DNA with *Kpn*I and *Sst*I to yield a 2.4 kb fragment which includes the 300 bp cDNA insert (see Fig. 2*A*). This was separated from other fragments on a preparative 0.6% agarose gel and after purification, nick-translated with [α^{32} P]dCTP to a specific activity of 1.7×10^7 c.p.m. μg^{-1}. After hybridization, filters were washed to a stringency of 0.1 ×SSC at 37 °C.

5), nor were antibodies already present in the probe against 42,000, 38,000 and 33,000 M_r contaminating proteins (compare lanes 2 and 3).

Antibody select is a rapid and convenient way to confirm or identify any foreign gene sequences expressed in bacteria. It provides an alternative to both hybrid selection of mRNA[18], which requires a large amount of mRNA from the parent organism, and immunization of mice with the fusion protein, followed by immuno-identification of the parent protein in extracts[13,19]. This latter approach is slow and we find that fusion proteins do not always elicit a strong immune response. Antibody select has the added advantage that the antibody probe used in the initial identification of the clones provides the immunoglobulins for the confirmation step. It also provides a way to purify from complex sera antibodies against defined regions of a single antigen molecule.

The clones and their hybrid protein are stable during growth in *E. coli*. Their inserts, which can all be excised with *Eco*RI, hybridize strongly to a total cDNA probe (made from blood-stage parasite poly(A)$^+$ RNA) and give an identical fragment of approximately 300 bp (data not shown). We have therefore studied one clone, representing a small fraction of the protein coding sequence in detail. We can detect the p190 message in total poly(A)$^+$ RNA extracted from mixed blood stages of the parasite. In Northern blots of denaturing gels[20] it has an apparent length of 6.7 kilobases (kb) (Fig. 4*b*), which agrees with the estimate that a coding sequence of at least 5 kb would be required for a 190,000 M_r protein.

The gene can be detected in total genomic DNA. When cut with *Eco*RI, it reveals a single major band which hybridizes strongly to the probe (Fig. 4*a*). Interestingly, when we compare DNA from three different isolates, we find a small but significant difference between Kl (4.5 kb) and two others, MAD20 and the

```
                  10        20        30        40        50
   GAATTCCAGTTTAATTTATTAAGAGCAAAATTAAATGATGTATGTGCTAATGATTAT
   GluPheGlnPheAsnLeuLeuArgAlaLysLeuAsnAspValCysAlaAsnAspTyr

        60        70        80        90       100       110
TGTCAAATACCTTTCAATCTTAAAATTCGTGCAAATGAATTAGACGTACTTAAAAAACTT
CysGlnIleProPheAsnLeuLysIleArgAlaAsnGluLeuAspValLeuLysLysLeu

       120       130       140       150       160       170
GTGTTCGGATATAGAAAACCATTAGACAATATTAAAGATAATGTAGGAAAAATGGAGATT
ValPheGlyTyrArgLysProLeuAspAsnIleLysAspAsnValGlyLysMetGluIle

       180       190       200       210       220       230
ACATTAAAAAAAATAAAAAAACCCATAGAAAATATAAATTGAATTAATTTGAAGAAAGTG
ThrLeuLysLysIleLysLysProIleGluAsnIleAsn***

       240       250       260       270       280       290
TAAGAAAACAATTTGATTAAAAATTAAGAATTGCCAACTAAAAAAAAAAAAAAAAAAAAA

AAAAAGGAATTC
```

Fig. 5 Nucleotide sequence of λp190-1 cDNA. Sequence determination was carried out by the chain termination method[32] after subcloning *Eco*RI fragments of λp190-1 cDNA into M13mp9 (ref. 33) in both orientations. The putative polyadenylation signal is underlined. The reading frame is shown in phase with β-galactosidase. The two *Eco*RI linkers are indicated by a line above the sequence.

genetically pure clone Tak9/96 (4.7 kb). Kl and Tak9/96 are from Thailand[10,21], whilst MAD20 is from Papua, New Guinea[3]. This result may be particularly important as MAD20 and Tak9/96 differ from Kl with respect to the antigenic properties of p190[2,3].

We have estimated the frequency of the cloned p190 sequence in the *P. falciparum* DNA from the intensity of the 4.5 kb band in Southern blots of total genomic digests. Standard copy-number analysis[22,23] using the λp190-1 clone suggests that the number of copies of the p190 sequence per parasite genome is between one and five (data not shown). The part of the gene in p190-1 does not contain tandem repeats (see below and Fig. 5) as has recently been reported in coding sequences for *P. falciparum* S-antigens[13] and *P. knowlesi* circumsporozoite protein[12].

Sequencing studies (Fig. 5) in this laboratory on the p190-1 insert reveals a single open reading frame encoding 70 amino acids in phase with β-galactosidase, terminating with a UGA codon followed downstream by two other stop codons. The clone has a run of 26 A residues at its 3′ terminus. In addition, the sequence ATTAAA starts 24 bases upstream from the first terminal adenine, the expected position for a polyadenylation signal. This function has recently been attributed to the above sequence in several different systems[24-26]. We therefore suggest that the cloned sequence encodes the 3′-terminus of the p190 mRNA and the C-terminus of the polypeptide.

Our conclusion affects the interpretation of the mechanism by which p190 is processed from a primary product of 190,000 M_r to apparently smaller products. Examination of the parasite proteins reacting to the antibodies selected by the p190 clone reveals that in addition to p190, large product bands are also found (Fig. 3, lanes 3, 5). This strongly suggests that epitopes in the C-terminus are not removed by processing. The simplest interpretation of our result is that processing removes the N-terminus of the p190 polypeptide.

We have been unable to detect in the polypeptide encoded in p190-1 epitopes defined by monoclonal antibodies, including 2.2 and 7.3. This may simply reflect the fact that p190-1 contains less than a tenth of the total coding sequence. An alternative explanation is that the C-terminus of p190 cannot elicit an immune response because it is sequestered inside the parasite, as the monoclonal antibodies were obtained after immunization Hwith a whole parasite preparation[2].

The present report describes a cloned gene for a *P. falciparum* protein known to be both strongly immunogenic in man and a candidate for a subunit vaccine against malaria. We now have clones with larger p190 sequences which will test whether, HHlike the native protein (and its homologue in *P. yoelii*[5]), p190 synthesized in bacteria can elicit a protective response against blood stages of the parasite.

We thank David Finnegan, Clare Lister and Andrew Coulson for help and advice on sequencing, John Pugh, David Walliker, Jana McBride and Neil Willetts for discussions and materials, Jackie King, Neil Bone, Ines Calligari and Marija Komarica for technical assistance, Betty McCready for typing the manuscript, and MRC for support.

Received 19 March; accepted 26 July 1984.

1. Hall, R. *et al. Molec. biochem. Parasit.* **11**, 61–80 (1984).
2. Hall, R. *et al. Molec. biochem. Parasit.* **7**, 247–265 (1983).
3. McBride, J. S., Walliker, D. & Morgan, G. *Science* **217**, 254–257 (1982).
4. Holder, A. A. & Freeman, R. R. *J. exp. Med.* **156**, 1528–1538 (1981).
5. Holder, A. A. & Freeman, R. R. *Nature* **294**, 361–364 (1981).
6. Boyle, D. B., Newbold, C. I., Smith, C. C. & Brown, K. N. *Infect. Immun.* **38**, 94–102 (1982).
7. Holder, A., Freeman, R. R. & Newbold, C. I. *Molec. biochem. Parasit.* **9**, 191–196 (1983).
8. Epstein, N. *et al. J. Immun.* **127**, 212–217 (1981).
9. Deans, J. A. *et al. Clin. exp. Immun.* **49**, 297–309 (1983).
10. Thaithong, S. & Beale, G. H. *Trans. R. Soc. trop. Med. Hyg.* **75**, 271–273 (1981).
11. Thaithong, S. *et al. Trans. R. Soc. trop. Med. Hyg.* **78**, 242–245 (1984).
12. Ozaki, L. S. *et al. Cell* **34**, 815–822 (1983).
13. Coppel, R. L. *et al. Nature* **306**, 751–756 (1983).
14. Young, R. A. & Davis, R. W. *Proc. natn. Acad. Sci. U.S.A.* **80**, 1194–1198 (1983).
15. Kemp, D. J. *et al. Proc. Natn. Acad. Sci. U.S.A.* **80**, 3787–3791 (1983).
16. Hyde, J. E. *et al. Molec. biochem. Parasit.* **10**, 269–285 (1984).
17. Zabin, I. & Fowler, A. V. in *The Operon* (eds Miller, J. H. & Reznikoff, W. S.) 89–121 (Cold Spring Harbor, New York, 1978).
18. Maniatis, T., Fritsch, E. F. & Sambrook, J. in *Molecular Cloning*, 329–349 (Cold Spring Harbor, New York, 1982).
19. MacKay, I. *et al. Proc. natn. Acad. Sci. U.S.A.* **78**, 4510–4514 (1981).
20. Hyde, J. E., Zolg, J. W. & Scaife, J. G. *Molec. biochem. Parasit.* **4**, 283–290 (1981).
21. Rosario, V. *Science* **212**, 1037–1038 (1981).
22. Lis, J. T., Prestidge, L. & Hogness, D. S. *Cell* **14**, 901–919 (1978).
23. Langsley, G., Hyde, J. E., Goman, M. & Scaife, J. G. *Nucleic Acids Res.* **11**, 8703–8717 (1983).
24. Jurg, A., Sippel, A. E., Crez, M. & Schutz, G. *Proc. natn. Acad. Sci. U.S.A.* **77**, 5759–5783 (1980).
25. Hagenbuchle, O., Borez, R. & Young, R. A. *Cell* **21**, 179–187 (1980).
26. Mostov, K. E., Friedlander, M. & Blobel, G. *Nature* **308**, 37–43 (1984).
27. Chandler, H. M. *et al. J. immun. Meth.* **53**, 187–194 (1982).
28. Stanley, K. K. *Nucleic Acids Res.* **11**, 4077–4092 (1983).
29. Towbin, H., Staehelin, T. & Gordon, J. *Proc. natn. Acad. Sci. U.S.A.* **76**, 4350–4354 (1979).
30. Laemmli, U. K. *Nature* **227**, 680–685 (1970).
31. Hope, I. A. *et al. Nature* **308**, 191–194 (1984).
32. Sanger, F., Nicklen, S. & Coulson, A. R. *Proc. natn. Acad. Sci. U.S.A.* **74**, 5463–5467 (1977).
33. Messing, J. & Vieira, J. *Gene* **19**, 269–276 (1982).

Human antisera detect a *Plasmodium falciparum* genomic clone encoding a nonapeptide repeat

Michael Koenen*, Artur Scherf†, Odile Mercereau‡, Gordon Langsley‡, Lise Sibilli‡, Philippe Dubois‡, Luis Pereira da Silva‡ & Benno Müller-Hill†

* ZMBH, 6900 Heidelberg, Im Neuenheimer Feld 364, FRG
† Institut für Genetik der Universität zu Köln, 5000 Köln 41, FRG
‡ Institut Pasteur, Paris 75015, France

Plasmodium falciparum causes malaria infections in its human host. Its wide distribution in tropical countries is a major world health problem. Before a vaccine can be produced, the identification and characterization of parasite antigens is necessary. This can be achieved by the cloning and subsequent analysis of genes coding for parasite antigens[1-4]. Recently established cDNA banks allow the expression of cDNA derived from the simian parasite _Plasmodium knowlesi_[5] and _P. falciparum_[6,7] in _Escherichia coli_. Recombinants encoding parasite antigens have been identified by immunodetection in both banks. Two of them contain repetitive units of 11 (ref. 7) or 12 (ref. 5) amino acids. We describe here the construction of an expression bank made directly from randomly generated fragments of _P. falciparum_ genomic DNA. We detect several clones which react strongly with human African immune sera. One clone expresses an antigenic determinant composed of occasionally degenerated repeats of a peptide nonamer.

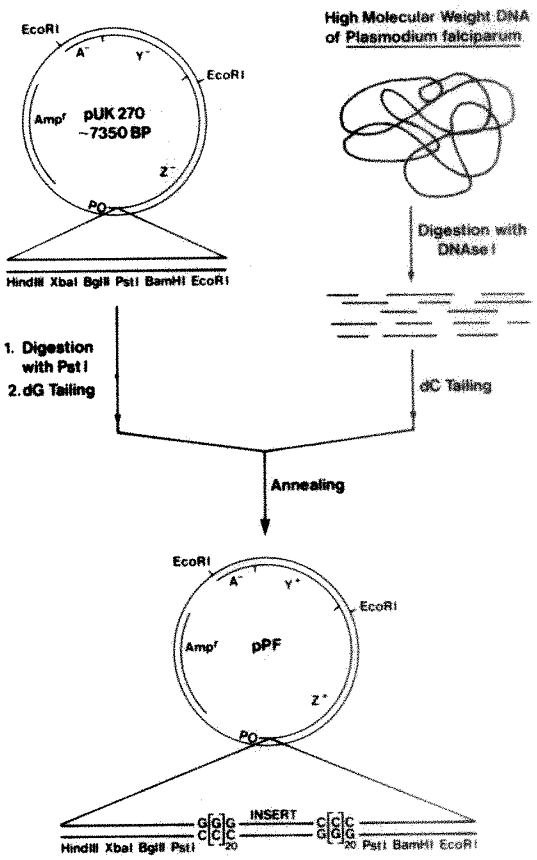

Fig. 1 Cloning of genomic DNA from *P. falciparum* in the expression vector pUK270. The vector pUK270 carries the *lacZ* and *lacY* genes with six unique restriction sites and a frameshift mutation in the promoter proximal part of the *lacZ* gene. Introduction of DNA inserts into the *Pst*I site after dG/dC tailing may overcome the frameshift mutation. Such plasmids will confer a Lac$^+$ phenotype on *E. coli* hosts which carry a deletion in the *lacZ* gene[8]. Such Z$^+$ clones can be isolated either as lactose-positive colonies on lactose minimal agar or as blue colonies on rich plates containing isopropyl-1-thio-β-D-galactoside as inducer and 5-bromo-4-chloro-3-indolyl-β-D-galactoside as indicator. The vector carrying no insert gives a pale blue colour to *E. coli* strains carrying a *lac* deletion on lactose indicator plates but does not allow growth on lactose plates. The lactose-positive recombinants express the inserted DNA as part of the N-terminus of β-galactosidase. Such chimaeric antigen-producing clones can be easily identified if antibodies directed against the expressed antigen are available[8]. Here we have modified the immunoenzymatic detection method described previously[8]. We have used nitrocellulose filters placed on lactose agar for colony replication and growth. Colonies grown on filters were lysed by dipping the filters for 1 min in chloroform at room temperature. Chloroform was removed from the filter by exposure to air for 5 min at 37 °C. Polyvinyl chloride sheets (80 mm diameter) were coated with antibodies and saturated with serum albumin[10]. We used IgG raised in rabbits immunized with Triton X-100 soluble *P. falciparum* asexual blood-stage antigens. The antibody-coated sheets were placed on the lysed colonies. After incubation for 1 h at 4 °C, the sheets were taken off and soaked in wash solution containing 0.5% Triton X-100 for 20 min. The adhering cell debris was removed by squirting with a 20-ml syringe containing wash solution over the sheets. To remove the last traces of cell debris the sheets were placed once more in fresh wash solution. The immunocomplexes were identified as described previously[8]. We used Kemp's method[6], which needs less antibody, to screen the Lac$^+$ colonies with a pool of four human African sera with high IFA titres directed against *P. falciparum* (gift of Professor Mannweiler). The mixture of antisera was cleared of antibodies directed against *E. coli* with sonicated extracts of *E. coli*. Immunocomplexes were detected with iodinated Protein A from *S. aureus*[6]. The lysed colonies were incubated with the treated human antisera after a ×25 dilution.

a

```
                  5'.... GnGGA GAG GTT GTG CCT
Repeat  1. GAA GAA GTT GTT GAA GAA GTT GTG CCT
        2. ... ... T.A ... ... ... ... ..A ..A
        3. .T. ... C.A ..A ... ... ... ..A ...
        4. .T. ... C.A ..A ... ... ... ..A ..A
        5. ..G ... C.A ... ... ..G ... A.A ...
        6. ... ... A.. ..G ... ... ... A.A ...
        7. ... ... ..C ... ... ... ..A ..A ...
        8. ..G ... A.A ... ... ... ..G A.A ...
        9. ... ... T.A A.. ... ... ... ... ..A
       10. .T. ... C.A T.A ... ... ... A.A ..A
       11. .T. ... ..A T.A ... ..T ... A.A ...
       12. ... ... ... ... ... ... ... A.A ..A
       13. ... ... A.. A.. ... ... ... A.A ...
       14. ... ... A.. A.. ... ..G .CG A.A ..A
       15. .T. ... A.. ... .....G ... A.A ..A
       16. ... ..T A.. ... ... ... ... A.A ..A
       17. ... ... A.. ... ... ..T ... A.A ..A
       18. ... ... ... ... ... ... ... A.A ...
       19. ... ... ... ... ... ... ... ..A ..A
       20. ... ... T.A ..A ... ... ... A.A ..A
       21. ... ... C.A ... ... ..G ..G A.A ...
       22. ... ... ... CC. ... ..G ... ..A ..A
       23. GAA GAA CTC Cn ....3'
```

b

```
                           --- Glu Val Val Pro
Repeat  1. Glu Glu Val Val Glu Glu Val Val Pro
        2. ... ... Leu ... ... ... ... ... ...
        3. Val ... Leu ... ... ... ... ... ...
        4. Val ... Leu ... ... ... ... ... ...
        5. ... ... Leu ... ... ... ... Ile ...
        6. ... ... Ile ... ... ... ... Ile ...
        7. ... ... ... ... ... ... ... ... ...
        8. ... ... Ile ... ... ... ... Ile ...
        9. ... ... Leu Ile ... ... ... ... ...
       10. Val ... Leu Leu ... ..  ... Ile ...
       11. Val ... ... Leu ... Asp ... Ile ...
       12. ... ... ... ... ... ... ... Ile ...
       13. ... ... Ile Ile ... ... ... Ile ...
       14. ... ... Ile Ile ... ... Ala Ile ...
       15. Val ... Ile ... ... ... ... Ile ...
       16. ... Asp Ile ... ... ... ... Ile ...
       17. ... ... Ile ... ... Asp ... Ile ...
       18. ... ... ... ... ... ... ... Ile ...
       19. ... ... ... ... ... ... ... ... ...
       20. ... ... Leu ... ... ... ... Ile ...
       21. ... ... Leu ... ... ... ... Ile ...
       22. ... ... ... Pro ... ... ... ... ...
       23. Glu Glu Leu ---
```

Fig. 2 *a*, DNA sequence of the insert of clone pPF11-1; *b*, the derived protein sequence.

We digested high-molecular weight DNA from the Palo Alto Uganda (FUP) strain[4] of *P. falciparum* with DNase I. Fragments of 50–1,000 base pairs (bp) were separated on a polyacrylamide gel and cloned into the 5′ end of the *lacZ* gene by dG/dC tailing (see Fig. 1 legend). We used the vector pUK270 that carries in the non-essential 5′ end of the *lacZ* gene several unique restriction sites. These sites introduce a frameshift into the *lacZ* gene which renders the *Z*, *Y* and *A* genes phenotypically Z$^-$, Y$^-$ and A$^-$. After cutting the vector with *Pst*I, dG-tailing and annealing with genomic fragments, only recombinants allowing read-through or restart in phase are phenotypically Lac$^+$. We identified these positive recombinants and isolated and screened 10,000 Lac$^+$ clones with antisera (Fig. 1). We screened the clones with rabbit antiserum, obtained after immunization with Triton-

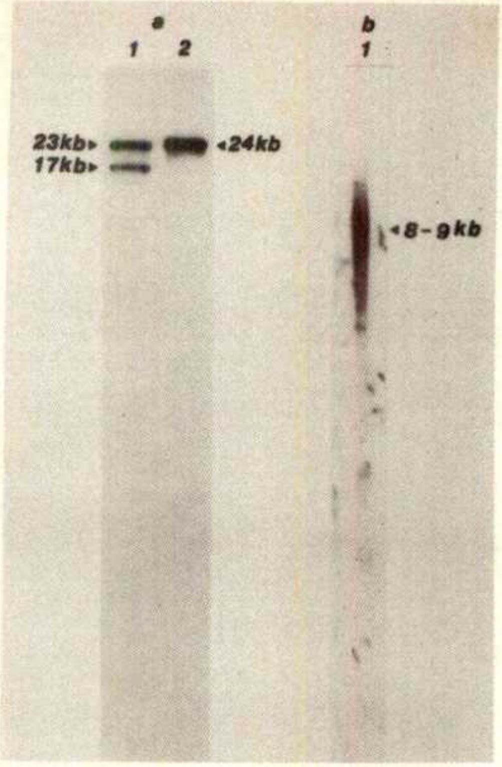

Fig. 3 *a*, Hybridization of genomic DNA of *P. falciparum* (FUP strain) with the 620-bp insert of clone pPF11-1. The genomic DNA (2 μg DNA per track) was cut with *Eco*RI (track 1) and *Hin*dIII (track 2). The DNA was fractionated on a 0.8% agarose gel, and transferred from the gel to nitrocellulose paper[13], hybridized with ^{32}P-labelled pPF11-1 probe, and autoradiographed. *b*, Hybridization of polyadenylated mRNA isolated from *P. falciparum* (blood stage) with the 620-bp insert of clone pPF11-1. 1.5 μg of polyadenylated mRNA was fractionated on a 1% agarose–formaldehyde gel, transferred to nitrocellulose paper, hybridized, washed and autoradiographed[15].

extracted proteins from *P. falciparum* asexual blood stages, using an immunoenzymatic technique[8–10]. Colonies producing antigen are visualized directly; we identified 36 positive clones with the rabbit antibodies.

We then screened 10,000 Lac$^+$ recombinants with a mixture of human sera from adult Africans living in areas endemic for malaria. Here, we visualized immunocomplexes with iodinated Protein A from *Staphylococcus aureus*[6]. Several positive clones were identified, most of them identical to those previously detected with the rabbit antisera. We present here the analysis of one antigen-producing clone, pPF11-1, which reacts strongly with both the rabbit and the human antisera in both tests. It produces a β-galactosidase fusion protein of about 140,000 molecular weight (MW) which is found in cytoplasmic extracts as a stable soluble protein and accounts for approximately 10% of the total protein. This clone contains 620 bp of *P. falciparum* genomic DNA. An insert of this length is consistent with the increase in size of the β-galactosidase fusion protein.

We next determined the complete sequence of the insert by the method of Maxam and Gilbert[11], and we found a 27-bp repeat running throughout the entire fragment. DNA sequence analysis reveals that only one reading frame contains no stop codons (Fig. 2). This frame codes for the ideal sequence Glu-Glu-Val-Val-Glu-Glu-Val-Val-Pro, but shows little similarity with the 12-amino acid repeat reported for the CS protein of *P. knowlesi*[5] or the 11-amino acid repeat found in *P. falciparum* S-antigen[7]. There is some variation in our polypeptide sequence as alanine, isoleucine or leucine can replace valine and aspartic acid or valine can replace glutamic acid. We conclude that the polypeptide probably exists as an α-helix, possibly interrupted by the prolines. The representation of this presumed α-helix according to Schiffer and Edmundson[12] reveals alternating amphipathic nonapeptides separated by proline residues, which suggests a superstructure of intertwined α-helices.

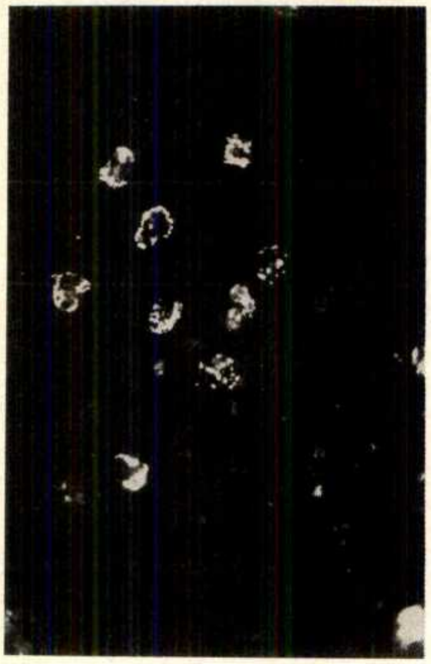

Fig. 4 Indirect immunofluorescence of *P. falciparum* antigen with anti-pPF11-1 antibodies. Thin smears of cultured parasites were fixed by acetone. The parasites were incubated with a 1/20 dilution of mouse antiserum raised against SDS-denatured 11-1 proteins and then revealed by fluorescein-conjugated anti-mouse IgG rabbit antibodies. Examination by phase-contrast microscopy (not shown) indicates that the immunofluorescence is not associated with the mature intracellular parasite but with the surrounding red blood cell membrane.

The pattern generated when pPF11-1 was hybridized[13] to FUP genomic DNA (Fig. 3*a*, track 2) demonstrates homology to a single *Hin*dIII fragment of approximately 24 kilobases (kb). We can identify two *Eco*RI fragments of 23 and 17 kbbbb (Fig. 3*a*, track 1), and single large *Bam*HI, *Aha*III, *Nde*I, *Hin*fI and *Bgl*II fragments. Sequences homologous to pPF11-1 are found in DNA extracted from a Thai isolate, K1 (ref. 14), and clone T9.96 (ref. 15)(data not shown). Our finding that the inside of pPF11-1 contains no *Eco*RI site, whereas two *Eco*RI fragments are observed in both FUP and T9.96[15] DNA, suggests that the repeated sequence spans more than 620 bp. Furthermore, a transcript of blood-stage *P. falciparum* of approximately 8–9 kb is identified[16] using pPF11-1 DNA as a probe (Fig. 3*b*). A mRNA of this apparent size could encode a protein of approximately 250,000 MW.

We raised rabbit and mice antisera against the purified fusion protein. In late trophozoites and schizont-infected red blood cells (RBC), a parasite protein can be detected by indirect immunofluorescence using these sera. The combination of phase-contrast and fluorescence microscopy indicates that the protein is located in patches associated with the membrane of the infected RBC (Fig. 4) and is not detected in ring-infected RBC or in merozoites. Using the same sera we are unable to immunoprecipitate an antigen from boiled culture supernatant in conditions where immune monkey serum immunoprecipitates an S-antigen of 200–220,000 MW. Preliminary data suggest that the 11-1 antigen has a higher molecular weight and is a minor constituent of the parasite protein. Several antigens are associated with the surface of erythrocytes infected with late stage parasites: schizont-infected cell agglutination antigen[17] which undergoes antigenic variation may be related to sequestration on endothelial cells[18]. We are currently investigating whether pPF11-1 is an antigen of this type.

Finally, concerning the difference between the commonly used cDNA expression banks (see refs 5–7) and our genomic expression bank, in a cDNA bank the most commonly expressed gene products are overrepresented. In searching for cDNA coding for a rare protein, the overrepresented cDNAs of frequent gene products have to be accounted for. In a genomic bank all genes are equally represented, therefore only one bank is needed for one organism. In cDNA there is a bias for clones coding for the C-terminal end of the particular protein; a genomic bank shows no such bias.

We thank Professor Mannweiler for the gift of the human sera, Dr J. Scaife for the K1 and T9.96 parasite DNA, Dr M. Cramer for iodination of Protein A, Dr A. Ullmann for purification of the fusion protein, Sigrid Quester, Evelyne Brunet, Micheline Guillote for technical assistance and Thierry Blisnick for growing the parasites. G.L. is a MRC/INSERM exchange fellow. This work was supported by the Deutsche Forschungsgemeinschaft through Schwerpunkt Gentechnologie and Institut Pasteur Production.

Received 13 April; accepted 26 July 1984.

1. Brown, G. V., Anders, R. F., Mitchell, G. F. & Heywood, P. F. *Nature* **297**, 591–593 (1982).
2. Gysin, J., Dubois, P. & Pereira da Silva, L. *Parasit. Immun.* **4**, 421–430 (1982).
3. Hall, R. *et al. Molec. biochem. Parasit.* **7**, 247–265 (1983).
4. Dubois, P. *et al. Proc. natn Acad. Sci. U.S.A.* **81**, 229–232 (1984).
5. Godson, G. N., Ellis, J., Suec, P., Schlesinger, D. H. & Nussenzweig, N. *Nature* **305**, 29–33 (1983).
6. Kemp, D. J. *et al. Proc. natn. Acad. Sci. U.S.A.* **80**, 3787–3791 (1983).
7. Coppel, R. L. *et al. Nature* **306**, 751–756 (1983).
8. Koenen, M., Rüther, U. & Müller-Hill, B. *EMBO J.* **1**, 509–512 (1982).
9. Rüther, U., Koenen, M., Sippel, A. E. & Müller-Hill, B. *Proc. natn. Acad. Sci. U.S.A.* **79**, 6852–6855 (1982).
10. Broome, S. & Gilbert, W. *Proc. natn. Acad. Sci. U.S.A.* **75**, 2746–2749 (1978).
11. Maxam, A. M. & Gilbert, W. *Meth. Enzym.* **65**, 499–560 (1980).
12. Schiffer, M. & Edmundson, A. E. *Biophys. J.* **7**, 121–135 (1967).
13. Southern, E. *J. molec. Biol.* **98**, 503–517 (1975).
14. Thaithong, S. & Beate, G. H. *Trans. R. Soc. med. Hyg.* **75**, 271–273 (1981).
15. Rosario, V. *Science* **212**, 1037–1038 (1981).
16. Langsley, G., Hyde, J. E., Goman, M. & Scaife, J. G. *Nucleic Acids Res.* **11**, 8703–8717 (1983).
17. Howard, R. J., Barnwell, J. W. & Kao, V. *Proc. natn. Acad. Sci. U.S.A.* **80**, 4129–4133 (1983).
18. Hommel, M., David, P. H., Olignio, L. D. & David, J. R. *Parasit. Immun.* **4**, 409–419 (1982).

Rearrangements of T-cell receptor gene *YT35* in human DNA from thymic leukaemia T-cell lines and functional T-cell clones

Barry Toyonaga, Yusuke Yanagi, Nicole Suciu-Foca*, Mark Minden & Tak W. Mak

The Ontario Cancer Institute and Department of Medical Biophysics, University of Toronto, 500 Sherbourne Street, Toronto, Ontario, Canada M4X 1K9
* Department of Pathology, College of Physicians and Surgeons, Columbia University, New York, New York 10031, USA

An essential property of the immune response is its ability to distinguish between self and non-self and to generate enormous diversity in antibody and T-cell immune responses. Although the genetic and molecular mechanisms responsible for antibody diversity have now largely been elucidated, the structure of the T-cell receptor and the diversification of the receptor repertoire have only recently become amenable to study. One approach has involved immunochemical studies of the protein precipitated by monoclonal antibodies which react specifically with the immunizing T-cell clones[1–3]. Another approach has been to clone and sequence a human[4] or a murine[5] T-cell specific message that may specify part of the T-cell receptor. We present here results of Southern blot analysis of non-T, immature T, and mature T-cell genomic DNA, and provide evidence that rearrangements of the *YT35* sequences do occur in the DNA of thymic leukaemia T cells. This suggests that *YT35* codes for at least part of the T-cell receptor and that rearrangements occur at this early stage of thymic ontogeny. Furthermore, DNA rearrangements are present in lymphocytes with phenotypic and functional characteristics of helper, killer, or suppressor T cells. We conclude that the three subpopulations of T cells operate via receptor molecules encoded by the same gene family.

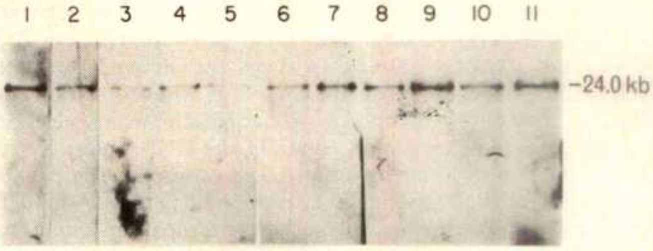

Fig. 1 Southern gel analysis of the T-cell receptor gene *YT35* in non-T-cell DNA. DNA was extracted from 11 independent samples of non-T cells and digested with 3 units of *Bam*HI per μg DNA overnight. DNA was then electrophoresed through 0.8% agarose gel as previously described[19]. DNA was transferred to nitrocellulose filters and hybridized to ^{32}P-dCMP-labelled nick-translated C35, a *Hpa*I (nucleotide 430) to *Eco*RV (nucleotide 1,087) subclone of *YT35* (ref. 4) by the method of Southern[6]. For detailed procedure, see ref. 19. Lane 1, DNA from granulocytes of a donor; lane 2, DNA from fibroblasts of the donor; lane 3, DNA from B-cell line RPMI 3638; lane 4, DNA from myeloid leukaemia cell line HL-60; lanes 5–11, DNAs from fibroblast cultures from seven different donors.

In order to determine the germ-line organization of the gene(s) corresponding to the putative T-cell receptor cDNA *YT35* and to estimate the frequency of DNA polymorphism among individuals, we have used Southern blot analysis[6] on 23 samples of genomic DNA extracted from fibroblasts (15 samples), B-cell lines (five lines), a bladder tumour cell line MGHU-1 and myeloid cell lines (two lines). The DNA samples were digested with the restriction enzyme *Bam*HI and probed with C35, a constant-region subclone of *YT35*. One 24-kilobase (kb) restriction fragment band was observed in each of the non-T cells examined (see Fig. 1). We also obtained similar results showing unchanging patterns and intensities of restriction fragment bands in non-T-cell DNA using four other restriction enzymes, *Bst*EII, *Hin*dIII, *Eco*RI and *Sph*I. These data establish that the non-T-cell DNAs from a variety of sources show no rearrangement of sequences corresponding to the putative T-cell receptor cDNA clone *YT35*. It also appears that DNA polymorphism between individuals is rare for sequences homologous to the *YT35* constant region.

To determine whether DNA rearrangements occur during or after intrathymic differentiation, we next investigated the rearrangement patterns of several thymic leukaemia lines. DNA was extracted from leukaemic T-cell lines and treated as described above. Our results show that DNA of non-T cells (Fig. 2*a*, lanes 4 and 5) contain the same restriction fragment band typical of germ-line DNA as summarized in Fig. 1. DNA from the thymic leukaemia cell lines (Fig. 2*a*, lanes 1, 2 and 3; Fig. 2*b*, lanes 2, 3 and 4) contains bands not found in the germ-line DNA lanes. When hybridization was carried out using the entire *YT35* cDNA, data consistent with DNA rearrangement in T-cell DNA were also observed, but the number of bands increased to 6 or 7 (Fig. 2*c*, lanes 2–4). In addition to the germ-line bands presented by the C35 probe, hybridization with the entire cDNA *YT35* probe reveals four new bands corresponding to the homologous variable gene segments.

Regulatory (helper and suppressor) and effector (killer) T-lymphocytes probably cooperate via complex interactions to establish a successful immune response, but the existence and relative role of the T-cell receptor in each of these subpopulations is unknown. In order to ascertain the presence of the T-cell receptor in functionally distinct T-cell subpopulations, we analysed four mature T-cell clones with helper, killer or suppressor function for possible gene rearrangements of sequences corresponding to the putative T-cell receptor clone *YT35*. All these T-cell clones were derived from the same individual and were generated by *in vitro* alloactivation against stimulating cells from a single donor[7,8].

The biological activities of these T-cell clones are summarized in Table 1. Total genomic DNA was extracted from these T-cell clones and from the autologous B-cell line derived from the same individual by Epstein–Barr virus transformation of peripheral blood B-lymphocytes. After digestion with restriction enzyme (*Eco*RI, *Bam*HI and *Hin*dIII), the DNA was analysed by the method of Southern using C35 as a probe. The results are similar for all the restriction enzymes used (Fig. 3). Although the B-cell bands (Fig. 3*a*, *b*, lane 1) retain a pattern similar to the germ-line DNA (Fig. 1), all four T-cell-clone DNA samples exhibit rearrangements of DNA homologous to *YT35* (Fig. 3*a*, *b*, lanes 2–5). Our results indicate that T-cell clones with helper, killer or suppressor activity exhibit gene rearrangement of sequences corresponding to the putative T-cell receptor gene *YT35*. The use of twin clones derived from the same individual excludes the possibility that the rearrangement is a reflection of an individual characteristic trait.

The results presented here are consistent with the somatic rearrangement of genomic T-cell DNA sequences corresponding to the putative human T-cell receptor cDNA clone *YT35*. The unchanging or germ-line restriction fragment band patterns found in the numerous non-T-cell DNA samples (Fig. 1) indicate

Table 1 Characterization of functional T-cell clones

Clone	Phenotype	T-cell functions		
		Blastogenic	CML	PFC formation
19	OKT4	DR1(r.086)	None	Helper
22	OKT4	DR1(r.083)	None	Helper
209	OKT4	DR1(r.083)	None	Suppressor
26	OKT8	None	B35	No effect
207	OKT4	DR1(0.83)	DR1	Helper

T-cell phenotype was determined by cytofluorimetric testing of reactivity with murine monoclonal antibody reacting with human T-cell surface antigens[16] (Ortho Diagnostic). Blastogenic response was determined in a 92-h ^{3}H-TdR incorporation assay. Cell-mediated lymphocytolysis (CML) was ascertained by ^{51}Cr-release assay[17]. Plaque-forming cells (PFC) induced by T-cell clones were tested as described[18].

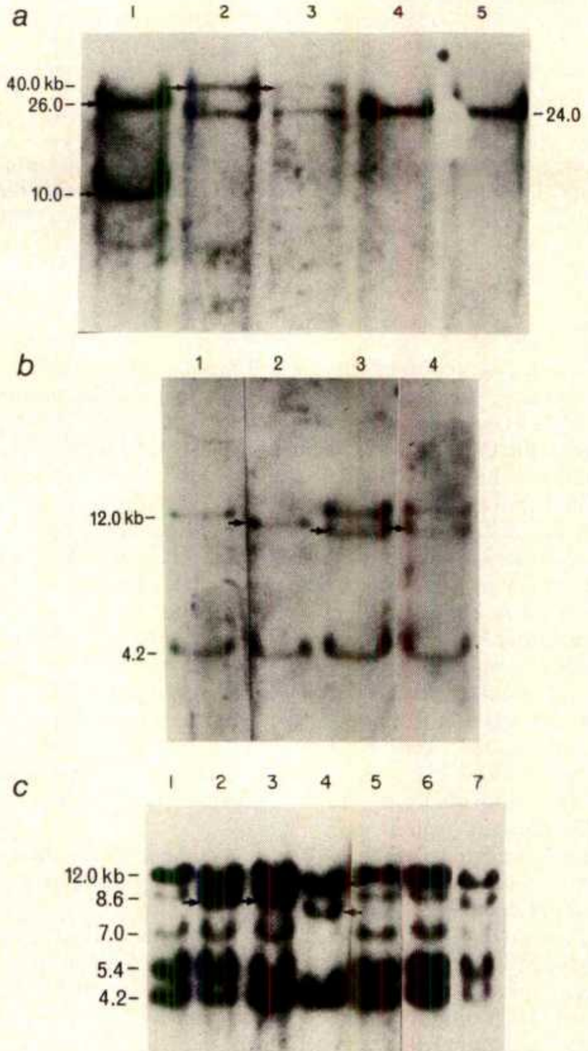

Fig. 2 Southern gel analysis of T-cell receptor gene *YT35* in DNA from thymic leukaemia lymphoblastic cell lines. DNA from thymic leukaemia cell lines MOLT-3, Jurkat and CEM, and control DNA from four non-T sources were analysed by Southern gel analysis (described in Fig. 1) using either the C35 constant-region probe (*a*, *b*) or the entire *YT35* cDNA (ref. 4) (*c*) as a probe. Arrows indicate rearranged bands. *a*, DNA digested with *Bam*HI and hybridized with C35 constant region as a probe. Lane 1, CEM; lane 2, Jurkat; lane 3, MOLT-3; lane 4, RPMI 3638; and lane 5, HL-60. *b*, DNA digested with *Eco*RI and hybridized with C35 constant region as a probe. Lane 1, fibroblast from a donor; lane 2, CEM; lane 3, Jurkat; lane 4, MOLT-3. *c*, DNA digested with *Eco*RI and hybridized with the entire *YT35* (ref. 4) as a probe. Lane 1, fibroblast from a donor; lane 2, MOLT-3; lane 3, Jurkat; lane 4, CEM; lane 5, RPMI 3638; lane 6, HL-60; lane 7, bladder tumour cell line MGJU-1.

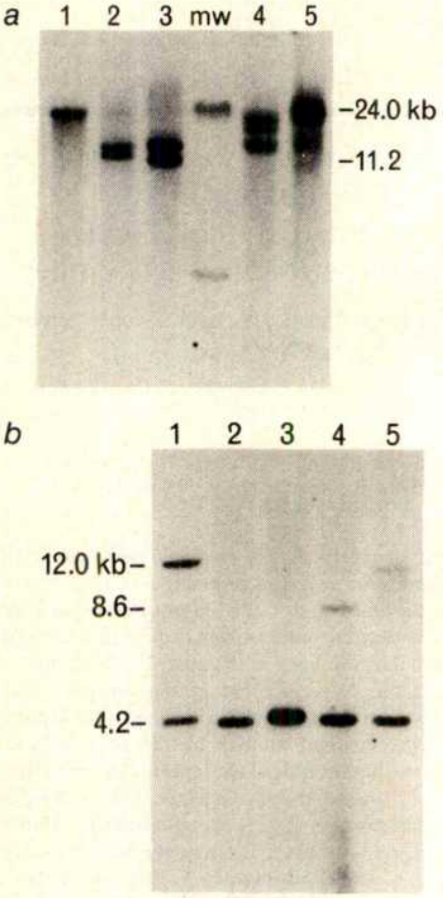

Fig. 3 Southern gel analysis of T-cell receptor gene *YT35* in DNA from five mature functional T-cell clones. DNAs and an autologous Epstein–Barr virus-transformed B-cell clone from the same individual were digested with *Eco*RI or *Bam*HI and examined by Southern gel analysis using C35 constant region as a probe (described in Fig. 1). *a*, *Bam*HI; *b*, *Eco*RI. Lane 1, LBCL (B-cell line); lane 2, clone 209 (suppressor); lane 3, clone 22 (helper); lane 4, clone 207 (helper and killer); lane 5, clone 19 (helper).

that DNA polymorphism is infrequent in genomic sequences homologus to *YT35*. The *YT35*-encoding protein thus resembles the κ light chains of mammalian immunoglobulin, where DNA polymorphism is not common[9]. It is possible that polymorphism gives rise to the inconstant restriction fragment band patterns of thymic leukaemic T-cell DNA (Fig. 2*a–c*), because we did not have the autologous non-T-cell DNA samples for comparison. To rule out this possibility, we observed DNA rearrangements in several mature T-cell clones where the autologous B cells from the same individual retain the germ-line patterns. These results (Fig. 3) suggest that DNA rearrangement in leukaemic T cells is not due to DNA polymorphisms among individuals. The increased complexity of the restriction band pattern observed on probing with the entire cDNA *YT35* (variable and constant regions) (Fig. 2*c*) implies the existence of multiple variable segments in the genome which is consistent with data analysing the germ-line genomic DNA (G. Siu *et al.*, unpublished observations). Thus, it appears that the generion of T-cell receptor diversity is accomplished by a rearrangement mechanism similar to that found in immunoglobulin production[10,11]. Immunoprecipitation of T-cell membrane glycoprotein by use of clonotypic monoclonal antibodies suggests the existence of two distinct chains in the T-cell receptor molecule[1–3]. *YT35* appears to code for one of these polypeptide chains, and further diversity can be expected to emerge through interactions with the other chain.

The non-germ-line patterns observed in monoclonal thymic leukaemia cell lines clearly indicate that rearrangement of the putative T-cell receptor gene *YT35* occurs during intrathymic differentiation in ontogenesis. Recent data demonstrate that the T-cell receptor for alloantigens is probably the most primitive one[12], and is also associated with the receptor for well-defined soluble antigens[13,14]. Our finding that helper, suppressor and cytotoxic T-cell clones exhibit rearrangement of DNA fragments corresponding to the *YT35* cDNA clone demonstrates that this gene codes for a receptor molecule which is present in all T-cell subpopulations. Furthermore, the level of mRNA expression of the cDNA *YT35* clone has been found to decrease following post-thymic differentiation of helper, suppressor and cytotoxic T cells[15]. Our data, combined with these findings, show that the *YT35* clone corresponds to a T-cell receptor gene and that rearrangement of this gene is involved in the diversification of the T-cell receptor repertoire.

Receptor gene rearrangement occurs in early ontogenetic stages of intrathymic differentiation, when T cells acquire the capacity to recognize both self and allogeneic MHC antigens. Rearrangement can also be found in helper, killer and suppressor T cells, suggesting that the three classes of cells operate via receptor molecules encoded by the same gene family. We hope that the isolation of the T-cell receptor gene from human and mouse will help in dissecting these complex interactions between lymphocytic and non-lymphocytic cells necessary for successful humoral and cytolytic immune responses.

We thank Beth Chin for technical assistance and Dr Leroy Hood for discussions and comments. This work is supported by the NCI of Canada, the MRC of Canada, and by grant NO1-A1-32505 from NIH. B.T. is a recipient of the Terry Fox Postdoctoral Fellowship, and Y.Y. is a fellow of the MRC of Canada.

Received 25 April; accepted 23 July 1984.

1. Acuto, O. *et al. Cell* **34**, 717–726 (1983).
2. Kappler, J. *et al. Cell* **34**, 727–737 (1983).
3. McIntyre, B. W. & Allison, J. P. *Cell* **34**, 739–746 (1983).
4. Yanagi, Y. *et al. Nature* **308**, 145–149 (1984).
5. Hedricks, S. M., Niëlsen, S. M., Kavaler, J., Cohen, D. T. & Davis, M. *Nature* **308**, 153–158 (1984).
6. Southern, E. M. *J. molec. Biol.* **38**, 503–517 (1975).
7. Suciu-Foca, N., Rohowsky, C., Kung, P. & King, D. W. *J. exp. Med.* **156**, 283–288 (1982).
8. Suciu-Foca, N., Rohowsky, C., Kung, P. & King, D. W. *Hum. Immun.* **9**, 37–47 (1984).
9. Korsmeyer, S. J. *et al. J. clin. Invest.* **71**, 301–313 (1983).
10. Honjo, T. *A. Rev. Immun.* **1**, 499–528 (1983).
11. Tonegawa, S. *Nature* **302**, 575–581 (1983).
12. Owen, F. L. *Immunology Today* **3**, 95–96 (1982).
13. Sredni, B. & Schwartz, R. H. *Nature* **287**, 855–857 (1980).
14. Abromson-Leeman, S. R. & Cantor, M. *J. exp. Med.* **158**, 428–437 (1983).
15. Yoshikai, Y. *et al. Nature* **310**, 506–508 (1984).
16. Suciu-Foca, N., Rohowsky, C., Kung, P. & King, D. W. *J. exp. Med.* **156**, 283–288 (1982).
17. Krensky, A. M., Reiss, C. S., Mier, J. W., Strominger, J. L. & Burakoff, S. J. *Proc. natn. Acad. Sci. U.S.A.* **79**, 2365–2369 (1982).
18. Fauci, A. S. & Pratt, K. R. *Proc. natn. Acad. Sci. U.S.A.* **73**, 3676–3679 (1976).
19. Yamamoto, Y. *et al. Proc. natn. Acad. Sci. U.S.A.* **78**, 6893–6897 (1981).

Identification of a diversity segment of human T-cell receptor β-chain, and comparison with the analogous murine element

Stephen P. Clark*, Yasunobu Yoshikai*, Sheryle Taylor*, Gerald Siu†, Leroy Hood† & Tak W. Mak*

* The Ontario Cancer Institute, and The Department of Medical Biophysics, University of Toronto, 500 Sherbourne Street, Toronto, Ontario, Canada M4X 1K9
† Division of Biology, California Institute of Technology, Pasadena, California 91125, USA

The humoral immune system antigen-binding proteins (immunoglobulins) are disulphide-linked heterodimers of light and heavy chains. The gene for the variable region which determines antigen specificity is assembled when one member from each of the dispersed clusters of variable (*V*) gene segments, diversity (*D*) elements (for the heavy chains only) and joining (*J*) segments rearrange and fuse during B-cell development (reviewed in ref. 1). Short recognition sequences adjacent to these elements appear to be involved in the recombination process. The cellular immune system antigen recognition proteins are receptors on the surface of T cells, which are composed of disulphide-linked α-chains and β-chains, each of which has a variable and constant region[2–4]. Recently, cDNA clones of the β-chain[5] mRNA have been isolated[6,7]; the genomic arrangement is very similar to immunoglobulin genes with multiple V_β genes[8], and two clusters of J_β segments, each of which is upstream from a constant-region gene segment[9]. The V_β and J_β segments have adjacent recombinational recognition sequences like the immunoglobulin elements. However, ~10 nucleotides of the cDNA clones between the V_β and J_β regions were not present in the corresponding genomic elements and may have been due to intervening D_β segments[8,10]. Here we describe a diversity element ($D_{\beta 1.1}$) in a region of high human–mouse homology about 650 bases 5′ to the first J_β cluster. Two transcripts which include sequences upstream of $D_{\beta 1.1}$ are found in the human thymus. This region may have some other function besides providing the β-chain with a diversity segment.

We have extended our previous sequence[8] of $J_{\beta 1}$, the first of the two human J_β clusters, from 750 bases 5′ to $J_{\beta 1.1}$ to 380 bases 3′ to $J_{\beta 1.2}$ (Fig. 1*a*). This cluster is about 4 kilobases (kb) 5′ to $C_{\beta 1}$. We identified what we believe to be a diversity element, $D_{\beta 1.1}$, 650 bases upstream from $J_{\beta 1.1}$. Its position with respect to the J_β cluster is similar to that of the murine immunoglobulin heavy-chain *D* element, D_{Q52} (ref. 11) and the equivalent human element, D_{HQ52} (ref. 12). However, there is no obvious homology between $D_{\beta 1.1}$ and the human or murine D_{Q52} element, other than the recombination signal sequences which flank the elements and the stretch of guanosine residues in the 3′ half of the protein coding region (comparisons not shown). $D_{\beta 1.1}$ has the typical recombination recognition heptamer and nonamer sequences[13,14] separated by 12 bases on the 5′ side and 23 bases on the 3′ side (Fig. 1*a*). This structure was expected because the germ-line V_β gene has a 23-base spacer between the two signal sequences and the *J* segments have a 12-base spacer (Fig. 1 and refs 8–10) and indicates that the β-chain follows the same 12/23 spacer rule for recombination that governs the

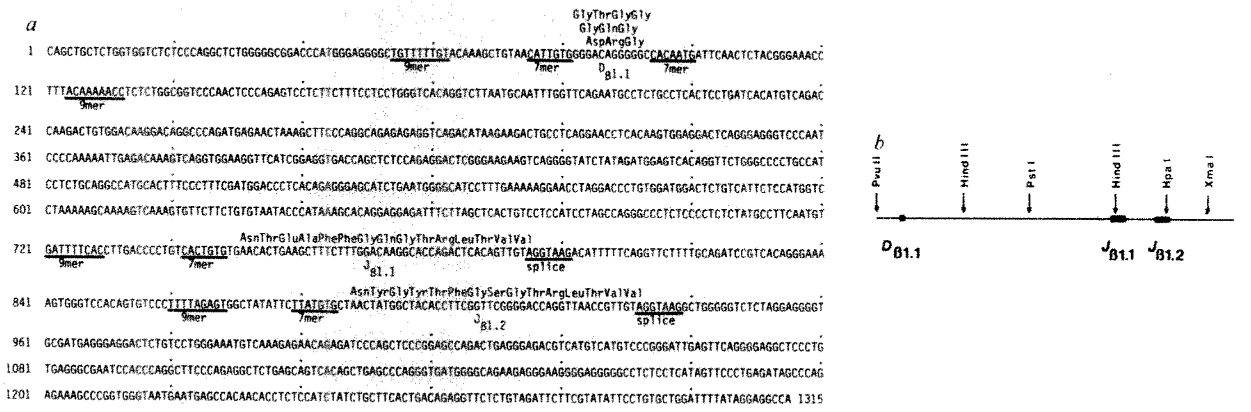

Fig. 1 The sequence which surrounds $D_{\beta 1.1}$, $J_{\beta 1.1}$ and $J_{\beta 1.2}$. *a*, The nucleotide sequence, with the $D_{\beta 1.1}$ element and the $J_{\beta 1}$ elements indicated and the translation products shown above the sequence. The heptamer and nonamer recombination signal sequences are underlined, as are the splice donor sites at the 3′ ends of the $J_{\beta 1}$ elements. *b*, A summary of the restriction sites used in sequencing and the positions of $D_{\beta 1.1}$ and the $J_{\beta 1}$ segments. The sequence was determined partly by the dideoxy chain-termination method[19] after cloning specific restriction fragments into the phage vector M13mp9 or M13mp10, and partly by the Maxam and Gilbert method[20] after 3′ end-labelling fragments at the *Xma*I site with [α-^{32}P]dCTP (Amersham) and the large (Klenow) fragment of *Esherichia coli* DNA polymerase I (New England Biolabs). All regions were confirmed by sequencing on both strands or using alternative procedures, and all restriction sites were sequenced across.

immunoglobulin genes[13,14]. Two elements can only rearrange and join if one has a 12-base spacer and the other a 23-base spacer between the recognition nonamer and heptamer sequences. However, the arrangement is different from the immunoglobulin heavy-chain *D* elements which have 12-base spacers on both the 5′ and 3′ sides. The reason for this difference, when the general organization of the β-chain elements so closely resembles that of the immunoglobulin heavy chain, is unknown but it may be a consequence of the evolution of the immune receptor family. It may be a part of a mechanism to allow the recombinatorial enzymes to distinguish between the T-cell receptor and immunoglobulin genes, or it may simply be a mechanism to allow greater flexibility in the structure of the variable region. The V_β gene segment (with the 23-base spacer) can attach directly to the J_β segment (with a 12-base spacer) without incorporating a D_β element at all (Y.Y. *et al.*, in preparation). Alternatively, it might also be possible to incorporate more than one *D* element into the rearranged β-gene.

The YT35 *D* element[8], $D_{\beta \mathrm{YT35}}$, and $D_{\beta 1.1}$ are not similar so they are probably members of distinct D_β families (comparisons not shown). Our cosmid clones of unrearranged DNA which contain about 20 kb 5′ to the $J_{\beta 1}$ cluster were analysed for other related D_β segments by probing with synthetic oligonucleotides complementary to $D_{\beta 1.1}$ and to $D_{\beta \mathrm{YT35}}$. No hybridization was observed, although the probes hybridized strongly to the positive controls (data not shown). This suggests that the D_β elements are dispersed much the same as the immunoglobulin *D* elements which are scattered over 80 kb 5′ to the J_H cluster[15]. The sequence presented in Fig. 1 was also searched by computer for human interspersed repetitive elements contained in the GenBank DNA sequences database, release 19.0, but none were found.

Northern blot analysis of T-cell RNA reveals two distinct bands that hybridize to a YT35 probe (Fig. 2). A constant-region probe detects a major band of 1.3 kb and a minor band of 1.0 kb in human thymus RNA and RNA from the leukaemic T-cell line MOLT-3 (ref. 16). The relative intensities of the two bands vary between experiments, as seen by comparing Fig. 2*a* and *b*, but the 1.3-kb band is always more intense. The C_β probe hybridizes to MOLT-3 and thymus RNA to the same extent, however, the YT35 V_β region probe hybridizes much more strongly to the 1.3-kb band of MOLT-3 than that of thymus (Fig. 2*a*), reflecting the heterogeneous mixture of *V*-region sequences found in the population of thymocytes, but does not detect the 1.0-kb band even after prolonged exposure. Thus, the 1.0-kb transcript contains no V_β sequences. To determine whether this species is the result of transcription initiating upstream of an aberrant or incomplete *D–J* rearrangement, a Northern filter was probed with the oligonucleotide D_βA30 as described in the legend to Fig. 2. Knowing the sequence of the 1.3-kb MOLT-3 message[6], we would not expect D_βA30 to hybridize to it. The two MOLT-3 bands that are observed after washing the filter and probing with this oligonucleotide may be due to traces of the C_β probe that remained on the filter, as the relative intensities of the bands are the same as when the C_β probe was used. For the thymus RNA, however, the 1.3-kb message hybridizes less strongly than the 1.0-kb message—the opposite of what is seen with the C_β probe—and a previously undetected transcript of ~0.8 kb appears. The 1.3-kb message is detectable partly because of hybridization to the 12 bases of coding region. The 0.8-kb species is not seen in the T-cell lines[16] MOLT-3 (Fig. 2*b*), Jurkat or CEM (data not shown). An oligonucleotide complementary to 40 bases immediately 5′ to the D_βA30 probe region also hybridizes to the 1.0-kb and 0.8-kb transcripts in thymus RNA (data not shown). These data indicate that at least some of the 1.0-kb transcripts initiate upstream from a $D_{\beta 1.1}$ element that has rearranged to be adjacent to a *J* segment but not to a V_β segment, as appears to occur in the mouse[17]. The lack of hybridization of D_βA30 to the MOLT-3 1.0-kb message suggests that it may be the result of rearrangement to some element other than $D_{\beta 1.1}$.

Figure 3 compares the sequences around $D_{\beta 1.1}$ with the murine $D_{\beta 1.1}$ and $D_{\beta 2.1}$ loci[17] and the similarities of the sequences in various regions are listed in Table 1. The $D_{\beta 1.1}$ elements have identical sequences, but the murine $D_{\beta 2.1}$ has an insert of two nucleotides. The high homology between human and murine $D_{\beta 1.1}$ (78% over 229 bases, which is as high as the homology between the coding regions of the human[6] and murine[7] C_β genes) was unexpected, considering the 85 Myr that these sequences have had to diverge since mammalian radiation[18]. Such conservation usually means that either the region encodes a protein with a conserved primary structure or that the region has a regulatory role. In addition, there may be overlapping functions. This extensive homology is probably not a requirement for general *D*-element rearrangement because the human and murine D_{Q52} immunoglobulin heavy-chain *D* elements do not have any similarity beyond the recombination recognition sequences (ref. 12 and our unpublished observations).

Sequences 5′ to the presumptive coding region of $D_{\beta 1.1}$ are present in the 1.0-kb transcript of immature thymocytes. Such transcripts are also found in the mouse[17]. An open reading frame extends upstream in the human and murine D_β segments, so it may be that these short transcripts encode a protein with

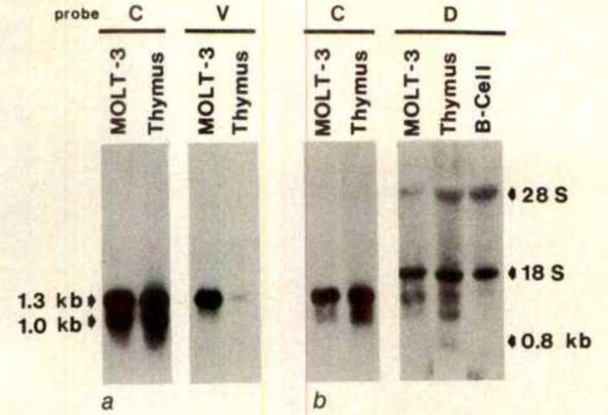

Fig. 2 Analysis of thymus and MOLT-3 RNA for transcripts containing V_β sequences, C_β sequences or 5′ $D_{\beta1.1}$ flanking sequences. RNA was extracted from the cells, electrophoresed and transferred to nitrocellulose membranes as previously described[6]. *a*, Hybridization of a YT35 constant- (*C*) or variable-specific (*V*) fragment. *b*, Hybridization with the YT35 constant-region probe (*C*).

Methods: *a*, The *C* or *V* fragment was gel-purified, nick-translated and hybridized to the nitrocellulose in hybridization solution (50% deionized formamide, 5×SSC (1×SSC is 150 mM NaCl, 15 mM Na citrate, *p*H 7.0), 50 mM sodium phosphate, 250 μg ml^{-1} salmon sperm DNA, 1×Denhardt's solution) and 1×10^6 c.p.m. per ml of probe at 40 °C for 16 h. The final wash was in 0.1×SSC, 0.1% SDS at 50 °C. *b*, The method for hybridization was as for *a*. After 80 h of autoradiography, the filter was washed three times in 0.1×SSC, 0.1% SDS at 90 °C, then exposed to film for 60 h to ensure complete removal of the probe. The 1.3-kb band was barely visible. The filter was then hybridized to the 30-base oligonucleotide probe D_βA30 (*D*; complementary to positions 93–64 in Fig. 1*a*, including 12 bases of $D_{\beta1.1}$ and 18 bases of the adjacent 5′ flanking region) which had been 5′ end-labelled with [γ-^{32}P]ATP (Amersham, specific activity 3,000 Ci mmol^{-1}) and T_4 polynucleotide kinase (Boehringer Mannheim). Hybridization was performed in hybridization buffer with 1×10^6 c.p.m. per ml at 37 °C for 16 h, then at 21 °C for 24 h. The filters were washed twice with 5×SSC at 21 °C and exposed for 10 days. The control lane of B-cell RNA shows that D_βA30 strongly hybridizes to 28S and 18S RNA, and that the 1.3-kb and smaller messages are specific to T cells.

Table 1 Homology between human and murine D_β elements and their flanking sequences

	Upstream of 5′ nonamer	Between nonamer recombination signals	Downstream of 3′ nonamer
Human $D_{\beta1.1}$ Murine $D_{\beta1.1}$	78%	90%	68%
Human $D_{\beta1.1}$ Murine $D_{\beta2.1}$	60%	75%	Random
Murine $D_{\beta1.1}$ Murine $D_{\beta2.1}$	54%	79%	Random

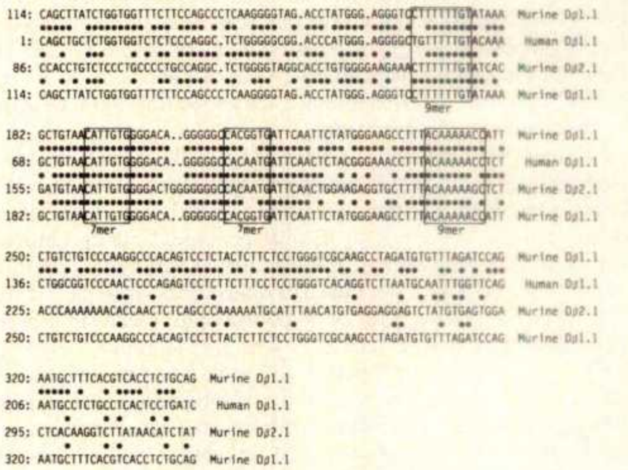

```
114: CAGCTTATCTGGTGGTTTCTTCCAGCCCTCAAGGGGTAG.ACCTATGGG.AGGGTCCTTTTTTGTATAAA  Murine Dβ1.1
  1: CAGCTGCTCTGGTGGTCTCTCCCAGGC.TCTGGGGGCGG.ACCCATGGG.AGGGGCTGTTTTTGTACAAA  Human Dβ1.1
 86: CCACCTGTCTCCCTGCCCCTGCCAGGC.TCTGGGGTAGGCACCTGTGGGGAAGAAACTTTTTTGTATCAC  Murine Dβ2.1
114: CAGCTTATCTGGTGGTTTCTTCCAGCCCTCAAGGGGTAG.ACCTATGGG.AGGGTCCTTTTTTGTATAAA  Murine Dβ1.1

182: GCTGTAACATTGTGGGGACA..GGGGGCCACGGTGATTCAATTCTATGGGAAGCCTTTACAAAAACCATT  Murine Dβ1.1
 68: GCTGTAACATTGTGGGGACA..GGGGGCCACAATGATTCAACTCTACGGGAAACCTTTACAAAAACCTCT  Human Dβ1.1
155: GATGTAACATTGTGGGGACTGGGGGGGCCACAATGATTCAACTGGAAGAGGTGCTTTTACAAAAAGCTCT  Murine Dβ2.1
182: GCTGTAACATTGTGGGGACA..GGGGGCCACGGTGATTCAATTCTATGGGAAGCCTTTACAAAAACCATT  Murine Dβ1.1

250: CTGTCTGTCCCAAGGCCCACAGTCCTCTACTCTTCTCCTGGGTCGCAAGCCTAGATGTGTTTAGATCCAG  Murine Dβ1.1
136: CTGGCGGTCCCAACTCCCAGAGTCCTCTTCTTTCCTCCTGGGTCACAGGTCTTAATGCAATTTGGTTCAG  Human Dβ1.1
225: ACCCAAAAAAACACCAACTCTCAGCCCAAAAAATGCATTTAACATGTGAGGAGGAGTCTATGTGAGTGGA  Murine Dβ2.1
250: CTGTCTGTCCCAAGGCCCACAGTCCTCTACTCTTCTCCTGGGTCGCAAGCCTAGATGTGTTTAGATCCAG  Murine Dβ1.1

320: AATGCTTTCACGTCACCTCTGCAG  Murine Dβ1.1
206: AATGCCTCTGCCTCACTCCTGATC  Human Dβ1.1
295: CTCACAAGGTCTTATAACATCTAT  Murine Dβ2.1
320: AATGCTTTCACGTCACCTCTGCAG  Murine Dβ1.1
```

Fig. 3 Comparison of the human $D_{\beta1.1}$ and the murine $D_{\beta1.1}$ and $D_{\beta2.1}$ regions. The murine sequences are from Siu *et al.*[17]. Solid circles indicate identity between adjacent sequences, and dots show where gaps have been introduced to improve the alignment. The relevant regions are marked.

unknown properties and functions. A prediction arising from this hypothesis is that there should be no homology 3′ of the D_β region, which would be deleted during recombination with a J_β segment. This is indeed seen when murine $D_{\beta2.1}$ is compared with the other two D_β elements, but not when the human and murine $D_{\beta1.1}$ elements are compared (Table 1). Perhaps the 0.8-kb transcript observed in the thymus includes regions 3′ to $D_{\beta1.1}$, or possibly there is some transcript being produced on the opposite strand, where there are long open reading frames in the human and murine $D_{\beta1.1}$ regions, but not in the murine $D_{\beta2.1}$.

The presence of a prominent and discrete transcript of 1.0 kb in immature but not mature T cells from both man (Y.Y. *et al.*, in preparation) and mouse[17] suggests that this message has a function during T-cell development. The frameshifts upstream from the D_β elements suggest that any proteins resulting from distinct incomplete *D–J* rearrangements would be quite different, so might be involved in the generation of, or selection for, receptor specificity. Unfortunately, knowledge of the molecular biology of the processes of T-cell ontogeny is scarce, so it is difficult to suggest a function for this RNA species or the protein it may encode. Further characterization of the 1.0-kb transcript may allude to some of these processes, and might indicate a reason for the strong homology around $D_{\beta1.1}$ between species.

We thank S. Horvath and M. Malissen for synthesizing and purifying, respectively, the 14-nucleotide oligomer complementary to the YT35 *D* region. S.P.C. and Y.Y. are recipients of awards from the MRC of Canada. This work was supported by the MRC of Canada and the National Cancer Institute of Canada.

Received 11 July; accepted 24 August 1984.

1. Tonegawa, S. *Nature* **302**, 575–581 (1983).
2. Acuto, O. *et al.* *Cell* **34**, 717–726 (1983).
3. Kappler, J. *et al.* *Cell* **34**, 727–737 (1983).
4. McIntyre, B. W. & Allison, J. P. *Cell* **34**, 739–746 (1983).
5. Acuto, O. *et al.* *Proc. natn. Acad. Sci. U.S.A.* **81**, 3851–3855 (1984).
6. Yanagi, Y. *et al.* *Nature* **308**, 145–149 (1984).
7. Hedrick, S. M., Nielsen, E. A., Kavaler, J., Cohen, D. I. & Davis, M. M. *Nature* **308**, 153–158 (1984).
8. Siu, G. *et al.* *Cell* **37**, 393–401 (1984).
9. Malissen, M. *et al.* *Cell* (in the press).
10. Chien, Y., Gascoigne, N. R. J., Kavaler, J., Lee, N. E. & Davis, M. M. *Nature* **309**, 322–326 (1984).
11. Sakano, H., Kurosawa, Y., Weigert, M. & Tonegawa, S. *Nature* **290**, 562–565 (1981).
12. Ravetch, J. V., Siebenlist, U., Korsmeyer, S., Waldmann, T. & Leder, P. *Cell* **27**, 583–591 (1981).
13. Early, P., Huang, H., Davis, M., Calame, K. & Hood, L. *Cell* **19**, 981–992 (1980).
14. Sakano, H., Maki, R., Kurosawa, Y., Roeder, W. & Tonegawa, S. *Nature* **286**, 676–682 (1980).
15. Wood, C. & Tonegawa, S. *Proc. natn. Acad. Sci. U.S.A.* **80**, 3030–3034 (1983).
16. Nagasawa, K. & Mak, T. W. *Cell. Immun.* **71**, 396–403 (1982).
17. Siu, G. *et al.* *Nature* **311**, 344–350 (1984).
18. Romero-Herrera, A. E., Lehman, H., Joysey, K. A. & Friday, A. E. *Nature* **246**, 389–395 (1973).
19. Sanger, F., Nicklen, S. & Coulson, A. R. *Proc. natn. Acad. Sci. U.S.A.* **74**, 5463–5467 (1977).
20. Maxam, A. M. & Gilbert, W. *Proc. natn. Acad. Sci. U.S.A.* **74**, 560–564 (1977).

Isolation of UV-resistant revertants from a xeroderma pigmentosum complementation group A cell line

Brigitte Royer-Pokora* & William A. Haseltine

Department of Pathology, Dana–Farber Cancer Institute,
Harvard Medical School, Boston, Massachusetts, USA

Xeroderma pigmentosum (XP) is an autosomal recessive disease. Cells cultured from XP patients are hypersensitive to the lethal effects of UV light[1–6]. Most XP cells are defective in an early stage in DNA repair of UV light-induced damage. The nature of the genetic defect of the XP syndrome has not been defined. To address this problem, we attempted to isolate UV-resistant cells from a cell line derived from an XP complementation group A (XPA) patient. By using a selection scheme capable of detecting one UV-resistant cell in a population of 10^8 cells, several UV-resistant clones were isolated at frequencies between 1×10^{-7} and 2×10^{-8}. Here we describe the isolation and initial characterization of these phenotypic revertants.

We used the cell line designated M1 which has been characterized with respect to its histocompatibility locus antigen (HLA) type, karyotype, isoenzyme profile, restriction map of the integrated simian virus 40 (SV40) genome, and its ability to function as a recipient in transfection experiments[7]. Multiple exposures to UV light were used to select for UV-resistant clones. The frequency of occurrence of UV-resistant clones in different experiments (listed in Table 1) was in the range 1×10^{-7} to 2×10^{-8}, regardless of whether the cells had been exposed to DNA under transfection conditions, subjected to mock transfection, or subjected to selection without previous treatment. The observation that the frequency of appearance of UV-resistant colonies was the same regardless of the previous treatment of the cells indicates that the frequency of reversion to a UV-resistant phenotype is substanitally higher than the frequency of DNA-mediated gene transfer of the wild-type *XPA* allele in the conditions used. We have been unable to repeat the results of Takano *et al.*[8] using their cell line as recipient, the same source of donor DNA, and the same selection conditions. In control experiments we found that the transfection frequency of a single-copy *gpt* gene integrated into HeLa cell DNA was 2×10^{-6} per 20 μg of high-molecular weight DNA, indicating that transfer of single-copy genes can be detected using the methods outlined here.

Several tests were done to determine whether the UV-resistant cell lines were derived from the original M1 UV-sensitive parent. The morphology, doubling time and cloning efficiency of the UV-resistant cell lines were indistinguishable from those of the M1 culture. In all cases tested, the restriction map of the integrated SV40 genome was the same as that of the M1 culture (Fig. 1). The isoenzyme profile, HLA type and the karyotype are also identical to those of the parental M1 cell line (Table 2). We conclude that the UV-resistant colonies derived in these experiments are phenotypic revertants of the M1 XPA culture.

The cytotoxic effect of UV-irradiation of several of the UV-resistant colonies was compared with that of normal and SV40-transformed human fibroblasts. Figure 2 shows that although D_0 varied somewhat from clone to clone, they all were within the normal range. (D_0 is the dose required to reduce survival by $1/e$ on the exponential portion of the survival curve.)

The ability of several cell lines to support the replication of UV-irradiated herpes simplex virus was examined[9]. The plating efficiency of UV-irradiated herpes simplex virus on the resistant cell lines is comparable with that on normal cell lines and distinctly different from that of the M1 cells (Fig. 3*a*). Similar results were obtained using UV-irradiated SV40 DNA in transfection assays[10]. One revertant cell clone, XP-RH10, was tested and found to resemble the normal cells rather than the M1 cell line. We conclude that the UV-resistant cell lines tested have recovered the ability to carry out host cell reactivation.

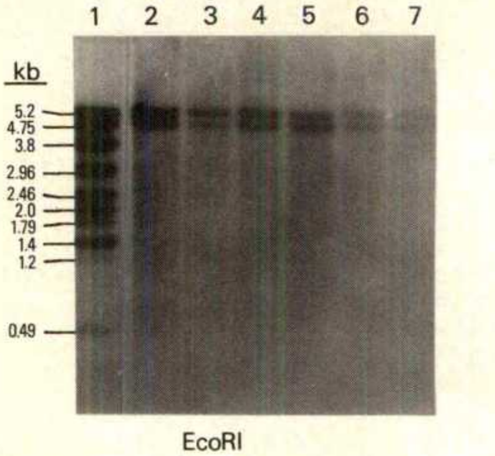

Fig. 1 Characterization of integrated SV40 DNA. DNA was isolated from the parental M1 cell line and from the revertants indicated below. The DNA was digested to completion with *Eco*RI and the sizes of the *Eco*RI DNA fragments determined by Southern blot analysis using SV40 DNA as probe, as described previously[7]. Lane 1, size markers (SV40 DNA digested with *Eco*RI, *Hha*I, *Pst*I, *Pvu*II, *Taq*I and *Hpa*II, as described elsewhere[7]). Lane 2, parental XP12RO-M1 clone; 3, XP-RE1; 4, XP-RH3; 5, XP-RH10; 6, XP-RG3; 7, XP-RG1.

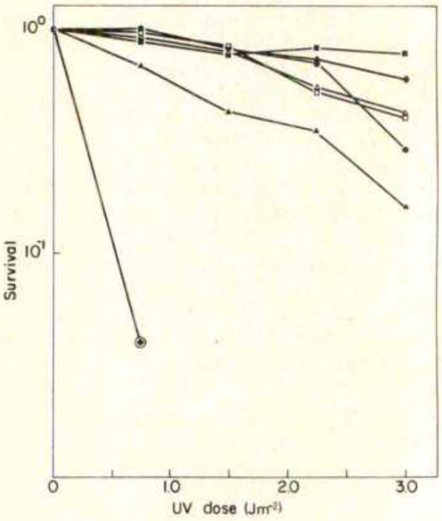

Fig. 2 Dose–response of M1 and revertant cell lines. ◈, XP12RO-M1; ▲, XP-RG1; ●, XP-RE1; □, XP-RH10; △, XP-RC12; ■, 1522, normal human fibroblasts; ◆, GM637, SV40-transformed fibroblasts. 1,000 cells were seeded per 60-mm dish and irradiated after 24 h under a layer of 1 ml Hank's buffer. After removal of the Hank's buffer, growth medium containing 15% serum was added. The medium was changed after 1 week and the plates were stained after 2 weeks. Colonies were counted and the relative survival determined as:

$$\frac{\text{number of colonies on UV-irradiated plates}}{\text{number of colonies on unirradiated plates}}$$

The relative survival values were found to be the same between experiments that were repeated at least three times for several of the clones. For the determination of D_0 values, plates were irradiated with higher doses of UV.

The ability of the cells to remove cyclobutane pyrimidine dimers from DNA can be measured by determining the number of UV-specific endonuclease-sensitive sites in DNA at several times post-irradiation. For this study, cells were irradiated with 2.5 J m^{-2}; DNA was extracted immediately and 24 h after

---

* Present address: Department of Haematology, Children's Hospital, Boston, Massachusetts 02115, USA.

Table 1 Frequency of occurrence of UV-resistant M1 clones

Experiment	Treatment	No. of cells used	No. of revertants	Designation of clones	Frequency
a	None	1×10^7	0		$<1\times10^{-7}$*
b	None	5.3×10^7	11	XP-RB1-XP-RB11	2×10^{-7}
c	None	3×10^8	11	XP-RC1-XP-RC11	3.6×10^{-8}
c	$CaPO_4$+DMSO	2.6×10^7	4	XP-RC12-XP-RC16	1.5×10^{-7}
e	$CaPO_4$+DMSO	1×10^7	2	XP-RE1, XP-RE2	2×10^{-7}
f	$CaPO_4$+DMSO	1×10^7	2	XP-RF1, XP-RF2	2×10^{-7}
g	XP DNA	1×10^7	2	XP-RG1, XP-RG2	ND†
k	XP DNA	5×10^6	0		$<2\times10^{-7}$*
h	Normal human DNA	1×10^7	9	XP-RH1-XP-RH9	9×10^{-7}‡
g		1×10^7	7	XP-RG3-XP-RG10	ND†
k		5×10^6	0		$<2\times10^{-7}$*
g	Mouse DNA	6.5×10^6	3	XP-RG11-XP-RG14	ND†‡
h	Mouse DNA	3×10^6	2	XP-RH10, XP-RH11	6×10^{-7}‡
k	Mouse DNA	3.5×10^6	0		$<8.5\times10^{-7}$*

To select for UV-resistant clones, 2×10^7 M1 cells were seeded at a density of 4×10^6 cells in large plates (245 cm^2). Selection was begun with a UV dose of 1 J m^{-2} 24 h after seeding. The selective pressure was maintained by exposure to 0.5 J m^{-2} every other day for 2 weeks. At the end of this time cells were exposed to 1 J m^{-2} and allowed to grow for 1 week. Surviving colonies were picked and tested for UV resistance. Only colonies having a $D_0>2.2$ were scored as resistant in this assay. Reconstruction experiments using M1 and SV40-transformed normal human cells demonstrate that this selection method can detect 1 in 10^8 UV-resistant cells. The frequency represents the number of UV-resistant colonies per initial number of cells plated. Between the start of transfection experiments and plating out for UV selection, the cells doubled two or three times. For different treatments, the same letter (*a*, *b*, *c*, *e*, *f*, *g*, *h* or *k*) indicates that the experiments were done at the same time, for example in expt *c*, one part of a pool of cells was subjected to UV selection alone and another part to calcium phosphate + dimethyl sulphoxide (DMSO) plus UV selection. In a typical transfection experiment, 5×10^5 cells were plated on 60-mm plates, then treated either with 20 μg DNA per plate or with $CaPO_4$ precipitate alone, or left untreated. DNA was left on the plates for 24 h. Cells were then treated with 10% DMSO for 10–20 min. The medium was changed every day for 5 days and cells were split to low density on day 6 (3×10^6–1×10^7 cells per dish, 245 mm^2). The next day UV selection was initiated as described above. In experiments *g* and *k*, cells were split the day after DMSO treatment and UV selection was initiated on day 3 after addition of DNA.

* No UV-resistant clones were obtained for the number of cells plated, therefore the frequency is less than the indicated number.

† ND, not determined. In this experiment the frequency could not be calculated, as the colonies obtained after UV selection were pooled and reseeded before a second round of UV selection.

‡ The clones were analysed for donor DNA by Southern blotting. In the case of clones transfected with mouse DNA, DNA from the revertant clones was analysed for repetitive mouse DNA as described by Grusella *et al.*[15]. No repetitive murine sequences were found in the UV-resistant cells. XP-RH1-XP-RH9 clones were transfected with normal human DNA ligated to pSV$_2$gpt DNA, which codes for resistance to mycophenolic acid (MPA). The clones contained neither pBR322 sequences nor additional SV40 sequences, and were not resistant to MPA (data not shown). These results indicate that the UV-resistant cells contained no transfected DNA.

Table 2 Karyotype and isoenzyme analysis of the parental XP clone and the UV-resistant (UV^r) revertants XP-RE1 and XP-RG1

	Parental SV40 XP12RO-M1 clone	UV^r clones XP-RE1 and XP-RG1
Cytogenetics		
Sex	Male	Male
Near-diploid count	44%	30%
Near-tetraploid count	56%	62%
Highly polyploid	0	2%
Marker A (3q$^+$)	+	+
Marker B (14q$^+$)	+	+
Isozymes		
LDH	Human	Human
G6PD	B	B
PGM1	1–2	1–2
PGM3	1	1
ESD	1	1
Me-2	1	1
Ak-1	1	1
GLO-1	1–2	1–2

The methods used for karyotype, isoenzyme and HLA type analysis have been described previously[7]. LDH, lactate dehydrogenase; G6PD, glucose 6-phosphate dehydrogenase; PGM1 and PGM3, phosphoglucomutase-1 and -3; ESD, esterase D; Me-2, malic enzyme, mitochondrial; Ak-1, adenylate kinase-1; GLO-1, glyoxylase 1.

exposure. The DNA was treated with the UV-specific endonuclease isolated from *Micrococcus luteus*[11]. The size of the DNA samples after such treatment was analysed on alkaline agarose gels and the extent of removal of cyclobutane pyrimidine dimers from the DNA was calculated using the procedures described by Sutherland[12]. Removal of dimers from the DNA of the revertants was not distinguishable from that of wild type cells by this test.

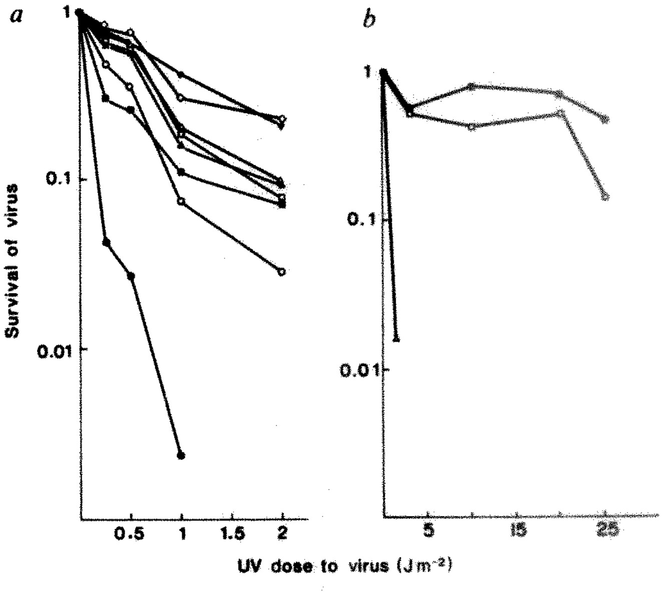

Fig. 3 Host cell reactivation of herpes virus (*a*) and SV40 (*b*). *a*: ●, XP12RO-M1; ○, XP-RE2; ■, GM637; □, SV80; ▲, XP-RE1; △, XP-RH10; ▼, XP-RH1; ◇, XP-RG3. For host cell reactivation of UV-irradiated herpesvirus, 7.5×10^5 cells were seeded on 35 mm plates. The following day, medium was removed and 0.2 ml of herpesvirus (UV-irradiated with the indicated doses) was added and the cells were incubated with the virus for 30 min at 37 °C. Then, 3 ml of medium containing 0.7% agar were added; 4–5 days later, when plaques were visible under the microscope, a fresh layer of medium containing agar and 0.015% neutral red was added. Plaques were counted either 24 or 48 h later. *b*: △, XP12RO-M1 cells; ●, CV-1 cells; □, XP-RH10. Host cell reactivation of UV-irradiated SV40 was done as described previously[10].

The ability of several of the isolates to undergo unscheduled DNA synthesis, both as measured by incorporation of ^{3}H-thymidine after irradiation of stationary cells and by counting grains overlying the nuclei, was determined as described by Royer-Pokora *et al.*[7]. These experiments showed that all the revertants tested (XP-RH10, XP-RG1, XP-RH2 and XP-RE1) were capable of unscheduled DNA synthesis.

Here we have demonstrated that phenotypic revertants can be isolated from the M1 (XP12RO) culture of XPA cells, in agreement with preliminary reports by others[13,14]. Phenotypic reversion may arise by several mechanisms including back mutation of the primary genetic defect, second-site compensatory mutations within the gene, suppression either by nonsense or missense suppressors, increased activity of a secondary pathway, or the overexpression of a defective gene product. The frequency of UV-resistant colonies observed in these experiments, between 1×10^{-7} and 2×10^{-8}, is comparable with reversion frequencies observed for other mutations. The observation that the revertants resemble the normal cells in all properties tested favours the possibility of a simple back mutation within the gene itself. Nonetheless, these experiments do not exclude other possible mechanisms of reversion. However, if phenotypic reversion has occurred by expression of a different repair mechanism, then this mechanism must resemble that which is defective in XPA cells with respect to certain biochemical properties, for example, excision of cyclobutane pyrimidine dimers.

The revertant cell lines isolated here should provide a convenient source of biological material for a future analysis of the defects of the XPA locus. These cell lines should be isogeneic with respect to all properties except for those encoded by the *XPA* locus itself.

We thank Debra Briggs for technical assistance, Judy Lippke for the *M. luteus* endonuclease preparation, Dr Betty Pancake for help with the herpes virus plaque assay, and Dr W. Peterson Jr for the cell characterization. This work was supported by NIH grant CA29294.

Received 12 June; accepted 10 July 1984.

1. Cleaver, J. E. & Bootsma, D. *A. Rev. Genet.* **9**, 19–38 (1975).
2. Robbins, J. H. *J. natn. Cancer Inst.* **61**, 645–656 (1978).
3. Setlow, R. B. *Nature* **271**, 713–717 (1978).
4. Friedberg, E. C., Ehman, V. K. & Williams, J. I. *Adv. Radiat. Biol.* **8**, 85–174 (1979).
5. Arlett, C. F. & Lehmann, A. R. *A. Rev. Genet.* **12**, 95–115 (1978).
6. Cleaver, J. E. *Int. J. Radiat. Biol.* **18**, 557–565 (1970).
7. Royer-Pokora, B., Peterson, W. Jr & Haseltine, W. *Expl Cell Res.* **151**, 408–420 (1984).
8. Takano, T., Noda, M. & Tamura, T. *Nature* **296**, 269–270 (1982).
9. Lytle, C. D., Aaronson, S. A. & Harvey, E. *Int. J. Radiat. Biol.* **22**, 159–165 (1972).
10. Abrahams, P. J. & Van der Eb, A. J *Mutat. Res.* **35**, 13–22 (1976).
11. Riazuddin, S. & Grossman, L. *Biol. Chem.* **252**, 6280–6286 (1977).
12. Sutherland, B. H. & Shih, A. G. *Biochemistry* **22**, 745–749 (1983).
13. Ganesan, A., Spivak, G. & Hanawalt, P. in *Manipulation and Expression of Genes in Eukaryotes* (eds Nagely, P., Linnane, A., W., Peacock, W. J. & Pateman, T. A. (Academic, Australia, 1982).
14. Thielmann, H. W. *et al. Int. J. Cancer* **31**, 687–700 (1983).
15. Grusella, T. F. *et al. Proc. natn. Acad. Sci. U.S.A.* **77**, 2829–2833 (1980).

Genetic effects of injection of Rous sarcoma virus DNA into polar plasm of early *Drosophila melanogaster* embryos

K. G. Gazaryan*, S. D. Nabirochkin†, A. G. Tatosyan‡, A. K. Shakhbazyan† & E. N. Shibanova†

* Institute of Molecular Genetics of USSR Academy of Sciences, Moscow 123182, USSR
† Moscow State University, Moscow 117234, USSR
‡ Cancer Research Centre, USSR Academy of Medical Sciences, Moscow 115478, USSR

Retroviral proviruses and the transposable elements of eukaryotic genomes are structurally similar[1–3]. The biological significance of eukaryotic transposable elements has not been examined extensively but it is known that, like prokaryotic transposons, these elements can induce mutations in adjacent genes and cause their transposition[4,5]. It is of interest to determine whether retroviral proviruses have the same mutagenic[6] and gene transposing ability as transposable elements, particularly because the retrovirus genome is assumed to have originated from transposable elements of lower eukaryotes[1]. The transfer of DNA sequences into animal zygotes or embryos by microinjection is a promising experimental approach for eluxidating their functions[7–11]: when foreign DNAs were introduced into a mouse germ line, mutations were induced[9–11] and at least in some mice, the mutation was caused by the insertion of a retroviral sequence[9,10]. We have introduced Rous sarcoma virus (RSV) DNA into a germ line of *Drosophila melanogaster*, and describe here the resultant genetic effects.

Retroviruses are evolutionarily remote from *Drosophila*. Nevertheless, when RSV was added to their food, *Drosophila* larvae and flies were found to carry such anomalies as necroses, tumours and chromosomal rearrangements. The progeny of these flies had recessive lethal mutations but no stable visible mutant lines were isolated, nor was the presence of the virus or its DNA detected in subsequent generations[12].

By using a microinjection technique, RSV or its cloned DNA fragment was injected into the polar plasm of *Drosophila* embryos at the stage when the nuclei of future germ cells migrate in that area (70–80 min post-oviposition, p.o.). We thus isolated a set of mutant lines in some of which the virus-specific sequence was detected by Southern blot hybridization. As this stage of embryogenesis takes only 10–15 min, we used a multi-dose injector[13] basically similar to that used by Spradling and Rubin[7], which allows ~1,000 microinjections per hour, so that several hundreds of synchronously laid eggs can be treated in a single experiment.

In the first series of experiments, we microinjected suspensions of 50–100 intact RSV infectious particles per embryo and among the F_2 progeny we observed some individuals with an altered eye structure, which gave rise to the *eye-deformed* mutant line[14,15]. Hybridization in solution revealed the presence of the virus-specific sequence in the DNA of the mutant flies (~1 copy of the viral genome per *Drosophila* haploid genome). It was unclear, however, whether the appearance of this mutation was accidental, or a result of the microinjection. In subsequent experiments (described below), we obtained a set of new mutant lines (Tables 1 and 2).

In some experiments we injected a fragment of RSV circular cDNA cloned in the pBR322 plasmid, pPrC 11 (see ref. 16 and the accompanying paper[17]). The use of this plasmid instead of RSV increased the yield of mutations (probably because in this way we introduced more DNA than can be formed in the embryonic cytoplasm by reverse transcription of the introduced viruses). The results of DNA analyses of several mutant lines are given in the accompanying paper[17]. The mutants analysed were: Dr-RSV^a, Dr-RSV^b (see Fig. 1*a*), Dr-RSV^c and Dr-PrC^d (see Fig. 1*b* and Table 2), the first three of which are allelic mutations that arose independently. The Dr-PrC^d mutant has a complex phenotype characterized by three types of wing anomaly: (1) dark, bubble-like wings; (2) wings with various outgrowths; and (3) wings spread out. We failed to isolate these in separate lines, as all three anomalies occurred in the progeny of each pair of flies originally carrying only one of the anomalies. It is interesting that the viral sequence is present in an unintegrated form (plasmid) in the DNA of Dr-PrC^d flies (ref. 17).

It is possible that the mutations observed in our experiments arose from genome rearrangements induced by exogenous DNA. If so, change in the level of recombination in the embryos at the stage of introduction of viral DNA might affect the mutation rate. To test this notion, we exposed the embryos to UV-light. We had found previously that irradiation of *Drosophila* embryos at stage 12 with short-wave (254 nm) UV light at 0.005 J cm^{-2}

Table 1 Results of microinjection of RSV or DNA preparations into embryos of *Drosophila melanogaster*

Material injected	No. of embryos injected	No. of surviving flies	Mutation found in F_2 progeny of a F_0 fly
RSV*	1,050	100	Dr-RSV^{a} (+)
RSV*	1,123	111	Dr-RSV^{b} (+) Dr-RSV^{c} (+)
pPrC 11*	640	96	Dr-PrC^{a} (?) Dr-PrC^{b} (−) Dr-PrC^{c} (−)‡ Dr-PrC^{d} (+)
pPrC 11†	280	30	Dr-UV^{a} (?)§ Dr-UV^{b} (?)
pPrC 11 + UV-irradiation†	1,050	21	Dr-UV^{c} (?)§ Dr-UV^{d} (?) Dr-UV^{e} (?) Dr-UV^{f} (?) Dr-UV^{g} (?)
pPrC 11 + UV-irradiation†	980	14	Dr-UV^{h} (?)§ Dr-UV^{i} (?) Dr-UV^{k} (?)
DNA from Oregon R (wild type)†	400	35	—
DNA from Oregon R + UV-irradiation†	890	40	—
DNA from Oregon R (wild type)*	790	85	—
Rat liver DNA*	700	79	—
pBR322*	850	91	—
Eagle's medium*	1,350	120	—
H_2O*	280	41	—

Eggs collected during a 15 min interval were used in each experiment. Either 50–100 infectious particles of RSV in Eagle's medium, or $2–4 \times 10^5$ copies of the pPrC 11 plasmid containing the RSV DNA insert (see ref. 16 and the accompanying paper[17]) or an adequate amount of other DNA (as indicated), all in 0.2–0.4 nl, were microinjected using a multidose injector[13] into the polar plasm of embryos at the 70–80 min p.o. (25 °C) stage. The flies (F_0) that developed from the embryos were crossed individually with wild-type Oregon R, and the progeny of each pair were intercrossed to obtain the F_2 generation. F_2 flies having an altered phenotype were individually crossed with wild-type Oregon R flies; the F_3 progeny of each pair were intercrossed, then F_4 individuals with anomalies were used to obtain stable mutant lines (lethals and non-heritable anomalies were discarded by the crossing procedure). Independently obtained mutants of similar phenotype were tested for allelism by the standard complementation procedure. Brackets enclose one complementation group. Symbols in parentheses represent the results of analysis of the DNA for the presence of the RSV sequence (see accompanying paper[17] and ref. 18): +, sequence was detected; −, sequence was not detected; ?, line not analysed.

* Embryos used were wild-type Oregon R.

† Embryos used were mutant stock *wsn*; embryos were totally irradiated with UV (254 nm, 0.005 J cm^{-2}) 1 h after the microinjection.

‡ Dr-PrC^{c} proved unstable, giving rise to Dr-PrC^{e} (see Table 2).

§ Dr-UV^{a}, Dr-UV^{c} and Dr-UV^{h} proved unstable: the mutants obtained from them are being analysed.

increased the yield of recombination in the *wsn* stock by ~80% (S.D.N., unpublished observations). UV-irradiation (0.005 J cm^{-2}) of *wsn* embryos that had been injected with pPrC 11 increased several fold the frequency of occurrence of the same mutation that had been induced by the plasmid without exposure to UV (Table 1).

We obtained 18 mutant lines, five of which were unstable (one new mutation appeared spontaneously in each of these). The mutagenesis is clearly selective, and certain loci are preferred; it is unclear, however, whether this depends on the loci themselves or whether it is determined entirely by the mutagen, because the molecular mechanism of the mutations remains obscure. Virus-specific sequences were detected in five of seven mutant lines analysed (including the *eye-deformed* line described previously[13,14]). However, there is no reliable evidence that the mutations actually resulted from the insertion of virus-specific

Table 2 Characteristics of mutant lines obtained after microinjection of RSV or its cloned DNA into early embryos of *Drosophila melanogaster*

Mutation	Phenotype	Type of mutation, chromosomal localization*
Dr-RSV^{a-c}	Tergites diminutive, with uneven edges (see Fig. 1*a*)	Recessive; chromosome 2; expressed in ♀ only
Dr-PrC^{a}	Wings showing disturbed venation, fusion of M_{4+5} and R_{1+2} veins	Expressed in ♂ only; decreased viability
Dr-PrC^{b}	Black body pigmentation	Recessive; chromosome 3; expressed in ♂ and ♀
Dr-PrC^{c}	Wings showing shiny oval spots	Recessive; chromosome 2; expressed in ♂ and ♀
Dr-PrC^{d}	Wings showing three phenotypic anomalies (see text and Fig. 1*b*)	Dominant; chromosome 2; expressed in ♂ and ♀
Dr-PrC^{e}†	Tergites very small, some lacking	Dominant; chromosome 2; expressed in ♂ and ♀
Dr-UV^{a-k}	Tergites diminutive with uneven edges, some arranged cross-wise	Recessive; chromosome 2; expressed in ♂ and ♀

* For chromosome analysis, the mutants were crossed with Oregon R and *Cy*/*Pm*; *Ubx*/*Sb*.

† Dr-PrC^{e} was found among 6th-generation flies of the Dr-PrC^{c} line (see Table 1).

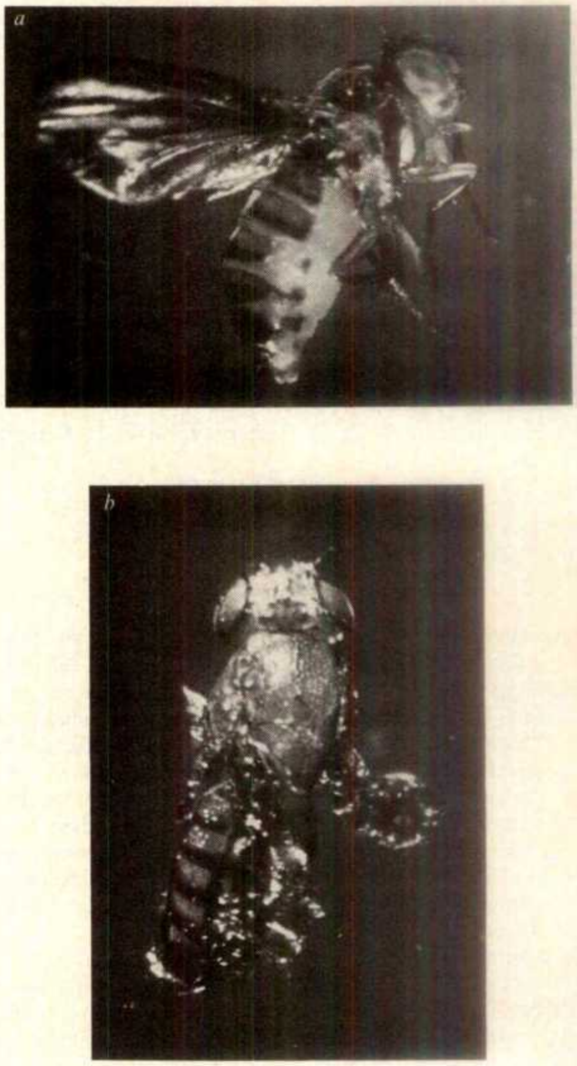

Fig. 1 Phenotypic appearance of flies of the mutant lines carrying the viral sequence (see accompanying paper[17]. *a*, Dr-RSV^{a}; *b*, Dr-PrC^{d} (the variant with outgrowths on the wings; see text).

sequences in the loci concerned, because our attempts to reveal the viral sequence in the polytene chromosomes, by hybridization *in situ*, were unsuccessful. We also considered the possibility that viral DNA derepressed endogenous elements of instability, activating them at their genomic sites or causing their transposition, a notion consistent with our major findings, namely that: (1) UV-irradiation, while increasing the general level of instability (gene recombinations), increases the frequency of plasmid-induced mutagenesis only at the locus which is already mutated without exposure to UV; (2) mutagenesis is highly selective, that is, some loci behave as 'hotspots' in the genome. It is clear, however, that some structural properties of RSV DNA are important in the development of these mutations because neither homologous DNA nor pBR32 showed any mutagenic effect (Table 1).

Received 19 April; accepted 11 July 1984.

1. Shimotohno, K. & Temin, H. M. *Cold Spring Harb. Symp. quant. Biol.* **45,** 719–730 (1981).
2. Skalka, A., Hishinuma, G. Ju. F., De Bona, P. J. & Astrin, S. *Cold Spring Harb. Symp. quant. Biol.* **45,** 739–746 (1981).
3. Majors, J. E. *et al. Cold Spring Harb. Symp. quant. Biol.* **45,** 731–738 (1981).
4. Dunsmuir, P., Brovein, W. J., Simon, M. A. & Rubin, G. M. *Cell* **21,** 575–579 (1980).
5. Tompson, J. N. & Woodruff, R. C. *Heredity* 47(3), 327–335 (1981).
6. Jenrins, N. A., Copeland, N. G., Taylor, B. A. & Lee, B. K. *Nature* **293,** 370–374 (1981).
7. Spradling, A. C. & Rubin, G. M. *Science* **218,** 341–347 (1982).
8. Rubin, G. M. & Spradling, A. C. *Science* **218,** 348–353 (1982).
9. Jaenisch, R. *Cell* **19,** 181–188 (1980).
10. Schnieke, A., Harbers, K. & Jaenisch, R. *Nature* **304,** 315–320 (1983).
11. Wagner, E. F., Covarrubias, L., Stewart, T. A. & Mintz, B. *Cell* **35,** 647–655 (1983).
12. Burdette, W. J. & Yoon, J. S. *Science* **154,** 340–341 (1967).
13. Gazaryan, K. G. & Shakhbazyan, A. K. *Drosoph. Inf. Serv.* **58,** 156 (1982).
14. Gazaryan, K. G. *et al. Dokl. Akad. Nauk SSSR* **258,** 1224–1227 (1981).
15. Gazaryan, K. G., Shakhbazyan, A. K., Sakharova, N. Yu. & Smirnova, S. G. *Drosoph. Inf. Serv.* **58,** 64–65 (1982).
16. Ambartzumian, N. S., Tatosyan, A. G. & Yenikolopov, G. N. *Molec. Biol.* (*USSR*) **16,** 1183–1188 (1982).
17. Tatosyan, A. G., Nabirochkin, S. D., Shakhbazyan, A. K., Gazaryan, K. G. & Kisseljov, F. L. *Nature* **311,** 394–395 (1984).
18. Gazaryan, K. G. *et al. Genetics* (*USSR*) **20,** 1237–1244 (1984).

Detection of virus-specific sequences in *Drosophila melanogaster* mutants induced by injection of RSV DNA into early embryos

A. G. Tatosyan*, S. D. Nabirochkin†,
A. K. Shakhbazyan†, K. G. Gazaryan† & F. L. Kisseljov*

* Institute of Cancerogenesis, Cancer Research Centre,
USSR Academy of Medical Sciences, Moscow 115478, USSR
† Institute of Molecular Genetics, USSR Academy of Sciences,
Moscow 123182, USSR

The injection of purified Rous sarcoma virus (RSV) (Prague strain) into *Drosophila melanogaster* (Oregon R line) eggs changes the fly phenotype in certain cases, and RSV-specific sequences can be identified in the *Drosophila* genome (ref. 1 and preceding paper[2]). Here we have used Southern blotting[3] to analyse in greater detail the proviral DNA present in several mutant lines of *D. melanogaster* produced by microinjection of intact RSV or plasmid DNA containing the viral insert. In certain populations of flies, RSV provirus was found to be incorporated into cellular DNA, and in one mutant family the unintegrated form of plasmid DNA was identified. Generally, the presence of injected genetic material in fly cells correlated with morphological changes in *Drosophila*.

DNA from mutant and wild-type lines was isolated by phenol extraction[1] and analysed by Southern blotting[3]; the morphological characteristics of the mutant *Drosophila* lines are described in detail in the accompanying paper[2]. Here we present restriction analyses of three of the mutant lines, which are quite different with respect to their viral sequence arrangements.

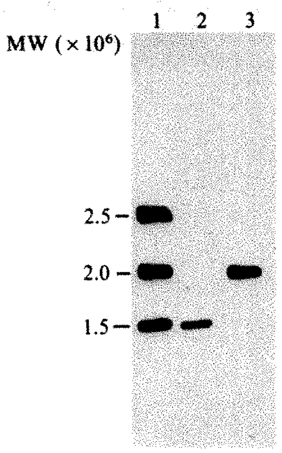

Fig. 1 Presence of RSV-specific sequences in the Dr-RSV^a genome. DNA was extracted from 1 g of flies (F_{8-10} generations) as described previously[1] and 15 µg were digested with *Eco*RI in standard conditions recommended by the supplier. Fragments were separated by electrophoresis on a 1% agarose gel. The DNA was denatured, transferred to nitrocellulose as described by Southern[3] and hybridization was performed in 50% formamide, 4×SSC at 41 °C. The probes (1.2×10^8 c.p.m. ^{32}P µg^{-1}) were: lane , RSV cDNA, prepared on 35S RSV RNA with calf thymus DNA as a primer[7]; lane 2, nick-translated pPrC-*gag* DNA containing the 1.5×10^6 dalton fragment of *Eco*RI-digested RSV provirus; lane 3, nick-translated pPrC-*src* DNA containing the 3′ part of the RSV genome located between the *Eco*RI and *Hin*dIII sites[4].

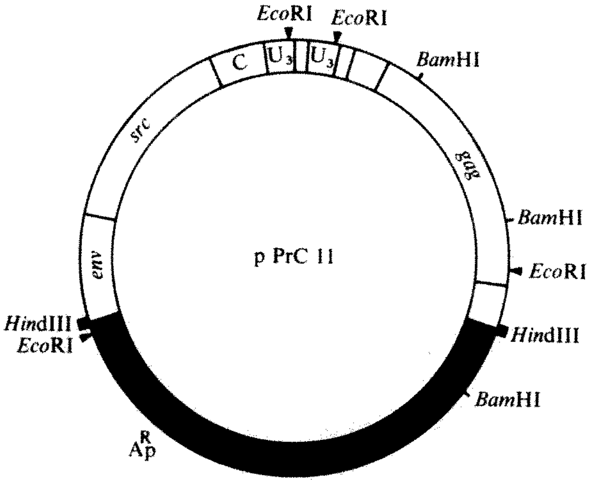

Fig. 2 Structure of pPrC 11 (ref. 4). Circular RSV (Prague strain) DNA was cloned on the *Hin*dIII site of pBR322. The total molecular weight of pPrC 11 is 6.9×10^6 daltons; the viral genome represents 4×10^6 daltons. This plasmid contains intact *src* and *gag* genes, two LTRs, the 5′ end of *pol* and the 3′ part of RSV *env* gene.

In the first restriction analysis, DNA was isolated from a mutant *D. melanogaster* population (designated Dr-RSV^a) induced by microinjection of purified RSV. The DNA was digested with *Eco*RI and, after immobilization on a nitrocellulose filter, either hybridized with total RSV cDNA or cloned fragments of viral genome containing *src* or *gag* sequences[4].

It is well known that *Eco*RI digestion of the RSV genome (Prague C strain) yields three major so-called internal fragments of molecular weight 1.5×10^6, 2×10^6 and 2.5×10^6. The two smaller fragments contain *gag* and *src* sequences respectively, while the 2.5×10^6 dalton fragment is localized in the middle of the genome and contains the *pol* gene and the 5′ part of *env*[5]. Figure 1 shows that a total DNA probe detected all three virus-specific fragments Hin the mutant line Dr-RSV^a (lane 1); the *gag* probe detected the 1.5×10^6 dalton fragment (lane 2); and the *src* probe the 2.0×10^6 dalton fragment (lane 3). These

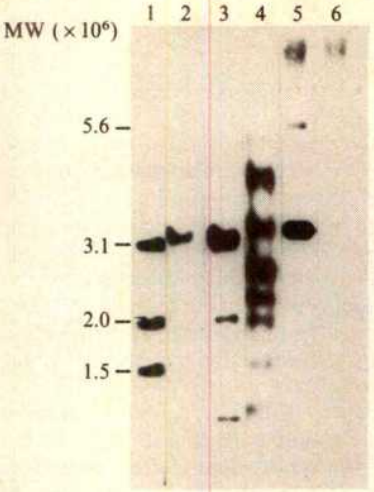

Fig. 3 The presence of pPrC 11 sequences in *Drosophila* 3A population and the Dr-PrC^d mutant line (F_{8-9} generations). 15 µg of DNA from each fly family were separated on a 1% agarose gel. Lanes 2, 3 and 5, Dr-PrC^d DNA; lanes 4, 6, *Drosophila* 3A DNA. Lane 1 contains 0.5 µg of pPrC 11 DNA. DNAs in lanes 1–4 were digested with *Eco*RI, DNAs in lanes 5 and 6 received no restriction endonuclease treatment. The probes were: lanes 1, 3–6, nick-translated pPrC 11 DNA; lane 2, RSV cDNA. Lanes 2 and 3 represent the same nitrocellulose filter which was hybridized first with RSV cDNA and, after dehybridization in 60% formamide at 70 °C, rehybridized with nick-translated pPrC 11 DNA.

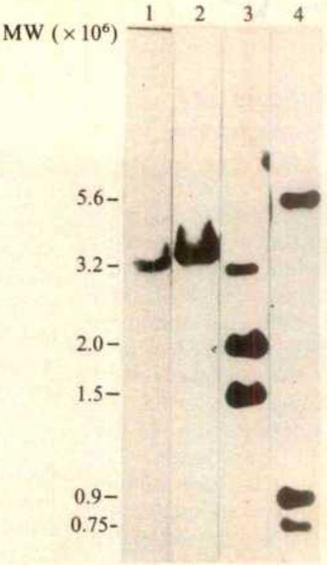

Fig. 4 Comparative restriction enzyme analysis of pPrC 11 and pDr 2A DNAs. 0.5 µg of each plasmid was digested with *Eco*RI (lanes 1 and 3) or *Bam*HI (lanes 2 and 4) then, after electrophoresis and blotting, hybridized with RSV cDNA. Lanes 1, 2, pDr 2A DNA; lanes 3, 4, pPrC 11 DNA.

data show that in this mutant *Drosophila* line, RSV provirus is co-linear with the well known genetic structure of the viral genome[5]. This DNA may persist in an integrated or extrachromosomal form, but our preliminary results with *Bam*HI and *Hin*dIII restriction lead us to suggest that provirus is associated with chromosomal DNA (data not shown).

The second example of interaction was observed on analysis of the DNA from the mixed progeny of 11 flies obtained after microinjection of bacterial plasmid pPrC 11 (*Drosophila* 3A family). pPrC 11 contains a fragment of circular RSV DNA with two long terminal repeats (LTRs) inserted in the *Hin*dIII site of pBR322 (Fig. 2). This fly population was not controlled by genetic analysis because we could not obtain a stable line. Compared with the Dr-RSV^a mutant line, the arrangement of virus-specific sequences in this population is much more complex (Fig. 3, lane 4) and essentially different from the genetic map of plasmid pPrC 11 (Fig. 2, Fig. 3, lane 1). These data show that plasmid DNA containing the viral insert can be integrated in the *Drosophila* genome. As we have been unable to obtain lines from such flies, we have not analysed further the integrated sequences.

Another example of interaction of pPrC 11 with the *Drosophila* genome was observed during analysis of the mutant line, Dr-PrC^d; this family consists of flies with dominant mutations influencing wing structure and producing three characteristic types (see accompanying paper[2]). Analysis of Dr-PrC^d DNA showed the presence of deleted plasmid DNA in which RSV sequences were observed. The main hybridization band after *Eco*RI digestion of fly Dr-PrC^d DNA was equivalent to a size of 3.2×10^6 daltons; the intensity of this band on autoradiography was much greater than that of other bands (Fig. 3, lanes 2, 3). On the basis of these results, we suggest that injected DNA may persist in fly cells of this population as an extrachromosomal element, and analysis of Dr-PrC^d DNA that had not been digested with restriction enzymes supported this suggestion. In this case, we also observed pPrC 11 sequences in the band of 3.4×10^6 daltons (Fig. 3, lane 5). In some experiments we found an additional band of 5.6×10^6 daltons, which may represent an open circular form of unintegrated DNA (Fig. 3, lane 5).

In an analogous experiment, DNA from the 3A family that had not been digested with restriction enzymes showed no indications of persistence in an unintegrated form (Fig. 3, lane 6).

We have tried to 'rescue' the unintegrated form by transformation of *Escherichia coli* HB101 strain with total DNA isolated from the mutant line, Dr-Pr^d (ref. 6). Ampicillin-resistant *E. coli* were produced which contained a new plasmid designated pDr 2A. The structure of this plasmid is essentially different from that of the original plasmid pPrC 11 (Fig. 4); its detailed structure will be described elsewhere, but it has a molecular weight of 3.4×10^6 daltons, and except for LTRs, it does not contain the main part of the RSV sequence. The possibility of insertion of *Drosophila* sequences into this plasmid has been excluded by blot hybridization experiments with DNA from the Oregon R line which gave negative results (data not shown), although we cannot exclude the possibility that a few oligonucleotide sequences from the *Drosophila* genome are scattered within this plasmid.

Our preliminary results suggest that injection of the pDr 2A plasmid into *Drosophila* embryos induced offspring carrying different mutations which produced great variations in phenotype. We conclude, therefore, that microinjection of RSV or its cloned DNA into *D. melanogaster* embryos can lead to different types of proviral DNA interaction with fly cells—persistence of the intact viral genome, integration of a rearranged viral genome and existence of the viral genome in an unintegrated form.

Received 17 April; accepted 11 July 1984.

1. Gasaryan, K. G. *et al. Dokl. Akad. Nauk SSSR* **258,** 1221–1227 (1981) (in Russian).
2. Gazaryan, K. G., Nabirochkin, S. D., Tatosyan, A. G., Shakhbazyan, A. K. & Shibanova, E. N. *Nature* **311,** 392–394 (1984).
3. Southern, E. M. *J. molec. Biol.* **98,** 503–513 (1975).
4. Ambartzumian, N. S., Tatosyan, A. G. & Yenikolopov, G. N. *Molec. Biol.* **16,** 4183–4188 (1982) (in Russian).
5. Taylor, J. M., Hsu, T. W. & Lai, M. M. *J. Virol.* **26,** 476–484 (1978).
6. Cohen, S. N., Chang, A. C. & Hsu, T. W. *Proc. natn. Acad. Sci. U.S.A.* **69,** 2110–2116 (1973).
7. Taylor, J. M., Illmensee, R. & Summer, J. *Biochim. biophys. Acta* **442,** 324–330 (1976).

21-1-87
A. Baker

15-Myr periodicity in the frequency of geomagnetic reversals since 100 Myr

MAZAUD *et al.*[1] have recently analysed geomagnetic reversal time scales, covering the past 100 Myr, and they concluded that the geomagnetic reversal rate has a 15-Myr periodicity superimposed on a monotonic function, which they modelled with a lorentzian function. However, because of the analysis procedure they used, the origin (and hence interpretation) of this periodicity must be questioned. The reversal frequency as a function of time was determined using a fixed-length, rectangular, sliding window: the estimated reversal rate for each position of the window being the number of reversals appearing within the window divided by the window length. Fixed-length sliding window techniques such as this are notorious for producing spurious frequencies when used to analyse time-sequenced data generated by a process which embodies a random element. This occurs because the random component typically has a fairly broadband spectral representation and the fixed-length window acts as a filter which allows through only certain frequencies.

McFadden and Merrill[2] have also analysed geomagnetic reversal time scales and found no indication of a 15-Myr periodicity in the reversal rate. Instead, they concluded that the geomagnetic reversal process is essentially a Poisson process and that since the Cretaceous Normal Polarity Interval the reversal rate has increased approximately linearly with time. Using a maximum likelihood method they concluded that λ, the reversal rate, is given approximately by

$$\lambda = \alpha + \beta t \qquad (1)$$

where $\alpha = 4.41 \pm 0.85\,(\mathrm{Myr}^{-1})$ and $\beta = -0.051 \pm 0.014\,(\mathrm{Myr}^{-2})$ with $t = 0$ now and increasing backwards in time. A Poisson process produces randomly distributed interval lengths, τ, between events (reversals) with probability density, $\rho(\tau)$, given by

$$\rho(\tau) = \lambda \exp(-\lambda\tau) \qquad (2)$$

Using a random number generator, random sequences of interval lengths have been generated from the distribution of equation (2) with λ given by equation (1), using the point estimates of $\alpha(4.41)$ and $\beta(-0.051)$. Analysis of such sequences by the method of Mazaud *et al.*[1], using as they did a window of 4 Myr, results in estimated λ curves strikingly similar to theirs. Autocorrelation of these λ curves (after subtraction of a linear component) gives periodicities very similar to that of Mazaud *et al.*[1], yet λ contains no periodic component. Using a 2-Myr window, a similar periodicity is still apparent but buried by the (expected) increased noise. Using an 8-Myr window the amplitude of the periodicity is decreased by the increased smoothing of the longer filter.

Thus, the evidence for the observed 15-Myr periodicity being a real geodynamo phenomenon may not be as convincing as the claim of Mazaud *et al.*[1], and the possibility that λ has simply increased linearly with time and that the observed periodicity is merely a by-product of the analytical technique must be strongly considered.

P. L. MCFADDEN
Division of Geophysics,
Bureau of Mineral Resources,
GPO Box 378,
Canberra ACT 2601,
Australia

1. Mazaud, A., Laj, C., de Sèze, L. & Verosub, K. L. *Nature* **304**, 328–330 (1983).
2. McFadden, P. L. & Merrill, R. T. *J. geophys. Res.* **89**, 3354–3362 (1984).

MAZAUD *ET AL. REPLY*—McFadden suggests that our report of a 15-Myr periodicity in the frequency of geomagnetic reversals arises from our use of a fixed-length, rectangular window to determine the number of reversals per unit time. We are well aware that the use of such a window can introduce apparent periodicities (even for random data) because the fixed-length window acts as a filter, permitting only certain frequencies to be seen. However, when such a filter does introduce spurious periodicities, the period is directly related to the window width. In our work, we used windows ranging from 1 to 10 Myr. Although the amplitude of our periodicities and the signal-to-noise ratio varied somewhat, the period itself was confined to the narrow range of 13–17 Myr. If the period had merely been the result of using a rectangular window, we would expect a much larger variation in its value.

We now turn to the more important and more interesting point of McFadden's comment, namely, the periodicity in his computer-generated time series. Following McFadden's method we produced over 50 different synthetic time series, which were then analysed by the fixed-length, rectangular-window method. Our goal was to determine whether all of the time series resulted in periodic oscillations of the same period. In our study, the answer was clearly no: while some of the time series did give rise to a distinct periodicity, this was not the general case. In fact, we found an nearly continuous range between time series which had well-defined periodicities and those in which no clear periodicity could be discerned. This result provides additional evidence that the periodicity which we observed in the reversal frequency did not arise from our method of analysing the data. However, it also shows that a completely random phenomenon can sometimes give rise to a periodic one. With regard to the frequency of geomagnetic reversals, we certainly cannot exclude the possibility that in this particular situation, the periodicity results from a probabilistic process. In this respect, McFadden's criticism has contributed to a deeper insight of our own data.

Finally, note that we never expected that our work should serve as the final word on the nature of the reversal process. The fact that McFadden and Merrill have reached a different conclusion only demonstrates that this is a complex problem whose final resolution requires further work.

ALAIN MAZAUD
Laboratoire de Stratigraphie (LA 319),
Université de Paris VI,
Tour 15–16, 4 Place Jussieu,
75230 Paris, Cedex 5, France

CARLO LAJ
Centre des Faibles Radioactivités,
Laboratoire Mixte CNRS-CEA,
91190 Gif-sur-Yvette, France

LAURENT DE SÈZE
Service de Physique des Solides
et Résonance Magnétique,
CEN-Saclay,
91191 Gif-sur-Yvette Cedex, France

KENNETH L. VEROSUB
Department of Geology,
University of California,
Davis, California 95616, USA

Matters Arising

Matters Arising is meant as a vehicle for comment and discussion about papers that appear in *Nature*. The originator of a Matters Arising contribution should initially send his manuscript to the author of the original paper and both parties should, wherever possible, agree on what is to be submitted. Neither contribution nor reply (if one is necessary) should be longer than 500 words and the briefest of replies, to the effect that a point is taken, should be considered.

LIBRARY [illegible]
Departments of
Chemical Engineering
Chemical Technology
Plastics and Rubber Technology

nature

21-1-87

Mr Gromyko and Mr Reagan

Last week's meeting in Washington seems to have something to do with future talks on arms control, but nobody knows quite what. The best hope is that Mr Reagan will redefine his policy.

MR Andrei Gromyko caused such a stir on his visit to Washington last week that observers could have been forgiven for thinking him a candidate for the US presidency. On the face of things, he has many of the essential attributes. He has been around for a long time and he is also an elderly gentleman. But his looks belie his age, suggesting that the longevity that comes with the successful exercise of power is on his side. He is also capable of those mercurial changes of mood that, in senior politicians, pass for inscrutability; a tough hardliner's speech at the United Nations on the Tuesday, an exit from the White House with his hands clasped in the traditional boxer's gesture of self-congratulation on the Thursday. By popping in and out of the United States like this, Mr Gromyko has cleverly changed the agenda of speculation from mundane questions such as whether interest rates will rise still further (and, if so, before or after the election) to simpler issues — what did he say to the real president (who is not quite as old), and in what tone of voice?

We shall have to wait until after the election to find out. It would have been no part of Mr Gromyko's purpose to help Mr Ronald Reagan to his re-election a month from now, for which reason it was never on the cards that a tangible agreement on anything would have emerged from last month's meeting. The Soviet Union has nothing to lose, and everything to gain, from postponing serious talk about East–West relations until after the election. But there was also, last week, much to be gained from emphasizing in the run-up to election-day the importance that the Soviet Union attaches to what politicians in the West may be tempted to say in the heat of an election campaign. Mr Gromyko, at least, will not have forgotten that President Reagan's previous election campaign was marked by repeated declarations that arms control negotiations then negotiated, Salt II in particular, were Soviet traps for the unwary. In the event, the first Reagan Administration took two years to learn that that position was untenable. Nothing could have been lost, and everything gained, by reminding the incumbent president of that waste of everybody's time and of the need to avoid a repetition of that error.

It is also in everybody's interest that the momentum of arms control negotiations should pick up again once the election result is known. On the assumption that Mr Reagan will not be a lame-duck president waiting for a successor to take office, the fallow period before the next inauguration day could be used constructively, especially if Mr Reagan should let slip during the election some strictly verbal promise likely to appeal to Mr Gromyko and his fellow-countrymen (not to mention many of Mr Reagan's). An undertaking that a moratorium on the testing of anti-satellite weapons would be a precondition of negotiations on these instruments would suit capitally. (Mr Reagan will have had a chance to let that carrot show in his speech this week to the United Nations.) The temptation to seem conciliatory must be huge. There will be no complaint if Mr Reagan should succumb to it.

Preparing the ground for negotiations on anti-satellite weapons is not however what matters most. Both Mr Reagan and Mr Gromyko should remember that. For practical purposes, the agenda for arms control in the next few years should not be determined by the imagined anxieties of statesmen on either side. The US Administration's ambitions for a star wars defensive system are not an immediate threat to stability, but a threat to the anti-ballistic missile treaty (part of the Salt process) ten years from now, a threat to stability twenty or thirty years from now — and a threat to everybody's pocket-book in the meantime. The immediate issues, however, have been what they have been for ten years — the needless investment in missile systems on both sides, their fluctuating imbalance and needless pieces of irrationality such as chemical weapons. The United States is right to have been insisting that these are the subjects crying for discussion.

Can the present administration, or a successor in the same mould, bring itself to consider these questions constructively? Mr Gromyko may also have been looking in Washington for guidance on that point. Nobody can say for sure, and indeed in the past few months, there have been disconcerting signs that too many senior officials in Washington are convinced (entirely against experience) that agreements with the Soviet Union are not worth the paper they are written on. That mood, or those people, will have to be exorcised if ever there is to be serious negotiation on arms control measures that will count. Fortunately, the election provides the president with an opportunity to redefine the basis for negotiations without spilling the blood of those who have helped him loyally in the past four years. The perennial problem of politicians running for office, that of making too many speeches with too little material, might be deftly solved by using an occasional speech to lead the White House out of its old-fashioned xenophobia. It would be ironical if Mr Gromyko had been putting Mr Reagan up to that old democratic trick. ☐

Nature and the Soviet Union

ON 22 November, *Nature* will publish a survey of science in the Soviet Union.

When the project was first planned, early in 1983, it was hoped to visit a number of institutes and laboratories in the Soviet Union, but repeated requests for assistance have now been met with the information that arrangements cannot be made until 1985. Accordingly, *Nature* would be glad to hear from scientists with recent first-hand experience of work in the Soviet Union, or of collaboration with Soviet scientists and/or institutes.

Those able to help are asked to write to the editor as soon as possible at one of the editorial offices in London, Tokyo and Washington. Please include a telephone number.

Anonymous correspondence will not be dealt with. All correspondence will be confidential unless otherwise agreed. Information will not be published without corroboration. On this occasion, *Nature* is exclusively concerned with content and texture of Soviet research, not with problems of dissent and emigration. ☐

Another culprit

The largest of the British research councils is not blameless for the plight of British research.

BRITISH self-contentment over the mechanism of research support has taken several hard knocks in the past few years, nowhere more conspicuously than over what is called the dual-support system, the mechanism by which public funds for academic research are channelled from two supposedly independent sources, the University Grants Committee (which is supposed to equip university departments to carry out research) and the five research councils (which then provide project funds on a selective basis). That the system has not been working as intended has been clear at least since the 1970s, although people differ in their diagnoses of what is wrong. Two years ago, the Merrison committee (commissioned jointly by the research councils and the grants committee) put most of the blame on the universities, but last month's forward strategy published by the University Grants Committee proudly took credit, on behalf of the universities, for roughly two-thirds of the cost of academic research with British public funds. The issue of which has been the weaker link is bound to be influential in the next few months, when the British Government will have to respond both to the grants committee's strategy document (probably early in 1985) and, more immediately, to the research councils' appeal (now lodged) for extra funds.

So where should the blame lie? The universities have been lackadaisical offenders for several years, adjusting to shrinking budgets by skimping on discretionary expenditure (among which research expenditure has been conspicuous), while the general increase of teaching loads casts doubt on the grants committee's assumption that something like 30 per cent of the university salary bill is a direct contribution to research. But the faults are not all on one side. The research councils are in their separate ways vulnerable to a variety of complaints, of which the most familiar is that so much of what they have to spend is committed to their own research institutes that they have too little to spend on newly arising projects. The research council responsible for the underlying welfare of British agriculture has been the most consistently pilloried on this count, but perhaps unfairly — many of its institutes are legacies from the distant past, not merely from the time, fifteen years ago, when prudence required that research councils should keep their fixed obligations to a minimum for the sake of flexibility. In any case, this line of defence continues, agencies with responsibility for research which is strategic in character (in Britain, medicine, the natural environment as well as agriculture) must seek some measure of continuity by institutionalizing parts of their programmes. The result, however, is the now notorious difficulty of effecting change. The problem for managers in the months ahead is to create room for manoeuvre.

Headhunting

In case there are doubts about the need, the curious circumstances of the British Government's difficulty in recruiting able people as heads of the research councils is a telling reminder of malaise. The post of chairman of the Natural Environment Research Council has been filled on a caretaker basis after one person to whom the job was offered stipulated "impossible conditions" — no doubt another way of referring to a demand for assurance about the council's future prospects and its chairman's freedom of action. The vacancy at the agricultural council, which has been put out to headhunters, is yet another sign that working researchers of distinction are unwilling to turn their backs on active science so as to administer the funds that help to keep other people active. The disincentive is that both research councils' funds are too meagre to serve their stated purposes and that an applicant for one of the top jobs cannot know in advance whether some of what there seems to be to spend will be snatched away from one year to the next.

This dilemma will be further sharpened in the next few months, when the government will be required to find a successor to Dr John Kingman, the chairman of the Science and Engineering Research Council who will be leaving less than a year from now to become vice-chancellor of the University of Bristol. On the face of things, this is the most attractive of all the top jobs. The council is the largest of all, with an annual budget equal to all the others put together. Moreover, this council differs from the others in that its terms of reference are explicitly to further the cause of academic science (which is why the council was not directly constrained by the Rothschild reorganization of 1973). Yet even this huge organization is now almost as hamstrung as the others. Only a few months ago, one of the council's own sub-committee's was wringing its hands over the tiny uncommitted sums of money available for spending on what was called "core" research — research in the physical sciences not tied to one of the council's national programmes of research in high-energy physics, astronomy, information technology or what have you. The difference is that while the strategically-orientated research councils can plead that their inflexibility has been wished upon them by historical accidents, the Science and Engineering Research Council has wished its problems on itself.

Costly trends

Over the years, several tendencies have been mistakenly allowed to perpetuate themselves, not the least of which is the growth of the share of the council's budget spent on central facilities ostensibly intended as services to academic science. The cost of the annual subscription to the CERN laboratory is the most conspicuous (and recently, the most contentious) of these costs, but is a declining proportion of the whole. Other facilities, such as the neutron spallation source in Berkshire (due to come on stream in November, six months late) are modest in scale (£18 million in capital cost) but justifiable against the background of possible cancellation chiefly by the argument (as at a recent council meeting) that completion would then cost next to nothing, and thus yield the cheapest machine of its kind anywhere in the world. The council's weakness for bricks, mortar and institutions is similarly evident; its agonized consideration a year ago of the question whether there should be two major observatories in Britain (Greenwich, Edinburgh) ending with the decision to keep both (as well as a castle near the Sussex coast). In recent years, the council seems to have found it difficult to make decisions.

Matters are further complicated by the council's way of dealing with the funds it has to spend. Everybody acknowledges that spending £250 million a year is difficult, but that simple consideration does not fully account for the council's predilection for distributing spending authority to four powerful committees (called boards) rolling logs for their own special interests. Weakly, the council has allowed (even encouraged) the growth of the board responsible for engineering research without providing much in the way of objective evidence that the pattern of academic engineering research resembles in any important way that common in other fields; the most charitable explanation is that engineering is politically popular (and that engineers are a turbulent group). It is especially iniquitous that the council should have parcelled out to its spending boards responsibility for the allocation of research studentships, the stipends by which graduate students are supported in Britain. The consequence is that by the allocation of research studentships to particular university departments (in whose gift their ultimate award to students rests), the boards are able to insulate themselves from suspicions that young people's estimation of what is interesting may be different from their own. In recent years, the council as a whole has further reduced its own freedom of manoeuvre by its willingness to set up earmarked funds (trendily called "directorates") to spend money on fashionable causes, biotechnology or information technology, as the fashion strikes.

To be fair, there have recently been signs that the council has occasionally seen the error of its ways. Within the past year, Dr Kingman has tried (and failed) to combine the two most powerful of his boards (nuclear physics and astronomy), hoping in the process that similar criteria would have applied in the two very different fields. It is now also firm council policy that the proportion of the council's budget spent on central facilities will in future decline from its peak (in 1982–83) of 37 per cent. There is no sign of repentance on the way in which research studentships are allocated, but that may yet come. In all this, the council's strongest defence is that even its comparatively large budget is far too small to accomplish everything it is supposed to do, and there is force in that claim. All the more reason, however, why the council should be more vigilant than in the past in creating some flexibility within the straitjacket it has made for itself. But that will be a thankless task, hardly the kind of job which people will be flocking to secure. ☐

European synchrotron source

Strasbourg and Grenoble battle for site

THE European Synchrotron Radiation Source (ESRS), a world-rank 5 GeV electron synchrotron first planned and championed in the late 1970s by the European Science Foundation (ESF), seems likely to be built at last, at Strasbourg on the Franco-German border. Or so the auguries suggested last week, in the midst of an extraordinary political and "scientific" battle now raging between the little tourist town of Strasbourg and the French alpine city of Grenoble, both potential sites for ESRS.

The battle is all the more extraordinary after the years ESRS has spent in the wilderness. The idea for an intense next-generation synchrotron radiation source was first canvassed in 1979, when ESF (a consortium of European research councils) began touting its technical study around Europe — without success. But now, partly as the result of a poll showing a potential ESRS user community of 2,000 scientists and 600 research groups in Europe, and much interest in industry, Cinderella has become the belle of the ball.

In the latest move, the French and German research ministers have reached a deal that will place ESRS in France and (as compensation) a "European trans-sonic wind tunnel" in Cologne, West Germany. (Britain was originally in the running for ESRS, but dropped out because of the high expenditure expected of successful bidders.)

Now, with the main battle settled in favour of France, the two regional governments that might benefit have raised the stakes by throwing money (and glossy brochures) at the project. Strasbourg, the home of ESF, has bid FF 100 million ((£85 million) to win the project, and Grenoble has offered FF 80 million (£65 million) towards the FF 900 million (£750 million) cost of the machine. If ESRS were built at Grenoble, it would go alongside the high-flux neutron beam facility, the Institut Laue-Langevin (ILL), which is insisting that the "scientific case" would favour such a link.

French regional, economic and scientific policy, however, favours Strasbourg. And this is a powerful force in Paris at present, with the government seeking to decentralize and to create new regional centres of excellence. Strasbourg is also more centrally located in Europe, which is why West Germany favours it. Although Britain would prefer Grenoble, its lack of cash gives it no leverage. The choice now rests with the French Goverment. Paris sources say that Strasbourg is the likely but not certain bet in a decision that should be taken in a few weeks.

On the scientific side, the battle for ESRS appears at first sight to be between the biologists (in whose discipline the University of Strasbourg and surrounding institutes excel) and the physicists (where Grenoble is on a level with Paris).

But do the biologists want the machine? Some say yes, some say no. The directorate of the major French research council, the Centre National de la Recherche Scientifique (CNRS), wants ESRS for the biologists and so favours Strasbourg, where CNRS already runs a centre for low-energy nuclear physics and a number of important laboratories in molecular biology and where it plans a major research centre in plant biology. Many individual CNRS biologists, however, have a different view: they would prefer that ESRS stayed with the physicists in Grenoble.

According to CNRS, a Strasbourg location for ESRS would help biologists (and chemists) to become more involved with the use of synchrotron radiation and break down interdisciplinary barriers. It would also contribute to the development of Strasbourg as a centre of European science, close to West Germany and Swiss centres. CNRS biologists are worried about having to help pay for a facility that in practice they will not use. They say their budget within CNRS is already tight, burdened as it is with more than their share of an existing French synchrotron source (LURE) at Orsay, whence their preference for Grenoble.

The director of the European Molecular Biology Laboratory (EMBL) at Heidelberg is said also to be in favour of Grenoble, where EMBL has a neutron scattering facility. ILL's own case is that its own work — the instrumentation as well as scientific interests — is similar but complementary to that of ESRS, so that a Grenoble site for ESRS (or "Maxwell Institute" as ILL has already dubbed it) would be more productive than at Strasbourg. ILL says there is room (just) on its compact site for the 772-metre-circumference synchrotron, and that vibration from the nearby autoroute should not be the nuisance once feared.

Grenoble's case is strong, but Strasbourg has politics on its side. No wonder that the French science minister, Hubert Curien, says that the decision "is not proving easy".

Robert Walgate

Marinov

Further threat of immolation

BRITISH diplomatic missions in Genoa (Italy) and Vienna (Austria) have been under siege in the past few weeks by Dr Stefan Marinov, the Bulgarian physicist now living in the West, with threats of self-immolation. Dr Marinov is protesting at the refusal of the Editor of *Nature* to publish three long scientific articles, one of which is a restatement of Marinov's theory of absolute space-time, another of which announces the design of a *perpetuum mobile*.

Dr Marinov first embarked on self-immolation in Genoa on 8 August, outside the British Consulate, but by his own account was held in conversation for half an hour by staff from the consulate and was compelled to flee when the staff sought the assistance of the police, knowing that he was present illegally in Italy (having been denied entry in 1980).

At a press conference held in Austria last week, Dr Marinov again announced his plan for self-immolation, this time outside the British Embassy in Vienna. On the telephone earlier this week, he said that he would take this step at 10 a.m. local time on 2 October but, on being informed of the appearance of this piece, said "Now I don't know whether to immolate myself tomorrow".

Dr Marinov's claims that Einstein's theory of special relativity is misplaced were first made in 1974 (*Czechoslovak J. Phys.* B24, 965; 1974), on the basis of an experiment carried out in Bulgaria that purported to show that the velocity of light is direction-dependent. Marinov has since claimed to have repeated the experiment. The paper describing that investigation, "New measurement of the Earth's absolute velocity with the help of the coupled shutters experiment", says that the experiment was carried out in his girl-friend's apartment, that the rotating shutters, functioning as a siren, disturbed the neighbours and that "after a couple of altercations, my girl-friend threw away from her apartment not only my apparatus but also me".

The two other papers submitted for publication are called "On the action and interaction of stationary currents" and "*Coup de grace* to special relativity and to something else". All three papers have now been published by Marinov in his book *The Thorny Way to Truth* (Part II).

Marinov's complaint against *Nature* is primarily that publication of these three papers has been refused, but also that "milliards of dollars" are being lost each day the world remains ignorant of his perpetual motion machine. Other matters in dispute are *Nature*'s refusal to publish an appeal to the late Yuri Andropov at the end of last year and, earlier, a manifesto called the "Ten Jena Commandments".

John Maddox

Canadian science

New brooms plan clean sweep

Ottawa

CANADA's science chiefs are expecting great things from their new progressive conservative minister, Thomas Siddon. With a professional engineering background and a PhD in aero-acoustics, Siddon is highly spoken of as a friend of science and may be the man to gain some much-needed political clout for his office as minister of state for science and technology.

One of the first signs of renewed emphasis on science may be the creation of a standing parliamentary committee to deal with technology development. And by all accounts the recent Wright Task Force report urging more demand-led research and development (see below) is being taken very seriously. While some science administrators admit to private doubts about the numbers, Siddon intends to deliver his party's pledge to double Canadian research and development to C$ 10,600 million within its first term of office.

Most of this increase needs to take place within industry. Canada suffers from being a "branch plant" economy — many companies based in the United States use Canada simply for warehousing and distribution — and this Siddon is determined to change. The activities of major companies will be examined and government investment and tax measures deployed to favour more innovation within the country. There is a strong feeling that trading competitors have been making gains from various forms of hidden assistance to their domestic industries, and the intention now is that Canada should use every fiscal measure permitted under the General Agreement on Tariffs and Trade to protect its home base.

One high priority is to revise the scientific research tax credits introduced earlier this year. That scheme, intended to help young high-technology companies that did not benefit from traditional tax incentives, has already proved an embarrassment: although a boon for investment dealers, it has cost the government significant revenue and has failed to generate innovation on the scale intended.

Changes can be expected at laboratories run by government departments and by the National Research Council (NRC), which cover everything from measurement standards to cancer research. A proposed manufacturing technology centre to be run by NRC was planned by Wright as representing "everything that is wrong with federal technology policy": industry was not consulted and the facility may be redundant before it is built. NRC's technology transfer programme has failed to make a real impact on Canadian industry, and Siddon wants to contract out some NRC work to make more productive use of the laboratories.

While most Canadian universities have science departments, subject cover is patchy and there is serious concern about the future supply of highly qualified manpower. Despite Siddon's obvious enthusiasm for development as opposed to research, he "can give an assurance" that federal support for university-based research will be "continued and expanded". But this will require difficult negotiations with provincial governments, which, though supposed to support education, have in practice ensured a creeping increase in the unit cost of research supported by the research councils. Siddon also wants to encourage academics to follow through development of important discoveries by promoting the idea that consultative work for industry as well as peer-reviewed academic publications can advance a university career.

Much of this ambitious programme will depend on what sort of influence Siddon can wield in cabinet. There is room only for improvement: science and technology has at different times had to share a minister with other departments and there have been 10 incumbents of the office since 1971. But Siddon, who was a critic of science and technology in the last parliament, has 5 years' parliamentary experience, making him almost a veteran in the cabinet. The traditional hewers of wood and drawers of water had better watch out. **Tim Beardsley**

Looking south

THE Canadian economy is beset with problems stemming from its historical reliance on natural resources and its poorly-developed indigenous industry: more than 50 per cent of manufacturing industry is foreign-owned, and the *per capita* budget deficit is much larger than that in the United States. Research and development accounts for only 1.28 per cent of the Gross National Product, less than half the figure in the United States, and by the latest unofficial estimates the proportion is actually decreasing.

One major difficulty is the lack of venture capital: unlike their entrepreneurial neighbours to the south, Canadians prefer to save their money than to put it at risk, and insurance is big business. Many banks refuse to make loans for commercial ventures unless the idea has previously been tried in the United States. Canada also lacks the defence-based industries of the United States.

A hard-hitting task force report released in July urged the government to stimulate private sector research by rationalizing and simplifying industrial support schemes, providing better tax incentives and redirecting government procurement policies. The task force, under the chairmanship of Douglas Wright of the University of Waterloo, said the federal government should pay the full cost of university research, thus eliminating the political dimensions of the present research support system under which indirect research costs ("overheads") are met by provincial governments. Cooperation between universities and industry should be strengthened by a flat-rate grant to universities undertaking industrial research and development by tax concessions for industrial companies making use of universities.

Wright was highly critical of Canada's federal laboratories, some of which are "struggling to find appropriate challenges". The suggested solution was that directors recruited from industry should be given authority to set goals for federal laboratories, encouraging them to contract out research as much as possible. A formal government response to Wright is in preparation. Tim Beardsley

---

Microscope acquired

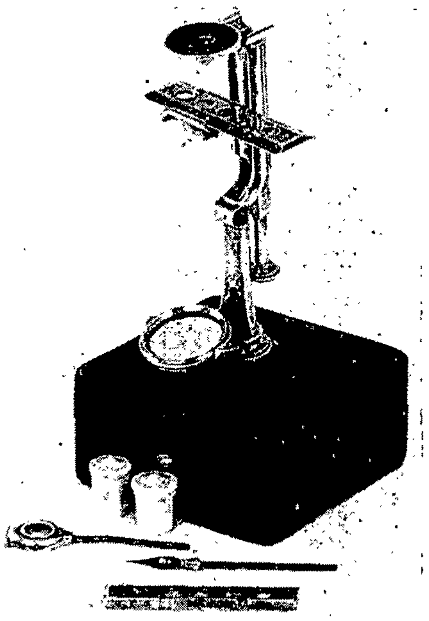

ONE of the earliest British scientific instruments to be designed, constructed and marketed outside London has just been acquired by Edinburgh's Royal Scottish Museum. The instrument, a 2-inch high silver microscope made in 1749, was a product of the workshop of John Clark, an Edinburgh goldsmith, jeweller and instrument maker. Although its eighteenth century purchaser would have been a Scots gentleman of leisure, desiring a novel curiosity, it was nevertheless the patronage of such customers that spurred instrument makers to develop the skills they would need to meet the demands of their first scientific and medical customers. The museum was assisted in making the purchase by the National Heritage Memorial Fund. □

European pollution

Towards lead-free auto fuel

Brussels

EUROPE is edging closer to a substantial reduction in exhaust pollution. But the ride has been far from smooth. Last week, the European Commission added the final flourish to proposals designed to phase lead out of petrol (gasoline). But only a few days earlier, West Germany announced its intention to apply US exhaust emission standards, which are twice as strict as those now in force in Europe, by 1989, rather than following the Commission's two-stage timetable.

With many of the 90 million cars on European roads expected to be running on super petrol by the early 1990s, the European Commission has ruled that the EEC countries should sell a single super-grade unleaded petrol from October 1989, although countries such as Italy and France, with a considerable market for small-engined cars, will still be able to sell a normal lower octane-rating unleaded petrol as well. (Unleaded petrol in Europe in fact means a lead content of between 0.01 and 0.02 grams per litre. The US content is 0.0135 grams per litre.)

Since both leaded and unleaded petrol will have to be available until old cars have been phased out, the super-leaded petrol will be marked with a red dye, to avoid mistakes in filling but also to make spot checks on "wilful misfuelling". The Commission feels price incentives should be encouraged, but this has so far been left to national governments.

Other technical specifications for the petrol (density, volatility, etc.) will be standardized by the European standards body, Le Comité Européen de Normalisation (CEN).

The proposals are the final touch to a series of European emission controls which environment ministers have to decide upon by the end of the year:

- Reducing the lead content of leaded petrol throughout the Community to 0.15 grams per litre, by 1989. Only two EEC countries, West Germany and Denmark, apply the minimum limit laid down by the 1978 EEC directive. But it is likely that the United Kingdom and the Netherlands will be allowed to impose that limit in 1986.
- Introducing unleaded petrol for new models of cars from 1989, and for all new cars sold from 1991 onwards.
- Imposing a limit of 5 per cent for benzene contained in the new petrol "cocktail" dictated by the removal of lead. Benzene is thought to be the source of a particularly toxic aromatic hydrocarbon in automobile exhausts. Some EEC countries would like the 5 per cent limit to apply to leaded petrol as well.
- Reducing other exhaust emissions (carbon monoxide, hydrocarbons, nitrous oxides) to Japanese and US standards in two stages by 1995.

Last June there appeared to be a consensus among environment ministers to adhere to the Commission's timetable. But more recently Denmark, Luxembourg and the Netherlands have seemed inclined to change to US standards in an earlier single move, and West Germany announced on 19 September that from 1 January 1989 new models of cars would have to be fitted with anti-pollution devices. The law would apply to 2-litre engines from 1988.

Whether West Germany will dare to go it alone is questionable, because of EEC rules on competition and free movement of goods. The European Commission is also doubtful about the tax incentives linked to the purchase of cars which are "environmentally friendly" (*Umweltfreundlich* in German), which could be seen as an unfair subsidy for the West German motor manufacturing industry.

While British and French car manufacturers have been quick to protest about unfair competition in Europe, West Germany fears competition just as much from the Japanese, whose ready-made models already fitted with catalytic converters for the home and US markets will, they fear, invade the West German market.

Meanwhile, Chancellor Helmut Kohl has also been severely criticized by the opposition parties for bowing to the industrial lobby, and delaying West Germany's original move to lead-free petrol scheduled for 1986.

West Germany's unilateral intentions have made a breach in the European consensus and could slow down progress on emission control in Europe unless ministers can reach a compromise before their meeting on 6 December.

Once the decision on these emission controls is taken, perhaps attention will be directed to the 10 million lorries and the 10 per cent of private cars that run on diesel fuel.

In addition to other pollutants (but not lead), diesel engines spew carcinogenic unburnt particulates (smoke) into the air. So far neither the United States nor Japan has been able to solve that problem either.

Anna Lubinska

Lead and pollution

Brussels

TWENTY per cent of air pollutants such as carbon monoxide, nitrous oxides and hydrocarbons come from the exhausts of motor vehicles. Permitted emission levels have been lowered four times since the European Community started regulating exhaust emissions in 1970.

The latest proposal involves reducing emissions in two stages to the very strict US and Japanese levels. These are as follows:

	Japan (grams per km)	United States (grams per mile)
Hydrocarbons	0.39	0.41
Carbon monoxide	2.7	3.4
Nitrous oxides	0.48	1.0

The first stage — by 1989 — aims at reducing emissions of carbon monoxide by 20 to 50 per cent (depending on the type of vehicle), hydrocarbons and nitrous oxides (which together form smog) by 20 to 40 per cent, and nitrous oxides alone by 30 to 45 per cent. Although emission levels in diesel-run cars are also to be reduced, they cannot be reduced to the same extent.

But the second stage, by 1995, requires the use of further technology. Although the development of lean-burn and fast-burn engines (which would produce less pollution in the first place) has been stepped up, the most efficient anti-emission pollution technology available today is the three-way catalytic converter. Fitted to the exhaust of a car, it chemically converts polluting exhaust emissions into the harmless components of the air we breathe: carbon dioxide, water, oxygen and nitrogen. Although research has been carried out into catalytic converters which have some tolerance of leaded petrol, their efficiency is limited.

Catalytic converters now in use are damaged by lead. Hence the need, even if lead were a doubtful health risk, to remove it from petrol. In order to fit "cats", which would reduce smog, in the early 1970s, the United States had to get rid of lead first. Europe has approached the problem from the opposite angle. Anna Lubinska

---

Weinberg *et al.* threat from animal lib

"Researchers beware!" was one of the immediate and somewhat unexpected British responses to the *Nature* conference on the molecular biology of cancer, at Boston two weeks ago. Within a week of the meeting, a document was widely distributed to laboratories in Britain, insisting that the paper presented by R. Weinberg ("Neoplasms as uncontrolled regenerative hyperplasia") would produce "horrible tissue trauma and wound healing experimentation. . . that must be publicly revealed, legally examined, morally questioned and humanely stopped".

Weinberg was accused of secretly communicating his "wretched and detestable experimentation" at a closed meeting rather than openly publishing it in the literature. How the Animal Liberation Front, the authors of the warning, intends to "punish those responsible" is unclear, but the organization claims that it will not tolerate the use of experimental animals in cancer research.

ICSU

Grand plans for global changes

Ottawa

THE International Council of Scientific Unions (ICSU) last week approved in principle a major international interdisciplinary research programme on interactions of the geosphere and the biosphere. The aim of the programme is to understand global change over long timescales, and in particular the influence of man on the environment.

Advocates of the venture, to be called the International Geosphere Biosphere Program (IGBP), argue that instruments now becoming available should be used in a coordinated fashion to monitor environmental changes that might affect human civilization as the Earth's population increases. Specific proposals are so far lacking; but the fate of carbon in the ocean and the long-term effects of high-yield agriculture on soils are likely to figure prominently.

But despite the laudable sentiments expressed last week by those seeking to avert possible environmental disaster, many were critical of what they saw as woolly thinking. Professor Tom Malone of the US National Academy of Sciences, a prominent champion of IGBP, promoted J. E. Lovelock's "Gaia" superorganism concept of the global environment, an idea most biologists find untenable. Speaker after speaker at a day-long symposium at last week's ICSU meeting emphasized the inter-relatedness of various facets of the geosphere and biosphere without specifying what new studies were needed.

Interestingly, some of the reactions heard last week may reflect the different styles of science in Europe and North America. One summary talk that featured a slide of starving children was privately criticized by some European delegates for using cheap tactics, while being praised for its effectiveness by American scientists. The second group argued that the purpose of the symposium was to stir delegates to action rather than to advance understanding.

The British Royal Society has been the leading the opposition to IGBP, believing that unless it was more carefully focused, the project could divert attention, and possibly resources, from existing international studies such as the World Climate Research Program. Some of the ideas canvassed for IGBP last week were nothing if not ambitious, with up to 50 dedicated Earth satellites being proposed. A compromise put forward by Academician V.V. Belousov of the Soviet Union and agreed by the general assembly calls for an *ad hoc* committee to work out specific proposals for IGBP in time for the next ICSU general assembly in 2 years' time. Sir Arnold Burgen, foreign affairs secretary of the Royal Society, said he was "quite happy" with Belousov's formula.

Everybody stresses that the programme is unlikely to produce data before the 1990s, and that the sort of long-term data acquisition needed will require a shift of attitudes from short-term fashionable projects towards more methodical data collection. But the success of International Geophysical Year in the late 1950s is being held up as an example of what might be achieved.

Tim Beardsley

Visas denied

THE Ottawa meeting of ICSU was marred by angry exchanges and protests by the Soviet delegation at the denial of entry visas to two Soviet representatives. A statement by the Canadian Ministry of External Affairs read out at the meeting said the government had ensured visas for "all *bona fide* scientists" to facilitate free association.

The two excluded Soviets were Dr V. K. Dobrosel'skii and Mr A.A. Kokoshin. Dobrosel'skii is, ironically a member of ICSU's standing committee on the free circulation of scientists. He is also widely rumoured to hold the rank of brigadier in the KGB (the Soviet secret police) and has previously been denied entry to other Western countries. Soviet delegates, insisted however, that Dobrosel'skii has several "outstanding" inventions to his credit. There was more puzzlement over the exclusion of Kokoshin, who is a member of ICSU's committee on science and technology in developing countries.

Most found the exclusions surprising and regrettable. There is no obvious rationale for a political reprisal by the newly elected Canadian Government, and some observers from Western nations believe Dobrosel'skii has genuinely worked for free movement of scientists regardless of what other positions he may hold. Everyone recognizes a grey area — ICSU has never consisted solely of active research scientists — and, as one US delegate observed, "we've some good scientists in the CIA" (Central Intelligence Agency). The assembly passed a resolution expressing its "deep concern" that entry visas were still being denied to scientists attending international meetings, singling out the governments of India, the Soviet Union and Canada. ICSU-sponsored activities will not be held in these countries until solutions have been found.

Visa problems also explain the Indian National Science Academy's decision to withdraw its offer to host the next ICSU general assembly; it has apparently been unable to secure the guarantee required by ICSU that scientists would be allowed entry visas. The 1986 general assembly will instead be held in Switzerland, but India may still be the host in 1988. Tim Beardsley

Drugs in athletics

Mortality of Soviet athletes

SUSPICIONS that the Soviet Union, and possibly some other socialist-bloc countries, routinely use anabolic steroids and other biochemicals in the training of athletes have now been fanned by an underground report which reached the West at the end of July, just in time for the Los Angeles Olympic Games. The report lists the names of 59 former Soviet Olympic competitors (including 26 medallists) from the 1952 games onwards, who have since died. The list, it is claimed, was compiled with the participation of Soviet athletes, many of whom fear for their own life-expectancy as a result of training procedures.

Although the list includes a few cases of accidental death not related to sports, the overall figures show a death rate of 17.1 per thousand competitors, whereas the corresponding figure for the United States over the same period is 4.5 per 1,000 and for the United Kingdom 2.1 per 1,000. Deaths occurred most frequently in the 41–50 age group (18), 31–40 (11) and under 30 (9). The death rate, according to these figures, has more than doubled since 1976, while remaining stable or even decreasing elsewhere.

We stick in doorways, and suffocate...
CCCP
BIRCH

The conclusion that these figures are related in some way to specifically Soviet training practices has been challenged by Michael Kessis, a physical education instructor in California who edits the *Soviet Sports Review* (a collection of translations from the Soviet sports press), but not, so far, by the Soviets themselves.

Thus, in a comment on "anti-Soviet" attitude in Los Angeles, *Literaturnaya Gazeta* did not deny the deaths but merely pointed out that Vsevolod Bobrov, the hockey-player, had been "approaching 60" when he died (he was in fact 57) and that Valerii Kharlamov (another hockey-player) and Valerii Popenchenko (a boxer) had died in "tragic accidents".

Apart from accidental victims, the

deceased athletes received no obituaries in the Soviet media, but the TASS correspondent in New York, Vladimir Kikilo, was able to confirm a number of the deaths. Given the uncertain provenance of the document, it would otherwise have been necessary to check its contents by a scan of the Soviet sporting press for the last recorded appearance of the listed competitors.

Mortality of Olympic medallists (1952–76*) by age group at time of death

Age	Soviet Union	United States	Germany (FRG & GDR)**
30 and under	9	7	3
31–40	11	1	3
41–50	18	4	4
51–60	7	1	2
61 +	1	1	0
Total deaths	46	14	12
Those dying in 1976–82	26	3	4
Total medallists	1,033	784	786
%Deaths	4.45	1.79	1.53

*The 1980 Moscow games are omitted from this survey due to the US boycott.

**Figures amalgamated because in 1952 East Germany did not compete and from 1956 to 1964 the two Germanies fielded a joint squad.

The ban on the use of anabolic steroids for athletes makes it difficult to obtain statistically significant data on their long-term effects. Earlier this year, however, *The American Journal of Sports Medicine* listed no fewer than twelve steroid-related disorders, ranging from testicular atrophy in males and virilization in females to hepatic dysfunction, hypertension, changes in cholesterol composition, tumours, changes in connective tissue and psychosis.

There have also been suggestions that the Soviets may be administering to their athletes carnitine (involved in fatty acid metabolism), potassium orotate (an intermediary in the biosynthesis of pyrimidine nucleotides) and inosine (also involved in pyrimidine nucleotide synthesis and in the formation and breakdown of high-energy phosphates). Such compounds could serve both as performance enhancers and to counteract the short-term side effects of steroids. The long-term effects of high dosages are, however, unknown.

The mortality report on Soviet athletes — if accepted abroad — could serve as a grim warning to athletes and trainers in other countries who might feel tempted to resort to unauthorized aids. The status of the document, however, is still far from decided. Attempts by the "Smolosky" human rights group in the United States to bring it to the attention of the International Olympic Committee in Los Angeles proved unsuccessful.

Part of the explanation for that may have been the absence of a Soviet Olympic team, which in turn is held by many in Eastern Europe as well as the West to have been caused by Soviet reluctance to submit athletes to the sophisticated drug tests installed at Los Angeles. **Vera Rich**

Heavy-ion research

European ambitions multiply

GANIL, the new French accelerator for heavy ions at Caen in Normandy, is to close down for January to save electricity. GANIL must save 12 per cent as its contribution to last year's budget cuts, but director Claude Detraz is not perturbed. "We're stopping in January when electricity is most expensive", he says, "and anyway we're finding we've got plenty to do when the machine's off."

In fact, Detraz is buoyant about the performance of his accelerator. He is even happy with his budget — which he believes to be quite sufficient to "sweep the field" in intermediate energy heavy-ion collisions. Detraz claims that GANIL is three years ahead of any other accelerator in performance and beam intensity and is making many interesting — and unexplained — discoveries. What GANIL needs, he says, is not money but a team of committed theorists to help explain the effects being revealed.

The accelerator at Caen is the latest of a clutch of European heavy-ion machines (others are in West Germany and Britain) dedicated to the study of the gross properties of nuclei rather than the structure of nucleons and other particles, with which high-energy physics is now preoccupied.

Detraz says he is enticing French theorists to GANIL with discoveries such as that of isolated excited states of the nucleus 100 MeV above the ground state (where previously only a continuum of states was expected), the apparent failure of thermodynamic models of the excited nucleus and strong forward scattering (a kind of nuclear transparency) at total nuclear energies above 40 GeV. Other GANIL products (detectable because of high beam intensity) are exotic neutron-rich nuclei such as nitrogen-23, neon-29 and neon-30 as well as highly-charged positron-emitting atoms. "It's a gold-mine", says Detraz.

GANIL, however, is not alone in the mine. In Britain, working another seam, the Nuclear Structure Facility (NSF) may have taken a lead in high-spin nuclear physics, where nuclei are spun to such angular momenta that Coriolis and centrifugal forces are comparable with nuclear forces. NSF is planning a major extension of its Van de Graaff accelerator, the largest in existence, by means of a superconducting linac.

In West Germany also, the heavy-ion laboratory (GSI) near Darmstadt is basking in the discovery of elements 108 and 109, and has won outline approval for a substantial extension. And Italy is building an advanced superconducting cyclotron in Milan, although the project was set back recently by the untimely death of its designer.

GANIL itself uses a pair of separated-sector cyclotrons to accelerate a wide range of nuclei from 100 MeV per nucleon (for light ions) up to 10 MeV per nucleon (for the heaviest). In low-energy nuclear accelerators (such as NSF), nuclei approach at velocities that are small compared with the internal velocities of their nucleons, so that internal structures are rearranged before collisions. At much higher energies (such as the GeV per nucleon available at Berkeley, California), on the other hand, collision velocity is much faster than the internal motions, and nuclei collide like bags of stationary separate particles. But at GANIL — the intermediate region — the velocities are roughly equal, so that simple approximations do not apply. Hence perhaps, the lack of enthusiasm of theorists, whom Detraz claims are nevertheless being won round by the challenge of GANIL.

NSF (at Daresbury, Cheshire) is making its mark because of its stable and turnable particle beams (a consequence of eletrostatic acceleration), the range of nuclei which can be accelerated ("virtually the whole periodic table" according to a Daresbury experimenter), and a superb detector of gamma-emission from high spin states which can discriminate against Compton-scattered radiation.

Daresbury now plans to abandon the original target of a 30 MV terminal voltage, to stay with the present 20 MV but to put all its effort into developing a superconducting linac stage after the Van de Graaff. This would give NSF the capability of colliding uranium with uranium. The proposal has not yet gone to the nuclear physics board of the Science and Engineering Research Council that would fund it, but the extension could be built segment by segment without increasing the budget, they say in Cheshire.

Meanwhile, GSI Darmstadt plans to add a synchrotron and a storage ring to its present UNILAC linac (which is capable of colliding nuclei at around 20 MeV per nucleon). The additions would bring GSI up to 1.3 GeV per nucleon at high intensity, making possible a search for new states of condensed nuclear matter. The GSI additions are all but finally approved, a federal government spokesman in Bonn said last week, with a decision due "before the end of the year".

With work in this field also at CERN (the European Organisation for Nuclear Physics near Geneva) and progress in Italy, the chauvinistic cry is getting louder in Europe that the old continent has taken "an unquestionable world lead" in nuclear matter studies. That, of course, was what the particle physicists were saying until President Reagan gave the go-ahead to the super-conducting super-collider now being built as an adjunct to the Stanford Linear Accelerator Center and which may steal a march on CERN's new large electron-positron storage ring. **Robert Walgate**

Japanese research

Companies go for basics

Tokyo

A BUILDING boom for basic research laboratories is under way in Japan — but neither the government nor the universities can take credit. Instead it is large private corporations that have begun to invest in academic research.

The latest is Meiji Milk Products, whose brand-new Institute for Basic Research in the Life Sciences, located in Odawara City, some 80 km from Tokyo, will be completed in the next few weeks. The initial outlay has run to 5,000 million yen ($21 million). Around 50 scientists will be employed, together with 50 support staff, to carry out research in eight divisions spanning the whole of molecular biology.

Before Meiji Milk came onto the scene, some fifteen other companies had opened basic research facilities this year alone. The biggest surge has come for the life sciences, with six new laboratories — and a demand for researchers that has sent head-hunters in search of Japanese working in US and European laboratories. Close behind come laboratories for new materials and electronics. Famous names include robot-builders Fanuc, whose factory, where robots build robots, was toured by Mrs Margaret Thatcher, the British Prime Minister, and Toshiba, with a new very large scale integrated circuit research laboratory. Almost all the new high-technology fields are represented: artificial intelligence, molecular memories and conducting polymers all have their new facilities.

At Meiji Milk's Meiji Institute of Health Science (which bears an "MIH" logo reminiscent of a certain US laboratory) there is no pressure at all to perform applied research for company products, according to Norio Nakatsuji, until recently at the MRC Mammalian Development Unit in London and now head of the new institute's developmental biology division. He also points out that recruiting highly qualified staff has proved easier than expected — some have given up tenured positions at universities to join the institute where, with new facilities (including four P2 and two P3 biological containment research laboratories) and generous budgets, there will be no limits on research.

The basic laboratory boom is a very recent phenomenon — only one such laboratory was set up in 1982 and seven in 1983 — but it seems likely to continue. Fifteen companies have already announced plans to set up basic facilities in the near future.

What exactly is the thinking behind the boom and why are corporations prepared to spend huge sums of money to set up these laboratories? Financial analysts admit to finding the trend quite puzzling. Increased prestige is one factor they all cite, adding that prestige is often reflected in higher stock market prices when plans for basic research facilities are announced. But the real factor seems to be an underlying feeling that Japanese corporations have drawn level with or passed their Western competitors in mastering applications of current technology, and must now look for the seeds of new technology in their own basic research rather than continuing to import ideas or to look for ideas in their own universities.

Barriers between universities and industry are said to be just too high for effective research cooperation, and the new laboratory boom has not been accompanied by a boom in either university endowments or research contracts at universities. Instead, corporations seem intent on giving select groups of their own researchers the kind of freedom that they would enjoy in universities.

Given this trend, it is likely that the difference between Japan, where industry pays two thirds of the total research and development bill, and countries like the United States, where it pays only 40 per cent, is likely to increase — and Japanese university laboratories will have finance, equipment and technical support far inferior to those of their industrial counterparts. **Alun Anderson**

Virus diseases

Immunogen for herpes, AIDS?

A DRUG developed as long ago as the early 1970s is now being hailed by its makers, Newport Pharmaceuticals of California, as a possible "new hope in herpes and AIDS". Unlike the recently introduced drug acyclovir, the "new" drug (inosine pranobex, new UK trade name Immunovir) acts by stimulating the patient's immune system, not directly against the virus.

Going by the results so far, however, it is either too early or too optimistic to welcome Immunovir as a major weapon against either genital herpes or AIDS (acquired immune deficiency syndrome, linked with human T-cell leukaemia virus type III). Clinical tests, carried out by Dr R.D. Miller and co-workers at the University of California's Irvine Medical Center, have indeed shown an effect on recurrence rate in genital herpes. In 35 patients given Immunovir tablets, 18 (51 per cent) had only 0 to 1 recurrence during the six-month study, compared with 8 of 41 (19 per cent) on placebo. The relatively high apparent response to placebo, inevitable when considering symptoms that recur at unpredictable intervals, makes it impossible to assess the efficacy of Immunovir until more clinical trials have been completed.

But the initial clinical trials do suggest that Immunovir significantly reduces viral shedding — the number of viruses present in the body's secretions. This raises the hope that the spread of herpes might be controlled by treating infected individuals. The US Center for Disease Control (CDC) estimates that there are between 5 and 20 million cases in the United States, with some 300,000 new cases each year. Herpes is not a notifiable disease in the United States, hence the uncertainty of CDC estimates. Dr Miller's own estimate is as high as 30 million cases.

Whatever the true figure, there is clearly a place for a drug that would both reduce discomfort (number of recurrences) in those with the disease and reduce the possibility of them passing it on. The makers of Immunovir claim that it is cheap enough (compared with extremely expensive antivirals) and safe enough to be used in such a role. No side effects have yet been found, it is claimed, although the drug is metabolized to uric acid so cannot be used in patients with gout or kidney disorders. For treating primary herpes, with the aim of a cure that would mean no further need for treatment, it seems likely that an antiviral drug such as acyclovir will be necessary.

Immunovir has not yet been used to treat patients with AIDS, although Dr Joyce Wallace and Dr J.G. Bekesi of Mount Sinai Hospital and the AIDS Medical Foundation, New York, have treated patients with "pre-AIDS". That condition is characterized by depression of the immune system and lymphadenopathy, and may or may not develop into AIDS as defined by CDC. In these patients, as in others given Immunovir, the number and activity of natural killer cells in the blood and the number of (antibody-stimulating) T-helper cells were increased.

Improvements in laboratory tests of immune function may not always be accompanied by a clinical response. But in the 16 pre-AIDS patients with significantly improved immune responses (of 20 treated), 5 reported a subjective improvement in symptoms and were well a year after the study. Clearly, as Dr Wallace stresses, it is too early to say whether Immunovir is likely to revolutionize the treatment of AIDS and pre-AIDS, although she is encouraged to carry out further trials, and a new trial is due to begin in London later this year.

Although publicity for Immunovir has centred mainly on herpes and AIDS, the drug has shown some promise in a variety of virus diseases — hepatitis, mumps, subacute sclerosing spondylitis and influenza among them. Initial results, however, seem to suggest that amelioration of symptoms is more likely than a complete cure. **Charles Wenz**

Australian science

Budget dismays even ministers

Canberra

IF they needed reminding of it, Australia's scientists had their political impotence brought sharply home to them when the federal budget was announced at the end of August. In a fiscal strategy aimed at promoting business confidence by reducing the budget deficit to $A6,745 million (£4,500 million) from last year's $A7,961 million, and smoothing the Labor Party's path to re-election by means of a small tax cut immediately before the federal polls (now tipped for November or December), the feebleness of the science lobby was made painfully obvious.

The science and technology minister, Mr Barrie Jones, is reported to have contemplated resignation from the ministry over the budget cuts to his portfolio, and later to have earned the prime minister's displeasure by hinting publicly that taxation would increase after the election. Beyond exhorting scientists to make the public more aware of the value of their work, Mr Jones did not elaborate on the tactical details of the successful science lobbying.

Including government appropriations for salaries, administration and major capital expenditure of $A596 million — a monetary increase of 1.6 per cent over the 1983–84 figure — funds totalling $A660 million will be available through the Department of Science and Technology, if industry subventions and earned revenue are taken into account. Complaining of the new budget's effect on morale, Dr Paul Wild, chairman of Australia's largest research group, the 7,000-strong Commonwealth Scientific and Industrial Research Organisation (CSIRO), reported that CSIRO's direct budget appropriation of $A322 million intends no provision for inflation in non-salary operating funds and that most areas of CSIRO research will face cuts of up to 4.3 per cent.

An estimated 180 CSIRO jobs will be cut, mostly those of young scientists in short-term non-tenured positions. Already, the staff of at least one CSIRO division have agreed to take leave without pay to bring down salary costs and minimize retrenchments. To keep things in perspective, though, the government has set aside $A30 million for Australia's defence of the America's Cup yacht race in 1987.

The science portfolio has suffered considerably compared with the others, which is especially disappointing given the importance accorded it in the national technological strategy. The government's total outlays, excluding health, represent an average monetary increase of 10.7 per cent across the whole economy. With a projected inflation rate of 6 per cent, the 1.6 per cent monetary increase for government-sponsored science and technology results in a net contraction of about 4.5 per cent in real terms.

At $A1,237 million, tertiary education commission grants for universities have kept pace with inflation and grants to colleges of technical and further education have increased by 23 per cent to $A307 million. The Australian Research Grants Scheme, however, has had its funds augmented by only $A3.5 million to $A26 million to meet grant applications for 1985 totalling $A65 million.

Budget provision for medical research grants has been increased by $A6 million to $A44 million. Defence science has an extra $A11 million, taking its budget to $A158 million. Support for the Bureau of Mineral Resources has increased from $A23 million to $A31 million.

An addition of $A150 million over five years to the research funds available for automobile design through the Australian Industrial Research and Development Incentives Board arises from the design facility of the Button car plan, formulated by Industry and Commerce Minister, Senator John Button.

Mr Jones is nevertheless bravely burying his disappointment by a recitation of the bright spots in the budget. Antarctic research and the Bureau of Meteorology are to enjoy considerable increases, and modest support will be given to marine sciences, the National Biotechnology Scheme, fifth generation computing and a new CSIRO Division of Information Technology. Nonetheless, the minister's exasperation could not be disguised. He remarked that in an election year, short-term political considerations will always displace the longer perspective necessary in science. **Jeffrey Sellar**

US election

Shoestring lobbies

Washington

IN an election campaign that has seen optometrists and freight-forwarders organize Political Action Committees (PACs) to channel money to candidates favourable to their causes, scientists seem almost strangely absent. The records of the Federal Election Commission reveal only a handful of PACs concerned with scientific issues, and these, by any standard, are woefully impoverished.

Organizers of science-oriented PACs blame their poor showing on an "ivory tower" attitude among scientists who refuse to see scientific interests as the basis for political organization, and on the "bad name" that PACs have received. The result of post-Watergate election reforms, PACs are the only legal means by which organizations not affiliated with a candidate can make campaign expenditures. Although PACs are allowed to contribute no more than $5,000 to any one candidate, there is no limit on the amount that can be spent on "independent" advertising opposing a candidate; PACs have come to be associated with such "negative advertising" campaigns.

The Science and Technology PAC, or SCITEC–PAC, which claims to represent the interests of research scientists most directly, has so far spent only $643 during this congressional election; it has made no campaign contributions at all this year. The organization's treasurer, David Garin, says that the group plans to donate a total of $1,000 to about a dozen candidates in the next three weeks. Garin said the average contribution to the PAC was $40 per person. (Corporations and labour unions are not permitted to contribute to PACs.)

At least two somewhat more successful PACs concentrate on space issues. The Campaign for Space, which has the stated aim of promoting a balanced manned and unmanned civilian space programme, including both construction of a space station and an increased programme of planetary exploration, has taken in about $40,000 for this election; the group plans to contribute $10,000 to congressional and senatorial races. The group has also endorsed the re-election of President Reagan, citing his support for the space station and Democratic challenger Walter Mondale's opposition to the shuttle when he was in the Senate.

The other space group, called SPACEPAC, has taken in $60,000 for the election, spending almost all of it so far on fund-raising costs. Its only campaign contribution has been one of $300 to Representative Don Fuqua, chairman of the House of Representatives Science and Technology Committee.

Thomas Frieling, executive director of the Campaign for Space, readily acknowledges that the small contributions of his and other science-related PACs cannot make much difference to the election results. But, he notes, even the "big league" PACs are limited to contributing $5,000 to election campaigns that cost hundreds of thousands of dollars in the House and millions in the Senate. Garin, of the SCITEC–PAC, suggested that the real significance of his contributions was that they represent an endorsement by a non-partisan group that has the interests of science at heart.

The one scientific professional society that has organized a PAC, the National Society of Professional Engineers, dwarfs these efforts; it has so far raised $200,000 for this election. And nobody else comes close to the American Medical Association's $3.6 million war-chest.

Stephen Budiansky

Peer review

Sir — The problems of peer review procedures deserve serious consideration, but the remedy proposed by M.C. Goodall (*Nature*, 23 August, p. 620), an effective appeal process, is not practicable. Grants committees have little difficulty in identifying outstanding or mediocre proposals; it is the predominant mass of attractive sound applications that cause the problems. In the "good old days", virtually all of these would have been supported. Today a large proportion fail, their fates being determined by slight variations in the (usually secret) scoring by various members of the committee. Mean scores determine a rank order which is the basis for allocating funding from the top of the order until the funds are exhausted.

It would be quite iniquitous to review at appeal a single application that had failed without also reviewing all the competing (even successful) applications, perhaps even including those that were successful. Who is to say that a second complete review would be any more just than the initial review? In a situation of diminished resources it has to be accepted (albeit reluctantly) that a considerable element of chance is an inescapable component of today's review procedures.

The only marginal improvement that might be worth considering would be a more sensitive scoring system in the critical region around the anticipated cut-off point. For example, at present one major grant award-body scores from 0 (bad) to 6 (outstanding) with a funding cut-off in the region of 3.7. In practice most good applications are scored either 3 or 4 by committee members and the mean score can be moved from one side of the cut-off point to the other by just one member altering a score from 3 to 4, or vice versa. If members could score in fractions in this region rather than integers they could exercise greater discrimination, giving a somewhat less chancy mean score.

Bryn Bridges
MRC Cell Mutation Unit,
University of Sussex,
Brighton BN1 9RR, UK

Nature bingo?

Sir — It occurs to me that the current "Bingo War" in Fleet Street may pose a serious threat to the maintenance of *Nature*'s circulation. May I therefore suggest a way in which this might be countered? I propose the institution of a new game entitled "Base Sequence". Each subscriber would be sent his own "DNA card" on which would be printed a unique sequence of 36 bases. Three or four tRNA anticodons would then be printed in each issue of *Nature* (possibly at the bottom of the contents page), the winner being the first reader to match up his base sequence with a complete set of complementary triplets, thus completing his peptide. Obviously frame-shifts and "spare" bases could not be allowed!

I feel certain that such a course of action would assure the future of the journal, the only possible disadvantage being the risk of attracting the eye of Rupert Murdoch or Robert Maxwell.

S.J. Publicover
293 Heeley Road,
Selly Oak,
Birmingham B29 6EL, UK

Brazilian science

Sir: — Your special offer for Brazilian scientists to purchase *Nature* is important not only in helping Brazilian scientists to keep themselves up to date in science, but also in calling attention to the isolation from the international scientific community of Brazilian scientists due to the present policy of budgetary restrictions for science and education. The faculty members of the Brazilian federal universities are involved in a national struggle for better working and teaching conditions. Among other facilities that are becoming inoperable, the libraries are at the moment incapable of renewing their subscriptions due to lack of money for education in addition to the restrictions on foreign exchange.

Marcello André Barcinski
Departamento de Biofísica Celular,
Instituto de Biofísica,
Universidade Federal do Rio de Janeiro,
21941 Rio de Janeiro, Brazil

Bio company launch

Sir — Since *Nature* has a long standing interest in promoting advances in biotechnology, we have chosen to make the first announcement of our new venture in your pages.

At a recent meeting of the American Society of Biological Chemists (ASBC, San Francisco, June 1983), we were amazed by the number of biochemists who are owners, co-owners or owned (as "consultants") by private enterprises. Our unbiased survey of participants at this meeting revealed the following (see figure).

At the time of Adam and Eve, less than 0.001 per cent of all living scientists were engaged in profit-yielding activities. Much later (see small blip in curve) a sizeable percentage of scientists convinced the public that lead could be transformed into gold. In the 1980s, this logic has been extremely successful[1,2]. There are a number of explanations for the rapid increase shown in the figure other than blatant greed including (1) new techniques for producing monoclonal antibodies; (2) gene cloning; (3) gullibility of the public.

At the San Francisco ASBC meeting, we were quite embarrassed not to have an official company business card, as did all our friends. Furthermore, when walking back to our sleazy hotel (Taylor Street, *et al.*) late one night, we were approached by two charming women asking "would you like a little company?" This encounter sparked our interest and we decided to start our own enterprise.

As indicated on our tastefully designed letterhead, Genasex was conceived. The response has been fantastic. In our travels, many scientists have expressed keen interest and overt jealousy. Suggestions arrive daily. One colleague advised changing our name from Genasex Ltd to Genasex Unlimited. A colleague from Milan offered to head an Italian subsidiary to be called Gen-italia, but we have postponed a decision on that.

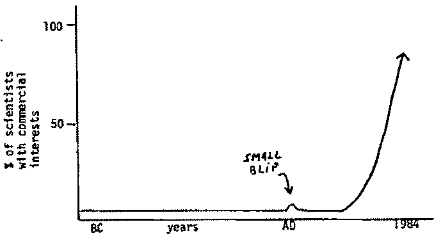

What products does our company produce? So far, none. The reasons for this policy include (1) our observation that many of the new biotechnological companies also produce no products; (2) of those who do, most are in the red; and (3) to use this company as an effective tax write-off, we must be careful not to be too successful.

Hitherto, our financial investment has been negligible. Naturally, we solicit readers' contributions and would certainly consider adding names to our board of directors. Our real hope is that another company, perhaps with a similar name, would offer to buy us in order to avoid the inevitable competition.

D. Malamud
J. Hanoune

Genasex Ltd,
c/o University of Pennsylvania,
Thomas W. Evans Museum
& Dental Institute,
4001 Spruce Street,
Philadelphia, Pennsylvania 19104, USA

1. Dow-Jones *et al.*, any day, any paper.
2. *Nature*, Index of Biotechnology Stocks, monthly reports.

Photocopying

Sir — J.D. St Aubyn (*Nature* **304**, 678; 1983) correctly stresses that it is publishers and not authors who are concerned about large-scale copying. In fact most reputable suppliers of tear sheets or photocopies, ourselves included, adhere to the requirements of the Copyright Clearance Center (CCC), so eliminating most of the administative copying.

The price of an authorized photocopy includes the CCC payment, I believe the British Lending Library has agreed to pay CCC fees on all photocopies mailed to the United States.

Eugene Garfield
Institute for Scientific Information,
University City Science Center, .
Philadelphia, Pennsylvania 19104, USA

Jumping the smoking gun

Are antibiotics in animal feed a threat to human health? Contrary to some opinions, the latest evidence put forward in the United States is inconclusive.

ALTHOUGH Western Europe has now banned the use of antibiotics as a growth-promoting additive in animal feeds, the United States has since 1977 — when a proposed ban was blocked by Congress — maintained that additional data are needed to justify such an action. Half of the 35 million tons of antibiotics manufactured each year in the United States end up in animal feed; not surprisingly, the prospect of a ban is not looked upon favourably by the pharmaceutical industry.

But neither is it by farmers. The evidence, as paradoxical now as it was when the growth effect was discovered in 1949, is nonetheless convincing that chickens, pigs and cattle do much better when fed subtherapeutic doses of antibiotics. Even when the animals show a significant percentage of resistant bacteria in the gut, the effect persists; chickens, for example, will gain weight as much as 10 per cent faster when fed antibiotics[1].

Balanced against this convincing economic benefit, however, is mounting concern about the spread of resistant organisms. The discovery that resistance can be conferred by mobile plasmids, and the appearance of certain resistant strains of gonorrhoea, *Haemophilus influenzae* and dysentery-causing organisms, has led to repeated calls for cutting back "inappropriate" use of antibiotics; a prime target is their use in animal feeds. The case has always been circumstantial: although it is known that resistance-conferring plasmids do occur in animal-borne microorganisms and that plasmids can readily be transmitted to other bacteria, there has been a lack of convincing proof that the end result actually is the production of resistant strains of human pathogens. A major complication in any effort to establish such a link is the other half of the US antibiotic production, the half that ends up in humans, not infrequently for reasons that range from the inappropriate (ingrown toenails) to the unethical (as placebos for treating colds).

Now, proponents of a ban claim to have found the smoking gun. A study published last month in the *New England Journal of Medicine*[2] traces an ampicillin–carbenicillin–tetracycline-resistant salmonella infection in 18 persons to a beef cattle herd that was the probable source of hamburger eaten by at least 13 of the patients. The cattle had been fed subtherapeutic amounts of chlortetracycline; no therapeutic doses had been administered. The bacteria in all of the patients showed identical resistance and contained a 38-kilobase *R* plasmid; and these bacteria were identical with salmonella isolated from the tissue of a dairy calf that died of scours on a farm adjacent to the beef feedlot. No samples of hamburger were tested, however. In an editorial in the same issue of *NEJM*[3], Stuart Levy of Tufts University, a longtime critic of the use of antibiotics in animal feed, asserts that this study establishes an "important missing link", and concludes that "the clarion is strong and clear".

But the clarion may sound differently, depending on where one is sitting. Salmonella is one of the few pathogens common to animals and humans; it is facile to point to this case as proof that subtherapeutic antibiotics in animals can lead to antibiotic-resistant diseases in humans. Salmonella is a dangerous organism whether it is resistant or not. It should never be present in meat, whether it is resistant or not. Treatment of salmonellosis does not involve the use of antibiotics. The entire story makes a stronger case for ensuring proper sanitation in meat processing and for cooking your hamburger than it does for banning antibiotics in cattle feed.

Even more to the point, 12 of the 18 patients had been taking antibiotics, most for questionable reasons, when they became ill. Three had taken the drugs without the direction of a physician, using pills left over from an earlier prescription or from a family-member's prescription; the others had had them prescribed for sore throats or bronchitis. Because the gastrointestinal symptoms appeared very rapidly after the patients began taking the drugs (usually a matter of 1–2 days), it seems likely that they already had an asymptomatic infection that flourished as soon as competing, non-resistant bacteria were wiped out by the antibiotics. The important conclusion that cannot be overlooked is that if those concerned had not been taking the drugs — and most of them probably should not — they would not have become ill. (Much is being made of the fact that one of the 18 patients died. According to the authors, he received his infection from an incompletely disinfected sigmoidoscope that had just been used on one of the salmonellosis patients.)

Rather than a "compelling" case for the banning of antibiotics from animal feed, as Levy would have it, the study begs the question whether animals are a significant generator of resistant human pathogens. Just as it has been insufficient merely to lay out the theoretical possibility that resistance in animal bacteria could be transferred to human pathogens (a possibility that no one disputes), so it is insufficient to demonstrate, however elegantly, that meat contaminated with resistant salmonella can make people ill. The real question is the extent to which resistance engendered in animal bacteria is responsible for the spread of resistance to strictly human pathogens, such as gonorrhoea. Levy's argument that we have to worry more about antibiotics fed to animals than antibiotics fed to humans because animals produce more faeces is unconvincing. The real missing link is the extent to which human pathogens have an opportunity to interact with animal pathogens and to acquire resistance plasmids. This is surely the limiting factor in determining the animal-feed contribution to resistant human pathogens. Speaking vaguely about the "environmental pool" of resistance plasmids makes little sense in the absence of an answer to this question.

One recent attempt to look at the big picture in fact suggests that there are mechanisms in the environment that indeed limit the spread of resistance. Barbara Atkinson and Victor Lorian have reviewed tests for resistance made on 43,250,000 bacterial samples in 242 hospitals from 1971 to 1982 and have found no overall increase in resistance to 15 different antibiotics during this period[4].

Indeed, the very fact that none of the bacteria residing in the gut of farm animals is resistant suggests that some equilibrium has been reached. If, in a couple of hundred thousand generations, bacteria have not become totally resistant in the face of assault by subtherapeutic antibiotics, is it merely complacency to assume they never will? It seems plausible that the energy cost to the bacteria of maintaining resistance plasmids is at least one countervailing force in the equilibrium equation.

If nothing else, all this should convince us that we do not risk imminent disaster by delaying regulatory action until we understand better the spread of resistance plasmids.

Stephen Budiansky

1. Dafwang, I.I., Bird, H.R. & Sunde, M.I *Poultry Sci.* 63, 1027-1032 (1984).
2. Holmberg, S.D. *et al.* *New Engl. J. Med* **311**, 617-622 (1984).
3. Levy, S.B. *New Engl. J. Med.* **311**, 663-665 (1984)
4. Atkinson, B.A. & Lorian, V. in *Am. Soc. Microbiol Meet.*, 7 March (1984); also *J. clin. Microbiol.* (in the press)

Materials science

Making fuel for inertially confined fusion reactors

from Robert W. Cahn

THE proceedings[1] have recently been published of the Third Topical Meeting of Fusion Reactor Materials, held in September 1983. The very varied and exhaustive papers on tokamaks and their numerous materials problems include nothing whatever on the design and fabrication of the fuel micropellets needed for inertially confined fusion (ICF) reactors. Indeed, ICF is not mentioned anywhere. What accounts for this absence?

The previous meeting in this biennial series (held in August 1981)[2], and a brief attempt to gaze into the future of fusion power, published in the same year[3], likewise had no mention of this important topic. If, however, we go back to the First Topical Meeting[4], held in January 1979, we find a group of nine papers concerned with ICF fuels, covering in considerable detail the position at that time concerning the design of the fuel microspheres, their fabrication and characterization, and the tricky problem of protecting the first wall of an ICF reactor from rapid series of mini-explosions. Why the near-total silence since then?

A very readable review paper on 'the special materials in laser fusion targets' has just been published[5]. The manuscript was received by the editor of *Res Mechanica* in April 1983, and the author states that he is presenting "the state of the technologies in making these materials, and problems encountered in their development, as of March 1980". So it seems, possibly because of the connection of these technologies and problems with the military uses of lasers, that a security blackout descended after March 1980. I have seen a reference to a "1980 Topical Conference on Inertial Confinement Fusion in San Diego" but no indication that the proceedings were published. Even with what we have, however — the 1979 papers and this 'postdated' 1980/1984 paper — it is possible to see the quite extraordinary complexity of the problems and techniques involved. Hendrick's[6] assertion that "pellet fabrication is not a trivial task as implied by some reports; it is also not the impossible task implied by others" is to be noted.

ICF reactors are designed on the basis of the inertial confinement principle — a huge energy pulse imparted by laser or particle beam implodes a spherical shell of frozen deuterium–tritium mixture with a view to satisfying the Lawson criterion and setting off a series of microthermonuclear fusion explosions, the heat from which is absorbed and utilized to make power. In their review paper Farnum and Fries[5] discuss the early stages of the development of a complex laser fusion target designed for maximum fusion yield when irradiated with 100 kJ of infrared light from a CO_2 laser with 1 ns pulses. The essential parts consist of a glass microballoon coated internally with a layer of deuterium–tritium fuel and externally with a dense 'pusher' layer, the whole separated by plastic foam from an external dense metal pusher layer which is itself coated by an ablative plastic layer which creates the 'rocket' effect.

The difficulties arise from the extreme precision needed in the sphericity, thickness uniformity of layers, smoothness of surfaces (to within a few nm) and uniformity of density, for instance of the plastic foam — and all this for microspheres usually well below 1 mm in external diameter. Microballoons can be bought commercially at $\$10^{-9}$ each, but their quality is hopelessly inadequate; the new paper outlines methods, starting either from liquid drops or from solid fragments in free fall, for making balloons with the requisite geometrical perfection. These thin shells can be filled with a gas mixture while in the gel state and then vitrified. (The method for turning the gas filling into a liquid spherical shell that is then frozen so rapidly that gravity has no time to distort it was described earlier[7]; this is really a kind of splat-quenching direct from the gas phase.) Problems connected with the buckling of the microballoons under gas pressure, and the effect of thin coatings on the buckling resistance, are discussed by Farnum and Fries.

The second part of their paper deals comprehensively with ways of making smooth uniform coatings of metals, polymers or a combination of these, by various forms of physical or chemical vapour deposition. These methods often depend for their efficacy on methods of levitating the spheres to be coated, either by systems of gas jets or even by whirling them around, during coating, in a form of synchrotron[6]. Remarkably perfect polymer coatings can now be produced; one method is to build up monolayers of 100 nm-diameter latex spheres under electrostatic attraction, discharge the layer and start again. Production of polymeric foam to the requisite specification, however, is still not possible to the necessary uniformity (or at least was not in 1980).

One of the rare publications to appear since 1980 that deal with ICF pellet (or 'target') production is a paper from Livermore National Laboratory describing the use of an array of gas microjets to levitate a pellet, to allow an ultrasmooth polymer surface layer to be made by plasma polymerization[8].

One curious technique that is not discussed in Farnum and Fries's paper is the approach to making thin flanged micro-hemispherical shells by methods based on microelectronic technology. For instance, starting from circular etch-windows in a silicon surface, hemispherical depressions of high perfection can be etched; these are then boron-doped by diffusion into a thin surface layer and etched from the back with an etchant that does not attack boron-rich silicon[9]. It is a striking tribute to the micromechanical precision of modern silicon handling that the necessary smoothness and sphericity can be attained in this manner.

Others have recently urged the use of metallic glass microballoons and this is exciting much interest[10,11]. Such hollow microspheres can be formed by exploiting the instabilities of hollow liquid jets. Microballoons of a dense Au-Pb-Sb glass have been made with surface smoothness and sphericity of a very high order. How such balloons are to be incorporated in a complete target is not disclosed. Such metallic glasses are known to be highly permeable to hydrogen and thus should not be difficult to fill with fuel. More generally, Lee has very recently outlined a range of other uses for metallic microballoons made from unstable hollow jets, including a rocket fuel[12]. A new technology seems to be emerging.

It would seem that a new generic name is required for the congeries of techniques which have been developed to make ICF fuel pellets — 'materials microtechnology' perhaps? When the full account of this work is published, it will be seen as an essential part of the history of modern materials science and technology. But we shall have to await wholesale declassification before we can know how successful the ICF approach to nuclear fusion currently is. Meanwhile, the interested reader is referred to a concise textbook[13] on thermonuclear fusion that discusses the essential characteristics of inertial confinement. □

1. Whitley, J.B. *et al.* (eds) *J. Nucl. Mat.* **122 & 123** (1984).
2. Nygren, R.E. *et al.* (eds) *J. Nucl. Mat.* **103** (1981).
3. Conn, R.W. *J. Nucl. Mat.* **100**, 139 (1981).
4. Wiffen, F.W. *et al* (eds) *J. Nucl. Mat.* **85 & 86** (1979).
5. Farnum, E.H. & Fries, R.J. *Res Mechanica* **10**, 87 (1984).
6. Hendricks, C.D. *J. Nucl. Mat.* **85 & 86**, 79 (1979).
7. Miller, J.R., Fries, R.J. & Press W.J. *J. Nucl. Mat.* **85 & 86**, 121 (1979).
8. Crane, J.K. *et al. J. Vac. Sci. Technol*, **20**, 129 (1982).
9. Wise, K.D., *et al. J. Nucl. Mat.* **85 & 86**, 103 (1979).
10. Lee, M.C., Kendall, J.M. & Johnson, W.L. *Appl. Phys. Lett.* **40**, 382 (1982).
11. Johnson, W.L. & Lee, M.C. *J. Vac. Sci. Technol.* A **1**, 1568 (1983).
12. Lee, M.C. paper presented at *5th Tut. Conf. on Rapidly Quenched Metals*, Würzburg, 3–7 Sept. 1984. To be published by North Holland.
13. Hagler, M.O. & Kristiansen, M. *An Introduction to Controlled Thermonuclear Fusion* (Lexington Books, Lexington M.A. 1977).

Robert W. Cahn was formerly Professor of Materials Science at the Univesity of Sussex and Professor of Metallurgy at the University of Paris-South. He can be contacted at 6 Storey's Way, Cambridge CB3 0DT.

Geology

Seismic reflections of the continental crust

from Simon L. Klemperer

A recent symposium* provided the opportunity for scientists from seventeen countries to discuss their most recent results on the structure of the deep continental crust using reflection seismology. Unusually for a technique used in pure science, reflection profiling was originally developed commercially for exploration of sedimentary basins, and therefore is available for immediate application without prohibitive developmental expense. The meeting demonstrated its versatility as a means to investigate a wide variety of geological issues in the crystalline rocks of the crust.

Many of the most dramatic successes of reflection seismology have come through tracing fault-plane reflections to surface outcrop. This has resulted in the discovery of major crustal features such as the Southern Appalachian overthrust, and the Outer Isles thrust. When basement reflections cannot be tied to information from surface exposures or boreholes, their interpretation may be ambiguous. The use of forward modelling, that is, estimating the expected reflection character from basement features observed at the surface, as a first step towards interpretation was demonstrated by J. Percival (Geological Survey of Canada) for the Kapuskasing granulite zone and the adjacent amphibolite-grade Wawa gneiss belt. He speculated that the irregular horizontal-to-discordant intrusive boundary between these metamorphic zones might appear as a Conrad discontinuity in a refraction experiment. Felsic-mafic layering in the granulite zone might be the cause of layered reflections in the lower crust, contrasting with the largely felsic (reflection-free?) gneiss belt above the granulites.

The origin of highly-reflective layered lower crust is obscure, and has attracted considerable speculation. Two contrasting theories were proposed with several workers arguing for magmatic processes, such as underplating of the crust, as the primary cause for the reflective layering with extensional shear or thrusting taking a secondary role.

By contrast D. Matthews (Cambridge University) proposed the existence of lamellae of hydration or of high pore-water pressure as the major cause of lower crustal reflectivity. The presence of water or graphite in the lower crust would reconcile the observed highly-conductive zones in the lower crust with data from laboratory experiments. Clearly, more detailed geophysical and geochemical modelling as well as more detailed geological mapping are called for.

Clear reflections at about Moho depth, or bands of reflections terminating at about Moho depth, are not uncommon on deep reflection profiles, particularly extensional terranes, as seen, for example, in the Consortium for Continental Reflection Profiling (COCORP) data from the Basin and Range, and in the British Institutes Reflection Profiling. Syndicate (BIRPS) data from the British marginal seas. Near-vertical reflection seismology does not accurately define volocities at Moho depths, but it is in terms of a velocity change that the Moho is conventionally defined. In the absence of velocity data, the reflection Moho must be picked on the basis of seismic character.

P. Barton (Cambridge Univesity) made use of the best available set of coincident refraction and near-vertical reflection profiles to show that in the North Sea, the reflection Moho, defined as the base to the reflective lower crust, coincides with the refraction Moho. By contrast, D. Okaya (Stanford University) asserted that in the Basin and Range, the base of the layered lower crust, or the reflection Moho, is not coincident with the refraction Moho, although in this case, the available reflection and refraction profiles are in different locations. A. Hirn (Institut de Physique du Globe), using wide-angle reflection and refraction data, and D. Matthews, using near-vertical reflection data, demonstrated the existence of Moho offsets along faults, causing sudden changes in Moho depth of several kilometers across narrow zones.

The reflection character of the Moho, where observed as discrete reflections, varies from complex layering to simple single reflections (L. Braile, Purdue University; R. Phinney, Princeton University). Braile suggested that the disparity between wide-angle reflections, on which the Moho may appear as a continuous boundary, and the near-vertical reflection Moho, which typically lacks horizontal continuity, could be due to fine-scale lamination of the Moho. D. Blundell (Chelsea College) used simple 3-D ray-tracing models to show how a single surface, suitably cross-folded into an egg-box structure, appears as a thick band of reflections on a stacked seismic section, due to interference of reflected arrivals from different directions. These complex reflection patterns show the need for 3-D surveys to constrain the direction from which reflected energy is returning.

Although most reflection profiling results so far have come from the crust, which is highly reflective relative to the mantle, several speakers discussed sub-crustal reflectors in the mantle. The most dramatic mantle structure imaged by near-vertical reflection seismology so far is the Flannan thrust, a Moho-offsetting fault north-west of Scotland, known to penetrate to at least 45 km, or 15 km below the Moho (D. Matthews). An experiment (DRUM: Deep Reflections from the Upper Mantle) to be conducted later this year, using long recording times, will have the potential to trace this structure, and to search for others, down to 180 km depth.

Sub-crustal structural complexity is also suggested by wide-angle reflections and refractions showing Moho offsets, or Moho doubling, beneath some Tibetan sutures and beneath the North Pyrenean fault (A. Hirn).

Many of the data shown were collected in programs for hydrocarbon and mineral exploration, nuclear waste disposal and earthquake fault hazard reduction, as well as for academic research. J. Oliver (Cornell University) described a plan for worldwide cooperation in undertaking a comprehensive reconnaissance of the earth's continental crust which might collect 200,000 km of deep seismic reflection profiles in a 20 year period. Although sounding impressive, this is in total only one-eighth of the mileage collected by the petroleum industry in a single year. In the United States, COCORP, now in its tenth year, has acquired nearly 6,000 km of crustal reflection data throughout the continent and there are more recent programmes including those of the United States Geological Survey (discussed by R. Hamilton), Virginia Polytechnic Institute (J. Costain), University of Wyoming (S. Smithson) and CALCRUST (P. Malin, University of California, Santa Barbara).

Programmes outside the United States include the Canadian LITHOPROBE (A. Green, Department of Energy, Mines and Resources) on the Quebec Appalachians and Vancouver Island, British Columbia; BIRPS (D. Matthews) which has recorded over 3,000 km of marine data circumscribing Great Britain; the Deutches Kontinentales Reflexions Program of Germany (DEKORP; R. Meissner, Kiel Institut für Geophysik); the French Etude Continentale et Océanique par Réflexion et Réfraction Sismique (ECORS; C. Bois, Institut Francais du Pétrole); the Australian continental reflection programme (F. Moss, Bureau of Mineral Resources) and others in New Zealand, China, India, Hungary, Czechoslovakia, Switzerland, Italy and Antarctica. Many of these groups have plans to expand their programmes considerably, and thus the global initiative outlined by Oliver should be attainable. ☐

Simon L Klemperer is in the Department of Geological Sciences, Cornell University, Ithaca, New York 14853, U.S.A.

---

*'Deep structure of the continental crust', 26-28 June, Cornell University, co-ordinated by Dr Muawia Barazangi.

Gene expression

Regulation by anti-sense RNA

from Andrew Travers

THE ability of two complementary strands of RNA to form a stable duplex offers a potentially powerful mode of regulating the biological function of RNA molecules. Thus the normal RNA transcript of a gene could be rendered inactive were it to form a duplex with an 'anti-sense' RNA transcript from part of the same DNA. The past year has produced some good examples of how bacteria employ such a form of control; moreover, the experimental manipulation of gene expression by double-stranded RNA in eukaryotic cells has recently been described.

In prokaryotes, a classic example of this type of control is the regulation of DNA replication of the plasmid ColE1. In this case, a short anti-sense transcript is believed to form a RNA–RNA duplex with the 5′ end of the replication primer and as a consequence to inhibit replication (Tomizawa, J. & Itoh, T. *Proc. natn. Acad. Sci. U.S.A.* **78**, 1981; Lacatena, R.M. & Cesareni, G. *Nature* **294**, 623; 1981). Mutations affecting either the structure or the amount of anti-sense RNA affect both copy number and plasmid incompatibility.

One example in the control of bacterial translation is the regulation of Tn*10* transposase production (Simons, R.W. & Kleckner, N. *Cell* **34**, 683; 1983). The discovery stemmed from the observation that the presence of a multicopy plasmid containing the insertion element IS*10* inhibits *in trans* transposition of a single-copy chromosomal Tn*10* element. IS*10* is itself essential for Tn*10* activity, providing the functions necessary for Tn*10* transposition. Simons and Kleckner found that they could delete all but 75 base pairs (bp) of the transposase-coding region of IS*10* and still retain multicopy inhibition, showing that the phenomenon does not require intact transposase protein. Intriguingly, the portion of the transposase gene required contains a promoter which directs transcription in the opposite direction to the transposase gene, producing a RNA molecule which overlaps and is complementary to 36 bases at the 5′ end of transposase mRNA. To determine the target of inhibition, Simons and Kleckner constructed two sets of IS*10*–*lacZ* fusions; in one set, the amino (5′)-terminal portion of the transposase gene with its cognate promoter was fused in frame to an appropriately engineered *β*-galactosidase gene; in the second set, an intact *lacZ* gene was fused to transposase promoter. Multicopy IS*10*-containing plasmids reduced expression of the fusion protein by more than 10-fold but that of the intact *lacZ* gene by less than 2-fold. Assuming that transcription originated from the transposase promoter in both cases, this result strongly suggests that regulation of transposase expression is exerted primarily by modulating translation and not transcription.

A similar situation has been described for the natural regulation of the production of the outer membrane protein encoded by the *ompF* gene (Mizuno, T. *et al. Proc. natn. Acad. Sci. U.S.A.* **81**, 1966; 1984). This protein is one of two major outer membrane proteins of *Escherichia coli* that serve as diffusion pores for small hydrophilic molecules. The total amount of these two proteins, OmpF and OmpC, remains constant but the proportion of the two varies, depending on the osmolarity of the medium. While characterizing the promoter of the *ompC* gene, Mizuno and his colleagues observed that a DNA fragment upstream of the promoter inhibited the production of OmpF protein when *ompF*$^+$ cells were transformed with a multicopy plasmid containing the fragment. They discovered that this DNA fragment encoded a small 174 base RNA, termed mic RNA (mRNA-interfering complementary RNA), which was transcribed in the opposite direction to the *ompC* gene. This RNA contains no open reading frames preceded by a ribosome-binding site and so is unlikely to encode a protein. It does, however, have extensive homology with the 5′ end of *ompF* mRNA, suggesting that the small RNA could form a stable hybrid with *ompF* mRNA. Since the region of homology includes the ribosome-binding site for *ompF* translation the obvious possibility is, again, that hybrid formation between the two RNA species inhibits translation initiation. A further characteristic of potential biological significance is the coordinate regulation of the *ompC* and mic RNA species which could provide an efficient mechanism for maintaining a constant total amount of OmpF and OmpC proteins.

For neither IS*10* transposase nor *ompF* protein production has the presence of a RNA–RNA duplex been directly demonstrated. Nevertheless, the fact that anti-sense RNA molecules can inhibit gene expression has been confirmed by engineering the production of such molecules for other genes. Coleman *et al.* (*Cell* **37**, 429; 1984) constructed plasmids that produce small RNA molecules complementary to the 5′ ends of the mRNA either for *E. coli* lipoprotein or for two other outer membrane proteins, OmpA and OmpC. In all cases expression of these anti-sense RNA species resulted in a substantial inhibition of expression of the target mRNA species. Significantly, anti-sense lipoprotein RNA also reduced expression of *ompC* mRNA and vice versa, a phenomenon consistent with the extensive homology between the 5′ regions of the two mRNA species.

The ability of anti-sense RNA to inhibit gene expression has been shown to be applicable to eukaryotes. Izant and Weintraub (*Cell* **36**, 1007; 1984) constructed a plasmid so that a promoter directed the transcription of a RNA complementary to the normal thymidine kinase (TK) transcript. When such plasmids together with a plasmid containing a normally expressed TK gene were injected into mutant mouse L cells that lacked TK, it was observed that the presence of the 'complementary' gene substantially reduced expression from the normal plasmid.

The extent to which this novel form of regulation of gene expression is utilized naturally in prokaryotes and eukaryotes remains to be established. Clearly, however, the potential for manipulating gene expression artificially by this mechanism is substantial and well worth exploiting. ☐

Andrew Travers is in the MRC Laboratory of Molecular Biology, Hills Road, Cambridge CB2 2QH.

Sedimentology

Control of dolomite formation

from M. Kastner

A PAPER on page 450 of this issue of *Nature* by Guanatilaka *et al.* describes a recent dolomite $[CaMg(CO_3)_2]$ formation in the subtidal zone of a shallow hypersaline lagoon in southern Kuwait[1]. The finding is of interest not only because it provides further insight into the mechanism of dolomite formation, but also because it has economic implications, dolomite being an important hydrocarbon reservoir, a host-rock for base-metals and associated with evaporites.

Dolomite, one of the three most common sedimentary carbonate minerals, has long perplexed sedimentologists, for two reasons. The first is that there are marked irregularities in its distribution with time. Thus, dolomite is a common, extensive and widespread rock-forming mineral in ancient sediments, in particular in late Precambrian and Palaeozoic times, but it is rather scarce in the Holocene. Between the Jurassic and Cretaceous the ratio of dolomitite (sedimentary rock composed essentially of dolomite) to limestone decreases rapidly and strikingly. Early explanations put forward for the scarcity of Holocene dolomitites were changes in the nature of plate tectonics, correlation with extensive shelf seas, and changes in the magnesium concentration in seawater (for example, refs 2–4), but none has proved satisfactory. The second puzzling aspect of dolomite distribution is that it seems to violate the laws of thermodynamics. Dolomite is the thermodynamically stable carbonate mineral in seawater; why, then, is it relatively scarce in the widespread Holocene marine carbonate sediments?

In the late 1950s and early 1960s several small deposits of Holocene penecontemporaneous dolomites were discovered in marine marginal, mostly supratidal, environments. Their location suggested that dolomite formation requires a molar Mg^{2+}/Ca^{2+} ratio higher than that of seawater (5.3). This theory dominated the literature until five years ago, since when dolomite has been discovered as an important constituent of many modern marine organic-rich sediments, for example, in the Gulf of California, the California borderlands, the shelf off Peru, the Japan trench and the Cariaco Basin off the coast of Venezuela. In the Gulf of California, dolomite forms actively from marine pore fluids with a molar Mg^{2+}/Ca^{2+} ratio of 3.0 (see, for example, ref. 5). Various new models of dolomitization have been proposed[6-8].

Recent experimental work[9,10] shows that the essential condition for dolomite formation is not a high Mg^{2+}/Ca^{2+} ratio, but a low concentration of sulphate ions. Sulphate ions are a major inhibitor of dolomitization of calcite and, to a significantly lesser extent, of aragonite. Mg^{2+}/Ca^{2+} ratios greater than about 0.7 favour dolomitization, but are not thermodynamically required at surface to near-surface temperatures and pressures. Marine sites conducive to dolomite formation are therefore those where dissolved sulphate concentrations are low. The most effective processes of sulphate removal from, or its dilution in, marine pore fluids are microbial sulphate reduction in organic-rich sediments and mixing of seawater with large volumes of freshwater. The high (28 millimoles) dissolved sulphate content of seawater also explains the scarcity of dolomite in thermodynamically highly-favourable environments, for example, in open marine carbonates. Other low-sulphate environments favouring the transformation of $CaCO_3$ into dolomite are $CaCO_3$-rich sediments or rocks exposed on land or within supratidal zones through which freshwater or a mixture of fresh- and seawater circulates, and chalks and limestones through which sulphidic hydrothermal mineralization solutions circulate.

The paper by Gunatilaka *et al*[1] is an important new study of Recent dolomite formation. On the basis of petrographical studies and chemical analyses of pore fluids, the authors suggest that dolomitization of micritic aragonite is promoted by a combination of partial bacterial reduction of sulphate dissolved in pore fluid and occasional near-schizohaline conditions through seasonal rainfall.

What is still puzzling is the paucity of dolomitites formed during the last 100–200 million years relative to their abundance in older sediments. It might be related to changes in the depositional environments of calcareous sediments, and hence to an increase of the calcite/aragonite ratio of the original calcareous sediments following the appearance of coccolithophoroids and foraminifers. On the other hand, the apparent abundance of Archaean dolomitites might indicate that the content of sulphate dissolved in the early oceans was relatively low. ☐

1. Gunatilaka, A., Saleh, A., Al-Teneemi, A & Nassar, N *Nature* **311**, 450 (1984).
2. Zenger, D.H. *J. geol. Education,* **20**, 107 (1972).
3. Boucot, A.J. in *Evolution and Extinction Rate Controls*, 28 (Elsevier, 1975).
4. Mottl, M.J. & Holland, H.D. *Am. geophys Union Trans* **56**, 1074 (1975).
5. Garrison, R.E., Kastner, M. & Zenger, D.H (eds) *Dolomites of the Monterey Formation and Other Organic-Rich Units* (Soc. Econ. Paleontol Mineral . Pac. Sect Spec. Publ., 1984).
6. Zenger, D.H., Dunham, J.B. & Ethington, R.L (eds) *Concepts and Models of Dolomitization* (Soc Econ Paleontol. Mineral. Spec. Publ. No. **28**, 1980).
7. Zenger, D.H. & Mazzullo, S.J (eds) *Dolomitization* (Benchmark Papers in Geology **65**, Hutchinson Ross Publ Co., 1982).
8. Land, L.H. *Dolomitization* (Am. Assoc Petrol. Geol . Education Course Notes Ser. No **24**, 1983)
9. Baker, P.A. & Kastner, M. *Science* **213**, 214 (1981)
10. Kastner, M. & Baker, P.A. in 1982/1983 *Yearbook of Science and Technology* (McGraw Hill, 1982).

M. Kastner is at the Scripps Institution of Oceanography, University of California, San Diego, La Jolla, California 92093.

Astronomy

Meteorites from Mars

[illegible]

from David W. Hughes

MUSEUMS around the world have about 2,500 meteorites in their collections. Where have they all come from? Various origins have been proposed, including the Moon, Mars and asteroids. In a recent paper, G.W. Wetherill of the Carnegie Institution of Washington examines the transport of meteoritic material from Mars to Earth.

Meteorites originate as parts of much larger parent bodies, which formed by a process of condensation and accretion, mixing, depletion, melting and loss of volatiles in the primordial Solar System nebula. The process was completed very quickly, about 4.6 × 10^9 years ago. Over the lifetime of the Solar System, the parent bodies have collided, producing fragments which are the meteorite precursors. The diversity of meteorite types suggests they are derived from about fifty parents which themselves differed in composition as a result of the different temperatures and pressures in the various regions of the primordial nebula. Once freed from their parents, the meteorites were exposed to cosmic-ray bombardment, which produced tracks of radiation-damaged material. Analysis of these tracks indicates that the parent-body collisions occurred typically 50 million years ago for the stony meteorites and 1,000 million years ago for the iron meteorites.

As their exposure ages are so short, some meteorite parents should still exist and be an observable class of celestial objects. Possible candidates are the Apollo and Amor asteroids. Alternatively, meteorites may be the debris of disintegrating cometary nuclei or they may have been ejected from Mars, Mercury and the Moon — the major negligible-atmosphere members of the inner Solar System.

Öpik predicted that only 0.2 per cent of meteorites were of lunar origin and suggested that even fewer would come from Mars (*Adv. Astr. Astrophys.* **4**, 301; 1966). Interest in the possibility of a martian origin for meteorites has recently been renewed, however, on account of three meteorite classes, the shergottites, chassignites and nakhlites. Their isotopic composition indicates that they crystallized as recently as 0.18–1.3 × 10^9 years ago. Even more unusual, they have a geochemical and petrological affinity to the rocks of the Earth's mantle. One shergottite, Elephant Morain, has trapped rare gases and nitrogen resembling the composition of the martian atmosphere.

Impact craters are being produced in the surfaces of all inner Solar System planets, including Mars. Crater-forming projectiles hit the planet at the rate of about 10^9 yr^{-1}. This produces about 10^{11} g of ejecta, most of which is melted, vaporized or pulverized and returns to the planetary surface.

In his recent paper (*Meteoritics* **19**, 1; 1984), Wetherill considers two models, for the transport of meteoritic material from Mars to Earth. In the large-body one, fragments larger than 15 m in diameter were ejected from Mars about 180 Myr ago, the shock metamorphism accompanying this ejection setting the isotopic dating clock. These bodies were then broken up by collisions with small asteroids and the fragments exposed to cosmic rays. The fragments subsequently hit Earth. In the small-body model, rocks smaller than 1 m are ejected from Mars and exposed to cosmic rays immediately after ejection. The major difference between the two models is the percentage of material that can be accelerated to greater than the martian escape velocity. Calculations show that only 0.03 per cent survives in the small-body case whereas a more unrealistic 0.4 per cent is predicted in the large-body model. Theoretical work on crater formation also indicates that only small bodies and those lying very near the planary surface will survive unaltered by the ejection process.

The orbits of the ejected bodies have relatively low eccentricities and inclinations and can exist, on average, between 5×10^6 and 100×10^6 years (depending on aphelion distance) before being hit by another minor body in the Solar System and broken up. Calculations show that of all the material that will hit the Earth from a specific martian event, 36 per cent will do so within 10^7 years. In the favoured small-body model, Wetherill suggests that the cosmic-ray exposure ages of the meteorites are equivalent to the transit time between Mars and Earth. The much longer isotopic age represents the time interval between the present day and the time of production of the specific region of Mars' surface that suffered the impact.

Similar calculations were made for Mercury ejector and it was found that 100 times fewer Mercury meteorites would finally hit the Earth.

What remains to be explained is the ratio between martian and lunar meteorites. The shergottite–nakhlite–chassignite class of meteorites represent 8 of the 2,000 distinct recovered stony meteorites. Only one certain lunar meteorite has been found, a 31 g rock found in the Allan Hills region of Antarctica and known as ALHA 81005. (There are two other 'possibles', both found by the Japanese near the Yamato Mountains in Antarctica.) Other things being equal, theory predicts that the influx of lunar meteorites will be at least several hundred times greater than that from Mars. By contrast, observations indicate that it is smaller by a factor of around 3. A possible explanation is that the orbital dynamics mitigates against lunar meteorites. More unlikely is the suggestion that it is due to a statistical quirk, there having been no large lunar cratering events for the last 10^5 years or more. Another possibility is that there is some special characteristic of the martian surface, the presence of volatiles for example, that facilitates the acceleration of impact-generated fragments to very high velocity.

Whatever the outcome, the importance of meteorites is obvious. The museums of the world contain about 200 tonnes of meteoritic material, of which 90 g are thought to come from the Moon, 70 kg from Mars and the rest from asteroids. Unfortunately, it seems that the only rigorous way of checking the martian origin is to go there and see. ☐

David W. Hughes is Senior Lecturer in Astronomy and Physics at the University of Sheffield, Sheffield S3 7RH.

Ecology

Forest history from pollen

from Peter D. Moore

POLLEN analysis has proved a useful tool for documenting vegetational changes over thousands of years. Carried out on a regional scale, with information collected from sites, such as large lakes and mires that have been carefully selected such that local vegetational events have little impact and local noise is minimal, the technique has supplied important information on climatic history[1]. To the ecologist, however, it is often the very local events that are of interest. Thus he will tend to choose small ponds, peat deposits and even organic humus layers accumulating on forest floors which receive their pollen input from the local vegetation canopy and in which regional changes in vegetation may be masked by the local flora. Such sites can provide a valuable record of local vegetational history and have recently been exploited for this purpose in many parts of the world.

Bradshaw has shown that in a forest, most pollen does not travel more than 20-30 m (ref.2), and recently, with the help of Jacobson, he has constructed a model relating the origin of pollen components to the diameter of the receptor site[3]. In a small 50 m diameter site, for example, 60–70 per cent of the pollen input is immediately local in origin.

The use of mor humus layers was pioneered in Denmark by Iversen[4,5], who found it a particularly useful technique for the detection of the impact of man on woodlands. His conclusion that *Ilex aquifolium*, holly, had been greatly favoured by man's modification of the Danish forests received further support from work on mor humus layers in the Netherlands by Stockmar[6]. This type of deposit has also proved useful for tracing the history of species that have limited powers of pollen dispersion and that are poorly represented in larger sites. Birks has shown that lime, *Tilia*, a tree which is known to have very local pollen deposition[7], has been abundant in Cumbrian limestone woodland in north-west Britain from about 6,000 years ago[8], while in southern England[9] and in Denmark[10], it declined following man's modification of the forests in AD 600–800 and AD 1650, respectively.

Outside the temperate zone of the Northern Hemisphere, relatively little advantage has been taken so far of the opportunities offered by small sites and mor humus layers. Recently, however, Macphail has done some important work in the wet sclerophyll forests of Tasmania. These forests are dominated by *Eucalyptus* species, often reaching heights of 30–40 m, with a high (20 m) shrub layer, consisting of many species, beneath the canopy. They are found in eastern and south western Australia. Their history is uncertain because of their apparent dependence on fire as a containing factor in succession: in the absence of fire, they may be subject to invasion by temperate rain forest trees. This dependence suggests that they may be a product of human activity and maintained by it.

Macphail has now approached this question by analysing the sediments of a small (8 × 18 m) kettle hole in Tasmanian wet *Eucalyptus* woodland[11]. The sediments have been buried by a landslip and date from the early Holocene (9,000 to 7,000 BP). The changes in the pollen stratigraphy of the site are associated mainly with a sequence of understorey species which can in part be explained in terms of climatic trends. Superimposed, however, is a pattern induced by fires, as indicated by charcoal frequency. A marked increase in fire frequency at about 7,200 BP is associated with Aboriginal activity in the area and this produced a distinct shift in the woodland composition in which the rain forest species, such as *Nothofagus*, which had previously been expanding, were set into decline. The involvement of fire and of man in the persistence of the wet sclerophyll forest is thus confirmed.

One further line of evidence is desirable if such studies are to be exploited to the full, namely the study of modern pollen rain in present-day forest types. In this way the varying properties of pollen production and dispersion in the trees and shrubs of the forest can be compensated for in the interpretation of fossil pollen spectra. Studies of this type in the European forests by Andersen[12] and Bradshaw[2] have proved very informative and one must look forward to the outcome of similar work on small sites in other parts of the world. ☐

1. Berglund, B.E. in *Background to Palaeohydrology: A Perspective* (ed. Gregory, K.J.) 237 (Academic, London, 1983).
2. Bradshaw, R.H.W. *J. Ecol.* 69, 45 (1981).
3. Jacobson, G.L. & Bradshaw, R.H.W. *Quat. Res.* 16, 80 (1981).
4. Iversen, J. *J. Ecol.* (Suppl.) 52, 59 (1964).
5. Iversen, J. *Oikos* (Suppl.) 12, 35 (1969).
6. Stockmar, J. *Palaeohistoria* 17, 38 (1975).
7. Keatinge, T.H. *Grana* 21, 171 (1982).
8. Birks, H.J.B. *New Phytol.* 90, 339 (1982).
9. Baker, C.A., Moxey, P.A. & Oxford, P.M. *Field Stud.* 4, 645 (1978).
10. Aaby, B. *Dansk. geol. Unders.* IIR, no. 114 (1983).
11. Macphail, M.K. *New Phytol.* 96, 131 (1984).
12. Andersen, S. Th. *Dansk. geol. Unders.* IIR, no. 96 (1970).

Peter D. Moore is Reader in Ecology in the Department of Plant Sciences, University of London King's College, 68 Half Moon Lane, London SE24 9JF.

Erratum

IN the course of editing the News and Views article by Malcolm Walter on 'Biased record of early life', (*Nature* 309, 512; 1984), an incorrect reference was introduced. The correct citation for ref.1 should have been to Hofmann. H.J. *J. Paleontol.* **50**, 1040 (1976) and not to Schopf, J.W. (ed.) *Earth's Earliest Biosphere: Its Origin and Evolution,* 543 (Princeton University Press, 1983).

Geophysics

Aurora seen in daylight

from Alan Johnstone

THE long-standing question of whether aurora occurs during the day as well as the night has just been answered in a most convincing way. The answer has actually been clear from indirect evidence for many years, because the electrons, which cause the aurora when they cascade into the upper atmosphere, produce many other detectable effects as they excite atmospheric molecules to emit their characteristic light. In fact, aurora occurs all round the magnetic pole in an oval offset towards the nightside. It is there during the summer days of midnight sun as well as during the long weeks of darkness in winter. Sunlight seems to have no influence on the occurrence of aurora. The difficulty until now has been that none of the methods used to detect aurora gives a picture of its structure.

The aurora cannot be seen in daylight because the brightness of scattered light (the blueness of the sky) overwhelms the much fainter light from the aurora. At ultraviolet wavelengths (below 200 nm), however, the background of scattered light is reduced both because the incoming solar radiation is weaker and because the radiation is totally absorbed by the atmosphere before penetrating it or being reflected from it.

Molecules excited by the impact of auroral electrons emit light at ultraviolet wavelengths, notably N_2 in molecular bands between 132.5 and 150 nm, and atomic oxygen with transitions at 130.4 and 135.6 nm. These emissions cannot be seen from the ground because they too are absorbed by the atmosphere. They can, however, be seen from above by instruments carried on satellites because they occur at such a height that the light can escape upwards without much attenuation.

The first auroral images in ultraviolet light, obtained in full sunlight by the American polar-orbiting spacecraft Hilat, have just been published (Meng & Huffman *Geophys. Res. Lett.* **4**, 135; 1984). As the instrument looks down from a height of 820 km it scans a strip 5,000 km long stretching from horizon to horizon across the satellite track. The forward movement of the satellite builds up a picture from a series of parallel lines just as a television tube does. The intensity in a band only 3 nm wide is measured by a spectrometer which covers the range of wavelengths from 110 to 190 nm. This narrow bandwidth improves the signal-to-background ratio when the spectrometer is set on the most prominent features in the auroral spectrum. The proof of the technique is in the picture below which shows a typical auroral structure, familiar from the nightside images.

Now that the restrictions on auroral images imposed by sunlight have been removed, the exciting possibility emerges of obtaining pictures of the aurora simultaneously at both ends of a geomagnetic field line. This would require recording by spectrometers on at least two satellites. A survey of the extent to which the aurora is conjugate would provide a great deal of information about the processes responsible.

Alan Johnson is in University College London Mullard Space Science Laboratory, Holmbury St Mary, Dorking, Surrey RH5 6NT.

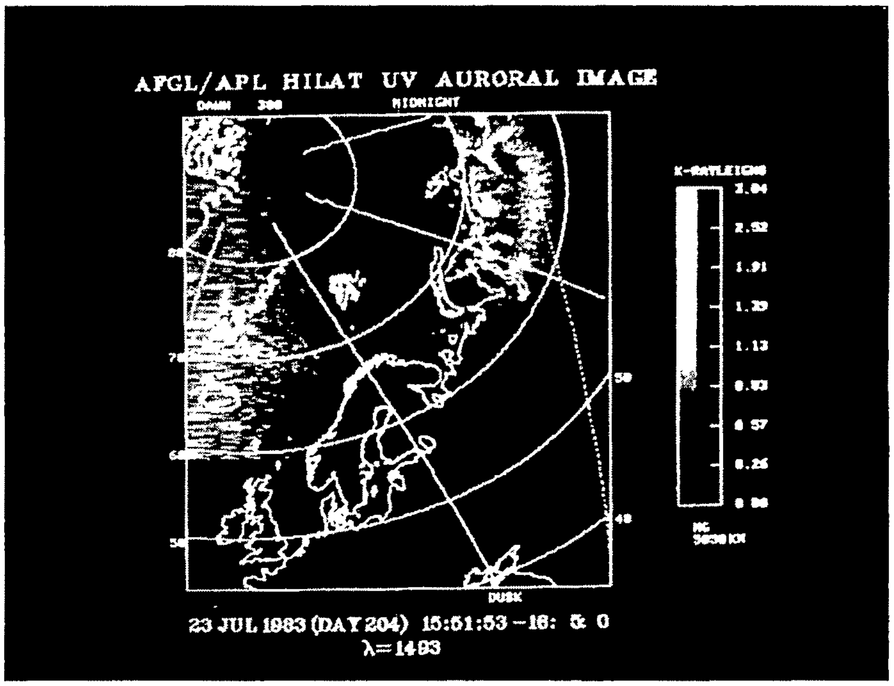
AFGL/APL HILAT UV AURORAL IMAGE
DAWN
MIDNIGHT
K-RAYLEIGHS
2.52
1.91
1.13
0.57
0.26
50
40
DUSK
23 JUL 1983 (DAY 204) 15:51:53 – 16: 5 0
λ=1493

Hilat auroral imagery over sunlit summer polar region. The nightside, under full sunlight in summer, of the auroral oval is over the arctic coast of the Soviet Union. The day-night terminator on the Earth's surface is indicated by the dotted line. The picture is in geomagnetic coordinate. The land mass above 80° geographic latitude is deleted in the picture.

Plant science

Molecular studies forge ahead

from John Ingle

EIGHT years and four meetings have passed since the first NATO/FEBS Advanced Study Institute provided a focus for the then fledgling science of plant molecular biology. The progress can honestly be described as dramatic. Research has progressed from the initial problems of DNA isolation and cloning, through nucleotide sequence analysis and vector construction to the use of site-directed mutagenesis for detailed study of regulatory and structural gene sequences. Physiological problems are now routinely addressed via the modulation of gene expression at both RNA and protein levels, and the transfer and efficient expression of tissue-regulated genes is an established fact. The impact and potential of molecular manipulations on the improvement of plants has attracted commercial interest in agricultural opportunities, a point amply illustrated by the strength and vigour of biotechnology company participation at a recent meeting*.

The initial focus of plant molecular biology on the chloroplast has largely continued, producing a detailed analytical description of its genome. Functional characterization of the genome has been less successful, depending largely on the use of heterologous *in vitro* systems, such as *Escherichia coli*. The development of an homologous transcription system and characterization of the RNA polymerase activities responsible for expression of chloroplast genes, together with the identification of chloroplast promoter elements, represents a major advance (W. Gruissem, University of California, Berkeley), but a chloroplast transformation system is still urgently needed.

For nuclear genes a welcome main trend

---

*'Molecular form and function of the plant genome'. NATO Advanced Studies Institute FEBS Advanced Course, 4-14 July, Renesse, The Netherlands.

is the increase in diversity of genes being studied and the improved detail of expression studies. The small subunit of ribulose bisphosphate carboxylase still dominates the field, offering an excellent experimental system for the study of such crucial problems as transport of proteins across membranes, regulation in response to light and expression of individual genes within a gene family. The complexity of gene expression, particularly at the post-transcriptional level, was indicated from a detailed study on the sulphur-rich albumin in pea seeds (T.J.V. Higgins, CSIRO, Canberra). In plants grown in sulphur-deficient conditions, accumulation of albumin is severely reduced and there is a low level of messenger RNA. This is due to destabilization of transcripts, which are synthesized at approximately the same rate as in control plants.

The complexity of the mitochondrial genome far exceeds that of the chloroplast, both in genetic and structural terms (D. Lonsdale, Plant Breeding Institute, Cambridge). The genome consists principally of circular DNA, and a master chromosome of 570 kilobase pairs (kbp) has been described in maize. The presence of several different repeated sequences within this circular molecule can result, however, in dramatic genome rearrangements through recombination, producing a variety of circular mitochondrial chromosomes. Mitochondria also possess small plasmids or episomes, which may be circular or linear. In the case of the linear episomes in the S male sterile cytoplasm, the terminal inverted repeats of the episomes share sequences with the circular chromosome such that recombination results in the linearization and fragmentation of the circular genome. The S-type mitochondrial genome therefore undergoes a dynamic flux between circular and linear chromosomal forms, and it is tempting to give these DNA rearrangements functional signficance, such as control of the male sterile phenotype.

Functional modification of the genome appears to be necessary for differentiation of nitrogen-fixing heterocysts in *Anabaena* (R. Haselkorn, University of Chicago). In vegetative non-fixing cells the *nif K* and *nif D* genes are separated by 10 kbp. This DNA is excised during the early stages of heterocyst differentiation, thereby bringing the genes into close proximity, and remains in the cell as a 10 kbp circle. These examples of mitochondrial DNA and *nif* DNA rearrangements, together with the genomic splicing mechanisms associated with immunoglobulin expression in animals, suggest that genome rearrangement may be a general feature of differentiation and development.

Commercial interest in improving plant varieties by genetic manipulation was well illustrated by excellent contributions on herbicide resistance. The 32,000-molecular weight ubiquinone-binding protein of photosystem II in the chloroplast was probably the most discussed protein of the meeting. A single amino acid change confers resistance to triazine herbicides, but the lack of a chloroplast transformation system has so far prevented its exploitation, except by cell fusion technology. The biochemical mechanisms involved in resistance to other herbicides, such as glutathione-*S*-transferase for chloroacetamides or triazines, 3-phosphoshikimate 1-carboxyvinyltransferase for glyphosate or acetolactate synthase for sulphonylureas, have been elucidated (R. Fraley, Monsanto, St Louis; L. Comai, Calgene, Davis; and S.C. Falco, Du Pont, Wilmington, respectively), and genes conferring resistance have been isolated and characterized from plants, bacteria and yeast. Some of these genes have been transferred to plants, but so far no resistant plants have been reported.

The successful transfer of the phaseolin gene from *Phaseolus* to sunflower has been followed up by transfer into tobacco. Regenerated tobacco plants have given the first clear indication of developmental regulation of a transferred gene since phaseolin, a seed storage protein, was produced in tobacco seeds but not in leaves, and the single copy of the gene appeared to be expressed to a similar level to that in *Phaseolus* seed (T.C. Hall, Agrigenetics, Madison). These results, together with a much improved 'leaf disk dip' for transformation of plant tissue (R. Fraley, Monsanto, St Louis) and the success of monocotyledon transformation by *Agrobacterium tumefaciens* (P. Hooykaas, University of Leiden), fully support the practical potential that has been envisaged for foreign gene expression in agricultural plants. □

John Ingle is Scientific Adviser to the Agricultural and Food Research Council, 160 Great Portland Street, London W1N 6DT.

Growth factors

The epidermal growth factor receptor gene and its product

from Tony Hunter

THE establishment of a direct mechanistic link between growth control and tumorigenesis has been a long-standing pipedream, but, within the last year, two such connections have been made. In both cases the connection is between the product of a known viral oncogene and a known cellular growth factor or its receptor. Late last year, the product of the v-*sis* gene was found to be closely related to platelet-derived growth factor (PDGF); and more recently, a remarkable similarity has been demonstrated between the product of the v-*erb*-B oncogene of avian erythroblastosis virus (AEV) and the receptor for epidermal growth factor (EGF)[1]. This homology and some partial protein sequence data for the EGF receptor have now enabled three groups to isolate cDNA clones for the EGF receptor mRNA and thus extend the characterization of the EGF receptor[2-4].

All three groups used as their primary source of EGF receptor mRNA the A431 human carcinoma cell line, which expresses 10–50 times more EGF receptors on its surface than most other cell lines do. The cloning of the EGF receptor mRNA has now helped to elucidate the normal structure and function of the receptor, its relationship to the v-*erb*-B oncogene product and several abnormalities associated with its expression in A431 cells.

EGF receptor protein structure

The EGF receptor was already known to be a 170,000–180,000 molecular weight (170–180K) glycoprotein with an intrinsic tyrosine-specific protein kinase which is stimulated upon binding EGF. From the primary amino acid sequence predicted from the nucleotide sequences of cDNA clones covering the entire coding region, the following picture of the EGF receptor now emerges (ref. 2 and see the figure). A signal peptide of 24 amino acids is cleaved from a precursor to yield a mature protein of 1,186 amino acids. The receptor can be divided figuratively into two parts: an NH_2-terminal region of 621 amino acids and a COOH-terminal domain of 542 amino acids, separated by a run of 26 preponderantly hydrophobic amino acids, which has been proposed to form a membrane-spanning domain[2,3]. The putative transmembrane domain is bounded on the cytoplasmic side by an extremely basic (9/15 residues) sequence, a feature which is common to many membrane-spanning segments.

From its sequence one would deduce that the N-terminal region is the external EGF-binding domain; it contains 51 cysteine residues, many of which must be involved in disulphide bonds, and 12 potential glycosylation sites, a number which fits well with the experimentally determined number of oligosaccharide chains[5]. The cysteines are clustered in two regions, each of about 170 amino acids (positions 132–313 and 446–612), which show similarities in the spacing of individual cysteines[2]. These might form a two-lobed structure with an EGF-binding cleft. This 'duplicated' structure could be involved in ligand-mediated receptor oligomerization.

The C-terminal region has strong sequence homology with the predicted v-*erb*-B gene product over a stretch of 250 amino acids starting at residue 694, about 50 amino acids from the proposed transmembrane domain. This region also shows homology to the catalytic domains of other protein kinases including the members of the *src* gene family of tyrosine-phosphorylating protein kinases. Thus it seems likely that this region comprises a cytoplasmic domain responsible for the tyrosine protein kinase activity of the receptor. The final 240 amino acids at the C-terminus of the EGF receptor show no homology with known proteins.

Gene structure and expression

Based on the sizes of the restriction enzyme fragments in placental DNA homologous with the various cDNA clones it can be deduced that the human EGF receptor gene is a large gene, greater than 50 kilobases (kb) in size[2]. All three groups find that the receptor gene is amplified in A431 cells, from 3- to 100-fold depending on the clone of cells analysed[2,4,6]. The amplification could in principle be responsible for the high level of EGF receptors found on these cells. Indeed, there does appear to be some correlation between the degree of amplification and the expression of EGF receptor both at the mRNA level and at the protein level[3,4]. The amplification may be associated with a translocation involving chromosome 7, to which the EGF receptor gene has been mapped[7,8], although the amplification of the gene is greater than that expected from the total number of copies of both normal and translocated chromosome 7 found in A431 cells[9]. The amplification does not seem to be a direct consequence of the translocation event since cells lacking the translocated chromosome have an amplified EGF receptor gene[4]. The structure of the amplified genes is similar to that of the normal gene, although there are minor differences[2,3].

The EGF receptor gene is expressed in the form of at least two mRNAs, with sizes of about 10 and 6 kb (refs 2–4). The exact relationship between these mRNAs is not yet known. The 6 kb RNA predominates but the ratio of the two RNAs differs between cell types. The structures of the overlapping cDNA clones[2] prove that the 6 kb RNA can encode the EGF receptor, but whether this is the case for the 10 kb RNA is uncertain. The two RNAs could well have similar 5′ ends and differ through virtue of alternate splicing pathways or poly(A) addition sites such that the 10 kb RNA carries a longer 3′-untranslated region.

In A431 cells a third EGF receptor-related mRNA is detected with a size of about 3 kb. The origin of this RNA is unclear but it is more common than the 6 kb RNA and might therefore arise from the amplified copies of the receptor gene, possibly as the result of an abnormal splicing event or some minor change in gene structure. This small RNA is all the more intriguing because its sequence corresponds to just the N-terminal half of the EGF receptor, including most of the EGF-binding region and a tail of 18 amino acids from an unknown source. Because the predicted protein lacks the transmembrane domain, it could well be secreted; and in fact, A431 cells have been observed to secrete just such an EGF-binding activity in the form of a 105–110K glycoprotein[5,10]. So far the 3 kb RNA and secreted protein have been detected only in A431 cells, and it will be interesting to see whether they are made by any normal cell type.

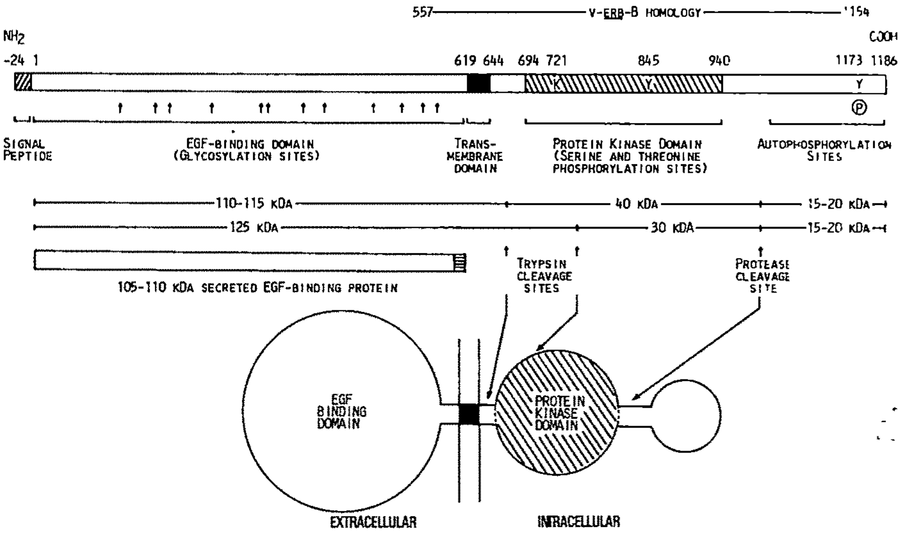

Relationship between the v-*erb*B gene (top), EGF receptor gene (middle) and EGF receptor protein (bottom), shown in linear form and as it might be organized in spanning the membrane of a cell.

Does the more extensive knowledge of the EGF receptor gene allow us to decide whether it is the c-*erb*-B gene as has been proposed? When amino acids 557–1,154 of the EGF receptor are compared with the v-*erb*-B gene product an overall homology of about 85 per cent is found, which rises to a striking 97 per cent homology in the protein kinase domain. The main difficulty in deciding on this basis whether the two genes are identical is that one is comparing the human EGF receptor with a chicken-derived oncogene potentially carrying point mutations. Human sequences homologous to the v-*erb*-B gene have been cloned[11]. They presumably arose from the c-*erb*-B gene, but no nucleotide sequence data are available to show whether it is a genuine identity rather than a close relationship. Chromosome-mapping results are consistent with the human c-*erb*-B-related sequence (chromosome 7 between 7p13 and 7q22)[12] and the human EGF receptor gene (chromosome 7 between 7p22 and 7qter)[7,8] being one and the same. On balance, therefore, it seems likely that the c-*erb*-B gene is the EGF receptor gene, but it is still formally possible that there are two related genes on chromosome 7 with homology in the protein kinase domain.

EGF receptor protein kinase

What is the evidence that the protein kinase activity of the receptor is located where the primary sequence predicts? There are several reports indicating that a fragment of 15–20K can be clipped proteolytically from the cytoplasmic domain of the EGF receptor leaving a 150K fragment which retains EGF-stimulated protein kinase activity. In the light of the sequence data, the 15–20 K fragment probably corresponds to the C-terminal region, which may be connected to the protein kinase domain by an exposed linker accessible to proteases. More extensive tryptic proteolysis of the purified receptor either in solution or bound to antibody gives rise to 30–40K and 110–125K fragments[5,13,14], presumably arising from the 150K C-terminally truncated receptor. The 110–125K fragment contains the EGF-binding site and all of the glycosyl side chains[13]. A report in this issue of *Nature* by Basu *et al.*[14] shows that the 40K fragment generated by trypsin treatment of receptor in solution retains about 30 per cent of the tyrosine protein kinase activity of the intact receptor. By contrast, the 30K fragment, which is the main species liberated by trypsin from EGF receptor bound to antibody, seems to lack tyrosine kinase activity[13]. The existence of alternate protease cleavage patterns for receptor in solution and bound to antibody might explain this difference.

The 40K fragment can both 'autophosphorylate' and phosphorylate exogenous substrates, but this activity is no longer regulated by EGF, nor does the fragment bind EGF[14]. The 40K fragment can be modified by the ATP analogue, 5′-*p*-fluorosulphonylbenzoyladenosine (FSBA), concomitant with the loss of protein kinase activity, as had previously been reported for the holoreceptor. In the case of the archetypal tyrosine protein kinase, $pp60^{v\text{-}src}$, FSBA inactivation is due to covalent modification of lysine 295 (ref. 15). This lysine is 16 residues downstream of the Gly-X-Gly-X-X-Gly sequence believed to be involved in nucleotide binding. Lysine 295 of $pp60^{v\text{-}src}$ is homologous to the ATP-binding lysine 71 in the cyclic AMP-dependent protein kinase and would correspond to lysine 721 in the EGF receptor or lysine 165 in the v-*erb*-B protein, both of which are 21 residues downstream of a Gly-X-Gly-X-X-Gly sequence. The likely location of the ATP-binding site, together with the results of Basu *et al.*, provide strong experimental support for the predicted location of the protein kinase domain within the EGF receptor. It is interesting to note that two of the retroviral tyrosine protein kinases can be cleaved by proteases to generate 30–40K fragments which retain tyrosine protein kinase activity[16,17]. Perhaps all tyrosine protein kinases which are members of the *src* family will prove to have such a protease-resistant catalytic domain.

Receptor phosphorylation

The sites of phosphorylation in the EGF receptor are of obvious interest because of intimations that its protein kinase activity may be regulated by phosphorylation. Based on sequence studies of phosphopeptides, Downward *et al.* [18] report in this issue of *Nature* that at least three out of four major 'autophosphorylation' sites are in the C-terminal 15–20K tail, suggesting an attractive model in which the C-terminal domain, by virtue of a flexible connection to the rest of the molecule, might be able to fold over and interact with the catalytic site.

Tyrosine 1,173, one of the autophosphorylation sites, corresponds to the only tyrosine detectably phosphorylated in intact cells in response to EGF[18,19]. Occupation of this site correlates with increased phosphotransferase activity towards exogenous substrates, perhaps because it results in the displacement of the C-terminal domain from the active site, thus allowing access to exogenous substrates. Two other autophosphorylation sites have been mapped close to the C-terminus (residues 1,068 and 1,148), but since these are only weakly phosphorylated in the cell, their significance is uncertain.

The C-terminal region of the EGF receptor, containing tyrosine 1,173, is missing from the v-*erb*-B genes of both strains of AEV. It is not clear whether the loss of this potentially regulatory region is a *sine qua non* for the oncogenic activation of the c-*erb*-B gene or whether it is simply a consequence of the recombination mechanism by which this gene was coopted. Examination of the structure of c-*erb*-B genes which have been activated by viral long-terminal-repeat promoter insertion[20] may well provide the answer to this question.

The retroviral tyrosine protein kinases all have a site of tyrosine phosphorylation in the catalytic domain, which can be autophosphorylated in vitro. In pp60$^{v\text{-}src}$ it is tyrosine 416, which aligns with an homologous tyrosine that is phosphorylated in the other retroviral tyrosine kinases. Tyrosine 416 of pp60$^{v\text{-}src}$ is homologous to tyrosine 845 within the protein kinase domain of the EGF receptor, yet apparently tyrosine 845 is not phosphorylated to a measurable extent in intact cells. The effect of this tyrosine phosphorylation on the activity of the retroviral protein kinases is variable, being minimal in the case of pp60$^{v\text{-}src}$ (ref.21), but of greater consequence for P140$^{gag\text{-}fps}$ (ref.22). Regardless of the functional significance of this phosphorylation it is somewhat surprising that autophosphorylation of tyrosine 845 in the EGF receptor is not observed.

In addition to tyrosine 1,173, the EGF receptor also has several sites of threonine and serine phosphorylation which are localized predominantly in the 30–40K proteolytic fragments and thus lie in the protein kinase domain[13]. The provenance of the protein kinases responsible for these phosphorylations is uncertain, nor is it known whether these modifications modulate receptor function. The EGF receptor can be phosphorylated *in vitro* by the cyclic AMP-dependent protein kinase[23,24], but this does not appear to alter its tyrosine protein kinase activity and there is no evidence that it is physiologically significant.

Two recent reports have indicated that the EGF receptor is also a substrate for the Ca^{2+}/phospholipid-dependent diacylglycerol-activated serine/threonine-specific protein kinase, C-kinase[25,26]. C-kinase appears to be the major receptor for the phorbol ester tumour promoters, such as 12-*O*-tetradecanoylphorbol-13 acetate (TPA), being activated upon binding phorbol esters. TPA enhances serine and threonine phosphorylation of EGF receptor in A431 cells, and at least one new site of threonine phosphorylation is evident[25,26]. This site is also phosphorylated when purified EGF receptor is incubated with purified C-kinase[25]. C-kinase-mediated phosphorylation of the EGF receptor in A431 cells leads to a diminished ability of EGF to stimulate its tyrosine protein kinase activity[25,27]. It is therefore intriguing that under some circumstances the same site is phosphorylated following EGF treatment[26]. Since EGF is known to increase the turnover of phosphatidylinositol, leading to formation of diacylglycerol, this effect of EGF may be mediated indirectly through an activation of C-kinase resulting from increased diacylglycerol production. Possibly the normal role of this phosphorylation is to act as a feedback mechanism to attenuate the response of the EGF receptor. Increased phosphatidylinositol turnover is a rather general effect of mitogen treatment, so it will be interesting to find out whether similar mechanisms exist for other growth factor receptors.

In fibroblasts TPA treatment leads to decreased EGF binding due to changes in either binding affinity or receptor number, while in A431 cells a class of very high-affinity receptors is lost. This effect, together with that on the tyrosine protein kinase activity of the receptor, indicates that phosphorylation of the cytoplasmic domain of the receptor by C-kinase can modulate communication between the extracellular EGF-binding domain and the protein kinase domain. From our own data, reported in this issue of *Nature*[28], the major site of threonine phosphorylation for C-kinase in the A431 cell EGF receptor is threonine 654, which lies in the basic region nine residues from the cytoplasmic end of the proposed transmembrane domain. Thus this threonine is situated between the extracellular domain and the protein kinase domain in an ideal position to affect interaction of the two domains.

An important issue raised by our new knowledge of the structure of the EGF receptor is how EGF binding transmits signals to the cytoplasm. It is not clear whether a protein chain which only traverses the plasma membrane once could transmit an allosteric signal. Potentially, oligomerization of the receptor in the membrane could be required, although one has to explain how EGF stimulates the phosphotransferase activity of the EGF receptor in solution. Another consideration is that the v-*erb*-B gene product, which lacks the majority of the extracellular domain, does not display overt tyrosine protein kinase activity. This implies that simple removal of the regulatory domain does not lead to constitutive activation of the catalytic domain. A comparison of the structures of the other receptors with inducible tyrosine protein kinase activities, such as the PDGF and insulin receptors, may give us a clue to the mechanism of signal transduction. The cloning and sequencing of these receptors is eagerly awaited. ☐

1. Downward, J. *et al. Nature* **307**, 521 (1984).
2 Ullrich, A. *et al. Nature* **309**, 418 (1984).
3. Xu, Y.-H. *et al. Nature* **309**, 806 (1984).
4. Lin. C.R. *et al. Science* **224**, 843 (1984).
5 Maynes, E.L.V. & Waterfield, M.D. *EMBO J.* **3**, 531 (1984).
6 Merlino, G.T. *et al. Science* **224**, 417 (1984).
7 Shimizu, N., Behzadian, M.A. & Shimizu, Y. *Proc. natn. Acad. Sci. U.S.A.* **77**, 3600 (1980).
8 Davies, R.L. *et al. Proc. natn. Acad. Sci. U.S.A.* **77**, 4188 (1980).
9. Shimizu, N. *et al. Somat. Cell molec. Genet.* **19**, 45 (1984).
10 Weber, W., Gill, G.N. & Spiess, J. *Science* **224**, 294 (1984).
11. Jansson, M., Philipson, L. & Vennström, B. *EMBO J.* **2**, 561 (1983).
12. Spurr, N.K. *et al. EMBO J.* **3**, 159 (1984).
13 Chinkers, M. & Brugge, J.S. *J. biol. Chem.* (in the press).
14. Basu, M., Biswas, R. & Das, M. *Nature* **311**, 477 (1984).
15. Kamps, M.P., Taylor, S.S. & Sefton, B.M. *Nature* **310**, 589 (1984).
16. Levinson, A.D., Courtneidge, S.A. & Bishop, J.M. *Proc. natn. Acad. Sci. U.S.A.* **78**, 1624 (1981).
17. Weinmaster, G., Hinze, E. & Pawson, T. *J. Virol.* **46**, 29 (1983).
18. Downward, J., Parker, P. & Waterfield, M.D. *Nature* **310**, 483 (1984).
19. Hunter, T. & Cooper, J.A. *UCLA Symp. molec. cell. Biol.* New Ser. 6, 369 (1983).
20. Fung, Y.K.T. *et al. Cell* **33**, 357 (1983).
21. Snyder, M.A. *et al. Cell* **32**, 891 (1983).
22. Weinmaster, G. *et al. Cell* **37**, 559 (1984).
23. Ghosh-Dastidar, P. & Fox, C.F. *J. biol. Chem.* **259**, 3864 (1984).
24. Rackoff, W.R., Rubin, R.A. & Earp, H.S. *Molec. cell. Endocr.* 34, 113 (1984).
25. Cochet, C. *et al. J. biol. Chem.* **259**, 2553 (1984).
26. Iwashita, S. & Fox, C.F. *J. biol. Chem.* **259**, 2559 (1984).
27. Friedman, B. *et al. Proc. natn. Acad. Sci. U.S.A.* **81**, 3034 (1984).
28. Hunter, T., Ling, N. & Cooper, J.A. *Nature* **311**, 480 (1984).

Tony Hunter is in The Molecular Biology and Virology Laboratory at the Salk Institute, San Diego, California 92138.

Malignant cell lines — why use APUDoma?

SIR — Several investigators have referred to our cell lines, COLO 320 and 321 as APUDomas (meaning "containing amine precursor uptake and decarboxylase activities"). These cell lines were derived from a carcinoma of the colon and are interesting because of their replication of c-*myc* oncogene[1]. Our description[2] of the cell lines included a list of cell products. The detection of several peptide hormones was subsequently interpreted by others as evidence that the cell line should be labelled "APUDoma".

Many diverse malignancies have been "frozen" in a stage of differentiation which results in activation of the genes for one or multiple peptide hormones[3]. There are probably malignant forms of every single kind of cell that could be labelled "APUDoma".

It seems reasonable that cell line designations should not be altered but that unique aspects of the cells should be noted if relevant to the work being described.

GEORGE E. MOORE
Department of Health and Hospitals,
Department of Surgical Oncology,
777 Bannock Street,
Denver, Colorado 80204-4507, USA

1. Alitalo, K. Schwab, M., Lin, C.C., Varmus, E.H. & Bishop, M.J. *Proc. natn. Acad. Sci. U.S.A.* 80, 1707-1711 (1983).
2. Quinn, L.A., Moore, G.E., Morgan, R.T. & Woods, L. *Cancer Res.* 39, 4914-4924 (1983).
3. Stevens, R.E. & Moore, G.E. *Lancet*, I, 118-119 (1983).

Mechanism for heritability of intelligence

SIR — I wish to suggest a partial answer to the important question of what mechanism in the central nervous system may account for the heritability of intelligence[1].

Although we are far from having a generally agreed definition of intelligence, let alone an understanding of the mechanism responsible, I believe that even now we can specify one necessary neurophysiological aspect of the variation in degree of intelligence and show that it has an appreciable degree of genetic determination. Whatever intelligence is, it must require communication, by nerve impulses, among different regions of the brain. These impulses are transmitted along nerve fibres and across synapses with the participation of many different proteins (including enzymes) and other molecules, such as neurotransmitters (which are synthesized by specific enzymes). These 'transmission proteins', like all proteins, are composed of polypeptide chains which are direct gene products.

There is great genetic diversity among humans (within races); half or more of structural gene loci are polymorphic, that is, they have two or more common alleles (genes) at that locus[2]. We consequently expect appreciable genetic variability among individuals for the genes specifying these 'transmission proteins'. In addition to this direct genetic variation in the structure, and hence the activity of these proteins, there is a second kind of genetically specified variation: differences, among normal individuals, in the amount (concentration) of each specific protein. In particular, whenever enzyme concentrations, for example, dopamine-β-hydroxylase and catechol-*O*-methyltransferase (which, respectively, synthesize and metabolize the neurotransmitter noradrenaline) have been studied genetically, they have been found to be under appreciable genetic control[3].

This genetic variability, both in structure and amount of transmission proteins is, of course, heritable from parent to offspring. This variability will affect nerve impulse transmission in the brain to some degree and in a variety of ways, such as in speed and accuracy. It therefore sets limits on information processing rates. Data from mice support this interpretation, directly showing heritability of nerve conduction velocity[4,5] and synaptic transmission time[6]. This genetic control of information processing is, I submit, a sufficient basis for asserting that there is significant genetic determination of variation in human intelligence.

I do not suggest of course, that such a mechanism would operate in isolation. I believe that in all societies, environment (in the broadest sense, beginning prenatally) also has very important effects (positive and negative) on human intelligence.

T. EDWARD REED
Departments of Zoology and Anthropology,
University of Toronto,
Toronto, Ontario, Canada M5S 1A1

1. Maddox, J. *Nature* 309, 579 (1984)
2. Nei, M. & Roychoudhury, A.K. *Evol. Biol* 14, 1-59 (1982).
3. Weinshilboum, R.M. in *Neurogenetics: Genetic Approaches to the Nervous System* (ed. Breakefield, X.O.) 257-282 (Elsevier, New York, 1979).
4. Hegmann, J.P., White, J.E., & Kater, S.B. *Behav. Genet.* 31, 121-131 (1973).
5. Reed, T.E. *Behav. Genet.* 13, 257-265 (1983).
6. Reed, T.E. *Behav. Genet.* (in press).

Atmospheric humidity in the nuclear winter

SIR — Recent calculations[1,2] and discussion of the possibility of a 'nuclear winter' consequent to widespread nuclear war may have ignored an important effect of atmospheric humidity. The nuclear winter is calculated[2] to be severe for wars in the late spring or summer. In those seasons, at most assumed targets the dew point is quite high, usually no less than 55°F (13°C). Soot from urban or forest fires would be produced intimately mixed in this humid air.

In order to reach the "nuclear winter" state this air is chilled. That portion of it which rises to the upper troposphere or higher reaches ambient temperatures when its rise stabilizes, in an hour or less; only on a much longer time scale does solar heating rewarm it. The remaining sooty air is below the warming influence of sunlight, and it cools to the low surface air temperatures calculated for the nuclear winter. In each case the air is cooled to a temperature at which the saturation water vapour pressure is far below the initial vapour content. The resulting condensate efficiently scavenges the soot aerosol, as in the precipitation cleaning of urban smog and the black rain observed after firestorms; precipitation removes both water and soot from the atmosphere.

Scavenging is unavoidable: in nuclear winter calculations the air begins warm and humid and ends cool and dry, a process which must efficiently purge it of its water vapour and aerosols. This effect has been ignored in the published calculations[1,2] because they begin by assuming a distribution of soot in the troposphere, and do not calculate condensation and scavenging. A quantitative understanding will require detailed calculation of rising sooty plumes and of condensation and scavenging both there and in the cooling troposphere.

JONATHAN KATZ
Department of Physics,
Washington University,
St Louis, Missouri 63130, USA

1. Turco, R.P., Toon, O.B., Ackerman, T., Pollack, J B & Sagan, D. *Science* 222, 1283-1300 (1983).
2. Covey, C., Schneider, S. H. & Thompson, S. L. *Nature* 308, 21-25 (1984).

DNA can be a selfish parasite

SIR — Evans[1] recently pointed out a "fatal flaw" in all evolutionary discussions of selfish or parasitic DNA. The problem, as outlined by Evans, is that any element which imposes *any* cost on its host will be eliminated by natural selection; this selection pressure can be counteracted only by a mechanism for horizontal transfer (presumably virus-like infection of cells) or by a high rate of *de novo* generation of new elements. The latter condition is highly unlikely and the former would imply that parasitic DNA is merely a new label applicable only to conventional viruses. I cannot agree with these conclusions.

I have already explored[2] in some detail the questions raised by Evans and the main conclusion is that parasitic DNAs can potentially spread very rapidly in natural populations despite the fact that they may also have significant negative effects on host fitness. A mechanism of horizontal spread is not necessary provided there is biparental inheritance of host genomes. This criterion is met in all sexually-reproducing, out-breeding higher eukaryotes. Parasitic elements capable of duplicate transposition are able to "colonize" new chromosomes at zygote formation. Thus, the elements can spread to new genomes by a means other than horizontal transfer. The general prediction of this model is that we expect a higher level of such parasites within the genomes of out-breeding higher eukaryotes than within the genomes of asexually reproducing prokaryotes. The experimental evidence is consistent with this prediction.

Other theoretical studies[3-5] have incorporated negative selection into models of selfish DNA and, recently, such a model[6] was applied explictly to the case of transposable P elements in *Drosophila*. P elements have a demonstrable negative effect on host fitness, yet they have spread rapidly within natural populations[7].

In conclusion, I believe that the remarks of Evans[1] are very pertinent to the question of parasitic DNA in some genomes but the situation is less restrictive than he describes for the case of the higher eukaryotes. I would say that parasitic DNA is not only possible but highly probable in these latter organisms. The evolutionary pressures on this DNA would indeed be of the type outlined by Doolittle *et al.*[8].

DONAL A. HICKEY

Department of Biology,
University of Ottawa,
Ottawa, Ontario,
Canada K15 0J8

1. Evans, R.V. *Nature* 310, 456 (1984).
2. Hickey, D.A. *Genetics* 101, 519-531 (1982).
3. Ohta, T. *Genet. Res.* 41, 1-15 (1983).
4. Charlesworth, B & Charlesworth, D. *Genet. Res.* 42, 1-28 (1983).
5. Langley, C.H., Brookfield, J.F.Y. & Kaplan, N. *Genetics* 104, 457-471 (1983).
6. Ginsburg, L.R., Bingham, P.M. & Yoo, S. *Genetcs* 107, 331-341 (1984).
7. Kidwell, M. *Proc. natn. Acad. Sci. U.S.A.* 80 1655-1659 (1983).
8. Doolittle, W.F. Kirwood, T.B.L. & Dempster, M.A.H. *Nature* 307, 501 (1984).

Primroses and self-fertilization

SIR — Bodmer's recent letter[1] concerning homostyle primroses raises some scientific issues on which we would like to comment. First, he suggests that it is important to explain why the self-fertile homostyle variant is confined to a few English populations; his model of a low rate of self-fertilization and a small viability disadvantage to homostyles[1,2] is intended to provide such an explanation in view of the absence of evidence for the large viability disadvantage of homozygous homostyles postulated by Crosby[3]. There is, however, no direct evidence that the primrose populations containing homostyles are tending towards a stable polymorphic equilibrium, as Crosby and Bodmer assume. As was previously pointed out[4], the polymorphism for homostyles in *Primula vulgaris* is a highly exceptional situation; most species of *Primula* are, of course, distylous and self-incompatible, but there are many in which homostyly has become fixed[5,6]. The same is true of other groups of distylous plants[7,8]. It is thus entirely possible that *P. vulgaris* is merely in a state of transient polymorphism, and that the homostyle variant is on its way to fixation, at least locally[4]. The model of a conflict between the advantage of fertility assurance of a self-fertile form and the disadvantage of inbreeding depression to its progeny can explain why homostyles become established only in some species or in some geographical areas of a species[4,9]; the biogeographic data on the distribution of homostyly are consistent with this model[4,6,8].

Second, Bodmer suggests that the selfing rate of homostyles may vary in time and space, so that our estimate[9] of a value of 0.92 for a single population in 1982 is not necessarily representative. We certainly agree with this, but would like to point out that there are two other independent estimates of the selfing rate for natural populations which give values of 0.93 (refs 10, 11); within the limits of sampling error, these estimates agree. Richards[12] has made clear the difficulties in interpreting Bodmer's low selfing rate estimate[2,13] for garden material, and in extrapolating this to natural populations. (As noted by Crosby[10], this estimate excluded data from a year (1955) in which the selfing rate was apparently unity). The weight of the empirical evidence is, we feel, in favour of a high selfing rate for homostyle primroses in nature.

J.G. PIPER
B. CHARLESWORTH
D. CHARLESWORTH

School of Biological Sciences,
University of Sussex,
Brighton, Sussex BN1 9QG, UK

1. Bodmer, W.F. *Nature* 310, 731 (1984).
2. Bodmer, W.F. *Phil. Trans. R. Soc.* B 242, 517-549 (1960).
3. Crosby, J.L. *Evolution* 3, 212-230 (1949).
4. Charlesworth, B. & Charlesworth, D. *Am. Nat.* 114, 499-513 (1979).
5. Ernst, A. *Oesterr. Bot. Z.* 100, 235-255 (1953).
6. Ernst, A. *Genetica* 27, 391-448 (1955).
7. Ray, P.M. & Chisaki, H.F. *Am. J. Bot.* 44, 537-544 (1957).
8. Baker, H.G. *Evolution* 20, 517-549 (1966).
9. Piper, J.G., Charlesworth, B. & Charlesworth, D. *Nature* 310, 50-51 (1984).
10. Crosby, J.L. *Heredity*, 13, 127-131 (1959).
11. Curtis, C.F. Jones & D.A. Curtis, J. *Heredity* (submitted).
12. Richards, A.J. *Nature* 310, 12-13 (1984).
13. Bodmer, W.F. *Heredity* 12, 363-370 (1958).

Herpes simplex transforming fragments

SIR — In the past twelve months, the subject of viral genes involved in immortalization and tumorigenic transformation has been reviewed at least three times in the News and Views section of *Nature*. Every time when reference was made to DNA tumour viruses, it was stated that genetically distinct functions for immortalization and malignant transformation have been demonstrated for two DNA viruses, polyoma virus and adenovirus. Mention was never made of the separable immortalizing and tumorigenic functions that have been identified in the genome of the human DNA virus herpes simplex type 2 (HSV-2).

The first report of escape from senescence and neoplastic transformation of early passage, nonestablished Syrian hamster embryo cells by a defined subgenomic fragment of HSV-2 DNA appeared in the spring of 1980[1]. Last autumn evidence was published[2] for the existence of two separate genetic functions within this defined fragment. One subfragment derived from the 64% left-hand end was shown to cause immortalization, whereas the other subfragment from the 36% right-hand end was demonstrated to cooperate with the left-hand subfragment in mediating tumorigenic transformation. What makes the HSV-2 data especially interesting is that the immortalizing DNA segment contains a region that exhibits homology to an interspersed middle-repetitive DNA sequence in mammalian cells[2,3]. I should like to bring these reports to the attention of *Nature* and its readers.

EMILE ZUCKERKANDL

Linus Pauling Institute
of Science and Medicine,
Palo Alto,
California 94306, USA

1. Jariwalla, F. J., Aurelian, L. & Ts'o, P.O.P. *Proc. natn. Acad. Sci. U.S.A.* 77, 2279 (1980).
2. Jariwalla, R. J., Aurelian, L. & Ts'o, P.O.P. *Proc. natn. Acad. Sci. U.S.A.* 80, 5902 (1983).
3. Peden, K., Mounts, P. & Hayward, G. S. *Cell* 31, 71 (1982).

Chinese sources no guide to Geminga

SIR — Pannekoek, in his study of Ptolemy[1], remarks "In studying the history of astronomy we are not learning something about the stars, but something about the astronomers". This statement is true for the Chinese records as well. The Chinese records are notorious for their inaccuracy and unreliability[2], and modern astronomers have been too keen to identify new sources with ancient recorded phenomena. Kukarkin *et al.*[3] list a good many identifications of ancient Chinese "nova" recordings with modern counterparts, and note that the vast majority of these is unfounded, and many (notably radiosources) are demonstrably wrong.

The reality of a phenomenon chronicled by the Chinese often has to be doubted[2], and the position is always uncertain (a famous example is the wrong position for the Crab nebula[4]). Rather than contribute to the spread of spurious identifications in the literature — once in existence, they die hard — Editors of scientific journals[5] would do well to show more restraint in publicizing such identifications. Bignami *et al.*[6] are justified in mentioning the Chinese record of AD 437; but its identification with Geminga can only be accepted if in addition to the positional coincidence (of necessity inaccurate) a much more precise temporal coincidence is established.

FRANK VERBUNT

Institute of Astronomy,
Madingley Road,
Cambridge CB3 0HA, UK

1. Pannekoek, *Vistas in Astronomy* I, 65 (1960).
2. Needham, J. *Science and Civilisation in China* Vol.3, 419 (1959).
3. Kukarkin B.V. *et al. General Catalogue of Variable Stars*, 3rd edn., III, 54-73, Moscow (1971).
4. Duyvendak, J.J.L., Mayall, M.U. & Oort, J.H. *PASP* 54, 91-104 (1942).
5. Maddox, J. *Nature* 310, 447 (1984).
6. Bignami, G.F., Caraveo, P.A. & Paul, J.A. *Nature* 310, 464-469.

REVIEW ARTICLE

Cellular automata as models of complexity

Stephen Wolfram

The Institute for Advanced Study, Princeton, New Jersey 08510, USA

Natural systems from snowflakes to mollusc shells show a great diversity of complex patterns. The origins of such complexity can be investigated through mathematical models termed 'cellular automata'. Cellular automata consist of many identical components, each simple, but together capable of complex behaviour. They are analysed both as discrete dynamical systems, and as information-processing systems. Here some of their universal features are discussed, and some general principles are suggested.

IT is common in nature to find systems whose overall behaviour is extremely complex, yet whose fundamental component parts are each very simple. The complexity is generated by the cooperative effect of many simple identical components. Much has been discovered about the nature of the components in physical and biological systems; little is known about the mechanisms by which these components act together to give the overall complexity observed. What is now needed is a general mathematical theory to describe the nature and generation of complexity.

Cellular automata are examples of mathematical systems constructed from many identical components, each simple, but together capable of complex behaviour. From their analysis, one may, on the one hand, develop specific models for particular systems, and, on the other hand, hope to abstract general principles applicable to a wide variety of complex systems. Some recent results on cellular automata will now be outlined; more extensive accounts and references may be found in refs 1-4.

Cellular automata

A one-dimensional cellular automaton consists of a line of sites, with each site carrying a value 0 or 1 (or in general $0, \ldots, k-1$). The value a_i of the site at each position i is updated in discrete time steps according to an identical deterministic rule depending on a neighbourhood of sites around it:

$$a_i^{(t+1)} = \phi[a_{i-r}^{(t)}, a_{i-r+1}^{(t)}, \ldots, a_{i+r}^{(t)}] \qquad (1)$$

Even with $k=2$ and $r=1$ or 2, the overall behaviour of cellular automata constructed in this simple way can be extremely complex.

Consider first the patterns generated by cellular automata evolving from simple 'seeds' consisting of a few non-zero sites. Some local rules ϕ give rise to simple behaviour; others produce complicated patterns. An extensive empirical study suggests that the patterns take on four qualitative forms, illustrated in Fig. 1:

(1) disappears with time;
(2) evolves to a fixed finite size;
(3) grows indefinitely at a fixed speed;
(4) grows and contracts irregularly.

Patterns of type 3 are often found to be self-similar or scale invariant. Parts of such patterns, when magnified, are indistinguishable from the whole. The patterns are characterized by a fractal dimension[5]; the value $\log_2 3 = 1.59$ is the most common. Many of the self-similar patterns seen in natural systems may, in fact, be generated by cellular automaton evolution.

Figure 3 shows the evolution of cellular automata from initial states where each site is assigned each of its k possible values with an independent equal probability. Self-organization is seen: ordered structure is generated from these disordered initial states, and in some cases considerable complexity is evident.

Different initial states with a particular cellular automaton rule yield patterns that differ in detail, but are similar in form and statistical properties. Different cellular automaton rules yield very different patterns. An empirical study, nevertheless, suggests that four qualitative classes may be identified, yielding four characteristic limiting forms:

(1) spatially homogeneous state;
(2) sequence of simple stable or periodic structures;
(3) chaotic aperiodic behaviour;
(4) complicated localized structures, some propagating.

All cellular automata within each class, regardless of the details of their construction and evolution rules, exhibit qualitatively similar behaviour. Such universality should make general results on these classes applicable to a wide variety of systems modelled by cellular automata.

Applications

Current mathematical models of natural systems are usually based on differential equations which describe the smooth variation of one parameter as a function of a few others. Cellular automata provide alternative and in some respects complemen-

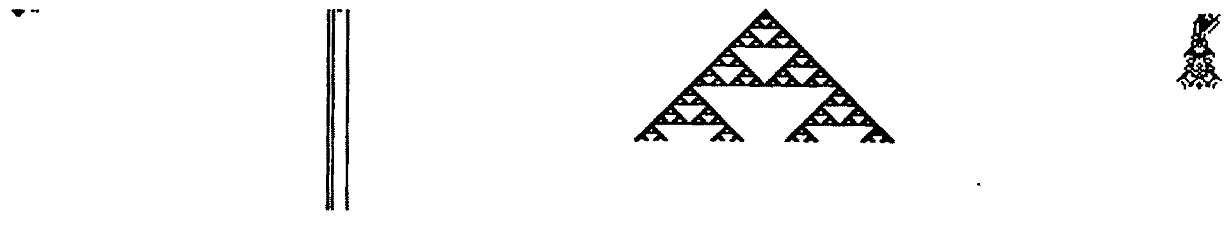

Fig. 1 Classes of patterns generated by the evolution of cellular automata from simple 'seeds'. Successive rows correspond to successive time steps in the cellular automaton evolution. Each site is updated at each time step according to equation (1) by cellular automaton rules that depend on the values of a neighbourhood of sites at the previous time step. Sites with values 0 and 1 are represented by white and black squares, respectively. Despite the simplicity of their construction, patterns of some complexity are seen to be generated. The rules shown exemplify the four classes of behaviour found. (The first three are $k=2$, $r=1$ rules with rule numbers[1] 128, 4 and 126, respectively; the fourth is a $k=2$, $r=2$ rule with totalistic code[2] 52.) In the third case, a self similar pattern is formed.

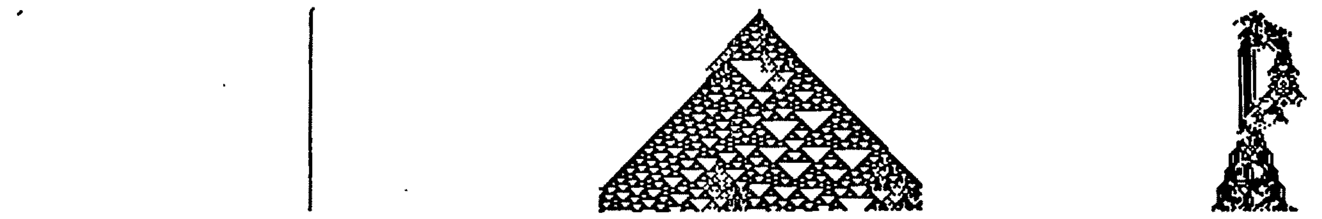

Fig. 2 Evolution of small initial perturbations in cellular automata, as shown by the difference (modulo two) between patterns generated from two disordered initial states differing in the value of a single site. The examples shown illustrate the four classes of behaviour found. Information on changes in the initial state almost always propagates only a finite distance in the first two classes, but may propagate an arbitrary distance in the third and fourth classes.

tary models, describing the discrete evolution of many (identical) components. Models based on cellular automata are typically most appropriate in highly nonlinear regimes of physical systems, and in chemical and biological systems where discrete thresholds occur. Cellular automata are particularly suitable as models when growth inhibition effects are important.

As one example, cellular automata provide global models for the growth of dendritic crystals (such as snowflakes)[6]. Starting from a simple seed, sites with values representing the solid phase are aggregated according to a two-dimensional rule that accounts for the inhibition of growth near newly-aggregated sites, resulting in a fractal pattern of growth. Nonlinear chemical reaction–diffusion systems give another example[7,8]: a simple cellular automaton rule with growth inhibition captures the essential features of the usual partial differential equations, and reproduces the spatial patterns seen. Turbulent fluids may also potentially be modelled as cellular automata with local interactions between discrete vortices on lattice sites.

If probabilistic noise is added to the time evolution rule (1), then cellular automata may be identified as generalized Ising models[9,10]. Phase transitions may occur if ϕ retains some deterministic components, or in more than one dimension.

Cellular automata may serve as suitable models for a wide variety of biological systems. In particular, they may suggest mechanisms for biological pattern formation. For example, the patterns of pigmentation found on many mollusc shells bear a striking resemblance to patterns generated by class 2 and 3 cellular automata (see refs 11, 12), and cellular automaton models for the growth of some pigmentation patterns have been constructed[13].

Mathematical approaches

Rather than describing specific applications of cellular automata, this article concentrates on general mathematical features of their behaviour. Two complementary approaches provide characterizations of the four classes of behaviour seen in Fig. 3.

In the first approach[2], cellular automata are viewed as discrete dynamical systems (see ref. 14), or discrete idealizations of partial differential equations. The set of possible (infinite) configurations of a cellular automaton forms a Cantor set; cellular automaton evolution may be viewed as a continuous mapping on this Cantor set. Quantities such as entropies, dimensions and Lyapunov exponents may then be considered for cellular automata.

In the second approach[3], cellular automata are instead considered as information-processing systems (see ref. 15), or parallel-processing computers of simple construction. Information represented by the initial configuration is processed by the evolution of the cellular automaton. The results of this information processing may then be characterized in terms of the types of formal languages generated. (Note that the mechanisms for information processing in natural system appear to be much closer to those in cellular automata than in conventional serial-processing computers: cellular automata may, therefore, provide efficient media for practical simulations of many natural systems.)

Entropies and dimensions

Most cellular automaton rules have the important feature of irreversibility: several different configurations may evolve to a single configuration, and, with time, a contracting subset of all possible configurations appears. Starting from all possible initial configurations, the cellular automaton evolution may generate only special 'organized' configurations, and 'self-organization' may occur.

For class 1 cellular automata, essentially all initial configurations evolve to a single final configuration, analogous to a limit point in a continuous dynamical system. Class 2 cellular automata evolve to limit sets containing essentially only periodic configurations, analogous to limit cycles. Class 3 cellular automata yield chaotic aperiodic limit sets, containing analogues of chaotic or 'strange' attractors.

Entropies and dimensions give a generalized measure of the density of the configurations generated by cellular automaton evolution. The (set) dimension or limiting (topological) entropy for a set of cellular automaton configurations is defined as (compare ref. 14)

$$d^{(x)} = \lim_{X\to\infty} \frac{1}{X} \log_k N(X) \tag{2}$$

where $N(X)$ gives the number of distinct sequences of X site values that appear. For the set of possible initial configurations, $d^{(x)} = 1$. For a limit set containing only a finite total number of configurations, $d^{(x)} = 0$. For most class 3 cellular automata, $d^{(x)}$ decreases with time, giving, $0 < d^{(x)} < 1$, and suggesting that a fractal subset of all possible configurations occurs.

A dimension or limiting entropy $d^{(t)}$ corresponding to the time series of values of a single site may be defined in analogy with equation (2). (The analogue of equation (2) for a sufficiently wide patch of sites yields a topologically-invariant entropy for the cellular automaton mapping.) $d^{(t)} = 0$ for periodic sets of configurations.

$d^{(x)}$ and $d^{(t)}$ may be modified to account for the probabilities of configurations by defining

$$d_\mu^{(x)} = -\lim_{X\to\infty} \frac{1}{X} \sum_{j=1}^{k^X} p_j \log_k p_j \tag{3}$$

and its analogue, where p_j are probabilities for possible length X sequences. These measure dimensions may be used to delineate the large time behaviour of the different classes of cellular automata:

(1) $d_\mu^{(x)} = d_\mu^{(t)} = 0$
(2) $d_\mu^{(x)} > 0,\ d_\mu^{(t)} = 0$
(3) $d_\mu^{(r)} > 0,\ d_\mu^{(t)} > 0$

As discussed below, dimensions are usually undefined for class 4 cellular automata.

Information propagation

Cellular automata may also be characterized by the stability or predictability of their behaviour under small perturbations in initial configurations. Figure 2 shows differences in patterns generated by cellular automata resulting from a change in a

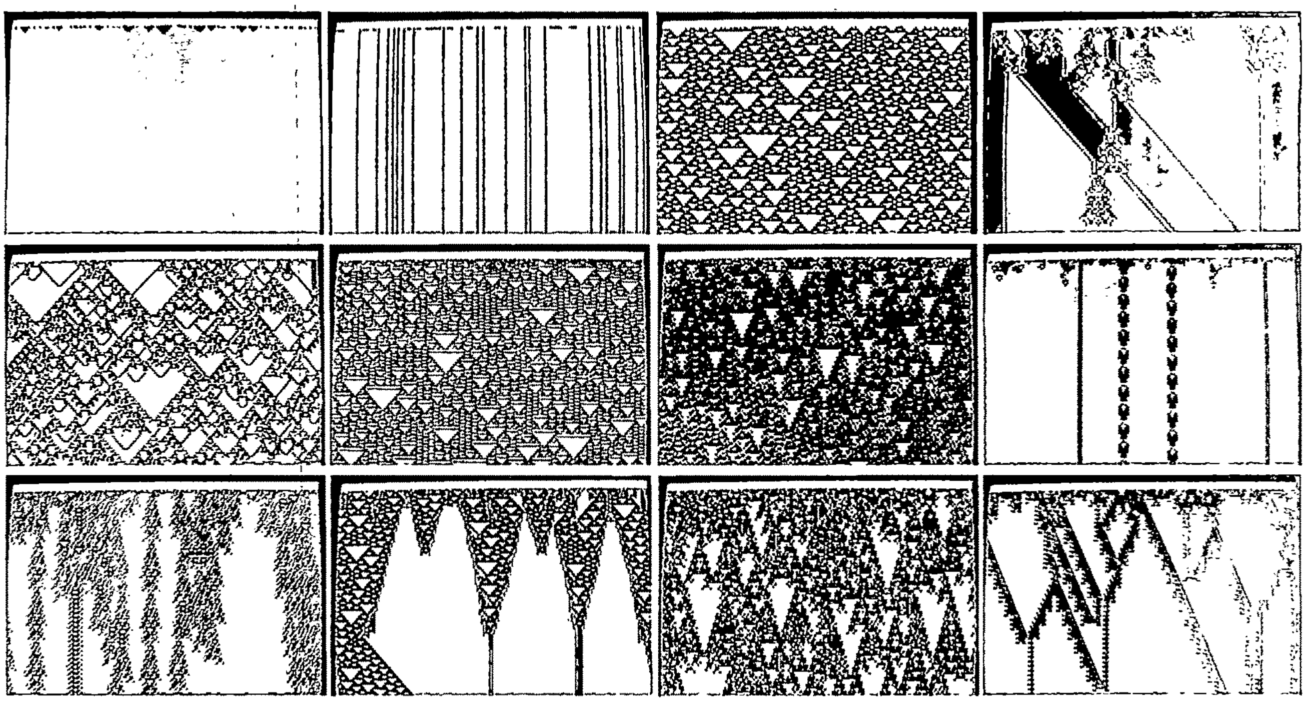

Fig. 3 Evolution of various cellular automata from disordered initial states. In many cases, ordered structure is seen to be generated. The first row of pictures show examples of the four qualitative classes of behaviour found. (The rules shown are the same as in Fig. 1.) The lower two rows show examples of cellular automata with $k=5$ (five possible values for each site) and $r=1$ (nearest neighbour rules). Site values 0 to 4 are represented by white, red, green, blue and yellow squares, respectively. (The rules shown have totalistic codes 10175, 566780, 570090, 580020, 583330, 672900, 5694390, 59123000.) The 'orange' discoloration is a background, not part of the pattern.

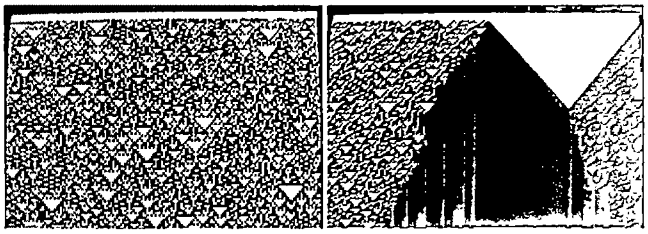

Fig. 4 Evolution of multiple phases in cellular automata. Pairs of sites are shown combined: 00 is represented by white, 01 by red, 10 by green and 11 by blue. Alternate time steps are shown. Both rules simulate an additive rule (number 90) under a blocking transformation. In the first rule (number 18), the simulation is attractive: starting from a disordered initial state, the domains grow with time. In the second rule (number 94), the simulation is repulsive: only evolution from a special initial state yields additive rule behaviour; a defect is seen to grow, and attractive simulation of the identity rule takes over.

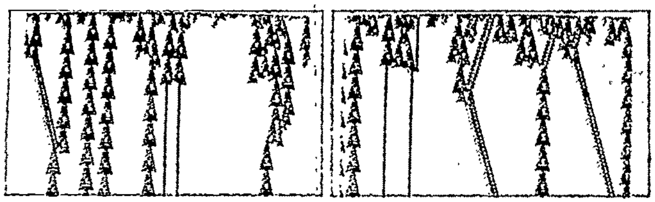

Fig. 5 Examples of the evolution of a typical class 4 cellular automaton from disordered initial states. This and other class 4 cellular automata are conjectured to be capable of arbitrary information processing, or universal computation. The rule shown has $k=3$, $r=1$, and takes the value of a site to be 1 if the sum of the values of the sites in its three-site neighbourhood is 2 or 6, to be 2 if the sum is 3, and to zero otherwise (totalistic code 792).

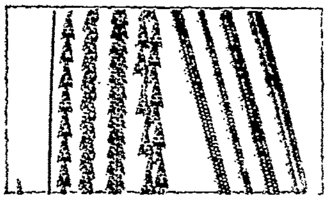

Fig. 6 Persistent structures generated in the evolution of the class 4 cellular automaton of Fig. 5. The first four structures shown have periods 1, 20, 16 and 12 respectively; the last four structures (and their reflections) propagate: the first has period 32, the next three period 3, and the last period 6. These structures are some of the elements required to support universal computation.

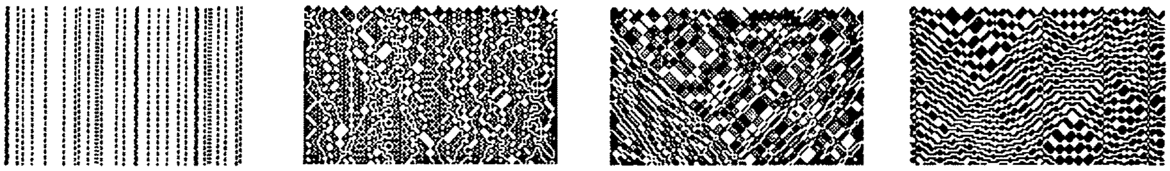

Fig. 7 Evolution of some cellular automata with reverisble rules. Each configuration is a unique function of the two previous configurations. (Rule numbers 4, 22, 90 and 126 are shown.) As initial conditions, each site in two successive configurations is chosen to have value 1 with probability 0.1.

single initial site value. Such perturbations have characteristic effects on the four classes of cellular automata:

(1) no change in final state;
(2) changes only in a finite region;
(3) changes over an ever-increasing region;
(4) irregular changes.

In class 1 and 2 cellular automata, information associated with site values in the initial state propagates only a finite distance; in class 3 cellular automata, it propagates an infinite distance at a fixed speed, while in class 4 cellular automata, it propagates irregularly, but over an infinite range. The speed of information propagation is related to the Lyapunov exponent for the cellular automaton evolution, and measures the degree of sensitivity to initial conditions (see ref. 16). It leads to different degrees of predictability for the outcome of cellular automaton evolution:

(1) entirely predictable, independent of initial state;
(2) local behaviour predictable from local initial state;
(3) behaviour depends on an ever-increasing initial region;
(4) behaviour effectively unpredictable.

Information propagation is particularly simple for the special class of additive cellular automata (whose local rule function ϕ is linear modulo k), in which patterns generated from arbitrary initial states may be obtained by superposition of patterns generated by evolution of simple initial states containing a single non-zero site. A rather complete algebraic analysis of such cellular automata may be given[17]. Most cellular automata are not additive; however, with special initial configurations it is often possible for them to behave just like additive rules. Thus, for example, the evolution of an initial configuration consisting of a sequence of 00 and 01 digrams under one rule may be identical to the evolution of the corresponding 'blocked' configuration consisting of 0 and 1 under another rule. In this way, one rule may simulate another under a blocking transformation (analogous to a renormalization group transformation). Evolution from an arbitrary initial state may be attracted to (or repelled from) the special set of configurations for which such a simulation occurs. Often several phases exist, corresponding to different blocking transformations: sometimes phase boundaries move at constant speed, and one phase rapidly takes over; in other cases, phase boundaries execute random walks, annihilating in pairs, and leading to a slow increase in the average domain size, as illustrated in Fig. 4. Many rules appear to follow attractive simulation paths to additive rules, which correspond to fixed points of blocking transformations, and thus exhibit self similarity. The behaviour of many rules at large times, and on large spatial scales, is therefore determined by the behaviour of additive rules.

Thermodynamics

Decreases with time in the spatial entropies and dimensions of equations (2) and (3) signal irreversibility in cellular automaton evolution. Some cellular automaton rules are, however, reversible, so that each and every configuration has a unique predecessor in the evolution, and the spatial entropy and dimension of equations (2) and (3) remain constant with time. Figure 7 shows some examples of the evolution of such rules, constructed by adding a term $-a_i^{(t-1)}$ to equation (1) (ref. 20 and E. Fredkin, personal communication). Again, there are analogues of the four classes of behaviour seen in Fig. 3, distinguished by the range and speed of information propagation.

Conventional thermodynamics gives a general description of systems whose microscopic evolution is reversible; it may, therefore, be applied to reversible cellular automata such as those of Fig. 4. As usual, the 'fine-grained' entropy for sets (ensembles) of configurations, computed as in equation (3) with perfect knowledge of each site value, remains constant in time. The 'coarse-grained' entropy for configurations is, nevertheless, almost always non-decreasing with time, as required by the second law of thermodynamics. Coarse graining emulates the imprecision of practical measurements, and may be implemented by applying almost any contractive mapping to the configurations (a few iterations of an irreversible cellular automaton rule suffice). For example, coarse-grained entropy might be computed by applying equation (3) to every fifth site value. In an ensemble with low coarse-grained entropy, the values of every fifth site would be highly constrained, but arbitrary values for the intervening sites would be allowed. Then in the evolution of a class 3 or 4 cellular automaton the disorder of the intervening site values would 'mix' with the fifth-site values, and the coarse-grained entropy would tend towards its maximum value. Signs of self-organization in such systems must be sought in temporal correlations, often manifest in 'fluctuations' or metastable 'pockets' of order.

While all fundamental physical laws appear to be reversible, macroscopic systems often behave irreversibly, and are appropriately described by irreversible laws. Thus, for example, although the microscopic molecular dynamics of fluids is reversible, the relevant macroscopic velocity field obeys the irreversible Navier–Stokes equations. Conventional thermodynamics does not apply to such intrinsically irreversible systems: new general principles must be found. Thus, for cellular automata with irreversible evolution rules, coarse-grained entropy typically increases for a short time, but then decreases to follow the fine-grained entropy. Measures of the structure generated by self-organization in the large time limit are usually affected very little by coarse graining.

Formal language theory

Quantities such as entropy and dimension, suggested by information theory, give only rough characterizations of cellular automaton behaviour. Computation theory suggests more complete descriptions of self-organization in cellular automata (and other systems). Sets of cellular automaton configurations may be viewed as formal languages, consisting of sequences of symbols (site values) forming words according to definite grammatical rules.

The set of all possible initial configurations corresponds to a trivial formal language. The set of configurations obtained after any finite number of time steps are found to form a regular language[3]. The words in a regular language correspond to the possible paths through a finite graph representing a finite state machine. It can be shown that a unique smallest finite graph reproduces any given regular language (see ref. 15). Examples of such graphs are shown in Fig. 8. These graphs give complete specifications for sets of cellular automaton configurations (ignoring probabilities). The number of nodes Ξ in the smallest graph corresponding to a particular set of configurations may

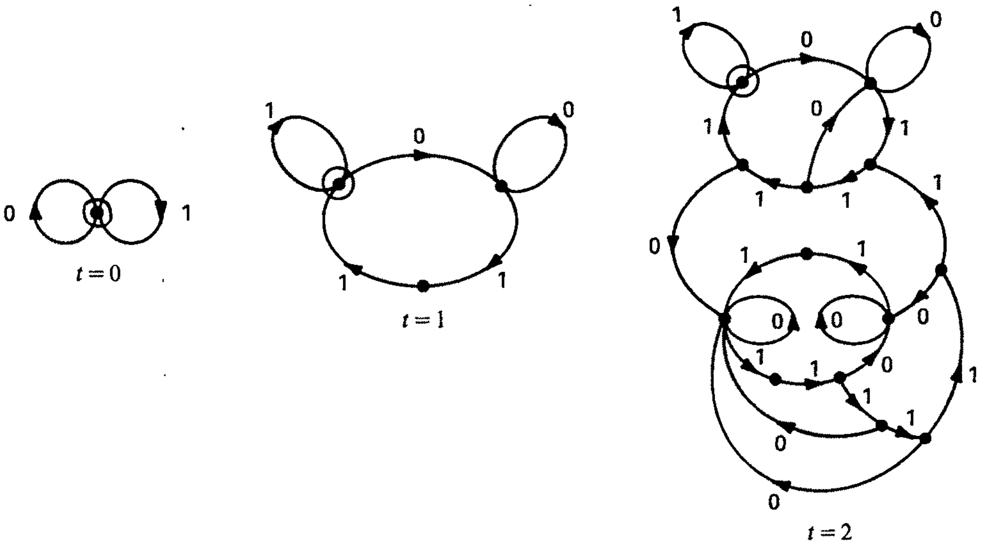

Fig. 8 Graphs representing the sets of configurations generated in the first few time steps of evolution according to a typical class 3 cellular automaton rule ($k=2$, $r=1$, rule number 126). Possible configurations correspond to possible paths through the graphs, beginning at the encircled node. At $t=0$, all possible configurations are allowed. With time, a contracting subset of configurations are generated. (After one time step, for example, no configuration containing the sequence of site value 101 can appear.) At each time step, the complete set of possible configurations forms a regular formal language: the graph gives a minimal complete specification of it. The number of nodes in the graph gives a measure of the complexity Ξ of the set, viewed as a regular language. As for other class 3 cellular automata, the complexity of the sets grows rapidly with time; for $t=3$, $\Xi=107$, and $t=4$, $\Xi=2{,}867$.

be defined as the 'regular language complexity' of the set. It specifies the size of the minimal description of the set in terms of regular languages. Larger Ξ correspond to more complicated sets. (Note that the topological entropy of a set is given by the logarithm of the algebraic integer obtained as the largest root of the characteristic polynomial for the incidence matrix of the corresponding graph. The characteristic polynomials for the graphs in Fig. 7 are $2-\lambda$ ($\lambda_{\max}=2$), $1-\lambda+2\lambda^2-\lambda^3$ ($\lambda_{\max}\simeq 1.755$) and $-1+\lambda-\lambda^2+2\lambda^3-4\lambda^4+\lambda^5+3\lambda^6-5\lambda^7+3\lambda^8-3\lambda^9+5\lambda^{10}-6\lambda^{11}+4\lambda^{12}-\lambda^{13}$ ($\lambda_{\max}\simeq 1.732$), respectively.)

The regular language complexity Ξ for sets generated by cellular automaton evolution almost always seems to be non-decreasing with time. Increasing Ξ signals increasing self-organization. Ξ may thus represent a fundamental property of self-organizing systems, complementary to entropy. It may, in principle, be extracted from experimental data.

Cellular automata that exhibit only class 1 and 2 behaviour always appear to yields sets that correspond to regular languages in the large time limit. Class 3 and 4 behaviour typically gives rise, however, to a rapid increase of Ξ with time, presumably leading to limiting sets not described by regular languages.

Formal languages are recognized or generated by idealized computers with a 'central processing unit' containing a fixed finite number of internal states, together with a 'memory'. Four types of formal languages are conventionally identified, corresponding to four types of computer:

- Regular languages: no memory required.
- Context-free languages: memory arranged as a last-in, first-out stack.
- Context-sensitive languages: memory as large as input word required.
- Unrestricted languages: arbitrarily large memory required (general Turing machine).

Examples are known of cellular automata whose limiting sets correspond to all four types of language (L. Hurd, in preparation). Arguments can be given that the limit sets for class 3 cellular automata typically form context-sensitive languages, while those for class 4 cellular automata correspond to unrestricted languages. (Note that while a minimal specification for any regular language may always be found, there is no finite procedure to obtain a minimal form for more complicated formal languages: no generalization of the regular language complexity Ξ may thus be given.)

Computation theory

While dynamical systems theory concepts suffice to define class 1, 2 and 3 cellular automata, computation theory is apparently required for class 4 cellular automata. Examples of the evolution of a typical class 4 cellular automaton are shown in Fig. 5. Varied and complicated behaviour, involving many different time scales is evident. Persistent structures are often generated; the smallest few are illustrated in Fig. 6, and are seen to allow both storage and transmission of information. It seems that the structures supported by this and other class 4 cellular automata rule may be combined to implement arbitrary information processing operations. Class 4 cellular automata would then be capable of universal computation: with particular initial states, their evolution could implement any finite algorithm. (Universal computation has been proved for a $k=18$, $r=1$ rule[22], and for two-dimensional cellular automata such as the 'Game of Life'[22,23].) A few per cent of cellular automaton rules with $k>2$ or $r>1$ are found to exhibit class 4 behaviour: all these would then, in fact, be capable of arbitrarily complicated behaviour. This capability precludes a smooth infinite size limit for entropy or other quantities: as the size of cellular automaton considered increases, more and more complicated phenomena may appear.

Cellular automaton evolution may be viewed as a computation. Effective preidiction of the outcome of cellular automaton evolution requires a short-cut that allows a more efficient computation than the evolution itself. For class 1 and 2 cellular automata, such short cuts are clearly possible: simple computations suffice to predict their complete future. The computational capabilities of class 3 and 4 cellular automata may, however, be sufficiently great that, in general, they allow no short-cuts. The only effective way to determine their evolution from a given initial state would then be by explicit observation or simulation: no finite formulae for their general behaviour could be given. (If class 4 cellular automata are indeed capable of universal computation, then the variety of their possible behaviour would preclude general prediction, and make explicit observation or simulation necessary.) Their infinite time limiting behaviour could then not, in general, be determined by any finite computational process, and many of their limiting properties would be formally undecidable. Thus, for example, the 'halting problem' of determining whether a class 4 cellular automaton with a given finite initial configuration ever evolves to the null configuration would be undecidable. An explicit simulation could determine only whether halting occurred before some fixed time, and not whether it occurred after an arbitrarily long time.

For class 4 cellular automata, the outcome of evolution from almost all initial configurations can probably be determined only by explicit simulation, while for class 3 cellular automata this is the case for only a small fraction of initial states. Nevertheless, this possibility suggests that the occurrence of particular site value sequences in the infinite time limit is in general undecidable. The large time limit of the entropy for class 3 and 4 cellular automata would then, in general, be non-computable: bounds on it could be given, but there could be no finite procedure to compute it to arbitrary precision. (This would be the case if the limit sets for class 3 and 4 cellular automata formed at least context-sensitive languages.)

While the occurrence of a particular length n site value sequence in the infinite time limit may be undecidable, its occurrence after any finite time t can, in principle, be determined by considering all length $n_0 = n + 2rt$ initial sequences that could evolve to it. For increasing n or t this procedure would, nevertheless, involve exponentially-growing computational resources, so that it would rapidly become computationally intractable. It seems likely that the identification of possible sequences generated by class 3 and 4 cellular automata is, in general, an NP-complete problem (see ref. 15). It can, therefore, presumably not be solved in any time polynomial in n or t, and essentially requires explicit simulation of all possibilities.

Undecidability and intractability are common in problems of mathematics and computation. They may well afflict all but the simplest cellular automata. One may speculate that they are widespread in natural systems, perhaps occurring almost whenever nonlinearity is present. No simple formulae for the behaviour of many natural systems could then be given; the consequences of their evolution could be found effectively only by direct simulation or observation.

I thank O. Martin, J. Milnor, N. Packard and many others for discussions. The computer mathematics system SMP[24] was used during this work. The work was supported in part by the US Office of Naval Research (contract No. N00014-80-C-0657).

1. Wolfram, S. *Rev. Mod. Phys.* **55**, 601–644 (1983).
2. Wolfram, S. *Physica* **10D**, 1–35 (1984).
3. Wolfram, S. *Commun. Math. Phys.* (in the press).
4. Wolfram, S. *Cellular Automata* (Los Alamos Science, Autumn, 1983).
5. Mandelbrot, B. *The Fractal Geometry of Nature* (Freeman, San Francisco, 1982).
6. Packard, N. Preprint, *Cellular Automaton Models for Dendritic Growth* (Institute for Advanced Study, 1984).
7. Madore, B. & Freedman, W. *Science* **222**, 615–616 (1983).
8. Greenberg, J. M., Hassard, B. D. & Hastings, S. P. *Bull. Amer. Math. Soc.* **84**, 1296–1327 (1978).
9. Vichniac, G. *Physica* **10D**, 96–116 (1984).
10. Domany, E. & Kinzel, W. *Phys. Rev. Lett.* **53**, 311–314 (1984).
11. Waddington C. H. & Cowe, R. J. *J. theor. Biol.* **25**, 219–225 (1969).
12. Lindsay, D. T. *Veliger* **24**, 297–299 (1977).
13. Young, D. A. *A Local Activator–Inhibitor Model of Vertebrate Skin Patterns* (Lawrence Livermore National Laboratory Rep., 1983).
14 Guckenheimer, J. & Holmes, P. *Nonlinear Oscillations, Dynamical Systems, and Bifurcations of Vector Fields* (Springer, Berlin, 1983).
15. Hopcroft, J. E. & Ullman, J. D. *Introduction to Automata Theory, Languages, and Computation* (Addison-Wesley, New York, 1979).
16. Packard, N. Preprint, *Complexity of Growing Patterns in Cellular Automata* (Institute for Advanced Study, 1983).
17. Martin, O, Odlyzko, A. & Wolfram, S. *Commun. Math. Phys.* **93**, 219–258 (1984).
18. Grassberger, P. *Physica* **10D**, 52–58 (1984).
19. Lind, D. *Physica* **10D**, 36–44 (1984).
20. Margolus, N. *Physica* **10D**, 81–95 (1984).
21. Smith, A. R. *Journal of the Association for Computing Machinery* **18**, 339–353 (1971).
22. Berlekamp, E. R., Conway, J. H. & Guy, R. K. *Winning Ways for your Mathematical Plays* Vol. 2, Ch. 25 (Academic, New York, 1982).
23. Gardner, M. *Wheels, Life and other Mathematical Amusements* (Freeman, San Francisco, 1983).
24. Wolfram, S. *SMP Reference Manual* (Computer Mathematics Group, Inference Corporation, Los Angeles, 1983).

ARTICLES

Orientation of *in situ* stresses in the oceanic crust

Robin L. Newmark*†, Mark D. Zoback‡ & Roger N. Anderson*

* Borehole Research Group, Lamont-Doherty Geological Observatory, and † Department of Geological Sciences, Columbia University, Palisades, New York 10964, USA
‡ Branch of Tectonophysics, US Geological Survey, Menlo Park, California 94025, USA

Two in situ *measurements of principal stress directions have been made in DSDP Holes 504B, south of the Costa Rica Rift on the Nazca plate, and 597C, west of the East Pacific Rise on the Pacific plate. In both cases, the orientations of* in situ *principal stresses determined from borehole breakouts are consistent with the stress directions inferred from intraplate earthquakes located near the sites.*

WELLBORE breakouts are intervals of borehole elongation which are caused by preferential spalling in a zone where the circumferential compressive stress is greatest[1], and in which the average azimuth of the long dimension is consistent in a given well or field[2,3]. Stress-induced wellbore breakouts form at an azimuth perpendicular to the maximum horizontal principal stress direction[1]. Wellbore breakouts have been reported in wells from several parts of North America[2–15] but there have been problems in their identification (see ref. 16). There now seems to be ample evidence that breakouts can be used as a reliable indicator of the orientation of the horizontal principal stresses. Here, we use specially processed borehole televiewer data to study the detailed shape of breakouts (see ref. 1).

Borehole televiewer reflectivity records have previously been used in the study of fractures intersecting wellbores at depth (see ref. 17), for identifying lithostratigraphical features in deep ocean boreholes (see refs 18, 19), and in identifying zones of borehole breakout[1,20,21].

Experimental data

Evidence of the orientation of the contemporary *in situ* stress field can be found at two DSDP (Deep Sea Drilling Project) sites in the oceanic crust (Fig. 1). DSDP Site 504 is located 200 km due south of the Costa Rica Rift and about 350 km north-west of the Peru-Chile Trench. DSDP Site 597 is located about 1,800 km west of the East Pacific Rise and 2,000 km east of Tahiti.

During DSDP Leg 83, the DV *Glomar Challenger* completed drilling Hole 504B to a depth of 1,350 m, 1,000 m of which was into basement[22] (Fig. 1). The upper 100 m of basement[19] is composed mainly of pillow basalts and thin flow units of seismic layer 2A. The next 550 m of pillows, breccias and flows is a site of intense fracturing, and contains extensive secondary alteration; it is thought to be seismic layer 2B. The bottom 350 m of the hole is composed mainly of massive, 'welded' units, or sheeted dykes, and is the upper part of seismic layer 2C.

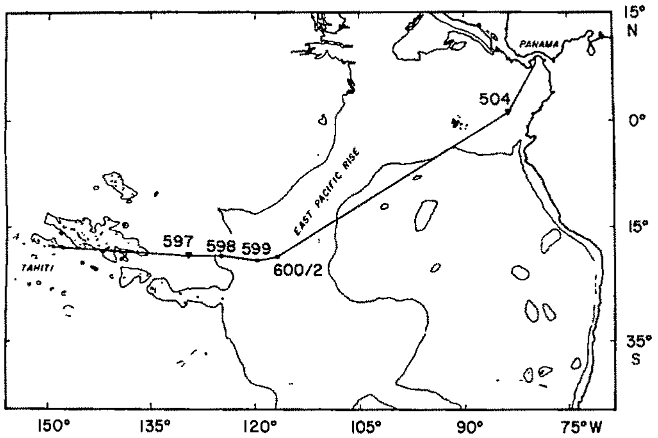

Fig. 1 Location of DSDP Sites 504 and 597 along ship track for DSDP Leg 92.

Borehole televiewer (BHTV) images run in Hole 504B suggested the presence of breakouts at many intervals down the hole. Our breakout analysis of the BHTV records was confined to the lower 350 m of the hole, because the borehole walls in the lower part of the hole are relatively smooth (apart from the breakout intervals), in comparison to the washed out, pitted and broken nature of the wellbore in the upper zones of pillows and breccias. For analysis of the BHTV records, cross-sectional travel-time images were produced every few centimetres in breakout zones in the lower 350 m of the hole. These form 360° caliper images of the wellbore. The criteria which were used to confirm the breakouts included: (1) the wellbore should have two bands of spalling, separated by 180°±20°; and (2) evidence of the same cross-sectional outline and orientation should persist over several (>4) consecutive rotations of the tool's acoustic transducer, indicating breakout continuity of several centimetres for each measurement.

Figure 2*b* shows a reflectivity record of a 5 m-long interval from Hole 504B which is oriented with respect to magnetic north. Hard, smooth surfaces produce white zones (high-amplitude reflectance), and fractures, voids and soft material, which would absorb much of the signal, produce dark zones (low-amplitude reflectance). The vertical, dark bands seen at azimuths of about 120° and 300° are breakout zones. Figure 2*c* shows a cross-sectional, 360° caliper view of the breakout at a depth of 944 m into basement which was made by plotting the travel time of the reflected acoustic pulse as a function of azimuth.

In all, 65 measurements of orientations of breakouts which conformed to the above listed criteria were made in the records obtained in the lower 350 m of Hole 504B. Figure 3*b* shows examples of breakout cross-sections at other depths through this depth interval. The azimuths (with respect to magnetic north) of the midpoints of each breakout zone are plotted against depth in Fig. 3*a*. The mean azimuths are N112E ± 16° (±s.d.) and N296E ± 16°, with a mean separation of 184° ± 11°. This indicates an average maximum horizontal compressional stress oriented at N24E magnetic, which, when corrected for magnetic declination (4.5° east), results in a maximum horizontal stress direction of N20E ± 16° at the site.

During DSDP Leg 92, as part of a hydrogeology investigation (Fig. 1), a series of holes was drilled at sites which form a west–east transect across the western flank of the East Pacific Rise, at 19° South. Hole 597C, a re-entry hole, was drilled 91 m into the 28.5-Myr-old crust, generated at the now-extinct but fast-spreading Galapagos Rise. Massive flows appear to comprise the entire sequence. This is supported by both the BHTV amplitude records and the core recovery which ranged up to 94%. Only one small fragment which might possibly be a pillow margin was recovered[23]. The caliper logs indicate that the borehole has few abrupt changes in diameter, and the BHTV amplitude records show the wellbore as having a generally uniform and solid appearance, with few zones of low reflectivity.

In some intervals, zones of borehole breakout oriented NNE–SSW were identified. Because of the otherwise smooth and solid character of the wellbore, the presence of breakouts is readily recognized in travel-time processing of the BHTV records (Fig. 3*d*). In all, 18 measurements of breakout orientations were made in the BHTV records from the upper 50 m of basement in Hole 597C (Fig. 3*c*, *d*). Unlike the measurements from Hole 504B, each of these measurements was made using data from only two rotations of the tool because cold formation temperatures slowed the speed of tool rotation. The azimuths (with respect to magnetic north) of the midpoints of each breakout zone are plotted against depth in Fig. 3*c*. The mean azimuths are N30E

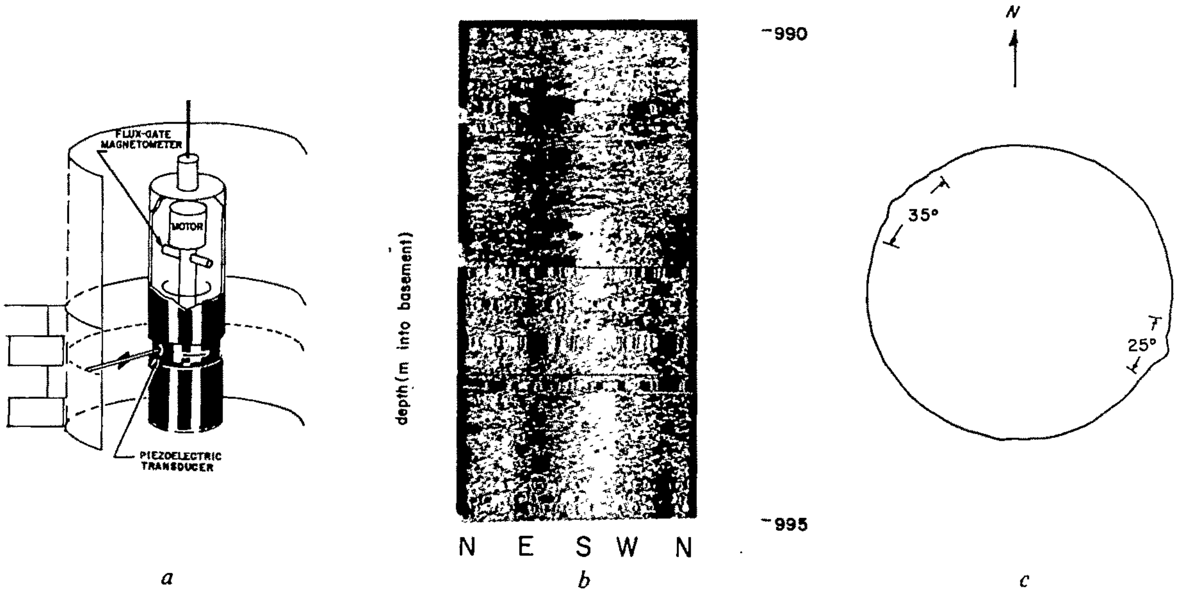

Fig. 2 *a*, Schematic of the borehole televiewer. The televiewer contains a rotating piezoelectric transducer which emits and receives an ultrasonic pulse 600 times a revolution as it rotates three times per s[33]. The amplitude of the reflected acoustic pulse can be plotted on a three-axis oscilloscope as a function of beam azimuth and vertical position in the hole, producing an image of wellbore reflectivity, or smoothness. The travel time of the reflected acoustic pulse can be plotted as a function of beam azimuth, which results in a detailed cross-sectional image of the wellbore. A fluxgate magnetometer triggers the scope trace at magnetic north so that the orientation of observed features can be determined. *b*, Amplitude, or plan-view borehole televiewer record of 5 m of Hole 504B. Width across image is about 1 m. Dark vertical bands oriented ESE–WNW are breakout zones. *c*, Cross-section of Hole 504B at a depth of 944 m into basement, showing breakout.

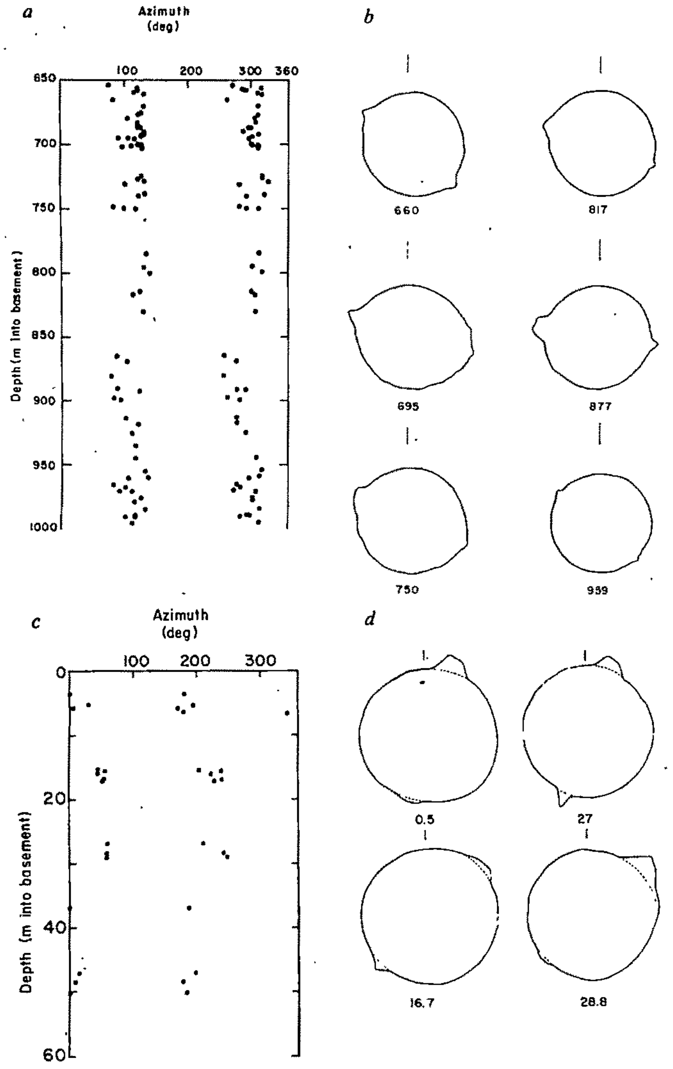

Fig. 3 Azimuths (with respect to magnetic north) of the mid-points of borehole breakouts plotted against depth in *a*, Hole 504B; *c*, Hole 597C. Mean azimuths are N112E and N296E ± 16° (*a*) and N30E and N208E ± 25° (*c*). Examples of breakout cross-sections in *b*, Hole 504B; *d*, Hole 597C. Vertical lines indicate true north. Numbers indicate depth in metres into basement.

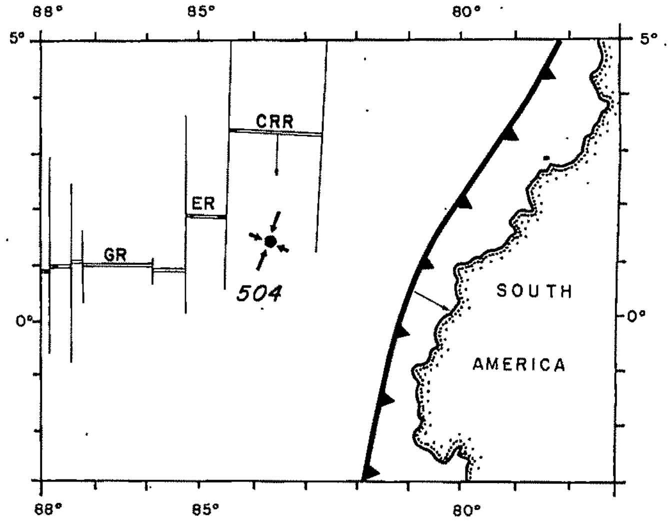

Fig. 4 Stresses near Site 504. Heavy arrows indicate the principal horizontal compressive stress directions determined from breakout directions at Hole 504B. Light arrows show the direction of ridge-push force from the Costa Rica Rift and the direction of the slab-pull force from the Peru–Chile Trench. Double lines indicate the ridge axis of the Cocos–Nazca spreading system and hatched line is the Peru–Chile Trench[32]. CRR, Costa Rica Rift; ER, Ecuador Rift; GR, Galapagos Rift.

and N208E ± 25°, with a mean separation of 178°. This indicates an average maximum horizontal compressional stress direction of N121E magnetic, which, when corrected for magnetic declination results in a maximum horizontal stress oriented N110E ± 25° at the site.

Discussion

DSDP Hole 504B is located 200 km due south of the east–west-trending Costa Rica Rift and about 350 km NW of the NE–SW-trending Peru–Chile Trench. Ridge push from the Costa Rica Rift should produce a southward compression at the site. The net slab pull, or the sum of driving and resisting slab forces, should produce southeastward extensional stresses at the site (Fig. 4).

As shown in Fig. 4, the observed maximum principal horizontal stress direction is oriented almost parallel to the north–south compression expected from a ridge-push force from the Costa Rica Rift. This would seem to suggest the dominance of the ridge-push force at this site. However, the slab pull force associated with subduction of the Nazca plate along the Peru–Chile Trench is expected to generate east-southeast-oriented extensional stresses. Because the observed direction of least principal stress is N110E, it is nearly parallel to the predicted direction of trench pull. Thus, it is not clear from the orientation of the principal horizontal stresses at Hole 504B whether ridge push, or trench pull, is the dominant mechanism controlling the *in situ* stress field. In any event, this direction is consistent with focal mechanism solutions of earthquakes located near the site, which exhibit a dominant NNE–SSW P-axis orientation[24].

DSDP Hole 597C is located ~1,800 km west of the East Pacific Rise (Fig. 1). Ridge push from the East Pacific Rise should produce west-northwest-oriented compression at the site. As can be seen in Fig. 5, the maximum horizontal compression at Site 597C is parallel to both the relative and absolute plate motion vectors for the Pacific plate, both of which are consistent with an interpretation of a dominant ridge-push force acting at the site.

The shaded areas in Fig. 5 indicate the local range of uncertainty in identifying the Okal and Bergeal 'J' line[25] which separates lithosphere generated at the Galapagos Rise before the Miocene ridge jump from lithosphere generated at the East Pacific Rise. It is a line of age discontinuity and may represent a zone of weakness in the plate. Because the ridge jump was accompanied by a change in the azimuth of spreading, the J line separates lithosphere with differing tectonic orientations. Fracture zones trend N250E in the older lithosphere and N290E in the younger lithosphere.

The anomalous intraplate seismicity in this area graphically demonstrates a change in the consistency of stress orientations inferred from intraplate earthquakes located in crust on either side of the J line. Focal mechanism solutions of several intraplate earthquakes located in the general vicinity of Site 597 are shown in Fig. 5 (refs 24, 26–29).

LI2, GB4 and GB5 correspond to Okal *et al.*'s[26] regions A, B and C, respectively. Each of these clusters has horizontal dimensions of ≤50 km. All solutions indicate focal depths of ≤5 km. A seismic network in French Polynesia has provided a detailed account of the seismicity in these regions over the past several years[26].

At LI2, activity is characterized by swarms, mostly with strike-slip solutions with some normal component. The P axes are oriented WNW–ESE which is nearly parallel to both the current relative and absolute plate motion vectors. There is no evidence of related local bathymetric features.

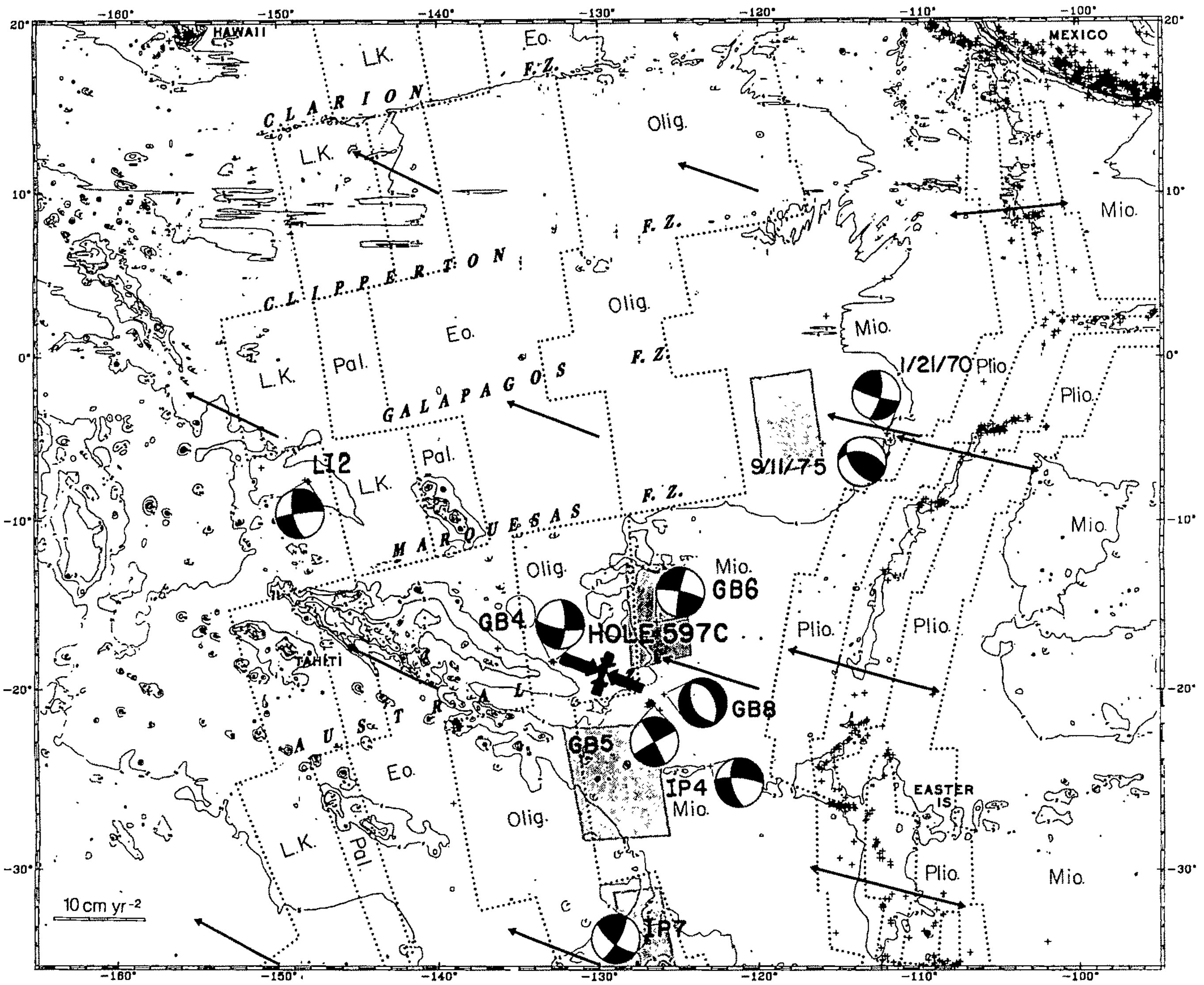

Fig. 5 Stresses near Site 597C. Heavy arrows indicate the principal horizontal stress directions determined from breakout directions at Hole 597C. Light single-headed arrows indicate the absolute Pacific plate motion, and light double-headed arrows show relative Pacific–Nazca plate motion[34]. The trend of the East Pacific Rise is shown by crosses which mark the locations of earthquakes with $m_b > 4.5$ mag and recorded by more than 10 stations by the International Seismological Centre between 1963 and 1979 [35]. Focal mechanism solutions are discussed in the text.

At GB4, activity occurred as discrete events through time, again mostly characterized by strike-slip solutions with some normal component. There were 12 events with body-wave magnitudes of up to 5.5 during 15 yr.

At GB5, there was a 3-yr swarm of intense activity from 1976 to 1979, with over 96 events—mostly characterized by strike-slip solutions, but unlike at LI2 or GB4, with some thrust component. This swarm was followed by a 3-yr period of quiescence when there was no activity with magnitude >4. In July 1983, a mainshock–aftershock pair of events occurred only 65 km away at GB8, with a purely normal solution, at depths of 15–20 km. There is no evidence of related local bathymetric features in the area.

IP4 is the site of one of the largest normal faulting events known in young oceanic lithosphere, with a body-wave magnitude of 6.8. Its epicentre lies north-west of a major seamount to which this activity may be related. IP7 is located in the range of uncertainty of the J line.

The focal mechanism solutions of earthquakes located in older crust (LI2 and GB4) indicate P axes oriented WNW–ESE, which are consistent with the interpretation of a dominant ridge-push force acting on the plate. However, focal mechanism solutions of events located at sites near the J line or in younger crust show more diverse orientations of P axes. At GB5 and GB8, events occurred with normal, thrust and strike-slip mechanisms, within 3 yr and 65 km.

Our Site 597 is located in crust just older than the J line and indicates a dominant stress orientation which is consistent with the stress regime inferred by the intraplate events in older crust. This is particularly satisfying because our measurement was made only in the upper 50 m of the oceanic crust.

Conclusions

Most events far from plate boundaries indicate compressive stresses which are thought to result from the gravitational force due to lithospheric thickening with age, or ridge-push force. However, both compressional and extensional events occur in young lithosphere. Various authors[29–31] have proposed ages of from 10 to 35 Myr for the transition between the near-ridge tectonic regime which may be dominated by local forces and the stress regime in stable plate interiors characterized by horizontal compression. Site 597 seems to be located very close to this transition zone west of the East Pacific Rise.

To date, two *in situ* measurements of principal stress orientations have been made in DSDP holes: at Hole 504B, south of the Costa Rica Rift on the Nazca plate and at Hole 597C, west of the East Pacific Rise on the Pacific plate. In both cases, the orientation of *in situ* principal stresses determined from borehole breakouts have been consistent with the stress directions inferred from intraplate earthquakes near the sites. The important point of this work is the demonstration that stress orientations can be reliably determined from borehole breakouts in the oceanic crust. With the advent of a new phase of deep ocean drilling, we are confident that these measurements, routinely made in boreholes at locations oriented with respect to major plate boundaries, will allow us to define more clearly the state of stress in the upper oceanic crust and the relationships between the driving forces of plate tectonics.

We thank the officers, crews and scientific party of the DV *Glomar Challenger* Legs 83 and 92, without whose diligence and hard work the televiewer logs could not have been successfully completed. Larry Mastin, Gray Jensen and several other people at the USGS provided invaluable technical assistance. Terry Engelder and Daniel Fornari greatly improved the content of this paper. This work was supported by NSF grants OCE 78-27026 and OCE 81-10919, Office of Naval Research contracts T0-0098 and T0-0132, scope HH and Joint Oceanographic Institutions Inc. contract JOI-66-84. Lamont-Doherty Geological Observatory contribution number 3702.

Received 29 March; accepted 11 July 1984.

1. Zoback, M. D., Moos, D. & Anderson, R. N. *J. geophys. Res.* (submitted).
2. Cox, J. W. *11th A. Logging Symp. Soc. Prof. Well Log Anal.*, Los Angeles (1970).
3. Babcock, E. A. *Bull. Am. Ass. petrol. Geol.* **62**, 1111–1126 (1978).
4. Schafer, J. N. *The Log Analyst*, 10–23 (Society of Professional Well Log Analysts, 1980).
5. Brown, R. O., Forgotson, J. M. & Forgotson, J. M. Jr *Soc. Petrol. Eng. Pap. SPE 9269, 55th A. Meet.*, Dallas (1980).
6. Gough, D. I. & Bell, J. S. *Can. J. Earth Sci.* **18**, 638–645 (1981).
7. Gough, D. I. & Bell, J. S. *Can. J. Earth Sci.* **19**, 1358–1970 (1982).
8. Springer, J. E. & Thorpe, R. K. *Pap. UCRL-87018 at Int. Conf. on* In-Situ *Testing of Rock and Soil Masses*, Santa Barbara (1981).
9. Bell, J. S. & Gough, D. I. *Earth planet. Sci. Lett.* **45**, 475–482 (1979).
10. Bell, J. S. & Gough, D. I. *US geol. Surv. Open-File Rep.* 82–1075, 539–557 (1982).
11. Plumb, R. A. *EOS* **63**, 1118 (1982).
12. Healy, J. H., Hickman, S. H., Zoback, M. D. & Ellis, W. L. Preprint, US Geological Survey.
13. Hickman, S. H., Healy, J. H., Zoback, M. D., Svitek, J. F. & Bretcher, J. E. *EOS* **63**, 1118 (1982).
14. Gough, D. I., Fordjor, C. K. & Bell, J. S. *Nature* **305**, 619–621 (1983).
15. Fordjor, C. K., Bell, J. S. & Gough, D. I. *Can. J. Earth Sci.* **20**, 1445–1455 (1983).
16. Blumling, P., Fuchs, K. & Schneider, T. *Phys. Earth planet. Int.* **33**, 250–254 (1983).
17. Seeburger, D. A. & Zoback, M. D. *J. geophys. Res.* **87**, 5517–5534 (1982).
18. Zoback, M. D. & Anderson, R. N. *Nature* **295**, 375–379 (1982).
19. Newmark, R. L., Anderson, R. N., Zoback, M. D. & Moos, D. *Init. Rep. DSDP* Leg **83** (in the press).
20. Hickman, S. H., Healy, J. H. & Zoback, M. D. *J. geophys. Res.* (submitted).
21. Newmark, R. L., Zoback, M. D. & Anderson, R. N. *Init. Rep. DSDP* Leg **83** (in the press).
22. Anderson, R. N. *et al. Nature* **300**, 594–598 (1982).
23. Leinen, M. *et al. Init. Rep. DSDP* Leg **92** (in the press).
24. Bergman, E. A. & Solomon, S. C. *J. geophys. Res.* (submitted).
25. Okal, E. A. & Bergeal, J. M. *Earth planet. Sci. Lett.* **63**, 113–122 (1983).
26. Okal, E. A., Talandier, J., Sverdrup, K. A. & Jordan, T. H. *J. geophys. Res.* **85**, 6479–6495 (1980).
27. Okal, E. A. *J. geophys. Res.* (submitted).
28. Dziewonski, A. M. & Woodhouse, J. H. *J. geophys. Res.* **88**, 3247–3272 (1983).
29. Wiens, D. A. & Stein, S. *J. geophys. Res.* (submitted).
30. Sykes, L. R. & Sbar, M. L. *Nature* **245**, 298–302 (1973).
31. Wiens, D. A. & Stein, S. *Tectonophysics* (submitted).
32. *Plate-Tectonic Map of the Circum-Pacific Region, Southeast Quadrant* (American Association of Petroleum Geologists, 1981).
33. Zemanek, J., Glen, E. E. Jr, Norton, L. J. & Dardwell, R. L. *Geophysics* **35**, 254–269 (1970).
34. Minster, J. B. & Jordan, T. H. *J. geophys. Res.* **83**, 5331–5354 (1978).
35. Haxby, W. F. & Weissel, J. K. *J. geophys. Res.* (submitted).

Mantle upflow under North America and plate dynamics

D. I. Gough

Institute of Earth and Planetary Physics, and Department of Physics, University of Alberta, Edmonton, Alberta, Canada T6G 2J1

In the development of plate dynamics there are two fundamental questions. First, do the plates slide over a passive asthenosphere, or are they driven by a convecting upper mantle? Second, are all ocean ridges passive, pull-apart plate margins, or do some lie above upcurrents in the mantle and in that sense become active margins? The combination of stress orientations in the crust of North America with other geophysical and geological information favours an active mantle interpretation, both for the North American plate and for the mantle upflow which lay beneath the East Pacific Rise in Tertiary times and which now lies beneath the western United States.

THE fundamental hypothesis of plate tectonics, that the Earth has a strong outer shell, or lithosphere, made up of a small number of quasi-rigid plates, is now well established. Earthquakes occur mainly along, and are used to locate, plate boundaries. Linear marine magnetic anomalies and earthquake mechanisms have been used to construct a detailed picture of the motions of the plates. The next step is to develop a similarly satisfactory account of the forces driving the plates. In this development of plate dynamics, an important question is whether the plates slide over a passive weak layer, or asthenosphere, under gravitational forces acting only on the plates themselves, or are driven by convection in the mantle through the asthenosphere as a coupling layer. In the latter case, one would expect to find active ocean ridges driven by upcurrents in the mantle, probably with rapid spreading rates; and probably also passive ridges where slower spreading is driven only by gravity acting on the plates. In the past 30 Myr, the boundary between the North American plate and adjacent plates under the Pacific Ocean has undergone a complex evolution. This article brings together a wide range of geological, geophysical and geochemical information to show that there is now an upward flow of mantle material under the western United States. The implication is that active convection in the mantle is driving the Pacific plate and maintaining compressive stress, in a NE–SW direction, in the North American plate.

Two well-known reconstructions[1,2] of the Cenozoic tectonic evolution of the Pacific–North American plate boundary started with a continuous subduction along the western margin of the continent, the Farallon Plate between that subduction and the East Pacific Rise (EPR) with its associated transform faults, and the Pacific Plate west of the EPR. After the first contact of the EPR and its transform faults with the subduction, some 30 Myr BP, triple junctions migrated to the south-east and north-west and replaced the subduction with the San Andreas transform fault system. In this process, the oceanic Farallon Plate disappeared, except its remnants the Gorda, Juan de Fuca and Explorer plates north of 40° N and the Cocos plate south of 23° N, all of which are still being subducted under North America.

For the present purpose I adopt this widely accepted model of the sequence of plate interactions over the past 50 Myr. If (as Atwater[2] assumed) the EPR had been a passive, pull-apart

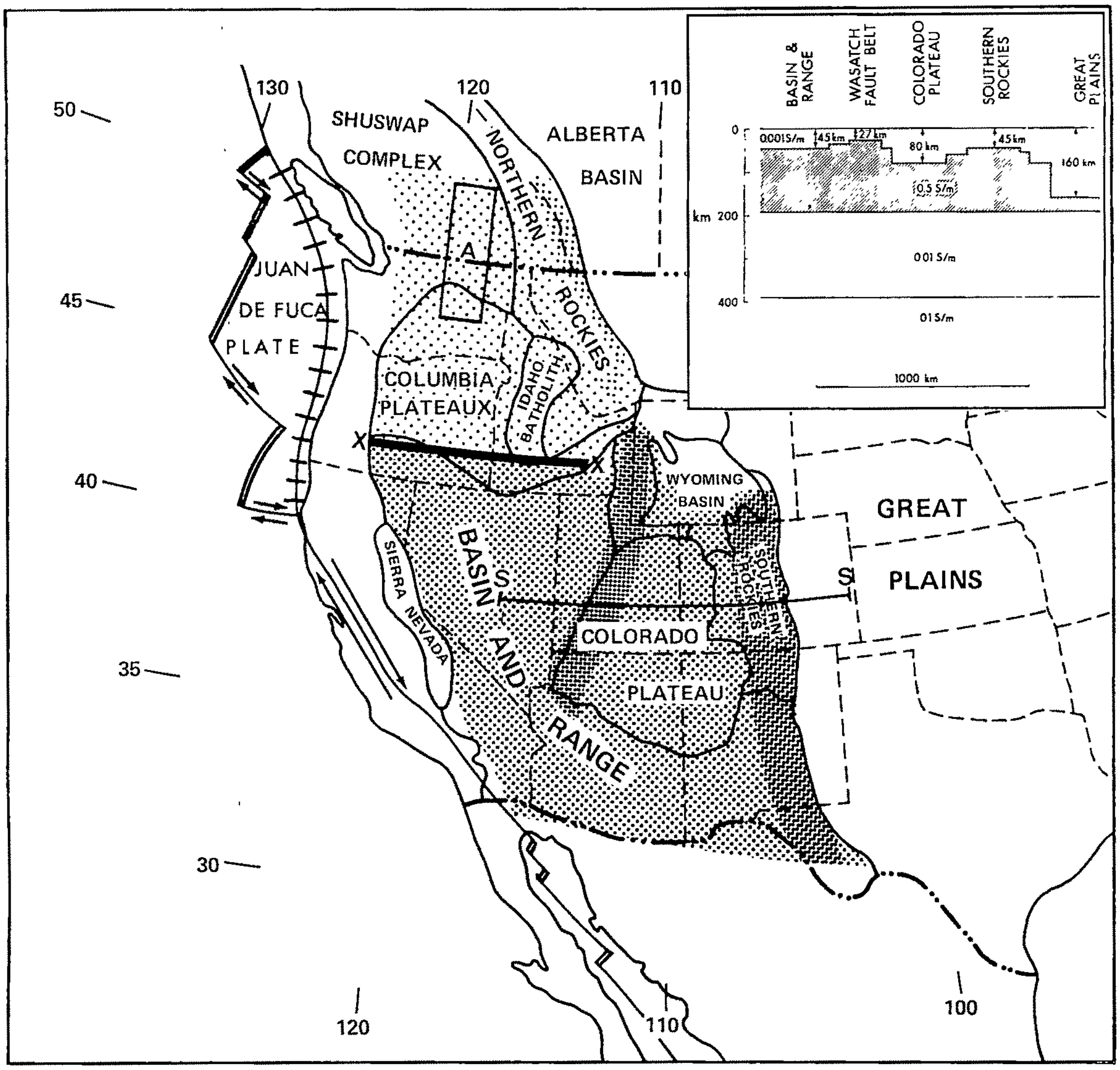

Fig. 1 The density of strippling on the map indicates variations of electrical conductance of an upper mantle layer. It is also believed to show partial melting. The section shows a model of conductive structure[26] along the east–west section SS. Major tectonic provinces are indicated.

margin, its replacement with the San Andreas Fault would not imply any marked thermal aftereffects within the continent. But if the EPR of Cenozoic times lay above a mantle upflow, such an upflow might now be present under the western US. Either possibility is consistent with earlier models[1,2] of the kinematics of the plates.

High temperatures and partial melting

There is abundant geophysical and geological evidence that temperatures in the upper mantle west of the undisturbed North American craton are higher than those beneath it. The boundary of the high-temperature régime lies at the eastern front of the Rocky Mountains[3,4]. West of this boundary the cratonic rocks of the Southern Rockies and Colorado Plateau (Fig. 1) have been uplifted in the Laramide orogeny[5], largely as a result of heating of the underlying upper mantle. The topographic uplift itself is highly significant as an indicator of the high-temperature region. Such features as the Colorado Plateau and the Grand Canyon show uplift of 3–4 km, and many mountains in the western US are peneplaned in this range of elevation. The igneous petrology of the region is even more significant. West and south of the Colorado Plateau the Basin and Range Province, and the Columbia Plateaus further north, are dominated by volcanic rocks of two types. Calc-alkaline andesitic volcanics were extruded in late Cretaceous and early Tertiary times, up to about 30 Myr BP (ref. 6). This epoch corresponds to the subduction regime in Atwater's[2] scheme, before the most easterly ridge segment reached the trench. The earlier, andesitic vulcanism can, therefore, be ascribed to ascent of melt from the downgoing plate on the model of Ringwood and Green[7], as shown in detail by Christiansen and Lipman[8]. Uplift of the Southern Rockies and Colorado Plateau probably occurred largely at that stage[5]. After 25 Myr BP basaltic vulcanism dominated the Basin and Range Province and Columbia Plateaus[8]. The basalts were extruded in great volume in an extensional stress field with most faults trending north–south. All of these observations receive a clear explanation if a mantle upflow, formerly feeding an active ridge at the EPR, lay under the Basin and Range Province after replacement of the ridge and trench with the San Andreas fault system. This is the explanation long held by J. Tuzo Wilson (ref. 9 and personal communications) and myself. Others[8,10] have preferred to regard the extensional fractures and basaltic extrusions as the result of oblique shearing transmitted from the San Andreas faults. This is probably the best account possible if one assumes that the EPR of early Tertiary times was a passive, pull-apart margin.

Regional variations of heat flow from the mantle confirm the thermal structure indicated by the volcanic rocks[3,4]. Seismology and electromagnetic geophysics reinforce the regional variations and add information in the depth dimension. For brevity the continent east of the Rocky Mountains is termed the 'craton', the region west of the craton the 'western region' within which lies the Basin and Range Province. Teleseismic P and S waves arriving vertically are delayed in the western region compared with the craton[11–13] in such a way as to show that the rigidity modulus is reduced much more than the bulk modulus under the western region[14], which would be the case if partial melting were present in the upper mantle there. Seismic refraction shows that the uppermost mantle, just under the crust, transmits P_n waves with lower velocities in the western region than in the craton, with the lowest velocities in the Basin and Range Province. Results from long seismic refraction lines show the presence of a marked low-velocity layer for P waves in the upper mantle under the western region[15–17], but not under the craton. In a representative recent model[18], the low-velocity layer lies in the depth range 65–200 km. Recent studies of attenuation of P and S teleseismic waves[19] have confirmed large variations under the US, with greatest attenuation under the western region including, but not confined to, the Basin and Range Province, and lowest attenuation under the north central shield of the craton. Seismological studies, therefore, define a region in which the elastic body wave velocities are reduced, and their amplitudes attenuated through anelastic response, in a layer in the upper mantle under the western region, in general, and the Basin and Range Province, in particular.

Observations of natural time variations of the geomagnetic field, with two-dimensional arrays of recording magnetometers, can be used to discover and map rock structures of anomalously high electrical conductivity[20]. Figure 1 summarizes the results of the first three such studies with arrays of magnetometers[21–24]. The density of stippling on the map gives a qualitative indication of the conductance (=conductivity × thickness) of the anomalously conductive layer. This is confined to the region west of the craton, with high conductance under the Basin and Range Province and the Colorado Plateau, and still higher conductance under the Southern Rockies and Rio Grande Rift (where Schmucker[25] first found a highly-conductive ridge in the upper mantle) and under the Wasatch Front mountains of Utah. The magnetovariation fields alone give poor discrimination in depth, and other physical parameters are usually invoked to constrain the depths of models of conductivity. Figure 1 (inset) shows a model obtained by Porath[26] on the assumption that the conductive layer is identical with the seismic low-velocity layer. It shows one, non-unique model which fits the magnetovariation fields along the section SS at latitude 38° N. The section and map can be used together to gain an impression of conductive structure under the western region. Recent magnetotelluric soundings[27,28] have verified that high conductivities occur at lower crustal depths, in general agreement with the section shown.

I have shown elsewhere[29] that the electrical conductivity distribution is highly correlated with heat flow and with the seismic low-velocity, high-attenuation layer. The conductivities required to model the magnetovariation fields are very high, and consistent with ionic conduction in a melt fraction in interconnected rock pores[30]. While there are several other ways in which rocks can be highly conductive[31], in the western US the close association of electrical conductivity with the seismic low-velocity layer, and with high heat flow, makes it very probable that the conductive layer is, in fact, a layer of the uppermost mantle containing a molten mineral fraction[32]. It is thus reasonable to regard Fig. 1 as a map and section of partial melting in the uppermost mantle. Shankland and others[33] have examined the properties required in a porous rock containing a melt fraction, to account for the electrical conductivities and seismic parameters observed.

Thus, there is substantial evidence for widespread partial melting in a layer, roughly 150 km thick, in the upper mantle under much of the US in a region bounded to the east by the east front of the Rocky Mountains and to the west by the Sierra Nevada. Furthermore, in this layer the rigidity modulus and estimates of Q are reduced, compared with the craton. As a first approximation, the crust and the lithosphere may be treated as equivalent in the region of partial melting, and are represented as such in Fig. 3.

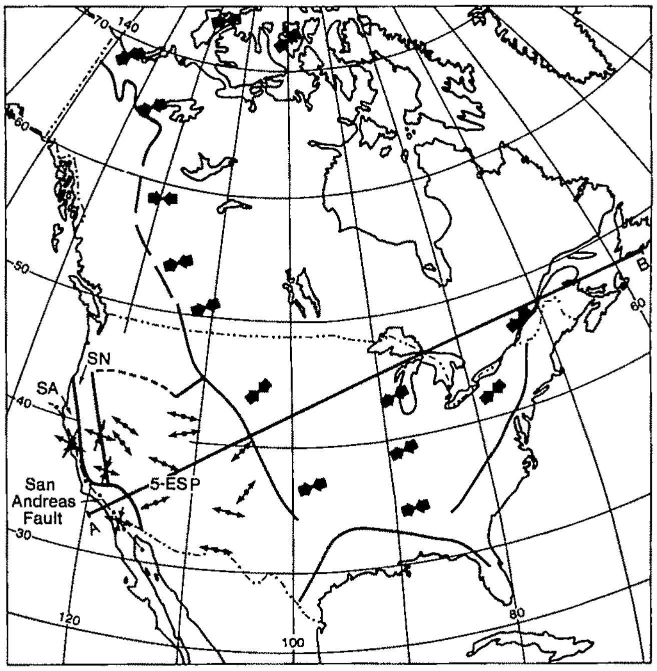

Fig. 2 Stress orientations in North America. Pairs of broad arrows show the directions of the greater horizontal principal stress in the craton. Two-headed arrows indicate the directions of the lesser horizontal principal stress in five extensional stress provinces (5-ESP). SN, Sierra Nevada stress province; SA, San Andreas stress province. Data sources: US and eastern Canada, ref. 37; western Canada, ref. 42; Arctic Islands, ref. 49. AB marks the great circle of the section in Fig. 3.

Mass transport of heat by an upflow of mantle material, formerly under the EPR and now under the continent, provides an explanation of all of the phenomena discussed above. However, heat was carried up in ascending melt from the former subduction, until about 20 Myr ago. There is now a crust ~30 km thick which can transmit heat only by conduction, and its thickness may have varied with time. It is therefore difficult to show that the existing layer of partially molten rock could not be a remnant from melt which came up from the plate before subduction ended. The change in character of the volcanics, from andesitic to basaltic composition, is difficult for proponents of the 'remnant' view but is not in itself conclusive. An entirely different line of evidence has become available which, I believe, resolves the ambiguity.

Stress orientations in North America

The orientation of the stress tensor in the Earth's crust, within a tectonic plate, contains important information on the forces driving that plate. In general, one principal stress is approximately vertical, that is, normal to the free surface; and fractures produce normal faults if σ_1 is vertical, strike-slip faults if σ_2 is vertical and thrust faults if σ_3 is vertical[34], where $\sigma_1 \geq \sigma_2 \geq \sigma_3$ are the principal stresses. For plate tectonics, special interest lies in the orientation and magnitudes of the two horizontal principal stresses, denoted S_H and S_h, with $S_H \geq S_h$. Crustal stress can be investigated by means of field studies of recent movements on faults and of igneous intrusions[35], and through overcoring strain relief techniques, hydraulic fracture experiments and earthquake source mechanisms[36]. Using these methods in a study of crustal stress in the conterminous United States, Zoback and Zoback[37] have delineated 14 stress provinces. Within each province the directions and relative magnitudes of the horizontal principal stresses are nearly constant. The largest of these is their Mid-Continent Stress Province, which extends from the east front of the Rocky Mountains of Colorado and Wyoming to New England and the Atlantic provinces of Canada.

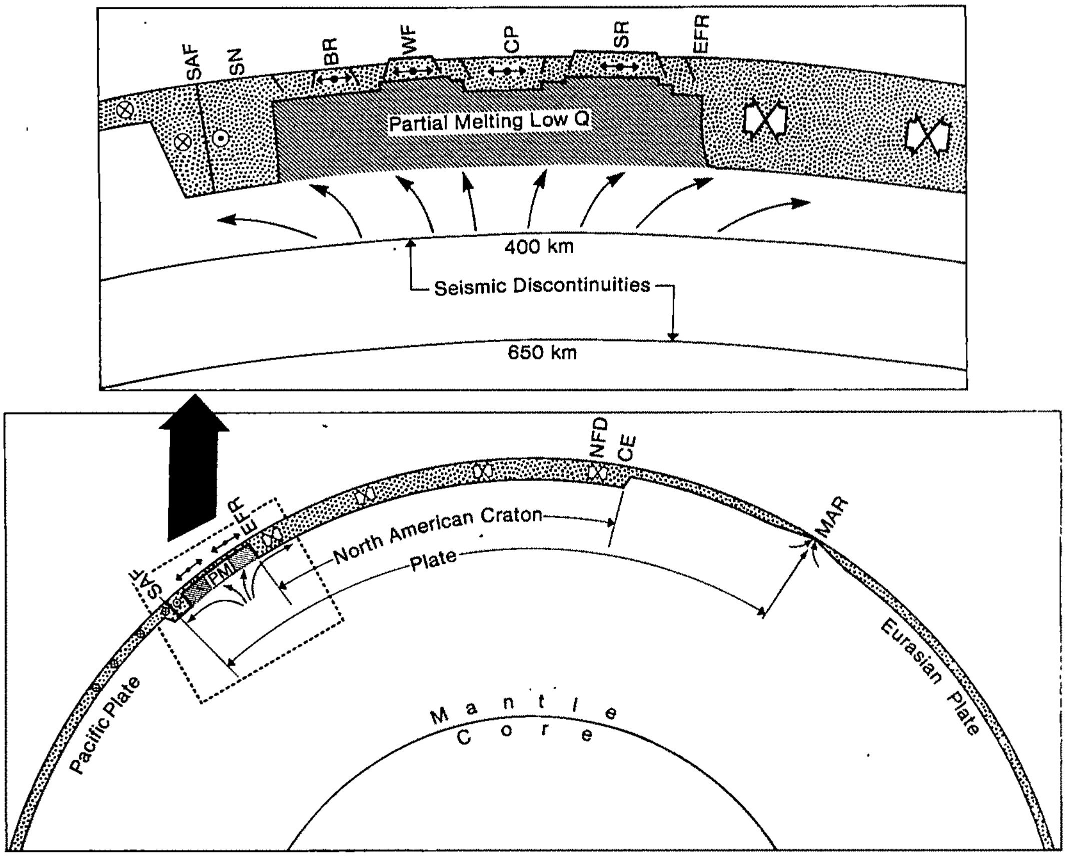

Fig. 3 A cartoon section, without radial exaggeration, along great circle AB in Fig. 2. The lithosphere is stippled. Stress symbols correspond to those in Fig. 2. SAF, San Andreas Fault; EFR, East Front of the Southern Rocky Mountains; NFD, Newfoundland; CE, continental edge; MAR, Mid-Atlantic Ridge. In the inset, SN, Sierra Nevada; BR, Basin and Range Province; WF, Wasatch Front; CP, Colorado Plateau; SR, Southern Rockies.

This province is characterized by a NE–SW direction of S_H, which is often greater than the vertical stress[37–40]. Recently, this stress province has been shown to extend through the western Canadian sedimentary basin to the Arctic coast at the Mackenzie River delta, and is probably coextensive with the old craton of North America[41,42]. The extension has been made through the recognition that a class of fractures in the walls of oil-wells, known as breakouts[43,44], are shear fractures which result from amplification by the oil-well of the stress difference in a stress field with $S_H \neq S_h$ (refs 45–47). According to this hypothesis[45,46], the fractures elongate the section of the borehole with its long axis aligned with the lesser horizontal stress S_h. It has been verified by comparing the stress orientations from the breakouts with other indicators of stress orientation in five stress provinces[41,42,46–48], and is widely accepted.

Directions of S_H in the craton are shown in Fig. 2 by pairs of arrows: each pair represents between 3 and 30 stress directions. Cox[49] has given breakout orientations from 15 oil wells in the Arctic Archipelago, of which 13 show the same NE–SW orientation of S_H as elsewhere in the craton. He has also determined the azimuths of breakouts in numerous wells in Quebec, which give S_H directions similar to the most easterly pair of arrows in Fig. 2.

The North American craton is under a stress field with remarkably uniform NE–SW orientations of S_H. As remarked elsewhere[37,42], this strongly suggests northeastward traction on the base of the plate. Such traction would arise if the plate were sliding to the south-west and experiencing viscous drag from a passive asthenosphere[37], or if northeastward flow in the underlying mantle were pushing the plate, again by viscous drag[42]. The latter case would apply if a divergent upcurrent were present in the mantle beneath the region west of the Rocky Mountains. The stress orientation in the craton cannot discriminate between these two possibilities.

The key to the problem is provided by the stress field in the region between the east front of the Rocky Mountains and the Sierra Nevada. Double-headed arrows in Fig. 2 represent directions of S_h, each from several stress orientations given by Zoback and Zoback[37], in five of their stress provinces showing east–west extensional stress. These extensional stress provinces include the Basin and Range, Colorado Plateau and Rio Grande Rift. In all of them the dominant fault type is normal, which requires σ_1 to be vertical and $\sigma_3 \equiv S_h$. It is not implied that east–west tensile stress exists except very near the surface; σ_3 is probably a small compression in most localities. A normal-fault type of stress field is what is required for uplift of the Colorado Plateau and Southern Rockies, and for development of the horst and graben topography of the Basins and Ranges.

This normal-faulting, extensional stress field is also what would be expected above an upcurrent in the mantle. It is, in fact, the stress field in the oceanic crust at ridges. Figure 3 shows an attempt to present this visually, for which purpose I have assumed lithosphere thicknesses of 250 km under the craton and 70 km below the sea floor. The thick cratonic lithosphere is controversial but the present argument does not depend on it. In the western region I suggest, in Fig. 3, that the seismic low-velocity, electrical high-conductivity uppermost mantle has reduced strength, and is essentially part of the asthenosphere. This is probably too simple but again is not essential to the argument.

The extensional stress field, between the Great Plains and the Sierra Nevada, cannot be understood by assuming that the North American plate is sliding over a passive asthenosphere to the south-west. On that model one would expect NE–SW compression to continue to the vicinity of the Sierra Nevada or even to the San Andreas fault system. Indeed if the lithosphere is thin above the western region (as shown in Fig. 3) one would expect the concentration of stress in it to produce increased NE–SW compression there. Instead, there is an extensional stress field. This requires vertical pressure from below which makes σ_1 vertical in the crust, as observed. Note that upward pressure exists now, as stresses propagate with the speeds of seismic waves. While the melt in the upper mantle could conceivably be a remnant from the subduction regime, say 25 Myr BP, it is difficult to believe that the uplift stress from such a melt remnant would not have been relieved in 25 Myr when postglacial isostatic rebound times are shorter by a factor of 1,000.

The change from andesitic to basaltic volcanics ~25 Myr ago fits the hypothesis that a mantle upcurrent was overridden by the continent then. The stress pattern indicates that there is now upward pressure. Recent evidence[50] from surface wave velocities indicates low velocities of vertically polarized shear waves at depth 250 km under the presently spreading EPR and the San Andreas and Queen Charlotte Islands transform fault regions, with resolution insufficient to discriminate between the San Andreas fault and the Basin and Range Province. These three observations strongly support continuing mantle upflow under the continent. Other evidence, noted earlier, strongly suggests such upflow but can be explained otherwise.

Implications for plate dynamics

The prime question for plate dynamics is what form convection takes. Even if the plates slide over a passive asthenosphere, propelled by gravity sliding[51] from the ridges ('ridge push') and, where there is a subducted leading edge which has not reached 650 km depth, by the excess weight of the subducted plate[52] ('trench pull') there is convection with some undefined return path. This simplest model cannot, however, account for the persistence of upflow under western North America.

Convection in the mantle is required to move the plates and various types are under examination. Simplicities in the distribution of the tectonic plates[53] and in geoid highs and lows[54–56] suggest deep mantle circulation, and whole-mantle convection is a model still favoured by some[57]. However several lines of geochemical and geophysical evidence increasingly indicate a stratified mantle with change of chemical composition at the seismic discontinuity near depth 650 km (refs 58–62). Whereas convection may be expected both below and above the 650-km level, the two convective patterns may be independent or weakly coupled[56]. Clearly, the upper mantle circulation will be of greater relevance to plate dynamics. Many models of convection in a 650-km layer describe square cells of comparable width which could not drive a plate thousands of kilometres wide. However, Houseman has shown[63] that convection cells of large width-to-depth ratio are possible if they are driven by a horizontal temperature difference such as would be expected between the mantle beneath an ocean ridge and a subduction. Anderson[58] has suggested alternatives to the various simplifying assumptions often adopted on convection. He suggests that melting may be more effective in producing the density change that drives convection rather than thermal expansion.

Evidence has been presented to show that an upward flow in the upper mantle, formerly under the EPR, is now under the Basin and Range and Colorado Plateau region of western North America. The mantle upflow may extend to western Canada, and the strip of low S_V velocity in Anderson's tomographic maps[50] suggests that it does. This would be consistent with the uniformity of stress orientation in the craton into the Arctic islands (Fig. 2). If the mantle upflow is present as I have argued, there are two points of interest related to convective models.

First, the upflow continued while the subducted plate (now the root of the Sierra Nevada) passed over it. It must, therefore, come from a depth near the 650 km discontinuity, as a minimum.

Second, the convective circulation has survived the effects of the continent overriding its upward limb for ~25 Myr. If one applies Houseman's type of convection, the operative temperature difference is that between colder mantle below the subductions on the north-west side of the Pacific, and hotter mantle, formerly below the EPR, now below western North America. Note that the upflow is not under the craton, whose great thickness of poorly-conducting lithosphere would probably change the flow rapidly[58]. With the thin crust of the Basin and Range Province as conductive cover, the upflow may have boundary conditions not too different from those of the Rise sea floor.

It is not implied that all ocean ridges lie above convective upcurrents in the mantle. Spreading rates of ridges vary, and *a priori* it seems possible that fast-spreading ridges such as the EPR lie above divergent mantle flow which drives them; whereas slowly-spreading ridges like the Mid-Atlantic Ridge may not be driven and may approximate to the pull-apart model. Gravity sliding will operate in both types, and even under a passive ridge partial melt will ascend, because its density is less than the mean value for the upper mantle, to form new lithosphere. In this case, however, the flow beneath the ridge will be convergent and only the sliding lithosphere itself exhibits divergent motion.

Conclusions

Observations of topography, seismology, heat flow, electromagnetic geophysics, petrochemistry and the orientation of the stress tensor in the crust, combine to support the view that an upcurrent exists in the mantle below western North America. This, in turn, implies that during the Tertiary, the EPR was a ridge of the active type, driven by a divergent upcurrent in the underlying mantle. Other ridges are probably of the passive type, but this has not been demonstrated.

For plate dynamics, a principal implication is that at least some tectonic plates are actively driven by mantle circulation. An interesting possibility is that the Pacific Plate is being driven by mantle convection towards the subductions which form its northwestern boundary. In such a system, if substantiated, the upward limb of the convection would lie under the EPR of southern and tropical latitudes, and under western North America.

I thank W. I. Gough for many discussions during the development of the ideas in this paper. This research has been supported by the Natural Sciences and Engineering Research Council of Canada.

Received 25 May; accepted 18 July 1984.

1. McKenzie, D. P. & Morgan, W. J. *Nature* **224**, 125–133 (1969).
2. Atwater, T. *Bull. geol. Soc. Am.* **81**, 3513–3536 (1970).
3. Roy, R. F., Blackwell, D. D. & Decker, E. R. in *The Nature of the Solid Earth* (ed. Robertson, E. C.) 506–543 (McGraw-Hill, New York, 1972).
4. Sass, J. H., Lachenbruch, A. H., Munroe, R. J., Greene, G. W. & Moses, T. H. *J. geophys. Res.* **76**, 6376–6413 (1971).
5. Gilluly, J. *Am. J. Sci.* **265**, 306–331 (1967).
6. Lipman, P. W., Prostka, H. J. & Christiansen, R. L. *Phil. Trans. R. Soc.* **A271**, 217–248 (1972).
7. Ringwood, A. E. in *The Earth's Crust and Upper Mantle* (ed. Hart, P. J.) 1–17 (American Geophysical Union Monogr. 13, 1969).
8. Christiansen, R. L. & Lipman, P. W. *Phil. Trans. R. Soc.* **A271**, 249–284 (1972).
9. Jacobs, J. A., Russell, R. D. & Tuzo Wilson, J. *Physics and Geology* 2nd edn, 438 ff. (McGraw-Hill, New York, 1974).
10. Hamilton, W. & Myers, W. B. *Rev. Geophys.* **4**, 509–550 (1966).
11. Cleary, J. R. & Hales, A. L. *Bull. seism. Soc. Am.* **56**, 467–489 (1966).
12. Doyle, H. A. & Hales, A. L. *Bull. seism. Soc. Am.* **57**, 761–771 (1967).
13. Herrin, E. & Taggart, J. *Bull. seism. Soc. Am.* **58**, 1325–1337 (1968).
14. Hales, A. L. & Doyle, H. A. *Geophys. J.R. astr. Soc.* **13**, 403–416 (1967).
15. Johnson, L. R. *J. geophys. Res.* **72**, 6309–6325 (1967).
16. Archambeau, C. B., Flinn, E. A. & Lambert, D. G. *J. geophys. Res.* **74**, 5825–5865 (1969).
17. Helmberger, D. & Wiggins, R. A. *J. geophys. Res.* **76**, 3229–3245 (1971).
18. Burdick, L. J. *J. geophys. Res.* **86**, 5926–5936 (1981).
19. Der, Z. A., McElfresh, T. W. & O'Donnell, A. *Geophys. J.R. astr. Soc.* **69**, 67–99 (1982).
20. Gough, D. I. & Ingham, M. R. *Rev. Geophys. Space Phys.* **21**, 805–827 (1983).
21. Reitzel, J. S., Gough, D. I., Porath, H. & Anderson, C. W. III *Geophys. J.R. astr. Soc.* **19**, 213–235 (1970).
22. Porath, H., Oldenburg, D. W. & Gough, D. I. *Geophys. J.R. astr. Soc.* **19**, 237–260 (1970).
23. Camfield, P. A., Gough, D. I. & Porath, H. *Geophys. J.R. astr. Soc.* **22**, 201–221 (1971).
24. Porath, H., Gough, D. I. & Camfield, P. A. *Geophys. J.R. astr. Soc.* **23**, 387–398 (1971).
25. Schmucker, U. *J. Geomagn. Geoelectr.* **15**, 193–221 (1964).
26. Porath, H. *J. geophys. Res.* **76**, 2643–2648 (1971).
27. Hermance, J. H. & Pedersen, J. *J. geophys. Res.* **85**, 3899–3912 (1980).
28. Wannamaker, P. E. *Trans. Am. geophys. Un. Abstr.* **61**, 941, (1980).
29. Gough, D. I. *J. Geomagn. Geoelectr.* **26**, 105–123 (1974).
30. Chan. T., Nyland, E. & Gough, D. I. *Nature phys. Sci.* **244**, 89–91 (1973).
31. Shankland, T. J. *Phys. Earth planet. Inter.* **10**, 209–219 (1975).
32. Shankland, T. J. & Waff, H. S. *J. geophys. Res.* **82**, 5409–5417 (1977).
33. Shankland, T. J., O'Connell, R. J. & Waff, H. S. *Rev. Geophys. Space Phys.* **19**, 394–406 (1981).
34. Anderson, E. M. *The Dynamics of Faulting* 2nd edn (Oliver and Boyd, Edinburgh, 1951).
35. Nakamura, K., Jacob, K. H. & Davies, J. N. *Pageophysics* **115**, 87–112 (1977).
36. Zoback, M. D. & Haimson, B. C. *U.S. geol. Surv. Open-file Rep.* 83–1075 (1982).
37. Zoback, M. L. & Zoback, M. D. *J. geophys. Res.* **85**, 6113–6156 (1980).
38. Sbar, M. L. & Sykes, L. R. *J. geophys. Res.* **82**, 5771–5786 (1977).
39. Lo, K. Y. *Can. Geotech. J.* **15**, 371–381 (1978).
40. Herget, G. *Rock Mech.* **6**, 53–64 (1974).
41. Fordjor, C. K., Bell, J. S. & Gough, D. I. *Can. J. Earth Sci.* **20**, 1445–1455 (1983).
42. Gough, D. I., Fordjor, C. K. & Bell, J. S. *Nature* **305**, 619–621 (1983).
43. Cox, J. W. *Proc. 11th A. Logging Symp. Soc. Professional Well Log Analysts* (1970).
44. Babcock, E. A. *Bull. Am. Ass. petrol. Geol.* **62**, 1111–1126 (1978).
45. Bell, J. S. & Gough, D. I. *Earth planet. Sci. Lett.* **45**, 475–482 (1979).
46. Hottman, C. E., Smith, J. H. & Purcell, W. R. *J. Petrol. Technol.* **31**, 1477–1484 (1979).
47. Gough, D. I. & Bell, J. S. *Can. J. Earth Sci.* **19**, 1358–1370 (1982).
48. Gough, D. I. & Bell, J. S. *Can. J. Earth Sci.* **18**, 638–645 (1981).

49. Cox, J. W. *Proc. 24th A. Logging Symp. Soc. Professional Well Log Analysts*, Paper J (1983).
50. Anderson, D. L. *EOS* **65**, 147–148 (1984).
51. Hales, A. L. *Earth planet. Sci. Lett.* **6**, 31–34 (1969).
52. Elsasser, W. M. in *The Application of Modern Physics to the Earth and Planetary Interiors*, (ed. Runcorn, S. K.) 223–246 (Wiley, New York, 1969).
53. Kanasewich, E. R., Havskov, J. & Evans, M. E. *Can. J. Earth Sci.* **15**, 919–955 (1978).
54. Gough, D. I. *Earth planet. Sci. Lett.* **34**, 360–364 (1977).
55. Crough, S. T. & Jurdy, D. M. *Earth planet. Sci. Lett.* **48**, 15–22 (1980).
56. Le Pichon, X. & Huchon, P. *Earth planet. Sci. Lett.* **67**, 123–135 (1984)
57. Kenyon, P. M. & Turcotte, D. L. *J. geophys. Res.* **88**, 6403–6414 (1983).
58. Anderson, D. L. *Science* **223**, 347–355 (1984).
59. Jeanloz, R. & Thompson, A. B. *Rev. Geophys. Space Phys.* **21**, 51–74 (1983)
60. Jacobsen, S. B. & Wasserburg, G. J. *J. geophys. Res.* **84**, 7411–7427 (1979)
61. De Paolo, D. J. *Geochim. cosmochim. Acta* **44**, 1185–1196 (1980)
62. O'Nions, R. K. & Oxburgh, E. R. *Nature* **306**, 429–431 (1983)
63. Houseman, G. *Geophys. J.R. astr. Soc.* **75**, 309–334 (1983).

Stimulation of 3T3 cells induces transcription of the c-*fos* proto-oncogene

Michael E. Greenberg & Edward B. Ziff

Kaplan Cancer Center and Department of Biochemistry, New York University Medical Center, 550 First Avenue, New York, New York 10016, USA

*Transcription of the c-*fos *proto-oncogene is greatly increased within minutes of administering purified growth factors to quiescent 3T3 cells. This stimulation is the most rapid transcriptional response to peptide growth factors yet described, and implies a role for c-*fos *in cell-cycle control. Transformation by c-*fos *may result from a temporal deregulation of this control.*

ABERRANT expression of a variety of normal cellular genes (proto-oncogenes) can transform a normal cell into a tumour cell[1–3]. Several of these genes encode protein products which are homologous to either a growth factor or a growth factor receptor. For example, the *sis* oncogene of the simian sarcoma virus displays striking homology with platelet-derived growth factor (PDGF)[4,5], a small polypeptide that stimulates the growth of connective tissue cells[2]. A portion of the sequence of the epidermal growth factor receptor is virtually identical to another oncogene (*erb-B*) carried by avian erythroblastosis virus[6]. Moreover, several growth factor receptors, including those for PDGF[7–9], epidermal growth factor (EGF)[10,11] and insulin[12,13], as well as 10 different oncogene protein products[3], share functional homology in that they are all associated with tyrosine kinase activity.

Much of the information about growth factors and their receptors has been obtained by stimulating BALB/c-3T3 fibroblast cells whose growth has been arrested by serum starvation to undergo a synchronous progression through the cell cycle by the addition of serum[14]. In the absence of serum, 3T3 cells enter a state (G_0) in which cell division and growth stop and many metabolic processes are reduced[1]. The addition of serum initiates a complex series of events (G_1 phase), which culminates 14–20 h later in DNA synthesis (S phase) and cell division[14]. PDGF is the serum component that renders 3T3 cells competent to undergo DNA synthesis[15–18], although additional components such as EGF and the somatomedins (progression factors) seem to be necessary to maintain cell viability[19–23]. PDGF interacts with the external surface of cells by binding to a specific receptor protein in the plasma membrane[24] which activates a receptor–associated tyrosine kinase activity[7–9,25]. Almost nothing is known, however, about the mechanisms by which these membrane changes lead to nuclear events such as the activation of specific cell-cycle genes and ultimately DNA replication.

The availability of cloned DNA probes for a variety of cellular genes has made it possible to examine the transcriptional events resulting from growth factor stimulation. Several virally encoded transforming proteins have normal cellular homologues that function in cell-cycle regulation[4–6], suggesting that in general, proto-oncogenes might be involved in cell-cycle control. Such a possibility is supported by recent experiments[26,27] demonstrating a cell-cycle dependence of the expression of the proto-oncogene c-*myc* mRNA. This gene encodes a nuclear protein[28] whose abnormal expression has been implicated in a wide variety of naturally occurring tumours[29–37].

The c-*onc* genes, particularly those encoding nuclear antigens, might be differentially regulated at the transcriptional level during cell-cycle progression. We therefore examined the extent of transcription of 17 different c-*onc* genes as a function of their position in the cell cycle, using a nuclear run-off transcription assay[38,39]. We report here that stimulation of BALB/c-3T3 cells with defined growth factors induces a rapid transient increase in the transcription of the proto-oncogene c-*fos*, the normal cellular homologue of the transforming gene of FBJ-osteosarcoma virus[40–42]. c-*fos* is a nuclear protein[43] of unknown function which is expressed at high levels in extra-embryonal tissues[44,45].

Analysis of c-*onc* transcription

We measured the effect of a mitogenic signal on the transcription of a range of different c-*onc* genes using isolated nuclei from BALB/c-3T3 cells (Fig. 1). The nuclear run-off transcription assay was used to measure the level of transcription of specific genes in a variety of cell types[39,40,46–50]. In this assay, new RNA transcripts are not initiated, but transcripts which are already initiated are faithfully elongated, giving a reasonably accurate measure of the level of transcription at the time of cell lysis[38,39,51].

Nuclei isolated from BALB/c-3T3 cells between 0 and 24 h after serum stimulation show a striking increase in the transcription of two genes, c-*fos* and actin, within 15 min of the initial stimulation of quiescent BALB/c-3T3 cells (Figs 1*a*, 2). c-*fos* transcription transiently increases more than 15-fold very soon after stimulation, returning to its initial levels within 30 min. No further changes in c-*fos* transcription are observed as the 3T3 cells continue to progress through the cell cycle from G_1 to S phase. The alteration in actin transcription appears more complex. The initial increase and subsequent decrease in actin transcription parallels that of c-*fos*. After about 60 min, however, actin transcription begins to increase again (Fig. 1*a*). This increase may correspond to the actin mRNA increase seen within 4 h of serum addition to growth-arrested 3T3 cells[27,52]. These initial experiments use an actin cDNA plasmid that does not distinguish which of the several different cross-hybridizing actin genes[53,54] display the cell-cycle dependent regulation of expression.

We also observe a small but reproducible increase in c-*myc* transcription after serum stimulation (Figs 1*a*, 2), which peaks approximately 2 h after stimulation and decreases significantly within 4 h. This experiment suggests that the previously reported growth-factor induced changes in c-*myc* mRNA[26,27] are at least in part controlled at the level of transcription. In addition, the transcription of c-*myb* (encoding another nuclear antigen[55]) appears to increase in parallel with c-*myc* (Fig. 1*a*). This result is inconclusive, however, because the c-*myb* plasmid DNA that was used, pVM2, also contains flanking cellular and viral sequences.

The increases in the transcription of c-*fos* and actin precede

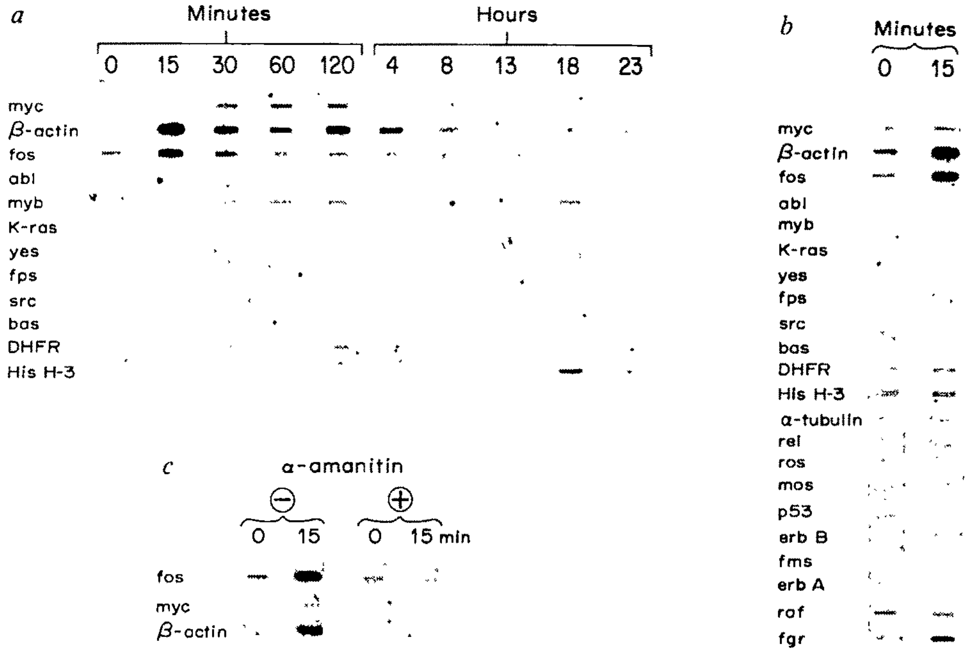

Fig. 1 Transcriptional analysis of c-*onc* genes after stimulation of BALB/c-3T3 cells. c-*onc* gene plasmids bound to nitrocellulose were hybridized with ^{32}P-labelled run-off transcripts from nuclei isolated at different times after serum addition to confluent, growth-arrested BALB/c-3T3 cells. ***a***, 23-h time course experiment analysing the transcription of 12 different genes. Increased transcription of c-*fos* and β-actin occurs within 15 min of serum addition, increased c-*myc* transcription occurs after 2 h and increased histone H3 transcription after 18 h. The changes in transcription are not due to hybridization of labelled RNA transcripts to non-specific DNA such as pBR322 sequences. No significant hybridization of ^{32}P-labelled RNA was detected for *onc* plasmid DNAs such as v-*abl* which contains a complete sequence of pBR322. Furthermore, when c-*fos* and actin sequences were cleaved from the pBR322 vector with restriction enzymes, Southern blotted and probed with ^{32}P-labelled RNA transcripts, significant hybridization to c-*fos*- or actin-specific fragments was detected but no hybridization to pBR322 sequences occurred (data not shown). The possibility that the actin and c-*fos* transcription signal is the result of cross-hybridization between these two genes was ruled out by a competition experiment in which preincubation of ^{32}P-labelled run-off transcripts with the actin plasmid, did not deplete the level of RNA transcripts hybridizing to pv-fos-1 (data not shown). ***b***, Analysis of the transcription of 22 different genes in growth-arrested 3T3 cells (0) and cells stimulated with calf serum for 15 min (15). ***c***, Transcription of c-*fos*, c-*myc* and β-actin was measured in isolated nuclei in the presence (+) or absence (−) of 1 μg ml^{-1} α-amanitin. Nuclei were isolated from growth-arrested 3T3 cells (0) or 3T3 cells stimulated with calf serum for 15 min (15).

Methods: Cell culture: BALB/c-3T3 A31 cells obtained from the American Type Culture Collection were passaged to a density of 9×10^5 cells per 175-cm^2 tissue culture flask in 25 ml Dulbecco's modified Eagle's medium (DMEM) supplemented with 10% calf serum (Gibco), and allowed to grow to confluence over a period of 7–8 days at 37 °C, 10% CO$_2$. After 7 days in culture, the confluent monolayers had depleted the medium of serum growth factors and the 3T3 cells had growth arrested and entered a G$_0$ state as described previously[14]. The cells were then stimulated to progress synchronously through the cell cycle by removing the depleted medium and replacing it with fresh DMEM containing 15% calf serum. Early passage BALB/c-3T3 cells were used for all experiments. Nuclear run-off transcription assay: Medium was removed from one 175 cm^2 tissue culture flask of BALB/c-3T3 cells, the cells were washed three times with ice-cold phosphate-buffered saline (PBS), scraped in PBS and pelleted at 500*g* for 5 min. The cell pellet (1×10^7 cells) was resuspended in 1 ml NP40 lysis buffer (10 mM Tris-HCl *p*H 7.4, 10 mM NaCl, 3 mM MgCl$_2$, 0.5% (v/v) NP40), incubated for 5 min on ice and centrifuged at 500*g* for 5 min. The supernatant was removed and used for the isolation of polyadenylated RNA. The nuclear pellet was washed once with 2 ml NP40 lysis buffer and centrifuged at 500*g*. The supernatant was discarded, the nuclei were resuspended in 100 μl 50 mM Tris-HCl *p*H 8.3, 40% (v/v) glycerol, 5 mM MgCl$_2$, 0.1 mM EDTA and frozen in liquid N$_2$. The nuclei were thawed for the run-off transcription assay and mixed with 100 μl reaction buffer (10 mM Tris-HCl *p*H 8.0, 5 mM MgCl$_2$, 300 mM KCl, 0.5 mM each of ATP, CTP, and GTP and 100 μCi of [α-^{32}P] UTP (760 Ci mmol^{-1}, NEN) and reacted at 30 °C for 30 min. The ^{32}P-labelled RNA was isolated as described elsewhere[39] with different conditions for hybridization to filters. Before ethanol precipitation, ^{32}P-labelled RNA was treated with a final concentration of 0.2 M NaOH for 10 min on ice. The solution was neutralized by the addition of HEPES (acid free) to a final concentration of 0.24 M and the RNA was precipitated with ethanol. After centrifugation, the ^{32}P-labelled RNA pellet was resuspended in 10 mM *N*-tris(hydroxymethyl)methyl 2-aminoethanesulphonic acid (TES), *p*H 7.4, 0.2% SDS, 10 mM EDTA at 5×10^6 c.p.m. ml^{-1}. This RNA solution was mixed with an equal volume of 10 mM TES *p*H 7.4, 0.2% SDS, 10 mM EDTA, 600 mM NaCl and 2 ml of the RNA solution was hybridized at 65 °C for 36 h to DNA immobilized on nitrocellulose. In a given experiment, each filter was hybridized with the same number of c.p.m. ^{32}P-labelled RNA. After the hybridization the filters were washed with several changes, 2×SSC (1×SSC = 0.15 M NaCl, 0.0125 M Na citrate *p*H 7) for 2 h at 65 °C and incubated at 37 °C in 2×SSC with 10 μg ml^{-1} RNase A for 30 min. The filters were then washed again in 2×SSC at 37 °C for 1 h, air dried and exposed to Kodak SB-5 X-ray film. For binding to nitrocellulose, plasmids were linearized by restriction enzyme digestion and the DNA was denatured by incubation with 0.2 M NaOH for 30 min at room temperature, followed by neutralization with 10 volumes of 6×SSC. The DNA was spotted onto nitrocellulose using the Schleicher and Schuell slot blot apparatus. 10 μg DNA was applied per slot. The plasmids used were provided by Dr Inder Verma (pvfos-1, v-*fos*[61]), Dr Larry Kedes (human β-actin-1, β-actin[54]), Dr Kenneth Marcu (pM-c-*myc*-54, c-*myc*[62]), Dr David Baltimore (pAB3sub3, v-*abl*[72]), Dr J. Michael Bishop (pVM 2, v-*myb*[72]; perb-A, v-erb-A[74], perb-B probe F, v-erb-B[74], pSRA, v-*src*[75]), Dr Edward Scolnick (Merck, Sharpe and Dohme) (pHiHi-3, v-Ki-*ras*[76]), Dr Hidesaburo Hanafusa (pFSV, v-*fps*[77]), Dr George Vande Woude (pMS1, c-*mos*[78]), Dr Howard Temin (peco-rel, v-*rel*[79]), Dr Keith Robbins (pv-fgr1000, v-*fgr*[80]), Dr Lui-Hai Wang (pv-ros, v-*ros*[81]), Dr U. Rapp (pv-rafE-H, v-*raf*[82]), Dr Charles Scherr (pSM3, v-*fms*[83]), Dr Steven Tronick (pHB1, v-*bas*[84]), Dr M. Yoshida (pY73, v-*yes*[85]), Dr Nicholas Cowan (pmcα-1, α-tubulin, unpublished), Dr Arnold Levine (pp53-208, p53[86]), Dr Robert Schimke (pDHFR11, dihydrofolate reductase[87]) and Dr Nathaniel Heintz (pHh5B, hisH-3[88]).

that of c-*myc* (Fig. 1) and occur during the time interval in which the 3T3 cells are becoming growth-factor independent[19,22,23]. All these changes occur as the 3T3 cells progress from G$_0$ to G$_1$ and before the initiation of cellular DNA synthesis at ~14 h after serum stimulation, measured by the incorporation of ^{3}H-thymidine into trichloroacetic acid (TCA) precipitable counts (Fig. 2). In similar conditions many other c-*onc* genes including c-Ki-*ras* whose viral counterpart encodes a GTP binding protein[56,57] and c-*abl* which encodes a tyrosine kinase[58], displayed barely detectable levels of transcription at all times after serum stimulation (Fig. 1*a*). Other sequences such as those for α-tubulin were transcribed at a low but constant level throughout the cell cycle and the transcription of the histone H3 gene was observed to increase at the time of DNA synthesis as reported previously (Fig. 1*a*)[47–49].

When 22 different genes were tested (Fig. 1*b*) only 3, c-*fos*, actin and an additional gene, c-*fgr* (ref. 59), exhibited a change in transcription 15 min after serum stimulation. c-*fgr* is the

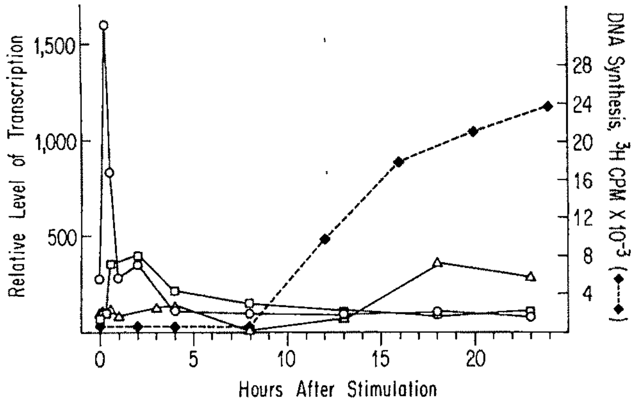

Fig. 2 Quantitation of transcriptional activation after stimulation of BALB/c-3T3 cells. The relative amounts of ^{32}P-labelled nuclear run-off transcripts hybridized to c-*fos* (○), c-*myc* (□) and histone H3 (△) plasmids bound to nitrocellulose, were determined by quantitative densitometric scanning of autoradiographs from Fig. 1*a*[89] (arbitrary units). DNA synthesis was measured after stimulating growth-arrested BALB/c-3T3 cells to divide by the addition of 15% calf serum as described in Fig. 1 legend. The incorporation of [*Me*-^{3}H]thymidine into DNA (■) was measured by pulse labelling cells with 90 μCi [*Me*-^{3}H]thymidine (2.0 Ci mmol^{-1}) for 2 h at the indicated times after serum stimulation. The medium was removed, cells washed three times with ice-cold PBS, and lysed with 0.2 M NaOH. An aliquot of the cell lysate was precipitated with TCA, collected on Whatman GF/A glass fibre filters and counted in toluene/omnifluor scintillation fluid. In all the experiments reported in Figs 1–6, serum stimulation of quiescent BALB/c-3T3 cells resulted in a 20–80-fold increase in the incorporation of ^{3}H-thymidine into TCA precipitable counts.

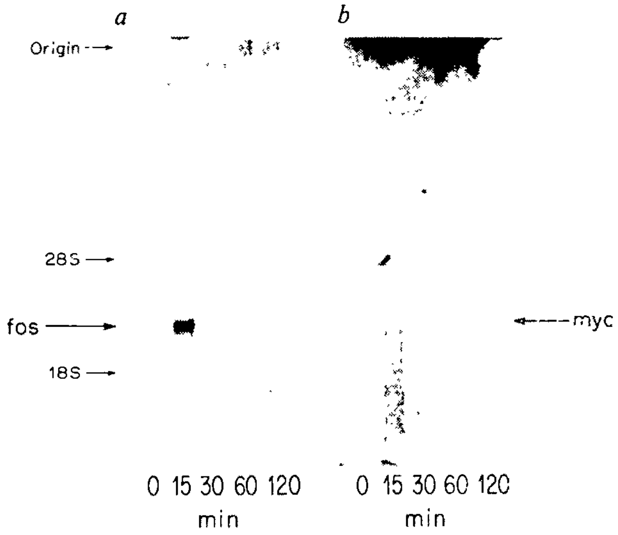

Fig. 3 Kinetics of c-*fos* and c-*myc* mRNA induction after serum stimulation of BALB/c-3T3 cells. Polyadenylated cytoplasmic RNA from 3T3 cells, isolated at various times after serum stimulation, was fractionated on a formaldehyde–agarose gel, transferred to nitrocellulose, hybridized with ^{32}P-labelled pv-fos-1 (*a*) or pM-c-myc-54 (*b*) plasmids, and after washing exposed to SB-5 X-ray film. **Methods:** Polyadenylated RNA was isolated from the post-nuclear supernatant (see Fig. 1 methods). The supernatant (4 ml, from 4×10^7 cells) was mixed with 0.2 ml 0.2 M vanadyl ribonucleoside complex (BRL) and centrifuged at 10,000*g* for 10 min at 4 °C. The supernatant was then mixed with 4 ml 0.2 M Tris-HCl *p*H 7.5, 0.44 M NaCl, 2% SDS, 25 mM EDTA containing 0.8 mg proteinase K (Worthington) and incubated at 37 °C for 30 min. After phenol and chloroform extractions, RNA was precipitated with ethanol. Pelleted RNA was resuspended in 10 mM Tris-HCl *p*H 7.4, 10 mM EDTA, 0.2% SDS, denatured by heating to 65 °C for 5 min and RNA (~50 μg) applied to a 0.5-ml poly(U) Sepharose column as described previously[90]. The polyadenylated RNA was fractionated on a 1% formaldehyde agarose gel and transferred to nitrocellulose following the procedure of Cheng-Kiang *et al.*[91]. The RNA bound to nitrocellulose was prehybridized overnight with buffer containing 1% glycine, 50% formamide, 5×SSC, 50 mM NaH_2PO_4 *p*H 6.5, 250 μg ml^{-1} sonicated salmon sperm DNA, 1 × Denhardt's solution (1% Ficoll, 1% polyvinylpyrrolidone, 1% bovine serum albumin). The hybridization was carried out for 12–16 h in 10 ml 50% formamide, 2×SSC, 40 mM NaH_2PO_4 *p*H 6.5, 200 μg ml^{-1} salmon sperm DNA, 0.8×Denhardt's, 10% dextran sulphate, 10 mM EDTA, 0.1% SDS, with 1×10^8 c.p.m. ^{32}P-nick-translated plasmid (4×10^8 c.p.m. per μg DNA)[92].

normal cellular homologue of v-*fgr*, the transforming gene of Gardner–Rasheed feline sarcoma virus. The v-*fgr* DNA we used as a probe is a hybrid gene containing a portion of actin as well as a tyrosine kinase sequence[60]. Therefore, the increased hybridization in the v-*fgr* slot (Fig. 1*b*) probably reflects increased actin transcription. c-*fgr* tyrosine kinase gene transcripts may, however, also change.

Several control experiments were performed to establish the fidelity of the run-off transcription assay. The increased transcription of c-*fos* and actin within 15 min of serum addition is not simply due to an increase in overall transcription efficiency, because the transcription of a variety of other genes is unaffected by serum stimulation (Fig. 1*b*). Also, no reproducible differences in the total number of counts incorporated into RNA in isolated nuclei are observed during progression of 3T3 cells through the cell cycle (data not shown). Genes such as histones and actin display a cell-cycle dependent change in transcription consistent with previous results[27,47–49,52], further indicating that the isolated nuclei retain their transcriptional fidelity. The increased c-*fos*, c-*myc* and actin transcription seems to be the result of increased RNA polymerase II utilization, as α-amanitin completely blocked the transcription of these genes (Fig. 1*c*).

The plasmids used to measure c-*fos* and c-*myc* were oncogene specific. The pv-fos-1 probe contains sequences entirely from the v-*fos* coding region and sequence homology to the corresponding c-*fos* sequences is >99%[42]. pv-fos-1 recognizes a unique *Eco*RI restriction fragment in mouse DNA[61], making it unlikely that our transcription assay has detected repetitive sequences due to cross-hybridization. Furthermore, the pv-fos-1 plasmid hybridizes to a discrete 2.2 kilobase (kb) mRNA which is the size of c-*fos* mRNA[44]. Moreover, c-*fos* lacks homology with any known cellular sequence[42], making it unlikely that the observed increase in the transcription of both c-*fos* and actin reflects a homology between these two genes as appears to be the case for actin and v-*fgr*.

It was more difficult to establish the specificity of the c-*myc* transcriptional signal. The pM-c-myc-54 plasmid used to measure c-*myc* transcriptional levels is a mouse cDNA, composed of the three c-*myc* exons inserted into the *Pst*I site of pBR322[62]. This plasmid recognizes a c-*myc*-specific fragment and two c-*myc*-homologous sequences[62]. Although it is possible that the increased transcription observed using the c-*myc* probe is a result of increased transcription from one of these homologous c-*myc*-like sequences, this appears unlikely as the pM-c-myc-54 plasmid detects a discrete c-*myc* mRNA of 2.4 kb which displays the expected cell-cycle dependent change in expression.

Stimulation of c-*fos*

To determine whether the increased transcription of specific genes after serum addition is followed by an increase in cytoplasmic mRNA, we isolated cytoplasmic RNA from quiescent and stimulated cells and analysed polyadenylated species (Fig. 3*a*). A prominent band of 2.2 kb appears 15 min after stimulation with a molecular weight equivalent to c-*fos* mRNA[44]. The 2.2 kb mRNA level is highest 15 min after serum addition and decreases below detection within 60 min; the half life is thus very short.

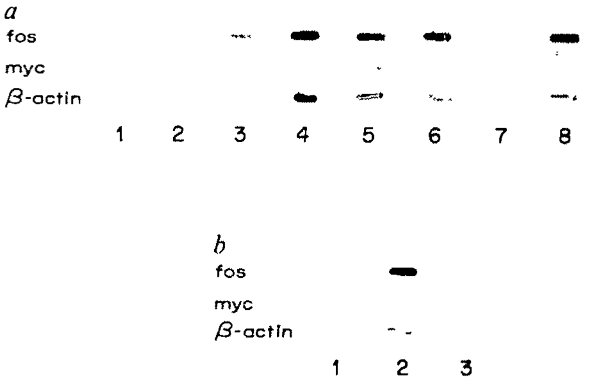

Fig. 4 Transcriptional activation after stimulation of BALB/c-3T3 cells with defined growth factors. 3T3 cells were grown to confluence and growth arrested as described in Fig. 1 legend. ***a***, The medium was removed and cells were incubated for 15 min with: lane 1, the same depleted medium; lane 2, DMEM without calf serum; lane 3, DMEM containing 0.5% calf serum; lane 4, DMEM containing 15% calf serum; lane 5, DMEM containing 2.5 U ml^{-1} partially purified porcine PDGF (Speywood); lane 6, DMEM containing 0.1 $\mu g\,ml^{-1}$ fibroblast growth factor (Collaborative Research); lane 7, DMEM containing 10 $\mu g\,ml^{-1}$ insulin (Sigma); lane 8, DMEM containing 0.26 $\mu g\,ml^{-1}$ TPA (Sigma). ***b***, The medium was removed and cells were incubated for 15 min with: lane 1, the same depleted medium; lane 2, DMEM containing 1.0 unit ml^{-1} homogeneous porcine PDGF; lane 3, DMEM containing 0.1 $\mu g\,ml^{-1}$ EGF (Collaborative Research). After stimulation with growth factor, cells were collected, nuclei isolated and run-off transcription assays performed. The ^{32}P-labelled RNA transcripts were hybridized with pv-fos-1, pM-c-myc-54 and pHβ-actin plasmids immobilized on nitrocellulose as described in Fig. 1 legend. The radioactivity was visualized by autoradiography. 1 U of PDGF is the amount of growth factor needed per ml of DMEM to yield 50% maximal incorporation of ^3H-thymidine into DNA in confluent growth-arrested Swiss 3T3 cells[93].

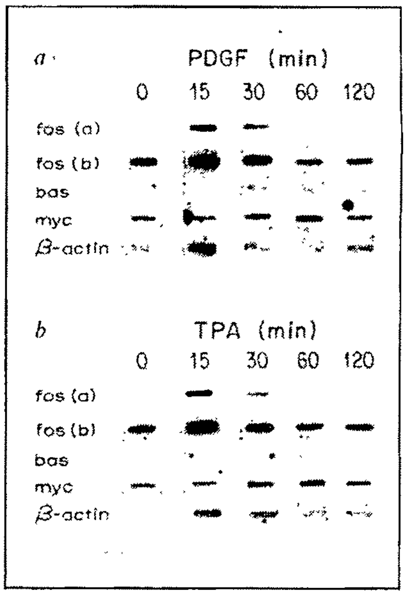

Fig. 5 Kinetics of c-*fos* transcriptional activation after stimulation of BALB/c-3T3 cells with PDGF and TPA. Nuclei were isolated from serum starved cells and 3T3 cells stimulated for 15, 30, 60 and 120 min with homogeneous porcine PDGF. *a*, 1 U ml^{-1} DMEM; *b*, TPA 0.26 $\mu g\,ml^{-1}$ DMEM. ^{32}P-labelled RNA transcripts were prepared as described in Fig. 1 legend and were hybridized with pv-fos-1, pbas, pM-c-myc-54 and pHβ-actin DNA immobilized on nitrocellulose. The radioactivity was visualized by autoradiography. c-*fos*(a) filters were exposed for 18 h; c-*fos*(b), c-*bas*, c-*myc* and β-actin filters exposed for 5 days.

The kinetics of c-*fos* mRNA induction are quite different from c-*myc*. Consistent with previous results[26,27], virtually no c-*myc* mRNA is detectable in the cytoplasm until 2 h after serum addition, at which point a substantial increase in the 2.4 kb c-*myc* mRNA (Fig. 3*b*) is observed.

We next tested the ability of specific purified growth factors to induce the transcription of the c-*fos* gene. When growth-arrested 3T3 cells are incubated in serum-free medium, no change in the level of c-*fos* transcription is observed (Fig. 4*a*, lane 2). If the serum-free medium is supplemented with various factors at concentrations that effectively generate the competence phase of the mitogenic response (Fig. 4)[19-22,63], a reproducible increase in c-*fos* transcription is observed within 15 min. Hormones that do not significantly stimulate competence in BALB/c-3T3 cells, but do maintain cell viability[21], cause no significant change in c-*fos* transcription (Fig. 4). In contrast with c-*fos*, the level of transcription of most other genes is not detectable after 15 min of treatment, although c-*myc* transcription is induced by PDGF and 12-*O*-tetradecanoylphorbol-13-acetate (TPA) within 1 h of growth factor addition (Fig. 5). Actin transcription is also stimulated with these purified factors in parallel with c-*fos* although the level of stimulation appears to be less than that observed using whole serum (Fig. 4). The kinetics of c-*fos* stimulation are identical when cells are treated with PDGF (Fig. 5*a*), TPA (Fig. 5*b*) or serum (Fig. 1*a*). The increased levels of c-*fos* nuclear transcripts are apparent as early as 5 min after serum addition; the c-*fos* transcription level peaks after 10 min, and begins to decrease by 15 min (Fig. 6).

Conclusions

The stimulation of c-*fos* transcription within 5 min of treatment of quiescent 3T3 cells with PDGF is the earliest transcriptional event known to occur in these cells in response to a growth factor; in other cells, factors such as glucocorticoid hormones have been shown previously to stimulate the transcription of murine mammary tumour virus genes with equally rapid kinetics[64].

The increased transcription of c-*fos* and c-*myc* genes is quickly followed by a substantial increase in the respective mRNAs. The transcriptional changes in c-*fos* and c-*myc* do not appear as large as the concomitant alterations in mRNA, perhaps because of differences in the sensitivity of the two assays, or because of changes in c-*fos* and c-*myc* mRNA stability. We have not established whether the cell-cycle dependent changes in expression result in comparable changes in the levels of the respective protein products. In the case of c-*fos*, this question is particularly significant because expression of the c-*fos* protein may be regulated by sequences at the 3′ end of the mRNA which, in some conditions, appear to inhibit translation of the RNA into protein[65].

The rapid activation and subsequent repression of c-*fos* transcription coupled with the short half life of the c-*fos* mRNA could explain why the mRNA is expressed during a very brief interval, ~30 min, of the G_0/G_1 transition and also why c-*fos* mRNA has been barely detectable in many nonsynchronized cell types[44]. If all cycling cells were to exhibit a transient increase in c-*fos* each time they pass through G_1, for a total of 15 min (~1/100th of the cell cycle), then in an asynchronous population of cells the levels of c-*fos* would be as much as 100-fold lower than the levels detected 15 min after synchronously stimulating cells to divide.

Our finding that the transcription of a proto-oncogene is rapidly stimulated in response to a growth signal raises questions about the role of this gene in the normal cell cycle, oncogenesis and transcriptional induction; for example, how a growth factor such as PDGF acts externally on the plasma membrane to induce gene transcription within 5 min. PDGF binding to its receptor activates a tyrosine kinase, which suggests that a protein modification such as phosphorylation could be involved in the transmission of the growth signal to the nucleus. This idea is

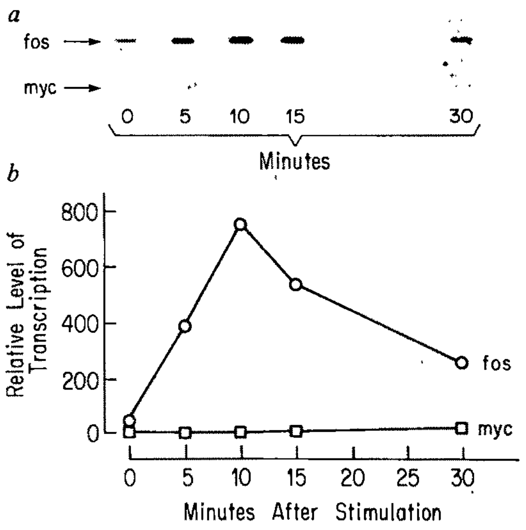

Fig. 6 Kinetics of c-*fos* transcriptional activation after serum stimulation of BALB/c-3T3 cells. Nuclei were isolated from serum starved 3T3 cells and from 3T3 cells stimulated with 15% calf serum for 5, 10, 15 and 30 min. ^{32}P-labelled RNA run-off transcripts were prepared as described in Fig. 1 legend and were hybridized with pv-fos-1, pM-c-myc-54 and pHβ-actin DNA immobilized on nitrocellulose. *a*, Radioactivity visualized by autoradiography; *b*, relative signal intensities calculated by densitometric scanning of the autoradiographs.

supported by the observation that TPA, which activates both protein kinase C[66,67] and tyrosine kinase[68–70], also activates c-*fos* and c-*myc* transcription.

Although the time course of activation of the c-*fos* and actin genes can be clearly distinguished from c-*myc*, it is not known whether c-*fos* or actin activation is a prerequisite for activating c-*myc* or other genes. PDGF induces c-*myc* mRNA levels even in the presence of protein synthesis inhibitors[26], suggesting that the prior stimulation of c-*fos* may not be required to induce c-*myc* transcription. Our kinetic experiments suggest that different factors may be involved in the regulation of c-*fos* and c-*myc* and that these genes may be members of two distinct classes of inducible genes. By differential screening of a cDNA library prepared from cells stimulated with PDGF for 4 h, a set of induced genes have been identified[71] into which c-*myc* may fall[25]. c-*fos* may be a member of a new class of early response genes, with actin and other unidentified genes; they could have a crucial role in committing a cell to enter G_1. Unlike c-*fos*, some of the genes might not produce a dominant transforming phenotype and therefore might not be detected by current assays for oncogenes.

We speculate that an early response gene such as c-*fos*, whose deregulation can result in cell transformation and uncontrolled proliferation, might be a gene that directly controls normal cell growth, for example by activating the cells' progression from G_0 into G_1. Nevertheless, a direct effect of c-*fos* expression on cell-cycle progression remains to be shown. The activation of c-*fos* may be necessary for commitment to DNA replication and cell division, but it appears not to be sufficient. c-*fos* transcription is activated by competence factors in the absence of progression factors (Fig. 4); these conditions will generate an initial mitogenic signal but are not sufficient to induce cellular DNA synthesis[19–22].

A variety of different mechanisms have been proposed to explain how normal cellular oncogenes might be altered so that they cause transformation, such as the overproduction of a normal gene or the mutation of a c-*onc* gene[3]. One proposal is that expression of high levels of c-*fos* protein in an inappropriate cell type might result in transformation[65]. Our finding that c-*fos* exhibits cell-cycle dependent changes in transcription supports a different possibility, that transformation by c-*fos* results at least in part from a deregulation of its temporal control. The expression of c-*fos* throughout the cell cycle rather than during a specific stage of the G_0/G_1 transition may be one mechanism of transformation. The continuous expression of c-*fos* might prevent a cell from ever entering a quiescent state, thus yielding a population of continually dividing cells.

We thank Drs Paul Stroobant and Michael Waterfield for providing the purified PDGF, Dr Robert Brackenbury for assistance with the densitometric scanning and Drs Nicholas Cowan and Peter D'Eustachio for their critical reading of the manuscript. This work was supported by ACS grant MV-75, and GM 30760 from the US NIH. E.B.Z. is the recipient of ACS Faculty Research Award FRA 207. M.E.G. was the recipient of a postdoctoral fellowship from the Damon Runyon-Walter Winchell Cancer Fund.

Received 18 July; accepted 11 September 1984.

1. Pardee, A. B., Dubrow, R., Hamlin, J. L. & Kletzien, R. F. *A. Rev. Biochem* **47**, 715–750 (1978).
2. Stiles, C. D. *Cell* **33**, 653–655 (1983).
3. Bishop, J. M. & Varmus, H. E. in *RNA Tumour Viruses, Molecular Biology of Tumour Viruses* (eds Weiss, R., Teich, N., Varmus, H. E. & Coffin, J.) 999–1108 (Cold Spring Harbor Laboratory, New York, 1982).
4. Waterfield, M. D. *et al. Nature* **304**, 35–39 (1983).
5. Doolittle, R. F. *et al. Science* **221**, 275–277 (1983).
6. Downward, J. *et al. Nature* **307**, 521–527 (1984).
7. Ek, B., Westermark, B., Wasteson, A. & Heldin, C.-H. *Nature* **295**, 419–420 (1982)
8. Nishimura, J., Huang, J. S. & Deuel, T. F. *Proc. natn. Acad. Sci. U.S.A.* 79, 4303–4307 (1982).
9. Cooper, J. A., Bowen-Pope, D. F., Raines, E., Ross, R. & Hunter, T. *Cell* **31**, 263–273 (1982).
10. Ushiro, H. & Cohen, S. *J. biol. Chem.* **255**, 8363–8365 (1980).
11. Hunter, T. & Cooper, J. A. *Cell* **24**, 741–752 (1981).
12. Kasuga, M., Zick, Y., Blithe, D. L., Crettaz, M. & Kahn, C. R. *Nature* **298**, 667–669 (1982).
13. Petruzzelli, L. M. *et al. Proc. natn. Acad. Sci. U.S.A.* **79**, 6792–6796 (1982).
14. Todaro, G. J., Lazar, G. K. & Green, H. *J. cell. comp. Physiol.* **66**, 325–334 (1965).
15. Antoniades, H. N., Scher, C. D. & Stiles, C. D. *Proc. natn. Acad. Sci. U.S.A.* **76**, 1809–1813 (1979).
16. Deuel, T. F. *et al. J. biol. Chem.* **256**, 8896–8899 (1981).
17. Heldin, C. H., Westermark, B. & Wasteson, A. *Proc. natn. Acad. Sci. U.S A.* **76**, 3722–3726 (1979).
18. Raines, E. W. & Ross, R. *J. biol. Chem.* **257**, 5154–5160 (1982).
19. Pledger, W. J., Stiles, C. D., Antoniades, H. N. & Scher, C. D. *Proc. natn. Acad. Sci. U.S.A.* **74**, 4481–4485 (1977).
20. Stiles, C. D. *et al. Proc. natn. Acad. Sci. U.S.A.* **76**, 1279–1283 (1979).
21. Scher, C. D., Hendrickson, S. L., Whipple, A. P., Gottesman, M. M. & Pledger, W. J. *Cold Spring Harb. Conf. Cell Proliferation* **9**, 289–303 (1982).
22. Vogel, A., Raines, E., Kariya, B., Rivest, M.-J. & Ross, R. *Proc. natn. Acad. Sci. U.S.A.* **75**, 2810–2814 (1978).
23. Singh, J. P., Chaikin, M. A., Pledger, W. J., Scher, C. D. & Stiles, C. D *J. Cell Biol.* **96**, 1497–1502 (1983).
24. Glenn, K., Bowen-Pope, D. F. & Ross, R. *J. biol. Chem.* **257**, 5172–5176 (1982).
25. Frackelton, A. R., Tremble, P. M. & Williams, L. T. *J. biol. Chem.* **259**, 7909–7915 (1984).
26. Kelly, K., Cochran, B. H., Stiles, C. D. & Leder, P. *Cell* **35**, 603–610 (1983).
27. Campisi, J., Gray, H. E., Pardee, A. B., Dean, M. & Sonenshein, G. E. *Cell* **36**, 241–247 (1984).
28. Hann, S. R., Abrams, H. D., Rohrschneider, L. R. & Eisenman, R. N. *Cell* **34**, 789–798 (1983).
29. Hayward, W. S., Neel, B. G. & Astrin, S. M. *Nature* **290**, 475–480 (1981).
30. Collins, S. & Groudine, M. *Nature* **298**, 679–681 (1982).
31. Dalla-Favera, R., Wong-Staal, F. & Gallo, R. C. *Nature* **299**, 61–63 (1982).
32. Alitalo, K. *et al. Proc. natn. Acad. Sci. U.S.A.* **80**, 100–104 (1983).
33. Taub, R. *et al. Proc. natn. Acad. Sci. U.S.A.* **78**, 7837–7841 (1982).
34. Dalla-Favera, R. *et al. Proc. natn. Acad. Sci. U.S.A.* **79**, 7824–7827 (1982).
35. Marcu, K. B. *et al. Proc. natn. Acad. Sci. U.S.A.* **80**, 519–523 (1983).
36. Shen-Ong, G. L. C., Keath, E. J., Piccoli, S. P. & Cole, M. D. *Cell* **31**, 443–452 (1982).
37. Slamon, D. J., de Kernion, J. B., Verma, I. M. & Cline, M. J. *Science* **224**, 256–262 (1984).
38. McKnight, G. S. & Palmiter, R. *J. biol. Chem.* **254**, 9050–9058 (1979).
39. Groudine, M., Peretz, M. & Weintraub, H. *Molec. cell. Biol.* **1**, 281–288 (1981).
40. Finkel, M. P., Biskis, B. O. & Jinkins, P. B. *Science* **151**, 698–701 (1966).
41. Curran, T., MacConnell, W. P., van Straaten, F. & Verma, I. M. *Molec. cell. Biol.* **3**, 914–921 (1983).
42. Van Beveren, C., van Straaten, F., Curran, T., Muller, R. & Verma, I. M. *Cell* **32**, 1241–1255 (1983).
43. Curran, T., Miller, D. A., Zokas, L. & Verma, I. M. *Cell* **36**, 259–268 (1984).
44. Muller, R., Slamon, D. J., Tremblay, J. M., Cline, M. J. & Verma, I. M. *Nature* **299**, 640–644 (1982).
45. Muller, R., Verma, I. M. & Adamson, E. D. *EMBO J.* **2**, 679–684 (1983)
46. Clayton, D. F. & Darnell, J. E. *Molec. cell. Biol.* **3**, 1552–1561 (1983).
47. Delisle, A. J., Graves, R. A., Marzluff, W. F. & Johnson, L. F. *Molec. cell. Biol.* **3**, 1920–1929 (1983).
48. Alterman, R.-B. M. *et al. Molec. cell. Biol.* **4**, 123–132 (1984).
49. Stein, G. S. *et al. Cold Spring Harb. Symp. quant. Biol.* **42**, 1107–1119 (1977).
50. Leys, E. J., Crouse, G. F. & Kellems, R. E. *J. Cell Biol.* **99**, 180–187 (1984).
51. Marzluff, W. F. *Meth. Cell Biol.* **19**, 317–331 (1978).
52. Riddle, V. G. H., Dubrow, R. & Pardee, A. B. *Proc. natn. Acad. Sci. U.S.A.* **76**, 1298-1302 (1979).
53. Cleveland, D. W. *et al. Cell* **20**, 95–105 (1980).
54. Gunning, P. *et al. Molec. cell. Biol.* **3**, 787–795 (1983).
55. Klempnauer, K.-H., Symonds, G., Evan, G. I. & Bishop, J. M. *Cell* **37**, 537–547 (1984).
56. Scolnick, E. M., Papageorge, A. G. & Shih, T. Y. *Proc. natn. Acad. Sci. U.S.A.* **76**, 5355–5359 (1979).
57. Willingham, M. C., Pastan, I., Shih, T. Y. & Scolnick, E. M. *Cell* **19**, 1005–1014 (1980).
58. Wang, J. Y. J., Ledley, F., Goff, S., Lee, R., Groner, Y. & Baltimore, B. *Cell* **36**, 349–356 (1984).
59. Naharro, G. *et al. J. Virol.* **47**, 611–619 (1983).

60. Naharro, G., Robbins, K. C. & Reddy, E. P. *Science* **223**, 63–66 (1984).
61. Curran, T., Peters, G., Van Beveren, C., Teich, N. M. & Verma, I. M. *J. Virol.* **44**, 674–682 (1982).
62. Stanton, L. W., Watt, R. & Marcu, K. B. *Nature* **303**, 401–406 (1983).
63. Frantz, C. N., Stiles, C. D. & Scher, C. D. *J. cell. Physiol.* **100**, 413–424 (1979).
64. Ringold, G. M., Yamamoto, K. R., Bishop, J. M. & Varmus, H. E. *Proc. natn. Acad. Sci. U.S.A.* **74**, 2879–2883 (1977).
65. Miller, A. D., Curran, T. & Verma, I. M. *Cell* **36**, 51–60 (1984).
66. Castagna, M. *et al. J. biol. Chem.* **257**, 7847–7851 (1982).
67. Yamanishi, J. *et al. Biochem. biophys. Res. Commun.* **112**, 778–786 (1983).
68. Bishop, R., Martinez, R., Nakamura, K. D. & Weber, M. J. *Biochem. biophys. Res. Commun.* **115**, 536–543 (1983).
69. Gilmore, T. & Martin, G. S. *Nature* **306**, 407–490 (1983).
70. Cooper, J. A., Sefton, B. M. & Hunter, T. *Molec. cell. Biol.* **4**, 30–37 (1984).
71. Cochran, B. H., Reffel, A. C. & Stiles, C. D. *Cell* **33**, 939–947 (1983).
72. Goff, S. P., Gilboa, E., Witte, O. N. & Baltimore, D. *Cell* **22**, 777–785 (1980).
73. Klempnauer, K.-H., Gonda, T. J. & Bishop, J. M. *Cell* **31**, 453–463 (1982).
74. Vennstrom, B. & Bishop, J. M. *Cell* **28**, 135–143 (1982).
75. DeLorbe, W. J., Luciw, P. A., Goodman, H. M., Varmus, H. E. & Bishop, J. M. *J. Virol.* **36**, 50–61 (1980).
76. Ellis, R. W. *et al. Nature* **292**, 506–511 (1981).
77. Shibuya, M. & Hanafusa, H. *Cell* **30**, 787–795 (1982).
78. Oskarsson, M., McClements, W. L., Blair, D. G., Maizel, J. V. & Vande Woude, G. F. *Science* **207**, 1222–1224 (1980).
79. Wilhelmsen, K. C. & Temin, H. M. *J. Virol.* **49**, 521–529 (1984).
80. Naharro, G. *et al. J. Virol.* **47**, 611 (1983).
81. Neckameyer, W. S. & Wang, L.-H. *J. Virol.* **50**, 914–921 (1984).
82. Rapp, U. R. *et al. Proc. natn. Acad. Sci. U.S.A.* **80**, 4218–4222 (1983).
83. Donner, L., Fedele, L. A., Garon, C. F., Anderson, S. J. & Sherr, C. J. *J. Virol.* **41**, 489–500 (1982).
84. Andersen, P. R., Tronick, S. R. & Aaronson, S. A. *J. Virol.* **40**, 431–439 (1981).
85. Kitamura, N., Kitamura, A., Toyoshima, K., Hirayama, Y. & Yoshida, M. *Nature* **297**, 205–208 (1982).
86. Oren, M. & Levine, A. J. *Proc. natn. Acad. Sci. U.S.A.* **80**, 56–59 (1983).
87. Chang, A. C. Y. *et al. Nature* **275**, 617–624 (1978).
88. Zhong, R., Roeder, R. G. & Heintz, N. *Nucleic Acids Res.* **11**, 7409–7425 (1983).
89. Edelman, G. M. and Chuong, C.-M. *Proc. natn. Acad. Sci. U.S.A.* **79**, 7036–7040 (1982).
90. Frazer, N. W. & Ziff, E. *J. molec. Biol.* **124**, 27–51 (1978).
91. Cheng-Kiang, S., Wolgemuth, D. J., Hsu, M.-T. & Darnell, J. E. *Cell* **28**, 575–584 (1982).
92. Rigby, P. W. J., Dieckmann, M., Rhodes, C. & Berg, P. *J. molec. Biol.* **113**, 237–251 (1977).
93. Lopes-Rivas, A., Stroobant, P., Waterfield, M. D. & Rozengurt, E. *EMBO J.* **3**, 939–944 (1984).

Differentiation of F9 teratocarcinoma stem cells after transfer of c-*fos* proto-oncogenes

Rolf Müller & Erwin F. Wagner

European Molecular Biology Laboratory, Postfach 10.2209, 6900 Heidelberg, FRG

Transfer of mouse or human c-fos *proto-oncogenes into F9 teratocarcinoma stem cells results in expression of* c-fos *mRNA and protein. This is accompanied by the appearance of morphologically altered cells which express several specific markers characteristic of differentiated cells, suggesting that* c-fos *plays a role in cellular differentiation.*

RECENT analyses of the structure of retroviral oncogenes and of the expression of their cellular homologues (c-*onc* genes or proto-oncogenes) strongly support the hypothesis that the products encoded by such genes are directly linked with cellular growth control[1–6]. Amino acid sequence homologies suggest that the c-*sis* gene probably encodes the platelet-derived growth factor[1,2] and the c-*erb-B* gene product appears to be identical to the epidermal growth factor receptor[3]. Expression analyses have shown that the c-*myc* gene product may be associated with the initiation of normal cellular proliferation: high levels of c-*myc* transcripts were detected specifically during the early G_1 phase of the cell cycle when either quiescent lymphocytes[4] or fibroblasts[5] were stimulated to proliferate. In agreement with these conclusions, c-*myc* expression was seen to be down-regulated when teratocarcinoma stem cells (F9)[5] or immature haematopoietic cells (HL60)[6] were induced to differentiate into non-proliferative cell types. Terminal differentiation of HL60 cells was also accompanied by a decrease of c-*myb* expression[6].

Another category of c-*onc* genes appears to be represented by c-*fos* whose gene product may be associated with functions in differentiated cells[7–10]. Transcription of c-*fos* at high levels was detected during prenatal development in specific tissues, notably amnion and visceral yolk sac and mid-gestation fetal liver[7–10]. The level of c-*fos* expression in the fetal membranes increased markedly at late stages of gestation[8]. In postnatal tissues, expression of c-*fos* at high levels was observed only in haematopoietic cells[10]. In cells of the monomyelocytic lineage high levels of c-*fos* mRNA were detected specifically at late stages of differentiation[10].

We have started to introduce c-*fos* genes into a variety of different cell types and into fertilized mouse eggs in order to analyse a potential function of the c-*fos* gene product in differentiation processes. We describe here the results of a study using 'nullipotent' F9 teratocarcinoma stem cells[11] as recipients for the introduction of c-*fos* genes. Teratocarcinoma stem cells have been used as a model system to study differentiation and development[12], and the introduction of selectable and nonselectable genes into various established embryonal carcinoma cell lines has been accomplished[13]. F9 stem cells do not differentiate spontaneously in culture[11], but treatment with retinoic acid and dibutyryl cyclic AMP can lead to endoderm-like differentiation[14,15]. Depending on culture conditions, parietal or visceral endoderm-like cells are formed in the presence of the chemical inducers, as judged by the expression of several specific differentiation markers. It has also been shown that nerve growth factor can induce adrenergic neuronal differentiation in F9 cells treated with retinoic acid and dibutyryl cyclic AMP[16]. We show here that the expression of either the human or mouse c-*fos* gene following DNA-mediated gene transfer into F9 stem cells results in a drastic alteration of cell morphology and proliferative potential associated with the onset of expression of several differentiation markers.

Morphological alteration of F9 cells

In F9 stem cells, the level of c-*fos* expression is normally very low[17]. To analyse whether an increased expression of the c-*fos* gene product affects the differentiation state of these cells, either

Table 1 Quantitative evaluation of transfection experiments

DNA	Ratio c-*fos*: pSV2-neo (μg)	Total no. of colonies†	Fraction of morphologically altered colonies (%)
c-*fos* (human) + pSV2-neo	10:10	300	15
c-*fos* (human) + pSV2-neo	15:5	85	30
c-*fos* (human) + pSV2-neo	20:1	80	70
c-*fos* (mouse) + pSV2-neo	20:1	100	50
c-*fos* (human) digested with *Nco*I* + pSV2-neo	5:5	75	0
c-*fos* alone	10	0	0
pSV2-neo alone	5	75	0

* Cleaves within c-*fos* coding region.

† Values are from at least two independent experiments and are expressed per 10^6 transfected cells.

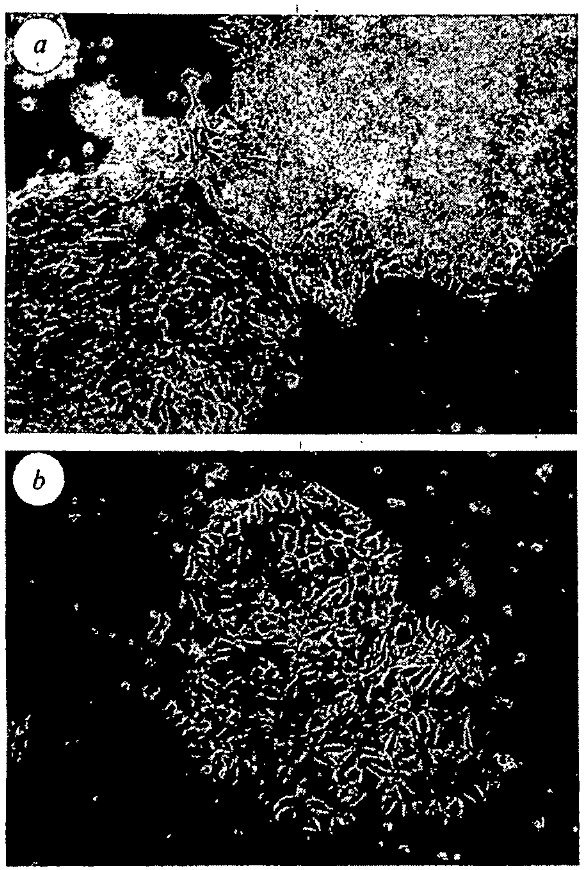

Fig. 1 Phase-contrast microscopy of F9 cells 10 days after co-transfection of c-*fos* and pSV2-neo and selection in G418-containing medium. *a*, The upper right colony is a typical F9 stem cell clone whereas in the lower left side, part of a characterisic c-*fos*-altered F9 clone is visible. *b*, A c-*fos*-altered F9 cell clone with the typical flat, epithelial-like morphology.

Method: DNA transfections were performed essentially as described[31,33,34]. The CaPO$_4$-precipitated DNA (20 μg human c-*fos* plasmid and 1 μg pSV2-neo) was added to 10^6 F9 cells and selection with G418 (1 mg ml^{-1}) was started 48 h later. Photographs were taken at magnification × 100.

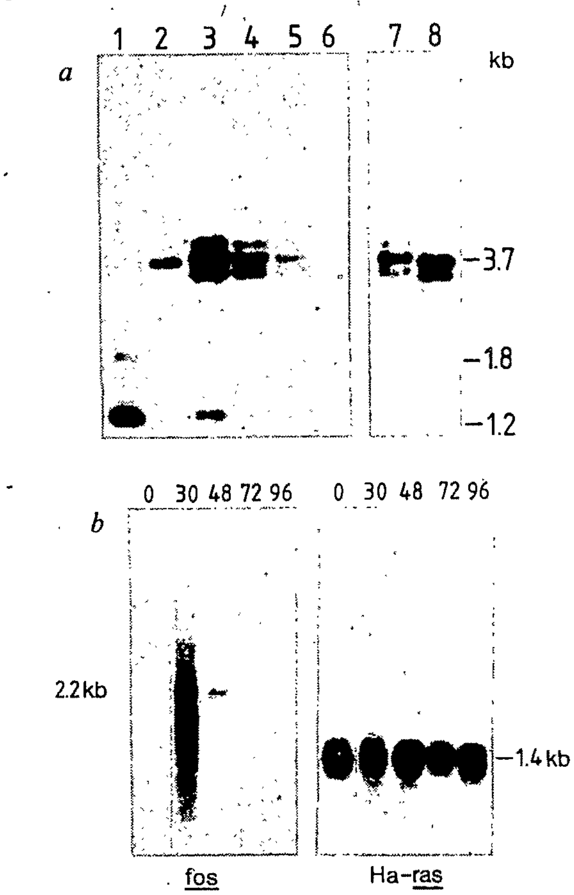

Fig. 2 *a*, Presence of exogenous c-*fos* DNA sequences in c-*fos*-altered F9 cells, 12 days after co-transfection of the human c-*fos* gene and pSV2-neo and subsequent selection in geneticin-containing medium. DNAs were digested with *Pvu*II and analysed by Southern blotting[21] using a v-*fos*-specific probe. Lane 1: normal F9 cells, 10 μg DNA; lane 2: normal human fibroblasts, 10 μg DNA; lanes 3–6: c-*fos*-altered F9 cells (experiment I, transfection of 10 μg c-*fos* and 10 μg pSV2-neo), 3 μg, 1 μg, 0.3 μg and 0.1 μg DNA (from left to right); lane 7, same as lane 3, but shorter exposure to facilitate comparison with lane 8 which contains c-*fos*-altered F9 cells (experiment II, transfection of 20 μg c-*fos* and 1 μg pSV2-neo). *b*, c-*fos* transcripts in transfected F9 stem cells. Poly(A)$^+$ RNA was isolated[35] 0, 30, 48, 72 and 96 h after transfecting 20 μg of the mouse c-*fos* plasmid[18] onto 10^6 F9 cells, separated on formaldehyde-containing agarose gels (8 μg per lane) and analysed by Northern blotting for transcripts hybridizing to a v-*fos* or v-Ha-*ras*-specific probe, respectively, as described[8,35,37]. The Ha-*ras*-specific probe was used to show that the pattern of expression observed with the *fos* probe was not due to quantitative or qualitative differences in the RNA samples analysed. After longer exposure of the same blot hybridized to the v-*fos*-specific probe, 2.2-kb transcripts were clearly visible at 96 h.

the human[18] or the mouse[19] c-*fos* gene and a plasmid (pSV2-neo)[20] containing a bacterial neomycin resistance gene were co-transfected into F9 stem cells. After selection in geneticin(G-418) containing medium for about 8–10 days, two types of colonies were detected with both c-*fos* genes: clones of cells showing the normal F9 stem cell morphology and colonies of greatly enlarged, flat cells growing in an epitheloid fashion (Fig. 1*a*, *b*). The maximum clone size of these morphologically altered cells was about 400 cells, although colonies consisting of less than 10 cells were also observed. No proliferative activity (as judged by clonal expansion) could be detected after 10–12 days in selective medium, whereas geneticin-resistant F9 stem cell clones continued to grow. The fraction of morphologically altered colonies was clearly dependent on the ratio of c-*fos*/pSV2-neo DNA used for transfection (Table 1). No clone of morphologically altered cells was obtained when the neomycin plasmid was transfected alone, or when the c-*fos* plasmid was cleaved within the coding region of c-*fos* prior to co-transfection (Table 1). No biological effect on F9 stem cells has been observed on transfer and expression of v-*myc* and v-*src*, which were linked to the metallothionein promoter region (M. Karin, personal communication). These results strongly suggested that the introduction of intact c-*fos* genes was responsible for the observed morphological alteration of F9 stem cells.

To obtain further evidence in support of this conclusion, DNA from transfected cultures was analysed for the presence of exogenous c-*fos* sequences (about 14 days after co-transfection of the normal human c-*fos* gene and the pSV2-neo plasmid). On digestion with *Pvu*II, the v-*fos*-specific probe used in this study recognized a fragment of 3.7 kilobases (kb) in human DNA and two fragments of 1.8 and 1.2 kb in mouse DNA (Fig. 2*a*). When mass cultures containing approximately 50% morphologically altered colonies were analysed by the Southern blot procedure[21], an average value of at least 20–50 copies per cell was determined for the exogenous human c-*fos* genes (Fig. 2*a*). When DNA from transfected, but morphologically normal, F9 cell clones was analysed by the same technique, only few intact copies of exogenous c-*fos* sequences were detected (R.M. and E.W., unpublished observation). These results suggest that c-*fos* expression in the morphologically altered F9 cells may result from low-level transcription of many exogeneous c-*fos* genes (see below).

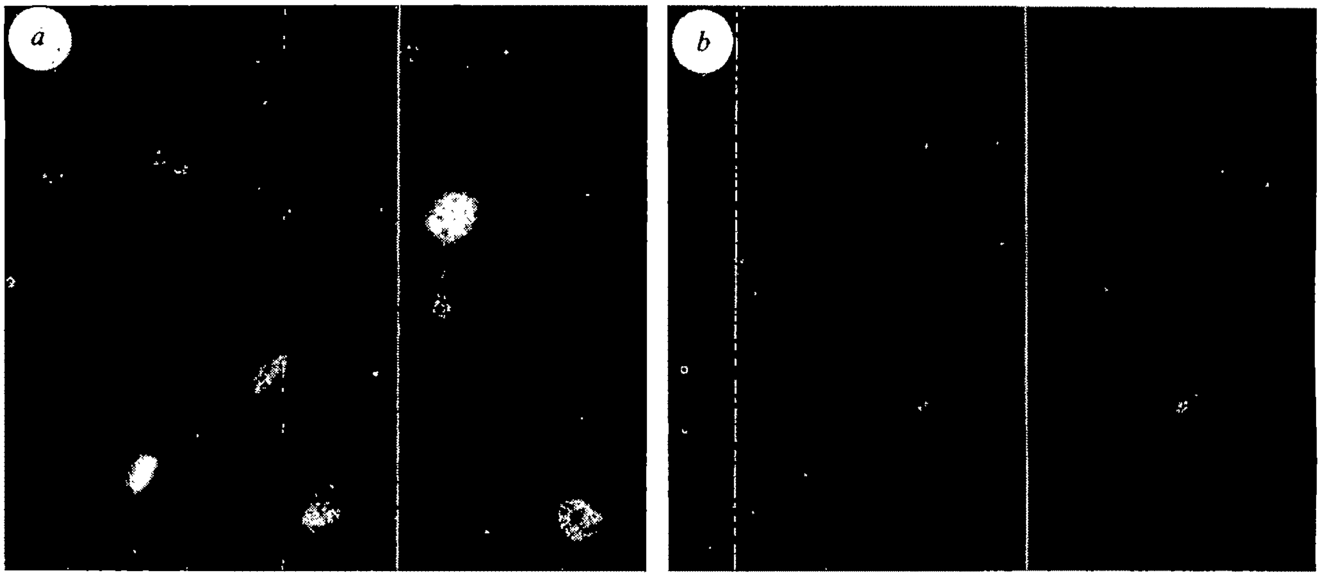

Fig. 3 Expression of c-*fos*-related nuclear protein in c-*fos*-altered F9 cells, 12 days after co-transfection of the human c-*fos* gene and pSV2-neo and subsequent selection in geneticin-containing medium. Double-antibody immunfluorescence using *fos*-specific TBRS[22,23] and a rhodamine isothiocyanate-conjugated sheep anti-rat-IgG antibody (provided by J. Adamkiewicz, University of Essen, FRG) was carried out on *p*-formaldehyde-fixed and Triton-permeabilized cells as described by Curran *et al.*[23]. *a*, *fos*-specific TBRS showing a clear nuclear staining[23]; *b*, preimmune serum showing only non-specific cytoplasmic fluorescence. Similarly, no specific nuclear staining was observed with TBR serum on normal F9 stem cells (not shown). Two different areas of the same culture are shown in both *a* and *b*.

Increased expression of c-*fos* mRNA

To examine whether the c-*fos*-induced morphological alteration was associated with elevated expression of c-*fos* mRNA, we analysed total poly(A)$^+$-containing RNA from cultures at different times after transfection of the mouse c-*fos* gene (thus including in the analysis all cells which had not taken up DNA). High levels of c-*fos*-related transcripts relative to untransfected F9 cells could be detected as early as 30 h after transfection (Fig. 2*b*). In addition to the normal c-*fos* mRNA of 2.2 kb, which has previously been described to be present in various mouse and human tissues[7–10], transcripts of heterogenous size producing a smear of c-*fos*-containing RNA were observed (Fig. 2*b*). At later times the level of c-*fos*-related RNA decreased and the c-*fos* transcripts predominantly occurred as normal 2.2-kb mRNA (Fig. 2*b*). These changes in the level and size of c-*fos* transcripts are apparently not due to variations in the RNA preparations, as neither quantitative nor qualitative changes could be observed when the same RNA blot was hybridized to a v-Ha-*ras*-specific probe (Fig. 2*b*). Our observations on c-*fos* expression might therefore reflect the elimination of extrachromosomal c-*fos* sequences or of unstable c-*fos* integration sites which could produce aberrant transcripts. The decrease of c-*fos* expression at later times could also occur because normal F9 stem cells may have a growth advantage over those cells which have taken up and express exogenous c-*fos* genes. Our results, however, demonstrate that c-*fos* sequences, on transfection into F9 stem cells, are transcribed at significant levels, leading to an over-expression of c-*fos* mRNA that is similar in size to the normal transcript.

Expression of c-*fos* protein

Exogenous c-*fos* genes transferred by transfection into F9 cells are transcriptionally active (Fig. 2*b*), but *Nco*I cleavage in the *fos* coding region abolishes this activity of the human c-*fos* gene (Table 1). These observations suggest that the altered F9 cell morphology may be induced by the c-*fos* protein. Using a tumour-bearing rat serum (TBRS), it has been reported recently that both v-*fos* and c-*fos* gene products are expressed as nuclear phosphoproteins in virus-transformed fibroblasts and in primary cultures of late-gestation mouse amnion cells, respectively[22,23]. This *fos*-specific antiserum was used here to investigate whether c-*fos* protein was expressed in the morphologically altered F9 cells. Because of the relatively low number of c-*fos*-altered F9 cells available, this analysis was only possible by using an *in situ* immunostaining procedure. As shown by immunofluorescence (Fig. 3), a strong nuclear staining was detected in most of the morphologically altered F9 cells. Only relatively weak nonspecific cytoplasmic staining (no nuclear fluorescence) was observed when either TBRS was used on normal F9 stem cells or when non-immune serum was applied to c-*fos*-altered F9 cells (Fig. 3). Therefore, our findings strongly suggest that c-*fos*

Table 2 Differentiation markers of c-*fos*-altered F9 cells compared with those of F9 stem cells, trophoblastic cells and endodermal cells

	Marker					
Cell type	TROMA-1[25,26]	TROMA-3[25,26]	Laminin[25,26]	AFP[26]	Fibronectin[25]	Deposited collagen type IV[26,27]
F9 stem cells	–	–	–	–	(+)	(–)
c-*fos*-transformed F9 cells	+	+	–	–	(+)	(+)*
Trophoblastic cells	+	+	–	–	?	?
Primitive endoderm	?	?	+	–	+	+
Parietal endoderm	+	(+)	+	–	–	+
Visceral endoderm	+	–	(+)	+	+	(+)

–, No expression detectable; (+), low level of expression; +, high level of expression (–, (+) and + correspond to –, +, more than one + in ref. 26).
* Variation among different clones from very low to high levels.

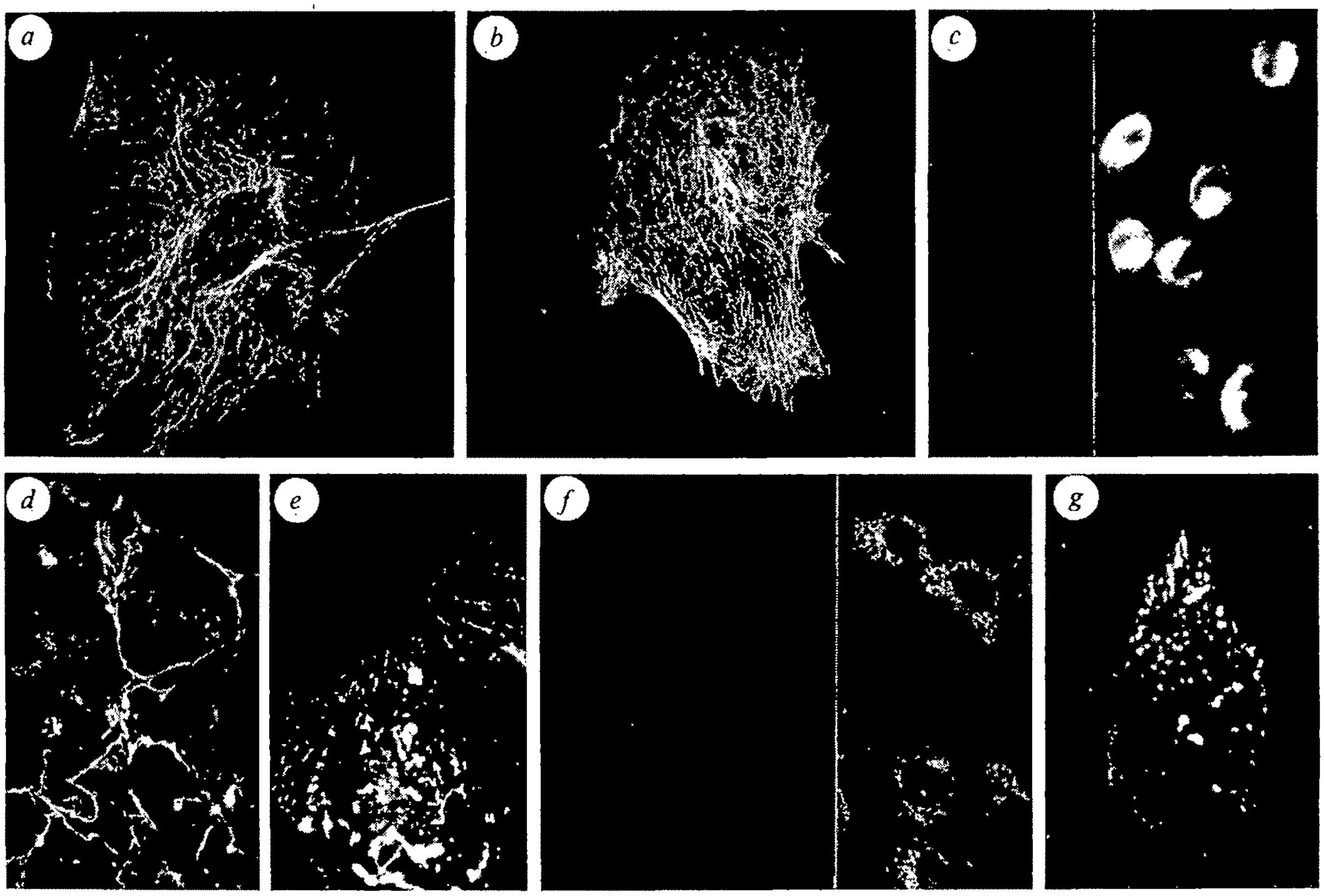

Fig. 4 Expression of differentiation markers in c-*fos*-altered F9 cells 12 days after co-transfection of the human c-*fos* gene and pSV2-neo and subsequent selection in geneticin-containing medium. Cells were fixed with Sante Marie reagent (ethanol/glacial acetic acid, 99:1 v/v) (*a–f*) or *p*-formaldehyde (*g*) and processed by double-antibody immunofluorescence as described elsewhere[38]. *a*, *b*: Mouse monoclonal antibodies TROMA-1 (*a*) and TROMA-3 (*b*) recognizing intermediate filaments[25] (provided by R. Kemler, Tübingen, FRG) on c-*fos*-altered F9 cells. *c*, Rabbit antiserum against AFP in c-*fos*-altered F9 cells (left) and in rat hepatoma cells (DTH2) as a positive control (right) (cells obtained from D. Paul, Hamburg, FRG; antiserum provided by E. Adamson, La Jolla, California). *d*, *e*: Rabbit antiserum against collagen type IV (given by K. von der Mark, Martinsried, FRG) on c-*fos*-altered F9 cells. *d*, Shows a clone of cells; *e* shows two single cells. *f*, Mouse monoclonal antibody against laminin (obtained from R. Kemler, Tübingen, FRG) on c-*fos*-altered F9 cells (left) and on the parietal endoderm-like teratocarcinoma cell line PYS-2 (as a positive control, right). *g*, Rabbit antiserum against hamster fibronectin (provided by H. Beug, EMBL; originally obtained from R. Hynes, MIT, Boston) on a c-*fos*-altered F9 cell. The second antibody was as in Fig. 3 (in *a*, *b*, *f*) or rhodamine isothiocyanate-conjugated sheep anti-rabbit IgG (Dakopatts, Hamburg, FRG) (*c*, *d*, *e*, *g*). Microscopic magnification ×400.

protein is synthesized in morphologically altered F9 cells. This observation is of particular relevance because other cell types may not efficiently express unmodified transfected c-*fos* genes[24]. Although these data do not yet prove a causative role for c-*fos* protein in the morphological alteration of F9 stem cells, such a function seems possible because c-*fos* mRNA was detected as early as 30 h after transfection. Thus, it seems that c-*fos* expression preceeds morphological alteration rather than vice versa.

Expression of differentiation markers

To investigate the nature of the morphologically altered F9 cells in further detail, we analysed the expression of a variety of differentiation markers in these cells. These studies were particularly designed to include those markers known to be switched on in F9 cells induced to differentiate by retinoic acid treatment[14,15,25–27]. The most dramatic change we observed was the appearance of an ordered intermediate filament network in the morphologically altered F9 cells (Fig. 4*a*, *b*). This network, which is entirely absent from normal F9 stem cells (data not shown; see ref. 25), was recognized by two monoclonal antibodies reacting with different intermediate filament components: TROMA-1 (Fig. 4*a*) and TROMA-3 (Fig. 4*b*). These antibodies have both been reported to bind to intermediate filament proteins, which are first detectable in tropho-ectodermal cells of the blastocyst[25]. While TROMA-1 antibodies also react strongly with both visceral and parietal endodermal cells, the specificity of TROMA-3 is more pronounced; this antibody shows a positive reaction (though weaker than TROMA-1) only on parietal endoderm (Table 2)[25,26]. In addition, both antibodies react with the primitive gut and fetal liver as well as with the mesoderm and endoderm-derived epithelia in adult animals. Although our results obtained with TROMA-1 and TROMA-3 already suggest the alteration by c-*fos* of F9 stem cells into an epithelioid cell type (in accord with the change in cell morphology; Fig. 1), the analysis of a larger number of differentiation markers was required to obtain a clearer picture of the cell type represented by the c-*fos*-altered F9 cells.

Figure 4*c*, *f* shows that the endodermal markers α-fetoprotein (AFP; expressed in visceral endoderm[26]) and laminin (expressed predominantly in parietal endoderm[26]) could not be detected in the morphologically altered F9 cells, although cell lines serving as positive controls showed strong reactions: the parietal endoderm-like cell line PYS-2[25] (Fig. 4*f*) and retinoic acid-induced F9 cells (data not shown) with monoclonal anti-laminin antibodies (Fig. 4*f*), and the rat hepatoma cell line DTH2 (D. Paul, personal communication) with anti-AFP serum (Fig. 4*c*).

Two other extracellular matrix proteins were found to be deposited in the morphologically altered F9 cells, fibronectin

(Fig. 4*g*) and collagen type IV (Fig. 4*d*, *e*)[26,27]. Fibronectin was detected as extracellular patches of protein (Fig. 4*g*) and as deposits on the plastic surface of the culture dish (not shown) at levels similar to that found in F9 stem cells. Collagen type IV was found in an intracellular form (Fig. 4*d*), in extracellular fibres within cell clones (Fig. 4*d*) and in patches on single cells (Fig. 4*e*). The pattern and level of collagen type IV expression was subject to some variation when different clones were compared.

Conclusions

Mouse and human c-*fos* genes are expressed in a stage-, tissue- and cell type specific fashion which has led to the hypothesis that products encoded by these c-*onc* genes may have a role in cellular differentiation processes[7–10]. One approach for testing this hypothesis is to transfer transcriptionally active genes into various undifferentiated cell types, in particular stem cells and fertilized eggs, and to analyse the biological effect of the exogenous gene products. In the present study we have shown that the introduction via transfection of c-*fos* genes into F9 teratocarcinoma cells gives rise to colonies of cells which are morphologically distinct from F9 stem cells, and which possess phenotypic properties characteristic of differentiated cells. The c-*fos*-altered F9 cells share several markers with trophoblastic and endodermal cells (in particular the intermediate filament proteins TROMA-1 and TROMA-3 as well as collagen type IV; Table 2)[25,26]. On the other hand, several markers diagnostic of retinoic acid-induced F9 cells and characteristic of either parietal endoderm (laminin)[25,26] or visceral endoderm (α-fetoprotein)[26] are not expressed in the c-*fos*-transfected, differentiated F9 cells. Thus, it seems that the differentiation pathways promoted by retinoic acid and c-*fos* are distinct events. Whether the c-*fos*-transfected F9 cells represent a normal cell type that has not yet been identified or whether an aberrant type of differentiation is triggered by c-*fos* is unknown. It is also possible that c-*fos* induces the expression of a particular set of genes, and that the acquisition of a terminal stage of differentiation requires the expression of another set of genes not controlled by c-*fos*. Nevertheless, our findings provide the first evidence that transfer of a single cellular gene can promote a cellular differentiation process, either by inducing differentiation in uncommitted stem cells or by conferring on committed cells present in the mass population of F9 cells the ability to pass through a predetermined differentiation pathway, for example by providing a maintenance function specifically required by differentiated cells.

Another intriguing aspect of this study is that c-*fos* sequences introduced into F9 stem cells were found to be expressed at both the mRNA and protein levels (Figs 2*b*, 3). Recently, it has been shown that c-*fos* genes transferred into fibroblastic cells are not efficiently expressed unless part of the 3′-untranslated region is removed from the transfected gene[24]. Such control mechanisms apparently do not exist in amniotic cells and, as shown here, also seem to be absent from c-*fos*-induced differentiated F9 cells. F9 stem cells could thus represent an invaluable tool for investigating the mechanims controlling c-*fos* mRNA and protein expression.

Our present observations, taken together with previous findings on c-*fos* expression in normal development, suggest a participation of the c-*fos* gene product in specific cellular differentiation processes. However, it should be emphasized that such a putative role of c-*fos* would not necessarily preclude its association with growth control mechanisms, a function suggested by the fact that the inappropriate expression of c-*fos* can lead to neoplastic transformation (uncontrolled cell proliferation)[24]. It is noteworthy that both differentiation-inducing properties and growth-promoting activities have been observed for nerve growth factor[16] and the v-*abl* gene product[28,29].

To elucidate the nature of the c-*fos*-altered F9 cells in greater detail, it is important to obtain larger numbers of these differentiated cells; this might be achieved by improving culture conditions (for example, to compensate for a possible requirement of the c-*fos*-altered cells for specific factors), by introducing 'immortalizing' genes[30,31] into the differentiated cells (to overcome a possible block of cell proliferation associated with terminal differentiation) or by using c-*fos*- gene constructs, allowing regulation of expression via inducible promoters[32] (in case the constitutive expression of high levels of c-*fos* expression is detrimental to the cell). To address these problems, we are currently introducing c-*fos* genes under the control of the metallothionein promoter[32] into various other stem cells and fertilized mouse eggs, either alone or together with the gene coding for the polyoma virus large-T antigen[30]. By using such inducible c-*fos* gene constructs, it may also be feasible to examine whether the promotion of differentiation by c-*fos* requires the selection of pre-existing committed cells in the mass population of F9 stem cells.

We thank E. Adamson, H. Beug, T. Curran, R. Kemler, K. von der Mark and R. Hynes for gifts of specific antibodies; T. Curran, R. Ellis, D. A. Miller and I. M. Verma for oncogene-specific probes and cloned c-*fos* genes; B. Adkins, K. von der Mark, H. Ponta and U. Rüther for valuable discussions and suggestions; M. Vanek for technical assistance and B. Blanasch for help in preparation of the manuscript.

Received 29 May; accepted 6 July 1984.

1. Waterfield, M. D. *et al. Nature* **304,** 35–39 (1983).
2. Doolittle, R. F. *et al. Science* **221,** 275–277 (1983).
3. Downward, J. *et al. Nature* **307,** 521–527 (1984).
4. Kelly, K., Cochran, B. H., Stiles, C. D. & Leder, P. *Cell* **35,** 603–610 (1983).
5. Campisi, J., Gray, H. E., Pardee, A. B., Dean, M. & Sonenshein, G. E. *Cell* **36,** 241–247 (1984).
6. Westin, E. H. *et al. Proc. natn. Acad. Sci. U.S.A.* **79,** 2194–2198.
7. Müller, R., Slamon, D. J., Tremblay, J. M., Cline, M. J. & Verma, I. M. *Nature* **299,** 640–644 (1982).
8. Müller, R., Verma, I. M. & Adamson, E D. *EMBO J.* **2,** 679–684 (1983).
9. Müller, R., Tremblay, J. M., Adamson, E. D. & Verma, I. M. *Nature* **304,** 454–456 (1983).
10. Müller, R., Müller, D. & Guilbert, L. *EMBO J.* **3,** 1887–1890 (1984).
11. Bernstine, E. G., Hooper, M. L., Grandchamp, S. & Ephrussi, B. *Proc. natn. Acad. Sci. U.S.A.* **70,** 3899–3903 (1973).
12. Mintz, B. & Fleischman, R. A. *Adv. Cancer Res.* **34,** 221–278 (1981).
13. Wagner, E. F., Rüther, U. & Stewart, C. L. in *The Impact of Gene Transfer Techniques in Eucaryotic Cell Biology* (Springer, Berlin, in the press).
14. Strickland, S. & Mahdavi, V. *Cell* **15,** 393–403 (1978).
15. Hogan, B. L. M., Taylor, A. & Adamson, E. *Nature* **291,** 235–237 (1981).
16. Liesi, P., Rechardt, L. & Wartiovaara, J. *Nature* **306,** 265–267 (1983).
17. Müller, R. *Cold Spring Harb. Conf. Cell Prolif.* **10,** 451–468 (1983).
18. van Straaten, F., Müller, R., Curran, T., van Beveren, C. & Verma, I. M. *Proc. natn. Acad. Sci. U.S.A.* **80,** 3183–3187 (1983).
19. Van Beveren, C., van Straaten, F., Curran, T., Müller, R. & Verma, I. M. *Cell* **32,** 1241–1255 (1983).
20. Southern, P. J. & Berg, P. *J. molec. appl. Genet.* **1,** 327–341 (1982).
21. Southern, E. M. *J. molec. Biol.* **98,** 503–517 (1975).
22. Curran, T. & Teich, N. M. *J. Virol.* **42,** 114–122 (1982).
23. Curran, T., Miller, A. D., Zokas, F. L. & Verma, I. M. *Cell* **36,** 259–268 (1984).
24. Miller, A. D., Curran, T. & Verma, I. M. *Cell* **36,** 51–60 (1984).
25. Boller, K. & Kemler, R. *Cold Spring Harb. Conf. Cell Prolif.* **10,** 39–49 (1983).
26. Kahan, B. & Adamson, E. D. *Cold Spring Harb. Conf. Cell Prolif.* **10,** 131–141 (1983).
27. Adamson, E. D., Gaunt, S. J. & Graham, C. F. *Cell* **17,** 469–476 (1979).
28. Waneck, G. L. & Rosenberg, N. *Cell* **26,** 79–89 (1981).
29. Witte, O. N. *Curr. Topics Microbiol. Immun.* **103,** 127–146 (1983).
30. Rassoulzadegan, M. *et al. Proc. natn. Acad. Sci. U.S.A.* **80,** 4354–4358 (1983).
31. Houweling, A., van der Elsen, P. & van der Eb., A. *Virology* **105,** 537–550 (1980).
32. Karin, M. *et al. Nature* **308,** 513–519 (1984).
33. Graham, F. L. & van der Eb, A. J. *Virology* **53,** 456–467 (1973).
34. Wagner, E. F. & Mintz, B. *Molec. cell. Biol.,* **2,** 190–198 (1982).
35. Müller, R. *et al. Molec. cell. Biol.* **3,** 1062–1069 (1983).
36. Curran, T., Peters, G., van Beveren, C., Teich, N. M. & Verma, I. M. *J. Virol.* **44,** 674–682 (1982).
37. Lehrach, H., Diamond, D., Wozney, J. M. & Boedtcher, H. *Biochemistry* **16,** 4743–4751 (1977).
38. Adamson. E. D. & Grover, A *Cold Spring Harb. Conf. Cell Prolif.* **10,** 69–81 (1983).

Accretion disk limit cycle mechanism in twin-degenerate interacting binaries

J. K. Cannizzo

Department of Astronomy, University of Texas, Austin,
Texas 78712, USA

The twin-degenerate interacting binary stars are thought to consist of two pure helium white dwarfs in close orbit. The candidates are G61-29 (also GP Com), HZ 29 (also AM CVn) and, tentatively, PG1346+082[1]. Large variations in the optical light of PG1346+082 suggest variable accretion onto the star gaining mass. Such behaviour in the light curves of the classical dwarf novae is thought to be caused by either episodic mass overflow from the mass-losing star[2,3] or the instability in the accretion disk[4,5]. Here we investigate the latter mechanism, and explore the non-thermal equilibrium limit cycle behaviour of the accretion disk expected for a twin-degenerate interacting binary system.

G61-29 is a system containing two white dwarfs orbiting each other with a period of 46.5 min. Nather *et al.*[6] interpret this system as consisting of a low-mass white dwarf transferring matter to its more massive companion through the inner lagrangian point. They find that the hydrogen-to-helium ratio is at least a factor of 1,500 lower than its solar value. It is also generally accepted that HZ 29 consists of two white dwarfs in close proximity[7-9]. The rate of mass transfer is thought to be orders of magnitude higher than for G61-29 (refs 6, 8). If the mass-losing star is also a low-mass white dwarf in contact with its Roche lobe, the orbital period would be of the order of 1/2 h, given the size considerations for white dwarfs.

Smak[10] has pointed out that the disk limit cycle mechanism[11-17] hypothesized to account for the recurrent bursts seen in dwarf novae should also be applicable to twin-degenerate Hinteracting binaries. This instability mechanism results from changes in the vertical disk structure which occur when the midplane temperature is near the peak in the Rosseland opacity. For a density of $\rho = 10^{-7}$ g cm^{-3} this peak occurs at $T \approx 15{,}000$ K for solar composition material[18] and $T \approx 30{,}000$ K for pure helium material[19]. The effective temperature of the disk corresponding to the onset of instability is $T_{\rm eff} \approx 6{,}500$ K for the former[11-17] and $T_{\rm eff} \approx 9{,}000$ K for the latter[10]. A comparison of vertical structure computations[10,20] shows that in pure helium disks the instability occurs at a surface density which is a factor of 7.5 larger than that in disks composed of solar matter because of the higher temperatures.

The strongest evidence for dwarf nova-like nature of these objects is the resemblance of their spectra to those seen in the classical dwarf novae. The eruption spectra of dwarf novae show strong absorption lines and their light curves exhibit flickering. In HZ 29 one sees[8,9] He absorption lines and flickering. Also, emission features are seen in dwarf novae during the quiescent periods between the outbursts—just as one sees[6] emission lines of He in G61-29.

Preliminary observations of PG1346+082 appear to be at least consistent with the notion that it too contains two helium white dwarfs orbiting at close range (D. E. Winget, and R. E. Nather, personal communications). The average spectrum of PG1346+082 is devoid of hydrogen and strongly resembles that of HZ 29. As in HZ 29 the absorption features are shallower than those seen in lone white dwarf spectra. Observations of this object are preliminary and no light curves have been published. However, variations of 2–3 mag seen in the optical light from this system seem to hint at episodic disk flow onto the accreting star. Were this true, one would be faced with the prospect that $\dot{M}_{\rm T}$ does, in fact, lie in an 'unstable' range[10]. What would be the expected amplitudes, durations, and recurrence times for bursts produced in such a system?

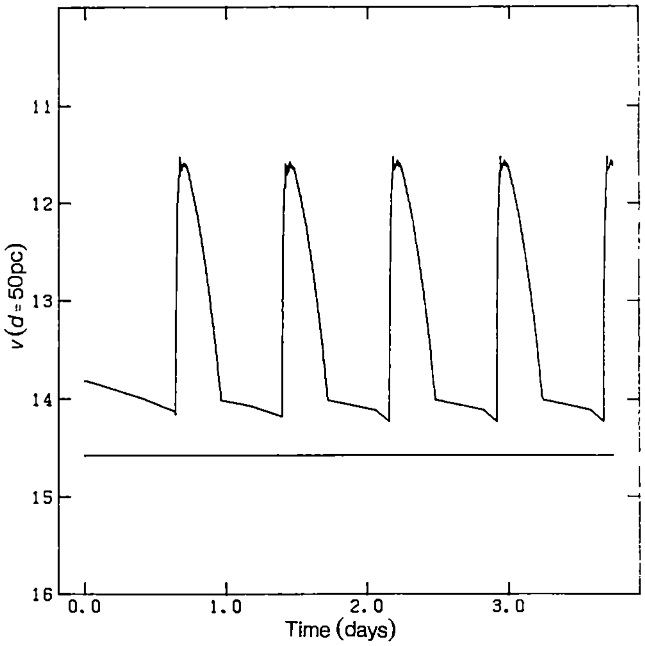

Fig. 1 A series of bursts for $\alpha_{\rm cold} = 0.05$, $\alpha_{\rm hot} = 0.2$, and $\dot{M}_{\rm T} = 5 \times 10^{-10}\ M_\odot\,{\rm yr}^{-1}$. The horizontal line represents the light from a typical white dwarf. The vertical axis is in units of apparent visual magnitude. The system quickly relaxes to a periodic behaviour with widely separated bursts occurring.

In an attempt to answer these questions we have employed a generalized time-dependent, non-thermal equilibrium accretion disk model developed for studying the classical dwarf novae. The mathematical formulation is similar to that being used elsewhere[20,21-24]. The exact method used[25] involves the α parameterization for the viscosity and consists of simultaneously solving for the temporal evolution of surface density and disk temperature.

Preliminary comparisons of theory with observation[25,26] using dwarf novae systems seem to demand $\alpha_{\rm cold} \approx 0.05$ and $\alpha_{\rm hot} \approx 0.2$. We take the inner disk edge to be at 5×10^8 cm, and the outer edge at 4×10^9 cm. Mass is added to the disk at a constant rate at 2.5×10^9 cm—an appropriate injection radius for $P = 1/2$ h. A radial grid of 40 points is used. At the inner edge we set $\Sigma = 0$, and at the outer edge we set $v_{\rm r} = 0$ (where $v_{\rm r}$ is the radial flow speed). We assume a face-on disk in computing the light curves presented below.

We use the opacities of Heubner *et al.*[19] which characterize matter with the composition $X = 0$, $Z = 0.001$ (where X is the hydrogen mass fraction and Z is the metal mass fraction). Power law scalings for the critical surface densities associated with the limit cycle are taken from computations using solar composition material[16]. These surface densities have to be multiplied by 7.5 for the helium-rich matter considered here.

We have computed a series of bursts for a wide range of values of the secondary mass transfer rate $\dot{M}_{\rm T}$. Figures 1 and 2 show a series of bursts for representative low and high values of $\dot{M}_{\rm T}$. The horizontal line represents the luminosity of a white dwarf with effective temperature, $T_{\rm eff} = 30{,}000$ K and radius $r_{\rm wd} = 5 \times 10^8$ cm. The varying curve gives the disk contribution. We take the distance to be $d = 50$ pc. In quiescence the optical depth through the disk vertically is $\tau \approx 1$ at all radii, and the disk temperature is $T \approx 10{,}000$ K. In outburst, the disk effective temperature varies between about 20,000 K and 50,000 K. The optical flux from the disk rises about two magnitudes in going from quiescence to outburst.

Even for very low $\dot{M}_{\rm T}$ we still find bursts occurring. For $\dot{M}_{\rm T} = 2 \times 10^{-11}\ M_\odot\,{\rm yr}^{-1}$ (corresponding to G61-29) the bursts

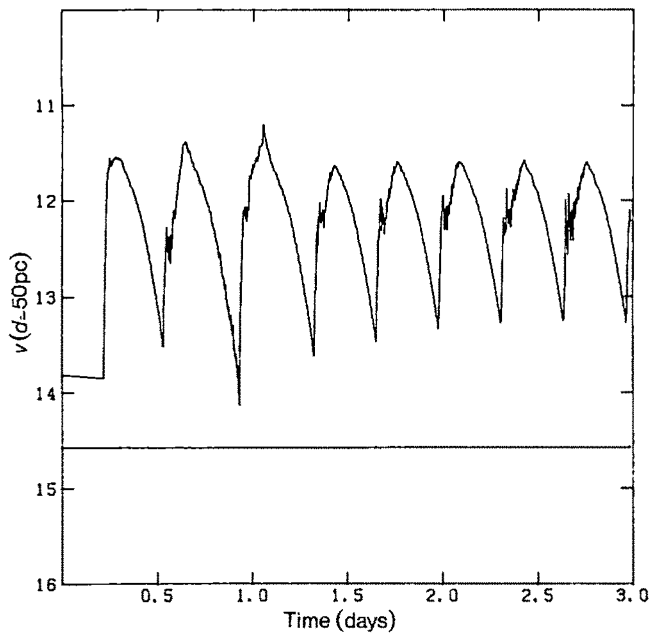

Fig. 2 A series of bursts for $\dot{M}_T = 1.5\times10^{-9}\,M_\odot\,\mathrm{yr}^{-1}$. Other parameters are as in Fig. 1. After three bursts the system settles to a repetitive pattern with closely spaced bursts.

happen once every 10 days and last about 5 h. Hence for the parameters chosen we predict a duty cycle of about 2%. So far this system has only been seen in the 'low' state. As $\dot{M}_T$ is increased the interval between bursts decreases but the duration of the burst itself increases slightly. The bursts shown in Fig. 1 for which $\dot{M}_T = 5\times10^{-10}\,M_\odot\,\mathrm{yr}^{-1}$ occur about once every 16 hours. There is still a sizeable quiescent period. Figure 2 depicts the system behaviour for $\dot{M}_T = 1.5\times10^{-9}\,M_\odot\,\mathrm{yr}^{-1}$. The bursts now occur so rapidly that the inner part of the disk is still in the high state when the next burst is initiated at larger radii. For even higher $\dot{M}_T$ the inner disk is always in the high state. Only the outer disk alternates between the low and high states. The disk light oscillates within a few tenths of a magnitude of $m_v = 12$. For $\dot{M}_T$ corresponding to HZ 29 the entire disk is in steady-state.

The burst amplitudes to be expected in a helium twin-degenerate interacting binary system are about three magnitudes, or less if $\dot{M}_T$ is large. The time between bursts is hard to predict from a theoretical standpoint without knowing $\dot{M}_T$. Indeed, a knowledge of the recurrence time should place limits on $\dot{M}_T$. If bursts are seen in one of these systems, the disk apparent magnitudes presented here should enable one to infer a distance, given an assumption for the disk inclination.

I thank Don Winget, Ed Nather, Rick Hessman, and Matt Wood for bringing PG 1346 + 082 to my attention and for discussing the existing observations of this object. I also thank Don Winget for making available the Heubner *et al.*[19] opacities, Doug Lin and Greg Shields for discussions involving the nonthermal equilibrium model, and especially Craig Wheeler for useful discussions of accretion disk physics and critical reading of this manuscript. This research was supported in part by NASA grant NSG 7232.

Received 10 April; accepted 10 July 1984.

1. Nather, R. E. in *NATO Conference on Interacting Binary Stars* (University of Cambridge press, in the press, 1983).
2. Bath, G. T. *Nature phys. Sci.* **246**, 84–87 (1973).
3. Bath, G. T. *Mon. Not. R. astr. Soc.* **171**, 311–328 (1975).
4. Osaki, Y. *Publs astr. Soc. Jap.* **26**, 429–436 (1974).
5. Hoshi, R. *Prog. theor. Phys.* **61**, 1307–1319 (1979).
6. Nather, R. E., Robinson, E. L. & Stover, R. J. *Astrophys. J.* **244**, 269–279 (1981).
7. Faulkner, J., Flannery, B. P. & Warner, B. *Astrophys. J. Lett.* **175**, L79–L83 (1972).
8. Patterson, J., Nather, R. E., Robinson, E. L. & Handler, F. *Astrophys. J.* **232**, 819–825 (1979).
9. Solheim, J.-E., Robinson, E. L., Nather, R. E. & Kepler, S. O. *Astrophys. J.* (in the press, 1984).
10. Smak, J. *Acta astr.* **33**, 333–337 (1983).
11. Meyer, F. & Meyer-Hofmeister, E. *Astr. Astrophys.* **104**, 0–L12 (1981).
12. Meyer, F. & Meyer-Hofmeister, E. *Astr. Astrophys.* **106**, 34–42 (1982).
13. Smak, J. *Acta astr.* **32**, 199–211 (1982).
14. Smak, J. *Acta astr.* **32**, 213–224 (1982).
15. Cannizzo, J. K., Ghosh, P. & Wheeler, J. C. *Astrophys. J. Lett.* **260**, L83–L86 (1982).
16. Cannizzo, J. K. & Wheeler, J. C. *Astrophys. J. Suppl.* **55**, 367–388 (1984).
17. Faulkner, J., Lin, D. N. C. & Papaloizou, J. *Mon. Not. R. astr. Soc.* **205**, 359–375 (1983).
18. Cox, J. P. & Giuli, R. T. *Principles of Stellar Structure*, 397 (Gordon and Breach, New York, 1968).
19. Heubner, W. F., Mertz, A. L., Magee, N. H. & Argo, M. F. *Los Alamos Scient. Rep.* LA-6760-M (1977).
20. Smak, J. *Astrophys. J.* (in the press, 1984).
21. Mineshige, S. & Osaki, Y. *Publs astr. Soc. Jap.* **35**, 377–396 (1983).
22. Mineshige, S. & Osaki, Y. *Publs astr. Soc. Jap* (submitted).
23. Papaloizou, J., Faulkner, J. & Lin, D. N. C. *Mon. Not. R. astr. Soc.* **205**, 487–513 (1983).
24. Meyer, F. & Meyer-Hofmeister, E. *Astr. Astrophys.* **132**, 143–150 (1984).
25. Cannizzo, J. K. thesis, Univ. Texas, Austin (1984).
26. Smak, J. *Publs astr. Soc. Pacif.* **96**, 5–18 (1984).

Boltzmann's ultraviolet cutoff and Nekhoroshev's theorem on Arnold diffusion

Giancarlo Benettin*, Luigi Galgani† & Antonio Giorgilli‡

* Dipartimento di Fisica dell'Università-Padova, Gruppo Nazionale di Struttura della Materia del CNR, Unità di Padova, Via Marzolo 8, Padova, Italy
† Dipartimento di Matematica dell'Università-Milano, Via Saldini 50, Milano, Italy
‡ Dipartimento di Fisica dell'Università, Milano, Via Celoria 16, Milano, Italy

The greatest difficulty with classical statistical mechanics may be the fact that some degrees of freedom do not seem to attain the energy expected from the equipartition principle. This is typical of the vibrational modes in molecules and of the high frequencies in the electromagnetic radiation (problem of the ultraviolet cutoff). Boltzmann[1] had the intuition that an explanation might be provided if each degree of freedom were to have a characteristic relaxation time until equilibrium, and that such a time should greatly increase with frequency; he spoke in terms of relaxation times of days or centuries. This possibility was seriously considered by Rayleigh and Jeans[2], but they could not produce a clear classical mechanism to explain the freezing of the high frequency degrees of freedom; so, the equilibrium concept of the ultraviolet cutoff provided by quantum mechanics was accepted, and Boltzmann's hypothesis was forgotten. Here we point out that a general framework for understanding the ultraviolet cutoff in Boltzmann's dynamical sense in a classical context seems to be provided by Nekhoroshev's[3] theorem on Arnold diffusion.

The Komogorov–Arnold–Moser (KAM) theorem[4–9] on the existence of invariant tori in nearly integrable Hamiltonian systems was stated in 1954, the same year in which Fermi *et al.*[10] found that a classical nonlinear string did not relax to equilibrium within the time then available to the computer. In the KAM theorem one concentrates on results which are valid for infinite times, and this imposes a strong limitation to the set of initial data, which are restricted to the complement of a dense open set. This is a serious obstacle to a physical interpretation. In Nekhoroshev's theorem, however, where the evolution of the system is considered only for finite (but large) times, one obtains estimates which are valid in open sets of phase space, and not only on the invariant tori.

Nekhoroshev considers an analytical Hamiltonian $H(I, \phi) = H^0(I) + \varepsilon H^1(I, \phi)$ for a system with s degrees of freedom, where $I = (I_1, \dots, I_s)$ and $\phi = (\phi_1, \dots, \phi_s)$ are action-angle variables, H^1 is 2π-periodic in $\phi_1, \dots, \phi_s$, $\varepsilon \ll 1$ is a perturbative parameter, and H^0 satisfies certain 'steepness conditions' (for example, H^0 is convex). Then his main theorem continues:

Let $0 < \varepsilon < \varepsilon^0$. Then for every solution $I(t)$, $\phi(t)$ of the system with Hamiltonian $H^0 + \varepsilon H^1$ one has

$$|I(t) - I(0)| < \mathscr{I}\varepsilon^b \qquad (1)$$

for all $t \in (0, T)$, where

$$T = \tau \frac{1}{\varepsilon} \exp\left(\frac{1}{\varepsilon}\right)^a \qquad (2)$$

with suitable positive constants a, b depending on H^0, $\mathscr{I}$ and τ being natural units, of action and time respectively, entering the problem.

Here $|\cdots|$ is the Euclidean norm in R^s. The actions are thus 'frozen' up to very long times, which increase exponentially with decreasing ε, if the perturbation is small enough. The dimensional constants $\mathscr{I}$ and τ are widely arbitrary, and, as often used in the mathematical literature, they were set equal to unity in Nekhoroshev's paper.

But what interests us here is his extrapolation to systems of coupled harmonic oscillators. In such cases, one considers a Hamiltonian of the form

$$H(p, q) = \sum_{j=1}^{s} \tfrac{1}{2}\omega_j(p_j^2 + q_j^2) + \sum_{k \geq 3} H^{(k)}(q)$$

where $p = (p_1, \ldots, p_s) \in R^s$ and $q = (q_1, \ldots, q_s) \in R^s$ are cartesian coordinates around an elliptic equilibrium point, the constants $\omega_1, \ldots, \omega_s$ being the harmonic frequencies and $H^{(k)}$ a polynomial of order k in the variables q; no small parameter ε is needed in the Hamiltonian, and the smallness is measured in terms of the Euclidean distance from the fixed point. As the quadratic part of the Hamiltonian does not satisfy the steepness conditions required in Nekhoroshev's theorem, one adapts the Hamiltonian by a preliminary change of variables which is the same used to apply KAM theorem[8]. Specifically, we assume that among the harmonic frequencies $\omega_1, \ldots, \omega_s$ there are now low-order resonances, that is, a positive integer l exists such that no relations of the form $\sum_{j=1}^{s} k_j\omega_j = 0$ are satisfied, $k_1, \ldots, k_s$ being integers with $0 < |k_1| + \cdots + |k_s| \leq l$. Then, through a sequence of $l-2$ Birkhoff's transformations, and using the new variables I, ϕ, where $I_j = \frac{1}{2}(p_j^2 + q_j^2) + \cdots$, theHamiltonian takes the form $H'(I, \phi) = H^0(I) + H^1(I, \phi)$, where H^0 is in general, steep and H^1 starts with terms of order $|I|^{l/2}$. One has to take into account the fact that any Birkhoff's transformation produces a restriction of the domain around the fixed point where the new Hamiltonian is defined; thus, for any given set of harmonic frequencies, one could, in principle, find an optimal l. In any case, the new Hamiltonian H' can be defined for small enough actions, say for $|I| < A$, with a given 'critical action' A. Then one can apply the theorem quoted above, and still obtain the estimates in equations (1) and (2), the only difference being that ε has to be replaced by a quantity ε_{eff} depending on the initial data and defined by

$$\varepsilon_{\text{eff}} = \left(\frac{|I(0)|}{A}\right)^{l/2}$$

This is given in Nekhoroshev's paper with A set equal to unity.

Such a mathematical result seems strongly to indicate that the high frequency degrees of freedom are frozen. Indeed, let us consider a very special initial condition, such that only one oscillator, say the jth one, is excited, that is, one has $I_i(0) = 0$ for $i \neq j$. In terms of the harmonic energies E_j of the oscillators with harmonic frequencies ω_j, because of the relation $E_j = \omega_j I_j$ which holds in a first approximation, one has then

$$\varepsilon_{\text{eff}} \simeq \left(\frac{|E_j(0)|}{A\omega_j}\right)^{l/2},$$

and the theorem guarantees that such oscillator is 'frozen', that is, it has small fluctuations of energy, up to a time T_j which, as seen from equation (2), is exponentially increasing with frequency. In this sense, the theorem seems to provide a general mechanism for freezing of the higher frequencies, as advocated by Boltzmann. In addition, this actually occurs for energies below some critical energies proportional to frequency. The latter posssibility was indeed conjectured more than 10 yr ago, on the basis of an analogy of critical energy with quantum zero-point energy, taking into account the adiabatic invariance of the action[11–12].

There are several limitations to these considerations. First, the class of initial conditions to which Nekhoroshev's theorem directly applies is not broad enough, because one also ought to consider initial conditions with some oscillators below, and others above, the respective thresholds. Furthermore, in the KAM theory, and thus also in Nekhoroshev's theorem, there are extremely small lower estimates for the thresholds, even for situations with few degrees of freedom as, for example, in molecules. This difficulty is enhanced for most systems of interest in statistical mechanics, which involve many degrees of freedom, because such lower estimates tend rapidly towards zero as the number of degrees of freedom tends to infinity (in the thermodynamic limit). In this connection, we note that the available lower estimates in KAM theory are highly non-optimal; in addition, it seems that the estimates of the thermodynamic limit would be improved if they were restricted to special classes of physically-relevant perturbations, such as those corresponding to short-range interactions (low connectance, in the terminology of refs 13, 14); in particular, this should be the case for systems of particles coupled by typical molecular potentials, such as the Lennard–Jones potential. This is supported by some results we have obtained using classical perturbation theory, which appear to agree with the indications given, since several years, by numerical computations[15–23].

Thus, we conclude that the most general theorem available in classical perturbation theory, strongly supports the intuition of Boltzmann of almost a century ago, and deserves serious consideration. In any case, the relevance of metaequilibrium states has been often pointed out. This is illustrated by the physics of spin temperatures, where the system considered, that of nuclear spins, appears to have temperatures quite different from the temperature of the supporting system, that is the lattice, and from the temperature of the surrounding radiation field, just because "the internal thermal equilibrium time of the elements of the system is short compared to the time during which appreciable energy is lost or gained from other systems"[24]. In such cases, for example, the first time is of the order of 10^{-5} s, while the relaxation time to the lattice is often of the order of many minutes or even days. Analogous situations are also met in connection with the rotational and the vibrational degrees of freedom of molecules, where a different temperature is often reported for any degree of freedom[25].

For a discussion of other problems related to the questions mentioned above, see refs 26–29.

Note added in proof: A first result proving the applicability of Nekhoroshev's theorem in the thermodynamic limit for short-range interactions, at least in a special case, has been independently obtained by C. E. Wayne[30].

Received 9 April; accepted 31 July 1984.

1. Boltzmann, L. *Nature* **51,** 413–415 (1895).
2. Langevin, P. & De Broglie, M. *La Theorie du Rayonnement et les Quanta* (Gauthier-Villars, Paris, 1912).
3. Nekhoroshev, N. N. *Russ. Math. Surv.* **32,** 1–65 (1977).
4. Kolmogorov, A. N. *Dokl. Akad. Nauk. SSSR* **98,** 527–530 (1954).
5. Arnold, V. I. *Russ. Maths. Surv.* **18,** 9–36 (1963); **18,** 85–191 (1963)
6. Moser, J. in *Proc. int. Conf. on Functional Analysis and Related Topics*, 60–67 (University of Tokyo Press, 1969).
7. Gallavotti, G., in *Scaling and Self-Similarity in Physics* (ed. Froelich, J.) 359–426 (Birkhauser, Boston, 1983).
8. Poeschel, J. *Commun. Pure Apl. Math.* **35,** 653–695 (1982).
9. Benettin, G., Galgani, L., Giorgilli, A. & Strelcyn, J.M. *Nuovo Cimento* **79B,** 201–223 (1984).
10. Fermi, E., Pasta, J. & Ulam, S., in *Fermi E., Collected Works* Vol. 2, 978–988 (Accademia Nazionale dei Lincei, Roma, 1965).
11. Cercignani, C., Galgani, L. & Scotti, A. *Phys. Lett.* **A38,** 403–404 (1972).
12. Galgani, L. & Scotti, A. *Riv. Nuovo Cimento.* **2,** 189–209 (1972).
13. Gardner, M. R. & Ashby, W. R. *Nature* **228,** 784 (1970).
14. Froeschle, C. *Phys. Rev.* **A18,** 277–281 (1978).
15. Bocchieri, P., Scotti, A., Bearzi, B. & Loinger, A. *Phys. Rev.* **A2,** 2013–2019 (1970)
16. Diana, E., Galgani, L., Casartelli, M., Casati, G. & Scotti, A. *Theor Math. Phys.* **29,** 1022–1027 (1976).
17. Casartelli, M., Diana, E., Galgani, L. & Scotti, A. *Phys. Rev.* **A13,** 1921–1925 (1976)
18. Galgani, L. & Lo Vecchio, G. *Nuovo Cimento* **52B,** 1–14 (1979).
19. Benettin, G. & Galgani, L. *J. stat. Phys.* **27,** 153–169 (1982).

20. Benettin, G., Lo Vecchio, G. & Tenenbaum, A. *Phys. Rev.* **A22**, 1709–1719 (1980).
21. Benettin, G. & Tenenbaum, A. *Phys. Rev.* **A28**, 3020–3029 (1983).
22. Fucito, F., Marchesoni, F., Marinari, E., Parisi, G., Peliti, C., Ruffo, S. & Vulpiani, A. *J. Phys. (Paris)* **43**, 707–713 (1982).
23. Livi, R., Pettini, M., Ruffo, S., Sparpaglione, M. & Vulpiani, A. *Phys. Rev.* **A28**, 3544–3552 (1983).
24. Ramsey, N. F. in *A Critical Review of Thermodynamics* (eds Stuart, E. B. *et al.*) (Mono, Baltimore, 1970).
25. Burnett, G. M. & North, A. M. *Transfer and Storage of Energy by Molecules* Vol. 2 (Wiley, London, 1969).
26. Galgani, L. & Benettin, G. *Lett. Nuovo Cimento* **35**, 93–96 (1982).
27. Galgani, L. *Annls Fond. L. Broglie* **8**, 19–64 (1983).
28. Crovini, L. & Galgani, L. *Lett. Nuovo Cimento* **39**, 210–214 (1984).
29. Bocchieri, P. & Loinger, A. *Lett. Nuovo Cimento* **2**, 41–42 (1971).
30. Wayne, C. E. Preprint (University Park, Pennsylvania, 1984).

Maximum entropy signal processing in practical NMR spectroscopy

Sibusiso Sibisi*, John Skilling*, Richard G. Brereton†, Ernest D. Laue† & James Staunton†

* Department of Applied Mathematics and Theoretical Physics,
Silver Street, Cambridge CB3 9EW, UK
† University Chemical Laboratory, Lensfield Road,
Cambridge CB2 1EW, UK

NMR spectroscopy is intrinsically insensitive, a frequently serious limitation especially in biochemical applications where sample size is limited and compounds may be too insoluble or unstable for data to be accumulated over long periods. Fourier transform (FT) NMR was developed by Ernst[1] to speed up the accumulation of useful data, dramatically improving the quality of spectra obtained in a given observing time by recording the free induction decay (FID) data directly in time, at the cost of requiring numerical processing. Ernst also proposed that more information could be obtained from the spectrum if the FID was multiplied by a suitable apodizing function before being Fourier transformed. For example (see ref. 2), an increase in sensitivity can result from the use of a matched filter[1], whereas an increase in resolution can be achieved by the use of gaussian multiplication[1,3], application of sine bells[4–8] or convolution difference[9]. These methods are now used routinely in NMR data processing. The maximum entropy method (MEM)[10] is theoretically capable of achieving simultaneous enhancement in both respects[11], and this has been borne out in practice in other fields where it has been applied. However, this technique requires relatively heavy computation. We describe here the first practical application of MEM to NMR, and we analyse ^{13}C and ^{1}H NMR spectra of 2-vinyl pyridine. Compared with conventional spectra, MEM gives considerable suppression of noise, accompanied by significant resolution enhancement. Multiplets in the ^{1}H spectra are resolved better leading to improved visual clarity.

For a given FID, many spectra can be produced which are consistent with the data—too many for easy comprehension. Nevertheless, we must, in practice, select just a single spectrum. It has been shown[12,13] that MEM is the only generally consistent selection procedure. We maximize the entropy (negative information content)

$$S = -\int f(\nu)\log f(\nu)\,\mathrm{d}\nu \quad (f \text{ normalized to } \textstyle\int f\,\mathrm{d}\nu = 1)$$

of the spectrum $f(\nu)$ of oscillator number densities, and in this way can select the spectrum which has the minimum of structure and hence fewest artefacts. Note that the '$f \log f$' formula used here differs from the '$\int \log f(\nu)\,\mathrm{d}\nu$' entropy form commonly used[14–16] in maximum entropy time-series analysis. The latter form produces a spectrum which gives greatest flexibility (maximum entropy) to individual samples from a time-series constrained by autocorrelation data. In NMR by contrast, we observe the FID time-series directly, and we are interested in the spectrum $f(\nu)$ as an object in its own right. For both these reasons, we should use the $f \log f$ form[17]. NMR data analysis is akin to radio interferometry[18,19], where $f \log f$ is also appropriate, but NMR has the advantage of being free of peripheral arguments such as that about the role of the statistics of radio photons[20].

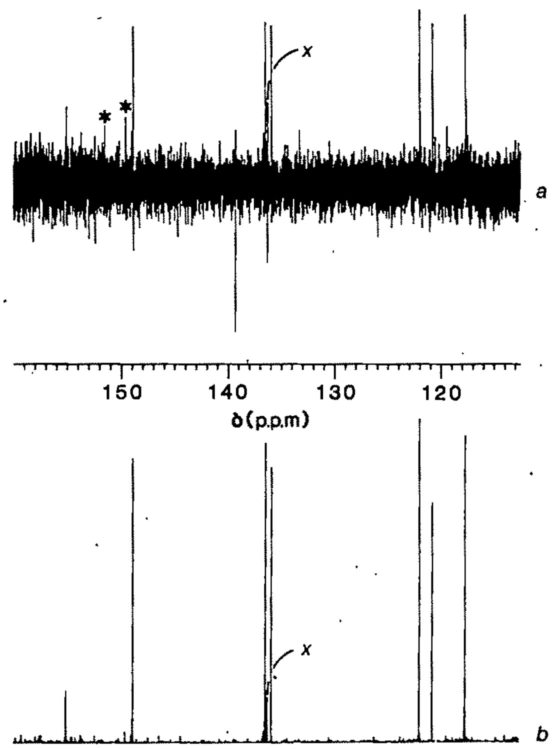

Fig. 1 *a*, Conventional Fourier transform of the ^{13}C FID produced by a pulse of 1.6 μs on a sample of 2-vinyl pyridine in CDCl$_3$. *b*, MEM spectrum from the same FID. ×, Instrumental artefact, attributed to imperfect transmitter gating.

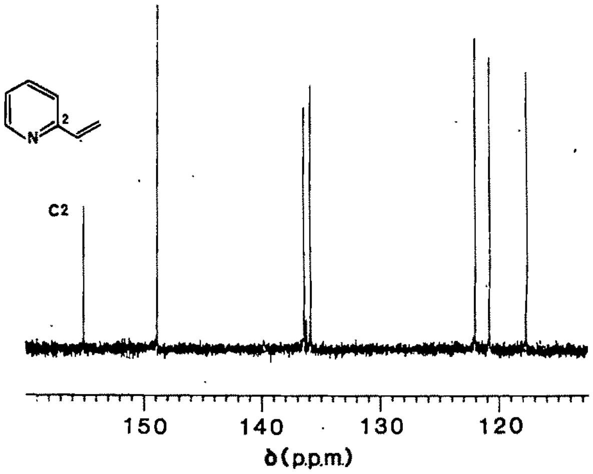

Fig. 2 Conventional Fourier transform of the ^{13}C FID produced by a pulse of 13 μs.

Note that MEM produces a spectrum which has to fit the data, in the sense that the distribution of oscillators would produce a FID not significantly different from the actual data. Conventional methods of processing, such as direct or apodized Fourier transforms, give spectra which lack this property.

The ^{13}C data for 2-vinyl pyridine in CDCl$_3$ were recorded on a Bruker WM-250 instrument using the manufacturer's quadrature phase cycling and quadrature detection mode. We present results for a noisy test spectrum determined using a short pulse

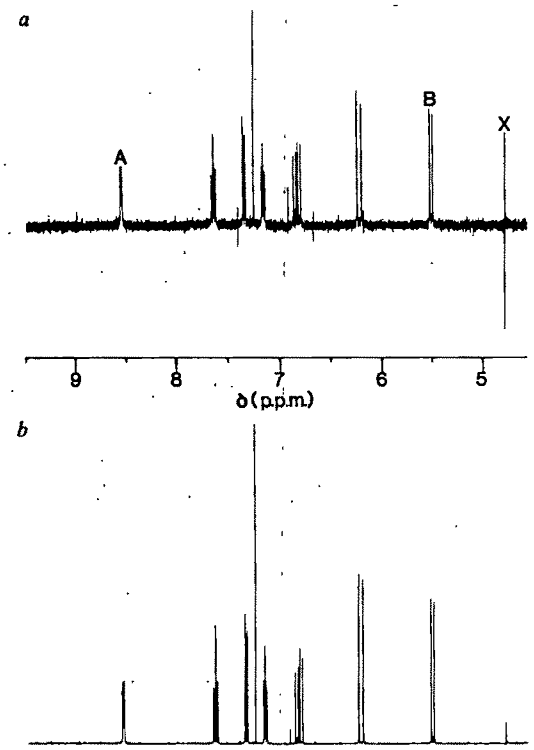

Fig. 3 *a*, ¹H spectrum of 2-vinyl pyridine produced by conventional Fourier transform. *b*, Corresponding MEM spectrum.

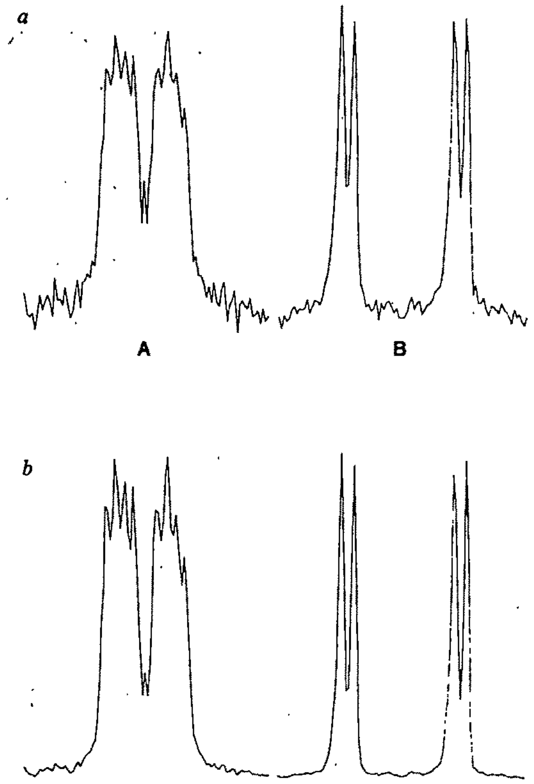

Fig. 4 *a*, Expansions of the multiplets A and B in the conventional spectrum (Fig. 3*a*). *b*, Expansions of the multiplets A and B in the MEM spectrum (Fig. 3*b*).

time (1.6 μs). We corrected the baseline of the FID and converted it from quadrature to cosine form[21] over 8,192 points before zero filling to 16,384 points. The Cambridge MEM algorithm[22] was used to find the two principal phase parameters, by maximizing the entropy over both the spectrum and these parameters simultaneously. The phase parameters were then used for both the conventional FT and MEM spectra shown in Fig. 1.

In the conventional FT spectrum, Fig. 1*a*, the signals assigned to C-3, C-4, C-5, C-6, C-7 and C-8 are reasonably clear of the noise, but the signal from C-2 is only marginally higher than some of the noise peaks (marked with asterisks). In the corresponding MEM spectrum obtained from the same data (Fig. 1*b*), noise is dramatically decreased, so that the peak for C-2 appears much more convincing. The reliability of the lines shown in the MEM spectrum can be assessed by comparison with a control FT spectrum (Fig. 2) produced from the same sample, using a longer pulse time (13 μs) to increase the signal-to-noise ratio. This proves that the C-2 line picked out by maximum entropy is a true signal, as opposed to the noise peaks marked with asterisks in Fig. 1*a*. The ability of MEM to discriminate in favour of real signals, and against noise of similar intensity, was reproduced in three other test spectra determined in the same conditions.

The ¹H data were recorded in a similar manner on a Bruker WH-400 instrument. We selected a moderately noisy spectrum to give a clear comparison between MEM and conventional procedures. Figure 3*a* shows the conventional Fourier spectrum, and Fig. 3*b* the corresponding MEM spectrum. In addition to the obvious suppression of noise, MEM has also sharply reduced the instrumental artefact, X. Two representative multiplets, A and B, are plotted on expanded scales in Fig. 4*a* (conventional) and Fig. 4*b* (MEM). The multiplets are appreciably sharper and better resolved in the MEM spectrum. Although not dramatic, this effect shows that suppression of noise is by no means accompanied by a loss of resolution, so that the technique should be of value in processing spectra that are crowded as well as noisy.

These results demonstrate that MEM provides a potentially important addition to the range of techniques currently available for producing NMR spectra. Details of the Cambridge MEM algorithm used to produce these spectra will be published elsewhere[22]. The disadvantage of MEM is the extra computing involved, amounting to about 1 min on a IBM3081 mainframe computer. The algorithm requires eight times the store and about 30 times the central processing time of an ordinary Fourier transform. Further work is in progress on the application of MEM to ¹H and ²H NMR spectra, and also on the more sophisticated approach in which a two-dimensional map is reconstructed from one-dimensional data[11].

We thank the SERC and St John's College, Cambridge, for financial support, and Drs J. D. Mersh and J. K. M. Sanders for use of their data transfer software. We also thank Dr Sanders for helpful comments.

Received 17 May; accepted 24 July 1984.

1. Ernst, R. R. *Advances in Magnetic Resonance* Vol. 2, 1–135 (Academic, New York, 1966).
2. Lindon, J. C. & Ferrige, A. G. *Prog. Nucl. Magn. Reson. Spectrosc.* **14,** 27–80 (1980).
3. Ferrige, A. G. & Lindon, J. C. *J. magn. Reson.* **31,** 337–340 (1978).
4. De Marco, A. & Wüthrich, K. *J. magn. Reson.* **24,** 201–204 (1976).
5. Gueron, M. *J. magn. Reson.* **30,** 515–520 (1978).
6. Clin, B., De Bony, J., Lalanne, P., Biais, J. & Lemanceau, B. *J. magn. Reson.* **33,** 457–463 (1979).
7. Lohmann, J. A. B. *J. magn. Reson.* **38,** 163–167 (1980).
8. Brereton, R. G., Garson, M. J. & Staunton, J. *J. magn. Reson.* **43,** 224–233 (1981).
9. Campbell, I. D., Dobson, C. M., Williams, R. J. P. & Xavier, A. V. *J. magn. Reson.* **11,** 172–181 (1973).
10. Gull, S. F. & Daniell, G. J. *Nature* **272,** 686–690 (1978).
11. Sibisi, S. *Nature* **301,** 134–136 (1983).
12. Shore, J. E. & Johnson, R. W. *IEEE Trans. Inform. Tech.* IT-26, 26–37 (1980); IT-29, 942–943 (1983).
13. Livesey, A. K. & Skilling, J. *Acta crystallogr.* A (in the press).
14. Burg, J. P. thesis, Stanford Univ. (1975).
15. Ulrych, T. J. & Bishop, T. N. *Rev. Geophys. Space Phys.* **13,** 183–200 (1975).
16. Fougere, P. *J. geophys. Res.* **82,** 1051–1054 (1977).
17. Skilling, J. & Gull, S. F. *SIAM Am. Math. Soc. Proc.* **14,** 167–189 (1984).
18. Scott, P. F. *Mon. Not. R. astr. Soc.* **194,** 25P–29P (1981).
19. Tuffs, R. J. thesis, Cambridge Univ. (1984).
20. Frieden, B. R. *J. opt. Soc. Am.* **73,** 927–938 (1983).
21. Redfield, A. G. & Kunz, S. D. *J. Magn. Reson.* **19,** 250–254 (1975).
22. Skilling, J. & Bryan, R. K. *Mon. Not. R. astr. Soc.* (in the press).

High $^3He/^4He$ ratio in ocean sediments

M. Ozima, M. Takayanagi, S. Zashu & S. Amari

Geophysical Institute, University of Tokyo, Tokyo 113, Japan

Two decades ago, Merrihue[1] reported $^3He/^4He$ ratios of $>10^{-4}$ in ferromagnetic separates from a Pacific deep ocean red clay and concluded that the high ratio is due to extraterrestrial debris amounting to ~1% of the sediment. A decade later Krylov *et al.*[2] compiled $^3He/^4He$ isotopic data on ocean sediments measured in the Soviet Union and observed that the $^3He/^4He$ ratio is generally higher in pelagic sediments where the sedimentation rate is lower. They suggested that the high $^3He/^4He$ ratio was attributable to extraterrestrial materials which were concentrated in slowly accumulating ocean floor. However, these important discoveries were almost completely neglected until we re-examined the problem. We have measured 39 sediments from 12 different sites, 10 sites from the western to central Pacific and two sites from the Atlantic Ocean. We find $^3He/^4He$ ratios $>5\times10^{-5}$ for six sites, well above the values generally observed in common terrestrial materials. The very high $^3He/^4He$ ratio in the sediments is probably due to input of extraterrestrial materials. Input of stratospheric dust of $\lesssim1$ p.p.m., which corresponds to a fallout rate of ~2,000 tons per year, can explain the observation.

All the sediments that we studied are piston-cored samples. While two Atlantic sediments (DSDP samples) are of Cretaceous age[3,4], all the Pacific samples are of Quaternary or, at most, of late Tertiary age[5,6]. Petrographical descriptions and other data of the samples are given either in a DSDP Initial Report[3,4] or in the Preliminary Report for the *Hakuho Maru* cruise[5,6]. All the Pacific and Atlantic samples are very fine-grained typical pelagic sediment. A few hundred milligrams of a sample were hand-picked from a sediment core (diameter, 5 cm), which had been stored with a thick plastic cover (Pacific samples). Sediments were almost completely dried out and consolidated. Before gas extraction, samples were heated in vacuum at ~150 °C to reduce surface air contamination. No further treatment of the samples, such as cleaning was attempted.

The detailed experimental procedures for the gas extraction and the mass spectrometric analysis are described elsewhere[7]. Helium isotopic measurements were done with a resolution of 600 and ^3He peak was completely resolved from HD and H_3. The measured $^3He/^4He$ isotopic ratio was calibrated against an air helium isotopic ratio, which was measured repeatedly during the sample runs. The mass spectrometer has a dual collector for simultaneous measurements of ^3He and ^4He. Neither the mass spectrometer nor the extraction system have been used previously to analyse extraterrestrial materials. With these precautions, we believe that the measured helium isotopic ratios are satisfactorily free from interference or contamination effects, or from mass discrimination.

Table 1 shows the experimental data. The principle uncertainty in the experimental results comes from the correction for the hot blank. We assigned 50% of the hot blank as a possible error, in addition to the analytical error in the mass spectrometry, the latter being generally much less than the former. Because the variation in the hot blank throughout the experimental period was <10%, a possible error of 50% of the hot blank would be an overestimation. Except for Ar, there was too little of the other noble gases to allow reliable quantitative or isotopic analyses. In most cases the $^{40}Ar/^{36}Ar$ ratio is significantly higher than the atmospheric ratio, that is 295.5.

Measurements made on samples taken from the same level in a core (~1 cm apart in the same level) (KH75-3-5-2: levels 100 and 860 cm) show considerable difference both in the He content and in the isotopic ratio. The above consideration of the error estimation suggests that this difference is primarily due to sample heterogeneity owing to the small size (~100 mg) used for the experiment.

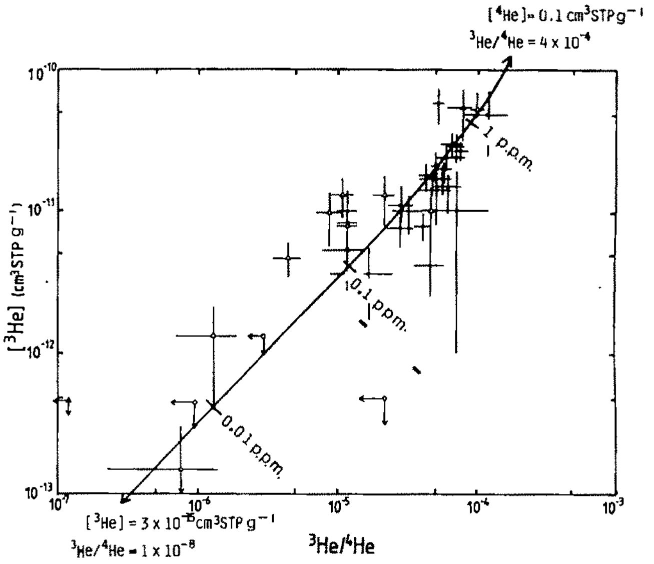

Fig. 1 ^3He content in sediments is plotted against $^3He/^4He$ ratio. The curve indicates the mixing between He in the cosmic dust ($^4He = 0.1\ cm^3STP\ g^{-1}$, $^3He/^4He = 4\times10^{-4}$) and in the sediments ($^3He = 3\times10^{-15}\ cm^3STP\ g^{-1}$, $^3He/^4He = 10^{-8}$). Numbers on the curve indicate the degree of the contamination (in p.p.m.) of the cosmic dust in sediments. △, KH-80-3; ○, KH68-4; ●, KH75-3-5; □, KH-75-3-11; ◇, DSDP.

Although the few data available make it difficult to draw a general conclusion on the distribution of $^3He/^4He$ ratios in ocean sediments, there appears to be no clear correlation between isotopic ratio and geography. However, it should be noted that high $^3He/^4He$ value ($>5\times10^{-5}$) is common in the Pacific sediments. Except for diamonds[8], the highest $^3He/^4He$ ratio ever reported for terrestrial materials is 5.2×10^{-5} for Hawaiian olivine xenoliths[9], the values for common terrestrial rocks such as granites being $\ll5\times10^{-5}$ (ref. 10). ^3He production in the Earth is practically negligible[11]. It is also difficult to attribute the high $^3He/^4He$ ratio to some artificial nuclear fallout or debris, as samples were taken at more than two different levels in a core considerably deeper than the seabed and in several cases the deeper level showed the higher $^3He/^4He$ ratio. Because extraterrestrial materials have $^3He/^4He$ ratios generally higher than 10^{-4} with high helium content ($^4He \geq 10^{-5}\ cm^3STP\ g^{-1}$)[10], it is reasonable to assume input of some extraterrestrial materials to the sediments to account for their high $^3He/^4He$ ratios ($>5\times10^{-5}$). This assumption is supported by the following observation.

Figure 1 shows the $^3He/^4He$ ratio plotted against ^3He content. There appears to be a clear positive correlation between them which can be explained by the mixing of some materials with a high ^3He content and $^3He/^4He$ ratios with sediment which has a generally low He content[12]. We can imagine either meteorite fragments or cosmic dust as possible contaminants. If meteorite fragments were produced by meteoritic impact on the Earth, the occurrence of high $^3He/^4He$ in ocean sediment must be sporadic. The observation of a common high $^3He/^4He$ ratio in ocean sediments, not only in the lateral but also in the vertical sections, contradicts the sporadic meteorite impact theory. Also, an impact would result in severe helium loss from the meteorite debris. Hence, we favour the cosmic dust origin for the anomalously-high $^3He/^4He$ ratio in the sediments.

If global fallout of cosmic dust were responsible for the high $^3He/^4He$ ratio as well as to the high ^3He content, we would expect an inverse relationship between the concentration of the cosmic dust and the sedimentation rate, because in the high accumulating region, the fallout cosmic dust must be diluted by terrestrial materials. Figure 2 shows the ^3He content plotted against the sedimentation rate (taken from refs 3–6). Two Atlan-

Table 1 Experimental data

			Hot blank		Sediments		
Sample*	Locality (water depth)	Weight (g)	^{3}He (10^{-11} cm^{3}STP g^{-1})	^{4}He (10^{-7} cm^{3}STP g^{-1})	^{3}He (10^{-11}cm^{3}STP g^{-1})	^{4}He (10^{-7}cm^{3}STP g^{-1})	^{3}He/^{4}He (10^{-6})
KH68-4-15	11°59′N						
220–222.5 cm	169°58′W	0.131	0.07	0.42	5.8±1.6	10.8±2.0	53±5
520–522.5 cm	(5,050 m)	0.116	0.07	0.62	1.0±0.4	8.2±1.3	12±2
790–792.5 cm		0.131	0.05	0.53	0.8±0.3	7.0±1.4	12±2
KH68-4-18	1°60′N						
203–205.5 cm	170°01′W	0.099	0.04	0.23	0.4±0.3	0.8±0.2	47±21
506 cm	(5,470 m)	0.133	0.08	0.55	1.5±0.6	2.4±0.4	63±15
979 cm		0.106	0.12	0.66	1.0±0.9	1.4±0.3	73±49
KH68-4-20	2°28′S						
527 cm	170°00′W	0.117	0.10	0.61	1.4±0.6	2.7±0.4	52±14
990 cm	(5,130 m)	0.106	0.08	0.48	1.1±0.5	1.9±0.3	58±17
KH75-3-5-2	26°01′N						
4–5 cm	150°00′E	0.110	0.10	0.58	0.4±0.2	2.1±0.1	17±8
100–101 cm (a)	(5,850 m)	0.135	0.04	0.42	1.8±0.4	4.1±0.3	44±7
100–101 (b)		0.151	0.05	0.32	1.1±0.4	3.7±0.7	29±5
205–206 cm		0.150	0.05	0.45	0.8±0.2	2.7±0.2	29±6
296–298 cm		0.157	0.03	0.34	0.8±0.2	2.5±0.2	32±6
378–379 cm		0.118	0.06	0.58	1.7±0.4	3.4±0.2	49±9
408–411 cm		0.0296	0.19	0.82	0.5±0.2	1.8±0.8	30±22
418 cm		0.121	0.05	0.54	1.0±0.3	3.0±0.2	33±8
513–517 cm		0.138	0.04	0.44	3.0±0.6	4.1±0.2	72±10
612 cm		0.144	0.04	0.38	1.7±0.4	2.9±0.2	58±10
620–623 cm		0.135	0.03	0.23	1.5±0.3	1.9±0.2	78±8
713–717 cm		0.142	0.06	0.53	2.1±0.5	4.2±0.3	51±8
813–815 cm		0.136	0.06	0.47	2.4±0.5	3.9±0.2	61±9
859–862 cm (a)		0.118	0.06	0.48	3.0±1.1	4.4±0.8	67±12
859–862 cm (b)		0.0335	0.14	0.89	3.1±1.5	2.6±0.3	119±43
890–891 cm		0.149	0.04	0.39	2.4±0.4	3.4±0.1	72±10
KH75-3-11-2	32°59′N						
218–220 cm	153°29′E	0.0221	0.06	1.03	NM§	2.75±0.92	<3
864–866 cm	(5,650 m)	0.133	0.04	0.62	0.13±0.1	10.5±2.2	1.3±0.6
KH80-3-18	32°44.9′N						
397 cm	158°17.6′E	0.140	0.18	0.35	0.09±0.09	3.1±0.1	3±3
529–531 cm	(2,640 m)	0.140	0.07	0.56	0.53±0.25	4.4±0.8	12±4
KH80-3-22	31°16.2′N						
403 cm	153°42.9′E	0.128	0.05	0.52	0.47±0.13	10.4±0.7	5±1
500–501 cm	(5,750 m)	0.144	0.06	0.45	0.95±0.40	10.8±2.3	9±2
KH80-3-22	13°44.3′N						
200–201 cm	148°37.9′E	0.118	0.06	0.77	0.79±0.27	6.7±1.1	12±2
550–552 cm	(5,800 m)	0.118	0.08	0.60	5.2±2.1	6.6±1.3	79±17
KH80-3-28	11°03.3′N						
200–201 cm	151°34.6′E	0.125	0.07	0.51	1.3±0.4	12.3±2.3	11±2
600–601 cm	(5,800 m)	0.114	0.08	0.44	1.3±0.5	6.0±1.0	22±4
1,049–1,051 cm		0.141	0.6	0.49	5.3±1.7	5.1±0.9	105±14
KH80-3-30	9°50.6′N						
999–1,003 cm	153°13.5′E	0.122	0.08	0.56	1.0±0.5	2.1±0.4	47±15
	(5,480 m)						
Leg 43-386-42-3	31°11.21′N						
30–31 cm	64°14.94′W	0.223	0.0039	0.054	0.0065±0.0158	0.099±0.011	7±15
109–110 cm	(4,782 m)	0.174	0.005	0.16	0.009±0.008	1.9±0.1	0.47±0.44
Leg 43-387-30-1	32°19.2′N						
140–141 cm	67°40.0′W	0.197	0.015	0.14	NM§	NM§	<0.3
	(5,117 m)						

* About 100 mg of sample was handpicked from a sediment core at the designated interval (depth from the water bottom for the Pacific samples and depth at respective core section for the Atlantic samples).

† ^{3}He/^{4}He ratio is calibrated against air helium ^{3}He/^{4}He ratio to reduce a mass fractionation effect.

‡ Errors in ^{3}He and ^{4}He consist of 50% of the hot blank and 1σ in the mass spectrometry, the former being much larger than the latter.

§ A fraction of the extracted gas was introduced into a mass spectrometer. Hence, only the isotopic ratio was measured and the helium amounts were not measured (NM).

tic samples are quite isolated from Pacific samples. This may be due to helium-loss from the Atlantic samples, because they are older by a factor of 100 than the Pacific sediments. Ignoring the Atlantic samples, there still seems to be an approximately inverse relation between the ^{3}He content and the sedimentation rate. If we assume uniform fallout rate of cosmic dust and also that the initial ^{3}He content in sediment is negligible, then the ^{3}He concentration in the sediment, which can be taken as a measure of the amount of cosmic dust input, can be expressed as a function of sedimentation rate (r) and flux of the cosmic dust fallout (f),

$$(^3\mathrm{He})_{\mathrm{sed}} = \frac{\alpha f}{\rho r} \qquad (1)$$

where α and ρ denote respectively the concentration of ^{3}He in the extraterrestrial material and density of the sediment. For the

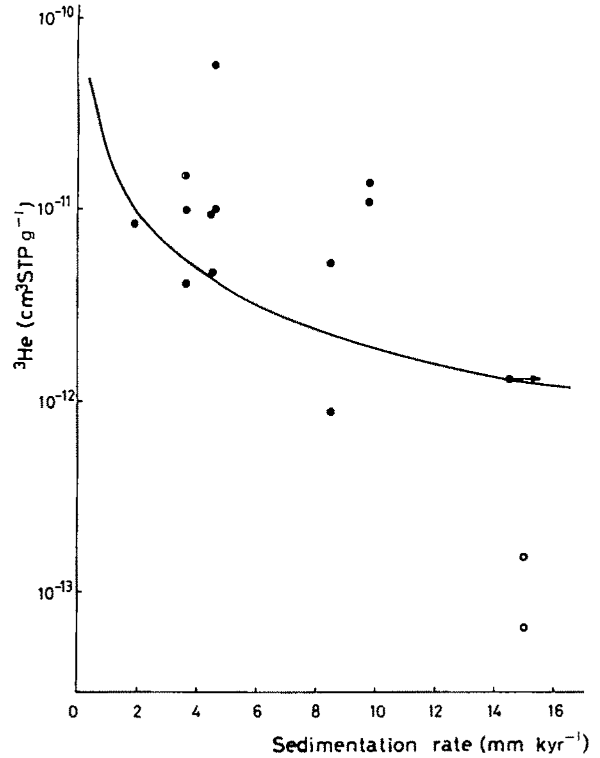

Fig. 2 ^{3}He content plotted against sedimentation rate. ○, The Atlantic DSDP samples which are of Cretaceous age. The Pacific samples (●) show an approximately inverse relationship between ^{3}He content and sedimentation rate. The curve is constructed by assuming uniform fallout rate (2,000 tons yr^{-1}) of cosmic dust ($^4\text{He} = 0.1$ cm^{3}STP g^{-1}, $^3\text{He}/^4\text{He} = 4\times10^{-4}$).

^{3}He concentration in the cosmic dust, we take the value measured for stratospheric cosmic dust (~10-μm diameter size), that is $\alpha = 4\times10^{-5}$ cm^{3}STP g^{-1}. Putting $\alpha = 4\times10^{-5}$ cm^{3}STP g^{-1} and $\rho = 2$ g cm^{-3} in equation (1), we can construct a family of curves corresponding to different values of f. Figure 2 shows a curve corresponding to $f = 4\times10^{-10}$ g cm^{-2} yr^{-1}, which approximates the data. The value $f(=4\times10^{-10}$ g cm^{-2} y$^{-1})$ corresponds to a cosmic dust fallout rate of about 2,000 tons yr^{-1}. The value may be favourably compared with the estimate made on satellite, radio and visual observations of about a few hundred tons per year for particle size below 10 μm in diameter[13], considering the large uncertainty in the estimates of the fallout rate and the helium content of the cosmic dusts. Cosmic dust which has a diameter greater than 10 μm may not be important in the helium inventory of sediments, because the larger grains are likely to lose helium due to atmospheric impact heating[14]. Because various factors such as the non-uniform fallout rate of the cosmic dust, heterogeneity in their ^{3}He content and He-loss from the cosmic dust particles all act to disturb the simple inverse relation between ^{3}He content and sedimentation rate, it is quite normal to observe only an approximate inverse relation if the cosmic dust fallout is indeed responsible for the high $^3\text{He}/^4\text{He}$ ratio. Hence, we believe that it is the approximate inverse relationship and not the random relationship between the ^{3}He content and sedimentation rate which is significant and that this relationship is attributable to the global cosmic dust fallout.

Assuming that the cosmic dust is responsible for the high $^3\text{He}/^4\text{He}$ ratio, Fig. 1 also shows a mixing curve between the cosmic dust and the sediment. For the cosmic dust, we take $^4\text{He} = 0.1$ cm^{3}STP g^{-1} (ref. 14) and assume solar-wind implanted helium, that is, $^3\text{He}/^4\text{He} = 4\times10^{-4}$. For the uncontaminated sediments, we assumed a typical crustal value of 10^{-8} for $^3\text{He}/^4\text{He}$ ratio[11] and $^4\text{He} = 3\times10^{-7}$ cm^{3}STP g^{-1} (ref. 12). The choice of the values for the sediments is not crucial. In fact, changing the value by a factor of 100 does not significantly alter the mixing curve. Figure 1 shows that <1 p.p.m. input of the cosmic dust can account for the observed high $^3\text{He}/^4\text{He}$ as well as the high ^{3}He content. A preliminary study to search for extraterrestrial materials was made on sample KH75-3-5-2. Microscopic examination did not show any such evidence. Neutron activation analyses showed slightly higher Ni (200–600 p.p.m.) and Co contents (100–200 p.p.m.), but Cr (30–50 p.p.m.) is slightly lower than that observed in common crustal rocks. We could not detect Ir. Note that because of the very significant difference in He isotopic ratios of extraterrestrial and terrestrial materials, the method is potentially very useful for identifying input of the former to ocean sediments.

In the case of sample KH75-3-5-2 (total core length ≈9 m), there seems to be a progressive increase both in the ^{3}He content and $^3\text{He}/^4\text{He}$ ratio with increasing depth. This may be due either to the change in the cosmic dust fallout rate, or to that in the sedimentation rate, or to the both.

We thank Professor K. Kobayashi and Dr T. Furuta for Pacific sediments and helpful comments.

Received 16 April; accepted 25 July 1984.

1. Merrihue, C. *Ann. N.Y. Acad. Sci.* **119**, 351–367 (1964).
2. Krylov, A. Ya., Mamyrin, B. A., Silin, Yu. I. & Khabarin, L. V., *Geochem. Int.* **10**, 202–205 (1973).
3. *Init. Rep. DSDP.* **43**, 19–321 (1979).
4. *Init. Rep. DSDP* **43**, 323–391 (1979).
5. Kobayashi, K., Tonouchi, S., Furuta, T. & Watanabe, M., *Bull. Ocean Res. Inst. Univ. Tokyo* No. 13, 1–148 (1980).
6. *Prelim. Rep. of the Hakuho Maru Cruise* KH80-3, 209 (Ocean Research Institute, University of Tokyo, 1981).
7. Ozima, M., Zashu, S. & Nitoh, O. *Geochim. cosmochim. Acta*, **47**, 2217–2224 (1983).
8. Ozima, M. & Zashu, S. *Science* **219**, 1067–1068 (1983).
9. Kaneoka, I. & Takaoka, N. *Earth planet. Sci. Lett.* **39**, 382–386 (1978).
10. Ozima, M. & Podosek, F. A. *Nobel Gas Geochemistry*, 367 (Cambridge University Press, 1983).
11. Tolstikhin, I. N. in *Terrestrial Rare Gases*, (eds Alexander, E. C. Jr & Ozima, M.) 33–62 (Japan Science Society Press, 1978).
12. Podosek, F. A., Honda, M. & Ozima, M. *Goechim. cosmochim. Acta* **44**, 1875–1884 (1980).
13. Hughes, D. W. in *Cosmic Dust* (ed. McDonnell, J. A. M.,), 123–185 (Wiley, New York 1978).
14. Rajan, R. S. *et al. Nature* **267**, 133–134 (1977).

Occurrence of subtidal dolomite in a hypersaline lagoon, Kuwait

A. Gunatilaka, A. Saleh, A. Al-Temeemi & N. Nassar

Department of Geology, Kuwait University, Box 5969, Kuwait

We report here the discovery of subtidal dolomite in a shallow hypersaline lagoon during a study of Recent carbonate and evaporite sediments in the Al-Khiran region of southern Kuwait in the northern part of the Arabian Gulf (Fig. 1). Diagenetic dolomites are known from a variety of geographical locations and a spectrum of environmental conditions[1–6]. Although many occurrences of subaqueous dolomite have been documented[1–4], none has been reported from the subtidal areas of extensive Recent marine carbonate environments. The Al-Khiran dolomites show complex polyhedral crystal habits and a composition which ranges from $Ca_{51}Mg_{49}$ to $Ca_{56}Mg_{44}$. We postulate that a partial removal of dissolved sulphate ions (by bacterial reduction) from the interstitial waters of the sediments, the moderate Mg^{2+}/Ca^{2+} ratios of the hypersaline waters and the occasional near-schizohaline conditions in the lagoon may be responsible for the formation of this dolomite.

The small Al-Khiran lagoon is the remnant of a much larger body of water which is now partly infilled and dry (Fig. 1), and is connected to the Arabian Gulf by a small tidal channel. The maximum spring tidal range is ~2.2 m and the lagoon drains out almost completely only two or three times each year. Most of the time there is at least 0.50 m of water in the lagoon, and its floor is colonized by a sparse cover of *Halodule* plants. Lagoon salinities are fairly uniform throughout most of the year (42–44‰) and occasionally rise to 50–52‰ in the hottest months (July–August). The average summer and winter air temperatures

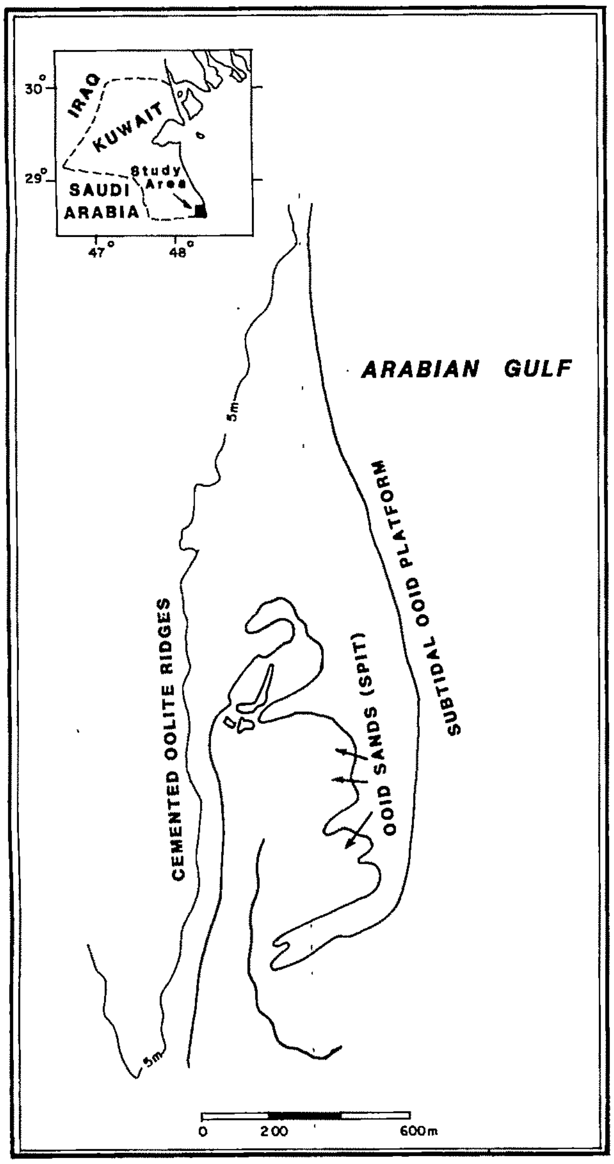

Fig. 1 The Al-Khiran lagoon and location of the study area.

are 45-47 °C and 12-15 °C, respectively. Water temperatures may exceed 30 °C in the summer and fall to as low as 8 °C in the winter months. Rainfall averages 100-120 mm yr^{-1}, but ranges up to 300 mm yr^{-1}.

The lagoon sediments are mostly a mixture of pellet muds and biodegraded skeletal material with some ooids (5–8%) and average ~70% aragonite. A representative lithological section (from cores) is shown in Fig. 2. The entire sediment column to a depth of more than 100 cm is highly reducing and organic-rich. Many samples from the lagoon bottom were analysed by X-ray diffraction and all contained diagenetic dolomite; it is most common in the upper 5 cm of the cores but occasionally is found at depths of 8–10 cm. The average dolomite content is 3.6% by weight of the total carbonate fraction and ranges from 3.2 to 4% (as determined by recalculation from 12 chemical analyses; the margin of error is too high when determining low dolomite contents by X-ray methods). The molar composition of dolomite was determined by measuring the peak shift of the (104) dolomite reflection relative to the (101) quartz reflection (internal standard)[7]; the standard error of the mean is ±0.20 mol% $CaCO_3$ in dolomite for seven replicates. Dolomite composition averages $Ca_{51.8}Mg_{48.2}$ (range is Ca_{51} to Ca_{56}, based on 22 analyses). The dolomites are all Ca-rich and poorly ordered and have diffraction characteristics typical of naturally occurring early diagenetic 'dolomites'[7,8].

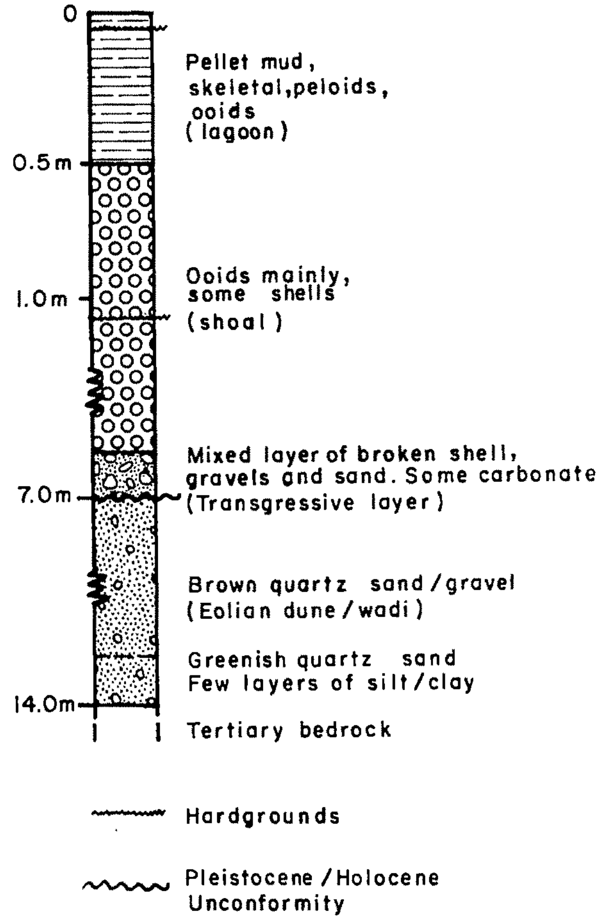
0
Pellet mud, skeletal, peloids, ooids (lagoon)
0.5m
Ooids mainly, some shells (shoal)
1.0m
Mixed layer of broken shell, gravels and sand. Some carbonate (Transgressive layer)
7.0m
Brown quartz sand/gravel (Eolian dune/wadi)
Greenish quartz sand Few layers of silt/clay
14.0m
Tertiary bedrock
Hardgrounds
Pleistocene/Holocene Unconformity

Fig. 2 Representative lithological section of the lagoon showing stratigraphical framework and depositional environments.

Scanning electron microscope (SEM) examination of several of these samples reveals that the dolomite crystals are well developed with complex polyhedral crystal habits, and range in size from <1 μm to ~5 μm (Fig. 3). They are found most commonly as clusters within minute 'solution' cavities on the surfaces of pellets and, less frequently, within the aragonitic needle mud fraction. Surprisingly, the development of the unit rhomb alone is very rare. The most common crystal form is the unit rhomb bevelled by a pair of triangular-shaped basal pinacoids (0001; 000$\bar{1}$) which may be equally or subequally (asymmetrically) developed in a given crystal (Fig. 3). Less commonly, various other vicinal facets develop, modifying the rhombic symmetry. Although X-ray analysis does not indicate the presence of any gypsum, the scanning electron micrographs do show trace quantities of microcrystalline, euhedral gypsum crystals in the sediment.

The concentrations of Mg and Ca in lagoon surface and squeezed interstitial waters were determined by standard atomic absorption methods and sulphate concentration was measured by a turbidimetric method[9]. Carbonate alkalinity was determined by acid titration. All analyses were performed with reference to standard seawater to ensure good precision and accuracy. The results are summarized in Table 1.

The data indicate moderate Mg/Ca ratios, but more important from the point of view of dolomite formation is the reduced levels of dissolved sulphate in the pore fluids compared with surface waters; this is due to the high degree of microbial sulphate reduction within the sediments which prevents large-scale build-up of SO_4^{2-} concentrations. The alkalinity of the reduced pore waters is slightly higher than that of surface waters, but we do not consider this significant, particularly because there was a lapse of ~30 h between collection and analysis (most critical for alkalinity).

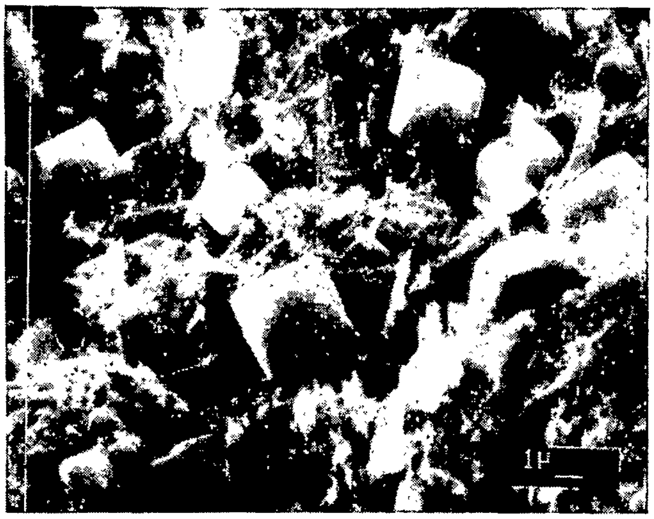

Fig. 3 Scanning electron micrograph of subtidal dolomite crystals from the Al-Khiran lagoon. The sample is from 7 cm depth in the core. Note the polyhedral crystal habits and particularly the unit rhomb modified by basal pinacoids.

In the winter months of 1982–83, ~240 mm of rainfall were recorded in the area, with one thunderstorm accounting for 128 mm in 18 h. The latter episode diluted and flushed the lagoon waters temporarily, but significantly, bringing it down to ~16‰ salinity (and possibly much lower as salinity was measured the day after the thunderstorm subsided) and producing mild schizohaline conditions. Freshwater flushing of hypersaline environments can be an important process in dolomite formation[10]. Freshwater flushing, however, does not markedly reduce the Mg/Ca ratio of the lagoon waters from its normal hypersaline values; if this were the case, the reduction of sulphate ion levels in the sediments (through microbial activity and/or by producing schizohaline conditions) could be more important than high Mg/Ca ratios or high salinities for dolomite formation[11]. Baker and Kastner suggest[11] that high concentrations of SO_4^{2-} ions suppress efficient dolomite nucleation in subtidal or open marine environments, and may be one of the kinetic barriers preventing large-scale dolomite precipitation from seawater, despite the fact that it is the thermodynamically preferred carbonate phase.

Based on the vast amount of data already available, it seems that high Mg/Ca ratios and salinities of pore waters should generate dolomites that are near stoichiometric in composition, and as the Mg/Ca ratio and salinities decrease the dolomites should depart from ideal stoichiometry[6]. The Al-Khiran data seem to agree with this general premise. However, other factors may be involved in determining stoichiometric behaviour[6].

The presence of dolomite in the top few centimetres of the sediments indicates that it formed in the very recent past of the lagoon and with the advent of quiet water conditions (pellet muds). The ooid sands below the dolomite represent the open and high-energy conditions of a shoal environment. Furthermore, the presence of patchy subtidal hardgrounds would act as a barrier for flushing and downward movement of potentially dolomitizing fluids. This difference between the nature of the lagoon now compared with earlier times shows the importance of the environment in dolomite genesis.

Dolomitization is a very complex process and opinion is divided as to the mechanisms involved in formation of diagenetic dolomites[2,3,4,6,10,11]. What is the mechanism operating during Recent dolomite genesis in an environment of reduced sulphate concentration and moderate Mg/Ca ratios, with the possible influence of occasional schizohaline conditions in the lagoon? Mass balance calculations indicate that with Mg/Ca ratios of 5.2–6.3 and average porosities in similar sediments, more dolomite should form than is observed in Al-Khiran. Massive dolomitization, however, (even in sabkhas) depends on more complex hydrodynamic behaviour of pore fluids in a sediment column (Al-Khiran sabkhas show Mg/Ca values of 10–14, yet the dolomite levels are rarely above 8%). Hence, the Mg/Ca ratio argument appears to be a geochemically weak one. However, moderate Mg/Ca values may be essential to stabilize the dolomite once it is formed[4]. Thus, the low SO_4^{2-} ion concentrations in the pore fluids are the most likely controlling factor in dolomite genesis. In fact, the effects of sulphate reduction on carbonate alkalinity are regarded by some authors as a critical factor for carbonate precipitation[4,11]. We do not imply that the dolomite is a direct precipitate from lagoon waters; rather, the textural evidence from scanning electron microscopy demonstrates that it may be a replacive, cement phase, having formed at the expense of micritic aragonite (Fig. 3).

Table 1 Carbonate alkalinity and levels of SO_4^{2-}, Ca and Mg in lagoon surface and interstitial waters

	Surface waters	Reduced pore waters
SO_4^{2-} concentration (M)	0.030–0.036 (0.034)	0.020–0.028 (0.025)
Carbonate alkalinity (M)	0.0033–0.0034 (0.0033)	0.0036–0.0041 (0.0037)
Mg^{2+}/Ca^{2+} ratio (molar)	5.2–6.3	5.4–6.2

Values are the range (mean).

It is instructive to compare Al-Khiran with other geochemically similar environments of Recent dolomite formation. Subtidal dolomite has not been reported from the Trucial Coast lagoons of the southern Arabian Gulf[12,13], where schizohaline conditions are probably never achieved (only 30–40 mm rainfall yr^{-1}). In contrast, Al-Khiran experiences slight drops in salinity every year during the wet season and mild schizohaline conditions at least once every few years, particularly during neap-tidal phases when the volume of water in the lagoon is considerably reduced. In the extremely evaporitic and stratified Solar Lake[4], dolomite formation is seasonal and the driving mechanism is the very efficient seepage-reflux of Mg-rich hot brines, which also explains why it forms at depth and not at the surface of the sediments. The dolomite here too is a replacement following aragonite. The occurrence of dolomite in Naxos[3] represents an example of dolomitization in much milder environmental conditions. These two cases and Al-Khiran have one common geochemical feature, that is, the reduction in sulphate ion levels of the potentially dolomitizing fluids, with a dramatic increase in carbonate alkalinity in the case of the Solar Lake[4]. Thus, a combination of water dynamics and fluid compositions could account for these occurrences.

An important implication of this study is that in a prograding coastline, there could be two generations of dolomite in the sediments, having formed either during the subtidal lagoonal phase and/or during the later supratidal sabkha phase by flood-recharge and refluxing, and it may not be possible to distinguish between them. We hope that such dolomite occurrences will encourage carbonate geologists to reinterpret at least some of the literature on dolomite.

We thank Dr D. Shearman for valuable suggestions. This research was made possible by a grant from the Kuwait University Research Council.

Received 14 February; accepted 11 May 1984.

1. Muller, G. Irion, G. & Forstner, K. *Naturwissenschaften* **59**, 158–164 (1972).
2. Bathurst, R. G. C. *Carbonate Sediments and their Diagenesis* (Elsevier, Amsterdam, 1975).
3. Koppenol, W. H. *et al.* in *VI Colloq. on Geology of the Aegean*, Athens Vol. 6(3), 985–994 (1977).
4. Aharon, P., Kolodny, Y. & Sass, E. *J. Geol.* **85**, 27–48 (1977).
5. Zenger, D. H. & Mazullo, S. J. *Dolomitization* (Benchmark Pap. in Geol. No. 65; Hutchinson and Ross, London, 1982).
6. Zenger, D. H., Dunham, J. B. & Ethington, R. L. in *Concepts and Models of Dolomitization* (SEPM spec. Publ. 28, 1980).
7. Goldsmith, J. R. & Graf, D. L. *J. Geol.* **66**, 678–693 (1958).
8. Land, L. S. in *Concepts and Models of Dolomitization*, 87–110 (SEPM Spec. Publ. 28, 1980).
9. Tabatabai, M. A. *J. Sulphur Inst.* **10**(1), 11–13 (1974).
10. Folk, R. L. & Land, L. S. *Bull. Am. Ass. petrol. Geol.* **59**, 60–68 (1975).
11. Baker, P. A. & Kastner, M. *Science* **213**, 214–216 (1981).
12. Butler, G. P. *J. sedim. Petrol.* **39**, 70–89 (1969).
13. Patterson, R. J. & Kinsman, D. J. J. *Bull. Am. Ass. petrol. Geol.* **66**, 28–43 (1982).

Cobalt in pore waters of marine sediments

David Heggie & Tim Lewis

Graduate School of Oceanography, University of Rhode Island, Kingston, Rhode Island 02881, USA

During early diagenesis on the sea floor, metal-recycling processes exert important controls on the preservation rates and distributions of metals in marine sediments. The elucidation of internal recycling processes, therefore, is important in understanding trace-metal mass balances in the oceans. Recent measurements of cobalt in seawater[1] suggest that cobalt is scavenged from the deep sea and hence follows biogeochemical pathways similar to manganese. We present here measurements of cobalt in pore waters of marine sediments and find that cobalt was released into pore waters in the sub-oxic sediment zone during dissolution of sedimentary manganese oxides (Table 1, Fig. 1). Solid-phase cobalt concentrations in surface (oxic) sediments, above the pore water remobilization horizon, are almost double those measured in the deep (anoxic) sediment zone (Table 2, Fig. 1). The sediment and pore water distributions indicate that a large fraction of sedimentary cobalt is recycled with manganese between oxic and sub-oxic pore waters and redeposited in surface (oxic) sediments.

Pore water samples were obtained from the Hatteras Abyssal Plain and Continental Rise sites of the western Atlantic and from the San Clemente Basin off southern California (Table 1). Sediments from gravity and box cores were loaded into polyethylene tubes and pore waters separated by centrifuging at 13,000 r.p.m. for 5 min (20,800*g*). Pore waters were filtered through precleaned 0.4-μm polycarbonate filters and acidified to *p*H ~ 2 in precleaned polyethylene vials. Cobalt was determined by direct-injection atomic absorption spectrometry on a Perkin Elmer 5000 with Zeeman background correction capability[2]. The detection limit for 60 μl injections was ~2.5 nmol kg^{-1} and precision is ±10% at concentrations of 10–50 nmol kg^{-1}. The technique is not sensitive enough to detect the cobalt levels measured in seawater[1].

The concentrations of cobalt, manganese, nitrate and ammonia in pore waters are listed in Table 1. We use nitrate and ammonia data to infer the 'redox' character of the sediments[3]. The depth of the nitrate maximum indicates the approximate depth of penetration of bottom water oxygen into the sediments[4] and, therefore, oxic sediments. Nitrate depletions below the maximum measured, and the appearance of

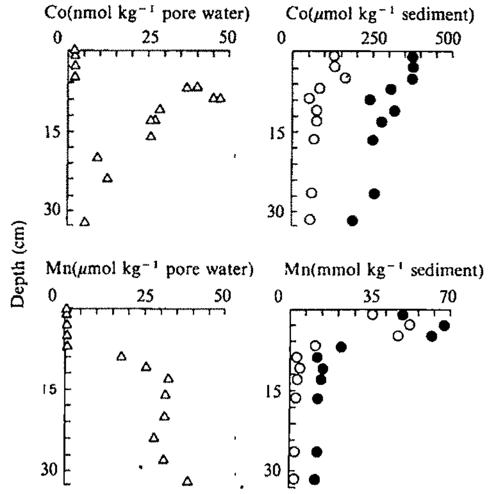

Fig. 1 Co and Mn pore water and sediment concentrations from Hatteras Continental Rise, core BC-4. ○, Leach; ●, total.

Table 1 Pore water concentrations

Depth (cm)	NO_3 (μmol kg^{-1})	NH_3 (μmol kg^{-1})	Mn (μmol kg^{-1})	Co (nmol kg^{-1})
HAP SC3; 32°34.0′ N, 69°49.7′ W; depth 5,330 m				
BW	22.5	0.9	<0.5	<2.5
0–2	24.6	9.3	<0.5	<2.5
4–6	21.7	3.4	<0.5	<2.5
8–10	32.5	6.5	1.6	18
12–14	33.3	8	<0.5	<2.5
16–18	35.4	12.2	<0.5	<2.5
25–30	35.6	5.7	<0.5	<2.5
35–40	34.5	8	<0.5	<2.5
50–55	32.3	4.5	1.1	<2.5
HAP PC11; 32°29.2′ N, 70°59.9′ W; depth 5,330 m				
BW	22.9	1.9	<0.5	<2.5
0–3	28.4	4.7	<0.5	<2.5
3–5	28.7	5.1	<0.5	<2.5
5–10	28.7	3.4	<0.5	<2.5
15–20	29.4	2.4	<0.5	<2.5
30–35	26.4	3.8	<0.5	<2.5
40–45	23	4	<0.5	<2.5
50–55	20.9	3.3	<0.5	<2.5
60–65	17.5	3.2	<0.5	<2.5
80–85	8.1	4.3	<0.5	<2.5
HCR BC4; 36°21.4′ N, 71°34.2′ W; depth 4,175 m				
BW	21.6	0.5	<0.5	<2.5
0–2	30.9	8.1	<0.5	<2.5
2–4	30.7	3.9	<0.5	<2.5
4–6	22.5	3.6	<0.5	<2.5
6–8	8.3	3.1	0.8	37.1
				40.2
8–10	3.5	6.5	17.8	47.3
				45.4
10–12	3.5	11.7	25.6	28.8
12–14	3.5	16.5	32.5	26.7
				26
14–18	3.9	21.2	31.6	26
18–22	3.9	40.8	31.4	9.3
22–26	2.9	—	28.3	12.6
26–30	4.4	62.0	31.4	
30–34	3.7	—	38.7	5.6
HCR GC5; 36°19.8′ N, 71°27.1′ W; depth 4,200 m				
BW	20.8	0.5	<0.5	<2.5
0–2	19.9	4.8	<1	<2.5
2–4	3.3	4.2	6	8.9
4–6	2.5	8.6	17.3	24.6
6–8	2.2	13.5	20.7	22.4
8–10	2.5	17.4	21.2	20.8
15–17	0.5	39	19.7	12.4
30–32	0.5	54.6	19.7	13.6
45–47	0.5	81.4	16.7	7.6
63–65	0.5	97	17.3	5.6
78–80	0.5	106	16.1	3.8
93–95	0.5	146.2	17	<2.5
106–108	0.5	159.5	20.2	<2.5
121–123	0.5	195.6	14.2	<2.5
148–150	0.5	227.6	15.9	<2.5
163–165	0.5	252.7	15.2	<2.5
178–180	0.5	275.6	13.1	<2.5
SCB-2; *32°33.1′ N, 118°0.8.1′ W; depth 1,930 m				
BW	42.3		0.01	<2.5
0.6	0.2		7.4	<2.5
1.9	0.2	No data	39.6	7
5	0.2		85.2	9.1
6.6	0.2		117.9	15.1
8.2	0.2		129.5	12.4
11.2			171.9	10
14			123.2	7.1
17.5			105.2	7.2

HAP, Hatteras Abyssal Plain; HCR, Hatteras Continental Rise; SCB, San Clemente Basin. Reported Co and Mn Atlantic bottom water (BW) concentrations do not reflect 'true' bottom waters. However, we emphasize that we are not able to distinguish differences between bottom waters and surface sediment (oxic) pore water concentrations. Co and Mn were measured in Atlantic Bottom waters (H. Windom, personal communication) at 20 pmol kg^{-1} and <1 nmol kg^{-1} respectively at depths of 3,800–5,600 m. We have measured the reported Mn content from San Clemente Basin of 10 nmol kg^{-1} on several cruises to this area. Co has been measured[1] at 27 pmol kg^{-1} in coastal Pacific waters at 1,900 m depth.

Table 2 Sediment concentrations

Depth (cm)	Total Mn	Leach Mn	Total Co	Leach Co
	(mmol kg^{-1} dry sediment)		(μmol kg^{-1} dry sediment)	
1	49.4	36.0	376.5	130.2
3	67.8	52.7	379.4	133.3
5	62.2	47.3	375.8	165.7
7	22.7	11.2	308.4	86.1
9	12.1	3.2	242.9	53.5
11	14.4	4.8	321.2	78.9
13	13.8	3.7	280.3	77.4
16.5	12.1	3.2	254.7	70.0
26.5	12.1	2.7	261.5	66.5
31.5	11.2	2.6	196.1	61.6

All data are corrected for % $CaCO_3$. A USGS rock standard GSP-1 and an in house Pacific pelagic sediment standard A3A were analysed along with BC-4 samples. Reported[20] Co and Mn concentrations for GSP-1 are 6 p.p.m. and 0.04 wt % Mn, respectively, compared with our analyses of 6.5 ± 1.0 p.p.m. Co and 0.03 wt % Mn. Similarly, reported concentrations of standard A3A (A. Graybeal, personal communication) are 66 ± 6 p.p.m. Co and 6.6 ± 0.1 wt % Mn, while our data are 58 ± 5 p.p.m. Co and 6.7 ± 0.1 wt % Mn.

Table 3 Comparisons of pore water cobalt and manganese fluxes with surface sediment excess metal accumulation rates, Hatteras Continental Rise, core BC-4

Core and metal HCR BC-4	Excess metal accumulation rate: Pore water flux (nmol cm^{-2} yr^{-1})	'Total'	'Leach'
		(nmol cm^{-2} yr^{-1})	
Mn	160	113	109
Co	0.5	0.3	0.2

Pore water flux $= \phi D_s\, dc/dz$. The 'average' concentration gradient (dc/dz) between oxic and sub-oxic sediments has been estimated between depths 5–13 cm and 5–11 cm for Mn and Co respectively. ϕ is porosity (0.7) and D_s is the bulk sediment diffusion coefficient[21] (D_s for Mn and Co are 57 and 63 cm^2 yr^{-1} respectively) obtained from the ionic diffusion coefficient[22] corrected to *in situ* temperatures (2°C) and further corrected for porosity and a formation resistivity factor[21] of 2.5. We estimate a 50% uncertainty in the pore water flux calculations. 'Excess' metal accumulation rate $= \Delta C \times D \times S$. ΔC is the concentration difference between mean surface oxic zone (<7 cm) metal concentrations and asymptotic concentrations in anoxic zone sediments for both 'total' and 'leach' metal digestions and extracts respectively. The *in situ* dry bulk density (D) was estimated[23] at 0.32 and the sedimentation rate estimated from the down-core $CaCO_3$ profile[24], from core GC-5, at 10 cm kyr^{-1}.

manganese in the pore waters, indicate the sub-oxic zone of sediments[3]. Rapidly rising ammonia, produced during sulphate reduction[3,5], indicates anoxic sediments.

We find that pore water cobalt concentrations are undetectable (<2.5 nmol kg^{-1}) in oxic zone sediments of Hatteras Abyssal Plain cores PC-11 and SC-3 (Table 1). However, cobalt concentrations rise rapidly from these concentrations in the oxic zone to maximum concentrations of 25–50 nmol kg^{-1} in the manganese reduction zone of Hatteras Continental Rise sediments BC-4 and GC-5. Pore water cobalt and manganese are shown for one core, BC-4, in Fig. 1. Similarly, in the San Clemente Basin pore water cobalt rises to 15 nmol kg^{-1} in the manganese reduction zone. Cobalt has been found adsorbed onto the surfaces of manganese oxide phases[6–8] and oxidized there to Co(III) (refs 9, 10). The data presented here indicate that cobalt is released to pore waters during reductive dissolution of manganese oxides. The shape of the cobalt profile indicates that cobalt in pore waters is diffused towards the sediment–seawater interface and is removed from pore waters to surface oxic sediments. The maximum cobalt concentration appears at shallower depths than the maximum manganese concentration, an unexpected result if cobalt and manganese undergo congruent dissolution. While we cannot explain this observation, cobalt in pore waters may diffuse further than manganese towards surface oxic sediments before it is removed to the solid phase. Cobalt concentrations decrease below the observed maximum in the sub-oxic sediment zone to near undetectable levels measured in anoxic sediments at depths <100 cm in Hatteras Continental Rise cores BC-4 (Fig. 1), and GC-5 (Table 1). Decreasing cobalt concentrations probably result from the precipitation of insoluble cobalt sulphides[11], formed during sulphate reduction which begins at shallow depths (~10 cm) in Hatteras Continental Rise cores.

Sediment samples for 'total' metal analyses were digested in an aqua-regia–hydrofluoric acid mixture[12,13]. Extracts of weakly bound or leachable metals were prepared by shaking sediment samples in ammonium oxalate–oxalic acid[14] mixtures. 'Total' metal digestions and 'leach' extracts were analysed for cobalt and manganese by flameless and flame atomic absorption spectrometry respectively. The analytical precision of 'total' and 'leach' cobalt analyses was respectively ±12% and ±5% over the concentration ranges reported here. 'Total' and 'leach' cobalt and manganese from the Hatteras Continental Rise core BC-4 are also shown in Fig. 1 and summarized in Table 2. Cobalt concentrations are highest in the top <7 cm of sediments and decrease sharply to near asymptotic concentrations at depths near 11 cm. Cobalt enrichments in the core tops are similar to the sediment manganese distributions (Fig. 1). However, while the top/bottom enrichment of sedimentary 'leach' manganese is near 10-fold, that of cobalt is only near two-fold. The processes of manganese release to sub-oxic pore waters and reprecipitation in surface oxic sediments, resulting in an enriched zone in oxic sediments, have been well documented[3,15–18]. The data presented here show that cobalt is recycled during dissolution and reprecipitation of sedimentary manganese oxides between sub-oxic and oxic sediments and pore waters. The recycling processes result in a surface sediment cobalt trap.

We now focus on the recycling between oxic and sub-oxic sediment zones and test the coherence of the pore water and sediment data shown in Fig. 1. First, we calculate the flux of dissolved metal diffusing upward from the cobalt remobilization zone in sub-oxic sediments to surface oxic sediments. Then, we compare this flux with the accumulation rate of 'excess' metal in surface sediments. 'Excess' metal is defined as the difference between the mean metal sediment content in the top 7 cm of oxic sediment and the asymptotic metal concentration in anoxic sediments (Table 2). The calculations are summarized in Table 3 and indicate that for both manganese and cobalt, the 'excess' accumulation rate of metal calculated from the 'leach' sediment data accounts for most 'excess' metal accumulation calculated from 'total' sediment concentrations. These 'excess' metal accumulation rate estimates are comparable with the upward flux of metal through pore water to surface oxic sediments, indicating that the recycling of metal between pore waters and surface sediments is in an apparent steady state and is a contemporary oceanographic feature. A measure of the extent of metal recycling between sediments and pore fluids is provided by comparing the dissolved manganese (160 nmol cm^{-2} yr^{-1}) and cobalt (0.5 nmol cm^{-2} yr^{-1}) fluxes upward through pore waters (Table 3) with the mean total manganese (160 nmol cm^{-2} yr^{-1}) and cobalt (1.1 nmol cm^{-2} yr^{-1}) sedimentation rates (mean total metal content × sedimentation rate × *in situ* dry density) in the top 7 cm of sediments. (Note the distinction between total mean sedimentation rate used here and 'excess' accumulation rate defined in Table 3.) These comparisons suggest that large fractions of the solid phase cobalt and the manganese settling into the remobilization zone are recycled through pore waters to surface oxic sediments at this rapidly sedimenting Continental Rise site.

During early diagenesis in sediments the behaviour of cobalt is, therefore, similar to that of nickel[19]. Both cobalt and nickel are released to pore waters in the manganese reduction zone and recycled between oxic and sub-oxic sediments and pore waters. This type of recycling is in contrast to that of copper where remineralization occurs primarily in the oxygen reduction zone, and most copper is recycled between oxic sediments and pore waters and overlying deep oceanic waters[19].

We thank D. Graham, R. Beach and E. Saravo for assistance during sample processing and M. Bender, L. Jacobs, J. Murray and C. Martin for comments. This work was supported by Knolls Atomic Power Lab. NPD 81-0472-AF, 82-0839-AN, Sandia Labs contract 16-9963 and NSF grants 82-19671 and 81-01830.

Received 22 March; accepted 7 August 1984.

1. Knauer, G. A., Martin, J. H. & Gordon, R. M. *Nature* **297**, 49–51 (1982).
2. Fernandez, F. J., Meyrs, S. A. & Slavin, W. *Analyt. Chem.* **52**, 741–746 (1980).
3. Froelich, P. N. *et al. Geochim. cosmochim. Acta* **43**, 1075–1090 (1979).
4. Bender, M. L., Fanning, K. A., Froelich, P. N., Heath, G. R. & Maynard, V. *Science* **198**, 605–609 (1977).
5. Richards, F. A. in *Chemical Oceanography* Vol. 1 (eds Riley, J. P. & Skirrow, G.) 611–645 (Academic, New York, 1965).
6. Murray, J. W. *Geochim. cosmochim. Acta* **39**, 505–519 (1975).
7. Hem, J. D. *Chem. Geol.* **21**, 199–218 (1978).
8. Burns, R. G. *Geochim. cosmochim. Acta* **40**, 95–102 (1976).
9. Murray, G. W. & Dillard, J. G. *Geochim. cosmochim. Acta* **43**, 781–787 (1979).
10. Dillard, J. D., Crowther, D. L. & Murray, J. W. *Geochim. cosmochim. Acta* **46**, 755–759 (1982).
11. Kremling, K. *Mar. Chem.* **13**, 87–108 (1983).
12. Bernas, B. *Analyt. Chem.* **40**, 1682–1686 (1968).
13. Dymond, J. *et al. Bull. geol. Soc. Am.*, 3355–3372 (1973).
14. Heath, G. & Dymond, J. *Bull. geol. Soc. Am.* **88**, 723–733 (1977).
15. Li, Y-H., Bischoff, J. & Mathieu, G. *Earth planet. Sci. Lett.* **7**, 265–270 (1969).
16. Calvert, S. E. & Price, N. B. *Earth planet. Sci. Lett.* **16**, 245–249 (1972).
17. Lynn, D. C. & Bonatti, E. *Mar. Geol.* **3**, 457–474 (1965).
18. Bender, M. L. *J. geophys. Res.* **76**, 4212–4215 (1971).
19. Klinkhammer, G. P. *Earth planet. Sci. Lett.* **49**, 81–101 (1980).
20. Flanagan, F. J. *U.S. geol. Surv. Prof. Pap.* 840 (1976).
21. Ullman, W. G. & Aller, R. C. *Limnol. Oceanogr.* **27**, 552–556 (1982).
22. Li, Y-H. & Gregory, S. *Geochim. cosmochim. Acta* **38**, 703–714 (1974).
23. Lyle, M. W. & Dymond, J. *Earth planet. Sci. Lett.* **30**, 164–168 (1976).
24. Balsam, W. *Palaeogeogr., Palaeoclimatol., Palaeocol.* **35**, 215–240 (1981).

Contribution of gaseous sulphur from salt marshes to the global sulphur cycle

P. A. Steudler & B. J. Peterson

The Ecosystems Center, Marine Biological Laboratory, Woods Hole, Massachusetts 02543, USA

Salt marshes have high rates of sulphide production due to dissimilatory sulphate reduction[1,2]; and because their anaerobic sediments are exposed to the atmosphere, they are thought to be important sites of biogenic sulphur emission[3,4]. We report here a synthesis of the results of an annual set of monthly flux measurements of hydrogen sulphide (H_2S), dimethyl sulphide (DMS), carbonyl sulphide (COS), carbon disulphide (CS_2) and dimethyl disulphide (DMDS) from a *Spartina* marsh and an adjacent tidal creek. Dimethyl sulphide and H_2S were the predominant gases released from the *Spartina* marsh (49% and 35% of the total, respectively) while H_2S was the major gas (71%) emitted from the creek site. We suggest that the short-lived sulphur gases released from marshes may have an important role in local atmospheric sulphur budgets. Globally, saline marshes may release a total of 1.7 Tg S yr^{-1} (1 Tg = 10^{12} g) into the atmosphere, which includes more than double the quantity of two important long-lived sulphur gases, COS and CS_2, needed to sustain the stratospheric sulphate layer.

Gaseous sulphur flux measurements were made using a FEP Teflon flow-through chamber[5] which covered the sediment or water surface. Ambient air was continuously drawn through the chamber at a velocity of 0.12 m s^{-1} and the difference between the gaseous sulphur concentrations in the chamber input and output air was used to determine the net uptake or release of the sulphur gases. This chamber design allowed the sulphur gases in the incoming ambient air to interact with the grass, sediment, or water surfaces so that net fluxes (emission minus uptake) were measured.

The volatile sulphur compounds were collected in the field from the chamber input and output air streams with glass tube traps packed with the solid adsorbents Molecular Sieve 5A and Tenax GC[6]. The chamber air streams were sampled at 40–100 cm^3 min^{-1} for 1–2 h depending on the anticipated sulphur concentrations for the sampling date. In the laboratory, the sulphur species were thermally desorbed from the trap, separated by temperature programming a Chromosil 330 column (10 foot × $\frac{1}{8}$ inch) and the amounts measured by a sulphur specific flame photometric detector[6]. Trap recoveries were determined with humid air (30–95% RH) to mimic field conditions.

We measured the gaseous sulphur fluxes during 1979 and 1980 from a short *Spartina alterniflora* marsh[5] and from an adjacent tidal creek (our unpublished work) in Great Sippewissett Marsh, Falmouth, Massachusetts. The sulphur fluxes from the *Spartina* site were measured with the grass intact and the chamber sealed to the peat surface. The fluxes from the creek site were obtained with a chamber which either rested on the creek sediment or floated on the surface of the tidal water. Each sampling usually consisted of a series of 1-h flux measurements made continuously for two consecutive tidal cycles (26 h) to obtain a daily flux estimate. The samplings were done at least once a month from February through December at the marsh site and from May through December at the creek site. We assumed that there were negligible releases in January from the *Spartina* site. Emission rates from the creek site for March and April were assumed to be equal to the rate measured in May. The creek site was ice covered (15 cm) in January and February so that flux measurements were not possible. We assumed negligible releases for those two months. We did not structure the sampling design to examine specifically the effects of the diurnal or tidal cycles on the emissions, but we included a variety of tidal and day-night regimes to obtain unbiased annual flux estimates.

Dimethyl sulphide and H_2S were the major components released from the *Spartina* site while H_2S was the major compound released from the creek site (Table 1). We calculated the annual sulphur emissions from Great Sippewissett marsh by weighting equally the daily fluxes from the *Spartina* and creek sites and then extrapolating to monthly fluxes. Maximum emission of each of the individual sulphur gases did not coincide but occurred from July through October (Fig. 1). Emissions during the summer and autumn months (June through October) accounted for 73% of the total release. We estimated a total emission from the marsh of ~4.5 g S m^{-2} yr^{-1} with H_2S (48%) and DMS (33%) the predominant sulphur gases emitted.

As the major gases released from marshes are short-lived compounds, H_2S, DMS and DMDS, the rapid tropospheric oxidation of these gases might be expected to produce elevated atmospheric levels of SO_2 and SO_4 in the vicinity of marshes. This could be important in locations where marshes constitute a large fraction of the land area. For example, Reisinger and Crawford[7] have hypothesized that marshes in the southern coastal US have an important role in the atmospheric sulphate concentrations in the Tennessee Valley.

Comparison of salt marsh sulphur fluxes with other biogenic sulphur sources (Table 2) indicates that marshes have the highest areal gaseous sulphur emissions with rates at least 10- to 100-fold greater than the emissions from oceans or inland soils. We estimated the inland soil emissions (Table 2) using the data reported by Adams *et al.*[8] from an extensive survey of sulphur fluxes from eastern US soils. We combined the average measured fluxes, which included some seasonal measurements (April through November), from 29 locations for seven different non-swamp (aerobic) soil orders and took the mean values. We also

Table 1 Annual gaseous sulphur emissions from the *Spartina* and tidal creek sites (g S m^{-2} yr^{-1})

	Spartina site	Tidal creek
H_2S	2.05	2.32
DMS	2.87	0.16
COS	0.30	0.34
CS_2	0.16	0.20
DMDS	0.42	0.25
Total	5.80	3.27

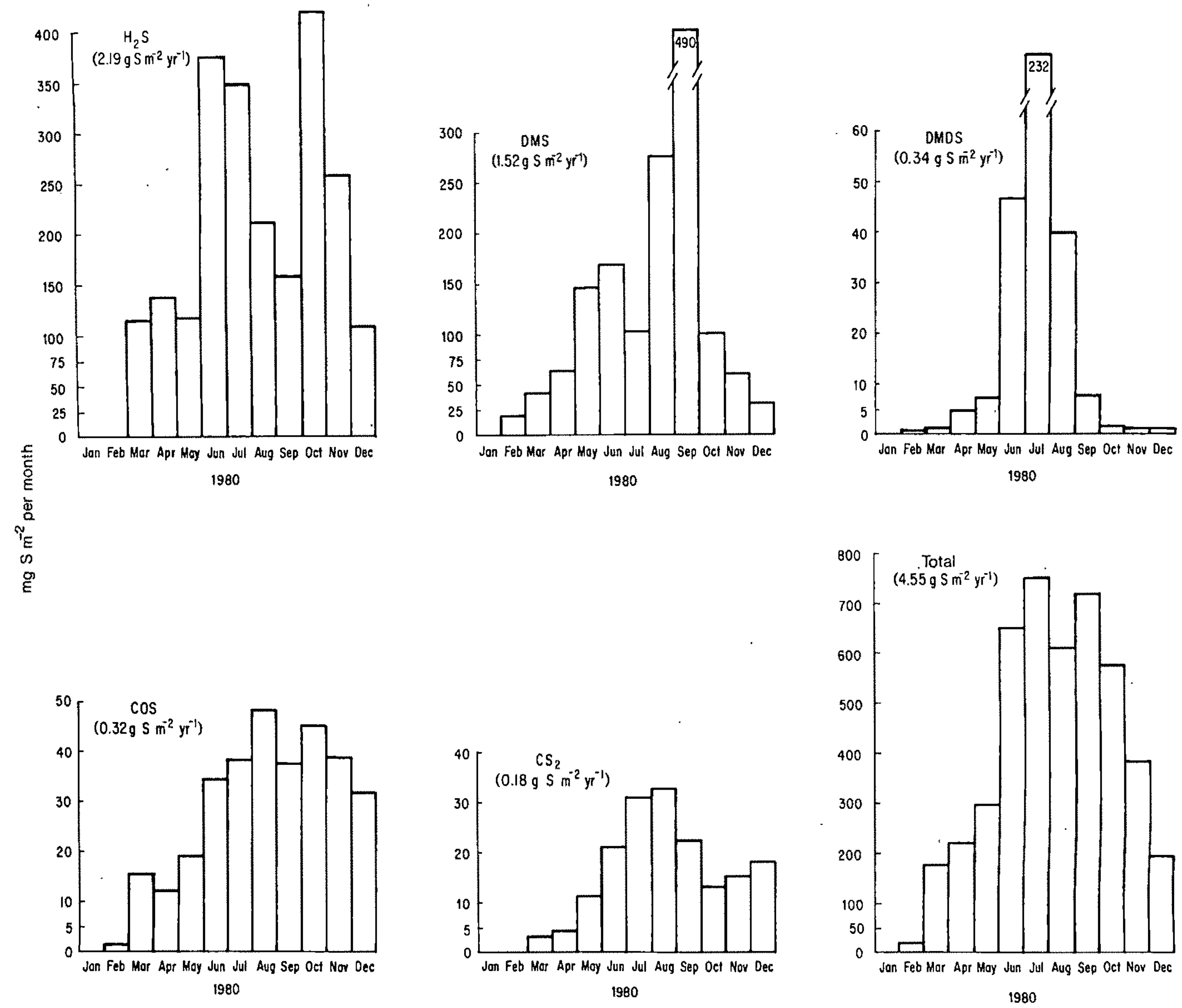

Fig. 1 Annual cycle of monthly fluxes for the individual sulphur gases and the total monthly release for Great Sipperwissett Marsh. Note that the flux rate scales are different.

adjusted each of the mean annual fluxes by increasing them two-fold (D. F. Adams, personal communication) because the data reported for inland soils were believed to represent minimum values[9].

A global estimate of the biogenic sulphur released from saline marshes can be calculated if we assume that: (1) all marshes have the same emission rates as Sippewissett Marsh; (2) the global marsh area[10] is 3.8×10^{11} m^2; (3) marshes are divided equally into vegetated areas and open-water areas of creeks and channels. We estimate that marshes release a total of 1.7 Tg S yr^{-1} to the troposphere of which 81% are the short-lived species H_2S (0.83 Tg S) and DMS (0.58 Tg S) with the remainder as DMDS (0.13 Tg S), COS (0.12 Tg S) and CS_2 (0.07 Tg S). Our value of 1.7 Tg S for the total global release from marshes is about half the 4.1 Tg S estimated by Aneja *et al.*[11] for the mean average global emission from saline marshes. In comparison, releases from the coastal regions which includes marshes, estuaries and coastal waters given in the most recent global budgets[12,13] range from 5 to 12 Tg S yr^{-1}. Thus, marshes by our estimate could contribute between 14 and 34% of the coastal estimates. Emissions from estuarine and coastal waters also contribute to the coastal region flux but the sulphur speciation and rates of release would probably be different than the sulphur gases emitted from marsh creek waters with more DMS[14] and much less H_2S released. However, there have not been any detailed emission studies from estuarine or coastal waters to verify this hypothesis. Recent estimates of the total global biotic release[13,15,16] range from 32 to 103 Tg S yr^{-1}. Marshes, therefore, would contribute only a small portion (1.6–5.4%) to the global biogenic emission.

Table 2 Annual gaseous sulphur emissions from natural sources

Source	Sulphur compound (g S m^{-2} yr^{-1}) H_2S	DMS	COS	CS_2	DMDS	Total
Oceanic	—	0.105[16]	0.0011[25,26]	0.00083[27]	—	0.1069
Inland non-swamp soils (derived from ref. 8)	0.0970	0.0070	0.0156	0.0232	0.0016	0.1444
Salt marshes (this paper)	2.19	1.52	0.32	0.18	0.34	4.55

While the emissions of COS and CS_2 are only a minor fraction (9.6%) of the total gaseous sulphur release they may have an important role globally. One reason is because COS and CS_2 are long-lived sulphur species with tropospheric lifetimes of ~1 yr and 1 month, respectively. Carbonyl sulphide, the most abundant sulphur gas in the atmosphere[17], has been proposed by Crutzen[18] to be the dominant sulphur source for the stratospheric aerosol layer during non-volcanic periods. An additional atmospheric source of COS results from the photooxidation of some portion of the CS_2 in the troposphere[19] because photooxidation of CS_2 yields one molcule each of COS and SO_2. Table 3 inventories COS, CS_2 and total sulphur emissions from natural sources including our estimate from marshes. The continental soil emissions were calculated using a global area[20] of 120.5×10^{12} m^2 (excluding lakes, streams, swamps, rocks, ice and sand) and the data in Table 2. We used 367.1×10^{12} m^2 as the global area of the oceans[16]. We estimate that marshes may release a total of 0.16 Tg S yr^{-1} (COS and CS_2 converted to COS) to the troposphere. The release from marshes is approximately two-fold larger than the quantity needed to maintain the stratospheric sulphate aerosol, but inland soils appear to be an even larger source.

We believe there is a global natural release of ~5.6 Tg S yr^{-1} as COS plus CS_2 (Table 3) which is in good agreement with several recent estimates of the total annual emission (natural plus anthropogenic) of ~5 Tg S (refs 12, 21). Thus, natural and, especially, biogenic sources appear to dominate the global atmospheric COS plus CS_2 cycle. Inland soils appear to be the major biotic source of COS plus CS_2 (84%) to the troposphere with about 4.7 Tg S yr^{-1} released from this source (Table 3). Our estimate of 3.2 Tg S yr^{-1} for the biogenic emission of CS_2 falls within the range of 1.5–5.8 Tg S calculated for a total global CS_2 source by Wine *et al.*[19] from atmospheric CS_2 abundances and modelling. If all the CS_2 is converted to COS, this would increase the natural tropospheric COS source to a maximum of ~4.0 Tg S yr^{-1} available for reaction with OH (ref. 22), long wavelength photodissociation[23] and other sinks or for transport of ~0.08 Tg S yr^{-1} to the stratosphere. Our estimate of 2.4 Tg S yr^{-1} for the direct COS emission from biogenic sources is much larger than the 0.5 Tg S yr^{-1} estimated by Turco *et al.*[21] to arise from biospheric processes. The difference in the estimates is due to our inclusion of recent data on the releases from marshes and soils and the change of the oceans from a sink to a source of these gases.

From the data in Table 2, we calculate that there is a global biogenic release of ~58 Tg S yr^{-1} to the atmosphere (Table 3). This value is well within the three-fold range of 32–103 Tg S yr^{-1} cited previously. Our global biogenic estimate is about half the recently calculated global anthropogenic SO_2 emission of 113 Tg S yr^{-1} (ref. 12). Biogenic oceanic emissions might be as large as 39 Tg S yr^{-1} predominately as DMS (98%) while inland soils may release ~17 Tg S yr^{-1} mostly as H_2S (67%). Ryaboshapko[12], in a recent global sulphur budget, calculated an annual bioemission from the land surface of 16 Tg S which is very close to our soils flux value (Table 3). Our estimate of the H_2S flux from soils of 11.7 Tg S yr^{-1} compares well with the 14 Tg S of H_2S estimated by Delmas *et al.*[24] to be emitted from aerobic soils. Our estimates suggest that oceanic DMS fluxes might be the single largest natural source (66%) of biogenic sulphur to the lower troposphere.

Emission of gaseous sulphur compounds from salt marshes are higher, per unit area, by one or two orders of magnitude than emissions from other ecosystems. However, because of the small global area of salt marshes, gaseous sulphur emissions from this source appear to contribute a minor fraction to the global emissions. Saline marsh releases of the short-lived sulphur gases (DMS, H_2S and DMDS) may have an important role in the atmospheric sulphur cycle on a local scale where the areal extent of marshes is large. Biotic emissions seem to be the dominant global source of long-lived sulphur gases, COS and CS_2, with a major fraction of the release originating from inland soils. Additional measurements of sulphur gas emissions from coastal oceans, soils (especially tropical soils) and forests are needed to refine the global biogenic emission estimates.

Table 3 Global release of COS, CS_2 and total sulphur emissions from natural sources (Tg S yr^{-1})

Source	COS	CS_2	Total sulphur emissions
Oceans[25–27]	0.40	0.30	39.2
Wild fires in temperate and boreal forests[28]	0.01	—	—
Inland non-swamp soils	1.88	2.80	17.4
Salt marshes	0.12	0.07	1.7
Volcanoes and fumaroles[29]	0.01	—	—
Total	2.42	3.17	58.3

We thank W. Kijowski, D. Juers, R. Howarth, J. Dacey, F. Bowles, B. Howes, D. Goehringer, H. Sladovich, S. Pilling, F. Lipshultz, B. Behrens, A. Friedlander, T. Duncan. A. McElroy, J. Fownes and J. Gale for assistance in field sampling and labroatory analyses. Financial support was provided by NSF grant no. DEB 78-03557 and DEB 81-04701.

Received 29 March; accepted 7 August 1984.

1. Howarth, R. W. & Teal, J. *Limnol. Oceanogr.* **24,** 999–1013 (1979).
2. Howarth, R. W. & Giblin, A. *Limnol. Oceanogr.* **28,** 70–82 (1983).
3. Conway, E. J. *Proc. R. Acad. Sci.* **A48,** 119–159 (1943).
4. Hitchcock, D., *Chemosphere* **3,** 137–138 (1975).
5. Steudler, P. A. & Peterson, B. J. *Atmos. Envir.* (in the press).
6. Steudler, P. A. & Kijowski, W. *Analyt. Chem.* **56,** 1432–1436 (1984).
7. Reisinger, L. M. & Crawford, T. L. *J. Air Pollut. Control Ass.* **30,** 1230–1231 (1980).
8. Adams, D. F., Farwell, S. O., Robinson, E., Pack, M. R. & Banesberger, W L. *Envir. Sci. Technol.* **15,** 1439–1498 (1981).
9. Adams, D. F., Farwell, S. O., Robinson, E. & Pack, M. R. *EPRI Rep.* EA-1516 (Electric Power Research Institute, Palo Alto, 1980).
10. Woodwell, G. M., Rich, P. H. & Hall, C. A. S. in *Carbon and the Biosphere* (eds Woodwell, G. M. & Pecan, E. V.) 221–240 (AEC Symp. 30, US Department of Commerce, 1973).
11. Aneja, V. P., Aneja, A. P. & Adams, D. F. *J. Air Pollut. Control Ass.* **32,** 803–807 (1982).
12. Ryaboshapko, A. G. in *The Global Biogeochemical Sulfur Cycle: SCOPE 19* (eds Ivanov, M. V. & Freney, J. R.) Ch. 4 (Wiley, New York, 1983).
13. Ivanov, M. V. in *Some Perspectives of the Major Biogeochemical Cycles SCOPE 17* (ed. Likens, G. E.) 61–78 (Wiley, New York, 1981).
14. Barnard, W. R., Andreae, M. O., Watkins, W. E., Bingemer, H. & Georgii, H. W. *J. geophys Res.* **87,** 8787–8793 (1982).
15. Granat, L., Rodhe, H. & Hallberg, R. O. in *Nitrogen, Phosphorus and Sulfur–Global Cycles: SCOPE 7* (eds Svensson, B. H. & Oderlund, S.) 89–134 (Ecological Bulletins No. 22, Stockholm, 1976).
16. Andreae, M. O. & Raemdonck, H. *Science* **221,** 744–747 (1983).
17. Rodhe, H. & Isaksen, I. *J. geophys. Res.* **85,** 7401–7409 (1980).
18. Crutzen, P. J. *Geophys. Res. Lett.* **3,** 73–76 (1976).
19. Wine, P. H., Chameides, W. L. & Ravishankara, A. R. *Geophys. Res. Lett.* **8,** 543–546 (1981).
20. Whittaker, R. H. & Likens, G. E. in *Carbon and the Biosphere* (eds Woodwell, G. M. & Pecan, E. V.) 281–302 (AEC Symp., 30, US Department of Commerce, 1973).
21. Turco, R. P., Whitten, R. C., Toon, O. B., Pollack, J. B. & Hamill, P. *Nature* **283,** 283–286 (1980).
22. Ravishankara, A. R., Kreutter, N. M., Shah, R. C. & Wine, P. H. *Geophys. Res. Lett.* **7,** 861–864 (1980).
23. Turco, R. P., Cicerone, R. J., Inn, E. C. Y. & Capone, L. A. *J. geophys. Res.* **86,** 5373–5377 (1981).
24. Delmas, R., Baudet, J., Servant, J. & Baziard, Y. *J. geophys. Res.* **85,** 4468–4474 (1980).
25. Rasmussen, R. A., Khalid, M. A. K. & Hoyt, S. D. *Atmos. Envir.* **16,** 1591–1594 (1982).
26. Ferek, R. L. & Andreae, M. O. *Geophys. Res. Lett.* **10,** 393–396 (1983).
27. Liss, P. S. in *The Major Biogeochemical Cycles and their Interactions SCOPE 21* (eds Bolin, B. & Cook, R. B.) 411–426 (Wiley, New York, 1983).
28. Crutzen, P. J., Heidt, L. E., Krasnec, J. P., Pollack, W. H. & Seiler, W. *Nature* **282,** 253–256 (1979).
29. Cradle, R. O. *Rev. Geophys. Space Physiol.* **18,** 746–752 (1980).

Functional neuronal replacement by grafted striatal neurones in the ibotenic acid-lesioned rat striatum

O. Isacson, P. Brundin, P. A. T. Kelly[*], F. H. Gage & A. Björklund

Department of Histology, University of Lund, Biskopsgatan 5,
S-223 62 Lund, Sweden

In rats, striatal neuronal destruction by so-called excitotoxic amino acids, kainic acid or ibotenic acid (IA) produce neuropathological and neurochemical changes in the basal ganglia[1–4] which resemble those seen in patients with Huntington's chorea[5,6]. Such lesioned animals show a behavioural syndrome which is reminiscent of the cardinal symptoms of the disease[7–12], accompanied by a substantial increase in local cerebral metabolic activity in several striatal target structures within the extrapyramidal motor system[13–15]. The study was designed to explore the potential of grafted fetal striatal neurones implanted into the IA-lesioned striatum to compensate for the structural, neurochemical, metabolic and behavioural defects of IA-lesioned rats. Extending previous studies[16,17], we report here that such striatal implants can significantly ameliorate the lesion-induced locomotor hyperactivity and at least partly normalize the metabolic hyperactivity in the extrapyramidal neuronal system.

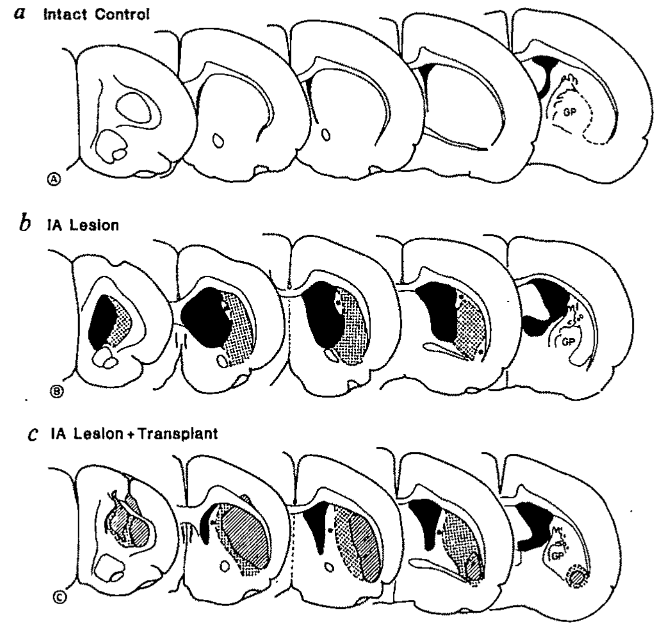

Fig. 1 Camera lucida drawings of a normal control rat (*a*), an IA-lesioned rat (*b*) and an IA-lesioned and grafted rat (*c*) 11 weeks after the lesion. The double-cross-hatched areas represent the scar tissue, the asterisks the areas of neuronal sparing and the black areas the lateral ventricle. The graft tissue in *c* is represented by the single-cross-hatched area. GP, globus pallidus.

Methods: 53 Female Sprague–Dawley rats, 180–200 g in weight, were used in this study. 13 Rats were unoperated controls; the remaining 40 were anaesthetized with methohexital barbiturate (Lilly) and mounted in a stereotaxic frame. Part of the cranium anterolateral to bregma was carefully removed by drilling, and a total of 20 μg of IA (Natural Products Ltd) in 1 μl of phosphate buffer (*p*H 7.4) was injected at four stereotaxically defined sites in the right caudate-putamen (A 0.4, L 3.9, V 5.3; A 0.4, L 3.1, V 4.0; A 1.3, L 3.1, V 4.4; A 1.3, L 2.0, V 4.3; all coordinates in mm, anterior and lateral coordinates from bregma, ventral coordinates from dural surface). Each of the four 0.25-μl microinjections was performed over a total of 10 min before the needle was slowly withdrawn. 5–7 Days after the IA lesion, 20 of the rats were selected at random to receive implantations of cell suspensions prepared from primordial striatum taken from rat fetuses of 13–15 days gestational age, as described previously[16]. Primordial striatal tissue was collected in 0.6% glucose in saline at room temperature and then transferred to a similar glucose solution with the addition of 0.1% trypsin (crude type II, Sigma), in which incubation took place at 37 °C for 15–20 min. At the end of the incubation period the trypsin medium was removed and the tissue rinsed four times with fresh glucose–saline solution. The tissue pieces were then mechanically dissociated with a fire-polished Pasteur pipette (diameter ~1 mm) in a volume equivalent to 10 μl per two striatal primordia. 1 μl suspension was injected over 1 min at each of the four sites which had previously received IA. After each injection the needle was left in position for an additional 2 min before being slowly withdrawn.

Our experimental rats (Fig. 1) was divided into three groups. One group, consisting of five lesioned, five lesioned and grafted and seven unoperated control rats, was used for measurements of local glucose utilization, according to the autoradiographic ^{14}C-2-D-deoxyglucose (^{14}C-2-DG) method of Sokoloff *et al.*[18]. We also used these brains for histology and morphometry of the grafts and the host striatal structures. The second group, consisting of six lesioned and five lesioned and grafted rats, was used for measurements of glutamic acid decarboxylase (GAD)[19] in the graft and the host striatum on the lesioned and control sides. The third group, consisting of nine lesioned, ten lesioned and grafted and six control rats, was used for analysis of locomotor activity.

The IA lesion caused an average reduction of ~65% in the volume of the head of the caudate-putamen accompanied by an average sevenfold increase in the volume of the lateral ventricle at the same cross-sectional levels (Fig. 1). The Klüver–Barrera stain revealed a severe loss of striatal neurones; only about 5–10% of the original volume of the head of the caudate-putamen showed sparing of neurones. The remaining tissue was virtually free of stainable neurones and had the appearance of a glial scar penetrated by the seemingly undamaged fibre bundles of the internal capsule. The spared neurones occurred as a rim along the ventricular surface and along the external capsule in the caudal aspects of the lesion (Fig. 1*b*). The nucleus accumbens and the tail of the caudate-putamen were only marginally affected; in most cases there were only minor signs of cell damage along the needle tracks in the cortex. Probably as a secondary consequence of the lesion[6,20], both globus pallidus and pars reticulata of the substantia nigra underwent a marked shrinkage on the lesioned side[20,21].

The GAD assay revealed an average depletion of the γ-aminobutyric acid (GABA) synthesizing enzyme concentration of 58% in the head of the caudate-putamen encompassing the lesion, from 76.9 ± 5.5 to 32.3 ± 8.4 nmol per h per mg protein. Taking into account the volume reduction of the caudate-putamen, we estimated the depletion of the total GAD content in the head of the caudate-putamen to be ~85%.

The striatal implant had an average volume of about 4 mm^3 (range 2–7 mm^3), which resulted in an average increase of 50% in the lesioned caudate-putamen volume. The amount of caudate tissue with signs of sparing, and the volume of the scar tissue were very similar in the lesion and the lesion + graft groups (5% compared with 6%; and 28% compared with 31%, respectively; Fig. 1*b*, *c*). Microscopically, the implant appeared as one or several neurone-rich cell masses sometimes extending along the needle tracks up into the overlying cortex (Fig. 1*c*). In the animals taken for neurochemical analysis, we found that the GAD level of the graft tissue was as high as that of the normal caudate-putamen (83.4 ± 9.0 nmol per h per mg protein), and in a parallel immunohistochemical study[21] the striatal grafts contained many of the chemically identified neurone types normally present in the neostriatum.

In the ^{14}C-2-DG autoradiography (Table 1), we found that the IA lesion caused a 60% reduction in glucose utilization throughout the lesioned caudate-putamen. The partially spared medial portion displayed smaller reductions (22%), while the

---

[*] Present address: Wellcome Surgical Institute, University of Glasgow, Glasgow HG61 1QH, UK.

Table 1 Transplant-induced effects on regional ^{14}C-2-deoxy-D-glucose utilization in the awake IA-lesioned rat

Structures	Intact	Ibotenate lesion		Ibotenate lesion + striatal transplant	
		Ipsilateral	Contralateral	Ipsilateral	Contralateral
Host caudate-putamen					
Medial	68±1	53±6*	87±2*	49±4*	75±2†
Lateral	68±1	28±2*	87±2*	30±3*	74±1*†
Tail	68±1	69±8	81±4*	64±2	71±1†
Primary striatal targets					
Globus pallidus	42±2	53±1*	55±3*	45±2†	51±2*
Entopeduncular nucleus	42±2	56±3*	47±4	49±3*	43±1
Substantia nigra, reticulata	41±1	61±3*	53±3*	58±2*	51±3*
Substantia nigra, compacta	52±1	59±2*	59±3*	56±1*	57±2*
Secondary striatal targets					
Subthalamic nucleus	63±1	74±2*	75±3*	66±3†	71±2*
Lateral habenula	89±2	103±7*	100±5*	106±4*	105±1*
Ventrolateral thalamus	64±1	75±4*	79±4*	71±2*	74±2*
Ventromedial thalamus	79±2	79±3	91±2*	76±2	86±2*
Superior colliculus, deep	64±1	75±1*	76±2*	68±1†	71±2*†
Associated motor and limbic areas					
Nucleus accumbens	66±2	76±2*	81±2*	67±3†	73±3*†
Ventral tegmental area	39±1	50±2*	49±2*	43±2†	44±2
Nucleus ruber	54±3	67±2*	69±2*	65±2*	65±3*
Mesencephalic raphe	73±1	—	71±4	—	77±2
Sensorimotor cortex	79±1	89±7*	97±4*	83±3	91±1*
Anterior cingulate cortex	79±2	87±5	93±6	77±4	86±4
Pontine nuclei	52±1	56±3	55±3	54±1	54±1
Cerebellar hemisphere	51±3	56±2	57±2	52±2	52±2
Cerebellar nuclei	67±4	79±3*	79±3*	74±2	74±2
White matter	31±2	34±2	31±2	32±2	32±2

Local ^{14}C-2-deoxy-D-glucose utilization after unilateral IA lesion ($n=5$) or IA lesion plus striatal suspension grafts ($n=5$). A group of seven age- and weight-matched unoperated female rats served as the control group. No side-to-side differences were observed within any brain structure in the intact animals, so the two sides were pooled to provide a single control value. Structures measured were sampled according to Schwartz and Sharp[31]. No transplant-induced effects were observed in other brain areas.

Methods: Under light halothane anaesthesia (1% in a 7:3 $N_2O_2:O_2$ gas mixture), both femoral arteries and one femoral vein were cannulated. Groin incision sites were infiltrated with local anaesthetic (xylocaine) and sutured. A loose-fitting plaster cast was applied around the lower body and hind legs, taking care not to impair thoracic movements, and the cast was taped to lead weights. Thus restrained, anaesthesia was discontinued and at least 2 h were allowed to elapse before proceeding with the experiments. The measurement was initiated with a 30-s intravenous injection of 0.5 ml ^{14}C-labelled 2-deoxy-D-glucose (125 μCi kg^{-1}, NEN). Over the subsequent 45 min, a total of 14 timed arterial blood samples were collected and the plasma separated from the cellular fraction by immediate centrifugation. Aliquots of the plasma were taken for measurement of glucose levels (10 μl) and ^{14}C concentrations (20 μl). At the end of 45 min the animals were decapitated and their brains were rapidly dissected and frozen in isopentane at −50 °C. Autoradiograms were prepared from ~150 coronal cryostat sections (20 μm) from each brain mounted on glass coverslips. The sections were placed in a light-tight X-ray cassette, together with a set of seven ^{14}C-containing plastic standards (concentrations 48–1,061 nCi per g tissue equivalents) in close apposition to a sheet of X-ray film (Kodak SB-5) for 7 days. The processed films were analysed densitometrically using a Leitz TAS plus computerized densitometer. Local cerebral glucose utilization was calculated according to Sokoloff *et al.*[18].

* Significantly different from intact control value ($P<0.05$); †, significantly different from IA lesion alone ($P<0.05$). One-way analysis of variance with post-hoc Neuman–Keuls test. No symbol indicates $P>0.05$.

spared tail of the caudate was unaffected. In contrast to the ipsilateral decreases, the contralateral caudate-putamen displayed increased mean glucose utilization values of between 19 and 28% over intact control levels in the different caudate regions measured. All major primary and secondary projection areas of the neostriatal efferents (Fig. 2) showed significant uni- or bilateral increases in glucose use. The strongest increases were seen in the pars reticulata of the substantia nigra (+49% and 29% on the ipsi- and contralateral sides, respectively), in the globus pallidus (+26% and 29%), in the subthalamic nucleus (+18% and 19%) and in the deep superior colliculus (+17% and 18%). Bilateral increases were seen also in several areas functionally associated with the extrapyramidal motor system, such as the ventral tegmental area, nucleus accumbens, sensorimotor cortex and nucleus ruber, whereas other cortical and brain-stem regions remained unaffected.

The striatal implant proper exhibited a significant ^{14}C-2-DG utilization of 69±3% of the intact control neostriatum. The implant does not influence glucose use in the surrounding, lesioned or spared areas of the host caudate-putamen, although the contralateral increases in glucose use in animals with IA lesions alone were attenuated enough to be no longer significantly different from the intact controls (Table 1).

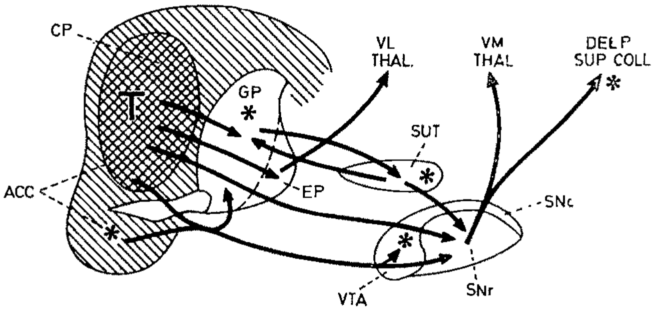

Fig. 2 Principal arrangements of the major output pathways from the caudate-putamen and nucleus accumbens. Those primary and secondary targets which exhibited graft-induced reductions in ^{14}C-2-DG utilization are marked by asterisks. ACC, nucleus accumbens; CP, caudate-putamen; EP, entopeduncular nucleus; GP, globus pallidus; SN, substantia nigra (c, compacta, r, reticulata); SUT, subthalamic nucleus; VL and VM Thal, ventrolateral and ventromedial thalamic nuclei; VTA, ventral tegmental area.

The hypermetabolic responses in the primary and secondary striatal projection areas were normalized by the implant ipsilaterally in the globus pallidus and subthalamic nucleus and bilaterally in the deep superior colliculi († in Table 1; * in Fig. 2). In the functionally associated areas, a significant transplant-induced effect was also seen in the VTA and nucleus accumbens. No transplant-induced effects were observed elsewhere in the brain.

Locomotor activity was measured in two different tests (Table 2). Previous studies[8,10] have shown that rats with excitotoxic striatal lesions are hyperactive only when tested during their active period at night (when rats normally express about 90% of their diurnal locomotor activity[22]) or under food deprivation. Consistent with these reports, the IA-lesioned animals in the present study were significantly hyperactive in the open field when tested overnight under temporary (24 h) food and water deprivation. In agreement with previous findings[17], the locomotor hyperactivity was compensated for completely in the animals with IA lesions plus striatal transplants ($P < 0.01$). These effects were also confirmed when locomotor activity was measured in rotometer bowls (Table 2); the individual scores recorded in the two tests were highly correlated ($r = 0.8$; $t = 5.05$). The rotometer test showed, moreover, that although the unilateral IA lesion caused spontaneous turning behaviour (in the direction towards the lesion) during the first few days after lesion, the motor asymmetry was no longer evident in any of the lesioned or grafted groups by 10–12 weeks after the operation.

The present results thus demonstrate that the striatal suspension grafts not only survive and differentiate within the host neostriatum previously depleted of its constituent neurones by IA, but that they are also capable of compensating for the nocturnal locomotor hyperactivity and the extrapyramidal metabolic hyperactivity seen in the unilaterally IA-lesioned animals. The exact mechanism of these transplant-induced effects are unknown. Previous experiments with implants of catecholamine-producing cell systems[23–28] have provided evidence that intracerebral grafts can exert their functional effects in the host brain both via direct axonal connections with previously denervated elements in the host target, and via a more diffuse release of the active compound into the host tissue or the cerebrospinal fluid. Both these mechanisms seem consistent with our present results. It thus seems possible that the striatal implants could exert a neurohumoral-like effect either on spared neurones in the caudate-putamen, or on parts of the nucleus accumbens in the neighbourhood of the graft, or perhaps even on more distant sites via a diffuse release of active compounds into the cerebrospinal fluid in the adjoining lateral ventricle. Alternatively, the grafted neurones might function via fibre connections established with striatal neurones in the host, either, for example, via a local fibre outgrowth into the spared portions of the striatum or nucleus accumbens, or via fibres growing over somewhat longer distances to reach, for example, the globus pallidus. Evidence for such effects of the striatal implants will, however, require further studies on the connectivity of the grafted neurones.

Table 2 Transplant-induced effects on locomotor activity of IA-lesioned rats

Groups	Overnight activity (total photocell counts)	Overnight turning in rotometer	
		Total half-turns	Side-bias (% turns in ipsilateral direction)
Control	7,232±380	142.0±28.7	44.8±9.6
IA lesion	12,273±1,842*	336.0±49.4*	58.7±8.2
IA lesion +transplant	6,485±467†	170.0±27.2†	49.8±8.2

Overnight locomotor activity measured in enclosed automated activity boxes (50 × 50 cm), connected to a microprocessor. Values represent the mean total photocell counts ±s.e.m. over a 13-h test period (1830–0730 h). 10–11 weeks after IA lesion and transplantation, rats from the three groups were randomly selected for activity tests. Before the test session, rats were temporarily deprived of food and water for 24 h (see text). Statistical analysis: one-way analysis of variance, $F = 7.25$, post-hoc Neuman–Keuls. Overnight locomotor activity was measured in rotometer bowls of diameter 55 cm. Values represent the total number of half-turns ± s.e.m. over an 11-h period (1830–0530 h). Rats were temporarily deprived of food and water for 2–5 h before testing. Statistical analysis, one-way analysis of variance, $F = 6.33$, post-hoc Neuman–Keuls. Side-bias is expressed as turns in the ipsilateral direction to IA lesions divided by the total number of turns. Values show mean per cent ± s.e.m. for each group. One-way analysis of variance, $F = 0.59$.

* $P < 0.05$ compared with control; † $P < 0.05$ compared with IA lesion.

The increased glucose utilization seen in several primary and secondary neostriatal target areas in the IA-lesioned animals indicates that the neostriatum normally exerts an inhibitory tonic action on the functional activity of these structures. Interestingly, it has previously been shown that the increases in glucose utilization induced by excitotoxic lesions of the neostriatum can be attenuated by systemic injections of the GABA receptor agonist, muscimol[29], and that it is possible to modify locomotor activity in rats by local administration of GABA receptor-active drugs directly into the globus pallidus[30]. Against this background it may be sufficient for the striatal implants to reinstate a tonic and relatively nonspecific inhibition over the striatal output structures (perhaps via release of GABA or other neuromodulators from the graft) in order to compensate for the lesion-induced metabolic and locomotor hyperactivity in the IA-lesioned animals. More complex striatum-dependent behaviours, may, by contrast, require both temporally and spatially patterned cortical inputs and are thus less likely to be influenced by the implants unless they are capable of establishing ordered and relatively specific afferent and efferent connections with the host brain. Whether this will be possible to achieve with striatal implants is an interesting topic for further investigation.

This work was supported by grants from the Swedish MRC (04X-3874), the NIH (AG03766), the European Science Foundation and the Royal Society of London.

Received 29 May; accepted 8 August 1984.

1. Coyle, J. T. & Schwarcz, R. *Nature* **263**, 244–246 (1976).
2. McGeer, E. G. & McGeer, P. L. *Nature* **263**, 517–519 (1976).
3. Schwarcz, R. & Coyle, J. T. *Brain Res.* **127**, 235–249 (1977).
4. Schwarcz, R. *et al. Expl Brain Res.* **37**, 199–216 (1979).
5. Bruyn, G. W. *Prog. Brain Res.* **55**, 445–464 (1982).
6. Bird, E. D. *A. Rev. Pharmac. Tox.* **20**, 533–551 (1980).
7. Mason, S. T. & Fibiger, H. C. *Brain Res.* **155**, 313–329 (1978).
8. Mason, S. T. & Fibiger, H. C. *Neuropharmacology* **18**, 403–407 (1979).
9. Sanberg, P. R. & Fibiger, H. C. *Expl Neurol.* **66**, 444–466 (1979).
10. Dunnett, S. B. & Iversen, S. D. *Behav. Brain Res.* **2**, 189–209 (1981).
11. Dunnett, S. B. & Iversen, S. D. *Behav. Brain Res.* **1**, 497–506 (1980).
12. Pisa, M., Sanberg, P. R. & Fibiger, H. C. *Expl Neurol.* **74**, 633–653 (1981).
13. Kimura, H., McGeer, E. G. & McGeer, P. L. *J. neural Transmission Suppl.* **16**, 103–109 (1980).
14. Wooten, G. F. & Collins, R. C. *Brain Res.* **201**, 173–184 (1980).
15. Kelly, P. A. T., Graham, D. I. & McCulloch, J. *Brain Res.* **233**, 157–172 (1982).
16. Schmidt, R. H., Björklund, A. & Stenevi, U. *Brain Res.* **218**, 347–356 (1981).
17. Deckel, A. W., Robinson, R. G., Coyle, J. T. & Sanberg, P. R. *Eur. J. Pharmac.* **93**, 287–288 (1983).
18. Sokoloff, L. *et al. J. Neurochem.* **28**, 897–916 (1977).
19. Fonnum, F., Storm-Mathisen, J. & Walberg, F. *Brain Res.* **20**, 259–275 (1970).
20. Krammer, E. B. *Brain Res.* **196**, 209–219 (1980).
21. Dawbarn, D. *et al. Brain Res.* (submitted).
22. Glick, S. D. & Cox, R. D. *Brain Res.* **150**, 149–161 (1978).
23. Björklund, A., Dunnett, S. B., Stenevi, U., Lewis, M. E. & Iversen, S. D. *Brain Res.* **199**, 307–333 (1980).
24. Freed, W. J. *et al. Ann. Neurol.* **8**, 510–519 (1980).
25. Björklund, A., Stenevi, U., Dunnett, S. B. & Iversen, S. D. *Nature* **289**, 497–499 (1981).
26. Freed, W. J. *et al. Nature* **292**, 351–352 (1981).
27. Björklund, A., Stenevi, U., Schmidt, R. H., Dunnett, S. B. & Gage, F. H. *Acta physiol. scand. Suppl.* 522, 1–8 (1983).
28. Dunnett, S. B., Björklund, A. & Stenevi, U. *Trends Neurosci.* **6**, 266–270 (1983).
29. Kelly, P. A. T. & McCulloch, J. *Br. J. Pharmac.* **76**, 290 (1982).
30. Mogenson, G. J. & Nielsen, M. A. *Brain Res. Bull.* **11**, 309–314 (1983).
31. Schwartz, W. J. & Sharp, S. R. *J. comp. Neurol.* **177**, 335–360 (1978).

The neostriatal mosaic: compartmentalization of corticostriatal input and striatonigral output systems

Charles R. Gerfen

Developmental Neurobiology Laboratory, The Salk Institute,
La Jolla, California 92037, USA and
*Laboratory of Neurophysiology, National Institute of Mental
Health, Bethesda, Maryland 20205, USA

The striatum (caudate-putamen) of the basal ganglia in the mammalian forebrain is a mosaic of two interdigitating, neurochemically distinct compartments. One type, the 'patch' compartment, is identified by patches of dense opiate receptor binding[1,2], and is enriched in enkephalin- and substance P-like immunoreactivity[3]. The other compartment, the 'matrix', has a high acetylcholinesterase activity[2,4], and is shown here to have a dense plexus of fibres displaying somatostatin-like immunoreactivity. The present study demonstrates the two compartments have distinct connections, using a method that concurrently reveals striatal input, output and neurochemical systems in the rat. Patches receive inputs from the prelimbic cortex (a medial frontal cortical area with direct 'limbic' inputs from the amygdala[5] and hippocampus[6,7]); they also project to the substantia nigra pars compacta (the source of the nigrostriatal dopaminergic system). Conversely, the matrix receives inputs from sensory and motor cortical areas[8]; here it is shown to project to the substantia nigra pars reticulata (the source of the non-dopaminergic nigrothalamic and nigrotectal system[9,10]). Also, an intrinsic striatal somatostatin-immunoreactive system is described that may provide a link between the two compartments. The striatal patch and matrix compartments thus appear to be functionally distinct and interactive parallel input–output processing channels.

The input-output organization of the striatum was examined using a method that concurrently demonstrates corticostriate systems (*Phaseolus vulgaris* leucoagglutinin (PHA-L) anterograde tracing[11]), striatonigral projection neurones (fluorescent retrograde tracer Fast blue[12]), and either the striatal patch (with enkephalin- or substance P-immunoreactivity[3]) or matrix (with somatostatin-immunoreactivity[13]) compartments. The anterogradely transported plant lectin PHA-L was injected iontophoretically into the right prelimbic cortex of eight female albino rats, as previously described[11]. These animals were also injected with 50 nl of the retrogradely transported fluorescent tracer Fast blue (in a 2.5% suspension) into the right substantia nigra. The animals received a left intraventricular injection of 75–100 μg colchicine 8 days after the tracer injections and 2 days later were perfused under chloral hydrate anaesthesia with 0.9% saline followed by 4% formaldehyde in 0.1 M acetate buffer (*p*H 6.5) and then 4% formaldehyde in 0.1 M borate buffer (*p*H 9.5) (ref. 14). The brains were removed and stored overnight in the last solution plus 20% sucrose. Coronal 30-μm-thick sections were cut on a freezing microtome, and sections through the substantia nigra examined to reconstruct the site of the Fast blue injections. The other sections were incubated overnight at 4 °C in 0.4% Triton X-100 plus 2% normal goat serum (NGS) in 0.02 M potassium phosphate-buffered saline (KPBS, *p*H 7.4), and then incubated at 4 °C for 24–48 h in a 1:1,000 dilution of guinea pig antisera directed against PHA-L in KPBS plus 2% NGS. These sections were then rinsed in KPBS and incubated at 4 °C for 24–48 h in rabbit antisera directed against either substance-P (1:3,000, a gift of M. Brown), Leu-enkephalin (1:2,000, Immunonuclear, Inc.), or somatostatin[13] (SS28 (1–12), 1:5,000 + SS28, 1:2,000, a gift of R. Benoit). After rinsing for 30 min, the primary antisera were localized by incubating the sections in a mixture of affinity purified fluorescein-labelled goat anti-guinea pig IgG (GAGP-FITC, 1:100, Cappel) and affinity purified tetramethylrhodamine-labelled goat anti-rabbit IgG (GAR-TRITC, 1:100; Sigma) in KPBS plus 0.3% Triton X-100 and 2% NGS for 45 min. Sections were examined with a Nikon fluorescent microscope. Sections incubated with one or the other labelled antisera demonstrated no cross-reactivity with the inappropriate primary antisera. Preadsorption of each antiserum with 1 mg ml^{-1} of the homologous

---

* Present address.

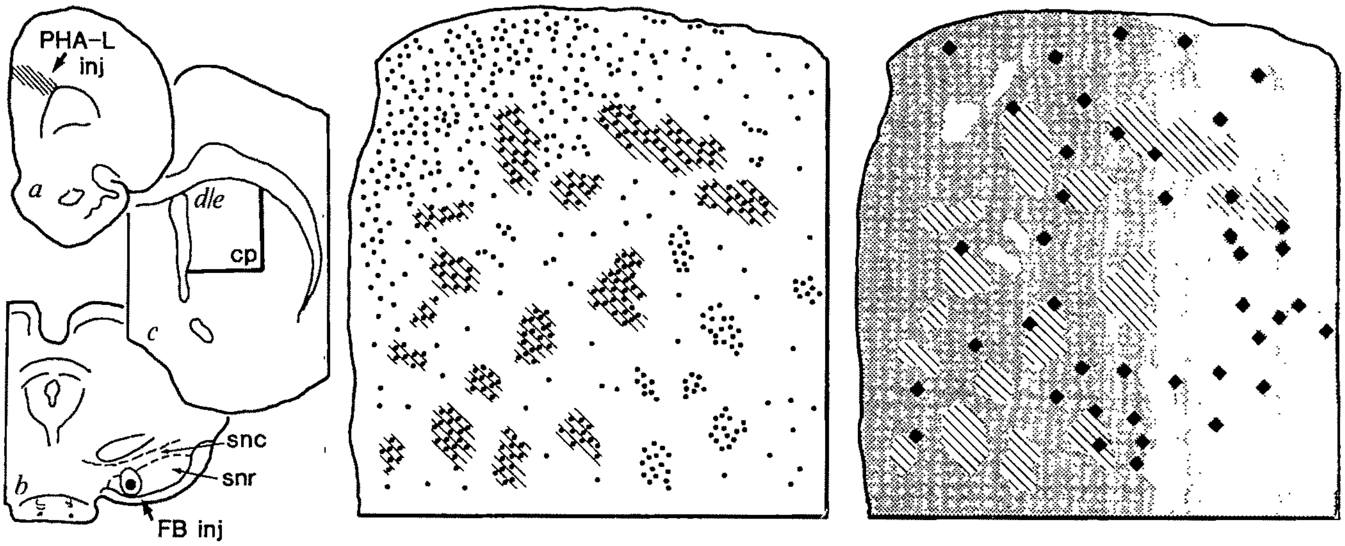

Fig. 1 Diagrammatic representation of labelling in coronal sections from case CSI-4. *a*, The location of PHA-L injection site (PHA-L inj) in the prelimbic cortex shown by hatching. *b*, The location of the Fast blue injection (FB inj) centred in the ventro-medial substantia nigra pars reticulata (snr) with spread into the pars compacta is marked (O). The area within the medio-dorsal caudate-putamen (cp) outlined in section *c* is enlarged in *d* and *e*. *d*, Retrogradely labelled striatonigral projection neurones (dots) are most heavily concentrated in the most medio-dorsal area. Their distribution here is relatively homogeneous, but ventral distribution is in discrete clusters, some of which are co-extensive with patches of labelled corticostriate afferents marked with hatching. *e*, The concurrent localization of somatostatin-immunoreactive cell bodies (diamonds) shows that such neurones are located both within and around patches of PHA-L labelled corticostriatal input (hatching), but that somatostatin-immunoreactive fibres (shaded area) appear to be limited to the matrix zone complementary to such patches. In this example, the prelimbic input is primarily to the medial half of the striatum; in two other cases where the PHA-L injection was into a more-rostral part of the prelimbic cortex, and labelled corticostriate inputs are distributed to the patches in the lateral half of the striatum.

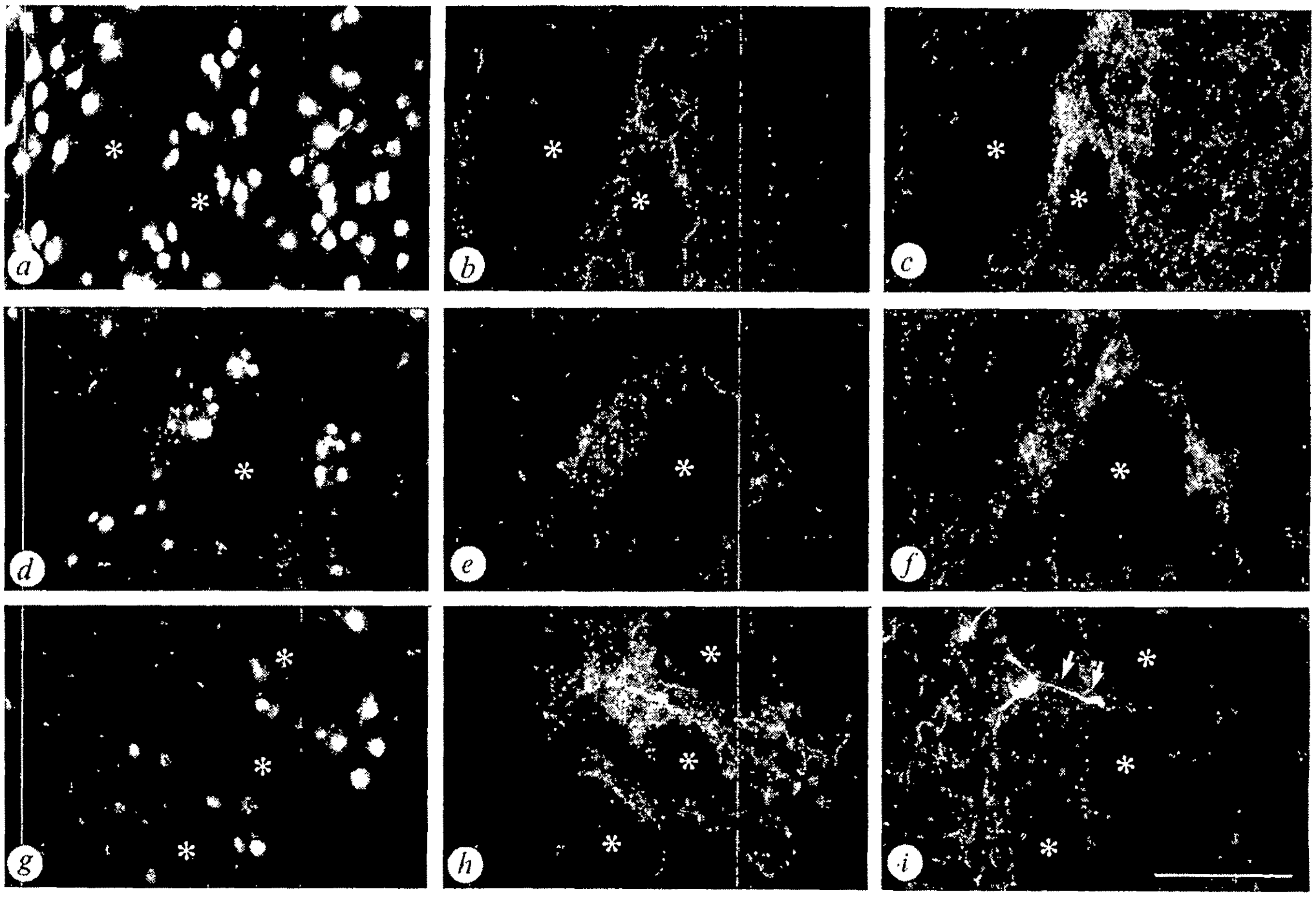

Fig. 2 Photomicrographs of striatal areas in three sections, *a–c*, *d–f*, and *g–i*, from case CSI-4 showing concurrent localization of striatonigral projection neurones labelled with the fluorescent marker Fast blue (*a*, *d*, *g*); patches of corticostriate input labelled with PHA-L (*b*, *e*, *h*) demonstrated with fluorescein-labelled goat anti-guinea pig IgG (GAGP-FITC) and Leu-enkephalin (*c*), substance-P (*f*), and somatostatin-like (*i*) immunoreactivity demonstrated with tetramethylrhodamine-labelled goat anti-rabbit IgG (GAR-TRITC). In each section the three labels are separately revealed with the appropriate epifluorescent excitation filters (e.f.) and barrier filters (b.f.) of the following wavelengths: true blue (e.f., 330–380; b.f., 420), FITC (e.f., 460–485; b.f., 515–545) and TRITC (e.f., 535–550; b.f., 580). Asterisks mark unlabelled cortico-fugal fibre tracts used as landmarks to compare the relative distribution of the labelled structures in the same field. The striatal area *a–c* lies in the medio-dorsal striatum. Fast blue labelled neurones (*a*) are present both within the corticoreceptive (*b*)/Leu-enkephalin-immunoreactive rich (*c*) patch and in the surrounding matrix compartment. The area in another section (*d–f*) is in a more ventral part of the striatum, where a cluster of retrogradely labelled striatonigral neurones (*d*) is co-extensive with a patch of PHA-L labelled corticostriate fibres and terminals (*e*) and a patch of substance P-immunoreactivity (*f*). In an adjacent section (*g–i*), in the same area of the striatum as *d–f*, a cluster of retrogradely labelled striatonigral neurones is observed (*g*), co-extensive with labelled corticostriate afferents (*h*) which are distributed complementary to the surrounding matrix of somatostatin-like immunoreactive fibres and terminals (*i*). A single somatostatin immunoreactive neurone is observed at the border of the corticoreceptive patch area with a dendrite (arrows) the end of which is enlarged due to focal aberration) that extends into the patch area away from the somatostatin fibre plexus in the matrix. Scale bar, 100 μm.

peptide completely blocked specific staining in the neostriatum.

In six cases, PHA-L injections were localized to different 300-μm-wide areas in the prelimbic cortex[5] (Fig. 1*a*). Projections distributed throughout the striatum but restricted to the striatal patch system are seen when the results of these injections are combined. In the example shown in Figs 1 and 2, labelled corticostriate fibres and terminals are distributed in discrete patches, 5–15 per section, of diameter 100–400 μm and spread throughout the dorso-ventral and rostro-caudal extent of the medial half of the striatum. In this example, the Fast blue injection is centred in the medial substantia nigra pars reticulata with tracer spreading dorsally into the pars compacta (Fig. 1*b*). In the medio-dorsal striatum, retrogradely labelled neurones are homogeneously distributed in both the patch areas co-extensive with labelled prelimbic corticostriate inputs and in the complementary matrix (Figs 1*d*, 2*a–c*). Ventral to this area, labelled striatonigral projection neurones are distributed in discrete clusters (Fig. 2*d*, *g*) co-extensive with the patches of labelled corticostriate terminals (Fig. 2*e*, *h*). These patches (Fig. 2*b*, *e*) are always co-extensive with patches of strong Leu-enkephalin-immunoreactivity (Fig. 2*c*) and substance P-immunoreactivity (Fig. 2*f*). In a third series of sections, a somatostatin-immunoreactive fibre plexus appears only in the matrix compartment (Figs 1*e*, 2*g–i*). Somatostatin-immunoreactive neurones are present in both patches and matrix and often dendrites from matrix-labelled neurones extend into the patches. Labelled axons of patch somatostatin-immunoreactive neurones project into the surrounding matrix, where they ramify into a fibre plexus which has numerous 'terminal-like' swellings. Somatostatin immunoreactivity was never observed in Fast blue labelled striatal projection neurones.

To obtain a more detailed view of the distribution of retrogradely labelled striatonigral projection neurones relative to the striatal compartments, 12 animals were injected with 35 nl of Fast blue into the substantia nigra. Colchicine was administered intraventricularly in a dose of 75 μg on the sixth post-injection day and the animals were killed on the eighth day, when the brains were processed as described above. Cases were classified as having injections restricted primarily to the pars compacta ($n=3$), pars reticulata ($n=3$), or with equal spread into both

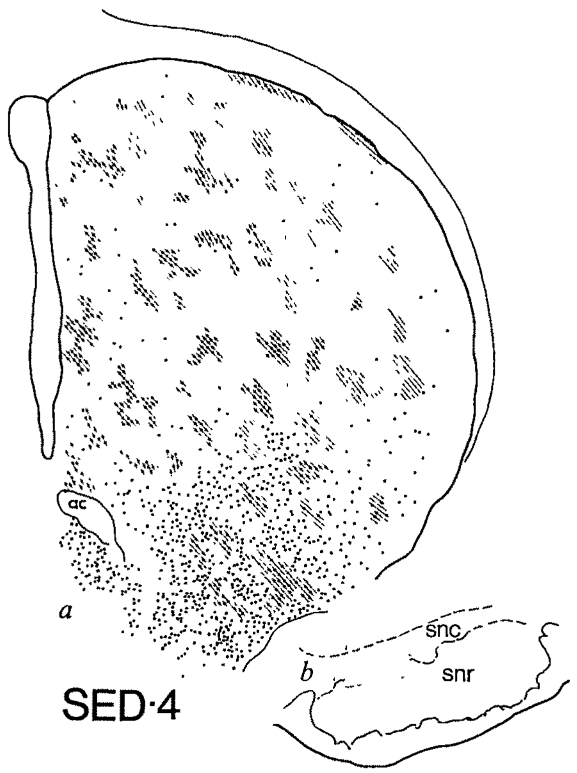

Fig. 3 *a*, A frontal section through the anterior striatum from case SED-4 onto which are mapped the distribution of substance P-like immunoreactive rich patches (hatching) and striatonigral projection neurones (dots), that are retrogradely labelled following an injection of Fast blue into the substantia nigra pars compacta (snc), shown diagrammatically in *b*. snr, Substantia nigra pars reticulata. Note that in the ventral striatum, labelled neurones are distributed in both the striatal patch and matrix compartments (see text), whereas dorsal to this area, labelled neurones are distributed in clusters that are co-extensive with patches of strong substance P-immunoreactivity.

areas ($n = 6$). Figure 3 shows the distribution of retrogradely labelled neurones relative to patches of substance P-immunoreactivity in one experiment in which the injection was centred in the medial pars compacta (snc, Fig. 3*b*). Labelled neurones are most densely distributed in the ventral striatum in both the patch and matrix compartments; outside this ventral zone and extending to the dorsal border of the striatum, labelled neurones are distributed preferentially in clusters co-extensive with patches of substance P-immunoreactivity. This pattern was evident throughout the rostrocaudal extent of the striatum and was typical in cases where injections were centred in the pars compacta. By contrast, when injections were centred in the pars reticulata, labelled neurones are most densely distributed in the matrix compartment throughout the dorsal striatum. However, the effective injection site cannot be determined using retrograde tracers, so these results must be viewed cautiously. In a recent study[15] (and C.R.G., in preparation) using PHA-L anterograde tract tracing, the dorsal striatum has been shown to give rise to a split nigral projection, one to the pars compact and a separate, denser one to the ventral pars reticulata. This result, combined with the retrograde data presented here, suggests that the projection neurones in the dorsal striatal patches are the source of fibres that innervate the pars compacta. These conclusions are consistent with ultrastructural data which demonstrate convergence of inputs from both the dorsal and ventral striatum onto pars compacta neurones[16].

Classical studies have linked the basal ganglia to sensorimotor function via the movement disorders produced by Parkinson's disease and Huntington's chorea[17]. More recently, involvement of this neural system in affective disorders such as schizophrenia has been suggested[18]. These dual functions of the striatum are thought to be regionally segregated to a ventral or 'limbic' striatal region that mediates striatal involvement in affective behaviour, and a dorsal or 'nonlimbic' striatal region involved in sensorimotor function[19,20]. The topographic organization of certain striatal input–output systems supports this view. The dorsal striatum, composed of the dorso-lateral part of the caudate-putamen, receives neocortical inputs from sensorimotor areas[21,22] and projects to the dorsal pallidum and substantia nigra pars reticulata[23,24]; the latter nucleus provides inputs to the thalamus, tectum and midbrain tegmentum[9,10]. The ventral striatum[19–21], composed of the nucleus accumbens, adjacent ventral caudate-putamen, and olfactory tubercle, receives limbic inputs from the amygdala and allocortex[5,6,19,21] and projects to the ventral extension of the pallidum (the substantia innominata, lateral preoptic area and lateral hypothalamus)[20,25]. Interactions between these striatal subsystems occurs via the convergence of their transynaptic output pathways to the thalamus[9,26] and the midbrain tegmentum[9,25,27], or via ventral striatal input to the substantia nigra pars compacta[23–25,28], which provides the nigrostriatal dopaminergic 'feedback' system to the dorsal striatum.

Recently the boundaries of the limbic striatum have been expanded to include the most medial part of the dorsal striatum, which receives inputs from the amygdala[21] and cingulate cortex[29]. However, these findings do not address the issue of possible interaction of limbic and non-limbic inputs within any given striatal district. The present results show that the prelimbic cortex, which receives direct limbic inputs from the amygdala[5] and hippocampus[6,7], projects to the patches throughout the striatum including the dorsolateral part that receives sensorimotor cortical inputs[8,21]. In this striatal region, sensory and motor cortical areas preferentially project to the matrix[8]. This suggests that, on the basis of extrinsic connections, the striatal patch and matrix are functionally distinct compartments. Furthermore, it is shown here that the striatal projection neurones in the patches project to the substantia nigra pars compacta whereas those in the matrix project to the substantia nigra pars reticulata. The somatostatin-immunoreactive intrinsic system provides a possible link between the two striatal compartments, with neurones in the patches providing inputs to the surrounding matrix areas. These findings suggest that the striatal patch and matrix compartments comprise a system of intermixed and interactive functionally distinct parallel input–output processing channels that are overlaid on the more classically recognized topographically ordered dorsal (non-limbic) and ventral (limbic) segregation of striatal connectivity and function[19–21,30].

The author acknowledges the gifts of antisera from Drs R. Benoit and M. Brown, the technical assistance of R. Butcher and the photographic assistance of K. Trulock. This study was supported by an NIH postdoctoral fellowship (NS-06813) to C.R.G. and by NIH grants EY-03653 and NS-16980 to Dr W. M. Cowan.

Received 19 October 1983; accepted 20 July 1984.

1. Pert, C. B., Kuhar, M. J. & Snyder, S. H. *Proc. natn. Acad. Sci. U.S.A.* **73**, 3729–3733 (1976).
2. Herkenham, M. & Pert, C. B. *Nature* **291**, 415–418 (1981).
3. Graybiel, A. M., Ragsdale, C. W. Jr., Yoneoka, E. S. & Elde, R. D. *Neuroscience* **6**, 377–397 (1981).
4. Graybiel, A. M. & Ragsdale, Jr, C. W. *Proc. natn. Acad. Sci. U.S.A* **75**, 5723–5726 (1978).
5. Krettek, J. E. & Price, J. L. *J. comp. Neurol.* **172**, 687–722 (1977).
6. Swanson, L. W. *Brain Res.* **217**, 150–154 (1981).
7. Donoghue, J. P. & Parham, C., *J. comp. Neurol.* **217**, 390–404 (1983)
8. Donoghue, J. P. & Herkenham, M. *Soc. Neurosci. Abstr.* 9, 15 (1983)
9. Gerfen, C. R., Staines, W. A., Arbuthnott, G. W. & Fibiger, H. C. *J. comp. Neurol.* **207**, 283–303 (1982).
10. Vincent, S. R., Hattori, T. & McGeer, E. G. *Brain Res.* **151**, 159–164 (1978)
11. Gerfen, C. R. & Sawchenko, P. E. *Brain Res.* **290**, 219–238 (1984).
12. Bentivoglio, M., Kuypers, H. G. J. M., Catsman-Berrevoets, Loewe, H. & Dann, H. *Neurosci. Lett.* **18**, 25–30 (1980).
13. Morrison, J. H., Benoit, R., Magistretti, P. J. & Bloom, F. E. *Brain Res.* **262**, 344–351 (1983)
14. Berod, A., Hartman, B. K. & Pujol, J. F. *J. Histochem. Cytochem.* **29**, 844–850 (1981)
15. Gerfen, C. R. *Soc. Neurosci. Abstr.* **9**, 16 (1983).
16. Somogyi, P., Bolam, J. P., Totterdell, S. & Smith, A. D. *Brain Res.* **217**, 245–263 (1981)
17. Denny Brown, D. *The Basal Ganglia* (Oxford University Press, 1962)
18. Stevens, J. R. *Archs gen. Psychiat.* **29**, 177–189 (1973).
19. Heimer, L. & Wilson, R. D. in *Golgi Centennial Symp.* (ed. Santini, M.) 177–193 (Raven, New York, 1975).

20. Mogenson, G. J., Swanson, L. W. & Wu, M. *J. Neurosci.* **3,** 189–202 (1983).
21. Kelley, A. E., Domesick, V. B. & Nauta, W. J. H. *Neuroscience* **7,** 615–630 (1982).
22. Webster, K. E. *J. Anat.* **95,** 532–544 (1961).
23. Tulloch, T. F., Arbuthnott, G. W. & Wright, A. K. *J. Anat.* **127,** 425–441 (1978).
24. Grofova, I. in *The Neostriatum,* 37–51 (Pergamon, Oxford, 1979).
25. Nauta, W. J. H., Smith, G. P., Faull, R. L. M. & Domesick, V. B. *Neuroscience* **3,** 385–401 (1978).
26. Swanson, L. W. *J. comp. Neurol.* **167,** 227–256 (1976).
27. Swanson, L. W., Mogenson, G. J., Gerfen, C. R. & Robinson, P. *Brain Res.* **295,** 161–178 (1984).
28. Swanson, L. W. & Cowan, W. M. *Brain Res.* **92,** 324–330 (1975).
29. Beckstead, R. M. *J. comp. Neurol.* **184,** 43–62 (1979).
30. Graybiel, A. M. & Ragsdale, C. W. Jr *Prog. Brain Res.* **51,** 239–283 (1978).

Intraneuronal generation of a pyridinium metabolite may cause drug-induced parkinsonism

S. P. Markey, J. N. Johannessen, C. C. Chiueh, R. S. Burns & M. A. Herkenham*

Laboratory of Clinical Science and *Laboratory of Neurophysiology,
National Institute of Mental Health, NIH, Bethesda,
Maryland 20205, USA

The compound 1-methyl-4-phenyl-1,2,3,6-tetrahydropyridine (MPTP) induces an irreversible neurological syndrome in man[1,2] and monkey[3] which is similar to idiopathic Parkinson's disease in its clinical, pathological, neurochemical and pharmacological response properties. MPTP is selectively neurotoxic to the dopaminergic regions of the brain, destroying neurones in the substantia nigra (A8 and A9 cells, nigrostriatal system) but not the ventral tegmental area (A10 cells, mesolimbic system)[3]. Selective dopamine depletion and nigral cell loss after MPTP treatment has also been reported recently in the mouse[4]. The mechanism by which a peripherally administered, low-molecular weight compound exerts permanent but selective toxic effects on dopamine systems in the brain may be relevant to parkinsonian syndromes induced by other toxins and to the disease process in idiopathic Parkinson's disease. We report here that MPTP is oxidized in the brain to a pyridinium species (a compound with potent herbicidal activity) and, in the monkey, is trapped intraneuronally. Furthermore, we demonstrate that this enzymatic oxidation is blocked *in vivo* in the mouse by a monoamine oxidase inhibitor, a condition which also blocks the neurotoxicity[5], indicating that the oxidative metabolism of MPTP is required for its neurotoxic effect.

Radiolabelled [1-^{14}C]MPTP was prepared by reacting ^{14}C-methyl iodide (2 mCi, 5.4 mg) with 4-phenylpyridine (10 mg) in dichloromethane at room temperature for 24 h, followed by reduction of the dried residue in aqueous solution with excess $NaBH_4$, using the method of Lyle[6]. The product, [1-^{14}C]MPTP, was extracted into hexane, dried and reconstituted in ethanol for injection. Alternatively, excess 1-methyl-4-phenylpyridinium iodide (5.4 mg) was reduced with NaB^3H_4 (77.8 Ci mmol^{-1}, 0.24 mg) in aqueous base at room temperature for 2 h and the product, 2,6-$^3H_2$-MPTP (38 Ci mmol^{-1}), extracted into hexane, dried and reconstituted in ethanol.

Four rhesus monkeys were injected intravenously with various combinations of $^3H_2$-MPTP, ^{14}C-MPTP and unlabelled MPTP and killed between 1 and 20 days after injection (Table 1). After a lethal dose of pentobarbital, the brains were removed and bisected in the sagittal plane. The right half was rapidly frozen and processed for autoradiography in the coronal plane. The left half was dissected using gross anatomical landmarks and the pieces frozen and retained for chemical studies. Dissected regions were homogenized in water (1:4 w/v) and either solubilized with Protosol (NEN) for counting or extracted with ethanol for counting and HPLC of radioactive materials, as described in Fig. 1 legend. Twenty-eight adult male mice (NIH Swiss Webster, 20–22 g) were also used. Seven mice were injected intraperitoneally (i.p.) with saline and seven with pargyline

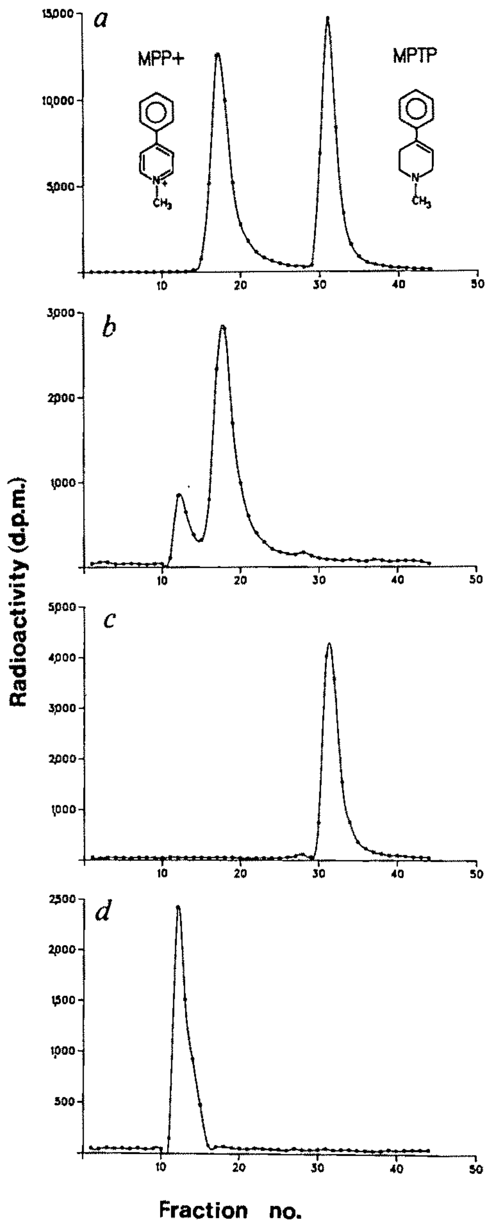

Fig. 1 *a*, Elution profiles of ^{3}H-MPTP and ^{14}C-MPP$^+$. *b*, Elution profile of radioactivity extracted from the brain of monkey BZ9. The predominant ^{3}H peak extracted from the monkey brain co-eluted with MPP$^+$ (fractions 16–24). The elution profile in *c* is that of hexane-extractable ^{3}H-labelled material obtained after $NaBH_4$ reduction of 50 μl of an ethanol extract. This reduced compound eluted as a single peak coincident with MPTP. The radiochromatogram in *d* is for cerebrospinal fluid from monkey BZ9 taken at the time of killing. The absence in CSF of MPP$^+$, which predominates in brain, is indicative of the intraneuronal trapping of MPP$^+$.

Methods: Monkey BZ9 was injected with $^3H_2$-MPTP and killed 24 h later. The left half of the brain was regionally dissected and homogenates were prepared as described in the text. An extract containing the radioactivity was prepared by adding an equal volume of ethanol to a small aliquot (0.5 ml) of an aqueous homogenate, vortexing thoroughly, then centrifuging at 16,000*g* for 15 min. Samples (50 μl) of a representative extract were then injected into an HPLC system consisting of a 5 μ, 25 cm, C-18 reverse-phase column with a mobile phase of acetonitrile/100 mM sodium acetate (60:40, v/v) containing 0.1% triethylamine (final *p*H 5.6) at a flow rate of 1.0 ml min^{-1}; 44 fractions were collected at 15-s intervals and counted in 10 ml Aquasol (NEN) at an efficiency of 46%. Recovery of injected radioactivity was 100%, in all cases.

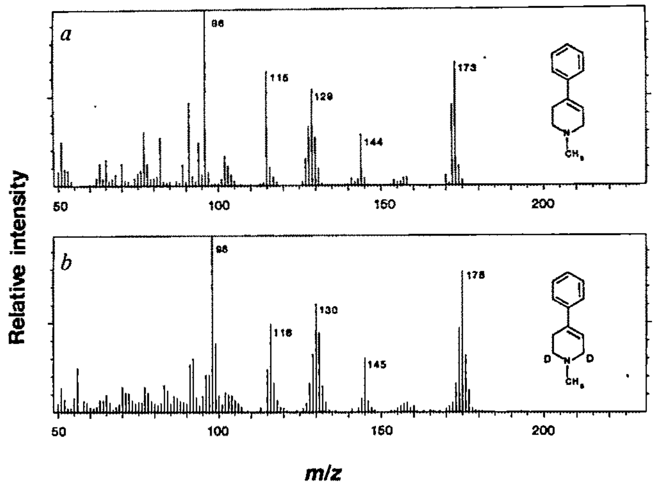

Fig. 2 *a*, Mass spectrum of authentic MPTP. *b*, Mass spectrum of metabolite reduced with NaB^2H_4 which was extracted from brain tissue of a monkey treated with MPTP.

Methods: One-half of the brain of a rhesus monkey (tissue weight 39.1 g) which died 17 days after the last of five daily injections of MPTP (0.33 mg per kg per day, total dose 9.6 mg) was homogenized in 5 vol. water. This homogenate was extracted with an equal volume of ethanol and the protein precipitated by centrifugation at 23,000*g* for 20 min. The supernatant was washed three times with 2 vol. hexane, then reacted with 1.78 g of NaB^2H_4 at room temperature for 30 min. The resulting product was extracted into hexane (two extractions with equal volumes of hexane), then concentrated to a volume of 5 ml by a series of forward and backward extractions of decreasing volume. A small quantity of decane (40 µl) was added to the final 5 ml of hexane, which was then evaporated to 40 µl under a gentle stream of N_2. This solution (0.5 µl) was inected into a 30 m × 0.322 mm DB-1 fused silica gas chromatographic column directly coupled to the ion source of a Finnigan 3200 quadrupole mass analyser.

(10 mg per kg); after 1 h both groups of mice were injected i.p. with MPTP (10 mg per kg) and 7.7 µCi [1-^{14}C]MPTP. Pairs of mice (control and pargyline-pretreated) were killed by spinal dislocation 5, 10, 20, 30, 40, 60, 120 and 240 min after the latter injection. The brains were rapidly removed, frozen on dry ice, and stored at −20 °C until extracted and assayed by HPLC, as described in Fig. 3 legend. In a separate experiment, two groups of seven mice were treated as above, but injected with unlabelled MPTP alone, and killed 10 min later. The brains were removed and rapidly frozen, then stored until assayed by gas chromatography–mass spectrometry (GC–MS). Briefly, $^2H_5$- or $^2H_{10}$-internal standards were added to brain homogenates, basified, and MPTP extracted into toluene. Reducible metabolites were assayed as $^2H_2$-MPTP after reduction with sodium borodeuteride and toluene extraction. The organic extracts were derivatized with isobutyl chloroformate to form a stable derivative with excellent chromatographic properties, and assayed by determining the ratio of ions from unlabelled MPTP ($m/z = 202$), reducible metabolites ($m/z = 204$), and internal standards ($m/z = 206$ or 210).

The persistence of large amounts of radioactivity in the rhesus monkey brains was apparent from the percentages of administered radioactivity found in each brain (Table 1). In the case of monkey BZ9, 0.99% of the total injected dose was recovered from the brain after 24 h, whereas ~0.2% still remained after 20 days in monkey 28. From a log plot of the ^3H data from four monkeys, a terminal-phase half life of 10 days was estimated. Virtually all of the radioactive material present in the monkey brains was ethanol-extractable from an aqueous tissue homogenate (98–99%). Measurements in 16 dissected brain regions from each monkey indicated that the pattern of radioactivity observed in the monkey brain at 24 h was consistent for at least 20 days. Furthermore, the use of a toxic dose did not affect the pattern observed with a tracer dose (for example, monkey BZ9 versus monkey 678).

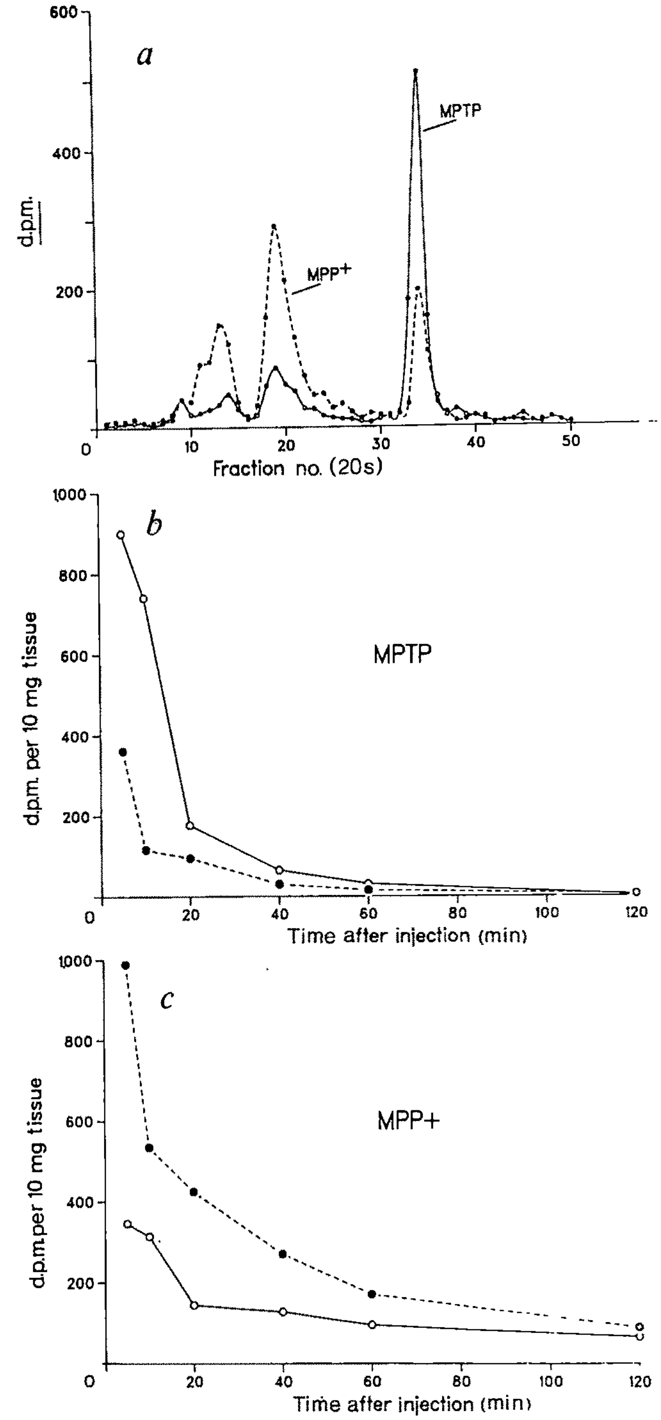

Fig. 3 Effect of pargyline pretreatment on MPTP metabolism in mice. ---●---, Control mice; —○—, pargyline-pretreated. The total radioactivity contained in the MPTP peak and MPP$^+$ peak (*a*) was summed for each mouse brain extract and the totals plotted against the time after injection (*b* and *c*). Pargyline pretreatment increased the levels of MPTP at all times, while blocking the enzymatic conversion to MPP$^+$.

Methods: Fourteen adult male mice (NIH Swiss Webster, 20–22 g) were used in this experiment. Half were injected i.p. with 0.2 ml saline and half with 10 mg per kg pargyline in 0.2 ml saline; after 1 h all animals were injected i.p. with 0.2 ml of a saline solution containing 0.2 mg MPTP (10 mg per kg) and 7.7 µCi ^{14}C-labelled MPTP. Pairs of mice (control and pargyline-pretreated) were killed by spinal dislocation 5, 10, 20, 40, 60, 120 and 240 min after the latter injection. The brains were rapidly removed, frozen on dry ice, and stored at −20 °C until used. Frozen brains were weighed, then homogenized in 4 vol. distilled water. A 0.5-ml aliquot of each homogenate was added to an equal volume of ethanol, vortexed, then centrifuged at 14,000*g* for 10 min. The radioactive components in the supernatant were separated by HPLC as described for Fig. 1.

Table 1 Amounts of radioactivity injected and survival times for four monkeys used in the study

Monkey	BZ9	910E	28	678
Weight (kg)	6.85	7.25	6.15	6.70
Dose of $^3H_2$-MPTP (mCi per animal)	9.3	1.15	1.15	0.75
Dose of ^{14}C-MPTP (mCi per animal)	–	0.41	0.41	0.49
Total MPTP dose (mg per kg)	Trace	0.19	0.22	0.90
Survival time after injection (days)	1	10	20	5/10*
% Of injected ^3H in brain	0.99	0.32	0.18	0.47
% Of injected ^{14}C in brain	–	0.40	0.22	0.24

* $^3H_2$-MPTP was injected 5 days after ^{14}C-MPTP. Total survival time was 10 days.

Figure 1*b* shows the HPLC analysis of a brain extract taken 24 h after a single injection of $^3H_2$-MPTP (monkey BZ9). The elution profile remained constant regardless of either the brain region examined or the time since injection of MPTP. The major MPTP metabolite, which eluted as a single peak somewhat more polar than MPTP, always accounted for ~80% of the total radioactivity. To isolate and identify this metabolite, we considered expected routes of MPTP metabolism including *N*-demethylation, ring hydroxylation and protein alkylation[7]. The solubility properties of the monkey brain metabolite precluded protein alkylation. HPLC comparison of authentic *N*-dealkylated or 4-phenylhydroxylated standards indicated that the monkey brain metabolite is intermediate in polarity. We then considered the pyridinium oxidation product of MPTP, 1-methyl-4-phenylpyridine (MPP$^+$)(shown below).

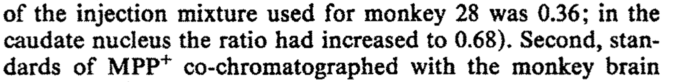

Several lines of evidence have confirmed the presence of MPP$^+$ in the brains of monkeys treated with MPTP. First, formation of this product would require partial loss of ^3H from [2,6-$^3H_2$]MPTP, but would preserve the 1-^{14}C label, causing an increased ^{14}C:^3H ratio. We observed this in monkeys which had received double-labelled MPTP (for example, the ^{14}C:^3H ratio of the injection mixture used for monkey 28 was 0.36; in the caudate nucleus the ratio had increased to 0.68). Second, standards of MPP$^+$ co-chromatographed with the monkey brain metabolite (Fig. 1*a*). Treatment of radiolabelled monkey brain extract with $NaBH_4$ quantitatively converted the metabolite into a hexane-extractable base which co-chromatographed with MPTP (Fig. 1*c*). Finally, sufficient metabolite to analyse by GC–MS was isolated (see Fig. 2 for details) from the brain tissue of a monkey which died 17 days after treatment with MPTP (1.65 mg per kg). Reduction of the metabolite with NaB^2H_4 yielded a product determined by mass spectrometry to be $^2H_2$-MPTP, the reduction product of the quaternary amine MPP$^+$ (Fig. 2). Thus, in monkey brain, MPTP is oxidized to MPP$^+$, which is retained in the brain for over 20 days.

Our experiments in mice provide evidence that the metabolism of MPTP is, in fact, required for the expression of neurotoxicity. Heikkila *et al.* have demonstrated that MPTP depletes neostriatal dopamine and destroys nerve cells in the zona compacta of the substantia nigra in mice[4]. This neurotoxicity can be blocked with monoamine oxidase (MAO) inhibitors including pargyline (see accompanying paper[5]). We found that pargyline decreased the oxidation of MPTP with a resultant increase in brain levels of MPTP and decreased concentrations of MPP$^+$ (Fig. 3). After 10 min, the ratio of MPTP to MPP$^+$ was 0.2 and 2.4 in the saline-pretreated and the pargyline-pretreated mouse brain, respectively, indicating the effectiveness of metabolic blockade. This observation was quantified in two groups of mice killed 10 min after injection with MPTP (10 mg per kg i.p.). Assay of MPTP and MPP$^+$ indicated higher levels of MPTP in the brains of pargyline-pretreated mice than in saline controls (188 ± 27 as opposed to 67 ± 13 ng per mg tissue ±s.e.m.; $P<0.01$ using Student's *t*-test). Conversely, the MPP$^+$ levels were significantly lower in the brains of pargyline-pretreated than in saline-pretreated mice (63 ± 8 compared with 144 ± 17 ng per mg tissue; $P<0.01$). Thus, pargyline blocks the oxidation of MPTP, but does not impair its entry to the brain. The fact that higher concentrations of MPTP were found at all times in the brains of pargyline-pretreated animals (Fig. 3*b, c*) indicates that MPTP cannot induce neurotoxicity without biotransformation. At times greater than 2 h, neither MPTP nor MPP$^+$ was present in appreciable amounts in the mouse brain, in marked contrast to the persistence of MPP$^+$ in the monkey brain. This difference in the persistence of MPP$^+$ may account for the difference in dose required to produce neurotoxicity in the mouse compared with the monkey (10 daily injections of 30 mg per kg produce only 80% neostriatal dopamine depletion in the mouse[4] whereas in

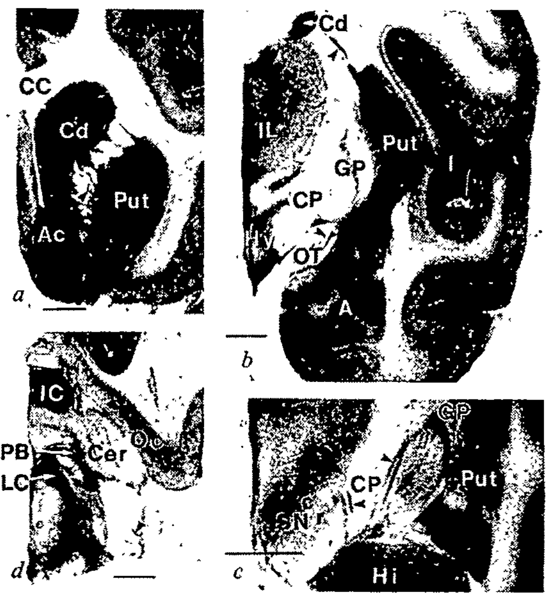

Fig. 4 Silver grain autoradiographic images of the brain of a monkey 24 h after treatment with $^3H_2$-MPTP. Cryostat-cut brain sections (30 μm) from monkey BZ9 were thaw-mounted onto slides, dried quickly at 60 °C and apposed to ^3H-sensitive film (3H-Ultrofilm, LKB) for 5 weeks. After developing, the sections were counterstained with Thionine (not shown) to allow comparison of morphology with autoradiographic localization patterns. The films show that the walls of arteries accumulate the label densely (arrowheads indicate examples), white matter and the globus pallidus (GP)(*b*) very little, and other grey matter structures by varying amounts. Computer-assisted densitometry confirmed the relative radioactive densities derived from liquid scintillation counting of digests or extracts of dissected brain regions, and added further details. Densest labelling occurred in the locus coeruleus (LC) and lateral parabrachial nucleus (PB)(*d*); within the thalamus the intralaminar nuclei (IL)(*b*) were selectively dense; the entire neostriatum, including the n. accumbens (Ac), was moderately dense (*a*); the cerebral cortex showed lower and rather invariant levels of density; the substantia nigra had still lower density—the substantia nigra reticulata as low as the GP (*c*). A, amygdala; CC, corpus callosum; Cd, caudate; Cer, cerebellum; CP, cerebral peduncle; Hi, hippocampus; Hy, hypothalamus; I, insular cortex; IC, inferior colliculus; Oc, occipital cortex; OT, optic tract; Put, putamen; SN, substantia nigra (c, compacta; r, reticulata). Scale bar, 3 mm.

the monkey, five daily injections of 0.33 mg per kg result in a 97% depletion[3]).

Oxidation of MPTP to MPP^+ in the primate provides a facile intracellular trapping mechanism similar to that proposed by Bodor *et al.* for site-specific drug delivery of dihydropyridines[8]. Evidence for the intracellular trapping mechanism comes from several observations. First, the radioactivity in the monkey brain was not uniformly distributed, but correlated with cytoarchitecture as illustrated by autoradiographic images of the brain from monkey BZ9 (Fig. 4). High concentrations of radioactivity were observed in the caudate nucleus, putamen, hypothalamus, nucleus accumbens (n. accumbens) and the parabrachial nuclei, while low levels were seen in white matter (for example, corpus callosum) and globus pallidus. Second, the radioactivity in cerebrospinal fluid (CSF) taken from the $^3H_2$-MPTP-treated monkey (BZ9) at the time of killing was lower than in any brain tissue, and the HPLC profile showed a total absence of MPP^+ (Fig. 1*d*). Finally, the MPP^+ persisting in all of the treated monkeys was easily extracted into water on homogenization and remained in solution after protein precipitation, indicating trapping as opposed to covalent binding to intracellular proteins.

In the monkey, the localization of high concentrations of MPP^+ in non-lesioned brain regions (for example, n. accumbens) suggests that the generation of MPP^+ does not ensure cell death[9]. The properties of nigrostriatal dopamine neurones which render them more sensitive to the toxic effects of MPTP are unknown, but the selectivity may be dose- and time-dependent. Burns *et al.*[3] clearly demonstrated temporary alterations in serotonergic and noradrenergic function following MPTP injection in the monkey.

We have demonstrated that MPP^+ is formed from MPTP in both monkey and mouse brain. This process is necessary for the expression of neurotoxicity in the mouse as evidenced by decreased metabolic formation of MPP^+ and increased MPTP concentrations in the brain in conditions which inhibit neurotoxicity. Whether MPP^+ is a selective toxin or the oxidation process forming MPP^+ is neurotoxic is unknown. The former notion is supported by the fact that MPP^+ was previously developed as a selective herbicide (Cyperquat, Gulf Oil Company), although never marketed; it has been reported to have animal toxicity (50% lethal dose in rat, 35 mg per kg, oral)[10]. Alternatively, the dehydrogenation of MPTP may produce toxic intermediates (for example, free radicals, dihydropyridines, *N*-oxides, hydrogen peroxide) within nigrostriatal neurones, a mechanism proposed for other neurotoxins and for Parkinson's disease[11]; this alternative is supported by the clinical observation that inhibition of monamine oxidase by deprenyl prolongs the life of patients with idiopathic Parkinson's disease by slowing the disease process[12]. Thus, there may be neurotoxic events common to both MPTP toxicity and Parkinson's disease. Regardless of whether it is the process or the product that is important, the study of the cellular consequence of the metabolic conversion of MPTP to MPP^+ appears relevant to our understanding of the pathogenesis of Parkinson's disease.

We acknowledge helpful discussions with Drs I. J. Kopin and D. M. Jacobowitz, the collaboration of Drs N. Castagnoli and R. E. Heikkila, and the technical assistance of C. Markey, M. Shih and R. Sherman.

Received 28 November 1983; accepted 15 August 1984.

1. Davis, G. C. *et al. Psychiat. Res.* **1,** 249–254 (1979).
2. Langston, J. W., Ballard, P., Tetrud, J. W. & Irwin, I. *Science* **219,** 979–980 (1983).
3. Burns, R. S. *et al. Proc. natn. Acad. Sci. U.S.A.* **80,** 4546–4550 (1983).
4. Heikkila, R. E., Hess, A. & Duvoisin, R. C. *Science* **224,** 1451–1453 (1984).
5. Heikkila, R. E., Manzino, L., Cabbat, F. S. & Duvoisin, R. C. *Nature* **311,** 467–469 (1984).
6. Lyle, R. E., Nelson, D. A. & Anderson, P. S. *Tetrahedron Lett.* 553–557 (1962).
7. Ward, D. P. *et al. Drug Metab. Disposit.* **10,** 690–695 (1982).
8. Bodor, N., Farag, H. H. & Brewster, M. E. III *Science* **214,** 1370–1372 (1981).
9. Jacobowitz, D. M., Burns, R. S., Chiueh, C. C. & Kopin, I. J. *Psychopharmac. Bull.* **20,** 416–422 (1984).
10. Swartzbek, R. A. *Proc. 12th Br. Weed Control Conf.* Vol. 2, 851–856 (1974).
11. Cohen, G. *Neurotoxicology* **5,** 77–82 (1984).
12. Birkmeyer, W., Knoll, J., Riederer, P. & Youdim, M. B. H. *Mod. Probl. Pharmacopsychiat.* **19,** 170–176 (1983).

Protection against the dopaminergic neurotoxicity of 1-methyl-4-phenyl-1,2,5,6-tetrahydropyridine by monoamine oxidase inhibitors

Richard E. Heikkila, Lawrence Manzino, Felicitas S. Cabbat & Roger C. Duvoisin

Department of Neurology, University of Medicine and
Dentistry of New Jersey-Rutgers Medical School, Piscataway,
New Jersey 08854, USA

1-Methyl-4-phenyl-1,2,5,6-tetrahydropyridine (MPTP) causes degeneration of the dopaminergic nigrostriatal pathway in several animal species, including humans[1,2], monkeys[3,4] and mice[5–7]. Changes observed after MPTP administration include marked decrements in the neostriatal content of dopamine and its major metabolites, dihydroxyphenylacetic acid and homovanillic acid, and a greatly diminished capacity of neostriatal synaptosomes to take up ^{3}H-dopamine[5,6]. In contrast, there is no pronounced loss of serotonin in the neostriatum or of dopamine and its metabolites in other brain areas in MPTP-treated animals. The oxidative metabolism of MPTP to 1-methyl-4-phenyl pyridine, a positively charged species, has been suggested as a critical feature in the neurotoxic process[8]. Moreover, in rat brain preparations, the monoamine oxidase (MAO) inhibitor pargyline and the specific MAO-B inhibitor deprenil can prevent the formation of 1-methyl-4-phenyl-pyridine from MPTP, while the specific MAO-A inhibitor clorgyline has no such effect[9], suggesting that MAO, and specifically MAO-B, is responsible for the oxidative metabolism of MPTP. We now report that pargyline, nialamide and tranylcypromine, which inhibit both MAO-A and MAO-B, when administered to mice before MPTP, protect against MPTP-induced dopaminergic neurotoxicity. Deprenil is also protective, but clorgyline is not. Our data are consistent with the premise that MAO-B has a crucial role in MPTP-induced degeneration of the nigrostriatal dopaminergic neuronal pathway.

Male, Swiss-Webster mice weighing 25–35 g were injected intraperitoneally with pargyline, deprenil, clorgyline, tranylcypromine or nialamide and subsequently received MPTP.

As Table 1 shows, 3 days after the last of five injections of MPTP, 30 mg per kg, the mean neostriatal content of dopamine (2.4 μg per g) fell markedly compared with the mean control value (10.7 μg per g). Animals given pargyline or nialamide alone had dopamine levels somewhat higher than control values, while the neostriatal dopamine content in mice receiving pargyline or nialamide before MPTP was similar to that in mice receiving the MAO inhibitors alone. The differences in dopamine levels between mice receiving MPTP alone and those receiving the MAO inhibitors plus MPTP were highly significant ($P < 0.001$). Thus, MPTP was non-toxic in the mice pretreated with either pargyline or nialamide. Similar results were obtained in mice killed 7 days after the last MPTP injection.

MPTP administration to mice also caused a pronounced decrement in the neostriatal content of the major metabolites of dopamine—dihydroxyphenylacetic acid (DOPAC) and homovanillic acid (HVA)—which was evident at both 3 and 7 days after the last MPTP injection, as has previously been reported[5–7]. This effect was probably due to the neurotoxic effects of MPTP. Mice treated with pargyline or nialamide, alone or before MPTP, also showed marked reductions in neostriatal levels of DOPAC and HVA. This latter effect was probably due to the residual inhibition of MAO by pargyline and nialamide, both of which are known to cause a long-lasting and irreversible inhibition of MAO. DOPAC and HVA are both formed from the enzymatic actions of MAO on the ethylamine side chain of dopamine and their levels should thus be diminished as long as MAO activity is decreased[10]. Any protective effect of pargyline

Table 1 The effects of pargyline or nialamide pretreatment on the MPTP-induced effects in mouse brain

MAOI	Treatment	Assay time (days)	*n*	Dopamine	DOPAC (μg per g tissue)	HVA	^{3}H-dopamine uptake (fmol per mg tissue)	% Of control
—	—	—	8	10.7 ± 1.2	4.7 ± 0.9	2.3 ± 0.5	814 ± 227	100
Pargyline	—	3	3	13.3 ± 0.3	2.7 ± 0.4	1.6 ± 0.3	838 ± 50	103
Nialamide	—	3	3	14.5 ± 1.5	1.8 ± 0.3	1.2 ± 0.2	823 ± 99	101
—	MPTP	3	5	2.4 ± 0.8	1.8 ± 0.3	1.3 ± 0.3	360 ± 40	44
Pargyline	MPTP	3	5	13.0 ± 1.4	2.2 ± 0.3	1.4 ± 0.3	784 ± 80	96
Nialamide	MPTP	3	3	12.8 ± 1.1	1.5 ± 0.4	1.3 ± 0.3	764 ± 106	94
Pargyline	—	7	3	14.4 ± 1.1	2.2 ± 0.6	1.6 ± 0.3	765 ± 91	94
Nialamide	—	7	3	15.2 ± 1.2	1.8 ± 0.3	0.9 ± 0.1	645 ± 154	79
—	MPTP	7	4	3.5 ± 0.4	1.5 ± 0.6	1.2 ± 0.1	359 ± 60	44
Pargyline	MPTP	7	5	13.7 ± 1.1	2.1 ± 0.2	1.5 ± 0.2	750 ± 63	92
Nialamide	MPTP	7	4	10.5 ± 3.1	1.2 ± 0.2	1.0 ± 0.2	624 ± 175	77

Parameters studied were levels of dopamine and its metabolites in mouse neostriatum and the capacity of a mouse synaptosomal preparation to accumulate ^{3}H-dopamine. The mice were treated with 15 mg per kg of pargyline or nialamide and subsequently given intraperitoneal injections of MPTP, 30 mg per kg (0.17 mmol per kg), dissolved in distilled water with the *p*H adjusted to 8.5 by dilute hydrochloric acid. Other mice received the MAO inhibitor alone, MPTP alone or no injections. Injection volumes were 1.0 ml per 100 g body weight. Levels of dopamine, serotonin and their metabolites were assayed in the neostriatum at various times after the last injection. The mice were stunned by a blow to the head, the brains removed and the neostriata rapidly dissected out. The paired neostriata were then weighed and homogenized in 0.3 M sucrose. An aliquot of this homogenate was diluted with an equal volume of 0.2 M perchloric acid containing dihydroxybenzylamine as an internal standard. The samples were centrifuged at 27,000*g* for 15 min and the supernatant used for assays[11]. A Bioanalytical Systems LC-304T liquid chromatograph connected to a Kipp and Zonen dual pen recorder was used for the assays. The operating potential was 750 mV, the temperature 25 °C; full scale on the detector was usually set to 1.0 nA. A Biophase ODS 5 μm column (Bioanalytical Systems) was used for all separations, with a flow-rate for the mobile phase of 1.5 ml min^{-1}. The mobile phase was made up as follows: 35 ml of acetonitrile was added to 965 ml of 0.15 M monochloroacetate buffer at *p*H 3.0 containing 193 mg of sodium octyl sulphate. This mixture was filtered and degassed, tetrahydrofuran (18 ml) was carefully added, and the mobile phase capped until use. The samples were injected into the liquid chromatograph and data calculated from standard curves run the same day based on five or six data points in the same concentration range as that present in the tissue. Levels of dopamine and its major metabolites DOPAC and HVA, and serotonin and its major metabolite 5-hydroxyindoleacetic acid were calculated on the basis of the original tissue weight and the results expressed in μg per g of tissue ± s.d. In some experiments, in the remaining 0.3 M sucrose homogenate, a synaptosomal preparation was made and the uptake of 2 nM ^{3}H-dopamine (30.2 Ci mmol^{-1}, NEN) was measured as described previously[12]. All data were calculated as fmoles of ^{3}H-dopamine accumulated per mg of tissue used ± s.d. and the data expressed as a per cent of control. Statistical analyses were done using Student's *t*-test.

or nialamide against MPTP, based on metabolic profiles, would therefore be masked by their capacity to inhibit MAO. These data indicate that decrements in levels of dopamine metabolites cannot by themselves always serve as a marker for determining whether toxicity to dopaminergic systems has occurred.

Table 1 also shows that neostriatal synaptosomes prepared from MPTP-treated mice had a greatly diminished capacity to take up ^{3}H-dopamine compared with control preparations. This observed decrement was the same (56%) at both 3 and 7 days after the last MPTP injection, indicating clearly that there was no recovery in MPTP-treated mice during this time[6,7]. In contrast to this marked decrement in ^{3}H-dopamine uptake, the ^{3}H-dopamine uptake in neostriatal synaptosomal preparations from mice pretreated with pargyline or nialamide before MPTP was relatively close to or only slightly below control values (Table 1), as was ^{3}H-dopamine uptake in mice treated with pargyline or nialamide alone. The difference in ^{3}H-dopamine uptake between mice receiving MPTP alone and those receiving the MAO inhibitors plus MPTP were significant (*P* values ranged from <0.05 to <0.001).

Six injections of MPTP produced a very large fall in the neostriatal content of dopamine, evident at both 5 and 12 days after the last MPTP injection (Table 2). The differences in neostriatal dopamine content between control and MPTP-treated animals were highly significant ($P < 0.001$). MPTP treatment also caused large decrements in the neostriatal content of DOPAC and HVA (Table 2). The MAO-B inhibitor deprenil was completely protective against the MPTP-induced dopaminergic neurotoxicity (Table 2). Levels of dopamine and its metabolites in animals receiving deprenil plus MPTP did not

Table 2 The effects of deprenil or clorgyline pretreatment on the MPTP-induced decrements in the neostriatal levels of dopamine and its metabolites

MAOI	Treatment	Assay time (days)	*n*	Dopamine	DOPAC (μg per g tissue)	HVA
—	—	—	7	11.7 ± 1.1	3.6 ± 1.0	2.7 ± 0.5
Deprenil	—	5	4	13.1 ± 2.4	3.0 ± 0.4	2.8 ± 0.7
Clorgyline	—	5	4	13.8 ± 0.9	2.5 ± 0.6	1.6 ± 0.3
—	MPTP	5	5	2.7 ± 0.6	1.2 ± 0.3	1.3 ± 0.4
Deprenil	MPTP	5	5	13.2 ± 1.4	2.4 ± 0.3	2.4 ± 0.4
Clorgyline	MPTP	5	5	4.9 ± 2.6	1.0 ± 0.3	1.0 ± 0.2
Deprenil	—	12	3	12.6 ± 1.0	2.9 ± 0.7	2.3 ± 0.5
Clorgyline	—	12	3	12.7 ± 1.4	2.5 ± 0.4	1.8 ± 0.1
—	MPTP	12	3	2.9 ± 0.8	1.4 ± 0.2	1.5 ± 0.4
Deprenil	MPTP	12	6	12.6 ± 1.3	2.3 ± 0.4	2.1 ± 0.3
Clorgyline	MPTP	12	3	4.6 ± 2.6	1.3 ± 0.2	1.4 ± 0.2

The mice were treated with the MAO-inhibitor at 10 mg per kg on days 1 and 8, and with 30 mg per kg of MPTP on days 1, 2, 3, 8, 9 and 10. On days 1 and 8, the MPTP was given 30 min after the MAO-inhibitor. The mice were then killed either 5 or 12 days after the last MPTP injection (on days 15 and 22, respectively). The data represent the mean value ±s.d.

differ significantly from levels in mice receiving deprenil alone ($P > 0.1$). However, in contrast to these protective effects of deprenil, the MAO-A inhibitor clorgyline, in identical conditions, failed to protect against MPTP-induced toxicity. Thus, dopamine levels were not significantly different in mice receiving MPTP alone and those given clorgyline plus MPTP ($P > 0.1$).

These data clearly demonstrate that two general MAO inhibitors, pargyline and nialamide (Table 1), and the specific MAO-B inhibitor deprenil (Table 2), effectively protect against the neostriatal dopaminergic neurotoxicity of MPTP in Swiss-Webster mice. We have obtained similar protective effects of these three MAO inhibitors against MPTP-induced toxicity in C57BL mice. In other experiments in Swiss-Webster mice, tranylcypromine, another inhibitor of both MAO-A and MAO-B, also protected against MPTP dopaminergic neurotoxicity. For example, neostriatal dopamine levels in mice receiving three MPTP injections of 30 mg per kg, with assays done 4 days after the last injection, were 4.4 ± 1.8 µg per g tissue ($n = 7$). In contrast, mice pretreated with 15 mg per kg of tranylcypromine 30 min before the MPTP injections had a neostriatal dopamine level of 13.3 ± 1.9 µg per g ($n = 6$). Neostriatal dopamine levels in control mice and in mice receiving only tranylcypromine were 12.3 ± 1.3 µg per g ($n = 8$) and 14.0 ± 0.4 µg per g ($n = 3$), respectively.

Our data are thus consistent with the premise that pargyline, nialamide, tranylcypromine and deprenil protect against the neurotoxic actions of MPTP by preventing the enzymatic formation of active metabolites of MPTP catalysed by MAO-B. However, it would be incautious to conclude that the prevention by these MAO inhibitors of the oxidative metabolism of MPTP is the sole mechanism for the observed protection. Nevertheless, the data have several important implications. First, they show that the mouse is an extremely useful small animal in which to study the mechanism of action of MPTP. Second, if the mouse data can be extrapolated to the monkey or human, a good working hypothesis would be that treatment with pargyline, nialamide, deprenil or other drugs capable of inhibiting MAO-B might counteract the neurotoxic actions of MPTP in the monkey or human. Third, and perhaps most important, if there is any relationship between the mechanism for the induction of MPTP-induced parkinsonism in experimental animals and Parkinson's disease in humans, investigators should be aware of a potential role for MAO in human parkinsonism.

We thank Drs S. P. Markey, N. Castagnoli, A. Trevor for many helpful discussions and also for sharing experimental observations before publication. This work was supported by a grant from the USPHS and by a gift from the United Parkinson Foundation.

Received 2 April; accepted 21 June 1984.

1. Davis, G. C. *et al. Psychol. Res.* **1**, 249–254 (1979).
2. Langston, J. W., Ballard, P., Tetrud, J. W. & Irwin, I. *Science* **219**, 979–980 (1983).
3. Burns, R. S. *et al. Proc. natn. Acad. Sci. U.S.A.* **80**, 4546–4550 (1983).
4. Langston, J. W., Forno, L. S., Rebert, C. S. & Irwin, I. *Brain Res.* **292**, 390–394 (1984).
5. Heikkila, R. E., Cabbat, F. S., Manzino, L. & Duvoisin, R. C. *Fedn Proc.* **43**, 743 (1984).
6. Heikkila, R. E., Hess, A. & Duvoisin, R. C. *Science* **224**, 1451 (1984).
7. Hallman, H., Olson, L. & Jonsson, G. *Eur. J. Pharmac.* **97**, 133–136 (1984)
8. Markey, S. P., Johannessen, J. N., Chiueh, C. C., Burns, R. S. & Herkenham, M. A. *American College of Neuropsychopharmacology Meeting*, Abstr., 69 (1983).
9. Chiba, K., Trevor, A. & Castagnoli, N. *Biochem. biophys. Res. Commun* **120**, 574–578 (1984).
10. Neff, N. H. & Goridis, C. *Adv. Biochem. Psychopharmac.* **5**, 307–323 (1972)
11. Mayer, G. S. & Shoup, R. E. *J. Chromatogr.* **255**, 533–544 (1983).
12. Gershanik, O., Heikkila, R. E. & Duvoisin, R. C. *Brain Res.* **261**, 358–360 (1983)

Monoclonal antibodies against carbohydrate differentiation antigens identify subsets of primary sensory neurones

J. Dodd, D. Solter* & T. M. Jessell

Department of Neurobiology, Harvard Medical School, Boston, Massachusetts 02115, USA
* The Wistar Institute of Anatomy and Biology, Philadelphia, Pennsylvania 19104, USA

Dorsal root ganglion (DRG) neurones transmit cutaneous sensory information from the periphery to the spinal cord. Within the dorsal horn of the spinal cord, classes of sensory fibres that are activated by different cutaneous stimuli terminate in separate and highly restricted laminae[1–3]. Although the developmental events resulting in the laminar organization of sensory afferent terminals have not been defined, it is likely that interactions between surface molecules on DRG and dorsal horn neurones are involved in the generation of afferent synaptic connections. The identification of surface antigens that distinguish functional subclasses of DRG neurones would represent a first step in establishing the existence and nature of such molecules. We report here that monoclonal antibodies directed against carbohydrate differentiation antigens[4,5] identify cytoplasmic and cell surface molecules expressed selectively by functional subsets of DRG neurones.

We used monoclonal antibodies to preimplantation murine embryos and human embryonal carcinoma cells, which recognize the developmentally-regulated stage-specific embryonic antigens, SSEA-3 and SSEA-4[6–8]. These antigens have been characterized as overlapping carbohydrate epitopes on globo-series glycolipids[8] (Table 1). Their presence in primary sensory neurones is demonstrated by indirect immunofluorescence on frozen or aldehyde-fixed sections of adult rat DRG and spinal cord. Incubation of DRG sections with anti-SSEA-3 or anti-SSEA-4 results in the labelling of neuronal cell bodies (Fig. 1*a*, *b*) and sensory axons within the DRG and dorsal roots (Fig. 1*a*–*d*), with no detectable staining of non-neuronal elements. Intense SSEA-3 and SSEA-4 immunoreactivity occurs within the cytoplasm of DRG neurones and in association with the neuronal plasma membrane. Anti-SSEA-3 labels 9% and anti-SSEA-4 labels 11% of all DRG neurones (Table 2*a*), the majority of these being of intermediate and large diameter (30–60 µm). The percentage of immunoreactive neurones is constant in the DRG at cervical, thoracic and lumbar levels and there is no obvious topographical organization of labelled neurones within the DRG. SSEA-3 and SSEA-4 epitopes are also expressed by subpopulations of neurones in cranial sensory ganglia (Table 3), and are detected in subpopulations of DRG neurones in the mouse, cat and squirrel monkey (data not shown). A more complete description of SSEA distribution in primary sensory neurones will be reported elsewhere.

To determine the relationship between SSEA-3$^+$ and SSEA-4$^+$ DRG neurones in the rat, we used subclass-specific second antibodies that distinguish anti-SSEA-3 (a rat IgM) from anti-SSEA-4 (a mouse IgG3) on single sections of the DRG. Most immunoreactive DRG neurones are SSEA-3$^+$/SSEA-4$^+$ (Fig. 1*f*, *g*; Table 2*a*); a few small-diameter neurones are, however, solely SSEA-3$^+$ and many large-diameter neurones are solely SSEA-4$^+$ (Table 2*a*). Double labelling has shown that SSEA-3$^+$, SSEA-3$^+$/SSEA-4$^+$ and SSEA-4$^+$ neurones are distinct from the DRG neurones that express the peptide transmitters substance P and somatostatin[9]. Sequential immunofluorescence and histochemical staining demonstrate that SSEA-3$^+$, SSEA-3$^+$/SSEA-4$^+$ and SSEA-4$^+$ neurones are also distinct from those that express the fluoride-resistant acid phosphatase isoenzyme (FRAP)[10,11].

Table 1 Stage-specific embryonic antigen carbohydrate structure

Antibody	Epitope	Immunogen	Ref.
Anti-SSEA-3	GalNAcβ1→3 Galα1→4Gal	4–8 cell stage murine embryos	7, 8
Anti-SSEA-4	NeuAcα2→3 Galβ1→3GalNAc	2102Ep teratocarcinoma	8

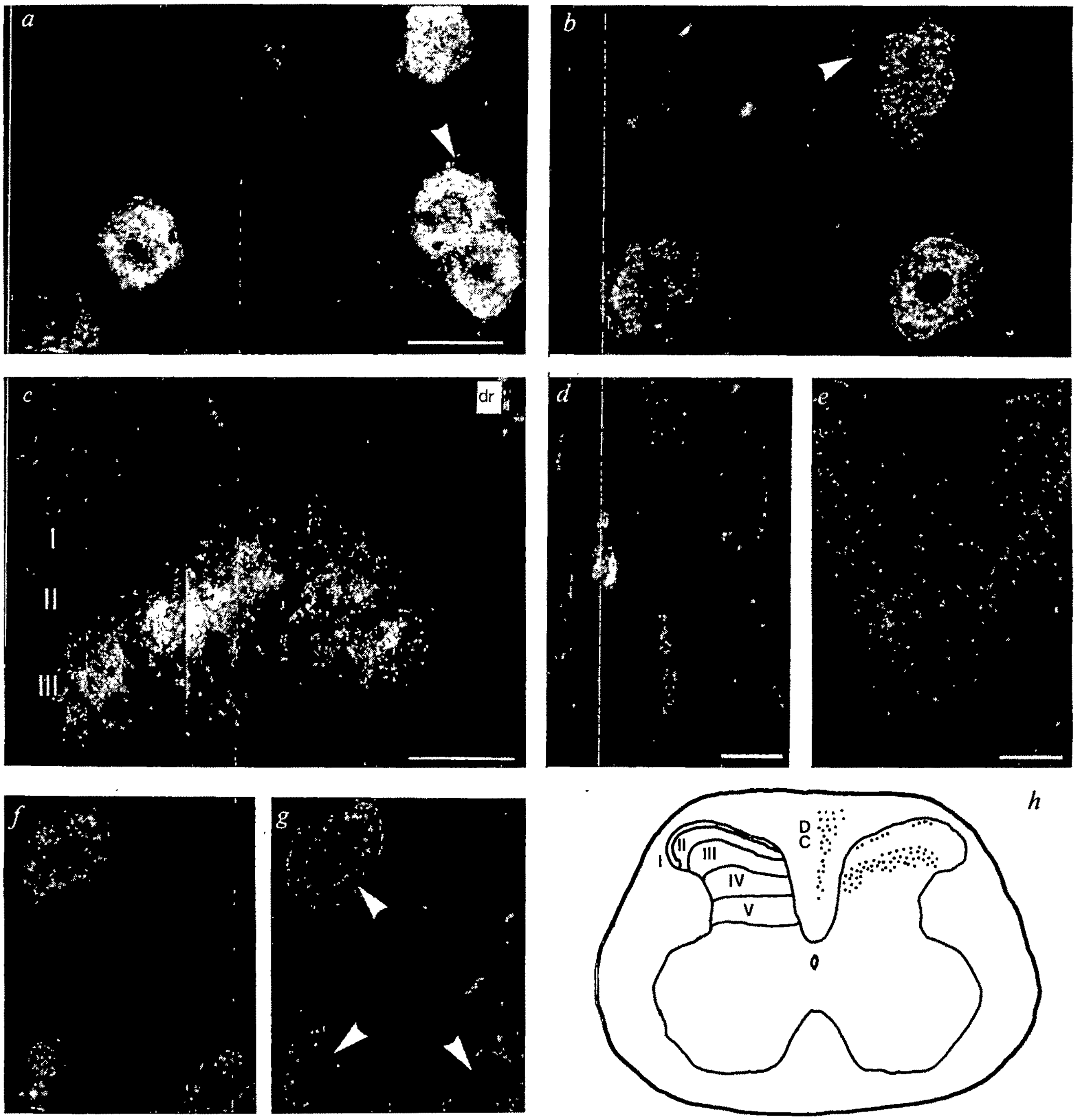

Fig. 1 Expression of SSEA epitopes by subpopulations of primary sensory neurones. Anti-SSEA-3 (*a*) and anti-SSEA-4 (*b*) produced bright, cytoplasmic labelling of a subpopulation of neurones in sections of DRG (arrows indicate stained axons). *c*, SSEA-4$^+$ fibres and terminals are found in a dense band in lamina III of the dorsal horn, with scattered fibres projecting into lamina IV. Immunoreactive afferent fibres can also be seen in cross-section, overlying the medial dorsal horn. In addition, SSEA-4$^+$ afferents are present in the dorsal root (dr) seen here in cross-section. In *c* and *h*, I, II, III, IV and V represent the location of the Rexed's laminae. *d*, SSEA-3$^+$ fibres are shown in a longitudinal section through a dorsal root. *e*, The distribution of SSEA-3$^+$ fibres in a transverse section through the dorsal columns. *f*, *g*, A single section of DRG was incubated with anti-SSEA-3 and anti-SSEA-4 and the distribution of the two antibodies was visualized using subclass-specific antibodies coupled to different fluorophores. *f*, Three DRG neurones that express SSEA-3; *g* shows the presence of SSEA-4 in the same neurones (arrows). Control experiments indicated that neither cross-reactivity of the antibodies nor barrier filter leakage contributed to this result. *h*, A diagram of a coronal section of the rat spinal cord, shows the laminar distribution of the central processes of SSEA-3$^+$ and SSEA-4$^+$ DRG neurones. SSEA-3$^+$ and SSEA-4$^+$ fibres were found predominantly in lamina III with a sparse representation in lamina I, a dense region of staining at the medial border of laminae III and IV and stained fibres in the cuneate and gracile fasciculi (DC). Scale bars: *a*, *b*, *f*, *g*, 40 μm; *c*, 80 μm; *d*, 10 μm; *e*, 150 μm.

Methods: Rat tissues were fixed by cardiac perfusion with 50 ml ice-cold saline followed by 500 ml ice-cold 4% paraformaldehyde in 0.1 M phosphate buffer, *p*H 7.2. Cryostat sections (10 μm) were incubated with anti-SSEA ascites fluid, diluted 1:100 to 1:300 in phosphate-buffered saline (PBS: 0.1 M PB in 0.9% saline) containing 10% fetal calf serum and 0.2% Triton X-100, *p*H 7.2 (16 h; 4 °C). *a–e*, Sections were washed with PBS containing 2% normal goat serum (PBS/NGS), incubated with fluorescein isothiocyanate (FITC) goat anti-mouse IgM or IgG (Tago, Inc. and Boehringer-Mannheim, respectively) diluted 1:75 in PBS/NGS for 30 min at room temperature. Sections were then washed in PBS/NGS and coverslipped in 50% glycerol in 0.1 M sodium carbonate buffer, *p*H 9.0, containing 0.4 mg ml^{-1} *p*-phenylenediamine (Sigma). *f*, *g*, Following incubation with anti-SSEA, sections were washed in PBS/NGS and incubated in PBS/NGS containing FITC-goat anti-mouse IgM, 1:75 and unconjugated rabbit anti-mouse IgG3, 1:30 (Litton Bionetics), for 30 min at room temperature. Sections were then washed again in PBS/NGS and incubated with FITC-goat anti-mouse IgM, 1:75 plus rhodamine-goat anti-rabbit IgG, 1:200 (Tago), for 30 min at room temperature. Sections were then washed and coverslipped as described above.

Table 2 Expression of SSEAs by rat DRG neurones

a, Cytoplasmic staining in adult rat DRG neurones *in situ*

Antigen	% Immunoreactive neurones	% Overlap
SSEA-3	9 ($n = 7868$)	68 SSEA-4$^+$
SSEA-4	11 ($n = 4789$)	55 SSEA-3$^+$

b, Surface staining of DRG neurones in culture

Antigen	% Immunoreactive neurones	% Overlap
SSEA-3	7 ($n = 1060$)	84 SSEA-4$^+$
SSEA-4	14 ($n = 1775$)	40 SSEA-3$^+$

Table 3 Expression of SSEAs in primary sensory neurones

	% SSEA-3	% SSEA-4
Dorsal root ganglion	9	11
Trigeminal ganglion	20	35
Petrosal ganglion	15	15
Jugular ganglion	<5	10
Nodose ganglion	60	>90

The distribution of molecules bearing the SSEA-3 and SSEA-4 epitopes in the central nervous system was examined by indirect immunofluorescence on 10 μm coronal sections taken at 100 μm intervals from the caudal brain stem to the olfactory bulb. We do not find SSEA-3$^+$ or SSEA-4$^+$ neuronal cell bodies within the CNS. In the spinal cord and brain stem, SSEA-3$^+$ and SSEA-4$^+$ immunoreactive fibres and terminals are restricted to regions that receive primary afferent input. In the dorsal horn of the spinal cord, a few labelled fibres and terminals are found in lamina I (Fig. 1*h*), whereas the tract of Lissauer and lamina II are devoid of immunoreactive fibres (Fig. 1*c*, *h*). The greatest density of labelled fibres occurs in lamina III (Fig. 1*c*) and the medial region of lamina IV (Fig. 1*h*). SSEA-3$^+$ and SSEA-4$^+$ fibres are also present in the dorsal columns (Fig. 1*e*) and in the gracile and the external cuneate nuclei. No immunoreactive fibres are observed on the lesioned side of the spinal cord in animals unilaterally deafferented 3 weeks previously by section of the dorsal roots. These results indicate that all SSEA-3$^+$ and SSEA-4$^+$ fibres within the dorsal horn of the spinal cord derive from sensory neurones within DRG.

The precise laminar arrangement of the central terminals of cutaneous afferent fibres in the rat has not been mapped in detail. The laminar cytoarchitecture and the distribution of peptide-containing sensory terminals in the rat dorsal horn are, however, similar to those in cat and primate[12,13], and we have found the laminar distribution of SSEA-3$^+$ and SSEA-4$^+$ that fibres in the dorsal horn is similar in rat, cat and squirrel monkey (J.D., T.M.J. and E. R. Perl, unpublished observations). In cats and primates, the terminal arbors of several classes of low threshold afferents are known to overlap within laminae III and IV[1]. Our observations are therefore consistent with the presence of SSEA-3 and SSEA-4 epitopes on low-threshold hair follicle afferents and mechanoreceptors[14,15]. The absence of labelled terminals in lamina II indicates that unmyelinated primary afferents do not express the SSEA-3 and SSEA-4 epitopes.

The SSEA-3 and SSEA-4 carbohydrate sequences are also expressed on the surface of DRG neurones. Approximately 7% of neonatal rat DRG neurones maintained in dissociated cell culture exhibit SSEA-3 immunoreactivity on neuronal somata and processes (Fig. 2*a*, *b*; Table 2*b*), and the SSEA-4 epitope is present on 14% of cultured DRG neurones (Fig. 2*c*, *d*; Table 2*b*). Dual-colour labelling with subclass-specific second antibodies reveals that the relationship between SSEA-3 and SSEA-4 epitopes on the surface of cultured DRG neurones is similar to that observed in the cytoplasm of DRG neurones *in situ*: over 80% of SSEA-3$^+$ DRG neurones in culture are SSEA-4$^+$ and, conversely, 40% of SSEA-4$^+$ neurones are SSEA-3$^+$ (Table 2*b*). SSEA-3$^+$ and SSEA-4$^+$ DRG neurones may correspond to the population of cultured sensory neurones that are labelled with antiserum to the globo-series glycolipid, globoside[16].

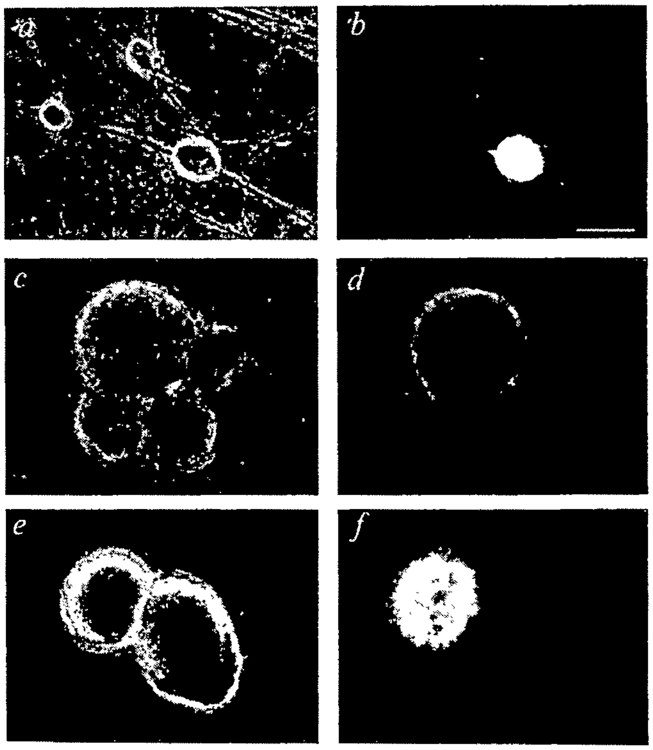

Fig. 2 Expression of SSEA epitopes on the surface of cultured DRG neurones. *a*, Phase micrograph showing three DRG neurones and a plexus of neuronal processes. *b*, Fluorescence micrograph of the field shown in *a*: one of the three neurones expresses intense SSEA-3 immunoreactivity on its cell soma and processes. *c*, Phase-contrast micrograph showing four DRG neurones. *d*, Fluorescence micrograph of the field shown in *c*; one of the neurones expresses SSEA-4 immunoreactivity. *e*, Phase-contrast micrograph of two adult rat DRG neurones. *f*, Immunofluorescent micrograph of the field shown in *e*, in which only one neurone expresses intense SSEA-3 immunoreactivity. Scale bar: *a*, *b*, 30 μm; *c*, *d*, 20 μm; *e*, *f*, 20 μm.

Methods: DRG neurones were isolated from neonatal rats and maintained in dissociated cell culture for periods of 14–42 days using previously described methods[26]. Non-neuronal cells were eliminated from DRG cultures by treatment with cytosine arabinoside (10 μM) for 24–48 h soon after plating. Live cultures were washed in HEPES-buffered balanced salt solution (BSS) supplemented with glucose and 0.1% bovine serum albumin. Cultures were then incubated with anti-SSEA ascites fluid diluted 1 : 100 to 1 : 200 in buffered BSS containing 1% NGS. FITC-labelled second antibodies were diluted in buffered BSS and used as described in the legend to Fig. 1.

We excluded the possibility that the cell surface expression of SSEA-3 and SSEA-4 epitopes is a result of maintaining DRG neurones in culture, by labelling adult rat DRG neurones immediately after dissociation. Many of these neurones are also SSEA-3$^+$ and SSEA-4$^+$ (Fig. 2*e*, *f*), but the low cell yields obtained after mechanical dissociation of adult DRG neurones preclude determination of the percentage of labelled cells.

The SSEA-3 and SSEA-4 epitopes are associated with glycolipids and glycoproteins on murine embryos and human embryonal carcinoma cells[6,8]. SSEA-3 and SSEA-4 immunoreactivity in fixed sections of DRG and spinal cord is abolished by chloroform–methanol treatment (1 : 1, 15 min) whereas peptide and protein antigens, recognized by other monoclonal antibodies, are not affected by identical treatment. Moreover, preincubation of sections with 10 mM sodium periodate for 30 min at room temperature, substantially reduced SSEA-3 and SSEA-4 immunoreactivity. These observations suggest that in sensory neurones, both epitopes are associated, at least in part, with glycolipids.

Our results suggest that subpopulations of DRG neurones involved in the processing of low threshold cutaneous stimuli can be identified by the surface expression of globo-series carbohydrates. In preliminary experiments, we have detected the SSEA-3 and SSEA-4 epitopes on some DRG neurones in 16-day rat embryos, soon after final mitosis[17]. Therefore, anti-SSEA antibodies may provide specific probes to examine early development and differentiation of this class of DRG neurones. Several other monoclonal antibodies have recently been generated against carbohydrate sequences expressed on the surface of embryonic or transformed cells[18,19]. We have found that some of these carbohydrate determinants are expressed selectively on subsets of DRG neurones distinct from those that express SSEA-3 and SSEA-4 epitopes[20], suggesting that many subclasses of DRG neurones may be characterized by differences in cell surface carbohydrate expression.

Cell surface carbohydrates have been implicated in intercellular adhesion and recognition in early embryos and embryonal carcinoma cells[21–23], and in neuronal adhesion during embryonic development[24,25]. Molecules bearing SSEA-3, SSEA-4 and other carbohydrate determinants could therefore be involved in the development and specification of sensory connections in the dorsal horn of the spinal cord.

This work was supported by a grant from NIH, NS 20116; by grants from the McKnight Foundation, the Muscular Dystrophy Association, the National Multiple Sclerosis Society and by a Dupont Faculty Award to T.M.J. J.D. was a Sloan Foundation Fellow and was supported by the Muscular Dystrophy Association and the National Multiple Sclerosis Society. D.S. was supported by NIH grant HD-12487. We thank P. N. Hamilton for technical assistance and B. B. Knowles, S. C. Landis and W. D. Matthew for helpful discussions.

Received 10 May; accepted 19 July 1984.

1. Brown, A. G. *Organization in the Spinal Cord* (Springer, Berlin, 1981).
2. Light, A. R. & Perl, E. R. *J. comp. Neurol.* **186**, 133–150 (1979).
3. Rethelyi, M. *J. comp. Neurol.* **172**, 511–528 (1977).
4. Solter, D. & Knowles, B. B. *Curr. Top. dev. Biol.* **13**, 139–165 (1979).
5. Feizi, T. *Trends biochem. Sci.* **6**, 333–335 (1981).
6. Shevinsky, L. H., Knowles, B. B., Damjanov, I. & Solter, D. *Cell* **30**, 697–705 (1982).
7. Kannagi, R. *et al. J. biol. Chem.* **258**, 8934–8942 (1983).
8. Kannagi, R. *et al. EMBO. J.* **2**, 2355–2361 (1983).
9. Hokfelt, T. Johansson, O., Ljungdahl, A., Lundberg, J. M. & Schultzberg, M. *Nature* **284**, 515–530 (1980).
10. Nagy, J. I. & Hunt, S. P. *Neuroscience* **7**, 89–97 (1982).
11. Dodd, J. *et al. Cold Spring Harbor Symp. quant. Biol.* **48**, 685–695 (1983).
12. McClung, J. R. & Castro, A. J. *Expl Neurol.* **58**, 145–148 (1978).
13. Nagy, J. I. & Hunt, S. P. *J. comp. Neurol.* **218**, 145–158 (1983).
14. Brown, A. G., Rose, P. K. & Snow, P. J. *J. Physiol., Lond.* **272**, 779–797 (1977).
15. Brown, A. G., Fyffe, R. E. W. & Snow, P. J. *J. Physiol., Lond.* **307**, 385–400 (1980).
16. Raff, M. C. *et al. Brain Res.* **174**, 283–308 (1979).
17. Lawson, S., Caddy, K. W. T. & Biscoe, T. J. *Cell. Tissue Res.* **153**, 399–413 (1974).
18. Magnani, J. L. *Biochem. Soc. Trans.* **12**, 543–545 (1984).
19. Feizi, T. *Biochem. Soc. Trans.* **12**, 545–549 (1984).
20. Jessell, T. M. & Dodd, J. *Phil. Trans. R. Soc.* (in the press).
21. Grabel, L. B., Singer, M. S., Rosen, S. D. & Martin, G. R. *Cold Spring Harb. Conf. Cell Proliferation* **10**, 145–161 (1983).
22. Shur, B. D. *Cold Spring Harb. Conf. Cell Proliferation* **10**, 185–195 (1983).
23. Bird, J. M. & Kimber, S. J. *Devl Biol.* **104**, 449–460 (1984).
24. Edelman, G. M. *et al. Cold Spring Harb. Symp. quant. Biol.* **48**, 515–526 (1983).
25. Rutishauser, U. *Cold Spring Harb. Symp. quant. Biol.* **48**, 501–514 (1983).
26. Yamamoto, M., Steinbusch, H. W. M. & Jessell, T. M. *J. Cell Biol.* **91**, 142–154 (1981).

Pattern of presynaptic nerve activity can determine the type of neurotransmitter regulating a postsynaptic event

Nancy Y. Ip & Richard E. Zigmond*

Department of Pharmacology, Harvard Medical School, Boston,
Massachusetts 02115, USA

The mammalian superior cervical ganglion has been the classical preparation for studying cholinergic transmission between neurones[1–3]. Recently, however, evidence has been presented showing that, in addition to the postsynaptic changes mediated via nicotinic and muscarinic receptors, there is a non-cholinergic component to transmission in this ganglion[4,5], as in frog paravertebral ganglia[6,7]. In the rabbit superior cervical ganglion, Ashe and Libet recorded a late, slow excitatory postsynaptic potential in response to preganglionic nerve stimulation in the presence of nicotinic and muscarinic antagonists[4]. We have found, in the rat superior cervical ganglion, that a postsynaptic biochemical consequence of preganglionic nerve stimulation, namely the acute activation of tyrosine 3-monooxygenase (tyrosine hydroxylase, TH; EC 1.14.16.2), is mediated in part by acetylcholine and in part by a non-cholinergic neurotransmitter[5]. The regulation of this enzyme activity is of particular interest because it catalyses the rate-limiting step in the biosynthesis of the postganglionic neurotransmitter, noradrenaline. In the present paper, we report that the relative importance of cholinergic and non-cholinergic transmission in the regulation of TH activity varies with the pattern of electrical stimulation of the preganglionic nerve trunk.

Male Sprague Dawley rats (160–200 g) were used in all studies. The rats were killed by cervical dislocation and their superior cervical ganglia rapidly removed, desheathed and maintained *in vitro* at 37 °C as previously described[5]. The preganglionic nerve trunk of one ganglion was stimulated via a suction electrode, and the effectiveness of the stimulation was monitored throughout the stimulation period by recording, via a second suction electrode, the compound action potentials elicited in the postganglionic internal carotid nerve. Except where noted, the current intensity used was twice that required to give a maximum compound action potential. Contralateral control ganglia from the same animals were maintained in similar conditions but were not stimulated. To initiate the measurement of the rate of tyrosine hydroxylation, brocresine (150 μM), an inhibitor of dopa decarboxylase, was added to the incubation medium 2 min before stimulation was begun. At the end of the stimulation period, stimulated and control ganglia were individually homogenized. The respective incubation media were added to the homogenates, and the combined samples were chilled on ice and then centrifuged for 2 min in a Beckman Microfuge. The supernatants were stored at −20 °C before determination of their dopa content by high performance liquid chromatography with electrochemical detection as described elsewhere[5,8]. We have shown previously (1) that dopa is not detectable in ganglia incubated in the absence of brocresine, (2) that dopa accumulation in the presence of brocresine is blocked by 3-iodo-tyrosine, an inhibitor of TH, and (3) that dopa, once accumulated, is stable under our incubation conditions for at least 30 min. Thus dopa accumulation is a valid measure of tyrosine hydroxylation in this preparation[8].

Preganglionic nerve stimulation at 10 Hz for 30 min resulted in about a 5-fold increase in dopa synthesis (Fig. 1). Addition of the nicotinic antagonist, hexamethonium (3 mM) and the muscarinic antagonist, atropine (6 μM) to the incubation medium inhibited the increase in dopa synthesis by 50% (Fig. 1). The concentration of hexamethonium used completely blocked the compound action potentials normally recorded during preganglionic nerve stimulation (data not shown), and the concentration of atropine used has been shown by others to block the muscarinic postsynaptic electrophysiological responses elicited by such stimulation[9,10]. However, in the presence of both of these antagonists, nerve stimulation still produced a significant (approximately 3-fold) increase in dopa synthesis. When the preganglionic nerve was stimulated with 10 Hz bursts (10 Hz for 1 out of every 6 s) for 30 min, dopa

---

* To whom correspondence should be addressed.

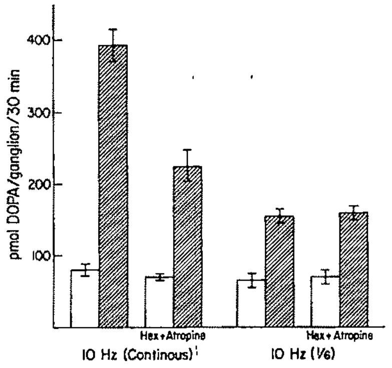

Fig. 1 Effect of cholinergic antagonists on the increase in dopa synthesis produced by preganglionic nerve stimulation. Ganglia were stimulated for 30 min either at 10 Hz continuously or at 10 Hz for 1 out of every 6 s. Hexamethonium (Hex, 3 mM) and atropine (6 μM) were added to certain preparations 10 min prior to the beginning of stimulation. The data represent the mean ±s.e.m. of 4–6 ganglia. Control ganglia, open bars; stimulated ganglia, hatched bars.

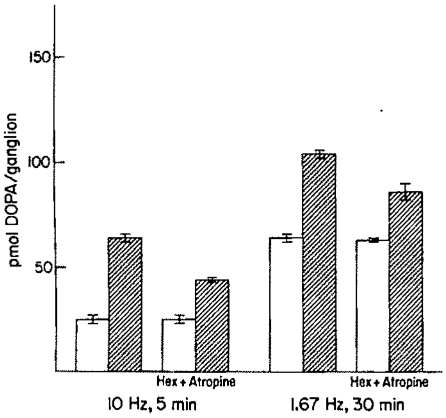

Fig. 2 Evidence for cholinergic and non-cholinergic regulation of tyrosine hydroxylase activity during continuous preganglionic nerve stimulation. Ganglia were stimulated at 10 Hz for 5 min or at 1.67 Hz for 30 min. Hexamethonium (Hex, 3 mM) and atropine (6 μM) were added to certain preparations 10 min before stimulation. The data represent the means ±s.e.m. of 4–5 ganglia. Control ganglia, open bars; stimulated ganglia, hatched bars.

synthesis was elevated by 2.4-fold (Fig. 1). Under these conditions, the increase in dopa production was not lessened at all by the addition of hexamethonium and atropine (Fig. 1). On the other hand, the compound action potentials were blocked by these antagonists under both stimulation conditions (data not shown).

The pharmacology of the acute transsynaptic regulation of TH differs under these two stimulation conditions. These results indicate that the increase in TH activity following continuous stimulation at 10 Hz is partially mediated by acetylcholine and partially by a non-cholinergic transmitter, as we have previously reported[5]. However, the increase in TH activity produced by stimulation with 10 Hz bursts is mediated entirely by a non-cholinergic mechanism. The two patterns of nerve stimulation examined differ in two respects; that is, in the total number of pulses delivered (which is six times greater in the continuous pattern) and in the temporal distribution of the pulses. The effects of two other stimulation conditions were examined to determine if one of these factors is particularly important in determining whether or not a cholinergically mediated stimulation of dopa synthesis occurs. Under each of these conditions, the same number of pulses was delivered as in the 10 Hz burst pattern. Preganglionic nerve stimulation at 10 Hz for 5 min increased dopa synthesis by 2.5-fold (Fig. 2). This effect of nerve stimulation was decreased by 43% by adding hexamethonium and atropine (Fig. 2). Continuous stimulation at 1.67 Hz for 30 min led to a smaller (62%) increase in dopa synthesis, which was reduced by 42% by the addition of the cholinergic antagonists (Fig. 2).

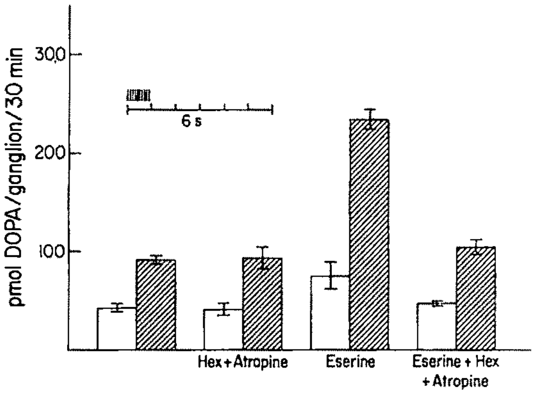

Fig. 3 Effects of physostigmine (eserine) and cholinergic antagonists on the increase in dopa production following "discontinuous" stimulation. Ganglia were stimulated at 10 Hz for 1 out of every 6 s for 30 min. Eserine (20 μM) and/or hexamethonium (Hex, 3 mM) and atropine (6 μM) were added to certain preparations 10 min before stimulation was begun. The current intensity used was that required to give a maximum compound action potential. In this experiment, the incubation medium used was Earle's balanced salt solution. In all other experiments reported in this paper, Kreb's bicarbonate buffer was used. The data represent the mean ±s.e.m. of 3–5 ganglia. Control ganglia, open bars; stimulated ganglia, hatched bars. The stimulation pattern is shown diagrammatically at the top of the figure.

These data suggest that the temporal distribution, rather than the number, of impulses is the important factor in determining the occurrence of a cholinergically mediated increase in TH activity. Perhaps preganglionic nerve stimulation for brief periods (for example 1 s) followed by prolonged periods of inactivity (for example 5 s) does not provide a sustained enough cholinergic stimulation of the postganglionic neurones to elevate TH activity. Acetylcholine is rapidly cleared from the synaptic region following a nerve impulse[3,11], due to activity of the enzyme acetylcholinesterase and to diffusion away from the synaptic cleft. Such a rapid removal of acetylcholine may be essential for its role in transmitting electrophysiological information as the continuous presence of a cholinergic agonist can lead to desensitization of the action potential triggering mechanism in sympathetic ganglia, as it does at the neuromuscular junction[12]. However, a brief exposure to an agonist, although suitable for triggering action potentials, may not be suitable for a sustained activation of an enzyme like TH. To investigate whether the degradation of acetylcholine prevents the expression of a cholinergic component in the regulation of TH during discontinuous nerve stimulation, ganglia were stimulated with 10 Hz bursts in the presence or absence of the acetylcholinesterase inhibitor, physostigmine. In agreement with the data reported in Fig. 1, stimulation with this discontinuous pattern produced about a 2-fold increase in dopa synthesis, which was completely resistant to cholinergic antagonists (Fig. 3). Addition of physostigmine (20 μM) to the incubation medium significantly elevated the rate of dopa synthesis in both control and stimulated ganglia (Fig. 3). These effects of physostigmine were completely blocked by hexamethonium and atropine (Fig. 3). Physostigmine thus causes the expression of a cholinergic component of TH regulation during discontinuous nerve stimulation, either by increasing the amount of acetylcholine in the synaptic cleft, or by prolonging the duration of cholinergic stimulation or by both.

We do not know yet which transmitter is responsible for the non-cholinergic elevation of TH activity. So far, after screening a large number of peptides and other transmitter candidates, we have found that secretin, vasoactive intestinal peptide (VIP) and PHI (which refers to a 27-amino acid peptide that has a histidine at the N-terminal and an isoleucine amide at the

C-terminal) can mimic this non-cholinergic effect of nerve stimulation[13,14]. Many other peptides tested, including glucagon, substance P, methionine-enkephalin, luteinizing hormone releasing hormone, and angiotensin had no effect on TH activity. The idea that certain neuropeptides may function as neurotransmitters in specific autonomic ganglia is now widely accepted[15]. Although we have not yet established that the non-cholinergic elevation of TH activity produced by preganglionic nerve stimulation is mediated by a neuropeptide, it is interesting to note that one characteristic of the electrophysiological effects of peptides, which has been commonly observed, is their long duration (for example, changes in resting potential lasting for a minute or longer, see refs 7, 16 for examples). Such a time course is compatible with our finding that the non-cholinergic (but not the cholinergic) regulation of dopa synthesis is present during a bursting pattern of nerve stimulation. Thus the postsynaptic consequences of a neuropeptide, unlike that of acetylcholine, might be sustained throughout the interburst interval. The magnitude of peptidergic postsynaptic effects may also be affected by the pattern of nerve stimulation. Thus, in certain peptidergic neurones, such as the VIP-containing parasympathetic neurones innervating the cat submandibular gland and the vasopressin- and oxytocin-containing neurones of the hypothalamo-hypophyseal system, the release of peptides is greater when impulses are delivered in high frequency bursts, rather than continuously at the same average frequency[17,18]. Perhaps a similar mechanism accounts for the fact that while the non-cholinergic component of TH regulation is present during continuous stimulation at a low frequency (1.67 Hz), its magnitude appears to be enhanced by delivering the same number of impulses intermittently in bursts at a higher frequency (10 Hz for 1 out of every 6 s) (Figs 1 and 2). Significantly, studies on the physiological discharge pattern in sympathetic neurones have demonstrated that the electrical activity *in vivo* often occurs in brief bursts separated by periods of inactivity[3,19]. Perhaps, in certain conditions (for example certain types of stress) a more continuous pattern of preganglionic nerve activity occurs, thus activating a second (cholinergic) mechanism for elevating noradrenaline synthesis.

Recent studies on the colon demonstrate that the nature of the tissue response to nerve stimulation (that is, whether vasodilation or contraction of the colon occurs) is dramatically altered by changing the pattern of stimulation[20]. These responses may well be mediated by different neurotransmitters. In the present study, we have found that the pattern of stimulation determines the relative importance of different transmitters in regulating a single postsynaptic response, namely the stimulation of catecholamine biosynthesis.

This research was supported by US PHS grant NS 12651 from the National Institutes of Health. N.Y.I. is a postdoctoral trainee of the US PHS (NS 07009) and R.E.Z. is a recipient of a Research Scientist Development Award (MH 00162) from the National Institute of Mental Health.

Received 25 April; accepted 10 July 1984.

1. Feldberg, W. & Gaddum, J. H. *J. Physiol., Lond.* **81**, 305–319 (1934).
2. Eccles, R. M. *J. Physiol., Lond.* **117**, 181–195 (1952).
3. Skok, V. I. *Physiology of Autonomic Ganglia* (I Shoin, Tokyo, 1973).
4. Ashe, J. H. & Libet, B. *J. Physiol., Lond.* **320**, 333–346 (1981).
5. Ip, N. Y., Perlman, R. L. & Zigmond, R. E. *Proc. natn. Acad. Sci. U.S.A.* **80**, 2081–2085 (1983).
6. Nishi, S. & Koketsu, K. *J. Neurophysiol.* **31**, 109–121 (1968).
7. Jan, L. Y. & Jan, Y. N. *J. Physiol., Lond.* **327**, 219–246 (1982).
8. Ip, N. Y., Perlman, R. L. & Zigmond, R. E. *J. Pharmac. exp. Ther.* **223**, 280–283 (1982).
9. Libet, B. *Fedn Proc.* **29**, 1945–1956 (1970).
10. McIsaac, R. J. *J. Pharmac. exp. Ther.* **200**, 107–116 (1977).
11. Volle, R. L. *Pharmacology of Ganglionic Transmission* (ed. Kharkevich, D. A.) 385–410 (Springer, Berlin, 1980).
12. Brown, D. A. *Pharmacology of Ganglionic Transmission* (ed. Kharkevich, D. A.) 185–235 (Springer, Berlin, 1980).
13. Ip, N. Y., Ho, C. K. & Zigmond, R. E. *Proc. natn. Acad. Sci. U.S.A.* **79**, 7566–7569 (1982).
14. Ip, N. Y., Baldwin, C. & Zigmond, R. E. *Peptides* **5**, 309–312 (1984).
15. Burnstock, G. *et al. Neurosci. Res. Prog. Bull.* **17**, 383–486 (1979).
16. Tsunoo, A., Konishi, S. & Otsuka, M. *Neuroscience* **7**, 2025–2037 (1982).
17. Andersson, P-O. *et al. J. Physiol., Lond.* **322**, 469–483 (1982).
18. Gainer, H. in *Comparative Endocrinology* (eds Gaillard, P. J. & Boer, H. H.) 293–304 (Elsevier/North-Holland Biomedical, Amsterdam, 1978).
19. Iggo, A. & Vogt, M. *J. Physiol., Lond.* **150**, 114–133 (1960).
20. Andersson, P-O., Bloom, S. R. & Järhult, J. *J. Physiol., Lond* **334**, 293–307 (1983).

Giant synaptosomes

J. A. Umbach, C. B. Gundersen* & P. F. Baker†

Department of Physiology, King's College London, Strand,
London WC2R 2LS, UK

* Department of Biophysics, University College London, Gower Street,
London WC1E 6BT, UK

Investigations using synaptosomes, pinched-off nerve ending particles from brain[1,2], have greatly improved our knowledge of presynaptic function. However, these structures, like most nerve endings, are too small to be penetrated with microelectrodes. We have treated synaptosomal preparations from rat brain with a neutral protease and obtained fused structures large enough to be recorded from directly with microelectrodes; we report here that these particles (30–250 μM in diameter) contain mitochondria and structures resembling synaptic vesicles, morphological features characteristic of synaptosomes. These 'giant synaptosomes' have resting membrane potentials in the range −45 to −76 mV, are depolarized by increasing concentrations of K^+, show responses to a variety of neuroactive substances and exhibit active membrane responses to depolarizing current pulses. These results suggest that this preparation will be of value in further studies of nerve terminal function.

Synaptosomal fractions were prepared from the brains of Wistar rats (25–100 g) using differential and sucrose gradient centrifugation as described[1], except that the initial homogenization step was performed by hand. The synaptosomal pellet from one brain was dispersed in approximately 0.5 ml of sucrose (0.32 M); neutral protease (dispase, Boehringer-Mannheim) was then added to a concentration of 0.1–0.2 mg ml^{-1}. The mixture was incubated for 30–40 min at 20–23 °C and samples were examined for fused synaptosomes using a light microscope. The number of giant particles formed (Fig. 1*a*) was in the range of 0–4 per preparation of synaptosomes. Giant particles failed to form in about half of the preparations.

Electron microscope investigation of these particles is difficult, mainly because of the low success rate of their formation. Nevertheless, the interior of the particles is nearly devoid of electron-dense material (Fig. 1*b*, *c*). Clustered along the limiting membrane there are mitochondria and occasional vesicles or clusters of vesicles of 40–60 nm diameter. Of the 10 particles examined in this way, none has contained ribosomes, rough endoplasmic reticulum or nuclei, which suggests that cell bodies do not participate in the genesis of these structures. The 40–60 nm vesicles could be synaptic vesicles, which along with mitochondria, are features typical of synaptosomes[1]. Also consistent with the interpretation that these giant particles derive from synaptosomes is the fact that similar structures have not been obtained either using the P_2 (crude mitochondrial fraction of Gray and Whittaker[1]) or the myelin or mitochondrial fractions from the sucrose gradients used to isolate the synaptosomes. Provisionally, we will call the fused structures giant synaptosomes.

For electrophysiological investigation, the giant synaptosomes were first incubated in a solution of 190 mM potassium phosphate (*p*H 7.2), 10 mM NaCl, 2 mM $MgCl_2 \cdot 7H_2O$ and 10 mM glucose. After 10 min, the particles were transferred to physiological saline [135 mM NaCl, 5 mM KCl, 2 mM $CaCl_2$, 1 mM $MgCl_2$, 0.5 mM Na_2HPO_4, 1 mg ml^{-1} glucose and 20 mM HEPES (*p*H 7.2 with NaOH] and impaled with conventional microelectrodes (20–40 MΩ filled with 3M KCl). On electrode insertion, resting potentials in the range −45 to −76 mV (mean −55 mV; $n = 26$) were obtained (Fig. 2*a*). Giant synaptosomes were usually depolarized in a nernstian fashion by increasing concentrations of KCl (Fig. 2*a*, *b*). However, synaptosomes with a resting potential smaller than −50 mV often showed less than

---

† To whom correspondence should be addressed.

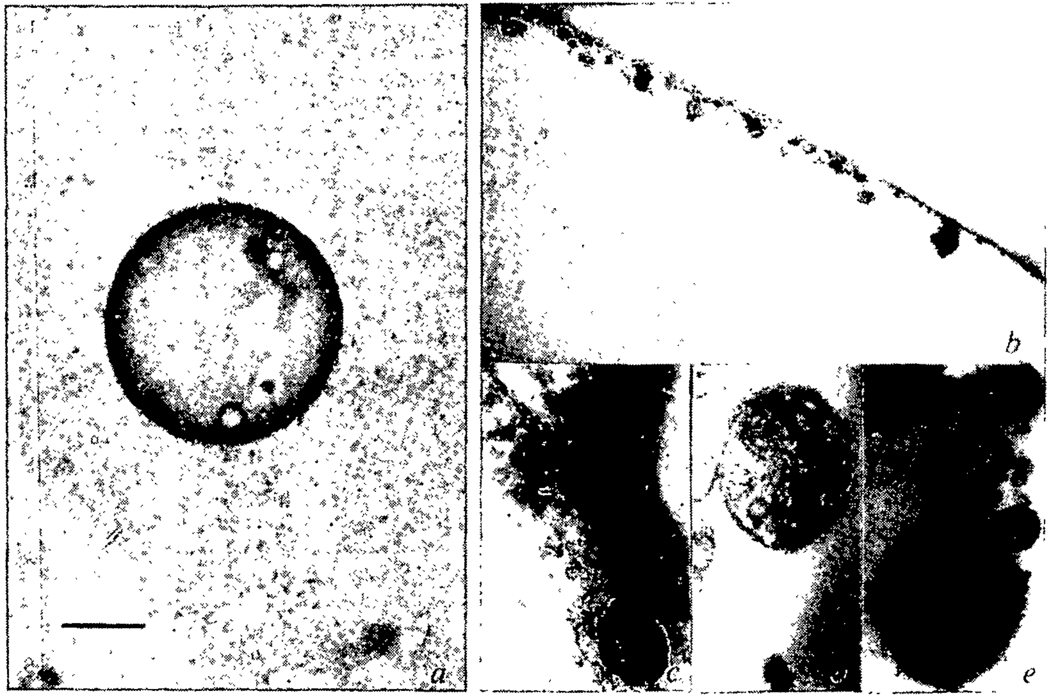

Fig. 1 *a*, Light micrograph of a giant synaptosome. The hazy material in the background represents unfused elements of the synaptosomal fraction. *b*, Electron micrograph showing the outer border of a giant synaptosome. Along the limiting membrane are structures which may represent small mitochondria and dense-cored vesicles. Note the lack of electron-dense organelles towards the interior of the particle. *c*, *d*, Examples of mitochondria found along the limiting membrane of giant synaptosomes. *e*, Cluster of vesicles, which may include synaptic vesicles, found near the surface membrane of a giant synaptosome. Scale bar corresponds to: 50 μm (*a*), 500 nm (*b*, *c*); 200 nm (*d*); 150 nm (*e*). **Methods:** Samples were processed for electron microscopy as follows. At 4 °C: 1-h wash in physiological saline, 4–6 h of fixation in 6% glutaraldehyde in 0.1 M cacodylate buffer (*p*H always at 7.4). At 20 °C: four 1-h washes with 0.2 M cacodylate buffer, 4–8 h postfixation in 2% osmium tetroxide in 0.1 M cacodylate buffer, two 1-h washes with 0.2 M cacodylate buffer, dehydration in a graded ethanol series followed by four 1-h rinses in 100% ethanol. Samples were transferred first to propylene oxide (two 15-min exposures), then to 1 : 1 propylene oxide/epon (12 h) followed by evaporation of the propylene oxide and finally to epon (three 30-min changes, followed by incubation overnight at 60 °C). Throughout this procedure (except when in epon) samples were rotated slowly. Sections were cut and stained with uranyl acetate and alkaline lead citrate for viewing in a JEOL electron microscope.

LIBRARY [illegible]
Department [illegible]
Chemical [illegible]
Chemical Technology
Plastics and Rubber Technology

nernstian responses to changes of external K^+ concentration. Equimolar replacement of either extracellular Cl^- by isethionate or Na^+ by choline had little effect on the resting membrane potential. These data suggest that K^+ permeability is the major determinant of the resting membrane potential in these structures.

Insertion of a second electrode into the giant synaptosome revealed that the interior was isopotential. When passing current through one electrode, a voltage response was recorded by the second electrode (Fig. 3). In many of the giant synaptosomes, depolarizing current pulses elicited a regenerative, transient spike which was graded with the stimulus intensity. This regenerative response was affected by changes in either external Ca^{2+} or Na^+ (Fig. 3*a*, *b*). The spike could be partially blocked by either Co^{2+} or tetrodotoxin (TTX) (Fig. 3*c*, *d*) and completely eliminated in the presence of both of these substances (Fig. 3*e*). Application of veratrine (100 μg ml^{-1}) depolarized the giant synaptosomes ($n = 3$) by 25–30 mV. Recovery of the membrane potential after veratrine required long wash-out periods (> 10 min). These data suggest that voltage-gated channels for Na^+ and Ca^{2+} are present in the plasma membrane of the fused synaptosomes. A pronounced hyperpolarization was usually

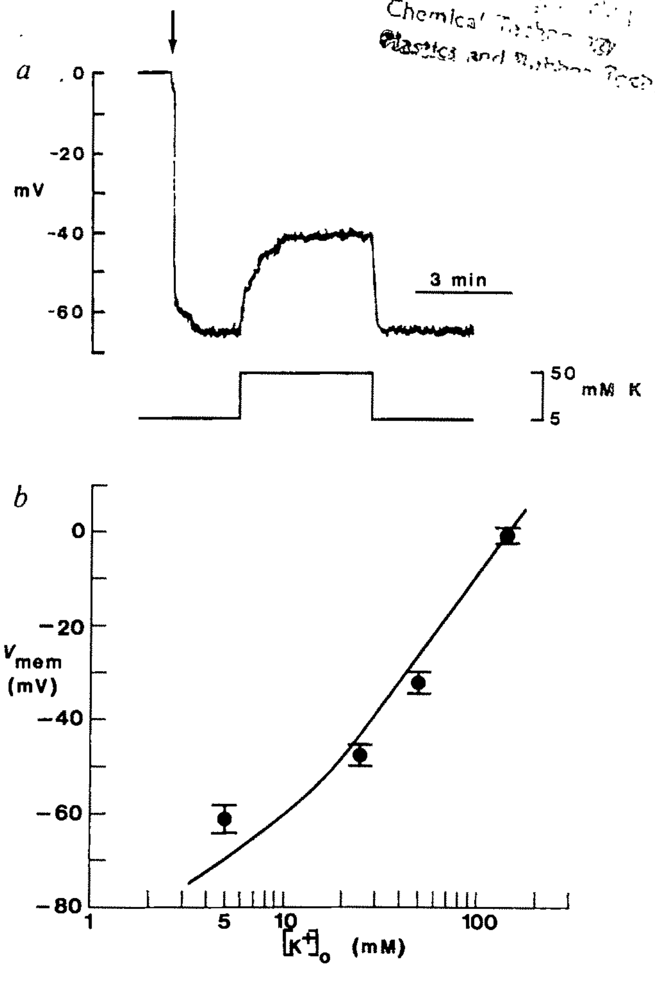

Fig. 2 *a*, Membrane potential records from a giant synaptosome. A giant particle was impaled (arrow) while in physiological saline ($K^+ = 5$ mM). Subsequently, the K^+ concentration of the medium was increased to 50 mM (by isotonic substitution for NaCl). The membrane potential was fully recovered on removal of high K^+. Temperature, 22 °C. *b*, Plot of membrane potential (V_{mem}) against extracellular K^+ concentration. Results are the mean±s.e.m. of nine experiments. The curve was calculated using the equation: $V_{mem} = 2.3\,(RT/F)\log([K]_o + \alpha[Na]_o) + B$, for $B = 48$ mV and $\alpha = 0.025$ (see ref. 8). B is equivalent to $-2.3(RT/F)\log([K]_i + [Na]_i)$, and is treated as a constant by assuming that the internal cation concentration does not change; α is equivalent to (P_{Na}/P_K), the permeability ratio between Na and K ions.

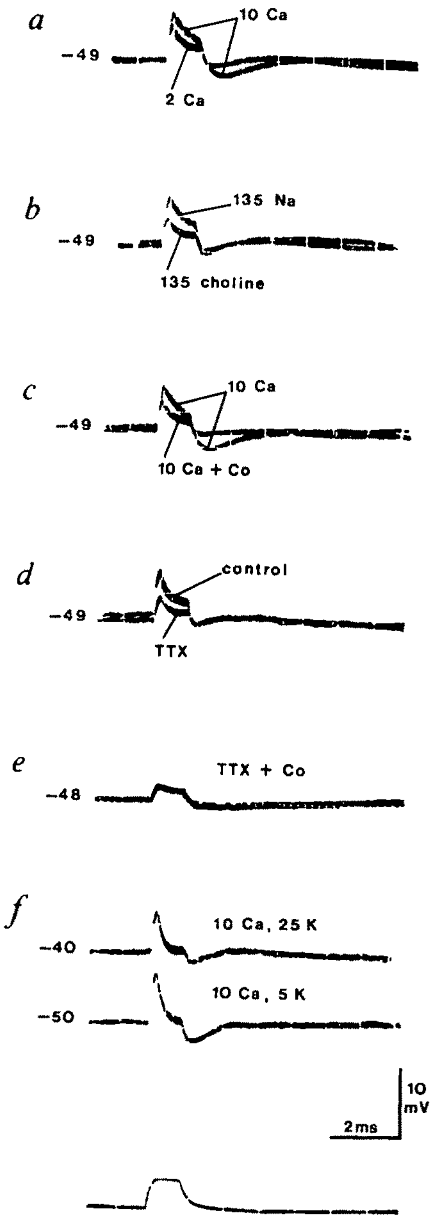

Fig. 3 Voltage records obtained during depolarizing current pulses. A single giant synaptosome was exposed to solutions of different composition as indicated: *a*, Physiological Ringer's with normal (2 mM) or high (10 mM) $CaCl_2$ (NaCl reduced to maintain tonicity). *b*, Physiological Ringer's with normal (135 mM)NaCl or replacement of NaCl by choline chloride. *c*, High calcium Ringer's (see *a*) or high calcium Ringer's plus 10 mM $CoCl_2$ (NaCl reduced to maintain tonicity). *d*, Normal Ringer's or normal Ringer's plus 1 μg ml^{-1} tetrotoxin (TTX). *e*, Normal Ringer's plus 1 μg ml^{-1} TTX and 10 mM $CoCl_2$. *f*, High calcium Ringer's containing normal (5 mM) or raised (25 mM) KCl (NaCl was altered to maintain tonicity). Resting potential is indicated to the left of each trace. An example of the 100 nA current pulse used to elicit these responses is shown at the bottom of the figure. Temperature, 20 °C.

observed at the offset of the stimulus (Fig. 3). This afterhyperpolarization was dependent on the concentration of extracellular calcium (Fig. 3*a*), attenuated in high K^+ solutions (Fig. 3*f*) and could be blocked by extracellular Co^{2+} (Fig. 3*c*). TTX minimally affected this hyperpolarization (Fig. 3*d*). These results are consistent with the presence of a calcium-activated K^+ conductance in these structures.

In many experiments the giant synaptosomes were sensitive to several neuroactive substances. Individually, glutamate, acetylcholine (ACh), serotonin and noradrenaline elicited depolarizing responses (Fig. 4). However, with some synaptosomes ACh induced a hyperpolarization (Fig. 4*e*). Both of these ACh responses were reversibly blocked by equimolar atropine (data not shown). Note that the concentrations of the substances used in Fig. 4 are 10^{-4}–10^{-2} M. However, the threshold concentration for eliciting these effects was usually 10^{-5}–10^{-4} M.

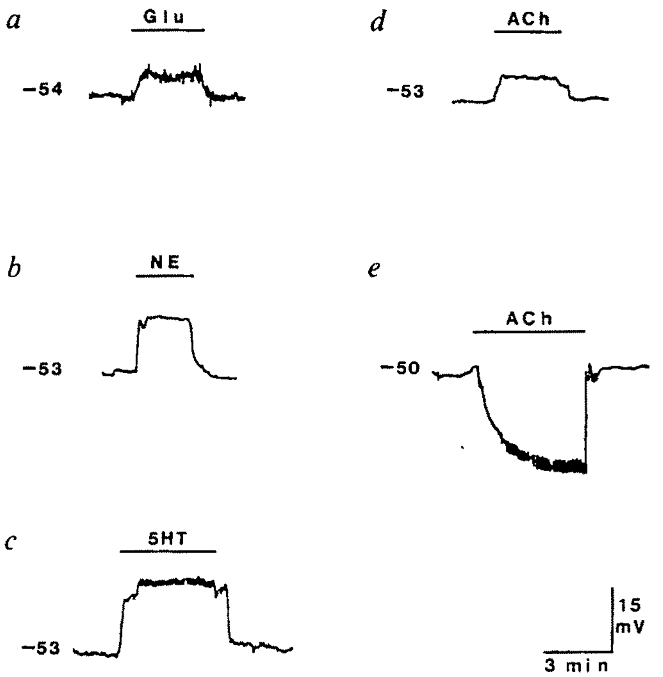

Fig. 4 Membrane response of giant synaptosomes on addition of putative neurotransmitters to the bathing medium. *a*, Glutamate 10^{-4} M); *b*, noradrenaline (10^{-3} M); *c*, serotonin (10^{-2} M); *d*, acetylcholine (10^{-2} M); and *e*, acetylcholine (10^{-2} M). Records *a* and *d* from separate giant synaptosomes; *b*, *c* and *e* from the same giant synaptosome. Resting potentials are given to the left of each trace. Temperature, 22 °C.

The above results are consistent with the suggestion that the giant particles derive from the fusion of a large number of synaptosomes. These particles retain (1) mitochondria and structures resembling synaptic vesicles, (2) a stable resting potential, (3) voltage-activated Na^+ and Ca^{2+} channels and Ca^{2+}-activated K^+ channels and(4) electrical responses to putative neurotransmitter agents. These are all properties expected of presynaptic nerve terminals[1–5]. Moreover, we failed to obtain similar structures either from crude synaptosome fractions or the other fractions from the sucrose gradient. However, we cannot exclude the possibility that both postsynaptic and non-synaptosomal elements may be involved in the formation of the particles that we obtained. Future use of antibodies that specifically recognize nerve terminals (see ref. 4) will be of value in clarifying this point.

Preparations of mammalian brain synaptosomes are heterogeneous with respect to the neurotransmitter and transmitter receptors carried by individual synaptosomes[5]. Thus, it is likely that the giant synaptosomes are obtained by the fusion of a similarly mixed population of particles. This line of reasoning suggests that studies of these particles might best be performed using populations of synaptosomes that are enriched in a particular class of nerve ending (for example, cholinergic, adrenergic). Extending this to the present data, we suggest that the high concentration of the putative neurotransmitters required to evoke the responses recorded in Fig. 4 may derive from the relative paucity of appropriate receptors on these hybrid particles. Alternatively, it may be that such presynaptic receptors do not become operational until a high concentration of the appropriate substance is present. This preparation should allow one to distinguish between these two explanations.

The preparation of these giant particles entailed the exposure of synaptosome preparations to dispase. Protease treatments have occasionally been found to encourage the fusion of other types of structures[6]. While we cannot exclude the possibility that dispase modified some of the membrane properties associated with the giant particles, we note that proteases are often used without detriment to prepare membranes for single-channel recording (see ref. 7). As such, this preparation may be used advantageously to study the characteristics of single channels and receptors in the nerve terminal membrane.

Assuming that these structures represent the fusion of large numbers of synaptosomes, one would expect a large dilution (on the basis of surface area/volume considerations) of the particle's cytoplasmic constituents by the sucrose medium in which fusion took place; this notion is consistent with the meagre amount of electron-dense material observed within these particles. However, the attendant dilution of the internal ionic milieu raises the question of how the resting potential of these particles is established. The data of Fig. 2 indicate that K^+ is the principal contributor to the resting membrane potential. Further studies should elucidate how this ion gradient is generated and maintained.

We thank Professor R. Miledi for encouragement, support and laboratory facilities, Mrs Carol Limbrick for electron microscope examination of specimens and Dr D. Knight for helpful discussions. This research was carried out during the tenure of a Muscular Dystrophy Association postdoctoral fellowship to J.A.U. We thank the MRC for support.

Received 12 June; accepted 19 July 1984.

1. Gray, E. G. & Whittaker, V. P. *J. Anat.* 96, 79–88 (1962).
2. DeRobertis, E., delraldi, A. P., Rodriguez, G. & Gomez, J. *J. biophys. biochem. Cytol.* 9, 229–235 (1961).
3. Starke, K. *A. Rev. Pharmac. Tox.* 21, 7–30 (1981).
4. Reichardt, L. F. & Kelly, R. B. *A. Rev. Biochem.* 52, 871–922 (1983).
5. Jones, D. G. *Synapses and Synaptosomes* (Chapman & Hall, London, 1975).
6. Zimmerman, U. *Biochem. biophys. Acta.* 694, 227–277 (1982).
7. Sakmann, B. & Neher, E. (eds) *Single-Channel Recording* (Plenum, New York, 1983).
8. Blaustein, M. P. & Goldring, J. M. *J. Physiol., Lond.* 247, 589–615 (1975).

42,000-molecular weight EGF receptor has protein kinase activity

Mitali Basu, Rupamanjari Biswas & Manjusri Das

Department of Biochemistry and Biophysics, University of Pennsylvania, Philadelphia, Pennsylvania 19104, USA

The epidermal growth factor (EGF) receptor and other growth factor receptors have been shown to possess tyrosine-specific protein kinase activity[1–5]. Before the demonstration of kinase activity in growth factor receptors, tyrosine kinases of molecular weight (MW) 60,000 (60K) were found to be encoded by the *src* oncogene and other oncogenes related to *src*[6–8]. Our earlier work on intracellular processing of the EGF receptor[9], a 170,000-MW polypeptide, provided evidence for proteolytic separation of well defined structural domains, and suggested to us the possibility of separating functional domains by limited proteolysis. The isolation of such kinase domains should facilitate comparison of the receptor/kinase with other well characterized kinases including those of oncogene origin. We report here the identification of a catalytically functional 42K kinase derived proteolytically from the isolated human EGF receptor. This fragment, comparable in size to pp60^{src}, carries the kinase ATP-binding site, and functions catalytically even after detachment from the EGF-binding site and the major autophosphorylation region.

We used 5′-fluorosulphonylbenzoyl[^{14}C]adenosine(5′-*p*-FSO$_2$bz[^{14}C]A) to screen for kinase site-containing fragments in tryptic digests of the solubilized purified receptor[10,11]. This ATP analogue irreversibly modifies ATP-binding sites[12–14], and inhibits phosphorylation of both the solubilized purified receptor and a receptor-derived peptide fragment (see below).

Treatment of the freshly purified EGF receptor preparation with 50 μM 5′-*p*-FSO$_2$bz[^{14}C]A at 20 °C for 30 min resulted in radiolabelling of two bands of 170K and 150K (Fig. 1*a*, lane *a*). Measurement of radioactivity in the 170K and 150K bands revealed incorporation of 0.5–0.7 mol of 5′-*p*-SO$_2$bz[^{14}C]A per mol, indicating ~1 ATP-binding site per mol of receptor molecule (measured in terms of EGF-binding sites).

Pretreatment of the receptor with 2 μg ml^{-1} trypsin at 20 °C for 30 min, followed by incubation with 5′-*p*-FSO$_2$bz[^{14}C]A, resulted in the appearance of radiolabel in two bands of 150K and 42K (Fig. 1*A*, lane *b*). Pretreatment with higher concentrations of trypsin (5 μg ml^{-1} and 9 μg ml^{-1}) resulted in covalent radiolabelling of only a single sharp band of 42K (Fig. 1*A*, lanes *c*, *d*). Only the 42K peptide and no other peptide smaller than 150K carried the affinity label.

The total amount of ^{14}C-label incorporated into the three bands (170K, 150K and 42K) was the same for trypsin-treated and untreated receptor preparations. Thus, the single kinase site of the receptor polypeptide is quantitatively recovered in the 42K fragment.

Experiments were done to determine whether the pre-labelled intact receptor would generate, on trypsin treatment, a ^{14}C-labelled 42K peptide (Fig. 1*B*). After labelling of the intact receptor with 5′-*p*-FSO$_2$*bz*[^{14}C]A, the unreacted reagent was removed and the preparation treated with 5 μg ml^{-1} trypsin. Amost all the radiolabel originally present in the intact receptor band appeared in the 42K band (Fig. 1*B*). Thus, the receptor is the precursor of the 42K peptide, and this peptide retains the full kinase ATP-binding activity of the receptor.

The ATP analogues, AMP-PNP and 5′-*p*-FSO$_2$bzA, at a concentration of 1 mM, abolished labelling with 50 μM 5′-*p*-FSO$_2$bz[^{14}C]A by more than 90% (Fig. 1*C*). Labelling was also abolished by pretreatment with *N*-ethylmaleimide or heat (Fig. 1*C*).

It would be interesting to know whether the 42K fragment, like other protein kinases, is capable of autophosphorylation. Phosphorylation of the purified receptor with [γ-^{32}P]ATP gave a major band of labelling at 170K and a minor band at 150K (Fig. 2*A*, lane *a*). When phosphorylation was preceded by a 30 min exposure of the receptor to 2 μg ml^{-1} trypsin, the 170K band largely disappeared (Fig. 2*A*, lane *b*). Trypsin-induced conversion of the 170K form to the 150K form was associated with a large loss (>90%) of autophosphorylation sites (although, as indicated above, there was no loss of ATP-binding sites). Pretreatment of the receptor with higher concentrations of trypsin (5 and 9 μg ml^{-1}), followed by incubation with [γ-^{32}P]ATP, resulted in the labelling of a single sharp band of 42K (Fig. 2*A*, lanes *c*, *d*). Only the 42K peptide, and no other peptide smaller than 150K carried the ^{32}P label.

The phosphorylation that occurs on the 42K fragment as well as on the 170K/150K receptor involves tyrosine residues only (studied by standard phosphoamino acid analysis). Also, a tyrosine kinase-specific substrate, Arg-Arg-Leu-Ile-Glu-Asp-Ala-Glu-Tyr-Ala-Ala-Arg-Gly[15], was phosphorylated by the 42K peptide at a rate of 0.7 mol peptide phosphorylated mol^{-1} min^{-1} (not shown). (The rate for the intact 170K receptor was 2.5 mol peptide phosphorylated mol^{-1} min^{-1}. These results support the conclusion that the 42K peptide is an active tyrosine kinase. Several ATP analogues or pretreatment with *N*-ethylmaleimide or heat completely abolished the autophosphorylation of the 42K peptide (Fig. 2*B*). It is significant that the active sites in both the intact receptor protein and the 42K tryptic fragment exhibit similar reactivity with the reagents. The inhibitory effects of the ATP analogues could be abolished with excess [γ-^{32}P]ATP. The results described above indicate that the 42K fragment carries the kinase ATP-binding site and that it can be phosphorylated in the unfractionated tryptic digest.

Is the fragment a self-sufficient catalytic entity? We investigated the activity of the 42K fragment after electrophoretic fractionation of the trypsin digest on non-denaturing (SDS-free) gels (Fig. 2*C*). The unproteolysed receptor (170K/150K, form) was recovered largely in gel slice 2 and the 42K fragment in slice 6; these, together with the other slices, were incubated with [γ-^{32}P]ATP and the phosphorylated species were subsequently visualized by SDS-gel electrophoresis and autoradiography (Fig.

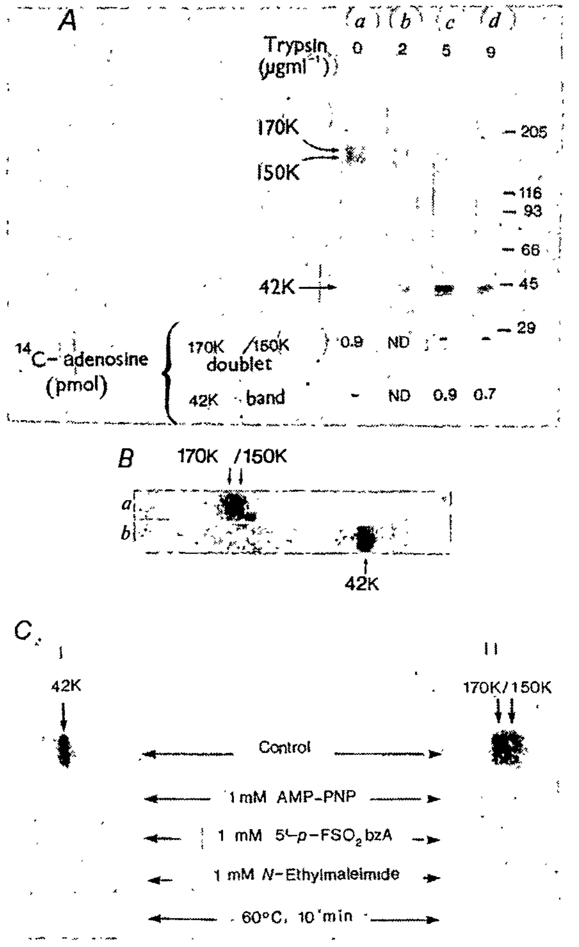

Fig. 1 Affinity labelling of EGF receptor fragments with a ^{14}C-ATP analogue monitored by SDS-polyacrylamide gradient gel electrophoresis. *A*, Trypsinization of the receptor, followed by incubation with 5'-p-FSO$_2$bz[^{14}C]A. *B*, Trypsin fragment of the pre-labelled receptor. *C*, Effect of inhibitors of EGF receptor kinase on ^{14}C affinity labelling of the 42K peptide.

Methods: *A*, Receptor (1.5 pmol, see below) was incubated at 20 °C for 30 min with the indicated amounts of trypsin (crystalline, tosylphenylethylchloromethylketone-treated; Sigma) in 20 μl of 20 mM HEPES *p*H 7.4, 10% glycerol, 0.2% Triton X-100. Trypsin action was stopped by adding 1 μl soybean trypsin inhibitor solution (10 mg ml^{-1}) to all tubes, followed by the addition of 5 μl of solution containing 20 mM HEPES *p*H 7.4, 5 mM MnCl$_2$. Labelling was initiated by adding 1 μl of a 1.25 mM solution of 5'-*p*-FSO$_2$bz[^{14}C]A (50 Ci mol^{-1}; NEN) in dimethylformamide. After incubation at 20 °C for 30 min, the reaction was stopped by adding rapidly in succession 2 μl of 10 mg ml^{-1} bovine serum albumin (BSA) and 1 ml of ice-cold 10% trichloroacetic acid (TCA). The precipitate was dissolved in SDS sample buffer and subjected to 5–20% polyacrylamide gradient SDS-gel electrophoresis. After staining and destaining, the gels were prepared for fluorography by immersion in dimethyl sulphoxide (DMSO) containing 2,3'-diphenyloxazole. The gels were then autoradiographed for 40 days using Kodak X-Omat AR films and Dupont Cronex Lightening Plus intensifying screens. After autoradiography, the regions of the dried gel containing the 170K/150K doublet or the 42K band were cut out and counted using toluene-based scintillation fluid. Adjacent regions of the dried gel were similarly counted to determine background radioactivity. In these counting conditions the specific radioactivity of 5'-*p*-FSO$_2$bz[^{14}C]A was ~100 c.p.m. pmol^{-1}. *B*, Intact receptor (4 pmol) was labelled with 50 μM 5'-*p*-FSO$_2$bz[^{14}C]A as described above, then the mixture (100 μl) was diluted with 10 ml of 20 mM HEPES *p*H 7.4, 10% glycerol, 0.2% Triton X-100, and concentrated by Amicon ultrafiltration (using PM-30 filters) to 0.2 ml. The dilution and filtration–concentration steps were repeated three times. The ^{14}C-labelled receptor, free of excess reagent, was incubated without (*a*) or with (*b*) or 5 μg ml^{-1} trypsin at 20 °C for 30 min. TCA-precipitable proteins were subjected to electrophoresis and autoradiography. *C*, Receptor (1.4 pmol) was either treated with 5 μg ml^{-1} trypsin (I) or untreated (II), then incubated in the conditions indicated, followed by incubation with 50 μm 5-*p*-FSO$_2$bz[^{14}C]A as described for *A*. Labelled proteins were isolated by acid precipitation and visualized by electrophoresis and autoradiography. Receptor isolation method: Plasma membranes were isolated from 2×10^8 human A431 epidermoid carcinoma cells as described[10,11] using Ca^{2+} and Mg^{2+}-free solutions. The membranes (2 mg protein) were stirred at 20 °C for 30 min with 1 ml of a solution containing 20 mM HEPES *p*H 7.4, 10% glycerol, 1% Triton X-100, and 10 μg ml^{-1} leupeptin. After centrifugation at 100,000*g* for 70 min, the supernatant was added to 0.5 ml of packed EGF–agarose containing 0.4 mg of covalently bound EGF[10,11]. After stirring at 20 °C for 30 min, the gel pellet was washed four times at 4 °C with 2 ml of a solution containing 10% glycerol and 0.2% Triton X-100, and the receptor eluted by stirring the washed gel three times (10 min at 4 °C each time) with 1 ml of 5 mM ethanolamine solution *p*H 10, containing 10% glycerol and 0.2% Triton X-100, and immediately brought to *p*H 7.0 with 0.05 M HCl[10]. The amount of receptor present was estimated by Scatchard analysis of ^{125}I-labelled EGF binding data, assuming a 1 : 1 complex of EGF and receptor. Recoveries varied from 40 to 60% of the input solubilized activity. The K_d binding to ^{125}I-labelled EGF was ~25 nM.

2*B*). The 42K fragment, separated in this way from the uncleaved receptor and from other receptor fragments, displayed kinase and autophosphorylating activity. These results confirm that the 42K peptide carries the entire self-sufficient kinase active site.

We investigated the relationship of the 42K fragment and the major autophosphorylation locus. Over 90% of the kinase activity sites (measured by labelling with the ^{14}C-labelled ATP analogue) in the intact receptor are recovered in the 42K peptide (Fig. 1). In contrast, only 5% of the autophosphorylation sites (measured by [γ-^{32}P]ATP labelling) are retained in the 42K peptide (Fig. 2*A*). The major autophosphorylation locus seems to lie in a 15K fragment that is cleaved off during the conversion of the 170K receptor to the 150K form (Fig. 2*D*). We know that the purified intact 170K receptor can maximally incorporate 6 mol of phosphate per mol of receptor. The phosphate-accepting tyrosine residue retained in the 42K peptide appears to be a minor site whose probability of phosphorylation is low, that is, the ^{32}P-phosphate incorporation is less than would be expected, given the presence in the peptide of one site which can be labelled. The observed low ^{32}P-phosphate incorporation could be due to previous occupancy of the tyrosine site with phosphate.

We next investigated the relationship of the 42K peptide to the EGF-binding site. Autophosphorylation of the 42K peptide was not stimulated by EGF (Fig. 3), and the peptide did not bind EGF, seen by the following assays: (1) covalent attachment of ^{125}I-EGF[16–18]; (2) polyethylene glycol assay[1]; (3) competitive inhibition of receptor binding to EGF–agarose.

We examined whether the 42K peptide represents an adventitious protein in the receptor preparation, or pre-exists as a separable subunit of the receptor. Analysis of the receptor by sucrose density gradient centrifugation revealed the presence of only a 7.7S kinase activity peak that on labelling with [γ-^{32}P]ATP, showed only a 170K major/150K minor doublet band. Thus, the 42K kinase is not present in unproteolysed receptor preparations as a separate or bound (active) entity.

Can the 42K protein pre-exist, either separately or bound to the receptor, in a catalytically inactive form that becomes active on trypsinization? This possibility is excluded by the precursor–product relationship shown in Fig. 1*B*. In these experiments, the ATP-binding site in the 170K receptor, covalently labelled with a ^{14}C-ATP analogue, appeared quantitatively in the 42K peptide.

These results suggest that the EGF receptor has three kinds of functional sites—the EGF-binding site, the protein kinase catalytic site and the major autophosphorylation site(s), located on separate domains. Tryptic processing of the EGF receptor results initially in the generation of an EGF-binding peptide of 150K which retains the kinase/ATP-binding site and a minor autophosphorylation site, but which has lost the major tyrosine-

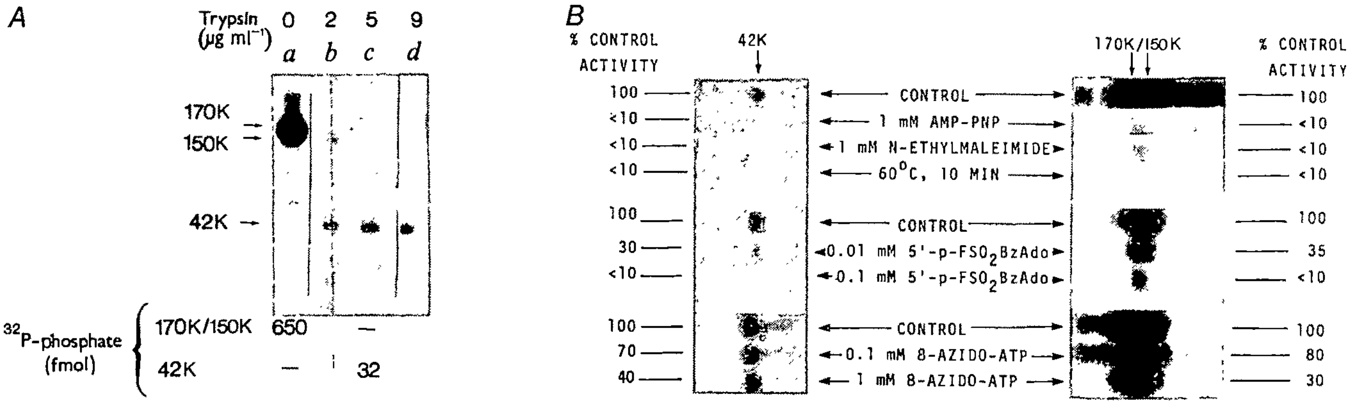

Fig. 2 Phosphorylation of the 42K fragment. *A*, Trypsinization of the receptor followed by incubation of fragments with [γ-^{32}P]ATP. *B*, Effect of inhibitors of EGF-receptor kinase on autophosphorylation of the 42K peptide. *C*, Autophosphorylating activity in gel slices after non-denaturing electrophoresis. *D*, Action of trypsin on the ^{32}P-phosphorylated receptor.

Methods: *A*, Receptor (0.2 pmol) was incubated at 20 °C for 30 min with 10 μl of 20 mM HEPES *p*H 7.4, 10% glycerol, 0.2% Triton X-100 containing the indicated amounts of trypsin; the reaction was stopped by adding 1 μl soybean trypsin inhibitor solution (10 mg ml^{-1}) and 5 μl of a solution containing 80 mM HEPES *p*H 7.4 and 4 mM $MnCl_2$. Phosphorylation was initiated by adding 5 μl of 60 μM [γ-^{32}P]ATP (70 c.p.m. fmol^{-1}). After 30 min at 20 °C, the reaction was stopped by rapid successive additions of 2 μl BSA (10 mg ml^{-1}) and 1 ml ice-cold 10% TCA. The precipitate was subjected to electrophoresis and autoradiography. *B*, Trypsin (5 μg ml^{-1}) digested (I) or undigested (II) receptor (0.1 pmol) was incubated with the indicated reagents at 20 °C for 30 min, or was heated at 60 °C for 10 min. This was followed by a 30 min incubation with 15 μM [γ-^{32}P]ATP. Labelled proteins were isolated by acid precipitation and visualized by electrophoresis and autoradiography. *C*, Receptor (2 pmol) was incubated at 20 °C for 30 min with 80 μl of 20 mM HEPES *p*H 7.4, 10% glycerol, 0.2% Triton X-100 containing trypsin at different concentrations (0, 2, 5 and 9 μg ml^{-1}). After stopping the reaction with 10 μg of soybean trypsin inhibitor, the samples were subjected to non-denaturing 5–20% polyacrylamide gradient gel electrophoresis in the cold (4 °C) at *p*H 8.8 for 9 h (25 mA, 300–400 V). The Triton X-100-containing SDS-free gel and buffer systems used were essentially the same as those of Cohen *et al.*[10]. After the run, each of the four lanes was cut into 11 slices. To each slice was added 0.2 ml of a solution containing 5 μM[γ-^{32}P]ATP, 1 mM $MnCl_2$, 50 mM HEPES *p*H 7.4, and 10 μg of soybean trypsin inhibitor. After incubation at 4 °C for 8 h, then at 37 °C for 30 min in a shaking bath, the liquid was transferred to an Eppendorf tube, together with an additional 0.7 ml of 20 mM HEPES *p*H 7.4, which had been used to rinse the gel slice. Proteins were precipitated by rapid successive additions of 2 μl of 10 mg ml^{-1} BSA and 0.1 ml of 100% TCA. The precipitate was subjected to SDS-gel electrophoresis and autoradiography as described for *A*. The relatively high activity of the 42K band here may be due to its greater stability or elutability compared with the 170K/150K receptor. *D*, Intact receptor (2 pmol) was labelled with 15 μM [γ-^{32}P]ATP at 20 °C for 30 min, as described for *A*. The mixture (100 μl) was then diluted 200-fold with ice-cold 20 mM HEPES *p*H 7.4, 10% glycerol, 0.2% Triton X-100 and concentrated to 100 μl by Amicon ultrafiltration. Aliquots of the concentrate (20 μl) were incubated without (*A*) or with (*B*) 2 μg ml^{-1} trypsin at 20 °C for 30 min, and the TCA-precipitable proteins were subjected to electrophoresis and autoradiography.

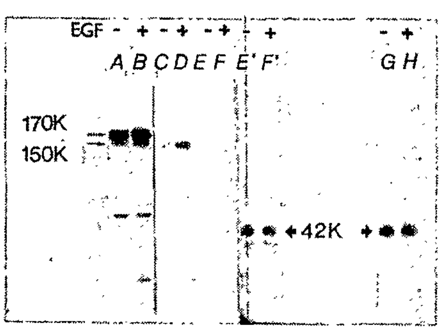

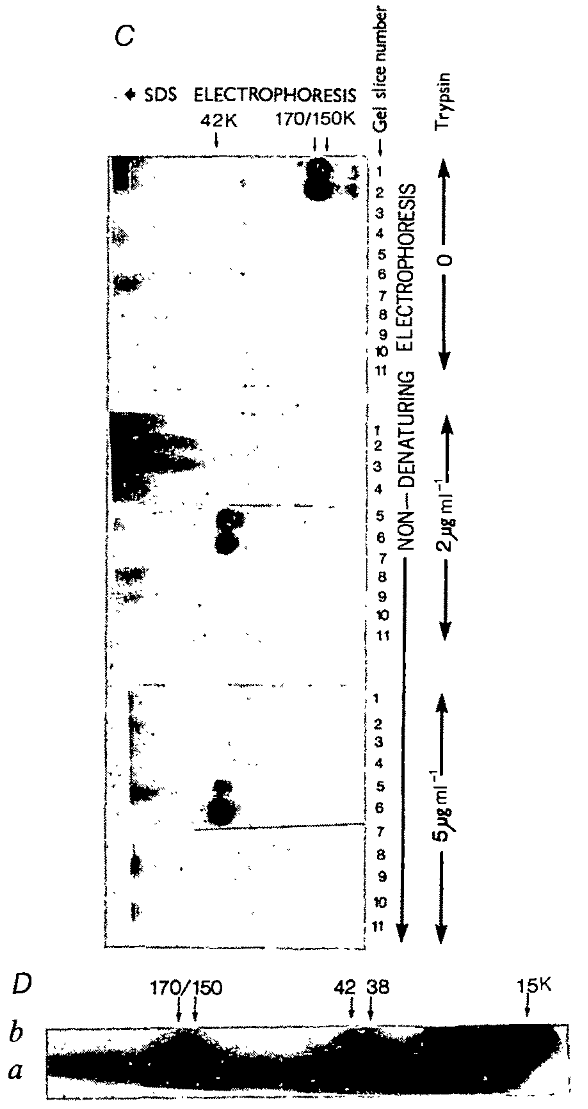

Fig. 3 Lack of effect of EGF on 42K peptide autophosphorylation. *A–F*, Crude Triton X-100 extracts of A431 membrane containing 0.1 pmol of receptor in 10 μl of 20 mM HEPES, 10% glycerol, 0.2% Triton X-100 were treated with different concentrations of trypsin at 20 °C for 30 min (lanes *A*, *B*: no trypsin; *C*, *D*: 3 μg ml^{-1} trypsin; *E*, *F*, *E'*, *F'*: 10 μg ml^{-1} trypsin). Action of trypsin was stopped with 1 μl of soybean trypsin inhibitor solution (10 mg ml^{-1}). The mixtures were incubated with (+) or without (–) 200 μM EGF at 20 °C for 10 min after which phosphorylation with 15 μM [γ-^{32}P]ATP and 1 mM $MnCl_2$ was allowed to proceed at 20 °C for 5 min. Lanes *E'* and *F'* represent longer autoradiographic exposures for the 10 μg ml^{-1} trypsin-treated crude extract samples. *G*, *H*, Purified receptor (0.1 pmol) treated with 5 μg ml^{-1} trypsin was incubated at 20 °C for 10 min either with (*H*) or without (*G*) 200 μM EGF, then phosphorylated with 15 μM[γ-^{32}*P*]ATP and 1 mM $MnCl_2$ at 20 °C for 5 min. TCA-precipitable radioactivity was subjected to electrophoresis and autoradiography.

containing phosphate acceptor domain of 15–20K. Further action of trypsin on the 150K peptide separates the kinase domain from the EGF-binding domain; a resultant 42K peptide retains both the kinase/ATP-binding site and the minor phosphate acceptor site and is catalytically functional. Note that similarly sized 30–45K phosphorylatable fragments have been described for $pp60^{src}$ and other oncogene kinase[19,20]. These findings and the recent demonstration of sequence homology between parts of the EGF receptor and the product of v-*erb-B*[21], suggest that some of the tyrosine kinase oncogene products may be generated by activation of the genomic segment encoding the kinase domain of EGF receptor. Also, there exists the possibility that such tyrosine kinases may be generated by cellular processing of the EGF receptor, resulting in a loss of the control normally exerted by EGF/ligand binding.

We thank Ms Laura Mattes for preparing A431 plasma membranes, and Drs Walter Englander and Charles Scher for reading the manuscript. This work was supported by NIH grants AM-25819 and HD-17896 and Research Career Development Award AM-00693 (to M.D).

Received 24 April; accepted 24 July 1984.

1. Cohen, S., Carpenter, G. & King, L. *J. biol. Chem.* **255**, 4834–4842 (1980).
2. Ushiro, H. & Cohen, S. *J. biol. Chem.* **255**, 8363–8365 (1980).
3. Kasuga, M., Zick, Y., Blithe, D. L., Crettaz, M. & Kahn, C. R. *Nature* **298**, 667–669 (1982).
4. Roth, R. A. & Cassel, D. J. *Science* **219**, 299–301 (1983).
5. Heldin, C. H., Ek, B. & Ronnstrand, L. *J. biol. Chem.* **258**, 10054–10061 (1983).
6. Erikson, E. & Erikson, R. L. *Cell* **21**, 829–836 (1980).
7. Hunter, T. & Sefton, B. M. *Proc. natn. Acad. Sci. U.S.A.* **77**, 1311–1315 (1980).
8. Bishop, J. M. *Cell* **32**, 1018–1020 (1983).
9. Das, M. & Fox, C. F. *Proc. natn. Acad. Sci. U.S.A.* **75**, 2644–2648 (1978).
10. Cohen, S., Ushiro, H., Stoscheck, C. & Chinkers, M. *J. biol. Chem.* **257**, 1523–1539 (1982).
11. Das, M., Knowles, B., Biswas, R. & Bishayee, S. *Eur. J. Biochem.* **141**, 429–434 (1984).
12. Colman, R. F., Pal, P. K. & Wyatt, J. L. *Meth. Enzym.* **46**, 240–249 (1977).
13. Hixson, C. S. & Krebs, E. G. *J. biol. Chem.* **256**, 1122–1127 (1981).
14. Buhrow, S. A., Cohen, S. & Staros, J. V. *J. biol. Chem.* **257**, 4019–4022 (1982).
15. Pike, L. J., Gallis, B., Casnellie, J. E., Bornstein, P. & Krebs, E. G. *Proc. natn. Acad. Sci. U.S.A.* **79**, 1443–1447 (1982).
16. Linsley, P. S., Das, M. & Fox, C. F. in '*Membrane Receptors*' Vol. B11 (eds Jacobs, S. & Cuatrecasas, P.) 87–113 (Chapman & Hall, London, 1981).
17. Bishayee, S., Feinman, J., Michael, H., Pittenger, M. & Das, M. *Proc. natn. Acad. Sci. U.S.A.* **79**, 1893–1897 (1982).
18. Das, M., Biswas, R., Basu, M. & Bishayee, S. *Cancer Res.* **44**, 3539-3545 (1984).
19. Levinson, A. D., Courtneidge, S. A. & Bishop, J. M. *Proc. natn. Acad. Sci. U.S.A.* **78**, 1624–1628 (1981).
20. Brugge, J. S. & Darrow, D. *J. biol. Chem.* **259**, 4550–4557 (1984).
21. Downward, J. *et al. Nature* **317**, 521–527 (1984).

Protein kinase C phosphorylation of the EGF receptor at a threonine residue close to the cytoplasmic face of the plasma membrane

Tony Hunter*, Nicholas Ling† & Jonathan A. Cooper*

* Molecular Biology and Virology Laboratory and
† Laboratories for Neuroendocrinology, The Salk Institute,
PO Box 85800, San Diego, California 92138, USA

The receptor for epidermal growth factor (EGF) is a 170,000–180,000 molecular weight single-chain glycoprotein of 1,186 amino acids[1]. Its sequence suggests that it has an external EGF-binding domain, formed by the NH_2-terminal 621 amino acids, linked to a cytoplasmic region by a single membrane-spanning segment[1]. In the cytoplasmic portion, starting 50 residues from the membrane, there is a 250-residue stretch similar to the catalytic domain of the *src* gene family of retroviral tyrosine protein kinases[1], and, indeed, a tyrosine-specific protein kinase activity intrinsic to the receptor is stimulated when EGF is bound[2–5]. Increased tyrosine phosphorylation of cellular proteins, detected in A431 cells following EGF binding[6,7], may be important in the mitogenic signal pathway. Tumour promoters such as 12-*O*-tetradecanoyl-phorbol-13-acetate (TPA), counteract this increase[8,9], as well as causing loss of a high affinity class of EGF binding sites[9]. The major receptor for TPA has been identified as the serine/threonine-specific Ca^{2+}/phospholipid-dependent diacylglycerol-activated protein kinase, protein kinase C[10–14]. By substituting for diacylglycerol, TPA stimulates protein kinase C. Protein kinase C phosphorylates purified EGF receptor at specific sites, and this reduces EGF-stimulated tyrosine protein kinase activity[8]. TPA treatment of A431 cells increases serine and threonine phosphorylation of the EGF receptor at the same sites[8,15], which suggests that the reduction of EGF-receptor kinase activity in TPA-treated cells is a consequence of the receptor's phosphorylation by the kinase. We have attempted to identify these phosphorylation sites and show here that protein kinase C phosphorylates threonine 654 in the human EGF receptor. This threonine is in a very basic sequence nine residues from the cytoplasmic face of the plasma membrane in the region before the protein kinase domain; it is thus in a position to modulate signalling between this internal domain and the external EGF-binding domain.

Although treatment of A431 cells with TPA causes increased phosphorylation of the receptor on both threonine and serine residues, the only change detectable by tryptic peptide mapping is the appearance of three new phosphothreonine (PThr)-containing phosphopeptides, peptides X, Y and Z (Fig. 1), which are also the sites phosphorylated by protein kinase C *in vitro*[8]. We therefore concentrated on identifying these sites of threonine phosphorylation in the EGF receptor. Because the v-*erb-B* gene product is very similar to part of the EGF receptor[16], and reasoning that the phosphorylation sites would lie in the cytoplasmic region of the protein, we scanned the predicted v-*erb-B* protein sequence[17] for likely sites of threonine phosphorylation. Many protein kinases select their target amino acids through recognition of the primary sequence neighbouring the hydroxyamino acid, with positively or negatively charged amino acids being the key determinants in such sequences. Although it is not known whether protein kinase C is similar in this regard, it will phosphorylate many basic proteins *in vitro* such as histone H1, high mobility group (HMG) proteins and myelin basic protein[18–21]. We therefore focused on threonines with highly charged environments. Thr 98 of the predicted v-*erb-B* protein is contained in the sequence Arg-Arg-Arg-His-Ile-Val-Arg-Lys-Arg-Thr-Leu-Arg-Arg (Fig. 2); if it were phosphorylated, the limit tryptic digest of this sequence would yield the peptide PThr-Leu-Arg. Our experiments on separations of peptides on cellulose thin layers by electrophoresis and chromatography suggest that the mobility of this peptide would be very similar to that of peptide X in the EGF receptor. Peptide X is not susceptible to digestion by *Staphylococcus aureus* V8 protease (cleavage at Glu), *Pseudomonas fragi* protease (cleavage at Asp and cysteic acid) or chymotrypsin (cleavage at Phe, Tyr and Trp). We therefore synthesized the peptide PThr-Leu-Arg (Fig. 1). This peptide co-migrates precisely with peptide X in our standard two-dimensional separation conditions (Fig. 1); the complete predicted sequence of the human EGF receptor[1] shows that the sequence surrounding Thr 654 is identical to that in the equivalent region of the v-*erb-B* protein (Fig. 2). Because residues 654–656 are the only place in the EGF receptor from which Thr-Leu-Arg can be generated by trypsinolysis[1], peptide X must correspond to residues 654–656.

We next investigated peptides Y and Z. We suspected that they might be related to peptide X, as they were not susceptible to digestion by *S. aureus* V8 or *P. fragi* proteases or chymotrypsin, and their two-dimensional mobilities could be accounted for by the addition to peptide X of one and two extra basic residues respectively. The sequence embedding Thr 654 is likely to give rise to products with additional basic residues at either terminus of the limit digest peptide due to the inability of trypsin to act as an exopeptidase. To test whether all three peptides indeed form a nested set, we synthesized a 24 amino acid peptide corresponding to residues 87–110 of the predicted v-*erb-B* protein (this is identical to the sequence of the EGF receptor between residues 643 and 666 except for the first two residues, and contains one threonine and no serines). This peptide is phosphorylated *in vitro* by a purified preparation of protein kinase C (Fig. 3*a*). The only detectable phosphoamino acid in the resultant labelled phosphopeptide is PThr (Fig. 3*b*). Two-

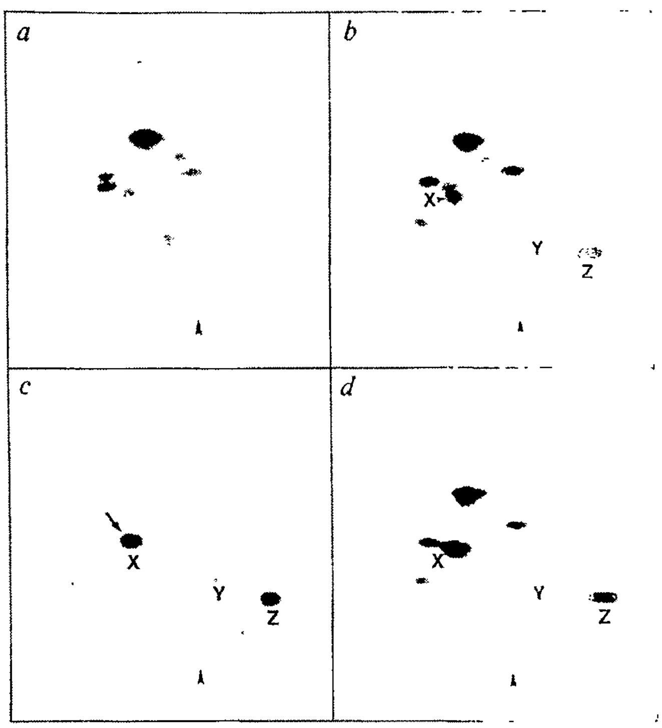

Fig. 1 Tryptic phosphopeptides of A431 cell EGF receptor and synthetic v-*erb-B* peptide. *a*, 700 Cerenkov c.p.m. tryptic digest of ^{32}P-labelled EGF receptor from untreated A431 cells (72 h). *b*, 900 Cerenkov c.p.m. tryptic digest of ^{32}P-labelled EGF receptor from TPA-treated A431 cells together with 1 μg PThr-Leu-Arg (72 h). *c*, 1,000 Cerenkov c.p.m. tryptic digest of ^{32}P-labelled phosphorylated synthetic peptide with 1 μg PThr-Leu-Arg (24 h). *d*, 900 Cerenkov c.p.m. tryptic digest of ^{32}P-labelled EGF receptor from TPA-treated A431 cells plus 400 Cerenkov c.p.m. tryptic digest of ^{32}P-labelled phosphorylated synthetic peptide (72 h). The positions of peptides X, Y and Z previously shown to be phosphorylated by protein kinase C are indicated. PThr-Leu-Arg, where present, was detected by staining with ninhydrin. Its position is given by a diagonal arrow on panel *c*, while in panel *b* it migrates with the spot arrowed X. **Methods:** Two subconfluent 5-cm dishes of A431 cells were labelled with 1 mCi ^{32}P-orthophosphate for 16 h, then one culture was treated with 100 ng ml^{-1} TPA dissolved in dimethyl sulphoxide for 60 min and the other with an equivalent amount of dimethyl sulphoxide before isolation of the EGF receptor by immunoprecipitation as described previously[8]. Tryptic peptides were prepared from ^{32}P-labelled EGF receptor as outlined previously[30]. The peptide Tyr-Leu-Arg-Arg-Arg-His-Ile-Val-Arg-Lys-Arg-Thr-Leu-Arg-Arg-Leu-Leu-Gln-Glu-Arg-Glu-Leu-Val-Glu-NH_2 was synthesized using a Beckman 990 synthesizer and purified by ion exchange and partition chromatography. The peptide was homogeneous on HPLC analysis and had the expected amino acid composition. This peptide was phosphorylated by protein kinase C as follows. Peptide at a final concentration of 0.2 mM was incubated at 30 °C for 10 min in 20 μl of a buffer containing 20 mM HEPES, *p*H 7.4, 10 mM $MgCl_2$, 0.5 mM $CaCl_2$, 5 mM dithiothreitol, 60 μg ml^{-1} phosphatidylserine and 6 μg ml^{-1} diolein together with 10 μCi [γ-^{32}P]ATP (3,000 Ci mmol^{-1}, Amersham) and 0.05 units kinase C purified from rat brain by a modification of the procedure of Kikkawa *et al.*[31] including DE52 cellulose chromatography, Ultragel ACA 34 filtration and hydroxyapatite chromatography steps. The protein kinase C preparation had a specific activity of ~150 U mg^{-1} at 22 °C using histone HI as substrate. The phosphorylated peptide was isolated by electrophoresis for 35 min at 1 kV on a 100-μm cellulose thin layer plate. 3×10^5 Cerenkov c.p.m. of peptide were recovered following elution and 10^4 c.p.m. digested with 2 μg trypsin in 10 μl 0.025 M NH_4HCO_3 for 2 h at 37 °C. The peptide PThr-Leu-Arg was synthesized as follows. tBOC-phosphothreonine was prepared by treatment of 100 μmoles D,L-phosphothreonine (Sigma) with 200 μmoles tBOC-azide (Aldrich) in 500 μl water/dimethylformamide/pyridine (25:25:1) for 24 h at 23 °C. The tBOC-PThr was recovered by stepwise elution from DE52 cellulose with ammonium acetate *p*H 4.5. tBOC-PThr, which eluted at 0.5 M, was desalted following lyophilization by gel filtration on Sephadex G-15 in water (yield of free acid 10%). 6 μmoles tBOC-PThr were coupled to 6 μmoles Leu-Arg (Bachem) in water (*p*H adjusted to 5.0) with 10 μmoles 1-ethyl-3(3-dimethylamino propyl)carbodiimide (Calbiochem-Behring) for 16 h at 23 °C. Following deblocking with trifluoroacetic acid for 30 min at 23 °C, the major product was separated from PThr and Leu-Arg by electrophoresis at *p*H 4.7 for 30 min at 1 kV on a 100-μm cellulose thin layer plate (yield 5%). This peptide contained phosphate and had the expected amino acid composition. The resultant samples were analysed on a 100-μm cellulose thin layer plate by electrophoresis at *p*H 8.9 for 20 min at 1 kV (horizontal dimension, with a centre origin (arrowhead) and anode to the left) and chromatography (vertical dimension)[30]. Exposure times are measured with an intensifying screen at −70 °C.

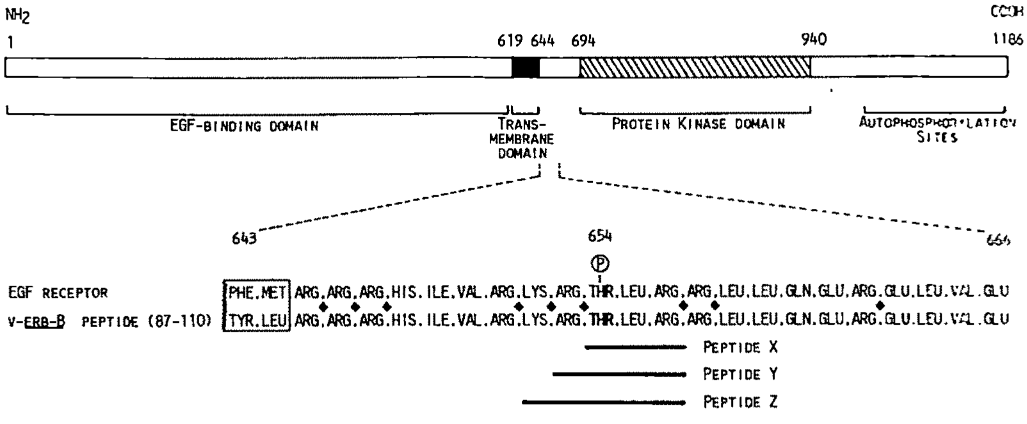
NH2
COOH
1
619 644 694
940
1186
EGF-BINDING DOMAIN
TRANS-MEMBRANE DOMAIN
PROTEIN KINASE DOMAIN
AUTOPHOSPHORYLATION SITES
643
654
666
Ⓟ
EGF RECEPTOR
PHE.MET ARG.ARG.ARG.HIS.ILE.VAL.ARG.LYS.ARG.THR.LEU.ARG.ARG.LEU.LEU.GLN.GLU.ARG.GLU.LEU.VAL.GLU
V-ERB-B PEPTIDE (87-110)
TYR.LEU ARG.ARG.ARG.HIS.ILE.VAL.ARG.LYS.ARG.THR.LEU.ARG.ARG.LEU.LEU.GLN.GLU.ARG.GLU.LEU.VAL.GLU
PEPTIDE X
PEPTIDE Y
PEPTIDE Z

Fig. 2 Schematic diagram showing the site of protein kinase C phosphorylation in the EGF receptor. The receptor is depicted as a bar, with amino acid numbers given above taken from the sequence of Ullrich *et al.*[1]. The proposed transmembrane domain is filled, while the protein kinase domain is hatched. The sequence of the human EGF receptor from residues 643 to 666 is shown with the homologous sequence from the v-*erb-B* gene product aligned below[1,17]. The v-*erb-B* sequence shown is that of the synthetic peptide used in Figs 1 and 3. The two residues at the cytoplasmic end of the proposed transmembrane domain are boxed at the left-hand side of these sequences. Note that the EGF receptor and v-*erb-B* sequences differ only in these two residues. Potential sites of trypsin cleavage are marked as diamonds between the two sequences. The heavy bars below the sequences indicate the deduced structures of peptides X, Y and Z.

dimensional separation of a tryptic digest of this phosphopeptide shows three peptides with mobilities very similar to peptides X, Y and Z, which co-migrate with those peptides on analysis of a suitable mixture (Fig. 1).

The precise structures of peptides Y and Z were determined by Edman degradation of ^{32}P-labelled peptides obtained from a digest of the phosphorylated synthetic peptide. After each cycle, a fraction of the sample was analysed by electrophoresis, without removal of the cleaved NH_2-terminal residue. All the radioactivity is released from peptide X at cycle 1 as expected (Fig. 3*c*), but the majority of the radioactivity is not released from peptide Y until cycle 2 (not shown). Sequential cycles convert peptide Z to peptide Y and then to peptide X (Fig. 3*c*) Prolonged digestion of peptide Z with a vast excess of trypsin also converts it inefficiently into peptide X (not shown). We therefore deduce that the structures of peptides Y and Z are Arg-PThr-Leu-Arg and Lys-Arg-PThr-Leu-Arg respectively.

The phosphorylation of the synthetic v-*erb-B* peptide by protein kinase C requires both Ca^{2+} and phospholipid (not shown). The K_m for peptide in this reaction was approximately 5 µM and the V_{max} 5 µmol per min per mg (Fig. 3*a*). This high affinity suggests that protein kinase C recognizes predominantly primary sequence determinants in its substrates. The sequence in the EGF receptor is the first described for a site phosphorylated by protein kinase C *in vivo*. It will be possible to produce synthetic variants of this sequence to identify residues which are important for recognition by the kinase. In myelin basic protein, the site has features similar to that in the EGF receptor, with basic residues at positions two and eight to the NH_2-terminal side of the phosphorylated Ser 115 (ref. 22). A synthetic peptide based on this sequence serves as a good substrate for protein kinase C (R. S. Turner, J. F. Kuo and B. E. Kemp, personal communication). Similarly, Ser 24 phosphorylated in HMG 17 is preceded by basic residues at positions 1, 2, 7 and 9 (ref. 21), and Ser 35 phosphorylated in histone H1 by basic residues at positions 2, 3, 4, 8 and 9 (ref. 18). Thus, protein kinase C appears to belong to the growing number of protein kinases which favour basic residues in the vicinity of their substrate hydroxyamino acid. These include the cyclic AMP- and cyclic GMP-dependent protein kinases, myosin light-chain kinase, phosphorylase kinase and the multi-functional calmodulin-dependent protein kinase.

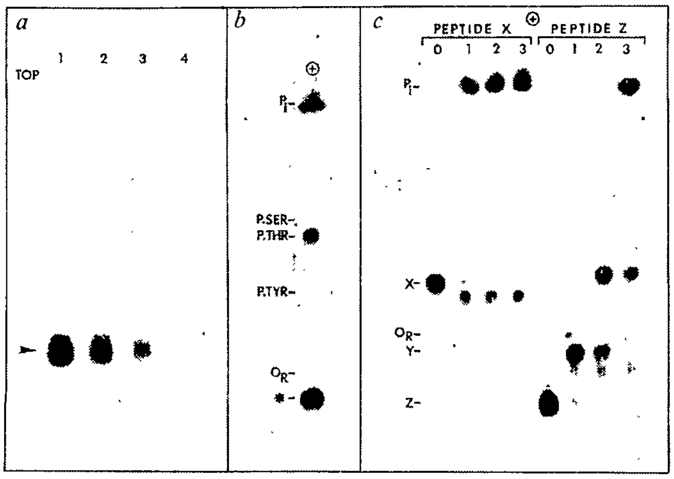

Fig. 3 Phosphorylation of synthetic peptide. ***a***, Synthetic peptide at the following concentrations was phosphorylated as described in Fig. 1 legend except that the final concentration of $[\gamma\text{-}^{32}\text{P}]$ATP was 10 µM (specific activity 10 µCi $nmol^{-1}$) and the incubation time at 30 °C was 4 min: lane 1, 3.0 µM; lane 2, 1.5 µM; lane 3, 0.75 µM; lane 4, no peptide. The reactions were stopped by the addition of EGTA to 2 mM and freezing. One µl of each sample was analysed by SDS-polyacrylamide electrophoresis on a gel containing 25% acrylamide, 0.05% bisacrylamide. The dried gel was exposed to X-ray film for 2 h. The arrowhead indicates the position of the phosphorylated peptide which co-migrated with marker glucagon (3,500 molecular weight). The band in lane 1 contained 1.7×10^3 Cerenkov c.p.m. ***b***, ^{32}P-labelled synthetic peptide (1,500 Cerenkov c.p.m.) was hydrolysed in 6 M HCl for 1 h at 110 °C and then analysed by electrophoresis at *p*H 3.5 (origin indicated O_R, anode at top) on a 100-µm cellulose thin layer plate for 30 min at 1 kV with internal phosphoamino acid standards. The plate was exposed to X-ray film for 12 h at −70 °C with an intensifying screen. The positions of the marker phosphoserine (P.SER), phosphothreonine (P.THR) and phosphotyrosine (P.TYR) detected by staining with ninhydrin are given. Also indicated are the positions of orthophosphate (P_i) and a phosphopeptide (*) which was identified as PThr-Leu by co-migration with synthetic PThr-Leu. ***c***, Purified ^{32}P-labelled peptides X and Z (7,000 and 13,000 Cerenkov c.p.m. respectively) were taken through three cycles of Edman degradation as follows. Peptides were dissolved in 40 µl pyridine/water (50:50) containing 5% phenylisothiocyanate and incubated at 45 °C for 30 min. The reactions were then extracted twice with 200 µl heptane/ethyl acetate (10:1) and twice with 200 µl heptane/ethyl acetate (2:1). The organic phases were discarded and the aqueous phases were lyophilized. The residues were taken up in 50 µl trifluoroacetic acid and incubated at 45 °C for 10 min to cleave the NH_2-terminal amino acid from the peptide. The trifluoroacetic acid was removed *in vacuo* and the residues were dissolved in 20 µl H_2O. Five µl were sampled and the remainder was taken through two further cycles in identical fashion with the equivalent of one-quarter of the original material being sampled at each stage. One-third of the samples from each cycle and an equivalent amount of untreated peptide were analysed by electrophoresis at *p*H 8.9 (origin indicated O_R, anode at top) for 20 min at 1 kV on a 100-µm cellulose thin-layer plate. The plate was exposed to X-ray film for 12 h at −70 °C with an intensifying screen. The positions of peptides X, Y and Z and orthophosphate (P_i) are indicated. Lane 0, starting material; lane 1, sample after first cycle; lane 2, sample after second cycle; lane 3, sample after third cycle. The acid-catalysed cyclization reaction of a phenylisothiocyanate-reacted peptide possessing an NH_2-terminal phosphothreonine or phosphoserine leads to the elimination of much of the phosphate during the cleavage rather than the formation of an anilinothiazolinone derivative. The minor spot migrating just below the position of peptide X may be anilinothiazolinone phosphothreonine. Note that the analysis of this type of experiment will be more complicated if the peptide contains a group reactive with phenylisothiocyanate in addition to the α-NH_2 group.

Very little is known about physiological substrates for protein kinase C. TPA-induced serotonin release from platelets correlates well with protein kinase C-mediated phosphorylation of a 40,000 molecular weight protein[23]. The EGF receptor, however, is the first example where phosphorylation by protein kinase C of a purified protein has been shown to have a functional consequence. The normal role of the protein kinase C-mediated phosphorylation of the receptor may be to act as a feedback mechanism to attenuate the response to EGF either by blocking kinase activation or by decreasing EGF binding affinity[9]. The feedback would be modulated via diacylglycerol whose concentration rises as a result of EGF-induced turnover of phosphatidylinositol[24]. This is in agreement with the increased phosphorylation of the receptor at the protein kinase C-specific sites in EGF-treated A431 cells[15].

We have shown here that there is a single major threonine phosphorylation site for protein kinase C in the EGF receptor at position 654. Our previous measurements indicate that up to 35% of receptor molecules are phosphorylated at this threonine in response to either phorbol ester or indole alkaloid tumour promoters[8]. The active form of kinase C is largely membrane associated, where it is bound to phospholipids and either its natural activator diacylglycerol or a substitute activator such as TPA[25]. The position of Thr 654 spaced nine amino acids from the cytoplasmic side of the proposed membrane-spanning segment puts it in an ideal position to be phosphorylated by protein kinase C. The 50 residues between the membrane and the start of recognizable homology with the tyrosine protein kinases may act as a 'linker' between the EGF-binding domain and the protein kinase domain, and as such might be involved in signal transmission between the two upon EGF binding.

It is not known how the binding of EGF increases the activity of the receptor tyrosine protein kinase. There could be a direct allosteric conformational change induced by EGF binding, although it is unclear how this might be transmitted across the membrane. Alternatively EGF-dependent clustering of the receptor may be required for activation. Because the basic residues in the 'linker' are likely to interact with the phosphate head groups of plasma membrane phospholipids, the introduction of a phosphate group in this region with its potential as an alternative charge acceptor could well have significant effects on both tyrosine protein kinase activity and EGF binding, whatever mechanism is involved. Our results suggest that alteration of Thr 654 or neighbouring residues by site-directed mutagenesis and the use of antibodies recognizing this region may further our understanding of signal transduction.

As TPA markedly reduces EGF binding to many mitogenically responsive cell types[26-29], it is of interest to determine whether protein kinase C mediates threonine phosphorylation of the EGF receptor in such cell types in a manner similar to A431 cells. An investigation of whether v-*erb-B* proteins are phosphorylated at the equivalent site also seems warranted.

We thank Jill Meisenhelder for her help, our colleagues for their encouragement and Gordon Gill for the preparation of kinase C used in these studies. This work was supported by USPHS grants CA-17096, CA-28485, HD-09096 and AM-18811 from the NIH.

Received 11 July; accepted 23 August 1984.

1. Ullrich, A. *et al. Nature* **309**, 418-425 (1984).
2. Cohen, S., Carpenter, G. & King, L. E. *J. biol. Chem.* **255**, 4834-4842 (1980).
3. Ushiro, H. & Cohen, S. *J. biol. Chem.* **255**, 8363-8365 (1980).
4. Buhrow, S. A., Cohen, S. & Staros, J. V. *J. biol. Chem.* **257**, 4019-4022 (1981).
5. Cohen, S. *et al. J. biol. Chem.* **257**, 1523-1531 (1982).
6. Hunter, T. & Cooper, J. A. *Cell* **24**, 741-752 (1981).
7. Gill, G. N. & Lazar, C. S. *Nature* **293**, 305-307 (1981).
8. Cochet, C. *et al. J. biol. Chem.* **259**, 2553-2558 (1984).
9. Friedman, B. *et al. Proc. natn. Acad. Sci. U.S.A.* **81**, 3034-3038 (1984).
10. Niedel, J. E., Kuhn, L. J. & Vandenbark, G. R. *Proc. natn. Acad. Sci. U.S.A.* **80**, 36-40 (1983).
11. Castagna, M. *et al. J. biol. Chem.* **257**, 7847-7851 (1982).
12. Leach, K. L., James, M. L. & Blumberg, P. M. *Proc. natn. Acad. Sci. U.S.A.* **80**, 4208-4212 (1983).
13. Ashendel, C. L., Staller, J. M. & Boutwell, R. K. *Biochem. biophys. Res. Commun.* **111**, 340-345 (1983).
14. Parker, P., Stabel, S. & Waterfield, M. D. *EMBO J.* **3**, 953-959 (1984).
15. Iwashita, S. & Fox, C. F. *J. biol. Chem.* **259**, 2559-2567 (1984).
16. Downward, J. *et al. Nature* **307**, 521-527 (1984).
17. Yamamoto, T. *et al. Cell* **35**, 71-78 (1983).
18. Nishizuka, Y. *et al. Adv. cyclic Nucleotide Res.* **9**, 209-220 (1978).
19. Takai, Y. *et al. J. biol. Chem.* **254**, 3692-3695 (1979).
20. Wise, B. C. *et al. J. biol. Chem.* **257**, 8489-8495 (1982).
21. Ramachandran, C. *et al. J. biol. Chem.* (in the press).
22. Turner, R. S. *et al. J. Neurochem.* (in the press).
23. Sano, K. *et al. J. biol. Chem.* **258**, 2010-2013 (1983).
24. Sawyer, S. T. & Cohen, S. *Biochemistry* **20**, 6280-6286 (1981).
25. Kraft, A. S. & Anderson, W. B. *Nature* **301**, 621-623 (1983).
26. Lee, L.-S. & Weinstein, I. B. *Science* **202**, 313-315 (1978).
27. Shoyab, M., DeLarco, J. E. & Todaro, G. J. *Nature* **279**, 387-391 (1979).
28. Salomon, D. S. *J. biol. Chem.* **256**, 7958-7966 (1981).
29. King, A. C. & Cuatrecasas, P. *J. biol. Chem.* **257**, 3053-3060 (1982).
30. Hunter, T. & Sefton, B. M. *Proc. natn. Acad. Sci. U.S.A.* **77**, 1311-1315 (1980).
31. Kikkawa, U. *et al. J. biol. Chem.* **257**, 13341-13348 (1982).

Autophosphorylation sites on the epidermal growth factor receptor

J. Downward, P. Parker & M. D. Waterfield

Department of Protein Chemistry, Imperial Cancer Research Fund, Lincoln's Inn Fields, London WC2A 3PX, UK

The epidermal growth factor (EGF) receptor is a tyrosine-specific protein kinase with autophosphorylating activity[1–4]. A 300 amino acid-long region of the receptor's cytoplasmic domain matches (35–90 % homology) sequences of transforming proteins from the *src* family[5] and includes a putative nucleotide binding site[6]. Several of the *src* transforming proteins have tyrosine kinase activity[7], but v-*erb-B*, which appears to be a truncated EGF receptor, is virtually identical to the receptor over this region and yet lacks detectable kinase activity[8,9]. To locate possible acceptor sites in the v-*erb-B* protein, we have mapped these sites in the human EGF receptor. We report here that three tyrosine sites near the C-terminus are phosphorylated *in vitro*. In intact cells, we find that EGF stimulates phosphorylation of several sites, the tyrosine 14 residues from the C-terminus being modified the most extensively. The equivalent site is absent in the v-*erb-B* protein of avian erythroblastosis virus (AEV) and may influence tyrosine kinase activity[10,11].

Knowledge of the complete primary structure of the human HEGF receptor[5] is used here to map the tyrosine acceptor sites for the receptor kinase autophosphorylation activity. We purified EGF receptors from detergent lysates of A431 cells using R1 monoclonal immunoaffinity chromatography and performed *in vitro* autophosphorylation by addition of [γ-^{32}P]ATP to immobilized receptor while in an immune complex[12] in the presence or absence of EGF (Fig. 1). After tryptic digestion of the receptor, peptides were resolved by reverse-phase HPLC. We found that phosphate-labelled peptides (P1, P2 and P3; Fig. 1*a*) eluted at three distinct acetonitrile concentrations as reported previously[13]. The most hydrophobic peptide, P3, was partially resolved into two components, a and b. Thin-layer electrophoretic analysis of acid hydrolysates[14] from either receptor or purified peptides demonstrated that tyrosine was the only amino acid phosphorylated *in vitro* in the conditions used. Only the rate of phosphorylation seemed to be altered by EGF, because identical peptides were phosphorylated in its presence or absence over longer incubation times (Fig. 1*b*).

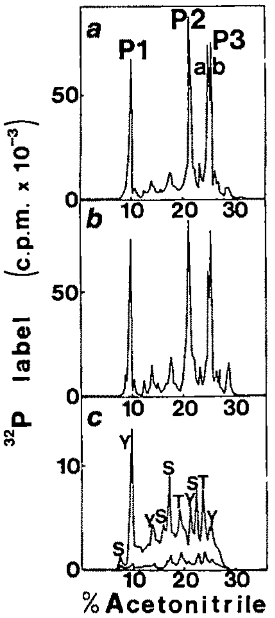

Fig. 1 Tryptic phosphopeptide maps of EGF receptor from A431 cells. ***a***, EGF receptor was purified from A431 cells as described previously[12]. Autophosphorylation was performed with 150 μg receptor as washed immunocomplex with monoclonal antibody R1–Sepharose. The receptor was incubated for 1 h at 20 °C in 1 μg ml^{-1} EGF, 150 mM NaCl, 1 mM MnCl$_2$, 50 mM HEPES *p*H 7.4, 0.1 % Triton X-100. [γ-^{32}P]ATP was then added (20 μM, specific activity 690 c.p.m. pmol^{-1}) for 10 min. Reagents were then removed by filtration and the receptor washed, eluted, fully reduced and alkylated, further purified by gel permeation chromatography, digested with trypsin and run on reverse-phase HPLC at *p*H 2.0, all as described previously[12]. Fractions (0.3 ml) were collected at a flow rate of 1.5 ml min^{-1} and a gradient of 1 % acetonitrile min^{-1}. The ^{32}P-phosphate label in each fraction was determined by counting Cerenkov radiation and is plotted against the percentage acetonitrile in the fraction. ***b***, Same as *a* except that autophosphorylation was performed in the absence of EGF (replaced by 1 μg ml^{-1} bovine serum albumin, BSA). The length of the incubation in the presence of [γ-^{32}P]ATP was increased to 60 min. ***c***, Two subconfluent 15-cm dishes of A431 cells were labelled for 14 h, each with 5 mCi ^{32}P-orthophosphate in Eagle's medium containing 5 % normal phosphate concentration and 0.5 % fetal calf serum. Upper line, 1 μg ml^{-1} EGF was added to one dish for 10 min before lysis in 100 mM HEPES *p*H 8.5, 50 mM NaF, 1 mg ml^{-1} BSA, 1 mM Na$_3$VO$_4$, 10 mM NaP$_i$ *p*H 8.5, 5 mM *p*-nitrophenylphosphate, 100 mM NaCl, 1 mM EGTA, 1 % Triton X-100, 10 mM benzamidine, 50 μg ml^{-1} phenylmethylsulphonyl fluoride, 10 μg ml^{-1} soybean trypsin inhibitor. Kinase activities were inhibited by chelation of divalent metal ions. The extract was clarified by centrifugation, then 50 μg of R1–Sepharose added for 90 min at 4 °C. The immobilized antibody was washed thoroughly and receptor eluted as described[12]. The *in vivo* labelled receptor was then mixed with 150 μg of unlabelled purified EGF receptor as a carrier and processed as described in *a*. The phosphoamino acid content of each peak was determined by partial acid hydrolysis and thin-layer electrophoresis[14]; the predominant phosphoamino acid is given above each peak. Lower line, the second dish was processed as above except the cells were not treated with EGF before lysis (replaced by 1 μg ml^{-1} BSA). Both dishes had the same cell density before labelling. The amount of receptor immunoprecipitated was the same from each plate as determined by Coomassie blue staining of SDS-polyacrylamide gels.

To characterize the kinase autophosphorylation sites used *in vivo*, we labelled A431 cells with ^{32}P-phosphate (Fig. 1). We fractionated tryptic phosphopeptides by HPLC and determined the phosphorylated amino acids by thin-layer electrophoresis[14]. Ten distinct phosphopeptides were found, four containing phosphotyrosine, four phosphoserine and two phosphothreonine. In previous reports, fewer phosphopeptides were detected[15]. Three

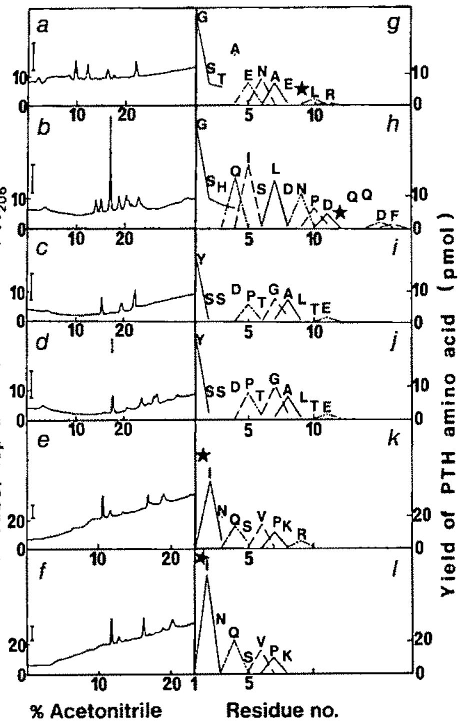

Fig. 2 Purification and sequencing of phosphopeptides. *a*, The fractions labelled Pl in Fig. 1*a* were pooled and applied to a Synchropak RPC 18 reverse-phase HPLC column (4.6×75 mm; Synchrom, Linden, Indiana) run in 10 mM ammonium acetate buffer at *p*H 6.5 with a linear gradient of acetonitrile of 1 % min^{-1} at 1.5 ml min^{-1}. Fractions (0.3 ml) were collected and counted for Cerenkov radiation. The absorbance of the eluate at 206 nm was monitored (the bar represents 0.01 absorbance units). 310 pmol of labelled phosphate were loaded onto the column. *b*, The fractions HHlabelled P2 in Fig. 1*a* were run as described above for *a*; 360 pmol were loaded. *c*, Fractions labelled P3a in Fig. 1*a* were run as in *a*; 220 pmol were loaded. *d*, Fractions labelled P3b in Fig. 1*a* were run as in *a*; 270 pmol were loaded. *e*, The fractions corresponding to P3a from a second identical preparation of *in vitro* labelled EGF receptor were digested with *Staphylococcus aureus* V8 protease (1 μg in 10 μl in 50 mM ammonium bicarbonate, *p*H 7.5 for 24 h at 37 °C). The resulting mixture of peptides was separated by reverse-phase HPLC at *p*H 2.0 (ref. 12). Fractions (0.3 ml) were collected. The linear gradient was 0.5% acetonitrile min^{-1}. The bar represents 0.01 absorbance units. *f*, The fractions corresponding to P3b were digested and separated as in *e*. *g*, The fractions containing the peak of phosphate label from *a* were pooled; the 70 pmol of phosphate label present were divided into two halves which were sequenced on gas phase sequencers[21,22]. The yield of PTH amino acid (identified above the peak by the one-letter code) is plotted against cycle number of the Edman degradation. *h*, Sequence of the phosphopeptide from *b*; 45 pmol of phosphate label were loaded for each sequencer run. *i*, Sequence of phosphopeptide from *c*; 25 pmol phosphate label loaded. *j*, Sequence of phosphopeptide from *d*; 30 pmol phosphate label loaded. *k*, Sequence of phosphopeptide from *e*; 85 pmol phosphate label loaded. *l*, Sequence of phosphopeptide from *f*; 105 pmol phosphate label loaded. * Phosphotyrosine residues.

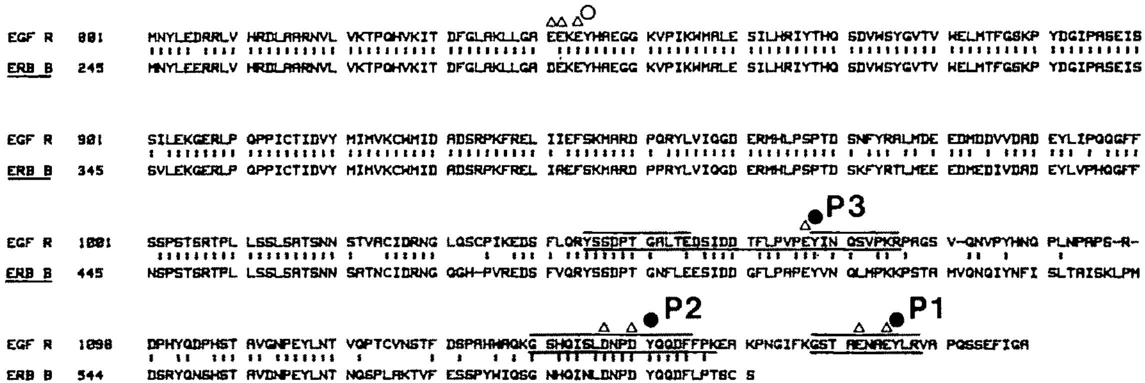

```
EGF R   801   MNYLEDRRLV HRDLAARNVL VKTPQHVKIT DFGLAKLLGA EEKEYHAEGG KVPIKWMALE SILHRIYTHQ SDVWSYGVTV WELMTFGSKP YDGIPASEIS
ERB B   245   MNYLEERRLV HRDLAARNVL VKTPQHVKIT DFGLAKLLGA DEKEYHAEGG KVPIKWMALE SILHRIYTHQ SDVWSYGVTV WELMTFGSKP YDGIPASEIS

EGF R   901   SILEKGERLP QPPICTIDVY MIMVKCWMID ADSRPKFREL IIEFSKMARD PQRYLVIQGD ERMHLPSPTD SNFYRALMDE EDMDDVVDAD EYLIPQQGFF
ERB B   345   SVLEKGERLP QPPICTIDVY MIMVKCWMID ADSRPKFREL IAEFSKMARD PPRYLVIQGD ERMHLPSPTD SKFYRTLMEE EDMEDIVDAD EYLVPHQGFF

EGF R   1001  SSPSTSRTPL LSSLSATSNN STVACIDRNG LQSCPIKEDS FLQRYSSDPT GALTEDSIDD TFLPVPEYIN QSVPKRPAGS V-QNVPYHNQ PLNPAPS-R-
ERB B   445   NSPSTSRTPL LSSLSATSNN SATNCIDRNG QGH-PVREDS FVQRYSSDPT GNFLEESIDD GFLPAPEYVN QLMPKKPSTA MVQNQIYNFI SLTAISKLPM

EGF R   1098  DPHYQDPHST AVGNPEYLNT VQPTCVNSTF DSPAHWAQKG SHQISLDNPD YQQDFFPKEA KPNGIFKGST AENAEYLRVA PQSSEFIGA
ERB B   544   DSRYQNSHST AVDNPEYLNT NQSPLAKTVF ESSPYWIQSG NHQINLDNPD YQQDFLPTSC S
```

Fig. 3 The alignment of the phosphate acceptor regions of the EGF receptor with the v-*erb-B* protein sequence. (Sequence of the EGF receptor from ref. 5, sequence of the v-*erb-B* protein from AEV-H, from ref. 10.) The tyrosine residue at 845 (○) in the EGF receptor sequence is homologous to the pp60$^{v\text{-}src}$ phosphoacceptor site[19]. ●, EGF receptor phosphorylation sites P1, P2 and P3; △, acidic residues at phosphorylation sites. The peptide sequences determined in Fig. 2 are overlined, the predicted complete sequence of each tryptic phosphopeptide is underlined. The last four residues of the v-*erb-B* protein are derived from the viral *env* gene[10].

of the four phosphotyrosine peptides co-chromatograph at two different *p*Hs with peptides P1, P2 and P3 (data not shown). Addition of EGF to intact cells caused a general increase (5-fold) in the extent of receptor phosphorylation with a marked selective increase (10-fold) in the extent of labelling of peptide P1 (Fig. 1*c*). This is a considerably larger stimulation than that reported previously, which may be due to the use of protease inhibitors that prevented loss of sites near the C-terminus.

To locate the phosphorylation sites, pmol amounts of phosphate-labelled peptides were purified[12] and sequenced[16,17] (Fig. 2). In each case we located our established sequence in the amino acid sequence of the EGF receptor (Fig. 3). At the ninth degradation cycle of P1, we recovered no phenylthiohydantoin (PTH) amino acid although the cDNA sequence predicted a tyrosine residue. In gas phase sequencing, phosphotyrosine PTH cannot be detected[18]. Because we knew that the phosphate in this peptide occurs in phosphotyrosine and that the peptide only contains one tyrosine residue, the phosphate could be assigned unequivocally to residue nine. Similarly, we assigned residue 12 as phosphotyrosine in P2. Peptides P3a and P3b gave the same sequence up to residue 11; however, none of the residues assigned was a phosphotyrosine that was presumably carboxy-terminal to this sequence. We digested peptides P3a and P3b with *Staphylococcus aureus* V8 protease and purified (Fig. 2*e*, *f*) and sequenced (Fig. 2*k*, *l*) the resulting phosphopeptides. P3a had an additional C-terminal arginine residue compared with P3b and the N-termini could be assigned as phosphotyrosine.

Thus the major *in vitro* autophosphorylation sites of the EGF receptor are assigned as follows: P3, tyrosine 1,068; P2, tyrosine 1,148; and P1, tyrosine 1,173. Each of these residues is immediately preceded by an amino acid residue with an acidic side chain. These sequences are similar to most of the tyrosine phosphorylation sites described previously[19,20]. Tyrosine 1,173 is the site selectively phosphorylated *in vivo* while tyrosines 1,148 and 1,068 are autophosphorylation sites used to a lesser extent *in vivo*. A third minor *in vivo* tyrosine autophosphorylated peptide has not yet been located. The major autophosphorylation site that is selectively phosphorylated *in vivo* (P1) is 14 residues from the carboxy-terminus of the EGF receptor and is not found in the v-*erb-B* protein from the *erb-B* gene of AEV (AEV-H) which is fused at the carboxy-terminus to four residues of the viral *env* protein (Fig. 3)[10]. Therefore, v-*erb-B* is probably terminated prematurely with respect to the cellular sequences from which it is derived. P1 has the same neighbouring V8 protease and trypsin cleavage sites as predicted for the major *in vivo* autophosphorylation site of the EGF receptor[21]. The autophosphorylation sites P1, P2 and P3 used *in vitro* do not correspond to the tyrosine phosphorylated in one member of the *src* family, pp60$^{v\text{-}src}$ (ref. 19), which would be tyrosine 845 in the EGF receptor. These sites are not shared with any other members of the *src* family of oncogene products except v-*erb-B*.

The absence of the site homologous to P1 in the v-*erb-B* protein may contribute to the failure to detect kinase autophosphorylation activity in AEV-transformed cells. C-terminal truncation can influence tumorigenicity since the deletion mutant AEV-H, td-130, which has a large C-terminal truncation, will induce sarcomas but not erythroblastosis in chickens[10]. On the other hand, avian leukosis virus can induce erythroblastosis by insertion of a viral long terminal repeat into c-*erb-B* with consequent N-terminal trunction but presumably without affecting the C-terminus of the protein product[22]. As yet the significance of EGF receptor tyrosine autophosphorylaton is unclear despite work performed on two other members of the *src* family, pp60$^{v\text{-}src}$ (ref. 23) and p130$^{gag\text{-}fps}$ (ref. 24); it remains to be seen if either or both amino- and carboxy-terminal truncations of the receptor are essential for generation of a transforming signal.

Received 13 June; accepted 31 August 1984.

1. Cohen, S., Ushiro, H., Stoscheck, C. & Chinkers, M. *J. biol. Chem.* **257,** 1523–1531 (1982).
2. Buhrow, S. A., Cohen, S. & Staros, J. V. *J. biol. Chem.* **257,** 4019–4022 (1981).
3. Cohen, S., Fava, R. A. & Sawyer, S. T. *Proc. natn. Acad. Sci. U.S.A.* **79,** 6237–6241 (1982).
4. Buhrow, S. A., Cohen, S., Garbers, D. L. & Staros, J. V. *J. biol. Chem.* **258,** 7824–7827 (1983).
5. Ullrich, A. *et al. Nature* **309,** 418–425 (1984).
6. Kamps, M. P., Taylor, S. S. & Sefton, B. M. *Nature* **310,** 589–592 (1984).
7. Bishop, J. M. *A. Rev. Biochem.* **52,** 301–354 (1983).
8. Hayman, M. J. *et al. Cell* **32,** 579–588 (1983).
9. Privalsky, M. L. *et al. Cell* **32,** 1257–1267 (1983).
10. Yamomoto, T. *et al. Cell* **35,** 71–78 (1983).
11. Privalsky, M. L., Ralston, R. & Bishop, J. M. *Proc. natn. Acad. Sci. U.S.A.* **81,** 704–707 (1984).
12. Downward, J. *et al. Nature* **307,** 521–527 (1984).
13. Cassel, D., Pike, L. J., Grant, G. A., Krebs, E. G. & Glaser, L. *J. biol. Chem.* **258,** 2945–2950 (1983).
14. Ushiro, H. & Cohen, S. *J. biol. Chem.* **255,** 8363–8365 (1980).
15. Hunter, T. & Cooper, J. A. *Cell* **24,** 741–752 (1981).
16. Hewick, R. M., Hunkapiller, M. W., Hood, L. E. & Dreyer, W. J. *J. biol. Chem.* **256,** 7990–7997 (1981).
17. Waterfield, M. D., Scrace, G. & Totty, N. in *Practical Protein Biochemistry* (ed. Darbre, A.) (Wiley, New York, in the press).
18. Cooper, J. A., Sefton, B. M. & Hunter, T. *Meth. Enzym.* **99,** 387–402 (1983).
19. Smart, J. E. *et al. Proc. natn. Acad. Sci. U.S.A.* **76,** 6013–6017 (1981).
20. Patschinsky, T., Hunter, T., Esch, F. S., Cooper, J. A. & Sefton, B. M. *Proc. natn. Acad. Sci. U.S.A.* **79,** 973–977 (1982).
21. Hunter, T. & Cooper, J. A. *UCLA Symp. molec. cell. Biol.* **6,** 360 (1983).
22. Fung, Y-K. T., Lewis, W. G., Crittenden, L. B. & Kung, H-J. *Cell* **33,** 357–368 (1983).
23. Snyder, M. A., Bishop, J. M., Colby, W. W. & Levinson, A. D. *Cell* **32,** 891–901 (1983).
24. Weinmaster, G., Zoller, M. J., Smith, M., Hinge, E. & Pawson, T. *Cell* **37,** 559–568 (1984).

Isolation of the closed circular form of the transposable element Tc*1* in *Caenorhabditis elegans*

A. M. Rose* & T. P. Snutch†

* Department of Medical Genetics, University of British Columbia, Vancouver, Canada V6T 1W5
† Department of Biological Sciences, Simon Fraser University, Burnaby, Canada V5A 1S6

The mobilization of Tc*1*, a transposable element in the genome of the roundworm *Caenorhabditis elegans*, has been investigated. Genomic blot hybridization has shown that Tc*1* exists in very different numbers in the genomes of two closely related strains of *C. elegans*[1,2]: there are ~30 copies of Tc*1* in the Bristol strain, whereas in the Bergerac strain there are 200–300. Most of these Tc*1* elements are structurally highly conserved[1–3] although there exists a second form which contains a *Hin*dIII restriction site (Tc*1* (*Hin*) form) and comprises ~10% of the population[4]. Excision of Tc*1* from its chromosomal location in the Bergerac strain is indicated by the presence, on genomic blots, of a minor band corresponding to the size of the uninserted restriction fragment[1,5,6]. Here we describe the recovery of extrachromosomal linear and closed circular copies of Tc*1* from the Bergerac strain, presumably a result of Tc*1* excision.

We initially looked for a Tc*1* transcription product using Northern blots containing RNA isolated from two strains of *C. elegans*. RNA preparations from the Bergerac strain contained Tc*1*-hybridizing sequences (Fig. 1). Attempts to demonstrate that the Tc*1*-hybridizing material was RNA revealed that this material was resistant to alkali hydrolysis and ribonuclease digestion, but sensitive to restriction enzyme digestion. These results indicated that extrachromosomal copies of Tc*1* had co-precipitated with RNA in the extraction conditions used here[7]. The Tc*1*-hybridizing material was observed in the Bergerac strain, but not in the Bristol strain, although the methods used would probably not have detected the 10-fold lower levels that would be expected in the Bristol strain. Some Tc*1*s from the Bristol strain have been cloned and found to have restriction maps identical to those isolated from the Bergerac strain, indicating that they are potentially functional elements (N. Mawji, unpublished results). The presence of extrachromosomal Tc*1* is not limited to the Bergerac strain; it has also been detected in other wild-type and laboratory strains of *C. elegans* (data not shown).

To investigate the Tc*1*-hybridizing material further, DNA was isolated by CsCl–ethidium bromide ultracentrifugation from the Bergerac strain. Individual fractions were collected from the gradient, electrophoresed on agarose gels, blotted onto nitrocellulose, and tested for the presence of Tc*1*-hybridizing material (Fig. 2). A large amount of Tc*1*-hybridizing material is present in the fractions corresponding to the genomic DNA. This material presumably represents the 300 or so copies of Tc*1* that are integrated throughout the genome. There is also a band in the region of the gradient which corresponds to linear copies of extrachromosomal Tc*1* (fractions 3, 4). Below the main genomic band on the gradient, a minor band containing Tc*1*-hybridizing material was detected in fractions 5 and 6. Restriction digestion was used to demonstrate that the material in fractions 5 and 6 is in fact closed circular Tc*1*.

The Tc*1*-hybridizing material in fractions 5 and 6 from the CsCl gradient, corresponding to a linear fragment of 950 base pairs (bp), was purified on an agarose gel and analysed by gel electrophoresis. In the undigested sample, two bands of Tc*1*-hybridizing material were apparent (Fig. 3, lane 1). The major band has an apparent size of 950 bp, consistent with its being a closed circular molecule the size of Tc*1* (1,610 bp). The minor band presumably consists of nicked circles that were generated after isolation of the closed circular material from the gradient fractions. When digested with *Cla*I, an enzyme that has a single cleavage site in Tc*1*, a single band of ~1,600 bp is observed (data not shown). When digested with *Xho*I, a band of ~1,400 bp is observed (Fig. 3, lane 2). *Xho*I digests Tc*1* at two

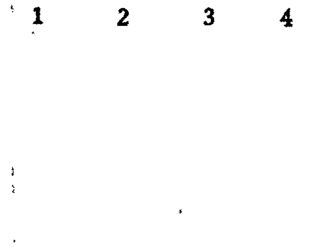

Fig. 1 Autoradiograph of Tc*1*-hybridizing material detected in RNA preparations: lanes 1, 2, Bristol strain; lanes 3, 4, Bergerac strain.

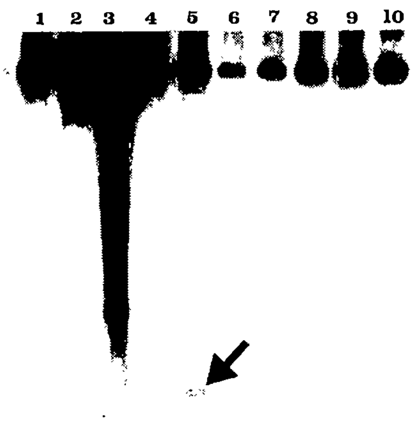

Fig. 2 Isolation of extrachromosomal closed circular and linear copies of Tc*1*. Bergerac DNA was prepared[1] and centrifuged on a CsCl-ethidium bromide equilibrium gradient[5]. Fractions were collected and the DNA recovered and electrophoresed on a 0·8% agarose gel. DNA was transferred to nitrocellulose[9] and hybridized with ^{32}P-labelled Tc*1* (*Hin*) DNA. Filters were hybridized overnight and autoradiographed for 5 days using Kodak Blue Brand film. Lane numbers correspond to CsCl gradient fraction numbers. The arrow indicates the closed circular Tc*1*.

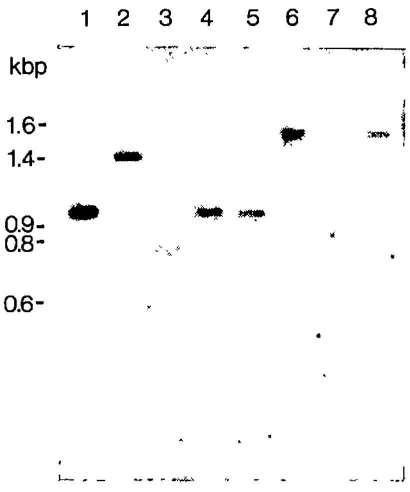

Fig. 3 Autoradiograph of restriction digests of the extrachromosomal Tc*1*-hybridizing material. Before digestion, the extrachromosomal Tc*1* from the CsCl fractions was further purified to remove the high-level contamination of chromosomal Tc*1* seen in Fig. 2. Agarose gel fractions corresponding to sizes of either 1,610 bp (linear) or 950 bp (closed circular) were electroeluted and electrophoresed in a 0.8% agarose gel. Lane 1, undigested material from CsCl fractions 5 and 6. Lanes 2-5, restriction digests of this material: *Xho*I (lane 2); *Hin*fI (lane 3); *Hin*dIII (lane 4); *Eco*RI (lane 5). Lane 6, undigested material from CsCl fraction 3. Lanes 7, 8, restriction digests of this material with *Xho*I and *Eco*RI, respectively. The sizes of the fragments are indicated at the left-hand side in kilobase pairs (kbp).

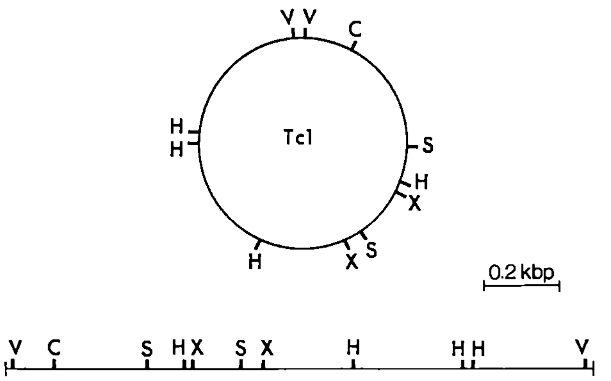

Fig. 4 Restriction map of closed circular and linear Tc*1*: V, *Eco*RV; X, *Xho*I; H, *Hin*fI; S, *Sal*I. Tc*1* lacks *Eco*RI and *Hin*dIII sites.

sites, 220 bp apart, thus a *Xho*I digest of a linear Tc*1* molecule would give three fragments of 890, 500 and 220 bp. The observed fragment of 1,400 bp is predicted for a circular molecule closed at the inverted repeats. The enzyme *Eco*RV, which cuts once in each of these inverted repeats, shifts the size from 950 bp to just under 1,600 bp as predicted (data not shown). Digestions with other restriction enzymes also generated fragments of the sizes predicted assuming a closed circular Tc*1* molecule was being digested (Fig. 3). No *Eco*RI or *Hin*dIII sites could be detected in the extrachromosomal material (lanes 4 and 5), as expected from the published restriction maps of Tc*1* (refs 1, 3). If the Tc*1* (*Hin*) form[4] was present in proportion to its chromosomal representation, ~10% of the molecules would be expected to linearize with *Hin*dIII.

Lane 6 of Fig. 3 contains material of 1,600 bp from fraction 3 of the CsCl gradient that had been purified on an agarose gel, and corresponds to linear copies of extrachromosomal Tc*1*. Restriction digestion of this material with *Xho*I gave a 890-bp fragment (lane 7); a fragment of this size is predicted if the DNA contains linear molecules of Tc*1* with unique ends at the inverted repeats (see above and restriction maps of linear and closed circular Tc*1* shown in Fig. 4). The large number of linear molecules detected is intriguing, but their significance to Tc*1* transposition is unclear.

We have demonstrated the recovery of extrachromosomal copies of Tc*1* from the Bergerac strain of *C. elegans*. High-frequency excision of Tc*1* from somatic tissue has been demonstrated previously[6] and is presumably the source of the extrachromosomal linear and closed circular Tc*1*s demonstrated here. At present we have no evidence linking the events of excision and closing of linear Tc*1*s to heritable events, such as the mutations that result from reintegration of Tc*1* into germ-line chromosomes. Indeed, high-frequency excision has been shown to be limited to somatic tissue[6]. The role of either the linear or closed circular molecules in the transposition process in *C. elegans* and other organisms is unknown. Extrachromosomal copies of the *copia* family of transposable elements in *Drosophila melanogaster* have been described[8], but their role in transposition is unknown. *Copia* transposable elements have direct terminal repeats, in contrast to Tc*1* elements which have inverted repeats; thus, the conditions and mechanisms by which these two transposable elements circularize are presumably different. *Copia* elements can be mobilized by hybrid dysgenic crosses, but it is unknown whether the closed circular form is involved. Tc*1*, on the other hand, appears to be constitutively excising in the Bergerac strain. The generation of new mutations resulting from excision or integration of Tc*1* is being investigated in our laboratories.

We thank Dr D. L. Baillie for valuable discussion and financial support and N. Mawji and K. Beckenbach for technical assistance. This research was supported by grants from the NCI (Canada) to A.M.R. and D.L.B.; the MRC (Canada) to A.M.R.; NSERC to Dr. D. L. Baillie; and an NSERC scholarship to T.P.S.

Received 4 May; accepted 17 July 1984.

1. Emmon, S. W., Yesner, L., Ruan, K. & Katzenberg, D. *Cell* **32** 55-65 (1983).
2. Liao, L. W., Rozenzweig, B. & Hirsh, D. *Proc. natn. Acad. Sci. U.S.A.* **80**, 3585-3559 (1983).
3. Rosenzweig, B., Liao, L. W. & Hirsh, D. *Nucleic Acids Res.* **11**, 4201-4209 (1983).
4. Rose, A. M., Harris, L. J., Mawji, N. & Morris, W. J. *Can. J. Biochem. Cell Biol.* (in the press).
5. Rose, A. M., Baillie, D. L., Candido, E. P. M., Beckenbach, K. A. & Nelson, D. *Molec. gen. Genet.* **188**, 286-291 (1982).
6. Emmons, S. W. & Yesner, L. *Cell* **36**, 599-605 (1984).
7. Snutch, T. P. & Baillie, D. L. *Can. J. Biochem. Cell Biol.* **61**, 480-487 (1983).
8. Flavell, A. J. & Ish-Horowicz, D. *Nature* **292**, 591-595 (1981).
9. Smith, G. E. & Summers, M. D. *Analyt. Biochem.* **109**, 123-129 (1980).

Sex and drugs . . . and science

John Treherne

Strong Medicine. By Arthur Hailey.
Michael Joseph with Souvenir Press/Doubleday: 1984.
Pp.430. £9.95, $16.95.

From the writer who brought to millions the glitter of *Hotel*, the drama of *Airport*, the intrigue of *The Moneychangers*, this immensely powerful novel takes the reader deep into the heart of the pharmaceutical industry where millions of dollars and millions of lives hang on every decision ... and into the heart and mind of an unforgettable woman.

THE manifest enthusiasm of Mr Hailey's publishers for his latest production even extends to sending a review copy to *Nature*. Evidently they hope to reach the hearts and minds of the scientific community, as well as selling the film rights. Their optimism is not entirely misplaced. There is widespread public and professional concern about the activities of international pharmaceutical companies; readers of the 9 August issue of this journal will recall Carl Djerassi's angry review of Gary Gereffi's book on the drugs industry and the Third World, under the headline "Making drugs (and soaking the poor?)".

There might be doubts about the depth of Mr Hailey's fictional study, but there can be none about the swiftness with which he grapples with his subject. In the Prologue we are "up forward in first class" on a Boeing 747 amidst caviare and champagne — next year (i.e. 1985). Eight lines down the first page, Celia de Grey, the international drugs tycoon, reminds her handsome, supportive husband, Dr (of medicine) Andrew Jordan, that *certain deaths may be drug-related*. Two pages later we are back in New Jersey in 1957. The harassed young Dr J. (attending the critically ill wife of a factory hand in a thunderstorm), gets very cross with Celia, the beautiful saleswoman from Felding-Roth Pharmaceuticals, who obligingly returns to the hospital with an untested drug called Letromycin. She rivets the doctor with blazing eyes and persuades him to administer Letromycin — and saves his patient. After this Celia never looks back: she is gratefully embraced by and, within another page, married to Dr J. ("a quiet civil wedding with a few close friends and relatives"); she persuades Felding-Roth *not* to market Thalidomide, has a baby, flings her weight about at sales conferences, has another baby and by 1963 is on the fast track at Felding-Roth.

The break-neck passage of time is signalled by the regular insertion of tense paragraphs seemingly culled from *Keesing's Contemporary Archives*. In 1972 ("The rock-music cult called 'Woodstock Nation' flared briefly, then burned out") Celia is despatched to Britain to nose out any local pharmacological talent. Between shopping trips to Harrods, she finds her way along Tennis Court Road to "Cambridge University's Biochemistry Building", there to seek the brilliant young Martin Peat-Smith who is in close pursuit of a memory-enhancing brain peptide, which, he hopes, will "perhaps eliminate mental ageing altogether". Celia is appalled by the gloomy squalor of what seems to be embarrassingly like a contemporary Cambridge research laboratory, is hardly mollified to be told that Fred Sanger once worked upstairs, but is much taken by Peat-Smith who is swiftly translated to the luxurious Felding-Roth laboratory at Harlow. There he gets to work to isolate Peptide 7, sacks the tight-lipped sadistic animal technician Gertrude Tilwick, seduces her beautiful replacement, Yvonne, and, eventually, Celia herself. There are quite a lot of spicy bits: Peptide 7 is not only an elixir but, it turns out, a powerful aphrodisiac *and*, apparently, a slimming agent.

Not surprisingly, Peptide 7 is an instant success; long lines form at pharmacy counters and Felding-Roth is well on the way to an increase in revenue of six hundred million dollars. Peat-Smith is elected to the Royal Society and there are rumours of a knighthood and a Nobel Prize. Meanwhile, Felding-Roth achieve another coup with Hexin W (a drug of rather vague pharmacological properties), the brainchild of the unpleasant Dr Vincent Lord who was very put out by the success of Peptide 7.

Unfortunately, Hexin W is discovered to have nasty side-effects and poor Celia (now the boss of Felding-Roth) is soon in trouble with the Federal Drug Administration and the persistent and unscrupulous Senator Donahue, who is intent on her destruction. Nevertheless, she manages a brief trans-Atlantic dash, next year (i.e. 1985), to witness Peat-Smith's investiture at Buckingham Palace. Yvonne (Lady Peat-Smith), looking lovelier than ever thanks to Peptide 7, is naturally very disappointed at not meeting Princess Diana, but excited by the prospect of Sir Martin's New-Blood post at Cambridge.

And that is where we came in, 400 pages before, with poor Celia returning to America to face the music. Will the Felding-Roth code of practice stand up to scrutiny by a Senate investigative committee?

Arthur Hailey's latest offering will doubtless help to relieve the tedium of many an uncritical hour up forward with caviare and back in economy class with a hamburger. Despite the cardboard characters and a strong-bronzed-arms-and-yielding-breasts approach, *Strong Medicine* does make the attempt to write about important issues in a surprisingly fair and even-handed fashion; for most readers it will probably constitute their only extensive reading on this matter of vital public concern. So we should, indeed, be grateful to the creator of Celia de Grey, Gertrude Tilwick, Peptide 7 and the nubile Lady Peat-Smith. ☐

John Treherne is University Reader and Honorary Director of the Agriculture and Food Research Council's Unit in the Department of Zoology, University of Cambridge. He is author of several novels, the most recent of which, The Trap, *will be published early next year by Jonathan Cape.*

Making scents

C.T. David

Chemical Ecology of Insects.
Edited by W.J. Bell and R.T. Cardé.
Chapman & Hall/Methuen: 1984.
Pp. 524. £30.

THE subject of chemical ecology embraces everything of ecological significance that is mediated in any way by olfaction or taste. It thus encompasses a vast amount of information and a great range of different behaviours. A full account of the area would be expected to include material about pheromones, about chemical influences on interactions with other organisms — the finding of plant and animal hosts by smell, for example, and in prey detection and predator avoidance — and also about reactions to other chemicals in the environment.

It would seem that any book which attempted to cover the effects of all of these semiochemicals would be superficial; but *Chemical Ecology of Insects* proves that need not be the case. The editors have provided us with a selection of detailed and interesting chapters — starting with mechanisms of chemoreception; leading on through odour dispersal, insect orientation mechanisms to distant odour sources, plant-host finding, plant-herbivore relations, predators and parasites, chemical protection (including a long chapter on mimicry which seems more to do with "visual" than with chemical ecology), and spacing and aggregation; and ending with chapters on the pheromones of bark beetles and social insects. The only serious omission is of a discussion of the relations of insects to vertebrates.

Such a range of material cannot be dealt with in detail here. So I will concentrate, quite invidiously, on one of the many good chapters in the book, and on the only bad feature.

Almost every other book covering insect pheromones discusses the maximum distance of effective pheromone communication on the basis of estimates of the time-averaged pheromone concentration at different distances downwind from the emitter, using three assumptions — that insects have a constant threshold for response to pheromone; that the response time of the insects is long compared to the time of passage past them of the turbulently dispersed puffs of pheromone; and that the wind direction is constant. All of these assumptions are wrong. In their chapter on odour dispersal, Elkington and Cardé give an excellent appraisal of the problem. They discuss the limits of time-average models, put forward other models, and assemble much experimental evidence to produce better ways of estimating the area from which insects might be attracted to an odour source.

The bad feature is the index. There are 324 entries only, quite inadequate for a book of this length. Publishers should not need to be told that ancillary features such as this make all the difference between a book being read and it being left untouched in the library. ☐

C.T. David is a Research Fellow in the Agriculture and Food Research Council's Insect Physiology Group, Imperial College at Silwood Park, Ascot, Berkshire.

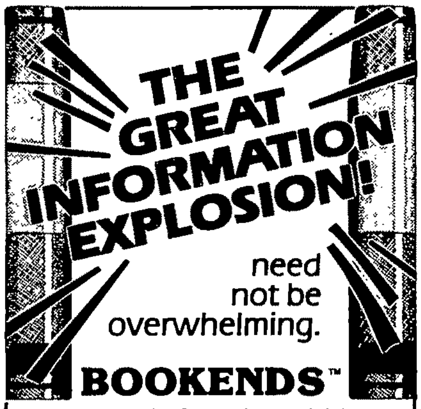

can prevent the frustration and delay which is otherwise inevitable when searching for elusive reference information in your bulging files. BOOKENDS lets you "put your finger" on specific information, articles, magazine or books almost instantly in your database. BOOKENDS lets you rearrange this data in virtually any configuration to create professional bibliographies. It edits like a word processor. It's the way of the Eighties to save, retrieve and format.

BOOKENDS™

The Reference Management Software System
is available for Apple computers for $124.95.

Apple is a trademark of Apple Computer, Inc.

Sensible Software, Inc.®
24011 Seneca, Oak Park, MI 48237
(313) 399-8877

Circle No.06 on Reader Service Card.

Political resources

Stephen Cotgrove

Development and the Environmental Crisis: Red or Green Alternatives?
By Michael Redclift.
Methuen: 1984. Pp. 149. Hbk £9.50, pbk £4.25.

WHAT is the connection between feminism, ecology and Marxism? And how, in association, might they save the environment of the underdeveloped world? It is these questions that Michael Redclift sets out to examine.

Marxists, however, have little to say about man's relations with nature — in general they see environmental problems as the outcome of the predatory and exploitative character of capitalism, and nature as an inexhaustible resource. So one wonders why Redclift spends so much of his short book exposing the inadequacies of Marxism. And while it is true that radical thinking and the emergence of new political parties has brought together an uneasy coalition of feminists, ecologists, anarchists and liberals in a search of an alternative to market-dominated, ecologically damaging and consumer-orientated industrialization, this book lacks an analysis of the constituencies from which such movements are drawn and their potential as bases from which political challenges may grow. It is a pity that the political dimension of environmental protection is explored within a somewhat partisan selection of political ideas.

Nevertheless we do need reminding that the environmental crisis is a global one and cannot be divorced from the conceptualization and analysis of development and the problems of the South. In his discussion of technology and the control of resources (Chapter 6), Redclift argues strongly that technologies are not politically neutral, either in their origins or consequences. The "Green Revolution" did not simply increase crop yields. It also

> redistributed income and wealth, materially affected land tenure institutions, introduced new marketing arrangements . . . and disrupted the ecology of natural resources [p.107].

Wealthy farmers who have access to credit and are better able to buy fertilizers and machinery flourish, and the gap between large and small farmers widens. By contrast, research in farming systems is intended to benefit those who employ their own resources and to increase yields without the same social consequences. Again, water technology

> provides opportunities for entrepreneurship which have important distributive consequences . . . In much of South Asia the control over water exercised by bureaucracies has enabled them to wield considerable political power [p.31].

The central lesson of *Development and the Environmental Crisis* is that protection of the remaining forests, and improvement in crop yields and in irrigation, are not simply technical questions which can be solved by conservation strategies. Both development and environmental protection are inextricably tied up with vested interests and the political and institutional arrangements which they support. But this book is unfortunately short on strategies which offer hope, and its style and organization tend to obscure the importance of the message. ☐

Stephen Cotgrove is Professor of Sociology at the University of Bath.

Questions of the Quaternary

D. Q. Bowen

Late-Quaternary Environments of the United States. Vol. 1 The Late Pleistocene, edited by Stephen C. Porter. Vol. 2 **The Holocene,** edited by H.E. Wright Jr.
University of Minnesota Press/Longman: 1984. Vol. 1 pp. 407, $45, £45. Vol. 2 pp. 277, $45, £45.

THESE two volumes arise from a series of meetings between American and Russian scientists, at Moscow and Baku (1976), New York and Salt Lake City (1978), and Irkutsk and Yakutsk (1980), sponsored by a co-operative agreement in environmental protection. Volume 1 covers the period 25,000 to 10,000 years ago, Vol. 2 10,000 years ago to the present. Both are subdivided into sections with specialist chapters.

To a large extent environments in the United States were climatically controlled by the Laurentide ice-sheet, not least during its decay. H.E. Wright Jr shows how the persisting ice, until 6,500 years ago in Labrador, may have caused increased seasonality in climate beyond its borders. Herein may be the explanation for the disharmonious faunas and floras of the late-glacial and early Holocene. Such increased seasonality and a picture of the time-transgressive response of natural systems to the forcing effect of climatic change (whereby the United States was transformed from a full glacial into a full interglacial state), form the background to the complex set of questions examined in the books. Here readers will be grateful to the editors for their helpful introductions.

Resolution of the issues, however, relies on adequate evidence and good-quality dating control. Almost inevitably, in a terrain as large and diverse as the United States, both will be uneven. Thus there is a contrast between the middle west — with its impressive isopol maps showing the development of Holocene vegetation (described here by Webb *et al.*) — and the west where detailed work on well-dated sites (Baker) is still required. The deficiency is remedied in part by the successful studies on packrat (*Neotoma*) middens (Spaulding *et al.*), though this work too needs to be extended beyond the south-west.

In a similar vein, the advance of montane ice is less well documented than that of the continental ice-sheet: in general the onset and decline of montane glaciation runs ahead of the continental ice-sheet, no doubt because of the lagged response of the latter to climatic change.

Of further importance in establishing time-transgressive events for use in climatic modelling are data showing falling pluvial lake levels some 13,000 years ago in the southern Basin and Range, but not until the end of the Pleistocene farther north (Smith and Street-Perrot). It is difficult to disagree with R.G. Barry in his call for the collection of even more accurately dated data as a prelude to realistic modelling of the contemporary atmosphere.

All will welcome the first major synthetic treatise on the Holocene — from the latest assembly of palaeoecological data on vegetational history (discussed, for example, by Heusser), at first colonizing, later in dynamic equilibrium and subsequently coping with a cooling which culminated in renewed montane glaciation (Burke and Birkland); to models of alluvial history reconciling vegetation and climate (Knox); to the pragmatic and careful evaluation of Kutzbach on climatic change; and to a review of archaeology (Aikens).

These two volumes follow in the tradition of *The Quaternary of the United States* (Princeton University Press, 1965). But times have changed. The books focus on the past 25,000 years only, a necessity arising from the vast array of data available, but also because of the relatively good dating controls available for that period. The restriction is also in part a response to the high level of sophistication now demanded of Quaternary data. This places the earlier Wisconsinan (last glaciation) and Last Interglacial in a somewhat depressing light, to say nothing of the Quaternary *terra incognita* before that time. Perhaps it will be one of the many triumphs of the present volumes that, as well as catalysing further work on the late Quaternary, they may focus some attention on the seemingly intractable problems of that earlier time — without the solution of such problems, the absence of a full explanation of the dynamics of atmospheric–oceanic–continental interaction through time will continue to frustrate full understanding of even the late Quaternary and the projection of its climatic trends to the future. Happily these new volumes will provide a visionary nudge forward along these highways. ☐

D.Q. Bowen is Professor of Physical Geography, The University College of Wales, Aberystwyth.

Alternative forms in bioenergetics

Hans V. Westerhoff

Physics of Bioenergetic Processes.
By L.A. Blumenfeld.
Springer-Verlag: 1984. Pp.132. DM 70, $27.20.

RATHER than writing a much-needed handbook on our knowledge of physics as applied to bioenergetics, Professor Blumenfeld claims that enzymic catalysis cannot be satisfactorily accounted for by the current principles of physical chemistry. He rejects the relevance of one of those principles — the Eyring equation — for enzyme reactions, as it assumes equilibrium between the transition state complex and substrate-plus-enzyme. Experimental evidence is reviewed indicating that shortly after undergoing a chemical transition from E to E^-, the conformation of an enzyme may still correspond to the equilibrium conformation of state E. Because this conformation generally does not correspond to the most stable conformation for state E^-, the enzyme will relax to a new conformation, E^{-*}. The transition state, says Blumenfeld, thus cannot be described as having an enzyme in a conformation defined by its chemical state. As an alternative, he proposes to describe conformational relaxation in mechanical terms.

In the usual — and quite successful — approach, the two states E^{-*} and E are just included as separate states in the description. It is characteristic of the book as a whole that Blumenfeld does not explain why such a treatment would fail.

The author also calculates that, for a gas engine of molecular dimensions, the information-energy needed to move the piston at zero rate would exceed the amount of work done. Thus molecular machines could not operate reversibly. Here, the flaw in the argument lies in the strictly mechanical interpretation of reversibility; reversibility merely implies that the ensemble (time) average of the piston movement is zero. Individual pistons may fluctuate rapidly. A similar snag is evident in Blumenfeld's alternative theory for energy transduction, which at the level of a single particle in a quantum mechanical box uses Newton's action = –reaction law.

The review sections in the book provide new information only where they describe results previously published in Russian. That information is useful, but it is clear that the *internal* inconsistencies in the chemiosmotic coupling theory suggested by Blumenfeld exist only in his interpretations of that theory. With respect to external inconsistencies, it is not news that the chemiosmotic theory does not survive all experimental tests.

Although slow conformational changes may prove to have a role in bioenergy transduction, Blumenfeld's assertion that already established physical chemical theories could not account for them is unconvincing. His alternative theory is even less so.

Hans V. Westerhoff is a visiting scientist at the National Institutes of Health, Bethesda, Maryland.

Selected theory

Mark Ridley

Conceptual Issues in Evolutionary Biology: An Anthology.
Edited by Elliott Sober.
MIT Press: 1984. Pp.725. Hbk $40, £38; pbk $19.95, £18.95.

WHAT is our modern philosophy of evolution? To judge from the generous, and, I think, representative selection of previously published works in Elliott Sober's anthology, it is mainly concerned with the "designful" properties of organisms — their adaptations — and with Darwin's explanation of adaptation, natural selection.

The most damaging philosophical criticism of Darwin's theory is that it does not explain adaptation at all. Natural selection, in Spencer's form, "the survival of the fittest", has often been said to be a circular argument; but all the relevant authors in this anthology would disagree. The point is here most clearly made by Gould. "Fitness" has two meanings: the number of offspring on average left by a type, and how well designed, in the engineer's sense, the type is. The fitness of an eye can be considered optically as well as reproductively, and in Darwin's theory the latter is the cause (but not the criterion) of the former. If anything, I found five papers spread through 80 pages too large a dinner, but this is the one part of a subject, often criticized for its interminable and sterile controversies, on which all the professionals now agree. Let us indulge the celebration.

If natural selection does explain adaptation, we can proceed to three more questions. For the benefit of what kind of entities does natural selection produce adaptations? How well adapted are those entities? What kind of explanation is it? Now the disagreement begins. The first question is professionally phrased as "What is the unit of selection?". The main answers on offer are the gene, the organism and the group; and the main controversy concerns Williams and Dawkins's argument in favour of the gene. Fifteen pages of Dawkins (no Williams) stand against 95 from Gould, Lewontin, Sober and Wimsatt who variously argue for selection at "higher levels"; but unfortunately the main arguments for Williams and Dawkins's position are nowhere explained. The Dawkins paper (on the "extended phenotype") aims to extend, rather than defend, his case, and his critics, although they describe (sometimes even fairly) the theory they oppose, do not pause to expound it.

The argument, in condensed form, is this. The unit of selection will be, in a sense, the unit of heritability, because natural selection cannot act on non-heritable entities. Organisms are not inherited, because they die; "higher genetic levels" are not inherited, because they are broken and recombined: the unit of heritability will be something smaller, which Williams and Dawkins have chosen to call (and *define* as) the gene. If, in the kind of complex situations that Wimsatt, Sober and Lewontin discuss, that unit is longer than a cistron, then the gene (in Williams and Dawkins's sense) is longer than a cistron too.

In practice, however, Williams and Dawkins do not apply their argument to the problems of population genetics, but use it to think about what kind of adaptations will be favoured in particular environments. That application is strictly circumscribed. Williams and Dawkins have not been trying to explain everything in biology solely in terms of genes. Wimsatt, however, directs his criticism against a hopelessly ambitious theory of genic selection, which he has practically pumped up into *ex DNA omnia*:

> T2: (Dynamical thesis): Processes at the genetic level determine (and are the primary and ultimate) explanations for processes at all higher levels.

It is quite easy to make mincemeat of this, especially if "genetic level" is identified with a single genic locus. Wimsatt only needs to argue "that understanding evolutionary processes requires the invocation of causal mechanisms and nomic regularities" concerning things other than genes, for his work of destruction, against T2, to succeed. Against Williams and Dawkins, however, he is rather wide of the mark.

Actually, because genes are propagated in sets by the thousand through organismic agency, the selection of genes often produces organismic adaptations. There is broad agreement that organismal (rather than genic or group) adaptation is common, the disagreement being mainly about whether organismal adaptation is caused by the selection of genes or "higher levels". But either way we can ask how important the theory of natural selection is by asking how well adapted organisms are. If adaptation is uncommon, and imperfect, natural selection may remain its proper explanation, but will be unimportant. The five authors here (Lewontin, Gould, Oster, E.O. Wilson, Maynard Smith) all agree that organisms are only imperfectly adapted, because the range of genetic variation available for selection is limited. The argument is strong, and not (so far as I know) doubted by anyone; which is only unfortunate for Lewontin and Gould, who would discover an orthodoxy of "adaptationists" (all of whom believe organisms to be perfectly adapted), portray them in caricature, and analyse them with Marxist absurdities.

Sober remarks in his preface that it is difficult to distinguish the science from the philosophy in this anthology. For the most part I would agree; but only for the most part. In the sections that discuss whether theories are true, the science is indeed generally indistinguishable from the philosophy, and there are numerous scientific authors. The distinction could be made; but only superficially, by language and style (I could not help noticing the philosophers are more long-winded than scientists, but perhaps that is only the selection). Two sections, however, deal not with the validity, but with the nature, of theories — these are on functional explanation (teleology) and the reduction (or not) of Mendelian principles to molecular genetics — and they are entirely written by philosophers. Only, it would seem, when philosophical argument is used to criticize theories do scientists become seriously interested.

The final section takes leave from the theory of natural selection. Mayr, and Sokal and Crovello, discuss the nature of species — whether reproductively ("biologically") or phenetically defined — and Hennig, Hull, Felsenstein and Farris discuss the three main schools of classification.

I often wonder who buys these anthologies. They are usually too expensive for individuals; but why on earth should a library buy a selection of papers it already possesses? I think *Conceptual Issues in Evolutionary Biology* may be an exception. Most of its contents originally appeared in philosophical journals that are not subscribed to by biological libraries: but they should all interest biologists who enjoy thinking about the theory of evolution. And every biological library in the world, I hope, eagerly serves that species of reader.

Mark Ridley is Astor Junior Research Fellow of New College, University of Oxford, and author of The Explanation of Organic Diversity *(Oxford University Press, 1983).*

Keeping cool

H.M. Rosenberg

Matter at Low Temperatures.
By P.V.E. McClintock, D.J. Meredith and J.K. Wigmore.
Blackie: 1984. Pp.258. Hbk £19.75; pbk £10.25.

IT IS time that we had a new introduction to low temperature physics, and this book fits the bill very satisfactorily. Each of the three authors is well-schooled in the cryo-arts and together they have produced a unified text in decent English, with the occasional felicitous turn of phrase that made me pause and smile.

The book assumes a background of undergraduate physics, but the first three chapters gently remind the older reader of certain essentials. For the final-year undergraduate and the beginning graduate student (by whom the book will probably be most used) they will act as a useful revision.

The authors begin by introducing the general principles of low temperature physics, with particular emphasis on the third law of thermodynamics, the effects of zero point energy and macroscopic quantization. The next two chapters deal with lattice vibrations and electrons, respectively, and in each case the differences between the behaviour of crystalline and of amorphous materials is well brought out. The meat of the book comes next in accounts of superconductivity, liquid helium 4 and liquid helium 3 (including the properties of mixtures of ^{3}He and ^{4}He). In each case a simple phenomenological introduction is given as well as an outline of the current theory—with ample references for those who need a more detailed theoretical treatment. The final section of each of these chapters attempts to bring the reader up to date (to 1983) with developments in the most recent fields of interest—the properties of one-dimensional conductors and the search for other boson and fermion fluids.

The last two chapters cover more practical matters. Chapter 7 gives a good outline of experimental methods — ^{4}He and ^{3}He cryostat design, the dilution refrigerator, magnetic and Pomeranchuk cooling — and there is a helpful discussion on thermometry for various purposes. Finally, the authors turn to the applications of low temperature physics, the major emphasis, of course, being on superconductivity (high field electromagnets, the application of Josephson effects in computer elements, squids and other devices). This concluding chapter ends with a brief account of the uses of liquified gases themselves, including the interesting application of superfluid ^{4}He as a couplant in the acoustic microscope and as a non-reacting surface in the neutron bottle.

All in all, this is a good useful text. Not only that, it is enjoyable to read—an unusual and refreshing attribute. □

H.M. Rosenberg is Reader in Physics at the Clarendon Laboratory, University of Oxford, and a Fellow of St Catherine's College.

New in paperback: Jonathan Slack's *From Egg to Embryo* published by Cambridge University Press, price £9.95, $24.95. For review see *Nature* **306**, 294 (1983).

New for neuroscience

With the meeting of the American Society for Neurosciences this week, we feature a range of products to interest the neurosciences expert, including a new assay for monitoring tricyclic antidepressants.

● A new HPLC assay that monitors the five major tricyclic antidepressants and active metabolites simultaneously in serum or plasma has been introduced by Waters Associates. The Waters HPLC assay of the tricyclic antidepressants (TCAs) simultaneously monitors amitriptyline, imipramine, desipramine, nortriptyline, doxepin and their clinically relevant metabolites in the same assay without cross reactivity. The assay has been evaluated for interference, correlation with GC and linearity and takes just 12 minutes. Full documentation is provided in a method book. The TCA Assay was designed for Waters QA-1 Analyzer, an HPLC system providing convenient push-button operation. With the same instrument, technicians can perform assays of other psychotropic agents such as tetracyclics, butyrophenones, phenothiazines, benzodiazepines and other therapeutic drugs.
Circle No. 100 on Reader Service Card.

● The recent 'hole-poke' program developed for Columbus Instruments animal activity meters, monitors simultaneously eight animal cages equipped with "hole-poke" boards. Each time an animal pokes its nose into one of the 16 holes located in the cage's floor, it interrupts two crossing infrared beams. Information about interruption is decoded by the Apple III computer which keeps track of the number of pokes in each hole, the time an animal spent with its nose in the particular hole, as well as totalized number of pokes and time spent "poking" for each animal cage. The "hole-poking" method is an established procedure for testing an animal's exploratory behaviour, a valuable indication of animal brain functions. Information collected by an Apple II computer is periodically printed and stored on the disc. The same system can be used to monitor animal feeding activity with feeders (food dishes) located underneath a "holed" floor. When monitoring animals' feeding, computer results will correspond to numbers of visits to the feeders and time spent eating. Animal food preferences are easily established from computer records. "Hole-poke" systems can be applied in neurotoxicology, experimental psychology, development of new drugs, as well as studying nutrition. Other Apple II computer programs from Columbus Instruments allow plotting of animal's movements, number of rearings, animal rotational behaviour and separation of stereotypic from ambulatory activity.
Circle No. 101 on Reader Service Card.

● LDC/Milton Roy is pleased to announce a new interface package for the CI-10 computing integrator to an Apple II or Apple IIe computer. The new interface allows all CI-10 functions to be accessible from the Apple Keyboard. In addition, any CI-10 file (slice files, peak files or method files) can be loaded from the CI-10 to the Apple for further data manipulation or enhancement by the Apple. This additional capability of the LDC/Milton Roy CI-10 is designed for ease of use and provides the user with an independent chromatography integration channel for the Apple computer. Up to 15 CI-10 computing integrators can be networked from one IEEE board.
Circle No. 102 on Reader Service Card.

● Two new models in its 700 Series laboratory XY recorder are being introduced by Allen Datagraph, Inc. Model 720 offers eleven ranges in X and Y and accepts Option 30, which provides digital control of the recorder and annotation of plots. Model 725 has eleven ranges plus a built-in time base. These new models extend the usefulness of the basic XY recorder in OEM and laboratory applications. The 700 Series' standard features include Pad-load paper supply, DC servo operation, sealed feed back potentiometers and low drift circuitry. These recorders offer fibre-tip pens, optional carrying case, English or metric calibration and a digital interface option.
Circle No. 103 on Reader Service Card.

● Wheaton Instruments announces the new Wheaton Biostir low profile heavy duty magnetic stirrer designed for use with Wheaton Celstir suspension culture flasks; it will accept one vessel up to 8 litres in size. The solid state speed control provides a speed range of 25 to 350 r.p.m. even with wide fluctuation in line voltage. The unit features a powerful alnico magnet for increased efficiency and the low profile cabinet conserves incubator space. For added protection, the circuit board has been coated with a special sealant so that the Biostir low profile stirrer can be used in high humidity incubators.
Circle No. 104 on Reader Service Card.

● Scientific Systems, Inc., now offers a pneumatically-actuated version of its 3XL Injection Valve, designed to permit automated and manual use of the valve. Available for both internal and external loop operation, the pneumatically-actuated 3XL provides load-to-inject times of 1/10 second at 50 psi. On the internal loop version, switching from one sample loop to another takes only 15 seconds. The valve has several unique design features that maximize efficiency. A straight flow path from the sample loop to the column prevents sample flow disruption and maintains a more symmetrical and efficient peak shape. To minimize band dispersion, the 3XL allows direct coupling of standard size columns to the valve. An event marker aids data handling.
Circle No. 105 on Reader Service Card.

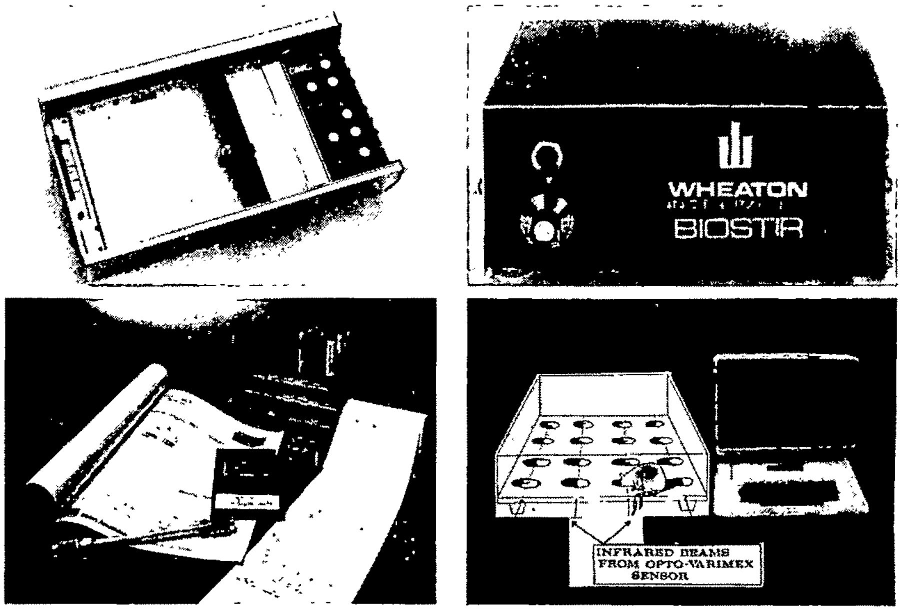

Allen Datagraph Model 720 recorder (top left), Wheaton Instruments' Magnetic Stirrer (top right), Waters' HPLC assay for monitoring antidepressants (bottom right) and 'hole-poke' program for monitoring animal behaviour from Columbus Instruments (bottom right).

● Dekasol from ICN Biomedicals Inc. is a powerful concentrated solution formulated for the rapid control of radioactive contamination. Dekasol removes radioactive particles from surfaces by a two-way action. It will sequester metallic ions which contaminate surfaces, and, because of its high detergent action, will lift and suspend contamination particles. The contamination is then easily rinsed away with water. For routine use, Dekasol is diluted 20 to 50 fold and can be used on virtually any type of surface; it is mild enough to be used on skin.
Circle No. 106 on Reader Service Card.

1-1-57
A. Bates

● A new patch clamp stimulator is now available from the Medical Systems Corporation. This unit, model S-100, is a low-noise pulse generator which is specifically designed for use with extra cellular patch clamps. When functioning as a stimulator, the S-100 provides voltage pulses (jumps) to the patch membrane. These same pulses can also be used as test pulses to measure the resistance of the patch pipette. The S-100 can be operated in a "free running" mode, in which it provides repetitive pulses to the patch; or in a "single shot" mode, in which it is triggered manually or externally. The output pulses of the S-100 are always paired and the first and the second pulse have independently adjustable magnitude and duration. Both unipolar and bipolar output pulses are available. The Model S-100 also functions as a simulator of single channel activity with a pseudo-random channel generator included for control and simulation of patch activity. Medical Systems Corporation is a specialist in the development and marketing of instruments used in electrophysiology.
Circle No. 107 on Reader Service Card.

ADVERTISEMENTS

PHORBOL ESTERS
TOOLS FOR CELL BIOLOGY AND CANCER RESEARCH

LC SERVICES CORPORATION
165 New Boston Street
Woburn MA 01801
(617) 938-1700

Circle No. 27 on Reader Service Card.

AUTHORS WANTED BY N.Y. PUBLISHER

A well-known New York subsidy book publisher is searching for manuscripts worthy of publication. Fiction, non-fiction, poetry, juveniles, travel, scientific, specialized and even controversial subjects will be considered. If you have a book-length manuscript ready for publication (or are still working on it), and would like more information and a free booklet, please write:

Vantage Press, Dept. D-69
516 W. 34th St., New York, N.Y. 10001

Circle No. 28 on Reader Service Card.

World Precision Instruments' Series 10000 micromanipulator (left) and Dekasol solution for the control of radioactive contamination from ICN.

● From World Precision Instruments Inc. the Model DVC1000 Dual Voltage clamp provides continuous measurement of the transepithelial currents while voltage clamping two separate membranes (one membrane as a control and the second membrane as the test material) at zero volts or at a preset voltage difference. This procedure allows the study of membrane permeability and ion transport under different experimental conditions.
Circle No. 108 on Reader Service Card.

● Hydraulic coupling of the fine control on World Precision Instrument Inc.'s new Series 10000 micromanipulators virtually eliminates vibration associated with touching the micromanipulator during adjustment. Hydraulic movements feature backlash-free operation and typically exhibit drift of less than 1 micron in a twenty-four hour period. Model 10000 can be fitted with one, two, or three hydraulic movements and offers 0.2 micron resolution for fine control. Coarse adjustment is manually controlled and has a resolution of 0.1 mm. Model 10,000 micromanipulators with hydraulic drives are available in right and left-handed versions and are supplied ready to use.
Circle No. 109 on Reader Service Card.

● The new Series 200 X-Y Recorder, featuring Houston Instrument's patented capacitance rebalance position transducer, operates without the friction and electrical noise associated with slide-wire potentiometers. The Series 200 performs with high speed and accuracy and can meet the needs of both educational and industrial users, with applications ranging from materials testing to compound analysis. By flipping a switch, users may select one of eleven input ranges on pen (Y) and beam (X) axis, starting at 1mV/inch, or one of eight beam (X axis) speed levels, ranging from 200 seconds/inch to 1 second/inch. A slew rate of more than 30 inches/second ensures high fidelity recording of test and measurement data.
Circle No. 110 on Reader Service Card.

● The Multipoint Recorder/Logger (MRL) from the Esterline Angus Instrument Corporation provides analog trend recording, digital (alphanumeric) data logging or a combination of both and a comprehensive choice of user-programmable performance functions offered in a multipoint recorder/logger. Simplified, programming is accomplished through a colour-coded panel keyboard. Programmable features include: mode of operation, chart speed, scan interval, peak or valley detection, printout/output time, scale limits, engineering units, real time clock and calendar, and three alarm setpoints per channel in standard or failsafe mode.
Circle No. 111 on Reader Service Card.

● A new microprocessor controlled osmometer, the Multi-Osmette from Precision Systems, performs freezing point determinations of osmolality on up to 24 samples. The new instrument accepts micro samples in disposable plastic tubes, calibrates automatically, makes the determination of osmolality, and with an optional printer, provides a fully annotated record for each sample. The complete cycle is activated by a single button. Automatic processing of multiple samples can free as much as an hour of technician's time, and a printed record eliminates questions of identification of results; use of inexpensive disposable plastic sample tubes eliminates the problems of glassware washing and breakage. When stat determinations are required, the automatic cycle can be interrupted. One or more stat samples can be introduced and run, after which the autocycle is resumed. Operation of the automatic sampler changer is simple, with easy operation for single samples when desired.
Circle No. 112 on Reader Service Card.

These notes are based on information provided by the manufacturers. For further details circle the appropriate numbers on the Reader Service Card bound inside the journal.

nature

21-1-87
A. Datta

A council ripe for abolition

The British research council with responsibility for the natural environment could with profit be dismembered into smaller pieces.

THOSE who read the account of the collapse of the British Geological Survey's reason for existence on p.499 should prudently also refer to last week's complaint of maladministration at the Science and Engineering Research Council (*Nature* 4 October, p.397) and to the opinion expressed two months ago (*Nature* 26 July, p.261) that the British research enterprise is either bankrupt or about to become so. The circumstance in which an organization employing 1,000 professional geologists should be compelled, at least during the present financial year, to reduce to one-third its geological surveying is a scandal by any standards. If resources had been wasted on such a scale by a joint-stock company, and if they had been measurable in money terms, the people responsible would have been sacked. Because, in this case, the waste can be assessed only intangibly, by the frustration and disappointment of those concerned, by the lack of what they might have done and by the contagious effects of their sunken morale on other professional people, there is every likelihood that under the British system, the villains responsible will still be mentioned in future lists of public honours.

The origins of the scandal are clear. The Geological Survey of Britain began work in 1835, a short while after the Reform Bill of 1832 and a full three decades before *Nature* began appearing every week. For most of its history, the survey was administratively untouched, but in the early 1960s, what with the rhetoric of Mr Aneurin Bevan (since dead) on the need for a thorough exploration of what lies beneath Britain, and the fashionable preoccupation with tidiness, it was inevitable that a government committee (under the late Sir Graham Sutton) should advocate setting up a research council concerned with the natural environment. The original idea was that the council should bring together the old geological survey, the Meteorological Office and various bits and pieces so as to forge an entirely novel instrument for multi-interdisciplinary investigation of the natural world, straddling ecology, the oceans and the atmosphere (not to mention the pollution thereof) as well as the solid Earth.

The Natural Environment Research Council (NERC) was already in a sense a failure when it came into being in 1967. The Meteorological Office had used its influence with the defence departments to opt out, with the result that the geological survey was the largest operational function with which NERC was involved. For many years, the new council did its best to combat the then expansionist tendencies of the geological survey (renamed for a time the Institute of Geological Sciences). Since the British Government's enthusiastic but uncomprehending adoption of the Rothschild recipe for the organization of civil science in 1973, the council has steadily won that battle.

Starting with the Rothschild precedent that government departments should pay for research they find worthwhile, NERC has sent the British Geological Survey (BGS) out into the market place, bidding for whatever odd jobs oil companies and minerals companies have wanted done. Nobody has ever examined the propriety of the accounting principles on which BGS has been able to win this business while still enjoying overhead support from NERC. The conflicts of interest that must arise when an agency whose prime function is to compile a public data bank (a geological survey) is also compelled to do jobs for private companies in return for cash have not been considered seriously. And NERC seems never to have asked the broader question whether a country such as Britain needs a geological survey (the answer must be yes) and, if so, how it should be managed.

For those concerned, there are inevitably extenuating circumstances. NERC, from the outset fearful that one of its operational tails (the geological survey) would wag the dog (itself), and distract it from the general support of the Earth sciences, has consistently and properly been seeking to quarry more funds from its budget for the support of academic science. The survey, on the other hand, has fought hard and often arrogantly in defence of its unspecific goal of mapping the subsurface of the United Kingdom in a manner and to a timetable of which it is the principal arbiter. The trouble, for NERC, is that much else of its business is organized into independently operational units, but without clear objectives of what the operations are intended to achieve by when. There is, for example, a British Antarctic Survey (with a post-Falklands doubled budget), an Institute of Oceanography lacking formal connections with academic oceanographic research and an Institute of Terrestrial Ecology whose work (mostly good) is more easily described than its function understood. NERC has been beastly about the annual budget to all these organizations, no doubt winning other false economies like those effected at BGS. But NERC's failure to bring about a radically different pattern after nearly twenty years, exacerbated by the government's failure to recruit a full-term successor to Sir Hermann Bondi as NERC's chairman, points to a simpler solution.

Why not simply disband the Natural Environment Research Council, finding more suitable homes for the laboratories in its charge? That task should not be nearly as formidable as it seems. The geological survey is necessary and could be continued securely if it were the principal responsibility of a ministry, probably the Department of the Environment. The Institute of Oceanography should be integrated with academic research, while the ecology institute (three laboratories) should become the research arm of the Nature Conservancy Council (which, once, some parts of it were). It is not altogether a joke to argue that the British Antarctic Survey might go to the Foreign and Commonwealth Office.

Reorganizations such as these are no doubt more easily carried out with scissors and paste than on the ground but, for NERC and its masters, there seems no alternative to making the attempt. There is, however, a serious difficulty — what should be done with NERC's small but slowly-growing support for academic science? The obvious solution is to transfer this important rump to the Science and Engineering Council (SERC). The obvious snag is that SERC is not immune from precisely the kinds of troubles that afflict NERC, and is in any case already so huge that it dominates the whole British system for the support of civil science. Transferring responsibilities elsewhere (biology to the Medical Research Council, engineering to a new council as British engineers are forever asking) would not suffice. Transferring SERC's central facilities intended for university use to some trust that would use them on a European footing would be the ideal, but would not easily be traded off against the right of access to comparable facilities elsewhere. But while both NERC and SERC are in need of radical change (dismemberment and reform for the sake of flexibility respectively) the present is as good an opportunity as any to attempt this task.

Australia's problem

Mr Bob Hawke's government must be positive about its support for research.

AUSTRALIA'S Labor Government has chosen the oddest way in which to prepare for the impending election, most probably in December. During two years of office, Mr Bob Hawke and his colleagues have been more or less committed to the view that Australia needs to make a special effort in industrial innovation if it is to be successfully dragged into the modern world. The prophet of change has been Mr Barry Jones, minister of science and technology in Mr Hawke's government, whose book *Sleepers, Wake!* has indeed stirred many Australians from their contentment. So why is it that in Mr Hawke's pre-election budget, published just over a month ago (see *Nature* 4 October, p.405) Mr Jones's department has fared worse than any other? The cash increase does not match inflation, so that the resources available will actually be reduced. So what will happen now, both to Mr Jones and to his policy?

Australia, with a population half that of California, is economically the victim of its rich natural resources. For decades, Australians have been arguing the toss about the efforts they should make to add value to the primary products, in agriculture and minerals, which as exports have bought modest prosperity for what used to be the most successful practitioners of Western ways in the South and West Pacific. The standard political response has been to restrict overseas investment in Australian primary production, and to protect Australian manufacturing industry (which has never seriously caught on) from outside competition. Mr Jones's tract was meant as a plea for more adventurous initiatives. Why not recognize that the world is changing, and becoming more dependent on the self-conscious application of technology? Why not put the country's sophisticated technical community to better use, both by means of links with novel industries but even in traditional fields such as agriculture (as by the self-conscious encouragement of biotechnology)? And why not (because there is no choice) confess that Australia must make its way in the world in partnership and competition with the other economies of the Pacific basin, which include Japan as well as California?

While some of Mr Jones's tub-thumping has occasionally been naive, it is a shame that he has not been listened to more attentively, both by his colleagues in the government and by the technical community. The trouble with Australia, whatever the political labels its governments may be wearing, is that it is deeply conservative. (Changing governments is permissible, but changing the ways in which people earn their livings is something else.) This cast of mind is reflected in the pattern of Australia's research effort, which is substantial (for a primary producer). The Commonwealth Scientific and Industrial Research Organization (CSIRO) is eminently suited to the improvement of traditional agriculture and the more effective exploration for minerals (with substantial side-interests in such fields as solar energy), but is so heavily institutionalized that it cannot be the radical force that radical Mr Jones has been looking for. During his spell in office, Mr Jones has done his best to loosen the bonds of Australian self-satisfaction, and there have been some signs of success. But these do not amount to the radical change for which Mr Jones has been working.

What will happen next is anybody's guess. Mr Hawke may not be re-elected, in which case Mr Jones's ambition will for a time be forgotten, but that is not what the pollsters say. In the hope of salvaging something from the disappointments on the technical front during the past two years, it is reported that Mr Hawke is planning a great administrative initiative — some kind of super-ministry that will unite the Australian Government's responsibilities for research and for the support of industry. That will be a strictly cosmetic device, and one that must be meaningless on the eve of an election. It would be more profitable for Australia and for the present government, even at this late hour, if Mr Hawke and Mr Jones could work out a less negative plan than that implicit in the budget, whose objective seems to be to teach the technical community a lesson the hard way — cutting back on resources through existing channels with the unrealistic objective of forcing people into partnership with an industrial sector notoriously unwilling to spend resources on research. The government is right not to try to back winners in a horse-race not yet devised, but wrong to think it can conjure industrial support of research simply by cutting back on what it spends itself. Far better, in reality, to embark on selective support for imaginative work at the universities and CSIRO institutes, so providing a showcase of what may already be available. A sum of money not much greater than the \$A30 million set aside for the defence of the America's Cup would go a long way to help. □

Conservation cheers

The tide is running in favour of British conservation.

THE British conservation movement, a little to everybody's surprise (its own included) is in good spirits. So much is clear from the tone of the tenth annual report of the Nature Conservancy Council (published on Tuesday), which gives an account of a frustrating year without undue wringing of the hands. Evidently the council's confidence has been reinforced by what others active in the field have been saying. The House of Lords committee which a few months ago pointed to the conflict of interest between agriculture and conservation, and asked that it should be redressed, has been good for people's morale. The Countryside Commission, like the Nature Conservancy Council a statutory body with formal functions defined by the Countryside Act (1981), has also been strong and sensible about the importance of the appearance of landscapes of all kinds. Already the council appears to have forgotten last year's rows, when the then chairman found that the government's refusal to renew his appointment did not excuse him from his duty to support an agriculture minister in a confrontation with farmers angry that ploughing a marsh in Somerset might be forbidden.

The most astounding development, however, is the noises being made by the National Farmers' Union, hitherto hot-gospellers of hedgerow destruction (with financial help from the British Government), contour violation by access roads (again grant-aided in the hill regions that are most easily damaged) and the replacement of traditional buildings by metallic barns designed to be seen from as far away as possible. The union's officials are now talking about the need to abate the rush for farm production by some consideration for conservation. Even if, as may be possible, the farmers have not repented of their ways but have merely calculated that it will be the worse for them if they alienate all countrygoers, the development has been a heartening surprise. The danger now is that people will be lulled into complacency.

One obvious trap stands out from the Nature Conservancy Council's report, which repeats the now familiar tale of its difficulties in administering the section of the Countryside Act allowing the designation of "Sites of Special Scientific Interest". When properly designated, sites cannot be altered radically by their owners (who may nevertheless have to be compensated for income forgone, or even bought out). The practical difficulty is that the council, with its small staff, cannot cover the ground as quickly as it wishes or as prudence requires. In the three years since the act became law, a third of 4,000 sites have been dealt with, but those remaining include some of the hardest cases. The council is now complaining of loopholes in the law, but it should seriously consider whether it should not restrain its ambitions for notifying so many sites. It has other powers (to protect species or create nature reserves) which might often serve the same purpose. If the tide of opinion is flowing in the right direction, there is less need to hurry. And it is asking for trouble to urge, as in this week's report, that there should be nationally agreed percentages of consumption of temperate foodstuffs to serve as permanent targets for the farming community. □

Genetic manipulation

Rifkin strikes against gene transfer experiments

Washington

ANTI-genetic engineering activist Jeremy Rifkin once again thrust recombinant DNA research in the United States under the spotlight of national attention last week. Rifkin's lobbying organization, the Foundation on Economic Trends, together with the Humane Society of the United States, has filed a suit in the district court here to halt gene-transfer experiments being carried out in livestock by the US Department of Agriculture (USDA). The plaintiffs allege that the experiments are a violation of the ethical canons of civilization and represent a new form of cruelty to animals.

Don't say Rifkin AND Hollywood didn't warn you....

The experiments entail injecting fusion genes that include the DNA structural sequence of the human growth hormone into the fertilized eggs of sheep and pigs. When similar experiments are done with mice, some of the resulting animals express the human gene, and so grow larger and faster than normal mice (see *Science* **222**, 809; 1983). The new work is a collaborative effort between Dr Ralph Brinster of the University of Pennsylvania Veterinary School and a group under Dr Vernon Pursel at USDA's agricultural research centre at Beltsville, Maryland.

While the human origin of the growth hormone sequence doubtless added to the public's fascination, Rifkin makes clear that his objects apply to transferring any foreign genetic material into the germ line of a species. It would be morally objectionable to transfer animal genes to humans, Rifkin says, and it is similarly objectionable to transfer human genes to animals. Furthermore, the biological stability of the species would be threatened if farmers switched in large numbers to "super animals" containing genes from other species. Rifkin believes there would be undesirable economic and evironmental consequences of the general use of genetically engineered livestock, with small farmers being forced out of the market and higher prices being passed on to the consumer. The Humane Society of the United States argues that physiological imbalances in genetically engineered animals would cause suffering.

Brinster, evidently feeling besieged, was trying to avoid the press last week, but wants the public to understand the possible benefits from the research. Apart from the prospect of better and cheaper meat and other animal products, gene transfer experiments hold great potential for cancer research, especially with Leder's recent demonstration that transgenic animals can inherit a propensity for particular cancers.

The human growth hormone sequence was used simply because it is well studied and is easier to detect in mice than the rat sequence originally used (see *Nature* **300**, 611; 1982). Despite the difficulties of working with opaque eggs, the livestock system is working well. Brinster declines, however, to discuss preliminary findings until definitive results are ready for publication. So far "several hundred" eggs have been injected with the growth hormone fusion gene; if successful, the experiments will allow further work on the processing of gene products, because livestock animals provide larger tissue samples than mice.

USDA officials concede that Rifkin's challenge will probably be pursued by the court, but they have not yet studied the litigation in detail. Whichever side loses in the first round of the action is certain to appeal, and the case could drag on for a long time.

The three causes of action cited by the plantiffs refer to the creation of federal common law nuisance and violations of the National Environmental Policy Act and the Administrative Procedure Act. In essence, the claim is that USDA's animal breeding programme is at odds with policies approved by Congress in other areas, and that USDA has not adequately considered other strategies or the impacts of its programmes. Rifkin is also trying to introduce an amendment to the guidelines used by the Recombinant DNA Advisory Committee of the National Institutes of Health, which would restrict research in the area and which due to be discussed later this month. In the meantime, the research continues. **Tim Beardsley**

Dutch universities

Small print conceals more cuts

THE Dutch universities will feel the pinch again next year, despite ministry of education figures that make it appear that university research spending has increased substantially. The ministry has achieved this sleight of hand by recalculating the time a university teacher spends on research.

In the 1970s, the ministry assumed that natural scientists in the Netherlands spent 36 per cent of their time on research — and their salaries were debited from the research budget in proportion. In 1985, however, the assumption will be very different; research time is estimated to be 44 per cent of duties on average, varying from 18 per cent in academic hospitals to 61 per cent in mathematics.

The result in the nominal university science budget is that what appears to be an increase, from Dfl 1,452 million (£341 million) in 1984 to Dfl 1,796 million (£418 million) in 1985, is actually a decrease in real terms. If the budget is calculated using the 36 per cent research time figure, and compared at constant prices with the 1980 figures, it appears that the 1983 budget was just 93 per cent of the 1980 figure, the 1984 budget 92 per cent and next year down to 91 per cent. Of course the new calculations (which put the 1985 university research figure at 114 per cent of that in 1980, at constant prices) do not make more money available to research, and by raising the apparent budget make it more vulnerable to the threat of cuts at cabinet level. However, the re-calculation was merely for administrative convenience, and not a policy matter, a government spokesman said last week. The new research-time figures are based on careful surveys of what Dutch researchers actually do, and are not pulled out of a hat. Interestingly, though, they conflict with lower fractions generally assumed in other countries. In Britain, for instance, the University Grants Committee estimates research time to be just over 30 per cent of duties. **Robert Walgate**

- Total Dutch spending on research and development will increase slightly next year to Dfl 8,132 million (£1,890 million), according to recent government predictions. Government spending will be Dfl 3,882 million (£903 million), a slightly lower fraction of the Gross National Product (GNP) (0.97 per cent) than last year (0.98 per cent), but still larger than in the years 1980-83 (0.90-0.93 per cent). Industry will spend Dfl 3,800 million (£884 million), the government estimates, and another Dfl 450 million (£105 million) will go to international projects.

Dutch research spending is therefore below the European Economic Community average as a fraction of GNP, but only 3 per cent of the Dutch research and development budget is spent on defence. This compares with 33 per cent in France. **Casper Schuuring**

French medical institutes

Twelve-year rule begins to bite

THE French medical research council, INSERM, is approaching its twentieth anniversary — and a time of testing. A government attempt to stop ageing laboratory directors sleeping at their posts, known as the "12-year rule", takes effect next year — when all who have been directors for 12 years or more must resign. Thus 60 out of 250 INSERM directors must go or reapply, which may explain why protests over the "bureaucratic" rule have been more bitter at INSERM than at any other French research council affected.

At the Centre National de la Recherche Scientifique (CNRS), for example, there has been little resistance — perhaps because, despite its size and age, CNRS has only 50 directors affected by the rule. This is attributable to physicists who often change directorships voluntarily before the 12 years are up, and to biologists who have been applying a policy of group concentration and reorganization, thus anticipating directorship problems. Altogether, CNRS seems naturally to have shown more of the flexibility that the 12-year rule is intended to encourage.

Flexibility will come, even at INSERM. Director-general Philippe Lazar is privately delighted that the "majority" of the 60 affected directors have not yet reapplied (with revitalized research programmes), as they are entitled to do by mid-November. This should give him some fun next year, when he will be able to reallocate this research potential according to new priorities now being defined by his advisory science council.

At INSERM, there were two kinds of resistance to the rule: from conservatives, whom — broadly speaking — the rule was designed to shift; and from a group of first-rate directors who are likely to remain directors after reapplication, but who deplore the paperwork and time involved. But among the latter, many have found the exercise of redefining 12-year research programmes "refreshing", Lazar claims.

Lazar, a medical statistician, has set out to refresh INSERM since he took over in 1982. "The image of the ivory tower has gone", he says. The 12-year rule is important to him because it makes it possible for directorships to change hands without the slur of explicit negative judgement on the incumbents.

Another major change at INSERM during Lazar's term has been a shift towards health service research, one outcome of an "honest review of strengths and weaknesses" instituted by Lazar and completed this summer. Some of the changes expected by next spring include:

- The creation of a new scientific committee (there are at present eight) in "the human and social sciences applied to health" with the objective of establishing new research fields and units.
- A general reorientation of priorities for new units established by INSERM, and a similar reorientation of INSERM external grants.
- An improved recruitment system for new scientists — with 60 new posts next year.

Several problems remain unsolved, however. There should be more foreign experts in review committees, Lazar admits, but "we shouldn't expect that foreign experts will do miracles". In INSERM itself, there are "silent experts" who refuse to judge their colleagues, but that is changing. And while INSERM (like the whole of France) is hamstrung by the total lack of postdoctoral fellowships, plans are under way at the research ministry to introduce a fellowship system.

Otherwise, the resolution of one old problem may mean less cash for French biologists. In its early days, INSERM competed openly with CNRS for the best biologists, to the benefit of many. But under a new agreement between the councils, that boon will end. Laboratories which have been jointly funded for no good policy reason will now have to adhere either to CNRS or INSERM, probably with a consequent loss of funds after a four-year transition period.

But to replace the past *ad hoc* joint support, there will now be three clear structures for collaboration: a few (10–20) existing common laboratories where the basic research goals of CNRS clearly overlap with the medical goals of INSERM; new "concerted development units" where INSERM and CNRS wish actively to set up joint action and "allied units" where, for example, CNRS staff may be working in an INSERM laboratory, or vice versa.

Thus clarity is entering the INSERM–CNRS relationship for the first time in twenty years, and French biomedical belts may tighten as a result. **Robert Walgate**

Soviet geology

Deep boreholes yield data-harvest

ON 7 September 1984, drilling operations began on a projected 15-km borehole through the Ukrainian crystalline shield from a site at Novoivanovka, near Krivoi Rog. This drilling project, involving more than 150 research institutes and "production collectives", marks a new stage in the Soviet deep borehole programme — the sinking of deep shafts specifically related to the search for metals.

Soviet interest in deep boreholes dates back to the beginning of the 1960s when the United States was planning to drill a "mohole" into the oceanic crust down to the Mohorovicic discontinuity between crust and mantle. Soviet plans have concentrated on drilling of several deep boreholes (12,000–15,000 km) at carefully chosen sites — the Kola peninsula, the Kura depression in Azerbaijan, the Urals, the Caspian depression and one of the Kuriles. At the outset, however, Soviet drilling technology was insufficiently advanced to reach the proposed depths. Oil drillings averaged less than 2,000 metres in depth, and the few shafts that passed the 4,000-metre mark were considered exceptional.

Not until May 1970 could work be started on the first deep hole, at a site 8 km north of Zapolyarnyi on the Kola peninsula, while the second, at Saatly in Azerbaijan, was started only in June 1977. Special drilling rigs developed by the Uralmash plant differ from US deep-drilling equipment in that the string remains virtually stationary while the bit, a miniature turbodrill, rotates. The special-purpose instruments, capable of withstanding high pressures and temperatures, include a miniaturized motor, developed by students at the Kaunas Polytechnic Institute, which can drill and analyse rock samples at depths of over 11,000 metres.

Already the programme has yielded interesting results. Samples from the Kola borehole have revealed in the Baltic shield aqueous solutions of carbon dioxide and helium at depths of 6,000 metres, the expected granite-basalt boundary at approximately 7,000 metres was found not to exist and the angle of inclination of beds which form outcrops of 45° was found to remain the same at increasing depths, contrary to the expectation that the inclination would increase. Fossilized microorganisms were found in strata believed to be 2,000 million years old. Fossils from the Saatly hole (shells and small corals) have confirmed that there had once been a shallow sea in that area.

In the Kola borehole the temperature at the 12,000-metre mark (on 28 December, 1983) was above 200°C, instead of the expected 100 to 120°. In the Saatly hole, the temperature at 7,500-metres was 140°C, less than expected, suggesting that there is no deep magmatic activity in the Kola depression.

The practical implications of the data have proved more valuable than expected. In the Kola borehole, traces of copper, lead, zinc, cobalt and nickel have been found far deeper than predicted, so the programme has been extended to include a further 20 holes in ore and hydrocarbon bearing localities. Boreholes in oil/gas-bearing regions will include sites in the Tyumen region, the Kuban, the north Caucausus, the Caspian depression and the Timan-Pechora region. The four metal-ore sites will be in the Urals, near Noril'ski in Uzbekistan and at Novoivanovka.

Vera Rich

Polish universities

Autonomy beyond reach

POLISH universities opened last week in somewhat gloomy circumstances. The Party daily, *Trybuna Ludu*, greeted the new term by observing that "for several years, the intellectual activity of the academic milieu has been declining" and has failed to produce "fresh achievements significant in world standards".

At the same time, the paper gave a strong hint that the autonomy of the universities was, essentially, part of an implicit bargain by which the university authorities, in their turn, assumed "co-responsibility" to prevent university self-governance being used as a cloak for "harmful" actions.

Neither of these criticisms is unexpected. The declining standards of Polish science have been repeatedly discussed, explained and excused in the Polish press during the past year, and may fairly be summed up as the result of the hierarchical planning of research during the Gierek regime (when every research project had, officially, to relate to a carefully graded ladder of "problems" of the national economy). But, now, all foreign currency for the purchase of equipment and journals has suddenly been cut off. The situation is so bad, a working party of the Polish Academy of Sciences warned last month, that without an immediate injection of hard currency, Polish science could come to a complete halt.

University autonomy has also been a contentious issue during the past year. The chief clash was over the election of university rectors, when three rectors-elect were vetoed by the Minister for Science, Higher Education and Technology, Dr Benon Miskiewicz; when the Warsaw University electoral college refused to accept his decision, its functions were suspended for six months and the minister let it be understood that he would appoint a rector of his own choosing. Yet when the university opened last week, the outgoing rector, Dr Kazimiedrz Dobrowolski, presided over the beginning-of-term ceremonies and, in his inaugural address, expressed the hope that the university would soon have a new rector, chosen by the electoral college.

It is now thought that Dr Dobrowolski came to an agreement with the minister during the vacation, by which he would continue in office until 15 February 1985, and that the electoral college would elect his successor when its term of suspension expires in February. But none of this has appeared in the Polish press, and there is no certainty that, even if there is another election, the minister will not again intervene if the choice is too "daring".

The issues of autonomy and of research standards are, in fact, related, since one of the major demands for academic autonomy formulated in the Solidarity period was the right of universities to determine their own research programmes, independently of state priorities. But even the autonomy granted by the 1982 Higher Education Act (considerably less far-reaching than was originally hoped for) is not always easy to implement. In a recent interview in *Polibyka* the rector of the Jagiellonian University of Krakow, Dr Józef Gierowski, noted that university self-government cannot be invoked to deal with the bottom-heavy structure of academic teaching staff, where too few assistants and junior lecturers are prepared to qualify themselves for professional posts.

The university, he explained, "being as it were a continuation of the function of the welfare state", is obliged to employ "scientific workers", for whom the PhD degree represents the "peak of their capacity or ambition". (Senior academic staff in Poland must hold the higher degree of *doctor habilitatus*). The only success for "autonomy" in dealing with such people is the acceptance of the principle that they must resign if they do not get their doctorate within eight years.

Polityka, which, although less liberal than before Martial Law, still enjoys considerable prestige, has during the past year given considerable space to problems of science and education. Recently it has been particularly concerned with the training of Poland's future scientific workforce, covering such issues as the falling interest among university entrants in the technical engineering sciences, the challenge of the "third wave", the relevance of "new maths" in primary schools, and the practice, recently introduced in some schools, of a longer school-day with Saturdays free.

Vera Rich

US-Japanese education

One man's meat, another's poison

Tokyo

JAPAN and the United States have agreed to set up a joint 30-member council to compare their educational systems from May of next year. The move comes not before time, for both nations have been worrying about the weaknesses of their respective systems (helped along by reports of emerging IQ differences) and envying the strengths — real and imagined — of the other's.

At the Washington meeting between Japan's Education Secretary Yoshiro Mori and US Secretary of Education Terrel H. Bell that gave approval to the council, Bell, reflecting growing US desires for a return to a more disciplined educational system, lavished praise upon Japan's tough *juku* (private cramming school) system, saying that the United States "must have *juku* because the Japanese are so productive".

A horrified Mori then had quickly to explain that the Japanese Government, reflecting growing desires for a more liberal educational system, regards private cramming schools, at which some students spend four hours a night, as an evil produced by the terrible competition for entry to leading universities and high schools, and hopes to do away with them. Later, Bell, well known as a supporter of increased homework in US schools, admitted that he had not actually known what *juku* were but what he really wanted was a longer school day "which is a supervised, studying, tutoring, *juku*-type thing" (*sic*).

The US-Japan council will have its first meeting in Tokyo and will have a special panel looking at problems of science and mathematics education — of particular concern to the United States. Experts from the United Kingdom, France and Germany are also to be invited.

Shortly before Mori's meeting with Bell, Japan's Prime Minister, Yasuhiro Nakasone, finally succeeded, after six months of Diet wrangling (see *Nature* **308**, 678 and **309**, 739; 1984), in inaugurating the special council which is to spend three years devising reforms of Japan's education system.

Despite vociferous protests from the socialist and communist parties, the council has been handpicked by Nakasone and is answerable directly to him. Only two school-teachers are among the council's 25 members (average age 60) and there are no representatives from the nation's biggest teachers' organization, the Japan Teachers Union, which virtually ensures that conflict will continue. The post of president of the council has, however, gone to a well known liberal, Professor Michio Okamoto, until recently president of Kyoto University. Nakasone has asked the council to take speedy action on the biggest problem — the university entrance examination — and to seek "diversity" in the education system.

Exactly what diversity means is likely to cause considerable debate. In the present straight "one-track" educational system, completely unstreamed groups study the same subjects and try the same examinations, with only total scores deciding how a distinguished university faculty can be entered (and thus often what subject is studied). The liberals would replace it with one in which students have freedom to follow their own interests and receive an education tailored to their own particular abilities, but what the left wing fears is that "diversity" will simply mean increasing the scale of divisions between top quality (and expensive) private schools and the poorer state schools: an effective return to a pre-war system where elites were selected for special training at an early age.

Alun Anderson

Japanese universities

Broadcasting for degrees

Tokyo

JAPAN'S first broadcasting university — the University of the Air (Hoso Daigaku) — is poised to go into action: its buildings and facilities are just being completed in Chiba City, near Tokyo, after an initial expenditure of 10,000 million yen (US$420 million). Application forms for the enrolment of its first 10,000 students will be available in a few weeks. Test broadcasts will start at the same time, beginning with programmes explaining what the university has to offer and how to apply for entry.

Once in full operation in April next year, the University of the Air will become the first broadcasting university in the world to have its own specially dedicated television and radio channels, each carrying lectures from 6 a.m. to midnight seven days a week. Adding to this generous helping of learning the 18 hours of school, documentary and language programmes broadcast each day by the national television corporation (NHK)'s Channel 3, there will be a little over 250 hours of television tuition available each week — enough, perhaps to satisfy even the Japanese thirst for education. The university's programmes will, however, be available only to those in the area around Tokyo, for plans to broadcast directly by satellite fell through and conventional transmitters are being used; the rest of the country will have to wait another five years for the service.

Support for the establishment of a broadcasting university resulted partly from the calls for fundamental educational reform after the 1960s student unrest. At Tokyo University, the centre of the trouble, teaching was totally disrupted, the entrance examinations had to be cancelled (losing a year's student intake) and the general public were treated to television coverage of the nation's young elite flinging "Molotov cocktails" from the university tower at riot police below.

With the ending of the troubles, no fundamental reform of university education was carried out, but some new educational projects did get under way: the new "American" style university at Tsukuba (see *Nature* **305**, 371; 1983); a pair of colleges to which school-teachers can return for two years of "refresher" graduate-level training at the government's expense (provided they can pass the tough entrance examination) and, now, the University of the Air.

Despite the Y10,000 million government expenditure on the university and the fact that the Ministry of Education, Culture and Science (MESC) will pay its operating budget, the government will have no direct legal control over the university, for Japanese law guarantees independence of the mass media. Instead, the university is run by a foundation, and its staff, unlike those of a normal university, will not be civil servants.

And although the university buildings are right alongside a new National Centre for the Development of Broadcasting Education, a part of MESC from which the university is renting its broadcasting studios, the university building has been kept just a few metres away to demonstrate its separateness. Only a corridor connects the two. But this arrangement has not fully satisfied the socialist opposition parties, and courses such as sociology and education which can encourage critical thinking about government policy are certain to be carefully watched.

The overall teaching system has much in common with other broadcasting universities. Set texts accompany lectures which are broadcast several times a week at different times of day, tests and reports are sent by mail and face-to-face teaching and end of term examinations given at six regional study centres. Success in the examinations gains credits towards the 124-credit total, and minimum of four years' study, needed to gain a degree. A typical two-credit course requires the understanding of a 120-page book and 15 accompanying 45-minute lectures: it is expected that students will average five broadcast lectures a week plus three hours of lectures at study centres.

Three main disciplines are to be offered: science in everyday life, industrial and social studies, and humanities and natural sciences, but within this framework there is to be considerable choice of specialized subjects after fundamental studies have been completed. Of the 10,000 students to be enrolled to begin with, 4,000 are expected to take a degree course (high-school graduation is the only requirement) and the remainder to take a few subjects for a short period. A full degree course will not be free, although at a total cost of Y750,000 ($3,000) it will be cheap compared with attendance at a university.

Around 50 professors have been chosen to run the university and will be backed up by an equal number of associate and assistant professors. Not having civil servant status, however, the junior staff will be employed on renewable five-year contracts rather than given tenure. Some 100 guest lecturers will also be brought in from other universities on contract to make particular television and radio programmes.

Efforts will be made to ensure that the University of the Air degree is a real degree and not a second-class qualification. To this end, the university is now trying to arrange for credits to be transferable to and from other universities. If this proves successful, given the notorious lack of interchange of students between conventional universities, it will be a remarkable achievement in its own right.

Alun Anderson

US basic research

Cheer and gloom at war

Washington

SHARPLY contrasting views on US university research were aired at a meeting held last week by the American Council on Education. Dr Edward David Jr, president of Exxon Research and Engineering and a former presidential science adviser, told the conference, held at the University of Georgia at Athens, that the growing links between university research and industry were "a promising picture for the future". But Professor William McElroy, professor of biology at the University of California at San Diego, said universities were facing "almost a disaster" in research support.

In his opening speech, David argued that the public's desire to create jobs based on new science, together with the power of new instruments, will lead to more cooperation between universities and private research institutions: industry has been the fastest growing source of support for university research since 1970. But David was concerned that manpower competition from large federal projects in defence and space might crowd out the civilian sector.

McElroy said bluntly that such optimistic views "do not stand up against the facts". Despite constant-dollar increases in federal university research support since 1972, the escalating cost of doing research has meant that the same money now buys less. The amount spent per grant has decreased substantially, and it is becoming harder to find money for research projects: five years ago, a merit rank of 3 on a scale from 1 to 5 would have been sufficient to ensure support from the National Institutes of Health, but now a rank of 1.5 would be insufficient. And McElroy commented that industrial support for university research is concentrated in relatively few universities.

McElroy's remarks echo comments made recently by Donald Kennedy, president of Stanford University, in a letter to Dr George Keyworth, director of the White House Office of Science and Technology Policy. Kennedy wrote that undercapitalization of teaching and research laboratories is causing problems in retaining faculty, while the need for renovations of research facilities had "reached crisis proportions".

University research is the subject of a major study nearing completion in the White House science office, chaired by David Packard, president of Hewlett-Packard. The study is rumoured to back the case for more generous support of basic science by federal agencies. And the Department of Defense is already preparing to step up its programme of unclassified research in universities.

Tim Beardsley

British geology

Strategic survey grinding to halt

GEOLOGICAL surveying of Britain by the British Geological Survey (BGS) has almost ground to a halt this year. Because of over-dependence on short-term contracts and the cost of its recent centralization at a site in Keyworth, Nottinghamshire, strategic surveys of land are running at only 30 per cent of last year's activity.

At the same time, BGS seems to have lost its old friends. Private industry is complaining about its function and performance, BGS has no long-term commitment from government departments that use its services and, unlike most national surveys, it has no direct responsibility to a government minister for strategic surveys and information management. With its parent body, the Natural Environment Research Council (NERC), itself under severe financial pressure, BGS has an uncertain future.

The decline of the land survey activities comes at a bad time. Since 1835, BGS and its predecessors have been preparing geological maps of the United Kingdom at 1:50,000 scale (1 inch to 1 mile), with more detailed mapping following later. Although most of the United Kingdom has been mapped at 1:50,000, at least 25 per cent of the maps are obsolete, according to BGS. Moreover, at the more detailed 1:10,000 scale, large areas of the country remain unmapped, partly because of concentration on regions important for economic or development reasons.

After the survey was attached to the newly-formed NERC, in 1965, it accumulated a wide range of new responsibilities: overseas activities, geochemistry, geophysics, seismology, geomagnetism, mineral and water resources. When, in 1973, the Rothschild "customer–contractor" principle was accepted by the British Government, a portion of BGS funds were transferred to government departments. By 1979, the land survey activites were financed and controlled by a consortium — 60 per cent NERC, 30 per cent Department of Environment, 5 per cent Department of Trade and Industry, 5 per cent Department of Energy. Meanwhile, other parts of the survey were so heavily engaged on commissioned work that three quarters of the survey's funds came from the customer departments.

Although cutbacks by government departments began in 1980, the first major blow to the land survey was struck in 1982 when the Department of the Environment withdrew from the consortium as well as from other activities, replacing that commitment by a series of short-term (six months) contracts whose allocations were not made until after the start of the financial year. The Department of Energy, meanwhile, transferred its consortium support to deep geological research related to onshore hydrocarbons assessment.

These developments left the land survey almost entirely dependent on NERC. The latest blow, earlier this year, was a cut by NERC in BGS science funds of £1 million (about 10 per cent) made necessary because of NERC's severe financial shortage. Because short-term BGS commissioned contracts draw on this science budget, and because the recent move to Keyworth has entailed relocation expenses, the result has been a 70 per cent decrease in the funds available for scientific work. Now, routine activities such as geomagnetic monitoring are threatened while the land survey programme has been curtailed to 30 per cent of last year's when, according to the director of BGS, Professor Malcolm Brown, this programme needed to be doubled.

BGS budget £ million 1984–85 prices

		1982 –83	1983 –84	1984 –85
NERC	Science Vote	63.1	65.1	65.9
	Commissioned income	30.8	26.4	23.7
BGS	Science Vote	9.8	10.4	9.2
	Commissioned	18.5	16.9	14.9

BGS Staff numbers:
1973: 757 **1979:** 1,156 **1985** Target: 920

There are those, inside and outside BGS, who conclude from this catalogue of misfortune that the Rothschild system was the biggest disaster to hit the survey since its foundation. There are others who say that BGS's problems are more fundamental.

Perhaps the strongest criticisms come from local government and private industry, which charge that the survey is simply not providing an adequate supply of basic geological information needed for planning purposes, for example. And the move to Keyworth will exacerbate the situation, the critics say, by rendering the available information less accessible. But BGS intends to maintain its London library until 1986 at least, and thereafter to maintain a London information centre with two BGS scientists and a duplicate supply of key geological maps and reports.

Many of the private companies are deeply irked that, as they maintain, BGS is in effect a state-subsidized competitor for short-term contracts which is too heavily engaged in such work to provide British industry with basic services. It is hard to document the charge, but staff at BGS concede that customers will tend to benefit from the large infrastructure available to support contracts placed with BGS.

Staff at BGS are all too aware of the backlog in the publication of maps and memoranda. One explanation is the diversion of resources and funds to other activities. It is estimated that one map at 1:50,000 scale now requires anything up to £1 million to produce from scratch. In fact, the survey has about 50 geological memoirs in preparation, some of which might be published for as little as £20,000, but the money cannot be found.

Another contributory factor, put forward by a visiting group commissioned by NERC to assess BGS, is that while the collapse of the land survey consortium was much to blame, BGS administration of the preparation of reports and maps was inadequate — a charge also made by the previous visiting group a few years earlier. A long-term response to such criticisms, but one of BGS's top priorities, is the establishment of a national computerized database — a massive task, particularly now that strategic surveys use geophysical as well as geological techniques to prepare maps.

Complaints against BGS are offset by industry's acknowledgement of the value of services such as the provision of minerals intelligence and general commodity expertise. In 1981, minerals and quarrying (including oil) accounted for 18 per cent of UK production, and BGS supplies information ranging from distributions of potash horizons based on North Sea drilling to details of small barytes mines.

Ultimate — and, in many people's opinion, excessive — control of BGS rests with NERC. Academic geologists and those working for other national surveys are surprised, even outraged that the director of BGS has to refer to NERC headquarters each new appointment to his staff, for instance. Similarly, every decision relating to the purchase of computing equipment is referred to NERC's central division. Coincidentally, computing problems have been highlighted by a decision by the Department of Energy to cancel its contract with NERC for computing services associated with its continental shelf programme, and by a recent internal NERC report which recommended some decentralization of computing power.

NERC says its control of manpower, budget and the scientific programme of BGS stems from its accountability to Parliament. But NERC is aware of the backlog in the preparation of maps and memoranda, and has proposed that resources might be diverted within BGS for the work.

In short, there is general agreement that the function of BGS which is most in demand — the provision of basic information about the geology and natural resources of the United Kingdom — has, for a number of reasons, virtually fallen by the wayside. Some members of other national surveys suggest that BGS should be wrested from NERC and made responsible to a "minister for natural resources". As no such post exists in the United Kingdom at present, this radical proposal is unlikely to be realized, at least unless NERC itself is disbanded. Given the tight budgets within which BGS is operating, however, it is hard to see that a simple redistribution of its internal resources can have a significant impact on a central problem.

Philip Campbell & Peter Gambles

UK atomic energy

Putting research out to contract

THE UK Atomic Energy Authority (AEA) may soon be dead, but long live atomic energy in the United Kingdom. That seems to have been the mood at Britain's nuclear establishments last week, in the wake of the publication a week ago of a set of proposals for reorganization that will eventually saddle electricity consumers and other users with much of the cost of applied research in nuclear energy.

The new arrangements have been put to the Secretary of State for Energy, Mr Peter Walker, by an anonymous committee of officials from the department. The good news for AEA is that the committee has shrunk back from the notions that the authority should be dispensed with ("an authoritative body of expertise . . . will continue to be required") or transferred to the private sector (which is "not realistic").

Big changes are nevertheless intended. The committee recommends that a greater share of AEA's research should be paid for by the electricity industry, and that other research commissioned by the Department of Energy should be paid for on the "customer-contractor" basis.

The case for some continuing support for nuclear research is that the "government's policy that [Britain] should have a significant nuclear power programme for the foreseeable future" makes some kind of research programme necessary, while the "unique nature of nuclear power and public perceptions of it" will require continuing public support for programmes of research going beyond strictly commercial interests.

On the authority's specific research programmes, the official committee recommends that the electricity industry should shoulder a larger proportion of the cost of fast reactor design as research gives way to development, that work on thermal reactors should be paid for exclusively by the electricity generators, that there should be further discussion about sharing the cost of nuclear safety research, but that the nuclear waste programme should continue to be paid for centrally.

The committee says that the "underlying programme" of research has been of benefit to user organizations but that, on the principle that present customers are "proxies for future customers", they should now begin to contribute towards the cost of this research.

The next step in the unwinding of AEA's dependence on public funds is that the minister should decide whether to accept the proposals his officials have put to him, which will in turn depend on negotiations between the potential customers (which may be unwilling to pay for service hitherto free) and the potential contractor (which may also be an unwilling partner).

The Department of Energy is nevertheless hoping that the outstanding issues of who pays what will be settled within a few months, which would have the advantage that much of the cost of the British nuclear research programme would disappear from the government's expenditure accounts before the beginning of the next financial year in April. Another specific recommendation of the committee, which has been generally accepted, is that AEA should in future be managed as a "trading fund", a public corporation subject to the accounting rules that apply to private companies (and carrying the freedom to borrow from the banks). But this arrangement will require legislation, so the formalities are likely to be delayed.

In the authority, officials and staff members say they "have seen this coming for a long time". There are grounds for optimism that, in the short run, the authority (which already supports a third of the research at its largest establishment at Harwell through outside contracts) will be able to maintain the present level of activity. The dangers may come later, when customers for its research services may spend their contract money on quite different things. ☐

UNESCO

One friend for M'Bow

MR Amadou-Mahtar M'Bow, director-general of the United Nations Educational, Scientific and Cultural Organization (UNESCO), went last week to Strasbourg to defend his beleaguered organization's record before the Assembly of the Council of Europe. And while he had little success in convincing delegates that UNESCO's house is in order, the Council of Europe agreed that its secretariat should go ahead with plans to increase cooperation between the two organizations.

This move may stem from a fraternal feeling between UNESCO and the Council, both of which were set up after the Second World War as institutional symbols of peace and goodwill. Now UNESCO is in trouble, accused of mismanagement, and threatened with the withdrawal of the United States, the Council wishes to come to its aid. In fact, there have been regular contacts between the two organizations since 1952, when the first cooperation agreement was signed, and the plans in hand are merely to extend the contacts a little. The new agreement is to cover areas of common interest such as communications (satellites and copyright questions), cultural development and North-South cooperation. The vexed issue of "a new world information order" for news reporting is not among topics for discussion.

Even so, the mere presence of M'Bow at the Council's building in Strasbourg was too much for conservative group members of the assembly, who issued a declaration deploring the invitation to him. But this need not deter M'Bow from returning later this month, when the plans for extended cooperation will be on the agenda.

At the assembly last week, M'Bow had to field questions on the morale of UNESCO staff; on the American General Accounting Office report which attacked UNESCO spending and 70-per-cent overheads; on the political nature of a UNESCO mission to Afghanistan; and on the "new world information order". The conclusion: that the UNESCO crisis is "very deep", said an observer.

Nevertheless M'Bow may count the meeting a success if increased cooperation between the Council and UNESCO does materialize. The 21 Council of Europe states between them pay 33 per cent of UNESCO's budget. The United States pays only a quarter. **Robert Walgate**

Australian array

Canberra

CONSTRUCTION work has begun at Culgoora, New South Wales (NSW), on the $A32 million Australia Telescope, which, if ultimately linked with other Australian radio antennas, would possess a baseline thousands of kilometres across, making it complementary to the large radio arrays planned in the Northern Hemisphere.

The Australia Telescope will comprise two arrays of individual radiotelescopes. The Compact Array will consist of six mobile antennas each of 22 metres diameter and locatable at 37 stations along a 6-km east-west line at Culgoora. The Long Baseline Array will combine the 64-metre radiotelescope at Parkes (NSW) with one or more of the Compact Array antennas and a seventh 22-metre antenna at Siding Spring (NSW). Its 319-km baseline will permit an angular resolution of 0.02 second of arc at a frequency of 10 gigahertz, a performance that could be improved on by linkage to telescopes at Fleurs, Hobart, Alice Springs and Carnarvon, and to the 64-metre radiotelescope of the National Aeronautics and Space Administration at Tidbinbilla, which is already linked with Parkes in preparation for the 1986 Voyager fly-by of Uranus.

Approximately half the overall capital cost will be taken up by the new Cassegrain antennas, which will incorporate feed horns designed for simultaneous observation in more than one frequency band. Both arrays are due for completion by 1988, and will be operated as a national facility by the Radiophysics Division of the Commonwealth Scientific and Industrial Research Organization (CSIRO).

Jeffrey Sellar

Italy

New hope for research council

SCIENTIFIC hearts are beating faster in Italy this week, as real hopes emerge of genuine reform of Italy's major but chaotic research council, the Consiglio Nazionale delle Ricerche (CNR). Last week the Italian Parliament ended eight years of colourful Neapolitan presidency of CNR by appointing a dynamic Milanese enzymologist, Professor Luigi Rossi Bernardi, to the next four-year presidential term. With Rossi Bernardi at the helm, the control of CNR passes from the underdeveloped south of Italy to the better-organized and industrial north: certainly the most fundamental event in Italian science politics for some time.

However, Rossi Bernardi is fully aware of the magnitude of his task. "Don't promise too much", he warned last week. Rossi Bernardi knows CNR from inside as a past president of the CNR medicine and biology committee. He identifies the key issue as that of quality: the proper allocation of resources, posts and promotions on the basis of scientific merit rather than custom or seniority. This means confronting interests, inevitably a political job. But Rossi Bernardi has powerful political friends, in the socialist prime minister Bettino Craxi, in the Christian Democrat research minister Luigi Granelli (both Milanese) and in the Christian Democrat party itself (which nominated him). He belongs to no political party, and says he will manage CNR "as a scientist", with the sole objective of improving the quality of CNR-supported science; but it will certainly be no hindrance to him to have friends in the right places. It will help also, said a colleague, that he comes from a medical department, medics being "the strongest mafia — in the best sense — in the Italian universities".

Rossi Bernardi is regarded as a proven organizer, both in his earlier work at CNR and his department in Milan. He is not greatly concerned, he says, with the total budget of CNR — which will grow 10 per cent next year, roughly in line with inflation. "The real problem is how the money is spent", he says.

Rossi Bernardi must also cut through the usual trip-wires with which Italian administration likes to entangle itself, such as a law recently passed which allows CNR institutes (and other state organizations) to hold as fluid funds only four per cent of their annual budgets, the rest remaining in the state treasury. The rule was originally designed to stop misappropriation, but its effect has been catastrophic, as CNR institutes are now having to request additional funds almost weekly from Rome. "We are at a standstill all over Italy", says one Naples biologist.

Another problem facing Rossi Bernardi is the fact that something like half of all CNR scientists have published nothing for five years (according to a survey he instituted two years ago). And the council languishes under a law which treats scientists as the most routine kind of civil servant, inhibiting promotion on merit (substituting seniority) and all but forbidding appointments into CNR at high level (as laboratory directors, for example). "It's a very, very hard job", says Rossi Bernardi.

Robert Walgate

US Army research

Expelled think-tank finds Rand

Los Angeles

THE US Army's new think-tank, given the cold shoulder by faculty of the California Institute of Technology earlier this year, has at last found a home. Within the next few months, the Arroyo Center will move from its present quarters at the Jet Propulsion Laboratory (JPL, administered by Caltech) to the Rand Corporation, located in another part of greater Los Angeles.

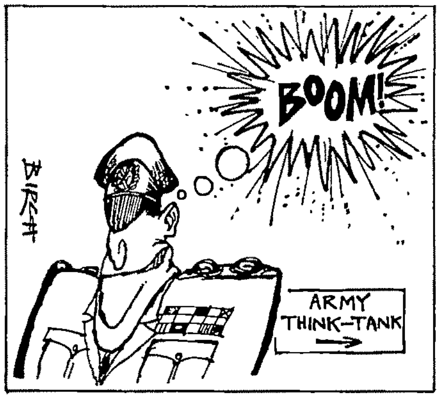

Rand has been home to the US Air Force's think-tank since the Second World War. "We don't see that there's a conflict", said Donald Rice, Rand's president and chief executive officer, who said that "for decades" Rand has been working for both the Air Force and the office of the Secretary of Defense as well as several other components of the Department of Defense, the Army and the Navy included.

Both the Navy and the Air Force have independent think-tanks, and the Army two years ago decided that it also needed one. The centre's charter is to examine long-term issues involving defence strategies, military operations, resource management and advanced technology as they affect the future Army.

As the centre began to set up shop last spring under Caltech's wing, the faculty balked. A majority said it was inappropriate for the university to lend its name and reputation to an organization that would lobby on behalf of military interests. Although it was acknowledged that many faculty members work on defence matters, it was argued that the university as a whole should not.

Caltech president, Marvin Goldberger, was criticized, but quickly forgiven, for having let the arrangement take place without prior faculty approval. The centre was moved to the nearby JPL campus and asked to look for another home.

At Rand, the Arroya Center will become a fifth division joining Project Air Force and other national security research, domestic research and the Institute for Civil Justice.

Sandra Blakeslee

Nature index of biotechnology stocks

12-Month high	12-Month low	Company	Close previous month	Close 28 September	Change
14	6	**Biogen (Switzerland)**	8	8	0
2	1	**Bio-Logicals (Canada)**	1¼	1¼	0
14⅜	6½	**Bio-Response (USA)**	9½	7¾	-1¾
14⅛	9¼	**Cetus (USA)**	11⅜	11	-⅜
10⅜	4¼	**Collaborative Research (USA)**	6¼	5⅝	-⅝
19⅞	11½	**Damon (USA)**	14½	14⅝	+⅛
26¼	11¾	**Enzo-Biochem (USA)**	14¼	14½	+¼
10⅛	4¼	**Flow General (USA)**	5⅜	5¼	-⅛
42¼	28⅜	**Genentech (USA)**	33¼	30¾	-2½
10¾	4½	**Genetic Systems (USA)**	6⅞	6¾	-⅛
17¼	8¼	**Genex (USA)**	12	9¾	-2¼
23	11	**Hybritech (USA)**	14¼	13¼	-1
16¼	7¼	**Molecular Genetics (USA)**	10¼	7¾	-2½
15½	8¼	**Monoclonal Antibodies (USA)**	10	10¾	+¾
60⅞	32⅛	**Novo Industri A/S (Denmark)**	37¼	33⅜	-3⅞
22¾	14½	**Pharmacia (Sweden)**	19	17⅞	-1⅛

Closing prices are for the last Friday of the month. For over-the-counter stocks, bid price is quoted; for stocks on the American and New York exchanges, the transaction price. *Nature*'s weighted index of biotechnology stocks stood at **139** on 28 September, compared with **149** a month earlier. Data from E.F. Hutton, Inc.

Persistence of miracles

SIR — A leading article in *Nature* (19 July, p. 171), quite rightly questioned whether "science has nothing to say" on the subject of miracles; but it was surely wrong in attributing to science the dogma that "miracles do not occur". In scientific laws we describe, as best we can, the pattern of precedent we observe in the sequence of natural events. While our laws do not prescribe what must happen, they do prescribe what we ought to expect on the basis of *precedent*. If by a "miracle" we mean an unprecedented event (and the resurrection of Christ is certainly described as such), then science says that miracles ought not to be expected on the basis of precedent. What science does not (and cannot) say, of course, is that the unprecedented does not (or cannot) occur.

If, as Christians have traditionally believed, the whole spatio-temporal sequence of events that make up our world owes its being to our Creator, then it is thanks to Him that our scientific explanations normally prove as reliable as they do. But by the same token, nothing whatever in our observations of "normal precedent" can make it impossible for the Creator to bring about a totally unprecedented event, if His overall purpose for His creation requires it. Christians believe that the resurrection of Christ was just such an event. We do no good to the cause of science by pretending that there are scientific grounds for denying that it could have happened.

To say this, however, is not to suggest that we should go soft on "mischievous reports of all things paranormal, from ghosts to flying saucers", as *Nature*'s leader writer seemed to fear. For the Christian believer, baseless credulity is a sin — a disservice to the God of truth. His belief in the resurrection does not stem from softness in his standards of evidence, but rather from the coherence with which (as he sees it) that particular unprecedented event fits into and makes sense of a great mass of data. Some of these data are historical, some derived from the cumulative experience of Christians down the ages, including himself. So his faith is not groundless. There is clearly no inconsistency in believing (with astonishment) in a unique event so well attested, while remaining unconvinced by spectacular stories of "paranormal" occurrences that lack any comparable support.

Both wishful thinking and wishful unthinking are evils, and it will not do to tumble into one for fear of the other. We cannot dogmatically exclude the ever-present possibility that the truth about our world is stranger than we have imagined.

DONALD M. MACKAY
*Department of Communications
and Neuroscience,
University of Keele,
Keele, Staffordshire ST5 5BG, UK*

SIR — Your leading article "Miracles do not happen" (*Nature* 19 July, p.171) appears to contradict itself at least twice. First you urge critical rigour for evaluating a particular miracle, the turning of water into wine by Jesus. I agree. But then you baldly state: "Miracles... do not occur — a definition by exclusion of the concept". You apparently mean that they are excluded from all factual discourse, not just from science, since the latter would be agreeing with the very notion you wish to oppose — that science has nothing to say about miracles. Finally, you state that religious belief "on other grounds" is unexceptionable.

But why insist on critical rigour for evaluating particular miracles, if *by definition* they do not occur? And how can you find religious belief "unexceptionable" if you deny (by definition!) some of its key tenets. It is not only the grounds of belief that are at issue here, but the content.

Your concern not to license "mischievous reports of all things paranormal" is no doubt motivated in the interest of scientific truth, but your strategy of defining away what you find unpalatable is the antithesis of scientific. It is disheartening that *Nature* should sell its empiricist birthright for the stale soup of *a priori* rationalism.

P.G.H. CLARKE
*Institut d'Anatomie,
Rue du Bugnon 9,
1011 Lausanne, Switzerland.*

SIR — Jeremy Marshall (*Nature* 30 August, p. 722) would like scientists to behave themselves and stop questioning miracles, as a sort of act of gratitude for his consent to "believe that evolution has occurred". He objects to scientists concerning themselves with miracles because this subject "is outside the bounds of proper scientific inquiry".

Unfortunately, miracles are sometimes invoked to explain natural phenomena on a nonscientific basis. Creationists have been particularly adept in the use of this device. Conclusions about miracles have been repeatedly reached by scientists on a scientific basis, and are not necessarily an invasion of theology. In turn, scientific inquiry into natural phenomena often reveals facts that seem sufficiently miraculous to excite admiration and awe from scientists and theologians alike.

THOMAS H. JUKES
*University of California,
Berkeley, California 94720, USA*

BioNet and GenBank

SIR — A few points in your recent news article "Limited access to BioNet" (30 August, p. 717) require clarification. The article confuses two separate projects funded by the US Government: the GenBank project, which is the national genetic sequence data bank in the United States funded by several institutes of the National Institutes of Health (NIH) and other government agencies; and BioNet, a computing resource for molecular biologists also supported by NIH.

GenBank is a contract jointly run by the Los Alamos National Laboratory and Bolt Beranek and Newman, Inc. to collect, maintain, distribute and provide computer access to nucleic acid sequences and related data. It is this work which is performed in close collaboration with the parallel effort here at EMBL in Heidelberg. The task of data collection is in fact shared between the EMBL and GenBank groups, and data are exchanged on a regular and unrestricted basis.

BioNet is a project managed by Intelligenetics, Inc. to provide molecular biologists with computing resources, including analysis software, communications facilities, and databases accessible by computer network. (Two of the databases so provided are those produced by the GenBank and EMBL efforts.) Limitations on BioNet access are necessary because it is, at present, implemented on a single computer of finite capacity.

It should be stressed that these limitations apply to use of the BioNet computing facility, not to availability of the GenBank and EMBL databases. Both databases are available worldwide, in various forms, to anyone.

GREG H. HAMM
*European Molecular Biology Laboratory,
Postfach 10.2209,
Meyerhofstrasse 1,
6900 Heidelberg, FRG*

Nuclear power

SIR — J.R. Ravetz complains (*Nature* 9 August, p. 446) that *Nuclear Power Technology*, reviewed by Sir Alan Cottrell (*Nature* **309**, 545; 1984), contains no reference to weapons technology. As deputy editor of that book I should explain that it is about nuclear power technology, not nuclear weapons technology.

While nuclear power stations and some nuclear weapons draw their energy from the same fundamental phenomenon, namely nuclear fission, the staff of the Atomic Energy Authority, by whom the material for the book was written, are not competent to write about nuclear weapons.

I am sure Mr Ravetz would not expect to see high explosives technology discussed in a book on oil-fired power stations, although the energy source is common to both.

R. H. FLOWERS
*Fuel Processing Directorate,
UK Atomic Energy Authority,
Harwell, Oxon OX11 0RA, UK*

Ethics, ethical committees and animal experimentation

from David Britt

Will the establishment of local review committees for animal experiments in Britain modify attitudes of researchers and the public?

THREE years ago, editorial comment in this journal advocated the establishment of institutional committees to scrutinize proposals for experiments on animals in a way that has proved useful in the regulation of genetic manipulation and research involving human subjects (*Nature* **293**, 173-174; 1981). The committees were seen as a means of bringing together persons with differing views on animal use in an attempt to resolve practical issues of animal experimentation in a less arbitrary manner than legislation seemed to offer. Correspondence on the subject published in subsequent issues revealed a favourable reaction to the idea but this has not been translated into a rush to set up such committees in the United Kingdom. Many British research institutions have committees devoted to the supervision of laboratory animal facilities but few, if any, of these consider the ethics of proposed animal usage and are therefore avoiding the issues which the *Nature* editorial wished to see addressed.

There is a notable reluctance among British scientists to discuss the moral implications of animal experimentation, possibly because, by and large, they are uncomfortable in the area of philosophical (especially ethical) debate. As long as their work is within the law, what research scientists do is very much their own responsibility and perhaps ethical issues are a matter for individual conscience rather than open debate? The growing interest and concern of a broad section of the rational general public renders this position untenable today. Some scientists have the arrogant notion that only they can fully appreciate and weigh the issues, so that discussion with others is pointless. Other scientists and scientific administrators apparently entertain the hope that by adopting a 'low profile' approach to public concern, it will fade away. In each case the scientific community is denying any responsibility to be accountable to the public for its actions and activity.

At an individual level, is there also, perhaps, an underlying fear that too deep a questioning may reveal to the scientist the weakness of the philosophical basis on which his current, permissive position is founded?

Elsewhere in the world, scientists have been less inhibited in the debate on the ethics of using animals in experimentation and have even invited participation by the public at large. One reason often advanced for the lack of similar initiatives here is that some proponents of animal rights issues have adopted illegal, even violent, means to further their cause and thus alienated themselves from rational opinion. However, it is quite wrong to suppose that the same spectrum of personal attitudes to animal experimentation is not to be found elsewhere, even if the practical expression of extreme views antagonistic to research on animals is qualitatively different. Why this difference exists offers a fascinating area for study in social psychology, but the present situation in Britain may not be totally unrelated to the aloofness and conservatism of our scientific establishment. It is time for scientists involved in research with animals to confide in, and consult with, the general public — at least those sections of it which can be objective while maintaining a genuine concern that unnecessary suffering should not be inflicted.

If introduced to British research institutions, animal experiment review committees would assist in establishing a valuable dialogue between scientists and the lay public. Further, they would provide the scientific community with the chance to reveal its own concern for the welfare of laboratory animals and their humane, non-profligate use, thus allaying public disquiet, often fanned by inaccurate, emotional propaganda from extremist sources. Lay input might encourage scientists to be more reflective in their management and use of animals and in experimental procedures. This has happened in Sweden, for example, without discouragement of worthwhile scientific investigation.

Ethical review in Sweden

In July 1979, local ethical committees for the review of animal experiments became mandatory in Sweden. Six committees were established, one for each of the country's University regions, to cover experiments in all research institutions using laboratory animals: academic, government and commercial. An additional committee was formed to review experiments on animals to be conducted by the military authorities, with members screened for security purposes. All the committees were made responsible to a board of the Ministry of Agriculture which still regulates the scheme and provides a secretariat and funds for essential expenses of committee members. Membership of the committees comprises equal numbers of individuals from three categories: research scientists, animal/laboratory technicians and lay persons. The sanctioning of such a high degree of participation by the general public is one of the boldest (some would argue, most reckless) aspects of the scheme. The largest committees, at Stockholm and Uppsala, have total memberships of 45, the smallest only 15. Volunteer scientist and technician members are solicited from all relevant institutions in each region; the lay members are nominated by animal welfare societies or local government agencies.

From the outset, attempts were made to ensure that the creation of an unwieldy bureaucratic monster would be avoided. Two aspects of committee organization have helped to achieve this. First, all experiments are graded (initially on a five-point scale, later simplified to two) for the degree of animal suffering likely to be imposed, and application for review is essential only for those, a minority, in which significant suffering is envisaged. In this way, the workload of the committee remains manageable. However, details of all experiments involving animals are notified to the committee, which may disagree with the grading. Second, each experimental protocol for review is discussed by the investigator and a subcommittee of only three members — one from each category — and referral of the project to consideration by the full committee is only necessary if agreement cannot be reached by the small group. Details of all projects submitted for review and sub-committee decisions are made available to all committee members. It is usual for the full committee to meet only two or three times a year.

Generally, reaction among scientists is favourable although the consensus is that the maximum usefulness of the committees has yet to be realized. There are criticisms that the three-year trial period in Uppsala was inadequate to allow potential problems to be identified and complaints that the decision to introduce review committees on a national basis was inspired more by political expediency than by scientific or humanitarian aims.

Scientific members of the committees are recruited from among the most experienced and senior research personnel. Such individuals are frequently overburdened with meetings of committees of various kinds. Any change which threatens to increase the time to be allocated to the work of the ethical committees will deter recruitment but this may be offset as the committees grow in influence and prestige.

Technician members have been accused by anti-vivisectionist groups in the country of refraining from expressing criticism of research proposals through timidity. Where the technicians feel themselves to be in a subordinate role to the scientists there may be truth in this accusation. On the other hand, many scientists and lay members of the committees of more moderate persuasion, feel that technician representatives have a vital contribution to make through their intimate knowledge of experimental procedures and good practice in animal care, often helping the committees to frame improvements to protocols.

Lay persons volunteering for membership of the committees have a concern for animal welfare in common but differ in their attitudes to animal experimentation. Some are unable to accept that there is any justification for the use of animals in biomedical research. It is difficult to understand why these individuals elect to serve on committees responsible, ultimately, for sanctioning animal experiments — at least those which are thoughtful, well-designed and both sparing and humane in their use of animals. Because they seek nothing less than the total abolition of experiments involving animals, anti-vivisectionists must remain frustrated by the activities of the committees. If they are members of one of the committees, their philosophical position demands that they must withhold consent from any protocol, even one which may have been improved at the recommendation of fellow members to ensure greater humanity in the treatment of animals. If their wish is to disrupt research effort, this also is frustrated, because all they can hope to achieve is a prolongation of debate in committee and delay in the onset of experiments before a majority decision allows the work to proceed.

Regrettably, ethical review committees in Sweden are presently facing serious problems. It is proving difficult to obtain suitable volunteers for membership and meetings are not always well attended. This is a serious indictment of the system because it suggests that the work of the committees is not highly valued. The problem has been exacerbated by the action of anti-vivisectionist members who have caused more and more lengthy, and circular, debate and prolonged meetings.

Proposals for radical reform of the system are currently being investigated by the Swedish Ministry of Agriculture. Included is a recommendation that each committee should be limited to a total of nine persons, the same three categories of membership to be retained but each with only three representatives. This is seen as a means of reducing administrative costs and overcoming problems of recruitment as well as facilitating the arrangement of meetings, but the idea attracts little support outside the Ministry except in so far as it promises to squeeze out participation by anti-vivisectionists. It is unlikely that this small committee could be representative of all relevant institutions within each University region and the necessary reduction in range of expertise available for consultation would also be detrimental. Because anti-vivisectionist groups wield considerable political influence in Sweden, attempts to exclude them from the committees may well be unsuccessful.

Professor Karl Johan Öbrink from the Biomedical Centre at Uppsala, one of the chief architects of the ethical review system, is also concerned about the present state of the committees and their future. He is critical of the emphasis on control which has become dominant with the codifying of the system in law and since administration of the committees became the responsibility of the Ministry of Agriculture Board. As originally conceived, the committees were to be advisory bodies encouraging consultation between investigators and other experts, with the aim of securing improvements in research design and ensuring the rational, humane use of experimental animals. In spite of misgivings about present arrangements, he remains totally convinced of the value of this kind of ethical review.

There was controversy earlier this year when a technician representative on the committee serving the Lund/Malmö region resigned after complaining that the committee system was powerless in offering protection to animals and implying that some scientists were unnecessarily callous in their use of experimental animals. This individual holds a responsible position within the University of Lund and is respected for his knowledge and experience in laboratory animal science. He is completely opposed to the views of the anti-vivisectionists, who he condemns as being largely responsible for the ineffectiveness of the committees, but, extraordinarily, finds himself advancing arguments which echo those of the opponents of animal research. He believes that the presence of anti-vivisectionists on the committees inhibits scientists and technician members from criticizing protocols which their expert knowledge, experience or intuition persuade them are suspect, because they fear exposure of these criticisms to the media with public discredit to the investigator and institution concerned. Unsound proposals thus pass unchallenged (except, perhaps, by lay members) with the implication that unnecessary suffering may be caused to animals in these investigations. This assertion says little for the moral integrity of the scientists and technicians involved and it also seems odd that by suggesting modifications to unsatisfactory projects the committee should create unfavourable publicity for the scientific community. However, it is conceivable that insensitive media treatment of such incidents might prove damaging.

The greatest threat to the usefulness of the Swedish committees is posed by the strength of the anti-vivisectionist lobby. It is regrettable that, by striving for the unattainable, that is, immediate abolition of the use of animals for experimentation, the anti-vivisectionists are hampering the amelioration of animal suffering that is possible now. The results of this activity in Sweden have wider implications, for the bold gesture which introduced the national system of ethical review as an essential prerequisite for animal experiments has attracted international attention. By reducing the efficiency of the commmittees or threatening their continued existence, the Swedish anti-vivisectionists fuel critics of the scheme elsewhere who are anxious to discredit the initiative in an effort to prevent the introduction of similar schemes in their own countries.

Review in North America

In the United States scientists are currently attempting to come to terms with new guidelines on laboratory animal welfare proposed by the National Institutes of Health (NIH), the major grant-awarding body for biomedical research in the country (*NIH Guide for Grants and Contracts* Vol. 12 No. 5; 1984). One of the major proposals requires the appointment at each research institution of an Animal Research Committee (ARC). It will consider both care and use of animals, and is required to review any research proposal in which animals are likely to be exposed to severe pain or distress. Most controversial is the directive that at least one committee member must be unconnected with the institution — in effect, a representative of the general public.

The commonly held view is that practices recommended in the document could be established before the end of this year and institutions throughout the country are producing plans to ensure conformity with the requirements. Other funding agencies traditionally defer to the NIH in matters of this kind, so failure to comply could deprive a research institution of any money from external sources. The grant-awarding bodies in the United States are the chief arbiters of what research may be carried out there and how. They have set standards which aspiring grantees have had to fulfil, including, for prospective users of experimental animals, standards of animal care and management. However, there have been a few highly publicised incidents of malpractice which suggest that the regulations require strengthening and the new guidelines are, in part at least, a response to this adverse publicity.

Some US research institutions have already, voluntarily, established committees with responsibilities similar to those outlined. A few even have lay members (often representatives of animal welfare societies) but these are exceptional. Their development has been due to the concern and enthusiasm of one or more staff members, not necessarily research scientists themselves. Ethical review was pioneered in America at Colorado State University, Fort Collins, largely through the efforts of Bernard E. Rollin, the forceful professor of philosophy, who developed a keen interest in animal rights issues and taught an ethics course to undergraduate veterinary students. The appreciation of the relevance of considering the morality of Man's use of animals which this engendered has so pervaded the University that concern for the treatment of experimental animals there quite naturally found expression in the careful consideration of experimental protocols by a committee of peers. This committee has not included participation from outside the University but plans are now in hand to change this in line with the NIH requirements.

The veterinary staff at Colorado State University gave good support to Professor Rollin's initiative. In other parts of the United States, laboratory animal veterinarians have since taken a lead in organizing similar review committees, if only to strengthen their own hands in securing improvements in maintenance and use of experimental animals. Generally, however, the veterinary profession has shown little collective concern for animals in research, preferring, as a Washington representative of the American Veterinary Medical Association (AVMA) recently remarked, "to remain neutral on the issue". There is a special AVMA committee on Animal Welfare which includes the welfare of laboratory animals in its remit and a postgraduate Diploma in Laboratory Animal Medicine has been developed which is gaining increasing acceptability as a suitable qualification for veterinarians employed in this young but expanding specialization. However, while there can be no doubt of the commitment of individual members of the profession to the cause of laboratory animal welfare, concerted effort to ensure needed improvements and reform are lacking, as if the profession is unsure of its ground in appearing to criticize colleagues in science or medicine.

One way in which ethical concern for experimental animals is expressed is by ensuring that only competent staff are employed in their care and maintenance. Competence is achieved through experience and training, so the provision of a training course for US veterinarians responsible for experimental animal facilities is a valuable contribution to laboratory animal welfare. The appointment of veterinarians with these specialist skills is a measure of the concern of an institution for the well-being of its animals — as is the minimal or complete lack of veterinary cover found in some large research institutions in the United States and, of course, in other countries.

The training of biomedical researchers in the specific skills of caring for and using experimental animals efficiently and humanely is just as important a consideration but courses are much less formalized, or even non-existent. This deficiency is not unique to the United States.

Potential members of an animal research review committee may also benefit from some training and with remarkable alacrity the Scientists Center for Animal Welfare (SCAW) in Washington has anticipated this in a series of workshops offering help on the setting up and running of the committees along the lines of the NIH proposals. The first of three workshops planned for 1984 was held in Baltimore in May. Eighty-five of the ninety participants who completed a questionnaire after the meeting thought that committee review of research proposals for animal welfare concern was "very important". None opposed review. Most of the respondents were research scientists, veterinarians or animal care technicians. Although the group was highly selected, the survey results provide evidence of a positive attitude among American scientists and their colleagues to Animal Care and Use Committees as an important means of improving laboratory animal welfare.

The NIH recommendations offer potential for such improvement but they present several problems which institutional heads and administrators will have to consider carefully as they formulate their response. Among questions which the planners will need to ask in the context of the individual circumstances of each institution, the following are likely to be significant:

(1) Will the volume of research proposals present the committee with an excessive workload — a distinct possibility in major centres. (If only selected protocols are reviewed, will demand for public accountability be satisfied?)

(2) Will the ARC consider matters of ethical concern only or ethics and scientific merit of the projects? The two are so interconnected — animal research which is badly conceived scientifically is necessarily unethical — that consideration of both seems inevitable.

(3) Will ARC decisions be arrived at by consensus or on a majority vote? (That is, how much influence will the lone, extra-institutional member carry?)

(4) How will the ARC confirm that investigators comply with its decisions? (Will there be any follow-up, reporting back, committee inspections or monitoring procedures?)

(5) Will there be any attempt to standardize ARC policy and criteria for decision making between institutions?

(6) What will be the legal status of ARCs?

(7) Will investigators have a right of appeal against decisions of the ARC?

(8) Concerning the non-institutional member: what kind of person should be selected? What should be the terms of the appointment? Should he/she be remunerated? How can the need for confidentiality be reconciled with conscience to protect (i) the interests of the institution and (ii) the integrity of the lay member.

The current proposals allow research institutions to select the outside member(s), but they will want to appoint persons from the community with sufficient objectivity to be credible as representatives of public opinion.

Several of the problems listed above have already been faced in Sweden and in Canada, where institutional Animal Care Committees have been in existence for several years. In Canada, such committees are a feature of all institutions in which experimental animals are used. Their responsibilities include the sanctioning of all work involving animals (in teaching, field studies, research and trials), ensuring high standards of animal care and the review of research protocols. In Ontario and Alberta, the committees are mandated through provincial legislation. The Canadian Council on Animal Care (CCAC), an authoritative body within the Association of Universities and Colleges in Canada, has recommended terms of reference and guidelines to which the committees conform. Periodically, site visitors are arranged by CCAC to assess the efficiency of each institution's committee and help effect standardization on a federal basis. It is recommended that membership should include lay persons to represent community interests; lay person also serve on assessment panels for site visits. Existing lay members of Animal Care Committees represent major animal welfare societies or are members of professions: law, education, the church. The committees should be primarily concerned with the ethical aspects of the suggested procedures and the property of suggested methodologies, since grant-awarding agencies use peer review to confirm the scientific merits of projects seeking financial support.

The Canadian Federation of Humane Societies, representing 36 member organizations, and somewhat akin to Britain's RSPCA, provides an effective mouthpiece for public animal welfare concerns in Canada. Its view is pragmatic on the issue of using animals in experiments, but there is a growing tendency, within the Federation, to question the continuing need for their use in biomedical research. It is fully supportive of the institutional Animal Care Committees and distributes publications to guide their members.

There is no shortage of animal welfare groups in the United States,one or more of which might adopt a similar role to that of the Canadian Council on Animal Care in providing oversight of the new committees when established, perhaps in conjunction with officers of NIH. Support similar to that provided by the Canadian Federation of Humane Societies would help to ensure the effectiveness of the American committees.

Lessons for Britain?

How relevant is all this to the situation in Britain? It is naive to suppose that a regulatory or advisory system which proves valuable in one country can be transposed to another with similar expectations. Equally, it is foolish to ignore interesting developments in other parts of the world which are relevant to one's own situation. Successes and failures of overseas initiatives can inform and guide the planners of suitable indigenous approaches. This is not to deny that there are major historical, cultural, legislative and logistical differences between the countries included in this discussion which create formidable barriers to the easy exchange of ways of tackling common problems.

One difference which is frequently advanced to suggest that Britain has nothing to learn from groups overseas in respect of animal welfare, is that legislation for the protection of animals in Britain predates that of any other modern State. The importance of this tends to be overemphasized and other nations have not been so tardy as is sometimes supposed. Sweden's first animal protection act, for example, dates back to 1944 and it is arguably more relevant to the present day than the British legislation formulated in 1876, no matter how amenable to reinterpretation that law may have proved.

Because of this misconception — that all other countries are 'starting from scratch' in animal protection — regulations which the latter introduce are interpreted as being nothing more than attempts to bring themselves 'up to our level'. In fact, the practical and philosophical expression of concern for improvements in laboratory animal welfare in countries like Sweden and Canada has outstripped legislative provision here — even if the ethical awareness of some scientists and others involved with laboratory animals in Britain remains as keen as that of their counterparts anywhere in the world.

The present British regulatory system is applauded as a model of rationality and efficiency by some and described as wholly inadequate by others. The latter group includes not only the hard-line opponents of animal experimentation but scientists working within the system. Wherever the truth lies, future Government legislation, based on an appraisal of the current system, promises to significantly tighten controls. But, no matter how stringently the law may be drawn and no matter how rigidly it may be enforced, at the interface between the scientist and his subject, only the attitudes of the scientist are important. A heightened awareness by experimenters of the responsibilities associated with the use of animals and increased sensitivity to their needs and their capacity to suffer will achieve much more for laboratory animal welfare than new legislative measures (although legislation to encourage the introduction of institutional review bodies here to help achieve these desirable changes would seem appropriate!). These were the kind of thoughts which prompted the Uppsala experiment and which make the Fort Collins initiative so important, where the ethos of these institutions has developed to permit the expression of a rational, caring approach to the use of animals in research.

The committees in Sweden and North America (existing and planned) are answerable directly to the institution chief or administrative head and contain very senior staff as members. As a tangible benefit to the institution, they provide an important public relations service by ensuring compliance by institution personnel with existing national and local regulations on the care and the use of experimental animals. Beyond this, they provide a guarantee that only 'clean' work is undertaken, this assessment having been reached not merely by the scientists alone. The attraction of such guarantees to institution chiefs is obvious and, equally, it is important to the prestige of the committees that they are seen to stem from the highest institutional authority. The same recognition will be critical to the success of any similar committees which may be developed in Britain.

We can profit from the problems which have occurred in Sweden by avoiding some of the pitfalls. The anti-vivisection movement in Britain is proportionally smaller than its Swedish counterpart. The Nordic Society Against Painful Experiments on Animals (Nordiska Samfundet mot Plågsamma Djurförsök, NSPD) has a membership of 38,000 in a country with a total population of only 8.5 million. Furthermore, so evenly divided is the country politically that 70,000 votes could change the government. In such a situation, any sizeable pressure group can exert considerable political influence and this power is used astutely by NSPD. To deny representation of minority, extremist groups opposed to animal experiments on ethical committees in Britain would not be thought tendentious. Here convinced opponents of animal research will not be favourably impressed by the introduction of research review procedures. Certainly for the law-breakers, the situation has gone beyond the stage at which participation in this sort of constructive dialogue is possible.

In Sweden and America there is still opportunity for discussion and compromise between groups of all shades of opinion. Once this ground is lost, it is unlikely to be regained — which is why attempts to exclude Swedish anti-vivisectionists from the ethical committees may have retrograde effects.

Several factors seem to favour the introduction of local ethical committees to Britain and, if forthcoming legislation follows the recommendations of the 1983 Government White Paper, *Scientific Procedures on Living Animals* (HMSO, cmnd 8883), this will strengthen the case for their establishment, in defining a role for them in careful scrutiny of applications for project licences before submission to the Home Office.

We have available through the Home Office Inspectorate, an excellent means of supervising institute-based ethical committees and ensuring a desirable measure of inter-institutional standardization. By close liaison with the committees, inspectors could exert their own influence more effectively in the regions. Undoubtedly, the collaboration and support of the Inspectorate will be vital to the successful functioning of the committees.

Major animal welfare groups in Britain favour the concept of local ethical committees and can be relied upon to participate in any initiatives to establish these bodies — providing that they are more than window dressing for research institutions.

Perhaps an Uppsala-type experiment is necessary here before British scientists will be persuaded of the value of the animal research review process in the context of University activities. This will be considered more fully at a meeting being convened in the University of Liverpool on 1st and 2nd October in response to a demand from scientists for improvements and alternatives to animal experimentation.

Scientists will groan at the prospect of 'yet another committee', but if the protestations of genuine concern for animal welfare which are frequently voiced by animal experimenters mean anything, then priority must be given to this kind of provision. ☐

David P. Britt was awarded a Churchill Trust Travelling Fellowship (1984) to study ethical monitoring of animal experiments in North America and Sweden. He is at the Department of Veterinary Parasitology, Liverpool School of Tropical Medicine, Pembroke Place, Liverpool L3 5QA, UK.

Thunder and electric storms

A neat measurement of the stratospheric electrostatic fields throws light on the link between solar activity and terrestrial climate.

CAREFUL readers of the scientific literature are forgivably suspicious of articles that refer to the very distant past. The sceptical will ask whether the authors of such an article have sinister motives for ignoring recent work, and will probably dismiss the possibility that they have managed to resuscitate an important problem whose trail runs cold before, say, 1980. So what is to be made of the contribution now published by R.H. Holzworth and T. Onsager of the University of Washington (Seattle) and P. Kintner and S. Powell of Cornell University to the problem of atmospheric electrostatic fields? Their paper (*Phys.Rev.Lett.* **53**, 1398; 1984) manages one reference to a regular paper (by Holzworth) after 1980, but is mostly spattered with references dating from the 1920s and earlier.

Holzworth *et al.* have nevertheless managed to break new ground, and in a stimulating fashion. What they have done is to equip two balloons so as to measure the electrostatic field in the Earth's atmosphere at an altitude of 26 km. The balloons were released from New Zealand in March last year, and allowed to drift for two weeks eastwards across the Pacific at a latitude of 45°S. The lateral separation between the balloons was never less than 750 km. The objective was to compare the electric field strength at two such widely separate locations. The conclusion that the two records are very similar, but that fluctuations of field strength from day to day are much greater than expected, have an important bearing on the understanding of atmospheric electricity.

One of the obvious early references in Holzworth *et al.* is to C.T.R. Wilson, whose design of the closed chambers that became the workhorses of early cosmic-ray measurements was originally part of an investigation of atmospheric electricity. What Wilson knew was simple — that thunderstorms consistently carry positive electric current upwards in the atmosphere and that near the surface of the Earth, the electric field strength (the gradient of electric potential), while variable, can amount to several hundred volts per metre. Wilson had the wit to recognize that the cumulative effect of thunderstorms must be to some degree offset by a less spectacular but continuous downward electric current, for the electrical potential between the surface of the Earth (negatively charged) and a presumed upper conducting layer (the ionosphere) cannot increase indefinitely.

But how can the atmosphere conduct electricity, even at the low rate suggested by the observations? Wilson was the first to show that the production of ions by cosmic rays is the essential mechanism for rendering the bulk of the atmosphere conducting. The potential difference between the surface of the Earth and the ionosphere is typically no more than some tens of thousands of volts — the large potential gradient near the surface quickly trails off with increasing altitude as cosmic-ray ionization increases the conductivity of the atmosphere — at 26 km Holzworth *et al.* measure fields of less than 1 V m^{-1}.

The immediate significance of the new balloon measurements is that they have demonstrated a technique for measuring electrostatic fields beneath the ionosphere that is bound to become established if sparsely used. From this first batch of data, the conductivity at 26 km seems virtually constant for days on end, while the electrostatic fields measured by the two balloons, even when separated by up to 3,000 km, are identical to within 10 per cent for most of the time (perhaps 70 per cent of the 16 days of common observation). That is understandable if, indeed, the field at 26 km can be likened to the electrostatic field between two parallel conducting plates, one the ionosphere and the other the ocean surface.

For then, given the high conductivity of the upper and lower surfaces, the relaxation of the distribution of charge must be rapid. The local effects of thunderstorms carrying positive charge into the stratosphere would be quickly dissipated. Holzworth *et al.* point out that there nevertheless seems to be a daily variation of field strength at 26 km, at least when 10-minute records for consecutive days are averaged together, with a possibly shallow maximum of field strength at 20h Universal Time. The records, however, show no drift in the timing of the diurnal variation with the eastward passage of the two balloons across the Pacific, which provisionally gives the lie to theories that the global pattern of the vertical electrostatic field is fixed in relation to the position of the land masses on the surface of the Earth.

The chief interest of these data, according to their authors, is the enormous variation in the pattern of the vertical electrostatic fields measured by each balloon on different days. Field strengths are generally less at local morning than after noon, but otherwise the variability is so great that one day's record is unrecognizably different from the next's. The inference, which is important, is that there must be substantial fluctuations (perhaps by a factor of two) in the global vertical current in the atmosphere, and on time-scales of the order of 10 minutes, perhaps themselves the consequences of fluctuations of thunderstorm activity near the surface of the Earth.

While Holzworth (among others) has previously been responsible for vertical field measurements at altitudes up to 30 km, the twin balloon measurement seems to be the first of its kind. Evidently the conclusion that there are large short-term fluctuations of the global electrostatic field could not have been sustained by measurement with a single balloon (for local thunderstorms might always have been responsible). One obvious benefit that lies ahead is a more detailed correlation of the global field fluctuation with observed thunderstorm activity (presumably anywhere in the world). The point is obviously important because, while there seems little dispute about the correlation between thunderstorm activity and the strength of the electric field, the degree to which the former may be excited by the latter, involving as it does the non-linear dynamics of condensation in cumulus clouds, remains to be settled.

So does the possibility that the electrostatic field beneath the ionosphere may provide a physical link between sunspot activity and terrestrial climate. Ralph Markson has argued that solar activity, by affecting the cosmic-ray flux and thus the conductivity of the atmosphere, might influence the occurrence of thunderstorms (*Nature* **273**, 103; 1978), but by a mechanism which has been disputed (L.C. Hale, *Nature* **278**, 373; 1979) and which again hangs on the degree to which electric fields and thunderstorms are mutually stimulating.

Unfortunately, given the short-term global fluctuations of the vertical field, it is by no means clear how quickly careful monitoring of the electrostatic field by an *in situ* measurement will be feasible, and how quickly that will yield direct evidence bearing on the question whether solar activity and terrestrial weather are in any way linked by atmospheric electric fields. At least another sunspot cycle will go by before matters are cleared up.

John Maddox

Cosmology

Cosmologists in the dark

from Joseph Silk

IN their continuing quest to unravel the true nature of the Universe, cosmologists are beginning to pursue a most bizarre trail. Never mind that the Universe contains more mysteries than a whole galaxy of astronomers could ever unravel. Now we are learning that all the clues may be heralding a false dawn. What we see may have little to do with the true distribution of matter in the Universe. If galaxies formed only in specially-selected regions, then much of our painstakingly-acquired knowledge of the large-scale structure of the Universe, based on decades of observations with the largest telescopes available, may as well be discarded.

Could the Universe really be fooling us so effectively? The search for the holy grail of elementary particle physics, an ultimate theory of the unification of the fundamental forces of nature, has provided a persuasive argument. One of the successful outcomes of this approach has been the development of grand unification theories (GUTs) which incorporate the electromagnetic and nuclear (weak and strong) forces. Many GUTs exist, and some have a property of profound cosmological importance. There is likely to be a phase transition, associated with the spontaneous breaking of symmetry between strong and electroweak forces, in which sufficient entropy is liberated to trigger an epoch of exponential expansion. This inflation of the Universe can explain several outstanding cosmological conundrums, including the isotropy of the Universe and the origin of the fluctuations from which galaxies formed. One of its most remarkable predictions, however, is that the Universe should be, almost precisely, flat. If spatial curvature is negligible, the Universe will expand at a rate that barely overcomes its self-gravitational attraction. It will continue to expand, slowly decelerating, into the remote future.

In such a situation, simple application of Einstein's or even Newton's theory of gravity, if suitably generalized, to the expanding Universe leads one to infer a critical density of matter that our observed Universe must contain. This is equal to $3H_0^2/8\pi G$, where G is Newton's constant of gravity and H_0 is Hubble's constant for the linear expansion of the Universe, and amounts, very roughly, to an average density of about three atoms per cubic metre.

To compare what we actually see with this prediction, it is convenient to define the cosmological density parameter Ω to be the ratio of the actual density to its critical value, above which the Universe would eventually recollapse. Inflation predicts that $\Omega=1$ to within 1 part in 10^4. However, astronomers are almost unanimous in their assertion that the density of all observed matter amounts to $\Omega \approx 0.1$, with a factor of two or so uncertainty. The loophole for reconciling the observed Universe with the inflationary theory is that a component, even a dominant one, of the mass density that is uniform over the scale of galaxy clusters or superclusters would be very difficult to detect. Certainly, such a smooth backdrop has no direct influence on the dynamics of galaxies or those of galaxy clusters, which provide the principal means for determining Ω.

The evolution of the observed large-scale structure does depend very sensitively, however, on the distribution of an underlying dark component of matter. Gravitational instability, by which small density fluctuations in the early Universe have amplified into galaxies and galaxy clusters, would have been quenched had the dominant mass distribution always been, for example, very hot and consequently very uniform. On the other hand, if astronomers' measurements of $\Omega \approx 0.1$ are taken literally, one encounters a severe problem in understanding the extreme isotropy of the cosmic microwave background radiation. Recently reported by Juan Uson and David Wilkinson of Princeton University to be isotropic to 3 parts in 10^5 on an angular scale of 4.5 arc min, the background radiation should sample the seed fluctuations in the matter distribution at the epoch when the radiation was last being scattered. Lowering Ω reduces the effectiveness of gravity in amplifying these fluctuations, and to obtain the observed structures, one would infer for the most plausible models correspondingly larger ripples in the microwave background than are seen. With $\Omega = 1$, this problem need not arise.

A workshop devoted to increasing our understanding of the evolution of the large-scale structure of the Universe, and lasting eight months, has just ended at the Institute for Theoretical Physics in Santa Barbara, California. One of the most significant outcomes was a scheme for reconciling the dynamic measurements of Ω with a dense universe. The idea, developed most fully by J. Bardeen (University of Washington) and N. Kaiser (University of California, Berkeley), is that galaxy formation occurs only in a biased subset of the real Universe, at points where the critical density is particularly high. Consider a random field of density fluctuations (a three-dimensional analogue of the pattern of waves on the ocean surface) with power on both large and small scales. Suppose that the bright galaxies form only at the peaks of the density fluctuations. It turns out that the large-scale structure of the galaxy distribution can be much more pronounced than that of the underlying distribution. One way to visualize this is to imagine filtering noise with a low bandpass filter: the surviving intensity peaks tend to be more strongly correlated than the unfiltered distribution. A similar mechanism has been applied by Kaiser to explain the anomalously large clustering of rich clusters of galaxies.

A precise physical mechanism for producing such a bias has not so far been worked out. It is likely to involve feedback of energy by the first galaxies to form. Since the largest peaks on any given scale collapse first, one could readily imagine that some form of negative feedback, suppressing later formation of galaxies, might lead to a plausible biasing mechanism. A scheme of biased galaxy formation resolves many of the outstanding problems of the large-scale structure of the Universe. The weakly correlated dark matter leads to predictions of low galaxy peculiar velocities, in accord with astronomical measurements, and the spatial correlations predicted for the galaxies resemble what is observed.

As for galaxies, galaxy groups and clusters, the presence of gravitationally dominant dark matter within their luminous confines seems to be an observational fact. A second theme to emerge from the Santa Barbara workshop and one that is reviewed on page 517 of this issue by Blumenthal *et al.* is that cold dark matter gives rather a good fit to the prescription for our Universe. This dark matter, which consists of hypothesized weakly-interacting elementary particles such as photinos or axions, was sufficiently cold in the early Universe that fluctuations developed by gravitational instability over a wide range of scales, down to and even below that of a typical galaxy. The massive neutrino is the prototype of a species of weakly-interacting particles that would have been sufficiently hot, when freely streaming at the speed of light, to have erased all substructure on scales below those of great galaxy clusters. A hot dark matter scenario for galaxy formation has several unpalatable features, most of which arise from the constraint imposed by the near uniformity of the Universe on large scales. This model guarantees that the first scales to have undergone collapse and allowed galaxy formation to occur could only have done so at what seems to be an unacceptably recent epoch. Cold particle models, on the other hand, undergo hierarchical clustering at a relatively early stage, small scales condensing first, followed by successively larger-mass scales.

The cold particle-dominated universe appears to provide a satisfactory understanding of the distribution of dark matter on scales from those of dwarf galaxies to those of the great clusters of galaxies. Combined with a biasing mechanism, it reconciles the inflationary prediction of a universe at critical density with the astronomers' Universe. Even the distribution of fluctuations predicted by the inflationary theory is, according to Blumenthal *et al.*, reflected in the characteristic distribution of galaxy masses and densities. What remains to be shown is whether the giant voids in the galaxy distribution, such as that in Bootes, and the enormous aggregates of galaxies, such as that in the Serpens-Virgo region some fifty million megaparsecs across, can be reconciled with such a theory. One of the most tantalizing aspects of the currently moribund idea of a universe dominated by massive neutrinos was that it naturally predicted the presence of large filaments and sheets of galaxies, separated by huge voids. It may not be so easy for a cold particle-dominated universe to meet the same challenge. ☐

Joseph Silk is in the Astronomy Department, University of California, Berkeley, California 94720.

Astrophysics

Oscillations of degenerate stars

from Arthur N. Cox

RECENTLY there has been renewed interest in the oscillations of degenerate dwarf stars. Very-low-luminosity variations were first seen in the white dwarf HL Tau-76 by Landolt some 20 years ago[1], and since then, luminosity variations with periods ranging from hundreds to thousands of seconds have been detected in many other white dwarfs. The past few months have seen several predictions confirmed by new observational discoveries, and the scope of our research and understanding of degenerate star oscillations greatly expanded.

The stars that have stimulated the interest are very small, with radii ranging from 1 - 10 per cent of the radius of our Sun, only slightly bigger than that of the Earth, and a probable mass of 0.6 solar masses (M_0). Their mean density is therefore very high, about 10^6 g cm^{-3}, implying the presence of electron degenerate matter throughout most of their mass. Because degenerate matter conducts heat easily, white dwarf stars have core temperatures as low as 10^7 K or less and, thus, are much cooler than any other stars except the lower-mass very-faint red dwarfs. White dwarfs produce no nuclear energy because any potential fuels, such as hydrogen and helium, are found only in their cool surface layers, so their luminosity is low. Because of their very small size and low luminosity (less than 1 per cent of that of our Sun) it has taken billions of years for the surfaces of these stars to cool to their current temperatures, typically 10,000 K.

Stellar evolution theory predicts that stars with masses of up to at least 6 *M*. evolve to become white dwarfs (see the figure). As these stars burn their initially copious supply of hydrogen to helium and the helium to carbon, oxygen and neon in a growing electron-degenerate core, they expand and increase in luminosity, to become red giants or supergiants. When they have reached a radius of perhaps 100 or more solar radii, they lose mass, sometimes to produce planetary nebula shells, by shedding all but the CNONe core resulting from the hydrogen and helium burning. The remaining core has a surface temperature typically of 150,000 K and a luminosity of 10,000 solar luminosities. Because the stars have lost the layers in which nuclear processes take place, they can no longer produce any new energy to sustain their luminosity and they rapidly (within no more than 10,000 - 100,000 years) become very small and hot. Finally, slow cooling turns these hot dwarfs into faint white dwarfs after millions of years.

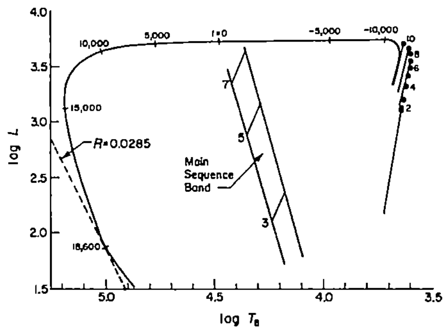

Hertzsprung–Russell diagram where luminosity is plotted versus the surface temperature, showing the evolution of a 0.6 *M*. star (adapted from ref.10). The initial increasing luminosity tracks for stars of 3, 5, and 7 *M*. are indicated as the main sequence band. The final stages of nuclear burning of the 0.6 *M*. star result in 10 helium shell flashes where the luminosity is greatly increased for durations of hundreds of years. These are marked at the very coolest surface temperatures where the mean emitted luminosity is still increasing with time. Zero time is arbitrarily set at the moment when the surface temperature increases to 30,000 K. The track represents hot dwarfs (upper left), turning as they slowly cool to become very faint white dwarfs (below the bottom of the figure). The minimum radius of the hot dwarfs is 0.0285 solar radius, and later this radius decreases as the conventional white dwarf is formed.

Many hot luminous stars have been discovered and very recently five of them have been found to show 5 - 30 minute period variations in their luminosity of a few per cent (ref.2 and H.E. Bond & A.D. Grauer, personal communication). These stars constitute a new class of variable, called PG variables, after the first studied PG1159-035 which is perhaps the hottest variable star in the sky. Oscillations of these stars are thought to result from the periodic ionization of carbon and oxygen in their surface layers. While they oscillate, the stars deviate from their spherical shape, hence their classification as nonradial pulsators. Last year, Starrfield *et al.* predicted that the stars would pulsate in nonradial g modes only if about half of the mass of their outer pulsation-driving layers was oxygen, and helium comprised only a small fraction[3]. Now, a large oxygen abundance has been verified spectroscopically[4]. Observations of helium at the stars' surfaces, however, indicate incomplete loss of this fuel. If there is enough helium, another shell flash may occur during the stars' evolution. Further studies of the longer-period K1-16 planetary nebula central star listed in the Kohoutek catalogue are underway to see what pulsations would be predicted at earlier and cooler stages of this luminous stellar evolution.

The same cyclical ionization of hydrogen and helium that drives the pulsations of Cepheids also causes the much cooler and older ZZ Ceti stars, the classical white dwarfs, to pulsate. The κ and γ effects drive motions by both blocking and hiding the radiative luminosity at key compressed phases of the pulsation cycle. At subsequent phases, the radiation is allowed to flow more strongly so that the oscillations are driven as the stars re-expand.

A further intriguing class of variable stars is the DB white dwarfs. These stars have helium-rich atmospheres and, probably, helium-rich pulsation-driving layers with temperatures of 100,000 K or more. They do not have hydrogen ionization driving, but they do have the driving mechanisms from the ionization of helium. Winget *et al.* predicted that these helium stars should pulsate in nonradial modes[5], and recently this has been confirmed in three cases (ref.6 and H.E. Bond & A.D. Grauer, personal communication).

What does the future hold in store? Several groups[7-9] have predicted that radial pulsations in high overtones should occur in white dwarfs. Perhaps the next observational discovery will be that these approximately 1-second oscillations also exist.

1. Landolt, A.U. *Astrophys. J.* **153**, 151 (1968)
2. Bond, H.E., Grauer, A.D., Green, R.F. & Liebert, J.W. *Astrophys. J.* **279**, 751 (1984).
3. Starrfield, S.G., Cox, A.N., Hodson, S.W. & Pesnell, W.D. *Astrophys. J. Lett.* **268**, L27 (1983).
4. Sion, E.M., Liebert, J. & Starrfield, S.G. *Astrophys. J.* (in the press).
5. Winget, D.E., Van Horn, H.M., Tassoul, M., Hansen, C.J. & Fontaine, G. *Astrophys. J. Lett.* **268**, L33 (1983).
6. Winget, D.E. Robinson, E.L., Nather, R.E. & Balachandran, S. *Astrophys. J. Lett* **279**, L15 (1984)
7. Cox, A.N., Hodson, S.W. & Starrfield, S.G. *Lect. Notes Phys.* **125**, 458 (1980).
8. Saio, H., Winget, D.E. & Robinson, E.L. *Astrophys. J.* **265**, 982 (1983).
9. Starrfield, S.G., Cox, A.N., Hodson, S.W. & Clancy, S.P. *Astrophys. J.* **269**, 645 (1983).
10. Iben, I. & Renzini, A. *A. Rev. Astron. Astrophys.* **21**, 271 (1983).

Arthur N. Cox is a Fellow of the Los Alamos National Laboratory, PO Box 1663, Los Alamos, New Mexico 87545.

Vaccines

In search of novel immunogens

from Peter Newmark

To judge by a recent meeting*, empiricism and tradition still offer at least as much to the production of new vaccines as rationalism and peptides. But the possibility of basing new vaccines on synthetic peptides that correspond to immunogenic parts of a pathogen's structure is acting as a great stimulus to immunochemists and their allies.

The initial problem with the peptide approach to vaccines is to identify immunogenic peptides. Were it possible to do that from no more than the amino acid sequence of a protein, life would be easy. But, although it is possible to predict crudely which segments of a sequence will form the surface of a folded protein, and although such segments, in peptide form, are likely to be antigens, they will not necessarily be immunogenic, in the sense of evoking a sufficient immune response to neutralise the pathogen. Moreover, it is inevitable that many, and probably most, immunogenic sites on a protein are not composed of contiguous amino acids but rather of amino acids that are juxtaposed by protein folding and so cannot readily be mimicked by a synthetic peptide.

For the most part, immunogenic peptides have been identified by screening candidates with monocloncal antibodies that neutralize the relevant pathogen *in vitro*. A promising new technique, requiring neither prior peptide synthesis nor sequence information was described by J. Nunberg (Cetus Corporation). The cloned gene of an immunogenic protein of a pathogen (feline leukaemia virus in the first case) is cut into random short fragments by DNase 1. The fragments are cloned into Lambda phage 'Charon 1b' in such a way that they are expressed. Phage colonies are screened with a monoclonal antibody that neutralises the pathogen. Those that react with the antibody must be expressing an antigenic peptide from an inserted gene fragment which is then sequenced (see *Proc. natl. Acad. Sci. U.S.A.* **81**, 3675; 1984). In that way, Nunberg reported, it had been possible to identify a 14-amino acid immunogen of the envelope protein of feline leukaemia virus. The corresponding synthetic peptide was able to compete with the virus for antibody. Moreover, when attached to a carrier and used to vaccinate guinea pigs, the peptide elicited a partial immunogenic response which was markedly enhanced by subsequent administration of a low dose of killed virus. An efficacy trial of this approach to a vaccine against feline leukaemia virus in cats is now being set up.

E. A. Emini (Merck Sharp and Dohme) reported a roundabout, but revealing, identification of immunogenic sites on the hepatitis A virus, a relative of poliovirus. Starting from the fact that antibodies against hepatitis A virus demonstrate some cross-reactivity with peptides representing major immunogenic sites on the VP1 protein of poliovirus type 1, and taking into account the observation that these peptides could prime animals to respond to a sub-immunogenic inoculum of hepatitis A virus, Emini expected to find that certain sequences within the VP1 of hepatitis A virus closely matched those of the poliovirus peptides. But the relevant cDNA sequences (J. Hughes, Merck Sharp and Dohme; B. Baroudy, National Institutes of Health, Bethesda) revealed no such match. Nor was there a concordance in the calculated secondary structures of the two VP1s. Only when a comparative analysis of the predicted surface features of the two proteins was made, was a striking similarity observed. Based on this comparison of 'shape', Emini *et al.* have synthesized a hepatitis A virus peptide, monoclonal antibodies against which have virus neutralising activity, mostly cross-react with the virus and in some cases compete with antibodies in the sera of humans infected with hepatitis A virus. These data underline the importance of the 'shape' of the surface of immunogenic proteins and explain why much effort is being invested into an understanding of 'shape' and its determinants.

Another way to investigate the relationship between structure and immunogenicity is to document any differences in sequence between a virus that can be neutralised by a monoclonal antibody and any genetic variants that resist neutralization. The expectation would be that resistance is the result of mutations within the sequences that encode antibody-binding regions of the protein. However, D. Diamond (State University of New York, Stony Brook) reported that expectations were confounded in the case of poliovirus type 1. Two regions within its VP1 protein have been identified as antibody binding sites but virus variants that resist neutralization have amino acid changes elsewhere on VP1 or even on VP2 or VP3 proteins. Presumably, within the virus proper, the mutated amino acids are either juxtaposed to the identified antibody binding sites or affect conformation at a distance.

Also intriguing were the sequence comparisons of an attenuated strain of poliovirus type 3 (used in the Sabin-type vaccine), its parent and some strains that are revertant in terms of their neurovirulence (J. Almond, Leicester University). The attenuated strain had ten base changes from its parent, only three of which give rise to amino acid changes. Contrary to expectation, none of these three is consistently of the parental type in the revertants; the only consistent base reversion is in a non-coding position. By recovering the poliovirus from sequential nappies of a vaccinated child the same base reversion has been documented to occur within 36 h of vaccination with the attenuated strain. Clearly the reversion is strongly selected for — but why?

A whole session of the meeting was devoted to the possible resurrection of vaccination with vaccinia virus, using it to carry and express a wide variety of immunogens. This possibility was recently put in its proper perspective in these columns by J. Beale (6 September p.12), and F. Fenner (John Curtin School of Medical Research, Canberra) provided more perspective at the meeting. Both commented that the known, though very infrequent, complications of smallpox vaccination could be a barrier to the return of vaccinia inoculation. But R. Buller (National Institutes of Health, Bethesda) described some parameters by which the virulence of vaccinia virus can be reduced if the thymidine kinase gene of the virus is used as the target for insertion of new immunogen genes.

In a novel application of the vaccina approach H. Koprowski (Wistar Institute) reported that vaccinia virus recombinants containing the gene for the immunogenic glycoprotein of rabies virus are able to protect experimental animals against an intracerebral challenge by the virus. K. Cremer (National Institutes of Health, Bethesda) reported that intradermal inoculation of mice with vaccinia virus carrying the gene for glycoprotein D of herpes simplex virus type 1 provided protection against both type 1 and type 2 virus and also inhibited latent ganglionic infection by type 1 virus. And E. Paoletti (New York State Department of Health, Albany) described inoculation experiments using a vaccinia virus in which the genes for immunogens of hepatitis B, herpes simplex and influenza viruses had been inserted at different sites; each provoked an antibody response, demonstrating the potential of vaccinia virus as a polyvalent vaccine.

Another approach to new polyvalent vaccines was described by P. Valenzuela (Chiron Research Laboratories). The idea is to recombine the gene of a second immunogen with that of hepatitis B surface antigen (HBsAg) so that the second immunogen is assembled into, and presented on, the HBsAg particles that engineered yeast and mammalian cells produce. As an initial step in that direction, the gene for glycoprotein D of herpes simplex virus has been recombined with that of HBsAg and a lysate of yeast containing the recombinant has been shown to react with antibodies against both proteins.

Ironically perhaps, the recombinant was made by inserting the herpes gene into the

---

*'Modern Approaches to Vaccines', Cold Spring Harbor, 12–16 September, arranged by R. Chanock and R. Lerner. The proceedings will be published in January 1985.

'pre-S' sequence that precedes the 'S' sequence of HBsAg and encodes a 55 amino acid extension which is poorly represented in serum HBsAg particles and is not found in yeast HBsAg particles because only the S gene has been engineered into yeast. The irony is that the pre-S encoded extension may be too important to be ignored or disrupted according to S. Kent (California Institute of Technology). Data he presented suggest that the pre-S extension is more immunogenic than the S gene product; that it should be included in hepatitis B vaccines; that a synthetic peptide corresponding to the amino terminus of pre-S might itself be the basis of a vaccine; and that antibodies against the peptide will find diagnostic uses. Note, however, that serum and yeast HBsAg particles have been shown to protect chimpanzees against hepatitis B virus challenge, as has vaccinia virus carrying the S gene (see J. Beale *op.cit.*)

Space forbids mention of many other diseases for which a modern (sometimes not so modern) approach to a vaccine was reported. It should , however, be recorded that a session and a half was devoted to the prospects of a malaria vaccine and to the repetitive sequences within most of the potential malaria immunogens; the bulk of what was reported has recently been discussed in these columns (27 September, p.300 and 16 August, p.541). ☐

Peter Newmark is Deputy Editor of Nature.

Biological aerodynamics

Flight of fancy planned for the largest pterosaur

from Kevin Padian

AT one time, pterosaurs, the 'flying reptiles' of the Mesozoic era, seemed relatively simple to understand. They were considered to be bat-like inferior prototypes of birds, incapable of flapping flight or of efficient locomotion on land, no more than an early experiment in vertebrate flight. The giant *Pteranodon*, with its 7 m wingspan, seemed to be at the upper limit of any flying creature's size. Their replacement by the 'real masters' of the air, the birds and the bats, could easily be explained by a factor as trivial as a change in the average wind speed at the end of the Cretaceous (Bramwell, G.R. & Whitfield, C.D. *Phil. Trans. R. Soc.* B**267**, 503; 1974).

Recent work has called for a re-evaluation of these bizarre animals; none more so than the discovery of the giant *Quetzalcoatlus northropi* (Lawson, D.A. *Science* **187**, 947; 1975) which, with a wingspan currently estimated at 11 m, was 50 per cent larger than *Pteranodon.* This remarkable beast was responsible for a recent gathering* of over 30 engineers, aerodynamicists, palaeontologists and inventors in Pasadena, California, to discuss the possibility of building an accurate radio-controlled flying model of the creature. The purpose of such a venture would be not only to challenge the potential of ornithopter technology, but also to use the problems posed to the aerodynamicist to illuminate the biological limitations of the largest animal ever known to fly.

Before any accurate flying model of a pterosaur can be built, it will be necessary to have as complete a picture of these animals as possible. Much of the conference was therefore devoted to reviewing the most recent findings.

We now know that pterosaurs' wings were attached, not bat-like to the feet, but to the pelvis, to give a much more attenuate planform (Wellnhofer, P. *Abh. bayer. Akad. Wiss.* **141**, 1; 1979); the resultant wing loading resembles closely that of modern fliers (Padian, K. *Discovery* **14**, 20; 1979). All pterosaurs, except the largest ones (like the largest birds), were active fliers; their wings were fully folded when they walked on the ground, which they did bipedally: their forelimbs are functionally homologous to those of their closest relatives, the dinosaurs and birds, not to those of the bats (Padian, K. *Paleobiology* **9**, 218; 1983).

Recent models have treated the wing membrane as if it billowed with no internal structure, and ignored the probability that most pterosaurs having a wingspan of less than 3m seldom glided or soared, but flapped continually. Moreover, finely preserved specimens of *Rhamphorhynchus*, from the Late Jurassic of West Germany, show a series of fine, intercalated and stiffened striae permeating the entire wing membrane (Wellnhofer, *op. cit.*). This arrangement resembles the structural elements in the wings of birds (feather shafts) and bats (fingers), and suggests a role in maintaining the shape of the wing. The striae may have helped to determine the camber of the wing, although the details of their muscular control, including the extent to which the wing may have been collapsed without losing its aerodynamic integrity in flight, are not known.

Some idea must also be had of the dimensions and mobility of the animal to be modelled. This is complicated by the bimodal distribution of *Quetzalcoatlus* specimens. Thus there are around 20 partially-preserved 'small' individuals, with wingspans of about 5.5 m. Taken collectively, they provide a complete three-dimensional picture of nearly every wing element (Langston, W. *Scient. Am.* **244**, 122; 1981). Then there is the giant specimen, known initially from its tree-like 50 cm long humerus. Each of its incomplete skeletal elements is approximately twice the length of its homologue in the 'small' form, although its shape is much more robust. Doubling the dimensions of the smaller form is not adequate for some parts of the body, including the torso, of which there are very few remains. Body length can be extrapolated from the few dorsal vertebrae preserved, but body weight is more difficult to determine and estimates range from 50 to 100 kg; until a scale replica of the animal can be built from preserved material, a weight of about 65 kg has been provisionally accepted. The wing area must depend on the length of the body, and seems to have been about 8.13 m^2; this yields a wing loading of approximately 0.8 g cm^{-2}. *Quetzalcoatlus* had an aspect ratio of about 15 which, although high by the standards of natural fliers, is significantly lower than that of *Pteranodon* and other smaller seagoing pterosaurs. No living or man-made flier is an exact analogy for pterosaurs, although ultralight sailcraft may serve the purpose (McMasters, J. *NASA Conf. Pap.* **2085** (II); 1979).

The practical problems of replicating the flight of such an animal in a radio-controlled soarer-ornithopter are just beginning to be addressed. The first is that *Quetzalcoatlus*, like all pterodactyloid pterosaurs, had no tail, so pitch control will be complicated. Its neck and head were, by contrast, remarkably long, each about 2 m, while its entire torso was much shorter and its legs did not trail far behind the body. How far the neck could have been retracted or bent, if at all, is an important problem for paleontologists and has implications for engineers for calculating the centre of mass. The long neck and head form a powerful lateral moment arm, but also create a large amount of inherent instability; some sort of balancing mechanism up front will be necessary to control this. There are also logistic problems in trying to construct joints that can, for example, trim the wings and adjust pitch, while also supplying power for climbing flight.

The aim of the project is to launch the model from the Air and Space Museum of the Smithsonian Institution, from where it will fly across the Mall, climbing under its own power, circle the Washington Monument and return. To add realism, it has been suggested the model might pause in its flight, swoop down to snatch a small child from the crowd, carry it aloft, and consume it. For the present, mercifully, that objective seems to be beyond the technological capabilities of the field of Robotics. ☐

Kevin Padian is Assistant Professor of Paleontology at the University of California, Berkeley, California 94720.

---

*9–10 July 1984, organized by Paul MacCready and sponsored by the National Air and Space Museum, Washington.

Geophysics

Continental interior in view

from Roger N. Anderson

ANOTHER frontier of geological exploration may at last be yielding to curiosity and advancing technology. After the great geological expeditions to the Moon, and dramatic discoveries of the ocean floor made over the last twenty years, the attention of a surprisingly large number of geologists worldwide is turning back to the original geological problem: the internal workings of the continents.

We know very little about how the continents form and deform. What we infer comes from remote-sensing with the use of classical geophysical and geochemical techniques such as seismology, gravity, petrology and minerology. But the sources of these observations are always at the surface. Although we can build elaborate models of the continental interiors, we shall never be able to verify these concepts without looking inside the continents. Experiments to this end are now being planned in several countries. The tool used to sample the inside of the Earth is the drillbit.

A remarkable coincidence of planning means that several countries will begin programmes of deep crustal drilling in 1986. German plans, outlined by E. Seibold at a conference* earlier this year, are to drill to at least 7 km through the Hycenian overthrust in the Black Forest. The aim is to understand how huge masses of rock could have slid several hundred kilometres over only slight slopes in the geological past. High pore pressures are suspected essentially to have floated these masses over other rock, but not a single measurement of pore pressure is yet available from such a shear zone. Scientists in Sweden, the United States, France, Austria and Japan are also planning to begin deep continental drilling in 1986.

Why are so many national programmes focusing on the drillbit at about the same time? Technology is probably the major driving factor. The international oil industry has developed in the drillbit a remarkable technology ideally suited for geological purposes as well as for hydrocarbon exploration. F. Schuh (Atlantic Richfield), for example, presented the conference with an entirely feasible design for a 50,000 foot well into crystalline rock. Several speakers (including G. Olhoeft and B. Dennis, US Geological Survey; P. Lysne, Sandia; M. Mathews, Los Alamos) offered a staggering array of geophysical and geochemical measurements and *in situ* experiments that can now be accomplished in a deep hole. It is now possible to measure accurately the pore pressure, permeability, electrical and thermal conductivity, sonic, ultrasonic and seismic character of the wellbore as well as the exact chemical composition of the rock and pore fluids that are being drilled through.

It was not just these visions of technology that captured imaginations at the conference but also the accomplishments of continental drilling projects already well underway. Although not in attendance, the Russians dominated this phase of the meeting. They have been drilling deep into the continent for over 10 years, and at one hole on the Kola peninsula, they have made extraordinary discoveries. The current dogma holds that the deep crust is void of minerals and fluids because fractures, abundant at the surface, cannot remain open to fluid flow at great pressures. The Russians have found just the opposite: at 13 km depth, they encountered open fractures, mineralization and abundant evidence of fluid transport. They even discovered liquid sulphur, which is hydrolysed in the drilling mud to form sulphuric acid which eats away their drillbit.

The highlight of the conference was P. Robinson's (Dalhousie University) report of results from an international group, supported by Canada, the UK and US, that is drilling through the Troodos Ophiolite on Cyprus. Deep penetration of the pillow basalts and underlying sheeted dike complex, has shown that Troodos is made neither from ordinary sea floor, nor from back-arc basin sea floor as has long been thought, but is instead the inside of an island arc. Moreover, M. Salisbury (Scripps Institution of Oceanography), using technology supplied by the British company British Plaster Board, has conducted a complete suite of geophysical measurements inside the hole, or logs. This revealed that the internal plumbing of an island arc produces layered structures almost identical to the crustal layers of the ocean floor. Hence the mistaken origin of the complex.

By August 1984, this collaboration had drilled to within 180 m of the MOHO, the seismic discontinuity between the Earth's crust and mantle. The penetration of that barrier — originally the aim of the Deep Sea Drilling Project — now looks likely to be achieved first by the Troodos drilling project. We eagerly await information on what lies beneath it.

The conference ended with an air of great optimism. Participants had heard from Bob Luth (Sandia) of a greater than 1 m penetration of magma inside Kiluea Volcano, Hawaii, and from W. Elders (University of California, Riverside) that drilling was about to begin in the 350°C waters of the Salton Sea geothermal area. Our understanding of the Earth was revolutionized by plate tectonics, which arose from exploration of the ocean floor. The exploration of the interior of the continents promises to further that understanding by a similar degree. □

Roger N. Anderson is in the Lamont-Doherty Geological Observatory of Columbia University, Palisades, New York 10964.

---

*'Observation of the continental crust through drilling', supported by the US Department of Energy, Geological Survey and National Science Foundation, held in Tarrytown, New York, 20–25 May, 1984.

Archaeology

Kin-groups in Megalithic burials

from C.J. Scarre

MEGALITHIC tombs are among the most impressive neolithic monuments of western Europe, and a principal source of information about social organization in that period. Communal burial was the prevalent rite and in cases in which a tomb has not suffered too severely from the attentions of nineteenth-century antiquarians or been destroyed by a landowner, the archaeologist can expect to find large quantities of human remains. Despite their evident potential, however, analyses of such bone assemblages all too often fail to go beyond estimating the number and stature of the individuals represented and commenting on any obvious traces of injury and disease. How much more information this material holds is vividly demonstrated by the recent work at La Chaussée-Tirancourt, where the study of osteological abnormalities has allowed a series of distinct burial populations to be identified which may correspond to the different kin-groups using the tomb.

La Chaussée-Trancourt lies a few kilometres west of Amiens and is a megalithic monument of the '*allée couverte*' type, with a burial chamber 9 m long and 2 m wide. By careful excavation over several years, Claude Masset and his team have recovered the remains of 356 individuals, 60 in layer V towards the bottom of the chamber and almost 300 in layer III higher up[1] (see figure). Within layer V, four separate 'zones' of burials were identified, while in layer III the human remains were concentrated in 'cases', which probably had originally been compartments or containers of wood or other organic material long since perished. At the end of its use the tomb was sealed by a substantial deposit of chalk and earth, on the surface of which fierce fires were lit, leaving a thick layer of ash. Curiously, the customary megalithic capstones are absent in this instance: the roofing of the chamber before the final

21-1-87 A. Eatle

burning must instead have been of wood or thatch. Objects associated with the burials and radiocarbon dates from the layer of ash suggest that the monument was used actively between the late third and early second millenia BC.

Recently, Masset[2], Amaya Rodriguez Hernandorena[3] and Pascal Sellier[4] have carried out detailed analyses of the human material recovered from the tomb, concentrating on four bones (tibia, femur, humerus and calvarium) and on some fifty discrete (that is, non-metric) characters that are probably genetically determined. In both of the principal burial layers, the distribution of the characters among different parts of the tomb chamber was found to be significantly non-random (see figure).

In layer V, the remains from zones 2 and 4 form a single group chacterized by a high incidence of incrustation of the humeral trochloea. Zone 1 is distinguished by the rarity of a third trochanter on the femur, a feature fairly common in the layer as a whole, and by an unusually high frequency of hypotrochanterian fossae. These and similar abnormalities allow the burials in layer V to be divided into three distinct populations: zones 1, 2 and 3/4.

Layer III shows a comparable, though somewhat more complex, patterning as the cases provide eight separate burial units. Case ω is distinguished by the frequency of an additional articular facet on the tibia. Cases ε, β and ζ share the absence of an olecranian perforation in females and the common presence of a hypotrochanterian fossa, but only case ε has a relatively high incidence of incrustation of the humeral trochlea.

The presence of the same abnormalities in the bone assemblages of layers III and V suggest that the populations of the two layers were probably related, though some characters are more common in one than in the other, and the individuals in layer III are on the whole less robust and closer to the norm than those in layer V.

A recent study argues that megalithic tombs of the *allée couverte* type in north eastern France served as community foci for populations living in scattered hamlets or farmsteads round about, the burial of members of the different households in the central tomb operating as a crucial mechanism of social integration[5]. At La Chaussée-Tirancourt, the concentration of individual abnormalities in the different zones and cases suggest that each of these units was reserved for a separate kin or household group. This reservation of particular parts of the chamber for specific kin-groups may have persisted throughout the life of the tomb, since, for instance, incrustation of the trochlea is a common feature of humeri from the south-central sector both in layer III and in layer V. The spatial arrangement of the burials of related individuals in the tomb therefore reflects the scatter of family or household groups in their small settlements.

The research on the bone material from La Chaussée-Tirancourt clearly demonstrates the potential use of genetically-dependent osteological abnormalities for improving our understanding of prehistoric burial practices. It is hoped that the excavation currently being conducted by Masset at Méréaucourt, another northern French *allée couverte*, will amplify the picture and throw further light on the social organization of the populations that used these monuments. ☐

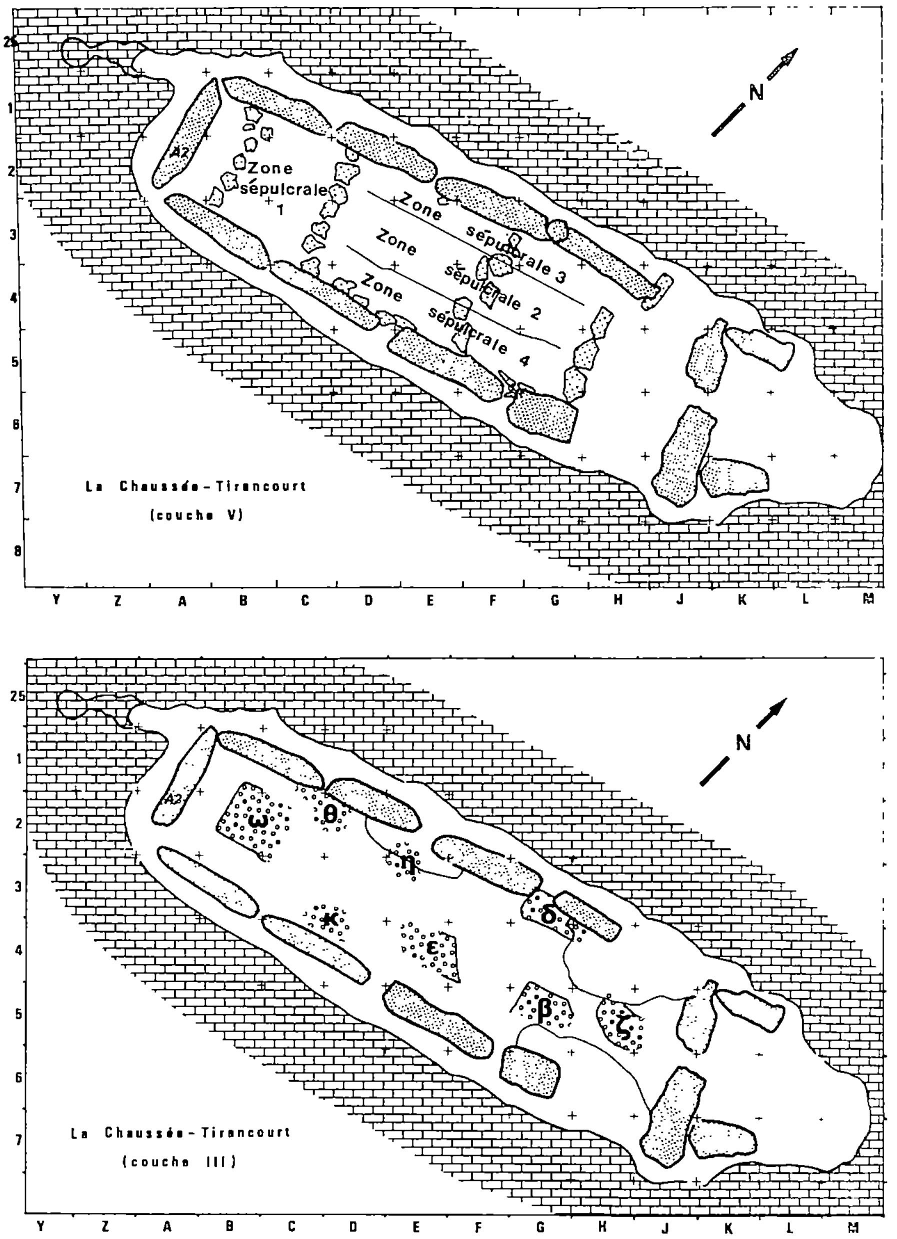

The megalithic tomb of La Chaussée-Tirancourt, showing the arrangement of the burials of the two principal layers in 'zones' (layer, V, top) and in 'cases' (layer III, bottom). From ref. 2 and reproduced by permission of C. Masset.

---

100 years ago

PROF. Ira Remsen testified to the utility of valence. He remarked that there were two ways of teaching: one by giving all the principal theories first, and the other giving the facts and then the theories — which latter he considered the best method. He had come to the conclusion that valence should never be mentioned until all the important properties of a compound are known. In regard to its value to young students, he thought its use was dangerous until they fully understood its meaning. He believed that the value of valence had been magnified, and that it was better to study the reactions of compounds, and the methods for their synthesis, and the manner of breaking-up.

Mr A.H. Allen said that many formulae that showed the structure of compounds according to the valence of the elements do not give any idea of the true constitution of these compounds as ascertained from their properties.

---

1. Masset, C. *Antiquity* 46, 297 (1972).
2. Masset, C. *Arch. Suisses d'Anthropologie gen.* 43(2), 223 (1979).
3. Rodriguez-Hernandorena, A. *Etude des Humérus, Fémurs et Tibias de la Chaussée-Tirancourt (sépulture Seine-Oise-Marne de la Somme)* (diploma, Ecole Pratique des Hautes Etudes, 3ème section, Paris, 1983).
4. Sellier, P. *Les Caractères Non-métriques du Calvarium Humain. Application à l'étude d'une Population Archéologique* (thesis, Univ. Paris VI, 1983).
5. Howell, J.M. *Settlement and Economy in Neolithic Northern France* (British archaeol. Rep., Oxford, 1983).

C.J. Scarre can be contacted at 28 Priory Road, Cambridge CB5 8HT.

Parkinson's disease

Clues to aetiology from a toxin

from Solomon H. Snyder

UNTIL recently Parkinson's disease was one of few neurological conditions whose pathophysiology was presumed to be 'solved'. Degeneration in the corpus striatum, which regulates motor activity, leads to rigidity, difficulty in moving, and tremors of the limbs. Hornykiewicz, in 1960, showed that the neurotransmitter dopamine is depleted from the corpus striatum of affected patterns[1] and Cotzias later developed a therapy based on orally administered L-DOPA, the amino acid precursor of dopamine[2]. At the same time, histochemical studies showed that the major dopamine pathway in the brain has cell bodies in the substantia nigra with axons ascending to terminate in the corpus striatum[3]. An animal model of Parkinson's disease soon followed: when injected into the vicinity of the substantia nigra, 6-hydroxydopamine, which is readily oxidized in cells to a toxic quinone, selectively accumulates through a pump-like mechanism exclusive to dopamine neurones with the result that the nigrostriatal dopamine pathway is destroyed.

This model, however, sheds no light on the aetiology of Parkinson's disease and may not even be adequate as a model of the human disease, since Parkinsonian brains show damage in areas other than the substantia nigra, including the noradrenaline-containing locus coeruleus. Several recent papers, two of them just published in *Nature*[4,5] show how a new animal model, based on the toxicity of 1-methyl-4-phenyl-1,2,3,6-tetrahydropyridine (MPTP), may overcome both shortcomings.

The toxin was originally implicated through a bizarre detective story. In the late 1970s a chemistry graduate student suddenly developed severe Parkinsonian symptoms, which were peculiar because of the patient's youth and the abrupt onset of the disease. The diagnosis was confirmed, following the patient's death from a drug overdose, when an autopsy revealed selective degeneration of the substantia nigra. Astute research scientists at the National Institutes of Mental Health in Bethesda learned that the patient had been synthesizing, for illicit sale, a close relative of the well-known opiate, meperidine. Chemical analysis of samples recovered from the patient's basement laboratory revealed contaminants, especially MPTP[6]. Subsequently, Californian investigators identified several patients with virtually identical clinical symptoms who had also taken preparations containing MPTP[7].

These cases have prompted speculation that MPTP or similar environmental toxins might 'cause' most cases of Parkinson's disease[8]. Direct ingestion may not be necessary: recently a 37-y-old chemist developed serious irreversible Parkinson's disease while using MPTP as a synthetic intermediate[9], but without ever ingesting it. Inhalation or skin contact may have sufficed to elicit the condition. Since MPTP itself is not toxic to cells, it is presumably converted to a more chemically reactive form. This fits the well-documented observation that cigarette smokers are less prone to Parkinson's disease than non-smokers[10,11], in the sense that carbon monoxide, which accumulates in the tissues of smokers, may detoxify active intermediates produced from MPTP and related agents. If Parkinson's disease is due to environmental toxins, one need not expect the sudden onset that follows MPTP ingestion, nor would chronic, lifelong exposure be required. Instead, initial damage to the substantia nigra, which might occur early in life, combined with the natural decrease with age of the dopamine-containing cells in the substantia nigra, could suffice to produce symptomatic Parkinsonism.

Several workers have used MPTP to develop an animal model of Parkinson's disease and have found species differences that have provided important clues to the mechanisms of toxicity. Unlike rats and guinea pigs[12-15], rhesus monkeys[12] and squirrel monkeys[16] given MPTP develop clinical Parkinsonian symptoms and show selective destruction of the substantia nigra. MPTP also produces irreversible depletion of striatal dopamine in mice[17-19].

MPTP can be oxidized by mitochondrial enzymes such as monoamine oxidase and possibly aldehyde dehydrogenase to 1-methyl-4-phenylpyridine (MPP^+), a charged pyridinium derivative[20], which is chemically reactive and toxic to tissues. It is detectable in the brain for prolonged periods after *in vivo* administration of MPTP [4]. An impressive link between the oxidation and neurotoxicity of MPTP has been reported by Heikkila and associates[5] who show that its neurotoxicity in mice can be prevented by pretreatment of the animals with monoamine oxidase-inhibiting drugs, which also block the conversion of MPTP to MPP^+.

But how does one explain the selective effect of MPTP on brain structures such as the substantia nigra and corpus striatum? Although MPP^+ is formed to a similar extent in all areas of the brain[12], species variations in recently identified receptor-like binding sites for MPTP may help provide an answer. MPTP binds with high affinity ($K_D = 2 \times 10^{-8}$M) to receptors in brains of numerous species. By autoradiographic techniques one can visualize MPTP receptors. In human brain they are most highly concentrated in the substantia nigra and corpus striatum[21] but we[21] and others[22] find substantially fewer receptors in the same regions of rat brain. Species variations in nigrostriatal receptor density thus may account for the lesser toxicity of MPTP in rats. Both human and rat brain have MPTP receptors in several other areas. One site of particularly high receptor density is the locus coeruleus. This localization fits well with the marked changes in noradrenaline metabolism that follow MPTP treatment of rats[13,14] and monkeys[12], with the pronounced changes in accumulation of 2-deoxyglucose by the locus coeruleus in MPTP-treated rat and guinea pig[23] and with the degeneration of the locus coeruleus in Parkinson's disease.

The most recent revelation in the MPTP story comes from Parsons and Thomas C. Rainbow (a leader in autoradiographic studies of neurotransmitter receptors, who met an accidental death on 6 September 1984). They compared by autoradiography the localizations of binding sites for ^{3}H-MPTP and for the monoamine oxidase inhibitor ^{3}H-pargyline[24], which selectively labels the type B isozyme of monoamine oxidase. Localizations of the two binding sites were virtually identical, indicating that the MPTP receptor may be the type B enzyme monoamine oxidase itself.

These findings not only reinforce the role of monoamine oxidase in MPTP actions, but also raise the intriguing possibility that the selective receptor binding sites that have been reported for diverse drugs might be enzymes rather than receptors for endogenous neurotransmitters. The very discrete localizations observed for monoamine oxidase suggest a more selective role for this enzyme in brain function than was previously suggested. ☐

1. Hornykiewicz, O. *Pharmac. Rev.* **18**, 925 (1966).
2. Cotzias, C.G., Van Woert, M.H. & Schiffer, L.M. *New Engl. med. J.* **276**, 374 (1967).
3. Ungerstedt, U. *Acta physiol. scand. Suppl.* **367**, 1 (1971).
4. Markey, S.P., Johannessen, J.N., Chiueh, C.C., Burns, R.S. & Herkenham, M.A. *Nature* **311**, 464 (1984).
5. Heikkila, R.E., Manzino, L., Cabbat, F.S. & Duvoisin, R.C. *Nature* **311**, 467 (1984).
6. Davis, G.C. *et al. Psychiat. Res.* **1**, 249 (1979).
7. Langston, J.W., Ballard, P., Tetrud, J.W. & Irwin, I. *Science* **219**, 979 (1983).
8. Calne, D.B. & Langston, J.W. *Lancet* **ii**, 1457 (1983).
9. Langston, J.W. & Ballard, P.A. *New Engl. med. J.* **309**, 310 (1983).
10. Kessler, I.L. *Adv. Neurol.* **19**, 355 (1978).
11. Baumann, R.J. *et al. Neurology* **30**, 839 (1980).
12. Burns, R.S. *et al. Proc. natn. Acad. Sci.* **80**, 4546 (1983).
13. Chiueh, C.C. *et al. Eur. J. Pharmac.* **100**, 189 (1984).
14. Enz, A., Hefti, F. & Frick, W. *Eur. J. Pharmac.* (in press).
15. Steranka, L.R., Polite, L.N., Perry, K.W. & Fuller, R.W. *Res. Commun. Substance Abuse* **4**, 315 (1983).
16. Langston, J.W., Forno, L.S., Rebert, C.S. & Irwin, I. *Brain Res.* **292**, 390 (1984).
17. Hallman, H., Olson, L. & Jonsson, G., *Eur. J. Pharmac.* **97**, 133 (1984).
18. Wallace, R.A., *et al. Life Sci.* **35**, 285 (1984).
19. Heikkila, R.E., Hess, A. & Duvoisin, R.C. *Science* **224**, 1451 (1984).
20. Chiba, K., Trevor, A. & Castagnoli, Jr., N. *Biochem. biophys. Res. Commun.* **120**, 574 (1984).
21. Javitch, J.A., Uhl, G.R. & Snyder, S.H. *Proc. natn. Acad. Sci. U.S.A.*, **81**, 4591 (1984).
22. Wieczorek, C.M., Parsons, B. & Rainbow, T.C. *Eur. J. Pharmac.* 98, 453 (1984).
23. Palacios, J. & Wiederhold, K. *Brain Res.* **301**, 187 (1984).
24. Parsons, B. & Rainbow, T. *Eur. J. Pharmac.* **102**, 375 (1984).

Solomon H. Snyder is in the Departments of Neuroscience, Pharmacology and Experimental Therapeutics, Johns Hopkins School of Medicine, Baltimore, Maryland 21205.

Similarity between p15E of murine and feline leukaemia viruses and p21 of HTLV

SIR — Retroviral infections of a number of animal species are frequently associated with immunosuppression. The hydrophobic retroviral transmembrane protein p15E is highly conserved among type C and type D retroviruses[1]. This protein may contribute to the immunosuppression associated with retroviral infections since it inhibits *in vitro* lymphocyte transformation in man[2], cats[3] and mice[4] and increases tumour incidence in cats given feline sarcoma virus[5]. The mechanism for the inhibition of human lymphocyte transformation by p15E was shown to be due to suppression of interleukin-2 (IL-2) production[6]. We have demonstrated *in vitro* suppression of human monocyte function[6] and *in vivo* inhibition of murine macrophage accumulation to inflammatory foci by p15E from murine leukaemia virus (MuLV)[7] or by tumour-associated proteins which are antigenically related to p15E[6,8].

Human T-cell leukaemia-lymphoma virus (HTLV) is the designation for a family of T-lymphotropic, exogenous type C retroviruses which have been isolated in a number of countries[9-13]. These viruses have been linked as aetiological agents to certain types of leukaemias and lymphomas and to the acquired immunodeficiency syndrome (AIDS)[14-16]. It has recently been reported that the polymerase gene products of HTLV, MuLV and avian Rous sarcoma virus are partially homologous in their amino acid sequence[17]. Since immunosuppression often accompanies the HTLV-associated T-cell malignancies and is characteristic of AIDS, we hypothesized that HTLV-viruses might have, in addition to their lymphocytopathic effects, other features in common with immunosuppressive MuLV and feline leukaemia viruses (FeLV). We therefore compared the amino acid sequences for p15E of Friend[18], Moloney[19], AKV[20], and Gross[21] murine leukaemia viruses (FLV, MoLV, AKV, GLV), FeLV[22], and mink-cell focus-forming viruses of Moloney[23] and AKR[24] origin (MMCF, AMCF) with the sequences of the envelope proteins of HTLV-I[25] and HTLV-II[26]. The sequences were analysed for homology using the PROTHOM computer program developed by Fristensky *et al.*[27].

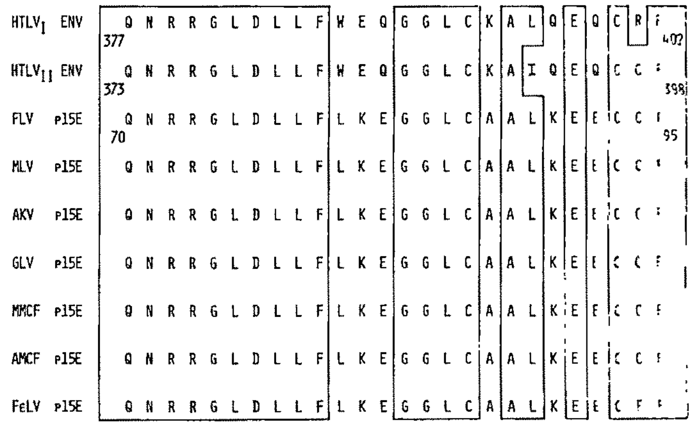
HTLV$_I$ ENV Q N R R G L D L L F W E Q G G L C K A L Q E Q C R F
377
402
HTLV$_{II}$ ENV Q N R R G L D L L F W E Q G G L C K A I Q E Q C C F
373
398
FLV p15E Q N R R G L D L L F L K E G G L C A A L K E E C C F
70
95
MLV p15E Q N R R G L D L L F L K E G G L C A A L K E E C C F
AKV p15E Q N R R G L D L L F L K E G G L C A A L K E E C C F
GLV p15E Q N R R G L D L L F L K E G G L C A A L K E E C C F
MMCF p15E Q N R R G L D L L F L K E G G L C A A L K E E C C F
AMCF p15E Q N R R G L D L L F L K E G G L C A A L K E E C C F
FeLV p15E Q N R R G L D L L F L K E G G L C A A L K E E C F F

Amino acid sequence homology between p21 of HTLV-I and HTLV-II and p15E of murine and feline leukaemia viruses. Residue 377 of the RTLV-I envelope and 373 of the HTLV-II envelope both correspond to residue 65 of the p21 protein.

As shown in the figure above there is a significant degree of homology (73%) between the various p15E proteins and HTLV-1 and HTLV-II which occurs in a 26-amino acid sequence located in the p21 region of HTLV. It is particularly noteworthy that the first 10 amino acids in this region are identical and that this region of homology occurs in almost the same region of the p15E and p21 molecules. The homology begins at residue 70 in p15E and at residue 377 of the HTLV-I envelope protein and at residue 373 of the HTLV-II envelope protein which both correspond to residue 65 of the p21 transmembrane protein[26].

The significance of such a well conserved region occurring in murine, feline, and human retroviruses is not yet clear. However, since dramatic immunosuppression is often associated with these viruses and purified p15E is immunosuppressive in a variety of systems, it will be particularly important to determine whether p21 of HTLV can also inhibit immune functions.

GEORGE J. CIANCIOLO
ROBERT J. KIPNIS
RALPH SNYDERMAN

Howard Hughes Medical Institute,
Department of Medicine,
Duke University Medical Center,
Durham,
North Carolina 27710, USA

1. Thiel, H.-J., Broughton, E.M., Matthews, T.J., Schafer, W. & Bolognesi, D.P. *Virology* **111**, 270-274 (1981)
2. Copelan, E.A. *et al. J. Immun.* **131**, 2017-2020 (1983).
3. Mathes, L., Olsen, R.G., Hebebrand, L.C., Hoover, E.A. & Schaller, J.P. *Nature* **274**, 687-689 (1978).
4. Fowler, A.K., Twardzik, D.R., Reed, C.D., Weislow, O.S. & Hellman, A. *Cancer Res.* **37**, 4529-4531 (1977).
5. Mathes, L.E. *et al. Cancer Res.* **39**, 950-955 (1979).
6. Cianciolo, G.J., Hunter, J., Silva, J., Haskill, J.S. & Snyderman, R. *J. clin. Invest.* **68**, 831-844 (1981).
7. Cianciolo, G.J., Matthews, T.J., Bolognesi, D.P. & Snyderman, R. *J. Immun.* **124**, 2900-2905 (1980).
8. Cianciolo, G.J., Lostrom, M.E., Tam, M. & Snyderman, R. *J. exp. Med.* **158**, 885-900 (1983).
9. Poiesz, B.J., Ruscetti, F.W., Gazdar, A.F., Bunn, P.A., Minna, J.D. & Gallo, R.C. *Proc. natn. Acad. Sci. U.S.A.* **77**, 7415-7419 (1980).
10. Gallo, R.C. *et al. Cancer Res.* **43**, 3892-3898 (1983).
11. Haynes, B.F. *et al. Proc. natn. Acad. Sci U.S.A.* **80**, 2054-2058 (1983).
12. Miyoshi, I. *et al. Nature* **296**, 770-771 (1981).
13. Popovic, M. *et al. Science* **219**, 856-859 (1983).
14. Gallo, R.C. *et al. Science* **224**, 501-503 (1984).
15. Popovic, M., Sarngadharan, M.G., Read, E. & Gallo, R.C. *Science* **224**, 497-500 (1984).
16. Sarngadharan, M.G., Popovic, M., Bruch, L., Schupbach, J. & Gallo, R.C. *Science* **224**, 506-508 (1984).
17. Patarca, R. & Haseltine, W.A. *Nature* **309**, 288 (1984).
18. Koch, W., Hunsmann, G. & Fredrich, R. *J. Virol.* **45** 1-9 (1983).
19. Shinnick, T.M., Lerner, R.A. & Sutcliffe, J.G. *Nature* **293** 543-548 (1981).
20. Lenz, J., Crowther, R., Straceski, A. & Haseltine, W. *J. Virol.* **423** 519-529 (1982).
21. DesGroseillers, L., Villemur, R. & Jolicoeur, P. *J. Virol.* **47**, 24-32 (1983).
22. Elder, J.H. & Mullins, J.I. *J. Virol.* **46**, 871-880 (1983).
23. Bosselman, R.A., van Straaten, F., Van Beveren, C., Verma, I.M. & Vogt, M. *J. Virol.* **44**, 19-31 (1982).
24. Kelley, M. *et al. J. Virol.* **45**, 291-298 (1983).
25. Seiki, M., Hattori, S., Hirayama, Y. & Yoshida, M. *Proc. natn. Acad. Sci. U.S.A.* **80**, 3618-3622 (1983).
26. Sodroski, J. *et al. Science* **225**, 421-424 (1984).
27. Fritensky, B., Lis J. & Wu, R. *Nucleic Acids Res.* **10**, 6451-6463 (1982).

Islet activating protein analogous to p21 *ras*?

SIR — In a recent article on mutant *ras* protein and cell transformation, Rob Newbold considered the significance of new findings about p21 *ras* function and activation. In particular, similarities between p21 *ras* and the guanine nucleotide binding proteins which are responsible for stimulation and inhibition of adenylate cyclase were emphasized and an analogy drawn with the action of cholera toxin on G_S protein GTPase, implying that p21 *ras* might act in an analogous manner to cholera toxin, which exerts a strong proliferative stimulus on certain mammalian cells in culture.

I suggest that the analogy with cholera toxin is dubious in view of the fact that rat cells transformed by Kirsten sarcoma virus have been shown to contain less cyclic AMP and lowered adenylate cyclase activity. Therefore a closer analogy may be with the action of islet activating protein which reacts with Gi proteins to inhibit adenylate cyclase and reduce cyclic AMP. This would imply that decreased cyclic AMP assists proliferation.

R. K. RALPH

Department of Cell Biology,
The University of Aukland,
Private Bag, Aukland, New Zealand

1. Newbold, R. *Nature* **310**, 628-629 (1984).
2. Carchman, R.A., Johnson, G.S., Pastan, I & Scolnick, E M. *Cell* **1**, 59-64 (1974).
3. Anderson, W. B., Gallo, M. Pastan, I *J biol. Chem.* **249**, 7041-7048 (1974)
4. Gilman, A. *Cell* **36**, 1577-1579 (1984).

Heritable IQ — a reason to bother

SIR — The recent article from Teasdale and Owen[1] prompts one to wonder about IQ genes. If intelligence is substantially heritable, is it determined by genes in a positive sense, such that better allelic combinations of IQ genes produce more intelligent people? This may seem to be the most parsimonious explanation, but parsimony is in the eye of the beholder.

That simple genetic mechanisms can account for conspicuously low IQ stirs no controversy (such as, phenylketonuria, Down's syndrome, Tay-Sachs), and most would agree that relatively mild homozygotic conditions can depress the IQ of afflicted persons (children who suffer from sickle cell anaemia or cystic fibrosis may test lower for IQ, on average, simply because they miss a great deal of school). Does this mean that such children have genetically heritable IQ? Does it mean, in the formal sense, that the disparity in IQ between them and normal children is attributable to variance in genes? Of course, it means exactly that — and yet the genes for beta haemoglobin and regulation of mucous production are not "IQ genes".

I am certain that my results on an IQ test would suffer if I were tested while I had a head cold. Imagine two boys reared in the same environment who are genetically identical except that one has an inherited sensitivity to ragweed. If they lived in a high ragweed area, such that the allergic one suffered from chronic congestion, would it be surprising to find that he tests slightly lower for IQ? Intelligence is a summary performance indicator, as distinct from an isolated component indicator (like how well a person's brain works), in the sense that suboptimal performance in any subsystem can have a negative impact. Variability in intelligence is perhaps analogous to the variability in horse power of a group of nominally identical engines, where quality of fuel represents the environmental component and fine tuning represents the genetic component. Performance is maximized when an engine is tuned for its operating conditions. A set of engines tuned in the tropics will not perform as well as when transported to Toronto. The question becomes, to what degree does the distribution of non-optimal non-IQ-genes account for heritable IQ?

The relative optimality of a gene is often environmentally specified. Teasdale and Owen, like others before them, found that the heritable component of IQ could be determined by segregation of a few alleles. ("The results for intelligence conform closely to what would be predicted by a simple polygenic model of genetic transmission . . . "). There are two ways this could happen: (1) there may be a universal handful of IQ genes that segregate appropriately, or (2) in any given environment, there may be a handful of genes for each of any one of hundreds of traits that can have a negative impact on IQ, and some of those handfuls segregate appropriately. If the former is the case, one wonders why alleles for superior IQ are not closer to fixation. Is there polymorphism for IQ because there were evolutionary environments in which intelligence was selected against?

Think about breathing through your nose in a steam bath. This is a genuine problem. Indeed, if you have a relatively long, thin, hairy nose (as typifies people from temperate zones and/or high altitudes — like Swedes and Ethiopians) it can be virtually impossible to pull enough air through that nose. But observe the steam bath breathing behaviour of someone with a wide, short, hairless nose (as typifies blacks and orientals indigenous to tropical wetlands). These people can breath superhumid air through their nose with no problem. Under the extreme condition of a steam bath, nose shape so strongly affects breathing efficiency that you can feel the difference by mechanically flaring your nostrils. Humans take over 10 million breaths a year. I submit that if we were all reared in steam baths, people with wide, short, hairless noses would have slightly higher mean IQ. This scenario is not silly because real noses in the real world are very differently adapted to conditions of humidity or dust. Among American racial and ethnic groups, only blacks and non-Japanese orientals have a conspicuous prevalence of lung disease[3]. Dust and airborne microorganisms can be a serious health hazard[4]. Noses have evolved accordingly.[5-7]

Can differences in nose shape (inherited) account for differences between black and white American IQ? It would be ridiculous to think so, but it should be considered equally ridiculous to assume that such factors have no effect. What about skin colour? More sunlight is required by dark skin to synthesize the same amount of vitamin D. Just as dark skin prevents hypervitaminosis-D in the tropics, so light skin facilitates D synthesis in temperate zones[8-10]. The question becomes, how many such factors are there? Dozens? Hundreds? More than enough to account for the portion of IQ variance which is heritable? Quite possibly. But this is not why the question is important.

The question is important because there are many factors that something could be done about if we knew what they were. People with dark skin in dark climates can get some extra sunshine. People with non-dust-trapping noses can have humidifiers in their homes during winter and take care to wear a dust mask when doing a dusty job. Unfortunately, looking for genetic differences that incidentally affect IQ is politically unacceptable because such investigations tacitly acknowledge the existence of such differences.

It may seem naive to think that things like clean air and sunshine could ameliorate genetic differences that contribute to differences in IQ. Fortunately, naivete is also in the eye of the beholder.

JOHN HARTUNG
Department of Anesthesiology,
Downstate Medical Center,
State University of New York,
New York 11203, USA

1. Teasdale, T.W. & Owen, D.R. *Nature* **309**, 620-622 (1984).
2. Hartung, J. *Curr. Anthropol* **21**, 131-132 (1980).
3. Damon, A. *Am J. Phys. Anthrop.* **22**, 375-382.
4. Cohen, D. Arai, S.F. & Brain, J.D. *Science* **204**, 514-517 (1979).
5. Newman, M.T. *Am. Anthropol.* **55**, 311-327 (1953).
6. Biasutti, R. *Razze e Popoli della Terra* (Unione Tipografico-Edi Traice, Torino, 1959).
7. Wolpoff, M.H. *Am. J. Phys. Anthrool.* **29**, 405-423 (1968).
8. Loomis, W.F. *Science* **157**, 501-506 (1967).
9. Haddad, J.G. & Hahn T.J. *Nature* **244**, 515-516 (1973).
10. Robertson, I., Glekin, B.M., McIntosh, W.B., Lakhani, A. & Dunnigan, M.G. *Proc. Nutr. Soc.* **41**, 243-250 (1982).

Raising the tone of DNA sequences

SIR — We assessed the potential for gene jingles following a lunchtime conversation two years ago. Hayashi and Munkata (*Nature* **310**, 96; 1984) appear to have used a purely arbitrary pitch-to-base assignment and ignored the complementary DNA strand altogether. We chose the notes D, A, F sharp, D, but have given some thought to base assignment of which there are 24 possibilities. We felt the complementary base triplet of each codon should produce a 'complementary' tune. Rather naively, we suspect, in musical terms, we took as complementary the quasi-mirror image of the notes on the stave (on the left of the figure). Eight of the possible 24 pitch-to-base assignments meet this requirement, but the assignment used by Hayashi and Munkata does not (on the right).

One of us (M.P.) sent short recorded DNA tunes to the other for the final selection of the pitch-to-base assignment by ear. No one assignment stood out as best, but the tunes of the promoter region CCAAT box were more pleasing musically than the 9-base repeat of collagen.

We are working towards the first public performance of 'Variations on a Cryptic Splice Junction' and the correspondence has given us renewed enthusiasm.

MARCUS PEMBREY
Mothercare Unit of Paediatric Genetics,
Institute of Child Health,
30 Guilford Street,
London WC1 1GH

DAVID HART

8 Chester Street,
London SW1, UK

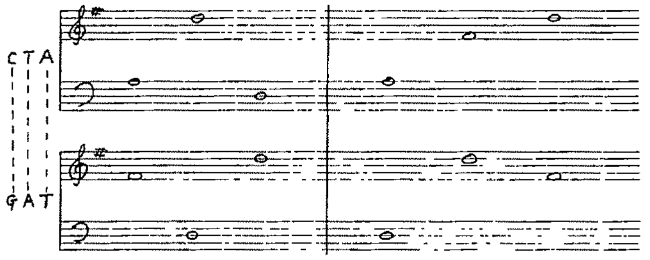

Base pairing by Pembrey and Hart (left) and Hayashi and Munkata (right).

Formation of galaxies and large-scale structure with cold dark matter

George R. Blumenthal* & **S. M. Faber***

* Lick Observatory, Board of Studies in Astronomy and Astrophysics, University of California, Santa Cruz, California 95064, USA

Joel R. Primack†§ & **Martin J. Rees**‡§

† Stanford Linear Accelerator Center, Stanford University, Stanford, California 94305, USA
‡ Institute of Theoretical Physics, University of California, Santa Barbara, California 93106, USA

The dark matter that appears to be gravitationally dominant on all scales larger than galactic cores may consist of axions, stable photinos, or other collisionless particles whose velocity dispersion in the early Universe is so small that fluctuations of galactic size or larger are not damped by free streaming. An attractive feature of this cold dark matter hypothesis is its considerable predictive power: the post-recombination fluctuation spectrum is calculable, and it in turn governs the formation of galaxies and clusters. Good agreement with the data is obtained for a Zeldovich ($|\delta_k|^2 \propto k$) spectrum of primordial fluctuations.

WHY are there galaxies, and why do they have the sizes and shapes that we observe? Why are galaxies clustered hierarchically in clusters and superclusters, separated by enormous voids in which bright galaxies are almost entirely absent? And what is the nature of the invisible mass, or dark matter, that we detect gravitationally roundabout galaxies and clusters but cannot see directly in any wavelength of electromagnetic radiation? Of the great mysteries of modern cosmology, these three may now be among the ripest for solution.

Because there is evidence that the mass of dark matter in the Universe exceeds that of the visible matter by at least an order of magnitude[1], the third question may hold the key to the first two. We now consider the hypothesis that the dark matter is cold[2-7], that is, that its thermal velocity is cosmologically negligible in the early Universe.

Most modern theories of the origin of structure in the Universe assume that the extreme inhomogeneity of the present Universe grew gravitationally from initially very small density fluctuations[8,9]. One hypothesis extensively explored[10-12] is that the dark matter (DM) consists of neutrinos of mass ~30 eV. Because these particles are noninteracting for $t \gtrsim 1$ s but are still relativistic at $t \sim 1$ yr when galaxy-size masses first come within the horizon ($R_{\text{horizon}} = ct$), they would freely stream away, smoothing out fluctuations of horizon size or smaller. We refer to such particles as hot DM, and to the phenomenon just mentioned as damping by free streaming. The mass of the neutrinos inside the horizon when they first become nonrelativistic is roughly $10^{15}\ M_\odot$, about the mass of a supercluster ($M_\odot$ is the solar mass). This is consequently the mass of the first structures to collapse gravitationally in a neutrino-dominated Universe.

It is also possible that the DM consists of elementary particles that decoupled thermally from the big bang much earlier than neutrinos. It can be shown that such particles would have lower number density today, and thus could be more massive (~1 keV) and become nonrelativistic sooner than neutrinos[13,14]. We refer to this as warm DM. The first structures to form in such a Universe would weigh about $10^{11}\ M_\odot$, about the mass of a typical galaxy[15-17].

In contrast, in a Universe dominated by cold DM, the free streaming damping mass is, by definition, smaller than galaxy masses. Below, we will discuss possible particle physics candidates for cold DM and explain why we believe it is more plausible that the Universe is dominated gravitationally by cold DM than by ordinary matter (baryons) or hot or warm DM. We next consider galaxy formation in the cold DM picture, and show that galaxy and cluster data compare favourably with the predictions of this model. We then discuss the extent to which the data constrain the cosmological density in the cold DM picture, and the evolution of superclusters and voids. The cold DM hypothesis seems to lead to a remarkably attractive theory for galaxy formation and to account for large-scale structure at least as well as any competing theory.

Evidence that dark matter is cold

Cold DM consists of particles having negligible thermal velocity with respect to the Hubble flow and having nongravitational interactions that are much weaker than the weak interactions[3,4]. A popular cold DM candidate is the axion[18], a pseudoscalar field proposed originally to avoid large CP (constant parity) violation in the strong interactions (which would imply, for example, much too large a value for the neutron electric dipole moment)[19-21]. Instanton effects generate a nonzero axion mass at the quark deconfinement temperature ($T \sim 10^2$ MeV), below which the axions act as a nonrelativistic, massive, pressureless fluid. The requirement that the axion density be less than the critical density implies that the axion mass $m_a \geqslant 10$[illegible] eV (refs 22-24), while the longevity of helium burning stars implies that $m_a < 10^{-1}$ eV (ref. 25). Thus, if axions exist, they may be cosmologically important, and, for $m_a \approx 10^{-5}$ eV, they would be gravitationally dominant. If axions comprise the dark halo of our Galaxy, laboratory experiments have recently been proposed that could detect them[26].

Another cold DM candidate particle is the photino, the spin $\frac{1}{2}$ supersymmetric partner of the photon. Photinos are thought to be the lightest supersymmetric particle, with $m_\gamma \gtrsim 0.5$ GeV (the lower limit corresponding to cosmological critical density)[27]. As photino annihilation at high temperatures is incomplete, the remnant photinos can, because of their large mass, contribute a critical density today.

A third cold DM candidate is black holes[28,29] of mass $10^{-16}\ M_\odot \leqslant M_{\text{BH}} \leqslant 10^6\ M_\odot$, the lower limit implied by the non-observation of γ rays from black hole decay by Hawking radiation, and the upper limit required to avoid disruption of galactic disks and star clusters[30,31]. Stronger but more controversial upper limits are $M_{\text{BH}} < 10^2\ M_\odot$ from dwarf spheroidal haloes[32] and $M_{\text{BH}} < 10^{-2}\ M_\odot$ from the non-observation of focusing of quasar cores[33].

---

§ Permanent addresses: Santa Cruz Institute of Particle Physics, University of California, Santa Cruz, California 95064, USA (J.R.P.); Institute of Astronomy, Madingley Road, Cambridge CB3 0HA, UK (M.J.R.).

Another exotic cold DM candidate, recently proposed by Witten, is "nuggets" of u-s-d symmetric quark matter[34]. There is thus no shortage of cold DM candidate particles—although there is no direct evidence that any of them actually exists. Our motivation for considering the hypothesis that the Universe is dominated by cold DM is twofold. First, there is more than a little evidence against baryonic, hot, and warm DM. Moreover, a cold DM Universe correctly predicts many of the observed properties of galaxies, including their range of masses, irrespective of the identity of the cold particle.

The most conventional assumption might be that DM is baryonic, since we know that baryons pervade the Universe. There are, however, three arguments that make a nonbaryonic form of DM more plausible. First, if DM consists of baryons, it must be clumped into objects with mass $\ll M_\odot$ to avoid nuclear burning and the emission of too much radiation[35], and there is no compelling theory for the formation of such a large density of objects of planetary mass or smaller. The difficulties with other possible forms of baryonic dark matter have been reviewed elsewhere[36]. The second argument involves the observed deuterium abundance, $D/H = (1\text{-}4)\times 10^{-5}$ (by number), which provides a lower limit on the primordial D abundance because deuterium is readily consumed but not produced in stars. This then corresponds to an upper limit for the baryonic density parameter (ratio of baryon density to critical density) of $\Omega_b \leq 0.035h^{-2}\,(T_0/2.7)^3$ (ref. 37), where T_0 is the present temperature of the microwave background radiation and h is Hubble's constant expressed in units of $100\ \text{km s}^{-1}$ Mpc. (Observationally, $1/2 \leq h \leq 1$.) However, there is also strong observational evidence that the total density parameter $\Omega \geq 0.1$. Therefore a baryon dominated Universe ($\Omega = \Omega_b$) is consistent with the deuterium limit only for Ω and h very near their observational lower limits. Finally, the existence of galaxies and clusters today requires that perturbations in the density must have become nonlinear before the present epoch. In a baryonic Universe, for adiabatic perturbations at recombination, this implies present-day fluctuations in the microwave background much larger than the present observational upper limits[38,39]. For baryonic DM, this problem can be avoided if the primordial fluctuation spectrum is isothermal rather than adiabatic, contrary to grand unified models of baryosynthesis[40,41], or if there is significant reheating of the intergalactic medium after recombination[42]. For nonbaryonic DM, on the other hand, the predicted fluctuations in the microwave background can be consistent with the observations as the fluctuations in the baryon-photon fluid are small at recombination and only later grow to the same size as fluctuations in the DM.

The neutrino dominated picture of galaxy formation also has serious weaknesses. Studies of nonlinear clustering (on scales $\lambda < 10$ Mpc) show that supercluster collapse must have occurred quite recently, at redshift $z_{sc} < 2$ (refs 43, 44). This is also consistent with a study of streaming velocity in the linear regime ($\lambda > 10$ Mpc), which indicates $z_{sc} < 0.5$ (ref. 45). However, the best limits on galaxy ages coming from globular clusters and other stellar populations, plus the possible association of QSOs with galactic nuclei, indicate that galaxy formation took place before $z = 3$ (ref. 46). This is inconsistent with the neutrino 'top-down' theory, in which superclusters form before galaxies rather than after them.

Another problem with the neutrino picture is that large clusters of galaxies can accrete neutrinos more efficiently than ordinary galactic haloes, which have lower escape velocities. One-dimensional numerical simulations predict that the ratio of total-to-baryonic mass M/M_b should be ~ 5 times larger for clusters ($\sim 10^{14}\,M_\odot$) than for ordinary galaxies ($M \sim 10^{12}\,M_\odot$)[47]. While there is evidence that mass-to-light ratio M/L does increase with scale, there is also considerable evidence that the more physically meaningful ratio of total-to-luminous mass M/M_{lum} remains constant from large clusters through groups of galaxies, binary galaxies, and ordinary spirals. (M_{lum}, which is the mass visible in galactic stars and gas plus hot, X-ray emitting gas, is $\leq M_b$, as an unknown fraction of the baryons is

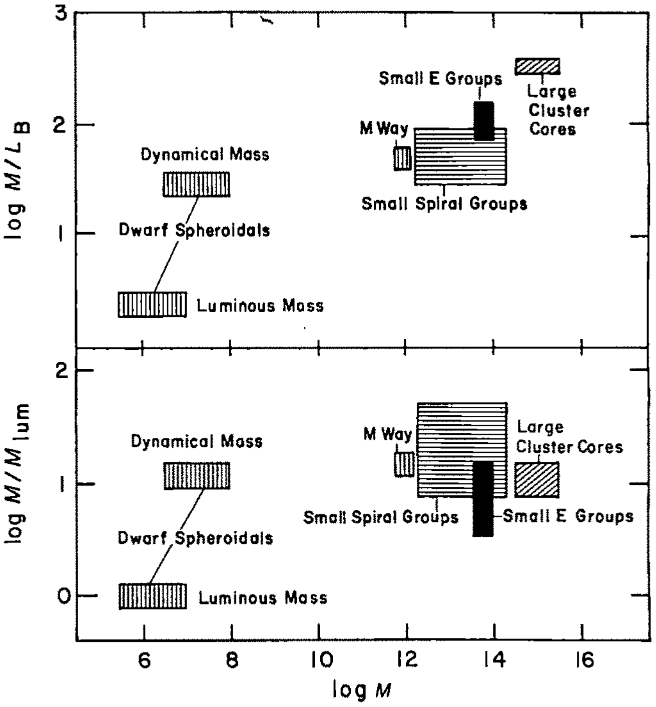

Fig. 1 Mass-to-light ratio, M/L_B, and total-to-luminous mass, M/M_{lum}, for structures of various size in the Universe. The data come from Table 1. Although M/L_B increases systematically with mass, the more physically meaningful ratio M/M_{lum} appears to be constant on all scales within the errors. If the velocity dispersion data for the dwarf spheroidal galaxies are interpreted to imply heavy haloes, the upper estimates result. The lower estimates follow from assuming that all the mass is visible. We believe the former estimate to be more realistic.

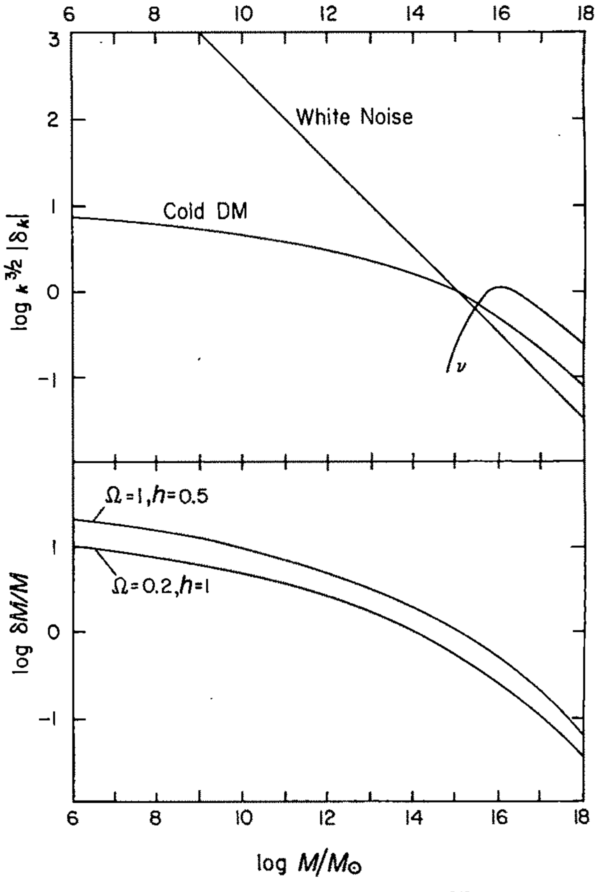

Fig. 2 Density fluctuations as a function of mass. *a*, $k^{3/2}|\delta_k| = \delta\rho/\rho(M)$, where $M = 4\pi^4\rho_0/3k^3$, for isothermal white noise ($n=0$), and adiabatic Zeldovich ($n=1$) neutrino[16] and cold DM spectra. *b*, r.m.s. mass fluctuation within a randomly placed sphere containing mass M for cold DM, $n=1$, and ($\Omega=1$, $h=0.5$), ($\Omega=0.2$, $h=1$).

invisible—for example, in the form of diffuse ionized intergalactic gas at $T \sim 10^4$ K.) This is illustrated in Table 1 and Fig. 1, where we have plotted observed data for M/L and $M/M_{\rm lum}$. The fact that the total-to-luminous mass of rich clusters is similar to that of galaxies including their massive haloes, even though the clusters' mass-to-light ratio is larger, is due mainly to the different stellar population in the E and S0 galaxies in rich clusters plus the large contribution of X-ray emitting gas to $M_{\rm lum}$. In very rich clusters such as Coma, there is perhaps ~2–5 times as much mass in hot gas as there is in stars.

Finally, preliminary velocity dispersion data for Draco, Carina, and Ursa Minor[48-50] as well as theoretical arguments[51] suggest that a significant amount of DM may reside in dwarf spheroidal galaxies. Because of the low velocity dispersion of dwarf galaxies, phase space constraints give a lower limit of $m > 500$ eV for the mass of particles comprising this DM[32]. The present velocity dispersion estimates are uncertain owing to possible stellar oscillations, mass outflow, and binary motions, but these effects can be discovered and eliminated with careful monitoring. Taken at face value, however, the existing mass limit of 500 eV would rule out neutrinos completely.

Although warm DM provides a natural (free streaming) scale for ordinary galaxies, it cannot account for massive haloes in dwarf spheroidals even though the warm DM mass is actually, if barely, consistent with the phase space constraint. This is because free streaming damps out fluctuations with mass $<10^{11}\,M_\odot$, so dwarf galaxies with mass $\sim 10^7\,M_\odot$ can form in this picture only by the fragmentation of much larger scale galactic masses. Because dwarf galaxies with escape velocity $\sim 10\,{\rm km\,s^{-1}}$ would capture only a small fraction of the warm DM particles, whose velocity dispersion would be $\sim 100\,{\rm km\,s^{-1}}$, typical of ordinary spirals, one would expect $M/M_{\rm lum}$ to be much smaller in dwarf galaxies than in spirals. However, the dynamical mass data on dwarf spheroidals shown in Fig. 1 suggest a similar value for the ratio of total-to-luminous mass. In view of the great importance of dwarf spheroidal haloes to constraints on warm as well as hot DM, it is clearly urgent to continue the monitoring programme on velocity dispersions mentioned above.

Recently proposed models having two or more kinds of possibly unstable DM[52-58] may be easier to reconcile with observations than models with one stable DM species, in part because of their additional adjustable parameters. Such models are, however, beyond the scope of this paper.

Galaxy formation with cold dark matter

The key features of galaxy formation in the cold DM picture are these: the DM fluctuation spectrum at recombination is determined by a small number of physical parameters; after recombination (at $z_{\rm rec} \approx 1{,}300$) the amplitude of the baryonic fluctuations rapidly grows to match that of the DM fluctuations; smaller-mass fluctuations grow to nonlinearity and virialize, and then are hierarchically clustered within successively larger bound systems; and finally the ordinary matter in bound systems of total mass $\sim 10^{8-12}\,M_\odot$ cools rapidly enough within the DM haloes to form galaxies, while larger mass fluctuations form clusters.

To calculate the growth of initially small perturbations and their ultimate gravitational collapse into condensed systems, one must first determine an initial spectrum for density perturbations in the very early Universe. We assume here that the initial fluctuations are adiabatic, which is consistent with fashionable particle theories in which a small excess of baryons over antibaryons is generated by the decay of supermassive grand unified theory particles[40,41]. Then the mass (or energy) density at any point can be written as $\rho(r,t) = \rho_0(1+\delta)$, where $\rho_0(t)$ is the average density in the Universe and δ represents the fractional density perturbation in the synchronous gauge. If the fluctuation spectrum is characterized by a power law distribution, then the r.m.s. fluctuation on mass scale M can be written $\delta \propto M^{(-1/2)(-n/6)}$, which corresponds to a Fourier power spectrum $|\delta_k|^2 \propto k^n$. Alternatively, we can characterize the perturbations on mass scale M when that mass scale crosses (first comes within) the horizon as $\delta_{\rm H} = \varepsilon(M/M_0)^{-\gamma}$, where M_0 is the present horizon mass and $n = 6\gamma + 1$. To avoid having too much power on either large or small scales requires $\gamma \approx 0$, which corresponds to $n \approx 1$. Limits on the large-scale variation of the microwave background further imply $\varepsilon \lesssim 10^{-4}$. The case $n = 1$ is commonly referred to as the constant curvature or (Harrison-Peebles-) Zeldovich[59-61] spectrum, and is predicted in inflationary models. It has recently been shown that not only inflation but also $\varepsilon \approx 10^{-4}$ can be arranged in suitably fine-tuned grand unified theories[62-64]. The Zeldovich spectrum also arises automatically if the fluctuations are due to cosmic strings[65,66]. We show below that $n = 1$ is, furthermore, in best agreement with galaxy and cluster data.

The first study of the growth of cold DM fluctuations was the numerical calculation of Peebles[2], who included cold DM, photons, and ordinary matter. Two of us (G.R.B. and J.R.P.)[3-[illegible]] extended these numerical calculations to include three massless neutrino species. Fluctuations having mass $M < M_{\rm eq} = 2 \times 10^{5}\,(\Omega h^2)^{-2}\,M_\odot$ cross the horizon when the Universe is still radiation dominated, that is, when $z > z_{\rm eq} = 2.5 \times 10^4\,\Omega h^2$. After such fluctuations cross the horizon, their neutrino components dissipate by free streaming, and the remaining photon and charged particle perturbations oscillate as an acoustic wave (whose amplitude is ultimately damped by photon diffusion for[67] $M < M_{\rm Silk} \approx 3 \times 10^{13}\,\Omega_{\rm b}^{-1/2}\Omega^{-3/4}h^{-5/2}M_\odot$). As a result, the main driving terms for the growth of cold dark matter fluctuations $\delta_{\rm DM}$ decrease, and consequently $\delta_{\rm DM}$ begins to grow only very slowly until the Universe becomes (dark) matter dominated at $z_{\rm eq}$, after which $\delta_{\rm DM} \propto a = 1/(1+z)$ until $z \approx \Omega^{-1}$. This stagnation of the growth of DM fluctuations between the epochs of horizon crossing and matter domination is called 'stagspansion'[3-7].

Because fluctuations with $M < M_{\rm eq}$ grow very little during the stagspansion era and as fluctuations on all scales grow at essentially the same rate after the Universe becomes matter dominated, an initial Zeldovich spectrum, $\delta_{\rm DM} \propto M^{-2/3}$, evolves to a much flatter spectrum for $M < M_{\rm eq}$ by the time of recombination. In Fig. 2 we plot the resulting cold DM fluctuation spectrum at present (ignoring the nonlinear evolution which is important for $\delta \gtrsim 1$, as discussed below; thus the plotted spectrum δ_k is larger than the spectrum at recombination by a constant factor). The quantity plotted in Fig. 2*a*, $k^{3/2}|\delta_k|$, roughly

Table 1 $M/L_{\rm B}$ and $M/M_{\rm lum}$ on various mass scales

Unit	M*	$M/L_{\rm B}$†	$M_{\rm gas}/M_{\rm lum}$	$M/M_{\rm lum}$
Large clusters	$10^{15}\,M_\odot$	316 ± 40‡	$0.84^{+0.0[illegible]}_{-0.1[illegible]}$§	8.4 [illegible]
Small E-dominated groups	5×10^{13}	83^{+80}_{-10}‖	$0.61^{+0.1[illegible]}_{-0.1[illegible]}$	5.4 [illegible]
Small spiral-dominated groups	2×10^{13}	40^{+50}_{-10}¶	0(?)	$14.2^{+[illegible]6}_{-6}$ #
Whole Milky Way	10^{12}**	50††	0(?)	14‡‡
Dwarf spheroidals§§				
Stellar masses	10^{5-7}	2.5	0	1
Dynamical masses	10^{6-8}	30	0	12

* Total mass including dark matter. $H = 50\,{\rm km\,s^{-1}\,Mpc}$.

† Mass-to-light ratio on B(0) magnitude system as described in ref. 1.

‡ From ref. 120.

§ $M_{\rm gas}/M_{\rm lum}$ is calculated as the product of two factors: $(M_{\rm gas}/M) \times (M_{\rm lum}/M)^{-1}$. $M_{\rm gas}/M = 0.10^{+0.02}_{-0.05}$ from ref. 121 for 14 X-ray clusters. Formal clusters have been increased to allow for the unknown gas distribution outside the core and possible settling of gas relative to galaxies or vice versa. $M_{\rm lum}/M$ is $(M_* + M_{\rm gas})/M$, where M_*/M is the fractional mass in stars. It may be calculated as $(M/L_{\rm B})_*(M/L_{\rm B})^{-1}$, where $(M/L_{\rm B})_*$ is the stellar mass-to-light ratio. For E and S0 galaxies in large clusters, $(M/L_{\rm B})_*$ appears to be about 6 (ref. 1).

‖ $L_{\rm V}$, $M_{\rm gas}$, and M from ref. 122 based on five groups. $L_{\rm V}$ corrected to B(0) system based on data provided by Kriss (personal communication). Comparison with Beers *et al.*[123] suggests that M may be underestimated by a factor of two. Quoted errors take this into account.

¶ From ref. 1.

# From ref. 72; includes baryonic mass in stars and neutral gas.

** Mass assumed to be 1/3 total mass of Local Group[1].

†† B(0) luminosity from ref. 1.

‡‡ $M_{\rm lum}$ from ref. 124.

§§ Basic data from ref. 51. Upper line assumes that only stars are present. Lower line includes excess dark matter, based on mean dynamical masses of Faber and Lin[51] and Aaronson *et al.*[48-50].

represents the spatial density fluctuation δ as a function of total mass $M=4\pi^4\rho_0/3k^3$. Also sketched are the fluctuation spectra in the hot DM scenario and in an isothermal scenario with white noise fluctuations. Note that the hot DM model requires more power on large scales today to form superclusters by $z\approx 2$. Figure 2*b* shows cold DM fluctuation spectra plotted in another form, $\delta M/M$, which represents the r.m.s. mass fluctuation within a randomly-placed sphere of radius R containing mass M. Following Peebles[2], we have normalized the curves so that, at the present epoch, $\delta M/M=1$ at $R=8h^{-1}$ Mpc.

Even though baryonic fluctuations do not grow (and are damped for $M<M_{\rm Silk}$) before recombination, after recombination the baryons 'fall into' the DM perturbations so that quickly $\delta_b=\delta_{\rm DM}$ (refs 68, 69). This will occur if $\Omega_{\rm DM}\delta_{\rm DM}\gg\Omega_b\delta_b$, as we expect, and if the baryonic fluctuation mass exceeds the baryonic Jeans mass[6] $M_{J,b}\sim 10^6\,\Omega_b\Omega^{-3/2}h^{-1}(T_b/T)^{3/2}M_\odot$, where T_b is the temperature of the baryonic gas and T is the photon temperature. On scales smaller than this, the pressure of the baryonic gas prevents it from developing the same density contrast δ as the cold DM. The value of T_b/T is kept close to unity for $z>100$ by the coupling of the residual free electrons with the radiation, but for smaller z it falls off approximately as $(1+z)$. This means that at $z\approx 10$, $M_{J,b}$ may be as small as $\sim 10^3\,M_\odot$.

At any mass scale M, when the fluctuation $\delta M/M$ approaches unity, nonlinear gravitational effects become important. The fluctuation then separates from the Hubble expansion, reaches a maximum radius, and begins to contract. Spherically symmetric fluctuations, for example, contract to about half their maximum radii. During this contraction, violent relaxation due to the rapidly varying gravitational field converts enough potential energy (PE) into kinetic energy (KE) for the virial theorem, $\langle PE\rangle=-2\langle KE\rangle$, to be satisfied. After virialization, the mean density within a fluctuation is roughly eight times the density corresponding to the maximum radius of expansion[8].

As the cold-DM fluctuation spectrum $\delta M/M$ is a decreasing function of M, smaller mass fluctuations will, on the average, become nonlinear and begin to collapse at earlier times than larger mass fluctuations. Smaller mass fluctuations are themselves typically clustered within larger mass perturbations, which go nonlinear later. This hierarchical clustering of smaller systems into larger and yet larger gravitationally bound systems begins at the baryon Jeans mass, $M_{J,b}$, and continues until the present. The baryonic substructures within larger mass clusters will then be disrupted by virialization of the clusters unless significant mass segregation between baryons and DM has occurred before cluster virialization. Hence, to maintain their existence as a separate substructure, the baryons must cool and gravitationally condense within their massive DM haloes before virialization occurs on larger scales[70].

Figure 3 shows the baryonic number density n_b plotted against temperature T (or halo velocity dispersion) for virialized spherically symmetric protocondensations resulting from an initial Zeldovich spectrum of cold DM fluctuations. The simplifying assumption of sphericity is not expected to be an unreasonable approximation for hierarchical clustering. Two cases are considered: $\Omega=1$ and $h=0.5$ (solid lines in Fig. 3), and $\Omega=0.2$ and $h=1$ (dashed lines). The curves assume that the protocondensations have virialized, but that the baryons have not yet cooled and condensed. The curves labelled 1σ assume that for each mass scale, $\delta M/M$ has the r.m.s. value; those labelled 2σ correspond to fluctuations $\delta M/M$ twice as great; and so on. For given total mass M, the distribution of values of $\delta M/M$ spreads out along lines of constant M (light diagonal lines in Fig. 3). We have also shown in Fig. 3 the present positions of clusters and groups of galaxies and of individual galaxies, including dwarf spheroidals. Note that different types of galaxies, the Hubble sequence, are spread out in this diagram.

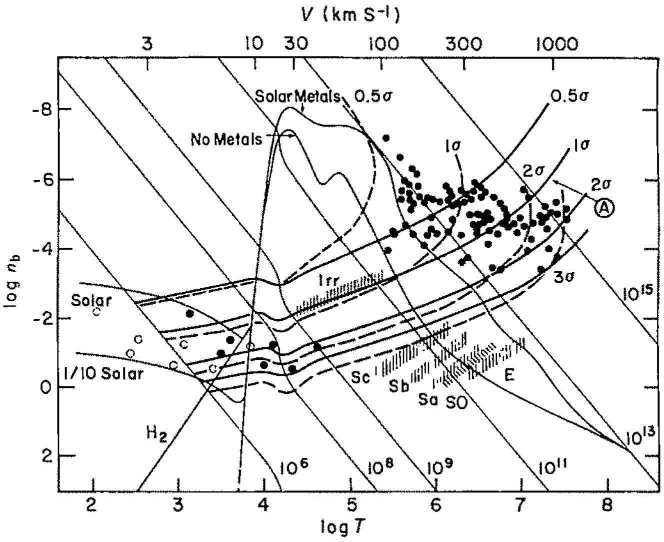

Fig. 3 Baryon density n_b versus three-dimensional, r.m.s. velocity dispersion V and virial temperature T for structures of various size in the Universe. The quantity T is $\mu V^2/3k$, where μ is mean molecular weight ($\approx$0.6 for ionized, primordial H+He) and k is Boltzmann's constant. Dots at upper right represent nearly all groups and clusters within 5,000 km s^{-1} in the CfA catalogue[82]. Baryon density is obtained from total density assuming $\rho_b/\rho=0.1$ (see Table 1), where ρ is defined as $M/(4\pi R_{\rm vir}^3/3)$, M is total mass, and $R_{\rm vir}$ is GM/V^2. Catalogue groups are chosen to exceed a minimum threshold luminosity density. Their minimum baryon density should thus fall on a horizontal line, slightly modified by the higher M/L of rich clusters, as is observed. Point A represents Abell clusters of richness 2 and 3 studied by Dressler[120]. Here $R_{\rm vir}=3.0\,R_{\rm eff}$, valid for a de Vaucouleurs cluster profile[125]. The quantity T for clusters corresponds to central velocity dispersion, with the arrow indicating the effect of the falloff in velocity dispersion at large radii observed in the Coma cluster[126,127]. For galaxies, $M_{\rm lum}$ is set equal to $(M_{\rm lum}/L_B)\times L_B$, where L_B is blue luminosity. Assumed values of $(M_{\rm lum}/L_B)$: E=8, S0=6, Sa=4, Sb=2.5, Sc=1.5, Dw. Irr=1.00, Dw. Spheroidal=2.5 (all but the last are based on $h=0.5$). Galaxy radii are approximate virial radii, assuming that the baryonic components of galaxies are self-gravitating (to obtain a radius consistent with the definition used for groups and clusters above). To achieve this, isophotal radii from various sources have been appropriately scaled, as follows: E–Sb, $R_{\rm vir}=R_{25}$ (refs 128–131); Sc, $R_{\rm vir}=1.24\,R_{25}$ (ref. 132); Dw–Irr, $R_{\rm vir}=1.24\,R_H$ (ref. 133); Dw–Sph. $R_{\rm vir}=0.70\,R_{\rm tid}$ (ref. 51). Velocities: E–S0, $V=\sqrt{3}\times\sigma$ (nucleus) (refs 129, 134); Sa–Sc, $V=v_{\rm rot}^{\rm max}$ (refs 130, 131, 132); Dw–Irr, $V=1/2$ FWHM (Δv) (ref. 133), corrected for inclination. Dw Spheroidals are plotted twice; open circles, $M=2.5\,L_B$ (stars only) and $V=(GM/R_{\rm vir})^{1/2}$; large dots, $M=30\,L_B$ (stars plus dark matter[48–51]), with V as before. Light diagonal lines represent the masses of self-gravitating bodies with the indicated values of n_b and T and assuming $\rho_b=0.1\rho$. The discontinuities near 10^4 K are due to the effects of H and He ionization. Cooling curves[78,135,136] (medium lines) separate regions where cooling is efficient ($\tau_{\rm cool}<\tau_{\rm dyn}$, lower region) from regions where it is inefficient ($\tau_{\rm cool}>\tau_{\rm dyn}$, upper region). All curves assume a residual electron fraction after recombination of 10^{-4}, consistent with $\Omega_b/\Omega=0.1$. Model curves represent the equilibria of structures that collapse dissipationlessly from the cold dark matter initial fluctuation spectra of Fig. 2 with $n=1$. DM haloes and groups and clusters of galaxies should lie on these curves, whereas the baryon components of galaxies should lie below due to baryonic dissipation. The curves labelled $v\sigma$ refer to fluctuations with $\delta M/M$ equal to v times the r.m.s. value shown in Fig. 2. Heavy curves: $\Omega=1$, $h=0.5$; dashed curves: $\Omega=0.2$, $h=1$. Model curves appear to pass through groups and clusters in about the right place, and the horizontal spread in T is roughly as expected for a gaussian distribution in $\delta M/M$. Baryon components of galaxies lie below the loci for dissipationless collapse and generally within the region where strong baryonic cooling is expected. Dwarf spheroidal galaxies lie near the beginning of the clustering hierarchy and may be typical of the earliest structures to collapse (see ref. 73). Hubble types are spread out along different loci, perhaps due in part to different baryon collapse factors (Es larger, Irrs smaller) and in part to intrinsic differences in initial $\delta M/M$ (see also Fig. 4).

Baryonic cooling moves structures downward in Fig. 3, below the model curves. Baryons can radiatively cool through collisional excitation of atoms and molecules, and by Compton cooling off the cosmic background radiation; Fig. 3 correspondingly includes the medium solid curves labelled 'No metals' and 'Solar metals', 'H_2', and 'Compton'. Below these curves the baryonic cooling time is shorter than the dynamical time and above them the reverse is true[71]. Figure 3 immediately shows that, while the Hubble sequence of galaxies shows strong evidence for baryonic cooling and dissipation (core condensation in heavy haloes), dwarf spheroidals are only marginally able to cool, and groups and clusters of galaxies have too long a cooling time to have dissipated much energy on their scale[72,73].

On average, for the cold DM fluctuation spectrum, what range of total masses yields baryon condensation within a massive halo? Let us first consider large galaxies. Naively, Fig. 3 suggests that there is an upper bound for galactic masses of $M \leqslant 10^{12}\ M_\odot$, where the baryonic cooling time for gas of primordial composition begins to exceed the dynamical time. More massive galaxies could form in dense regions, where perhaps an early generation of Population III stars enriched the remaining baryonic gas with metals. Actually, the situation is likely to be more complicated, with many large galaxies formed by the merger of smaller ones. The resulting galaxy mass distribution arises from competition between hierarchical clustering and decreasing galaxy collision cross-sections due to dissipation, and it is thus difficult to calculate reliably. Regarding the smallest galaxies, collisional excitation of atomic hydrogen provides a lower limit of $M \geqslant 10^8\ M_\odot$, corresponding to virialized baryonic temperature $T_b \geqslant 10^4$ K. This range of protogalactic total masses, $10^8\ M_\odot \leqslant M \leqslant 10^{12}\ M_\odot$, encompasses virtually all the mass that is observed to comprise galaxies. For protogalaxies in this mass range, the velocity dispersion of the baryons will initially remain nearly constant ($T \approx$ constant) as they condense within the gravitational potential of the virialized (and presumably roughly isothermal) DM halo. When the baryon density increases enough that their gravitational potential dominates that of the halo, the baryons' velocity dispersion will rise as they continue to dissipate energy and condense. Baryonic contraction is finally halted by rotation and perhaps, in some protogalaxies, by star formation (see below).

The collapse of fluctuations with mass $M > 10^{13}\ M_\odot$ leads to clusters of galaxies in this picture. In clusters, only the outer parts of member galactic haloes are stripped off by collisions—the inner baryonic cores are able to contract to form the observed stellar systems. More of the baryons in the richest clusters are observed to be in the form of hot gas than in galaxies, as we have already mentioned in connection with Fig. 1. Perhaps this is because rich clusters tend to contain high-density cores, which collapse early, simultaneously with many of the galaxies they contain.

Can the cold DM picture account for the wide range of morphologies displayed by clusters of galaxies in X-ray[74] and optical-band[75] observations, ranging from regular, apparently relaxed configurations to complex, multicomponent structures? Preliminary results are encouraging. In particular, simulations show that large central condensations form quickly and can grow by subsequent mergers to form cD galaxies if most of the DM is in haloes around the baryonic substructures, as expected for cold DM, but not if the DM is distributed diffusely[76,77].

What happens to small clouds whose baryonic mass M_b lies in the range $M_{J,b} < M_b < 10^{7\text{-}8}\ M_\odot$ and for which $T_b < 10^4$ K after virialization? For a primordial element abundance, the molecular cooling time (primarily due to H_2) is less than the dynamical time for fluctuations that satisfy

$$M_b > M_{C,b} \approx 4.1 \times 10^6 (\Omega h^2)^{-0.917} \left(\frac{Y_e}{10^{-4}}\right)^{-0.625} \left(\frac{\Omega_b}{0.1\Omega}\right)^{-1.04} \times \left(\frac{1+z_t}{10}\right)^{-2.75} M_\odot$$

where z_t is the redshift of maximum expansion of the fluctuation. (This result uses the cooling rates given by Yoneyama[78] and assumes the simple 'top hat' model of collapsing fluctuations. It corrects an equation given in ref. 17.) The quantity Y_e, the fraction of free electrons, is essentially the fraction that escapes recombination as the universe cools below ~1,000 K, and is roughly $10^{-4}(\Omega_b/0.1)^{-1}\Omega^{1/2}h^{-1}$. Systems with $M_b < M_{C,b}$ will persist as pressure supported clouds until they are disrupted by the virialization of larger scale clusters. Clouds having $M_b > M_{C,b}$ can dissipate energy and collapse, although the influence of rotation and the efficiency of fragmentation are poorly understood. The end product may be an irregular or dwarf spheroidal galaxy. Other possibilities such as a protoglobular cluster or one or more very massive objects (VMOs) would require greater contraction and are likely to be inhibited by angular momentum.

Moreover, it is unclear what fraction of the original baryonic mass can be retained by such small clouds rather than expelled. There is—despite the uncertainties—a strong probability that energy output from fragmented subsystems can influence the gas that remains uncondensed, thereby exerting a feedback on further condensation. In particular, UV emission from massive or supermassive stars can photoionize the remaining diffuse baryons, raising T_b up to 10^4 K. If such stars radiate a fraction q_{UV} of their Eddington luminosity in Lyman continuum photons, then the entire baryonic medium can be ionized even by a mass fraction of stars as low as $\sim 3 \times 10^{-5}/q_{UV}$. If the baryonic gas is re-ionized in systems with total mass $M \leqslant 10^6\ M_\odot$, the baryons become so hot that they flow out of the cloud, whose gravitational field is not strong enough to bind them.

This may explain the origin of dwarf spheroidal galaxies, with $10^6\ M_\odot < M < 10^8\ M_\odot$, which show little evidence of dissipation in Fig. 3. As the baryons in these systems begin to condense through molecular cooling, if fragmentation and star formation are very efficient the baryons quickly turn into stars and condensation ceases. On the other hand, if a fraction of the baryons fragment into stars having strong UV luminosity, the remaining baryons are heated until they leave the system, and dissipation will again cease. The apparent absence of dissipation in dwarf spheroidals could also be due to stripping of their baryons in encounters with more massive systems[32], which would move the dwarfs upward in Fig. 3.

In the cold DM scenario, globular clusters are probably not primordial objects. For one thing, there is no evidence that they have massive haloes (although, as Peebles[79] points out, there is not much direct contrary evidence either). Furthermore, if truly primordial, they should be distributed in the Universe like DM whereas, at least within galaxies, they seem to have dissipated and condensed like the other baryonic matter. However, the existence of 'standard objects' inside galaxies with mass $\sim 10^6\ M_\odot$ demands some explanation. In the model discussed here, there is a natural mass scale of order $M_{g,b} \sim M_{Gal,b}(T_{virial}/10^4\ K)^{-2}$, where $M_{Gal,b}$ is the baryonic mass within a galaxy; $M_{g,b}$ is the Jeans mass of a cloud at 10^4 K in pressure balance with protogalactic gas at the virial temperature[80]. During the dissipation phase of galaxy formation, the gas might be likely to have a two-phase structure with a hot phase at T_{virial} and a cool phase at $\sim 10^4$ K, in which case subcondensations of mass $M_{g,b}$ would be expected with density contrast $\approx T_{virial}/10^4$ K. We identify these with protoglobular clusters (noting that the considerations of Fall and Rees[81] could further limit the mass range).

Galaxies and clusters

While the n_b–T plot (Fig. 3) is useful for comparing data and predictions with the cooling curves, it is also useful to consider total mass M versus T, as in Fig. 4. This avoids having to take into account the differing amounts of baryonic dissipation suffered by various galaxies. The heavy solid and dashed curves again correspond to the $n = 1$ cold DM spectrum, for ($\Omega = 1$, $h = 0.5$) and ($\Omega = 0.2$, $h = 1$) respectively. It is striking that galaxies in the M–T diagram lie along lines of roughly the same slope as these curves. This occurs because the effective slope of the $n = 1$ cold DM fluctuation spectrum in the galaxy mass range is $n_{eff} \approx -2$, which corresponds to the empirical Tully-Fisher and Faber-Jackson laws: $M \propto v^4$. The light dashed lines in Fig. 4 are the postvirialization curves for primordial fluctuation spectra with $n = 0$ (white noise) and $n = 2$. The $n = 1$ (Zeldovich) spectrum is evidently the one that is most consistent with the data.

The points in Fig. 4 represent essentially all of the clusters identified by Geller and Huchra[82] in the CfA catalogue within 5,000 km s^{-1}. The cluster data lie about where they should on the diagram, and even the statistics of the distribution seem roughly to correspond to the expectations represented by the 0.5, 1, 2, and 3σ curves. Note that the galaxies and clusters are neatly separated by the Compton cooling line of Fig. 3, suggesting that the era of galaxy formation ceased in the Universe when Compton cooling off microwave background photons became inefficient (J. E. Gunn, personal communication).

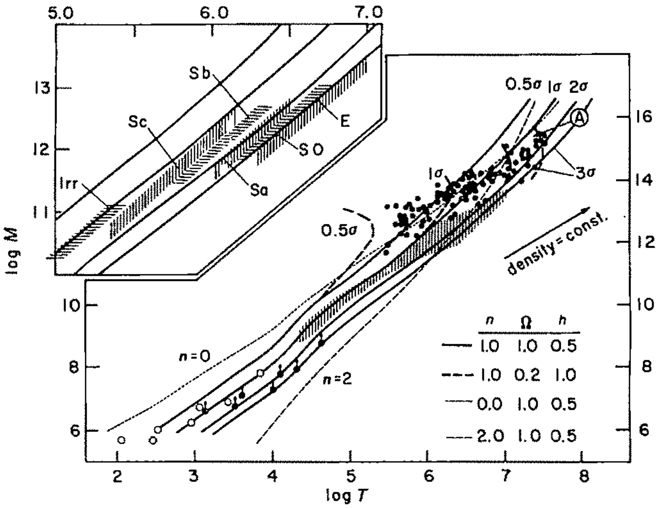

Fig. 4 Total mass M versus virial temperature T. Data sources and symbols are as in Fig. 3. M for groups and clusters is total dynamical mass. For galaxies, M is assumed to be 10 $M_{\rm lum}$ (see Fig. 3 legend). If Dw spheroidals actually have $M/L_{\rm B}=30$, they may have suffered baryon stripping[32], in which case M is a lower limit (arrows). Details of the region occupied by massive galaxies are shown in the inset, upper left. In addition to the $n=1$ models from Fig. 3, two 1σ curves for $n=0$ and $n=2$ are also shown (light dashes). Either set of curves for an $n=1$ (Zeldovich) spectrum provides a good fit to the observations over 9 orders of magnitude in mass. Curves with $n=0$ and $n=2$ do not fit as well. The apparent gap between galaxies and groups and clusters in Fig. 3 (which stems from baryonic dissipation) vanishes in this figure, and the clustering hierarchy is smooth and unbroken from the smallest structures to the largest ones. The Fisher–Tully and Faber–Jackson laws for galaxies ($M\propto V^4$ or T^2) arise naturally as a consequence of the slope of the cold DM fluctuation spectrum in the mass region of galaxies. Groups and clusters are distributed around the $n=1$ loci about as expected. The apparent upward trend among the groups is not physically meaningful but arises from their selection as density enhancements above a minimum threshold (see caption, Fig. 3, and constant-density arrow, this figure). The exact locations of galaxies are uncertain. In particular, the temperatures of Es and S0s may be overestimated owing to the use of nuclear rather than global velocity dispersions. The masses of Dw. Irrs may also be too low owing to neglect of mass in H_2. Taken at face value, however, the data suggest that early-type galaxies (Es and S0s) arise from high-$\delta M/M$ fluctuations, whereas late-type galaxies (Scs and Irrs) arise from low-$\delta M/M$ fluctuations. Groups and clusters appear to fill a wider band than galaxies. If real, this difference may indicate that low-$\delta M/M$ fluctuations on the mass scale of galaxies once existed but did not give rise to visible galaxies. This suggests further that galaxy formation, at least in some regions of the Universe, may not have been fully complete and that galaxies are therefore not a reliable tracer of total mass. The sharp demarcation line between galaxies and clusters corresponds to the Compton cooling limit in Fig. 3 and suggests that galaxy formation ceased when Compton cooling off the microwave background became inefficient.

Note that spiral galaxies lie roughly along the 1σ curve while elliptical galaxies lie along the 2σ curve. Although this displacement is not large compared with the uncertainties, it is consistent with the fact that more than half of all galaxies are spirals, while only ~15% are ellipticals. We have suggested elsewhere[83] that, in hierarchical clustering scenarios, the higher σ fluctuations will develop rather smaller angular momenta, as measured by the dimensionless parameter $\lambda(=JE^{1/2}G^{-1}M^{-5/2})$. This difference seems to exist with either white noise or a flatter spectrum, but to be larger in the latter case. If high σ fluctuations have little angular momentum, their baryons can collapse by a large factor in radius, forming high-density ellipticals and spheroidal bulges, as shown in Fig. 3. Because, with a flat spectrum, higher σ fluctuations occur preferentially in denser regions destined to become rich clusters (the statistics of such correlations can be treated[84] by the methods of Peebles[6]), one expects to find more ellipticals there—as is observed. Indeed, the rich clusters lie along the same 2 and 3σ curves in Fig. 4 as do the elliptical galaxies.

Presumably the collapse of the low-λ protoelliptical galaxies is halted by star formation well before a flattened disk can form, yielding a stellar system of spheroidal shape. The mechanism governing the onset of star formation in these systems is unfortunately not yet understood, but may involve a threshold effect which sets in when the baryon density exceeds the DM halo density by a sufficient factor[70,72]. Disks (spirals and irregulars) form from more typical higher-λ protogalaxies, which, for a given mass, are larger and more diffuse than their protoelliptical counterparts. The collapse of disks thus occurs through a relatively slow infall of baryons from ~10^2 kpc, and is halted by angular momentum. Infall from such distances is consistent both with the extent of dark haloes inferred from observations and with the high angular momenta of present-day disks ($\lambda\sim 0.4$)[85,86]. The location of galaxies in Fig. 3 is consistent with these ideas if the baryons in all galaxies collapsed in radius by roughly the same factor, about an order of magnitude, but less for late-type irregulars and more for early-type Es and spheroidal bulges.

It has been theorized that the Hubble sequence originates in the distribution of either the initial angular momenta[87,88] or else the initial densities[89] of protogalaxies. However, if overdensity and angular momentum are linked, with the high-σ fluctuations having lower λ, then these two apparently competitive theories become opposite sides of the same coin.

Consider finally the difference in Fig. 4 between the solid and dashed lines. The dashed lines, representing a lower-density Universe ($\Omega=0.2$), curve backward at the largest masses and lie far away from the circle representing the cores of the richest clusters, Abell classes 2 and 3. Because these regions of very high galaxy density contain at least several per cent of the mass in the Universe, the circle should lie between the 2 and 3σ lines (assuming gaussian statistics). It does so for the solid ($\Omega=1$) lines, but not for the dashed lines. At face value, this is evidence favouring an Einstein–de Sitter Universe for cold DM. However, there are at least two reasons why this argument should not be taken too seriously. First, the velocity dispersions represented by the Abell cluster circle in Fig. 4 correspond to the cluster cores. The model curves on the other hand refer to the entire virialized cluster, over which the velocity dispersion is considerably lower (as indicated schematically by the arrow attached to the circle in Fig. 4). Second, the assumption of spherical symmetry used in obtaining both sets of curves is only an approximation. The initial collapse is probably often quite anisotropic—more like a Zeldovich pancake than a sphere. It is, therefore, preferable to compare these data with N-body simulations than with the simple model represented by the curves in Fig. 4. Until this becomes possible we do not believe that the data in Fig. 4 allow a clear-cut discrimination between the $\Omega=0.2$ and $\Omega=1$ cases, especially if the Hubble parameter h is allowed to vary simultaneously within the observationally allowed range, as we have assumed.

Cosmological density

The most straightforward interpretation of the approximate constancy of $M/M_{\rm lum}\approx 10$ from galaxy through rich cluster scales (Fig. 1) is that dark matter clusters with galaxies. This is precisely what cold DM is expected to do. One then expects the density parameter $\Omega=(M/M_{\rm lum})\Omega_{\rm galaxies}\approx 10\times 0.02=0.2$, in agreement with $\Omega=0.2\times 1.5^{\pm 1}$ from the cosmic energy equation and the stability of clustering[90].

The value $\Omega\approx 0.2$ is consistent with all reliable measurements and furthermore gives an age for the Universe, t_0, consistent with globular cluster age estimates[91] ($\geq$15 Gyr) if $h\leq 0.6$. The observed abundance of deuterium plus helium-3 implies a lower limit[37] $\Omega_{\rm b}h^2\geq 0.01$, which is also consistent with $\Omega=0.2$ and $\Omega_{\rm b}\approx 0.02$ if $h\geq 0.7$.

Another argument favouring $\Omega=0.2$ for cold DM is based on preliminary N-body results[92], which indicate that superclusters and voids form on the observed scale for $\Omega=0.2$, but on too small a scale for $\Omega=1$ unless the Hubble constant is unrealistically small. However, this conclusion follows from comparing the N-body mass autocorrelation function $\xi_{\rm m}(r)$ with the observed galaxy autocorrelation function $\xi_{\rm g}(r)$. This is justified only if the galaxies are a good tracer of mass—if $M/L\approx$ constant. This is certainly not true for rich clusters, as illustrated in the top part of Fig. 1 and in Table 1, where M/L for very rich clusters is roughly six times larger than it is for small groups and for the Milky Way (including its DM halo). This means that some of the actual small-distance-mass autocorrelation is not included in the galaxy autocorrelation function; that $\xi_m(r)$ is steeper for $r \leq 1$ Mpc than $\xi_g(r)$. This effect is in the right direction to bring the $\Omega = 1$ N-body simulations into consistency with observations. Note that galaxy velocity dispersion averages also underestimate the actual mass-weighted velocity dispersion, because the high-velocity, dense regions of rich clusters are under-represented in the counts. This effect is also compatible with higher Ω.

The absence of measurable fluctuations in the cosmic microwave background also restricts Ω, because in a low-Ω Universe there is less growth of fluctuations both before and after recombination. The latest limits[38,39] on $\Delta T/T$ require $\Omega \geq 0.2h^{-4/3}$ (refs 93, 94), unless the Universe was reionized after recombination.

Both prejudice and the inflationary hypothesis favour the Einstein-de Sitter value $\Omega = 1$. (Actually, inflation implies more generally that $\Omega = 1 - \Lambda/3H^2$, where H is Hubble's constant and Λ is the cosmological constant[95], but we assume here that $\Lambda = 0$.) For $\Omega = 1$, $t_0 = 6.5h^{-1}$ Gyr, so consistency with globular cluster age estimates requires the Hubble constant to be perhaps unrealistically small. As we have discussed, the Zeldovich ($n = 1$) spectrum of primordial adiabatic fluctuations, which also follows from inflation, is compatible with models of galaxy formation in the cold DM scenario. Of course, the Zeldovich spectrum does not necessarily entail inflation. Moreover, inflation does not necessarily imply $\Omega = 1$: if there is a great deal of inflation, then, of course, Ω is very close to unity (assuming vanishing cosmological constant); but if we speculate that greater amounts of inflation are increasingly unlikely, then our horizon might happen to lie in a patch with $\Omega = 0.2$.

Could $\Omega = 1$ in the cold DM model? Based on Fig. 1, this could happen only if M/M_{lum} increases substantially on scales larger than rich clusters. Perhaps galaxy formation is suppressed in the voids, and the resulting luminosity contrast is so strong, for reasons we do not yet understand, that $M/L > 1{,}500$ there (see below). Alternatively, if the virial mass of clusters of galaxies is significantly underestimated, as suggested recently by Kaiser, and if galactic haloes extend much further than ~70 kpc, then the ratio M/M_{lum} may be substantially underestimated in Fig. 1, leading to a larger value for Ω. If galaxy formation is inefficient so that only large-overdensity perturbations can form galaxies—a possibility suggested by Fig. 4—the $\Omega = 1$, cold DM N-body simulations[92] can be brought into agreement with observations[96,97]. We conclude that a straightforward interpretation of the evidence summarized above favours $\Omega \approx 0.2$ in the cold DM picture, but that $\Omega = 1$ is not implausible.

Note that the cold DM model may require some means of suppressing galaxy formation in voids for $\Omega \approx 0.2$ as well as for $\Omega = 1$. This is required in the latter case to hide most of the mass. In a low-Ω Universe, on the other hand, large, very underdense regions cannot form by gravitation alone[98,99]; and galaxy formation must be suppressed somehow in regions of moderately low density if the density of galaxies in voids is less than one-quarter of the average density, the quoted upper limit for the Boötes void[100,101]. Suppression of galaxy formation may occur partly because of the substantial difference at $z < \Omega^{-1}$ between $\langle \rho \rangle$ and ρ_c in a low-density Universe.

Superclusters and voids

Recent, accurate redshift measurements of several thousand galaxies have revealed the presence of voids with linear dimensions ranging up to $\sim 50h^{-1}$ Mpc that are almost completely empty of bright galaxies. Most galaxies are concentrated in irregularly shaped, flattened, or elongated superclusters (see ref. 102 for fuller discussion and references). Two related observations are particularly interesting for their possible bearing on the origin of this large scale structure: a correlation of galaxy type with galaxy number density[103,104] and, possibly, a correlation between the orientation of cluster major axes and the direction to neighbouring clusters within $\sim 15h^{-1}$ Mpc (ref. 105).

In the hot DM picture, the fluctuation spectrum is rather sharply peaked at masses $\sim 4 \times 10^{15}$ (30 eV/m)^2. The suppression of smaller scale structure results in an essentially pressure-free collapse on the supercluster scale, with the formation of sharp caustics—Zeldovich pancakes[106,107]. If galaxies form only in the densest regions, where the shocked baryons have cooled sufficiently[108,109], most of the Universe would be essentially devoid of galaxies. Simulations[110] also show large-scale cluster orientation correlations resembling those observed. On the other hand, the rapid evolution of the autocorrelation function requires that the pancakes form at $z \leq 2$, which is uncomfortably recent if smaller structures including galaxies must form subsequently.

The cold DM scenario avoids this latter problem because galaxies and clusters would already have formed by the time of supercluster collapse. Would superclusters and voids arise in a cold DM Universe? There are good reasons to believe that pancakes, filaments, and voids would indeed form, and preliminary indications from N-body simulations suggest that they do[92,111]. The cold and hot DM fluctuation spectra are identical on the very largest scales, differing only in that the latter is cut off below $\sim 10^{15}$ $M_\odot$ by neutrino free streaming and normalized larger above this scale (see Fig. 2a). The presence of already-formed and partially-virialized substructure in the cold DM case causes supercluster collapse to be less dissipative than in the neutrino picture because the caustics are thickened and because a smaller fraction of the baryons remains as cold, uncondensed gas. Nevertheless, as Dekel[112] has shown, persistent flattened or elongated structures can form even in the absence of dissipation as a result of continued expansion in directions orthogonal to the collapse. Indeed, the sharp caustics and highly dissipative shocks in the neutrino picture may produce superclusters that are too flat compared with the observations, even when gravitational interactions with neighbouring superclusters are taken into account.

Another related difference between hot and cold DM is that the hot DM Universe is predicted to have a rather simple cellular structure while the cold DM Universe probably has a considerably richer structure, perhaps more like that observed. In particular, the sizes of superclusters and voids in the cold case should span a fairly broad range. This will be an important test of the models when enough galaxy redshift data become available to indicate the statistics of the void distribution.

What should one expect to find in the voids? In the hot DM picture, all galaxies form from the dense gas along the caustics. Hence, the centres of voids should be entirely empty of galaxies and should contain only low-density DM and hot primordial gas (heated by radiation from pancake shocks and too dilute to have cooled)[113]. In the cold DM picture, one might at first suppose that galaxies form more or less uniformly in space, with their density subsequently enhanced by gravitational clustering and the pancake distortion of the Hubble flow. One would then expect to find galaxies in the voids, although with lower density than in superclusters.

In a low-density Universe, both analytical calculations[98,99] and N-body simulations[92] suggest that large regions having $\rho/\langle \rho \rangle \leq 0.2$ cannot form by gravitational clustering alone. Nonetheless, large regions with few bright galaxies may actually be more likely in a low density cold DM Universe, for the following reason. On average, large galaxies form late when the average density has dropped well below the critical density. Larger initial fluctuations are thus required to form large galaxies in low-density regions. But larger fluctuations are statistically less likely in low-density regions with the flat, cold DM spectrum. This suppresses formation of large galaxies in moderate-size voids, and formation of clusters in larger voids[84].

In addition, feedback from nongravitational processes could amplify the number density contrast of bright galaxies compared with the underlying density of dark and baryonic matter. For example, at $z \sim 10$ the average density is highest where pancakes will later occur. This is where most of the earliest galaxies and rich clusters form, and these will be the regions earliest enriched in metals. Radiation from these early galaxies (and quasars, and possibly Population III stars or VMOs) could heat the gas in lower density regions, raising the Jeans mass, as discussed above, and suppressing small galaxy formation. Indeed, if this early radiation has a hard enough spectrum and heats the gas sufficiently rapidly, it could raise the gas temperature throughout the Universe to 10^6 K and essentially halt galaxy formation outside pancakes. One of us (M.J.R.) has recently discussed[114] processes for suppressing galaxy formation in protovoids. Finally, explosive shocks could also enhance galaxy formation in denser regions[115]. Although the efficacy of all these processes is uncertain and needs further investigation, we conclude that the existence of large regions in which the density of bright galaxies is low is probably not a serious problem for the cold DM picture.

Now let us briefly discuss the two types of correlations mentioned above. The observed correlation of galaxy type with galaxy number density[103,104] can, at least partly, be understood as a consequence of the greater statistical likelihood of large-σ fluctuations in regions of greater density (protoclusters), together with the effect discussed above that results in higher-σ fluctuations acquiring lower angular momenta on average and becoming elliptical galaxies or spheroidal bulges. There is also an environmental effect: lower-σ fluctuations yield dark haloes that are physically larger and more diffuse than higher-σ fluctuations. Disks, which form from such fluctuations, thus form slowly, by infall of gas from large radii within these extended haloes. Because large haloes have correspondingly large collision cross-sections, few disks can form in regions of high galaxy number density. In dense regions, the halo gas is stripped by collisions and is mixed with enriched gas from galactic winds to become the hot intergalactic medium observed in X rays. It will be interesting to investigate these effects with N-body simulations and a more detailed theory of galaxy formation.

Regarding the second type of correlation, Binggeli[105] has found that the position angles of nearby, elongated Abell clusters are within 45° of the direction to the nearest cluster, provided the two clusters are separated by $\leq 15h^{-1}$ Mpc. He found a similar, though less significant, correlation between the position angle of the brightest cluster galaxy's major axis and the direction to the nearest cluster. In the hot DM picture, where superclusters form before clusters and galaxies, such correlations arise naturally. Indeed an N-body simulation[110] has shown that such correlations also occur, but more weakly, even with a fluctuation spectrum having an adiabatic peak at $\sim 10^{15}\ M_\odot$ superimposed on an $n = 0$ spectrum, so that rich clusters and superclusters form almost simultaneously. However, a preliminary analysis[116] of cold DM N-body simulations finds Bingelli-type correlations only if $\Omega h \leq 0.2$.

It is important to find other observationally accessible information that can discriminate between cosmological models. The large-scale velocity fields of superclusters should be rather different in the hot and cold DM schemes because of the much greater dissipation in the former. With new instruments it will also be possible to study the $z < 2$ evolution of superclustering of quasars and of Lyα absorbing clouds, and perhaps the density and composition of the gas in voids.

It was once hoped that percolation analysis of the large scale galaxy distribution could help to distinguish between different cosmological models.[11,117]. However, when this analysis is applied to the CfA galaxy data, the results are found to be a sensitive function of the depth of the survey[118]. Moreover, realistic N-body simulations of isothermal and adiabatic scenarios (that is, with accurate treatment of gravitational interactions on small as well as large scales) have nearly identical percolation properties[110,119]. Better statistical tests are needed to compare objectively the large-scale distribution of matter in models and observations.

Conclusions

We have shown that a Universe with ~ 10 times as much cold dark matter as baryonic matter provides a remarkably good fit to the observed Universe. This model predicts roughly the observed mass range of galaxies, the dissipational nature of galaxy collapse, and the observed Faber-Jackson and Tully-Fisher relations. It also gives dissipationless galactic haloes and clusters. In addition, it may also provide natural explanations for galaxy-environment correlations and for the differences in angular momenta between ellipticals and spiral galaxies. Finally, the cold DM picture seems reasonably consistent with the observed large-scale clustering, including superclusters and voids. In short, it seems to be the best model available and merits close scrutiny and testing.

We thank Dick Bond, Jim Bardeen, Marc Davis, Avishai Dekel, George Efstathiou, Mike Fall, Carlos Frenk, Margaret Geller, Jim Gunn, Jim Peebles, Nicola Vittorio, and Simon White for valuable conversations. In addition, J.R.P. acknowledges the hospitality of the Max Planck Institute for Physics and Astrophysics, Munich during the summer 1983. This work was supported by the Department of Energy under contract no. DE-AC03-76SF00515 and by NSF grants AST-82-11551 and PHY-81-15541. This is Lick Observatory Contribution No. 436.

1. Faber, S. M. & Gallagher, J. S. *A. Rev. Ast. Astrophys.* **17**, 135–187 (1979).
2. Peebles, P. J. E. *Astrophys. J. Lett.* **263**, L1–L5 (1982).
3. Primack, J. R. & Blumenthal, G. R. *Formation and Evolution of Galaxies and Large Structures in the Universe* (eds Audouze, J. & Tran Thanh Van, J. 163–183 (Reidel, Dordrecht, 1983).
4. Primack, J. R. & Blumenthal, G. R. *4th Workshop on Grand Unification* (eds Weldon, H. A., Langacker, P. & Steinhardt, P. J.) 256–288 (Birkhauser, Boston, 1983).
5. Primack, J. R. & Blumenthal, G. R. *Clusters and Groups of Galaxies* (eds Mardirossian, F., Giuricin, G. & Mezzetti, M.)(Reidel, Dordrecht, in the press).
6. Peebles, P. J. E. *Astrophys. J.* **277**, 470–477 (1984).
7. Blumenthal, G. R. & Primack, J. R. Preprint (SLAC-PUB-3388, 1984).
8. Peebles, P. J. E. *The Large Scale Structure of the Universe* (Princeton University Press, 1980).
9. Efstathiou, G. & Silk, J. *Fundm. Cosmic Phys.* **9**, 1–138 (1983).
10. Lyubimov, V. A. *et al. Phys. Lett.* **B94**, 266–268 (1980).
11. Zeldovich, Ya. B., Einasto, J. & Shandarin, S. F. *Nature* **300**, 407–413 (1982).
12. Shandarin, S. F., Doroshkevich, A. G. & Zeldovich, Ya. B. *Sov. Phys. Usp.* **26**, 46–76 (1983).
13. Pagels, H. R. & Primack, J. R. *Phys. Rev. Lett.* **48**, 223–226 (1982).
14. Olive, K. A. & Turner, M. S. *Phys. Rev.* **D25**, 213–216 (1982).
15. Blumenthal, G. R., Pagels, H. & Primack, J. R. *Nature* **299**, 37–38 (1982).
16. Bond, J. R., Szalay, A. S. & Turner, M. S. *Phys. Rev. Lett.* **48**, 1636–1639 (1982).
17. Bond, J. R. & Szalay, A. S. *Astrophys. J.* **274**, 443–468 (1984).
18. Ipser, J. & Sikivie, P. *Phys. Rev. Lett.* **50**, 925–927 (1983).
19. Peccei, R. & Quinn, H. *Phys. Rev.* **D16**, 1791–1797 (1977).
20. Weinberg, S. *Phys. Rev. Lett.* **40**, 223–226 (1978).
21. Wilczek, F. *Phys. Rev. Lett.* **40**, 279–282 (1978).
22. Preskill, J., Wise, M. & Wilczek, F. *Phys. Lett.* **120B**, 127–132 (1983).
23. Abbott, L. & Sikivie, P. *Phys. Lett.* **120B**, 133–136 (1983).
24. Dine, M. & Fischler, W. *Phys. Lett.* **120B**, 137–141 (1983).
25. Fukugita, M., Watamura, S. & Yoshimura, M. *Phys. Rev. Lett.* **48**, 1522–1525 (1982).
26. Sikivie, P. *Phys. Rev. Lett.* **51**, 1415–1417 (1983); erratum **52**, 695 (1984).
27. Ellis, J., Hagelin, J. S., Nanopoulos, D. V., Olive, K. & Srednicki, M. *Nucl. Phys. B* **238**, 453–476 (1984).
28. Stecker, F. W. & Shafi, Q. *Phys. Rev. Lett.* **50**, 928–931 (1983).
29. Freese, K., Price, R. & Schramm, D. N. *Astrophys. J.* **275**, 405–412 (1983).
30. Carr, B. J. *Commts Astrophys.* **7**, 161–173 (1978).
31. Lacey, C. G. *Formation and Evolution of Galaxies and Large Scale Structures in the Universe* (eds Audouze, J. & Tran Thanh Van, J.) 351–360 (Reidel, Dordrecht, 1984).
32. Lin, D. N. C. & Faber, S. M. *Astrophys. J. Lett.* **266**, L21–L25 (1983).
33. Canizares, C. R. *Astrophys. J.* **263**, 508–517 (1982).
34. Witten, E. *Phys. Rev.* **D30**, 272–285 (1984).
35. Carr, B. J., Bond, J. R. & Arnett, W. D. *Astrophys. J.* **277**, 445–469 (1984).
36. Hegyi, D. J. & Olive, K. A. *Phys. Lett.* **126B**, 28–32 (1983).
37. Yang, J., Turner, M. S., Steigman, G., Schramm, D. N. & Olive, K. A. *Astrophys. J.* (in the press).
38. Uson, J. M. & Wilkinson, D. T. *Astrophys. J. Lett.* **277**, L1–L4 (1984).
39. Uson, J. M. & Wilkinson, D. T. *Inner Space/Outer Space* (eds Kolb, E. W. *et al.*) (University of Chicago Press, in the press).
40. Weinberg, S. *Astrophysical Cosmology: Proc. Study Week on Cosmology and Fundamental Physics* (eds Brück, H. A., Coyne, G. V. & Longair, M. S.) 503–528 (Pontifical Scientific Academy, Vatican, 1982).
41. Kolb, E. W. & Turner, M. S. *A. Rev. Nucl. Part. Sci.* **33**, 645–696 (1983).
42. Rees, M. J. *The Very Early Universe* (eds Gibbons, G., Hawking, S. & Siklos, S.) 29–58 (Cambridge University Press, 1983).
43. Frenk, C., White, S. D. M. & Davis, M. *Astrophys. J.* **271**, 417–430 (1983).
44. Dekel, A. & Aarseth, S. *Astrophys. J.* **283** (in the press).
45. Kaiser, N. *Astrophys. J. Lett.* **273**, L17–L20 (1983).
46. Faber, S. M. *Proc. 1st ESO-CERN Symp., Large Scale Structure of the Universe, Cosmology, and Fundamental Physics* (in the press).
47. Bond, J. R., Szalay, A. S. & White, S. D. M. *Nature* **301**, 584–585 (1983).
48. Aaronson, M. *Astrophys. J. Lett.* **266**, L11–L15 (1983).
49. Aaronson, M. & Cook, K. *Bull. Am. astr. Soc.* **15**, 907 (1983).
50. Cook, K., Schechter, P. & Aaronson, M. *Bull. Am. astr. Soc.* **15**, 907 (1983).
51. Faber, S. M. & Lin, D. N. C. *Astrophys. J. Lett.* **266**, L17–L20 (1983).
52. Davis, M., Lecar, M., Pryor, C. & Witten, E. *Astrophys. J.* **250**, 423 (1981).
53. Hut, P. & White, S. D. M. *Nature* **310**, 637–644 (1984).
54. Doroshkevich, A. G. & Khlopov, M. Yu. *Mon. Not. R. astr. Soc.* (in the press).
55. Turner, M. S., Steigman, G. & Krauss, L. M. Preprint (Fermilab, 1984).
56. Primack, J. R. & Roncadelli, M. Preprint (SLAC-PUB-3304, 1984).
57. Shafi, Q. & Stecker, F. W. Preprint (Bartol Research Foundation, 1984).
58. Gelmini, G., Schramm, D. N. & Valle, J. W. F. Preprint (CERN-TH-3865, 1984).
59. Harrison, E. R. *Phys. Rev.* **D1**, 2726–2730 (1970).
60. Peebles, P. J. E. & Yu, J. T. *Astrophys. J.* **162**, 815–836 (1970).
61. Zeldovich, Ya. B. *Mon. Not. R. astr. Soc.* **160**, 1P–3P (1972).

62. Shafi, Q. & Vilenkin, A. *Phys. Rev. Lett.* **52**, 691–694 (1984).
63. Steinhardt, P. J. & Turner, M. S. Preprint (Fermilab, 1984).
64. Quinn, H. R. & Gupta, S. *Phys. Rev.* **D29**, 2791–2797 (1984).
65. Zeldovich, Ya. B. *Mon. Not. R. astr. Soc.* **192**, 663–667 (1980).
66. Vilenkin, A. *Phys. Rev.* **D24**, 2082–2089 (1981).
67. Bond, J. R., Efstathiou, G. & Silk, J. *Phys. Rev. Lett.* **45**, 1980–1984 (1980).
68. Doroshkevich, A. G., Zeldovich, Ya. B., Sunyaev, R. A. & Khlopov, M. Yu. *Soviet Astr. Lett.* **6**, 252–256 (1980).
69. Chernin, A. D. *Soviet Astr.* **25**, 14–16 (1981).
70. White, S. D. M. & Rees, M. J. *Mon. Not. R. astr. Soc.* **183**, 341–358 (1978).
71. Rees, M. J. & Ostriker, J. P. *Mon. Not. R. astr. Soc.* **179**, 541–559 (1977).
72. Faber, S. M. *Astrophysical Cosmology: Proc. Study Week on Cosmology and Fundamental Physics* (eds Brück, H. A., Coyne, G. V. & Longair, M. S.) 191–234 (Pontifical Scientific Academy, Vatican, 1982).
73. Silk, J. *Nature* **301**, 574–578 (1983).
74. Forman, W. & Jones, C. *Ann. Rev. Astr. Astrophys.* **20**, 547–585 (1982).
75. Geller, M. J. & Beers, T. C. *Proc. Astr. Soc. Paci.* **94**, 421–439 (1982).
76. Thuan, T. X. & Romanishin, W. *Astrophys. J.* **248**, 439–459 (1981).
77. Cavaliere, A., Santangelo, P., Tarquini, G. & Vittorio, N. *Clusters and Groups of Galaxies* (eds Mardirossian, F., Giuricin, G. & Mezzetti, M.) (Reidel, Dordrecht, in the press).
78. Yoneyama, T. *Publ. Astr. Soc. Jap.* **24**, 87–98 (1972).
79. Peebles, P. J. E. Preprint (Princeton Univ., 1984).
80. Fall, S. M. & Rees, M. J. (in preparation).
81. Fall, S. M. & Rees, M. J. *Mon. Not. R. astr. Soc.* **181**, 37P–42P (1977).
82. Geller, M. & Huchra, J. *Astrophys. J. Suppl.* **52**, 61–87 (1983).
83. Faber, S. M., Blumenthal, G. R. & Primack, J. R. *Astrophys. J. Lett.* (submitted).
84. Blumenthal, G. R., Faber, S. M. & Primack, J. R. (in preparation).
85. Efstathiou, G. & Jones, B. J. T. *Mon. Not. R. astr. Soc.* **186**, 133–144 (1979).
86. Fall, S. M. & Efstathiou, G. *Mon. Not. R. astr. Soc.* **193**, 189–206 (1980).
87. Sandage, A., Freeman, K. C. & Stokes, N. R. *Astrophys. J.* **160**, 831–844 (1970).
88. Efstathiou, G. & Barnes, J. *Formation and Evolution of Galaxies and Large Scale Structures in the Universe* (eds Audouze, J. & Tran Thanh Van, J.) 361–377 (Reidel, Dordrecht, 1984).
89. Gott, J. R. & Thuan, T. X. *Astrophys. J.* **204**, 649–667 (1976).
90. Davis, M. & Peebles, P. J. E. *Astrophys. J.* **267**, 465–482 (1983).
91. Sandage, A. *Proc. 1st ESO-CERN Symp., Large Scale Structure of the Universe, Cosmology, and Fundamental Physics* (in the press).
92. Davis, M., Efstathiou, G., Frenk, C. & White, S. D. M. (in preparation).
93. Bond, J. R. & Efstathiou, G. Preprint (NSF-ITP-84-79, 1984).
94. Vittorio, N. & Silk, J. Preprint (U. Cal. Berkeley, 1984).
95. Peebles, P. J. E. Preprint (Princeton Univ., 1984).
96. Kaiser, N. *Inner Space/Outer Space* (eds Kolb, E. W. *et al.*) (University of Chicago Press, in the press).
97. Bardeen, J. *Inner Space/Outer Space* (eds Kolb, E. W. *et al.*) (University of Chicago Press, in the press).
98. Hoffman, G. L., Salpeter, E. E. & Wasserman, I. *Astrophys. J.* **268**, 527–539 (1983).
99. Hoffman, Y. & Shaham, J. *Astrophys. J. Lett.* **262**, L23–L26 (1982).
100. Kirshner, R. F., Oemler, A., Schechter, P. L. & Schectman, S. A. *Astrophys. J. Lett.* **248**, L57–L60 (1981).
101. Kirshner, R. F., Oemler, A., Schechter, P. L. & Schectman, S. A. *Early Evolution of the Universe and its Present Structure, IAU Symp.* No. 104 197–202 (1983).
102. Oort, J. H. *A. Rev. Astr. Astrophys.* **21**, 373–428 (1983).
103. Dressler, A. *Astrophys. J.* **236**, 351–365 (1980).
104. Postman, M. & Geller, M. J. *Astrophys. J.* **281**, 95–99 (1984).
105. Binggeli, B. *Astr. Astrophys.* **107**, 338–349 (1982).
106. Zeldovich, Ya. B. *Astr. Astrophys.* **5**, 84–89 (1970).
107. Arnold, V. I., Shandarin, S. F. & Zeldovich, Ya. B. *Geophys. Astrophys. Fluid Dyn.* **20**, 111 (1982).
108. Bond, J. R., Centrella, J., Szalay, A. S. & Wilson, J. R. *Formation and Evolution of Galaxies and Large Structures in the Universe* (eds Audouze, J. & Tran Thanh Van, J.) 87–93 (Reidel, Dordrecht, 1984).
109. Shapiro, P. R., Struck-Marcell, C. & Melott, A. L. *Astrophys. J.* **275**, 413–429 (1983).
110. Dekel, A., West, M. J. & Aarseth, S. J. *Astrophys. J.* **279**, 1 (1984)
111. Melott, A., Einasto, J., Saar, E., Suisalu, I., Klypin, A. A. & Shandarin, S. F. *Phys. Rev. Lett.* **51**, 935–938 (1983).
112. Dekel, A. *Astrophys. J.* **264**, 373–391 (1983).
113. Doroshkevich, A. G., Shandarin, S. F. & Zeldovich, Ya. B. *Comm. Astrophys.* **9**, 265–273 (1982).
114. Rees, M. J. *Clusters and Groups of Galaxies* (eds Mardirossian, F., Giuricin, G. & Mezzetti, M.) (Reidel, Dordrecht, in the press).
115. Ostriker, J. P. *Astrophysical Cosmology: Proc. Study Week on Cosmology and Fundamental Physics* (eds Brück, H. A., Coyne, G. V. & Longair, M. S.) 473–493 (Pontifical Scientific Academy, Vatican, 1982).
116. Dekel, A. *8th Johns Hopkins Workshop on Current Problems in Particle Theory* (eds Domokos, G. & Kovesi-Domokos, S.) (World Scientific Publishing, Singapore, in the press).
117. Shandarin, S. F. *Soviet Astr. Lett.* **9**, 104 (1983).
118. Barrow, J. D. & Bhavsar, S. P. *Mon. Not. R. astr. Soc.* **205**, 66 (1983)
119. Dekel, A. & West, M. J. Preprint (NSF-ITP-84-44, 1984).
120. Dressler, A. *Astrophys. J.* **226**, 55–69 (1978).
121. Jones, C. & Forman, W. *Astrophys. J.* **276**, 38–55 (1983).
122. Kriss, G. A., Cioffi, D. F. & Canizares, C. R. *Astrophys. J.* **272**, 439–448 (1983)
123. Beers, T. C., Geller, M. J., Huchra, J. P., Latham, D. W. & Davis, R. J. *Astrophys. J.* (in the press).
124. Gunn, J. E. *Astrophysical Cosmology* (eds Brück, H. A., Coyne, G. V. & Longair, M. S.) 233–259 (Pontifical Scientific Academy, Vatican, 1982).
125. Young, P. J. *Astr. J.* **81**, 807–816 (1976).
126. Kent, S. M. & Gunn, J. E. *Astr. J.* **87**, 945–971 (1982).
127. Kent, S. M. & Sargent, W. L. W. *Astr. J.* **88**, 697–708 (1983)
128. de Vaucouleurs, G., de Vaucouleurs, A. & Corwin, H. R. *2nd Reference Catalogue of Bright Galaxies* (University of Texas, Austin, 1976).
129. Dressler, A. & Sandage, A. R. *Astrophys. J.* **265**, 664–680 (1983).
130. Rubin, V. C. *Internal Kinematics and Dynamics of Galaxies* (ed. Athanassoula, E.) 3–6 (Reidel, Dordrecht, 1983).
131. Rubin, V. C., Ford, W. K., Thonnard, N. & Burstein, D. *Astrophys. J.* **261**, 439–456 (1982).
132. Burstein, D., Rubin, V. C., Thonnard, N. & Ford, W. K. *Astrophys. J.* **253**, 70–85 (1982)
133. Thuan, T. X. & Seitzer, P. O. *Astrophys. J.* **231**, 680–687 (1979)
134. Tonry, J. & Davis, M. *Astrophys. J.* **246**, 680–695 (1981).
135. Raymond, J. C., Cox, D. P. & Smith, B. W. *Astrophys. J.* **204**, 290–292 (1976)
136. Dalgarno, A. & McCray, R. A. *A. Rev. Astr. Astrophys.* **10**, 375–426 (1972)

ARTICLES

Ultrahigh gradient particle acceleration by intense laser-driven plasma density waves

C. Joshi*, W. B. Mori*, T. Katsouleas*, J. M. Dawson*,
J. M. Kindel† & D. W. Forslund†

* University of California Los Angeles, California 90024, USA
† Los Alamos National Laboratory, Los Alamos, New Mexico 87545, USA

Space-charge waves driven by resonantly beating two laser beams in a high-density plasma can produce ultrahigh electric fields that propagate with velocities close to c*. By phase-locking particles in such a wave, particles may be accelerated to very high energies within a very short distance.*

DURING the past four decades, we have witnessed an increase of six orders of magnitude in the output energy of high-energy accelerators, while the cost per MeV has been reduced by a factor of 16 per decade. But can this progress continue? Current accelerators, such as the Stanford linac, have accelerating fields of 200 keV cm^{-1}. However, for particle energies beyond 10 TeV, one had to invent schemes that can produce fields of at least 10 MeV cm^{-1}. In any particle accelerator scheme, the basic requirement for obtaining particles with ultrahigh energies is an intense longitudinal electric field that interacts with particles for a long time. Since highly relativistic particles move nearly at the speed of light c, the energy gained by the particles, $\int E \cdot dl$, is maximum if the field is made to propagate with the particles. Extremely large electric fields propagating with phase velocities close to c can be produced by space charge waves in a plasma (ionized gas). The maximum electric field that can be produced by such a wave is approximately $\sqrt{n_e}$ V cm^{-1}, where n_e is the plasma electron density per cm^3. Thus for plasma densities in the range 10^{16}–10^{20} electrons cm^{-3}, the longitudinal electric fields E_L, can be as large as 10^8–10^{10} V cm^{-1}. We now show that such high-gradient, high-phase velocity plasma density waves can be driven by intense laser beams. If particles could be phase-locked in such waves, this scheme has the potential for accelerating particles to ultrahigh energies in very short distances.

Theory

If an intense laser beam is propagated in a plasma, then in certain conditions, the transverse electric field of the laser (which may reach values of 10^9–10^{10} V cm^{-1}) can be very effectively transformed into a longitudinal electric field of a plasma density wave. In the laser accelerator scheme known as the 'Plasma beat wave accelerator' proposed by Tajima and Dawson[1,7], such a plasma wave can be driven by beating two colinear laser beams, with frequencies and wavenumbers (ω_0, k_0) and (ω_1, k_1), in a plasma resonantly, such that the frequency and the wavenumber of the plasma wave are

$$\begin{aligned}\omega_{\text{epw}} &= \omega_0 - \omega_1 \\ k_{\text{epw}} &= k_0 - k_1\end{aligned} \qquad (1)$$

To achieve the ultrahigh accelerating gradients, high-density plasmas ($10^{16} < n_e < 10^{20}\ \text{cm}^{-3}$) must be used. Also, because the laser of frequency ω_0 cannot penetrate a plasma whose density exceeds the critical density n_c, corresponding to the plasma frequency $\omega_P = \omega_0$, plasmas with densities less than the quarter critical density must be used. Physically, the plasma wave consists of regions of space charge, which propagate with a phase velocity v_{ph} that is equal to the group velocity of the beat wave $v_g = c(1 - \omega_p^2/\omega_0^2)^{(1/2)}$. These arise because the spatial intensity gradient of the beat wave envelope, which is in the direction of propagation, exerts a periodic force (ponderomotive force) on the plasma at wavenumber k_{epw}. The plasma wave is thus an electrostatic wave with $\mathbf{E}_{\text{epw}}$ parallel to $\mathbf{k}_{\text{epw}}$.

When two parallel propagating laser beams beat in a plasma resonantly, the plasma density fluctuations grow rapidly. Using fluid equations it can be shown that for $v_0/c \ll 1$, the plasma wave electric field, which is proportional to the perturbed density, initially grows in time with a growth rate

$$\delta = \left(\frac{1}{4}\frac{v_0(0)}{c}\frac{v_0(1)}{c}\omega_p\right) s^{-1} \qquad (2)$$

where $[v_0(0, 1)]/c = eE_{(0,1)}/m\omega_{(0,1)}c$ is the normalized oscillatory velocity of an electron in the laser field. Wavebreaking is approached when the perturbed density becomes as large as the initial density; however, to reach this limit the plasma wave must remain in phase with the beat wave. As the plasma wave grows, the relativistic effect on the frequency mismatch becomes important[2] and the plasma wave saturates at a lower amplitude given by

$$\varepsilon = \frac{eE_{\text{epw}}}{m\omega_{\text{epw}}c} = \left(\frac{16}{3}\frac{v_0(0)}{c}\frac{v_0(1)}{c}\right)^{1/3} \qquad (3)$$

Once the saturation amplitude is reached, the plasma wave amplitude actually begins to decrease, if this process alone acts to sustain the plasma wave[3].

As the plasma wave is an electrostatic wave, we can use Poisson's equation, $E_{\text{epw}} = 4\pi e n_e/k_{\text{epw}}$, to estimate the maximum electric field that we might expect if we assume that the perturbed electron density is equal to the initial density (the so-called cold plasma wavebreaking limit $\varepsilon = 1$). As the plasma wave is propagating at relativistic speed, the Lorentz transformation gives the maximum energy gained by an electron with initial energy $\gamma_{\text{ph}}mc^2$ as $2\gamma_{\text{ph}}^2 mc^2$ or (n_c/n_e) MeV in a distance $2\gamma_{\text{ph}}^2 c/\omega_p$. Here, $\gamma_{\text{ph}} = (\omega_0/\omega_p)$. For a given laser wavelength, the maximum energy gained increases as the plasma density is reduced but because the electric field scales as $\sqrt{n_e}$ it takes longer and longer to obtain this energy.

In a practical accelerator, we cannot use wavebreaking electric fields because as the electric field approaches this value it 'traps' background plasma electrons and begins to accelerate them. It also develops harmonics. Both of these effects are not desirable if we wish to accelerate an externally-injected bunch of electrons. Computer simulations (described below) show that a coherent plasma wave, without any significant number of self-trapped particles, can be generated with electric fields of the order of 10% of the wavebreaking electric field. If we require that the minimum value of the longitudinal field be 10 MeV cm^{-1}, this leads to a minimum plasma density of 10^{16} cm^{-3}. Using a CO_2 laser to excite a beat wave in such a plasma, gives maximum particle energies of ~100 MeV. The physical reason for this limit on the maximum energy is the dephasing of particles and the electric field of the correct polarity (which only exists for half-a-wavelength of the plasma wave in the wave frame). Although for a given plasma density the maximum energy scales inversely with square of the laser wavelength λ, it becomes increasingly difficult to keep the laser beam focused at shorter wavelengths because the Rayleigh length scales as λ. In a single stage, therefore, the best that can probably be achieved is to accelerate electrons to a few GeV using a laser with wavelength in the micrometre range.

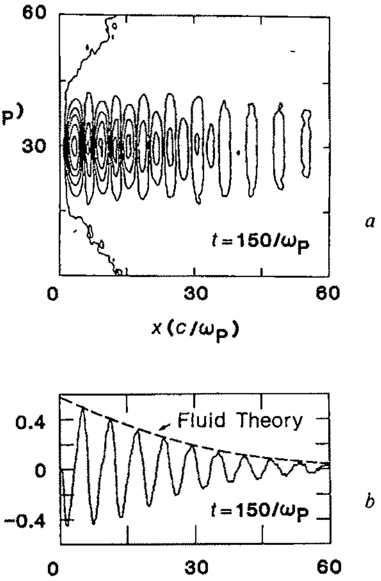

Fig. 1 Potential contours of the space-charge density wave driven by the two laser beams at time $150/\omega_p$ (*a*) section through the centre of the longitudinal electric field of the plasma wave (*b*). The dotted line in *b* shows a comparison of the rate of plasma wave build-up as predicted by the fluid theory with that obtained in these two-dimensional simulations.

To obtain higher energies, one has to be prepared for multistaging or invent a scheme for phase-locking the particles in the wave so that they do not out run the wave. One such scheme will be described later.

Simulations

Computer simulations were carried out using the two-dimensional fully relativistic, electromagnetic particle code WAVE[4] to study the above described acceleration mechanism in a self-consistent manner. A typical WAVE simulation has 10^6 electrons and 10^6 ions. From the particle positions and velocities, charge densities and current densities are found. Then Maxwell's equations are used to calculate the electric and magnetic fields or equivalently the forces on the particles. Equations of motion are used, to calculate new particle locations and velocities and then the process is repeated.

The results of a typical two-dimensional simulation are depicted in Figs 1-3. The parameters for this simulation were as follows: two laser beams $\omega_0 = 5\omega_p$ and $\omega_1 = 4\omega_p$, each with an r.m.s. intensity of $v_0 = 0.4\ c$, a transverse intensity profile of $\cos^2 y$ and a beam width of 30 c/ω_p were injected into a homogeneous plasma 60 c/ω_p long and 60 c/ω_p wide with a temperature of 2.5 keV. The laser beams had a cubic rise from zero to maximum intensity in $300/\omega_p$ after which the laser intensity remained constant. The ion-to-electron mass ratio was 1,836 and temperature ratio was 1. Thus for an IR laser with wavelengths 9.6 μm and 12 μm the parameters were: a hydrogen plasma with $n_e \sim 4.9 \times 10^{17}$ cm^{-3}, laser risetime ~7.6 ps, laser intensity ~2×10^{15} W cm^{-2}, beam width ~25 wavelengths and system length ~50 wavelengths. The simulation parameters were chosen to study both the beat wave driven plasma wave and other competing one- and two-dimensional effects.

The simulation results can be categorized into two time regimes. The first, during the risetime of the laser pulse when

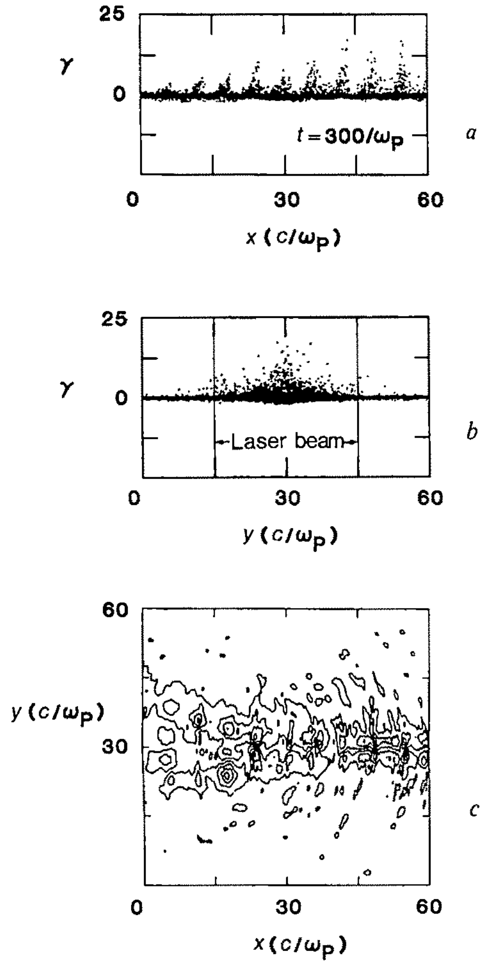

Fig. 2 Phase space plot (momentum in the x direction) of the plasma electrons shows that at time $300/\omega_p$, trapped electrons are accelerated in every wavelength of the plasma wave which represents an accelerating 'bucket' (*a*). Particles have larger energies on the right-hand side as they have seen an accelerating field for a longer time. The maximum particle energies of $\gamma = 25$ are in good agreement with theory. In the transverse direction, although the laser beam is 30 c/ω_p wide, most particles are confined to a narrow region down the centre of the accelerating wave (*b*). Contours of the self-consistent magnetic field at time $t = 300/\omega_p$ generated by the accelerating trapped particles (*c*). This field exerts a radial force on the trapped particles confining them in a small region down the axis and also forces the return current to flow on the outside of the region where it exists.

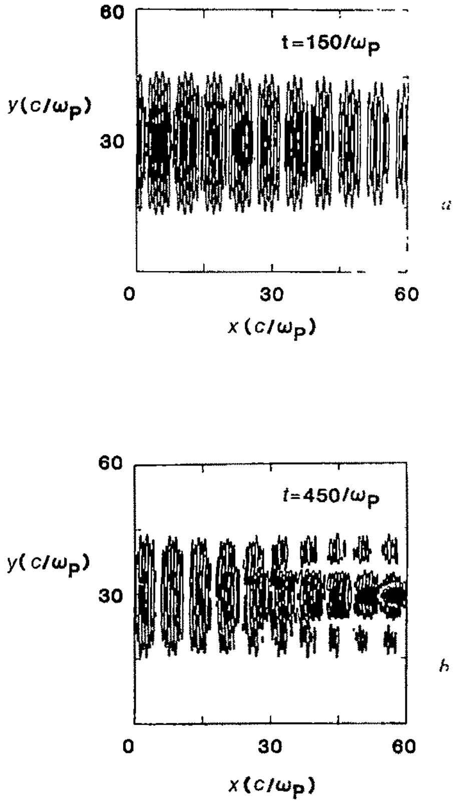

Fig. 3 Contour plot of the beat pattern produced by two colinearly-propagating laser beams in the plasma at time $150/\omega_p$ (*a*) and at $450/\omega_p$ (*b*). The x and y dimensions are in units of c/ω_p. Clear evidence for laser beam self-focusing is seen at the later time from the converging inner contours. As a result of self-focusing, the plasma is pushed out and the space-charge wave accelerating the particles disrupts.

a very coherent plasma wave grows and reaches saturation and the second after the peak of the laser pulse ($300/\omega_p$) when competing phenomena come into play.

Figure 1*a* shows the contour plot of the potential of the plasma density wave at $150/\omega_p$. According to the fluid theory, the plasma wave should reach peak amplitude at this time. The plasma wave wavefronts in the contour plot are seen to be planar. A section through the centre of the transverse axis of the longitudinal electric field plot is shown in Fig. 1*b*. An extremely coherent plasma wave builds up rapidly in time/space and saturates at $\varepsilon \simeq 0.5$, in excellent agreement with the value expected from the fluid theory. By $300/\omega_p$, the longitudinal electric field becomes non-planar as the laser beams begin to self-focus. Fluid theory would predict that one saturation is reached, the plasma wave amplitude decreases but simulations show that a 'plasma wave' with greatly reduced coherence persists driven by the multiple Raman forward scattering.

Figure 2*a* shows that the electrons trapped at an earlier time, when the plasma wave field was intense and coherent, have by time $300/\omega_p$ approached maximum energies. Accelerated particles leaving the right-hand boundary of the plasma (not shown here) have maximum energies of $\gamma = 25$, in reasonable agreement with theory. Here $\gamma = (1-\beta^2)^{-1/2}$ is the usual relativistic scaling factor. More important, however, is the fact that although the laser beam and, therefore, the plasma wave is 30 c/ω_p wide, most of the accelerated particles are collimated within 10 c/ω_p of the centre (Fig. 2*b*). The accelerating particles remain highly collimated because the trapped particles give rise to an azimuthal magnetic field which, in turn, exerts a radial force on the particles keeping them tightly focused. The contour plot of this self-generated magnetic field which can reach megagauss magnitudes is shown in Fig. 2*c*. The maximum field is in the regions where bunches of electrons are accelerated. The accelerated particles constitute a flow of charges or current which leaves the plasma positively charged, thus driving a return current of colder particles in the opposite direction. In the simulations the return current is found to flow predominantly on the outside of the region bounded by the self-generated magnetic field.

These two-dimensional simulations also allowed us to investigate competition between the beat wave driven plasma wave and Raman back- and side-scattering. To allow the growth of large angle side-scattering the transverse dimension of the beam was made periodic. Even in relatively cold plasmas ($T_e \sim$ 200 eV), where Landau damping is expected to be weak, Raman backscatter is not found to be a problem under two-frequency illumination. Small angle (from the forward direction) side-scatter can occur, effectively making the desired plasma wave non-planar. This gives rise to a radial component of the electric field; however, the self-generated magnetic field tends to keep the trapped particles focused in the centre of the plasma wave as discussed above.

Figure 3*a* shows the laser beat wave contours at $150/\omega_p$ as the beams propagate from left to right. Contrast this with laser

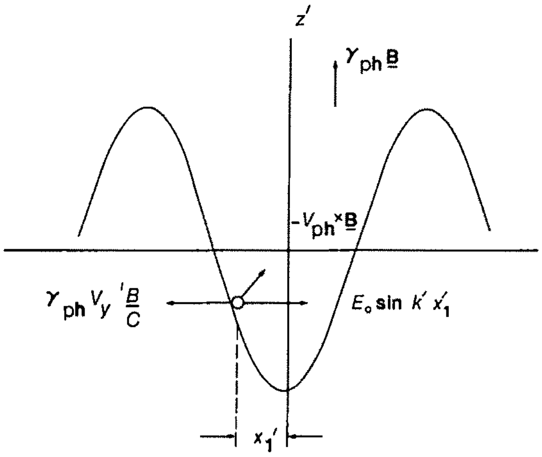
z'
$\gamma_{ph}\underline{B}$
$-V_{ph}\times\underline{B}$
$\gamma_{ph}V_y'\frac{\underline{B}}{c}$
$E_0 \sin k' x_1'$
x_1'

Fig. 4 In the phase stabilization scheme, Surfatron, a perpendicular magnetic field is applied to the wavevector of the longitudinal space-charge wave. In the wave frame, a trapped particle comes to an equilibrium position against the side of the potential well where the 'trapping' and 'de-trapping' forces balance: $E_0 \sin k'_{epw} x' = \gamma_{ph}B$. The energy gained by the particle in the direction of the wave is simply $\gamma_{ph}Bx$.

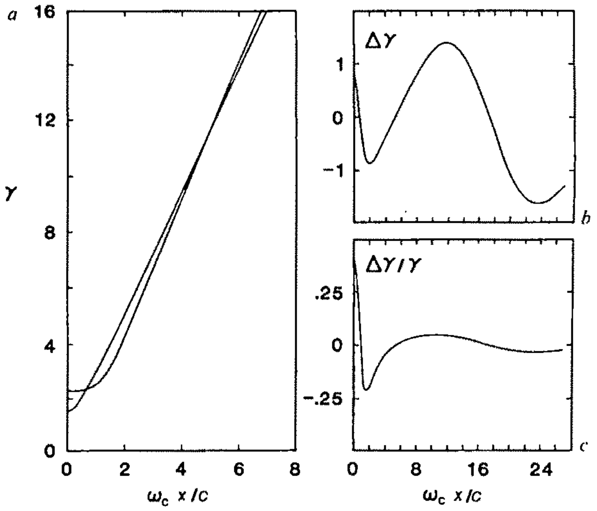

Fig. 5 *a*, Energy gain (γ) plotted against distance for two Surfatron particles of different initial velocities ($0.8c$ and $0.9c$). In *b*, energy separation ($\Delta\gamma$) of the particles remains roughly constant, while in *c*, $\Delta\gamma/\gamma$ decreases rapidly. $V_{ph}/c = .9$, $cE/B = 2.5$, $\omega/\omega_c = 9$. ω_c is the nonrelativistic electron cyclotron frequency.

beam contours at $450/\omega_p$ (Fig. 3*b*). Although the outer contours are still the same size, the contours at the beam centre are seen to 'self-focus' to a smaller size. We have determined that this self-focusing is due to two effects: intensity-dependent refractive index (relativistic self-focusing) and transverse intensity gradient (ponderomotive self-focusing). Whether the beam self-focuses as a whole or breaks up into smaller filaments depends on the transverse size and the intensity profile of the laser beams. In any case, catastrophic self-focusing is an undesirable phenomenon because it tends to push the plasma out and create a channel of low density, thereby destroying the resonance condition for driving the plasma wave and terminating the accelerating process.

Two-dimensional simulations of the beat wave build-up have been encouraging and given results that are consistent with predictions of the fluid and single particle theories. Although there are many competing instabilities in the plasma, these occur on a longer time scale; and plasma wave coherence can be maintained over typically tens of plasma wave wavelengths at the front of the laser pulse, which continually moves into unperturbed plasma. If the laser pulse is longer than this, then wave-particle and wave-wave interactions heat up the plasma to temperatures of hundreds of keV at the back of the laser pulse and make it extremely turbulent. Thus, extremely short laser pulses on the order of a few picoseconds are probably most effective in this acceleration scheme. Such short pulses will also inhibit other instabilities such as the stimulated Brillouin scattering.

Phase-stabilization

The limit on energy gain of a particle in the Plasma beat wave accelerator can be overcome if a magnetic field of appropriate strength, $\gamma_{ph}B < E_{epw}$, is applied perpendicular to the plasma wave (Fig. 4). This accelerates particles parallel to the phase fronts of the accelerating wave, which, in turn, provides a force keeping the particles in phase with the wave[5]. In principle, therefore, particles can gain energy at rate

$$\frac{\Delta U}{\Delta x} = 0.1\left[\frac{B_{KG}}{n_{16}\lambda_\mu}\right](n_{16})^{1/2}\ \mathrm{GeV\,cm^{-1}} \qquad (4)$$

in the direction of the wave and the accelerated particles move at an angle $\tan\theta = 3\times10^{-3}\sqrt{n_{16}\lambda_\mu}$ with respect to the wavevector of the plasma wave. Here B_{KG} is the applied magnetic field in kilogauss, n_{16} is the plasma density in units of $10^{16}\ \mathrm{cm^{-3}}$ and λ_μ is the laser wavelength in micrometres. The quantity in the square bracket must be $<\varepsilon$ to prevent the detrapping by the magnetic field. Because the particles move at an angle with respect to the plasma wave, the width of the plasma wave necessary to accelerate the particles to the desired energy can be rather large. Fortunately, the plasma wave width (and hence the energy required to excite it) can be reduced considerably by beating the electromagnetic waves at a finite angle (optical mixing) rather than colinearly[6]. One possible limitation associated with finite angle optical mixing is that, while the particles move at $\sim c$, the laser energy propagates through the plasma with the particles at v_g. In a device of length L the particles move ahead with respect to the laser pulse by a distance $\Delta L = \omega_p^2 L/\omega_0^2$. Thus the plasma wave coherence must be maintained over a distance ΔL behind the leading edge of the laser pulse. We have carried out one-dimensional (one spatial, three velocites) particle simulations, which confirm the above scaling laws. Two-dimensional computer simulations are being carried out to test the phase-locking and cross-field acceleration concept when the plasma wave is driven by finite angle optical mixing, but this technique has the promise of utilizing the high gradients of space-charge plasma waves for obtaining ultrahigh energies. For example, using a 100-kG magnetic field across a $10^{19}\ \mathrm{cm^{-3}}$ plasma and a 1-μm laser, particles may be accelerated to 100 GeV in a device that is only 3.16 m long.

Laser and plasma requirements

While there is a tremendous promise for $>10\ \mathrm{MeV\,cm^{-1}}$ acceleration gradients in this scheme, there are technological obstacles between the concept and a realizable working system. The laser needed for a TeV class accelerator based on this concept will exceed the capability of fusion lasers (presently the largest laser systems) in the areas of peak power, pulse width, repetition rate, and the need for the power to be delivered in a single diffraction limited beam. Considerable work is also needed in the areas of focusing and optical transport of such high peak power leaser beams.

An estimate of the laser power required can be obtained from energy balance arguments. The longitudinal electric field of the plasma wave represents an energy density

$$W_{epw} = \frac{E_{epw}^2}{8\pi} \simeq 500\, n_{16}\varepsilon^2\ \mathrm{J\,cm^{-3}} \qquad (5)$$

Because the group velocity of the plasma wave, $3v_e^2/v_{ph} \ll c$, we assume that the laser pulse excites the plasma wave only in the volume through which it propagates. To avoid significant pump depletion, the total energy in the laser beams must be much greater than that in the plasma wave.

The problem of producing plasmas (particularly with a cross magnetic field) with densities between $10^{16} < n_e < 10^{20}$ cm^{-3} and with the required length and homogeneity will also require considerable attention. At high intensities that are necessary in this scheme, the requirement that plasma frequency be exactly equal to the difference frequency may be relaxed, but this issue needs careful investigation.

Prospects for ultrahigh energies

High-phase velocity space charge waves in a plasma have the potential for producing the high accelerating gradients that are necessary for a new generation of particle accelerators. Whether this scheme can be used to accelerate particles to ultrahigh energies depends on how well the phase stabilization (Surfatron) scheme can be made to work in practice. Particular problems are pump depletion, filamentation of the laser and injected particle beams, and the effect of self-generated magnetic fields on the accelerating particles.

On the positive side, the Surfatron scheme would produce a compact accelerator with a high quality beam. The energy spread, $\Delta\gamma/\gamma$ would be small because approximately half of the injected particles quickly form accelerating 'buckets' that are narrow in phase space near the equilibrium point. In the wave frame this is where $\gamma_{\mathrm{ph}}B$ is equal to the local longitudinal electric field. Thus all the particles gain energy at nearly the same rate, the one given by equation (4). The bunch length of the final beam as well as $\Delta\gamma/\gamma$ is thus expected to be extremely small, as shown in Fig. 5.

The number of accelerated particles N can be estimated from the consideration of the energy balance[6]:

$$N = 2\times10^{10}\frac{\text{laser energy (kJ)}}{\text{particle energy (GeV)}}\,\varepsilon\alpha\lambda_{\mu}\, n_{16} \qquad (6)$$

where factor α is the ratio of particle energy to wave energy.

The zero-order motion of the particles in the Surfatron scheme is approximately a straight line, and thus synchrotron radiation loss turns out not be to be a problem. The radiation loss due to high-order bounce motion[5] and due to oscillation in the laser field, as well as other loss mechanisms such as Coulomb scattering and bremsstrahlung radiation, are also not thought to be serious problems.

Finally, the acceleration scheme is still at an embryonic stage for a reliable estimate to be made of its potential total efficiency from wall power (ac) to beam power. The severest limitation, one that is common to all laser acceleration schemes, is the a.c.-to-laser beam efficiency. If we optimistically assume this to be 10% then using our simulations as a guide we may be able to achieve a total efficiency between 10^{-3} and 10^{-4}.

We thank Professor F. F. Chen and Dr C. E. Clayton for valuable comments and discussions. This work was supported at UCLA by DOE contract DE-AM03-76SF00034, NSF grant ECS 83-10972 and LLNL University Research Program and at LANL by the DOE.

Received 11 May; accepted 6 August 1984.

1. Tajima T. & Dawson, J. M. *Phys. Rev. Lett.* **43**, 267-270 (1979).
2. Rosenbluth, M. N. & Liu, C. S. *Phys. Rev. Lett.* **29**, 701-705 (1972).
3. Joshi, C., Tajima, T., & Dawson, J. M., Baldis, H. A. & Ebrahim, N. A. *Phys. Rev. Lett.* **47**, 1285-1288 (1981).
4. Morse, R. L. & Neilson, C. W. *Phys. Fluids* **14**, 830-840 (1971).
5. Katsouleas, T. & Dawson, J. M. *Phys. Rev. Lett* **51**, 392 (1983).
6. Katsouleas, T., Joshi, C., Mori, W. B. & Dawson, J. M. *Proc. 12th int. Conf. on High Energy Accelerators* (Fermilab, Batavia, 1982).
7. Cohen, E. I., Kaufman, A. N. & Watson, K. M. *Phys. Rev. Lett* **29**, 581-584 (1972).

Is there a climatic attractor?

C. Nicolis

Institut d'Aéronomie Spatiale de Belgique, 3 avenue Circulaire, 1180 Bruxelles, Belgium

G. Nicolis

Faculté des Sciences de l'Université Libre de Bruxelles, Campus Plaine, Boulevard du Triomphe, 1050 Bruxelles, Belgium

Much of our information on climatic evolution during the past million years comes from the time series describing the isotope record of deep-sea cores. A major task of climatology is to identify, from this apparently limited amount of information, the essential features of climate viewed as a dynamic system. Using the theory of nonlinear dynamic systems we show how certain key properties of climate can be determined solely from time series data.

EXPERIMENTAL data have essentially two roles in the process of modelling. First, they parameterize the equations postulated by the modeller. Second, they set constraints to be satisfied by the model. For instance, a reasonable model of Quaternary glaciations should reproduce the general aspects of a palaeotemperature time series as deduced from ice or deep-sea core data and, in particular, should exhibit the characteristic time scales of 100,000, 41,000 and 22,000 yr (ref. 1). In either case, however, the information drawn from the data will remain esentially one-dimensional. Thus, starting from the time series of a certain variable one may construct a power spectrum or a histogram which, despite their interest, do not provide any hint about the additional variables that may affect the evolution. We show here that experimental data contain far richer information which, independent of any particular model, can be used to 'resurrect' the multivariable dynamics of a system starting from a time series pertaining to a single variable.

We should first comment on the status of a time series from the standpoint of the theory of dynamical systems. Let $X_0(t)$ be the time series available from the data, and $\{X_k(t)\}$, where $k=0, 1, \ldots n-1$, the full set of variables actually taking part in the dynamics. $\{X_k\}$ is expected to satisfy a set of first-order nonlinear equations, whose form is generally unknown but which, given a set of initial data $\{X_k(0)\}$, will produce the full details of the system's evolution. It is instructive to visualize this evolution in an abstract multi-dimensional space spanned by these variables, the phase space. An instantaneous state of the system becomes a point, say P, in this space, whereas a sequence of such states followed as time varies defines a curve, the phase space trajectory (see Fig. 1). As time grows and transients die out, the system is expected to reach a state of permanent regime, not necessarily time-independent. In phase space, this will be reflected by the convergence of whole families of phase trajectories towards a subset of phase space (C in Fig. 1), such that the system subsequently remains trapped therein. We refer to this invariant set as the attractor.

The interest of the phase space description of a system lies primarily in the fact that the nature of the attractors provides extensive information on the time behaviour of the variables and on the nature of their coupling. For instance, a point

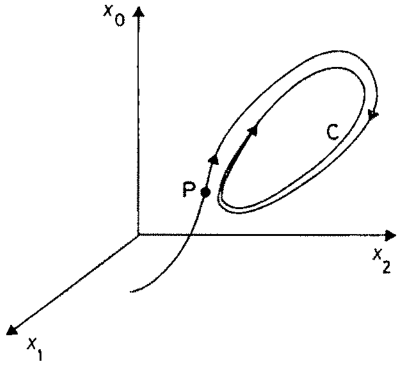

Fig. 1 Typical phase space trajectory emanating from point P and converging to a periodic attractor, represented by curve C.

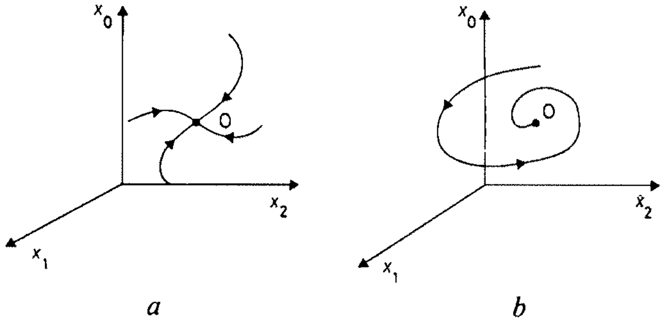

Fig. 2 Two different approaches to a steady state, represented by point 0 in phase space (point attractor). *a*, Monotonic approach; *b*, approach through damped oscillations.

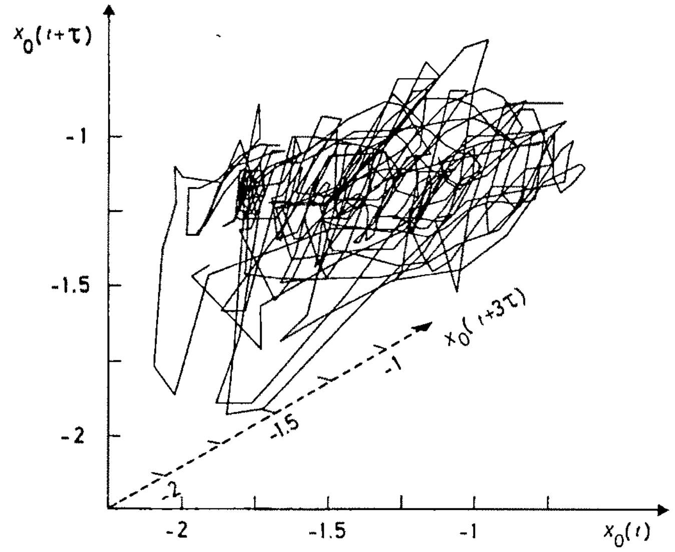

Fig. 3 A view of the climatic attractor embedded in a three-dimensional phase space. The result utilizes about 500 equidistant values of X_0. These are inferred from the oxygen isotope record obtained from the V28-238 deep sea core of Shackleton and Opdyke[4] and extended over the past million years, following an interpolation available from the data bank of the University of Louvain[7]. The value of the shift τ adopted in drawing the figure is $\tau = 2$ kyr.

attractor (point 0 in Fig. 2*a*, *b*) implies that the transient-free behaviour of the system will be time-independent. In addition, if the attractor is approached in the way shown in Fig. 2*a* the transients will die out monotonically, whereas a spiral approach like that in Fig. 2*b* indicates that transients perform damped oscillations. An attractor in the form of a closed curve (C in Fig. 1) implies, on the other hand, that the system will perform sustained oscillations in time with an intrinsically-determined period and amplitude. Finally, multiperiodic motions with incommensurate frequencies are represented in phase space by high-dimensional attracting toroidal surfaces. In each of the above cases, the character of the attractor also gives an indication of the minimum number of variables that should be involved in the description. Thus, for the zero-dimensional attractors of Fig. 2 ($d = 0$) we need, respectively, at least one variable ($n = 1$) for Fig. 2*a* and two variables ($n = 2$) for Fig. 2*b*. For the one-dimensional attractor of Fig. 1 ($d = 1$) we need at least two variables ($n = 2$), and for the simplest quasi-periodic phenomenon we need at least a two-dimensional torus ($d = 2$) embedded in a three-dimensional phase space ($n = 3$).

So far we have argued in terms of attractors which are points, lines or surfaces or, in more technical terms, smooth topological manifolds characterized by an integer dimensionality. In recent years, it has been firmly established that geometrical objects exist which are not topological manifolds. Such constructions, which have a non-integer dimensionality, are known as fractals[2]. The theory of dynamical systems and some experimental results from fluid dynamics and chemical kinetics provide us with many examples of fractal attractors[3]. The importance of the latter stems from the fact that they model irregular, time-dependent phenomena, characterized by two features, both of which are shared by the climatic system: a marked sensitivity to initial conditions; and the appearance of large dispersions from a mean motion similar to a stochastic process, even though the underlying dynamics is perfectly deterministic. Note that the dimensionality of an attractor, fractal or smooth, is bound to be a number smaller than the number of variables present in the evolution.

Climatic attractor

We shall establish the existence of an attractor associated with the long-term climatic evolution of the past million years and determine its dimensionalty. Knowing the characteristics of this climatic attractor automatically gives us information on the minimum number of variables that must be introduced into the description.

Our starting point is the oxygen isotope record obtained from the equatorial Pacific deep-sea core V28–238 (refs 4, 5), which is one of the best climatic records available, because the sediment accumulated at a fairly regular rate[6].

Let $X_0(t)$ be the corresponding time series[7]. Because the n variables $\{X_k(t)\}$ satisfy a set of first-order differential equations, successive differentiation in time reduces the problem to a single (generally highly nonlinear) differential equation of nth order for one of these variables. Thus, instead of $X_k(t)$, $k = 0, 1, \ldots, n-1$, we may consider $X_0(t)$, the variable supplied by the time series data, and its $n-1$ successive derivatives $X_0^{(k)}(t)$, $k = 1, \ldots, n-1$, to be the n variables of the problem spanning the phase space of the system[8]. Now, both X_0 and its derivatives can be deduced from the single time series pertaining to $X_0(t)$, as provided by the data. We see, therefore, that, in principle we have sufficient information at our disposal to go beyond the one-dimensional space of the original time series and to unfold the system's dynamics into a multidimensional phase space.

Actually, as suggested originally by Ruelle[9], instead of $X_0(t)$ and $X_0^{(k)}(t)$ it will be easier to work with $X_0(t)$, and the set of variables obtained from it, by shifting its values by a fixed lag τ. We, therefore, consider from now on the phase space defined by the variables :

$$X_0(t), X_0(t+\tau), \ldots, X_0(t+(n-1)\tau) \qquad (1)$$

For a typical choice of τ these variables are expected to be linearly independent, and this is all one needs to define properly a phase space. A simple example illustrating how an unshifted function can give rise to a linearly independent one by a simple shift is provided by the polynomials $X_0(t) = t^2$, $X_0(t+\tau) = t^2 + 2t\tau + \tau^2$. These two functions are indeed independent, as

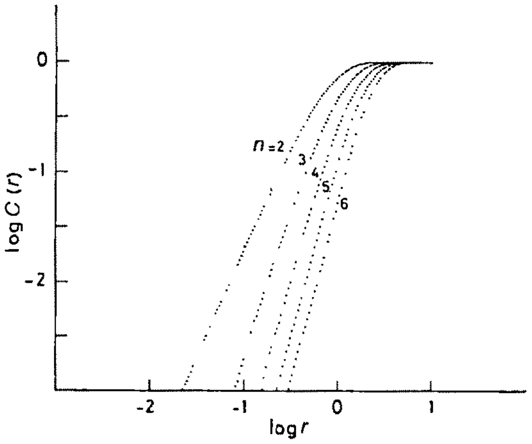

Fig. 4 Distance dependence of the correlation function on the climatic attractor. Note the existence of an extensive range of linearity, from which the dimensionality of the attractor can be inferred. Parameter values as in Fig. 3, except that $\tau = 8$ kyr.

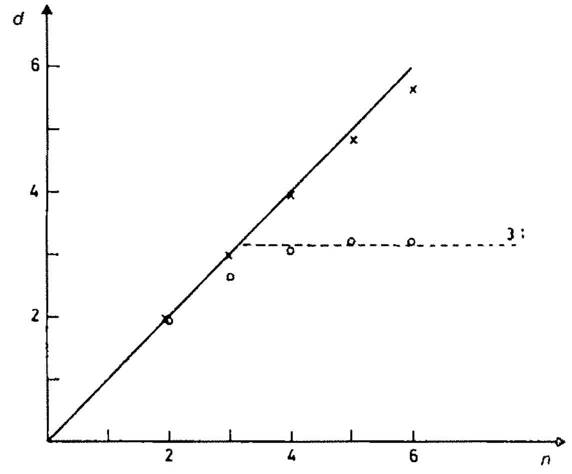

Fig. 5 Dependence of dimensionality, d on the number of phase space variables, n for the climatic attractor (O) and for a white noise signal (×) for the same parameters as in Fig. 4. Notice the saturation to a plateau value of ~3.1 in the first case, and the $d \sim n$ relationship in the second case.

the second polynomial contains terms of first and zero degree in t, which are absent in the first one.

Before describing the procedure that will enable us to obtain quantitative information on the nature of the climatic attractor and, in particular, on its dimensionality we present, in Fig. 3, a characteristic view of this object in a three-dimensional phase space. This view clearly exhibits the complexity of the underlying motion. However, the data are too coarse to draw any conclusion from this figure alone. It will be our task to characterize the complexity of the dynamics more sharply and, in particular, to assess its similarities and differences with random noise. Note that similar phase portraits have been constructed from experimental data pertaining to chemical kinetics[10].

Analytical procedure

We now describe briefly a recently proposed procedure[11,12] which allows the indentification of some salient features of the phase space portrait of a dynamical system. Consider a set of N points on an attractor embedded in a phase space of n dimensions, obtained from a time series:

$$\begin{aligned}&X_0(t_1), \ldots, X_0(t_N)\\ &X_0(t_1+\tau), \ldots, X_0(t_N+\tau)\\ &\vdots\\ &X_0(t_1+(n-1)\tau), \ldots, X_0(t_N+(n-1)\tau)\end{aligned} \tag{2}$$

For convenience we introduce a vector notation: $\mathbf{X}_i$ which stands for a point of phase space whose coordinates are $\{X_0(t_i), \ldots, X_0(t_i+(n-1)\tau)\}$.

A reference point $\mathbf{X}_i$ from these data is now chosen and all its distances $|\mathbf{X}_i - \mathbf{X}_j|$ from the $N-1$ remaining points are computed. This allows us to count the data points that are within a prescribed distance, r from point $\mathbf{X}_i$. Repeating the process for all values of i, one arrives at the quantity

$$C(r) = \frac{1}{N^2} \sum_{\substack{i,j=1\\ i\neq j}}^{N} \theta(r - |\mathbf{X}_i - \mathbf{X}_j|) \tag{3}$$

where θ is the Heaviside function, $\theta(x) = 0$ if $x < 0$, $\theta(x) = 1$ if $x > 0$. The non-vanishing of this quantity measures the extent to which the presence of a data point $\mathbf{X}_i$ affects the position of the other points. $C(r)$ may thus be referred to as the (integral) correlation function of the attractor.

Suppose that we fix a given small parameter ε and we use it to define the site of a lattice which approximates the attractor. If the latter is a line, the number of data points within a distance r from a prescribed point should be proportional to r/ε. If it is a surface, this number should be proportional to $(r/\varepsilon)^2$ and, more generally, if it is a d-dimensional manifold it should be proportional to $(r/\varepsilon)^d$. We expect, therefore, that for r, relatively small $C(r)$ should vary as

$$C(r) = r^d \tag{4}$$

In other words, the dimensionality d of the attractor is given by the slope of the log $C(r)$ versus log r in a certain range of values of r:

$$\log C(r) = d|\log r| \tag{5}$$

This property remains valid for attractors of fractal dimensionality.

The above results suggest the following algorithm (a similar procedure has also been proposed in the context of fluid dynamics[13,14]):

(1) Starting from a time series, we can construct the correlation function, equation (3), by considering successively higher values of the dimensionality n of phase space.

(2) Deduce the slope d near the origin according to equation (5) and see how the result changes as n is increased.

(3) If d reaches a saturation limit beyond some relatively small n, the system represented by the time series should possess an attractor. The saturation value d_s will be regarded as the dimensionality of the attractor. The value of n beyond which saturation is observed will provide the minimum number of variables necessary to model the behaviour represented by the attractor.

Application to climatic data

This procedure has been applied to the analysis of the data pertaining to core V28–238. Figure 4 gives the dependence of log $C(r)$ versus log r for $n = 2$ to $n = 6$. We see that there is indeed an extended region over which this dependence is linear, in accordance with equation (5). Figure 5 (points in circles) shows that the slope reaches a saturation value at $n = 4$, which is about $d_s = 3.1$. The same plot also shows the way in which d varies with n if the signal considered is a Gaussian white noise: there is no tendency to saturate. In fact, in this case d turns out to be equal to n. It should be emphasized that the above results are independent of the choice of the time lag τ, provided that the latter is of the order of magnitude of the times scales pertaining to the long-term climatic evolution, and the linear independence of the variables is secured.

The existence of a climatic attractor of low dimensionality shows that the main feature of long-term climatic evolution may be viewed as the manifestation of a deterministic dynamics, involving a limited number of key variables. The fact that the attractor has a fractal dimensionality provides a natural explanation of the intrinsic variability of the climatic system, despite its deterministic character[15]. Moreoever, it suggests that despite the pronounced peaks of spectra in the frequencies of the orbital forcings, the actual behaviour is highly non periodic[16]. A new interpretation of variance spectra of the ice volume record is, therefore, necessary.

Conclusion

We have identified a number of intrinsic properties of the climate assuming it to be dynamical system, using only the time series obtained from the data.

Our results do not anticipate the validity of any particular model of climatic evolution. Rather, they set a number of constraints that should be satisfied by a model. In particular, they suggest that models involving four variables could already provide a description of the salient features of the system.

Our approach could be applied to many other problems in which naturally occurring complex systems are probed through time series. Within the context of atmospheric physics and climatotology, one important example is the blocking transition. Another promising field of application are biological rhythms like the heart beat or the electroencephalogram[17]. In the long run, it may be hoped that fractal dimensionality could become for such systems a useful characterization of their specificity as well as a measure of their complexity.

We thank P. Pestiaux for providing the time series of the V28-238 core and P. Bergé for an enlightening discussion. The work of C.N. is supported, in part, by the EEC under contract no. STI-004-J-C(CD).

Received 2 May; accepted 27 July 1984.

1. Berger, A. L. (ed.) *Climatic Variations and Variability: Facts and Theories* (Reidel, Dordrecht, 1981).
2. Mandelbrot, B. *Fractals: Form, Chance and Dimension* (Freeman, San Francisco, 1977).
3. Helleman, R. (ed.) *Ann. N.Y. Acad. Sci.* **347**, 1981.
4. Shackleton, N. J. & Opdyke, N. D. *Quat. Res.* **3**, 39–55 (1973).
5. Shackleton, N. J. *et al. Nature* **307**, 620–623 (1984).
6. Imbrie, J. *et al.* in *Milankovitch and Climate* (eds Berger, A. L. *et al.*) (Reidel, Dordrecht, 1984).
7. Berger, A. L. & Pestiaux, P. *Tech. Rep.* No. 28, (Institut of Astronomy and Geophysics, Catholic University of Louvain, 1982).
8. Packard, N. H., Crutchfield, J. P., Farmer, J. D. & Shaw, R. S. *Phys. Rev. Lett.* **45**, 712–716 (1980).
9. Ruelle, D. in *Nonlinear Phenomena in Chemical Dynamics*, (eds Pacault, A. & Vidal, C.) (Springer, Berlin, 1981).
10. Roux, J. C., Simoyi, R. H. & Swinney, H. L. *Physica* **8D**, 257–266 (1983).
11. Grassberger, P. & Procaccia, I. *Physica* **9D**, 189–208, 1983.
12. Grassberger, P. & Procaccia, I. *Phys. Rev. Lett.* **50**, 346–349 (1983).
13. Brandstäter, A. *et al. Phys. Rev. Lett.* **51**, 1442–1445 (1983).
14. Malmaison, B., Atten, P., Berge, P. & Dubois, M. *J. phys. Lett.* **44**, 897–902 (1983).
15. Lorenz, E. N. *Tellus* **36A**, 98–110 (1984).
16. Le Treut, H. & Ghil, M. *J. geophys. Res.* **88**, 5167–5190, 1983.
17. Babloyantz, A., Nicolis, G. & Nicolis, J. S. (in preparation).

Structure of the nucleosome core particle at 7 Å resolution

T. J. Richmond, J. T. Finch, B. Rushton, D. Rhodes & A. Klug

MRC Laboratory of Molecular Biology, University Postgraduate Medical School, Hills Road, Cambridge CB2 2QH, UK

The crystal structure of the nucleosome core particle has been solved to 7 Å resolution. The right-handed B-DNA superhelix on the outside contains several sharp bends and makes numerous interactions with the histone octamer within. The central turn of superhelix and H3 · H4 tetramer have dyad symmetry, but the H2A · H2B dimers show departures due to interparticle associations.

THE nucleosome is the primary repeating unit of DNA organization in chromatin[1-3]. Extensive digestion of chromatin with micrococcal nuclease releases the nucleosome core, a small, well-defined particle which has been crystallized. The particle mass (~206 kilodaltons) is equally distributed between 146(±2) base pairs (bp) of DNA and an octamer formed by two each of the histone proteins, H2A, H2B, H3 and H4 (the outer histone H1 and the linker DNA having been removed during nuclease digestion[4]). The crystals first obtained were of limited order and gave a picture of the particle to 20 Å resolution[5]. We later prepared better crystals which diffracted to about 5 Å, having a single particle in the asymmetric unit[6]. We describe here the three-dimensional structure of the nucleosome core particle at 7 Å resolution determined by X-ray diffraction and multiple isomorphous replacement. This advance was achieved by improved diffractometry, control of the crystal unit cell parameters by adjustment of hydration, and derivatives prepared from multi-heavy atom cluster compounds.

The nucleosome core crystals have previously been investigated by several structural methods. Electron microscopy and X-ray diffraction techniques were initially used to obtain electron density maps in the principal projections, suggesting that the particle had the shape of a disk 57 Å thick and 110 Å in diameter. The DNA appeared to be wound around the histone core in 1.8 turns of a flat superhelix with a pitch of 28 Å[5]. Using neutron diffraction in conjunction with contrast matching[7,8], the DNA and protein components were seen as separate densities in projections at 25 Å resolution. The three-dimensional shape of the octamer alone was determined to a resolution of 20 Å by image reconstruction from electron micrographs of negatively stained, ordered aggregates[9]. The assignment of histone locations on the resulting low-resolution map relied on DNA–histone[10,11] and histone–histone (for references, see ref. 12) proximities obtained from chemical cross-linking experiments, and the neutron experiments fixed the orientation of the DNA superhelix on the octamer. The suggested division of the octamer into two H2A · H2B dimers residing on opposite faces of a H3 · H4 tetramer agrees well with the pattern of dissociation found in earlier physicochemical studies[13,14]. The tetramer (proteolysed) and octamer have also been crystallized in the absence of DNA, but structures have not yet been reported[15,16].

The electron density map at the higher resolution of 7 Å described here reveals many new structural features. The DNA is not bent uniformly into the superhelix, but exhibits several regions of tight bending or possible kinking, adjacent to points of substantial contact with histones H3 and H4. The histone–DNA interactions occur on the inside of the superhelix; the protein density does not seem to embrace the outside of the

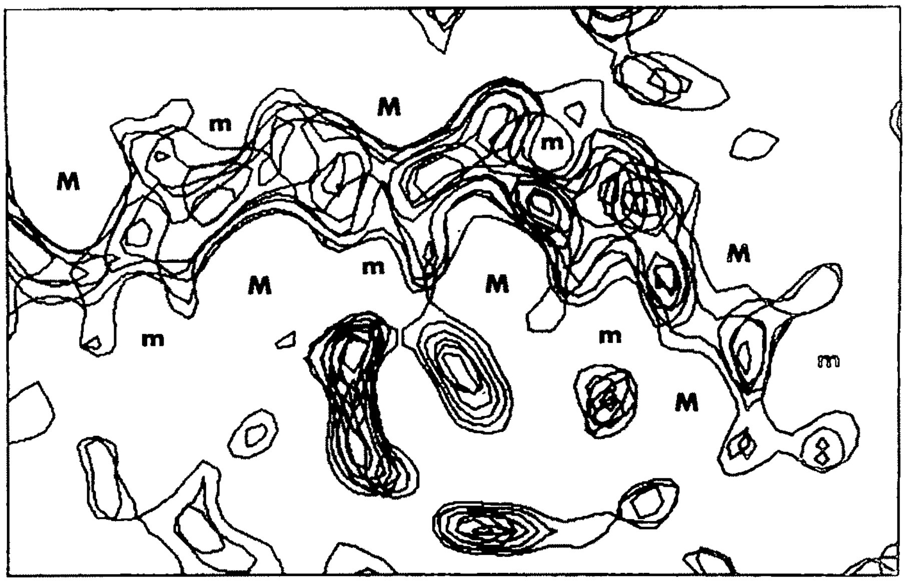

Fig. 1 Electron density of an arc of the DNA superhelix, showing two turns of the double helix. Alternating major (M) and minor (m) grooves are indicated. Three sections (−10 to −12) of the map, 1.73 Å apart, were stacked to show a slice through the double helix. The density seen below the arc of DNA is part of H2B[1].

DNA nor protrude between the turns of the superhelix. Protein domains are now visible, consistent with the earlier histone assignments, and the location of histone H3 has been confirmed by a heavy atom label. Non-crystallographic dyad symmetry relates the halves of the H3·H4 tetramer and the central turn of DNA superhelix; the dyad symmetry, however, does not extend to the same degree to the two H2·H2B dimers, due to interactions between adjacent particles in the crystal.

X-ray analysis and map interpretation

Nucleosome cores from beef kidney were prepared and crystallized as described previously[6]. The space group is $P2_12_12_1$, with one particle of 206,000 daltons per asymmetric unit. The unit cell dimensions of the crystals are dependent on the mean length of the core DNA in a particular preparation[6,17]. The *b*-axis dimension shows the greatest variability, about 4 Å per base-pair increment. The cell dimensions also depend on the degree of hydration, and we found that the crystalline order was increased by shrinkage to an essentially stable optimum state. Thus in 20% 1,6-hexanediol, the *b*-axis length decreases from 200 Å to 184 Å, and the order increases by about 1 Å in resolution in all directions, although the fall-off in intensity remains anisotropic. As a test for particle integrity, DNase I digestion was carried out in the presence of hexanediol, and the positions and frequencies of cutting were found to be unaffected except for minor deviations near the ends of the DNA. Naked DNA would be unwound by about 3% in screw angle at the alcohol concentrations used here[18]. No change in the high angle X-ray pattern[6] characteristic of B-form DNA was detected.

A variation of ±1.5% in the *b*-cell dimensions between different crystals was compensated by adjusting the alcohol concentrations over the range 21–27% to systematically obtain cell dimensions of $a = 107.5$, $b = 184$, $c = 110.5$ Å. The crystal was mounted in a solution containing low gelling temperature agarose which set on cooling to maintain constant hydration during data collection at 4 °C and to keep it fixed in position. The glass capillaries were gently tapered at one end to provide a good fit to the rod-shaped crystals, thereby minimizing X-ray absorption; this was less overall in this method than in conventional mounting techniques, and resulted in a deviation of typically ±5% about the capillary axis.

X-ray diffraction data were collected with a modified four-circle, Hilger–Watts diffractometer mounted on an Elliot rotating anode GX13 X-ray source, using well collimated beams to ensure accurate data at low resolution. For each dataset, the 3,800 reflections from 35 Å to 7 Å and their Friedel mates were measured twice using a partial peak scan method followed by profile fitting analysis to yield the integrated intensities (T.J.R., in preparation). In total, 64 crystals were used for the three datasets. The merging *R*-factors for the amplitudes were 0.05–0.06 over all crystals and symmetry equivalents for a dataset. A crystal was abandoned after one of several reference reflections had decayed by 20% of its initial intensity.

Two heavy atom derivatives were used to determine the phases by the method of multiple isomorphous replacement. Cluster compounds containing several heavy atoms were used in order to overcome the difficulties imposed by the large asymmetric unit and fall-off in the diffraction intensity. The first was tetrakis(acetoxymercuri)methane (TAMM)[19] used at 2 mM and solubilized in 20 mM glycylglycine. TAMM bound to essentially a single site as determined from difference Patterson projections. The second heavy atom cluster, di-μ-iodo, bis(diaminoethyl-*N*,*N*′)diplatinum(II) (PIP) was used at 0.1 mM and found to bind at three major and several minor sites which were located by difference Fourier projections using the phases generated from the TAMM derivative. The *R*-factors for the scaling of the TAMM and PIP datasets to the native dataset were 0.12 and 0.17, respectively. The heavy atom parameters were refined against the centric data using the F_{hle} procedure[20], and resulted in phasing power factors, f_H/E, for the two derivatives of 1.55 and 1.72, respectively (f_H is the r.m.s. calculated heavy atom contribution to the structure factor, and E is the r.m.s. closure error). The figures of merit over all the data were 0.543 for the selected enantiomorph and 0.529 for the opposite hand.

The major and minor grooves of the DNA (or conversely the phosphodiester backbones) are clearly visible as alternating cusps in the electron density map over all the expected length of the DNA, thus defining the DNA superhelix (Fig. 1). Several rods of strong density (presumably α-helices) are seen on the inside of the DNA superhelix, each belonging to discrete regions of electron density, which appear to define the histone domains in a manner consistent with the assignments deduced from the low-resolution map[9] and chemical cross-linking data[10–12]. Thus the order of the main histone contacts from end to end of the DNA superhelix is: H2A, H2B, H4, H3, H3, H4, H2B, H2A. The density at the interfaces between histones cannot, however, be assigned unambiguously at this resolution, and we have ignored any dovetailing that might exist, particularly between H3 and H4. The particle dyad axis (see below) was determined by comparing prominent features in the histone tetramer and the grooves of the central turn of the DNA superhelix.

As a check on the assignments, the volumes of the DNA and of the individual histone domains were estimated by summing the relevant contour areas over all sections. The fractional volume of the crystal occupied by the core particle is 0.35 as

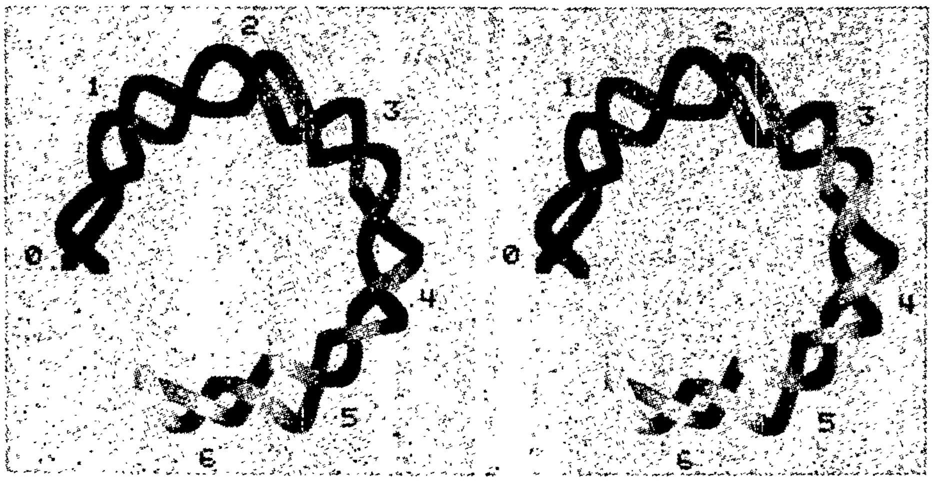

Fig. 2 The folded DNA double helix represented by the course of the phosphodiester backbones. Only one turn of the DNA superhelix as viewed down the superhelix axis is shown for clarity (as a stereopair). The points of intersection of the phosphodiester chains with each map section were joined by cubic spline fitting[56] to produce the two smooth curves shown. The superhelix is oriented such that the molecular dyad axis is horizontal and passes through the minor groove facing outward at position 0. The other positions where the minor groove faces outward are numbered accordingly. The same orientation of the dyad axis is used in Figs 2–6.

compared with a calculated value of 0.40. This agreement is as good as can be expected, as the contour level (55% of the difference between maximum and minimum peak heights) which should be chosen for the boundaries will depend on unknown factors such as small variations in particle position and orientation and local disorder in the histone N-terminal segments[21]. The counterions associated with the DNA and protein would also affect the partial specific volumes.

The core particles are pseudo-hexagonally packed in layers as described previously[6,17]. Most of the contacts between particles are made by DNA–DNA interactions, with one important exception. The H2A · H2B dimers on each flat face of the particle associate with the DNA of an adjacent particle in a head-to-tail fashion along the *b*-direction in the layers. Presumably nuclease trimming of the nucleosome has freed a DNA binding site on each dimer, making it available for interparticle associations. There is also a protein–protein interaction ($H3^2$–$H2B^1$) between layers of the crystals.

The DNA double helix and superhelix

The DNA double helix is in a right-handed B-form (see also ref. 6) and folded into a left-handed superhelix (Fig. 2). About 12 turns of the DNA double helix are clearly visible; the last half turn on each end is indistinct owing to the variable length of the DNA and crystal packing effects. As before[9], we mark the distance along the DNA by numbers from −7 to +7 (from end to end), taking as origin the point where the dyad axis passes through the double helix at the middle of the nucleosomal DNA. The minor groove faces directly outward from the particle at this point, position 0 (Fig. 3*a*), which corresponds to site 7 of the DNase I cutting pattern[22,23]. The positions of the integral numbers correspond approximately to the sites of attack (the local maxima in the frequency of cutting) by the enzyme DNase I[24]. These sites consist of pairs of cuts staggered by 1–3 bp on the two DNA strands[25].

The DNA has on average about 7.6 turns of double helix in a complete superhelical turn. As a result of this periodicity, the adjacent turns of the superhelix are arranged with a minor groove approximately opposite a major groove. The pitch of the superhelix is ~30 Å for the central turn measured between positions −3.8 and +3.8, but reaches a minimum value of 25 Å between positions −2.5 and +5.0. The pitch of the double helix measured along an arc of the superhelix is about 35 Å. At the resolution described here, the actual number of nucleotides per double helical turn cannot be determined. The precise nature of the distortions in the DNA should be apparent when the data to 5 Å resolution are included, as the phosphates should then be visible.

The DNA double helix does not take up a perfectly regular superhelical path as it winds around the histone octamer, but is bent fairly sharply or possibly kinked at several locations (Fig. 2). The DNA bend in the region of position +1 is itself not in direct contact with the histones, but bridges between an extensive histone interaction at position +0.5 on one side and lesser contacts on the other. A similar bend occurs at position +4, apparently due to the DNA–histone contact at position +3.5. The symmetrically related positions at −1 and −4 show similar DNA bending. These regions of high curvature are apparently unlike previously proposed kinks (for example, ref. 26), as the departure from good stacking is apparently spread over several base pairs. Despite the evident ovaloid shape of the superhelix as viewed down its axis (Fig. 2), its diameter (measured between axes of the double helix across the particle) is fairly constant at 86 ± 4 Å.

Because the widths of the major and minor groove seemed to depend on the degree of bending (Fig. 2), we measured them at both the inside and outside surfaces of the double helix at several sites which are exceptionally clear in the map. At period +1 for example, the minor groove width increases from 7 Å on the inside of the particle to 13 Å on the outside. Similarly, the major groove widths are 11 Å and 20 Å. The major groove appears to be more compressed than the minor groove on the inside of the most highly curved regions.

The positions of tightest DNA bending (±1, ±4) correlate well with the sites of greatest 'protection' from DNase I digestion[24] and enhanced reactivity with dimethyl sulphate[27]. Because no obvious protein density is seen extending around the outside of the DNA, it appears that the reduced nuclease cleavage rates do not arise through simple steric hindrance, but rather from distortions in the DNA conformation, or from a reduction of its flexibility due to tight binding by the histones. It has been shown for a double helical oligonucleotide of defined sequence that the cleavage rate for DNase I depends on the local variation in the screw of the double helix[28,29]. Conformational differences along the nucleosome superhelix might indeed lead to relative enhancements of nuclease cleavage rate and also of chemical reactivity. Dimethyl sulphate labelling of purines shows altered reactivity at only two bases as compared with free DNA[27], and these are located in the inward-facing major groove free of protein at positions ±1, where the double helix is sharply bent, and in the minor groove in contact with histone at ±0.5.

The histone octamer and DNA interactions

As mentioned above, features in the protein part of the map are clustered and correspond to the eight individual histone molecules. The assignment of histone H3 is confirmed by the location of the major binding site for the TAMM heavy atom cluster. This label falls precisely on the particle dyad axis (Fig. 3*a*), suggesting that this tetravalent compound bridges between two invariant sulphydryl groups, one from each H3. These are known to be close enough to form a disulphide bond[30]. Even though there are two −SH groups in each bovine H3, we can

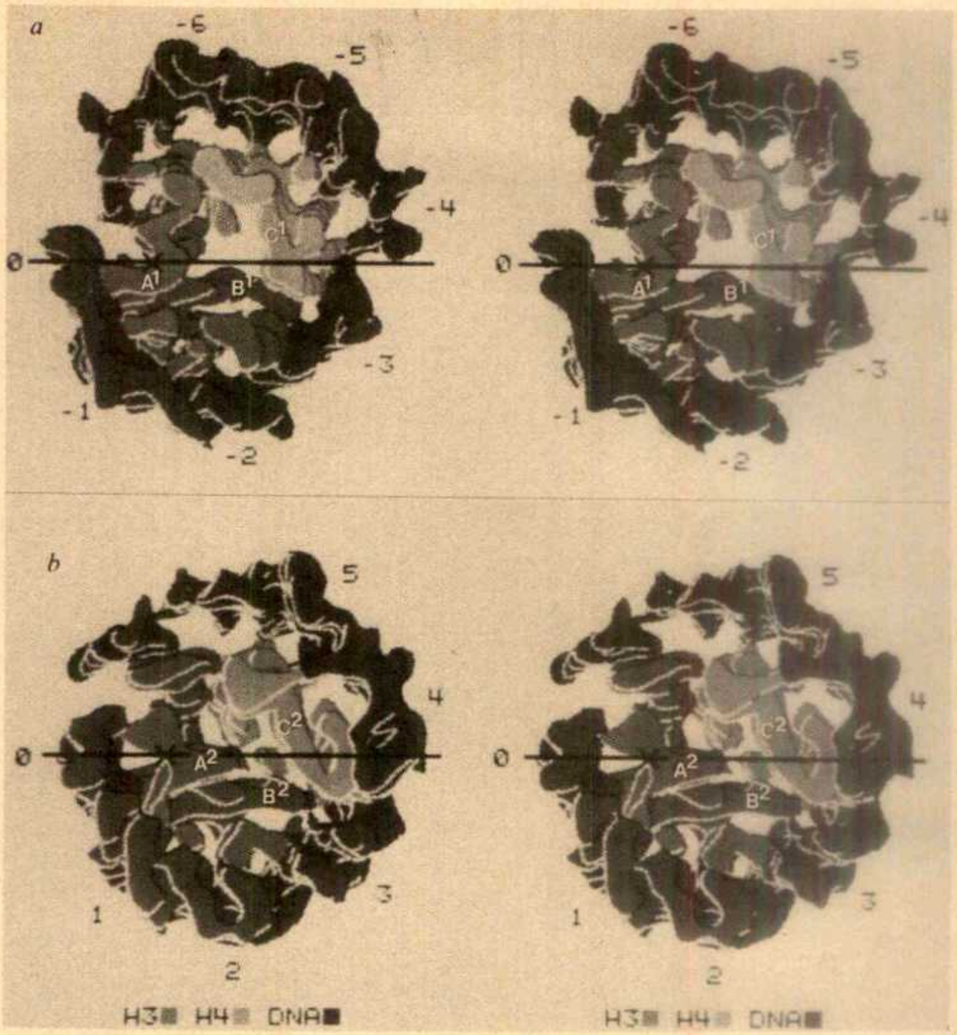

Fig. 3 The two halves of the H3·H4 tetramer and the central turn of the DNA superhelix, both viewed from inside outwards. The map is presented in the form of a stereo-pair of a computer-generated model and has here been sliced into two 15 Å thick slabs parallel to the flat faces of the core particle: *a*, sections −12 to −3; *b*, sections −1 to 6. The alternating groove structure of the DNA is seen particularly clearly from positions 0 to +4 in *b*. The half-tetramer in *b* has been rotated 180° about the dyad axis to give the same view as in *a*: thus the arc 1 to 4 fits against the arc −7 to −3 in the other half. The position of the molecular dyad axis was determined from the rods of histone density labelled B^1 and C^1, and B^2 and C^2. Some of the contours in the histone core have been removed to allow these rods to be seen. The TAMM heavy atom cluster site on the H3 dimer is indicated by a bold X.

be certain that cysteine 110 is the labelled group, because the level of mercurial binding and the intensity distribution in the X-ray patterns from TAMM-reacted crystals of bovine core particles are the same as those from chicken erythrocytes (data not shown), which contain only the two cysteine 110 residues. As can be seen in Figs 3 and 4, the heavy atom site lies between two rods of electron density ~20 Å long (A^1 and A^2) which abut the minor grooves of the DNA at sites −0.5 and +0.5. The H3 densities fold back from the DNA at these positions and extend across the particle for ~35 Å in long rods of density (B^1 and B^2).

Two other rod-like features ~35 Å in length (C^1 and C^2) are visible in the same map sections, but appear to be disconnected from the features defining the H3 region. Therefore, they are likely to be part of the H4 molecules. Shorter pieces of density fold back from the ends of these rods, and make substantial contact with the DNA minor grooves at positions −3.5 and +3.5. These grooves lie on either side of the particle dyad axis at the point where it passes between the two turns of the superhelix. Histones H4 also appear to make minor contacts with the outer superhelical turns of DNA from positions ±4 to ±5.

The two pairs of rod-like density, B^1C^1 and B^2C^2, prominent in the tetramer region, were aligned to determine the orientation of the non-crystallographic dyad symmetry axis (Fig. 3). Other features in the H3·H4 histone tetramer and the central turn of the DNA superhelix are well related by this dyad axis.

DNA–protein contacts are made on nearly every turn of the DNA double helix and are confined to the inner surface of the superhelix. If each such histone contact contained a positive charge, the degree of phosphate charge neutralization thereby afforded would be consistent with the value of 20% derived from the analysis of melting of core particle DNA[31]. If any parts of the histones larger than, say, an extended chain are bound to the outer surface of the DNA, they are disordered in the crystals because there are no places in the 7 Å map where the DNA grooves on the outside of the particle are obscured by protein density. The spaces between the turns of the superhelix are also free from obvious protein density.

In contrast to the tetramer, the pair of H2A·H2B dimers clearly depart from dyad symmetry in the crystals. The whole core particle forms the asymmetric unit, so that the two copies of each histone are not constrained to identical environments. Being on the outer surface of the particle, the H2A·H2B dimers are more susceptible to disturbance by crystal packing forces than is the internally located H3·H4 tetramer.

The $H2A^1 \cdot H2B^1$ dimer is a striking feature of the electron density map. The $H2B^1$ domain contains an ~40 Å long rod of density, D^1 (Fig. 5). Contacts with minor grooves are made at positions −3.5, −4.5 and −6.5 whereas the protein density runs roughly parallel with the major groove at −5. The $H2A^1$ domain extends over the DNA at position 0 to the outer edge of the core particle, and is bound to the major groove at site −3.5 of the DNA on the neighbouring particle (Fig. 5).

The second copy of the dimer is less well ordered and has apparently turned (anticlockwise from the position in Fig. 6) about a point in $H2B^2$ such that the body of $H2A^2$ is shifted by ~10 Å from the position which is symmetrically equivalent to $H2A^1$. This departure from symmetry may represent an intermediate position of this dimer during a quaternary structural change relative to the H3·H4 tetramer. Like $H2A^1$, $H2A^2$ is associated with the DNA at position −7 on an adjacent particle in the crystal. In order to make this DNA interaction, the

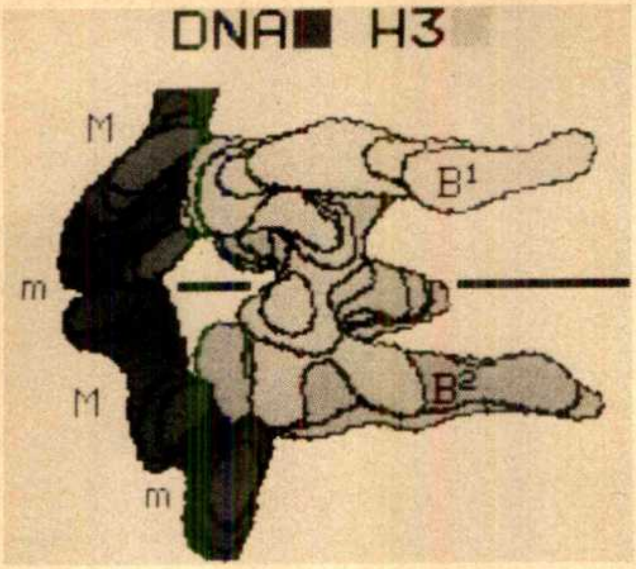

Fig. 4 The H3 dimer and its contact with the middle region of the superhelix. The terminal regions of the long rods, presumably α-helices, make extensive contacts with the minor grooves of the DNA one-half turn of the double helix away on either side of the dyad axis, represented by the solid line. The minor groove faces away from H3 on the dyad.

$H2A^2 \cdot H2B^2$ contacts with the tetramer must be rearranged as compared with $H2A^1 \cdot H2B^1$.

Linker DNA and H1 binding

Nucleosomes which are nearest neighbours along the course of the DNA in chromatin are connected by the linker DNA; its path in chromatin is unknown and may vary. In the core particle structure determined here, the spaces to either side of the DNA at position 0 are blocked by H2A molecules (Fig. 6). If this is also true in solution, the linkers, which would in a nucleosome extend beyond positions −7 and +7, could not simply follow the smooth superhelical course set by the central turn of DNA, as has been suggested[5,32]. The H2A molecules extend to the outer edge of the particle, and are likely to cause the linkers to make angles of roughly 50° to 60° with the molecular dyad axis. Chromatin containing very short linker lengths (that is, 0–10 bp) would then require the DNA to bend sharply or kink, perhaps as seen on the core particle itself. It could be argued that in solution the H2A · H2B dimers take up a more central position in the particle and do not protrude over position 0, but this would entail a major distortion on the diametrically opposite side of the superhelix at position ±4, which we consider unlikely.

This proposed arrangement of the DNA one double helical turn beyond the observed ends of the core particle DNA suggests how H1 may be bound on the nucleosome. Electron microscopy studies of H1-containing and H1-depleted chromatin[33] and the isolation of the chromatosome (which contains H1 and an additional 20 bp of DNA[34]) indicate that H1 is associated with both ends of the superhelix as they make the transition into the linker region. The three DNA segments −7 to −8, +7 to +8, and −1 to +1 would form, when viewed edge-on down the dyad axis, a three-sided cavity, which would provide a reasonable binding site for the H1 globular domain[35]. The core histones that would be closest to H1 are the H2A molecules, as was indicated from chemical cross-linking studies[36,37].

Biological implications

The arrangement of the histones and their degrees of contact with the DNA are suggestive of the roles of the different histones in the assembly of the nucleosome[9,17]. The most substantial contacts are made between the H3 · H4 tetramer and the central turn of the DNA superhelix, and, as was foreseen[9], account for the fact that the tetramer alone can protect about 80 bp of DNA against cleavage by micrococcal nuclease[38,39]. Weaker interactions also occur between the tetramer and the outer turns of the superhelix and explain how the tetramer alone can also organize ~140 bp into a loose nucleosome-like particle[40,41]. The H2A · H2B dimers add to each exposed face of the tetramer, binding to the DNA of the last half turns of the superhelix and increasing the overall stability of the nucleosome.

The H3 dimer within the tetramer binds to DNA in a way which superficially resembles the DNA binding model suggested for the sequence-specific proteins from prokaryotes (for example, cro repressor[42], catabolic activator protein[43] and the N-terminal fragment of λ *c*I repressor[44]). These proteins form dimers whose dyad symmetry axis could align with a local dyad axis in the DNA structure as we have found for the H3 dimer, but the details may differ. For the prokaryotic proteins, a pair of α-helices may contact the edges of the bases in the major grooves of the DNA one half turn to either side of the dyad, whereas, in the case of the H3 dimer, the ends of presumptive α-helices lie against the minor grooves of the DNA one-half turn of the double helix away from the central dyad axis (Fig. 4). Another variation is seen in the complex of the *Eco*RI restriction enzyme and its specific DNA recognition sequence. The protein and DNA are oriented as for the H3 dimer–DNA interaction, but dimerically related α-helices contact the bases in an expanded major groove facing inward on the dyad[45].

Fig. 5 The $H2A^1 \cdot H2B^1$ dimer and outer half turn of the DNA superhelix, viewed from the inside. The stretch of DNA from its end position at −7 to position −3.5 is shown: the groove structure in the region −4 to −5 is very clear. The $H2B^1$ domain includes a number of distinct features such as the partly buried rod of density (D^1) crossing the length of the domain, and a piece of density running roughly in the major groove at position −5. The point on the $H2A^2$ domain which contacts the DNA of the adjacent particle (in the horizontal direction) at position −3.5 is indicated by the X. This contact is repeated along the crystallographic two-fold screw axis in the *b*-direction.

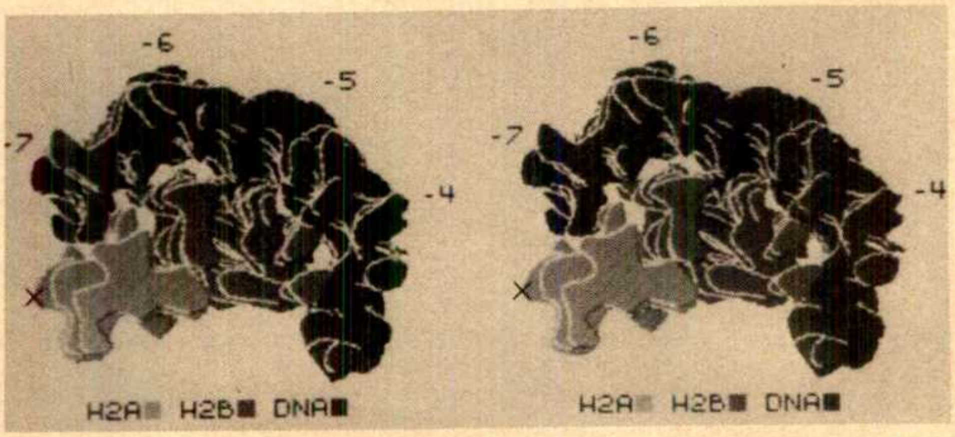

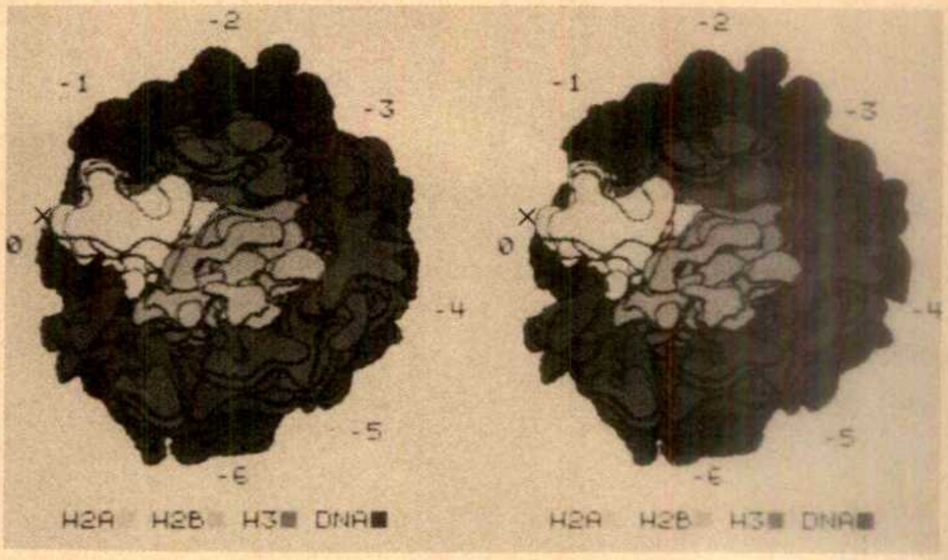

Fig. 6 The location of the $H2A^1 \cdot H2B^1$ dimer in the nucleosome core particle. The entire core particle is shown (sections −21 to +13) to illustrate that $H2A^1$ is positioned over the central turn of the DNA superhelix near position 0. The point marked X is the same as in Fig. 5.

The sharp bends in the DNA path on the nucleosome suggest a structural explanation for the observation that certain DNA sequences are specifically positioned on the histone octamer[46,47], a phenomenon that has been called nucleosome phasing[48] (but see ref. 49). It may be that on account of their relative flexibility, certain short nucleotide sequences are preferentially accommodated at the sharp bends, whereas others may be preferentially excluded[50,51] because of their stiffness. The interplay of these preferences in different regions of a DNA sequence of roughly nucleosome length could result in fixing it at a favoured position. This mode of positioning would not depend directly on specific interactions between the histones and certain base pairs, although it does not, of course, exclude them.

The compact structure that the genomic DNA attains in the nucleosome is essential for chromosome segregation during mitosis, yet the nucleosome cannot be a static structure throughout the cellular processes of transcription and replication. Several recent studies indicate that the histone octamer of transcriptionally active chromatin dissociates from the DNA[52] or takes on an altered structure[53,54]. In the crystal structure, one of the H2A·H2B dimers appears to have moved due to an interaction of H2A with the DNA of another particle. This suggests how the nucleosome might disassemble in response to an alteration in the path of the linker DNA joining nucleosomes in chromatin, perhaps in response to the passage of DNA or RNA polymerase. It seems possible that the dimer would dissociate from the tetramer, while both oligomers maintain separate contact with the DNA. The movement of the H2A·H2B dimer with respect to the histone tetramer is of particular interest in view of the report of a complex formed between RNA polymerase II and nucleosome core particles enriched in transcribed DNA sequences, because this complex lacks one of the dimers[55].

We thank S. J. Lippard and T. O'Halloran for their gifts of the TAMM and PIP heavy atom cluster compounds, the preparation and use of which will be described elsewhere in a joint communication (S.J.L., T.O'H., T.J.R. and A.K., in preparation).

We dedicate this paper to Dr Max Perutz on the occasion of his 70th birthday.

Received 30 May; accepted 27 July 1984.

1. Kornberg, R. D. *A. Rev. Biochem.* **46**, 931–954 (1977).
2. McGhee, J. D. & Felsenfeld, G. *A. Rev. Biochem.* **49**, 1115–1156 (1980).
3. Klug, A. *Symposium on Nucleic Acid Res.* (eds Mizobuchi, K., Watanabe, I. & Watson, J. D.) 91–112 (Academic, New York, 1983).
4. Noll, M. & Kornberg, R. D. *J. molec. Biol.* **109**, 393–404 (1977).
5. Finch, J. T. *et al. Nature* **269**, 29–36 (1977).
6. Finch, J. T. *et al. J. molec. Biol.* **145**, 757–769 (1981).
7. Finch, J. T., Lewit-Bentley, A., Bentley, G. A., Roth, M. & Timmins, P. A. *Phil Trans. R. Soc.* **B290**, 635–638 (1980).
8. Bentley, G. A., Finch, J. T. & Lewit-Bentley, A. *J. molec. Biol.* **145**, 771–784 (1981).
9. Klug, A., Rhodes, D., Smith, J., Finch, J. T. & Thomas, J. O. *Nature* **287**, 509–516 (1980).
10. Mirzabekov, A. D., Shick, V. V., Belyavsky, A. V. & Bavykin, S. G. *Proc. natn. Acad. Sci. U.S.A.* **75**, 4184–4188 (1978).
11. Shick, V. V., Belyavsky, A. G., Bavykin, S. G. & Mirazebekov, A. D. *J. molec. Biol.* **139**, 491–517 (1980).
12. Thomas, J. O. & Kornberg, R. D. *FEBS Lett.* **58**, 353–358 (1975).
13. Kornberg, R. D. & Thomas, J. O. *Science* **184**, 865–868 (1974).
14. Eickbush, T. H. & Moudrianakis, E. N. *Biochemistry* **17**, 4955–4964.
15. Lattman, E., Burlingame, R., Hatch, C. & Moundrianakis, E. N. *Science* **216**, 1016–1018 (1982).
16. Burlingame, R. & Moundrianakis, E. N. *Science* **216**, 1016–1018 (1984).
17. Richmond, T. J., Finch, J. T. & Klug, A. *Cold Spring Harb. Symp. quant. Biol.* **47**, 493–501 (1983).
18. Lee, C-H., Misuzawa, H. & Kakefuda, T. *Proc. natn. Acad. Sci. U.S.A.* **78**, 2838–2842 (1981).
19. Lipka, J. J., Lippard, S. J. & Wall, J. S. *Science* **206**, 1419–1421 (1979).
20. Dodson, E. J. in *Crystallographic Computing Techniques* (ed. Ahmed, F. R.) 259–268 (Munksgaard, Copenhagen, 1976).
21. Cary, P. D., Moss, T. & Bradbury, E. M. *Eur. J. Biochem.* **89**, 475–482 (1979).
22. Lutter, L. C. *J. molec. Biol.* **117**, 53–69 (1977).
23. Sollner Webb, B. & Felsenfeld, G. *Cell* **10**, 537–547 (1977).
24. Lutter, L. C. *J. molec. Biol.* **124**, 391–420 (1978).
25. Lutter, L. C. *Nucleic Acids Res.* **6**, 41–56 (1979).
26. Crick, F. C. & Klug, A. *Nature* **255**, 530–533 (1975).
27. McGhee, J. D. & Felsenfeld, G. *Proc. natn. Acad. Sci. U.S.A.* **76**, 2133–2137 (1979).
28. Lomonossoff, G. P., Butler, P. J. G. & Klug, A. *J. molec. Biol.* **149**, 745–760 (1981).
29. Dickerson, R. E. & Drew, H. R. *J. molec. Biol.* **125**, 535–543 (1981).
30. Camerini-Otero, R. D. & Felsenfeld, G. *Proc. natn. Acad. Sci. U.S.A.* **74**, 5519–5523 (1977).
31. McGhee, J. D. & Felsenfeld, G. *Nucleic Acids Res.* **8**, 2751–2769 (1980).
32. McGhee, J. D., Nichol, J. M., Felsenfeld, G. & Rau, D. C. *Cell* **33**, 831–841 (1982).
33. Thoma, F., Koller, Th. & Klug, A. *J. Cell Biol.* **83**, 403–427 (1979).
34. Simpson, R. T. *Biochemistry* **17**, 5524–5531 (1978).
35. Allan, J., Hartman, P. G., Crane-Robinson, C. & Aviles, F. X. *Nature* **288**, 675–679 (1980).
36. Boulikas, T., Wiseman, J. M. & Garrard, W. T. *Proc. natn. Acad. Sci. U.S.A.* **77**, 127–131 (1980).
37. Thomas, J. O. & Khabaza, A. J. A. *Eur. J. Biochem.* **112**, 501–511 (1980).
38. Camerini-Otero, R. D., Sollener-Webb, B. & Felsenfeld, G. *Cell* **8**, 333–347 (1976).
39. Stockley, P. G. & Thomas, J. O. *FEBS Lett.* **99**, 129–135 (1979).
40. Thomas, J. O. & Oudet, P. *Nucleic Acids Res.* **71**, 611–623 (1979).
41. Simon, R. H., Camerini-Otero, R. D. & Felsenfeld, *Nucleic Acids Res.* **5**, 4805–4818 (1978).
42. Anderson, W. F., Ohlendorf, D. H., Takeda, Y. & Matthews, B. W. *Nature* **290**, 754–758 (1981).
43. McKay, D. B. & Steitz, T. A. *Nature* **290**, 744–749 (1981).
44. Pabo, C. O. & Lewis, M. *Nature* **298**, 443–447 (1982).
45. Frederick, C. A. *et al. Nature* **309**, 327–331 (1984).
46. Chao, M. W., Gralla, J. & Martinson, H. G. *Biochemistry* **18**, 1068–1074 (1979).
47. Simpson, T. R. & Stafford, D. W. *Proc. natn. Acad. Sci. U.S.A.* **80**, 51–55 (1983).
48. Zachau, H. G. & Igo-Kemenes, T. *Cell* **24**, 597–598 (1981).
49. Kornberg, R. D. *Nature* **292**, 579–580 (1981).
50. Kunkel, G. R. & Martinson, H. G. *Nucleic Acids Res.* **9**, 6869–6888 (1981).
51. Prunell, A. *EMBO J.* **1**, 173–179 (1982).
52. Ness, P. J., Labhart, P., Banz, E., Koller, Th. & Parish, R. W. *J. molec. Biol.* **166**, 361–381 (1983).
53. Andersson, K., Mahr, R., Bjorkroth, B. & Daneholt, B. *Chromosoma* **87**, 33–48 (1982).
54. Prior, C. P., Cantor, C. R., Johnson, E. M., Littau, V. C. & Allfrey, V. G. *Cell* **34**, 1033–1042 (1983).
55. Baer, B. & Rhodes, D. *Nature* **301**, 482–488 (1983).
56. Hayes, J. G. & Halliday, J. *J. Instn Maths. Appl.* **14**, 89–103 (1974).

Different modes of Ca channel gating behaviour favoured by dihydropyridine Ca agonists and antagonists

Peter Hess, Jeffry B. Lansman & Richard W. Tsien

Department of Physiology, Yale University School of Medicine, New Haven, Connecticut 06510, USA

Single cardiac transmembranous Ca channels have three modes of gating behaviour in the absence of drugs, expressed as current records with brief openings (mode 1), with no openings because of channel unavailability (mode 0 or null mode) and with long-lasting openings and very brief closings that appear only rarely (mode 2). The dihydropyridine Ca agonist Bay K 8644 enhances Ca channel current by promoting mode 2, while the Ca antagonists nitrendipine and nimodipine inhibit the current by favouring mode 0.

DIHYDROPYRIDINES such as nifedipine and nitrendipine are among the newest and most interesting of the many agents that modify Ca channel activity in excitable cells[1,2]. As therapeutic agents, they have already gained wide use in the treatment of cardiovascular disorders[3-6]; as specific ligands, they open the way towards eventual biochemical purification and reconstitution of Ca channels[7-10]. Questions about the mechanism of their action have been raised by the discovery of 'Ca agonists', such as Bay K 8644 and CGP 28 392 (refs 11, 12), which increase cardiac contractility and divalent cation influx[11-16] even though they are dihydropyridines and thus very similar in structure to nifedipine and other 'Ca antagonists'. How can such closely related compounds produce effects that seem so diametrically opposite? Here we report analysis of Ca agonist and Ca antagonist effects on Ca channel activity of single heart cells and single Ca channels. We find that Bay K 8644 increases the chances that the channel will show a mode of gating marked by long opening and brief closing events. The same type of gating can be seen occasionally in the absence of drug. On the other hand, nitrendipine and nimodipine exert their Ca antagonist effect by increasing the proportion of sweeps where the channel fails to open. The results provide an explanation for partial agonist or antagonist actions; in particular, we find that the effects of nitrendipine include a Ca agonist component.

Methods

Single ventricular cells were obtained from guinea pig or frog hearts by enzymatic dispersion[17,18], and whole cell membrane current recordings were made under voltage clamp conditions using suction pipette methods of Lee *et al.*[19] (guinea pig) or Hamill *et al.*[20] (frog). Patch clamp recordings of single Ca channel activity were made from cell-attached patches on guinea pig ventricular cells[21,22] with patch pipettes containing 110 mM $BaCl_2$, 10 mM glucose and 10 mM HEPES (titrated with $Ba(OH)_2$ to *p*H 7.5). The cells were bathed in a solution containing 10 mM KCl, 140 NaCl, 1 mM $MgCl_2$, 10 mM glucose and 10 mM HEPES (titrated with NaOH to *p*H 7.5). In some of the experiments, the external solution also contained 0.5 mM EGTA. Current signals were filtered with an eight-pole Bessel filter with a cut-off frequency (3 dB) of 1 kHz, and sampled at 5 kHz. Automated analysis of the digitized signals was carried out with procedures similar to those previously described[21,22]. The analysis program disregarded open or closed periods that lasted up until the time of repolarization. The figures show results from patches containing only one channel, as judged by the absence of a multiple conductance level. All experiments were carried out at room temperature (22 °C).

Ca channel current in single cells

The Ca agonist compound Bay K 8644 strongly enhanced Ca channel current in both guinea pig and frog ventricular cells. With 10 mM external Ca, and test depolarizations from −60 mV to +10 or +20 mV, 1 μM Bay K 8644 increased the peak inward current by 3.0 ± 0.3 fold (s.e.m.) in guinea pig myocytes ($n = 6$) and 4.05 ± 0.52 fold in frog ventricular cells ($n = 7$). Bay K 8644 at 10 μM gave no greater enhancement than at 1 μM; half-maximal effects were obtained at concentrations of 30–100 nM. At maximally effective doses, Bay K 8644 increased whole cell Ca channel current within seconds, and in all cases the enhancement was sustained.

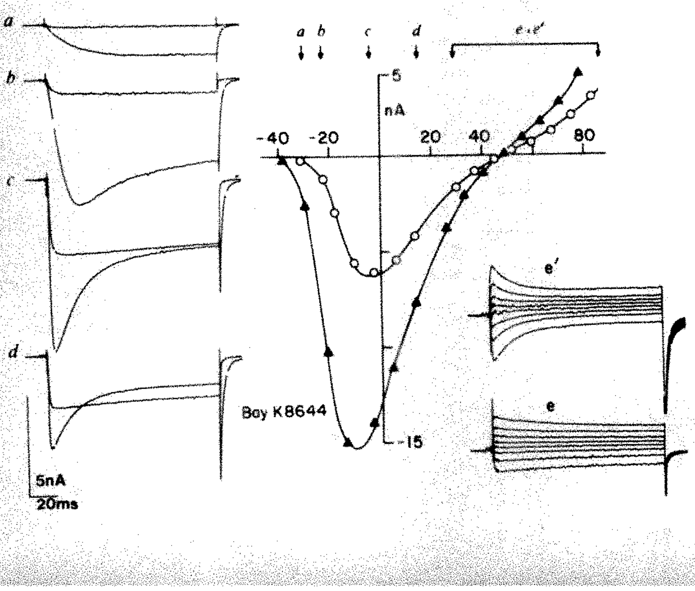

Fig. 1 Voltage-dependent effect of Bay K 8644 on Ca channel currents carried by Ba^{2+}. Single guinea pig ventricular cells were studied with a suction pipette for voltage clamp and internal dialysis[19]. Each panel shows current signals evoked by step depolarizations from a holding potential of −60 mV, in the absence of drug (smaller peak current, more rapidly decaying tail current), and in the presence of 1 μM Bay K 8644 (larger peak current, more slowly decaying tail current). *a–d*, Depolarizations to within 1 mV of −31, −23, −3, and +15 mV. *e*, *e'*, Families of records taken over the voltage range between +27 and +80 mV to show reversal of Ca channel current with Bay K8644 (*e'*) and in control (*e*). The current-voltage diagram plots peak current against test potential. Series resistance compensation for 0.75 MΩ out of a total pipette resistance of 0.9 MΩ. Linear leak currents and capacity currents have been subtracted from the current signals. External solution contained (mM) 10 $BaCl_2$, 85 Cs-aspartate, 2.85 $MgCl_2$, 5 glucose, and 10 HEPES titrated with CsOH to *p*H 7.4. Internal dialysate contained (mM) 75.5 Cs-aspartate, 75.5 Cs-phosphate, 5 glucose, and 10 HEPES titrated with CsOH to *p*H 7.0. Cell 205G.

The Ca agonist altered the voltage- and time-dependence of Ca channel currents carried by either Ca^{2+} or Ba^{2+}. The analysis of Ba current (charge carried by Ba^{2+}) is somewhat simpler because of the absence of Ca-induced Ca channel inactivation[23]; Figure 1 illustrates the effect of Bay K 8644 (5 μM) on Ba current in a whole-cell suction pipette recording from a guinea pig myocyte. The agonist-induced enhancement of peak current was largest at weak depolarizations (where the current was small in the absence of drug) and became progressively smaller with increasing depolarization. For example, the enhancement was ~10-fold at −31 mV (*a*) and only ~1.8-fold near +80 mV (*e*, *e*′). As the current–voltage relationship indicates, the current through the Ca channel reversed near +50 mV (due to a balance of Ba influx and Cs efflux[24]) and the reversal potential remained unchanged with agonist.

The time-dependence of Ba current through Ca channels was also changed by the Ca agonist. In the presence of Bay K 8644, the current showed a greater tendency to decay. As the depolarizing pulse grew stronger, the enhancement of decay was so great that the agonist current signal was smaller than the control record by the end of the pulse, regardless of the polarity of the current (*d*, *e*, *e*′). Inward tail currents also decayed more slowly following a repolarizing step.

The pronounced changes in kinetics suggest that Ca channel gating is modified by Bay K 8644. To investigate this possibility, we carried out patch clamp recordings of single Ca channel activity.

Long-lasting channel openings

Activity of single Ca channels was recorded from cell-attached patches on guinea pig ventricular cells with 110 mM Ba in the pipette as the charge carrier (Fig. 2*a*, *b*). Ca channel activity was seen in the form of brief pulses of inward current in the absence of drug as in previous studies[21,25]. The test depolarization was kept small enough to give large, easily resolved unitary currents. Exposure of the cell to Bay K 8644 did not detectably alter the amplitude of the unitary event, but it produced a striking change in the pattern of channel opening. In many of the sweeps, the channel spent the majority of its time open, rather than closed; channel openings were very much prolonged; channel closings were abbreviated. As a result of these effects, the average current signal in the presence of agonist (Fig. 2*d*) was about 11-fold greater than its amplitude before drug (Fig. 2*c*). This response was typical of results from five patches, and reflected the whole-cell response at comparably weak depolarizations (Fig. 1*a*) in the degree of enhancement and in the absence of a drug-promoted relaxation of inward current.

When the agonist effect was large, and the drug dose was at a maximally effective concentration as in Fig. 2*b*, a substantial fraction of sweeps still contained no detectable openings or only rapidly flickering openings like those found in the absence of drug. Such sweeps are easily differentiated from sweeps with long openings and short closings. The combination of both types of behaviour provides an interesting clue to the agonist's mechanism of action.

Sweep-to-sweep variations in behaviour are illustrated for the same experiment by plotting the probability of a channel being open (*p*) for each sweep (Fig. 3*a*,*b*). The value of *p* was obtained by integrating over a period when the current signal was steady (see Fig. 3 legend). In the control run (Fig. 3*a*), *p* was less than 0.20 in all but one of the sweeps. After exposure to Bay K 8644, changes in *p* were immediate and well-maintained throughout the 15 min exposure to the drug (Fig. 3*b*). In the presence of the agonist, the distribution of *p* values is strikingly bimodal: over the range between $p = 0.5$ and $p = 1.0$ a new group of *p* values appears; however, between $p = 0$ and $p = 0.5$, the distribution remains similar to that in the absence of drug (Fig. 3*c*, *d*).

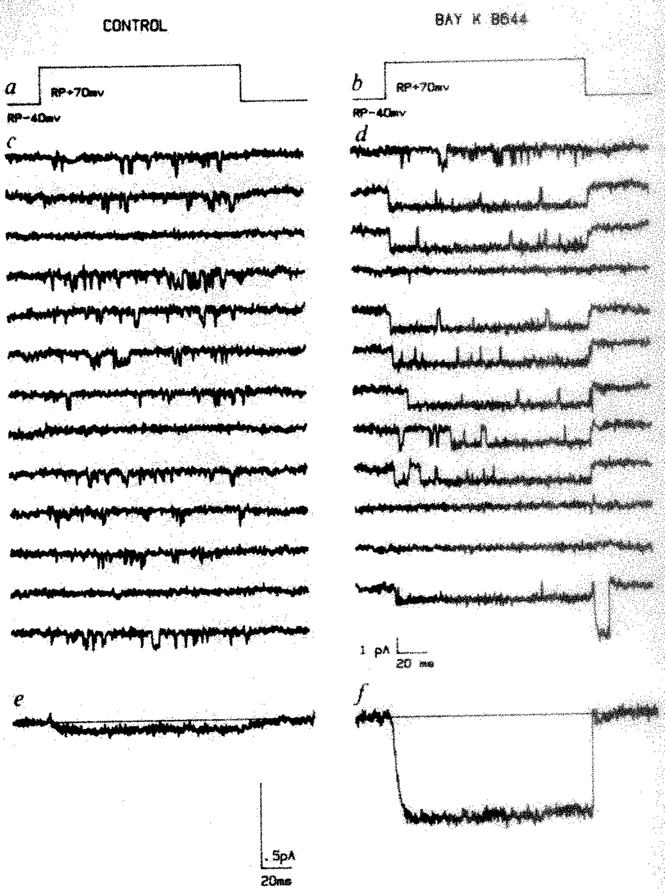

Fig. 2 Patch clamp recording of single Ca channel activity in the absence (left column) and presence of 5 μM Bay K 8644 (right column). Cell-attached patch. *a*, *b*, Voltage protocol RP, resting potential ~ −60 mV as determined by measurement of open channel current-voltage relations (data not shown). Pulses were applied once every 3 s. *c*, *d*, Representative current signals (consecutive sweeps). Linear leak and capacity currents have been subtracted. *e*, *f*, Averaged current signals from all the sweeps in each run (vertical scale is different in *c*, *d*). Cell 6A.

Sweeps with low *p* and high *p*

Taking advantage of the bimodal distribution of *p* values, we separated records taken in the presence of Bay K 8644 into two groups of records for analysis of the kinetics of opening and closing: 'low *p*' sweeps with $p < 0.3$, and 'high *p*' sweeps with $p > 0.65$ (Fig. 4). The behaviour of low *p* sweeps in the presence of agonist is very similar to that in the absence of drug (Fig. 4, left and middle columns). Both of these open time histograms are fitted by a single, rapidly decaying exponential ($T \sim$ 0.5–0.6 ms). Both of the shut time distributions are well-fitted by the sum of two exponentials as described elsewhere[21,22]. The mean latency-to-first opening is similar in both cases (21 ms control, 19 ms for low *p* sweeps in Bay K 8644). The percentage of sweeps with no openings is also very similar (132/420 = 31% in control and 42/127 = 33% for the low *p* sweeps after agonist).

The behaviour of the high *p* sweeps is strikingly different. The open time histogram shows a predominance of long openings (mean value ~20 ms), as expected from the records illustrated in Fig. 3. The distribution fits a single exponential reasonably well, except for a surplus of brief openings in the first few bins, which may reflect imperfect exclusion of the low *p* behaviour with its much greater density of open events per unit time. The shut time distribution is fitted by the sum of two exponentials, as in the other two cases, but the mean closed time is much briefer. Similarly, the cumulative histogram of latency-to-first opening is biased towards shorter times. The combination of longer openings and shorter closings accounts for the extremely high values of *p*.

The results from this patch were representative of a total of three experiments with 5–10 μM Bay K 8644. In an experiment with 100 nM drug, the high *p* sweeps showed similar open and closed time distributions; the proportion of high p sweeps was simply lower than with maximally effective doses of drug.

Multiple modes of channel gating

The analysis is consistent with the idea that the Ca channel switches between different modes of channel gating. Figure 5*a* presents our working hypothesis. We use the terms mode 0, mode 1, and mode 2 to refer to the three distinct forms of gating behaviour. Mode 1 is characterized by brief (~1 ms) openings occurring in rapid bursts. The most obvious form of gating in the absence of drug, it has been the main focus of single channel recordings up to now[21,22]. The probability of openness in this mode is relatively low at membrane potentials where the unitary current is easily resolved, although it must be remembered that p can approach levels as high as 0.7 at stronger depolarizations[21,25]. The observed distributions of open and shut times have been interpreted in terms of two closed states (C1, C2) and one open state (O) (see refs 21, 22, 26). Mode 2 can be distinguished by relatively long-lasting channel openings (~20 ms) and typically brief closings. Probability of channel openness is typically high (>0.7) even at relatively negative test potentials. The distributions of open and closed times in Fig. 4, right column are compatible with a C1-C2-O scheme, with very different values of rate constants than those appropriate for mode 1.

Although mode 2 behaviour is most easily studied after administration of Ca agonist, it can also be seen in the absence of drug. For example, Fig. 3*a* shows a sweep with a p value of ~0.85; this sweep has openings lasting 3.6, 9.5, 10.8, 3.2, 0.6, and 77.5 ms, typical of what we define as mode 2. The sweep was the only one out of 420 that clearly showed long openings. In a total of 11 patches with one or two channels, sweeps with long openings and unusually high p typically appeared at a rate of about 1%, with a wide range (0.4–11%). Figure 5*b–e* illustrates the behaviour of the patch with the highest incidence of sweeps showing intrinsic mode 2 behaviour. Two main points can be made. First, sweeps with high p appear significantly clustered in time (Fig. 5*b*). Second, sweeps with high p in the absence of agonist show a pattern of channel opening and closing (Fig. 5*d*) very similar to that found in the presence of agonist (Fig. 2*b*). For example, in the experiment illustrated in Fig. 5 the mean open time in the high p sweeps was 16.4 ms, close to the ~20 ms time constant of the slow exponential in Fig. 4*f*. Similarly good agreement was found in other experiments: average values for the mean open time of high p sweeps were 19.0 in control (93 sweeps, 7 cells) and 18.2 in the presence of Bay K 8644 (338 sweeps, 4 cells).

Mode 0 or null mode refers to a condition or conditions where the channel is unavailable for opening. It is expressed by sweeps showing no openings, in excess of those empty sweeps expected from the C1-C2-O kinetics of mode 1. Voltage-dependent inactivation is one factor that increases the proportion of time a channel spends in mode 0. However, we found an excess of null sweeps even with holding potentials negative enough to achieve maximal removal of voltage-dependent inactivation.

The distinction between mode 0 and 1 can be demonstrated in at least two ways. The cumulative histogram of first latency (Fig. 4*d*) levels off at about 70%. This runs contrary to a simple C1-C2-O model, which predicts that the saturating level should be 100% (eventually, the channel should reach the open state long enough for an event to be detected). As the curve falls 30% short of certainty it appears that the channel was simply unavailable for opening at the test potential 30% of the time.

Another way of distinguishing mode 0 from mode 1 relies on the histogram of p values, as in Fig. 3*c* for example. The first two bins of the histogram largely represent sweeps for which no openings could be detected. When these sweeps are disregarded, the remaining distribution rises smoothly to a peak at the fifth bin and then falls smoothly, as might be expected for a single type of gating behaviour, namely mode 1.

By either of these criteria, the vast majority of patches in our experiments show an appreciable number of null sweeps in excess of those expected from C1-C2-O kinetics. A similar excess has been observed, but not commented on by other investigators (for example, ref. 27). Like sweeps showing mode 2 behaviour, null sweeps show a tendency to follow each other (see Fig. 5 legend).

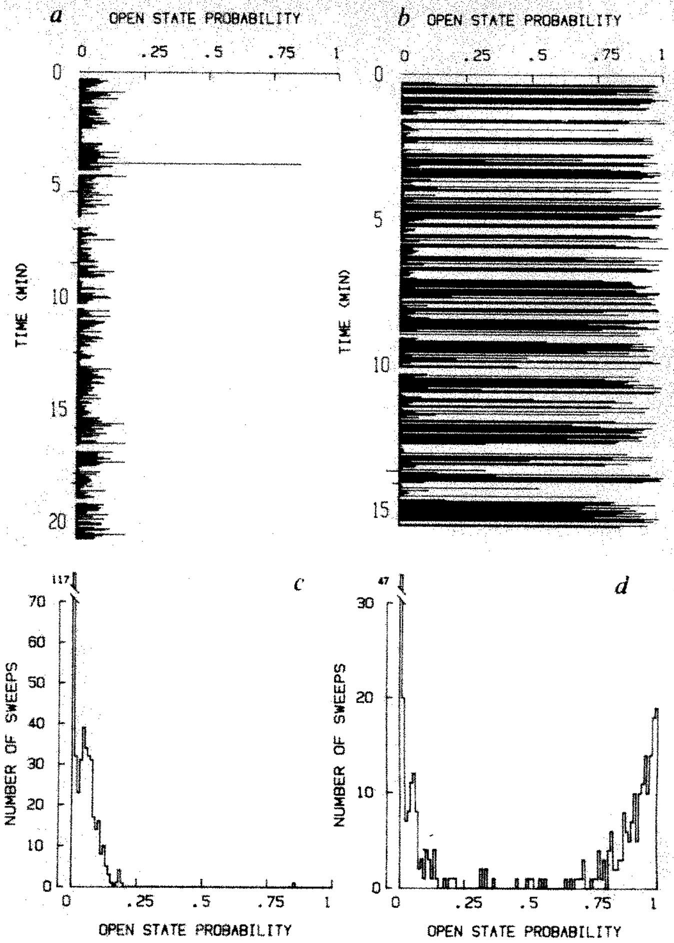

Fig. 3 Influence of Bay K 8644 on probability of channel openness (p) during individual sweeps. Control (left), 5 μM Bay K 8644 (right). In *a* and *b*, p is plotted against time. Gaps along the time axis indicate sweeps used to measure leak conductance or sweeps marred by noise interference. *c*, *d*, Histograms of p values for the runs shown in *a*, *b*. Each bin is 0.008 wide. For each sweep, steady-state values of p were determined as $p = \langle I \rangle / i$, where i is the unitary current, and $\langle I \rangle$ is the steady-state value of current, averaged over a period from 22 ms after the depolarizing step until the end of the pulse. Sweeps with no detectable openings ('nulls') have near-zero values of p, and show up in the first few bins. For example, in panel *c*, bins 1 to 5 contain 108, 18, 4, 1 and 1 nulls respectively; if the null sweeps had been excluded from the histogram in *c*, the distribution of p values would rise to a single peak and fall smoothly.

Mechanism of agonism and antagonism

The identification of different modes of Ca channel gating leads naturally to a hypothesis for the mechanism of action of dihydropyridine (DHP) Ca agonists and antagonists (Fig. 5*a*). We propose that the binding of these drugs does not plug the pore, but favours one or more modes of gating instead. Within a mode, the kinetics of gating transitions need not be different when DHP occupies its binding site (see Fig. 6). Pure agonist effects arise when mode 2 is specifically favoured, and pure antagonist effects result when mode 0 is preferentially stabilized; these extremes encompass a wide range of intermediate possibilities for 'partial agonist' or 'partial antagonist' effects[34].

We observed effects of 5–15 μM nimodipine consistent with the above hypothesis for a pure antagonist: at these drug concentrations we found that the reduction of the averaged current

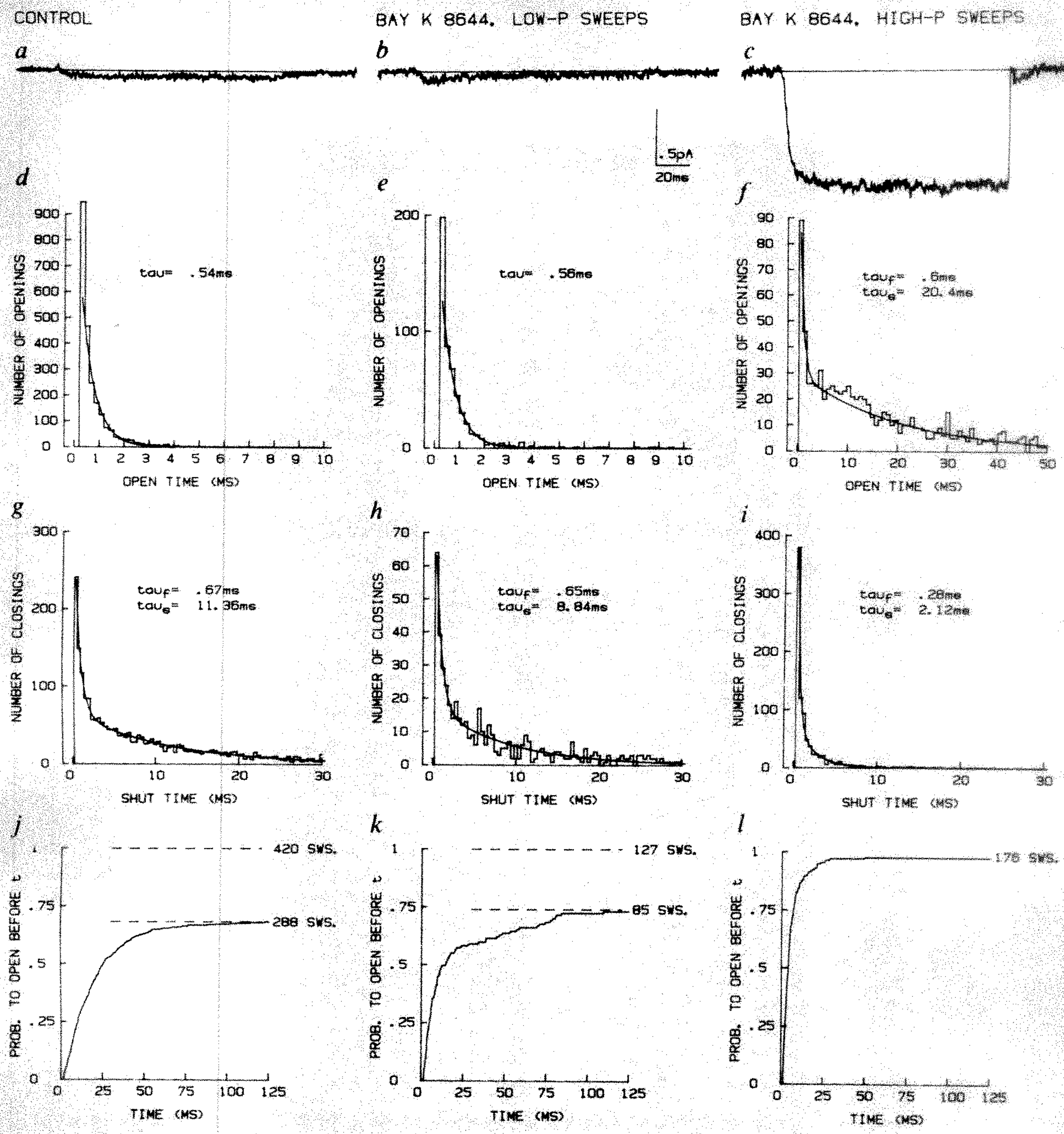

Fig. 4 Effect of Bay K 8644 on Ca channel kinetics. Left column, analysis of all sweeps from the control run; middle column, all sweeps from agonist run with $p < 0.3$; right column, all sweeps from agonist run with $p > 0.65$. The rows show averaged current records (first row), distributions of open times (second row), closed times between openings (third row), and cumulative distributions of the latency to first opening (fourth row). Smooth curves in panels *d* and *e* are single exponentials (the fits ignore the first bin of the histogram data). Smooth curves in panels *f–i* are sums of two exponentials. Fits were obtained by minimizing χ^2, using a computer program provided by Dr R. S. Kass.

was caused by an increase of the proportion of sweeps with no openings, whereas we found no clear evidence for a change in open or closed time distributions.

Mixed effect of nitrendipine

Although nitrendipine is generally assumed to be pure antagonist, we found that the net inhibitory effect of this dihydropyridine is the resultant of agonist as well as antagonist components. Figure 6 illustrates the response of a single Ca channel to 5 μM nitrendipine, a partially inhibitory dose in the presence of the 110 mM Ba (ref. 24). The control run included a large number of empty sweeps, as well as sweeps with bursts of flickery openings (mode 1), and sweeps with long openings, some lasting beyond the repolarizing step (mode 2, not shown). Nitrendipine altered channel activity in several ways. As with nimodipine, the proportion of sweeps with detectable openings was greatly decreased. This is evident from the plot of cumulative latencies to first opening (Fig. 6*g*), which levels off at a level roughly half that of control. When a more complete reduction of inward current was obtained at 10 μM nitrendipine in other experiments, the proportion of empty sweeps approached 100%. We attribute these effects to stabilization of mode 0, in line with a pure antagonist action.

Other aspects of the nitrendipine response were rather surprising. (1) The percentage of sweeps with $p > 0.5$ was not decreased; (2) a larger percentage of sweeps contained long openings, and the distribution of open times was prolonged (Fig. 6*e*), (3) closed times were abbreviated (Fig. 6*f*); (4) latencies-to-first opening were shortened (Fig. 6*a*). In all of these respects, nitrendipine resembles Bay K 8644.

The agonist-like effect of nitrendipine is most clear at the time of peak inward current. The peak amplitude of the averaged

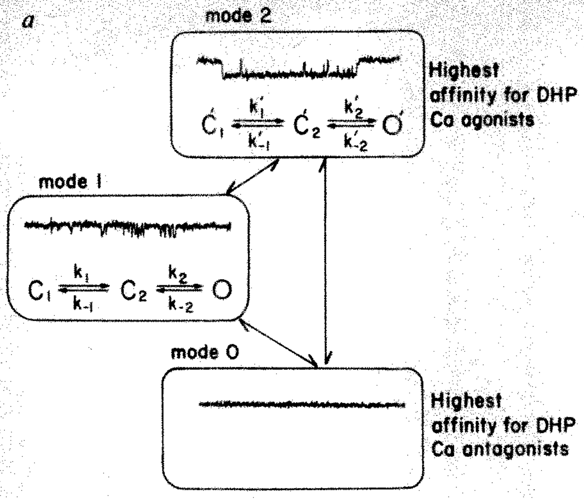
a
mode 2
$C'_1 \underset{k'_{-1}}{\overset{k'_1}{\rightleftharpoons}} C'_2 \underset{k'_{-2}}{\overset{k'_2}{\rightleftharpoons}} O'$
Highest affinity for DHP Ca agonists
mode 1
$C_1 \underset{k_{-1}}{\overset{k_1}{\rightleftharpoons}} C_2 \underset{k_{-2}}{\overset{k_2}{\rightleftharpoons}} O$
mode 0
Highest affinity for DHP Ca antagonists

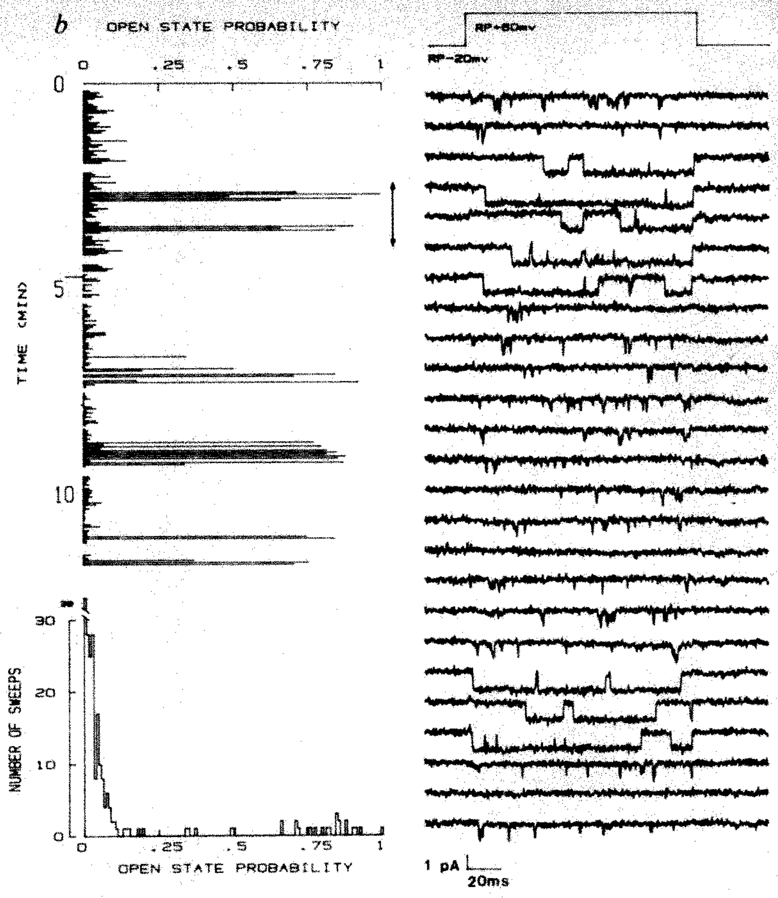

Fig. 5 *a*, Hypothetical modes of Ca channel gating. In the absence of drug, transitions between modes are assumed to be much slower than gating reactions within modes; details of inter-mode connections are left unspecified and require further study. At the test potentials studied, mode 1 and mode 2 are distinguished by qualitatively different patterns of opening and closing. This is put in terms of a kinetic model for Ca channel gating with two closed (C1, C2) and one open (O) state: rate constants for transitions between the states are assigned different values depending upon the mode. No gating reactions are depicted for mode 0 because it represents condition(s) in which the channel is unavailable for opening at the test depolarization. Since voltage-dependent inactivation is one factor that biases the channel towards mode 0, the rate constants for transitions to and from mode 0 are presumably voltage-dependent. The voltage-dependence of transitions between mode 1 and mode 2 is not known. *b–d*, Spontaneous appearance of sweeps with long-lasting openings and high *p* in the absence of drug. Experimental conditions as in Fig. 2*a*. RP ≃ −55 mv. *b*, probability of channel openness during 250 sweeps at 0.33 Hz. Gaps correspond to measurements of leak current with weak depolarizing pulses. *c*, Histogram of *p* values for the set of sweeps shown in *b*. In 31 sweeps, no openings were detected by the analysis program. *d*, Representative current records associated with the depolarizing pulse shown above. Twenty-five records were taken sequentially during the period marked in *b*, illustrating the tendency for mode 2 activity to occur in clusters of consecutive sweeps. The incidence of high *p* sweeps following immediately after a previous high *p* sweep was (11/21) = 52%, significantly higher than the overall incidence of high *p* sweeps (21/198) = 11% (χ^2, $P < 0.0001$). The incidence of null sweeps immediately after a preceding null sweep was (8/29) = 29%, significantly higher than the overall incidence of null sweeps, (30/198) = 15% (χ^2, $P < 0.05$). Cell 5F. In the presence of Bay K 8644, sweeps with high *p* values also tended to follow each other. For example, in the run shown in Fig. 3*b*, the incidence of high *p* sweeps was (176/316) = 56% while the incidence of high *p* sweeps following a previous high *p* sweep was (118/176) = 67%. This difference is also highly significant, $P < 0.0005$).

current remains almost unchanged (compare Fig. 6*c*, *d*), despite a doubling of the number of empty sweeps; this can only mean that *p* increased in the non-empty sweeps. The increase in *p* is associated with an increase in the number of long openings relative to the number of short openings (Fig. 6*e*). The overall inhibitory action of nitrendipine is more obvious toward the end of the depolarization since the average current decays more quickly in the presence of the drug (Fig. 6*f*). Individual records show a corresponding tendency for openings to occur towards the beginning of the pulse and not towards the end. When the faster decay of mean current was first observed with global current recordings[24,28], it was attributed to open channel block[24]. We now favour the interpretation that the faster decay results from antagonist-promoted inactivation (see below).

Activity of other dihydropyridines

Nitrendipine is not exceptional in its mixed effects. For example, nifedipine is used widely for its inhibitory action, but it can increase cardiac contractility at low doses[11,29]. The drug CGP 28 392 has agonist effects on contractile activity in heart and smooth muscle[12] and Ca fluxes in cultured cells[16] but its presence partially occludes the stimulatory effect of Bay K 8644 (ref. 16). Bay K 8644 itself is probably not a pure agonist. Sanguinetti and Kass[25] have reported that this drug increases Ca channel current in Purkinje fibres when the holding potential is negative, but reduces it when the holding potential is positive to −40 mV. We have seen similar effects of holding potential on the effects of Bay K 8644 in single ventricular cells. A partial antagonist effect may also be involved in the acceleratory effect of Bay K 8644 on Ba current decay with stronger depolarizations (Fig. 1).

Conclusions

Although this work began with an analysis of the effects of Ca agonists and antagonists, the experiments led us to some unexpected conclusions about the fundamental properties of Ca channels. We believe that the strikingly long openings seen with Bay K 8644 are not a new form of gating, but an intrinsic form of gating (mode 2) whose likelihood is merely enhanced by the drug. Without the agonist-promoted activity as a guide, the intrinsic mode 2 activity might be overlooked, since it appears only rarely in most experiments, and contributes only a small number of events per sweep to histograms of open or closed times. But once attention is focused on the mode 2 pattern of long openings and short closings, even single sweeps of this type of activity can be easily picked out. The distinction between mode 1 and mode 2 is particularly clearcut at weak depolarizations where the open probability in mode 1 is low.

Our results provide an attractive explanation for how structurally similar dihydropyridines can exert seemingly opposite effects on Ca influx. They argue against the idea that the inhibitory action of nitrendipine and other Ca antagonists reflects a

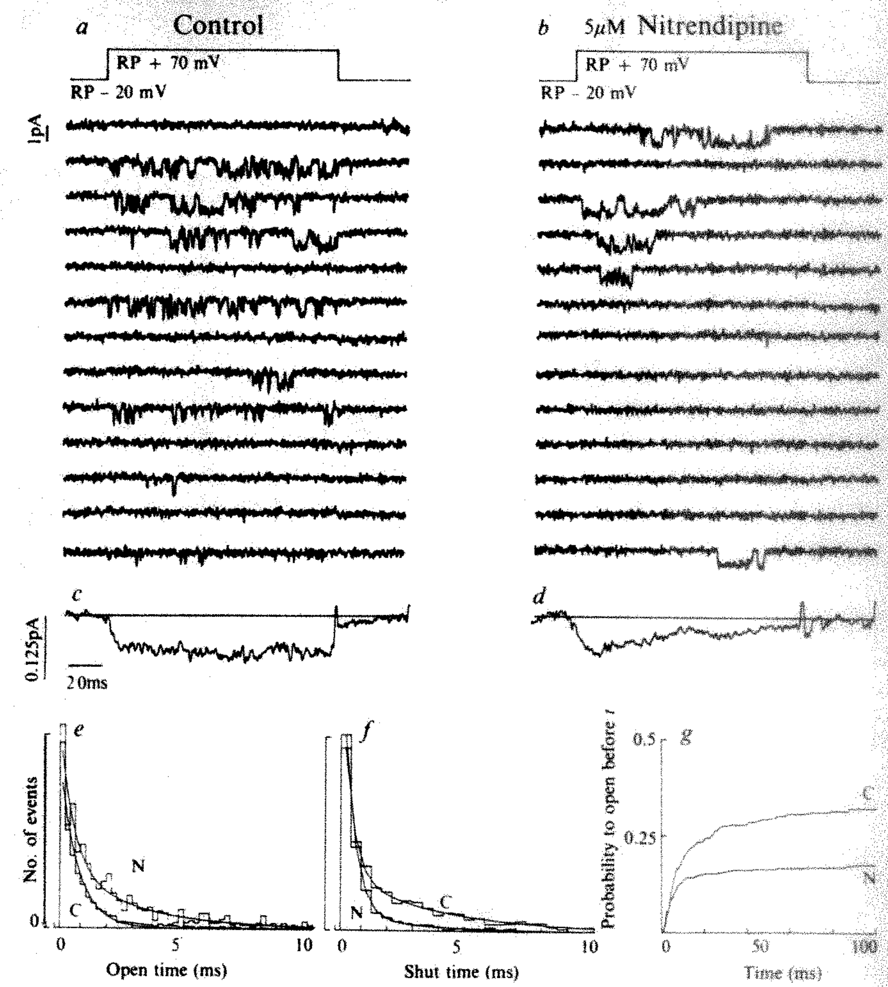

Fig. 6 Effect of nitrendipine on the activity of a single channel. Experimental conditions as in Fig. 2*a*. RP ≈ −60 mv. *a*, *b*, Representative groups of consecutive sweeps in the absence (*a*) and presence of 5 μM nitrendipine (*b*). Voltage clamp protocol shown above the current traces, *c*, *d*, Averaged currents from run *a* (409 sweeps) and run *b* (414 sweeps). *e*, Superimposed distributions of open times. Control data (C) fitted by a single exponential ($T = 0.8$ ms), nitrendipine data (N) fitted by the sum of two exponentials ($T_f = 0.75$ ms, $T_s = 3.2$ ms). Full-scale is 700 and 100 openings for control and nitrendipine respectively. *f*, Superimposed distributions of closed times, fitted by sum of two exponentials (control: $T_f = 0.38$ ms, $T_s = 3.63$ ms; nitrendipine: $T_f = 0.42$ ms, $T_s = 2.57$ ms). Full scale is 600 and 300 closings for control and nitrendipine respectively. *g*, Superimposed cumulative distributions of latencies to first opening. The distribution of open times in nitrendipine (*e*) consisted of a fast exponential component as in control ($T \sim 0.75$ ms), plus an additional slow component. The time constant of the slow component (3.2 ms) falls short of the ~20 ms time constants characteristic of mode 2 activity in control and with Bay K 8644. The cause for this discrepancy is not clear. We cannot exclude the possibility that nitrendipine not only influences the proportion of sweeps the channel spends in mode 2, but also affects the kinetics of opening and closing within mode 2. Another explanation is that openings of nitrendipine-bound channels are cut short by an accelerated inactivation reaction (transition from mode 2 to mode 0), which acts in parallel with the closing reaction within mode 2 (O − C2) and thereby increases the overall closing rate above its normal value.

physical plugging of the Ca channel pore. A simple binding and plugging hypothesis can be excluded since a nitrendipine molecule cannot plug the channel and show agonist-like activity at the same time; separate binding sites for nitrendipine's antagonist and agonist actions seem highly unlikely since Bay K 8644 competes for all of the nitrendipine binding sites[30]. The results point instead to modulation of gating as the mechanism of DHP agonist or antagonist action. The changes in gating revealed by the single channel analysis help to explain earlier observations in single cell or multicellular cardiac preparations. All lines of evidence support the idea that inactivation and the inhibitory effects of DHP Ca antagonists reinforce each other. Thus, (1) nitrendipine speeds the decay of Ba current through Ca channels in both whole cell[27] and unitary current recordings (Fig. 6), as if drug binding promotes mode 0. (A similar acceleration is seen with Bay K 8644 at stronger test depolarizations (Fig. 1), and is tentatively attributed to the drug's partial antagonist action.) (2) Nitrendipine[24] and nisoldipine[28] act to slow recovery from inactivation following a depolarizing pulse. (3) Steady depolarizations that inactivate Ca channels strongly promote nisoldipine's inhibitory effect[28]. (4) Like voltage-dependent inactivation[21,25], the inhibitory effect of DHP antagonists is expressed as an increase in the percentage of empty sweeps at the single channel level (Fig. 6).

Our hypothesis provides a simple explanation of partial agonist or partial antagonist effects, and a framework for classifying the 7,000 or more dihydropyridine compounds that remain less well studied than nifedipine or nitrendipine. It will be interesting to see if any of these molecules behaves as a pure agonist or antagonist, exclusively stabilizing mode 2 or mode 0. It is important to remember that the range of possibilities is not limited to a one-dimensional scale between agonism and antagonism, since stabilization of three modes needs to be taken into account. In addition to the ideal agonist and ideal antagonist, one might imagine a compound that exclusively stabilizes mode 1, and thereby opposes effects of both agonists and antagonists.

The mechanism of transitions between modes is not known. The clustering of mode 2 activity indicates that switching can be relatively slow and raises the question of whether the transition between modes is an expression of a covalent modification of the channel protein. For the moment, we can only say that the modulatory process is probably not cyclic AMP-dependent protein phosporylation, since the effect of agonist is quite different than that produced by elevation of cyclic AMP with isoprenaline[25,27] or 8-bromo-cyclic AMP[22]. Unlike Bay K 8644, isoprenaline slows both the activation and inactivation of Ba currents through Ca channels[18,27] but it does not by itself slow significantly the decay of inward tails[18]; it does not induce mode 2 activity, but it modifies the rate constants within mode 1 (refs 21, 22, 25). Isoprenaline-induced increases in the number of functional channels[18] might be accounted for by a recruitment of channels from mode 0 to mode 1.

Like the cardiac cells described here, sensory neurones from chick dorsal root ganglion and neuroblastoma cells show a mixture of modes 0, 1 and 2, and an enhancement of mode 2 behaviour with Bay K 8644 (refs 31, 32). The apparently widespread existence of the gating modes and their positive response to Ca agonist gives new reason to wonder whether dihydropyridines have endogenous counterpart(s) that up- or down-modulate Ca channels (compare ref. 11).

We thank Drs R. W. Aldrich, C. J. Cohen, A. P. Fox, R. A. Janis, Y. Kurachi, M. C. Nowycky, A. Scriabine and B. Sakmann for helpful discussions, and the USPHS and the Miles Institute for support.

Note added in proof: After submission of this manuscript and publication of preliminary communications of this work[14,31], prolonged openings of cardiac Ca channels in the presence of DHP Ca agonists have been reported[35,36].

Received 6 March; accepted 10 July 1984

1. Reuter, H. *Nature* **301**, 569-574 (1983).
2. Tsien, R. W. *A. Rev. Physiol.* **45**, 341-358 (1983).
3. Fleckenstein, A. *Calcium Antagonism in Heart and Smooth Muscle* (Wiley, New York, 1983).
4. Flaim, S. F. & Zelis, R. *Calcium Blockers* (Urban and Schwarzenberg, Baltimore, 1982).
5. Schwartz, A. & Taira, N. (eds) *Circ. Res.* **52** (Suppl., part II), 1-181 (1983).
6. Scriabine, A. (ed.) *Nitrendipine* (Urban and Schwarzenberg, Baltimore, 1984).
7. Curtis, B. M. & Catterall, W. A. *J. biol. Chem.* **258**, 7280-7283 (1983).
8. Venter, J. C. *et al. J. biol. Chem.* **258**, 9344-9348 (1983).
9. Norman, R. I., Borsotto, M., Fosset, M. & Lazdunski, M. *Biochem. biophys. Res. Commun.* **111**, 878-883 (1983).
10. Glossmann, H. & Ferry, D. R. *Naunyn-Schmiedeberg's Arch. Pharmac.* **323**, 279-291 (1983).
11. Schramm, M., Thomas, G., Towart, R. & Franckowiak, G. *Nature* **303**, 535-537 (1983).
12. Truog, A. G. *et al.* in *Calcium in Biological Systems* (eds Rubin, R. P., Weiss, G. B. & Putney, J. W. Jr. (Plenum, New York, 1984).
13. Sanguinetti, M. C. & Kass, R. S. *Biophys. J.* **45**, 394a (1984).
14. Hess, P., Lansman, J. B. & Tsien, R. W. *Biophys. J.* **45**, 394a (1984).
15. Cohen, C. J. & Chung, M. *Biophys. J.* **45**, 394a (1984).
16. Freedman, S. B. & Miller, R. J. *Proc. natn. Acad. Sci., U.S.A.* (in the press).
17. Kao, R. L. *et al. Archs Biochem. Biophys.* **203**, 587-599 (1980).
18. Bean, B. P., Nowycky, M. C. & Tsien, R. W. *Nature* **307**, 371-375 (1984).
19. Lee, K. S., Akaike, N. & Brown, A. M. *J. Neurosci. Meth.* **2**, 51-78 (1980).
20. Hamill, O., Marty, A., Neher, E., Sakmann, B. & Sigworth, F. J. *Pflügers Arch. ges. Physiol.* **391**, 85-100 (1981).
21. Cavalie, A., Ochi, R., Pelzer, D. & Trautwein, W. *Pflügers Arch. ges. Physiol.* **398**, 284-297 (1983).
22. Cachelin, A. B., dePeyer, J. E., Kokubun, S. & Reuter, H. *Nature* **304**, 462-464 (1983).
23. Marban, E. & Tsien, R. W. *Biophys J.* **33**, 143a (1981).
24. Lee, K. S. & Tsien, R. W. *J. Physiol., Lond.* (in the press).
25. Reuter, H., Stevens, C. F., Tsien, R. W. & Yellen, G. *Nature* **297**, 501-504 (1982).
26. Fenwick, E. M., Marty, A. & Neher, E. *J. Physiol., Lond.* **331**, 599-635 (1982).
27. Brum, G., Osterrieder, W. & Trautwein, W. *Pflügers Arch. ges. Physiol.* **401**, 111-118 (1984).
28. Sanguinetti, M. C. & Kass, R. S. *Circ. Rec.* submitted.
29. Himori, N., Ono, H. & Taira, N. *Jap. J. Pharmac.* **26**, 427-435 (1976).
30. Janis, R. A., Sarmiento, J. G., Maurer, S. C., Bolger, G. T. & Triggle, D. J. *J. Pharm. exp. Ther.* (in the press).
31. Fox, A. P., Hess, P., Lansman, J. B., Nowycky, M. C. & Tsien, R. W. *J. Physiol., Lond.* **353**, 75P (1984).
32. Fox, A. P., Nowycky, M. C. & Tsien, R. W. *Soc. Neurosci. Abs.* **10**, 526 (1984).
33. Lee, K. S. & Tsien, R. W. *Nature* **302**, 790-794 (1983).
34. Glossmann, H., Lin, T., Rombusch, M. & Ferry, D. R. *FEBS Lett.* **160**, 226-232 (1983).
35. Ochi, R., Hino, N. & Niimi, Y. *Proc. Jap. Acad. Ser.* B **60**, 153-156 (1984).
36. Kokubun, S. & Reuter, H. *Proc. natn. Acad. Sci. U.S.A.* **81**, 4824-4827 (1984).

LETTERS TO NATURE

Relic interstellar grains in Murchison meteorite

Jongmann Yang & Samuel Epstein

Division of Geological and Planetary Sciences, California Institute of Technology, Pasadena, California 91125, USA

Isotopic analyses of hydrogen, carbon and nitrogen in meteorites provide important information about the origin and history of these elements both in meteorites and in the Solar System. Here we show that, in the Murchison meteorite, the D/H ratios of hydrogen are unusually high in several separates and in one case up to 30 times the cosmic value of 2×10^{-5}. Many phases show high $^{13}C/^{12}C$ ratios, up to 2.5 times the terrestrial value of 0.011. These ^{13}C-rich and D-rich components of the two chemical elements are not correlated. Also they are heterogeneously distributed, suggesting that different components in the meteorite originated from different astrophysical sites and at different times. The D-rich hydrogen in the meteorite is probably due to molecules formed by ion–molecule reactions in interstellar clouds while the tiny amount of ^{13}C-rich carbon is probably due to nucleosynthesis in red giant stars as suggested by Swart *et al.*[1]. Both of these heavy-isotope enriched components survived homogenization in the accumulation and subsequent history of the meteorites.

Following studies of isotopic compositions and concentrations of hydrogen and carbon in acid residues from various types of meteorites, we have shown[2] that: (1) Many primitive carbonaceous and non-carbonaceous meteorites contained HCl–HF insoluble organic matter with high D/H ratios, $>30\times10^{-5}$, suggesting enrichment of deuterium in the molecules by means of isotopic exchange reactions with cosmic hydrogen[3-5] below 150 K. (2) All the meteorites that have been analysed contained inorganic hydrogen which was soluble in HCl–HF solutions. This hydrogen uniformly had a D/H ratio of about 14×10^{-5}, similar to terrestrial hydrogen. This suggests that the D/H ratio in this inorganic component was determined in the solar nebula at a minimum temperature of ~200 K by isotopic exchange reactions between molecules and cosmic hydrogen gas. (3) Three unequilibrated meteorites (Semarkona, Bishunpur and Renazzo) showed another extremely anomalous component of acid soluble organic hydrogen with $D/H \simeq 170\times10^{-5}$, more than 80 times higher than the D/H ratio of cosmic hydrogen. This suggests that meteorites contain organic matter that formed well below 100 K in interstellar clouds before formation of the solar nebula because the temperatures attributed to the solar nebula are much higher than 100 K.

Carbon, on the other hand, showed no obvious ^{13}C anomalies, other than a $\delta^{13}C$ enrichment of about 60‰ due to the presence of carbonates[2,6,7]. δ indicates the variation in isotopic ratios relative to standards in ‰. Standards for hydrogen, carbon and nitrogen are ocean water, PDB and air, respectively. However, a tiny fraction of the carbon, was found to be resistant to various chemical reagents and resistant to combustion below 800 °C. This carbon was a new component in the meteorite and its $^{13}C/^{12}C$ ratio was greater than all carbon previously found on the Earth and in the meteorites[1,8,9]. This carbon has a $^{13}C/^{12}C$ ratio of at least twice that of the Earth.

The aim of the present study was to determine how the new ^{13}C-rich carbon might relate in origin to the D-rich hydrogen and to the $^{15}N/^{14}N$ ratio of nitrogen. Murchison meteorite was powdered and aliquots of the samples were demineralized by reaction with HCl–HF solutions. The resulting residue, designated CF, was then treated with various chemicals to remove certain components of the residue and separated by particle size (see Table 1) to try to concentrate the exotic mineral phases and the interstellar relic grains. Gas samples of hydrogen, carbon and nitrogen were analysed by standard stable isotope ratio mass spectrometric techniques and reported in the usual δ notations.

Concentrations and isotopic data of hydrogen, carbon and nitrogen are given in Table 1. For the bulk sample the hydrogen is dominated by hydrogen from inorganic sources whose δD value is about −50‰. The $\delta^{13}C$ value of the total carbon is about −2.4‰ but the presence of heavier carbon is apparent from the CO_2 given off at the combustion above 500 °C ($\delta^{13}C=27‰$). The D/H data of the CF residue show that all inorganic hydrogen is removed by HCl–HF acid and a deuterium-rich organic material dominates the residue (Fig. 1*a*).

Two residue samples (CFOc, CFOf) resulting from the oxidation of CF residue by reagent H_2O_2 contain an unusually high $^{13}C/^{12}C$ ratio carbon which is oxidized to CO_2 above 800 °C. The $\delta^{13}C$ ranges between 500 and 1,200‰. In principle, such high $\delta^{13}C$ values can be produced by isotope exchange reactions at very low temperatures[10] that exist in the interstellar media. In such circumstances, one might expect that there would be a much greater heterogeneity in the $\delta^{13}C$ values in the organic residues and that a much larger fraction of the organic acid residue would be relatively enriched in ^{13}C. Therefore, it is the tiny amount of ^{13}C-rich component that makes it a good candidate for a red giant origin. On the other hand, large fractions of the organic residues have high δD values. As we have argued previously, such δD values for a large fraction of the organic residues could only be obtained by ion–molecule reactions occuring in the interstellar medium.

The finer grain fraction (CFOf) has a hydrogen and carbon content per gram of bulk meteorite a factor of 10 times higher than the coarser grain fraction (CFOc). Compared with CFOc, CFOf has a higher C/H ratio of 2.76 and a higher $^{13}C/^{12}C$ ratio of up to 0.025 but a lower D/H ratio by a factor of two. Perhaps

Table 1 The concentrations and isotopic compositions of hydrogen, carbon and nitrogen released by stepwise oxidation–pyrolysis of bulk and various acid residues of Murchison meteorite

	T†	H_2		CO_2		N_2		
Sample*	(°C)	(μmol g^{-1}‡)	δD	(μmol g^{-1}‡)	$\delta^{13}C$	(μmol g^{-1}†)	$\delta^{15}N$	C/H§
Bulk	300	1,738	−48	310	1.6			0.089
51.9 mg	350	454	−47	250	−3.9			0.28
	500	820	−51	840	−7.9			0.51
	900	217	−80	120	27.0			0.29
	1,100	~20	−48	~1	27.6			—
	Total	3,250	−51	1,530	−2.4			0.23
CF	300	47.9	463	42	−3.9			0.44
4.79%	350	10.0	562	68	−10.4			3.39
20.5 mg	500	1.5	607	129	−20.7			42
	800	<0.1	—	7.3	−8.3			>38
	1,100	<0.1	—	~0.5	~22			—
	Total	59.4	483	246	−14.5			2.07
CFOc	(250)	1.49	1,042	0.71	−9.5			0.24
0.39%	(300)	0.73	1,104	0.33				0.22
20.1 mg	(350)	0.74	1,708	0.65	−11.9			0.44
	700	5.97	2,584	33.5	−6.5	0.23	−13.2	2.81
	800	0.49	2,213	0.23	176	<0.02	—	0.22
	900	~0.09	~2,853	0.11	508			0.47
	1,100	~0.04	—	0.77	184			~6.1
	Total	9.56	2,144	36.3	0.2			1.90
CFOf	(250)	16.7	268	11.2	−19.2			0.34
1.18%	(300)	6.0	—	5.0	−19.3			0.42
35.1 mg	(350)	6.9	791	6.2	−20.9			0.45
	350	19.5	992	17	−20.9			0.43
	500	28.2	1,008	76	−21.9			1.35
	700	12.6	888	98	−22.0			3.90
	800	7.9	823	71	−22.0	1.5	−20.8	4.51
	900	4.1	826	68	−22.6	1.2	−28.7	8.24
	800	1.9	930	221	−21.9	1.3	−21.6	58
	900	0.09	1,111	0.04	~703	<0.02	—	~0.2
	1,100	<0.006	—	0.05	~1,220	<0.02	—	—
	Total	104	806	574	−21.7			2.76
CFOfN(I)	(250)	0.56	−45	0.65	−23.6	<0.01	—	0.58
0.12%	(350)	0.26	41	0.73	−24.1	<0.01	—	1.38
7.2 mg	500	3.25	309	46.2	−30.6	0.19	−170	7.12
	700	0.18	158	3.9	22.6	0.02	33.5	10.7
	800	<0.01	~600	0.09	985	<0.01	—	—
	1,100	<0.01	~700	0.05	~1,480	<0.01	—	—
	Total	4.25	240	51.6	−23.2			6.03
CFOfN(II)	(350)	0.51	−158	1.02	−25.9	<0.06	—	1.0
0.12% 0.6 mg	700	1.31	57	42.7	−22.7	0.23	—	16
CFOfNf	(350)	3.5	124	5.4	−25.1	<0.01	—	0.78
~0.17%	500	5.1	158	44.0	−25.0	0.17	6.7	4.36
5.0 mg	700	2.3	34	0.43	−20.6	<0.01	—	0.095
	800	<0.1	—	0.04	−24.5	<0.01	—	—
	1,100	<0.1	—	0.03	−25.5	<0.01	—	—
	Total	10.8	121	49.9	−25.0			2.31
CFP	(350)	0.10	23	0.09	—	<0.01	—	0.45
0.24%	500	0.24	214	6.72	−36.7	<0.01	—	14
11.0 mg	700	<0.1	—	1.79	−28.6	<0.01	—	—
	1,100	<0.1	—	0.16	977	<0.01	—	—
	Total	0.34	158	8.76	−16.3			13
P	(350)	150	−81	49	−28.4	0.7	—	0.16
34.3%	500	210	−79	20	−36.4	<0.1	—	0.049
129.8 mg	800	68	−101	0.40	81	0.14	—	0.003
	1,100	13	−117	~0.35	~573	0.1	—	0.013
	Total	440	−84	70	−27.1			0.080
PCF	(350)	0.44	~144	0.51	−22.6	<0.05	—	0.58
2.66%	700	<0.02	—	4.39	−31.7	~0.03	—	>60
8.2 mg	1,100	<0.02	>300	~0.22	~705	~0.03	—	—
	Total	0.44	~144	5.12	~1.1			5.8
CFS	300	101	691	99	−7.1			0.49
2.2%	800	76	785	450	−17.0			2.94
5.6 mg	900	4.8	659	0.44	320			0.05
	1,100	2.7	~594	~0.09	~630			—
	Total	185	728	550	−14.8			11.48

Eight acid treated residues (from CF to PCF) were prepared from aliquots of Murchison bulk powder. The procedures were basically similar to previous studies[2,12]. An aliquot of HCl–HF treated residue (CF) which contains sulphides, spinel, chromite and organic polymer was further treated with acetone, hexanes, CS_2, benzene, methanol, 6M NaOH and 30% H_2O_2. This residue, CFO, was separated into a very fine-grained colloidal phase in an H_2O solution (CFOf) and into a coarse-grained residue (CFOc). CFOf was black, its density was 1.25 and it contained the organic polymer, sulphides and spinel. Residue CFOc was grey and contained spinel, chromite and organic polymer. An aliquot of CFOf was treated with boiling NaOH–NaOCl and fuming HNO_3. Two new residues were produced. One (CFOfN) contained organic polymer, chromite and spinel settled out on centrifugation, and the other (CFOfNf) remained dispersed in the solution of HCl-acetone but was recovered by evaporation to dryness. It contained organic polymer, sulphides and spinel. An aliquot of CF was boiled in $HClO_4$ producing a residue, CFP which was white and contained spinel and chromite. To examine the chemical resistivity of trace quantities of ^{13}C-rich carbon present in Murchison, an aliquot of bulk Murchison was dissolved with boiling 70% $HClO_4$ producing a residue, *P* which was white and contained silicates and spinel. An aliquot of this residue *P* was further treated with HCl–HF. This residue PCF contained spinel and silicates. Residue CFS[2] which contained organic polymer, chromite, sulphides and spinel was prepared treating bulk Murchison with HCl–HF solution and with CS_2.

* Acid residues: C, HCl; F, HF; O, H_2O_2; N, HNO_3,; P, $HClO_4$; S, CS_2; f, finer grain fraction; c, coarser grain fraction. Weight percentage of the acid residue and amount of sample used for the analysis are also shown.

† Samples were heated in a quartz vacuum system for 1 h at each temperature in an oxygen atmosphere of ~5 mmHg except the underlined steps where the samples were heated for 4–18 h. *T* in parentheses represents the step where pyrolysis was made in the absence of oxygen. The pyrolyses steps were to analyse separately the terrestrial contamination.

‡ Yields are given in μmol g^{-1} of bulk Murchison.

§ Very low C/H ratios are mainly due to dominance of inorganic hydrogen and very high C/H ratios are due to carbon accumulated at lower temperature steps. Thus each C/H ratio at each *T* step should not be interpreted as a characteristic average C/H ratio of the organic matter decomposed at that temperature.

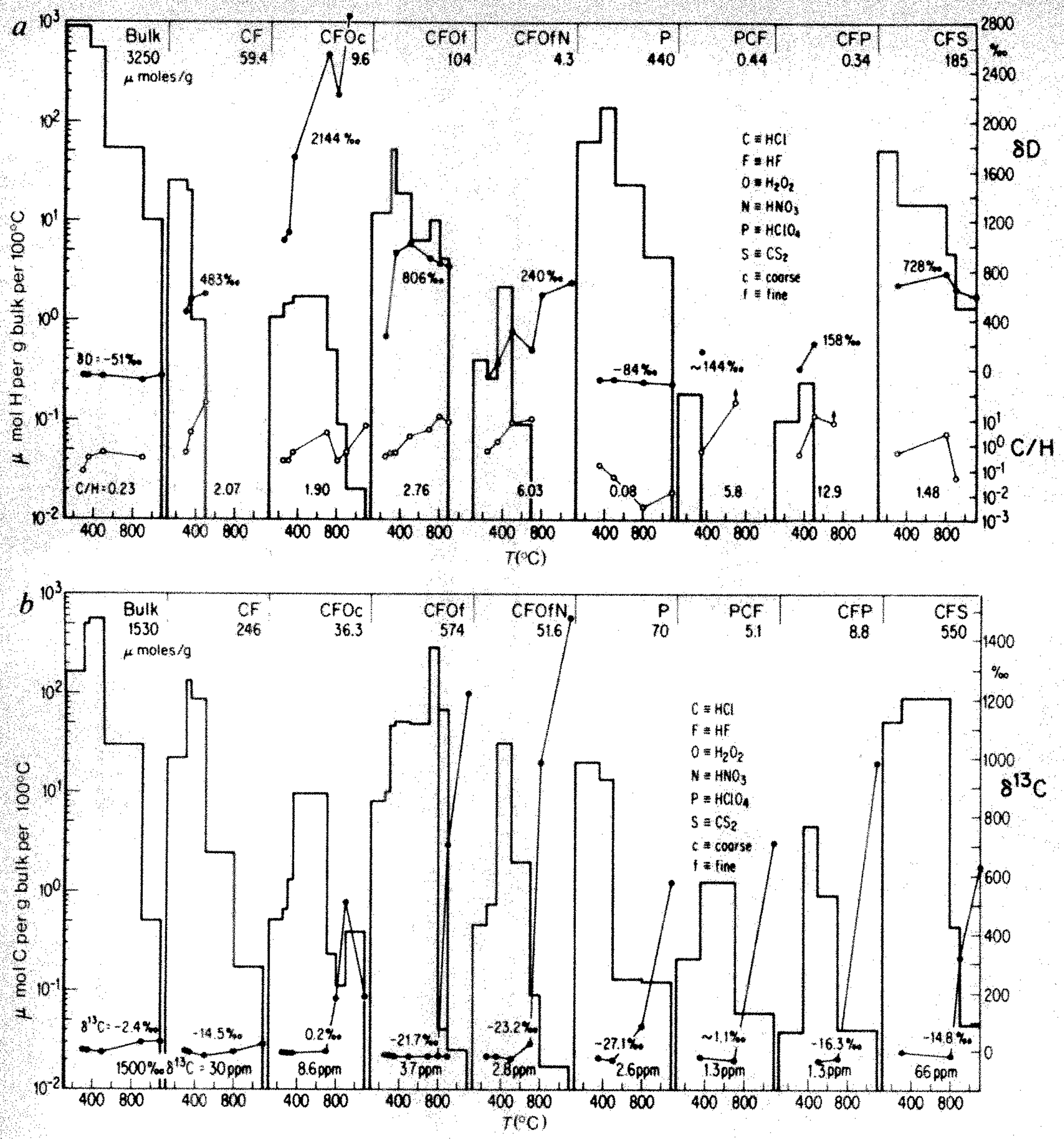

Fig. 1 *a*, A histogram showing the amount of hydrogen released by stepwise oxidations (pyrolysis for lower temperature steps up to 350 °C) of Murchison bulk and acid treated residue samples plotted against the releasing temperature. δD values (●) and C/H ratios (○) of the released gases are also shown. A sample (CFOc) which is composed primarily of spinel and chromite shows the highest δD values of 1,040–2,850‰. Perchloric acid treated samples (P, PCF, CFP) show much lower δD values. Also included are: values for the total H_2 (in μmol g^{-1}), its δD value and the C/H ratio of the total gases. *b*, The carbon released simultaneously with the hydrogen. The concentration of the total carbon, the $\delta^{13}C$ value of the total carbon and the amount of carbon which has $\delta^{13}C$ value of 1,500‰ in units of μg C per g of bulk sample are given.

this means that the CFOc residue, 60% of which is spinel, contains a larger fraction of the preserved interstellar organic matter. The CFOf residue, 70% of which is organic polymer, perhaps contains relatively more of the organic matter formed in the solar nebula at higher temperatures and thus has a lower D/H ratio. Note that HCl–HF residues of many meteorites that we previously examined[2] also contained large amounts of spinel and chromite.

A residue sample (CFOfN) formed by treating CFOf with boiling NaOH–NaOCl solution and fuming HNO_3 shows extremely high $\delta^{13}C$, up to ~1,480‰, and a C/H ratio of 6.0 (Table 1). If it can be assumed that the total carbon in each residue is composed of two carbon sources with nominal $\delta^{13}C$ values of 1,500‰ and −30‰, then residues CF, CFOc, CFOf and CFOfN contain respectively 30, 9, 37 and 3 p.p.m. of the isotopically-heavy carbon component (Fig. 1*b*).

The concentration and $\delta^{15}N$ of nitrogen was also measured for residue samples (Table 1). In the case of the CFOfN sample, most of the nitrogen was released at the 500 °C combustion temperature and the $\delta^{15}N$ value for this N_2 was −170‰, lower than for any other fraction. Our data for total nitrogen (0.21 μmol g^{-1}, $\delta^{15}N = -151‰$) for this sample checks well with the value of Lewis *et al.*[11] (0.16μmol g^{-1}, $\delta^{15}N = -205‰$). There is no correlation between this light nitrogen and isotopically-heavy carbon. Lewis *et al.* came to the same conclusion from their study of acid residues from Allende and Murchison meteorites. They suggested that light nitrogen was produced by neucleosynthesis which is responsible for CCF–xenon. We now suggest an alternative explanation for the −170‰ nitrogen. There seems to be some relationship between the δD and $\delta^{15}N$ in our residues. Thus, the isotopic composition of the nitrogen and the deuterium may be attributable to ion–molecule reactions in the interstellar medium.

Another technique was used to try to isolate the ^{13}C-rich carbon in the residues. The CF residue was boiled in 70% $HClO_4$ and labelled as CFP. The CFP sample contained a concentration of 0.16 μmol g^{-1} of carbon whose $\delta^{13}C$ is 977‰. These are comparable with that observed for residues CFOf and CFOfN (Table 1). However, the CFP residue contained much less total hydrogen and total carbon and almost no nitrogen compared with residues CFOf and CFOfN. Thus perchloric acid is very effective in removing most of organic material but not the very heavy carbon. We, therefore, conclude that the ~1,500‰ $\delta^{13}C$ carbon is not associated with hydrogen and nitrogen. It is quite possible that this small carbon fraction is in a carbide form such as Fe_3C and SiC, or is present as some high-temperature carbon grain such as diamond. Also this result suggests that the low ^{15}N nitrogen and the ^{13}C-rich carbon do not come from the same source.

The perchloric treatment was repeated on an aliquot of Murchison bulk sample. This procedure destroyed 95% of the carbon but the remaining residue (P) contained a heavy carbon component whose $\delta^{13}C$ is ~570‰. This sample, however, contains a large amount of inorganic hydrogen with a characteristic δD value of −80‰, confirming that the hydrogen in this sample is dominantly inorganic. The perchloric acid treatments (P, PCF,

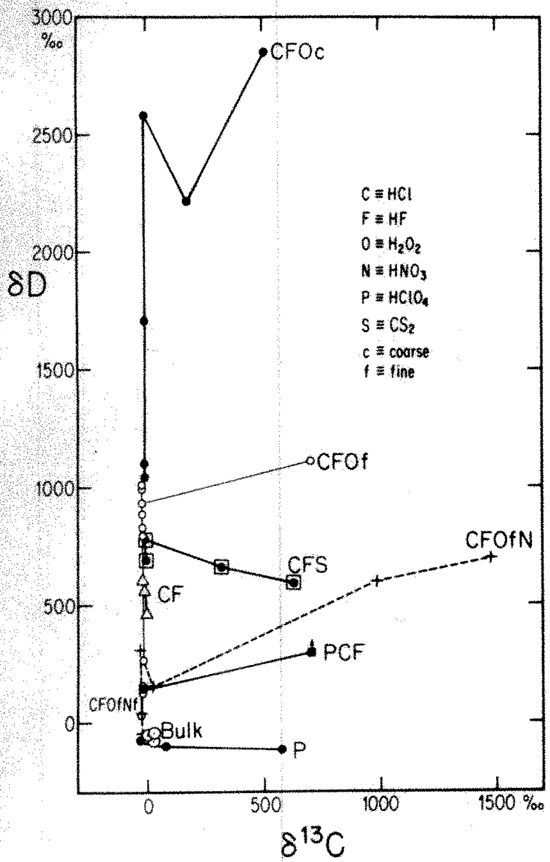

Fig. 2 A plot of the δD against the $\delta^{13}C$ of hydrogen and carbon released by oxidation of Murchison samples. Carbon with high $\delta^{13}C$, up to 1,480‰, was found in the CFOfN residue. This residue consists mostly of carbon with some chromite, spinel and sulphides. There is no clear correlation between the high δD hydrogen and the high $\delta^{13}C$ carbon in the various release patterns and in the various residues, suggesting that they are located in different minerals or different grains. Note that all samples except bulk, CF and CFOfNf have a high $\delta^{13}C$ component which is released on oxidation at high temperatures. The carbon with high $\delta^{13}C$ values compared with the total carbon is preferentially resistant to all chemicals we have used.

CFP) show that the ^{13}C-rich carbon comes from a different source to the deuterium.

We have compared the $\delta^{13}C$ values with δD values of coexisting carbon and hydrogen extracted from various components. This is shown in Fig. 2. The most striking feature of this plot is that the $\delta^{13}C$ values initially recorded up to temperatures of 800 °C are on average about −20‰ whereas the δD values of the hydrogen cover an enormous range of −80 to +2,600‰. On the other hand, at the higher temperature range of extraction of the carbon where $\delta^{13}C$ values range up to 1,500‰, the accompanying hydrogen has relatively smaller up and down variations in δD values. It is difficult to assign a common chemical origin of the meteorite to the D-rich hydrogen and the ^{13}C-rich carbon. The previously mentioned perchloric acid experiments suggested a similar conclusion.

Our experimental procedures will probably add contaminents of low values of δD and $\delta^{13}C$. Consequently, our high $\delta^{13}C$ and δD values are probably minimum values and we hope that procedures will eventually be perfected to allow measurement of the pristine δD and $\delta^{13}C$ values. In the case of hydrogen, the higher the δD values for the extracted hydrogen, the more confident we can become about the proposal that the organic matter and its isotopic composition originated from an interstellar medium due to ion-molecule hydrogen isotopic exchange reactions.

Thus, unusually high $\delta^{13}C$ carbon can be isolated by treating the Murchison meteorite with certain reagents due to the preferential destruction of the ^{12}C-rich components. The fine-grained acid residue (CFOf) contains the highest concentration of the ^{13}C-rich carbon. The ^{13}C-rich component has special chemical properties which will allow its isolation and identification.

The δD of hydrogen does not correlate with the $\delta^{13}C$ of carbon. The coarse-grained acid residue (CFOc) contains hydrogen of the highest D/H ratio while the $\delta^{13}C$ enrichment is relatively modest. The acid residue (CFOfN) which contains the highest ^{13}C-rich component has only modest D enrichment. If the D-rich component is formed by ion-molecule isotope exchange reactions in the interstellar dust clouds, the ^{13}C-rich component is not associated with the deuterium enrichment. This adds credibility to the suggestion by Swart *et al.*[1] regarding the red giant origin of the ^{13}C-rich component in the meteorite.

The fact that the ^{13}C-rich component survived the post accumulation history of Murchison without losing its high ^{13}C value supports our previous assertion[2] that the $\delta^{13}C$ of the major part of the organic carbon in the meteorite is representative of the carbon in the interstellar medium. In addition, the presolar origin of the ^{13}C-rich component in the acid residues of the meteorites agrees with the suggestion that the high D/H ratios observed in the organic matter in the meteorites were due to the preservation of the presolar material. After the D-rich organic matter was incorporated into the meteorite the post-accumulation history for the organic matter should have been sufficiently mild to allow its preservation and its availability for our examination.

We thank Dr I. R. Kaplan for nitrogen analyses, J. Ruth for technical assistance, and Dr E. Olson for a specimen of Murchison meteorite. This research was funded by NASA (NGL-05-002-190) and by NSF (EAR-7816873).

Received 16 May; accepted 24 July 1984.

1. Swart, P. K., Grady, M. M., Pillinger, C. T., Lewis, R. S. & Anders, E. *Science* **220**, 406–410 (1983).
2. Yang, J. & Epstein, S. *Geochim. cosmochim. Acta* **47**, 2199–2216 (1983).
3. Watson, W. D. *Rev. Mod. Phys.* **48**, 513–552 (1976).
4. Geiss, J. & Reeves, H. R. *Astr. Astrophys. J.* **93**, 189–199 (1981).
5. Robert, F. & Epstein, S. *Geochim. cosmochim. Acta* **46**, 81–95 (1982).
6. Clayton, R. N. *Science* **140**, 192–193 (1963).
7. Smith, J. W. & Kaplan, I. R. *Science* **167**, 1367–1370 (1970).
8. Kerridge, J. F. *Lunar planet. Sci. Conf.* **13**, 381–382 (1982).
9. Yang, J. and Epstein, S. *Meteoritics* **18**, 429–430 (1983).
10. Langer, W. D., Graedel, T. E., Frerking, M. A. & Armentrout, P. B. *Astrophys. J.* **277**, 581–604 (1984).
11. Lewis, R. S., Anders, E., Wright, I. P., Norris, S. J. & Pillinger, C. T. *Nature* **305**, 767–771 (1983).
12. Alaerts, L., Lewis, R. S. & Anders, E. *Geochim. cosmochim. Acta* **43**, 1399–1415 (1979).

Improved positive-ion composition measurements in the upper troposphere and lower stratosphere and the detection of acetone

G. Hauck & F. Arnold

Max-Planck-Institut für Kernphysik, PO Box 103 980,
D-6900 Heidelberg, FRG

Atmospheric ion composition measurements were recently extended downwards to the lower stratosphere and upper troposphere following development of a new aircraft-borne mass spectrometer technique. Perhaps the most interesting aspect of these measurements is that they can serve as a powerful tool for neutral trace gas detection in passive chemical ionisation mass spectrometry (PACIMS). However, the measurements, in particular those of positive ions, suffer from a poor mass resolution which complicates ion identification and the PACIMS application. Here we report improved positive-ion composition measurements in the lower stratosphere and upper troposphere, using an improved aircraft-borne mass spectrometer with higher mass resolution and sensitivity than hitherto achieved.

The experimental method is essentially similar to one used for our previous measurements[1,2], but with four modifications:

Table 1 Positive ion masses obtained from high-resolution spectra taken in flights F4 and F5 at 11,280 m altitude

Mass	Ion
28 ± 1	HCO^+
	H^+HCN
32 ± 1	H^+CH_3OH
37 ± 1	$H^+(H_2O)_2$
50 ± 1	$H^+CH_3OH \cdot H_2O$
55 ± 1	$H^+(H_2O)_3$
59 ± 1	$H^+(CH_3)_2CO$
64 ± 1	$H^+CH_3COH \cdot H_2O$
	$H^+C_2H_5OH \cdot H_2O$
	$H^+CH_3OCH_3 \cdot H_2O$
	$H^+HCOOH \cdot H_2O$
73 ± 1	$H^+(H_2O)_4$
77 ± 1	$H^+(CH_3)_2CO \cdot H_2O$
88 ± 1	$H^+CH_3OH(H_2O)_2$
114 ± 1	$H^+(CH_3)_2CO(H_2O)_3$
126 ± 1	$H^+(H_2O)_7$

Tentative ion identifications are also given. Instead of H_2O, ions may contain an ammonia molecule although this seems to be less likely.

(1) a larger quadrupole mass spectrometer (rod diameter, 0.8 cm; rod length, 20 cm) providing higher mass resolution and ion transmission; (2) on-axis ion sampling providing a higher sampling efficiency; (3) an ion-dissociation mode allowing for fragment ion studies; (4) a high-frequency glow discharge ion source working at ambient gas pressure and allowing for in-flight calibration and testing.

The modified instrument will be described in detail elsewhere together with laboratory simulation studies; here the ion-dissociation mode will be briefly discussed. After passing through the mass spectrometer inlet hole (diameter, 0.01 cm), located at the tip of a conically-shaped sampling electrode onto which the incoming gas stream is directed, atmospheric ions are electrically extracted from the high-density gas jet forming behind the inlet hole. During extraction they undergo energetic collisions with gas molecules stimulated by the electric field established between the four-pole rods and the sampling cone. As a result, efficient collisional breakup of the ambient cluster ions occurs and thus only fragments, naked- or weakly-clustered 'cores', of the ambient complex cluster ions are ultimately mass analysed and detected.

Typically, the sampling cone is kept at ground potential and the four-pole field axis is several tens of volts, depending on mass resolution. This ion dissociation mode offers two advantages, a larger sentitivity and a better 'core ion' identification. Upper tropospheric positive ions are expected[2] to be heavily hydrated (~6–7 H_2O-ligands) and, therefore, very massive. Fragmentation leads to much smaller ions, which are more successfully transmitted through the four-pole rods (particularly at high mass resolution) and easier to identify.

A few important characteristics of the new instruments are: mass range, 0–1,000 AMU; smallest mass peak width at half peak amplitude $\Delta m = 1$ AMU; sensitivity, ~0.1 ion counts per ion cm^{-3} (depending on mass resolution).

The new instrument has been flown twice (flights F4 and F5) on board a twin jet research aircraft (type FALCON 20) of the DFVLR (Deutsche Forschungs- und Versuchsanstalt für Luft- und Raumfahrt) over the FRG. The flights took place during daytime on 25 November 1983 (F4) and 24 February 1984 (F5). Maximum altitudes of 11,280 m were reached in both flights while the local tropopause heights were 11,900 m (F4) and 9,750–10,036 m (F5). High mass-resolution positive-ion data were obtained only at the float height (11,280 m) where sufficiently long integration times were available and they thus relate to the uppermost part of the troposhere (F4) and the lowermost part of the stratosphere (F5). Lower mass-resolution data obtained in the height region down to 5,300 m will not be discussed here.

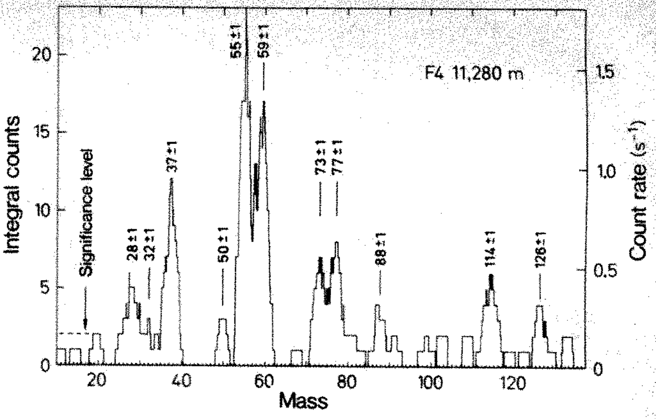

Fig. 1 Positive ion mass spectrum as obtained in flight F4 at 11,280 m altitude. A 2σ significance level is indicated. Total integration time, 640 s.

A typical positive-ion mass spectrum ($\Delta m = 3$ AMU) as measured in F4 at 11,280 m is shown in Fig. 1. As confirmed by the larger mass range, but lower mass-resolution studies, made in F4 at the same height, all major positive ion peaks fall into the mass range shown by the spectrum. Among these, 55 ± 1 and 59 ± 1 are most prominent peaks followed by 37 ± 1, 73 ± 1, and 77 ± 1. A compilation is given in Table 1 along with tentative ion identification. The ions 37 ± 1, 55 ± 1, and 73 ± 1 may readily be identified as proton hydrates ($H^+(H_2O)_n$; $n = 2, 3, 4$) which were previously found in the stratosphere[3–5] and which are expected[6,7] to form quickly at the tropopause from primary positive ions produced by galactic cosmic-ray ionization. In view of the mass uncertainty of ±1 AMU, which is mainly due to poor ion counting statistics, it is also possible that the core ion is NH_4^+ instead of H_2O.

The size distribution of the observed $H_3O^+(H_2O)_n$ or $NH_4^+(H_2O)_n$ clusters peaks at n equal to 2 which is quite different from the distribution of ambient $H_3O^+(H_2O)_n$ ions[2] which should peak at around n equal to 6 and 7. Thus, there is clear evidence for massive electric field-induced dissociation which greatly facilitates the identification of other observed ions.

To improve mass identification of the most prominent peaks observed in F4 (55 ± 1 and 59 ± 1), a much higher mass resolution ($\Delta m = 1$ AMU) was used in F5. However, most of the mass range had to be sacrificed for the high-resolution study to gain integration time for the mass range of interest (50–71 AMU), and thereby to offset the lower sensitivity associated with higher resolution. The portion of the spectrum scanned in the high-resolution mode ($\Delta m = 1$ AMU) of F5 is shown in Fig. 2 along with a lower resolution ($\Delta m = 3$ AMU) spectrum of the same flight. Surprisingly, the spectrum is quite different from that shown in Fig. 1 with 55 ± 1 being virtually absent. However, peak 59 is present, and its mass can be unambiguously identified. The large mass range, low-resolution studies made in F5 reveal that peak 59 is the most prominent one in the entire mass range, and that only minor peaks of other ions are present.

To identify ion 59, the following arguments should be considered: (1) the ion seems to be an unhydrated 'core ion' as no fragment having a mass of 41 is observed; (2) the hydrate of 59 seems to have a stability which is similar to the stability of $H_3O^+(H_2O)_3$ or $NH_4^+(H_2O)_3$ as suggested by the similarity of the ratios 77 ± 1/59 and 73 ± 1/55 ± 1; (3) ion 59 is probably a fragment of ions formed by the reaction of $H_3O^+(H_2O)_n$ with an atmospheric trace gas which possesses a proton affinity sufficiently larger than that of H_2O (165.3 kcal mol^{-1})[8].

If correct, the first argument immediately suggests protonated acetone $H^+(CH_3)_2CO$ which is rather stable due to the large proton affinity of acetone (193.8 kcal mol^{-1})[8]. Unfortunately, the bond energy of $H^+(CH_3)_2CO \cdot H_2O$ is not known and, therefore, the second argument cannot be checked. However, bond

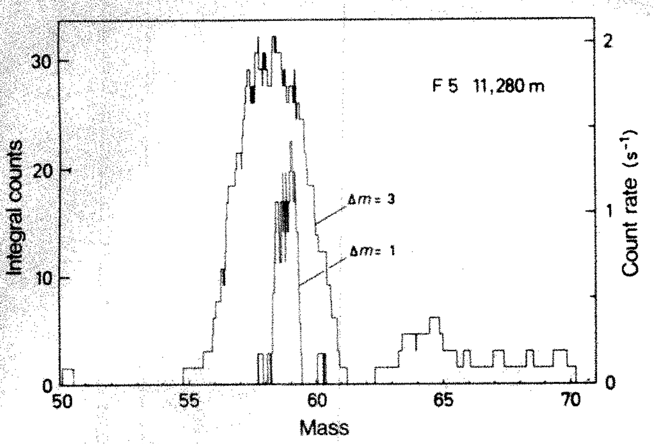

Fig. 2 Portions of positive ion mass spectra with different peak widths at half-peak amplitude, Δm, of 3 and 1 AMU obtained during flight F5 and 11,280 m altitude. Total integration times, 100 and 410 s.

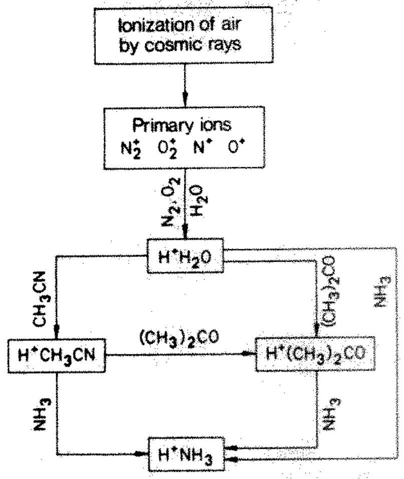

Fig. 3 Simplified reaction scheme for major positive core ions in the upper troposphere and lower stratosphere.

energies for hydrates of large core ions similar to $CH_3CH_2CO^+$ have been measured in the laboratory[8] and were found to be around 17 kcal mol^{-1} which is, in fact, the same bond energy as $H_3O^+(H_2O)_3$ (ref. 8).

High-pressure flow reactor studies, recently carried out at our laboratory, have revealed that at an ambient pressure of 200 mbar (corresponding to an altitude of around 11.000 m), $H^+(CH_3)_2CO(H_2O)_n$ clusters are severely dissociated with $H^+(CH_3)_2CO$ being the most prominent fragment ion. It was also found that the fragmentation behaviour was similar to that of $NH_4^+(H_2O)_n$ clusters, which are less strongly bonded than $H_3^+O(H_2O)_n$ clusters (the bond energy for $NH_4^+H_2O$ is only 17.2 kcal mol^{-1})[8].

Thus, protonated acetone seems the most likely identification of peak 59. The strongest argument, however, comes from CIMS measurements[9], also made on flight F5, which reveal the presence of substantial amounts of acetone vapour at 11,280 m (acetone volume mixing ratio, 100 parts per 10^{12}, p.p.t.). Considering the latter acetone abundance one would expect acetone containing clusters to be the most dominant ions, which was in fact the case in F5. From a comparison of the CIMS-and the present ambient ion measurements we can conclude that the $H^+(CH_3)_2CO$ ions are not due to acetone contamination[9].

If peak 59 was protonated acetone, it seems likely that observed ion families, other than $H_3O^+(H_2O)_n$, are also represented primarily by their naked cores ($n = 0$). This is to be expected since such ions, including NH_4^+ usually have much smaller hydration energies compared with H_3O^+. Thus 55 ± 1 is probably $H_3O^+(H_2O)_2$ and not $NH_4^+(H_2O)_2$.

Of the other observed ions (Fig. 1), 33 ± 1 may be identified as protonated methanol or formaldehyde with 50 ± 1 possibly being its hydrate. The ion 28 ± 1 may be attributed to HCO^+ which could be a fragment of protonated acetone[9]. Tentative identifications for the remaining minor peaks are included in Table 1 and will not be further discussed here. Positive ions with masses 29, 31 and 33 are also present in the CIMS spectra of F5 (ref. 9).

From the above, it seems that much more acetone vapour must have been present at 11,300 m in F5 compared with F4. Considering a typical rate coefficient of 2×10^{-9} cm^3 s^{-1} for reaction of acetone with $H_3O^+(H_2O)_n$ clusters, and an ion–ion recombination lifetime of 130 s acetone abundances of about 1 p.p.t.v. (F4) and ≥ 20 p.p.t.v. (F5) have been estimated[1,2]. However, if the ions 37 ± 1, 55 ± 1 and 73 ± 1 (F4) were not $H_3O^+(H_2O)_n$, but $NH_4^+(H_2O)_n$ clusters, the above steady-state treatment would not apply.

Acetone vapour measurements at ground level (typically 500 p.p.t.v.) have recently been reported by Penkett[10] using a GC–MS technique. Destruction of acetone (S. Penkett, personal communication) by OH-reaction (lifetime ~1,300 h) and photolysis (lifetime of ~500 h), although being sufficiently slow, allow efficient vertical mixing of acetone. However, heterogeneous removal may also operate in the troposphere and, unfortunately, very little is known about this potential acetone sink. Sources of acetone seem to be photo-oxidation of C_3H_8 or higher aliphatic hydrocarbons[10,11], preferably through OH-reaction.

Finally, we consider an implication of the present data for lower stratospheric ammonia abundances. If peak 59 is, in fact, protonated acetone, the ammonia abundances at 11,280 m must have been very low for both F4 and F5. This is because $H^+(CH_3)_2CO(H_2O)_n$ clusters should react efficiently with ammonia. Using a steady-state treatment analogous to the one discussed above, the upper limits to the ammonia abundance at 11,280 m are estimated to be ~1 p.p.t.v. (F4) and ~0.05 p.p.t.v. (F5).

From the preceding discussion, a simplified picture of the ambient positive-ion chemistry emerges (Fig. 3). Primary ions formed by cosmic ray ionization of air are quickly converted to H^+H_2O 'core' ions which are strongly hydrated (~6–7 H_2O ligands). Reactions of H^+H_2O 'cores' with the large proton-affinity trace gases acetonitrile and acetone which are almost equal around the tropopause[9], lead to corresponding H^+CH_3CN and $H^+(CH_3)_2CO$ 'cores'. Incorporation of these molecules into the clusters may also lead to mixed clusters. At lower heights, ammonia vapour[12,13] becomes abundant enough to convert most of the $H^+(CH_3)_2CO$ 'cores' to H^+NH_3. Above the tropopause, acetone seems to decrease more rapidly than acetonitrile and ultimately has such a low abundance in the middle stratosphere that H^+CH_3CN conversion becomes inefficient, as suggested by the observed[4] dominance of H^+CH_3CN cores around 25-km altitude. At even higher altitudes (upper stratosphere), the acetonitrile abundance becomes low enough to prevent efficient transformation of H^+H_2O cores. It is not known at which heights the transitions from dominant H^+NH_3 to $H^+(CH_3)_2CO$ and from $H^+(CH_3)_2CO$ to H^+CH_3CN cores occur.

Future ion composition measurements should be extended downwards in altitude to search for clusters containing H^+NH_3 and other cores with large proton-affinity molecules. Thus *in situ* ion composition measurements may also become a powerful tool for tropospheric trace-gas detection.

We thank E. E. Ferguson, P. Crutzen, D. Ehhalt and D. Griffith for helpful discussions, the technical staff of the MPI-K, particularly K. Oberfrank and the Flugbereitschaft of the DFVLR for assistance. This project was funded by the Bundesministerium für Forschung und Technologie through GSF.

Received 8 May; accepted 9 July 1984.

1. Heitmann, H. & Arnold, F. *Nature* **306**, 747–751 (1983).
2. Arnold, F., Heitmann, H. & Oberfrank, K. *Planet Space Sci.* (in the press).
3. Arnold, F. & Henschen, G. *Nature* **275**, 521–522 (1978).
4. Henschen, G. & Arnold, F. *Geophys. Res. Lett.* **8**, 999 (1981).
5. Arijs, E., Ingels, J. & Nevejans, D. *Nature* **271**, 642–644 (1978).
6. Ferguson, E. & Arnold, F. *Accts. chem. Res.* **14**, 327 (1981).

7. Arnold, F. in *Atmospheric Chemistry*, (ed. Goldberg, E. D.) (Springer, Heidelberg, 1982).
8. Kebarle, P. *A. Rev. Phys. Chem.* **445**, (1977).
9. Arnold, F., Oberfrank, K. & Hauck, G. *Planet. Space Sci.* (submitted).
10. Penkett, S. in *Atmospheric Chemistry* (ed Goldberg, E. D.) (Springer, Heidelberg, 1982).
11. Niki, H. in *Atmospheric Chmistry*, (ed. Goldberg, E. D.) (Springer, Heidelberg, 1982).
12. Georgii, H. W. & Müller, W. J. *Tellus* **16**, 1–2 (1974).
13. Georgii, H. W. & Lenhard, U. *Pageophysics* **116**, (1978).

Microdomains observed at the ferroelectric/paraelectric phase transition of barium titanate

L. A. Bursill & Peng Ju Lin

School of Physics, University of Melbourne, Parkville, 3052,
Victoria, Australia

The physical properties of barium titanate have been thoroughly studied because of fundamental interest in its singular ferroelectric properties and the wide variety of applications[1]. Inelastic neutron and X-ray diffraction studies suggest that the atomic mechanism for the phase transition from the paraelectric (cubic) to ferroelectric (tetragonal) phases lies somewhere between the extremes of 'displacive' and 'order–disorder' models[1,2]. Analysis of the 'central-peak' phenomena[2,3] has led to microdomain models, while molecular dynamic computer studies for ferrodistortive and antiferrodistortive phase transitions predict travelling clusters of locally-ordered regions, with slowing-down and increasing cluster size close to the critical temperature[4]. Direct evidence for the occurrence of microdomains has been obtained by *in situ* electron microscopy of the transition.

Slices (200 μm) of a crystal of $BaTiO_3$ were mechanically thinned parallel to a pseudocubic face. These were chemically thinned using orthophosphoric acid and sandwiched between two 75-mesh grids. Specimens were observed in a Gatan double-tilting heating–cooling goniometer ($-180 < T < 150$ °C) in a JEOL-100CX electron microscope. Images were recorded as a function of temperature using standard photographic techniques as well as a television camera with videotape recorder.

The room-temperature observations closely followed the results of Tanaka and Honjo[5]. Thus 90° domains of a–c and a–a type occurred frequently (see ref. 6, Fig. 2). On heating above 120–130 °C, a faint contrast appeared between existing domain walls (Fig. 1). Approximately equal areas of light and dark contrast occurred, with periodicity ~425 ± 25 Å. Dots of contrast and wavy lines occurred with ill-defined orientation and connectivity. This 'microdomain' contrast could be enhanced (Fig. 1) by tilting off the [001] zone axis by a few degrees and using the *hh*0 systematic row diffraction condition (L.A.B. and P.J.L., in preparation). For a wedge-shaped crystal (Fig. 2) the microdomain periodicity varied systematically with crystal thickness, ranging from ~250 Å in the thinnest areas, to ~1,200 Å for a crystal thickness of ~1,000 Å. Displacing or focusing the electron beam did not change the gross features of the pattern and no sideways movements of the microdomains could be induced. This behaviour is quite distinct from that of a–c or a–a ferroelectric domain walls, which could be induced to move sideways quite readily by moving or focusing the electron beam. Closer examination of videotapes showed fluctuations within microdomain contrasts (see arrowed positions in Fig. 3). Thus, for specimens thermally equilibrated at temperatures in the range 130–140 °C, small patches of darker contrast (~40–60 Å diameter) could be seen to transfer across the domain walls between adjacent dark contrast spots or stripes. The overall periodicity and texture of the microdomains were maintained, but they clearly possessed a dynamic character on a finer (20–40 Å) scale. Such movements, detectable at 25 frames s^{-1}, probably contribute to the diffuse appearance of the microdomain wall contrast. Such fluctuations were not simply due to small tilts during observation, as judged from the stability of bend extinction contours.

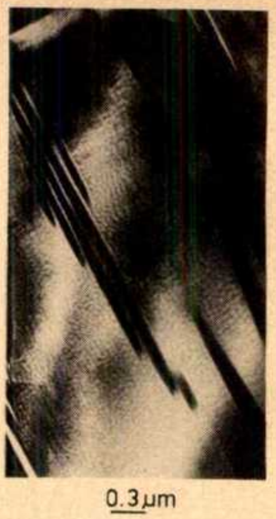

Fig. 1 Microdomain contrast within ferroelectric domains in a $BaTiO_3$ crystal observed at 120–130 °C (pseudocubic projection axis). Note equal areas of light and dark contrast with periodicity ~425 Å.

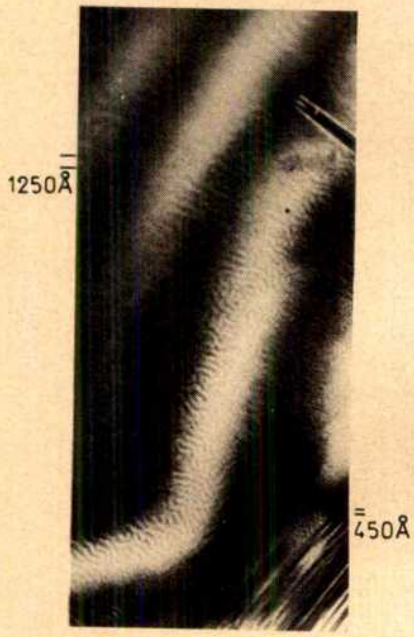

Fig. 2 Thickness dependence of microdomain periodicity in wedge-shaped crystal of $BaTiO_3$ (pseudocubic projection).

Attempts were made to establish systematic relationships between microdomain size and/or fluctuation frequency and temperature. These were not conclusive. On cooling the specimens from 140 °C to room temperature, the microdomains sometimes disappeared at ~100–120 °C but sometimes remained stable to ~60–80 °C. They did not occur at room temperature. The stability of microdomains on cooling appeared to be related to the topology of the specimen, in particular to elastic bending, and to the cooling rate. There was no systematic variation of domain size on cooling, and the microdomains probably disappear suddenly rather than gradually. The onset temperature was more sharply defined, being 127 °C for three different experiments, indicating reproducible behaviour. In other experiments the onset temperature varied between 130 and 150 °C. Thus exceptionally flat and extensive wedge-shaped thin edges, which were initially free of a–c or a–a domain walls, were strongly

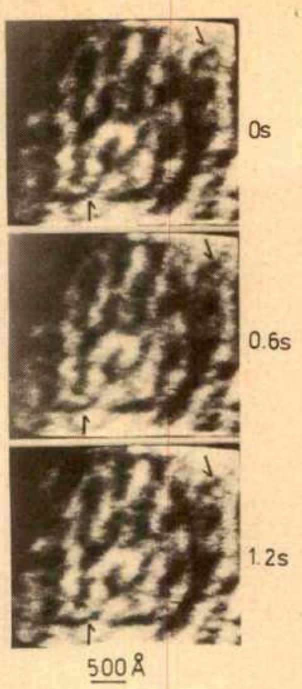

Fig. 3 Time sequence from videotape recording showing fluctuations in microdomains at 140 °C (25 frames per s). Note transfer of small (50-Å diameter) areas of darker contrast between adjacent microdomains, whereas the overall domain periodicity and topology is essentially maintained.

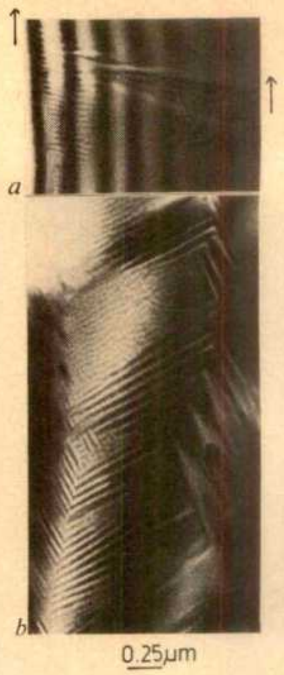

Fig. 4 *a*, Divergence of a–c domain wall at 140 °C, creating a slab containing microdomains bounded by inclined boundaries. Note one-dimensional nature of microdomains, lying parallel to existing a–c wall. *b*, Elements of two-dimensional short-range-ording of microdomains, apparently imposed by topology of coexisting a–c ferroelectric domain walls.

resistant to microdomain nucleation, even up to the maximum available temperature (150 °C).

Microdomain nucleation was clearly demonstrated for such a wedge-shaped crystal which contained only a single a–c domain wall. This wall remained quite stable until 140 °C and then suddenly diverged to create a slab containing microdomains bounded on either side by fault fringe contrast (Fig. 4*a*). Slight changes in the incident beam illumination angle were then enough to cause this slab to expand or contract, following movement of the incident beam. The microdomain texture often showed topology apparently determined by that of existing a–c or a–a domains. Thus for Fig. 4*a* the microdomains form essentially a one-dimensional array, parallel to the existing (011) wall, whereas in Fig. 4*b* some elements of two-dimensional short-range order appear to be imposed by orthogonal (011) and $(01\bar{1})$ a–c domain walls. The fine scale of the latter sometimes appears as a precursor to microdomain formation. In other areas (see Figs 1 and 2), the microdomains do not show preferred orientations.

Dark-field observations of the microdomains will be discussed elsewhere (unpublished work), as will other results for domain wall kinetics, recorded for $-180\,°\mathrm{C} \leq T \leq 150\,°\mathrm{C}$. These also concern the tetragonal/orthorhombic (5 °C) and orthorhombic/trigonal phase transitions. Distinctive behaviour often occurred at thin edges and cracks.

The observed mechanism of microdomain formation, by a–c or a–a wall divergence, and the fine-scale fluctuations involving transfer of one-ferroelastic orientation between adjacent microdomains should add more reality to molecular dynamical[4] and other theoretical approaches to the understanding of structural phase transitions[2].

The structure of the microdomains and hence contrast mechanisms have not been determined. Five important new observations need to be explained: (1) apparently equal volumes of bright and dark contrasts appeared in every case recorded; (2) the microdomains did not readily interact with the electron-beam, whereas a–c and a–a domain walls in the tetragonal phase move readily on focusing or translating the incident beam; (3) the microdomain contrast is relatively very weak compared with normal 90° domain wall contrast; (4) the microdomain walls are relatively diffuse and subject to fine-scale fluctuations; and (5) microdomains may coexist with normal a–c or a–a domain walls, often showing topology apparently related to the latter.

The following tentative interpretation of the structural mechanism for the ferroelectric/paraelectric phase transition is based on these observations. We propose that the bright and dark microdomains contain a structure intermediate between that of the well-known[1] tetragonal and cubic forms of $\mathrm{BaTiO_3}$. This transition structure could simply be a tetragonal distortion of the cubic phase. This would allow domain formation and give reasonable changes in background contrast across the microdomain walls (L.A.B. and P.J.L., in preparation). It should also be paraelectric, so that there is no electrical interaction between the incident beam and the microdomain walls. The transitional phase could also be ferroelastic, with noncentrosymmetric displacements of the oxygen atoms with respect to the cubic phase, but retaining zero electric dipole moment. Such a structural mechanism is respresented in Fig. 5. Clearly, the tetragonal distortion may take different orientations with respect to the cubic (or tetragonal) axes, but to minimize elastic strain overall, equal volumes of symmetrically equivalent domains should occur. The coexistence of a–c or a–a ferroelectric domains in the tetragonal phase, together with microdomains of the transitional phase (Fig. 4*b*), occurs over a range of temperatures, and a strong influence of the former on the topology of the latter is to be expected, as the structural difference involves small atomic displacements within virtually identical tetragonal unit cells (Fig. 5).

Our observations (Fig. 3) give some insights into the question of microdomain dynamics. The observation of a sharp onset temperature for microdomain formation (Fig. 3), rather than a gradual coarsening with increasing temperature, suggests that some modification of the models used for molecular dynamical calculations is required.

The present work has obvious limitations. First, the restriction to $T \leq 150\,°\mathrm{C}$ meant that it was not possible to study the stability of microdomains within the cubic phase. The molecular dynamic computations may then be more appropriate, with behaviour

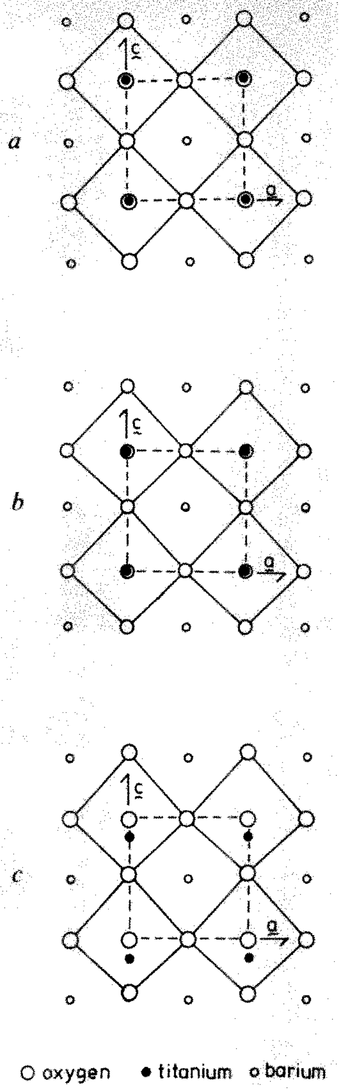

Fig. 5 Structural relationships between cubic (*a*), transitional (*b*) and tetragonal (*c*) phases of $BaTiO_3$.

quite different from that within the tetragonal phase. Second, the observed thickness dependence of microdomain periodicity (Fig. 2) indicates that at least some of the observed behaviour may not be characteristic of the bulk. Further studies using higher voltage instruments are required.

Clearly, transmission electron microscopy may be used to study some aspects of critical fluctuation phenomena associated with structural phase transitions. The present *in situ* studies have provided insights into the ferroelectric/paraelectric transition in barium titanate and the techniques used should have much wider applicability, even given that there may be some limitations, especially with regard to the applicability of the results for bulk crystals. However, many future device applications, and hence fundamental interests, are likely to involve thin films.

This work was supported by the Australian Research Grants Committee and the University of Melbourne. P.J.L. thanks the Education Department of China for permission to visit Melbourne. We thank Dr A. E. C. Spargo and P. Hanan (University of Melbourne) for assistance.

Received 12 June; accepted 14 August 1984.

1. Lines, M. E. & Glass, A. M. *Principles and Applications of Ferroelectrics and Related Materials* Ch. 8 (Clarendon, Oxford, 1977).
2. Cowley, R. A. & Bruce, A. D. *Adv. Phys.* **29,** 1–321 (1980).
3. Müller, K.-A. *Non-Linear Phenomena at Phase Transitions and Instabilities* (ed. Riste, T.) 1–34 (Plenum, New York, 1981).
4. Schneider, T. & Stoll, E. *Phys. Rev.* **B13,** 1216–1237 (1976); **B17,** 1302–1322 (1978).
5. Tanaka, M. & Honjo, G. *J. phys. Soc. Jap.* **19,** 954–970 (1964).

Invariant and changing transitional field configurations in a sequence of geomagnetic reversals

Jean-Pierre Valet & Carlo Laj

Centre des Faibles Radioactivités, Domaine du CNRS,
Avenue de la Terrasse, 91190, Gif-sur-Yvette, France

In the past few years, the increasing number of detailed records of geomagnetic transitions has provided new and important information about the behaviour of the Earth's magnetic field during a reversal. Surprisingly, however, no attempt has been made to obtain information about the evolution of the transitional field characteristics over a long period of time. We report here the results of a palaeomagnetic study of four different geomagnetic reversals, three of which are successive, recorded at different stratigraphical levels of two Upper Tortonian marine clay sections in western Crete (Greece). This sequence represents ~1.5 Myr of geomagnetic field history. The results obtained suggest that the process of reversal from either starting polarity may remain invariant for a long period of time, then change rather abruptly between successive reversals.

The two sections investigated are situated 5 km apart in the Kastelli basin in western Crete, near the villages of Potamida and Skouloudhiana. A careful correlation between these two sections, among others, has been established by a previous extensive bio- and magnetostratigraphical study of late Miocene sediments in Crete[1]. The location of the two sections is shown schematically in Fig. 1, together with the corresponding correlated polarity sequences. Correlation with the geomagnetic time scale shows that the two sections combined cover the time interval between 7.4 and 5.3 Myr, and that the four reversals studied here are spread over a time interval of ~1.5 Myr (ref. 1).

Some of the results obtained from these two sections have already been reported[2–4]. We add here new results for the normal–reversed (N–R) KS 05 transition. Moreover, extensive resampling has allowed us to obtain further transitional palaeomagnetic directions, so that all the palaeomagnetic records may be classified as category A, as defined by Fuller *et al.*[5].

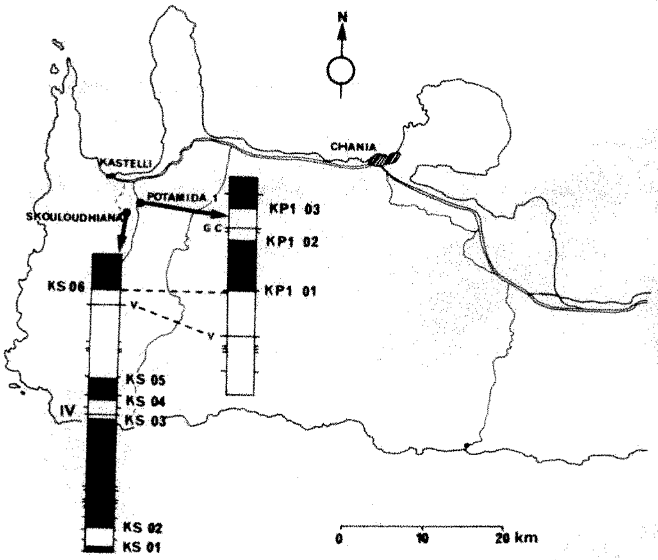

Fig. 1 Map showing the location of Potamida and Skouloudhiana sections together with the biomagnetostratigraphical correlation of the corresponding polarity sequences adapted from ref. 1. GC, First occurrence datum (FOD) of *G. conomiozea* group; V, FOD of *G. menardii* form 5; IV, last occurrence datum of *G. menardii* form 4.

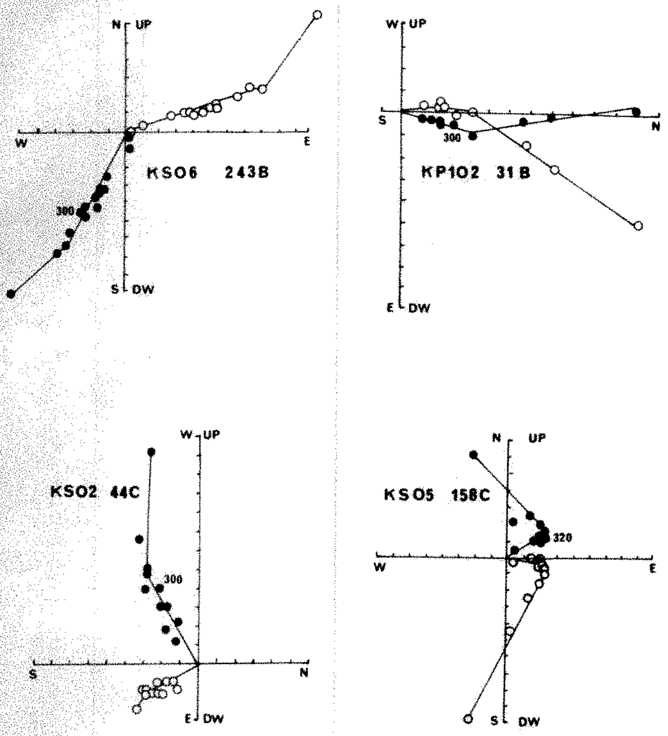

Fig. 2 Typical thermal demagnetization diagrams of samples from KS 02, 05, 06 and KP1 02 transition zones. ●, Declination data; ○, inclination data.

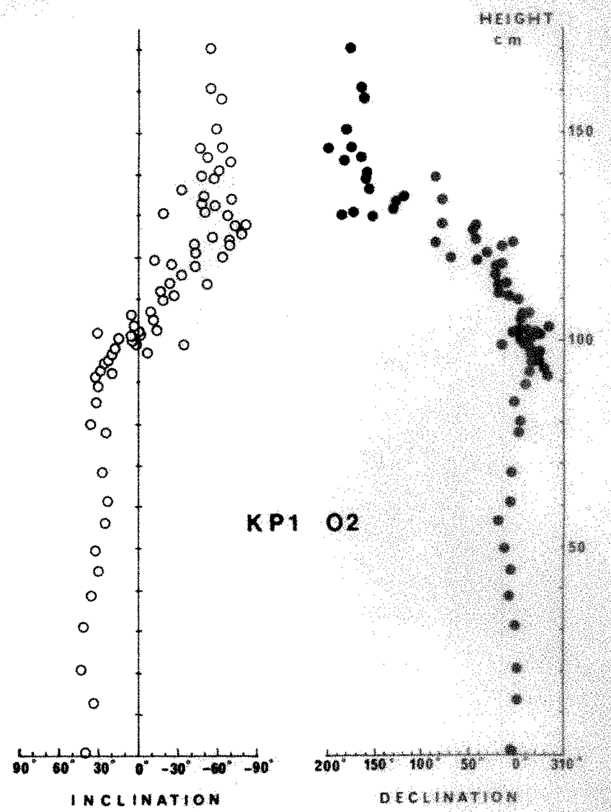

Fig. 3 Detailed declination/inclination record relative to the (N–R) KP1 02 transition in the Potamida 1 section.

The sampling was done using standard palaeomagnetic techniques, with either water or compressed air as a coolant. Care was taken to determine the exact relative stratigraphical position of the cores in each transitional zone. Repetitive measurements yielded identical results within 0.5 cm. The exact stratigraphical height of the different samples obtained from each core was calculated using a computer program which took into account the usual orientation parameters of the core, its stratigraphical position and even the width of the diamond saw used to cut the cores. The magnetic properties of the clays have been carefully investigated to check that there are no changes in the magnetic or sedimentary mineralogy over the different transitional zones. Isothermal remanent magnetization (IRM) measurements show that, in all cases, magnetite is the main magnetic mineral, with a very small amount of a mineral of higher coercivity, presumably haematite, also generally present.

The anisotropy of the magnetic susceptibility has also been measured at different horizons of the two sections. In both cases, the magnetic fabric is described by an oblate ellipsoid with a very moderate (1.05) degree of anisotropy. In Skouloudhiana, the mean $K_{\min}$ axis is perfectly perpendicular to the bedding plane (inclination $I = 88.5°$) while the $K_{\max}$ axes of the individual samples show no preferential orientation in this plane. In Potamida 1, the well grouped $K_{\min}$ axes dip slightly in a northeasterly direction and there is a preferential north–south trend of the $K_{\max}$ axes. The magnetic lineation $(3(K_{\max} - K_{\text{int}})/(K_{\max} + K_{\text{int}} + K_{\min}))$ is, however, very small (0.014), so that in both sections the results indicate a planar undisturbed sedimentary fabric.

Stepwise thermal demagnetization of all samples has been used and the magnetization was measured with either a Digico spinner magnetometer or a three-axis LETI cryogenic magnetometer. For the most weakly magnetized samples, and in particular for all the samples of the KS 05 transition, the double precision procedure of Vandenberg[6], involving four independent measurements for each sample, was used with the cryogenic magnetometer. In spite of this procedure, some of the demagnetization diagrams can hardly be judged to be linearly decreasing. These diagrams which represent ~30% of the total in KS 05, were not taken into account in the final results. No such problems were encountered for the other transitions.

Typical demagnetization diagrams of samples from four different reversals are shown in Fig. 2; these are plotted relative to transitional samples so that they correspond to the lowest natural remanent magnetization (NRM) and most delicate part of each transition. It can be seen that, apart from a secondary, probably viscous, component removed at low temperature (≤ 250 °C), only a single stable component of magnetization is present.

The magnetic susceptibility of samples from each transition was monitored during progressive demagnetization using a susceptibility bridge. No changes of more than a factor of three were found between room temperature and 500 °C, indicating that no major mineralogical transformations had affected the magnetic materials.

Palaeomagnetic directions were obtained by hand fitting a straight line through the last points of the demagnetization plots. As an example, the complete declination–inclination record for transition KP1 02 is shown in Fig. 3.

In all the sediments, the mean inclination of the samples situated well outside the transition zones is about 8–10° shallower than that expected at the site latitude on the basis of a geocentric axial dipole. This is a general property, not only of Potamida and Skouloudhiana[1,2], but also of all sediments of the same nature throughout the Hellenic sedimentary arc[7]. A correction of this error using a formula such as $\tan I' = f \tan I$ (ref. 8) does not, however, significantly change estimates of the virtual geomagnetic pole (VGP) paths[2] and we have therefore worked with uncorrected measurements.

From the directions obtained from the demagnetization diagrams, the successive VGP positions have been calculated for the five transitions. The results are shown in Fig. 4 together

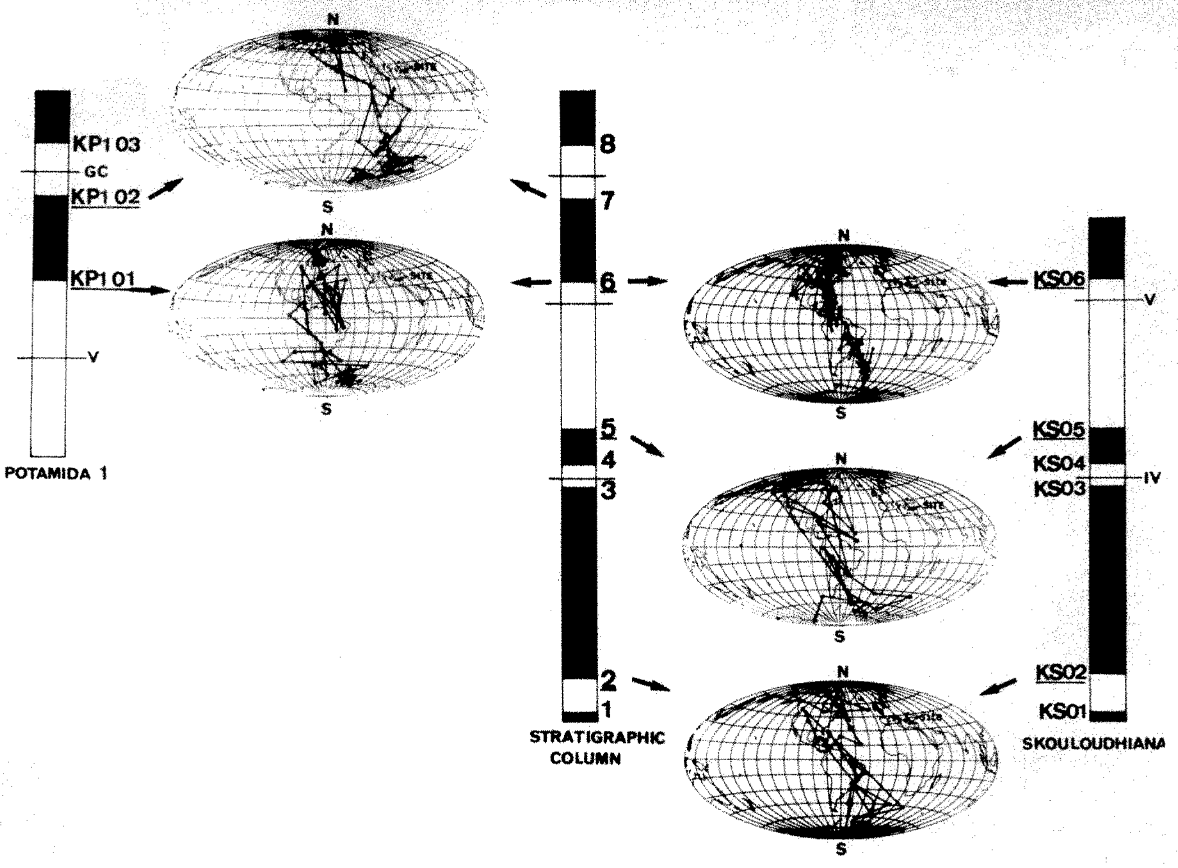

Fig. 4 VGP paths of the five polarity transitions (north VGPs for the R–N and south VGPs for the N–R transitions). The composite total stratigraphical column in the centre gives the stratigraphical position of the transitions. The VGP paths of the lower three transitions are identical within noise limits, while the upper one differs by ~60° long.

with the stratigraphical position of the reversals. To compare directly the VGP paths corresponding to transitions of opposite sense, we have plotted in Fig. 4 the north VGPs associated with R–N transitions and the south VGPs associated with the N–R transitions, as suggested by Hoffman[9].

It can be seen from Fig. 4 that, within noise limits, the VGP paths associated with the transitions KS 06 and KP1 01, which represent the record of the same transition in the two sections, are identical. This, of course, is a condition that must be fulfilled if transitional VGP paths from the two sections are to be compared; the fact that it is suggests that differences in the VGP paths of other transitions are probably a result of changes in the reversal mechanism and not of distortion in the sampled sections.

The main result (Fig. 4) is that the north-VGP paths associated with the two (R–N) transitions, and the south-VGP path for the (N–R) transition in Skouloudhiana, are identical. In spite of significant scatter, which is a consequence of the low magnetization of the sediments for the two lower transition zones, even an east to west migration of the intermediate VGPs can be recognized in these plots as already noted by Hoffman[9]. The directional field variation at the site during this (N–R) transition is thus identical to that associated with the R–Ns except for a change in sign. (This situation is exactly opposite to a standing field situation which requires identical transitional field along with sign, but is consistent with a flooding model.)

On the other hand, the south-VGP path relative to the upper (N–R) transition in Potamida 1 is significantly different, being about 60° of longitude away from the other paths.

The marine sediments used in this study have an average sedimentation rate of $\sim$4–5 cm kyr^{-1} (ref. 1). Therefore, they may not record changing field directions as faithfully as rapidly deposited lake sediments or, indeed, volcanic rocks. These sediments have, however, proved to be a faithful record of the direction of the steady magnetic field to within a few degrees[1,7]. It is, thus, very difficult to imagine that poor remanence acquisition processes for a rapidly changing field, such as long integration times for the locking-in of the remanence, would modify the general features of the reversal records. In particular, we cannot think of any process which would result in antipodal reversal paths for the different transition senses. This feature, in contrast, can be taken as proof of the reliability of the palaeomagnetic records.

These results, therefore, suggest that the process of reversal from either starting polarity remained unchanged during the time interval of 1.2–1.3 Myr, corresponding to the first three reversals[1]. A change then occurred in the period between the two upper reversals. This change must have occurred rather abruptly, because these two reversals are separated by <250,000 yr (ref. 1).

Similarities, or even coincidence, of VGP paths of different transitions, recorded in different, but geographically close, sites, have already been reported[10–12]. Hoffman has even suggested, on the basis of four Cenozoic transitions in the western US that because of particular conditions in the core, only a very limited number of possible reversal configurations might be liable to occur with finite probability at any epoch, so that only particular ones will be frequently observed in time[13]. The results reported here are, however, the first to suggest that the mechanism of reversal is invariant over a long period of time, confirming previously reported results[3].

Moreover, these results from the upper Tortonian epoch cannot be reconciled with the standing field model. It is thus interesting that a set of two successive palaeomagnetic reversals obtained by Bogue and Coe from slightly younger (5.6–4.5 Myr) lava flows in Kauai yield, in contrast, very similar paths[14]. These authors have noted that unless the standing field or the flooding process can, at least occasionally, change from reversal to reversal, neither model can explain all the available transition data. The present results, together with those from Kauai, suggest that such changes in the reversal process might occur not only from reversal to reversal but also between different epochs, so that a particular process might be more effective during a particular period of time.

In this respect, the results from the (R–N) KP1-03 transition would be quite interesting. Indeed its age is 5.6 Myr (ref. 1), so that it could eventually provide a link between the results from Crete and those from Kauai. Unfortunately the sediments in the KP1 03 transition zone are weakly magnetized and furthermore a ferrugineous level is present in this zone[1]. Thus, such measurements would be quite difficult to achieve.

We thank Cor Langereis for invaluable field assistance, H. Zijderveld for many helpful discussions, and K. Hoffman for detailed comments and suggestions. The Director General of the Institute of Geological and Mining Research (IGME) in Athens provided the necessary permits. C. Kissel, S. Sen and M. Villeger helped with the sampling. This work was supported by the French CNRS ATP Géologie et Géophysique des Océans.

Received 24 April; accepted 20 July 1984.

1. Langereis, C. G., Zachariasse, W. J. & Zijderveld, J. D. A. *Mar. Micropaleont* **8**, 261–281 (1983–84).
2. Valet, J. P., Laj, C. *Earth planet. Sci. Lett.* **54**, 53–63 (1981).
3. Valet, J. P., Laj, C. & Langereis, C. G. *Nature* **304**, 330–332 (1983).
4. Valet, J. P. & Laj, C. *Nature* **309**, 90–91 (1984).
5. Fuller, M., Williams, I. & Hoffman, K. A. *Rev. Geophys. Space. Phys.* **2**, 179–203 (1979).
6. Vandenberg, J. *Tectonophysics* **98**, 29–41 (1983).
7. Laj, C., Jamet, M., Sorel, D. & Valente, J. P. *Tectonophysics* **86**, 45–67 (1982).
8. King, R. F. *Mon. Not. R. astr. Soc. Geophys. Suppl.* **7**, 115 (1955).
9. Hoffman, K. A. *Nature* **309**, 90 (1984).
10. Mankinien, E. A., Donnely-Nolan, J. M., Gromme, C. S. & Hearn, B. C. Jr. *U.S. geol. Surv. Prof. Pap.* **1141**, 67–82 (1981).
11. Liddicoat, J. C. *Phil. Trans. R. Soc.* A**306**, 121–128 (1982).
12. Dodson, R. *et al. Geophys. J. R. astr. Soc.* 373–412 (1978).
13. Hoffman, K. A. *Earth planet. Sci. Lett.* **44**, 7–17 (1979).
14. Bogue, S. W. & Coe, R. S. *Nature* **295**, 399–401 (1982).

Density of the ocean crust

R. L. Carlson & G. S. Raskin

Department of Geophysics and Geodynamics Research Program,
Texas A&M University, College Station, Texas 77843, USA

The density structure and average density of the oceanic crust have implications for various geological and geophysical problems, including interpretations of gravity data, the variation of lithospheric bouyancy in relation to age, and role and fate of the crust in subduction. But no systematic evaluation of oceanic crustal density has been made and estimates range from 2.85 to 3.0 Mg m^{-3} (refs 1–3). We have made an evaluation based on seismic refraction data in combination with drilling results, laboratory studies of seismic properties of oceanic and ophiolitic rocks, and ophiolite lithostratigraphy. Our preferred value for the mean density of the oceanic crust is 2.89±0.04 Mg m^{-3}.

Seismic refraction data provide the most important constraints on the structure and composition of the oceanic crust. (Seismic models and their interpretation in terms of composition are given in refs 4, 5.) Over the past decade or so, simple three-layer velocity-structure models have given way to more detailed multilayer models, and synthetic seismogram modelling has led to more sophisticated 'gradient' models.

Synthetic seismogram models indicate that the upper 2 km of igneous basement (layer 2) is characterized by strong vertical velocity gradients, with P-wave velocities ranging from <4 km s^{-1} at the top to >6 km s^{-1} at the bottom of the interval. Layer 2 may, nevertheless, be subdivided into layers (2a, 2b, 2c), though these regions may not be homogeneous or separated by distinct discontinuities[5,6]. The rapid increase of velocity with depth in layer 2 may be attributed to several factors: (1) velocities in the upper 200–400 m of the section are significantly reduced by large-scale porosity (produced, for example, by collapsed pillows,.and lava tubes)[7–9]; (2) there is a systematic decrease of grain-boundary porosity with depth[10–12]; and (3) metamorphic grade increases with depth; greenschist facies mineral assemblages (chlorite, epidote, actinolite, albite) are associated with layer 2c in hole 504B (ref. 9). In contrast to layer 2, velocity gradients in oceanic layer 3 are low (0.0–0.1 S^{-1}). The velocity at the top of the unit is typically 6.7–6.8 km s^{-1}, but the internal structure of layer 3 is apparently variable. In some cases, the gentle gradient extends to the Moho; in others the layer may be subdivided into two (or more) units[4,5,13]. The transition from crustal to mantle velocities generally occurs over an interval of ~1 km.

The oceanic crust can be approximated by a layered sequence, having an average density given by

$$\rho_{\mathrm{avg}} = \frac{1}{T}\sum_{i=1}^{n} \rho_i t_i;\ T = \textstyle\sum_{i=1}^{n} t_i \qquad (1)$$

where ρ_i and t_i are the density and thickness of the ith layer, respectively, n is the total number of layers and T is the total thickness of the sequence. The number of layers and their thicknesses may be taken directly from seismic velocity-structure models; the problem is to find a means of estimating the layer densities. We have approached this problem in three ways.

Some ophiolites, at least, are now believed to be slices of oceanic crust and upper mantle. The velocity structures of the Semail Ophiolite, Oman and the Bay of Islands Complex, Newfoundland, for example, have been reconstructed on the basis of laboratory studies[14–16]. The principal lithologies present in the 'crustal' sections of ophiolites are basalts, diabases, gabbros and their metamorphic equivalents. A much simplified lithologic sequence, viewed from the top downward, consists of extrusive, generally pillowed, basalts (1–1.5 km thick), sheeted diabase dykes (1–1.5 km), and a high-level isotropic gabbro sequence (up to 1 km), which grades downward into a 3–5-km thick sequence of mafic, layered gabbros (hornblende, pyroxene, and olivine gabbro, troctolite, and so on) in which the ultramafic component typically increases with depth. The mafic gabbros are commonly, but not always, interlayered with ultramafic cumulates in the lower part of the 'crustal' section.

The velocity structures of ophiolites are similar to the velocity structure of the oceanic crust[14,15,17]. In ophiolites, 'layer 2' is characterized by strong velocity gradients which extend well into the sheeted dykes and reflect the combined effects of a systematic increase in metamorphic grade (zeolite to upper greenschist facies) and a systematic decrease in grain-boundary porosity with depth[14–17]. Velocities typical of oceanic layer 3 are encountered in the middle to lower part of the dyke sequence, where upper greenschist assemblages give way to those of lower amphibolite grade. The velocity gradient below this level is relatively low, and differences between ophiolites in the amount of modal olivine present in the lower part of the gabbro sequence account for the observed variability of layer 3 velocity structures[16].

In method 1, to estimate crustal density, we assume that layer 2 consists of basalts and dyke rocks in about equal proportions. The upper part of layer 3 is taken to consist of gabbro and metagabbro, with denser, olivine gabbros occurring in the lower half the layer. Neglecting the effect of interlayered ultramafic rocks in the lowermost part of the crustal section, we have used

Table 1 Densities of ophiolite samples

Lithology		No. of samples	Density (Mg m^{-3})
Metabasalt, basalt and spilite	(B)	34	2.73±0.09
Diabase and metadiabase	(D)	31	2.85±0.07
Metagabbro	(MG)	27	2.90±0.07
Gabbro and olivine gabbro	(G+OG)	38	2.95±0.07
Metagabbro, gabbro and olivine gabbro	(G+MG+OG)	65	2.93±0.07

Table 2 Summary of average velocity-structure models and density structures

Model				Method 1		Method 2	Method 3
Ref.	Layer	Thickness (km)	Velocity (km s^{-1})	Lithology*	Density (Mg m^{-3})	Density (Mg m^{-3})	Density (Mg m^{-3})
24	2	1.71 ± 0.75	5.07 ± 0.63	B + D	2.79 ± 0.08	2.63 ± 0.15	2.75 ± 0.09
	3	4.86 ± 1.42	6.69 ± 0.26	G + MG + OG	2.93 ± 0.07	2.91 ± 0.04	2.91 ± 0.04
	Mean				2.89 ± 0.06	2.84 ± 0.06	2.87 ± 0.04
25	2	1.49 ± 0.98	5.19 ± 0.69	B + D	2.79 ± 0.08	2.66 ± 0.16	2.77 ± 0.10
	3	4.62 ± 1.30	6.81 ± 0.16	G + MG + OG	2.93 ± 0.07	2.93 ± 0.03	2.93 ± 0.03
	Mean				2.90 ± 0.06	2.86 ± 0.06	2.89 ± 0.04
4	2	1.39 ± 0.5	5.04 ± 0.69	B + D	2.79 ± 0.08	2.62 ± 0.17	2.75 ± 0.10
	3	4.97 ± 1.25	6.73 ± 0.19	G + MG + OG	2.93 ± 0.07	2.92 ± 0.04	2.92 ± 0.04
	Mean				2.90 ± 0.06	2.85 ± 0.05	2.88 ± 0.04
4	2	1.6	4.4	B + D	2.79 ± 0.08	2.45 ± 0.03‡	2.64 ± 0.01‡
Sonobouy Type I	3a	1.2	6.4	MG	2.90 ± 0.07	2.87 ± 0.03	2.91 ± 0.01
	3b	4.8	7.1	G + OG	2.95 ± 0.07	2.97 ± 0.03	2.97 ± 0.03
	Mean				2.91 ± 0.05	2.84 ± 0.02	2.89 ± 0.02
4	2	1.6	4.4	B + D	2.79 ± 0.08	2.45 ± 0.03	2.64 ± 0.01‡
Sonobouy Type II	3a	3.0	6.8	MG	2.90 ± 0.07	2.93 ± 0.03	2.93 ± 0.03
	3b	2.6	7.5	G + OG	2.95 ± 0.07	3.01 ± 0.01	3.01 ± 0.02
	Mean				2.89 ± 0.04	2.85 ± 0.02	2.89 ± 0.01
6	2a	0.3 ± 0.1	3.74 ± 0.50	B	2.73 ± 0.09	2.21 ± 0.22	2.49 ± 0.14
Atlantic	2b	1.0 ± 0.1	5.13 ± 0.38	B + D	2.79 ± 0.08	2.64 ± 0.09	2.76 ± 0.06
	2c	1.0 ± 0.3	6.05 ± 0.22	D	2.85 ± 0.07	2.82 ± 0.05	2.87 ± 0.03
	3	4.97 ± 1.25†	6.83 ± 0.21	G + MG + OG	2.93 ± 0.07	2.93 ± 0.04	2.93 ± 0.04
	Mean				2.89 ± 0.05	2.85 ± 0.04	2.88 ± 0.03
6	2a	0.4 ± 0.1	3.47 ± 0.35	B	2.73 ± 0.09	2.08 ± 0.18	2.41 ± 0.11
Pacific	2b	0.8 ± 0.1	5.28 ± 0.39	B + D	2.79 ± 0.08	2.68 ± 0.09	2.78 ± 0.05
	2c	0.9 ± 0.4	6.12 ± 0.18	D	2.85 ± 0.07	2.83 ± 0.04	2.88 ± 0.02
	3	4.97 ± 1.25†	6.90 ± 0.17	G + MG + OG	2.93 ± 0.07	2.94 ± 0.03	2.94 ± 0.03
	Mean				2.89 ± 0.05	2.85 ± 0.03	2.89 ± 0.03
13	2a	0.38	5.30	B + D	2.79 ± 0.08	2.68 ± 0.03‡	2.78 ± 0.01‡
	2b	1.93	6.10	D	2.85 ± 0.07	2.83 ± 0.03	2.88 ± 0.01
	3a	1.55	6.86	MG	2.90 ± 0.07	2.94 ± 0.03	2.94 ± 0.03
	3b	3.15	7.06	G + OG	2.95 ± 0.07	2.96 ± 0.03	2.96 ± 0.03
	Mean				2.90 ± 0.04	2.90 ± 0.01	2.92 ± 0.01

* Abbreviations as in Table 1.

† Thickness of layer taken from the average structure of Christensen and Salisbury[4].

‡ Calculated standard deviations do not include the effect of variability in crustal structure.

published water-saturated bulk densities[14–17] to estimate the mean densities of pertinent combinations of rock types given in Table 1.

Assigning densities to velocity structure models on the basis of ophiolite lithostratigraphy neglects the large-scale porosity of layer 2a (refs 7, 8), and is based on a lithologic model which is only loosely tied to the velocity structure. A preferable approach is one in which layer densities can be calculated from a statistically-valid, functional relationship between formation density and seismic velocity.

Assuming that the variation of grain properties is small relative to the difference between the properties of the grains and those of the pore medium (seawater), we may combine the theoretical density and time-average relations for two-component systems, to obtain a velocity/density function

$$\rho = a + b/V_p \qquad (2)$$

Fitting this equation to the laboratory densities and P-wave velocities (measured at 100 MPa) of samples recovered by the Deep Sea Drilling Project and from ophiolites[14–21] (Fig. 1) yields

$$\rho(\mathrm{Mg\,m^{-3}}) = (3.81 \pm 0.02) - (5.99 \pm 0.11)/V_p(\mathrm{km\,s^{-1}}) \qquad (3)$$

with a coefficient of determination (r^2) of 0.86 and an r.m.s. error of 0.07 Mg m^{-3}. Equation (3) describes the velocity/density relation for oceanic rocks very well.

In method 2 layer densities are calculated from seismic velocities according to equation (3). The relation does not account for increasing confining pressure, but the effect of pressure (above 100 MPa) on density and velocity is relatively small. Equation (3) reflects the effects of grain-boundary porosity and metamorphic grade, but also includes effects of alteration[18–19], which is not representative of oceanic basalts. This method also fails to account for large-scale porosity. Thus method 2 may be applied to deeper levels of the crust where porosity is low, but cannot be applied with confidence to oceanic layer 2.

Seismic velocities in porous media depend on the shapes of the voids as well as the properties of the matrix and pore medium. Because the shapes of large-scale voids in layer 2 are unknown, there are likely to be large uncertainties in the any postulated relationship between velocity and density or porosity[5]. We have, therefore, taken the simplest possible approach of calculating the coefficients of equation (2) from the properties of an average, zero-porosity basalt and the properties of seawater ($\rho = 1.025$ Mg m^{-3}; $V_p = 1.5$ km s^{-1}). The average bulk-grain densities of oceanic basalts range from 2.9 to 3.0 Mg m^{-3} (refs 7, 10, 12); we estimate the properties of a typical, zero-porosity basalt to be $\rho = 2.03 \pm 0.06$ Mg m^{-3} and $V_p = 6.65 \pm 0.20$ km s^{-1}. The velocity/density relation is then

$$\rho(\mathrm{Mg\,m^{-3}}) = (3.50 \pm 0.2) - (3.79 \pm 0.1)/V_p(\mathrm{km\,s^{-1}}) \qquad (4)$$

The velocity/density relation for the porous basalt formation (equation (4)) and for the laboratory data (equation (3)) are shown in Fig. 2.

Also shown in Fig. 2 are velocities and densities estimated from downhole logging in igneous basement at a number of

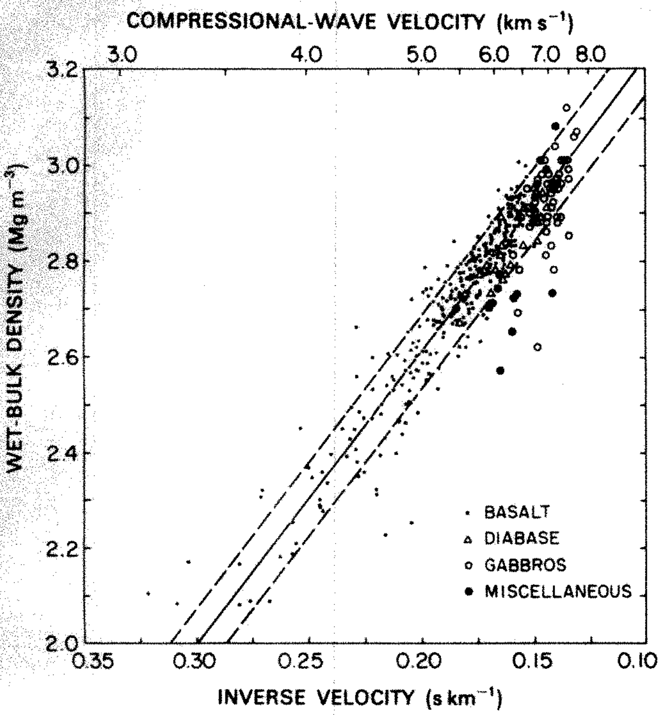

Fig. 1 Compressional-wave velocity versus wet-bulk density of basalts, diabases and gabbroic rocks sampled from ophiolites and recovered from the sea floor by drilling. Also included are some rock types (including serpentinites and amphiliolites) thought to be present but not abundant in the oceanic crust. Solid line represents least-squares fit (equation 3). Dashed lines represent standard error. The r.m.s. misfits to basalt, diabase and gabbro data taken separately range from 0.04 to 0.08 Mg m^{-3}.

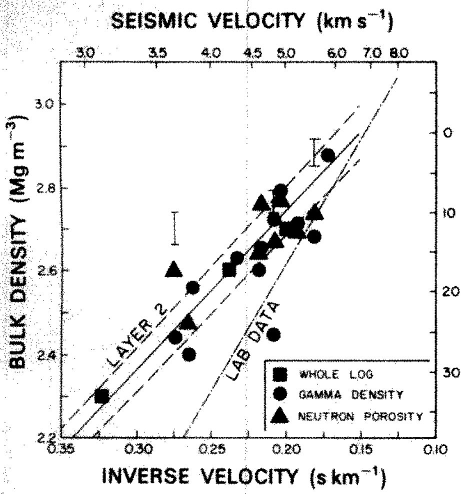

Fig. 2 Approximate velocity–density–porosity relation for a porous basalt formation (layer 2) and best-fitting relation for laboratory data. Also shown are formation velocities, densities and porosities estimated from downhole logs. Bars indicate porosities estimated from wide-spacing resistivity data[23].

DSDP sites. Some of the data are from published reports[8,11,22]. We have made additional, preliminary analyses of logs from holes 504B (Leg 83), 556, 558 and 564. The velocities shown are averages from sonic logs. Gamma–gamma density, neutron porosity and electrical resistivity data[23] have been used to estimate densities and porosities. The neutron porosity values have been corrected for pressure and bound water content as described by Kirkpatrick[8]. Some of the data points represent averages over the entire logged interval; in other cases (such as, Leg 83, 504B) the data points represent different intervals such as layers 2a, 2b and 2c. While we must emphasize that our interpretations of the logs are preliminary, and, therefore, subject to (presumably) minor changes, we find that the data correspond quite well with the predicted relation. The r.m.s. misfits of equation (4) to the log values of density and porosity are 0.06 Mg m^{-3} and 4%, respectively. Insofar is it does agree with available downhole logging data, equation (4) represents a valid means of estimating both the porosity and the density of layer 2 from seismic refraction data.

A particularly important point is that equation (4) predicts markedly higher densities than does the velocity–density relation based on laboratory measurements (equation (3)). For a seismic velocity of 5.0 km s^{-1}, the difference is ~0.15 Mg m^{-3}, for a velocity typical of layer 2a, about 3.75 km s^{-1}, the difference is 0.3 Mg m^{-3}. Thus the common practice of using laboratory data to estimate formation densities from seismic velocities may lead to serious errors when the porosity of the layer is greater than the grain-boundary porosity of the rocks.

In method 3, we have accounted for large-scale porosity of layer 2a by calculating layer densities according to equation (4) when the seismic velocity is <6.65 km s^{-1}. Thus, in general, equation (4) applies to oceanic layer 2. For velocities >6.65 km s^{-1} (layer 3), we have used equation (3).

Any of the three methods outlined above can be applied to an individual refraction survey. Because our objective is to estimate the average density of the oceanic crust, we have used several average velocity structures: three 'standard' three-layer models[4,24,25]; the type I and II sonobouy models of Christensen and Salisbury[4], in which layer 3 is subdivided into two units (3a and 3b); the Atlantic and Pacific multilayer models proposed by Houtz and Ewing[6]; and a four-layer model suggested by Purdy[13] for crust 140 Myr old. The velocity structures, estimated layer densities and mean crustal densities are summarized in Table 2.

A remarkable feature of the results is that the different velocity-structure models yield such similar mean crustal densities: the range of values found by method 1 is 2.89–2.91 Mg m^{-3}, the range for method 2 is, in general, 2.84–2.86 Mg m^{-3}, and most of the densities calculated by method 3 are in the range 2.88–2.90 Mg m^{-3}. Mean crustal densities estimated by methods 1 and 3 are also remarkably similar; the average difference is <0.01 Mg m^{-3}. Method 2 yields mean densities which are systematically lower by ~0.03 Mg m^{-3}. Having calculated the density structures by these methods, the problem is to select the best model.

Method 3 is preferable to the other methods because densities are calculated from the seismic structure, and the large-scale porosity of layer 2 is taken into account. Equation (4) used to estimate the density of layer 2 is also in good general agreement with the results of downhole logging in igneous basement (Fig. 2). Furthermore, the density structures calculated by this method are consistent with the inferred variation of physical properties with depth in the oceanic crust.

Large-scale porosity is generally restricted to the uppermost 400 m (layer 2a) of the section. Below that depth, the porosity is markedly reduced (layer 2b), and below 1,000 m (layers 2c and 3) porosity is apparently restricted to the grain boundaries[6,11,13,23]. Consequently, calculated layer densities (Table 2) should correspond to the densities of corresponding lithologies. Calculated layer 3 densities agree with the mean density of oceanic gabbros (2.93 ± 0.07 Mg m^{-3}). The density of the lower part of layer 2 (2.88) is higher than the mean (2.85 Mg m^{-3}), but agrees with the modal value (2.88 Mg m^{-3}) for diabases. The mean densities of different suites of oceanic basalts range from 2.79 to 2.80 Mg m^{-3} (refs 7, 10, 12). The range of calculated layer 2 mean densities (not included in Table 2) is 2.80–2.75 Mg m^{-3}. These values range downward from the mean for basalts and diabases because of the porosity of layer 2a, but the effect of porosity on the average density of layer 2 is reduced because the porous region occupies only ~20% of the layer thickness.

Thus, we conclude that density structures calculated by method 3 are representative of *in situ* densities in the oceanic crust. A reasonable mean density is 2.89 ± 0.04 Mg m^{-3}. Even if we assume that 500 m of ultramafic cumulates having a density of 3.20 Mg m^{-3} should be included, the mean crustal density is only 2.91 Mg m^{-3}. The proposed existence of a low-velocity layer of partially serpentinized periodotites at the base of the crust[26] would not significantly affect its density because the density of periodotites containing 50% serpentine is ~2.9 Mg m^{-3} (ref. 27). Including a 500-m blanket of sediments having a mean density of 2.0 Mg m^{-3} reduces the density of the entire crust to ~2.85 Mg m^{-3}.

This research was supported by Office of Naval Research Contract N-00014-80-C-0013. N. L. Carter's suggestions substantially improved the manuscript. Texas A&M Geodynamics Research Program contribution no. 44.

Received 11 May; accepted 31 July 1984.

1. Watts, A. B. *J. geophys. Res.* **83**, 5989–6004 (1978).
2. Molnar, P. & Atwater, T. *Earth planet. Sci. Lett.* **41**, 330–340 (1978).
3. Pennington, W. D. *Tectonophysics* **102**, 377–398 (1984).
4. Christensen, N. I. & Salisbury, M. H. *Rev. Geophys. Space Phys.* **13**, 57–86 (1975).
5. Spudich, P. & Orcutt, J. *Rev. Geophys. Space Phys.* **18**, 627–645 (1980).
6. Houtz, R. & Ewing, J. *J. geophys. Res.* **81**, 2490–2498 (1976).
7. Hyndman, R. D. & Drury, M. J. *J. geophys. Res.* **81**, 4042–4052 (1976).
8. Kirkpatrick, R. J. *J. geophys. Res.* **84**, 178–188 (1979).
9. Anderson, R. N. *et al. Nature* **300**, 589–594 (1982).
10. Hamano, Y. *Init. Rep. DSDP Legs* **51, 53** Part 2, 1457–1466 (1980).
11. Salisbury, M. H. *et al. Init. Rep. DSDP Legs* **51, 53** Part 2, 1579–1597 (1980).
12. Karato *et al. Init. Rep. DSDP Leg* **69**, 675–682 (1981).
13. Purdy, G. M. *Geophys. J. R. astr. Soc.* **72**, 115–137 (1983).
14. Salisbury, M. H. & Christensen, N. I. *J. geophys. Res.* **83**, 805–817 (1978).
15. Christensen, N. I. & Smewing, J. D. *J. geophys. Res.* **86**, 2545–2556 (1981).
16. Christensen, N. I. & Salisbury, M. H. *Geophys. J. R. astr. Soc.* **68**, 675–688 (1982).
17. Christensen, N. I. *Tectonophysics* **47**, 131–157 (1978).
18. Christensen, N. I. & Salisbury, M. H. *Earth planet. Sci. Lett.* **15**, 367–375 (1972).
19. Christensen, N. I. & Salisbury, M. H. *Earth planet. Sci. Lett.* **19**, 461–470 (1973).
20. Fountain, D. M. *et al. Mar. Geol.* **19**, M75–M80 (1975).
21. Carlson, R. L. & Wilkens, R. H. *Geodyn. Ser.* **11**, 127–136 (1983).
22. Cann, J. R. & Von Herzon, R. P. *Init. Rep. DSDP Leg* **69**, 281–299 (1981).
23. Becker, K. *et al. Nature* **300**, 594–598 (1982).
24. Raitt, R. in *The Sea* Vol. 3 (ed. Hill, M. N.) 85–102 (Wiley, New York, 1963).
25. Shor, G. G. in *The Sea* Vol. 7 (ed. Maxwell, A.) 3–27 (Wiley, New York, 1971).
26. Lewis, B. T. R. & Snydsman, W. *Nature* **266**, 340–344 (1977).
27. Carlson, R. L. *et al. Earth planet. Sci. Lett.* **51**, 171–180 (1980).

Growing season precipitation from D/H ratios of Eastern White Pine

J. R. Lawrence* & J. W. C. White

Lamont-Doherty Geological Observatory of Columbia University, Palisades, New York 10964, USA

The search for climatic information from the hydrogen and oxygen isotope analysis of tree rings has produced mixed results[1–6]. Systematic changes in the D/H ratio with changing climate have been demonstrated[7], although relationships between climate change and the D/H ratio in tree rings from a single tree have been claimed, the interpretation of these data still causes controversy. Here we report that there is a strong correlation between both the D/H ratio of summer rain and tree ring cellulose from Eastern White Pine (*Pinus strobus* L.), and the amount of precipitation between May and August.

There are three major difficulties in interpreting the isotope composition of tree ring cellulose. (1) Organic matter is isotopically inhomogeneous[4,7–11]. (2) Complex biological, biochemical and hydrological processes take place during the growth of a tree[7,12–15]. (3) Isotope variations in precipitation from year to year at a single location have not been clearly related to temperature changes, except perhaps for those that accompany significant changes in the polar ice caps[16–18]. We have avoided the problem of the isotopic inhomogeneity of organic matter by analysing only carbon-bound hydrogen from cellulose[7]. Our studies of the complex isotopic fractionations resulting from biological, biochemical and hydrological processes in Eastern White Pine are reported elsewhere[19,20]. They demonstrate that the average hydrogen isotope composition of rain that falls during the growing season, May-August, can be found in tree rings of Eastern White Pine growing under highly restricted water supply conditions. Such trees mostly use soil moisture obtained from summer precipitation and therefore retain only a summer climate signal.

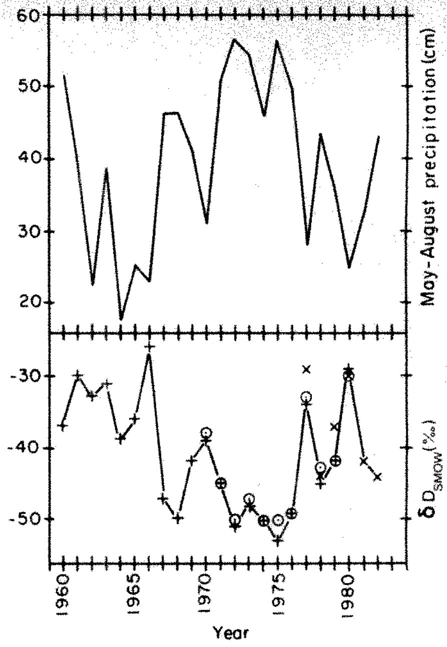

Fig. 1 Average amount of precipitation for the period May–August for five meteorological stations (Mohonk Lake, Poughkeepsie, Ellenville, Gardiner and Rosendale) plotted as a function of time. The δD values of rain and carbon-bound hydrogen from tree rings of two Eastern White Pine trees are also plotted. One tree covers the period 1960–80 (+), the other the period 1970–80 (○) and the rain from 1977–82 (×). The correlation coefficients between the δD values and the amount of May to August precipitation are −0.76, −0.93 and −0.88 respectively.

One climate signal that has been observed from stable isotopes in the precipitation from lower latitudes, is the inverse relationship between the δD and $\delta^{18}O$ of rain and the amount of precipitation. ($\delta D = [(D/H \text{ sample})/(D/H \text{ SMOW} - 1)] \times 10^3$, where SMOW is standard mean ocean water.) This 'amount effect' was observed by Dansgaard[21] when evaluating monthly precipitation samples obtained and analysed by the International Atomic Energy Agency (IAEA). He observed that isotopic ratios were "low in rainy months and high in months with sparse rain". He stated: "this 'amount effect' is found all the year round at most tropical stations, and in the summer time at mid latitudes", this rain being predominantly produced by convective storms. We also detected this amount effect during the present investigation.

Our sampling location, Mohonk Lake, New York, is located ~130 km north of New York City on the Schawangunk ridge on the west side of the Hudson Valley near New Paltz, New York. The two Eastern White Pine trees studied are located on a talus slope where groundwater has not been detected in the tree sap[20]. The trees are ~5 m high, 60 cm in diameter and >200-yr old.

The δD values of the rings from these trees together with the unweighted average δD value of all the individual rainfalls between May and August are plotted as a function of time in Fig. 1. One tree (no. 1) covers the period 1960–80, the other tree (no. 2) 1970–80 and the rains from 1977 to 1982. Also shown in Fig. 1 is the total amount of rain that fell between May and August of each year. These quantities represent the averages of five rain recording stations in the vicinity of Mohonk Lake.

An inverse relationship can be seen between the amount of precipitation and the isotope data (Fig. 1): years of high precipi-

---

* Present address: Department of Geological Sciences, University of Houston, Texas 77004, USA.

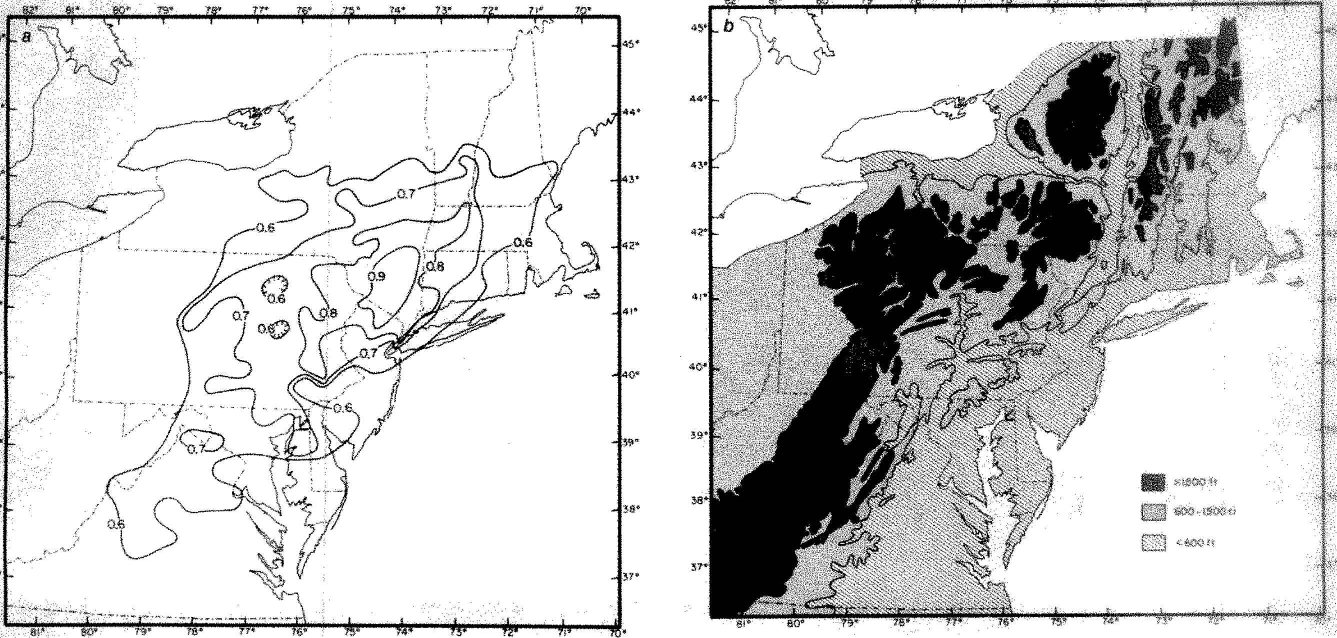

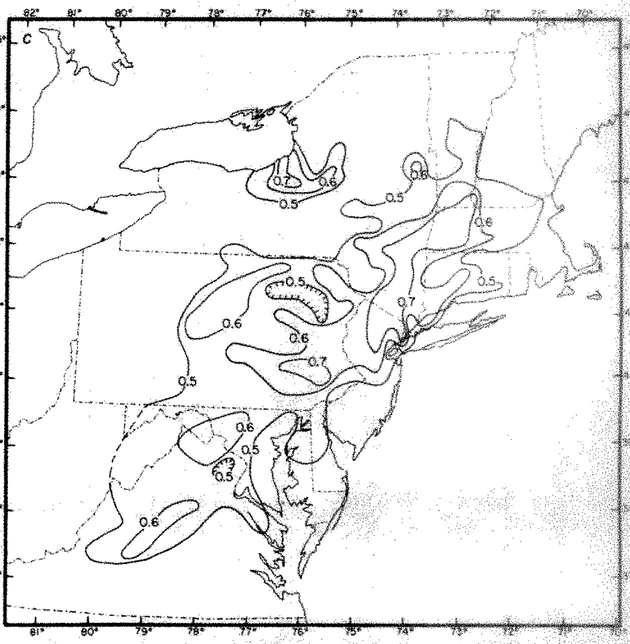

Fig. 2 *a*, Contours of correlation coefficients between the average amount of precipitation for May to August for the five stations given in Fig. 1 for the period 1960–82 and the amount of precipitation for the same time period for 181 stations around the northeastern US. After reduction in the degrees of freedom for persistence in the time series[22] the correlation coefficient contours, 0.6 and 0.7, are significant to better than the 95% confidence level. The contours >0.7 are significant to better than the 99% confidence level. *b*, The topography of the northeastern US showing elevation breaks at 600 and 1,500 feet. *c*, Contours of correlation coefficients between the δD values of carbon-bound hydrogen in the tree rings of the tree covering the period 1960–80 (see Fig. 1) and the average δD value (unweighted) of rainfall from May to August for the years 1981 and 1982 (23 δD values for the period 1960–82) and the amount of rain for May to August at 181 meteorological stations around the northeast US for the same 23-yr period. After reduction for the degrees of freedom in the time series[22] the correlation coefficient contours shown are significant to better than the 95% confidence level.

tation are marked by low δD values and vice versa. There is excellent agreement between the separate isotope data sets. The correlation coefficient between the mean δD value of the rain and the amount of precipitation for the 6 yr when samples were collected is −0.88. For the tree where 11 rings were analysed, the correlation coefficient is −0.93. For the tree covering 21 yr the correlation coefficient is −0.76. Each of these three paired sets of data were checked for persistence (autocorrelation)[22]. After reduction in the number of degrees of freedom, the three correlation coefficients were found to be significant to better than the 95%, 99% and 99% confidence levels respectively. The precipitation data show that the early 1960s had low rainfall whereas the mid-1970s had high rainfall. The isotope data only provide an indication of rainfall amounts during the warmer months, but there was a severe drought during the early 1960s, and during the mid-1970s the climate was wet, as demonstrated by the high level of reservoirs at the time[23]. Individual years of low rainfall during the relatively wet periods stand out—see 1980, 1977 and 1970 in Fig. 1.

The correlation coefficient between the δD of the tree rings and the amount of precipitation during the growing season applies to the immediate area around Mohonk Lake. To get a better idea of the regional extent of this isotope–precipitation relationship, additional correlations were attempted with meteorological stations around the northeastern US. First, the average May to August precipitation amounts from the five stations in the vicinity of Mohonk Lake for the period 1960–82 were correlated with precipitation amounts for the same 4 months and 23 yr for stations around northeastern US. A total of 181 correlation coefficients were calculated. The results (shown in Fig. 2*a*) show that topography and proximity to the ocean may be important (Fig. 2*b*). Correlations drop markedly near the ocean and are generally lower over mountain areas. Lower-lying areas excluding near shore areas have higher correlation coefficients.

A similar regional correlation picture (Fig. 2*c*) was constructed using the isotope data from tree 1 for the period 1960–80 and 2 yr (1981 and 1982) of rain isotope data. The isotopic results for this 23-yr period were correlated with precipitation during May–August for the same 181 stations as used in the precipitation correlations. The patterns are very similar to those observed in Fig. 2*a*.

Our results suggest that δD values of carbon-bound hydrogen from tree rings of Eastern White Pine growing in water-restricted conditions can be used to study past summer precipitation patterns. The region covered by our studies is primarily the

Hudson Valley and bordering areas. Because the relationship between the δD values of rain and the amount of precipitation during the growing season should apply to other areas in the eastern US, isotopic studies of trees in such areas might also reveal distinctive precipitation patterns with time. Combining results from several trees in different areas would then not only give variations of growing-season precipitation for individual areas but would also give the historical distribution of precipitation in both a spatial and temporal sense. Such a picture would be useful for understanding long-term changes in atmospheric circulation particularly for the warmer months of the year.

The isotope technique for obtaining climate information from tree rings of Eastern White Pine has certain advantages including that the hydrogen isotope climate signal is derived from the precipitation itself, and thus contains information about atmospheric processes. Future research will give a better picture of the causes of changes in the isotope ratios. For example, it has been shown that the isotopic composition of precipitation is influenced by the positions of storm tracks[24]. Oxygen isotopic analyses of Eastern White Pine when combined with hydrogen isotope analyses show considerable promise in providing a relative humidity signal[19]; the use of both isotopes should therefore prove highly valuable. The combined use of these isotope techniques with standard ring width techniques looks even more promising.

This research was supported by grants ATM 79-18920, ATM 81-16371 and ATM 83-13954 from the Climate Dynamics Section of the NSF. We thank E. R. Cook, D. Stockton, G. Jacoby, and J. Jouzel for helpful critical comments. Lamont-Doherty Geological Observatory contribution no. 3706.

Received 3 May; accepted 13 August 1984.

1. Schiegl, W. E. *Nature* **251,** 582–584 (1974).
2. Wilson, A. T. & Grinsted, M. J. *Nature* **257,** 387–388 (1975).
3. Libby, L. M. *et al. Nature* **261,** 284–288 (1976).
4. Epstein, S. & Yapp, C. J. *Earth planet. Sci. Lett.* **30,** 252–261 (1977).
5. Gray, J. & Thompson, P. *Nature* **262,** 481–482 (1976).
6. Yapp, C. J. & Epstein, S. *Earth planet. Sci. Lett.* **34,** 333–350 (1977).
7. Epstein, S., Yapp, C. J. & Hall, J. H. *Earth planet. Sci. Lett.* **30,** 241–251 (1976).
8. Wilson, A. T. & Grinsted, M. J. *Earth planet. Sci. Lett.* **36,** 246–248 (1976).
9. Epstein, S. & Yapp, C. *Nature* **266,** 477–478 (1977).
10. Libby, L. M. & Pandolfi, L. J. *Nature* **266,** 478 (1977).
11. Gray, J. & Thompson, P. *Nature* **270,** 708–709 (1977).
12. Wigley, T. M. L., Gray, B. M. & Kelly, P. M. *Nature* **271,** 92–93 (1978).
13. Wilson, A. T. *Nature* **271,** 93 (1978).
14. Gray, J. & Thompson, P. *Nature* **271,** 93–94 (1978).
15. Libby, L. M. & Pandolfi, L. J. *Nature* **271,** 94 (1978).
16. Dansgaard, W. & Tauber, H. *Science* **166,** 499–502 (1969).
17. Epstein, S., Sharp, R. P. & Gow, A. J. *Science* **168,** 1570–1572 (1970).
18. Dansgaard, W., Johnsen, S. J., Clausen, H. B. & Langway, C. C. Jr in *Late Cenozoic Glacial Ages* (ed. Turekian, K. K.) 37–56 (Yale University, New Haven, 1971).
19. White, J. W. C. thesis, Columbia Univ. (1983).
20. White, J. W. C., Cook, E. R., Lawrence, J. R. & Broecker, W. S. *Geochim. cosmochim. Acta* (in the press).
21. Dansgaard, W. *Tellus* **16,** 436–468 (1964).
22. Dawdy, D. R. & Matalas, N. C. in *Handbook of Applied Hydrology* (ed. Chow, V. T.) 87 (McGraw-Hill, New York, 1964).
23. Cook, E. R. & Jacoby, G. C. Jr *Science* **198,** 399–401 (1977).
24. Lawrence, J. R., Gedzelman, S. D., White, J. W. C., Smiley, D. & Lazov, P. *Nature* **296,** 638–640 (1981).

Induction of hair growth by implantation of cultured dermal papilla cells

C. A. B. Jahoda*, K. A. Horne & R. F. Oliver

Department of Biological Sciences, University of Dundee,
Dundee DD1 4HN, UK

Mammalian hairs are formed by differentiation and keratinization of cells produced in the epidermal matrix (Figs 3, 4). Using the rodent vibrissa follicle as a model[1], transplantation studies have shown that the dermal papilla, a discrete population of specialized fibroblasts, is of prime importance in the growth of hair[2,3]. Papillae induce hair growth when implanted into follicles[4,5] and can interact with skin epidermis to form new hair follicles[6]. When grown in culture, papilla cells display singular morphological and behavioural characteristics compared with connective tissue cells from other skin sources[7,8]. We report here that serially cultured adult papilla cells can induce the growth of hair when implanted into follicles which otherwise would not grow hairs. This finding presents an opportunity to characterize properties distinguishing the papilla cell population from other skin fibroblasts, and, more specifically, those which control hair growth. The eventual application of this work to human hair replacement techniques can also be envisaged.

We have cultured dermal papillae from adult rats. When the cells reach confluence, they form aggregates (Fig. 1) and can be serially cultured[7,8]. We have shown previously that discrete, freshly dissected papillae induce hair growth when implanted into the bases of follicles from which the lower halves with their original papillae have been removed[4]. Such follicles (Fig. 2) would not otherwise produce hairs[4,9,10]. In the present studies, we used similarly prepared follicles to evaluate the inductive capacity of cultured papilla cells when implanted as pellets into the bases of follicles from which the lower halves had been removed. Skin fibroblasts of early passage numbers (1–4) were used as control implants. After 4 weeks, hairs emerged from 28 (53%) of the follicles which had received papilla cells of early passage numbers (1–3), and those follicles kept under observation produced generations of hairs in a normal cyclic fashion.

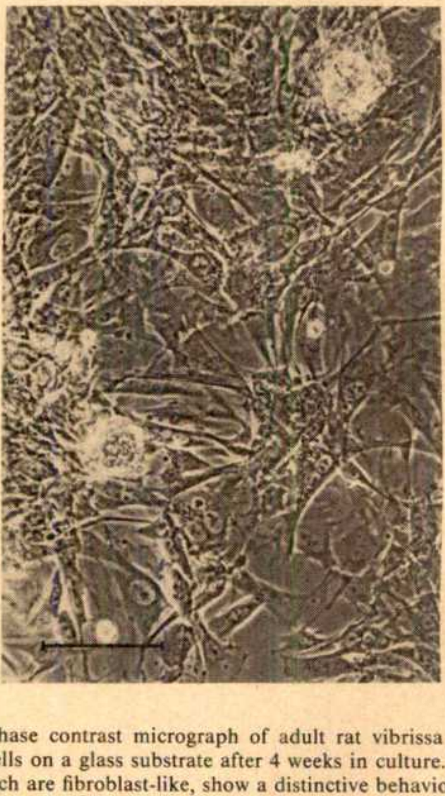

Fig. 1 Phase contrast micrograph of adult rat vibrissa dermal papilla cells on a glass substrate after 4 weeks in culture. Papilla cells, which are fibroblast-like, show a distinctive behaviour both in explant culture[7] and after passaging[8] and, in contrast to skin fibroblasts, tend to form clumps or aggregates on reaching confluence. Using a stereoscopic microscope, intact, epidermal cell-free dermal papillae dissected from the lower regions of vibrissa follicles, which had been excised from the upper lip of adult inbred hooded PVGC rats, were cultured as described previously[7,8]. Between 5 and 30 papillae were cultured at any one time as explants in Cruickshank culture chambers at 37 °C in an atmosphere of 5% CO_2–95% air in Eagle's minimal essential medium (Gibco) supplemented with 15–20% fetal calf serum (Gibco). The medium was changed every 3 or 4 days and on reaching confluence the cells were serially transferred to 35-mm dishes. Adult skin fibroblasts, derived from skin explants, were similarly grown in culture. Scale bar, 100 μm.

---

* Present address: Laboratoire de Zoologie, Université de Grenoble I, France.

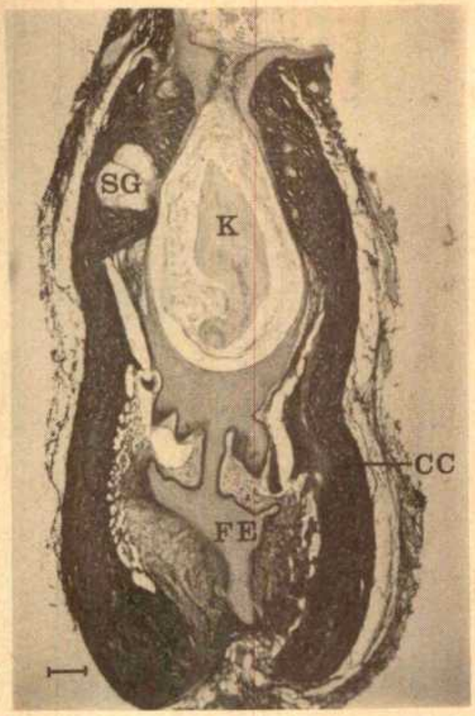

Fig. 2 Longitudinal section of a control vibrissa follicle from which approximately the lower half of the follicle has been removed. No subsequent hair growth has occurred and, near the bottom, remaining follicular epidermis (FE) has reverted to a solid column of outer root sheath cells. A loose plug of keratin (K) is visible near the top of the follicle adjacent to the sebaceous gland (SG). Vibrissa follicles are enclosed by a thick collagenous capsule (CC) the cut edge of which can be seen at the bottom. Vibrissa follicles, which are clearly arranged in a well defined pattern[9], were exposed by reflecting the whisker pad on the upper lip and the follicles selected for operation were identified. Lengths of follicle, including the entire bulb and enclosed papilla, were removed with a transverse cut to leave half or less of the upper region of each follicle *in situ* and the pad was stitched back into position[4]. An identical procedure was used to prepare follicles to receive either cultured papilla cell or fibroblast implants. Following biopsy, follicles were serially sectioned for histological examination. Scale bar, 100 μm.

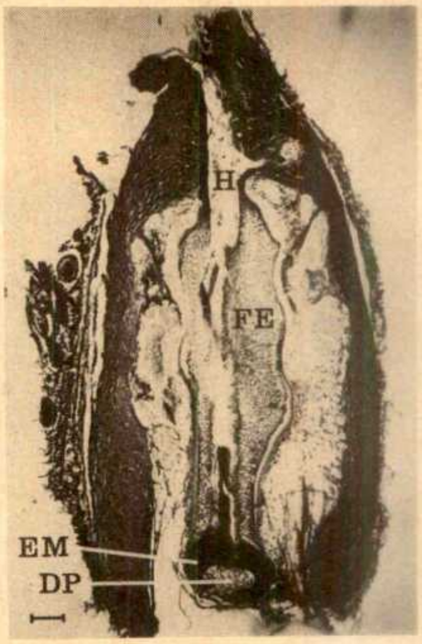

Fig. 3 The upper half of a vibrissa follicle into the base of which cultured dermal papilla cells had been implanted. Follicular epidermis (FE) has become organized around the new dermal papilla (DP) and has formed a basophilic epidermal matrix (EM) which is actively producing hair (H). Papilla cells scraped from culture dishes and divided into small pellets were inserted into the bases of the exposed follicular epidermis following removal of the lower halves of the follicles. Scale bar, 100 μm.

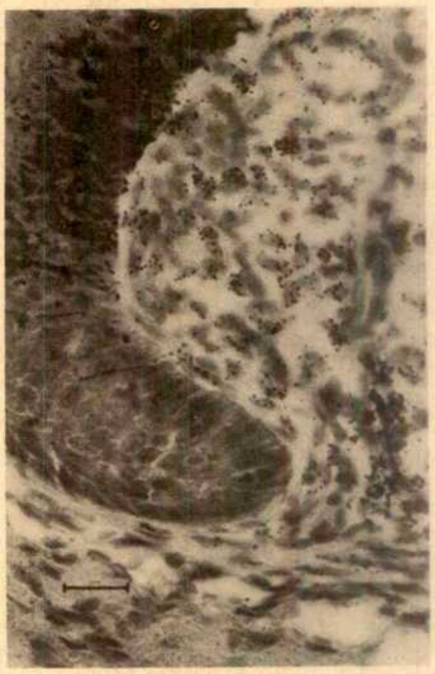

Fig. 4 Autoradiograph showing detail of the bulb region of a follicle actively growing hair 28 days after implantation of papilla cells which had been labelled in culture with a total dose of 2 μCi of ^{3}H-labelled thymidine. Labelling is restricted to cells in the dermal papilla and its basal stalk with no evidence of labelling in the surrounding connective tissue cells. Part of the epidermal matrix is shown on the left-hand side. Scale bar, 20 μm.

In contrast, no hairs emerged either from amputated follicles which had not received papilla cell implants (Fig. 2) or from follicles into which cultured skin fibroblasts had been implanted.

Histological examination revealed the presence of a new bulb at the site of papilla cell implantation, with an epidermal matrix organized around a discrete dermal papilla (Fig. 3). Further evidence that the new papilla originated from implanted papilla cells was obtained by autoradiographic examination of follicles where implanted papilla cells were labelled with ^{3}H-thymidine (Fig. 4). Thus we have shown that the original papilla cell mass can form a functional dermal papilla which interacts with follicular epidermis, resulting in the organization of a new, hair-producing bulb. By demonstrating that cultured papilla cells retain their ability to elicit hair growth, the specific properties of papilla cells which operate to modulate follicular epidermal cell activity and thus control the growth of hair can now be analysed and characterized *in vitro*. One such approach would be to compare profiles of the characteristics of papilla cells of early passage numbers (1–3) with those of later passage number cells (10–15), which appear to lose their inductive ability, and with skin fibroblasts. Work is in progress to determine the stage at which the functional capacity of papilla cells in culture is irretrievably lost.

With the recent culture of follicular epidermal cells[11], it will be possible also to study the influence of papilla cells (which retain some of their *in situ* traits when grown alone in culture[8]) on epidermal proliferation and differentiation. Although it has been shown that epidermal and dermal cell suspensions from newborn mouse skin are capable of reforming hair follicles when transplanted into adult animals[12], it is unclear whether at this stage of skin development all dermal cells are still capable of being involved in follicle reformation. We suggest that in adult animals, skin fibroblast cells from non-follicular dermis are incapable of performing the same role as dermal papilla cells.

Finally, recent advances in cell culture of individual dermal and epidermal follicle components have importance for the study of human hair disease and hair loss as well as for dermal–epidermal interactions. In particular the culture of human hair dermal papilla cells[13] means that, for example, the effects of hormones on the dermal component can now be examined. Our demonstration that dermal papilla cells which have divided can still promote active hair growth, and our recent finding that cultured papilla cells can induce hair follicle formation when associated with non-hair-forming embryonic epidermis (C.A.B.J., unpublished data), raises the possibility of using cell culture techniques to increase dermal papilla cell numbers as part of a human hair transplant process.

We thank Mr G. Coghill for performing the autoradiography. This work was supported by MRC studentship.

Received 6 February; accepted 3 August 1984.

1. Cohen, J. *J. Embryol. exp. Morph.* **9,** 117–127 (1961).
2. Oliver, R. F. in *The Skin of Vertebrates* (eds Spearman, R. I. C. & Riley, P. A.) 199–210 (Academic, London, 1980).
3. Oliver, R. F. & Jahoda, C. A. B. in *Hair Research* (eds Orfanos, C. E., Montagna, W. & Stuttgen, G.) 18–24 (Springer, Berlin, 1981).
4. Oliver, R. F. *J. Embryol. exp. Morph.* **18,** 43–51 (1967).
5. Ibrahim, L. & Wright, E. A. *Nature* **265,** 733–734 (1977).
6. Oliver, R. F. *J. Embryol. exp. Morph.* **23,** 219–236 (1970).
7. Jahoda, C. A. B. & Oliver, R. F. *Br. J. Derm.* **105,** 623–627 (1981).
8. Jahoda, C. A. B. & Oliver, R. F. *J. Embryol. exp. Morph.* **79,** 211–224, 1984.
9. Oliver, R. F. *J. Embryol. exp. Morph.* **15,** 331–347 (1966).
10. Oliver, R. F. *J. Embryol. exp. Morph.* **16,** 231–244 (1966).
11. Weterings, P. J. J. M., Vermorken, A. J. M. & Bloemendal, H. *Expl Cell Res.* **139,** 439–443 (1982).
12. Worst, P. K. M., Mackenzie, I. C. & Fusenig, N. E. *Cell Tissue Res.* **225,** 65–77 (1982).
13. Messenger, A. G. *Br. J. Derm.* **110,** 685–689 (1984).

Monoclonal antibodies define differential *ras* gene expression in malignant and benign colonic diseases

A. Thor, P. Horan Hand, D. Wunderlich, A. Caruso, R. Muraro & J. Schlom

Laboratory of Tumor Immunology and Biology,
National Cancer Institute, National Institutes of Health, Bethesda,
Maryland 20205, USA

DNAs of some human tumours can transform NIH 3T3 fibroblast cells[1–7], thus demonstrating the transforming potential of human *ras* genes (Hu-*ras*^{Ha}, Hu-*ras*^{Ki}, and Hu-*ras*^{N}, respectively Harvey, Kirsten and neuroblastoma *ras* genes). Only a small percentage of a given type of human carcinoma, however, scores positive in this assay system[8–10]. Activation of *ras* and subsequent transformation of NIH 3T3 cells are either by a point mutation in the *ras* gene[11–18] or enhanced expression of the normal, or proto-onc, *ras* gene[19–21]. If the transformation of a given human tumour involves the enhanced expression of the normal or cellular *ras* gene and the resulting gene product, the tumour DNA would probably score negative in the NIH 3T3 transfection assay. In human colon carcinoma, for example, lesions at position 12 of Hu-*ras*^{Ki} have been found[8,21]. None of nine colon carcinomas obtained at biopsy, however, contain the *ras* lesion at this position, using a Hu-*ras*^{Ha} probe[22]; one other colon carcinoma does appear to contain amplified proto-onc *ras*[21], and other colon carcinomas do have increased levels of *ras* RNA[23]. There are at least three explanations for these observations. Either very few colon carcinomas contain point-mutated *ras*, the lesion in the majority of colon carcinomas is at a position other than 12, or *ras* activation in many colon carcinomas involves the enhanced expression of either the point-mutated or proto-onc form of a *ras* gene. We have now used monoclonal antibodies directed against a synthetic peptide reflecting sequences of the human T24 *ras* gene product to define *ras* p21 protein expression in a spectrum of colonic disease states. Immunohistochemical analyses of individual cells within tissue sections reveal differences in *ras* p21 expression in colon carcinomas compared with normal colonic epithelium, benign colon tumours and inflammatory or dysplastic colon lesions. Our data suggest that *ras* p21 expression is correlated with depth of carcinoma within the bowel wall, and is probably a relatively late event in colon carcinogenesis.

Monoclonal antibodies directed against human tumour-associated antigens have proved extremely useful in understanding the human neoplastic process and in defining differences between human malignant and normal cell populations. Immunohistochemical techniques using formalin fixed tissue sections and monoclonal antibodies have been used to identify different cell populations within a given tumour mass, which is particularly useful in the study of human carcinomas, such as colon carcinoma.

We have developed recently a series of monoclonal antibodies that are immunoreactive with the human *ras* 21,000 molecular weight (MW) gene product, p21. The immunogen used was a synthetic peptide reflecting positions 10–17 of the Hu-*ras* protein product from the T24 bladder carcinoma[24]. The antibodies designated RAP (for *ras* peptide) one to five[24], react with both the T24 Hu-*ras* peptide and the Hu-*ras*^{Ha} peptide (which differ in a single amino acid at position 12 of the p21 molecule, Val for Gly, respectively[17]) using solid phase radioimmunoassays. They also immunoreact with a 21,000 MW protein in both T24 bladder carcinoma cells[15] and rat mammary tumours containing activated *ras*[25,26]. We have shown also that denaturation of cell extracts or tissue sections with formalin or glutaraldehyde enhanced detection of *ras* p21 by the RAP monoclonal antibodies[24]; this was expected, as the amino acids at positions 10–17 are predicted to sequester within the tertiary structure of the p21 molecule[27,28]. We report here studies using the RAP antibodies to determine whether any biological correlations exist between enhanced *ras* p21 expression (either the point-mutated

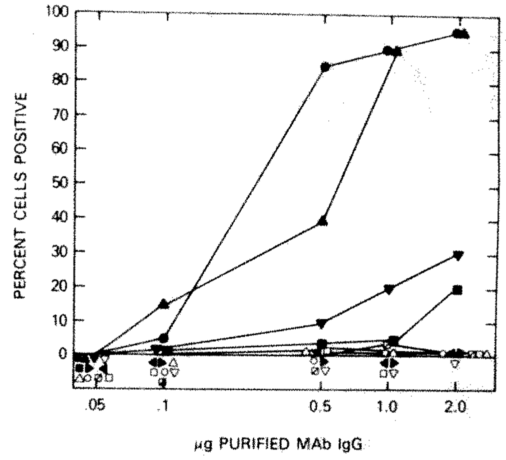

Fig. 1 Titration of purified antibody RAP-5 (in μg purified IgG per 200 μl) with formalin fixed colonic tissues. Serial sections of adenocarcinomas of the colon (solid symbols), tubulovillous adenomas (open and slashed squares), tubular adenomas (open triangles) and normal colonic epithelium (open circles) were assayed for *ras* p21 using the ABC immunoperoxidase technique[49,50] and purified IgG[51] of RAP-5. (Histologically, tubular adenomas demonstrate branching tubules embedded in the lamina propria, and tubulovillous adenomas are mixtures of tubular and villous patterns[43]). The % of positive cells is a semiquantitative value (evaluated twice independently) determined by tumour cells scoring *ras* positive divided by the total tumour cells × 100 (for carcinomas and adenomas), and the % normal colonic epithelial cells is determined by dividing *ras* positive epithelial cells by the total number of normal colonic epithelial cells × 100. For all tissues used in this study a control IgG2a isotype identical primary antibody (UPC-10)[52] was used at the same immunoglobulin concentrations as the RAP antibodies and no positivity was demonstrated.

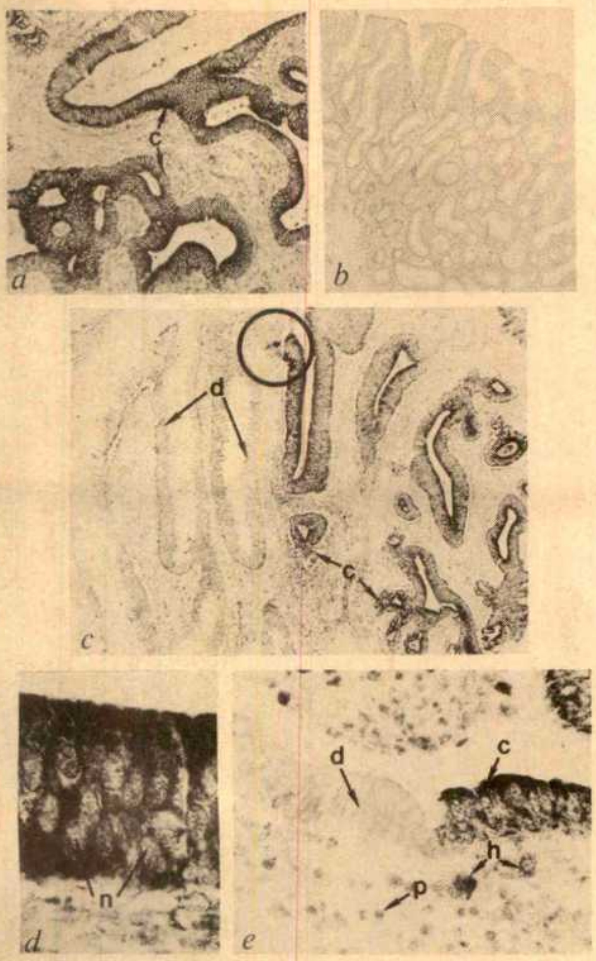

Fig. 2 Immunoperoxidase staining of colon lesions by RAP-1. RAP-1 (at a 1:8 dilution of supernatant fluid) was reacted with formalin fixed paraffin embedded human tissues using the ABC immunoperoxidase method. *a*, Adenocarcinoma of the colon (invasive, ×130). The dark regions reflect the reaction of the diaminobenzidine substrate and thus antibody binding to cytoplasmic *ras* p21 in carcinoma (c) cells. The lighter region is the haematoxylin counter stain, showing no antibody reactivity. *b*, Tubulovillous adenoma (×38). Dysplastic colonic epithelium, stroma and a mixed inflammatory mononuclear cell infiltrate are negative. *c*, Colonic adenocarcinoma (×130); mild dysplasia (d) and invasive carcinoma (c) arising in a patient with a 20-yr history of ulcerative colitis. Weak basal positivity with RAP-1 of mildly dysplastic cells is seen (circle) adjacent to strongly staining cells which are severely dysplastic and/or carcinoma *in situ*. *d*, A higher magnification (×540) of *c* demonstrating cells expressing large quantities of *ras* p21 with disorganized architecture and enlarged anaplastic nuclei (n) in the zone of severe dysplasia and/or carcinoma *in situ*. *e*, A transition zone (other than seen in *d*) of mild dysplasia (d), adjacent to carcinoma *in situ* (c) expressing high levels of *ras* p21. Note the negative submucosal stroma and plasma cells (p) and the positive histiocytes (h) (×540).

or proto-onc form) within individual cell types in a spectrum of colonic disease states.

5 μm-thick sections of formalin fixed colon carcinomas were assayed for Hu-*ras* p21 content using purified immunoglobulin preparations of monoclonal antibody RAP-5 and the ABC immunoperoxidase method. Using a 40-fold range of purified antibody and serial sections of tumours, four of the six colon carcinomas are clearly positive for *ras* p21 expression (Fig. 1). The cell type expressing *ras* in these sections is the malignant epithelium (Fig. 2*a*), with the number of positive carcinoma cells ranging from 20% to 90% (Fig. 1); the number of reactive cells could be reduced in a linear fashion by decreasing the concentration of the RAP antibody used. Colonic stroma and smooth muscle are negative for *ras* p21. Normal colonic mucosa from carcinoma patients (when seen within the same section containing carcinoma cells) is either negative for reactivity with RAP-5 at all immunoglobulin concentrations used, or demonstrates less than 1% of normal epithelial cells expressing *ras* p21. Normal colonic epithelium from a non-cancer patient also contains less than 1% positive cells at all RAP-5 concentrations (Fig. 1).

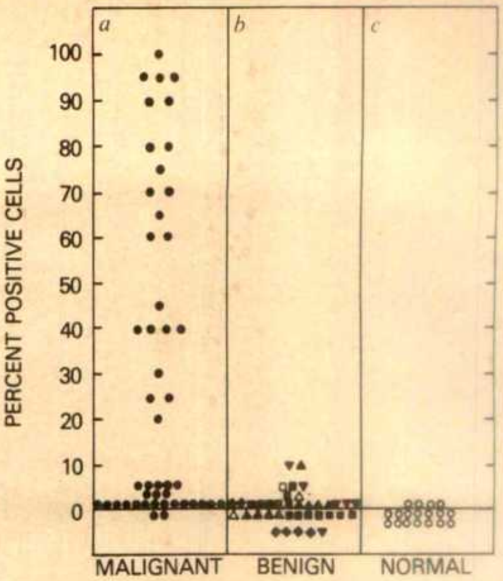

Fig. 3 Reactivity of RAP-1 with various colonic disease states. RAP-1 (at a 1:8 dilution of supernatant fluid) was reacted with formalin fixed 5-μm sections of colonic adenocarcinomas (*a*, closed circles), diverticulitis (*b*, inverted triangles), tubular adenomas (*b*, squares), tubulovillous adenomas (*b*, triangles), ulcerative colitis (*b*, diamond), hamartomatous polyp (*b*, open square), inflammatory bowel disease, not otherwise specified (*b*, open triangle), and normal colon (*c*, open circles), using the ABC immunoperoxidase method. Each symbol represents a tumour or tissue from a different patient. The % positive cells denotes the number of tumour cells scoring *ras* p21 positive divided by the total number of tumour cells × 100 in carcinomas and benign tumours (*a*, *b*) and denotes the number of epithelial cells scoring *ras* p21 positive divided by the total number of epithelial cells × 100 in diverticulitis and inflammatory bowel disease (*b*) and normal colon (*c*). RAP-1 and RAP-5 gave similar results in these studies.

Four benign colon tumours (two tubular and two tubulovillous adenomas) were also assayed for *ras* p21 expression using identical RAP-5 concentrations and assay conditions to those described above. Both types of lesions have been implicated as potentially premalignant[29,30], with a higher incidence of carcinoma arising from tubulovillous adenomas[31-33]. The tumour cells from all four polyps assayed are either negative for RAP binding or contain only a few cells positive over the 40-fold range of antibody concentrations used (Figs 1 and 2*b*).

To further define if biological correlations exist in *ras* p21 expression, 47 colon carcinomas, 38 benign colon tumours, inflammatory or dysplastic colon lesions, and 18 specimens of normal colon from non-cancer patients were examined for reactivity with antibody RAP-1. Of the 47 carcinomas, 45 contain some *ras* positive carcinoma cells; however, a distinction could be observed (Fig. 3*a*) with 23/47 (49%) of the tumours from individual cancer patients containing greater than 20% of tumour cells expressing *ras* p21 at the antibody concentration used. In contrast, 4 of the 18 normal colon samples from non-cancer patients contain ≤1% positive cells with the remainder scoring negative (Fig. 3*c*). Several types of benign, dysplastic or inflammatory colon lesions were also assayed (Fig. 3*b*). Of these 38 lesions, 36 are either negative for *ras* p21 expression or contain ≤5% of tumour or epithelial cells scoring positive, with the remaining two lesions containing 10% positive cells. We conclude that at the RAP antibody concentration and conditions used for these assays, enhanced *ras* p21 expression can be observed (using >20% cells positive as an arbitrary criterion, Fig. 3) in 23 of 47 colon carcinomas, as opposed to none of 38

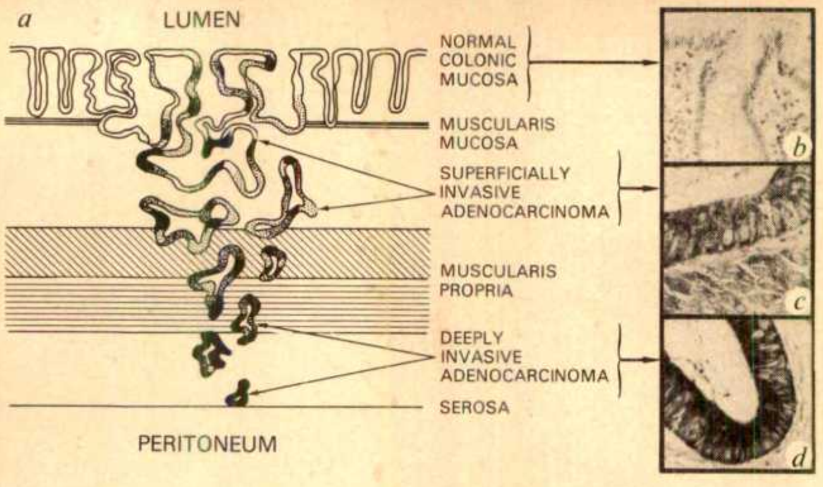

Fig. 4 Correlation between depth of colon carcinoma invasion and *ras* p21 expression. *a*, Schematic representation of a serial section of the bowel wall with the various histological layers, dysplastic and carcinomatous structures identified. Representative immunoperoxidase staining of these various structures with RAP-1 is depicted by the strong (dark) expression of *ras* p21 in deeply invasive glands versus the lesser amount of *ras* p21 expression (lighter shading) in more superficial glands. *b*–*d*, The different areas of a single tissue section containing all areas represented schematically in *a*. *b*, Normal colonic mucosa (×220). The epithelium and stroma are negative. There is a weak reactivity of tissue histiocytes. *c*, Superficially invasive adenocarcinoma (×330). Tumour cell heterogeneity and weak reactivity for *ras* p21 are demonstrated *d*, Deeply invasive adenocarcinoma (×220). Subserosal tumour demonstrates intense expression of *ras* p21.

benign colon tumours, dysplastic or inflammatory lesions, or 18 normal colon specimens (all from different patients). The immunoassays reported here should be termed 'group specific' for Hu-*ras*, in that they identify determinants shared by a group of related genes (Ha, Ki, N) within a given species[34]. The development of additional immunological reagents to 'class specific' and 'type specific' epitopes reflecting the more variable regions of this gene family, and molecular probes reflecting these variable regions, will be required to answer questions as to which tumours or cells within a given tumour mass are expressing a specific *ras* gene.

Much antigenic heterogeneity has been observed within most human carcinomas using monoclonal antibodies directed against several distinct tumour associated antigens[35]. We find that virtually all colon carcinoma specimens also vary in the per cent of tumour cells within a given tumour mass expressing *ras* p21 (Fig. 3*a*). It is interesting that *ras* activation defined by DNA transfection occurs in only one of five melanoma cell lines derived from independent metastatic foci of a single patient[36]. We used RAP-5 to examine five metastatic lesions from two colon carcinoma patients whose primary tumours were positive for *ras* p21 expression (40% and 80% of tumour cells, respectively). All five metastatic lesions (to ovary, liver, omentum and two lymph nodes) also displayed antigenic heterogeneity, with levels ranging from 5% to >90% of cells scoring positive for *ras* p21 expression. There are several possible explanations for this observed heterogeneity in *ras* expression. (1) The assays used may not be sensitive enough to detect low levels of *ras* expression in some cells; (2) the cell cycle may influence p21 expression (as seen in other tumour-associated antigens[37] and *ras*[38]); (3) the milieu of individual tumour cells or tumour cell clusters including autocrine, paracrine and/or endocrine factors may influence *ras* expression; (4) *ras* may not be involved in the aetiology of colon cancer; its expression could be an effect of the neoplastic process in some cells or lesions. Alternatively, it may be involved in the initial transformation event, but other mechanisms of conferring immortality may come into play in the approximately 10 to 30 years that elapse between the initial cell transformation and the detection and removal of a carcinoma mass[39,40].

There is much evidence that many carcinomas arise from premalignant disease states such as adenomas, familial adenomatous polyposis, or ulcerative colitis[41–43]. If such a multistep process is involved in colon carcinogenesis, it would be of interest to determine where in this process enhanced *ras* expression is detected. Figure 2 shows examples of invasive carcinoma in a pseudopolyp of an ulcerative colitis patient (Fig. 2*c*, *e*). The dysplastic epithelial cells of the pseudopolyp here react weakly with the RAP antibody. In contrast, adjacent cells (which are more severely dysplastic and/or carcinoma *in situ*) express comparatively high levels of *ras* p21. We conclude that *ras* activation, at least in these carcinomas, may be a relatively late event in the transformation process[10,44,45].

The degree of malignancy (potential for metastasis) of a colon carcinoma correlates with the depth of tumour invasion through the bowel wall (from the muscularis mucosa to the serosa) (Fig. 4*a*)[46–48]. This invasion may occur via the infiltration of individual tumour cells through the stromal elements and musculature of the bowel wall; these cells are believed to subsequently divide and form individual tumour cell clusters with various degrees of glandular organization. We identified specimens from three colon cancer patients in which benign colonic mucosa, as well as the depth of invasion of tumour cell clusters, could be evaluated for each patient. In these samples, normal colonic mucosa are either negative or express extremely low levels ($\leq 1\%$ of cells) of Hu-*ras* p21 (Fig. 4*b*). Superficially invasive carcinoma cells show intermediate levels of Hu-*ras* p21 (Fig. 4*c*), whereas deeply invasive tumour cell clusters (Fig. 4*d*) show the highest levels of *ras* p21 in the tumour mass. Thus, in each of the three cases in which the depth of individual dysplastic and malignant tumour cell clusters could be evaluated, enhanced Hu-*ras* p21 expression detected by RAP-1 correlate with depth of tumour invasion.

Whether *ras* gene activation is actually involved in the aetiology of human colon cancer remains to be proven. The immunological studies reported here do, however, provide evidence that *ras* p21 is differentially expressed in many malignant colon carcinomas compared with benign colon tumours, dysplastic or inflammatory lesions and normal colon. Furthermore, enhanced *ras* expression appears to correlate with the depth of invasion (presumed degree of malignancy) in at least some colon carcinoma lesions, and also appears to be a relatively late event, at least within some lesions, in the multi-step process of colon carcinogenesis.

We thank K. McNaughton, A. Sloan, M. Ballard, J. Knapp, D. Poole, M. Taylor, E. Smith, P. Freeman and L. Otsby for technical assistance and Dr M. Weeks for helpful discussions.

Received 13 April; accepted 26 July 1984.

1. Pulciani, S. *Proc. natn. Acad. Sci. U.S.A.* **79,** 2845–2849 (1982).
2. Parada, L. F., Tabin, C. J., Shih, C. & Weinberg, R. A. *Nature* **297,** 474–478 (1982).
3. Shimizu, K. *et al. Proc. natn. Acad. Sci. U.S.A.* **80,** 2112–2116 (1983).
4. Hall, A., Marshall, C. J., Spurr, N. K. & Weiss, R. A. *Nature* **303,** 396–400 (1983).
5. Shimizu, K., Goldfarb, M., Perucho, M. & Wigler, M. *Proc. natn. Acad. Sci. U.S.A.* **80,** 383–387 (1983).
6. Der, C., Krontiris, T. & Cooper, G. *Proc. natn. Acad. Sci. U.S.A.* **79,** 3637–3640 (1982).
7. Shih, C. & Weinberg, R. A. *Cell* **29,** 161–169 (1982).
8. Pulciani, S. *et al. Nature* **300,** 539–542 (1982).
9. Feig, L. A., Bast, R. A. Jr, Knapp, R. C. & Cooper, G. M. *Science* **223,** 698–700 (1984).
10. Land, H., Parada, L. F. & Weinberg, R. A. *Science* **222,** 771–777 (1983).
11. Santos, E., Tronick, S. R., Aaronson, S. A., Pulciani, S. & Barbacid, M. *Nature* **298,** 343–347 (1982).
12. Nakano, H. *et al. Proc. natn. Acad. Sci. U.S.A.* **81,** 71–75 (1984).
13. Capon, D. J. *et al. Nature* **304,** 507–513 (1983).
14. Der, C. J. & Cooper, G. M. *Cell* **32,** 201–208 (1983).
15. Tabin, C. J. *et al. Nature* **300,** 142–148 (1982).
16. Santos, E. *et al. Science* **223,** 661–669 (1984).
17. Taparowsky, E. *et al. Nature* **300,** 762–765 (1982).
18. Reddy, E. P., Reynolds, R. K., Santos, E. & Barbacid, M. *Nature* **300,** 149–152 (1982).
19. Chang, E. H., Furth, M. E., Scolnick, E. M. & Lowy, D. R. *Nature* **297,** 479–483 (1982).
20. DeFeo, D. *et al. Proc. natn. Acad. Sci. U.S.A.* **78,** 3328–3332 (1981).
21. McCoy, M. S. *et al. Nature* **302,** 79–81 (1983).

22. Feinberg, A. P., Vogelstein, B., Droller, M. J., Baylin, S. B. & Nelkin, B. D. *Science* **220,** 1175–1177 (1983).
23. Slamon, D. J., deKernion, J. B., Verma, I. M. & Cline, M. J. *Science* **224,** 256–262 (1984).
24. Horan Hand, P. *et al. Proc. natn. Acad. Sci. U.S.A.* **81,** 5227–5231 (1984).
25. Sukumar, S., Notario, V., Martin-Zanca, D. & Barbacid, M. *Nature* **306,** 658–661 (1983).
26. Cho-Chung, Y. S. & Huang, F. L. in *Proc. 16th Miami Winter Symp.*, 142–143 (ICSU Press, Miami, 1984).
27. Wierenga, R. K. & Hol, W. G. J. *Nature* **302,** 842–844 (1983).
28. Pincus, M. R. *et al. Proc. natn. Acad. Sci. U.S.A.* **80,** 5253–5257 (1983).
29. Muto, T., Bussey, H. R. J. & Morson, B. C. *Cancer* **36,** 2251–2270 (1975).
30. DeVita, V. T. Jr, Hellman, S. & Rosenberg, S. A. *Cancer: Principles and Practice of Oncology*, 647–650 (Lippincott, Philadelphia, 1982).
31. Spratt, J. S., Ackerman, L. V. & Moyer, C. A. *Ann. Surg.* **148,** 682–698 (1958).
32. Castleman, B. & Krickstein, H. I. *New Engl. J. Med.* **267,** 469–475 (1962).
33. Fung, C. H. K. & Goldman, H. *Am. J. clin. Path.* **53,** 21–25 (1970).
34. Shih, T. Y. & Weeks, M. O. *Cancer Invest.* **2,** 109–123 (1984).
35. Horan Hand, P., Nuti, M., Colcher, D. & Schlom, J. *Cancer Res.* **43,** 728–735 (1983).
36. Albino, A. P., LeStrange, R., Oliff, A. I., Furth, M. E. & Old, L. J. *Nature* **308,** 69–72 (1984).
37. Kufe, D. W. *et al. Cancer Res.* **43,** 851–857 (1983).
38. Campisi, J., Gray, H. E., Pardee, A. B., Dean, M. & Sonenshein, G. E. *Cell* **36,** 241–247 (1984).
39. Spratt, J. S. & Ackerman, L. V. *Am. Surg.* **27,** 23–28 (1961).
40. Welin, S., Youker, J. & Spratt, J. S. *Am. J. Roentgenol., Radium Ther. nucl. Med.* **90,** 673–687 (1963).
41. Bussey, H. J. R. *Familial Polyposis Coli* (Johns Hopkins University Press, Baltimore, 1975).
42. Edwards, F. C. & Truelove, S. C. *Gut* **5,** 15–22 (1964).
43. DeVita, V. T., Jr, Hellman, S. & Rosenberg, S. A. *Cancer: Principles and Practice of Oncology*, 674–675 (Lippincott, Philadelphia, 1982).
44. Land, H., Parada, L. F. & Weinberg, R. A. *Nature* **304,** 596–602 (1983).
45. Needleman, S. W., Yuasa, Y., Srivastava, S. & Aaronson, S. A. *Science* **222,** 173–175 (1983).
46. Dukes, C. E. *J. Path. Bact.* **50,** 527–539 (1940).
47. Cass, A. W., Million, R. R. & Pfatt, W. W. *Cancer* **37,** 2861–2865 (1976).
48. Molson, B. C. & Dawson, I. M. P. *Gastrointestinal Pathology*, 664–665 (Blackwell, Oxford, 1979).
49. Nuti, M. *et al. Int. J. Cancer* **29,** 539–545 (1982).
50. Hsu, S-M., Raine, L. & Fanger, H. J. *Histochem. Cytol.* **29,** 577–580 (1981).
51. Colcher, D. *et al. Cancer Res.* **43,** 736–742 (1983).
52. Potter, M. *Physiol. Rev.* 631–719 (1972).

T3-Ti receptor triggering of T8+ suppressor T cells leads to unresponsiveness to interleukin-2

Armand Bensussan, Oreste Acuto, Rebecca E. Hussey, Claudio Milanese & Ellis L. Reinherz

Division of Tumour Immunology, Dana-Farber Cancer Institute and the Departments of Medicine and Pathology, Harvard Medical School, Boston, Massachusetts 02115, USA

T3-associated disulphide linked heterodimers (Ti_n) comprised of clonally unique α-chains of molecular weight (MW) 49,000–54,000 and β chains of MW 43,000 have been identified as the antigen receptors on human cytotoxic effector and inducer T-lymphocytes[1–3]. Crosslinking of Ti molecules by either the appropriate nominal antigen/MHC specificity or anti-clonotypic monoclonal antibody results in clonal expansion of such cells via induction of IL-2 receptor expression, endogenous IL-2 release and IL-2-IL-2 receptor interaction[4]. To determine whether analogous antigen receptor molecules and autocrine growth mechanisms are utilized by suppressor T-cells[5–7], we produced an anti-clonotypic monoclonal antibody against a non-cytotoxic T8+ suppressor T-cell, T8AC6, which defines a T3-associated disulphide-linked heterodimer of similar molecular weight to the above clonotypes. We find that T3-Ti triggering of suppressor clones (T8AC6, T8AC7 or T8RW) does not result in IL-2 production or T-cell proliferation and in contrast to inducer clones, also leads to a transient IL-2 unresponsive state. We suggest that such T3-Ti receptor mediated autoregulation of suppressor T-cell growth is necessary in the facilitation of initial inducer T-cell activation following antigenic perturbation.

We derived human suppressor T-cells T8AC6 and T8AC7 by stimulating autologous peripheral blood mononuclear cells (PBMC) of a healthy ragweed antigen (RWAGE) atopic donor with an MHC restricted/RWAGE-antigen specific inducer T-cell termed RW17C[3] and cloned in a two-layer agar system as previously described[8]. This strategy was employed because earlier studies indicated that such stimulation results in both autoreactive T4+ amplifier T-cells and noncytotoxic T8+ clones[8]. A third suppressor clone (T8RW) was obtained from direct stimulation of PBMC with RWAGE at the end of the fall hay fever season. We propagated these T-cell clones *in vitro* with IL-2 and irradiated autologous PBMC for more than 14 months, maintaining stable phenotype (T1+T3+T4−T8+T11+T12+) and function. To determine whether the T8+ clones were capable of suppressing the secretion of immunoglobulin by a combination of B-cells and RW17C T-cells stimulated with RWAGE, we added increasing numbers of T8AC6, T8AC7 or T8RW to the autologous T-B-cell mixture consisting of 5×10^4 T4+RW17C T-cells in the presence of RWAGE. This mixture produces 18 μg ml^{-1} of IgG without additional cells (Fig. 1). In the absence of RW17C, B-cells with or without RWAGE produces less than 200 ng of IgG per ml (data not shown). Addition of increasing numbers of T8+ cells results in marked suppression of IgG secretion. For example, when as little as 6.2×10^3 cloned T8-cells were added, IgG secretion is reduced to 6–9 μg ml^{-1}, a reduction of more than 50%, and is reduced further when 12.5–50×10^3 T8+ T-cells were added.

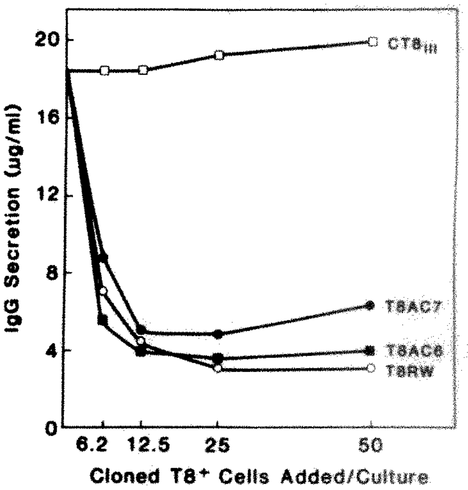

Fig. 1 Regulatory activities of T8+ T-cell clones. Human T8+ T-cells T8AC6 and T8AC7 were derived by stimulating PBMC of a healthy atopic donor with an irradiated autologous antigen/MHC restricted T4+ inducer RW17C and cloning in a semi-solid system as described previously[8]. T8RW was obtained by an identical technique from RWAGE stimulated PBMC of the same donor. Individual colonies were expanded in liquid culture by restimulating with irradiated (5,000 rad) autologous PBMC and IL-2 containing supernatants. Further cloning was performed (×2) by limiting dilution technique at 0.3 cells per well. Clones were maintained in IL-2 and also placed on irradiated autologous PMBC on a feeder layer every 3 weeks. $CT8_{III}$ is an extensively characterized alloreactive T8+ T-cell clone derived from the same donor and was utilized as a control[1]. Varying numbers of T8+ cloned cells (6.2×10^3 to 50×10^3) were added to a culture consisting of 50×10^3 autologous B cells (E rosette negative PBMC treated with anti-T4, anti-T8, anti-Mo1 and rabbit complement)[16], 2.5×10^3 macrophages, 50×10^3 RW17C and the specific antigen RWAGE (final concentration: 5 μg ml^{-1}) (Worthington Diagnostics[3]). The cultures were performed in a total volume of 0.2 ml in 96 well round-bottomed microtitre plates (Costar) in RPMI 1640 (Gibco) containing 10% FCS (M.A. Bioproducts). After 7 days' incubation at 37 °C in a humidified atmosphere containing 7% CO_2 in air, the wells were harvested by pooling the cells and supernatants from triplicate wells and storing at −20 °C prior to assay of IgG synthesis. Solid phase RIA was performed as previously described[18].

To eliminate the possibility that the inhibition of immunoglobulin production is due to an unspecific crowding effect of cells in the culture system, an autologous alloreactive cytotoxic T-cell clone, $CT8_{III}$, was added to the mixture of RW17C T-cells and B-cells. In contrast to the effect of the three other clones (T8AC6, T8AC7 and T8RW), increasing $CT8_{III}$ concentration has no effect on IgG secretion by RW17C and B-cells (Fig. 1). We conclude that the suppressive activity of T8+ clones in this system is not mediating via a trivial crowding mechanism.

We then investigated whether clonotypic structures on T8+ suppressor T-cell clones were similar to those identified on T4+ inducer clones and class I and class II specific CTL clones. We

Table 1 Influence of various monoclonal antibodies on IL-2 proliferative responses of clones T8AC6 and T4AC3

	Pretreatment of clone T8AC6					
Stimulus	Medium	Anti-T3	Anti-Ti_5	Anti-Ti_6	Anti-T4	Anti-T8
Medium	480	398	456	506	511	413
IL-2	27,312	5,301	6,205	29,312	28,049	28,506
	Pretreatment of clone T4AC3					
Stimulus	Medium	Anti-T3	Anti-Ti_5	Anti-Ti_6	Anti-T4	Anti-T8
Medium	140	153	190	192	201	141
IL-2	16,912	26,281	17,412	27,266	18,733	17,854

3×10^4 T8AC6 or T4AC3 cells were incubated in round-bottomed microtitre wells (Costar) with either media or monoclonal antibody (final dilution 1:1,000 in culture medium). 30 h later, purified 0.5 IL-2 U ml^{-1} (provided by Dr K. A. Smith, Dartmouth Medical School) was added[4]. After 24 h at 37 °C in humidified atmosphere containing 7% CO_2 in air, individual wells were pulsed with 0.2 μCi of ^{3}H-TR (Schwarz-Mann), collected 18 h later on a MASH II apparatus (M. J. Bioproducts) and ^{3}H-TdR incorporation was then measured in a β scintillation spectrometer. Each value represents the mean of triplicate samples with standard derivations in all experiments <15%. Anti-Ti_5 and anti-Ti_6 are the anti-clonotypic antibodies directed against T8AC6 and T4AC3, respectively. These IgG1 subclass monoclonal antibodies were also purified from malignant ascites with protein A Sepharose (Pharmacia) and coupled to swollen CnBr activated Sepharose 4B beads (Pharmacia) at 5 mg ml^{-1} for induction of clonal proliferation and IL-2 production[4]. Proliferative responses of 3×10^4 T8AC6 or 3×10^4 T4AC3 were as follows: (i) T8AC6: + medium, 392 c.p.m.; + Sepharose-linked anti-T3, 282 c.p.m.; + Sepharose-linked anti-Ti_5 314 c.p.m.; + Sepharose-linked anti-Ti_6, 416 c.p.m.; + Sepharose-linked anti-T4, 402 c.p.m.; + Sepharose-linked anti-T8, 511 c.p.m. (ii) T4AC3: + medium, 153 c.p.m.; + Sepharose-linked anti-T3, 19,373 c.p.m.; + Sepharose-linked anti-Ti_5, 198 c.p.m.; + Sepharose-linked anti-Ti_6, 15,219 c.p.m.; + Sepharose-linked anti-T4, 202 c.p.m.; + Sepharose-linked anti-T8, 186 c.p.m. To quantitate the amount of IL-2 secreted by T8AC6, T8AC7, T8RW, and T4AC3 after stimulation with Sepharose-linked anti-T3, a previously described murine T-cell proliferative assay was employed[4]. Specifically, 10^5 T-lymphocytes were incubated overnight at 37 °C with Sepharose-linked anti-T3 in a final volume of 0.5 ml. The supernatants were then collected, passed through 0.45 μ filters and added 1:1 (v/v) to 5×10^4 murine PHA T-lymphoblasts. After 18 h of culture, individual wells were pulsed for 24 h with 0.2 μCi of ^{3}H-TdR, mashed and counted. A standard curve obtained with serial dilutions of purified human IL-2 was used to quantitate the amounts of lymphokine produced by the various T-cell clones. Supernatants generated from T8AC6, <0.01 U ml^{-1}; T8AC7, <0.01 U ml^{-1}; T8RW, <0.01 U ml^{-1}; T4AC3, >0.20 U ml^{-1}.

developed a series of monoclonal antibodies directed at the T8AC6 suppressor T-cell clone by standard fusion techniques[9], and selected hybridoma cultures containing antibody reactive with T8AC6 but unreactive with Laz 509 (an autologous EBV transformed line). Supernatant from one individual hybridoma of approximately 800 tested contained antibody (anti-Ti_5, IgG1 murine isotype subclass) which did not react with resting or activated T-cells or a series of additional T8+ suppressor clones derived from the same individual ($n = 15$). This hybridoma was cloned and recloned by limiting dilution in the presence of feeder cells; malignant ascites were then developed.

Solubilized membrane preparations were obtained from the ^{125}I labelled T8AC6 clone in order to characterize the surface structure recognized by anti-Ti_5. SDS-PAGE electrophoresis of the molecule precipitated by anti-Ti_5 from ^{125}I labelled-T8AC6 in reducing conditions shows two bands of a 49,000 and 43,000 MW corresponding to the α- and β-chain respectively (Fig. 2, lane *a*). In nonreducing conditions this structure appears as a single band of 90,000 MW (Fig. 2, lane *c*), which demonstrates that the Ti_5 structure is a disulphide-linked heterodimer. The 90,000, 49,000 and 43,000 molecular weight species are not present in control immunoprecipitates with an irrelevant anticlonotype, anti-Ti_6 (Fig. 2, lanes *b* and *d*). Anti-Ti^5 does not precipitate material from a second T8+ suppressor clone T8AC7, derived from the same donor, thus confirming its non-crossreactive anticlonotypic specificity (data not shown).

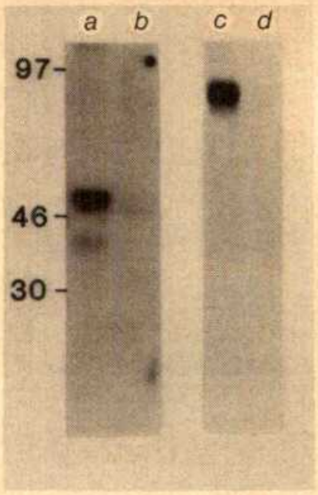

Fig. 2 SDS-PAGE of anti-Ti_5 immunoprecipitates from surface ^{125}I-labelled T8AC6 cells. Cells were surface labelled with ^{125}I (NEN) using a standard lactoperoxidase method[10]. Briefly, 2×10^7 viable, cells were washed with RPMI 1640, resuspended in PBS, and labelled with1 μCi ^{125}I for 15 min at room temperature, followed by the addition of 100 μl NaI (1 mol l^{-1}). Labelled cells were then harvested and washed three times in cold RPMI 1640. Cell lysate was prepared by resuspending the cell pellet in 300 μl RIPA buffer, *p*H 7.5, containing 1% Triton X-100, phenylmethylsulphonyl fluoride, and trypsin inhibitor and agitated for 40 min at 4 °C. Cell lysates were stored at −70 °C before use. Immune precipitations were carried out using preformed complexes of rabbit anti-mouse Ig and specific monoclonal antibody[19]. They were then washed 4 times with RIPA buffer as above and dissolved in SDS-polyacrylamide gell electrophoresis (SDS-PAGE) sample buffer and loaded onto separate slots on a 10% polyacrylamide slab gel. Identical aliquots of immune precipitates were run in reduced and nonreduced conditions. Gels were dried and radiolabelled precipitates were visualized using standard methods. *a*, Anti-Ti_3, reduced; *b*, negative control complex (anti-Ti_6, an irrelevant anticlonotypic antibody), reduced; *c*, anti-Ti_5, nonreduced; *d*, negative control complex (anti-Ti_6), non-reduced.

Previous studies with cytotoxic T cell clones indicate that the Ti structure is linked to the monomorphic 20,000 and 25,000 MW T3 molecules and comodulates with them[10]; we have therefore attempted to determine whether a similar noncovalent association exists between the Ti molecules on suppressor cells and T3. We preincubated T8AC6 cells with anti-T3 for 24 h at 37 °C and then washed them to remove free monoclonal antibodies. We subsequently analysed cell reactivity by indirect immunofluorescence (Epics V cell sorter) with a panel of monoclonal antibodies. Before modulation, we found that all T8AC6 cells are reactive with anti-T3 and anti-Ti_5 (Fig. 3). After modulation with anti-T3, however, T3 expression is reduced by 95%. Anti-T3 induced modulation also results in removal of the Ti_5 molecule, indicated by loss of anti-Ti_5 reactivity. This is not a non-specific effect, as we observe that T8 surface expression is not influenced by this process and IL-2 receptor expression (shown by anti-IL-2 R, a monoclonal antibody directed at the IL-2 receptor and with an identical distribution to anti-Tac) is enhanced. Our findings imply that suppressor T-cells have antigen receptor structures similar to those found on inducer and cytotoxic T-cells (T3-Ti molecular complexes).

We show here that the outcome of a given immune response is dependent on the relative number of T8+ suppressor and T4+ inducer T-cells (see also ref. 11). It is thus important to determine the signals required for T8+ suppressor T-cell growth. Earlier studies have shown that soluble or Sepharose bound anti-Ti (or anti-T3) monoclonal antibodies, like physiological ligand, enhanced proliferative responses of inducer and cytotoxic T-cells to purified IL-2 by inducing an increase in their surface IL-2 receptor expression[4]. Moreover, Sepharose-bound anti-Ti (or anti-T3) or physiological ligand triggers

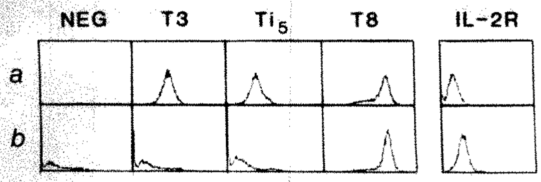

Fig. 3 The Ti structure of the T8+ T-cell suppressor clone T8AC6 comodulates with T3. T8AC6 cells were preincubated with media (*a*) or the monoclonal antibody anti-T3 (*b*) (final dilution 1:300) for 24 h at 37 °C and subsequently washed several times prior to analysis. Phenotypic analysis was performed by indirect immunofluorescence with fluorescence conjugated goat anti-mouse $F(ab')_2$ IgG. Samples were analysed with monoclonal antibodies (see designations above indicated histogram) on an Epics V cell sorter[10]. 10,000 cells were analysed in each sample. Each histogram displays the number of cells (ordinate) versus the intensity of fluorescence (abscissa) expressed on a logarithmic scale. The negative control used to determine background fluorescence was a 1:300 dilution of ascites derived from a nonreactive hybridoma (neg).

endogenous clonal IL-2 production in the absence of macrophages or feeder cells, leading subsequently to T-cell proliferation. This suggests that induction of IL-2 receptor expression, but not IL-2 release occurs with minimal T3-Ti receptor crosslinking and that antigen-induced proliferation of these cells is mediated through an autocrine pathway involving endogenous IL-2 production, release and subsequent binding to IL-2 receptors. We have performed similar experiments using T8+ suppressor T-cells. The representative T8+ suppressor clone (T8AC6) proliferates as well as the T4+ inducer clone T4AC3 to purified IL-2 (measured by ^{3}H-TdR incorporation) (Table 1). In the presence of soluble anti-T3 antibody, however, the IL-2 response of T8AC6 was virtually abolished (5, 301 vs. 27,312 cpm). Similarly, soluble anti-Ti_5 greatly reduces IL-2 responsiveness of T8AC6. An irrelevant anti-clonotype, (anti-Ti_6), or anti-T4 or anti-T8 antibodies have no effect on subsequent IL-2 responsiveness by T8AC6, and anti-Ti_5 has no effect on the response of the T4AC3 clone to IL-2. Hence the effects on T8 suppressor clones are specific and non-toxic. Furthermore, although the appropriate anti-clonotype and anti-T3 antibody inhibit IL-2 responsiveness of T8+ suppressor cells, they also enhance the IL-2 response of T4AC3 T4 inducer cells as previously observed (16,912 to 26,281-27,266 c.p.m.)[10]. This enhancement was observed at all anti-T3 and anti-Ti_6 antibody concentrations tested (10^{-2}-10^{-4} dilutions), and in either 0.1, 0.5 or 1 U ml^{-1} of IL-2. The inhibition of IL-2 responsiveness following soluble anti-T3 or anti-Ti preincubation of suppressor T-cells is not secondary to a failure of IL-2 receptor expression (Fig. 3).

One possible explanation of the inhibition is that such T3-Ti triggering results in an autoregulatory antagonist functional activity, in which case even T3-Ti receptor crosslinking with Sepharose-bound antibody would not initiate cell growth. We find that such Sepharose-bound anti-T3 and appropriate anti-Ti antibodies induce T4AC3 but not T8AC6 proliferation (Table 1). These antibodies stimulate IL-2 production from T4AC3 but not T8AC6, T8AC7 or T8RW. As crosslinking of T3/Ti molecules on suppressor T-cells does not result in autologous IL-2 production and clonal proliferation, it is not surprising that the same T8+ suppressor T-cells are unable to proliferate to the irradiated RW17C inducer T-cell utilized in the initial cloning procedure, autologous macrophages or B-cells (with or without RWAGE). The absence of a measurable proliferative response makes determination of the specificity and the target of an individual suppressor clone difficult. We plan experiments on regulation of immunoglobulin production with suppressor clones and isolated autologous and allogeneic lymphoid populations to address this issue.

Our results described here suggest that suppressor T-cells proliferate to IL-2 but that triggering of the T3-Ti complex on suppressor T-cells (with or without crosslinking) induces a state of IL-2 hyporesponsiveness. We also find that this refractory period is transient, persisting for only three to four days. Thus, the growth response of anti-Ti (or anti-T3)-treated T8AC6 compared to anti-T8-treated (control) T8AC6 cells is reduced by 80% at 24 h, 60% at 48 h, 30% at 72 h and 0% at 96 h. Such autoregulation of suppressor T-cell growth[12,13] may be necessary to facilitate inducer T-cell activation following initial antigenic pertubation. Once antigen is eliminated and T3-Ti stimulation abates, inducer T-cell-derived IL-2 can mediate clonal T8+ suppressor cell growth. Persistent amplification of the immune response would result in further T8+ suppressor cell expansion and hence appropriate termination of induction. Our future experiments will attempt to determine the targets and mechanism of suppression, and the relationship of the T3-Ti complex to any putative suppressor effector molecules which abolish immunoglobulin production in this or other unrelated systems[6,14,15]. We will also attempt to determine whether other types of suppressor T-cells are governed by similar mechanisms of growth regulation[16,17]. We thank Mr John Daley and Mr Herb Levine for technical assistance with the Epics V cell sorter. This work was supported by NIH grants R01 NS17182 and R01 AI19087-01. A.B. is a recipient of a research support grant from the French Medical Research Foundation.

Note added in proof: Monoclonal antibodies and heteroantisera have now been produced to clonotypes on T8RW and T8AC7 and precipitate characteristic disulphide-linked heterodimers.

Received 1 May: accepted 16 July 1984.

1. Meuer, S. C. *et al. Nature* **303**, 808-810 (1983).
2. Acuto, O. *et al. J. exp. Med.* **158**, 1368-1373 (1983).
3. Meuer, S. C. *et al. Science* **222**, 1239-1242 (1983).
4. Meuer, S. C. *et al. Proc. natn. Acad. Sci. U.S.A.* **81**, 1509-1513 (1984).
5. Cantor, H. F. *et at. J. exp. Med.* **143**, 1391-1401 (1976).
6. Fresno, M. *et al. J. exp. Med.* **153**, 1246-1259 (1981).
7. Sy, M. S. *et al. J. exp. Med.* **153**, 1415-1421 (1981).
8. Bensussan, A. *et al. J. exp. Med.* **159**, 559-576 (1984).
9. Kohler, G. & Milstein, C. *Nature* **256**, 495-497 (1975).
10. Meuer, S. C. *et al. J. exp. Med.* **157**, 705-719 (1983).
11. Reinherz, E. L. *et al. Eur. J. Immun.* **10**, 570-572 (1980).
12. Gershon, R. K. *et al. J. exp. Med.* **153**, 1533-1546 (1981).
13. Green, J. R. *et al. Eur. J. Immun.* **11**, 973-986 (1981).
14. Tanaguichi, M., Takei, I. & Tada, T. *Nature* **283**, 227-228 (1980).
15. Kapp, J. A., Sorensen, C. M. & Pierce, C. W. *Prog. Immun.* **5**, 871-880 (1983).
16. Benacerraf, B. & Germain, R. N. *Immun. Rev.* **38**, 70-119 (1978).
17. Lamb, J. R. & Feldman, M. *Nature* **300**, 456-458 (1982).
18. Reinherz, E. L. *et al. J. Immun.* **128**, 463-468 (1982).
19. van Agthoven, A. C. *et al. Eur. J. Immun.* **11**, 18-21 (1981).

A Ca-dependent Cl^- conductance in cultured mouse spinal neurones

David G. Owen, Menahem Segal & Jeffery L. Barker

Laboratory of Neurophysiology, National Institute of Neurological and Communicative Disorders and Stroke, National Institutes of Health, Bethesda, Maryland 20205, USA

Long-lasting conductance changes triggered either by brief (millisecond) electrical stimuli and/or entry of calcium ions have been observed in a variety of excitable tissues[1-4]. The electrical consequences of these events depend on the ion conductance affected and on the ion concentration gradient across the membrane, while the long-lasting nature of the change sustains the cell at either sub- or supra-threshold levels for activation of regenerative action potentials. We report here that many cultured mouse spinal neurones exhibit a voltage-activated chloride conductance that lasts for seconds and is dependent on extracellular calcium, $[Ca^{2+}]_o$. This conductance may repolarize and stabilize the cell at a level subthreshold for generating action potentials, thus complementing the functional roles of Ca-dependent K^+ conductances[5-8].

Neurones were cultured from the embryonic mouse spinal cord according to methods published previously[9]. After 3-4 weeks in culture, we studied the cells at 23 °C with intracellular recording and two-electrode voltage-clamp techniques (Fig. 1). Most of our experiments used CsCl-filled microelectrodes and bathing media containing tetraethylammonium (TEA) in order

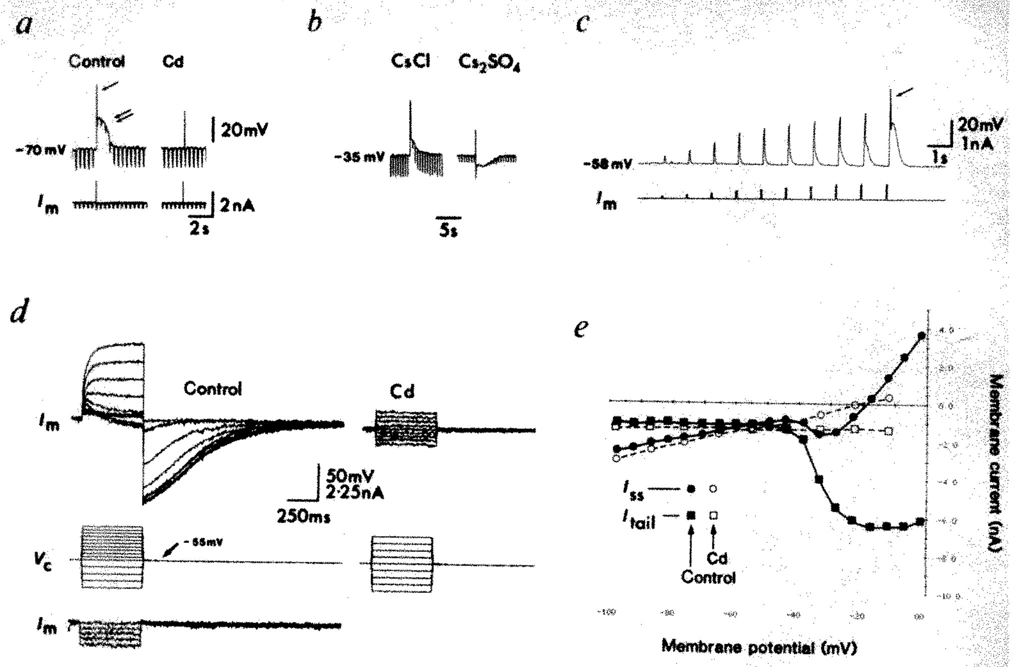

Fig. 1 A slow Ca^{2+}- and Cl^--dependent conductance is present in cultured mouse spinal neurones. ***a***, Records made using a KCl-filled electrode. Left trace: A 50-ms depolarizing current step evokes a Ca spike (single arrow) and long-lasting ('slow') afterdepolarization (double arrow). Voltage deflections in response to constant-amplitude hyperpolarizing current pulses (I_m) reveal an increase in membrane conductance during the afterdepolarization. Right trace: Both events are abolished when 0.2 mM Cd^{2+} is applied by pressure ejection. ***b***, Voltage responses to 50-ms depolarizing current steps at a holding potential (maintained with d.c. current injection) of −35 mV. A depolarizing response is recorded with a CsCl-filled electrode (left trace) while a hyperpolarizing response is triggered with Cs_2SO_4-filled electrodes (right trace). Downward voltage deflections are in response to hyperpolarizing constant current injections and indicate sizeable increases in membrane conductance during both responses. ***c***, Voltage responses (upper trace) recorded with a CsCl-filled electrode in response to depolarizing constant current steps of increasing amplitude (I_m). Activation of the long-lasting depolarizing response occurs in a graded manner and precedes the generation of a Ca spike (indicated by single arrow). ***d***, Voltage-clamp analysis of the same cell shown in *c* using two CsCl-filled electrodes. Membrane currents (I_m) in response to voltage commands (V_c) in normal bathing medium (left) and in the presence of Cd (right). For clarity, control current records (left) are separated according to the polarity of the commands, with responses to hyperpolarizing command voltage steps shown in the lower traces and responses to depolarizing steps in the upper traces. Voltage commands and data acquisition were controlled with a PDP-11/23 computer. Current and voltage were digitized at 250 Hz and for display purposes individual data points are connected by lines. ***e***, Current–voltage (I–V) relationships for data obtained from *d*. Currents were measured at the end of the 500-ms voltage steps (steady-state currents, I_{ss}) and immediately after returning to the holding potential (I_{tail}), in the presence and absence of 0.1 mM Cd^{2+}. In all these experiments, microelectrodes contained either 3 M KCl, 3 M CsCl or 3 M Cs_2SO_4. The bathing medium consisted of (mM): 121 NaCl, 2.5 KCl, 4 $MgCl_2$, 4 $CaCl_2$, 5 HEPES, 10 glucose, 20 TEA-Cl and 0.5–1.0 µM TTX.

to block all outward potassium conductances[10,11]. In these conditions, 27 of 33 cells expressed the conductance described below, whereas with KCl-filled electrodes the conductance was detected less frequently (10 of 43 cells).

The conductance response was routinely elicited with brief depolarizing current steps to potentials more depolarized than −45 mV. When recording with KCl-filled electrodes, the response was usually associated with a 15–30 mV depolarization (from resting potentials of −60 to −70 mV) lasting a second or more and usually preceded by a rapid (about 100 ms) Ca^{2+} spike (Fig. 1*a*). Both the Ca^{2+} spike and the slow after-depolarization were eliminated by local application of cadmium (Fig. 1*a*) or cobalt ions. The polarity of the voltage change associated with the conductance response was sensitive to the counteranion in the microelectrode. A slow depolarizing conductance was consistently triggered in cells recorded with CsCl-filled electrodes, whereas a long-lasting hyperpolarizing response could be triggered in cells when recording with Cs_2SO_4-filled electrodes (Fig. 1*b*). The Cl^- gradient across the membrane is therefore important in determining the polarity of the response. A Ca-dependent action potential was not a prerequisite for triggering the conductance response, as activation of the slow depolarization frequently occurred in a graded manner and at membrane potentials negative to the threshold for generating a Ca-dependent action potential (Fig. 1*c*). The steady-state current–voltage (I–V) relationship (where the steady-state current was measured at the end of each 500-ms voltage step) of cells bathed in TEA and tetrodotoxin (TTX) and voltage-clamped with CsCl-filled electrodes was nonlinear over the range of membrane potentials −45 mV to 0 mV (Fig. 1*d*, *e*). Following voltage steps to potentials more depolarized than −45 mV, inward-going 'tail' currents were detectable on returning to the holding potential. Both the nonlinear properties of the steady-state I–V curve and the tail currents were eliminated in solutions nominally free of Ca^{2+} (not shown) or by application of either Cd^{2+} (Fig. 1*d*, *e*) or other Ca^{2+} conductance antagonists, including manganese, Co, nickel and D600, suggesting that Ca^{2+} entry is required for activation of the conductance.

The time-dependent currents generated during the depolarizing commands ('on response') and subsequent tail currents ('off response') probably reflect activation of a single ion conductance mechanism, because analysis of responses to voltage-clamp double-step protocols reveals that the I–V relations and reversal potentials (E_{rev}) for both 'on' and 'off' current responses are the same. E_{rev} cannot be measured directly in the recording conditions normally used (Cl^--loaded cells) because E_{rev} lies within the potential range for activation of the conductance. Extrapolated 'instantaneous' I–V relations of pairs of I (steady-state and tail currents) and V measurements taken from the data in Fig. 1*d*, however, give a reversal potential of −17.6 mV (s.e.m. = 0.8 mV, $n = 7$ pairs) and the result for a constant activation step (not shown) was −19.6 mV (s.e.m. = 0.2 mV, $n = 7$ pairs). The steady-state I–V relationship is linear in the −20 to 0 mV range and the amplitudes of the corresponding tail currents are maximal (Fig. 1*e*), suggesting that the conductance is fully activated in this range. The intercept of the I–V relationship over this range with either the passive I–V relations (extrapolated from data in the −79 mV to −55 mV range) or the I–V relationship in the presence of blocking concentrations of Cd^{2+} is −17 mV (Fig. 1*e*). This is consistent with our estimate of E_{rev} above. When maximally activated from a holding potential of −55 mV, the magnitude of the Ca-dependent conductance evoked in Fig. 1*d* was 150 nS (calculated from tail currents and assuming E_{rev} is −17 mV). This Ca-dependent conductance did not inactivate appreciably during depolarizing steps to between −20 and −10 mV for up to 10 s, as evidenced by the constancy of tail current amplitudes following depolarizing commands maintained for this period of time (not shown). Activation at −10 mV could be described by an exponential function with a single time constant of 70 ms (from tail current measurements). The decay of tail currents following repolarization of the membrane from the activation potential reflects deactivation of the

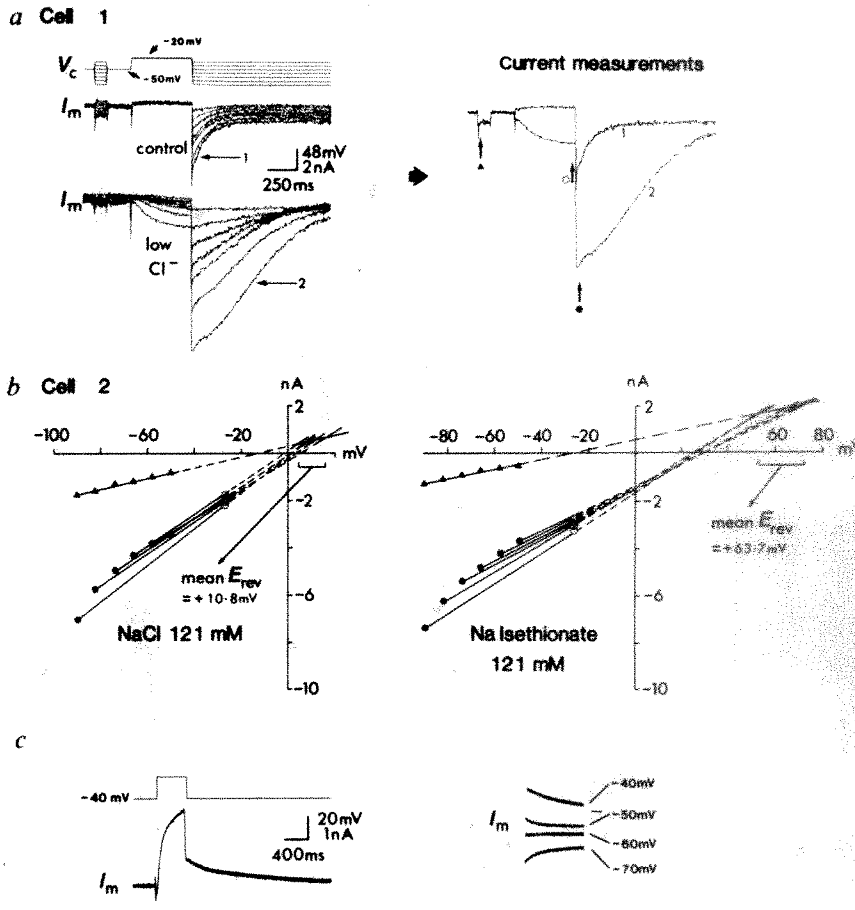

Fig. 2 Time-variant currents remaining in cells bathed in TTX and TEA and after Cs injection are sensitive to E_{Cl}. ***a***, Left panel, upper trace: a typical double-voltage-step protocol used to derive estimates of the reversal potential (E_{rev}) of tail currents evoked by a constant activation (depolarizing) voltage step. A series of *I* responses to *V* steps is superimposed. Middle trace: superimposed current responses, in normal bathing medium containing 158 mM Cl⁻. Lower trace: current responses obtained when Na isethionate was pressure-applied in the vicinity of the cell to reduce $[Cl^-]_0$ from 158 mM to about 37 mM. Right panel: two current records in response to the same voltage command are superimposed to emphasize the difference between the responses recorded in control (trace 1) and low $[Cl^-]_0$ (trace 2). When $[Cl^-]_0$ is reduced, current developed during the depolarizing step is reversed in direction, the tail current increases in amplitude and its decay slows. Current measurements were made as indicated by the arrows. Time-invariant or leak current is represented by triangles and instantaneous currents for the activated conductance state are represented by the open and closed circles. Instantaneous *I*-*V* relations were extrapolated to their intercept with that extrapolated from leakage or passive conductances in *b*. Use of such pairs of currents to make this estimate was justified by the identity of the conductance underlying the two components (I_{ss} and I_{tail}) and also necessitated by the lability inherent in both activation and driving force parameters. For example, the steady-state current during depolarization (○) was not necessarily constant, particularly in low $[Cl^-]_0$ (*a*, left panel, lower trace). *I*-*V* plots of the type shown in *b* revealed a progressive collapse of the driving force in this cell when bathed in low [Cl⁻] but with no apparent change in the degree of activation (not shown). ***b***, Leak *I*-*V* plots (currents measured before depolarizing voltage step: triangles) and chord *I*-*V* relationships (circles) following activation of the conductance with a depolarizing voltage step. Currents were sampled as indicated in *a*. These data were obtained from another cell for which the driving force was more stable and for which E_{rev} for GABA-activated currents was also calculated to monitor changes in the Cl⁻ gradient across the membrane. Left panel: E_{rev} in normal medium ($[Cl^-]_0 = 158$ mM) is estimated to be +10.8 mV (s.e.m. = 1.4 mV, $n = 6$ *I*-*V* pairs). Right panel: ambient NaCl was displaced by close application of Na isethionate in the vicinity of the recorded cell to reduce $[Cl^-]_0$, theoretically to a minimum of 37 mM. E_{rev} now extrapolates to +63.7 mV (s.e.m. = 3.2 mV, $n = 6$ *I*-*V* pairs), a change which somewhat exceeds that predicted from the Nernst relationship (that is, +37 mV), for a conductance involving solely Cl⁻ and assuming that the effective $[Cl^-]_0$ at the membrane is 37 mM. The shift in E_{rev} for GABA-activated current in this cell was about +40 mV (not shown). ***c***, Tail currents invert at about −60 mV when recording with Cs_2SO_4-filled electrodes. Left: activation of a slowly developing outward current by a command voltage step to −20 mV. Similar current responses in other cells were abolished in 0.2 mM Cd^{2+}. Right: tail currents measured, in the same cell, at different membrane potentials (indicated) following an activating (depolarizing) command voltage step. The polarity of the tail current reverses at about −60 mV.

conductance, since instantaneous *I*-*V* plots from varying times during tails indicate a progressive reduction in the membrane conductance rather than a change in the driving force for the current. Deactivation is apparently voltage-sensitive, being faster at more hyperpolarized potentials (Fig. 2*a*) and slower during prolonged or intense activation or with increased $[Ca^{2+}]_0$. This is consistent with the regulation of conductance by Ca^{2+} entry and saturation of Ca-sequestering mechanisms during prolonged or strong depolarizing commands.

This conductance mechanism superficially resembles Ca-dependent K^+ conductances recorded in a variety of excitable membranes in its apparent voltage-sensitivity, time course of activation and relative lack of inactivation[12,13]. The reversal potential for the current response is not consistent with a K^+-selective mechanism, however, nor is it consistent with a pure Ca^{2+} current, which would be expected to reverse at quite positive potentials[14]. E_{rev} is in fact identical to that of γ-aminobutyric acid (GABA)-activated Cl⁻ currents recorded in the same cells[15]. Ca-dependent 'nonspecific' cation currents, described for other preparations[16-18], also reverse in this potential region (about 0 mV).

We used a double-voltage-step protocol in different ionic conditions to estimate E_{rev} for tail currents (Fig. 2*a*). Neither complete replacement of extracellular Na^+ with choline, nor raising $[K^+]_0$ from 2.5 mM to 25 mM, nor raising $[Ca^{2+}]_0$ from 4 mM to 20 mM altered E_{rev} measured in this way. We did find, however, that replacement of much of the extracellular Cl⁻ by the impermeant anion isethionate[19] altered current responses evoked during depolarizing commands, changed the amplitude and time-course of tail currents (Fig. 2*a*) and shifted the estimated E_{rev} in a depolarizing direction (Fig. 2*b*). Replacement of Cl⁻ with isethionate also shifted E_{rev} for GABA-activated currents in a depolarizing direction in the same cell (not shown). Similar sizeable shifts in estimates of E_{rev} have been recorded using methane sulphonate to replace Cl⁻. Furthermore, tail currents, measured following activating voltage steps, using SO_4^{2-}-filled electrodes (without loading the cell with Cl⁻), reverse in polarity at −60 mV (Fig. 2*c*), which corresponds well with E_{Cl} in these cells[20]. E_{rev} averaged −1.7 mV (s.e.m. = 3.5 mV, $n = 20$ from 7 cells) when Cl⁻-filled electrodes were used and −44 mV (s.e.m. = 2.3 mV, $n = 9$ from 8 cells) when SO_4^{2-}-filled electrodes were used. These findings taken together are consistent with the hypothesis that the conductance involves primarily, if not exclusively, Cl⁻.

Ca-dependent Cl⁻ conductance mechanisms have been reported in toad oocyte[21] and salamander photoreceptor membranes[22] but their functional roles in these cells are unclear. Ca-dependent depolarizing shifts have also been observed in vasopressinergic neurones cultured from the mammalian hypothalamus[1]. In our experiments, it was necessary to eliminate some of the K^+ conductances in order to reveal the Ca-dependent Cl^- conductance. Activation of K^+ conductances attenuates spread of depolarizing current injections, indicating that the Cl^- conductance may be electrotonically distant from the current-passing microelectrode. Presumably, membrane depolarization increases intracellular Ca^{2+} concentration, $[Ca^{2+}]_i$, by activating Ca^{2+} conductances in plasma (and/or cisternal) membranes. It is well established that Ca^{2+} conductances are present at terminals in the vertebrate central nervous system, where they participate in transmitter release. If the Ca-dependent Cl^- conductance is also present at nerve endings, and provided that E_{Cl} is similar at terminals and cell bodies[20], then activation of the conductance at this level, by depolarization and/or Ca^{2+} entry, may serve to repolarize the terminal region, thus limiting transmitter release.

We thank Joann Mazzetta for culturing spinal cord neurones, Drs Amy MacDermott and David Lange for helpful criticism and Mary Ann Bragg for typing the manuscript.

Received 7 February; accepted 3 August 1984.

1. Legendre, P., Cooke, I. M. & Vincent J.-D. *J. Neurophysiol.* **48**, 1121–1141 (1982).
2. Dichter, M. A. & Fischbach, G. D. *J. Physiol., Lond.* **267**, 281–298 (1977).
3. Fukada, J., Fischbach, G. D. & Smith, T. G. Jr *Devl Biol.* **49**, 412–424 (1976).
4. MacDonald, J. F. & Schneiderman, H. H. *Brain Res.* **296**, 350–355 (1984).
5. Barrett, E. F. & Barrett, J. N. *J. Physiol., Lond.* **255**, 737–774 (1976).
6. Aldrich, R. W., Getting, P. A. & Thompson, S. H. *J. Physiol., Lond.* **291**, 531–544 (1979).
7. McAfee, D. A. & Tarowsky, P. J. *J. Physiol., Lond.* **290**, 507–523 (1979).
8. Barrett, E. F., Barrett, J. N. & Crill, W. E. *J. Physiol., Lond.* **304**, 251–276 (1980).
9. Ransom, B. R., Neale, E., Henkart, M., Bullock, P. N. & Nelson, P. G. *J. Neurophysiol.* **40**, 1132–1150 (1981).
10. Adams, P. R. in *Advances in Physiological Sciences* Vol. 4 (ed. Salankim, J.) 135–138 (Pergamon, New York, 1981).
11. Puil, E. & Werman, R. *Can. J. Physiol. Pharmac.* **59**, 1280–1284 (1981).
12. Brown, D. A., Griffith, W. H. & Halliwell, J. V. *J. Physiol., Lond.* **324**, 63P (1982).
13. Segal, M. & Barker, J. L. *J. Neurophysiol.* (in the press).
14. Reuter, H. & Scholz, H. *J. Physiol., Lond.* **262**, 17–47 (1977).
15. Barker, J. L., McBurney, R. N. & MacDonald, J. F. *J. Physiol., Lond.* **322**, 365–387 (1982).
16. Lansman, J. B. *Biophys. J.* **41**, 61a (1983).
17. Colquhoun, D., Neher, E., Reuter, H. & Stevens, C. F. *Nature* **294**, 752–754 (1981).
18. Yellen, G. *Nature* **296**, 357–359 (1982).
19. Chesnoy-Marchais, D. *J. Physiol., Lond.* **342**, 277–308 (1983).
20. Barker, J. L. & Ransom, B. R. *J. Physiol., Lond.* **280**, 331–354 (1978).
21. Barish, M. E. *J. Physiol., Lond.* **342**, 309–325 (1983).
22. Bader, C. R., Bertrand, D. & Schwartz, E. A. *J. Physiol., Lond.* **331**, 253–284 (1982).

The agonist effect of dihydropyridines on Ca channels

A. M. Brown, D. L. Kunze & A. Yatani

Department of Physiology and Biophysics, University of Texas
Medical Branch, Galveston, Texas 77550, USA

Dihydropyridines (DHP) have great potential for clinical use because of their inotropic and vasomotor effects. The mechanism of action is unknown although Ca currents have been implicated[1,2]. Here we report measurements of single channel and whole cell cardiac Ca currents after application of two DHP agonists BAY K 8644 and CGP 28 392. Whole cell Ca currents from individual myocytes were increased and the 50% effective doses (ED_{50}) were similar to those reported for contractility in rabbit aorta and guinea pig heart[1] and catecholamine release from cat adrenal glands[3]. The measured ED_{50} was also consistent with the apparent dissociation constant (K_d) of a high affinity binding site present in cardiac sarcolemmal vesicles[4–7]. We propose that the molecular basis for these results is an increase in the probability that a single Ca channel, having opened and closed, will subsequently re-open during membrane depolarization. At high concentrations of BAY K 8644 and in the presence of 96 mM Ba, different effects are observed, primarily a marked prolongation of open time[8].

Neonatal rat and adult guinea pig ventricular cells were prepared using the methods of refs 9 and 10 respectively. The guinea pigs (300–500 g in weight) were anaesthetized with pentobarbital (50 mg per kg body weight)) and the ascending aorta was cannulated *in situ* under artificial respiration before removing the heart[11]. The enzyme solution used for dispersion was washed out with 'power soup'[12].

Whole cell currents were recorded using the blown-out patch clamp method[13] and single channel Ca currents were recorded using the patch gigaseal method in the cell-attached configuration[13]. Cardiac action potentials were recorded in five experiments with standard intracellular microelectrodes. For whole cell Ca currents, the extracellular fluid (in mM) was: NaCl 135, KCl 5.4, $CaCl_2$ 1.8, $MgCl_2$ 1.0, glucose 10, HEPES 5.0 (*p*H was adjusted to 7.4 with NaOH). The intracellular pipette contained (in mM), KOH 110, aspartic acid 110, KCl 20, HEPES 5, EGTA 0.2, ATP 2 and the *p*H was adjusted to 7.3 with KOH. The Ca patch pipette contained (in mM): $CaCl_2$ 40, tetraethylammonium chloride (TEACl) 20, KCl 5.5, glucose 20, 4-aminopyridine (4-AP) 5.0, Tris-HCl 55. The *p*H was adjusted to 7.4 with KOH. The Ba patch pipette contained (in mM): $BaCl_2$ 96, HEPES 10 (*p*H 7.4). All experiments were done at room temperature (20–22 °C).

Both agonists at low concentrations produced dose-dependent increases in the duration of the ventricular action potential with no changes in the resting potential (Fig. 1*D*). At an action potential of 0 mV, the duration was increased by as much as 25% whereas at half-peak amplitude the duration was increased by a factor of two or more. The effects occurred within 1 min and were usually complete within 5 min (Fig. 1*E*). The effects of the agonists were reversible after 15–20 min of washing. The effect of BAY K 8644 (10^{-7} M) on whole cell peak Ca currents was an increase between −20 and +30 mV (Fig. 2*A*) and similar values were obtained when Cs was substituted for K in the

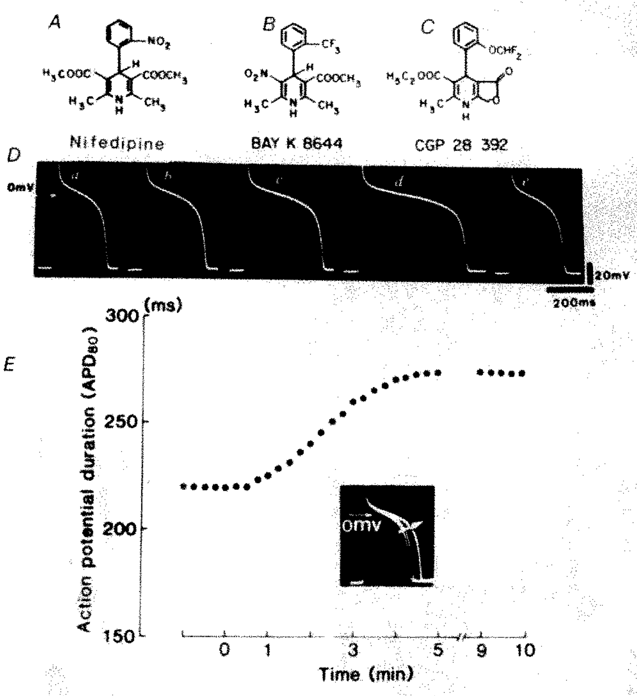

Fig. 1 *A–C*, Chemical structures of nifedipine, BAY K 8644 and CGP 28 392. The difference between dihydropyridines with antagonist effects and those with agonist effects is that the former have two freely rotating ester groups whereas the latter have only one. The difference between BAY and CGP is that a nitro group replaces an ester group in BAY and one ester group is locked into a rigid ring structure in CGP. *D*, *E*, The effects of BAY on the action potential (AP) of single isolated adult guinea pig ventricular cells. *D*, Dose-dependent changes; *a*, control; *b*, 5×10^{-9} M; *c*, 5×10^{-8} M; *d*, 5×10^{-7} M and *e*, recovery 15 min after washing. The major effect is a prolongation of AP duration. *E*, The time course of the changes in AP measured at 80% repolarization (APD_{80}) produced by 5×10^{-9} M BAY. The inset shows the AP before and 1, 3, 5 and 10 min after adding the drug. Stimulation occurred every 15 s.

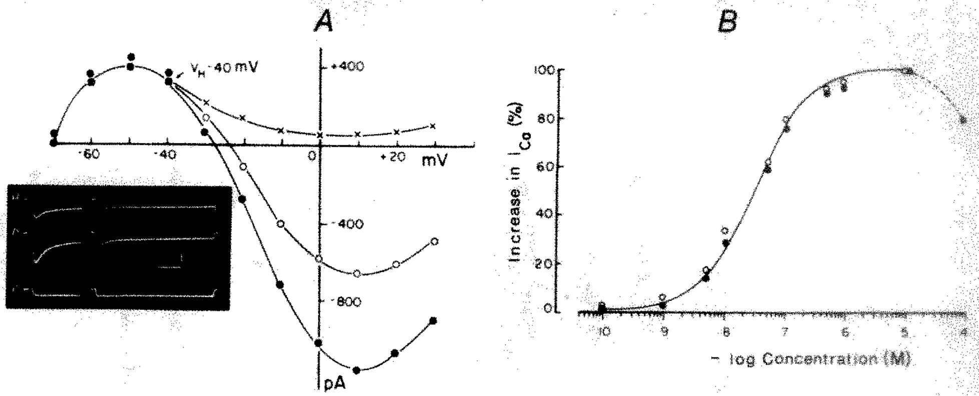

Fig. 2 *A*, Effects of BAY K 8644 (10^{-7} M) on Ca current and peak *I–V* curve of single adult guinea pig ventricular myocytes. ○, Control; ●, plus BAY K 8644 (10^{-7} M); X, plus Co. The holding potential (V_H) was −40 mV and steps were applied every 10 s. The inset shows the currents in response to steps from −40 to +10 mV before and after drug (*a*, *b*) and after blocking calcium current with 3 mM Co (*c*). There are two time bases, left, 10 ms; right, 100 ms. Current calibration was 500 pA. The outward holding current is produced by using a holding potential which is less negative than the zero current potential; it is carried by the inward rectifier. Ca currents for the dose–response curves were measured as the difference in inward current before and after addition of Co. *B*, Dose–response curves of maximum Ca current in adult guinea pig for the CGP agonist (○) and the BAY agonist (●). Each point is the mean value of seven cells for BAY and five cells for CGP. S.E. values were $< \pm 10\%$ for both agents. The solid line extends only to the peak I_{Ca} and is the theoretical curve for one to one agonist–receptor interactions. ED_{50} is 3×10^{-8} M. Similar results were obtained in neonatal rat myocytes. The maximum increase produced by BAY was three- to fourfold whereas that produced by CGP was twofold.

intracellular pipette. At doses of 10^{-7} M or greater, the effects for BAY K 8644 but not CGP 28 392 appeared to be larger at negative test potentials. Inactivation from the peak was quicker, the steady current was larger and tail currents were prolonged. As results of this kind have been attributed to loss of potential control[14], we investigated these effects using neonatal myocytes, which have smaller currents and simpler geometry due to the absence of T-tubules[15]. The bath solution (in mM) was: $CaCl_2$ 5, TEACl 20, KCl 5.5, 4-AP 5, Tris-HCl 90, glucose 20; *p*H was adjusted to 7.3 with KOH. The pipette solution (in mM) was: CsOH 110, aspartic acid 110, CsCl 20, HEPES 5, EGTA 1, ATP 2; *p*H was adjusted to 7.3 with CsOH. The currents were controlled in these cells and in these conditions, a voltage-dependence of drug action was not observed. Nevertheless we cannot exclude a voltage-dependent effect in adult cells. The effects of alteration in the state of the channel were investigated in inactivated and rested channels. To study steady-state inactivation, holding potentials as negative as −70 mV were required. This could reactivate Na currents which were abolished at the usual holding potential of −40 mV. To avoid this, tetrodotoxin (TTX) was added in doses of 5×10^{-5} M to completely block Na currents[16]. Steady-state inactivation measured using prepulses of several seconds duration combined with test pulses to either +10 or −10 mV was unaffected by agonists. We did not observe the blocking action reported for syncytial cardiac Purkinje preparations[17] at the ED_{50} using holding or conditioning potentials of −40 mV.

The effects were specific for Ca currents. The inward rectifier current activated by hyperpolarizing potentials to −100 mV and the outward currents activated at potentials above +20 mV were unaffected. The *β*-blocker propranolol at a concentration of 5×10^{-6} M had no effect; thus *β*-receptors which when activated by noradrenaline also increase Ca currents in these cells[18,19] were not involved. The Ca currents were eliminated by the specific DHP Ca antagonist nitrendipine in doses of 10^{-5} M or by substitution of Co for Ca extracellularly. The dose–response curves for both agonists were similar (Fig. 2*B*). At lower doses the effects were reversible; at higher doses recovery was partial. This may be partially due to the fact that Ca currents in small cells run down with time[20,21]. A maximum effect at an agonist concentration of 10^{-5} M was also observed when contraction of aortic smooth muscle or heart[1] or noradrenaline release[3] was used as the observable response.

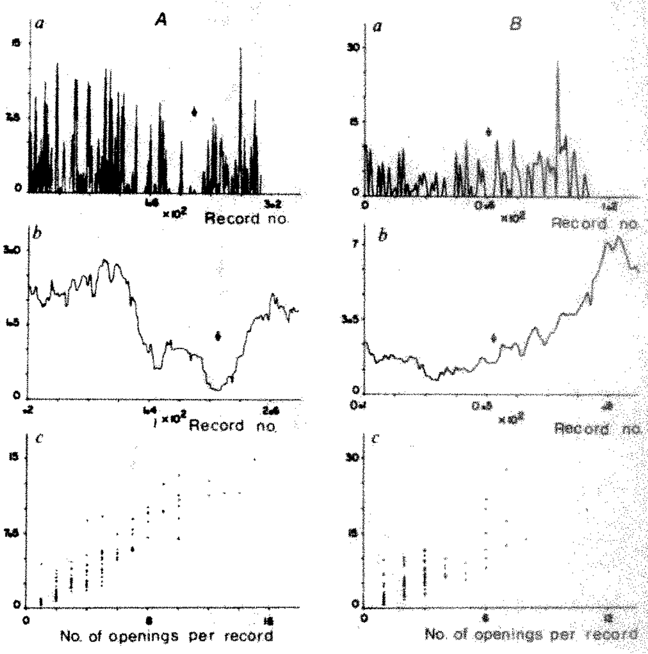

Fig. 3 Single channel activity from two cell-attached patches on neonatal rat ventricular myocytes during control and after addition (marked by arrows) of BAY K 8664 (*A*) and CGP 28 392 (*B*) in doses of 5×10^{-7} M. The patch pipette contained 40 mM Ca. In *B*, the potential step was applied at 0.25 Hz for 70 ms. Resting potential, V_R, estimated (from whole cell mesurements) was −50 mV. The patch potential was −20 mV, and the step potential (V_{step}) was +50 mV. In *A* the step was 100 ms in duration, holding potential was −20 mV, and V_{step} was 40 mV; repetition rate was 0.2 Hz. Records were low pass filtered at 1 kHz using a zero phase, nonringing, digital filter; sampling rate was 50 μs per point. *a*, Percentage of open time against the record number. *b*, Smoothed versions of *a*, where smoothing is done by averaging at each point the surrounding 41 and 21 points in *A* and *B* respectively. Note that in *B*, rundown during control was small whereas in *A* it was substantial. *C*, The relationship between the percentage of open time (ordinate) and number of openings per record (abscissa). The data were fitted by linear regressions with $r = 0.84$ and 0.69, respectively. The slopes correspond to open times per opening of 0.88 and 1.0 ms in *A* and *B* respectively. Large deviations due to prolonged openings are not present.

To examine the mechanism of action at a molecular level, we studied single Ca channels. The trials consisted of up to 500 identical voltage steps 50–500 ms duration delivered at intervals of 4–12 s. Long periods of recording during control were associated with a progressive loss of activity and it was useful to construct a trace by trace 'diary' of the single channel activity. The diary consisted of measurements of the percentage of open time per record and the number of openings per record (Fig. 3). Figure 3 shows that in control experiments the activity was cyclic; it also confirms the occurrence of rundown. Addition of agonist was always associated with a large increase in activity although the cyclical pattern persisted. Similar results were observed in three additional experiments. At an agonist

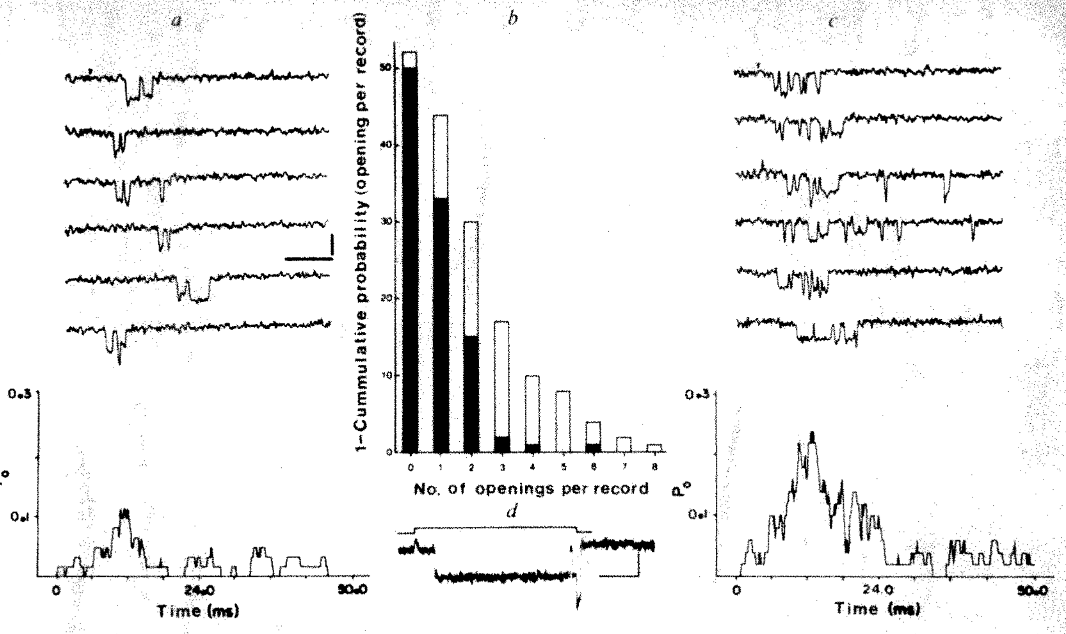

Fig. 4 Effects of agonist CGP 28 392 on single channel Ca currents (*a*, control; *c*, after drug). Control traces are representative of record numbers 25-65 and traces after drug are representatives of record numbers 80-120 shown in Fig. 3*B*. Arrows indicate onset of potential step. There were two channels in this patch (sixth trace in *a*, third trace in *c*). Bars are 0.4 pA and 15 ms. Linear components of capacitance and leakage have been subtracted. *c* was taken 3 min after addition of 5×10^{-7} M CGP 28 392 to the bath. Below *a* and *c* are the averaged currents for the record numbers referred to above—P_0 is the opening probability. *b*, Agonist effect on the distributions of openings per trace. ■, Control; □, plus CGP 28 392 (5×10^{-7} M). The ordinate is 1− the cumulative discrete probability density function of the number of openings per record. *d*, Effect on a single channel of 10^{-5} M BAY. Pipette contained isotonic Ba. V_H was the resting potential of −50 mV, V_{step}, +40 mV, pulse duration 100 ms. Calibration, 1 pA and 20 ms. Slope conductance calculated from the closure following return of the voltage step was 30 pS, which is about 20% greater than the usual value in isotonic Ba (ref. 18).

concentration of 5×10^{-7} M with 40 mM Ca in the patch pipette, the relationship between percentage of open time and number of openings per record was monotonic and highly correlated. In 1,536 events there was no evidence of greatly prolonged open times such as those observed in Fig. 4*d*. Unitary amplitudes were unchanged and the major effect was an increase in the average number of openings per sample due to the fact that re-openings became more frequent (Fig. 4). When the individual single channel records were summed and averaged, they increased and decreased in the same way as the whole cell currents, and the increase due to agonist was consistent with the increase observed in whole cell current recordings (Fig. 4). The open time distributions were fitted by a single exponential function and were unaffected by agonist. The mean value of open time was 1.36 ± 0.76 ms ($n=815$) for the control experiments and 1.47 ± 0.98 ms ($n=721$) for agonist when holding potential (V_H) = resting potential (V_R) −20 to −40 mV and the voltage step (V_{step}) was +30 to +60 mV.

The mean values for waiting times (latencies to first opening) were unchanged. The openings occurred in bursts as already reported[20,22-24], and these gave rise to short and long closed times. The burst duration and gaps within bursts were unaffected and the mean closed times were also unchanged. Although increased re-opening should reduce the mean closed times, for pulsed data, the last closed times were not determined. More of the longer closed times are discarded in the control experiment so that the drug effect is obscured. When high agonist concentrations (10^{-5} M) were used with 96 mM Ba in the patch pipette, repetitive activity was markedly intensified and greatly prolonged openings appeared[8] (Fig. 4*d*). These events gave a bimodal distribution to the plots of percentage open time versus number of openings per record.

Bath applications of nitrendipine in doses which blocked the whole cell current responses also blocked the single channel responses. It is not surprising that DHPs gain access to the membrane patch via extra-patch membrane as these agents are highly lipophilic. However, it is not known whether equilibrium conditions for drug distribution are attained in the patch.

The effects on single channels were due to an increase in the probability of re-opening. We cannot exclude an increase in the number of activatable Ca channels, but the results suggest that much of the increase in whole cell current is attributable to the increased probability of re-opening. Two possibilities are that progression to an absorbing inactivated state was inhibited or that re-opening from a closed state was enhanced. The absence of an effect on steady-state inactivation might favour the latter interpretation. The concentrations we used indicate that the effects were mediated by the high-affinity binding sites. In these circumstances the agonists did not change channel structure sufficiently to increase unit conductance or duration in the open state. The dramatic changes observed at 10^{-5} M concentrations of agonist[8] indicate a considerable change in channel structure and might be mediated by the low-affinity binding sites described for these agents[4,6]. They might also be associated with the falling phase of the dose-response curves.

We thank Dr A. Scriabine (Miles Laboratories) and Dr G. Weiss (Ciba-Geigy) for supplies of the agonists. This work was supported in part by NIH grants NS 11453 and HL 25145.

Received 24 April; accepted 25 July 1984.

1. Schramm, M., Thomas, G., Towart, R. & Franckowiak, G. *Nature* **303**, 535-537 (1983).
2. Glossman, H., Ferry, D. R., Lübbecke, F., Mewes, R. & Hofmann, F. *Trends pharmac. Sci.* **3**, 431-437 (1982).
3. Garcia, A. G. *et al. Nature* **309**, 69-71 (1984).
4. Janis, R. A., Rampe, D., Sarmiento, J. G. & Triggle, D. J. *Biochem. biophys. Res. Commun.* (in the press).
5. Sarmiento, J. G., Janis, R. A., Rampe, D. & Triggle, D. J. *Fedn Proc.* **43**, 448 (1984).
6. Vaghy, P. L., Grupp, I. L., Grupp, G. & Schwartz, A. *Circulation Res.* (in the press).
7. Grupp, I. L. *et al. Fedn Proc.* **43**, 937 (1984).
8. Hess, P., Lansman, J. B. & Tsien, R. W. *Biophys. J.* **45**, 394a (1984).
9. Mark, G. E. & Strasser, F. F. *Expl Cell Res.* **44**, 217-233 (1966).
10. Powell, T., Terrar, D. A. & Twist, V. W. *J. Physiol., Lond.* **302**, 131-153 (1980).
11. Taniguchi, J., Kokubun, S., Noma, A. & Irisawa, H. *Jap. J. Physiol.* **31**, 547-558 (1981).
12. Isenberg, G. & Klockner, U. *Pflügers Arch. ges. Physiol.* **395**, 6-18 (1982).
13. Hamill, O. P., Marty, A., Neher, E., Sakmann, B. & Sigworth, F. J. *Pflügers Arch. ges. Physiol.* **391**, 85-100 (1981).
14. Johnson, E. A. & Lieberman, M. *A. Rev. Physiol.* **33**, 479-532 (1971).
15. Moses, R. L. & Kasten, F. H. *Cell Tissue Res.* **203**, 173-180 (1979).
16. Josephson, I., Sanchez-Chapula, J. & Brown, A. M. *Circulation Res.* **54**, 157-162 (1984).
17. Sanguinetti, M. C. & Kass, R. S. *Biophys. J.* **45**, 394a (1984).
18. Reuter, H., Stevens, C. F., Tsien, R. W. & Yellen, G. *Nature* **297**, 501-504 (1983).
19. Cachelin, A. B., de Peyer, J. E., Kokubun, S. & Reuter, H. *Nature* **304**, 462-464 (1983).
20. Fenwick, E. M., Marty, A. & Neher, E. *J. Physiol., Lond.* **331**, 599-635 (1982).
21. Hagiwara, S. and Ohmori, H. *J. Physiol., Lond.* **336**, 649-661 (1983).
22. Lux, H. D. & Nagy, K. *Pflügers Arch. ges. Physiol.* **391**, 252-254 (1981).
23. Brown, A. M., Camerer, H., Kunze, D. L. & Lux, H. D. *Nature* **299**, 156-158 (1982).
24. Cavalié, A., Ochi, R., Pelzer, D. & Trautwein, W. *Pflügers Arch. ges. Physiol.* **398**, 284-297 (1983).

Immunochemical tests of acetylcholine receptor subunit models

Jon Lindstrom*, Manuel Criado*,
Susan Hochschwender*, J. Lawrence Fox†
& Virender Sarin†

* The Salk Institute for Biological Studies, PO Box 85800, San Diego, California 92138, USA
† Department of Molecular Biology, Abbott Laboratories, Abbott Park, North Chicago, Illinois 60064, USA

Acetylcholine receptors of fish electric organs and mammalian skeletal muscle comprise four structurally homologous glycoprotein subunits in the mole ratio $\alpha_2\beta\gamma\delta$ (refs 1–4). All four subunits have leader sequences and are exposed on both sides of the membrane[5,6]. From amino acid sequencing, three groups[5,7,8] have predicted that each subunit has four hydrophobic α-helical transmembranous domains. Because the N-terminus of each subunit is thought to remain on the extracellular surface after cleavage of the leader sequence, this model predicts that the N- and C-termini are both on the extracellular side. An alternative model proposed by two other groups[9,10] predicts that there is, in addition, a fifth amphipathic transmembranous domain which would place the C-terminus on the cytoplasmic side. Here, using anti-subunit sera and monoclonal antibodies and their reaction with synthetic subunit peptides, we demonstrate that the C-terminus is in fact on the cytoplasmic surface. We also show that, contrary to other predictions[11], the most hydrophilic sequence on the extracellular domain of α-subunits is not the main immunogenic region.

More than half of the antibodies made against native acetylcholine receptors (AChR) are directed at a small part of the extracellular surface of the α-subunits called the main immunogenic region (MIR)[12–14]. It has been reported that the most hydrophilic part of an amino acid sequence is usually a prominent antigenic determinant[15]. Therefore, it has been suggested that the most hydrophilic sequence on the predicted extracellular domain of α-subunits would form the main immunogenic region, although we show here that this is not correct.

Peptides were synthesized corresponding to the N- and C-terminal 10 amino acids of each subunit (except for δ, where the C-terminal peptide extended from C-3 to C-12 because of synthetic difficulties with the penultimate cysteine) and to the predicted main immunogenic region on the α-subunit (residues 159–169; ref. 11) (Bachem). At the unnatural terminus of each peptide, a tyrosine was added so that the peptides could be labelled with ^{125}I.

Anti-receptor monoclonal antibodies from our library (refs 12–14 and unpublished data) and antisera to native receptor from *Torpedo californica* and its purified denatured subunits were tested for reaction with these ^{125}I-labelled synthetic peptides (see Table 1). The results indicate that the N-termini of the chains are negligible immunogens in the intact receptor. Antisera to SDS-denatured receptor subunits also showed negligible reactions with the N-termini, however, the C-termini of the β-, γ- and, to some extent, δ-subunits were significantly immunogenic. Comparison of the titres of these anti-subunit sera to intact receptor (all $\sim 2.5\ \mu$M) with their titres against C-terminal peptides suggests that ~20% of antibodies to β-subunits, ~6% of antibodies to γ-subunits, and ~0.4% of the antibodies to δ-subunits are directed at the C-terminus. Titres against intact receptor were measured by indirect immune precipitation in units of mol α-bungarotoxin binding sites bound per litre of solution, and converted to approximate molar concentration of antibody by assuming that all of the receptors were present as dimers (containing four binding sites) and dividing the titre by four. Titres against peptides were measured by indirect immune precipitation in units of mol peptide bound per litre of solution, and converted to approximate molar concentration of antibody by assuming that peptides were bound to both of the antibody binding sites and dividing the titre by two. The fraction of antibodies to the C-terminus was calculated by dividing the concentration of antibodies to the peptide by the concentration of antibodies to the intact receptor. Three monoclonal antibodies to β-subunits were found which recognized the C-terminus. These monoclonal antibodies were initially selected by S. Tzartos *et al.* and were used in refs 16–18. They are the result of the fusion of spleen cells from rats immunized with β-subunits with the mouse myeloma S194 as previously described[12–14]. Their subclasses are 163-IgM, 170-IgG2a and 172-IgG1.

Antibodies which bound to C-termini were tested to determine whether they bound to the extracellular surface or the cytoplasmic surface of the receptor. Receptor-rich membrane vesicles from *Torpedo* electric organ are sealed rightside-out[19], but can be permeabilized using saponin or lithium diiodosalicylate (LIS)[20]. The ability of native or permeabilized vesicles to adsorb antibodies to the C-termini was tested (Fig. 1, Table 2). These results clearly demonstrate that the C-termini of β-, γ- and δ-subunits are on the cytoplasmic surface of the receptor and are accessible to antibody binding only when receptor-rich membrane vesicles have been permeabilized to permit entry of the antibody molecules. Pretreatment of the vesicles with saponin (0.3% or 3%) also permitted the vesicles to adsorb antibodies to the C-termini (Fig. 1). Previously, we found 11 monoclonal antibodies to receptor which required saponin to bind to receptors in the postsynaptic membrane of muscle and then showed

Table 1 Reaction of antibodies with synthetic peptides from receptor subunits

	[(Antibody c.p.m. divided by blank c.p.m.) − 1]								
	α_{1-10}	$\alpha_{159-169}$	$\alpha_{428-437}$	β_{1-10}	$\beta_{460-469}$	γ_{1-10}	$\gamma_{480-489}$	δ_{1-10}	$\delta_{490-499}$
Anti-AChR serum	0	0	0	0	0	0	7	0	0
Anti-α serum	0	3	0	0	0	0	0	0	0
Anti-β serum	0	0	0	0	44	0	0	0	0
Anti-γ serum	0	0	0	0	3	0	147	0	1
Anti-δ serum	0	0	0	0	0	0	30	0	2
18 Anti-α antibodies	0	0	0						
6 Anti-MIR antibodies		0							
40 Anti-β antibodies				0	0				
mAb 163				0	78				
mAb 170				0	41				
mAb 172				0	182				
10 Anti-γ antibodies						0	0		
20 Anti-δ antibodies								0	0

Peptides were labelled with ^{125}I to specific activities of about 3×10^{18} c.p.m. mol^{-1} by the same basic procedure reported for labelling α-bungarotoxin[30]. After dilution to 1×10^{-9} M (in 0.5% Triton X-100, 100 mM NaCl, 10 mM NaN_3, 10 mM Na phosphate buffer *p*H 7.5), triplicate 1-ml aliquots were incubated overnight with 5 µl of antisera or 2 µl of monoclonal antibody plus 3 µl of normal rat serum. After precipitation with goat anti-rat IgG, the washed pellets were counted. Normal rat serum was used as a blank. MIR, main immunogenic region.

Table 2 Inhibition of antibody binding to C-terminal peptides by receptor in various forms

	% Inhibition of binding by 3×10^{-8} M AChR		
	Native vesicles	LIS-permeabilized vesicles	Soluble receptor
Anti-β serum	0	68	71
Anti-β mAb 163 (IgM)	3	11	31
Anti-β mAb 170 (IgG)	0	74	55
Anti-β mAb 172 (IgG)	0	52	59
Anti-γ serum	0	39	45
Anti-δ serum	0	44	85

Inhibition experiments were conducted as described for Fig. 1.

by electron microscopy using colloidal gold-labelled anti-antibody that in every case the antibodies bound to the cytoplasmic surface of the membrane[16]. Saponin treatment was less effective than LIS treatment (Fig. 1). This observation can be explained[20] by the fact that saponin only makes holes in the membrane through which antibodies can enter the vesicle, whereas LIS not only disrupts the vesicle, but also removes a protein (molecular weight 43,000) which is known to associate with the cytoplasmic surface of β-subunits[21]. This observation further supports our proposal that antibodies to the C-termini of the subunits bind to the cytoplasmic surface of the receptor. To test this conclusion further, we prepared antisera against the C-terminal peptides of all four subunits and showed that LIS-extracted but not native receptor-rich vesicles could adsorb those antisera[22].

Our results conclusively demonstrate that models[4,7,8] which place the C-termini of receptor subunits on the extracellular surface of the postsynaptic membrane are incorrect. Those models[9,10] which propose a fifth amphipathic domain may be correct. R. Stroud and co-workers have reached a similar conclusion using electron microscopy to localize binding of antisera to the C-terminus of δ-subunits (personal communication). A fifth amphipathic transmembranous domain is especially appealing because it provides a hydrophilic surface for lining the cation channel through the receptor, which must have a hydrophilic surface to accommodate the high flow rate of hydrated cations known to occur through the channel[23].

It was proposed that the main immunogenic region of the receptor is formed by the most hydrophilic sequence of the α-subunits (amino acids 161-166)[11]. However, Table 1 shows that the synthetic peptide α 159-169 reacts only slightly with antisera to α-subunits and not at all with antisera to native receptor or with a collection of monoclonal antibodies to the main immunogenic region which react with denatured α-subunits. The main immunogenic region is a conformation-sensitive region—antibodies to it react better with native receptor than with SDS-denatured α-subunits. However, as these antibodies react with denatured α-subunits, they should bind to a synthetic peptide corresponding to the main immunogenic region. Therefore, the sequence α 159-169 does not form the main immunogenic region. Juillerat *et al.* recently reached a similar conclusion[24].

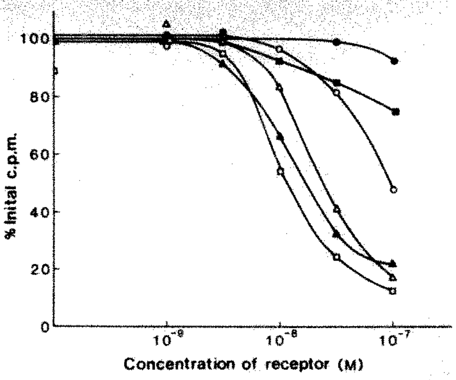

Fig. 1 Inhibition of binding of monoclonal antibody 172 to the ^{125}I- labelled C-terminal peptide of β-subunits. ●, Native vesicles; ■, native vesicles plus saponin; ○, *p*H 11 extracted vesicles; ▲, soluble receptor; △, *p*H 11 and Li diiodosalicylate (LIS)-extracted vesicles; □, denatured soluble receptor. Native receptor-rich membrane vesicles[19] were permeabilized with 0.3% saponin[16], or extracted with *p*H 11[29], or extracted first with *p*H 11 and then with 10 mM LIS[20]. Affinity-purified solubilized receptor[30] was denatured with 1% SDS and then diluted to 0.15% SDS in 0.5% Triton X-100. Triplicate 1-ml aliquots of ^{125}I-labelled C-terminal peptide at 1×10^{-10} M (in 100 mM NaCl, 10 mM NaN_3, 10 mM Na phosphate *p*H 7.5) were mixed with the indicated concentrations of receptor (measured as α-bungarotoxin binding sites[30]). Antibody was added overnight at a concentration of 2×10^{-10} M (measured as α-bungarotoxin binding sites precipitated per litre) in the presence of 5 μl of normal rat serum as carrier, then goat anti-rat IgG was added. The resulting pellet was washed and counted.

To test this conclusion further, a larger peptide from the same region of the α-subunit (amino acids 152-167) was synthesized and coupled to keyhole limpet haemocyanin by glutaraldehyde, for use as an immunogen. Spleen cells from an immunized rat were fused with S194 mouse myeloma cells as previously described[12,13,19] to produce a hybridoma secreting a monoclonal antibody designated mAb 236 (M.C. *et al.*, in preparation). This antibody bound to α-subunits but not to β-, γ- or δ-subunits

Table 3 Competition between monoclonal antibody to α 152-167 and monoclonal antibodies to MIR for binding to AChR in an ELISA

	Additivity index (raw data)			
	mAb 236	mAb 6	mAb 35	mAb 203
mAb 236 (anti-α 152-167)	(0.50 ± 0.04)	82 (0.80 ± 0.03)	96 (0.99 ± 0.08)	97 (1.34 ± 0.12)
mAb 6 (anti-*Torpedo* MIR)		(0.38 ± 0.04)	11 (0.51 ± 0.05)	−32 (0.42 ± 0.02)
mAb 35 (anti-eel MIR)			(0.53 ± 0.04)	−12 (0.61 ± 0.04)
mAb 203 (anti-human MIR)				(0.86 ± 0.06)

Receptor was bound to microtitre dishes (Immulon 1, Dynatech) by adding 50 μl per well of a 2×10^{-8} M solution in 0.01 M Na bicarbonate buffer, *p*H 9.5 overnight at 4 °C. Unreacted sites on the plates were quenched by adding 200 μl of 0.5% bovine serum albumin in 5% Tween 20 for 15 min. This was followed by four washes with the same solution. Monoclonal antibodies at concentrations chosen to just saturate this assay after overnight incubation at 4 °C, were added in the same solution. Monoclonal antibody binding was measured using a monoclonal antibody to rat IgG κ-chains (MAR 18.5) (ref. 26) coupled to glucose oxidase[27]. The raw data shown are the absorbance in the ELISA for each monoclonal antibody or combination of monoclonal antibodies corrected by subtracting the absorbance of blank wells. The additivity index (AI)[28] is calculated as follows: $AI = 100\ ((2A_{1+2}/A_1 + A_2) - 1)$ where A_1 is the absorbance with the first monoclonal antibody alone, A_2 is the absorbance with the second monoclonal antibody alone, and A_{1+2} is the absorbance with the two monoclonal antibodies together. A low value of the additivity index indicates that the two monoclonal antibodies cannot bind simultaneously and compete for binding, whereas a value near 100 indicates that both monoclonal antibodies can bind to receptor simultaneously and do not compete for binding. Combinations of monoclonal antibodies to the main immunogenic region (MIR) give low values of the additivity index. The absorbance in the ELISA of combinations of either mAb 6 or mAb 35 with mAb 203, is close to the absorbance of mAb 6 or mAb 35, probably because mAb 6 was made against receptor from *Torpedo* electric organ[12], and mAb 35 was made against receptor from *Electrophorus* electric organ[13], whereas mAb 203 was made against receptor from human muscle[14], thus monoclonal antibodies 6 and 35 have higher affinity for the *Torpedo* receptor which was used as the antigen in this assay. Combinations of mAb 6, 35 or 203 with mAb 236 raised to the synthetic peptide α 152-167 give absorbances approximating the sum of the absorbances of the monoclonal antibodies added individually, showing that monoclonal antibodies bound to the MIR do not impair binding of mAb 236 to α 152-167.

bound to enzyme-linked immunosorbent assay (ELISA) wells (data not shown). Similarly, this antibody bound to intact receptor by ELISA and this binding was inhibited by both the synthetic peptides α 159-169 and α 152-167. Using this system, we tested whether mAb 236 competed for binding to the receptor with antibodies to the main immunogenic region. Table 3 shows that monoclonal antibodies to the main immunogenic region compete with each other for binding to receptor, whereas mAb 236 and monoclonal antibodies to the main immunogenic region can bind to receptors simultaneously. This shows that not only is the sequence 161-166 not the main immunogenic region, it is not even immediately contiguous to this region.

The studies described here reveal that predicting protein structure from cDNA sequences (the method used to predict the two alternative models[4,7-10] investigated here) is difficult and that immunochemical techniques are a useful approach for testing the predictions of such studies. Further studies with anti-peptide antibodies and other methods will be required to refine models of subunit structure and to account for the conformation changes which have been detected during the maturation and assembly of receptor subunits[25].

We thank John Cooper, Doug Schneider and Lorene Langeberg for technical assistance and the NIH (NS11323), the Muscular Dystrophy Association, the McKnight Foundation, the Alexander S. Onassis Public Benefit Foundation, and the Los Angeles and California Chapters of the Myasthenia Gravis Foundation for support. S.H. is supported by a Muscular Dystrophy Association postdoctoral fellowship.

Received 26 March; accepted 8 August 1984.

1. Lindstrom, J., Merlie, J. & Yogeeswaran, G. *Biochemistry* **18**, 4465-4470 (1979).
2. Reynolds, J. A. & Karlin, A. *Biochemistry* **17**, 2035-2038 (1978).
3. Raftery, M., Hunkapiller, M., Strader, C. & Hood, L. *Science* **208**, 1454-1457 (1980).
4. Conti-Tronconi, B., Hunkapiller, M., Lindstrom, J. & Raftery, M. *Proc. natn. Acad. Sci. U.S.A.* **79**, 6489-6493 (1982).
5. Noda, M. *et al. Nature* **302**, 528-532 (1983).
6. Anderson, D. & Blobel, G. *Proc. natn. Acad. Sci. U.S.A.* **78**, 5598-5602 (1981).
7. Claudio, T., Ballivet, M., Patrick, J. & Heinemann, S. *Proc. natn. Acad. Sci. U.S.A.* **80**, 1111-1115 (1983).
8. Devillers-Thiery, A., Giraudat, J., Bentaboulet, M. & Changeux, J. P. *Proc. natn. Acad. Sci. U.S.A.* **80**, 2067-2071 (1983).
9. Guy, R. *Biophys. J.* **45**, 249-261 (1983).
10. Finer-Moore, J. & Stroud, R. *Proc. natn. Acad. Sci. U.S.A.* **81**, 155-159 (1984).
11. Noda, M. *et al. Nature* **299**, 793-797 (1982).
12. Tzartos, S. & Lindstrom, J. *Proc. natn. Acad. Sci. U.S.A.* **77**, 755-759 (1980).
13. Tzartos, S., Rand, D., Einarson, B. & Lindstrom, J. *J. biol. Chem.* **256**, 8635-8645 (1981).
14. Tzartos, S., Langeberg, L., Hochschwender, S. & Lindstrom, J. *FEBS Lett.* **158**, 116-118 (1983).
15. Hopp, T. & Woods, K. *Proc. natn. Acad. Sci. U.S.A.* **78**, 3824-3828 (1981).
16. Sargent, P., Hedges, B., Tsavaler, L., Clemmons, L., Tzartos, S. & Lindstrom, J. *J. Cell Biol.* **98**, 609-618 (1983).
17. Swanson, L. *et al. Proc. natn. Acad. Sci. U.S.A.* **80**, 4532-4536 (1983).
18. Gullick, W. & Lindstrom, J. *Biochemistry* **22**, 3801-3807 (1983).
19. Elliott, J. *et al. Biochem. J.* **185**, 667-678 (1980).
20. Froehner, S., Douville, K., Klink, S. & Culp, W. *J. biol. Chem.* **258**, 7112-7120 (1983).
21. Burden, S., DePalma, R. & Gottesman, G. *Cell* **35**, 687-692 (1983).
22. Ratnam, M. & Lindstrom, J. *Biochem. biophys. Res. Commun.* **122**, 1225-1233 (1984).
23. Lewis, C. & Stevens, C. *Proc. natn. Acad. Sci. U.S.A.* **80**, 6110-6113 (1983).
24. Juillerat, M., Barkas, T. & Tzartos, S. *FEBS Lett.* **168**, 143-148 (1984).
25. Merlie, J. P. & Lindstrom, J. *Cell* **34**, 747-757 (1983).
26. Lanier, L. L., Gutman, G. A., Lewis, D. E., Griswold, S. T. & Warner, N. L. *Hybridoma* **1**, 125-131 (1982).
27. Johnson, R. & Nakamura, R. in *Immunoassays: Clinical Laboratory Techniques for the 1980s* 141-156 (Liss, New York, 1980).
28. Friguet, B., Djavadi-Ohaniance, L., Pages, J., Bussard, A. & Goldberg, M. *J. immun. Meth.* **60**, 351-358 (1983).
29. Neubig, R., Krodel, E., Boyd, N. & Cohen, J. *Proc. natn. Acad. Sci. U.S.A.* **76**, 690-694 (1979).
30. Lindstrom, J., Einarson, B. & Tzartos, S. *Meth. Enzym. immunochem. Tech.* **74**, 432-460 (1981).

Photoreceptor-specific degeneration caused by tunicamycin

Steven J. Fliesler, Laurence M. Rapp & Joe G. Hollyfield

Cullen Eye Institute, Baylor College of Medicine, Houston, Texas 77030, USA

The antibiotic tunicamycin inhibits the biosynthesis of *N*-acetylglucosaminylpyrophosphoryl polyisoprenol[1-3], a key intermediate in the formation of the asparagine-linked oligosaccharides of glycoproteins[4]. The effects of tunicamycin have been studied in various biological systems[5], primarily with the aim of elucidating the role of the carbohydrate moieties in the cellular function of glycoproteins[6]. Rhodopsin, the visual pigment of retinal rod photoreceptor cells, is a membrane glycoprotein which consists of a single polypeptide chain (opsin) to which a chromophoric prosthetic group (11-*cis*-retinaldehyde) and two asparagine-linked oligosaccharide chains are covalently attached[7]. The glycosylation of opsin can be blocked with tunicamycin *in vitro* in conditions where polypeptide synthesis is only slightly decreased[8,9]. We have reported[9] that tunicamycin can disrupt the normal assembly of rod outer segment membranes *in vitro* without significantly inhibiting the biosynthesis or intracellular transport of opsin. Here we report that intraocular injection of tunicamycin produces a photoreceptor-specific degeneration characterized by (1) progressive shortening of rod outer segment, (2) decreased electroretinogram amplitudes, (3) cessation of rod outer segment membrane assembly, and (4) eventual photoreceptor cell death.

Frogs (*Rana pipiens*, 20-25 g each) were maintained at 23°C under cyclic lighting (12 h light-12 h dark) in a metabolic incubator. In each animal, one eye was injected with 1.0 μg of tunicamycin (Calbiochem; in 10 μl dimethyl sulphoxide (DMSO)); the contralateral (control) eye was injected with 10 μl DMSO alone. At various times (1, 4, 8 and 20 days), animals were dark-adapted, immobilized, and electroretinogram (ERG) measurements were performed as described previously[10]. The light intensity necessary to obtain a criterion *b*-wave response of 30 μV was defined as the threshold (I_t, expressed in −log units). Following ERG measurements, animals were exposed to normal room illumination for 1 h and the eyes were then removed and processed for light microscopy[11].

No differences between the control and tunicamycin-injected eyes were observed with respect to maximal *b*-wave amplitude one day after injections (Fig. 1*a*,*b*). However, a small increase in threshold was observed in tunicamycin-injected eyes relative to controls: $\Delta I_t = 0.6$ (Fig. 1*a*,*b*). By day 4, a tunicamycin-induced decrease in maximal *b*-wave amplitude to 73.6% of control (Fig. 1*d*) and increase in threshold, $\Delta I_t = 1.6$ (Fig. 1*c*,*d*) were clearly evident. Further decreases in the maximal *b*-wave amplitude to 31.6% of control (Fig. 1*f*) and increases in threshold to $\Delta I_t = 3.4$ (Fig. 1*e*, *f*) were observed by day 8. During the time course of the decrease in maximal *b*-wave amplitude, the ERG *a*-wave amplitude also declined progressively. Finally, no ERG responses could be elicited from eyes 20 days after the tunicamycin injection (Fig. 1*h*), in contrast to control eyes (Fig. 1*g*). Linear regression analyses of ERG amplitudes as a function of post-injection time indicated that the decrease in maximal *a*-wave and *b*-wave amplitudes occurred at a rate of approximately 5% per day (correlation coefficient, 0.98), relative to controls.

The extent of retinal degeneration induced by tunicamycin was assessed by light microscopy. One day after the tunicamycin injection, no gross morphological changes were apparent relative to contralateral controls (Figs 2*a*, 3). However, by 4 days post-injection (Figs 2*b*, 3), rod outer segments in tunicamycin eyes (29.1 ± 3.7 μm) were reduced in length by nearly 23% ($P < 0.05$, $n = 3$) relative to those of controls (37.9 ± 5.5 μm). Furthermore, retinal pigment epithelium cells in the tunicamycin-injected eyes were laden with phagosomal debris (arrows in Fig. 2*b*). Eight days after the tunicamycin injection, photoreceptor degeneration had progressed markedly (Figs 2*c*, 3). Rod outer segments in the tunicamycin-injected eyes (21.8 ± 1.1 μm) were shortened to 48% of control length ($P < 0.001$, $n = 3$). The retinal pigment epithelium cells exhibited several pathological features, including hypertrophy and rounding, clustering of pigment granules in the apical cytoplasm, retraction of apical

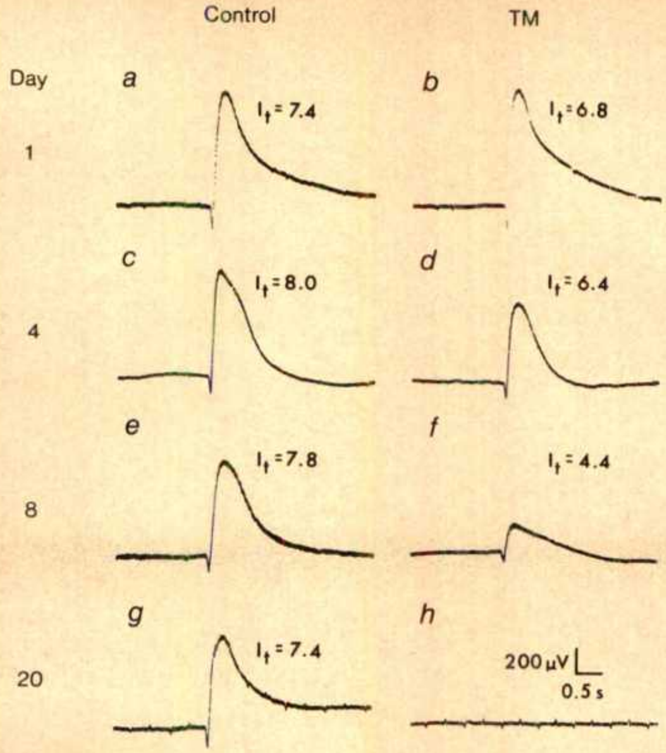

Fig. 1 Electroretinogram (ERG) recordings obtained following intraocular injection of frogs with DMSO (control: *a*, *c*, *e*, *g*) or tunicamycin (TM: *b*, *d*, *f*, *h*).

Methods: Groups of frogs (3 per time point) were anaesthetized by immersion in 0.5% MS-222 (Sigma) and injected in one eye with a tunicamycin solution (1 μg, in 10 μl DMSO) and in the contralateral eye with DMSO (10 μl). Injections (in the vitreous, at the pars plana) were performed under a dissecting microscope, using a Hamilton syringe fitted with a 32-gauge needle. Dark adaptation, immobilization by injection with curare and isoproteranol, and ERG measurements were perfomed as described previously[10]. Data from the experimental and control eyes are shown for a single animal representative of the group at the given post-injection time. Threshold values (I_t, in −log units) are given in each panel.

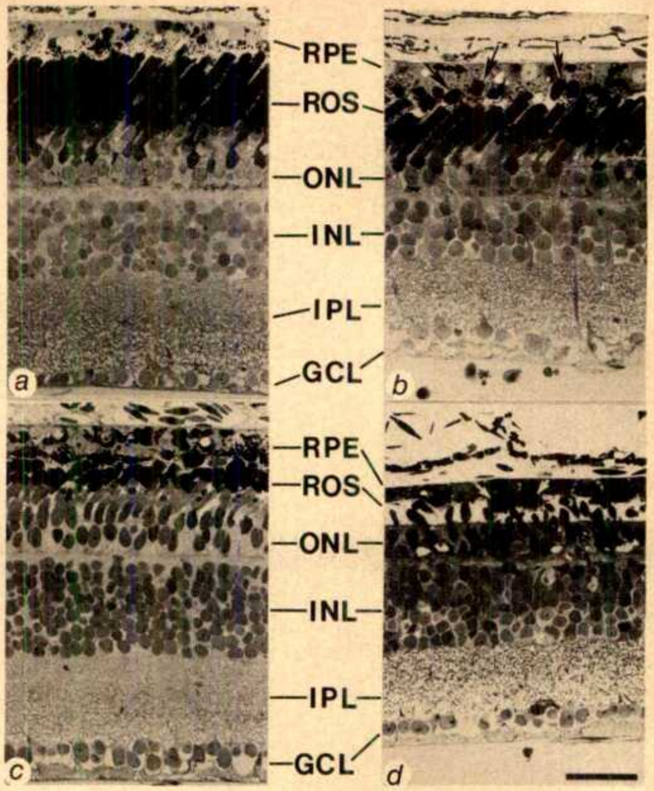

Fig. 2 Light micrographs of retinas from tunicamycin-injected eyes. Frogs were killed at (*a*) 1, (*b*) 4, (*c*) 8 and (*d*) 20 days following intraocular injection of tunicamycin, ~1 h after initial exposure to light. Fixation and processing of tissue for light microscopy was carried out as described previously[11]. RPE, retinal pigment epithelium; ROS, rod outer segment; ONL, outer nuclear layer; INL, inner nuclear layer; IPL, inner plexiform layer; GCL, ganglion cell layer. Retinas from control eyes (not shown) exhibited morphology comparable to that shown in *a* at all post-injection times. Apparent differences in retinal cell layer thickness reflect normal regional variations and do not represent significant changes as a function of time following injection of tunicamycin (see Fig. 3*A*). Monocytes are present in the vitreous, proximal to the ganglion cell layer (*b*). Phagosomes (black arrows, *b*) of unusually large size and number are evident within the apical cytoplasm of retinal pigment epithelium cells. Migratory pigmented cells (white arrows, *d*) can be seen within the subretinal space; note the absence of rod outer segment debris in the subretinal space.

microvilli, and accumulation of densely staining cytoplasmic inclusions. At 20 days post-injection, the morphology of the retinal pigment epithelium and photoreceptor layer of the retina in the tunicamycin-injected eyes was highly degenerate (Figs 2*d*, 3). Although many of the remaining rods in the tunicamycin-injected eyes retained some outer segment material, the rod outer segments were disoriented and were reduced in length by 73% ($P < 0.001$, $n = 3$) relative to controls. The lack of accumulated rod outer segment debris in the subretinal space and the engorged appearance of the retinal pigment epithelium indicated that phagocytosis continued after the injection of tunicamycin.

Rod outer segments exhibited a progressive and significant decrease in length as a function of post-injection time, at a rate of about 4% per day (correlation coefficient, 0.97). Even during the most advanced stages of photoreceptor degeneration, there was no significant thinning of other retinal layers (Fig. 3*A*; $P > 0.3$, $n = 3$). However, there was a progressive and selective loss of photoreceptor cells with time, resulting in nearly a 30% decrease ($P < 0.02$, $n = 3$) in the density of nuclei in the outer nuclear layer by day 20, relative to controls (Fig. 3*B*). Also, we did not observe any preferential loss of rod versus cone photoreceptors, as indicated by a relatively constant rod/cone ratio at all post-injection times.

Light microscopic autoradiography was performed after systemic labelling of the animals with ^{3}H-leucine to determine the incorporation of radiolabelled proteins into rod outer segment membranes, as indicated by the formation of a band of silver grains over the base of the rod outer segments. The apical displacement of these bands was measured from the base of the rod outer segments as a function of time (Fig. 4). One day following intraocular injection, bands of silver grains were observed in retinas from both tunicamycin-injected and control eyes approximately 2.0 μm from the base of the rod outer segments. In control eyes the displacement of these bands towards the distal tips of the rod outer segments progressed linearly at a rate of 0.92 μm per day, in good agreement with previous determinations of rod outer segment renewal rates for this animal[12]. In contrast, no further rod outer segment band displacement was observed in autoradiograms of tunicamycin-injected eyes throughout the experimental time course. These results indicate that renewal of rod outer segment membranes ceased some time within the first 4 days after the tunicamycin injection.

The photoreceptor cells are the most distal to the vitreous with respect to the other retinal cell types, and thus it is possible that the tissue concentration of tunicamycin in the photoreceptor layer was lower than in the other retinal cell layers. Therefore, it is remarkable that the degenerative changes were restricted to the photoreceptor cells, while the effects of tunicamycin on other retinal neurones were apparently negligible. The selective effect of tunicamycin on the photoreceptor cells may be due to the fact that their oxidative metabolic rate is similar to that of neoplastic cells[13], which have been shown to be extremely sensi-

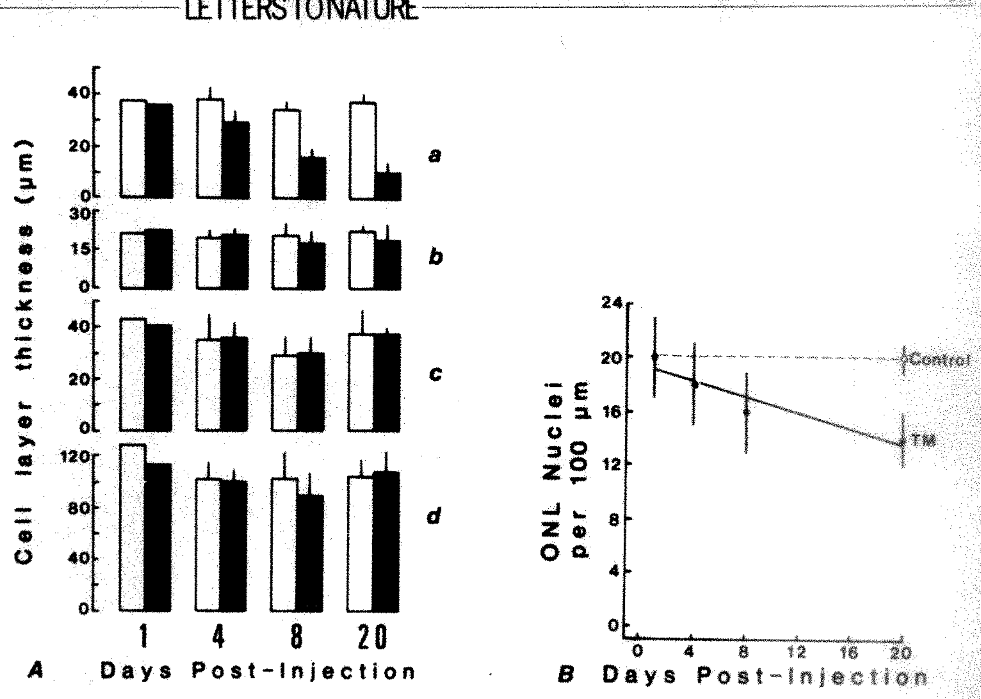

Fig. 3 Morphometric analysis of retinal cell layers as a function of time following intraocular injections with DMSO (control) or tunicamycin (TM). Measurements were made using a light microscope (×25 lens) coupled to a Zeiss Videoplan image analysis system via a video camera. Data represent the mean ±s.d. of 3 retinas for each condition; 5 random regions were analysed per retinal section and 15-20 individual measurements were performed per region. *A*, Length of rod outer segments (*a*) and thickness of the outer nuclear layer (*b*), inner nuclear layer (*c*), and the entire retinal expanse measured from the outer limiting membrane to the inner limiting membrane (*d*). Open bars, controls; shaded bars, TM. *B*, Quantitation of photoreceptor nuclei in the outer nuclear layer (ONL) (per 100 µm linear expanse) in tunicamycin-injected eyes (●) and controls (○). Linear regression analysis indicated the rate of photoreceptor cell loss to be about 1.6% per day (correlation coefficient, 0.90).

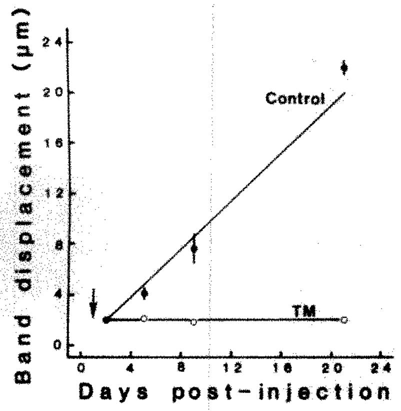

Fig. 4 Displacement of bands of silver grains in autoradiograms of rod outer segments as a function of post-injection time. **Methods:** Frogs were injected systemically with L-[4, 5-^{3}H] leucine (Amersham; 130 Ci mmol^{-1}; 10 µCi per g body weight) in the dorsal lymph sack. After 24 h (indicated by arrow), intraocular injection with DMSO (●) or tunicamycin (○) was performed (see Fig. 1 legend), permitting sufficient time for the assembly of several radiolabelled disk membranes in the basal portion of the rod outer segments before the introduction of the drug. At various times (2, 5, 9 and 21 days after ^{3}H-leucine injection), animals were killed approximately 1 h after initial exposure to light and the eyes were processed for light microscopic autoradiography[11]. Band displacement from the base of the rod outer segments was measured using a light microscope (×100 oil immersion lens) coupled to a Zeiss Videoplan image analysis system via a video camera. Quantitative analysis was performed as described in Fig. 2 legend. Linear regression analysis of the control (DMSO) points gave a slope of 0.92 µm per day (correlation coefficient, 1.00), corresponding to a daily renewal equivalent to 2.2% of the length of the rod outer segment.

tive to very low concentrations of tunicamycin[14]. In addition, the relative activity of the lipid-intermediate pathway for glycoprotein biosynthesis in the retina is greatest in the photoreceptor layer[15]. Therefore, tunicamycin might be expected to exert its inhibitory effects most prominently in the photoreceptor cells. Alternatively, the relative affinity of the uptake system for tunicamycin may be higher in photoreceptors than in other retinal cells.

These results are reminiscent of the kinds of pathological features observed in human rod–cone dystrophies, including retinitis pigmentosa[16–20]. A feature of these progressive blinding disorders is the selective deterioration of the photoreceptor cells, with the initial degeneration of the outer segments followed by pyknosis and cell death. The molecular etiology underlying these inherited retinal dystrophies remains unknown. These results suggest the novel possibility that a defect in the lipid-intermediate glycosylation pathway may be involved in one or more of these disorders. In this regard, we have recently obtained evidence which indicates grossly abnormal protein glycosylation in the rod photoreceptors of a human retina from a patient with an inherited chorioretinal degeneration resembling sectoral retinitis pigmentosa[21]. We are currently pursuing biochemical investigations to determine which retinal glycoproteins are affected during the tunicamycin-induced photoreceptor degeneration, as well as more detailed microscopic studies to assess potentially subtle ultrastructural changes which may occur in photoreceptors and other retinal cells during early times following intraocular injection of tunicamycin.

This work was supported by grants from the National Institutes of Health (NIH/NEI), the National Retinitis Pigmentosa Foundation (Baltimore), and the Retina Research Foundation (Houston). We thank Ms Janis Rosenthal and Mrs Mary E. Rayborn for technical assistance.

Received 24 April; accepted 25 July 1984.

1. Takatsuki, A., Kohno, K. & Tamura, G. *Agric. biol. Chem.* **39**, 2089–2091 (1975).
2. Tkacz, J. S. & Lampen, J. O. *Biochem. biophys. Res. Commun.* **65**, 248–257 (1975).
3. Lehle, L. & Tanner, W. *FEBS Lett.* **71**, 167–170 (1976).
4. Struck, D. K. & Lennarz, W. J. in *The Biosynthesis of Glycoproteins and Proteoglycans* (ed. Lennaz, W. J.) 35–83 (Plenum, New York, 1980).
5. Tamura, G. (ed.) *Tunicamycin* (Japan Scientific Societies, Tokyo, 1982).
6. Olden, K., Parent, J. B. & White, S. *Biochim. biophys. Acta* **650**, 209–232 (1982).
7. Hargrave, P. A. in *Progress in Retinal Research* Vol. 1 (eds Osborne, N. & Chader, G.) 1–51 (Pergamon, New York, 1982).
8. Plantner, J. J., Poncz, L. & Kean, E. L. *Archs Biochem. Biophys.* **201**, 527–532 (1980).
9. Fliesler, S. J., Rayborn, M. E. & Hollyfield, J. G. *J. Cell Biol.* **97**, 413a (1983).
10. Rapp, L. M. & Basinger, S. F. *Vision Res.* **22**, 1097–1103 (1982).
11. Hollyfield, J. G., Rayborn, M. E., Sarthy, P. V. & Lam, D. M. K. *J. comp. Neurol.* **188**, 587–598 (1979).
12. Young, R. W. *Invest. Ophthalmol. vis. Sci.* **15**, 700–725 (1976).
13. Graymore, C. N. in *Biochemistry of the Eye* (ed. Graymore, C. N.) 645–735 (Academic, New York, 1970).
14. Yamada, K. M. & Olden, K. in *Tunicamycin* (ed. Tamura, G.) 119–144 (Japan Scientific Societies, Tokyo, 1982).
15. Fliesler, S. J., Tabor, G. A. & Hollyfield, J. G. *Expl Eye Res.* (in the press).
16. Kolb, H. & Gouras, P. *Invest. Ophthalmol. vis. Sci.* **13**, 487–498 (1974).
17. Szamier, R. B. & Berson, E. L. *Invest. Ophthalmol. vis. Sci.* **16**, 947–962 (1977).
18. Szamier, R. B., Berson, E. L., Klein, R. S. & Meyers, S. *Invest. Ophthalmol. vis. Sci.* **18**, 145–160 (1979).
19. Rayborn, M. E., Moorhead, L. C. & Hollyfield, J. G. *Opthalmology* **89**, 1441–1454 (1982).
20. Bunt-Milam, A. H., Kalina, R. E. & Pagon, R. A. *Invest. Ophthalmol. vis. Sci.* **24**, 458–469 (1983).
21. Hollyfield, J. G., Frederick, J. M., Tabor, G. A. & Ulshafer, R. J. *Ophthalmology* **91**, 191–196 (1984).

Recombinant vaccinia virus primes and stimulates influenza haemagglutinin-specific cytotoxic T cells

J. R. Bennink*, J. W. Yewdell*, G. L. Smith†, C. Moller* & B. Moss†

* The Wistar Institute, 36th Street at Spruce, Philadelphia, Pennsylvania 19104, USA
† Laboratory of Viral Diseases, National Institute of Allergy and Infectious Diseases, NIH, Bethesda, Maryland 20205, USA

The ability of vaccinia virus to accept and express cloned genes[1–3] encoding immunologically important proteins of unrelated viruses[4–9] and malarial parasites[10] has suggested a novel approach to the development of live vaccines. Vaccinia virus recombinants retain infectivity and stimulate synthesis of specific antibodies to the cloned gene products in vaccinated animals. Moreover, animals inoculated with recombinants expressing the influenza virus haemagglutinin (HA)[7], the hepatitis B virus surface antigen[11], and type 1 herpesvirus glycoprotein D[8] were protected against subsequent challenge with the corresponding virus. For maximal effectiveness, vaccines should produce cellular as well as humoral immunity. We now report that a vaccinia virus recombinant, expressing the influenza HA, primes and stimulates a specific murine cytotoxic T-lymphocyte (CTL) response. Histocompatible cells infected with this recombinant also serve as targets for CTLs. These properties make vaccinia virus a unique tool for studying cell-mediated immunity and enhance the attractiveness of this vector for production of live vaccines.

The construction of the vaccinia virus recombinant H2-VAC (formerly referred to as vInf1) expressing the HA gene of influenza virus A/Jap/305/57 (H2N2) (JAP) has been described previously[7]. The HA gene was inserted next to a vaccinia virus transcriptional start site so that the authentic translational initiation and termination codons of the influenza gene were used. Tissue culture cells infected with the recombinant virus synthesized an HA polypeptide of the correct size that was glycosylated and transported to the cell surface[7,9]. The latter feature suggested that histocompatible cells infected with the recombinant virus might serve as targets for influenza virus-specific CTLs. To test this directly, P815 cells (a mastocytoma line derived from DBA/2 (*H-2*^{d}) mice) were infected and used as targets in a ^{51}Cr-release assay. CTLs derived from BALB/c (*H-2*^{d}) mice previously inoculated with JAP and restimulated with JAP-infected autologous splenocytes were able to lyse both JAP- and H2-VAC-infected cells (Fig. 1). In contrast, only background levels of cell lysis were observed using targets infected with wild-type vaccinia virus (Fig. 1). Control experiments verified that the latter were effectively lysed by CTLs prepared from vaccinia virus-infected mice (not shown). These results confirm our previous evidence that the HA is expressed on the surface of cells infected with recombinant vaccinia virus and further demonstrate that the HA can interact with class I major histocompatibility complex molecules in a manner sufficient for recognition by CTLs.

We next examined the ability of the recombinant vaccinia virus to restimulate *in vitro* splenocytes derived from BALB/c mice primed 3 weeks earlier by infection with JAP. Figure 2 shows that CTLs stimulated by H2-VAC were able to efficiently lyse cells infected with JAP or H2-VAC itself but not cells infected with an influenza B virus or wild-type vaccinia virus. As anticipated, we repeatedly found no detectable anti-influenza virus CTL activity when wild-type vaccinia virus was used for stimulation (not shown).

Further experiments demonstrated that the recombinant vaccinia virus could also prime for an influenza virus-specific CTL response. BALB/c mice were inoculated with recombinant or wild-type vaccinia virus; after 4 weeks, splenocytes were stimulated *in vitro* with JAP. Figure 3*a* shows that the recombinant virus was able to prime for an influenza virus-specific CTL response, whereas influenza virus-specific priming did not occur when mice were inoculated with wild-type vaccinia virus (Fig. 3*b*). Note that CTLs induced by H2-VAC priming and JAP secondary stimulation lysed cells infected with H2-VAC and

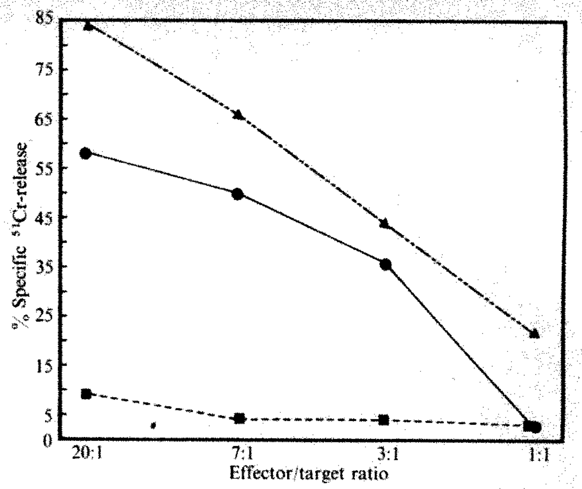

Fig. 1 Lysis of H2-VAC-infected target cells (–●–) by anti-influenza virus-specific CTLs. BALB/c splenocytes for *in vitro* stimulation were obtained from mice 2–4 weeks after intraperitoneal immunization with allantoic fluid containing 200 haemagglutinating units of JAP. Primed spleen cells (5×10^7) were cultured for 6 days in the presence of 2.5×10^7 autologous spleen cells infected with JAP at a multiplicity of 100 egg infectious doses (EID) per cell, then tested in a standard ^{51}Cr-release assay. P815 cells were infected with vaccinia virus WR isolate (- -■- -) or recombinant H2-VAC at a multiplicity of 10–100 plaque-forming units (PFU) per cell or with JAP (——▲——) at 10–100 EID per cell for 1 h[18]. After washing, cells were incubated for 6 h (JAP infection) or 15 h (vaccinia infection), then incubated for 1 h with ^{51}Cr at 37 °C, washed twice and dispensed into wells of microtitre plates (10^4 cells per well). Effector cells from *in vitro* cultures were added at various ratios, and after 4 h incubation at 37 °C, one-half of the culture supernatant was removed for determination of the concentration of released ^{51}Cr by γ counting. Per cent specific release was determined as follows: experimental release – spontaneous release (no CTLs) divided by total release (in the presence of detergent) – spontaneous release. Spontaneous release values were: JAP, 28%; H2-VAC, 14%; and wild-type vaccinia virus, 18%.

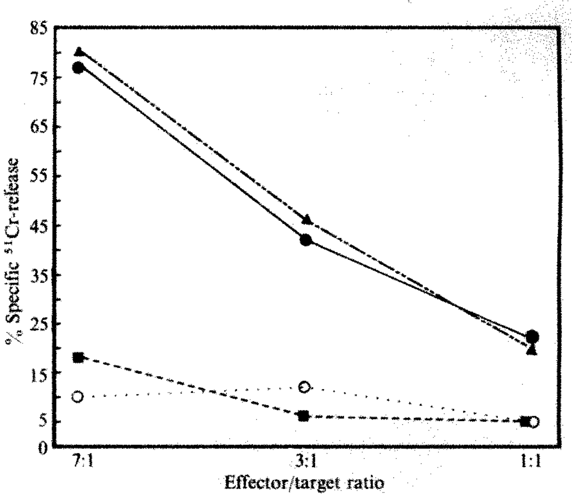

Fig. 2 Stimulation of JAP-primed CTLs by H2-VAC. Splenocytes from BALB/c mice primed with JAP were cultured for 6 days in the presence of BALB/c spleen cells infected with the recombinant H2-VAC virus (10 PFU per cell). ^{51}Cr-release assays were performed on P815 cells as described in Fig. 1 legend. Spontaneous release values were: JAP (——▲——), 18%; H2-VAC (-●-), 16%; wild-type vaccinia virus (--■--), 14%; and B/Lee (··○··), 39%.

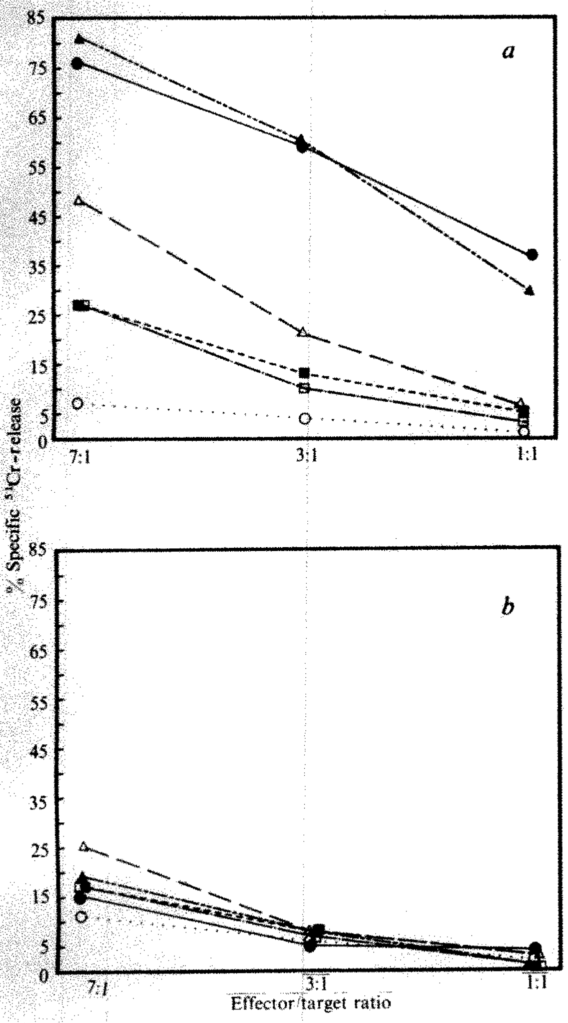

Fig. 3 *a*, *b*, Priming for an anti-JAP-specific CTL response by H2-VAC. Splenocytes were obtained from BALB/c mice 2–4 weeks after intravenous immunization with 10^7 PFU of the vaccinia recombinant H2-VAC (*a*) or the wild-type WR isolate of vaccinia virus (*b*). Primed splenocytes were restimulated *in vitro* with JAP-infected splenocytes. Target cells were prepared as described in Fig. 1 legend except that, after infection, all targets were incubated for 6 h before labelling with ^{51}Cr. Spontaneous release value for all targets was <13%. Targets: —●—, H2-VAC; - -■- -, wild type vaccinia virus; ——▲——, JAP; ··○··, B/Lee; —△—, PR8; —·□—·, HK.

JAP to a similar extent—this demonstrates that at least a significant proportion of these cells are specific for the HA. It is also apparent that cells infected with influenza A viruses of other subtypes [A/PR/8/34 (H1N1) (PR8) and A/HK/107/68 (H3N2) (HK)] were lysed at levels significantly greater than observed with B/Lee-infected cells. This could be due to cross-reactive recognition of heterosubtypic haemagglutinins by anti-JAP HA CTLs[12], in which case the better killing of PR8-infected cells could reflect the higher amino acid homology between JAP and PR8 haemagglutinins compared with JAP and HK haemagglutinins[13]. Alternatively, the observed cross-reactive lysis could be due to CTLs specific for other viral components whose *in vitro* stimulation depends on the presence of HA-specific T-helper cells primed by H2-VAC inoculation. In either case, it is important that priming for CTLs able to lyse cells infected with influenza viruses of H1N1 and H3N2 subtypes was not observed consistently between experiments; this, and the relatively small cross-reactive response, suggests that it may be due to stimulation of relatively infrequent T-cell clonotypes. Finally, as anticipated from the preceding experiments, virus priming and stimulation with H2-VAC alone resulted in the generation of JAP-specific CTLs (Fig. 4).

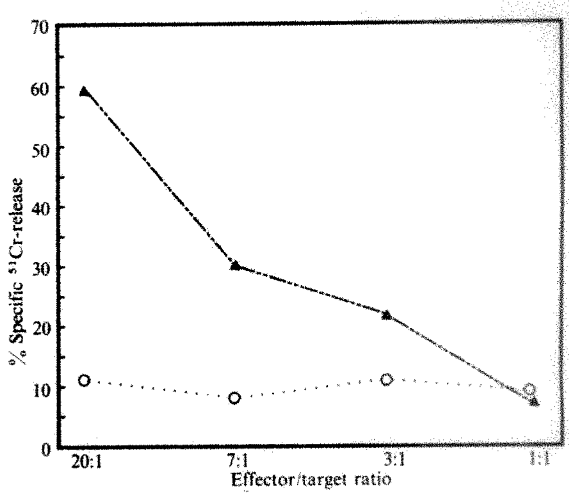

Fig. 4 Generation of anti-JAP-specific CTLs by priming and stimulation with H2-VAC. Splenocytes from BALB/c mice primed with H2-VAC were cultured for 6 days in the presence of BALB/c spleen cells infected with H2-VAC and tested for cytotoxic activity. Target cells were prepared as described in Fig. 1 legend. Spontaneous release values were: JAP (——▲——), 18%; B/Lee (··○··), 35%.

These data are of practical importance in two respects. First, we have shown that cells infected with a recombinant vaccinia virus can serve as excellent targets for CTLs specific for the product of the inserted gene. This, coupled with a wide host cell range, makes recombinant vaccinia virus an excellent tool for determining which viral antigens are recognized by CTLs, a question which remains unanswered for almost all viruses. The ability of vaccinia virus to accommodate large amounts of inserted DNA[14] means that it would even be possible to include multiple viral genes or viral and major histocompatibility complex genes in the same vaccinia virus vector. Second, regarding the potential use of recombinant vaccinia viruses as live vaccines, we have shown that these vaccines will probably efficiently prime recipients for secondary CTL responses. Although the role of CTLs in host defence against viral infection remains to be precisely defined[15], present evidence suggests that they reduce replication and dissemination of at least some viruses[16,17]. This property of recombinant vaccinia viruses may offer a significant advantage over subunit or inactivated vaccines, which do not, in general, prime for anti-viral CTL responses.

This work was supported by NIH grants AI 14162, AI 20338, AI 13989 and NS 11036.

Received 11 May; accepted 15 August 1984.

1. Panicali, D. & Paoletti, E. *Proc. natn. Acad. Sci. U.S.A.* **79**, 4927–4931 (1982).
2. Mackett, M., Smith, G. L. & Moss, B. *Proc. natn. Acad. Sci. U.S.A.* **79**, 7415–7419 (1982).
3. Mackett, M., Smith, G. L. & Moss, B. *J. Virol.* **49**, 857–864 (1984).
4. Smith, G. L., Mackett, M. & Moss, B. *Nature* **302**, 490–495 (1983).
5. Smith, G. L., Mackett, M. & Moss, B. in *UCLA Symp. molec. cell. Biol. new Ser.* (eds Hamer, D. & Rosenberg, M.) 543–554 (Liss, New York, 1983).
6. Panicali, D., Davis, S. W., Weinberg, R. L. & Paoletti, E. *Proc. natn. Acad. Sci. U.S.A.* **80**, 5364–5368 (1983).
7. Smith, G. L., Murphy, B. R. & Moss, B. *Proc. natn. Acad. Sci. U.S.A.* **80**, 7155–7159 (1983).
8. Paoletti, E., Lipinskas, B. R., Samsonoff, C., Mercer, S. & Panicali, D. *Proc. natn. Acad. Sci. U.S.A.* **81**, 193–197 (1984).
9. Smith, G. L., Mackett, M., Murphy, B. R. & Moss, B. in *Modern Approaches to Vaccines* (eds Chanock, R. & Lerner, L.) (Cold Spring Harbor Laboratory, New York, in the press).
10. Smith, G. L., Godson, B. N., Nussenzweig, V., Nussenzweig, R. S. & Moss, B. *Science* **224**, 397–399 (1984).
11. Moss, B., Smith, G. L., Gerin, J. L. & Purcell, R. H. *Nature* **311**, 67–69 (1984).
12. Braciale, T. J., Braciale, U. L., Henkel, T. J., Sambrook, J. S. & Gething, M. *J. exp. Med.* **159**, 341–354 (1984).
13. Winter, G., Fields, S. & Brownlee, G. G. *Nature* **292**, 72–75 (1981).
14. Smith, G. L. & Moss, B. *Gene* **25**, 21–28 (1983).
15. Zinkernagel, R. M. & Doherty, P. C. *Adv. Immun.* **27**, 51–77 (1979).
16. Yap, K. L., Ada, G. L. & McKenzie, I. F. C. *Nature* **273**, 238–239 (1978).
17. Lin, Y. & Askonas, B. A. *J. exp. Med.* **154**, 225–234 (1981).
18. Yewdell, J. W., Frank, E. & Gerhard, W. *J. Immun.* **126**, 1814–1819 (1981).

Transposition without duplication of infecting bacteriophage Mu DNA

Rasika M. Harshey

Research Institute of Scripps Clinic,
Department of Molecular Biology, 10666 North Torrey Pines Road,
La Jolla, California 92037, USA

Most models of DNA transposition invoke replication of the transposable element[1], but it is not clear whether a 'co-integrate' is an obligatory intermediate in the pathway leading to the production of simple insertions during transposition. Such an intermediate can be accounted for only by a replicative transposition scheme. Bacteriophage Mu is a temperate phage that can either lysogenize or lyse its host[2], and it encodes at least two modes of transposition as judged by the end-products generated by the process. During the lytic development of the integrated prophage, co-integrates are the predominant end-products[3]; transposition is coupled to replication during this phase[4]. A small number of simple insertions are also produced during the lytic growth[3], but during transposition from the infecting phage into the host chromosome, simple insertions are the main end-products[5]. Conditions can be found where the choice between the two kinds of end-products depends on a delicate balance between the essential transposition functions encoded by Mu[6]. Experiments[7,8] have suggested that the simple insertions which arise during transposition from the infecting phage may do so without Mu DNA replication. Here I demonstrate using an infecting phage with completely methylated DNA, a *dam*$^-$ (DNA adenine methylase) host and a combination of restriction enzymes that can cut either fully methylated or unmethylated DNA but not hemi-methylated DNA, that transposition of the phage DNA into the host chromosome does not involve a duplication of its DNA. This result may also have significance for other transposons[9] that do not appear to go through a co-integrate intermediate during transposition[10].

The *dam* gene of *Escherichia coli* codes for an enzyme that methylates the N-6 position of deoxyadenosine residues in DNA[11]. The methylated sequence, GATC, is cleaved by the restriction enzyme *Dpn*I. Another enzyme, *Mbo*I, cleaves the same sequence, but only if the sequence is unmethylated; however neither enzyme will cleave a hemi-methylated sequence[12]. I have used this property to design a strategy for investigating the state of replication of infecting Mu DNA, when it transposes into its host chromosome.

Phage [(Mu *cts* 62 445-5, *gin*$^-$(G+)][13] were methylated by growing them in a strain of *E. coli* containing the cloned *dam* gene (p *dam* 118)[14]. The DNA was digested with *Dpn*I (data not shown) to show that it was completely methylated. These phage were then used to infect a *dam*$^-$ *E. coli* host. At various times after infection, total *E. coli* DNA was isolated and checked for integration of Mu (Fig. 1*A*). Integration can be detected 8 min after infection (the exact time of detection of integration varies, being as early as 4 min in some experiments). Chromosomal DNA was then separated from unintegrated Mu DNA by non-equilibrium centrifugation on a sodium chloride gradient (Fig. 1*A*, lane *d*). Digestion of the integrated Mu DNA with *Hin*dIII showed that the two central *Hin*dIII fragments present in the phage DNA still remained, but the terminal *Hin*dIII fragments present in the phage DNA had disappeared, to be replaced by a smear, as would be expected from molecules that had transposed from the phage DNA into many different sites in the chromosome (Fig. 1*B*). The integrated DNA was also digested with *Eco*RI which releases larger terminal fragments. Again, only the central fragment could be detected (data not shown). Using these criteria, contamination from free phage DNA was judged to be <0.5%.

DNA isolated 8 min post-infection was digested with *Mbo*I and *Dpn*I respectively (Fig. 2*a*, *b*). Integrated Mu DNA is resistant to the action of *Mbo*I but completely digested by *Dpn*I, showing that no replication of the DNA had occurred during its transposition. However, this DNA is capable of further rounds of transposition as seen by the digestion pattern 15 min post-infection. Figure 2*c* shows that some of the integrated DNA is resistant to both *Mbo*I and *Dpn*I whereas some has become susceptible to *Mbo*I, indicating that a fraction of the integrated Mu DNA has gone through one round of replication (become hemi-methylated and hence resistant to both enzymes) and even two rounds (become unmethylated and hence sensitive to *Mbo*I). By 30 min post-infection, most of the integrated Mu

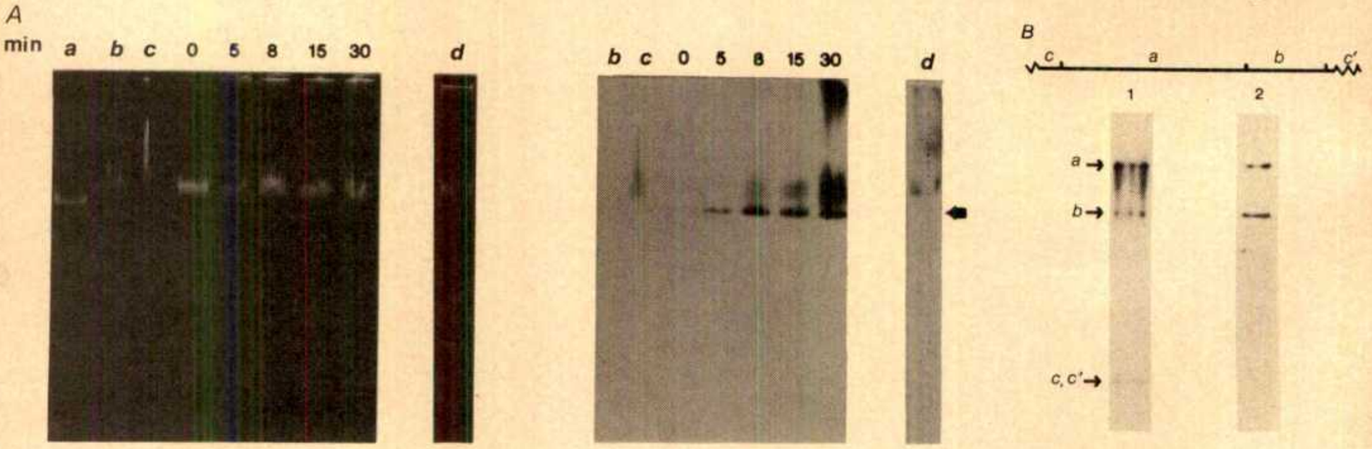

Fig. 1 Chromosomal integration of infecting Mu DNA. *A*, Total *E. coli* DNA (GM119) isolated at various times after phage infection was run on a 0.35% agarose gel, transferred to nitrocellulose and probed with radiolabelled Mu DNA. The left panel shows the ethidium-bromide stained fluorescence and the right panel the autoradiogram of the gel. Lane *a*, DNA isolated from phage; lane *b*, control *E. coli* DNA; lane *c*, DNA from a Mu lysogen. 0 to 30 indicate the time in minutes after infection at which total *E. coli* DNA was isolated. Lane *d*, DNA from the 8 min time point, separated from free phage DNA as described below. The arrow indicates the position of free phage DNA. *B*, Schematic diagram showing the distribution of *Hin*dIII sites in Mu 445-5. ~ represents heterogeneous host sequences. *a*, *b* Represent the internal fragments and *c* and *c'* the terminal fragments. *c* and *c'* are similar in size and band as a doublet. Lane 1, the *Hin*dIII digestion pattern of DNA from 445-5 phage, and lane 2 that from integrated Mu DNA 8 min post-infection.

Methods: Cells (GM119, *dam*, *dcm*-6) were grown to a cell density of 2×10^8 per ml at 37 °C. They were pelleted, resuspended on ice in buffer containing 20 mM Tris, 200 mM NaCl, 2 mM $CaCl_2$, 20 mM $MgCl_2$, *p*H 7.5. Phage were added at a multiplicity of infection (MOI) of 5, mixed gently for 1–2 min and diluted into pre-warmed broth at 37 °C. Cells were left shaking at 37 °C and at various times aliquots were withdrawn and total DNA isolated as described elsewhere[4]. Integrated Mu DNA was separated from the free phage DNA by running not more than 100 µg of total DNA over 10–30% NaCl gradients in 10 mM Tris, 1 mM EDTA *p*H 7.5, spun in a SW41 rotor, 25 °C, 37,000 r.p.m. for 3 h. High molecular weight DNA pelleted; it was recovered, redigested with pronase, re-extracted with phenol and precipitated with ethanol.

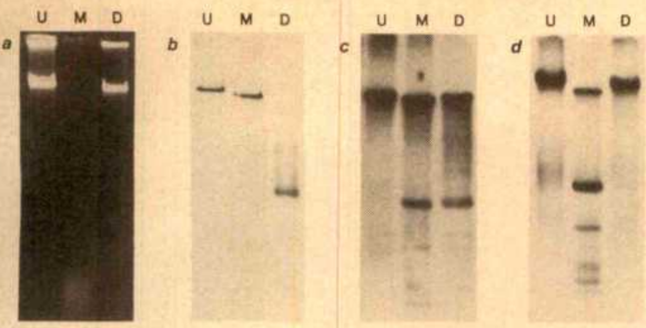

Fig. 2 *Mbo*I and *Dpn*I digestion pattern of integrated Mu DNA Agarose gels (0.5%) were run as in Fig. 1. *a*, Ethidium-bromide stained fluorescence of DNA 8 min post-infection. The DNA was digested with *Mbo*I (lane M) (New England Biolabs) or *Dpn*I (lane D) (Boehringer Mannheim) according to manufacturer's specifications. Control lanes contain undigested DNA (lane U). *b*, Autoradiogram of the same gel. *c*, Autoradiogram of DNA isolated 15 min post-infection and treated as in *a*. *d*, Autoradiogram of DNA isolated 30 min post-infection and treated as in *a*.

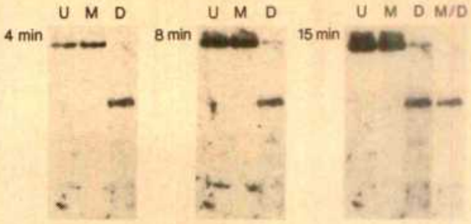

Fig. 3 *Mbo*I and *Dpn*I digestion pattern of integrated Mu DNA isolated from a dam^- strain carrying *him*AΔ82 (RH300). Agarose gels (1%) were run as in Fig. 1. Lanes U, M and D refer to undigested controls, *Mbo*I and *Dpn*I cleaved samples, respectively. The patterns for 4 min, 8 min and 15 min post-infection are shown.

DNA is resistant to *Dpn*I (Fig. 2*d*). These results are consistent with observations that by 30 min after phage induction, Mu DNA is actively undergoing replicative transposition[4,15].

Although most of the integrated Mu DNA appears to be digested with *Dpn*I 8 min after infection, showing that integration had occurred without replication, it would nevertheless be expected that 170 base pairs (bp) or ~0.46% of Mu DNA would still remain linked to *E. coli* DNA, as the first *Dpn*I sites occur 56 bp from the left end and 114 bp from the right end of Mu. A densitometric tracing of the autoradiogram in Fig. 2*b* indicates, however, that about 4% of the integrated DNA remains resistant to *Dpn*I (data not shown). There are several possible explanations of this result, the simplest being that some of the integrated molecules had already entered the subsequent pathway of replicative transposition. To eliminate this possibility, infections were performed into a dam^- host strain carrying *him*AΔ82, a mutation which allows infecting Mu to integrate normally but which does not support the subsequent lytic growth of the phage[16]. In this experiment, integration could be detected as early as 4 min post-infection. The integrated DNA, as in the previous experiment, was susceptible to *Dpn*I, but remained so even 15 min post-infection (Fig. 3). However, 4–8% of the DNA still remained resistant to the enzyme at every time point studied. To test the possibility that this fraction represented a subpopulation of molecules that transposed using the replicative mode, the DNA was double-digested with *Mbo*I and *Dpn*I (Fig. 3, 15 min, lane M/D). If such a subpopulation existed, this fraction would have been hemi-methylated for the entire length of Mu, and would have remained in the high molecular weight region of the gel. However, the *Dpn*I resistant material in lane D no longer remained in the high molecular weight DNA fraction in lane M/D, indicating that it represents partial replication of some or all the integrated Mu molecules. Such replication could be unrelated to the transposition process itself; for example, it could occur by passive replication of the integrated Mu DNA by the *E. coli* replication machinery, or it could be an essential feature of the transposition mechanism which generates simple insertions. It is known, for example, that Mu integration generates a 5-bp duplication at the target site[17,18], which is proposed to arise by a staggered break at the site of insertion and which is subsequently repaired[19]. Some degree of nonspecificity in this process might lead to repair synthesis extending beyond the 5 bp and into Mu sequences. I favour this latter explanation because if the former had been the case, one would have observed an increase in the *Dpn*I resistant material with time, and this did not occur.

Our results indicate that Mu DNA transposition from an infecting phage into the chromosome of its host occurs without a duplication of its genome, in sharp contrast to its subsequent transposition events which are replicative[4]. This then raises questions of what factors govern the choice of the transposition pathway, either simple insertions or co-integrates. One obvious candidate is the physical state of the DNA (although phage DNA is linear, after infection it can be isolated as a non-covalently-closed circular DNA–protein complex[20]). Another possibility is a differential regulation of transposition functions[6]. It is possible that the state of DNA in turn influences the expression of specific proteins.

During the transposition of Tn*3*, the occurrence of an intermediate co-integrate state which is resolved by a site-specific recombination system to produce simple insertions[21], led to the proposal that co-integrates are intermediates in all DNA transpositions[22]. The results reported here prove that is not so. They do not, however, rule out the possibility that there are other circumstances in which simple insertions could arise by a replicative pathway[1].

When determining the molecular mechanism of a non-replicative transposition reaction, the fate of the donor molecule on which the transposable element resides (in the case of infecting Mu, the heterogeneous *E. coli* sequences at its ends) must be considered. The donor molecule may be repaired after the element has 'jumped' out, or may not be repaired. If unrepaired, it would result in the destruction of the donor (either event would be irrelevant for the survival of the infecting Mu phage)[9]. Such a suicidal, non-replicative mode of DNA transposition may explain the occurrence of chromosomal breaks associated with the movement of some transposable elements[23]. One may then raise general questions about the evolutionary significance of replicative versus non-replicative mechanisms for DNA transposition and why different movable elements make the choices they do.

I dedicate this paper to the memory of Ahmad Bukhari. I thank M. Jayaram for many discussions and Richard Lerner for his support. This work was supported by grants from the NSF (PCM8203174) and the NIH (GM33247-01).

Received 14 May; accepted 3 August 1984.

1. Bukhari, A. I. *Trends biochem. Sci.* **6**, 56–60 (1981).
2. Bukhari, A. I. *A. Rev. Genet.* **10**, 389–411 (1976).
3. Chaconas, G., Harshey, R. M., Sarvetnick, N. & Bukhari, A. I. *J. molec. Biol.* **150**, 341–359 (1981).
4. Ljungquist, E. & Bukhari, A. I. *Proc. natn. Acad. Sci. U.S.A.* **74**, 3143–3147 (1977).
5. Chaconas, G., Kennedy, D. L. & Evans, D. *Virology* **128**, 48–59 (1983).
6. Harshey, R. M. *Proc. natn. Acad. Sci. U.S.A.* **80**, 2012–2016 (1983).
7. Leibart, J. C., Ghelardini, P. & Paolozzi, L. *Proc. natn. Acad. Sci. U.S.A.* **79**, 4362–4366 (1982).
8. Akroyd, J. E. & Symonds, N. *Nature* **303**, 84–86 (1983).
9. Berg, D. E. in *DNA Insertion Elements, Plasmids and Episomes* (eds Bukhari, A. I., Shapiro, J. A. & Adhya, S. L.) 205–212 (Cold Spring Harbor Laboratory, New York, 1977).
10. Kleckner, N. *A. Rev. Genet.* **15**, 341–404 (1981).
11. Marinus, M. G. & Morris, R. N. *J. Bact.* **114**, 1143–1150 (1973).
12. Vovis, G. F. & Lacks, S. *J. molec. Biol.* **115**, 525–538 (1977).
13. Chow, L. T., Kahmann, R. & Kamp, D. *J. molec. Biol.* **113**, 591–609 (1977).
14. Brooks, J. E., Blumenthal, R. M. & Gingeras, T. R. *Nucleic Acids Res.* **11**, 837–851 (1983).
15. Razzaki, T. & Bukhari, A. I. *J. Bact.* **122**, 437–442 (1975).
16. Miller, H. I. & Freidman, D. I. *Cell* **20**, 711–719 (1980).
17. Allet, B. *Cell* **16**, 123–129 (1979).
18. Kahmann, R. & Kamp, D. *Nature* **280**, 247–250 (1979).
19. Grindley, N. D. F. & Sherratt, D. J. *Cold Spring Harb. Symp. quant. Biol.* **43**, 1257–1261 (1978).
20. Harshey, R. M. & Bukhari, A. I. *J. molec. Biol.* **167**, 427–441 (1983).
21. Gill, R., Heffron, F., Dougan, G. & Falkow, S. *J. Bact.* **136**, 742–756 (1978).
22. Shapiro, J. A. *Proc. natn. Acad. Sci. U.S.A.* **76**, 1933–1937 (1979).
23. McClintock, B. *Cold Spring Harb. Symp. quant. Biol.* **16**, 13–47 (1951).

Effect of protein packing structure on side-chain methyl rotor conformations

A. A. Kossiakoff*†‡ & S. Shteyn†

* Department of Pharmaceutical Chemistry, School of Pharmacy, University of California, San Francisco, California 94143, USA
† Department of Biology, Brookhaven National Laboratory, Upton, New York 11973, USA

Protein molecules undergo a series of conformational fluctuations ranging in degree from atomic vibrations to transient denaturation, even in physiological conditions[1,2]. The rotational motions of amino acid side chains form an important subset of the types of fluctuation a protein can undergo. NMR[3–7] and molecular dynamics[8–10] have shown that methyl groups in proteins are not held in fixed positions, but spin rapidly around their rotor axes. The question then arises as to whether methyl groups in proteins predominantly adopt the 'staggered' conformation, favoured by the intrinsic barrier to rotation of these groups, or whether cooperative packing effects in the folded protein perturb the average configurations to higher torsional energy. We report here an investigation of the rotational conformations of the methyl groups of aliphatic side chains in the protein crambin by neutron diffraction. We find that in the time-averaged structure of this protein, the majority of methyl rotors adopt the staggered conformation. This is consistent with rotation being a quantized event consisting of rapid reorientations of ~120° steps to positions of highest stability. The fact that the local environment does not dictate the low energy state of methyl groups suggests that within the seemingly close-packed interior structure of a protein, mutual packing accommodation occurs as a consequence of the inherent flexibility and small packing defects in protein structures.

Neutron diffraction is an ideal method for investigating methyl group conformation because it allows direct observation of hydrogen atom positions in neutron density maps, and also measurement of the time-averaged structure and thus identification of the lowest energy conformer. Previously, neutron diffraction of trypsin demonstrated that high-resolution data and a well refined phasing model are a prerequisite of any type of detailed methyl rotor analysis[11]. Crambin, a small protein consisting of a single polypeptide chain of 46 amino acid residues[12,13], with 27 terminal methyl groups, therefore makes an ideal candidate for this type of study. Data are obtained from a neutron structure analysis at 1.4 Å resolution. Details of the experimental procedures have been reported previously[14].

Figure 1 shows examples of methyl group neutron densities from the crambin analysis. These densities are taken from a difference map with the density contribution of the methyl carbon subtracted (see Fig. 1). It is clear that for most cases, unambiguous rotor orientations can be assigned from maps of this quality. The rotor density profiles can be displayed graphically by density plots (Fig. 2). These profiles plot the density sampled every 10° around the rotation axis at the stereochemically appropriate location for a possible methyl hydrogen position. Most profiles show a pattern for hydrogen positions every 120° around the rotation axis, which indicates a high degree of order. However, there are a significant number of cases that are disordered by crystallographic criteria. This does not necessarily indicate rotational disorder alone, but could be a function of the inherent vibrational motion of the parent methyl carbon itself and hence of the entire methyl group.

The least well ordered methyl group pictured is Ala 45 CB (Fig. 1*d*). Its corresponding rotor density plot (Fig. 2, symbol +), however, shows a symmetrical profile from which a 'preferred' orientation can be identified. We find in several instances that although the fine structures of this type of curve showed varying degrees of asymmetry (presumably due to residual phasing error), the overall shapes of the profiles generally indicated a systematic trend of peaks and valleys. The rationale in assigning a specific orientation to a rotor is because the peaks and valleys usually appear at intervals of 120°, irrespective of their relative amplitudes. Since no bias was introduced into the maps, the probability of this pattern occurring by chance is remote.

The identification of the highest populated rotor orientation of each methyl group can be assigned most accurately by a 3-fold averaging procedure. In theory, the shape of the resulting

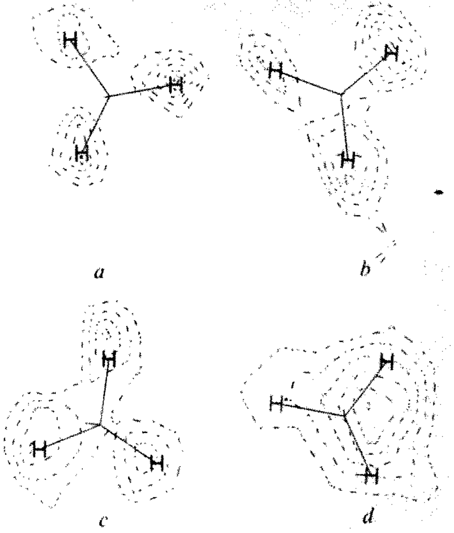

Fig. 1 Sections of the neutron difference Fourier map showing methyl hydrogen densities for several representative methyl groups. The groups shown are: *a*, Ala 24; *b*, Thr 21; *c*, Thr 28; and *d*, Ala 45. Because of the unique scattering characteristics of neutrons by hydrogen atoms, hydrogen atom positions appear in neutron density maps as negative peaks. No phase information about the methyl hydrogens was included in the model; therefore, hydrogens appear in the difference map at their true positions but at reduced density (≃1/2 weight). This crambin analysis represents the first time that methyl hydrogens have ever been observed at atomic resolution in a Fourier density map.

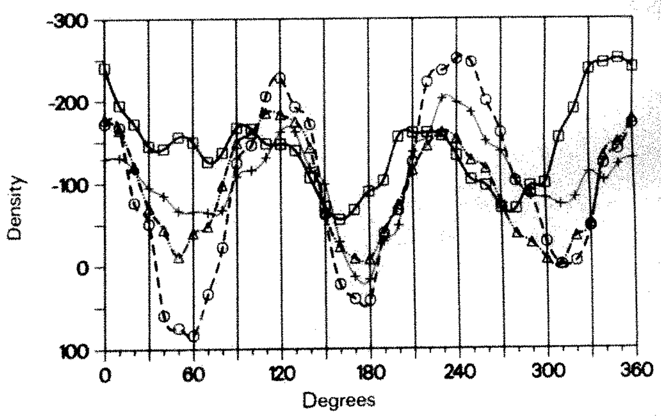

Fig. 2 Examples of representative methyl rotor plots calculated by sampling the map densities in incremental steps around the rotor axes. □, Val 15 CGI; △, Thr 21; ○, Ala 27; +, Ala 45. These plots are derived by calculating a series of possible methyl hydrogen positions at points differing by a rotational increment of 10° and then sampling the observed density at each point in the difference map. Many of the rotor plots have a 3-fold symmetrical pattern, which is due to real structural features since there is no inherent bias in the phasing to produce the 3-fold character. The torsion angle for a staggered conformation is defined here as 0°, 20°, 240° (this corresponds to the usual convention of 60°, 180°, 300°).

---

‡ Present address: Genentech, Inc., 460 Point San Bruno Blvd, South San Francisco, California 94080, USA.

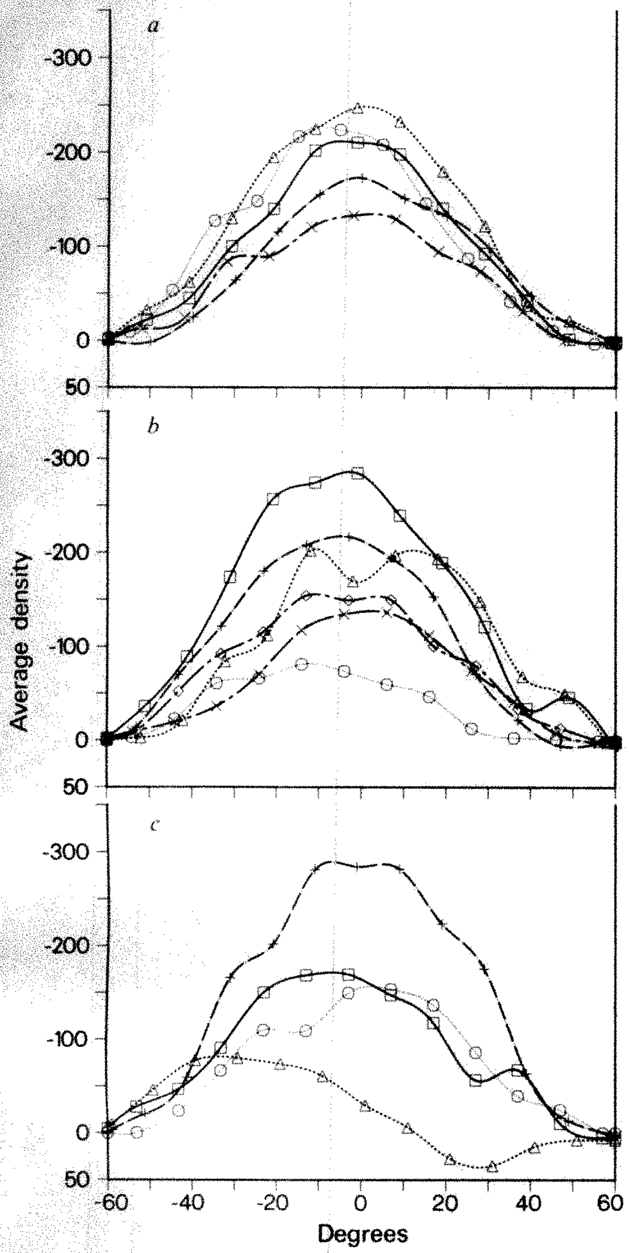

Fig. 3 Rotationally averaged rotor plots for alanine (*a*), threonine (*b*) and valine (*c*). *a*, Ala CB: □ 9, ○ 24, △ 27, + 38, × 45; *b*, Thr CG2: □ 1, ○ 2, △ 21, + 28, × 30, ◇ 39; *c*, Val CG1: □ 8, △ 15; CG2: ○ 8, + 15. Plots were calculated by averaging densities at points separated by 120° in the Fig. 2 type plots (0°, 120°, 240°; 10°, 130°, 250°, etc.). The position of the density maximum defines the group's torsional angle. The staggered conformation is defined as 0°. Plots were placed on the same relative scale by adjusting the lowest average density point for each individual group to be at 0. Effects on the methyl densities due to the inherent vibrational motion of the parent carbon atoms were corrected for by an empirical procedure. This was done by developing an empirical function relating the expected attenuation of the methyl peak density to the vibrating motion (B factor) of the parent carbon atom.

profile curve (Fig. 3) provides useful information on the rotor's characteristic minimum energy, the height and breadth of the curve indicating the rotor's degree of order. Interpretation of these plots, even at the high resolution (1.4 Å) and phasing accuracy ($R = 0.17$) of this analysis, has distinct limitations. Model studies indicate that while the resolution is sufficient to assign precisely the orientation of rotor groups when a position is highly occupied, attempts to discriminate between localized vibrational or static disorder effects are not warranted[15].

Rotationally averaged plots for three representative side-chain types, alanine, threonine and valine, are shown in Fig. 3. Taken together, these plots clearly suggest that the preferred conformations in the large majority of cases is closely staggered. There are, however, a few exceptions to this general observation. The clearest example of this is the CG1 rotor of Val 15 (△, Fig. 3*c*) which is displaced by about 25° from the staggered orientation. This deviation is likely to represent a real effect and not an artefact because the symmetrical nature of the density peaks, each of which is displaced by about 20–30°, is very systematic (□, Fig. 2). We believe this occurs because the CG1 methyl hydrogens make van der Waals' contact with a portion of a symmetry-related molecule in the crystal packing lattice. On the other hand, methyl groups at all other similar intermolecular contact regions do have staggered conformations, so no single generalization applies to these types of interactions.

A significant finding of this study is that a majority of the rotor density plots have distinctive 3-fold symmetry. We suggest that well-defined energy minima for methyl groups exist in protein molecules. (Similar findings were obtained from a trypsin analysis[11], but because the study was done at lower resolution (1.8 Å) the interpretation of the density plots was less definitive.) The staggered conformation of the methyl hydrogens is consistent with the staggered conformations seen around side-chain carbons in high-resolution protein structures determined by X rays. This is a general observation described in many studies. Experimental observations from NMR (showing rapid rotatory motions) together with the neutron diffraction results described here (indicating highly preferred orientations) show that methyl rotations are 'quantized' in 120° steps about a position of highest stability. The lifetime in any particular orientation is short in absolute terms, but it is much longer than times spent in the rotational transition from one 3-fold energy minimum to the next.

The experimental observations presented here address an important question about protein packing. Examination of space-filling models of proteins shows that the groups contained in the interior core are usually extremely close-packed with regard to neighbouring atoms and seemingly have little room to manoeuvre. It might be expected, therefore, that a number of the methyl groups on aliphatic side chains could be forced out of their stable rotatory conformations by packing considerations. Both the crambin and trypsin[16] analyses, however, show that such situations are rare. This implies that the inherent 'breathing' of the protein and its small but numerous packing defects[17,18] allow the methyl groups to adopt the low energy conformation defined by their intrinsic barrier to rotation.

We thank Dr M. Teeter for assistance in the crambin analysis, J. Shpungin and Dr B. P. Schoenborn for technical assistance, and Drs A. Kossiakoff, R. Levy and G. Rose for advice during the preparation of the manuscript. A.A.K. thanks Genentech, Inc. for support during part of the work. Research at Brookhaven National Laboratory under the auspices of the US Department of Energy was supported by NIH grant GM29616.

Received 13 April; accepted 26 July 1984.

1. Gurd, F. N. & Rothgeb, T. M. *Adv. Protein Chem.* **33**, 73–165 (1979).
2. Karplus, M. & McCammon, J. A. *A. Rev. Biochem.* **53**, 263–300 (1983).
3. Wagner, G., DeMarco, A. & Wüthrich, K. *Biophys. Struct. Mech.* **2**, 139–158 (1976).
4. Wüthrich, K. in *Nuclear Magnetic Resonance in Biological Research—Peptides and Proteins* (North-Holland, Amsterdam, 1976).
5. Campbell, I. D., Dobson, C. M. & Williams, R. J. P. *Proc. R. Soc.* **B189**, 503–509 (1975).
6. Oldfield, E., Norton, R. S. & Allerhand, A. *J. biol. Chem.* **250**, 6368–6380 (1975).
7. Wittebort, R. J., Rothgeb, T. M., Szabo, A. & Gurd, F. R. N. *Proc. natn. Acad. Sci. U.S.A.* **76**, 1059–1063 (1979).
8. McCammon, J. A. & Karplus, M. *Biopolymers* **19**, 1375–1405 (1980).
9. McCammon, J. A. & Karplus, M. *Proc. natn. Acad. Sci. U.S.A.* **76**, 3585–3589 (1979).
10. Lipari, G., Szabo, A. & Levy, R. M. *Nature* **300**, 197–198 (1982).
11. Kossiakoff, A. A. & Spencer, S. A. *Biochemistry* **20**, 6462–6474 (1981).
12. Teeter, M. M., Mazer, J. A. & L'Italien, J. J. *Biochemistry* **20**, 5437–5443 (1981).
13. Hendrickson, W. A. & Teeter, M. M. *Nature* **290**, 107–113 (1981).
14. Teeter, M. M. & Kossiakoff, A. A. in *Neutrons in Biology, Basic Life Sciences* **27**, 335–348 (Plenum, New York, 1984).
15. Kossiakoff, A. A. *Meth. Enzym.* (in the press).
16. Kossiakoff, A. A. *A. Rev. Biophys. Bioengng* **12**, 159–183 (1983).
17. Lumry, R. & Rosenberg, A. *Colloques natn. Cent. natn. Rech. scient.* **246**, 53–63 (1975).
18. Richards, F. M. *Carlsberg Res. Commun.* **44**, 47–63 (1979).

'Z-RNA'—a left-handed RNA double helix

Kathleen Hall, Phillip Cruz, Ignacio Tinoco Jr, Thomas M. Jovin* & Johan H. van de Sande*†

Chemistry Department and Laboratory of Chemical Biodynamics, University of California, Berkeley, California 94720, USA
* Abteilung Molekulare Biologie, Max Planck Institut für Biophysikalische Chemie, D-3400 Göttingen, FDR

In contrast to double-stranded DNA, there has so far been little evidence that double-stranded RNA can undergo major conformational transitions. We have investigated the conformation in different conditions of the double-stranded RNA molecule poly(G-C)·poly(G-C), by NMR, circular dichroism and absorbance spectroscopy. We report here evidence obtained by these different spectroscopic techniques that poly(G-C)·poly(G-C) undergoes a transition from the A-form to a left-handed Z-form in conditions of high ionic strength and at temperatures above 35 °C. This conformational transition may be of relevance to the biological situations in which double-stranded RNA occurs, such as in ribosomes and in some viruses.

Figure 1 shows the phosphorus NMR spectra of three forms of poly[r(G-C)]·poly[r(G-C)]. There are two forms of RNA that are identified by ^{31}P-NMR in the lower salt concentrations, one in 10 mM HEPES where the resonances are separated by 0.40 p.p.m. (Fig. 1*a*) and the other in 3 M $NaClO_4$ where the separation is 0.50 p.p.m. (Fig. 1*b*). In contrast, the spectrum of poly[r(G-C)]·poly[r(G-C)] in 6 M $NaClO_4$ at 45 °C shows a much larger separation of 1.33 p.p.m. (Fig. 1*c*). This pattern is similar to that seen by Patel *et al.*[1] for poly[d(G-m^{5}C)] and poly[d(G-C)] double strands.

The large separation of the phosphorus resonances is characteristic of Z-form DNA[1,2]. The two well-separated ^{31}P resonances have been assigned[3] to the CpG and GpC residues, which in the crystallographic dinucleotide repeat unit have greatly different phosphodiester torsion angles[4]. This produces a zig-zag form with two distinct chemical and magnetic environments for the phosphorus. Our data suggest that the poly[r(G-C)]·poly[r(G-C)] has adopted a Z-form; this conformation will be referred to as Z-RNA.

We have used transient proton nuclear Overhauser effect (NOE) measurements to investigate the conformation about the glycosidic bond. NOE arises from through-space dipolar interactions between spins, and can be observed as a change in intensity of one peak upon irradiating another. These spins must be spatially proximal, as the magnitude of the NOE falls off as $1/r^6$, where r is the distance between the spins. In the Z-DNA structure as determined by X-ray crystallography[4], the guanosine residues adopt a *syn* conformation about the glycosidic bond, and in this form, the guanosine H-8 (GH8) and guanosine H-1' (GH1') protons are only 2.2 Å apart. The guanosine residues adopt an *anti* conformation in A- and B-form, however, and the GH8 to GH1' distance increases to greater than 3.5 Å. Patel *et al.*[1] showed that in low salt, the only NOE from an aromatic proton in poly[d(G-C)]·poly[d(G-C)] was from the cytosine H-6 (CH6) to its neighbouring cytosine H-5 (CH5); these protons are separated by only 2.4 Å. When the polymer was placed in 4 M salt, in addition to the CH6 to CH5 NOE, an NOE was observed between the GH8 and GH1', indicating a transformation to *syn*.

Figure 2*a* shows the proton NMR spectrum of poly[r(G-C)]·poly[r(G-C)] in 6 M $NaClO_4$, 10 mM phosphate, $pD = 7$ at 45 °C. Only resonances due to the GH8 and CH6 protons appear in the region between 7 and 8 p.p.m., and the peak at 7.82 p.p.m. has been assigned to the GH8 using deuterium exchange at high temperature. The GH8 shows a large NOE to a resonance at 5.7 p.p.m., which is assigned to the GH1' (Fig. 2*b*). The presence of this NOE shows that the guanosine residues adopt the *syn* conformation. These NOE measurements, together with the phosphorus NMR data, provide the basis for designating the high salt form of poly[r(G-C)]·poly[r(G-C)] as Z-RNA. The CH6 proton also shows a large NOE (Fig. 2*c*) to a peak at 5.17 p.p.m., which has been assigned to the neighbouring CH5.

Figure 3*a* shows the proton NMR spectrum of poly[r(G-C)]·poly[r(G-C)] in 3 M $NaClO_4$, 10 mM $NaPO_4$, $pD = 7$, at 45 °C. Deuterium exchange at high temperature was used to assign the resonance at 7.51 p.p.m. to the GH8 proton. In the

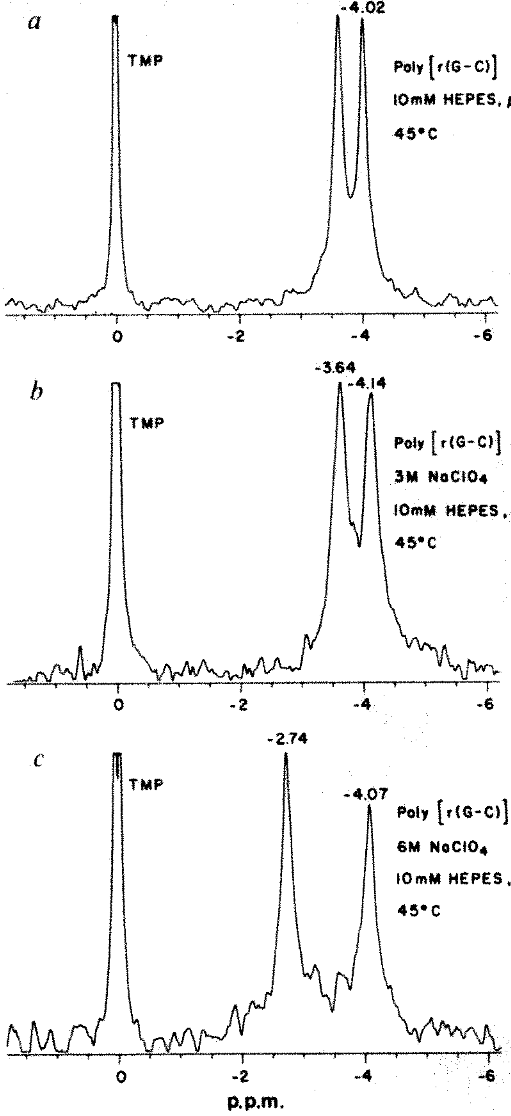

Fig. 1 Phosphorus NMR spectra of poly[r(G-C)]·poly[r(G-C)] in three ionic strengths at 45 °C. *a*, Poly[r(G-C)]·poly[r(G-C)] with no added $NaClO_4$. *b*, Poly[r(G-C)]·poly[r(G-C)] in 3 M $NaClO_4$. *c*, Poly[r(G-C)]·poly[r(G-C)] in 6 M $NaClO_4$.

Methods: The polymer was prepared using *Escherichia coli* RNA polymerase on a poly[d(I-C)]·poly[d(I-C)] template[12]. Polymer size was determined by polyacrylamide gel electrophoresis in denaturing conditions. Size markers of simian virus 40 *Hinf* I digests were used for comparison. The size distribution ranged from 40 to 800 nucleotides, most being 150–500 nucleotides. The DNA template was removed by DNase I digestion; removal was complete as assessed by optical melting and CD data. Spectra were obtained at 81.75 MHz on the UCB-200 spectrometer (200 MHz proton), using broad-band proton decoupling. Each sample contained approximately 30 mM (in nucleotides) of the polymer, 10 mM HEPES, *p*H 7.0, 0.1 mM EDTA; chemical shifts are referenced to the internal standard, trimethyl phosphate (TMP).

---

† Present address: Department of Medical Biochemistry, University of Calgary, Calgary, Alberta, Canada T2N 4N1.

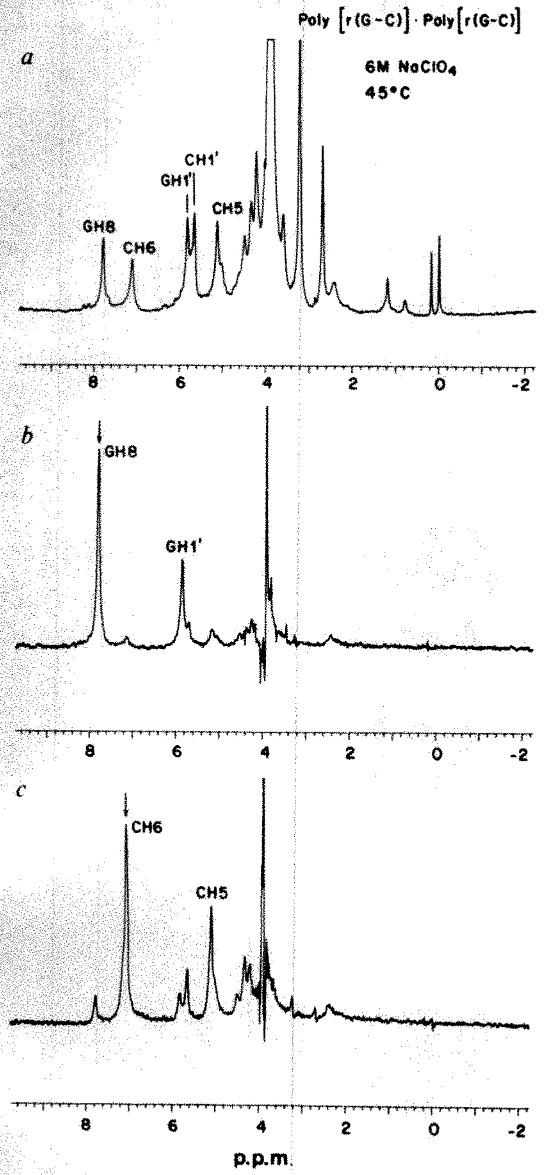

Fig. 2 Proton NMR spectra at 500 MHz of poly[r(G-C)]·poly[r(G-C)] (~30 mM in nucleotides) at 45 °C in 6 M $NaClO_4$, 10 mM phosphate buffer, *p*H 7.0, and ~0.1 mM EDTA. Chemical shifts are referenced to the internal standard trimethylsilyl propionate (TSP). Spectra were obtained on the JEOL GX-500 instrument at the Stanford University NMR Center. *a*, Spectrum in D_2O. The large narrow resonances below 5 p.p.m. correspond to residual solvent protons, EDTA and reference TSP. *b*, Transient NOE difference spectrum obtained by irradiating the GH8 proton (indicated by an arrow) with a 50-ms saturation pulse before obtaining the spectrum. The difference spectrum represents the spectrum with an on-resonance presaturation pulse subtracted from the spectrum with the presaturation pulse 10 kHz off resonance. A large NOE to the GH1′ is observed. The reverse experiment (not shown) results in NOE to the GH8 proton on irradiation of the GH1′. *c*, Transient NOE difference spectrum obtained by irradiating the CH6 proton (indicated by an arrow) as described above. A large NOE can be seen to the CH5 proton. Irradiation of the CH5 proton results in a large NOE to the CH6 (not shown).

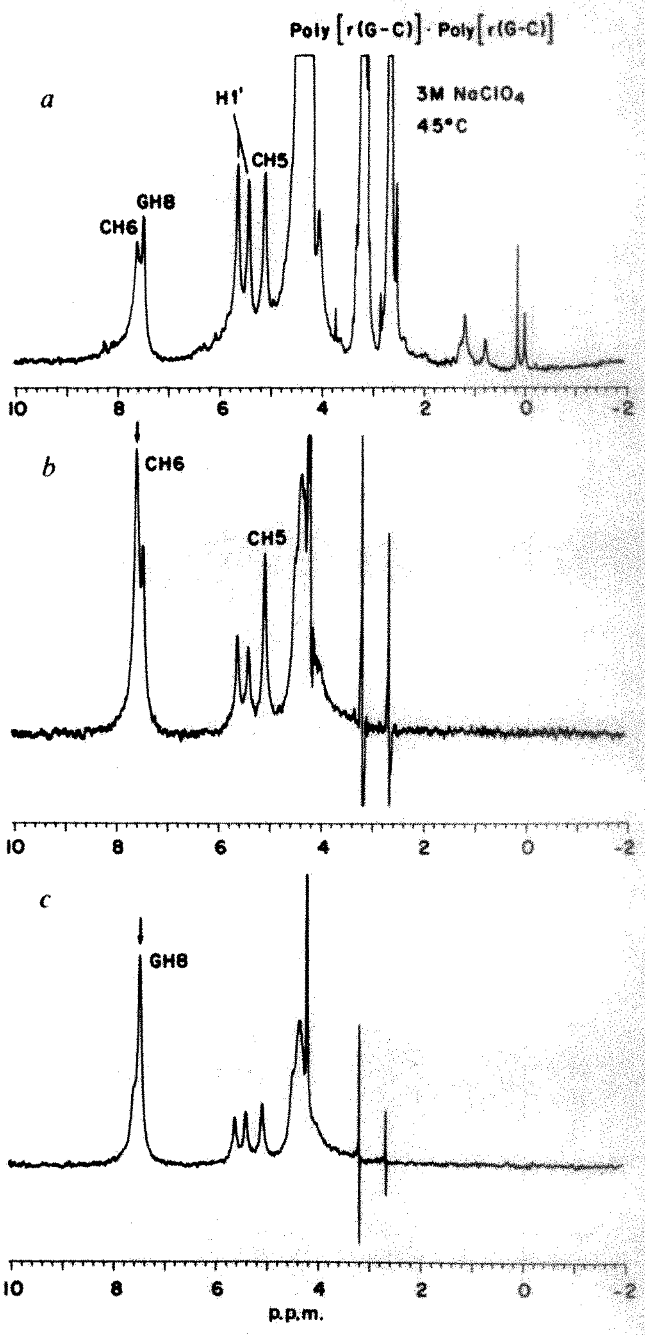

Fig. 3 Proton NMR spectra of poly[r(G-C)]·poly[r(G-C)] in 3 M $NaClO_4$. All other conditions are as described in the legend to Fig. 2. *a*, Spectrum at 500 MHz in D_2O. *b*, Transient NOE difference spectrum obtained by irradiating the CH6 proton (indicated by an arrow) as explained in Fig. 2 legend. A large NOE to the CH5 is observed. *c*, Transient NOE difference spectrum obtained by irradiating the GH8 proton (indicated by an arrow). Only small NOEs due to spin diffusion are observed.

A-form, exchange is extremely slow; this is in contrast to the Z-form, which exchanges more rapidly. Therefore, to promote deuterium exchange, the poly[r(G-C)]·poly[r(G-C)] was heated to 80 °C for several hours in 1 mM Na phosphate, 0.1 mM EDTA.

Figure 3*b*, *c* shows the NOE difference spectra of poly[r(G-C)]·poly[r(G-C)] in 3 M $NaClO_4$ that result upon irradiation of the peaks at 7.63 and 7.51 p.p.m., respectively. Saturating the CH6 peak at 7.63 p.p.m. results in a large NOE to a peak at 5.11 p.p.m.; this peak has been assigned to CH5. When the GH8 peak at 7.51 p.p.m. was irradiated, only several small NOEs were observed, indicating that guanosine is in the *anti* conformation. It is seen from the NOE spectra that there is a significant amount of spin diffusion among the various protons. This was also seen with poly[d(G-C)] (ref. 1) and can to some extent be diminished by shortening the duration of the saturation pulse. It was not entirely eliminated in these experiments, however, and appears as small NOEs in all the spectra.

The absorption and the circular dichroism (CD) spectra of two forms of RNA (Fig. 4) corroborate the NMR conclusions. The Z-RNA absorption spectrum (6 M $NaClO_4$, 45 °C) has a

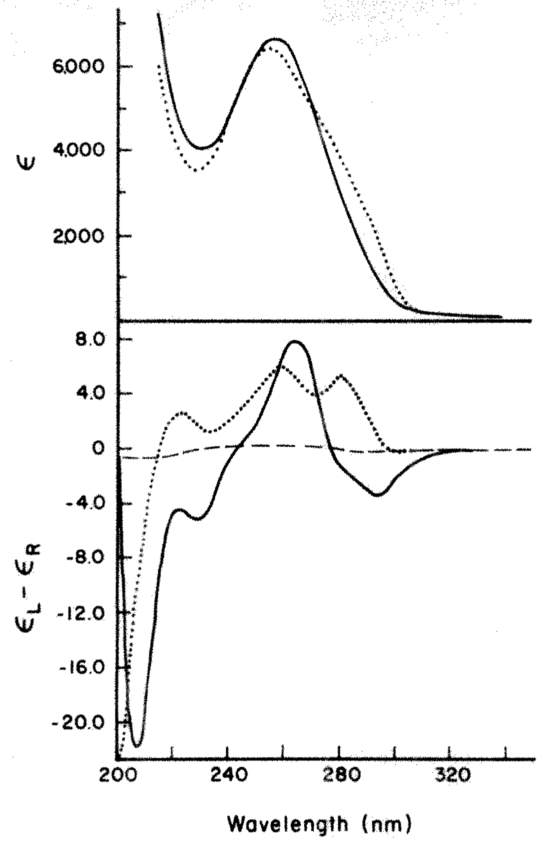

Fig. 4 Absorption (top) and CD (bottom) spectra of two forms of poly[r(G-C)]·poly[r(G-C)]. Absorption spectra were measured with a Gilford model 250 spectrophotometer; CD spectra were measured with a JASCO J500C spectropolarimeter. Both instruments have thermoelectric cell blocks. The absorbance and CD were measured in 10 mM phosphate, *p*H = 7.0, 6 M $NaClO_4$ at 22 °C (solid line) and 45 °C (dotted line). An extinction coefficient of 6,560 at 260 nm was used for the poly[r(G-C)] at 22 °C (ref. 6). The CD spectrum at 22 °C is similar, but not identical to the spectrum seen in buffer alone. It is identical to that for the polymer in 3 M $NaClO_4$. At 45 °C, 6 M $NaClO_4$ the CD spectrum is identical to that seen in conditions of lower perchlorate and higher temperatures, and is similar to that in 20% (v/v) ethanol in 4.8 M $NaClO_4$.

shoulder at 290 nm; this is very similar to the spectrum of Z-DNA (ref. 5). Two types of CD spectra are seen for poly[r(G-C)]. The first is represented by the spectrum at 6 M $NaClO_4$, 22 °C. It is identical to the CD spectrum in 3 M $NaClO_4$ and is similar to a CD spectrum measured in 10 mM sodium phosphate (not shown) which matches the CD spectrum of Gray *et al.*[6] in 1 mM Na phosphate, 0.1 mM EDTA, *p*H 7.8. These CD spectra are all presumed to be from an A-type conformation of the poly[r(G-C)] (ref. 7). Because the CD spectrum of the polymer in 6 M $NaClO_4$, 22 °C and 3 M $NaClO_4$ are identical, we used the latter solvent at 45 °C for NMR experiments; at 22 °C the NMR linewidths are too broad for analysis. The CD spectra in dilute phosphate differ from those in $NaClO_4$ by a small change in the band at 285 nm. This band is particularly sensitive to solvent, and diminishes at high ionic strength. This CD band may be correlated with the small differences in phosphorus resonances between the RNA in 10 mM HEPES and in 3 M $NaClO_4$.

The CD spectrum in 6 M $NaClO_4$, 45 °C is very different from the others, and is identified as that of Z-RNA. The CD remains positive in the region above 215 nm. The negative bands above 280 nm and below 240 nm in A-RNA change sign in Z-RNA; the positive band near 260 nm remains positive.

The transition temperature for the A- to Z-RNA transition is a function of the solvent conditions. In 6 M $NaClO_4$, the transition temperature is ~35 °C; in 4.8 M, it is ~45 °C; in 4 M, ~80 °C; in 3 M, it is above 80 °C and not measurable in our instrument. The addition of ethanol to the perchlorate solution decreases the transition temperature, so that in 4.8 M $NaClO_4$/20% ethanol, the RNA is in Z-form at room temperature. This temperature dependence of the transition to Z-RNA form is analogous to that of poly[d(G-C)]·poly[d(G-C)]. For that polynucleotide, the Z-form is favoured at higher temperatures in LiCl or ethanol/water solutions[1,8,9]. However, we have found that solvents which will cause a B to Z transition in poly [d(G-C)], such as 4 M NaCl or 1 M $MgCl_2$, do not cause an A to Z transition in poly[r(G-C)]. This is consistent with the work of Westerink *et al.*[10] and Uesugi *et al.*[7] who found no Z transition in these salt solutions for r(G-C) oligonucleotides.

The kinetics of the transition also vary with the solvent and the temperature. In 6 M $NaClO_4$, a temperature shift from 22 °C to 35 °C results in an A- to Z-RNA transition which takes ~1 h. The reverse transition occurs over 5 h. A temperature shift from 22 °C to 45 °C (or addition of 20% (v/v) ethanol and concomitant dilution to 4.8 M $NaClO_4$), however, produces the Z-RNA form in ~10 min, although again the reverse transition on lowering the temperature from 45 °C to 22 °C takes several hours.

This is the first major conformational change reported for a double-stranded RNA; it shows that RNA has conformational lability, contrary to current belief. It is consistent with the finding of Uesugi *et al.*[11] that r(C-m^{8}G-C-m^{8}G) exists in a Z-like structure. The transition to Z-form RNA requires more extreme conditions than the transition to Z-form DNA. However, in analogy to Z-DNA, other more physiological environments may be found to favour Z-RNA, and other RNA sequences may also undergo the transition. In any case one should now consider conformations other than A-form when considering double-stranded regions of RNA in ribosomes, viruses and other RNA-protein complexes.

We thank Professor Michael Chamberlin and his laboratory for providing us with RNA polymerase as well as advice on the synthesis and purification of poly[r(G-C)]·poly[r(G-C)]. We also thank Dr Dave Wilbur for assistance on the GX-500 spectrometer at Stanford. The proton NMR experiments were performed at Stanford University NMR Center, which is supported by NSF grant GP23633 and NIH grant RR00711. The work at Berkeley was supported in part by NIH grant GM10840 and the US Department of Energy, Office of Energy Research, under contract 03-82ER60090.000.

Received 4 June; accepted 9 August 1984.

1. Patel, D. J., Kozlowski, S. A., Nordheim, A. & Rich, A. *Proc. natn. Acad. Sci. U.S.A.* **79,** 1413–1417 (1982).
2. Patel, D. J., Canuel, L. L. & Pohl, F. M. *Proc. natn. Acad. Sci. U.S.A.* **76,** 2508–2511 (1979).
3. Jovin, T. M. *et al. Cold Spring Harb. Symp. quant. Biol.* **47,** 143–154 (1983).
4. Wang, A. H.-J. *et al. Science* **211,** 171–176 (1981).
5. Pohl, F. M. & Jovin, T. M. *J. molec. Biol.* **67,** 375–396 (1972).
6. Gray, D. M., Liu, J.-J., Ratliff, R. L. & Allen, F. S. *Biopolymers* **20,** 1337–1382 (1981).
7. Uesugi, S. *et al. J. biol. Chem.* **259,** 1390–1393 (1984).
8. van de Sande, J. H. & Jovin, T. M. *EMBO J.* **1,** 115–120 (1982).
9. Hall, K. B. & Maestre, M. F. *Biopolymers* (in the press).
10. Westerink, H. P., van der Marel, G. A., van Boom, J. H. & Haasnoot, C. A. G. *Nucleic Acids Res.* **12,** 4323–4338 (1984).
11. Uesugi, S. *et al. J. Am. Chem. Soc.* **106,** 3675–3676 (1984).
12. Hall, K. B., Cruz, P. & Chamberlin, M. F. *Archs Biochem. Biophys.* (in the press).

Erratum

Dynamics of meltwater discharge from Northern Hemisphere ice sheets during the last deglaciation

R. H. Fillon & D. F. Williams

Nature **310,** 674–677 (1984)

IN the above letter, the last four lines of the penultimate paragraph on p. 676 ('anomaly areas... $\delta^{18}O_{sw}$ anomaly') are a repetition from a previous paragraph. The correct four lines read:

amount of meltwater discharged into the Canadian Current before 13 kyr BP according to our calculations. This excess may reflect an early marine-drawdown phase of North American deglaciation[4,23].

Preformation to punctuation

Colin Patterson

Evolution: The History of an Idea. By Peter J. Bowler.
University of California Press: 1984. Pp. 412.
Hbk $34.45, £23.95; pbk $12.60, £8.75.

I CAME to this excellent book with vague misgivings, remembering the tedium of Henry Fairfield Osborn's *From the Greeks to Darwin*, or Edward Clodd's *Pioneers of Evolution*. No need to worry, for neither is cited in Peter Bowler's massive 54-page bibliography, and history of science is long past relentless progress towards today's truth, as chronicled in those older works. But Bowler does say that

> A few years ago, it would have been difficult to write a history of evolutionism except from the perspective that the modern form of Darwinism represents a triumphant climax to the process.

To my real surprise, I learned from Bowler's bibliography that his book has no real competitor — there is no modern, general history of evolutionism. The closest competitors, I suppose, are D.R. Oldroyd's *Darwinian Impacts* (Open University Press, 1980), and Ernst Mayr's magnum opus, *The Growth of Biological Thought* (Harvard University Press, 1982). In his opening chapter Bowler notes, and denies, the distinction between "internalist" and "externalist" historians of science, the first studying the "objective process of scientific discovery", the second looking at "how society reacted". He argues that the distinction disappears once we realize that scientific knowledge is not purely objective; perhaps, but one would have to rate Oldroyd's book as more externalist than Bowler's, and Mayr's as more internalist. Both are more difficult going. Bowler aims at readers with no background in either biology or history, especially students in history of science, but I believe that most biologists and many other scientists could read him with pleasure and profit.

The book is finely and carefully balanced, as exemplified by the arrival of *On the Origin of Species* exactly midway through the text, so that half the book is pre-1859, and half after that date. Bowler has particular strengths in both halves, for he has published in history of biology from seventeenth-century theories of reproduction to twentieth-century genetics, notably in books on nineteenth-century palaeontology (*Fossils and Progress*; Science History Publications, 1976) and on "anti-selectionism" around 1900 (*The Eclipse of Darwinism*; Johns Hopkins University Press, 1983). Throughout the book, I was struck by the way Bowler compresses complicated ideas into a page or two, and still finds space for illuminating comment: someone who can do this even for so thoroughly studied a figure as Darwin (for example on pp. 142–146) is doing excellent work.

There are two technical blemishes, the first trifling, of the kind it pleases pedants to discover — the portrait on the dust-jacket, said to be of J.B.S. Haldane, is his father J.S. The second blemish, more intrusive, is Bowler's usage of the word "hierarchy", a vital and recurring concept in the history of evolution. He uses "hierarchy" to mean linear sequence, as in the "chain of being" or a chain of command, where the general's orders pass down the military hierarchy to the private. But in biology today, "hierarchy" entails the inclusion relation, so that the higher includes the lower rather than outranks it: this usage is definitive in taxonomy, but also general in ontogenetic theory and other fields invoking theories or processes of branching. Bowler's idiosyncratic or old-fashioned usage leads to apparently nonsensical statements such as "Linnaeus' system [of classification]...does not imply a hierarchical ranking" or "Cuvier's reluctance to accept hierarchical classification"—here the notion of branching, or inclusion, is seen as the antonym of hierarchy.

The book ends with a chapter on "The Modern Debates", picking out four or five areas of controversy. Surprisingly neutralism, and the associated "molecular clock", get no mention here. Indeed, neutralism receives very short shrift in the book, three passing mentions, one of which is mistaken:

> If the survival of the fittest were necessarily true, it would be impossible for anyone to imagine that it was false—yet there have been theories of evolution based on random factors that deny the superior reproductive power of the fit.

The mistake here is to equate natural selection with change (directional selection), whereas neutralists emphasize the dominance of stabilizing selection, which resists change. Neutral theory seems to me to deserve at least as much space as punctuated equilibrium, which gets a very fair hearing, and modern Creationism, which gets 11 pages. But one point in those pages deserves thought:

> It may sound paradoxical, but the only way creationists can be forced to expose their own extraordinary theory to close analysis is if evolutionists concede that they cannot prove their own case. It is only by admitting the lack of certainty inherent in any theory that we can shift the argument to a new level.

Bowler occasionally slips from that noble level, as with "The true story of the horse's evolution has turned out to be rather more complicated" and similar comments implying access to the truth on human evolution. But all in all, I salute what I believe is a superb job. □

Colin Patterson is Senior Principal Scientific Officer in the Palaeontology Department, British Museum (Natural History), London.

Records of the early metazoans

Steven M. Stanley

The Dawn of Animal Life: A Biohistorical Study.
By Martin F. Glaessner.
Cambridge University Press: 1984.
Pp. 244. £25, $49.50.

FOR nearly a century after Darwin published *On the Origin of Species*, the nature of Precambrian life was debated fruitlessly in a climate of empirical uncertainty. Early fossil finds were continually announced and continually debunked, so that in any given year some claims were alive but clearly vulnerable to rejection.

During the 1950s and 1960s, the discovery of four types of Precambrian and earliest Cambrian fossils altered the picture dramatically, adding greatly to the temporal range of palaeontological inquiry. The four new fossil groups were single cells preserved in fine-grained sedimentary rocks; imprints of soft-bodied animals; tiny skeletal fossils slightly older than the first Cambrian trilobites; and trace fossils (tracks, trails and burrows). Of the four, single cells have often been seen as the most exciting finds, partly because their record extends some 2×10^9 years further back in time than the record of multicellular life. In many ways, however, the study of Precambrian cells has been disappointing: increase in cell size and surface complexity about 1.4×10^9 years ago point to the primary expansion of eukaryotes at this time, but the fossil record reveals little about the biological nature of earlier prokaryotic cells. The early metazoan record has been far more revealing, and we must welcome Martin Glaessner's publication of a book that focuses on this record, pulling together our knowledge, while briefly reviewing Precambrian microfossils. Glaessner, a pioneer in the study of Precambrian metazoans, has kept abreast of new developments, including many in the Soviet Union that have gone largely unnoticed elsewhere.

As might be expected, Glaessner devotes about half of his book to the spectacular

Ediacara soft-bodied fauna of Australia, which he first elucidated in 1958 and 1959, and to similar but less rich faunas that have since been discovered in many other parts of the world. The treatment of these faunas is the most comprehensive yet and is perhaps weakened only by the paucity of photographs — written descriptions of important morphological and preservational features leave the reader no recourse but to seek illustrative material among the other works cited in the book. In Glaessner's interpretation, the Ediacara fauna is dominated by medusoid and sea-pen-like coelenterates as well as annelids and arthropods. Unfortunately, the book was published too soon for the author to respond to Professor A. Seilacher of Tübingen, who is currently challenging these taxonomic assignments. Perhaps the need for a response will prompt Professor Glaessner to provide another review with plentiful photographs of high quality. Glaessner's global reviews of Late Precambrian trace fossils and Tommotian (earliest Cambrian) shelly fossils are also comprehensive and authoritative, though unfortunately they are even less well illustrated.

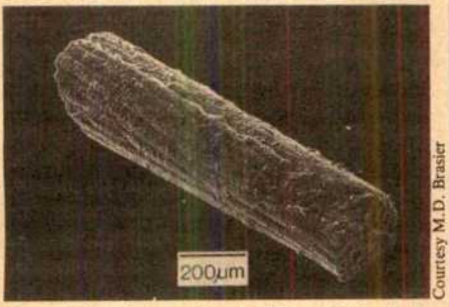

Courtesy M.D. Brasier

Part of the picture of early life — *Coleoloides typicalis*, a calcareous tubular fossil from the earliest Cambrian Hyolithes Limestone of Nuneaton, UK.

A nagging question that remains in Precambrian palaeontology is: when did the metazoans actually originate? Trace and body fossils reveal the presence of metazoans in considerable diversity after the end of the Varangian glaciation, about 6.5×10^8 years ago, but what about an earlier history? Glaessner concludes that the metazoan record extends to about 1×10^9 years before the present, but the evidence he cites is meagre and equivocal. If some of the alleged trace fossils are real, the suppression of metazoan diversification for several hundred million years remains one of the greatest puzzles in palaeontology.

Although Glaessner has been unable to shed much light on this problem, his book does provide a unique, up-to-date evaluation of Late Precambrian life. It should expand the knowledge of all palaeontologists, save a few specialists, and serve as a basis for graduate seminars on the early diversification of metazoan life. □

Steven M. Stanley is Professor of Paleobiology at The Johns Hopkins University.

Gauge theories with a difference

Graham G. Ross

Quarks and Leptons: An Introductory Course in Modern Particle Physics.
By Francis Halzen and Alan D. Martin.
Wiley: 1984. Pp. 396. Hbk £35.45, $31.95; pbk £12.50, $13.75.
Gauge Theories of the Strong, Weak, and Electromagnetic Interactions. Frontiers in Physics.
By Chris Quigg.
Benjamin-Cummings/Addison Wesley: 1984. Pp. 334. $42.95, £33.60.
Gauge Theory of Elementary Particle Physics.
By Ta-Pei Cheng and Ling-Fong Li.
Clarendon: 1984. Pp. 450. Hbk £35, $39.95; pbk £15.
Gauge Theories of Strong and Electroweak Interactions.
By P. Becher, M. Böhm and H. Joos.
Wiley: 1984. Pp. 306. £28, $54.95.

IT IS indicative of the state of high energy physics that four textbooks should appear together covering broadly the same ground. In recent years gauge field theories have emerged for the strong and the weak interactions, complementing quantum electrodynamics, the remarkably successful theory of the electromagnetic interaction. A large amount of experimental data has now accumulated consistent with the predictions of these theories, culminating with the detection of the gluons (the strong interaction partners of the photon) and of the $W^\pm$ and Z intermediate vector bosons (the weak interaction partners of the photon).

After the success of these theories there has been something of a lull in theoretical activity, leaving time for reflection and organization. The four books reviewed here are products of this period and all introduce the subject of local gauge field theories and their application in particle physics. However each book has a character of its own and addresses a different level of audience.

Pitched at an introductory level is the book by Halzen and Martin. It acquaints the reader with the nature of the fundamental interactions and the fundamental building blocks of matter, quarks and leptons, and is at its best in the explicit treatment of the use of Feynman rules to calculate physical processes at tree level. Many worked examples are given (with all the steps) and the text is supplemented by a large number of instructive problems; together, these features should enable readers with no prior knowledge in the subject to calculate simple processes for themselves.

The treatment of fermions and the early introduction of a chiral basis for Dirac matrices is clear and thorough, but somewhat less successful is the treatment of the group theory which falls short of being really useful. Beyond the tree level the book is, possibly necessarily, less explicit. While I was disappointed that the introduction of local gauge theories and the Lagrangian formalism was left to the penultimate chapter — too late for a thorough treatment — I liked this book in general. Above all it should prove to be a *useful* part of an introductory course in particle physics.

In many ways, Chris Quigg starts where Halzen and Martin leave off. After a nice introduction to quarks, leptons and gauge bosons, local gauge field theories are introduced via the Lagrangian formalism. In the main, the reader is expected to be able to calculate Born graphs, leaving space for a fuller discussion of quantum chromodynamics (QCD — the gauge theory of the strong interactions) and of spontaneously broken gauge theories used in describing the weak interactions.

There is a good discussion of radiative corrections in QCD, well motivated by explicit calculations and leading to a Feynman graph analysis of the leading log summation, but it stops short of the renormalization group analysis needed to justify and simplify this summation. The general emphasis is on explicit physical applications, the book containing good coverage of deep inelastic scattering, $\gamma\gamma$ scattering and e^+e^- annihilation. The treatment of the electroweak theory is easy to follow but is only at tree level; no attempt is made to present a loop calculation in a spontaneously broken gauge theory. The book ends with a brief but helpful discussion of the extension to grand unified theories, in particular to SU(5). Throughout problems are set, carefully chosen to augment and illustrate the textual discussion, while the extensive reference list will help readers delve further into particular topics. Overall this is a good introductory book, with plenty of physical insights, and will repay study.

By far the longest book of the four is that by Cheng and Li. It is also the most ambitious in terms of the subject matter covered, with emphasis more on the theoretical aspects. Part One covers the formal aspects of field theory, group theory and chiral symmetry in strong interactions, as well as the construction of local gauge field theories, their Feynman rules and the calculation of radiative corrections. All this should be useful to theoretical students with some prior knowledge for it neatly summarizes a vast subject. Because of its wide scope, however, there is necessarily little time for elaboration and I think this part would be heavy going for a newcomer to the field. Renormalization and the renormalization group are discussed in detail and this aspect of the book would complement the more physical analysis in terms of Feynman graphs presented, for example, by Quigg.

In Part Two, Cheng and Li move on to

QCD and the electroweak theory. I particularly appreciated inclusion of an explicit treatment of loop calculations in a spontaneously broken gauge theory, and also the detailed discussion of the Kobayashi–Maskawa matrix, CP violation and neutrino masses. All in all the book contains a lot of goodies, including grand unification and nonperturbative aspects of gauge theories; but, again, one probably needs some experience to appreciate them, for often an historical approach is followed which hinders the logical development of the subject. For example, a detailed discussion of the role of light-cone singularities in the Bjorken scaling region precedes the more modern and more physical momentum space Feynman graph analysis. Also there are no set problems to guide the reader. Ideally, then, Cheng and Li's book should be read after one (or both!) of the more introductory texts discussed above.

The fourth book, by Becher, Böhm and Joos, is a translation of the German edition which first appeared in 1981. It is different in character to the others, delving deeper into the theory of the renormalization of the gauge field theory. This is more in the nature of an advanced text or review for an experienced theoretician and contains extensive discussions, without full details of intermediate steps, of perturbative and nonperturbative aspects of QCD. The account of the electroweak theory, on the other hand, is briefer but more straightforward with a nice discussion of the high energy behaviour of Yang–Mills gauge theories.

Although the four texts reviewed here have as a general theme the gauge theories of the fundamental interactions, they vary widely in their demands on the reader. To a large extent they complement one another, and together represent a substantial improvement in the literature surveying modern particle physics. □

Graham G. Ross is in the Department of Theoretical Physics at the University of Oxford.

Pastures of muscle physiology

D.R. Wilkie

Muscles, Reflexes, and Locomotion.
By Thomas A. McMahon.
Princeton University Press: 1984. Pp.331. Hbk $50, £50; pbk $15, £12.50.

THIS is a brilliant book. Dr McMahon's original training as an engineer is an excellent one for a physiologist; in both branches of science we are concerned with machines that must function in an optimal way. Here we are provided with a clear and accurate summary of many of the mathematical aspects of muscular function that otherwise demand a laborious appraisal of a large number of original papers. Our understanding (and diligence) are repeatedly challenged by the examples and questions to be found at the end of every chapter.

McMahon's wide and scholarly approach to his subject, and his limpid and often witty style of writing, enable him to illuminate a whole range of topics ranging in physical scale (though not necessarily in complexity!) from the mode of operation of the individual cross-bridges thought to generate mechanical power at the molecular level, to the problems inherent in designing an elephant and in building a "tuned" running track on which athletes have consistently produced improved performances.

Naturally I do not agree with every word in the book. For example, McMahon writes (p.35) "The discovery of a process which apparently absorbs heat, like the mechanism of a refrigerator, provided a great deal of entertainment in the muscle literature for years". Alas he does not make it nearly clear enough for my liking that the "entertainment" resulted in deep confusion which lasts to this day. There are no circumstances in which a muscle acts as a refrigerator, which is a machine that moves heat from a lower to a higher temperature by the continued application of mechanical or electrical power. Nor can I see how a "unifying principle" (p.79) is provided by the non-uniformity of sarcomere lengths. The question of the instability of stretched muscle fibres, whose tension–length curve has a negative slope, has been discussed for many years yet remains controversial. In whole anatomical muscles (rather than in isolated single fibres) an important role, probably a stabilizing one, may well be played by the connective tissue between the fibres which is plentiful and unlikely to be arranged at random. Microanatomical studies are much needed; until they have been carried out, comparison between isolated muscle fibres and intact anatomical muscle demands great caution.

The biochemical aspects of muscular function are touched on only lightly (nobody should expect everything!) but McMahon is careful to differentiate between the chemical processes and the physical energy — heat and work — that results from them. A widespread failure to make this distinction is at the root of the continuing confusion about a topic introduced on page 211, that of positive and negative work. In movements of a whole animal, the function of muscles as brakes *absorbing* mechanical work is almost as important as their function as motors *producing* mechanical work. Unlike mechanical brakes, however, the muscles consume fuel in performing their braking action and even in sustaining a static load. To pursue the mechanical analogy further, a motor car can stop indefinitely on a hill by applying the brake and stopping the engine. A muscle must rev the engine and slip the clutch. The definition of "efficiency" given in Eqn 8.3 is ambiguous concerning positive and negative signs, though they can be inferred from the left-hand lines in Fig. 8.21 which do indicate negative values of "efficiency". This is formally correct though perhaps not very helpful. I hope that this section will make the topic as clear to the uninitiated as I know it to be to the author himself.

The last chapter, "Effects of Scale", is a delight to read and may well come as a surprise to biologists who work on subjects other than muscular contraction. Experimentally, we find in animals of different size a large number of functions that depend in a highly regular way on body weight, but in hardly a single case is there a satisfactory physical or biochemical explanation for the dependence. McMahon explores various possibilities in a way that is both instructive and entertaining. The relationship between metabolic rate and body weight is the best-established of such laws and is referred to briefly on page 279. It is known to apply to living creatures over a weight range of 10^{18}, a respectable number even by astronomical standards, yet it totally lacks an adequate explanation. This seeming vacuum is a constant source of irritation to all biologists who concern themselves with such issues. Presumably because of their recent publication dates, no references are given to the fuller analyses of the problems of scale given in the beautifully-illustrated books by McMahon and John Tyler Bonner (*On Size and Life*; W.H. Freeman, 1983) and by Knut Schmidt-Nielsen (*Scaling: Why is Animal Size so Important?*; Cambridge University Press, 1984).

Students of muscle physiology at all levels will benefit from reading *Muscles, Reflexes, and Locomotion*. Not only is it a compact source of information, but a novel, comprehensive and readable book which tempts one to browse in the wider pastures opened up by Dr McMahon. □

D.R. Wilkie is Jodrell Research Professor of Physiology at University College London.

New in paperback

- *The Enchanted Ring: The Untold Story of Penicillin* by John C. Sheehan (reviewed in *Nature* **300**, 126; 1982). Publisher is MIT Press, price is $6.95, £7.25.
- *Quarks: The Stuff of Matter* by Harald Fritzsch (reviewed in *Nature* **306**, 508; 1983). Publisher is Penguin, price is £4.95.
- *W.H. Hudson: A Biography* by Ruth Tomalin, first published by Faber & Faber and reviewed in *Nature* **301**, 446; 1983. Publisher of the paperback is Oxford University Press, price is £3.95.
- *Man and the Natural World: Changing Attitudes in England 1500–1800* by Keith Thomas (reviewed in *Nature* **303** 641; 1983). Publisher is Penguin, price is £4.95.

21-1-87
A. Bates

Job prospects in the United States

from Richard Pearson

With the United States' economic boom continuing, and the rate of job generation far outstripping that of other Western economies, what are the job prospects for life scientists and engineers?

PROJECTING future employment levels is notoriously difficult, yet for occupations requiring many years of training and experience, insights into future employment patterns and imbalances can show where significant adjustments might be needed in labour market and training policies. Any forecasts, however, can only be as good as the assumptions on which they are based, and these need to involve assessments of future levels of economic and investment activity, and technological and productivity changes.

Although scientists, engineers and technicians account for only a small fraction of the US workforce (less than 5 per cent), they have a disproportionate role in economic growth, technical innovation and national security and are a key area of concern. A key role for the governmental National Science Foundation (NSF) in Washington is to provide information on the availability, both current and projected, of such scientific and technical resources in the United States. A recent NSF study looks at the ability of the labour force to fuel the expected 45 per cent increase in defence expenditure over the period 1982 to 1987 (see Table 1). A series of scenarios was used, looking at the implications of high and low growth rates in Gross Domestic Product between 2 and 4 per cent per year, and of two defence expenditure scenarios averaging 3 and 8 per cent per year growth.

Table 1 Projected US employment changes for the years 1982–87

	Employment (thousands)		
	1982	1987 (low growth)	1987 (high growth)
Computer scientists	219	287	303
Other scientists	508	556	585
Engineers	1,140	1,296	1,423
Technicians	1,468	1,649	1,760

Values for 1982 are 'actual', and those for 1987 are projected. Source: *Projected Response of the Science Engineering, and Technician Labor Market to Defense and Non-Defense Needs: 1982–87* (National Science Foundation, Washington, 1984).

Growth in demand for scientific engineering and technician (SET) manpower is expected to grow by between 2.6 and 4.1 per cent per year, a rate of growth higher than for employment generally (up 1–2.4 per cent per year). This increasing demand is driven not only by the strong performance of high technology industries, with their high concentrations of SET manpower, but more importantly by the diffusion of technology throughout the economy, which has led to a significant shift in staffing patterns towards SET employment. Interestingly, although each scenario focuses on rather different sets of assumptions, the projected range of SET requirements is rather more restricted, never varying by more than 5 per cent from the average 1987 projected value in any of the major occupational categories (Table 1). This is in part because SET manpower is only a small proportion of all jobs in the economy but also because productivity increases at a much faster rate under the high growth scenario, with the productivity gains counterbalancing the employment impact of economic growth which in turn reduces the need for additional SET manpower.

There were nearly 750,000 university degree level science jobs in the US economy in 1982 and this figure was expected to grow by between 116,000 (3 per cent per year) and 161,000 (4.1 per cent per year) jobs over the period to 1987. Both these figures represent a slow-down in the 8.7 per cent average annual growth rate over the period 1977–1982. The key determinants of these growth patterns are shown to be primarily economy-related, with the key driving forces for increased scientific jobs being the service sectors, particularly research and development laboratories, consulting firms and computer establishments.

The engine of this growth in science jobs seems to be the computer, with computer systems analysts, an occupation first recognized officially in the 1970 census, accounting for about 300,000 people in 1987, regardless of the scenario followed, with half of them employed in business services. The growth in these jobs will average about 6 per cent per year, the net growth being 70,000–85,000 jobs over the five years. Computer specialists are expected to dominate science jobs in 1987, increasing their share over the period from 34 to 55 per cent, with psychologists, chemists and mathematicians being the other largest groups.

Of the physical sciences, physics has the fastest growth at 1.4 to 3 per cent per year with growth for chemists being rather lower, at 1.5–2.5 per cent, a figure similar to that for geologists. Mathematical science is projected to have rather faster growth at 2.2–3.5 per cent per year but the total job gain will only be 5,000–10,000 jobs overall. In the life sciences, agricultural jobs barely keep pace with overall employment growth, and while the number of jobs for biological scientists will grow rather faster, the total job gain will be only about 5,000–10,000 extra jobs.

By way of contrast, engineering shows an overall growth of between 2.6 and 4.5 per cent with aeronautical/astronautical employment rising by a massive 5.9–11.1 per cent per year, a gain of 22,000–45,000 jobs. Electronics is the other major growth occupation, and although it shows rather less spectacular growth of between 3.9 and 5.1 per cent, the expected gains of between 69,000 and 94,000 jobs match the absolute growth in jobs for computer systems analysts.

As well as considering possible demand, NSF also makes corresponding supply projections, taking account of such factors as new entrants to the labour force, occupational mobility, immigration, and deaths and retirements. The model projects that supply will exceed demand under all the scenarios for all science occupations; for example, there could be three people seeking every job. However, significant shortages are indicated for aeronautical/astronautical engineers and electronic engineers, together with particularly large shortages in the computer speciality fields. These projections, however, assume no major forms of labour force adjustment such as increased salaries, reduced hiring standards, significant mobility from other occupations or increased immigration. One particular concern is the possibility that industry may be so attractive that the universities will be unable to attract enough talented people for research.

Labour market adjustments are expected to alleviate the likely level and impact of shortages in the above disciplines, and also mitigate the size of surpluses. But NSF's main concern is that the larger the adjustment needed, the greater the impact on and likely lowering of the quality of the workforce. This could induce productivity and quality losses in the short term, while hindering longer-term supply of skilled manpower if the academic sector cannot retain graduate students or its existing faculty. Already many specialists in information technology are leaving academic posts for industry. However, for many of those seeking a science-linked job, employment prospects are declining and may continue to deteriorate for the next few years. Occupational mobility and retraining will then become higher priorities for the individual seeking secure employment. ☐

Richard Pearson is at the Institute of Manpower Studies, Mantell Building, University of Sussex, Brighton BN1 9RF, UK.

nature

21-1-87
A. Latter

Targets for future arms control

Before East-West talks on arms control resume, there is a strong case for an examination of what the two sides should be aiming at — even for an agreement on the subject.

PREDICTABLY, not much has been heard of arms control in the past few weeks. For all the importance rightly attaching to the question how best to reach an accommodation between the Soviet Union and the United States on the range of issues left suspended at Geneva a year ago, it was never likely that the US electorate would let the presidential election be determined by the answers of the different candidates. And there is a sense in which the indifference is well-placed. Even if a re-elected President Reagan should be discovered to be more flexible than he has sometimes seemed to be, as on issues such as negotiation from strength, everybody knows that it takes two to make an equitable agreement — and nobody knows what the putative partners in negotiation are now thinking. But a new president, whatever his virtues, would be no more able to conjure agreement out of thin air, and would in any case have to spend time learning what kind of agreement would be acceptable. So what can people, in the United States and elsewhere, hope to be doing while waiting for the dust to settle?

The simple but important task that needs to be taken up is that of defining a stable and possibly attainable goal for arms controllers in the medium term, say by the end of the century. Such an exercise is not as academic as it seems, for there is a sense in which proposals for new arms control agreements between the Occidental super-powers or within larger groupings, reasonable enough in themselves, turn out to be insubstantial when set against the pattern of changing military technology and the complexity of the world in which international conflicts of interest must be supposed to continue to exist. This is the spirit in which the notion of a comprehensive ban on nuclear testing, desirable (and nearly attainable) in the early 1960s, would no longer be safe (on its own), let alone feasible. Similarly, because the Salt agreements (both I and II, the latter and the more important never ratified) say nothing about missiles of intermediate range, strategists have been stuffing Europe with SS-20, Pershing and cruise missiles.

These disheartening developments are not as surprising as they appear. This side of that utopian state of affairs in which international conflicts of interest have been subsumed in universal sweetness and light, no single arms control agreement of the kinds now talked about at negotiations can on its own be stable. A comprehensive test-ban treaty would survive only until one of the participants considered its position had been undermined by the development of other military technologies than those for bomb construction. The Non-Proliferation Treaty, which mercifully still holds, would not have much value if it were not backed up by a whole array of political restraints on potential bomb-makers, but would not last long if more than one or two of its signatories defected. Nuclear-free zones in Europe would probably survive for as long as the countries directly concerned agreed not to change their external relationships significantly. And even the design of a more general package of arms control measures to limit the damage that the superpowers may inflict on themselves (and others) requires, for stability, a clear understanding of what political changes will be allowed without bringing the whole agreement tumbling down.

Put directly, the problem is this. Is there any arms control regime that can be expected in Europe to survive, say, the transfer of one Central European state from one alliance to its opponent? As a corollary, is it possible to conceive of a regime for nuclear arms control in Europe that will allow conventional wars to proceed conventionally? And if not, what understandings about political change must accompany what the arms controllers agree? These important questions have been given far less attention than they deserve.

But do not the Helsinki agreements (on European security) serve just such a purpose? They formally require of signatory governments such liberality in regulation of people's freedom that, if the agreements were enforced, many potential international conflicts would never surface. The trouble, as the world knows, is that the Helsinki agreements are a dead letter, especially in Eastern Europe. But an attempt to breathe new life into them, perhaps by new administrations in the United States and the Soviet Union, would not be a waste of time.

The safest assumption (which some would think wild) is that Helsinki could yield, by 2000, an understanding that moderately paced political change would be permitted among the lesser allies of major powers, perhaps against a background of steady economic improvement (also one of the Helsinki objectives). Whatever the permissible pace of change agreed, it is unthinkable that either side would agree to the entire abandonment of nuclear weapons within Europe, while even some European states (France, for example) would think twice on that subject. The best realistic bet is that great-power deterrence would persist, but preferably based on relatively invulnerable submarines, and that nuclear warheads actually based in Europe would be limited to, say, a score on each side. Inspection and verification could be by means of human inspectors (one per warhead) and by tight control of military nuclear explosives. Such a force of warheads would have the limited purpose of helping defence against overwhelming conventional attack, and of alerting allies.

In such a setting, chemical weapons (more attractive to the generals as weapons in conventional wars) could and should be outlawed, while the regulation of nuclear facilities within Europe could obviously be enormously simplified. For the intercontinental powers, the accompaniment of this regime would plainly be such a tight restriction of strategic warheads — say 100 — that only bases in invulnerable submarines would make sense. In such a regime, it would obviously be sensible to aim at a cut-off of military production — no skin off the noses of the major powers but a help against proliferation. There are two views of this prospect — one that it is a cowardly over-modest goal at which to aim, the other that it is idealistically ambitious. The second opinion, unfortunately, is nearer the truth. □

New academic tests

British universities have to share funds for research. Self-choice is best.

BRITISH universities seem to have embarked on their new academic year in a mood blended of resignation and combativeness. After several years of shrinking budgets, and after a summer filled with threats that there is worse to come, even the hope of a period of stagnation, called "level funding" in the trade, seems almost too much to ask for. But, since the appearance of the University Grants Committee strategy document a few weeks ago (*Nature* 20 September, p. 193) some university administrators and their academic colleagues have indulged the fancy that the government is about to relent. What has happened is simply that the grants committee has taken a more robust view than in recent years of the universities' problems, and declared itself sympathetic to their needs. Specifically, it has made it plain that it does not passively accept that the universities can bend ever more pliantly to the government's demands (to train more engineers, for example) on a fixed budget. But as the experience of recent years has shown, even the strongest case may not prevail against a government strapped for cash. Lord Flowers, chairman of the Committee of Vice-Chancellors and Principals, was right to remind his constituents a week ago that this is not a "battle won, but a battle joined".

Euphoria is contagious, but dangerous. The debate arranged for 25 October in the House of Commons, on which many hopes are pinned, is almost certain to be a disappointment for the universities. Having lost their political friends in the 1970s, they are unlikely to be much comforted if the government's political opponents seize on what has been done to them as yet another stick with which to beat the administration over the head; or if, as seems likely, the government disarms criticism of its handling of British higher education in the past five years by a show of generosity, perhaps by promising an increase of the budget for university equipment. The test that those in higher education should apply to what is said in the House of Commons is that of whether the debate reveals an understanding that higher education (not just in universities) is a national resource and an economic and social necessity, not just a way of insulating a bunch of academic layabouts from the rigours of the labour market. (Tenure irrationally remains everybody's *bête noire*.)

Meanwhile, the universities have work of their own to do. The grants committee's document is rhetorically encouraging but full of pitfalls for the unwary or the indolent. Thus nothing substantial is said about the chief iniquity of the past three years — the imposition of student quotas that individual universities might exceed only at the risk of being penalized financially. The inference is that the grants committee will not in future enforce the rules its predecessor committee promulgated, which is a welcome development. The result should be that many universities will be able to make more economical use of the resources at their disposal by allowing departments starved of students to operate at full capacity. The snag, also only implicit in what the grants committee says, is that individual institutions will find themselves engaged in a complicated attempt to second-guess the grants committee. Taking in more students may help financially, if only at the margin, but may hazard an institution's capacity to compete for research support in future, but under a set of rules that has yet to be defined.

The issue is complicated and potentially contentious. The grants committee acknowledges, perhaps even overestimates, the importance of its financial support to the conduct of academic research in Britain. And now, when it is generally agreed that the dual mechanism of research support (from the committee and, in parallel, by means of project grants from research councils) has broken down, the committee says that it will in future be more discriminating between universities. All that makes sense, if only because, on paper, the present system provides all institutions with the general support that should enable them to compete for project grants in circumstances in which it is also generally understood that some are more able to compete successfully than others. Indeed, the grants committee has, over the years, implicitly trimmed its sails to this wind by being more generous to some universities than others while declining to say why, no doubt in the knowledge of the ructions there would be if universities had grounds for thinking that research support was being "earmarked", a synonym for the act of telling universities what to do and thus a gross intrusion into academic freedom.

So by what criteria will the grants committee discriminate among British universities in the provision of research support? By all accounts, the question has not been settled. All that the committee has said in public is that it will devise criteria that are distinct from those followed by the research councils in their provision of (mostly) project grants. Obviously that makes sense, for otherwise it would be just as well to replace the research councils as a whole by the grants committee. But what other yardsticks than peer-review, and a general sense of "timeliness and promise", can there be?

Here is one interesting and subversive way in which the grants committee might choose to solve the problem it has set itself. Why not, to begin with, take universities' own estimation of the reasons why they deserve research support? At first, the result would be that universities would share the research component of the grants committee's budget in much the same proportions as at present, and so might be tempted to assume that nothing had changed. But in making a case for research support, the prudent among them would be compelled to explain why their research proposals should be taken seriously. And the consequences of that could be enlivening. For it would turn out that universities that were capable internally of discriminating between good and less good research would be more likely to succeed in the second round of the proposed competition. And those which had the flair to spot new lines of promising research at an early stage, and the willingness to commit internal resources to their support, would be found to emerge with extra kudos from such competitions. So, properly handled, the grants committee's ambition to devise alternative criteria for assessing research support may turn out to provide two of the benefits conspicuous by their absence in recent years from the British system — internal mechanisms for deciding what backing should be given to what research, and opportunities by which institutions can improve their standing by their own wit. That such a system would also lend substance to the notion that universities are autonomous institutions even in the uncomfortable sense of that word is not the least of its attractions. □

Irish disunity

Bombs apart, Anglo-Irish talks are hopeful. Education deserves attention.

THE unsuccessful attempt to assassinate the British cabinet last week will have one important and beneficent consequence — that of further stimulating the search for an accommodation between the governments of Ireland and the United Kingdom over the Ulster problem. By all accounts, the weeks preceding the bombing of the Brighton hotel in which four people were killed were cheerful times for the officials labouring on the details of an agreement. What seems to have happened, on the British side, is that one minister, Mr James Prior, has been replaced (at his own request) by another, Mr Douglas Hurd. In the nature of this, the most disheartening job in British politics, new policies require new men, who usually have only one chance at a solution. Mr Prior's chief initiative, the consultation between Irish politicians called a forum, was less successful than it might have been because of the absence of the Ulster nationalists and the intransigence of the Irish nationalists. Within the same framework, Mr Hurd appears to be putting his energy into the building of common institutions, the touchstone of Irish hopes two years ago.

While it is remarkable (but unremarked) that many Irish institutions (rugby football and the administration of lighthouses, for example) have survived Irish partition, it tends to be forgotten that Irish higher education has preserved many of the appearances of commonality. As European citizens, Irish students can enter British universities without paying the penal fees exacted from other foreigners, but the Irish Government will not help with maintenance costs. Roman Catholic students from Ulster tend to seek higher education south of the border, when they are welcomed as if Irish. There is the basis for a deal between the two governments on this trade in young people's aspirations, as well as for an understanding that, for the purposes of research, the two countries should count as one. That should be at least one part of the package of proposals Mr Hurd is hoping to have assembled by next month. □

Fast reactors

Japanese plans delayed despite Clinch River bonus

Tokyo

JAPAN'S fast breeder reactor (FBR) research programme is running into financial difficulties, despite the recent gift of Y200-million-worth of unwanted research equipment and instruments from the US Government's abandoned Clinch River project.

The difficulties are caused by a massive increase in estimates of the construction costs for Monju, a 300-MW sodium-cooled prototype FBR to be constructed near Tsuruga in Fukui Prefecture. Monju is the key project in the FBR development programme and a major step forward from the 100-MW experimental reactor Joyu, which went critical in 1977.

Ground clearance operations have begun at the Monju site after several years of geological and seismic surveys. But construction costs have now risen from the 1980 estimate of Y400,000 million (US$1,600 million) to around Y590,000 million ($2,500 million). Responsibility for the project rests with the Power Reactor and Nuclear Fuel Development Corporation, a large research organization attached to the Science and Technology Agency. Funds for the project are not, however, entirely provided by the government, around 20 per cent coming, under a 1980 agreement, from privately-owned electricity utilities, largely through a power source development tax.

Now, the Science and Technology Agency wants to pass on a third of the extra costs to the utilities. They, however, have refused point blank to increase their contribution, arguing that any further funds could be found only by increasing electricity charges — something the government is anxious to avoid.

The shortage of funds is likely to hit the project hard next year when construction should move into top gear so as to finish by 1990. At present, given that the Japanese Government is already running an enormous budget deficit, the most likely option is to postpone the completion date by up to 5 years and to slow down the rate of construction to match availability of funds.

The pessimism over completing Monju on time comes just as the federation of electric power companies and the big five nuclear construction companies have launched a new Y6,000 million ($25 million) study project to choose the basic design for Monju's successor, a 1,000-MW demonstration reactor expected to be ready by the end of the century. The three-year study will aim to make the choice between a loop type design, in which heat from the primary sodium coolant is transferred to a secondary liquid sodium system outside the reactor, and a tank type in which the heat exchanger is located inside the reactor. The two reactor types are being researched by groups led by Mitsubishi and Hitachi–Toshiba respectively.

The key to success is to find some way to cut the enormous construction costs of the FBR, currently estimated at around two and a half times that of a conventional light water reactor. One way in which this will be tackled is through a joint US–Japanese project, agreed in principle this week, to perfect methods of driving the sodium coolant by electromagnetic forces rather than by a conventional pump.

Technical specifications for the reactor are to be examined by the French company Novatome, for although enthusiasm for FBRs remains great in Japan, the technology is still a long way behind that of France. The French began operation of a 250-MW prototype FBR, the Phénix, in 1972 (at the same time as a similar reactor at Dounreay in the United Kingdom) and expect to have Super-Phénix — the world's first demonstration FBR — ready by 1985, some 15 years ahead of any Japanese competitor.

Alun Anderson

Danish physics

Niels Bohr on a shoestring

Copenhagen

THE Niels Bohr Institute for nuclear and particle physics in Copenhagen, which celebrates the centenary of Bohr's birth next year, is in dire straits because of opposition to nuclear power in Denmark. That, at least is the opinion of one of its professors, nuclear theorist Aage Winther. For the result is poor student enrolment in physics at the University of Copenhagen (of which the Niels Bohr Institute is a part), and some departments with five physics lecturers per student. Because university research funds are distributed in rough proportion to student numbers, these are hard times for the Bohr Institute.

There have been no new research posts at the institute for seven years. With a staff of 50, the institute needs one or two posts a year to keep alive, Winther reckons. A clutch of retirements begins in five years' time, but meanwhile, the institute needs perhaps 10–15 new staff. Will it happen? Winther throws up his hands in a gesture of doubt. Sad news for a city that gave its name to the statistical interprepation of quantum mechanics and for the institute that housed Europe's first cyclotron. The Niels Bohr also began the European Organization for Nuclear Research (CERN), now based near Geneva, as a theoretical group in 1951.

The trouble lies not only with the opposition of the young to things nuclear and the fashion (as Winther describes it) for the new biology. The Danish university system, in which the Niels Bohr is enmeshed, is in something of a mess. First degrees typically take 8–10 years to complete, with some students stretching out their time to the age of 34. After such a long first degree, there are very few postgraduate students.

Also, as in many countries, research funds have been pared down "to the level of counting pencils and erasers". The goverment expected the universities to perform major surgery on themselves, says Winther. "But how can we do that with our democratic structures?" All university committees have 25 per cent representation from students and 25 per cent from technicians, says Professor Teder Olesen Larsen, chairman of the national science policy advisory committee. "With such a broad structure the only decisions the universities can take are decisions to do nothing."

Thus the Niels Bohr Institute and many other important laboratories in Denmark's universities, have been submerged — except where they can fight for special support. This is often distributed by the government in "cigar boxes", a Danish phrase for special-purpose funds administered separately from the 10 per cent or so of research money that comes through the Danish research council system. Thus when essential moneys were allocated for the re-instrumentation of Danish laboratories, the money came from a "cigar box", where research council priorities were not easy to take into account. With so many special funds, the Danish research support system has now become "Kafkaesque", says Olesen Larsen.

The Niels Bohr is hoping to insulate itself from these problems in two ways. First it has negotiated a deal with the government that will give it more funds than its low student intake would normally entail. But the money will go in a lump to the university administration, and it is yet to be seen whether it comes the institute's way, says a cynical Winther. But as a second string, the Niels Bohr is hoping to raise more external support — which, with 50 mostly foreign visiting scientists, is already large. "We hope to make a success of our 100th anniversary celebration next year", says Winther, "by appealing to our external benefactors". Among them have been the US Ford Foundation and National Science Foundation; the Nishima Foundation of Japan; and the Italian national institute for nuclear physics (INFN). They should expect a few discreet Danish knocks on their doors next year.

Robert Walgate

European biotechnology

Community seeks new funds

Copenhagen

THE Governments of Austria, Switzerland and Sweden have asked the European Commission if they may join in the European Economic Community's next biotechnology programme, even though none of them belongs. The decision rests with the European Council of Ministers but the signs are that the applicants will be refused.

If so, this would be an inauspicious start to the 154-million-ECU (£130 million) five-year programme, which has as yet not an ECU (European currency unit) to call its own. The research plan, called the "Research Action Programme" (RAP) in biotechnology, has been conceived as a development and sixfold amplification of an existing Community biotechnology programme devoted to agriculture and food, the "Biomolecular Engineering Programme" (BEP). BEP has had "a tremendous impact" on developing collaboration among European research groups in plant sciences, said one senior participant speaking at a meeting last week to take stock of the programme.

Others, however, claim that while BEP has certainly been good for Europe, its benefits — new collaborations — will fade away when BEP ends (in March 1986) unless new funds are found to pay the costs of travel, meetings, training and materials now supported under BEP. Participants point to an earlier successful programme on photosynthesis, which collapsed when the programme finished.

One of the successes claimed for BEP last week is that work on the mitochondrial DNA of plants is now more advanced in Europe than elsewhere, partly as a result of the collaborations that have been supported. Without claiming sole credit, officials were gratified last week to hear from Professor Jeff Schell and his colleague Professor Marc van Montagu that *Agrobacterium* plasmids can be cloned into a monocotyledonous plant, *Asparagus officianalis*.

It seems to be agreed that BEP is responsible for the stimulation of *Agrobacterium* research in Europe and for establishing joint research programmes between groups that would otherwise have been working independently and in duplication. "The money has been better spent than it would have been in separate national programmes", said one participant.

BEP and, by extension, its successor, is not, however, without critics. Professor Schell, of Cologne and Ghent, doyen of the *Agrobacterium* vector for introducing foreign genes into plants, considered that the funds available (15 million ECU from Brussels) have been too thinly spread, but fears that if there were a massive increase in the budget, the money might be wasted among the undeserving masses.

Commission officials say, however, that the objectives of the new programme are different, and that in the plant sciences, the best groups and programmes have already been identified. RAP would develop the programme, but also support initiatives in bioreactor technology (in particular for multi-enzyme, multi-phase and co-factor-requiring reactions), vaccines, hormones, gene transfer in animals, microbiology, the methodology of animal cell cultures (for monoclonal antibodies), new methods for toxicological testing and other fields of "basic, pre-competitive" research.

Whether funds for the new programme will materialize is, however, still an open question. France, West Germany and the United Kingdom are objecting to the cost, even though all governments gave outline approval last April. Now the European Commission is trying to persuade ministers to open their purses by quoting the poor opinion of European biotechnology expressed by the US congressional Office of Technology Assessment, published in January this year (see *Nature* **307**, 402; 1984).

Robert Walgate

Danish collaboration

Europe seems long way south

Copenhagen

THE Danish minister for education and science, Mr Bertel Haarder, is to make a strong protest at the next European council of research ministers at the way in which France and Germany appear to have decided between themselves where to put the proposed European Synchrotron Radiation Source (see *Nature* 4 October, p.399), trading a trans-sonic wind tunnel for Cologne against the ESRS for Strasbourg or Grenoble.

Denmark had offered to site ESRS at the Risø atomic research centre, and had offered DKr 350 million (£25 million) to help pay for it. But now Denmark feels its proposal was not properly assessed.

"We are very very upset", said Professor Teder Olesen Larsen, chairman of the Danish advisory council for science policy, last week. As well as Haarder's protest in Brussels, Denmark is to raise the issue at the annual general meeting of the European Science Foundation (ESF) in Strasbourg in November.

The ESRS project has been managed by ESF since 1979, and site proposals should have been assessed and compared by an ESF technical committee. In Denmark, it is now felt that this scientific assessment never took place, or at least was not taken seriously. A detailed Risø proposal has still not received a reply said Olesen Larsen.

The Risø proposal is generally believed in Denmark to have been technically excellent, and to have had a good chance of success if purely scientific criteria had been involved. "We would be very disappointed if a decision was reached by Franco-German agreement", said Olesen Larsen. "We are not going to be dictated to in that way." The French research minister, Hubert Curien "has a responsibility" at the very least to put the Franco-German proposal before the ESRS technical committee. If nothing is done to heal wounds there could be "very strong and nearly disastrous consequences for ESF", Olesen Larsen said.

According to Professor Alan Mackintosh, an ex-director of Risø now at the University of Copenhagen, Denmark has a good record in synchrotron radiation research. Indeed, the latest design of ESRS was coordinated by a Dane, Professor Bronislav Buras, at the European Organization for Nuclear Research (CERN) near Geneva. The Nordic countries are also dismayed that they have never had a major European research facility (except the ionospheric laboratory, EISCAT). The complainants are, however, more reticent about the urgent domestic case for Risø as a site. It is one of those big laboratories originally devoted to nuclear research that needs to find new goals. ESRS would have suited it very nicely.

Risø's problems have been sharpened by the tacit Danish Government decision to abandon all hope of developing nuclear power stations in the light of the recent vote by the Social Democratic Party (SDP) (now opposing the centre-right coalition government) against nuclear power. Taking SDP together with the centre ("Radical") party, there is probably now a majority in the Danish Parliament against all nuclear development. For the first time in years, the Danish Prime Minister failed to refer to a nuclear future for Denmark in the opening speech to Parliament this month.

Another question-mark to place against Danish interest in ESRS could be the Danish commitment to another European institution, the European Molecular Biology Laboratory (EMBL) at Heidelberg. Denmark has kept its continued membership of EMBL in doubt now for three years — and that doubt will continue if Olesen Larsen's science policy committee has its way. A committee of biologists had recommended in August that Denmark should finally announce its long-term confidence in and commitment to EMBL, which costs the country DKr 3 million (£210,000) a year; but the committee has rejected that advice, and instead advised Minister Haarder to leave the matter open for another three years — and meanwhile encourage more Danish molecular biologists to use the laboratory. Haarder has yet to decide which advice to take.

Robert Walgate

Japanese conservation

Aphrodisiacs and whales excepted

Tokyo

PRINCE Philip, Duke of Edinburgh, visiting Tokyo in his capacity as president of the World Wildlife Fund, has called upon Japan to take more vigorous action to abide by the Washington Convention — which regulates international trade in endangered species. His comments add to savage criticism of Japan's disregard of threatened species voiced at last week's Asian Pacific regional meeting of the convention — and comes when the Japanese Government is in a quandary over what to do about the cuts in whaling quotas agreed earlier this year by the International Whaling Commission (IWC).

The regional meeting of the convention on international trade in endangered species, held in Kuala Lumpur, ended with the adoption of a resolution severely criticizing Japan for failing to enforce the convention, which permits trading in endangered species only when official permission has been given by both exporting and importing countries. Japan is one of the signatories but has never actually enforced the regulations properly.

Critics at Kuala Lumpur pointed out that, despite the great efficiency with which Japan controls the import of manufactured goods, no experts are provided at customs offices who can check the status of a species or the validity of documents showing where animals have come from. The result is that Japanese traders have found it easy to deal in a range of endangered species — in a recent case, it was found that extremely rare lion tamarins (*Leontopithecus rosalia*) had been brought from Brazil with forged permits — as well as being able to sell large quantities of ivory, furs and tropical fish.

On top of lax adminstration of existing regulations, the Japanese Government has excluded from control 14 species recognized as endangered by the convention on the grounds that they are "vital for domestic industry". Chief among the excluded species is the musk deer, which has now been exterminated in most of India and is found in only a few isolated areas of the Himalayan states of Nepal, Sikkim and Bhutan.

Despite the real risk of extinction, the enormous prices that Japanese dealers will pay for the male deers' musk gland meant that around 3,500 adult male deer were killed last year. Probably four times that number of deer died when the young animals and females that fall into poachers' traps are included. All this to supply the ingredients for a traditional Chinese medicine of very doubtful efficacy.

The Kuala Lumpur meeting's resolution is not on its own expected to have much influence; it had been expected and discounted in advance by the Japanese. A representative was sent only to the first day of the two-week meeting. Later, financial restrictions were claimed to have prevented fuller attendance. Of the other 16 Asian-Pacific member countries, only Iran was absent.

Prince Philip, on his visit to Japan, also said he tended to the pessimistic view that whale stocks are declining rather than the optimistic view, taken by the Japanese, that commercial whaling can be continued without pause, and he argued that continued Japanese hunting of sperm whales would run "counter to the world consensus of opinion".

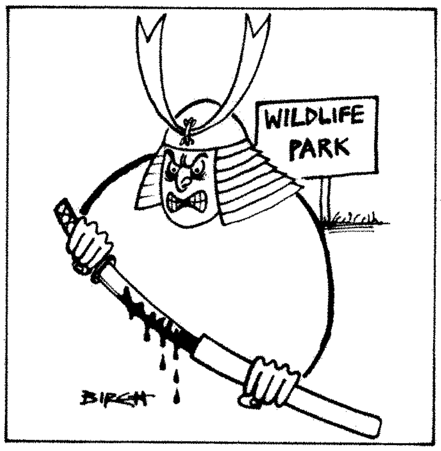

But the Japanese Government has already decided to permit sperm whale hunting in Japan's coastal waters on the grounds that it is a domestic matter. And, last week, the decision was made "in principle" to join the Soviet Union and Brazil in objecting to the cut in the minke whale quota agreed at the IWC meeting earlier this year (see *Nature* **310**, 440; 1984). The objection will not, however, actually be lodged, and Japan will not actually break the quota agreement, until all attempts have been made to persuade the US Government not to retaliate by cutting fish quotas in US waters, as the United States has said it will do to any country disregarding IWC agreements.

A decision is unlikely to be reached until after the US presidential election in November. Right now, anyway, fisheries agreements are not a popular topic in Japan. Not only are talks with the Soviet Union over salmon fisheries stalled, but Japan has just been accused of systematic violation of US fishery quotas in the North Pacific region. The Alaskan office of the US Department of Commerce's National Oceanic and Atmospheric Administration has claimed that the Japanese fishing fleet has been deliberately misleading US observers placed on-board fishing boats and has been using secret telegraph codes to broadcast the presence of patrol boats.

It is expected that Prince Philip will raise conservation issues when he meets Prime Minister Yasohiro Nakasone later this week.

Alun Anderson

US patents

Dying Congress aids innovation

Washington

THE 98th United States Congress ground to an inglorious halt last Friday after a frantic series of eleventh-hour compromises between the House of Representatives and the Senate that still left several major items of legislation unfinished and hence abandoned. Drafters worked around the clock, and such was the confusion that military jets had to be used to ferry back to Washington senators who, keen to start campaigning in their home states, had left the capital before a final vital vote authorizing next year's budget deficit.

Among last week's casualties were the Export Administration Act, which might have established a new framework for the control of high-technology exports but which resisted last-ditch efforts to reconcile House and Senate views, and the controversial Simpson–Mazzoli immigration bill.

But there were also successes. Manufacturers of "generic" pharmaceuticals won a last-minute battle in the Senate to strike out a section of the 1984 Patent Law Amendments Act that would have extended the scope of US process patents to cover products made outside the United States. At present, there is no straightforward way in US law (in contrast with the position in Europe) to prevent a "copycat" manufacturer from using a home-patented process abroad and then importing the end product for sale. As first drafted, the bill would have put a stop to that, but the generic manufacturers argued successfully that they would be prevented from conducting safety tests for their products if foreign suppliers were unwilling to testify before US courts about their manufacturing processes.

The bill as approved does, however, include measures to help inventors working in companies or universities. A new device, the Statutory Invention Registration (SIR), will enable an inventor to stake his claim for patent rights at little cost and without a full patent examination. An SIR would become "prior art", thus preventing a patent claim by a later inventor, and could be upgraded to a full patent later.

Another provision in the bill would alter the definition of prior art to exclude private communications between members of a research team, thus making it easier for team members to claim patent rights. Inventors will not have to work together to be able to claim joint inventorship, and different claims made by different inventors will all be entitled to the benefits of the earliest filing date. The bill would also establish a national commission on innovation and productivity to examine inventors' rights in relation to their employers.

Tim Beardsley

Soviet astronomy

Astrophysics in space

FRANCE is to build a 1-tonne gamma-ray telescope and imaging system to be launched by the Soviet Union aboard an Astron satellite in 1987. The project, which has been under discussion for some time, is covered by a special protocol signed earlier this month in Samarkand during the regular annual meeting of the Franco-Soviet working group on cooperation in space.

The announcement from Samarkand suggests that the name Astron, at present denoting the astrophysical satellite launched on 23 March 1983, is to become the name of a series. The first is basically a Venera-15 backup, stripped of its navigation gear and course-correction motor. The satellite carries an optical telescope (the largest to be orbited so far), an ultraviolet telescope, a spectrometer (produced by the Marseilles laboratory of space astronomy) working in the 1,100 to 3,500 Å range and an X-ray telescope-spectrometer in the 6 to 0.5 Å range. A high apogee (200,000 km) orbit is used to eliminate interference from the Earth's radiation belt and corona.

French participation in Astron-1 is confined to the X-ray study of normal stars and extended surfaces. The more spectacular results have, however, come from the Soviet part of the programme although — in the case of the anomalous behaviour of the X-1 Hercules X-ray signal — the observations were confirmed by the European Exosat satellite. X-1 Herculis is a double star consisting of the visible HZ-Herculis and a neutron star (the X-ray source). In the course of an observation session on 30 July 1983, the X-ray signal was found to have vanished, although visual observations from the Byurakan and Crimean observatories found no significant changes in the optical brightness curve. This suggested that the loss of signal was due to some change in the accretion disc of the neutron star, possibly in the angular distribution of the radiation. During a subsequent observation session on 1 March 1984, the signal was found to be back to normal.

Other surprises have included the anomalous spectrum of 73 Draconis (in which the content of heavy elements (lead, tungsten and uranium) was considerably higher than theoretical predictions and the ultraviolet observations of the double stars SS-Auriga and SS-Andromeda, which indicated that the "hot" components have dimensions only a few per cent of the radius of the Sun. Also unexpected were the results of the occlusion of "fast burster" MXB 1728-34 by the Moon on 16 August, 1983, which suggested that, during the occlusion, the source had emitted constant X-radiation, not the expected sequence of discrete pulses.

Astron is a major research project, involving a number of high-level Soviet institutes. It is therefore not surprising that these results have been given wide publicity in the general Soviet press, which claims every result as a major breakthrough. One newspaper even suggested that the work on 73 Draconis would lead to a greater understanding of the origin of metals.

It is also surprising that there are frequent errors in these popular reports. Thus the "hot" components of SS-Andromeda and SS-Auriga were said to have a temperature of 100,000K (not 60,000K), the lead and tungsten content of 73 Draconis have been described as "100,000 times higher than in the Solar System" and, on one occasion, TASS distinguished itself by locating the Astron telescope not in orbit but at the Byurakan observatory in Armenia. **Vera Rich**

DR César Milstein, one of this year's winners of the Nobel prize for physiology and medicine (see p.601).

US health research

NIH further subdivided

Washington

CONGRESS last week approved a controversial research extension act for the National Institutes of Health (NIH) that creates three new institutes and for the first time sets out policy and general research directives for NIH component institutes. The bill was passed in the face of stiff opposition from NIH, which wanted to retain their existing freedom to set their own research priorities. The director of NIH, Dr James Wyngaarden, fears that the creation of new institutes will only add to bureaucracy and said that NIH will have to "find ways of accommodating" to the bill.

The principal change is the splitting of the National Institute for Arthritis, Diabetes, Digestive and Kidney Diseases into a new National Institute of Arthritis and Musculoskeletal and Skin Diseases and a separate National Institute for Diabetes, Digestion and Kidney Diseases. Part of the reason for the split appears to be the wish of private fund-raising organizations to have their favourite diseases incorporated into the name of an NIH institute. In addition, Congress has voted to create a new National Institute of Nursing: as politicians, congressmen are doubtless aware that few things are so likely to endear them to their electorates as the creation of a new medical institute.

Wyngaarden says the new institutes will create administrative costs without significantly benefiting the target areas: the work proposed for the new arthritis institute, costing $80–100 million a year, is currently being carried out by the existing parent institute. The new act contains no special authorization for new bureaucratic costs. And the proposed research in nursing could best be done through existing mechanisms, according to Wyngaarden. But whatever the frustrations of a Congress that likes to involve itself in research administration, the ever-popular NIH have little to complain about on budget; this year Congress has allocated $5,000 million to NIH, a hefty increase on last year and way above the administration's request. But Congress does seem concerned about the threat of charlatanism. The legislation approved last week formalized for the first time the need for peer review of NIH research contracts and grants, and also requires administrators to set up mechanisms for investigating "substantial" scientific fraud. **Tim Beardsley**

Health ethics

THE House and Senate also agreed last week to establish a Congressional Ethics Advisory Commission to study human genetic engineering and fetal research. The commission, to be modelled on Congress's Office of Technology Assessment, will report on scientific developments to Congress and the public, supported by a 14-strong biomedical ethics advisory committee.

The commission is seen as the US answer to the Warnock Committee in Britain, although it is expected to be more permanent.

Two studies are specifically mandated: whether the stringent federal protections for fetuses are appropriate for research, and the ethical implications of developments in genetic engineering technology that might be applied to humans.

As things stand, NIH are in practice barred from supporting research on *in vitro* fertilization and embryo transfer, and right-to-life ideologues in the administration who ally themselves to the Moral Majority are content to see things stay that way. The creation of the new commission is seen by its supporters as a vital first step towards new policy development.

Tim Beardsley

Acid rain

Parliament in power row

AN almost unprecedented row about acid rain has broken out between the Central Electricity Generating Board (CEGB), the monopoly generator of electricity in England and Wales, and the House of Commons Select Committee on Energy. The board's chairman, Sir Walter Marshall, last week complained that the select committee had "unfairly" pilloried his organization in a report on acid rain published a month ago (*Nature* 13 September, p. 94).

The House of Commons report differs from others on the subject including that earlier this year from the House of Lords, in the directness of its attack on CEGB, which is at one point accused of "ignorance or a deliberate attempt to mislead". That comment was the committee's response to CEGB's argument that forest damage in West Germany is now thought to be caused by ozone, whose formation in the troposphere is stimulated by nitrogen oxides in the presence of sunlight.

Readers of the published report are likely, on reflection, to agree with Marshall that CEGB has been misunderstood, while it also seems that the committee's complaint at the supposed inadequacy of the board's research programme does not assign proper credit for what is being done. Apart from basic research, its board is supporting studies of combustion systems intended to bring reductions of acid emissions of all chemical compositions.

Marshall last week repeated CEGB's position on the steps that could be taken to reduce emissions of sulphur dioxide, saying that "if reducing CEGB sulphur dioxide emissions would solve real environmental problems in the most cost-effective way, we will get on with the job despite the costs". He quoted estimates that the retro-fitting of flue-gas desulphurizing plant to a large generating station might cost £140 million.

According to Marshall's statement last week, the problem of control of nitrogen oxides (NO_x) is different and more difficult. Combustion systems designed to increase thermal efficiency by burning combustible material close to boiler walls will actually increase the production of NO_x, for which reason such a boiler fitted with specially designed burners is to be put in trials beginning in 1986. But CEGB is also planning to carry out trials with a corner-boiler at its Fiddler's Ferry power station. Each experiment will cost about £2 million.

The outcome of the dispute between the nationalized industry and the House of Commons committee is hard to predict. Although the committee seems in part to have reflected a general opinion that "something should be done", it is the British Government and the European Commission that will eventually determine policy.

Marshall himself, who was made a freeman of the City of London last week, is unlikely to be accused of a breach of parliamentary privilege, even though it is customary for people in his position to leave their defence to the appropriate government department. ☐

Health advice

Berkeley goes into business

Los Angeles

DEAR SUBSCRIBER ELECT,

AND NOW THERE IS, AT LAST, AN AUTHORITATIVE NEWSLETTER DEALING WITH THE SUBJECT OF HEALTH AND NUTRITION THAT IS DESIGNED TO KEEP YOU WELL AND MAKE YOU MORE WELL. HOW AUTHORITATIVE? AS AUTHORITATIVE AS THE UNIVERSITY OF CALIFORNIA, BERKELEY, SCHOOL OF PUBLIC HEALTH CAN MAKE IT.

So begins a solicitation recently mailed to two million households throughout the United States to pay $15 a year (soon to be $18) for yet another health publication. But this, according to its promoters, is different.

"Every last word" of each article is approved by the faculty of the Berkeley School of Public Health, says the school's dean, Joyce Lashoff. The faculty's goal in this unusual endeavour, Dr Lashoff says, is to "put current information about health and nutrition in perspective".

In so doing, the School of Public Health stands to make a substantial profit. "They'll do very well", says New York-based publisher Rodney Friedman, who first proposed the idea and raised the venture capital to launch the project. The contract says the school receives 5 per cent of all gross billings, which translates, with regular subscriptions at $18 per year, into $75,000 for every 100,000 subscriptions. The publishers' ultimate goal is to attract 250,000 subscribers, when the School of Public Health would earn more than $180,000 a year for giving its expert opinions and final editing to the newsletter. University of California budgets have suffered cutbacks in recent years, Mr Friedman said, and the public health school will be able to spend the money from its newsletter venture as it sees fit.

The United States market for health and nutrition news seems insatiable. Over 30 magazines and a dozen newsletters publish hundreds of articles each month on how to prevent, cure or cope with illness. Much of the information, according to a recent survey by the American Council on Science and Health, is poor if not dishonest.

The credibility of the Berkeley School of Public Health stands behind the newsletter, participants say. The eight-page publication, called the *Wellness Newsletter*, aims to give specific advice, written in a short, "palatable" format, on how to improve or enhance health.

A few other universities publish monthly health newsletters, but they are said to be disease-oriented and not written for a broad consumer audience. Nor do individual departments profit so directly from the endeavours. Other academic departments in other institutions may want to keep an eye on the California project as a model for increasing budgets to train graduate students and buy equipment, the objectives which the Berkeley School of Public Health has set itself for the disposal of the income it hopes the project will generate.

Sandra Blakeslee

Chip pirates hit

Washington

SEMICONDUCTOR chip manufacturers last week succeeded in their goal of protecting circuit designs against "chip piracy" — unauthorized sale and distribution of a copied device. Congress finally approved a bill that for the first time grants copyright protection for the masks used to manufacture semiconductor circuits.

The United States dominates the chip supply industry, a world market estimated to be worth $16,000 million a year in 1983. The manufacturers' complaint has been that a chip costing millions of dollars to develop can be copied photographically and "reverse engineered" for as little as $50,000, thus denying designers the incentive to innovate. US dominance of the industry has been achieved only through massive research and development efforts: in 1982, average research and development expenditure in the US semiconductor industry amounted to over 10 per cent of sales value, with capital investment over 14 per cent.

Circuit designs, however much careful work they represent, rarely meet the standards of inventiveness needed for patent protection. And, because chips are so easily copied, trade secrecy does not help either. The new bill, the Semiconductor Chip Protection Act, commanded widespread support in Congress and is likely to be signed into law very soon. It provides "mask works" (in whatever physical form) protection against unauthorized copying for 10 years. (Other copyright designs can be protected for up to 100 years.) The bill also breaks new ground in allowing copyright of a utilitarian design; in previous copyright law, only non-functional aspects of design have been covered, a change that appears to have troubled the Copyright Office. The impact on the semiconductor manufacturing industry will be immediate: chip piracy is already big business in some parts of the world.

Tim Beardsley

Israeli aid

Hidden cooperation revealed

Rehovot

AFTER a decade of discreet silence, Israel's programme of scientific and technical cooperation with developing nations has suddenly surfaced. Last month, the International Cooperation Department of the Foreign Ministry announced that Israel had hosted 28,000 trainees from developing countries between 1958 and 1983, and during that same period some 8,500 Israeli experts had worked overseas.

The programme really began in 1957, when Israel helped to create Ghana's Black Star Shipping Line and to organize Ghana's Trade Union Congress. In the years that followed, cooperation flourished on many levels.

During that period, Israel worked not only with national governments but even with some liberation movements, for example training nurses from underground groups in Mozambique and Angola. Although most developing countries cut off diplomatic relations with Israel after the Yom Kippur War in 1973, it now appears that cooperation has continued with most of them, but quietly.

The emphasis of these programmes has always been on agriculture, but experience has shown that transferring technical know-how is much easier than transferring social forms. The so-called "Rehovot Approach" to integrated rural planning, has, however, proved itself in many developing countries. The aim of this approach, taught so far to 1,000 students from 50 countries at the Rehovot Settlement Study Centre, is to make life in rural areas more attractive so as to stem the flood of country people to urban slums.

The seven-month course, four months of which are spent in Israel, concentrates on the creation of new jobs as well as of a network of economic, social and community services. Comprehensive plans have been prepared for the Lampang Region of Thailand, the Neru Region in central Kenya and several places in Latin America. One group of Israeli experts is now working in Fiji on plans for a multipurpose rural services centre and the development of rural cooperatives, in collaboration with no fewer than 20 Fijians who have studied in Israel.

In medicine, Israel no longer provides a full-scale six-year course in medicine for students from developing countries, but instead a one-year course in public health and an MA course in community medicine. Much of the effort is concentrated in ophthalmology, as the result of which a dozen African countries have advanced eye clinics. Feasibility studies are first carried out by Israeli physicians; local doctors and nurses are brought to Israel for specialized training and, finally, expatriate Israelis are seconded to this clinic for a couple of years.

As might be expected in a country with enormous financial problems, there are people in Israel who question the wisdom of spending money on cooperation with nations which often do not have diplomatic relations with Israel, and which regularly vote against Israel in the United Nations. Mr Johanan Bein, director of the Foreign Ministry's International Cooperation Department, is philosophical. He says that the total cost of the programme is not large and that more than half of Israel's costs are borne by other countries, mainly in Western Europe, which sub-contract work in fields such as arid-zone agriculture.

Bein also notes that a few African countries, including Zaire and Liberia, have recently re-established diplomatic relations, and that in others without formal links, such as Nigeria, the Ivory Coast and Ghana, Israeli companies are now involved in development programmes much larger than the Israeli Government could have mounted. There are also hopes of a further political payoff, illustrated by the fact that among the 13,000 students from 100 nations who have participated in labour studies programmes run by Israel's General Federation of Labour, there are now 37 secretary-generals of union federations, 300 chairmen or secretary-generals of individual unions, over 150 members of parliament and several dozen ministers, including three prime ministers.

Politics apart, there is also a sense of mission. Forty years ago, chemist Chaim Weizmann, due to become Israel's first president, was corresponding with Maung Kyi (deputy secretary of the Burmese National Planning Department) and with a number of Indians, including Jawaharlal Nehru, about possible scientific cooperation between the Jewish State on the one hand, and India and Burma on the other. Even at the lowest point in relations between Israel and the governments of developing countries in 1973, when most of her long-time friends had turned their backs on her, Golda Meir, then prime minister, said that political disagreements were "no excuse for disowning or belittling . . . an attempt on the part of one country to better human life in other countries". **Nechemia Meyers**

Israelis visiting China

Rehovot

AMBIGUITY continues to attend the status of Israelis making scientific visits to the People's Republic of China. So much is clear from the experience of Dr Smil Ruhman, professor at the Weizmann Institute, at the First International Conference on Computers and their Applications in Beijing this summer.

Although Ruhman was an invited speaker listed (with his affiliation) on the programme, he notes that Israel was not listed among the overseas countries participating in a report on the conference published in the *China Daily*. Technically, this may have been correct, because Ruhman entered China on a US passport, having dual nationality.

Others, such as Mordhay Avron, have been less fortunate. Invited by the organizers of the 11th International Seaweed Symposium to give a talk at Qingdao in June 1983, and listed in the official programme, Avron was told to apply for a visa in some country with which China has diplomatic relations. In the event, he was told by the Chinese Embassy in the United States that a visa could not be issued there and, eventually, by the conference organizer, Dr Tseng, that the invitation to speak was conditional on possession of a visa.

Ironically, Ruhman has returned from China brimming with enthusiasm for the opportunities for collaboration, in which, he says, Israel has some distinctive developments to offer the Chinese. He, like many others, hopes that Chinese policy on passports will change. Nechemia Meyers

Democratic elitism

CHINA, as part of its policy of reversing the anti-intellectual attitudes of the Cultural Revolution, has inaugurated a scheme of state awards for "the promotion of scientific and technological advances". State prizes for science are a feature of most socilist societies, but the Chineses regulations, promulgated last month, contain a unique feature — the decision of the adjudicators is not final.

According to the recommended procedure, the names of the winners chosen by a special examination committee must be published at least three months before the awards are conferred. Complaints against the winners may be lodged within that period. Such complaints will then be investigated by "appraisal units", who will then report back to the examining committee for a final decision. If no complaints are sustained, the winners will receive their prizes.

There are three classes of award, each consisting of a citation and medal together with a sum of money (15,000 yuan — £5,000 — for a first class award, down to 5,000 yuan for a third class). Provision is also made for a "special-class" award, of greater (but unspecified) monetary value, for a "scientific and technological advance that makes special contributions to socialist modernization".

In the case of joint achievements, the cash is to be divided "rationally" according to the contributions of individual team members to the project, with those who made greater contributions getting the greater rewards. "It is impermissible", the regulations warn "to practise egalitarianism." • Vera Rich

In defence of CERN

SIR — May an observer well acquainted with US and European particle physics comment on the report of social scientists Ben Martin and John Irvine on the achievements of CERN, the European High Energy Laboratory in Geneva (*Nature* 6 September, p.4)? I find this report unfairly biased against CERN.

When European high-energy accelerator research on a large scale began in 1960, CERN was a completely novel social experiment. There was almost no tradition of "big science" in Europe, and no experience of international scientific management. Nevertheless, within less than 24 years, CERN had developed into the world's leading laboratory in this field.

Why then do Martin and Irvine consider CERN's performance disappointing? They concentrate their attention on sensational peak discoveries, in which respect CERN has contributed only in recent decades. But science does not consist of discoveries that make headlines in newspapers. The bulk of science consists of a broad front of painstaking investigations, leading to ever deeper insights. They are the soil from which striking discoveries can develop. In this respect, CERN has made many contributions to which Martin and Irvine give only passing attention.

It is true that some of the peak discoveries, in particular the so-called *c* (charm) and *b* (bottom) quarks, could have been found at the intersecting storage rings (ISR) at CERN. Other "sensational" discoveries, the violation of parity, the Ω-minus and the two types of neutrinos, which CERN is blamed for missing, were made in the United States before or at a time when research had barely started at CERN. But even if one insists on counting the lucky events of that type, CERN did not fare so badly during the second half of its research period. It discovered a new form of radioactivity, the so-called neutral currents, the well-advertised quanta of the weak interaction and probably a sixth quark (*t*, for top) as well.

Martin and Irvine ascribe the latest achievements to a recent change of spirit due to the present director. It is true that Herwig Schopper vigorously supported the last phases of the conversion of the super proton synchrotron (SPS) as a proton–antiproton collider, and the subsequent successful research. However, Martin and Irvine do not seem to appreciate that the conversion of an accelerator and the preparation of such giant experiments take much longer than the three and a half years of Schopper's directorship. The daring spirit and the technical inventiveness that have led to these achievements date from much earlier times. They are a proof of the opportunities given to individual scientists, which Martin and Irvine consider to have been too restricted at CERN. They also show a steady growth of this institution towards its present world supremacy, that started long ago.

The comparison with Fermilab in the United States is unfairly presented. True enough, several great discoveries were made at that laboratory, such as the existence of a fifth quark. But it was the CERN accelerator that was able to produce sharp and intense muon and neutrino beams with which the so-called structure functions of protons and neutrons were determined with astounding accuracy. Moreover, the important "EMC-effect" was discovered, which has led to a new view of the role of quarks in the atomic nucleus. One of the main purposes of those accelerators was the production of usable secondary muon and neutrino beams, in which CERN was much more successful than Fermilab inspite of the latter's four-year lead. Why do Martin and Irvine not appreciate these successes? Why do they consider them to be dull physics?

CERN's contributions to the physics of nuclear structure are almost completely neglected in Martin and Irvine's report. CERN has the most advanced isotope separation device (Isolde) attached to its synchro-cyclotron, where many new unstable nuclei have been discovered and studied. Recently, a low-energy source for antiprotons was constructed (LEAR) which provides unique opportunities for the study of antiproton interactions.

The success of CERN is based to a large extent upon a circumstance that has been a surprise for people who have observed the development of physics in the past half century. The United States was assumed to the superior in engineering and instrumentation, as demonstrated by the development in the 1930s of cyclotrons, synchrotrons, linear accelerators, bubble chambers and so on. But the quality of the engineer-physicists at CERN turned out to be at least as high. They succeeded in constructing accelerators of unusual reliability and flexibility under the leadership of the late Sir John Adams. Some have ascribed this to over-conservative design, but it helped greatly in the exploitation of the machines. Thus it allowed the luminosity of the intersecting storage rings to reach more than ten times the design value, and it facilitated the production of the intense muon and neutrino beams. Finally, it made possible the fast conversion of the 400 GeV accelerator into a proton–antiproton collider, the success of which hung on one of the imaginative devices invented and implemented at CERN by Simon Van der Meer — the so-called stochastic cooling of the antiproton beam, destined to be used in future colliders everywhere in the world.

Furthermore, CERN engineer-physicists led by Kjell Johnson constructed the intersecting storage rings at a time when laboratories in the United States did not dare to take on this difficult task. CERN designed and built the first two colliders for protons, the ISR and the proton–antiproton collider in the SPS tunnel. The effect has been to pioneer a new style of experimentation which has now been taken up by other centres of particle research all over the world. CERN continues the tradition with the large electron–positron collider LEP.

The Martin–Irvine report does not make much of these achievements and also all but ignores the many new ideas for instrumentation spawned at CERN, such as the multiwire proportional chamber and the vacuum ultraviolet imaging device. Both innovations are not only significant advances in detecting particles, but have important applications in medicine and in other sciences.

High-energy physics is an international endeavour, more so than most other scientific activities. There is a constant exchange of physicists and engineers between CERN, the United States and other countries. It does not make much sense to consider progress in this field as a competition between two continents. It is a collective achievement of all participating nations. The CERN effort has contributed essential ingredients. Particle physics would not be what it is without CERN's impetus, without its technical innovations and without its studies and discoveries, even if some of them have not made newspaper headlines.

Last and by no means least, CERN represents the United States of Europe in fundamental physics. It became an active symbol of the spirit of European unity. That is no mean achievement. It serves as the University of Europe for high-energy physics, and brings together the many individual universities in Europe in scientific collaborations of unprecedented magnitude and complexity often involving also universities and institutes of the United States, Eastern Europe and Asia.

In spite of the obvious difficulties which such international collaborations entail, CERN has developed into the foremost high-energy laboratory of the world, as is strikingly confirmed by the recent US panel report on New Facilities for the US High Energy Physics Program, in which it was stated that "the European facilities frequently provide a better level of support and/or a larger number of opportunities than the American equivalents".

How can such an institution be given "Poor Marks for Enterprise"?

VICTOR F. WEISSKOPF

Massachusetts Institute of Technology,
Cambridge, Massachusetts 02139, USA

Victor Weisskopf was director of CERN from 1961 to 1965.

SIR — Robert Walgate's enthusiasm (see *Nature* 6 September, p.4) for the assessment of CERN carried out by two social scientists from Sussex, Irvine and Martin, is misplaced. Most would agree with one conclusion reached by Martin and Irvine, that since the end of the 1960s CERN has been either the leading or next to leading laboratory in the world of particle physics. But their claims to have developed a powerful new tool of assessment in scientific research are exaggerated and their use of it is misleading.

Originally, Martin and Irvine advertised their method as one of "converging partial indicators", based on the questionable assumption that if a variety of uncertain measures appear to agree, the result is reliable. Having applied this method to CERN and found that the indicators do not converge, they nonetheless continue by "interpreting" the non-convergence. Here they rely on an opinion poll of physicists, so the new method boils down to a peer review interpreted by social scientists.

The authors base their main conclusions on a selection of so-called "crucial" experiments. This is hardly the way a serious history of the extraordinary progress in particle physics over the past ten or fifteen years will eventually be written. Such an approach traps the unwary into supposing all other results are negligible, and is a travesty of the basis on which scientific understanding advances. CERN is given credit for the discovery of the weak neutral current, which opened the door for the Glashow–Salam–Weinberg unified theory of the electromagnetic and weak forces and set the stage for much of what has followed. But this discovery did not win a place in the "top eleven" selected by citation analysis.

The method clearly fails seriously in not giving proper weight to several other CERN results of fundamental and lasting importance. For example, experiments at the intersecting storage rings discovered that the strong interactions of the proton are due to point-like constituents; deep inelastic neutrino experiments showed that the weak interactions of the proton also involve point-like "partons" and, when put together with the electron scattering results from the electron linear accelerator (SLAC) at Stanford, demonstrated that the partons are quarks. High-energy neutrino experiments found departures from point-like scattering of a kind attributable to the effects of the quark–quark forces, providing early support for quantum chromodynamics, the now established theory of the strong interaction.

Nevertheless, it is an accepted view that over the decade 1969 to 1978, US laboratories would have appeared more often in a list of top experiments than Europe. Why? Because Martin and Irvine have set themselves the objective of judging CERN, they have no device but to attribute this difference in performance to some inadequacy of managements and physicists at CERN. Unsupported by evidence, they even attribute what they regard as CERN's poorer performance to its being an international laboratory with scientific advisory commitees accountable to national interests. Anyone with the slightest acquaintance with the ways CERN's scientific programme is handled knows there is no such interference; in making this inference Martin and Irvine display such a total ignorance of how CERN actually works that it must invalidate any other conclusions they reach.

With all their great effort of hindsight, Martin and Irvine are yet blind to the single most significant factor in the Europe-United States comparison in the 1970s: the electron-positron collider (SPEAR) at Stanford, together with SLAC, was responsible for the major part of the difference in score on which they hang their case. All will agree that SPEAR was, supremely, the best type of machine for the physics of the 1970s; once this factor is allowed for, the differences are not significant.

No doubt, in retrospect, some decisions of the CERN management and actions of some physicists if differently made could have led to greater success. But this can be said of most scientific endeavours — including those in the United States. What Irvine and Martin seem unable to understand, and what makes their analysis so misleading, is that in research of this nature, until the experiments are done, noone knows which is the best choice. This is why the "methodology" of Martin and Irvine could not have predicted the remarkable success of Stanford in the 1970s.

The authors conclude that after the 1970s, CERN's performance has improved. We are given no "explanation" for this, which the analysis of the preceding years would not have foretold. Their naivety makes any views they express irrelevant to the assessment of any future enterprise such as LEP.

J.H. MULVEY

University of Oxford,
Nuclear Physics Laboratory,
Keble Road,
Oxford OX1 3RH, UK

Mental arithmetic

SIR — I was surprised to read in David Singmaster's review[1] of Steven B. Smith's book, *The Great Mental Calculators*, that the mental calculation of the square root of 51 is considered to be so difficult.

I have just calculated the answer to be 7.14142842854216; the last two digits should be 85 I believe. To perform this calculation I have to write down the number (in fact 510,000,000,000 is easier, giving the required answer $\times 10^5$), and also write down and see my growing answer. I have been able to do this for quite some time, but have not developed the capacity, it being of somewhat limited use!

To calculate 1/97 to 96 decimal places, another example given by Dr Singmaster, seems quite easy, and I can multiply three-digit numbers in my head (again, provided they are written down), with a fairly high success rate. From these examples, I could match Alexander Aitken, one of the prodigies cited in the review, but not George Bidder. Indeed I have never thought in terms of logs, as did Bidder — Taylor or Maclaurin series presumably? However I would think that compound interest calculations could be achieved fairly easily by use of suitable binomial coefficients.

As a postdoctoral biochemist I rarely have any call to use such mathematical abilities. But I am astounded that they are thought to be so rare.

BRIAN COOPER

c/o Department of Medicine,
University of Bristol,
Bristol Royal Infirmary,
Bristol BS2 8HW, UK

1. *Nature* **310**, 79 (1984).

Animal rights

SIR — In his article "Animal rights lobby cashes in" (*Nature* 13 September p.95) Marcus Chown points out that it is more than a year since the Government White Paper on animal experiments appeared. Neither in your article nor in recent articles and letters in *The Times* is mention made of certain wording relating to pain which I believe may be responsible for misunderstanding and anxiety. Mr Chown quotes the present rule "if an animal is found to be suffering severe pain which is likely to endure, it shall at once be killed". That is not unfortunately the whole story. Every licence to experiment on living animals carries a list of conditions. The passage quoted is from paragraph 3(b) of these conditions. 3(a) states that if an animal is suffering pain which is either severe or is likely to endure, and *if the main result of the experiment has been attained*, the animal shall forthwith be painlessly killed (italics mine). It is this which gives rise to problems and leads those of a suspicious mind to say that there is always a let-out. An experimenter faced with the loss of valuable experimental material might be tempted to hang on for a few more days until the experiment has been completed, with consequent suffering. This wording must be clarified. An important purpose of future legislation must be to allay public suspicion or disquiet and there must be no suggestion of an easy escape. Paragraph 3(c) of the conditions states that if an Inspector believes that an animal is suffering "considerable" pain he can direct it to be painlessly killed. We thus have pain described as "severe" and "considerable". Since it is impossible to give a clear definition of pain in animals, these terms are of doubtful value. Nevertheless the more moderate animal welfare organizations are right on insisting on some clarification of the "pain condition" and some attempt to balance possible suffering against possible benefits is not unreasonable.

R. BARER

Department of Anatomy and Cell Biology,
University of Sheffield,
Sheffield S10 2TN, UK

Prizes (at last) for immunology

This week's Nobel prize comes less than 10 years after monoclonal antibodies, already produced commercially as diagnostic reagents. But in that decade, immunology has been transformed.

SOME Nobel prizes are inevitable, the only question being when the nomination will rise to the top of the pile. This year's prize for César Milstein must have been close to the top for at least three years. Nor does it come as any great surprise that Georges Köhler is the second of the three winners of this year's prize for Physiology and Medicine, for he and Milstein jointly discovered the principle of producing monoclonal antibodies. Less predictable is the third winner, Niels Jerne. But to immunologists, Jerne is the great man of influential ideas.

Köhler and Milstein published their paper on "Continuous cultures of fused cells secreting antibody of predefined specificity" in August 1975 (*Nature* **256**, 495). It described how the fusion of a single lymphocyte-secreting antibody with a single bone marrow tumour (myeloma) cell resulted in a hybrid cell with the antibody-producing capacity of the lymphocyte and the immortality of the malignant cell. Their antibody-producing cells came from the spleens of mice immunized with red blood cells from sheep, so that the fused cell lines (hybridomas) each secreted an antibody directed against the sheep cells. Köhler and Milstein emphasized that they could not tell whether similar results would be obtained with other antigens but, obviously believing they could, finished their paper by saying: "It is possible to hybridize antibody-producing cells from different origins. Such cells can be grown *in vitro* in massive cultures to provide specific antibody. Such cultures could be valuable for medical and industrial use."

They were right. Specific antibodies, now known as monoclonal antibodies, are an essential tool of much biomedical research and are of great commercial and medical value. The therapeutic use of monoclonal antibodies is still at an early stage, but they are already invaluable aids to diagnosis and screening. A good example is in blood grouping, where hybridomas established by Milstein are now the basis for the production of monoclonal antibodies on a sufficient scale to replace human sera in ABO blood typing in the United Kingdom.

César Milstein was born in Argentina in 1927, and was on the staff of the Instituto Nacional de Microbiologica in Buenos Aires until 1963, taking time out to obtain a PhD at Cambridge in 1960 as a British Council Fellow. In 1963, he left Argentina to join the staff of the Medical Research Council Laboratory of Molecular Biology in Cambridge, where he has been ever since. He now heads the Protein and Nucleic Acid Chemistry division, which he previously co-directed with Dr Fred Sanger — twice a Nobel Laureate, now retired.

Milstein has always worked on the structure, genetics and evolution of antibody molecules. Perhaps the best known of his "pre-monoclonal" papers is that in *Nature New Biology* **239**, 117; 1972, which demonstrated that the light chain of antibodies is first produced as a larger precursor molecule, whose extra sequence serves as a signal for the process of attachment to, and secretion through, the lymphocyte membrane, during which it is cleaved off. This was probably the first firm evidence to support the signal sequence hypothesis of Blobel and Sabatini.

In 1974, Georges Köhler, then a 27-year-old West German at the Basel Institute of Immunology, obtained an EMBO grant to work at Cambridge with Milstein. His chief interest was the development of antibody-producing cell lines to allow the analysis of the rates of mutation of their antibody genes and so to study the role of somatic mutation in the generation of antibody diversity. It was not by design that monoclonal technology emerged from this research, and the relative contributions of Köhler and Milstein to the discovery is a matter of controversy. The pair have shared some minor prizes, but both the Wolf prize (an Israeli's answer to Nobel) in medicine and the Sloan prize of the General Motors Cancer Research Foundation went to Milstein alone. The Nobel committee has obviously decided that Köhler played a substantial part in the discovery. Köhler returned to the Basel institute in 1976, becoming a permanent member in 1980; he has maintained his interest in the mechanism of antibody diversity. Next March he becomes co-director of the Max Planck Institute of Immunology in Freiburg.

When Köhler returned to Basel it was still under the direction of Niels Jerne, the founding director of the Basel Institute of Immunology, from which he retired in 1980. Jerne was born in Denmark in 1911, started life as a student of physics but soon switched to medicine. From 1943 to 1956 he was at the Danish State Serum Institute and there began his studies on antibodies. He had spells of a few years in Geneva (for the university and World Health Organization), as a visitor at the California Institute of Technology, at the University of Pittsburgh and as director of the Paul Ehrlich Institute in Frankfurt. Technically, his most important paper of that period is probably the description of the plaque-forming assay (*Science* **140**, 405; 1963), a test that allows the quantitation of antibody-producing cells of a particular specificity among a mixed population.

In 1969 when Hoffmann-La Roche founded the Basel Institute of Immunology, Jerne became its first director. During his tenure as director, he became ever more widely acknowledged as the father of several influential, if not always correct, ideas in immunology. In particular he was involved in the theory of antibody selection by antigen — the doctrine that antigens do not instruct the immune system to manufacture new antibodies, but rather select the relevant antibody-producing cell from a pre-existing pool.

Jerne's network theory of immunology, an outcome of his analytical approach to a subject bedevilled by murky observations and operational definitions, was at its most influential about a decade ago. It was based on the fact that antibodies can themselves serve as antigens, Jerne postulated that any antigen would set off a train of events, with each antibody acting also as an antigen and thus linking cells of the immune system in a network since their antigen-binding sites were almost certain to recognize one of the antibodies produced in the course of the response. But in spite of strong experimental evidence in support of the network theory, it remains difficult to determine whether the regulation of most immune responses is substantially controlled in this way.

This year's prizes will be thought well deserved. They will be seen as further justification of the British Medical Research Council's support of basic research at its Laboratory for Molecular Biology in Cambridge. Milstein joins Aaron Klug, Francis Crick, James Watson, Max Perutz and John Kendrew as well as Sanger (twice), whose work at Cambridge brought them a trip to Stockholm. The prizes will also no doubt be seen in certain quarters as a justification of Hoffmann-La Roche's wisdom in founding a basic research institute. But above all this year's Physiology and Medicine prize demonstrates how theory, experiment, curiosity and serendipity can produce not only great scientific insight but what is certain to turn out to be tremendous benefits to mankind.

Peter Newmark

Mineralogy

A continent in a grain of sand

from Bruce W. Sellwood

FOR well over sixty years the abundance, identities and assemblages of minerals in sandstones have been used in the determination of sediment provenance in order to reconstruct the geography, climate and geology of sediment source terrains of the past. Recently, it has been realized that sandstone composition is to a large degree also governed by plate tectonics. Provenance studies of modern sedimentary systems have previously been carried out on the scale of individual basins, but not for a whole continent. Now on page 645 of this issue, Potter describes the mineralogy of sands from the beaches of South America, and interprets it in terms of the palaeotectonics of the continent.

In ancient systems, the petrography of sandstones has been used in the interpretation of the geotectonic regimes of depositional basins, such as a passive continental margin or a fore-arc basin, and of source areas,despite the fact that sand is recycled from older sandstones. Geotectonic interpretations rely heavily on observations and assumptions of the probable composition of typical terrestrial terrains. It is argued that quartz-rich sediments are associated typically with passive continental margins and that quartz-poor sediments are mostly of volcanic origin in magmatic arcs. Sediments of intermediate quartz content are generally believed to be associated with active continental margins and orogenic belts while arkosic (feldspar-rich) sands are often derived from uplifted basement rocks adjacent to rifts and wrench faults. Other factors, such as climate and the length and vigour of streams, are considered to tune the ultimate composition of deposited sands.

The validity of these palaeotectonic models can be tested only in terms of large-scale modern investigations and this is the significance of Potter's study. He chose South America because it has a well-developed active margin on its west coast, a passive margin on its east coast, with transcurrent motions affecting only the Caribbean border zones. Although lacking significant continental glaciation it exhibits major climatic belts lying transverse to the Andes. Potter's is the first report on the petrography of sands from within the same environmental regime (beaches) around an entire continent and thus is highly significant, even though the results come from only about 200 samples.

Much of the sediment arriving on continental beaches is derived from rivers and Potter argues that its mineralogy is likely to have been extensively modified by abrasion. Furthermore, if the mineralogy of beach sands closely relates to the tectonic setting of adjacent land areas, then that of the local river sediments is likely to be even more closely related. The results of the study confirm the predictions of earlier workers (for example, Dickinson, W.F.R. & Suczek, C.A. *Bull. Am. Ass. petrol. Geol.* **63**, 2164; 1979). On its leading margin (the Pacific coast), quartz comprises only 19 per cent of the mineral and so is subordinate to rock fragments and feldspar, while on the trailing margin (Atlantic coast) it comprises, on average, 96 per cent of the mineral, even where mountains of Precambrian crystalline rocks border the coastline.

Some anomalous patterns exist, however, indicating that results from ancient sequences must be interpreted with some caution. Although sited on a trailing margin, the Argentine coast from Rio de la Plata to Tierra del Fuego has an Andean (leading-margin) composition, being dominated by volcanic rock fragments. This is partly because Pategonia is too narrow to allow abrasive processes to be completed and partly because the coastal bedrock is itself immature young sediments recently derived from the rising Andes.

This work thus confirms the view that the detrital mineralogy of ancient sandstones may be used successfully in the reconstruction of palaeoplate settings.

Although the predicted patterns of mineralogical provinces are generally confirmed in the study, further questions need to be answered. For example, what subtle effects does climate have on the rate of degradation of certain types of rock and mineral species during transport? In what way does the interaction between relief, transport distance and rainfall favour either the elimination or preservation of unstable grains? And to what extent do the boundaries between mineralogical provinces coincide with major physiographical features such as large river mouths?

Potter's study is merely a first step, doing for grains on a continental scale what clay mineralogists have already done for mudrocks on a global scale (Griffin, G.M., Windom, H. & Goldberg, E.D. *Deep Sea Res.* **15**, 433; 1968). As Potter observes, if his models stand up to further scrutiny, the next stage will be deduction of sand composition over all types of environment of an entire continent (or palaeocontinent). Because the depositional maturity of sediments is a key factor in their behaviour during burial, predictive models based on studies such as Potter's bear directly on the assessment of regional porosity and permeability trends in hydrocarbon reservoir rocks. ☐

Bruce W. Sellwood is a Lecturer in Geology at the University of Reading, Whiteknights, Reading RG6 2AB.

Astronomy

Nemesis for Nemesis?

from Mark E. Bailey

LAST spring, great interest and excitement were generated by the idea that a hypothetical companion star of the Sun, called Nemesis by some, could trigger the periodic sequence of extinction events found in the fossil record[1-5]. Now, only six months later, another collection of papers on the same subject (see pages 635-642) gives what amounts to a considered reflection on the model.

Interest in Nemesis began about a year ago[4], following the claim by Raup and Sepkoski to have identified a regular 26-Myr periodicity in the fossil record, with a confidence level of better than 99 per cent. The evidence that the sequence of events was periodic was further strengthened by an independent analysis of the cratering record[3], which produced a period and phase for the cyclicity agreeing with that of the fossil record. These arguments for strict periodicity in the geological record can be challenged at a number of points[5], although the independent evidence for rough periodicity as, for example, in the sense that the solar sunspot cycle is 'periodic', is probably less easily denied[6-8].

But if the cratering and extinction record is strictly periodic, which will be settled only by further detailed research on the geological front, it is clearly important to devise explanations, and this is the spirit in which the Nemesis proposal was made. Thus, it was argued, the orbital period of the hypothetical companion should give the strict periodicity required, while its gravitational influence on the comets in a hypothetical dense inner core of the Oort cloud might produce periodic comet showers in the manner outlined by Hills[9]. The further possibility that Nemesis (or Planet X) might show up in the Infrared Astronomical Satellite data also gave piquancy and a certain urgency to the debate.

In the papers published in this issue of *Nature*, the Nemesis proposal is extended and shown, in fact, to be quite incapable of producing the strictly periodic sequence of extinction events for which it was originally designed. The stability of the orbit has been investigated by Torbett and Smoluchowski[10], whereas Hills[11] and Hut[12] show in particular that when stellar perturbations and the overall tidal field of the Galaxy are included, the orbital period should drift towards larger values by about 15 per cent or more over the 250-Myr time scale considered by Raup and Sepkoski. The probably dominant effects of giant molecular cloud perturbations would further reinforce this conclusion, and cast serious doubt on the likely survival of such a solar companion for the age of the Solar System[10,13]. Of course, it is conceivable that the star might have been recently captured or scattered to its present orbit from a more tightly bound state with much shorter period, but these suggestions beg many questions. In any case, as shown by Hut[12], it appears that the Nemesis proposal — if correct — does not predict a constant interval between extinctions. A re-analysis of the fossil record may agree with this new prediction[2], but this has not yet been carried out.

The alternative, that extinctions are quasi-periodic, was explored last April in two papers[14,15] and is now reviewed in detail by Clube and Napier[13], who argue strongly against the Nemesis proposal and come down in favour of a galactic connection, as they have advocated for some time[6,7,16].

In view of these developments, one might possibly be excused for regarding this episode of hypothesis followed by near-retraction as yet another example of the explosion in the volume of the literature, and of the over-rapid publication of speculative ideas. Previous commentaries[4,5] already hinted at this, and it is therefore perhaps not wholly out of place to consider the point further. Although some cynicism is doubtless justified and can easily be understood, to hold such a view exclusively is, in my opinion, to miss the point. It is often the case in astronomy, and no doubt other subjects, that the various pieces of a puzzle can be assembled in a number of ways and still explain the same data. Indeed, it is an important part of a theorist's job to do just that, and provided the proposed hypotheses take all the facts into account and are not obviously so contrived as to be subject to Occam's razor, the more possibilities the better. This in spite of the reality that no more than one can be true. Science often progress by mistakes and it is therefore too easy simply to dismiss speculative suggestions as a kind of non-science.

In the present case, the argument for Nemesis causing mass extinctions is indeed highly speculative since it assumes the existence of the star, the presence of a dense inner core to the Oort cloud, the regularity of the extinction cycles and the possibility that impacts trigger extinctions. Yet whatever the final decision about the existence of the star, the benefits of the suggestion have already outweighed any temporary nuisance or adverse reaction it may originally have caused. For example, the shape of the Oort cloud and the stability of comet-like orbits under the perturbing action of passing stars, gas clouds and the Galaxy, are crucial to an understanding of cometary origins. Moreover, the papers now published have a clear connection with studies of binary stars and of their long-term orbital stability, while the connection between these kinds of problem and studies of open star clusters has already been noted[17].

On the geological front, I am less qualified to judge, but if the Nemesis saga has served only to increase general awareness that cometary impacts may frequently occur, then it will have been beneficial. Ten years ago the idea was hardly considered, and even last year, at the Brighton meeting of the British Association for the Advancement of Science, it was dismissed. Yet the most conservative Oort cloud model predicts some cometary impacts, and presumably they do have some influence worth exploring.

Finally, if the extinction sequences should somehow be shown to be strictly periodic, it may be worth noting that there is already a new variant on the Nemesis theme[18] — in which comet showers are still predicted to be periodic. To mix two metaphors, though there may be smoke without fire, perhaps even the darkest clouds have silver linings. ☐

1. Whitmire, D.P. & Jackson, A.A. *Nature* **308**, 713 (1984).
2. Davis, M., Hut, P. & Muller, R.A. *Nature* **308**, 715 (1984).
3. Alvarez, W. & Muller, R.A. *Nature* **308**, 718 (1984).
4. Maddox, J. *Nature* **308**, 685 (1984).
5. Hallam, A. *Nature* **308**, 686 (1984).
6. Napier, W.M. & Clube, S.V.M. *Nature* **282**, 455 (1979).
7. Clube, S.V.M. & Napier, W.M. *Q. Jl. R. astr. Soc.* **23**, 45 (1982); *Earth planet. Sci. Lett.* **57**, 251 (1982).
8. McCrea, W.H. *Proc. R. Soc.* **A375**, 1 (1981).
9. Hills, J.G. *Astr. J.* **86**, 1730 (1981).
10. Torbett, M. & Smoluchowski, R. *Nature* **311**, 641 (1984).
11. Hills, J.G. *Nature* **311**, 636 (1984).
12. Hut, P. *Nature* **311**, 638 (1984).
13. Clube, S.V.M. & Napier, W.M. *Nature* **311**, 635 (1984).
14. Rampino, M.R. & Stothers, R.B. *Nature* **308**, 709 (1984).
15. Schwartz, R.D. & James, P.B. *Nature* **308**, 712 (1984).
16. Clube, S.V.M. & Napier, W.M. *Mon. Not. R. astr. Soc.* **208**, 575 (1984).
17. Wielen, R. in *IAU Symp.* **113**, (in the press).
18. Whitmire, D.P. & Matese, J.J. *Nature* (submitted).

Mark Bailey is in the Department of Astronomy, University of Manchester, Manchester M13 9PL.

Behavioural ecology

Optimal foraging theory tested

from Jared M. Diamond

A KEY postulate of behavioural ecology is that animals practise 'optimal foraging'. That is, animals forage for food in a way that maximizes some function such as the rate of energy gain[1,2]. A paper by Carpenter *et al.* describes an ingenious experiment designed to test the theory of optimal foraging[3].

Consider the territory size of an animal attempting to maximize its daily net energy gain. Optimal foraging theory argues that a territory yields benefits (especially food resources), which increase in proportion to territory size up to a ceiling set by an individual's food-processing abilities or time constraints. An increase in territory size also incurs increased costs of travel time and territorial defence against intruders. Supposedly, individual energy-maximizing animals can both assess and achieve an optimal territory size at which the difference between the benefits and costs represents a maximal rate of energy intake.

While much animal behaviour is roughly consistent with this view, it has proved very difficult to devise quantitative tests of the optimality principle in the field. A suitable test would require measuring an animal's rate of net energy intake (approximated by its rate of weight gain) as a function of the parameter putatively optimized (for example, territory size). One could then examine whether the rate of weight gain does peak at intermediate territory sizes, and whether individuals adjust territory size towards this optimal value.

How could one perform such a test? Periodically capturing a wild animal to weigh it has the obvious drawbacks that one can rarely count on capturing an individual at fixed intervals, and the disturbance associated with capture is likely to influence the results. The ideal solution would be to induce an animal to weigh itself repeatedly. It is this task of persuasion that has recently been achieved by F. Lynn Carpenter, David C. Paton and Mark A. Hixon, working with rufous hummingbirds (*Selasphorus rufus*) of western North America[3].

Like most other migratory hummingbird species, the rufous faces severe energetics problems. In July and August of each year the birds migrate at least 3,000 km south, along mountain ranges, from their breeding grounds (Oregon to Alaska) to their wintering grounds in southern Mexico[4]. To fuel their flight, these 3-g birds stop en route, defend feeding territories and gain at least 1.5 g of fat in 1–2 weeks before resuming migration. At this season, migration in the mountains is risky: rain, hail and wind often prevent feeding, destroy the flowers that serve as nectar sources and even endanger the birds themselves. Thus, individuals should be selected to make few stops, and to fatten up quickly and maximize daily net energy gain while on stopover, so as to complete the migration as quickly as possible.

In order to obtain exclusive access to the nectar of flowers[5,6], hummingbirds engage in two types of fierce competition for territories. First, territory-owning hummingbirds spend much time and energy driving off intruding hummingbirds and sometimes bees, hawkmoths and butterflies which drink the same nectar ('interference competition')[7]. Second, territory holders start off each day by depleting the nectar in the flowers at the periphery of their territories[8]. Since intruders mainly try to rob peripheral flowers and return to sites where they were previously successful, early-morning peripheral foraging by the territory owner spoils the territory for intruders ('exploitation competition').

In 1979, Carpenter and her colleagues tested a model of optimal territory size[9] by covering half the flowers in a hummingbird's territory with plastic bags[10]. They found that within one day the bird increases its territory size to maintain the original number of defended flowers, and then abandons the extra area when the bagged flowers are unbagged on the next day. This experiment shows that the benefit gained from territory size is control of food, and that hummingbirds are capable of measuring their nectar intake or nectar resources. The experiment does not assess, however, whether the preferred flower supply is optimal, as defined by maximization of weight gain.

In 1980 the following direct test was devised. A hummingbird spends about 75 per cent of each hour quietly perched on one or two preferred twigs while clearing its crop of nectar between foraging bouts. Carpenter and colleagues replaced these twigs with a Pesola spring balance, modified to carry a perch on top and to function by being depressed from above rather than stretched from below. The bird accepted this perch, thereby enabling Carpenter *et al.* to sit with a telescope outside the territory boundaries and periodically read off the bird's weight to ±50 mg. In 1982 the spring balance was exchanged for a Mettler electronic balance whose pan had been replaced by a perch. With the resulting weighing accuracy of ± 10 mg, the biologists could detect a hummingbird's weight gain in a single foraging bout or its weight loss on defaecation.

As an example of the results, consider bird WP, who was first observed on 23 July as a lean individual weighing 3.1 g. On 27 and 28 July WP had a relatively small territory containing 1,970 flowers and gained weight at the low rate of 0.10–0.15 g per day. On 29 July WP nearly doubled its territory size to 3,320 flowers and increased its weight gain to 0.25 g per day. The following day it relinquished half of the extra flowers to achieve its maximal rate of weight gain of 0.35 g per day, and it maintained this territory for another day. It thus reached a weight of 4.6 g by the morning of 1 August and took off on migration.

The results with WP and other rufous hummingbirds reveal that the birds adjust their territory size by trial and error until they have maximized the rate of weight gain[3]. Territories that are either too large or too small yield reduced rates. Hence, this system supports two basic postulates of optimal foraging theory: the birds can detect changes in energy intake, or a correlate of it, and they apparently adjust territory size to maximize energy intake. More generally, however, this study offers a method of repeatedly weighing a wild animal without disturbance. With further ingenuity the field balance technique could be applied to other animal species that periodically return to one or a few preferred sites. Such regular weighings of wild animals could elucidate behavioural, physiological and ecological problems, such as ones related to foraging, water loss and reproduction. The new method may provide a breakthrough in field biology. ☐

1. Pyke, G., Pulliam, H. R. & Charnov E. *Q. Rev. Biol.* **52**, 127 (1977).
2. Krebs, J. & Davies, N. *Behavioural Ecology* (Sinauer, Sunderland, Massachusetts, 1978).
3. Carpenter, F. L., Paton, D. & Hixon, M. *Proc. natn. Acad. Sci. U.S.A.* **80**, 7259 (1983).
4. Phillips, A. *Condor* **77**, 196 (1975).
5. Kodric-Brown, A. & Brown, J. *Ecology* **59**, 285 (1978).
6. Gass, C. *Can. J. Zool.* **57**, 914 (1979).
7. Carpenter, F. L. *Am. Zool.* **19**, 1105 (1979).
8. Paton, D. & Carpenter, F. L. *Ecology* (in the press).
9. Hixon, M. *Am. Nat.* **115**, 510 (1980).
10. Hixon, M., Carpenter, F. L. & Paton, D. *Am. Nat.* **122**, 366 (1983).

Jared M. Diamond is Professor of Physiology at the University of California School of Medicine, Los Angeles, California 90024.

Developmental biology

Autocrine control of growth?

from C.D. Stiles

IN the 'autocrine growth' scenario for malignant transformation, popularized by Todaro, DeLarco and others[1], cancer is initiated when a cell begins to produce a growth factor for which it has receptors and to which it is responsive. When this factor binds to receptors on the cell from which it has been secreted, a self-perpetuating automitogenic response is triggered. Within this context, autocrine growth is seen as a perversion of normal information flow, it being tacitly understood that growth factors, like conventional hormones, function normally in the paracrine or endocrine modes — that is, they communicate between heterologous tissues and are synthesized at some distance from the target cell. A letter in this issue of *Nature* challenges this precept; in it, Seifert *et al.* describe the developmentally regulated synthesis of a growth factor that may normally function in the autocrine mode[2].

Ironically, platelet-derived growth factor (PDGF) serves as the point of departure for the studies of Seifert *et al.* It is recent insights into the molecular biology of this molecule (reviewed in ref. 3) that provide the strongest support for the autocrine theory of malignancy. High-affinity receptors for PDGF are confined to a well-defined subset of animal tissues — only fibroblasts, glia and arterial smooth muscle cells display them, and only these cells show a growth requirement for PDGF in culture. Last year, the c-*sis* oncogene was shown to direct synthesis of a functional PDGF subunit. As expression of this gene is (almost) exclusively confined to cells derived from connective tissue neoplasms, it can be concluded that synthesis of the sis protein (PDGF) *in vivo* provides a selective advantage only to cells that express PDGF receptors.

Seifert *et al.* report that cultured aortic smooth muscle cells isolated from 13 – 18-day-old rat pups secrete a growth factor that competes with authentic human PDGF for binding to fibroblasts. This cellular PDGF-like material (which they term PDGF-c) is recognized by anti-PDGF immunoglobin and is mitogenic for 3T3 cells. Comparable smooth muscle cells isolated from adult rats secrete little, if any, PDGF-c. The inability of adult cells to generate PDGF-c does not merely reflect the passage of time or cell divisions, because the pup smooth muscle cells continue to secrete PDGF-c during 20 passages in culture and over a 6-month interval. The authors conclude that synthesis of PDGF-c is developmentally regulated. They speculate that the substantial increase in both the number of smooth muscle cells and the thickness of the connective tissue matrix of the rat aorta, that occurs within the first three months, reflects an automitogenic response to PDGF-c.

Synthesis and secretion of PDGF-c by pup smooth muscle draws attention to a broader body of literature on the production of growth factors either by normal diploid cell cultures derived from embryos or by embryonal carcinoma cell lines. Substances identical to, or closely related to, nerve growth factor, transforming growth factors and colony-stimulating factor are synthesized by these cells[4-6]. Two recent studies echo the developmental control observed by Seifert *et al.* First, Nissley, Rechler and their co-workers have shown that diploid fibroblast cultures derived from neonatal rats secrete the neutral form of insulin-like growth factor (IGF-II) which seems to modulate growth *in utero*. Comparable cultures established from adult rats secrete the basic form (IGF-I) which is the dominant factor in skeletal development of juveniles and adults[7]. Second, Clemmons has noted that while fetal fibroblast cultures secrete a functional homologue of PDGF, comparable cultures derived from human donors aged three or more do not[8]. Though Clemmons did not have the PDGF radioreceptor assay at his disposal, it seems plausible that the mitogen he observed is the PDGF-c described by Seifert *et al.* The plethora of growth factors secreted by embryonic cells, the developmental control of their production and the early appearance of growth factor receptors in embryogenesis[9] support a popular prejudice that the serum growth factors, scrutinized so thoroughly within the context of tumour biology, may play pivotal roles in developmental growth and morphogenesis.

The new twist provided by Seifert *et al.* is the suggestion that 'embryo-derived growth factors' function normally in the autocrine mode. On first consideration the concept is aesthetically distasteful. Why should a developing tissue secrete a growth factor to stimulate its own proliferation? Surely the process could be controlled more stringently from within the cell at some point subsequent to the events governed by growth factors and their receptors. A teleological rationale may be contained within the biological need to amplify weak chemical signals — the *raison d'etre* of membrane-bound receptors for hormones and growth factors. It is worth noting that normal embryo fibroblast cultures typically require less serum for growth than do established lines of the 3T3 genre, an observation consistent with the view that embryonic cultures respond to the growth factors they produce. Furthermore, another growth factor, interleukin-2, seems normally to function in the autocrine mode[10].

The interface between growth factors and development remains even less than tenuous. Nonetheless, if recent observations can be extended, the implications are wide indeed. Growth factor receptors and other components of the 'mitogenic cascade' may be vestiges of an automitogenic apparatus used in development. By switching off the gene encoding an automitogen and activating the same gene at some distal site, the developmental machinery may be neatly converted to the paracrine mode. In this state, it could promote cell proliferation 'on demand' during adult life in, for example, wound healing, erythropoiesis and immunogenesis. Switching errors in adult life would manifest themselves as proliferative disorders — keloids, psoriasis, atherosclerosis and, of course, neoplasia. ☐

1. Todaro, G.J. *et al. Cold Spring Harbor Conf. Cell Prolif.* **6**, 113 (1979).
2. Siefert, R.A., Schwartz, S.M. & Bowen-Pope, D.F. *Nature* **311**, 669 (1984).
3. Stiles, C.D. *Cell* **33**, 653 (1983).
4. Young, M. *et al. Science* **187**, 361 (1975).
5. Stewart, C.C. & Lin, H.S. *J. reticuloendothel. Soc.* **23**, 143 (1983).
7. Adams, S.C. *et al. Nature* **302**, 150 (1983).
8. Clemmons, D.R. *J. cell. Physiol.* **114**, 61-67 (1983).
9. Adamson, E.D. & Meek, J. *Devl Biol.* **102**, 62 (1984).
10. Cantrell, D.A. & Smith, K.A. *Science* **224**, 1312 (1984).

C.D. Stiles is in the Department of Microbiology and Molecular Genetics, Harvard Medical School and the Dana-Farber Cancer Institute, Boston, Massachusetts 02115.

Biophysics

Many guises in Bristol

from Maxine Clarke

There probably never was an adequate definition of biophysics. Perhaps there never will be. That, at least, seemed to be one inevitable conclusion of the 8th International Congress of Biophysics held in Bristol, 29 July — 4 August, at which it became clearer than ever just how many biological questions have recently been annexed by biophysicists.

For example, T. Wiesel (Rockefeller University) presented one classic physiological study in the guise of biophysics in reporting how electron microscopy has been used to demonstrate axonal spread of peroxidase-stained neurones throughout several hierarchical levels of organisation in the visual cortex. Physiological experiments on monkey photoreceptors (D. Baylor, Stanford University) show that both rods and cones have identical properties to those deduced by psychophysical studies in man. Many other biological questions, from how ion channels are gated to how microtubules cause cilia to beat, were similarly addressed in biophysical fashion.

To anyone with a primary interest in the structure of cells and organelles, it was very obvious that improvements in electron microscopy and synchrotron radiation measurements had contributed greatly to progress since the 7th congress, three years ago. An optical diffraction pattern taken from an electron microscope image contains information about the phases as well as the amplitudes of the reflections. This inherent advantage of electron microscopy over X-ray diffraction techniques has been limited by problems in the resolving power of the method, but the use of low electron dose to eliminate beam damage to the specimen and the development of cryomethods which do not require staining of the specimen are solving some of the problems. Such improvements enabled E. Kellenberger (University of Basel) to show that the bacterial cell envelope has a periplasmic gel of regular thickness between the inner and outer membranes, with the nucleoids (bacterial DNA) much freer than originally thought. The dependence of nucleoid structure on environmental conditions is now being measured by a freeze-substitution technique. J.L. Carrascosa (Universidad Autónoma de Madrid) produced a 2.2 nm-resolution three-dimensional image of the head-to-tail connection (neck region) of the 029 bacteriophage by tilting a two-dimensional hexagonal array of necks and performing a Fourier analysis of differently angled views of the section. The inner region of the neck was identified as the part interacting with the DNA; it has 6-fold symmetry and the proteins constituting this and the 12-fold outer neck region have been assigned.

Improvements in synchrotron radiation techniques have enabled some of the predictions of the crossbridge theory of muscle contraction to be confirmed for the first time. A two-dimensional detector allows a difference pattern between relaxed and contracting muscle to be produced. H. Huxley (MRC laboratory of Molecular Biology, Cambridge) reported an increase of the actin (thin filament) reflections on contraction; this result is the necessary outcome of the attachment of crossbridges from the thick to the thin filaments but had not been visualized previously. His group has also found that the part of the diffraction pattern that arises from the calcium-binding proteins changes before the part that is related to the crossbridges. This confirms the hypothesis that calcium binding has a structural consequence which must express itself in the muscle filaments before the crossbridges can produce force. In a different approach to elucidating the mechanism of contraction, Y. Goldman (University of Pennsylvania) described an ambitious attempt to link the biochemical rate constants of the muscle's ATPase, derived from solution studies of muscle proteins, with the force-producing properties of the fibres. Caged ATP, an inert molecule which can be photolysed to ATP with UV light after its infusion into a muscle fibre, is used in this approach. Several of the kinetically intermediate reactions in the ATPase in muscle fibres are similar to those in solution, so that the particular step in the biochemical pathway affected by force can now be sought.

Innumerable other topics, ranging from atomic interactions in proteins to the role of biophysics in university teaching courses, were discussed at the meeting. The main virtue of the conference lay in the manner in which a review of a huge number of topics, via sessions centred around either a biological problem or a physical technique, was arranged. This was particularly valuable for highlighting old problems which might now be solved using new methods. Individual sessions did not necessarily provide a balanced view of the field under discussion, but that is always likely to remain the case at the International Congress. The annual meeting of the US Biophysical Society attracts universal attendance and is established as the forum for comprehensive discussions in a large number of subjects. This is more difficult to achieve in a nomadic meeting in which there is a necessarily random sampling of a much wider population. However, for those biophysicists with time and desire to expand their education, looking for a new problem or interested in new methods, the International congresses remain a valuable venue. ☐

Maxine Clarke is an assistant editor of Nature.

Geology

Submersible study of the East Pacific Rise

from members of the Geocyarise expedition

ON 5 March 1984 the French research vessel *Nadir* docked at Manzanillo, Mexico, at the end of a highly successful leg of diving operations on the East Pacific Rise using the submersible *Cyana*. Several key sites between 11° and 13°N were explored, with the specific aim of studying hydrothermal processes.

Previous investigations by French vessels had established, near 12°50′N, the existence of a narrow zone (less than 200 m wide and 20 km long) of intense hydrothermal activity believed to be due to the presence of a shallow magma reservoir beneath the axis. The East Pacific Rise in this vicinity is conspicuously asymmetric, with off-axis seamounts on one side and linear normal faults on the other. Geological reconnaissances were carried out on four seamounts located 4 km west of the rise axis near 11°30′N(A), 18 km west of the axis at 12°38′N(B), 6 km east of the axis at 12°43′N(C) and 6 km east of the axis at 12°50′N(D).

Seamounts A and C, which are structurally similar and rise less than 400 m above the surrounding sea floor at 2,700 m, were explored extensively. Linear north–south aprons some 500 m long and less than 100 m in relief extend south from the eastern and western margins of both seamounts. Extensive hydrothermal deposits found on seamount C during a *Cyana* dive in 1982. On this leg, highly-altered fragile hydrothermal edifices several metres high were found around an apron of seamount A. Its western flank consisted of a vertical fault scarp with extensive piles of talus at its foot composed of sulphide boulders and fragments of massive flows. Extensive areas of Fe oxides, hydroxides and thick (> 2 cm) Fe–Mn crusts were encountered during dives from the southern foot of the seamount to its top.

Three dives confirmed the existence of a massive sulphide field capped with ochreous oxidation products on the western limb of an apron of seamount C. Hydrothermal material extends at least 800 m down the south flank of the seamount from its top and some 500 m in an east–west direction along the 2,600 m isobath. Assuming the deposit to be, on average, 3 m thick and to have a density of 3.0 g cm^{-3}, its mass is conservatively estimated to be more than 2×10^6 tonnes. Metal contents in the deposit are in the range 20–40 per cent Fe, 1–3 per cent Cu and less than 1 per cent Co. This deposit differs from those on the adjacent Rise axis in its massive appearance, its relative depletion in zinc sulphide and its abundance of hydrated silica. The smaller size (<50 m diameter) and richer metal (Cu and Zn) content of the Rise axis deposits suggest a faster deposition at a higher temperature than occurred for the seamount deposit. The age of the deposit on seamount C is unknown, although the lack of sediment cover indicates a relatively recent origin. The crust on which the seamount lies is approximately 100,000 years old. The occurrence of fresh pillow flows partially covering some of the ochreous hydrothermal products indicates off-axis volcanic activity. Interestingly, near the base of the seamounts at 2,700 m depth the pillow flows are almost entirely covered by pelagic sediment.

A semicircular volcanic structure located between seamount C and the rise axis showed evidence of recent off-axis hydrothermal activity. A diffuse white fluid was exiting from hydrothermal edifices on top of a volcanic peak (<50 m in height) made up of fresh sheet flows, and a large amount of ochreous sediment with slumped boulders of massive sulphide was observed at its base.

Two dives took place on the eastern margin of the axial graben near 12°50′N in order to study the alteration and mode of emplacement of sulphide precipitates at recently active hydrothermal sites. A field of green-coloured altered pillows and flows mixed with sulphide boulders, which formed piles of talus at the foot of a 30 m high fault scarp, was observed. Along the wall was an extensive stockwork of sulphide filled veins (<50 m wide) within altered country rock containing chlorite–smectite–sulphide assemblages typical of low-grade metamorphism.

The offset spreading centre discovered by Macdonald and Fox (*Nature* **301**, 55; 1983) at 12°53′N was the target for another dive. The eastern segment seemed relatively old, with flows and pillows partially covered by sediment. The western ridge is marked by a small graben (some 10 m deep and 30 m wide) containing fresh lobated flows but discontinuous along the axis. The sporadic occurrence of *Galathea* and brachyuran crabs indicated hydrothermal activity nearby. Proceeding northwards along the western axis the basaltic flows become fresher in appearance (very shiny glassy surfaces) and ochreous sediments more common, suggesting increasing hydrothermal activity. By contrast, the eastern ridge at the same latitude is apparently inactive and being tectonically disrupted.

The first electrical resistivity measurements of the seabed to be made from a submersible were carried out by T.J.G. Francis of the Institute of Oceanographic Sciences, UK. At each site an electrical cable 50 m long was laid along the bottom. Current was passed between electrodes 30 m apart by means of a 12 V battery within the submersible and voltages were detected by Ag–AgCl potential electrodes. The resistivity of the pillow lava terrain was about 40 times that of seawater, in good agreement with downhole logging measurements in DSDP drill holes. The resistivity of the sulphide deposit was between one and two orders of magnitude less than that of the pillow basalts. At one site the seabed was approximately twice as conductive as the seawater and preliminary measurements suggest the sulphides could be of the order of 15 m thick. Self potentials were observed associated with the sulphide deposit.

Electrical potentials were also measured in the water column in order to determine whether hydrothermal fluids exiting from the seabed create masses of water with a different (redox) potential from the adjacent water mass. This experiment, devised by F. Avedik of CNEXO-COB, consisted of measuring the potential difference between one non-polarizing electrode held at 150 m depth and another lowered to the ocean floor at a depth of 2,600–2,900 m. Negative anomalies with amplitudes of 6–8 mV were observed next to the sea floor, some of which extended up to 500–600 m above the bottom. This type of measurement could prove to be a useful way of detecting the presence of hydrothermal activity. ☐

Contributors to this article were R. Hekinian, F. Avedik, D. Bideau and Y. Fouquet from the Centre Océanologique de Bretagne, Brest, France; T.J.G. Francis of the Institute of Oceanographic Sciences, Wormley, Surrey, UK; J.M. Franklin of the Geological Survey of Canada, Ottawa, and W.D. Nesteroff of the Université Pierre et Marie Curie, Paris.

100 years ago

THE PRIME MERIDIAN CONFERENCE

THE Prime Meridian Conference at Washington on Monday adopted the Greenwich line as the universal prime meridian. Only one vote — that of St. Domingo — was given against its adoption; but the representatives of France and Brazil declined to vote.

To the American resolution for adopting the Greenwich line, Mr. Fleming (Canada) moved an amendment to the effect that the Conference should adopt the 180th degree of longitude east from Greenwich as the prime meridian; but the other British delegates opposing the proposition, it was lost. M. Lefaivre (France) said the Greenwich was not a scientific meridian, and that it implied no progress in any science, but was merely a commercial standard. Since, therefore, nothing would be gained to science by adopting Greenwich, France could not make a sacrifice of her own meridian, and incur the vast expense consequent upon the adoption of a new one, because she would thereby gain no advantage whatever. Sir William Thomson said that it was purely a matter of convenience, and that Greenwich answered the world's convenience better than any other standard meridian.

From *Nature* **30**, 603, 16 October 1884.

Space programmes

Details of Soviet cosmodrome from space shuttle photographs

from Grant H. Thomson

EVIDENCE that the Soviet Baikonur Cosmodrome is situated at 63.3°E, 46.0°N has already been provided by the remote-sensing Landsat multispectral and return-beam vidicon systems. But that evidence has recently been supplemented by two colour photographs (NASA 84-HC20 and 84-HC-22) obtained using a hand-held camera, with 100 mm and 250 mm lenses, during the flight of STS-9, *Columbia* (1983-116A), in December 1983. Although the ground-resolution of the photography is not particularly good, it is sufficient to add some useful up-to-date detail to maps published by observers of the Soviet space programme.

So far as is known, the Soviet authorities have not yet published, for general reference, a map of the Tyuratam area showing the cosmodrome. They have, however, announced the geographical coordinates of the manned-spaceflight launch pads at 65.5°E, 47.3°N, and press briefings for the Apollo–Soyuz Test Project have the launch site as 66.0°E, 47.8°N, presumably based on Soviet information. These coordinates place the Baikonur Cosmodrome well to the north-east of the extensive launch facilities just north of the old town of Tyuratam. Recently, former CIA official and photo-interpretation expert, Dino Brugioni, has explained how U-2 photography enabled the site to be located, following intelligence reports in the 1950s of a missile site somewhere south of the Aral Sea (*Air Force Mag.*, 108; March 1984). In the absence of any Soviet acknowledgement at the time of such a facility, a war-time German map, showing Tyuratam as a nearby railway station, provided the name by which the cosmodrome has become widely known in the West.

The STS-9 photographs indicate extensive disturbance of the steppe over an area in excess of 150 km², in region C of the accompanying map, which is based on photography. Most noticeable in this area are the three very large new buildings (A) which, because of their size, are probably vehicle assembly buildings. The approximate dimensions of one of these buildings is 220 m × 190 m × 23 m; another is 220 m × 80 m × 35 m; the third has dimensions 155 m × 110 m × 23 m. At B, approximately 2 km to the north-east of these three buildings, the shadow of what is possibly the new heavy-lift vehicle, once referred to as Type G, can be seen. From the solar elevation and the length of the shadow, the vehicle would appear to be more than 90 m tall, in good agreement with Vick's speculation (*Spaceflight* **25**, 159; 1984).

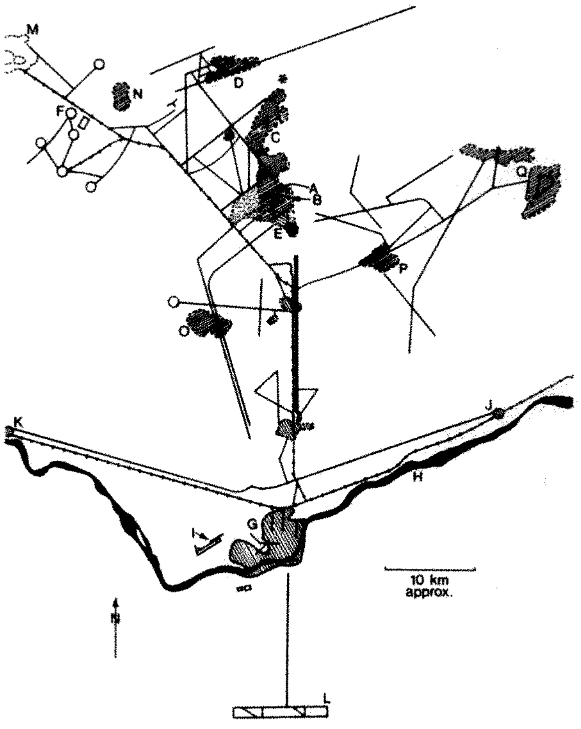

A, Probable new vehicle assembly building. B, Possible new heavy-lift vehicle. C, New area showing signs of construction, including a launch pad. D, New runway and supporting facilities. E, Possible Soyuz assembly facilities. F, Military launch area. G, Tyuratam old town and new city of Leninsk. H, Syr Dar'ya river. I, Airport. J, Diirmentobe. K, Bay-Khoza. L, Possible air defence airfield. M, Possible old quarry site. N, Possible technical site. O, Possible technical site. P, Probable technical site. Q, Possible technical site and/or launch-pad facilities.

Map of the Soviet Baikonur Cosmodrome at Tyuratam constructed from photographs taken from the space shuttle *Columbia*.

There is a V-shaped feature in the northern part of area C, strongly suggestive of a large new launch pad and associated flame-pit. Its size and probable recent construction suggest that it could be the launch facility for the new heavy-lift vehicle. Area E is shown on Vick's maps as facilities for the long-serving A-vehicle (*The Illustrated Encyclopedia of Space Technology*, 39, Salamander, 1981; and *Soviet Space Programs: 1976-80*, Pt 1, 48, US Govt Printing Office, Washington DC, 1982).

A new runway is under construction at D, in the more northerly part of the cosmodrome. At the time the photographs were taken, this was some 5 km long and may not yet have been completed. Extending from and in line with the runway, in the direction of the typical launch azimuth, is a track across the steppe, approximately 20 km long, that may indicate future development. Buildings and signs of construction activity in an area on the north side of the runway are thought to be the Soviet 'spaceplane'.

The ground in the area N shows some evidence of disturbance compared with the surrounding steppe, possibly indicating some work in progress at that site. The terrain in the area M appears very uneven, unlike the rolling or fairly flat surrounding region. This could have been a quarry site and a rectangular structure, approximately 250 m long, can be seen at the north-west limit of the area.

Area F has been identified by Vick as a military launch complex (*Soviet Space Programs: 1976-80*), and possible sites of launch pads or silos are marked with circles. An unidentified rectangular feature, 1,400 m × 750 m, can be seen close to the south-west side of the railway. Sites O and Q show extensive activity, with Q thought to include launch-pad facilities at the end of the railway line. The nature of the large area immediately to the south-east is uncertain, although extensive linear features can be seen. At least two sizeable structures can be seen at P which, although not fully recognizable, is likely to be a technical site.

Just less than 20 km south of Tyuratam are what appear to be parallel runways. If this interpretation is correct, they are likely to be part of an air defence system which almost certainly will have been provided for the cosmodrome. The location would provide airspace clear of the launch complex.

Although the photographs do not provide great detail, they clearly show the extensive activity now in progress at the Baikonur Cosmodrome and provide a good guide for the West to the Soviet authorities' intention of continuing with their investment in space programmes. ☐

Grant H. Thomson is in the Kettering Group and can be contacted at 4 Lullington Garth, Boreham Wood, Herts WD6 2HE.

Astrophysics

Neutrinos and the Sun

from Virginia Trimble

NOTHING can replace real data from a working scientific experiment. This was the most important lesson to be learned by the participants in the Homestake Neutrino Conference*. Among the questions addressed, for which there either are, or should be such data, were the following. (1) What is the flux of neutrinos hitting the Earth? (2) How does it depend on time and neutrino energy? And (3) what is the Sun doing in addition to (or instead of) making neutrinos? In short, the answers are, for (1), still puzzlingly low; for (2), possibly variable with an 11 yr period; and for (3), perhaps stirring its interior, probably driving its magnetic field with a dynamo at the base of the convection zone, and, just maybe, showing a solar activity cycle as far back as 700,000,000 yr.

First the incident flux. There cannot be a physicist, astronomer, or chemist who has not heard of Raymond Davis Jr and his 100,000 gallons of cleaning fluid (C_2Cl_4) in the depths of the Homestake Mine. The experiment was designed to permit recovery of a few atoms of ^{37}Ar, resulting from the decay of ^{37}Cl driven by neutrinos from the Sun. The counting rate from the recovered atoms has persisted for more than a decade in being about one-third of what theorists predict from solar neutrinos alone (observed production rate 0.39 ± 0.05 atoms per day = 2.1 ± 0.26 SNU, after subtracting the current best estimates for assorted backgrounds). There is now no serious doubt about the atoms' identity: they not only have the chemistry and decay energy of ^{37}Ar but also have its half life (J. Rowley, Brookhaven National Laboratory). But the fraction of ^{37}Ar production that should be attributed to backgrounds from cosmic-ray secondaries has become less certain. Two backgrounds are important, muons and neutrinos. E. Fireman (Center for Astrophysics) is currently checking the muon background adjacent to Davis's tank using several thousand gallons of potassium hydroxide. The rationale behind his experiment is that cosmic-ray particles can be expected to make ^{37}Ar from ^{39}K at about the same rate as from ^{37}Cl, whereas neutrinos will make far less. His 1σ limits on particle production of ^{37}Ar are currently 0.20 ± 0.20 atoms per day, consistent either with the standard best estimate of 0.08 atoms per day or with the entire observed rate of 0.47. Longer runs should tighten the error bars considerably. The flux of cosmic ray-produced neutrinos can easily be checked only by e–ν scattering at energies $\gtrsim 10$ MeV (because of interference from still other kinds of backgrounds at lower energies) using multi-tone water Čerenkov detectors. At least five of these are now operating and producing consistent results (T. Stanov, Bartol Research Foundation). The detector in Kamioka, Japan, however, has seen a considerable excess of low-energy neutrino-like events. If these result from stopped muons and the same flux hits the perchlorethylene tank, it will produce 0.37 ^{37}Ar per day, essentially the observed level.

An estimate of neutrino flux as a function of energy is vital for deciding whether the low flux at Homestake is due to a minor flaw in the solar model (affecting only the high-energy B^8 neutrinos), neutrino oscillations during propagation (which might reduce the flux at all energies by about a factor of three), or some major defect in modern astrophysical theory (for example, stars do not derive their energy from fusion and so do not produce any neutrinos at all). Apart from the Davis result, there are currently only upper limits, mostly several orders of magnitude above predicted values and pertaining to fluxes made by high-energy cosmic rays (P. Sokolsky, University of Utah) or stellar collapses (A. Burrows, SUNY) rather than by the Sun.

Contributions on the time-dependence of neutrino flux were rather more intriguing. Rowley's simultaneous plot of the ^{37}Ar production rate and sunspot numbers since 1970, particularly the coincidence of the very high run nos 27 and 71 with the giant flare of 4 August 1972 (another indicator of solar activity) strongly suggested a correlation. A. V. Kopylov (Institute for Nuclear Studies, Moscow) pointed out that the present data are not inconsistent with constant ^{37}Ar production rate, and R. Lingenfelter (University of California, San Diego) sketched out calculations eliminating the most obvious sort of connection: energetic particles from a large solar flare produce neutrino secondaries at a rate too low by 10^6 to affect the Homestake experiment. Nonetheless, the possibility of correlated time-dependence is clearly worthy of further study. It is therefore particularly disturbing that the Brookhaven experiment will have to be wound down over the next fiscal year unless a new source of support is found.

Several promising experiments are under construction. The Institute for Nuclear Studies, Moscow (N.V. Gavrin, A.V. Kopylov) has 25 tonnes of gallium metal on hand, and more available, and a chamber ready and lined with iron and concrete shielding at 3,500 m depth at Baksan. The group hopes for construction in 1985 and counting in 1986. ^{71}Ga (ν, e) ^{71}Ge has a low enough threshold to see neutrinos from ordinary pp reactions. The same group is also working on both a scaled-up ^{37}Cl experiment (five times Davis's volume; the equipment is ready, but the chamber still needs to be dug) and ^{7}Li(ν, e)^{7}Be (for which they have tested recovery and counting techniques for a 12-litre tank and are ready to try 200 l). The Cl experiment should provide a high enough count rate to see any solar cycle variations unambiguously, and, with patience, annual ones, while the Li experiment is sensitive to CNO cycle and pep neutrinos, thus testing different details of nuclear and solar physics.

MPI Heidelberg (W. Hampel) intends to continue a gallium experiment, in the form of $GaCl_3$, despite Brookhaven's withdrawal from the collaboration. They have tested germanium recovery and counting in a 1.25 tonne tank and envisage a 30 tonne experiment at an existing European site. L.S. Peak (University of Sydney) reported that his group is about to install its first 10 tonne module of a projected 100 tonne water Cerenkov detector to look for a ν–e scattering at the Broken Hill mine. In practice, this is sensitive only to B^8 neutrinos, owing to high backgrounds at low energies, but it is otherwise totally different from the Cl experiment and can yield approximate directional information, separating the Sun from other sources.

Models of the solar interior designed to reduce the predicted neutrino flux are numerous and often rather *ad hoc*. G. Michaud (University of Montreal) and E. Schatzman (University of Nice) reviewed the effects of turbulent diffusion. If this provides a diffusion coefficient about 100 times that expected from ordinary molecular diffusion, then fresh hydrogen coming in reduces the necessary central temperature slightly and hence the predicted flux by about the requisite factor of three. Energy to drive the turbulence and mixing can be drawn from the build-up of burnable ^{3}He just outside the solar core (I. Roxburgh, University of London). One price paid is a 30 per cent increase in main-sequence lifetimes for low-mass stars, and thus some difficulty in interpreting the Hertzsprung–Russell diagrams of globular clusters. A partial compensation is a better understanding of lithium abundances on the surface of old stars.

Efforts to probe the central temperature, composition, rotation and magnetic field distribution (all of which can affect neutrino production) of the solar interior using frequencies of *g*-mode oscillations would seem premature. G. Isaak (University of Birmingham), whose group has collected much of the solar surface velocity data concerned, does not believe that these modes have yet been unambiguously identified. The *p*-modes have been seen in considerable detail, but are only informative about the solar core after the dominant contributions from the envelope have been understood and subtracted.

Nonetheless, *p*-modes may already have

---

*Lead, South Dakota, 23-25 August.

21-1-87
A. Batter

resolved one uncertainty. P. Gilman (High Altitude Observatory) reviewed the discrepancy between solar dynamo models with driving in the convection zone and models for convective driving of the solar differential rotation. The former require angular frequency to increase inwards (to make active zones migrate to lower latitudes through the solar cycle), while the latter require angular frequency to decrease inwards. The observed *p*-mode-splitting strongly favours ω decreasing inwards (see Duvall, T.L. Jr *et al. Nature* **310**, 22; 1984). Gilman suggested an alternative site for dynamo driving at the base of the convection zone, where ω seems to be rising again with depth.

Finally, P. Foukal (Atmospheric and Environmental Research Inc.) showed fragmentary sunspot, auroral and ^{14}C data suggestive of a roughly 11 yr solar activity cycle for several hundred years before the late-seventeenth-century turn-off (the Maunder minimum). And, in what was perhaps the greatest surprise of the meeting, he showed photographs of a pre-Cambrian varve sequence discovered by George Williams of Broken Hill Proprietary. Varves are layers deposited in periglacial lakes when rapid spring–summer melting and sediment transport alternate with quiet winter settling of silt. The annual layers showed additional banding with periods ranging from 9 to 14 yr and averaging 11.2 yr over a 20,000 yr sequence. This strongly suggests an influence by the solar cycle some 700,000,000 yr ago. There's nothing quite like real data, but you can never be sure where it's going to come from. ☐

Virginia Trimble is Visiting Professor of Astronomy at the University of Maryland, College Park, Maryland 20742, and Professor of Physics at the University of California, Irvine, California 92717.

Invertebrate neurophysiology

Sodium channels in muscle

from P.R. Stanfield

INFORMATION in the nerve fibres of both vertebrates and invertebrates is signalled by means of action potentials that are generated by an inward movement of sodium ions through channels (Na channels) which are selective and dependent upon membrane potential. Similar channels characterize most of the skeletal muscle fibres of vertebrates, where the all-or-nothing action potentials they produce trigger contraction by releasing calcium ions from an intracellular store in the sarcoplasmic reticulum. In contrast, invertebrate muscles have seemed to lack sodium channels, showing instead an electrical excitability that depends on the presence of calcium channels in the muscle fibre membrane and is either graded or all-or-nothing in nature. This calcium-dependent pattern of electrical excitability has been seen as phylogenetically older than the pattern in vertebrate muscle and Ca channels are themselves believed to be evolutionarily older than Na channels[1].

The generalization that invertebrate muscles lack Na channels has recently been challenged by Lawrence Schwartz and Walter Stühmer[2], who have used electrophysiological techniques to show that the striated muscle fibres of the planktonic arrow worm, *Sagitta elegans*, possess Na channels and certain other properties that make them very like skeletal muscle fibres of vertebrates. *Sagitta* was chosen because it belongs to the phylum Chaetognatha and in turn to the deuterostome branch of coelomate animals, the branch to which the vertebrates also belong.

In discussing their data, Schwartz and Stühmer argue that, since Na action potentials are always more rapid events than those depending on Ca^{2+}, they permit a more rapid switching on and off of muscle activation. The advantages of a rapid switch may have provided part of the selection pressure that led to the expression of Na-channels in muscle as well as in nerve. The rapid muscular responses required of a successful predator like *Sagitta* may account for its adoption of Na channels. The alternative, however, is that they are the bequest of an evolutionary ancestry shared with the chordates, and that the Na action potential in muscle is a deuterostome trait.

If this is a deuterostome trait, it is not a universal property among the group, nor is it limited to them. Indeed, since Na channels of very consistent properties are almost universal in nerve, it is possible that their expression in muscle has arisen independently in a number of groups. Thus, the tunicates (urochordates) lack muscle Na channels, while *Amphioxus* (among the cephalochordates) possesses them; these protochordates have therefore been seen as transitional between non-chordates that lack muscle Na channels and the vertebrates[1]. Furthermore, among the vertebrates, lack of Na channels lives on in smooth muscle and also in the slowly-contracting tonic skeletal muscle fibres, found in frog and, for example, in the extraocular muscles of certain mammals. Moreover, protostomes (the other branch of the coelomates) can also have muscle Na channels, for these have now been demonstrated in an evolutionary ancient group of arthropods, the scorpions[3].

While muscle fibres of the scorpion and of *Sagitta* both give brisk twitch-like contractions in response to Na-dependent action potentials, they are very different in other ways. First, in scorpion, the Na action potential is followed by a brief train of Ca-dependent ones[3], an electrical behaviour that has not been described in other muscles. Second, blockage of Ca channels or removal of external Ca^{2+} blocks contraction in the scorpion, in spite of the presence of a well-developed cellular store of Ca^{2+}. This dependence on external Ca^{2+} is commonly found in invertebrate muscles that lack Na channels. In *Sagitta*, as in vertebrate muscle, removal of external Ca^{2+} seems not to block contraction[2].

The presence of Na-channels in scorpion muscle may raise the question of whether Ca-dependent excitability really is the older form. There remains little doubt that it is, and arguments from ontogeny support the position. During development, vertebrate muscles go through a stage where they possess only Ca action potentials. And even in adult muscle, Ca channels are retained at a high density. In addition, in the tunicates, whose muscles lack Na channels, these channels are lacking in all cells in the initial stages of development (though they are present in the unfertilized egg) and are never expressed in presumptive muscle cells. Indeed, these cells acquire their mature pattern of ionic permeability very early in embryonic life, and at much the same stage at which Na channels first appear in presumptive nerve cells[4].

To confuse the picture, certain muscle fibres seem to have the potential but not usually the stimulus to express Na channels. Thus denervation of tonic muscle fibres of the frog leads to the development of Na action potentials; since reinnervation suppresses them again, some trophic effect of nerve seems to be involved[5]. Denervation of crayfish muscle has similar results[6].

At the end of their article, Schwartz and Stühmer challenge comparative physiologists to use new methods to investigate muscle cells hitherto inaccessible to electrophysiological attack. Since it was in a crustacean muscle that the first evidence for the Ca channel was obtained[7], since the pattern of evolution of muscle excitability turns out to be complex, and since a comparative approach will help sort out the poorly understood problem of excitation–contraction coupling[3], there is a strong case for a wide survey. ☐

1. Hagiwara, S. *Membrane Potential-dependent Ion Channels in Cell Membranes, Phylogenetic and Developmental Approaches* (Raven, New York, 1983).
2. Schwartz, L. & Stühmer, W. *Science* **225**, 523 (1984).
3. Gilly, Wm.F. & Scheuer, T. *J. gen. Physiol.* **84**, (in the press).
4. Hirano, T., Takahashi, K. & Yamashita, N. *J. Physiol. Lond.* **347**, 301 (1984).
5. Miledi, R., Stefani, E. & Steinbach, A.B. *J. Physiol. Lond.* **217**, 737 (1971).
6. Lehouller, J., Cuadras, J. & Bruner, J. *Neuroscience Lett.* **37**, 227 (1983).
7. Fatt, P. & Katz, B. *J. Physiol., Lond.* **120**, 171 (1953).

P.R. Stanfield of the Department of Physiology at Leicester University is currently in the Department of Biological Sciences, Purdue University, West Lafayette, Indiana 47907.

The nature of tumour cell proliferation

SIR — The comments by Erika Coward[1] on the origins of malignancy were interesting though not entirely novel. Clearly, cancer is not just a matter of abnormal proliferation and it would seem necessary to invoke lesions which do more than alter the levels of regulators otherwise one would merely have hyperplasia. Nevertheless, it is equally evident that the major, and possibly only, defect which is common to all transformed cells is that they replicate when they should not do so. Such an effect can be induced in a variety of ways, each of which could produce a unique functional change, while operating through the same mechanism[2]. The ability to totally inhibit proliferation would be a major advance but it might not overcome the effects of the altered properties, for example, increased hormone production.

Bell[3], has considered some aspects of altered proliferation consequent upon changes in the levels of regulators, both inhibitory and nitrogenic. On the other hand, as a result of my deliberations on the nature of proliferation processes[2,4], I have suggested[5,6] that the aberrant behaviour of cancer cells in most cases is due to an altered threshold with respect to regulator levels — decreased with respect to mitogens, raised for inhibitors. (A threshold is required by the cell cycle concept I have developed[2,5], although it may vary in magnitude and can be zero in particular instances. Its existence provides an explanation for cell density inhibition of proliferation while an altered threshold accounts for the often observed effect thereon of the malignant transformation, namely the ability of such cells to attain much higher densities[5].) At the same time, I also briefly considered the effects of altered levels of regulators on surrounding normal tissue cells[5].

There is no evidence that tumour cells in general proliferate faster than the corresponding normal cells. However, although taking different approaches, both Bell and I concluded that a critical tumour size might exist above which the growth may increase more rapidly than hitherto (one possible explanation for latency). My studies[5] also indicated the possibility that tumours of limited growth potential might arise as a result of lesions which increase the uptake[7] or binding of regulators, whereas those affecting thresholds could (depending on the magnitude of the change) yield tumours more malignant with respect to growth potential.

A question of major importance to Coward's considerations, however, is whether or not regulation *in vivo* is ever effected by a single agent. Culture studies clearly indicate that the replicative ability of cells can be affected by a wide range of normal agents, including various hormones. Recent studies have emphasized that transformation is often associated with positive growth factors (mitogens) rather than inhibitors. I have proposed a mechanism for the interaction of regulators[2] and, on that basis, suggested[6] (in contrast to the chalone approach) that attempts be made to control the proliferation of tumour cells by the use of a combination of such agents rather than just one (thereby limiting side effects on the replication of normal cells). However, the available data fail to indicate which regulators should be used, and at what concentrations, in any particular instance. It would thus still seem necessary to establish suitable regimes by trial and error, as is the usual procedure.

Another problem is that of heterogeneity in the cells of a tumour. Such heterogeneity implies that the response to growth regulators will also be heterogeneous[5]. As a consequence, treatment by the methods proposed by Coward and by myself, are likely to meet the same limitations in this direction as present approaches. On the other hand, they may be less toxic for the patient and might not produce the opposing adaptive responses.

Interestingly, accompanying Coward's letter was another by Schleifer *et al.*[8] on the effects of psychological factors on the immune response. That brings to mind the old issue of whether or not the mental state can affect tumour formation and development, a topic about which there has been much (often subjective) discussion. There is much data showing that various hormones can regulate cell proliferation, both negatively and positively. It thus seems reasonable to accept that any process modulating hormonal levels, such as stress, is potentially able to modify tumour growth rate (if not transformation), although the actual dependencies are likely to be complex and individualistic.

D. A. GILBERT
University of the Witwatersrand,
Johannesburgh, 2001,
South Africa

1. Coward, E. *Nature* **310**, 455 (1984).
2. Gilbert, D.A. *Biosystems* **10**, 227-233 (1978).
3. Bell, G.I. *Science* **192**, 369-372 (1976).
4. Gilbert, D.A. *S. Afr. J. Sci.* **77**, 541-546 (1981).
5. Gilbert, D.A. *Biosystems* **9**, 215-228 (1977).
6. Gilbert, D.A. *S. Afr. J. Sci.* **78**, 48-49 (1978).
7. Holley, R.W. *Nature* **258**, 487-490 (1975).
8. Schleifer, S.J., Keller, S.E. & Stein, M. *Nature* **310**, 456 (1984).

Machine-readable DNA sequences

SIR — Hayashi and Munakata[1] suggest that the four bases in DNA might be represented by four musical notes. We prefer a graphic representation, where the four bases are displayed in a line extension format: values attributed to the four bases G,A,T and C being +2, +1, -1 and -2. In the example (below), 100 nucleotides of coding sequence from a recent paper[2] have been converted into this format: significant features of the sequence ("TATA" transcription signal — in fact TATTAT here; start site of transcription; translation initiation codon ATG) are indicated.

Such a presentation has several interesting features. First, particular sequence patterns are readily discernible: purine (A,G) rich stretches appear exclusively above the line and pyrimidine (C, T) stretches below. G/C and A/T rich regions have extended and retracted aspects respectively. Second, restriction sites appear (usually) as simple rotationally-symmetrical patterns which are rapidly picked out by the eye. Third, it takes little time to determine, for instance, that the dinucleotide pair *C followed by G* is, as expected, depleted. Fourth, to convert to the complementary strand the diagram need only be rotated through the horizontal axis.

Such a line extension format is inherently machine-readable, and may permit suitably equipped readers to transfer sequences directly from the printed page to an information retrieval system.

R. LATHE
R. FINDLAY
AFRC Animal Breeding Research Organisation,
West Mains Road,
Edinburgh, UK

1. Hayashi, K. & Munakata, N. *Nature* **310**, 96 (1984)
2. Gillies, S.D. *et al. Nature* **310**, 594 (1984)

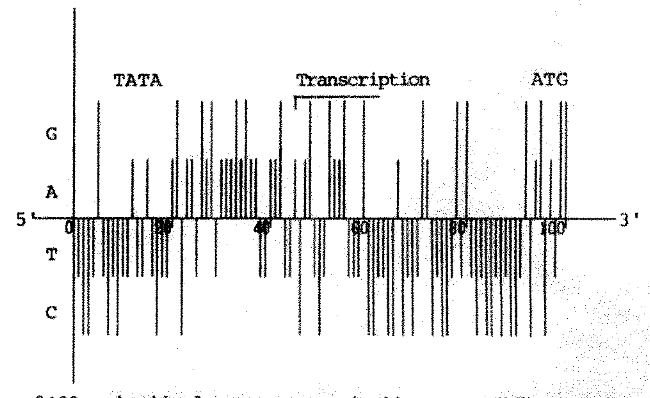

A sequence of 100 nucleotides from a mouse major histocompatibility complex gene, E_β

NATURE VOL. 311 18 OCTOBER 1984 REVIEW ARTICLE

Organizing centres for three-dimensional chemical waves

Arthur T. Winfree
Department of Biological Sciences, Purdue University, West Lafayette, Indiana 47907, USA
Steven H. Strogatz
Division of Applied Sciences, Harvard University, Cambridge, Massachusetts 02138, USA

Excitable media propagate periodic waves of chemical activity. In three dimensions, they resemble scrolls rotating about axes where reactions are not periodic. These axes close in rings which may be linked and knotted, in ways limited by an exclusion principle.

NONLINEAR waves are conspicuous in a variety of biologically and chemically excitable media. Waves of excitation propagate at uniform speed and mutually annihilate in collisions in the Belousov-Zhabotinsky reagent[1-8], in retinal[9] and cortical[10-12] nerve nets, where they may underlie neuromotor pathologies such as epilepsy, in heart muscle[13-16] where they are involved in life-threatening arrhythmias, and in aggregations of social amoebae[17-20] where they coordinate normal development. These waves commonly appear as involute spirals radiating from tiny rotating activity patterns, here called 'organizing centres'. In three-dimensional media, spirals are still seen, now as cross-sections through a scroll-shaped wave[3-5,21-28]. The scroll emanates from its central organizing axis, which typically forms a closed ring. The simplest form of organizing centre is an 'untwisted scroll ring'[1-4,21-28] or 'toroidal vortex'[29]. We present here a chemical/topological exclusion principle that predicts a quantized hierarchy of other, topologically distinct organizing centres and delimits the initial conditions required for their experimental realization[22-28]. We now review the published theoretical, computational, and experimental evidence concerning these three-dimensional reaction-diffusion structures.

Scroll rings

Periodicity is the central principle of all these arrangements of waves. Throughout any region organized by a spiral wave (Fig. 1), each point cycles periodically through activity, refractoriness, quiescence, and activity again. Hence we may describe a snapshot of the pattern in terms of the spatial distribution of phase. The phase, ϕ, of a point means the fraction of a cycle elapsed since the last wavefront excited that point. We represent the phase geometrically as a point on an abstract cycle, the unit circle S^1.

Description of spiral patterns in terms of phase entails a weird topological consequence: there must be a 'phase singularity' in the medium[1-3,23,30]. To prove this, first consider any closed path C enclosing the spiral's inner portions (Fig. 2). In one circuit of C, phase changes through exactly one full cycle. In mathematical terms[1,31], the map $\phi|_C: C \rightarrow S^1$ has winding number $W = \pm 1$. To conclude the proof, a theorem of topology[31] asserts that since $W \neq 0$, phase cannot be assigned continuously throughout any disk bounded by C. The most localized discontinuity possible is a phaseless point surrounded by all phases of the cycle: a phase singularity. The immediate neighbourhood of the singularity is a rotating pattern of chemical activities, the pivot of the rotating spiral wave, and the centre from which it radiates.

Because even a thin layer of excitable medium has finite thickness, the ostensibly flat spiral is actually a cross-section of a three-dimensional wave shaped like a scroll. This wave emerges from a filament of singularity. The filament has no physical substance; it cannot be strained out of the liquid like a strand of spaghetti. It represents merely the locus of intersection between two surfaces of uniform chemical concentration[1,3,21-23]. As such, it typically closes in a ring (unless interrupted by the physical boundaries of the medium as in Fig. 2). This predicted exact closure was confirmed experimentally by reconstruction of the fixed wave from serial sections[28,32] and by recent direct video recording during the uninterrupted reaction[4], as well as by computer simulation from the equations of local kinetics and molecular diffusion[3,29]. In the Belousov-Zhabotinsky reagent, these scroll rings persist through about a hundred rotations of the scroll, shrinking slowly at a rate which increases with the curvature of the singular filament[4,21,29,32].

A symmetric caricature of the observed scroll ring is shown in Fig. 3*a*, which depicts a snapshot of the expanding wavefront of excitation. In the next instant, the front would advance a uniform distance at every point and the ring would shrink slightly.

Twists and links

New topologically distinct possibilities exist for scroll ring closure. Imagine forming the ring by bending a straight segment of scroll, then sealing its ends together to preserve continuity (Fig. 3*b*). We might instead have given the straight scroll a 360° twist (Fig. 3*c*), or even have tied knots in it before joining its ends. These structures are indistinguishable locally: in each, a short segment along the singular filament is indistinguishable from a segment of the scroll ring of Fig. 3*a*. Because that untwisted, unknotted scroll ring is viable, local considerations suggest that twisted and knotted rings might be comparably stable.

However, global topology forbids most of these otherwise-plausible organizing centres. Consider, for example, the once-twisted scroll ring (built on the pattern of Fig. 3*c*) that has evolved to fill a cube of the medium. The winding number argument used above to detect a singularity reveals that this solitary once-twisted ring cannot exist: it must be threaded by another singular filament. To prove this, we evaluate the winding number along the inner equator of the invisible torus that confines Fig. 3*b* and *c*. As shown in Fig. 4, W is the number of twists locked into the planar scroll ring. Because $W \neq 0$, any surface bounded by that equator must be punctured by a singular filament[1,24,31].

In a computer-generated image[24,27,28] of the fully evolved wave (Fig. 3*d*), spirals emanate from the singular ring and collide awkwardly along a gnarled helicoidal surface, whose axis is the topologically-inferred phase singularity. This image was constructed by placing an involute spiral in each half-plane extending radially from the ring's axle, and then twisting it through 360° while swinging the plane once about the axle. Gomatam[5] has also shown analytically that such a screw

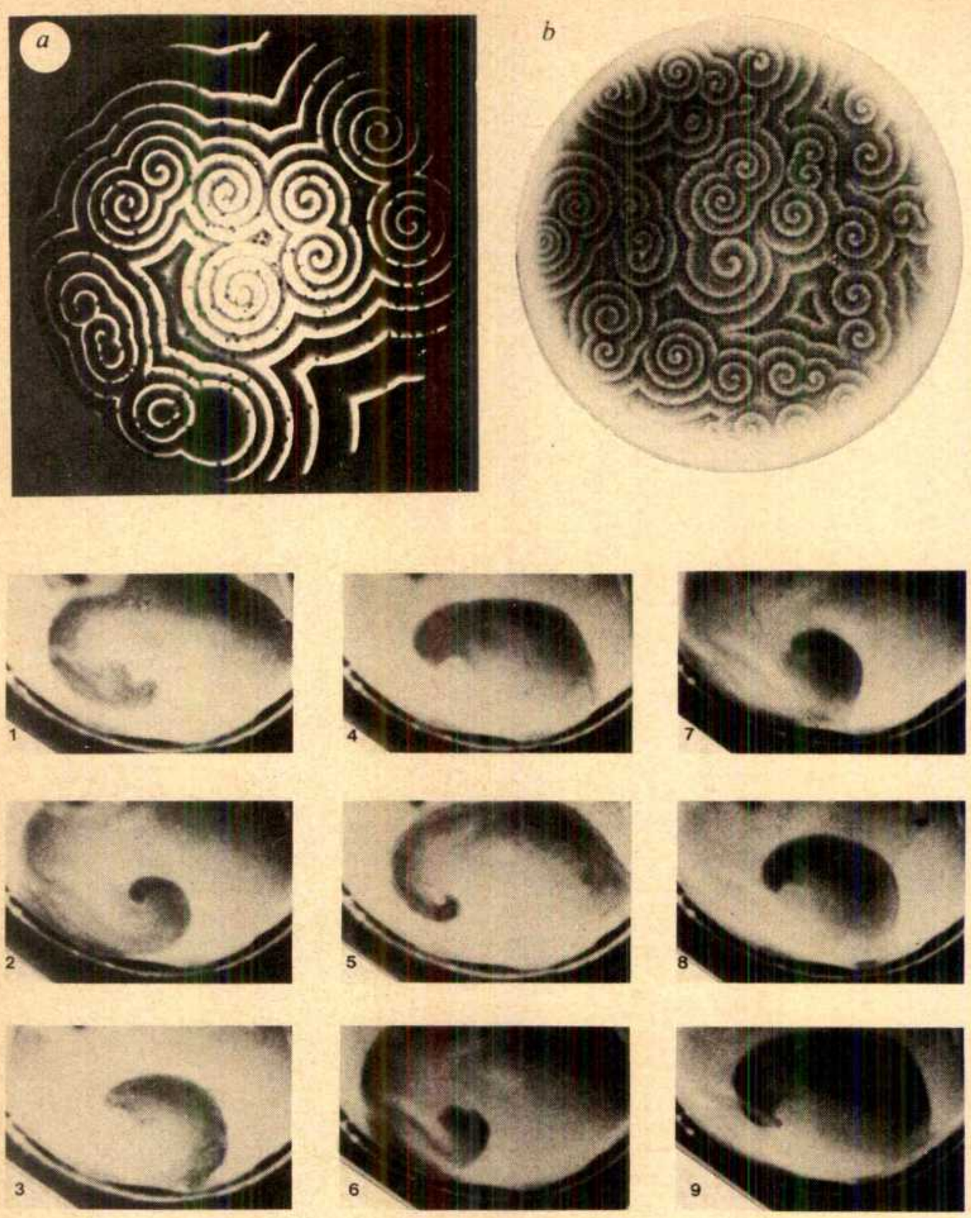

Fig. 1 Rotating spiral waves in excitable media. *a*, Transmitted light photograph of the chemical reagent originated by Belousov[42], and modified[2,7,21]. Waves radiate from spiral centres at a few mm min^{-1}, the spirals turning in about 1 min. The liquid layer is 1 mm deep; the field of view spans 90 mm. *b*, Dark-field photograph of a monolayer of *Dictyostelium discoideum* cells. Cells refract light differently when responding to a pulse of cyclic adenosine monophosphate. The instantaneous loci of this response are spirals rotating once in ~5 min as waves propagate at a few mm min^{-1}. The field of view spans 90 mm (with permission from Newell[20]). *c*, Successive photographs of the retina of a chicken taken by ambient light at intervals of 40 s. The dark area consists of cells recovering behind a wavefront of spreading depression. The front moves ~3 mm min^{-1}, rotating once in 3 min (twice in this mosaic). The field of view is 11 mm × 7.5 mm. (Adapted with permission from Gorelova and Bures[9]).

surface is a solution to linearized reaction–diffusion equations. Because physical rotation is equivalent to time evolution for this particular solution[24], we can animate the intricately rotating, propagating, and self-colliding wavefront by merely spinning it about its vertical axle (ref. 28, and our videotape).

However, there are two reasons why this symmetric solution is best regarded as a limiting extreme of a physically more realistic case. First, observation shows that stable spiral waves in excitable media always radiate outwards from their singularity; here they have been allowed to converge to the axial singularity in Fig. 3*d*. Second, to avoid ending the wave along an unphysical edge, the symmetries of Fig. 3*d* require it to extend to infinity in all directions, in violation of the realistic requirement that waves propagate at finite speed.

The practically realizable (but analytically less convenient) alternative is a pair of identical linked twisted scroll rings. Each provides the necessary threading singularity for the other. Figure 5*a* represents this organizing centre with the horizontal ring viewed nearly edge-on, while the other, regarded as arbitrarily large, is vertical, but hidden behind an interface where waves from each source collide. In Fig. 5*a*, viewports are opened in the horizontal scroll wave as it approaches collision a finite distance from the much larger vertical source ring. Realism is improved in Fig. 5*b* by giving both rings identical radii. Figure 5*b* presents a schematic of comparably sized rings, interlinked by their mutual rotation.

This mated pair of linked scroll rings exists in two mirror-image isomers, each with both singularities left-twisted (as here) or right-twisted. Either can be constructed from toroidal surfaces of uniform chemical concentration[23,24]. Experimental methods to contrive such initial conditions in an excitable medium are suggested elsewhere[23,24]. If its laboratory synthesis is successful the pair of linked twists will be the second observed organizing centre.

Exclusion principle

The allowed anatomy of an organizing centre is quantized by an exclusion principle, derived from both chemical and topological requirements. Away from boundaries of the medium, surfaces of uniform concentration must be disjoint, closed, and orientable; infinite concentration gradients are forbidden; singular filaments must be wave sources, not sinks; and far from the organizing centre, concentrations must approach quiescent uniformity[23]. The exclusion principle then states[26] that any realizable organizing centre must satisfy the constraints that:

$$\sum_{j=1}^{R} L_{ij}N_j = 0 \text{ for each } i = 1, 2, \ldots, R \qquad (1)$$

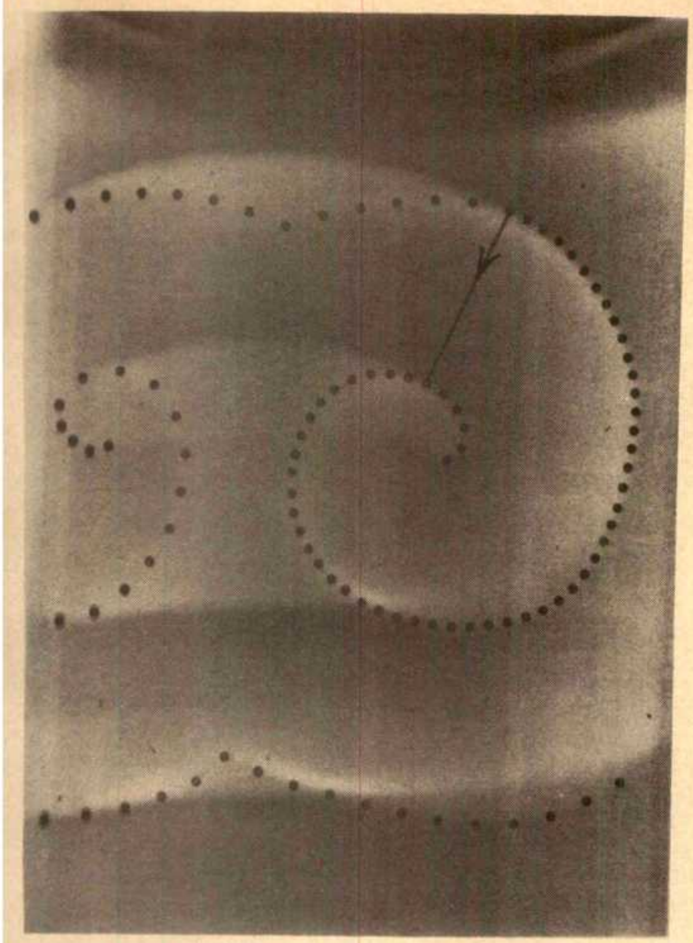

Fig. 2 Untwisted scroll wave and singular filament. A scroll wave in modified[4] Belousov–Zhabotinsky reagent is outlined in dots added to the photograph. Its spiral cross-section is exposed where it encounters the glass wall. A closed curve is traced 360° along this spiral with no change of phase (the chain of closely-spaced dots) then radially through one full wave (the line segment) passing through one full cycle of phase. It is accordingly linked by a singular filament: the scroll's source. (Reproduced with permission from Welsh *et al.*[4].)

where R is the number of constituent rings or knots[25], N_j is the positive number of spiral arms emanating from ring j (the singularity's "topological charge"[6]), L_{ij} is the linking number of rings i and j, and L_{ii} is the linking number of ring i with an imaginary ring traced along the wavefront infinitesimally nearby. These equations dictate the unique integer number L_{ii} of revolutions of the spiral wave required along each ring: $N_i L_{ii}$ must be equal and opposite to the sum of that ring's signed linkages with each of the other rings, counted with multiplicities N_j. L_{ii} is a sum of two real numbers called[25,33,34] the 'twist' (an integral of the spiral's gyration around the ring) and the 'writhing' (which depends only on the shape of the filament itself, and is zero for planar rings).

For a solitary ($R = 1$) ring or knot, the principle requires $L_{ii} = 0$. Thus, it predicts that a solitary scroll ring cannot contain net twist, as proved earlier by winding number arguments, and a solitary scroll knot must be twisted by an amount equal and opposite to its writhing number[25,26,34]. An untwisted ring pair cannot link. A pair of rings may contain equal twists if appropriately linked. For organizing centres composed of more than one ring, equation (1) specifies the set of quantum numbers, N_j, L_{ij}, and L_{ii} compatible with the known constraints. There may be additional constraints forbidding some organizing centres allowed by equation (1).

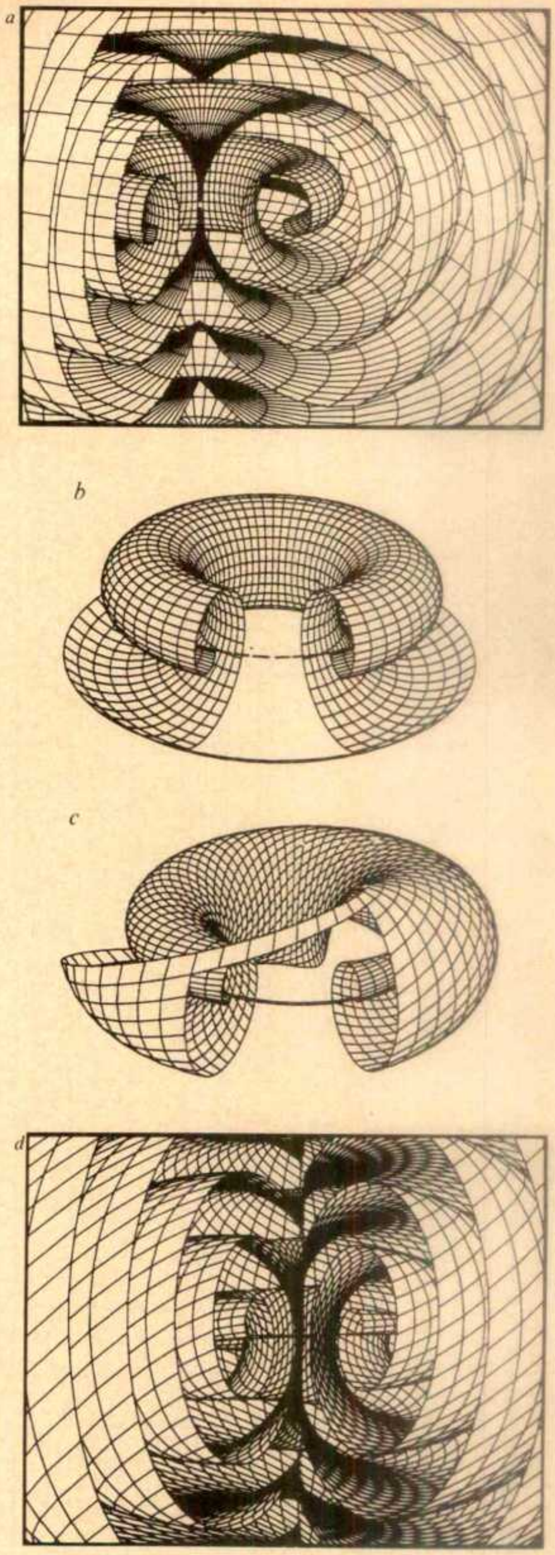

Fig. 3 Computer images of untwisted and twisted scroll rings. *a*, The inner lamina of an untwisted scroll ring wave fill the field of view. Their source is a horizontal circle of phase singularity, the front's inner edge. To aid in visualization, wavefronts are made transparent within a wide sector reaching to the internal symmetry axis along which wavefronts collide. (Reproduced from ref. 28.) *b*, At the same scale, we show as much of *a* as fits inside a torus around the singular ring. The wave's edge is a closed ring. *c*, As in *b* but the contents of the invisible torus are given one full 360° left twist around the circumference. The outer edge of this wave (where it terminates on striking the torus) is still a closed ring, but it now links the torus. *d*, As in *a*, but the wave field is extrapolated from *c* rather than from *b* to fill space. A phase singularity linking the torus is unavoidable. Here it is depicted as the unphysical focus of converging waves. (Reproduced from ref. 28.)

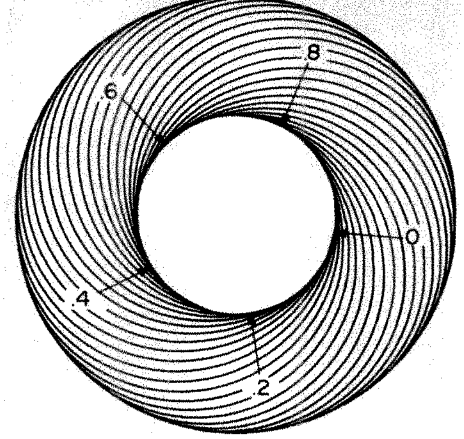

Fig. 4 Successive wavefront positions on a twisted scroll ring. Closed contours of fixed phase on an imaginary toroidal shell enclosing a uniformly once-twisted scroll ring. Only half of each contour is visible. A disk plugging the hole in the toroid touches these phase contours in serial order, spanning one cycle around the disk's boundary. Since $W \neq 0$, the disk must contain a phase singularity[31]. Applying the same argument to every diaphragm bounded by the toroid's inner equator, we detect an unforeseen singular filament threading the twisted scroll ring[1,24].

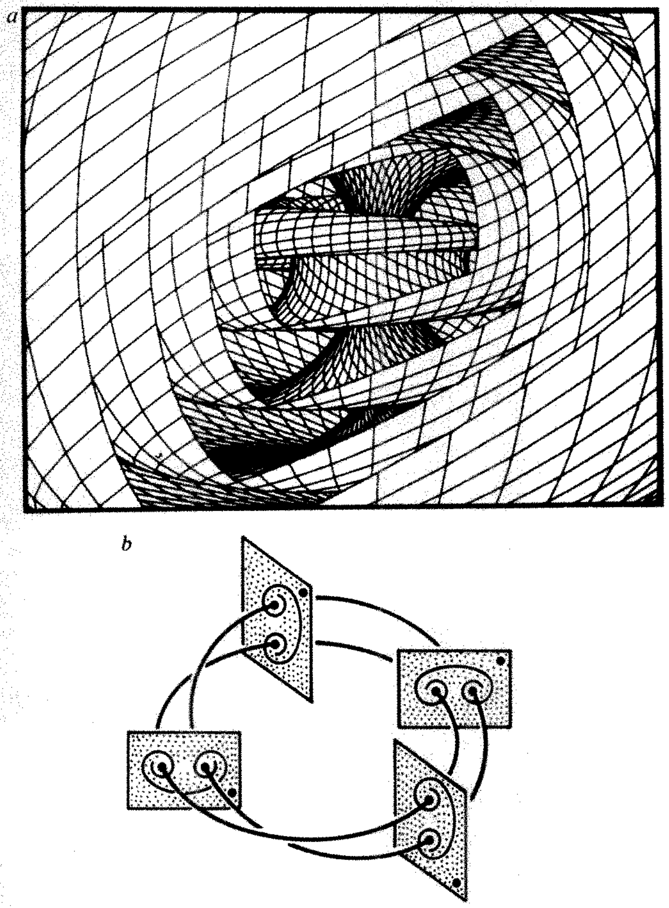

Fig. 5 Mutually linked pair of left-twisted scroll rings. *a*, As in Fig. 3*d*, a once-twisted scroll wave radiates from a horizontal source ring (exposed through a succession of windows). But here the wavefront stops short of collision with itself along an unphysical 'sink'. Rather, it collides with the outgoing wave from the much larger vertical twisted scroll ring hidden in the interior. (Reproduced from ref. 28.) *b*, A mirror-image pair of spirals is transported around a circular path to sweep out a pair of adjacent scrolls. Four local cross-section planes are shown. The pair is rotated as it is transported, so that each scroll is left twisted and the two are mutually linked. Waves emerging from the pair in each cross-section plane eventually join in rings. (Reproduced from ref. 24.)

Transmutation

Solitary scroll rings tend to contract towards their centres of curvature[4,21,29]; it seems likely that the twisted rings of more complex organizing centres do the same. Unless neighbouring filaments repel one another[22], organizing centres in media without boundaries must then eventually decay, leaving behind only quiescent uniformity. (Assuming that there are boundaries, a ring retains the alternative of opening into a scroll wave with an uncurved and stable axis.) Elementary decay processes[3,21] can only involve fission or fusion of rings. It is possible to envision such events in terms of continuous deformation of concentration fields[26]. The result in each case is a rearrangement of quantum numbers which alters R by ±1 and preserves identities (equation (1)). One allowable transmutation pathway regresses from a solitary trefoil knot to a linked pair of twisted scroll rings to a solitary untwisted scroll ring to an unlinked pair of scroll rings or to spatial homogeneity ('vacuum'). The latter two transmutations have already been observed in a chemically-active medium[37]. Presumably they can also occur in reverse, including the final transmutation to/from the vacuum state. In particular, mechanisms for creating scroll rings *ex nihilo* may have practical importance in biologically excitable media such as heart muscle[38].

Conclusion

We envisage a hierarchy of organizing centres ordered by the number of constituent rings. Loosely analogous to the Periodic Table, this hierarchy contains atoms made of scroll rings, much as in the "vortex atom" notion of Thomson and Helmholtz[39,40]. At each level, diverse isotopes are distinguished by mutual linkage and knotting of rings. Atomic structure is defined by integer quantum numbers, restricted by an exclusion principle. Fission and fusion transmute the elements. However, the geometric periodism peculiar to organizing centres imposes on them a more complex hierarchy than the rows and columns of the Periodic Table.

Attempts are under way to synthesize some of the missing organizing centres, and to observe organizing centres in diverse excitable media. Solitary scroll rings, at least, have been reported in chemically-active media[4,32] and in thick cardiac muscle[38].

Organizing centres could be biologically significant. They emit waves of short period comparable with the absolute minimum attainable, the medium's refractory period. Because waves mutually annihilate in collisions, higher frequency sources eventually dominate slower ones, including normal pacemaker centres, thus usurping control. Although modified by the inhomogeneities of biological media, such organizing centres may be involved with the pathological waves of spreading depression and epilepsy[9-12], and of cardiac fibrillation and sudden death[13-16,38,41].

A.T.W. thanks the NSF for grant CHE-810322, the US Department of Energy and Los Alamos National Laboratory for hospitality and Cray-1 computer time in summer 1983, Mel Prueitt for GRAFIC software and instruction.

1. Winfree, A. T. *The Geometry of Biological Time* (Springer, New York, 1980).
2. Winfree, A. T. *Science* **175**, 634-636 (1972).
3. Winfree, A. T. *Scient. Amer.* **230**(6), 82-95 (1974).
4. Welsh, B., Gomatam, J. & Burgess, A. *Nature* **304**, 611-614 (1983).
5. Gomatam, J. *J. Phys.* **A15**, 1463-1476 (1982).
6. Agladze, K. & Krinsky, V. I. *Nature* **296**, 424-426 (1982).
7. Zaikin, A. N. & Zhabotinsky, A. M. *Nature* **225**, 525-527 (1970).
8. Tyson, J. J. *The Belousov-Zhabotinsky Reaction, Springer Lecture Notes in Biomathematics* Vol. 10 (ed. Levin, S.) (Springer, Berlin, 1976).
9. Gorelova, N. A. & Bures, J. *J. Neurobiol.* **14**, 353-363 (1983).
10. Bures, J., Buresova, O. & Krivanek, J. *The Mechanism and Application of Leao's Spreading Depression of Electroencephalographic Activity* (Academic, Prague, 1974).
11. Koroleva, V. I. & Bures, J. *Brain Res.* **173**, 209-215 (1979).
12. Bures, J., Buresova, O., & Koroleva, V. I. in *Neurophysiological Mechanisms of Epilepsy* (ed. Okujava, V. M.) 120-130 (Metsnierba, Tblisi, 1980).
13. Krinsky, V. I. *Pharm. Ther.* **B3**, 539-555 (1978).
14. Janse, M. J., van Capelle, F. J., Morsink, H. & Kleber, A. G. *Circ. Res.* **47**, 151-165 (1980).
15. Allessie, M. A., Bonke, F. I. M., & Schopman, F. J. G. *Circ. Res.* **333**, 54-62 (1973).
16. van Capelle, F. J. L. & Durrer, D. *Circ. Res.* **47**, 454-466 (1980).
17. Bonner, J. T. *The Cellular Slime Molds* (Princeton University Press, 1967).
18. Gerisch, G. *Current Topics in Developmental Biology* Vol. 3 (eds Moscona, A. & Monroy, A.) 157-197 (Academic, New York, 1968).
19. Tomchik, K. N. & Devreotes, P. N. *Science* **212**, 433-446 (1981).

20. Newell, P. C. in *Fungal Differentiation: a Contemporary Synthesis* (ed. Smith, J.) 43 (Dekker, New York, 1983).
21. Winfree, A. T. *Science* **181**, 937-939 (1973).
22. Winfree, A. T. in *Oscillations and Travelling Waves in Chemical Systems* (eds Field, R. J. & Burger, M.) (Wiley, New York, 1984).
23. Winfree, A. T. & Strogatz, S. H. *Physica* **8D**, 35-49 (1983).
24. Winfree, A. T. & Strogatz, S. H. *Physica* **9D**, 65-80 (1983).
25. Winfree, A. T. & Strogatz, S. H. *Physica* **9D**, 333-345 (1983).
26. Winfree, A. T. & Strogatz, S. H. *Physica* **10D** (in the press).
27. Strogatz, S. H., Prueitt, M. L., & Winfree, A. T. *IEEE Comput. Graphics Appl.* **4**, 66-69 (1984).
28. Winfree, A. T. *Physica* **10D** (in the press).
29. Panfilov, A. & Pertsov, A. M., *Dokl. Akad. Nauk. USSR* **274**, 1500-1503 (1984) (in Russian).
30. Berry, M. V. in *Les Houches Lecture Series* Vol. 35 (eds Bahian, R., Kleman, M., & Poirer, J.-P.) 453-543 (North Holland, Amsterdam, 1981).
31. Munkres, J. R. *Topology: A First Course* 357-360 (Prentice-Hall, Englewood Cliffs, 1975).
32. Winfree, A. T. *Faraday Symp. chem. Soc.* **9**, 38-46 (1974).
33. Crick, F. H. C. *Proc. natn. Acad. Sci.* U.S.A. **73**, 2639-2643 (1976).
34. Fuller, F. B. *Proc. natn. Acad. Sci.* U.S.A. **68**, 815-819 (1971).
35. Pohl, W. F. *Math. Intelligencer* **3**, 20-27 (1980).
36. Bauer, W. R., Crick, F. H. C., & White, J. H. *Scient. Am.* **243**(7), 118-133 (1980).
37. Welsh, B. thesis, Glasgow College of Technology (1984).
38. Medvinsky, A. B., Pertsov, A. M., Polishuk, G. A., & Fast, V. G. in *Electrical Field of the Heart* (eds Baum, O, Roschevsky M. & Titomir, L.) 38-51 (Nauka, Moscow, 1983) (in Russian).
39. Helmholtz, H. *Phil. Mag. Suppl.* **33**, 485-510 (1867).
40. Thomson, W. I. *Phil. Mag.* **34**, 15-24 (1867).
41. Winfree, A. T. *Scient. Am.* **248**(5), 144-161 (1983).
42. Winfree, A. T. *J. chem. Educ.* **61**, 661-663 (1984).

ARTICLES

India–Eurasia collision chronology has implications for crustal shortening and driving mechanism of plates

Philippe Patriat & José Achache

Institut de Physique du Globe de Paris, Université Paris 6, Laboratoire de Géomagnétisme et Paléomagnétisme, 4 Place Jussieu, 75005 Paris, France

The motion of the Indian plate is determined in an absolute frame of reference and compared with the position of the southern margin of Eurasia deduced from palaeomagnetic data in Tibet. The 2,600 ± 900 km of continental crust shortening observed is shown to have occurred in three different episodes: subduction of continental crust, intracontinental thrusting and internal deformation, and lateral extrusion. The detailed chronology of the collision and plate reorganizations in the Indian and Pacific oceans supports the hypothesis that slab-pull is a dominant driving mechanism of plate tectonics.

THE collision between the Indian and Eurasian continents is considered to be one of the major tectonic events of Cenozoic time. It has resulted in ~2,000 km of north–south crustal shortening within continental Eurasia[1]. Several models have been proposed for the mechanism of this shortening: continuous deformation, multiple continental underthrusting, eastward propagating extrusion or mosaic tectonics[2–5]. Convergent plate motion still occurs between India and Eurasia and is evidenced in particular by active tectonics beneath the Himalayas, in Tibet and in south-central Asia[6–8].

The continental effects of the collision have been extensively studied, in particular during the 1980–83 French–Chinese cooperation programme in Tibet[5–9]. Geological or geophysical observations on land can only give bounds on the age of the initial collision. For instance, structural observations along the Yarlung Zangbo suture zone (YZSZ) in Tibet (in the vicinity of Lhasa) show the ophiolites to have been obducted before the end of the Eocene (before 40 Myr)[9]. Such a young upper bound is also indicated by petrological and geochronological data on igneous rocks in Tibet. Indeed, the youngest granodiorites observed near Lhasa are dated at 41 Myr (ref. 10) and thus may be consistent with the subduction of oceanic crust beneath Tibet until at least 45 Myr, assuming up to 4 Myr for the transit and cooling of magma in the crust. An older age for the initial collision has been proposed from geological evidence and seafloor spreading data[11]. It is suggested that it began, at least in the Ladakh area, before the middle Eocene (near 53 Myr).

On the other hand, only a few studies have analysed the consequences of the collision on plate tectonics. In an early analysis of seafloor spreading in the Indian ocean, Molnar and Tapponnier[12] interpreted a decrease in the rate of northward drift of India near 40 Myr as indicative of the India–Eurasia collision. Using more detailed data, this slowing of the Indian plate has been associated with the decrease in spreading rate on the Eastern Indian ridge near anomaly 22 time (~50 Myr)[13–15]. Following Molnar and Tapponnier[12], several authors have related this change in spreading rate to the collision between the two continental masses[16,17]. However, the change in India–Africa relative motion observed at anomaly 20 (44 Myr) has been considered elsewhere as indicative of this collision[17]. Also, evidence for an important plate reorganization in the north-eastern Indian Ocean after anomaly 20 time has recently been put forward and interpreted as a consequence of the collision[18].

Here we use a more comprehensive set of marine magnetic anomalies in the central Indian Ocean, in the vicinity of the triple junction[19] to determine the detailed motion of the Indian plate since anomaly 32 time (late Upper Cretaceous) and to clarify the chronology of the collision. The relative position of India with respect to Eurasia is computed using a procedure originally proposed by Patriat *et al.*[17]. It is then compared with its absolute position with respect to the hotspot frame of reference. This latter absolute motion is compared with recently determined palaeomagnetic poles in Ladakh, Tibet and Thailand[1,20–22] in order to determine the northern extent of India before the collision. The present data are combined with a recent interpretation of the northeastern Indian Ocean[18] to provide a complete reconstruction of the Indian plate before, and immediately after, the India–Eurasia continental collision. The relative importance of the driving forces of plate tectonics is then discussed taking into account these reconstructions.

Age of the India–Eurasia collision

In the past 15 yr, an extensive survey has been performed in the Indian Ocean using ships *Gallieni* and *Marion Dufresne* (see ref. 23). This survey has allowed a detailed interpretation of marine magnetic anomalies in the Central Indian Basin, the Crozet Basin and the Madagascar Basin[19,23] (Fig. 4*b*). These anomalies were generated at the accreting boundaries between the India, Antarctica and Africa plates, which meet at the Rodriguez triple junction. The simultaneous study of seafloor spreading on both flanks of these three ridges in the vicinity of the triple junction has allowed a complete and consistent

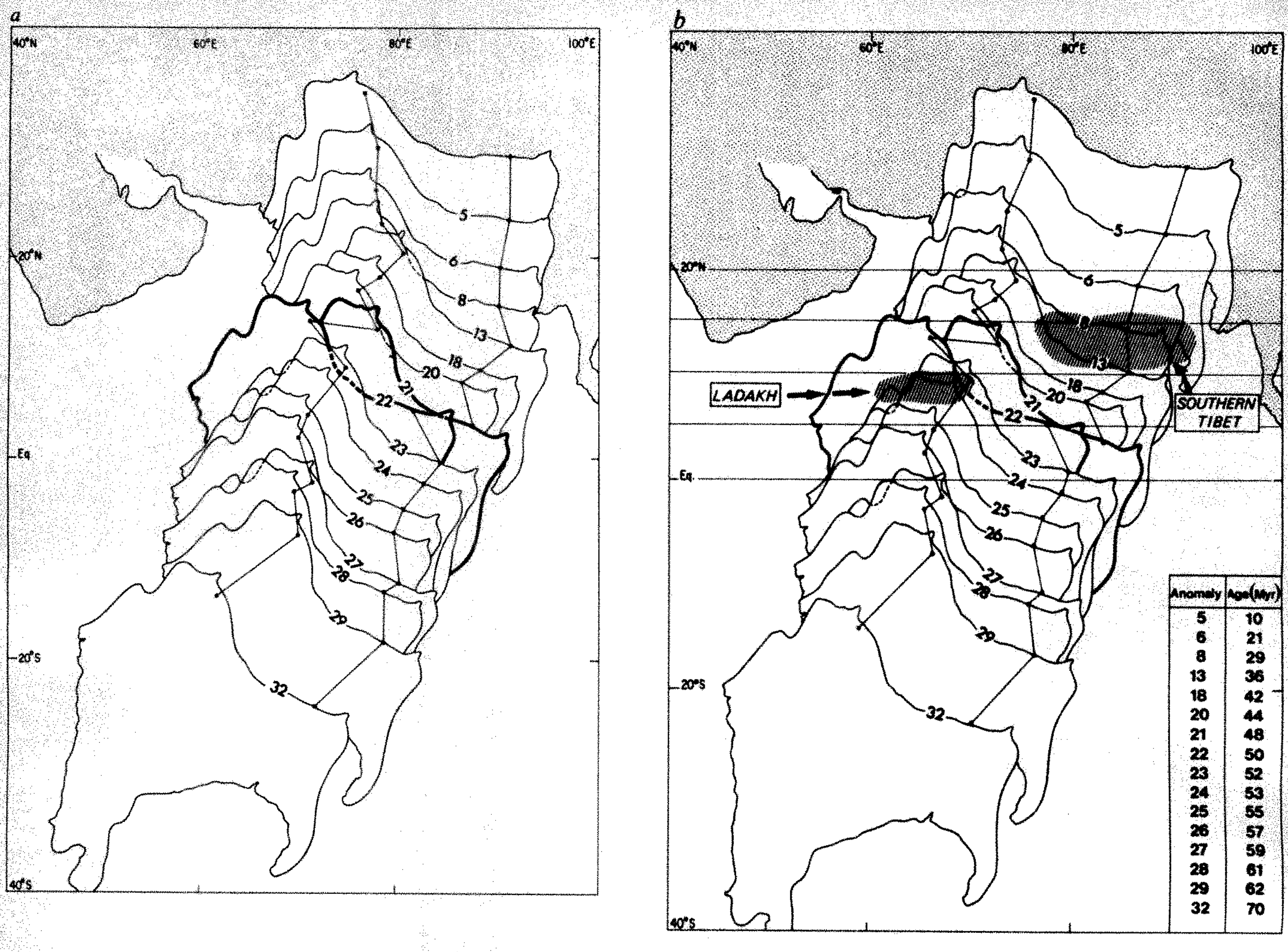

Fig. 1 Cenozoic northward drift of India. The northern limit of the Indian continent is taken as the present position of the Indus–YZSZ. The passive margins are drawn at the 500-m isobath (represented at anomaly 32 time). Also plotted is the motion of two points located on the Indian continent near the northern margin: in Ladakh (34°34′ N, 76°7′ E) and on the suture zone near the present position of Lhasa (29°20′ N, 91° E). The position of the northern margin of India is emphasized at the time of initial collision with the southern margin of Eurasia (anomalies 22 and 21). *a*, Relative motion of India with respect to Eurasia, kept arbitrarily fixed in its present position. *b*, Absolute motion of India in the hotspot frame of reference. The positions of southern Tibet and Ladakh before collision deduced from palaeomagnetic data, are also indicated for comparison.

reconstruction of the relative motion of the plates from anomaly 34 time (83 Myr) to the present[19].

Figure 1*a* represents the successive positions of India since anomaly 32 time (70 Myr) with respect to the Eurasian plate which is kept arbitrarily fixed in its present position (Table 1). The position of India at a given time is obtained by combining the rotation of India with respect to Africa, determined from magnetic anomalies in the Indian Ocean[19], with the rotation of Africa with respect to Eurasia, deduced from magnetic anomalies in the Atlantic Ocean[24–26]. Figure 1*b* shows the successive positions of India with respect to the hotspot frame of reference (Table 2). Here, India is, as before, first restored in its position with respect to Africa but then Africa is rotated in its position with respect to the hotspot reference frame at a given time[27].

The two reconstructions of Fig. 1 are very similar. It confirms that during the Cenozoic, the Eurasian plate underwent only a small clockwise rotation with respect to the Earth's mantle. This is evidenced by the apparent polar wander path (APWP) of this plate between 60 Myr and the present[28–30] and also by hotspot tracks analysis[27]. In addition, the location of the Euler pole for this rotation implies very little latitudinal displacement of the plate in the vicinity of the collision zone[1,30].

One can observe on Fig. 1 three successive phases in the drift history of India. First, down to anomaly 23 (52 Myr) India was drifting northward with a mean velocity of 15 to 20 cm yr^{-1}. Then, between anomaly 23 and anomaly 13 (36 Myr) the motion of India became rather erratic showing several changes in direction while the mean northward velocity was reduced to <10 cm yr^{-1}. Finally, from anomaly 13 to the present, India resumed a stable northward direction of convergence with respect to Eurasia with a constant rate of <5 cm yr^{-1}.

The decrease of the mean velocity of India is seen in Fig. 2 where the rate of convergence between India and Eurasia is computed at two arbitrary points and plotted as a function of time, assuming two particular orientations of the plate boundary (subduction). Before anomaly 22 (50 Myr), the rate varied between 15 and 25 cm yr^{-1}; it then decreased until anomaly 18 (42 Myr) (or 13, depending on the orientation of the trench), where it reached a stable value of ~ 4 cm yr^{-1}.

The sudden velocity drop after anomaly 22 is more clearly observed directly on the evolution of spreading rates at the eastern and central Indian ridges (Fig. 3). Indeed, on both spreading centres bordering the Indian plate, one observes a sharp decrease in spreading rate between anomalies 22 and 21. On the central Indian ridge, the velocity decrease seems to have occurred slightly later in the vicinity of the Vema fracture zone (Fig. 3*a*). This should be atrributed to the uncertainties in the reconstruction of plate motion in this area, also suggested by the frequent changes in the azimuth of spreading near anomaly 22 time (Fig. 3*b*) and due to the proximity of the pole of rotation.

These changes in the direction of spreading coincide with the surprisingly erratic behaviour of India, indicated in Fig. 1, at the time of anomalies 22 and 21. The Indian plate seems to have

Table 1 Euler poles of India–Eurasia relative motion during the Cenozoic

Age (Myr)	Anomaly	Lat. (°N)	Long. (°E)	Angle (°)
10.21	A5	16.6	37.6	7.44
20.98	A6	18.5	33.3	12.85
29.22	A8	16.9	34.8	17.74
36.47	A13	13.3	40.7	23.82
41.81	A18	17.7	37.0	26.98
44.40	A20	20.7	34.0	28.44
47.69	A21	16.0	35.0	33.27
49.68	A22	26.0	24.0	30.50
51.62	A23	18.1	28.7	36.44
53.03	A24	19.0	25.8	38.37
55.25	A25	20.1	22.1	40.81
56.92	A26	19.8	20.7	43.17
59.31	A27	16.2	22.7	48.67
60.57	A28	17.3	20.6	49.47
62.49	A29	14.9	21.5	54.65
70.62	A32	18.8	13.3	60.72

The rotation at A32 between India and Africa is obtained by combining the India–Antarctica and Antarctica–Africa rotations.

Table 2 Euler poles of India absolute motion during the Cenozoic

Age (Myr)	Anomaly	Lat. (°N)	Long. (°E)	Angle (°)
10.21	A5	27.7	31.1	7.83
20.98	A6	30.6	24.9	13.93
29.22	A8	28.6	26.0	19.13
36.47	A13	24.1	32.0	24.74
41.81	A18	26.8	29.2	27.51
44.40	A20	29.1	26.5	28.80
47.69	A21	23.0	28.7	32.50
49.68	A22	33.2	16.1	30.59
51.62	A23	24.2	22.4	35.22
53.03	A24	24.5	19.3	36.91
55.25	A25	25.2	14.9	39.30
56.92	A26	24.6	13.3	41.48
59.31	A27	20.2	15.7	46.18
60.57	A28	21.1	13.2	47.01
62.49	A29	18.1	14.2	51.52
70.62	A32	20.6	3.4	57.53

The rotation at A32 between India and Africa is obtained by combining the India–Antarctica and Antarctica–Africa rotations.

undergone, during this period, several successive important shifts in its direction of motion (absolute or relative to Eurasia). Since the momentum of a plate can always be neglected[31], such shifts must be explained by successive changes in the balance of forces applied to the plate. The time constant for these changes is too short to allow a significant modification of the body or surface forces acting on the entire plate like gravitational sliding (ridge-push) or viscous drag. Thus, the shifts observed should rather be related to modifications at the plate boundaries. Following earlier studies, we suggest that the directional shifts and velocity decrease of the Indian plate observed at anomalies 22 and 21 time are likely to be associated with the closure of the Neotethys to the north of India and thus to indicate the onset of the collision of India with the southern margin of Eurasia.

Reconstructions based on magnetic anomalies 22 and 21 on both sides of the central Indian ridge are subject to some uncertainties. However, anomaly 21 is also well identified on the two flanks of the eastern and western Indian ridges, and the rotation of India with respect to Africa determined on the central Indian ridge is in close agreement with the combined rotation of India with respect to Antarctica and of Antarctica with respect to Africa. This confirms that even when uncertainties are taken into account, the shifts in plate motion direction described above cannot be avoided in the reconstructions. Thus, although a precise description of the actual motion of India between anomalies 23 and 21 time cannot be achieved, the shifts observed must be considered as significant and indicative of a peculiar and major event, such as the beginning of a continental collision.

Palaeomagnetic data in Tibet

In Fig. 1*b*, the position of the northern margin of India in the hotspot frame of reference is compared with the palaeoposition of the southern margin of Eurasia deduced from palaeomagnetic studies. It has been shown that the two frames of reference used for this comparison, the axial geomagnetic dipole field and the hotspot frame, have remained fixed within 5°–10° of each other, in the past 60 Myr (refs 27, 29). Furthermore, the consistency between the palaeomagnetically-determined latitude of India and its absolute position derived from oceanic magnetic anomalies and hotspot track analysis is confirmed by recent palaeomagnetic work in Tibet, on the northern margin of India[22]. This study of Eocene limestones, sampled to the south of the YZSZ, reveals two different components of magnetization. A primary component of Lower Eocene age indicates a palaeolatitude for the northern margin of India, in the vicinity of Lhasa, of 2.5°±4° S. Our present reconstruction places the sampled area at anomaly 26 time (the age of the magnetization) at a palaeolatitude of about 6° S (Fig. 1*b*). A secondary post-collisional component is also revealed by the study of Besse *et al.*[22] and indicates a palaeolatitude of 6°±5° N. This is again very consistent with our reconstructions which show the collision to have occurred in the area of Lhasa near 5° N (Fig. 1*b*).

Two palaeomagnetic poles have been derived for southern Tibet in the area of Lhasa for late Cretaceous and Palaeocene time[1]. Southern Tibet was accreted to the southern margin of Eurasia before the late Jurassic[5] and, therefore, indicates the position of this margin since that time. The late Cretaceous pole, derived from Albian–Aptian red beds, places the margin near Lhasa at a palaeolatitude of 11.5±3° N. The early Cenozoic pole has a slightly larger confidence limit associated with the large timespan of volcanic emplacement (ages range at least

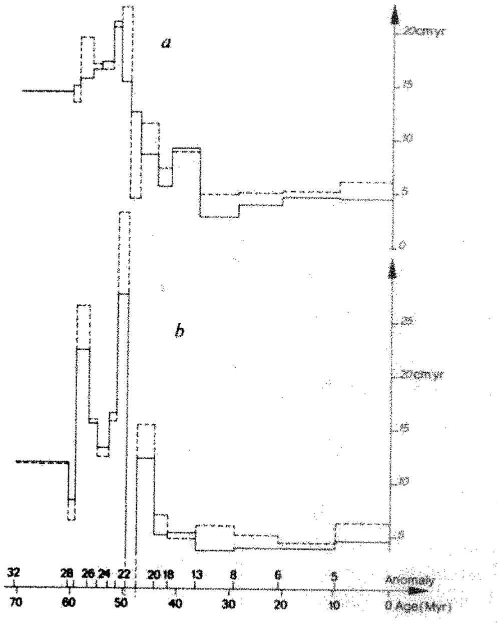

Fig. 2 Computed rate of convergence between the Indian and the Eurasian plates during the Cenozoic, at two arbitrary points (5° N, 75° E, solid line; 5° N, 90° E, dashed line) along two particular directions. It indicates the rate of subduction perpendicular to the trench for a subduction zone located near the southern margin of Eurasia and trending N120 E (*a*) or east–west (*b*).

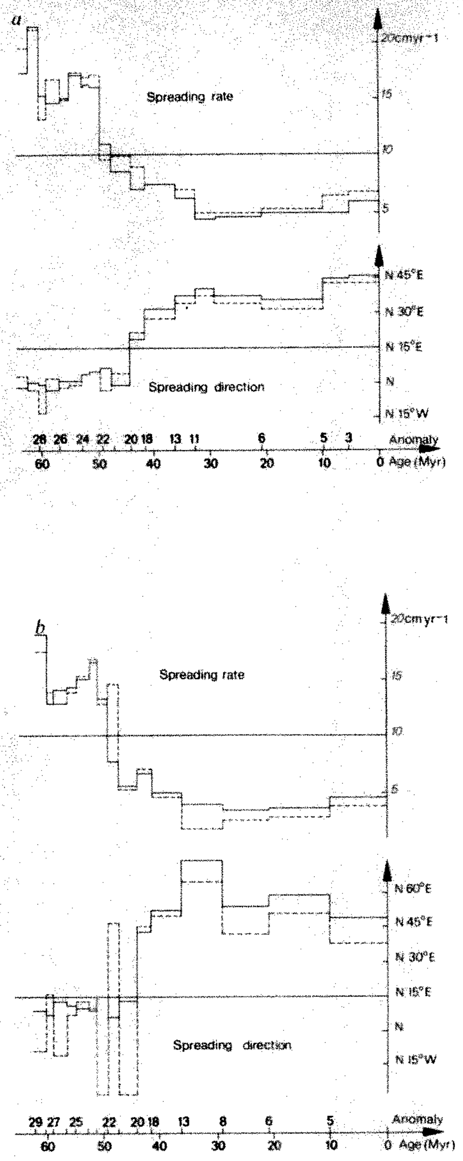

Fig. 3 Measured rate and direction of spreading at two accreting boundaries of the Indian plate during the Cenozoic. *a*, Eastern Indian ridge, in the vicinity of the Rodriguez triple junction (solid line) and near the Amsterdam fracture zone further east (dashed line). *b*, Central Indian ridge, in the vicinity of the triple junction (solid line) and near the Vema fracture zone further north (dashed line). The important shifts in spreading direction near the Vema fracture zone are related to the proximity of the reconstructed poles of rotation at the time of the collision (anomalies 22 and 21).

from 60 Myr (ref. 32) to 48 Myr (ref. 33)), secular variation of the Earth's magnetic field and the possible occurrence of Cenozoic deformation within southern Tibet[1,34]. This younger pole indicates a palaeolatitude of 13±6.5° N for the southern margin of Eurasia.

Another palaeomagnetic pole has been derived in Tibet, north of the Indus–YZSZ, for Palaeocene–Eocene time in the Ladakh area[20]. The Ladakh intrusives have been interpreted as the batholitic foundation of an island arc[35,36]. The remanent magnetization recorded in these intrusives indicates a palaeolatitude between 7 and 10° N and is considered to have been acquired shortly before 50 Myr.

It can be seen on Fig. 1*b* that the northern margin of India collided with the Ladakh island arc before anomaly 24 (53 Myr). It is not until anomaly 22 (50 Myr), however, that the first significant change in the direction of motion occurred on the Indian plate. This confirms that such a collision between a large continent and an offshore island arc is unlikely to significantly alter the motion of the plate.

In contrast, one observes on Fig. 1*b* that at anomaly 22 time, the northern margin of India near Lhasa still lay about 7° south of the southern margin of Eurasia (southern Tibet). Since Argand[37], several estimates of crustal shortening have been proposed for the Indian continent and accounted for, either by continental subduction beneath Tibet along the YZSZ, or by underthrusting within India (along the Main Central thrust (MCT), Main Boundary thrust (MBT) or Kangmar thrust. See, for example, refs 5, 38). The reconstruction proposed here implies between 400 and 1,000 km of continental shortening between India and southern Tibet, at the longitude of Lhasa. Uncertainties are taken from the position of India at anomalies 23 and 20 (see Fig. 1) and are thus likely to be overestimated.

Driving mechanism of plates

The analysis of seafloor spreading on the central and eastern Indian ridges reveals that the decrease in spreading rate at anomaly 22 is followed at anomaly 20 by a consistent and significant change in the direction of spreading (Fig. 3). A more detailed analysis of magnetic anomalies in the Central Indian Basin and the Crozet Basin reveals that this change in spreading direction did not occur synchronously along the entire eastern Indian ridge. Instead, the change seems to have propagated eastward along the ridge. Anomaly 20 is parallel to the new direction of spreading near the triple junction but is still parallel to older anomalies further east[19]. The change in spreading direction on the central Indian ridge was accompanied by a jump of the spreading centre. This is evidenced by the existence in the Madagascar Basin, near Ile Maurice, of a fossil spreading centre which ceased spreading just before anomaly 20 time[19].

Liu *et al.*[18] have re-analysed magnetic anomalies in the north-western Wharton Basin, south of Sumatra. They have recognized a fossil spreading centre. The existence of this fossil ridge was first reported by McDonald[39] who observed a series of basement highs beneath the sedimentary cover of the Nicobar Fan. This accreting plate boundary which separated India from Australia in the early Cenozoic, before the India–Eurasia collision, ceased its spreading shortly after anomaly 20 time[18].

Cande and Mutter[40] have re-identified the oldest magnetic lineations between Australia and Antarctica. They propose that initial rifting between the two continents took place between 110 and 90 Myr but seafloor spreading occurred at a very low rate of <1 cm yr^{-1} until anomaly 21, where it reached a value of 2 cm yr^{-1}. After anomaly 20, this spreading rate suddenly increased significantly to a value of 5.5 cm yr^{-1}.

All these observations indicate the occurrence of a global plate reorganization in the Indian Ocean which seems to have started near the Indian triple junction immediately before anomaly 20, near 45 Myr, and to have been completed before the formation of anomaly 19, near 43 Myr. Figure 4 represents the plate configuration in the Indian Ocean at anomaly 24 time (53 Myr), that is before the beginning of the collision (Fig. 4*a*), and at anomaly 18 time (42 Myr), when the plate reorganization had been completed (Fig. 4*b*). The reconstruction of the spreading centre between India and Australia is based on the new identification of magnetic anomalies in the Wharton Basin[18]. The central and western Indian Ocean are reconstructed from the identification of magnetic anomalies described in Patriat[19]. Finally, the whole reconstruction is rotated in an absolute position with respect to the hotspot frame of reference. This allows the comparison with palaeopositions deduced from palaeomagnetic studies.

The position of the southern margin of Eurasia is given by palaeomagnetic data in Tibet (see above) and Thailand. Mesozoic poles for the Indochina block indicate an early Tertiary palaeolatitude for this block between 15 and 20° N (ref.

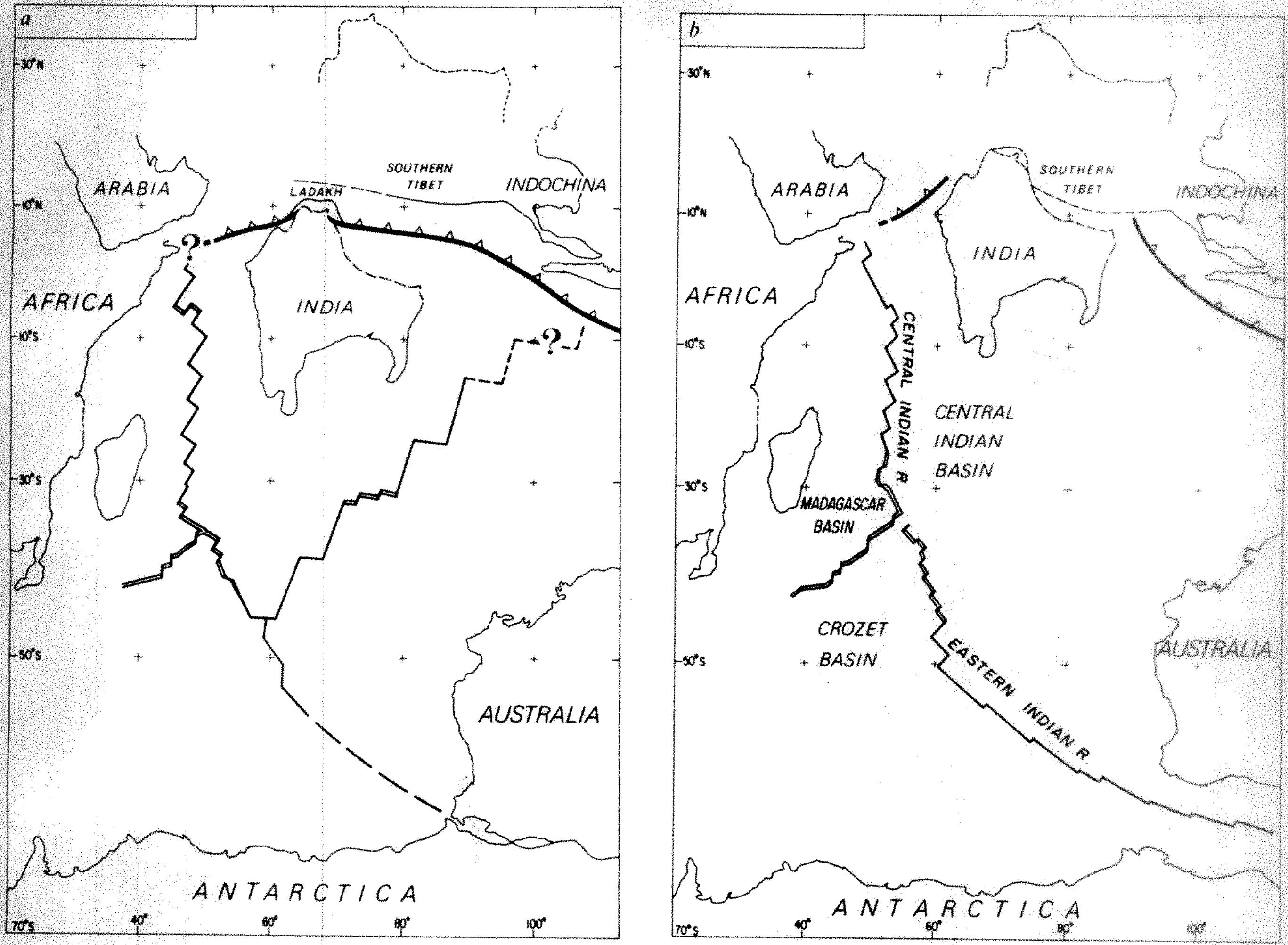

Fig. 4 Plate reconstruction of the Indian Ocean in an absolute frame of reference (hotspot and axial geomagnetic field), before the India–Eurasia collision (at anomaly 24 time, *a*) and immediately after the end of the plate reorganization which followed the collision (at anomaly 18 time, *b*). The contours of Arabia, Africa, Madagascar, Antarctica and Australia were digitized at the 2,500-m isobath. The contours of India were taken at the 500-m isobath (because of the thick series of deltaic sedimentary deposits) and along the Indus–YZSZ to the north (dashed line). The southern margin of Eurasia is reconstructed from palaeomagnetic data (southern Tibet, Ladakh and Indochina–Thailand). The present position of the Indus–YZSZ is also shown for comparison (dashed line). Double lines represent the position of spreading centres reconstructed from identified magnetic anomalies[18,19]. The position of other spreading centres is more speculative and may be subject to revision. The subduction zone (barbed line) is located after the distribution of Upper Mesozoic granites in Tibet and southeastern Asia. Euler poles for the motion of Australia with respect to Antarctica are taken from ref. 51. The overlap in the reconstruction at anomaly 24 between Australia and Antarctica is consistent with the model of propagating rift and continental breakup of Courtillot[50].

21). This study also indicates an approximate 20° clockwise rotation of Indochina with respect to Eurasia since the collision, thus allowing Indochina to be restored to its pre-collision position (Fig. 4*a*). The subduction zone is located along the southern margin of Eurasia as suggested by the occurrence of Upper Mesozoic granites (see ref. 30). Although, as discussed above, ~700 km of crustal shortening is likely to have occurred within the Indian continent, the northern limit of India before the collision is indicated by the Indus–YZSZ in Fig. 4*a*.

The slab-pull force associated with subduction zones is a dominant force controlling the direction of motion of a plate[41,42]. Indeed, the sequence of events associated with the collision and the plate reorganization are all very consistent with this hypothesis. First, as discussed above, the dramatic decrease of the Indian plate velocity at anomaly 22 time (50 Myr) is associated with the closure of the Neotethys in Tibet. This event affected >50% of the total length of subducting boundary of the plate (Fig. 4*a*). However, the northward motion of India continued until anomaly 20 time (44 Myr) when a new regime of plate tectonics was established in which India and Australia became a single plate. This 5-Myr delay between the initial contact (closure of the Neotethys) and this major plate reorganization corresponds, as seen in Fig. 1, to the subduction of 300–500 km of Indian continental crust beneath Tibet. This value is in agreement with earlier estimates of the amount of continental crust which can be subducted in a trench[43] suggesting that the plate reorganization did not occur until subduction had nearly stopped beneath Tibet, when the slab-pull force acting on the Indian plate along the colliding boundary was balanced by the buoyancy of the subducted continental crust. This is further indicated by the convergence rate between India and Eurasia which continues to decrease rapidly until anomaly 20 time and keeps a nearly constant values afterwards (Fig. 2).

As shown in Fig. 4*b*, India and Australia have become part of the same plate after anomaly 20 time. A counterclockwise rotation of India with respect to Eurasia is observed since that time (Fig. 1). This rotation is also indicated by palaeomagnetic studies on DSDP cores in the Indian Ocean[44] and on the Deccan Trapps in India[45] and is matched in southern Tibet by a similar counterclockwise rotation with respect to Eurasia[1]. This is in agreement with the fact that the suturing of India against Eurasia had been completed by anomaly 20 time. The distribution of subducting boundaries bordering the new larger Indian plate, essentially the New Guinea and Java trenches, is consistent with the observed counterclockwise rotation in the late Cenozoic in the hypothesis of a driving mechanism dominated by slab-pull forces. Furthermore, this rotation of the Indian plate is likely to imply the onset of a convergent relative motion at the India–Pacific plate boundary. Indeed, one observes the creation in the early Tertiary of several thousands of kilometres of new subduction zones along the southwestern boundary of the Pacific plate (Tonga–Kermadec, Macquarie; see refs 41, 46). The bend observed in the Hawaian–Emperor seamount chain has been interpreted as evidence for a change in the absolute motion of the Pacific plate and shown to be consistent with the redistribution of slab-pull forces acting on this plate[41].

The bend in the Hawaian–Emperor chain occurred near 42 Myr. Thus, the time lag between the onset of a convergent motion between the two plates (the end of the plate reorganization in the Indian Ocean) and the creation of new slabs acting on the plate (and producing the change in the direction of plate motion evidenced by the bend) is of the order of 2 Myr. McKenzie[47] has shown that the creation of a new trench may be considered as a finite amplitude instability which develops in an elastic plate only for a horizontal convergence greater than 180 km (for a slab dipping at 45°). For a typical relative plate velocity of 10 cm yr^{-1}, the 2-Myr time lag observed corresponds to a horizontal convergence of the order of 200 km.

The observed chronology of events during the plate reorganization also suggests that ridge-push associated with the thermal structure of plates is not a dominant driving force and that seafloor spreading is a passive phenomenon. Indeed, the change in spreading direction of the Indian plate seems to occur in the vicinity of the triple junction before spreading ceased in the eastern Indian basin. The new direction of spreading on the central and eastern Indian ridges tends to be more parallel to the ridge between India and Australia, and thus, the termination of spreading at this ridge seems to be a consequence rather than a cause of the plate reorganization.

Crustal shortening mechanisms

Palaeomagnetic studies in Tibet have shown the existence of 1,900 ± 850 km of shortening within Eurasia since the collision[1]. The present comparison of palaeomagnetic data and reconstructions based on magnetic anomalies document an additional 700 ± 300 km of convergence between India and southern Tibet. Thus, the total north–south shortening resulting from the collision between India and Eurasia amounts to 2,600 ± 900 km.

The last shift observed on India's motion occurred at anomaly 13 time (Fig. 1). This could be regarded as an artefact of our reconstructions since the finite rotations for the closure of the Atlantic Ocean were computed at anomalies 24 and 13 (see ref. 17). However, this shift appears both in the motion of India relative to Eurasia (Fig. 1*a*) and relative to the hotspot frame of reference (Fig. 1*b*). It thus seems to indicate an actual change in the motion of the Indian plate. The motion observed between anomalies 18 and 13 corresponds to several hundred kilometres of left lateral strike-slip motion between India and Eurasia in addition to north–south shortening. Tectonic studies in Tibet have shown the frequent occurrence of a large component of strike-slip motion along thrust faults and suture zones[5] (YZSZ, Bangong–Nujiang suture, Yangbajain thrust, MCT). In addition, palaeomagnetic studies have shown internal deformation to occur in Tibet, in the vicinity of large thrust faults[1,34]. The present observations suggest that strike-slip motion and penetrative deformation may have been contemporaneous with reverse faulting during the early phase of the collision.

After anomaly 13, transverse motion is no longer observed and >1,500 km of shortening still occurred within Eurasia while India moved steadily northward and rotated counterclockwise[1]. This change near anomaly 13 may be interpreted as a change in the mechanism of shortening of Eurasia. The oldest magnetic lineations in the South China Sea have been identified as anomaly 11 (32 Myr)[48]. Following Courtillot[49], we interpret the magnetic quiet zone as the consequence of continental rifting. Initial rifting is thus likely to have begun near anomaly 13 in the South China Sea. Tapponnier *et al.*[3] have related this rifting with the occurrence of left lateral strike-slip motion along the Red River fault which allowed the rotating extrusion of the Indochina block out of the way of the Indian indenter.

Thus, we suggest that the crustal shortening which followed the collision occurred in three episodes. First, from the initial collision to anomaly 20, say from 50 to 44 Myr, shortening occurred mainly by subduction of ~400 km of Indian continental crust beneath southern Tibet. This initial phase terminated when the buoyant resistive force opposed the subduction. Then, from anomaly 20 to anomaly 13 time, between 44 and 37 Myr, shortening continued essentially through crustal thickening by continental underthrusting and internal deformation. During this second phase, left lateral strike-slip motion was also taking place and the total associated north–south shortening is of the order of 300 km. Finally, since that time, shortening within Eurasia has been mostly taken up by block rotation and lateral extrusion along large left-lateral strike-slip faults as proposed by Tapponnier *et al.*[3,4]. This last phase was initiated by activation of the Red River fault and associated rifting in the South China Sea.

Of course, the three mechanisms must have overlapped. In particular, during the last phase, lateral extrusion occurred first along the Red River fault shifting afterwards to the Altyn Tagh fault. During the transition the two other shortening mechanisms must have been active to allow the northward movement of India. In addition, seismic observations indicate that underthrusting is currently observed south of the Himalayas (MBT). However, the present data seem to indicate that during each episode, one particular mechanism dominated. Therefore, if we assume that during the third phase some 80% of the shortening results from lateral extrusion, this mechanism accounts for more than 1,500 km of north–south convergence of India and Eurasia. Because the two other mechanisms account for ~1,100 km of the total shortening, lateral extrusion appears to have been the most efficient in deforming the continent.

Conclusion

The analysis of Cenozoic magnetic anomalies in the Indian Ocean confirms that the collision between India and Eurasia began at anomaly 22 time, that is 50 Myr ago. This age is consistent with all previously available bounds given by geological or geochronological observations. In particular, it is very consistent with the age of volcanics in the Lhasa area. A K–Ar study on an ignimbrite indicates an age of 48.5 ± 1.5 Myr (ref. 33). Also, several $^{39}\text{Ar}/^{40}\text{Ar}$ analyses on andesites show an important grouping of ages at 50 Myr (ref. 50). The collision with the Ladakh island arc probably occurred earlier, near 54 Myr, but it does not seem to have affected the motion of the Indian plate.

A comparison with palaeomagnetic data in southern Tibet (the southern margin of Eurasia before the collision) shows that 'greater' India extended between 500 and 1,000 km further north than the present northern limit of the Indian continent (the YZSZ). The total continental shortening of India and Eurasia produced by the collision is 2,600 ± 900 km and seems to have occurred in three successive phases.

The termination of subduction beneath Tibet at 44 Myr (anomaly 20 time) produced a change in the direction of motion of the Indian plate. This resulted in the termination of spreading between India and Australia which became attached, and a sudden increase in the spreading rate between Australia and Antarctica[18,40]. This plate reorganization in the Indian Ocean preceded the shift in the direction of absolute motion of the Pacific plate evidenced by the bend of the Hawaian-Emperor chain. This shift may therefore be interpreted as a consequence of the India–Eurasia collision. Finally, the relative chronology of this plate reorganization, which is well constrained by the present study, is very consistent with the hypothesis that the slab-pull force associated with subduction zones is a dominant driving mechanism of plate tectonics.

This work has benefited from many discussions with C. Jaupart. This is IPGP contribution no. NS 776.

Received 1 May; accepted 25 July 1984.

1. Achache, J., Courtillot, V. & Zhou, Y. X. *J. geophys. Res.* (in the press).
2. Dewey, J. F. & Burke, K. C. *J. Geol.* **81,** 683–692 (1973).
3. Tapponnier, P., Peltzer, G., Le Dain, A. Y., Armijo, R. & Cobbold, P. *Geology* **10,** 611–616 (1982).
4. Tapponnier, P., Peltzer, G. & Armijo, R. *Proc. geol. Soc. Lond.* (in the press).
5. Allègre, C. J. *et al. Nature* **307,** 17–22 (1984).
6. Tapponnier, P. & Molnar, P. *J. geophys. Res.* **82,** 2905–2930 (1977).
7. Tapponnier, P. & Molnar, P. *J. geophys. Res.* **84,** 3425–3459 (1979).
8. Armijo, R., Tapponnier, P., Mercier, J. L. & Han, T. G. *EOS* **63,** 1093 (1982).
9. Tapponnier, P. *et al. Nature* **294,** 405–410 (1981).
10. Schärer, U., Xu, R. H. & Allègre, C. J. *Earth planet. Sci. Lett.* (in the press).
11. Powell, C. McA. & Conaghan, P. J. *Earth planet. Sci. Lett.* **20,** 1–12 (1973).
12. Molnar, P. & Tapponnier, P. *Science* **189,** 419–426 (1975).
13. Sclater, J. G. & Fisher, R. L. *Bull. geol. Soc. Am.* **85,** 683–702 (1974).
14. Schlich, R. *Mem. Hors Ser. Soc. Geol. Fr.* **6** (1975).
15. Johnson, B. D., Powell, C. McA. & Veevers, J. J. *Bull. geol. Soc. Am.* **87,** 1560–1566 (1976).
16. Powell, C. McA. in *Pakistan Geodynamics Project* (eds Farah A. & DeJong, K. A.) 5–24 (Geological Survey of Pakistan, 1979).
17. Patriat, P. *et al. Bull. Soc. geol. Fr.* **2,** 363–373 (1983).
18. Liu, C. S., Curray, J. R. & McDonald, J. M. *Earth planet. Sci. Lett.* **65,** 331–342 (1983).
19. Patriat, P. thesis, Univ. Paris 6 (1983).
20. Klootwijk, C. T. *et al. Earth planet. Sci. Lett.* **44,** 47–64 (1979).
21. Achache, J. & Courtillot, V. *Earth planet. Sci. Lett.* (in the press).
22. Besse, J., Courtillot, V., Pozzi, J. P., Westphal, M. & Zhou, Y. X. *Nature* **311,** 621–626 (1984).
23. Schlich, R. in *Ocean Basins and Margins* Vol. 6 (eds Nairn, A. E. M. & Stehli, F. G.) 51–147 (Plenum, New York, 1982).
24. Olivet, J. L. thesis, Univ. Paris 6 (1978).
25. Bonnin, J. thesis, Univ. Paris 6 (1978).
26. Olivet, J. L., Bonnin, J., Beuzart, P. & Auzende, J. M. *Cinematique de l'Atlantique Nord et Central* (CNEXO, Paris, 1982).
27. Morgan, J. W. *Tectonophysics* **94,** 123–139 (1983).
28. Irving, E. *Nature* **270,** 304–309 (1977).
29. Harrison, C. G. A. & Lindh, T. *Nature* **300,** 251–252 (1982).
30. Achache, J. Courtillot, V. & Besse, J. *Earth planet. Sci. Lett.* **63,** 123–136 (1983).
31. McKenzie, D. P. & Sclater, J. G. *R. Astr. Soc. Geophys. J.* **25,** 437–528 (1971).
32. Maluski, M., Proust, F. & Xiao, X. C. *Nature* **298,** 152–154 (1982).
33. Westphal, M., Pozzi, J. P., Zhou, Y. X., Xing, L. S. & Chen, X. Y. *Geophys. J. R. astr. Soc.* **73,** 507–521 (1983).
34. Achache, J. thesis, Univ. Paris 7 (1984).
35. Frank, W., Gansser, A. & Trommsdorff, K. *Schweiz, miner. petrogr. Mitt.* **57,** 89–113 (1977).
36. Andrieux, J. & Brunel, M. *Mem. Hors Ser. Soc. Geol. Fr.* **8,** 189–207 (1977).
37. Argand, E. *Int. Geol. Congr. Rep. Sess.* **13,** 170–372 (1924).
38. Powell, C. McA. & Conaghan, P. J. *Geology* **4,** 727–731 (1975).
39. McDonald, J. M. thesis, Univ. California San Diego (1977).
40. Cande, S. C. & Mutter, J. C. *Earth planet. Sci. Lett.* **58,** 151–160 (1982).
41. Gordon, R. G., Cox, A. & Harter, C. A. *Nature* **274,** 752–755 (1978).
42. Peterson, E. T. & Seno, T. *EOS* **64,** 843 (1983).
43. Molnar, P. & Gray, D. *Geology* **7,** 58–62 (1979).
44. Klootwijk, C. T. & Pierce, J. W. *Nature* **282,** 605–607 (1979).
45. Klootwijk, C. T. in *Pakistan Geodynamics Project* (eds Farah, A. & de Jong, K. A.) 41–80 (Geological Survey of Pakistan 1979).
46. Rona, P. A. & Richardson, E. S. *Earth planet. Sci. Lett.* **40,** 1–11 (1978).
47. McKenzie, D. P. in *Am. geophys. Un. Maurice Ewing Ser.* **1,** 57–61 (1977).
48. Taylor, B. & Hayes, D. *Am. geophys. Un. Monogr.* **23,** 9–104 (1980).
49. Courtillot, V. *Tectonics* **1,** 239–250 (1982).
50. Coulon, C., Maluski, M. & Wang, S. C. *Int. Symp. on Geology of the Himalayas, Abstr.* Chengdu China (1984).
51. Weissel, J. K., Hayes, D. A. & Herron, E. M. *Mar. Geol.* **25,** 231–277 (1977).

Palaeomagnetic estimates of crustal shortening in the Himalayan thrusts and Zangbo suture

J. Besse*, V. Courtillot*, J. P. Pozzi*, M. Westphal† & Y. X. Zhou‡

* Laboratoire de Géomagnétisme et Paléomagnétisme (CNRS ERA922), Institut de Physique du Globe de Paris, and UER Sciences Physiques de la Terre, Universités de Paris 6 et 7, 4 Place Jussieu, 75230 Paris Cedex 05, France
† Institut de Physique du Globe de Strasbourg, 67084 Strasbourg Cedex, France
‡ Ministry of Geology, Beijing, PR China

This article reports new palaeomagnetic results from precisely-dated late Palaeocene limestones from the former northern margin of the Indian subcontinent, now in Tibet, between the major Himalayan thrusts and the India–Tibet suture zone. Convergence in the suture and intracontinental thrusting can be estimated separately and are respectively found to be of the order of 550 km (±650 km) and 400 km (±400 km). Comparison with kinematic models derived from magnetic anomalies constrains the age of the collision at about 50 Myr.

CRUSTAL shortening in major orogenic belts involves, in addition to folding, one or several modes of deformation: subduction of continental crust in the wake of pre-existing oceanic subduction, and sideways escape of crustal blocks along major strike-slip faults (see refs 1–4). A direct measurement of the amount of shortening is often not possible and the relative contributions of each mode have remained highly controversial, particularly in the case of the world's largest orogen, the Himalayan range and associated Tibetan plateau[5–9]. Palaeomagnetism remains the only indirect means of obtaining quantitative estimates.

Continental collision of India with southern Tibet, at that time the southern active margin of Eurasia, occurred in the late Palaeocene–Eocene. The rough original estimate of the age of collision was based on the drastic change in relative motions observed in magnetic anomalies from the Indian Ocean[10]. Large-scale continental shortening followed, firstly, along the original Indus–Zangbo suture zone and then to the south of the suture, along newly developed major continental thrusts such as the Main Central thrust (MCT) and Main Boundary fault (MBF) south of the High Chain, or the recently identified Kangmar thrust (KT) to the north of the High Chain[3,11]. The amount of convergence along the suture remained essentially unknown, and estimates of convergence along the intracontinental thrusts were a cause of great controversy, ranging from 200 km or less[8] to >1,500 km (ref. 6 and see also refs 5, 7, 9). A study of middle Cretaceous red beds and Palaeocene–Eocene volcanics from southern Tibet (Lhasa Block) has recently constrained the total amount of post-80 Myr (and, with some uncertainty on age, post-60–50 Myr) convergence between India and southern Tibet o 1,400±900 km (ref. 4).

Geological setting

During the first (1981) and the third (1983) French–Chinese geoscience expeditions to Tibet, we sampled an outcrop of early Cenozoic shallow marine sediments deposited on the northern margin of India (Fig. 1). The series starts with grey limestones rich in foraminifera (*Nummulites, Orbitolites*) and dated as Thanetian to Illerdian (that is between 50 and 60 Myr, ref. 12). The shallow water depositional environment is clearly demonstrated by algae and polyps. The limestones are conformably overlain by reddish fine-grained sandstones, witnessing the progressive rise of the Indian margin above water level. The entire sequence lies conformably over Cretaceous limestones and shales and appears to be analogous to the Spiti sequences in Ladakh[13]; it is folded in a large synclinorium, trending 110° N and verging south (Fig. 2). The entire unit is located structurally to the north of the MBF, MCT (and High Chain) and to the south of the KT and Zangbo suture (Fig. 1).

Age determination and palaeomagnetic results

Oriented hand samples were taken near Dingri (Figs 1, 2) in limestones (sites XPP 24, 25; XPB 62, 63) and sandstones (site XPB 60). Accurate biostratigraphical age determinations were made by Feinberg, ages and faunas being scaled to the Contessa section in Italy[14]. Deposition of the limestones was found to

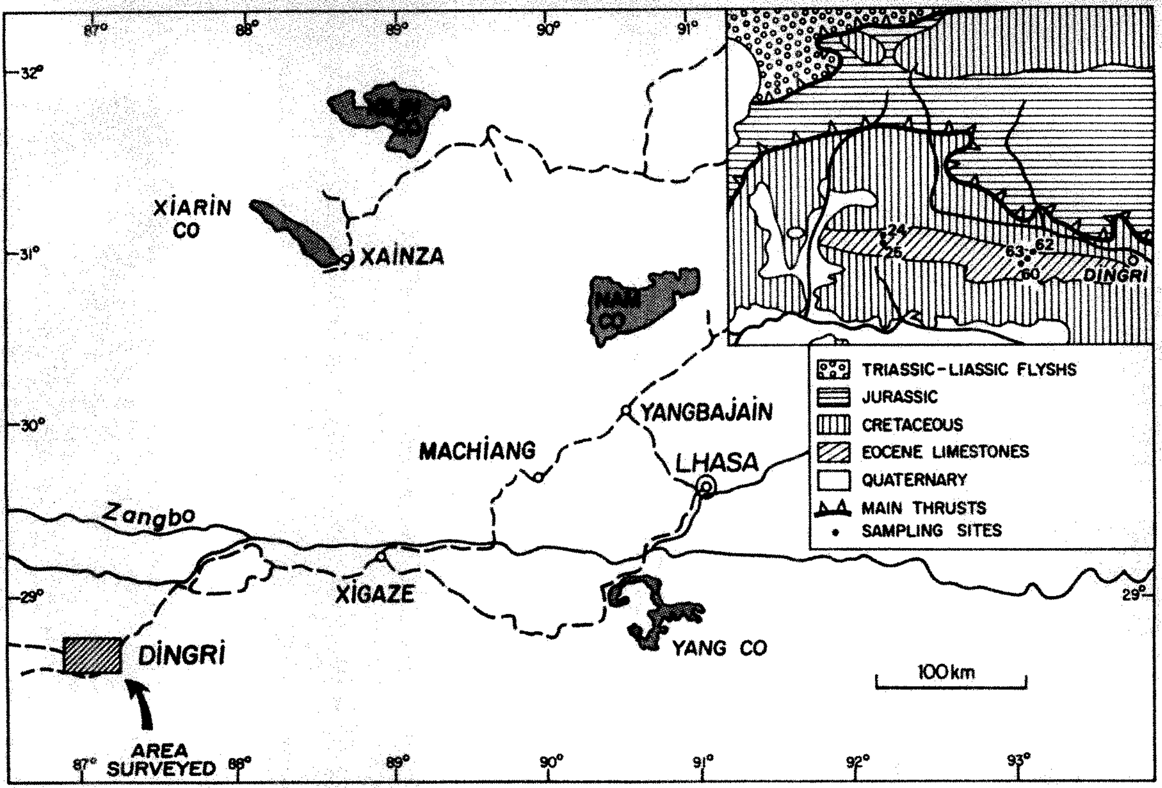

Fig. 1 Geographical map of the sampling area and schematic geological map (inset, after refs 11, 13).

have occurred strictly between anomalies 26 and 25. A comparison of various magnetic polarity time scales[14–16] leads to an age of 57 ± 1 Myr. Specimens were cored from the samples in the laboratory and demagnetized by step-heating followed by cooling in approximately field-free space (20 nT), or by using alternating fields (AF). Magnetic measurements were done with a two-component CTF cryogenic magnetometer. Most samples had weak multicomponent magnetizations which were separated with a modified version of Kirshvink's principal component analysis[17].

Only three limestone sites provided reliable directions. The magnetization of specimens from site 25 fell below 5×10^{-6} A m^{-1} at 200 °C. Typical vector demagnetization plots are given in Fig. 3. Two distinct components (A and B) are clearly indicated for the limestone specimens. Component B disappears after heating at 250–300 °C. The mean direction for sites 24, 62 and 63 is declination, $D = 14°$, inclination $I = 11.5°$ ($\alpha_{95} = 11.5°$) before bedding correction. This is significantly different from either the present geomagnetic direction ($D = 0°$, $I = 43°$) or the dipole direction ($D = 0°$, $I = 48°$) at the sampling sites (lat. 29° N, long. 87° E). Applying the bedding correction increases the scatter of the mean direction. This indicates a secondary (post-folding) remagnetization. Note that the points do not follow a Fisherian distribution: the scatter in declination is approximately twice the scatter in inclination (Fig. 4). Component A has unblocking temperatures between 300 and 500 °C and the demagnetization path points to the origin (Fig. 3). The principal carrier of remanence A is thus probably a (titano-) magnetite. Both normal and reverse polarities are observed and a positive fold test is obtained (Table 1, Fig. 4). The resulting mean direction $D = 337.6°$, $I = -4.5°$ ($\alpha_{95} = 14.6°$) is thus pre-folding and probably of primary origin.

The single sandstone site (no. 60) also showed a multicomponent magnetization, with a more complicated behaviour. A scattered component with high-unblocking temperatures (500–640 °C), probably carried by haematite, is close to the A component of limestones after application of a bedding correction (Table 1: $D = 339°$, $I = -10°$, $\alpha_{95} = 24°$). Beyond 620–640 °C, the progressive build-up of viscous remanent magnetization prevents a close study of the final steps of demagnetization. Depending on the lithology of the samples, two components with medium-unblocking temperatures were observed. One, found

Table 1 Palaeomagnetic results

	Component A							Component B							Component C						
	Corrected for bedding				Uncorrected			Corrected				Uncorrected			Corrected				Uncorrected		
	N	$\%n$	D	I	D	I	α_{95}	N	$\%n$	D	I	D	I	α_{95}	N	$\%n$	D	I	D	I	α_{95}
Site 24	5	100	335	−9	335	11	16	17	100	20	−20	20	17	7							
Site 25	No characteristic direction																				
Site 60	6	50	329	−10	323	30	24	7	0	29	−22	27	13	13	7	100	313	−47	328	−2	7.5
Site 62	10	23	344	−9	338	41	10	11	30	16	−41	13	10	22							
Site 63	7	15	334	4.5	310	−46	17	5	15	15	77	19	7	17							
Site mean	$D = 335.5$, $I = -5.9$ $K = 76$, $\alpha_{95} = 10.6$				$D = 327.3$, $I = 11$ $K = 4$, $\alpha_{95} = 50.4$			$D = 20.7$, $I = -8.0$ $K = 3$, $\alpha_{95} = 71.9$				$D = 17.2$, $I = 11.8$ $K = 84$, $\alpha_{95} = 10.1$ Palaeolatitude $\lambda = 6° \pm 5°$									
Mean C+A	$D = 154.0°$, $I = 5.1°$, $K = 83$, $\alpha_{95} = 8.4°$, palaeolatitude $= -2.5° \pm 4°$																				

N is the number of samples, $\%n$ is the percentage of samples of normal polarity.

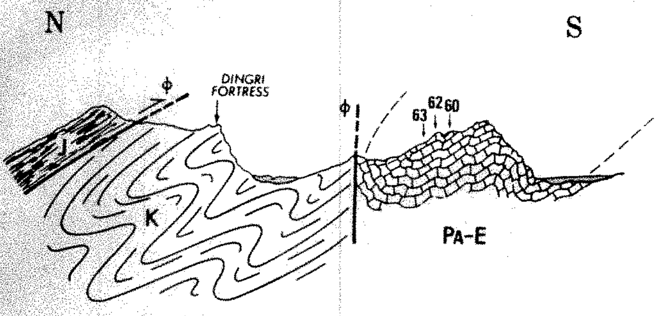

Fig. 2 Simplified cross-section going through sites 60–63. Site 60 is in sandstones, 62 and 63 are in limestones.

Table 2 New apparent polar wandering path for India and expected palaeolatitudes in Dingri (lat. 29° N, long. 87° E)

Age (Myr)	Anomaly no.	Pole lat. (°N)	Pole long. (°E)	Palaeolatitude in Dingri (°)
70	32	47.5	301	−22.5 (S)
62	29	41.2	293	−16
61	28	46.1	292.5	−12
59	27	46.6	294.5	−10
57	26	52	293	−6
55	25	55	293.5	−3
53	24	56.4	298	−0.6
52	23	58	300	1.3 (N)
50	22	64.6	294.3	6.3
48	21	66	306	4.6
44	20	64.4	303	7.2
42	18	64.8	303	8
36	13	67	308	11
29	8	73	301	14.5
21	6	77.7	300	18.5
10	5	83	304	23

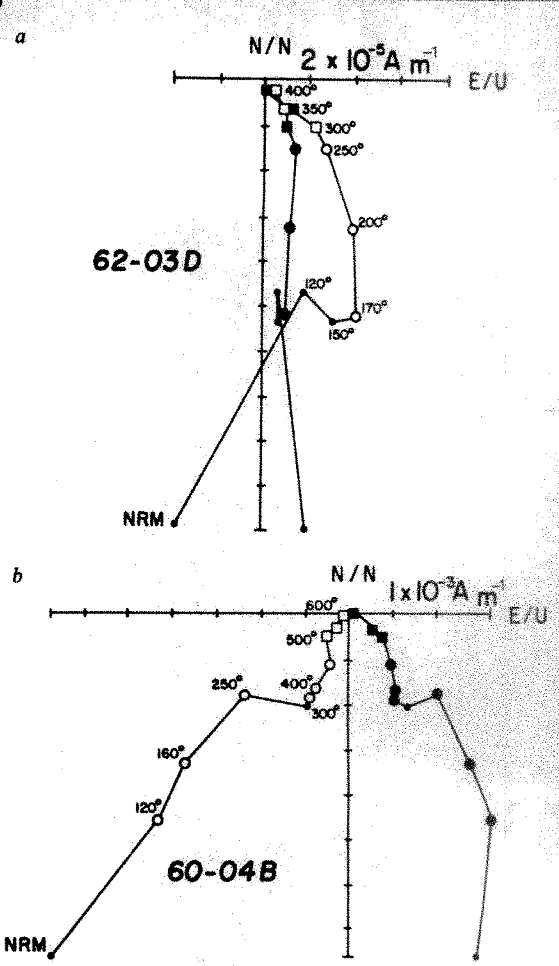

Fig. 3 Typical thermal demagnetization diagrams in geographical coordinates for *a*, a limestone (62-03D) and *b*, a sandstone (60-04B) specimen. Open symbols are for horizontal components, closed symbols are for the component in the north–south vertical plane. Circles are for the lower-temperature B component (remagnetization) and squares for the high-temperature (primary) A component.

between 120 and 450 °C, is close to component B before bedding correction (Table 1: $D = 27°$, $I = 13°$, $\alpha_{95} = 13°$). More interestingly, a second component (C) is found to be $D = 328°$, $I = -2°$ ($\alpha_{95} = 7.5°$) before bedding correction, which is close to component A after bedding correction. The medium-to-high unblocking-temperature components are also revealed by the converging circles method of Hoffman and Day[18] and occur as (alternate) discontinuous linear segments on the vector diagrams, generating a characteristic 'Christmas-tree' pattern (Fig. 3). Both normal and reversed directions are found, often intermediate between directions A and B before and after bedding correction. Secondary components may have an unblocking-temperature spectrum that extends to high temperatures and may be responsible for the scatter of the high-temperature component. These observations (particularly component C), together with the scatter in declination of the B component of limestones, suggest that part of the (re)magnetization was acquired during folding, and part shortly after folding.

The combined high-temperature component A for all sites passes a positive fold test[19] at the 99% level (Table 1). The previous discussion leads us to interpret it as being primary and to assign it the age of 57 ± 1 Myr. The depositional palaeolatitude at that time was then 2.5° S ± 4°, close to and slightly south of the Equator. On the other hand, the B component is a remagnetization, acquired at 6° N ± 5°, during the end or immediately after folding (the age of which is as yet unknown): the fold test is negative at the 99% level. The precise mechanism of overprinting remains unknown although it may be related to the growth of new magnetic minerals, induced by solution transfer under stress.

APWP of India

The determination of continental shortening in the MBT and MCT requires that our data be compared with palaeomagnetic data of similar age from the Indian shield. Such data are unfortunately not available. However, two indirect estimates of the Indian apparent polar wander path (APWP) are available. One determination is based on inclinations from DSDP cores[20], for which, however, no declination control is available. As a result, true palaeolatitudes are systematically underestimated[20]. The lacking declination data are supplemented by magnetic anomaly data. The resulting APWP for India for the period 70–0 Myr (ref. 20) is shown in Fig. 5, together with error circles which are probably underestimates. We redetermined the 60 Myr pole, which is of particular importance here, by discarding highly suspicious results from DSDP sites 215 (basalts) and 217 (sediments).

Because a perfect calibration in age is fundamental here, a new Indian APWP (late Cretaceous and Cenozoic) can be derived on the basis of a detailed study of magnetic anomalies in the Indian Ocean[21] combined with the 'absolute' motion of Africa (with respect to hotspots) deduced by Morgan[22] (see also ref. 23). The new APWP is shown in Fig. 5 and the corresponding palaeomagnetic directions expected for Dingri are listed in Table 2. It is not easy to determine error bars for these estimates. Magnetic anomaly reconstructions contribute an error of the order of 2° (P. Patriat, personal communication, and refs 24, 25), which is not isotropic, and hotspot positions contribute ~2° (as estimated in ref. 25), yielding a total error of about 3°. On the other hand, the age control is excellent[21].

The two APWP estimates are not significantly different after 50 Myr. From 50 to 70 Myr, they are systematically offset (rotated) one with respect to the other, by ~10°. If this difference is significant, it may arise for several reasons, such as systematic

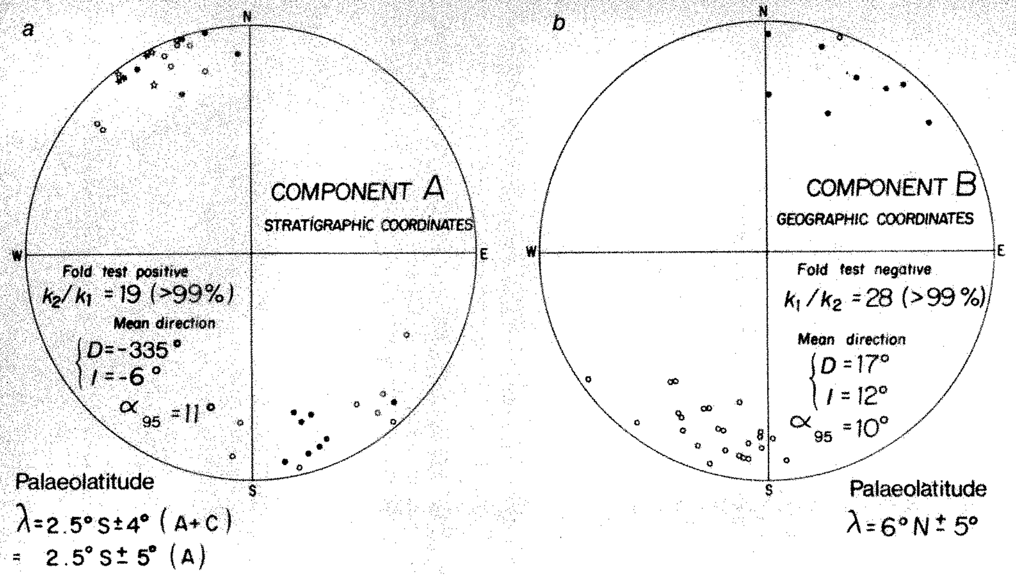

Fig. 4 Stable magnetic directions for all Dingri specimens. A and B (directions in stratigraphical coordinates) are shown as circles, C (in geographical coordinates) as stars (see text and Table 1).

differences between the geocentric axial dipole and hotspot reference frames[25] or more likely from errors in generating the DSDP curve. The only available 70 Myr Deccan trapps palaeomagnetic pole[20] does not resolve this dilemma, as it falls about halfway between the two APWPs (Fig. 5).

Continental convergence and collision

We are now in a position to generate palaeolatitude against time plots for points of the northern margin of India (Fig. 6), namely the former northern edge of continental India, and points now located near Dingri and to the south of it before convergence on the MBF and MCT. Using the data of refs 21, 23, the new APWP for India implies 3.5° ± 4° of convergence south of Dingri (Fig. 6). The DSDP path leads to a larger value of 5.5° ± 4.5°. These values are deduced from the 57-Myr old A component of magnetization. The error estimates are, as usual in palaeomagnetic studies, at the 2σ level and include errors on palaeomagnetic determinations and kinematic reconstructions. Further geological constraints help in reducing them: because we know that convergence definitely occurred between Dingri and India, the latitude difference cannot be negative or even smaller than ~1°, the smallest possible amount of underthrusting in the MBF and MCT.

Using the APWP, one can then generate the latitude history of Dingri as it moved together with stable India before the collision (Fig. 6). When this curve intersects the palaeolatitude for the B remagnetization, the age of this remagnetization is obtained: we interpret this age as the end of folding of the Dingri series, related to blocking of the Zangbo suture due to continental crust subduction. We find this age to be 50 Myr (that of magnetic anomalies 22–23). When error bounds are included for the palaeolatitudes of both magnetizations A and B and the

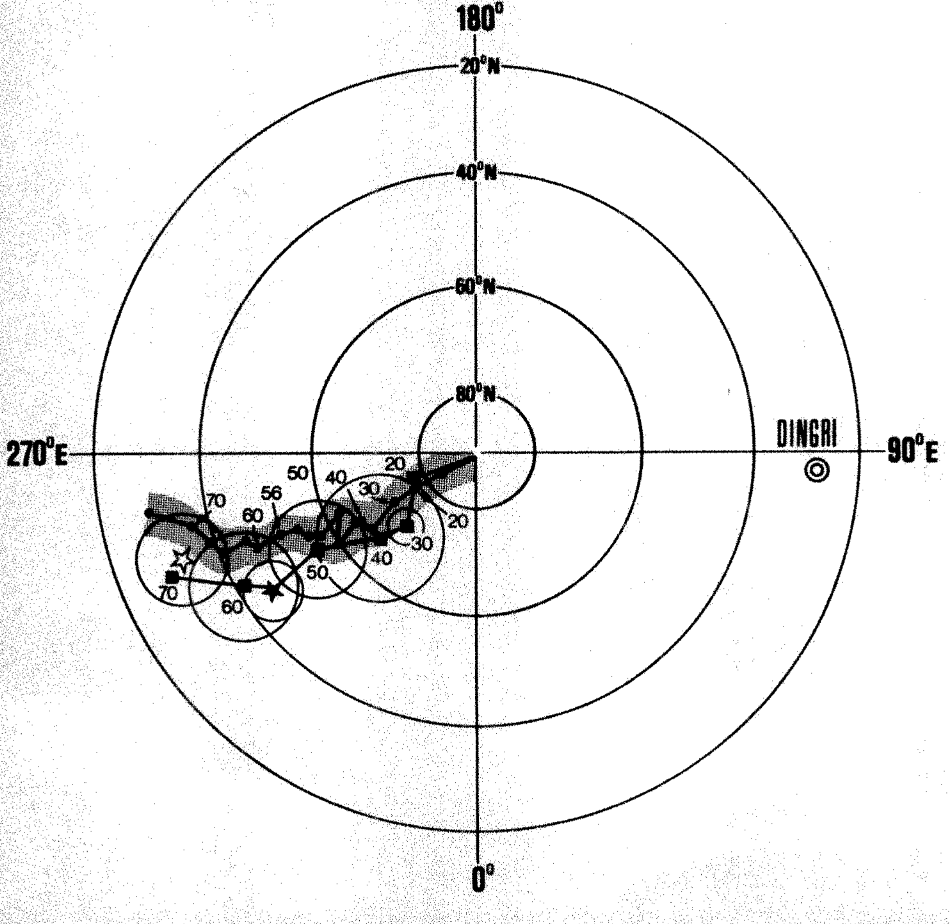

Fig. 5 Two estimates of the APWP for India. ■, From DSDP cores[20]; ●, based on Indian Ocean magnetic anomalies (see refs 21, 23, text, and Table 2); ★, A DSDP pole for 57 Myr, recomputed from ref. 20 (see text); ☆, a 70 Myr Deccan traps pole[20].

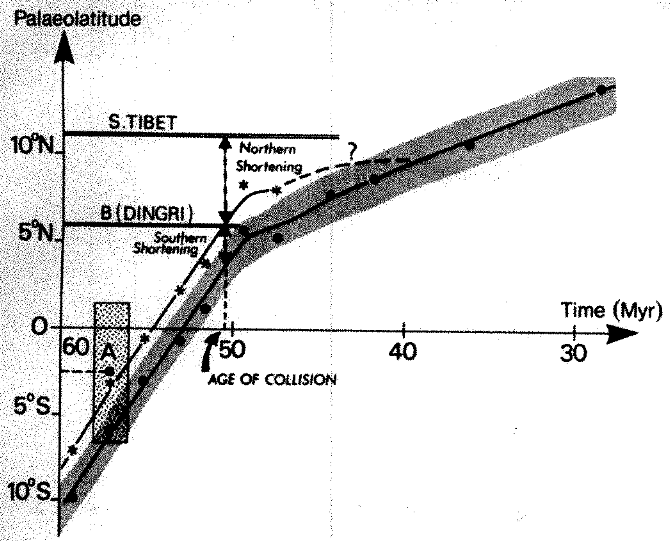

Fig. 6 The northward drift of a point now at Dingri following the motion of cratonic India, as deduced from the data of Fig. 5 and Table 2, is shown as a thick line with error estimates shaded. The primary (A) magnetization for Dingri, also shown with a shaded error box, provides an estimate for crustal shortening in the MBF and MCT to the south. The northward drift of Dingri (thick curve through A parallel to the Indian motion) intersects the B remagnetization, giving the age of the collision and, by comparison with data from southern Tibet[4], the amount of crustal shortening in the Zangbo suture. Error estimates for those are omitted for clarity but are given in the text.

kinematic history of India, this age is found to range between 36 and 59 Myr. However, an age older than 57 Myr (deposition at Dingri) is geologically impossible. An age as young as 36 Myr implies the unlikely combination of (2σ) error bars, with the palaeolatitude of the B component at 10° N and the amount of convergence in the MBF and MCT reduced strictly to zero. The most probable age is unlikely to be older than 53 Myr or younger than 47 Myr (Fig. 6). The age of anomaly 22 happens to be that at which the relative and absolute motions given by Patriat and Achache[23] suddenly slow down and exhibit an erratic azimuthal behaviour which these authors also associate with the collision. Finally, the palaeolatitude of Dingri at 50 Myr can be compared with that of southern Tibet as determined by Achache *et al.*[4], thus yielding an estimate of convergence in the Kangmar thrust and Zangbo suture: 5° ± 6°. The uncertainty on this estimate is still rather large, and further age determinations from the Tibetan (60–40 Myr) volcanics will be helpful. Preliminary results from the ophiolitic complex and flysh series near Xigaze on the Zangbo suture[26] seem to indicate a remagnetization close to 6° N ± 8° which might have been acquired at the same time and under the same circumstances as remagnetization B at Dingri. This might indicate that the 5° estimate of convergence in the Zangbo is on the high side, but further work is needed to refine this analysis. Figure 6 can be complemented by tracing back the motion of the northernmost continental boundary of India before the collision. A schematic series of sections (Fig. 7) also displays the sequence of events before and immediately after the collision. The northern margin of India passed the Equator in the vicinity of Dingri around 56 Myr ago and emergence of Dingri occurred around 55 Myr. The collision (in the sense defined above) occurred around 50 Myr. The deformation history that followed may be deduced from the values presented here and previously published tectonic scenarios[1–4,23]. Approximately 500 km of continental crust (or less) was subducted in the Zangbo before the suture was choked. Part of this may correspond to folding of the Dingri and Xigaze[3,13] series and thrusting (around 40–20 Myr?) on the Kangmar thrust, and the estimate of subducted continental lithosphere might be reduced to a classical value around 300 km (refs 23, 27). When the suture became blocked (around 45 Myr? see refs 1, 2, 23), motion was transferred to the MCT and then MBF, much of the 400 km of convergence determined above occurring by thrusting between 45 and 35 Myr (refs. 28, 29). The amount of folding should, however, be subtracted from these values. Also, thrusting still proceeds to the south of the MBT and elsewhere[9,30]. Propagating extrusion tectonics may have started concurrently to the north of the suture and may account for over two-thirds of the total Cenozoic convergence between India and Asia[1–4].

We thank H. Feinberg for biostratigraphical age determinations and P. Patriat for providing Indian Ocean data. This work was carried out within the Cooperative Research Project of the Chinese Ministry of Geology, Chinese Academy of Sciences, French Centre National de la Recherche Scientifique and Institut National d'Astronomie et de Géophysique. This is IPGP contribution no. 782.

Received 6 June; accepted 20 August 1984.

1. Tapponnier, P., Peltzer, G. & Armijo, R. *Proc. geol. Soc. Lond.* (submitted).
2. Tapponnier, P., Peltzer, G., Le Dain, A. Y., Armijo, R. & Cobbold, P. *Geology* **10**, 611–616 (1982).
3. Allègre, C. J. *et al. Nature* **307**, 17–22 (1984).

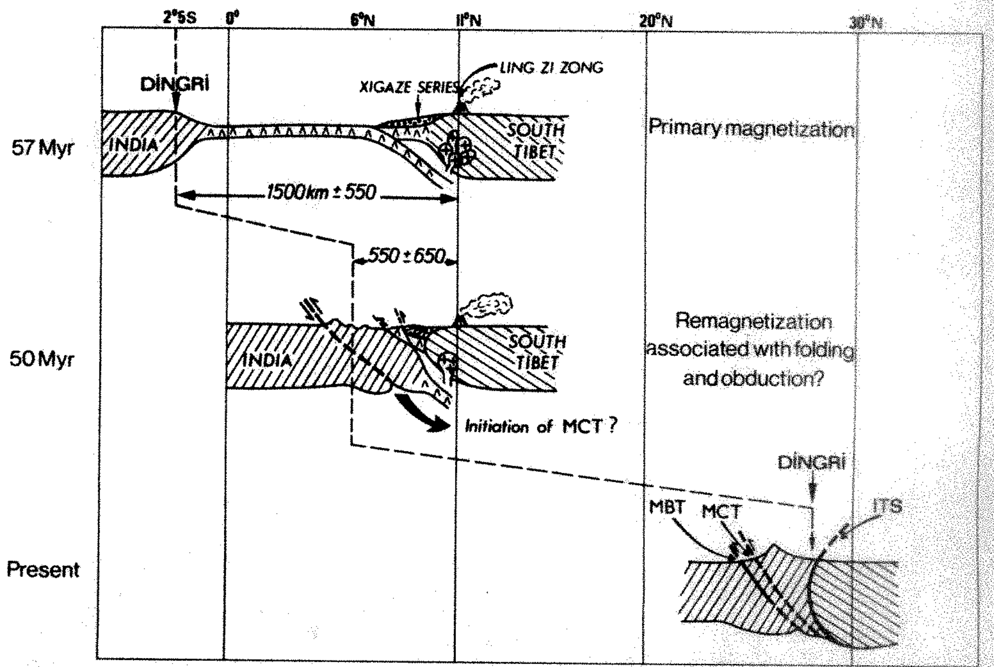

Fig. 7 Geodynamic evolution of the India–South Tibet collision assuming that the mean palaeolatitudes are exactly correct (compare with Fig. 6).

4. Achache, J., Courtillot, V. & Zhou, Y. X. *J. geophys. Res.* (in the press).
5. Argand, E. *C.r. Congr. Géol. Int.* **13,** 171–372 (1924).
6. Powell, C. & Conaghan, P. J. *Earth planet. Sci. Lett.* **20,** 1–12 (1973).
7. Lyon-Caen, H. & Molnar, P. *J. geophys. Res.* **88,** 8171–8191 (1983).
8. Gansser, A. *Geology of the Himalayas* (Wiley–Interscience, London, 1964).
9. Ni, J. & Barazangi, M. *J. geophys. Res.* **89,** 1147–1163 (1984).
10. Molnar, P. & Tapponnier, P. *Science* **189,** 419–426 (1975).
11. Burg, J. P. thesis, Univ. Montpellier (1983).
12. Bassoulet, J. P. *et al* in *Résultats de la Coopération franco–chinoise au Tibet (mission 1980)* (eds Mercier, J. L. & Guangquin, Li) (CNRS, in the press).
13. Tapponnier, P. *et al. Nature* **294,** 405–410 (1981).
14. Lowrie, W. *et al. Bull. geol. Soc. Am.* **33,** 414–432 (1982).
15. Schlich, R. *et al. Bull. Soc. Géol. Fr.* **21,** 57–63 (1979).
16. Cox, A. V. in *A Geologic Time Scale* (eds Harland, W. B. *et al.*) 63–84 (Cambridge University Press, 1982).
17. Kirshvink, J. L. *Geophys. J. R. astr. Soc.* **62,** 699–718 (1980).
18. Hoffman, K. A. & Day, R. *Earth planet Sci. Lett.* **40,** 433–438 (1978).
19. McElhinny, M. W. *Geophys. J. R. astr. Soc.* **8,** 338–340 (1964).
20. Klootwijk, C. T. & Radhakrishnamurty, C. in *Paleoreconstruction of the Continents* (eds McElhinny, M. W. & Valencio, P. A.) (American Geophysical Union, 1981).
21. Patriat, P. thesis, Paris Univ. (1983).
22. Morgan, J. W. *Tectonophysics* **94,** 123–139 (1983).
23. Patriat, P. & Achache, J. *Nature* **311,** 615–621 (1984).
24. Stock, J. M. & Molnar, P. *Geology* **11,** 697–701 (1983).
25. Harrison, C. G. A. & Lindh, T. *Nature* **300,** 251–252 (1982).
26. Pozzi, J. P. *et al. Earth planet. Sci. Lett.* (in the press).
27. Molnar, P. & Gray, D. *Geology* **7,** 58–62 (1979).
28. Brunel, M. thesis, Univ. Paris VII (1983).
29. Schärer, U., Xu, R. H. & Allègre, C. J. *Earth planet. Sci. Lett.* (in the press).
30. Armijo, R. *et al. EOS* **63,** 1093 (1982).

Molecular cloning and expression of cDNAs for the human interleukin-2 receptor

Warren J. Leonard*, Joel M. Depper*, Gerald R. Crabtree†, Stuart Rudikoff‡, Janet Pumphrey‡, Richard J. Robb§, Martin Krönke*, Penny B. Svetlik*, Nancy J. Peffer*, Thomas A. Waldmann* & Warner C. Greene*

* Metabolism Branch, † Laboratory of Pathology and ‡ Laboratory of Genetics, National Cancer Institute, Bethesda, Maryland 20205, USA
§ E.I. du Pont, de Nemours and Co., Glenolden, Philadelphia 19036, USA

We have purified the human T-cell growth factor (interleukin-2) receptor and have cloned, sequenced and expressed cDNAs corresponding to this receptor. We identify one gene, but two interleukin-2 receptor mRNAs which differ in their polyadenylation signals. We have isolated an additional cDNA that may correspond to an alternatively spliced mRNA that lacks a 216 base segment and appears to encode an altered membrane protein which cannot bind interleukin-2.

INTERLEUKIN-2 (IL-2 or T-cell growth factor) is a lymphokine synthesized and secreted by some T cells following activation with antigen or mitogen in the presence of monocyte derived interleukin-1[1]. IL-2 permits long-term growth *in vitro* of T-cell populations serving helper and cytotoxic functions[2-4]. It also augments natural killer cell activity[5], and is being evaluated for possible therapeutic effects in patients with the acquired immunodeficiency syndrome and select neoplasms. IL-2 has been biochemically characterized[6], molecularly cloned[7-9], and is known to be encoded by a single gene[10,11] on human chromosome 4.

In order to exert its biological effects, IL-2 must interact with specific high-affinity membrane receptors[12]. This interaction is critical to the evolution of a normal immune response. IL-2 receptors are not expressed in resting T cells, but they are expressed rapidly following activation with antigen or mitogen. Thus, in contrast to most other hormone–receptor systems, this is an example where both ligand and receptor must be induced. IL-2 receptors are not present in most human leukaemic T-cell lines, but are expressed uniformly in high numbers in human T-cell leukaemia/lymphoma virus-I (HTLV-I)[13,14] infected T cells[15], and it is possible that these receptors may be involved in the uncontrolled growth of these cells.

The IL-2 receptor has been identified as an $M_r = 55,000$ glycoprotein on normal activated peripheral blood T cells[16-18]. These receptors are composed of a peptide precursor of $M_r = 33,000$ (p33). This precursor is cotranslationally modified to a p35/p37 doublet by *N*-linked carbohydrate addition, and then modified in the Golgi apparatus to the $M_r = 55,000$ form. Mature receptors contain *N*-linked and *O*-linked carbohydrate and sialic acid, and are both sulphated and phosphorylated. The receptors on some, but not all HTLV-I infected T-cell lines, vary slightly in mobility on SDS polyacrylamide gels. For example, the receptor on HUT-102B2 cells appears 5,000 daltons smaller than the receptor on normal activated peripheral blood T cells[17,19]. These receptors share the same sized p33 and p35/p37 precursor forms, and the basis for their size difference is the result of altered post-translational modifications, including the amount of sialic acid and sulphate added.

Elucidation of IL-2 receptor structure, function and regulation of expression will improve our understanding of the early events of T-cell activation, including the mechanisms of membrane signal transduction. The availability of cDNA probes to the IL-2 receptor also allows further study of the relationship of these receptors to the adult T-cell leukaemia.

Purification and cloning of receptor

Using anti-Tac, an anti-IL-2 receptor monoclonal antibody[16,19,20], we purified the IL-2 receptor on an immunoaffinity column (Fig. 1). The purified protein, but not control eluates, blocked over 98% of human IL-2 induced proliferation of a mouse cytotoxic T lymphocyte line, suggesting that it indeed possesses IL-2 binding activity (data not shown).

We next determined the N-terminal 29 amino acids of the IL-2 receptor by a combination of sequencing unlabelled purified receptor on a gas phase sequenator and receptor biosynthetically labelled with ^{35}S-methionine, ^{35}S-cysteine, ^{3}H-leucine, ^{3}H-proline, or ^{3}H-aspartic acid on a modified Beckman spinning cup sequenator (Table 1).

An oligonucleotide probe of 17 nucleotides and 64-fold degeneracy homologous to the (−)cDNA strand was synthesized, corresponding to the sequence Cys-Asp-Asp-Asp-Pro-Pro (amino acids three to eight). The 17mer was end-labelled with ^{32}P-ATP and polynucleotide kinase, and hybridized to Northern blots of HUT-102B2 mRNA to confirm that the 17mer identified at least one mRNA species. In fact, we detected two mRNAs approximately 1,500 and 3,500 bases long (data not shown).

A cDNA library (see Fig. 2 legend) was constructed in λgt10 from HUT-102B2 cell mRNA according to the protocol of T. St John, J. Rosen and H. Gershenfeld (unpublished data), except that size-fractionated double-stranded cDNA was purified

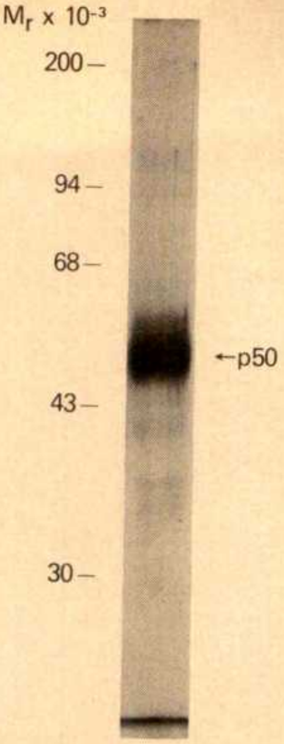

Fig. 1 Purification of IL-2 receptor protein. Anti-Tac and control UPC10 immunoaffinity columns were prepared by coupling purified anti-Tac and UPC10 monoclonal antibodies to cyanogen bromide-activated Sepharose (Pharmacia). Approximately 8×10^{10} HUT-102B2 cells were grown in 10% fetal bovine serum/RPMI medium, collected by ultrafiltration, washed twice in phosphate buffered saline and solubilized in 100 ml extraction buffer (10 mM Tris *p*H 7.4, 0.15 M NaCl, 100 μg ml^{-1} phenylmethylsulphonyl fluoride (PMSF), 0.5% NP40) for 45 min on ice with periodic vortexing. An additional 100 ml of extraction buffer was then added and the cells solubilized for an additional 30 min on ice. Extracts were then centrifuged in a Beckman Ti60 rotor at 37,000 r.p.m. for 30 min at 4 °C. The top lipid layer was discarded and the supernatant collected and stored in aliquots in liquid nitrogen. For each protein preparation, 10 ml aliquots of the extracted cells were passed over a UPC10 column four times, and then over an anti-Tac column three times. The anti-Tac column was washed with 40 ml extraction buffer, 40 ml of 10 mM Tris *p*H 7.5, 0.5 M NaCl, 0.5% NP40, 25 ml of 10 mM Tris *p*H 7.5, 0.1% NP40, and then 10 ml of 10 mM Tris *p*H 7.5. The anti-Tac column was eluted with 3 ml of 2.5% (v/v) acetic acid. The eluted protein was lyophilized, resuspended in 100 μl water and 5 μl analysed on SDS-polyacrylamide gels under reducing conditions: gels were silver stained to assess yield and purity[38]. The columns were then washed extensively and stored in extraction buffer.

Table 1 Sequence of IL-2 receptor

H$_2$N-Glu-$\overset{*}{\text{Leu}}$-$\overset{*}{\textit{Cys}}$-$\overset{*}{\textit{Asp}}$-$\overset{*}{\textit{Asp}}$-$\overset{*}{\textit{Asp}}$-$\overset{*}{\textit{Pro}}$-$\overset{*}{\textit{Pro}}$-Glu-

Ile-$\overset{*}{\text{Pro}}$-His-Ala-Thr-Phe-Lys-Ala-$\overset{*}{\text{Met}}$-Ala-

Tyr-Lys-Glu-Gly-Thr-$\overset{*}{\text{Met}}$-$\overset{*}{\text{Leu}}$-Asn-$\overset{*}{\text{Cys}}$-Glu

Human IL-2 receptor from HUT-102B2 cells (purified using the anti-Tac affinity column) was subjected to automated Edman degradation on a gas phase sequenator and samples analysed by HPLC. Some positions were determined or confirmed by sequencing receptor biosynthetically labelled with ^{3}H-aspartic acid, ^{3}H-leucine or ^{3}H-proline, or with ^{35}S-methionine or ^{35}S-cysteine. For incorporation of radioactive amino acids, cells were grown in the presence of amino acid free RPMI, 5% fetal bovine serum (as a source of unlabelled amino acids) and 1-5 mCi of the radiolabelled amino acid. For aspartic acid, labelling was performed in the presence of 1 mM amino oxyacetic acid, as suggested by Coligan *et al.*[37]. All radioactive amino acids used were the highest specific activity available from Amersham and/or New England Nuclear. *, The positions determined or confirmed by radiolabelled sequencing. The positions italicized represent the amino acids on which the oligonucleotide DNA sequence was based. The 17mer was synthesized and provided to us by Drs Rama M. Belagaje and J. Paul Burnett of Lilly Research Laboratories.

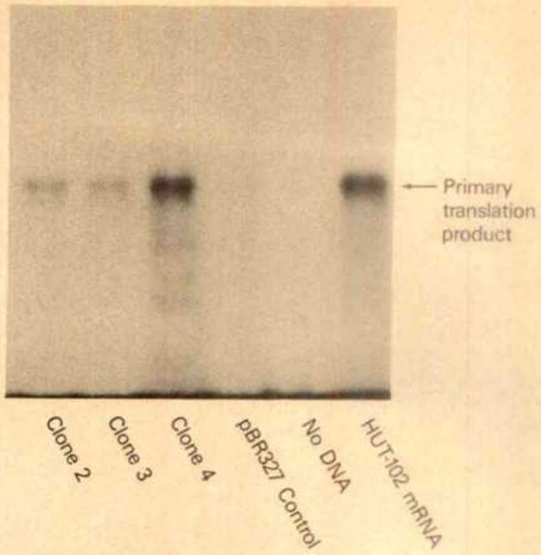

Fig. 2 Preparation of a rabbit heteroantiserum, identification of the primary translation product for the IL-2 receptor, screening of the cDNA library and selective hybridization. Purified IL-2 receptor protein (approximately 3–5 μg) was divided into equal aliquots, one boiled in 1% SDS for 5 min and one not treated, each emulsified with an equal volume of complete Freund's adjuvant, and injected subcutaneously into multiple sites in a New Zealand white female rabbit. The rabbit was boosted (analogous injections in complete Freund's adjuvant) at six weeks. The rabbit was phlebotomized weekly and the ability of the serum to block ^{3}H-anti-Tac binding to activated T cells and to precipitate the IL-2 receptor was assessed. The antiserum specifically precipitated the same 50,000 M_r band from HUT-102B2 cells as did anti-Tac (data not shown) and did not appear to specifically identify any other proteins. Total cellular RNA was isolated from HUT-102B2 cells by the method of Chirgwin *et al.*[39]. The poly(A) fractions were isolated on oligo (dT)-cellulose (Collaborative Research) and translated for 2 h at room temperature in a wheat germ cell-free translation system as described by Gordon *et al.*[40]. The translation mix was then boiled in 2% SDS by the method of Mostov *et al.*[41], cooled to room temperature, diluted to five times the original volume with final concentrations of 1 × phosphate-buffered saline, 1% Triton X100 and 100 μg ml^{-1}PMSF. The mix was cleared with normal rabbit serum and Cowan I strain staphylococcus[42], immunoprecipitated with the heteroantiserum or preimmune serum as previously described and electrophoresed on a gel (sixth lane)[19]. The cDNA library consisted of 2.4 million recombinant phage. 500,000 phage from the library were amplified and approximately 200,000 recombinant phage from the amplified library were screened with the ^{32}P-kinased 17mer. Phage plaques were bound to nitrocellulose as described by Benton and Davis[43], prehybridized overnight at 50 °C in 6 × NET (1 × NET is 0.15 M NaCl, 0.001 M EDTA, 0.015 M Tris, *p*H 7.5), 5 × Denhardts, 0.5% NP40, 200 μg ml^{-1} salmon sperm DNA and then hybridized with the 17mer for 24–48 h in the same buffer containing 10% dextran sulphate. Filters were washed four times for 5 min in 6 × SSC on ice, then for 1 min at 50 °C, and then transferred immediately to 6 × SSC on ice, blotted dry and autoradiographed. Selective hybridization was performed[22] with cDNA inserts from three phage clones subcloned into pBR322: pIL2R2, pIL2R3, and pIL2R4, and with pBR327 and omission of DNA as controls. DNA was linearized by digestion with *Sal*I prior to binding to nitrocellulose, HUT-102B2 mRNA was selectively hybridized, translated, and precipitated with the anti-IL-2 receptor heteroantiserum (first five lanes).

on glass silica mesh[21] rather than by electroelution. In HUT-102B2 cells, IL-2 receptors account for approximately 0.05% of total cellular *de novo* protein synthesis[16].

Eleven clones with inserts of 900–2,300 bases were identified by the 17mer as true positives. Inserts from three of the phage clones were subcloned into the *Eco*RI site of pBR322 (clones denoted pIL2R2, pIL2R3, and pIL2R4, with 900, 2,300, and 1,600 bases, respectively) to facilitate large-scale preparation of inserts. We performed selective hybridization experiments by the method of Maniatis *et al.*[22]. All three recombinant plasmids hybridize mRNA that, when translated in a wheat germ cell-free translation system and immunoprecipitated with a rabbit heteroantiserum to the IL-2 receptor, yield the same sized primary translation product precipitated directly from translations with HUT-102B2 mRNA (Fig. 2). In contrast, control pBR327 and nitrocellulose without DNA added does not selectively hybridize to the IL-2 receptor mRNA. These data confirm that clones 2, 3 and 4 are receptor-associated clones.

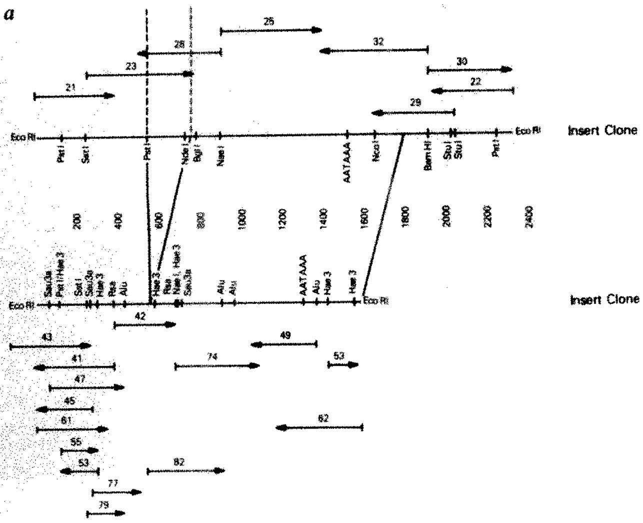

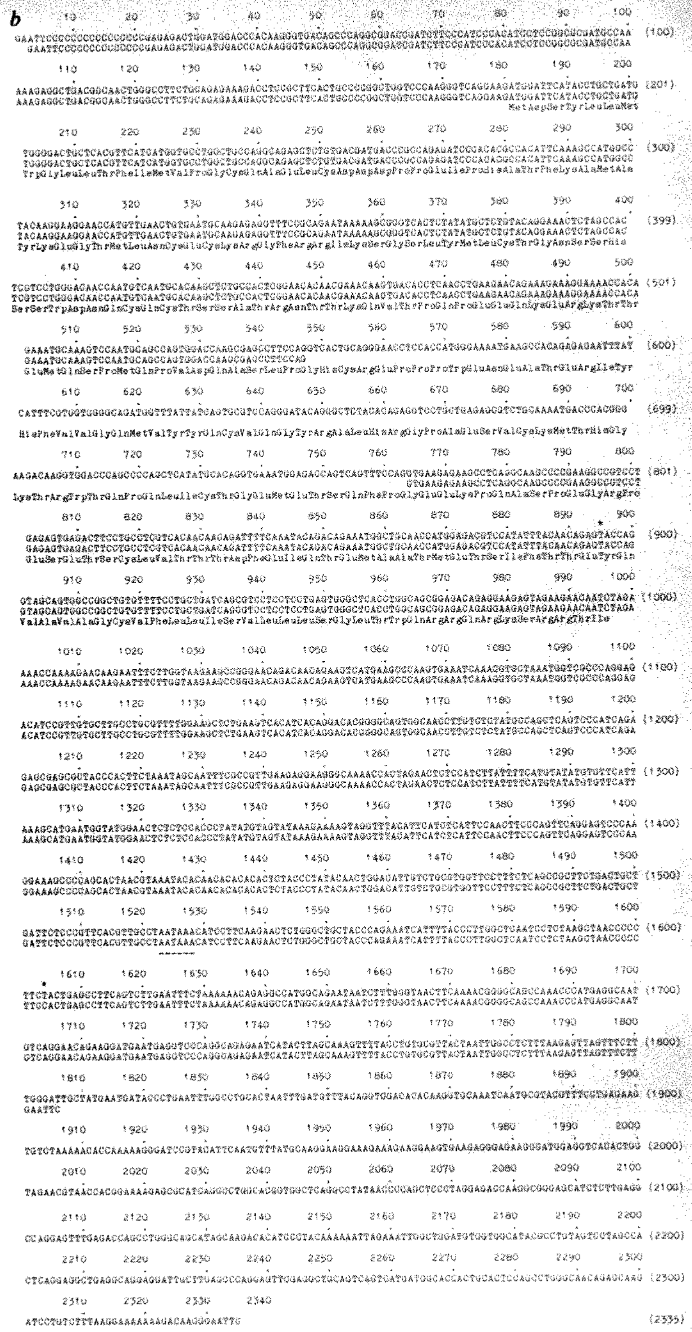

Fig. 3 Restriction map, sequencing strategy, DNA sequence and corresponding protein sequence of IL-2 receptor cDNA. *a*, Restriction map of cDNA inserts of pIL2R3 (clone 3) and pIL2R4 (clone 4). Note the location (vertical dashed lines) of the splicable segment in pIL2R3 that is not present in pIL2R4. Clone 3 was directionally cloned into M13 phage using *Eco*RI, *Sst*I, *Nae*I, *Bam*HI, and *Stu*I restriction sites. Clone 4 was sequenced using four base restriction enzymes *Rsa*I, *Hae*III, *Alu*I, and *Sau*3aI. *b*, DNA and protein sequences for the IL-2 receptor. The DNA sequences of clones 3 (top row) and 4 (second row) are shown with deduced amino acid sequence (third row). The N-terminal amino acid (glutamic acid) and the AATAAA polyadenylation signal which may be used in the 1,500 base mRNA are underlined. The T at 895 (under the asterisk) in one of four sequencing runs was a C. We cannot distinguish with certainty whether position 1,604 (under the asterisk) is a C or a T, which may represent a difference between the two clones.

Sequence of pIL2R3 and pIL2R4 cDNA inserts

The inserts of pIL2R2, pIL2R3 and pIL2R4 were subcloned into M13 bacteriophage and their complete nucleotide sequences by the dideoxy chain termination method[23-25]. The restriction maps and sequencing strategy of pIL2R3 and pIL2R4 inserts (Fig. 3*a*) and the DNA sequences for each (Fig. 3*b*) are shown. We analysed and compared the DNA sequences on an IBM system 370 computer using the program described by Queen and Korn[27] and with the assistance of Dr M. Kanehisa on a Vax computer (Digital Equipment Corporation). Clones 2, 3 and 4 each contain long open reading frames, including the 87 bases corresponding to the 29 amino acids determined by protein sequencing. The N-terminal amino acid of the mature receptor is located at base 244. There are three potential initiator ATGs in the correct reading frame at amino acid positions −21, −15, and −7 (bases 181-183, 199-201, and 223-225, respectively). Preliminary data from sequencing of an ^{35}S-methionine labelled primary translation product suggest that the initiation site is at amino acid −21. All clones had C-tails at the 5′ end added during cDNA synthesis (St John, Rosen and Gershenfeld, unpublished data), but lacked 3′ poly(A) tails. We hypothesize that the poly(A) tails and a part of the 3′ untranslated region may have been lost due to 5′ to 3′ exonuclease activity on the first strand cDNA during second-strand synthesis, since the holoenzyme DNA polyermase I instead of the Klenow fragment is used in the protocol.

Analysis of the sequence of clones 3 and 4 reveals that they differ in two principal ways. First, clone 4 encodes a smaller peptide (179 amino acids; 20,070 daltons) than does clone 3 (251 amino acids; 28,437 daltons). These proteins share the same amino- (base 244) and carboxy- termini (TAG at 997-999 in clone 3) and both contain 2 potential N-linked glycosylation sites (asparagines at bases 388-390 and 445-447), but clone 4 lacks 216 bases (72 amino acids) in the middle of the protein coding region. In clone 3, this region is present and is bounded by the sequence TTCCAGGT on both sides (bases 542-549 and 758-765), and therefore is a segment flanked by a typical messenger RNA donor and acceptor splice site[27,28]. Second, clone 3 extends further 3′ than clone 4, but neither clone reaches a terminal polyadenylation signal sequence (AATAAA).

Expression of IL-2 receptor cDNA

We predict a molecular mass for the IL-2 receptor of 33,000 daltons based on apparent M_r on SDS gels for the putative

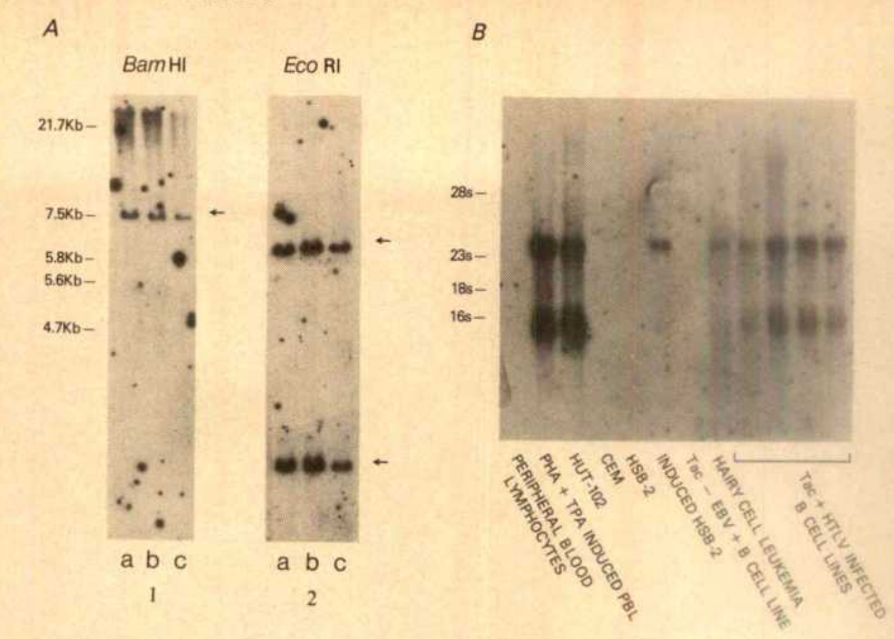

Fig. 4 *A*, The IL-2 receptor appears to be encoded by a single-copy gene. DNA from human placenta (lane *a* of each panel) and tonsils (lanes *b* and *c* of each panel) was digested with *Bam*HI and *Eco*RI, transferred to nitrocellulose, and hybridized with nick-translated pIL2R2. The blotted DNA was provided by Dr Ajay Bakhshi. DNA was digested with *Bam*HI (panel 1) and with *Eco*RI (panel 2). *B*, IL-2 receptor mRNA expression in various lymphoid cell types. 10 μg of poly(A)$^+$ RNA from each indicated cell type was electrophoresed on a formaldehyde gel, transferred to nitrocellulose and hybridized with nick-translated pIL2R3.

peptide precursor. It seems probable that clone 3, which encodes the larger protein product, is the correct one, despite the variability that can exist in migration of different proteins on SDS gels due to variable association with SDS up to the theoretical level of 1.4 g SDS per gram of protein. To test this hypothesis, we expressed each of the cDNAs in COS-1 cells using the expression vector pcEXV-1, which places the cDNA under the control of the Simian virus 40 (SV40) early promoter and SV40 enhancer sequences (Table 2). Cells transfected with control pBR322 do not bind either ^{3}H-IL-2 or ^{3}H-anti-Tac, whereas cells transfected with the insert from pIL2R3 bind both ^{3}H-IL-2 and ^{3}H-anti-Tac. This binding is specific, as it was completely blocked by excess unlabelled IL-2 and anti-Tac. The receptor on these cells has an apparent M_r of 50,000, apparently identical to the receptor on HUT-102B2 cells, and smaller than the receptor on PHA activated T cells (M_r of 55,000). Transfection with pcEXV-1 containing the clone 4 insert, which encodes a smaller protein than clone 3, does not result in the expression of IL-2 receptors (Table 2). As both expression vector constructs were active transcriptionally, these data demonstrate that clone 3 encodes a functional IL-2 receptor and that clone 4 does not.

A single gene encodes IL-2 receptor

We next evaluated the number of genes corresponding to the IL-2 receptor by hybridizing nick-translated ^{32}P-pIL2R2 to genomic DNA digested with *Eco*RI and *Bam*HI. pIL2R2 has an insert corresponding to bases 1–937 and therefore lacks the C-terminal region of the protein and the 3′ untranslated region. We identified two fragments in the *Eco*RI digests, the larger of which is 5,800 bases long with a third faint band of 10,000 bases (Fig. 4*A*). In the *Bam*HI digests, we identified a major 7,500-base fragment and a second less intense more diffuse band of over 25 kilobases (kb). Hybridization with full-length IL-2 receptor cDNA reveals *Eco*RI genomic fragments of 10, 5.8, 2.4 kb and two smaller fragments, and *Bam*HI fragments of 25 and 7.5 kb. These data suggest a single copy gene, but do not exclude a recently duplicated gene.

mRNA expression and HTLV-I infection

Using an IL-2 receptor cDNA, we find that the pattern of expression of IL-2 receptor mRNA parallels the expression of Tac antigen. Resting Tac-negative peripheral blood T cells contain few, if any, IL-2 receptor mRNA copies (Fig. 4*B*, lane 1). However, Tac-positive peripheral blood T cells activated with phytohaemagglutinin (PHA) plus phorbol myristate acetate (PMA) (Fig. 4*B*, lane 2), and HTLV-I-infected HUT-102B2 cells (Fig. 4*B*, lane 3), contain two mRNAs (approximately 1,500 and 3,500 bases), which hybridize to nick-translated IL-2 receptor cDNA. Tac-negative CEM and HSB-2 acute lymphocytic leukaemic T-cell lines do not contain IL-2 receptor mRNA; induction of Tac expression on HSB-2 cells with PMA[29], however, is associated with the appearance of IL-2 receptor

Table 2 Expression of IL-2 receptors in COS-1 cells

	Experiment 1		Experiment 2	
Transfected plasmid	Unlabelled IL-2 added	^{3}H-IL-2 d.p.m. bound	Unlabelled anti-Tac added	^{3}H-anti-Tac d.p.m. bound
pBR322	−	25	−	60
pBR322	+	17	+	150
pcEXV-1-IL2R3	−	562 ± 11	−	28,588 ± 1,548
pcEXV-1-IL2R3	+	62 ± 18	+	261 ± 0
pcEXV-1-IL2R4	−	12 ± 10	−	252 ± 9
pcEXV-1-IL2R4	+	12 ± 3	+	171 ± 39

0.5 μg of clone 3 or 4 insert were ligated to 0.25 μg of *Eco*RI digested and alkaline phosphatase treated pcEXV-1 (provided by Drs J. Miller and R. Germain). The plasmid was transformed into competent cells and recombinant plasmids with the inserts in the correct orientations selected. 5 μg of each recombinant plasmid or of control pBR322 were transfected into COS-1 cells using calcium-phosphate precipitation. The cells were grown overnight, media changed, and then grown for 48 h. The cells were washed, incubated for 90 min at 4 °C with RPMI 1640 medium containing 3% fetal bovine serum and tested for expression of IL-2 receptors. In experiment 1, 45,000 d.p.m. of ^{3}H-IL-2 with or without a 500-fold excess of unlabelled IL-2 were added. In experiment 2, 194,000 d.p.m. of ^{3}H-anti-Tac with or without a 1,000-fold excess of anti-Tac were added. The cells were then washed four times in medium containing fetal bovine serum and dissolved in 1 ml 0.1 M NaOH. The cell-associated radioactivity was then determined. The machine background of 44 d.p.m. has been subtracted from each data point. Data are expressed as mean d.p.m. bound ± standard deviation determined from duplicate plates. For reference, HUT-102B2 cells, which have approximately 300,000 total (high plus low affinity) IL-2 receptors per cell, bound either 1,160 of 6,500 d.p.m. of ^{3}H-IL-2 or 34,500 of 92,100 d.p.m. of ^{3}H-anti-Tac added per 10^6 HUT-102B2 cells.

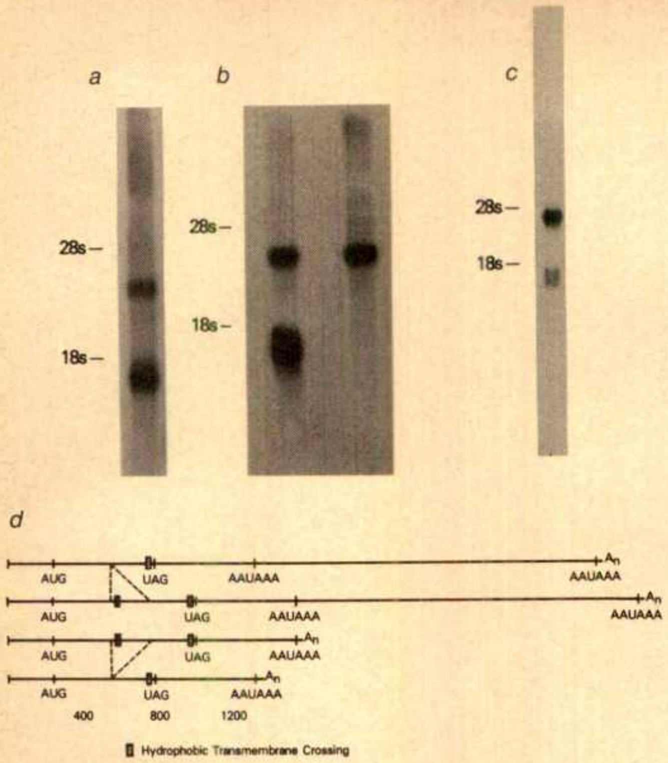

Fig. 5 *a*, Hybridization to HUT-102B2 mRNA with ^{32}P-labelled *Pst*I-*Nde*I segment from pIL2R3. Washes were performed in 0.1 × SSC, 0.1% SDS at 52 °C. *b*, Hybridization to HUT-102B2 mRNA with ^{32}P-labelled pIL2R3 (left lane) or *Nco*I-*Eco*RI 3′ segment of pIL2R3. *c*, Hybridization of ^{32}P-labelled pIL2R3 to mRNA from PHA activated normal T cells. Note that the smaller mRNA appears to be a doublet. *d*, Four possible mRNAs from the IL-2 receptor gene. The top two mRNA (3,300 and 3,500 bases, corresponding to clones 4 and 3, respectively) utilize the same AAUAAA but differ in that the 3,300-base mRNA splices out and the 3,500-base mRNA retains a 216-base segment. The third and fourth are like the second and first, respectively, except that they utilize a more proximal AAUAAA. The third mRNA represents the 1,500-base mRNA retaining the region and the fourth has lost the region and is similar to the 3,300-base mRNA (doublet in *c*).

mRNA. The induced HSB-2 cells express the two mRNAs in significantly different relative quantities. A Tac-negative Epstein-Barr virus (EBV)-transformed B-cell line is negative, but Tac-positive hairy-cell leukaemia cells[30] and Tac-positive HTLV-infected EBV negative B-cell lines (provided by Drs D. Longo and D. Mann) express both IL-2 receptor mRNAs. These data provide a pattern of mRNA expression consistent with our knowledge of which cells react with anti-Tac and express IL-2 receptors, and demonstrate that even in B cells, HTLV-I infection is associated with IL-2 receptor mRNA expression.

We next attempted to determine how the 1,500- and 3,500-base mRNAs differ. A *Pst*I/*Nde*I segment probe from clone 3 (bases 552–729), which contains most of the 216-base pair segment spliced from clone 3 to generate clone 4, hybridizes to both the 1,500- and 3,500-base mRNAs (Fig. 5*a*). These data suggest that both mRNAs contain the segment and that neither corresponds to clone 4. From the sequence and expression data, which together indicate that nonsplicing of the 216-base pair region correlates with IL-2 receptor expression, we hypothesize that both the 1,500- and 3,500-base mRNAs are capable of encoding functional IL-2 receptors. In support of our hypothesis, when mRNA is size-fractionated on a methyl mercuric hydroxide gel, the gel sliced, and RNA contained in the slices translated and immunoprecipitated, the correct primary translation product is identified from either the 1,500- or 3,500-base mRNAs (data not shown).

Both clones 3 and 4 contain two AATAAA sequences corresponding to the potential polyadenylation addition signal present in eukaryotic mRNAs (the first is in the coding region, bases 351–356, and the second is 3′ to the coding region, beginning at base 1,523 in clone 3, and is underlined in Fig. 3*b*). In addition, there is an AATAAA-like sequence (ATTAAA) at bases 1,298–1,303. These AATAAAs apparently are not utilized in clones 3 and 4, as no poly(A) tails are noted and the cDNAs continue 3′ to the AATAAA sites. The functional AATAAAs in clones 3 and 4 are presumably 3′ to the ends of our clones. The *Nco*I-*Eco*RI (Fig. 5*b*) and *Bam*H1-*Eco*R1 3′ fragments of clone 3 (bases 1,642–2,335 and 1,921–2,335, respectively) hybridize only to the 3,500-base mRNA. Thus, we propose that the difference in size of the IL-2 receptor mRNAs is the result of using different polyadenylation signal sequences. In the *Bam*HI-*Eco*RI region, there are two sets of repeated sequences (2,080–2,113 is 82% homologous to 2,213–2,247, and 2,115–2,137 is 87% homologous to 2,279–2,301), although the significance of this finding is unclear. Clone 4 does not arise from either message noted, but its mRNA is identical to that of clone 3 except that the splicable segment has been removed. Such an mRNA (approximately 3,300 bases) would not be resolved from the 3,500-base mRNA corresponding to clone 3 on the Northern blot.

Conclusions

The IL-2 receptor sequence described here has been compared with the Biomedical Research Foundation and Los Alamos databases; no significant homology was found to other known proteins or DNA sequences. Lack of homology to HTLV-I excludes the possibility that this virus encodes the IL-2 receptor. We have shown previously that the primary translation product and other precursor forms of the IL-2 receptor expressed on HUT-102B2 cells are identical in size to those of PHA lymphoblasts, but that there are differences in post-translational processing[17]. Point mutations may thus exist which distinguish these two receptors.

Sequencing of the cDNAs suggests the possibility of alternate mRNA splicing, wherein a 216 base, 72 amino acids long, internal region of the protein may be excised. Whether this region is retained or removed, the encoded protein uses the same initiation and termination sites and shares the identical protein sequence except in the region of splicing. Alternate mRNA splicing has been implicated in the control of gene expression in a variety of different cellular systems. For example, the splicing of alternative exons results in the synthesis of membrane versus secreted forms of immunoglobulin δ and μ genes at different stages in B-lymphocyte maturation[31,32]. Similarly, transcripts from the calcitonin gene are alternatively spliced in neural tissue to produce a calcitonin gene-related peptide which is distinct from the product found in thyroid tissue[33]. Transcripts from the α-amylase and c-*myc* genes in different tissues are differentially processed without altering the protein product[34]. The rat and human γ-fibrinogen genes can be spliced alternatively in the same cell to produce proteins with different functions[35]. Splicing of a segment within the coding region of the IL-2 receptor mRNA appears to change the function of the resultant protein. Transfection of the unspliced cDNA clone in COS-1 cells results in the expression of membrane receptors capable of binding both purified radiolabelled IL-2 and anti-Tac. Transfection of the spliced form of the cDNA, however, does not result in the expression of IL-2 receptors, even though specific mRNA is detected in the transfected cells (data not shown). We assume that this mRNA is translated into protein product that does not bind IL-2, but thus far we have not been able to precipitate the 'spliced' protein product from either surface iodinated or ^{35}S-methionine biosynthetically labelled COS-1 cells. It is also possible that the mRNA is unstable, ineffectively translated, or that the resulting protein product is rapidly degraded. Nevertheless, these data suggest that IL-2 receptor expression may not be regulated solely at the level of transcription, but rather also through post-transcriptional changes in mRNA processing. We cannot exclude the possibility that clone 4 represents a cloning artefact, but the presence of typical mRNA splice signals makes this less likely.

We hypothesize that the four different mRNAs may exist in two pairs, with one of each pair retaining and one lacking the splicable region (Fig. 5*d*). The doublet in the 1,500-base mRNA (Fig. 5*c*) is consistent with the presence of a spliced mRNA, but could also be due to utilization of the ATTAAA sequence.

The DNA sequence of clone 3 permitted us to deduce the entire protein sequence of the human IL-2 receptor. The carboxy-terminus of the protein encoded by these mRNAs contains a stretch of positively charged basic amino acids (6 of the terminal 13 amino acids are arginines or lysines), which we presume to be intracytoplasmic. This region contains one serine and one threonine, which may serve as potential phosphorylation sites[17]. This region is preceded by a hydrophobic region 19 amino acids long which could readily form a transmembrane region (Fig. 5*d*). Both these regions are typical for membrane proteins[36]. There is a second hydrophobic region which is included in the splicable region. Although it is conceivable that this region represents a second transmembrane crossing, the presence of amides (histidine and glutamines) makes this unlikely. If this were a second transmembrane crossing, the two N-linked glycosylation sites would be intracytoplasmic, which is without precedent. It is possible that this region may represent a fold in the protein, a loop into but not through the membrane, or may be important in binding IL-2, which itself has hydrophobic regions. Presumably both of the potential *N*-linked glycosylation sites in the protein are used, as we have identified previously two discrete *N*-linked precursor forms with apparent M_rs of 35,000 and 37,000[16]. In addition, there are numerous serine and threonines immediately extracytoplasmic to the transmembrane region which may serve as the potential *O*-linked glycosylation sites which exist in this protein[16]. The mechanism of signal transduction by this receptor remains unclear, especially in view of the very short cytoplasmic tail (13 amino acids long) which would appear too short to mediate an enzymatic activity. Whether the ligand itself communicates the signal to the cell or whether other proteins serve as subunits in a receptor complex, as has been suggested[16,19], is under further investigation.

Note added in proof: Preliminary S_1 nuclease protection assays suggest that HUT-102B2 cells contain both the spliced and unspliced forms of mRNA indicated in Fig. 5*d*. Since submission of this paper, Wano *et al.*[44] have characterized IL-2 receptors on HUT-102B2 cells and PHA lymphoblasts, with findings similar to those in refs 16–19.

Received 1 June; accepted 17 August 1984.

1. Morgan, D. A., Ruscetti, F. W. & Gallo, R. C. *Science* **193,** 1007–1008 (1976).
2. Watson, J. *J. exp. Med.* **150,** 1510–1519 (1979).
3. Coutinho, A., Larsson, E.-L., Gronvik, K.-O. & Andersson, J. *Eur. J. Immun.* **9**, 587–592 (1979).
4. Gillis, S., Baker, P. E., Ruscetti, F. W. & Smith, K. A. *J. exp. Med.* **148,** 1093–1098 (1978).
5. Shaw, J., Monticone, V. & Paetkau, V. *J. Immun.* **120,** 1967–1973 (1978).
6. Robb, R. J., Kutny, R. M. & Chowdhry, V. *Proc. natn. Acad. Sci. U.S.A.* **80,** 5990–5994 (1983).
7. Taniguchi, T. *et al. Nature* **302,** 305–309 (1983).
8. Clark, S. C. *et al. Proc. natn. Acad. Sci.* (*U.S.A.*) **81,** 2543–2547 (1984).
9. Devos, R. *et al. Nucleic Acids Res.* **11,** 4307–4323 (1983).
10. Fujita, T., Takeoka, C., Matsui, H. & Taniguchi, T. *Proc. natn. Acad. Sci U.S.A.* **81,** 1634–1638 (1983).
11. Holbrook, N. J. *et al. Proc. natn. Acad. Sci. U.S.A.* **81,** 1634–1638 (1984).
12. Robb, R. J., Munck, A. & Smith, K. A. *J. exp. Med.* **154,** 1455–1474 (1981).
13. Poiesz, B. J., Ruscetti, F. W., Reitz, M. S., Kalyanaraman, V. S. & Gallo, R. C. *Nature* **294,** 268–271 (1981).
14. Kalyanaraman, V. S. *et al. Proc. natn. Acad. Sci. U.S.A.* **79,** 1653–1657 (1982).
15. Depper, J. M., Leonard, W. J., Krönke, M., Waldmann, T. A. & Greene, W. C. *J. Immun.* (in the press).
16. Leonard, W. J., Depper, J. M., Robb, R. J., Waldmann, T. A. & Greene, W. C. *Proc. natn. Acad. Sci. U.S.A.* **80,** 6957–6961 (1983).
17. Leonard, W. J. *et al. J. biol. Chem.* (in the press).
18. Leonard, W. J., Depper, J. M., Waldmann, T. A. & Greene, W. C. in *Receptors and Recognition, Ser. B,* Vol. 17 (ed. Greaves, M.) 45–66 (1984).
19. Leonard, W. J. *et al. Nature* **300,** 267–269 (1982).
20. Uchiyama, T., Broder, S. & Waldmann, T. A. *J. Immun.* **126,** 1393–1397 (1981).
21. Vogelstein, B. & Gillespie, D. *Proc. natn. Acad. Sci. U.S.A.* **76,** 615–619 (1979).
22. Maniatis, T., Fritsch, E. F. & Sambrook, J. in *Molecular Cloning* 330–333 (Cold Spring Harbor Laboratory, New York, 1982).
23. Sanger, F. & Coulson, A. R. *J. molec. Biol.* **94,** 414–418 (1975).
24. Sanger, F., Coulson, A. R., Banell, B. G., Smith, A. J. H. & Roe, B. *J. molec. Biol.* **143,** 161–178 (1980).
25. Crabtree, G. R., Comeau, C., Fowlkes, D. & Kant, J. A. *J. molec. Biol.* (in the press).
26. Queen, C. L. & Korn, C. J. *Meth. Enzym.* **65,** 595–609 (1980).
27. Breathnach, R., Benoist, C., O'Hare, K., Gannon, F. & Chambon, P. *Proc. natn. Acad. Sci. U.S.A.* **75,** 4853–4857 (1978).
28. Catterall, J. F. *et al. Nature* **275,** 510–513 (1978).
29. Greene, W. C. *et al. J. Immun.* **133,** 1042–1047 (1984).
30. Korsmeyer, S. J. *et al. Proc. natn. Acad. Sci. U.S.A.* **80,** 4522–4526 (1983).
31. Early, P. *et al. Cell* **20,** 313–319 (1980).
32. Maki, R., Roeder, W., Traunecker, A., Raschke, W. & Tonegawa, S. *Cell* **25,** 353–365 (1981).
33. Rosenfeld, M. G., *Nature* **304,** 129–135 (1983).
34. Young, R. A., Hagenbuchle, O. & Schibler, U. *Cell* **23,** 451–458 (1981).
35. Crabtree, G. R. & Kant, J. A. *Cell* **31,** 159–166 (1982).
36. Weinstein, J. N., Blumenthal, R., van Renswoude, J., Kempf, C. & Klausner, R. D. *J. Membrane Biol.* **66,** 203–212 (1982).
37. Coligan, J. E., Gates, F. T. III, Kimball, E. S. & Maloy, W. L. *Meth. Enzym.* **91,** 413–434 (1983).
38. Merrill, C. R., Goldman, D., Sedman, S. A. & Ebert, M. H. *Science* **211,** 1437–1438 (1981).
39. Chirgwin, J. M., Przybyla, A. E., MacDonald, R. J. & Rutter, W. J. *Biochemistry* **18,** 5294–5299 (1979).
40. Gordon, J. I. *et al., J. biol. Chem.* **257,** 971–978 (1982).
41. Mostov, K. E., Kraehenbuhl, J. P. & Blobel, G. *Proc. natn. Acad. Sci. U.S.A.* **77,** 7257–7261 (1980).
42. Kessler, S. W. *J. Immun.* **115,** 1617–1624 (1975).
43. Benton, W. D. & Davis, R. W. *Science* **196,** 180–182 (1977).
44. Wano, Y. *et al. J. Immun.* **132,** 3005–3010 (1984).

Molecular cloning of cDNA encoding human interleukin-2 receptor

Toshio Nikaido, Akira Shimizu, Norio Ishida, Hisataka Sabe, Keisuke Teshigawara*, Michiyuki Maeda†, Takashi Uchiyama‡, Junji Yodoi* & Tasuku Honjo

Department of Medical Chemistry, *Institute for Immunology, †Chest Disease Research Institute and ‡Department of Internal Medicine, Kyoto University, Faculty of Medicine, Sakyo-ku, Kyoto 606, Japan

The human interleukin-2 (IL-2) receptor was purified by affinity chromatography using the anti-Tac monoclonal antibody, and its N-terminal amino acid sequence was determined. Complementary DNA clones were isolated and sequenced to reveal the primary structure of the IL-2 receptor precursor, which has 272 amino acid residues. The receptor is separated into two domains by a putative 19-residue transmembrane region. Two mRNAs (1.4 and 3.5 kilobases) hybridizing to the cDNA clone were found in human T cells bearing the IL-2 receptor. The cDNA directed synthesis of the IL-2 receptor in COS cells.

THE physiological proliferation of T lymphocytes (T cells) requires a specific interaction between a hormone-like peptide, T-cell growth factor (TCGF)[1] or interleukin-2 (IL-2)[2], and its cell-surface receptor[3-6]. Human IL-2, a peptide of ~14,000 molecular weight (M_r)[7], produced by activated T cells, allows the continuous *in vitro* proliferation of T cells bearing the IL-2 receptor. The immunological activation of G_0-phase T cells, which fail to receive the growth signal by the ligand, requires not only the presence of IL-2 but also expression of the IL-2 receptor. Experiments from several laboratories[8,9] have

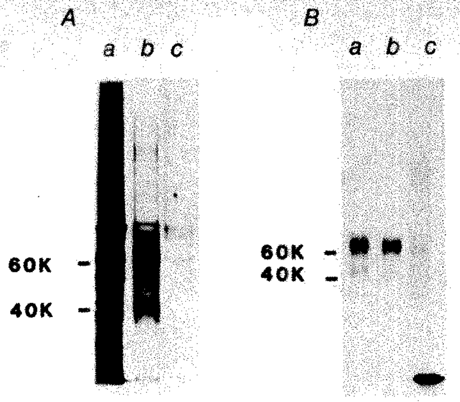

Fig. 1 Purification of the Tac antigen and IL-2 receptor. *A*, SDS-polyacrylamide gel electrophoresis of purified Tac antigen. *a*, Effluent fraction of anti-Tac-Sepharose column (20 μg); *b*, eluted fraction of anti-Tac-Sepharose column (0.1 μg); *c*, buffer alone (to show staining background). *B*, SDS-polyacrylamide gel electrophoresis of the IL-2 receptor of MT-1 cells surface-labelled with ^{125}I-NaI. *a*, Eluate from IL-2-Affigel-10 column (4,250 c.p.m.); *b*, eluate from anti-Tac-Sepharose column (5,200 c.p.m.); *c*, total extracts (4,800 c.p.m.).

Methods: *A*, MT-1 cells (5×10^9 cells) were solubilized with buffer (10 mM Tris-HCl, *p*H 7.4, 0.15 M NaCl, 1% NP40, 1 mM phenyl methyl sulphonyl fluoride (PMSF)). The lysates were absorbed successively with bovine serum albumin-conjugated Sepharose 4B and immunoglobulin (human and mouse)-conjugated Sepharose 4B. The effluent fractions of the solubilized materials were applied to a column (0.5×2 cm) of the anti-Tac antibody coupled with Sepharose 4B (5 mg protein ml^{-1} beads). After extensive washing of the column with PMSF-free solubilizing buffer and a high-salt buffer (10 mM Tris-HCl, *p*H 7.4, 1% NP40, 1 M NaCl), the Tac antigen was eluted with 0.2 M sodium citrate buffer, *p*H 2.6, containing 1% NP40. The eluate was neutralized with 2 M Tris and rechromatographed with an anti-Tac-Sepharose column. An aliquot of the eluted material was precipitated with 10% trichloroacetic acid and run on a 7.5% SDS-polyacrylamide gel[6], analysed with silver stain. *B*, MT-1 cells were labelled with ^{125}I using lactoperoxidase[6]. The solubilized materials were purified by a column of anti-Tac-Sepharose or Affigel-10 conjugated with IL-2 synthesized by recombinant DNA in *Escherichia coli* (1.8 mg IL-2 per ml gel). Eluates from each column and the original extracts were run on a 7.5% SDS-polyacrylamide gel autoradiographed.

Table 1 Expression of Tac-2 cDNA in COS-7 cells

DNA		Antibody	% Positive	MFI
pKCR·Tac-2·A	Expt 1	X5563	1.4	18.8
		Anti-Tac	22.9	56.3
	Expt 2	X5563	1.6	20.2
		Anti-Tac	16.8	46.5
pKCR·Tac-2		X5563	1.4	19.0
		Anti-Tac	7.3	30.4
pKCR·Tac-2·Ai		X5563	3.5	23.4
		Anti-Tac	3.4	24.3
pKCRH2		X5563	1.0	18.5
		Anti-Tac	3.1	24.9

COS-7 cells[46] (500,000) maintained in Dulbecco's minimal essential medium (DMEM) with 5% fetal calf serum (FCS) were seeded onto disposable tissue culture dishes. Medium was washed after 20 h. 4 h later, the cells were supplemented with 1/10th volume of transfection mixtures each containing 40 μg ml^{-1} of the plasmid DNA indicated[47,48]. After 12 h incubation, cells were exposed to 2.5% glycerol in DMEM at room temperature for 1 min, washed and further incubated in DMEM with 8% FCS for 48 h at 37 °C[45]. The cells were collected and stained with anti-Tac monoclonal antibody and fluoresceinated goat anti-mouse antibody (Cappel) as described elsewhere[17]. As paired control experiments, a murine myeloma protein, X5563, replaced anti-Tac antibody. The expression of Tac antigen on the cells were determined by flow cytometry using Spectrum III (Ortho). MFI, mean fluorescence intensity.

demonstrated that antigenic stimulation induces temporal expression of the IL-2 receptor on resting T cells as well as cloned T-cell lines, indicating that the antigen-mediated regulation of the IL-2 receptor expression has an essential role in the clonal expansion of the antigen-specific T cell. As most peripheral as well as thymic T cells do not carry the receptor *in vivo*, the regulatory expression of the IL-2 receptor appears to be a safeguard against a catastrophic spread of the T-cell proliferation by an immunogenic stimulus.

By contrast, an excessive number of IL-2 receptor molecules are expressed on leukaemic cells[10,11] of adult T-cell leukaemia (ATL) endemic in parts of Japan and the Caribbean[12-14]. The leukaemic T cells and the T-cell lines established from these patients contain the DNA sequence of a unique C-type retrovirus, human T-cell leukaemia virus (HTLV)[15] or adult T-cell leukaemia virus (ATLV)[16]. A monoclonal antibody (anti-Tac) produced by using ATL cells as antigens[17], recognizes determinants associated with the IL-2 receptor[18,19]. The number of IL-2 receptors of normal T cells is reduced by interaction with the anti-Tac antibody (down-regulation)[20]. This down-regulation is another abnormal feature of IL-2 receptor expression of ATL cells[11]. This aberrant and excessive expression of the IL-2 receptor might be related to leukaemogenic proliferation of ATL cells[21-23], thus the structure of the IL-2 receptor and regulation of its expression appear to be essential for elucidation of molecular mechanisms of ATL cells. Biochemical analyses of the IL-2 receptor is facilitated by the recent availability of purified IL-2 and monoclonal antibodies recognizing determinants associated with the human and rodent IL-2 receptors[8,9,24-26]. The receptor molecules in these species appear to be similar glycoproteins of about 55,000-60,000 M_r as assessed by mobility in SDS-polyacrylamide gels. Intracellular precursor molecules of the human receptor have smaller molecular sizes, of ~40,000 (refs 5, 6).

IL-2 receptor sequence

We purified the Tac antigen (the putative IL-2 receptor) from an ATL cell line MT-1 (ref. 27) by affinity chromatography with the anti-Tac monoclonal antibody. We find two components of MT-1 of 60,000-65,000 M_r and 40,000-45,000 M_r (Fig. 1*A*). The broad precipitated bands on our gels were essentially the same as those of material internally labelled with ^{35}S-methionine as described previously[5,6]. Pulse-chase experiments have clearly demonstrated that the lower molecular component is a precursor to the surface receptor[5,6]. We also obtained the identical two components by purification with Sepharose conjugated with IL-2 (Fig. 1*B*); we thus confirm here the previous conclusion that the Tac antigen is present on the IL-2 receptor molecule.

The molecular size difference of the two components is thought to be due to different extents of glycosylation; we therefore sought to determine the N-terminal amino acid sequence of the affinity-purified material containing the two components (Fig. 2*A*). We find a unique amino acid sequence from the mixture of the two components, which indicates the identity of the peptide moieties of the two components, although we cannot exclude the possibility that the N-terminus of one of the components is blocked. Short oligonucleotides (14 bases) corresponding to residues 4-8 (Asp-Asp-Asp-Pro-Pro) were synthesized as a probe for screening cDNA libraries.

cDNA clones

A cDNA library complementary to poly(A)$^+$ mRNA of MT-1 cells was constructed and screened with the ^{32}P-labelled 14-base oligonucleotides. The synthetic probes hybridized with three out of 4×10^5 colonies of the MT-1 cDNA library. In the second screening, two of the three candidates hybridized with the probes. After isolation and propagation of the two colonies designated Tac-1 and Tac-2, we cut out the inserts by double digestion with *Hin*dIII and *Pvu*II; both inserts hybridize with the oligonucleotide probes. Restriction site mapping and nucleotide sequence determination show that the two clones are identical, except that the Tac-2 is 16 bases longer at its 5′ end than Tac-1.

The complete nucleotide sequence (1,308 base pairs, bp) of the Tac-2 insert was determined according to the strategy shown

A

```
        1           5                   10                  15                  20
a.  Glu-Leu-X-Asp-Asp-Asp-Pro-Pro-Glu-Ile-Pro-His-Ala-Thr-Phe-Lys-Ala-Met-Ala-Tyr-Lys
```

b. $5'\quad \mathrm{GA}^{\mathrm{T}}_{\mathrm{C}}\ \mathrm{GA}^{\mathrm{T}}_{\mathrm{C}}\ \mathrm{GA}^{\mathrm{T}}_{\mathrm{C}}\ \mathrm{CC}^{\substack{\mathrm{T}\\ \mathrm{C}}}_{\substack{\mathrm{G}\\ \mathrm{A}}}\ \mathrm{CC}\quad 3'$

c. $3'\quad \mathrm{CT}^{\mathrm{A}}_{\mathrm{G}}\ \mathrm{CT}^{\mathrm{A}}_{\mathrm{G}}\ \mathrm{CT}^{\mathrm{A}}_{\mathrm{G}}\ \mathrm{GG}^{\substack{\mathrm{A}\\ \mathrm{G}}}_{\substack{\mathrm{C}\\ \mathrm{T}}}\ \mathrm{GG}\quad 5'$

B

```
               ↓
AACTCCTGACTCCGATAGAGACTGGATGGACCCGCAAGGGTGGCAGCCCAGGCGGACCGATCTTCCCATCCCACATCCTCCGGCGCGATGCCAAAAAGAG      100

                                                                                          -21
                                                                                    MetAspSerTyrLeuLeuMetTrpGl
GCTGACGGCAACTGGGCCTTCTGCAGAGAAAGACCTCCGCTTCACTGCCCCGGCTGGTCCCAAGGGTCAGGAAGATGGATTCATACCTGCTGATGTGGGG      200

                                            -1 +1                                                          20
yLeuLeuThrPheIleMetValProGlyCysGlnAlaGluLeuCysAspAspAspProProGluIleProHisAlaThrPheLysAlaMetAlaTyrLys
ACTGCTCACGTTCATCATGGTGCCTGGCTGCCAGGCAGAGCTCTGTGACGATGACCCGCCAGAGATCCCACACGCCACATTCAAAGCCATGGCCTACAAG      300

                                                             40
GluGlyThrMetLeuAsnCysGluCysLysArgGlyPheArgArgIleLysSerGlySerLeuTyrMetLeuCysThrGlyAsnSerSerHisSerSerT
GAAGGAACCATGTTGAACTGTGAATGCAAGAGAGGTTTCCGCAGAATAAAAAGCGGGTCACTCTATATGCTCTGTACAGGAAACTCTAGCCACTCGTCCT      400

                    60                                                                  80
rpAspAsnGlnCysGlnCysThrSerSerAlaThrArgAsnThrThrLysGlnValThrProGlnProGluGluGlnLysGluArgLysThrThrGluMe
GGGACAACCAATGTCAATGCACAAGCTCTGCCACTCGGAACACAACGAAACAAGTGACACCTCAACCTGAAGAACAGAAAGAAAGGAAAACCACAGAAAT      500

                                         100                                                           120
tGlnSerProMetGlnProValAspGlnAlaSerLeuProGlyHisCysArgGluProProProTrpGluAsnGluAlaThrGluArgIleTyrHisPhe
GCAAAGTCCAATGCAGCCAGTGGACCAAGCGAGCCTTCCAGGTCACTGCAGGGAACCTCCACCATGGGAAAATGAAGCCACAGAGAGAATTTATCATTTC      600

                                                             140
ValValGlyGlnMetValTyrTyrGlnCysValGlnGlyTyrArgAlaLeuHisArgGlyProAlaGluSerValCysLysMetThrHisGlyLysThrA
GTGGTGGGGCAGATGGTTTATTATCAGTGCGTCCAGGGATACAGGGCTCTACACAGAGGTCCTGCTGAGAGCGTCTGCAAAATGACCCACGGGAAGACAA      700

                    160                                                                 180
rgTrpThrGlnProGlnLeuIleCysThrGlyGluMetGluThrSerGlnPheProGlyGluGluLysProGlnAlaSerProGluGlyArgProGluSe
GGTGGACCCAGCCCCAGCTCATATGCACAGGTGAAATGGAGACCAGTCAGTTTCCAGGTGAAGAGAAGCCTCAGGCAAGCCCCGAAGGCCGTCCTGAGAG      800

                                         200                                                           220
rGluThrSerCysLeuValThrThrThrAspPheGlnIleGlnThrGluMetAlaAlaThrMetGluThrSerIlePheThrThrGluTyrGlnValAla
TGAGACTTCCTGCCTCGTCACAACAACAGATTTTCAAATACAGACAGAAATGGCTGCAACCATGGAGACGTCCATATTTACAACAGAGTACCAGGTAGCA      900

                                                             240
ValAlaGlyCysValPheLeuLeuIleSerValLeuLeuLeuSerGlyLeuThrTrpGlnArgArgGlnArgLysSerArgArgThrIleEnd
GTGGCCGGCTGTGTTTTCCTGCTGATCAGCGTCCTCCTCCTGAGTGGGCTCACCTGGCAGCGGAGACAGAGGAAGAGTAGAAGAACAATCTAGAAAACCA      1,000

AAAGAACAAGAATTTCTTGGTAAGAAGCCGGGAACAGACAACAGAAGTCATGAAGCCCAAGTGAAATCAAAGGTGCTAAATGGTCGCCCAGGAGACATCC      1,100

GTTGTGCTTGCCTGCGTTTTGGAAGCTCTGAAGTCACATCACAGGACACGGGGCAGTGGCAACCTTGTCTCTATGCCAGCTCAGTCCCATCAGAGAGCGA      1,200

GCGCTACCCACTTCTAAATAGCAATTTCGCCGTTGAAGAGGAAGGGCAAAACCACTAGAACTCTCCATCTTATTTTCATGTATATGTGTTCATTAAAGCA      1,300

TGAATGGTA_150                                                                                              1,400
```

Fig. 2 Nucleotide and amino acid sequences of the IL-2 receptor. *A*, Partial amino acid sequence of human IL-2 receptor. *a*, N-terminal 21 residues of human IL-2 receptor; *b*, possible nucleotide sequences for amino acid residues 4–8, deduced from the protein sequence; *c*, synthesized oligonucleotides complementary to the deduced nucleotide sequence. *B*, Nucleotide and predicted amino acid sequences of the IL-2 receptor. Nucleotides are numbered at right and amino acids are numbered throughout. Residue one corresponds to the N-terminal amino acid residue of the protein sequence. Overline, sites of potential asparagine-linked glycosylation; black bar, underline, poly(A) addition signal; vertical arrow, origin of Tac-1 clone.

Methods: *A*, IL-2 receptor molecules (2 μg, ≈50 pmol) purified by chromatography with the anti-Tac–Sepharose column were analysed with an automatic protein sequencer[35] (Applied Biosystem Inc.). 31 N-terminal amino acid residues were obtained; the first 21 residues were identical (two separate analyses of the same sample). Mixture of 32 possible oligonucleotides (14 bp) complementary to mRNA encoding residues 4–8 were constructed by an automatic DNA synthesizer (Applied Biosystem Inc.). *B*, Restriction fragments isolated with 5% polyacrylamide gel electrophoresis and labelled with [γ-^{32}P]dATP by T4 polynucleotide kinase. Labelled fragments were digested with suitable restriction enzymes, and fragments labelled at one end were isolated with 5% polyacrylamide gel electrophoresis. End-labelled fragments were sequenced according to the method of Maxam and Gilbert[36].

in Fig. 3. The amino acid sequence deduced from the nucleotide sequence contained a stretch matching with the N-terminal 21 amino acid residues of the IL-2 receptor protein (Fig. 2). The complete 272-amino acid sequence reveals several characteristic features of the IL-2 receptor precursor. First, there is a hydrophobic signal peptide of 21 residues common to many secretory or membrane-bound glycoproteins, although the sequence *per se* is unique to each protein.

Second, the IL-2 receptor consists of a 251-residue protein of 28,463 M_r which is slightly smaller than the apparent M_r (40–45 × 10^3) of the intracellular precursor protein purified using the anti-Tac antibody (Fig. 1). The slight difference might be explained if the anti-Tac antibody-immunoreactive precursor protein has already been partly glycosylated at serine or threonine residues (*O*-glycosylation), giving a higher apparent M_r than the primary translation product[5,6]. The high content of serine and threonine residues (19 and 27 residues respectively) and the presence of many clusters of these residues in the protein sequence are consistent with the previous findings that the IL-2 receptor protein is highly *O*-glycosylated. The apparent size difference determined by migration in an SDS-polyacrylamide gel between the precursor and mature membrane protein is mostly due to *O*-glycosylation rather than *N*-glycosylation, as tunicamycin, an inhibitor of the *N*-glycosylation, reduced the size of the mature IL-2 receptor only slightly[6]. There are two possible *N*-glycosylation sites.

Third, the IL-2 receptor molecule has a putative hydrophobic transmembrane domain of 19 residues (residues 220–238). The N-terminal and C-terminal portions may correspond to the extra- and intracytoplasmic domains, respectively, analogous with the epidermal growth factor (EGF) receptor[28]. Another hydrophobic region occurs at residues 118–135. The hydrophobicity of this region is less prominent than that of other transmembrane regions and the amino acid sequence is different.

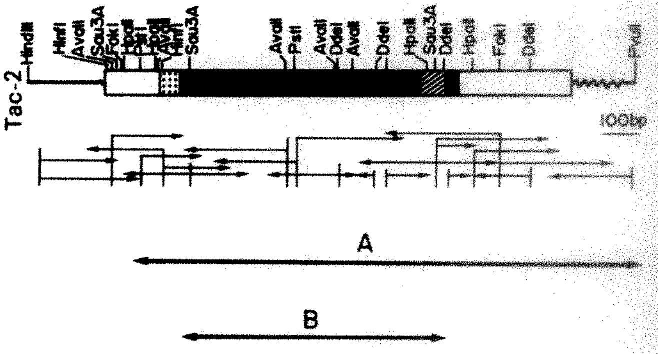

Fig. 3 Restriction cleavage site map of Tac-2 clone and strategy for nucleotide sequence determination. Clone DNAs were cleaved with restriction enzymes and relative locations of cleavage sites were determined. Solid lines, vector; zig-zag lines, oligo-GC (or AT) tails. Black rectangle, coding region; open rectangle, untranslated region; dotted rectangle, signal peptide sequence; hatched rectangle, putative transmembrane region. Direction of mRNA transcription is from left to right. Horizontal arrows show regions and directions of sequencing. Fragment A indicates the insert of pKCR·Tac-2·A (Fig. 5). Fragment B shows probe used for Northern blot hybridization experiments (Fig. 4*A*).

Methods: Cytoplasmic mRNA from MT-1 cells was isolated as described previously[37]. Poly(A)$^+$ mRNA was obtained using oligo(dT)-cellulose. cDNA synthesis and cloning into plasmid were carried out according to Okayama and Berg[38] with a slight modification. Colony screening was performed[39,49] and the probe radiolabelled by phosphorylation using T4 polynucleotide kinase and [γ-^{32}P]ATP to a specific activity of 500 c.p.m. pmol^{-1}.

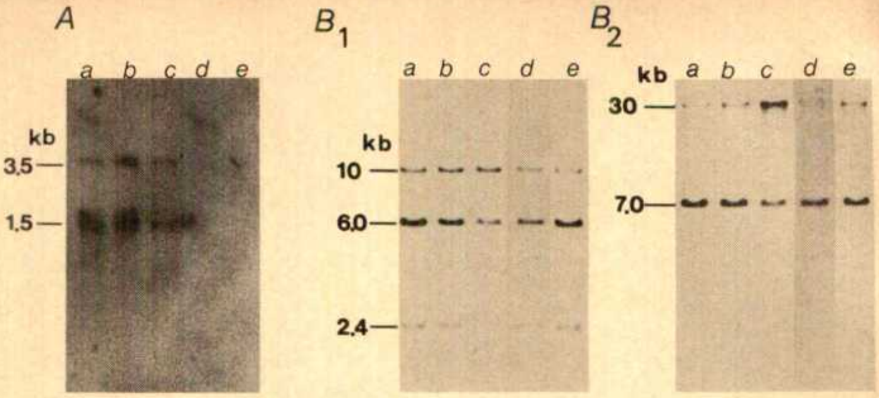

Fig. 4 Analyses of mRNA and DNA of T cells by Tac-2 probe. *A*, Northern blot analysis of IL-2 receptor mRNA. Origins of RNA are: *a*, ATL-2; *b*, MT-1; *c*, YT stimulated with a conditioned medium; *d*, MOLT-4; and *e*, RPMI 8866. MT-1 and ATL-2 were ATLV-positive T-cell lines established from ATL patients. MOLT-4 and YT were ATLV-negative leukaemic cell lines. RPMI 8866 is a human B-cell line. *B*, Southern blot analysis of the IL-2 receptor gene. Origins of DNA are: *a*, Hut-102; *b*, MT-2; *c*, MT-1; *d*, ATL-2; and *e*, human placenta. Restriction enzymes used are: 1, *Eco*RI; 2, *Bam*HI.

Methods: *A*, Poly(A)$^+$ RNAs were prepared from various cell lines[37]. Five μg of poly(A)$^+$ mRNAs were subjected to electrophoresis in a 1.2% agarose gel, which was blotted to a nitrocellulose filter[40]. The filter was hybridized with ^{32}P-labelled fragment B (Fig. 3) of the Tac-2 clone. DNA probe was labelled by nick-translation[41]. *B*, High molecular weight DNAs were prepared from human placenta and established human lymphoid cell lines[42]. DNAs were cut with *Eco*RI or *Bam*HI, electrophoresed in a 0.6% agarose gel and transferred to nitrocellulose filters according to Southern[43]. The filters were hybridized with ^{32}P-labelled *Hin*dIII-*Pvu*II fragment of Tac-2 clone as described elsewhere[44].

mRNA species

Cells stained by the anti-Tac antibody always reversibly bind IL-2, supporting the assumption that the Tac antigen is the IL-2 receptor. This has gained further support by the close correlation between the presence of the Tac-2 mRNA clone sequence and expression of the IL-2 receptor. We assessed the amount of mRNA complementary to the Tac-2 clone in poly(A)$^+$ RNA preparations of various human lymphoid cell lines by the Northern hybridization technique using the 600-bp *Sau*3A fragment (fragment B in Fig. 3) of the Tac-2 clone as probe. Significant amounts of the Tac-2 sequence are present in the ATL cell lines constitutively expressing the IL-2 receptor (ATL-2[30] and MT-1) (Fig. 4*A*). The expression of this gene has been shown in an ATLV-negative human leukaemic cell line YT which had been stimulated to express the IL-2 receptor[29]. As expected, we find little mRNA hybridizing to the Tac-2 insert in non-stimulated YT cells (data not shown).

It is interesting that there are two species (about 1.4 and 3.5 kilobases, kb) of the IL-2 receptor gene transcripts in human T cells. ATL-2 and MT-1 contain an additional mRNA species of 1.6 kb. We show here that the Tac-2 clone, which contains the 1.4-kb insert probably complementary to the 1.4-kb mRNA, is active for expression of the IL-2 receptor in COS cells. We do not know, however, whether the 3.5-kb RNA encodes a functionally active protein. The two mRNAs may encode IL-2 receptors with different affinities for IL-2 (D. A. Cantrell and K. A. Smith, unpublished). The difference could also be accounted for by two alternative poly(A) addition sites as shown in membrane-form immunoglobulin mRNAs[31].

Multiple genomic DNA segments hybridize to the Tac-2 probe (Fig. 4*B*). Human placental DNA contains three *Eco*RI fragments (10, 6 and 2.4 kb) hybridizable to the IL-2 receptor cDNA, and *Bam*HI digestion of human DNA yields two fragments, 30 and 7 kb. The number of bands and relative intensity of each band are the same in ATLV-infected cells and human placenta DNA, suggesting that there is neither amplification nor gross rearrangement of the IL-2 receptor gene in these cell lines (Fig. 4).

The 1.35-kb *Pst*I-*Pvu*II fragment (fragment A in Fig. 3) of the Tac-2 clone has been recloned into an expression vector pKCRH2 (ref. 32). We used the recloned plasmid designated pKCR·Tac-2·A (Fig. 5*a*) to transfect COS cells. After 48 h the cell surface is stained with the anti-Tac monoclonal antibody. Approximately 23% of transfected cells expressed the Tac antigen (Table 1). The pKCR vector and pKCR·Tac-2·Ai containing fragment A in the reverse orientation were used as controls, which are all negative. We also tested the transfected cells for ^{3}H-labelled IL-2 binding (specific activity 25,000 c.p.m. U^{-1}, provided by K. Smith)[3]. COS cells transfected with pKCR·Tac-2·A express on average 2,000 molecules of the IL-2 receptor

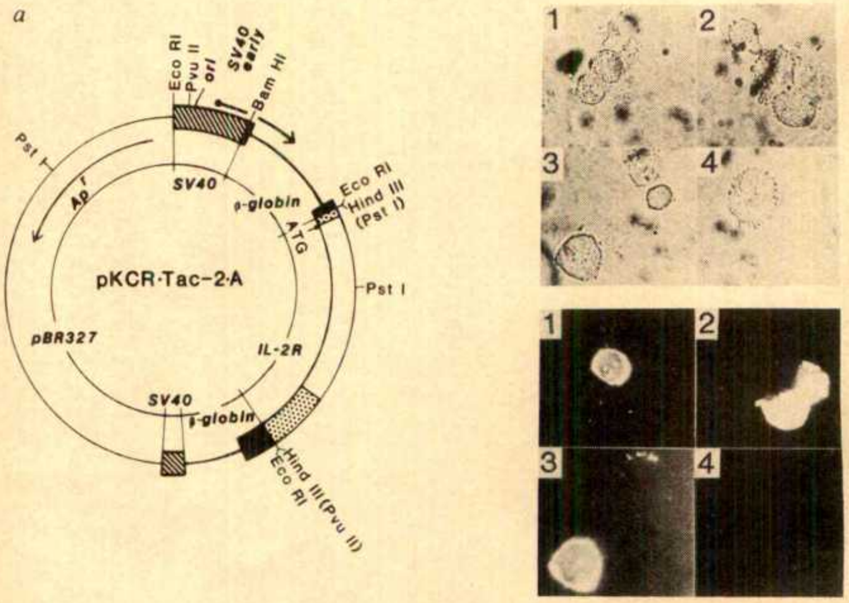

Fig. 5 Structure of expression vector containing Tac-2 cDNA and Tac antigen expression in COS cells. *a*, Structure of pKCR·Tac-2·A. Fragment A of Tac-2 clone (Fig. 3) was isolated by partial *Pst*I cleavage followed by *Pvu*II digestion and ligated with *Hin*dIII linkers after filling single-stranded ends with T4 DNA polymerase. The fragment was cleaved with *Hin*dIII and ligated with pKCRH2 plasmid[32] cleaved with *Hin*dIII (gift of M. Mishina). Recombinant plasmids were cloned and those containing fragment A inserted with the same and reverse orientations relative to the β-globin gene were designated pKCR·Tac-2·A and pKCR·Tac-2·Ai, respectively. A similar recombinant containing the *Hin*dIII-*Pvu*II fragment was also constructed and designated pKCR·Tac-2. Open rectangles, coding sequences; closed rectangles, non-coding sequences of Tac-2; closed boxes, β-globin sequences; hatched rectangles, simian virus 40 sequences; solid line, β-globin gene introns and pBR327; arrow, the origin and direction of transcription; Ori, origin of replication. *b*, *c*, Tac antigen expressed on COS cells. Methods as described in Table 1. DNAs used were pKCR·Tac-2·A (1–3) and pKCRH2 (4). The same fields were observed by phase-contrast (*b*) and fluorescence (*c*) microscopes.

per cell whereas ATL-2 expresses about 8,000 molecules per cell. Our results unequivocally demonstrate that the Tac-2 sequence encodes the IL-2 receptor.

Discussion

The amino acid sequence of the IL-2 receptor does not have any significant homology with any known eukaryotic genes (or oncogenes). Cloning of the IL-2 receptor gene will, however, allow new insights into the physiological function and mechanism by which the IL-2 and its receptor system regulates T-cell proliferation. These include elucidation of the three-dimensional structures of the ligand and receptor which can be produced in large quantities in *E. coli* or mammalian cells, and the molecular mechanisms of signal transmission via surface receptor in the hormone and lymphokine systems, via mutants of the IL-2 receptor gene.

Cloning of the IL-2 receptor gene will also allow us to test several hypotheses proposed for the mechanism of leukaemogenesis of ATL triggered by ATLV, which has no typical oncogene sequence[33]. The excessive numbers of IL-2 receptor on ATL cells may be similar to aberrant expression of the EGF receptor on certain transformed cell lines such as A431 (ref. 34). The homology between the *erb-B* oncogene and the cytoplasmic domain of the EGF receptor[28] has strengthened the hypothesis[21-23] that an excessive amount of the IL-2 receptor might alter the normal growth control of T cells. This can be directly tested by transfection of human T-cell lines by the IL-2 receptor cDNA clone. We can also examine whether the IL-2 receptor gene in ATL cells has any mutations. A unique lymphokine secreted from ATL cells, ATL-derived factor (ADF), enhances the expression of the IL-2 receptor[30]. ADF may be responsible for the continued expression of the IL-2 receptor in many ATLV-positive T-cell lines. It is of interest to know whether ADF is able to induce transcription of the IL-2 receptor gene in human T cells.

We thank Japan Scientific Instrument Co. (JSIC) and Dr I. Kubota (Suntory Ltd) for amino acid sequence determination, JSIC for oligonucleotide synthesis, Dr K. Kato (Takeda Chemical Co.) for supply of IL-2 and Affi gel-conjugated IL-2, Dr T. Miyata for computer analysis of the sequence, and Dr M. Okada, Mr Y. Tagaya and Dr T. Noma for technical assistance. This investigation was supported by grants for special promotion of science from Ministry of Education, Science and Culture of Japan.

Received 28 June; accepted 17 July 1984.

1. Morgan, D. A., Ruscetti, F. W. & Gallo, R. C. *Science* **193,** 1007–1008 (1976).
2. Smith, K. A. *Immun. Rev.* **51,** 337–357 (1980).
3. Robb, R. J., Munck, A. & Smith, K. A. *J. exp. Med.* **154,** 1455–1474 (1981).
4. Cantrell, D. A. & Smith, K. A. *J. exp. Med.* **158,** 1895–1911 (1983).
5. Leonardt, W. J. *et al. Proc. natn. Acad. Sci. U.S.A.* **80,** 6957–6961 (1983).
6. Wano, Y. *et al. J. Immun.* (in the press).
7. Taniguchi, T. *et al. Nature* **302,** 305–309 (1983).
8. Hemler, M. E. *et al. Proc. natn. Acad. Sci. U.S.A.* **81,** 2171–2175 (1984).
9. Yachie, A. *et al. J. Immun.* **131,** 731–735 (1983).
10. Hattori, T. *Blood* **58,** 645–647 (1981).
11. Tsudo, M., Uchiyama, T., Uchino, H. & Yodoi, J. *Blood* **61,** 1014–1016 (1983).
12. Yodoi, J., Takatsuki, K. & Masuda, T. *New Engl. J. Med.* **290,** 572–573 (1974).
13. Uchiyama, T. *et al. Blood* **50,** 481–492 (1977).
14. Takatsuki, K. *et al. Gann. Monogr. Cancer Res.* **28,** 13–22 (1982).
15. Poiesz, B. Z. *et al. Proc. natn. Acad. Sci. U.S.A.* **77,** 7415–7419 (1980).
16. Himuma, Y. *et al. Proc. natn. Acad. Sci. U.S.A.* **78,** 6476–6480 (1981).
17. Uchiyama, T., Broder, S. & Waldmann, T. A. *J. Immun.* **126,** 1393–1397 (1981).
18. Leonard, W. J. *et al. Nature* **300,** 267–269 (1982).
19. Robb, R. J. *et al. J. exp. Med.* **158,** 1332–1337 (1983).
20. Tsudo, M. *et al. J. Immun.* **129,** 592–595 (1982).
21. Yodoi, J., Uchiyama, T. & Maeda, M. *Blood* **62,** 509–510 (1983).
22. Gallo, R. C., Wong-Staal, F., Greene, W. C. & Waldmann, T. M. *Blood* **62,** 510–511 (1983).
23. Yodoi, J. & Honjo, T. *Molec. biol. Med.* (in the press).
24. Osawa, H. & Diamanstein, T. *J. Immun.* **30,** 51–55 (1983).
25. Malek, T. R., Robb, R. J. & Shevach, E. M. *Proc. natn. Acad. Sci. U.S.A.* **80,** 5694–5697 (1983).
26. Osawa, H. & Diamantstein, T. *J. Immun.* **132,** 2445–2450 (1984).
27. Moyoshi, I. *et al. Gann* **71,** 155–156 (1980).
28. Downward, J. *et al. Nature* **307,** 521–527 (1984).
29. Yodoi, J. *et al.* in *Thymic Hormones and Lymphokines 83'* (ed. Goldstein, A. L.) (Plenum, New York, in the press).
30. Yodoi, J. *et al.* in *Cancer Cells Vol.* 3 (eds Gallo, R. C., Essex, M. E. & Gross, L.) (Cold Spring Harbor Laboratory, New York, in the press).
31. Ishida, N. *et al. EMBO J.* **9,** 1117–1123 (1982).
32. Mishina, M. *et al. Nature* **307,** 604–608 (1984).
33. Seiki, M., Hattori, Y., Hirayama, Y. & Yoshida, M. *Proc. natn. Acad. Sci. U.S.A.* **80,** 3618–3622 (1983).
34. Haigler, H. T., Ash, J. F., Singer, S. J. & Cohen, S. *Proc. natn. Acad. Sci. U.S.A.* **75,** 3317–3321 (1978).
35. Hewick, R. M., Hunkapiller, M. W., Hood, L. E. & Dreyer, W. J. *J. biol. Chem.* **256,** 7990–7997 (1981).
36. Maxam, A. M. & Gilbert, W. *Meth. Enzym.* **65,** 499–560 (1980).
37. Aviv, H. & Leder, P. *Proc. natn. Acad. Sci. U.S.A.* **69,** 1408–1412 (1972).
38. Okayama, H. & Berg. P. *Molec. Cell Biol.* **2,** 161–170 (1982).
39. Hanahan, D. & Meselson, M. *Gene* **10,** 63–67 (1980).
40. Thomas, P. D. *Proc. natn. Acad. Sci. U.S.A.* **77,** 5201–5205 (1980).
41. Maniatis, T., Jeffrey, A. & Kleid, D. G. *Proc. natn. Acad. Sci. U.S.A.* **72,** 1184–1188 (1975).
42. Yaoita, Y. & Honjo, T. *Biomed. Res.* **1,** 164–175 (1980).
43. Southern, E. M. *J. molec. Biol.* **98,** 503–517 (1975).
44. Honjo, T. *et al. Cell* **18,** 559–568 (1979).
45. Nielsen, D. A. *et al. Proc. natn. Acad. Sci. U.S.A.* **80,** 5198–5202 (1983).
46. Gluzman, Y. *Cell* **23,** 175–182 (1981).
47. Graham, F. L. & Van der Ev, A. J. *Virology* **52,** 456–467 (1973).
48. Wigler, M. *et al. Proc. natn. Acad. Sci. U.S.A.* **76,** 1373–1376 (1979).
49. Wallace, R. B. *et al. Nuclear Acids Res.* **9,** 879–894 (1981).

LETTERS TO NATURE

Terrestrial catastrophism—Nemesis or Galaxy?

S. V. M. Clube

Department of Astrophysics, South Parks Road,
Oxford OX1 3RQ, UK

W. M. Napier

Royal Observatory, Blackford Hill, Edinburgh EH9 3HJ, UK

The ~30 Myr periodicity associated with the Sun's motion through the central plane has been linked to geomagnetic reversals[1,2], biological extinctions[3] and crater ages[4–6]. This periodicity is consistent with galactic theories of terrestrial catastrophism[1,5]. It has been suggested, however, that the periodicity is controlled by a hypothetical stellar companion of the Sun ('Nemesis') in a highly eccentric orbit of arbitrarily chosen period which periodically upsets the Oort cloud[7,8]. Although the idea appears superficially attractive, there has been little or no attempt to relate it to what is already known about the Oort cloud and the environment in which the Sun–Nemesis system would have to exist. Thus, the inferred phase of the Nemesis cycle is inconsistent with such evidence as there may be for a recent disturbance (~5 Myr) of the Oort cloud, namely the apparent non-equilibrium distributions of perihelia[1] and 1/*a* (ref. 9) and the enhancement of the short-period comet population[10,11] (compare ref. 12). It also discounts the generally high glacial, magnetic and orogenic activity on Earth within this period and the Sun's recent passage through Gould's belt[10,13]. However, the most serious problem is reconciling the approximately constant time-averaged cratering rate for the last ~3,000 Myr (ref. 14) and the stability of the proposed system.

The long-period comet system is dynamically unstable, over the lifetime of the Solar System, against the perturbing action of molecular clouds[15–17]. Since the proposed companion star has an aphelion distance $Q \simeq 180{,}000$ AU (that is, $P \simeq 30$ Myr) as against ~40,000–50,000 AU for long-period comets, one expects its orbit to be unstable *a fortiori*. On the impulse approximation the specific energy change ΔE of the companion resulting from a change Δv in its velocity v relative to the Sun is

$$\Delta E = \tfrac{1}{2}(v + \Delta v)^2 - \tfrac{1}{2}v^2$$

or

$$\Delta E = v.\Delta v + \tfrac{1}{2}(\Delta v)^2 \qquad (1)$$

Considering only the random component $v.\Delta v$, Oort[18] derived an expression for the specific energy fed into a body of separation Q from the Sun in $t \times 10^9$ yr, as a result of encounters with

Table 1 Energy injected by various perturbers

Perturber	Energy, Δv^2 $[(\text{cm s}^{-1})^2]$
GMCs with $M = 2\times10^5\,M_\odot$, $\nu = 40\,\text{kpc}^{-3}$	3.8×10^9
Molecular clouds with $M = 2\times10^4\,M_\odot$, $\nu = 400\,\text{kpc}^{-3}$	9.6×10^9
Stars	4.2×10^9
Σ	17.6×10^9
Energy required for escape	0.9×10^8

point masses. Modifying[15] to allow for the effect of penetrating encounters with molecular clouds of mass M solar masses, radii R AU and number density ν kpc^{-3}, one finds

$$\sum \Delta v^2 = 740\nu\left(\frac{M}{2.21\times10^5 M_\odot}\right)^2 \times\left(\frac{Q}{R}\right)^2\left(\frac{t}{4.5\times10^9\,\text{yr}}\right)10^8 \qquad (\text{cms}^{-1})^2 \tag{2}$$

The energy injected by various perturbers over 4.5×10^9 yr is listed in Table 1. According to Sanders[19] recent determinations of the mass of the molecular cloud system agree to within a factor ~2, whilst the column density of molecular clouds is $\sim5M_\odot\,\text{pc}^{-2}$ at the solar distance, the mass-averaged mean mass of giant molecular clouds (GMCs) being $\sim5\times10^5\,M_\odot$. The first two entries in Table 1 each correspond to a column density $\simeq1\,M_\odot\,\text{pc}^{-2}$ and are therefore below the extreme lower limit of mass allowed by the data. There is also considerable substructure within GMCs, which adds substantially to the energy injected: thus GMCs ($\sim10^5$–$10^6\,M_\odot$) appear to comprise aggregates of molecular clouds ($\sim10^4\,M_\odot$). We consider here three extreme models which are likely to encompass all reasonable possibilities: GMCs are uniform throughout their interiors (rows 1+3); GMCs do not exist, only molecular clouds (rows 2+3); GMCs comprise molecular clouds as substructure (rows 1+2+3). It seems that even with the most conservative assumption the energy injected into the Sun/Nemesis binary by molecular clouds and stars is at least an order of magnitude greater than its binding energy and that the system could not survive in its postulated state for 4.5×10^9 yr. Most probably, the sum of the injected energies is ~200 times that required to eject the companion star from the Solar System. The probable survival time can be found from equation (1) by equating the energy input to the binding energy whence it is found that, in the most likely case of rows 1+2+3, the formal survival time is ~50 Myr. Considering only the effect of uniform GMCs (rows 1+3), the survival time is found to be ~100 Myr. The rate of energy input is decreased by a factor ~1.5–2 allowing for the exponential z-distribution of molecular clouds[16], and increased by factors ~2 and ≥2 allowing for gravitational focussing and a more gaseous past Galaxy respectively[17].

The dissolution time τ of a binary system has been derived also by Chandrasekhar[20] neglecting the random component in (1) and considering only the systematic unbinding term $\frac{1}{2}(\Delta v)^2$. Adjusting his formula slightly to allow for the high eccentricity of Nemesis, one finds

$$\tau \simeq \frac{7\times10^{13}}{\nu M Q^{3/2}}\times10^9\,\text{yr} \tag{3}$$

yielding similar survival times, for example $\tau\sim100$ Myr for uniform GMCs with $\nu\simeq40\,\text{kpc}^{-3}$ and $M = 2\times10^5\,M_\odot$. Putting these two effects together (equation (1)), it is evidently unlikely that the Sun–Nemesis system will survive the Galactic environment for more than two or three revolutions.

In addition to the disruptive influence of encounters with molecular clouds and stars, the somewhat lesser effect of the Galaxy's smoothed-out mass distribution has to be considered. The disturbing potential due to the Galaxy is $\phi = -\frac{1}{2}(\alpha x^2 + \gamma z^2)$, with $\alpha\sim1.6\times10^{-30}\,\text{s}^{-2}$, $\gamma\sim-4.8\times10^{-30}\,\text{s}^{-2}$, in a heliocentric rotating coordinate system with x-axis directed towards the galactic anticentre, y-axis in the direction of rotation and z-axis towards the north galactic pole[21]. The critical Hill surface, beyond which orbits around the Sun are unstable, is roughly a tri-axial ellipsoid with $x_{\text{max}}\simeq300{,}000$ AU, $y_{\text{max}}\simeq200{,}000$ AU, $z_{\text{max}}\simeq150{,}000$ AU. Thus with aphelion ~180,000 AU, the orbit of Nemesis is barely if at all stable. Take the orbit to be roughly rectilinear, let χ represent the angle between orbit and x-axis, and consider the perturbing forces acting on the companion while its radius vector $r > a \simeq 10^5$ AU, which will hold for about half the orbital period. Over this time, the x-component of the galactic field satisfies $\ddot{x} = \partial\phi/\partial x \geqslant \alpha a\cos\chi$, whence $|\dot{x}| \geqslant (\alpha a\cos\chi)T/2$. With $a\simeq1.5\times10^{18}$ cm, $T\simeq9\times10^{14}$ s, $\cos\chi\simeq\frac{1}{2}$ one obtains $|\dot{x}|\gtrsim0.05\,\text{km s}^{-1}$. Likewise $|\dot{z}|\geqslant0.15\,\text{km s}^{-1}$. These perturbations should be compared with the aphelion velocity of Nemesis, $\sim0.03\,\text{km s}^{-1}$, and the circular velocity at 180,000 AU, $\sim0.07\,\text{km s}^{-1}$. It is clear that the velocity vector of the companion star will be grossly perturbed around its aphelion: the binary system would not in general maintain the high eccentricity necessary for Oort cloud perturbations and indeed might not survive even a single revolution. Thus, the Galaxy's smoothed-out mass distribution is also an important factor, though if one were to (1) overlook molecular cloud perturbations; and (2) adopt a binary configuration with major axis close to the galactic plane, it is possible such a system might survive for $\geqslant1\times10^9$ yr. Note also that the proposed binary characteristics are very rare or absent amongst observed systems. Thus among binaries with solar type primaries, only ~1% have periods in excess of 0.3 Myr, the computed periods amongst common proper motion pairs ranging from 3.5 to 820,000 yr with mean 67,000 yr and median 3,100 yr. Furthermore, only ~3% of binaries have eccentricities ≥0.75. These facts are of course consistent with disruption by molecular clouds and the Galaxy.

Received 3 July; accepted 22 August 1984.

1. Clube, S. V. M. & Napier, W. M. *Mon. Not. R. astr. Soc.* **208**, 575–588 (1984).
2. Negi, J. G. and Tiwari, R. K. *Geophys. Res. Lett.* **10**, 713–716 (1983).
3. Raup, D. M. and Sepkoski, J. J. *Proc. natn. Acad. Sci. U.S.A.* **81**, 801–805 (1984).
4. Seyfert, C. K. & Sirkin, L. A. *Earth History and Plate Tectonics* (Harper Row, New York, 1979).
5. Rampino, M. R. & Stothers, R. B. *Nature* **308**, 709–712 (1984).
6. Alvarez, W. & Muller, R. A. *Nature* **308**, 718–720 (1984).
7. Whitmire, D. P. & Jackson, A. A. *Nature* **308**, 713–715 (1984).
8. Davis, M., Hut, P. & Muller, R. A. *Nature* **308**, 715–717 (1984).
9. Yabushita, S. *Mon. Not. astr. Soc.* **204**, 1185–1191 (1983).
10. Napier, W. M. & Clube, S. V. M. *Nature* **282**, 455–459 (1979).
11. Clube, S. V. M. & Napier, W. M. *Mon. Not. R. astr. Soc.* (in the press).
12. Fernandez, J. A. & Jockers, K. *Repts. Progr. Physics* **46**, 665–772 (1983).
13. Clube, S. V. M. & Napier, W. M. *Earth planet. Sci. Lett.* **57**, 251-262 (1982).
14. Hartmann, W. K. *Icarus* **24**, 181-187 (1975).
15. Clube, S. V. M. & Napier, W. M. in *Highlights of Astronomy* Vol. 6 (ed. West, R.) 355-362 (Reidel, Dordrecht, 1983).
16. Bailey, M. E. *Mon. Not. R. astr. Soc.* **202**, 603–633 (1983).
17. Napier, W. M. & Staniucha, M. *Mon. Not. R. astr. Soc.* **198**, 723–735 (1982).
18. Oort, J. H. *Bull. astr. Inst. Netherl.* **11**, 91–110 (1950).
19. Sanders, D. B., Solomon, P. M. & Scoville, N. Z. *Astrophys. J.* **276**, 182–203 (1984).
20. Chandrasekhar, G. A., *Astrophys. J.* **99**, 54–58 (1944).
21. Antonov, V. A. & Latyshev, I. N. in *The Motion, Evolution of Orbits, and Origin of Comets* (eds Chebotarev, G. A. *et al.*) 341-345 (Reidel, Dordrecht, 1972).

Dynamical constraints on the mass and perihelion distance of Nemesis and the stability of its orbit

J. G. Hills

T-6, Theoretical Division, Los Alamos National Laboratory,
Los Alamos, New Mexico 87545, USA

It has been suggested[1,2] that the observed periodic extinction of species at intervals of 26 Myr (ref. 3) may be catalysed by a hypothetical stellar companion of the Sun, Nemesis, with an orbital period of 26 Myr. The passage of a stellar companion through the inner comet cloud[4] will fill the loss cone of these comets and cause a comet shower to enter the planetary system. It has been estimated that about 20–30 comets will hit the Earth during a shower, which

lasts less than a million yr. Such Earth impacts would produce considerable environmental stress and may lead to widespread extinction of species[4]. I now investigate the effect of Nemesis on the comets in the inner comet cloud. This is used to determine the minimum required mass of Nemesis and its minimum required perihelion distance. The effect of passing stars on the stability of the orbit of Nemesis is investigated, and the probability of its having passed within the planetary system estimated.

My previous calculations[4] were for a passing star in a hyperbolic orbit with an impact velocity of 30 km s^{-1}, which is very much greater than the orbital velocity of a long-period comet. This allowed an impulse approximation to be used. However, Nemesis has an orbit similar to that of the comets in the outer, steady-state or Oört comet cloud, so its orbital velocity is similar to that of the comets which it perturbs. A series of exact three-body calculations are used to determine the amount by which Nemesis perturbs the orbits of the comets in the inner cloud.

I consider comets having semimajor axes of 4,000 AU, which is about the maximum semimajor axis of the comets needed to produce a death shower. In the computer calculations, Nemesis is assumed to be a black dwarf with a mass of either $M_N = 0.05\ M_\odot$, or $M_N = 0.005\ M_\odot$. If the orbital period of Nemesis is 26 Myr and its mass is 0.05 $M_\odot$, the semimajor axis of its orbit is $a_N = 89{,}200$ AU by Kepler's Third Law.

Because of the large semimajor axis of its orbit, Nemesis crosses the orbits of comets having semimajor axes of 4,000 AU at very nearly the parabolic speed. This means that the pericentre passage of Nemesis can be well approximated by modelling it as an object in a hyperbolic orbit with a velocity at infinity of 0.1 km s^{-1}, which is an order of magnitude less than its orbital velocity at pericentre passage. This approximation allowed me to use my massive, very accurate computer code which was originally applied to encounters between a binary system and a stellar intruder (refs 5, 6 and refs therein). The calculations used a representative comet orbit with a semimajor axis $a_c = 4{,}000$ AU and an eccentricity $e_0 = 0.999$ (see Table 1).

The loss cone comets are long-period comets which pass within the orbits of Jupiter and Saturn at perihelion. Such comets are lost by their ejection into hyperbolic orbits in a time comparable with the original orbital period of these long-period comets[5,6]. They are not present unless perturbations by passing stars have deflected fresh comets into the loss cone within the previous orbital period. The latter situation occurs in the steady-state for comets in the classical Oört cloud[4] (comets with semimajor axis, $a_c > 2\times10^4$ AU). Comets with semimajor axis $< 2\times10^4$ AU only have their loss cones filled episodically by passing stars. An intense comet shower enters the planetary system whenever a close stellar passage occurs[4].

To fill the loss cone of the comets in the inner cloud requires that the mean change in their pericentre distance $\langle\Delta q\rangle$ exceed the semimajor axis of the orbit of Saturn or $\langle\Delta q\rangle > 9.5$ AU. Table 1 shows that for a Nemesis mass of $M_N = 0.05\ M_\odot$ and for comets with semimajor axes $a_0 = 4{,}000$ AU, this requires that the closest approach of Nemesis, its pericentre distance, be $<2.6\ a_0 = 1.04\times10^4$ AU. Since the semimajor axis of Nemesis is $a_N = 89{,}200$ AU, this requires that its orbital eccentricity be at least $e_N \geq (1 - R_{min}/a_N) = 0.88$.

The orbit of Nemesis has been greatly perturbed by passing stars, so the probability of its having a given eccentricity is dictated by conditions of statistical equilibrium rather than by its initial eccentricity. The probability of its having an eccentricity e or greater at some arbitrary time is given by[4]

$$P_e = (1 - e^2) \tag{1}$$

For $e = 0.88$, we note that $P_e = 0.23$. Invoking the Ergodic Hypothesis that a time average for one object produces the same distribution as an ensemble average over many objects, we anticipate that ~23% of the time its orbital eccentricity is high enough for Nemesis to induce an intense comet shower at its pericentre passage. For a fixed value of Nemesis's pericentre distance q_N, the mean change in the pericentre distance of the comets with $a_c = 4{,}000$ AU scales as

$$|\Delta q_c| \propto \frac{M_N^2}{M_\odot + M_N} \tag{2}$$

in the impulse approximation. In this approximation, we expect that a Nemesis with $M_N = 0.005\ M_\odot$ would produce a $|\Delta q_c|$ about 96 times smaller than a Nemesis with $M_N = 0.05\ M_\odot$. The scatter in the exact numerical results of Table 1 are fairly large, but they indicate that the lower-mass Nemesis produces a $|\Delta q_N|$ about twice that prediced by scaling from $M_N = 0.05\ M_\odot$ using the impulse approximation.

Applying the scaling law given by equation (2) to the data in Table 1, we can find $|\Delta q_c|$ for other possible masses of Nemesis. Table 2 shows, as a function of M_N, the maximum value of q_N that would still allow the perturbations by Nemesis to fill the loss cones at pericentre passage (that is, still result in $|\Delta q| \geq 9.5$ AU).

If we correct for the small breakdown in the scaling law indicated by the computer calculations for $M_N = 0.005\ M_\odot$, we see that a Nemesis with a mass $M_N = 0.01\ M_\odot = 10$ Jupiter masses may be close to the minimum required mass, but a Nemesis with $M_N = 0.005\ M_\odot$ is well below the minimum mass.

When the loss cone is filled, the fraction of the comets of semimajor axis a_c which have pericentre distances of q_c or less is $F_l = 2q_c/a_c$, for $q_c \ll a_c$ (ref. 4). Here F_l is also the fraction of the comets of semimajor axis a_c which are lost per orbital period due to the perturbations by Jupiter and Saturn if $q_c \leq 9.5$ AU. The fraction of the comets of a given semimajor axis surviving N loss cone fillings is given by

$$F_N = [1 - (2q/a_c)]^N \tag{3}$$

If the loss cone of the inner cloud comets were filled at every perihelion passage of Nemesis for the past 4.6×10^9 yr then $N = N_0 = 177$ assuming the orbital period of Nemesis has remained constant at 2.6×10^7 yr. For comets with $a_c = 4{,}000$ AU and $q_c \leq 9.5$ AU, $F_N = 0.43$ for $N = 177$. In this case, more than half these comets would be lost. However, the orbit of Nemesis is severely perturbed by passing stars. The factor P_e in Table 2 is the fraction of the time that its orbit is eccentric enough and

Table 1 Relaxation of comet orbits by Nemesis

p/a_0	R_{min}/a_0	$\Delta q/(\text{AU})$	N
$M_N = 0.05\ M_\odot$			
2.5	0.134	84.8	100
5.0	0.531	134	551
9.0	1.68	149	551
10.0	2.06	79	551
11	2.47	12.8	551
12	2.91	4.1	100
15	4.41	1.7	100
20	7.41	0.7	100
$M_N = 0.005\ M_\odot$			
5.0	0.554	2 3	551
9.0	1.75	7.4	551
10.0	2.14	1.3	551
11.0	2.57	0.54	551

$V = 0.1$ km s^{-1}; $a_0 = 4\times10^3$ AU; $e_0 = 0.999$. Impact parameter p, and closest approach $R_{min} = q_N$ are shown in units of the semimajor axis of the comet orbit. $\langle\Delta q\rangle$ is the mean change in the pericentre distance of the comets.

Table 2 Maximum perihelion distance of Nemesis

$M_N/M_\odot$	$q_{max}(a_0)$	q_{max} (AU)	e_{min}	P_e	$1-F_N$
0.015	1.7	6,800	0.92	0.15	0.12
0.02	2.1	8,400	0.91	0.17	0.13
0.05	2.6	10,400	0.88	0.21	0.16
0.10	4.0	16,000	0.85	0.27	0.20
0.20	7.4	30,000	0.66	0.60	0.40

e_{min} is the minimum orbital eccentricity of Nemesis required by q_{max}. P_e gives the fraction of the time during which its eccentricity exceeds e_{min}.

Table 3 Change in orbit of Nemesis due to stellar intruders

p/q_N	Ni/Encounter	$\Delta q_N/q_N$	Δq_N/AU	$\Delta p/p_N$
0.1	0.46	0.717	3,200	0.1333
0.2	1.8	0.205	914	0.0559
0.5	11.5	0.080	357	0.0413
1.0	46	0.049	219	0.0102
1.5	104	0.044	198	0.0103
2.0	184	0.020	89	0.0025

p/a_N is the impact parameter in units of the semimajor axis of the orbit of Nemesis. N_i shows the average number of stellar intruders that pass within distance p/a_N of the Sun within one orbital period of 26 Myr. This was scaled from the results given in ref. 4. Δq_N is the change in the pericentre distance per encounter listed in units of the original pericentre distance and in units of AU. $\Delta p/p_N$ gives the average fractional change in the orbital period of Nemesis due to the passage of a single solar mass intruder.

its perihelion distance short enough to allow Nemesis to fill the loss cone of comets with $a_c = 4{,}000$ AU. The number of loss cone fillings is $N = N_0 P_e = 177 P_e$ for these comets. The last column of Table 2 shows $F_L = 1 - F_N$, the fraction of the comets in the inner cloud that have been lost.

I simulated 5,400 encounters between solar-mass stars and the Sun–Nemesis system at an impact velocity of $30\ \mathrm{km\ s^{-1}}$. Here Nemesis is assumed to have a mass of $0.05\ M_\odot$, its orbital semimajor axis is taken as $a_N = 89{,}200$ AU, and its eccentricity is taken as $e_N = 0.95$. Because the impact velocity is much higher than the orbital speed of the Nemesis–Sun system, gravitational focusing is not important and the closest approach of a stellar intruder to the Sun is very nearly its impact parameter. At each of six different impact parameters, p, 900 different simulations were made. None of these 5,400 encounters led to the intruder knocking Nemesis into a hyperbolic orbit. (However, molecular clouds may perturb Nemesis more than passing stars[7,8].)

While most stars are less massive than the Sun and would produce smaller perturbations per encounter than shown in Table 3 (the perturbations in period are proportional to the intruder mass), the large number of stellar encounters per orbital period of Nemesis ensures that at least one star having a mass equal to or larger than the Sun passes within distances $(p/a_N) = 0.5$ per orbital period. This requires that the average minimum change, $\langle \Delta q_N \rangle$, in pericentre distance q_N suffered by Nemesis per orbital period is at least as large as that resulting from an individual star of solar mass passing within distance $p/a_N = 0.5$. Dividing the value of Δq_N in Table 3 by the value of $q_{\max}$ in Table 2, we see that the variation in $\Delta q_N/q_N$ per orbital period of Nemesis must be at least 5% for $M_N = 0.015\ M_\odot$ and about 2% for $M_N = 0.1\ M_\odot$. If Nemesis has a low mass, we can expect fairly large variations in the strength of the comet showers at consecutive perihelion passages. Because of the large number of intruders, we can expect at least one or more intruder of solar mass to approach within distance $p/a_N = 0.5$ of the Sun during each orbital period of Nemesis. The fractional change in the period of Nemesis per orbital period is at least 4%. This can either be an increase or a decrease in the orbital period. After $N = 10$ revolutions the walk-away change in period should be at least 4% $N^{1/2} = 13\%$.

A more disastrous situation than a comet shower would arise if Nemesis were perturbed into an orbit that takes it into the planetary system. In this case, it may strip some planets directly from the Solar System. It would leave the remaining planets in highly eccentric orbits which would produce a fast-moving, dangerous situation[9].

By the Ergodic Hypothesis the time-averaged properties of one object follows the same distribution as an ensemble average over many objects. The fraction of the time that Nemesis spends with a pericentre distance of q_N or less is $F_l = 2q_N/a_N$. For $q_N = 40$ AU and $a_N = 89{,}200$ AU, $F_l = 9 \times 10^{-4}$. As the average change in the pericentre distance, $\langle \Delta q_N \rangle$, of Nemesis per orbital period is much larger than the value of q_N considered, the probability of its entering the planetary system per pericentre passage is 9×10^{-4}. For $N = 177$ pericentre passages, the total probability that it has entered the planetary system is

$$P_N = 1 - (1 - F_l)^N = 1 - (1 - 2q_N/a_N)^N$$
$$= 0.15 \qquad (4)$$

Obviously, this catastrophe did not occur, but the probability is high enough to be interesting.

Nemesis itself may be responsible for the termination of the planetary system at Pluto. If comets formed in the solar nebula just outside the orbit of Pluto, they could have been ejected into the comet cloud by Nemesis. However, the comets may have formed in the outer part of the proto-Sun in the inner comet[4,10–12].

Nemesis may not be the only massive object in the Oört Cloud. However, the fact that the planets have survived in nearly planar, circular orbits indicates that they have not been greatly perturbed since the dissipation of the solar nebula. It is unlikely that any massive object has plunged through the planetary system since its formation. A massive object with a semimajor axis of 2×10^4 AU, that is, one at the inner edge of the Oört or steady-state comet cloud, would have a loss cone $F_l = 2q/a_0 = 4.5$ times larger than that of Nemesis. Its orbital period would be about 0.1 that of Nemesis, so it has made $N \cong 1.7 \times 10^3$ orbital revolutions. Using equation (4) we find that the probability of its having entered within the orbit of Saturn to be about 80%. The lack of apparent damage to the planetary system points to the unlikelihood of their being any massive objects in the inner edge of the Oört Cloud. A Nemesis with a semimajor axis of 9×10^4 AU is dangerous to life on Earth, but a Nemesis at the inner edge of the Oört Cloud would probably have produced a catastrophe of truly cosmogonical proportions.

Received 24 April; accepted 4 July 1984.

1. Davis, M., Hut, P. & Muller, R. A. *Nature* **308,** 715–717 (1984).
2. Whitmire, D. P. & Jackson, A. A. *Nature* **308,** 713–715 (1984).
3. Raup, D. M. & Sepkoski, J. J. *Proc. natn Acad. Sci. U.S.A.* **81,** 801–806 (1984).
4. Hills, J. G. *Astr. J.* **86,** 1730–1740 (1981).
5. Hills, J. G. *Astr. J.* **88,** 1269–1283 (1983).
6. Hills, J. G. *Astr. J.* **88,** 1857–1867 (1983).
7. Napier, W. M. & Staniucha, M. *Mon. Not. R. astr. Soc.* **198,** 723–735 (1982).
8. Bailey, M. E. *Mon. Not. R. astr. Soc.* **204,** 603–633 (1983).
9. Hills, J. G. *Nature* **225,** 840–842 (1970).
10. Hills, J. G. *Astr. J.* **87,** 906–910 (1982).
11. Hills, J. G. & Sandford, M. T. II *Astr. J.* **88,** 1519–1521 (1983).
12. Hills, J. G. & Sandford, M. T. II *Astr. J.* **88,** 1522–1530 (1983).

How stable is an astronomical clock that can trigger mass extinctions on Earth?

Piet Hut

Institute for Advanced Study, Princeton, New Jersey 08540, USA

The periodicity in mass extinctions observed in the fossil record[1,2] may be driven by an astronomical clock consisting of a companion star to the Sun[3,4]. Each perihelion passage of the companion star would result in an enhanced rate of arrival of comets in the inner planetary system, some of which could collide with the Earth and perturb the atmosphere strongly enough to cause a catastrophic extinction of many, if not most, species[5,6]. A similar periodicity has been observed in the cratering rate on the Earth[7,8]. On Earth, the dating of both mass extinctions and crater formation is subject to observational uncertainties. In the heavens, too, we should not expect the 'double star clock' to be perfect, because of the influence of the galactic tidal force field and the perturbations of passing stars. On the basis of orbit calculations reported below, I expect the irregularity in the period of revolution over the past 250 Myr to be at least 10%, and more likely around 20%. This suggests that even completely accurate dating of mass extinctions and crater impacts should not be expected to yield perfectly sharp peaks in the power spectrum of a Fourier analysis.

The present results have been derived from an extensive series of numerical orbit calculations (including 10^7 stellar encounters) the details of which will be published elsewhere. These calculations take into account the perturbations of passing field stars as well as the galactic tidal field on the orbit of a double star; additional perturbations are caused by occasional passages close to molecular clouds and through spiral arms. The first two types of perturbations, stars and galactic tides, act continuously. The galactic tidal field has a nearly constant strength over the orbit of the Sun, and passing stars appear in large numbers: every million years the Sun encounters many different stars some of which actually pass through the orbit of the solar companion. Because of their intermittent character, the effects of molecular clouds and spiral arms are less important on a 250 Myr time scale on which the extinction record is well documented; these will be discussed in more detail elsewhere.

The strongest component of the tidal force acts perpendicular to the galactic plane, where the gradient of the galactic force field is steepest, and has a restoring character. The tidal force in the direction to the galactic centre is smaller by about a factor of six, and tends to pull a wide double star further apart. This radial force is composed of two parts, one of which stems from the radial gradient in the galactic force field and the other from the centrifugal force in the coordinate system rotating with the Sun in its path around the Galaxy. Another important effect in the rotating frame of reference is the Coriolis force acting in the galactic plane perpendicular to the motion of the companion. I have modelled all these effects in a linearized approximation, which is sufficiently accurate[9].

Each field star passing close to the double star exerts a perturbing force which acts over a time interval much shorter than the orbital period of the binary, by a factor typically of the order a few hundred. Therefore, I have used the impulsive approximation, where the perturbing force is taken to act instantaneously at one point in the binary orbit. This approximation saves a factor of nearly 100 in computer time, and gives 1 Myr worth of orbit integration, featuring about 100 stellar encounters, every few seconds (rather than minutes[10]) of central processing unit time on a VAX 11/780 computer.

To understand the relative importance of both types of perturbations, I consider first the galactic tidal field only, neglecting passing stars, and orient the major and minor axes of the orbit along two of the three principal axes of the tidal field. For each of these six choices, I have computed many orbits, all starting with the same eccentricity $e = 0.7$, but with different values for α, the length of the semi-major axis, to find an orbit with a periodicity of 26 to ~28 Myr (Kepler's third law is a poor approximation in the presence of strong tidal forces). The numerical values for the components of the tidal force have been computed from recent estimates at Oort's A and B constants ($A = 16$ and $B = -11$, in km s^{-1} kpc^{-1}, refs 11, 12) together with the inferred mass density in the solar neighbourhood which includes the unobserved galactic disk material[3], while the Coriolis forces follow from the inferred galactic rotation frequency[11,12].

Figure 1*a* shows the largest tidal perturbations which occur for orbits with their major axis perpendicular to the galactic plane and minor axis perpendicular to the direction of the galactic centre (so that the galactic tidal force is purely restoring, which shortens the orbital period and therefore requires a larger, less stable orbit to satisfy a given orbital period). Figure 1*b* shows the most regular orbit, which lies in the galactic plane with its major axis pointing to the galactic centre.

Orbits parallel to the galactic plane are not affected by the strongest component of the tides, and thus are more regular and have a smaller amplitude than orbits which feel the compressive but overstabilizing tidal field component perpendicular to the galactic disk. Both effects suggest that a search for the companion star might have a higher chance of success at lower galactic latitudes (even though crowding is worse there), because (1) the fossil record as well as crater ages are more compatible with the regularity of Fig. 1*b* than with Fig. 1*a*, and (2) the smaller excursions in Fig. 1*b* make the orbit less vulnerable to perturbations by passing stars, which I now discuss.

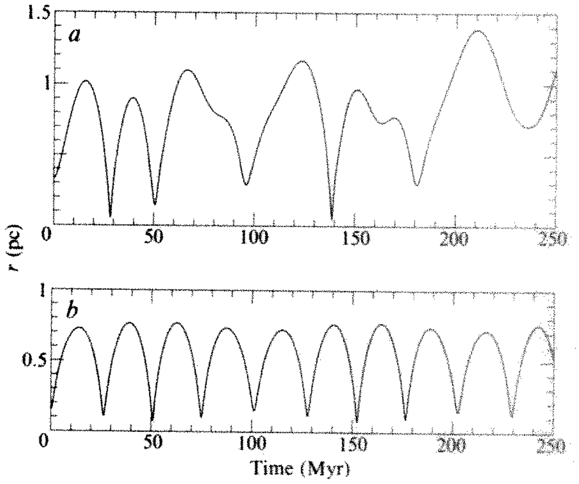

Fig. 1 The separation between the Sun and companion star under the perturbing influence of the galactic tidal field, in parsecs (1 pc = 206,000 AU). *a*, For an orbit perpendicular to the galactic plane; *b*, for an orbit in the plane.

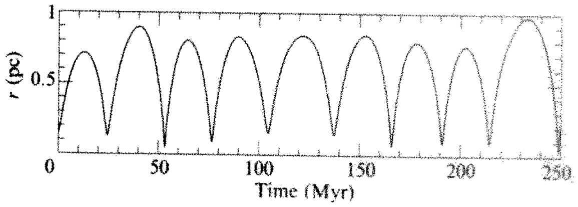

Fig. 2 The separation between Sun and companion star under the combined perturbing influences of passing stars as well as the galactic tidal field, for an orbit with the same initial conditions as in Fig. 1*b*.

I have immersed a double star in a field of passing stars, most of which cause only a tiny perturbation even when they cross the binary's orbit, because the total momentum transfer is proportional to the time spend in the encounter (typically only 0.1–1% of the orbital period). For the distribution of field stars I have accurately modelled the solar environment, using 10 discrete mass classes in the range 0.25–20 $M_\odot$, each with their particular observed number density and velocity dispersion[11,12], with a total mass density of 0.06 $M_\odot$ pc^{-3} (0.02 $M_\odot$ pc^{-3} of which resides in light stars of 0.25 $M_\odot$, to model the unseen disk material; a choice of 0.05 $M_\odot$ pc^{-3} in the form of 0.1 $M_\odot$ stars would have given a similar cumulative effect). The procedure for generating the properly weighted random distributions of orbital elements has been described previously[10] using a Monte Carlo approach to obtain scattering cross-sections in the gravitational three-body problem.

Figure 2 shows an orbit which starts out with exactly the same initial conditions as in Fig. 1*b*, but which is now subject to stellar perturbations as well as to the galactic tidal field. Note the fluctuations in the time intervals between successive close approaches (perihelion passages) of the companion, spanning a range 23 to ~34 Myr. This suggests that even completely accurate dating of mass extinctions and crater impacts should not be expected to yield perfectly sharp peaks in the power spectrum of a Fourier analysis. A more sensitive test of the hypothesis of an unseen solar companion follows rather from the prediction of a tight correlation between individual periods of enhanced cratering rates and periods of mass extinction (several authors have argued that an alternative explanation can be given using the Sun's periodic motion perpendicular to the

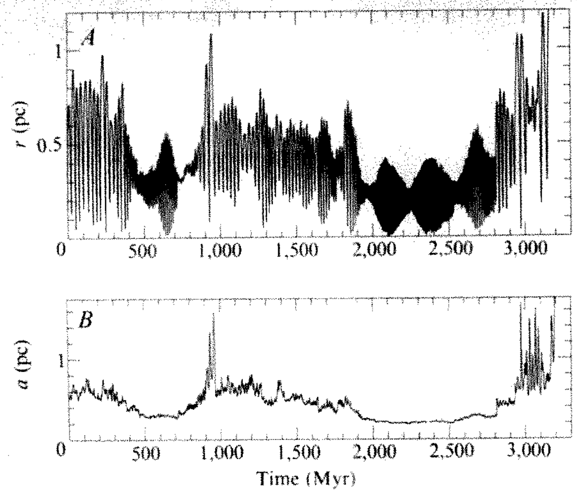

Fig. 3 *A*, The same orbit as in Fig. 2, followed until final dissolution around AD 3,200,000,000. *B*, The evolution of the semi-major axis of the orbit in *a*. The noise in the perturbations has a fine structure down to 0.01 Myr.

galactic plane[8,14]; however, it is hard to understand why both extinctions and cratering seem to occur when the Sun is furthest away from the galactic plane[1,7]). Although the intermediate time intervals cannot be predicted individually, their probability distribution can be obtained from orbit calculations, which thereby provide additional constraints.

Also note in Fig. 2 the significant scatter in the distance of closest approach. The number of comets directed into the inner planetary system at these times is strongly dependent on this distance, although for small perihelion distances a saturation effect might occur if the loss cone is filled completely[3,4]. This could naturally explain why some mass extinctions have been so much more dramatic than others[1,2]. The term 'loss cone' is used in analogy with plasma physics, where a mirror machine has a cone-shaped region in velocity space from which the plasma can escape. For the gravitational application the region in velocity space from which comets are lost is really bounded by a loss hyperboloid-of-one-sheet[15]; this is sufficiently less euphonious that the term loss cone is preferable as long as it is understood to refer to a strictly hyperboloid geometry.

I have computed several hundred orbits, each starting with a revolution period 26 to ~28 Myr, and with an initial distribution isotropic in space. As mentioned above, the orbits parallel to the galactic plane live longer than those perpendicular to the plane. About half of the total sample of orbits dissolved within 1,000 Myr, in agreement with analytical estimates[16-18]. A more quantitative discussion has to include the complicated dependence of the dissolution rate on the orientation of the orbit with respect to the Galaxy, and lies beyond the scope of the present letter. These half lives decrease if the effects of molecular clouds and spiral arms are taken into account, but the decrease is sensitively dependent on the distribution of molecular clouds, which is observationally less well determined than that of the field stars. A realistic guess for the final life time would be a value larger than 500 Myr, because (1) the Sun is, at present, ~1 kpc closer to the galactic centre than on average, and (2) the Sun has an unusually low velocity perpendicular to the galactic plane at present (Wielen, personal communication). Both effects strongly diminish the influence of giant molecular clouds which are concentrated towards the galactic plane and towards the galactic centre, in contrast with results by other authors[18-20]. A detailed analysis of orbit calculations which include these effects will be published elsewhere.

With a half life of 1,000 Myr, survival times of a few 1,000 Myr still occur frequently. Figure 2 shows a double star orbit which lasts for 3,200 Myr, as plotted in Fig. 3*A*, to illustrate the richness of the spectrum of perturbations. The final breakup of the double star occurs after a random walk in orbital parameter space, through the combined influence of more than 100,000 individual encounters with field stars. These perturbations can be seen more clearly in Fig. 3*B*, which plots the semi-major axis a of the orbit. Typically, every 10,000 yr another field star begins an encounter (included in the numerical calculations whenever it occurs within a distance of five times the semi-major axis) each of which lasts for a 100,000 yr. Occasionally a large jump occurs, which can be caused in any of three different ways; the passing star can be extra massive, come extra close or move extra slowly, in each way increasing the total momentum transfer.

The noise in Fig. 3*B* is strongly dependent on the size of the orbit. For $a < 0.3$, on the right-hand side of Fig. 3*B*, the jitter has died down by nearly an order of magnitude. This is because fewer stars pass close to a tighter orbit, and larger perturbations are required significantly to affect a tighter and therefore more energetic orbit. During these lulls in stellar perturbations, the galactic tidal field makes itself visible in the slow modulation of the eccentricity with a period of about 300 Myr, as can be seen in the rising and falling of the amplitude of the excursions in r on the right-hand side of Fig. 3*A*.

The closest encounter in Fig. 3*A* brings the companion to a distance of 800 AU from the Sun, by AD 2,100,000,000. Encounters much closer than that are rare during the lifetime of the Solar System, as I have found from orbit calculations starting at an initial separation of 0.1 pc (resulting in a half life of ~5,000 Myr). This suggests that a planetary system can indeed survive the presence of a distant solar companion, as the expected induced eccentricity for the orbits of the outer planets is <0.01 (ref. 21), even if the companion would come in as close as 200 AU. A detailed study of the perturbations on the planets would nevertheless, be very interesting; it would probably not put very stringent restrictions on the hypothesis of a solar companion, but it might explain the ill-understood irregularities in the planetary system.

Figures 2 and 3 chart only one of the many possible future evolutions of the orbit of a solar companion. Each individual orbit calculation yields vastly different results, since the passing stars exert a stochastic perturbing force on the double star. These perturbations are unpredictable on a short time scale and difficult to treat analytically, even using the average for longer time scales, because of the complicated interference with the galactic tidal field. Each of the different future evolutions which I have calculated as starting with the initial conditions of Fig. 1*b* are equally likely to occur, as are many others starting from different initial conditions (but with the same initial orbital period of 26 to ~28 Myr).

The evolution of the hypothetical solar companion can be summarized as follows: the original orbital period at the time of the formation of the Solar System was probably in the range 1 to ~5 Myr, much shorter than the present value of 26 to ~28 Myr; and the final escape of our companion star might take place relatively soon, on a time scale of the order of 1,000 Myr.

After completing this work I received a preprint by Smoluchowski and Torbett[22], whose calculations of tidal disturbances of comets agree with the present paper.

I acknowledge interesting discussions with many colleagues, especially Luis Alvarez, Walter Alvarez, John Bahcall, Haldan Cohn, Ivan King, Myron Lecar, Eugene Shoemaker, Fred Whipple, Roland Wielen, Richard Muller, Scott Tremaine and Alar Toomre. This work was supported in part by NSF grant PHY-8217352.

Received 24 April; accepted 15 June 1984.

1. Raup, D. M. & Sepkoski, J. J. *Proc. natn Acad. Sci.* **81**, 801–805 (1984).
2. Fischer, A. G. & Arthur, M. A. *Soc. Econ. Paleont. Miner., Spec. Publ.* **25**, 19–50 (1977).
3. Davis, M., Hut, P. & Muller, R. A. *Nature* **308**, 715–717 (1984).
4. Whitmire, D. P. & Jackson, A. A. *Nature* **308**, 713–715 (1984).
5. Alvarez, L. W. *Proc. natn Acad. Sci.* **80**, 627–642 (1983).
6. Silver, L. T. & Schultz, P. H. (eds) *Geol. Soc. Am. Spec. Pap.* **190** (1982)
7. Alvarez, W. & Muller, R. A. *Nature* **308**, 718–720 (1984).
8. Rampino, M. R. & Stothers, R. B. *Nature* **308**, 709–712 (1984).
9. Aarseth, S. J. *Vistas Astr.* **15**, 13 (1973).
10. Hut, P. & Bahcall, J. N. *Astrophys. J.* **268**, 319–341 (1983).

11. Mihalas, D. & Binney, J. *Galactic Astronomy* (Freeman, San Francisco, 1981).
12. Bahcall, J. N. & Soneira, R. M. *Astrophys J. Suppl.* **44**, 73–110 (1980).
13. Bahcall, J. N. *Astrophys J.* **276**, 169–181 (1984).
14. Schwartz, R. D. & James, P. B. *Nature* **308**, 712–713 (1984).
15. Cohn, H. & Kulsrud, R. M. *Astrophys. J.* **226**, 1087–1108 (1978).
16. Heggie, D. C. *Mon. Not. R. astr. Soc.* **173**, 729–787 (1975).
17. Retterer, J. M. & King, I. R. *Astrophys J.* **254**, 214–220 (1982).
18. Bailey, M. E. *Mon. Not. R. astr. Soc.* **204**, 603–633 (1983).
19. van den Bergh, S. *J. R. Soc. Can.* **76**, 303–308 (1982).
20. Napier, W. M. & Staniucha, M. *Mon. Not. R. astr. Soc.* **198**, 723–735 (1982).
21. Hut, P. & Paczynski, B. *Astrophys J.* (in the press).
22. Smoluchowski, R. & Torbett, M. Preprint, University of Texas, Austin.

Orbital stability of the unseen solar companion linked to periodic extinction events

Michael V. Torbett

Department of Terrestrial Magnetism, 5241 Broad Branch Road, NW,
Washington, DC 20015, USA

Roman Smoluchowski

Departments of Astronomy and Physics, University of Texas
Austin, Texas 78712, USA

Recent suggestions of astronomical causes for the closely periodic extinction events in the geological record[1] and the possible periodicities in the cratering record[2] have involved two basic ideas. First, it has been suggested[3–5] that the oscillations of the Solar System through the galactic plane with semi-periods of the order of 30 Myr make possible close encounters with giant molecular clouds, or sub-units thereof, which are expected to scatter Oort cloud comets into the terrestrial zone. Second, it has been suggested[6,7] that a low-mass, and as yet unseen, companion to the Sun, tentatively named Nemesis, is in an eccentric orbit ($e \sim 0.7$), such that perihelion passages bring it through the postulated dense inner Oort cloud[8]. Perturbations of cometary bodies there result in scattering of some 10^9 comets into the terrestrial zone. Those that impact the Earth are assumed to loft dust into the atmosphere, causing climatic chaos[5,9]. To achieve the period that matches the best estimates for the intervals between extinction events, semimajor axes in the range 9×10^4–1×10^5 AU are required. Whether such orbits are indeed stable over the lifetime of the Solar System is not known. We present here evidence from three-dimensional numerical modelling that only orbits with a limited range in inclination with respect to the galactic plane are formally stable for the required length of time. Perturbations bypassing stars and molecular clouds may make even these orbits unstable.

Calculations were done using Cowell's method employing a fourth-order Runge–Kutta integration scheme in an inertial reference frame in orbit about the Galaxy, which is approximated as a point mass of $1.3\times10^{11}\ M_\odot$ at a distance of 8.22 kpc from the Sun to give a galactic rotation velocity of $\sim$250 km s^{-1}. Tidal perturbations in the radial direction due to the Galaxy as well as Coriolis forces are thus automatically included. Superimposed on these forces is the vertical component of the gravitational field of the galactic disk, taken from the results of Bahcall[10] and given per unit mass as

$$f(z) = 2.565\times10^{-11}\,z - 1.66\times10^{-16}\,z^3\ \mathrm{cm\ s^{-2}} \qquad (1)$$

where z is in parsecs. Hence, the companion is subject to the 'gravitational compression shock' during its excursions through the galactic disk. Moreover, since the semi-period of this motion ($\sim$30 Myr) is comparable with the orbital period (26–29 Myr), resonant accumulation of the perturbations can become significant, eventually leading to disruption of the system.

The calculational procedure was as follows. The Sun–companion barycentre was given initial conditions corresponding to a circular orbit about the galaxy with an initial height above the plane equal to that expected for its oscillation amplitude ($\sim$100 pc). The initial inclination with respect to the galactic plane of the companion's orbit was adjusted to yield a resultant mean inclination, i, which was stepped from 0° to 180° in intervals of 10°. During the course of a typical run, the scatter in the inclination amounted to $\sim$10°. The companion and the Sun were then given initial conditions so as to produce a semimajor axis, a, such that the mean interval between perihelion passage was in the range 25–30 Myr and eccentricity, e, in the range such that perihelion passage occurred within the inner Oort cloud. To achieve the proper period, it was necessary to vary considerably the semimajor axis due to the strength of the perturbations relative to the solar attraction at the separation required. Values of 10^{-1} and $10^{-2}\ M_\odot$ for the mass of Nemesis were both investigated, with negligible differences in the results.

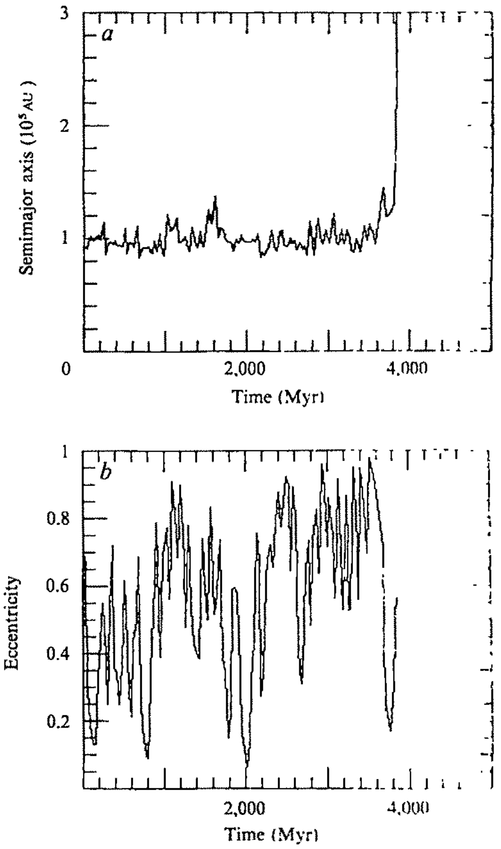

Fig. 1 *a*, Semimajor axis and *b*, eccentricity as functions of time for Nemesis in an orbit about the Sun inclined at an angle $i_0 = 40°$ with respect to the galactic plane. System becomes unstable within the age of the Solar System.

The results indicate that for inclinations $i \gtrsim 30°$ the orbits are unstable with the system being disrupted within the age of the Solar System. This is true for both prograde and retrograde orbits. A representative case is illustrated in Fig. 1 where a and e are plotted as a function of time for $i \sim 40°$. Orbits with larger values of inclination than shown in Fig. 1 become unstable even sooner. For example, at $i \sim 90°$, the system is disrupted within 500 Myr. For inclinations $i \lesssim 30°$ the orbits appear stable although irregular as shown in Fig. 2 where a and e are again plotted as a function of time. Orbits with high galactic inclination are less stable than low inclination orbits since the vertical tidal field of the disk is 3 or 4 times stronger than is the radial galactic tide at the Sun's position. Thus, inclined orbits sense stronger perturbations than do orbits lying in the plane. This leads to more chaotic trajectories for the inclined case as can be seen by comparison of Figs 1 and 2. Hence, since the orbits with periods corresponding to extinction intervals verge on the margin of stability[11], the near-resonant match of orbital period with

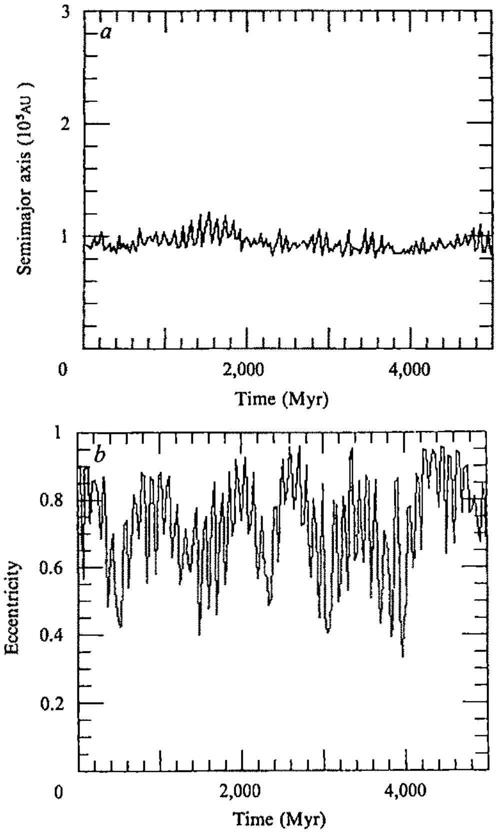

Fig. 2 *a*, Semimajor axis and *b*, eccentricity as functions of time for Nemesis with galactic inclination $i_0 = 30°$. Orbit is formally stable for the age of the Solar System, although irregular.

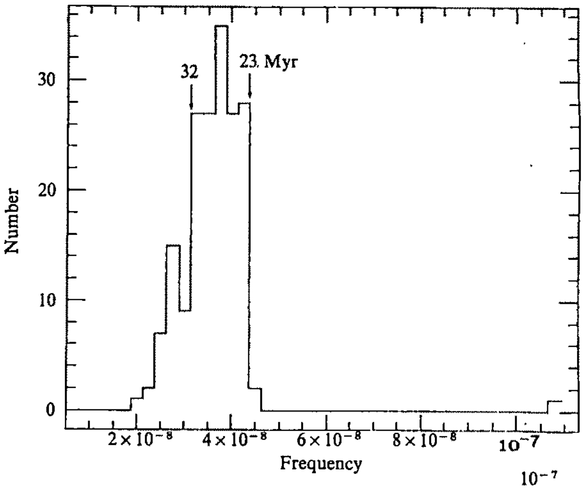

Fig. 3 Histogram of the inverses of the intervals between perihelion passage for prograde orbit of Nemesis for the case depicted in Fig. 2. Note the scatter in the intervals from 23 to 32 Myr. Thus strict periodicities should not be expected in fossil or crater records.

the semi-period of the Sun's oscillation about the galactic plane leads to disruptive accumulation of perturbations.

Figure 3 shows a histogram of the inverses of the intervals between perihelion passage for the case shown in Fig. 2. It is clear that the intervals vary widely within limits greater than the 25–30 Myr inferred from the data. This chaotic nature of the permitted direct orbits makes the causal connection of periodic extinctions with regularly timed astronomical events less compelling. Retrograde orbits with $i < \sim 30°$ seem, however, to be considerably more stable because in this case Coriolis forces tend to increase rather than decrease stability. This results in the range of the limits for intervals between perihelion passage being factors of 2–3 smaller than in the prograde case and within the limits of the data. Thus, the scatter in orbital period can be reduced by assuming a retrograde orbit for Nemesis. Hence, if Nemesis exists, it may be in retrograde orbit; but even then, strict periodicities should not be expected even in perfectly dated fossil records. These results indicate that orbits for the companion that are inclined at more than 30° to the galactic plane are not allowed and suggests that the search for Nemesis should be concentrated towards the plane of the galaxy. This limit on the range of permissible galactic inclinations excludes orbits in the plane of the ecliptic, which makes an angle of ~60° with the galaxy. It is not impossible, however, that an orbit originally in the ecliptic could have been perturbed to lie near the plane of the galaxy by close encounters of passing stars or molecular clouds.

Perturbations by passing stars or molecular clouds may make even the low-inclination orbits unstable. Stability analysis[12] of companion orbits subject to stellar perturbations and the galactic tides, while neglecting the 'gravitational compression shock' due to the vertical oscillations, indicates lifetimes for Nemesis of the order of 10^9 yr which is consistent with our analysis. In addition, the randomizing effect of stellar perturbations on the orbital elements will change low-inclination orbits into high-inclination ones leading to disruption. Perturbations by molecular clouds may, however, deliver the most serious blow to stability. Numerical modelling[13] of the effect of molecular cloud passages on cometary orbits indicates that for close encounters a large fraction of the orbits will be disrupted. Preliminary analysis from a current numerical study (Torbett, M. V. & Smoluchowski, R., in preparation) shows that, for the expected encounter distances from, and velocities relative to, $10^5 M_\odot$ clouds, a large fraction (>50%) of the orbits for Nemesis will be disrupted. This is in reasonable agreement with arguments based on balancing the tidal force of the cloud against the binding force.

Hence, at best, the existence of an appropriately positioned companion should be viewed as a highly temporary, low-inclination, and probably retrograde phenomenon. At worst, the instabilities induced by the galactic tides and molecular cloud passage make the companion hypothesis untenable.

M.V.T. acknoweldged helpful discussions with Linda Stryker and Kirk Borne. R.S. is supported in part by NASA grant NSG 7505 suppl. 5.

Received 29 May; accepted 15 August 1984.

1. Raup, D. M. & Sepkoski, J. J. *Proc. natn. Acad. Sci. U.S.A.* **81**, 801–805 (1984).
2. Alvarez, W. & Muller, R. A. *Nature* **308**, 718–720 (1984).
3. Rampino, M. R. & Stothers, R. B. *Nature* **308**, 709–712 (1984).
4. Schwartz, R. D. & James, P. B. *Nature* **308**, 712–713 (1984).
5. Clube, S. V. M. & Napier, W. M. *Mon. Not. R. astr. Soc.* **208**, 575–588 (1984).
6. Whitmire, D. P. & Jackson, A. A. *Nature* **308**, 713–715 (1984).
7. Davis, M., Hut, P., & Muller, R. A. *Nature* **308**, 715–717 (1984).
8. Hills, J. G. *Astr. J.* **86**, 1730–1740 (1981).
9. Alvarez, L. W., Alvarez, W., Asaro, F., & Michel, H. V. *Science* **208**, 1095–1105 (1980).
10. Bahcall, J. N. *Astrophys. J.* **276**, 169–181 (1984).
11. Smoluchowski, R. & Torbett, M. V. *Nature* **311**, 38–39 (1984).
12. Hut, P. Preprint (Univ. California, Berkely 1984).
13. Napier, W. M. & Staniucha, M. *Mon. Not. R. astr. Soc.* **198**, 723–735 (1982).

Nitryl perchlorate as the essential intermediate in the thermal decomposition of ammonium perchlorate

Andrew K. Galwey & Mohamed A. Mohamed*

Department of Chemistry, The Queen's University of Belfast,
Belfast BT9 5AG, UK

Because of its use as a solid propellant and more generally in pyrotechnic systems, the thermal decomposition of ammonium perchlorate (AP) has been extensively studied. The breakdown of this salt is complicated, an exceptional feature being that the low-temperature (<~570 K) decomposition is incomplete

---

* Permanent address: Department of Chemistry, Faculty of Science, Assiut University, Qena, Egypt.

(~30%), yielding a residual solid with a composition and crystal structure very similar to those of the original reactant. Extensive rate measurements and kinetic analyses[1-5] have produced two alternative general hypotheses of reaction mechanisms[5], in which rate control has been attributed to steps involving the transfer of either a proton[4] or an electron[6]. In the present study, we have found that the addition of various inorganic nitrates reduces the induction period to reaction and increases the extent of the low-temperature decomposition of AP. The measured rate of decomposition was close to that estimated for reaction involving nitryl perchlorate (NO_2ClO_4) as an intermediate and we have detected small quantities (~0.08%) of an oxidized nitrogenous species in partly reacted AP. We therefore propose a novel reaction mechanism in which NO_2ClO_4 is the essential intermediate in the thermal decomposition of ammonium perchlorate.

Our investigation of the possible rôle of oxidized nitrogen in promoting AP decomposition represents an attempt to characterize the chemical steps involved in breakdown of the relatively stable (at ~500 K) perchlorate ion, ClO_4^-. Khairetdinov and Boldyrev[5] have pointed out that the present reaction, involving sublimation, occurs 300-350 K below the corresponding temperatures for reactions of other alkali perchlorates. Perchloric acid is sufficiently stable to survive sublimation and it is suggested that the low-temperature reaction may be incomplete due to accumulation of the relatively more stable acid hydrates, $H_3^+O\ ClO_4^-$, $H_5^+O_2\ ClO_4^-$, etc., on the walls of the channels eroded in the reactant crystals during decomposition. We have attempted to identify the intermediates involved in these reactions and the interactions that culminate in ClO_4^- disintegration.

It is known that ammonium salts of certain strongly oxidizing anions yield NH_4NO_3 on decomposition[2] and that the same compound, NH_4NO_3, reduces the induction period to AP reaction. The formation of N_2 and N_2O during AP decomposition[2] can be explained by the intervention of nitrite and nitrate respectively, involving a mechanism generally similar to that recently proposed[7] for the breakdown of $(NH_4)_2Cr_2O_7$. At least one other type of additive containing oxidized nitrogen—nitrophenol-formaldehyde polymers—has been shown[8] to accelerate AP breakdown. Oxidized nitrogenous species thus appear to merit particular consideration as intermediates.

We made isothermal kinetic studies of the decomposition of AP alone and with added NH_4NO_3 or $Mg(NO_3)_2 \cdot 6H_2O$, both of which readily melted on heating to reaction temperature. Comparative yield-time data for N_2+O_2 evolution (in a conventional accumulatory apparatus[3] using a 78 K refrigerant trap) during the low-temperature reaction[2] for consecutive experiments, in identical conditions, showed that both additives significantly reduced the induction period to reaction. Figure 1*a* shows typical results for the decomposition at 495 K of AP by itself and initially covered with molten NH_4NO_3 (most of which was rapidly volatilized out of the reaction vessel soon after the start of the reaction). The additive markedly reduced the induction period (from 120 to 40 min) and appreciably increased the reaction rate (by about 1.5 times) but it did not change significantly the final yield of product gases (N_2+O_2).

Figure 1*b* shows the relative activities of four different inorganic nitrates in promoting the decomposition of AP powder at 503 K. Three of the additives (NH_4^+, K^+ and Mg^{2+} nitrates) caused approximately similar reductions in the time to onset of reaction. The ammonium salt was the most effective of this group, however, in accelerating the overall rate of reaction, presumably because removal by distillation occurred less readily here and volatilization temporarily distributed the additive to all surfaces of the compacted powder reactant. Systematic variations in the proportion of added $Mg(NO_3)_2 \cdot 6H_2O$, between 1 and 25%, showed that the kinetic characteristics did not vary widely from the curve shown in Fig. 1*b*, but the total yield of gaseous products (N_2+O_2) was always greater than that obtained from the pure salt. Silver nitrate was identified as being a particularly active catalyst for AP decomposition, causing the most rapid onset of reaction and the greatest increase in rate of decomposition.

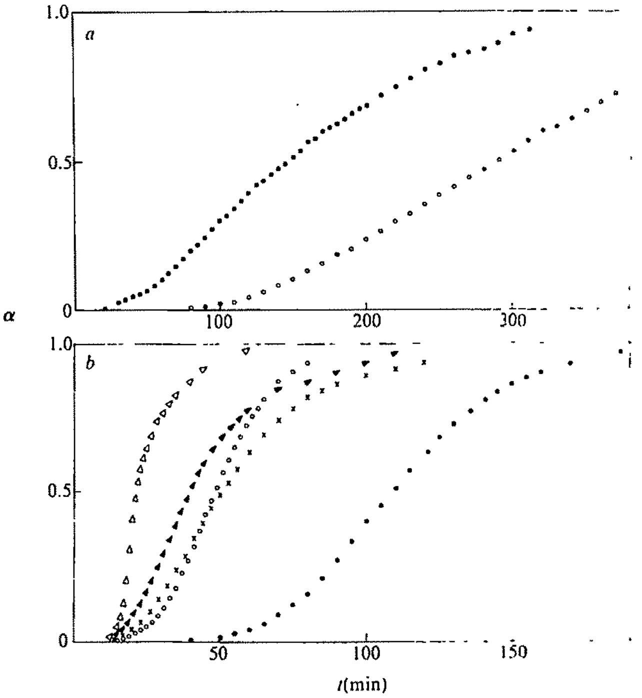

Fig. 1 *a*, Curves of comparative fractional reaction (*α*) against time for the isothermal (495 ± 1 K) decomposition of single crystals of AP measured for evolution of N_2+O_2 (78 K trap) in identical conditions in a constant-volume system. One crystal was reacted 'as prepared' (○); the other was 'promoted' by the addition of NH_4NO_3 (●), which resulted in a reduction of the induction period and an increase in the reaction rate. *b*, Comparative *α*-time curves for the decomposition of AP powder mixtures crushed with 10% (by weight) of various nitrates: NH_4NO_3 (○), $Mg(NO_3)_2 \cdot 6H_2O$ (▲), KNO_3 (×), $AgNO_3$ (△), and no additive (●). All four additives reduced the induction period, accelerated the maximum rate of reaction and increased the extent of reaction. The silver salt was the most active catalyst. The reactant mixtures containing nitrate and AP were crushed in a pestle and mortar before reaction.

Microscopic inspection of large single crystals after partial (≤10%) decomposition, initiated with either added NH_4NO_3 or $Mg(NO_3)_2 \cdot 6H_2O$, showed that the reaction was initially rapidly established over the entire surface of the AP reactant, in contrast to the well known development of individual, approximately hemispherical nuclei during reactions of unpromoted single crystals[2]. The same conclusion was reached on scanning electron microscope examination of cleavage surfaces traversing reacted zones, exposed after the partial decomposition of large single crystals. Representative textures are shown in Fig. 2*a*,*b* for an exposed cleavage section of an AP crystal after 10% decomposition initiated by adding $Mg(NO_3)_2 \cdot 6H_2O$. A continuous layer of decomposed salt, with approximately constant thickness, has developed below the original crystal surface; this contrasts with the generation of separated reaction zones (nuclei) during reactions of the salt in the absence of additives: the edge of a discrete nucleus and a zone of unnucleated surface are evident (Fig. 2*c*).

Previous observations[3] have shown that the yield of gaseous products (N_2+O_2) by a second successive AP decomposition is ~10% that of the first. Here we have repeated this observation and have also shown that the addition of NH_4NO_3 to a decomposed crystal, followed by the restoration of reaction conditions (510 K), results in a marked increase in the extent of the second reaction, to ~50%. This demonstrates the ability of the nitrate to promote AP decomposition.

Previous analytical measurements have detected NO_3 in partly decomposed AP[9] and in the sublimate[2]. We have measured the amount of oxidized nitrogen in partially (50%) decomposed AP by two methods: first, by reaction with brucine[10] in sulphuric acid, followed by spectrophotometric determination of absorption at 405 nm, and second, by the (less accurate)

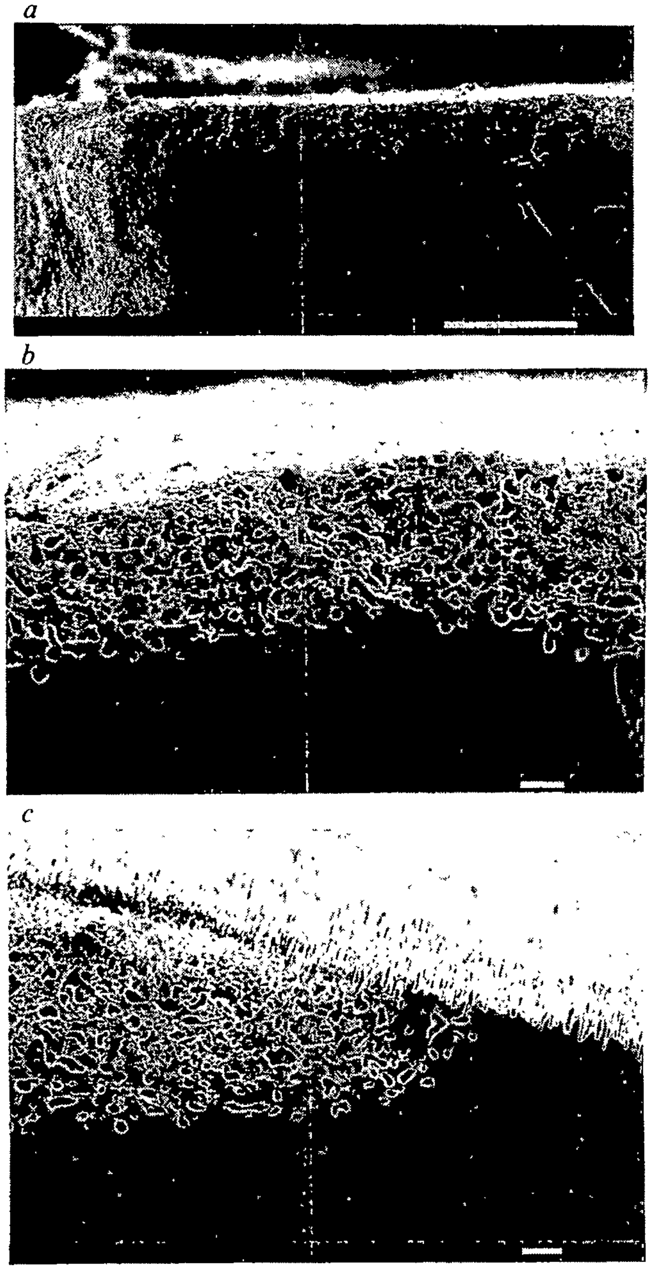

Fig. 2 Scanning electron micrographs of decomposition zones, revealed in section by cleavage of single crystals after 10% reaction. *a*, *b*, The reaction in this crystal was initiated by addition of $Mg(NO_3)_2 \cdot 6H_2O$, which melted immediately on heating. The decomposed layer is of almost constant thickness and is developed below the total surface. *c*, In reaction of the pure salt, discrete nuclei were formed; the boundary edge of one of these is shown here. Although reaction has not occurred in the crystal beyond the nucleus, the surface is extensively grooved. Scale bars (white): *a*, 100 µm; *b*, *c*, 10 µm.

colorimetric method as ammonia with Nessler's reagent (after removal of ammonia by boiling with alkali, followed by reduction with Devarda's alloy). While the low concentration of the active intermediate present precludes its specific identification (as NO_3^- or NO_2^+), repeated determinations gave reproducible evidence that the amount of oxidized nitrogen present corresponded to 0.08 ± 0.04% NO_2ClO_4. (This choice of intermediate anticipates the conclusion reached in our mechanistic discussion below.) The quantities of oxidized nitrogen detected in the residual salt[9] and in the sublimate[2] were less, corresponding to ~0.01 and ~0.02% NO_2ClO_4, respectively.

It seems probable that nitrate present during decomposition under the oxidizing, acidic[2,5] and probably dehydrating conditions prevailing within the reaction zones must be in the form NO_2ClO_4 (ref. 11). Nitryl perchlorate, therefore, is identified as the reaction intermediate as it is unstable at reaction temperature[11,12] and its presence can be maintained by dynamic equilibrium through ammonia oxidation by the active oxygen species resulting from ClO_4^- breakdown. NH_3 and/or NH_4^+ reacts with products of ClO_4^- disintegration to yield NO_2^+ which combines with a reactant anion and, on decomposition, the cycle continues.

In this mechanism, the difficult perchlorate ion breakdown step is explained by the formation and rupture of covalent bonds, as such perchlorates are less stable[13] than the more ionic compounds:

$$O_2N^+ + OClO_3^- \rightarrow [O_2N{-}O{-}ClO_3] \rightarrow [O_2N^+O] + ClO_3^-$$

The unstable $[O_2N^+O]$ may rapidly, perhaps concurrently, disintegrate, yielding $N^+O + O_2$ (or 2O); $NOClO_4$ is also a product of NO_2ClO_4 decomposition[11]. The chlorate ion is known to be unstable under reaction conditions[5] and capable of oxidizing NH_3 and/or NH_4^+ since NH_4NO_3 is a product of NH_4ClO_3 decomposition[2].

We estimate, by extrapolation of published[12] kinetic data, that decomposition of NO_2ClO_4 at 503 K would proceed from 20% to 80% in 0.10 min. At 50% reaction, our powder samples of AP reactant contain 0.08% NO_2ClO_4. For this dynamic equilibrium concentration of intermediate and estimated reaction rate, we calculate, by direct proportions, that the time required to complete the low-temperature (503 K) rate process (30% AP weight loss) is ~70 min. The corresponding time estimated from the middle section of the curve for AP powder in Fig. 1*b* is ~85 min. In view of the uncertainties in our calculations, this agreement is unexpectedly close and provides strong evidence that the NO_2ClO_4 decomposition step is rate-controlling in AP decomposition. (The similarly estimated[14] value for NH_4NO_3 decomposition is larger, and less attractive here because it does not result in ClO_4^- breakdown.)

In the kinetic argument presented above, we have not considered the phase within which the NO_2ClO_4 decomposes. If this intermediate is present as a solid, geometric controls may be expected to operate[15]. However, it is known that NO_2ClO_4 is volatile[11] at reaction temperature, though here confined within the pores of the reaction zone, and its melting point may be depressed by eutectic formation with the other perchlorates present (NH_4ClO_4, $HClO_4$, $NOClO_4$). It seems probable, therefore, that reaction occurs in local melted droplets (fusion nuclei[15]). Evidently, the concurrent oxidation of ammonia and the presence of hydrogen-containing products does not significantly affect the rate of decomposition of the NO_2ClO_4 intermediate. We also note that the activation energy for AP decomposition[1-4] is close to that[11,12] reported for NO_2ClO_4 (130 kJ mol^{-1}), which provides a further indication that the same rate-controlling process operates in both reactions. This similarity is not, however, a proof of mechanism because the same value has also been reported[16] for the breakdown of $Cl_2O_7(+H_2O \rightleftharpoons 2HClO_4)$, another covalent molecule. Thus, this temperature coefficient of reaction may be characteristic of the common step, the bond rupture: $O{+}ClO_3$.

The internal structures of zones of decomposed salt (nuclei), revealed by cleavage section after reaction, were identical in the pure salt and following initiation by NH_4NO_3 (Fig. 3*a* and *b*, respectively) or $Mg(NO_3)_2 \cdot 6H_2O$. This is evidence that the additive does not change the mechanism and is consistent with the view that promotion involves the conversion of NO_3^- to NO_2^+, which thereafter participates in the chemical sequence described above.

Each pore in the reacted salt (~0.2–0.5 µm diameter) evidently resulted from the irregular progress of an active droplet of NO_2ClO_4, and the rounding of these internal surfaces provides further indication of the participation of a fluid or molten reaction phase. The larger holes, up to 5 µm diameter, and

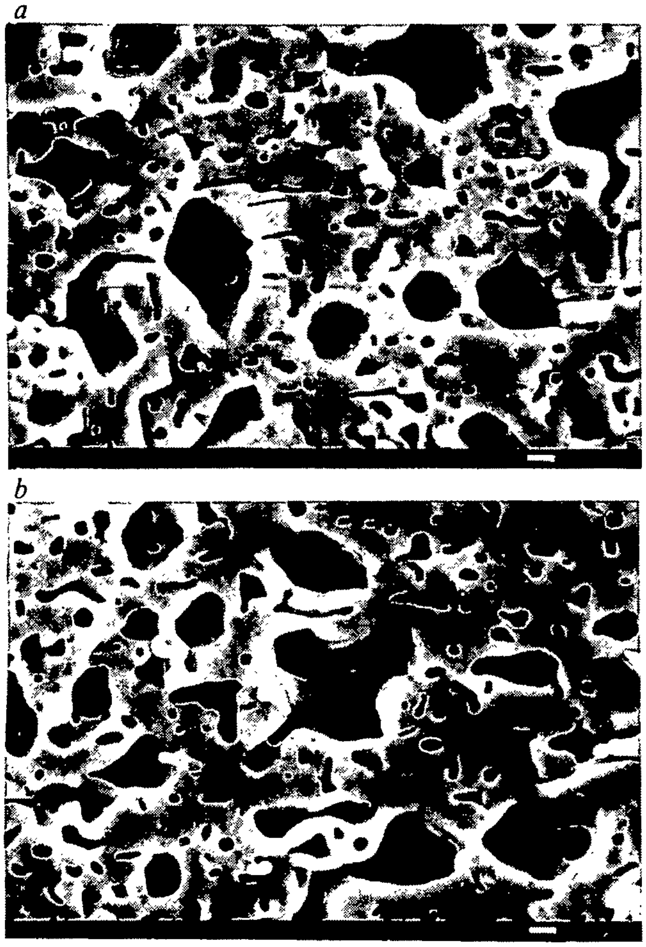

Fig. 3 Scanning electron micrographs showing cleavage sections of decomposed regions of AP in *a*, a pure crystal and *b*, a crystal in which the reaction was initiated by NH_4NO_3. No difference in texture could be discerned in a series of careful comparisons of many areas of both types. We suggest that the texture of the decomposed salt is that of reactant remaining after penetration by the irregular migration of small particles of an active phase within or around which decomposition occurs, presumably including NO_2ClO_4 intermediate and possibly in the form of liquid. Enhanced reaction occurs when droplets coalesce, resulting in the larger pore spaces. Scale bars, 1.0 μm.

evidently linked by two or more pores, may be ascribed to a marked enhancement of reaction when two active reaction droplets meet during their irregular wanderings. Perhaps there is temporary growth of the active reaction zone by bubble or froth formation. As nuclei grow hemispherically, there must also be division of active droplets[17] into two or more which thereafter progress independently. Unfortunately, the identification of the distribution of NO_2ClO_4 within partly decomposed crystals was impracticable as it hydrolyses so readily.

The reaction mechanism described above does not take into account the initiation of reaction in pure AP, where no source of oxidized nitrogen is available. Although we have not yet studied in detail the slow reactions occurring during the induction period, we have observed that nucleus generation often occurs within grooves on roughened surfaces (see, for example, Fig. 2*c*). Such surface retexturing occurs during sublimation and presumably is accompanied by other slower decomposition reactions, such as Cl_2O_7 breakdown[16], capable of oxidizing ammonia. Any volatile NO_2ClO_4 produced can only participate in nucleus growth when it is effectively retained within pores and channels, progressively formed at the inner surfaces of grooves. Thus again[17,18] we identify nuclei as specialist structures developed particularly to retain (temporarily) a fluid participant in the chemical change. Salt that is undecomposed after passage of active liquid droplets occurs because sites of enhanced reactivity have been removed and further intermediate cannot be produced in sufficient local concentration to generate a new reaction zone. The addition of NH_4NO_3, however, was capable of initiating some further decomposition of the residue.

This mechanism can also explain the ability of certain compounds to act as catalysts for AP decomposition. NH_4ClO_3 yields[2] NH_4NO_3, shown here to be active in promoting AP decomposition. Permanganate and chromium-containing[7] anions may participate similarly by oxidizing ammonia, the reduced oxyanion being reoxidized through ClO_4^- breakdown.

We thank J. McCrae and R. Reed for advice on obtaining and interpreting the electron micrographs. M.A.M. thanks the Egyptian Government and the ORS Award Schemes for Scholarships held during this research.

Received 16 April; accepted 11 September 1984.

1. Jacobs, P. W. M. & Whitehead, H. M. *Chem. Rev.* **69**, 551-590 (1969)
2. Bircumshaw, L. L. & Newman, B. H. *Proc. R. Soc.* **A227**, 115-132 (1954), 228-241 (1955).
3. Galwey, A. K. & Jacobs, P. W. M. *Proc. R. Soc.* **A254**, 455-469 (1960)
4. Davies, J. V., Jacobs, P. W. M. & Russell-Jones, A. *Trans. Faraday Soc.* **63**, 1737-1748 (1967).
5. Khairetdinov, E. F. & Boldyrev, V. V. *Thermochimica acta* **41**, 63-86 (1980).
6. Owen, G. P., Thomas, J. M. & Williams, J. O. *Trans. Faraday Soc.* **70**, 1934-1943 (1974)
7. Galwey, A. K., Pöppl, L. & Sundara Rajam. *JCS Faraday Trans.* I **79**, 2143-2151 (1983).
8. Girdhar, H. L., Arora, A. J. & Malik, G. N. *Indian J. Chem.* **21A**, 353-356 (1982).
9. Pai Verneker, V. R., Kishore, K. & Varadaraju, U. V. *Combust. Flame* **45**, 137-146 (1982).
10. Snell, F. D. *Photometric and Fluorometric Methods of Analysis: Non-metals* 546 (Wiley, New York, 1981).
11. Solymosi, F. *Structure and Stability of Salts of the Halogen Oxyacids in the Solid Phase*, 329-342 (Wiley, London, 1977).
12. Maycock, J. N. & Pai Verneker, V. R. *J. phys. Chem.* **72**, 4004-4009 (1968).
13. Solymosi, F. *Structure and Stability of Salts of the Halogen Oxyacids in the Solid Phase*, 174 (Wiley, London, 1977).
14. Smith, R. D. *Trans. Faraday Soc.* **53**, 1341-1345 (1957).
15. Galwey, A. K. *Thermal Analysis 7th int. Conf.*, Kingston, Ontario 38 53 (Wiley, London, 1982).
16. Fisher, I. P. *Trans. Faraday Soc.* **64**, 1852-1857 (1968).
17. Galwey, A. K. & Pöppl, L. *Phil. Trans. R. Soc.* **A311**, 159-182 (1984)
18. Galwey, A. K., Spinicci, R. & Guarini, G. G. T. *Proc. R. Soc.* **A378**, 477-505 (1981)

South African modern beach sand and plate tectonics

Paul Edwin Potter

H. N. Fisk Laboratory of Sedimentology, Department of Geology, University of Cincinnati, Cincinnati, Ohio 45221, USA

South America is the ideal continent for baseline studies on how the framework composition of modern sands relates to reconstruction of palaeoplates—it has well-defined active and passive margins, great contrasts in climate and relief and is free of continental glaciation (Fig. 1). I report here petrographical studies of its beach sands which show two active margin associations rich in volcanics and plagioclase—one along its Pacific coast and one along the Argentine coast—and two associations rich in quartz—a passive margin association from Argentina to Trinidad and a moderately, quartz-rich association along the Caribbean coast. Tectonic control is thus overwhelming but complications exist along the Argentine coast where a dry, narrow continent permits active margin sand to mantle a passive margin. Another surprising result is that quartz-rich sands border the crystalline rocks of much of the Sera do Mar in Brazil.

Sandstone has long been used[1] to help identify the tectonic setting of ancient basins for many reasons. It is present in almost every basin, including some of the very oldest, and it occurs in almost every sedimentary environment with the possible exception of the abyssal plains of some deep sea basins. Each grain also carries its own provenance history, which is easy to study with both microscope and microprobe. However, the idea that the petrographic study of 10–30 sandstone samples from an ancient basin, perhaps a sample of only 10^{-12} to 10^{-16} of its entire volume, can reveal a plate tectonic setting, and thus infer major crustal processes, may be considered audacious.

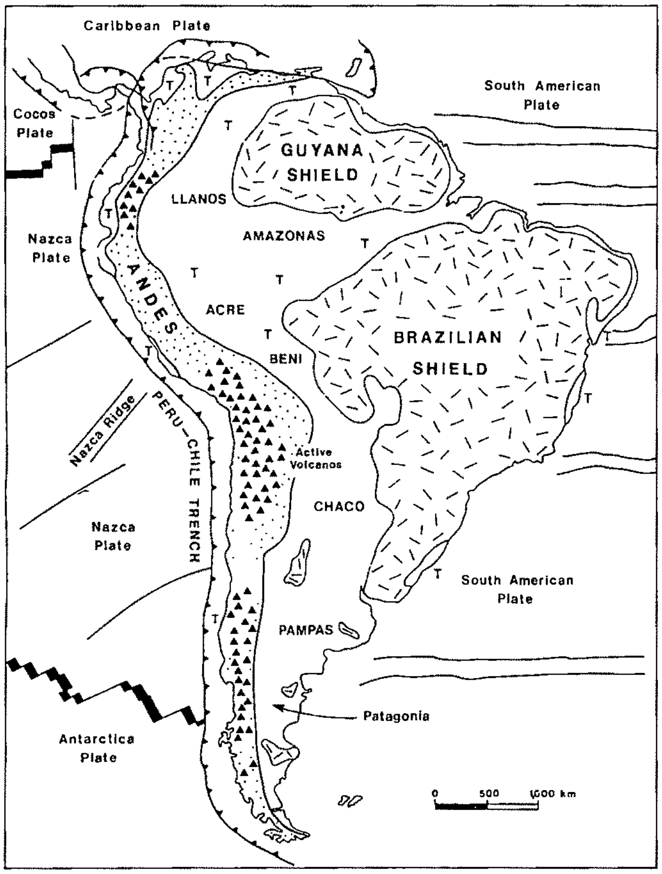

Fig. 1 Major tectonic elements of South America and adjacent ocean basins.

Present themes of the plate tectonic control on framework mineralogy come from studies of Mesozoic and Cenozoic basins[2–7] supplemented by studies of modern deep sea[8–11] and alluvial sands[12–15]. More than 40 papers on the plate tectonic interpretation of sandstone mineralogy have appeared since 1970, and virtually all of these recognize three different major tectonic settings with seven to nine subdivisions using standard compositional triangles (Fig. 2).

South America, the fourth largest continent, forming 12% of all the Earth's land surface, is the most elegantly asymmetric of all the continents from a plate tectonic standpoint—the entire west coast is an active margin, all of the eastern coast from Tierra del Fuego to Trinidad is a passive margin and only its Caribbean border, where translation seems important—is moderately complex (Fig. 1). South America is also free of continental glaciation; continent-wide provenance studies of modern sands are difficult to interpret where Pleistocene continental glaciation was widespread, because it blurs the continent-wide distribution pattern of sand. The climate of South America ranges from arid, with extremely dry deserts along coastal Peru and Chile, through temperate to tropical, with up to 10 m of rainfall in northwestern Colombia. Furthermore, major climatic trends are transverse to the Andes. Physiographic contrasts are equally impressive. The Andes Mountains, the world's longest mountain range with a length of almost 9,500 km, have towering peaks, an average elevation second only to that of the Himalayas, and many high, vast, dry plateaus. Additionally, South America has sweeping plains and low plateaus—some dry and grass covered, some covered by vast jungles. Also present along much of the Brazilian coast are jungle covered mountains composed of Precambrian rocks that rise from a narrow coastal plain. The coastal physiography and climate for the entire continent is summarized in ref. 16.

Another reason to study South America is that there are data available on the petrography and chemistry of the modern river sands of the Amazon and Tocantins basins[14], an area that covers about 40% of South America plus some for the Magdalena, Orinoco, Parniba do Sul, Paraná and Sao Francisco rivers[15], as well as for small rivers on the Peruvian coast. Together these river sands come from basins that drain about 65% of the continent. There are also published data on deep-sea and shelf sands of the Peru–Chile trench bordering South America[17] in addition to the sands of Atlantic shelf[18].

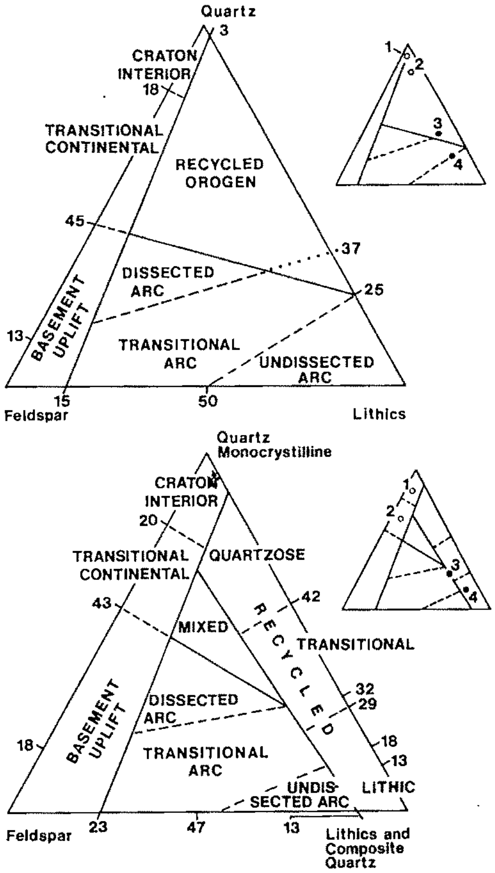

Fig. 2 Plate tectonic classification of sandstone mineralogy (after ref. 6, Fig. 1). Numbers in the small triangles indicate: 1, average composition of passive margin sands from the Rio de Plata to Trinidad; 2, beach sands from Trinidad westward along the Caribbean coast; 3, Argentine beach sands; and 4, the sands of South America's Pacific coast (see Fig. 3).

This study reports on the first-ever effort to study petrographically the sand of a single environment, the beach, around an entire continent. The technique used in sampling the beach sands of South America was based on that of Du Rietz[19], who showed how the petrology and chemistry of modern Baltic beaches become more mature as litoral drift transports sand away from the southern edge of the Baltic Shield.

Why study modern beaches? The beach is the interface between marine and non-marine environments so that all marine sands have passed through it and, with recycling, perhaps the same is true for many, if not most, ancient sandstones. Because the beach environment is one of high kinetic energy, it provides a strong test of another factor: modification of framework mineralogy by abrasion. In other words, if petrologists can correctly identify the tectonic setting of a landmass from its beaches, surely they could do so from its fluvial sands. Also, the beach is an easy environment to reach and sample—an important factor when an entire continent with a coast line of 50,000 km is to be sampled. More than 200 samples of beach sand were collected in 116 field days. Beaches were selected at points of convenient access and the 27 samples reported here were selected because of their geographical representation of each major mineral association.

Where possible, fine- to medium-sand was collected to best match the dominant size classes with midpoints of 177 and 350 mm (2.5 and 1.5ϕ) as reported by Shea[20] based on his compilation of 11,212 analyses chiefly of onshore sands and sandstones, but including some sands from modern continental shelves. These two size classes include ~35% of his present average grain-size distribution. Because grain sizes of samples in this study are coarser than those of most deep-sea sands, more rock fragments with their greater provenance information can be expected than in studies of typical fine-grained, deep-sea sands derived from the same source. To avoid the pitfalls of studying only a narrow size fraction and missing important diagnostic grains[21], the entire sand was impregnated and studied using standard counting procedures[15] after staining for potash feldspar.

Contrasts in the beach sands of South America are dramatic as judged by variations of quartz (Q), feldspar (F), and rock fragments (Rf) and dominant types of rock fragments (Fig. 3). Beach sands of South America's leading margin, the Pacific coast, have an average Q:F:Rf ratio of 19:13:68, whereas the continent's trailing margin coastline from the Rio Plata to Trinidad, a coastline bordering the Brazilian and Guyana Shields, averages 95:3:2, a staggering difference which is even more impressive when it is realized that mountains composed of Precambrian crystalline rocks border much of the South Atlantic coastline of Brazil. A petrographical count of each size fraction from a beach at Huacho in Peru and one from Natal in Brazil confirm these contrasts (Fig. 4). Downstream increase in quartz content in both the Amazon and Orinoco rivers effectively eliminates significant Andean contributions to beach sands from the mouth of the Amazon to Trinidad (Fig. 5). The rock fragments of the two major mineral associations are also totally different—volcanics predominate along most of the Pacific coast whereas rare alterites and igneous and metamorphic grains are characteristic of beach sands between Rio de la Plata and Trinidad.

Two smaller mineral associations are present and both are of great interest. All the Argentine coast from Rio de la Plata to Tierra del Fuego has an Andean, leading edge composition only slightly more mature than that of Pacific beach sands—the Q:F:Rf ratio averages 33:15:52—and again volcanics are its dominant rock fragments. Although the entire Argentine coast is a trailing margin, its beach sands have a leading edge composition because Patagonia is narrow and its bedrock near the coast is largely Tertiary molasse itself derived from the Andes. In addition, rainfall is scant, thus minimizing increase in maturity downstream from the Andes. One important implication immediately follows—use of sandstone mineralogy alone to identify palaeoplate setting can result in tectonic misclassification unless the basin's characteristics and regional setting are also considered.

The fourth and smallest association occurs from Trinidad to the mouth of the Magdalena River in Colombia. Here beach sands have an average Q:F:Rf composition of 78:5:17, although locally rock fragments are more abundant. This predominance of quartz—as along the southwestern coast of Brazil—is surprising given the proximity of metamorphic highlands close to the horeline. Dominant rock fragments are metamorphics derived from the Venezuelean Andes.

Preliminary results based on thin section study of light minerals indicate four major mineral associations for South American beaches: two immature leading edge associations and two trailing margin association, one from the Rio de la Plata to Trinidad and the other along the Caribbean coast from Trinidad to the Magdalena River. Compositionally, west coast beaches plot on the boundary between undissected and transitional arc of Dickinson and others[6] and Argentine beaches plot as a recycled orogen (back arc basin), although near the boundary to transitional arc; Venezuelan beaches plot as a recycled orogen near the boundary of the craton–interior field and beaches from the Rio de la Plata to Trinidad plot in the craton–interior field (Fig. 2, inset). Thus my preliminary results confirm the fields suggested by Dickinson and others[6].

These preliminary results pose several interesting questions: Where a leading edge of a continent becomes narrow, its

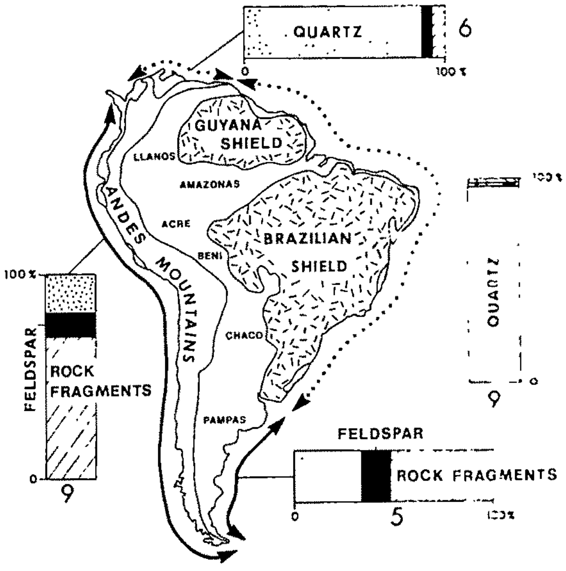

Fig. 3 Major, broad, mineral associations of South American beach sands.

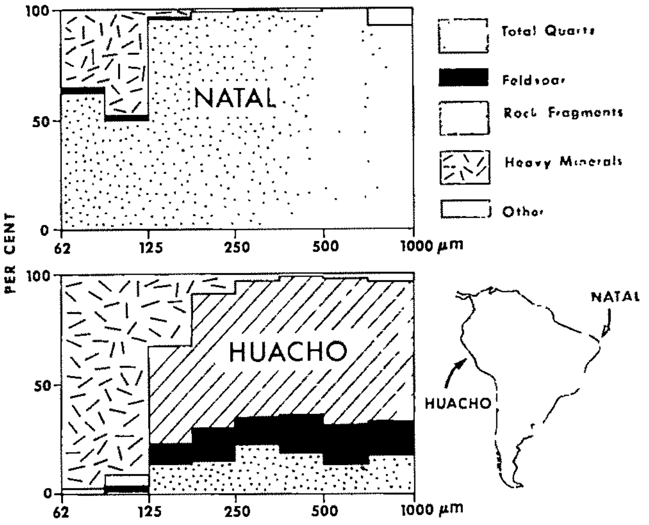

Fig. 4 Fraction analysis of beach sand at Huacho, Chancay Province, Peru and Natal, Rio Grande do Norte, Brazil shows great contrast in composition between each size grade.

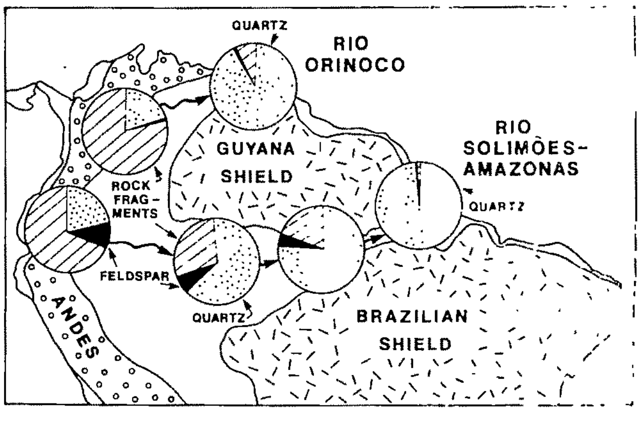

Fig. 5 Downstream increase in compositional maturity—more quartz and fewer rock fragments—in Orinoco and Solimões–Amazonas Rivers. Data for Solimões–Amazonas from ref. 14

characteristic composition can also occur on its 'backside', passive margin, especially where a dry climate prevails, as in Patagonia in Argentina. What implications does this have for the palaeogeographic reconstructions of ancient basins? How will a wet versus dry climate on the backside of a continent affect the mineralogy of its sandy detritus reaching the sea?

Abrasion on the beaches of South America's western leading edge does not reduce our perception of the towering land mass on shore; on the other hand, the low feldspar content of beaches bordering Brazil's Serra do Mar commonly gives little hint of these Precambrian mountains. Would this be true if the coastal climate were arid rather than humid?

Why do some of the continent's larger rivers show such a great change in mineralogy from Andean source to Atlantic mouth? Would this happen if their river basins had a subarctic, temperate or arid climate?

How commonly do the boundaries of major mineral provinces along a continental margin coincide with the mouth of a large river and produce contrasts like that on opposite sides of the Rio de la Plata, whose estuary separates sand of leading edge composition in Argentina from sand of trailing margin composition in Uruguay?

How carefully can we recognize subprovinces along the Andean leading edge, either on- or offshore, and relate them to onshore geology?

The effect of tectonic control on sandstone composition seems to be overwhelming, but how much relief is needed to overcome the effects of high rainfall? Could there be areas where we could sample a 'controlled experiment'?

As more samples are reported from modern beach sands and the adjacent offshore, how well will they agree? Will onshore sands have a different composition than their bordering shelf or deep seas?

Are we near the stage in regional studies of modern sands that we can deduce the sand composition of an entire continent? If so will computer modelling add a new dimension to provenance studies in the not too distant future.?

This research was funded by NSF grant EAR-80-18209. I received much help in every coastal country of South America, which will be fully acknowledged when final results are published but, until then, I thank W. R. Dickinson (University of Arizona) L. J. Suttner and A. Basu (Indiana University), K. O. Emery (Woods Hole Oceanographic Institute) and J. Barry Maynard, (University of Cincinnati) for helpful advice.

Received 30 January; accepted 22 June 1984.

1. Krynine, P. D. *Geologia* 1st Pt **2**, 537–561 (1942).
2. Dickinson, W. R. *Rev. Geophys. Space Phys.* **8**, 813–860 (1970).
3. Dickinson, W. F. & Suczek, C. A. *Bull. Ass. petrol. Geol.* **63**, 2164–2182 (1979).
4. Ingersoll, R. V. & Suczek, C. A. *J. sedim. Petrol.* **49**, 1217–1228 (1979).
5. Dickinson, W. R. *Bull. Am. Ass. petrol. Geol.* **66**, 121–137 (1982).
6. Dickinson, W. R. *et al. Bull. geol. Soc. Am.* **94**, 222–235 (1983).
7. Schwab, F. L. *Geology* **3**, 487–490 (1975).
8. Harrold, P. J. & Moore, J. C. in *Init. Rep. DSDP Leg* **31**, 507–514 (1975).
9. Stewart, R. J. *Bull. Am. Ass. petrol. Geol.* **87**, 793–808 (1976).
10. Valloni, R. & Maynard, J. B. *Sedimentology* **28**, 75–83 (1981).
11. Maynard, J. Barry, Valloni, R. & Yu, Ho-Shing in *Trench and Fore-Arc Sedimentation* (ed. Leggett, J. K.) 551–561 (Geological Society, London, 1982).
12. Suttner, L. J. Basu, A. & Mack, G. H. *J. sedim. Petrol.* **51**, 1235–1246 (1981).
13. Davies, D. K., Vessell, R. K., Miles, R. C., Foley, M. G. & Bonis, S. B. *Can. Soc. Petrol. Geol. Mem.* **5**, 61–84 (1978).
14. Franzinelli, E. & Potter, P. E. *J. Geol.* **91**, 23–39 (1983).
15. Potter, P. E. *J. Geol.* **86**, 423–449 (1978).
16. Psuty, N. P. & Mizobe, C. in *Encyclopedia of Earth Sciences* Vol. 15 (ed. Schwartz, M. L.) 765–770 (Hutchinson Ross, Stroudsburg, Pennsylvania, 1982).
17. Yerino, L. N. & Maynard, J. B. *Sedimentology* **31**, 83–89 (1984).
18. Damuth, J. E. & Fairbridge, R. W. *Bull. geol. Soc. Am.* **75**, 1131–1156 (1970).
19. DuReitz, T. *Geol. För. Förh.* **75**, 381–395 (1953).
20. Shea, J. H. *J. sedim. Petrol.* **44**, 985–1003 (1974).
21. Van Andel, Tj. H. *Provenance, Transport and Deposition of Rhine Sediments* (Veenman, Wagenigen, 1950).

A new method for environmental analysis of particle size distribution data from shoreline sediments

N. R. J. Fieller*, D. D. Gilbertson† & W. Olbricht‡

* Department of Probability and Statistics, University of Sheffield, Sheffield S3 7RH, UK
† Department of Prehistory and Archaeology, University of Sheffield, Sheffield S10 2TN, UK
‡ Abteilung für Mathematik, Ruhr-Universität Bochum, D-4630 Bochum, FRG

The study of particle size distributions is commonly used to investigate sedimentary processes and environments. Originally such work concentrated on typifying these distributions by their sample moments, while more recent statistical studies have proposed fitting parametric models to sample data and then using the resulting parameter estimates. We have investigated the use of log-hyperbolic and skew log-Laplace models to distinguish between beach and dune sands, with the aim of classifying the depositional environment of some mesolithic middens. We found that the former models were unsatisfactory for various numerical and physical reasons, while the latter provide a simple and robust method which is useful for the classification of sand sediments.

Barndorff-Nielsen[1,2] and Bagnold and Barndorff-Nielsen[3,4] demonstrated the statistical and geological advantages of using log-hyperbolic distributions to interpret particle size distributions. The method eliminated[1] the mathematical arbitrariness and unreliable assumption of normality associated with the use of low-order moment measures (such as, mean, median, skewness, kurtosis and developments of them[5–7], and (2) used a mathematical distribution that had been directly related to the geological processes of transportation and deposition responsible for the sediments[3,4]. Four parameters were utilized to describe the log-hyperbola: ϕ, γ, μ and δ (Fig. 1). Bagnold[1–4] suggested that the gradient ϕ was related to the significance in the particle size distribution of saltation, and that the gradient γ corresponded to the significance of coarser grains which 'creep'.

We have employed this statistical procedure to characterize the particle mass-size distributions with data obtained at $\frac{1}{2}\phi$ intervals obtained by standard procedures[8,9] from coastal beach, salting and dune environements in the Inner Hebrides, Libya and South Wales; and, in particular, to identify the depositional environments, and hence the palaeogeography, represented by shell sands of unknown origins obtained in trial pits and cores beneath late mesolithic shell middens investigated on the east coast of Oronsay, Inner Hebrides[10–13] (Fig. 2). In this latter study, samples were taken from along four transects crossing several depositional environments.

The fitting of the log-hyperbola was satisfactorily achieved both on our reworking of the published Bagnold and Barndorff-Nielsen[2,3] data and on a substantial proportion of our own data[14]. However, in four out of our 15 attempts to use this procedure no numerically stable solution was obtained. Detailed numerical investigation of these four cases revealed that the likelihood function was virtually flat with respect to the parameter δ. The physical explanation is that there are many different log-hyperbolic distributions, differing only in curvature at the peak of the distribution, which fit the data equally well. This arises because of the coarse sequence of sieves used in the collection of our data: $\frac{1}{2}\phi$ rather than the $\frac{1}{4}\phi$ intervals used in the Bagnold and Barndorff-Nielsen data. The transition from 'fine-grade fraction' to 'coarse-grade fraction' typically occurs over a range rather less than $\frac{1}{2}\phi$. Consequently, if the peak of the distribution occurs close to a mesh size of any of the sieves, then the available data provide little information on the value of this parameter δ which essentially measures the curvature of the distribution at its peak. Use of alternative numerical techniques, in particular the programs used by Barndorff-Nielsen and his colleagues[15], did not alleviate the numerical problem. Note also that the computation, using any of the numerical

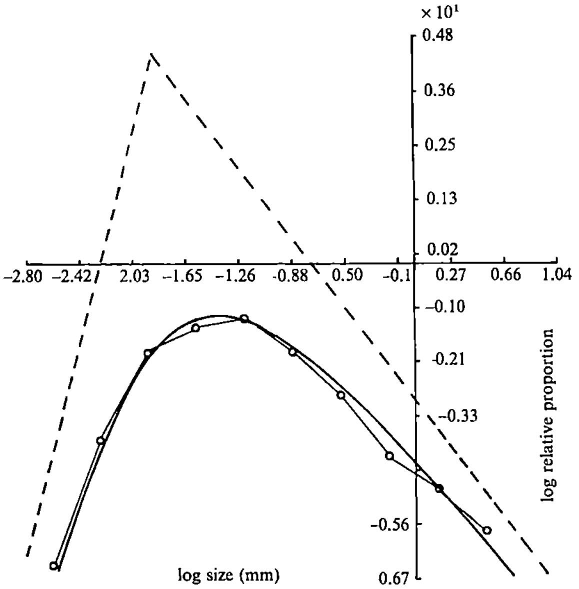

Fig. 1 Sample TUS1-6 and fitted log-hyperbolic distribution. The asymptotes to the hyperbola are shown as dashed lines. The four parameters of the distribution ϕ, γ, μ and δ are defined, respectively, as the arc-tangents of the acute angles made by the two asymptotes with the horizontal, the abscissa of the point of intersection of the asymptotes, and the difference (divided by $\sqrt{\phi\gamma}$) in ordinates of the point of intersection of the asymptotes and the maximum of the hyperbola.

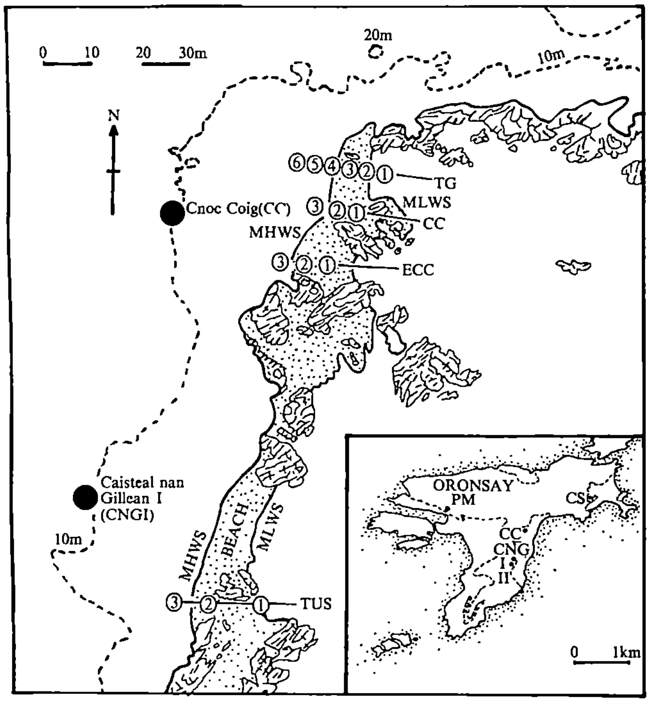

Fig. 2 Sample provenance on beach and dunes, Oronsay, Inner Hebrides and the location of the mesolithic middens and mid-Holocene shoreline (inset, after Jardine[10]). Middens: CC, Cnoc Coig; CNG I and II, Caisteal nan Gillean I and II; CS, Cnoc Sligeach; PM, Priory Midden.

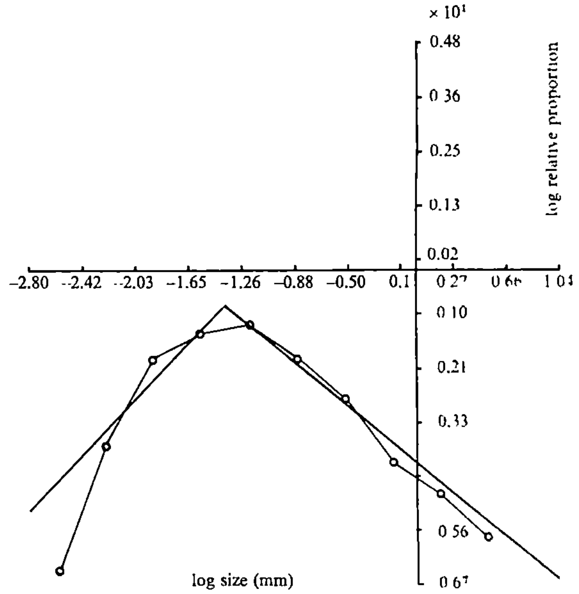

Fig. 3 Truncated skew log-Laplace distribution fitted to particle size distribution TUS1-6. The three parameters of the distribution α, β and μ are defined, respectively, as the reciprocals of the arc tangents of the acute angles made by the two lines with the horizontal axis and the abscissa of their point of intersection.

techniques, proved prohibitively expensive for application to the large number of samples involved in our study.

Another physical explanation of our difficulties is that the sand samples we dealt with were typically less 'pure' than those described by Barndorff-Nielsen[1-3]. Many of our samples were taken from less ephemeral locations, and many were indeed from archaeological sites, and might, therefore, have been subject to diagenetic and pedological changes.

To cope with these problems, we have fitted a distribution which is essentially described by two straight lines instead of a hyperbola when the mass-size distribution is plotted on log-log axes (Fig. 3). Statistically this was achieved by fitting a skew log-Laplace distribution using the program LAPSKEW.FTN[16]. This distribution was truncated to allow for the finite number of sieves and the inevitable grouping of the distribution at the upper and lower ends. The skew log-Laplace distribution can be regarded as the limiting form of the log-hyperbolic distribution obtained by letting the parameter δ tend to zero. It is conveniently parameterized by parameters, α, β and μ. Where α and β correspond to the reciprocals of ϕ and γ, and corresponds directly to the parameter μ of the log-hyperbolic distribution. LAPSKEW.FTN utilizes a modified Davidon-Fletcher-Powell algorithm[17] for determining the values of α and β for fixed μ and then a grid search for determining μ.

To illustrate the effectiveness of this approach, we have calculated and plotted values of α, β and μ for modern and mid-Holocene sand samples associated with mesolithic shell middens near the eastern shore of the Hebridean island of Oronsay (Fig. 2). Two-and three-dimensional plots of all possible combinations of the parameters have been generated, archived[9,18], and inspected. The equivalents of Friedman's[5,6] plots of standard deviation against mean; skewness against mean and skewness against variance have also been plotted as $\alpha^2+\beta^2$ against μ; α/β against μ and α/β against $\alpha^2+\beta^2$. Most of these plots present the same pattern of results and conclusions as for the case of α versus μ.

The plot of α versus μ, shown in Fig. 4*a*, reveals two clear clusters distinguished by their bay of origin. Both the mesolithic and modern samples have higher values of μ (the 'typical' grain size) at Caisteal nan Gillean (CNG) locations than at Cnoc Coig (CC) locations. Second, the values of α clearly separate modern dunes from beach sands at each location.

More detailed examination of one location—the modern environments and mesolithic sediments of CC—shown in Fig. 4*b*, indicate other important trends. Sediment samples from each transect CC, ECC and TG (Figs 2 and 4*c*) show a systematic variation in the values of α and μ from lower, via mid-beach into upper-beach and dune sands. Presumably this reflects the impact of the changing character of the transportational and depositional processes affecting the sediment.

The transects themselves are arranged in a clockwise rotation (with increasing μ and α values) from transects ECC through CC to TG (Figs 2 and 4*c*). This corresponds to, and is

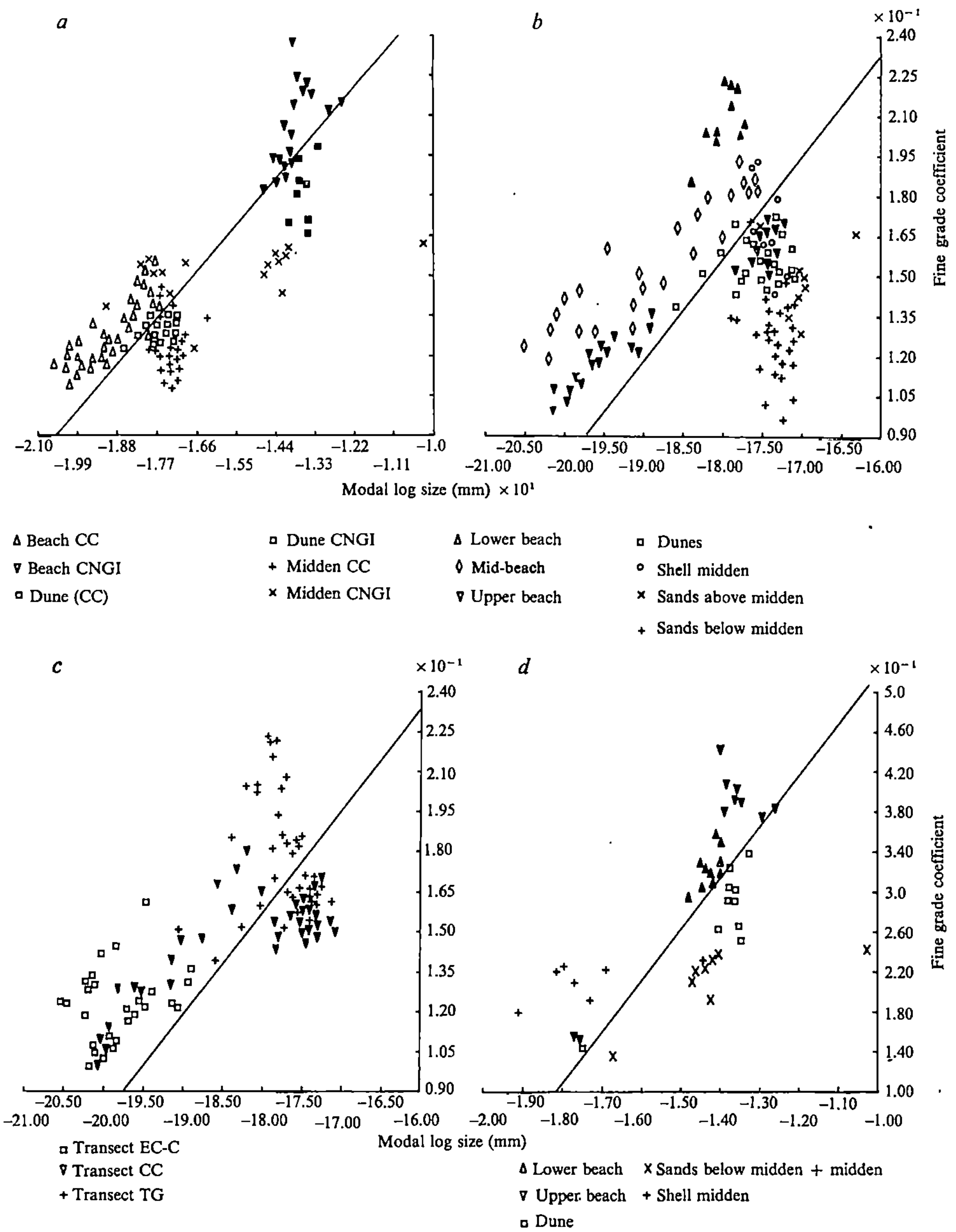

Fig. 4 Scattergrams showing the plots of modal log grain size and fine-grade coefficient of beach, dune and midden sands and the linear discriminant functions[19] separating modern beach and dune sediments at; *a*, eastern Oronsay: *b*, Cnoc Coig (showing midden samples); *c*, Cnoc Coig (distinguishing transects); *d*, Caisteal nan Gillean.

presumably the result of, a gradient from the exposed coastal locations to the relatively sheltered ECC with its protecting offshore rock bars and skerries.

In some cases, sands from the base of the dune and back of the beach are scarcely distinguishable in terms of their mass-size distribution. In practice, the components of this transitional zone are often difficult to separate in this field. The graphs of the linear discriminant functions[19] separating modern beach and dune sands (Fig. 4*b*, *c*) generally corroborate and clarify these patterns.

The sands immediately above and below the mesolithic CC shell midden are principally dune sands, but some plot in a position indicating that they might represent the actual beach/dune transitions. The sands of previously unknown origins obtained by coring beneath the midden are seen to be dune sands (Fig. 4*b*). These data have archaeological and palaeogeographical significance, as it was anticipated that the middens had accumulated on beach sand associated with the mid-Holocene sea-level maximum[10].

The sands obtained from interstices between the shells of the actual CC midden form a further distinct cluster straddling the upper beach/dune base transition. This suggests that (1) the middens were located at that position and/or (2) these particle mass-size distributions reflect sand introduced on animals, shellfish and seaweed gathered from the foreshore and/or introduced by feet and hands after harvesting activities. The sands within the CNGI shell midden (Fig. 4*d*) resemble more closely deposits found on the modern mid-beach, rather than upper beach, suggesting that the second group of explanations might be more applicable in this case.

This case study has concentrated on plots of α versus μ. In other cases, our unpublished work indicates the value of inspecting three-dimensional plots of α against β against μ. Single plots of β against μ have also provided adequate environmental discrimination in other situations. The more complex studies representing the equivalents of mean, skewness, variance and so on have not yielded notable additional information.

The data indicate that fitting skew log-Laplace distributions to particle mass-size distributions can provide a sensitive tool for the characterization and discrimination of depositional process and environments in coastal locations. The method is simple and cheap in computational terms: it can even be quickly approximated 'by hand'. It is statistically robust and has been used successfully with data obtained at $\frac{1}{2}\phi$ intervals facilitating notable savings in laboratory analyses. It retains the important assets of being directly comparable with the log-hyperbolic distribution, and consequently the slope parameters of the skew log-Laplace distribution may also be directly related to geological processes. It makes no assumptions of an underlying normal particle size distribution, but reliably describes important attributes of particle mass-size distributions.

We thank Mrs D. A. Y. Timmins for particle mass-size distribution data; Drs G. W. Jardine and P. A. Mellars for discussions; D.D.G. acknowledges the financial support for field work from the University of Sheffield research grant nos 359, 561, and 710 and W.O. acknowledges receipt of a scholarship from the Studienstiftung des deutschen Volkes.

Received 29 May; accepted 14 August 1984.

1. Barndorff-Nielsen, O. *Proc. R. Soc.* A353, 401-419 (1977).
2. Barndorff-Nielsen, O. *et al. Sedimentology* 29, 53-65 (1982).
3. Bagnold, R. A. & Barndorff-Nielsen, O. *Sedimentology* 27, 199-207 (1980).
4. Bagnold, R. A. *The Physics of Blown Sand and Desert Dunes* (Methuen, London, 1941).
5. Friedman, G. M. *Sedimentology* 26, 3-32 (1979).
6. Friedman, G. M. *Sedimentology* 26, 859-862 (1979).
7. Folk, R. L. *Sedimentology* 6, 73-93 (1966).
8. Timmins, D. A. Y. thesis, Univ. Sheffield (1981).
9. Fieller, N. R. J., Gilbertson, D. D., Olbricht, W. & Timmins, D. A. Y. *A Computer-Compatible Archive of Sedimentological Data from Oronsay, Inner Hebrides* (Department of Prehistory and Archaeology, University of Sheffield Archive No. 2, 1983).
10. Jardine, W. G. *Nature* 267, 138-140 (1977).
11. Mellars, P. A. *The Early Postglacial Settlement of Northern Europe: An Ecological Perspective* (Duckworths, London, 1978).
12. Mellars, P. A., Wilkinson, M. R. & Fieller, N. R. J. *Proc. prehist. Soc.* 46, 19-44 (1980).
13. Mellars, P. A. *The Mesolithic Shell Middens of Oronsay* (Monographs the Department of Prehistory and Archaeology, University of Sheffield, 1984).
14. Olbricht, W. thesis, Univ. Sheffield (1982).
15. Ledet Jensen, J. *Maximum Likelihood Estimation of the Hyperbolic Parameters from Grouped Observations* (Res. Rep. No. 91, Department of Theoretical Statistics, University of Aarhus, 1983).
16. Fieller, N. R. J. *FORTRAN Program LAPSKEW. FTN* (Department of Probability and Statistics, University of Sheffield, 1982).
17. Walsh, G. R. *Methods of Optimization* (Wiley, London, 1975).
18. Fieller, N. R. J., Gilbertson, D. D., Olbricht, W. & Timmins, D. A. Y. *Atlas of Multi-colour Two- and Three-Dimensional Graphs of Particle Size Distribution form Colonsay and Oronsay using Parameters from Estimated Skew log-Laplace Distributions* (Department of Prehistory and Archaeology, University of Sheffield, Archive No. 3 (1984).
19. Mardia, K. V., Kent, J. T. & Bibby, J. M. *Multivariate Analysis* (Academic, London, 1979).

Effect of benthic mixing on the information content of deep-sea stratigraphical signals

Paul Schiffelbein

Scripps Institution of Oceanography, La Jolla, California 92093, USA

Benthic mixing or bioturbation affects sediments in various ways, including: (1) the production of trace fossils, (2) mechanical and/or chemical alteration of the sediment, and (3) filtering or smearing stratigraphical signals[1]. Because mixing alters both the slopes and amplitudes of any recorded events, some knowledge of the process is essential for the correct interpretation of the signals. In view of recent trends towards high-resolution stratigraphy[2,3] and signal unmixing[4-6], the frequency characteristics of the benthic mixing filter must be understood to determine which types of signals can be detected after mixing. Analyses of ash and tektite profiles in deep-sea cores from various geographical regions indicate that even signals from cores having sedimentation rates as high as 7 cm kyr^{-1} will show severe attenuation of frequencies higher than 0.35 cycles kyr^{-1} (periods shorter than 2.9 kyr) resulting in loss of ability to resolve closely-spaced events. Most signals will experience much more serious high-frequency attenuation, however. The severity of high frequency loss is directly related to sedimentation rate ($R = 0.97$ for the cores examined), suggesting that this is the most important variable to take into account when considering a core for palaeoceanographic or palaeoclimatic study.

Several models have been developed to explain the filtering suffered by stratigraphical signals as they pass through the sediment mixed layer[7-9]. They express the mixing function (system impulse response) in terms of physical parameters, usually mixed-layer thickness and a diffusion coefficient, which determines the rate of transfer of material through the mixed layer. All previous workers have treated benthic mixing as a linear time-invariant system. In fact, there are several reasons why the process is expected to vary with time. Productivity, and hence sedimentation rate, varies as a function of climate. The number of benthic organisms (and hence mixing intensity), should depend on the amount of organic matter reaching the sediments[10]. Because the time-varying aspects of the mixing system are not well characterized, however, simplification is necessary.

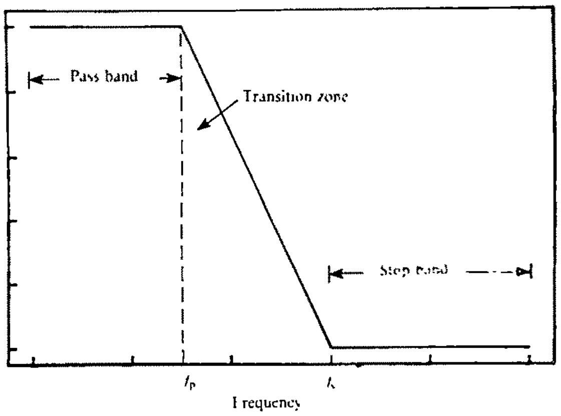

Fig. 1 Aspects of a lowpass filter. f_p and f_s are the passband and stop-band cutoff frequencies, respectively

The output and the input of a linear time-invariant system are related by the convolution integral[11]. A frequency response approach is generally used to identify such a system, which is accomplished by taking the Fourier transform of the convolution equation. The system is then represented as

$$G(\omega) = H(\omega)F(\omega)$$

where $G(\omega)$, $H(\omega)$, and $F(\omega)$ are, respectively, the Fourier transforms of the output (filtered) signal, the impulse response, and the input signal. $H(\omega)$ is called the system transfer function, as it completely describes input and output relationships[12]. Most natural processes, including benthic mixing, involve smoothing or lowpass filters, meaning that the low frequencies are passed through, while the high frequencies are attenuated. Characteristics of a typical lowpass filter are shown in Fig. 1. The passband extends from zero frequency to the cutoff frequency f_p. The stopband extends from the cutoff frequency f_s to the Nyquist frequency. The region between f_p and f_s is the transition region.

Many volcanic ash and tektite profiles have been measured in deep-sea sediment cores from a broad range of geographical areas[13-17]. These profiles represent system impulse response functions due to the instantaneous nature of the inputs. Officer and Lynch[18] compiled 16 of these profiles, which were then fit to theoretical mixing profiles using the model of Guinasso and Schink[9]. These profiles were thus parameterized in terms of mixed layer thickness d and diffusion coefficient D. These parameters and a truncated series solution of the mixing equation[18] can be used to regenerate the mixing profiles. The regenerated curves offer an advantage over the measured profiles when investigating the mixing transfer function in that counting noise and mixing heterogeneity are effectively smoothed out. The power spectrum of each mixing function is calculated to determine the frequency characteristics of the transfer functions.

In practice, the passband cutoff frequency is usually defined as the halfpower point[19], that is the frequency at which one half of the input signal power is attenuated (−3 dB). As an example, the mixing function from core RC17-126, is shown in Fig. 2. The halfpower point (−3 dB) is at a frequency 0.14 cycles kyr (f_p). Frequency response decreases ('rolls off') at roughly 10 dB per octave (an octave refers to a doubling of frequency). The benthic mixing filter analyses for the 16 profiles are summarized in Table 1, and −10 dB (signal attenuated one order of magnitude) points are provided to give some idea of filter roll-off. Most stratigraphical signals (such as, oxygen isotopes) do not have a signal-to-noise ratio >10 dB (ref. 20), so these numbers also give some idea of an absolute attenuation frequency (f_s).

The f_p values shed some light on the affects of benthic mixing on stratigraphical signals, as they span well over an order of magnitude. Even in the cases of minimal signal attenuation, all wavelengths $\leq$3,000 yr are substantially attenuated. This level of filtering will smooth out rapid transitions or transients (such as glacial–interglacial transitions), and obscure the relationships of closely-spaced events. This is true even when sedimentation rates are high (for example, 7 cm kyr^{-1} in cores V19-28 and V19-29). Most deep-sea cores used for palaeoceanographic or palaeoclimatic analysis tend to have sedimentation rates of the order of 1–2 cm kyr^{-1}. Mixing filters in Table 1 corresponding to cores of this type have a passband cutoff at a period of roughly 10,000–20,000 yr. While filters of this severity would not obscure Milankovitch or orbital frequencies (20 kyr–100 + kyr), they will lead to some reduction in the amplitudes of these spectral peaks[21] and will certainly make the results of any high-resolution study (sampling every 500–1,000 yr) questionable, unless there were some sort of signal restoration (deconvolution).

A relationship between sedimentation rate and mixed layer thickness has been observed in equatorial Pacific box cores[22], suggesting a link between the amount of benthic mixing activity, primary productivity of the overlying surface waters, and the consequent flux in surface sediments. A strong correlation between sedimentation rate and mixed layer thickness would not be expected in areas with terrigenous influx, or in areas not so strongly controlled by biogenous sediment production. Using radiotracers in cores from diverse geographical areas, DeMaster and Cochran[23] found no systematic relationship between depth of mixing or mixing rate and sedimentation rate. A similar statement can be made for the cores listed in Table 1.

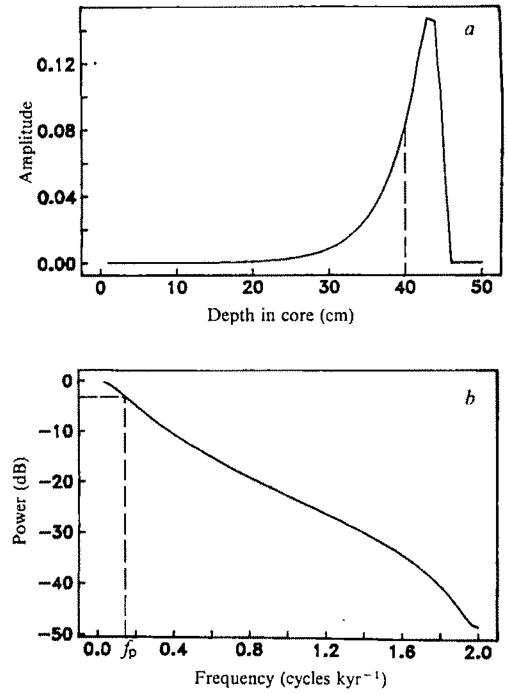

Fig. 2 Mixing function from core RC17-126. *a*, The impulse-response function, or time-domain representation of the filter, as easured from volcanic ash concentrations down core. Tracer impact depth was set arbitrarily at 40 cm (vertical dashed line). Vertical scale is in arbitrary units, and reflects unit-area normalization of the curve. *b*, The frequency-domain representation of the filter. Passband cut-off frequency (f_p) is taken to be the half-power (−3 dB) point.

The values in Table 1 suggest that sedimentation rate is the variable with the most direct influence of f_p, and hence the information contained in a deep-sea core. A linear regression of f_p values against sedimentation rates for the 16 entries in Table 1 yielded the equation $f_p = 0.05\, v$, with a correlation coefficient of 0.97. Rewriting in terms of period, and rearranging, yields $v(\text{cm kyr}^{-1}) = 20.0/\text{period (kyr)}$. This equation, based on the half-power points from the benthic mixing filters examined, can be used to find the appropriate minimum sedimentation rate required to ensure recovery of a given signal period (or frequency). To recover a signal of period 4 kyr, for example, requires a minimum sedimentation rate of about 5 cm kyr^{-1}. Many 'high-resolution' studies hope for better resolution than this, yet rarely use cores having such high sedimentation rates. Even if the −10 dB points are used to construct an equation ($f_{-10\,\text{dB}} = 0.14\, v - 0.01$; $R = 0.97$), in the hope that the 10 dB of lost gain can be restored by deconvolution, a sedimentation rate of 2 cm kyr^{-1} still yields a resolution of only ~4 kyr. Resolving a period of 1 kyr requires a core having a sedimentation rate of roughly 7 cm kyr^{-1}. That benthic mixing places severe restrictions on the time resolution of data recovered from deep-sea cores has long been appreciated[24], but the quantitative effects of mixing on signal recovery have received little attention. Hence, sampling of deep-sea cores often proceeds on arbitrary or intuitive grounds, usually with an optimistic idea of stratigraphical resolution. Sedimentiation rate is seen to be the primary control and limiting factor on signal resolution in deep-sea cores. Unless there is some way of increasing the signal-to-noise ratio (such as signal stacking), and/or a core of extremely high sedimentation rate is used, there is little to be gained from

Table 1 Benthic mixing filter characteristics

		Time-domain filter*		Frequency-domain filter	
Core	Sedimentation rate v(cm kyr^{-1})	Mixed layer thickness d (cm)	Diffusion coefficient D (cm^2 kyr^{-1})	f_p (−3dB point) (cycles kyr^{-1})	−10 dB point (cycles kyr^{-1})
V19-28	7.0	8	30	0.37	1.000
V19-29	7.0	10	20	0.33	0.83
E48-23	2.5	5	9	0.20	0.56
V27-19	2.25	8	6	0.13	0.32
RC17-126	2.0	6	8	0.14	0.37
V16-76	1.51	15	20	0.039	0.11
RC9-58	1.0	12	8	0.037	0.095
V19-153	0.75	13	3	0.031	0.068
V19-297	0.7	16	40	0.015	0.046
RC9-137	0.64	16	8	0.016	0.046
RC9-143	0.51	18	6	0.011	0.033
V29-39 (ash)	0.5	7	1	0.036	0.083
V29-39 (tektite)	0.5	8	2	0.027	0.072
V29-40 (ash)	0.5	12	5	0.017	0.047
V29-40 (tektite)	0.5	14	4	0.016	0.041
V16-70	0.22	13	2	0.007	0.019

* The values in these columns are from ref. 18. Approximation values rather than optimization values were used since approximation equations were employed to reconstruct the impulse responses.

very closely-spaced samples in constructing downcore stratigraphies.

My work on benthic mixing has been supported by the US Office of Naval Research (contract no. N00014-80-C-0440). I thank W. H. Berger and H. R. Thierstein for reviewing the manuscript and for helpful suggestions.

Received 9 March; accepted 2 August 1984.

1. Hanor, J. S. & Marshall, N. F. in *Trace Fossils* (ed. Perkins, B. F.) 127–135 (SEPM, Tulsa, 1971).
2. Berger, W. H., Killingley, J. S. & Vincent, E. *Oceanol. Acta* **1**, 203–216 (1978).
3. Kennett, J. P. & Shackleton, N. J. *Science* **188**, 147–150 (1975).
4. Berger, W. H., Johnson, R. F. & Killingley, J. S. *Nature* **269**, 661–663 (1977).
5. Berger, W. H. *Deep-Sea Res.* **25**, 473–480 (1978).
6. Jones, G. A. & Ruddiman, W. F. *Quat. Res.* **17**, 148–172 (1982).
7. Goldberg, E. D. & Koide, M. *Geochim. cosmochim. Acta* **26**, 417–450 (1962).
8. Berger, W. H. & Heath, G. R. *J. mar. Res.* **26**, 134–143 (1968).
9. Guinasso, N. L. & Schink, D. R. *J. geophys. Res.* **80**, 3032–3042 (1975).
10. Somayajulu, B. L. K., Sharma, P. & Berger, W. H. *Mar. Geol.* **54**, 169–180 (1984).
11. Graupe, D. *Identification of Systems* (Van Nostrand Reinhold, New York, 1972).
12. Peled, A. & Liu, B. *Digital Signal Processing* (Wiley, New York. 1976).
13. Glass, B. P. *Earth planet. Sci. Lett.* **6**, 409–415 (1969).
14. Glass, B. P., Baker, R. N., Storzer, D. & Wagner, G. A. *Earth planet. Sci. Lett.* **19**, 184–192 (1973).
15. Ruddiman, W. F. & Glover, L. K. *Bull. geol. Soc. Am.* **83**, 2817–2836 (1972).
16. Ruddiman, W. F. *et al. Sedim. Geol.* **25**, 257–276 (1980).
17. Ruddiman, W. F. & McIntyre, A. *Palaeogeogr. Palaeoclimatol. Palaeoecol.* **35**, 145–214 (1981).
18. Officer, C. B. & Lynch, D. R. *Mar. Geol.* **52**, 59–74 (1983).
19. Otnes, R. K. & Enochson, L. *Digital Time Series Analysis* (Wiley-Interscience, New York, 1972).
20. Schiffelbein, P. & Hills, S. *Palaeogeogr. Palaeoclimatol. Palaeoecol.* (in press).
21. Goreau, T. J. *Nature* **287**, 620–622 (1980).
22. Berger, W. H. & Killingley, J. S. *Mar. Geol.* **45**, 93–125 (1982).
23. DeMaster, D. J. & Cochran, J. K. *Earth planet. Sci. Lett.* **61**, 257–271 (1982).
24. Emiliani, C. *J. Geol.* 538–578 (1955).

Pre-Columbian age for North American *Corispermum* L. (Chenopodiaceae) confirmed by accelerator radiocarbon dating

J. L. Betancourt*, A. Long*, D. J. Donahue†, A. J. T. Jull† & T. H. Zabel†

* Department of Geosciences and † NSF Accelerator Facility for Radioisotope Analysis, University of Arizona, Tucson, Arizona 85721, USA

Criteria for recognizing alien (historically introduced) plants in continental floras are largely inferential, involving range disjunctions, absence in the first botanical records for a region, pioneer status in secondary successions ('weedy habit'), and, to a lesser extent, the fossil record. Decisions on whether a species is native or introduced commonly appear in local and regional floras. In a few cases, the plant's occurrence in the fossil record has reversed its presumed alien status[1]. Ironically, the appearance of assumed introduced species in prehistoric contexts could also be taken as an index of modern contamination due to stratigraphical mixing. We now present conclusive evidence for the prehistoric occurrence of *Corispermum* L. (Chenopodiaceae), a herbaceous annual growing on sandy soils throughout western North America, where it was previously reported as adventive from Eurasia. The use of tandem accelerator mass spectrometry (TAMS) for direct radiocarbon measurement of seeds eliminates problems with stratigraphical mixing and using this method we verify a pre-Columbian age for *Corispermum*.

The genus *Corispermum* is best represented in the semi-deserts of Eurasia. *Corispermum hyssopifolium* L. and *C. nitidum* Kit ex. Schult. are the two Eurasian species that today occur in North America, thought to have been introduced at the time of European settlement. *Corispermum hyssopifolium* has been regarded as endemic to southern Russia and adventive or partly indigenous in central and southern Europe. It is the most widely distributed species in North America. *Corispermum hyssopifolium* and *C. nitidum* are the only species reported in modern floras of Alaska and the Yukon, but at least five species with no recognized Old World synonyms have been described from type specimens in the Rocky Mountain states, US. Three of these species, *C. villosum* Rydb., *C. emarginatum* Rydb., and *C. marginale* Rydb., were described at the turn of the century by Rydberg[2]. His reputation for taxonomic splitting[3] may have influenced some workers in synonymizing his and other North American species with *C. hyssopifolium* or *C. nitidum*[4,5]. Further confusion results from at least one worker assigning alien status to one of the North American species (*C. villosum*) which Rydberg described[6].

The suggestion in many North American floras that *C. hyssopifolium* arrived only recently seems peculiar in view of early historical records from what was then remote wilderness. John Richardson found it on the shores of the Great Slave Lake, western Canada in 1821[7]. In the 1870s, Joseph T. Rothrock collected *C. hyssopifolium* in Colorado[8]. Hence, it is not surprising that an extensive record for pre-Columbian *Corispermum* has emerged in areas where early botanists first collected it.

Table 1 summarizes select localities and direct or associated conventional dates for *Corispermum* seeds in fossil contexts from northwest Canada, Alaska, and the Colorado Plateaus in the United States. The seeds are very distinctive and may resemble ticks to the unaccustomed eye (*Cori* = bug, Greek; *spermum* = seed, Latin). Seeds are oval in outline, flat and slightly concave-convex, with a persistent encircling wing. The base of the wing is emarginate or rounded, and the apical end bears two minute, toothlike style bases[9] (Fig. 1). Average seed dimensions are 5×4×0.5 mm. An attempt to distinguish species of *Corispermum* based on seed size and morphology from modern voucher specimens yielded erratic results, though in some cases fossil and modern seeds of a particular species are close facsimiles (Fig. 1*c* and *d*).

Fossil contexts for *Corispermum* seeds include alluvium[10,11], cave fill[12,13], human and herbivore coprolites[12,14], archaeological sites[12,13,15–17], and fossil packrat (*Neotoma*) middens[18–20]. Direct evidence for *Corispermum*'s role in the prehistoric human diet include its presence in human coprolites, as parched seeds in hearths, and some 80 cm^3 of seeds cached in a Mimbres pottery jar from Swartz Ruin, New Mexico. Associated ages in the various contexts range from >38,000 yr BP in the Yukon to <1,000 yr BP in archaeological sites on the Colorado Plateaus. Four of the localities contained sufficient seeds from a single context to allow direct radiocarbon measurements by TAMS. The mass of the seeds in these samples ranged from 5 to 17 mg per sample (8–15 seeds per sample). We followed routine radiocarbon dating procedures, by pretreating each sample with 1 M HCl, then 2% NaOH, again with HCl, and finally washing it thoroughly with distilled water. Target preparation involved first, pyrolysis *in vacuo*, then heating the carbonized material with powdered iron under argon to form a spheroid of cast iron. Details of target preparation and radiocarbon measurement procedures are given elsewhere[21]. All four of the direct dates generally agree with the associated ages of the samples. The oldest direct dates for *Corispermum* are 9,970 ± 460 yr BP for the Canadian and Alaskan sites and 14,500 ± 600 yr BP for the Colorado Plateaus.

A pre-Columbian age for *Corispermum* and the present discontinuity in its range between Siberia and Alaska raise questions about points of origin, dispersal routes, arrival times, and subsequent evolution in North America. In the late Cenozoic, the most reasonable dispersal route would have been from northeastern Siberia across the Bering Land Bridge to Alaska. The presence of *Corispermum* seeds in herbivore dung, tentatively assigned to *Mammuthus*, from Cowboy Cave[12] and Bechan Cave[14] in southeastern Utah, suggests one mode of dispersal. In the Yukon, associated dates from alluvium containing *Corispermum* seeds indicate an arrival time >38,000 yr BP. The best candidates for the Yukon and Alaskan records are probably *C. hyssopifolium* and *C. nitidum*, the only species presently in the region and the ones that were assumed to be recent European introductions. Beringian phytogeographers, taxonomists, and palaeoecologists disagree about the timing for intermingling of

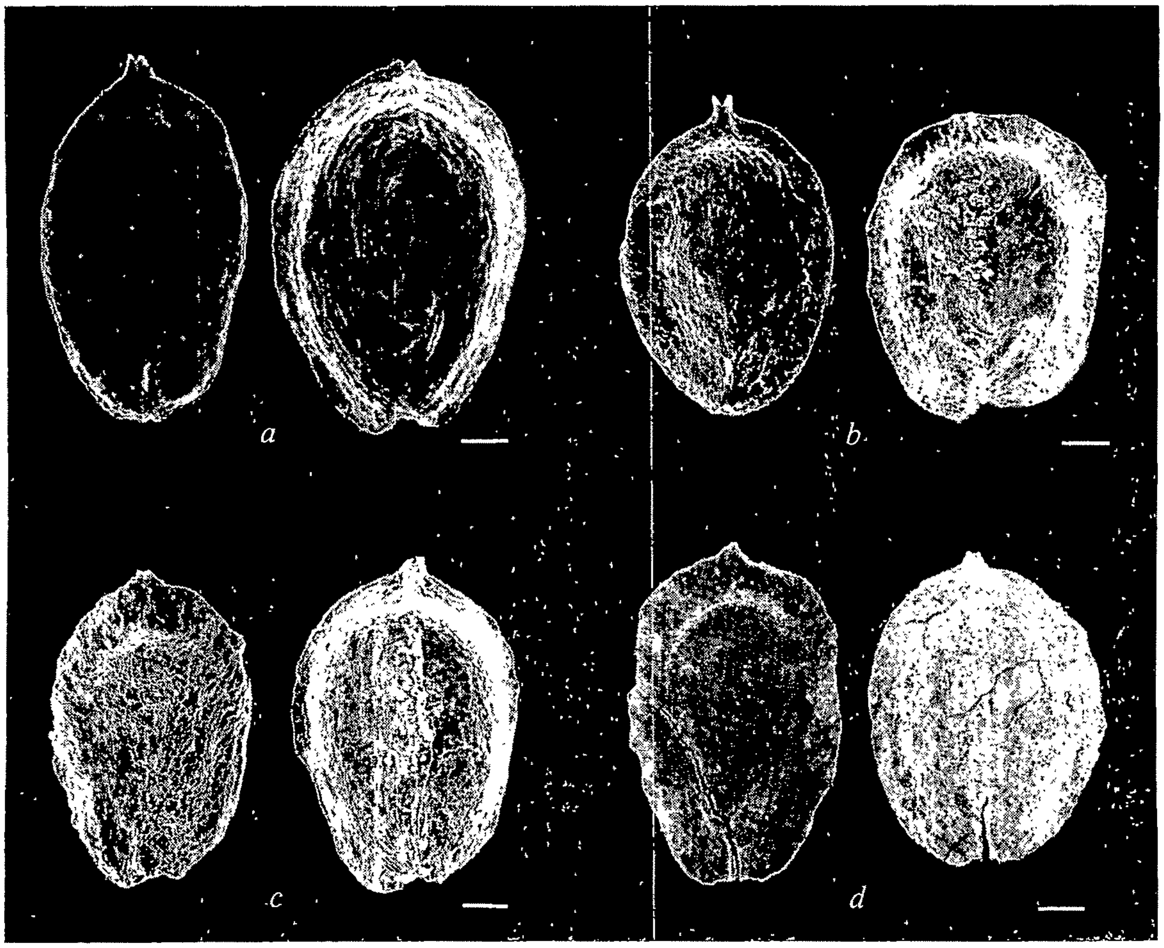

Fig. 1 Scanning electron micrographs of modern (*a–c*) and fossil (*d*) *Corispermum* seeds. Convex surfaces are shown on the left and concave ones on the right for each pair of seeds. Scale bars, 500 μm. *a*, Modern seeds of *C. hyssopifolium*; *b*, modern seeds of *C. nitidum*; *c*, modern seeds of *C. villosum*; *d*, fossil seeds from *Neotoma* midden in northwestern New Mexico. Seeds from this midden were directly dated by accelerator mass spectrometry to 3,880±240 yr BP. Note the similarity between *d* and *c*, a North American species with no Eurasian synonym.

Table 1 Select fossil localities for *Corispermum* in North America

Area	Site	Lat.	Long.	Context	Associated age (yr BP)	Direct age (yr BP)	Ref. for associated age
Yukon Territory, Canada	Bell Basin, Upper Porcupine River	66°56.7′ N	137°42.5′ W	Alluvium	>38,000 (GSC-2274)	None	10
Northwest Territory, Canada	Great Bear River	64°56.5′ N	125°29.75′ W	Alluvium	10,600±260 (GSC-2328)	9,970±460 (A-3748)	10
Arctic Coastal Plain, Alaska, USA	Ikpikpuk River	69°43.0′ N	154°53.0′ W	Alluvium	9,670±130 (I-11,073) 9,430±160 (I-13,174)	9,100±350 (A-3900)	11
Northern Arizona, USA	Grand Canyon, Shinumo no. 1	36°00.0′ N	112°29.0′ W	*Neotoma* midden	13,660±160 (A-1321) 12,070±600 (A-1444)	14,500±600 (A-3539)	18
Northwestern New Mexico, USA	Chaco Canyon, Gallo Wash no. 2	36°00.0′ N	108°00.0′ W	*Neotoma* midden	4,480±90 (A-1833)	3,880±240 (A-3364)	20
Southeastern Utah, USA	Cowboy Cave	38°19.0′ N	110°12,0′ W	Cave fill, human and herbivore coprolites	13,040±440 (A-1654) through 1,495±60 (SI-2425)	None	12
Southeastern Utah, USA	Bechan Cave	37°40.0′ N	110°45.0′ W	Herbivore coprolites	>11,670±300 (A-3212)	None	14

Associated ages are based on conventional radiocarbon dating of other organic material in same context as *Corispermum*. Direct ages were obtained by TAMS analyses of *Corispermum* seeds. All dates are in radiocarbon years before present. Radiocarbon laboratory numbers are enclosed in parentheses.

eastern and western steppe floras[22]. Because *Corispermum* may have undergone adaptive radiation and speciation after its arrival, perhaps within the past 2 Myr, its taxonomic and evolutionary status in North America should be critically re-examined.

Finally, plants of questionable origin are often herbaceous and thus contribute little biomass in depositional environments. More often than not, there is insufficient material (<1 g of carbon) for conventional β-counting methods. Hence, we anticipate application of direct radiocarbon determinations by TAMS, useful for samples of just a few milligrams, as a routine investigative tool to resolve questions about alien or native status for other problematical plants in the fossil record.

This work was funded in part by National Geographic Society grant 2410-81. The NSF Accelerator Facility for Radioisotope Analysis at the University of Arizona is supported by NSF Regional Instrumentation grant CHE 78-118576. We thank J. Matthews, R. Nelson, V. Bohrer, M. Toll, T. R. Van Devender, W. G. Spaulding, and O. K. Davis for loan of specimens or information about *Corispermum*, H. Hull for taking the scanning electron micrographs, T. Linick and L. Warneke for analytical support, and R. M. Turner and O. K. Davis for helpful reviews.

Received 19 June; accepted 13 August 1984.

1. Byrne, R. & McAndrews, J. H. *Nature* **253**, 726-727 (1975).
2. Rydberg, P. A. *Bull. Torr. Bot. Club* **24**, 191-192 (1897); **30**, 247 (1903); **31**, 404 (1904).
3. Weber, W. A. in *The Quaternary of the United States* (eds Wright, H. E. Jr & Fry, D. G.) 453-468 (Princeton University Press, 1965).
4. Dorn, R. D. *Manual of the Vascular Plants of Wyoming* (Garland, New York, 1977).
5. Hitchcock, C. L., Cronquist, A., Ownbey, M. & Thompson, J. W. *Vascular Plants of the Pacific Northwest: Part 2* (University of Washington Press, Seattle, 1964).
6. Martin, W. C. & Hutchings, C. R. *A Flora of New Mexico* (Cramer, 1980).
7. Hulten, E. *Flora of Alaska and Neighbouring Territories* (Stanford, California, 1968).
8. Rothrock, J. T. in *Report upon Geographical and Geological Surveys West of the One-hundredth Meridian* Vol. 6, 238 (US Government Printing Office, Washington DC, 1878).
9. Martin, A. C. & Barkley, W. D. *Seed Identification Manual* (University of California, Berkeley, 1961).
10. Matthews, J. V. Jr in *Paleoecology of Beringia* (eds Hopkins, D. M., Matthews, J. V. Jr, Schweger, C. E. & Young, S. B.) 127-150 (Academic, New York, 1982). Radiocarbon dates published in London, J. A. & Blake, W. Jr *Geol. Surv. Can. Pap.* 80-87 (1980)
11. Nelson, R. E. thesis, Univ. of Washington, Seattle (1982).
12. Jennings, J. *Univ. Utah Anthropol. Pap.* **104**, 1-224 (1980).
13. Donaldson, M. L. *Univ. Kansas Mus. Anthr. Pap.* **53**, 136-166 (1983).
14. Davis, O. K., Agenbroad, L., Martin, P. S. & Mead, J. I. *Carneg. Mus. Nat. Hist. Spec. Publ.* 8 (in the press).
15. Dennis, A. & Harlan, A. in *Archaeological Investigations at Antelope House* (eds Morris, D. P. *et al.*) (US National Park Service, Washington, DC, in the press)
16. Donaldson, L. and Toll, M. S. *Navajo Nat. Pap. Anthropol.* **14**, 1099-1179 (1983).
17. Pippin, L. C. thesis, Washington State Univ., Pullman (1979).
18. Van Devender, T. R. & Mead, J. I. *J. Ariz. Nev. Acad. Sci.* **11**, 16-22 (1976).
19. Betancourt, J. L. & Davis, O. K. *Quat. Res.* **21**, 56-64 (1984).
20. Betancourt, J. L. & Van Devender, T. R. *Science* **214**, 656-658 (1981)
21. Jull, A. J. T., Donahue, D. J., Zabel, T. H. *Nucl. Instrum. Meth.* **218**, 509-514 (1983).
22. Hopkins, D. M., Matthews, J. V. Jr, Schweger, C. E. & Young, S. B. *Paleoecology of Beringia* (Academic, New York, 1982).

Seabird colony distributions suggest competition for food supplies during the breeding season

R. W. Furness

Department of Zoology, University of Glasgow,
Glasgow G12 8QQ, UK

T. R. Birkhead

Department of Zoology, University of Sheffield,
Sheffield S10 2TN, UK

There is long-standing disagreement over the way in which seabird populations are regulated[1]. They may be regulated by density-dependent mortality during winter as a consequence of food shortage[2–4], shortage of nest sites[5–7], social factors[8], or not regulated at all[9]. Ashmole[10,11] argued that for tropical seabirds, density-dependent mortality of adults outside the breeding season is most unlikely because intraspecific competition for food close to the colony would result in prey depletion, causing adults to travel increasing distances for food as colony size increased. Breeding numbers could be regulated through a density-dependent reduction in reproductive output resulting from reduced rates of provisioning of chicks. This mechanism may not apply to seabird colonies in higher latitudes, however, because seasonal production might provide superabundant food supplies during the breeding season. Recent studies of the quantity of food consumed by breeding seabirds[12–15] suggest that prey depletion also occurs in temperate regions and invites a critical test of Ashmole's hypothesis. We present here an analysis of interactions between spatial distribution and size of seabird breeding colonies and provide support for Ashmole's suggestion that seabird numbers may be limited by intraspecific competition for food around colonies during the breeding season.

We tested the idea of prey depeletion by considering spatial distribution and sizes of seabird colonies, as a direct demonstration would require an expensive marine sampling programme. If Ashmole's model is correct, then in an area of uniform mean productivity, colony size should be strongly and negatively related to the number of competitors from other colonies which are feeding within the foraging range used by members of the colony.* Such a relationship would not be predicted by any of the other models. Indeed, if numbers were limited by nest sites, one might expect large colonies to be spatially aggregated (the opposite trend), as geologically similar islands will tend to occur together. Further, there is no reason to expect that any pattern in the distribution of islands should affect all four data sets.

Table 1 Correlations between seabird colony size and numbers at other colonies within a given range

Species	Range (km)	Mean no. of colonies within range	Correlation	*P*
Gannet	100	0.8	−0.92	<0.001
(12 colonies)	150	0.8	−0.92	<0.001
	200	1.0	−0.47	NS
	300	1.8	−0.51	NS
Puffin	50	0.7	−0.56	<0.05
(15 colonies)	100	2.5	−0.81	<0.001
	150	4.9	−0.88	<0.001
	200	6.6	−0.74	<0.001
	250	9.0	−0.58	<0.05
Shag	20	2.0	−0.45	<0.05
(27 colonies)	30	3.5	−0.54	<0.01
	40	4.9	−0.48	<0.05
	50	6.4	−0.58	<0.01
	60	7.2	−0.66	<0.001
	70	8.1	−0.32	NS
	80	9.3	−0.24	NS
Kittiwake	20	1.5	−0.55	<0.01
(22 colonies)	30	3.3	−0.49	<.05
	40	4.9	−0.67	<0.001
	60	8.8	−0.36	NS
	80	11.7	−0.32	NS
	100	14.5	−0.08	NS

Competition for food is a function of the density of conspecifics, which is proportional to the square root of the number of birds, so we have used square root transformations of numbers. NS, not significant.

Reliable census data for all colonies of a species in a restricted area of relatively uniform oceanography and productivity are scarce. We have analysed four sets; for gannets (*Sula bassana* (L.)), puffins (*Fratercula arctica* (L.)), shags (*Phalacrocorax aristotelis* (L.)) and kittiwakes (*Rissa tridactyla* (L.)) in parts of Britain and Ireland. To restrict our analysis to areas of relatively uniform oceanography, we considered the smallest possible

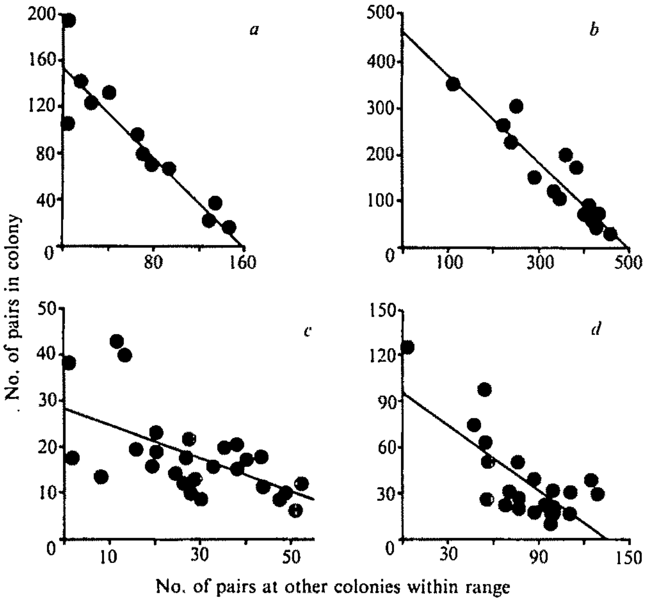

Fig. 1 Relationships between sizes of colonies and numbers at other colonies within a specific shortest sea distance for gannets, 100 km (*a*); puffins, 150 km (*b*); shags, 30 km (*c*); and kittiwakes, 40 km (*d*).

geographical area compatible with the need for an adequate sample size. For gannets, we used the most recent census data[16-18] for each colony founded before 1960 in Scotland, Ireland and Wales. We did not include colonies in England, France or the Faeroes; the first two are in an oceanographically different water mass[19], and the last is the only colony which is still heavily exploited by man as well as being distant from the colonies under consideration. We also ignored the four colonies founded in the 1970s because these are too young to have increased beyond a very small number of pairs and so are likely to be well below their optimum numbers. There is a high negative correlation for ranges of 100 km and 150 km. For greater ranges the correlation tends towards zero (Table 1). The highest correlation occurs where most colonies have only one other colony within their range and this leads to statistical difficulties of interpretation because points are not independent. This problem was overcome by carrying out 999 randomizations of colony sizes. None resulted in a correlation greater than that observed.

For puffins we took census data directly[20] and considered all colonies of over 1,000 pairs in Scotland north of 57°30′N, a total of 15 colonies holding over 97% of the Scottish puffin population[20]. There is a high negative correlation for ranges of 100-200 km (Table 1).

For shags we included all colonies of 40 pairs or more in Orkney and Shetland[21] (>95% of the Orkney and Shetland total[21]) and for kittiwakes we examined 1981 census data for Shetland[22]. Patterns for these species (Table 1) are similar to those already described. Species with shorter foraging ranges are more likely to be influenced by local variations in marine productivity; our assumption that mean productivity is uniform is a weakness of this test of Ashmole's hypothesis, but the fact that strong correlations do exist in spite of this strengthens our confidence in the result.

For puffins, and to a lesser extent for shags and kittiwakes, correlations over the shortest ranges are poorer than those over slightly greater ranges, partly due to the small number of colonies within the shortest range (Table 1). The tendency also arises because for short ranges the size of a colony may be influenced by the presence of a large colony just outside the range considered, whereas for large ranges the additional influence of a colony outside the range is very much less.

The strong negative relationships imply that seabird colony sizes are strongly influenced by numbers of conspecifics competing for food near to the colony. This interpretation is strengthened by the fact that the relationships are most pronounced over distances which match the foraging range of the species. Normal maximum foraging ranges of shags are 10-30 km[23,24], for kittiwakes 40-60 km[24], for puffins 10-150 km[24,25] and for gannets 100-150 km[16], while the closest relationships occur respectively over ranges of 30-60 km, 20-40 km, 100-200 km and 100-150 km (Fig. 1).

Numbers of nest sites may restrict the size of some particular colonies, but the distribution and size of other colonies usually compensates for this to raise the overall species' density to that limit set by food availability during the breeding season. The mechanism for the regulation of colony size is presumably through variations in recruitment in relation to colony breeding performance, possibly resulting from the tendency of young to recruit into their natal colony; however, recruitment processes in seabirds are poorly understood.

Received 15 June; accepted 20 August 1984.

1. Birkhead, T. R. & Furness, R. W. *Symp. Br. Ecol. Soc.* (Blackwell, London, in the press).
2. Lack, D. *The Natural Regulation of Animal Numbers* (Oxford University Press, 1954).
3. Lack, D. *Population Studies of Birds* (Oxford University Press, 1966).
4. Lack, . *Proc. XIV int. Orn. Congr.* **14,** 3-42 (1967).
5. Potts, G. R., Coulson, J. C. & Deans, I. R. *J. Anim. Ecol.* **49,** 465-484 (1980).
6. Duffy, D. C. *Auk* **10,** 680-688 (1983).
7. Manuwal, D. A. Thesis, Univ. Calif. Los Angeles (1972).
8. Wynne-Edwards, V. C. *Animal Dispersion in Relation to Social Behaviour* (Oliver & Boyd, Edinburgh, 1963).
9. Nelson, J. B. *Seabirds Their Biology and Ecology* (Hamlyn, London, 1980).
10. Ashmole, N. P. *Ibis* **103b,** 458-473 (1963).
11. Ashmole, N. P. *Avian Biology* Vol. 1, 112-286 (Academic, London, 1971).
12. Wiens, J. A. & Scott, J. M. *Condor* **77,** 439-452 (1975).
13. Furness, R. W. *J. Anim. Ecol.* **47,** 39-53 (1978).
14. Furness, R. W. & Cooper, J. *Mar. Ecol. Prog. Ser.* **8,** 243-250 (1982).
15. Schneider, D. & Hunt, G. L. *Mar. Biol.* **67,** 337-344 (1982).
16. Nelson, J. B. *The Sulidae: Gannets and Boobies* (Oxford University Press, 1978).
17. Murray, S. *Scott. Birds* **11,** 205-211 (1981).
18. Dennis, R. H. *Scottish Birds Annual Birds Reports* (Scottish Ornithologists' Club, 1979-83).
19. Bary, B. McK. *J. Fish. Res. Bd Can.* **20,** 789-815 (1963).
20. Harris, M. P. *Br. Birds* **69,** 239-264 (1976).
21. Cramp, S., Bourne, W. R. P. & Saunders, D. *The Seabirds of Britain and Ireland* (Collins, London, 1974).
22. Richardson, M. G. *Shetland Bird Report for 1982,* 54-64 (Shetland Bird Club, 1983).
23. Potts, G. R. *J. Anim. Ecol.* **38,** 53-102 (1969).
24. Pearson, T. H. *J. Anim. Ecol.* **37,** 521-552 (1968).
25. Harris, M. P. & Hislop, J. R. G. *J. Zool., Lond.* **185,** 213-236 (1978).

Excitatory amino acids directly depolarize rat brain astrocytes in primary culture

C. L. Bowman* & H. K. Kimelberg*†

Division of Neurosurgery* and Departments of Anatomy† and Biochemistry†, Albany Medical College, Albany,
New York 12208, USA

L-glutamic acid (L-Glu) and L-aspartic acid (L-Asp) are considered to be major excitatory amino acid transmitters, causing depolarization and excitation of neurones in the mammalian central nervous system (CNS)[1,2]. These responses have been thought to be an exclusively neuronal property as the excitatory amino acids either did not affect the potential of electrophysiologically unresponsive glial cells[3,4], or when an effect was seen, it was attributed to changes in external [K$^+$] (refs 5, 6). Here we report that L-Glu directly depolarizes immunocytochemically-identified astrocytes in primary culture. L- or D-Asp and kainic acid (KA) also depolarized these cells while none or minimal changes in the resting membrane potentials were found in response to *N*-methyl-D-aspartate, D-glutamate, taurine, L-glutamine or to the inhibitory amino acids γ-aminobutyric acid (GABA) and glycine. We conclude that the membrane potential of astrocytes can no longer be thought of as being responsive only to K$^+$ and that the electrophysiological effects of excitatory amino acids *in situ* may not be exclusively a neuronal property.

When astrocytes were bathed in a solution of L-Glu (10^{-4} M), rapid depolarization was detected, followed by a slow repolariz-

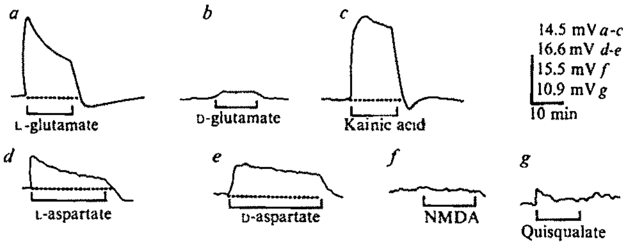

Fig. 1 *a*–*g*, Membrane potential responses of cultured astrocytes to excitatory amino acids and other agonists. NMDA, *N*-methyl-D-aspartate. Final concentrations of all additions were 10^{-4} M and perfused for the times marked on the figures. Dashed lines indicate pre-addition baseline. The temperature ranged between 35–37 °C and was maintained by heating the room. Membrane potentials of the cells shown before addition of the amino acids were *a*, −85; *b*, −87; *c*, −78; *d*, −56; *e*, −70; *f*, −86; *g*, −64 mV. Recordings shown in *a*–*g* are from separate cells. All cells responded to L-Glu (10^{-4} M).

Methods: Astrocytes were grown as primary cultures from neonatal rat brains as described previously[10,11,15,28], with the exception that the brain tissue was dissociated using a neutral protease (Dispase II, Boehringer-Mannheim)[29]. These cultures show ≥90% staining of the cells[10,28,29] for the astrocyte marker GFAP[8,9]. Membrane potentials were measured using standard electrophysiological recording techniques as previously described[11,15]. Microelectrodes were filled with 0.5 M K_2SO_4, buffered with 5 mM HEPES, *p*H 7.2 instead of KCl-filled electrodes as we have found that the use of K_2SO_4-filled microelectrodes allowed us to record from the cells for longer periods of time. The bathing medium consisted of 122 mM NaCl, 2.8 mM KCl, 1.2 mM KH_2PO_4, 1.3 mM $CaCl_2$, 0.4 mM $MgSO_4$, 10 mM D(+) glucose and 25 mM HEPES adjusted to *p*H 7.4 with NaOH (total [Na^+] was 140 mM and total [K^+] was 4.5 mM). The electrophysiological recordings were made under conditions of continuous perfusion using a Nikon Diaphot inverted microscope equipped with Hoffman modulation contrast optics as previously described[11]. The bathing medium and stock solutions (10 mM) of the amino acids were made in glass distilled water 1 to 2 h before use. L-glutamic acid hydrochloride was obtained from Sigma Chemical Co., St Louis, Missouri.

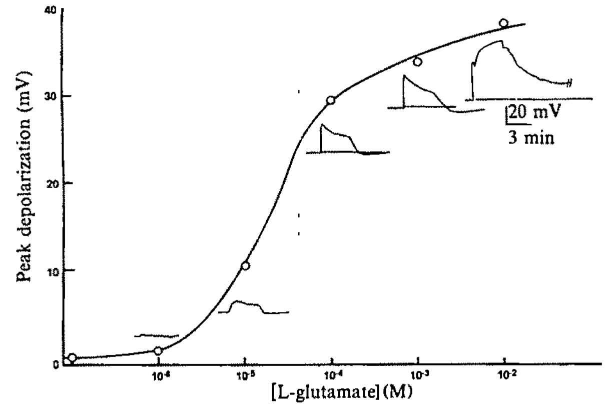

Fig. 2 Depolarizing responses to varying concentrations of L-glutamate. Initial peak depolarizations are plotted. Representative examples of the responses obtained at different concentrations are shown. Records are from a single cell. Other conditions are as in Fig. 1.

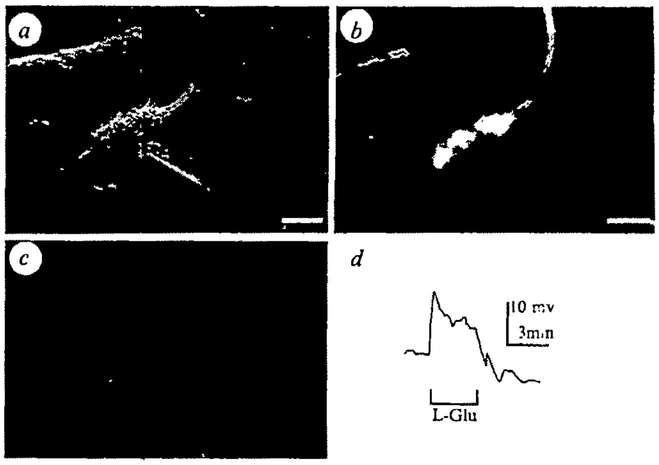

Fig. 3 Cells that are depolarized by L-Glu contain glial fibrillary acidic protein. *a*, Impaled cell viewed through Hoffman modulation contrast. Electrode is visible impaling cell from right-hand corner *b*, Same cell after fixation and staining for GFAP, viewed through fluorescent optics. Filamentous staining is clearly visible in processes. Bar in *a* and *b* represents 20 μM. *c*, Fluorescent micrograph of another coverslip where the primary antibody was absorbed with bovine GFAP. *d*, L-Glu (10^{-4} M) induced depolarization from same cell as in *a* and *b*. Resting membrane potential was −42 mV

Methods: Cells were recorded from as described in Fig. 1. The impaled cells were then photographed, an area on the underside of the coverslip was marked with a diamond object marker (Leitz) and photographs of the mark were made[11]. This procedure allowed us to identify the impaled cell after staining for GFAP After all recordings, photographs and marks were made the coverslip was removed and the cells stained for GFAP as described previously[11,28]. A monoclonal antibody (Amersham) directed against GFAP was used as the primary antibody. It was specified as being positive only for glial cells in human and rat brain and did not react with a variety of other tissues. The second antibody was goat anti-mouse IgG conjugated with fluorescein. Using a Nikon Labophot microscope the areas containing the impaled cells were identified by means of the marks previously made with the diamond object marker and the impaled cells identified using the photographs. Fluorescent micrographs were then taken of these cells. Controls were established by omitting the primary antibody, or by absorbing the primary antibody with bovine GFAP and were all negative (*c*). Also, neuronal primary cultures from rat hippocampus[30] did not stain using this monoclonal antibody.

ation in the continued presence of L-Glu (Fig. 1*a*). The removal of L-Glu resulted in a rapid repolarization which was followed by a transient hyperpolarization and then a slower recovery to the baseline membrane potential (Fig. 1*a*). The mean magnitudes of the L-Glu (10^{-4} M) induced depolarization, repolarization and hyperpolarization were 19±7 mV (mean ±s.d., 48 cells), 8±4 mV (48 cells) and 4±3 mV (46 cells) respectively. The resting membrane potentials were −71±10 mV (48 cells). We have observed an L-Glu induced depolarization in all cells (48 in total) tested from six different primary cell cultures. The age of these cultures ranged from 21 to 36 days. Perfusion of D-Glu (10^{-4} M, 4 cells) resulted in only a small depolarization (Fig. 1*b*) showing that the L-Glu-induced depolarization was stereospecific. Bathing the cells with KA (10^{-4} M, 7 cells), L-Asp (10^{-4} M, 3 cells) or D-Asp (10^{-4} M, 2 cells) also resulted in a depolarization of the resting membrane potential (Fig. 1*c*, *d* and *e*). The magnitude of the KA-induced depolarization was usually equivalent to that seen for L-Glu whereas the effect of L- or D-Asp was generally less. *N*-methyl-D-aspartate (NMDA) (10^{-4} M, 3 cells) and quisqualate (QA) (10^{-4} M, 5 cells) were without effect, or only minimally effective (≤4 mV) (Figs. 1*f*, *g*). The inhibitory amino acids, glycine (10^{-4} M, 10 cells), GABA (10^{-4} M, 4 cells), taurine (10^{-4} M, 3 cells) and the L-glutamate metabolite L-glutamine (10^{-4} M, 3 cells) had no effect on the membrane potentials (data not shown). The lack of effect of GABA may not be surprising as only a non-neuronal low affinity [^{3}H]-flunitrazepam binding site has been found in cultured glial cell membranes[7].

Figure 2 shows the responses from a single cell and demonstrates that the 50% effective concentration (EC_{50}) of the L-Glu-induced depolarization was approximately 50 μM. The shape of the response was altered at the highest concentration tested (10^{-2} M), with the appearance of a second slower depolarization that overcame the normal pattern of partial repolarization in the presence of L-Glu and a slower repolarization after removal of L-Glu (compare responses to 10^{-2} M L-Glu with 10^{-4} M L-Glu in Fig. 2). Similar results were obtained from another cell.

Since at least 90% of the cells in our cultures stain for glial fibrillary acidic protein (GFAP), and intermediate filament

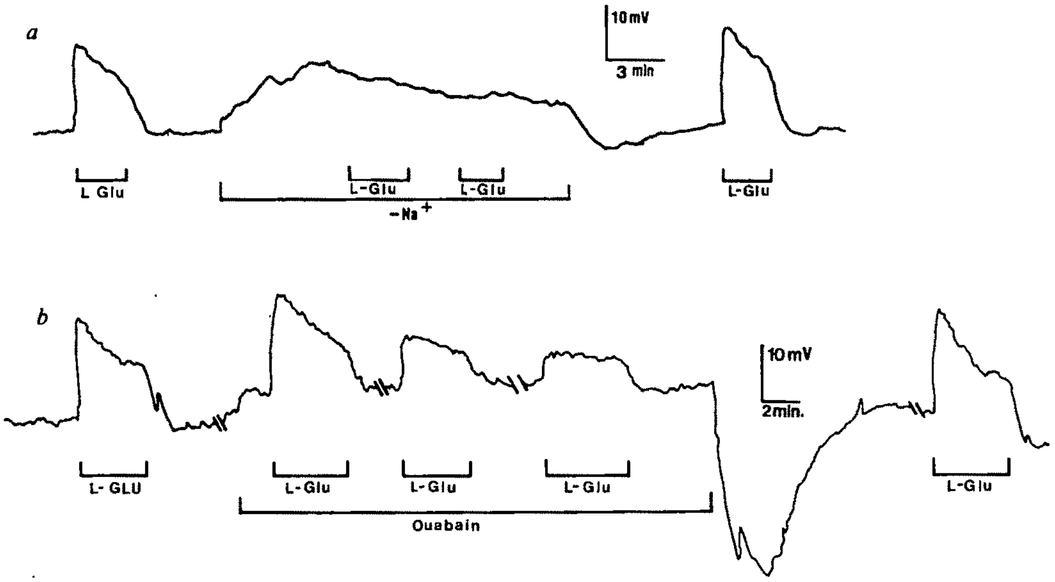

Fig. 4 The L-Glu induced depolarization requires external Na$^+$. [L-Glu] was 10^{-4} M. *a*, L-Glu response in normal Na$^+$ medium (see Fig. 1) and in the absence of Na$^+$ ($-$Na$^+$). In the latter case, Na$^+$ was replaced mole for mole by choline. In the absence of impalement removal of Na$^+$ either did not alter the electrode potential or at most changed it by 1-2 mV. Resting membrane potential of this cell was −72 mV. *b*, Effect of 1 mM ouabain on the L-Glu induced depolarization. The breaks in the tracings represent approximately 2 min. Resting membrane potential for this cells was −70 mV.

protein considered specific for astrocytes[8,9], and since the cells have essentially linear current-voltage characteristics[10,11], we considered it unlikely that all our electrophysiological recordings were from any contaminating neuronal cells. However, because it is well-established that L-Glu depolarizes and excites neurones and as previous investigators had found no evidence for a direct electrophysiological effect of L-Glu on mammalian glial cells *in vivo*[3] or *in vitro*[4-6], we determined whether the cells in our cultures depolarized by L-Glu were astrocytes by post-staining such cells for GFAP. Figure 3 shows a cell depolarized by L-Glu and showing positive staining for GFAP. Similar results were found in 2 other cells. Therefore, we conclude that astrocytes in our primary cultures are directly depolarized by L-Glu.

Astrocytes in primary culture show Na$^+$-dependent high affinity uptake of L-Glu[12,13]. Thus, an electrogenic uptake of L-Glu with Na$^+$ might be partially or wholly responsible for the depolarization. Alternatively, the L-Glu induced response could be the result of an increased Na$^+$ conductance. To test these alternatives we investigated the effect of removing external Na$^+$ on the L-glu-induced response. Removal of Na$^+$ (replaced with choline) alone resulted in a depolarization, initially of 14 mV which then repolarized by 6 mV (see Fig. 4*a*). We have previously reported [11,14] a depolarizing response to omission of external Na$^+$ in primary astrocyte cultures which we suggested could be partly due to inhibition of an electrogenic Na$^+$/K$^+$ pump and/or a secondary consequence of other effects of no external Na$^+$, such as modification of intracellular *p*H due to inhibition of Na$^+$/H$^+$ exchange. In the absence of external Na$^+$, perfusion of L-Glu had no further effect on the resting membrane potential (Fig. 4*a*). Subsequent addition of Na$^+$ and re-perfusion of L-Glu resulted in a normal L-Glu-induced depolarization identical to that seen before removal of external Na$^+$ (Fig. 4*a*). Similar results were obtained when Na$^+$ was replaced with arginine (data not shown). These results show that external Na$^+$ is required for the L-Glu induced depolarization. Because we found that the L-Glu-induced depolarization is not affected by tetrodotoxin (10^{-6} M) (data not shown) an involvement of veratridine-induced Na$^+$ channels that we have recently observed in these cells[11], is unlikely.

Although the present data do not allow us to distinguish between an electrogenic Na$^+$-dependent L-Glu uptake mechanism, or activation of an L-Glu receptor resulting in a depolarizing conductance change to Na$^+$, both mechanisms should involve an inward movement of Na$^+$. Thus, the repolarization in the continued presence of L-Glu could involve activation of an electrogenic Na$^+$/K$^+$ ATPase due to an increase in $[\mathrm{Na}^+]_i$. To test for this possibility, we studied the effect of ouabain on the L-Glu-induced response (Fig. 4*b*). Perfusion of L-Glu immediately after addition of ouabain showed no immediate change in the L-Glu induced depolarization and repolarization (Fig. 4*b*). With continued exposure to ouabain, however, there was a progressive decrease in the size of the initial depolarization due to L-Glu and the subsequent repolarization. This is likely to be a result of the gradual dissipation of the Na$^+$ gradient that occurs in these cells in response to ouabain[15]. Thus, the repolarization is not directly involved with activation of an electrogenic Na$^+$/K$^+$ pump, which should have been immediately inhibited by ouabain. Possible alternative mechanism for the repolarization could include receptor desensitization or an increased K$^+$ conductance. However, the Na$^+$/K$^+$ pump in these cells clearly has an electrogenic component as shown by the small initial, ouabain induced depolarization (4 mV) and by the large (30 mV) transient hyperpolarization seen when ouabain was removed (Fig. 4*b*). This large transient hyperpolarization is presumably caused by Na$^+$ loading of the cells in the presence of ouabain, causing increased activation of the electrogenic component of the Na$^+$/K$^+$ pump after removing the ouabain[16].

The L-Glu-induced depolarization of cells shown to contain GFAP, the block of this response by Na$^+$ removal, and the depolarization caused by L- or D-Asp and KA all show that astrocytes in primary culture are directly depolarized by excitatory amino acids via a Na$^+$-dependent mechanism. This conclusion differs from that inferred from previous studies both *in vivo* and *in vitro*, where depolarization of glial cells was either not seen after L-Glu application[3,4], or, when it was observed, was ascribed to increased external K$^+$ released from stimulated neurones[5,6]. However, the depolarization caused by L-Glu of non-excitable cells in guinea pig cortical slices, also attributed to increased external concentration of K$^+$, was followed by a distinct hyperpolarization[17]. This is similar to the response we have invariably observed in cultured astrocytes, suggesting that this effect may indeed occur in the mammalian CNS *in situ.* Also, L-glutamate-induced depolarization of non-mammalian glial cells from axon-free *Necturus* optic nerve[18] and Schwann cells of axon-free squid giant nerve fibre sheaths[19] has also been observed suggesting that this response is a highly conserved glial property. The present findings of amino acid-induced depolarization of astrocytes in culture can now be added to a growing list of neurotransmitter induced effects in glial cultures of which the majority have been identified by changes in cellular cyclic AMP content or by ligand binding studies[20-24]. However, α-adrenergic receptor induced depolarization of glia in explant cultures[25] or of astroctyes in primary cultures[26] has also been observed, as well as a tetrodotoxin-sensitive, veratridine-induced Na$^+$ channel in primary astrocyte cultures[11]. It thus appears that the membrane potential of astrocytes, and other glial cells[18,19], can no longer be thought of as being responsive only to changes in external K^+ concentrations[27].

This work was supported by grants NS19492 from NINCDS and BNS 821873 from NSF to H.K.K. We thank Dr J. Huston for bovine GFAP, Dr G. Banker for neuronal hippocampal cultures and Dr P. Del Vecchio for use of his Nikon Labophot microscope and goat anti-mouse IgG. We thank Drs C. J. Frangakis (Sterling-Winthrop Research Institute, Rensselaer, New York), D. O. Carpenter, J. ffrench-Mullen, D. Martin, N. T. Slater, J. Swann and R. Waniewski (New York State Division of Research Laboratories, Albany, New York) for helpful comments. We also thank Mrs M. V. Frangakis for growing the cell cultures and Mrs E. P. Graham for typing the manuscript.

Received 3 April; accepted 23 July 1984.

1. Watkins, J. C. & Evans, R. H. *A. Rev. Pharmac. Tox.* **21**, 165-204 (1981).
2. Watkins, J. C. in *Glutamate: Transmitter in the Central Nervous System* (eds Storm-Mathisen, J. & Johnston, B. W.) 1-24 (Wiley, Ltd., Chichester, 1981).
3. Krnjevic, K. & Schwartz, S. *Expl Brain Res.* **3**, 306-319 (1967).
4. Wardell, W. M. *Proc. R. Soc.* **165**, 326-361 (1966).
5. Hosli, L., Andres, F. & Hosli, E. *Neuroscience* **4**, 1593-1598 (1979).
6. Hosli, L. & Hosli, E. in *Glutamine, Glutamate and GABA in the Central Nervous System* (eds Hertz, L., Kvamme, E., McGeer, E. G. & Schousboe, A.) 441-455 (Alan R. Liss, Inc., New York, 1983).
7. McCarthy, K. D. & Harden, T. K. *J. Pharmac. exp. Ther.* **216**, 183-191 (1981).
8. Bignami, A., Dahl, D. & Rueger, D. in *Advances in Cellular Neurobiology* (eds Fedoroff, S. & Hertz, L.) 285-310 (Academic, London 1980).
9. Eng, L. F. in *Proteins of the Nervous System* (eds Bradshaw, R. & Schneider, D.) 85-117 (Raven, New York, 1980).
10. Kimelberg, H. K. Cell *Molec. Neurobiol.* **3**, 1-16 (1983).
11. Bowman, C. L., Kimelberg, H. K., Frangakis, M. V., Berwald-Netter, Y. & Edwards, C. *J. Neurosci.* **4**, 1527-1534 (1984).
12. Schousboe, A., Svenneby, G. & Hertz, L. *J. Neurochem.* **29**, 999-1005 (1977)
13. Fonnum, F. *J. Neurochem.* **42**, 1-11 (1984).
14. Kimelberg, H. K. *et al.* in *Head Injury: Basic and Clinical Aspects* (eds Grossman, R. & Gildenberg, P. L.) 31-44 (Raven, New York, 1982).
15. Kimelberg, H. K., Bowman, C. L., Biddlecome, S. & Bourke, R. S. *Brain Res.* **177**, 533-550 (1979).
16. Thomas, R. C. *Physiol. Rev.* **52**, 563-594 (1972).
17. Constanti, A. & Galvin, M. *Brain Res.* **153**, 183-187 (1978).
18. Tang, C.-M. thesis. Univ. Pennsylvania (1982).
19. Villegas, J. in *Dynamic Properties of Glia Cells* (eds Schoffeniels, E., Franck, G., Hertz, L. & Tower, D. B.) 207-215 (Pergamon, New York, 1978).
20. Van Calker, D. & Hamprecht, B. in *Advances in Cellular Neurobiology* Vol. 1 (eds Fedoroff, S. & Hertz, L.) 31-67 (Academic, New York, 1980).
21. Evans, T., McCarthy, K. D. & Harden, T. K. *J. Neurochem.* **43**, 131-138 (1984)
22. Ebersolt, C., Perez, M. & Bockaert, J. *J. Neurosci. Res.* **6**, 643-652 (1981)
23. Repke, H. & Maderspach, K. *Brain Res.* **232**, 206-211 (1982).
24. Trimmer, P. A., Evans, T., McCardy, M. S. & Harden, T. K. *J. Neurosci.* **4**, 1598-1606 (1984).
25. Hosli, L., Hosli, E., Zehntner, C., Lehmann, R. & Lutz, T. W. *Neuroscience* **7**, 2867-2872 (1982).
26. Hirata, H., Slater, N. T. & Kimelberg, H. K. *Brain Res.* **270**, 358-362 (1983)
27. Kuffler, S. W., Nicholls, J. G. & Orkand, R. K. *J. Neurophysiol.* **29**, 768-787 (1966)
28. Kimelberg, H. K., Stieg, P. E. & Mazurkiewicz, J. *J. Neurochem.* **39**, 734-742 (1982)
29. Frangakis, M. V. & Kimelberg, H. K. *Neurochem. Res.* **9**, 1685-1694 (1984)
30. Banker, G. A. & Cowan, W. M. *Brain Res.* **126**, 397-425 (1977)

Millisecond activation of transducin in the cyclic nucleotide cascade of vision

T. M. Vuong*, M. Chabre* & L. Stryer†

* Département de Recherche Fondamentale, Laboratoire de Biologie Moléculaire et Cellulaire, Centre d'Etudes Nucléaires-Grenoble, Bôite Postale 85X, F38041 Grenoble, France
† Department of Cell Biology, Stanford University School of Medicine, Stanford, California 94305, USA

Cyclic GMP has been implicated as a messenger molecule involved in visual transduction[1]. Photoexcited rhodopsin (R*) binds to a multisubunit membrane protein called transducin (T) and stimulates the exchange of a bound GDP molecule for GTP. This leads to the release of the α-subunit of T with bound GTP (T_α–GTP), which activates a cyclic GMP phosphodiesterase[2–6]. The question arises as to whether the hydrolysis of cyclic GMP that results from activation of the phosphodiesterase is sufficiently rapid to be involved in visual excitation, which occurs on a time scale of ~2 s in the single-photon limit[7]. Previous studies have suggested that the cyclic GMP phosphodiesterase is activated in less than 100 ms at moderate light levels[3,8,9]. We report here light scattering studies of magnetically orientated frog rod outer segments which show that a molecule of R* catalyses the activation of a molecule of T in about 1 ms. Thus, hundreds of molecules can be activated within the response time of vision in the single-photon limit, and the formation of T_α–GTP is fast enough for it to be a key step in visual transduction.

The near-infrared turbidity of rod outer segment (ROS) suspensions changes following excitation with a visible light pulse[10–16]. Kühn and co-workers[8] delineated three types of scattering changes by using reconstituted disk membranes containing different amounts of transducin: (1) an R* signal due to the bleaching of rhodopsin, (2) a binding signal due to the association of R* with T-GDP and (3) a dissociation signal due to the release of T-GTP from R* following GTP-GDP exchange. We have further analysed the physical basis and kinetics of the dissociation signal which is of interest because it arises from an amplified event in the cyclic nucleotide cascade. We magnetically oriented frog ROS fragments in a 6-kG field at 45° to an infrared beam (Fig. 1). We achieved a high degree of orientation because of the large diamagnetic anisotropy of the multiple transmembrane α-helices of rhodopsin[17–18]. The lattice spacing (29.5 nm) and intensities of the first four meridional orders of diffraction of these fragments are virtually the same as those of intact ROSs[19–20]. The lamellar organization of disks and the orientation of these ROS fragments (Fig. 1) allowed us to obtain new information concerning the activation of transducin. The amplitude dA of the light scattered at right angles on the left and right sides by a volume element dV located at P is given by the product of the scattering power $f(\mathbf{x})\,dV$ and a phase factor:

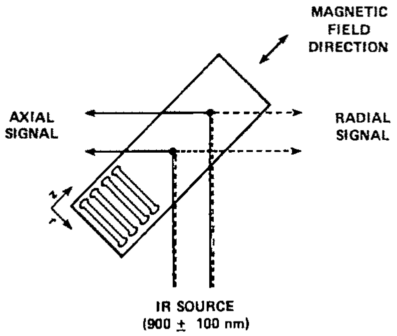

Fig. 1 Scattering geometry. ROS fragments in a 1-cm path length quartz cuvette were magnetically oriented at 45° to the incident 900±100 nm IR beam (900±100 nm). The intensity of light scattered at right angles to the incident beam was monitored by photodiodes located on the left and right sides by photovoltaic positive-intrinsic-negative diodes whose output was amplified, digitized and stored in 512 channels. The instrument response time was 0.1 ms. A photographic flash unit fitted with a 500-nm interference filter and a series of neutral density filters provided 0.5-ms light pulses to excite the sample via a light guide from below the curvette. ROSs obtained from the retinas of freshly dissected dark-adapted frogs (*Rana pipiens* and *Rana catesbieana*) were fragmented by being injected three times through a constricted 22-gauge hypodermic needle. This treatment made the plasma membrane sufficiently leaky to enable GTP to gain entry. These ROS fragments retained the native stacking of disks as judged by neutron scattering (measurement performed at ILL, Grenoble). A photodiode in the forward direction monitored the transmitted light intensity. The 500-nm excitation flash came from below via a light guide. Only axial changes (along the z direction) are seen by the detector on the left, whereas only radial changes (along the r direction) are seen by the detector on the right. The paths of the incident and scattered beams from scattering centres x and x' are shown

$$dA(\text{left}) = f(\mathbf{x}) \exp\left[-4\pi i z \sin(\pi/4)/\lambda\right] dV \quad (1)$$

$$dA(\text{right}) = f(\mathbf{x}) \exp\left[-4\pi i r \sin(\pi/4)/\lambda\right] dV \quad (2)$$

where z and r are the axial and radial coordinates, respectively, and λ is the wavelength of incident light. Now let dV move in the axial (z) direction from position $\mathbf{x}$ to $\mathbf{x}'$. It is evident from equations (1) and (2) that dA(left) will change because of the z-dependence of the exponential phase factor term, whereas

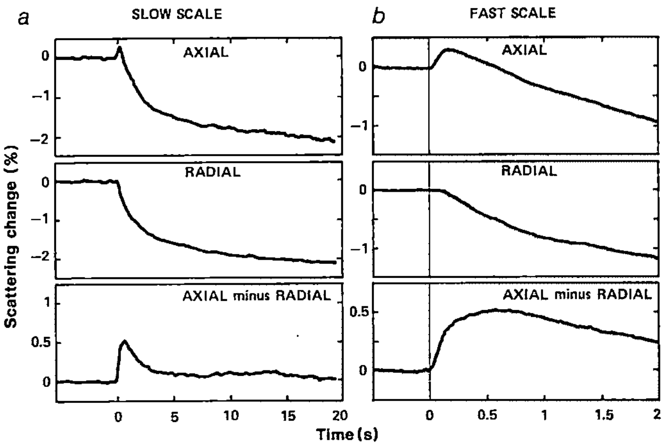

Fig. 2 Kinetics of the axial and radial light scattering changes and of their difference. A light pulse at $t=0$ produced $R^*=3.4\times10^{-4}$ (mol fraction). The sample contained about 10^6 ROS fragments (obtained from one retina) in 2 ml Ringer's solution (102 mM NaCl, 2.7 mM KCl, 1.9 mM $CaCl_2$, 2.1 mM $MgSO_4$, 2 mM $NaHCO_3$, 0.36 mM NaH_2PO_4, *p*H 7.4), 0.5 mM GTP, 23 °C. *a*, Slow time scale; *b*, fast time scale. The axial signal has a fast and a slow component whereas the radial signal has only the slow component. The slow scattering decrease has the same magnitude (2%) and decay time (4 s) in both axial and radial signals. *a*, *b* Bottom panels, axial signal minus the radial signal showing the rapid axial component alone. This signal has a rise time (initial time constant of the rising phase) of 100 ms and a decay time (initial time constant of the falling phase) of 4 s.

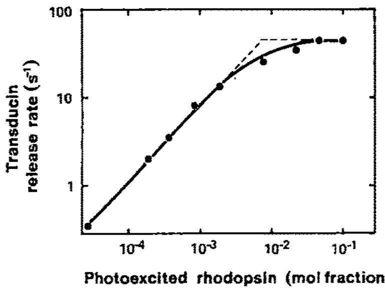

Fig. 3 Dependence of the transducin release rate on the mol fraction of photoexcited rhodopsin. GTP concentration, 0.5 mM. The release rates were determined from the slopes of the rise of the axial minus radial signals (for example, the bottom panel of Fig. 2*b*).

d*A*(right) will stay the same. Conversely, if d*V* is moved along the radial direction, d*A*(right) will change, whereas d*A*(left) will stay the same because the optical path length is unaltered. Thus, the detector on the left side monitors displacements in the axial direction only, whereas the one on the right side monitors displacements in the radial direction only. A displacement of molecules within the ROS fragment can be distinguished from a loss of molecules into the large aqueous space surrounding the fragments. In that event, $f(x)$ will be less and so d*A*(left) and d*A*(right) will decrease equally. A loss of scattering material from ROS fragments also leads to an increase in the intensity of transmitted light as monitored by a detector in the forward direction. A more detailed discussion of the characteristics of this θ-2θ scattering experiment is given elsewhere[24].

The light scattering changes produced by a light pulse forming 3.4×10^{-4} R* in the presence of 0.5 mM GTP are shown in Fig. 2. The axial signal is a combination of two components: a fast, transient scattering increase and a slow scattering decrease. The radial signal, in contrast, shows only a slow scattering decrease (Fig. 2). This slow decrease exhibits a lag of the same duration as the rise of the rapid axial signal.

The rapid axial increase in scattering probably arises from the release of transducin from the disk membrane surface into the inter-disk space following its activation to the GTP form. The decrease in scattering seen in both the radial and axial signals is probably due to the loss of soluble transducin from the ROS fragments. This loss of scattering material reduces the contrast between the ROS fragment and the surrounding medium by decreasing the refractive index of the fragment and slightly increasing that of the medium. Hence, a general decrease in scattering is observed in all directions. We will refer to the rapid axial increase as the release signal and to the slow decrease as the loss signal. The loss signal is 20-30 times larger than the release signal because the 900-nm incident beam is more effective in probing changes occurring on the scale of hundreds of nanometres than of a few nanometres. Several lines of evidence support this interpretation. (1) The release signal and loss signal show the same dependence on nucleotide and R* as does the activation of transducin. GTP or a hydrolysis-resistant analogue such as GTPγS or GppNHp is required for the appearance of both signals. ATP, GDP and GMP are ineffective. The amount of R* needed to elicit these signals is much less than the amount of transducin, indicating that R* has a catalytic role in the generation of these signals. (2) A release of transducin into the inter-disk space would give the observed exclusively axial signal because such a movement changes the *z* but not the *r* coordinate of the scattering units. (3) A loss of transducin from the ROS fragments would decrease the axial and radial scattering equally, as observed, because such a movement removes scattering material and thereby lowers the scattering density. (4) Complementary information was obtained by monitoring the intensity of transmitted light with a detector in the forward direction. An increase in the relative intensity of transmitted light having the same time course and amplitude as the loss signal was observed. This increase is the complement of the decrease observed by the left and right detectors, confirming that this signal is due to the loss of scattering material (T-GTP) from the ROS fragments. (5) Supernatants of ROS fragment suspensions illuminated in the presence of GTPγS contained all three subunits of transducin, as shown by SDS-polyacrylamide gel electrophoresis. In the absence of GTPγS or illumination, transducin remained bound to the ROS fragments, as expected from previous studies[21]. (6) Small ROS fragments (<10 μm in length) separated from large ones by centrifugation display a more rapid loss signal, as would be expected if their plasma membranes were rendered more leaky by extensive shearing. The kinetics of the release signal, in contrast, are independent of fragment size. (7) The loss signal exhibits a lag that matches the rise of the release signal. These signals are coupled because transducin must be released into the inter-disk space before it can leak out of the ROS fragment.

The loss signal corresponds to the dissociation signal observed by Kühn *et al.*[8] in their light scattering study of isotropic suspensions of homogenized bovine ROSs. The kinetics of their dissociation signal (~100 ms) was more rapid than the kinetics of our loss signal because of the small size and absence of a barrier to diffusion in their photoreceptor fragments.

The rise time of the release signal depends on the concentration of photoexcited rhodopsin. The rate of release *k*, expressed in units of mol fraction transducin released per s, is given by $k=\beta/\alpha$, where β is the maximal slope of the rise of the release signal (measured from the axial minus radial signal and expressed in units of % scattering change per s), and α is its maximal amplitude (% scattering change) in saturating conditions (1% bleach and 0.5 mM GTP). The dependence of the transducin release rate on the concentration of R* is shown in Fig. 3. The release rate is linearly proportional to R* at low light levels, ranging from $0.35\ s^{-1}$ at $R^*=3.6\times10^{-5}$ to $13\ s^{-1}$ at $R^*=1.8\times10^{-3}$. The number of molecules of transducin activated by a molecule of R* can be calculated from the slope of the linear region of the release rate versus R* plot. A release rate of $1\ s^{-1}$ at $R^*=10^{-4}$ corresponds to 1,000 molecules of transducin activated per s per molecule of R*, because the molar ratio of rhodopsin to transducin is 10. Thus, a molecule of transducin is activated to the GTP form by a molecule of R* in ~1 ms. At high light levels, the release rate becomes independent of R*, reaching a maximal value of $45\ s^{-1}$, which corresponds to a rise time of 22 ms. This limit is imposed by a step after the formation of metarhodopsin II, the photolytic intermediate that serves as R* (refs 22, 23), which occurs in 2 ms in our experimental conditions (23 °C).

It is of interest to compare the rate of activation of transducin with the kinetics of visual excitation. In the single-photon limit, the closure of sodium channels and consequent hyperpolarization of the plasma membrane are relatively slow, occurring in times of 1-2 s[7]. Extrapolation of our measurements to the single-photon limit shows that a single molecule of R* can activate 500 molecules of transducin in 0.5 s. Hence, the activation of transducin to the GTP form and its release into the inter-disk space occur sufficiently rapidly to enable T-GTP to serve as an amplified intermediate in visual excitation.

This work was supported by research grants from the National Eye Institute and the National Institute of General Medical Sciences (to L.S.) and the Comité des Membranes Biologiques, DGRST (to M.C.). T.M.V. was the recipient of an NIH training grant award (GM-07276).

Received 21 May; accepted 15 August 1984.

1. Miller, W. H. & Nicol, G. D. *Nature* **280**, 64-66 (1979).
2. Bitensky, M. W., Wheeler, G. L., Yamazaki, A., Rasenick, M. M. & Stein, P. J. *Curr. Topics Membrane Transport* **15**, 237-271 (1981).
3. Liebman, P. A. & Pugh, E. N. *Curr. Topics Membrane Transport* **15**, 157-170 (1981).
4. Fung, B.K.-K., Hurley, J. B. & Stryer, L. *Proc. natn. Acad. Sci. U.S.A.* **78**, 152-156 (1981).
5. Stryer, L. *Cold Spring Harb. Symp. quant. Biol.* **48**, 841-852 (1984).
6. Hurley, J. B. & Stryer, L. *J. biol. Chem.* **257**, 11094-11099 (1982).
7. Baylor, D. A., Lamb, T. D. & Yau, K.-W. *J. Physiol., Lond.* **288**, 589-611 (1979).
8. Kühn, H., Bennett, N., Michel-Villaz, M. & Chabre, M. *Proc. natn. Acad. Sci. U.S.A.* **78**, 6874-6877 (1981).
9. Bennett, N. *Eur. J. Biochem.* **123**, 133-139 (1982).
10. Bignetti, E., Cavaggioni, A., Fasella, P., Ottonello, S. & Rossi, G. L. *Molec. cell. Biochem.* **30**, 93-99 (1980).
11. Harary, H. H., Brown, J. E. & Pinto, L. H. *Science* **202**, 1083-1085 (1978).
12. Hofmann, K. P. & Emeis, E. *Biophys. Struct. Mech.* **8**, 23-34 (1981).
13. Hofmann, K. P., Schleicher, A., Emeis, D. & Reichert, J. *Biophys. Struct. Mech.* **8**, 67-93 (1981).
14. Hofmann, K. P., Uhl, R., Hofmann, W. & Kreutz, W. *Biophys. Struct. Mech.* **2**, 61-77 (1976).
15. Reichert, J. & Hofmann, K. P. *Biophys. Struct. Mech.* **8**, 95-105 (1981).
16. Uhl, R., Hofmann, K. P. & Kreutz, W. *Biochim. biophys. Acta* **469**, 113-122 (1977).
17. Chabre, M. *Proc. natn. Acad. Sci. U.S.A.* **75**, 5471-5474 (1978).
18. Worcester, D. L. *Proc. natn. Acad. Sci. U.S.A.* **75**, 5475-5477 (1978).
19. Saibil, H., Chabre, M. & Worcester, D. *Nature* **262**, 266-270 (1976).
20. Yeager, M., Schoenborn, B., Engelman, D., Moore, P. & Stryer, L. *J. molec. Biol.* **137**, 315-348 (1980).
21. Kühn, H. *Nature* **283**, 587-589 (1980).
22. Bennett, N., Michel-Villaz, M. & Kühn, H. *Eur. J. Biochem.* **127**, 97-103 (1982).
23. Emeis, D., Kühn, H., Reichert, J. & Hofmann, K. P. *FEBS Lett.* **143**, 29-34 (1982).
24. Vuong, T. M. thesis, Stanford Univ. (1984).

Electrogenic Na–Ca exchange in retinal rod outer segment

King-Wai Yau & Kei Nakatani

Department of Physiology and Biophysics, University of Texas Medical Branch, Galveston, Texas 77550, USA

Previous work has suggested that a Na–Ca exchanger may have a key role in visual transduction in retinal rods[1–10]. This exchanger is thought to maintain a low internal free Ca^{2+} concentration in darkness[4–10] and to contribute to the rod's recovery after light by removing any internally released Ca^{2+} (refs 1, 2, 6–8). Little else is known about this transport mechanism in rods. We describe here an inward membrane current recorded from single isolated rods which appears to be associated with such external Na^+-dependent Ca^{2+} efflux activity. External Na^+, but not Li^+, could generate this current; high external K^+ inhibited it while small amounts of La^{3+} (10 μM) completely abolished it. The exchanger can also transport Sr^{2+}, but not Ba^{2+} or other divalent cations. The exchange ratio was estimated to be $3Na^+ : 1Ca^{2+}$. As well as demonstrating clearly the Na–Ca exchanger in the rod outer segment, our experiments also cast serious doubt on the commonly held view that light simply releases internal Ca^{2+} to bind to and block the light-sensitive conductance.

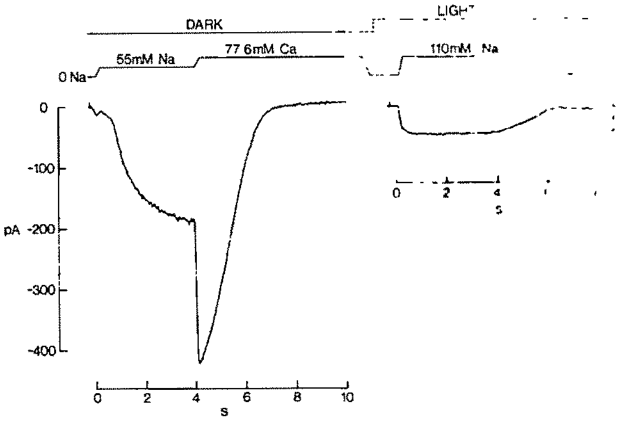

Fig. 1 Electrogenic Na^+-dependent Ca^{2+} efflux, or Na-Ca exchange, recorded from a toad rod after Ca^{2+} loading. Under infrared light a piece of retina from a dark-adapted toad (*Bufo marinus*) was finely chopped in Ringer's solution, yielding some isolated rods with intact outer and inner segments[7]. Membrane current from one of these rods was recorded by sucking its inner segment into a close-fitting glass pipette containing Ringer's solution while its outer segment was rapidly perfused[6,8,9]. Recordings were made with a current-to-voltage converter connected to the suction pipette. Time courses of solution changes, as indicated by junction currents[7], were ~200 ms and are shown above the sweeps. The valve controlling solution changes was operated pneumatically and with electronic timing so that the solution changes could be exactly reproduced many times. The exchange current was measured as the difference in recorded current on restoring Na^+ to a Na^+-free solution, done in light before and after the Ca^{2+} load. The light-sensitive current in darkness was obtained as the difference between total current recorded in darkness (light-sensitive current plus junction current) and junction current recorded in a repeated run in light. Outward membrane current across the outer segment is plotted upwards on the ordinate scale. All solutions except the isotonic (77.6 mM) Ca^{2+} solution contained ~1 μM buffered Ca^{2+}, with the following composition (in mM): 110 Na^+ or choline in partial or full substitution, 2.5 K^+, 1.5 Mg^{2+}, 0.093 Ca^{2+}, 119.7 Cl^-, 2 Mg-EDTA, 5 TMA (tetramethylammonium)–HEPES, 5 dextrose, *p*H 7.6. The isotonic Ca^{2+} solution contained (in mM): 77.6 $CaCl_2$, 5 TMA–HEPES, 5 dextrose, *p*H 7.6. The time lapse between Ca^{2+} loading and subsequent extrusion was ~26 s. Recordings were low pass-filtered at 100 Hz, 8-pole; room temperature. Steady light for junction current and exchange current measurements delivered about 800 photons (500 nm) $\mu m^{-2}\ s^{-1}$, unpolarized. Dark Ca^{2+} loading was 588 pC, or $\sim 1.8 \times 10^9$ Ca^{2+} ions.

We recorded the Na–Ca exchange current from an isolated, dark-adapted rod after its outer segment was loaded with Ca^{2+} (Fig. 1). Ca^{2+} loading was readily achieved as the light-sensitive conductance was highly permeable to divalent cations, especially after initial exposure to a Na solution containing low Ca^{2+} (refs 7, 9, 10). In order to isolate the exchange current, the recording was made normally in the presence of light which completely shut off the light-sensitive conductance; this conductance is thought to be the only ionic conductance in the plasma membrane of the outer segment[11,12]. The current, which was inward and transient, was seen only after the outer segment was loaded with Ca^{2+}, and not with monovalent cations such as Na^+, K^+ or Li^+. However, loading with Sr^{2+} (but not Ba^{2+} or other divalent cations such as Mg^{2+} or Mn^{2+}) also induced a similar current. We observed detectable but substantially smaller inward currents when much smaller Ca^{2+} or Sr^{2+} loads were effected by omitting the initial exposure to low external Ca^{2+} before introducing isotonic Ca^{2+} or Sr^{2+}.

The size of the current depends on the transmembrane electrochemical gradients for both Na^+ and Ca^{2+}, and the total charge transfer due to the current appears to depend only on the Ca^{2+} load (Fig. 2). These observations suggest that the current is associated with electrogenic Na^+-dependent Ca^{2+} efflux rather than ion movement through a novel membrane conductance being turned on by a rise in internal Ca^{2+} (ref. 13). The inward direction of the current suggests that more than two Na^+ ions enter the outer segment in exchange for each Ca^{2+} ion extruded. Assuming that the Ca^{2+} load is entirely removed

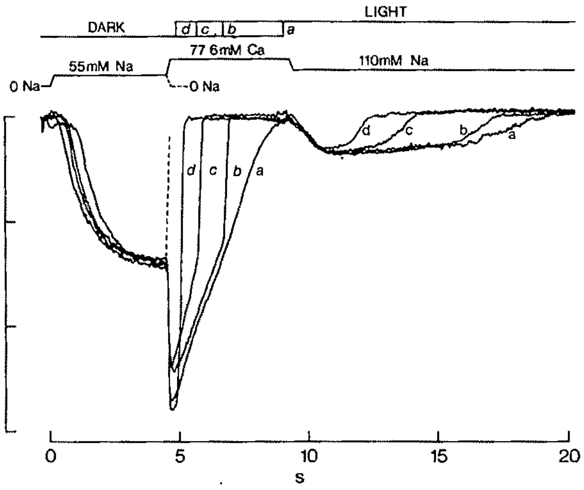

Fig. 2 Dependence of Na-Ca exchange current on size of Ca^{2+} load. The Ca^{2+} load was controlled by light which completely shut off the dark Ca^{2+} influx at various times, as shown by traces *a*–*d*. All records are from the same cell. All solutions and experimental conditions were the same as in Fig. 1, the only other difference being that the Na^+-free solution was not interposed between the 77.6 mM Ca^{2+} and the 110 mM Na^+ solutions in order to minimize the time lapse between Ca^{2+} load and subsequent extrusion. The broken line indicates the time course of decline of the Na^+ current if 0 Na^+ 110 mM Choline is introduced instead of 77.6 mM Ca^{2+}. The Ca^{2+} loads (Q_{load}) were *a*, 562; *b*, 404; *c*, 230; and *d*, 139 pC, equivalent to $\sim 1.7 \times 10^9$, 1.2×10^9, 6.9×10^8 and 4.2×10^8 Ca^{2+} ions respectively. The charge ratios $Q_{load}/Q_{exchange}$ were *a*, 2.38; *b*, 2.02; *c*, 1.87; and *d*, 2.43 (mean 2.18). This ratio is related to the stoichiometry (n) of the exchange (that is, n Na^+ : 1 Ca^{2+}) by $Q_{load}/Q_{exchange} = 2/(n-2)$. Hence n was 2.92. From 18 experiments the average value of n was 2.94 ± 0.10 (±s.d.). (In Figs 1 and 3, n was not computed because of the relatively long time between Ca^{2+} loading and readmission of external Na^+ (26–111 s). Other experiments have indicated that a long time lapse tends to allow some of the Ca^{2+} influx to slowly leave the outer segment via an alternative route, most probably by diffusion into the inner segment (see also ref. 8).) Steady light delivered 300 photons (500 nm) μm^{-2} s^{-1}, unpolarized; this produced $\sim 4.5 \times 10^3$ photoisomerizations s^{-1}, assuming an effective collecting area of 15 μm^2 (see ref. 22). Light itself should also trigger some Ca^{2+} efflux even in the absence of Ca^{2+} loading[1,2,8]. From estimates obtained by others[1,2,8], this additional efflux even at high light intensities is unlikely to be over 10^7 Ca^{2+} ions s^{-1}, corresponding to an inward exchange current of ~1.6 pA. However, most of this current should already have been subtracted from the records because each record was obtained as the difference between two runs in the same light conditions (Fig. 1 legend). As the exchange current induced by a Ca^{2+} load as reported here is typically 30–40 pA, the error introduced to the above analysis by the light-triggered Ca^{2+} efflux should be less than a few per cent.

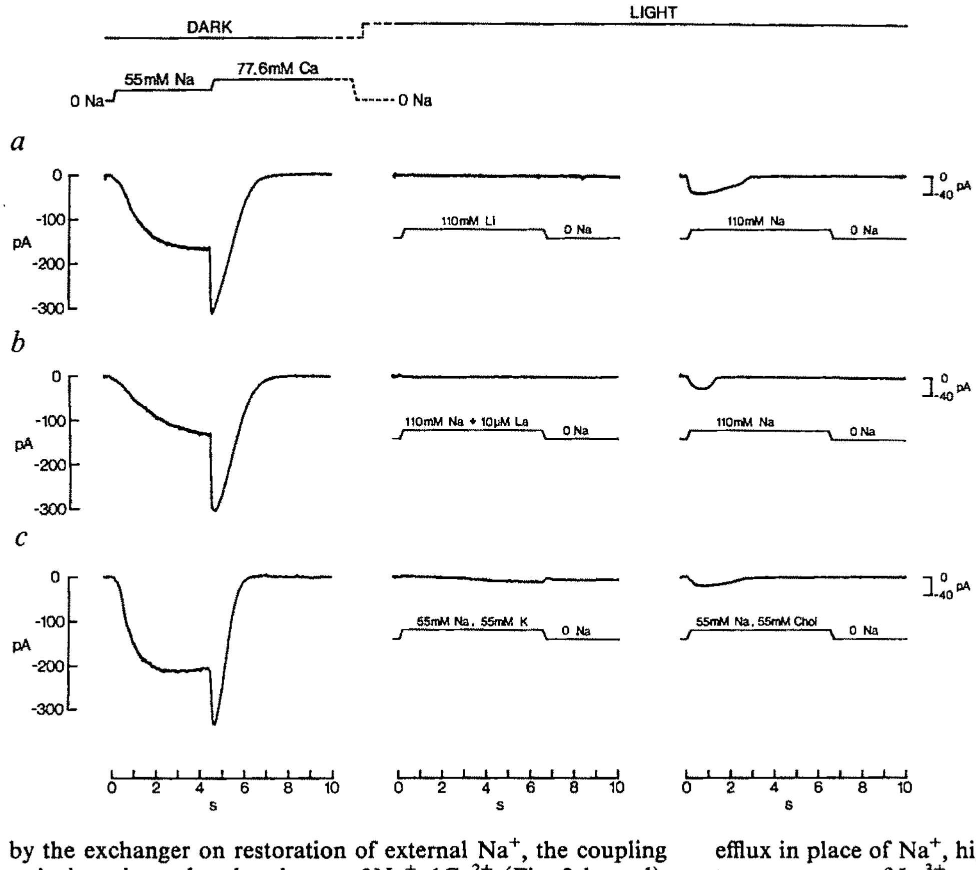

Fig. 3 Effects of external Li^+, La^{3+} and K^+ on the Na-dependent Ca^{2+} extrusion. Three different cells in *a*, *b* and *c*. In each experiment, the test solution containing Li^+, La^{3+} or high K^+ was followed by a control Na^+ solution. *a*, *c*, Na^+ (including 0 Na^+) and Li^+ solutions identical in composition to those in Fig. 1 with a buffered Ca^{2+} concentration of ~1 μM. *b*, Na^+ solutions contained nominally (that is, unbuffered) zero Ca^{2+} as follows (in mM): 110 Na^+, 2.5 K^+, 1.6 Mg^{2+}, 0 Ca^{2+}, 115.7 Cl^-, 5 TMA-HEPES, 5 dextrose, pH 7.6. Time lapse between Ca^{2+} load and admission of test solution: *a*, 37 s; *b*, 57 s; *c*, 33 s. Time lapse between Ca^{2+} load and admission of control Na^+ solution: *a*, 73 s; *b*, 111 s; *c*, 51 s. Steady light delivered 800 Photons (500 nm) μm^{-2} sec^{-1}, unpolarized.

by the exchanger on restoration of external Na^+, the coupling ratio is estimated to be close to 3Na^+ : 1Ca^{2+} (Fig. 2 legend). Since the Ca^{2+} loading and the subsequent extrusion by the exchanger could be repeated reversibly many times on the same cell, the above assumption seems reasonable. It has previously been suggested[2] that an uncoupled Ca^{2+} efflux might also exist at the outer segment; such a mechanism should generate an outward membrane current, however, which we have not detected. If present, this uncoupled Ca^{2+} efflux probably saturates at very low capacity and produces an outward current too small to be detected in our experimental conditions. The exchange ratio of 3 Na^+ : 1 Ca^{2+} is similar to some estimates obtained from other types of cells[14,15].

We have examined several properties of this exchange current (Fig. 3) and found that external Li^+ cannot support the Ca^{2+} efflux in place of Na^+, high external K^+ inhibits the efflux, and trace amounts of La^{3+} completely abolish it. These results confirm indirect evidence from earlier experiments about the actions of these ions on rods[4–7,9,10,16] and they suggest also that this exchanger in rods may share some similar properties with that found elsewhere, for example squid axon[17,18].

One striking feature of the Na-Ca exchanger in rods is its large Ca^{2+} pumping capacity. In the experiment of Fig. 1, for example, calculations show that the Ca^{2+} influx during exposure to isotonic Ca^{2+} should have increased the total Ca^{2+} concentration within the outer segment by ~2 mM; yet it took the exchanger only seconds to remove this excess Ca^{2+} and allow recovery of the cell. We observed rather similar effectiveness in pumping when a normal (1 mM) instead of low Ca^{2+} concentration was present externally during Ca^{2+} extrusion. In normal circumstances, when the steady Ca^{2+} influx through the light-sensitive conductance in darkness is likely to be relatively small[9,10], the exchanger should run well below its maximal capacity.

Collective evidence so far[4,5,7,9,10,19-21] has clearly indicated that a rise in internal Ca^{2+} somehow leads to the blockage of the light-sensitive conductance. In view of this, it is rather surprising that the large Ca^{2+} current in, for example, Fig. 1 switches off relatively slowly despite a peak influx of as many as 10^9 Ca^{2+} ions s^{-1}; thus, the current declines only by ~50 % after 1.4×10^9 Ca^{2+} ions have entered. It might be argued that Ca^{2+} buffering within the rod outer segment is so extremely rapid and powerful as to be able to maintain low internal free Ca^{2+} despite this very large influx. This, however, seems highly unlikely because we found that much smaller Ca^{2+} loads in the same conditions also led to a large increase in exchange current in darkness (data not shown), suggesting a rapid rise in free Ca^{2+} within the outer segment. Internal Ca^{2+} most probably does not act by binding directly to and blocking the conductance, or perhaps it requires additional cellular substrates to express fully its blocking action. In contrast, the large Ca^{2+} current could be completely shut off within ~300 ms by light at an intensity causing about 5×10^3 photoisomerizations s^{-1} in the rod outer segment (Fig. 2). From other estimates[1,2,8], any rise in internal free Ca^{2+} triggered by the light during this period is probably only ~10^7 ions, far less than that caused by the Ca^{2+} influx through the light-sensitive conductance. This suggests that the ability of light to block the conductance results from its modulation of other cellular substrates which act more directly or perhaps more effectively on the conductance.

We thank Professors Alan Hodgkin, Denis Baylor, L. E. Moore and Drs Peter McNaughton and Brian Nunn for discussions. We also thank Dr Kenneth Nielsen for help in computer programming. This work was supported by the US National Eye Institute and the Retina Research Foundation, Houston, Texas.

Received 12 June; accepted 14 August 1984.

1. Yoshikami, S., George, J. S. & Hagins, W. A. *Nature* **286**, 395–398 (1980).
2. Gold, G. H. & Korenbrot, J. I. *Proc. natn. Acad. Sci. U.S.A.* **77**, 5557–5561 (1980).
3. Schnetkamp, P. P. M., Daemen, F. J. M. & Bonting, S. L. *Biochim. biophys. Acta* **468**, 259–270 (1977).
4. Fain, G. L. & Lisman, J. E. *Prog. Biophys. molec. Biol.* **37**, 91–147 (1981).
5. Bastian, B. L. & Fain, G. L. *J. Physiol., Lond.* **330**, 331–347 (1982).
6. Yau, K.-W., McNaughton, P. A. & Hodgkin, A. L. *Nature* **292**, 502–505 (1981).
7. Hodgkin, A. L., McNaughton, P. A., Nunn, B. J. & Yau, K.-W. *J. Physiol., Lond.* **350**, 649–680 (1984).
8. Schröder, W. H. & Fain, G. L. *Nature* **309**, 268–270 (1984).
9. Yau, K.-W. & Nakatani, K. *Nature* **309**, 352–354 (1984).
10. Hodgkin, A. L., McNaughton, P. A. & Nunn, B. J. *J. Physiol., Lond.* (in the press).
11. Baylor, D. A. & Lamb, T. D. *J. Physiol., Lond.* **328**, 49–71 (1982).
12. Baylor, D. A. & Nunn, B. J. *J. Physiol., Lond.* (in the press).
13. Meech, R. W. *A. Rev. Biophys. Bioengng* **7**, 1–18 (1978).
14. Blaustein, M. P. & Hodgkin, A. L. *J. Physiol., Lond.* **200**, 497–527 (1969).
15. Blaustein, M. P. in *Electrogenic Transport: Fundamental Principles and Physiological Implications* (eds Blaustein, M. P. & Lieberman, M.) 129–147 (Raven, New York, 1984).
16. Cervetto, L. & McNaughton, P. A. *J. Physiol., Lond.* **341**, 75–76P (1983).
17. Blaustein, M. P. & Russell, J. M. *J. Membrane Biol.* **22**, 285–312 (1975).
18. Baker, P. & McNaughton, P. A. *J. Physiol., Lond.* **276**, 127–150 (1978).
19. Hagins, W. A. & Yoshikami, S. *Expl Eye Res.* **18**, 299–305 (1974)
20. Brown, J. E., Coles, J. A. & Pinto, L. H. *J. Physiol., Lond.* **269**, 707–722 (1977).
21. MacLeish, P. R., Schwartz, E. A. & Tachibana, M. *J. Physiol., Lond.* **348**, 645–664 (1984).
22. Baylor, D. A., Lamb, T. D. & Yau, K.-W. *J. Physiol., Lond.* **288**, 612–634 (1979).

Abrogation of resistance to bone marrow transplantation by induction of specific tolerance in natural killer cells?

Martin Waterfall, Lee S. Rayfield & Leslie Brent

Department of Immunology, St Mary's Hospital Medical School, Paddington, London W2 1PG, UK

Hybrid resistance describes the capacity of first generation (F_1) hybrids between certain mouse strains to inhibit the growth of tumour or haematopoietic cells of parental origin[1,2]. The cells that appear to mediate this phenomenon differ from classical T and B lymphocytes in several respects. For example, they are unusually radioresistant[3], show no immunological memory[4], are present in thymectomized[5] or congenitally athymic[6] mice, and are not functional until about 3 weeks after birth[3,4]. These characteristics suggest that the effectors are natural killer (NK) cells[7]. Although most of the evidence implicating NK cells in hybrid resistance is circumstantial, the experiments of Warner and Dennert[8] are more direct in that they show that resistance can be restored to mice with a congenital or induced defect in NK activity by the infusion of cells belonging to an NK clone. Conversely, treatment of mice with an antibody to NK cells abrogated hybrid resistance to parental bone marrow grafts[9]. Both NK cells and the effectors of hybrid resistance are generally considered to be nonspecific. We have now investigated this assumption by attempting to prevent hybrid resistance by neonatal tolerance induction with parental strain antigens. Our data indicate that hybrid resistance can be abrogated by this means and that the tolerance is specific and transferable with Thy-1⁺ spleen cells.

Groups of (CBA/Ca × C57BL/Gr)F_1 hybrid mice ($H\text{-}2^{k/b}$) received varying doses of adult C57BL/Gr bone marrow cells intraperitoneally within 24 h of birth and were tested 2–3 months later for their capacity to resist the engraftment of parental or F_1 hybrid bone marrow cells following lethal whole body irradiation (8.0 Gy). The 'take' of the grafts was assessed by the incorporation of ^{125}I-labelled 5-iodo-2′-deoxyuridine in the recipient spleens (see Fig. 1 legend for experimental details).

Hybrid resistance is clearly demonstrated in Fig. 1. Normal F_1 recipients of C57BL bone marrow failed to incorporate significant levels of the label (Fig. 1*c*) compared with mice that had received syngeneic F_1 cells (Fig. 1*a*). The neonatal inoculation of C57BL cells had no effect on the engraftment of F_1 cells (Fig. 1*b*) but prevented rejection of C57BL cells (Fig. 1*d*). Although in this experiment the take of C57BL bone marrow cells was virtually the same as that of F_1 cells, it tended to be lower in most other experiments (see Fig. 2). Neonatal exposure to parental strain bone marrow antigens thus had a profound effect on the development of hybrid resistance. Unexpectedly, cells from the SJL/J strain ($H\text{-}2^s$), which are likewise rejected by (CBA × C57BL)F_1 mice (Fig. 1*e*), were unaffected by the tolerance (Fig. 1*f*). This result, which has been obtained consistently in eight separate experiments, shows conclusively that the tolerance mechanism operative in this system is strain specific and suggests that haematopoietic resistance is mediated by more than one population of effector cells.

The dose of cells inoculated neonatally varied between 1.0 and 4.0×10^7. The data in Fig. 1 were based on 1.5×10^7 cells, but in the other seven experiments 4.0×10^7 cells were used; we have found that 1×10^7 cells are inadequate (data not shown). Female recipients were generally more resistant to tolerance induction: 1.5×10^7 induced tolerance in only some females but 4×10^7 secured tolerance in all.

Three attempts to break tolerance by the adoptive transfer of 10^8 normal syngeneic F_1 hybrid spleen cells were unsuccessful, suggesting that tolerance is maintained by active suppression. We therefore injected 10^8 spleen cells from tolerized mice into normal syngeneic F_1 animals to ascertain whether tolerance in hybrid resistance is transferable. The cell recipients were irradiated 6 days after cell transfer and received the indicator bone marrow grafts on the following day (see Fig. 2 legend). As found in previous experiments, hybrid resistance to C57BL grafts was abrogated by neonatal tolerance induction (Fig. 2, compare *a*, *b* and *c*). The adoptive transfer of cells from tolerant donors conferred unresponsiveness to C57BL (Fig. 2*d*) but not to SJL (Fig. 2*e*) cells. Pretreatment of the cells with a monoclonal anti-Thy-1.2 antibody and complement completely prevented the transfer of tolerance (Fig. 2*f*), showing that Thy-1⁺ cells, presumably T lymphocytes, are required. Similar results have been obtained in three other experiments.

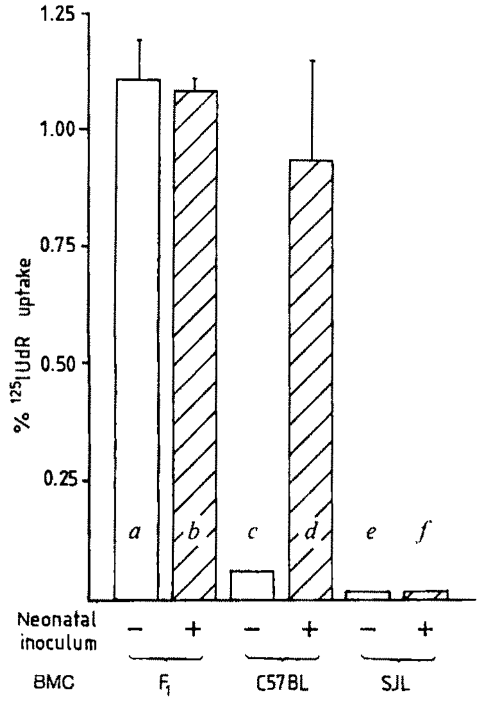

Fig. 1 Abrogation of hybrid resistance in (CBA×C57BL)F_1 hybrid mice by the neonatal inoculation of C57BL bone marrow cells (BMC). 8-12-week old hybrid mice that had received 1.5×10^7 C57BL bone marrow cells intraperitoneally (i.p.) within 24 h of birth (groups *b, d, f*) were used to measure hybrid resistance. Groups of four male mice were exposed to 8.0 Gy whole body X-irradiation and given intravenously (i.v.) 5×10^5 bone marrow cells from F_1 hybrid (*b*), C57BL (*d*) or SJL (*f*) donors (tolerized animals shown as hatched bars in this and other figures). Controls were provided by non-tolerized and sex and age-matched F_1 hybrids (*a, c, e*) given the same types of cells, respectively. Engraftment of donor cells was assessed by measuring the incorporation of ^{125}I-labelled 5-iodo-2′-deoxyuridine (^{125}IUdR) in the recipient spleens[17] as follows. Five days after bone marrow cell transplantation, the mice were given a single i.p. dose of 25 μg 5-fluorodeoxyuridine to decrease the availability of endogenous thymidine. This was followed 1 h later by 0.5 μCi ^{125}IUdR i.p. Spleens were removed 18-24 h later and counted in a Packard γ spectrometer. ^{125}IUdR uptake was calculated as the % of total radioisotope injected. Geometric means and standard deviations of the arithmetic means are shown for each group. In some experiments (though not in the experiment shown here), engraftment of parental CBA cells was also evaluated: such data were always comparable to the syngeneic controls.

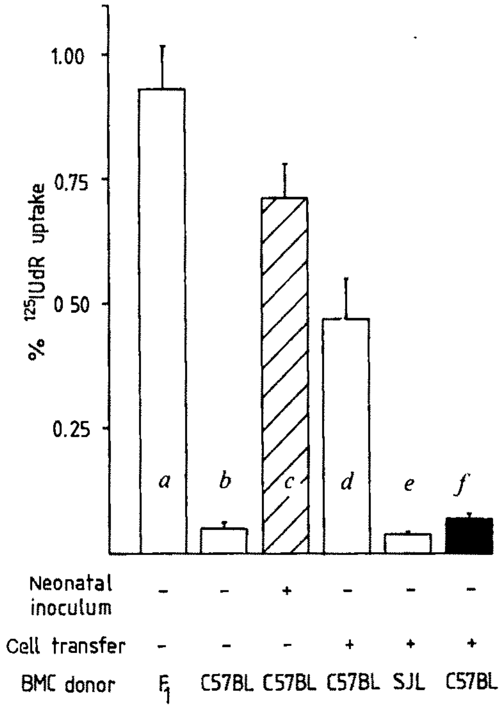

Fig. 2 Suppression of hybrid resistance by the adoptive transfer of spleen cells from tolerant mice. Tolerant F_1 hybrid donors were prepared as described in Fig. 1 legend except that the tolerizing inoculum consisted of 4×10^7 C57BL bone marrow cells. 10^8 spleen cells from tolerized donors were injected i.v. into normal adult (CBA×C57BL)F_1 mice 6 days before lethal whole body irradiation (groups *d-f*), followed 1 day later by 5×10^5 C57BL bone marrow cells given i.v. Group *f* received spleen cells that had been pretreated by two exposures to a monoclonal IgM anti-Thy-1 antibody and guinea pig complement[16]. Control mice were either normal (*a, b*) or neonatally tolerized (*c*) F_1 hybrids. Resistance to engraftment by C57BL (*b-d, f*) or SJL (*e*) cells was assessed by ^{125}IUdR uptake (see Fig. 1 legend) and compared with controls given syngeneic bone marrow cells (*a*). All groups comprised four mice.

Our study raises the question of the antigens involved in hybrid resistance. Genetic analysis by Cudkowicz and Nakamura[10] has shown that in certain mouse strains the expression of hybrid resistance is controlled by a number of *Hh* (haematopoietic histocompatibility) loci, some of which are linked to *H-2*, the major histocompatibility complex (MHC) of the mouse. *Hh* products seem to be expressed only in homozygous inbred strains. Both C57BL and SJL strains express products of the *Hh-1* locus which are thought to be highly cross-reactive, if not identical[11]. The specificity we have encountered is therefore all the more intriguing. One important difference between the antigenic relationship of the two strains to their hybrid hosts is that SJL cells are completely histoincompatible, whereas C57BL cells are not. It could therefore be argued that mechanisms other than those mediating NK activity are involved in hybrid resistance to allogeneic haematopoietic grafts, although it is generally accepted that the effectors responsible for resistance to allogeneic haematopoietic grafts in lethally irradiated animals are similar, if not identical, to those causing the rejection of parental cells[7].

In this connection, we have shown in two experiments (Fig. 3) that (CBA×SJL)F_1 bone marrow cells are not rejected by normal (CBA×C57BL)F_1 mice, indicating that conventional

Fig. 3 Resistance of (CBA× C57BL)F_1 hybrid mice to haematopoietic grafts presenting SJL strain MHC antigens. Engraftment of bone marrow cells was determined in groups of four 8-12-week old (CBA× C57BL)F_1 hybrids following lethal irradiation and reconstitution with 5×10^5 bone marrow cells from syngeneic (group *a*), SJL (*b*) or (CBA×SJL)F_1 (*c*) mice as described in Fig. 1 legend.

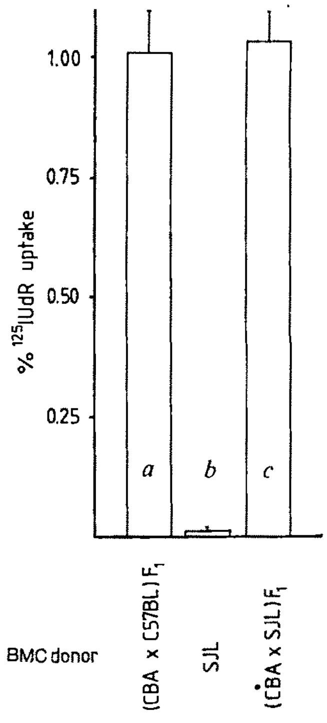

SJL MHC antigens are unlikely to be the target of resistance. Another approach was to examine resistance to parental grafts in (C57BL×SJL)F_1 hybrids. In an early experiment we found that such hybrids accepted C57BL bone marrow cells following tolerance induction with C57BL cells but retained resistance to bone marrow from SJL mice (the other parental strain). However, other experiments on these lines showed such marked variability in the take of both parental and even of syngeneic F_1 hybrid cells that we cannot have confidence in this result.

Our experiments show that T lymphocytes can suppress hybrid resistance, but we have not excluded the possibility that resistance to parental and allogeneic bone marrow cells is mediated by the same nonspecific NK effector and that specificity is imparted by suppressor lymphocytes. Were this the case, it would be expected that SJL cells would take when transplanted in the same inoculum with C57BL cells, to (CBA×C57BL)F_1 hybrids that had been tolerized with C57BL antigens. Figure 4 illustrates that this is not the case. Here we have used two doses of bone marrow cells (2.5×10^5 and 2.5×10^6) to increase the sensitivity of the assay. SJL cells at the higher dose were mixed with C57BL cells at the lower dose and inoculated into tolerized (CBA×C57BL)F_1 recipients. The take of this mixture (Fig. 4*h*) was not significantly different from the take of 2.5×10^5 C57BL cells alone (Fig. 4*g*). If exposure to C57BL antigens had caused the activation of a suppressor cell specific for C57BL, which then acted on a nonspecific effector, the take of cells in group *h* should have been greater than that in group *d* (2.5×10^6 C57BL cells in normal recipients) and approaching the level of incorporation observed in group *b* (2.5×10^6 F_1 cells). These experiments therefore favour the notion that the effectors for SJL and C57BL are distinct in their specificity.

We believe this to be the first demonstration that hybrid resistance can be prevented by neonatal tolerance induction and that specific Thy-1^+ suppressor cells can apparently regulate the activity of NK cells *in vivo*. The specificity of the effector cells is compatible with the earlier report by Cudkowicz and Bennett[3] that adult (C3H×C57BL)F_1 hybrids (H-$2^{k/b}$) become specifically unresponsive to H-2^b bone marrow cells after multiple immunization with C57BL spleen cells. It is at variance with the recent observation (ref. 11 and I. Nakamura, personal communication) that homozygous H-2^s and H-2^b lymphoid cells were equally effective in abrogating resistance to C57BL bone marrow cells when given to (C57BL/6×DBA/2)F_1 adult mice shortly before irradiation and reconstitution. However, this apparent lack of specificity could be due to the use of a hybrid (H-$2^{b/d}$) different from that used by Cudkowicz and Bennett and by us (H-$2^{k/b}$): whereas the latter recognizes at least two epitopes of Hh antigens, one common to H-2^b and H-2^s strains and the other unique to H-2^s, the former may recognize only the common epitope. Unresponsiveness to the common determinant in (C57BL/6×DBA/2)F_1 mice could therefore be expected to allow the take of H-2^s as well as of parental grafts. Alternatively, the suppression rather than the effector mechanism might have been nonspecific in the system described by Nakamura.

It could be argued that the specificity of the NK cells is imparted by naturally occurring antibody, based on the model of Chow *et al.*[12] for NK surveillance against syngeneic tumours. Such an interpretation is virtually ruled out by the observation that hybrid resistance is intact in mice depleted of B lymphocytes by the neonatal administration of anti-μ antibody[13].

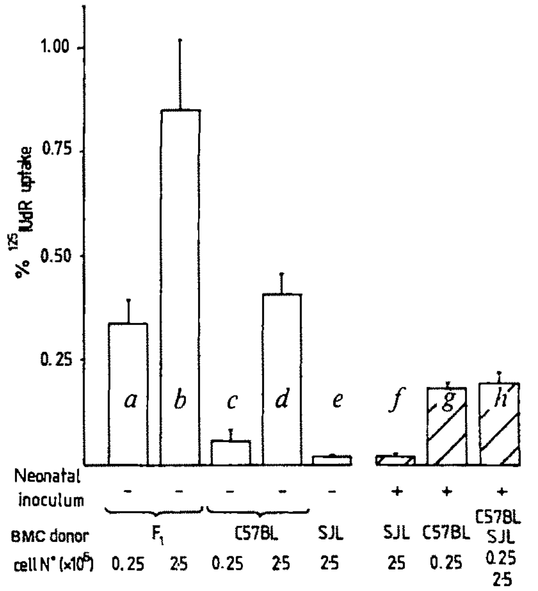

Fig. 4 Resistance of (CBA×C57BL)F_1 hybrid mice, tolerized neonatally to parental C57BL Hh antigens, to allogeneic SJL bone marrow cells injected as a mixture with C57BL bone marrow cells. (CBA×C57BL)F_1 mice tolerant to C57BL bone marrow cells were prepared as described in Fig. 2 legend (groups *f*–*h*). Groups of four 8–10-week old (CBA×C57BL)F_1 hybrids were lethally irradiated (8.0 Gy) and given i.v., 24 h later, bone marrow cells from F_1 (*a*, *b*), C57BL (*c*, *d*, *g*) or SJL (*e*, *f*) donors. Groups *a*, *c* and *g* were given 2.5×10^5 and groups *b*, *d* and *e* 2.5×10^6 cells. Group *h* received a mixture of 2.5×10^5 C57BL and 2.5×10^6 SJL cells. Engraftment was assessed 5 days after reconstitution as described in Fig. 1. Although we were unable to include SJL→SJL controls in this experiment to show that the SJL bone marrow cells take normally in susceptible hosts, we have found in five other experiments that this is indeed the case.

In conclusion, our evidence shows that resistance to parental and allogeneic haematopoietic grafts is mediated by different effector cell populations, presumed to be subpopulations of NK cells. Moreover, the effectors involved in hybrid resistance can be controlled by specific suppressor T cells. Our demonstration of specificity in hybrid resistance probably accounts for the unexplained finding by Warner and Dennert[8] that cloned NK cells from C57BL/6 mice did not establish resistance against C57BL/6 bone marrow grafts in NK-deficient (C57BL/6×C3H)F_1 hybrids (H-$2^{b/k}$), despite the fact that resistance to allogeneic BALB/c grafts (H-2^d) was restored.

Our model should enable us to examine the effect of tolerance induction on the activity of NK cells *in vitro*, as well as on the progression of syngeneic tumours, some of which seem to be subject to NK cell surveillance[8,14]. Finally our results make it highly probable that the transplantation of allogeneic bone marrow grafts *in utero*[15,16] should not be thwarted by fetal NK activity.

We thank the Wellcome Trust for their support of L.S.R. and the MRC for M.W.'s postgraduate studentship. We also thank Ms Beverley Whittle, Mrs Ellen Yanez and Mr M. Gevaux for their assistance and Professor W.L. Ford for helpful comments.

Received 4 June; accepted 23 August 1984.

1. Cudkowicz, G. & Stimpfling, J. H. *Immunology* **7**, 291–306 (1964).
2. Cudkowicz, G., Rossi, R. B., Haddad, J. C. & Friend, C. *J. natn. Cancer Inst.* **48**, 997–1003 (1972).
3. Cudkowicz, G. & Bennett, M. *J. exp. Med.* **134**, 1513–1528 (1971).
4. Lotzova, E. *Expl Hemat.* **5**, 215–235 (1977).
5. Cudkowicz, G. & Bennett, M. *J. exp. Med.* **134**, 83–102 (1971).
6. Bonmassar, E., Campanile, F., Houchens, D., Crino, L. & Goldwin, A. *Transplantation* **20**, 343–346 (1975).
7. Lotzova, E. in *Natural Cell-mediated Immunity against Tumors* (ed. Herberman, R. B.) 1117–1120 (Academic, New York, 1980).
8. Warner, J. F. & Dennert, G. *Nature* **300**, 31–34 (1982).
9. Lotzova, E., Pollack, S. B. & Savary, C. A. in *NK Cells and Other Natural Effector Cells* (ed. Herberman, R. B.) 1535–1540 (Academic, New York, 1982).
10. Cudkowicz, G. & Nakamura, I. *Transplantn Proc.* **15**, 2058–2063 (1983)
11. Nakamura, I. *Prog. Immun.* **5**, 1219–1222 (1983).
12. Chow, D. A., Wolosin, L. B. & Greenberg, A. H. *J. natn. Cancer Inst* **67**, 445–453 (1981).
13. Brodt, P., Kongshavn, P., Vargas, F. & Gordon, J. *J. reticuloendothel. Soc.* **30**, 283–289 (1981)
14. Haller, O., Hansson, M., Kiessling, R. & Wigzell, H. *Nature* **270**, 609–611 (1977)
15. Brent, L., Rayfield, L. S. & Modell, B. *Transplantn Proc.* **14**, 538–540 (1982).
16. Rayfield, L. S. & Brent, L. *Eur. J. Immun.* **14**, 308–313 (1984).
17. Iorio, A. M., Neri, M., Paola, E. & Bonmassar, E. *Transplantation* **32**, 355–363 (1981)

Characterization of cDNA for precursor of human luteinizing hormone releasing hormone

Peter H. Seeburg & John P. Adelman

Department of Molecular Biology, Genentech, Inc., 460 Point San Bruno Boulevard, South San Francisco, California 94080, USA

Human reproduction is controlled by the hypothalamic–pituitary–gonadal axis laid down early in fetal development. Luteinizing hormone releasing hormone (LHRH), also termed gonadotropin releasing hormone (GnRH), is a decapeptide[1,2] and is a key molecule in this control circuit. It is produced by hypothalamic neurones, secreted in a pulsatile manner into the capillary plexus of the median eminence and effects the release of luteinizing hormone and follicle stimulating hormone from gonadotropic cells in the anterior pituitary[3]. The peptide may have further functions, including behavioural ones[4], as LHRH or LHRH-like immunoreactivity has been found in gonadal tissue[5,6], placenta[7,8] and the central nervous system[9,10], and exogenously administered LHRH is shown to affect behaviour[11,12]. To investigate the biosynthesis of LHRH, we have now isolated cloned genomic and cDNA sequences encoding the precursor form of LHRH, the existence of which had been suggested from chromatographic studies of hypothalamic[8,13] and placental[8] extracts. These DNA sequences code for a protein of 92 amino acids in which the LHRH decapeptide is preceded by a signal peptide of 23 amino acids and followed by a Gly-Lys-Arg sequence, as expected for enzymatic cleavage of the decapeptide from its precursor[14–16] and amidation[17] of the carboxy-terminal of LHRH.

A genomic library was used in preference to cDNA libraries to initially screen for LHRH-encoding DNA sequences. The most important reasons for this choice were the anticipated low abundance of LHRH messenger RNA, the possibility of a very long 3′ untranslated region, and the unknown location of the decapeptide coding unit within the mRNA. Figure 1 shows the probe strategy used to screen the genomic library; it is described in the corresponding legend. Although a similar approach using a single long probe has led to the successful isolation of several genes[18–20], the available amino acid sequence in these cases had comprised more than 20 residues. The LHRH-coding sequences would only be isolated successfully if all members of the pool of long probes (Fig. 1 legend) were present, and if the correct nucleotide choices were incorporated into a sufficient number of the third-codon positions. To determine the pool composition and sequence, the oligonucleotide mixture was analysed by cloning in a phage M13 vector[21] (see Fig. 2 legend). Figure 2 shows the results of this analysis and demonstrates that, most importantly, all the nucleotide combinations of the long probes were represented. Thus, in spite of several deletions predominantly within the Tyr codon and a single nucleotide insertion in the same codon, the quality of the oligonucleotide mixture was considered satisfactory for screening a genomic library.

The probing of 10^6 λ phage containing human genomic DNA[22] produced ~300 positives with signal strengths ranging from barely visible to very strong. Only one of them hybridized to both the long and short probes. Figure 3 shows the analysis of this clone; the same single restriction fragments are seen to hybridize with both sets of oligomers (Fig. 3*a*). Figure 3*b* shows a sequencing gel indicating the hybridizing region. The amino acid sequence derived from the nucleotide sequence shows that this DNA indeed codes for the LHRH peptide. The DNA sequence also predicted the expected C-terminal Gly residue necessary for amidation[17] followed by a Lys-Arg processing site[14]. Although such a processing site had been expected to, but does not, precede LHRH (see Fig. 1), and although our long probes also differed in five nucleotides from the actual LHRH coding region (compare Figs 1 and 4), the sequence homology of these probes was sufficient to find the correct gene.

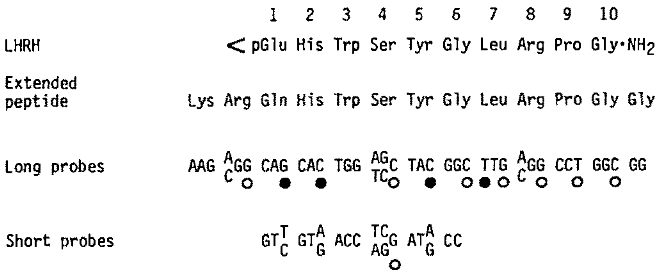
1 2 3 4 5 6 7 8 9 10
LHRH
< pGlu His Trp Ser Tyr Gly Leu Arg Pro Gly·NH2
Extended peptide
Lys Arg Gln His Trp Ser Tyr Gly Leu Arg Pro Gly Gly
Long probes
AAG A/C GG CAG CAC TGG AG/TC C TAC GGC TTG A/C GG CCT GGC GG
Short probes
GT T/C GT A/G ACC TC/AG G AT A/G CC

Fig. 1 Synthetic oligodeoxynucleotides for the isolation of LHRH coding sequences. The amino acid sequence of LHRH(1–10) (refs 1, 2) is shown with a conjectural sequence for part of the LHRH precursor (extended peptide). The three additional amino acid residues were incorporated on the assumption that LHRH is preceded in its precursor protein by a processing site in the form of a pair of basic amino acids[14] and that a Gly residue donates its amino group during C-terminal amidation[17]. The pyro-Glu is thought to be derived from Gln[44]. Based on this extended peptide sequence, a pool of eight oligonucleotides (long probes, 5′→3′) was synthesized[45] to be used as probes for the screening of a human genomic library. The degeneracy of these probes allowed for the two codon types for Arg (AGPu and CGX) and Ser (AGPy and TCX), but for only one of any two or four choices for all third-codon positions. The single choice of TTG for the Leu codon was based on evolutionary arguments[46]. The pool of 16 heptadecamers with a sequence complementary to that coding for amino acids 1–6 of LHRH (short probes, 3′→5′) was used to further select between the large number of genomic clones that hybridized with the long probes (J.P.A. *et al.*, in preparation). Filled circles represent one of two, and open circles one of four possible nucleotides in third-codon positions.

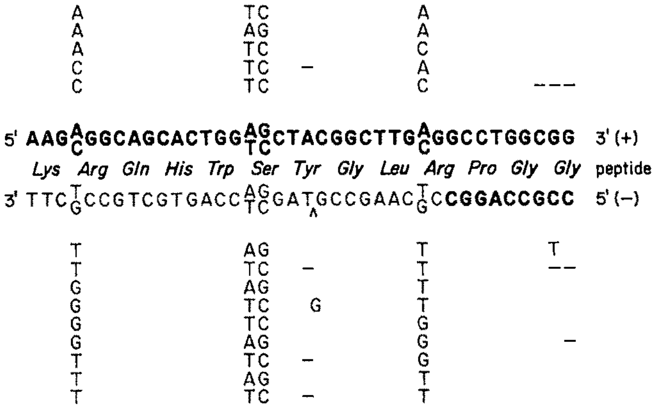
5′ AAG A/C GGCAGCACTGG AG/TC CTACGGCTTG A/C GGCCTGGCGG 3′ (+)
Lys Arg Gln His Trp Ser Tyr Gly Leu Arg Pro Gly Gly peptide
3′ TTC T/G CCGTCGTGACC AG/TC GATGCCGAAC T/G CCGGACCGCC 5′ (−)

Fig. 2 Analysis of long probes. The double-stranded DNA shown is composed of the synthetic 38-mer pool (+) coding for the extended LHRH peptide (Fig. 1) and a complementary nonameric primer (both in bold print), together with the rest of the complementary strand (−) generated by enzymatic DNA synthesis (normal print). This DNA was molecularly cloned and 14 clones were sequenced. Only nucleotides in degenerate positions are shown above and below the double-stranded DNA. Hyphens denote missing nucleotides. The position of a GMP insertion found in the Tyr codon in one of the cloned DNAs is indicated.

Methods: 20 pmol of 5′-phosphorylated long probes were annealed with 40 pmol of 5′-phosphorylated nonameric primer in 40 µl of 20 mM Tris-HCl *p*H 7.5, 100 mM NaCl, 6 mM $MgCl_2$, 0.1 mM EDTA, 100 µM each of dATP, dGTP, dCTP, dTTP, at 14 °C for 15 min. DNA synthesis was initiated by the addition of 5 U *Escherichia coli* DNA polymerase I (large fragment, Boehringer Mannheim) and allowed to proceed for 30 min at 14 °C. Following phenol extraction and ethanol precipitation, the DNA was incubated for 2 h at room temperature with 10 ng *Sma*I-cleaved M13 mp10 RF-DNA[48] in 20 µl containing 50 mM Tris-HCl *p*H 8, 10 mM $MgCl_2$, 0.1 mM EDTA, 10 mM β-mercaptoethanol, 0.5 mM rATP and T4 DNA ligase (New England Biolabs). The ligation mixture was used to transform competent *E. coli* JM103 cells[21]. Recombinant phage was grown, single-stranded phage DNA prepared and sequenced using dideoxynucleoside triphosphates as described[21,47].

Because of the possible presence of introns in the gene, we isolated the corresponding cDNA to elucidate the complete structure of the LHRH precursor protein.

A 600-base pair (bp) DNA restriction fragment obtained from the genomic clone and containing the LHRH coding sequence (J.P.A. *et al.*, in preparation) was used as a probe to screen a large cDNA library constructed in λ phage[23]. As human hypothalami were not available to us, the cDNA was derived from human placental tissue where LHRH synthesis has been shown to occur[24]. Two hybridizing clones were isolated which contained cDNA inserts of ~1,500 and 800 bp in length. Figure 4 shows the complete nucleotide sequences of both cDNAs, together with the deduced amino acid sequence of the LHRH precursor protein.

The most prominent feature of the cDNA is a very long 5′ untranslated region of >1,000 nucleotides. A similarly sized 5′ region has been described for the human preproenkephalin B gene[25] but seems otherwise to be a rare phenomenon. As LHRH is expressed in various tissues, transcription of the precursor gene from different tissue-specific promoters[26] might be invoked to account for the presence of such an extended 5′ region in the placental cDNA[26,27]. The trivial explanation, that the clone is derived from an unspliced nuclear RNA, can be refuted because two introns present in the gene had been clearly removed (J.P.A. *et al.*, in preparation). The smaller of the two cloned cDNAs has ~400 nucleotides of 5′ untranslated sequence which also contain the best consensus splice acceptor site[28] (nucleotides 960-974), making the possibility of a partially spliced version unlikely. The very low abundance of the corresponding mRNA in placental tissue has so far precluded the use of Northern analysis[29] to establish the correct length of its 5′ region. Furthermore, complete co-linearity of this region with the established genomic sequence (J.P.A. *et al.*, in preparation) excludes artefacts which might have been introduced during reverse transcription and molecular cloning.

The largest open reading frame (nucleotides 1,063-1,350) specifies the coding sequence for LHRH and translates into a peptide of molecular weight ~10,000 with characteristics of a precursor for a polyfunctional protein (for review see ref. 30). This reading frame is terminated by an ochre stop codon and followed by 160 nucleotides of a 3′ untranslated region containing an AATAAA sequence for polyadenylation[27] shortly upstream of the poly(A) tail. The actual start of translation within the open reading frame is unclear. The first ATG initiation codon (position 1,063) is followed by an in-frame ATG four codons downstream. This second ATG, but not the first, is followed by a purine and preceded by an A at position −3, as is the case with most eukaryotic initiation codons[31]. We therefore consider this latter ATG at position 1,075 to be the most likely start codon for initiation of the synthesis of the LHRH precursor protein although it involves a violation of the rule which specifies that the first ATG should bear this function[32]. It is possible that both ATGs are involved in the initiation of protein synthesis, resulting in a low translational efficiency[31].

The first 23 amino acids form a typical signal sequence containing a hydrophobic middle section[33]. The putative signal sequence ends in two serine residues followed by the expected decapeptide sequence for LHRH[1,2]. Cleavage of the signal peptide results in an amino-terminal glutamic residue which spontaneously or enzymatically undergoes cyclization to pyro-Glu, the modified amino-terminus of LHRH[1,2]. The decapeptide sequence is followed by a glycine, the standard donor of the amino group for C-terminal amidation[17]. A Lys-Arg cleavage site is present for enzymatic processing, as is found in many precursors to neuroendocrine peptides[30]. Thus, the isolated cDNAs code for a true precursor protein to LHRH which features a direct linkage of signal sequence to biologically active peptide reminiscent of the situation in the precursor for vasopressin[34].

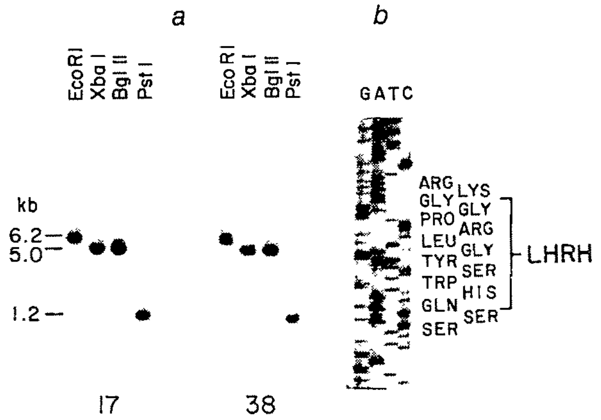

Fig. 3 Identification of a cloned human genomic DNA segment carrying LHRH coding sequences. Sequential screening of a human genomic library[22] with two pools of oligomers (long (38) and short (17) probes; see Fig. 1) yielded one isolate the DNA of which hybridized with both oligomeric probes. *a*, Southern analysis[40] of the DNA digested with four restriction endonucleases (*Eco*RI, *Xba*I, *Bgl*II, *Pst*I). DNA fragment sizes in kilobase pairs (kb) are indicated on the left and were assessed using *Hin*dIII-cleaved λ DNA (BRL). *b*, A sequencing gel (G, A, T, C) across the region of hybridization with both oligomer pools. The amino acid sequence encoded by the nucleotide sequence in this region is indicated.

Methods: 10^6 λ phage containing human genomic DNA were screened on duplicate filters using the long probes (see Fig. 1) which had been phosphorylated to a specific activity of 10^7 c.p.m. per pmol. Hybridization was at 37 °C in the presence of 30% formamide using 10^7 c.p.m. per filter. Filters were washed in 3×SSC (1×SSC = 0.15 M NaCl, 0.015 M Na-citrate) at 37 °C and exposed to X-ray film. Phage from 300 small areas corresponding to the number and location of positive signals were replated on individual plates and probed with long and short probes (Fig. 1). Short probe hybridization was at room temperature in the presence of 20% formamide and corresponding filters were washed at the same temperature in 5×SSC. DNA from the single isolate which hybridized with both pools of oligomers was cleaved with restriction enzymes and DNA fragments characterized by Southern[40] analysis using the two oligonucleotide pools as probes under the conditions specified above. A 1,200-bp DNA fragment containing the hybridizing region was cloned into phage M13 mp18 RF-DNA and recombinant single-stranded DNA was sequenced using primed DNA synthesis in the presence of dideoxynucleoside triphosphates[21,47].

The remainder of the LHRH precursor consists of a peptide of 56 amino acids, the function of which is unknown. It does not contain any sites for *N*-glycosylation (Asn-X-Thr/Ser) and no homologies were found when the sequence was compared with other known hypothalamically produced precursors to neuroendocrine peptides[34-37]. Interestingly, the C-terminus of this peptide consists of the sequence Lys-Lys-Ile, which may represent an enzymatic cleavage site for further processing. It is likely that the resulting peptide of 53 amino acids is released together with LHRH, possibly to complement the biological function of the decapeptide in ways not yet understood. It might be a carrier protein of LHRH in analogy with neurophysins[34,38] or it could be involved in the release of follicle-stimulating protein (FSH) from pituitary gonadotrophs, a process for which an agent other than LHRH has been invoked[39].

The LHRH precursor produced in placenta and hypothalamus is probably the same, as antisera raised against a synthetic peptide derived from its sequence can be used to stain rat hypothalamic LHRH-producing neurones (H. Phillips *et al.*, in preparation). In addition, Southern analysis[40] of the human genome using the cloned cDNA as a probe did not reveal the presence of related genes (J.P.A. *et al.*, in preparation). The two other hypothalamic releasing factors for which cloned cDNAs exist, namely growth hormone releasing factor and corticotropin releasing factor, are also encoded by single genes[36,37]. However, the molecular weight of 10,000 (10K) for prepro-LHRH as deduced from the cloned cDNA is much smaller than the 28K precursor reported from *in vitro* translation and immunoprecipitation of rat hypothalamic mRNA[41]. There are two possible

```
                      5' - AGGGCTTTATGTGAGGATTTTTAAAAATTACCATTAAAAAAAAAAAAGCATAGTCCATTTGCAGTATAATTTAC     74

CAGCAGGAAAGATTTCAATGTCCTGGAAAAATTCCCTATAAAAAGGAAGATAGGAAAACAGAAAAGTCACAGTACTCAACCTACTTCAAGGGAAGATTGA   174

GATCTTTTTGGCTCTCTGCCTCTAAACAGGTAAAAGGCTTTGTATTATTTCTAGCACGAGTTTTTCTTCTTTAGATTGCATGCTATTGTATGTCTACAGG   274

GCATTTGACAGCCCAAGGGCTAAATCCAGGTGTGACGGTATCTAATGATGTCCTGTCCTTCACTGTCCTTGCCATCACCAGCCACAGAGATCCAGGCTTT   374

GGGGACTCCCACAGCTTATCGACCAGTGTTTGATTTAGTTTTTAGCCTCTTTCCCATCAAATGAAAATTAACTTGGAGACACATTTCATTAGAAAATTAG   474

AGGCCCCCTTGGCTAGGAAGGCATCTGGTCTGGGACTAACTACTTTGAACAGTGTTGAGTCCTCTCTCCCACAGATGGTTCAGCCAGCAGTAATGCTAGG   574

CAAGACTGAAGGATAAATAGAAAAATGTCATTAGTACCATGGGGTAGCCATGTAATGTCAAGCAATTTTATATTAGCCAGAGATTCCTAGTAGGAGCTAC   674

        ┌→                 T
TTTTCTTAACAGATGACTCAGTTCTCTCTATCTCAGGAATGAAAGAGTTGAAGACCAATCCACAACAGGGGAAATGTTAAGGCAAAATGATGAACTTGAT   774

AAGGGATGAATTATGGGGTTTGGATAACCAAACAATAAAAATAAAAGTATAGACTATTTTAGTACTAAAAAGGTCCTGAACATGTGAGCTTAAGTACTCA   874

TTTTGTCCCCAGTGGCTAAGAAACTAAAGGCAAGCCAGCAAGTGTCTCTGAGTTTCAGTGTCTGTATGTAAAAACTGACTCTGACTTCCATCTTCTGCAG   974

                         C                                                                     ___
GGTTAGTGATACAGATGCTAGCTTTTTCACTAAAGAGGTCTTTTAGTTTATACTCAACCTTGTCTGGATCTAATTTGATTGTGCATTCATGTGCCTTAGA  1,074


-23         -20                                         -10                                 -1
met lys pro ile gln lys leu leu ala gly leu ile leu leu thr ser cys val glu gly cys ser ser
ATG AAG CCA ATT CAA AAA CTC CTA GCT GGC CTT ATT CTA CTG ACT TCG TGC GTG GAA GGC TGC TCC AGC          1,143

|---------------- LHRH ---------------|
  1                                   10                                      20
gln his trp ser tyr gly leu arg pro gly gly|lys arg|asp ala glu asn leu ile asp ser phe gln
CAG CAC TGG TCC TAT GGA CTG CGC CCT GGA GGA|AAG AGA|GAT GCC GAA AAT TTG ATT GAT TCT TTC CAA          1,212
                                        ___


                        30                                      40
glu ile val lys glu val gly gln leu ala glu thr gln arg phe glu cys thr thr his gln pro arg
GAG ATA GTC AAA GAG GTT GGT CAA CTG GCA GAA ACC CAA CGC TTC GAA TGC ACC ACG CAC CAG CCA CGT          1,281
   ↑


            50                                      60                              69
ser pro leu arg asp leu lys gly ala leu glu ser leu ile glu glu glu thr gly gln¦lys lys¦ile END
TCT CCC CTC CGA GAC CTG AAA GGA GCT CTG GAA AGT CTG ATT GAA GAG GAA ACT GGG CAG¦AAG AAG¦ATT TAA      1,353
                                       ↑

ATCCATTGGGCCAGAAGGAATGACCATTACTAACATGACTTAAGTATAATTCTGACATTGAAAATTTATAACCCATTAAATACCTGTAAATGGTATGAAT  1,453

TTCAGAAATCCTTACACCAAGTTGCACATATTCCATAATAAAGTGCTGTGTTGTGAATG - polyA 3'
                                    ______
```

Fig. 4 Amino acid and nucleotide sequence of prepro-LHRH and its cDNA as isolated from human placental tissue. Numbers for amino acids appear within the sequence, whereas nucleotide numbers are given on the right-hand side. The nucleotide sequence is that of the longer cDNA clone. The shorter cDNA starts at nucleotide 683 (see horizontal arrow) and nucleotide differences between the two cDNAs (positions 702, 997) are indicated. The overlined ATG indicates an alternative translational initiation codon. The Lys-Arg processing site for the precursor sequence is boxed and the glycine involved in carboxy-terminal amidation is underlined. A second possible processing site at the C-terminus of the precursor protein is shown by a hyphen. Arrows indicate interruptions due to introns in the corresponding genomic DNA sequence (J.P.A. *et al.*, in preparation). The AATAAA polyadenylation signal[27] is underlined.

Methods: Polyadenylated RNA (10 μg) from human placental tissue was converted into double-stranded cDNA using standard procedures[49]. The cDNA was cloned using phage λgt10 as a vector according to published methods[23]. 1.5×10^6 recombinant phage were obtained and screened using a DNA fragment isolated from the genomic clone (Fig. 3) and labelled[50] to a specific activity of 10^8 c.p.m. per μg. Two hybridizing λ clones were isolated and found to contain cDNA inserts of ~1,500 and 800 bp, respectively. These cloned cDNAs were sequenced using single-stranded recombinant M13 DNA as templates for the primed DNA synthesis in the presence of dideoxynucleoside triphosphates[21,47].

explanations for this discrepancy. It can be argued that the protein seen by immunoprecipitation is not the LHRH precursor, especially as the competition by unlabelled LHRH used in the experiments[41] may not be a reliable means of identification. Alternatively, the 28K precursor could give rise to the hypothalamically expressed LHRH, whereas the placenta might produce a smaller protein. If this is the case, different LHRH-encoding genes would be expressed in hypothalamus and placenta, or different sets of exons spliced in a tissue-specific fashion[42] from the same primary gene transcript.

Although the genomic analysis (see above) might be taken to indicate the existence of only one LHRH gene—and its expression in both hypothalamus and placenta—it should be stressed that different genes for LHRH need only be homologous in their DNA encoding the decapeptide. Homology over such a small region might not be detected using cDNA probes, as shown by the related sequences for proopiomelanocortin[15] and preproenkephalin A (ref. 16) and B (ref. 43). Isolation of cDNA coding for hypothalamically-produced LHRH will reveal which of the alternatives outlined above is correct.

We thank Mark Vasser and Kim Dinkelspiel for the synthesis of the oligodeoxynucleotides used in this study, Joel S. Hayflick for his help in the DNA sequence analysis, Drs Karoly Nikolics and Anthony Mason for critically evaluating this manuscript and Jeanne Arch for helping in preparing it.

Received 13 June; accepted 15 August 1984.

1. Matsuo, H. *et al. Biochem. biophys. Res. Commun.* **43,** 1334–1339 (1971).
2. Burgus, R. *et al. Proc. natn. Acad. Sci. U.S.A.* **69,** 278–282 (1972).
3. Schally, A. V. *et al. Biochem. biophys. Res. Commun.* **43,** 393–401 (1971).
4. Moss, R. L. *Fedn Proc.* **36,** 1978–1983 (1977).
5. Ying, S. Y., Ling, N., Bohlen, P. & Guillemin, R. *Endocrinology* **108,** 1206 (1982).
6. Bhasin, S., Heber, D., Peterson, M. & Swerdloff, R. *Endocrinology* **112,** 1144–1145 (1983).
7. Khodr, G. S. & Siler-Khodr, T. M. *Science* **207,** 315–317 (1980).
8. Gautron, J. P., Pattou, E. & Kordon, C. *Molec. cell. Endocr.* **24,** 1–16 (1981).
9. Silverman, A. J. & Krey, L. C. *Brain Res.* **157,** 233–246 (1976).
10. Samson, W. K. *et al. Neuroendocrinology* **31,** 66–72 (1980).
11. Moss, R. L. & McCann, S. M. *Science* **181,** 177–179 (1973).
12. Pfaff, D. W. *Science* **182,** 1148–1150 (1973).
13. Millar, R. P., Ashnelt, C. & Rossier, G. *Biochem. biophys. Res. Commun.* **74,** 720–726 (1977).
14. Steiner, D. F. *et al. Ann. N.Y. Acad. Sci.* **343,** 1–16 (1980).
15. Nakanishi, S. *et al. Nature* **278,** 423–427 (1979).
16. Gubler, U. *et al. Nature* **295,** 206–208 (1982).
17. Bradbury, A. F., Finnie, M. D. A. & Smyth, D. G. *Nature* **298,** 686–688 (1982).
18. Anderson, S. & Kingston, B. *Proc. natn. Acad. Sci. U.S.A.* **80,** 6838–6842 (1983).
19. Jaye, M. *et al. Nucleic Acids Res.* **11,** 2325–2335 (1983).
20. Ullrich, A. *et al. EMBO J.* **3,** 361–364 (1984).
21. Messing, J., Crea, R. & Seeburg, P. H. *Nucleic Acids Res.* **9,** 309–321 (1981).
22. Lawn, R. M. *et al. Cell* **15,** 1157–1163 (1978).
23. Huynh, T., Young, R. & Davis, R. in *Practical Approaches in Biochemistry* (ed. Grover, D.) (IRL Press, Oxford, in the press).
24. Tan, L. & Rousseau, P. *Biochem. biophys. Res. Commun.* **109,** 1061–1071 (1982).
25. Orihawa, S. *et al. Nature* **306,** 611–614 (1983).
26. Young, R. A., Hagenbuchle, O. & Schibler, U. *Cell* **23,** 451–458 (1981).
27. Proudfoot, N. J. & Brownlee, G. G. *Nature* **263,** 211–214 (1976).
28. Breathnach, R. *et al. Proc. natn. Acad. Sci. U.S.A.* **75,** 4853–4857 (1978).
29. Lehrach, H., Diamond, D., Wozney, J. M. & Boedtker, H. *Biochemistry* **16,** 4743–4751 (1977).
30. Douglass, J., Civelli, O. & Herbert, E. *A. Rev. Biochem.* **53,** 665–750 (1984).
31. Kozak, M. *Nature* **308,** 241–246 (1984).
31. Kozak, M. *Nucleic Acids Res.* **9,** 5233–5252 (1981).
33. Perlman, D. & Halvorson, H. O. *J. molec. Biol.* **167,** 391–409 (1983).
34. Land, H., Schutz, G., Schmale, H. & Richter, D. *Nature* **295,** 299–303 (1982).
35. Shen, L. P., Pictet, R. L. & Rutter, W. J. *Proc. natn. Acad. Sci. U.S.A.* **79,** 4575–4579 (1982).
36. Furutani, Y. *et al. Nature* **301,** 539–540 (1983).
37. Gubler, U. *et al. Proc. natn. Acad. Sci. U.S.A.* **80,** 4311–4314 (1983).
38. Chauvet, M. T., Chauvet, J. & Acher, R. *Eur. J. Biochem.* **69,** 475–485 (1976).
39. McCann, S. M. *Neuroendocrinology* **31,** 355–363 (1980).
40. Southern, E. *J. molec. Biol.* **98,** 503–517 (1975).
41. Curtis, A. & Fink, G. *Endocrinology* **112,** 390–392 (1983).
42. Amara, S. G. *et al. Nature* **248,** 240–244 (1982).
43. Kakidani, H. *et al. Nature* **298,** 245–249 (1982).
44. Smyth, D. G., Stein, W. H. & Moore, S. *J. biol. Chem.* **238,** 227–234 (1963).
45. Crea, R. & Horn, T. *Nucleic Acids Res.* **8,** 2331–2348 (1980).
46. Sherwood, N. *et al. Proc. natn. Acad. Sci. U.S.A.* **80,** 2794–2798 (1983).
47. Sanger, F., Nicklen, S. & Coulson, A. R. *Proc. natn. Acad. Sci. U.S.A.* **74,** 5463–5467 (1977).
48. Messing, J. & Vieira, J. *Gene* **19,** 269–276 (1982).
49. Maniatis, T., Fritsch, E. F. & Sambrook, J. *Molecular Cloning,* 211–217 (Cold Spring Harbor Laboratory, New York 1982).
50. Taylor, J. M., Illmensee, R. & Summers, J. *Biochim. biophys. Acta* **4,** 324–330 (1976).

Developmentally regulated production of platelet-derived growth factor-like molecules

Ronald A. Seifert, Stephen M. Schwartz & Daniel F. Bowen-Pope

Department of Pathology, SM-30, School of Medicine,
University of Washington, Seattle, Washington 98195, USA

Platelet-derived growth factor (PDGF) is thought to mediate the proliferation of smooth muscle cells in injured arteries, and may be involved in the pathogenesis of atherosclerosis[1]. PDGF-like molecules from non-platelet sources may also play a role in the regulation of cell activity in other circumstances. Transformation of cells by a wide range of oncongenic agents appears to activate a cellular gene encoding a PDGF-like molecule[2-6], possibly accounting for the ability of transformed cells to grow without addition of exogenous mitogens[7-12]. We show here that a molecule (PDGF-c) which can compete with ^{125}I-PDGF for binding to PDGF receptors is secreted by cultured rat aortic smooth muscle cells (rASMC) isolated from 13 to 18-day-old rats (pups) but not from three-month-old animals (adults). Thus, production of PDGF-c appears to be developmentally regulated and may be a factor in the more rapid proliferation of rASMC and synthesis of connective tissue components which occurs during growth of the aorta *in vivo*.

Pup rASMC secrete into their culture medium an average of 170 times (Range 77-1,100×) more PDGF-c than do adult rASMC (Table 1). This difference is consistently observed for two separate isolates (pup and adult) of rASMC from each of three different rat strains. Prior adsorption of pup rASMC-conditioned medium with goat anti-PDGF IgG covalently coupled to Sepharose-4B completely abolishes the ability of pup rASMC-conditioned medium to reduce ^{125}I-PDGF binding to human fibroblasts (data not shown), demonstrating that pup rASMC PDGF-c is antigenically related to PDGF. Pup, but not adult, rASMC continue to produce PDGF-c during 20 passages in culture over a period of at least six months. These data suggest that the critical events occurring *in vivo* between the ages of two weeks and three months is not a mere consequence of the passage of time or number of cell divisions. Pup rASMC-conditioned medium is mitogenic for 3T3 fibroblastoid cells (Fig. 1), whereas adult rASMC-conditioned medium is nonmitogenic or only weakly so (data not shown). Stimulation of DNA synthesis by added PDGF or pup rASMC-conditioned medium is, however, completely prevented by simultaneous addition of goat anti-PDGF IgG (Fig. 1). Comparable amounts of non-immune goat IgG have no effect. We conclude from these results that pup rASMC PDGF-c is mitogenic as well as antigenically similar to PDGF.

Table 1 Rate of PDGF-c production by rASMC

Rat strain	Rate of PDGF-c production (ng per equiv.) Pup	Adult
Sprague–Dawley		
Isolate 1	1.13	0.036
Isolate 2	1.09	0.01
Wistar Kyoto		
Isolate 1	1.92	0.002
Isolate 2	2.25	0.004
Spontaneous hypertensive rat		
Isolate 1	3.48	0.003
Isolate 2	0.48	0.006
Average ± *s.d.*	1.73 ± 1.07	0.01 ± 0.013

Aortic smooth muscle cells were placed into culture as described elsewhere[36]. The PDGF-c concentration in media conditioned (Ref. 6 for method) by two different isolates of rASMC obtained from 13- to 18-day-old or 3-month-old rats of three strains (Sprague–Dawley, Wistar Kyoto, and the spontaneously hypertensive rat) was determined by radioreceptor assay[18,37] using volumes of conditioned medium resulting in an approximately 50% decrease in specifically bound ^{125}I-PDGF (radiolabelled as previously described[13,37]). The results were normalized by expressing production rate as ng PDGF-c per equivalent (where an equivalent equals 1 ml medium conditioned by 1×10^6 cells for 48 h). The tabulated values are the averages of at least two, and in most cases three or more, determinations of PDGF-c concentration.

Isolates of pup rASMC possess considerably fewer binding sites for ^{125}I-PDGF compared with adult rASMC; the binding which does occur increases linearly over the ^{125}I-PDGF concentration range tested (Fig. 2). This binding may be to a previously unrecognized PDGF-binding site with a dissociation constant substantially greater than that of the PDGF mitogen receptor. At concentrations of ^{125}I-PDGF near to the apparent dissociation constant of the PDGF mitogen receptor (6.6×10^{-12} M), adult rASMC isolates bind 11-26 times more ^{125}I-PDGF than pup rASMC from the same strain (Fig. 2). We also measured ^{125}I-PDGF binding to human foreskin fibroblasts (6.5×10^4 receptors/cell) and to A431 carcinoma cells (no detectable receptors/cell), for comparison with rASMC (Fig. 2*a*).

PDGF-receptor complexes are rapidly internalized at 37 °C, resulting in a marked reduction in membrane receptors available for binding subsequently added ligand[13-17], a process referred to as down regulation[18,19]. Since pup rASMC secrete PDGF-c, any PDGF receptors produced by these cells may be continuously down regulated by endogenously produced PDGF-c. To examine this possibility, we determined the effect of PDGF and rat pup PDGF-c on the binding properties of test cells (Table 2). Human fibroblasts preincubated at 37 °C with PDGF or pup rASMC-conditioned medium (which contains PDGF-c) retain very few binding sites for ^{125}I-PDGF. The level of ^{125}I-PDGF binding to adult rASMC preincubated with PDGF or pup rASMC-conditioned medium was reduced to levels approaching that of pup rASMC (Table 2). Medium conditioned

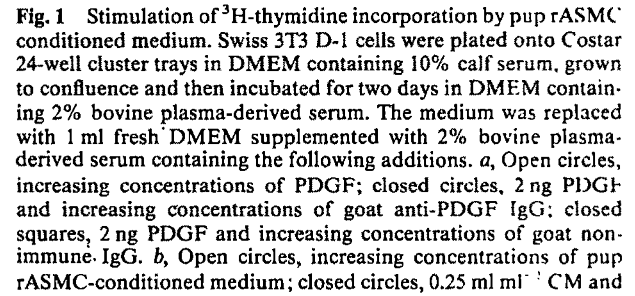

Fig. 1 Stimulation of ^{3}H-thymidine incorporation by pup rASMC conditioned medium. Swiss 3T3 D-1 cells were plated onto Costar 24-well cluster trays in DMEM containing 10% calf serum, grown to confluence and then incubated for two days in DMEM containing 2% bovine plasma-derived serum. The medium was replaced with 1 ml fresh DMEM supplemented with 2% bovine plasma-derived serum containing the following additions. *a*, Open circles, increasing concentrations of PDGF; closed circles, 2 ng PDGF and increasing concentrations of goat anti-PDGF IgG; closed squares, 2 ng PDGF and increasing concentrations of goat non-immune IgG. *b*, Open circles, increasing concentrations of pup rASMC-conditioned medium; closed circles, 0.25 ml ml^{-1} CM and increasing concentrations of goat anti-PDGF IgG closed squares, 0.25 ml ml^{-1} CM and increasing concentrations of goat non-immune IgG [Monospecific antiserum to pure PDGF was prepared in a goat. (Elaine Raines, personal communication). IgG was prepared by sodium sulphate precipitation and DEAE chromatography]. The cells were incubated with test substance for 19 h, 37 °C and then ^{3}H-thymidine incorporation determined as described previously[13]. Results are expressed as the ratio of ^{3}H-thymidine incorporation by cells exposed to test mixtures to incorporation by untreated cells. The plotted values are the means of triplicate determinations from a representative experiment. The pup rASMC-conditioned medium was produced by cells isolated from 16-day-old Sprague-Dawley rats and contained 3.06 ± 0.54 (*s.d.*) ng ml^{-1} PDGF-c. CM, conditioned medium.

Table 2 PDGF receptor expression by rASMC and human fibroblasts after exposure to pup rASMC-conditioned medium or PDGF

Cell type	Test substance (amt per ml)	Specific ^{125}I-PDGF binding (c.p.m. per 10^6 cells)
a Human fibroblasts	0	34,300
	2 ng PDGF	0
	1 ml Pup CM	2,400
	1 ml Adult CM	20,500
b Pup rASMC	0	900
c Adult rASMC	0	5,400
	2 ng PDGF	1,400
	1 ml Pup CM	2,600
	1 ml Adult CM	5,900

Pup rASMC-conditioned medium was obtained from cells isolated from 18-day-old Sprague-Dawley rats and contained 1.12 ng ml^{-1} of PDGF-c. Adult rASMC-conditioned medium was obtained from cells isolated from 3-month-old spontaneously hypertensive rats and contained 0.026 ng ml^{-1} PDGF-c. Human adult foreskin fibroblasts were prepared as for the radioreceptor assay[18,37] and rASMC were plated onto Costar 24-well cluster trays in DMEM containing 20% fetal bovine serum, grown to confluence, then incubated in DMEM containing 2% bovine plasma-derived serum. Two days later the cells were exposed to 1 ml binding medium, 1 ml binding medium containing 2 ng ml^{-1} PDGF, or 1 ml rASMC-conditioned medium supplemented with 0.025 M HEPES, *p*H 7.4 for 4 h, 37 °C. The cells were washed three times with binding rinse and then exposed for 2 h, 4 °C to 1 ml binding medium containing 0.5 ng ml^{-1} ^{125}I-PDGF. Specifically bound radioactivity was determined as described in Fig. 2 legend, and cell counts were obtained from parallel cells treated with binding medium alone. Numbers are the mean of triplicate wells from a representative experiment. Since pup rASMC do not express detectable high affinity receptors for ^{125}I-PDGF (see Fig. 2) they were only examined for their ability to bind ^{125}I-PGDF following exposure of the cells to binding rinse alone. CM, conditioned medium.

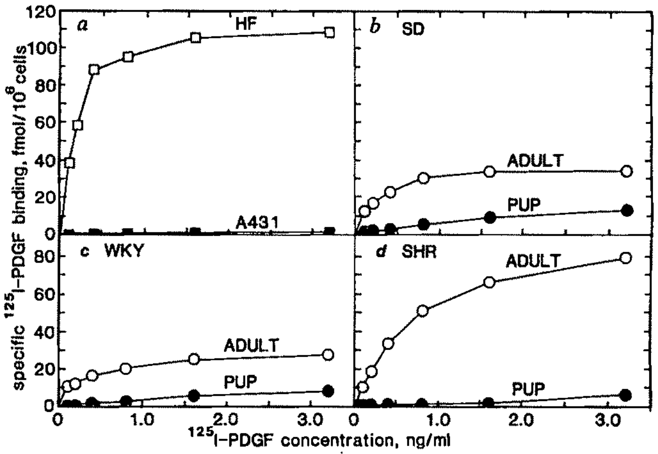

Fig. 2 Specific binding of ^{125}I-PDGF to rASMC. Cells were plated onto 24-well trays in Waymouth's medium containing 10% or 20% bovine serum or in DMEM containing 10% or 20% fetal bovine serum. After cells had grown to near confluence the media were replaced with DMEM supplemented with 2% PDGF-deficient calf serum (CMS-I; see ref. 38) or 2% bovine plasma-derived serum, and assayed for ^{125}I-PDGF binding 2 to 3 days later as previously described[13,37]. Cell counts were obtained from cells treated in a parallel fashion but with binding medium alone and nonspecifically bound c.p.m., determined by exposing cells to ^{125}I-PDGF and an excess of unlabeled, partially-purified PDGF (5-40 μg ml^{-1}, the equivalent of 50 to 400 ng ml^{-1} purified PDGF), was subtracted to determine the amount of specifically bound ^{125}I-PDGF. The plotted values represent the average amount of ^{125}I-PDGF binding to three or more different isolates of rASMC from each age (except for SHR pup, $n = 2$). HF, human fibroblasts; A431, human carcinoma cells; SD, Sprague-Dawley; WKy, Wistar Kyoto; SHR, spontaneously hypertensive rat.

by adult rASMC (which does not contain PDGF-c) had a minimal effect on ^{125}I-PDGF binding to human fibroblasts and no effect on its binding to adult rASMC. Therefore, PDGF-c production by pup rASMC may account for our inability to detect high affinity PDGF receptors on pup rASMC.

We find that adult and pup rASMC express approximately 1.0×10^4 ^{125}I-EGF binding sites per cell with an estimated k_D of 6.7×10^{-10} M (data not shown). There was no detectable difference in the number of EGF receptors expressed by pup and adult rASMC, unlike the PDGF receptor. Pup rASMC-conditioned medium contains no detectable (less than 0.4 ng/ml) EGF-like binding competitor activity as determined by radioreceptor assay (data not shown). The ability of anti-PDGF IgG to completely abolish the stimulation of DNA synthesis by 3T3 cells caused by pup rASMC-conditioned medium (Fig. 1), also indicates that these cells do not secrete biologically significant amounts of non-PDGF-like mitogens for 3T3 cells. Therefore, it appears that the mitogen-related phenotypic differences between adult and pup rASMC are relatively specific for PDGF and do not reflect general differences in mitogen receptor number or in production of growth factors.

A similar phenomenon may occur in human fibroblasts since Clemmons[23] has reported that, in platelet-poor plasma, normal human fetal fibroblasts secrete a factor which enhances their own growth. This does not occur in fibroblasts from three-year-old donors. Pup rASMC, but not adult rASMC, secrete a PDGF-like mitogen and express fewer detectable PDGF receptors. This is consistent with our suggestion that rASMC synthesize the PDGF mitogen receptor at all developmental stages and only pup rASMC synthesize a PDGF-c which provides a constant mitogenic stimulation, resulting in down regulation of their own PDGF receptors. That pup rASMC can respond to the PDGF-c they produce is indicated by the ability of PDGF to stimulate [^{3}H]thymidine incorporation in some, but not all, isolates of pup rASMC (data not shown). Nilsson *et al.*[20] have also reported that rASMC obtained from 5-day-old donors and cultured in serum-free medium respond to added PDGF with increased DNA synthesis and more rapid growth. Thus we suggest that pup rASMC may regulate their growth properties by producing a growth factor (PDGF-c) to which they themselves respond—that is, an autocrine mechanism first proposed to explain the growth properties of transformed cells[21,22].

The basic structure of the rat aorta is already developed at birth[24,25]. From birth until three months of age, however, there is a substantial increase in cell number[26-30] and the amount of connective tissue matrix components[24-27]. PDGF-c could be responsible for these changes since PDGF has been shown to stimulate the growth of cultured smooth muscle cells[13,31-33] and enhance the production of connective tissue components *in vitro*[34,35]. PDGF-c may thus provide an example of autocrine stimulation of growth operating during normal development and which can be inappropriately activated during neoplastic transformation.

We thank Linda Mohai and Karen Tittle for technical assistance and Anna Choi and Jan Fullenwider for typing the manuscript. This research was supported by NIH grants HL 18645 and HL 29873 and a grant from R. J. Reynolds Industries, Inc.

Received 18 May; accepted 6 August 1984.

1. Ross, R. & Glosmet, J. A *New Engl. J. Med.* **295**, 369-377; 420-425 (1976).
2. Deuel, T. F., Huang, J. S., Huang, S. S., Stroobant, P. & Waterfield, M. S. *Science* **221**, 1348-1350 (1983).
3. Heldin, C.-H., Westermark, B. and Wasteson, Å. *J. cell. Physiol.* **105**, 235-246 (1980).
4. Dicker, P., Pohjanpelto, P., Pettican, P. & Rozengurt, E. *Expl Cell Res.* **135**, 221-227 (1981).
5. Nister, M., Heldin, C.-H., Wasteson, Å. & Westermark, B. *Ann. N.Y. Acad. Sci.* **397**, 25-33 (1982).

6. Bowen-Pope, D. F., Vogel, A. & Ross, R. *Proc. natn. Acad. Sci. U.S.A.* **81**, 2396-2400 (1984).
7. Holley, R. & Kiernan, J. *Proc. natn. Acad. Sci. U.S.A.* **60**, 300-304 (1968).
8. Clarke, G. D., Stoker, M. G. P., Ludlow, A. & Thornton, M. *Nature* **227**, 798-801 (1970).
9. Dulbecco, R. *Nature* **227**, 802-806 (1970).
10. Curie, G. A. *Br. J. Cancer* **43**, 335-343 (1981).
11. Scher, C. D., Pledger, W. J., Martin, P., Antoniades, H. & Stiles, C. D. *J. cell. Physiol.* **97**, 371-380 (1978).
12. Graves, D. T., Owen, A. J. & Antonaides, H. N. *Cancer Res.* **43**, 83-87 (1983).
13. Bowen-Pope, D. F. & Ross, R. *J. biol. Chem.* **257**, 5161-5171 (1982).
14. Heldin, C.-H., Westermark, B. & Wasteson, Å. *Proc. natn. Acad. Sci. U.S.A.* **78**, 3664-3668 (1981).
15. Heldin, C.-H., Wasteson, Å. & Westermark, B. *J. biol. Chem.* **257**, 4216-4221 (1982).
16. Huang, J. S., Huang, S. S., Kennedy, B. & Deuel, T. F. *J. biol. Chem.* **257**, 8130-8136 (1982).
17. Williams, L. T., Tremble, P. & Antoniades, H. N. *Proc. natn. Acad. Sci. U.S.A.* **79**, 5867-5870 (1982).
18. Carpenter, G. & Cohen, S. *J. Cell Biol.* **71**, 159-171 (1976).
19. Aharonov, A., Pruss, R. M. & Herschman, H. R. *J. biol. Chem.* **253**, 3970-3977 (1978).
20. Clemmons, D. R. *J. cell. Physiol.* **114**, 61-67 (1983).
21. Nilsson, J., Ksiazek, T., Heldin, C.-H. & Thyberg, J. *Expl Cell Res.* **145**, 231-237 (1983).
22. Sporn, M. B., Newton, D. L., Roberts, A. B., DeLarco, J. E. & Todaro, G. J. in *Molecular Actions and Targets for Cancer Chemotherapeutic Agents* (eds Sartorelli, A. C., Lazo, J. S. & Bertino, J. R.) 541-554 (Academic, New York, 1981).
23. Sporn, M. B. & Todaro, G. J. *New Engl. J. med.* **303**, 878-880 (1980).
24. Paule, W. J. *J. Ultrastruct. Res.* **8**, 219-235 (1963).
25. Cliff, W. J. *Lab. Invest.* **17**, 599-615 (1967).
26. Berry, C. L., Looker, T. & Germain, J. *J. Anat.* **113**, 1-16 (1972).
27. Looker, T. & Berry, C. L. *J. Anat.* **113**, 17-34 (1972).
28. Gerrity, R. G. & Cliff, W. J. *Lab. Invest.* **32**, 585-600 (1975).
29. Olivetti, G., Anversa, P., Melissari, M. & Loud, A. V. *Circulation Res.* **47**, 417-424 (1980).
30. Bucher, B., Travo, P., Laurent, P. & Stoclet, J. C. *Cell biol. Internat. Reports* **6**, 113-123 (1982).
31. Ross, R., Glomset, J. A., Kariya, B. & Harker, L. *Proc. natn. Acad. Sci. U.S.A.* **71**, 1207-1210 (1974).
32. Rutherford, R. B. & Ross, R. *J. Cell Biol.* **69**, 196-203 (1976).
33. Witte, L. D. *et al. Circ. Res.* **42**, 402-409 (1978).
34. Burke, J. M. & Ross, R. *Expl Cell Res.* **107**, 387-395 (1977).
35. Narayanan, A. S. & Page, R. *J. biol. Chem.* **258**, 11694-11699 (1983).
36. Gordon, D. & Schwartz, S. M. *Circulation Res.* (submitted).
37. Bowen-Pope, D. F. & Ross, R. *Meth. Enzym.* **109** (in the press).
38. Vogel, A., Raines, E., Kariya, B., Rivest, M.-J. & Ross, R. *Proc. natn. Acad. Sci. U.S.A.* **75**, 2810-2814 (1978).

A novel transforming gene in a human malignant melanoma cell line

R. A. Padua, N. Barrass & G. A. Currie

Marie Curie Memorial Foundation, Research Institute, The Chart,
Oxted, Surrey RH8 0TL, UK

Cellular transforming genes can be detected in human tumours by DNA-mediated transfection into NIH 3T3 mouse fibroblasts[1,2]. The activated transforming genes have been, in most cases, members of the *ras* gene family, of which the most frequently found is the c-Ki-*ras* oncogene[3–7] and least frequently the c-Ha-*ras* gene[8–10]. An increasing number of studies has identified the presence of activated N-*ras* (which has no known viral homologue) in human tumour cell lines[11–18]. Furthermore, other transforming genes, distinct from the *ras* gene family, have been reported in B- and T-cell lymphomas[19,20]. The activation of c-Ha-*ras* and N-*ras* has been described in some cell lines derived from cases of human malignant melanoma[21]. Here we describe the presence of transforming activity in the DNA from a human melanoma cell line which shows weak homology with members of the *ras* oncogene family.

High-molecular weight DNA prepared from established melanoma cell lines was used to transform NIH 3T3 cells by the calcium phosphate co-precipitation method[22]. Table 1 shows the results of these transfection assays. The foci observed were collected and grown to confluence, then DNA was extracted and analysed by Southern blotting[23] for human repetitive sequences using Blur 8 (ref. 24), a clone of human *Alu* sequences (Fig. 1), and total human DNA (data not shown). Positive results were obtained for foci derived from lines NKI4, MeWo and Mel Swift. (The Mel Swift line was subsequently found to contain an activated N-*ras* gene and will be reported separately.) DNA from NKI4 and MeWo transformants was further analysed by Southern blotting and hybridization to clones containing v-Ha-*ras* (BS9)[25], v-Ki-*ras* (HiHi-3)[26] and N-*ras* (pAT8.8)[14]. In addition, these DNA samples were blotted and hybridized to probes specific for the following oncogenes: B-*lym*, v-*abl*, v-*sis*, v-*erb*, v-*fes*, v-*fgr*, v-*fms*, v-*fps*, v-*fos*, v-*mos*, v-*myb*, v-*myc*, v-*raf*, v-*src* and v-*yes*. In each case the hybridization pattern obtained was identical to that of normal NIH 3T3 DNA. DNA from serially transformed foci (second cycle transfectants) from NKI4 showed a conserved 16-kilobase (kb) *Eco*RI fragment containing *Alu* sequences (Fig. 1).

Primary and secondary transformants from NKI4 were grown in soft agar (0.3% Noble) and colonies were detected after 2 weeks. Plating efficiencies well in excess of 10% were observed whereas control NIH 3T3 cells had negligible colony-forming efficiencies. Colonies were picked from the soft agar cultures and grown to confluence in liquid medium. DNA was extracted and Southern analysis demonstrated that the *Alu* sequences associated with NIH 3T3 transformation were conserved in cells displaying the anchorage-independent phenotype.

DNA was isolated from a secondary transformant of the NKI4 cell line and enriched for the 16-kb *Eco*RI fragment by size fractionation. This fragment was cloned into λ L47 and one clone was characterized in detail (λNK/16). Hybridization of λNK/16 to clones containing v-Ha-*ras* (BS9), c-Ha-*ras*[10] (pT24-C3), Ki-*ras* (HiHi-3) and N-*ras* (pAT 8.8) under low stringency showed that λNK/16 has some homology with HiHi-3 and c-Ha-*ras* (Fig. 2). Weak hybridization was observed when BS9 was probed with λNK/16 (Fig. 2, lane *b*), but there was clearer evidence of conserved sequences between λNK/16 and BS9 when the λNK/16 clone was probed with BS9 (Fig. 3, lanes *d*, *e*). There was no apparent hybridization of λNK/16 probe to the first exon of N-*ras* (Fig. 2, lane *d*) and λNK/16 failed to hybridize with a probe specific for the first exon of N-*ras* (data not shown). As the first exon of the known *ras* genes is highly

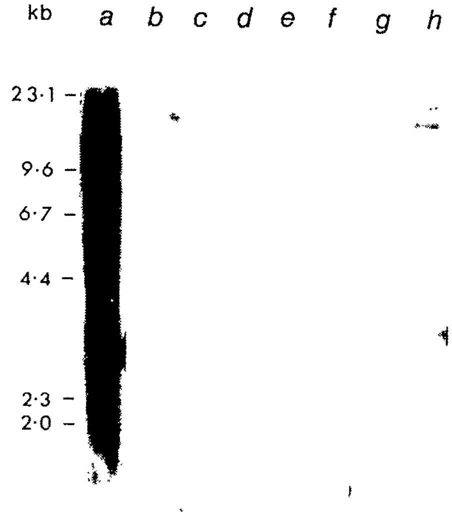

Fig. 1 Detection of human repetitive sequences. 20 μg of high-molecular weight DNA isolated from primary and secondary transformants were digested with *Eco*RI, electrophoresed in horizontal 0.8% agarose gels and blotted onto nitrocellulose filters[23]. The filters were hybridized in stringent conditions[29] to 10^6 c.p.m. ml^{-1} ^{32}P-labelled 0.3-kbp cloned repetitive sequence DNA purified from plasmid Blur 8 (ref. 24; specific activity 2-4×10^8 c.p.m. μg^{-1}). Filters were washed with 0.6×SSC, 0.1% SDS at 60 °C for 1 h. NKI4 transformants: lane *a*, primary focus; lanes *b*-*f*, secondary foci; lane g, NIH 3T3; lane *h*, EJ secondary focus. *Hin*dIII-digested λ cI857 DNAs served as molecular weight markers.

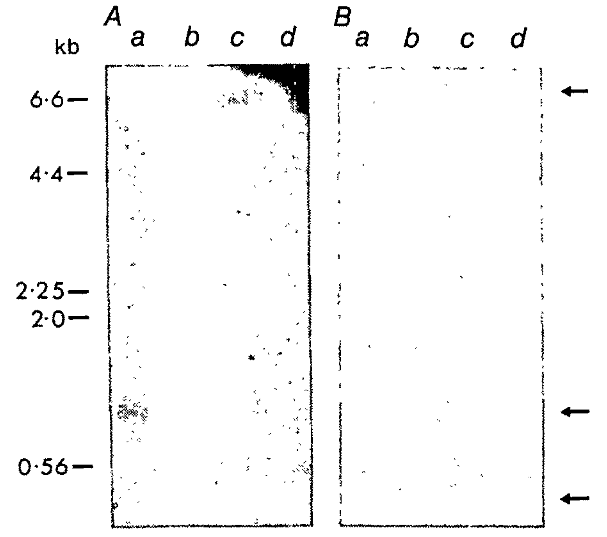

Fig. 2 Hybridization of λNK/16 to members of the *ras* gene family. Lane *a*, v-Ki-*ras* (Hi-Hi 3)[26]; *b*, v-Ha-*ras* (BS9)[25]; *c*, c-Ha-*ras* (pT24-C3)[10]; *d*, N-*ras* (*Pvu*II fragment containing exon 1). Arrows indicate positions of cloned insert DNAs. *Hin*dIII-digested λ *c*1857 DNAs were used as molecular weight markers. 10 μg (per lane) of cloned DNA were analysed by Southern blotting and hybridization to the purified insert of λNK/16 clone under: *A*, low stringency conditions of 30% formamide, 6×SSC, 1×Denhardt's at 42 °C and washed in 2×SSC, 0.1% SDS at 60 °C for 1 h, or *B*, high stringency conditions[23] and washed in 0.1×SSC, 0.1% SDS at 60 °C.

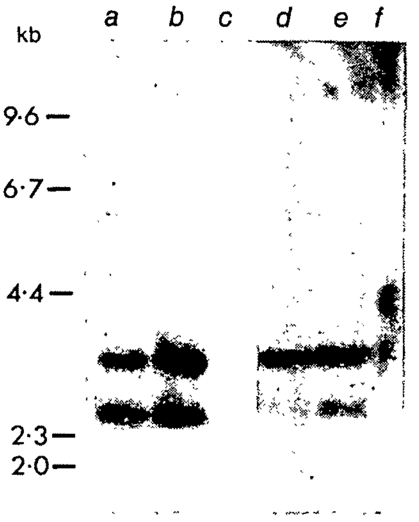

Fig. 3 Detection of human repetitive and *ras*-related sequences in λNK/16. 1 μg of cloned DNA was digested with *Kpn*I and *Pvu*II, electrophoresed on 0.8% agarose gels and blotted onto nitrocellulose filters. Lanes *a–c* were hybridized to Blur 8 in conditions of high stringency as described in Fig. 1 legend. Lanes *d–f* were hybridized to BS9 (v-Ha-*ras*) in conditions of low stringency as described in Fig. 2 legend. Lanes *a*, *d*, λNK/16 insert; *b*, *e*, λNK/16 clone; *c*, *f*, λL47 *Hin*dIII-digested λ *c*1857 DNAs served as molecular weight markers.

conserved, we conclude that λNK/16 must contain divergent sequences which show similarity to the HiHi-3, BS9 and pT24-C3 clones. Hybridization to these clones was lost in high stringency conditions (Fig. 2*B*).

The λNK/16 clone was also hybridized in high stringency conditions to Southern filters containing the plasmid clones of those viral oncogenes mentioned above and to clones of the following cellular and viral oncogenes: v-*ski*, v-*ets*, v-*rel*, c-*sis*, c-*myc*, c-*myb* and c-*mos*. In each case, the plasmid clone had been digested with the restriction endonuclease(s) which separated the oncogene-specific fragment(s) from the remainder of the clone under electrophoresis. No hybridization was observed with the coding sequences of these clones. In conditions of low stringency, faint hybridization was seen with the 1.9-kb pSA17 v-*abl* clone, but this was probably due to the presence of mouse sequences in the clone[27]. The λNK/16 clone detects fragments of 5.5 and 6.5 kb in *Eco*RI-digested human DNA and of 5.0 and 7.0 kb in *Eco*RI-digested dog DNA in high stringency conditions. This suggests that λNK/16 contains conserved sequences. Furthermore, λNK/16 also detects a human transcript of 3.5 kb on Northern blot analysis.

λNK/16 probably contains only part of the gene as it does not cross-hybridize with all of the *ras* gene clones tested. Exon 1 of N-*ras*, for example, is not detected at all. Furthermore,

Table 1 Transforming activity of DNA from melanoma tumours and cell lines

	Transformation frequency, foci per μg DNA (no. foci/no. flasks)		
	1st cycle	2nd cycle	3rd cycle
Controls			
3T3	0.03 (127/195)	ND	ND
Human peripheral blood leukocytes	0.05 (54/52)	ND	ND
Human placenta	0.02 (12/25)	ND	ND
Salmon sperm	0.03 (2/10)	ND	ND
EJ (bladder carcinoma)	0.13 (95/37)	>1.2 (>704/29)	>1.6 (>1,275/40)
Melanoma cell lines			
Mel 2a	0.05 (26/24)	ND	ND
Mel 28	0.01 (4/14)	ND	ND
Mel 57	0.03 (17/33)	ND	ND
Mel 64	0.05 (9/9)	ND	ND
RPM I 5966	0.03 (17/29)	ND	ND
Mel Swift	0.04 (25/36)	0.16 (62/19)	0.16 (16/5)
MeWo	0.03 (26/33)	0.13 (76/30)	0.13 (13/5)
NKI4	0.04 (29/33)	0.12 (49/20)	0.12 (63/26)

NIH 3T3 cells were seeded at 3×10^5 per 25 cm^2 flask and 24 h later exposed to 20 μg DNA as a calcium phosphate precipitate[22]. Foci were counted 3 weeks after transfection. ND, not determined (when the 1st cycle transfectants contained no detectable human DNA, no further transfections were performed).

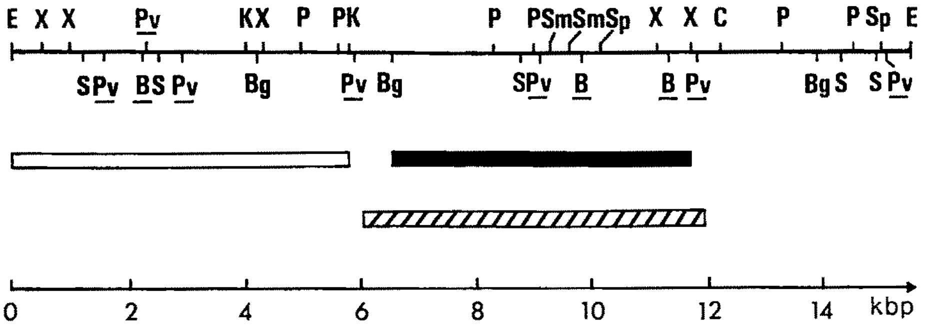
E X X Pv KX P PK P PSmSmSp X X C P PSp E
SPv BS Pv Bg Pv Bg SPv B B Pv BgS SPv
0 2 4 6 8 10 12 14 kbp

Fig. 4 Restriction map of λNK/16. Restriction endonuclease sites are as follows: B, *Bam*HI; Bg, *Bgl*II; C, *Cla*I; E, *Eco*RI; K, *Kpn*I; P, *Pst*I; Pv, *Pvu*II; Sm, *Sma*I; Sp, *Sph*I; S, *Sst*I; X, *Xba*I. Underlined enzymes are incompletely mapped. *Hin*dIII and *Sal*I did not cut within the clone. Solid bar indicates regions hybridizing to human DNA. Open bar indicates the region containing mouse-related sequences. Hatched bar indicates region of homology with the v-Ha-*ras* (BS9) probe.

λNK/16 is not active in the NIH 3T3 transfection assay—this lack of biological activity of λNK/16 indicates that the entire activated gene has not been cloned. Comparison of the restriction map of λNK/16 (Fig. 4) with those of the five known human *ras* genes (c-Ha-*ras*1, c-Ha-*ras*2, c-Ki-*ras*1, c-Ki-*ras*2 and N-*ras*[15,28]) indicates that the sequences showing homology with *ras* are likely to be novel. Thus, we have demonstrated a weak homology of λNK/16 with the *ras* gene clones (and not with any other cloned oncogenes), but proof that this gene is a member of the *ras* family must await sequence analysis.

We thank David Hughes, Althea Smallwood, Frederick Rayment, Julia Roberts and Jonathan Fletcher for technical assistance, and Dr Margaret Knowles for help with the biological assays. The cell lines Mel 2a, Mel 57, RPMI 5966, Mel Swift, MeWo and NKI4 were provided by Dr J. Embleton. Our use of NKI4 was by courtesy of Dr Jan de Vries. NIH 3T3 cells were provided by Demetrios Spandidos. Cloned oncogene probes were provided by Drs S. Aaronson, D. Baltimore, M. Bishop, G. Cooper, T. Curran, R. Gallo, A. Hall, J. Neil, D. Lowy, M. Nunn, M. Oskarsson, U. Rapp, C. Sherr, E. Stavnezer, N. Teich and M. Yoshida.

Received 16 July; accepted 30 August 1984.

1. Weinberg, R. A. *Adv. Cancer Res.* **36**, 149-163 (1982).
2. Cooper, G. M. *Science* **218**, 801-806 (1982).
3. Der, C. J., Krontiris, T. G. & Cooper, G. M. *Proc. natn. Acad. Sci. U.S.A.* **79**, 3637-3640 (1982).
4. Pulciani, S. *et al. Nature* **300**, 539-542 (1982).
5. McCoy, M. S. *et al. Nature* **302**, 79-81 (1983).
6. Shimizu, K. *et al. Proc. natn. Acad. Sci. U.S.A.* **80**, 2112-2116 (1983).
7. Cooper, C. S. *et al. Cancer Res.* **44**, 1-10 (1984).
8. Pulciani, S. *et al. Proc. natn. Acad. Sci. U.S.A.* **79**, 2845-2849 (1982).
9. Parada, L. F., Tabin, C. J., Shih, C. & Weinberg, R. A. *Nature* **297**, 474-478 (1982).
10. Santos, E., Tronick, S. R., Aaronson, S. A., Pulciani, S. & Barbacid, B. *Nature* **298**, 343-347 (1982).
11. Marshall, C. J., Hall, A. & Weiss, R. A. *Nature* **299**, 171-173 (1982).
12. Shimizu, K., Goldfarb, M., Perucho, M. & Wigler, M. *Proc. natn. Acad. Sci. U.S.A.* **80**, 383-387 (1983).
13. Murray, M. J. *et al. Cell* **33**, 749-757 (1983).
14. Hall, A., Marshall, C. J., Spurr, N. K. & Weiss, R. A. *Nature* **303**, 396-400 (1983).
15. Taparowsky, E., Shimizu, K., Goldfarb, M. & Wigler, M. *Cell* **34**, 581-586 (1983).
16. Eva, A., Tronick, S. R., Gol, R. A., Pierce, J. H. & Aaronson, S. A. *Proc. natn. Acad. Sci. U.S.A.* **80**, 4926-4930 (1983).
17. Souyri, M. & Fleissner, E. *Proc. natn. Acad. Sci. U.S.A.* **80**, 6676-6679 (1983).
18. Gambke, C., Signer, E. & Moroni, C. *Nature* **307**, 476-478 (1984).
19. Lane, M., Sainten, A. & Cooper, G. M. *Cell* **28**, 873-880 (1982).
20. Diamond, A., Cooper, G. M., Ritz, J. & Lane, M. *Nature* **305**, 112-116 (1983).
21. Albino, A. P., Le Strange, R., Oliff, A. I., Furth, M. & Old, L. J. *Nature* **308**, 69-72 (1984).
22. Graham, F. L. & Van der Eb, A. *J. Virol.* **52**, 456-461 (1973).
23. Southern, E. M. *J. molec. Biol.* **98**, 503-517 (1975).
24. Rubin, C. M., Houck, C. M., Deininger, P. L. & Schmid, C. W. *Nature* **284**, 372-374 (1980).
25. Ellis, R. W. *et al. J. Virol.* **36**(2), 408-420 (1980).
26. Ellis, R. W. *et al. Nature* **292**, 506-511 (1981).
27. Dale, B. & Ozanne, B. *Molec. cell. Biol.* **1**, 731-742 (1981).
28. Chang, E. H., Gonda, M. A., Ellis, R. W., Scolnick, E. M. & Lowy, D. R. *Proc. natn. Acad. Sci. U.S.A.* **79**, 4848-4852 (1982).
29. Wahl, G. M., Stern, M. & Stark, G. R. *Proc. natn. Acad. Sci. U.S.A.* **76**, 3683-3687 (1979).

An artefact explains the apparent association of the transferrin receptor with a *ras* gene product

Joe Harford

Laboratory of Biochemistry and Metabolism, National Institute of Arthritis, Diabetes and Digestive and Kidney Diseases, National Institutes of Health, Bethesda, Maryland 20205, USA

There is substantial evidence implicating *ras* genes in a number of human neoplasms[1]. The *ras* genes of several human tumours[2–6] display mutational changes which are likely to be responsible for their transforming activity. Normal cells also express *ras* genes[7], over-expression of which can induce cellular transformation[8]. *ras* genes encode proteins of ~21,000 molecular weight (MW) (p21)[9] that are localized to the inner surface of the plasma membrane[10,11]. Much effort is being focused on the elucidation of the physiological function of *ras*-encoded proteins in normal and transformed cells, concentrating on interactions between p21 and other cellular elements. Recently, Finkel and Cooper[12] reported that p21 in extracts of human bladder carcinoma cells is involved in a molecular complex with the transferrin receptor of these cells. This report aroused considerable interest, particularly as expression of the transferrin receptor has been linked to cell proliferation[13–15]. I present here evidence that the apparent association of p21 and the transferrin receptor is an artefact of the immunoprecipitation technique[12].

Transferrin is an iron-binding protein present in serum at concentrations of 2-4 mg ml^{-1} (ref. 16). The human transferrin receptor can be solubilized in buffers containing non-ionic detergents with the retention of transferrin-binding activity[15,17,18] and the receptor has been purified by affinity chromatography on Sepharose to which transferrin was covalently linked[19]. When immune serum is used for coating the staphylococcal protein A-Sepharose (Pharmacia) to be used in immunoprecipitation, I observe that serum proteins other than IgG can become associated nonspecifically with the resin. Notably, some transferrin remains with the protein A-Sepharose even after extensive washing with buffers containing Triton X-100. When such coated and washed resin is boiled in sample buffer for SDS-polyacrylamide gel electrophoresis, the released proteins revealed by silver staining of the gel included albumin and transferrin in addition to the predominant heavy and light chains of IgG (data not shown). Polypeptides having the molecular weights of albumin and transferin are not observed when uncoated protein A-Sepharose is similarly boiled and analysed. Thus, protein

A-Sepharose coated with immune serum is in effect an affinity column for the transferrin receptor.

The observations that led Finkel and Cooper[12] to conclude that the transferrin receptor is associated with the *ras* gene product are consistent with inadvertent affinity purification of the transferrin receptor during p21 immunoprecipitation. To test this hypothesis, protein A-Sepharose coated in various ways was added in the absence of additional antibodies to a lysate of ^{35}S-methionine-labelled T24 bladder carcinoma cells. No band corresponding to the 90,000-MW transferrin receptor subunit was found to be associated with uncoated protein A-Sepharose (Fig. 1, lane *b*). This lysate does contain labelled transferrin receptor, demonstrated by inclusion of a monoclonal antibody (B3/25, Boehringer Mannheim) which recognizes the transferrin receptor (Fig. 1, lane *a*). B3/25 is bound by protein A and thus no coating of the resin is needed for immunoprecipitation of the transferrin receptor. Precoating of the protein A-Sepharose with an IgG fraction of rabbit anti-rat IgG (Cappel) results in an increase in antibody-independent association of several radioactive polypeptides from the cell lysate; most notably a band appears having the molecular weight of the transferrin receptor subunit (Fig. 1, lane *c*). This is most likely to occur as a result of transferrin present in the IgG fraction used to coat this resin. Indeed, when whole rabbit serum against rat IgG (Cappel) is used for coating the protein A-Sepharose, a significant increase is seen in the amount of receptor bound by the resin (Fig. 1, lane *d*), reflecting the higher transferrin content of the coating substance. The inclusion of rat anti-*ras* monoclonal, Y13-238 (a gift of M. Furth) results in the immunospecific binding of radiolabelled p21 from the lysate (Fig. 1, lane *e*), but no increase in the amount of transferrin receptor associated with the resin. Finkel and Cooper[12] used normal rat serum as a negative control for the rat anti-*ras* monoclonal antibodies. Therefore, the effect of normal rat serum was examined in the present study. When 20 μl of normal rat serum are used in place of the anti-*ras* antibody, not only is p21 no longer present but the transferrin receptor also disappears (Fig. 1, lane *f*). This latter effect is probably the result of transferrin in the normal rat serum. This rat serum transferrin seems able to compete with the rabbit transferrin on the coated resin, preventing the affinity binding of the transferrin receptor. In support of this contention, human diferric transferrin (100 μg ml^{-1}) also eliminates the receptor band when added to serum-coated protein A-Sepharose in the absence of additional antibodies (Fig. 1, lane *h*). It has long been recognized that extensive species cross-reactivity exists in the interaction of transferrin and its receptor[20,21]. The addition of anti-*ras* monoclonal together with 20 μl of normal rat serum yields the expected result; p21 is immunoprecipitated by the anti-*ras*, but the transferrin receptor was prevented from interacting with the serum-coated protein A-Sepharose by the transferrin in the normal rat serum (Fig. 1, lane *g*). To demonstrate conclusively that the T24 lysate contained active transferrin receptor capable of being affinity purified, a portion of the labelled lysate is exposed to Sepharose covalently linked with human diferric transferrin (a gift of G. Ashwell). After washing and boiling the transferrin-Sepharose in analogy to the immunoprecipitations, the major polypeptide seen on the SDS gel is the 90,000-MW transferrin receptor subunit (Fig. 1, lane *i*). Addition of transferrin to the lysate prevents this intentional affinity chromatography of the receptor on transferrin-Sepharose (Fig. 1, lane *j*).

All our observations are consistent with the absence of any direct association between p21 and the transferrin receptor. When anti-*ras* is added in the absence of normal rat serum, p21 is precipitated with no increase in the amount of resin-associated transferrin receptor (compare Fig. 1, lanes *d* and *e*). Likewise, when anti-*ras* is added in the presence of normal rat serum, p21 is precipitated but there is no *ras*-specific precipitation of the transferrin receptor (compare lanes *f* and *g*). Unfortunately, Finkel and Cooper[12] used conditions analogous to lane *f* as a negative control for an anti-*ras* immunoprecipitation analogous

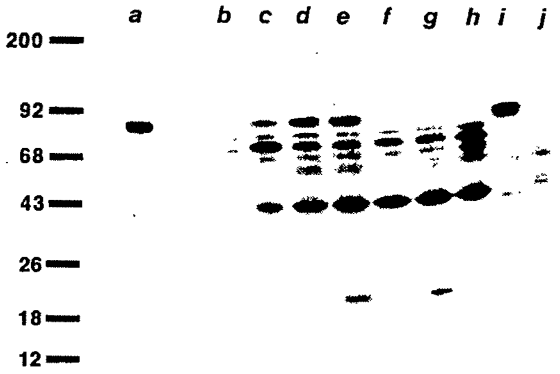

Fig. 1 Electrophoretic analysis of samples from the lysate of ^{35}S-methionine-labelled T24 cells. Lane *a*, material bound by an anti-transferrin receptor monoclonal antibody using uncoated protein A-Sepharose; lane *b*, material bound by uncoated protein A-Sepharose alone; lane *c*, material bound protein A-Sepharose coated with an IgG fraction of rabbit anti-rat immunoglobulin serum; lane *d*, material bound by protein A-Sepharose coated with rabbit anti-rat immunoglobulin serum; lane *e*, anti-*ras* monoclonal antibody added to lane *d* conditions; lane *f*, normal rat serum added to lane *d* conditions; lane *g*, anti-*ras* monoclonal antibody plus normal rat serum added to lane *d* conditions; lane *h*, transferrin added to lane *d* conditions; lane *l*, material bound by transferrin-Sepharose; lane *j*, transferrin added to lane *l* conditions. Numbers to the left of the gel represent molecular weights × 10^{-3} of marker polypeptides.

Methods: Human bladder carcinoma cells (T24) at 75% confluence were labelled in 100-mm culture dishes for 18 h by incubation with 400 μCi ml^{-1} ^{35}S-methionine (Amersham) in 2.5 ml RPMI 1640 medium containing 10% fetal bovine serum and 10% of the normal amount of methionine. The labelled cells were washed twice with 10 ml ice-cold phosphate-buffered saline and then scraped into cell lysis buffer (2 ml per dish) consisting of 0.125 M NaCl, 1 mM $CaCl_2$, 1 mM $MgCl_2$, 1% Triton X-100, 3 trypsin inhibitory units per ml aprotinin (Calbiochem), 0.2 M Tris-HCl, *p*H 7.4. The cells were then homogenized with 20 strokes of a Dounce homoginizer (Kontis, pestle B) and clarified by centrifugation at 30,000*g* for 20 min. The resultant supernatant fluid was used for immunoprecipitations and affinity chromatography. Each sample contained 5×10^7 trichloroacetic acid-precipitable c.p.m. in a volume of 500 μl. All reactions were performed in 1.5-ml Eppendorf tubes. Lysates were first incubated for 1 h at 4 °C with 25 μl of staphylococcal protein A-Sepharose beads (as a 25% suspension in lysis buffer) that had been coated with rabbit anti-rat immunoglobulin serum (Cappel) and washed extensively (5 times, 15 volumes) with phosphate-buffered saline. This resin was removed by centrifugation and the preadsorbed lysate incubated for 1.5 h at 4 °C with no addition (lanes *b*, *c*, *d*, *i*) or after addition of 10 μl anti-transferrin receptor monoclonal antibody B3/25 (lane *a*), 2 μl anti-*ras* monoclonal Y13-238 (lane *e*), 20 μl normal rat serum (lane *f*), 2 μl of anti-*ras* monoclonal Y13-238 plus 20 μl normal rat serum (lane *g*), or 100 μg ml^{-1} human diferric transferrin (lanes *h*, *j*). Following these incubations, 25 μl (as a 25% suspension in lysis buffer) of either uncoated protein A-Sepharose (lanes *a*, *b*) or protein A-Sepharose previously coated with an IgG fraction of rabbit anti-rat immunoglobulin serum (lane *c*), protein A-Sepharose previously coated with rabbit anti-rat immunoglobulin serum (lanes *d*-*h*), or transferrin-Sepharose (3 mg human diferric transferrin per ml resin) (lanes *i*, *j*) were added and the Eppendorf tubes tumbled for 1.5 h at 4 °C. The resins were washed by seven cycles of brief centrifugation and resuspension in 1 ml of cell lysis buffer. The final pellet was boiled in the sample buffer and analysed on 10-20% linear gradient polyacrylamide slab gel using the buffer system of Laemmli[22]. The gel was treated with 1 M sodium salicylate for fluorography before drying and exposure to Kodak X-ray film at −70 °C.

to lane *e*. When these lanes are compared in isolation, the presence of the transferrin receptor in the immunoprecipitate appears to be *ras*-specific.

Transferrin-laden normal rat serum is clearly an inappropriate control for monoclonal antibodies collected by salt precipitation from ascites fluid or from culture fluid of hybridoma cells grown in medium with or without 10% fetal bovine serum[11]. Finkel and Cooper[12] also observed that transferrin added to the lysate eliminated the transferrin receptor band from anti-*ras* immune precipitates and proposed a transferrin-mediated conformational change in the receptor that disrupted the interaction with p21. They also suggested that a disruption of the p21-receptor complex by an anti-transferrin receptor monoclonal antibody was responsible for the fact that p21 was not co-precipitated by anti-receptor. The effect of transferrin and the asymmetrical co-precipitation are both explained more simply by the inadvertent affinity chromatography of the receptor demonstrated here. Loss of co-precipitation of the receptor on 'exhaustive precipitation' with anti-*ras*[12] may be due to the difference in the nature of the binding of the transferrin receptor to the resin in the absence and presence of anti-receptor antibodies. Only biologically active receptor can be bound by virtue of its affinity for the transferrin present on coated protein A-Sepharose. No such dependence on activity applies, however, in the binding of receptor by anti-receptor antibody. Thus, any loss of biological receptor activity during extraction or handling would result in transferrin receptor that could no longer become associated with coated protein A-Sepharose by affinity chromatography but which would still be precipitated with anti-receptor antibody. Partial inactivation of the receptor may also account for the high variability (5-50%) in the molar amounts of transferrin receptor apparently co-precipitated by anti-*ras*[12]. It is unsurprising that several anti-*ras* monoclonal antibodies apparently co-precipitated the transferrin receptor[12] because the association of the receptor with the coated proteinA-Sepharose is independent of the presence of the anti-*ras* (Fig. 1, lanes *b-d*). Using the methodologies of Finkel and Cooper[12] with normal rat serum as a control, addition of other monoclonal antibodies against any protein in the lysate would yield results suggesting that the transferrin receptor is co-precipitated specifically.

The results of Finkel and Cooper[12] have been reproduced here but additional controls support the lack of any molecular complex between p21 and the transferrin receptor. Although the 90,000 MW polypeptide observed[12] is the transferrin receptor, its presence in immunoprecipitates is demonstrated to be independent of anti-*ras*. I have shown here that it is due to inadvertent affinity chromatography resulting from the presence of transferrin on the coated protein A-Sepharose used in immunoprecipitation.

I thank E. Chang for her gift of T24 cells, M. Furth for the anti-*ras* monoclonal antibody, G. Ashwell for preparation of transferrin-Sepharose, and G. Ashwell, E. Chang and R. D. Klausner for discussions and comments.

Received 18 July; accepted 2 August 1984.

1. Cooper, G. M. & Lane, M. A. *Biochim. biophys. Acta* (in the press).
2. Tabin, C. J. *et al. Nature* **300**, 143-149 (1982).
3. Reddy, E. P., Reynolds, R. K., Santos, E. & Barbacid, M. *Nature* **300**, 149-152 (1982).
4. Taparowsky, E. *et al. Nature* **300**, 762-765 (1982).
5. Der, C. J. & Cooper, G. M. *Cell* **32**, 201-208 (1983).
6. Yuasa, Y. *et al. Nature* **303**, 775-779 (1983).
7. Langbeheim, H., Shih, T. Y. & Scolnick, E. M. *Virology* **106**, 292-300 (1980).
8. Chang, E. H., Furth, M. E., Scolnick, E. M. & Lowy, D. R. *Nature* **297**, 479-483 (1982).
9. Ellis, E. W. *et al. Nature* **292**, 506-511 (1981).
10. Willingham, M. C., Pastan, I., Shih, T. Y. & Scolnick, E. M. *Cell* **19**, 1005-1014 (1980).
11. Furth, M. E., Davis, L., Fleurdelys, B. & Scolnick, E. M. *J. Virol.* **43**, 294-304 (1982).
12. Finkel, T. & Cooper, G. M. *Cell* **136**, 1115-1121 (1984).
13. Judd, W., Poodry, C. A. & Strominger, J. L. *J. exp. Med.* **152**, 1430-1435 (1980).
14. Goding, J. W. & Burns, G. F. *J. Immun.* **127**, 1256-1258 (1981).
15. Trowbridge, I. S. & Omary, M. B. *Proc. natn. Acad. Sci. U.S.A.* **78**, 3039-3043 (1981).
16. Putnam, F. W. in *The Plasma Proteins* Vol. 1 (ed. Putnam, F. W.) 265-316 (Academic, New York, 1975).
17. Wada, H. G., Hass, P. E. & Sussman, H. H. *J. biol. Chem.* **254**, 12629-12635 (1979).
18. Klausner, R. D. *et al. J. biol. Chem.* **298**, 4715-4724 (1983).
19. Enns, C. A., Shindelman, J. R., Tonik, S. E. & Sussman, H. H. *Proc. natn. Acad. Sci. U.S.A.* **78**, 4222-4225 (1980).
20. Harris, D. C. & Aisen, P. *Biochemistry* **14**, 262-268 (1975).
21. Huebers, H., Csiba, E., Josephson, B., Huebers, E. & Finch, C. A. *Proc. natn. Acad. Sci. U.S.A.* **78**, 621-625 (1981).
22. Laemmli, U.K. *Nature* **227**, 680-685 (1970).

FINKEL AND COOPER COMMENT—Since learning of the above results we have repeated our experiments with additional controls. We concur with Harford that our findings are explained by the artefact he describes and, therefore, do not indicate an interaction between transferrin receptor and *ras* proteins.

T. FINKEL
G. M. COOPER

Laboratory of Molecular Carcinogenesis,
Dana-Farber Institute,
44 Binney Street,
Boston,
Massachusetts 02115, USA

Primary structure of human transferrin receptor deduced from the mRNA sequence

C. Schneider*, M. J. Owen†, D. Banville & J. G. Williams

Imperial Cancer Research Fund, Mill Hill Laboratories,
Burtonhole Lane, London NW7 1AD, UK
† The Tumour Immunology Unit, Imperial Cancer Research Fund,
Department of Zoology, University College London, Gower Street,
London WC1E 6BT, UK

In vertebrates all iron is taken up via the carrier protein transferrin[1]. The carrier first binds its receptor and the receptor–ligand complex is then internalized via coated pits[2–4]. The transferrin receptor is a transmembrane glycoprotein (apparent molecular weight (MW) 180,000) composed of two disulphide-bonded subunits (each of apparent MW 90,000)[1,5,6]. It contains three N-linked glycan units and is post-translationally modified with both phosphate and fatty acyl groups[5,7]. Here we have determined the nucleotide sequence of the coding region of the human transferrin receptor mRNA and from this deduced the amino acid sequence of the protein. The receptor does not contain an N-terminal signal peptide but there is a membrane-spanning segment 62 amino acids from the N-terminus. It therefore has a somewhat unusual configuration with a small N-terminal cytoplasmic domain and a C-terminal extracellular domain of 672 amino acids.

The clone pTR48 contains a 2-kilobase (kb) cDNA insert derived from the human transferrin mRNA[8]. Using this clone as a probe, a set of five overlapping cDNA clones was isolated containing, in total, 5 kb of sequence derived from the human transferrin receptor mRNA (Fig. 1). The mRNA is slightly over 5 kb long (ref. 9 and C.S., unpublished) thus this set of clones probably spans most of the length of the mRNA. We have used primer extension (Fig. 2) to show that the insert in clone pTR36 terminates only 20(±2) nucleotides from the 5′ end of the mRNA. The nucleotide sequence of the inserts in the set of cDNA clones was determined and is presented in Fig. 3. There is an open reading frame which extends from nucleotide 33 to nucleotide 2,544. The first available initiation codon in this reading frame is at position 264 and translation using this codon

---

* Present address: EMBL, Mayerhofstrasse 1, 6900 Heidelberg, FRG

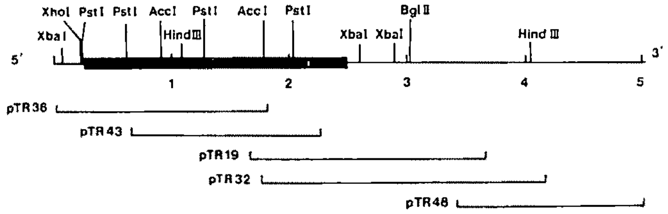

Fig. 1 Molecular cloning of human transferrin receptor cDNA sequences. The cDNA clone pTR48 was prepared using the orthodox 'hairpin cleavage' technique and shown by hybrid selection to contain human transferrin receptor sequences[8]. The complete nucleotide sequence of the cDNA clone was established using the dideoxy technique and the orientation of the insert was deduced by hybridization of cDNA to single-stranded DNA from one of the recombinant clones used in establishing the sequence. Analysis of the transferrin receptor mRNA by Northern transfer (data not shown) indicated that it was ~5 kb long, and the nucleotide sequence of the cDNA insert showed that it was derived from a noncoding region of the mRNA. An oligomer containing 18 nucleotides of sequence from very near the 5' end of the insert in pTR48 (given by Dr I. Stabinsky) was used to prime cDNA synthesis with ~5 μg of immune-enriched mRNA from MOLT-4 cells. This mRNA was derived from immune-selected polysomes in which transferrin receptor mRNA was estimated to constitute between 5 and 10% (by mass) of the mRNA population. Double-stranded (ds) DNA was prepared from the RNA-DNA hybrid using RNase H and the DNA polymerase I holoenzyme exactly as described by Gubler and Hoffman[21]. dsDNA >1,600 nucleotides long was selected by agarose gel electrophoresis and inserted into a pBR322-based vector, p2732K (J. Monahan, unpublished) by homopolymer tailing. The library of ~10,000 cDNA clones was screened by hybridization with a restriction fragment from near the 5' end of the insert in pTR48. Approximately 500 clones gave a positive signal and clones pTR19 and pTR32 were purified and used to screen for cDNA clones containing sequences more proximal to the 5' end of the mRNA. The entire set of overlapping cDNA clones shown was isolated in this way and yielded the indicated restriction map for a DNA copy of the human transferrin receptor mRNA. The map agrees precisely with that published recently by Kühn *et al.*[9]. Based on our estimate of the size of the mRNA, it seemed likely that the clone pTR36 would contain sequences from very near the 5' end of the mRNA and this was confirmed by primer extension (Fig. 2). (Given the method of construction of the clones, all of them might be expected to share a common 3' terminus—that is, the sequence of the oligonucleotide primer. However, only clone pTR32 has a terminus in the expected position. We believe this may be due to random priming because a very large excess of oligomer was used in the cDNA synthesis. This will not affect our sequence analysis because the region of overlap between clones is large and sequences across the termini were in each case established independently from another clone.)

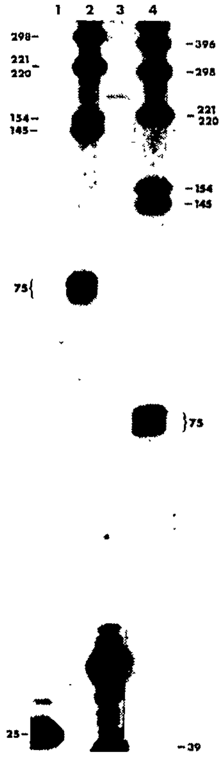

Fig. 2 Analysis of the 5' terminus of the human transferrin receptor mRNA by primer extension. The conditions for the hybridization of the DNA primers to the RNAs and the extension reactions were as described by Devine *et al.*[22] except that the temperature of the hybridization step was 55 °C. The first primer used was a single-stranded 25-nucleotide *Hha*I-*Xba*I fragment derived from within the 5'-noncoding region of the pTR36 transferrin receptor cDNA clone (Fig. 1) labelled at its 5' end with [γ-^{32}P]-ATP and T4 polynucleotide kinase. Lane 1 shows an extension product of 64±2 nucleotides obtained with this primer and an RNA preparation immune-selected with a preparation of anti-transferrin receptor antibody as described by Schneider *et al.*[8]. Identical extension products were obtained using total placental RNA or size-selected (≥5 kb) placental RNA preparations (data not shown). The second primer was a single-stranded 39-nucleotide *Xho*I-*Hae*III fragment derived from the beginning of the coding region of the transferrin receptor cDNA clone (Fig. 1), similarly labelled at its 5' terminus with [γ^{32}-P]-ATP and T4 polynucleotide kinase. Lane 3 shows the extension product of 250±2 nucleotides obtained with this primer and a size-selected (≥5 kb) total placental RNA preparation. Identical extension products were obtained with immune-selected RNA or total placental RNA (data not shown). The size markers in lane 2 were loaded at the same time as the sample in lane 1. The size markers in lane 4 were loaded at the same time as the samples in lane 3. The lengths of the extended products obtained independently with these two primers demonstrate that the start of the human transferrin receptor mRNA is no more than 20±2 nucleotides upstream from the start of the cloned cDNA.

generates a polypeptide 760 amino acids long. The deduced molecular weight is in very good agreement with that predicted by translation of the mRNA[8,10] and the position of the presumptive transmembrane segment is precisely that expected (see below). Confirmation that this is the correct reading frame is provided by the amino acid sequence of two tryptic peptides (J. Downward, G. Scrace, R. Sutherland, M. Greaves and M. Waterfield, unpublished data) which are found in our predicted amino acid sequence at the positions indicated in Fig. 3 legend. The 5'-noncoding region of the mRNA is therefore somewhat longer than average (280±2 nucleotides); it is also a little unusual in that there is an ATG trinucleotide upstream of the initiation codon. There are, however, precedents for both these features (reviewed in ref. 11) and the complete concordance with the expected protein structure suggests strongly that we have identified the correct N-terminus.

The 3'-noncoding region is also much longer than that of the average eukaryotic mRNA. We cannot determine the precise length of this region because pTR48, the 3'-proximal clone, does not contain sequences derived from the poly(A) tail. It must, however, terminate very near to the end of the mRNA because the total length of the established nucleotide sequence closely approximates the length of the mRNA. Hence, the 3' noncoding region is >2,466 nucleotides long. Again, this is not without precedent and it is intriguing that the epidermal growth factor (EGF) receptor also displays such a feature[12]. It is also interesting that the 3'-noncoding region contains several AATAAA sequence elements which are not used (Fig. 3).

Inspection of the receptor's predicted primary sequence reveals a stretch of 26 predominantly nonpolar amino acids with a sequence of nine hydrophobic residues in the centre (residues 63–88). When a hydropathicity plot (see Fig. 3 legend) was used to predict hydrophilic and membrane-embedded regions, this segment was the only convincing potential transmembrane segment. It would span, in an α-helical conformation, the 40 Å nonpolar part of the lipid bilayer (Fig. 4). The sequence, however, resides at the N-terminal end of the protein; no hydrophobic stretch is apparent at the C-terminal end. As the majority of the receptor is located at the external face of the bilayer, the receptor must be oriented with its N-terminus on the cytoplasmic side; this is in contrast to most membrane proteins which span the membrane close to the carboxy-terminus, exposing it on the cytoplasmic side (for review see ref. 13). A similar orientation has, however, also been found for several glycoproteins including the chicken asialoglycoprotein receptor, human erythrocyte band 3 protein and the murine and human Ia-associated invariant chain[14-17]. The sequence of the putative transmembrane domain of the transferrin receptor permits multiple interactions within the lipid bilayer, as several residues are capable of forming hydrogen bonds. Also, a cysteine residue, which may

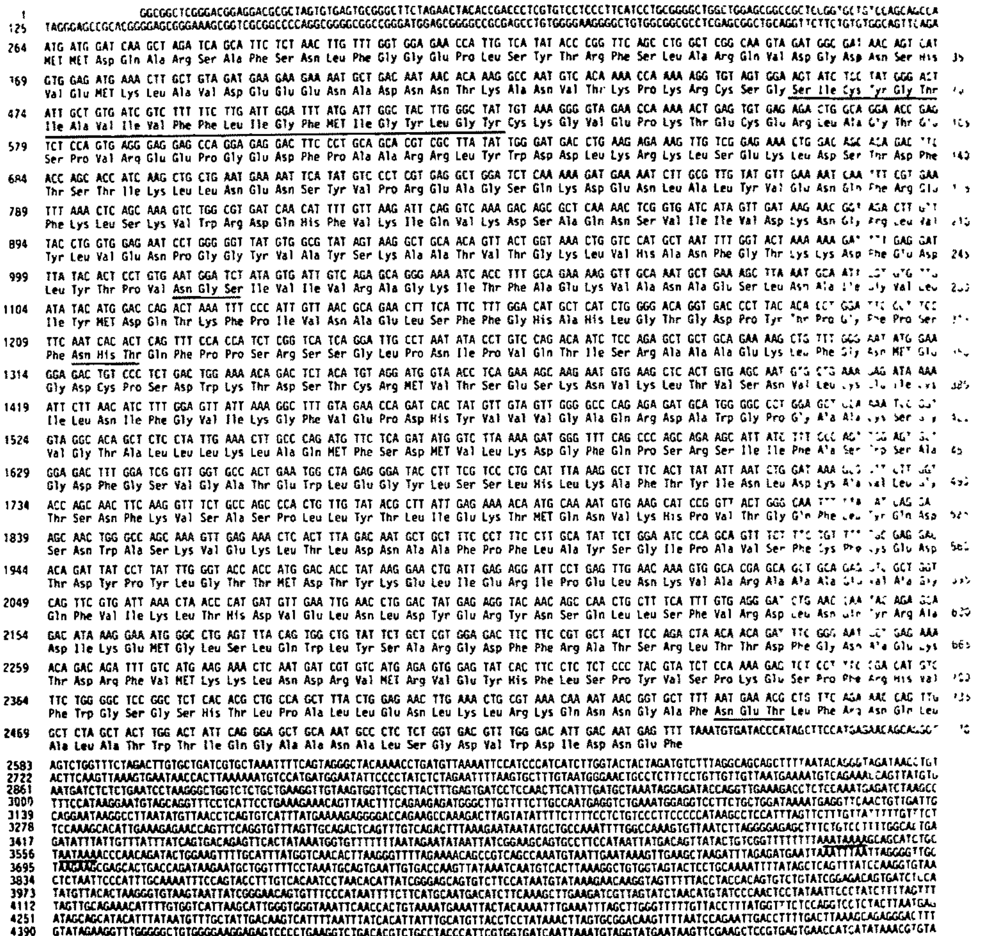

Fig. 3 Nucleotide sequence of the cDNA clones. The entire nucleotide sequence was determined using the dideoxy method of Sanger[27] but the sequence around the 5′-proximal *Xba*I site was confirmed using the chemical procedure of Maxam and Gilbert[28]. This was considered necessary because of difficulty in reading the DNA sequence near the homopolymer tails when using the synthetic procedure. Approximately half the sequence was determined from randomly sheared fragments of DNA inserted into the M13 mp8 vector[23] or the pEMBL vector[24], the remainder of the sequence was determined from ordered deletion series which were generated by random DNase I cleavage and re-circularization. Two procedures were used, one involving the addition of restriction enzyme linkers (D. Ish-Horowicz, personal communication) and the other involving blunt end-ligation to the *Sma*I site in pEMBL8+. The entire sequence of the 5′-noncoding region and that of the coding region was determined in both strands and the majority of the sequence of the 3′-noncoding region was also determined in both strands. The sequence of each nucleotide was determined on average 4.3 times. Note the presence of stop codons in all three frames at positions 24, 30 and 43. The ATG indicated is the first in-frame initiation codon downstream of the stop codon at nucleotide 30 and several lines of evidence (see text) suggest this to be the correct N-terminus. Confirmation that this is the correct reading frame derives from the sequence of two tryptic peptides: Ser-Ser-Gly-Leu-Pro-Asn-Ile-Pro-Val-Gln starting at position 326, and Arg-Arg-Leu-Tyr-Trp-Asp-Leu-Lys starting at position 121. The transmembrane segment (see text) between amino acids 63 and 88 is underlined, as are the positions of the three extracellular glycosylation sites (see text) at amino acids 251, 317 and 727, and the two unused AATAAA elements. A hydropathicity plot was performed on the predicted polypeptide sequence using a method similar to that of Kyte and Doolittle (ref. 25 and M. Green, personal communication). The protein sequence was compared with all proteins in the National Biomedical Research Foundation database using the search program of Wilbur and Lipmann[26]. The parameters used in the data base search were *k*-tuple length = 3, window size = 20, gap penalty = 2. The length-corrected scores for the degree of homology with the EGF precursor and with the chicken transferrin precursor were 4.0E and 3.3E, respectively. A copy of this sequence has been placed in the EMBL data base.

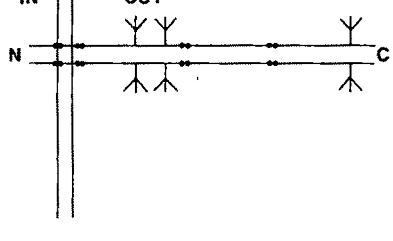

Fig. 4 Proposed structure and membrane orientation of the human transferrin receptor. The receptor is depicted as spanning the plasma membrane close to its N-terminal end, exposing it in the cytoplasm. It contains three glycan units linked to asparagine. The positions of the cysteine residues (●) are indicated.

act as the site of fatty acylation via a thioester bond[18], is present within the bilayer sequence. Since the receptor exists as a dimer in the plasma membrane, self-interactions of the transmembrane segments within the lipid bilayer could help to stabilize the dimer structure; alternatively, they could contribute to associations with other proteins which might be important in receptor function.

The putative transbilayer sequence is preceded (at the N-terminal end) by a cluster of basic residues (Lys-Pro-Lys-Arg). This sequence is found on the cytoplasmic side of the transmembrane segments of virtually all membrane glycoproteins thus far characterized; it has been referred to as a stop-transfer sequence and may interact with the polar phospholipid headgroups[19].

The cytoplasmic domain comprises 62 amino acids and contains four serine residues which can act as acceptors for phosphate modification. This domain is large compared with those of other membrane proteins (3 to ~35 residues long)[13]. However, it is considerably shorter than the corresponding domain of the human EGF receptor, which comprises 542 amino acids[12].

The extracellular domain, which contains the transferrin binding site, comprises 648 amino acids. This domain contains three of the five possible sites for asparagine-linked glycosylation (Asn-X-Ser/Thr). As endoglycosidase digestion experiments have indicated that the receptor contains three N-linked glycan units, all three of these asparagines must be glycosylated.

Eight cysteine residues are distributed throughout the transferrin receptor sequence. Four cysteines are found in the region of the transbilayer peptide; two flank the peptide, one resides within the putative transbilayer sequence, and one is located close to the bilayer on the extracellular side. The remaining cysteines are present in two clusters in the extracellular domain (Fig. 4). It is unknown whether any of these cysteine residues form intrachain disulphide bridges. However, at least one must form the interchain disulphide bond(s) between the two 90,000-MW receptor subunits. Protein biochemical data suggest that the intersubunit disulphide bond(s) must lie close to the cell membrane, as trypsin treatment releases a non-disulphide-linked, 70,000-MW fragment from the cell surface[5]. It is unlikely that the cysteine (residue 62) on the cytoplasmic domain is disulphide-bonded due to the strong reducing environment of the cytoplasm. The cluster of three cysteines close to or in the bilayer are, therefore, the most likely candidates for making an interchain disulphide bond.

The amino-terminus of the transferrin receptor contains no obvious signal sequence. This observation is consistent with *in vitro* translation experiments in which the size of the primary translation product is indistinguishable from that of the endoglycosidase H-treated polypeptide synthesized in the presence of microsomes[10]. The lack of an N-terminal cleavable signal sequence is not unprecedented. No such signal sequence has been identified in the Ia-associated invariant polypeptide, which also has the reverse orientation in the plasma membrane[17]. Similarly, the secreted glycoprotein ovalbumin has been shown to contain an internal signal sequence[20]. It is possible that the transbilayer sequence of the human transferrin receptor performs the dual function of acting as a signal sequence and of anchoring the protein in the plasma membrane.

When the amino acid sequence of the transferrin receptor was used in a search of the Dayhoff data base, no strong homology with any known protein was revealed. There is some homology with the EGF precursor and with the chicken transferrin precursor, but the degree of homology is very low (see Fig. 3 legend). Similarly, a search of a more specialized data base containing a comprehensive collection of oncogene sequences (G. Scrace, personal communication) revealed no strong homologies.

We thank Hiro Mahbubani for technical assistance, Michael Green for performing secondary structure analysis of the protein, and I. Stabinsky for providing the synthetic oligonucleotide described in the text. We also thank G. Scrace, J. Downward, R. Sutherland, M. Greaves and M. Waterfield for allowing us access to protein sequence data in advance of publication, and Rita Harris and Brenda Marriott for their help in preparing the manuscript. C.S. is on leave of absence from the Institute of Biochemistry, University of Trieste, Trieste 34127, Italy.

Received 30 July; accepted 7 September 1984.

1. Newman, R., Schneider, C., Sutherland, R., Vodinelich, L. & Greaves, M. *Trends biochem. Sci.* **1**, 397–400 (1982).
2. Hopkins, C. R. & Trowbridge, I. S. *J. Cell Biol.* **97**, 508–521 (1983).
3. Dautry-Varsat, A., Ciechanover, A. & Lodish, H. F. *Proc. natn. Acad. Sci. U.S.A.* **80**, 2258–2262 (1983).
4. Goldstein, J. L., Anderson, R. G. W. & Brown, M. S. *Nature* **279**, 679–685 (1979).
5. Schneider, C., Sutherland, R., Newman, R. & Greaves, M. *J. biol. Chem.* **257**, 8516–8522 (1982).
6. Trowbridge, I. S. & Omary, M. B. *Proc. natn. Acad. Sci. U.S.A.* **78**, 3039–3043 (1981).
7. Omary, M. B. & Trowbridge, I. S. *J. biol. Chem.* **256**, 12888–12892 (1981).
8. Schneider, C., Kurkinen, M. & Greaves, M. *EMBO J.* **2**, 2259–2263 (1983).
9. Kühn, L. C., McClelland, A. & Ruddle, F. H. *Cell* **37**, 95–103 (1984).
10. Schneider, C., Assen, U., Sutherland, R. & Greaves, M. F. *FEBS Lett.* **158**, 259–264 (1983).
11. Kozak, M. *Nucleic Acids Res.* **9**, 5233–5252 (1981).
12. Ullrich, A. *et al. Nature* **309**, 418–425 (1984).
13. Lodish, H. F., Braell, W. A., Schwartz, A. L., Straus, G. J. A. M. & Zilberstein, A. *Int. Rev. Cytol.* **12**, 247–307 (1981).
14. Drickamer, K. L. *J. biol. Chem.* **256**, 5827–5839 (1981).
15. Drickamer, K. L. *J. biol. Chem.* **253**, 7242–7248 (1978).
16. Singer, P. A. *et al. EMBO J.* **3**, 873–877 (1984).
17. Claesson, L., Larhammar, D., Rask, L. & Peterson, P. A. *Proc. natn. Acad. Sci. U.S.A.* **80**, 7395–7399 (1983).
18. Kaufman, J. F., Krangel, M. S. & Strominger, J. L. *J. biol. Chem.* **259**, 7230–7238 (1984).
19. Blobel, G. *Proc. natn. Acad. Sci. U.S.A.* **77**, 1496–1500 (1980).
20. Braell, W. A. & Lodish, H. F. *J. biol. Chem.* **257**, 4578–4582 (1982).
21. Gubler, U. & Hoffman, B. J. *Gene* **25**, 263–269 (1983).
22. Devine, J. M., Tsang, H. & Williams, J. G. *Cell* **28**, 793–800 (1982).
23. Messing, J. & Vieira, J. *Gene* **19**, 269–276 (1982).
24. Dente, L., Cesareni, G. & Cortese, R. *Nucleic Acids Res.* **11**, 1645–1655 (1983).
25. Kyte, J. & Doolittle, R. F. *J. molec. Biol.* **157**, 105–132 (1982).
26. Wilbur, W. T. & Lipmann, D. *Proc. natn Acad. Sci. U.S.A.* **800**, 726–730 (1983).
27. Sanger, F., Nicklen, S. & Coulson, A. R. *Proc. natn. Acad. Sci. U.S.A.* **74**, 5463–5467 (1977).
28. Maxam, A. M. & Gilbert, W. *Methods Enzymol.* **65**, 499–560 (1980).

Three-dimensional structure of an antigenic mutant of the influenza virus haemagglutinin

M. Knossow*‡, R. S. Daniels†, A. R. Douglas†, J. J. Skehel† & D. C. Wiley*

* Department of Biochemistry and Molecular Biology,
Harvard University, Cambridge, 02138, USA
† National Institute of Medical Research, Mill Hill,
London NW7 1AA, UK

Antigenic variation in the haemagglutinin (HA) glycoprotein of influenza virus is associated with recurrent epidemics of respiratory disease in man (for review see ref. 1). We have examined the size of structural changes necessary to alter the antigenicity of HA by determining the three-dimensional structure of the HA from an antigenic mutant containing a single amino acid substitution which was selected by growth of virus in the presence of monoclonal antibodies. Here we present evidence that the simple addition of an amino acid side chain which results in only minor local distortions of the structure of the HA is sufficient structural alteration for a virus to escape neutralization by a monoclonal antibody. Our results also demonstrate that single amino acid substitutions can cause only local changes in the HA structure, verifying the assumption made in several studies to locate antigenic sites on the HA[2–5] and other molecules[6,7], and indicate that proposals[8,9] of large conformational changes to account for variations in HA antigenicity are unnecessary in this case. The structure of the variant antigen has independently been successfully predicted (M. Karplus, personal communication).

An antigenic variant, V3a, was selected by growing the parent (X31) virus[10] in the presence of a neutralizing monoclonal antibody, HC3a, as described previously[11,12]. Table 1 shows that while haemagglutination by the parent virus is inhibited by HC3a ascitic fluid at a dilution of 1:12,800, the variant virus V3a is not inhibited at a 1:100 dilution of the fluid. A similar result was obtained in enzyme-linked immunosorbent antibody binding assays, in which parent virus and V3a mutant virus bound antibodies at ascitic fluid dilutions of 1:100,000 and 1:100, respectively.

The amino acid sequence of the entire V3a HA was determined by sequencing the viral RNA using methods described previously[13,17,18]; only one nucleotide change was observed, G to A, at nucleotide 514 which, when translated into amino acids, established that V3a has an aspartic acid at position 146 in the HA1 polypeptide instead of the glycine in the parental sequence[19].

Isomorphous crystals of V3a were grown under conditions in which the X31 HA crystallizes[14]. (This has been observed for all of four single amino acid variants tested to date.) We collected 76,840 unique X-ray reflections to 3.0 Å resolution on 1° oscillation photographs recorded at 4 °C by methods described previously[15]. Partially recorded reflections (≥50%) were included in the data set after adjustment by the post-refinement pro-

---

‡ Present address: Laboratoire de Physique, Centre Pharmaceutique, 92290 Chatenay-Malabry, France.

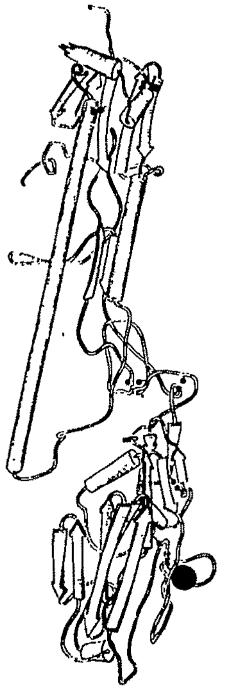

Fig. 1 A schematic diagram of a monomer of the haemagglutinin from the 1968 Hong Kong influenza virus[15], showing the location of the single mutation, Gly to Asp 146.

cedure[16]. The symmetry R factor (see Fig. 2 legend) on fully recorded reflections is 0.11 and on all reflections more than half recorded, 0.14. The parent and variant structure factors were scaled together using a Wilson statistics curve (R scale $= (F_{\mathrm{obs\,V3}} - F_{\mathrm{obs\,X31}})/(F_{\mathrm{obs\,X31}}) = 0.161$) and a difference Fourier was calculated to 3 Å resolution using phases from the refined model (see Fig. 2 legend for details).

The difference Fourier averaged about the molecular 3-fold axis shows nine peaks above the 5σ level. The largest peak is 12σ and is at the location expected for an aspartic acid side chain if it were added to Gly 146 (Fig. 2*b*); the next highest peak is $<6\sigma$. Similar results with fewer noise peaks were observed on a difference Fourier calculated with a shell of data from 10 to 6 Å resolution.

The coordinates of the aspartic acid were obtained from model building on a $2F_0 - F_c$ map after refining native coordinates against V3a data. The O^{δ} of the carboxylate of Asp 146 appears within 3.0 Å of the N^{ε} of Arg 141, forming an apparent hydrogen bond. No other distortion of the external loop (amino acids 139–147) or of other features of the protein are observed, with the exception of a small (less than 1 Å) adjustment in the position of the side chain of arginine 141, presumably to accommodate the hydrogen bonding geometry required by the aspartic acid.

The structure of the variant HA suggests two possible mechanisms for the decreased affinity of the monoclonal antibody for the mutant HA: (1) The difference in the properties (shape, polarity and/or charge) of the aspartic acid and glycine side chains may directly affect the binding affinity. (2) The aspartic acid 146–arginine 141 interaction may stabilize the local structure of the site to which the monoclonal antibody binds, which would decrease the binding affinity if the antibody needed to locally distort or denature the site for tight binding. The former possibility corresponds to the classical 'static' view of an antibody–antigen complex, while the latter would apply if the free energy decrease on binding to a distorted site were greater than that required to distort the site. Present knowledge about the state of an antigen when 'seen' by immunogenic lymphocytes during the generation of an immune response and about the structure of an antigen–antibody complex leaves both possibilities feasible. In the case of V3a, the electrostatic charge of the Asp side chain would lead to unfavourable charge interactions (the burying of an unpaired charge) in complexes with antibodies against the parent (Gly).

Although multiple amino acid substitutions in the HA appear to be necessary for a virus to acquire the potential to cause an epidemic[2], single amino acid substitutions in the HA are sufficient for a virus to escape neutralization by monoclonal antibodies[11]. The three-dimensional structure of the HA of an antigenic variant presented here indicates that the substitution of an aspartic acid for a glycine, without any significant changes in the positions of the atoms in the rest of the HA molecule, is a sufficient alteration to reduce by three orders of magnitude the binding of a monoclonal antibody. The absence of other structural changes in the variant HA, in turn, proves that the monoclonal antibody used to select this variant must bind directly to the region of the HA surface designated site A by Wiley *et al.*[2].

Since submitting this manuscript we have found that H. H.-L. Shih, J. Brady and M. Karplus (unpublished) have independently and with no prior knowledge of our results successfully predicted the structural changes in the mutant V3a, relative to the parent protein. Using a perturbation approach making use of the empirical energy function program CHARMM[23], they calculated a conformational potential energy surface[24] for the aspartic acid side chain in the presence of the rest of the protein Energy refinement[23] of the low energy conformations on this surface yielded side chain torsion angles for Asp 146 with ±20° of the X-ray results. Further, the prediction of an adjustment

Table 1 Haemagglutination-inhibition reactions of X31 virus and antigenic mutant V3a

	Monoclonal antibody				
Virus	HC3a	HC31	HC101	HC83	HC263
X31	12,800	6,400	12,800	6,400	25,600
V3a	>100	6,400	12,800	6,400	25,600

Haemagglutinin-inhibition reactions were done by standard procedures. The values shown are the reciprocals of the highest dilutions of the antibodies at which haemagglutination was inhibited The specificities of the different monoclonal antibodies are defined by the amino acid substitutions observed in antigenic variants of X31 virus that the individual antibodies select. Thus, antibody HC3a selects mutants with amino acid substitutions at residue 146; HC31 at residue 198; HC101 at residue 63; HC83 at residue 193; and HC263 at residue 158. All monoclonal antibodies tested, other than HC3a which was used to select V3a, react with X31 and V3a equally.

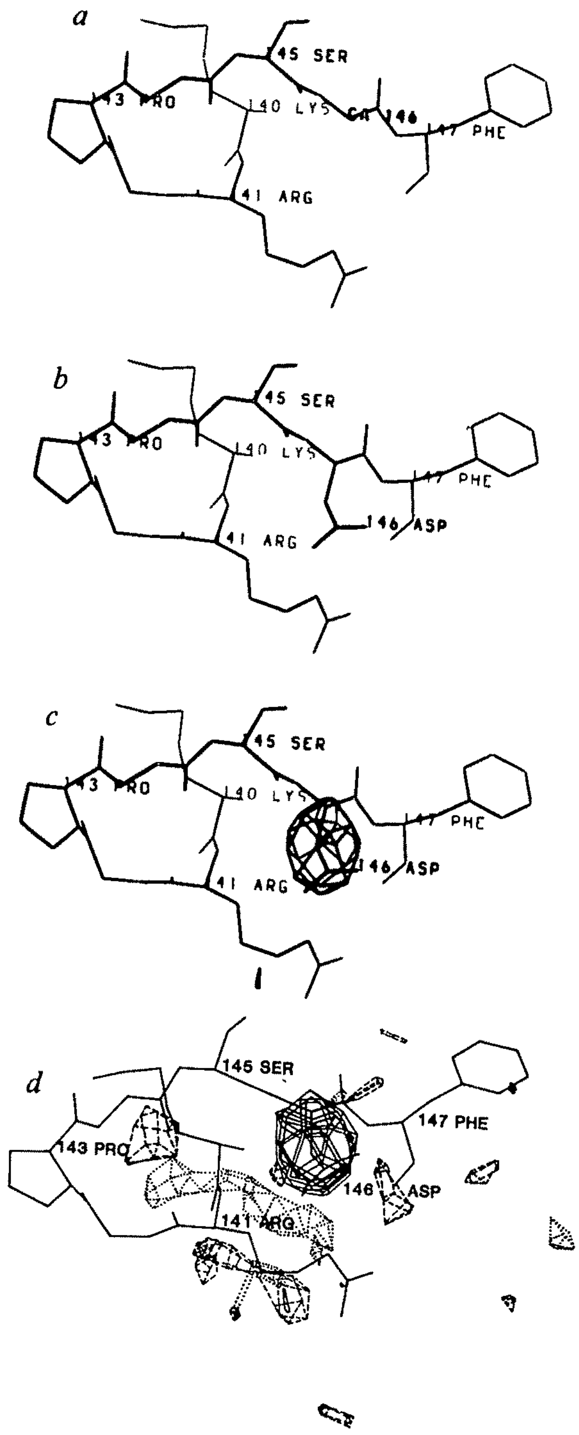

Fig. 2 *a*, Structure of the amino acid 140-147 loop which contains a glycine at position 146 in the parent HA. Atomic coordinates for the parent structure[15] were obtained by model building (I. A. Wilson and D.C.W.) on a version of the BILDER program[20] modified by Robert Ladner. These were refined to an *R* factor of 0.26 after six cycles of restrained least-squares refinement[21] where the contribution of the structure factor to the least-squares equation was evaluated by the gradient-curvature method on a difference map (ref. 22 and M. Lewis and D. Rees, personal communication). ($R = \Sigma|s_iI_{hi} - \bar{I}_h|/\Sigma\bar{I}_h$) where s_i = scale factor (including film temperature factor) for crystal *i*, and I_{hi} = intensity of reflection *h* of crystal *i*.) Exact 3-fold symmetry was imposed on the HA trimer in the crystallographic asymmetric unit by refining only a monomer's coordinates from 3-fold averaged difference maps. An overall *B* factor of 14 was used. Details of the refinement will be published elsewhere. *b*, The coordinates of the 140-147 loop of the antigenic variant V3a showing the location of the Asp (for Gly) substitution. Note that no conformational changes are observed between *a* and *b*. The V3a loop coordinates were obtained from model building on a $2F_0 - F_c$ map after refining the X31 coordinates (minus the loop) against the V3a data. *c*, The V3a difference map (F_{obs} V3a $- F_{obs\,X31}$) showing the 12σ peak at Asp 146. The only significant difference is at the position expected by the addition of the Asp 146 side chain instead of Gly 146 in the wild type. The difference Fourier was calculated using observed parent and variant structure factors with the refined phases described for *a*. *d*, The same as *c* with additional positive (dashed) and negative (dotted) contours at the noise level, 3σ. The interpretable 3σ peaks are a ridge of difference density indicating a small shift in the position of the side chain of Arg 141, which is within hydrogen bonding distance of Asp 146. (This figure was produced with an Evans and Sutherland PS-300 on the version of FRODO written by J. W. Pflugrath, M. A. Saper, B. Bush and A. Jones.)

in the position of Arg 141 to improve the hydrogen bond to the carboxyl group of Asp 146 led to our finding its displacement in the experimental difference map. Details of the method and results will be given separately.

We thank David Stevens and Rose Gonsalves for assistance, Eugene Brown of Genetic Institute for synthesizing one of the oligonucleotide primers, and acknowledge support from NIH AI 13654 (D.C.W.). M.K. was the recipient of fellowship DRG-542 from the Damon Runyon-Walter Winchell Cancer Fund. We also thank Henry H.-L. Shih, John Brady and Martin Karplus for allowing us to quote from their unpublished results predicting the structure of the single-site mutant

Received 25 April; accepted 14 June 1984.

1. Webster, R. G. & Laver, W. G. in *Influenza Viruses and Influenza* (ed. Kilbourne, E. D.) 270-314 (Academic, New York, 1975).
2. Wiley, D. C., Wilson, I. A. & Skehel, J. J. *Nature* **289**, 373-378 (1981).
3. Caton, J. J., Brownlee, C. C., Yewdell, C. A. & Gerhard, W. *Cell* **31**, 417-427 (1982).
4. Daniels, R. S., Douglas, A. R., Skehel, J. J. & Wiley, D. C. *J. gen. Virol.* **64**, 1657-1662 (1983).
5. Daniels, R. S. *et al.* in *The Origin of Pandemic Influenza Viruses* (eds Laver, G. W. & Chu, C. M.) (Elsevier, New York, in the press).
6. Colman, P. M., Varghese, J. N. & Laver, W. D. *Nature* **303**, 41-44 (1983).
7. Evans, D. M. A., Minor, P. D., Schild, G. S. & Almond, J. W. *Nature* **304**, 459-462 (1983).
8. Laver, W. G., Air, G. M. & Webster, R. G. in *Genetic Variation Among Influenza Viruses* (ed. Nayak, D. P.) 283-295 (Academic, New York, 1981).
9. Webster, R. G. & Laver, W. G. *Virology* **104**, 139-148 (1980).
10. *Bull. Wld Hlth Org.* **45**, 119-124 (1971).
11. Laver, W. G., Air, G. M., Dophiede, T. A. & Ward, C. W. *Nature* **283**, 454-457 (1980).
12. Skehel, J. J. *et al. Proc. natn. Acad. Sci. U.S.A.* (in the press).
13. Rogers, G. N. *et al. Nature* **304**, 76-78 (1983).
14. Wiley, D. C. & Skehel, J. J. *J. molec. Biol.* **112**, 343-347 (1977).
15. Wilson, I. A., Skehel, J. J. & Wiley, D. C. *Nature* **289**, 368-373 (1981).
16. Winkler, F. K., Schutt, C. E. & Harrison, S. C. *Acta crystallogr.* **A35**, 901-911 (1979).
17. Sanger, F., Nicklen, S. & Coulson, A. R. *Proc. natn. Acad. Sci. U.S.A.* **74**, 5463-5467 (1977).
18. Patel, T. P. *et al. Nucleic Acids Res.* **10**, 5605-5620 (1982).
19. Verhoeyen, M. *et al. Nature* **286**, 771-776 (1980).
20. Diamond, R. in *Biomolecular Structure, Conformation, Function and Evolution* Vol. 1 (ed. Srinivasan, R.) 567-588 (Pergamon, Oxford, 1980).
21. Hendrickson, W. A. & Konnert, J. in *Biomolecular Structure, Function, Conformation, and Evolution* Vol. 1 (ed. Srinivasan, R.) 43-47 (Pergamon, Oxford, 1980).
22. Cochran, W. *Acta crystallogr.* **4**, 408-411 (1951).
23. Brooks, B. *et al. J. comp. Chem.* **4**, 187-217 (1983).
24. Gelin, B. R. & Karplus, M. *Biochemistry* **18**, 1256-1268 (1979).

Errata

A general circulation model of water isotope cycles in the atmosphere

S. Joussaume, J. Jouzel & R. Sadourny

Nature **311**, 24-29 (1984)

In this article, the order of the authors was incorrect. It appears correctly above.

Sequential late Cenozoic structural disruption of the northern Himalayan foredeep

D. W. Burbank & R. G. H. Raynolds

Nature **311**, 114-118 (1984)

The above article was published with the name of the third author spelt incorrectly as Reynolds.

Much ado about CO_2

John S. Perry

Man-Made Carbon Dioxide and Climatic Change: A Review of the Scientific Problems.
By P.S. Liss and A.J. Crane.
Geo Books, Regency House, 34 Duke Street, Norwich NR3 3AP, UK: 1983. Pp.127. Hbk £8.50, $17; pbk £3.95, $7.80.
Carbon Dioxide — Emissions and Effects (Report No. ICTIS/TR18).
By Irene M. Smith.
IEA Coal Research, 14-15 Lower Grosvenor Place, London SW1W 0EX: 1982. Pp.132. £10 (IEA countries), £20 (elsewhere).
Climate and Energy Systems: A Review of their Interactions.
By Jill Jäger.
Wiley: 1983. Pp.231. £19.95, $39.95.
Our Threatened Climate: Ways of Averting the CO_2 Problem through Rational Energy Use.
By Wilfrid Bach.
Reidel: 1983. Pp.368. $29, Dfl. 95, £24.25.

THE Niagara of writings on carbon dioxide, of which a sampling of the output over the past year or so forms the basis for this review, suggests that the gas is becoming an essential nutrient not only for green plants but for a large segment of the scientific community as well. Indeed, Roger Revelle — who, with Hans Suess, once termed man-made emissions of CO_2 a "geophysical experiment" — now wryly muses about the CO_2 "cottage industry". What is all the fuss about?

The following is an attempt to compress a large bookcase into a paragraph. The Earth's carbon is distributed among crustal sediments, the ocean, a thin layer of living materials, a wisp of CO_2 in the air and millions of years' accumulation of fossilized organic material in the forms of coal, oil and gas. By burning the fossil matter and by converting carbon-rich forest to thinly vegetated agricultural land, we move carbon atoms into the atmosphere in the form of CO_2. Some of these atoms find new homes in the ocean or the living biota, but about half seem to stay in the air. Globally, we are injecting more than 5×10^9 tonnes of carbon into the environment each year, and the atmosphere's carbon dioxide concentration — now about 340 parts per million by volume — is increasing by about 1 ppm per year. This would be no great matter, except for the fact that CO_2 is a good radiator and absorber of thermal (infrared) radiation. Thus, increasing airborne CO_2 increases the effectiveness of the cool upper layers of the atmosphere as radiators and absorbers, and reduces the direct export of radiant energy from the Earth's surface to space. The lower atmosphere and surface must thus run at a higher temperature to make good the planet's energy accounts with the Sun and the cosmos. Altered heating and higher mean temperatures mean changes in climate, changes that must concern a world whose food supply depends on what Paul Waggoner has termed "the annual lottery of the weather". Is fossil fuel like tobacco, then: convenient and pleasant to burn, but with nasty long-term consequences?

To assess the issue, one must systematically explore every link in a long chain of processes. The marvellously complex nature of that chain has inspired increasing numbers of authors to try to sum up various findings and attempt a synthesis of the structure as a whole. The four volumes addressed here fall into this category. As in the classic *Rashomon* tale, each witness sees the scene through a filter of his own experience and background and tells a somewhat differently tinted story.

Liss and Crane, both associated with the electric power industry, follow a straightforward path through the major scientific questions attending CO_2 to their implications for future energy production from fossil sources. The authors' expositions of crucial physical processes such as ocean chemistry and radiation are clear, concise and accurate. Indeed, their analysis of the mechanics of the greenhouse effect is by a long mile the best short account in print. Irene Smith, writing for the coal and energy community, presents an objective and meticulously documented review that favours scientific results over methods and response strategies over unanswered questions. Jill Jäger takes a virtually orthogonal tack; after a notably complete essay on climate and carbon dioxide, she systematically assesses the connections between all aspects of energy production and climate. Her discussions of particulates, of solar and renewable energy sources, and of the effects of climate on the energy sector are particularly valuable. Finally, like his colleagues, Wilfrid Bach reviews the elements of the problem, but he never strays far from a path to its solution. Thus he focuses on the human society that is the source of CO_2 emissions, that must bear the consequences and that alone can devise means to cope with them. (In passing, it should be said that Jill Jäger contributes to this collection not only as author of her own book and translator of Bach, but also as the prolific J. Williams who appears in the notably comprehensive bibliographies of all of the books.)

Despite their diverse approaches, the authors converge in their assessments. Indeed, their findings differ little from those of another recent volume about which I can hardly claim an unbiased view — *Changing Climate*, a report of the US National Academy of Sciences published in 1983.

- *How will the atmospheric CO_2 change?* This depends mostly on how much energy future populations will want and where they will get it. Forecasting approaches are diverse and predictions for the distant future span a wide range. Liss and Crane simply extrapolate constant growth rates, while Smith, Jäger and Bach review a number of forecasts, tending to favour the projections of the International Institute for Applied Systems Analysis. Jäger's discussion is particularly thorough, taking into account, for example, the logistical and sociopolitical obstacles to burning huge amounts of coal. Allowing for the uncertainties in the disposition of excess carbon by the ocean and atmosphere, all projections show rapid growth in airborne CO_2 as we move into the twenty-first century. Using an economic model in a Monte Carlo simulation, Nordhaus (in the NAS report) projected a probable doubling of airborne CO_2 in the third quarter of the century, with a broad band of uncertainty that comfortably envelopes the other studies.
- *What effects will there be on climate?* Numerical models of the climate system indicate that a doubled concentration of atmospheric CO_2, if maintained indefinitely, would produce a mean global warming of around 3°C. Regional changes in weather and precipitation would be more marked, but models cannot yet identify them reliably. It does seem that the poles would warm more than the tropics, and that mid-latitude summers would be longer, warmer and thus drier. Analogies with past and contemporary climate — carefully reviewed by Jäger — provide useful insights but no definite conclusions. Changes will be slowed and complicated by the heat buffering of the oceans, and other radiation-absorbing trace gases injected anthropogenically may add to the influence of CO_2. A particularly good discussion of the latter area is presented by Bach.
- *What are the implications of these changes?* In a warmer world, sea water will expand, glaciers will melt and sea level will rise (70 cm in a century according to the NAS study). Changes in weather will influence almost every aspect of human life — energy demand, agriculture, water resources, fisheries, settlement patterns, health and recreation, to follow Bach's exhaustive taxonomy. Especially troublesome are possible changes in

precipitation, evaporation and runoff that might affect the availability of water for irrigation. All of the authors see these changes as potentially serious, but only Bach agrees with a recent assessment by the US Environmental Protection Agency (*Can We Delay a Greenhouse Warming?*, which was also published last year) that the implications are unequivocally catastrophic.

- *What should we do?* If we side with all of the authors except Bach, giving weight to the huge uncertainties and the adaptive capabilities of life on Earth, then the wise course is to be alert for signs of nasty consequences (none is yet evident), to take sensible steps to reduce damage to the environment, and to develop a range of alternative options for energy supply and for living in a changing climate. If we share Bach's assessment then a much more active policy is called for. He proposes aggressive energy conservation measures, reforestation, soil conservation and the expeditious development of renewable energy resources. In the short term, the cautious and activist prescriptions may differ little in their practical effect, and by the end of the century, the NAS report proposes, we will know a lot more if we keep up the pace of research. In the meantime, the implementation of elements of Bach's prescription can only be to the good — fear of climate change, like fear of cancer, may lead us into healthier habits that could spare us from many other hazards.

Reading these books leads one to conclude that the CO_2 "cottage industry" is serving the public well by clearly illuminating the complexities of this web of scientific and social issues. Others in the business have different strengths. In a popular vein, John Gribbin's *Future Weather and the Greenhouse Effect* (Delacorte, 1982) has much to recommend it, if its more mystical elements are disregarded. Wilfrid Bach and colleagues have given us two earlier and excellent reviews — *Man's Impact on Climate* (Elsevier, 1979) and *Carbon Dioxide: Current Views and Developments in Energy/Climate Research* (Reidel, 1983). Societal aspects were explored by W.W. Kellogg and R. Schware in *Climate Change and Society* (Westview, 1981), while a detailed scientific analysis was orchestrated by Gordon J. MacDonald (*The Long-Term Impacts of Increasing Atmospheric Carbon Dioxide Levels*; Ballinger, 1982). A most comprehensive review, edited by William C. Clark, is *Carbon Dioxide Review: 1982* (Clarendon, 1982). And the NAS report, *Changing Climate*, a compendium of reviews, original contributions and synthesis, has already been mentioned.

The books of current vintage contribute much to this literature, and all can be recommended. Both Jäger and Bach are distinctive and important additions. Jäger's comprehensive view of climate through the prism of energy is unique and illuminating. Bach, though regrettably impeded by abominable computer typesetting, presents an impressively scholarly and exhaustive treatment. While his road leads to but one conclusion, it is broad and solidly built.

The next few years will bring further contributions. The US Department of Energy will soon release an assessment of the knowledge and conclusions emanating from its massive research programme, and an international effort is laying the groundwork for a 1985 intergovernmental conference. Thus, as was observed in the NAS report, while CO_2 may be a worrisome issue, it may also be a healthy stimulus which forces us to address seriously the long-term maintenance of our planetary home. □

John S. Perry is Staff Director of the Board on Atmospheric Sciences and Climate of the US National Academy of Sciences.

"Beluga or White Whale", from William Scoresby's *An Account of the Arctic Regions, with a History and Description of the Northern Whale-Fishery*, (1820). The illustration is reproduced from *Voyage into Substance: Art, Science, Nature, and the Illustrated Travel Account, 1760-1840*, by Barbara Maria Stafford, recently published by MIT Press. Price is $39.95, £41.75.

Cells: bags of water or blobs of jelly?

D.A.T. Dick

In Search of the Physical Basis of Life.
By Gilbert N. Ling.
Plenum: 1984. Pp. 791. $79.50, £67.57.

QUANTITATIVE membrane theories, such as those of Boyle and Conway and the Hodgkin–Katz–Goldman equation, achieved spectacular success in the 1940s. These, along with Hodgkin and Keynes's demonstration of rapid potassium diffusion in the squid axon, induced a widespread view among physiologists that the cell is simply a membrane-bounded bag. In it, so the story ran, is a fairly homogeneous, aqueous soup of proteins and inorganic ions, the composition and electrical potential of which is controlled by the membrane. By contrast, a heterodox group of physiologists — led in particular by Troschin in Russia and by Ling in the United States — has maintained that the cell is essentially a blob of jelly, held together by controlled intermolecular forces between protein molecules to which water and the ionic constituents are variably bound. This view, called by Ling the association–induction theory, has been pursued to the extent of denying any significant role to the cell membrane.

Neither of these extreme stances is of course correct. In addition to the ample evidence for the function of the cell membrane, it is now known that the cellular matrix possesses a structure of microtubules and microfilaments (see for example *J. Cell Biol.* **99**, No. 1, Pt 2; 1984), that in some cells the distribution of ions (particularly sodium and potassium) is not uniform within the cell, and that at least some cellular water is bound. Thus there is sore need of an impartial review of alternative theories of the cell.

Dr Ling's book is divided into five sections, the first of which surveys concepts in cell physiology in a historical framework (here the most important chapter is the fifth which deals with the evidence for and against the membrane theory of the cell). The second section gives a full account of Ling's association–induction theory, particularly in relation to the control of the sodium, potassium and water contents of the cell. The third is largely devoted to the experimental work of Ling and his colleagues in support of the association–induction theory, while the fourth gives an account of mitochondria, muscle and epithelial transport, usually rejecting conventional physiological views and reinterpreting the data in terms of the association–induction hypothesis. The final section describes recent work on protein synthesis, growth and differentiation, and cancer, and offers speculative interpretations of these phenomena again based upon the association-induction hypothesis.

Dr Ling describes his book as "at once a monograph, a science history tract, and a textbook". A monograph, it certainly is, but it has little of the objective judgement and impartiality normally associated with a history or a textbook. For example there are 106 references to the work of Dr Ling while some quite distinguished cell physiologists are represented by a couple of citations only. A distinctive historical feature is a series of portraits, most of them of justly prominent figures but with some bizarre omissions (and inclusions); often one cannot help feeling that the space occupied by the photograph would have been better employed by a more adequate treatment of the work of the scientist portrayed. For example Ling's survey of the sodium-potassium ATPase of the cell membrane, embracing the work of J.C. Skou, E.T. Dunham, I.M. Glynn, R.L. Post and S.L. Bonting, occupies but a page and a half.

Dr Ling appears to be constitutionally an advocate, rather than a judge, and he has set out to win his case by presenting every conceivable argument in support of his own position and giving the other side inadequate and unbalanced treatment. This is a pity. Since the 1950s majority views of the cell have moved significantly nearer to those of Dr Ling, but in this book he harms his own case by overstatement. What we need now is a judge, not an advocate. □

D.A.T. Dick is Cox Professor of Anatomy in the University of Dundee.

From the laboratory to the clinic

W. F. Bynum

Science and Medicine in France: The Emergence of Experimental Physiology, 1790–1855.
By John E. Lesch.
Harvard University Press: 1984. Pp.276. $25, £22.

A SCIENTIST's proclaimed self-image may conceal as much as it reveals. Isaac Newton likened himself to a boy playing on the seashore, "diverting myself in now and then finding a smoother pebble or a prettier shell than ordinary, whilst the great ocean of truth lay all undiscovered before me". This is a charming image, but one which hardly does justice to Newton's complex psychology, or to his belief that he had seen into the heart of things. François Magendie compared himself to "a rag-pricker: with my spiked stick in my hand and my basket on my back, I traverse the field of science and I gather what I find". Equally charming this, but equally inadequate as an account of Magendie's philosophy of discovery. Certainly he did not possess the philosophical sophistication of his pupil Claude Bernard (1813–1878), by whom this statement of Magendie was recorded and who rather liked to cast his teacher into the role of John the Baptist as foil to himself as Messiah. But Magendie (like Bernard) was concerned with the dialectic between basic science and clinical medicine, and it is this which is a central theme in John Lesch's book.

Magendie (1783–1855) was a child of the French Revolution, a product and a participant in the "hospital medicine" which, particularly after the reorganization of the Paris Medical School in 1794, came to dominate French medical education. This form of clinical medicine was firmly rooted in the hospital, where medical students were to be based from the first day of their education and where they were to "read little, see much, do much". The high priests of hospital medicine — Corvisart, Laennec, Louis — stressed the importance of the local lesion as opposed to the generalized symptom, the lesion to be discovered by careful physical diagnosis (made more systematic after Corvisart popularized percussion and Laennec invented the stethoscope) and confirmed by autopsy. Every hospital physician was to be his own pathologist, permitting diseases such as phthisis, pneumonia and typhoid to be conceptualized in terms of more constant lesion than more variable symptom. For many doctors of the French school, the sciences of physics, chemistry, physiology and even microscopy were "accessory" rather than "basic" to the medical enterprise: accessory and potentially dangerous, for they encouraged speculation and system-building in advance of the "facts" demonstrable by pathological anatomy.

This aspect of "hospital medicine" has been elucidated in books such as E.H. Ackerknecht's *Medicine at the Paris Hospital, 1794–1848* (The Johns Hopkins University Press, 1967) and Michel Foucault's *Birth of the Clinic* (published in English translation by Tavistock in 1973). But while Lesch recognizes the cogency of their work, the value of his own lies in its patient examination of an equally rich tradition in early-nineteenth-century French medicine: a tradition which recognized the value of experimental science. He scrutinizes three sciences, chemistry, pharmacology and physiology, in each of which Magendie was a key figure.

A critical chemical tradition in French science dates back to the formation (in 1776) of the Société Royale de Médecine and to the rigorous attempt by prominent members of that Society, especially Antoine Fourcroy (1755–1809), to apply the newer analytical methods of chemistry to isolate and identify the active ingredients of common medical preparations. From the turn of the century the discovery of plant alkaloids—including emetine, strychnine, codeine, quinine and morphine—had demonstrated the value of the "analytical method", and had provided Magendie with the justification for producing his own *Formulaire* (1821), a therapeutic manual based on the notion of pure substances rather than polypharmic preparations. In using the word "pharmacology" in 1805, J.B.G. Barbier (1776–1865) had insisted that the pharmacologist had to be both chemist (to identify the active substance) and physiologist (to elucidate its precise actions). It was particularly in the latter guise that Magendie pursued his experimental investigation of strychnine, prussic acid and ipecacuanha. His relations with the Paris hospitals were chequered, but various clinicians helped him in his researches; and, in 1830, he became director of a women's ward in the Hôtel Dieu, where he was able to conduct more systematic clinical trials.

Magendie's clinical work (some of it simply attempting to cope with the seriously ill, as in the 1832 cholera epidemic when this most gifted experimentalist of his generation treated 594 cholera victims between March and August) reminds us of the complexity of the relationship between science and medicine during the period. The interplay between the two can be seen in Magendie's concept of "pathological physiology", for much of his most famous research—on the cerebro-spinal fluid, on the functions of the posterior and anterior roots of the spinal nerves, on localization within the central nervous system—was laboratory based but clinically informed. Lesch establishes continuity between the methods and problems of the late Magendie and the early Bernard, just as he also sees important legacies for Magendie from the experimental work of Xavier Bichat (1771–1802).

Much of Lesch's monograph consists of rather detailed expositions of the experimental chemical, pharmacological and physiological results obtained by French medical scientists of Magendie's era. Some of this may be of specialist historical interest. But the general problem he addresses—what place has experimental science in medicine?—is one of great topicality. Our own answers may not be the same as those proposed in nineteenth-century France, but Lesch's book does illuminate an important historical moment in that continuing dialogue.

W.F. Bynum is at the Wellcome Institute for the History of Medicine, London.

●Subscription rates were omitted from the review of the journal *Molecular Biology & Medicine* (*Nature* 311, 318, 1984). Published by Academic Press, and rates for 1985: institutional £60 (UK), $100 (elsewhere); personal £30 (UK), $50 (elsewhere).

Meeting of minds in a magnetic field

Robert S. Coe

Geomagnetism of Baked Clays and Recent Sediments.
Edited by K.M. Creer, P. Tucholka and C.E. Barton.
Elsevier Scientific: 1983. Pp. 324.
Dfl. 125, $53.25.

K.M. Creer and his co-editors frankly confess to holding "mixed views about the publication of symposium proceedings". Such pessimism was misplaced; to my mind, they have succeeded admirably in avoiding the pitfalls that doom most books of this genre to a limited readership and transient life.

Several factors have contributed to the success of this volume. First, the subject of geomagnetism has entered one of those periods in which the various sub-disciplines are bubbling with excitement and appear to be converging on common (but as yet dimly perceived) ground. Satellites such as MAGSAT have revolutionized the business of global measurement and description of the present geomagnetic field, cryogenic magnetometers have greatly increased the rate that data about the ancient geomagnetic field can be obtained from weakly magnetized rocks, and computers have immeasurably improved our ability to store and manipulate data and perform the calculations required for increasingly sophisticated models of geodynamos. Geomagnetists are now talking to palaeomagnetists; theory is meeting observation and experiment.

Secondly, the Fourth Assembly of the International Association of Geomagnetism and Aeronomy held in 1981 in Edinburgh—including the Symposium on Time Scales of Secular Variation, from which the core of papers published in this volume is drawn—was graced with an unusual number of truly fine contributions, and came at a time when the subject is manageable in scope and sorely in need of review. The main reason, however, that this book is definitely more than just another symposium volume lies in the clear effort taken by the editors to achieve a logical organization, adequate coverage and balance, and a semblance of uniformity of style.

The central theme is the behaviour of the geomagnetic field over the past several tens of thousands of years, as deduced from the remanent magnetization of baked clays and lake sediments. The 33 contributions (by 40 authors) are grouped into four chapters, the first of which contains brief and often interesting critiques of the most relevant magnetization processes, including thermoremanent magnetization, detrital remanent magnetization and shear remanent magnetization. The second consists of similar treatments of selected dating techniques (palynology, radiocarbon, tree-rings and varves, lead-210 and thermoluminescence).

The third chapter is the longest and most highly developed. It is distinguished by a particularly clear and informative review of techniques for archaeointensity determination by M.J. Aitken; by summaries of archaeomagnetic results up to 1981 for Greece, Bulgaria and Yugoslavia, Egypt, the Near East, the USSR, China, Japan, the United States, Peru and Australia; and by a perceptive analysis of global intensities for the past 50,000 years by M.W. McElhinny. The final chapter consists of presentations of palaeomagnetic data—many of which show encouraging consistency—of lake sediments from Europe, North America, Argentina and Australia, and cave sediments from Europe, as well as reviews of mathematical techniques for analysis of directional data as a function of depth or time. Throughout the book, the various topics are woven together by means of introductory sections and occasional summary discussions within each chapter. An "Epilogue" by the editors, containing their own analysis, interpretation and conclusions, also helps to unify the book and is a stimulating contribution in its own right.

One can always find things to complain about. I found myself wishing at times that the coverage were more encyclopaedic, and resolving to get my eyes examined because of the small camera-ready type-face with commas that are almost indistinguishable from full points. While it is impossible for a symposium volume to have the same intellectual impact as a book written by one or a few excellent scientists who are also excellent writers, this is about as close as you can get; newcomers can read it as a detailed and relatively unbiased introduction to the field, and practising specialists will find it a handy reference for quite some years. Simply put, it is one of the most effective multi-author works that I have encountered in the earth sciences. ☐

Robert S. Coe is a Professor in the Department of Earth Sciences at the University of California, Santa Cruz.

Instruments of change

Alan Braithwaite

Microcomputers and Laboratory Instrumentation.
By David J. Malcolme-Lawes.
Plenum: 1984. Pp. 246.
$35, £29.75.

MOST scientists and technologists are now faced with the challenge of the microprocessor chip. It is present in all types of instrumentation, to control the mechanics and optimize parameters, and also to collect and process data. It is still possible to lead the quiet life of an alchemist, but the march of progress means that sooner or later almost everyone in a laboratory will have to wrestle with a new language — the language of the computer — and with sophisticated instruments employing arrays of chips.

Programming languages are not too difficult to learn. They use an understandable syntax, and there are numerous books on the topic. The hardware presents more of a problem but, surprisingly, there are few accounts of the subject as it applies to scientific instrumentation and intended for the practising scientist. David Malcolme-Lawes has written such a text. It sets out to present in clear, understandable terms the overall concept of microcomputer systems, microprocessors and various logic chips incorporated into digital and interfacing circuitry. Further, many computers are used for collection of data from detectors and transducers, and also to control instrument functions, switches, relays, heaters and so on, and these principles too are explained both in general terms and in more detail, including the logic required to buffer and interface digital signal buses and interconnect equipment. For the more enterprising readers there is also a chapter on system design concepts and the construction of interfaces and microcomputer equipment.

It is quite possible to read the book selectively to obtain an overview, but the main purpose is to cover all the necessary background concepts relating to the nature and handling of instrument and transducer signals, microcomputer systems and interfacing concepts. Overall, the writing reflects the teaching experience of the author, as does the inclusion of a large number of diagrams to supplement the text — in this subject in particular, a picture is indeed worth a thousand words.

The net result is a well-presented, readable book which provides a sound introduction to microcomputers in the laboratory and also to the principles and concepts of microprocessor systems and interfacing. Scientists and technologists seeking to get to grips with new technological developments, and students for whom laboratory instrumentation is part of their course, will find it very helpful. My only plea is that the publishers should consider issuing a paperback edition; I think they would find it worth their while. ☐

Alan Braithwaite is a Senior Lecturer in Analytical Chemistry in the Department of Physical Sciences, Trent Polytechnic, Nottingham.

BOOKS RECEIVED

Mathematics

Calculus: Basic Concepts and Applications. By R.A. ROSENBAUM and G. PHILIP JOHNSON. *Cambridge University Press: 1984. Pp.422. ISBN 0-521-25012-9. £12.50, $24.95.*

Mathematical Essays in Honor of Su Buchin. C.C. HSIUNG (ed.). *World Scientific: 1983. Pp.276. ISBN 9971-950-98-7. £26.35.*

Multifacetted Modelling and Discrete Event Simulation. By BERNARD P. ZEIGLER. *Academic: 1984. Pp.372. ISBN 0-12-778450-0. £25.50; $42.50.*

Nonparametric Functional Estimation. By B.L.S. PRAKASA RAO. *Academic: 1983. Pp.522. ISBN 0-12-564020-X. $70.*

The Umbral Calculus. By STEVEN ROMAN. *Academic: 1984. Pp.193. ISBN 0-12-594380-6. $35.*

Unified Integration. By E.J. McSHANE. *Academic: 1983. Pp.607. ISBN 0-12-486260-8. $55.*

Astronomy

Astrodynamics 1983. Advances in the Astronautical Sciences, Vol. 54 Parts I & II. T.G. TSENG *et al.* (eds). *American Astronautical Society: 1984. Pp.653 & 1,330. Hbk ISBN 0-87703-190-7, 0-87703-190-8; pbk ISBN 0-87703-191-6, 0-87703-191-6. Np.*

Connected Components in Binary Images: The Detection Problem. By CHRISTIAN RONSE and PIERRE A. DEVIJVER. *Wiley: 1984. Pp.165. ISBN 0-86380-016-5. £24.*

Interstellar Chemistry. By W.W. DULEY and D.A. WILLIAMS. *Academic: 1984. Pp.264. ISBN 0-12-223360-3. £29, $45.*

The Solar System. By ROMAN SMOLUCHOWSKI. *Scientific American Books: 1984. Pp.173. ISBN 0-7167-1492-2. $27.95.*

Technology

Advances in Cryogenic Engineering Materials, Vol.30. A.F. CLARK and R.P. REED (eds). *Plenum: 1984. Pp.998. ISBN 0-306-41704-9. Np.*

Atmospheric Turbulence: Models and Methods for Engineering Applications. By HANS A. PANOFSKY and JOHN A. DUTTON. *Wiley: 1984. Pp.397. ISBN 0-471-05714-2. £47.45, $66.45.*

Flexible Assembly Systems. Assembly by Robots and Computerised Integrated Systems. By A.E. OWEN. *Plenum: 1984. Pp.231. ISBN 0-306-41527-5. Np.*

Science, Technology and Society Today. MICHAEL GIBBONS and PHILIP GUMMETT (eds). *Manchester University Press: 1984. Pp.198. Hbk ISBN 0-7190-0905-7; pbk ISBN 0-7190-0878-6. Hbk £11.50; pbk £4.50.*

Chemistry

Advanced Organic Chemistry 2nd Edn. Part A: Structure and Mechanisms. By FRANCIS A. CAREY and RICHARD J. SUNDBERG. *Plenum: 1984. Pp.726. Hbk ISBN 0-306-41087-7; pbk ISBN 0-306-41198-9.*

Analysis Using Glass Electrodes. By PETER W. LINDER, RALPH G. TORRINGTON and DAVID R. WILLIAMS. *Open University Press: 1984. Pp.148. ISBN 0-335-10420-7. £20.*

75th Jubilee Conference on Helium — 4. J.G.M. ARMITAGE (ed.). *Wiley: 1983. Pp.211. ISBN 9971-966-23-9. £20.75.*

Molecular Diffusion and Spectra. By WILLIAM T. COFFEY, MYRON W. EVANS and PAOLO GRIGOLINI. *Wiley: 1984. Pp.378. ISBN 0-471-87539-2. £47.50.*

Organometallic Chemistry, Vol.12. F.G.A. STONE and E.W. ABEL (eds). *Royal Society of Chemistry: 1984. Pp.498. ISBN 0-85186-601-8. £82.*

Reactions of Small Transient Species: Kinetics and Energetics. A. FONTIJN and M.A.A. CLYNE (eds). *Academic: 1983. Pp.488. ISBN 0-12-262040-2. £49.80, $89.*

Room Temperature Phosphorimetry for Chemical Analysis.•By TUAN VO-DINH. *Wiley: 1984. Pp.304. ISBN 0-471-87884-7. £47.50.*

Solid-Liquid Separation. JOHN GREGORY (ed.). *Wiley: 1984. Pp.363. ISBN 0-470-20021-9. £32.50.*

Surfactants in Solution, Vols 1 & 2. K.L. MITTAL and B. LINDMAN (eds). *Plenum: 1984. Pp.705, 1,432. ISBN 0-306-41483-X; 0-306-41484-8. Np.*

Theilheimer's Synthetic Methods of Organic Chemistry. A.F. FINCH (ed.). *Karger: 1984. Pp.620. ISBN 3-8055-3817-0. $346.25.*

Topics in Carbon-13 NMR Spectroscopy. GEORGE C. LEVY (ed.). *Wiley: 1984. Pp.282. ISBN 0-471-09857-4. £54.65, $57.50.*

Physics

Advances in Liquid Crystals, Vol. 6. GLENN H. BROWN (ed.). *Academic: 1983. Pp.268. ISBN 0-12-025006-3. $80.*

Classical Mechanics: A Course of Lectures. By A.K. RAYCHAUDHURI. *Oxford University Press: 1984. Pp.210. ISBN 0-19-561343-0. £7.50.*

The Creation of Quantum Mechanics and the Bohr-Pauli Dialogue. Studies in the History of Modern Science 14. *Reidel: 1984. ISBN 90-2771648-X. $34.50.*

The Dynamic World of Physics. By ROBERT T. DIXON. *Charles E. Merrill: 1984. Pp.560. ISBN 0-675-20093-8. Np.*

Foundations of Quantum Mechanics in the Light of New Technology. S. KAMEFUCHI *et al.* (eds). *Physical Society of Japan: 1984. Pp.377. ISBN 4-89027-001-9. Np.*

Fusion: An Introduction to the Physics and Technology of Magnetic Confinement Fusion. By WESTON M. STACEY. *Wiley: 1984. Pp.260. ISBN 0-471-88079-5. £39.50.*

Isotope Shifts in Atomic Spectra: Physics of Atoms and Molecules. By W.H. KING. *Plenum: 1984. Pp.208. ISBN 0-306-41562-3. $37.50.*

Methods in Radiative Transfer. WOLFGANG KALKOFEN (ed.). *Cambridge University Press: 1984. Pp.450. ISBN 0-521-25520-8. £25, $49.50.*

Perspectives in Nuclear Physics at Intermediate Energies. S. BOFFI, C. CIOFI DEGLI ATTI and M.M. GIANNINI (eds). *Wiley: 1984. Pp.546. ISBN 9971-966-32-8. £49.*

Physical Sciences and History of Physics. Boston Studies in the Philosophy of Science, Vol.82. R.S. COHEN and M.W. WARTOFSKY (eds). *Reidel: 1984. Pp.259. ISBN 90-277-1615-3. $39.50.*

Secondary Ion Mass Spectrometry SIMS IV. Springer Series in Chemical Physics 36. A. BENNINGHOVEN *et al.* (eds). *Springer-Verlag: 1984. Pp.502. ISBN 3-540-13316-X/0-387-13316-X. $38.50.*

Statistical Physics & Chaos in Fusion Plasmas. C.W. HORTON and L.E. REICHL (eds). *Wiley: 1984. Pp.361. ISBN 0-471-88310-7. £80.75.*

Symplectic Techniques in Physics. By VICTOR GUILLEMIN and SHLOMO STERNBERG. *Cambridge University Press: 1984. Pp.468. ISBN 0-521-24866-3. £32.50, $49.50.*

Earth Sciences

Catchment Experiments in Fluvial Geomorphology. T.P. BURT and D.E. WALLING (eds). *Geo Books: 1984. Pp.608. Pbk ISBN 0-86094-137-X. Pbk £28.50.*

Chemistry of Particles, Fogs and Rains Acid Precipitation Series Vol. 2. JACK L. DURHAM (ed.). *Butterworth: 1984. Pp.262. ISBN 0-250-40567-9. Np.*

Constitution of the Earth's Interior. J. LELIWA-KOPYSTYNSKI and R. TEISSEYRE (eds). *Elsevier: 1984. Pp.368. ISBN 0-444-99646-X. $83, Dfl. 195.*

Deposition Both Wet and Dry. Acid Precipitation Series Vol. 4. BRUCE B. HICKS (ed.) *Butterworth: 1984. Pp.197. ISBN 0-250-40569-5. Np.*

Direct and Indirect Effects of Acidic Deposition on Vegetation. Acid Precipitation Series Vol. 5. RICK A. LINTHURST (ed.). *Butterworth: 1984. Pp. 117. ISBN 0-250-40570-9. Np.*

Early Biotic Responses to Advancing Lake Acidification. Acid Precipitation Series Vol. 6. GEORGE R. HENDREY (ed.) *Butterworth: 1984. Pp.173. ISBN 0-250-40571-7. Np.*

Erosion and Sediment Yield: Some Methods of Measurement and Modelling. R.F. HADLEY and D.E. WALLING (eds.) *Geo Books: 1984. Pp.218. Hbk ISBN 0-86094-158-2; pbk ISBN 0-86094-141-8. Hbk £13.50; pbk £9.*

Geography & Population: Approaches and Applications. JOHN I. CLARK (ed.) *Pergamon 1984. Pp.245. Hbk ISBN 0-08-028781-6, pbk ISBN 0-08-028780-8. Pbk £6.95, $11.50.*

Geological Aspects of Acid Deposition. Acid Precipitation Series Vol. 7. OWEN P. BRICKER (ed.) *Butterworth: 1984. Pp.143. ISBN 0-40572 5. Np*

Groundwater as a Geomorphic Agent. R. G. LAFLEUR (ed.). *Allen & Unwin: 1984 Pp 390 ISBN 0-04-5517069-5. £30, $50*

Handbook on the Physics and Chemistry of Rare Earths, Vol. 6. K.A.G. SCHNEIDNER and L. EYRING (eds). *North-Holland 1983. Pp 604 ISBN 0-444-86592-6. $119.25.*

Ice Sheets and Climate. By J. OERLEMANS and C.J. VAN DER VEEN. *Reidel 1984 Pp 217 ISBN 90-277-1709-5. $34.50.*

London Illustrated Geological Walks. By ERIC ROBINSON. *Scottish Academic Press 1984 Pp 97 ISBN 0-7073-0350-8. Pbk £4 95*

Materials Science of the Earth's Interior. ICHIRO SYNAGAWA (ed.). *Reidel 1984 Pp 653 ISBN 90-277-1649-8. $120.*

Meterological Aspects of Acid Rain. Acid Precipitation Series Vol. 1. CHANDRAKANT M. BHUMRALKAR (ed.). *Butterworth 1984 Pp 243 ISBN 0-250-40566-0. Np*

Mineral Resources Appraisal: Mineral Endowment, Resources, and Potential Supply. Concepts, Methods and Cases. By DEVERLE P. HARRIS. *Oxford University Press: 1984. Pp 445 ISBN 0-19 854456-[illegible] £37.50.*

Modelling of Total Acid Precipitation Impacts. Acid Precipitation Series Vol. 9. JERALD L. SCHNOOR (ed.). *Butterworth: 1984 Pp 222 ISBN 0 250 40573 1 Np.*

Satellite Sensing of a Cloudy Atmosphere. Observing the Third Planet. ANN HENDERSON-SELLERS (ed.). *Taylor & Francis: 1984 Pp 340 ISBN 0-85066-254-0. £18.*

Scandinavia: A New Geography. By BRIAN JOHN *Longman: 1984. Pp.365. Pbk ISBN 0-582-48950-4 Pbk £11.95.*

SO_2, NO and NO_2 Oxidation Mechanisms. Atmospheric Considerations. Acid Precipitation Series Vol. 3. JACK G. CALVERT (ed.) *Butterworth 1984 Pp.254. ISBN 0-250-40568-7 Np*

Environmental Sciences

Air Monitoring Methods for Industrial Contaminants. DAVID A. HALLIDAY (ed.) *Biomedical Publications, Box 495, Davis, California 95617: 1983. Pp.428. ISBN 0-931890-12-8 Np*

Chlorinated Dioxins and Dibenzofurans in the Total Environment. By GANGADHAR CHOUDHARY, LAWRENCE H. KEITH and CHRISTOFFER RAPPE. *Butterworth: 1984 Pp 416 ISBN 0-250-40604-7. £42.*

Handbook of Air Pollution Technology. SEYMOUR CALVERT and HAROLD M. ENGLUND (eds). *Wiley: 1984. Pp 1066 ISBN 0-471-08263-5 £71.20, $74,95.*

Hazardous Waste Land Treatment. KIRK W. BROWN, GORDON B. EVANS and BETH D. FRENTRUP (eds). *Butterworth: 1983 Pp 692 ISBN 0-250-40636-5. £48.*

Identification and Analysis of Organic Pollutants in Air. LAWRENCE H. KEITH (ed.) *Butterworth 1984. Pp.486. ISBN 0-250-40575-X £55*

Liquid Chromatography in Environmental Analysis. JAMES F. LAWRENCE (ed.). *Wiley 1984 Pp 374 ISBN 0-89603-045-8. £48.75*

Toxic Contaminants in the Great Lakes. JEROME O. NRIAGU and MILAGROS S. SIMMONS *Wiley 1984. Pp.527. ISBN 0-471-89087-1 £90.25.*

Biological Sciences

Advances in Cyclic Nucleotide and Protein Phosphorylation Research Vol. 16. SAMUEL J. STRADA and W. JOSEPH THOMPSON (eds) *Raven: 1983. Pp.460. ISBN 0-89004-779-0 $62*

Advances in Cyclic Nucleotide and Protein Phosphorylation Research, Vol. 17A. PAUL GREENGARD *et al.* (eds). *Raven: 1983 Pp 182 Pbk ISBN 0-89004-881-9. Pbk $22.*

Advances in Enzyme Regulation, Vol. 22. By GEORGE WEBER. *Pergamon: 1984. ISBN 0-08-031498-8. £93.75, $150.*

Aging and Recovery of Function in the Central Nervous System. STEPHEN W. SCHEFF (ed.). *Plenum: 1984. Pp.221. ISBN 0-306-41525-9. Np.*

Amphibian Morphogenesis. By HAROLD FOX. *Humana Press: 1984. Pp.320. ISBN 0-89603-043-1. $59.50.*

Applications of Optimal Control Theory in Biomedicine. By GEORGE W. SWAN. *Marcel Dekker: 1984. Pp.285. ISBN 0-8247-7192-3. SwFr. 151.*

Bailey's Textbook of Microscopic Anatomy, 18th Edn. By DOUGLAS E. KELLY, RICHARD L. WOOD and ALLEN C. ENDERS. *Williams & Wilkins: 1984. Pp.909. ISBN 0-683-04568-7. £35.*

The Bee-Eaters. By C.H. FRY. *T. & A.D. Poyser: 1984. Pp.304. ISBN 0-85661-037-2. £19.60.*

Bio-Energy: Technology, Thermodynamics and Costs. By DAVID BOYLES. *Wiley: 1984. Pp.158. ISBN 0-85312-637-2. £16.50.*

Biological Regulation and Development: Volume 3B Hormone Action. ROBERT F. GOLDBERGER and KEITH R. YAMAMOTO (eds). *Plenum: 1984. Pp.312. ISBN 0-306-41442-2. $42.50.*

Biology of Knowledge: The Evolutionary Basis of Reason. By RUPERT RIEDL. *Wiley: 1984. Pp.252. ISBN 0-471-10309-8. £26.*

The Birds of China. By RODOLPHE MEYER DE SCHAUENSEE. *Oxford University Press: 1984. Pp.602. ISBN 0-19-858602-7. £35.*

Butterflies East of the Great Plains. An Illustrated Natural History. By PAUL A. OPLER and GEORGE O. KRIZEK. *Johns Hopkins University Press: 1984. ISBN 0-8018-2938-0. $49.50.*

Cephalopod Life Cycles. Vol. 1 Species Accounts. P.R. BOYLE (ed.). *Academic: 1983. Pp.516. ISBN 0-12-128001-5. £70, $120.*

Developmental Control in Animals and Plants, 2nd Edn. C.F. GRAHAM and P.F. WAREING (eds). *Blackwell Scientific: 1984. Pp.519. Pbk ISBN 0-632-00758-3. Pbk £18.50.*

Drug and Alcohol Abuse: A Clinical Guide to Diagnosis and Treatment. 2nd Edn. By MARC A. SCHUCKIT. *Plenum: 1984. Pp.267. ISBN 0-306-41457-0. Np.*

Early Ancestry and Evolution of the Higher Plants. By P.J. FAULKS. *D. McLean, 32 Market Place, Coleford, Gloucestershire, GL16 8AA: 1983. Pp.96. Hbk ISBN 0-946252-07-6; pbk ISBN 0-946252-08-4. Hbk £10.95; pbk £4.95.*

Effects of Pollutants at the Ecosystem Level. PATRICK J. SHEEHAN (eds.). *Wiley: 1984. ISBN 0-471-90204-7. £31.90.*

Energy Balance and Temperature Regulation. By M.W. STANIER, L.E. MOUNT and J. BLIGH. *Cambridge University Press: 1984. Pp.152. Hbk ISBN 0-521-25827-8; pbk ISBN 0-521-27727-2. Hbk £17.50, $29.95; pbk £7.50, $12.95.*

Essential Haematology, 2nd Edn. By A.V. HOFFRAND and J.E. PETTIT. *Blackwell Scientific: 1984. Pp.274. ISBN 0-632-01196-3. Pbk £8.50.*

Essentials of Immunology. By W.H. HILDEMANN. *Elsevier: 1984. Pp.146. ISBN 0-444-00805-5. $19.50.*

Feathered Friends. By IAN NIALL. *Chatto & Windus: 1984. Pp.170. ISBN 0-7011-2772-4. $9.95.*

Fetal Alcohol Syndrome and Fetal Alcohol Effects. By ERNEST L. ABEL. *Plenum: 1984. Pp.246. ISBN 0-306-41427-9. Np.*

Frankia Symbioses. Developments in Plant and Soil Sciences, Vol. 12. A.D.L. AKKERMANS *et al.* (eds). *Martinus Nijhoff: 1984. Pp.258. ISBN 90-247-2967-X. Dfl 130, $50, £33.*

Fundamentals of Plant Pathology, 2nd Edn. By DANIEL A. ROBERTS and CARL W. BOOTHROYD. *W.H. Freeman: 1984. Pp.448. ISBN 0-7167-1505-8. $29.95.*

Genes and Antigens of Parasites: A Laboratory Manual, 2nd Edn. C.M. MOREL (ed.). *Instituto Oswaldo Cruz, Rio de Janeiro, Brazil: 1984. Pp.580. ISBN 85-85033-01-0. Np.*

Genetic Aspects of Speech and Language Dsorders. CHRISTY L. LUDLOW and JUDITH A. COOPER (eds). *Academic: 1984. Pp.221. ISBN 0-12-459350-X. $29.*

The Genetic Code and Protein Biosynthesis, 2nd Edn. Studies in Biology No. 83. By BRIAN F. C. CLARK. *Edward Arnold: 1984. Pp.76. Pbk ISBN 0-7131-2887-9. Pbk £3.20.*

Hallucinogens: Neurochemical, Behavioural, and Clinical Perspectives. BARRY L. JACOBS (ed.). *Raven: 1984. Pp.247. ISBN 0-89004-990-4. $61.50.*

Handbook of Neurochemistry, 2nd Edn. Volume 6, Receptors in the Nervous System. ABEL LAJTHA (ed.). *Plenum: 1984. Pp.668. ISBN 0-306-41411-2. Np.*

Handbook of Vegetation Science. Sampling Methods and Taxon Analysis in Vegetation Science. R. KNAPP (ed.). *Dr. W. Junk: 1984. Pp.370. ISBN 90-6193-185-1. $67.50, £39.25.*

Histone Genes: Structure, Organization and Regulation. GARY S. STEIN, JANET L. STEIN and WILLIAM F. MARZLUFF (eds). *Wiley: 1984. Pp.494. ISBN 0-471-89615-2. £78.70.*

Human Intestinal Microflora in Health and Disease. David J. HENTGES (ed.). *Academic: 1983. Pp.568. ISBN 0-12-341280-3. $65.50.*

Immunity to Parasites: How Animals Control Parasite Infections. By DEREK WAKELIN. *Edward Arnold: 1984. Pp.165. ISBN 0-7131-2889-5. Pbk £7.50.*

International Review of Cytology, Vol.83. G.H. BOURNE and J.F. DANIELLI (eds). *Academic: 1983. Pp.304. ISBN 0-12-364483-6. $42.*

Intestinal Toxicology. Target Organ Toxicology Series. CAROL M. SCHILLER (ed.). *Raven Press: 1984. Pp.251. ISBN 0-89004-841-X. $68.50.*

Investigation of Membrane-Located Receptors. ERIC REID, G.M.W. COOK and D.J. MORRÉ (eds). *Plenum: 1984. Pp.558. ISBN 0-306-41499-6. $75.*

The Kidney and Body Fluid in Health and Disease. SAULO DLAHR (ed.). *Plenum: 1984. Pp.593. Pbk ISBN 0-306-41660-3. Np.*

Leukemia Reviews International, Vol.2. MARVIN A. RICH (ed.). *Marcel Dekker: 1984. Pp.184. ISBN 0-8247-7157-5. SwFr 113.*

Leukotriene Syntheses: A New Class of Biologically Active Compounds Including SRS-A. By FEODOR SCHEINMANN and JOHN ACKROYD. *Raven: 1983. Pp.100. ISBN 0-89004-897-5. $30.*

Macrophage Activation. Contemporary Topics in Immunobiology 13. DOLPH O. ADAMS and MICHAEL G. HANNA (eds). *Plenum: 1984. Pp.262. ISBN 0-306-41536-4. $39.50.*

A Manual on Methods for the Assessment of Secondary Productivity in Fresh Waters, 2nd Edn. JOHN A. DOWNING and FRANK H. RIGLER (eds). *Blackwell: 1984. Pp.501. ISBN 0-632-00616-1. £27.50.*

Manual Specialization and the Developing Brain. GERALD YOUNG *et al.*(eds). *Academic: 1983. Pp.412. ISBN 0-12-773140-7. $48.*

Mechanisms of Migration in Fishes. JAMES D. MCCLEAVE *et al.* (eds). *Plenum: 1984. Pp.574. ISBN 0-306-41676-X. Np.*

Mechanisms of Morphological Evolution. A Combined Genetic, Developmental and Ecological Approach. By WALLACE ARTHUR. *Wiley: 1984. Pp.275. ISBN 0-471-90347-7. £19.*

Membranes and their Cellular Functions, 3rd Edn. By J.B. FINEAN, R. COLEMAN and R.H. MICHELL. *Blackwell Scientific: 1984. Pp.227. ISBN 0-632-01204-8. Pbk £9.80.*

Methods in Enzymology, Vol.98. Biomembranes. SIDNEY FLEISCHER and BECCA FLEISCHER (ed.). *Academic: 1983. Pp.688. ISBN 0-12-181998-1. $73.*

Methylation of DNA. Current Topics in Microbiology and Immunology. T.A. TRAUTNER (ed.). *Springer-Verlag: 1984. Pp.176. ISBN 3-540-12849-2/ 0-387-12849-2. DM 88, $32.90.*

The Microbe 1984. Part 1 Viruses. B.W.J. MAHY and J.R. PATTISON (eds). *Cambridge University Press: 1984. Pp.344. ISBN 0-521-26056-6. £30, $59.50.*

The Microbe 1984. Part II Prokaryotes and Eukaryotes. D.P. KELLY and N.G. CARR (eds). *Cambridge University Press: 1984. Pp.349. ISBN 0-521-26057-4. £30.*

Migration and Mobility: Biosocial Aspects of Human Movement. A.J. BOYCE (ed.). *Taylor & Francis: 1984. Pp.378. ISBN 0-85066-243-9. £16.*

Molecular Biology and Pathogenesis of Coronaviruses. P.J.M. ROTTIER *et al.* (eds). *Plenum: 1984. Pp.409. ISBN 0-306-41616-6. Np.*

Nervous System, Endocrine System and Infusion Therapy. J.C. PETRIE (ed.). *Elsevier: 1984. Pp.370. ISBN 0-444-80529-X. $96.25, Dfl.250.*

The Neurohypophysis: Physiological and Clinical Aspects. SEYMOUR REICHLIN (ed.). *Plenum: 1984. Pp.224. ISBN 0-306-41642-5. $32.50.*

Oligodendroglia. WILLIAM T. NORTON (ed.). *Plenum: 1984. Pp.351. ISBN 0-306-41547-X. Np.*

Photoreceptors. A. BORSELLINO and L. CERVETTO (eds). *Plenum: 1984. Pp.373. ISBN 0-306-41629-8. $55.*

Physiological Correlates of Human Behaviour Vol.3. Individual Differences and Psychopathology. ANTHONY GALE and JOHN A. EDWARDS (eds). *Academic: 1984. Pp.298. ISBN 0-12-273903-5. $48.*

Plant Life in the Devonian. By PATRICIA G. GENSEL and HENRY N. ANDREWS. *Praeger: 1984. Pp.380. ISBN 0-03-062002-3. $29.95.*

Plant Variation and Evolution, 2nd Edn. By D. BRIGGS and S.M. WALTERS. *Cambridge University Press: 1984. Pp.412. Hbk ISBN 0-521-25706-9; pbk ISBN 0-521-27665-9. Hbk £30, $59.50; pbk £9.95, $17.50.*

Posttranslational Covalent Modifications of Proteins. B. CONNOR JOHNSON (ed.). *Academic: 1984. Pp.424. ISBN 0-12-387560-9. $37.*

Progressive Spinal Muscular Atrophies. International Review of Child Neurology Series. INGRID GAMSTORP and HARVEY B. SARNAT (eds). *Raven Press: 1984. Pp.243. ISBN 0-89004-952-1. $60.*

Quantum-Mechanical Tunnelling in Biological Systems, 2nd Edn. By D. DEVAULT. *Cambridge University Press: 1984. ISBN 0-521-24904-X. £22.50.*

Rabbits. By MICHAEL LEACH. *Adam & Charles Black: 1984. Pp.25. ISBN 0-7136-2387-X. £3.50.*

Recent Advances in Immunology. ASUMAN Ü. MÜFTÜOĞLU and NEFISE BARLAS (eds). *Plenum: 1984. Pp.241. ISBN 0-306-41515-1. Np.*

Reflux Nephropathy Update: 1983. Contributions to Nephrology, Vol. 39. C.J. HODSON, R.H. HEPTINSTALL and J. WINBERG (eds). *Karger: 1984. Pp.388. ISBN 3-8055-3807-3. $59.50, DM 119.*

Regulation of Target Cell Responsiveness, Vol. 2. KENNETH W. McKERNS, ASBJØRN AAKVAAG and VIDAR HANSSON (eds). *Plenum: 1984. Pp.548. ISBN 0-306-41501-1. $75.*

The Reticuloendothelial System: A Comprehensive Treatise. Vol. 6 Immunology. JOSEPH A. BELLANTI and HERBERT B. HERSCOWITZ (eds). *Plenum: 1984. Pp.347. ISBN 0-306-41421-X. $55.*

The Reticuloendothelial System: A Comprehensive Treatise. 7A Physiology. SHERWOOD M. REICHARD and JAMES P. FILKINS (eds). *Plenum: 1984. Pp.411. ISBN 0-306-41422-8. Np.*

Subcellular Biochemistry. Vol. 10. DONALD B. ROODYN (ed.). *Plenum: 1984. Pp.552. ISBN 0-306-41528-3. Np.*

Thermal Physiology. J.R.S. HALES (ed.). *Raven: 1983. Pp.607. ISBN 0-89004-331-0. $84.50.*

White Cell Mechanics: Basic Science and Clinical Aspects. HERBERT J. MEISELMAN, MARSHALL A. LICHTMAN and PAUL L. LACELLE (eds). *Alan R. Liss: 1984. Pp.328. ISBN 0-8451-0306-7. £52.*

General

Policy and Development of Energy Resources. T. L. SHAW *et al.* (eds). *Wiley: 1984. Pp.247. ISBN 0-471-10537-6. £19.95.*

The Pond. Oxford Scientific Films. By GERALD THOMPSON *et al. Collins: 1984. Pp.256. ISBN 0-00-219145-8. £12.95.*

The Primal Place. By ROBERT FINCH. *W.H. Norton: 1984. Pp.243. ISBN 0-393-01623-4. £12.50, $18.00.*

Russian–English Translators' Dictionary: A Guide to Scientific and Technical Usage. 2nd edn. By MIKHAIL ZIMMERMAN. *Wiley: 1984. Pp.544. ISBN 0-471-90218-7. Np.*

Seaborn. By NEVILLE DRURY. *Tabb House: 1984. Pp.156. ISBN 0-907018-21-1. £6.95.*

In Search of Ancient Astronomies. E. C. KRUPP (ed). *Penguin: 1984. Pp.281. ISBN 0-14-00-5481-2. £4.95.*

Sport Science. Physical Laws and Optimum Performance. By PETER J. BRANCAZIO. *Simon & Schuster: 1984. Pp.400. ISBN 0-671-45584-2. $18.95.*

Starting from Scratch. J. D. HARE. *J. D. Hare: 1983. Pp.25. $3.00.*

State of the World. By LESTER R. BROWN *et al. W. W. Norton: 1984. Pp.252. ISBN 0-393-01835-0. £13.95, $19.50.*

Surfactants in Solution: Volume 3. K. L. MITTAL and B. LINDMAN (eds). *Plenum: 1984. Pp2173. ISBN 0-306-41475-6. Np.*

Vegetation in Civil and Landscape Engineering. By D. H. BACHE and I. A. MACASKILL. *Granada: 1984. Pp.317. ISBN 0-246-11507-6. Np.*

For the biochemistry laboratory

New ideas in this selection include a simple stopped-flow kinetics system for standard laboratory spectrophotometers and spectrofluorimeters.

- Schwarz/Mann Biotech's new Ultra-Pure grade of caesium chloride is 99.999% pure, specifically designed for use in sensitive density gradient determinations. In using the density gradient technique the optical density of the gradient medium should be as close to zero as possible, particularly when studying nucleoproteins. This new pure caesium chloride has an optical density that is inded near zero across the ultraviolet spectrum, and most critically from 260 to 280 nm.
Circle No. 100 on Reader Service Card.

- The Swiss balance manufacturer Precisa has introduced three new analytical balances featuring enlarged weighing ranges. These instruments offer a weighing capacity of 120 g, 160 g or 200g. Readability is 0.1mg. The 120A, 160A and 200A balances also feature a capacity- or tare-availability indicator.
Circle No. 101 on Reader Service Card.

- Specially designed for the electrophoresis of nucleic acids on horizontal agarose gels, the GNA-100 'mini-submarine', and GNA-200 'submarine' from Pharmacia are injection moulded, state-of-the-art units. Gel trays and lids are made of UV-transparent material; electrodes are robust titanium-based rods and a wide selection of gel combs is available.
Circle No. 102 on Reader Service Card.

- Clontech's Lamda (λ) gt11 immunoscreening kit (CLIK) offers well-characterized control components for screening λ gt11 expression libraries with antibody probes to assure that the proper conditions for antigen detection are used. CLIK includes λ gt11 chicken ovalbumin clone, λ gt11 phage, rabbit anti-ovalbumin serum, and biotinylated goat anti-rabbit IgG. The detection of bound primary antibody using biotinylated anti-IgG is extremely sensitive. False positives are rarely found.
Circle No. 103 on Reader Service Card.

- The Nicool LM 10 manufacturerd by the Harris Manufacturing Co. is designed for freezing biological specimens in cryotubes or straws. Manually operated and using liquid nitrogen as a refrigerant, and Nicool LM 10 is approximately 23 inches tall and 10 inches wide. Samples are placed at a specified level above the liquid nitrogen and freezing rates are obtained proportionately to the speed of the fan. Specimens can be plunged into the liquid nitrogen without opening the chamber. The electrical service is 110 volts.
Circle No. 104 on Reader Service Card.

- Scientific Systems, Inc. produces a low cost HPLC gradient system, featuring the Model 230 gradient control, the Model 210 Guardian, and two Model 200 LC pumps. Built around SSI's proven single-piston rapid refill pump, this system offers the chromatographer a sophisticated analytical instrument at low cost. The Model 200 delivers precise flows from 0.05 to 9.99 ml per min at pressures up to 6,000 p.s.i. and includes a compensation control that adjusts for the compressibility variations of different mobile phases. The Guardian enhances the operation of the pumps, acting as a pulse damper, a pressure monitor, high and low pressure limit circuits and a prime purge valve. The gradient control is a microprocessor-based unit designed to interface directly with the Model 200 (or other pumps having frequency-controlled flow rates).
Circle No. 105 on Reader Service Card.

- Based on the stopped-flow technique, the Hi-Tech SFA-11 rapid kinetics accessory reduces the fastest reaction half-life measurable with a UV/Vis spectrophotometer or spectrofluorimeter from several minutes to well under a second. Two precisely thermostatted 200μl shots of reagents can be readily mixed to fill the observation cell in less than 20 ms and thus half-lives down to less than 0.5s may be measured. The potential thermostatting range is 5 to 80°C. The observation cell can be fitted in seconds to any instrument that accommodates 10 mm cells/cuvettes. It has both 2 and 10 mm optical pathlengths selected by rotating the cell through 90° in the cell holder.
Circle No. 106 on Reader Service Card.

- The Microsyn ultrasonic processor is designed specifically for high intensity work in small volumes offering rapid powerful disruption of 250 μl to 10ml of material. Stable high-intensity power is generated at the titanium probe tip by a PZT crystal piezoelectric converter. The standard probe is lightweight with the lower 100 mm maintained at 3.2 mm diameter for insertion into long narrow sample tubes. Interchangeable probe tips offer 4.8 mm diameter for larger volume processing and a subminiature 2.4 mm diameter for delicate micro work. Power is supplied to the probe via a flexible lead connected to a compact free-standing generator module allowing the probe to be used on the bench or built into a processing system if required. The Microsyn ultrasonic processor is produced by Life Science Laboratories.
Circle No. 107 on Reader Service Card.

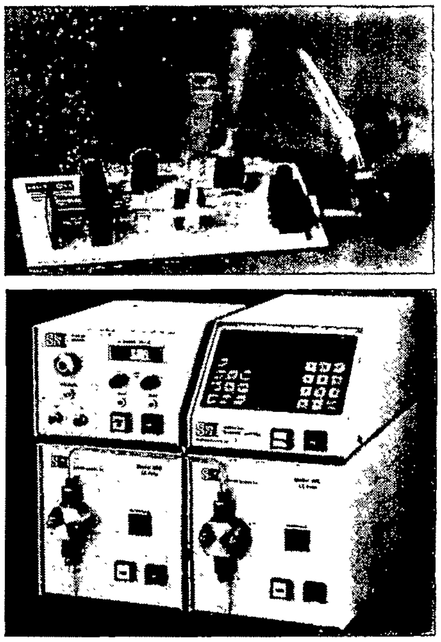

The Hi-Tech rapid kinetics accessory (top) and the SSI HPLC gradient system.

- A new compact radioisotope camera for the visualization of radioactive distributions of tritium and carbon-14 labelled compounds on TLC and paper chromatograms is now being produced by Birchover Instruments Ltd of Letchworth. The instrument uses a high resolution scanning spark chamber detector to produce a Polaroid print approximately ⅓ full size of the radioactive separations with exposure times of between 20 to 120 min, reducing considerably the evaluation time as compared with autoradiography which would require 3 to 21 days for a comparable result. A print projector for projecting the Polaroid print back so that radioactive areas can be quickly marked out on to the original radiochromatogram is an integral part of the bench top instrument.
Circle No. 108 on Reader Service Card.

- Imperial Laboratories (Europe) Ltd. of Salisbury has developed a serum-free lymphocyte culture medium for cytogenetics. This medium, Iscove's modification of Dulbecco's MEM, has the folic acid level reduced from the normal 4.00mg to 0.01mg per litre. Imperial Laboratories will undertake the production of cell culture media to customers' specifications in addition to supplying their range of standard media and sera. The medium was developed in conjunction with the Wessex Regional Cytogenetics Unit at Salisbury General Hospital.
Circle No. 125 on Reader Service Card.

● Ten purified homologues of tunicamycin are now available from Boehringer Mannheim Biochemicals. Each homologue exhibits a different degree of inhibition of glycosylation and overall protein synthesis. Thus, using a purified homologue rather than a standard commercial preparation of tunicamycin (mixtures of these homologues), achieves a much greater precision of inhibition. The levels of inhibition of protein synthesis by tunicamycin homologues and glycosylation are dependent on the system and growth conditions. Selection of the homologue with the desired inhibitory effects will be largely empirical.
Circle No: 109 on Reader Service Card.

● From LKB Instruments, Inc., comes a new pamphlet on the bioluminescent assay of NADH and NADPH. Application Note 506 offers a useful summary of the current state of the art, plus two generalized bioluminescent assay protocols, and a selected bibliography of applications in enzyme and metabolite analysis. The light produced by these luminescence methods is from two purified forms of bacterial luciferase specific for either NADH or NADPH. Measurement of light is simple as the quick flash problem has been solved by the monitoring reagents. In the applications section 14 dehydrogenases and other enzyme references are listed.
Circle No. 110 on Reader Service Card.

ADVERTISEMENT

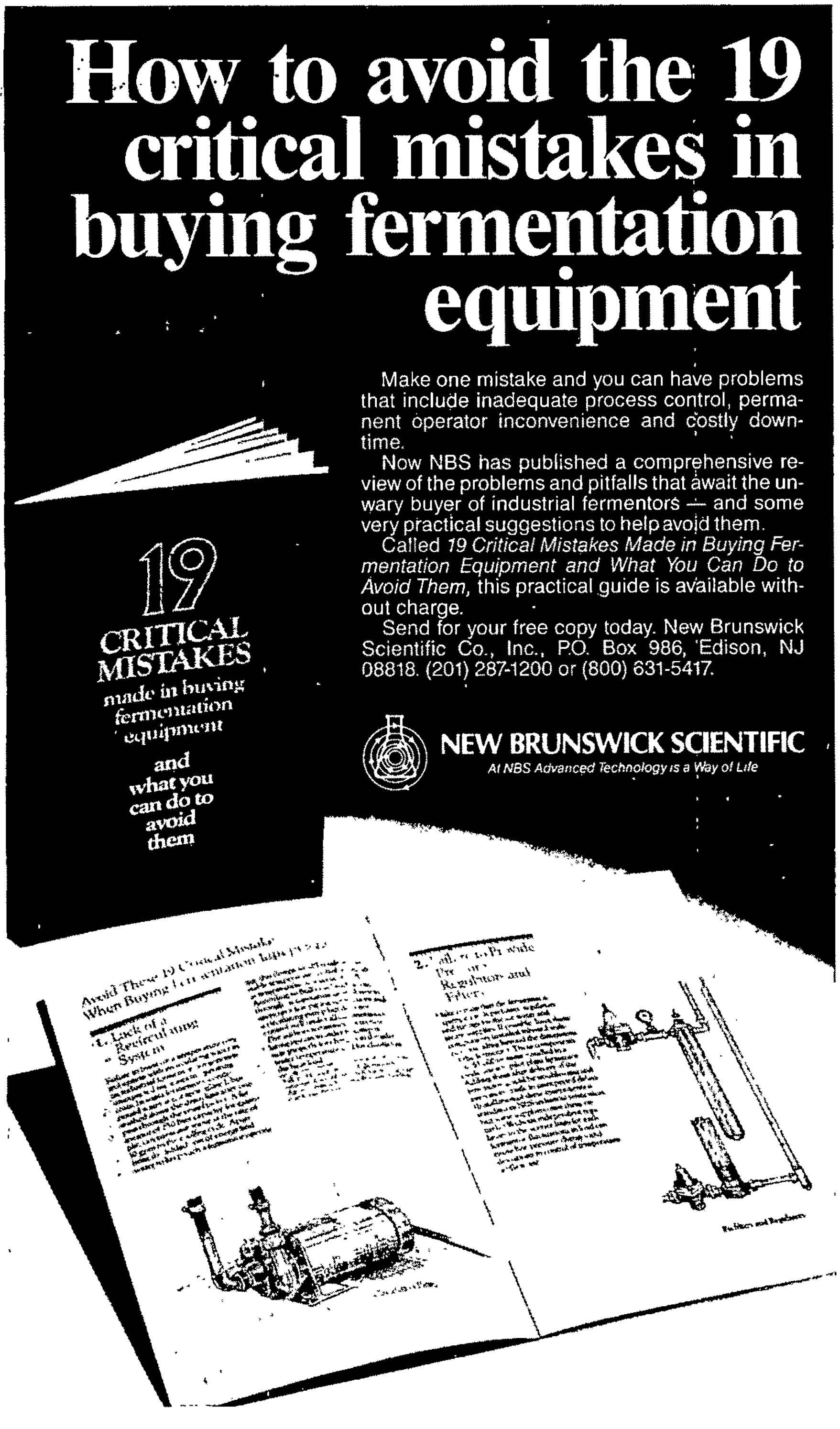
19
CRITICAL MISTAKES
made in buying fermentation equipment
and what you can do to avoid them
Avoid These 19 Critical Mistakes When Buying Fermentation Equipment
1. Lack of a Recirculating System

How to avoid the 19 critical mistakes in buying fermentation equipment

Make one mistake and you can have problems that include inadequate process control, permanent operator inconvenience and costly downtime.

Now NBS has published a comprehensive review of the problems and pitfalls that await the unwary buyer of industrial fermentors — and some very practical suggestions to help avoid them.

Called *19 Critical Mistakes Made in Buying Fermentation Equipment and What You Can Do to Avoid Them,* this practical guide is available without charge.

Send for your free copy today. New Brunswick Scientific Co., Inc., P.O. Box 986, Edison, NJ 08818. (201) 287-1200 or (800) 631-5417.

NEW BRUNSWICK SCIENTIFIC
At NBS Advanced Technology is a Way of Life

Circle No.13 on Reader Service Card.

● The Bio-Rad Bio-Gel TSK SP-5PW cation exchange HPLC column offers the advantages of high resolution, high sample loads, and high recoveries of biological activity in protein and peptide analysis. Unlike silica-based ion-exchange HPLC columns, the SP-5PW column, with its resin based packing, permits a *p*H operating range of 2—12. This wide *p*H range gives flexibility in optimizing protein separations and simplifies column cleanup procedures. Either acid (0.1M HCl) or base (0.1M NaOH) washes may be used to clean the column. The 1,000 Å pore size of the SP-5PW matrix enables the column to separate proteins with molecular weights as high as 10^6. The column has a capacity of 1-5 mg for the protein of interest.
Circle No. 111 on Reader Service Card.

A new system for applying samples for electrophoresis—the Practiga from Shandon

● The Shandon Pratiga system is a new application system for electrophoresis, designed for separations on cellulose acetate membranes including serum proteins, haemoglobins, lipoproteins and isoenzymes. The Pratiga system performs up to 48 separations in one run using 'Dispocards' which 'stroke' the sample onto the applicator ensuring even deposition everytime. The sample is applied in a long narrow rectangle, regarded as the best geometric form for optimum scanning and sample evaluation. There are no capillary effects or globules of sample on the side of the applicator avoiding the inherent design faults of conventional wire-type applicators.
Circle No. 112 on Reader Service Card.

● World Precision Instrument Inc.'s new S7000A modular microelectrode system combines proven technology with latest advances. Features include ultra-stability, low noise, and ± 100 volt compliance. Mainframes are available in either single or four channel designs, and modules are available for ionophoresis, electrometer, and a voltage/patch clamp. Each module is supplied with one probe of the end-user's choice.
Circle No. 113 on Reader Service Card.

- Tissue, organs, tumours and coatings can be rapidly disintegrated using Heat Systems-Ultrasonics' ultrasonic debrider, and the resulting homogenate is removed in the same operation. Liquids such as water, saline, acid, or solvents travel down the centre of the needle and flood the tip. Intense ultrasonic energy disrupts any solid matter near the tip, even bone. Simultaneously, the fluidized mass or tissue is sucked through the needle and exits at the rear of the probe. Both ultrasonic energy and liquid flow are controllable. The probe is 6 inches long and available in three tip diameters: 3/8 in, 1/8 in, and 0.010 in.

Circle No. 114 on Reader Service Card.

- A new 5 mm Radial-Pak cartridge with Waters Nova Pak C$_{18}$ packing for high sensitivity HPLC analyses is now on the market. The cartridges allow HPLC analyses with the efficiency (100,000 plates per metre) to separate acids, neutrals and amines within the same mixture. Used with Waters Radial Compression Separation Systems (RCSS), Waters Radial-Pak cartridges are low cost, flexible-wall HPLC 'columns'. When radially compressed in a RCSS module, the cartridge provides a stable column bed which results in longer life, typically three times longer than a conventional steel column. Nova Pak C$_{18}$ is a 4-μm spherical packing featuring an exclusive bonding end-capping process which provides a stable and durable stationary phase for wide selectivity of all compound classes.

Circle No. 115 on Reader Service Card.

- The Miniultrasart from Sartorius is a self-contained ultrafiltration module with a 20,000 molecular weight cutoff membrane. The Miniultrasart offers high flux rates and long service life and is specially suited for depyrogenation of water and other liquids, and concentration/fractionation of macromolecules.

Circle No. 116 on Reader Service Card.

- A new bulletin from Bio-Rad describes 7 carbohydrate analysis HPLC columns, each specially tailored to separate a specific class of carbohydrate, and discusses ways to optimize separations with each column. Topics discussed include selecting the proper column, solvent selection, organic modifier concentrations, and optimizing column temperature and flow rate.

Circle No. 117 on Reader Service Card.

ADVERTISEMENT

Liposomes

A new laboratory instrument (LIPOPREP®-GD-1) is available for the **reproducible** preparation of extremely homogeneous, unilamellar liposomes of controllable size. The instrument permits the **simultaneous use of five different lipid mixtures** and provides extensive versatility. Applications range from membrane reconstitution, remodelling of cellular functions, liposome drug delivery systems, microanalysis of drugs and metabolites, to antibody targeting, clinical diagnostic assays, and genetic engineering.
For details write to:
DIANORM-Geräte, P.O. Box 126, D-8 München 65, FRG.

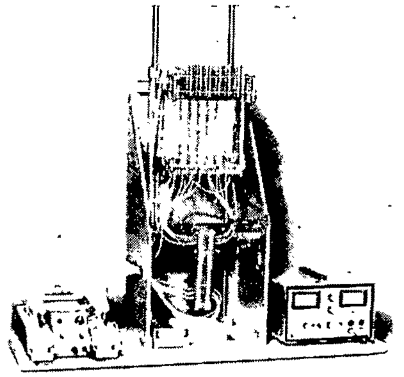

The Isoprep isoelectric focusing apparatus.

- The latest LC 5001 amino acid analyser, available from Astra Scientific International, features a high pressure fluid delivery/sample injection system for efficient column packings and an automatic reaction coil flush for emergency and scheduled instrument shut-downs. A microprocessor controls the entire analytical protocol with eight user-defined programs. Chromatographic separations require only 45 min for protein hydrolysates and 95 min for biological fluids. An adjustable temperature-gradient profile fine tunes chromatographic separations, and standard features include dual HPLC pumps, a refrigerated compartment for storage of samples, eluents, and reagent, dual-channel photometer, and dual-channel recorder.

Circle No. 118 on Reader Service Card.

- A new line of plastic, disposable serological pipettes featuring continuous dispensing tips for accurate fluid delivery is now available from Bellco Biotechnology. Made of high clarity polystyrene with crisp, fine line graduations and large numbering for easier reading, the pipettes' pulled tips provide smooth internal wall surfaces which cannot trap and hold back fluid when dispensing. They are calibrated for accurate delivery with dispensing accuracy rated within ±2%. Bellco plastic serological pipettes are compatible with all standard pipetting devices, and are available in four sizes to suit most laboratory needs. The four sizes are: 1 ml with 0.01 ml graduations; 2 ml with 0.01 ml graduations; 5 ml with 0.1 ml graduations; and 10 ml with 0.1 ml graduations. All are provided with cotton plugs and packed in sterile individual wrappers, or sterile canister packs.

Circle No. 119 on Reader Service Card.

- The Hamilton Microlab 1000 diluter/dispenser is capable of carrying out standard curves with up to 10 diluting steps in one program. In addition, it has the following optional functions: serial diluting, serial pipetting, multiple pick-up, serum distribution, diluter function, double diluter, dispensing and repetitive dispensing. Up to 50 programs can be stored and retrieved. On the sample side syringes of 50μl to 5 ml and on the diluting side from 50μl up to as much as 25 ml can be used as required.

Circle No. 120 on Reader Service Card.

- The Medical Products Division of Ionics, Incorporated has introduced a new recirculating isoelectric focusing system for separation of proteins. IsoPrep systems can be used to separate synthesized peptides and enzymes on a preparative scale and is scalable for production of genetically engineered proteins. The IsoPrep system separates proteins of close *p*I's under the influence of applied d.c. electrical current. It uses porous membranes to form multiple compartments, each with a different *p*H. The membranes prevent convection but allow the proteins to migrate freely until they reach a channel with *p*H equal to their respective isoelectric points and concentrate there to be collected.

Circle No. 121 on Reader Service Card.

- The Nytran membrane from Schleicher & Schuell is a modified, positively charged nylon-66 solid support medium for use in nucleic acid and protein transfers. The new membrane offers a high binding capacity that allows for complete immobilization of all samples. It gives low backgrounds and has the ability to bind nucleic acids at low molecular weight, making it especially suited for electrophoretic transfers. It is also suitable where re-probing is necessary.

Circle No. 122 on Reader Service Card.

- Tresyl-activated Sepharose 4B is a pre-activated affinity medium for the immobilization of small ligands and proteins. The new medium can accomplish easy and reproducible coupling through both thiol and amino functional groups. Coupling capacity is affected only by the nature of the ligand, the temperature, and the *p*H. Since the active coupling groups of this affinity medium are stable to hydrolysis, unused swollen gel can be stored for at least one month. Tresyl-activated Sepharose 4B, from Pharmacia is supplied in 15g pack sizes which yields approximately 60ml of gel.

Circle No. 123 on Reader Service Card.

- Dionex's new amino acid analysis systems are claimed to bring more speed, reliability, and simplicity to amino acid analysis. Based on a new pellicular cation exchange resin, it combines the specificity of ion-exchange chromotography with the speed and simplicity of reversed phase HPLC methods. Conventional cation exchange resins require long separation and equilibration times (60–90 min total analysis time). Reversed phase methods, while offering fast run times, suffer from sample matrix interferences, instability of pre-column derivatives and short column life. Dionex's new cation resin operates at ambient temperature in a completely non-metallic system using very dilute, non-citrate eluants. Hydrolysate analyses are completed in less than 30 min.

Circle No. 124 on Reader Service Card.

These notes are based on information provided by the manufacturers. For further details circle the appropriate numbers on the Reader Service Card bound inside the journal.

21-1-87
A. Batty

ANNOUNCEMENTS

Awards

The **Medical Research Council** UK annually awards Senior Research Leave Fellowships and Senior Clinical and Non-Clinical Fellowships. For further details contact the Grants Section, MRC, 20 Park Crescent, London W1N 4AL, UK.

Applications are invited by the **International Foundation for the Promotion of Nutrition Research and Nutrition Education (ISFE)**, Zug, Switzerland for the 1985 ISFE Prize on research into new approaches to the prevention and/or treatment of obesity. Conditions of entry for the Sfr. 15,000 award are obtainable from the President of the Foundation, Professor Dr J.C. Somogyi, Niedelbadstrasse 82, 8803, Ruschlikon, Switzerland.

The **International Association of Gerontology** has announced that the 2nd Sandoz Prize for Gerontological Research (worth 20.000 SFr) will be presented in July 1985. Further information from Dr Leo Abisch, International Association of Gerontology "Sandoz Prize for Gerontological Research", Box 4043, CH-4002 Basle, Switzerland.

The **Scientific Council of the International Centre for Theoretical Physics**, Trieste, Italy is again offering an annual prize of US $1,000. For further information contact the 1984/1985 Prize Committee, International Centre for Theoretical Physics, PO Box 586, 34100 Trieste, Italy.

For details of the International Research Awards offered by the **World Population Council** on Determinants of Fertility in Developing Countries, contact the Program Manager, The Population Council, 1 Dag Hammarskjold Plaza, New York, New York 10017, USA.

The **National Science Foundation** (US) Alan T. Waterman Award Committee has issued a call for nominations of candidates for its tenth annual award intended to give recognition to outstanding US researchers under 35 in any field of science, mathematics or engineering. Additional information from the Executive Secretary for the Committee, Mrs Lois J. Hamaty, NSF, Washington D.C. 20550, USA.

Appointments

Mr Roger Courtney has been appointed as head of the Technology and Innovation Directorate of the Energy Efficiency Office the Department of Energy, UK.

Dr K.J. Treharne, Head of the Plant Sciences Division at the Long Ashton Research Station, Bristol University, is now to take over as Director; he has also been appointed to a Chair and the Headship of the Department of Agriculture and Horticulture within the University.

Alan Watson, Reader in Particle Cosmic Physics in the Department of Physics and Dean of the Faculty of Science at Leeds University, has been appointed a Professor of Physics at the University.

Mr Don Metz, currently Deputy Secretary with the Department of Territories and Local Government in Canberra, Australia, has been appointed as the new Director General of the Commonwealth Agricultural Bureaux — the first Director not to be resident in the United Kingdom.

Ms Gill Glass has been appointed Managing Director of Bachem UK, the British branch of Bachem Inc., USA.

Mr F. Edward Gustafson and **Mr William F. Hendershot** have been elected as vice-presidents of Miles Laboratories Inc., Indiana, USA.

Dr. Muroni, currently president of the University Corporation for Atmospheric Research in Boulder, Colorado, has been nominated to a six-year term as a member of the National Science Board, Washington D.C., USA.

Dr. Charles Elachi has been named manager of the Earth and Space Sciences Division of the Jet Propulsion Laboratory, NASA, California.

Meetings

22-26 October, **European Wind Energy Conference and Exhibition**, Hamburg, FRG (H.S. Stephens & Associates, European Commercial and Technical Conferences, Agricultural House, 55 Goldington Road, Bedford MK40 3LS, UK).

29 October-1 November, **Second International Conference on Computers in Science**, Washington D.C., USA (Computers in Science, Scherago Associates, Inc., 1515 Broadway, New York, New York 10036, USA).

14 November, **Meeting on High Complexity Displays**, London (The Meetings Officer, The Institute of Physics, 47, Belgrave Square, London SW1X 8QX, UK).

15 November, **Seminar on Plan for Computer Integrated Manufacturing**, London, UK (The Manager — Conferences and Exhibitions, The Institution of Production Engineers, Rochester House, 66 Little Ealing Lane, London, W5 4XX, UK).

15-17 November, **3rd Epileptology Meeting — The Epileptic and His Family**, Coimbra, Portugal (Dra. Margarida Santiago, Clinica Neurológica, Bloco Hospital de Celas, H.U.C. 3000 Coimbra, Portugal).

20 November, **Paper on Technological Change — The Effect on People at Work**, London (The Manager — Conferences and Exhibition, The Institution of Production Engineers, Rochester House, 66 Little Ealing Lane, London W5 4XX, UK).

22 November, **Hockley Memorial Lecture on Communications and Propaganda**, London, UK (Secretary, Institute of Scientific and Technical Communicators, 17 Bluebridge Avenue, Brookmans Park, Hatfield, Hertfordshire AL7 9RY).

26-28 November, **2nd International Conference and Exhibition on New Technology and the Food and Drink Industries**, Bristol, UK (Mr David Jones, New Technology & the Food & Drink Industries Conference, Brintex Limited, 178-202 Great Portland Street, London W1N 6NH, UK).

27-28 November, **11th Mammalian Molecular and Biochemical Genetics Workshop**, London, UK (Dr G. Bullfield, Genetics Group, AFRC Poultry Research Centre, Roslin, Midlothian EH25 9PS, UK).

4 December, **International Conference on Hybridomes**, Paris, France. (INNOBIO, Scientific Association for Biotechnology Advancement, 26 Rue Guynemer, 75006 Paris, France).

17-19 December, **Annual Conference of the Society for Research into Higher Education**, London (SRHE, University of Guildford, Surrey GU2 5XH, UK).

3-5 January, **2nd International Conference on Clinical and Basic Factors Influencing Bone Growth**, Los Angeles, USA (Prof A.D. Dixon, School of Dentistry and Medicine, Dental Research Institute, Center for Health Sciences, University of California Los Angeles, Los Angeles, California 90024, USA).

12-16 January, **Keystone Summit on Allergy, Immunology, Pulmonology, and ENT**, Colorado, USA (Ms Helga Cole, National Jewish Hospital and Research Center/National Asthma Center, 3800 East Colfax Avenue, Denver, Colorado 80206, USA).

14-15 January, **2nd Annual International Symposium on Sample Preparation and Isolation Using Bonded Silicas**, Philadelphia, USA (Mr Lane Yago, Symposium Coordinator, Analytical International Inc., 24201 Frampton Avenue, Harbor City, California 90710, USA).

21-22 January, **Symposium on Pediatric Pharmacology**. Ahmedabad, India (Professor S.M. Mansuri, Chairperson, Department of Pharmacology, B.J. Medical College, Amedabad 380016, Gujarat, India).

22 January, **Meeting on Radiological Protection Measurements and Their Traceability**, London (Prof. J.H. Martin, Programme Committee Secretary, Department of Medical Biophysics, Blackness Laboratory, University of Dundee, Dundee DD1 4HN, UK).

18-21 February, **International Conference on Health Hazards and Biological Effects of Welding Fumes and Gases**, Copenhagen, Denmark (Mr Richard M. Stern, WHO/EURO, 8 Scherfigsvej, DK-2100 Copenhagen Denmark).

22-24 February, **International Symposium on Conceptual Issues in Environmental Archaeology**, Oxford, UK (Conceptual Issues in Environmental Archaeology, Department of Geography, University of Strathclyde, Livingstone Tower, 26 Richmond Street, Glasgow G1 1XH, UK).

nature

21-i-87
R. Bates

Causes of the British disease

Economists are once more glooming about the British economy, but looking for remedies in the wrong places.

JUST over a decade ago, the then Conservative British Government under Mr Edward Heath took fright that the unemployment rolls appeared to be growing inexorably and an inflationary budget was hastily put together out of season. There was hardly time to tell whether its intended effect — the creation of jobs — would have become reality, for the Heath Government was voted out of office after a bruising confrontation with the British coalminers' union. Now, with another Conservative Government in office, there is again a miners' strike (not fully effective), the pound sterling is trading more cheaply against other currencies than ever before and, this time, unemployment is twice what it was when Mr Heath took fright. Inevitably, people wring their hands in anxiety, even despair. What has gone wrong? And what can be done to put things right?

Most answers to these questions are political, usually in the partisan sense, and that, in the long run, is the language in which they will have to be answered. But there is also an sense in which the problem of the British economy is a model, not an especially uplifting model, for the way in which economic systems should be managed in times of rapid technological change. The curious feature of the British example is that it has been fully analysed and thoroughly discussed for at least the past forty years (since the end of the Second World War), and that even now, nobody is quite sure of what should be done. The government of the past five years believes that sound money is an essential part of any solution (which is probably true), and recently has taken to saying that a more flexible job market would also help (which is probably also true, but only up to a point). The chief opposition party, on the other hand, says that the chief need is to create more jobs, and is plainly envious of the way in which deficit financing of the Reagan Government's operations seems to have gone hand-in-hand with a revival of economic activity in the United States. The obvious difficulty is that the objectives at which the political parties have set their sights may be parts of a solution to the problems that afflict the British economy, but cannot be the whole of one.

Changes

That the post-war decades would be times of rapid change was apparent from the outset. That they would also be decades of rapid social change was also obvious, and was foreseen. The agenda for most speculations about what may happen to Britain was set in the five hectic years to 1950, a period of unprecedented and unmatched change. While voluntarily giving the notion of being the hub of an empire, the British embarked on two enlightened schemes — universal high-school education and a social security system and a health service to go with it — embodying the principle that bad luck (including ill-health) should not overwhelmingly determine the conditions in which people lived and died. During the same five years, several major industries (railways, coal, electricity generation and supply) were nationalized. (Steel and water came later, telecommunications were an outgrowth of Rowland Hill's Victorian Post Office and will be half-turned over to the private sector only next month.) It tends now to be forgotten, even in Britain, that from this earliest post-war period, government committees were repeatedly forecasting desperate shortages of trained technical people, and pleading that something should be done about the scale as well as the quality of technical education.

In retrospect, this heady period of social and administrative change was lived through with too little calculation of what the costs might be. Throughout the 1950s, while economic growth picked up, taxation grew even faster, with the result that a succession of Conservative governments presided over the personal impoverishment of most of those who had voted them into power. This was nevertheless a period of great optimism about the way in which technology would soon make Britain prosperous again — nuclear power would be dirt cheap, civilian jet airliners would fill the skies and there would even be thermonuclear power for succeeding decades to enjoy. The truth became plain only in the winter of 1962–63, when much of Britain went without electricity for weeks on end because the weather was appalling and the demand could not be met. There had already been the Italian miracle to remind the British how easily pride of place in some economic league table can be lost by erosion at the rate of one or two per cent a year. In the circumstances, it is only natural that the Wilson Government of 1964 should have promised prosperity by stimulated technological revolution — and that it should have failed because the money supply ran away from it.

Mistakes

Throughout this now long period, two categories of mistakes have been consistently perpetuated. First, in spite of the lip-service paid by governments of all colours to the importance of technical education as a basis for the prosperity of the modern state, too little has been done to turn the dictum into a reality. Qualitatively, the system has hardly changed in half a century. Young people are still required to choose at high-school the directions in which they will follow intellectual pursuits, with the consequence that many of the most able people follow careers which are only peripheral to present needs, while those who take the technical route have a lopsided education. Now, half a century later, there are signs that this may change. Quantitatively, however, there is great confusion. The present happens to be a time when there are obvious shortages of technical skills, and of general engineering knowledge, but there have as often been times when British governments and their advisers have been willing to leave what they considered well alone. In the circumstances, it is unremarkable that those technical people who work in industry are badly rewarded and undervalued. The common wry comment, that Britain is skilled at invention but poor at exploitation, is too often considered an entirely unconnected circumstance.

The other consistent mistake is the assumption, to which all governments are prone, that there are some features of the working of an industrial economy that are best decided by civil servants, not by those who earn their livings in industry or even by market forces. The most memorable follies of this kind date from the 1960s, when the Wilson Government embarked on schemes for cementing mergers between successful and less successful companies when it would have been cheaper, and simpler, to let the latter go to the wall. The curious circumstance is that similar transgressions of good sense occur even under the present government, which is almost un-British in its belief that business failure is merely the other side of the coin of success. Only two weeks ago, the Bank of England saved from bankruptcy a bank that should have been allowed to go to the wall. The same government is doing everything it can to encourage the growth of a few high-technology sectors without recognizing that they are unlikely to succeed unless there is a climate in which intermediate technology can also prosper. But as if to show its even-handedness, the government also goes to great trouble to ensure that its chosen sunrise industries fall flat on their faces needlessly. Thus it is that the two most experienced operators, Rediffusion and Visionhire, last week pulled out of the nascent cable industry, the brave new industry of 1982, because the terms of operating licences have been made unduly onerous.

The consequences of all this are evident. The free market in manufactured goods and value-added services is both hamstrung and feather-bedded. Why should the labour market be singled out for exceptional efficiency, with all the political trouble (and inequity) that would cause? But the civil service, acting as proxy entrepreneur, makes mistakes whose cost is never counted, but which can be measured by the collective impoverishment. But these are the circumstances in which, in a mobile world, people who think they can better themselves elsewhere are up and off. The cost to Britain of the shiploads of those who have left for good, convinced that Britain has nothing much to offer, is incalculable.

It is in the circumstances no wonder that the word has got about that Britain is not serious about its talk of joining the modern world. What sense can it make that a government seeking to sponsor a new industry should cripple it with artificial conditions that prevent it from being viable? Or that it should delegate decisions such as whether there should be another nuclear power station in Britain, not to the nationalized industry that would build and operate the plant, but to a one-man tribunal (with two advisers) sitting daily in Suffolk for the past two years? Would it not be better that the government should tackle the problems that nobody else has the power to tackle, such as the reform of public education? And should it not from time to time make speeches that give some hint that it is not entirely overwhelmed by the despondency about the future which, for want of evidence to the contrary, must be the general conviction. ☐

Argument too formal

The US National Academy has a new journal on public policy, which deserves to succeed.

AFTER more than a decade of introspection, the National Academy of Sciences in Washington has published the first issue of its journal concerned with the general implications of its members' professional work. *Issues in Science and Technology* is as handsome a publication as would be expected, given both the sources (the National Academy of Engineering and the Institute of Medicine are also partners in the venture) but also the ambition — to provide a regular (quarterly) commentary on important issues and related public policies that will compare in influence with publications such as *Foreign Affairs*. The Fall 1984 issue deals with some of the issues certain to be recurrent themes in the years ahead — ballistic missile defence, the cost of health care and the regulatory impediments to the application of technical innovation (specifically, the introduction of air bags as safety devices in impacting automobiles). At $6.00, the first issue is a good read, or at least an interesting one.

What will follow next is, naturally, not necessarily determined by this first advertisement of what the academies have in mind. Next time, for example, there will be no need to reprint the article by Daniel Yankelovich, the social pollster, retailing a simple account of why public disenchantment with science and technology has been growing since the 1960s. (The influence of articles on this same theme has not, unfortunately, been recorded.) Arms control is, however, certain to be a recurrent theme, and the first issue includes a pair of opposing articles, by Dr George A. Keyworth and Dr Sydney Drell, on star wars and related matters. Most people will find this a valuable summary of influential opinions on the subject.

So haven't the academics been brave, venturing so far from academic ways? That is what the blurbs suggest. The trouble is that neatly counterbalanced articles are less a way of helping to form opinion than to inform it. If *Issues* is to win the influence it seeks, it will at some stage have to climb down off this fence, not so as to be partisan but to avoid the appearance of seeking equal time within every pair of covers. And it will have to carry regular book reviews, not just thumbnail sketches of them. But the enterprise is brave; we shall all be better off it it succeeds. ☐

Truth will out (if late)

The departure from the United States of a once-German rocket engineer is a chilling lesson.

THE surprising announcement last week that Arthur Rudolph, who designed the Saturn V rocket, had left the United States and given up his US citizenship to avoid deportation as a Nazi war criminal should be enough to convince the most dedicated pragmatists of the moral contradictions in the recruitment of Nazi scientists at the close of the Second World War. More than a hundred Nazi scientists and technicians were then whisked to the United States in an effort to exploit Germany's commanding expertise in rocketry at that time — and, perhaps of greater importance to the US military commanders who directed the operation, to prevent Nazi experts from falling into the hands of the Soviets, as many nonetheless did.

The United States was plainly eager to overlook the obvious fact that these scientists had, with no apparent moral qualms, fully supported and enthusiastically worked for the Nazi regime; scientists are always called upon to build weapons for their country during wartime, the easy rationalization went, and these scientists just happened to be in the wrong country. It was not their fault; they were just following orders. And, mass memory being what it is, few in the United States seem to have been genuinely troubled that their space programme was partly run by the men who built the V-2. A rare dissent was registered in the 1960s by satirical songwriter Tom Lehrer, who summed up the amorality of the rocket scientists with his biting irony, ascribing to Wernher von Braun the opinion that where the rockets came down was "not my department".

The Rudolph case offers a reminder that really should not be needed that Nazi Germany was not just another country at war. Rudolph's job as director for production of the V-2 made him not only a collaborator with the German war effort, but with the most enormous of the Nazi horrors as well. The workers in the underground factory that produced the V-2 were slave labourers and concentration camp inmates. Of the 60,000 prisoners who passed through the Dora-Nordhausen concentration camp adjacent to the factory, one-third died. The Justice Department now says that Rudolph "participated in the persecution" of these labourers, who were worked 12 hours a day, starved, forced to sleep on bare rock in the tunnels and beaten.

The United States Government did not require 40 years to discover these facts. Rudolph was interrogated by US Army investigators in 1947, on that occasion giving contradictory answers to questions about treatment of prisoners, ultimately acknowledging that he had witnessed the execution of 12 prisoners accused of sabotage. But only the establishment in 1979 of a special office within the Justice Department, charged with investigating suspected war criminals in the United States, seems to have led to the recent action against Rudolph.

There is another reminder in this story. As much as researchers (and, it seems particularly, university administrators) like to maintain that science is not to be judged by its "end use", there are exceptions. Scientific research is a neutral, amoral enterprise only in a free society, one with a democracy capable of exercising social judgement over the propriety of end uses. In the absence of such social judgement, scientists have an obligation to exercise a personal moral judgement, to think through the consequences of their actions. ☐

British research council

Science council looks for projects to cut

THE British Science and Engineering Research Council (SERC) decided at its council meeting last week that it must withdraw from some of the research fields it supports. The council has given itself until February to decide how the pattern of its activities should be reshaped. "Major acts of surgery" are on the cards, according to Professor John Kingman, chairman of the council, speaking after the council meeting.

By Kingman's account, the council is now at a "turning point" in its affairs. Since this time last year, when the British Government refused the request from the Advisory Board for the Research Councils (ABRC) to provide more money for research, Kingman says the council has seen trouble coming. While the total research budget has been formally indexed against inflation, Kingman says that for various reasons it is being eroded by several per cent a year.

Among the council's immediate difficulties is a demand by ABRC that it should contribute £7 million towards the cost of reorganization at the Agricultural and Food Research Council, which is having to close a number of institutes under financial pressure. Kingman says he is "bitterly disappointed" that no extra help has been provided on this account. But the council has also been further hit by a decline in the value of sterling in the past few months, and by improvements of some university salaries (to which many postdoctoral stipends are tied).

Kingman says that with this project, the choice is between uniform cuts across the board and "more radical decisions" that will entail pulling out of some activities. For much of the past year, a group of council members and officials has been considering what steps of this kind might be taken, and what the financial savings would be. One conclusion is that a decision to shut down an institution or to abandon a research programme will yield full savings only over a period of five years. This is why, Kingman says, the impending cuts are meant to increase flexibility only in the 1990s.

For the time being, nobody is prepared to guess what will be cut. At pains to forestall the rumour mills, Kingman last week emphasized that the period between now and February will be used for a re-examination of the research programmes supported by the council's four spending boards (responsible for nuclear and high-energy physics, astronomy and space, engineering and general science). Each board will be expected by February to have "gone back to square one", and to present a new case for its claim on council funds. Kingman says that at last week's council meeting, he asked for and was given an assurance by the four board chairmen that they accept the need for a radical reappraisal.

The task of listing projects and institutions that might be abandoned, and of working out the savings that may result, will fall on SERC officials overseen by a steering group appointed by the council. It seems to be accepted that there will be no time for full consultation with those affected before decisions must be made in February, although Kingman says that there will still then be a need for individual boards to choose between options that will have been presented to them.

This tight timetable, which may be changed, is conditioned by the need that the council should disclose to ABRC its spending plans by next April, at the beginning of the next financial year. SERC hopes that the Kendrew committee's recommendation on continued membership of CERN (the European Organization for Nuclear Research) will be available by February, but "if not we shall have to do our own study". Pulling out of high-energy physics would "be an easy option" but could not give the council the flexibility it needs — it would merely "buy time" for perhaps five years.

Kingman is not hopeful that significant economies can arise from changed relationships with other research councils. He considers that there should be a closer relationship between SERC and the Natural Environment Research Council, however, and that ABRC should give thought to British support for research in biology. Economies through European collaboration accrue only when partners have money to contribute to joint projects.

Although the British Government's allocation of funds for 1985–86 and thereafter could still be increased above the amount forecast last December, nobody seems to think it likely that there will be a last-minute change of heart. Kingman last week also complained that last year's agreement with the Treasury about compensation for the depreciation of sterling, which yielded £7 million out of a total shortfall of £10 million, would have to be negotiated all over again this year, perhaps this time unsuccessfully.

The council seems to be entirely serious in its intentions. Professor Kingman last week quoted ABRC evidence to a House of Commons committee in support of his estimate that SERC would be £70 million short by the end of the decade (in a budget then estimated at £280 million a year). He said nevertheless that he welcomed the strategy document from the University Grants Committee, promising increased selectivity if "the other half of the dual-support system were properly managed".

On the question whether the council could have made its decisions sooner, Kingman said the investigation of what might be done had started a year ago, but that council would then probably have been unable to accept the need for the tough decisions it had now, in worsened circumstances, recognized to be necessary.

John Maddox

Medical shoestring pared down

A FURTHER drawing-in of horns in support for academic research in Britain is forecast in a letter from the secretary of the UK Medical Research Council (MRC), Sir James Gowans, to vice-chancellors of British universities. The letter, published last week, says that the council has no choice but to reduce the funds available for meeting project grant applications in the coming financial year by 7.5 per cent. Programme grants, used for supporting longer term projects, sometimes of a more open-ended character, are to be reduced by 25 per cent, while the funds available for paying stipends to postgraduate students and trainees will be reduced by no less than 30 per cent.

The council's letter, an unusual advertisement of its financial problems, explains that part of the reason for the substantial cut in prospect is the contribution, of about £2 million, that MRC will be required to make to the cost of reorganizing the Agricultural and Food Research Council. But it seems that the extra cost of university salaries, which affect the council's budget for expenditure already agreed by increasing automatically the salaries of research fellows, will cost the council more than £1 million next year.

As might be expected, the council's letter says that these further economies are made with regret. It also says that if there is some alleviation in the financial position, perhaps because the government accepts its case that its budget should be increased, it may be possible to increase the sums available for next year.

The surprise is that the council should have gone so far as to say that its case for extra money has been urged on the government, in the persons of the Prime Minister, Mrs Margaret Thatcher, and the Secretary of State for Education and Science, Sir Keith Joseph, by the secretary of MRC and its chairman, Lord Jellicoe. From the evidence of the latter now published, the meetings were particularly joyless even as these occasions go.

John Maddox

US Congress sweeps up remaining bills

ASATs, agriculture and antitrust

Washington

AMONG the last-minute business that the US Congress completed before adjourning to hit the campaign trail was the resolution of three long-standing issues in science policy and arms control:

Antisatellite weapons

MOVED to act by the absence of any discernible leadership on this issue from the White House, Congress imposed its own moratorium on testing of the new US antisatellite device, a small nonexplosive rocket launched from an F-15 fighter. The Air Force has so far conducted only one test of the weapon, which on that occasion did not carry a warhead. (The warhead, which has been described as a "smart rock", technically the Miniature Homing Vehicle, manoeuvres into the target satellite and disables it simply by ramming it.) The congressional ban is on testing against a live target — seen as the critical step in proving the weapon.

Under the compromise finally worked out between the House of Representatives, which had wanted a one-year ban, and the Senate, which favoured only a requirement that the President should convey to Congress certain assurances that the testing was necessary, no tests are allowed before 1 March of next year. After that, and before tests can begin, the President will have to certify that tests are necessary to prevent harm to national security, that they are consistent with the anti-ballistic missile (ABM) treaty and will not irreversibly harm chances for negotiation of an antisatellite weapons (ASAT) limitation treaty, and that an effort is being made in good faith to negotiate such limitations with the Soviet Union.

The law also provides for a 15-day waiting period after the President's certifications, during which time Congress could presumably vote to extend the moratorium — although any such vote would be subject to the President's veto. And no more than three tests against a target will in any case be permitted during the 1985 fiscal year, which ends on 30 September 1985.

Technical or political reasons, or a combination of the two, have delayed the second planned test, which has been expected for some time. In this test, the weapon, with warhead, will be shot at an imaginary target in space. Rumour has it that this test will occur within the next few weeks.

The limitations passed by Congress are a small but nonetheless important step — it is the first time that Congress has legislated on arms control. Representative George Brown (Democrat, California), a principal sponsor of the moratorium, said the measure "provides a *de facto* arms control agreement" that buys time "to get negotiations back on track".

No limitations have, however, been imposed on the US Air Force's budget for procuring the weapons. Congress approved $74 million for that purpose. The research and development budget is $133 million.

Agriculture

THE catch-all appropriations bill passed by Congress, which will keep the government operating until the end of the 1985 fiscal year, includes a generous budget for the habitually impoverished competitive grants programme for agricultural research. Created in 1977 as a alternative to the formula-funding system — long criticized for its absence of peer review and its exclusion of non-land-grant colleges — the programme has been held to a mere $17 million by those in Congress — notably Representative Jamie Whitten (Democrat, Mississippi) — who saw it as a threat to business as usual.

This year, Congress agreed to $46 million, close to the $50 million requested by the administration. Efforts by Whitten to keep up the appearance of a budget increase while undermining its substance were, however, modestly successful. Within the $46 million is $7.5 million earmarked by Whitten for specific programmes, apparently transferred wholesale from "special grants" — congressionally-mandated research that the US Department of Agriculture has never cared for and which are finally being eliminated this year. Thus while the general area of plant sciences was voted an increase of $1.5 million from last year's $15 million, $1.7 million was set aside for special projects in soybeans, acid precipitation and alcohol fuels. A new area of "pest sciences" turns out to be devoted completely to three special projects, with $1 million apiece: studies of boll weevil, pine bark beetle and gypsy moth. And of the $4.5 million appropriated for a new area of animal sciences, $3 million is committed to special projects.

Real gains were, however, made in the creation of a new $20 million biotechnology area, with no strings attached. The human nutrition area will receive $2 million, as before.

The director of the competitive grants programme, Ed Kendrick, says that although the incorporation of the special projects into the programme will take some careful planning, all the money will be awarded on a competitive basis.

Most attention now will turn to the budget for the next fiscal year, due next February. The first substantial increase in competitive grants for several years is bound to whet the appetites of their advocates.

Requests for proposals in the new programme area will be announced in mid-November.

Antitrust exemption

HIGH-technology companies in the United States have been pressing for an exemption from antitrust laws that would allow them to collaborate on research without fear of landing in court. The inevitable comparisons with Japan were heard over and over again at congressional hearings least spring. Legislation signed by the President on 11 October confers a degree of protection upon such joint ventures, although it stops far short of the blanket exemption that industry had hoped for.

Under the principal antitrust statutes, a company engaged in anticompetitive practices can be sued by a competitor for three times the competitor's actual monetary damages. The bill just enacted limits that to actual damages in the case of joint ventures in research and development, so long as the companies entering into such collaborations disclose their activities in advance to the federal government.

The government will print a notice in the *Federal Register* listing the parties and a general description of their activities; although more specific information will have to be supplied to the government, those details will be protected against release to the public.

The theory behind the new law is that although joint ventures in research and development have never been illegal *per se*, the threat of triple damages has made companies overly cautious. And, in turn, companies involved in such ventures are likely to toe the line if they know that the Justice Department is keeping an eye on them.

The new law provides another protection for joint research and development ventures by allowing courts to award attorneys' fees to defendants who are the victim of frivolous lawsuits.

Whether the law will be the tonic to US industry that its high-technology advocates claim is questionable. For one thing, joint research and development ventures have almost never been the target of antitrust actions anyway. In the past 25 years, only four cases have been brought; and none of these questioned the joint collaboration *per se*.

The best known case was brought by the Justice Department against the major US auto-makers, which had collaborated on pollution control research (which was not illegal) but then allegedly conspired to delay the introduction of that technology. In another famous case, a photographic company sued over a joint research venture that Kodak had entered into with virtually all other photographic companies, excluding only the plaintiff in the case.

Stephen Budiansky

Carlsberg Foundation

Research rides on beer sales

SOME countries have natural resources; so does Denmark. It has beer. And Danish beer benefits science for, strangely enough, the United Carlsberg and Tuborg breweries are run by five professors for the profit of research. And since conservative Danes drink nothing but Carlsberg and Tuborg, and since the breweries have been investing effectively in breweries abroad (Britons now drink more Carlsberg than the Danes), the Carlsberg Foundation has been doing well.

In fact, the Carlsberg Foundation for Research has increased its spending by 20–25 per cent a year for the past four years, and it now disburses annually as much as the Danish natural sciences research council. A fair fraction of the foundation's money goes to the humanities, but that still leaves a fine sum for science, from astronomy to microbiology. Yet, says foundation secretary Niels Petri, most of the recent increases have been taken up in "supporting unemployed scientists". And future growth is threatened by new tax laws.

Beer also pays for the Carlsberg Laboratory, supported directly by the breweries as a tax-break, which is free to range (in style) over much basic agricultural and molecular biology. In the past, the laboratory was responsible for the first cloning of a microorganism (E. Christian Hansen's pure yeast cultures), S.P.L. Sørensen's concept of *p*H, Linderstrøm-Lang's concepts of protein structure and function and — they say — Schmidt's discovery of eel migration and Winge's discovery of sexuality in yeast. More recently, the laboratory did less well, but now in quite extraordinary new premises there appears to be something of a refermentation at the Carlsberg.

"Recruiting? We've never had to do any", says Carlsberg Laboratory director of physiology, Professor Carl von Wettstein. According to a Danish student, a scientist can get to work at the Carlsberg only "by invitation". The laboratory, however, has few permanent jobs. Of the 150 researchers at the laboratory at any one time, many will be postdoctoral people from abroad working on foreign money.

"But we get more results per kronor than any other institution in Denmark", claims von Wettstein. And the fact that he has to apply for outside money, from the European Communities for example, is proof that the laboratory is not over-generously supported, he says.

The only problem of working at the Carlsberg, say researchers there, is a strict requirement to publish in the house journal *Carlsberg Research Communications*, which has a circulation of only 400. But, says von Wettstein, the good work gets out anyway; the journal is critically refereed; it is not so affected by fashions as other journals; and it can report steps in major projects that take years to complete, as in the Carlsberg work on chlorophyll synthesis. "This was very fashionable in the 1960s, then everyone dropped it because it was too difficult. But we carried on and published in our journal."

In spite of acknowledged successes, some observers say the foundation could be more adventurous in the way it uses its funds. The five professors who direct it have considerable power to influence the directions of Danish science, but they usually walk in strict step with the research councils. Moreover, foreign beer sales are levelling off, and Petri expects the foundation's funds to level off next year, quite apart from possible tax changes aimed at a number of foundations somewhat less charitable than the Carlsberg.

Robert Walgate

Synchrotron radiation

THE French and West German governments have agreed to place the European Synchrotron Radiation Source (ESRS) at Grenoble, in the foothills of the French Alps, and not at Strasbourg as previously predicted by French government and scientific sources. This will put ESRS alongside the extremely successful high neutron flux beam reactor of the Institut Laue Langevin, and the announcement (last Friday) has been greeted with enthusiasm as making scientific sense.

Whether it makes political sense, however, is unclear. According to the announcement, ESRS will be a Franco-German facility; but the outline diagnosis of the synchrotron was done not just by France and Germany but also by the United Kingdom, Italy, Denmark, Sweden and Finland, two of which (Denmark and Italy) had put in firm site proposals.

Denmark has protested about apparent French hijacking of the project. All seven countries had been paying the costs of a study under the auspices of the European Science Foundation (ESF) to bring up ESRS, originally designed in 1979, to modern standards. The 300-page draft of the new design was sent to officials of the seven countries earlier this month, and a meeting of the ESRS intergovernmental programme committee (under ESF) is due to take place in Brussels tomorrow (Friday), ostensibly to discuss that design.

A French government spokesman on Monday was, however, unable to explain the relationship between the Franco-German ESRS decision and the ESF committee. Would ESRS be solely for the use of France and Germany? "France believes in creating a 'European space for research' " he said, quoting Prime Minister Laurent Fabius, "so ESRS will be open to all Europe". Robert Walgate

Genetic manipulation

Agency tries out regulations

Washington

THE US Environmental Protection Agency (EPA) last week formally announced its interim policy on field tests of microbial pesticides (*Federal Register* 49, 40659–40661; 1984). Citing a "higher degree of uncertainty in predicting ecological impacts" of microbial as opposed to chemical pesticides, EPA will in future require 90 days' advance notice of field tests of "genetically altered or manipulated" organisms, or of those not indigenous to the test area. Hitherto, field tests of pesticides on plots smaller than 10 acres have been exempted from the notification requirement.

Industrial companies seem pleased with EPA's efforts to regulate in this area. The Monsanto Corporation has already given notice of its intention to carry out field experiments that will be controlled under the new policy; Robert Conken, director of registrations for the company, said the rules would satisfy the public's demand for regulation without impeding research.

As expected, EPA will not require a formal "Experimental Use Permit" for every test. Under the new policy, companies will, however, need to provide EPA with complete information about the proposed test, including details of the ecology and physiological tolerances of the test organism, as well as a complete description of the manipulations performed and their expected results. The agency will also require proposals for monitoring any spread of the microorganism and evaluating potential adverse effects, together with methods for disposal of exposed materials. The test will be allowed to proceed if EPA raises no objection in the 90-day notification period.

There were, however, some questions raised by industry about the scope of the new policy. Conken asked how a company should determine whether an organism is "non-indigenous" and so within the new guidelines: would an organism that occurs naturally elsewhere in the same state, for example, be counted as indigenous? There is similar uncertainty about the meaning of "genetically altered or manipulated" — the question being whether organisms obtained through artificial selection, for example, are included. But many of the questions are likely to be answered quite soon, when EPA produces a policy statement that will also cover releases of genetically-engineered or non-indigenous organisms other than pesticides. The agency plans to use the existing Toxic Substances Control Act for non-pesticides (see *Nature* 23 August, p.613). And EPA officials stress that no decisions in this area should be regarded as final: the agency is by its own admission feeling its way, and comments are invited on how the regulations should be improved. **Tim Beardsley**

US space station

Anxieties abound in Europe

THE British Government is steeling itself for a decision on whether or not Britain should participate, at an estimated cost of £40 million a year, in the development of the US manned space station. But it can expect little direct financial help from British industry, which considers that investment in such a long-range project is a matter for the government. Such was the general feeling of participants at a symposium staged two weeks ago by the Department of Trade and Industry (DTI) to sound out the views of industry and science.

Another first for Britain—the only nation to send an I.O.U. into space!
S.E.R.C.

For the British Government, part of the problem is that space spending will have to increase because of the demands of the European Space Agency (ESA). The agency's Horizon 2000 study earlier this year recommended an increase of the science budget by 7 per cent a year over five years. Britain now contributes £13 million a year, based on the Gross National Product. Failure to pay the proposed 40 per cent increase by 1990 could exclude Britain from a series of ambitious ESA projects, including a new X-ray observatory, a submillimetre orbiting telescope and a probe to return samples from a comet or asteroid.

The need for extra cash will embarrass the Science and Engineering Council (SERC), whose fixed budget is already under strain and which is already considering whether to strengthen support for general research at the expense, for example, of high-energy physics. Ironically, SERC finds itself facing the prospect of a shortfall in space funds at a time when an internal review group, under the chairmanship of Sir Mark Richmond, is about to recommend greater use of ESA by Britain's space scientists.

By the time science ministers meet in Paris to discuss the long-term goals of ESA, in January next year, Britain's European partners will expect a reaction to both new demands for funds. But, before then, the British Government needs to be convinced of the economic potential of a space station. At the DTI symposium, PA Technology attempted to do just this, presenting the results of a study on the industrial processes that stand to benefit from a microgravity environment. It pinpointed two principal areas: the fabrication of defect-free semiconductor crystals and the preparation of extra large protein crystals. PA Technology says that the latter could benefit the enzyme business by allowing molecular structures to be defined quickly and efficiently.

Even so, British high-technology companies are sceptical of the benefits and of the speed with which they would emerge. The cost of the space station is estimated at $8,000 million (1982 prices); the United States hopes that 15–20 per cent will be contributed by Europe and Japan.

PA Technology also argued at the DTI symposium that participation in the space station would stimulate industrial research in areas such as robotics, computer design and materials manufacture. British Aerospace has endorsed this view, presenting, at the DTI symposium, specific plans for an unmanned platform, launched by the US shuttle, to which Britain might contribute 40 per cent of the cost. This plan would complement rather than duplicate the US manned space station, says the company, which claims that the National Aeronautics and Space Administration has already responded enthusiastically to the suggestion.

Elsewhere in Europe, there are more subversive views. Strong bodies of opinion in West Germany and Italy are pushing for an independent European space station, perhaps to work in conjunction with a US platform. This idea, called Columbus, is being widely discussed within ESA and reflects a feeling abroad in Europe that greater autonomy is necessary. Buoyed by the successes of Ariane and Spacelab, many aerospace companies are eager to show that they can function independently of the United States.

The United States expects firm proposals for European collaboration in the space station by the end of 1985, and will want to know how the work would be divided between participating nations, which may include Japan and Canada as well as European states, acting either independently or in concert through ESA, by mid-1986.

Marcus Chown

UK Australian nuclear tests

Inquiry stirs fallen dust

ON 16 October, the president of the Royal Commission inquiring into British nuclear testing in Australia, Mr Justice James McClelland, urged that if the British Government wished to have its views accurately represented, it would be well advised to appear before the commission. The newly-installed British High Commissioner to Australia, Sir John Leahy, had earlier expressed concern about the recent public allegations that the British authorities had disregarded the safety of aborigines and atomic personnel.

The present official silence, Sir John said, must not be interpreted as tacit admission to the charges laid, that the decision to present evidence would be taken in London and that it would depend upon "how the commission goes about its business in future". Mr Justice McClelland replied that the Royal Commission could not be expected to forbid publication of allegations discomfiting to the British Government.

So far the allegations claim that unprotected servicemen flew sorties through radioactive clouds, that they decontaminated aircraft after the tests, that servicemen had buried the corpses of aborigines found on the range, that mentally-retarded civilians were placed in bunkers near a Maralinga blast in 1956 (see *Nature* **310**, 90; 1984) and that servicemen were used as guinea pigs (see *Nature* **309**, 199; 1984), a claim stressed by counsel for the British Nuclear Test Veterans Association.

On 3 October, the three royal commissioners also heard an account of the discovery and attempted decontamination of a family of four aborigines who, it was alleged, had camped for a few days in the Marcoo bomb crater seven months after the 1956 Maralinga blast, in apparent contradiction to a report in January 1983 of the same event by the Australian Ionizing Radiation Advisory Council (AIRAC). Servicemen who had witnessed the event were told by a British officer that disclosure would result in court-martial and possibly the firing squad.

The commission's charter includes investigation of the safety measures taken before, during and after the tests, whether health had been affected, and the nature and size of the devices tested in the twelve major explosions and an unknown number of "minor trials" known as Rats, Kittens, Ayres, Tims and Vixens.

Last week, the federal government refused a request from the Australian Nuclear Veterans for legal aid to challenge the credentials of royal commissioner Mrs Jill Fitch. A conflict of interest arose, they asserted, from her continued membership of both the commission and AIRAC, since it was criticism by Professor Charles B. Kerr's committee in May this year of AIRAC's treatment of fall-out data which led to the commencement of the Royal Commission.

The commission is due to report in June 1985 and has applied to the British Government to take evidence in Britain later this year.

Jeffrey Sellar

European telecommunications

Community looks at strategy

Brussels

AFTER years of dithering, the member states of the European Economic Community have agreed to work together to strengthen Europe's telecommunications market. Meeting in Luxembourg on 15 October, industry ministers adopted two recommendations constituting a first step towards a telecommunications strategy.

First, all ten Community governments are to ensure that national telecommunications administrations consult before introducing new services. (The United Kingdom, in the throes of selling off half its nationalized industry, was at the outset rather embarrassed, but has now fallen in line.) Contacts already exist through the European Conference of Post and Telecommunications Administrations (CEPT) set up in 1959, but new services put into operation from 1985 would have to conform to standards now being laid down by the developing network of European standards bodies.

Six million ECU (European Currency Units) or $4.6 million have been granted by the Community to these bodies for a two-year programme for 1984–85 to define and certify European norms in the telecommunications field. Equipment other than terminals, such as digital transmission and switching systems, would have to conform to common standards from 1986.

The second recommendation would throw open to all member states procurement of both conventional terminals (telephone apparatus for mains telephone use, PABX, ordinary teleprinters) as well as telematic terminals.

On switching and transmission equipment, and conventional terminal equipment for which there are no common specifications, the recommendation is that at least 10 per cent of the annual value of orders should be opened up for tender throughout the Community.

French pleas that the market should be opened to the full have been resisted by the European Commission, which is wary of risking a flood of components from both other member states and beyond, as well as scaring member states off a move it has taken them four years to make.

As a technical pioneer, and still the world's biggest exporter of first-generation telecommunications (telex, telephone), with a trade surplus of $2,000 million a year, the Community recognizes its industry is at a turning point: how to develop a second- and third- generation market in telecommunications which can stand up to Japan and the United States.

The Community at present controls a 19 per cent slice of the world telecommunications equipment market, but growth to the end of the decade is forecast to be slower than in the rest of the world (6–7 per cent as opposed to 8 per cent in the United States and Japan). The Community's telecommunications sector represents 2 per cent of the Community's gross domestic product which, with innovation, could grow to 10 per cent by the year 2000.

The Commission, however, is looking further ahead. Telecommunications are already reckoned to affect 55 per cent of value-added services and 62 million jobs; according to the Commission, investments in telecommunications could double the turnover of the European economy.

Under the Community's telecommunications programme, informally adopted by ministers last May, aid to finance telecommunications in ill-favoured regions could be drawn from the regional fund, the European investment bank and the new Community lending instrument (which is tailor-made to encourage investments in such conditions).

These schemes are likely to figure on the agenda of the next council of industry ministers on 20–21 November, when there will probably also be a decision on a programme of telecommunications research and development. Twenty-five million ECU a year over a five-year period has been proposed for Research in Advanced Communications in Europe (RACE), to be financed jointly by the Commission, companies and research institutes, much along the lines of the computer research programme Esprit.

Meanwhile, the Commission plans to set up a number of analysis and forecasting groups to look after the development of new services such as integrated digital networks, cellular radio-telephone services, videocommunications and wide-bank trans-national networks. At the October meeting, industry ministers also found an extra 11 million ECU to extend the 1979–83 programme on standardization in data processing for a further two years.

Anna Lubinska

US policies offend Europeans

EUROPEAN optimism about the future of the new telecommunications strategy, as of other new industrial research and development programmes, is marred by anxiety about the effects of high-technology export restrictions by the United States.

There is speculation that the US 1976 Arms Export Control Act and the 1979 Export Administration Act will be tightened up by the new Congress when it reassembles next January.

Existing controls, justified on national security grounds by the US Administration, are suspected of giving US companies an unfair advantage over others.

At the informal dinner following the Industry Council on 15 October, the soon-to-retire EEC Commissioner for Industry and Research, Vicomte Etienne Davignon, told national ministers that the European Commission intends to draw up an inventory of US measures to restrict high-technology transfer and to assess the consequences for economic and industrial development in the Community. The objective of the study, which will be ready in six weeks, is to make it clear to the United States that security considerations and continued European economic and industrial development are not mutually exclusive.

There is particular concern in Europe at some of the recent measures by the US Administration to restrict the transfer of technology and the dissemination of scientific information, including restrictions on foreigners attending defence- or industry-oriented meetings and conferences, on the dissemination of certain published information, on the transfer of technical data regarding participants at private conferences to certain countries, stricter conditions for foreign scientists applying for entry visas and broadening the base for classified information.

More recently in Belgium, the United States attempted to block the export of agricultural machinery to the Soviet Union by the Pegard Company, on the grounds that it could be converted for military aims.

Anna Lubinska

North Sea records

A NEW centre for the storage of North Sea drilling records and cores was opened in Edinburgh last week by the junior energy minister, Mr Alec Buchanan-Smith. The centre will provide public access to core sections for sampling and inspection. Any oil company granted a drilling licence must make records and cores available, but only after an interval of five years.

According to Mr Buchanan-Smith, the first nine months of this year have seen more exploration and appraisal than any previous year. One hundred and forty wells had been drilled in the North Sea by the end of September, compared with last year's record total of 128.

The new centre will be administered on behalf of the Department of Energy by the British Geological Survey (BGS). The tasks of the 55 staff will include the provision of inspection facilities for the 40,000 core samples now housed, of which 50 per cent have been released for access. The associated borehole logs are stored in microfiche form. Samples of cores may be removed for experimental measurements subject to the approval of BGS, which says that the number of requests for access average about three a week. Apparently demand increases as deadlines for new licence applications approach. The annual cost of maintaining the centre is £120,000.

Philip Campbell

Thermonuclear fusion

Europe from hand to mouth

THE 1982–86 budget of JET, the Joint European Torus for fusion research at Culham in Oxfordshire, is running out ahead of time. Planned to last 60 months, the budget will last for only 46, until October next year. The reasons are inflation (the 1982–86 programme was fixed at 1982 prices) and high maintenance costs at JET, including £250,000 to rebuild JET shock absorbers after an accident earlier this year.

Despite the economic crisis in the European Communities, which pay 80 per cent of JET's bills, there is little concern at Culham that the extra money will not be found. Community programme budgets never allow for inflation, says JET budget director Peter Kind, and it is always assumed that shortfalls will be made good in the next programme. Even if the 1985–89 programme (overlapping the first by two years), now before the council of ministers, is not agreed until next spring, JET accounts for 1985 could be balanced.

Mr Kind also has a contingency plan. Since operations began a year ago, JET has been short-staffed, so that there has been a squeeze on design time for the JET "extension to full performance" (neutral beam and radiofrequency heating, tritium handling equipment and so on). It has therefore been difficult to keep up the rate at which contracts have been put out to industry. Kind thinks it will be possible to let purchasing slip by a couple of months, particularly on items needed only some years hence.

The high maintenance and operating costs are exactly those predicted by the JET design team, but double what the council of ministers allowed in 1982. So JET can say "we told you so". "We had allowed 5 per cent of the capital equipment costs (excluding buildings) a year for maintenance", says Kind, but the ministers allowed only 2.5 per cent. But since JET began operations, there have been "10–15 requisitions a day for items from £50 to £5,000, from nuts and bolts to vacuum seals", reaching a total of around £10 million over a year, compared with JET equipment costs of £175–£200 million in today's values.

The largest item, the £250,000 for new supports, came after a single unfortunate discovery: that when the oval-cross-sectioned plasma ring was at its maximum elongation, the plasma snaked up and down and escaped control. In this shot, the plasma finally shorted out through the vacuum wall with currents of several megamps, and jolted the vacuum chamber with forces of hundreds of tons-weight. The force shook the floor like an earthquake, and although JET was not seriously damaged (it is now a millimetre longer than before) it has been thought prudent to modify its support structure.

Otherwise, JET has been running well, and made one particularly tantalizing discovery in the last two weeks of its recent closedown (to introduce neutral beam heating). The team has found that a carbide layer a few molecules thick can be deposited on the inconel inner surface of the vacuum chamber by making a glow discharge in a mixture of methane and hydrogen gas, and that this layer dramatically reduces the amounts of metal impurities entering the chamber from the wall. As these high atomic-number impurities efficiently radiate heat from the plasma, it is important to control their number.

Until this work, it had appeared that impurities would be a bigger problem at JET than expected. The carbide layer may bring a striking improvement. And because the layer can be efficiently removed, controlled experiments can be attempted. The effect was also seen earlier at the TEXTOR torus at Jülich, West Germany, but not followed up. In any case, it should not be over-emphasized, says JET physicist Alan Gibson.

Meanwhile, JET staff are crossing their fingers that Europe will come up with the cash JET needs. "JET is the only really successful example of European co-operation anywhere", claims Kind, "so there is a considerable political will to keep us going." Moreover, the present Irish presidency of the European Commission has put the 1985–89 nuclear fusion programme near the top of its priorities for agreement by the end of this year.

One explanation may be that Ireland sees JET as one of the few problems it can solve. JET officials, however, note uneasily that less senior Irish representatives in Brussels who have been discussing the fusion programme have been, with Greece, among the most negative. Who means what should be clearer at the November and December meetings of the research council.

Robert Walgate

Conservation in Japan

Modest gain for UK royal

Tokyo

PRINCE Philip, Duke of Edinburgh, has wrung some modest concessions on conservation from the Government of Japan. In his capacity as president of the World Wildlife Fund (see also *Nature* 18 October, p.595), the prince was last week promised that steps would be taken to restrict the import of endangered wildlife species into Japan. But the six-day visit did not yield all the prince had asked for.

In a 20-minute meeting with the prince, Japan's Prime Minister Yasuhiro Nakasone said that he would consider the introduction of domestic legislation to prevent the illegal import of protected species. A task force to study the problem is to be set up immediately. Customs officers are also to receive training in detecting illegal imports — the lists of endangered species are long and complicated and some dealers have skilfully forged documents.

The Minister for International Trade and Industry, Hikosaburo Okonogi, also promised to introduce by next April a system that will require dealers in endangered species to produce export permits from the governments of the nations from which the species are claimed to have come.

Rather less was promised though, in dealing with the vexed question of the 14 endangered species — six species of whale, three species of turtle, three species of monitor lizard, the musk deer and the African saltwater crocodile — which Japan refused to include in a list of endangered plants and animals and their products when it first became a signatory of the Convention of International Trade in Endangered Species, the Washington Convention efforts to reduce the number of species on the list, but gave no clue as to how or when this might be done.

Interest was also shown in the prince's desire to have Japan stage a conference on the protection of nature on islands. Among the prince's stops on his six-day tour of Japan was the island of Amami Ōshima, one of a group of remote islands known as the "Galapagos of Japan" and containing many endemic species of mammal, including the Iriomoto wildcat and the Amami rabbit.

Prince Philip had also expressed, in very diplomatic terms, his reservations about Japan's plans to continue sperm whaling in coastal waters, despite the International Whaling Commission's agreement to ban all sperm whale hunting. The Japanese whaling fleet, however, left harbour last Friday to hunt for sperm whales. The Japanese Government is now waiting to see what will happen once a whale is caught — will the US Government carry out its threat to cut Japan's fishing quota in US waters? Japanese officials had earlier expressed confidence that the United States would not retaliate even if whales were caught. Talks on the issue in Washington last week, however, were inconclusive.

Quite separately, the US Department of Commerce also announced last week that it would give Japan only a quarter of the fish quota in US waters it had requested for the rest of this year because of evidence that the Japanese fishing fleet had systematically violated earlier agreements. Whether such action will be extended if sperm whales are caught will depend on the strength of the US conservation lobby.

Alun Anderson

Nobel prize

Merrifield wins in chemistry

THOSE who have followed the growth of peptide research over the past twenty years will have received with delight and no surprise the news of Bruce Merrifield's Nobel Prize for Chemistry. The simple solid phase technique for the chemical synthesis of peptides which bears his name has been adopted in scores, possibly hundreds, of research laboratories worldwide. The concept has been widely applied in other areas of research, notably in oligonucleotide synthesis, with important consequences for genetic engineering, and in structural studies including protein sequencing.

To understand the impact that Merrifield's technique has made upon the development of peptide synthesis itself, it is necessary first to sketch in the situation in the 1950s and earlier. Peptide chemistry was then in an expansive mood. Natural peptides with powerful and important biological action, such as the pituitary hormone oxytocin, were being isolated. These natural peptides were soon shown to consist of short chains of the same building blocks (the α amino acids) as constitute the proteins. The sequence of amino acids in these linear chains was soon determined and the stage was set for the understanding of biological activity in terms of these relatively simple sequences. The techniques of peptide synthesis — the chemical union of α amino acids into chains of defined sequence — had been growing steadily during this period but were slow and labour-intensive. They could barely meet the explosive demand from pharmacologists and others for synthetic natural peptides and their structural variants which could be used to correlate chemical structure and biological activity.

It was just at this time that Merrifield introduced the simplifying step in peptide synthesis which rapidly transformed the situation. Much of the labour in contemporary peptide synthesis was involved in the isolation, purification and characterization of reaction products after each chain extension. Merrifield reasoned that by attaching the first amino acid to an insoluble polymeric support, these isolation steps could be much simplified and speeded up. There were other chemical advantages which might also increase the efficiency of synthesis — a necessary concomitant since the polymeric system did not allow separation of the products of incomplete reactions. Most importantly, the process became amenable to mechanization.

Merrifield demonstrated these advantages convincingly in 1964 with a synthesis of the nonapeptide hormone bradykinin. The hormone was prepared singlehandedly in eight days, evidently in a highly pure form. By contemporary conventional methods, it could have occupied several skilled chemists for weeks or months.

The new technique of solid phase peptide synthesis was adopted with enthusiasm by biologists, sometimes beyond its immediate capabilities at this early stage in development. Organic chemists were slower to accept its advantages, some finding it in conflict with their rigorous classical training. Within the decade, the limitations and advantages were well recognized and solid phase peptide synthesis found and established a secure place alongside more conventional methods. The number of synthetic peptides prepared with its aid must now be counted in thousands.

By the mid-1970s, improved understanding of the solid phase system and numerous technical improvements allowed successful application to oligonucleotide synthesis. This was a timely development in view of the rapid strides in genetic engineering around this time. Again, synthetic DNA fragments became much more accessible using solid phase techniques. On the structure side, solid phase methods were developed for protein sequence analysis. Throughout organic chemistry, the concept of polymer-supported reagents and reactions has become commonplace. Although Merrifield confined his own activities to the peptide field in which he has continued to make massive contributions, many of these later developments must be attributed to his inspiration. The dream of automated synthesis of artificial proteins remains to be realized, but the impact of Merrifield's work is without question.

Robert C. Sheppard

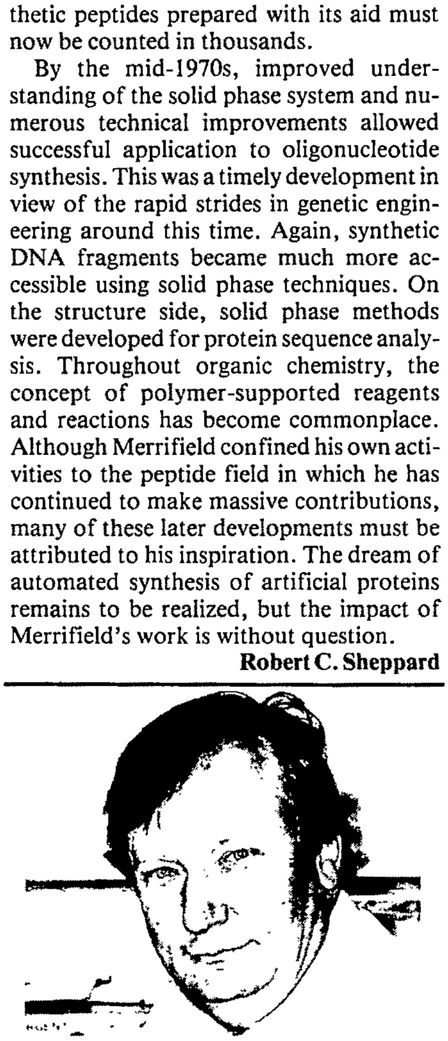

DR Carlo Rubbia, who shares this year's Nobel Prize for Physics (see p.701).

Animal welfare

Berkeley again in trouble

Washington

THE University of California at Berkeley is awaiting with more than the usual apprehension the result of an investigation by the US Department of Agriculture (USDA) into new allegations of animal welfare abuses. The reason: $41 million of state funds earmarked for a new life sciences building cannot be spent until the university is able to satisfy the state legislature that there will be no future violations of the Animal Welfare Act. The building is already well behind schedule, and a decision by USDA to prosecute would further delay construction until the case had been decided.

Last July, the university was fined $12,000 and ordered to correct long-standing deficiences in its treatment of laboratory animals at the Berkeley campus (see *Nature* 2 August, p.356). The university was still under an order to "cease and desist" from future violations when the latest allegations were made on 10 September. Complaints were made to USDA by animal welfare groups, which entered animal houses "surreptitiously" and photographed a monkey with a tumour on its face and rabbits with local infections around cranial implants. The USDA investigation started after a surprise inspection on 12 September.

The complaint about the monkey has been dropped because USDA found no evidence of lapses in veterinary care. The care given to the rabbits is now being scrutinized, and a decision on whether to prosecute is expected before the end of the month.

Both the university and the researcher involved, Dr Walter Freeman, maintain that the animals were at all times under adequate veterinary care and that there were no violations. A university spokesman, Mr Debley, said the university "had been told" that the second complaint would also be dropped.

The requirement that the university must demonstrate compliance with the Animal Welfare Act before using state funds for the new building was written into California's 1984 Budget Act. A report by the university on the steps taken to improve animal care since the court case this summer is now being reviewed by the state legislature. Ironically, the building that may now be delayed is needed partly to improve the Berkeley campus's animal facilities. On 28 September, the university postponed an appearance before the state public works board where it was to have pressed its case for the new building. The university says the decision to postpone the appearance was due to "administrative delays" that had nothing to do with the latest allegations.

Tim Beardsley

Progress at NERC

Sir — As the new chairman of the Natural Environment Research Council (NERC), and after 8 years as a council member, I was intrigued to read your article (*Nature* 11 October, p.498) on the British Geological Survey and the related leading article (p.493) advocating the disbandment of the council.

While you have correctly identified some of the problems with which the council has grappled in recent years, I am disappointed that you have not recognized more fully the progress the council has made in the context of a severe shortage of funds.

The objective of a research council is to foster high-quality science in institutes and universities. Achieving this requires, firstly, well-motivated scientists and support staff, and secondly, money to pay them and supply the necessary support services and equipment. In spite of the council's strenuous efforts to persuade the government that environmental sciences need and deserve more funds, these have not been forthcoming on the science vote. Indeed, in the areas of NERC interest, with the exception of Antarctic research, science vote money has shrunk in recent years. Equally significant is the substantial reduction of income from commissioned research sponsored by government departments.

In the face of these reductions, my council has been at pains to maintain the level of its support for university research and has attempted to find new sources of commissioned research funds with the private sector. Contrary to your editorial comments, this has been done in line with principles clearly laid down by the Treasury, is largely on a collaborative rather than a competitive basis and is leading to the successful transfer of knowledge and technology from basic research to industry.

It will not surprise you or your readers that I reject your proposed solution to NERC's present difficulties and believe it would benefit neither science nor the country. It is a solution we have already examined and dismissed because we believe there is a real need within the United Kingdom for an organization which can promote objective environmental research to provide a basis for sound industrial, economic and political policies.

In taking up the office of chairman of NERC, I intend to continue actively the programme of reorganization and structural change which is already in hand and which, I believe, will provide purposeful support for environmental science research — basic, strategic and applied — of benefit to industry and government.

I trust that you and your readers will continue to show interest in the development of NERC and be prepared to recognize achievements resulting from reorganization as it proceeds. I believe that NERC has a strong and vibrant contribution to offer the United Kingdom and the scientific community and that the environmental sciences deserves more than the emasculation you propose.

Hugh Fish

Natural Environment Research Council,
Polaris House, North Star Avenue,
Swindon SN2 1EU, UK

Telling all

Sir — In his article "Widespread aftereffects of nuclear war" (*Nature* 23 August, p. 621), Dr Edward Teller points out that we should not expose the general public to highly speculative theories of worldwide destruction. Instead we should tell people exactly what we know and do not know about the nuclear winter, "for only then can decisions affecting the well-being of Western societies be made on an intelligent basis". I think that the general public would be even more satisfied if the decisions could consider the well-being of all societies.

Tom Reuter

Department of Zoology,
University of Helsinki,
00100 Helsinki, Finland

US deficit

Sir — Your leading article "Election irrelevant" (13 September, p.92) wonders about the arithmetic of funding the US federal budgetary deficit.

In the fiscal year ending 30 September, this will be $172,000 million[1], but the trade deficit this year may exceed $130,000 million[2]. The dollars expatriated on current account are therefore sufficient to cover 130/172 or 75 per cent of the budgetary shortfall if reinvested on capital account directly or indirectly in American government securities.

Brian Potter

3305 Pottawattamie Trail,
Michigan City, Indiana 46360, USA

[1] *The Economist*, 15 September, 1984, p.24.
[2] *Ibid*, p.18.

Miracles

Sir — Berry *et al.* (see *Nature*, 19 July, p.171) must be born-again Baconians. This conclusion can be drawn from their statement that the laws of science are generalizations of experience and therefore cannot be applied to the examination of claims for miracles. Falsificationists would define the accumulations of scientific laws in terms of hypotheses that have so far survived empirical testing.

This subtle difference in emphasis suggests that the debunking of miracles is a job for a falsificationist whereas a neo-Baconian may be permitted the luxury of faith without being faced by a dilemma. It is however interesting to note that in fact professional illusionists appear to be better investigators of miracles than scientists, if the Yuri Geller investigation can be regarded as an exemplar of a rational examination of a claim for supernatural powers.

Berry *et al.* may therefore have arrived at a correct conclusion but for the wrong reasons. Alternatively, professional magicians perhaps may be regarded as conducting scientific research in the Popperian tradition when employed in the investigation of miracles.

Barrie Pearson

13 Knoll Cottage
Residential Park,
Winfrith, Dorchester,
Dorset DT2 8LD, UK.

Enough of Homer

Sir — M. Pulbrook (*Nature* **309**, 204; 1984), focusing on a parenthetic point I made within a quote-marked hypothetical question (*Nature* **307**, 590; 1984), has produced an interesting exegesis on black versus red Homeric wine — but the contrast I had in mind was red/*white*, or yellow. Compare the classicist W.B. Stanford, Commentary on *Odyssey*, 1947, Vol. 1, p. 355, line 196, Bk. IX: Homer "never mentions white or yellow wines". And *pace* Pulbrook, I did not assume that the key question in the wine-dark sea controversy is to "account for the redness of the sea": this surely is evident from my mention of many other aspects of the topic, formulaic devices, for example.

As the distant Homeric world-view and pattern of sensibility differ significantly from ours, our thinking about Homer's epics is easily subject to various colourations. And whatever the pros and cons of translating *οινοπα ποντον* as "wine-dark sea", the English phrase itself is viable and poetically very potent: to exemplify a facet, Kazantzakis once envied the relative monosyllabicality (!) of English.

This interdisciplinary international correspondence has been piquant. *Floreat Nature . . .*

Michael Macnamara

Philosophy Department,
University of South Africa,
PO Box 392,
Pretoria 0001, South Africa

Sir — Regarding your editorial note about this correspondence (*Nature* 12 July, p.95), the *literati* used to believe that the last word came from Stephen Dedalus when he spoke the winged words "snotgreen and scrotumtightening sea" (Joyce, J. *Ulysses*, Bodley Head, London, 1937).

Thank you nevertheless for your nostalgic revival of a dying culture, so aptly rounded by a scholarly note from Balliol.

Hilton Stowell

ERBP Laboratory,
120 Nature Creek SW,
Milledgeville, Georgia 31061, USA

● This correspondence is now closed — Editor, *Nature.*

CERN's first Nobel prize

Stockholm's recognition of the importance of the discovery of the intermediate vector bosons W *and Z is nicely tempered by an appreciation of the technical ingenuity which underlies it.*

CARLO Rubbia, Italian-born discoverer of the W and Z particles that carry the weak nuclear force, and Simon van der Meer, the Dutch accelerator designer without whom, says Rubbia, "we couldn't have done it", share the 1984 Nobel Prize for Physics. But neither is sitting back. They are, instead, separately at work on the proton–antiproton collider at the European Organization for Nuclear Research (CERN) near Geneva that won them the prize.

Rubbia is at present working flat out to exploit the collider to its utmost. There are two objectives. While the approximate masses and decay properties of the W and Z particles are now known, there is much detail yet to discover — such as the particles' lifetimes. Clearly, CERN would be well-advised to wring as much as possible from the machine before Stanford's Single Pass Collider (planned to produce a million Zs a year, compared with CERN's present few dozen) comes on line towards the end of 1987. But Rubbia and his colleagues have also been stimulated by hints from his "UA1" detector on the collider that all is not quite as expected at energies beyond the W and Z particles.

"Our chance is now" he says. Rubbia is pleased at finding the Ws and Zs, but clearly feels like an explorer who arrives at the South Pole and finds footprints in the snow — here, the footprints of Abdus Salam, Steven Weinberg and Sheldon Glashow whose "electroweak" unification predicted the presence and exact properties of the particles. "For me these anomalies — and I must be frank with you, we're not sure they're there — represent hope", he said last week. "We may be on the threshold of a whole new territority."

Rubbia has been the driving force behind the collider. "The road was very long", he said. "You have to be a hell of a persistent person. You have to be very stubborn." With two American colleagues, he first presented the idea, in 1976, to Robert Wilson, then director of Fermilab near Chicago, who rejected it. Rubbia, ebullient and outspoken, feels the reasons were partly personal. "I didn't get on with Wilson. He'd had enough of me." Fermilab went ahead instead with its Tevatron project, an upgrade to 1,000 GeV beams. (This was a lengthy project, involving the development of superconducting magnets, and it will not provide competition for the CERN collider before 1986-87 — when it will collide protons and antiprotons at 2,000 GeV total energy.)

The Rubbia project went ahead instead at CERN, assisted by the better vacuum in the CERN super proton synchrotron, through which the colliding proton and antiproton beams now circulate. In the poorer Fermilab vacuum, the beams would have been rapidly damped, and a new beam-tube would have been necessary. CERN also had van der Meer ("our best accelerator man"), whose essential contribution to the collider has been "stochastic cooling", a technique which allows an accumulation of antiprotons to collide with protons in the collider.

Stochastic cooling is much more than a technical *tour de force* but, on the face of things, is a violation of Liouville's theorem of statistical mechanics describing the motion of collections of particles. Only once before has a Nobel prize been awarded to an accelerator physicist — Ernest O. Lawrence, for his design of the cyclotron. The comparison of van der Meer with Lawrence is a measure of the stature of the Dutchman's achievement.

The problem van der Meer has solved is this. Antiprotons are formed in high-energy collisions of a proton beam with a target, and collected into a rough beam. But the particles so produced have a wide spread of velocities, and so could not be accelerated coherently in a synchrotron machine. The velocity spread has to be reduced or, in the jargon, the beam has to be "cooled". An earlier (1960s) Soviet solution (due to the late Gersh Budker of Novosibirsk) was to inject a "cool" (mono-energetic) beam of electrons to run alongside the protons: the electrons would "heat up" and the protons "cool" until the beams reached the same "temperature" (this thermodynamic analogy is exact). Then further cooling would be done with a new injection of electrons until the proton beam was sufficiently cool that it could be accelerated up to the 270 GeV planned in the collider (the super proton synchrotron). This idea worked, but proved too complicated to use in practice.

van der Meer's approach is different. Liouville's theorem has it that the crowd of points representing a collection of particles in phase space (embodying both momentum and position) will keep a constant density, whatever the external forces acting on it. According to Liouville, a beam is like toothpaste in a tube: if you squeeze it somewhere in phase-space, it must come out somewhere else. But "cooling" aims to increase phase-space density, by putting all the particles in a physic bunch in real space, each with the same momentum. How does van der Meer's cooling method get around this difficulty?

"I began thinking that if you can control a single particle perfectly in an accelerator, then why can't you control several?" he says. He developed the idea that an uncooled beam of particles is represented in phase space by points (one for each particle) with plenty of space between them, and that in principle these points can be squeezed closer to each other without changing the phase-space density around each point.

In practice, the technique is to control the fluctuations of the beam. Antiprotons are accumulated in a storage ring called the Antiproton Accumulator. Sensors detect deviations at one point on the ring, ultra-fast electronics calculate the necessary corrections and correcting signals are relayed to some point later in the trajectory. The process is possible — with both beam and signal travelling near the speed of light — because a chord of a circle is shorter than the circumference which it intercepts. This whole correction process takes a few tens of nanoseconds, and is repeated for each circuit of the beam. Roughly 24 hours are needed to accumulate and cool enough antiprotons for a collider run, but van der Meer is working on a new accumulator (ACOL) that will reduce this by a factor of ten.

ACOL will take its first beam only in May 1987. Meanwhile, Rubbia and his 130-strong UA1 collaboration* will try to get as much time and energy as possible to explore the "new territory".

Robert Walgate

***The UA1 group includes teams from West Germany (Aachen and Kiel), Austria (Vienna), CERN, the United States (Harvard, Riverside and Wisconsin), Finland (Helsinki), Italy (Padua and Rome), France (Annecy, Collège de France and Saclay), the Netherlands (Amsterdam) and the United Kingdom (Birmingham, Queen Mary College London and the Rutherford-Appleton Laboratory).**

Erratum

IN the penultimate paragraph of Stephen Budiansky's article "Jumping the smoking gun" (*Nature* 4 October, p.407), the statement that "none of the bacteria residing in the gut of farm animals is resistant" should have read "not all of the bacteria . . .".

Photoreception

Bovine-like rhodopsin in algae

from Howard C. Berg

THE outer segment of the light-sensitive retinal rod has long been the system of choice for work on phototransduction in vision, from the isomerization of 11-*cis* retinal to the transient closure of sodium channels in the plasma membrane. Recent advances have centred on amplification involving GTP–GDP exchange, on activation of phosphodiesterase and on hydrolysis of cyclic GMP (Stryer, L. *Cold Spring Harb. Symp. quant. Biol.* **48**, 841; 1983). To those of us who work on sensory transduction in microorganisms, for example on chemotaxis in bacteria, it seems remarkable that so much has been learned without the use of genetics. There is nothing like the right mutant to open the door to fresh discovery, to reveal an unsuspected component or process essential to the function of a complex biological machine. The report on page 756 of this issue that the green alga *Chlamydomonas* can see with the aid of a bovine-like rhodopsin foreshadows a renaissance in studies of eukaryotic photoreception.

Chlamydomonas is an aquatic organism about 10 μm in diameter that is propelled along a helical path by means of two anterior flagella. For photosynthesis, the cell uses blue and red light, which it detects using one chloroplast while for phototaxis, it uses blue-green light, which it detects with one lateral eye, or eyespot. It swims towards or away from a source of light, aligning the axis of its helical path with that of the beam. In 1980, Foster and Smyth argued that the eyespot is a directional antenna, comprising alternate layers of material of different refractive index, that enhances contrast on a layer of photoreceptor pigment in the overlying plasma membrane (*Microbiol. Rev.* **44**, 572). They noted that this antenna completes a 360° lateral scan of the environment every time the cell advances one helical turn. Using a phase-sensitive system that causes one flagellum to pull harder than the other when the output of this scan is non-uniform, the cell can correct its course and 'lock on to' the beam. On the basis of the phototactic action spectrum and other optical properties of the cell, they predicted that the photopigment would be a bovine-like rhodopsin.

Now Foster and his associates, using retinal analogues provided by Nakanishi's group, have proved the point. Phototaxis of a carotenoid-free mutant is restored on addition of suitable analogues, and the shifts in the action spectra parallel those seen in absorption spectra of bovine rhodopsins. The pigment protein clearly differs from bacteriorhodopsin, which works with different analogues and has different spectral properties.

Most steps of the sensory pathway remain to be worked out. Coupling to the flagella presumably occurs via changes in membrane potential, since such changes are observed, with the appropriate action spectrum, when a related green alga, *Haematococcus*, is exposed to light (Litvin, F.F., Sineshchekov, O.A. & Sineshchekov, V.A. *Nature* **271**, 476; 1978). The two flagella of *Chlamydomonas* have different sensitivities to calcium ions (Kamiya, R. & Witman, G. B. *J. Cell Biol.* **98**, 97; 1984), so voltage-sensitive calcium channels might be involved. Little is known about how light absorption generates changes in membrane potential. It is at the level of these early steps in phototransduction that we can expect to see the most significant advances.

Lest anyone should doubt the power of genetic and biochemical dissection in *Chlamydomonas*, look how it has broadened our understanding of the assembly, structure and function of the eukaryotic flagellum (Luck, D.J.L. *J. Cell Biol.* **98**, 789; 1984). Similar breakthroughs should now be possible in studies of eukaryotic photoreception. ☐

Howard C. Berg is in the Division of Biology, California Institute of Technology, Pasadena, California 91125.

Palynology

Andean guide to Pliocene–Quaternary climate

from J.R. Flenley

THE city of Bogota, 2,600 m up in the Colombian Andes, enjoys a remarkably level site, being built on the dry bed of a former lake. A resistivity survey has recently shown that the lake deposits are 800 m deep and have probably been accumulating continuously from well back in the Pliocene and throughout the Quaternary. This has provided a unique opportunity to obtain a complete land-based record of the climatic oscillations of the Quaternary to complement the existing deep-sea record. The results are contained in *Vegetational and Climatic History of the High Plain of Bogota, Colombia: a Continuous Record of the Last 3.5 Million Years* (Cramer, Liechtenstein; 1984), by H. Hooghiemstra.

The deep-sea record has been investigated by Nick Shackleton from Cambridge, and Neil Opdyke at Lamont-Doherty Geological Observatory. By oxygen isotope analysis of the shells of foraminifera from the ocean-bed ooze they have shown that there were numerous major climatic cycles in the past 1.6 Myr, that is since the Olduvai magnetic event which provides one possible definition of the Pliocene–Quaternary boundary. Oxygen isotopes, however, though giving an indication of the amount of ice in the world and of the palaeotemperature of the ocean surface, tell one little about ecological conditions on the continents. In that respect the continuous land-based record from Bogota is very important indeed.

The Bogota sediments have now been cored to a depth of 357 m. Fortunately they contain numerous bands of volcanic ash, which can be dated by the potassium–argon method, allowing it to be established that this part of the record covers the last 3.5 Myr. The monumental task of pollen-analysing this core fell to Henry Hooghiemstra and O.K. Hulshof, working with Tom van der Hammen at the Hugo de Vries Laboratorium in Amsterdam. After 1,230 pollen samples and 378 pollen and spore types, they graphed their results with a laser-beam plotter.

The resulting diagram has been divided into no less than 55 zones, representing 27 complete major climatic cycles, which can be correlated with those from the deep-sea record, and extend it much further back in time. The fluctuations in mean annual temperature are from <6°C to >15°C — so much for those who would write off Quaternary temperature change in the tropics. Some of the most marked fluctuations and some of the coolest temperatures occur in the Pliocene part of the record. It seems that the Late Tertiary was not the time of gently declining temperatures which it was once thought to be.

The great advantage of a land-based core over an ocean core is that it gives direct biogeographical and ecological information. The Isthmus of Panama and the Andes were formed relatively late in the Tertiary, before which it was almost impossible for taxa from North America to migrate into South America. In the Bogota record, we can actually see the arrival of the North American trees *Quercus* and *Alnus*. *Alnus* arrived in the Late Pliocene, about 2.9 Myr ago; *Quercus* appeared on the scene only 1.0 Myr ago. Such direct evidence of migration provides a factual basis for biogeography and offers essential tests for the hypotheses put forward by students of modern biogeographical distributions.

The major ecological cycle recorded is the alternation of rain forest elements with those from the paramo, the grass-dominated vegetation above the tree line. It is these alternations which provide the evidence for temperature fluctuation. Careful inspection of the pollen curves shows that no two cycles are precisely the same. *Alnus*, after its arrival, usually dominates the forest pollen, but the proportions of other forest trees such as *Podocarpus, Weinmannia, Hedyosmum, Rapanea* and *Miconia* vary rather widely and are constantly fluctuating. Some of these variations may indicate hydrological differences between the forest periods, but others could relate to the population biology of individual taxa or to complex ecological interactions. Two points emerge: there is no set pattern of succession in each forest period and there is no stable 'climax'. In fact the diagram is more an exhibition of continuous change than of any kind of stability; any idea of the rain forest as a stable museum-piece does not apply to these montane forests.

Is the Bogota record unique or can we hope to find similarly long undisturbed records elsewhere? In glaciated parts of the world it is clearly unlikely and in subtropical arid regions deposition may often have been interrupted by aridity and by deflation of sediments. It is therefore no accident that this valuable record is from the tropics. The Bogota lake happens to be dry, but there are other tropical lakes which are wet and almost certainly contain long records. The most likely examples are the East African Rift Valley lakes, although the tectonic lakes of the Sumatran Rift Valley also hold out much promise. What is needed now is an international coring project for tropical deep lakes. A start has been made by Dan Livingstone of Duke University, who plans to core the meteorite crater of Lake Bosumtwi in Ghana, and it would be tragic if the expertise to be gained so expensively in money and time at Bosumtwi were not to be more widely used.

The amount of laboratory work involved in analysing the Bogota core was enormous but that being generated by analysis of a 1,000 m core from Lake Biwa in Japan is positively daunting. How incongruous that the pollen analysis of cores obtained with such sophisticated technology is carried out with 'steam-age' manual preparation and optical microscopy. This is true not only for pure research, but also in the field of oil search where palynology is increasingly important. It seems odd that so few palynology laboratories put any effort into modernizing their techniques, and that research-funding bodies have not yet supported attempts to apply information technology in this challenging and commercially significant area. □

J. R. Flenley is in the Department of Geography, University of Hull, Hull HU6 7RX.

Evolution

Creationism in confusion

from Michael E. Howgate and Alan J. Lewis

THIS Saturday (27 October, 2.30pm, Conway Hall, Red Lion Square, London WC1) there is to be a debate between the Association for the Protection of Evolution (APE) and the Biblical Creation Society (BCS) whose talents were on display at an open day during the society's biennial conference*.

Evidently, BCS members range from 'young earthers' who are strict literalists and believe that the Earth was created in six days about 6,000 years ago, to 'mature earthers', who believe it was created about 6,000 years ago but looking much older. It even includes some who put forward the 'gap' theory, which proposes that geology happened sometime between the Fall of Adam and the Flood.

The open day was introduced by David Tyler, who set the tone by being very noncommittal about whether Hutton's classic unconformity at Siccar Point was due to the Flood. However, he was convinced that the presence of a basal breccia and a smoothly planed-off contact was due to some unnamed catastrophic event. Tyler is unusual for a creationist in that he does go into the field to look at the evidence, although he freely admits that his observations are interpreted in the light of 'the biblical constraints on (his) geological thinking'. Tyler, a young-earth theorist (and an organizer of the Open University Geology Club), disparages Uniformitarian geologists for relying on present-day observable analogies when interpreting past processes, but seems not to be averse to doing the same when using the Mount St Helens eruption as a convenient catastrophist analogy. As he is faced with a multiplicity of non-correlatable unconformities throughout the geological column, Tyler seems destined to arrive at the position of Baron Cuvier who, nearly two centuries ago, saw the necessity to interpose as many catastrophes as required in order to match up his catastrophism with the record of the rocks.

A surprising fillip for evolutionists was the discovery that BCS's top geneticist, Chris Darnbrough (Glasgow University) believes in evolution. However, his lecture *Genes, created but evolving* gave the game away. Far from his belief in the genetic mechanisms of evolution affecting his literalist faith in creation, Darnbrough believes that the 'Biblical kinds' of organisms have evolved, but only since the Flood.

In his keynote theological policy statement, Edgar Andrews, professor of materials at Queen Mary College, London, wisely distanced the BCS from US creationism, which he described as being ascriptural and anti-scriptural, as well as suffering from inconsistency. Andrews condemned the opportunist tactics of 'scientific creationism' for leaving the revealed word of God — the Bible — out of their arguments. More specifically, Andrews did not criticize the pseudoscience of the American creationists but concentrated his attack on their failure to appreciate fully the role of Christ Himself as the agency of Creation.

David Gower, reader in biochemistry at University College, London, gave a biblically uninterpreted account of recent advances in the study of olfaction. But in the finale to his lecture he opined that nasal biochemistry was firm evidence for creative design as opposed to natural selection. When tackled on the subject of inherent and genetic defects in olfaction and gustation as well as the lustful temptations presented by pheromones, Gower unenthusiastically admitted that his theological position impelled him to ascribe these faults to the Fall of Adam or to the agency of the Devil.

When a stalwart of the rival creationist organization, the Creation Science Movement, attacked the backsliding into theism of the BCS and asked for a show of hands in support of young-earth, six day, literalism, only one member of the panel of lecturers committed herself to this position. (Perhaps the presence of your Neodarwinist correspondents had an inhibiting effect on their forthrightness). It is to be hoped that at Saturday's debate with APE, the BCS protagonists will not hide the flame of their empirical predictions behind a bushel of theological diversions.

Michael E. Howgate of the Department of Zoology, University College London, WC1E 6BT and Alan J. Lewis of the Department of Electrical and Electronic Engineering, Brunel University, Uxbridge UB8 3PH, are founder members of APE.

*'Creation and Origins Study Conference', High Leigh, Hoddesdon, Herts, 23-26 July 1984.

100 years ago

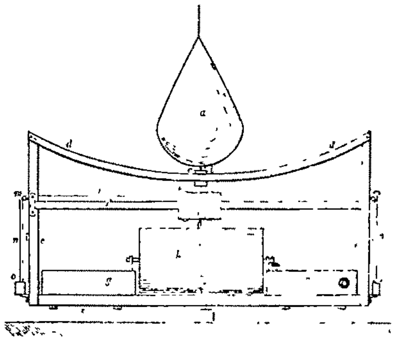

Fig. 4 Horizontal component of wave-path register for strong and destructive earthquakes.

From *Nature* **30**, 610, 23 October 1884.

Anthropology

Supertramps at sea

4630

from Jared M. Diamond and William F. Keegan

WHEN European navigators began 'discovering' the rest of the globe in the fifteenth century, they were surprised to find that technologically less advanced peoples had already settled many oceanic islands. The pattern of settlement is intriguing: in the tropical Pacific almost every habitable scrap of land, no matter how small or remote, was occupied, whereas in other oceans much larger and less remote islands, for example the Madeiras, Azores, Mauritius and Flinders, remained vacant. Recent archaeological work has shown that Pacific peoples colonized earlier, farther and at a lower level of overall technology than did Europeans, Africans and Amerindians. It is now possible to explain why this pattern should be so, and to draw interesting parallels between island colonization by man and that by birds and other animals.

While most Atlantic islands remained empty until thousands of years after the rise of Western civilization, stone-age hunter-gatherers reached the eastern Indonesian islands of Flores and Timor by 100,000 yr BP (ref.1), Australia and New Guinea by 50,000 yr BP (ref.1), the Bismarck Archipelago by 11,000 BP (ref.2) and the West Indies around 5,000 yr BP (refs.3,4). Madagascar was colonized by people from remote Indonesia rather than from nearby Africa, while the colonists of Hawaii and Easter Island stemmed ultimately from the west rather than from the closer Americas. The explanation for this unexpected pattern of settlement, put simply, is that the Pacific is endowed with far more islands than are other oceans.

One reason why both the area and distribution of islands are important factors for colonization is that close islands serve as stepping-stones to more remote islands. For instance, Polynesians or Caribbean Indians did not reach Easter Island or Cuba in a single leap from New Guinea or Venezuela, but via many intermediate islands. But stepping stones cannot be the whole explanation. To reach remote Pacific islands such as Easter Island, New Zealand and Hawaii, Polynesians had to cross stretches of open ocean of up to 3,500 km (refs 5,6), far greater than the distances from the nearest mainland to the Atlantic and Indian Ocean islands that Africans and Europeans failed to reach until modern times. This suggests that the availability and initial discovery of many habitable Pacific islands stimulated overwater colonization by humans. For similar reasons the bird species of New Guinea include many more superior overwater colonists than do the birds of South America or Africa. Thus, understanding of island colonization by humans[7,8] raises problems similar to the island biogeographical problems that have long fascinated students of plant and animal distributions[9].

For European navigators the effect of island availability on colonizing effort is obvious. Between 1400 and 1800 the discovery and expectation of habitable land catalysed further voyages dedicated to exploration and settlement. Egocentric Europeans have tended to assume, however, that only they explored consciously, while illiterate stone-age peoples must have reached islands by accidental drift voyages[10]. Archaeologists still believe this theory holds for the settlement of Australia and New Guinea from Indonesia. The first securely dated human remains from Australia/New Guinea (united to each other in the Pleistocene) date from around 50,000 yr BP (ref. 1), and there is no proof of a second wave of human colonization until the arrival of pigs, taro and dogs of Asian origin around 5,000–10,000 yr BP. In this case, the simplest interpretation is that one raft-load from Timor or the Moluccas survived after being swept to Australia/New Guinea[11], and that a similar accident did not happen again for 40,000 yr.

Portrait of a New Zealand man by F. Parkinson, on Cook's first voyage, 1768-71 (British Library).

By contrast, for the Mediterranean and Polynesia, archaeological research has shown that colonization could only have been purposeful. The presence of obsidian from the Aegean island of Melos on the Greek mainland demonstrates overwater voyaging in the eastern Mediterranean around 13,000 yr BP (ref.12). Yet mainlanders did not choose to begin settling eastern Mediterranean islands until the rise of agriculture and domestication first made self-sustaining human populations possible on the largest islands around 8,000 yr BP. Settlement gradually spread to smaller Mediterranean islands as subsistence techniques improved over the following five millenia[12].

In Polynesia, not only settlement but also discovery of many islands must have resulted from purposeful voyaging. Computer simulations and historical records show that there is essentially no chance of eastern Polynesia having been reached by accidental drift voyages[13,14]. Detailed studies of Polynesian navigational techniques[15], and the Hawaii-to-Tahiti sea trial of the reconstructed Polynesian canoe Hokule'a[16], have demonstrated that the exploration of the Pacific was within Polynesian voyaging capabilities. Polynesian islands were discovered during a series of upwind voyages that reached Fiji, Samoa and Tonga slightly before 1000 BC, the Marquesas around AD 300, and all other Polynesian islands over the following 500 yr (refs 5,6). Human introductions of crops and domestic animals throughout Polynesia provide abundant evidence that settlement as well as discovery was planned[17].

All this is not to say that prehistoric navigational skills were such as to ensure risk-free exploration and colonization. On the contrary, the settlement of Polynesia is estimated to have cost 500,000 Polynesian lives at sea, a number equal to Polynesia's standing population once settled[5]. The motivation of prehistoric voyagers was strong, however. Those few fifteenth and sixteenth century European navigators who returned alive told tales of wealth and habitable lands that triggered an explosive exodus of Europeans seeking these and other still-undiscovered lands. Similar reports of discovering empty islands must have driven the explosive wave of colonization in Polynesia between AD 300 and 800. With the occupation of all the Pacific's habitable islands, the main motivation for long-distance voyaging ceased, and it was only a memory by the time Europeans reached Polynesia.

---

1. White, J. & O'Connell, J. *A Prehistory of Australia, New Guinea, and Sahul* (Academia, Sydney, 1982).
2. Specht, J., Lilley, I. & Normu, J. *Aust. Archaeol.* 16, 92 (1983).
3. Rouse, I. & Allaire, L. in *Chronologies in New World, Archaeology* (eds Taylor, R. & Meighan, C.W.) 431 (Academic, New York, 1978).
4. Maggiolo, M. & Vega, B. *J. New Wld Archaeol.* 5, 33 (1982).
5. Jennings, J. *The Prehistory of Polynesia* (Harvard University Press, Cambridge 1979).
6. Kirch, P. *Adv. Wld Archaeol.* 1, 51 (1982).
7. Jones, R. in *Sunda and Sahul* (eds Allen, J. *et al.*) 317 (Academic, London, 1977).
8. Terrell, J. *Wld Archaeol.* 9, 62 (1977).
9. MacArthur, R. & Wilson, E. *The Theory of Island Biogeography* (Princeton University Press, 1967).
10. Sharp, A. *Ancient Voyages in Polynesia* (Angus & Robertson, Sydney, 1963).
11. Birdsell, J. in *Sunda and Sahul* (eds Allen, J. *et al.*) 113 (Academic, London, 1977).
12. Cherry, J. *Proc. Prehist. Soc.* 47, 41 (1981).
13. Levinson, M., Ward, R. & Webb, J. *The Settlement of Polynesia: a Computer Simulation* (University of Minnesota, Minneapolis, 1973).
14. Dening, G. in *Polynesian Navigation* (ed. Gordon, J.) 102 (Polynesian Society, Wellington, 1963).
15. Lewis, D. *We, The Navigators* (University Press of Hawaii, Honolulu, 1972).
16. Finney, B. *Science* 196, 1277 (1977).
17. Kirch, P. *Archaeol. Oceania* 17, 1 (1982).
18. Diamond, J. & Marshall, A. *Emu* 76, 187 (1976).
19. McGhee, R. *Am. Antiq.* 49, 4 (1984).

The patterns of distribution of Polynesians in the eastern and western Pacific contrast dramatically[5]. On archipelagos lacking other peoples (from Tonga eastwards, including New Zealand), the Polynesians occupied all islands. On tropical western Pacific archipelagos from the New Hebrides to the Carolines, which are shared with Melanesians and Micronesians, the Polynesians occupied only small or outlying islands. In the Solomons, for instance, Polynesians were confined to Rennell and six other outliers, while Melanesians were on all other islands. How could Polynesians have swept thousands of miles across the Pacific from eastern Polynesia to New Zealand and Rennell, without completing the last jumps of 1,000 and 100 miles respectively to Australia and the central Solomons?

The answer proves to be that Polynesians were excluded by established human populations on Australia and western islands other than small outliers: the Rennellese who reached the central Solomons are known to have been killed and eaten. For Australia, a similar exclusion is inferred from Polynesian-style stone axes found along the east coast. The distribution of Polynesians on Pacific islands is paralleled in detail by distribution of numerous bird, bat, lizard, snail and plant species (termed supertramps), which are similarly confined to outlying islands in western archipelagos by established related species[18]. Other cases of human supertramps excluded from mainlands are the Norse from Newfoundland by Amerindians[19] and West Indian Arawaks from Florida by other Amerindians. ☐

Jared M. Diamond is in the Department of Physiology and William F. Keegan in the Department of Anthopology at the University of California, Los Angeles, California 90024.

Astronomy

Chaotic spinning of Hyperion?

From Carl D. Murray

FOR many people the Solar System is a paradigm of ordered regular motion. Indeed, the origins of mechanics can be traced to the early attempts to explain the observed regularity in the motions of planets and satellites. However, according to recently published work by Jack Wisdom and Stanton Peale of the University of California, Santa Barbara, and François Mignard of CERGA, Grasse, the Solar System probably contains one permanent member, Saturn's satellite Hyperion, whose rotational behaviour is far from regular (*Icarus* **58**, 137; 1984).

A general feature of chaotic motion is that relatively simple equations can give rise to solutions with complicated unpredictable behaviour, the degree of chaos depending on a number of factors. The common analogy of a deterministic yet chaotic system is a pinball machine, where small changes in starting conditions can produce radically different results. Hyperion's orbital motion and its interaction with the satellite Titan are quite well understood, and apparently regular. What Wisdom, Peale and Mignard have investigated is the effect of Hyperion's unusual shape on its spin behaviour.

Most of the natural satellites in the Solar System exhibit what is known as synchronous spin-orbit resonance, that is, the satellite's spin period is approximately equal to its orbital period. The most familiar example of this configuation is the Earth–Moon system, resulting in the Moon always presenting the same face to the Earth. Such configurations are not due to chance but have arisen because of the effects of tides raised on the planet by the satellite, the time scale for the process depending on the mass of the satellite and its distance from the planet. For Hyperion, which is small, this time scale was known to be a significant fraction of the age of the Solar System, even before the Voyager missions, but observations had not produced a definitive spin period. In 1980 and 1981 Voyager images of Hyperion revealed a satellite with a highly irregular shape which has been variously described as resembling a cigar or hamburger (see the figure). Wisdom *et al.* show that it is this unusual shape which will probably prevent Hyperion from ever achieving a stable spin-orbit configuration.

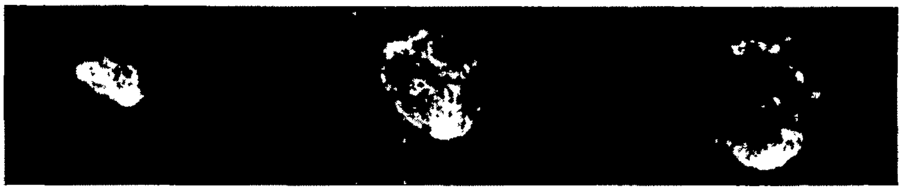

Three images of the saturnian satellite Hyperion from Voyager 2 spacecraft. (JPL and NASA.)

A spin-orbit resonance can occur when the ratio of the spin period to the orbital period is some simple fraction. Near-spherical objects can be trapped in a number of different spin-orbit resonances other than the synchronous one — the planet Mercury is actually in a 3/2 spin-orbit resonance. Each resonance occupies a well-defined region in the phase space and has a narrow chaotic region at its boundary. Only in this narrow region does the behaviour of the spin become unpredictable. If the satellite shape is irregular, with large differences in the principal moments of inertia, then nearby resonances start to overlap and the extent of the chaotic region dramatically increases. A criterion for the onset of chaos as a result of overlapping resonances was first developed by Chirikov (*Phys. Rep.* **52**, 263; 1979) in connection with work on plasma confinement. With parameters appropriate for Hyperion, Wisdom *et al.* show that the chaotic region around the synchronous state is so large that the 3/2 state vanishes and the 1/2 and 2 states are reduced to small islands of apparent stability in a sea of chaos. If Hyperion finds itself in this large chaotic region, its spin period will undergo essentially random variations over a few orbital periods. Nevertheless, Hyperion could still survive in the synchronous state provided that its spin axis remained perpendicular to the orbital plane. But Wisdom *et al.* have also carried out an attitude stability analysis and shown that the synchronous and 1/2 states are unstable to small displacements, resulting in a chaotic tumbling motion. Hyperion's only hope for a chaos-free existence is to enter the attitude stable 2 state. The probability of such an event is very low, however, so Wisdom *et al.* conclude that Hyperion will be found to tumble chaotically.

This naturally leads to the question of what evidence is available in the Voyager images to support a claim for the chaotic tumbling of Hyperion. Thomas *et al.* estimate a rotational period of 13 days (*Nature* **307**, 716; 1984), which, since the orbital period is 21 days, tends to confirm that Hyperion has yet to reach synchronous rotation. They also claim, however, that Voyager 2 images show a spin which is coherent over 61 days and that the derived spin period is consistent between the Voyager 1 and Voyager 2 photographs, even though the sequences were made 220 days apart. If Hyperion has maintained the same spin period for this length of time then the balance swings in favour of ordered rather than chaotic motion. Wisdom *et al.* argue, however, that if the spin is chaotic, with variations over a few orbital periods, then the standard technique of fitting observations made at different times to a constant period is not applicable. The conflicting evidence can only be resolved by an accurate determination of Hyperion's light curve.

Wisdom *et al.* give a convincing demonstration of how some of the techniques of modern dynamics can be applied to the Solar System. It remains to be seen whether or not the 'majestic clockwork' of Kepler and Newton has an unpredictable component.

Carl D. Murray is in the Theoretical Astronomy Unit, School of Mathematical Sciences, Queen Mary College, Mile End Road, London E1 4NS.

Plant engineering

More prospects for Ti plasmids

from M.H. Drummond

AGROBACTERIUM TUMEFACIENS causes crown gall tumours in some gymnosperms and most dicotyledonous angiosperms[1] by inserting its Ti plasmids into the nuclear genome of the infected plant; and agrobacterial Ti plasmids are now well established as vectors for introducing foreign genetic material into a wide range of higher plants[2,3]. This may ultimately make possible useful additions to the genomes of crop plants. Unfortunately the prospect for using Ti-based vectors in monocotyledonous plants has been gloomy because *A. tumefaciens* is not a pathogen for them, a matter of considerable regret since the monocots include the grass crops, which feed the greater part of mankind. On page 763 of this issue, however, Hooykaas-Van Slogteren *et al.* indicate that Ti plasmid DNA enters the cells of at least some monocot species, but is simply not oncogenic[4]. Vectors based on Ti plasmids may thus be useful in monocots after all.

The observation made by the Dutch group concerns the presence in plant tissue of opines. These metabolites are absent from normal tissue but are synthesised in large amounts in crown gall tissue by synthases encoded in T-DNA, the Ti plasmid segment that is integrated into the plant genome. The best known opines, octopine and nopaline, characterize the two principal varieties of Ti plasmid. Ti plasmid sequences outside the T-DNA segment encode oxidases that catabolize opines in the bacterium. Thus the plasmid both diverts the biosynthetic resources of the plant and enables its bacterial carrier to exploit the resulting opine pool as a very specific carbon and nitrogen source. This strategem has been termed genetic colonization. The ecological niche it creates is further enlarged by multiplication of opine-producing cells into a crown gall tumour. This is brought about by other T-DNA genes which perturb hormone metabolism in the plant cell, raising the level of both auxins and cytokinins[5]. The Ti plasmid vectors developed for genetic engineering can be 'disarmed' by deleting, or otherwise mutating, their oncogenic genes, in order to permit differentiation of engineered tissue into entire plants[3,6].

The Dutch group find that when certain ornamental monocots are infected with virulent strains of *A. tumefaciens,* opine synthesis ensues in the absence of any sustained neoplastic growth. Opine synthase genes are known to be under the control of eukaryotic regulatory sequences[7]. The remote possibility that they are being expressed by the bacterial cell in this system is excluded by the observation that no octopine synthesis is detectble when T-DNA transfer is blocked by a plasmid mutation, *virB*, outside the T-DNA[8]. The obvious interpretation is that T-DNA does enter the monocot cell, but fails to bring about oncogenesis. If so, Ti plasmids, far from being unsuitable for the genetic engineering of monocots, can be considered well-suited because already disarmed, although it remains to be seen whether the Dutch group's observations can be extended to the important grass crops.

The definitive experiment, demonstrating the presence of T-DNA sequences in monocot tissues by nucleic acid hybridization, remains to be carried out. Southern blotting is now used routinely to characterize DNA sequences inserted into dicot genomes[2,3,9], but this is more problematical for monocots because of difficulties in the culture of large amounts of transformed tissue without significant contamination by normal cells. In dicots the hormone autotrophy conferred by T-DNA facilitates the selection and growth of transformed tissue, and in many species the establishment of tissue culture lines from single cells is quite straightforward. This is not yet the case for monocots but other means of deriving monocot tissue enriched for cells containing inserted DNA should be feasible. For example, a Ti vector encoding neomycin phosphotransferase such as that constructed by Bevan *et al.*[9] could be used in combination with G418 drug selection in tissue culture. Neomycin resistance is expressed from the *nos* (nopaline synthase) promoter in this construct, which underlines the importance for monocot genetic engineering of the present demonstration that synthase genes are transcribed in the monocot genetic background.

If T-DNA is integrated into the monocot genome in its entirety, its failure to induce tumorigenesis must be accounted for. There are two obvious possibilities: either the oncogenic genes are not properly expressed, or their protein products fail to disrupt control of cell division. If the oncogenic genes are not transcribed, then comparing their regulatory regions with the *nos* or *ocs* (octopine synthase) promoters might bring to light differences between monocot and dicot promoter sequences. However, the Dutch group seem to favour the second possibility.

The work has one further interesting aspect. By illustrating nicely that oncogenesis is not an essential part of genetic colonization, it raises the question of whether other procaryotes have evolved similar stratagems for exploiting plant or animal hosts. To discover any that were a tenth as useful as Ti plasmids would be very exciting, but in the absence of any obvious pathogenic effect, how does one start looking? □

1. Elliot, C. *Manual of Bacterial Plant Pathogens* 2nd edn (Chronica Botanica, Waltham, 1951).
2. Herrera-Estrella, L. *et al. Nature* **310**, 115 (1984).
3. Barton, K.A. *et al. Cell* **32**, 1033 (1983).
4. Hooykaas-Van Slogteren, G.M.S., Hooykaas, P.J.J. & Schilperoort, R.A. *Nature* **311**, 763 (1984).
5. Akiyoshi, D.E. *et al. Proc. natn. Acad. Sci.* U.S.A. **80**, 407 (1983).
6. Zambryski, P. *et al. EMBO J.* **2**, 2143 (1983).
7. De Greve, H. *et al. J. molec. appl. Genet.* **1**, 499 (1983).
8. Hoekema, A. *et al. Nature* **303**, 171 (1983).
9. Bevan, M.W., Flavell, R.B .& Chilton, M-D. *Nature* **304**, 184 (1983).

M.H. Drummond is in the Agricultural and Food Research Council Unit of Nitrogen Fixation, University of Sussex, Brighton BN1 9RQ.

DNA recombination

Resolution of intermediates

from Nancy L. Craig

HOLLIDAY structures[1] are thought to join DNA duplexes by a reciprocal single-strand exchange and are thought to be intermediates in various pathways of genetic recombination (Fig. 1). They have been visualized by electron miscroscopy, but biochemical evidence in support of their role in recombination has been hard to come by. Now, proteins encoded by *Escherichia coli* phages are beginning to provide information about breakage and rejoining reactions that can mediate the formation and resolution of Holiday structures. Kemper *et al.*[2] and de Massy *et al.*[3] have characterized phage endonucleases that can specifically cleave Holliday structures *in vitro*, probably reflecting an important step in the resolution of Holliday intermediates in homologous recombination. And on page 721 of this issue, Hsu and Landy show that Holliday structures can be resolved *in vitro* to recombinant duplexes by the site-specific recombination machinery of phage lambda, providing strong evidence that Holliday structures are intermediates in this recombination pathway[4].

Integration of phage lambda into the *E. coli* chromosome occurs by reciprocal combination between *att*P(POP′), a ~240-base pair (bp) specific site in the phage chromosome, and *att*B(BOB′), a ~25-bp site in the bacterial chromosome[5] (see Fig. 2). The products of integrative recombination are the hybrid sites *att*L(BOP′) and *att*R(POB′) which flank the integrated prophage. Prophage excision occurs by reciprocal recombination between *att*L and *att*R, regenerating *att*P and *att*B. Each *att* site contains the same

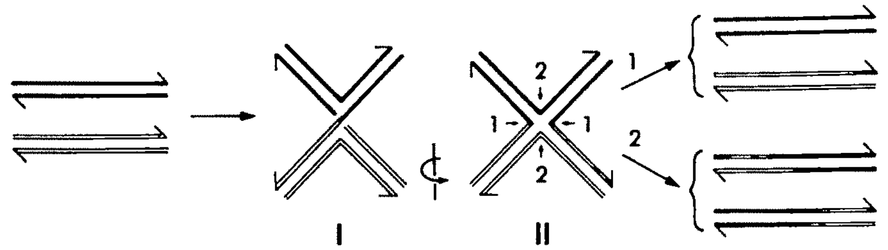

Fig. 1 Formation and resolution of a Holliday structure. The polarity of the strands in two DNA duplexes is indicated by the arrowheads. A Holliday structure (I) is formed by breakage, exchange and rejoining of a pair of strands of like polarity at equivalent positions. Rotation produces II, an isomer of I. A Holliday structure is resolved by breakage, exchange and rejoining of a pair of strands of like polarity at the branch point; the outcome depends on whether this occurs at positions 1 or 2.

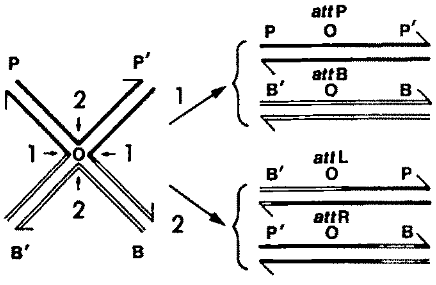

Fig. 2 Resolution of a Holliday intermediate in lambda site-specific recombination. A Holliday structure containing *att* sites is shown. P, P',B' and B are the main *att* sites. The branch point occurs in the core (O), a sequence common to all *att* sites. Resolution at positions 1 yields the products of excisive recombination, *att*P(POP') and *att*B(BOB'). Resolution at positions 2 yields the products of integrative recombination, *att*L(BOP') and *att*R(POB').

15-bp core (O), flanked by unique arms (P, P', B, B'); see Fig. 2. Integrative recombination requires Int, a lambda-encoded protein, and integration host factor (IHF), a host-encoded protein. Excisive recombination requires Int, IHF and Xis, another phage-encoded protein. These proteins are specific DNA-binding proteins and the *att* sites contain elaborate arrays of recognition sequences.

Using a method developed by Bell and Byers[6], Hsu and Landy[4] constructed pairs of *att* site-containing DNA duplexes with four non-homologous arms (Fig. 2) joined by a reciprocal single-strand exchange in the core. Incubation of these structures with purified Int resulted in their resolution to the products of excisive and integrative recombination. Both pairs of recombinants are observed because resolution can occur either at positions 1 or positions 2 of the Holliday structure (Fig. 2). These experiments suggest that natural Int-dependent recombination proceeds via the formation of a Holliday structure by a reciprocal single-strand exchange between the cores of *att* sites, followed by its resolution by a second reciprocal exchange.

The demonstration that Int alone can promote resolution emphasizes its central role in strand exchange and extends the finding that Int has specific topoisomerase activity which breaks and rejoins DNA at the junction-type Int recognition sequences in the cores of *att* sites[7]. Hsu and Landy show that resolution, like recombination, proceeds in the absence of a high energy cofactor and produces intact duplexes, features reflecting the action of a topoisomerase. Moreover, they also found that Int's capacity for resolution is specific to Holliday structures containing *att* site cores at the branch point. Int can resolve synthetic Holliday structures that lack distal segments of the arms of the *att* sites but does not resolve synthetic Holliday structures which lack the core. Thus, it is likely that Int topoisomerase mediates strand exchange by promoting sequence-specific breakage and rejoining reactions in the cores of *att* sites and that these reactions form and resolve Holliday structures. The action of topoisomerases may also underlie other site-specific recombination reactions[8,9].

What are the roles of the other components of the lambda site-specific recombination machinery? Hsu and Landy show that sequences in the *att* site arms which are essential for recombination are not required for resolution. This suggests that the interactions of IHB, Xis and Int with their recognition sequences in the arms of *att* sites are important in promoting the formation of a Holliday structure. The formation of such an intermediate is a multistep reaction in which recognition of the *att* sites by the recombination proteins and synapsis of the *att* sires precede the strand-exchange step, which is mediated by the interaction of Int with the core. The assembly of the *att* sites and recombination proteins into organized complexes[10] may facilitate these steps.

Hsu and Landy have also observed that, although an *att* site-containing a Holliday structure can be resolved by Int alone to the products of either integrative or excisive recombination, the relative efficiencies of these two reactions vary under different experimental conditions. This suggests that resolution may also be regulated by other components of the recombination machinery.

Formation and resolution of Holliday structures is also probably involved in strand exchange in homologous recombination. Study of the *E. coli recA* protein is revealing how Holliday structures can be formed during homologous recombination[11]. How can they be resolved? Purified endonuclease VII (endo VII), an enzyme encoded or regulated by coliphage T4 gene 49, cleaves Holliday structures *in vitro* by breaking pairs of DNA strands of like polarity at the branch point — that is, at positions 1 or positions 2 (see ref. 12). De Massy *et al.*[3] have now shown that phage T7 endonuclease I, which is the gene 3 product, has similar activity. It has now been shown that endo VII (refs 2 and 13) and endo I (ref. 3) cleave at the branch points of cruciforms which occur at short inverted repeats in supercoiled DNA. This result suggests that such cruciforms are useful analogues of Holliday structures and that these enzymes will also be useful as probes of cruciform structure.

The resolution of Holliday structures promoted by endo VII and endo I is significantly different from Int-promoted resolution. In contrast to Int, whose resolving capacity is limited to *att* site-containing Holliday structures, endo VII and endo I are capable of resolving Holliday structures that contain a variety of sequences, although endo VII has a modest sequence preference[2]. Furthermore, in contrast to Int, neither endonuclease promotes rejoining of the DNA strands they break. Thus, in homologous recombinations of bacteriophage DNA, resolution of Holliday intermediates to intact recombinant duplexes probably involves the action of other enzymes, for example, DNA ligase. It is also likely that endo VII and endo I participate only in the resolution step in recombination, whereas Int mediates both the formation and resolution of recombination intermediates.

Hsu and Landy provide the first physical evidence that Holliday structures are intermediates in phage lambda site-specific recombination. It will now be possible to dissect separately the formation and resolution of these intermediates. Although further work is needed to establish that endo VII and endo I participate directly in homologous recombination between phage DNA molecules *in vivo*, detection of activities that can resolve Holliday structures supports the hypothesis that these structures are recombination intermediates. Using the methods developed to detect the activity of endo VII and endo I towards Holliday structures, it should be possible to search for similar cellular activities.

1. Holliday, R. *Genet. Res.* 5, 282 (1964).
2. Kemper, B., *et al. Cold Spring Harb. Symp. quant. Biol.* 49 (in the press).
3. de Massy B., *et al. Cold Spring Harb. Symp. quant. Biol.* 49 (in the press).
4. Hsu P.L. & Landy, A. *Nature* 311, 721 (1984).
5. Weisberg, R. & Landy, A. in *Lambda II* (eds Hendrix, R., Roberts, J., Stahl, F. & Weisberg, R.) 211 (Cold Spring Harbor Laboratory, New York, 1983).
6. Bell, L. & Byers, B. *Proc. natn. Acad. Sci.* 76, 3445 (1979).
7. Craig, N. & Nash, H. *Cell* 35, 795 (1983).
8. Abremski, K., Hoess, R. & Sternberg, N. *Cell* 32, 1301 (1983).
9. Krasnow, M. & Cozzarelli, N. *Cell* 32, 1313 (1983).
10. Better, M., Chu, L., Williams, R. & Echols, H. *Proc. natn. Acad. Sci. U.S.A.* 79, 5837 (1982).
11. Radding, C. *A. Rev. Genet.* 16, 405 (1982).
12. Mizuuchi, K., Kemper, B., Hays, J. & Weisberg, R. *Cell* 29, 357 (1982).
13. Lilley, D. & Kemper, B. *Cell* 36, 413 (1984).

Nancy L. Craig is in the Department of Microbiology and Immunology, School of Medicine, University of California, San Francisco, California 94143.

Meteorology

Origins of stony-iron meteorites

from Edward R.D. Scott

ALTHOUGH most of the meteorites that fall on Earth are chondrites, more is known about the formation and parent bodies of the 15 per cent that come from bodies that were once largely molten. Three such igneous meteorites come from the surface of the Moon[1], eight may have come from Mars[2], and a large group — known as basaltic achondrites — may be pieces of 4 Vesta, the second or third largest asteroid[3,4]. But what is the origin of the variety of igneous meteorites known as stony-irons, which account for only seven per cent of falls of igneous meteorites but whose unusual mineralogy constitutes a major puzzle? New astronomical and theoretical studies indicate how and where the stony-iron meteorites may have formed in the asteroid belt.

Most igneous meteorites contain either less than 1% or greater than 99%, by weight, of metallic iron-nickel and other metallic phases. This is because the large density difference between molten iron and silicate ensures their rapid separation. By contrast, stony-irons usually contain 40–60 wt % iron-nickel (and always 20–80 wt %). In pallasites, the remainder is olivine $(Mg,Fe)_2SiO_4$, whereas in mesosiderites it is basaltic material, which lacks significant amounts of olivine.

How were large volumes of metal intimately mixed with massive amounts of mantle olivine or crustal basalts? For the pallasites, it is widely believed that metal from the core of a molten asteroid was forced into part of the surrounding olivine mantle as a result of cooling stresses, impacts and the weight of the mantle. But it is much more difficult to understand how mesosiderites formed. Petrological studies show that brecciated basaltic material from the surface of an asteroid was mixed with metallic iron-nickel without the inclusion of significant quantities of mantle olivine. At 1,000°C, the cooling rate of the mixture was about one degree per year but because the mesosiderites were eventually buried so deeply, their rate of cooling at 500°C was reduced by at least 10^5-fold and so was slower than that of any other type of meteorite.

Conventional models for the origin of mesosiderites attribute the mixing of metal and silicate to impacts between two igneously differentiated asteroids, and the slow cooling to subsequent accretion. However, R. Greenberg and C.R. Chapman[5] argue that the lack of olivine, the uniform cooling rates and the abundance of mesosiderites preclude such models and suggest instead that the mixing occurred within a single asteroid. In their scheme, a solid basaltic crust of a largely molten body sank towards the core-mantle interface when it was fractured by impacts because it was slightly denser than a liquid mantle beneath it. Liquid iron from the core penetrated the cold fractured blocks of crust so that the mixture cooled rapidly at high temperatures but much more slowly at low temperatures. Greenberg and Chapman suggest that pallasites formed in smaller bodies in which the olivine-rich mantles solidified before the crusts foundered.

Reviewing this and other proposed origins for mesosiderites, R. Hewins[6] concludes that no single model is wholly satisfactory. He finds that mesosiderite textures resemble those of rocks formed by impacts and believes that major collisions must have mixed metal and silicate. Hewins suggests that mesosiderites lack olivine because, unlike all known oxidized chondrites, their parent body never contained much olivine — an argument not favored by Greenberg and Chapman.

There has been no certain identification of asteroids with mesosiderite-like surfaces, although several S-type asteroids have been proposed as candidates. However, recent telescopic observations have revealed the existence of a new class of asteroids with surfaces that resemble those of pallasites. According both to D.P. Cruikshank and W.K. Hartmann[7] and to J.F. Bell and coworkers[8], infrared spectra of 246 Asporina, 289 Nenetta and 446 Aeternitas show the deep absorption bands of olivine and overall red colors that are consistent with the presence of a metal phase. Hence some asteroids of 50-100 km diameter have melted to form olivine-rich mantles that have since been exposed by collisional stripping of the crusts.

To learn more about the origins of mesosiderites and pallasites we must reach a much better understanding of the nature and distribution of the heat source, and of the movement of solid and liquid phases during melting and solidification. We need to know whether totally molten mantles of olivine-rich composition could be produced, and whether melting occurred after or during accretion in the asteroid belt. Theory and experiment will help to address these questions but to understand fully the origins of stony-irons we shall also need field studies of asteroids. □

1. Eberhardt, J. *Science News* **126**, 70 (1984).
2. McSween, H.Y. Jr, *Geology* **12**, 3 (1984).
3. Drake, M.J. in *Asteroids* (ed. Gehrels, T.) 765 (University of Arizona, 1979).
4. Chapman, C.R. *Planetary Report* **4**, 12 (1984).
5. Greenberg, R. & Chapman, C.R. *Icarus* **57**, 267 (1984).
6. Hewins, R.H. *J. geophys. Res. Suppl.* **88**, B257 (1983).
7. Cruikshank, D.P. & Hartmann, W.K. *Science* **223**, 281 (1984).
8. Bell, J.F., Hawke, B.R., Singer, R.B. & Gaffey, M.J. in *Lunar and Planetary Science* **XV**, 48 (Lunar and Planetary Institute, Houston 1984).

Edward R.D. Scott is in the Institute of Meteoritics, University of New Mexico, Albuquerque, New Mexico 87131.

Shiro Kakiuchi 1929–1984

SHIRO Kakiuchi of Osaka University Medical School, who died on 22 September, was a pioneer in many areas of cell regulation. During the mid 1960s he worked with T. E. Rall at Case Western Reserve in Ohio and made many contributions to cyclic nucleotide research during the formative years of this field. It was during this time that he began work on cyclic nucleotide phosphodiesterases. In 1970, soon after his return to Japan, Dr Kakiuchi revealed that a form of phosphodiesterase required the presence of an activator and that stimulation by the activator required Ca^{2+}-dependent protein activator that later came to be called calmodulin.

Kakiuchi realized the potential importance of the activator in other enzyme systems and in 1978 recognized that it was also the activator of myosin light chain kinases. Subsequently he isolated the protein from a variety of ciliates and invertebrates and discovered a calmodulin-dependent form of guanylate cyclase. In the same year, Kakiuchi found that calmodulin was partitioned between the soluble and particulate fractions of the cell, which led him to the discovery in 1980 that the only calmodulin-binding protein in the cytoskeleton of the red blood cell is spectrin. A year later he was the first to show the presence of a spectrin-like protein in other tissues and to purify the protein from brain. Also in 1981 he purified another calmodulin-binding protein from chicken smooth muscle and showed that it interacted with actin filaments.

This protein, which he called caldesmon, was subsequently named fodrin by US scientists. Caldesmon interacts with actin when the Ca^{2+} concentration is less than 1μM but with calmodulin at higher concentrations. This led to the hypothesis that calmodulin might control those proteins associated with actin in a 'flip-flop' mechanism depending on the Ca^{2+} concentration. The hypothesis was later extended to the Ca^{2+} regulation of microtubules when Kakiuchi showed that one of the microtubule-associated proteins, *tau*, was a Ca^{2+}-dependent calmodulin binding protein.

All of these experiments were pioneering efforts and each observation has been repeated and extended by numerous laboratories. As much as any one individual Shiro Kakiuchi was the father of the field of calmodulin research and an innovator in the study of its interaction with other regulatory proteins. He will be passionately missed by his many students, collaborators and friends. **A.R. Means**

21-1-87

Geomagnetic secular variation impulses

V. Courtillot & J. L. Le Mouël

Laboratoire de Géomagnétisme Interne et Paléomagnétisme (ERA CNRS 922), Institut de Physique du Globe, Université Paris 6 et UER Sciences Physiques de la Terre, Université Paris 7, 4 Place Jussieu 75230 Paris Cedex 05, France

The secular variation of the Earth's internal magnetic field changes on time scales of the order of a year. Such impulses occurred in 1969 and probably in 1913; they provide constraints on deep mantle conductivity, which appears to be rather low, and on the motions of the top of the fluid core, which are probably dominated by westward drift. Present data favour the existence of upwelling of core material at the core-mantle boundary. The impulses can be correlated with extrema in the Earth's rotation rate and interpreted in terms of electromagnetic core-mantle coupling.

THE study of temporal variations of the Earth's magnetic field has benefitted from observational advances in the past 5 yr. Secular variation of the geomagnetic field observed at the Earth's surface has been found to undergo rapid accelerations lasting less than a few years, a much shorter duration than had previously been recognized for signals generated in the Earth's core and having diffused through the electrically-conducting mantle. One such rapid and worldwide acceleration occurred in 1969; an earlier, less well documented, acceleration apparently occurred around 1913. The identification of these events was made possible by carefully assembled long data sets from magnetic observatories around the world. The centenary of the French Magnetic Observatory (St Maur-Val Joyeaux-Chambon La Forêt) provided the opportunity for a meeting to discuss recent progress on the origin and secular variation of the geomagnetic field. We now review evidence (in part presented at the meeting) for the occurrence of impulsive accelerations in geomagnetic secular variation. Also discussed are the implications of these events regarding deep mantle conductivity, their link with decade fluctuations in the rotation of the Earth, the case for core-mantle coupling and efforts to determine core motions.

Secular acceleration impulse of 1969

Short-period variations of the geomagnetic field are linked with electric currents flowing in the ionosphere and magnetosphere (thus having a primarily external origin), whereas longer-period variations are thought to be due to dynamo processes acting within the Earth's fluid metallic core. It was accepted until recently that the cutoff between the two was about 4 yr (see ref. 1). This cutoff was raised to more than 10 yr by Currie[2] and Alldredge[3], although it was recognized that signals with a clear external origin, such as the 11-yr solar cycle, fell close to this limit (see ref. 4). In a previous study[5] of observatory data for the period 1947-1972, we found no evidence for short-period signals that would have originated from the core. However, when attempting to separate the solar cycle from long-period internal variations, we noticed discrepancies in the correlation between variations seen on the horizontal versus vertical components, particularly between 1967 and 1972 (the date of the most recent data then available). These suggested that the effect could be due to a slight change in the second derivative of the 'true' internal secular variation. With data available up to 1977, it has been shown[6] that there had been an impulse in the third derivative of geomagnetic field components around 1969. The impulse was particularly spectacular in the east (Y) component of European observatories and was identified in at least 38 observatories from the Northern Hemisphere (Fig. 1).

Extremal secular variation behaviour had already been observed by Vestine[7] to have occurred around 1910. The concept of secular variation impulses was introduced by Walker and O'Dea[8], who found it convenient, for the purpose of correcting magnetic data to a given epoch, to approximate the secular variation by a constant value for a chosen interval. In this process, changes in constants from one interval to the next resulted in 'impulses'. These impulses were formerly attributed to the internal field (see refs 9, 10) but Alldredge[11] showed that the impulses were correlated with the sunspot cycle and resulted from an ill-chosen piecewise linear fit to the smooth external variations. We confirmed[5] that the slope breaks resulting in impulses coincided with extrema in the 11-yr variation.

The 1969 impulse is a completely different matter both in time evolution, geographical distribution and intensity, being an order of magnitude larger than the constructions of Walker and O'Dea. The original[6] presentation of the impulse was based on a representation of the field components themselves, which were interpreted in terms of two parabolic segments, with discontinuous curvature (that is second derivative) in 1969. This meant that the third derivative of the field components could be represented by a Dirac distribution. The parabolic representation was criticized by Alldredge[12] who suggested that the impulse might be an artefact of the fitting procedure. In response to this comment, Courtillot *et al.*[13] showed that displaying the data as first derivatives (computed simply from first-order finite differences) provided a very clear and convincing picture of the impulse (Fig. 1).

Parallel to the work done in Paris, a team led by Malin in Edinburgh observed, when preparing the 1975 World Magnetic Charts, the sudden change in secular acceleration of declination which occurred in 1969 in European observatories: Malin *et al.*[14] showed that the representation of secular variation as a function of time was to be preferred over that of the original data or of its second derivative. In the case of second-order finite differences, higher frequency noise is amplified together with harmonics of the solar cycle, in particular the harmonic with a period of 3.7 yr. Careful filtering can, however, reveal the step change in acceleration at the expense of time resolution (J. G. Gavoret, personal communication). Thus, together with Courtillot *et al.*[13], Malin *et al.*[14] concluded that data are well represented by a simple instantaneous change of slope between two linear segments and that the representation as "the sum of a series of sine curves of different frequency", proposed by Alldredge[12], "is an unnecessarily complicated and conceptually unhelpful way of regarding the phenomenon".

Working on first order differences for the X(north), Y and Z(vertical) annual mean values from 130 observatories, Chau *et al.*[15] and Le Mouël *et al.*[16] were able to confirm the worldwide and simultaneous character of the 1969 impulse. The amplitude of the step in the second time derivative was estimated from a least-squares fit of two linear segments to the data. The date of the impulse was determined by minimizing the r.m.s. residuals for impulse dates ranging from 1967 to 1972, and was found to be 1969. The worldwide distribution of impulse amplitude for each field component is shown in Fig. 2. Departure from the V shape in original observatory data may be due to remaining external signals, to problems in baseline control (up to 1970 most frequently in the Z component) and to more localized internal signals with a different behaviour, as is apparently the case under Central America and the Indian peninsula. In any case, the resulting picture is smooth and coherent.

Malin *et al.*[14] analysed the *D* (declination), *H* (horizontal intensity) and *Z* annual mean values for 184 worldwide observatories. They assumed that the magnetic field associated with the impulse was internal and performed a spherical harmonic analysis on 3-yr smoothed means, limiting the expansion to degree and order 6. Secular variation models were derived (by subtracting) for epochs 1963.5, 1965.5 and 1967.5, and for epochs 1971.5, 1973.5 and 1975.5, providing two estimates of secular acceleration, one centred on 1965.5, the other on 1973.5. Accelerations were derived by least-square fits of linear time functions to the secular variations, both before and after the impulse, and the resulting impulse amplitudes (1973.5 minus 1965.5 accelerations) truncated to degree and order 4 were given by Malin *et al.*[14]. The maps which can be derived from this truncated representation are in reasonable agreement with those of Le Mouël *et al.*[16], although differences exist. The largest amount of power in the Malin *et al.*[14] expansion is in the $n = 2$ terms. In a more recent analysis, Malin and Hodder[17] resumed the experiment for the components from 83 selected observatories, this time including the possibility for an external part in the field. The expansion was limited to degree and order 4. They found that most of the jerk is indeed of internal origin.

Inspection of the data from ref. 16 (see Fig. 2) reveals wide areas where the distribution of impulse elements are rather flat (such as central Asia for δX and δZ, or South America for δY) separated by narrow areas with steep gradients where sign changes occur (such as in northern Central America or South East Africa for δZ). Thus, an accurate description of the impulse distribution may require high-order spherical harmonics or a different representation; available data do not allow such a detailed expansion. However, the simplicity of the overall pattern demonstrated by the few and smooth zero-isolines of Fig. 2 favours the dominance of low (particularly $n = 2$) order terms[14,18].

Secular acceleration impulse of 1913

Following the identification of the 1969 impulse, it was natural to search for earlier occurrences of such a phenomenon that might have escaped identification. Vestine[7], for example, had noticed large changes in secular variation around 1910, and we noticed a sharp change in the secular acceleration of declination shortly after the beginning of this century at Val Joyeux ("Chambon"). Courtillot *et al.*[6] tentatively identify this event on the *Y* component of many observatories. Ducruix *et al.*[19] analysed annual mean values of *X*, *Y* and *Z* from 40 observatories in the Northern Hemisphere and 10 observatories in the Southern Hemisphere. They observed that for many observatories and many components secular variation roughly follows a linear trend between 1913 and 1969, which is preceded by a global break in the secular variation slope occurring around 1913 (Fig. 1). In certain areas, other internal variations of regional importance distort the simple piecewise linear (V) shape of the secular variation. Such is the case for the *Y* component in European observatories where an anomaly centred on 1925 renders the identification of the 1913 impulse more difficult. Ducruix *et al.*[19] outlined the zero isolines of the 1913 impulse for the three components. The geometry of the impulse is reminiscent of that for the 1969 impulse but with a reversal in sign. Secular variation may also have been linear between 1905 and 1913, but data for the early years of the century and last years of the previous century are too scarce, and sometimes too noisy, to allow a satisfactory global analysis of the event. The identification of impulses before 1910 is difficult. Only 19 observatories were in operation in 1900, 12 of them in western European countries. However, long homogeneous series of data such as that provided by Malin and Bullard[20] for London or that being prepared for Paris (J.L. Le M. *et al.*, in preparation) may help in searching for earlier events.

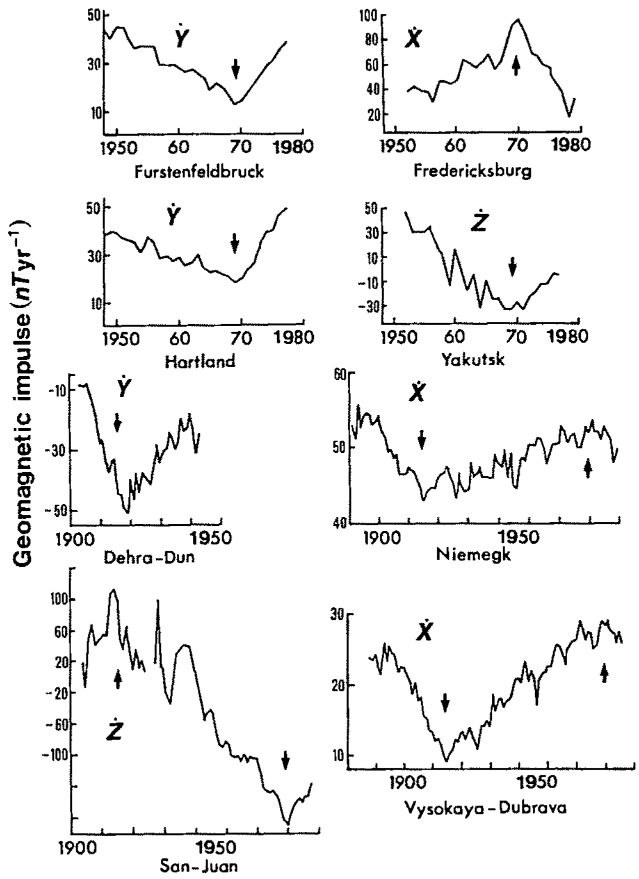

Fig. 1 Secular variation (first difference of annual mean values) of geomagnetic components *X*(north), *Y*(east) and *Z*(vertical) in widely-spaced observatories (from refs 13, 16 and 19). Furstenfeldbruck, Hartland and Niemegk are in Europe, Fredericksburg in the USA, Yakutsk and Vysokaya-Dubrava in the USSR, Dehra-Dun in India and San Juan in Puerto-Rico. The occurences of the ≈1969 and ≈1913 impulses are outlined by arrows.

Secular variation 1910–80

Ducruix *et al.*[19] and Gire *et al.*[18] conclude that the secular variation field can be modelled in a remarkably simple way from at least 1913; as a first approximation, each component of the secular variation can be represented as a two-segment broken line, with an apparently worldwide and synchronous break occurring in 1969 and probably an earlier one in 1913 (Fig. 3).

Using spherical harmonic coefficients provided by Hodder[21], Gire *et al.*[18] found that, between 1913 and 1969, the secular variation isovalue lines became wider apart and that the energy of secular variation was reduced by a factor 2. Between 1969 and 1980 the secular variation field recovered its strength and in 1980 the maps displayed strong similarities to those in 1912, except in the Far East where data are scarce. The linear model proposed by Gire *et al.*[18] accounts for more than 75% (in terms of energy) of the total secular variation observed for the *X* and *Y* components. Early values for the *Z* component are inaccurate and the piecewise linear model does not work as well.

Mantle conductivity

The classical way of probing the electrical conductivity of the Earth's mantle is to study transient geomagnetic variations of primary external origin and to separate the internal and external parts of the signal as it is observed at the Earth's surface (see ref. 22). The longer the period of the signal, the deeper its penetration depth. The identification of the solar-cycle variation and the separation of its internal and external parts have yielded some of the deepest estimates of mantle conductivity (down to ~1,500 km; refs 3-5, 23-28).

Another approach of the mantle conductivity problem uses the diffusion of magnetic signals generated in the Earth's core.

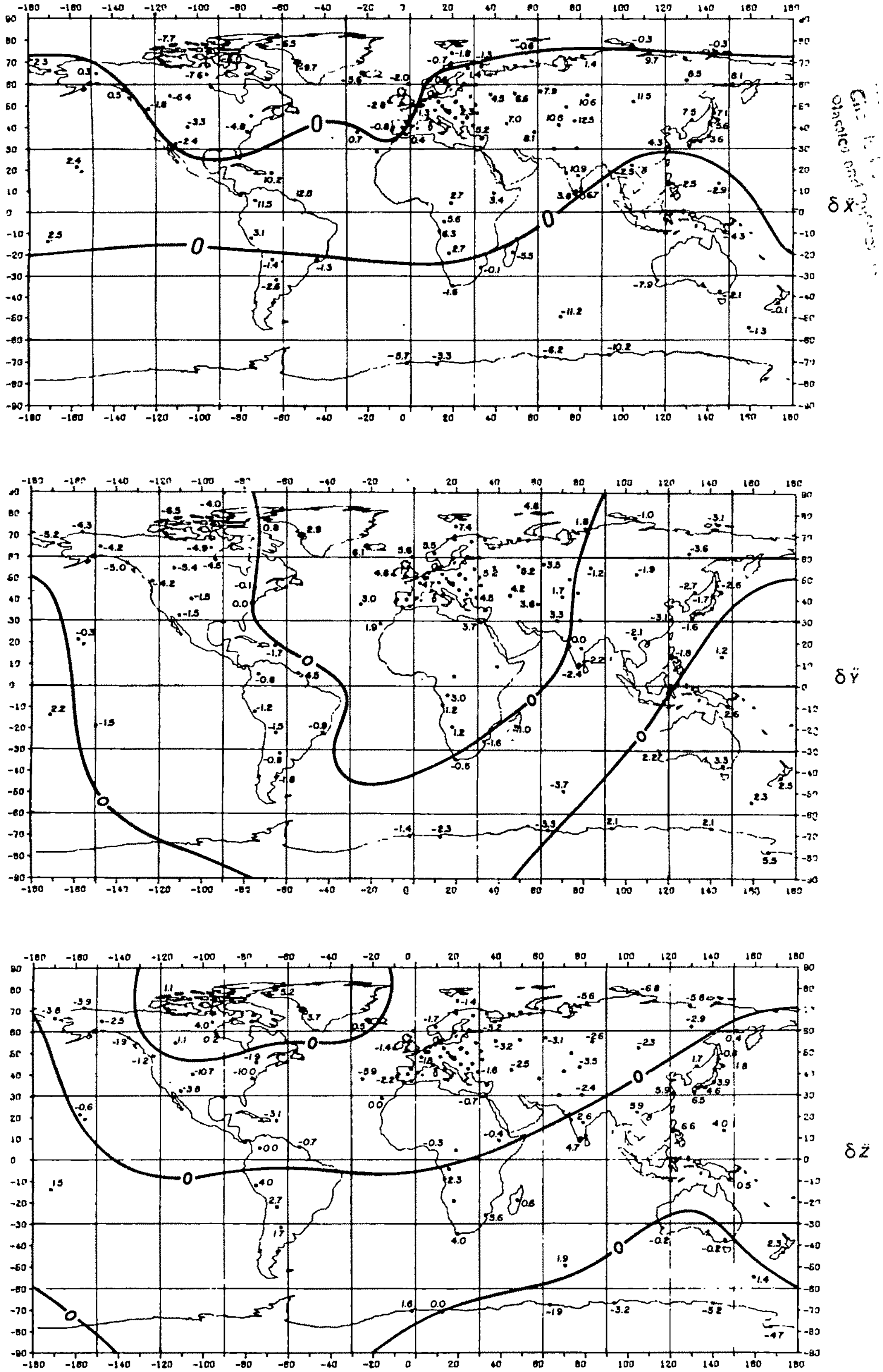

Fig. 2 Worldwide distribution of the $\delta\ddot{X}$, $\delta\ddot{Y}$ and $\delta\ddot{Z}$ components of the 1969 impulse with interpolated zero-isolines (in nT yr^{-2}, after ref. 16).

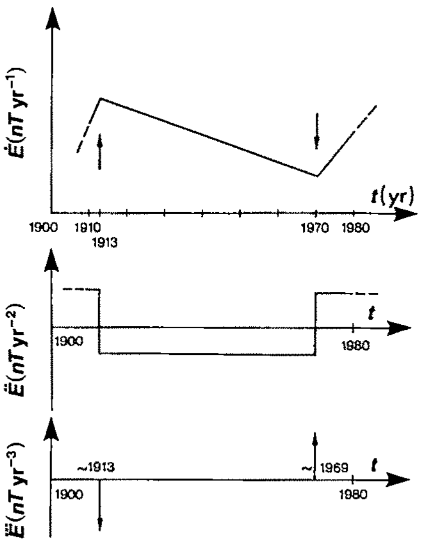

Fig. 3 A simple secular variation (first-time derivative) model for any geomagnetic element E involving two impulses in 1913 and 1969 and linear variations between the impulses. The second and third derivatives of E are also sketched.

Runcorn[9] used the "secular variation impulses" introduced by Walker and O'Dea[8] to infer an upper bound of the mean mantle conductivity, which he found to be of the order of $10^2\ \Omega^{-1}\ \mathrm{m}^{-1}$. McDonald[10] further studied the penetration of secular variation, including the 'impulses', through the mantle and derived a profile for the conductivity of the entire mantle, rising slowly from $30\ \Omega^{-1}\ \mathrm{m}^{-1}$ at 1,200 km depth to $200\ \Omega^{-1}\ \mathrm{m}^{-1}$ at the core-mantle interface. However, note that the impulses introduced by Walker and O'Dea are artefacts. Following the positive identification of the 1969 impulse, Achache *et al.*[29,30] resumed Runcorn's early analysis. These authors erroneously modelled the 1969 event as a second-order impulse, that is a step change in secular variation, and not acceleration[31]. The shape of the secular variation curves after 1969 was interpreted as part of the transient impulse response leading to a mean conductivity for the lower 2,000 km of the mantle of the order of $150\ \Omega^{-1}\ \mathrm{m}^{-1}$. This result was included in the global study of Achache *et al.*[28], who proposed a conductivity of the order of $300\ \Omega^{-1}\ \mathrm{m}^{-1}$ in the lower 700 km of the mantle.

Backus[31] has shown that when the radial component of the time-dependent magnetic field measured at the Earth surface is expanded in surface spherical harmonics, each spherical harmonic component of a given degree l observed at the surface is related to the same component at the Earth's core by a causal linear filter. Backus showed that the filter impulse response can formally be treated as a probability density function, whose mean τ_l and standard deviation σ_l are the delay time and smoothing time of the filter: the main effects of the lth mantle filter are to delay the input by τ_l yr and to smooth it in a gaussian way over σ_l yr. In principle, τ_l and σ_l can be evaluated from observations through spherical harmonic analysis, and thus they provide functions of (constraints on) mantle conductivity. Backus provided the way to apply mantle filter theory to an impulse of order p, that is, one for which the pth derivatives of geomagnetic components are Dirac distributions: if the impulse starts at the core surface at time t_0 and has an amplitude A_l, one can derive from the data the order p of the impulse, A_l, σ_l and $t_0+\tau_l$, but not t_0 and τ_l separately. Moreover, Backus stresses that each component of the field at a single location is a linear combination of the outputs for all degrees l and that if this composite signal is processed as if it were the output of a single filter, the resulting fictitious mixed filter can have a negative delay time τ_l and imaginary smoothing time σ_l. Applying the theory to the 1969 impulse as observed in Europe on the Y component (that is, the record on which the impulse was discovered and is particularly clear), Backus finds that $t_0+\tau = 1969.8 \pm 0.2$ (corrected from the original paper to account for the fact that annual mean values are centred on 1 July), $p=3$, $A = 5.0 \pm 0.3\mathrm{nT\,yr^{-2}}$ and $\sigma^2 = -2 \pm 1$ yr. Backus[31] concludes that harmonic mode mixing in Europe is probably responsible for the observed negative value of σ^2 (although a sunspot-related contribution or other source of noise remains a possibility). Even in the case where mode mixing does not occur, Backus remarks that the 1969 impulse permits values of σ as high as 2 yr with harmonics as high as order 4 and concludes that this is compatible with a lower mantle conductivity as high as several thousands of $\Omega^{-1}\ \mathrm{m}^{-1}$.

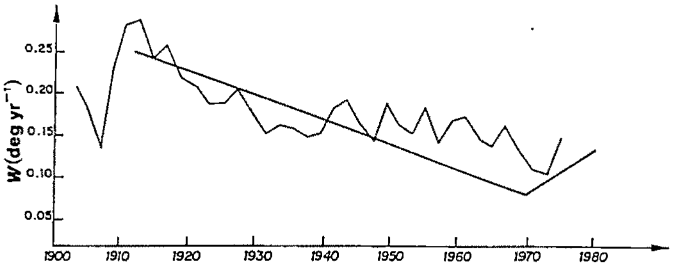

Fig. 4 Estimates of the westward drift rate computed for the period 1910–80 from a V-shaped model (straight lines, after refs 19 and 34) and using Hodder's[20,36] results (curved line).

Courtillot *et al.*[32] elaborated on Backus's[31] results and emphasized the fact that a sunspot-related signal could be responsible for the negative value of σ^2. They generated a synthetic curve, adding a typical sunspot signal to a pure third-order impulse, and found that the short data window available after the impulse indeed generated a sunspot related bias of σ^2, with a magnitude close to the observed one. Courtillot *et al.*[32] argued that the 1969 impulse is apparently worldwide and synchronous and that in many observatories, for many components, the transition from the pre-impulse to the post-impulse 'asymptotic' behaviour seems to take on the order of 1 yr. This led Courtillot *et al.*[32] to propose that harmonic mode mixing could be of minor importance.

Backus[31] showed that, for reasonable conductivity distributions, the ratio of smoothing time to delay time of a mantle filter has to lie between 0.3 and 0.8. Courtillot *et al.*[32] applied this constraint and pointed out that if σ, as they believe, is of the order of 1 yr, then τ must be <3 yr. Conversely, if the τ_l are indeed 13 yr, σ_l must be >4 yr (ref. 31 and G. Backus personal communication). Available data should allow a discrimination between $\sigma_l \leq 1$ yr and $\sigma_l \geq 4$ yr.

Using their preferred values of σ and the dominating spherical harmonic order $l=2$ of Malin and Hodder[17], together with Backus's[31] formalism, Courtillot *et al.*[32] pointed out that electrical conductivity must be $<300\ \Omega^{-1}\ \mathrm{m}^{-1}$ in 97% of the volume of the mantle. A precise determination of mantle filter coefficients will be required before any firmer statement can be made. The complex behaviour of the post-1970 solar magnetic effects (see ref. 27) and the poor geographical distribution of magnetic observatories may render a precise determination difficult.

Variations of westward drift rate

It has been known since the time of Halley (1692) that a significant part of the secular variation field can be accounted for by a westward rotation of the main field about the rotation axis of the Earth, known as westward drift (see ref. 33). Courtillot *et al.*[6] and Ducruix *et al.*[27] proposed that the 1969 impulse could be partly due to an enhancement of westward drift. Following Bullard *et al.*[33] and others, Le Mouël *et al.*[34] estimated the westward drift rate w by maximizing the contribution of the term $w\cdot\partial\mathbf{B}/\partial\phi$ (where ϕ is longitude) to secular variation $\dot{\mathbf{B}} = \partial\mathbf{B}/\partial t$. This estimate is:

$$w = \iint_S \dot{\mathbf{B}}\cdot\partial\mathbf{B}/\partial\phi\ \mathrm{d}S \Big/ \iint_S (\partial\mathbf{B}/\partial\phi)^2\ \mathrm{d}S$$

where the integrals are extended over the entire surface S of the Earth. Estimates can be made either directly from observatory data or spherical harmonic models of the fields **B** and $\dot{\mathbf{B}}$. In the last case, one can use the whole field or a single component[34]. Although results obtained with spherical harmonics were inaccurate and oversmoothed in time, they revealed a consistent pattern of decreasing westward drift from 1955 until 1970–75, increasing since then. Results were clearer with the raw observatory data, where the w variation displayed the characteristic V shape of the original recordings, with a minimum around 1970. The analysis was pushed further by Gire *et al.*[35] who used Hodder's[36] secular variation coefficients (Fig. 4). Gire *et al.* computed the energy spectrum of the geomagnetic field at the Earth's surface and noted that, regardless of the component being used to estimate w, the major contribution to this estimate came from multipoles with degree <4. The dominant contribution was found to come from the quadrupolar term P_2^2, as already discussed, for instance, by Yukutake[37], and to a lesser extent from P_2^1. Gire *et al.* further noted that estimates of w based respectively on Y, B, Z and X were always in the order $w_Y > w_B > w_Z > w_X$. They suggested, based on numerical experiments on existing field and secular variation models, that all these estimates were smaller than the actual w and that Y provided the best estimate. Errors on w_Y estimates in the numerical experiments were of the order of 20%.

The results (Fig. 4) confirm the regular decrease in w from 1950 to 1970, already pointed out by Harwood and Malin[25]. The decrease started around 1913 as shown by Hodder[36], and Gire *et al.*[18]. The increase that started in 1970 has now brought the westward drift rate back to its 1950 value.

Motions in fluid core

Secular variation and, in particular, westward drift may provide information on fluid core motions. To extract that information, *a priori* knowledge of the electrical conductivity of the core material is required. This conductivity is estimated to be of the order of 10^5–$10^6\ \Omega^{-1}\ \mathrm{m}^{-1}$ (see ref. 38), that is $\sim 10^3$–10^4 times larger than the estimated conductivity of the lower mantle. On the decade time scale, which is typical of secular variation, the core material is actually often considered to be a perfect conductor. Voorhies and Benton[39] have recently shown with MAGSAT data that this is an excellent approximation. In that case, the secular variation observed outside the core depends only on the motion **U** at the core-mantle boundary[40] (CMB), more precisely at the surface of the main stream of the upper core just below a transparent boundary layer[41]. Under this so-called frozen-flux approximation[41,42], the lines of force of the magnetic field are advected by motions at the surface of the main stream of the core. Many authors propose that the geomagnetic westward drift is due to the drift of the outer core layers with respect to the mantle. It is then tempting to associate secular variation impulses with corresponding impulses in the drift rate of the outer core. Another suggestion put forward by Hide[43–46] is that westward drift could be due to magnetohydrodynamic waves in the liquid core.

The horizontal velocity field at the CMB can be written as a sum of toroidal terms and of poloidal terms which characterize upwelling, that is exchange of material with the deeper regions of the core. The first toroidal term $t_1^0\theta_1^0$ characterizes the body rotation part of westward drift. The equation which relates **B**, $\dot{\mathbf{B}}$ and **U** is:

$$\dot{B}_r = -\mathrm{div}_S(B_r\mathbf{U}) \qquad (1)$$

where div_S is the surface divergence operator $(\nabla - \mathbf{r}(\mathbf{r}\cdot\nabla))$. Since the relative change in **B** is comparatively small in the time interval of decades considered here, we might indeed expect that secular impulses in $\dot{\mathbf{B}}$ be related to similar accelerations of **U**. To continue B_r and $\dot{B}_r$ downward from the surface of the Earth to the CMB, one often assumes that the mantle is a perfect insulator. Although this is clearly not the case, the mantle conductivity is sufficiently weak not to distort the core field significantly. Benton *et al.*[47,48] and Whaler and Gubbins[49,50] have continued B_r and $\dot{B}_r$ to the CMB under the assumption of an insulating mantle. Benton and Whaler[51] investigated the effects of the weakly-conducting mantle using a perturbation procedure and found that, at present, the errors in the core fields due to uncertainties in the higher-order terms of the surface field models are larger than the perturbations due to finite conductivity. Backus (ref. 31 and personal communication) has shown that, provided the delay time τ_l is about the same for individual modes, downward continued maps of B_r and $\dot{B}_r$ at the CMB actually describe the field there as it was τ_l yr before the time when geomagnetic variations occurred at the Earth surface.

Backus[42] showed that the determination of **U** from **B** is an ill-posed problem and that if one solution can be found, an infinity of other solutions can be built from it. However, several authors have recently attempted to use the rather simple and well-organized pattern of secular variation to estimate **U** using additional restricting assumptions.

Whaler[52] used equation (1) only at extrema of B_r on the CMB. She noted that if the upper core is stably stratified, that is, if there is no poloidal component in $\mathbf{U}(\mathrm{div}_S\mathbf{U} = 0)$, then these extrema must be points at which $\dot{B}_r$ is zero. Using the 1965.0 IGRF model ($N = 8$), Whaler noted that ($\dot{B}_r = 0$) contours pass remarkably close to extrema of B_r. She used a statistical argument to suggest that this observation is significant, implying a stably stratified layer at the top of the core. In more recent work, Whaler uses linear inverse theory in an attempt to estimate integrals of $\dot{B}_r$ inside spherical caps bounded by (B_r = constant) contours (ref. 53 and personal communication). With 318 data points from well-distributed long running permanent observatories, she finds that the error due to imperfect resolution far exceeds that due to mapping of the original data into the solutions and that a considerably larger data set would be needed to decide whether the core velocity field is purely toroidal. This conclusion is independantly sustained by work done by Benton *et al.*[48]. These authors show that the shape of null-flux curves ($B_r = 0$ contours) and the number and locations of critical points of B_r are a sensitive function of the truncation level of the spherical harmonic expansion.

Madden and Le Mouël[54] and Gire *et al.*[35] also expanded $\dot{B}_r$ in spherical harmonics at the CMB under the assumption of an insulating mantle and derive (from equation (1)) the linear equations which relate observations **b** (the vector of coefficients of the $\dot{B}_r$ spherical harmonic expansion) to the unknowns **u** (the vector of coefficients of the **U** expansion in elementary poloidal and toroidal harmonics modes):

$$\mathbf{D}\cdot\mathbf{u} = \mathbf{b} \qquad (2)$$

Alternatively, the data can be values of secular variation components at several observatories (140 in Madden and Le Mouël[54] analysis). Gire *et al.*[35] use both a generalized inverse approach[55,56] and a stochastic inverse approach[57] to solve equation (2). To reduce the fundamental non-uniqueness in the problem, both Madden and Le Mouël[54] and Gire *et al.*[54] restrict **U** to be a simple regular motion by damping the higher degree terms of the truncated expansion.

Gire *et al.*[35] concluded that the t_1^0 estimate is stable (stability being defined mathematically) and clearly dominates other terms. The estimate of the drift rate of the outer core layers is of the same order as values computed from observations of geomagnetic westward drift made at the Earth's surface. Estimates for t_1^0 in 1980 are between 0.15 and 0.20° yr^{-1} and are systematically higher than estimates in 1970 (between 0.05 and 0.10° yr^{-1}): this acceleration is thought to be linked with the 1969 impulse. This result had not been obtained in the earlier analysis of Madden and Le Mouël[54]. More recently, Gire *et al.* (personal communication) have extended the discussion to higher-order terms, and found that no term of degree higher than four is stable. Gire *et al.* constructed poloidal and toroidal motion models from these stable terms (Fig. 5) and found that between 1970 and 1980 the shape of the toroidal motion (clearly dominated by westward drift) does not change much but that its intensity increases by 70%. In contrast, the geometry of poloidal motions is different. The motion, which had slowed down in 1970, had returned to a stronger, more energetic state

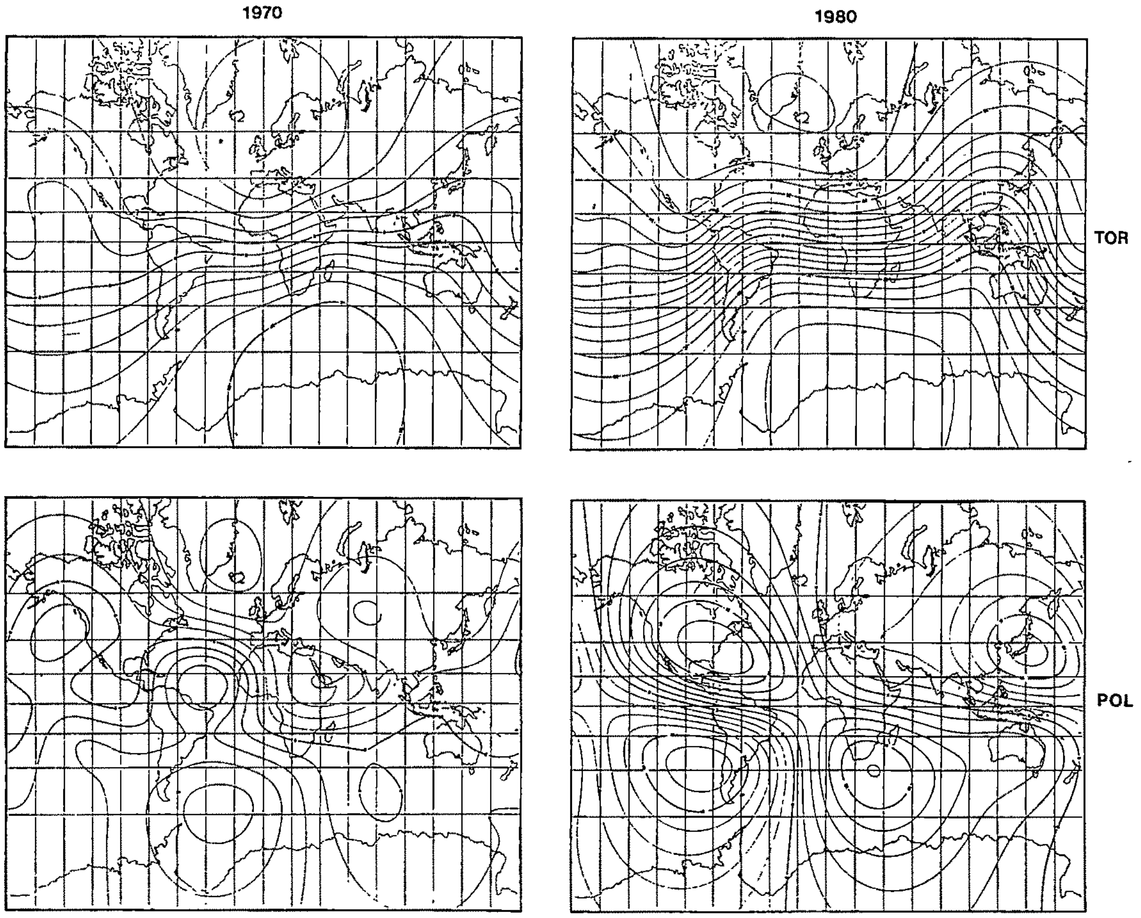

Fig. 6 Stable toroidal and poloidal motion models of Gire *et al.* (personal communication) for 1970 and 1980.

in 1980, the energy input probably being related to the 1969 impulse. Gire *et al.* are able to generate the observed secular variation field from either a purely poloidal or a purely toroidal motion, but this requires harmonics with considerably higher degree and much more energy than the low degree stable composite (toroidal + poloidal) motion. Whaler (personal communication) did not find an acceptable purely toroidal velocity field that would satisfy the surface geomagnetic secular variation data. Velocity fields which satisfied the original data to within their errors had considerable short-wavelength motion that could not possibly be resolved by the data. They were also unstable in the sense that small changes in the misfit between data and model produced very different velocity models.

Thus, parallel studies of recent geomagnetic secular variation suggest that the upper core is not stably stratified and that fluid upwelling exists at the CMB. Even if one is not yet ready to accept the velocity models of Fig. 5 as having actually something to do with real motions, these motions can still be considered as (in a way) the simplest phenomenological representation of the secular variation field.

Rotation of Earth

An up-to-date discussion of the Earth's rotation, in particular of its irregularities, has recently been given by Lambeck[58] (see also ref. 59). Hide[44] summarizes aspects of the problem that are relevant to atmosphere-mantle and core-mantle coupling. Small irregular changes in the rotation rate (or corresponding length of day, l.o.d.) can be attributed in part to atmospheric circulation: Hide *et al.*[60] and Barnes *et al.*[61] have shown that observed short-term changes in l.o.d. (with a period less than a few months and perhaps up to 1 yr) can be fully accounted for on the basis of angular momentum exchange of the mantle and atmosphere. On the other hand, the observed changes in l.o.d. of up to 5 ms on the decade time scale[62] cannot be associated with atmosphere-mantle coupling[58]. There is a general consensus that these variations originate in the Earth's core in relation to geomagnetic field generation and electromagnetic or mechanical core-mantle coupling. Hide[44] reviews the magnitudes of three kinds of horizontal stresses that couple the core to the mantle finding that viscous coupling is almost certainly inadequate. Electromagnetic coupling is sufficient (provided available estimates of relative electrical conductivities and field intensities are correct), although topographic coupling due to bumps on the core-mantle interface of about 1 km in height may be important[45,46]. Therefore, we may expect to find a correlation between geomagnetic indicators and changes in l.o.d. in the decade period range which is typical of secular variation. Vestine[7] was probably the first to give evidence that such a correlation might exist.

The discovery of the 1969 geomagnetic impulse has revived this topic. Courtillot *et al.*[6] noted a striking proximity between periods of intense secular acceleration changes, particularly impulses, and extrema in the l.o.d. variations. Le Mouël *et al.*[63] compared the secular variation of D in Europe and l.o.d. (with a sign error in their figure, see ref. 64) over the past 120 yr, and found a good correlation, with l.o.d. variations lagging geomagnetic variations by 10–15 yrs (Fig. 6). Le Mouël *et al.*[63] have suggested that secular variation impulses near 1900 (?), 1913, and 1969 should be linked with extrema of the l.o.d. curve near 1910, 1930 and 1980 (?): increased (decreased) westward drift is followed by increased (decreased) rotational velocity of the Earth. This correlation is the opposite of that proposed by Vestine[7], Runcorn (ref. 65 and personal communication) and more recently by Backus[31]. Backus has pointed out that Morrison's[62] l.o.d. data indicate that the angular position of the mantle suffered an impulse of order 3 in 1956 and suggested that both this event and the 1969 geomagnetic impulse may be caused by an impulse in westward drift: in that case, the magnetic effects would lag the rotational effects by some 13 yr, an increase in westward drift following a decrease in rotational velocity.

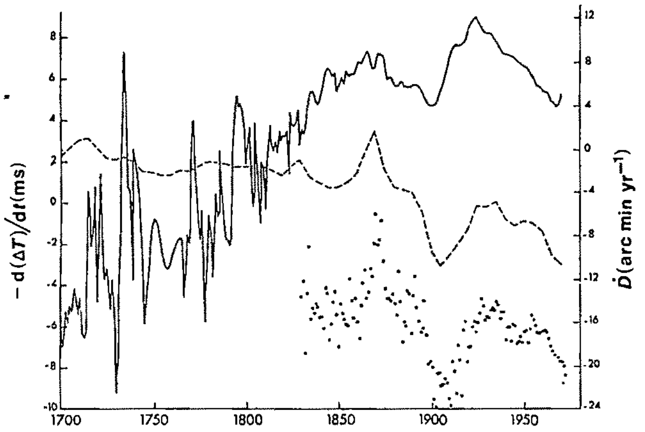

Fig. 6 Plot of the secular variation of declination $\dot{D}$ at Chambon La Forêt (solid curve) and of the excess length of day $-d(\Delta T)/dt$ (ref 62) (dashed curve) for the period 1700-1972 (see refs 63, 64 for the sign correction which is included here). Dots are annual means of excess l.o.d. from which the smooth dashed curve is derived[62]. For clarity they are displaced by 5 ms.

One way to assess the correlation is to investigate whether it extends back in the past. As already pointed out, the number of available observatories before 1900 is limited, but a preliminary analysis of the 1700-1870 period (ref. 63 and J.L. Le M. *et al.*, in preparation) seems to indicate that this was a time with no dramatic geomagnetic changes, no large accelerations of westward drift, and also no large changes in the acceleration of the Earth's rotation (Fig. 6). It may then be tentatively suggested that the correlation still holds qualitatively and that the eighteenth and nineteenth centuries were times when the core regime was more stable than in the present century.

Models of core–mantle coupling

Simple models of mechanical and electromagnetic core-mantle coupling can be constructed in an attempt to account roughly for the magnitude of l.o.d. and westward drift variations and for the correlation which is assumed to link the two. If one accepts the correlation which is suggested by Backus and Vestine, the fact that changes in westward drift rate follow l.o.d. changes and are of the same sign can be understood if one assumes convective mass exchange between a thin rigid shell, forming the top of the core, and the rest of the liquid core below it (called here a three-layer model). This model is similar to that originally proposed by Bullard[66] and later extended by Rochester[67]. The radial mass exchange exerts a torque on the outer core and (in the case of 1956 l.o.d. event studied by Backus) decelerates it. Electromagnetic coupling at the CMB in turn decelerates the mantle. The changes in rotational velocity of the mantle would immediately show as l.o.d. changes (a second-order impulse in mantle angular velocity in 1956), and be followed by geomagnetic changes, observed with a 13-yr mean delay due to diffusion of westward drift related signals through a rather strongly conducting mantle[31].

If, on the other hand, one follows the correlation suggested by Le Mouël *et al.*[63], one has to account for the discrepancy between the short time scale over which the geomagnetic impulse is established (1 yr) and the long delay after which the rotation of the mantle is altered (10-15 yr). We have also used a three-layer model[68], in which an impulsive torque (P) related to core convection is applied to the top core layer and a torque ($-P$) to the rest of the liquid core. When the torques exerted by Lorentz forces on the three part of this electromagnetic system are computed, a linear differential system for the rotations of the mantle and of the top and rest of the liquid core results. We[68] found that the solutions of this system depend exponentially on two time constants, one always short (<1 yr) and the other proportional to the ratio σ_c/σ_m of the core versus mantle conductivity. If this time constant can be identified with the 10-15 yr delay in changes of l.o.d., σ_c/σ_m is found to range from 500 to 1,000, in agreement with conductivity estimates discussed above. For (P) a first-order impulse (that is a step function), the l.o.d. suffers a second-order impulse, and the ratio $(\delta\omega_m)/(\delta\omega_0)$ of asymptotic amplitudes of rotational changes in the mantle and outer core layer following the impulse is found to depend only, in a first-order approximation, on the ratio of the outer core layer thickness h to the total core radius r_c. We found h to be of the order of 150 km. The radial velocity of fluid exchange between the outer and inner parts of the external core was found to be $\sim 10^{-6}$ ms^{-1}. Although this model provides a reasonable account for observations discussed by Le Mouël *et al.*[63], it is limited in that it does not include a quantitative treatment of magnetic field transport, particularly from the outer-inner core interface to the CMB. Thus, both an improved assessment of the l.o.d./geomagnetic correlation and more complete models of electromagnetic core-mantle coupling are required.

Runcorn (ref. 65 and personal communication) argues that irregular changes in l.o.d. may even be shorter than the present smoothing of the astronomical data indicates. If such impulsive torques indeed act on the mantle to provide changes in l.o.d., Runcorn points out that equatorial components of these torques may exist and excite the Chandler wobble. He proposes that such an impulse occurring in mid-1967 in the Chandler wobble supports this idea. It is not clear whether this event can be causally related to the 1969 geomagnetic impulse. On the other hand, Barnes *et al.*[61] showed that meteorological phenomena provide an important contribution to the excitation of polar motion.

Both Runcorn (personal communication) and Backus (ref. 69 and personal communication) note that the magnetic variations related to the 1969 impulse should be accompanied by a second-order impulse in the tangential component of the electric field on the ocean bottom, with an amplitude of the order of 10^{-8} Vm^{-1} yr^{-1}. Runcorn and colleagues (personal communication) have observed the occurrence in 1969 of step-like increases of d.c. potentials on long telegraph cables in the southwestern Pacific. These might arise from leakage currents associated with the core magnetic field and might be related to the geomagnetic impulse (Runcorn *et al.* in preparation).

Conclusion and perspectives

The reality of short-term (quasi-discontinuous) changes in the rate of internal geomagnetic secular variation has been confirmed by observational evidence in the past few years. The last worldwide impulse occurred in 1969 and may have been preceded by an event in 1913. The duration (of the order of 1 yr), intensity and geographical pattern of these impulses constrain values of deep mantle conductivity and the pattern of flow in the upper part of the fluid core. We suggest a correlation of geomagnetic westward drift and the l.o.d.; this correlation is still debated but would place important constraints on mechanisms of core-mantle coupling. It has also been proposed[70] that decade fluctuations of climate and l.o.d. are both correlated with geomagnetic changes, thus raising the possibility of a long-term influence of core motions on some climatic trends. In this process, angular momentum would be transferred from the core to the mantle and to the atmosphere.

Theoretical work[31] indicates the need for further observational work on both recognized impulses and earlier (seventeenth to nineteenth century) events, although the data base is scarce. Present data favour the existence of upwelling in the fluid upper core. Secular variation models which involve impulsive events separated by quiet phases are simpler, both in space and time, than previously expected and yet account for much of the energy of observed secular variation.

Progress on dynamo theory in coming years might be expected to come from detailed observational advances of two basic features of the geomagnetic field: impulses and reversals. The frozen-flux approximation, which is valid for impulses, might be extended to the 1,000-yr time scale which characterizes reversals. Much progress has been made on the description of individual reversals (see refs 71-73) and on the frequency of reversals (see refs 74, 75). The interests and frequency bands of specialists of geomagnetism and palaeomagnetism are converging in this endeavour.

This paper reviews published work on geomagnetic impulses and contributions to a meeting held on 27 September 1983 at the Institut de Physique du Globe in Paris on the occasion of the centenary of the French National Magnetic Observatory. Our review has greatly benefited from oral presentations made at the meeting, and from written communications sent after the meeting by G. Backus, R. Hide, W. Lowrie, T. Madden, S. Malin, K. Runcorn and K. Whaler. The meeting and paper are dedicated to the observers in magnetic observatories whose painstaking and often ill-recognized efforts in gathering data are essential for the kind of work described here. IPGP contribution NS793.

Note added in proof: M. McLeod (personal communication) has completed a detailed response to Alldredge's criticism[17] which fully vindicates our analyses[6,13] and those of Malin *et al.*[14,17]. The following conclusions from McLeod's work are worth noting: (1) The 1969 impulse is clearly real and of internal origin. The external coefficients of the s.h. expansion[17] appear to represent noise due to external currents unrelated to the impulse. Better estimates of internal s.h.c. are obtained. (2) The 1969 impulse can be as short as 1 yr in duration and its date of occurrence is found to be 1969.5.

1. Currie, R. G. *J. geophys. Res.* **71**, 4579-4598 (1966).
2. Currie, R. G. *Astrophys. Space Sci.* **21**, 425-438 (1973).
3. Alldredge, L. R. *J. Geomagn. Geoelectr.* **29**, 123-135 (1977).
4. Yukutake, T. *J. Geomagn. Geoelectr.* **17**, 287-309 (1965).
5. Courtillot, V. & Le Mouël, J. L. *J. geophys. Res.* **81**, 2941-2950 (1976).
6. Courtillot, V., Ducruix, J. & Le Mouël, J. L. *C. r. hebd. Séanc. Acad. Sci., Paris* **D287**, 1095-1098 (1978).
7. Vestine, E. H. *Proc. natn. Acad. Sci. U.S.A.* **38**, 1030-1038 (1952).
8. Walker, J. B. & O'Dea, P. L. *EOS* **33**, 797-800 (1952).
9. Runcorn, S. K. *EOS* **36**, 191-198 (1955).
10. McDonald, K. L. *J. geophys. Res.* **62**, 117-141 (1957).
11. Alldredge, L. R. *J. geophys. Res.* **80**, 1571-1578 (1975).
12. Alldredge, L. R. *C. r. hebd. Séanc. Acad. Sci., Paris* **B289**, 169-172 (1979); *J. geophys. Res.* **89**, 4403-4412 (1984).
13. Courtillot, V., Ducruix, J. & Le Mouël, J. L. *C. r. hebd. Séanc. Acad. Sci., Paris* **B289**, 173-175 (1979).
14. Malin, S. R. C., Hodder, B. M. & Barraclough, D. R. in *75th Anniversary Volume of Ebro Observatory*, (ed. Cardus, J. O.) (Tarragona, in the press).
15. Duyen Chau, Ducruix, J. & Le Mouël, J. L. *C. r. hebd. Séanc. Acad. Sci., Paris* **B293**, 157-160 (1981).
16. Le Mouël, J. L., Ducruix, J. & Duyen, C. *Phys. Earth planet. Inter.* **28**, 337-350 (1982).
17. Malin, S. R. C. & Hodder, B. M. *Nature* **296**, 726-728 (1982).
18. Gire, C., Le Mouël, J. L. & Ducruix, J. *Nature* **307**, 349-352 (1983).
19. Ducruix, J., Gire, C. & Le Mouël, J. L. *C. r. hebd. Séanc. Acad. Sci., Paris* **B296**, 1419-1424 (1983).
20. Malin, S. R. C. & Bullard, E. C. *Phil. Trans. R. Soc.* **A299**, 357-423 (1981).
21. Hodder, B. *Geophys. J. R. astr. Soc.* **65**, 763-776 (1981).
22. Lahiri, B. N. & Price, A. T. *Phil. Trans. R. Soc.* **237**, 509-540 (1939).
23. Alldredge, L. R. *J. geophys. Res.* **81**, 2990-2996 (1976).
24. Alldredge, L. R. *J. geophys. Res.* **82**, 5427-5431 (1977).
25. Harwood, J. M. & Malin, S. R. C. *Nature* **259**, 469-471 (1976).
26. Courtillot, V. & Le Mouël, J. L. *J. geophys. Res.* **84**, 4785-4790 (1979).
27. Ducruix, J., Courtillot, V. & Le Mouël, J. L. *Geophys. J. R. astr. Soc.* **61**, 73-94 (1980).
28. Achache, J., Le Mouël, J. L. & Courtillot, V. *Geophys. J. R. astr. Soc.* **65**, 579-601 (1981).
29. Courtillot, V., Ducruix, J., Le Mouël, J. L. & Achache, J. in *Mechanisms of Continental Drift and Plate Tectonics*, (eds Davies, P. A. & Runcorn, S. K.) 317-326, (Academic, New York, 1980).
30. Achache, J., Courtillot, V., Ducruix, J. & Le Mouël, J. L. *Phys. Earth planet. Inter.* **23**, 72-75 (1980).
31. Backus, G. *Geophys. J. R. astr. Soc.* **74**, 713-746 (1983).
32. Courtillot, V., Le Mouël, J. L. & Ducruix, J. *Geophys. J. R. astr. Soc.* **78**, 619-625 (1984).
33. Bullard, E. C., Freedman, C. F., Gellman, H. & Nixon, J. *Phil. Trans. R. Soc.* **A243**, 67-92 (1950).
34. Le Mouël, J. L., Ducruix, J. & Duyen, C. *Geophys. Res. Lett.* **10**, 369-372 (1983).
35. Gire, C., Le Mouël, J. L. & Madden, T. *Annls Geophys.* **2**, 37-46 (1984).
36. Hodder, B. *Nature* **306**, 136-137 (1983).
37. Yukutake, T. *J. Geomagn. Geoelectr.* **25**, 195-212; 231-235 (1973).
38. Jeanloz, R. *Scient. Am.* **249**, 40-49 (1983).
39. Voorhies, C. V. & Benton, E. R. *Geophys. Res. Lett.* **9**, 258-261 (1982).
40. Bondi, H. & Gold, T. *Mon. Not. R. astr. Soc.* **110**, 607-611 (1950).
41. Roberts, P. H. & Scott, S. *J. Geomagn. Geoelectr.* **17**, 137-151 (1965).
42. Backus, G. *Phil. Trans. R. Soc.* **A263**, 239-266 (1968).
43. Hide, R. & Stewartson, K. *Rev. Geophys. Space Phys.* **10**, 579-598 (1972).
44. Hide, R. *Phil. Trans. R. Soc.* **A299**, 233-234 (1982); *IUGG Chronicle*, (ed. Melchior, P.) (in the press).
45. Malin, S. R. C. & Hide, R. *Phil. Trans. R. Soc.* **A299**, 281-287 (1982).
46. Hide, R. *Q. Jl. R. Soc.* **96**, 579 (1970).
47. Benton, R. E., Muth, L. A. & Stix, M. *J. Geomagn, Geoelectr.* **32**, 615-626 (1979).
48. Benton, E. R., Estes, R. H., Langel, R. A. & Muth, L. A. *Geophys. Res. Lett.* **9**, 254-257 (1982).
49. Whaler, K. A. *Phil. Trans. R. Soc.* **A306**, 235-246 (1982).
50. Gubbins, D. *Phil. Trans. R. Soc.* **A306**, 247-254 (1982); *Geophys. J. R. astr. Soc.* **77**, 753-766 (1984).
51. Benton, E. R. & Whaler, K. A. *Geophys. J. R. astr. Soc.* **75**, 77-100 (1983).
52. Whaler, K. A. *Nature* **287**, 528-530 (1980).
53. Whaler, K. A. *Geophys. J. R. astr. Soc.* **78**, 453-474 (1984).
54. Madden, T. & Le Mouël, J. L. *Phil. Trans. R. Soc.* **A306**, 271-280 (1982).
55. Backus, G. & Gilbert, F. *Geophys. J. R. astr. Soc.* **16**, 169-205 (1968); *Phil. Trans. R. Soc.* **A266**, 123-192 (1970); *Geophys. J. R. astr. Soc.* **13**, 247-276 (1967).
56. Jackson, D. D. *Geophys. J. R. astr. Soc.* **28**, 97-110 (1972).
57. Jackson, D. D. *Geophys. J. R. astr. Soc.* **57**, 137-157 (1979).
58. Lambeck, K. *The Earth's Variable Rotation: Geophysical Causes and Consequences* (Cambridge University Press, New York, 1980).
59. Cazenave, A. thesis, Univ. Toulouse (1975).
60. Hide, R., Birch, N. T., Morrison, L. V., Shea, D. & White, A. A. *Nature* **286**, 114-117 (1980).
61. Barnes, R. T. H., Hide, R., White, A. A. & Wilson, C. A. *Proc. R. Soc.* **A387**, 31-73 (1983).
62. Morrison, L. V. *Geophys. J. R. astr. Soc.* **58**, 349-360 (1979).
63. Le Mouël, J. L., Madden, T. R., Ducruix, J. & Courtillot, V. *Nature* **290**, 763-765 (1981).
64. Courtillot, V., Le Mouël, J. L., Ducruix, J. & Cazenave, A. *Nature* **303**, 638 (1983).
65. Runcorn, S. K. *Phil. Trans R. Soc.* **306**, 261-270 (1982).
66. Bullard, E. C. *Mon. Not. R. astr. Soc., Geophys. Suppl.* **5**, 248-257 (1948).
67. Rochester, M. G. *Phil. Trans. R. Soc.* **252**, 531-555 (1960); *J. geophys. Res.* **17**, 4833-4836 (1962).
68. Le Mouël, J. L. & Courtillot, V. *Phys. Earth planet. Inter.* **24**, 236-241 (1981); *J. geophys. Res.* **87**, 4103-4108 (1982).
69. Backus, G. *Phys. Earth planet. Inter.* **28**, 191-214 (1982).
70. Courtillot, V., Le Mouël, J. L., Ducruix, J. & Cazenave, A. *Nature* **297**, 386-387 (1982).
71. Hoffman, K. *Rev. Geophys. Space Phys.* **21**, 614-620 (1983).
72. Valet, J. P., Laj, C. & Langereis, C. G. *Nature* **304**, 330-332 (1983).
73. Prévôt, M., Mankinen, E. A., Grommé, C. S. & Coe, R. S. *EOS* **63**, 921 (1982).
74. Lowrie, W. & Kent, D. V. *Earth planet. Sci. Lett.* **62**, 305-313 (1983).
75. Mazaud, A., Laj, C., de Sèze, L. & Verosub, K. L. *Nature* **304**, 328-330 (1983).

ARTICLES

Cell type-specific activation of actin genes in the early amphibian embryo

T. J. Mohun, S. Brennan, N. Dathan, S. Fairman & J. B. Gurdon

CRC Molecular Embryology Research Group, Department of Zoology, University of Cambridge, Downing Street, Cambridge CB2 3EJ, UK

Muscle actin genes are the earliest yet described to show cell type-specific activation in amphibian embryos. Gene-specific probes show that α-skeletal and α-cardiac actin genes start to be transcribed simultaneously at the end of gastrulation, but only in those regions of the mesoderm that subsequently form embryonic muscle. Their expression provides a molecular marker for early cell determination.

WITHIN a day of egg fertilization, most animal embryos comprise many morphologically distinct tissues and organ primordia, the arrangement of which remains essentially unchanged throughout all subsequent development[1]. In each region of the embryo, cells initiate distinct programmes of gene expression as they embark on diverse pathways of differentiation, the basic body plan of the embryo being laid down from the earliest times. As yet, however, almost nothing is known of the molecular mechanisms that underlie regional differences in cell fate within the early embryo. Classical theories suggest that the spatial pattern of early cell differentiation reflects the distribution of cytoplasmic factors or 'determinants' inherited by the early *a*

amino acid number		1 5		10	
cytoskeletal actin (γ)*		Ala Glu Glu Glu Ile Ala	ALA LEU VAL	Ile	ASP.....
cardiac actin*		Asp Asp Glu Glu Thr Thr	ALA LEU VAL	Cys	ASP.....
		Ala Glu Glu Glu Ile Ala		Ile	
pXlcA1 (Cytoskeletal)	....	GCA GAA GAA GAG ATT GCA	GCG CTC GTC	ATT	GAC.....
		Asp Asp Glu Glu Thr Thr		Cys	
pXlcA2 (Cardiac)	....	GAC GAC GAG GAG ACT ACC	GCC TTG GTG	TGC	GAC.....

amino acid number	265		270		294		356		
cytoskeletal actin (γ)*	....PHE	Leu	GLY MET GLU SER	Cys	GLY....ALA ASN	Thr	VAL ....ILE	Ser	LYS GLN.....
cardiac actin*	....PHE	Ile	GLY MET GLU SER	Ala	GLY....ALA ASN	Asn	VAL ....ILE	Ser	LYS GLN.....
		Leu		Cys		Thr		Ser	
pXlcA1 (Cytoskeletal)	....TTC	CTG	GGT ATG GAA TCC	TGT	GGC....GCC AAC	ACT	GTC ....ATC	AGC	AAG CAA ....
		Ile		Ala		Asn		Ser	
pXlcA2 (Cardiac)	....TTC	ATT	GGT ATG GAA TCT	GCC	GGT....GCC AAT	AAT	GTC ....ATC	AGC	AAA CAA.....
		Ile		Ala		Asn		Thr	
pXlcA3 (Skeletal)	....TTC	ATT	GGC ATG GAA TCT	GCT	GGC....GCC AAC	AAC	GTT ....ATC	ACC	AAG CAA.....

* consensus actin sequence for vertebrates

boxes indicate diagnostic amino acids

b

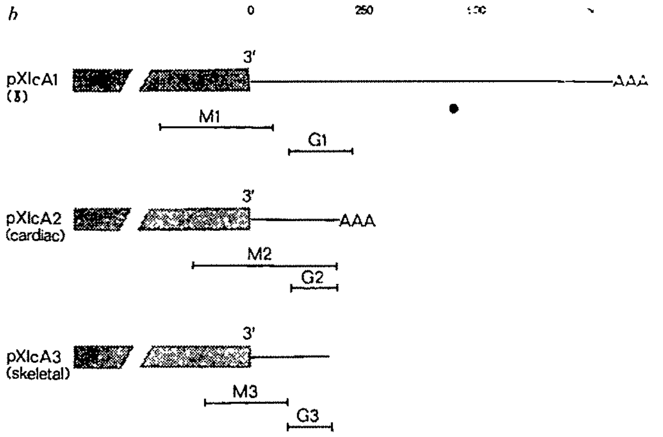

Fig. 1 Identification of *Xenopus* actin cDNAs. *a*, Portions of the nucleotide sequence for three *Xenopus* actin cDNAs, pXlcA1, pXlcA2 and pXlcA3, obtained using the dideoxy sequencing procedure[32,33]. These are aligned by comparing their coding capacity with the consensus polypeptide sequence of vertebrate γ-cytoskeletal and α-cardiac actins[9-13]. Amino acids diagnostic for particular actin protein types are boxed. Diagrams of each cDNA are shown in *b*. Amino acid coding regions are indicated by stippling. Subclones used in subsequent experiments are identified; M1, M2 and M3 contain the 3' terminal portions of protein coding sequence and an adjacent region of the untranslated mRNA trailer. These were used for S_1 nuclease protection experiments. G1, G2 and G3 comprise subclones for the mRNA 3'-untranslated region and provided gene-specific hybridization probes in RNA blot experiments.

blastomeres[2], but few of these have been demonstrated in any organism and none has been purified. The nature of determinants and the manner by which they regulate cell differentiation remain central problems for embryologists.

As a prerequisite for a molecular analysis of embryonic cell differentiation we have examined the expression of the actin multi-gene family in the amphibian embryo. It is well established that among vertebrates the several actin proteins are distributed in a tissue-specific manner[3,4]. The cytoskeletal actins are ubiquitous, whereas the sarcomeric actins are found only in muscle cells where they constitute a major component of the contractile apparatus. In amphibians, the morphological differentiation of cells that give rise to embryonic muscle occurs soon after neurulation[5,6] and the onset of muscle actin protein synthesis[7]. We report here that activation of amphibian α-cardiac and α-skeletal actin genes is coordinated at the end of gastrulation. Using mRNA-specific probes derived from *Xenopus laevis* α-cardiac, α-skeletal and γ-cytoskeletal actin cDNAs, we find that activation of both muscle-specific genes is precisely localized to certain regions within the mesoderm. In contrast, cytoskeletal actin gene transcription can be detected throughout the entire embryo.

Characterization of actin cDNAs

cDNA libraries from embryo RNA and adult skeletal muscle RNA were constructed as described elsewhere (T.J.M. *et al.*, in preparation) and screened for actin cDNA sequences using a chick β-actin cDNA[8] as probe. The entire DNA sequence of several positive recombinants was determined to establish the amino acid sequence of the actin that each cDNA encoded. Amongst vertebrates, the two cytoskeletal (designated β and γ) and four sarcomeric actins (α-cardiac, α-skeletal and two smooth muscle types) may be identified by characteristic differences in their polypeptide sequence[9-13]. Using these diagnostic differences, we obtained a tentative identification of three *Xenopus* cDNAs, pXlcA1-3. pXlcA1 codes for a protein identical to the consensus for vertebrate γ-cytoskeletal actins (Fig. 1*a*). Unlike other vertebrates, amphibians possess a variety of cytoskeletal actins that differ from both β-type and γ-type proteins[14]. pXlcA1 encodes the protein previously identified as 'type-8'. pXlcA2 and pXlcA3 match the consensus for muscle-type actins, pXlcA2 coding for α-cardiac actin and pXlcA3 encoding the related α-skeletal actin.

In addition to determining the coding capacity of each cDNA, we have examined the untranslated portions of their sequence (T.J.M. *et al.*, in preparation). We find no homology between any of the three cDNAs in their 3'-untranslated regions; therefore we constructed mRNA-specific hybridization probes for subsequent experiments (Fig. 1*b*).

Tissue-specific expression of actin mRNAs

We next sought the *in vivo* identity of the three actin cDNAs by determining in which adult tissues their equivalent mRNAs could be detected. RNA from a variety of adult frog tissues was hybridized with individual actin mRNA-specific single-stranded DNA probes M1, M2 and M3, derived from the cDNAs pXlcA1-3. Each probe, comprising several hundred nucleotides, includes the carboxy-terminus of the actin protein as well as a portion of the adjacent message-specific 3′-untranslated region subcloned into ml3mp8. Individual actin mRNAs were identified by the size of the S_1 nuclease-resistant fragments obtained (Fig. 2). As expected, the two muscle-type actin transcripts show distinct, tissue-specific patterns of expression consistent with the amino acid sequences they encode. mRNA corresponding to pXlcA2 is found exclusively in heart tissue (Fig. 2*a*), whilst the message-specific probe from pXlcA3 identifies transcripts only in skeletal muscle (Fig. 2*b*). We conclude that the clones pXlcA2 and pXlcA3 comprise α-cardiac and α-skeletal actin cDNAs respectively. The S_1 nuclease assay shows that α-cardiac and α-skeletal actin mRNAs are at least 50 times less abundant (if present at all) in non-muscle tissues. An equivalent survey demonstrates the presence of cytoskeletal actin transcripts complementary to pXlcA1 in all adult tissues examined (data not shown).

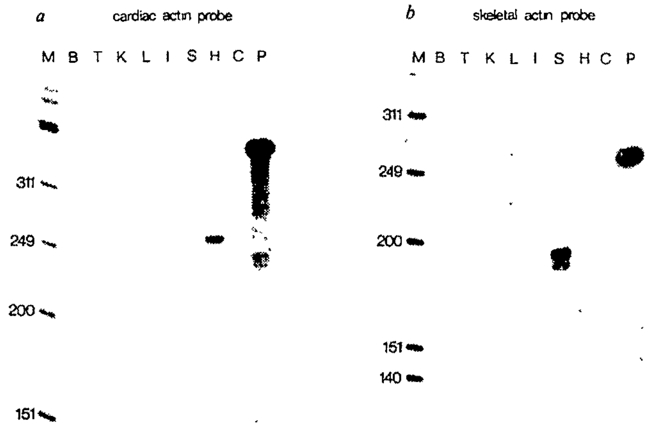

Fig. 2 Tissue-specific expression of actin genes. *a*, 250-nucleotide fragment obtained by protection of the α-cardiac probe M2 by α-cardiac mRNA; *b*, doublet of 185 and 190 nucleotides obtained by protection of the α-skeletal actin cDNA probe M3 by α-skeletal actin mRNA. RNA was prepared from various adult frog tissues and hybridized separately to the two probes M2 and M3 (see Fig. 1). DNA protected from subsequent digestion by S_1 nuclease was analysed by electrophoresis. The source of each RNA sample is indicated. B, brain; T, testes; K, kidney; L, liver; I, intestine; S, leg muscle; H, heart. Lanes 'P' and 'C' are controls using yeast tRNA for the hybridization, before and after S_1 digestion respectively. Size markers were provided by ΦX174 RF DNA digested with *Hin*fI (lane M). Each of the probes M2 and M3 contains 55 nucleotides of M13 sequence which is removed from all DNA/RNA hybrids by S_1 nuclease action. Protected fragments resulting from hybridization of the probes to their corresponding mRNAs are therefore significantly shorter than the input probes. The α-cardiac cDNA pXlcA2 contains an internal polyadenylation signal sequence 91 nucleotides upstream from the poly(A) tail (T.J.M. *et al.*, in preparation); our unpublished experiments indicate that this first polyadenylation signal predominates in transcript processing. Polyadenylation mostly occurs about 15 nucleotides downstream from this first pentanucleotide AAUAA and about 70 nucleotides upstream of the second polyadenylation site. Hence protection of the α-cardiac probe M2 (381 nucleotides) by α-cardiac mRNA yields a 250-nucleotide fragment (*a*). In addition, several fragments approximately 120–130 nucleotides long are protected by α-cardiac actin mRNA (not included in *a*, see Fig. 6). Experiments using end-labelled probes have demonstrated that these result from internal S_1 nuclease cleavage over a region of about five nucleotides in the middle of the actin cDNA portion of probe M2. Protection of the α-skeletal actin cDNA probe M3 (247 nucleotides) by α-skeletal actin mRNA results in a doublet of 185 and 190 nucleotides (*b*), presumably due to minor nibbling at the ends of the 190-base pair DNA/RNA hybrid by S_1 nuclease. RNA was extracted from various adult tissues by homogenization of frozen tissue in 3 M lithium chloride, 6 M urea, 0.5% SDS, 70 mM 2-mercaptoethanol, 10 mM sodium acetate, *p*H 5.0 (ref. 34). After precipitation overnight at 4 °C, the RNA was resuspended in 0.2% SDS, 100 mM sodium acetate, *p*H 5.0, extracted twice with phenol and chloroform and reprecipitated. Single-stranded hybridization probes were prepared using subclones M2 and M3 (see Fig. 1) inserted into the *Sma*I site of M13mp8 (ref. 35). Radioactive probes were excised by digestion with *Eco*RI. For S_1 nuclease protection analysis[36], 2.5 μg of total tissue RNA were hybridized with 100,000 c.p.m. of probe in 20 μl buffer (50% formamide, 1 mM EDTA, 0.4 M NaCl, 10 mM PIPES, *p*H 7.0) at 30 °C (25 °C below T_m for a DNA:DNA hybrid) overnight. Unhybridized material was digested with 100 units of S_1 nuclease (BRL) at 37 °C for 30 min. S_1-resistant DNA was collected by ethanol precipitation and analysed by electrophoresis on 6% acrylamide, 8.3 M urea gels.

Actin gene expression in embryos

In adult frog tissues, sarcomeric and cytoskeletal actin genes show distinct, tissue-specific patterns of regulation. To discover when these differences are first established, we have examined the levels of cytoskeletal, α-cardiac and α-skeletal actin mRNA in RNA extracted from early embryos using RNA blots and S_1 nuclease protection. We detect actin transcripts of three distinct sizes in neurula embryos using a chick β-actin cDNA probe (Fig. 3). To identify each size class and to determine their presence during the course of early development, we have constructed message-specific probes comprising 100–150 nucleotides of the 3′-untranslated sequence from each of the *Xenopus* actin cDNAs (subclones G1, G2 and G3; see Fig. 1). The specificity of each probe was confirmed by genomic Southern blots; each hybridized to a different subset of restriction fragments (data not shown). The three probes were then hybridized individually to nitrocellulose blots of embryonic RNA derived from several stages of early development (Fig. 3).

Our results confirm that *Xenopus* cytoskeletal and α-cardiac actin mRNAs are similar in size to their counterparts in other vertebrates. The cytoskeletal actin transcript of embryos comprises ~2,300 nucleotides whilst the α-cardiac transcript is ~1,600 nucleotides long and co-migrates with its α-skeletal counterpart (data not shown). An intermediate-sized transcript is also detected throughout early development and presumably encodes a further class of cytoskeletal actins. Even in early embryos, the cytoskeletal and muscle-specific actin genes show different patterns of expression. The α-cardiac actin transcripts and their α-skeletal counterparts are absent in the early stages of development, being first detected in neurula embryos. By contrast, a low, constant level of cytoskeletal actin mRNA was detected in all stages before gastrulation. In later stages, the levels of both cytoskeletal and sarcomeric actin mRNAs increase in a similarly dramatic manner.

The time of actin gene activation

Are the actin genes activated specifically during early embryogenesis or do they simply respond to a 'signal' that stimulates embryonic gene transcription in general? We have made careful estimates of the levels of all three actin mRNAs through development and compared their developmental profiles with those of other identified genes. By a quantitative S_1 nuclease protection assay using single-stranded probes radioactively labelled through their entire length, we have obtained a sensitivity 10-fold greater than that provided by RNA blots. We compared the signals derived from each RNA sample with those of a dilution series using tailbud RNA (stage 26), performing each measurement on RNA extracted from individual, staged embryos (see Fig. 4).

Both α-cardiac and α-skeletal actin mRNAs are first detected in stage 14 embryos which have just completed gastrulation, and the two mRNAs increase their subsequent levels in parallel. The observed actin mRNA development profiles diverge from the theoretical curve for a stable gene transcript at this stage, either because of specific activation of the actin genes at the end of gastrulation, or from a similarly timed and equally dramatic change in the kinetics of actin message turnover. From the specific activity of our probes, we believe that a stage 18 (neurula) embryo contains 10^7–10^8 α-cardiac transcripts; this number would be accumulated if the α-cardiac actin gene is single copy and activated in ~5% of cells at stage 13 (activated exclusively in the presumptive somatic mesoderm 1 h before the first transcripts are actually detected). For such a calculation, we assume that stable transcripts are synthesized at a rate of 10

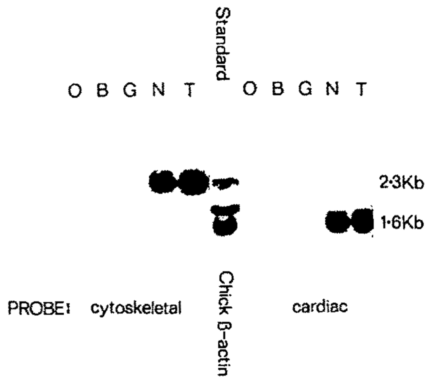

Fig. 3 Actin mRNA accumulation in early embryos. Total RNA was extracted from embryos at successive stages of development as previously described[34], resolved by electrophoresis using formaldehyde-agarose gels[37] and transferred to nitrocellulose[38]. The RNA blots were hybridized individually with mRNA-specific probes (G1 and G2) from the α-cardiac and cytoskeletal actin cDNAs (see Fig. 1 legend). Single-stranded, ^{32}P-labelled probes were synthesized[35] in M13mp8. A further blot containing RNA extracted from a neurula embryo was hybridized with the chick β-actin cDNA probe to serve as a standard that identifies all actin mRNA size classes. The figure is a composite from these experiments, using 10 μg of RNA from fully grown oocytes (O), blastula (B), gastrula (G), neurula (N) and tailbud (T) embryos. Sizes of hybridizing transcripts were estimated by comparison with ribosomal and transfer RNA markers.

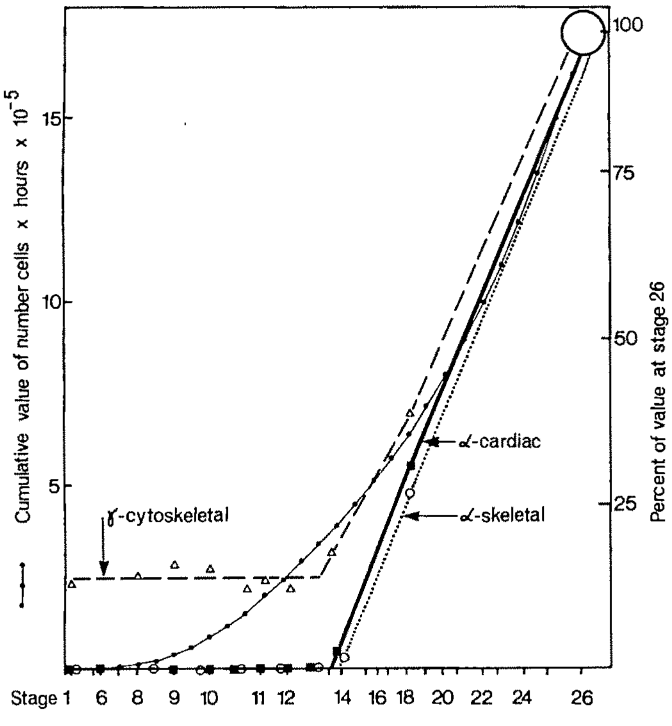

Fig. 4 Temporal changes in actin mRNA content during *Xenopus* development. Relative levels of accumulated actin message were assayed by S_1 nuclease protection as described in Fig. 2 legend, each experiment using the RNA from a single embryo. We confirmed that hydribidization signals increased in a linear fashion with input RNA by including a dilution series of RNA from several embryonic stages. Each point represents the average of several determinations in different experiments. These are plotted as a percentage of the value at stage 26. △- - -△, Cytoskeletal actin mRNA; ■—■, α-cardiac actin mRNA; ○···○, α-skeletal actin mRNA. A theoretical accumulation curve (●—●) (prepared by adding cumulatively the number of nuclei present at each hour of development) has been superimposed for comparison.

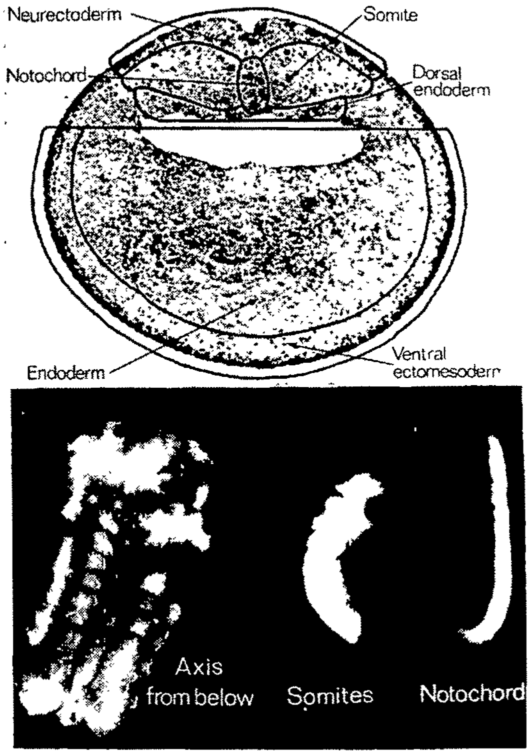

Fig. 5 Dissection of a stage 18 neurula embryo. A transverse section of a stage 18 neurula embryo (1.2 mm diameter) indicating the six fragments that were obtained by dissection, several of which are in the lower figure. After removal of endoderm, ventral ectomesoderm and dorsal endoderm, the remaining fragment (axis) is readily separated into somites, notochord and neurectoderm.

per gene per min[15]. Other genes active in early embryos commence transcription at varying times before muscle actin transcripts are first detected, irrespective of which RNA polymerase is involved[15-18]. Similarly, muscle actin gene activation occurs several hours after the levels of both newly synthesized and accumulated cytoplasmic poly(A)$^+$ RNA begin to increase[19]. We conclude that the sarcomeric actin genes are activated at stage 13, independently of any other gene so far identified.

The relatively constant level of the 2.3-kilobase (kb) cytoskeletal actin mRNA detected in all stages before gastrulation could result from *de novo* gene transcription or the inheritance of maternally derived message (or indeed a combination of both). Certainly by neurula stage, any pool of inherited cytoskeletal transcripts is supplemented by newly synthesized mRNA.

Regional actin gene expression

By the early neurula (stage 14), *Xenopus* embryos show morphological differentiation, possessing endoderm, mesoderm and ectoderm germ layers. The future anterior–posterior axis of the embryo is evident from the polarity of the elevated neural plate, formed by dorsal ectoderm; beneath it lies the notochord (the embryonic 'backbone') which segregates as a mid-dorsal strip from the mesoderm layer. On either side of the notochord, the thickened, dorsal regions of mesoderm largely comprise the precursors of embryonic muscle (the somites)[20]. We dissected neurula embryos (neural folds complete; stage 18) into six different pieces (Fig. 5) and used the RNA from each in the S_1 nuclease protection assay. All the pieces contain cytoskeletal actin mRNA in approximate proportion to their tissue mass (data not shown); α-cardiac and α-skeletal actin mRNA distribution is shown in Fig. 6. Strikingly, the sarcomeric actin transcripts are restricted almost exclusively to the somite region of the mesoderm and are completely absent from an equivalent amount of the adjacent notochord tissue. A minor signal is detected in the ventral ectomesoderm, possibly arising from the

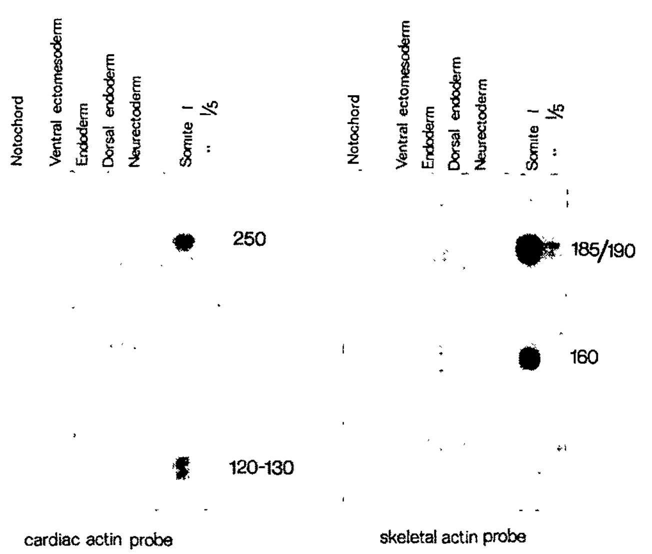

Fig. 6 Region-specific accumulation of muscle actin mRNAs. The six different embryo fragments (Fig. 5) were assayed for the presence of actin mRNAs by the S_1 nuclease protection procedure. α-Cardiac actin mRNA is detected by the presence of protected fragments 250 and 120–130 nucleotides long. α-Skeletal actin mRNA gives a major doublet 185 and 190 nucleotides long (see Fig. 2 legend), and a minor protected fragment about 160 nucleotides in length. This fragment results from partial cleavage of the probe M3 at an A+T-rich region (18 out of 20 bases are A or T). Cleavage in this region is variable, giving a prominent signal in this experiment but a very minor one in others (for example, Fig. 2*b*).

mesodermal component of this fragment which subsequently gives rise to the embryonic heart.

Muscle-gene activation is thus restricted to the mesoderm cell layer in early embryos. Furthermore, within the mesoderm the expression of these genes is precisely regionalized, because the most dorsal portion, the notochord, contains neither α-cardiac nor α-skeletal actin mRNA. We conclude that sarcomeric actin gene activity is restricted to the embryonic tissue from which muscle cells are later derived. Muscle actin mRNA accumulation commences very early in development, several hours before the morphological differentiation of muscle tissue. Developmental regulation of actin genes has also been studied in fruitflies[21,22] and sea urchins[23–25]. Several actin mRNAs are synthesized in these organisms, each with a distinct developmental profile. However, in contrast to amphibians, the appearance of muscle actin gene transcripts is a later embryonic event, coinciding with the formation of muscle-containing tissues in larval or metamorphosis stages.

Myogenesis and actin gene expression

The dorsal, flanking region of the mesoderm is irreversibly committed to embryonic muscle formation in the stage 10 gastrula *Xenopus* embryo[26], several hours before newly synthesized muscle proteins are first detected[7]. This may be a common feature of amphibian embryogenesis (see ref. 27). Our present results also show that mesoderm commitment occurs significantly before actin gene transcription and no major store of untranslated muscle actin transcripts is accumulated before α-actin protein is first synthesized in *Xenopus* embryos.

Muscle precursors, the embryonic somites, begin to appear a few hours after sarcomeric actin gene activation[5]. From stage 14 (actin gene activation) to stage 26 (tailbud embryo; 16 somites) the level of muscle actin mRNA increases over 20-fold, yet the total number of the cells in the embryo only doubles. Both somitic mesoderm and subsequent somite cells must therefore accumulate muscle actin transcripts over this period.

During the same interval, more lateral regions of mesoderm extend ventrally, eventually fusing along the midline to form the embryonic heart rudiment, thus being derived from a quite distinct region of the gastrula mesoderm from the somites. Somitic mesoderm accumulates similar amounts of both α-cardiac and α-skeletal muscle actin mRNA whilst immediately adjacent mesoderm cells and their derivatives (such as notochord) do not. This suggests that the initial events that regulate the actin multi-gene family distinguish muscle actin-encoding genes from their more distantly related cytoskeletal-type counterparts, whilst subsequent controls establish the final tissue specificity of the various muscle actin genes. Vertebrates seem to differ in the extent to which individual sarcomeric actin genes are expressed in each adult, muscle-containing tissue. The predominant muscle actin mRNA in adult mouse heart tissue (the α-cardiac form) provides about one-third of all the sarcomeric actin transcripts in fetal skeletal muscle[28]. This is replaced by α-skeletal actin mRNA in the skeletal muscle of newborn and adult mice. In neonatal rats, both α-cardiac and α-skeletal actin gene transcripts are present in heart tissue[29]. In man, both adult heart and skeletal muscle contain a significant proportion of each kind of sarcomeric actin message[30]. The initial activation of actin genes in early embryos from these species has not been documented.

Co-expression of α-cardiac and α-skeletal actin genes is not a transient phenomenon in early amphibian development, as we have detected roughly equivalent levels of each transcript in embryonic heart, somites and the myotomes of swimming tadpoles (stage 42) 3 days after fertilization (data not shown). It seems highly improbable that only one set of transcripts is utilized in each of these tissues and more likely that each functional embryonic organ uses both types of muscle actin protein in their contractile apparatus. If so, this raises an intriguing problem: why do adult muscle tissues express the sarcomeric actin genes in a tissue-specific manner if such complex regulation is unnecessary in larval stages?

Conclusions

The α-actin genes are the first identified genes known to be activated in a tissue-specific manner in the early amphibian embryo. Transcription of these genes is regulated in a cell type-specific manner, being restricted exclusively to those regions of the mesoderm that are committed to form embryonic muscle. The presence of muscle actin transcripts therefore offers a convenient molecular marker for these cells and their detection provides the basis of an assay for cytoplasmic factors involved in early cell determination[31].

This work was initiated in the MRC Laboratory of Molecular Biology, Cambridge. We thank Peter Gunning, Rob Maxson and Larry Kedes (Stanford University) for help in the construction of cDNA libraries. T.J.M. is a Royal Society Research Fellow in Biological Sciences. S.B. is the recipient of a USPHS National Research Service Award.

Received 28 March; accepted 9 August 1984.

1. Gerhart, J. C. in *Biological Regulation and Development* Vol. 2 (ed. Goldberger, R.) 133–316 (Plenum, New York, 1981).
2. Davidson, E. H. *Gene Activity in Early Development* (Academic, New York, 1976).
3. Pollard, T. D. & Weihing, R. R. *CRC crit. Rev. Biochem.* **2**, 1–65 (1974).
4. Buckingham, M. E. & Minty, A. J. in *Eucaryotic Genes: their Structure, Activity and Regulation* (eds Maclean, N., Gregory, S. P. & Flavell, R. A.) 365–395 (Butterworths, London, 1983).
5. Hamilton, L. *J. Embryol. exp. Morph.* **22**, 253–264 (1969).
6. Muntz, L. *J. Embryol. exp. Morph.* **33**, 757–774 (1975).
7. Ballantine, J. E. M., Woodland, H. R. & Sturgess, E. A. *J. Embryol. exp. Morph.* **51**, 137–153 (1979).
8. Cleveland, D. W. *et al. Cell* **20**, 95–105 (1980).
9. Vandekerckhove, J. & Weber, K. *FEBS Lett.* **102**, 219–222 (1978).
10. Vandekerckhove, J. & Weber, K. *Eur. J. Biochem.* **90**, 451–462 (1978).
11. Vandekerckhove, J. & Weber, K. *Differentiation* **14**, 123–133 (1979).
12. Fornwald, J. A., Kuncio, G., Peng, I. & Ordahl, C. P. *Nucleic Acids Res.* **10**, 3861–3976 (1982).
13. Kost, T. A., Theodorakis, N. & Hughes, S. H. *Nucleic Acids Res.* **11**, 8287–8302 (1983).
14. Vandekerckhove, J., Franke, W. W. & Weber, K. *J. molec. Biol.* **152**, 413–426 (1981).
15. Sargent, T. D. & Dawid, I. B. *Science* **222**, 135–139 (1983).
16. Woodland, H. R., Flynn, J. M. & Wyllie, A. J. *Cell* **18**, 165–171 (1979).
17. Newport, J. & Kirschner, M. *Cell* **30**, 675–686 (1982).
18. Shiokawa, K. *et al. Devl Biol.* **68**, 503–514 (1979).
19. Sagata, N., Shiokawa, K. & Yamana, K. *Devl Biol.* **77**, 431–448 (1980).
20. Nieuwkoop, P. D. & Faber, J. *Normal Table of* Xenopus laevis (North Holland, Amsterdam, 1967).
21. Sanchez, F., Tobin, S. L., Rdest, U., Zulauf, E. & McCarthy, B. J. *J. molec. Biol.* **163**, 533–551 (1983).

22. Fyrberg, E. A., Mahaffey, J., Bond, B. J. & Davidson, N. *Cell* **33**, 115-123 (1983).
23. Scheller, R. H. *et al. Molec. cell. Biol.* **1**, 609-628 (1981).
24. Shott, R. J., Lee, J. J., Britten, R. J. & Davidson, E. H. *Devl Biol.* **101**, 295-306 (1984).
25. Crain, W. R., Durica, D. S., Cooper, A. D., Van Doren, K. & Bushman, F. D. in *Muscle Development: Molecular and Cellular Control* (eds Pearson, M. & Epstein, H. F.) 97-105 (Cold Spring Harbor Laboratory, New York, 1982).
26. Slack, J. M. W. & Forman, D. *J. Embryol. exp. Morph.* **56**, 283-299 (1980).
27. Mohun, T. J., Tilly, R., Mohun, R. & Slack, J. M. W. *Cell* **22**, 9-15 (1980).
28. Minty, A. J., Alonso, S., Caravatti, M. & Buckingham, M. E. *Cell* **30**, 185-192 (1982).
29. Mayer, Y., Czosnek, H., Zeelon, P. E., Yaffe, D. & Nudel, U. *Nucleic Acids Res.* **12**, 1087-1100 (1984).
30. Gunning, P., Ponte, P., Blau, H. & Kedes, L. *Molec. cell Biol.* **3**, 1783-1791 (1983).
31. Gurdon, J. B., Brennan, S., Fairman, S. & Mohun, T. J. *Cell* (in the press).
32. Sanger, F., Nicklen, S. & Coulson, A. R. *Proc. natn. Acad. Sci. U.S.A.* **74**, 5463-5467 (1977).
33. Sanger, F., Coulson, A. R., Barrell, B. G., Smith, A. J. H. & Roe, B. A. *J. molec. Biol.* **143**, 161-178 (1980).
34. Auffray, C. & Rougeon, F. *Eur. J. Biochem.* **107**, 303-314 (1980).
35. Nasmyth, K. *Nature* **302**, 670-676 (1983).
36. Berk, A. J. & Sharp, P. A. *Cell* **12**, 721-732 (1977).
37. Lehrach, H., Diamond, D., Wozney, J. M. & Boedtker, H. *Biochemistry* **16**, 4743-4751 (1977).
38. Maniatis, T., Fritsch, E. F. & Sambrook, J. *Molecular Cloning: A Laboratory Manual* 202-203 (Cold Spring Harbor Laboratory, New York, 1983).

Resolution of synthetic *att*-site Holliday structures by the integrase protein of bacteriophage λ

Pei Ling Hsu* & **Arthur Landy**

Division of Biology and Medicine, Brown University, Providence, Rhode Island 02912, USA

Site-specific recombination of the bacteriophage λ genome into and out of the host bacterial genome is postulated to involve the formation of Holliday structure intermediates by reciprocal single-strand exchanges. Synthetic analogues of the predicted recombination intermediates are resolved in vitro *by the protein product of the λ* int *gene. Some of the structural features and reaction conditions for this genetic recombination can now be defined.*

INTEGRATION of the bacteriophage λ chromosome into a bacterial chromosome occurs by a reciprocal site-specific recombination between the phage *att*P site and the bacterial *att*B site. The resulting prophage *att* sites, *att*L and *att*R, are themselves able to recombine to regenerate *att*P and *att*B during excision of the viral genome (see refs 1, 2 for reviews). Both integrative and excisive recombination require the phage-encoded protein Int and the host-encoded protein IHF (integration host factor)[3,4]. Additionally, efficient excision requires the phage-encoded protein Xis[5,6]. Although purified Int protein is a type I topoisomerase that nicks and reseals pBR322 supercoiled DNA one strand at a time[3], no activity other than specific DNA binding has been found for purified IHF[1,4].

The *att*P site has 240 base pairs (bp)[7]; it contains a 15 bp 'common core' sequence (occurring in all four *att* sites)[8], three binding sites for IHF[1] and two classes of Int binding sites[9,10]. Essential DNA sequences to the left or right of the central 'core region' comprise the P arm and P′ arm respectively. (Similarly, in *att*B the essential left and right sequences are labelled B and B′ respectively.) The *att*B site is much smaller, extending approximately 5 bp to either side of the 15 bp common core[11]; it does not have any IHF recognition or arm-type Int binding sites. *att*B and *att*P do, however, have a similar junction-type Int binding site at each core-arm junction[10].

Int-dependent recombination does not involve any degradation or synthesis of DNA nor does it require any high-energy cofactors[4]. During recombination, the DNA strands are cut within the common core at position −3/−2 (from the centre of the core) in the 'top' strand and at position +4/+5 in the 'bottom' strand, to generate a 3′-protruding 7 bp stagger or overlap region[12], (referred to as O in POP′ and BOB′). Within the overlap region, DNA: DNA homology between the *att* sites is necessary for efficient recombination[13]. Genetic evidence suggests that at least some fraction of Int-dependent recombinants proceed via a single-strand exchange intermediate or Holliday structure[14,15].

Holliday structures, also referred to as χ-forms, are formed by the reciprocal exchange of single strands between two DNA duplexes[16-18]. They are thought to be intermediates in several recombination pathways, and would be resolved to recombinant products by a second cycle of nicking and re-ligating[19,20]. χ-

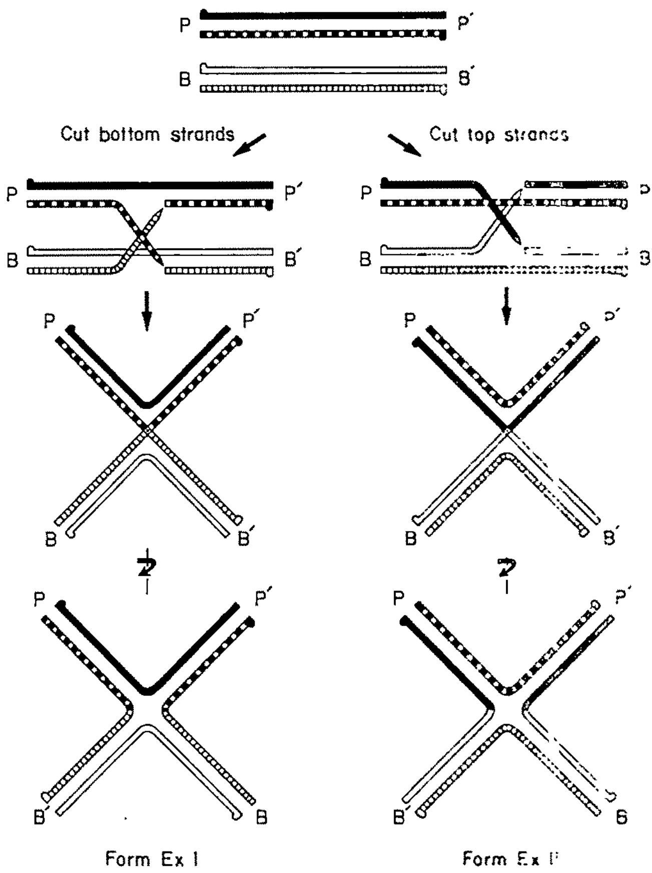

Fig. 1 Formation of Holliday structures (χ-forms) during λ site-specific recombination. The *att*P top (▬) and bottom (▨) strands and the *att*B top (▭) and bottom (⬚) strands have their 5′ termini indicated by a knob. The cutting and exchange of two bottom strands (left) results in form ExI, whereas the cutting and exchange of two top strands (right) results in form ExII. In the case where *att*L and *att*R are the parental DNAs (not shown here), the cutting and exchange of the two top strands would result in form ExI and the cutting and exchange of the two bottom strands would result in form ExII.

---

* Present address: Department of Pathology, University of Texas Health Science Center, Houston, Texas 77225, USA.

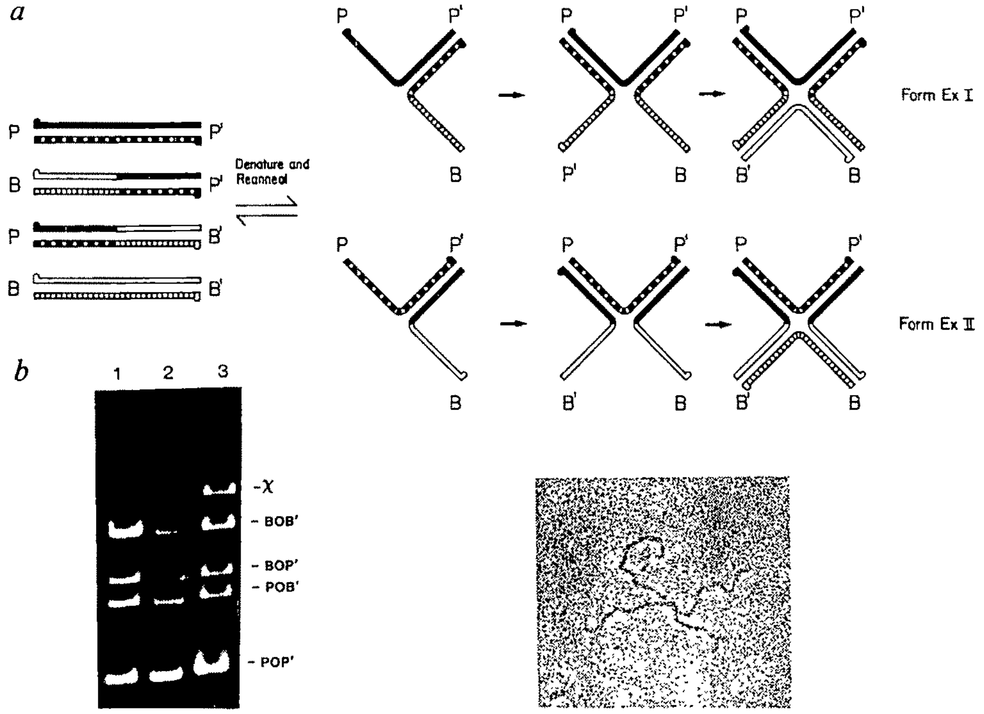

Fig. 2 Construction of forms ExI and ExII Holliday structures with a branch point in the common core region of the *att* site. Equivalent amounts of the four parental fragments, containing the POP', BOP', POB' and BOB' DNA sequences, were denatured and reannealed as described here. *a*, Schematic illustration of the stepwise formation of χ-structures during the reannealing process. Designations for the *att*P top (▬) and bottom (▪▪▪) strands and the *att*B top (▭) and bottom (▤) strands are also used to indicate the corresponding DNA strands in the prophage *att* sites BOP' and POB'. The 5' termini are marked with a knob. *b*, The ethidium bromide-stained agarose gel shows the four DNA restriction fragments before (lane 1) and after (lane 2) denaturation and after reannealing (lane 3). Electron micrograph shows DNA eluted from the gel band marked χ-form.

Methods: 40–120 pmol of restriction fragments in 0.8–1.0 ml were denatured and reannealed by one of the following two procedures: (1), the DNAs were denatured by boiling at 100 °C for 2 min in 1 mM Tris-HCl (*p*H 7.9), 0.1 mM EDTA, followed by rapid chilling in ice water. One-tenth volume of 20 × SSC (3 M NaCl, 0.3 M Na citrate) was added and the mixture was placed in a 65 °C water bath that was then allowed to equilibrate to room temperature overnight. (2), DNA restriction fragments in low melting agarose were heated at 68 °C until the agarose was melted and then placed at 37 °C. They were then denatured in 0.1 M NaOH for 5 min; after adding 1/2 vol of deionized formamide and neutralizing with acetic acid, they were incubated at 37 °C overnight. The χ-forms were purified by gel electrophoresis in 1% agarose at 1.8 V cm^{-1} in E* buffer (18 mM NaCl, 2 mM EDTA, 40 mM Tris, 20 mM sodium acetate, adjusted to *p*H 8.0 with acetic acid). DNA was electroeluted from the excised gel band and purified by elution from a BND cellulose column as described previously[42].

forms have been observed in *Escherichia coli* with phage[21–24] and plasmid DNAs[25], in yeast with 2 μ circle DNA[26] and in HeLa cells with adenovirus DNA[27]. In the Int-dependent pathway of λ it has not yet been possible to detect χ-form recombination intermediates. We report here an investigation of this aspect of the recombination reaction by construction of 'synthetic' Holliday structures that are structurally analogous to a reciprocal single-strand exchange intermediate in site-specific recombination.

Generation of Holliday structures

In forming Holliday structures (Fig. 1), the two DNA helices are first aligned with respect to their common core sequences. The cutting and reciprocal exchange of the two 'bottom' strands results in form ExI, and of the 'top' strands, form ExII. (We identify the individual DNA strands in each helix as either 'top' or 'bottom' in accordance with the convention of writing the four *att* sites as POP', BOB', POB' and BOP'; see Fig. 1.) In site-specific recombination, forms ExI and ExII are not conformational isomers—they cannot be interconverted without breakage and resealing of the DNA strands. This contrasts with Holliday structures generated in homologous recombination, where forms ExI and ExII are indistinguishable because both partners have the same DNA sequence.

We constructed 'artificial' Holliday structures (that is, without recombination) from four restriction fragments containing the POP', BOB', BOP' and POB' DNA sequences. A mixture of the four restriction fragments was denatured and reannealed in a manner analogous to that first used by Bell and Byers[26]. During renaturation, some of the single strands anneal with their original complement to regenerate the original restriction fragment. Alternatively, annealing between two strands originating from different restriction fragments (such as POP' and POB') generates a 'Y' structure comprising one duplex arm (such as P) and two single-stranded tails (such as P' and B'). Each of the single-stranded tails can further anneal with complementary sequences originating from a different restriction fragment, and this leads by analogous steps to formation of the four-armed Holliday structure (Fig. 2*a*).

Forms ExI and ExII comprise two different sets of DNA strands; from each restriction fragment one DNA strand is found only in ExI, for example, the top strand of POP', and the other strand is found only in ExII, for example, the bottom strand of POP' (see Fig. 2*a*). Thus, by starting with a POP' restriction fragment containing ^{32}P in only the top strand or the bottom strand, it is possible to label specifically either ExI or ExII respectively. In an alternative procedure it is possible to start with the isolated strands of each restriction fragment; then the appropriate combination of four (out of the total of eight) can be annealed to generate either ExI or ExII.

The χ-structure has a higher molecular weight than any of the other DNAs in the annealing mixture and is readily purified by agarose gel electrophoresis on the basis of its unique mobility (Fig. 2*b*). To prove that the unique slow-migrating band is indeed χ-form DNA, we eluted it from the gel and examined it in the electron microscope. At least 90% of the DNA has the expected χ-structure and arm lengths (see Fig. 2*c*). Furthermore, if eluted DNA was subjected to a second cycle of denaturation and renaturation, the four initial restriction fragments were recovered as expected. Finally, in the resolution experiments described below we were able to convert 100% of the χ-form DNA preparation into those linear products expected from cutting at the branch points of a simple χ-form structure.

Resolution of Holliday structures

A critical test of whether the synthetic χ-structures do correspond to intermediates of site-specific recombination is the ability of Int protein to resolve them to the expected linear products. Theoretically a synthetic *att* site Holliday structure might be resolved in either the integrative mode, generating *att*L

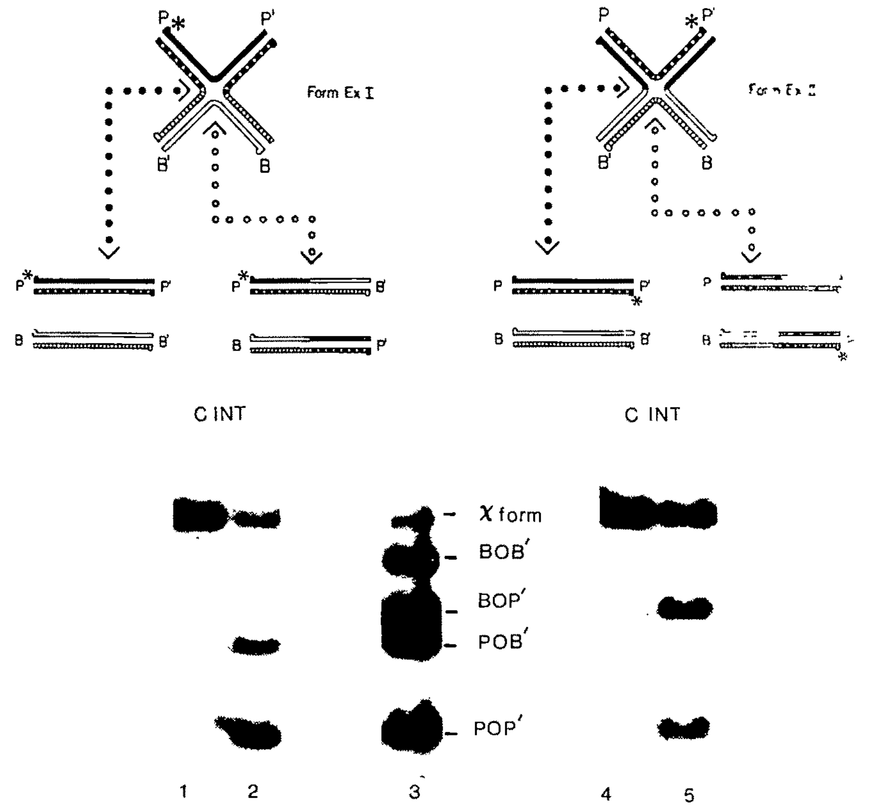

Fig. 3 Resolution of forms ExI and ExII by Int protein. The strands of the four *att* sites and the 5′ termini are designated as in Fig. 2. The positions of the unique ^{32}P label (*) in each χ-form that are expected after resolution are shown in the schematic diagram (see text). Lane 3 shows the positions of the χ-forms and the four restriction fragments used to make the χ-forms. Each labelled χ-form was incubated without (C) or with (INT) Int protein. Radioactive bands were visualized by autoradiography.

Methods: χ-Forms were constructed according to the first procedure described in Fig. 2 legend using the POP′ *Hin*dIII-*Bam*HI-492 fragment of pWR1, the BOB′ *Eco*RI-*Bam*HI-1740 fragment of pWR101, the BOP′ *Eco*RI-*Bam*HI-1210 fragment of pPH201 and the POB′ *Hin*dIII-*Bam*HI-1020 fragment of pPH202 (Table 1). The POP′ restriction fragment was labelled before denaturation with [γ-^{32}P]ATP and polynucleotide kinase at the *Hin*dIII site (for labelling form ExI) or at the *Bam*HI site (for labelling form ExII). Each reaction mixture (20 µl) contained 0.1 µg of ^{32}P-labelled form ExI or form ExII in 50 mM Tris-HCl (*p*H 7.9), 5 mM EDTA, 50 mM KCl and 6.25 mM spermidine. Incubation with 1 U of Int protein (purified by N. Hasan) was carried out at 25 °C for 60 min. (In these reaction conditions 1 U of Int plus 1 U of purified IHF[4,43] gives optimal recombination of 0.1 pmol supercoiled *att*P, pWR1, and 0.1 pmol of linear *att*B, pWR101.) The reactions were terminated with SDS (0.1% final) and electrophoresed on a 1% agarose gel as described for Fig. 2.

and *att*R (vertical cuts in ExI and ExII, Fig. 3) or in the excisive mode, generating *att*P and *att*B (horizontal cuts in ExI and ExII, Fig. 3). This resolution reaction is presumably equivalent to the second half of normal integrative or excisive recombination. In fact, in reaction conditions suitable for *in vitro* recombination, purified Int protein efficiently resolves both forms ExI and ExII into the expected linear products (Fig. 3).

Each χ-form is labelled with only one ^{32}P atom and, therefore, in each pair of products, only one will be radioactively labelled. Under these experimental conditions the resolution of form ExI yields approximately three times more *att*P than *att*R product, thus indicating a preference for the 'excisive mode' (cutting the bottom strands). On the other hand, resolution of form ExII yields approximately twice as much *att*L as *att*P product, thus indicating a preference for the 'integrative mode' (cutting the bottom strands). This is a good example of how an overall preference for cutting the bottom strand has opposite consequences for ExI (generating excision-type products) and ExII (generating integration-type products). The patterns and degree of preferential strand-cutting are significantly influenced by several experimental parameters (currently under investigation); this is a particularly interesting aspect of the reaction because of its relevance to directionality in site-specific recombination.

Following resolution, there is an additional band on alkaline denaturing gels, corresponding to full-length *att*R for ExI, and full-length *att*L for ExII (data not shown). This transfer of label from a POP′ strand to the corresponding strand of a prophage *att* site indicates the successful ligation of DNA strands during resolution.

Specificity and factors

The strand exchange in λ site-specific recombination resembles the relaxation of superhelical DNA by certain topoisomerases (including the type I topoisomerase activity of Int protein) in

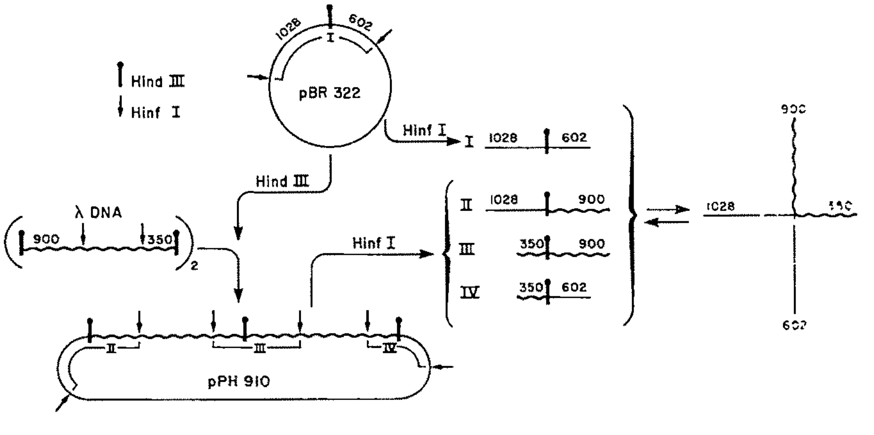

Fig. 4 Construction of a non-*att* Holliday structure. The *Hin*dIII fragment of λ DNA (〰〰), which extends from 57.0% to 52.4% on the λ map and does not contain an *att* site, was cloned as a tandem duplication into the *Hin*dIII site of pBR322 (———), to generate plasmid pPH910. Three *Hin*fI fragments of pPH910 were isolated for the χ-form construction: fragment II consists of the left pBR322-λ junction, fragment III of the head-to-tail junction of the two λ fragments, and fragment IV of the right λ-pBR322 junction. Fragment I is the pBR322 *Hin*fI fragment into which the λ DNA had been inserted. For each fragment, and for each arm of the χ-structure, the amount (base pairs) of pBR322 DNA or λ DNA is indicated.

Methods: The χ-form was generated by alkali denaturation and renaturation according to scheme (2) and purified by agarose gel electrophoresis as described in Fig. 2 legend.

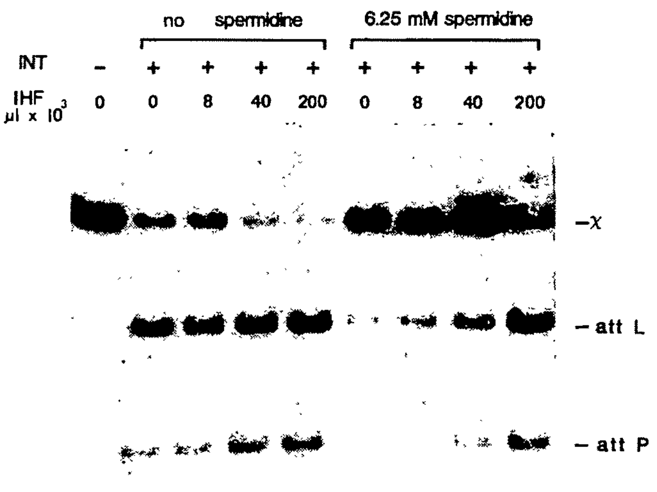

Fig. 5 Effect of IHF protein and spermidine on resolution. ^{32}P-labelled form ExII was constructed and isolated as described in Fig. 3 legend. The composition and processing of each resolution reaction was the same as described for Fig. 3 except that incubation with 0.2 U of purified Int protein was for 30 min. Purified IHF protein[4] (a gift from H. Nash) at 1 U μl^{-1} and spermidine were present as indicated.

that the DNA strands are broken and resealed in the absence of DNA synthesis and energy cofactors (see refs 28, 29 for reviews). This raises two points of interest: as the topoisomerase I activity of Int works efficiently with a substrate such as supercoiled pBR322 DNA[3], can it resolve a Holliday structure that does not contain an *att* site? Similarly, is the Holliday structure resolved by other DNA topoisomerases?

To address these questions, we constructed a Holliday structure that bears no *att* site DNA sequences (Fig. 4). This structure is not resolved into linear products by Int protein, either in conditions for *in vitro* recombination or conditions for the nicking-closing reaction. The addition of host factor also has no effect. We also tested the ability of three different topoisomerases to resolve the *att* site Holliday structure (these enzymes were a gift from Leroy Liu), HeLa cell topoisomerase I[29], T4 topoisomerase II[30,31] and calf thymus topoisomerase II, whose purification and properties (L. F. Liu, unpublished results) are identical to HeLa topoisomerase II[32]. In conditions where these enzymes relaxed approximately 30–70% of supercoiled DNA, we observed no resolution of Holliday structure (data not shown). We conclude that, in these experimental conditions, the ability of Int protein to resolve a Holliday structure is specific for the *att* site DNA sequences and is not merely a general property of DNA topoisomerases.

In an *in vitro* reaction, the integrative and excisive recombination functions of Int require the *E. coli*-encoded IHF protein and are strongly stimulated by the presence of spermidine. In contrast, the topoisomerase activity of Int does not require IHF protein and is inhibited by the addition of spermidine[3]. Int resolution of the Holliday structures is also independent of IHF

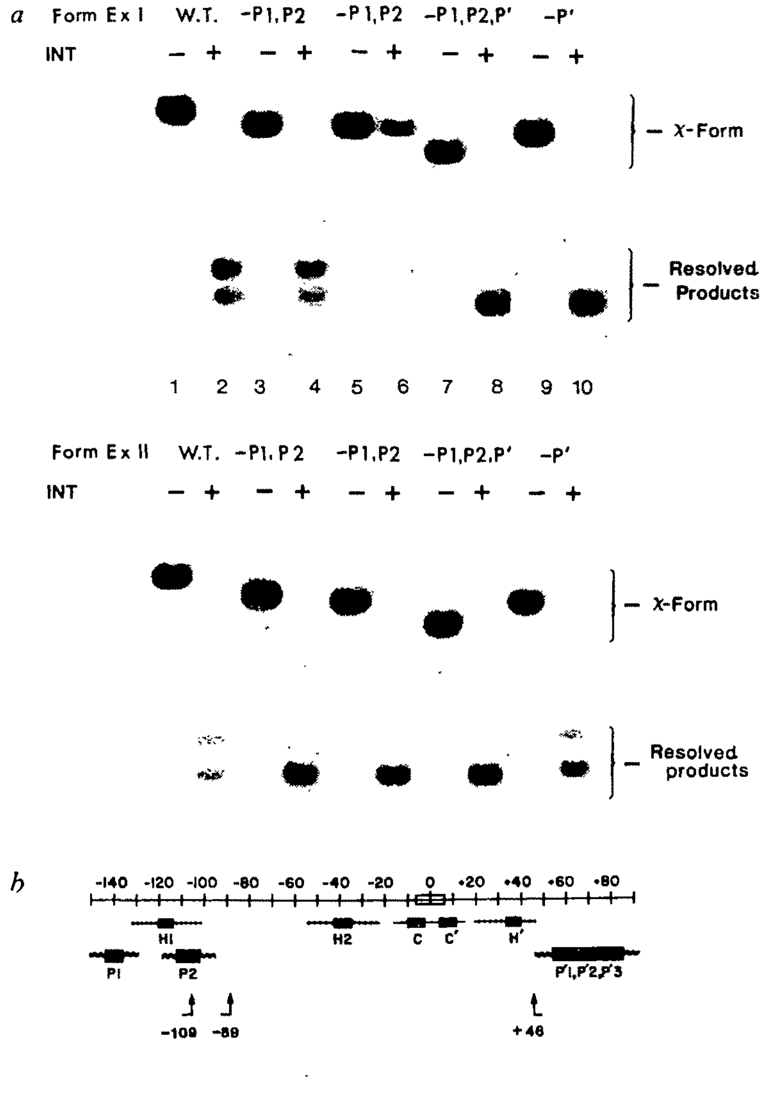

Fig. 6 Int resolution of χ-forms lacking one or more arm-type Int binding sites. χ-forms composed of intact *att* sites (W.T.) or lacking the indicated arm-type Int binding site(s) ($-$P1, P2, etc.) were constructed from the appropriate *Hin*cII restriction fragments (Table 1, using the second procedure in Fig. 2). *b*, The *att*P coordinates for the 15 bp common core (⊟); the consensus recognition sequences (—■—) and the approximate region of DNA covered (as determined by nuclease protection) for each of the following: the junction-type Int binding sites, C and C' (—■—■—), the arm-type Int binding sites P1, P2, P'1, P'2, and P'3 (—■—)[9,10], the IHF binding sites H1, H2 and H' (‖■‖)[1]. The endpoints of *att* DNA in the three deletions used to construct the different χ-structures are indicated ($-$109, $-$89 and +46) (see Table 1). Each χ-form was incubated in the absence ($-$) or presence (+) of purified Int protein in a 20-μl reaction that contained ~0.01 μg of χ-form, 0.5 μg of supercoiled pBR322 DNA and 1 U of purified Int. After electrophoresis of the reaction products, gels were stained with ethidium bromide (0.5 μg ml^{-1}) to visualize the nicking-closing activity of Int on the supercoiled pBR322 DNA. The expected levels of activity were observed in each case (data not shown). The ^{32}P-labelled χ-forms and resolution products were visualized by autoradiography. The size (in base pairs) of each labelled resolution product is as follows: BB', 940; BP', 1,077; BΔ', 886; PB', 1,114; ΔB', 972 (lane 4) and 952 (lanes 6 and 8). In this exposure of the autoradiogram, resolution products of similar size are not clearly resolved in several of the lanes; shorter exposures (and other gels) show that both resolution products are obtained in each reaction. The incomplete resolution observed in lane 6 of the upper gel is not typical; in other experiments in these conditions resolution is complete.

Methods: Reaction conditions, processing and gel electrophoresis were as for Fig. 3, with no spermidine. For ^{32}P labelling of forms ExI and ExII, the BOB' *Hin*cII fragment was first labelled at the 5' termini with polynucleotide kinase and then strand-separated by gel electrophoresis. The top strand of BOB' was incorporated into form ExI and the bottom strand into form ExII (see Fig. 2) by annealing with the other three restriction fragments (Table 1). The specific activity is the same for the entire form ExI family (or the entire form ExII family), because the ^{32}P label is always on the BOB' strand which is common to all five χ-forms (see Table 1).

protein (Fig. 3), resolving 95–100% of the Holliday structure to linear products in the absence of IHF. Int purified from the *him*A deletion mutant K5242 (ref. 33 and H. Miller, in preparation) is also efficient in resolution (data not shown). However, when limiting amounts of Int are used, IHF does stimulate resolution in a dose-dependent manner (Fig. 5). Spermidine inhibits resolution; omission of spermidine results in a three- to fivefold enhancement (Fig. 5). Thus, as might be expected, the requirements for the overall recombination reaction are greater than the requirements for the resolution phase.

Structural requirements

We have shown that the arm-type Int binding sites are essential for integrative recombination. The role of these sites, which are quite distant from the cross-over locus, is unclear (see Fig. 6, bottom)[7,9]. Are they required throughout the reaction or only involved in some phases? If the latter, are they required for synapsis between the recombining partners and possibly the initial strand exchange, or are they required for resolution of the recombinational intermediate? To address these questions, we have constructed Holliday structures lacking the P arm and/or P′ arm Int binding sites and asked which, if any, of these is an acceptable substrate in the resolution reaction.

Holliday structures containing various deletions of the P and/or P′ arms were constructed by annealing a ^{32}P-labelled separated strand of BOB′ with different combinations of the appropriate restriction fragments. Two families of χ-forms were constructed, representing forms ExI and ExII for each deletion analysed (Table 1). The restriction fragments and constructions were designed so that all of the arms in every χ-structure are perfect duplexes over their entire length.

In any one series of experiments (see Fig. 6), all of the χ-forms have the same specific activity. This is because the single ^{32}P atom in each χ-structure is donated by the same BOB′ restriction fragment which has been end-labelled and strand-separated before being distributed into the respective annealing mixtures. This protocol facilitates the comparison of resolution efficiencies under identical Int:DNA ratios. As an additional (internal) control, supercoiled pBR322 DNA was added to each reaction mixture to monitor the topoisomerase activity of Int.

In a 1-h incubation with χ-form, pBR322 supercoiled DNA and Int (present in a molar ratio of 1:20:30), approximately 70% of the supercoiled molecules are relaxed in all of the reaction mixtures. Concomitantly, Int protein resolves all of the Holliday structures with 95–100% efficiency, irrespective of the presence or absence of the arm-type Int binding sites (Fig. 6). For all Holliday structures in this form ExI family, resolution occurs in both the integrative and excisive modes. Similar results and efficiencies are obtained with the analogous family of form ExII Holliday structures. When the concentration of Int is lowered (χ-form:pBR322:Int at 1:20:10) so that χ-form resolution is reduced to ~30%, the resolution efficiency of Holliday structures with each of the deletions is still the same as the non-deleted form (data not shown). We conclude that the arm-type Int binding sites that are required for integrative recombination are dispensable for the resolution of Holliday structures resembling the cross-over region of recombining *att* sites.

Discussion

Does Int-dependent site-specific recombination proceed by a concerted mechanism in which both DNA strands on each partner are cut at the same time and then exchanged and re-ligated, or does it proceed in two distinct steps where first, only one strand on each partner is exchanged to generate a Holliday structure, and second, the single-strand exchange intermediate is resolved by a second cycle of nicking and re-ligation?

We have shown here that Holliday structures with their branch points in the common core region of the *att* site are efficiently

Table 1 Construction of different χ-form structures

χ-Forms Intact	Arm sites deleted −P1 −P2	 −P1 −P2	 −P′	 −P1 −P2 −P′	Plasmid	*att*	P arm or Δ arm	P′ arm or Δ′ arm	B arm	B′ arm
+					pWR1	PP′	−251(734)	+242(517)		
	+				pPH55	ΔP′	−109(592)	+242(517)		
		+			pPH56	ΔP′	−89(572)	+242(517)		
			+		pPH310	PΔ′	−251(734)	+46(326)		
				+	pPH5610	ΔΔ′	−89(572)	+46(326)		
+	+	+			pPH201	BP′		+242(517)	−560	
			+	+	pPH110	BΔ′		+46(326)	−560	
+			+		pPH202	PB′	−251(734)			+380
	+				pPH551	ΔB′	−109(592)			+380
		+		+	pPH561	ΔB′	−89(572)			+380
+	+	+	+	+	pWR101	BB′			−560	+380

χ-Forms with intact *att* sites or lacking one or more of the arm-type Int binding sites (as labelled), were constructed using the indicated (+) restriction fragments, one from each of the four classes (see Fig. 6). For example, to make a Holliday structure lacking the P1 and P2 sites, an isolated BOB′ strand from pWR101 was annealed with the ΔOB′-containing fragment of pPH551, the BOP′-containing fragment of pPH201 and the ΔOP′-containing fragment of pPH55. The plasmids from which the *att* site restriction fragments (*Hin*cII) are isolated are shown. The construction att sites (pWR1, pWR101, pPH201 and pPH202), or *att*P with distal deletions of the P and P′ arms (pPH55, pPH56, pPH310), has been described previously[7]. Transfer of the *att*P deletions to the other *att* sites was as follows: Int-dependent *in vitro* recombination was carried out (with an extract containing Xis) on head-to-tail heterodimer plasmids containing ΔOP′ and POB′; to make pPH551, the dimer consisted of pPH55 and pPH202, to make pPH561, the dimer consisted of pPH56 and pPH202. After recombination the DNA was digested with *Eco*RI, circularized and transformed into HB101. Plasmids containing the recombinant ΔOB′ site were identified by their restriction digestion patterns. For plasmids pPH110 (BOΔ′) and pPH5610 (ΔOΔ′) the Δ′ arm is the *Dde*-*Bam*HI fragment from pPH310. It was ligated through the *Dde* site in the core to the appropriate *Eco*RI-*Dde* fragment, from pPH201 for the B arm or from pPH56 for the Δ arm. The four *att* site arms are denoted P, P′, B and B′ as described in the text; any change (deletion) in one of the phage *att* site arms is denoted as Δ (corresponding to P) or Δ′ (corresponding to P′). The extent of phage *att* site sequence is indicated in base pairs from the centre of the core extending left (−) or right (+) (using the conventions of ref. 8) (see Fig. 6). The *Hin*cII restriction fragments chosen for these constructions also contain neighbouring pBR322 DNA, thus making it possible to generate physically longer (fully duplex) arms in the final χ-structure; numbers in parentheses indicate the total amount of DNA (phage DNA plus pBR322 DNA) in that arm of the χ-form. DNA from the region around the bacterial *att* site is indicated in base pairs (approximate) from the centre of the core extending left (−) or right (+)[8]; these numbers also indicate the total amount of DNA in that arm of the χ-form (that is, these arms do not have pBR322 sequences).

resolved by purified Int protein. In a mixed recombination reaction containing both χ-form (0.01 pmol) and *att*P and *att*B (0.1 pmol each), 1 U of Int and IHF give ~30% recombination between the *att* sites and ~90% resolution of the χ-form (data not shown). It seems highly unlikely that this unique substrate would be utilized in such a specific and efficient manner if it were not part of the normal recombination pathway. We infer that Int-dependent recombination most probably proceeds through a single-strand exchange Holliday intermediate. Resolution of this intermediate is probably very closely coupled with its formation, as suggested by the efficiency of χ-form resolution, the low frequency of branch migration observed in *in vivo* crosses[14,15] and the failure to find such forms accumulating during recombination. A mechanism that exchanges DNA strands one pair at a time is compatible with the type I topoisomerase activity of Int, and with the four-stranded DNA structure that has been proposed for synapsis[3,34].

The finding that purified Int protein efficiently resolves the Holliday intermediate in the absence of IHF (or Xis) substantiates its role in executing the cutting and ligating reactions of recombination[3,4,12,35]. Because IHF does not participate directly in the strand exchange reaction (resolution), its obligatory participation in integrative recombination is probably due to a role in the formation of Int-*att* complexes or in the synapsis of two *att* sites.

A striking feature of the Int resolution reaction is its specificity for *att* site DNA—in particular for the Int recognition sites at the core-arm junctions. Holliday structures lacking *att* site sequences are not resolved by Int. Of the known enzymes, only the T4-encoded endonuclease VII has also been shown to nick specifically at the branch points of χ-structures[36]. In contrast to the Int reaction, however, endonuclease VII is not sequence specific and does not appear to reseal the nicked DNA without the aid of DNA ligase.

We have shown here that resolution is efficient even with a Holliday structure lacking all the Int binding sites in the P and P′ arms and containing only the four Int binding sites at the core-arm junctions (Fig. 6). Because a Holliday structure lacking the junction-type sites is not resolved by Int (Fig. 4), we conclude that this family of Int recognition sites (C, C′, B and B′) is both necessary and sufficient for cutting and re-ligating DNA. The corollary of this conclusion is that the Int binding sites in the arms, although required for *att*P recombination, are not required for the cutting and re-ligation reaction. This is consistent with the finding that a single core-type Int binding sequence, even in non-*att* DNA, is sufficient for nicking by Int protein (ref. 35 and W. Ross and A.L., unpublished results). We infer that the Int sites in the arms function in synapsis of the recombining sites and/or formation of a presynaptic multimeric complex involving *att*P and the necessary proteins. In this context it is interesting that higher order complexes involving *att*P and approximately 10 Int monomers have been observed in the electron microscope[37,38] and nuclease digestion patterns[7,9,39] and topological transformations during recombination[40,41] suggest a wrapping of DNA around, or along the surface of, Int protein(s).

We have shown here that both forms ExI and ExII can be resolved in the integrative mode (producing *att*L and *att*R) or in the excisive mode (producing *att*P and *att*B). This suggests that in these experimental conditions either form ExI or form ExII could serve as an intermediate of either integrative or excisive recombination. Furthermore, as resolution can occur by cutting either pair of strands, there is the possibility that some attempts at recombination are abortive: if the same pair of strands is used for both the first and second cross-over, the original parents are restored. Thus, the overall efficiency of recombination between any two *att* sites could be determined not only by the formation of Holliday intermediates but also by the directionality of their resolution. In our experiments the relative efficiency of resolution was not the same in both directions, with either form ExI or form ExII. It will be interesting to determine how this directionality is influenced by reaction conditions and the various components of the recombination reaction.

We thank Noaman Hasan for purified Int protein, Howard Nash for purified IHF protein, Leroy Liu for the topoisomerases, David Straney for the electron microscopy and Breck Beyers for helpful advice. Lina Vargas and Shirley Rodrigues provided technical assistance. This work was supported by NIH grant AI13544.

Received 20 April; accepted 3 August 1984.

1. Nash, H. A. *A. Rev. Genet.* **15**, 143–167 (1981).
2. Weisberg, R. & Landy, A. in *Lambda II* (eds Hendrix, R. W., Roberts, J. W., Stahl, F. W. & Weisberg, R. W.) 211–250 (Cold Spring Harbor Laboratory, New York, 1983).
3. Kikuchi, A. & Nash, H. A. *Proc. natn. Acad. Sci. U.S.A.* **76**, 3760–3764 (1979).
4. Nash, H. A. & Robertson, C. A. *J. biol. Chem.* **256**, 9246–9253 (1981).
5. Abremski, K. & Gottesman, S. *J. biol. Chem.* **257**, 9658–9710 (1982).
6. Better, M., Wickner, S., Auerback, J., Williams, R. & Echols, H. *Cell* **32**, 161–168 (1983).
7. Hsu, P-L., Ross, W. & Landy, A. *Nature* **285**, 85–91 (1980).
8. Landy, A. & Ross, W. *Science* **197**, 1147–1160 (1977).
9. Ross, W. & Landy, A. *Proc. natn. Acad. Sci. U.S.A.* **79**, 7724–7728 (1982).
10. Ross, W. & Landy, A. *Cell* **33**, 261–272 (1983).
11. Mizuuchi, M. & Mizuuchi, K. *Proc. natn. Acad. Sci. U.S.A.* **77**, 3220–3224 (1980).
12. Mizuuchi, K., *et al. Cold Spring Harb. Symp. quant. Biol.* **45**, 429–437 (1981).
13. Weisberg, R., Enquist, L., Foeller, C. & Landy, A. *J. molec. Biol.* **170**, 319–342 (1983).
14. Enquist, L. W., Nash, H. A. & Weisberg, R. A. *Proc. natn. Acad. Sci. U.S.A.* **76**, 1363–1367 (1979).
15. Echols, H. & Green, L. *Genetics* **93**, 297–307 (1979).
16. Holliday, R. *Genet. Res.* **5**, 282–304 (1964).
17. Sigal, N. & Alberts, B. *J. molec. Biol.* **71**, 789–793 (1972).
18. Holliday, R. *Genetics* **78**, 273–287 (1974).
19. Dressler, E. & Potter, H. *A. Rev. Biochem.* **51**, 727–761 (1982).
20. Stahl, F. *Genetic Recombination. Thinking about it in Phage and Fungi* (Freeman, San Francisco, 1979).
21. Thompson, B. *et al. J. molec. Biol.* **91**, 409–419 (1975).
22. Benbow, R., Zuccavelli, A. & Sinsheimer, R. *Proc. natn. Acad. Sci. U.S.A.* **72**, 235–239 (1975).
23. Valenzuela, M. & Inman, R. *Proc. natn. Acad. Sci. U.S.A.* **72**, 3024–3028 (1975).
24. Thompson, B. J., Camien, M. N. & Warner, R. C. *Proc. natn. Acad. Sci. U.S.A.* **73**, 2299–2303 (1976).
25. Potter, H. & Dressler, D. *Proc. natn. Acad. Sci. U.S.A.* **73**, 3000–3004 (1976).
26. Bell, L. & Byers, B. *Proc. natn. Acad. Sci. U.S.A.* **76**, 3445–3449 (1979).
27. Wolgemuth, D. J. & Hsu, M. T. *Nature* **287**, 168–171 (1980).
28. Cozzarelli, N. R. *Science* **207**, 953–960 (1980).
29. Gellert, M. *A. Rev. Biochem.* **50**, 879–910 (1981).
30. Liu, L. F. & Miller, K. G. *Proc. natn. Acad. Sci. U.S.A.* **78**, 3487–3491 (1981).
31. Liu, L. F., Liu, C.-C. & Alberts, B. M. *Nature* **281**, 456–461 (1979).
32. Miller, K. G., Liu, L. F. & Englund, P. T. *J. biol. Chem.* **256**, 9334–9339 (1981).
33. Miller, H. I. & Friedman, D. I. *Cell* **20**, 711–719 (1980).
34. Nash, H. A., Mizuuchi, K., Enquist, L. W. & Weisberg, R. A. *Cold Spring Harb. Symp. quant. Biol.* **45**, 417–428 (1981).
35. Craig, N. & Nash, H. *Cell* **35**, 795–803 (1983).
36. Mizuuchi, K., Kemper, B., Hays, J. & Weisberg, R. *Cell* **29**, 357–365 (1982).
37. Hamilton, P., Yuan, R. & Kikuchi, Y. *J. molec. Biol.* **152**, 163–170 (1981).
38. Better, M., Chi, L., Williams, R. C. & Echols, H. *Proc. natn. Acad. Sci. U.S.A.* **79**, 5837–5841 (1982).
39. Davies, R. W., Schreier, P. H., Kotewicz, M. L. & Echols, H. *Nucleic Acids Res.* **7**, 2255–2273 (1979).
40. Nash, H. & Pollock, T. *J. molec. Biol.* **170**, 19–38 (1983).
41. Pollock, T. & Nash, H. *J. molec. Biol.* **170**, 1–18 (1983).
42. Rossi, J. J., Ross, W., Egan, J., Lipman, D. J. & Landy, A. *J. molec. Biol.* **128**, 21–47 (1979).
43. Nash, H. A. *Meth. Enzym.* **100**, 210–216 (1983).

Preferential utilization of the most J_H-proximal V_H gene segments in pre-B-cell lines

George D. Yancopoulos*, Stephen V. Desiderio†‡, Michael Paskind†‡, John F. Kearney§, David Baltimore†‡ & Frederick W. Alt*

* Department of Biochemistry and Institute for Cancer Research, Columbia University, College of Physicians and Surgeons, New York 10032, USA
† Center for Cancer Research and Department of Biology, Massachusetts Institute of Technology, Cambridge, Massachusetts 02139, USA
‡ Whitehead Institute for Biomedical Research, Massachusetts Institute of Technology, Cambridge, Massachusetts 02139, USA
§ The Cellular Immunobiology Unit of the Tumor Institute, Departments of Microbiology and The Comprehensive Cancer Care Center, University of Alabama, Birmingham, Alabama 35294, USA

The most J_H*-proximal* V_H *gene segments are used highly preferentially to form* V_HDJ_H *rearrangements in pre-B-cell lines. This result demonstrates that the rate at which immunoglobulin* V_H *gene segments recombine is influenced by their chromosomal organization, and that the initial repertoire of* V_H *genes expressed in pre-B cells is strikingly different from that seen in mature populations.*

THE genetic information encoding the murine immunoglobulin heavy chain variable (V) region is formed from the juxtaposition of members of three separate clusters of germ-line DNA elements: variable segments (V_H), diversity segments (D) and joining segments (J_H)[1,2]. Approximately 15 D segments are situated 1 to 80 kilobases (kb) upstream from a 2-kb region containing the four J_H segments[3-5], while the 100-200 V_H segments lie at an unknown distance 5′ to the D segments[6,7]. A complete V_HDJ_H variable region gene is assembled during the pre-B-cell stage of the murine B-lymphocyte differentiation pathway via an ordered two-step process: D to J_H joins occur first and on both chromosomes, followed by V_H to DJ_H rearrangement[6]. The tremendous diversity of antibody specificities is due, in part, to the large repertoire of V_H gene segments which are apparently randomly represented in the mature antibody population[8]. The murine V_H gene segments can be divided into approximately ten families based on nucleotide sequence homology; the members of each family are grouped together on the chromosome[9-12]. The relative locations of these families on chromosome 12 have recently been mapped[13]. Little is known about the developmental control of the rearrangement, and subsequent expression, of the many V_H regions. If the choice of V_H gene segments used in rearrangements were not random, it could be mediated by factors such as chromosomal location or recombination recognition sequence elements.

Transformation of murine fetal liver or adult bone marrow cells by Abelson murine leukaemia virus (A-MuLV) generates permanent cell lines which represent the pre-B stage of B-lymphocyte differentiation[6,14]. Fetal liver-derived transformants generally represent the earliest defined pre-B cell: null(non-immunoglobulin producing) cells which initially contain DJ_H complexes on both chromosomes, but which actively assemble complete V_HDJ_H complexes when propagated in culture[6]. Such cell lines will subsequently be referred to as V_H to DJ_H rearranging. The V_H to DJ_H joins which occur in such lines can be identified and isolated from appropriate cellular subclones[6,15,16]. Transformants isolated from bone marrow usually represent more mature pre-B cells which contain V_HDJ_H complexes on at least one allele upon isolation, but do not yet express light chain or have surface immunoglobulin[6,14]. The ability to study rearrangement outside of the animal, and in cells which lack surface immunoglobulin (sIg) upon isolation, provides a unique opportunity to examine the initial V_H usage pattern in the absence of antigenic or immunoregulatory selective forces acting *in vivo*. Thus, examination of the V_H segments used by such lines may identify developmentally important V_H rearrangement patterns that have not been observed previously.

Two V_H to DJ_H rearranging lines

To explore the possibility of a developmentally-related pattern of V_H segment utilization, we first characterized the V_H segments employed in six independent V_H to DJ_H joins that were identified in subclones of the V_H to DJ_H rearranging lines 22D6 and 4OE4[6,15]. Remarkably, the nucleotide sequence of the V_H portion of these rearrangements (Fig. 1) reveals that three use an identical V_H gene segment designated V_H81X (see sequence V_H81X(R) in Fig. 1; ref. 17), whereas the remaining three rearrangements use V_H gene segments closely related to V_H81X. The V_H81X gene segment and two of the related segments (designated V_HD6.96 and V_HE4.15, Fig. 1) appear to encode functional V_H regions, and the remaining V_H segment is a pseudogene (designated V_HE4.Psi; Fig. 1). These sequences all exhibit stronger nucleotide sequence homology (> 80%) to the MOPC21 V_H sequence than to V_H segments from other families (Fig. 1, Table 1), classifying them as members of the relatively small (approximately 10 members) V_H7183 gene family which has V_HMOPC21 as its prototype sequence[12]. Thus, the cell lines 22D6 and 4OE4 use a very limited set of the many V_H segments available.

J_H proximity of V_H81X and V_HE4.Psi

Because V_H81X was used at a particularly high frequency in the two V_H to DJ_H rearranging lines, it was chosen for further study. *Eco*RI-digested BALB/c liver DNA was assayed for hybridization to probes specific for V_H81X, V_HD6.96 and V_HMOPC21 (see Fig. 5 for preparation of probes) using the

Table 1 Comparison of % sequence homology in V_H coding regions

	V_HD6.96	V_HE4.15	V_HE4.Psi	V_HMOPC21	V_H141	V_H603	B1-8
V_H81X	83	87	86	81	59	57	55
V_HD6.96	—	96	88	85	ND	ND	ND
V_HE4.15		—	90	87	ND	ND	ND
V_HE4.Psi			—	88	ND	ND	ND

The sequences of V_H81X, V_HD6.96, V_HE4.Psi and V_HE4.15 are presented in Fig. 1. They are compared within the coding region to each other and to the previously published V_HMOPC21 sequence[10]. V_H81X is also compared to previously published V_H sequences[10] representative of the three V_H families immediately upstream to the V_H7183 family: V_H141 is representative of the V_HQ52 family, MCPC603 representative of the V_HS107 family, and the B1-8 sequence representative of the V_H558 family. ND indicates that the V_H segments were not compared.

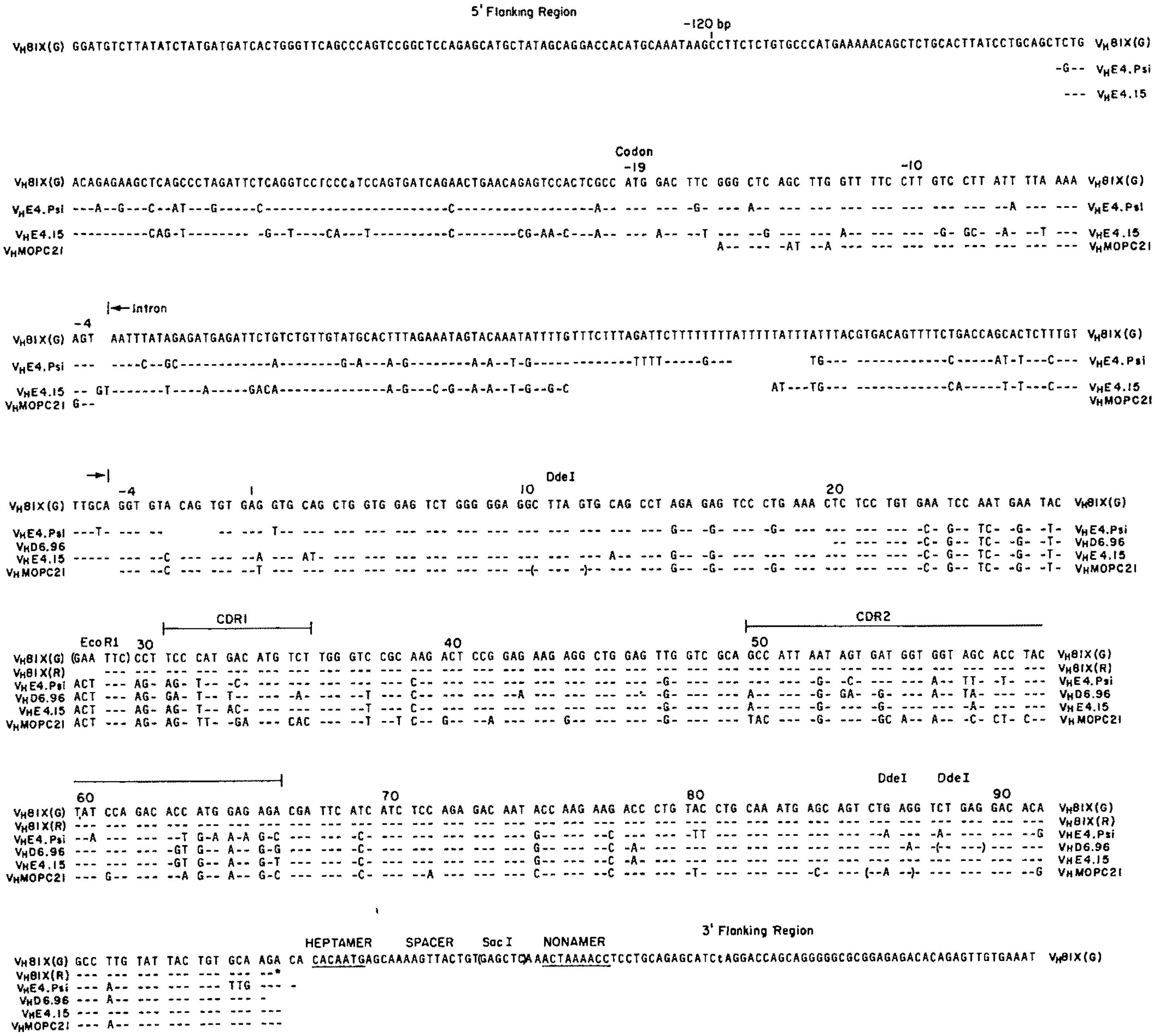

Fig. 1 Comparison of nucleotide sequences of V_H81X and related V_H segments. Rearrangements of V_H7183 segments were isolated from subclones of the V_H to DJ_H rearranging lines 22D6 and 40E4. V_H81X and V_HD6.96 rearrangements were isolated from the line 22D6-G2[6]. The V_HE4.Psi rearrangement was isolated from the line 40E4-2-26 and the V_HE4.15 rearrangement was isolated from the line 40E4-2-15[15]. Three additional rearrangements of V_H81X were isolated from two independent subclones of the line 40E4-2[15] and from the stably rearranged line 18-81A2[17]. The nucleotide sequence of the germ-line V_H81X segment (designated V_H81X(G)) was determined according to the strategy indicated in Fig. 3. The nucleotide sequence of the rearranged V_H81X segments was determined downstream from the *Eco*RI site located at codons 28–29, and often upstream from sites within the J_H region for confirmation. All four rearranged V_H81X sequences were identical and are represented by a single sequence (designated V_H81X(R)); the asterisk at the end of this sequence marks the point where the rearranged sequences begin to diverge due to heterogeneous recombination junctions with DJ_H complexes[15,17]. The nucleotide sequence of the V_HE4.Psi segment was determined from the bordering *Pst*I sites in the V_HE4.Psi-DJ_H3 rearrangement (see restriction map in Fig. 3). The V_HE4.15 rearrangement was sequenced from bordering *Pst*I sites[15]. The V_HD6.96 segment was sequenced downstream from the *Ava*II site indicated and upstream from the *Nae*I site located in the J_H4 region. The V_HMOPC21 sequence of a cDNA clone is that previously published by Bothwell *et al.*[10], and thus does not include the intron region. The V_H81X(G) sequence was used as a reference for comparison with the other sequences. A dash indicates identity and a blank within a sequence marks a deletion with respect to the corresponding bases in V_H81X(G). Changes occur in the V_H81X sequence which are invariant among all other V_H segments[8]: these include the lysine at codon 39, the leucine at codon 47, and the glutamic acid at codon 64. The V_H81X heptamer is unusual, corresponding only to that of the murine lambda light chain variable region, while the nonamer, although it differs by only one base from the consensus nonamer sequence, is unique[1,3,10,31-35]. V_HE4.Psi contains two deleterious mutations: a 7-base deletion causing a frameshift that occurs at codons −3 to −1, and a substitution creating a terminator at codon 60. All genomic cloning procedures were performed as previously described[6] and all DNA sequencing was performed by the standard Maxam and Gilbert procedure[36].

standard Southern blot procedure[18]. Under low stringency hybridization conditions all three probes identify the same set of germ-line *Eco*RI fragments (data shown for V_H81X, Fig. 2*a*, lane 2), presumably corresponding to fragments encoding the different members of the V_H7183 family. Under high stringency hybridization conditions the V_H81X probe preferentially identified a single 9.7-kb band (Fig. 2*a*, lane 3). A recombinant phage containing this fragment was isolated by screening a BALB/c germ-line DNA library with the V_H81X probe at high stringency (Fig. 3). Analysis of this recombinant clone yielded the sequence of the germ-line V_H81X segment (Fig. 1), and revealed that the 9.7-kb *Eco*RI fragment also contains the unrearranged V_HE4.Psi segment just downstream of the V_H81X segment (Fig. 3). Thus these two V_H segments are closely linked in the germ line.

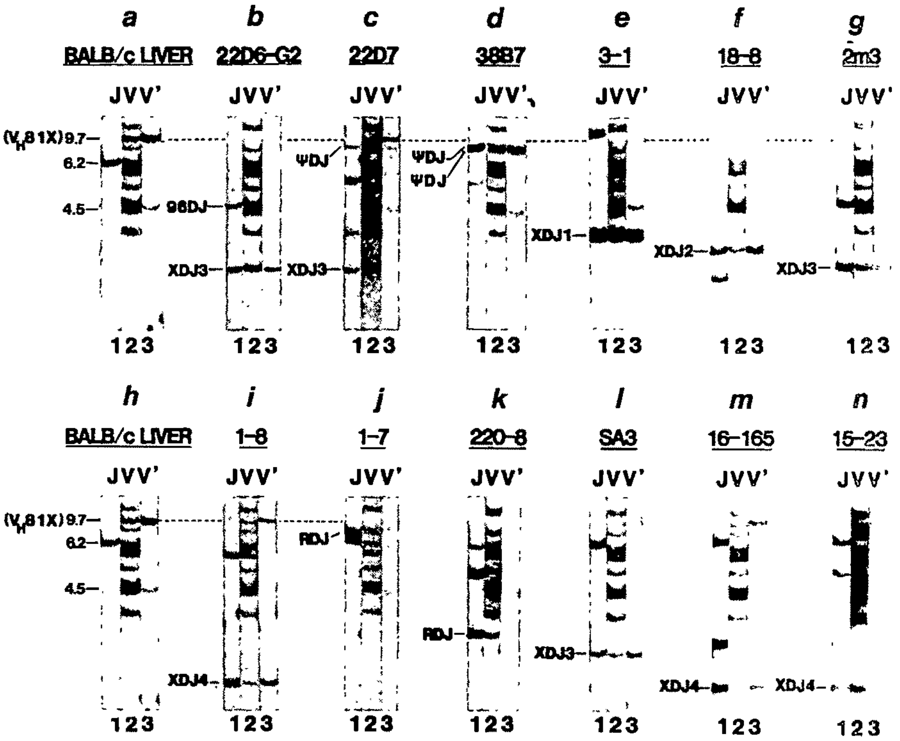

Fig. 2 Identification of V_H81X and related rearrangements in pre-B-cell lines. The derivation and growth of the A-MuLV-transformed cell lines[6,14] and the fetal liver hybridomas[20] have previously been described; other characteristics of the lines are indicated in Table 2. Approximately 10 μg DNA from the indicated sources were digested with *Eco*RI, fractionated on 1.0% agarose gels and transferred to nitrocellulose filters; duplicate blots were assayed for hybridization to either ^{32}P-labelled J_H (see ref. 6) or V_H81X (see Fig. 5) probes. Preparation of high molecular weight genomic DNA, restriction enzyme digests, agarose gel electrophoresis, nick-translations, DNA blotting and hybridizations were performed as described previously[17]. BALB/c liver DNA represents the unrearranged (germ-line) state of the immunoglobulin gene segments. The V_H81X filters were first washed at low stringency (2 × SSC, 68 °C) and then at high stringency (0.08 × SSC, 68 °C). The sizes of *Eco*RI fragments containing V_H81X and V_HE4.Psi rearranged to each of the J_H segments can be predicted from the germ-line restriction maps of the respective regions (see Fig. 3 for the germ-line V_H81X/V_HE4.Psi restriction map; ref. 2 contains the restriction map of the germ-line J_H region): for V_H81X the predicted sizes are 2.6, 2.3, 2.0 and 1.5 kb; for V_HE4.Psi the sizes are all greater than 7.8 kb, thus, a V_HDJ_H rearrangement hybridizing to the V_H81X probe at high stringency can be classified as a V_H81X-DJ_H or V_HE4.Psi-DJ_H rearrangement based on its size. V_HDJ_H rearrangements in which the V_H segment utilized has been classified as a V_H7183 family member are indicated on the figure (XDJ indicates a V_H81X rearrangement, ΨDJ a V_HE4.Psi rearrangement, 96DJ a V_HD6.96 rearrangement, and RDJ indicates that another member of the V_H7183 family was used in the rearrangement). Sizes indicated to the left on the figure are in kilobases. Lane 1: J_H probe (J); lane 2: V_H81X probe, low stringency (V); lane 3: V_H81X probe, high stringency (V').

The V_H7183 family has recently been shown to be the V_H gene family which maps closest to the J_H locus[13]. The line 22D6-G2 has utilized members of the V_H7183 family in V_HDJ_H rearrangements on both chromosomes (V_H81X and V_HD6.96; legend to Fig. 1). This line maintains at least one copy of all germ-line *Eco*RI fragments containing V_H7183 family members except for the 9.7-kb fragment which encodes V_H81X and V_HE4.Psi (compare Fig. 2*a* and *b*, lane 2). Because V_H to DJ_H joining occurs by a deletional mechanism (for example, ref. 6), this result implies that V_H81X/V_HE4.Psi are located 3′ to all other members of the V_H7183 family, and thus are the most J_H-proximal V_H segments yet characterized. This result was confirmed by analysis of many lines with two V_HDJ_H rearrangements: if at least one of the rearrangements utilized V_H81X or V_HE4.Psi (see below), the 9.7-kb germ-line *Eco*RI fragment containing these V_H segments is exclusively deleted (for example, Fig. 2*d*–*g*, *l*).

Utilization of J_H-proximal V_H segments

To determine whether preferential utilization of V_H81X and other members of the most J_H-proximal V_H family was characteristic of the pre-B-cell stage, we devised a simple hybridization assay to examine the V_HDJ_H rearrangements in a large number of lines. The four J_H segments lie within a single, germ-line 6.2-kb *Eco*RI fragment which hybridizes to a J_H probe prepared from the most 3′ portion of this germ-line fragment (Fig. 2*a*, lane 1). Assembly of a V_HDJ_H complex replaces the 5′ end of this germ-line J_H fragment, generating a novel *Eco*RI fragment which retains hybridization to the J_H probe, but which now also hybridizes to a probe homologous to the V_H segment utilized in the rearrangement (for example, Fig. 2*f*, top rearrangement). Under low stringency hybridization conditions, J_H-associated rearrangements utilizing any members of the V_H7183 family will hybridize with a V_H81X probe. Under high stringency conditions, only J_H-associated rearrangements of V_H81X itself will hybridize to the V_H81X probe; these rearrangements include V_HE4.Psi-DJ_H as well as V_H81X-DJ_H rearrangements because an *Eco*RI fragment containing a V_HE4.Psi-DJ_H rearrangement will retain an unrearranged V_H81X segment at its 5′ end (see Fig. 3). V_H81X-DJ_H and V_HE4.Psi-DJ_H rearrangements can, however, be differentiated according to the size of the *Eco*RI fragment bearing the rearrangement (see Fig. 2 legend). Any V_HDJ_H rearrangements not hybridizing to a V_H81X probe at low stringency must utilize V_H segments from more 5′ families. Because the organization of V_H segments has been most extensively characterized in BALB/c mice, all of the studies described below employed lines of BALB/c origin, except as noted.

Three V_H to DJ_H rearranging A-MuLV transformants were analysed: 22D6, 40E4 and 22D7. The rearrangements isolated from subclones of 22D6 and 40E4 have been described above (representative subclone 22D6-G2 shown in Fig. 2*b*). The third V_H to DJ_H rearranging line, 22D7, initially contained two DJ_H complexes[6], but accumulated sub-molar levels of two readily detectable V_HDJ_H rearrangements, one which utilized V_H81X and the other V_HE4.Psi (Fig. 2*c*). Thus all eight rearrangements characterized in these three V_H to DJ_H rearranging lines utilized gene segments from the V_H7183 family, with half of these rearrangements utilizing V_H81X. Fourteen A-MuLV transformants which had assembled V_HDJ_H rearrangements prior to isolation and which did not undergo further rearrangement during propagation (referred to as stably rearranged) have been assayed as described above. Of the 22 V_HDJ_H rearrangements identified in these lines[6], at least 10 utilized members of the V_H7183 family, predominantly V_H81X and V_HE4.Psi (Table 2, Fig. 2*d*–*k*). Several rearrangements did not use V_H segments which hybridized to the V_H81X probe (for example, the lower rearrangement in Fig. 2*f*). The V_H segments in five of these rearrangements were characterized by nucleotide sequence

Table 2 V_H segment utilization in the V_HDJ_H rearrangements of pre-B-cell lines

	V_HDJ_H rearrangements	Rearrangements using V_H7183 segments			Rearrangements using segments from more 5′ V_H families
	Total	V_H81X	V_HE4.Psi	Other	
Fetal liver-derived V_H to DJ_H rearranging lines					
22D6	2	1*	0	1*	0
40E4	4	2*	1*	1*	0
40E1		+		+	−
38B9		+		+	−
38B11		+		+	−
41B1		+		+	+
22D7	2	1	1	0	0
Fetal liver-derived stably rearranged lines					
38B7	2	0	2	0	0
FL	2	1	0	0	1
Marrow-derived stably rearranged lines					
298-13	0	0	0	0	0
220-8	2	0	0	1*	1*
AT1	1	0	0	1	0
2M3	2	1	0	?	?
230-238†	2	0	0	0	2
230-37†	2	0	0	0	2
223-18†	1	0	0	0	1*
18-48	0	0	0	0	0
1-7	2	0	0	1	1*
18-8	2	1*	0	0	1*
1-8	1	1	0	0	0
3-1	2	1	0	0	1
234-8†	2	0	0	0	2
298-8	2	0	0	1	1*
Fetal liver hybridomas BALB/c origin					
15-23	1	1	0	0	0
15-35	0	0	0	0	0
15-56	1	0	0	?	?
15-58	0	0	0	0	0
15-79	1	0	0	?	?
15-83	0	0	0	0	0
16-165	1	1	0	0	0
26-30	1	0	0	?	?
SJL × BALB/c origin					
SA1	1	0	0	?	?
SA2	1	0	0	?	?
SA3	2	1	0	?	?
ACZ	1	0	0	0	1
Totals	43	12	4	6+	14+

The data presented represent a composite of the DNA/RNA hybridization assays and the nucleotide sequence analysis presented in the paper. The number of V_HDJ_H rearrangements in the stably rearranged A-MuLV transformants was previously determined[6]. The number of rearrangements listed for the V_H to DJ_H rearranging lines 40E4 and 22D6 indicates the number of independent V_HDJ_H rearrangements molecularly cloned and characterized from subclones of these lines (see Fig. 1). The V_H to DJ_H rearranging line 22D7 was described in the text. The other V_H to DJ_H rearranging lines were analysed for RNA expression only; the expression data are listed as '+' or '−' under the appropriate column. For the stably rearranged lines, ? in the last two columns indicates that a V_HDJ_H rearrangement co-migrated with a germ-line V_H7183 fragment (for example, upper rearrangement in Fig. 2*g*), and thus it could not be determined if this rearrangement utilized a V_H7183 segment or a V_H segment from a more 5′ V_H family.

* Rearrangements which have been molecularly cloned and sequenced. These include five rearrangements which have utilized segments from families 5′ to the V_H7183 family (G.D.Y., T. K. Blackwell, K. Kruger, N. E. Kohl, R. dePinho, M. G. Reth & S.W.A., unpublished data): four different V_H segments from the very large V_H558 family were isolated in rearrangements from the lines 220-8, 223-18, 204-1-7 and 298-8 while the V_H segment in the rearrangement isolated from the line 18-8 corresponded to the prototype sequence of a more 5′ V_H family, V_H36-60[19]. The RNA assay (see Fig. 5) revealed that V_H segments from the V_HQ52 and V_HS107 families were utilized in at most one rearrangement each in the stably rearranged lines.

† Derived from C57L strain, identical in Igh *z* haplotype to BALB/c[12].

analysis (see Table 2); four were different members of the very large (up to 50 members) V_H558 family, and the other corresponded to the prototype sequence from one of the more 5′ V_H families, V_H36-60[19].

V_H expression in A-MuLV transformants

Both productive and non-productive rearrangements are expressed at the RNA level in A-MuLV transformed cell lines[17]; thus, definition of the V_H-specificity of the expressed RNA can be used to characterize the V_H segments rearranged in these lines. This approach, which can be used to screen efficiently many lines with several different probes, was used to further characterize V_H segment utilization within the V_H7183 family, and also to examine more readily V_H segment utilization from other families. Poly(A)-containing RNA prepared from 24 A-MuLV-transformed cell lines was slot-blotted onto nitrocellulose filters and assayed for hybridization to probes prepared from six different V_H segments: V_H81X, V_HD6.96 and V_HMOPC21, which are members of the V_H7183 family (see above); V_HQ52 and V_HS107, which represent the V_H families immediately upstream to the V_H7183 family[12,13]; and V_H1-7, a member of the V_H558 family (see legend to Figs 4, 5). Under

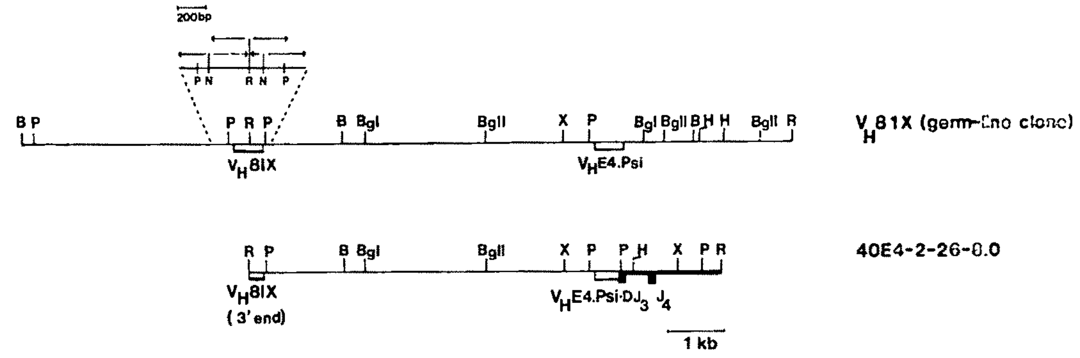

Fig. 3 Linkage of V_HE4.Psi and V_H81X in the germ line. A partial restriction map of a recombinant Charon 4A phage containing a 20-kb germ-line insert, including the 9.7-kb V_H81X/V_HE4.Psi-containing *Eco*RI fragment, is presented. This phage was isolated from a library of *Hae*III/*Alu*I partially digested BALB/c sperm DNA[37] as described in the text. An enlargement of the region surrounding the V_H81X segment is depicted above the map with arrows indicating the strategy utilized to obtain the V_H81X(G) sequence. The map of the cloned V_HE4.Psi rearrangement[15] is presented below the germ-line map, with the restriction maps aligned to demonstrate that the 5' region of the V_HE4.Psi rearrangement is identical to the 5' end of the 9.7-kb V_H81X-containing germ-line *Eco*RI fragment. The map diverges at the point of recombination of the V_HE4.Psi segment with the DJ_H region (the J_H region is indicated by the bold line). Partial nucleotide sequence analysis also confirmed the identity of the 5' ends of these two clones. The restriction sites are marked as follows: B, *Bam*HI; *Bgl*, *Bgl*I; *Bg*II, *Bgl*II; H, *Hin*dIII; N, *Nco*I; P, *Pst*I; R, *Eco*RI; *X*, *Xba*I.

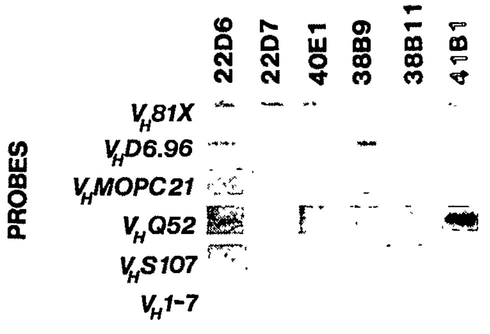

Fig. 4 V_H expression in V_H to DJ_H rearranging A-MuLV transformants. Poly(A)-containing RNA was prepared from the indicated sources as previously described[17]; 0.5 μg of this RNA was denatured in 6% formaldehyde, 50% formamide, 1× SSC at 68 °C for 10 min, a fourfold excess of 20× SSC was added, and the samples were then blotted onto nitrocellulose filters using a slot-blotting apparatus (Schleicher and Schuell-minifold II) The filters were baked, hybridized to probe, and washed as described previously[17]. Identical blots were hybridized with the ^{32}P labelled V_H-specific probes indicated (V_H7183 probes described in Fig. 5. the V_H1-7 segment was prepared from a rearrangement isolated from the A-MuLV transformant 204-1-7 (see Table 2) and is a member of the V_H558 family; all other V_H-specific probes extensively characterized by G.D.Y. and F.W.A., in preparation) Approximately 1.0 μg of total RNA prepared from 4-week spleens probed at high stringency served as positive control and is shown in far right in Fig. 5. The exposures depicted were washed at low stringency (1.0× SSC, 68 °C) except for the blot probed with V_H1-7 which was washed at high stringency (see Fig. 5) The probe for each set of samples is indicated on the left of the figure.

high stringency conditions these probes strongly hybridize only to identical or very homologous sequences whereas at low stringency they hybridize to additional, less closely related, members of their family (see Fig. 5 legend). Six V_H to DJ_H rearranging lines were assayed for V_H-specific expression. These lines contain subpopulations which have formed complete V_HDJ_H complexes in culture[6,14,15]. All six lines revealed low levels of expression of RNA sequences which hybridized to V_H81X and V_HD6.96 but not to V_HMOPC21 (Fig. 4; the RNA sequences which hybridized to the V_H81X and V_HD6.96 probes were the size of *u* mRNA—data not shown). Only one line, 41B1, expressed V_H sequences related to any of the other probes (Fig. 4). These results indicate that the V_H sequences expressed in these lines generally represent a subset of the V_H7183 sequences that are more closely related to V_H81X and V_HD6.96 than to V_HMOPC21. Fifteen stably rearranged A-MuLV transformants were assayed for V_H-specific expression (Fig. 5). Ten of these lines expressed V_H sequences from the V_H7183 family, of which five expressed V_H81X and five expressed sequences closely related to V_HD6.96 (Fig. 5, Table 2). Tested V_H probes representing families upstream of V_H7183 were expressed in many fewer lines than were V_H81X-related segments (Fig. 5, Table 2). This is consistent with the results described above.

In summary, 23 A-MuLV-transformed cell lines of BALB/c origin were analysed for V_H usage by nucleotide sequencing and DNA and/or RNA hybridization studies. The V_H to DJ_H rearranging lines almost exclusively used V_H7183 gene segments in rearrangements, whereas the stably rearranged lines preferentially utilized V_H7183 segments, but also used segments from other V_H families (Table 2).

V_H81X usage in fetal liver hybridomas

To show that preferential use of V_H81X and related V_H segments was not confined to A-MuLV-transformed cell lines, we examined a set of 12 fetal liver hybridomas that were derived from BALB/c or (BALB × SJL) F$_1$ mice[20]. We identified a total of 10 possible V_HDJ_H rearrangements in these lines by methods described previously[6] (the remaining J_H rearrangements were DJ_H complexes). Using the genomic DNA hybridization assay described above, we found that V_H81X was utilized in three of these rearrangements (Fig. 2*l*–*n*).

Structure of V_H81X

Characterization of the V_H segments utilized by pre-B-cell lines allowed identification and nucleotide sequence analysis of five members of the most J_H-proximal V_H family in the BALB/c mouse strain. V_H81X is the most highly divergent of these five related V_H segments; its sequence is striking in that changes occur at several positions which are invariant among all other V_H genes (see Fig. 1 legend). In particular, the replacement of the highly conserved tryptophan at codon 47 by leucine may disrupt the heavy chain structure and affect binding with light chain (M. Reth, personal communication). The recombination recognition sequences for V_H81X, which mediate V_H to DJ_H joining, are also quite distinctive (see Fig. 1 legend). It is notable that the V_H81X segments utilized in the four sequenced V_H81X-DJ_H rearrangements are identical to the germ-line V_H81X segment (Fig. 1). This result is consistent with a lack of selection for somatic mutants in the early developmental stages represented by these lines.

Chromosomal location and V_H utilization

Our studies have revealed a striking consistency in the pattern of V_H usage in pre-B-lymphocytic cell lines. A set of the most J_H-proximal V_H segments, typified by V_H81X, were highly preferentially rearranged in many A-MuLV transformants derived from both fetal liver and adult bone marrow. As discussed earlier, it is unlikely that selection for particular immunoglobulin specificities has influenced our results. It is also unlikely that our results represent an artefact related to the use of permanent cell lines; we have observed this phenomenon in both A-MuLV-

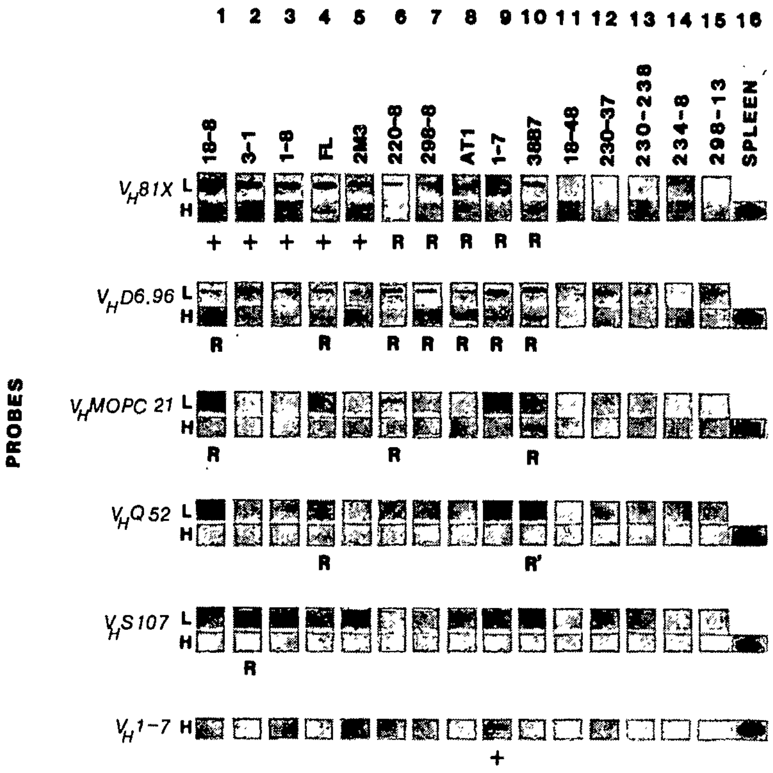

Fig. 5 V_H expression in stably rearranged A-MuLV transformants. Poly(A)- containing RNA was prepared from the indicated lines and processed as in Fig. 4. Exposures of blots washed at low (1.0× SSC, 68 °C) and high (0.1× SSC, 68 °C) stringency, as indicated for each probe, are shown. The blot probed with V_H1-7 was washed only at high stringency; this was because closely related unrearranged V_H gene segments have been found to be expressed in most pre-B-cell lines (G.D.Y. and F.W.A., in preparation). The V_HQ52 probe hybridizes to RNA from the line 38B7 because the V_HQ52 probe hybridizes to V_HE4.Psi sequences at low stringency (G.D.Y. and F.W.A., in preparation), not because of V_HQ52 expression. The hybridization to the V_H81X and V_HD6.96 probes has been determined to be of normal μ-size (data not shown). A '+' under a slot indicates that the V_H expressed by the line is completely homologous to the V_H fragment used as a probe, as judged by Southern hybridization data and by maintenance of hybridization even at high stringency. An 'R' under a slot indicates that a line expresses V_H sequences very closely related to the V_H fragment used as probe. An R' indicates low-level hybridization that may or may not be due to hybridization within a V_H family. Preparation of probes: The V_H81X fragment was prepared from the germ-line clone by digesting at the *Eco*RI and *Sac*I sites indicated by brackets in the V_H81X(G) sequence (Fig. 1) and purifying the approximately 220-bp fragment spanned by these sites. The V_HD6.96 fragment was prepared by digesting at the *Ava*II and *Dde*I sites indicated (Fig. 1) and isolating the intervening fragment. The V_HMOPC21 fragment was prepared from a cDNA clone by digesting at the *Dde*I sites indicated in the V_HMOPC21 sequence (Fig. 1) and isolating the approximately 200-bp fragment released. All fragments contained V_H coding regions only and spanned both hypervariable regions.

transformed pre-B cells and fetal liver (pre-B) hybridomas, and have recently confirmed these findings in studies of normal pre-B cells[21].

Examples of developmental control related to chromosomal organization are found with mammalian globin genes[22], silk moth chorion genes[23], and immunoglobulin genes[6,24]. Here we demonstrate that members of the most J_H-proximal V_H family (V_H7183) are rearranged preferentially in pre-B-cell lines. Furthermore, there is biased usage within the V_H7183 family: the most J_H-proximal segments (V_H81X/V_HE4.Psi) are used most frequently, while a subset of closely related segments (typified by V_HD6.96 and V_HE4.15) are used more frequently than the remaining members of the family (typified by V_HMOPC21). Although fetal liver-derived A-MuLV transformants almost exclusively utilize V_H segments from the V_H7183 family, V_H segments from more 5′ families are represented in approximately half the rearrangements made by marrow-derived A-MuLV transformants. Because the fetal liver-derived lines generally represent a less mature stage of pre-B-cell differentiation than marrow-derived lines[6], this result implies that the repertoire of expressed V_H segments expands during pre-B-cell development. Our data suggests that V_H segments from more 5′ families are randomly represented in rearrangements in pre-B-cell lines; many of these rearrangements used different members of the largest V_H family (V_H558), which may contain up to half of the entire V_H repertoire. The simplest mechanism for the preferential rearrangement of V_H7183 segments would involve their relative chromosomal location: for example, potential recombinases may recognize J_H-proximity in the context of one-dimensional scanning[5]. J_H-proximity is not, however, the sole determinant of preferential rearrangement because V_HE4.Psi is located 3′ to V_H81*X* and is used less frequently.

Functional significance of biased V_H usage

The distinctive amino acid sequence encoded by V_H81X has never been found to be expressed in lines representing mature cell types; furthermore, V_H7183 segments are rarely seen in the apparently random representation of V_H segments found in mature cell types[8]. This reveals a major difference in the repertoire of V_H segments expressed by precursor and mature B-cell populations. The apparently random and extremely diverse set of V_H segments expressed in mature populations could derive from an initial population expressing a biased repertoire by various methods. One such is selection against cells with V_H81X rearrangements occurring during pre-B-cell development; for example, if V_H81X-encoded heavy chains could not associate with light chains, sIg formation would be impossible. Alternatively, even if V_H81X was over-represented in the initial sIg$^+$ B-cell population, other clonotypes might be selectively expanded.

Although we have observed preferential V_H7183 segment rearrangement in strains other than BALB/c, in at least one strain V_H81X is not the most J_H-proximal segment (G.D.Y., M. G. Reth and F.W.A., unpublished data). Thus, different V_H segments may be preferentially rearranged in different strains. This preferential rearrangement may simply be a by-product of the recombinational mechanism, or the rearrangement of the most J_H-proximal V_H segments *per se* may be important in early B-cell differentiation, for example, by serving as a substrate for subsequent *V*-replacement mechanisms. On the other hand, expression of preferentially rearranged segments could play an important role in the developing immune system. Although there are no direct precedents for our results, many studies have suggested that the ability to respond to different antigens follows an ordered developmental sequence[25–30]. It has been shown that highly restricted sets of anti-DNP and anti-TNP antibodies (clonotypes) reproducibly appear during early murine ontogony[30]. Recently, Riley and Ogata (personal communication) have cloned the cDNA for one heavy chain involved in an early DNP response. The V_H segment utilized in the variable region coding for this heavy chain is, remarkably, far more homologous to V_HE4.15 and V_HD6.96 (greater than 95% homology to both) than to any V_H segment previously identified. Thus an antibody made early in development is encoded by a V_H segment which rearranges preferentially in early B-lymphoid cells, suggesting that programmed rearrangement may underlie the programmed appearance of clonotypes.

We thank T. K. Blackwell, M. G. Reth, C. Gee and especially R. Riblett and P. Brodeur for reagents, communication of unpublished results and critically reading this manuscript. This work was supported by American Cancer Society grants NP-393 (F.W.A.) and MV-34M(D.B.), NIH grants AI-20047(F.W.A.), CA16673 and AI14782(J.F.K.), CA-14051 (a core grant to S. Luria) and an award from the Searle Foundation (to F.W.A.). G. D. Y. was supported by NIH training grant GM-07367, S.V.D. is a fellow of the Jane Coffin Childs Memorial fund and F.W.A. is an Irma T. Hirschl Career Scientist.

Received 30 April; accepted 30 July 1984.

1. Early, P., Huang, H., Davis, M., Calame, K. & Hood, L. *Cell* **19**, 981-992 (1980).
2. Sakano, H., Kurosawa, Y., Weigert, M. & Tonegawa, S. *Nature* **290**, 562-565 (1981).
3. Sakano, H., Maki, R., Kurosawa, Y., Roeder, W. & Tonegawa, S. *Nature* **286**, 676-683 (1980).
4. Kurosawa, Y. & Tonegawa, S. *J. exp. Med.* **155**, 201-218 (1982).
5. Wood, C. & Tonegawa, S. *Proc. natn. Acad. U.S.A.* **80**, 3030-3034 (1983).
6. Alt, F. W. *et al. EMBO J.* **3**, 1209-1219 (1984).
7. Tonegawa, S. *Nature* **302**, 575-581 (1983).
8. Kabat, E. A., Wu, T. T., Bilofsky, H., Reid-Miller, M. & Perry, H. in *Sequences of Proteins of Immunoglobulin Interest* (NIH, Bethesda, 1983).
9. Kemp, D. J. *et al. J. molec. appl. Genet.* **1**, 245-261 (1981).
10. Bothwell, A. L. M. *et al. Cell* **24**, 625-637 (1981).
11. Loh, D. Y., Bothwell, A. L. M., White-Scharf, M. E., Imanishi-Kari, T. & Baltimore, D. *Cell* **33**, 85-93 (1983).
12. Brodeur, P. & Riblet, R. *Eur. J. Immun.* (in the press).
13. Brodeur, P., Thompson, M. A. & Riblet, R. *UCLA Symp. molec. cell. Biol. new Ser.* **18** (in the press).
14. Alt, F. W., Rosenberg, N., Lewis, S., Thomas, E. & Baltimore, D. *Cell*, **27**, 381-390 (1981).
15. Desiderio, S. V. *et al Nature* (in the press).
16. Yaoita, Y. *Nucleic Acids Res.* **11**, 7303-7316 (1983).
17. Alt, F. W., Rosenberg, N., Enea, V., Siden, E. & Baltimore, D. *Molec. cell Biol.* **2**, [illegible] (1982).
18. Southern, E. M. *J. molec. Biol.* **98**, 503-517 (1975).
19. Near, R. *et al. Proc. natn. Acad. Sci. U.S.A.* **81**, 2167-2171 (1984)
20. Burrows, P., LeJeune, M. & Kearney, J. F. *Nature* **280**, 838-840 (1979)
21. Blackwell T. K., Yancopoulos, G. D. & Alt, F. W. *UCLA Symp. molec. cell Biol. new Ser.* **19** (in the press).
22. Fritsch, E. F., Lawn, R. M. & Maniatis, T. *Cell* **19**, 959-972 (1980)
23. Eickbush, T. H. & Kafatos, E. C. *Cell* **29**, 633-643 (1982)
24. Marcu, K. B. *Cell* **29**, 719-721 (1982).
25. Silverstein, A. M., Uhr, J. W., Kraner, K. L. & Lukes, R. J. *J. exp. Med.* **117**, 799-812 (1963)
26. Sterzl, J. & Silverstein, A. M. *Adv. Immun.* **6**, 337-459 (1967)
27. Ivanyi, J. *Immunology* **28**, 1007-1013 (1975).
28. Lydyard, P. M., Grossi, C. E. & Cooper, M. D. *J. exp. Med.* **144**, 79-97 (1976)
29. Press, J. L. & Klinman, N. P. *Eur. J. Immun.* **4**, 155-159 (1974)
30. Klinman, N. R. & Press, J. L. *Fedn Proc.* **34**, 47-50 (1975)
31. Crews, S., Johanna, G., Huang, H., Calame, K. & Hood, L. *Cell* **25**, 59-65 (1981)
32. Givol, D. *et al. Nature* **292**, 426-430 (1981).
33. Ollo, R., Auffray, C., Sikorov, J. L. & Rougeon, F. *Nucleic Acids Res.* **9**, 4099-4109 (1981)
34. Kataoka, T., Nikaido, T., Miyata, T., Moriwaki, K. & Hongo, T. *J. biol. Chem.* **257**, 277-285 (1982).
35. Cohen, J. B. & Givol, D. *EMBO J.* **2**, 1795-1800 (1983).
36. Maxam, A. & Gilbert, W. *Meth. Enzym.* **65**, 419-460 (1980)
37. Davis, M. M. *et al. Nature* **283**, 733-739 (1980).

LETTERS TO NATURE

Rapid variability in optical polarization of the quasar-like object OJ287

Anjani K. Kulshrestha, U. C. Joshi & M. R. Deshpande

Physical Research Laboratory, Ahmedabad-380009, India

OJ287 (0851+20) is one of a small group of quasar-like objects, the BL Lac group. It has a featureless optical nonthermal continuum, a relatively flat radio spectrum, a high degree of linear polarization at radio and optical wavelengths, it is extremely compact and displays a strong rapid variability at all wavelengths. Rapid variations in the optical flux of OJ287 with a period of about 40 min were observed by Visvanathan and Elliot[1] and by Frohlich *et al.*[2]. At 1.25 μm even more rapid but non-periodic variations were reported by Wolstencroft *et al.*[3]. We report here observations of rapid and strong variations in the degree of linear polarization of the optical flux of OJ287. We conclude that if the radiation observed from the variable component was of synchrotron nature, then there must be a high degree of relativistic beaming in OJ287. On the other hand, if the variable flux is assumed to be the inverse-Compton scattered flux and relativistic effects are not invoked, OJ287 must have a very compact central source, probably a black-hole accretion-disk system.

The photopolarimetric observations of OJ287 in the ultraviolet, blue, visible, red and infrared (UBVRI) wavebands were made using the Minipol instrument[4], with GaAs detectors (cooled to dry ice temperatures), on the 1.55-m telescope of the University of Arizona at Mt Catalina on 10-12 January 1984. Normalized Stokes parameters, Q and U, and their errors were calculated from a least squares analysis of the data, and the degree of linear polarization ($P=(Q^2+U^2)^{1/2}/I$) and position angle ($\theta=\frac{1}{2}\tan^{-1}Q/U$) were calculated from these quantities, where I is the intensity. Sky observations were made approximately every 15 min and the results were obtained from the data corrected for sky background. Instrumental polarization was negligible in comparison with that of the source. Photometric calibrations were made on all nights by observing the star HR382.

Polarization in the R band was monitored from 09:10 to 09:50 UT on 10 January and from 09:55 to 10:50 UT on 11 January (Fig. 1). On 10 January, polarization dropped from 18 to 14% (standard error in polarization, $\sigma_p\approx0.8\%$) in about 20 min. During this interval the adjacent sky polarization varied very little (2.7-3.1%, $\sigma_p\approx1\%$). Two polarization peaks were observed on 11 January; first the degree of polarization dropped from 13% to 9% in about 20 min, and then it increased again to 14% in the next ~15 min. On 12 January, polarization was monitored in I band from 08:50 to 10:00 UT (Fig. 2). Three asymmetric saw-tooth shaped variations were observed. The polarization peaks were separated by about 25 min, and the degree of polarization varied from 12 to 16% ($\sigma_p\approx0.9\%$). In this interval, four sky observations were made; the sky polarization varied from 1.7 to 2.2%, and the variations in the sky brightness were <0.1 mag. The magnitude, linear polarization, and position angle measurements made in the UBVRI bands on the same date, just after the above-mentioned observations, are shown in Table 1. The observed wavelength-independence of the degree and orientation of polarization indicates that the variations

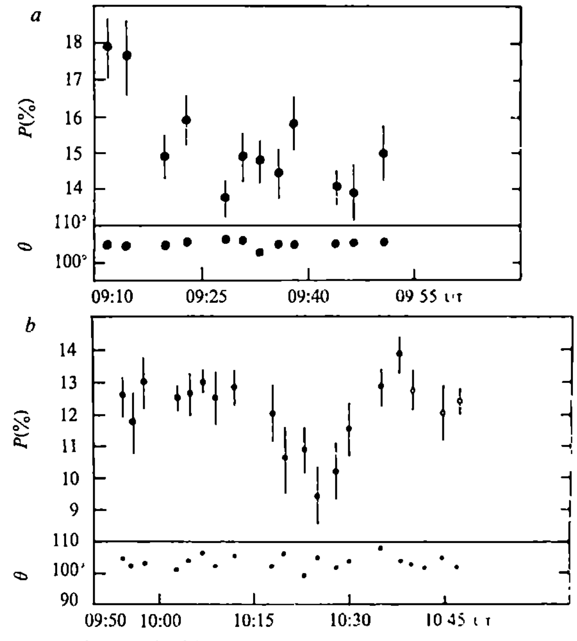

Fig. 1 Time variability of the percentage linear polarization (P) and the position angle (θ) of OJ287 in R band. *a*, 09:10-09:50 UT on 10 January 1984; *b*, 09:55-10:50 UT on 11 January 1984. The error bars have a total length of 2 s.d.

Table 1 Photopolarimetric observations of OJ287 on 12 January 1984

Waveband (λ)	Magnitude	P ($\pm\sigma_P$) (%)	θ ($\pm\sigma_\theta$) (deg)
U (0.36 μm)	14.3	13.4 (±0.8)	97 (±1.7)
B (0.44 μm)	15.1	13.6 (±0.6)	94 (±1.3)
V (0.55 μm)	14.6	13.5 (±0.4)	93 (±0.8)
R (0.7 μm)	14.0	14.6 (±0.8)	94 (±1.6)
I (0.8 μm)	13.3	13.7 (±0.4)	94 (±0.8)

observed in I band were present at least in the whole optical region, that is from U to I bands. The total optical flux, received at Earth, amounts to 2.77×10^{-11} erg s^{-1} cm^{-2}.

The general trend of the observed variations can be described as follows: the degree of polarization fluctuates by ~4% on a time scale of ~25 min; the variations are saw-tooth shaped with the rising edges much steeper compared to the falling ones, and these fluctuations recur at very short time-intervals.

The optical polarization of the star RY Tau was observed on 9 January for ~25 min and the degree of polarization was found to lie between 3.2 and 3.3% ($\sigma_p \approx 0.1\%$). The amplitudes of the observed variations in the polarization of OJ287 are very large (~4%) and, thus, these variations cannot be attributed to systematic instrumental effects.

For a source redshift of 0.306 (ref. 5), $H_0 = 75$ km s^{-1} Mpc^{-1} and $q_0 = 0$, the observed absolute optical luminosity equals 4.8×10^{45} erg s^{-1}. To produce variations in the degree of polarization by as much as 4%, the absolute luminosity of the variable component, L, should be $\geqslant 2\times10^{44}$ ergs s^{-1}. The observed period of 25 min corresponds to a variability time scale, τ, of ~19 min in the rest-frame of the source.

A severe Compton problem (the paradox first described by Hoyle *et al.*[6]) arises if we assume that the variable component was radiating by synchrotron process. This trouble can be removed by invoking bulk relativistic streaming. The requirement that the synchrotron lifetime of electrons be at least equal to the variability time scale gives the value of relativistic Doppler factor: $\delta \geqslant 15$, where $\delta = (1-\beta^2)^{1/2}/(1-\beta\cos\phi)$ where β is the bulk velocity in units of c, and ϕ is the angle between the direction of motion and the direction along the line of sight. An alternate way of overcoming the Compton problem is to assume that the observed radiation was coming from a very small instability, far from the central source, which derived its energy from the central source (in an unspecified way). Other mechanisms, such as small pitch angle coherent synchrotron emission[7] or the reacceleration of electrons[8], could eliminate the Compton problem. However, note that the models which can explain an isolated rapid variation are not necessarily capable of explaining this kind of rapidly recurring variations.

Rees[9] has shown that rapid periodic variations can be explained using models which invoke relativistic expansion, provided the source is optically thick. An interesting feature of this kind of expanding-source models is that in any outburst, at a given frequency, the source should brighten faster that it fades. This feature would fit to our data when both the variable and the basic synchrotron components of OJ287 were radiating in the same magnetic field configuration.

The other possibility is that the radiation observed from the variable component was inverse-Compton scattered flux from lower frequency photons. The particles which scatter the photons, themselves present some opacity to the photons and thus set a lower limit to the possible variability time scales for an outburst with given luminosity. On the basis of this type of consideration, Fabian[10] has derived a minimum time scale of variation, $\tau \geqslant L(\mathrm{erg\,s^{-1}})/2\times10^{42}\eta$, where η is the efficiency with which matter is converted to energy. Our data imply a value of $\eta \geqslant 10\%$. For the case of accretion onto massive black hole, such a high value of efficiency is possible only if the accreting material possesses anguar momentum[11]. If we consider the source to be isotropic and free from bulk relativistic motions, and if its luminosity does not significantly exceed the Eddington limit, due to emission of pulsar-type radiation, then by equating the luminosity of the variable component to Eddington luminosity and taking the appropriate radius of the accretion disk round a black hole to be about five times the Schwarzschild radius, the minimum value of possible variability time scales is ~1.3 min which is one-fifteenth of the observed time scale. The supermassive stars would give about 100 times more than this for the minimum time scales. Thus, our observations suggest that the central core of OJ287 is probably a black hole accretion-disk system.

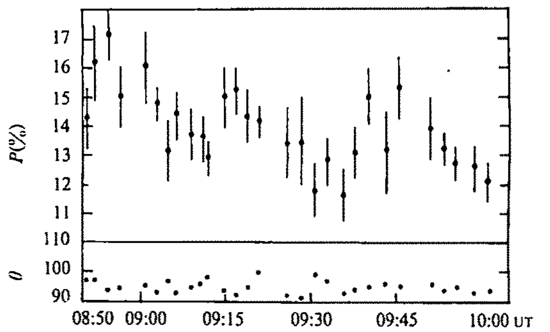

Fig. 2 Time variability of P and θ of OJ287 in I band, 08:50–10:00 UT on 12 January 1984.

We thank S. P. Pandya and P. V. Kulkarni for encouragement. Tom Gehrels and S. Tapia (Lunar and Planetary Laboratory, University of Arizona) made available Minipol and the telescope. This work was supported by Department of Space, Government of India.

Received 4 May, accepted 15 August 1984.

1. Visvanathan, N. & Elliot, J. L. *Astrophys. J.* **179,** 721–730 (1973).
2. Frohlich, A., Goldsmith, S. & Weistrop, D. *Mon. Not. R. astr. Soc.* **168,** 417–425 (1974).
3. Wolstencroft, R. D. Gilmore, G. & Williams, P. M. *Mon. Not. R. astr. Soc.* **201,** 479–485 (1982).
4. Frecker, J. E. & Serkowski, K. *Appl. Opt.* **15,** 605–606 (1976).
5. Miller, J. S., French, H. B. & Hawley, S. A. *Pittsburgh Conf. On BL Lac Objects* (ed. Wolfe, A. M.) 176–191 (University of Pittsburgh, 1978).
6. Hoyle, F., Burbidge, G. R. & Sargent, W. L. W. *Nature* **209,** 751–753 (1966).
7. Cocke, W. J. & Pacholczyk, A. G. *Nature* **265,** 608–609 (1977).
8. Cavaliere, A. & Morrison, P. *Astrophys. J. Lett.* **238,** L63–L66 (1980).
9. Rees, M. J. *Mon. Not. R. astr. Soc.* **135,** 345–360 (1967).
10. Fabian, A. C. *Proc. R. Soc.* **A366,** 449–459 (1979).
11. Pringle, J. E., Rees, M. J. & Pacholczyk, A. G. *Astr. Astrophys.* **29,** 179–184 (1973).

Outer-core geostrophic flow and secular variation of Earth's geomagnetic field

J. L. Le Mouël

Laboratoire de Géomagnétisme et Paléomagnétisme (ERA 922),
Institut de Physique du Globe, Tour 14, 4 Place Jussieu,
75230 Paris Cedex 05, France

In studies of the temporal variations of the main internal geomagnetic field (the secular variation or SV), it is usual to consider separately the variations of the dipolar and non-dipolar parts which appear to have different time constants. The mechanism that is generally invoked to explain the generation of SV is the advection of the lines of force of the main field by the highly conducting fluid at the top of the core. Such a mechanism involves the main field as a whole and it is not clear *a priori* why its two parts should behave separately. I show here that the Coriolis force will probably dominate the force budget at the top of the core and that, in such a case, the motion of the fluid involves the two parts of the field in a different way; in particular, the existing axial dipolar component is not re-engaged in the process which builds up the SV.

Let us consider the Navier-Stokes equation in the outer layers of the core:

$$\rho(\delta\mathbf{u}/\delta t + \mathbf{u}.\nabla\mathbf{u}) = -\nabla p + \mathbf{J}\times\mathbf{B} - 2\rho(\mathbf{\Omega}\times\mathbf{u}) + \rho\nu\Delta^2\mathbf{u} - \rho g\mathbf{n} \tag{1}$$

where ρ is the density, $\mathbf{u}$ the velocity, p the pressure, $\mathbf{J}$ the electric current density, $\mathbf{B}$ the magnetic field, $\mathbf{\Omega}$ the Earth's rotation, ν the kinematic viscosity, $\mathbf{n}$ the unit radial vector, g the gravity.

In the frozen-flux approximation, where the core fluid is considered to be a perfect conductor[1-5], the SV observed outside the core depends only on the (horizontal) motion $\mathbf{u}$ of the fluid at the core-mantle boundary, more exactly below a thin boundary layer. If the flow is assumed to be large scale, its velocity can be estimated from SV data: its order of magnitude U is found to be 10^{-4} m s^{-1} (see ref. 6; the value of 0.2^{0} yr^{-1} for the westward drift rate corresponds to 4×10^{-4} m s^{-1}). In this large-scale hypothesis, both the Rossby number R and the Ekman number E are quite small. Taking $L=10^{6}$ m as a characteristic horizontal length of $\mathbf{u}$, we have $R=U/\Omega L\simeq10^{-6}$ and $E=\nu/\Omega L^{2}\ll1$, whichever value we adopt for the poorly known kinematic viscosity of the core.

As for the time constant of $\mathbf{u}$, the SV field can change significantly—by half its value—in, say, 10 yr (refs 7, 8). But the acceleration term $\rho\delta\mathbf{u}/\delta t$ is fairly negligible ($<10^{-3}$) compared with the Coriolis force.

Let us now consider the Lorentz force $\mathbf{J}\times\mathbf{B}$. If the field is purely poloidal in the external layers of the core, $B\simeq5\times10^{-4}$ T, and we get: $|(\mathbf{J}\times\mathbf{B})|/|2\rho(\mathbf{\Omega}\times\mathbf{u})|\simeq B^{2}/2\mu\rho\Omega LU\simeq10^{-3}$. It is possible that a toroidal field also exists in the outer layers of the core, as often predicted by dynamo theory, and as is required for electromagnetic core-mantle coupling. But, even if this toroidal field does exist and is intense in the body of the core (up to 10 times the poloidal field), it is certainly less intense in the neighbourhood of the (nearly) insulating mantle. More precisely, let β be the ratio of the dominant part of the horizontal Lorentz force to the horizontal Coriolis force. It is easily shown that $\beta\simeq B_{r}B_{T}f(\theta)/(2\mu\rho\Omega lU\cos(\theta))$, where B_{r} is a typical value of the radial component of the poloidal field at the core-mantle boundary, B_{T} a typical value of the toroidal field $\mathbf{B}_{T}$ in the body of the core, l a characteristic vertical scale of $\mathbf{B}_{T}$. $f(\theta)$ depends on the variation of $\mathbf{B}_{T}$ with colatitude θ. If, as is generally assumed, $\mathbf{B}_{T}$ is antisymmetrical with respect to the Equator and vanishes on the Equator (for example, if $\mathbf{B}_{T}$ is a P_{2}^{0} toroidal field due to the differential rotation of the core in the presence of the axial dipolar field), $f(\theta)/\cos(\theta)\simeq1$. When $l=10^{6}$ m then β has approximately the same numerical value as B_{T} expressed in tesla, that is to say 5×10^{-2} in the most unfavourable case. If l is smaller, as suggested by Benton and Muth[9], due to the possibility of a strong gradient of B_{T} near the core-mantle boundary, β is, of course, larger. If not, or if the toroidal field is of the same order of magnitude as the poloidal one, the horizontal projection of equation (1) reduces nearly everywhere to the geostrophic approximation in its usual form:

$$2\rho(\mathbf{\Omega}\times\mathbf{u})_{\mathrm{H}}+\nabla_{\mathrm{H}}p=0 \qquad (2)$$

where H indicates horizontal. Equation (2) must be complemented by the radial component of equation (1) whose principal part is the hydrostatic equation. Then

$$\mathbf{u}=(2\rho\Omega\cos\theta)^{-1}\mathbf{n}\times\nabla_{\mathrm{H}}p \qquad (\theta\neq\pi/2) \qquad (3)$$

Let us now recall an important result due to Backus[3]. Let B_{r} be the radial component of the geomagnetic field $\mathbf{B}$ at the core-mantle boundary, $\dot{B}_{r}$ its time derivative. These quantities are related through the equation

$$\dot{B}_{r}=\mathrm{div}_{\mathrm{H}}(\mathbf{u}B_{r}) \qquad (4)$$

It follows directly that all motions of the form

$$\mathbf{u}=(B_{r})^{-1}(\mathbf{n}\times\nabla_{\mathrm{H}}\psi), \qquad (5)$$

where ψ is any well behaved function of longitude ϕ and colatitude θ, are in the so-called null space of $\mathbf{B}$ that is generate no secular variation $\dot{\mathbf{B}}$ from $\mathbf{B}$.

From equations (5) and (3), the geostrophic motion (3) is in the null space of the axial-dipole field: if, at a certain epoch, the geomagnetic field happens to be that of an axial dipole, it will remain axial dipolar and unchanged.

In general, at the core-mantle boundary,

$$B_{r}=\alpha_{1}^{0}\cos\theta+\Sigma_{n,m\neq1,0}(\alpha_{n}^{m}\cos m\phi+\beta_{n}^{m}\sin m\phi)\,P_{n}^{m}(\cos\theta)$$

Equation (4) being linear, it follows that the axial dipolar part of $\mathbf{B}$ is not involved in the generation of SV by the geostrophic motion $\mathbf{u}$. Let $\mathbf{B}_{1}$ denote the axial dipolar component of $\mathbf{B}$, $\mathbf{B}_{\mathrm{nda}}$ the non-dipolar-axial field, that is $(\mathbf{B}-\mathbf{B}_{1})$. The behaviour of SV can be summarized by the two equations

$$\dot{\mathbf{B}}_{1}=\mathbf{F}_{1}(\mathbf{u},\mathbf{B}_{\mathrm{nda}})$$

and

$$\dot{\mathbf{B}}_{\mathrm{nda}}=\mathbf{F}(\mathbf{u},\mathbf{B}_{\mathrm{nda}}) \qquad (6)$$

The fact that the existing axial dipolar field is not used in the process by which the field is changed provides a simple explanation of why the secular variation of this axial dipolar field (the geological field) does not involve the same time constant as the secular variation of the non-dipole field (all the better since the westward drift of the external layers of the core, which is sometimes considered as the prominent stable part of $\mathbf{u}$, does not generate any $\mathbf{B}_{1}$ from $\mathbf{B}_{\mathrm{nda}}$).

Let us now assume that the frozen flux approximation still holds for time spans of some thousands of years[10] and consider a reversal of the geomagnetic field: the non-dipole field cannot disappear during the process, otherwise the whole process would stop (equation (6)). Such an extrapolation to long time spans is certainly speculative. But, for time spans short enough for the frozen-flux approximation to hold, a geostrophic flow in the upper layers of the core implies some of the observed features of the secular variation of the geomagnetic field (my arguments in favour seem to fail only if the unobservable toroidal field is both very intense and rapidly varying near the core-mantle boundary).

I acknowledge fruitful discussions with R. Hide and G Backus. IPGP contribution 788.

Received 25 June; accepted 15 August 1984.

1. Bondi, H. & Gold, T. *Mon. Not. R. astr. Soc.* **110,** 607–611 (1950)
2. Roberts, P. H. & Scott, S. *J. Geomagn. Geoelectr.* **17,** 137–151 (1965)
3. Backus, G. E. *Phil. Trans. R. Soc.* A**263,** 239–266 (1968).
4. Hide, R. *Phil. Trans. R. Soc.* A**259,** 615–680 (1966).
5. Voorhies, C. & Benton, E. R. *Geophys. Res. Lett.* **9,** 258–261 (1982)
6. Kahle, A., Vestine, E. H. & Ball, R. *J. geophys. Res.* **72,** 1095–1108 (1967)
7. Gire, C., Le Mouël, J. L. & Ducruix, J. Nature **307,** 349–352 (1984)
8. Courtillot, V. & Le Mouël, J. L. *Nature* **311,** 709–716 (1984)
9. Benton, E. R. & Muth, A. L. *Phys. Earth Planet. Inter.* **20,** 127–133 (1979)
10. Gubbins, D. & Roberts, N. *Geophys. J. R. astr. Soc* **73,** 675–687 (1983)

Stress corrosion in a borosilicate glass nuclear wasteform

A. E. Ringwood & P. Willis

Research School of Earth Sciences, Australian National University,
Canberra 2601, Australia

Most current technologies for the incorporation of high-level nuclear wastes in borosilicate glass wasteforms on a large scale yield products characterized by marked internal stresses developed during cooling and also around crystalline inclusions. We discuss here a typical borosilicate glass wasteform which, when exposed to water vapour and water for limited periods, exhibits evidence of stress corrosion cracking arising from the interaction of polar OH groups with stressed glass surfaces. Glass wasteforms may experience similar stress corrosion cracking when buried in a geological repository and exposed to groundwaters over an extended period. This would increase the effective surface areas available for leaching by groundwater and could decrease the lifetime of

the wasteform. Conventional leach-testing methods are insensitive to the longer-term effects of stress corrosion cracking. We suggest that specific fracture-mechanics tests designed to evaluate susceptibility to stress corrosion cracking should be used when evaluating the wasteforms for high-level nuclear wastes.

The most important property which is used to characterize borosilicate glass wasteforms is their leaching performance in water and aqueous solutions. Most glasses which have been characterized by leach tests have been produced on a small scale in laboratory conditions. Melting is typically carried out under well-controlled conditions above the liquidus, so that there are no crystalline phases present. In many cases, the glasses have been annealed during cooling to eliminate internal stresses. The borosilicate glasses produced by current technologies for the immobilization of high-level nuclear waste (HLW) on a full engineering production scale differ from these 'ideal' laboratory-produced glasses in two important respects. First, they usually contain a few per cent of dispersed crystalline phases, arising either from incomplete solution of the HLW or from crystallization during slow cooling, after the glass has been poured into canisters[1,2]. Second, when HLW-glasses are cooled in commercial-sized canisters, they are subjected to thermal stresses which cause extensive cracking[3,4]. Typically, this leads to an increase in the surface area of the glass by about a factor of 10 (ref. 3). Moreover, the remaining domains of uncracked glass are themselves subjected to quite strong internal stress fields.

These characteristics are displayed by a sample of borosilicate glass containing about 25% of simulated HLW produced by the 'in-canister' melting process at the US Department of Energy plant at Savannah River, South Carolina. This technology is the accepted 'back-up' process for the joule-heated ceramic melter on-site. The chemical composition of this glass as determined by electron microprobe analysis is as follows: SiO_2, 46.0; TiO_2, 0.3; Al_2O_3, 4.2; Fe_2O_3, 14.8; MnO, 3.3; NiO, 1.5; CaO, 5.3; Na_2O, 15.2; $B_2O_3+Li_2O$, 9.4 wt%. Note, however, that the phenomena discussed here are not specific to glasses of any singular chemical composition, or produced by any one technology, but are generic to HLW glasses produced on a commercial scale by most current technologies because of the residual stresses which these processes induce in the final products.

The sample which was studied (Fig. 1) is bounded by generally conchoidal fracture surfaces. Small impacts readily cause spalling, demonstrating the existence of a pervasive state of internal stress. Numerous crystalline inclusions are visible. Large numbers of sharp cleavage steps are also present (Figs 1, 2). In many cases, cleavage steps propagate outwards from crystalline inclusions (Fig. 2).

Close examination of cleavage steps on surfaces of glass which have been exposed to the atmosphere for ~2 yr show that distinct cracks up to 5 mm long have formed at the base of many of the steps. In contrast, cracks beneath cleavage steps rarely occur on freshly fractured surfaces. The common occurrence of these cracks on surfaces which have been exposed to the atmosphere for an extended period suggests a causal relationship. Related observations and interpretation by Wiederhorn and others[5-8] suggests that the cracks have been caused by stress corrosion in the presence of atmospheric moisture. This phenomenon has been widely recognized in stressed glasses in the presence of polar solvents (such as, water) and also in the presence of atmospheric water vapour[5-8]. The basal corners of the cleavage steps represent sites of localized stress concentrations[9]. The stresses at these sites can be intensified by the pervasive thermal stresses present in the sample, arising from its cooling history. Polar atmospheric water molecules preferentially attack the glass at the sites of greatest stress concentration, causing stress corrosion cracks to develop and propagate[6-8].

Several years ago, Wiederhorn[5] drew attention to the potential importance of stress corrosion on the long-term performance of nuclear-waste glasses, but the significance of his contribution has been largely ignored. Nevertheless, if HLW glass experienced extensive stress-corrosion cracking over an extended period after burial in a geological repository, the effective area exposed to leaching would be greatly increased and the survival time of the glass correspondingly decreased. In these essentially unpredictable circumstances, the conventional methods of predicting long-term performance of glasses on the basis of short-term measurements of average leach rates of laboratory-prepared glasses with constant surface area, would be decidedly inadequate.

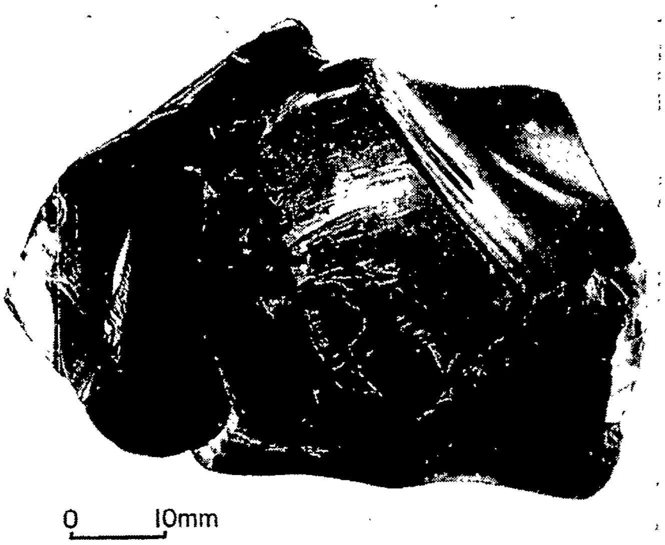

Fig. 1 Sample of borosilicate glass containing ~25% of simulated high-level US defence wastes, produced by in-canister melting at the Savannah River Laboratory of the US Department of Energy. Note the presence of abundant cleavage steps on some of the surfaces.

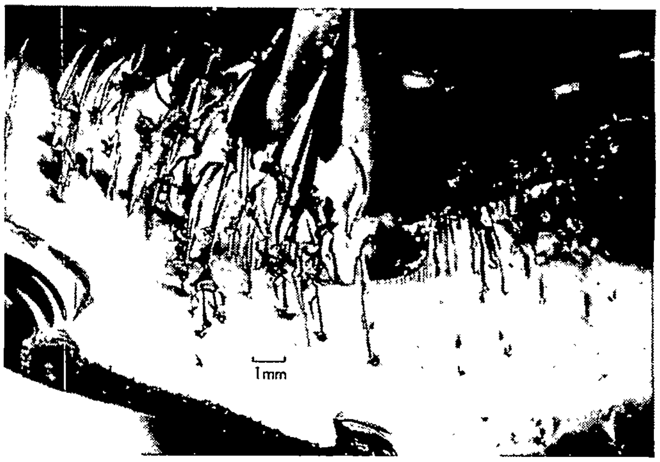

Fig. 2 Glass surface shows complex cleavage steps, mostly originating at crystalline inclusions. Some of these steps represent the outcrops of planar fractures containing iridescent air films.

Studies of polished and thin sections showed that the crystalline inclusions consisted of small spinels (mostly 30–100 μm), commonly sheathed by laths of acmitic pyroxene. The glass immediately surrounding the larger spinel crystals is sometimes observed to be optically anisotropic. This feature is apparently caused by stresses arising from differential thermal expansion coefficients of glass and crystals during cooling.

Samples of glass (dimensions, 1–3 cm) were removed from the interior of the specimen and polished to yield planar surfaces, free of any cracks. The samples were then placed in closed Teflon containers and immersed in 20 ml of deionized water at 95 °C for 25 days. At the conclusions of these treatments, the glasses were covered by loosely adhering iridescent films of hydrous oxides. These were easily removed by a minimal degree of polishing. The underlying surfaces of the glasses displayed several interesting features (Fig. 3).

The glass immediately surrounding the spinel crystals was selectively removed by leaching so that the spinels were surrounded by deep pits (Fig. 3*a*). We have already noted that the glass immediately next to some of the spinels is anisotropic, indicative of localized stress. The formation of pits around the spinels is believed to be caused by the higher intrinsic leachability of stressed regions. The samples also displayed systems of intersecting grooves which commonly radiated from, and linked spinel crystals. It seems possible that the development and location of these grooves is determined by the interaction of localized stress fields surrounding spinels and the pervasive state of thermally-induced stress which exists within the glass.

The fact that simple leaching of the smooth surfaces of a typical borosilicate glass causes the rapid development of grooves and pits has important implications for the long term behaviour of these glasses. As noted above, the glass is characterized by a pervasive residual thermal stress. The present experiments show that in the presence of water, grooves and pits develop quite rapidly. The effect of a tensile or shear stress of thermal origin will be to magnify the local stress intensity at the bases of the grooves or pits by a factor proportional to $1/\sqrt{R}$ where R is the local radius of curvature[7]. Thus, the bases of grooves and pits will dissolve more rapidly than plane surfaces and these features will propagate into the interior of the glass much faster than the average rate of surface dissolution. This process of inhomogeneous dissolution may lead ultimately to disintegration of the glass, with a large increase in the effective surface area which can be exposed to the attack of groundwater.

The development of grooves as seen in Fig. 3 seems to reflect a form of stress corrosion. These features may propagate steadily into the interior of the glass through preferential dissolution at their tips as discussed above. Alternatively, if the stress intensity within the glass should exceed a critical limit, they are likely to propagate catastrophically in stress corrosion cracks. In regions subjected to tensile stress, Si-O bonds are stretched and preferentially attacked by polar water molecules which become inserted between the silicon and oxygen atoms in the Si-O-Si glass network. In consequence, Si-O bonds are broken and replaced by Si-O-H|H-O-Si groupings where the vertical bar represents a rupture. This causes a crack to propagate inwards[8,10]. The propagation distance is primarily controlled by the stress intensity at the tip of the crack. With an isolated stress centre, the stress intensity decreases with distance and crack growth is ultimately halted. If, however, the entire specimen is also subjected to an overall tensile or shear stress exceeding the critical limit, the crack will propagate through the entire specimen. Alternatively, if there is a high spatial density of stress centres (see below), their localized crack propagation envelopes may intersect, with catastrophic consequences.

After burial in geological repositories, nuclear waste glasses are likely to be subject to additional critical stresses arising from the effects of radiation damage on included crystalline phases. Borosilicate glasses produced on a large scale for HLW immobilization frequently contain a few per cent of dispersed crystalline phases, including metallic alloys, a fluorite-type phase $Ce^{4+},REE^{3+}O_{2-x}$, spinels, silicates and molybdates[1,2] (where REE is the rare-earth element). The volume expansions exhibited by some of these crystalline phases after strong irradiation from α particles may be as high as several per cent, whereas glass does not usually expand beyond 1% (ref. 1). Localized stresses will be induced in the glass surrounding the damaged crystals. These stresses may greatly exceed the thermally-induced stresses around the spinel crystals in the present glass, which are caused by differential volume changes <1%.

In these circumstances, it seems that localized stresses around many of the larger (for example, ~50 μm) crystalline phases could eventually exceed the critical levels required for the initiation of stress corrosion cracking on surfaces, which are in contact with groundwater, or even with atmospheric water vapour. The capacity of nuclear waste glasses to withstand ultimate disintegration because of these factors is open to question.

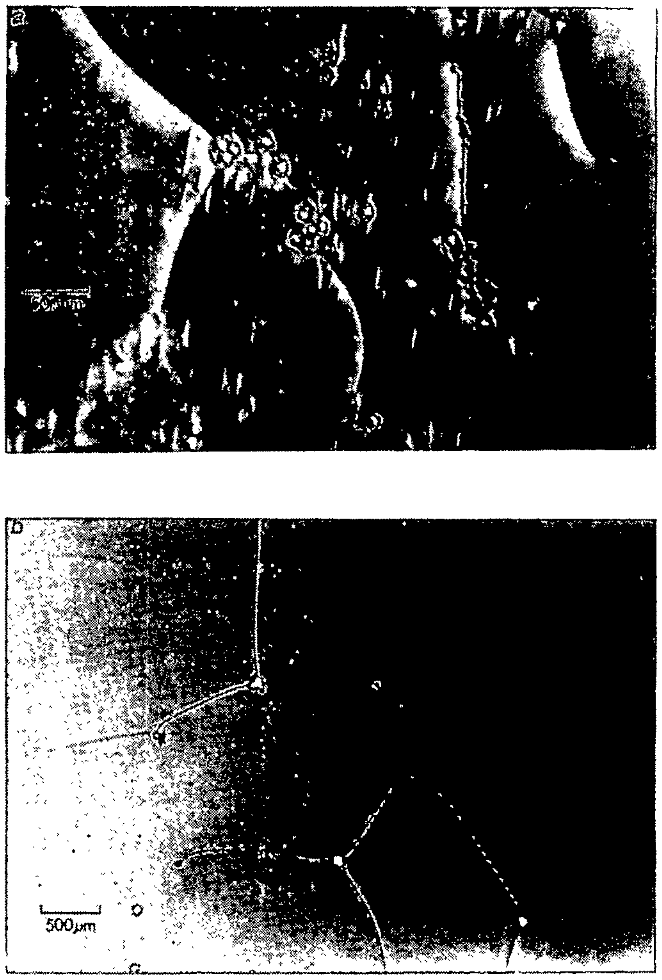

Fig. 3 Originally planar polished surfaces of glass sample from the interior of specimen after leaching. In *a*, spinel crystals now sit in deep pits formed by selective leaching of stressed envelopes. Note development of grooves associated with spinel crystals. These are believed to represent incipient stress corrosion cracking.

The considerations advanced above suggest that susceptibility to stress corrosion cracking should be an important criterion in the evaluation and selection of wasteforms for high level nuclear waste.

We thank Dr B. Lawn of the US Bureau of Standards for discussion and constructive criticism. The investigation was partially supported by a grant provided by the National Energy Development and Demonstration Program of the Commonwealth Department of Resources and Energy.

Received 20 February; accepted 25 July 1984.

1. Turcotte, R. P. & Roberts, F. P. in *Ceramic and Glass Radioactive Waste Forms* (eds Readey, D. & Cooley, C.) 65-82 (Summary of workshop at ERDA-Germantown, CONF 770-102, 1977).
2. Turcotte, R. P., Wald, J. W. & May, R. P. in *Scientific Basis for Nuclear Waste Management* Vol. 2 (ed. Northrup, C.) 141-146 (Plenum, New York, 1980)
3. Ross, W. A. in *Ceramic and Glass Radioactive Waste Forms* (eds Readey, D & Cooley, C.) 49-64 (Summary of workshop at ERDA-Germantown, CONF 770 102, 1977)
4. Laude, F., Vernaz, E. & Saint-Gauders, M. in *Scientific Basis for Nuclear Waste Management* Vol. 5, (ed. Lutze, W.) 239-247 (North-Holland, Amsterdam, 1982)
5. Wiederhorn, S. M. in *Ceramic and Glass Radioactive Waste Forms* (eds Readey, D & Cooley, C.) 215-234 (Summary of workshop at ERDA-Germantown, CONF 770-102, 1977).
6. Wiederhorn, S. M. & Bolz, L. H. *J. Am. ceram. Soc.* **53**, 543 (1970).
7. Wiederhorn, S. M., Fuller, E. & Thomson, R. *Met. Sci.* **14**, 450 (1980)
8. Michalske, T. & Freeman, S. *Nature* **295**, 511 (1982).
9. Swain, M., Lawn, B. R. & Burns, S. *J. Mat. Sci.* **9**, 175 (1974).
10. Lawn, B. R. *J. Am. ceram. Soc.* **66**, 83 (1982).

A novel ignition device for the internal combustion engine

A. J. J. Lee & F. J. Weinberg

Department of Chemical Engineering and Chemical Technology,
Imperial College of Science and Technology, London SW7 2BY, UK

Although the recent rapid proliferation of research into plasma jet ignition[1–16] has partly been prompted by the requirements of continuous combustion and pollutant removal[17–25], the main motive has been to extend the lean operability limit of the internal combustion engine. This trend to leaner mixtures has been stimulated by the need to improve engine emission characteristics and efficiencies. Because optimum conditions occur near the lean misfire limit, a plug providing increased rates of flame propagation and more effective and reliable ignition has been sought; pulsed plasma jets offer much promise but use too much power. In these devices, the igniting jet is generated by explosive gas expulsion through an orifice, engendered by a short-duration arc discharge to which the plasma medium is exposed while confined by the walls of a cavity within the plug. Such plasma jets, and particularly those fed with specific plasma media, have proved capable of extending the flammable fuel–air mixture range both at the fuel lean and at the rich limit, and increase the speed at which flames propagate following ignition. This is thought to be due to the generation of turbulence and free radicals. We report here the development and testing of an ignition plug based on two sparks at the extremities of an internal cavity. This design combines much of the effectiveness of a plasma jet with the small power consumption, and consequently low rates of wear, of a conventional sparking plug.

From the point of view of practical applicability, plasma jets suffer from a major shortcoming; they use appreciably larger amounts of energy than do conventional automobile ignition systems. This results not only in increased consumption of electrical power but also in much greater rates of electrode wear. The former may be improved by redesigning the electrical supply system for greater efficiency, as the small proportion of the total energy which eventually reaches the jet[10] is not inordinately larger than conventional spark energies. The latter, however, restricts plasma plug life to, at best, tens of hours. Thus we set out to design and test an ignition plug[26] which would combine some of the essential features of plasma jet ignition with the energy requirements of a conventional spark plug.

The essential features seem to be the production of a high-velocity gas jet which contains at least some regions or pockets of high-temperature gas within which active species, such as free radicals, reside. The spark channel itself, being at an extremely high temperature, is a sufficient source of the latter—without requiring the dissipation of a lot of energy in its creation. The main energy requirement in plasma jets (apart from losses due to the large currents used) seems to be associated with the generation and expulsion of the jet. If this could be contrived by drawing on the large amount of chemical energy in the fuel rather than on the electrical input, the major need for large amounts of electrical power would be removed. The plug design[26] in Fig. 1 achieves this aim as follows. Of the two sparks in series, the one at the base of the cavity is intended to ignite the flammable mixture compressed into the cavity by the advancing piston. The spark channel across the mouth of the cavity then rides on top of the ejected column of gas. For very lean mixtures, or fuels that are particularly difficult to ignite, small amounts of fuel or other substances which will promote reaction within the cavity may be introduced. Simple methods for providing the cavity with minute flows of gas, wetting it with small amounts of liquid fuel or furnishing it with solid hydride inserts have been developed in research on plasma jets[8,9,11,13].

Table 1 Extension of incendivity limits, both spark gaps broken down

Cavity parameters Length (mm)	Volume (mm^3)	Contents	% Limit extension Lower	Upper
10	31.4	Test mixture	9.5	2.7
10	31.4	Oxygen mixture	14	56

Table 2 Increase of flame speed

Cavity parameters Length (mm)	Volume (mm^3)	Contents	% Improvement Top spark only	Both sparks
1	3.14	Test mixture	47	64
2	6.28	Test mixture	48	59
4	12.6	Test mixture	42	63
7	22.0	Test mixture	55	74
10	31.4	Test mixture	45	80
1	3.14	Oxygen mixture	137	162
2	6.28	Oxygen mixture	132	200
4	12.6	Oxygen mixture	253	251
7	22.0	Oxygen mixture	282	270
10	31.4	Oxygen mixture	183	351

There is evidence of jet formation and some gas expulsion through the orifice even in the absence of a flammable mixture in the cavity. With a small cavity, even the small amount of energy that the internal spark imparts to its contents is sufficient to raise the temperature significantly, at least at atmospheric pressures. Thus if the spark energy were uniformly distributed across the 33 mm^3 of the cavity, a doubling in the absolute room temperature would require some 10 mJ. Of course, the energy release from a stoichiometric mixture is almost an order of magnitude higher, even at atmospheric pressure, whilst, at engine pressures, the electrical contribution to the ejection of the jet would be expected to be relatively insignificant.

Practical tests to help elucidate the mechanism included a study of what happens when the two electrode gaps are shorted out in turn. Ignition at the base of the flammable contents of the cavity first ejects reactants into the gas to be ignited and eventually flame, if that has not been quenched within the cavity. Discharge at the upper electrode gap alone corresponds to conventional spark ignition only if the cavity is not filled with a flammable mixture. If flame propagation into the cavity can occur then the spark channel finds itself in a jet of hot products—again unless the flame is quenched. Comparing the incendivity of the device in these various conditions with that of the two-discharge configuration gives much information on quenching and the mechanism by which the igniter functions generally. The quenching criterion is less restrictive in an engine than during tests at atmospheric pressure because quenching distance is inversely proportional to pressure. Quenching distance also decreases with increasing burning velocity and is about 10 times less for a stoichiometric mixture than at the limits of flammability. For this reason a series of experimental tests at atmospheric pressure were conducted with more vigorous flammable mixtures in the cavity to minimize quenching within it and simulate, in this respect, the most extreme engine conditions.

Before any fundamental work to optimize the plug design could be carried out, an opportunity arose to test the ignition device in a Ricardo experimental engine. It spite of the unoptimized cavity geometry, very promising reductions in burn times were obtained. As expected, these were greatest for the initial stages of propagation (8–9% during the first 10% of burn time) but were not inappreciable even when averaged over most of the flame travel (5–6% for 90% burn time).

In view of the difficulties encountered during engine experiments, more academic studies were carried out at atmospheric pressure with an adjustable plug (see Fig. 1*b*). This included provision for the feed of specific media as well as for variable cavity lengths and hence volumes. The most sensitive

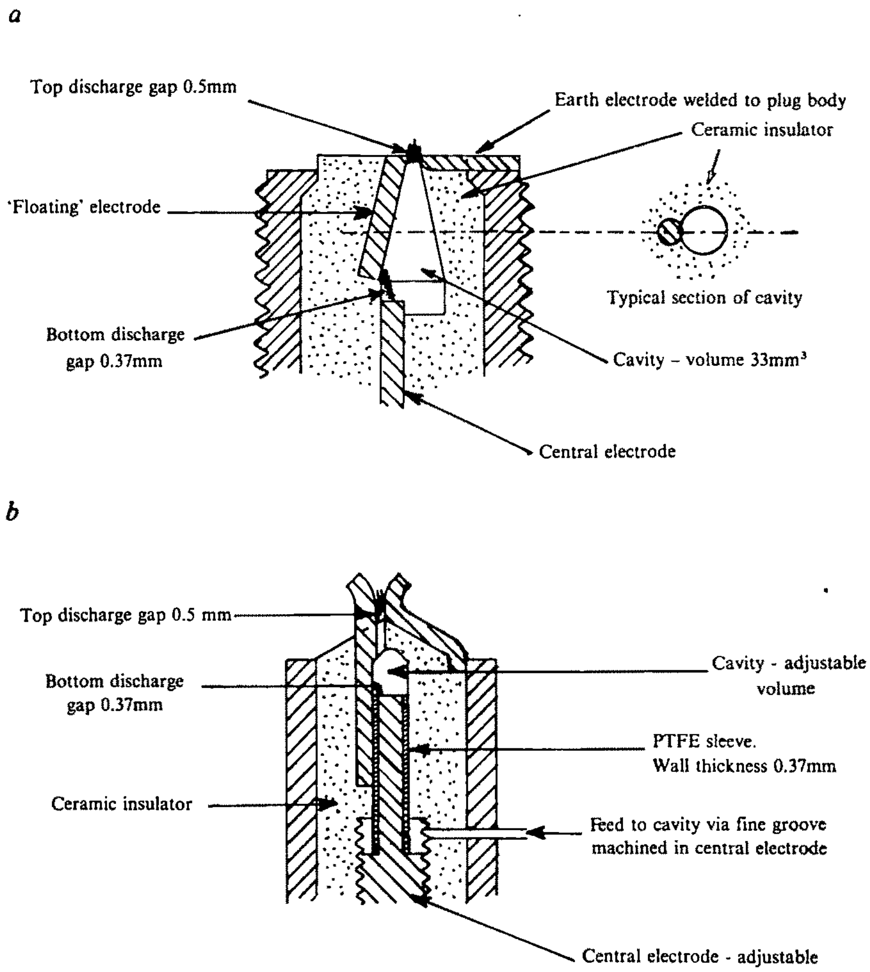
a
Top discharge gap 0.5mm
Earth electrode welded to plug body
Ceramic insulator
'Floating' electrode
Typical section of cavity
Bottom discharge gap 0.37mm
Cavity - volume 33mm^3
Central electrode
b
Top discharge gap 0.5 mm
Cavity - adjustable volume
Bottom discharge gap 0.37mm
PTFE sleeve. Wall thickness 0.37mm
Ceramic insulator
Feed to cavity via fine groove machined in central electrode
Central electrode - adjustable

Fig. 1 Sections of tops of plugs used for: *a*, engine tests; *b*, laboratory experiments.

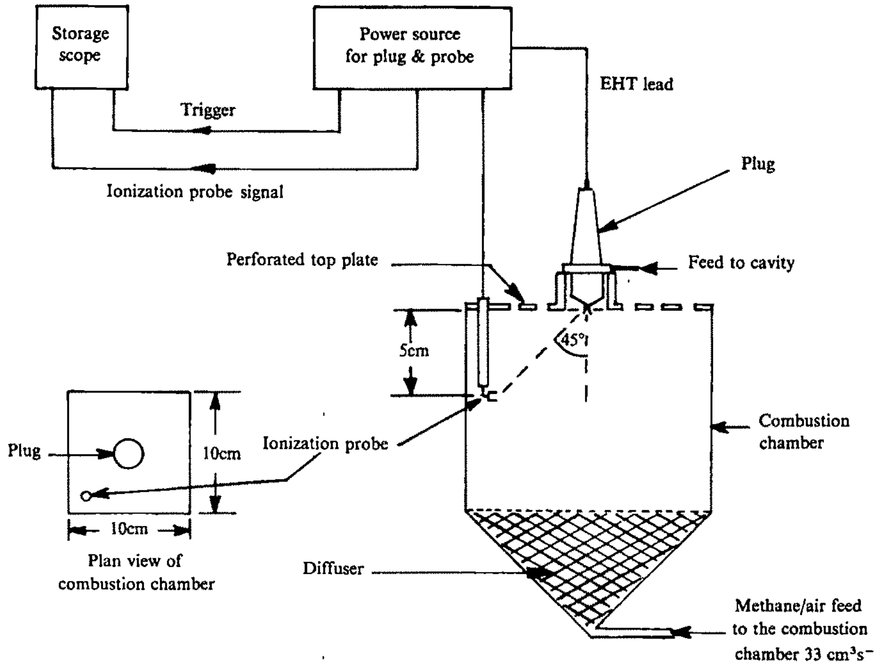

Fig. 2 Schematic of laboratory apparatus showing relative positions of plug and ionization probe.

measure[9,10,16,21] of incendivity,was found to be the stoichiometry of the leanest and richest mixtures which, when ignited at the centre of a vessel 10 cm square, would propagate flame all the way to the walls at least four times out of five. The other essential parameter is the speed of propagation of the flame. This was determined by measuring the time that the flame took to reach the ionization probe situated as shown in Fig. 2. The total stored energy available from the conventional ignition coil was of the order of 9 mJ.

The results for methane-air mixtures, based on several hundred firings, are listed in Tables 1 and 2. The 'percentage improvement' refers to the decrease in minimum or increase in maximum fuel concentration which could be ignited, or to the increase in flame speed, all compared with the results for a conventional spark plug with a 2-mm gap. 'Test mixture' in the cavity signifies that the feed is the mixture under test in the vessel. 'Oxygen mixture' refers to the feeding into the plug of oxygen bubbled through mixtures of acetone and isopropanol in a saturator. The fastest burning mixtures studied produced stoichiometric conditions within the cavity. The flow in these experiments is minute, $\sim$0.083 cm^3 s^{-1}, which is only sufficient to compensate for diffusion losses through the orifice and can have no appreciable effect on the composition of the test mixtures[16]; this was stoichiometric methane-air for all the burning velocity measurements.

The lower and upper limit determinations were obtained using a plug without the extended electrodes shown in Fig. 1*b*, to avoid the quenching which these surfaces seem to induce at the lower limit. The spark duration was of the order of 1 ms. When it was reduced to 0.1 ms, no extension of limits of incendivity was observed, except for the oxygen mixtures, presumably because the spark at the mouth of the cavity expired before the jetting action became effective. Results with the bottom spark only are not listed in Table 2 because no ignition was achieved with the test mixture in the cavity, whilst ignition occurred only sporadically and irreproducibly with the oxygen mixture. When ignition did occur, however, burn times were virtually the same as for the two-spark system.

The new ignition device can extend the limits of incendivity and the rates of flame propagation—both sets of results compare favourably with the performance of high-energy (several joules stored) plasma jets (see refs 9, 16). The very large extension of the rich flammability limit for the more vigorously burning plasma media agrees with the plasma jet studies of ref. 16 and, by analogy, may be expected to be accompanied by large reductions of soot generation. The two-spark system consistently achieves large improvements over conventional sparking plugs. When the cavity is filled with the stoichiometric oxygen-fuel mixture, ignition by the top spark alone can produce very similar results—at least for cavities of intermediate lengths. The same is true for ignition by the bottom spark alone, though this is erratic and often does not occur at all. These results make good sense because, in the case of ignition with the top spark, propagation into the cavity results in the expulsion of a hot product jet immediately; in contradistinction to the spark at the base of the cavity, which will eject cold reactants until the flame reaches the top of the cavity-if it is not quenched before then. Unless a second spark is present at the top to ignite this cold reactant jet, the generation of turbulence (cold) is the most the jet can achieve. As the gas expansion due to combustion has been dissipated by the time that the flame reaches the top of the cavity, following ignition at the base alone, (all the jet velocities are readily calculable in terms of burning velocity and flame area) this type of 'torch ignition' would only occur when unquenched flame is ejected.

It is not possible to simulate cavity quenching in engine conditions accurately by feeding the plug any specific mixture, if only because a practical igniter has to cope with various throttle openings. The stoichiometric fuel-oxygen mixture used here was designed to represent one extreme, with burning velocities in excess of any that are likely to be obtained in an engine. It may be that it is only in such extreme conditions that either of the single spark systems generates a jet approaching the performance of the double spark configuration. The effectiveness of the plug in various conditions will also depend on the cavity diameter and orifice geometry, and further studies of the influence of these parameters are in progress. However, although single sparks at the top or the bottom of the cavity can sometimes produce considerable improvements over conventional sparking plugs, the double spark system produces large improvements consistently. It offers the advantages which have been claimed for plasma ignition without drawing any more electrical power than conventional spark plugs currently used in internal combustion engines.

We thank Mr. E. L. Marshall (BP Research Centre, Sunbury) for engine tests, Dr Ivan Vince who participated in some of the experimental work and the Wolfson Foundation for financial support to A.J.J.L.

Received 14 June; accepted 13 August 1984.

1. Weinberg, F. J. *Inst. Mech. Eng. Symp. Combustion in Engineering*, Oxford, 65 (1983).
2. Waterson, K. thesis, Oxford Univ. (1973).
3. Topham, D. R., Smy, P. R. & Clements, R. M. *Combustion Flame* **25**, 187 (1975).
4. Wyczalek, F. A., Frane, D. L., Neuman, J. C. *SAE pap.* 750349 (1975)
5. Fitzgerald, D. J. *SAE Pap.* 76064 (1976).
6. Asik, J. R., Piatkowski, P., Foucher, M. J. & Rado, W. G. *SAE Pap.* 770355 (1977).
7. Dale, J. D., Smy, P. R. & Clements, R. M. *Combustion Flame* **31**, 173 (1978).
8. Weinberg, F. J., Hom, K., Oppenheim, A. K. & Teichman, K. *Nature* **272**, 341 (1978).
9. Orrin, J. E., Vince, I. M. & Weinberg, F. J. *18th Symp. int. on combustion* 1755 (The Combustion Institute, Pittsburgh (1981).
10. Carleton, F. B., Vince, I. M. & Weinberg, F. J. *19th Symp. int. on Combustion* 1523 (The Combustion Institute, Pittsburgh, 1982).
11. Tozzi, L. & Dabora, E. K. *19th Symp. int. on Combustion*, 1467 (The Combustion Institute, Pittsburgh, 1982).
12. Pitt, P. L. & Clements R. M. *Combust. Sci. Technol.* **55**, 555 (1982).
13. Grant, J. F., McIlwain, M. E. & Marram, E. P. *Combust. Sci. Technol.* **30**, 171 (1983).
14. Clements, R. M., Smy, P. R. & Dale, J. D. *Combust. Flame* **42**, 287 (1981).
15. Cetegen, B., Teichman, K. Y., Weinberg, F. J. & Oppenheim, A. K. *SAE Pap.* 80042 (1980).
16. Vince, I. M., Vovelle, C. & Weinberg, F. J. *Combust. Flame* **105**, 56 (1984).
17. Harrison, A. J. & Weinberg, F. J. *Proc. Soc.* **A321**, 95 (1971).
18. Kimura, I. & Imajo, M. *16th Symp. int. on combustion, 809* (The Combustion Institute, Pittsburgh, 1976).
19. Kimura, I., Aoki, H. & Kato, M. *Combustion Flame* **42**, 297 (1981).
20. Warris, A-M. thesis, Univ. London (Imperial College) (1983).
21. Warris, A-M. & Weinberg, F. J. *20th Symp. int. on Combustion* (The Combustion Institute, Pittsburgh, 1984).
22. Hilliard, J. C. & Weinberg, F. J. *Nature* **259**, 556 (1976).
23. Behbahani, H. F., Fontijn, A., Muller-Dethlefs, K. & Weinberg, F. J. *Combust. Sci. Technol.* **27**, 123 (1982).
24. Chan, A. K. F., Hilliard, J. C., Jones, A. R. & Weinberg, F. J. *J. Phys.* D**13**, 2309 (1980).
25. Behbahani, H. F., Warris, A-M. & Weinberg, F. J. *Combust. Sci. Technol.* **30**, 289 (1983).
26. British Patent Application No. 827009, PCT/GB/83/00253 (October 1982).

Climatic impact of explosive volcanic eruptions

P. M. Kelly & C. B. Sear

Climatic Research Unit, School of Environmental Sciences,
University of East Anglia, Norwich NR4 7TJ, UK

Major explosive volcanic eruptions inject ash and gas into the upper atmosphere, producing aerosol layers which can affect the global energy balance and climate[1]. Empirical studies have shown that major eruptions can produce a decrease in surface air temperature of up to a few tenths of a degree Celsius over the Northern Hemisphere land masses and that the effects may last for 2 or 3 yr (refs 2–4). This temperature decrease has been simulated by numerical models using realistic estimates of the nature of the aerosol cloud[1]. Previous empirical studies of volcanic effects have examined fluctuations in monthly, seasonal or annual climate data, but generally only at a frequency of one observation per year. This has rendered determination of the timing of the onset of effects during the first year impossible. Using continuous monthly surface air temperature for the Northern Hemisphere land masses, we resolve the month-by-month development and decay of the initial climatic impact. In the case of Northern Hemisphere eruptions, abrupt cooling occurs during the first two to three months, which is more rapid than previously assumed.

Dates of major eruptions during the study period, 1881–1980, were extracted from records of volcanic activity based on geological evidence[5,6], on anecdotal, geological and other evidence[7–10] and on conductivity (acidity) profiles from ice cores[11]. Nine events were selected for study (Table 1). The selection criteria are summarized in the notes accompanying Table 1. As this study is concerned primarily with the initial climatic impact, the volcanic events were stratified into Northern Hemisphere and Southern Hemisphere samples. During the first few months of its lifetime, a volcanic cloud will be restricted to the hemisphere of injection, even in the case of low-latitude volcanoes[12]. Two superposed epoch analyses were undertaken to define the Northern Hemisphere temperature response to the Northern Hemisphere and Southern Hemisphere eruptions. We used a recent compilation of monthly surface air temperatures[13] interpolated onto a regular grid from station observations before averaging over the Northern Hemisphere.

Superposed epoch analysis is commonly used in studies of the effects of volcanic activity on climate[2–4]. Taking the date of each eruption event as month zero, temperature data for succeeding months were averaged to produce the composite volcanic signals seen in Fig. 1. The value for month zero in the

Table 1 Volcanic events selected for study

Date Event (Month, year)	Lat.	Long.	VEI†	DVI†	Acidity†
Northern Hemisphere					
5, 1902 Pelée, Montagne (West Indies)	14.8° N	61.2° W	2×4	100	
5, 1902 Soufrière of St Vincent (West Indies)	13.4° N	61.2° W	4	300	
*10, 1902 Santa Maria (Guatemala)	14.8° N	91.6° W	6	600	
3, 1907 Ksudach (Kamchatka)	51.8° N	157.5° E	5	500	
6, 1912 Novarupta (Alaska Peninsula)	58.3° N	155.2° W	6	500	30
3, 1956 Bezymianni (Kamchatka)	57.1° N	160.7° E	5	30	
Southern Hemisphere					
8, 1883 Krakatau (Indonesia)	6.1° S	105.4° E	6	1000	55
6, 1886 Tarawera (New Zealand)	38.2° S	176.5° E	5	800	
4, 1932 Azul (Chile)	35.7° S	70.8° W	5	70	
3, 1963 Agung (Indonesia)	8.3° S	115.5° E	4	800	20

Several factors determine the climatic significance of a volcanic eruption. The explosivity of an eruption affects the height of injection and, in particular, whether or not the dust and gas enters the stratosphere where residence times are much longer than in the lower atmosphere. The dust ejected (which is largely silicate ash) affects the energy balance in the initial stages of the development of the volcanic cloud. The amount of sulphur is, however, considered to be a more critical measure of climatic significance[1]. The initial injection of sulphur gases is rapidly transformed into sulphate aerosols (secondary aerosol production) which have a greater effect on the energy balance and a longer residence time than the particulate injection.

All volcanic histories are prone to error because of the rudimentary nature of the historical data available and can only provide a crude classification of eruption size and climatic significance[9]. An objective synthesis of the available information has, therefore, been used to identify the events most likely to be of climatic importance. Well-dated events with a VEI of ⩾5 and/or a DVI of ⩾300 were selected.

* Not included in the superposed epoch analysis as effects are likely to be obscured by eruptions earlier in 1902.

† VEI, Volcanic explosivity index[5,6]; DVI, dust veil index[7,8,10], not weighted by extent of veil; acidity, global fallout (10^6 tons)[11]. Acidity estimates are not available for many of the eruptions.

Table 2 Monthly standard deviations (°C) of the Northern Hemisphere average surface air temperature data (1881–1980)

January	February	March	April	May	June
0.64	0.54	0.42	0.35	0.31	0.28
July	**August**	**September**	**October**	**November**	**December**
0.23	0.25	0.27	0.39	0.44	0.50

Northern Hemisphere composite shown in Fig. 1 corresponds to the average over the eruption months listed in Table 1; the value for month 1 is then the average of the temperature data for June 1902, April 1907, July 1912 and April 1956, and so on. The superposition, or compositing, clarifies the volcanic signal by averaging out features not common to the individual events. These are, presumably, caused by non-volcanic factors and can be considered to be noise.

To avoid biasing the results towards the winter months when the variability is greatest (Table 2), the data were standardized before compositing. Each monthly temperature value was divided by the appropriate long-term (100-yr) standard deviation after subtraction of the long-term monthly mean. We have repeated the analysis using unstandardized data and the general conclusions are not affected. To reveal the short-term response and avoid the effects of longer-term climatic changes, the data were then expressed as departures from the prevailing temperature level defined by the 12-month average for the period up to the eruption date (that is, month −12 to month −1). Use of longer averaging periods, of up to 5 yr, made little difference to the results.

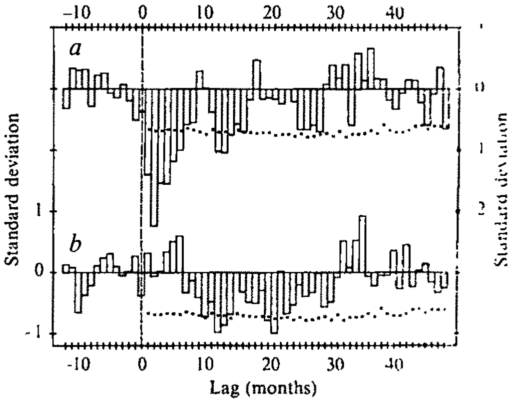

Fig. 1 Superposed epoch analyses of standardized monthly Northern Hemisphere surface air temperatures for the Northern Hemisphere eruption sample (*a*) and the Southern Hemisphere eruption sample (*b*). The data are expressed as deviations from prevailing temperature levels defined by the 12-month average for the period up to but not including the eruption date (month zero). To convert standard deviation units to °C, use Table 2. The near-horizontal line of dots indicates the one-tailed 5% significance level based on a Monte Carlo simulation. It should be noted that these data are largely representative of conditions over the land masses of the hemisphere as few data are available for ocean areas at present. Most of the eruptions studied took place during the early decades of the record for which the spatial coverage of the data is best over middle to high latitudes.

Statistical significance was tested using a Monte Carlo technique[14], so implicit account was taken of the particular statistical characteristics of the data under analysis (for example, systematic fluctuations caused by non-volcanic factors[15]). Values for months 1–48 were calculated as above using 1,000 sets of four randomly selected 'eruption' dates. The distribution of the resulting samples of 1,000 values was used to determine 5% significance levels separately for each of the 48 months. A one-tailed significance test was used, as it is generally accepted that surface cooling is the probable climatic effect[1].

The composite temperature departure sequences for the two samples are shown in Fig. 1. The Northern Hemisphere composite shows a marked response: a rapid decrease in temperature following month zero, with maximum cooling in month 2, then a slow recovery over the next couple of years. Temperatures return to the pre-eruption level during the third year. The maximum depression is about 2.2 s.d. corresponding to a cooling of ~1.4 °C in January and 0.5 °C in July. Individual departures during the first few months are clearly significant at the 5% level. The cumulative probability of the occurrence of a sequence of departures significant at the 5% level is, of course, extremely low. Statistically significant temperature depressions occur in all but six of the first 16 months and only three positive values occur during the first 28 months. The average depression over the first 12 months is between 0.3 and 0.4 °C depending on the month of the eruption. This agrees well with the results of previous analyses[1-4]. The duration of statistically significant effects is around 18 months, although cooling is still apparent through to the early stages of the third year.

The Southern Hemisphere composite exhibits a similar, but delayed, signal. As we are now considering the effects of Southern Hemisphere eruptions on Northern Hemisphere climate, the delay is to be expected. Persistent cooling is first apparent about month 7 and is strongest during year 2. Depending on the time of year, the maximum cooling in any one month ranges between 0.2 and 0.6 °C and the average cooling during year 2 is ~0.2 °C, rather less than is often cited in the cases of Krakatau and Agung. The termination of appreciable effects at the beginning of the third year is similar to that seen in the Northern Hemisphere composite.

The similarity of the signal revealed by the two independent samples, allowing for the delay in the case of Southern Hemisphere events, strongly supports the reality of the volcanic effect. Nevertheless, there is a need for further verification by repeating the analysis for earlier eruptions and on a Southern Hemisphere temperature average. At present, however, suitable data are not available.

The composite volcanic signals seen in Fig. 1 are statistical generalizations and their applicability to individual events is not necessarily straightforward because of the background climate variability or noise. Temperature departures following the individual volcanic events are shown in Figs 2 and 3. With the composites from Fig. 1 in mind, the outline of the volcanic signal can be seen in most of these sequences. The notable exception is the case of Tarawera. Interestingly, the magnitude of the maximum response, in terms of standard deviation units, is similar in all the individual sequences (except that of Tarawera) although the character and size of the associated stratospheric injections differed. The apparent duration of the climate response does, however, vary from event to event, although the point where the volcanic signal becomes indistinguishable from the background noise is difficult to determine.

The most striking feature of our results is the speed of the climate system's response. Contrary to general belief, the maximum impact occurs when the volcanic cloud is far from being hemispherically distributed. The time scale of the development of the aerosol cloud produced by the eruptions of El Chichón, Mexico, in April 1982[16] is relevant here. Satellite observations[12] of the stratospheric injection have shown that the aerosol cloud at 27 km reached maximum density in late May 1982 as particle growth rates were first balanced and then exceeded by sedimentation losses. The total mass of sulphate above 20 km reached a maximum about 15 weeks after the eruption[17]. Modelling of the chemistry involved suggests a similar 2-5-month gas-to-particle transformation time with maximum optical depths in lower northern latitudes occurring during summer 1982[18]. By the beginning of June 1982, the El Chichón aerosol cloud was homogeneous and circumglobal in longitudinal extent but limited in latitudinal span[12]. Turco *et al.*[19], modelling the net effect on hemispherically averaged vertical optical depth, find maximum departures occurring 1-3 months after the eruption, in agreement with our results. (Unfortunately, the exceptional warmth of 1981[13] and the onset of cooling in early 1982, before the El Chichón eruptions, renders identification of the actual surface air temperature response difficult[20].)

Nevertheless, it is surprising that surface temperatures, even over land, should respond so quickly to the volcanic forcing with little, if any, delay produced by the thermal inertia of the climate system. The mechanism whereby a localized disturbance in the energy balance can produce a swift response in surface air temperature of hemispheric significance (although not necessarily hemispheric extent) warrants further investigation. As Ellsaesser has noted[15], empirical studies concerning volcanic effects on climate tend to raise as many, if not more, questions than they answer. This is symptomatic of many studies of the causes of climatic change and is an almost inevitable byproduct of limited data availability and small sample size.

The strength of the immediate temperature response to volcanic injections revealed by our analysis may result in a limited predictive ability, and the accurate determination of the volcanic signal is relevant to the prompt detection of the climatic effects of increasing levels of atmospheric carbon dioxide[21]. We believe, however, that the major significance of this work lies in the fact that it challenges commonly held beliefs concerning the response time and the sensitivity of the climate system to external forcing.

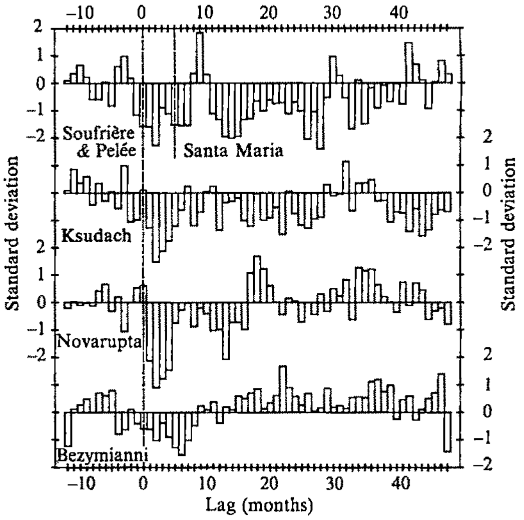

Fig. 2 Individual sequences of standardized monthly Northern Hemisphere temperatures following the eruption dates in the Northern Hemisphere sample (see Table 1). The data are expressed as deviations from prevailing temperature levels defined by the 12-month average for the period up to but not including the eruption date (month zero). To convert standard deviation units to °C, use Table 2.

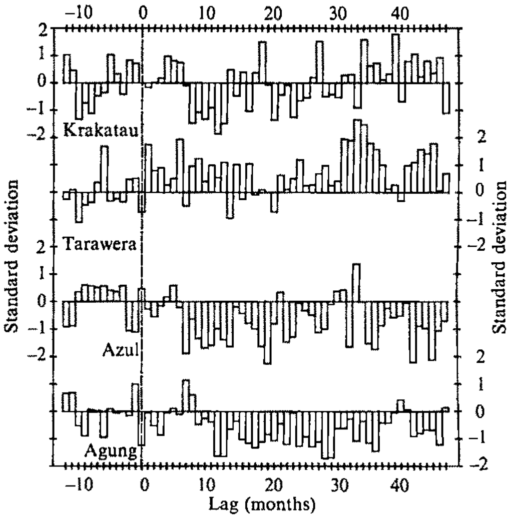

Fig. 3 Individual sequences of standardized monthly Northern Hemisphere temperatures following the eruption dates in the Southern Hemisphere sample (see Table 1). The data are expressed as deviations from prevailing temperature levels defined by the 12-month average for the period up to but not including the eruption date (month zero). To convert standard deviation units to °C, use Table 2.

Our results provide empirical support for the short response time suggested by recent attempts to simulate the climatic effects of a nuclear exchange[19,22].

This research was supported by US Office of Naval Research grant N0014-77-G-0074 and US Department of Energy contracts DE-ACO2-81EV10739 and DE-ACO2-79EV10098. C.B.S. was in receipt of a NERC Research Studentship. We thank all who commented on this research, particularly A. Robock, S. H. Schneider and T. M. L. Wigley, and acknowledge the inspiration of H. H. Lamb. E. M. Kelly provided programming assistance and the analyses were performed on 16-bit microcomputers.

Received 11 May; accepted 20 August 1984.

1. Newell, R. E. & Deepak, A. *Mount St Helens Eruptions of 1980: Atmospheric Effects and Potential Climatic Impact* (NASA, Washington, DC, 1982).
2. Mass, C. & Schneider, S. H. *J. Atmos. Sci.* **34**, 1995-2008 (1977).

3. Taylor, B. L., Gal-Chen, T. & Schneider, S. H. *Q. Jl. R. met. Soc.* **196**, 175-199 (1980).
4. Self, S., Rampino, M. R. & Barbera, J. J. *J. Volcanol. Geother. Res.* **11**, 41-60 (1981).
5. Simkin, T. *et al. Volcanoes of the World* (Hutchinson Ross, Stroudsberg, 1981).
6. Newhall, C. G. & Self, S. *J. geophys. Res.* **87**, 1231-1238 (1982).
7. Lamb, H. H. *Phil. Trans. R. Soc.* A **266**, 425-533 (1970).
8. Lamb, H. H. *Climate Monitor* **6**, 57-67 (1977).
9. Kelly, P. M. & Sear, C. B. in *Atmospheric Effects and Potential Climatic Impact of the 1980 Eruptions of Mount St Helens* (ed. Deepak, A.) 293-298 (NASA, Conf. Publ. no. 2240, Washington DC, 1982).
10. Lamb, H. H. *Climate Monitor* **12**, 79-80 (1983).
11. Hammer, C. U., Hausen, H. B. & Dansgaard, W. *Nature* **288**, 230-235 (1980).
12. Barth, C. A. *et al. Geophys. Res. Lett.* **10**, 993-996 (1983).
13. Jones, P. D., Wigley, T. M. L. & Kelly, P. M. *Mon. Weath. Rev.* **110**, 59-70 (1982).
14. Haurwitz, M. W. & Brier, G. W. *Mon. Weath. Rev.* **109**, 2074-2079 (1981).
15. Ellasaesser, H. W. Preprint UCRL-89161, (Lawrence Livermore National Laboratory, Univ. California, Livermore, 1983).
16. Robock, A. *Nature* **301**, 373-374 (1983).
17. Thomas, G. E., Jakosky, B. M., West, R. A. & Sanders, R. W. *Geophys. Res. Lett.* **10**, 997-1000, (1983).
18. Capone, L. A. *et al. Geophys. Res. Lett.* **10**, 1053-1056 (1983).
19. Turco, R. P., Toon, O. B., Ackerman, T. P., Pollack, J. B. & Sagan, C. *Science* **222**, 1283-1292 (1983).
20. Sear, C. B. & Kelly, P. M. *Climate Monitor* **11**, 134-139 (1982).
21. Klein, W. H. in *Carbon Dioxide Review: 1982* (ed. Clark, W. C.) 215-242 (Oxford University Press, 1982).
22. Covey, C., Schneider, S. H. & Thompson, S. L. *Nature* **308**, 21-25 (1984).

Nd–Sr isotopic and REE constraints on the genesis of hydrothermal manganese crusts in the Galapagos

N. Clauer*, P. Stille*, C. Bonnot-Courtois† & W. S. Moore‡

* Centre de Sédimentologie et Géochimie de la Surface, Université L. Pasteur, 67084 Strasbourg-Cedex, France
† Equipe de Recherche Associée 765, Université Paris Sud, Orsay, France
‡ Department of Geology, University of South Carolina, Columbia, South Carolina 29208, USA

Manganese oxide crusts from the Galapagos spreading centre, interpreted to be of hydrothermal origin, have Nd isotopic compositions and rare-earth element (REE) concentrations that approach seawater values as the age increases. Numerous authors[1,2] have cited hydrothermal processes along the mid-oceanic ridges to explain the composition of 'metalliferous' sediments. Other authors believe that these sediments, whether now located on a ridge axis or in some deep, were derived from hydrothermal activity near ridges and were modified during removal from these ridges[3–6]. Nd and Sr isotopic compositions as well as concentrations of REE and Cu, Ni and Co in hydrothermal Mn crusts of different ages from the Galapagos spreading area were determined to provide new information regarding the problem of the alteration behaviour with time of oceanic sediments. Our data suggest that hydrothermal crusts react with seawater and ultimately acquire the trace-element characteristics of hydrogeneous crusts.

During a 1972 oceanographic cruise to the Galapagos spreading axis[7], dredging in the axial valley recovered a 2–4 cm thick Mn crust (station D6) consisting of a surface grey-banded zone covering a dark, friable zone. The latter material is todorokite, whereas the former consists of a mixture of todorokite and birnesite. The basement age is 0.3 Myr as estimated from magnetic anomalies.

At a second station (D9) located on a ridge about 25 km north-east of D6, fragments of another manganese oxide crust were also recovered on a 2.4 Myr old basement. This crust consists of a dark, iron-stained, 2–4-mm thick surface zone covering 4–6 cm of massive, grey material. The outer layer is amorphous material, and the underlying 4–6 cm is a mixture of todorokite and birnesite. Samples analysed are identified in Table 1.

Previous studies[7] showed that the outer layer of the D9 crust was hydrogeneous, but that the 0.3-Myr old D6 and the 2.4-Myr old D9 crusts are of hydrothermal origin. This conclusion is supported by the high accumulation rates measured by ^{230}Th/^{234}U dating of the Mn crusts, as well as by the young basement age determined by magnetic anomalies. Thus the growth rate for the D6 crust is of the order of 1–2 mm kyr^{-1}, 1,000 times faster than the growth rate of hydrogeneous Mn deposits.

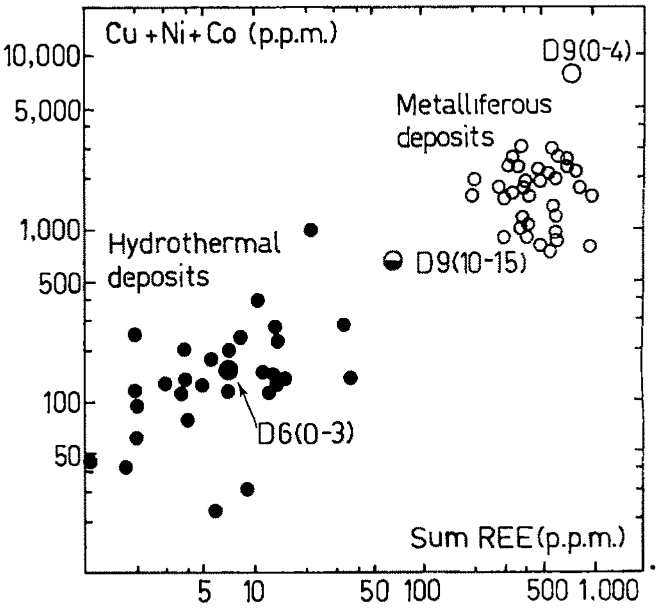

Fig. 1 Correlation between REE and Cu + Ni + Co concentrations in hydrothermal deposits and metalliferous sedimentary deposits. Data, characterized by smaller open and filled circles, are from ref. 10 corresponding to hydrothermal and metalliferous material from FAMOUS, Galapagos, Cyprus, Leg 54, Bauer deep, Marquesas zone, North Pacific[4,19–22].

A comparison of Cu + Ni + Co concentrations with REE concentrations (Fig. 1), provides a means of differentiating and characterizing hydrothermal and hydrogeneous Mn deposits. Hydrothermal deposits have REE and Cu, Ni and Co concentrations that are distinctly lower than those of hydrogeneous deposits. The data for the hydrothermal section of D9 fall in a region of the diagram that is intermediate between those of hydrogeneous deposits, here typified by its own outer coating, and those of hydrothermal deposits typified by the younger D6 crust.

In Fig. 2, the shale-normalized distribution of REEs[8] in the hydrothermally-formed D6 crust is quite similar to those of other hydrothermal deposits from the Galapagos[9] and from the FAMOUS area[10]. The crust shows a weak negative Ce anomaly and a slight increase in the heavy rare-earth elements (HREEs). The REE patterns of hydrothermally-formed parts of the D9 crust are significantly different from those of D6. Especially striking is the strong Ce anomaly and the marked similarity of the REE patterns to that of Pacific Ocean water and of authigenic marine sediments. The outer hydrogeneous layer of the same crust contains very high REE concentrations of about 765 p.p.m.; again the pattern shows a slight enrichment in the HREEs, but the negative Ce anomaly is less developed than in the hydrothermal portion.

The Sr isotopic ratios measured on 12 samples of the D6 and D9 crusts are remarkably constant. The average value is 0.70906 ± 4 (2σ mean) and thus agrees very well with present seawater Sr isotopic composition[11]. The Sr isotopic ratio of seawater measured in the hydrogeneous outer coating of D9 was as expected. For the hydrothermally-formed parts of the crust, however, we suggest either that the Sr originally had seawater-like ratios or more probably that exchanges with seawater occurred after the crust was formed.

Albarede *et al.*[12] measured the Sr isotopic compositions of hydrothermal waters and deposits from the East Pacific Rise

Table 1 Sr–Nd isotopic compositions* and Cu, Ni, Co and REE concentrations in the Mn crusts from the Galapagos spreading centre

Depth (mm)	Sr (p.p.m.)	$^{87}Sr/^{86}Sr$†	$^{143}Nd/^{144}Nd$‡	Cu (p.p.m.)§	Ni (p.p.m.)§	Co (p.p.m.)§	Cu+Ni+Co (p.p.m.)
Dredge D6							
0–3	969	0.70911±18	—	43	100	<23	<166
15–20	518	0.70917±13	0.512609±31	16	—	35	>51
30–36	364	0.70915±8	—	—	—	—	—
Dredge D9							
0–4	1,457	0.70915±5	0.512518±48 0.512520±40	936	6,300	909	8,145
0–4‖	3,213	0.70922±22	—	—	—	—	—
0–4¶	642	0.70909±11	—	—	—	—	—
10–15	599	0.70913±12		65	535	<50	<650
23–30	1,502	0.70894±13		—	—	—	—
23–30¶	262	0.70918±9	0.512499±50#	—	—	—	—
51–58	757	0.70914±10		—	—	—	—
51–58‖	2,327	0.70911±11		—	—	—	—
51–58¶	278	0.70918±7		—	—	—	—

	La	Ce	Nd	Sm	Eu	Tb	Yb	Lu	Total	La/Yb
Dredge D6										
0–3	2.55	2.74	1.5	0.33	0.12	0.09	0.52	0.10	8	4.9
30–36	2.96	4.07	2.1	0.42	0.15	0.12	0.39	0.07	10	7.6
Dredge D9										
0–4	219	281	178	37.3	9.40	6.80	27.9	5.40	765	7.8
10–15	23.3	8.17	19.5	3.83	1.25	1.00	5.82	1.13	64	4.0
51–58	29.7	7.60	32.5	6.40	1.98	1.60	5.46	0.98	86	5.4

* Uncertainties are 2σ mean.

† Ratios adjusted to 0.71022 mean value for the $^{87}Sr/^{86}Sr$ ratio of the NBS 987 standard.

‡ Normalized to $^{146}Nd/^{144}Nd = 0.7219$. $^{143}Nd/^{144}Nd = 0.51261 \pm 30$ for International Rock Standard BCR-1.

§ Values from ref. 16.

‖ Values of the solutions after weak leaching in 1M HCl.

¶ Values of the residues after weak leaching in 1M HCl.

# D9(10–58), no leaching.

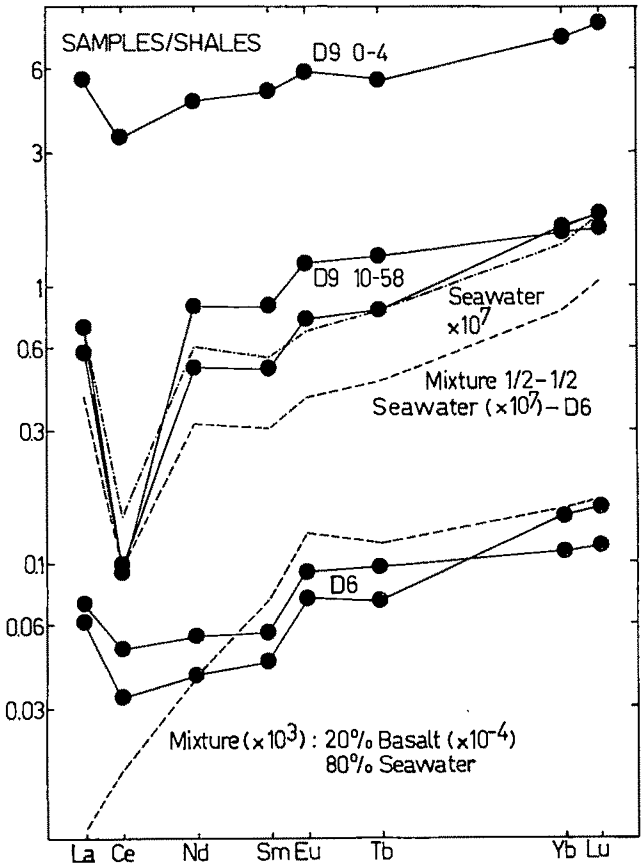

Fig. 2 Distribution patterns of the REE in the Mn-crusts from the Galapagos spreading centre. Seawater × 10^7.

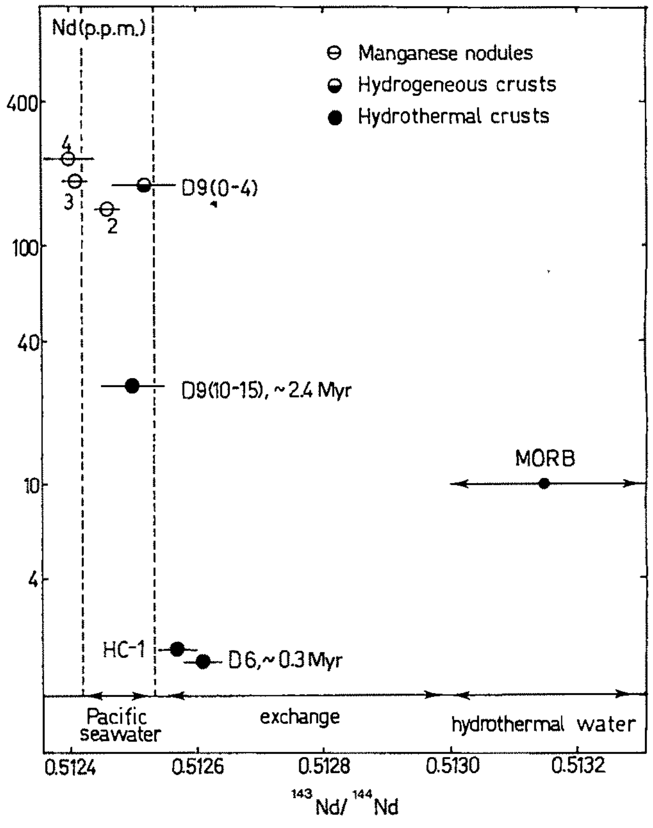

Fig. 3 $^{143}Nd/^{144}Nd$ plotted against Nd-concentrations. Hydrogeneous nodules 2–4 and hydrothermal crust HC-1 are from ref. 23. Nd isotopic composition values of Pacific seawater are from ref. 24.

(EPR) and showed that the hydrothermal system may be basically handled as a two component system in which endmembers are (1) the ambient seawater, and (2) a hot hydrothermal solution with $^{87}Sr/^{86}Sr$ ratio of 0.703, close to, but significantly higher than, the Sr isotopic ratio of the surrounding fresh basalts. Similar observations were made by Vidal and Clauer[13] in their combined Pb–Sr isotopic study of basalts and sulphides from the EPR. They found that the Sr isotopic compositions of the hydrothermally-formed sulphides were intermediate between those of basalt and seawater.

Based on these studies and the strong evidence for the hydrothermal origin of the D6 and lower parts of the D9 crusts, we suggest that originally both seawater and hydrothermal Sr were incorporated in the Mn crusts. Later, after a long exposure to seawater, the original Sr isotopic compositions changed to present seawater values.

This suggestion is supported by the Nd isotopic compositions and Nd concentrations obtained on D6 and D9 crusts (Fig. 3). The isotopic composition of hydrothermal water is suggested to be mid-ocean ridge basalt (MORB)-like. The hydrogeneous samples, including the outer coating of the D9 crust, are characterized by high Nd concentrations ranging between 150 and 300 p.p.m. and Nd isotopic compositions that are the same as Pacific ocean water and agree within error limits with those found by Goldstein and O'Nions[14] on the same D9 crust. In addition, the hydrothermal portion of the D9 crust has a seawater Nd isotopic composition, but its Nd concentration is intermediate between the data for the remaining hydrothermal and hydrogeneous Mn crusts. The two hydrothermal samples (HC-1 and D6) have very low Nd concentrations of <2 p.p.m. and Nd isotopic compositions that are higher than the upper limit for Pacific Ocean water. This observation indicates that the Nd in these deposits has a volcanogenic component.

Corliss[15] demonstrated that hydrothermal leaching of submarine basalts could supply all excess REEs in the hydrothermal and hydrogeneous crusts. His geochemical balance calculations further show that the REE concentrations in hydrothermal mineralizing solutions are significantly greater than the concentrations of the seawater reservoir. This is supported by new measurements on high temperature hydrothermal waters from the EPR by Michard *et al.*[16] who demonstrated that REE concentrations in hydrothermal fluids are approximately 1,000 times those of seawater.

Assuming that leaching of basaltic material is the main mechanism which produces excess REE in the hydrothermal solutions and that its Nd isotopic composition and REE distribution was similar to MORB, then ~15–20% of the total Nd in the hydrothermal Mn crust of D6 must have been derived from a magmatic source and 80% from Pacific seawater.

Because of the extremely low REE concentrations in seawater, its mixing with a basalt source in the above-mentioned proportions will still produce a basaltic REE pattern. However, as shown in Fig. 2 only the HREEs in the hydrothermal crust of D6 reflect a basaltic component. The strong light rare-earth element (LREE) depletion, typical for MORB, is not observed. Thus, if hydrothermal leaching of basalts was the main mechanism which accumulates REEs in the hydrothermal solutions it did not fractionate the HREE but it enriched the LREE relative to the HREE. This suggestion is in good agreement with the geochemical mass balance calculations of Corliss[15], which demonstrate that in hydrothermal leaching of basalts three times more Ce than Sm accumulates in the solutions. It also agrees with the statement of Michard *et al.*[16] who observed a large enrichment of LREE in hydrothermal waters relative to seawater.

The 2-Myr older hydrothermal portion of the D9 crust was possibly formed in different conditions than that of the D6 crust. A larger seawater or even detrital component might be responsible for the significantly lower Nd isotopic compositions and the REE concentrations that are higher than usual for hydrothermal deposits.

The strong similarity in REE patterns to those of ocean water might indicate that seawater rather than detrital sediments was responsible for modifying the chemical characteristics of these crusts with time. We, therefore, suggest that the REE patterns of D9 reflect mixing between a hydrothermal and a seawater pattern. The theoretical mixing REE pattern is shown in Fig. 2. If our suggestion is correct and the crust originally had a REE pattern similar to that of the 2 Myr younger D6 crust, then the material must have undergone extensive REE exchange with seawater, possibly by a diffusion process[17,18]. Such post-depositional processes seem to alter significantly the composition of elements and to erase the original hydrothermal signature.

We thank J. Abrecht, P. J. Patchett and J. R. O'Neil for helpful discussions and English corrections. This work was funded by a grant from the Swiss National Science Foundation to P.S.

Received 23 March, accepted 20 July 1984.

1. Bostrom, K. & Peterson, M. N. A. *Mar. Geol.* **7**, 427–447 (1969).
2. Bostrom, K. *Earth planet. Sci. Lett.* **9**, 348–354 (1970).
3. Bischoff, J. L. & Sayles, F. L. *J. sedim. Petrol.* **42**, 711–724 (1972).
4. Dymond, J., Corliss, J. B., Heath, G. R., Field, C. W. & Dasch, E. J. *Bull. geol. Soc. Am.* **84**, 3355–3372 (1973).
5. Bischoff, J. L. & Rosenbauer, R. J. *Earth planet. Sci. Lett.* **33**, 379–388 (1977).
6. Edmond, J. M. *et al. Earth planet. Sci. Lett.* **46**, 19–30 (1979).
7. Moore, W. S. & Vogt, P. R. *Earth planet. Sci. Lett.* **29**, 349–356 (1976).
9. Hoffert, M. *Sci. Géol. Mém. Stras.* **61**, 231 (1980).
8. Haskin, M. A. & Haskin, L. A. *Science* **154**, 507–509 (1966).
10. Bonnot-Courtois, C. *Mar. Geol.* **39**, 1–14 (1981).
11. Faure, G. in *Numerical Dating in Stratigraphy* (ed. Odin, G. S.) (Wiley, New York, 1982).
12. Albarede, F., Michard, A., Minster, J. F. & Michard, G. *Earth planet. Sci. Lett.* **55**, 229–236 (1981).
13. Vidal, Ph. & Clauer, N. *Earth planet. Sci. Lett.* **55**, 237–246 (1981).
14. Goldstein, W. L. & O'Nions, R. K. *Nature* **292**, 324–326 (1981).
15. Corliss, J. B. *J. geophys. Res.* **76**, 8128–8138 (1971).
16. Michard, A., Albarede, F., Michard, G., Minster, J. F. & Charlou, J. L. *Terra cognita* **3**, 169 (1983).
17. Krishnaswami, S. & Cochran, J. K. *Earth planet. Sci. Lett.* **40**, 45–62 (1978).
18. Moore, W. S. *et al. Earth planet. Sci. Lett.* **52**, 151–171 (1981).
19. Dymond, J., Corliss, J. B. & Heath, G. R. *Geochim. Cosmochim. Acta* **41**, 741–753 (1977).
20. Corliss, J. B., Lyle, M., Dymond, J. & Crane, K. *Earth planet. Sci. Lett.* **40**, 12–24 (1978).
21. Courtois, C. & Desprairies, A. C. R. *Somm. Soc. Geol. Fr.* **5**, 242–245 (1974).
22. Courtois, C. & Hoffert, M. *Bull. Soc. géol. Fr.* **19**, 1245–1251 (1977).
23. Piepgras, D. J., Wasserburg, G. J. & Dasch, E. J. *Earth planet. Sci. Lett.* **45**, 223–236 (1979).
24. Piepgras, D. J. & Wasserburg, G. J. *Earth planet. Sci. Lett.* **50**, 128–138 (1980).

Efficiency of petroleum expulsion from shale source rocks

D. Leythaeuser, M. Radke & R. G. Schaefer

Institute for Petroleum and Organic Geochemistry (ICH-5),
KFA-Jülich, PO Box 1913, D-5170 Jülich, FRG

The limited data available on the mechanism and the efficiency of the processes by which petroleum is expelled in the subsurface from source rocks into adjacent reservoir rocks are mostly qualitative[1,2]. We present here material balance-type comparisons of sample series extending from the centre portions of two adjacent hydrocarbon source rock units towards their outer edges[3], which enable expulsion efficiencies to be determined. In certain parts of the shale the expulsion efficiencies for total extract and its saturated and aromatic hydrocarbon fractions, have much higher values than previously thought (reaching up to 80% for the total extract) which increase towards possible secondary migration avenues. The expulsion is associated with fractionation effects, such as those based on polarity differences. Also, expulsion efficiencies were found to be related to the degree of hydrocarbon saturation of the pore system: they are higher for a rich, oil-prone source rock unit compared with a poorer quality one, which had generated less hydrocarbons.

Using geochemical techniques described elsewhere[4,5] 15 samples of conventional cores were analysed from a ~30-m thick organic matter-rich shale interval in the Kökelsumer Heide no. 1 well penetrating Upper Carboniferous coal-bearing strata in the northern Ruhr district, FRG. From the variation of its organic carbon content and kerogen composition[6] (as defined by the hydrogen index HI, ref. 7), this shale could be subdivided

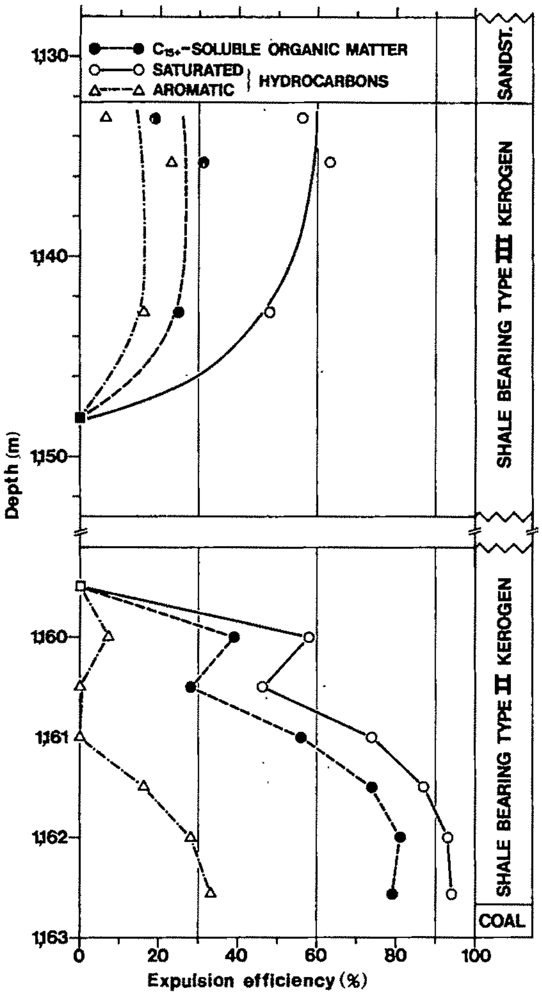

Fig. 1 Efficiency of expulsion of C_{15+}-soluble organic matter and saturated and aromatic hydrocarbons plotted against depth for the upper and lower depletion intervals of shale unit 1,132.5–1,162.6 m in the corehole Kökelsumer Heide No. 1, Ruhr district, FRG. The calculation of expulsion efficiencies[10,11] was based on the assumption that samples 1,148.1 m and 1,159.5 m have the hydrocarbon concentrations which resemble most closely those generated *in situ* (unmodified) for the upper and lower shale interval respectively.

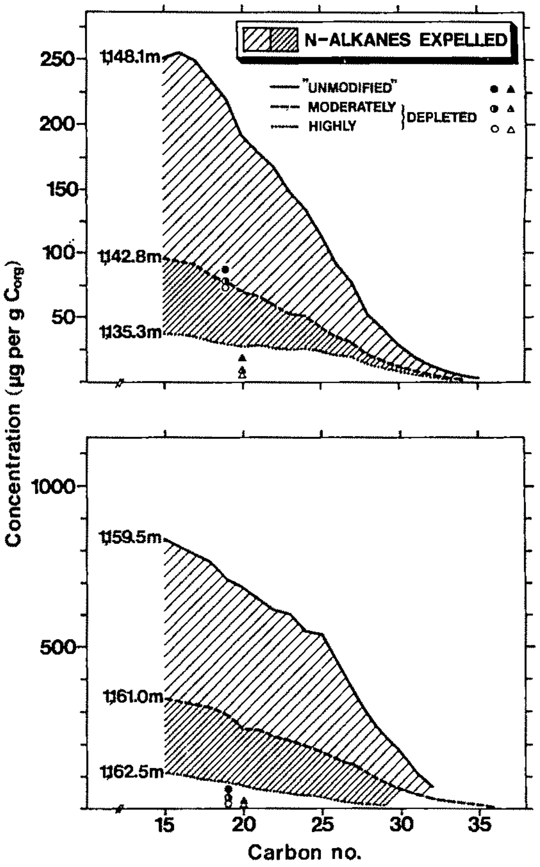

Fig. 2 Comparison of the absolute amounts of individual normal and isoprenoid alkanes (µg per g C_{org}) based on quantitative evaluation of the gas chromatograms for selected samples from the upper (1,148.1, 1,142.8 and 1,135.3 m) and lower depletion intervals (1,159.5, 1,161.0 and 1,162.5 m) of the shale unit shown in Fig. 1. The designation of samples as 'unmodified', 'moderately' and 'highly depleted' is explained in the text. Concentration differences between the three samples from each depletion zone represent hydrocarbon mixtures expelled from the indicated interval during primary migration. Circles, pristane; triangles, phytane.

into two intervals (Fig. 1, right hand column):

(1) From 1,132.5 to 1,158.0 m a medium grey shale with modest organic carbon content (mean, 0.8%) and bearing a hydrogen-lean type III kerogen[8] (mean HI 61.2 mg hydrocarbons per g organic carbon) was penetrated.

(2) From 1,158.0 to 1,162.6 m a black shale of high organic carbon content (mean, 3.9%) and bearing a hydrogen-rich, oil-prone type II kerogen[8] (mean HI, 175 mg per g organic carbon) occurs. Stratigraphically, this interval is the 'Katharina shale', which was deposited during a short marine transgression and directly overlies the Katharina coal seam[9].

Within each of these intervals the kerogen composition remains uniform except for the lowermost two samples of (2) where a high proportion of reworked and oxidized organic matter is thought to have been admixed with the type II kerogen[6]. Formation of petroleum hydrocarbons has advanced in both shales to beyond the peak generation stage as indicated by a maturity level of the organic matter equivalent to 1.1% mean vitrinite reflectance. The qualitative effects of hydrocarbon expulsion from the above-defined source rock intervals have been reported previously[6]. We now concentrate on quantifying some of these expulsion effects.

Samples from the upper and the lower edge of shale interval 1,132.5–1,162.6 m had systematic differences in concentration and composition of extractable hydrocarbons compared with samples from the centre[6]. Using an established concept[10,11] we now attempt to quantify these observations. For this purpose, the samples at 1,148.1 m and 1,159.5 m were assumed to have the hydrocarbon concentrations, which resemble most closely those generated *in situ* (that is, those within each shale unit relatively least affected by expulsion losses). They are referred to as the 'unmodified' samples, although they may also have lost some of their originally-generated hydrocarbons.

The percentage decrease in total extract and extractable hydrocarbons, shown in Fig. 1, for all samples closer to the upper and the lower shale contact respectively are interpreted as reflecting the expulsion efficiency. Over the uppermost 12-m and the lowermost 2.5-m intervals, the expulsion efficiencies for the total extract and its saturated and aromatic hydrocarbon fractions increase strongly towards the outer shale contacts: the edges of the shale have been preferentially depleted by expulsion. At any given depth level within both depleted intervals the expulsion efficiency is highest for the saturated hydrocarbons and lowest for the aromatic hydrocarbons; that of the total extracts is between the two. These trends are more regular in the lower depletion interval, where expulsion efficiencies increase within a narrow interval of only 2.5 m for the total extract to almost 90%, and for the saturated and aromatic hydrocarbons up to 94 and 33% respectively. The drainage avenue into which the expelled hydrocarbons were transported is obvious for the upper depletion zone (the overlying sandstone), while it is not as clear for the lower one. Several thin

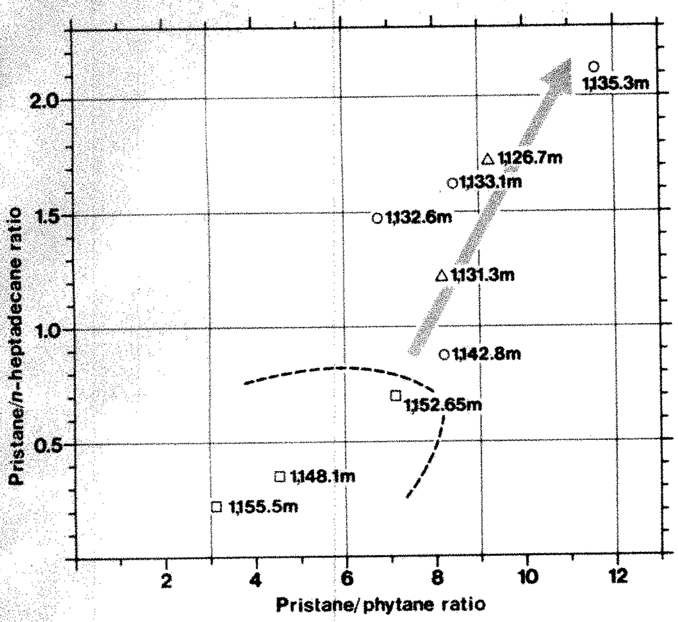

Fig. 3 Pristane/*n*-heptadecane plotted against pristane/phytane concentration ratios for all samples (identified by depth) from the type III kerogen-bearing source rock unit shown in Fig. 1. Note that the original composition largely preserved in the centre of this shale unit (squares) is altered more and more with increasing degree of hydrocarbon expulsion as indicated by the depleted samples (circles, from edge of this shale unit; triangles, thin, highly depleted shale interbeds from overlying sandstone unit). Arrow indicates the shift with increasing degree of expulsion.

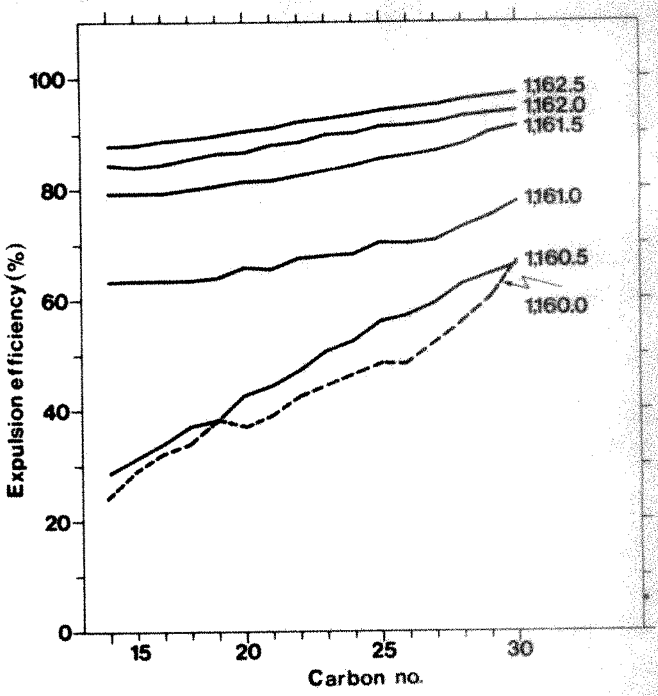

Fig. 4 Efficiencies of expulsion (as % of the unmodified sample 1,159.5 m) of individual *n*-alkanes as a function of carbon number and depth for all samples from the lower depletion interval (defined in Fig. 1), corehole Kökelsumer Heide No. 1, Ruhr district, FRG.

sandstone layers between 1,167.0 and 1,180.0 m are possible avenues because the Katharina coal seam shows a similarly severe depletion of hydrocarbons as previously observed nearby[12]. That the expulsion efficiencies are highest at 1,135.3 m within the upper depletion interval, and not at the shale/sandstone contact itself, suggests that increased depletion into a fracture zone between 1,135.0 and 1,135.2 m has occurred[6].

The conclusions reached from Fig. 1 support the hypothesis that primary migration is associated with chromatography-like fractionation effects according to polarity. Most importantly, however, the observations from Fig. 1 help to solve the controversy over whether primary migration of oil occurs as a separate phase, or dissolved in water. The major difference in maximum expulsion efficiency between the upper and the lower depletion interval (Fig. 1) supports an oil-phase migration mechanism. Based on the relationships between kerogen-types and hydrocarbon generation[1,2,8], it can be deduced that at the time of expulsion the oil saturation of the pore system must have been much higher in the lower source rock interval. More oil was generated there per unit pore volume due to the higher organic carbon content and the superior kerogen quality. In analogy with fluid flow in reservoir sandstones[13], relative permeability and hence expulsion rates for oil from source rock shales are believed to increase drastically if oil saturation of the pore fluid exceeds ~40% (ref. 14). As this value is clearly in excess of the solubility limit for oil in water (even at the maximum temperature and pressure conditions endured by this sequence) oil must have existed in the pore system as a separate phase in this rich source rock unit. While the expulsion efficiency for the total extract (which is indicative of the total oil) reached a maximum of 80% in the rich, lower source rock interval it reached only a maximum of 30% in the less prolific upper source rock interval. Due to the low concentration of organic carbon and the low hydrocarbon generation potential of the kerogen oil, saturation of the pore system must, even at peak generation stage, have remained very small, resulting in low values of the relative permeability and hence low expulsion rates for the oil.

The increasing expulsion of the saturated hydrocarbons in proximity to the upper and lower shale contact is shown by the data in Fig. 2. In comparison with the unmodified samples from 1,148.1 and 1,159.5 m, the samples closer to the outer shale contacts exhibit increasingly lower concentrations (μg per g C_{org}) of normal and isoprenoid alkanes. From the upper depletion interval, pristane is expelled to a lesser degree than its *n*-alkane isomer, as revealed by its gradual emergence over the *n*-alkane distribution envelope with increasing depletion. A corresponding effect cannot be observed in the lower depletion interval, because this source rock has, in accordance with its superior kerogen quality (type II), generated a hydrocarbon mixture with a very low relative proportion of pristane.

The compositional fractionation effects associated with expulsion of the saturated hydrocarbons from the upper depletion interval are shown in more detail in Fig. 3. The three samples analysed from the central portion of this source rock interval (1,148.1, 1,152.65 and 1,155.5 m) have the lowest pristane/*n*-heptadecane and pristane/phytane concentration ratios. With an increasing degree of hydrocarbon expulsion into the overlying carrier bed both compound ratios attain higher values, indicating a general depletion trend as shown in Fig. 3. Pristane is expelled less effectively than *n*-heptadecane and phytane, even less so. Furthermore, the ratios for the two thin source rock-type shales (at 1,131.3 and 1,126.7 m) interbedded in the overlying reservoir sandstone unit, and the sample 1,135.3 m near the fracture zone, imply the expected high degrees of hydrocarbon expulsion (Fig. 3). Both parameters have traditionally been used in petroleum geochemistry in a different way: the pristane/*n*-heptadecane ratio to monitor maturity progress[15] and the pristane/phytane ratio to indicate the organic facies[16-18]. We have also demonstrated here that regular changes, especially of the pristane/*n*-heptadecane ratio occurring over relatively narrow depth intervals, and independent of changes in kerogen-type, can be used to monitor the degree of hydrocarbon expulsion from the source rocks.

The efficiencies of expulsion of individual *n*-alkanes were quantified for the deeper interval utilizing the concept explained above (Fig. 4). For any given *n*-alkane in the molecular range C_{15}-C_{30}, the expulsion efficiency increases drastically from the slightly depleted samples at 1,160.0 m and 1,160.5 m, to the moderately depleted one at 1,161.0 m to the highly depleted samples between 1,161.5 and 1,162.6 m close to the lower contact of this shale unit. Among the latter samples the expulsion efficiencies of the *n*-alkanes vary between ~80 and 95%. The higher molecular weight *n*-alkanes have apparently been expelled to a greater extent. However, the trends shown in Fig. 4 are the result of several processes occurring in the sequence: initial hydrocarbon generation-expulsion-replenishment by subsequent hydrocarbon generation. Therefore, these trends could be explained if, after the main phase of expulsion, hydrocarbon generation continued and, due to the high maturity level of this source rock, mainly lower molecular weight alkanes were formed and added to the unexpelled remainder: erroneously low expulsion efficiencies are apparent from Fig. 4 for the lower molecular weight *n*-alkanes. This effect is observed best near the inner edge of the depletion interval (samples at 1,160.0 and 1,160.5 m); due to the more efficient expulsion of the alkanes generated later, the effect is increasingly obliterated towards the outer shale edge.

The values determined in this study for the expulsion efficiencies should not be considered as absolute. The values depend on whether the sample chosen contains the *in situ* generated hydrocarbon concentrations. It is possible that even the samples from the centre of both source rock units have expelled some of their generated oil. Nonetheless, our conclusions remain valid: the values of the expulsion efficiencies are minimum values and the relative differences in the degree of depletion within the shale edges remain the same.

The results of this study have implications for applied petroleum geochemistry. We have shown that, within an individual source rock body, expulsion efficiencies are variable: they change as a function of proximity to the carrier beds and migration avenues and vary with compound-type, molecular size and structure. It may, therefore, be difficult to select approximate mean values for the expulsion efficiencies of entire source rock units so as to calculate the amount of oil which migrated and possibly accumulated in the traps of a given exploration area. Previously reported values for the efficiency of petroleum expulsion from shale source rocks were much lower (10–15%)[1,2] than the ones documented in this study. However, as previous researchers used a completely different approach (hydrocarbon budget estimates for entire shale and reservoir rock volumes of whole basins), the expulsion efficiency values reported here may not contradict previous experiences. Further work utilizing the approach discussed above should document the natural range of variation of the thicknesses of the depleted edges of average source rock shales at different maturity stages. Another implication of the conclusions reached in this study concerns source rock/crude oil correlation: to establish genetic origins of crude oils more convincingly, an understanding of the nature of hydrocarbon expulsion processes and the associated compositional fractionation effects is required.

We thank the Ruhrkohle AG, Essen, for supplying the sample material, Dr A. S. Mackenzie (BP Research Centre) for a careful review and Dr D. H. Welte (KFA) for support and advice.

Received 19 April; accepted 14 August 1984.

1. Tissot, B. P. & Welte, D. H. *Petroleum Formation and Occurrence* (Springer, Berlin, 1978).
2. Hunt, J. M. *Petroleum Geochemistry and Geology* (Freeman, San Francisco, 1979).
3. Vandenbroucke, M. in *Advances in Organic Geochemistry 1971* (eds Gärtner, H. R. & Wehner, H.) (Pergamon, Oxford, 1972).
4. Radke, M., Sittardt, H. G. & Welte, D. H. *Analyt. Chem.* **50,** 663–665 (1978).
5. Radke, M., Willsch, H. & Welte, D. H. *Analyt. Chem.* **52,** 407–411 (1980).
6. Leythaeuser, D. & Schaefer, R. G. in *Advances in Organic Geochemistry 1983* (eds Schenck, P. A., de Leeuw, J. W. & Lijmbach, G. W. M.) (Pergamon, Oxford, in the press).
7. Espitalié, J. *et al. Rev. Inst. Fr. Petrol.* **32,** 23–42 (1977).
8. Tissot, B. P. *et al. Bull. Am. Ass. petrol. Geol.* **58,** 499–506 (1974).
9. Rabitz, A. *Fortschr. Geol. Rheinld. Westf.* **13,** 125–194 (1966).
10. Mackenzie, A. S. *et al. Nature* **301,** 506–509 (1983).
11. Leythaeuser, D. *et al. Bull. Am. Ass. petrol. Geol.* **68,** 196–219 (1984).
12. Altebäumer, A. M., thesis, Univ. Aachen (1983).
13. Craft, B. C. & Hawkins, M. F. *Applied Petroleum Reservoir Engineering* (Prentice-Hall, Englewood Cliffs, 1959).
14. Durand, B. *et al. Proc. 11th World Petroleum Congr.* **1,** 1–13 (1983).
15. Connan, J. & Cassou, A. M. *Geochim. cosmochim. Acta* **44,** 1–23 (1980).
16. Brooks, J. D., Gould, K. & Smith, J. W. *Nature* **222,** 257–259 (1969).
17. Lijmbach, G. W. M. *Proc. 9th World Petroleum Congr.* **2,** 357–369 (1975).
18. Didyk, B. M. *et al. Nature* **272,** 216–222 (1978).

Investigation of claims for interstellar organisms and complex organic molecules

Robert E. Davies*†, **Adelaide M. Delluva*** **& Robert H. Koch**†

*Laboratories of Biochemistry, Department of Animal Biology, School of Veterinary Medicine, and † Department of Astronomy and Astrophysics, University of Pennsylvania, Philadelphia, Pennsylvania 19104, USA

For many years, Hoyle, Wickramasinghe and their associates have examined interstellar (IS) absorption features in the ultraviolet, visible and infrared and 'identified' them with a variety of organic structures or organisms. Among these there have been generalized, pre-biotic molecules[1], polyoxymethylene whiskers[2], polysaccharides and hydrocarbons[3,4], tryptophan (and inferentially proteins)[5]—all claimed to be coatings on IS grains. In other cases, the grains[1,6] have been described as 10–100% alkanes, alkenes, alkynes or aromatics by mass. In extensions of these claims, the grains are supposed to be microorganisms (such as viruses and bacteria[7], algae[8], siliceous cells similar to diatoms[9], yeasts[10] or other eukaryotic cells[11]) in whole or in part. Finally, a case has been advanced for possible interstellar and interplanetary insects[11]. The 'identifications' in these and many other publications call into question the intrinsic origin of Earth life itself[12,13] and the uniqueness and validity of darwinian evolution[11]. We now report on ultraviolet spectra of specimens of the types cited by these workers and compare our results with infrared and ultraviolet data published previously. We conclude that the identifications claimed by Hoyle, Wickramasinghe and their colleagues are unwarranted.

The UV results are based on spectrophotometry with the OAO 2 and IUE spacecrafts. Accuracies for these measurements fall in the range ±5 to ±20% depending on the specific wavelength and star and on the observing circumstances. Speakers at a special meeting of the Royal Astronomical Society[14] noted that IUE spectra may be degraded over extended wavelength intervals (specifically near 280 nm)[5] and by saturation losses from over-exposure. The visible-band observations concern weak and diffuse absorption bands in the blue through the red and the accuracies of the measurements made on these bands are commonly of the order of ±10%. For the IR data beyond 2 μm, accuracy is improving very rapidly and, whether from ground (with its restricted wavelength coverage) or from an airborne observatory, is about ±5%. For all these data, spectral resolution (Δλ/λ) is of little consequence as the claims of Hoyle, Wickramasinghe and their colleagues all concern relatively broad

Table 1 Comparison of the Karim *et al.* absorption feature with present measurements of tryptophan near 280 nm

Wavelength (nm)	ΔA*	A†
310	0.00	0.00
300	+0.24	+0.04
290	+0.50	+0.52
280	+0.61	+0.61
270	+0.58	+0.55
260	+0.47	+0.37
250	+0.20	+0.18
240	0.00	+0.12
230	−0.02	+0.91
220	0.00	+3.71
210	+0.01	+2.47
200	+0.02	+2.56
190	+0.02	—
180	+0.02	—

* Karim *et al.*'s excess extinction after subtraction of graphite (0.02-μm radius spheres) extinction.

† Measured extinction due to tryptophan normalized to A=0.61 at 280 nm.

Table 2 Observed spectral absorption ratios for specimen materials

Material	λ (nm)†	λ′ (nm)‡	$(A_{\lambda'}/A_{\lambda})$
Tryptophan	280	220	6.1
Bovine serum albumin (BSA)	279	230	4.0
Trypsin (dry)*	279	200	32
RNase (in HCl)*	280	200	63
Aldolase (*p*H 7.4)*	280	200	50
E. coli (envelope protein in $NaHCO_3$)*	275	235	1.4
E. coli	260	220	1.7
E. coli (dry)	260	220	3.1
B. cereus (dry)	260	200	1.4
M13	258	200	27
Nuclear polyhydrosis virus (NPV)	260	200	15
M. luteus DNA	258	200	1.4
Calf thymus DNA	259	200	1.5
Merismopedia	260	200	1.7
Achnanthes brevipis	260	220	2.9
Chlorella	266	200	1.6

* Data taken from ref. 18.

† Wavelength in nm of measured peak absorption.

‡ Where λ′>200 nm, the sample has an absorbance, >2.000, which cannot be recorded accurately at wavelengths ⩾200 nm.

bands. We have already commented[15] on the treatment of the astronomical data set which Karim *et al.* claimed "confirms" the presence of proteinaceous material in grains[5]. In their Figs 3-5, Karim *et al.* noted the similarity of the absorption spectrum of tryptophan from 310 to 240 nm (including its peak at 280 nm) to a band, nominally freed of the contribution from IS graphite, derived from the ratios of UV spectra of distant, reddened stars to those of nearby comparison stars. Our comments referred to serious mismatches between the paired program and comparison stars and to the reasons why their detailed calculations of the residuum from a particular graphite absorption cannot be defended. However, this property of tryptophan cannot be used alone for identification; this is clear from a perusal of the 118-volume *Sadtler Standard Spectra Collection* which records the UV spectra from 300 to 200 nm of over 34,000 organic compounds. Hundreds of these spectra show peak absorptions with central wavelengths and bandwidths comparable with those of the feature singled out by Karim *et al.*[5]. Furthermore, they represent only a fraction of the several millions of organic compounds now known. Consequently, any particular peak is not specific for any particular molecule, and thus UV spectra alone cannot be used for identification although they may be used to exclude an identification with certainty.

We have, therefore, measured the UV absorbances (which in some cases include the effects of scattering) of some molecules and primitive life forms, including several types which Hoyle and Wickramasinghe have suggested or claimed to exist in IS space.

Absorption spectra were measured accurately from 320 to 235 nm or less in quartz cuvettes (1 cm light path) by means of a Bausch and Lomb Houston Instrument Omniscribe D-5000 strip chart recorder attached to a Varian DMS 90 UV-Visible Spectrophotometer. In all cases except tryptophan, whenever the lowest recorded value was above 200 nm this was because the absorbance had gone off scale (>2.0) and remained there at all wavelengths down to 200 nm. The region below 240 nm is where the excess absorbance of the Karim *et al.* feature has an absorbance of 0.02 or less. The absorption spectra were obtained for the amino acid tryptophan, the protein bovine serum albumin (BSA), the nucleic acids calf thymus DNA and *Micrococcus luteus* DNA, the bacteriophages M13 and ΦX174, the nuclear polyhedrosis virus (NPV) that attacks the wax moth *Galleria mellonella*, the Gram-positive bacterium *Bacillus cereus*, the Gram-negative bacterium *Escherichia coli* JM 103, the cyanobacterium (blue-green alga) *Merismopedia*, the diatom *Aehnanthes brevipis*, and the green alga *Chlorella*. The spectra for tryptophan, BSA, the DNAs, NPV, *E. coli* and *B. cereus* were also measured on thin films of the dry materials because there would be no free liquid water on interstellar grains.

Table 1 compares our experimental results for tryptophan with the excess extinction from Figs 3 and 5 of Karim *et al.* Disagreement between the two spectra is conspicuous at wavelengths below 240 nm. Our complete results appear in Table 2. For all specimens with an absorption peak in the region 290-250 nm that was different from that at 280 nm, the absorption ratios are even larger when calculated for a standard wavelength of 280 nm.

The results show that, whereas tryptophan and BSA in solution had peaks near 280 nm, every other sample of our materials had a peak near 260 nm that was clearly dominated by the nucleic acids present[16]; this does not agree with Karim *et al.*'s expectation[5] that organisms or their dry remains would have a peak of their UV absorption spectra at or near 280 nm. The effect of drying depended on the size and shape of the particles or crystals formed. For tryptophan, for example, differential scattering can change the position of the observed peak by tens of nanometres and also flatten it conspicuously. In general, absorption peaks are affected by the solvent and its *p*H—a phenomenon known as 'the universal redshift'[17].

For each one of the wet or dry specimens the absorption band from 210 to 200 nm was higher than the peak between 290 and 250 nm. This finding alone undermines the basis on which Karim *et al.* claimed[5] to have confirmed the presence of proteinaceous material on IS grains. This claim depended on the almost complete lack of absorption from 240 to 180 nm (see their Fig. 3) by the unknown material they believed responsible for their 280 nm peak. Figure 3 of Karim *et al.*[5] was normalized at both the 310 nm and 220 nm peaks. This 280 nm peak is the only one within the recorded range of wavelength. It follows that substances or organisms with higher absorbances below 240 nm than at 240 nm must be excluded. This property was found in dry tryptophan and in each of the other materials and organisms tested. For tryptophan in solution, a peak at 220 nm was followed by a shallow trough at 210 nm, then by higher absorbances at and below 200 nm—this particular detail also excludes the identification.

Setlow and Doyle[18] recorded the absorption spectra of dry samples of the protein trypsin and of aldolase and RNase from 310 to 185 nm. All these proteins had absorption peaks at 280 nm but absorbed (and scattered) the incident radiation much more effectively at and below 240 nm. The ratios of the molar absorption coefficients were 32, 50 and 63 for $\varepsilon_{200}/\varepsilon_{280}$ and 8.6, 12.5 and 13.6 for $\varepsilon_{220}/\varepsilon_{280}$. These ratios are so large that, if proteins were the source of the absorption, the contribution from graphite would be negligibly small and the curve for HD14250 and its comparison star in Fig. 3 of Karim *et al.* would not have the observed shape.

Although the higher absorption of tryptophan in solution at 230 nm (compared with that at 280m) was shown in Fig. 1 of Karim *et al.*[5], it was neglected in their Fig. 5 which compared "the excess extinction in the star HD14250 relative to graphite" (spheres of 0.02 μm radius). This comparison was given only from 310 to 245 nm where the curves fit but not for points below 240 nm and especially below 220 nm where the discrepancy becomes increasingly large. A similar objection follows from the papers[19,20] which Karim *et al.* cite concerning the proteins of tobacco mosaic virus and the envelope proteins of *E. coli*; these papers show a higher absorption for these proteins at or below 240 nm than at 280 nm. This peak is also claimed to confirm the proteinaceous material in grains[5] from dried bacteria and algae[8] and viruses[13].

Karim *et al.* state that "DNA has a strong absorption at 2,600 Å . . . but the DNA content of microorganisms is so small that prospects of detecting this particular absorption are not encouraging". However, the content of the various ribonucleic acids is very high[21] and the spectra of the corresponding ribo- and deoxyribonucleotides as well as nucleosides are essentially identical[16]. The molar absorption coefficients of the various nucleotides at 260 nm are greater[16] (≈9,000 to ≈15,000) than that of tryptophan ($\approx$5,000) at 280 nm. Furthermore, tryptophan comprises only 3 of the 336 amino acids in each *E. coli* envelope protein, but 25 of the amino acids are tyrosine and this moves the peak absorption to 275 nm (ref. 20). This accounts for *E. coli* and the other organisms enumerated above having peaks near 260 nm rather than 280 nm.

It is well known that the sterilization action spectrum of UV radiation from 300 to 220 nm parallels the absorption spectrum of bacteria[22,23] and that enzymes are inactivated by UV-induced damage to phenylalanine, tyrosine, tryptophan and cystine[24]. If tryptophan and these other amino acids were exposed to the interstellar UV, they would soon be destroyed. For example, the quantum yield for the production of ammonia, by 253.7-nm radiation, from tryptophan is 0.002 (ref. 24). If the amino acids were protected deep inside a grain covered by a polymeric coat, they could not be observed. However, a literature search failed to uncover any finding of tryptophan or any other indole derivative in either meteorites or IS clouds. One paper[10] concludes that the IR spectrum of the galactic centre source IRS7 contains strong evidence for bacterial grains on the basis of the IR spectrum of *E. coli*. However, from these results we have calculated that the same bacterial mass would cause an absorbance $\approx$100 times larger in the UV than in the IR and this has not been observed in the direction to any star. The same comparison excludes polysaccharides[25,26] associated with diatoms[9] and algae[8]. Finally, on the basis of experiments of Rosenbusch[20] and Setlow and Doyle[18], pure proteins in general[5,10] (including the major envelope protein of *E. coli*[20]) have a maximum UV absorbance at least 100 times larger than the highest IR absorbance. Because neither the required shape nor magnitude of the UV absorbances are observed, proteins are also excluded as explanation for these absorbances.

After this work was completed, Williams[27] and Hoyle and Wickramasinghe[28] published letters also describing the recent adverse comment[14] on the conclusions of Hoyle, Wickramasinghe and colleagues. Turner[29] expressed the need for much more stringent requirements than have recently been applied for molecular identification in the microwave region; although he is concerned only with highly resolved spectra, the same constraints apply even more forcibly to presently resolvable IR and UV molecular bands.

The M13 and *E. coli* JM 103 were gifts from Dr Roselyn Eisenberg; the DNA samples from Dr Phoebe S. Leboy; the other viruses and living organisms came from the Carolina Biological Supply Co., North Carolina.

Note added in proof: Greenberg's claim (see ref. 14) that the 280 nm feature[5] is spurious has now been published[30] together with summaries of papers given at the Royal Astronomical Society's Specialist Discussion, 'Are Interstellar Grains Bacteria?'[31]. Other adverse comments have appeared[32-35]. The response to these by Karim, Hoyle and Wickramasinghe[36,37] has in turn been answered by us[35].

Received 3 January; accepted 15 August 1984.

1. Hoyle, F. & Wickramasinghe, N. C. *Nature* **266**, 241-243 (1977).
2. Wickramasinghe, N. C. *Mon. Not. R. astr. Soc.* **170**, 11P-16P (1975).
3. Hoyle, F. & Wickramasinghe, N. C. *Nature* **270**, 323-324 (1977).
4. Hoyle, F. & Wickramasinghe, N. C. *Mon. Not. R. astr. Soc.* **181**, 51P-55P (1977).
5. Karim, L. M., Hoyle, F. & Wickramasinghe, N. C. *Astrophys. Space Sci.* **94**, 223-229 (1983).
6. Wickramasinghe, D. T. & Allen, D. A. *Nature* **287**, 518-519 (1980).
7. Hoyle, F. & Wickramasinghe, C. *Astrophys. Space Sci.* **65**, 241-244 (1979).
8. Hoyle, F. & Wickramasinghe, C. *Astrophys. Space Sci.* **66**, 77-90 (1979).
9. Hoyle, F., Wickramasinghe, N. C. & Al-Mufti, S. *Astrophys. Space Sci.* **86**, 63-69 (1982).
10. Hoyle, F., Wickramasinghe, N. C. Al-Mufti, S., Olavesen, A. H. & Wickramasinghe, D. T. *Astrophys. Space Sci.* **83**, 405-409 (1982).
11. Hoyle, F. & Wickramasinghe, C. *Evolution from Space*, 151-159 (Simon & Schuster, New York, 1981).
12. Hoyle, F. & Wickramasinghe, C. *Lifecloud The Origin of Life in the Universe*, 157-165 (Harper & Row, New York, 1978).
13. Hoyle, F. & Wickramasinghe, C. *Diseases from Space*, 1-11 (Harper & Row, New York, 1979).
14. Campbell, P. *Nature* **306**, 218-219 (1983).
15. Koch, R. H. & Davies, R. E. *Astrophys. Space Sci.* **100**, 425-426 (1984).
16. Lehninger, A. L. *Biochemistry* 2nd edn, 314 (Worth, New York, 1975).
17. Weber, G. & Teale, F. W. J. in *The Proteins* Vol. 3, 2nd edn (ed. Neurath, H.) 445-521 (Academic, New York, 1965).
18. Setlow, R. & Doyle, B. *Biochim. biophys. Acta* **24**, 27-41 (1957).
19. Taniguchi, M., Yamaguchi, A. & Taniguchi, T. *Biochim. biophys. Acta* **251**, 164-171 (1971).
20. Rosenbusch, J. P. *J. biol. Chem.* **249**, 8019-8029 (1974).
21. Feinberg, G. & Shapiro, R. *Life Beyond Earth*, 55 (Morrow, New York, 1980).
22. Gates, F. L. *J. gen. Physiol.* **14**, 31-42 (1930).
23. Davis, B. D., Dulbecco, R., Eisen, H. N. & Ginsberg, H. S. *Microbiology* 3rd edn, 1267 (Harper & Row, New York, 1980).
24. Setlow, J. K. *Compreh. Biochem.* **27**, 157-209 (1967).
25. Hoyle, F. & Wickramasinghe, N. C. *Nature* **268**, 610-612 (1977).
26. Hoyle, F., Olavesen, A. H. & Wickramasinghe, N. C. *Nature* **271**, 229-231 (1978).
27. Williams, D. A. *Nature* **306**, 420 (1983).
28. Hoyle, F. & Wickramasinghe, N. C. *Nature* **306**, 420 (1983).
29. Turner, B. E. *Astrophys. Lett.* **23**, 217-224 (1983).
30. Greenberg, J. M. *Observatory* **104**, 134-135 (1984).
31. *Observatory* **104**, 129-139 (1984).
32. McLachlan, A. & Nandy, K. *Observatory* **104**, 29-31 (1984).
33. Whittet, D. C. B. *Observatory* **104**, 159-160 (1984).
34. Savage, B. D. & Sitko, M. L. *Astrophys. Space Sci.* **100**, 427-429 (1984).
35. Duley, W. W. *Q. Jl R. astr. Soc.* **2**, 109-113 (1984).
36. Karim, L. M., Hoyle, F. & Wickramasinghe, N. C. *Astrophys. Space Sci.* **100**, 431-435 (1984).
37. Hoyle, F. & Wickramasinghe, N. C. *Astrophys. Space Sci.* **103**, 189-193 (1984).
38. Davies, R. E., Delluva, A. M. & Koch, R. H. in *The Search for Extraterrestrial Life—Recent Developments* (ed. Papagiannis, M. D.) Int. ast. Un. Symposium 112 (Reidel, Dordrecht, in the press).

Rejection of transplantable AKR leukaemia cells following MHC DNA-mediated cell transformation

Kam Hui, Frank Grosveld* & Hilliard Festenstein

Department of Immunology, The London Hospital Medical College,
Turner Street, London E1 2AD, UK
* Laboratory of Gene Structure and Expression,
National Institute for Medical Research, The Ridgeway,
Mill Hill, London NW7 1AA, UK

Major histocompatibility complex (MHC) class I molecules can function as specific target antigens in T-cell-mediated cytotoxity[1,2]. In addition, T cells can kill target cells through non-MHC antigens, for example, virally infected cells, if the target and effector cells express the same MHC class I antigens[2]. Consequently, quantitative and/or qualitative variations in the expression of the H–2/HLA antigens on the target cells could interfere with MHC-restricted immune reactions. We have reported that the AKR leukaemia cell line K36.16, a subline of K36 (ref. 3), on which the H–2K^k antigen cannot be detected, is resistant to T-cell lysis and grows very easily in AKR mice[4]. Other AKR tumour cell lines, like 369, which have a relatively large amount of H–2K^k on their surface, are easily killed by T cells *in vitro* and require a much larger inoculum to grow *in vivo*[4]. Monoclonal antibodies against H–2K^k, but not against H–2D^k, prevented the killing by T cells[4,5]. This suggests that some tumour cells grow *in vivo* because tumour-associated antigen(s) cannot be recognized efficiently by the host's immune system, due to the absence of MHC molecules which would function as restriction elements for T-cell cytotoxicity. We have tested this hypothesis by introducing the *H-2K^k* gene into the H–2K^k-deficient AKR tumour cell line K36.16 and have now demonstrated directly the biological relevance of H–2K^k antigen expression in the regulation of the *in vivo* growth of this tumour cell line.

Transformations were done by calcium phosphate co-precipitation[20] with a cosmid containing the *H-2K^k* gene (c27.2) and pTCF[6], the vector for the aminoglycosyl 3′-phosphotransferase gene (*agpt*), or pTCF alone. Between 8 and 20 transformants per 10^6 cells were selected in medium containing 800 μg ml^{-1} of the antibiotic G418. From over 300 transformants, we selected a series of clones that expressed different amounts of H–2K^k on the cell surface (see below). DNA and RNA were isolated from each of the selected transformants and analysed by Southern blot or S_1 nuclease protection analysis. Hybridization with a plasmid (vector) or an *H-2K^k* probe showed that each of the transformants contained one to three copies of the exogenous *H-2K^k* gene (data not shown). Figure 1 shows the level of *H-2K^k* mRNA determined by S_1 nuclease protection assay in the K36.16 tumour cells before and after transformation with *H-2K^k*. The negative control *H-2K^d* P_3-X63-Ag8 (Ag8) cells[7] (Fig. 1*b*) and the K36.16 cells show a low mRNA signal, probably due to incomplete S_1 digestion of RNA–DNA hybrids

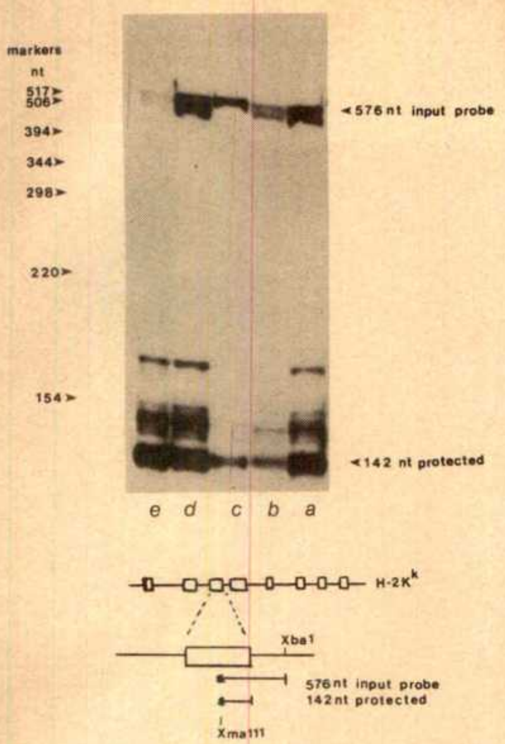

Fig. 1 S_1 nuclease protection analyses of mRNA isolated from the c27.2 transformants and control cell lines: *a*, 369 (H-2K^k, positive control); *b*, Ag8 (H-2K^d, and H-2K^k-negative control); *c*, K36.16; *d*, C27.2.2; and *e*, C27.2.3.

Methods: S_1 nuclease protection analysis was done using procedures described elsewhere[18,19]. The input probe is a 576-nucleotides (nt) *Xma*III-*Xba*I DNA fragment isolated from the third exon-intron boundary; 142 nt of this fragment are protected from S_1 nuclease digestion (S. Kvist, personal communication). 25 μg of total cytoplasmic RNA isolated from the different cell lines were hybridized overnight at 57 °C with the labelled DNA input probe. S_1 nuclease cleavage was at 37 °C for 2 h and electrophoretic separation was on 8 M urea-7% polyacrylamide gels, resulting in a 142-nucleotide protected fragment. Multiple protected bands shorter than 142 nt are due to overdigestion by S_1 nuclease.

formed between the DNA probe and mRNA molecules other than *H-2K^k*. The *H-2K^k*-transformed cells, however, show an increase of at least 20-fold of *H-2K^k* mRNA (Fig. 1*d*, *e*) to a level similar to that of the positive control, 369 (H-2K^k-positive) (Fig. 1*a*). This suggests that the absence of the H-2K^k antigen on the K36.16 cells is due to a failure to transcribe the *H-2K^k* gene efficiently, rather than any post-transcriptional event.

To demonstrate the presence of the H-2K^k antigen on the cell surface, we carried out radiobinding analysis with anti-H-2K^k monoclonal antibodies. Table 1 gives the results from only five *H-2K^k* DNA transformants and the control cell lines, because they cover a wide range of H-2K^k antigen expression on the cell surface and were subsequently used in experiments designed to evaluate the role of H-2K molecules in oncogenesis and host resistance to AKR leukaemias. All these cell lines express the same amount of H-2D^k, as expected (data not shown). In addition, a 45,000-molecular weight molecule was precipitated by anti-H-2K^k monoclonal antibody from ^{35}S-methionine-labelled lysates of one of the transformed clones. Competition by added unlabelled AKR (H-2K^k-positive) lysates specifially prevented the immunoprecipitation of this molecule (data not shown).

Because the H-2K^k antigen is important as a restriction element in T-cell-mediated killing of Gross virus tumours[4], we examined the ability of these transformed clones to induce tumours in syngeneic AKR and semi-syngeneic (AKR × BALB/c)F1 mice. Table 1 shows that inocula of 10^5 viable cells

Table 1 Radioimmunoassay and tumour inducibility of *H-2K^k*-transfected K36.16 cells

Transformant	Radiobinding (net c.p.m.)		No. of mice with tumours*	
K36.16	0	(0)	10/10	(10/10)
pTCF-K36.16	92	(21)	10/10	(10/10)
C27.2.1	364	(424)	0/10	(0/10)
C27.2.2	376	(529)	1/5	
C27.2.3	1,334	(1,073)	0/5	(0/5)
C27.2.4	257	(209)	4/5	
C27.2.5	230	(497)	0/5	
369	19,416	(6,350)		

For radiobinding, 5×10^5 cells were reacted with monoclonal antibodies as indicated. The anti-H-2K^k (refs. 15, 16) and anti-H-2D^k (ref. 15)-producing hybridoma cell lines were obtained from the American Type Culture Collection. The results are an average of two independent assays with anti-H-2K^k antibody 11.4.1 (ref. 15) (or 16-3-22S[16]) and are expressed as c.p.m. after subtraction of the background (200 c.p.m.) pTCF-K36.16 is a clone obtained by transformation of K36.16 with the vector pTCF alone. The positive control, 369, is an AKR leukaemia that expresses H-2 K^k antigen[4].

* 100,000 K36.16 tumour cells (in 0.1 ml phosphate-buffered saline, PBS) were injected subcutaneously (s.c.) into one thigh and the same number of c27.2 transfected clones into the other thigh of the recipient mouse. The diameters of the tumour masses were measured after 3 weeks. Mice were scored as positive for tumours when the diameters measured were 1.5–2.0 cm, whereas mice were scored as negative for tumours when the diameters observed were <0.6 cm. 3,000 K36.16 tumour cells were able to induce 100% tumour incidence in both AKR and (AKR × BALB/c)F1 mice in 14–20 days. The values for F_1 mice are given in parentheses.

Table 2 Induction of tumour by treatment of the transfected clones with monoclonal anti-H-2K^k antibody

Clone	Treatment of AKR recipients	No. of mice with tumours
C27.2.1	Anti-H-2K^k MoAb	3/5
C27 2 1	Anti-H-2K^b MoAb	0/5
C27.2.1	Culture medium	0/5
C27.2.3	Anti-H-2K^k MoAb	6/7
C27.2.3	Anti-H-2K^b MoAb	0/7

100,000 transfected clones treated with monoclonal antibody (MoAb) (anti-H-2K^k MoAb 16-3-22S[16] or anti-H-2K^b MoAb B8-24-3 (ref. 17) as indicated were injected s.c. into the thigh of one of the hind legs of the recipient, and K36.16 cells treated with the same antibody were injected into the other hind leg of the same mouse. This was followed by subsequent injections of the corresponding monoclonal antibody *in vivo* once every other day. The number of tumour incidences was recorded after 20 days. The K36.16 tumour cells were able to induce tumours in all cases.

Table 3 Mice immunized with the transfected clones reject a second challenge of the original K36.16 tumour cells

Mouse strain tested	Mice primed with clone	No. of mice with tumours
AKR	C27.2.3	0/5
AKR	C27.2.3 (mitomycin C)	4/5
(AKR × BALB/c)F1	C27.2.3	0/5
AKR	C27.2.2	0/5
AKR	C27.2.4	0/2
AKR	K36.16 (mitomycin C)	5/5

Mice were injected s.c. with 100,000 c27.2 transfected cells as indicated in Table 1. After 3–4 weeks, mice that did not show signs of tumours were given an additional dose (s.c.) of 100,000 K36.16 tumour cells. The number of mice with tumours was observed after 30 days. The K36.16 (mitomycin C) cells were treated with mitomycin C at 50 μg ml^{-1} 10^6 cells for 30 min at 37 °C, washed four times with PBS and subsequently injected s.c.

of the original K36.16 tumour cells and a clone of K36.16 tumour cells transformed with the vector pTCF alone, induced necrotic tumours within 20 days. However, inocula of 10^5 viable cells each of clones C27.2.1, C27.2.3 and C27.2.5 all failed to induce tumours in AKR and (AKR × BALB/c)F1 mice; these clones were able to induce tumours in all cases when the recipient AKR mice were irradiated (700 rad) before injection. Clones C27.2.2 and C27.2.4, which express relatively lower amounts of H-2K^k antigens (Table 1), were both able to induce tumours in some of the AKR mice. Interestingly, the diameters of the tumour masses which developed after inoculation of the latter clones were smaller (0.9–1.2 cm) and necrosis was absent even after 30 days. The oncogenicity of these transformed clones may thus be determined by: (1) the level of expression of the H-2K^k gene product in a particular transformant; (2) the ability of individual recipient mice to mount an efficient immune response against these inocula; and (3) the size of the inoculum needed to induce a tumour. When a higher dose of 5×10^6 viable cells was given, C27.1.1 and C27.2.3 were able to develop tumours in AKR mice (C27.2.5 was not tested). Conversely, clones C27.2.2 and C27.2.4 failed to induce tumours in AKR mice if a lower dose of 5×10^3 cells, instead of 10^5 cells, was given.

To prove that H-2K^k is the restriction element needed for the *in vivo* rejection of the transformed clones, C27.2.1 and C27.2.3 were first allowed to react separately with several different monoclonal antibodies (as shown by Table 2) before injection into the mice. The corresponding monoclonal antibodies were subsequently injected once every other day for 5 days. This procedure enabled the transformed clones to induce tumours in most AKR recipients (three out of five for C27.2.1, and six out of seven for C27.2.3; Table 2). Injection of the irrelevant anti-H-2K^b monoclonal antibody and culture medium were both ineffective.

To test whether the *H-2K*^{k} DNA-transformed clones can confer immunity, mice were injected with either the transformed clones, or mitomycin C-treated K36.16 tumour cells or C27.2.3 cells as indicated in Table 3. After 3 weeks, mice that did not show signs of tumours were again challenged with an additional 10^5 live K36.16 tumour cells. While only 3×10^3 K36.16 tumour cells always produced a tumour, the mice which had rejected the *H-2K*^{k}-transformed K36.16 clones were protected against a subsequent challenge of 10^5 live K36.16 tumour cells—this even included mice which had rejected the relatively low H-2K^k-expressing clone C27.2.4. Thus, once an efficient immune response was obtained, this protective immunity was as efficient as that elicited by the more immunogenic clones (for example, C27.2.3) against a subsequent challenge of the original K36.16 tumour cells. When the H-2K^k-positive C27.2.3 cells were prevented from dividing by treatment with mitomycin C before injection, their ability to induce protection against a second challenge of live K36.16 tumour cells was abrogated (Table 3).

These experiments raise several interesting questions. First, the importance of the expression of the H-2K^k product seems to be central to the host reponse to tumours. The examination of many AKR tumours showed that several of them had only a small amount of H-2K^k antigen on the surface[4]. These findings and those of others[8-11] suggest that the relative absence of the H-2K specificity provides such tumours with a selection advantage *in vivo*[12,13]. One might expect, as indeed is found, that the cell-mediated cytotoxicity of tumours which are H-2D-restricted would exhibit a relative absence of the *H-2D*-encoded products[14].

The results presented here strongly suggest that the selective loss of the H-2K^k restriction elements in K36.16 is caused by a 'switch-off' at the transcriptional level, rather than any changes in the amino acid sequences or any fault in the mechanism necessary for the insertion of the antigens in the cell membrane. Experiments to study the molecular basis of this suppression are in progress.

We thank M. Steinmetz for the cosmid c27.2; S. Kvist for providing unpublished information in preparing the *H-2K*^{k} DNA probe for the S_1 nuclease protection analysis; and C. O'Carroll for typing the manuscript. The '369' tumour line was provided by Peter Krammer. These studies were supported by the CRC and the MRC (UK).

Received 26 July; accepted 3 September 1984.

1. Schreffler, D. C. & David, C. S. *Adv. Immun.* **20,** 125–195 (1975).
2. Zinkernagel, R. M. & Doherty, P. D. *Adv. Immun.* **27,** 52–177 (1979).
3. Old, E. J., Boyse, E. A. & Stockert, E. *Cancer Res.* **25,** 813–819 (1965).
4. Festenstein, H. & Schmidt, W. *Immun. Rev.* **60,** 85–127 (1981).
5. Schmidt, W. & Festenstein, H. *Immunogenetics* **16,** 257–264 (1982).
6. Grosveld, F. G. *et al. Nucleic Acids Res.* **10,** 6715–6732 (1982).
7. Horbita, K. & Harris, A. W. *Expl Cell Res.* **60,** 61–70 (1970).
8. Baldani, P., Pogo, F., Gisselbrecht, S. & Komilsky, P. *J. exp. Med.* **158,** 1294–1306 (1983).
9. Eisenbach, L., Segal, S. & Feldman, M. *Int. J. Cancer* **32,** 113–120 (1983).
10. Gooding, L. R. *J. Immun.* **129,** 1306–1312 (1982).
11. Rogers, M. J., Gooding, L. R., Margulies, D. H. & Evans, G. A. *J. Immun.* **130,** 2418–2422 (1983).
12. Schrier, P. I., Bernards, R., Vaessen, R. T. M. J., Houweling, A. & van der Eb, A. J. *Nature* **305,** 771–775 (1983).
13. Bernards, R. *et al. Nature* **305,** 776–779 (1983).
14. Pierotti, M. A., Ballinaii, D., Colombo, M. P., Gragioli, L. & Parmiani, G. *Transplantn Proc.* **15,** 2068–2073 (1983).
15. Oi, V., Jones, P. P., Goding, J. W. & Herzenberg, L. A. *Curr. Topics Microbiol. Immun.* **81,** 115–129 (1978).
16. Ozata, K., Mayer, N. & Sachs, D. H. *J. Immun.* **124,** 533–540 (1980).
17. Kohler, G., Fischer Lindahl, K. & Hensser, C. *Immune System* **2,** 202–208 (1981).
18. Berk, A. J. & Sharp, P. A. *Cell* **12,** 721–732 (1977).
19. Weaver, R. F. & Weissmann, C. *Nucleic Acids Res.* **7,** 1175–1193 (1979).
20. Wigler, M. *et al. Cell* **16,** 777–785 (1979).

Insertion of *N* regions into heavy-chain genes is correlated with expression of terminal deoxytransferase in B cells

Stephen V. Desiderio*, George D. Yancopoulos†, Michael Paskind*, Elise Thomas*‡, Michael A. Boss*‡, Nathaniel Landau*, Frederick W. Alt† & David Baltimore*

* Whitehead Institute for Biomedical Research, Cambridge,
Massachusetts 02142, USA and Department of Biology,
Massachusetts Institute of Technology, Cambridge,
Massachusetts 02139, USA
† Columbia University, College of Physicians and Surgeons,
Department of Biochemistry, New York, New York 10027, USA

The variable regions of immunoglobulin heavy chains are encoded in the germ line by three discrete DNA segments: V_{H} (variable) elements, *D* (diversity) elements and J_{H} (joining) elements. During the differentiation of B lymphocytes, individual segments from each group are brought together by recombination to form the complete $V_{\mathrm{H}}DJ_{\mathrm{H}}$ variable region[1-8]. To understand these processes better, we have now isolated and sequenced molecular clones representing intermediates (DJ_{H} fusions) and final products (V_{H}-to-DJ_{H} joins) of heavy-chain gene rearrangement in two cell lines[9,10] that represent analogues of cells at early stages of B-lymphocyte differentiation[11-13]. Heavy-chain gene assembly in one cell line but not in the other is accompanied by the appearance of short nucleotide insertions at the recombinational junctions. The generation of such insertions is positively correlated with the expression of terminal deoxynucleotidyl transferase in these lines.

The two cell lines used in our study, 40E4 and 22D6, were produced by Abelson murine leukaemia virus (A-MuLV) transformation of BALB/c fetal liver at 13–14 and 17–19 days of gestation, respectively. These cell lines produce no detectable immunoglobulin[12]; they possess DJ_{H} rearrangements on both chromosomes and undergo further rearrangement during propagation[12-14]. Thus the 40E4 and 22D6 cell lines seem to represent the stage of differentiation during which lymphoid progenitor cells give rise to μ-positive pre-B cells.

Two clonal cell lines, 40E4-2 and 22D6-G, were isolated, carried in culture for about 25 generations and subcloned to generate sets of secondary clonal isolates. The clonal origin of these isolates was verified by analysis of the pattern of A-MuLV

---

‡ Present addresses: Tufts University, School of Veterinary Medicine, Boston, Massachusetts 02111, USA (E.T.); Celltech Ltd, Slough SL1 4DY, UK (M.A.B.).

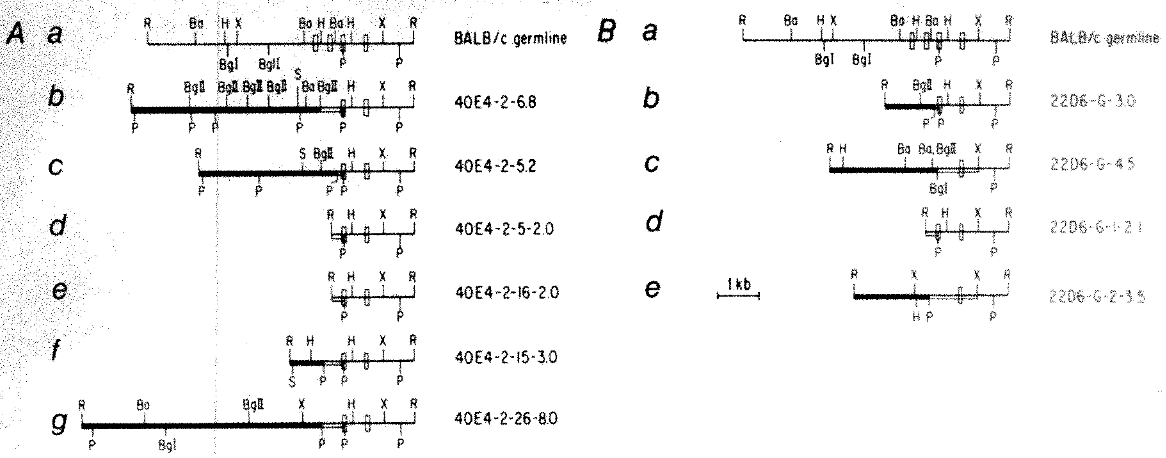

Fig. 1 Restriction maps of molecular clones representing J_H-associated rearrangements in derivatives of 40E4-2 and 22D6-G. *A*, Partial restriction maps of recombinants from 40E4-2 and its derivatives. *a*, Map of the 6.2-kb J_H-containing *Eco*RI fragment from the BALB/c germ line[3], shown for comparison. *b–f*, Restriction maps of the following J_H-associated rearrangements: *b*, 40E4-2-6.8; *c*, 40E4-2-5.2; *d*, 40E4-2-5-2.0; *e*, 40E4-2-16-2.0; *f*, 40E4-2-15-3.0; *g*, 40E4-2-26-8.0. Narrow lines represent regions of identity with the BALB/c germ-line map. Closed bars represent the minimal extent of novel DNA sequence; open bars designate the localization of the recombinant junctions. Restriction enzymes are abbreviated as follows: R, *Eco*RI; Ba, *Bam*HI; H, *Hin*dIII; X, *Xba*I; P, *Pst*I; Bgl, *Bgl*I; BglI, *Bgl*II; S, *Sac*I. *B*, Partial restriction maps of recombinants from 22D6-G and its derivatives: *a*, the BALB/c 6.2-kb germ-line *Eco*RI fragment; *b*, 22D6-G-3.0; *c*, 22D6-G-4.5; *d*, 22D6-G-1-2.1; *e*, 22D6-G-2-3.5. Regions of novel DNA sequence and locations of recombinant junctions are identified as in *A*.

Methods: Genomic DNA libraries for each of the A-MuLV-transformed parental cell lines and their derivatives were constructed in Charon 16A and screened for hybridization to a J_H probe[14]. J_H-containing bacteriophage insert fragments were subcloned into the *Eco*RI site of pBR322 and partial restriction maps were determined. The A-MuLV-transformed cell lines were produced as described by Rosenberg and Baltimore[9] and Waneck and Rosenberg[10]. Cell lines were cultured in RPMI-1640 medium supplemented with 10% heat-inactivated fetal calf-serum and 50 μM 2-mercaptoethanol. Primary subclones 40E4-2 and 22D6-G were derived from the 40E4 and 22D6 cell lines by limiting dilution to a concentration of 0.2 cells per microtitre well. These primary subclones were carried for 2 weeks in culture and secondary subclones were obtained by limiting dilution as described above. Preparation of genomic DNA, restriction enzyme digestion, agarose gel electrophoresis, radiolabelling of probes by nick-translation and DNA hybridization were performed as previously described[29]. Genomic DNA libraries were constructed in the bacteriophage vector Charon 16A[30]. Genomic DNA from 40E4-2, 40E4-2-26, 22D6-G or 22D6-G-2 was digested with *Eco*RI and ligated to Charon 16A DNA, which had previously been digested with *Eco*RI and dephosphorylated with calf intestinal phosphatase. Genomic DNA from 40E4-2-5, 40E-2-15, 40E4-2-16 or 22D6-G-1 was cut with *Eco*RI and fractionated on gradients of 10–40% sucrose containing 1 M NaCl, 20 mM Tris-Cl *p*H 8.0 and 10 mM EDTA. Centrifugation was performed at 24,000 r.p.m. and 20 °C for 24 h in the SW27 rotor. Fragments <2.5 kb long were selected from digests of 40E4-2-5, 40E4-2-16 and 22D6-G-1 genomic DNA; fragments <3.5 kb long were selected from the digest of 40E4-2-15 genomic DNA. These size-selected pools were ligated to Charon 16A DNA, prepared as described above. The products of ligation were encapsidated *in vitro* by the method of Sternberg *et al.*[31]. The resultant bacteriophage were propagated in *Escherichia coli* strain LE392. Plaques were screened for hybridization to the ^{32}P-labelled J_H probe by the method of Benton and Davis[32]. Bacteriophage positive for hybridization were isolated by three additional rounds of plaque purification. After initial propagation in Charon 16A, the J_H-containing *Eco*RI fragments were subcloned into the *Eco*RI site of pBR322.

proviral integration[15], which was identical among all members of each set of subclones (data not shown). Hybridization of J_H and D probes to DNA from both series of clonal cell lines showed that each parental line had two DJ_H rearrangements and that many subclones had lost one or both DJ_H-containing fragments but had acquired new fragments[14]. The new fragments generally hybridized well to the J_H probe but not to the D probe, suggesting that they might have arisen by appendage of V_H segments onto pre-existing DJ_H units.

To determine the structures of the J_H-associated rearrangements present in the 40E4-2 and 22D6-G cell lines and their derivatives, we carried out molecular cloning of each putative V_H-to-DJ_H rearrangement. The restriction maps of the fragments and their relationship to the J_H region of BALB/c germ-line DNA are shown in Fig. 1. In the 40E4-2 series, the original DJ_H rearrangements were near J_H3 and further rearrangements also occurred near J_H3. In 22D6-G, one rearrangement was near J_H4 and the other near J_H3; the subclones had secondary rearrangements near the same regions. The areas around these points of rearrangement were therefore chosen for DNA sequence analysis.

From its sequence, it is evident that the 5.2-kilobase (kb) J_H-containing *Eco*RI fragment from the 40E4-2 line had arisen by recombination between an SP2-type D segment[8] and J_H3 (Fig. 2*A*, *a–c*). The 5′ flank of the D region and part of its coding sequence are totally homologous to $D_{SP2.7}$ but, as is often found at DJ_H joints[2,5–8], some nucleotides were apparently lost from both the D and J_H potential coding sequences. Also, 7 nucleotides not represented in the $D_{SP2.7}$ or J_H3 germ-line sequences were found between D and J_H; they constitute an N region[16]. A similar analysis of the sequence in the 6.8-kb allele showed that it, too, consisted of part of D, part of J_H3 and an N region of 4 nucleotides (Fig. 2*B*). The exact germ-line sequence for this allele is not known, although it is most similar to $D_{SP2.3}$ (see Fig. 2*B*).

The alleles cloned from 22D6-G had also lost some coding sequence from J_H or D (Fig. 3*A*, *a–c*; *B*, *a–c*). Both D regions were identical to known germ-line D segments. The rearrangements differed from rearrangements in 40E4-2 in that all of the nucleotides near the joints could be accounted for by D and J_H germ-line sequences; no insertion of N regions seemed to have occurred.

The presence of the highly conserved[17] 3′ end of the V_H segment in all four secondary rearrangements of the 5.2-kb DJ_H-containing *Eco*RI fragment in 40E4-2 and both rearrangements in 22D6-G shows that all of these rearrangements involved recombination of V_H segments with pre-existing DJ_H segments (Figs 2*A*, *e–h*; 3*Ae*, *Bd*). All six of these V_H-to-DJ_H rearrangements have used closely related members of the V_H7183 gene family, of which the MOPC21 V_H gene is representative[18]. In all but one case, whenever a new band appeared in a subclone, the new fragment contained the DNJ_H structure characteristic of the fragment that had been lost (see Figs 2, 3), proving that a pre-existing DJ_H gives rise to a V_HDJ_H unit.

The junctions formed during V_H-to-DJ_H joining were similar in several respects to the junctions formed during D-to-J_H joining. First, there was loss of a variable number of nucleotides from the 5′ end of the DJ_H coding sequence. Second, variable numbers of nucleotides were lost from the 3′ ends of the V_H coding sequences. This was definitively observed in the

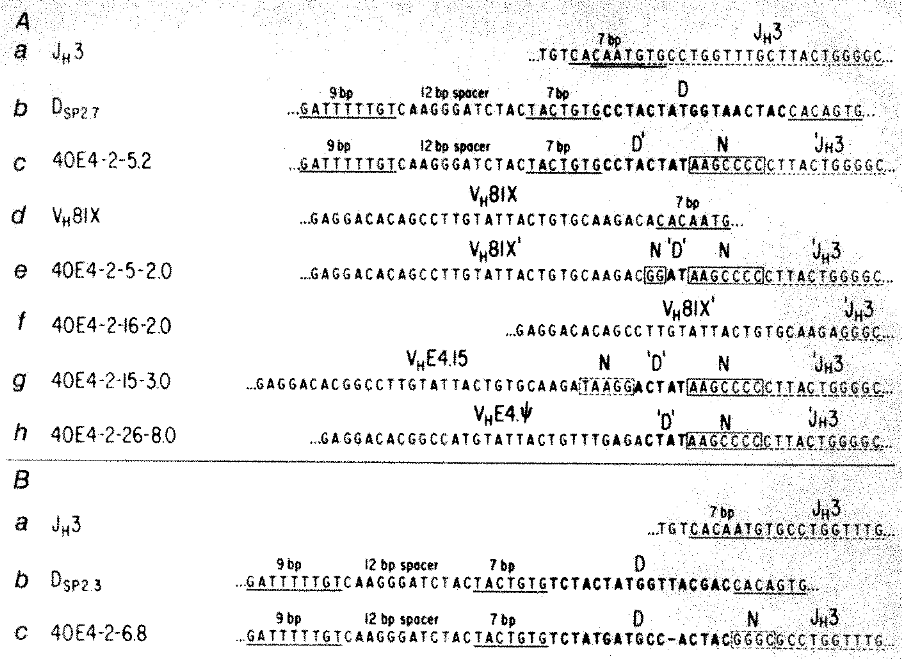
A
a J_H3
7 bp
J_H3
...TGTCACAATGTGCCTGGTTTGCTTACTGGGGC...
b $D_{SP2.7}$
9 bp
12 bp spacer
7 bp
D
...GATTTTTGTCAAGGGATCTACTACTGTGCCTACTATGGTAACTACCACAGTG...
c 40E4-2-5.2
9 bp
12 bp spacer
7 bp
D'
N
'J_H3
...GATTTTTGTCAAGGGATCTACTACTGTGCCTACTATAAGCCCCCTTACTGGGGC...
d V_H81X
V_H81X
7 bp
...GAGGACACAGCCTTGTATTACTGTGCAAGACACACAATG...
e 40E4-2-5-2.0
V_H81X'
N 'D'
N
'J_H3
...GAGGACACAGCCTTGTATTACTGTGCAAGACGGATAAGCCCCCTTACTGGGGC...
f 40E4-2-16-2.0
V_H81X'
'J_H3
...GAGGACACAGCCTTGTATTACTGTGCAAGAGGGC...
g 40E4-2-15-3.0
$V_HE4.15$
N
'D'
N
'J_H3
...GAGGACACGGCCTTGTATTACTGTGCAAGATAAGGACTATAAGCCCCCTTACTGGGGC...
h 40E4-2-26-8.0
$V_HE4.\psi$
'D'
N
'J_H3
...GAGGACACGGCCATGTATTACTGTTTGAGACTATAAGCCCCCTTACTGGGGC...
B
a J_H3
7 bp
J_H3
...TGTCACAATGTGCCTGGTTTG...
b $D_{SP2.3}$
9 bp
12 bp spacer
7 bp
D
...GATTTTTGTCAAGGGATCTACTACTGTGTCTACTATGGTTACGACCACAGTG...
c 40E4-2-6.8
9 bp
12 bp spacer
7 bp
D
N
J_H3
...GATTTTTGTCAAGGGATCTACTACTGTGTCTATGATGCC-ACTACGGGCGCCTGGTTTG...

Fig. 2 V_H–DJ_H assembly in the 40E4-2 A-MuLV transformant. ***A***, Primary and secondary rearrangement of the 5.2-kb J_H-containing *Eco*RI fragment from 40E4-2. Recombinant junctions in molecular clones of the primary (5.2 kb) and secondary rearrangements were localized by restriction mapping, and nucleotide sequences across the joints were determined by the method of Maxam and Gilbert[33]. *a*, *b*, Partial sequences of the germ-line J_H3 segment[3,7] and $D_{SP2.7}$ segments[8]. *c*, Sequence of the $D_{SP2.7}$-J_H3 fusion in clone 40E4-2-5.2. *d*, 3′-Terminal portion of the germ-line sequence of the V_H81X gene segment[18]. *e*, *f*, Sequences at the recombinant junctions of clones 40E4-2-5-2.0 and 40E4-2-16-2.0; these recombinants resulted from joining of V_H81X to the D-J_H3 fusion of 40E4-2-5.2. *g*, *h*, Sequences at the recombinant junctions of clones 40E4-2-15-3.0 and 40E4-2-24-8.0; these rearrangements are also the result of V_H-to-DJ_H joining. Sequences derived from J_H coding regions are indicated by a dashed underline; sequences derived from D regions are given in boldface type. Conserved heptamer and nonamer recognition sequences are indicated. Nucleotide regions not accounted for by germ-line V_H, D or J_H sequences (N regions) are enclosed in boxes and labelled N. Dotted boxes designate probable N regions in instances where the precise germ-line sequence of one recombination partner has not been determined (see text). Loss of nucleotides from the 5′ or 3′ side of a coding segment is designated by 'X or X′, respectively. ***B***, Primary rearrangement of the 6.8-kb J_H-containing *Eco*RI fragment from 40E4-2. The recombinant junction in the 6.8-kb fragment was localized by restriction mapping and the nucleotide sequence across the joint was determined as above. *a*, *b*, Partial sequences of the germ-line J_H3 and $D_{SP2.3}$ segments[8]. *c*, Sequence of the D-J_H3 fusion in clone 40E4-2-P-6.8. The D segment used is not identical to any known D segment, although it is similar to $D_{SP2.3}$. The hyphen indicates a gap introduced in the D coding region to maximize homology to $D_{SP2.3}$. Symbols used are defined in *A*.

recombinants 40E4-2-5-2.0 and 40E4-2-16-2.0 both of which used the V_H81X segment[18] and lost one and two nucleotides, respectively, from its 3′ end (Fig. 2*Ad*–*f*). Comparison with related V_H sequences[17] suggests that the V_H segment used in 40E4-2-15-3.0 has probably lost no nucleotides whereas the V_H segment used in 40E4-2-26-8.0 has lost at most one (Fig. 2*Ag*, *h*).

A third characteristic of V_H-to-DJ_H joining was that nucleotides not present in the germ-line sequences appeared at the V_H–DJ_H junction in at least one and probably two of the four secondary recombinants derived from 40E4-2. In 40E4-2-5-2.0, two dG residues appeared at the boundary between V_H81X and D, neither of which was present in the germ-line V_H81X segment or the parental DJ_H segment. Using related V_H segments[17] for comparison, it seems likely that five nucleotides (TAAGG) had been introduced at the V_H–DJ_H junction in 40E4-2-15-3.0 which were not encoded by either V_H or the parental DJ_H segment.

As in the 40E4-2 derivatives, the V_H–DJ_H junctions in the 22D6-G subclones exhibited variable loss of nucleotides from the V_H and DJ_H coding segments. In neither recombinant, however, did we find nucleotides at the V_H–DJ_H junction that could not be accounted for by the DJ_H or V_H sequences.

Comparison of the V_HDJ_H segments found in derivatives of 40E4-2 and 22D6-G revealed one obvious difference: recombinants from the 40E4-2 line commonly contained extra nucleotides not encoded by V_H, D or J_H segments whereas recombinants from the 22D6-G line did not. These N regions, which have also been found in DJ_H and V_HDJ_H fusions from terminally differentiated cell lines[5,6,8,16], vary widely in length and sequence and it therefore seems unlikely that each is encoded in the germ line. It has been suggested that extra nucleotides might be introduced at D–J_H and V_H–DJ_H junctions by the enzyme terminal deoxynucleotide transferase (TdT) during recombination[16]. This enzyme, which is present in several lymphoid lines[19], is capable of catalysing polymerization of deoxyribonucleotides onto the 3′-hydroxyl terminus of an oligonucleotide primer in the absence of a template[20]. In an attempt to correlate the expression of TdT in the 40E4-2 and 22D6-G lines with their ability to introduce extra nucleotides at the junctions of V_H, D and J_H segments, extracts prepared from these cell lines were assayed for TdT activity, as indicated by polymerization of dGTP onto an oligo(dA) primer[21,22]. In the presence of extract from 40E4-2 (16 μg protein), 10.0 pmol dGMP was incorporated into acid-precipitable material in 60 min at 37 °C, a level similar to that of the TdT-containing thymoma line, RL♂11. In contrast, we were unable to detect polymerization in the presence of an extract from 22D6-G cells (<0.2 pmol dGMP incorporated). Addition of extract from 22D6-G did not inhibit polymerization catalysed by the 40E4-2 extract. To confirm these results, the cell lines RL♂11, 40E4-2 and 22D6 (the parental line from which 22D6-G was cloned) were metabolically labelled with ^{35}S-methionine and extracts of these cells were assayed by immunoprecipitation with affinity-purified anti-TdT antibody. A protein of the size of TdT was precipitated from RL♂11 and 40E4-2 but not from 22D6 (Fig. 4). Also, a partial cDNA clone for TdT has been observed to hybridize to a 2.2-kb RNA species present in RL♂11 and 40E4-2 but not in 22D6 (N.L. and D.B., unpublished observations).

For five of the six V_H-to-DJ_H rearrangements that we examined, we were able to identify unambiguously in the parental cell the DJ_H segment that had participated in the rearrangement (in 40E4-2-16-2.0, V_H-to-DJ_H rearrangement resulted in deletion of the D–J_H junction). We have therefore shown directly that the DJ_H units found in these fetal liver-derived A-MuLV transformants are intermediates in V_HDJ_H assembly, as had been suggested by the results of hybridization assays reported previously[13,14,23]. All six V_HDJ_H rearrangements characterized here have placed the V_H coding sequence out of frame with respect to the J_H coding sequence. This could reflect the small sample size or it could be that cells containing productive rearrangements are lost, perhaps through a toxic effect of free heavy chain[24].

We found no evidence for somatic point mutation. Comparison of the 200-base pair (bp) portion of the V_H81X sequence present in molecular clones of three V_HDJ_H recombinants (40E4-2-5-2.0, 40E4-2-16-2.0 and 22D6-G-1-2.1) with the germ-line sequence of the gene segment, and similar comparisons involving J_H segments, failed to reveal any nucleotide differences[18]. This is consistent with other evidence that rather than occurring coincidentally with rearrangement[25,26] somatic point mutation occurs principally at later stages in B-lymphocyte

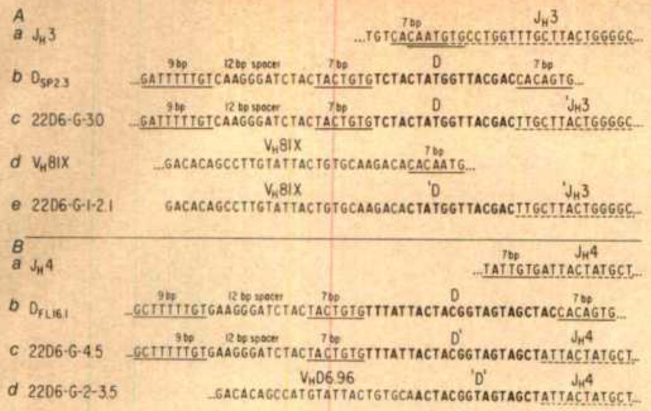
A
a J_H3
7bp
J_H3
...TGTCACAATGTGCCTGGTTTGCTTACTGGGGC...
b D_SP2.3
9bp
12bp spacer
7bp
D
7bp
...GATTTTTGTCAAGGGATCTACTACTGTGTCTACTATGGTTACGACCACAGTG...
c 22D6-G-3.0
9bp
12 bp spacer
7bp
D
'J_H3
...GATTTTTGTCAAGGGATCTACTACTGTGTCTACTATGGTTACGACTTGCTTACTGGGGC...
d V_H81X
V_H81X
7bp
...GACACAGCCTTGTATTACTGTGCAAGACACACAATG...
e 22D6-G-1-2.1
V_H81X
'D
'J_H3
GACACAGCCTTGTATTACTGTGCAAGACACTATGGTTACGACTTGCTTACTGGGGC...
B
a J_H4
7bp
J_H4
...TATTGTGATTACTATGCT...
b D_FL16.1
9bp
12 bp spacer
7bp
D
7bp
...GCTTTTTGTGAAGGGATCTACTACTGTGTTTATTACTACGGTAGTAGCTACCACAGTG...
c 22D6-G-4.5
9bp
12 bp spacer
7bp
D'
J_H4
...GCTTTTTGTGAAGGGATCTACTACTGTGTTTATTACTACGGTAGTAGCTATTACTATGCT...
d 22D6-G-2-3.5
V_HD6.96
'D'
J_H4
...GACACAGCCATGTATTACTGTGCAACTACGGTAGTAGCTATTACTATGCT...

Fig. 3 V_HDJ_H assembly in the 22D6-G A-MuLV transformant. ***A***, Primary and secondary rearrangement of the 3.0-kb J_H-containing *Eco*RI fragment from 22D6-G. Recombinant junctions were localized and sequence was determined as in Fig. 3. *a*, *b*, Partial nucleotide sequences of germ-line J_H3 (refs 3, 7) and $D_{SP2.3}$ (ref. 8) segments are shown. *c*, The sequence across the $D_{SP2.3}$–J_H3 junction found in clone 22D6-G-3.0. *d*, The 3′ terminal germ-line sequence of the V_H81X gene segment[18]. *e*, The sequence across the recombinant junction of clone 22D6-G-2.1; this recombinant is the result of rearrangement of V_H81X to the D–J_H3 fusion of 22D6-G-3.0. Symbols are defined in Fig. 2*A*. ***B***, Primary and secondary rearrangement of the 4.5-kb J_H-containing *Eco*RI fragment from 22D6-G. Recombinant junctions were localized and sequence was determined as in Fig. 3. *a*, *b*, Partial nucleotide sequences of germ-line J_H4 (refs 3, 7) and $D_{FL16.1}$ (ref. 8). *c*, Sequence of the $D_{FL16.1}$–J_H4 junction in clone 22D6-G-4.5. *d*, Partial sequence of the 22D6-G-2-3.5 recombinant, which was the product of recombination between a V_H segment and the DJ_H4 fusion of 22D6-G-4.5. Symbols are defined in Fig. 2*A*.

maturation that follow rearrangement. The consistent lack of somatic point mutation in rearrangements from the 40E4-2 line, which expresses TdT, implies that, contrary to a previous suggestion[27], the function of the enzyme in this line is not related to the process of generating somatic point mutants.

A role for TdT in the production of *N* regions[16] is strongly implied by the observation that *N* regions were present at four of six independent D–J_H or V_H–DJ_H junctions in the 40E4-2 line, which expresses TdT, but none was found among the four junctions examined in the 22D6-G line that lacks the enzyme.

An alternative hypothesis, that *N* regions are encoded by a set of germ-line genes, seems unlikely because of their extreme heterogeneity in length and sequence. Another argument against *N* regions being encoded stems from the observation that the *N*-region sequence GTGGGGGCC is found at the junction between D_{Q52} and J_H segments in the 18-81A-2 cell line[28]. The D_{Q52} segment is the most J_H-proximal *D* segment, occurring in the germ line about 700 bp to the 5′ side of J_H1. The nucleotide sequence from D_{Q52} to the J_H cluster has been determined previously[5]; this interval does not contain the 9-bp *N* region sequence of 18-81A-2. Thus, unless we invoke two acts of inversional recombination, so as to transpose a sequence originally 5′ to a site between D_{Q52} and J_H, we must conclude that the *N* region present at this D_{Q52}–J_H junction was not represented in the germ line. *N* regions are therefore likely to be synthesized *de novo* and TdT is likely the responsible enzyme.

We thank Keith Blackwell for advice and assistance in the isolation of the 22D6 rearrangements. S.V.D. is a fellow of the Jane Coffin Childs Memorial Fund for Medical Research. G.D.Y. is supported by NIH training grant AI-20047. F.A. is an Irma T. Herschel Career Scientist. This work was supported by ACS grant NP-393, NIH grant AI-20047 and a Searle Foundation award to F.A. and ACS grant IM-355 to D.B.

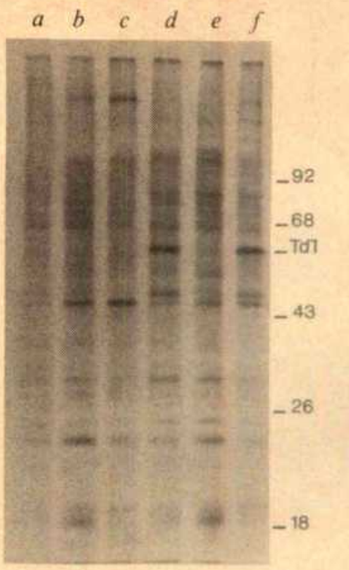

Fig. 4 Assay for terminal deoxynucleotidyl transferase by immunoprecipitation. TdT was assayed in metabolically labelled extracts from cell lines RL♂11 (lanes *a*, *d*), 22DG (lanes *b*, *e*) and 40E4-2 (lanes *c*, *f*), as described below. (Cell line 22D6 is the parent line from which clone 22D6-G was derived.) Immunoprecipitations were performed with normal rabbit serum (lanes *a*–*c*) or with rabbit anti-TdT antiserum (lanes *d*–*f*). The positions of molecular weight standards and their sizes ($\times 10^{-3}$) are indicated.

Methods: Cells (4×10^6) were labelled for 5 h at 37 °C in 2 ml methionine-free RPMI-1640 supplemented with 10% dialysed, inactivated fetal calf serum and 500 μCi ^{35}S-methionine. Cells were washed in PBS and lysed by addition of 1 ml RIPA buffer[34] containing 0.1 mM phenylmethylsulphonyl fluoride. Samples, containing 10^7 c.p.m. ^{35}S-labelled protein, were incubated with 5 μl normal rabbit serum for 1 h at 4 °C. Protein A-containing *Staphylococcus aureus* (25 μl of a 10% suspension) was added and incubation was continued for 30 min. Samples were cleared by centrifugation at 12,000*g* for 2 min. Precleared samples were incubated with 5 μl rabbit antiserum against calf TdT[35] or with 5 μl normal rabbit serum for 2 h at 4 °C. Protein A-containing *S. aureus* (25 μl of a 10% suspension) was added and incubation was continued for 30 min. RIPA buffer (1 ml) was added and samples were spun for 15 s at 12,000*g*. Pellets were washed twice with RIPA buffer. Immunoprecipitated protein was analysed by SDS-polyacrylamide gel electrophoresis and autoradiography.

Received 25 May; accepted 19 September 1984.

1. Tonegawa, S. *Nature* **302**, 575–581 (1983).
2. Early, P., Huang, H., Davis, M., Calame, K. & Hood, L. *Cell* **19**, 981–992 (1980).
3. Sakano, H., Maki, R., Kurosawa, Y., Roeder, W. & Tonegawa, S. *Nature* **286**, 676–683 (1980).
4. Bernard, O. & Gough, N. M. *Proc. natn. Acad. Sci. U.S.A.* **77**, 3630–3634 (1980).
5. Sakano, H., Kurosawa, Y., Weigert, M. & Tonegawa, S. *Nature* **290**, 562–565 (1981).
6. Kurosawa, Y. *et al. Nature* **290**, 565–570 (1981).
7. Gough, N. M. & Bernard, O. *Proc. natn. Acad. Sci. U.S.A.* **78**, 509–513 (1981).
8. Kurosawa, Y. & Tonegawa, S. *J. exp. Med.* **155**, 201–218 (1982).
9. Rosenberg, N. & Baltimore, D. *J. exp. Med.* **143**, 1453–1463 (1976).
10. Waneck, G. L. & Rosenberg, N. *Cell* **26**, 79–89 (1981).
11. Siden, E. J., Baltimore, D., Clark, D. & Rosenberg, N. E. *Cell* **16**, 389–396 (1979).
12. Alt, F., Rosenberg, N., Lewis, S., Thomas, E. & Baltimore, D. *Cell* **27**, 381–390 (1981).
13. Sugiyama, H. *et al. Nature* **303**, 812–815 (1983).
14. Alt, F. *et al.*, *EMBO J.* **3**, 1209–1219.
15. Goff, S., Gilboa, E., Witte, O. N. & Baltimore, D. *Cell* **22**, 777–785 (1980).
16. Alt, F. & Baltimore, D. *Proc. natn. Acad. Sci. U.S.A.* **79**, 4118–4122 (1982).
17. Kabat, E. A., Wu, T. T., Bilofsky, H., Reid-Miller, M. & Perry, H. *Sequences of Proteins of Immunological Interest* (U.S. Department of Health and Human Services, NIH, Bethesda, 1983).
18. Yancopoulos, G. D. *et al. Nature* **311**, 727–733 (1984).
19. Silverstone, A. E. *et al. Cold Spring Harb. Conf. Cell Proliferation* **5**, BA, 433–453 (1978).
20. Bollum, F. J. *Enzymes* **10**, 145–171 (1974).
21. Kung, P. C., Silverstone, A. E., McCaffrey, R. & Baltimore, D. *J. exp. Med.* **141**, 855–865 (1975).
22. McCaffrey, R. P., Smoler, D. F. & Baltimore, D. *Proc. natn. Acad. Sci. U.S.A.* **70**, 521–525 (1973).
23. Yaoita, Y. *et al.*, *Nucleic Acids Res.* **11**, 7303–7316 (1983).
24. Kohler, G. *Proc. natn. Acad. Sci. U.S.A.* **77**, 2197–2199 (1980).
25. Gearhart, P. J., Johnson, N. D., Douglas, R. & Hood, L. *Nature* **291**, 29–34 (1981).
26. Bothwell, A. L. M. *et al. Cell* **24**, 625–637 (1981).
27. Baltimore, D. *Nature* **248**, 409–411 (1974).
28. Alt, F., Rosenberg, N., Enea, V., Siden, E. & Baltimore, D. *Molec. Cell Biol.* **2**, 386–400 (1982).
29. Alt, F. W., Enea, V., Bothwell, A. L. M. & Baltimore, D. *Cell* **21**, 1–12 (1980).
30. Blattner, F. R. *et al. Science* **196**, 161–169 (1977).
31. Sternberg, N. T., Tiemier, D. & Enquist, L. *Gene* **1**, 255–280 (1977).
32. Benton, W. D. & Davis, R. W. *Science* **196**, 180–182 (1977).
33. Maxam, A. M. & Gilbert, W. *Meth. Enzym.* **65**, 499–560 (1980).
34. Gilead, Z. *et al. Nature* **264**, 263–266 (1976).
35. Silverstone, A., Sun, L., Witte, O. N. & Baltimore, D. *J. biol. Chem.* **255**, 791–796 (1980).

A rhodopsin is the functional photoreceptor for phototaxis in the unicellular eukaryote *Chlamydomonas*

Kenneth W. Foster*‡§, Jureepan Saranak*‡, Nayana Patel*, Gerald Zarilli†, Masami Okabe†, Toni Kline* & Koji Nakanishi†§

* Department of Pharmacology, Mt Sinai School of Medicine, City University of New York, New York, New York 10029, USA
† Department of Chemistry, Columbia University, New York, New York 10027, USA

Rhodopsin is a visual pigment ubiquitous in multicellular animals. If visual pigments have a common ancient origin, as is believed, then some unicellular organisms might also use a rhodopsin photoreceptor[1,2]. We show here that the unicellular alga *Chlamydomonas* does indeed use a rhodopsin photoreceptor. We incorporated analogues of its retinal chromophore into a blind mutant; normal photobehaviour was restored and the colour of maximum sensitivity was shifted in a manner consistent with the nature of the retinal analogue added. The data suggest that 11-*cis*-retinal is the natural chromophore and that the protein environment of this retinal is similar to that found in bovine rhodopsin, suggesting homology with the rhodopsins of higher organisms. This is the first demonstration of a rhodopsin photoreceptor in an alga or eukaryotic protist and also the first report of behavioural spectral shifts caused by exogenous synthetic retinals in a eukaryote. A survey of the morphology and action spectra of other protists suggests that rhodopsins may be common photoreceptors of chlorophycean, prasinophycean and dinophycean algae. Thus, *Chlamydomonas* represents a useful new model for studying photoreceptor cells.

Chlamydomonas is an aquatic organism of 10 μm diameter with a single eye and two flagella[3] which together guide the swimming cell in its light environment. A coloured quarter-wave-layered eyespot focuses incoming light onto an overlying patch of plasma membrane containing ~10^5 receptor pigment molecules and also prevents light from passing through the cell to the receptor pigment[2]. As the cell rotates while swimming, its eye conically scans a pattern of light which modulates conductance changes that control the steering of its flagella, thus forming a simple, but nevertheless complete visual system. All the essential elements of the photoreceptor cells of a multicellular animal are present[2].

Although there are many light-sensitive pigments, particularly in protists[4], the receptor pigments in the eyes of all multicellular animals studied so far contain 11-*cis*-retinal as the chromophore; in addition, some freshwater fish and amphibians use 11-*cis*-3,4-dehydroretinal as a second chromophore. We used the following rationale to check for the presence of a retinal chromophore in *Chlamydomonas*. If a retinal moiety were the chromophore, replacing it by other retinal analogues would shift the action spectrum (the relative sensitivity of the cells to different wavelengths of light) compared with the natural pigment; such a shift in action spectrum would prove the incorporation and function of retinal. Nonspecific binding of retinals to protein would not produce the anticipated shifts. The behaviour used to test the photoreceptor response was that of phototaxis[2,5]—the swimming of an aquatic cell towards or away from light.

Numerous retinal analogues have been bound to bovine opsin and bacteriorhodopsin *in vitro*[6-9] to give pigments absorbing at different wavelengths of light. At least four analogues have recently been shown to shift the behavioural action spectrum of *Halobacterium*[10,11] and a similar rationale using a riboflavin analogue was applied to determine the nature of the chromophore for phototropism in the fungus *Phycomyces*[12].

As with the *Phycomyces* studies in which a riboflavin auxotroph was used[12], we used a blind mutant incapable of synthesizing retinal in the dark to measure incorporation of analogues. As any mutant blocking carotenoid synthesis would also block retinal synthesis, we surveyed all carotenoid mutants we could obtain; as hypothesized, these are blind compared with wild type. We chose the mutant FN68 (Car-1) because of the comparative slowness of its light induction of carotenoids (K.W.F *et al.*, in preparation) and its 1,000–10,000-fold increased threshold sensitivities relative to wild type (compare Fig. 1*B*, *C* with *D*). The carotenoid biosynthesis of the mutant[13] is blocked in the dark at a step before phytoene. The mutant is negatively phototactic, that is, it normally swims away from light. The wild type (for carotenogenesis) (Car$^+$ *agg*$^-$ cell, designated FN13) was a negatively phototactic strain (derived from culture 806 of *Chlamydomonas reinhardtii* 137c(−); given by Robert Smyth).

We used threshold measurements of phototaxis (Fig. 1) to determine the sensitivity of the cells to a particular colour of light. The sensitivity or reciprocal of the threshold was plotted as a function of wavenumber (wavelength^{-1}) to give a phototaxis action spectrum for each analogue tested (Fig. 2*A*, *a*–*g*). Peaks were determined by fitting the data to a standard curve[14]. As in other animals, *trans*-retinol (vitamin A) and β-carotene function as well as retinal, while retinoic acid has no effect.

To provide a standard to determine the effect of the protein environment on a retinal analogue, a simple reference environment was needed. As it is known that the retinal in other rhodopsins is attached to the protein as a protonated Schiff base (SBH$^+$), the absorption of the analogue in that form, attached to a small compound such as *n*-butylamine in the solvent methanol, provides a useful reference. The difference (in wavenumber) between the absorption maximum of SBH$^+$ in methanol and those of the pigments has been defined as the opsin shift[15]. The action spectra maxima for *Chlamydomonas* are not only shifted towards the red away from the reference maxima provided by the protonated Schiff bases (SBH$^+$), but the trends of these opsin shifts (Fig. 3) are very similar to those encountered for bovine rhodopsins. The opsin shifts from the SBH$^+$ model vary over a narrow range, with the 9-*cis* analogues having a smaller opsin shift than the 11-*cis* analogues. In contrast, the shifts observed here are markedly different from those encountered with bacteriorhodopsin, which, unlike visual pigments, absorb at 570 nm and only accept *trans*- and 13-*cis*-retinals[16]. The natural or light-induced action spectra maximum for *Chlamydomonas* is at 503 nm, whereas the maxima resulting from *trans*- and 11-*cis*-retinal incorporation are at 505 and 501 nm, respectively (Fig. 2). As these values are within experimental error, it is likely that the retinals are isomerized in the dark (to 11-*cis* by an isomerase?). However, the maximum at 488 nm caused by incorporation of 9-*cis* is outside the range of error and parallels the 485 nm maximum of bovine 9-*cis* rhodopsin. These findings suggest that *Chlamydomonas*, a chlorophycean, has a pigment homologous to bovine rhodopsin. We suspect the existence of rhodopsins in other algae also (Fig. 4). These pigments show a variation in their maximum absorption wavelength, from 457 to 493 nm, which implies a similar variety of chromophore environments to those in multicellular animals. Although they are probably all rhodopsin-like pigments, the nature of the chromophores in the Prasinophyceae and Dinophyceae remains to be proven.

Our results involving incorporation of retinal analogues have established *Chlamydomonas* as a viable model for studies of rhodopsin photoreceptors. A major advantage of this system is that it is already widely used for the study of basal bodies[17], circadian rhythms[18,19] and flagellar architecture and function[20,21,38], among others. Furthermore, the visual pigment and ionic processing elements are readily accessible as they lie in the plasma membrane at the surface of the cell. The versatility of this genetically well-studied microorganism for the study of photoreception, together with the apparent close homology of its photoreceptor cells to those of multicellular organisms, make it an excellent model. Use of this simple unicellular system

---

‡ Present address: Physics Department, 201 Physics Building, Syracuse University, Syracuse, New York 13210, USA.

§ To whom reprint requests should be addressed.

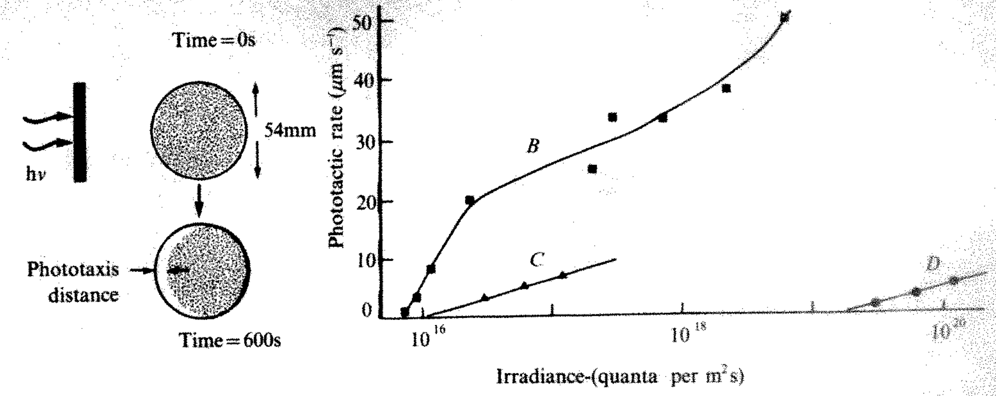

Fig. 1 *A*, The experimental set-up at time 0 and at 600 s. *B–D*, Dose–response curves, using 540 nm light with: *B*, FN13 cells (normal for carotenoids); *C*, FN68 cells and added 11-*cis*-retinal (25 μM); and *D*, FN68 cells without any added retinal.

Methods: FN68 cells were taken from slant cultures and grown on plates (salt, acetate Bacto-tryptone media with no yeast)[23]. These cells were transferred to HSM liquid (9.3 mM NH_4Cl, 81 μM $MgSO_4$, 0.1 mM $CaCl_2$, 8.27 mM K_2HPO_4, 5.3 mM KH_2PO_4, 15 mM Na acetate, plus trace elements[24]) and grown for 5–7 days in the dark at 18 °C. These vegetative cells were converted to gametes by nitrogen starvation in NMM (81 μM $MgSO_4$, 0.1 mM $CaCl_2$, 4.13 mM K_2HPO_4, 2.65 mM KH_2PO_4, plus trace elements[24]). On the day before the experiment, vegetative cells were centrifuged out at 1,500 r.p.m. for 3 min. The pellets were washed two or three times with NMM and resuspended in NMM to a concentration of $5\text{–}7\times10^6$ cells ml^{-1}. To the final NMM and cell suspension 25 μM of each retinal analogue and 0.025% α-tocopherol (as an antioxidant) were added. There was a dose-related effect of the analogues, and 25 μM was the lowest concentration that resulted in nearly full recovery with the most effective analogues. All analogues were transferred to methanol solvent immediately before addition to the cells. α-Tocopherol was also dissolved in methanol. The final concentration of methanol in the cell suspension was always <0.5%. Cells were left overnight for gametes to develop and incorporate the analogues. All cells were checked for motility and bacterial contamination. 4–5 ml of the cell suspension were poured into 54 mm diameter polystyrene Petri plates and placed at various distances from a stabilized quartz-iodide light source, the colour of which was selected with a series of interference filters. As the same set of filters was used for each analogue, the error in the comparative data is very small. To ensure a high degree of accuracy, two interference filters in series were used on the rapid fall-off in response to the red. Each light condition was measured with a 400 series Photodyne radiometer calibrated to ±5% for each wavelength. The energies were converted to absolute irradiances and corrected for the small amount of plate absorption. To measure action spectra, dose–response curves of phototactic rate versus light intensity were obtained. The distance travelled by the trailing edge of phototactic cells was measured for a 600-s period. Any effects of light scattering were minimized as light passed through the clear region created by cells swimming away from the light. The amount of opsin available may differ from day to day and the absolute sensitivity at all wavelengths may be changed; therefore, a complete action spectrum for one analogue was determined for one set of cells in one day. A control (undoped cells) was always included and measured for phototactic threshold. The procedure was repeated on a second or third day, if necessary, and all data points plotted with a common symbol for each day's set of data, as shown in Fig. 2. Unfortunately, in our mutant some induction of carotenoid and retinal synthesis (K.W.F. *et al.*, in preparation) occurs in the dark in the presence of retinals and retinal oxidation products (as also found in *Phycomyces*)[25]. However, we minimized oxidation by limiting exposure to light and oxygen and we added the analogues in optimum amounts; thus chemical induction did not interfere with out experiments. The slopes of the dose–response curves vary with wavelength as the conical scanning mechanism (see ref. 2 for details) results in a signal proportional to the magnitude of contrast modulation, which varies with wavelength. Therefore, we used the threshold for phototaxis rather than the intensity to give a standard response. Using this method, the presence of low concentrations of analogues, which contribute <0.001 absorbance units to the contrast modulation, has no effect on the action spectra. For threshold, we used the linear extrapolation to zero response, on a linear plot of phototactic rate as a function of the log of light intensity.

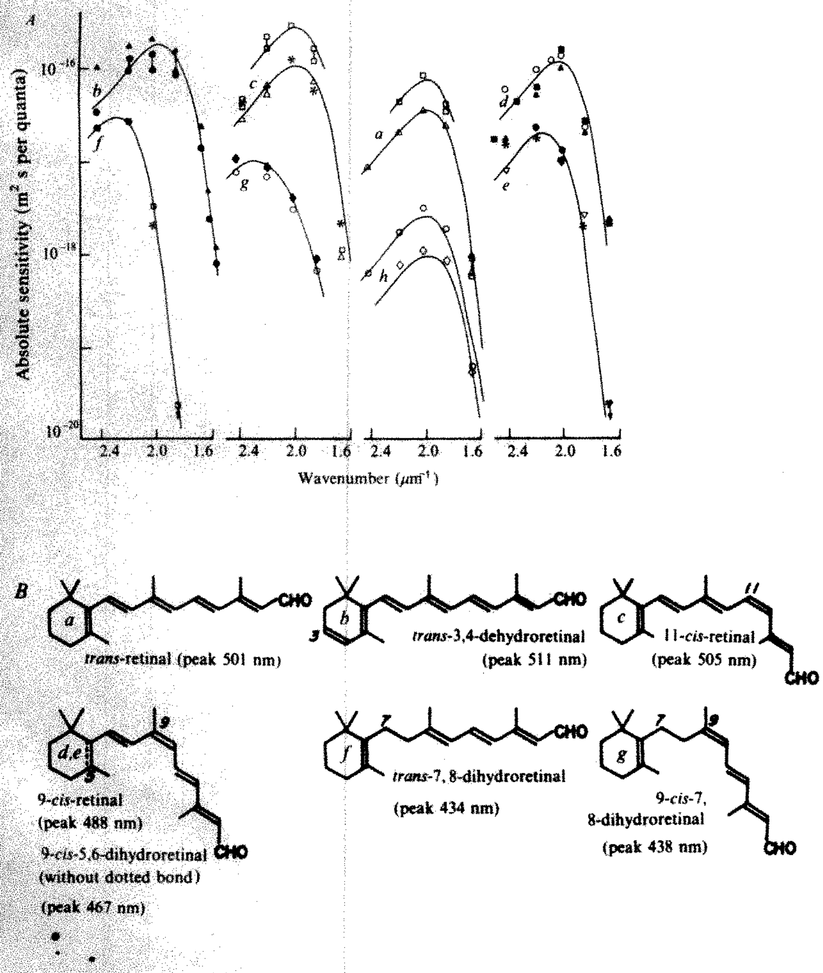

Fig. 2 *A*, The action spectra for different incorporated analogues. *B*, The structure and excitation maxima of the analogues: *a*, *trans*-retinal (peak 501 ± 5 nm); *b*, *trans*-3,4-dehydroretinal[26] (peak 511 ± 2 nm); *c*, 11-*cis*-retinal (peak 505 ± 6 nm); *d*, 9-*cis*-retinal (with dotted bond) (peak 488 ± 5 nm); *e*, 9-*cis*-5,6-dihydroretinal[27] (without dotted bond) (peak 467 ± 5 nm); *f*, *trans*-7,8-dihydroretinal[27] (peak 434 ± 3 nm); *g*, 9-*cis*-7,8-dihydroretinal[27] (peak 438 ± 5 nm); and *h*, light induced at 540 nm for 1.8×10^3 s at an irradiance of 4.2×10^{19} quanta per m^2 per s (upper curve) and 2.5×10^{19} quanta per m^2 per s (lower curve) (peak 503 ± 2 nm).

Methods: The action spectra were determined by the method described in Fig. 1 legend. log of sensitivity (reciprocal of threshold) on an absolute scale is plotted on the ordinate as a function of the wavenumber (wavelength^{-1}) (μm^{-1}, 10,000 cm^{-1}); when plotted in this way, the shape of the curve of rhodopsin excitation does not change despite shifts of maxima. The ordinate is given an absolute scale to compare the sensitivities of each analogue added at the same concentration. The absolute sensitivity of an analogue is a function of its affinity and quantum efficiency; we did not distinguish between these two parameters in this study. In some cases a second partial curve is drawn through a particular day's data because on that day the analogue's own absolute sensitivity was different. The data were fitted to a standard rhodopsin curve[14] (solid lines) and from this fit the peak wavelengths were obtained. The one exception is 9-*cis*-7,8-dihydroretinal (*g*) for which the curve is distorted by competition with the induced native chromophore (K.W.F. *et al.*, in preparation). To obtain the best estimate of the maxima of the data curve, however, a 1/6 component of natural chromophore was subtracted and the standard curve fitted to the result. In all other cases we are confident of complete dominance of the substitution.

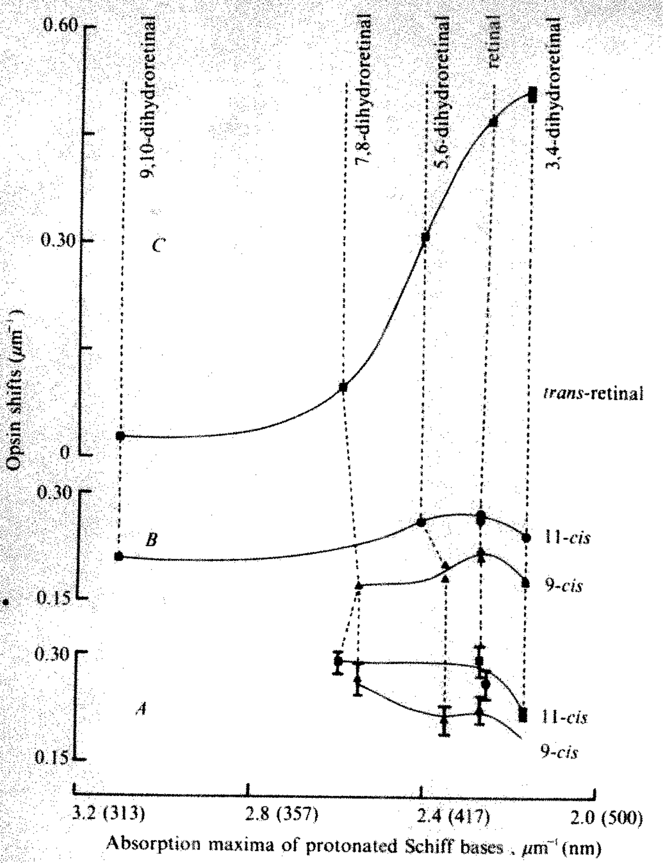

Fig. 3 Chromophore environments of *Chlamydomonas* rhodopsin (*A*), bovine rhodopsin (*B*) and bacteriorhodopsin (*C*). Retinal chromophores in rhodopsins are bound to opsin via a protonated Schiff base linkage, absorption maxima being considerably redshifted from those (in methanol) of protonated Schiff bases formed with *n*-butylamine (SBH^+). This redshift, reflecting the unique rhodopsin protein environment of retinal, expressed in wavenumbers (μm^{-1}, 10,000 cm^{-1}), is defined as the opsin shift[15]. Retinals nonspecifically bound to proteins in the SBH^+ form absorb at the SBH^+ wavelength[28], and in free solution in the UV. In *Chlamydomonas* the action spectra are again redshifted from the SBH^+ form and are fitted so well to the standard rhodopsin curve, so nonspecific protein attachment of retinals has no effect on phototaxis. For *Chlamydomonas* rhodopsin we define opsin shift to include the difference between the maxima of SBH^+ and those of its action spectra. An analogue added *trans* will probably be isomerized by the cell to 11-*cis*, but the SBH^+ values are nearly identical. Opsin shifts of the excitation maxima of *Chlamydomonas* phototaxis (*A*) and of absorption maxima of bovine rhodopsins (*B*) and bacteriorhodopsin (*C*) resulting from incorporation of various analogues are plotted against maxima of the corresponding SBH^+, expressed in μm^{-1}. Data points in the 9-*cis* (▲), 11-*cis* (●) and *trans* (■) series are connected laterally for clarity. The vertical dashed lines interconnect the double bond isomers of respective retinals. The values for the excitation maxima of *Chlamydomonas* are listed in Fig. 2 legend. The values for absorption maxima of SBH^+, bovine rhodopsins (RH) and bacteriorhodopsins (BR) are as follows: *trans*-retinal (*a* of Fig. 2*B*), SBH^+ 443 nm (ref. 29), BR 560 nm (ref. 15); *trans*-3,4-dehydroretinal (*b*), SBH^+ 460 nm (ref. 28), BR 603 nm (ref. 30) or 599 nm (ref. 31); 11-*cis*-3,4-dehydroretinal, SBH^+ 460 nm (assumed to be like *trans* as only a few nanometres different)[28], RH 517 nm (ref. 28); 9-*cis*-3,4-dehydroretinal, SBH^+ 460 nm (assumed to be like *trans*), RH 501 nm (ref. 28) or 500 nm (ref. 32); 11-*cis*-retinal (*c*), SBH^+ 440 nm (ref. 15), RH 498 nm (ref. 28) or 500 nm (ref. 15); 9-*cis*-retinal (*d*), SBH^+ 440 nm (ref. 15), RH 485 nm (ref. 15) or 487 nm (ref. 28); *trans*-5,6-dihydroretinal, SBH^+ 415 nm (ref. 28), BR 476 nm (ref. 15); 11-*cis*-5,6-dihydroretinal, SBH^+ 415 nm (assumed to be like *trans*), RH 465 nm (ref. 28); 9-*cis*-5,6-dihydroretinal (*e*), SBH^+ 425 nm (ref. 15), RH 465 nm (ref. 28) or 460 nm (ref. 15); *trans*-7,8-dihydroretinal (*f*), SBH^+ 385 nm (ref. 15), BR 400 nm (ref. 15); 9-*cis*-7,8-dihydroretinal (*g*), SBH^+ 392 nm (ref. 33), RH 420 nm (ref. 15); and *trans*-9,10-dihydroretinal, SBH^+ 322 nm (ref. 15), RH 345 nm (ref. 15), BR 325 nm (ref. 15).

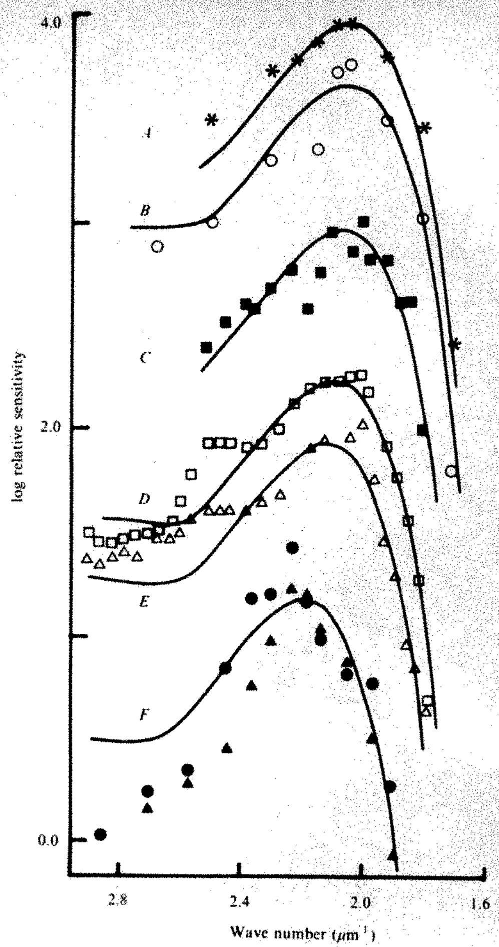

Fig. 4 Action spectra of algae taken from the literature. The most probable homologous characteristic to identify between alga eyes and those of multicellular organisms is an oriented rhodopsin-like protein formed in the plasma membrane regulating ion currents. The use of a photoreceptor at the quarter-wave position overlying a quarter-wave stack antenna in several algal classes (see ref. 2 for details) requires an oriented receptor for optimal functioning. On the grounds of morphology and action spectra, therefore, we have redrawn several action spectra from the literature: log of sensitivity (reciprocal of threshold or quantum efficiency) is plotted as a function of the wavenumber (wavelength^{-1}) (μm^{-1}, 10,000 cm^{-1}) as in Fig. 2*A*. To facilitate comparison, the data have been arbitrarily displaced on the ordinate and the same standard curve[14] has been horizontally shifted to best fit the data from the maximum to the red cut-off of sensitivity. We anticipate significant distortion in the action spectra above 2.3 μm^{-1} (to the violet side of 430 nm) due to activation of photosynthesis. *A*, The 'stop' response (*) of *Volvox aureus* (a chlorophycean) (peak 493 nm)[34]; *B*, the threshold positive phototaxis response (○) of *V. aureus* (peak 490 nm)[34]; *C*, the photoreceptor electrical potential (■) of *Haematococcus pluvialis* (a chlorophycean) (peak 483 nm)[35]; *D*, the threshold negative phototaxis response (□) of *Platymonas subcordiformis* (a prasinophycean) (peak 478 nm)[36]; *E*, the threshold positive phototaxis response (△) of *Pl. subcordiformis* (peak 472 nm)[36]; *F*, the stop response (▲) and positive phototaxis (recalculated) (●) of *Gymnodinium splendens* (a dinophycean) (peak 457 nm)[37].

should allow us to elucidate the active sites of protein interaction; transduction aspects; adaptation; signal processing; membrane, receptor and chromophore biosynthesis and maintenance; nutritional effects on the lipid environment of the receptor; and effects of cell homeostasis.

The use of eukaryotic rhodopsins as visual receptors may indeed be quite ancient and as common in several classes of algae as in higher animals. The use of molecular biology[22] to check for homology between the rhodopsins found throughout these algae and higher animals should prove exciting. •

We thank Dr Robert D. Smyth for discussions and the important suggestion that a rhodopsin might be the photoreceptor in *Chlamydomonas*. We also thank the NIH for support (grant EY 03760 to K.W.F. and N.P. and grant EY 01253 to K.N.) and the many who lent us equipment to make these experiments possible. W.-Y. Wang (University of Iowa) supplied the FN68 mutant.

Received 22 February; accepted 11 July 1984.

1. Foster, K. W. & Smyth, R. D. *Fedn Proc.* **39**, 2139 (1980).
2. Foster, K. W. & Smyth, R. D. *Microbiol. Rev.* **44**, 572–630 (1980).
3. Ehrenberg, C. G. *Die Infusionthierchen als Vollkommene Organismen*, Leipzig (1838).
4. Song, P.-S. *Photochem. Photobiol. Rev.* **7**, 77–140 (1983).
5. Greuet, C. *Année biol.* **21**, 97–141 (1982).
6. Balogh-Nair, V. & Nakanishi, K. in *New Comprehensive Biochemistry* Vol. 3 (ed. Tamm, Ch.) (Elsevier, Amsterdam, 1982).
7. Balogh-Nair, V. & Nakanishi, K. *Meth. Enzym.* **88**, 496–506 (1982).
8. Kropf, A., Whittenberger, B. P., Goff, S. P. & Waggoner, A. S. *Expl Eye Res.* **17**, 591–606 (1973).
9. Motto, M. G., Sheves, M., Tsujimoto, K., Balogh-Nair, V. & Nakanishi, K. *J. Am. chem. Soc.* **102**, 7947–7949 (1980).
10. Schimz, A., Sperling, W., Ermann, P., Bestmann, H. J. & Hildebrand, E. *Photochem. Photobiol.* **38**, 417–423 (1983).
11. Schimz, A., Sperling, W., Hildebrand, E. & Kohler-Hahn, D. *Photochem. Photobiol.* **36**, 193–196 (1982).
12. Otto, M. K., Jayaram, M., Hamilton, R. M. & Delbruck, M. *Proc. natn. Acad. Sci. U.S.A.* **78**, 266–269 (1981).
13. Wang, W.-Y. *Genetics* **91**, s134 (1979).
14. Knowles, A. & Dartnell, H. J. in *The Eye* Vol. 2B (ed. Davson, H.) 76 (Academic, New York, 1977)
15. Nakanishi, K., Balogh-Nair, V., Arnaboldi, M., Tsujimoto, K. & Honig, B. *J. Am. chem. Soc.* **102**, 7945–7947 (1980).
16. Oesterhelt, D. & Stoekenius, W. *Nature new Biol.* **233**, 149–152 (1971).
17. Huang, B., Ramanis, Z., Dutcher, S. K. & Luck, D. J. C. *Cell* **29**, 745–753 (1982).
18. Straley, S. C. & Bruce, V. G. *Pl. Physiol.* **63**, 1175–1181 (1979).
19. Goodenough, J. E., Bruce, V. G. & Carter, A. *Biol. Bull. mar. biol. Lab., Woods Hole* **161**, 371–381 (1981).
20. Hoops, H. J. & Witman, G. B. *J. Cell Biol.* **97**, 902–908 (1983).
21. Brokaw, C. J. & Luck, D. J. C. *Cell Motility* **4**, 131–150 (1983).
22. Nathans, J. & Hogness, D. S. *Cell* **34**, 807–814 (1983).
23. Nichelson-Guthrie, C. S. & Hudock, G. A. *J. gen. Microbiol.* **129**, 159–165 (1983).
24. Hutner, S. H., Provosoli, L., Schatz, A. & Haskins, C. P. *Proc. Am. phil Soc.* **94**, 152–170 (1950).
25. Eslava, A. P., Alvarez, M. I. & Cerdá-Olmedo, E. *Eur. J. Biochem.* **48**, 617–623 (1974).
26. Hubbard, R., Brown, P. K. & Bownds, D. *Meth. Enzym.* **33C**, 615–653 (1971).
27. Arnaboldi, M., Motto, M. G., Tsujimoto, K., Balogh-Nair, V. & Nakanishi, K. *J. Am. chem. Soc.* **101**, 7082–7086 (1979).
28. Blatz, P. E., Dewhurst, P. B., Balasubramaniyan, V., Balasubramaniyan, P. & Lin, M. *Photochem. Photobiol.* **11**, 1–15 (1970).
29. Erickson, J. O. & Blatz, P. E. *Vision Res.* **8**, 1367–1375 (1968).
30. Tokunaga, F. & Ebrey, T. G. *Biochemistry* **17**, 1915–1922 (1978).
31. Sperling, W. & Schimz, A. *Biophys. Struct. Mech.* **6**, 165–169 (1980).
32. Azuma, M., Azuma, K. & Keto, Y. *Biochim. biophys. Acta* **295**, 520–527 (1973).
33. Honig, B. *et al. J. Am. chem. Soc.* **101**, 7084–7086 (1979).
34. Schletz, K. *Z. Pflanzenphysiol.* **77**, 189–211 (1976).
35. Litvin, F. F., Sineshchekov, O. A. & Sineshchekov, V. A. *Nature* **271**, 476–478 (1978).
36. Halldal, P. *Physiologia Pl.* **14**, 133–139 (1961).
37. Forward, R. B. Jr *J. Protozool.* **21**, 312–315 (1974).
38. Lack, D. J. L. *J. Cell Biol.* **98**, 789–794 (1984).

Co-localization of neurotensin-like immunoreactivity and ^{3}H-glycine uptake system in sustained amacrine cells of turtle retina

Reto Weiler* & Alexander K. Ball

Department of Anatomy and Lion's Sight Centre, Faculty of
Medicine, The University of Calgary, Calgary, Alberta,
Canada T2N 4N1

Amacrine cells are axonless intrinsic neurones of the vertebrate retina which have cell bodies in the proximal inner nuclear layer and processes contributing to the synaptic network of the inner plexiform layer. They receive input from bipolar, interplexiform and other amacrine cells, and synapse onto these and ganglion cells[1,2]. Amino acid and monoamine transmitters are found in most retinal neurones[3], but peptide transmitters are exclusively located in amacrine cells[4]. Only one neuropeptide, amino acid or monoamine transmitter exists in any single amacrine cell population[4,5]. Coexistence of neuropeptides with classical transmitters has been demonstrated histologically in many neurones of the central nervous system[6], but the physiological relevance of these findings is unknown[7]. We report here evidence of such coexistence in retinal amacrine cells of the turtle, *Pseudemys scripta elegans*. Using combined immunocytochemistry and autoradiography, we have localized both neurotensin-like immunoreactivity and a high affinity uptake system for ^{3}H-glycine to the same amacrine cell, implying that this cell type may use both substances as neurotransmitters. We also present electrophysiological evidence that this type of amacrine cell responds to photic stimulation with a sustained and graded membrane depolarization.

We examined formalin-fixed frozen sections of turtle retina by the peroxidase-antiperoxidase method[8] and found neurotensin-like immunoreactivity in four different amacrine cell types (Fig. 1*a–d*)[9,10]. Two of these types occurred more frequently (Fig. 1*a*, *b*) than the other two (Fig. 1*c*, *d*). Type A cells (Fig. 1*a*) are large, with the soma located in the first row of amacrines. They sent a single primary process to the middle of the inner plexiform layer before branching in the proximal half of this layer. Type B cells (Fig. 1*b*) are smaller, with the soma located in the first or second row of amacrines. They stain much more intensely than type A cells. Beaded processes from type B cells extend along the inner nuclear-plexiform layer border for a short distance before dropping to the proximal half of the inner plexiform layer. Both cell types are identical to other neurotensin-like immunoreactive cells described recently[11]. Less frequent neurotensin-like immunoreactive cell types were found in the distal half of the inner plexiform layer (large pyramidal soma, Fig. 1*c*) and the ganglion cell layer, where a thick primary process extended into the middle of the inner plexiform layer before branching (Fig. 1*d*).

Somas of varying sizes in different rows of the inner nuclear layer accumulated ^{3}H-glycine (Fig. 1*e*). Labelling of the inner plexiform layer was diffuse, with no evident banding pattern. Some of the somas which accumulated ^{3}H-glycine also showed neurotensin-like immunoreactivity. We identified these somas as type B cells on the basis of their shape, location and the distribution of their processes. (Somas of type A cells are characterized by their single process, which does not branch until it reaches the proximal inner plexiform layer, whereas type B somas are characterized by several processes which branch immediately after leaving the soma; Fig. 1*a*, *b*.) The diffuse labelling pattern of ^{3}H-glycine uptake within the inner plexiform layer corresponds well with the branching pattern of type B cells. In thin sections (0.5 μm), the co-localization of the two markers in a type B soma was readily identifiable (Fig. 1*f*). Such preparations also confirmed that ^{3}H-glycine uptake and neurotensin-like immunoreactivity was co-localized in type B but not in type A cells (Fig. 1*f*). Although type B cells all accumulate ^{3}H-glycine, they make up only 7% of the ^{3}H-glycine-accumulating cells in the turtle retina. The co-localization of these two markers in one cell implies that this neurone uses both an amino acid and a neuropeptide as neurotransmitters. We also investigated the possible co-localization of neurotensin-like immunoreactivity with [^{3}H]-γ-aminobutyric acid and dopamine accumulation, but evidence of such coexistence could not be established.

In parallel experiments we used intracellular recording and staining techniques to examine the function of type B cells. The processes of most injected amacrine cells ($n = 47$) were either mono- or multi-stratified within the inner plexiform layer, covering 10–70% of it in transverse sections. This branching pattern differed in cells of only one group ($n = 6$), which had somas located in the proximal inner nuclear layer. A few processes from cells of this smaller group left the soma close to the inner nuclear-plexiform layer border, descending through the total inner plexiform layer and branching at different levels with an increasing density of fine branches in the proximal half (Fig. 2*a*). The six injected cells of this type were morphologically homogeneous, differing from one another only in the size of their receptive field. The size and location of the soma of these cells, and the diffuse pattern of their process distribution within

---

* Present address: Zoological Institute, University of Munich, Luisenstrasse 14, 8 Munich 2, FRG.

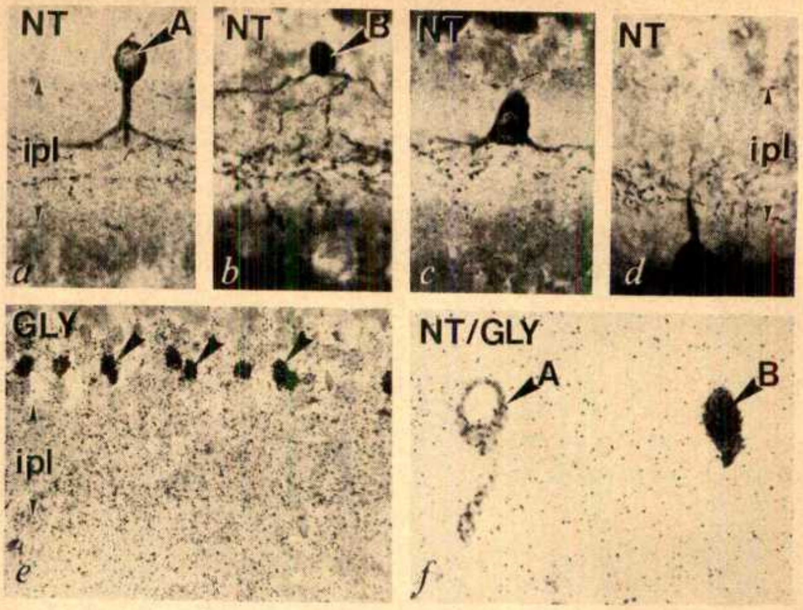

Fig. 1 *a*, Neurotensin (NT)-like immunoreactivity in a large amacrine cell of the turtle retina (A). A single primary process distributes fibres to the proximal half of the inner plexiform layer (ipl). Neurotensin-like immunoreactivity was localized using primary rabbit antiserum against neurotensin (dilution 1:1,000), goat anti-rabbit γ-globulin (Sigma) (dilution 1:20) and rabbit peroxidase-antiperoxidase complex (Miles) (dilution 1:50). Background staining was reduced with the addition of 1% normal goat serum (Sigma) to all reagents. *b*, Neurotensin-like immunoreactivity in a small amacrine cell of the turtle retina (B). Numerous processes distribute fibres to the proximal half of the inner plexiform layer. *c*, Neurotensin-like immunoreactivity in an interstitial cell of the turtle retina. The soma occupies the distal half of the inner plexiform layer and processes ramify in its proximal half. *d*, Neurotensin-like immunoreactivity in a displaced amacrine cell. A single primary process distributes fibres to the proximal half of the inner plexiform layer. *e*, Autoradiograph showing ^{3}H-glycine accumulation by several turtle amacrine cells (arrowheads). Labelling of the inner plexiform layer is diffuse. The section was overexposed (2 weeks) to emphasize glycinergic neurones and slightly counterstained with toluidine blue. *f*, Combined immunocytochemistry-autoradiography of neurotensin and ^{3}H-glycine uptake. Neurotensin-like immunoreactivity in the two major cell types encountered in turtle retina is indicated (A, B). Autoradiographic label is present over the type B cell showing that it also has a high affinity uptake system for glycine. The type A cell is not labelled. The section was exposed for 1 week and is not counterstained. *a*–*e*, ×318; *f*, ×650. Thickness of sections: *a*–*d*, 40 μm; *e*, *f*, 0.5 μm.

Methods: For combined autoradiography and immunocytochemistry, turtles (20 cm shell diameter) were injected with 25 μl ^{3}H-glycine (NEN), resulting in an estimated concentration of 3 μM at the retinal level. After 4 h, the retinae were fixed and processed for immunocytochemistry according to published procedures[18]. 40 μm-thick sections of resin-embedded retinae were used to localize neurotensin-like immunoreactive neurones and these sections were then re-cut at 0.5–2 μm[19] for autoradiography. Intracellular microelectrodes filled with Lucifer yellow or horseradish peroxidase were used to record intracellularly from amacrine cells in an eye-cup preparation. The histological procedures after dye injection were similar to those described elsewhere[9,20].

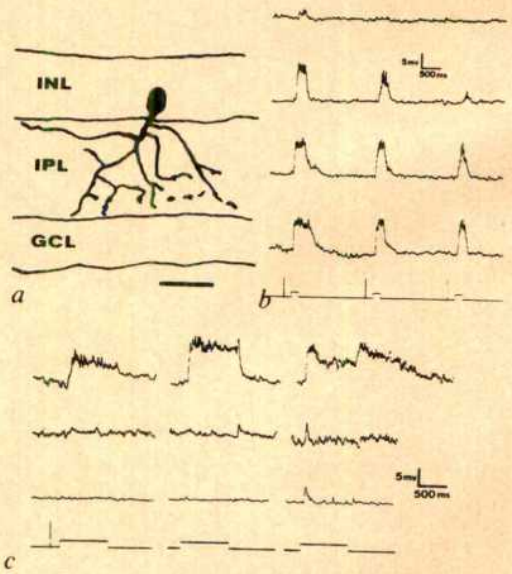

Fig. 2 *a*, Camera lucida drawing from transverse sections of an amacrine cell stained intracellularly with Lucifer yellow. Processes leave the soma close to the inner nuclear-plexiform layer border and ramify mainly in the proximal half of the inner plexiform layer. Scale bar, 25 μm. *b*, Photoresponses of the same cell to white light stimulation from a quartz-iodine lamp of increasing intensity (from left to right: 1.6×10^{-2}, 1.6×10^{2} erg s^{-1} cm^{-2}) and different size (from top to bottom: small spot 500 μm diameter, large spot 3,500 μm, annulus 3,500/1,200 μm). The signals were amplified with a WPI 707 amplifier and stored on a Racal tape recorder. *c*, Photoresponses of the same cell to different monochromatic stimuli (small spot, from left to right: 625, 530, 450 nm). The irradiance was attenuated from top to bottom by 6, 4, 3 and 2 log units. The photoresponses are univariant with maximal sensitivity at 625 nm.

the inner plexiform layer, was identical to that of type B cells. They responded to light at the centre of their receptive fields with graded depolarizations (Fig. 2*b*). This depolarization was most prominent with a spot diameter of 500 μm and with the light intensity attenuated by 2.5 log units. Repetitive oscillations varying over 1–5 mV shaped the response. The centre response, including the oscillations, could be abolished almost completely by increasing the diameter of the illuminated area by up to 1,000 μm to stimulate both the centre and periphery of the cell's receptive field (middle trace, Fig. 2*b*). The persistence of only small 'on' or 'off' responses, depending on the light intensity, suggested the presence of an antagonistic surround, but peripheral illumination by itself generally produced no response. Monochromatic illumination evoked univariant responses (Fig. 2*c*), with maximal sensitivity around 625 nm. These physiological properties are similar to those attributed to diffuse amacrine cells described elsewhere[9].

Our co-localization of neurotensin-like immunoreactivity and ^{3}H-glycine uptake may indicate that these two putative neurotransmitters, a neurotensin-like peptide and glycine, are released from the synaptic endings of type B cells in the inner plexiform layer. As such cells appear to be sustained-depolarizing amacrines with diffuse arborizations in the inner plexiform layer, these transmitters should be released in both distal and proximal levels (sublaminae a and b) of the layer during depolarization induced by illumination of the receptive field centre.

We do not yet have evidence for a physiological action of both glycine and neurotensin in the turtle retina. In the mudpuppy retina, however, glycine inhibits both on and off ganglion cells, whereas neurotensin excites these cells[12,13]. Because the dendrites of off-centre ganglion cells usually ramify in inner plexiform layer sublamina a and those of on-centre ganglion cells usually ramify in sublamina b[14–16], focal illumination should activate both neurotensin- and glycine-responsive mechanisms in both on- and off-centre ganglion cells. The electrophysiological findings in the mudpuppy retina are therefore in good agreement with the assumption of a release by a diffuse amacrine cell of neurotensin and glycine in both sublaminae.

If release and action of neurotensin and glycine within the turtle inner plexiform layer proves widespread, this would pose interesting questions about the role of neurotransmitters in visual information processing. Co-release as well as co-content of a peptide and a cooperatively acting conventional transmitter has been demonstrated elsewhere[17], but co-release of antagonistic transmitters is unprecedented. The type B amacrines may be capable of multiple actions on postsynaptic neurones in the inner plexiform layer. This may enable a simple pathway to create a complex response pattern in postsynaptic neurones, thus considerably increasing the functional potentialities of the neural network of the inner plexiform layer.

This work was carried out in the laboratories of Dr William K. Stell. We thank Dr Stell for criticism of this work and for reading the manuscript. This work was supported by grants to W. K. Stell and A.K.B. from the MRC of Canada, W. K. Stell, A.K.B. and R.W. from the Alberta Heritage Foundation for Medical Research and to R.W. from the Swiss Academy of Medicine.

Received 23 March; accepted 13 September 1984.

1. Dowling, J. E. & Werblin, F. *J. Neurophysiol.* **32**, 315-338 (1969).
2. Dowling, J. E. & Ehinger, B. *Science* **188**, 270-273 (1975).
3. Brecha, N. in *Chemical Neuroanatomy* (ed. Emson, P. C.) [illegible]-129 (Raven, New York, 1983).
4. Karten, H. J. & Brecha, N. *Nature* **283**, 87-88 (1980).
5. Stell, W. K., Marshak, D., Yamada, T., Brecha, N. & Karten, H. J. *Trends Neurosci.* **3**, 292-295 (1980).
6. Gilbert, R. F. T. & Emson, P. C. *Handbk Psychopharmac.* **16**, 519-556 (1983).
7. Hökfelt, T. *et al.* in *Neural Peptides and Neuronal Communication* (eds Costa, E. & Trabucci, M.) 1-23 (Raven, New York, 1980).
8. Sternberger, L. A. *Immunochemistry* (Wiley, New York, 1974).
9. Marchiafava, P. L. & Weiler, R. *Proc. R. Soc.* **B214**, 403-415 (1982).
10. Kolb, H. *Phil. Trans. R. Soc.* **B298**, 355-393 (1982).
11. Eldred, W. D. & Karten, H. J. *J. comp. Neurol.* **221**, 371-381 (1983).
12. Dick, E. & Miller, R. F. *Neurosci. Lett.* **26**, 131-135 (1981).
13. Miller, R. F., Frumkes, T. E., Slaughter, M. & Dacheux, R. F. *J. Neurophysiol.* **45**, 743-763 (1981).
14. Weiler, R. & Marchiafava, P. L. *Vision Res.* **21**, 1635-1638 (1981).
15. Famiglietti, E. V., Kaneko, A. & Tachibana, M. *Science* **198**, 1267-1269 (1977).
16. Nelson, R., Famiglietti, E. V. & Kolb, H. *J. Neurophysiol.* **41**, 472-483 (1978).
17. Olschowka, J. A. & Jacobowitz, D. M. *Peptides* **4**, 231-238 (1983).
18. Eldred, W. D., Zucker, C., Karten, H. J. & Yazulla, S. *J. Histochem. Cytochem.* **31**, 285-292 (1983).
19. Stell, W. K. & Lightfoot, D. O. *J. comp. Neurol.* **159**, 473-502 (1975).
20. Weiler, R. *Cell Tissue Res.* **195**, 515-526 (1978).

Interactions between enkephalin and GABA in avian retina

Carl B. Watt, Ying-yet T. Su & Dominic Man-Kit Lam

Cullen Eye Institute, Baylor College of Medicine,
Houston, Texas 77030, USA

In addition to conventional neurotransmitters such as acetylcholine, dopamine, glycine and γ-aminobutyric acid (GABA)[1,2], a number of peptide-immunoreactive substances have recently been localized in the vertebrate retina[3,4]. The functional roles of these retinal peptides and their interactions with conventional neurotransmitters are largely unknown. We have previously shown that exogenous opiates affect both the release of GABA and the firing patterns of ganglion cells in the goldfish retina[5], and we have now begun a systematic characterization of the opioid pathways in the chicken retina, because, among vertebrate retinas, avian retinas contain the highest concentration of enkephalins[6]. Monoclonal antibodies specific for enkephalin have been used to demonstrate that a subpopulation of enkephalin-containing amacrine cells exists in the chicken retina[6,7]. This retina also synthesizes Met^5-enkephalin and releases it on cell depolarization[6,8,9]. The enkephalin-induced inhibition of GABA release in goldfish retina[5] led us to examine whether similar interactions occur in chicken, and if so, whether enkephalins and GABA coexist in the same amacrine cells. Our results, presented here, indicate that exogenous enkephalins do indeed inhibit GABA release in the chicken retina. Surprisingly, we found that although some amacrine cells contain both enkephalin and GABA, others contain only one or the other.

The effect of opiates on K$^+$-stimulated release of pre-loaded GABA from GABA-accumulating amacrine cells of the chicken retina was examined by a method reported earlier[5,10,11]. As exogenous GABA is taken up by both horizontal cells and subpopulations of amacrine cells in the retina[12], the amount of ^{3}H-GABA accumulated into GABAergic horizontal cells was minimized by injecting ^{3}H-GABA directly into the vitreous humour of the eye *in situ*[11,12]. After 1 h, over 90% of the accumulated ^{3}H-GABA was localized in GABA-accumulating amacrine cells (C.B.W., Y.-Y.T.S. and D.M.-K.L., unpublished result; see also ref. 11). The release of ^{3}H-GABA from these cells by elevated external K$^+$ (50 mM) in the absence or presence of opioid analogues could then be measured in isolated retina[5]. Met^5-enkephalin inhibits K$^+$-stimulated release of ^{3}H-GABA in a dose-responsive manner (Fig. 1). This inhibition is mimicked by the enkephalin analogue [D-Ala^2,D-Leu^5]enkephalin (DADLE) and the opioid agonist morphine, but is reversed by the opioid antagonist naloxone. The maximal inhibition of ^{3}H-GABA release by an opiate we tested was ~40%.

A logical extension of this study was to examine the anatomical relationships between putative enkephalinergic and GABAergic amacrine cells in this retina. A direct approach was to visualize enkephalinergic and GABA-accumulating neurones in the same retinal section. We used immunocytochemistry of enkephalin immunoreactivity to visualize the enkephalinergic neurones[5,13-16]. The putative GABAergic neurones were localized by ^{3}H-GABA uptake *in vitro* followed by autoradiography, an appropriate choice as in other retinae we have shown that neurones possessing a high-affinity mechanism for GABA uptake also contain the enzyme for GABA biosynthesis, and are therefore likely to be GABAergic[17,18]. Thus, it is reasonable

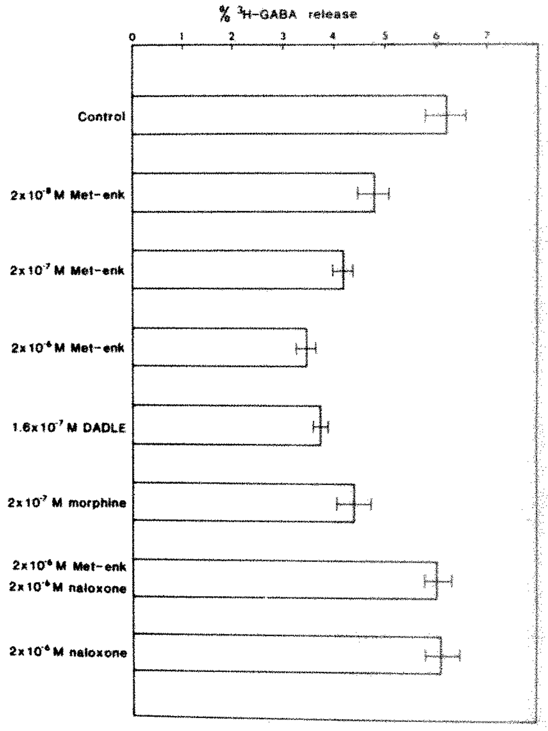

Fig. 1 Effects of opioid agonist and antagonist on K$^+$-stimulated ^{3}H–GABA release from GABA-accumulating amacrine cells of the chicken retina. One hour after an intravitreal injection *in vivo* with 50 μl Ringer's solution containing 40 μCi ^{3}H-GABA (specific activity 82.6 Ci mmol^{-1}), the injected eye was removed and the posterior eye cup bisected. The two pieces of retina were washed with excess oxygenated Ringer's solution for 30 min then incubated for 3 min with 1.5 ml of normal or K$^+$-rich (50 mM) Ringer's solution in the absence or presence of an opioid analogue, using a method previously described. The figure shows the percentage of ^{3}H-GABA released (radioactivity released/radioactivity present in the retina) in different conditions. Each bar represents the mean ± s.e.m. from at least three independent experiments of duplicate samples.

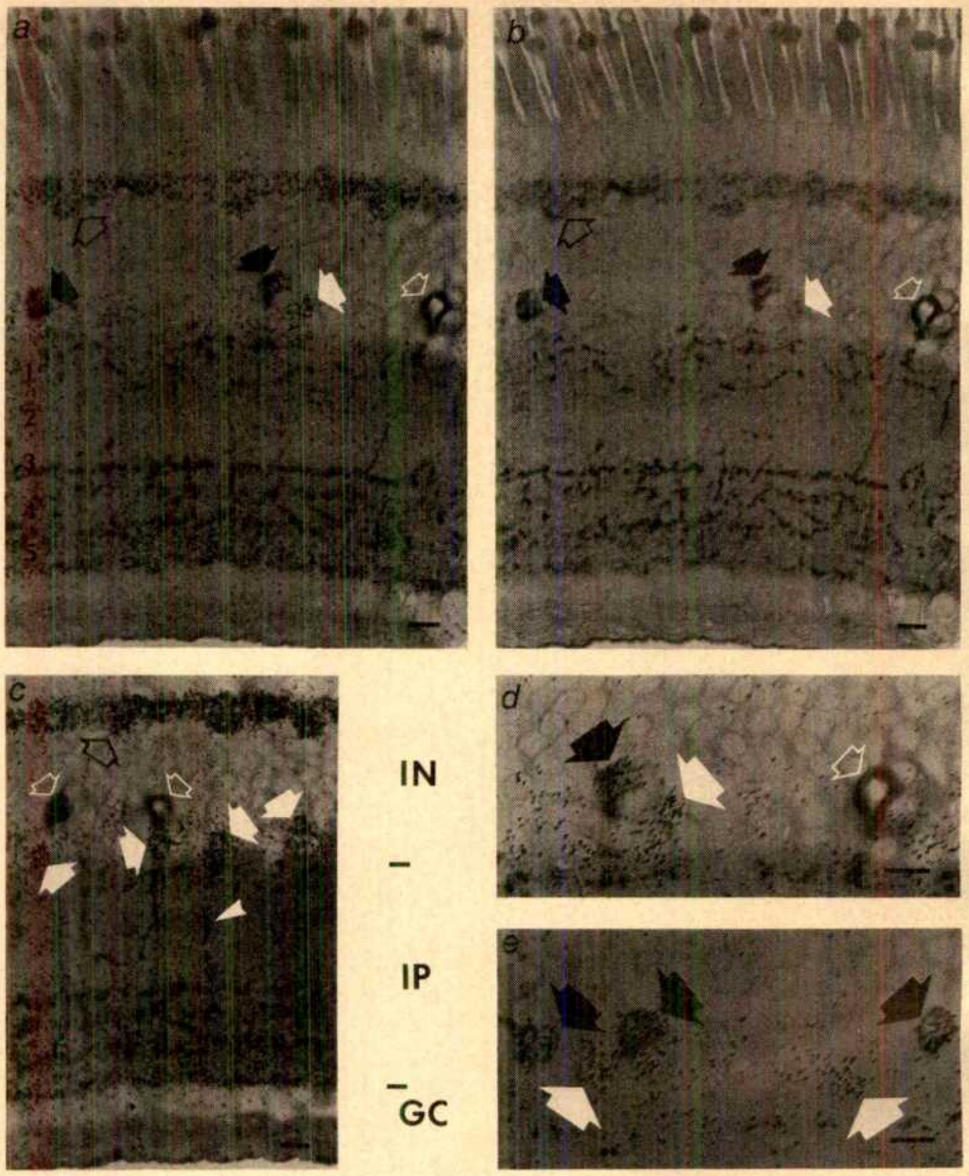

Fig. 2 Simultaneous localization of enkephalins (by immunocytochemistry) and ^{3}H-GABA uptake (by autoradiography) in the chicken retina. *a*, *b*, GABA-accumulating horizontal cells in chicken retina do not contain enkephalins. Double-labelled cells are denoted by solid black arrows; solid white arrows and open white arrows indicate cells labelled only for GABA or enkephalin, respectively. Open black arrows denote GABA-labelled horizontal cells. In *c* the white arrowhead indicates a GABA-labelled process within the inner plexiform (IP) layer. *d*, A higher magnification of the labelled cells in *a*. *e*, A higher magnification demonstrating typical double-labelled cells. IN, inner nuclear layer; GC, ganglion cell layer; 1–5 denotes distal to proximal sublayers of IP. Scale bar, 10 μm.

Methods: To visualize enkephalin-immunoreactive cells and GABA-accumulating neurones in the same retinal section, the retina was processed sequentially for autoradiography and immunocytochemistry. A piece of retina was isolated under room light and incubated for 10 min in 100 μl of an oxygenated Ringer's solution containing 10 μCi ^{3}H-GABA (specific activity 82.6 Ci mmol^{-1}). After incubation, the retina was rinsed for 1 min in unlabelled saline and placed in a cold fixative (4% parformaldehyde/0.1% glutaraldehyde in 125 mM phosphate buffer, *p*H 7.3) for 1 h and transferred to a fresh fixative (4% paraformaldehyde) overnight at 4 °C. Transverse sections (75 μm thick) of the ^{3}H-GABA–labelled retina were then cut with a vibratome and processed for enkephalin-immunoperoxidase staining at the light microscopic level. All steps were performed at room temperature and antibodies were diluted in phosphate-buffered saline (PBS, 20 mM phosphate buffer, 0.9% NaCl, *p*H 7.3) with 0.3% Triton X-100. Sections were first washed in 4% goat serum for 1 h, then incubated overnight in the primary antiserum (rabbit anti-Leu^5-enkephalin; batch A-206 from K.-J. Chang[6,15]) at a dilution of 1:1,000. After the incubation, the retinal sections were washed three times for 10 min with PBS and incubated in goat anti-rabbit IgG (1:20) for 3 h. After washing twice for 15 min in PBS, the sections were incubated in rabbit peroxidase–antiperoxidase (1:50) for 3 h, rinsed twice for 15 min in PBS, then transferred to the staining solution (10 ml PBS, 100 μl H_2O_2, 30 μg diaminobenzidine 4-HCl) for 4–7 min. After the post-staining wash and light microscopic examination, the sections were fixed overnight with 2% glutaraldehyde in 125 mM phosphate buffer. Retinal sections were subsequently embedded in plastic[13], and autoradiograms prepared routinely according to procedures described previously[18].

to assume that neurones in the chicken retina which accumulated ^{3}H-GABA are probably GABAergic.

Examination of retinal sections processed sequentially for immunocytochemistry and autoradiography shows that the GABA-accumulating horizontal cells (Fig. 2*a*, *b*, open black arrows) in chicken retina do not contain enkephalins. Our double-label technique also reveals that some amacrine cells contain both enkephalins and GABA (Fig. 2, solid black arrows), whereas some GABA-accumulating amacrine cells (solid white arrows) do not contain enkephalins and some enkephalinergic neurones (open white arrows) appearently do not take up GABA.

The present study, together with our earlier finding[5], indicates that in both chicken and goldfish retinae, enkephalins inhibit the K$^+$-stimulated release of GABA from putative GABAergic amacrine cells. Furthermore, electrophysiological studies of the goldfish retina[5] suggest that opiate systems affect the information received by on-centre ganglion cells, by direct or indirect interactions involving enkephalinergic and GABAergic amacrine cells in the proximal region (sublamina b) of the inner plexiform layer. In most vertebrate retinae, sublamina b has been associated mainly with the processing of on-centre information, whereas the distal region (sublamina a) is involved with off-centre information[19–21]. If this aspect of retinal organization is conserved in the chicken retina, then our observation that enkephalinergic and GABAergic processes overlap in the proximal region of the inner plexiform layer (Fig. 2) suggests that as in the goldfish retina[5], interactions in the chicken retina may also influence the outflow of information to on-centre ganglion cells.

The finding that some GABA-accumulating amacrine cells in the chicken retina do not contain enkephalins is not surprising, as earlier studies have shown that although there was primarily one type of morphologically distinct enkephalin-immunoreactive amacrine cell[6,7,13–16], on the basis of somatic positions, there were several types of GABA-accumulating amacrine cells in the chicken retina[6,12]. Similarly, the co-localization of GABA and enkephalins in the same amacrine cells is consistent with recent reports that certain peptides and transmitters coexist in the same neurones[22–27]. In particular, enkephalin has been found in putative dopaminergic, serotoninergic and cholinergic neurones[23], and enkephalin-immunoreactive substances have been recently detected in putative GABAergic neurones from cultured embryonic chick cerebral hemisphere[24].

The functional significance for peptide–transmitter coexistence is unknown, although numerous possibilities have been suggested[23–28]. One such suggestion is that in the parasympathetic system innervating the urinary bladder, enkephalin, which is co-localized with acetylcholine[25], may function as an inhibitory transmitter by blocking the presynaptic release of acetylcholine[26]. Our finding that enkephalin inhibits GABA release from putative GABAergic amacrine cells is consistent with this hypothesis. However, our morphological findings suggest that enkephalin may also inhibit GABA release from putative GABAergic amacrine cells that do not contain enkephalin. Electron microscope studies involving the simultaneous visualization of ^{3}H-GABA uptake and enkephalin immunocytochemistry are consistent with both mechanisms. Our preliminary results indicate that while there are synaptic structures which label for both enkephalin immunoreactivity and ^{3}H-GABA uptake, there also exist enkephalinergic processes which form synaptic contacts on ^{3}H-GABA–accumulating profiles (C.B.W., unpublished observations). Thus, our results suggest that (1) at synapses where enkephalin and GABA are released from the same structure in response to depolarization, enkephalin might inhibit further GABA release at that synapse via a presynaptic mechanism and (2) at certain other synapses, enkephalin might diminish GABA release by interacting with opiate receptors located on neurones which contain GABA but not enkephalin. Probably, the most interesting conclusion from our data is that even within a single class of neurones such as the retinal amacrine cells, a neuroactive peptide and a neurotransmitter may coexist in some cells and be localized individually in different subpopulations.

We thank Ms Patricia Glazebrook and Mr Alex Kogan for technical assistance, Dr K.-J. Chang for anti-enkephalin antiserum and Ms Pat Cloud for typing the manuscript. This work was supported by grants from the US NIH (EY02490 to C.B.W., EY03701 to Y.-Y.T.S. and EY02432 to D.M.-K.L.) and the Retina Research Foundation (Houston).

Received 13 April; accepted 23 July 1984.

1. Lam, D. M. K. *et al. Neurochem. Int.* **1,** 183–190 (1980).
2. Ehinger, R. *Vision Res.* **23,** 1281–1291 (1983).
3. Stell, W., Marshak, D., Yamada, T., Brecha, N. & Karten, H. *Trends Neurosci.* **3,** 292–295 (1980).
4. Brecha, N. in *Chemical Neuroanatomy* (ed. Emson, P. C.) 85–129 (Raven, New York, 1983).
5. Djamgoz, M. B. A., Stell, W. K., Chin, C. A. & Lam, D. M. K. *Nature* **292,** 620–623 (1981).
6. Watt, C. B., Su, Y.-Y. T. & Lam, D. M. K. *Prog. Retina Res.* (in the press).
7. Watt, C. B., Tavella, D., Su, Y.-Y.Y., Peng, Y. W. & Lam, D. M. K. *Soc. Neurosci. Abstr.* **9,** 282 (1983).
8. Su, Y.-Y. T. & Lam, D. M. K. *Soc. Neurosci. Abstr.* **9,** 289 (1983).
9. Su, Y.-Y. T., Su, S. & Lam, D. M. K. *Invest. Ophthal. vis. Sci.* **25** (Suppl.), 292 (1984).
10. Chin, C. A. & Lam, D. M. K. *J. Physiol., Lond.* **308,** 185–195 (1980).
11. Ayoub, G. S. & Lam, D. M. K. *J. Physiol., Lond.* (in the press).
12. Marshall, J. & Voaden, M. J. *Invest. Ophthal. vis. Sci.* **13,** 602 (1974).
13. Brecha, N., Karten, H. J. & Laverack, C. *Proc. natn. Acad. Sci. U.S.A.* **76,** 3010–3104 (1979).
14. Tornqvist, K., Loren, I., Hakanson, R. & Sundler, F. *Expl Eye Res.* **33,** 55–64 (1981).
15. Fukuda, M. *Cell. molec. Biol.* **28,** 275–283 (1982).
16. Ishimoto, I. *et al. Invest. Ophthal. vis. Sci.* **24,** 879–885 (1983).
17. Lam, D. M. K. *et al. Nature* **278,** 565–567 (1979).
18. Brandon, C., Lam, D. M. K. & Wu, J.-Y. *Proc. natn. Acad. Sci. U.S.A.* **76,** 3557–3561 (1980).
19. Famiglietti, E. V., Kaneko, A. & Tachibana, M. *Science* **198,** 1267–1269 (1977).
20. Stell, W. K., Ishida, A. T. & Lightfoot, D. O. *Science* **198,** 1269–1271 (1977).
21. Nelson, R., Famiglietti, E. V. & Kolb, H. *J. Neurophysiol.* **41,** 472–483 (1978).
22. Hokfelt, T., Johansson, O., Ljungdahl, A., Lunberg, J. M. & Schultzberg, M. *Nature* **284,** 515–521 (1980).
23. Lunberg, J. M. & Hokfelt, T. *Trends Neurosci.* **6,** 325–333 (1983).
24. Louis, J. C. *et al. J. Neurochem.* **41,** 930–938 (1983).
25. Kawatani, M. *et al. Neurosci. Lett.* **39,** 143–148 (1983).
26. Konishi, S., Teunoo, A. & Oteuka, M. *Nature* **294,** 80–82 (1981).
27. Weiler, R., Ball, A. K. & Stell, W. K. *Soc. Neurosci. Abstr.* **9,** 896 (1983).
28. Jan, Y. N. & Jan, L. Y. *Trends Neurosci.* **6,** 320–325 (1983).

Expression of Ti plasmid genes in monocotyledonous plants infected with *Agrobacterium tumefaciens*

G. M. S. Hooykaas-Van Slogteren, P. J. J. Hooykaas* & R. A. Schilperoort

MOLBAS Research Group, Department of Plant Molecular Biology,
Biochemical Laboratory, University of Leiden, Wassenaarseweg 64,
2333 AL Leiden, The Netherlands

When the bacterium *Agrobacterium tumefaciens* infects a fresh wound site on a dicotyledonous plant, it attaches to the plant cell wall and introduces a piece of its Ti plasmid DNA into the plant cell via an unknown mechanism[1–4]. This piece of Ti plasmid DNA (the T-DNA) becomes integrated in the nuclear genome of the plant cell and is transcribed into a specific number of different transcripts. The T-DNA renders the plant cell tumorous, and also codes for enzymes involved in the synthesis of certain tumour-specific compounds called opines. Any DNA segment inserted into the T-region of the Ti plasmid by genetic manipulation seems to be co-transferred to the plant cell by *A. tumefaciens*. Thus, the Ti plasmid offers great potential as a vector for the genetic engineering of plant cells. However, as monocots are not susceptible to tumour formation by *A. tumefaciens*, it is generally believed that the Ti plasmid can be used as a vector for dicotyledonous plants only[1–5]. This would severely limit the applicability of the Ti plasmid as a vector, as most commercially important crops are monocots. However, we report here data which indicate that the Ti plasmid may be a useful vector for transforming monocotyledonous plant species.

Infection of dicotyledonous plants with *A. tumefaciens* usually results in crown gall tumour formation, due to the expression of *onc* genes present in the T-DNA[6,7]. These *onc* genes enable crown gall cells to grow in the absence of the phytohormones auxin and cytokinin[6–8]. Recent evidence suggests that the *onc* genes in the T-DNA possibly code for enzymes that are directly involved in the biosynthesis of these hormones[9].

Tumorous plants can be derived from certain tobacco crown gall lines which spontaneously regenerate shoots. These shoots do not usually form roots, but they can develop into mature plants after grafting onto normal tobacco understems[10]. Superinfection of such plants with *A. tumefaciens* does not lead to tumour induction whereas infection with *A. rhizogenes*, which contains an Ri plasmid, results in the formation of an extensive swelling of the internodes having an infected wound rather than in the formation of a local tumour[10]. Similarly, infection of monocotyledonous plants with *A. tumefaciens* does not result in crown gall formation[11]. It is believed there is no T-DNA transfer to the tumour plant cells[12,13] or monocot cells[14], either because the bacterium cannot attach to the plant cell walls[12,14] or because of an abnormal phytohormone balance in such cells[14]. An alternative explanation is that T-DNA transfer did occur in these cases, but did not lead to tumour formation.

The opines octopine and nopaline are synthesized via enzymes that are encoded by T-DNA genes[15,16] which only have eukaryotic regulatory sequences for expression[17]. The detection of opines in plant cells is therefore direct evidence for the presence of T-DNA. To establish whether T-DNA is still transferred to and expressed in tumorous plants and monocots after infection with *A. tumefaciens*, we assayed for octopine and nopaline in plant material from infected wound sites via the method described by Otten and Schilperoort[18].

Grafted octopine tumour plants (from line TSO136)[19] were infected with *A. tumefaciens* strain LBA2318 (containing a nopaline Ti plasmid), strain LBA1020 (an Ri plasmid), and strain LBA2347 (carrying a nopaline Ti plasmid and an Ri plasmid). Infection with LBA2318 did not result in any swelling or tumour formation, but after infection with LBA1020 or LBA2347 small swellings were apparent (Fig. 1). Functions determined by the Ri plasmid thus stimulate the occurrence of swellings. Nopaline was detected in plant material isolated from the swellings

---

* To whom correspondence should be addressed.

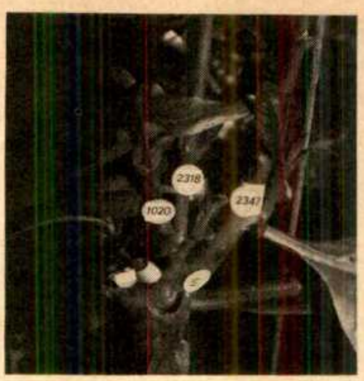

Fig. 1 Infection of a grafted crown gall shoot from line TSO136 with *A. tumefaciens* strains LBA1020, LBA2347 and LBA2318.

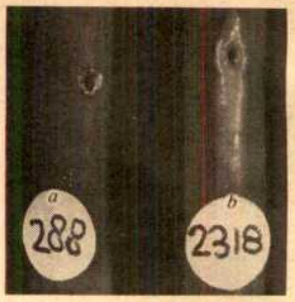

Fig. 2 Infection of *Narcissus* cv. 'Paperwhite' with avirulent *A. tumefaciens* strain LBA288 (*a*) and with virulent strain LBA2318 (*b*). Opine assays were performed as described elsewhere[18]. A small piece of tissue ($\sim 60\ \mathrm{mm}^3$) was extracted with 30 μl cold buffer, and the supernatant was mixed 1:1 with buffer and incubated for 60 min. At the start ($t=0$) and end ($t=60$) of the incubation period, 2-μl samples from the mix were spotted onto electrophoresis paper. After electrophoresis the paper was dried then stained with phenanthrene quinone reagent. Yellowish spots of guanidine compounds (such as arginine, octopine and nopaline) were visualized under long-wave UV. Tissues from both monocots and dicots (used as a control) infected with the nopaline strains LBA2318 or LBA2347 normally displayed a spot corresponding to nopaline at $t=0$ and $t=60$. In monocot or dicot tissues from plants infected with the octopine strains LBA1010 or LBA1023, a clear spot corresponding to octopine was visible only in the $t=60$ sample. This shows that in both infected dicot and monocot cells sufficient nopaline, but not enough octopine, accumulates for direct detection at $t=0$. Although octopine is not detected at $t=0$, octopine synthase activity is present which converts *in vitro* pyruvate and arginine into octopine so that at $t=60$ an octopine spot becomes visible. Neither octopine nor nopaline synthase activity was present in uninfected tissues from monocots or dicots, nor in tissues from plants infected with the avirulent strains LBA288 or LBA1516.

induced by LBA2347, which shows that the nopaline T-DNA from LBA2347 must have been introduced into the TSO136 crown gall cells. Therefore, we conclude that neither existing T-DNA, nor an altered phytohormone balance nor an altered cell wall are barriers to the transfer of T-DNA into the cells of the tumorous plant. The finding that introduction of a second copy of T-DNA into the tumorous shoots does not lead to tumour formation may be related to the abnormal phytohormone balance in the tumorous plants.

To determine whether monocots, which also do not show tumour formation after exposure to agrobacteria, can take up and express T-DNA after infection with *A. tumefaciens* we tested for production of opines in infected tissues. Two monocot species were selected for these studies, *Chlorophytum capense* (Liliaceae) and *Narcissus* cv. 'Paperwhite' (Amaryllidaceae). Plants of both species were infected with strain LBA2347. Fourteen days after infection small swellings were observed at the wound sites. After 21 days plant material from the wound sites always contained nopaline. In non-infected plant tissue neither octopine nor nopaline was detected. Following these positive results, infection tests were done on *Narcissus* cv. 'Paperwhite' with many different *A. tumefaciens* strains, LBA288 (Ti plasmid-cured; avirulent), LBA1516 (octopine Ti plasmid with a *vir*B mutation; avirulent), LBA1010 (octopine Ti plasmid), LBA2318 (nopaline Ti plasmid), LBA1023 (Ri plasmid plus octopine Ti plasmid), LBA2347 (Ri plasmid + nopaline Ti plasmid). After infection with the avirulent strains LBA288 and LBA1516 no swellings were formed, and in plant cells from wound sites infected with these strains, neither octopine nor nopaline was detected. After infection with any of the other strains small swellings were invariably formed (Fig. 2). In the case of the infection with LBA1010 or LBA1023, octopine was detected in the plant cells from the wound sites; in the case of infection with LBA2318 or LBA2347, nopaline was detected.

These results show for the first time both the occurrence of T-DNA transfer to cells of monocotyledonous plants, and the expression of the T-DNA genes for octopine and nopaline synthase in such cells. This latter finding suggests that the regulatory sequences which are essential for transcription and translation of the octopine and nopaline synthase genes in cells of dicots also function in monocots. This result is of great importance in the development of vectors with selectable markers for monocotyledonous plants.

Our results show that T-DNA transfer to monocots occurs from strains with a wild-type Ti plasmid, but not from strain LBA1516, which has a defect in one of its essential *vir* genes. Therefore it is likely that *A. tumefaciens* introduces T-DNA into cells of monocots and dicots via the same mechanism. Some years ago it was found that the attachment of *A. tumefaciens* to the plant cell wall is necessary for the bacterium to accomplish T-DNA transfer[20]. Our results suggest that *Agrobacterium* is able to attach to the cell walls of monocots. In support of this it has been shown recently that *A. tumefaciens* can attach to cells of *Asparagus officinalis* (a monocot)[21] which had not previously been found for other monocots[14]. The apparent discrepancy between these results might be explained by assuming that wounding can trigger transient changes in the cell walls of monocots which eventually enable *A. tumefaciens* to attach for a limited period of time.

T-DNA transfer to monocots is not accompanied by the induction of large crown gall tumours. The finding that the T-DNA genes for octopine and nopaline synthase are expressed in monocotyledonous plant cells suggests that the other T-DNA genes are also expressed in the monocot cells. Therefore the absence of proper tumour formation in monocots may be because monocot cells (like the octopine crown gall cells) do not respond to the products derived from the T-DNA encoded *onc* genes, perhaps because of peculiarities of their phytohormone metabolism.

We suggest that the Ti plasmid may emerge as a useful vector for monocotyledonous plants of the families Liliaceae and Amaryllidaceae. Further research is needed to establish whether crops from other monocot families (for example, Gramineae) can be transformed by the Ti plasmid. Nevertheless, our results have considerable implications for the biotechnology of a vast group of plant species of commercial interest.

We thank Drs A. Hoekema, L. Melchers and R. J. M. van Veen for critical reading of the manuscript.

Received 18 June; accepted 30 July 1984.

1. Kahl, G. & Schell, J. (eds) *Molecular Biology of Plant Tumors* (Academic, London, 1982).
2. Hooykaas, P. J. J. & Schilperoort, R. A. *Adv. Genet.* **22**, 209–283 (1984).
3. Ream, L. W. & Gordon, M. P. *Science* **218**, 854–859 (1982).
4. Schell, J. & Van Montagu, M. *Bio/Technology* **1**, 175–180 (1983).
5. Flavell, R. & Mathias, R. *Nature* **307**, 108–109 (1984).
6. Ooms, G., Hooykaas, P. J. J., Moolenaar, G. & Schilperoort, R. A. *Gene* **14**, 33–50 (1981).
7. Garfinkel, D. J. *et al. Cell* **27**, 143–153 (1981).
8. Braun, A. C. *Proc. natn. Acad. Sci. U.S.A.* **44**, 344–349 (1958).
9. Schröder, G., Waffenschmidt, S., Weiler, E. W. & Schröder, J. *Eur. J. Biochem.* **138**, 387–391 (1984).
10. Wullems, G. J., Molendijk, L., Ooms, G. & Schilperoort, R. A. *Cell* **24**, 719–727 (1981).
11. De Cleene, M. & De Ley, J. *Bot. Rev.* **42**, 389–466 (1976).
12. Lippincott, J. A. & Lippincott, B. B. *Science* **199**, 1075–1078 (1978).
13. Krens, F. A., Wullems, G. J. & Schilperoort, R. A. in *Structure and Function of Plant Genomes* (eds Ciferri, O. & Dure, L.) 387–408 (Plenum, New York, 1983).
14. Rao, S. S., Lippincott, B. B. & Lippincott, J. A. *Physiologia Pl.* **56**, 374–380 (1982).
15. Schröder, J. *et al. FEBS Lett.* **129**, 166–168 (1981).
16. Murai, N. & Kemp, J. D. *Proc. natn. Acad. Sci. U.S.A.* **79**, 86–90 (1982).
17. De Greve, H. *et al. J. molec. appl. Genet.* **1**, 499–512 (1983).
18. Otten, L. A. B. M. & Schilperoort, R. A. *Biochim. biophys. Acta* **527**, 497–500 (1978).
19. Van Slogteren, G. M. S., Hoge, J. H. C., Hooykaas, P. J. J. & Schilperoort, R. A. *Plant molec. Biol.* **2**, 321–333 (1983).
20. Lippincott, B. B. & Lippincott, J. A. *J. Bact.* **97**, 620–628 (1969).
21. Draper, J., MacKenzie, I. A., Davey, M. R. & Freeman, J. P. *Plant. Sci. Lett.* **29**, 227–236 (1983).

Defending the Earth

Eric Ashby

International Environmental Policy: Emergence and Dimensions.
By Lynton K. Caldwell.
Duke University Press: 1984. Pp.367. Hbk $37.50, £28.50; pbk $14.75, £11.90.

ON 1 January 1970 the word "biosphere" was incorporated into the public laws of the United States of America. The word appears in the preamble to the Environmental Policy Act, 1969. It was one of many incidents — Britain's Wildlife and Countryside Act 1981 is another — in what some people call a "new environmental paradigm": a worldwide change in assumptions and beliefs about our responsibility for the rest of nature.

Are such incidents evidence of the emergence of a new paradigm? Lynton Caldwell believes that they are, and that is what this book is about. No one is better qualified then he to write such a book because he combines a capacity to digest huge masses of published material (the references in this book cover 56 pages of small print) with a capacity to write clearly and pungently. He has already described the gestation and birth of a national decision, the law to protect the environment of the United States (*Science and the National Environmental Policy Act*, reviewed in *Nature* **303**, 354; 1983). Now he takes a far wider view and offers a "sketch-description" of international decisions about environmental policy.

Caldwell himself would wish the book to be called only a sketch-description. He emphasizes that he writes at a high level of generalization and that a detailed analysis would require many volumes. It would be dull, too, and Caldwell's account is not. The book can be put in perspective by recalling something Caldwell wrote over a decade ago. Americans (and it is true for Europeans too) live in a "hypertrophic society":

> The hypertrophic society has fallen victim to a social 'disease', an 'endocrine failure' followed by runaway metabolism and accelerating growth. The negative feedback and homeostatic mechanisms that contain and project a stable self-renewing society have been supplanted by the self-generating impetus of positive feedback [*National Resources Journal;* Vol. 11, No. 3 (1971)].

Social carcinoma: a grim diagnosis. Caldwell's present theme is that a minority of thoughtful people all over the world are now aware of this "disease" and their influence is sufficient to persuade governments to take steps, even at an international level, to arrest its erosion of the biosphere. His book describes these international conferences, treaties, agreements, declarations; and he evaluates them with detachment.

The environmental movement, which (Caldwell thinks) recruits more people than join the world's peace movements, is an example that not only individuals but whole nations can learn from experience. People learn about something from press and television (the link between sulphur emissions and acid rain, for instance). It may then become an "issue". This in turn brings pressures upon governments to do something about the issue, at first at national level to satisfy self-interest and then, though much less effectively, internationally. That there has been any success at all at international level is remarkable when one considers how intense is the dislike, suspicion and jealously even between nations that are political allies. The only justification for hoping that international co-operation may become less difficult lies in the evidence summarized in Caldwell's book, fortified by a faith that the environmental movement is not a transient enthusiasm but "an awakening of modern man to a new awareness of the human predicament on earth".

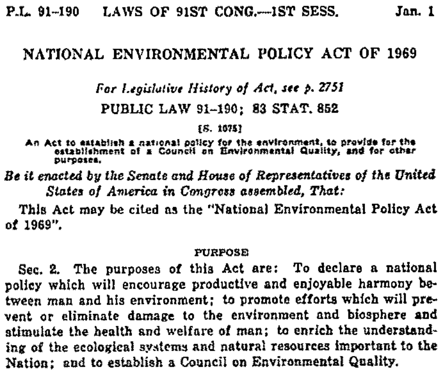

P.L. 91-190 LAWS OF 91ST CONG.—1ST SESS. Jan. 1

NATIONAL ENVIRONMENTAL POLICY ACT OF 1969

For Legislative History of Act, see p. 2751

PUBLIC LAW 91-190; 83 STAT. 852

[S. 1075]

An Act to establish a national policy for the environment, to provide for the establishment of a Council on Environmental Quality, and for other purposes.

Be it enacted by the Senate and House of Representatives of the United States of America in Congress assembled, That:

This Act may be cited as the "National Environmental Policy Act of 1969".

PURPOSE

Sec. 2. The purposes of this Act are: To declare a national policy which will encourage productive and enjoyable harmony between man and his environment; to promote efforts which will prevent or eliminate damage to the environment and biosphere and stimulate the health and welfare of man; to enrich the understanding of the ecological systems and natural resources important to the Nation; and to establish a Council on Environmental Quality.

Law of change? The opening passages of the National Environmental Policy Act, which came into effect 15 years ago.

We have heard all this before, in the overwrought style of *Blueprint for Survival.* But the contrast between that sort of clamorous rhetoric and Caldwell's calm diagnosis is as wide as the contrast between a layman's guess and a medical consultant's considered opinion. Let me first say something about the facts in Caldwell's book and then offer an opinion about the faith needed to interpret the facts.

The prime fact was the United Nations Conference on the Human Environment, in Stockholm in 1972. The importance of this was not the meeting itself but the decades of activity preceding it; that is what made a conference inevitable. The conference itself was tedious and at times degenerated into political wrangling. But it had two important consequences: the first, to put environmental policies permanently on the agenda for national and international discussion; the second to create the United Nations Environment Programme (UNEP) which, although its achievements over the past ten years have been modest, has undoubtedly helped to bring environmental policies within the ambit of international law.

Since 1972 millions of man-hours have been spent and tons of print have been produced to promote international environmental policy. You can get an idea of the scale of effort from the list of bodies (all with acronyms conveniently listed in the book) concerned with the issues: there are over 200 of them. Some promising agreements have been reached at a regional level: the environmental directives that are complied with (more or less) by member states in the European Community are an example. And on paper, at any rate, there are numerous treaties, for instance to control endangered species, to conserve wetlands used by migrating birds, to stiffen protection against products harmful to health (a United Nations Resolution (37/137) adopted in 1981 with one dissentient: the United States!), to monitor long-range air pollution, to prevent pollution from ships, to conserve the Antarctic.

But does all this paperwork really mean that the paradigm is changing? Yes-and-no is the answer I gather from Caldwell's book. Yes, because this is just the kind of activity one expects before a paradigm-shift and it has no precedent. No, because international law and policing cannot alone cope with the issues; there will need to be a *massive* consensus which puts long-range interests before short-term convenience, and as yet there is no sign of that.

This is how Caldwell points to the problem.

> For as long as it pays people to destroy living systems unnecessarily, to deplete nonrenewable resources, and to degrade the quality of the biosphere, they may be expected to do so except as influenced by social or political constraints.

He has no patience with reports that are "long on 'musts' and 'shoulds' and very short on 'hows'". But he would surely agree that he is pretty short on "hows" himself, though he does encourage those who have seen the light to press on, regardless of setbacks, to learn by experience and to recruit supporters. A radical, lasting shift in attitudes may take a century; progress in any one lifetime may seem disheartening; but we have had an International Geophysical Year, a Global Atmospheric Research Programme, and in many nations already there is a public conscience about the environment which politicians and industrial corporations disregard at their peril.

It is to these signs of glacial change that Caldwell attaches his faith. But it is a sombre faith, laced with doubt. Here (on p. 274) is his conclusion:

> Barring unforeseen events, the ecological quality of the environment for all living things seems almost certain to suffer a net decline in the decades ahead....It is difficult to believe that a change in human perceptions and values could occur on a scale and within a period of time to reverse this pessimistic conclusion. Yet human history has recorded abrupt and unpredicted changes in social behavior. Events of the decade 1972–82 suggest that peoples and their governments are...developing an appreciation of the consequences of continuing along the path of ecologically heedless exploitation of the earth.

And if they do heedlessly continue? In the essay I quoted at the beginning of this review Caldwell gives his answer. The task, he wrote, is to cure the patient of the disease of societal hypertrophy. If:

> we are unable to avoid disaster, some moral satisfaction may be gained by the knowledge that our failure was not a failure of nerve or will...the outcome may be tragic; but it will be neither disgraceful nor absurd.

Here is encouragement to continue what Caldwell calls the "Defense of Earth". □

Lord Ashby is a Fellow of Clare College, Cambridge. He was Chairman of the Royal Commission on Environmental Pollution from 1970 to 1973.

ADVERTISEMENT

Aquaculture and Fisheries Management

Edited by **D. H. Mills** and **R. Roberts** and published quarterly. Subscription rates for 1985 are £60.00 (UK), £72.00 (overseas), $108.00 (USA and Canada) post free.
0266 – 996X

This new journal has been developed from Fisheries Managements and is an international journal which will publish research papers and short communications on all aspects of aquaculture and fisheries management including practical and theoretical papers on the conservation of fresh water, estuarines and marine fish, the creation, development or management of commercial freshwater, estuarine and marine fisheries in all parts of the world.

Blackwell Scientific
Publications Ltd.
P.O. Box 88
Oxford

Circle No.29 on Reader Service Card.

Place for biography in chemistry

Colin A. Russell

Amedeo Avogadro: A Scientific Biography.
By Mario Morselli.
Reidel: 1984. Pp. 375. Dfl. 160, £40.75, $59.50.
Boussingault: Chemist and Agriculturist.
By F.W.J. McCosh.
Reidel: 1984. Pp. 280. Dfl. 140, £35.50, $53.50.

CHEMICAL biography is not much in fashion today. There was a time when history of chemistry dominated history of science, but for some years the pendulum has swung far in other directions, especially towards the ubiquitous social history of scientific ideas and institutions. As for biography, many potential writers have been frozen into immobility by fears of perpetuating the cult of the scientific "hero" which, in these iconoclastic and egalitarian days, wouldn't do at all.

Yet biography is not hagiography and there still is a place for studies of our chemical forefathers. Indeed it is now necessary to replace the ageing monographs of a previous generation and to deploy the resources and display the insights of modern scholarship. Hence Reidel's conception of a series of books on "Chemists and Chemistry" is timely and welcome. The first two volumes are about the Italian aristocrat whose hypothesis was once familiar to every elementary student of chemistry, Amedeo Avogadro (1776–1856), and the French chemist J. B. J. D. Boussingault (1802–1887). If the order is alphabetical we shall have to wait some time for the volume on Zsigmondy.

In the first two books of any new series it would be hard to find a pair that differ more strikingly than these. At an editorial level alone they are far from homogeneous; one has American spelling and notes at the ends of chapters; the other uses English spelling and consigns notes to the back of the book. The systems of referencing are also entirely different, as are the use of page-headings and various other details. Perhaps only the fastidious will care for such things, but no one can fail to notice considerable differences of treatment. In part, no doubt, this springs from the subjects themselves. Boussingault, relatively unknown to all but a handful of historians, is chiefly memorable for his contributions (that *is* the right word) to agricultural science. Avogadro has a certain deathless reputation for enunciating the hypothesis connecting gas volumes and molecular numbers, so pointing a way out of the impasse over atomic weights that plagued chemistry for over half a century.

In his long-awaited volume, Morselli first traces the complicated political history of Piedmont where for centuries Avogadro's ancestors had lived. Though geographically part of Northern Italy it was, for most of Avogadro's life, part of the far-flung Kingdom of Sardinia, as well as being for some years a dependency of Napoleonic France. We read of his legal studies at Turin during which he was seduced into science, and of his appointment to chairs in physics and mathematics at, first, Vercelli, and then Turin itself. The scene being set we are next conducted, chapter by chapter, on a tour of Avogadro's scientific papers and their subsequent reception (or lack of it). As the subtitle indicates this is a *scientific* biography. After the first chapter little is heard of the political, social and cultural roots of the science described and there is no systematic attempt to relate them. This is consistent with the author's declared perception of dangers in "overly relating them [scientific theories] to earlier philosophical and cultural movements" (p. 356).

By contrast McCosh gives a more or less chronological account of Boussingault's life, from his childhood in war-torn Paris, through his unconventional scientific education at a mining school near Lyon to his adventures as teacher and scientific consultant in South America. He later became a collaborator of Dumas at the Sorbonne, professor at the Conservatoire des Arts et Métiers in Paris and pioneer in experimental farming in Alsace. He also worked in metallurgy, air and water analysis and on the thermal decomposition of barium peroxide. All this, and more, is described in detail and the social and scientific elements are woven into one tapestry. However, even this approach does not always show how Boussingault's science reflected social and other values and one is often left with more questions than answers. One welcome emphasis is on education, both given and received. The conclusion that Boussingault failed to become "a truly great chemist" because "he suffered from the lack of a university training" (p. 13) is, however, much too simple. It implies a systematic approach that was by no means always provided by universities, and neglects the many highly successful chemists who were denied any kind of undergraduate teaching.

Both Morselli and McCosh have written thorough, well-researched books. The adventures of Boussingault in South America are particularly well-told and should be of interest to many political historians who do not habitually read *Nature*. All who teach chemistry at school and have to conjure with the name of Avogadro will find Morselli's book an admirable corrective to popular errors. Such include the notion that Avogadro's solution to the atomic weight problem was immediately accepted by grateful colleagues, or (contrariwise) that he was totally ignored in his lifetime because he was a lawyer, inarticulate or Italian. Nor can the howlers be perpetuated that he proposed in 1811 diatomic molecules for the common elementary gases, or that he was instantly rescued from oblivion by Cannizzaro at the Karlsruhe Congress of 1860.

Of these two books Morselli's makes the more telling points because the scientific and historiographic issues have such unusual complexity and importance. But it has less relevant and fewer illustrations than its companion volume and a number of minor textual irritations. Thus Davy (whom McCosh usually calls "Humphrey") was not a single-minded supporter of contact electrification (Morselli, p. 63), nor was he a lifelong disciple of Boscovich (p. 199). Kekulé was certainly not a "close friend" of Frankland (p. 233), was not called "Frederick" and did not produce the first edition of his *Lehrbuch* in 1867 (p. 266). Prout's *Bridgewater Treatise* appeared in 1834 (p. 182), not 1904 (p. 184).

It is to be hoped that future volumes in the series will benefit from more careful editorial attention. In one chapter of Morselli, for example, an article by Graebe is given no less than five different abbreviated titles, while McCosh's book is marred by an extremely high number of misprints. Other than these blemishes the main deterrent is the price. But to those who can afford them both books have much to tell of the rise of modern chemistry. □

Colin Russell is Professor of History of Science and Technology at the Open University.

Pieces of artificial intelligence

Wendy G. Lehnert

Artificial Intelligence: Tools, Techniques, and Applications.
Edited by Tim O'Shea and Marc Eisenstadt.
Harper & Row: 1984. Pp.497. Pbk $19, £12.95,

TRUE to their title, O'Shea and Eisenstadt have produced an anthology of papers dealing with the tools, techniques and applications of artificial intelligence. However, while the book is intended to serve as an introduction to the field, it should not be seen as a textbook. The 15 chapters have been written by different authors and no effort has been made to achieve a unified effect, each contribution being a self-contained introduction to its own topic. As such, therefore, the book cannot be compared to single-author texts, for example Patrick Winston's *Artificial Intelligence* (published by Addison-Wesley in 1984), nor does it attempt to provide the comprehensive coverage of the three volumes of *The Handbook of Artificial Intelligence* by A. Barr, P. Cohen and E.A. Feigenbaum (Pitman, 1981 and 1982). But viewed as a *collection* of introductory papers, it is reasonably solid.

Here students of AI will find well-presented material that is certain to motivate further delving into the literature. Among the topics covered are natural language, vision, robotics and expert systems, as well as introductions to the LISP and PROLOG programming languages. There is, too, an account of text processing, which really has nothing to do with AI but does show how AI techniques can be useful in spin-off applications.

There is also a chapter on how to get a PhD in AI, apparently aimed at graduate students who have no adviser. As a teacher, I found this contribution laudable in intent but irresponsible in practice. It gives the impression that a PhD in AI can be pursued by anyone with sufficient interest in the subject and access to adequate computing facilities. In fact, there are only a few computer science departments capable of supporting quality research in AI, and all such research is conducted in the context of organized projects. Since there is a very high demand for well-qualified people in AI, and a paucity of such people to go around, there is a grave danger that third-rate research will be accepted at lesser institutions for the sake of exploiting the bullish job market. A trend in this direction could hurt AI irreparably by destroying what delicate credibility has been established by more responsible research sites: a field that is as controversial and susceptible to media hype as AI cannot afford to make room for mediocre practitioners. So I fail to see how this chapter will help anyone, and I fear it will only serve to encourage borderline research.

That chapter apart, my reaction to the collection is largely positive. The various contributions grew out of a school which was aimed at both academic and industrial participants, so the book should be read in the same spirit with which one approaches a conference proceedings volume. The quality varies from paper to paper and readers are left to discover for themselves any unifying threads between topics. But given additional guidance to make more explicit the underlying principles of AI, the book does provide a good introductory background to the field. I would therefore suggest that teachers use it as a supplementary text, or as a source of selected readings, and it should certainly be included in any library intending to keep a comprehensive collection of the AI literature. □

Wendy G. Lehnert is an Associate Professor of Computer and Information Science at the University of Massachusetts.

Spasm? Or rigor?

Michael Spencer

Contractile Mechanisms in Muscle.
Edited by G.H. Pollack and H. Sugi.
Plenum: 1984. Pp. 921. $125, £106.25.

IN THE heady years of the 1960s, D.R Wilkie advertised a lecture on muscle with a jokey prospectus that started: "Available *now*. LINEAR MOTOR. Rugged and dependable: design optimized by world-wide field testing over an extended period" and ended with the laconic phrase "Good to eat". Optimism was in the air. Nobody knew exactly what made the filaments slide, but there was no shortage of ingenious hypotheses. As few of these could immediately be tested, imaginations roamed freely; among ideas discussed were crossbridges on springs, erectile crossbridges, contractile filaments and various wheezes involving forces at a distance.

As the 1970s dawned, the rocking crossbridge model emerged as front-runner with influential backing from the two Huxleys and others. It looked ideally suited to the simple four-stage kinetic scheme of Lymn and Taylor, with a powered change in the angle of attachment corresponding to one of the steps. It seemed inevitable that time-resolved studies by X-ray and other techniques would soon sort it all out, and Nobel-spotters made mental bets on the likely beneficiaries.

Then troubles began to mount, and nagging doubts to arise. X-ray work of ever-increasing sophistication and cost failed to reveal any obvious correlation with kinetics; and the kinetic schemes themselves became so complex that E.W Taylor once started a lecture by observing drily that we now knew less than we did two years earlier. Worst of all, a series of new experiments with fluorescent and EPR probes failed to provide any consistent evidence that the crossbridges rocked at all. Heretics who had temporarily been silenced began to raise their voices: was the supposed mainstream of muscle research really a blind channel? At the present time few workers are sure of anything any more, and there is a desperate feeling that although no alternative scheme is highly plausible, there is some vital feature missing from the crossbridge hypothesis.

Young post-doctorals just entering the field are less afflicted by self-doubt than their more world-weary elders, and for them there is no shortage of work: many types of muscle remain almost virgin territory, and there are fascinating new techniques to spend money on. So the flow of bulky conference reports continues unabated, and the volume under review is typical: it records the second international symposium on crossbridge mechanisms and contains around half-a-million words, ending with a ruminative summary (expressing due gratitude to the organizers) by one of the grand masters of the field. The fact that the conference took place more than two years ago is, however, significant: the reprehensible delay in publication has not in fact rendered most of the material obsolete, because progress just isn't that fast any more.

The main topics covered by the meeting were structural dynamics, including the curious affair of the shortening thick filaments in *Limulus*; mechanics, particularly tension transients and stiffness; and energetics. The text is enlivened by reports of verbal exchanges, such as this baffling dialogue:

A: Where you say A-band mass, you don't actually mean "mass" do you?
B: What would you have me say?
A: Whatever you mean — what *do* you mean?

or this outburst from an exasperated critic:

X: I mean you've just done the control, got the wrong results, and then persist in fitting your hypothesis?
Y: No . . .

A lot of effort at the conference went into reconciling the evidence from spectroscopic probes with the rocking crossbridge model: if the probes showed no motion, could they all have been attached (by sheer bad luck) to a portion of the myosin head that remained fixed to actin, while another unlabelled portion did the rocking? The need for detailed crystallographic structures of the relevant proteins was heavily emphasized; and there is now (two years later) a glimmer of hope that this may be achieved before the retirement dates of those who have devoted their lives to the crossbridge hypothesis.

It would be a mistake to belittle this obsession with molecular detail by comparing it with the fruitless debates of mediaeval theologians, as Graham Hoyle tends to do in his recent book (*Muscles and their Neural Control*, published by Wiley in 1983). If (dreadful thought) the crossbridge head turns out not to be the source of motion after all, then belated and more widespread attention will have to be given to iconoclastic ideas such as W.F. Harrington's contractile S-2 region, or to charge-effect hypotheses of the kind adhered to by G.F. Elliott. Neither of the last-named workers presented papers at the conference in question, but occasional references to their thoughts appear in the proceedings like Banquo's ghost at the feast in *Macbeth*.

It is imperative to resolve the uncertainties — not just for the satisfaction of those involved with muscle, but because motility is now seen to be of such universal importance in cell biology. The muscle proteins or their analogues are so widely distributed among cell types that a single basic mechanism seems rather likely, even though control systems vary considerably. It remains a central problem to find out exactly what goes on, and the present uncomfortable state of spasm in the field must surely soon be succeeded by purposeful movement. □

Michael Spencer has just given up being a Senior Research Fellow in the Department of Biophysics at King's College, University of London.

Starting with laser spectroscopy

G.R. Wilkinson

Foundations of Laser Spectroscopy.
By Stig Stenholm.
Wiley: 1984. Pp. 268. £40.95, $36.95.

ALTHOUGH the laser was invented before most of our undergraduates and postgraduates were born, laser spectroscopy is still a young and active area of research. Hence Dr Stenholm's book, which expounds upon the foundations of the subject, is likely to be widely read.

The author starts by establishing a notation and recalls the basic principles of electrodynamics and quantum mechanics. Following this introductory material is a chapter in which the response of the laser medium to strong electromagnetic fields is derived, and another which treats the physical basis of laser operation (this latter account might have been more useful if consideration of the working of some actual lasers had been included). The next chapter contains description of some applications to laser spectroscopy; here I found the treatment rather abstract for the average reader, who will have to look elsewhere for a review of the spectroscopy involved in lasers. Fluctuations are concisely introduced in Chapter 5, whilst finally field quantization and some of the simplest consequences are discussed. The book contains helpful comment and references at the end of each chapter.

The author, a theoretical physicist,

> intends this volume for beginning theorists and experimentalists who lack extensive training in algebraic manipulations, hence it contains more equations than are needed for readers more accustomed to mathematical sophistication.

This is indeed one of the book's most valuable features; however I am not sure that the claim that it can be used as a textbook for a course, even without previous knowledge of laser physics, is valid. For example it is disappointing to find that the author has left out mention of processes belonging to non-linear optics as these are so prominent at the present time.

Despite the misgivings that I have as a spectroscopist, this is undoubtedly an important book, and one which will not date quickly. Every worker in the field of laser spectroscopy should have access to a copy. □

G. R. Wilkinson is Professor of Physics at King's College, University of London.

ADVERTISEMENT

INSERM
Institut National de la Santé et de la Recherche Médicale

Cours pratique de génie génétique
Constitution de banques d'ADN génomique à l'aide de phages ou de cosmides
Edited by S. Wain-Hobson,
C. Bishop et A. Dejean
1984, Vol 118, 88 pages,
60 FF H.T.

Nouvelles techniques d'étude d'hémostase et de thrombose
Edited by S. Levy-Toledano
1984, Vol. 120, 128 pages,
75 FF H.T.

Méthodologie des études épidémiologiques et cliniques sur le diabète
Edited by Laure PAPOZ
1984, Vol. n° 122, 264 pages,
90 FF H.T.

Naître en France
Editeb by
C. RUMEAU-ROUQUETTE,
C. du MAZAUBRUN,
Y. RABARISON

1er titre de la collection
«Grandes enquêtes»
Coédition INSERM/DOIN
240 pages, 102,80 FF H.T

LES EDITIONS
INSERM

101, rue de Tolbiac
75654 Paris Cedex 13
France
Tél.: 584.14.41

Prepayment is required Bank cheque to the order of INSERM

Circle No.39 on Reader Service Card.

BOOKS RECEIVED

Technology

Advances in Cryogenic Engineering, Vol. 29. R.W. FAST (ed.). *Plenum: 1984. Pp. 1049. ISBN 0-306-41703-0. Np.*

Advances in Energy Systems and Technology, Vol. 4. PETER AUER and DAVID DOUGLAS (eds). *Academic: 1983. Pp. 213. ISBN 0-12-014904-4. $49.*

First European Conference on Coal Liquid Mixtures. INSTITUTION OF CHEMICAL ENGINEERS. *Pergamon: 1983. Pp. 415. ISBN 0-08-031397-3. £27, $48.50.*

Heterogeneous Reactions: Analysis, Examples, and Reactor Design. Vol. 2 Fluid–Fluid–Solid Reactions. By L.K. DORAISWAMY and M.M. SHARMA. *Wiley: 1984. Pp. 374. ISBN 0-471-05367-8. £59.35.*

Ion Exchange Technology. D. NADEN and M. STREAT (eds). *Ellis Horwood: 1984. Pp. 742. ISBN 0-85312-770-0. £45.00.*

Rainfall as the Basis for Urban Run-off Design and Analysis. Water Science & Technology, Vol. 16, Nos 8-9. PETER HARREMOES (ed.). *Pergamon: 1984. Pp. 368. ISBN 0-08-031506-2. £50.00.*

River Basin Management. Water Science & Technology, Vol. 16, Nos 5-7. D.H. NEWSOME and A.M.C. EDWARDS (eds). *Pergamon: 1984. Pp. 670. ISBN 0-08-031505-4. £75.00.*

Robots and Telechairs: Manipulators with Memory; Remote Manipulators; Machine Limbs for the Handicapped. By M.W. THRING. *Ellis Horwood: 1983. Pp. 298. ISBN 0-85312-274-1. £27.50.*

THRING. *Ellis Horwood: 1983. Pp. 298. ISBN 0-85312-274-1. £27.50.*

The Silicon Idol: The Micro Revolution and its Social Implications. By MICHAEL SHALLIS. *Oxford University Press: 1984. Pp. 188. ISBN 0-19-215877-5. £8.95.*

Stepping Motors and their Microprocessor Controls. By TAKASHI KENJO. *Oxford University Press: 1984. Pp. 244. ISBN 0-19-859326-0. £25.*

Treatise on Materials Science and Technology. Vol. 19 Experimental Methods Part B. HERBERT HERMAN (ed.). *Academic: 1983. Pp. 274. ISBN 0-12-341842-9. $45.*

Computer Science

The Computer Comes of Age: The People, the Hardware, and the Software. By R. MOREAU. *MIT Press: 1984. Pp. 227. ISBN 0-262-13194-3. £17.95.*

Computing in Applied Science. By WILLIAM J. THOMPSON. *Wiley: 1984. Pp. 325. ISBN 0-471-09355-6. £26.70.*

The Electronic Library. By KENNETH E. DOWLIN. *Mansell Publishing: 1984. Pp. 199. Pbk ISBN 0-918212-75-8. Pbk £21.*

The Robot Revolution. By TOM LOGSDON. *Simon & Schuster: 1984. Pp. 207. Pbk ISBN 0-671-46705-0. Pbk $9.95.*

SPSS/PRO For Dec Professional 350. *McGraw-Hill: 1984. Pp. 282. ISBN 0-07-046556-8. Np.*

Super-Computers and Parallel Computation. D.J. PADDON (ed.). *Oxford University Press: 1984. Pp. 258. ISBN 0-19-853601-1. £25.*

Text Processing. Cambridge Computer Science Texts 20. By A. COLIN DAY. *Cambridge University Press: 1984. Pp. 141. Hbk ISBN 0-521-24432-3; pbk ISBN 0-521-28683-2. £14, $29.95; pbk £5.95, $12.95.*

Biological Sciences

Advances in Lipid Research, Vol.20. RODOLFO PAOLETTI and DAVID KRITCHEVSKY (eds). *Academic: 1983. Pp.367. ISBN 0-12-024920-0. $48.50.*

Advances in Metabolic Disorders, Vol.10, CNS Regulation of Carbohydrate Metabolism. ANDREW J. SZABO (ed.). *Academic: 1983. Pp. 508. ISBN 0-12-027310-1. $65.00.*

Advances in Virus Research, Vol. 28. MAX A. LAUFFER and KARL MARAMOROSCH (eds). *Academic: 1983. Pp.478. ISBN 0-12-039828-1. $59.*

The Alkaloids: Chemistry and Pharmacology, Vol.22. ARNOLD BROSSI (ed.). *Academic: 1983. Pp.342. ISBN 0-12-469522-1. $50.00.*

Amino Acids: Biosynthesis and Genetic Regulation. KLAUS M. HERRMANN and RONALD L. SOMERVILLE (eds). *Addison-Wesley: 1983. Pp.453. ISBN 0-201-10520-9. $41.95.*

Anatomy and Physiology, 2nd Edn. By EDWIN B. STEEN and ASHLEY MONTAGU. *Harper & Row: 1984. Pp.406. Pbk ISBN 0-06-460190-0. Pbk £4.95.*

Ants. By PAT and HELEN CLAY. *Adam & Charles Black: 1984. Pp.25. ISBN 0-7136-2386-1. £3.50.*

The Bacterial Cell Surface. By STEPHEN M. HAMMOND, PETER A. LAMBERT and ANDREW N. RYCROFT. *Croom Helm: 1984. Pp.226. Hbk ISBN 0-7099-1229-3; pbk ISBN 0-7099-1267-6. Hbk £22.50; pbk £10.95.*

Badgers. By ERNEST NEAL. *Adam & Charles Black: 1984. Pp.25. ISBN 0-7136-2389-6. £3.50.*

Basic Marine Biology. By A.A. FINCHAM. *Cambridge University Press: 1984. Pp.157. Hbk ISBN 0-521-26421-9; pbk ISBN 0-521-26966-0. Hbk £20, $36; pbk £7.95, $14.95.*

Biological Foundations and Human Nature. The Katzir–Katchalsky Lecture Series. MIRIAM BALABAN (ed.). *Academic: 1983. Pp.243. ISBN 0-12-076150-8. $39.50, £28.*

Biological Macromolecules and Assemblies. Vol. 1: Virus Structures. FRANCES A. JURNAK and ALEXANDER MCPHERSON (eds). *Wiley: 1984. Pp.397. ISBN 0-471-87077-3. £69.25.*

Biological Oceanographic Processes, 3rd Edn. By TIMOTHY R. PARSONS, MASAYUKI TAKAHASHI and BARRY HARGRAVE. *Pergamon: 1984. Pp.330. ISBN 0-08-030765-5. £10.95, $19.75.*

Biology of Chrysopidae. M. CANARD, Y. SEMERIA and T.R. NEW (eds). *Dr W. Junk: 1984. Pp.288. ISBN 90-6193-137-1. Dfl. 150, £38.*

The Biology of Crustacea, Vol. 7. E. JOHN VERNBERG and WINONA B. VERNBERG (eds). *Academic: 1983. Pp.338. ISBN 0-12-106407-7. $45.00.*

Biology of Microorganisms, 4th Edn. By THOMAS D. BROCK, DAVID W. SMITH and MICHAEL T. MADIGAN. *Prentice/Hall: 1984. Pp.847. Pbk ISBN 0-13-078338-2. Pbk £14.95.*

Black Caribs: A Case Study in Biocultural Adaptation. Current Developments in Anthropological Genetics, Vol.3. MICHAEL H. CRAWFORD (ed.). *Plenum: 1984. Pp.395. ISBN 0-306-41308-6. £59.50.*

Cardiovascular Review 1984. By GERALD C. TIMMIS *et al. Academic: 1984. Pp.705. ISBN 0-12-691346-3. $44.*

Cellular Ageing. Monographs in Developmental Biology 17. H.W. SAUER (ed.). *Karger: 1984. Pp.278. ISBN 3-8055-3860-X. SwFr. 148, DM 177, $88.75.*

CMV: Pathogenesis and Prevention of Human Infection. STANDLEY A. PLOTKIN, SUSAN MICHELSON, JOSEPH S. PAGANO and FRED RAPP (eds). *Alan R. Liss: 1984. Pp.515. ISBN 0-8451-1057-8. £67.00.*

Coastal Waders and Wildfowl in Winter. P.R. EVANS, J.D. GOSS-CUSTARD and W.G. HALE (eds). *Cambridge University Press: 1984. Pp.331. ISBN 0-521-25928-2. £27.50, $54.50.*

Competition Models in Population Biology. By PAUL WALTMAN. *Wiley: 1984. Pp.77. Pbk ISBN 0-89871-188-6. Pbk £8.*

Comprehensive Endocrinology. The Pineal Gland. RUSSEL J. REITER (ed.). *Raven: 1984. Pp.394. ISBN 0-89004-314-0. $68.50.*

Current Topics in Eye Research Vol. 4. JOSE A. ZADUNAISKY and HUGH DAVSON (eds). *Academic: 1984. Pp.227. ISBN 0-12-153004-3. $73.00, £56.50.*

Current Topics in Membranes and Transport, Vol. 22: The Squid Axon. PETER F. BAKER (ed). *Academic: 1984. Pp.593. ISBN 0-12-153322-0. $89, £62.50.*

Cytology of the Central Nervous System. By DOROTHY L. ROSENTHAL. *Karger: 1984. Pp.206. ISBN 3-8055-3808-1. SwFr. 98, DM 117, $58.75.*

Development of Nerve Cells and their Connections. By W.G. HOPKINS and M.C. BROWN. *Cambridge University Press: 1984. Pp.137. ISBN 0-521-25344-6; pbk ISBN 0-521-27725-0. Hbk £16, $29.95; pbk £6.95, $13.95.*

Developmental Biology of Cultured Nerve, Muscle, and Glia. By DAVID SCHUBERT. *Wiley: 1984. Pp.315. ISBN 0-471-86592-3. £49.45.*

Disease Resistance in Plants, 2nd Edn. By J. E. VANDERPLANK. *Academic: 1984. Pp.194. ISBN 0-12-711442-4. $34.50, £24.50.*

Ecology and Evolutionary Biology: A Round Table on Research. GEORGE W. SALT (ed.). *University of Chicago Press: 1984. Pp.130. Pbk ISBN 0-226-73443-9. Pbk £6.75.*

The Ecology of Neotropical Savannas. By GUILLERMO SARMIENTO. Translated by OTTO SOLBRIG. *Harvard University Press. 1984. Pp.235. ISBN 0-674-22460-4. £19.10.*

Ecology of Saprotrophic Fungi. By R.C. COOKE and A.D.M. RAYNER. *Longman: 1984. Pp.415. ISBN 0-582-44262-1. £20.*

Ecosystem Homeostasis. By PREZEMYSŁAW TROJAN. *Dr. W. Junk: 1984. Pp.132. Pbk ISBN 90-6193-622-5. Pbk Dfl. 85, $32, £21.50*

The Endocrinology of Pregnancy and Parturition. Current Topics in Experimental Endocrinology, Vol 4. L. MARTINI and V.H.T. JAMES (eds). *Academic: 1983. Pp.290. ISBN 0-12-153204-6. $44.50.*

The Enzymes, 3rd Edn. Vol.16. Lipid Enzymology. PAUL D. BOYER (ed.). *Academic: 1983. Pp.783. ISBN 0-12-122716-2. $79.00.*

Essential Reproduction, 2nd Edn. By MARTIN JOHNSON and BARRY EVERITT. *Blackwell. 1984. Pp.367. ISBN 0-632-01258-7. £10.80.*

Evolution of Domesticated Animals. I. L. MASON (ed.). *Longman: 1984. Pp.452. ISBN 0-382-46046-8. £35.*

Evolutionary Ecology. B. SHORROCKS (ed.). *Blackwell Scientific: 1984. Pp.418. ISBN 0-632-01189-0. £25.80.*

Evolutionary Theory: Paths into the Future. J.W. POLLARD (ed.). *Wiley: 1984. Pp 271. ISBN 0-471-90026-5. £21.50.*

Fetal Endocrinology and Metabolism. Current Topics in Experimental Endocrinology, Vol. 5. L. MARTINI and V.H.T. JAMES (eds) *Academic: 1983. Pp.363. ISBN 0-12-153205-4. $48.00.*

Fish Physiology, Vol.9. W.S. HOAR, D.J. RANDALL and E.M. DONALDSON (eds). *Academic: 1983. Pp.477. ISBN 0-12-350429-5. $52.00.*

Fish Physiology, Vol.9, Part A. W.S. HOAR, D.J. RANDALL and E.M. DONALDSON (eds). *Academic: 1983. Pp.483. ISBN 0-12-350409-0. $59.00.*

Free Radicals in Biology, Vol. VI. WILLIAM A. PRYOR (ed.). *Academic: 1984. Pp 437. ISBN 0-12-566506-7. $75, £52.50.*

From Neuron to Brain, 2nd Edn. By STEPHEN W. KUFFLER, JOHN G. NICHOLLS and A. ROBERT MARTIN. *Sinauer: 1984. Pp.651. ISBN 0-87893-443-X. Np.*

Frontiers of Oral Physiology. Steroid Hormones in Saliva. D.B. FERGUSON (ed.). *Karger: 1984. Pp.162. ISBN 3-8055-3848-0. SwFr. 115, DM 138, $69.*

A Functional Biology of Free-Living Protozoa. By JOHANNA LAYBOURN-PARRY. *Croom Helm: 1984. Pp.218. Hbk ISBN 0-7099-1625-6; pbk ISBN 0-7099-1678-7. Hbk £16.95; pbk £8.95.*

Ganglioside Structure, Function, and Biomedical Potential. Advances in Experimental Medicine and Biology, Vol. 174. ROBERT W. LEDEEN, ROBERT K. YU, MAURICE M. RAPPORT and KUNIHIKO SUZUKI (eds). *Plenum: 1984. Pp.649. ISBN 0-306-41707-3. Np.*

Gastrointestinal Disorders of the Elderly. By LAWRENCE J. BRANDT. *Raven Press: 1984. Pp. 636. ISBN 0-89004-987-4. $80.50.*

Genetic Analysis of the Cell Surface. Receptors and Recognition, Series B, Vol. 16. P. GOODFELLOW (ed.). *Chapman & Hall: 1984. Pp.193. ISBN 0-412-25070-5. £27.50.*

Genetics and Development. By JAMES H. SANG. *Longman: 1984. Pp.398. Pbk ISBN 0-582-44681-3. Pbk £13.95.*

Growth and Maturation Factors, Vol. 2. GORDON GUROFF (ed.). *Wiley: 1984. Pp.340. ISBN 0-471-09708-X. £66.*

Handbook of the Birds of India and Pakistan, 2nd Edn. Vol. 4, Frogmouths to Pittas. By SALIM ALI and S. DILLON RIPLEY. *Oxford University Press: 1984. Pp.267. ISBN 0-19-561551-4. £19.50.*

Hydrobiology of the Mangal. Developments in Hydrobiology. FRANCIS DOV POR and INKA DOR (eds). *Dr W. Junk: 1984. Pp.264. ISBN 90-6193-771-X. Dfl. 180, £45.75.*

BOOKS RECEIVED

Immunologische Abwehr and Krebs. By JÜRGEN MILLECK. *Akademie-Verlag, Berlin: 1984. Pp.139. DM 48.*

Immunology of Anergy and Systemic Lupus Erythematosus. Progress in Allergy, Vol. 35. R.S. SCHWARTZ (ed.). *Karger: 1984. Pp.176. ISBN 3-8055-3824-3. DM 117, $58.75.*

In a Patch of Fireweed: A Biologist's Life in the Field. By BERND HEINRICH. *Havard University Press: 1984. Pp.194. ISBN 0-674-44548-1. £15.70.*

Infanticide: Comparative and Evolutionary Perspectives. GLENN HAUSFATER and SARAH BLAFFER HARDY (eds). *Walter de Gruyter: 1984. Pp.598. ISBN 0-202-02022-3. $34.95.*

International Review of Cytology, Vol. 81. G.H. BOURNE and J.F. DANIELLI (eds). *Academic: 1984. Pp.295. ISBN 0-12-364481-X. $39.50.*

International Review of Cytology, Vol. 89. G.H. BOURNE and J.F. DANIELLI (eds). *Academic: 1984. Pp.359. ISBN 0-12-364489-5. $49.50, £35.00.*

Intrahepatic Calculi. Progress in Clinical and Biological Research, Vol. 152. KUNIO OKUDA, FUMIO NAKAYAMA and JOHN WONG (eds). *Alan R. Liss: 1984. Pp.352. ISBN 0-8451-5002-2. £60.00.*

Introduction to Molecular Immunology, 2nd Edn. By ALFRED NISONOFF. *Sinauer: 1984. Pp.236. ISBN 0-87893-595-9. £12.80.*

Invertebrate–Microbial Interactions. Joint Symposium of The British Mycological Society and the British Ecological Society held at the University of Exeter, September 1982. J.M. ANDERSON *et al.* (ed.). *Cambridge University Press: 1984. Pp. 349. ISBN 0-521-25395-0. £40.00, $79.50.*

Lecture Notes on Coastal and Estuarine Studies. Vol. 6, Ecology of Barnegat Bay, New Jersey. MICHAEL J. KENNISH and RICHARD A. LUTZ (eds). *Springer-Verlag: 1984. Pp. 396. Pbk ISBN 3-540-90935-4/0-387-90935-4. Pbk DM 96, $37.70.*

The Leukotrienes: Chemistry and Biology. LAWRENCE W. CHAKRIN and DENIS M. BAILEY (eds). *Academic: 1984. Pp.308. ISBN 0-12-166750-2. $52.*

ADVERTISEMENT

Federal Biotechnology Funding Sources

Oskar R. Zaborsky, Ph.D.
Brenda K. Young

Vital information on U.S. government programs for:

- Research Scientists and Engineers
- R&D Administrators
- High-Tech Small Businessmen

This invaluable 262-page guide provides the most up-to-date information on extramural R&D programs.

It identifies and describes:

- 329 programs; within
- 33 federal departments and agencies; and
- 282 key contact individuals.

Federal Biotechnology Funding Sources
ISBN 0-931283-23-X
$69.95

For further information and ordering:

OMEC Publishing Company
1128 Sixteenth Street, N.W.
Washington, D.C. 20036
(202) 833-4161

Circle No. 46 on Reader Service Card.

Metabolism of Hormonal Steroids in the Neuroendocrine Structures. Serono Symposia Publications Vol. 13. F. CELOTTI, F. NAFTOLIN and L. MARTINI (eds). *Raven: 1984. Pp. 213. ISBN 0-89004-510-0. $49.*

Methods in Enzymology. Vol. 96 Biomembranes. SIDNEY FLEISCHER and BECCA FLEISCHER (eds). *Academic: 1984. Pp. 901. ISBN 0-12-181996-5. $79.*

Methods in Enzymology, Vol. 102. Hormone Action Part G, Calmodulin and Calcium-Binding Proteins. ANTHONY R. MEANS and BERT W. O'MALLEY (eds). *Academic: 1983. Pp. 336. ISBN 0-12-182002-5. $41.50.*

Methods for the Study of Marine Benthos, 2nd Edn. N.A. HOLME and A.D. McINTYRE (eds). *Blackwell: 1984. Pp. 387. ISBN 0-632-00894-6. £25.00.*

Mice. By RON WILSON. *Adam & Charles Black: 1984. Pp. 25. ISBN 0-7136-2388-8. £3.50.*

Molecular and Cellular Basis of Visual Acuity. S. ROBERT HILFER and JOEL B. SHEFFIELD (eds). *Springer-Verlag: 1984. Pp. 184. ISBN 3-540-90964-8/0-540-90964-8. DM 98, $38.50.*

Molecules and Evolution. By A. CULLINAN. *British Museum (Natural History): 1984. Pp. 17. Pbk ISBN 0-565-00858-7. Pbk £1.50.*

The Mollusca. Vol. 6 Ecology. W.D. RUSSEL-HUNTER (ed.). *Academic: 1983. Pp. 695. ISBN 0-12-751406-6. $69.*

Monoclonal Antibodies and Functional Cell Lines. ROGER H. KENNETT, KATHLEEN B. BECHTOL and THOMAS J. McKEARN (eds). *Plenum: 1984. Pp. 426. ISBN 0-306-41567-4. Np.*

Muscle and Nonmuscle Motility. Vol. 1. ALFRED STRACHER (ed.). *Academic: 1983. Pp. 372. ISBN 0-12-673001-6. $45.*

Muscle and Nonmuscle Motility, Vol. 2. ALFRED STRACHER (ed.). *Academic: 1983. Pp. 211. ISBN 0-12-673002-4. $34.50.*

Mutations in Man. GÜNTER OBE (ed.). *Springer-Verlag: 1984. Pp.327. ISBN 3-540-13113-2/0-387-13113-2. DM 116, $45.50.*

Myelofibrosis and the Biology of Connective Tissue. Progress in Clinical and Biological Research, Vol. 154. PAUL D. BERK, HUGO CASTRO-MALASPINA and LOUIS R. WASSERMAN (eds). *Alan R. Liss: 1984. Pp. 520. ISBN 0-8451-50004-9. £52.00.*

Neurobiology of the Trace Amines. Analytical, Physiological, Pharmacological, Behavioural and Clinical Aspects. ALAN A. BOULTON *et al.* (eds). *Humana Press: 1984. Pp. 624. ISBN 0-89603-063-6. $59.50.*

Neurocommunications: An Introduction. By I.C. WHITFIELD. *Wiley: 1984. Pp. 304. ISBN 0-471-10320-9. £17.*

Neuroendocrine Aspects of Reproduction. REID L. NORMAN (ed.). *Academic: 1984. Pp. 430. ISBN 0-12-521480-4. $46.*

Neuroendocrinology and Psychiatric Disorder. GREGORY M. BROWN, STEPHEN H. KOSLOW and SEYMOUR REICHLIN (eds). *Raven: 1984. Pp. 448. ISBN 0-89004-742-1. $73.50.*

Neuroimmunology. Serono Symposia Publications Vol. 13. PETER O. BEHAN and FEDERICO SPREAFICO (eds). *Raven: 1984. Pp. 500. ISBN 0-89004-963-7. $105.50.*

New Manual of Bryology. Vol. 1. RUDOLF M. SCHUSTER (ed.). *Hattori Botanical Laboratory, Miyazaki-ken 889-25, Japan: 1984. Pp. 626. ISBN 4-938163-3045. Np.*

General

Collins Guide to the Grasses, Sedges, Rushes and Ferns of Britain and Northern Europe. By RICHARD FITTER and ALASTAIR FITTER. *Collins: 1984. Pp.256. Pbk ISBN 0-00-219136-9. Pbk £5.95.*

Continuities and Discontinuities in Development. ROBERT N. EMDE and ROBERT J. HARMON (eds). *Plenum: 1984. Pp.418. ISBN 0-306-41563-1. Np.*

The Dynamics of Nuclear Proliferation. By STEPHEN M. MEYER. *University of Chicago Press: 1984. Pp.229. ISBN 0-226-52148-6. £17.*

Economic Perspectives on Acid Deposition Control. Acid Precipitation Series Vol.8. THOMAS D. CROCKER (ed.). *Butterworth: 1984. Pp.180. ISBN 0-250-40573-3. Np.*

European Mires. PETER MOORE (ed.). *Academic: 1983. Pp.384. ISBN 0-12-505580-3. £49; $75.*

Evaluation of Research and Development. Proceedings of the Seminar held in Brussels, Belgium, October 17–18, 1983. G. BOGGIO and E. SPACHIS-PAPAZOIS (eds). *Reidel: 1984. Pp.147. ISBN 90-277-1759-1. $27.*

The Food Scandal. By CAROLINE WALKER and GEOFFREY CANNON. *Century: 1984. Pp.190. ISBN 0-7126-0906-7. £7.50.*

A Generous Confidence. Thomas Story Kirkbride and the Art of Asylum-Keeping, 1840–1883. By NANCY TOMES. *Cambridge University Press: 1984. Pp.387. ISBN 0-521-24172-3. £27.50, $39.50.*

Health Information Systems: A Bibliography. By DONALD G. ZIEGENFUSS and JAMES T. ZIEGENFUSS. *Plenum: 1984. Pp.247. ISBN 0-306-65208-0. $85.*

Human Laterality. By MICHAEL C. CORBALLIS. *Academic: 1984. Pp.255. ISBN 0-12-188180-6. $29.*

Introduction to Wastewater Treatment Processes, 2nd Edn. By R.S. RAMALHO. *Academic: 1984. Pp.580. ISBN 0-12-576560-6. $57.*

John Muir Summering in the Sierra. ROBERT ENGBERG (ed.). *University of Wisconsin Press: 1984. Pp.160. Pbk ISBN 0-299-09624-6. Hbk £20.40; pbk £12.30.*

Machines that Think. ISAAC ASIMOV, PATRICIA S. WARRICK and MARTIN H. GREENBERG (eds). *Allen Lane: 1984. Pp.626. ISBN 0-7139-1685-0. £10.95.*

A Manual of Chemical and Biological Methods for Seawater Analysis. By TIMOTHY R. PARSONS, YOSHIAKI MAITA and CAROL M. LALLI. *Pergamon: 1984. Pp.173. Hbk ISBN 0-08-030288-2; pbk ISBN 0-08-030287-4. Pbk £5.50, $8.95.*

Marketing Health Behavior: Principles, Techniques and Applications. LEE W. FREDERIKSEN, LAURA J. SOLOMON and KATHLEEN A. BREHONY (eds). *Plenum: 1984. Pp.200. ISBN 0-306-41523-2. $24.50.*

Matrix and Finite Element Displacement Analysis of Structures. By D.J. DAWE. *Oxford University Press: 1984. Pp.565. ISBN 0-19-856211-X. £35.*

Micromorphology of Soils. By E.A. FITZPATRICK. *Chapman & Hall: 1984. Pp.433. ISBN 0-412-24200-1. £32.50.*

Minimum Steric Difference: The MTD Method for QSAR Studies. By Z. SIMON *et al. Wiley: 1984. Pp.173. ISBN 0-86380-015-7. £24.90.*

The Nature of the Beast: Are Animals Moral? By STEPHEN R.L. CLARK. *Oxford University Press: 1984. Pp.127. ISBN 0-19-283041-4. Pbk £2.95.*

Nonconventional Energy. G. FURLAN *et al.* (eds). *Plenum: 1984. Pp.796. ISBN 0-306-41466-X. $75.*

Otto Hahn: Ein Forscherleben unserer Zeit. By WALTHER GERLACH and DIETRICH HAHN. *Wissenschaftliche Verlagsgesellschaft mbH, Postfach 40, D-7000 Stuttgart 1: 1984. Pp.267. ISBN 3-8047-0757-2. DM 39.*

Review of Progress in Quantitative Nondestructive Evaluation. DONALD O. THOMPSON and DALE E. CHIMENTI (eds). *Plenum: 1984. Pp.682. ISBN 0-306-41678-6. Np.*

Septic-Tank Systems: A Consultant's Toolkit, Vols 1 & 2. By JOHN H. TIMOTHY WINNEBERGER. *Butterworth: 1984. Pp.222, 123. ISBN 0-250-40586-5, 0-250-40634-9. Hbk £30; pbk £19.50.*

Spatial Hearing. By JENS BLAUERT. *MIT: 1984. Pp.427. ISBN 0-262-02190-0. £36.*

Statistical Inference. By VIJAY K. ROHATGI. *Wiley: 1984. Pp.940. ISBN 0-471-87126-5. £44.50.*

Stellar Nucleosynthesis. CESARE CHIOSI and ALVIO RENZINI (eds). *D. Reidel: 1984. Pp.397. ISBN 90-277-1729-X. $55.*

Subrecursion: Functions and Hierarchies. By H.E. ROSE. *Oxford University Press: 1984. Pp.189. ISBN 0-19-853189-3. £22.50.*

The Śulbasūtras. By S.N. SEN and A.K. BAG. *Indian National Science Academy, New Delhi: 1983. Pp.293. $30.*

Sun Calender. By UNA JACOBS. *Adam & Charles Black: 1984. Pp.37. ISBN 0-7136-2411-6. £4.50.*

Teaching a Stone to Talk: Expeditions and Encounters. By ANNIE DILLARD. *Picador: 1984. Pp.177. ISBN 0-330-28341-3. Pbk £2.50.*

Test Tube Babies — A Christian View. By IAN DONALD *et al. Order of Christian Unity: 1984. Pp.98. Pbk ISBN 0-7289-0019-X. Pbk £2.95.*

New for immunology and assay

This week's feature covers new immunological products, reagents, sera, monoclonal antibodies and ELISA kits.

● A highly purified peroxidase especially developed as a marker enzyme for enzyme immunoassays is now available from Boehringer Mannheim. The salt-free lyophilizate has a specific activity of at least 250 U per mg (25°C) and a purity number higher than 3.0. The preparation may be used directly for the conjugation without pretreatment.
Circle No. 100 on Reader Service Card.

● The Biomedical Technologies, Inc. epidermal growth factor (EGF) radioreceptor assay kit is capable of measuring the levels of EGF, and also measures other EGF-like peptides from a variety of biological fluids. The term EGF-like peptides includes the peptides termed collectively transforming growth factor-α (TGF-α). The TGF-alpha proteins, including some proteins produced by transformed cell lines, compete equally for the EGF receptor. The assay measures EGF/TGF-α from a variety of species including mouse and human. Assay sensitivity. is 20 picograms per tube.
Circle No. 101 on Reader Service Card.

● Sanbio b.v. of the Netherlands has introduced a large range of monoclonal antibodies for indirect immunoperoxidase staining on tissues and enzyme-linked immunosorbent assay (ELISA) techniques. The series includes anti-human keratin, neurofilament, human chorionic gonadotropin, follicle stimulating hormone and glia fibrillary acidic protein, anti-human vimentin, thyroglobulin and blood vessel endothelium. Sanbio also produces a range of monoclonal antibodies: anti-human T cells and an anti-rat tubulin which will stain eukaryotic cells grown in cell culture as well as frozen sections of tissues. In the United States, Sanbio products are distributed by Accurate Chemical and Scientific Corporation.
Circle No. 102 on Reader Service Card.

● Tissue polypeptide antigen (TPA) is a protein associated with cytoskeletal intermediate filaments of internal epithelial (and hence carcinoma) cells. Rabbit anti-TPA antibody, supplied as 10ml of prediluted liquid, can be used for the specific staining of tumour cells in tissue sections using immuno-enzyme techniques. Monitoring serum TPA released by developing tumours using the Prolifigen RIA kit from Sangtec Medical is of use in the control of treatment and detection of recurrence in several types of cancer including breast and intestinal carcinomas. The kit is sufficient for 100 assay tubes. Products are available through Sangtec Medical in Stockholm and through distributors.
Circle No. 103 on Reader Service Card.

● What is claimed to be the first commercially available monoclonal antibody against choline acetyltransferase has been launched by Boehringer Mannheim. This antibody should be of considerable value in the study of the role of cholinergic neurones in the function of the central nervous system. The neurotransmitter synthesizing enzyme choline acetyltransferase is the only reliable marker for cholinergic cells. Immunological demonstration of this enzyme was possible only when highly purified choline acetyltransferase was available as an antigen in order to produce this monoclonal antibody.
Circle No. 104 on Reader Service Card.

● The factor VIII related antigen immunoperoxidase staining kit produced by Biomeda uses avidin–biotin immunotechnology. This immunohistochemical kit is designed to recognize the presence of this blood vessel-endothelial cell marker in paraffin-embedded and frozen tissue sections. The Histoscan-FX VIII kit yields a highly contrasting red colour in positively stained sections. The morphological characteristic of the tissue under study is revealed by the haematoxylin stain which is also part of the kit. The staining methodology using the avidin–biotin affinity cytochemistry (ABAC) gives outstanding staining of tissue sections, and allows very short but efficient incubation steps. The kit is available in two size configurations containing all basic reagents needed to stain either 50 or 150 tissue sections up to the mounting stage. The reagents forming these kits are supplied in a ready-to-use form and are contained in convenient dropper bottles which, for simplicity of use, are both colour and numerically coded.
Circle No. 105 on Reader Service Card.

● A new modular system has been introduced by A/S Nunc of Denmark for ELISA and other analyses. The MicroWell Module consists of a frame, into which different types of modules can be fixed to meet individual requirements. The module system is composed of 1 × 8 and 2 × 8 well modules with flat bottoms and 2 × 8 well modules with round bottoms. All three versions are available with high and with medium binding capacity. The frames and the wells of the modules have the same dimensions as a traditional 96-well plate and can thus be used in existing readers, dispensers, washers and so on. The well bottoms are protected against scratches, and selfstanding modules. The same frame is applicable for all the different types of modules. MicroWell Modules are supplied either as loose modules, empty frames or as modules mounted in frames.
Circle No. 106 on Reader Service Card.

● Antisera to human thyroglobulin and thyroid binding globulin (TBG) are the latest additions to Miles Scientific's line of undiluted hormone/protein antisera. These products are useful in a variety of procedures including gel diffusion, immunohistology and RIA. Anti-human thyroglobulin is a whole serum product enriched by the addition of a concentrated IgG fraction of the same antiserum. The antiserum is produced in sheep, using an antigen prepared from thyroid. Using the peroxidase–anti-peroxidase (PAP) technique, this antiserum has titres of approximately 1:100 against normal thyroid and 1:500 against secondary tumours following thyroidectomy. Anti-human thyroid binding globulin is also an IgG fraction-enriched antiserum. The antigen used is purified from human plasma.
Circle No. 107 on Reader Service Card.

One of the range of ELISA-based kits from Labsystems, this one designed for the diagnosis of cytomegalovirus infection. Circle number 110 for details.

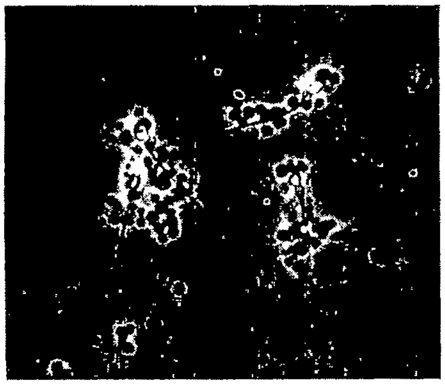

Detection of anti-sperm antibodies with Immunobead from Bio-Rad.

- A rosette-type assay using Bio-Rad's Immunobead reagent allows rapid and reliable detection of anti-sperm antibodies. The assay, performed in 30 minutes, requires only basic laboratory equipment and commercially available reagents. The test can be used either for detection of autoantibodies which are already bound to sperm in semen, or for detection of free anti-sperm antibodies in fluids such as seminal plasma, serum, follicular fluid, or cervical mucus.

Circle No. 108 on Reader Service Card.

- The Hamilton Microlab M liquid handling system features versatile program storage in a battery buffered memory, making it especially suitable for RIA work. Microlab 1000 is a dual syringe unit, ideal when high dilution ratios are required, and capable of repeat dispense and double dilutions. The most recent addition to the Hamilton range is the Microlab MT, for use with microtitre plates.

Circle No. 109 on Reader Service Card.

ADVERTISEMENTS

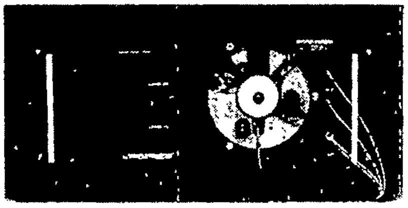

Liposomes

LIPOPREP® the equipment for the reproducible preparation of stable unilamellar liposomes of defined size in the range of 30-300 nm Ø with extremely narrow particle size distribution for e.g. the efficient incorporation of (therapeutic) agents incl antibodies.

DIANORM-Geräte, P.O. Box 126, D-8 München 65, FRG

Circle No.30 on Reader Service Card.

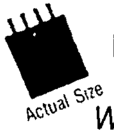

FM TELEMETRY TRANSMITTER

Smallest & Lightest Available (.5 Grams)
Transmits ECG, EEG, Pressure,
Temperature, Digital Data, Audio, Etc.!

Price—$449

Write for Fact Sheet

BIOTELEMETRICS, INC.
24650 CENTER RIDGE ROAD #135
WESTLAKE, OHIO 44145 • (216)835-5770

Circle No.51 on Reader Service Card.

- Five test kits, based on the ELISA technique, are available from Labsystems (UK) Limited. Tetanus IgG EIA kits provide for practical and convenient screening of tetanus antitoxin. The normal sensitivity is 0.1 mIU ml^{-1} but, if necessary, a more rapid less sensitive test may be performed by decreasing the incubation time to one hour. The CMV IgG EIA test kit allows accurate diagnosis of cytomegalovirus infections. The assay speeds up CMV antibody testing considerably, especially in large screening tests. A positive IgG test suggests previous infection. All the kits are based on solid phase enzyme immunoassay, automatic photometric reading and simple laboratory work. Each kit is complete with all the necessary reagents, sensitized Microstrips or cuvette blocks for the tests.

Circle No. 110 on Reader Service Card.

- A new cell marker, DiI-Ac-LDL (1,1′-dioctadecyl-1-3, 3′, 3′-tetramethyl-indocarbocyanine perchlorate acetylated low density lipoprotein) labels both vascular endothelial cells and macrophages. It can be used to identify and/or isolate these cells from mixed cell populations. When cells are labelled with DiI-Ac-LDL, the lipoprotein is degraded by lysosomal enzymes and the DiI (fluorescent probe) accumulates in the intracellular membranes; there is no effect on cell viability. DiI-Ac-LDL is available from Biomedical Technologies Inc. of Cambridge, Massachusetts.

Circle No. 111 on Reader Service Card.

- Leukotriene B_4 can now be measured accurately and conveniently in biological samples using a radioimmunoassay reagents system from Amersham International. The new product consists of ^{3}H-leukotriene B_4 tracer, high specificity antiserum and leukotriene B_4 standard. The measurement range is 12.5 to 400 pg per tube and sufficient reagents are supplied for 125 assay tubes. This permits the construction of a standard curve and the measurement of 53 unknowns in duplicate, but as unused reagents can be stored, a standard curve may be constructed on more than one occasion.

Circle No. 112 on Reader Service Card.

- The ImmunoReader NJ-2000 from Tissue Culture Services is a new approach to automated quantitative photometry. All operations are controlled by an advanced microprocessor which makes it possible to combine a number of standard modes with various parameters as requested by the user. As the NJ-2000 can read up to 15 microplates in sequence, it is suitable for clinical applications and permits a high volume of tests to be performed. Using a keyboard combined with digital displays, the NJ-2000 can be operated without specialized training and user-specific programs can be designed to suit individual analytical needs. Once created, the built-in memory in the NJ-2000 allows eleven programs to be stored for later retrieval when needed.

Circle No. 113 on Reader Service Card.

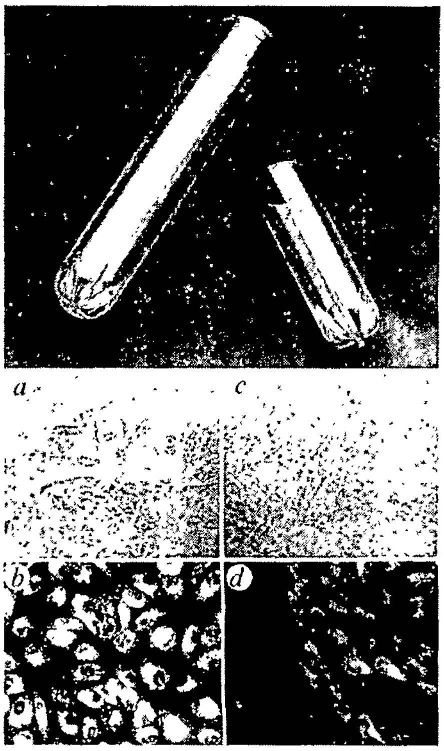

Top: Nunc's StarTube for ELISA and RIA. Bottom: Micrographs of cells labelled with the new cell marker from Biomedical Technologies. a, *Phase and* b, *fluorescence migrographs of a pure culture of bovine aortic endothelial cells.* c, *Phase and* d, *fluorescence micrographs of bovine aortic smooth muscle cells and endothelial cells.*

- The Nunc StarTube is a specialist tube for ELISA and RIA analyses. It is a round-bottomed polystyrene tube with six wings — a star — on the inside of the tube bottom. The purpose of the star is to increase the surface and thereby make it possible to adsorb greater amounts, more rapidly than is the case with traditional tubes. We have succeeded in increasing the surface by 50–100% dependent on the amount of liquid. The StarTube is manufactured from the same type of polystyrene as the Nunc-Immuno Plate I, and it can thus adsorb 400 ng immunoglobulins per cm^2 compared with a tube manufactured from ordinary polystyrene, which will only adsorb 100 ng per cm^2. The special design of the tube bottom makes it possible to reduce the time required for coating and incubation by about two-thirds without influencing the sensitivity of the analysis. The StarTube is available in two versions: 40 × 10.5 mm and 75 × 12 mm.

Circle No. 114 on Reader Service Card.

- Cellular Products, Inc. of Buffalo, New York and Cordis Laboratories, Inc., of Miami, Florida, have entered into an agreement to jointly produce and market test kits for the detection of antibodies to human T-lymphotrophic viruses (HTLV). Kits are available for both HTLV-I and the AIDS virus (HTLV-III). The system provides quantitative results in less than 3 hours at an approximate cost of $2.00 per determination.

Circle No. 115 on Reader Service Card.

- A new method for measuring levels of the immunosuppressant cyclosporin has been developed by Water Associates. The HPLC assay monitors cyclosporin in patients without cross-reactivity with its metabolites. Unlike RIA kits, the 15-min assay separates cyclosporin from its metabolites to allow better patient management. Samples are prepared in 30 min using a simple extraction procedure.
Circle No. 116 on Reader Service Card.

- The new electron microscopy grade colloidal gold probes from Janssen are virtually cluster-free immunogold particles with a narrow size distribution. EM-grade colloidal gold is available in four non-overlapping sizes, coupled to secondary antibodies of various specificities, or protein A. Light microscopy (LM) grade immunogold can be used in conjunction with epi-polarization (anti-mouse secondary antibody only) or with the ImmunoGold silver staining technique. An immunoblotting (BL) grade range has been developed for the immunochemical visualization of antigen-antibody reactions at the surface of blotting membranes.
Circle No. 117 on Reader Service Card.

- For use with glucose oxidase in immunohistochemical staining processes, Vector Labs has introduced several glucose oxidase substrate kits as companion reagents to Vecta stain ABC-GO immunohistochemical staining kits. Each substrate kit contains optimal concentrations of reagents in convenient dropper bottles and includes a mixing bottle for preparing the substrate solution. The colour of the reaction product depends on the tetrazolium salt supplied with the kit. Three kits are available with a choice of reaction product colours — black, red or purple-blue. The substrate kits include easy to follow instructions and sufficient stock solutions to prepare approximately 300 ml of substrate solution.
Circle No. 118 on Reader Service Card.

- Affinity purified anti-pig IgG (γ) and IgM (μ) are available from Kirkegaard and Perry of Gaithersburg, Maryland. These heavy chain specific polyclonal antibodies were isolated from goat antisera immunized with normal pig IgG or IgM and then affinity purified by exhaustive adsorption on pig IgM and IgG respectively to insure minimal cross-reactivity and high purity. Both antibodies are especially suited to high performance immunoassays that differentiate current and past infections by distinguishing pig IgG or IgM activity. These antibodies are available unlabelled and as peroxidase, phosphatase or fluorescein conjugates.
Circle No. 119 on Reader Service Card.

- Nycodenz Monocytes is a new medium from Nyegaard designed for the one-step isolation of monocytes from leukocyte rich plasma and whole blood. The method is claimed to yield monocytes of high purity (over 90%), good yield (over 60%) and good viability.
Circle No. 120 on Reader Service Card.

- The new 120-page catalogue from Miles Scientific includes an extensive range of immunochemicals. The other products listed are divided into separate sections including: Lectins, Blood Proteins, Polypeptides, Enzymes and Companion Reagents. The catalogue also includes description of LUX tissue culture labware and Lab-Tek general labware.
Circle No. 121 on Reader Service Card.

- The Tago range of antisera now includes goat antisera to human proteins; fluorescein conjugated IgG fractions; antibodies to mouse immunoglobulins; goat anti-rat IgG and goat F(ab′)2 fractions from pepsin-digested affinity isolated antibodies. Both affinity adsorption and affinity isolation are used to purify the Tago reagents.
Circle No. 122 on Reader Service Card.

- A wide range of Bio-Yeda biological products, including many immunochemicals, is now available in the United Kingdom through P & S Biochemicals of Liverpool. Bio-Yeda is a subsidiary of Yeda Research and Development Company of the Weizman Institute of Science in Israel. Amongst the variety of immunochemicals available are: monoclonal antibodies to human immunoglobulins, lactate dehydrogenase isozymes and T and B lymphocytes; monoclonals to DNP, mouse lymphocyte markers and many hormones and drugs; fluorescent and alkaline phosphatase conjugated monoclonals, and monoclonal peroxidase anti-peroxidase complexes. Antisera to almost 100 different human, animal and general cytoskeletal proteins are available. Other Bio-Yeda immunochemicals available include RID plates, IgG fractions of antisera, affinity purified antibodies , RIA/EIA reagents (plus RIA second antibodies) and protein A reagents.
Circle No. 123 on Reader Service Card.

- T-cell growth factor (TCGF, interleukin 2) has been added to Metachem's range of growth and attachment factors. The TCGF is from human leukocytes and is available in 5 ml quantities in sterile, lectin-free liquid containing a small amount of calf serum. The growth factor is stable for one year when stored at 4°C or for 3 days at room temperature.
Circle No. 124 on Reader Service Card.

- The new Imagen RSV test from Boots-Celltech Diagnostics provides an accurate diagnosis of respiratory synctial virus infection within 30 min. The Imagen RSV test is a rapid, simple direct immunofluorescence test utilizing monoclonal antibodies specific to RSV. This is the second product in the Imagen range to be made available, the first being the Imagen Chlamydia test which was launched earlier this year.
Circle No. 125 on Reader Service Card.

These notes are based on information provided by the manufacturers. For further details circle the appropriate numbers on the Reader Service Card bound inside the journal.

- Hybridoma reagents designed for the easy purification of monoclonal antibodies, titred interleukin 2 (in three purity levels), T-cell reagents and protein-A reagents are now available from Inter-Cell Technologies, Inc. of Somerville, New Jersey. Also available from Inter-Cell are antisera and IgG fractions to human and animal proteins and cells, a wide range of complement reagents, adsorbed antisera with improved specificity to individual cell populations and lymphocytes useful as starting matrials for lymphokine production or the isolation of lymphocyte subsets. In addition, Inter-Cell includes among its services custom immunological assays and antisera production.
Circle No. 126 on Reader Service Card.

- A new reagent for immunological research *in vitro* and in laboratory animals removes viability, infectivity and oncogenicity of the viruses (through photochemical inactivation of nucleic acid functions) to provide a new degree of experimental freedom. The reagents, from Lee Biomolecular, are provided in sterile lyophilized form having good shelf life, eliminating the need to propagate, inactivate and standardize viruses in the user's laboratory. More than seventy human and veterinary viruses are listed in the catalogue including herpes simplex, cytomegalovirus, Epstein–Barr and simian virus 40.
Circle No. 127 on Reader Service Card.

ADVERTISEMENT

Copies of articles from this publication are now available from the UMI Article Clearinghouse.

Yes! I would like to know more about UMI Article Clearinghouse. I am interested in electronic ordering through the following system(s)

☐ DIALOG/Dialorder ☐ ITT Dialcom
☐ OnTyme ☐ OCLC ILL Subsystem
☐ Other (please specify)________
☐ I am interested in sending my order by mail
☐ Please send me your current catalog and user instructions for the system(s) I checked above

Name________
Title________
Institution/Company________
Department________
Address________
City______ State____ Zip____
Phone (____)________

UMI Article Clearinghouse

Mail to: University Microfilms International
300 North Zeeb Road, Box 91 Ann Arbor, MI 48106

21-1-87 4630

A. Gatto,

ANNOUNCEMENTS

Meetings

17-18 December, **Meeting on Metal Ions, Free Radical Reactions and Disease,** London (Mr B. Halliwell, Department of Biochemistry, King's College, Strand, London WC2R 2LS, UK).

25 February-1 March, **36th Pittsburg Conference and Exposition on Analytical Chemistry and Applied Spectroscopy,** New Orleans, USA (Mrs Linda Briggs, Program Secretary, 437 Donald Road, Pittsburgh, Pennsylvania, 15235, USA).

26 February-8 March, **Winter Session on Disordered Systems and Biological Organization,** Les Houches, France (Mr G. Weisbuch, Centre de Physique, Univ. Scientifique et Medicale de Grenoble, Côte des Chavants, 74310 Les Houches France).

26-29 March, **3rd European Conference on Food Chemistry,** Antwerp, Belgium (Euro Food Chem. III, Flemish Chemical Society — Food Science Section, Dr P. Dirinck, Faculty of Agricultural Sciences, State University of Gent, Coupure Links 653, B-9000 Gent, Belgium).

27-29 March, **Symposium on the Oceanography of the Rockall Channel** organized by the Royal Society of Edinburgh and the Scottish Marine Biological Association, Edinburgh, UK (The Meeting's Secretary, The Royal Society of Edinburgh, 22,24 George Street, Edinburgh EH2 2PQ, UK).

31 March-4 April, **Meeting on Process Systems Engineering:** SPE '85 — The Use of Computers in Chemical Engineering, Cambridge, UK. The Institution of Chemical Engineers, 165-171 Railway Terrace, Rugby CV21 3HQ, UK).

31 March-5 April, **4th Pfefferkorn Conference on The Science of Biological Specimen Preparation for Microscopy and Microanalysis,** Las Vegas, USA (Dr. Om Johari, PO Box 66507, AMF O'Hare, Illinois 60666 USA).

10-12 April, Symposium on **Recent Advances in Medical and Physiological Imagery,** Harrow Middlesex, UK (Mr M. Goff, Thermographic Laboratory, Clinical Rsearch Centre, Watford Road, Harrow, Middlesex HA1 3UJ, UK).

15-19 April, **International Symposium on Biomineralization in Lower Plants and Animals,** Birmingham, UK (Dr Robert Riding, Biomineralization Symposium, Department of Geology, University College, Cardiff CF1 1XL, UK).

16-18 April, **International Meeting on Pregnancy Proteins in Animals,** Copenhagen, Denmark (Ms Ulla Salado-Jimena, Department of Pathology, Laboratory Animal Unit, Royal Veterinary and Agricultural University of Copenhagen, Bülowsvej 13, Dk-1870 Copenhagen V, Denmark).

22-26 April, **International Symposium-Workshop on Particulate and Multi-Phase Processes, & 16th Annual Meeting of the Fine Particle Society,** Miami Beach, USA (Mr T. Nejat Veziroglu, Director, Clean Energy Research Institute, University of Miami, PO Box 248294, Florida 33124, USA).

24-26 April, **International Symposium on Peptides and Ion Transport,** Florence, Italy (Organizing Secretary, Fondazione Giovanni Lorenzi, Via Monte Napoleone 23, 20121 Milan, Italy).

9-15 June, **21st Chemical Engineering Exhibition,** Frankfurt, FRG (Ms A. Bondaray, V.I.P. Business & Trade Fairs Travel Ltd, 42 North Audley Street, Grosvenor Square, London W1A 4PY, UK).

18-20 June, **Conference on Forest Decline,** Goslar, FRG (Verein Deutscher Ingenieure, Kommission Reinhaltan der Luft, POB 1139 D-4000 Düsseldorf 1, FRG).

The Institute of Physics, London, is holding a series of one-day meetings in London this autumn: 17 October, **Electronics Update;** 23 October, **Applications of Non-linear Analysis,** and **Resonator Sensor Systems;** 24 October, **Critical Phenomena in Magnetism and Low Temperature Physics;** 29 October, **Fundamental Aspects of Polymer Flammability;** 6 November, **Magnetic Thin Film Coatings for the Recording Media;** 8 November, **Low Temperature Techniques Course;** 14 November, **High Complexity Displays;** 21 November, **Drying and Curing;** 5 December, **Electrostatic Imaging;** 12 December, **Transient Annealing of Semiconductors;** 14 December, **Permanent Magnetic Materials and Applications.** Further information from The Meetings Office, The Institute of Physics, 47 Belgrave Square, London SW1X 8QX, UK.

The Scientists Center for Animal Welfare USA, are sponsoring three workshops on **Animals and the Scientist : Institutional Responsibilities,** and **"How to Run an Effective Animal Care and Use Committee,** in conjunction with the following universities: 11-12 October, Michigan State University, Lansing Michigan; 14-15 November, University of Southern California, Los Angeles; and 23-24 May 1985, Aspen Institute, Aspen, Colorado (Dr Barbara Orlans, Scientists Center for Animal Welfare, PO Box 9581, Washington D.C. 20016, USA).

Short courses

19-22 November, **Training Course in Fluid Rheology** (Mr L.J. Viney, Warren Spring Laboratory, Gunnels Wood Road, Stevenage, Hertfordshire SG1 2BX, UK).

10-12 December, **Yield of Cereals** (Warwick University, UK); 12-14 December, **Yield of Potatoes** (Warwick University, UK) and 5-7 February, **Yield of Sugar Beet** (Peterborough, UK). Further details form the Arable Unit, National Agricultural Centre, Stoneleigh, Kenilworth, Warwickshire CV8 2LZ, UK).

23 April-29 June 1985, **Understanding Climate** (Dr T.M.L. Wigley, Director, Climatic Research Unit, University of East Anglia, Norwich NR4 7TJ, UK).

6-25 January, **International Training Courses on Gene Transfer in Higher Eukaryotes,** Sofia, Bulgaria (Professor R.G. Tsanev, Institute of Molecular Biology, Bulgarian Academy of Sciences, 1113 Sofia, Bulgaria).

3-7 June 1985, **Second International Summer School on Mathematica Modelling in Physiology and Clinical Medicine,** University of Padua, Italy (E.R. Carson, Research Centre f Measurement and Information i Medicine, The City University, Northampton Square, London EC1, UK.

The Centre for Extension Studies, Loughborough University is organizing a programme of five modular short courses in 1985, leading to the University Diploma in Occupational Health and Safety Management (Mrs K. Gilbert, Centre for Extension Studies, Loughborough University of Technology, Loughborough, Leicestershire LE11 3TU, UK).

Miscellaneous

The Royal College of Pathologists is introducing a Final Examination in Clinical Cytogenetics open to medical and non-medical candidates. Further details are available form the Examinations Department of the Royal College of Pathologists, 2, Carlton House Terrace, London SW1Y 5AF, UK.

The International Commission on Zoological Nomenclature is calling for nominations for new members to replace staff who are retiring. Nominations should be sent by the end of December 1984 to The Secretary, International Commission on Zoological Nomenclature, British Museum (Natural History), Cromwell Road, London SW7 5BD, UK.

It was recently announced that the **British Computer Society** had been granted a Royal Charter by Her Majesty the Queen.

The **Nobeyama Radio Observatory (NRO)** has decided to make its 45m telescope available to foreign scientists from January — May 1985 and is calling for study proposals for its use. Those scientists having a Japanese co-investigator will be preferred although in a limited number of cases applications from those without Japanese co-investigators will also be accepted. The deadline for applications will be at the end of October 1984 and further details can be obtained from K. Akabane, Director, Nobeyama Radio Observatory, Nobeyama, Minamisaku, Nagano 384-13, Japan.

A **Trauma Research Center,** one of the largest of its kind in the world, has been established at the Hebrew University-Hadassah Medical School, Israel.

The **European Powder Metallurgy Federation** was formed earlier this year in Clermont Ferrand, Switzerland; further information from Mr Robert Wood, The Metals Society, 1 Carlton House Terrace, London SW1Y 5DB, UK.

Laboratory 85 will now form part of British Laboratory week to be held next year from 17-19 September at Olympia, London, UK.

Author Index for Volume 310

July – August 1984

4630

Issue no.	Issue date	Pagination
5972	5 July	1-86
5973	12 July	87-170
5974	19 July	171-260
5975	26 July	261-350
5976	2 August	351-438
5977	9 August	439-526
5978	16 August	527-610
5979	23 August	611-714
5980	30 August	715-810

Abney, J R. *See under* Braun, J., **310,** 316
Abraham, J. *See under* Lim, A T W., **310,** 61
Addadi, L. *See under* Weissbuch, L, **310,** 161
Adrian, R H. *See under* Woledge, R C., **310,** 170
Aharon, P. Erratum: Isotope studies of insular phosphates explain atoll phosphatization (*with* Veeh, H H) *Letter to Nature,***310,** 340
Aitken, M J. Geomagnetic intensity in Egypt and western Asia during the second millennium BC (*with* Allsop, A L, Bussell, G D, Winter, M B) *Letter to Nature,***310,** 305
Aldiss, D T. Early Jurassic pillow lavas and palynomorphs in the Karoo of eastern Botswana (*with* Benson, J M, Rundle, C C) *Letter to Nature,***310,** 302
Allen, R D. *See under* Brady, S T., **310,** 56
Allsop, A L. *See under* Aitken, M J., **310,** 305
Allègre, C J, *et al.*. Cold Gondwana, warm Tethys and the Tibetan Lhasa block: Reply, *Matters arising,***310,** 165
Altman, J. Neurobiology: Cross-section of the spinal cord, *News and views,***310,** 730
Anders, R F. *See under* Coppel, R L., **310,** 789
Anderson, A. Technopolis: Japan's tomorrow here today, *News,***310,** 5
  Motives for mobility, *News,***310,** 5
  Japanese research: Call for industrial university, *News,***310,** 90
  Ageing Japan: Riches make for longevity, *News,***310,** 92
  Japanese biotechnology: Search begins for superbugs, *News,***310,** 172
  Learning Japanese: Plans for language teaching, *News,***310,** 177
  Japanese research: New money for cancer, *News,***310,** 264
  Japanese nuclear power: Lawsuit dismissed, *News,***310,** 357
  Operation of power plants, *News,***310,** 357
  Japanese whaling: Will monitoring suffice when the hunting stops?, *News,***310,** 440
  Japanese cities: Neoaquapolis, *News,***310,** 444
  Nuclear shipping: Japan's vessel still adrift, *News,***310,** 531
  Japan to import US idea, *News,***310,** 531
  Japanese research: Ministry's ambitions still higher, *News,***310,** 614
  MITI's proposals, *News,***310,** 614
  Japanese space research: Halley probe on show, *News,***310,** 719
Anderton, B. *Book review of* Monoclonal antibodies (*by* Sikora, K, Smedley, H M,) **310,** 256
Andrew, E R. *Book review of* Nuclear magnetic resonance imaging: Basic principles (*by* Young, S W,) **310,** 803
  Book review of Magnetic resonance in medicine and biology (*by* Foster, M A,) **310,** 803
Andrews, D. Meteorology: Stratospheric planetary waves, *News and views,***310,** 185
Ang, V T Y. *See under* Nussey, S S., **310,** 64
Anstrom, J A. *See under* Raff, R A., **310,** 312
Antia, N H. Science in India, *Correspondence,***310,** 722
Antiochos, S K. *See under* Liang, E P., **310,** 121
Antoine, M. Intron-less globin genes in the insect *Chironomus thummi thummi* (*with* Niessing, J) *Letter to Nature,***310,** 795
Appelt, K. *See under* Tanaka, I., **310,** 376
Armelin, H A. Functional role for c-*myc* in mitogenic response to platelet-derived growth factor (*with* Armelin, M C S, Kelly, K, Stewart, T, Leder, P, Cochran, B H, Stiles, C D) *Article,***310,** 655
Armelin, M C S. *See under* Armelin, H A., **310,** 655
Arthur, M A. Stratigraphy: Carbon isotope anomalies?, *News and views,***310,** 450
Ashby, E. *Book review of* Empire of knowledge: The Academy of Sciences of the USSR (1917-1970) (*by* Vucinich, A,) **310,** 77
Ashcroft, W A. Major shear zones and autochthonous Dalradian in the north-east Scottish Caledonides (*with* Kneller, B C, Leslie, A G, Munro, M) *Letter to Nature,***310,** 760
Ashmore, J. Auditory physiology: Splitting hairs over hearing?, *News and views,***310,** 544
Asimov, I. The history of physics, *Book review by* Porter, R. **310,** 708
Atherton, P D. *See under* Phillips, M M., **310,** 554
Atherton, W A. From compass to computer, *Book review by* Cardwell, D S L. **310,** 342
Atkinson, W. *See under* Shorrocks, B., **310,** 310
Audley-Charles, M G. Cold Gondwana, warm Tethys and the Tibetan Lhasa block, *Matters arising,***310,** 165
Auteiltano, D J. *See under* Lim, A T W., **310,** 61
Axelrod, J. *See under* Mezey, E., **310,** 140
Axon, D J. *See under* Phillips, M M., **310,** 554
Babuska, V. *See under* Fyfe, W F., **310,** 537
Baer, R. DNA sequence and expression of the B95-8 Epstein-Barr virus genome (*with* Bankier, A T, Biggin, M D, Deininger, P L, Farrell, P J, Gibson, T J, Hatfull, G, Hudson, G S, Satchwell, S C, Séguin, C, Tuffnell, P S, Barrell, B G) *Article,***310,** 207
Bailey, J A. *See under* Aitken, D K., **310,** 660
Baker, P F. Cell biology: Multiple controls for secretion?, *News and views,***310,** 629
Balasubramanian, D. Mrs Malaprop at work, *Correspondence,***310,** 178
Bankier, A T. *See under* Baer, R., **310,** 207
Barber, J. Botany: Manipulation of photosynthesis, *News and views,***310,** 184
Barkenbus, J N. Nuclear building-down (*with* Weinberg, A M) *Correspondence,***310,** 95
Barklis, E. *See under* Chisholm, R L., **310,** 67
Barlow, J W. *See under* Lim, A T W., **310,** 61
Barnard, E A. *See under* Houamed, K M., **310,** 318
Barrell, B G. *See under* Baer, R., **310,** 207
Barron, E J. Continental distribution as a forcing factor for global-scale temperature (*with* Thompson, S L, Hay, W W) *Letter to Nature,***310,** 574
Barry, R A. *See under* Bendheim, P E., **310,** 418
Bartlett, P F. *See under* Wong, G H W., **310,** 688
Bastiani, M J. *See under* Thomas, J B., **310,** 203
Bate, M. *See under* Thomas, J B., **310,** 203
Battye, F. *See under* Wong, G H W., **310,** 688
Beardsley, T. Taxation: UK budget hits research councils, *News,***310,** 4
  US technology controls: Curbs on conference membership advocated, *News,***310,** 172
  Dispute over AIDS patent priority, *News,***310,** 174
  US space station: No enthusiasm in Congress, *News,***310,** 265
  Telescope for 1990s: Multiple choice on mirrors, *News,***310,** 265
  Nuclear waste: Ocean disposal recommended, *News,***310,** 354
  Burford in hot water, *News,***310,** 354
  US immigration: Reprieve by default for academics, *News,***310,** 355
  COCOM agreement on computers, *News,***310,** 355
  Koshland for *Science* post, *News,***310,** 356
  Cyclamates ban: Carcinogenicity claim questioned, *News,***310,** 442
  US manpower: Shortages of specialists foreseen, *News,***310,** 443
  US nuclear power: Silver lining shows for industry as demand grows, *News,***310,** 529
  Artificial fertilization: US Congress plans to act, *News,***310,** 533
  US environmental protection: Agency pleads for less support, *News,***310,** 616
  Satellite insurance: Shuttle to make good failure?, *News,***310,** 618
Becker, D M. *See under* Gascoigne, N R J., **310,** 387
Beemer, F A. How did retinoblastoma arise? (*with* Van Veelen, C W M, Staal, G E J) *Scientific correspondence,***310,** 731
Beier, R C. Homocysteine and arteriosclerosis, *Scientific correspondence,***310,** 18
Bell, G I. Sequence of a cDNA clone encoding human preproinsulin-like growth factor II (*with* Merryweather, J P, Sanchez-Pescador, R, Stempien, M M, Priestley, L, Scott, J, Rall, L B) *Letter to Nature,***310,** 775
  See under Tricoli, J V., **310,** 784
Bendheim, P E. Antibodies to a scrapie prion protein (*with* Barry, R A, DeArmond, S J, Stites, D P, Prusiner, S B) *Letter to Nature,***310,** 418
Bennett, J. Photosynthesis: Control of protein turnover by photosynthetic electron transport, *News and views,***310,** 547
Benson, J M. *See under* Aldiss, D T., **310,** 302
Bentley, J. Sea of subdued light, *Correspondence,***310,** 358
Benton, M. Vertebrate palaeontology: Rauisuchians and the success of dinosaurs, *News and views,***310,** 101
Berardelli, A. *See under* Dick, J P R., **310,** 407
Berg, H C. Random walks in biology, *Book review by* DeLisi, C **310,** 258
Berger, R. *See under* de Taisne, C., **310,** 581
Berggren, W A. **Editor,** Catastrophes and Earth history: The new uniformitarianism, *Book review by* Hallam, A **310,** 435
Berkovitch-Yellin, Z. *See under* Weissbuch, I., **310,** 161
Bernard, M. *See under* Chu, M-L., **310,** 337
Bernheim, A. *See under* de Taisne, C., **310,** 581
Besant, L X. Price of European journals (*with* Rechin, S) *Correspondence,***310,** 358
Blanco, A E. *See under* Coppel, R L., **310,** 789
Biggin, M D. *See under* Baer, R., **310,** 207
Bignami, G F. Evidence for an increasing 59-s period in the X-ray emission from Geminga (*with* Caraveo, P A, Paul, J A) *Article,***310,** 464
  See under Caraveo, P A., **310,** 481
Bijleveld, W. De Leidse Sterrewacht: Vier eeuwen wacht bij dag en bij nacht, *Book review by* Bosma, P B. **310,** 169
Bilbe, G. *See under* Houamed, K M., **310,** 318
Bisset, G W. *See under* Nussey, S S., **310,** 64
Blackburn, E H. *See under* Shampay, J., **310,** 154
Blakemore, R P. *See under* Mann, S., **310,** 405
Blakeslee, S. Britons never slaves?, *News,***310,** 177
  US space research: Moon beckons for NASA, *News* **310,** 718
Blandford, R. *See under* Narayan, R., **310,** 112
Blundell, T L. *See under* Travers, P., **310,** 235
Bode, M F. *See under* Graham, J R., **310,** 213
Bodmer, W F. *See under* Travers, P., **310,** 235
Boettiger, D. *See under* Spooncer, E., **310,** 228
Bohren, C F. Evidence for haematite particles at 60 km altitude (*with* Olivero, J J) *Letter to Nature,***310,** 216
Bolter, J D. Turing's man: Western culture in the computer age, *Book review by* Edge, D. **310,** 705
Bonner, T I. Molecular endocrinology: Vasopressin, tissue-specific defects and the Brattleboro rat (*with* Brownstein, M J) *News and views,***310,** 17
Bootsma, D. *See under* Westerveld, A., **310,** 425
Bosma, P B. *Book review of* De Leidse Sterrewacht: Vier eeuwen wacht bij dag en bij nacht (van Herk, G, Kleibrink, H, Bijleveld, W, *editors*) **310,** 169
Boublik, J. *See under* Lim, A T W., **310,** 61
Boulègue, J. *See under* Jedwab, J., **310,** 41
Bown, W H. Nuclear war – counting the cost, *Scientific correspondence,***310,** 455
Boyd, R J. A quantum mechanical explanation for Hund's multiplicity rule, *Letter to Nature,***310,** 480
Brady, S T. Gelsolin inhibition of fast axonal transport indicates a requirement for actin microfilaments (*with* Lasek, R J, Allen, R D, Yin, H L, Stossel, T P) *Letter to Nature,***310,** 56
Brannigan, A. *See under* Hunkapiller, M., **310,** 105
Braun, J. How a gap junction maintains its structure (*with* Abney, J R, Owicki, J C) *Letter to Nature,***310,** 316
Brickell, P M. Selfish ideologies (*with* Murphy, D) *Correspondence,***310,** 178
Briggs, J H. *See under* Aitken, D K., **310,** 660
Brigham-Grette, J. *See under* Sejrup, H P., **310,** 772
Brimblecombe, P. Atmospheric chemistry: Henry's Law confounded, *News and views,***310,** 11
Brinster, R L. *See under* Storb, U., **310,** 238
Brissenden, J E. Human chromosomal mapping of genes for insulin-like growth factors I and II and epidermal growth factor (*with* Ullrich, A, Francke, U) *Letter to Nature,***310,** 781
Brisson, N. Expression of a bacterial gene in plants by using a viral vector (*with* Paszkowski, J, Penswick, J R, Gronenborn, B, Potrykus, L, Hohn, T) *Letter to Nature,***310,** 511
Brookfield, J F Y. Apparent absence of transposable elements related

to the P elements of *D. melanogaster* in other species of *Drosophila* (*with* Montgomery, E, Langley, C H) *Letter to Nature,* **310**, 330
Brower, D J. Posterior-to-anterior transformation in *engrailed* wing imaginal disks of *Drosophila*, *Letter to Nature,* **310**, 496
Brown, D A. *See under* Houamed, K M., **310**, 318
Brown, G V. *See under* Coppel, R L., **310**, 789
Brown, M S. Workers at risk: Voices from the workplace, *Book review by* Hay, A. **310**, 80
Brown, R D. *See under* Matthews, H E., **310**, 125
Brownstein, M J. *See under* Bonner, T I., **310**, 17
Editor, Brain peptides, *Book review by* Phillips, M I. **310**, 256
Bryan, G W. *See under* Gibbs, P E., **310**, 494
Bud, H. *See under* Weiss, E H., **310**, 650
Budiansky, S. Soviet-US agreements: Reagan to review lapsed deals at last, *News,* **310**, 3
Genetic engineering: Rifkin strikes at corn this time, *News,* **310**, 3
More on creationism, *News,* **310**, 6
AIDS: Test companies chosen, *News,* **310**, 6
US astronomy: Kitt Peak and other observatories shaken up, *News,* **310**, 88
Mt Wilson telescope for axe, *News,* **310**, 88
US research budget: Spending plan remains intact, *News,* **310**, 89
US space weapons: ASAT deal in Congress, *News,* **310**, 173
Rows continue over US patent life, *News,* **310**, 176
Chinese census: Demographic transition under way, *News,* **310**, 177
Non-proliferation treaty: United States asks for more safeguards, *News,* **310**, 263
Pakistanis indicted, *News,* **310**, 263
Laboratory animals: Berkeley fined for violations, *News,* **310**, 356
Materials science: Academy backs synchrotron, *News,* **310**, 442
Star wars: Strategic weaknesses made plain, *News,* **310**, 530
Gasoline lead: Ruckelshaus makes a move, *News,* **310**, 532
US plutonium: Japan enjoys inside track, *News,* **310**, 533
Recombinant DNA: Prospect of new US regulation: Surprise welcome for EPA, *News,* **310**, 613
Industrial research: US tax credits a failure, *News,* **310**, 615
US election: Heads you win, tails you win: Prospects good for science, *News,* **310**, 717
Small space platforms favoured, *News,* **310**, 718
Voodoo on the campus, *News,* **310**, 718
Buffetaut, E. Palaeontology: Selective extinctions and terminal Cretaceous events, *News and views,* **310**, 276
Bull, J H. Heavily methylated amplified DNA in transformants of *Neurospora crassa* (*with* Wootton, J C) *Letter to Nature,* **310**, 701
Bullman, H. *See under* Weiss, E H., **310**, 650
Burkhalter, A. *See under* Katz, L C., **310**, 498
Bussell, G D. *See under* Aitken, M J., **310**, 305
Butcher, H R. Nature of blue galaxies in the cluster C1 1447+2619 (*with* Oemler, A) *Letter to Nature,* **310**, 31
Butler, F K. *See under* Reiman, E M., **310**, 683
Byrne, J. Constraints on the neutron lifetime from triton β decay, *Letter to Nature,* **310**, 212
Cahen, L. The geochronology and evolution of Africa, *Book review by* Grant, N K. **310**, 78
Caimi, P G. *See under* Piccoli, S P., **310**, 327
Calcagno, L. *See under* Foti, G., **310**, 126
Calvert, L D. *See under* Mishima, O., **310**, 393
Camilleri, J A. The state and nuclear power: Conflict and control in the Western world, *Book review by* Roth, E B. **310**, 342
Campbell, P. Atmospheric science: UK initiatives for change, *News,* **310**, 175
UK oceanography institute to close, *News,* **310**, 264
UK research: Catalogue of scarcity, *News,* **310**, 267
Where the cuts fall, *News,* **310**, 267
UK fast breeder: Accountants' worries, *News,* **310**, 355
Canizares, C R. *See under* Fabian, A C., **310**, 733
Capon, D J. *See under* McGrath, J P., **310**, 644
Caraveo, P A. *See under* Bignami, G F., **310**, 464
Exosat observation of the candidate X-ray counterpart of Geminga (*with* Bignami, G F, Giommi, P, Mereghetti, S, Paul, J A) *Letter to Nature,* **310**, 481
Carbone, E. A low voltage-activated, fully inactivating Ca channel in vertebrate sensory neurones (*with* Lux, H D) *Letter to Nature,* **310**, 501
Cardwell, D S L. *Book review of* From compass to computer (*by* Atherton, W A,) **310**, 342
Carrasco, A E. *See under* Shepherd, J C W., **310**, 70
Carswell, R. Astronomy: Quasar polarization properties, *News and views,* **310**, 186
Carter, W E. *See under* Robertson, D S., **310**, 572
Caruthers, M. *See under* Hunkapiller, M., **310**, 105
Cashmore, A. *See under* Herrera-Estrella, L., **310**, 115
Caskey, C T. *See under* Yang, T P., **310**, 412
Cazenave, A. Two distinct trends for cooling of the oceanic lithosphere, *Letter to Nature,* **310**, 401
Cedar, H. *See under* Rosenthal, A., **310**, 415
Chan, C S M. *See under* Walmsley, R M., **310**, 157
Chance, D. *See under* Yusef-Zadeh, F., **310**, 557
Chapman, C R. *See under* Kazazian, H H., **310**, 152
Charlesworth, B. *See under* Piper, J G., **310**, 50
Charlesworth, D. *See under* Piper, J G., **310**, 50
Chen, C-N. *See under* Silver, M S., **310**, 681
Chien, Y-h. *See under* Gascoigne, N R J., **310**, 387
See under Kavaler, J., **310**, 421
Chinault, A C. *See under* Yang, T P., **310**, 412
Chisholm, R L. Mechanism of sequential induction of cell-type specific mRNAs in *Dictyostelium* differentiation (*with* Barklis, E, Lodish, H F) *Letter to Nature,* **310**, 67
Chowdrey, H S. *See under* Nussey, S S., **310**, 64
Chown, M. Student benefits, *News,* **310**, 535
AIDS: London scare ends, *News,* **310**, 614
European fast reactors: UK committee critical of pact, *News,* **310**, 618
Open University help for women, *News,* **310**, 618
Medical education: New "private" school to open, *News,* **310**, 720
UK medical research: Funds scarce, *News,* **310**, 720
Christensen, A. *See under* Willumsen, B M., **310**, 583
Christensen, K. Role of soluble myosin in cortical contractions of *Xenopus* eggs (*with* Sauterer, R, Merriam, R W) *Letter to Nature,* **310**, 150
Christensen, S M. Editor, Quantum theory of gravity: Essays in honor of the 60th birthday of Bryce S DeWitt, *Book review by* Townsend, P. **310**, 804
Chupp, E L. Solar physics: New lease on life for the Solar Maximum Mission, *News and views,* **310**, 725
Clark, D H. Superstars: How stellar explosions shape the destiny of our Universe, *Book review by* Tayler, R J. **310**, 706
Clark-Lewis, I. *See under* Wong, G H W., **310**, 688
Clarke, M. Muscle contraction: Two states of attachment, *News and views,* **310**, 275
Biophysics congress: Stay-away hosts, *News,* **310**, 532
Claussen, M J. Water-vapour maser emission from galactic nuclei (*with* Heiligman, G M, Lo, K Y) *Letter to Nature,* **310**, 298
Clemens, M. Control of translation: Enzymes and toxins that regulate protein synthesis, *News and views,* **310**, 727
Clement, B M. Latitudinal dependency of geomagnetic polarity transition durations (*with* Kent, D V) *Letter to Nature,* **310**, 488
Cochran, B H. *See under* Armelin, H A., **310**, 655
Cohen, I R. *See under* Naparstek, Y., **310**, 241
Cohen, P. *See under* Hemmings, H C., **310**, 503
Cole, M D. *See under* Piccoli, S P., **310**, 327
Compton, R. *Book review of* Electroanalytical chemistry (*by* Vassos, B H, Ewing, G W,) **310**, 519
Connors, B W. Initiation of synchronized neuronal bursting in neocortex, *Letter to Nature,* **310**, 685
Conrad, M K. *See under* Lo, M M S., **310**, 792
Constanti, A. *See under* Houamed, K M., **310**, 318
Cooper, W. *Book review of* Random variables (*by* Rothschild, Lord,) **310**, 436
Coppel, R L. Immune sera recognize on erythrocytes a *Plasmodium falciparum* antigen composed of repeated amino acid sequences (*with* Cowman, A F, Anders, R F, Bianco, A E, Saint, R B, Lingelbach, K R, Kemp, D J, Brown, G V) *Letter to Nature,* **310**, 789
Cordova, L. *See under* Taylor, K A., **310**, 285
Cornish-Bowden, A. Molecular biology: No introns in insect globin genes, *News and views,* **310**, 724
Book review of Biochemical adaptation (*by* Hochachka, P W, Somero, G N,) **310**, 804
Cosmovici, C B. Detection of new molecules in the visible spectrum of Comet IRAS-Araki-Alcock (1983 d) (*with* Ortolani, S) *Letter to Nature,* **310**, 122
Cossman, J. *See under* Longo, D L., **310**, 505
Coutelle, A. *See under* Pautot, G., **310**, 133
Covey, C. *See under* Thompson, S L., **310**, 625
Cowan, J M A. *See under* Dick, J P R., **310**, 407
Coward, E. The origins of malignancy, *Scientific correspondence,* **310**, 455
Cowley, R A. *Book review of* Theory of structural transformations in solids (*by* Khachaturyan, A G,) **310**, 606
Cowley, S W H. Geophysics: The nightside magnetosphere, *News and views,* **310**, 543
Cowman, A F. *See under* Coppel, R L., **310**, 789
Cox, F E G. *Book review of* Genes and antigens of parasites: A laboratory manual, 2nd edn (Morel, C M *editor*) **310**, 608
Crawford, L. Tumour virology: Papilloma viruses and cervical tumours, *News and views,* **310**, 16
Crawley, M J. *Book review of* A new ecology: Novel approaches to interactive systems (Price, P W, Slobodchikoff, C N, Gaud, W S *editors*) **310**, 168
Croke, M E. *See under* Scott, R W., **310**, 562
Cronin, B. The citation process, *Book review by* Ravetz, J R. **310**, 607
Cullis, C A. Molecular botany: Plant cells under stress, *News and views,* **310**, 366
Dacey, J W H. *See under* Wakeham, S G., **310**, 770
Davies, B E. *See under* Elwood, P C., **310**, 138
Davies, D. Martin Goldman, *News,* **310**, 441
Davis, M M. *See under* Gascoigne, N R J., **310**, 387
See under Kavaler, J., **310**, 421
Day, B L. *See under* Dick, J P R., **310**, 407
Dayton, B. *See under* Tümer, O T., **310**, 214
De Robertis, E M. *See under* Shepherd, J C W., **310**, 70
DeArmond, S J. *See under* Bendheim, P E., **310**, 418
DeLisi, C. *Book review of* Random walks in biology (*by* Berg, H C,) **310**, 258
Deininger, P L. *See under* Baer, R., **310**, 207
Delhal, J. The geochronology and evolution of Africa, *Book review by* Grant, N K. **310**, 78
Desch, M D. Predictions for Uranus from a radiometric Bode's law (*with* Kaiser, M L) *Letter to Nature,* **310**, 755
Devlin, J J. *See under* Weiss, E H., **310**, 650
Dexter, T M. *See under* Spooncer, E., **310**, 228
de Crombrugghe, B. *See under* Yamada, Y., **310**, 333
de Haas, M P. *See under* Warman, J M., **310**, 305
de Taisne, C. Chromosomal localization of the human proto-oncogene *c-ets* (*with* Gegonne, A, Stehelin, D, Bernheim, A, Berger, R) *Letter to Nature,* **310**, 581
de Wet, W. *See under* Chu, M-L., **310**, 337
de Wit, J. *See under* Westerveld, A., **310**, 425
Di Virgilio, F. Protein kinase C activation of physiological proc in human neutrophils at vanishingly small cytosolic Ca^{2+} le (*with* Lew, D P, Pozzan, T) *Letter to Nature,* **310**, 691
Diamond, J. Evolution: DNA map of the human lineage, *News* *views,* **310**, 544
Diamond, J M. Island population biology: Possible effects of unr tricted pesticide use on tropical birds, *News and views,* **310**, 4
Evolutionary biology: Evolution of stable exploiter-victim syste *News and views,* **310**, 632
Diamond, R M. Angular velocity: a new dimension in nuclei (*w* Stephens, F S) *Review article,* **310**, 457
Dick, J P R. The corticomotoneurone connection is normal in P kinson's disease (*with* Cowan, J M A, Day, B L, Berardelli, Kachi, T, Rothwell, J C, Marsden, C D) *Letter to Nature,* **310**, 407
Dijk, J. *See under* Tanaka, I., **310**, 376
Ding, J-F. *See under* Chu, M-L., **310**, 337
Djerassi, C. *Book review of* The pharmaceutical industry and dependency in the Third World (*by* Gereffi, G,) **310**, 517
Dorn, R I. Cause and implications of rock varnish microchemical laminations, *Letter to Nature,* **310**, 767
Dreyer, W. *See under* Hunkapiller, M., **310**, 105
Dreyer, W J. *See under* Katz, L C., **310**, 498
Driscoll, C T. Short-term changes in the base neutralizing capacity of an acid Adirondack lake, New York (*with* Schafran, G C) *Letter to Nature,* **310**, 308
Druitt, T H. On the formation of calderas during ignimbrite eruptions (*with* Sparks, R S J) *Letter to Nature,* **310**, 679
Dudeney, J R. *See under* Rycroft, M J., **310**, 449
Dull, T J. Insulin-like growth factor II precursor gene organization in relation to insulin gene family (*with* Gray, A, Hayflick, J S, Ullrich, A) *Letter to Nature,* **310**, 777
Dumbell, K. *Book review of* Princes and peasants: Smallpox in history (*by* Hopkins, D R,) **310**, 608
Duncan, R. Editor, The encyclopaedia of medical ignorance: Exploring the frontiers of medical knowledge, *Book review by* Weatherall, D J. **310**, 257
Durham, A. *See under* Duvall, T L., **310**, 19
Duvall, T L. Rotational frequency splitting of solar oscillations (*with* Harvey, J W) *Article,* **310**, 19
Internal rotation of the Sun (*with* Dziembowski, W A, Goode, P R, Gough, D O, Harvey, J W, Leibacher, J W) *Article,* **310**, 22
Dziembowski, W A. *See under* Duvall, T L., **310**, 22
Earl, C. US nuclear waste: Widespread problem of disposal, *News,* **310**, 174
Edge, D. *Book review of* Turing's man: Western culture in the computer age (*by* Bolter, J D,) **310**, 705
Edwards, K. *See under* Shorrocks, B., **310**, 310
Edwards, R G. Parental consent over embryos (*with* Puxon, M) *Commentary,* **310**, 179
Elwood, P C. Greater contribution to blood lead from water than from air (*with* Gallacher, J E J, Phillips, K M, Davies, B E, Toothill, C) *Letter to Nature,* **310**, 138
Embleton, C. Editor, Geomorphology of Europe, *Book review by* Worsley, P. **310**, 709
English, L S. *See under* Gordon, J., **310**, 145
Erickson, R P. *See under* Kiel-Metzger, K., **310**, 579
Erlank, A J. *See under* Richardson, S H., **310**, 198
Euteneuer, U. Persistent, directional motility of cells and cytoplasmic fragments in the absence of microtubules (*with* Schliwa, M) *Letter to Nature,* **310**, 58
Evans, R V. Limits on the selfishness of DNA, *Scientific correspondence,* **310**, 456
Ewing, G W. Electroanalytical chemistry, *Book review by* Compton, R. **310**, 519
Fabian, A C. Cooling flows in clusters of galaxies (*with* Nulsen, P E J, Canizares, C R) *Review article,* **310**, 733
Fahrlander, P D. *See under* Stanton, L W., **310**, 423
Fahrner, K. *See under* Weiss, E H., **310**, 650
Falkner, F G. Correct transcription of an immunoglobulin κ gene requires an upstream fragment containing conserved sequence elements (*with* Zachau, H G) *Letter to Nature,* **310**, 71
Farrell, P J. *See under* Baer, R., **310**, 207
Fengel, D. *See under* Hut, P., **310**, 637
Feramisco, J R. *See under* Kamata, T., **310**, 147
Fillon, R H. Dynamics of meltwater discharge from Northern Hemisphere ice sheets during the last deglaciation (*with* Williams, D F) *Letter to Nature,* **310**, 674
Fink, G R. Genetics: Gene conversion in the absence of reciprocal recombination (*with* Petes, T D) *News and views,* **310**, 728
Firca, J. *See under* Hunkapiller, M., **310**, 105
Flavell, A J. Role of reverse transcription in the generation of extrachromosomal *copia* mobile genetic elements, *Letter to Nature,* **310**, 514
Flavell, R. *See under* Rosenthal, A., **310**, 415
Flavell, R A. *See under* Weiss, E H., **310**, 650
Fletcher, J O. Climatology: Clues from sea-surface records, *News and views,* **310**, 630
Flock, Å. Graded and nonlinear mechanical properties of sensory hairs in the mammalian hearing organ (*with* Strelioff, D) *Letter to Nature,* **310**, 597
Folland, C K. Worldwide marine temperature fluctuations 1856-1981 (*with* Parker, D E, Kates, F E) *Letter to Nature,* **310**, 670
Folsom, V. *See under* Gillies, S D., **310**, 594
Foster, M A. Magnetic resonance in medicine and biology, *Book review by* Andrew, E R. **310**, 803
Foti, G. Micrometre-sized polymer layers synthesized by MeV ions impinging on frozen methane (*with* Calcagno, L, Sheng, K L, Strazzulla, G) *Letter to Nature,* **310**, 126
Foulger, G. Anomalous focal mechanisms: tensile crack formation on

accreting plate boundary (*with* Long, R E) *Letter to*
*ture,*310, 43
Book review of Conceptual structures: Information process-
g in mind and machine (*by* Sowa, J F,) **310**, 437
ls, T J G. *See under* Freeman; T J., **310**, 130
ke, U. *See under* Brissenden, J E., **310**, 781
kel, R B. *See under* Mann, S., **310**, 405
ks, N P. Do general anaesthetics act by competitive binding to specific receptors? (*with* Lieb, W R) *Letter to Nature,* **310**, 599
eman, T J. Modelling radioactive waste disposal by penetrator experiments in the abyssal Atlantic Ocean (*with* Murray, C N, Francis, T J G, McPhail, S D, Schultheiss, P J) *Letter to Nature,* **310**, 130
rench, A P. *Book review of* Understanding relativity: Origin and impact of a scientific revolution (*by* Goldberg, S,) **310**, 606
Freney, J R. Editor, The global biogeochemical sulphur cycle, *Book review by* Rees, C E. **310**, 607
Friberg, P. *See under* Matthews, H E., **310**, 125
Fuks, Z. *See under* Naparstek, Y., **310**, 241
Funder, J W. *See under* Lim, A T W., **310**, 61
Fyfe, W F. The geology of nuclear waste disposal (*with* Babuska, V, Price, N J, Schmid, E, Tsang, C F, Uyeda, S, Velde, B) *Commentary,* **310**, 537
Förstel, H. Oxygen isotope ratios in plants: Reply, *Matters arising,* **310**, 166
Gage, K S. *See under* Nastrom, G D., **310**, 36
Gall, J G. Molecular genetics: Ciliates come of age, *News and views,* **310**, 453
Gall, S F. *See under* Williams, A G., **310**, 33
Gallacher, J E J. *See under* Elwood, P C., **310**, 138
Gallo, R C. *See under* Longo, D L., **310**, 505
Gardner, M. Wheels, life and other mathematical amusements, *Book review by* Singmaster, D. **310**, 521
Gascoigne, N R J. Genomic organization and sequence of T-cell receptor β-chain constant- and joining-region genes (*with* Chien, Y-h, Becker, D M, Kavaler, J, Davis, M M) *Article,* **310**, 387
Gaskell, C M. Astronomy: What triggers a quasar?, *News and views,* **310**, 102
Gati, E. *See under* Weissbuch, I., **310**, 161
Gaud, W S. Editor, A new ecology: Novel approaches to interactive systems, *Book review by* Crawley, M J. **310**, 168
Gazzaniga, M S. Editor, Handbook of cognitive neuroscience, *Book review by* Morton, J. **310**, 708
Gegonne, A. *See under* de Taisne, C., **310**, 581
Gehring, W J. *See under* Shepherd, J C W., **310**, 70
Geiger, S R. *See under* Woledge, R C., **310**, 170
Gelmann, E P. *See under* Longo, D L., **310**, 505
Gereffi, G. The pharmaceutical industry and dependency in the Third World, *Book review by* Djerassi, C. **310**, 517
Gibbs, P E. Calcium phosphate granules in muscle cells of *Nephtys* (Annelida, Polychaeta) - a novel skeleton? (*with* Bryan, G W) *Letter to Nature,* **310**, 494
Gibson, T J. *See under* Baer, R., **310**, 207
Giffin, C. *See under* Hunkapiller, M., **310**, 105
Gilbert, G N. *See under* Hunkapiller, M., **310**, 105
Gill, S J. Triple-point behaviour of human haemoglobin (*with* Richey, B) *Letter to Nature,* **310**, 160
Gillies, S D. Cell type-specific enhancer element associated with a mouse MHC gene, E_β (*with* Folsom, V, Tonegawa, S) *Letter to Nature,* **310**, 594
Gilliland, R L. Volcanic, CO_2 and solar forcing of Northern and Southern Hemisphere surface air temperatures (*with* Schneider, S H) *Letter to Nature,* **310**, 38
Gingerich, O. *Book review of* Cecilia Payne-Gaposchkin: An autobiography and other recollections (Haramundanis, K *editor*) **310**, 519
Glommi, P. *See under* Caraveo, P A., **310**, 481
Glashow, S L. *See under* Krauss, L M., **310**, 191
Glendenning, N K. Direct nuclear reactions, *Book review by* Hodgson, P E. **310**, 258
Glenn, L A. Verification limits for test-ban treaty, *Commentary,* **310**, 359
Godfrey, P D. *See under* Matthews, H E., **310**, 125
Goeddel, D V. *See under* McGrath, J P., **310**, 644
Goldberg, S. Understanding relativity: Origin and impact of a scientific revolution, *Book review by* French, A P. **310**, 606
Golden, L. *See under* Weiss, E H., **310**, 650
Goldstein, M. *See under* Mezey, E., **310**, 140
Gollahon, K A. *See under* Storb, U., **310**, 238
Gonda, T J. Expression of *myb*, *myc* and *fos* proto-oncogenes during the differentiation of a murine myeloid leukaemia (*with* Metcalf, D) *Letter to Nature,* **310**, 249
Good, I J. The impossibility of inductive probability, *Matters arising,* **310**, 434
Goodall, M C. Reform needed, *Correspondence,* **310**, 620
Goode, P R. *See under* Duvall, T L., **310**, 22
Goodman, C S. *See under* Thomas, J B., **310**, 203
Goodman, D S. Editor, The retinoids (two volumes), *Book review by* Goodwin, T W. **310**, 520
Goodwin, T W. *Book review of* The retinoids (two volumes) (Sporn, M B, Roberts, A B, Goodman, D S *editors*) **310**, 520
Gordon, J. Immortalized B lymphocytes produce B-cell growth factor (*with* Ley, S C, Melamed, M D, English, L S, Hughes-Jones, N C) *Letter to Nature,* **310**, 145
See under Tranchina, D., **310**, 314
Gorski, J. *See under* Long, E O., **310**, 233
Goto, M. *See under* Kijima, T., **310**, 45
Gough, D O. *See under* Duvall, T L., **310**, 22
Graham, J R. NGC3256: an emerging elliptical galaxy (*with* Wright, G S, Meikle, W P S, Bode, M F) *Letter to Nature,* **310**, 213
Grant, N K. *Book review of* The geochronology and evolution of Africa (*by* Cahen, L, Snelling, N J, Delhal, J, Vail, J R,) **310**, 78
Gratzer, W. Cell biology: More red than dead, *News and views,* **310**, 368
Gray, A. *See under* Dull, T J., **310**, 777
Greengard, P. *See under* Hemmings, H C., **310**, 503
Gregg, M C. *See under* Shay, T J., **310**, 282
Gregoriadis, G. Drug delivery: Old drugs in new clothing, *News and views,* **310**, 186
Grieve, R A F. Cretaceous-Tertiary extinctions: Physical evidence of impact, *News and views,* **310**, 370
Griffin, J. Homer's sea, *Correspondence,* **310**, 95
Griffin, R & R. Mt Wilson 100-inch telescope, *Correspondence,* **310**, 536
Grindlay, J E. *See under* Molnar, L A., **310**, 662
Gronenborn, B. *See under* Brisson, N., **310**, 511
Grosse-Wilde, H. *See under* Hohlfeld, R., **310**, 244
Grosveld, F. *See under* Rosenthal, A., **310**, 415
Grunberger, D. Molecular biology of mutagens and carcinogens, *Book review by* Venitt, S. **310**, 520
Grätzel, M. *See under* Warman, J M., **310**, 305
Guennoc, P. *See under* Pautot, G., **310**, 133
Gurney, J J. *See under* Richardson, S H., **310**, 198
Hall, G S. *See under* Hut, P., **310**, 637
Hallam, A. *Book review of* Catastrophes and Earth history: The new uniformitarianism (Berggren, W A, Van Couvering, J A *editors*) **310**, 435
Handa, T. *See under* Sofue, Y., **310**, 568
Hanke, D. Plant development: Antibodies to the rescue, *News and views,* **310**, 272
Hanson, G N. *See under* Shirey, S B., **310**, 222
Haramundanis, K. Editor, Cecilia Payne-Gaposchkin: An autobiography and other recollections, *Book review by* Gingerich, O. **310**, 519
Harris, J W. *See under* Richardson, S H., **310**, 198
Harrison, C. Holocene penguin extinction, *News and views,* **310**, 545
Harvey, J W. *See under* Duvall, T L., **310**, 19
See under Duvall, T L., **310**, 22
Hatfull, G. *See under* Baer, R., **310**, 207
Hawkesworth, C. *See under* Rogers, N., **310**, 187
Hawksworth, D L. Fungi in culture, *Scientific correspondence,* **310**, 18
Hay, A. *Book review of* Workers at risk: Voices from the workplace (*by* Nelkin, D, Brown, M S,) **310**, 80
Hay, W W. *See under* Barron, E J., **310**, 574
Hayashi, K. Basically musical (*with* Munakata, N) *Correspondence,* **310**, 96
See under Makino, R., **310**, 697
Hayes, J M. *Book review of* Microbial geochemistry (Krumbein, W E *editor*) **310**, 709
Hayflick, J S. *See under* Dull, T J., **310**, 777
Hayton, A F. Of plants and men, *Correspondence,* **310**, 178
Hedenquist, J W. Adiabatic boiling and ocean metal transport, *Scientific correspondence,* **310**, 636
Heiligman, G M. *See under* Claussen, M J., **310**, 298
Heininger, K. *See under* Hohlfeld, R., **310**, 244
Hemmings, H C. DARPP-32, a dopamine-regulated neuronal phosphoprotein, is a potent inhibitor of protein phosphatase-1 (*with* Greengard, P, Tung, H Y L, Cohen, P) *Letter to Nature,* **310**, 503
Hendry, J. Editor, Cambridge physics in the thirties, *Book review by* Pease, R S. **310**, 803
Herbert, E. *See under* Martens, G J M., **310**, 251
Herrera-Estrella, L. Light-inducible and chloroplast-associated expression of a chimaeric gene introduced into *Nicotiana tabacum* using a Ti plasmid vector (*with* Van den Broeck, G, Maenhaut, R, Van Montagu, M, Schell, J, Timko, M, Cashmore, A) *Article,* **310**, 115
Herscovitch, P. *See under* Reiman, E M., **310**, 683
Hester, L D. *See under* Lo, M M S., **310**, 792
Heyworth, M F. Basso continuo, *Correspondence,* **310**, 536
Hickmott, W. A weighty problem cracked, *Scientific correspondence,* **310**, 731
Hildebrand, B M. *See under* Yang, T P., **310**, 412
Hill, S M. *See under* Hulten, M., **310**, 456
Hirose, T. *See under* Nakayama, K., **310**, 699
Hochachka, P W. Biochemical adaptation, *Book review by* Cornish-Bowden, A. **310**, 804
Hodges, R. Archaeology: Diet in the Dark Ages, *News and views,* **310**, 726
Hodgson, P E. *Book review of* Direct nuclear reactions (*by* Satchler, G R,) **310**, 258
Book review of Direct nuclear reactions (*by* Glendenning, N K,) **310**, 258
Hoeijmakers, J H J. *See under* Westerveld, A., **310**, 425
Hogan, C. Cosmology: Cosmic strings and galaxies, *News and views,* **310**, 365
Hohlfeld, R. Autoimmune human T lymphocytes specific for acetylcholine receptor (*with* Toyka, K V, Heininger, K, Grosse-Wilde, H, Kalies, I) *Letter to Nature,* **310**, 244
Hohn, T. *See under* Brisson, N., **310**, 511
Hood, L. *See under* Hunkapiller, M., **310**, 105
Hook, R N. *See under* Phillips, M M., **310**, 554
Hopkins, D. *See under* Sejrup, H P., **310**, 772
Hopkins, D R. Princes and peasants: Smallpox in history, *Book review by* Dumbell, K. **310**, 608
Hornberg, C. High-affinity binding sites for abscisic acid on the plasmalemma of *Vicia faba* guard cells (*with* Weiler, E W) *Letter to Nature,* **310**, 321
Horvath, S. *See under* Hunkapiller, M., **310**, 105
Hoshino, H. Human T-cell leukaemia virus is not lysed by human serum (*with* Tanaka, H, Miwa, M, Okada, H) *Letter to Nature,* **310**, 324
Houamed, K M. Expression of functional GABA, glycine and glutamate receptors in *Xenopus* oocytes injected with rat brain mRNA (*with* Bilbe, G, Smart, T G, Constanti, A, Brown, D A, Barnard, E A, Richards, B M) *Letter to Nature,* **310**, 318
Hoult, D I. *See under* Silver, M S., **310**, 681
Howes, B I. *See under* Wakeham, S G., **310**, 770
Howgate, M. *Archaeopteryx*'s morphology, *Scientific correspondence,* **310**, 104
Hubbert, N L. *See under* Willumsen, B M., **310**, 583
Hudson, G S. *See under* Baer, R., **310**, 207
Huffman, C J. *See under* Raff, R A., **310**, 312
Hughes, D W. *See under* Tabor, M., **310**, 277
Hughes-Jones, N C. *See under* Gordon, J., **310**, 145
Hulten, M. Somatic gene mutation and breast carcinoma (with Rodgers, C S, Hill, S M), *Scientific correspondence,* **310**, 103; Correction, **310**, 456
Hunkapiller, M. A microchemical facility for the analysis and synthesis of genes and proteins (*with* Kent, S, Caruthers, M, Dreyer, W, Firca, J, Giffin, C, Horvath, S, Hunkapiller, T, Tempst, P, Hood, L) *Review article,* **310**, 105
Hunkapiller, T. *See under* Hunkapiller, M., **310**, 105
Hut, P. Can a neutrino-dominated Universe be rejected? (*with* White, S D M) *Review article,* **310**, 637
Hutson, V. *See under* Law, R., **310**, 104
Iagolnitzer, D. Wigner's phase-space density function, *Scientific correspondence,* **310**, 635
Inayama, S. *See under* Nakayama, K., **310**, 699
Infelta, P P. *See under* Warman, J M., **310**, 305
Inouye, S. Sequence-specific insertion of the *Drosophila* transposable genetic element *17.6* (*with* Yuki, S, Saigo, K) *Letter to Nature,* **310**, 332
Iosson, M. Peer revue, *Correspondence,* **310**, 96
Irvine, S J C. Semiconductor processing technology New prospects offered by photolytic deposition, *News and views,* **310**, 452
Irvine, W M. *See under* Matthews, H E., **310**, 125
Irving, E. Evidence against large-scale Carboniferous strike-slip faulting in the Appalachian-Caledonian orogen (*with* Strong, D F) *Letter to Nature,* **310**, 762
Isdale, P. Fluorescent bands in massive corals record centuries of coastal rainfall, *Letter to Nature,* **310**, 578
Ivanov, M V. Editor, The global biogeochemical sulphur cycle, *Book review by* Rees, C E. **310**, 607
Jackson, L G. *See under* Yang, T P., **310**, 412
Jacobs, J A. Reversals of the Earth's magnetic field, *Book review by* Tarling, D H. **310**, 436
Jaffe, L A. *See under* Turner, P R., **310**, 414
Jankovic, G M. The meaning of homology, *Scientific correspondence,* **310**, 635
Janouch, F. More visa trouble, *Correspondence,* **310**, 268
Jasperson, W H. *See under* Nastrom, G D., **310**, 36
Jay, M F. Erratum: Auditory receptive fields in primate superior colliculus shift with changes in eye position (*with* Sparks, D I) *Letter to Nature,* **310**, 340
Jedwab, J. Graphite crystals in hydrothermal vents (*with* Boulègue, J) *Letter to Nature,* **310**, 41
Jeffrey, R C. The impossibility of inductive probability, *Matters arising,* **310**, 433
Jenkins, J S. *See under* Nussey, S S., **310**, 64
Jenkinson, E J. *See under* Ready, A R., **310**, 231
Johnston, C I. *See under* Lim, A T W., **310**, 61
Jones, D. *See under* Rycroft, M J., **310**, 449
Joseph, R I. *See under* Silver, M S., **310**, 681
Joyce, G F. Chiral selection in poly(C)-directed synthesis of oligo(G) (*with* Visser, G M, van Boeckel, C A A, van Boom, J H, Orgel, L E, van Westrenen, J) *Letter to Nature,* **310**, 602
Jukes, T H. Alignment of base sequences, *Scientific correspondence,* **310**, 636
Kachi, T. *See under* Dick, J P R., **310**, 407
Kaiser, M L. *See under* Desch, M D., **310**, 755
Kaiser, N. Microwave anisotropy due to cosmic strings (*with* Stebbins, A) *Letter to Nature,* **310**, 391
Kalies, I. *See under* Hohlfeld, R., **310**, 244
Kamata, T. Epidermal growth factor stimulates guanine nucleotide binding activity and phosphorylation of *ras* oncogene proteins (*with* Feramisco, J R) *Letter to Nature,* **310**, 147
Kamin, L J. Not in our genes: Biology, ideology, and human nature, *Book review by* Medawar, P B. **310**, 255
Kamps, M P. Direct evidence that oncogenic tyrosine kinases and cyclic AMP-dependent protein kinase have homologous ATP-binding sites (*with* Taylor, S S, Sefton, B M) *Letter to Nature,* **310**, 589
Kates, F E. *See under* Folland, C K., **310**, 670
Katz, L C. Fluorescent latex microspheres, as a retrograde neuronal marker for *in vivo* and *in vitro* studies of visual cortex (*with* Burkhalter, A, Dreyer, W J) *Letter to Nature,* **310**, 498
Kavaler, J. *See under* Gascoigne, N R J., **310**, y387
Localization of a T-cell receptor diversity-region element (*with* Davis, M M, Chien, Y-h) *Letter to Nature,* **310**, 421
Kazazian, H H. Quantification of the close association between DNA haplotypes and specific β-thalassaemia mutations in Mediterraneans (*with* Orkin, S H, Markham, A F, Chapman, C R, Youssoufian, H, Waber, P G) *Letter to Nature,* **310**, 152
Keele, K D. Leonardo da Vinci's elements of the science of man, *Book review by* Kemp, M. **310**, 605
Keeley, J E. *Stylites*, a vascular land plant without stomata absorbs CO_2 via its roots (*with* Osmond, C B, Raven J A) *Letter to Nature,* **310**, 694
Keller, S E. *See under* Schleifer, S J., **310**, 456
Kelly, K. *See under* Armelin, H A., **310**, 655
Kemp, D J. *See under* Coppel, R L., **310**, 789
Kemp, D V. *See under* Spera, F J., **310**, 764

Kemp, M. *Book review of* Leonardo da Vinci's elements of the science of man (*by* Keele, K D,) **310**, 605
Kennedy, H E. Abstract policy, *Correspondence,* **310**, 96
Kent, D V. *See under* Clement, B M., **310**, 488
Kent, S. *See under* Hunkapiller, M., **310**, 105
Keynes, R J. Segmentation in the vertebrate nervous system (*with* Stern, C D) *Letter to Nature,* **310**, 786
Khachaturyan, A G. Theory of structural transformations in solids, *Book review by* Cowley, R A. **310**, 606
Kiek, S N. Earthquake prediction from *b*-values, *Scientific correspondence,* **310**, 456
Kiel-Metzger, K. Regional localization of sex-specific Bkm-related sequences on proximal chromosome 17 of mice (*with* Erickson, R P) *Letter to Nature,* **310**, 579
Kijima, T. A complex of copper (II)-montmorillonite with a modified cyclodextrin (*with* Tanaka, J, Goto, M, Matsui, Y) *Letter to Nature,* **310**, 45
Kilmister, C W. *Book review of* Number theory: An approach through history from Hammurapi to Legendre (*by* Weil, A,) **310**, 168
King-Hele, D G. Geopotential harmonics of orders 15 and 30 (*with* Walker, D M C) *Letter to Nature,* **310**, 218
Kingston, R. *See under* Ready, A R., **310**, 231
Kiss, J Z. *See under* Mezey, E., **310**, 140
Kitcher, P. *Book review of* Science and Creationism (Montagu, A *editor*) **310**, 167
Klar, A J S. Resolution of recombination intermediates generated during yeast mating type switching (*with* Strathern, J N) *Article,* **310**, 744
Kleibrink, H. De Leidse Sterrewacht: Vier eeuwen wacht bij dag en bij nacht, *Book review by* Bosma, P B. **310**, 169
Klein, H L. Lack of association between intrachromosomal gene conversion and reciprocal exchange, *Article,* **310**, 748
Kneller, B C. *See under* Ashcroft, W A., **310**, 760
Kohshima, S. A novel cold-tolerant insect found in a Himalayan glacier, *Letter to Nature,* **310**, 225
Kosslyn, S M. Ghosts in the mind's machine: Creating and using images in the brain, *Book review by* Sutherland, S. **310**, 344
Krauss, L M. Antineutrino astronomy and geophysics (*with* Glashow, S L, Schramm, D N) *Review article,* **310**, 191
Krieger, D T. Editor, Brain peptides, *Book review by* Phillips, M I. **310**, 256
Krumbein, W E. Editor, Microbial geochemistry, *Book review by* Hayes, J M. **310**, 709
Kung, H-F. *See under* Stacey, D W., **310**, 508
Kyte, F T. *See under* Smit, J., **310**, 403
Lachman, H M. Expression of c-*myc* changes during differentiation of mouse erythroleukaemia cells (*with* Skoultchi, A I) *Letter to Nature,* **310**, 592
Lagravère, C. Ring-opened alkylated guanine is not repaired in Z-DNA (*with* Malfoy, B, Leng, M, Laval, J) *Letter to Nature,* **310**, 798
Lahav, M. *See under* Weissbuch, I., **310**, 161
Lambrick, G H. *See under* Robinson, M A., **310**, 340
Langley, C H. *See under* Brookfield, J F Y., **310**, 330
Lasek, R J. *See under* Brady, S T., **310**, 56
Laughon, A. Sequence of a *Drosophila* segmentation gene: protein structure homology with DNA-binding proteins (*with* Scott, M P) *Article,* **310**, 25
Laurberg, S. *See under* Sunde, N., **310**, 51
Lautridou, J P. *See under* Wintle, A G., **310**, 491
Laval, J. *See under* Lagravère, C., **310**, 798
Law, R. Mutualism disagreement (*with* Hutson, V, Lewis, D H) *Scientific correspondence,* **310**, 104
Lawton, J H. Insects on plants: Community patterns and mechanisms, *Book review by* Wratten, S D. **310**, 343
Leaf, D S. *See under* Raff, R A., **310**, 312
Leder, P. *See under* Armelin, H A., **310**, 655
Leibacher, J W. *See under* Duvall, T L., **310**, 22
Leiserowitz, L. *See under* Weissbuch, I., **310**, 161
Lemen, J R. *See under* Sylwester, J., **310**, 665
Leming, T D. Zones of coastal hypoxia revealed by satellite scanning have implications for strategic fishing (*with* Stuntz, W E) *Letter to Nature,* **310**, 136
Lemischka, I R. *See under* Williams, D A., **310**, 476
Leng, M. *See under* Lagravère, C., **310**, 798
Leslie, A G. *See under* Ashcroft, W A., **310**, 760
Lester, H A. *See under* Nerbonne, J M., **310**, 74
Levi, I. The impossibility of inductive probability, *Matters arising,* **310**, 433
Levinson, A D. *See under* McGrath, J P., **310**, 644
Lew, D P. *See under* Di Virgilio, F., **310**, 691
Lewis, D H. *See under* Law, R., **310**, 104
Lewis, J. Developmental biology: On to the vertebrates, *News and views,* **310**, 724
Lewontin, R C. Not in our genes: Biology, ideology, and human nature, *Book review by* Medawar, P B. **310**, 255
Ley, S C. *See under* Gordon, J., **310**, 145
Liang, E P. Magnetic flare model of γ-ray bursts (*with* Antiochos, S K) *Letter to Nature,* **310**, 121
Liau, G. *See under* Yamada, Y., **310**, 333
Lieb, W R. *See under* Franks, N P., **310**, 599
Lim, A T W. Immunoreactive arginine-vasopressin in Brattleboro rat ovary (*with* Lolait, S J, Barlow, J W, Autelitano, D J, Toh, B H, Boublik, J, Abraham, J, Johnston, C I, Funder, J W) *Letter to Nature,* **310**, 61
Lingelbach, K R. *See under* Coppel, R L., **310**, 789
Little, P F R. Sequencing techniques: A close look at the genome, *News and views,* **310**, 369
Lo, K Y. *See under* Claussen, M J., **310**, 298
Lo, M M S. Monoclonal antibody production by highly specific electric field-induced cell fusion (*with* Tsong, T Y, Conrad, M K, Strittmatter, S M, Hester, L D, Snyder, S H) *Letter to Nature,* **310**, 792
Lodish, H F. *See under* Chisholm, R L., **310**, 67
Lolait, S J. *See under* Lim, A T W., **310**, 61
Londer, R. The coevolution of climate and life, *Book review by* Wigley, T M L. **310**, 517
Long, E O. Structural relationship of the SB β-chain gene to *HLA-D*-region genes and murine *I*-region genes (*with* Gorski, J, Mach, B) *Letter to Nature,* **310**, 233
Long, J. *See under* Tümer, O T., **310**, 214
Long, R E. *See under* Foulger, G., **310**, 43
Longair, M S. Astronomy: Galaxy evolution at late epochs, *News and views,* **310**, 13
Longo, D L. Isolation of HTLV-transformed B-lymphocyte clone from a patient with HTLV-associated adult T-cell leukaemia (*with* Gelmann, E P, Cossman, J, Young, R A, Gallo, R C, O'Brien, S J, Matis, L A) *Letter to Nature,* **310**, 505
Lonsdale, D M. *See under* Schardl, C L., **310**, 292
Loo, J-H. *See under* Raff, R A., **310**, 312
Lovell-Badge, R H. *See under* Mann, J R., **310**, 66
Lovlie, R. *See under* Sejrup, H P., **310**, 772
Lowry, D. Nuclear proliferation, *Correspondence,* **310**, 95
Lowy, D R. *See under* Willumsen, B M., **310**, 583
Lux, H D. *See under* Carbone, E., **310**, 501
Lyberis, N. *See under* Pautot, G., **310**, 133
Lynch, J M. *See under* Veal, D A., **310**, 695
Lyne, A G. Orbital inclination and mass of the binary Pulsar PSR0655+64, *Letter to Nature,* **310**, 300
Mach, B. *See under* Long, E O., **310**, 233
Mackintosh, A J. PhD glut in Japan, *Correspondence,* **310**, 619
Mackintosh, N J. Conditioning and associative learning, *Book review by* Shettleworth, S J. **310**, 801
Maddox, J. Patterns of developing embryos, *News and views,* **310**, 9
  UK electronics: Sleeping giant waking up?, *News,* **310**, 91
  UK agriculture: Shake-up for research, *News,* **310**, 93
  CERN comes out again on top, *News and views,* **310**, 97
  Immunology made accessible, *News and views,* **310**, 183
  US election: From frying-pan to Senate?, *News,* **310**, 356
  Relativity's most elaborate test, *News and views,* **310**, 363
  Whale-watching: Conservation goes commercial, *News,* **310**, 445
  Where cosmic rays come from?, *News and views,* **310**, 447
  Academic tenure: British rights to go, *News,* **310**, 530
  Malaria vaccine in sight?, *News and views,* **310**, 541
  Hunting for the missing mass, *News and views,* **310**, 627
  Continuing doubt on gravitation, *News and views,* **310**, 723
Maenhaut, R. *See under* Herrera-Estrella, L., **310**, 115
Mak, T W. *See under* Yoshikai, Y., **310**, 506
Makino, R. c-*myc* transcript is induced in rat liver at a very early stage of regeneration or by cycloheximide treatment (*with* Hayashi, K, Sugimura, T) *Letter to Nature,* **310**, 697
Malfoy, B. *See under* Lagravère, C., **310**, 798
Manchester, R N. Search for pulsed optical emission from the millisecond pulsar PSR1937+214 (*with* Peterson, B A, Wallace, P T) *Letter to Nature,* **310**, 569
Manjrekar, J. Policy on heritability of IQ, *Correspondence,* **310**, 268
Mann, J R. Inviability of parthenogenones is determined by pronuclei, not egg cytoplasm (*with* Lovell-Badge, R H) *Letter to Nature,* **310**, 66
Mann, S. Structure, morphology and crystal growth of bacterial magnetite (*with* Frankel, R B, Blakemore, R P) *Letter to Nature,* **310**, 405
Mansfield, D A. *See under* Palmer, T N., **310**, 483
Marcu, K B. *See under* Stanton, L W., **310**, 423
Markham, A F. *See under* Kazazian, H H., **310**, 152
Marsden, C D. *See under* Dick, J P R., **310**, 407
Marshall, C. Cancer: Functions of *ras* oncogenes, *News and views,* **310**, 448
Marshall, C J. Activation of c-Ha-*ras*-1 proto-oncogene by *in vitro* modification with a chemical carcinogen, benzo(*a*)pyrene diol-epoxide (*with* Vousden, K H, Phillips, D H) *Letter to Nature,* **310**, 586
Marshall, J H. Miracles, *Correspondence,* **310**, 722
Martens, G J M. Polymorphism and absence of Leu-enkephalin sequences in proenkephalin genes in *Xenopus laevis* (*with* Herbert, E) *Letter to Nature,* **310**, 251
Martin, J B. Editor, Brain peptides, *Book review by* Phillips, M I. **310**, 256
Martin, R D. *Book review of* Five new world primates: A study in comparative ecology (*by* Terborgh, J,) **310**, 707
Mason, S. Origins of life: Bounds to the amplification of biomolecular handedness, *News and views,* **310**, 546
Mathez, E A. Influence of degassing on oxidation states of basaltic magmas, *Review article,* **310**, 371
Matis, L A. *See under* Longo, D L., **310**, 505
Matsui, Y. *See under* Kijima, T., **310**, 45
Matthews, H E. A new interstellar molecule: tricarbon monoxide (*with* Irvine, W M, Friberg, P, Brown, R D, Godfrey, P D) *Letter to Nature,* **310**, 125
Matthews, K S. *See under* Sams, C F., **310**, 429
Max, E E. Molecular biology: New twist to DNA methylation, *News and views,* **310**, 100
May, R M. Ecology: Oceanic noise and fish stocks, *News and views,* **310**, 190
McConnell, H M. *See under* Weis, R M., **310**, 47
McElhinny, M W. The Earth's magnetic field, *Book review by* Tarling, D H. **310**, 436
McGinnis, W. *See under* Shepherd, J C W., **310**, 70
McGrath, J P. Comparative biochemical properties of normal and activated human *ras* p21 protein (*with* Capon, D J, Goeddel, D V, Levinson, A D) *Article,* **310**, 644
McMullen, M D. *See under* Storb, U., **310**, 238
McPhail, S D. *See under* Freeman, T J., **310**, 130
McQuay, H J. *See under* Pybus, A., **310**, 636
Medawar, P B. *Book review of* Not in our genes: Biology, id and human nature (*by* Lewontin, R C, Rose, S, Kamin, L J, 255
Medvedev, Z A. East-West relations, *Correspondence,* **310**, 7
Mehendale, H M. Science in India discussed, *Correspondenc* 8
Meikle, W P S. *See under* Graham, J R., **310**, 213
Melamed, M D. *See under* Gordon, J., **310**, 145
Mellor, A L. *See under* Weiss, E H., **310**, 650
Mereghetti, S. *See under* Caraveo, P A., **310**, 481
Merriam, R W. *See under* Christensen, K., **310**, 150
Merrill, R T. The Earth's magnetic field, *Book review by* Tarling, H. **310**, 436
Merryweather, J P. *See under* Bell, G I., **310**, 775
Metcalf, D. *See under* Gonda, T J., **310**, 249
Mewe, R. *See under* Sylwester, J., **310**, 665
Meyers, N. Israeli innovation: Biggest science park so far, *News,* **310**, 7
  Israeli universities: Faculty forced into salary cut, *News,* **310**, 176
Mezey, E. Increase of corticotropin-releaasing factor staining in rat paraventricular nucleus neurones by depletion of hypothalamic adrenaline (*with* Kiss, J Z, Skirboll, L R, Goldstein, M, Axelrod, J) *Letter to Nature,* **310**, 140
Michie, C A. The rotation of birds' eggs, *Scientific correspondence,* **310**, 635
Milani, A. Resonance locking between Jupiter and Uranus (*with* Nobili, A M) *Letter to Nature,* **310**, 753
Miller, D. *See under* Popper, K., **310**, 434
Miller, G H. *See under* Sejrup, H P., **310**, 772
Milligan, P R. *See under* White, A., **310**, 219
Milner, J. Different forms of p53 detected by monoclonal antibodies in non-dividing and dividing lymphocytes, *Letter to Nature,* **310**, 143
Mishima, O. 'Melting ice' I at 77 K and 10 kbar: a new method making amorphous solids (*with* Calvert, L D, Whalley, E) *Letter to Nature,* **310**, 393
Mitelman, F. Restricted number of chromosomal regions implicated in aetiology of human cancer and leukaemia, *Letter to Nature,* **310**, 325
Mittal, C K. Science in India discussed, *Correspondence,* **310**, 8
Miwa, M. *See under* Hoshino, H., **310**, 324
Mollison, D. Simplifying simple epidemic models, *Letter to Nature,* **310**, 224
Molnar, L A. Low-level radio flares from Cygnus X-3 (*with* Reid, M J, Grindlay, J E) *Letter to Nature,* **310**, 662
Montagnier, L. AIDS priority, *Correspondence,* **310**, 446
Montagu, A. Editor, Science and Creationism, *Book review by* Kitcher, P. **310**, 167
Montgomery, E. *See under* Brookfield, J F Y., **310**, 330
Moore, P D. Ecology: Rise and fall of palsa mounds, *News and views,* **310**, 188
  Book review of The European garden flora. Vol. II Monocotyledons (Part II) (Walters, S M, *et al. editor*) **310**, 344
  Photosynthesis: Novel carbon supply on land, *News and views,* **310**, 633
Moore, R A. *See under* Pybus, A., **310**, 636
Morabito, M. *See under* Chu, M-L., **310**, 337
Moran, J. Astronomy: Masers in the nuclei of galaxies, *News and views,* **310**, 270
Morel, C M. Editor, Genes and antigens of parasites: A laboratory manual, 2nd edn, *Book review by* Cox, F E G. **310**, 608
Morris, M. *See under* Yusef-Zadeh, F., **310**, 557
Morton, J. *Book review of* Handbook of cognitive neuroscience (Gazzaniga, M S *editor*) **310**, 708
Mudryj, M. *See under* Yamada, Y., **310**, 333
Mulkay, M. *See under* Hunkapiller, M., **310**, 105
Mulligan, R C. *See under* Williams, D A., **310**, 476
Munakata, N. *See under* Hayashi, K., **310**, 96
Munro, M. *See under* Ashcroft, W A., **310**, 760
Murphy, D. *See under* Brickell, P M., **310**, 178
Murray, C N. *See under* Freeman, T J., **310**, 130
Myers, J. *See under* Chu, M-L., **310**, 337
Nakanishi, S. *See under* Nakayama, K., **310**, 699
Nakayama, K. mRNA sequence for human cardiodilatin-atrial natriuretic factor precursor and regulation of precursor mRNA in rat atria (*with* Ohkubo, H, Hirose, T, Inayama, S, Nakanishi, S) *Letter to Nature,* **310**, 699
Naparstek, Y. Activated T lymphocytes produce a matrix-degrading heparan sulphate endoglycosidase (*with* Cohen, I R, Fuks, Z, Vlodavsky, I) *Letter to Nature,* **310**, 241
Narayan, R. Multiple imaging of quasars by galaxies and clusters (*with* Blandford, R, Nityananda, R) *Article,* **310**, 112
Nargeot, J. *See under* Nerbonne, J M., **310**, 74
Nastrom, G D. Kinetic energy spectrum of large- and mesoscale atmospheric processes (*with* Gage, K S, Jasperson, W H) *Letter to Nature,* **310**, 36
Nathan, D G. *See under* Williams, D A., **310**, 476
Nelkin, D. Workers at risk: Voices from the workplace, *Book review by* Hay, A. **310**, 80
Nerbonne, J M. New photoactivatabale cyclic nucleotides produce intracellular jumps in cyclic AMP and cyclic GMP concentrations (*with* Richard, S, Nargeot, J, Lester, H A) *Letter to Nature,* **310**, 74
Newbold, R. Cancer: Mutant *ras* proteins and cell transformation, *News and views,* **310**, 628
Niessing, J. *See under* Antoine, M., **310**, 795
Nityananda, R. *See under* Narayan, R., **310**, 112
Nobili, A M. *See under* Milani, A., **310**, 753

AUTHOR INDEX

an , J L. A single gene error of noradrenergic axon growth synchronizes central neurones, *Letter to Nature,* **310,** 409
t, J G. Aegean celebration, *News and views,* **310,** 9
in, Y. Excess ^{227}Ac in deep ocean water, *Letter to Nature,* **310,** [illegible]6
nen, P E J. *See under* Fabian, A C., **310,** 733
an', S S. Brattleboro rat adrenal contains vasopressin (*with* Ang, T Y, Jenkins, J S, Chowdrey, H S, Bisset, G W) *Letter to Nature,* **310,** 64
en, R L. *See under* Storb, U., **310,** 238
den, S J. *See under* Longo, D L., **310,** 505
eill, T. *See under* Tümer, O T., **310,** 214
ici, S. *See under* Yamada, Y., **310,** 333
dijk, H. *See under* Westerveld, A., **310,** 425
Odum, H T. Systems ecology: An introduction, *Book review by* Wiegeret, R G. **310,** 706
Oemler, A. *See under* Butcher, H R., **310,** 31
Ohkubo, H. *See under* Nakayama, K., **310,** 699
Okada, H. *See under* Hoshino, H., **310,** 324
Okun, L M. *See under* Yoshikami, D., **310,** 53
Olivero, J J. *See under* Bohren, C F., **310,** 216
Orgel, L E. *See under* Joyce, G F., **310,** 602
Orkin, S H. *See under* Kazazian, H H., **310,** 152
Ortolani, S. *See under* Cosmovici, C B., **310,** 122
Osmond, C B. *See under* Keeley, J E., **310,** 694
Owen, J J T. *See under* Ready, A R., **310,** 231
Owicki, J C. *See under* Braun, J., **310,** 316
Palmer, T N. Response of two atmospheric general circulation models to sea-surface temperature anomalies in the tropical East and West Pacific (*with* Mansfield, D A) *Letter to Nature,* **310,** 483
Papageorge, A G. *See under* Willumsen, B M., **310,** 583
Parker, D E. *See under* Folland, C K., **310,** 670
Parker, F S. Applications of infrared, Raman, and resonance Raman spectroscopy in biochemistry, *Book review by* Tsuboi, M. **310,** 345
Parr, R. Oxygen isotope ratios in plants, *Matters arising,* **310,** 166
Pastink, A. *See under* Westerveld, A., **310,** 425
Pastore, N. Canary before the pigeon, *Scientific correspondence,* **310,** 18
Paszkowski, J. *See under* Brisson, N., **310,** 511
Patel, P I. *See under* Yang, T P., **310,** 412
Paul, G S. The hand of *Archaeopteryx*, *Scientific correspondence,* **310,** 732
Paul, J A. *See under* Bignami, G F., **310,** 464
  See under Caraveo, P A., **310,** 481
Pautot, G. Discovery of a large brine deep in the northern Red Sea (*with* Guennoc, P, Coutelle, A, Lyberis, N) *Letter to Nature,* **310,** 133
Payne, A I. Tropical malaise, *Correspondence,* **310,** 358
Peachey, L D. *See under* Woledge, R C., **310,** 170
Pearson, R. *See under* Laughon, A., **310,** 25
  Is all science vocational?, *Employment,* **310,** 260
Pease, R S. *Book review of* Cambridge physics in the thirties (Hendry, J *editor*) **310,** 803
Peczkis, J. Nuclear war - counting the cost, *Scientific correspondence,* **310,** 455
Penrose, O. *Book review of* Order out of chaos: Man's new dialogue with nature (*by* Prigogine, I, Stengers, I,) **310,** 341
Penswick, J R. *See under* Brisson, N., **310,** 511
Perron, C. Relativistic ^{238}U ion tracks in olivine and cosmic-ray track studies, *Letter to Nature,* **310,** 397
Perry, R P. Gene regulation: What controls the transcription of immunoglobulin genes?, *News and views,* **310,** 14
Peterson, B A. *See under* Manchester, R N., **310,** 569
Petes, T D. *See under* Walmsley, R M., **310,** 157
  See under Fink, G R., **310,** 728
Pettersen, R C. Oil-shale petroporphyrin, *Scientific correspondence,* **310,** 18
Phillips, D H. *See under* Marshall, C J., **310,** 586
Phillips, K M. *See under* Elwood, P C., **310,** 138
Phillips, M I. *Book review of* Brain peptides (Krieger, D T, Brownstein, M J, Martin, J B *editors*) **310,** 256
Phillips, M M. Broad-line high-excitation gas in the elliptical galaxy NGC5128 (*with* Taylor, K, Axon, D J, Atherton, P D, Hook, R N) *Article,* **310,** 554
Piccoli, S P. A conserved sequence at c-*myc* oncogene chromosomal translocation breakpoints in plasmacytomas (*with* Caimi, P G, Cole, M D) *Letter to Nature,* **310,** 327
Piper, J G. A high rate of self-fertilization and increased seed fertility of homostyle primroses (*with* Charlesworth, B, Charlesworth, D) *Letter to Nature,* **310,** 50
Pisias, N G. Modelling the global climate response to orbital forcing and atmospheric carbon dioxide changes (*with* Shackleton, N J) *Letter to Nature,* **310,** 757
Popper, K. The impossibility of inductive probability: Reply (*with* Miller, D) *Matters arising,* **310,** 434
Porter, R. *Book review of* The history of physics (*by* Asimov, I,) **310,** 708
Potrykus, I. *See under* Brisson, N., **310,** 511
Pozzan, T. *See under* Di Virgilio, F., **310,** 691
Price, D. European Community: No decisions on research, *News,* **310,** 4
  European Community: Davignon quits as commissioner, *News,* **310,** 441
  Computers: IBM in Europe, *News,* **310,** 443
Price, G D. Mineralogy: The riches of silica revealed, *News and views,* **310,** 631
Price, N J. *See under* Fyfe, W F., **310,** 537
Price, P W. Editor, A new ecology: Novel approaches to interactive systems, *Book review by* Crawley, M J. **310,** 168
Priestley, L. *See under* Bell, G I., **310,** 775
Prigogine, I. Order out of chaos: Man's new dialogue with nature, *Book review by* Penrose, O. **310,** 341
Pring, D R. *See under* Schardl, C L., **310,** 292
Protheroe, R J. Clues from the photonuclear time scale on the nature of particle accelerators in Cygnus X-3 and Vela X-1, *Letter to Nature,* **310,** 296
Prusiner, S B. *See under* Bendheim, P E., **310,** 418
Puigdoménech, P. Biotechnology centres: Spanish self-consolation, *News,* **310,** 529
Pulbrook, M. Black as grapes, *Correspondence,* **310,** 95
Puxon, M. *See under* Edwards, R G., **310,** 179
Pybus, A. Opiates and sexual function (*with* Torda, T, McQuay, H J, Moore, R A) *Scientific correspondence,* **310,** 636
Quiocho, F A. Novel stereospecificity of the L-arabinose-binding protein (*with* Vyas, N K) *Article,* **310,** 381
  See under Sams, C F., **310,** 429
Rabson, A. *See under* Shearer, G M., **310,** 103
Raff, R A. Origin of a gene regulatory mechanism in the evolution of echinoderms (*with* Anstrom, J A, Huffman, C J, Leaf, D S, Loo, J-H, Showman, R M, Wells, D E) *Letter to Nature,* **310,** 312
Raichle, M E. *See under* Reiman, E M., **310,** 683
Rall, L B. *See under* Bell, G I., **310,** 775
  See under Tricoli, J V., **310,** 784
Ramirez, F. *See under* Chu, M-L., **310,** 337
Rampino, M R. Sulphur-rich volcanic eruptions and stratospheric aerosols (*with* Self, S) *Letter to Nature,* **310,** 677
Raven, J A. *See under* Keeley, J E., **310,** 694
Raven, P H. Bacterial problems, *Correspondence,* **310,** 96
Ravetz, J R. Nuclear power, *Correspondence,* **310,** 446
  Book review of The citation process (*by* Cronin, B,) **310,** 607
Ready, A R. Successful transplantation of deoxyguanosine-treated embryonic thymus expressing class II antigens across major histocompatibility barrier (*with* Jenkinson, E J, Kingston, R, Owen, J J T) *Letter to Nature,* **310,** 231
Reedy, M C. *See under* Taylor, K A., **310,** 285
Reedy, M K. *See under* Taylor, K A., **310,** 285
Rees, C E. *Book review of* The global biogeochemical sulphur cycle (Ivanov, M V, Freney, J R *editors*) **310,** 607
Reid, M J. *See under* Molnar, L A., **310,** 662
Reiman, E M. A focal brain abnormality in panic disorder, a severe form of anxiety (*with* Raichle, M E, Butler, F K, Herscovitch, P, Robins, E) *Letter to Nature,* **310,** 683
Rich, V. Soviet refusnik, *News,* **310,** 4
  Eastern bloc trade: Comecon sets store in science, *News,* **310,** 6
  Israeli science: Ministry's fate in voters' hands, *News,* **310,** 6
  Soviet emigré case not resolved, *News,* **310,** 89
  Chinese research administration: Relics of cultural revolution, *News,* **310,** 92
  Polish science: Administration changes afoot, *News,* **310,** 92
  Yugoslav dissent: Physicist's passport confiscated, *News,* **310,** 93
  Indo-Soviet yoga: Space exercises still up aloft, *News,* **310,** 94
  New Polish university proposed, *News,* **310,** 175
  Afghan students, *News,* **310,** 357
  Romanian technology: Neglected by West and East, *News,* **310,** 441
  Soviet Union: More institutional inefficiency, *News,* **310,** 444
  Sakharovs: More anxiety in West, *News,* **310,** 532
  Albanian universities: Old problems found anew, *News,* **310,** 616
  See under Walgate, R., **310,** 617
  Soviet education: What prospects for reform?, *News,* **310,** 719
  Polish geology: Government policy attacked, *News,* **310,** 721
  Palaeontology: Hungarian flint-mine found, *News,* **310,** 721
Richard, S. *See under* Nerbonne, J M., **310,** 74
Richards, A J. Plant ecology: The sex life of primroses, *News and views,* **310,** 12
Richards, B M. *See under* Houamed, K M., **310,** 318
Richardson, S H. Origin of diamonds in old enriched mantle (*with* Gurney, J J, Erlank, A J, Harris, J W) *Article,* **310,** 198
Richey, B. *See under* Gill, S J., **310,** 160
Rickinson, A. Virology: Epstein-Barr virus in epithelium, *News and views,* **310,** 99
Roberts, A B. Editor, The retinoids (two volumes), *Book review by* Goodwin, T W. **310,** 520
Roberts, K V. *See under* Duvall, T L., **310,** 19
Robertson, D S. Relativistic deflection of radio signals in the solar gravitational field measured with VLBI (*with* Carter, W E) *Letter to Nature,* **310,** 572
Robins, E. *See under* Reiman, E M., **310,** 683
Robinson, L J. Jumping the gun, *Correspondence,* **310,** 536
Robinson, M A. Erratum: Holocene alluviation and hydrology in the upper Thames basin (*with* Lambrick, G H) *Letter to Nature,* **310,** 340
Robock, A. Snow and ice feedbacks prolong effects of nuclear winter, *Letter to Nature,* **310,** 667
Roche, P F. *See under* Aitken, D K., **310,** 660
Rodgers, C S. *See under* Hulten, M., **310,** 456
Rogers, N. Earth science: New date for diamonds (*with* Hawkesworth, C) *News and views,* **310,** 187
Rose, K R. *See under* Schardl, C L., **310,** 292
Rose, S. Trouble whipping up, *Correspondence,* **310,** 178
  Not in our genes: Biology, ideology, and human nature, *Book review by* Medawar, P B. **310,** 255
Rosenthal, A. Regulated expression of an introduced MHC $H\text{-}2K^{bm1}$ gene in murine embryonal carcinoma cells (*with* Wright, S, Cedar, H, Flavell, R, Grosveld, F) *Letter to Nature,* **310,** 415
Rosewell, J. *See under* Shorrocks, B., **310,** 310
Roth, E B. *Book review of* The state and nuclear power: Conflict and control in the Western world (*by* Camilleri, J U A,) **310,** 342
Rothschild, Lord. Random variables, *Book review by* Cooper, W. **310,** 436
Rothwell, J C. *See under* Dick, J P R., **310,** 407
Rundle, C C. *See under* Aldiss, D T., **310,** 302
Ruschin, S. *See under* Besant, L X., **310,** 358
Rutishauser, U. *See under* Schlosshauer, B., **310,** 141
  Developmental biology of a neural cell adhesion molecule, *Review article,* **310,** 549
Rycroft, M J. Solar terrestrial physics: Global geospace study (*with* Smith, A J, Jones, D, Dudeney, J R, Shawhan, S D) *News and views,* **310,** 449
Saigo, K. *See under* Inouye, S., **310,** 332
Saint, R B. *See under* Coppel, R L., **310,** 789
Sams, C F. Predicted structure of the sugar-binding site of the *lac* repressor (*with* Vyas, N K, Quiocho, F A, Matthews, K S) *Letter to Nature,* **310,** 429
Sanchez-Pescador, R. *See under* Bell, G I., **310,** 775
Sank, V J. *See under* Silver, M S., **310,** 681
Sanyal, G. Science in India discussed, *Correspondence,* **310,** 8
Sapsai, A. East-West relations, *Correspondence,* **310,** 446
Satchler, G R. Direct nuclear reactions, *Book review by* Hodgson, P E. **310,** 258
Satchwell, S C. *See under* Baer, R., **310,** 207
Sauterer, R. *See under* Christensen, K., **310,** 150
Schafran, G C. *See under* Driscoll, C T., **310,** 308
Schardl, C L. Linearization of maize mitochondrial chromosomes by recombination with linear episomes (*with* Lonsdale, D M, Pring, D R, Rose, K R) *Article,* **310,** 292
Schell, J. *See under* Herrera-Estrella, L., **310,** 115
Schleifer, S J. Brain, behaviour and the immune system (*with* Keller, S E, Stein, M) *Scientific correspondence,* **310,** 256
Schliwa, M. *See under* Euteneuer, U., **310,** 58
Schlosshauer, B. Topological distribution of different forms of neural cell adhesion molecule in the developing chick visual system (*with* Schwartz, U, Rutishauser, U) *Letter to Nature* **310,** 141
Schmid, E. *See under* Fyfe, W F., **310,** 537
Schneider, S H. *See under* Gilliland, R L., **310,** 38
  The coevolution of climate and life, *Book review by* Wigley, T M L **310,** 517
  See under Thompson, S L., **310,** 625
Schrader, J W. *See under* Wong, G H W., **310,** 688
Schramm, D N. *See under* Krauss, L M., **310,** 193
Schultheiss, P J. *See under* Freeman, I J., **310,** 13[illegible]
Schwartz, U. *See under* Schlosshauer, B., **310,** 141
Scott, J. *See under* Bell, G I., **310,** 775
  See under Tricoli, J V., **310,** 784
Scott, M P. *See under* Laughon, A., **310,** 25
Scott, R W. Tissue-specific activation of a cloned α-fetoprotein gene during differentiation of a transfected embryonal carcinoma cell line (*with* Vogt, T F, Croke, M E, Tilghman, S M) *Article* **310,** 562
Sefton, B M. *See under* Kamps, M P., **310,** 589
Séguin, C. *See under* Baer, R., **310,** 207
Sejrup, H P. Amino acid epimerization implies rapid sedimentation rates in Arctic Ocean cores (*with* Miller, G H, Brigham-Grette, J, Lovlie, R, Hopkins, D) *Letter to Nature,* **310,** 772
Selden, A C. All Greek to me, *Correspondence,* **310,** 96
Self, S. *See under* Rampino, M R., **310,** 677
Sellar, J. UK nuclear tests: Another Australian inquiry, *News* **310,** 90
  Uranium: Australian exports continue, *News* **310,** 354
  Agent Orange: Australian study continues, *News* **310,** 533
Shackleton, N J. *See under* Wintle, A G., **310,** 491
  See under Pisias, N G., **310,** 757
Shampay, J. DNA sequences of telomeres maintained in yeast (*with* Szostak, J W, Blackburn, E H) *Letter to Nature* **310,** 154
Shapley, R M. *See under* Tranchina, D., **310,** 314
Shawhan, S D. *See under* Rycroft, M J., **310,** 449
Shay, T J. Turbulence in an oceanic convective mixed layer (*with* Gregg, M C) *Article,* **310,** 282
Shearer, G M. Semen polyamines in AIDS pathogenesis (*with* Rabson, A) *Scientific correspondence* **310,** 103
Sheetz, M P. *See under* Turner, P R., **310,** 414
Sheng, K L. *See under* Foti, G., **310,** 126
Shepherd, J C W. Fly and frog homoeo domains show homologies with yeast mating type regulatory proteins (*with* McGinnis, W, Carrasco, A E, De Robertis, E M, Gehring, W J) *Letter to Nature,* **310,** 70
Sherman, S M. *See under* Sur, M., **310,** 246
Shettleworth, S J. *Book review of* Adaptive behavior and learning (*by* Staddon, J E R,) **310,** 801
  Book review of Conditioning and associative learning (*by* Mackintosh, N J,) **310,** 801
Shields, R. Gene regulation: Throwing light on plant genes, *News and views,* **310,** 98
Shirey, S B. Mantle-derived Archaean monozodiorites and trachyandesites (*with* Hanson, G N) *Letter to Nature,* **310,** 222
Shore, M J. A seismic *Q*-profile for the lower mantle from short-period P waves, *Letter to Nature,* **310,** 399
Shorrocks, B. Interspecific competition is not a major organizing force in many insect communities (*with* Rosewell, J, Edwards, K, Atkinson, W) *Letter to Nature,* **310,** 310
Showman, R M. *See under* Raff, R A., **310,** 312
Shows, T B. *See under* Tricoli, J V., **310,** 784
Sibatani, A. PhD glut in Japan, *Correspondence,* **310,** 619
Sikora, K. Monoclonal antibodies, *Book review by* Anderton, B. **310,** 256
Silver, M S. Selective population inversion in NMR (*with* Joseph, R I, Chen, C-N, Sank, V J, Hoult, D I) *Letter to Nature,* **310,** 681
Silvertown, J. Plant life history: Death of the classic biennial, *News and views,* **310,** 271
Simmonds, H A. Two views on UK research, *News* **310,** 620
Singer, B. Molecular biology of mutagens and carcinogens, *Book review by* Venitt, S. **310,** 520
Singer, S F. Is the "nuclear winter" real?, *Commentary,* **310,** 625

Singmaster, D. *Book review of* Wheels, life and other mathematical amusements (*by* Gardner, M,) **310,** 521
Skirboll, L R. *See under* Mezey, E., **310,** 140
Skoultchi, A I. *See under* Lachman, H M., **310,** 592
Slack, J. Developmental biology: A Rosetta stone for pattern formation in animals?, *News and views,* **310,** 364
Slobodchikoff, C N. Editor, A new ecology: Novel approaches to interactive systems, *Book review by* Crawley, M J. **310,** 168
Smart, T G. *See under* Houamed, K M., **310,** 318
Smedley, H M. Monoclonal antibodies, *Book review by* Anderton, B. **310,** 256
Smit, J. Siderophile-rich magnetic spheroids from the Cretaceous-Tertiary Boundary in Umbria, Italy (*with* Kyte, F T) *Letter to Nature,* **310,** 403
Smith, A J. *See under* Rycroft, M J., **310,** 449
Smith, D C. Coesite in clinopyroxene in the Caledonides and its implications for geodynamics, *Article,* **310,** 641
Smith, S B. *Book review of* The great mental calculators: The psychology, methods, and lives of calculating prodigies past and present **310,** 79
Snelling, N J. The geochronology and evolution of Africa, *Book review by* Grant, N K. **310,** 78
Snyder, S H. *See under* Lo, M M S., **310,** 792
Sofue, Y. A radio lobe over the galactic centre (*with* Handa, T) *Letter to Nature,* **310,** 568
Somero, G N. Biochemical adaptation, *Book review by* Cornish-Bowden, A. **310,** 804
Sommerville, J. Molecular genetics: RNA polymerase I promoters and transcription factors, *News and views,* **310,** 189
Sonnabend, J A. Caution on AIDS viruses, *Scientific correspondence,* **310,** 103
Southwood, R. Insects on plants: Community patterns and mechanisms, *Book review by* Wratten, S D. **310;** 343
Sowa, J F. Conceptual structures: Information processing in mind and machine, *Book review by* Fox, J. **310,** 437
Spandidos, D A. Malignant transformation of early passage rodent cells by a single mutated human oncogene (*with* Wilkie, N M) *Article,* **310,** 469
Sparks, D L. *See under* Jay, M F., **310,** 340
Sparks, R S J. *See under* Druitt, T H., **310,** 679
Spencer, M. Bacterial motion: Surprises from halobacteria, *News and views,* **310,** 367
Spera, F J. Mass transfer rates along vertical walls in magma chambers and marginal upwelling (*with* Yuen, D A, Kemp, D V) *Letter to Nature,* **310,** 764
Spitzer, J J. A re-interpretation of hydration forces near charged surfaces, *Letter to Nature,* **310,** 396
Spooncer, E. Continuous *in vitro* generation of multipotential stem cell clones from src-infected cultures (*with* Boettiger, D, Dexter, T M) *Letter to Nature,* **310,** 228
Sporn, M B. Editor, The retinoids (two volumes), *Book review by* Goodwin, T W. **310,** 520
Staal, G E J. *See under* Beemer, F A., **310,** 731
Stace, C A. *See under* Diamond, R M., **310,** 457
Stacey, D W. Transformation of NIH 3T3 cells by microinjection of Ha-*ras* p21 protein (*with* Kung, H-F) *Letter to Nature,* **310,** 508
Staddon, J E R. Adaptive behavior and learning, *Book review by* Shettleworth, S J. **310,** 801
Stanton, L W. Nucleotide sequence comparison of normal and translocated murine c-*myc* genes (*with* Fahrlander, P D, Tesser, P M, Marcu, K B) *Letter to Nature,* **310,** 423
Stebbins, A. *See under* Kaiser, N., **310,** 391
Stehelin, D. *See under* de Taisne, C., **310,** 581
Stein, M. *See under* Schleifer, S J., **310,** 456
Stemplen, M M. *See under* Bell, G I., **310,** 775
Stengers, I. Order out of chaos: Man's new dialogue with nature, *Book review by* Penrose, O. **310,** 341
Stephens, F S. *See under* Diamond, R M., **310,** 457
Stern, C D. *See under* Keynes, R J., **310,** 786
Sternberg, M J E. *See under* Travers, P., **310,** 235
Stewart, I. Mathematics: Three conjectures in one blow, *News and views,* **310,** 729
Stewart, T. *See under* Armelin, H A., **310,** 655
Stiles, C D. *See under* Armelin, H A., **310,** 655
Stites, D P. *See under* Bendheim, P E., **310,** 418
Storb, U. High expression of cloned immunoglobulin κ gene in transgenic mice is restricted to B lymphocytes (*with* O'Brien, R L, McMullen, M D, Gollahon, K A, Brinster, R L) *Letter to Nature,* **310,** 238
Stossel, T P. *See under* Brady, S T., **310,** 56
Stout, J T. *See under* Yang, T P., **310,** 412
Strathern, J N. *See under* Klar, A J S., **310,** 744
Strazzulla, G. *See under* Foti, G., **310,** 126
Strelloff, D. *See under* Flock, Å., **310,** 597
Strittmatter, S M. *See under* Lo, M M S., **310,** 792
Strong, D F. *See under* Irving, E., **310,** 762
Strong, D R. Insects on plants: Community patterns and mechanisms, *Book review by* Wratten, S D. **310,** 343
Struhl, G. Developmental biology: A universal genetic key to body plan?, *News and views,* **310,** 10
Stuntz, W E. *See under* Leming, T D., **310,** 136
Suciu-Foca, N. *See under* Yoshikai, Y., **310,** 506
Sugimura, T. *See under* Makino, R., **310,** 697
Sunde, N. Brain grafts can restore irradiation-damaged neuronal connections in newborn rats (*with* Laurberg, S, Zimmer, J) *Letter to Nature,* **310,** 51
Sur, M. Development of X- and Y-cell retinogeniculate terminations in kittens (*with* Weller, R E, Sherman, S M) *Letter to Nature,* **310,** 246
Sutherland, S. *Book review of* Ghosts in the mind's machine: Creating and using images in the brain (*by* Kosslyn, S M,) **310,** 344
Sylwester, J. Variation in observed coronal calcium abundance of X-ray flare plasmas (*with* Lemen, J R, Mewe, R) *Letter to Nature,* **310,** 665
Szostak, J W. *See under* Shampay, J., **310,** 154
Szulmcjster, J. Science in India discussed, *Correspondence,* **310,** 8
Tabor, M. Modern dynamics and classical analysis, *Review article,* **310,** 277
Tanaka, H. *See under* Hoshino, H., **310,** 324
Tanaka, I. 3-Å resolution structure of a protein with histone-like properties in prokaryotes (*with* Appelt, K, Dijk, J, White, S W, Wilson, K S) *Article,* **310,** 376
Tanaka, J. *See under* Kijima, T., **310,** 45
Tang, T B. Electrical neutrality of atoms, *Scientific correspondence,* **310,** 635
Tarling, D H. *Book review of* The Earth's magnetic field (*by* Merrill, R T, McElhinny, M W,) **310,** 436
Book review of Reversals of the Earth's magnetic field (*by* Jacobs, J A,) **310,** 436
Tarney, J. *See under* Weaver, B L., **310,** 575
Tayler, R J. *Book review of* Superstars: How stellar explosions shape the destiny of our Universe (*by* Clark, D H,) **310,** 706
Taylor, K. *See under* Phillips, M M., **310,** 554
Taylor, K A. Three-dimensional reconstruction of rigor insect flight muscle from tilted thin sections (*with* Reedy, M C, Cordova, L, Reedy, M K) *Article,* **310,** 285
Taylor, S R. Planetary science: Source of the oldest lunar basalt, *News and views,* **310,** 98
Taylor, S S. *See under* Kamps, M P., **310,** 589
Teem, J M. Kitt Peak, *Correspondence,* **310,** 536
Teller, E. Widespread after-effects of nuclear war, *Commentary,* **310,** 621
Tempst, P. *See under* Hunkapiller, M., **310,** 105
Terborgh, J. Five new world primates: A study in comparative ecology, *Book review by* Martin, R D. **310,** 707
Tesser, P M. *See under* Stanton, L W., **310,** 423
Thomas, J B. From grasshopper to *Drosophila*: a common plan for neuronal development (*with* Bastiani, M J, Bate, M, Goodman, C S) *Article,* **310,** 203
Thomas, N. Two views on UK research, *Correspondence,* **310,** 620
Thompson, S L. *See under* Barron, E J., **310,** 574
Is the "nuclear winter" real? Reply (*with* Schneider, S H, Covey, C) *Commentary,* **310,** 625
Thorpe, S A. Oceanography: Probing beneath the waves, *News and views,* **310,** 274
Tiddens, H. *See under* Weiss, E H., **310,** 650
Tilghman, S. *See under* Scott, R W., **310,** 562
Timko, M. *See under* Herrera-Estrella, L., **310,** 115
Toh, B H. *See under* Lim, A T W., **310,** 61
Tonegawa, S. *See under* Gillies, S D., **310,** 594
Toothill, C. *See under* Elwood, P C., **310,** 138
Torda, T. *See under* Pybus, A., **310,** 636
Townsend, P. *Book review of* Quantum theory of gravity: Essays in honor of the 60th birthday of Bryce S DeWitt (Christensen, S M *editor*) **310,** 804
Toyka, K V. *See under* Hohlfeld, R., **310,** 244
Tranchina, D. Retinal light adaptation - evidence for a feedback mechanism (*with* Gordon, J, Shapley, R M) *Letter to Nature,* **310,** 314
Travers, P. Structural and evolutionary analysis of *HLA-D*-region products (*with* Blundell, T L, Sternberg, M J E, Bodmer, W F) *Letter to Nature,* **310,** 235
Tricoli, J V. Localization of insulin-like growth factor genes to human chromosomes 11 and 12 (*with* Rall, L B, Scott, J, Bell, G I, Shows, T B) *Letter to Nature,* **310,** 784
Trimble, V. Scientific articles: A controllable aspect of the information explosion?, *News and views,* **310,** 542
Astronomy: Nucleosynthesis in barium stars, *News and views,* **310,** 633
Tsang, C F. *See under* Fyfe, W F., **310,** 537
Tsong, T Y. *See under* Lo, M M S., **310,** 792
Tsuboi, M. *Book review of* Applications of infrared, Raman, and resonance Raman spectroscopy in biochemistry (*by* Parker, F S,) **310,** 345
Tsvelev, N N. *See under* Diamond, R M., **310,** 457
Tuffnell, P S. *See under* Baer, R., **310,** 207
Tümer, O T. γ Rays of 0.3-30 MeV from PSR0833-45 (*with* Dayton, B, Long, J, O'Neill, T, Zych, A, White, R S) *Letter to Nature,* **310,** 214
Tung, H Y L. *See under* Hemmings, H C., **310,** 503
Turner, P R. Fertilization increases the polyphosphoinositide content of sea urchin eggs (*with* Sheetz, M P, Jaffe, L A) *Letter to Nature,* **310,** 414
Tye, B-K. *See under* Walmsley, R W., **310,** 157
Ubell, R. *Book review of* The medical industrial complex (*by* Wohl, S,) **310,** 438
Ullrich, A. *See under* Dull, T J., **310,** 777
See under Brissenden, J E., **310,** 781
Uyeda, S. *See under* Fyfe, W F., **310,** 537
Vail, J R. The geochronology and evolution of Africa, *Book review by* Grant, N K. **310,** 78
Van Couvering, J A. Editor, Catastrophes and Earth history: The new uniformitarianism, *Book review by* Hallam, A. **310,** 435
Van Montagu, M. *See under* Herrera-Estrella, L., **310,** 115
Van Veelen, C W M. *See under* Beemer, F A., **310,** 731
Van den Broeck, G. *See under* Herrera-Estrella, L., **310,** 115
Vassos, B H. Electroanalytical chemistry, *Book review by* Compton, R. **310,** 519
Veal, D A. Associative cellulolysis and dinitrogen fixation by co-cultures of *Trichoderma harzianum* and *Clostridium butyricum* (*with* Lynch, J M) *Letter to Nature,* **310,** 695
Veeh, H H. *See under* Aharon, P., **310,** 340
Velde, B. *See under* Fyfe, W F., **310,** 537
Venitt, S. *Book review of* Molecular biology of mutagens and carcinogens (*by* Singer, B, Grunberger, D,) **310,** 520
Visser, G M. *See under* Joyce, G F., **310,** 602
Vlodavsky, I. *See under* Naparstek, Y., **310,** 241
Vogt, T F. *See under* Scott, R W., **310,** 562
Vousden, K H. *See under* Marshall, C J., **310,** 586
Vuas, N K. *See under* Sams, C F., **310,** 429
Vucinich, A. Empire of knowledge: The Academy of Sciences of the USSR (1917-1970), *Book review by* Ashby, E. **310,** 77
Vyas, N K. *See under* Quiocho, F A., **310,** 381
van Boeckel, C A A. *See under* Joyce, G F., **310,** 602
van Boom, J H. *See under* Joyce, G F., **310,** 602
van Duin, M. *See under* Westerveld, A., **310,** 425
van Herk, G. De Leidse Sterrewacht: Vier eeuwen wacht bij dag en bij nacht, *Book review by* Bosma, P B. **310,** 169
van Westrenen, J. *See under* Joyce, G F., **310,** 602
Waber, P G. *See under* Kazazian, H H., **310,** 152
Wakeham, S G. Dimethyl sulphide in a stratified coastal salt pond (*with* Howes, B I, Dacey, J W H) *Letter to Nature,* **310,** 770
Walbridge, E. Angle constraint for nuclear-pumped X-ray laser weapons, *Commentary,* **310,** 180
Walgate, R. Bombs and rockets, *News,* **310,** 443
French research: Agenda for a new minister, *News,* **310,** 534
Acid rain: Allies for UK government, *News,* **310,** 535
Mason's own view, *News,* **310,** 535
Particle physics: Higgs discovery at DESY?, *News and views,* **310,** 546
Visa protests: Who will go to Prague? (*with* Rich, V) *News,* **310,** 617
Particle physics: *Der Spiegel* makes trouble, *News,* **310,** 617
Uranium shipment: Soviet contract nobody wants, *News,* **310,** 720
Walker, D M C. *See under* King-Hele, D G., **310,** 218
Wallace, P T. *See under* Manchester, R N., **310,** 569
Walmsley, R M. Unusual DNA sequences associated with the ends of yeast chromosomes (*with* Chan, C S M, Tye, B-K, Petes, T D) *Letter to Nature,* **310,** 157
Walters, S M, *et al.*. **Editor,** The European garden flora. Vol. II Monocotyledons (Part II), *Book review by* Moore, P D. **310,** 344
Walton, D. Re-evaluation of Greek archaeomagnitudes, *Article,* **310,** 740
Warman, J M. Microwave probing of electronic processes in small particle suspensions (*with* de Haas, M P, Grätzel, M, Infelta, P P) *Letter to Nature,* **310,** 305
Weatherall, D. Gene transfection: A step nearer gene therapy?, *News and views,* **310,** 451
Weatherall, D J. *Book review of* The encyclopaedia of medical ignorance: Exploring the frontiers of medical knowledge (Duncan, R, Weston-Smith, M *editors*) **310,** 257
Weaver, B L. Empirical approach to estimating the composition of the continental crust (*with* Tarney, J) *Letter to Nature,* **310,** 575
Wegener, G. *See under* Hut, P., **310,** 637
Weil, A. Number theory: An approach through history from Hammurapi to Legendre, *Book review by* Kilmister, C W. **310,** 168
Weiler, E W. *See under* Hornberg, C., **310,** 321
Weinberg, A M. *See under* Barkenbus, J N., **310,** 95
Weis, R M. Two-dimensional chiral crystals of phospholipid (*with* McConnell, H M) *Letter to Nature,* **310,** 47
Weiss, E H. Organization and evolution of the class I gene family in the major histocompatibility complex of the C57BL/10 mouse (*with* Golden, L, Fahrner, K, Mellor, A L, Devlin, J J, Bullman, H, Tiddens, H, Bud, H, Flavell, R A) *Article,* **310,** 650
Weiss, R. Virology: Tissue-specific transformation by human T-cell leukaemia virus, *News and views,* **310,** 273
Weissbuch, I. Spontaneous generation and amplification of optical activity in α-amino acids by enantioselective occlusion into centrosymmetric crystals of glycine (*with* Addadi, L, Berkovitch-Yellin, Z, Gati, E, Lahav, M, Leiserowitz, L) *Letter to Nature,* **310,** 161
Weller, R E. *See under* Sur, M., **310,** 246
Wells, D E. *See under* Raff, R A., **310,** 312
Westerveld, A. Molecular cloning of a human DNA repair gene (*with* Hoeijmakers, J H J, van Duin, M, de Wit, J, Odijk, H, Pastink, A, Wood, R D, Bootsma, D) *Letter to Nature,* **310,** 425
Weston-Smith, M. Editor, The encyclopaedia of medical ignorance: Exploring the frontiers of medical knowledge, *Book review by* Weatherall, D J. **310,** 257
Whalley, E. *See under* Mishima, O., **310,** 393
White, A. A crustal conductor on Eyre Peninsula, South Australia (*with* Milligan, P R) *Letter to Nature,* **310,** 219
White, R H. Hydrolytic stability of biomolecules at high temperatures and its implication for life at 250°C, *Letter to Nature,* **310,** 430
White, R S. *See under* Tümer, O T., **310,** 214
White, S D M. *See under* Hut, P., **310,** 637
White, S W. *See under* Tanaka, I., **310,** 376
Wiegeret, R G. *Book review of* Systems ecology: An introduction (*by* Odum, H T,) **310,** 706
Wigley, T M L. *Book review of* The coevolution of climate and life (*by* Schneider, S H, Londer, R,) **310,** 517
Wilkie, N M. *See under* Spandidos, D A., **310,** 469
Williams, A G. A three-dimensional model of the fluid dynamics of radio-trail sources (*with* Gall, S F) *Letter to Nature,* **310,** 33
Williams, C. *See under* Chu, M-L., **310,** 337
Williams, D A. Introduction of new genetic material into pluripotent haematopoietic stem cells of the mouse (*with* Lemischka, I R, Nathan, D G, Mulligan, R C) *Article,* **310,** 476
Williams, D F. *See under* Fillon, R H., **310,** 674
Williamson, J D. Semen polyamines in AIDS pathogenesis, *Scientific correspondence,* **310,** 103
Willumsen, B M. The p21 *ras* C-terminus is required for transformation and membrane association (*with* Christensen, A, Hubbert, N

L, Papageorge, A G, Lowy, D R) *Letter to Nature,* **310**, 583
Wilson, K S. *See under* Tanaka, L, **310**, 376
Winter, M B. *See under* Aitken, M J., **310**, 305
Wintle, A G. Thermoluminescence dating of periods of loess deposition and soil formation in Normandy (*with* Shackleton, N J, Lautridou, J P) *Letter to Nature,* **310**, 491
Wohl, S. The medical industrial complex, *Book review by* Ubell, R. **310**, 438
Woledge, R C. Handbook of physiology: Section 10, Skeletal muscle (*with* Peachey, L D, Adrian, R H, Geiger, S R) *Letter to Nature,* **310**, 170
Wong, G H W. Inducible expression of H-2 and Ia antigens on brain cells (*with* Bartlett, P F, Clark-Lewis, I, Battye, F, Schrader, J W) *Letter to Nature,* **310**, 688
Wood, R D. *See under* Westerveld, A., **310**, 425
Wootton, J C. *See under* Bull, J H., **310**, 701
Worsley, P. *Book review of* Geomorphology of Europe (Embleton, C *editor*) **310**, 709
Wratten, S D. *Book review of* Insects on plants: Community patterns and mechanisms (*by* Strong, D R, Lawton, J H, Southwood, R,) **310**, 343
Wright, G S. *See un*[illegible] Graham, J R., **310**, 213
Wright, P B. Possible role of cloudiness in the persistence of the Southern Oscillation *Letter* [illegible] **310**, 128
Wright, S. *See under* Rosen[illegible] A., **310**, 415
Yamada, Y. Conservation of the sizes for one but not another class of exons in two chick collagen genes (*with* Liau, G, Mudryj, M, Obici, S, de Crombrugghe, B) *Letter to Nature,* **310**, 333
Yanagi, Y. *See under* Yoshikai, Y., **310**, 506
Yang, T P. Molecular evidence for new mutation at the *hprt* locus in Lesch-Nyhan patients (*with* Patel, P I, Chinault, A C, Stout, J T, Jackson, L G, Hildebrand, B M, Caskey, C T) *Letter to Nature,* **310**, 412
n, H L. *See under* Brady, S T., **310**, 56
shikai, Y. Presence of T-cell receptor mRNA in functionally distinct T cells and elevation during intrathymic differentiation (*with* Yanagi, Y, Suciu-Foca, N, Mak, T W) *Letter to Nature,* **310**, 506
hikami, D. Staining of living presynaptic nerve terminals with selective fluorescent dyes (*with* Okun, L M) *Letter to Nature,* **310**, 53
Y g, R A. *See under* Longo, D L., **310**, 505
Y g, S W. Nuclear magnetic resonance imaging: Basic principles, *ook review by* Andrew, E R. **310**, 803
Youflan, H. *See under* Kazazian, H H., **310**, 152
Yu D A. *See under* Spera, F J., **310**, 764
Yu S. *See under* Inouye, S., **310**, 332
Yu Zadeh, F. Large, highly organized radio structures near the galtic centre (*with* Morris, M, Chance, D) *Article,* **310**, 557
Zac, H G. *See under* Falkner, F G., **310**, 71
Zim J M. Absentees from Prague meeting, *Correspondence,* **310**, 9
Zimr, J. *See under* Sunde, N., **310**, 51
Zych, *See under* Tümer, O T., **310**, 214

Nature Indexes

AUTHOR indexes covering each successive volume of *Nature* appear once every two months and are printed as part of the journal. Author indexes have appeared in the following issues: 19 April (Vol. 307); 7 June (Vol. 308); 26 July (Vol. 309). At the end of the year, *Nature* publishes an annual author/subject index distributed separately from weekly issues of the journal. The next subject index will appear early in January 1985.

TWO NEW reliable, up-to-date and complete biotechnology information resources.

Essential aids for everyone concerned with both the old and new biotechnologies — will save you valuable time and money.

EXAMINE ON FREE APPROVAL WITHOUT COMMITMENT

Detailed information on every aspect of biotechnology worldwide

An indispensable guide to:

- ★ Products, services and research worldwide.
- ★ Companies worldwide.
- ★ Government and international agencies worldwide.
- ★ Information sources worldwide.

This **new** world directory, compiled by the eminent biotechnologist Dr. Jim Coombs, provides a mass of authoritative information about **the entire biotechnology industry worldwide.**

Unlike other directories, THE INTERNATIONAL BIOTECHNOLOGY DIRECTORY 1984 —

- is thoroughly international
- features a unique BUYER'S GUIDE to products, research and services
- covers both the old and new biotechnologies

4638

The Directory tells you:

- ★ Who your competition is, and what they are doing.
- ★ Who are potential customers and suppliers.
- ★ Where to buy equipment, chemicals and services.
- ★ Where culture collections are located and what cultures they hold.
- ★ Where to get plants built.
- ★ Who imports/exports biotechnology products in over 20 countries.
- ★ What consultancy services are available.
- ★ Which government departments are associated with biotechnology, and their programmes.

Authoritative author

Dr. Jim Coombs is a Member of the Organising Committee of Biotech 83 and of Bio-Energy 1984, and Scientific Secretary of the Third European Community Energy from Biomass Conference 1984. He is editor of *Biomass* and Joint Secretary of the BABA.

The Directory is designed for use across the whole biotechnology industry by scientists and researchers, sales managers, buyers and consultants. Here you will find: over 2,000 organisations — companies, universities and research centres — listed by country. Government agencies and programmes — listed by country. Societies and associations — listed by country. Databases, journals and newsletters — listed alphabetically. Products listed under more than 1,000 headings.

All compiled by Dr. Coombs from a vast array of sources then meticulously cross-checked to ensure the reliability of the data. Now available to you on FREE APPROVAL.

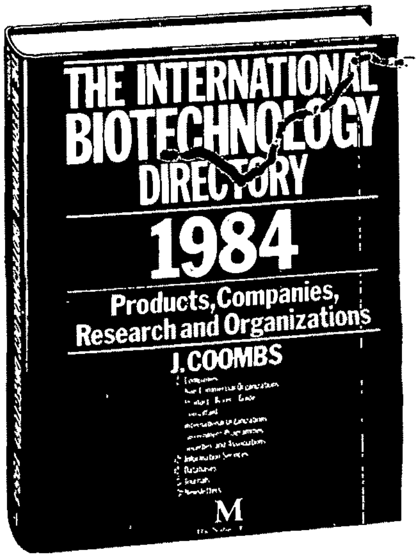
THE INTERNATIONAL BIOTECHNOLOGY DIRECTORY
1984
Products, Companies, Research and Organizations
J. COOMBS
M

Macmillan Hardcover 400pp
November 1983 ISBN 0 333 35140 1
£50.00/$100.00

The ONLY guide to the selection of cost-effective biotechnology information sources

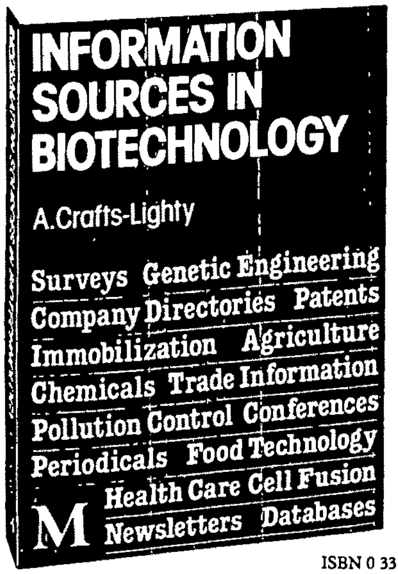
INFORMATION SOURCES IN BIOTECHNOLOGY
A. Crafts-Lighty
Surveys Genetic Engineering
Company Directories Patents
Immobilization Agriculture
Chemicals Trade Information
Pollution Control Conferences
Periodicals Food Technology
Health Care Cell Fusion
Newsletters Databases
M

Macmillan Paperback
320pp **September 1983**
ISBN 0 333 36178 4 **£40.00/$80.00**

Evaluates and assesses the whole range of information sources available.

- ★ covers both old and new technologies.
- ★ covers technical and commercial literature.
- ★ covers difficult and hard to trace sources.
- ★ includes over 20 at-a-glance evaluation tables.
- ★ provides an Index of publishers and their addresses.

Dr. Crafts-Lighty, Head of Information and Library Services at Celltech Limited, systematically and critically reviews all the important information sources:

• books • conferences • trade periodicals • research periodicals • computer databases • patents • market surveys • directories • organisations • secondary sources

'Information Sources in Biotechnology' is an invaluable guide to current technical, business and commercial biotechnology information sources for Researchers, Librarians, Information Officers, Businessmen, Investment Analysts, Investors, and Academic Researchers.

Send no money now.
Examine on FREE APPROVAL.

You can take both these new books for 30 days examination without commitment. Decide to keep either or both, then simply pay the accompanying invoice. If you are not completely satisfied, just return the book(s) in good condition within 30 days and that will be the end of the matter. Ensure prompt delivery by completing and returning the order form **now.**

Globe

Globe Book Services Limited,
Brunel Road, Houndmills,
Basingstoke, Hants RG21 2XS, England.
Telephone: Basingstoke (0256) 26222
A DIVISION OF MACMILLAN PUBLISHERS LTD.

The Nature Press,
15 E 26 Street, New York, N.Y. 10010.
Telephone: 212-532-4811

FREE APPROVAL ORDER FORM

To: Ian Jacobs, Globe Book Services Ltd.,
FREEPOST, Brunel Road, Houndmills,
Basingstoke, Hants RG21 2BR, England.
The Nature Press, 15 E 26 Street, New York.
N.Y. 10010. Credit card callers call toll-free
800-221-2123 (or in New York: 212-532-4811)

Please send me on 30 days FREE APPROVAL ______ copies of *The International Biotechnology Directory 1984* at £50.00/$100.00 each, and/or ______ copies of *Information Sources in Biotechnology* at £40.00/$80.00 each.

If I am not entirely satisfied, I may return the book(s) in good condition within 30 days and you will cancel my invoice.

Postage and packing
UK subscribers £2.00 (Overseas £3.00)
US Subscribers $1.50.

Tick preferred method of payment
☐ Bill me. I need send no money now.
☐ I enclose cheque for £/$______
☐ Charge my credit card on publication £/$______
☐ Visa ☐ Access/Mastercharge ☐ Am. Express ☐ Diners

Card No______
Expiry Date______

Signature ______
(Orders cannot be accepted without a signature.)

Name ______ (PLEASE PRINT)

Address ______

______

______

______

Postcode/Zip Code______
Books will be delivered to you on publication. N1

UK Subscribers POST TODAY — NO STAMP NEEDED